Virchows Arch (2001) 439:1–5
DOI 10.1007/s004280100401

ORIGINAL ARTICLE

**Andrea Tannapfel · Ulrich Stölzel · Erich Köstler
Steffi Melz · Matthias Richter · Volker Keim
Detlef Schuppan · Christian Wittekind**

C282Y and H63D mutation of the hemochromatosis gene in German porphyria cutanea tarda patients

Received: 6 September 2000 / Accepted: 20 December 2000 / Published online: 17 March 2001
© Springer-Verlag 2001

Abstract *Background and aims:* Patients with porphyria cutanea tarda (PCT) have a susceptibility to reversible inactivation of hepatocyte uroporphyrinogen decarboxylase, which can be triggered by alcohol, hepatitis C virus, and other agents. Inherited factors that may predispose to PCT include the C282Y mutation in the hemochromatosis (HFE) gene. *Methods*: We analyzed the hemochromatosis mutations C282Y and H63D in liver biopsies and serum samples of 190 German patients (mean age 48±12.5 years) with sporadic PCT. The hepatic iron concentration was determined within the liver tissue. Age-matched healthy blood donors (115 donors) served as controls. *Results*: The C282Y and H63D mutations were found in 75 (39%) and 85 (45%) of 190 patients with PCT, respectively. Twenty-two patients (12%) were homozygous for the C282Y mutation, and eighteen patients (9%) were compound heterozygotes, displaying both the C282Y and the H63D mutation. Within the control group, 3 of 115 patients were heterozygous for C282Y (3%) and 12 for H63D (10%). Serum and hepatic iron, ferritin, transferrin saturation, or liver enzymes did not differ significantly between patients with or without HFE mutations. *Conclusions*: The high frequency of homo- and heterozygosity for the C282Y and H63D alleles strongly suggests that these mutations are important predisposing factors for PCT in German patients.

Keywords HFE · Porphyria cutanea tarda · Control · German patients

A. Tannapfel · S. Melz · C. Wittekind (✉)
Institute of Pathology, University of Leipzig, Liebigstrasse 26, 04103 Leipzig, Germany
e-mail: tana@medizin.uni-leipzig.de
Tel.: +49-341-9715000, Fax: +49-341-9715009

U. Stölzel · M. Richter
Department of Gastroenterology, Dr. Drogula-Kliniken, 04720 Döbeln, Germany

E. Köstler
Department of Dermatology, Städtisches Klinikum Dresden-Friedrichstadt, 01008 Dresden, Germany

V. Keim
Clinic for Internal Medicine II, University of Leipzig, Ph.-Rosenthal-Strasse 27, 04103 Leipzig, Germany

D. Schuppan
Department of Medicine I, University of Erlangen-Nuremberg, Krankenhausstrasse 12, 91054 Erlangen, Germany

Introduction

Sporadic porphyria cutanea tarda (PCT) is associated with decreased activity of the enzyme uroporphyrinogen decarboxylase (URO-D) in the liver, leading to characteristic alterations of urinary heme precursors and to typical lesions on skin exposed to sunlight [5, 11, 13, 18, 19]. Hepatic siderosis and mild iron overload are common in PCT, and much evidence exists that iron is an essential inhibitory cofactor of URO-D in hepatocytes [13, 18, 19]. Furthermore, based on clinical studies, iron removal by means of phlebotomy is an efficient treatment of patients with PCT, resulting in a reversion of URO-D inhibition [18]. Alcohol, hormones, and drugs are well known trigger factors responsible for the precipitation of PCT and the associated hepatic alterations [5].

Recently, two findings renewed the discussion on PCT [2, 16, 17, 22]. First, a high proportion of antibodies to hepatitis C virus (HCV) has been reported in PCT patients, with an increasing gradient in HCV prevalence from Northern (8–10%) to Southern Europe (71–91%) [17, 22]. Thus, PCT has been considered a major extrahepatic manifestation of HCV infection in predisposed individuals from Southern Europe [2]. Although the relationship between HCV and PCT is strongly established, the details of the interaction are not yet clarified.

Second, a high frequency of the C282Y mutation in the HFE gene, the major genetic alteration in genetic hemochromatosis [9], has been found in PCT patients from Great Britain, Australia, Japan, Bulgaria and the United States (ranging from 44% to 52%) [2, 16,17, 22]. In an Italian study, however, the homozygous C282Y mutation

occurred as frequently in PCT patients as in control subjects (5%) [1], although the H63D mutation was found with a significantly increased frequency in PCT compared with controls [18, 19]. In Japanese and Bulgarian patients, no C282Y mutations were found [7, 9].

The studies presented so for have been based on a small number of patients [7, 9] and did not use healthy controls of the same local area for comparison of the frequencies of C282Y and H63D mutations. The aim of our study was, therefore, to investigate the role of C282Y and H63D mutations and indices of iron metabolism in German patients with PCT, among which only a low prevalence of HCV infection is observed. The results obtained were compared with the gene frequencies of age- and region-matched healthy German controls.

Patients and methods

PCT was diagnosed in special outpatient departments of dermatology clinics. We examined 190 consecutive patients with sporadic PCT (52 female and 138 male). Urinary porphyrins were separated by means of thin-layer chromatography and characterized using spectrophotometric absorption [4]. Using a questionnaire, daily alcohol consumption and intake of estrogens were recorded in all patients. Of the patients examined, 91 patients were found to have moderate alcohol consumption, and seven patients used oral contraceptives. At the time of serum sampling or liver biopsy, PCT was overt in all patients prior to medical treatment or venesection. Overt disease included typical skin lesions accompanied by characteristic proportions of urinary heme precursors. Clinical signs of hemochromatosis were not evident.

Serum samples were tested for anti-HCV by second generation enzyme-linked immunosorbent assay (ELISA; Abbott Laboratories, North Chicago, Ill.). In addition, all serum samples were tested for antibodies to HBcAg (anti-HBc) (ELISA; Abbott Laboratories), and anti-HBc-positive sera were further tested for antibodies to HBsAg (anti-HBs) and for HBsAg (ELISA; both by Abbott Laboratories). As a control group, randomly selected blood samples from 115 healthy volunteers of the same geographical area without any known liver or skin disease were used (median age 51 years; 61 male and 54 female).

In 32 cases, liver biopsies taken before therapy were available for histological analysis. The hepatic iron concentration was measured by means of atomic absorption spectrometry as described in the literature [15]. In our laboratory, the normal hepatic iron content is less than 2200 µg/g dry weight for men and less than 1600 µg/g dry weight for women. The upper range of normal for the hepatic iron index (HII), calculated as the tissue iron content (in µmol/g dry weight) divided by the patient's age (in years), is 1.0 µmol/g per year.

Genomic DNA was extracted from liver tissue and blood samples and used as template for a polymerase chain reaction (PCR)-based assay in which we tested the C282Y mutation and the H63D mutation. Amplification was performed with 150 ng of each oligonucleotide primer set and 2.5 U *Taq* polymerase (Boehringer, Ingelheim, Germany) in a final volume of 50 µl of the following solution: 0.5 mmol/l deoxynucleotide triphosphates, 67 mmol/l Tris, 16.6 mmol/l ammonium sulfate, 6.7 µmol/l ethylenediaminetetraacetic acid, 10 mmol/l β-mercaptoethanol, and 2 mmol/l $MgCl_2$. The primers for PCR amplification for the C282Y and H63D mutations were designed according to prepublished reports [14]: C282Y-forward (5′ TGG CAA GGG TAA ACA GAT CC 3′) and C282Y-reverse (5′ CTC AGG CAC TCC TCT CAA CC 3′), H63D-forward (5′ ACA TGG TTA AGG CCT GTT GC 3′), and H63D-reverse (5′ GCC ACA TCT GGC TTG AAA TT 3′).

Amplification was performed by annealing at 55°C for 2 min, extension at 72°C for 3 min, and denaturation at 95°C for 1 min. PCR products (sizes for C282Y and H63D: 388 bp and 200 bp, respectively) were digested with restriction enzymes *Rsa*I and *Mbo*I at 72°C. The C282Y mutation creates a new *Rsa*I restriction site, leading to two fragments (248 bp and 111 bp) for the wild type. Completeness of digestion was controlled with the invariant 248-bp fragment observed in all genotypes. The H63D mutation abolishes an *Mbo*I restriction site, resulting in two fragments (140 bp and 60 bp) for the wild type and no fragmentation (200 bp) for the homozygous mutant. Heterozygosity is characterized by the presence of both fragments. Digested PCR products were electrophoresed using 10% sodium dodecyl sulfate polyacrylamide gel electrophoresis (SDS-PAGE) and visualized with ethidium bromide staining. All PCR and digestion experiments were performed in triplicate.

The frequencies of the C282Y and H63D mutations in PCT patients were compared with the data obtained from the healthy controls and also with the reported control population frequencies in Germany [12, 17]. The significance of the differences between the frequencies of C282Y and H63D for PCT patients and controls was determined by $\chi 2$ analysis. Statistical significance of differences was determined using Student's *t*-test and Wilcoxon rank sum test. Comparisons between groups were performed following logarithmic transformation to normalize the distribution. The significance level was defined as $P<0.05$.

Results

Clinical and biochemical details of the 190 PCT patients included in our study are presented in Table 1. The C282Y mutation was present in 75 of 190 patients (39%). Fifty-three patients (28%) had a single copy of the C282Y mutation, whereas 22 patients (12%) were C282Y homozygotes. These patients had no clinical evidence of hemochromatosis. The frequency of the C282Y mutation was significantly increased in PCT subjects compared with controls (39% vs 3%, $P<0.001$). Of 190 patients, 82 (43%) of the PCT patients were found to be heterozygous for the H63D mutation, and three patients (2%) were H63D homozygotes. The frequency of any H63D mutation (homo- and heterozygous combined), was significantly higher in the PCT patients compared with the frequencies of 10% in our control group.

Eighteen patients with PCT were found to be compound heterozygotes, bearing both the C282Y and H63D mutations. Thus, the wild type for both HFE alleles was found in less than half of the 190 patients [$n=59$ (31%)] compared with 87% in the control group ($P<0.01$).

Within the control group, the C282Y mutation was found in 3 of 115 patients (3%), and 12 of them were heterozygous for H63D (10%). Homozygosity for C282Y or H63D was not found. Taken together, allele frequencies for the controls were comparable with those previously found in the German population [12, 15].

We found increased serum iron, ferritin, and transferrin saturation in the patients bearing the C282Y and H63D mutations. Thus, patients homozygous for C282Y, heterozygous for H63D, and compound heterozygous for C282Y and H63D exhibited a trend to higher levels of serum ferritin and iron concentrations relative to patients with the wild type of the HFE gene (Table 1). However, these differences were below statistical significance ($P=0.59$).

Table 1 Clinical and biochemical details of porphyria cutanea tarda (PCT) patients according to C282Y and H63D status. Data are presented as mean±SD unless specified otherwise. *HFE* haemochromatosis; *ALAT* alanine aminotransferase; *ASAT* aspartate aminotransferase; *Fe* iron; *WT* wild type, compound heterozygotes carrying each one allele with the C282Y and H63D mutations

	All patients	C282 Y heterozygotes (C282Y/WT)	C282Y homozygotes (C282Y/C282Y)	H63D heterozygotes (H63D/WT)	Compound heterozygotes (C282Y/H63D)	No HFE mutations (WT/WT)
Number of patients (%)	190	53 (28)	22 (12)	82 (43)[b]	18 (9)	59 (31)
Number of controls (%)	115	3 (3)	–	12 (10)	–	100 (87)
ALAT (range)[a]	1.12±0.64 (0.16–3.08)	1.06±0.60 (0.36–2.62)	1.01±0.59 (0.2–2.08)	1.07±0.61 (0.16–3.08)	1.32±0.67 (0.42–3.08)	1.19±0.66 (0.23–2.91)
ASAT (range)[a]	1.35±0.69 (0.22–5.25)	1.26±0.72 (0.22–3.08)	2.22±1.69 (0.32–5.25)	1.58±1.37 (0.22–5.12)	1.16±0.56	1.12±0.88 (0.27–4.96)
Transferrin saturation (%)[a]	47±18	55±19	61±19	44±13	52±14	45±18
Ferritin (µg/l) (range)[a]	882±782 (90–3581)	756±756 (90–2945)	1269±1158 (163–3581)	1048±927 (27–3582)	1176±1095 (28–2941)	826±667) (23–2497
Fe (µmol/l) [median±SD; (range)][a]	28.0±9.87 (4.6–52.0)	32.5±9.4 (15.6–52.0)	36.0±13.1 (13.8–48.2)	27.0±9.2 (6.5–51.9)	33.0±10.16 (16.4–51.9)	26.0±9.89 (4.60–48.00)

[a] Normal ranges: ALAT 117–350 nmol/s per liter; ASAT 117–450 nmol/s per liter; transferrin saturation 16–45%; ferritin 4–651 µg/l; Fe 7.2–21.5 µmol/l

[b] 82 patients were heterozygous for H63D, and three patients were homozygous

Table 2 Hepatic iron concentration according to C282Y and H63D status. Data are presented as mean±SD. *HII* hepatic iron index

	All patients	C282 Y heterozygotes (C282Y/WT)	C282Y homozygotes (C282Y/C282Y)	H63D heterozygotes (H63D/WT)	Compound heterozygotes (C282Y/H63D)	No HFE mutations (WT/WT)
Number of patients	32 (%)	12 (38%)	1 (3%)	19 (59%)	5 (16%)	1 (3%)
Transferrin saturation (%)[a]	45±15%	51±11%	58	42±16%	50±10%	45
Perl stain (medium range)[b]	2 (1–4)	2 (1–4)	4	3 (1–4)	3 (1–4)	2
HII[c]	0.99±0.62	0.58±0.31	1.54	1.16±0.68	1.43±0.54	0.94
Hepatic iron (µg/g)[d]	2256±852	2057±612	3097	3952±958	5251±1210	3546

[a] Normal ranges: transferrin saturation 16–45%

[b] Semiquantitative iron assessment (amount of stainable iron on a Perl's Prussian blue stain according to Scheuer et al [13]. 1 iron staining present in less than 25% of hepatocytes; 2 staining present in 25–75% of hepatocytes; 3 staining present in more than 75% of hepatocytes; 4 heavy staining present in almost all hepatocytes and also detectable in biliary epithelial cells

[c] HII: calculated as the tissue iron content (in µmol/g dry weight) divided by the patient's age (in years). Upper normal range is 1.0 µmol/g per year

[d] Normal range for hepatic iron content is less than 2200 µg/g dry weight for men and less than 1600 µg/g dry weight for women

In 32 patients, biopsy specimens were available. The HII showed only a trend for increased values in patients with HFE mutations which, due to the low number of specimens, did not reach statistical significance. Furthermore, we failed to observe a significant relationship between HII and serum iron parameters in terms of a correlation of both parameters (Table 2). Histological assessment revealed the classical abnormalities of PCT with mild fatty changes, focal necrosis, and inflammation and fibrotic portal tracts [4, 20] (Fig. 1). In some cases, birefrigent needle-shaped inclusions were observed under polarizing light, resembling uroporphyrin crystals. Iron deposits were observed predominantly within periportal hepatocytes and Kupffer cells. Semiquantitative assessment of iron content within the liver tissue according to Perl's [20] did not show any correlation to HFE gene mutation status, serum iron parameters, or biochemically defined hepatic iron content (Table 2).

In 28 patients (15%), antibodies against HCV were found. The frequencies of C282Y and H63D mutations were not related to HCV antibody status. Of these 28 patients, 7 were heterozygous for C282Y and eleven for

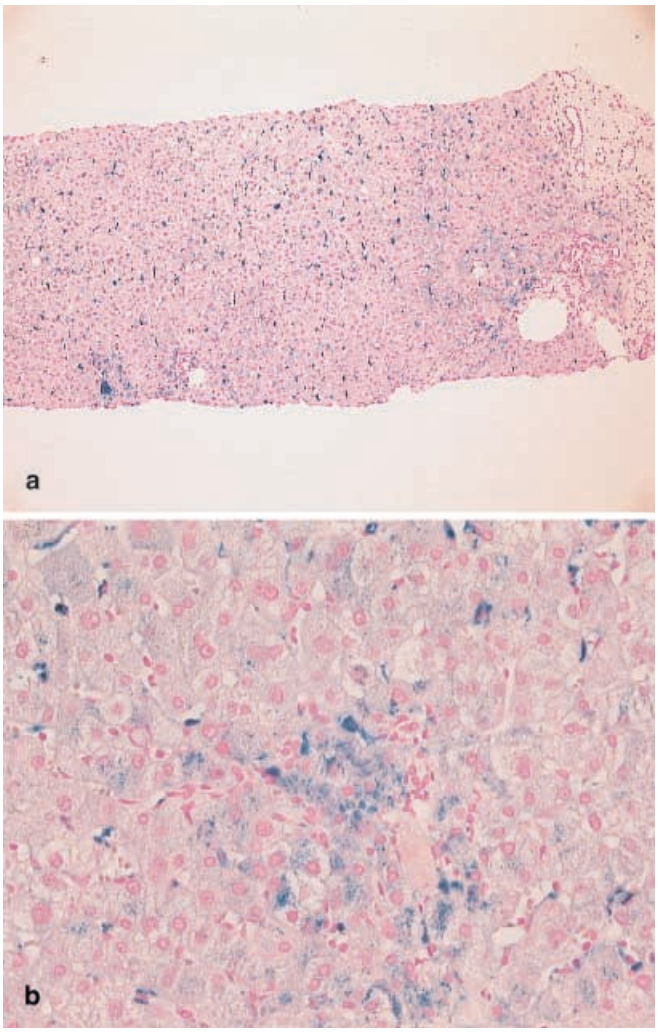


Fig. 1 Liver biopsy specimen from a patient with porphyria cutanea tarda, prior to therapy. Hemosiderosis within the hepatocytes and also within Kupffer cells is visible. Next to siderosis, mild fatty changes are also demonstrated

H63D compared with ten HCV-positive patients with the wild-type HFE gene. Patients with HCV infection displayed a trend for elevated liver enzymes [alanine aminotransferase (ALAT) and aspartate aminotransferase (ASAT)] compared with uninfected patients. There was no significant relationship between patient age or gender and C282Y or H63D status.

Discussion

In a large cohort of patients, we could show that the frequency of the C282Y and H63D mutation in PCT patients from Germany is highly increased compared with controls. Thus, 39% of our patients were either homozygous or heterozygous for the C282Y mutation. For the H63D mutation, 45% of our patients were found to be hetero- or homozygous and 9% were found to be compound heterozygous with both mutant alleles. The HFE gene mutation frequencies of our PCT patients were significantly above the frequency in a German control population found by us in this study and reported by others [12] with a prevalence of 3% and 3.9% for the C282Y, and 10% and 15% for the H63D mutation [12].

The frequency of the C282Y mutation in German PCT patients is, therefore, comparable with those observed in other countries. Previously published data from British, North American, and Australian patients indicated a prevalence of the C282Y mutation among PCT patients between 42% and 44% [5, 6, 7, 8, 9]. However, our observed rate of the H63D mutation of 45% is not only significantly higher than that of the normal population [12] but also significantly increased compared with that of PCT patients from other countries, with reported ranges from 3% up to 50% – the latter in 68 PCT patients from different geographical regions of Italy [18, 19]. The reason for these regional variations remains unclear. There is no evidence to suggest major differences in the frequency of iron overload or alcohol ingestion between patients from Germany and Italy, North America, Australia, or Great Britain. A possible explanation may be the differing prevalence of HCV infection in patients from these countries. HCV infection is a suggested trigger for PCT. Australian, North American, and Italian PCT patients showed a prevalence of HCV antibodies of 25% and 56% [2, 18, 19, 22], respectively, whereas in Germany, the prevalence of HCV antibodies in PCT patients is only 8% in a previous [21] and 15% in this study. These data support the hypothesis that, in Germany, other factors than HCV infection – namely the presence of HFE mutations – may play an important role in the precipitation of PCT.

Recent studies indicate a function of the normal HFE gene product in attenuating cellular iron absorption [24], possibly via physical interaction with the transferrin receptor [23]. Iron transportation into the duodenal crypt cells is regulated by the duodenal metal transporter called NRAMP-2 or divalent metal transporter 1 (DMT1). Thus, due to the lack of downregulation by the mutated HFE gene product, DMT1 mRNA expression is greatly enhanced in duodenal mucosa of patients with hereditary hemochromatosis and correlates with duodenal iron uptake [24]. One may speculate that in PCT patients with C282Y and/or H63D mutations, the increased hepatocellular iron concentration may trigger PCT, as it was hypothesized for chronic HCV infection, which predisposes for iron overload [14].

In our series, 18 patients were found to be compound heterozygotes for both HFE alleles, C282Y and H63D. These patients also displayed high liver enzymes, transferrin saturations, and ferritin levels. It has been reported that these compound heterozygotes also have an increased risk of developing clinical hemochromatosis [3, 8, 10]. However, neither the compound heterozygotes nor the C282Y or H63D homozygotes among our PCT patients met current clinical criteria for hereditary hemochromatosis.

Our data confirm previous hypotheses on the association between PCT and hemochromatosis and clearly establish the iron status as an important predisposing factor for the manifestation of PCT. However, it remains to be fully understood how iron overload and, in particular, the cellular modifications of the iron status secondary to HFE gene mutations, affect the activity of URO-D, the key enzyme of porphyrin metabolism that is compromised in PCT. Furthermore, it remains to be elucidated how the altered iron metabolism interacts with the other two common triggers for PCT and the associated liver disease – alcohol and viral hepatitis.

Acknowledgements We wish to thank Mrs Claudia Hänel for excellent technical assistance and Dr. Andreas Eichler for providing blood samples from healthy volunteers.

References

1. Beutler E, Gelbart TA (2000) Common intron 3 mutation (IVS3 –48c→g) leads to misdiagnosis of the c.845G→A (C282Y) HFE gene mutation. Blood Cells Mol Dis 26:229–233
2. Bonkovsky HL, Poh-Fitzgerald M, Pimstone N, Obando J, DiBisceglie AD, Tattrie C, Tortorelli K, LeClair P, Mercurio MG, Lambrecht RW (1998) Porphyria cutanea tarda, hepatitis C, and HFE gene mutations in North America. Hepatology 27:1661–1669
3. Brissot P, Moirand R, Jouanolle AM, Guyader D, Le Gall JY, Deugnier Y, David V (1999) A genotypic study of 217 unrelated probands diagnosed as "genetic hemochromatosis" on "classical" phenotypic criteria. J Hepatol 30:588–593
4. Doss M (1967) The quantitative separation of porphyrins and protohaemin as methyl esters by thin-layer chromatography. J Chromatogr 30:265–269
5. Doss M (1982) Hepatic porphyrias: pathobiochemical, diagnostic, and therapeutic implications. In: Popper H, Schaffner F (eds) Progress in liver disease, vol VII. Grune and Stratton, New York, pp 573–597
6. Feder JN, Gnirke A, Thomas W, Tsuchihashi Z, Ruddy DA, Basava A, Dormishian F, Domingo B Jr, Ellis MC, Fullan A, Hinton LM, Jones NL, et al (1996) A novel MHC class I-like gene is mutated in patients with hereditary haemochromatosis. Nat Genet 13:399–407
7. Furuyama K, Kondo M, Hirata K, Fujita H, Sassa S (1999) Extremely rare association of HFE mutations with porphyria cutanea tarda in Japanese patients. Hepatology 30:1532–1533
8. Gottschalk R, Seidl C, Loffler T, Seifried E, Hoelzer D, Kaltwasser JP (1998) HFE codon 63/282 (H63D/C282Y) dimorphism in German patients with genetic hemochromatosis. Tissue Antigens 51:270–275
9. Ivanova A, von Ahsen N, Adjarov D, Krastev Z, Oellerich M, Wieland E (1999) C282Y and H63D mutations in the HFE gene are not associated with porphyria cutanea tarda in Bulgaria. Hepatology 30:1531–1532
10. Jazwinska EC (1998) Hemochromatosis: a genetic defect in iron metabolism. Bioessays 20:562–568
11. Kushner JP, Barbuto AJ, Lee RG (1976) An inherited enzymatic defect in porphyria cutanea tarda: decreased uroporphyrinogen-decarboxylase activity. J Clin Invest 58:1089–1097
12. Merryweather-Clarke AT, Pointon JJ, Shearman JD, Robson KJH (1997) Global prevalence of putative heamochromatosis mutations. J Med Genet 34:275–278
13. Moran MJ, Fontanellas A, Brudieux E, Hombrados I, de Ledinghen V, Couzigou P, de Verneuil H, De Salamanca RE (1998) Hepatic uroporphyrinogen decarboxylase activity in porphyria cutanea tarda patients: the influence of virus C infection. Hepatology 27:584–589
14. Powell LW, Subramaniam VN, Yapp TR (2000) Haemochromatosis in the new millennium. J Hepatol 32:48–62
15. Press RD (2000) Iron beware: a common HFE gene polymorphism may prevent the accurate molecular diagnosis of homozygous hemochromatosis in low-risk, but not high-risk groups. Hepatology 31:540–542
16. Roberts AG, Whatley SD, Morgan RR, Worwood M, Elder GH (1997) Increased frequency of the haemochromatosis Cys282Tyr mutation in sporadic porphyria cutanea tarda. Lancet 349:321–323
17. Roberts AG, Whatley SD, Nicklin S, Worwood M, Pointon JJ, Stone C, Elder GH (1997) The frequency of hemochromatosis-associated alleles is increased in British patients with sporadic porphyria cutanea tarda. Hepatology 25:159–161
18. Sampietro M, Piperno A, Lupica L, Arosio C, Vergain A, Corbetta N (1998) High prevalence of the His63Asp HFE mutation in Italian patients with PCT. Hepatology 27:181–183
19. Sampietro M, Fiorelli G, Fargion S (1999) Iron overload in porphyria cutanea tarda. Haematologica 84:248–253
20. Scheuer PJ, Williams R, Muir AR (1962) Hepatic pathology in relatives of patients with haemochromatosis. J Pathol Bacteriol 84:53–64
21. Stölzel U, Köstler E, Koska C, Stöffler-Meilecke M, Schuppan D, Somasundaram R, Doss M, Habermehl K, Riecken O (1995) Low prevalence of hepatitis c virus infection in porphyria cutanea tarda in Germany. Hepatology 21:1500–1503
22. Stuart KA, Busfield F, Jazwinska EC, Gibson P, Butterworth LA, Cooksley WG, Powell LW, Crawford DHG (1998) The C282Y mutation in the haemochromatosis gene (HFE) and hepatitis C virus infection are independent cofactors for porphyria cutanea tarda in Australian patients. J Hepatol 28:404–409
23. Waheed A, Parkkila S, Saarnio J, Fleming RE, Zhou XY, Tomatsu S, Britton RS, Bacon BR, Sly WS (1999) Association of HFE protein with transferrin receptor in crypt enterocytes of human duodenum. Proc Natl Acad Sci USA 96:1579–1584
24. Zoller H, Pietrangelo A, Vogel W, Weiss G (1999) Duodenal metal-transporter (DMT-1, NRAMP-2) expression in patients with hereditary haemochromatosis. Lancet 353:2120–2123

Virchows Arch (2001) 439:6–13
DOI 10.1007/s004280100438

ORIGINAL ARTICLE

**Noriyoshi Fukushima · Kiyoshi Mukai
Michiie Sakamoto · Takahiro Hasebe
Kazuaki Shimada · Tomoo Kosuge · Taira Kinoshita
Setsuo Hirohashi**

Invasive carcinoma derived from intraductal papillary-mucinous carcinoma of the pancreas: clinicopathologic and immunohistochemical study of eight cases

Received: 31 August 2000 / Accepted: 12 February 2000 / Published online: 31 March 2001
© Springer-Verlag 2001

Abstract Most intraductal papillary-mucinous carcinomas (IPMCs) of the pancreas are resectable and curable, but some develop into frankly invasive carcinomas. We studied the clinicopathologic features of eight cases of invasive carcinoma derived from IPMC (IC-IPMC) of the pancreas. The patients were aged 54–75 years (mean, 66.6 years); six were male and two were female. The mean tumor size was 7.7 cm (range 5.5–10.5 cm). Two patients without lymph node metastasis had no peripancreatic invasion, and survived longer (115 and 20 months). Three out of four patients with extrapancreatic invasion died of their tumors or developed tumor recurrence within a year. One patient with evidence of liver and lymph node metastasis at the time of first surgery again showed metastatic tumor 21 months later. One patient died of another cause. We also performed a comparative study of the immunohistochemical features of IC-IPMCs in 9 IPMCs (including minimally invasive cases) and 15 ductal adenocarcinomas. CEA cytoplasmic positivity was observed in most of the IC-IPMCs (87.5%) and ductal adenocarcinomas (93.3%), but in only 1 IPMC (11.1%). The frequency of p53 nuclear staining in ductal adenocarcinoma (73.3%) was higher than in IPMC (33.3%) or IC-IPMC (37.5%). In conclusion, IC-IPMC with extrapancreatic invasion should be treated as ductal carcinoma because of its aggressive behavior after resection. Some IPMCs might progress to invasive carcinoma via pathways that are different from those followed by ductal adenocarcinomas.

Keywords Intraductal papillary-mucinous carcinoma · Pancreas · Invasive carcinoma · Immunohistochemistry

N. Fukushima (✉)
Clinical Laboratory Division, National Cancer Center Hospital, 5–1-1 Tsukiji, Chuo-ku, Tokyo 104–0045, Japan
e-mail: shirohas@ncc.go.jp
Tel.: +81-3-35422511, Fax: +81-3-32482463

K. Mukai · T. Hasebe
Pathology Division,
National Cancer Center Research Institute East, Kashiwa, Japan

M. Sakamoto · S. Hirohashi
Pathology Division, National Cancer Center Research Institute, Tokyo, Japan

K. Shimada · T. Kosuge
Hepato-biliary-pancreatic Surgery Division,
National Cancer Center Hospital, Tokyo, Japan

T. Kinoshita
Hepato-biliary-pancreatic Surgery Division,
National Cancer Center Hospital, East, Kashiwa, Japan

Present address:
K. Mukai, Tokyo Medical University, Tokyo, Japan

Introduction

Intraductal papillary-mucinous neoplasms (IPMNs) are mucus-producing neoplasms of the pancreas that lead to diffuse or segmental dilatation of the main and/or branch pancreatic ducts [3, 4, 5, 6, 7, 9, 10, 11, 13, 16, 19]. On the inner surfaces of the ectatic ducts there are papillary projections with abundant mucus. Most patients with IPMN are older males, and the prognosis is excellent with pancreatic excision only, even if the tumors are histologically malignant [3, 4, 5, 6, 7, 9, 10, 11, 13, 16, 19]. In contrast, ductal adenocarcinoma usually forms a firm mass with an ill-defined infiltrating margin at diagnosis, and its prognosis is dismal [5, 7, 8]. The incidence of ductal adenocarcinoma is slightly higher among men than women (the male/female ratio is 1.6), and four-fifths of the patients are 60–80 years of age [8]. Mucinous cystic neoplasms (MCNs) are defined as cystic tumors composed of mucin-producing columnar epithelium supported by “ovarian-type” stroma [3, 4, 5, 7, 17, 20, 21]. MCNs occur preferentially in the body and tail of the pancreas, and most lesions have no communication with the duct system. These tumors are found almost exclusively in middle-aged women [3, 4, 5, 7, 17, 20, 21]. Consequently, IPMNs are categorized differently from invasive ductal adenocarcinoma and MCNs.

The term "IPMN" histologically represents variable grades of lesions from adenoma to adenocarcinoma. Although minimal invasion may be seen in half or more of intraductal papillary-mucinous carcinomas (IPMCs), cases with extensive invasion are relatively rare [4, 6, 10, 11, 16]. Only a few reports have described the clinicopathologic findings of advanced cases of IPMC [6]. Such invasive cases of IPMC are called "invasive carcinoma derived from intraductal papillary adenocarcinoma" by the Japan Pancreatic Society [5].

In this report we present eight cases of invasive carcinoma derived from intraductal papillary-mucinous carcinoma (IC-IPMC). To clarify the clinicopathologic characteristics of these tumors, we also performed a comparative study of IC-IPMC, ductal adenocarcinoma and IPMC (including minimally invasive cases).

Materials and methods

We retrieved 17 cases of intraductal papillary-mucinous carcinoma, including invasive cases, from the files of the Diagnostic Pathology Laboratory, National Cancer Center Hospital and National Cancer Center Hospital East. We divided them into two groups according to the presence or absence of macroscopic invasion. Noninvasive and minimally invasive cases were classified as IPMC and were used for immunohistochemical comparison. Although the criterion of "minimally invasive" is obscure and a more precise definition needs to be established, we defined the group of minimally invasive cases as tumors in which invasive features were found only on microscopic examination. All of our minimally invasive cases showed only a few tumor glands around the noninvasive lesions.

Our subclassification of IPMNs as main-duct type, branch-duct type and combined type was based on the classification by Kuroda [9]. The factors concerned with tumor invasiveness, such as lymphatic, venous, perineural, serosal and retroperitoneal invasion, were evaluated according to the rule described in the Japan Pancreas Society Classification [5]. Lymphatic, venous and perineural invasion were classified into negative (-), slight (+), moderate (++) and marked (+++). Serosal (anterior pancreatic capsule) invasion and retroperitoneal invasion were classified into no evidence of invasion (-), invasion suspected (+), definite invasion (++) and invasion to the adjacent organs (+++).

Sections of formalin-fixed, paraffin-embedded tissue were subjected to immunohistochemistry by the avidin–biotin complex (ABC) method to characterize the tumor cells. We used antibodies against carcinoembryonic antigen (CEM010, Mochida, Tokyo; 1:500 dilution) and p53 (DO-7, Novocastra Laboratories, UK; 1:100 dilution). Carcinoembryonic antigen (CEA) immunoreactivity was evaluated as follows: negative (-), less than 10% of the tumor cells were immunoreactive; positive (+, apical), at least 10% of the tumor cells were immunoreactive and positive staining was localized at the apical region of the tumor cells; positive (++, both), at least 10% of the tumor cells were immunoreactive and the immunoreactivity was observed in both the apical region and the cytoplasm of the tumor cells. In IC-IPMC we evaluated CEA immunoreactivity in the intraductal component and the invasive components separately. The grade of p53 positivity was evaluated as follows: negative (-), less than 10%; positive (+), more than 10% of the cells had immunoreactive nuclei.

Results

Clinical characteristics

There were six male and two female patients with IC-IPMC, their ages ranging from 54 to 75 years with a

Table 1 Clinicopathologic features of the patients with invasive carcinoma derived from intraductal papillary-mucinous adenocarcinoma of the pancreas (*DM* diabetes mellitus, *Main* main-duct type, *Branch* branch-duct type, *Comb.* combined type, *CT* tumor was detected by computed tomography)

	Age	Sex	Portion	Size (cm)	Subtype	Clinical presentation
1	68	M	H	5.5×5	Main	Back pain
2	66	M	H	6.2×5×4.3	Branch	Epigastric pain
3	67	M	H	9.5×5×4.3	Comb.	Jaundice, weight loss
4	72	F	HBT	6.7×3	Main	Tumor, back pain
5	75	F	BT	10×3.2	Main	DM, tumor (CT)
6	67	M	H	5.5×3.5	Branch	Abdominal pain, appetite loss
7	54	M	BT	10.5×1.7×1.2	Main	Liver metastases (CT)
8	64	M	H	8×7.5×5.5	Santorini	Fatigue, jaundice

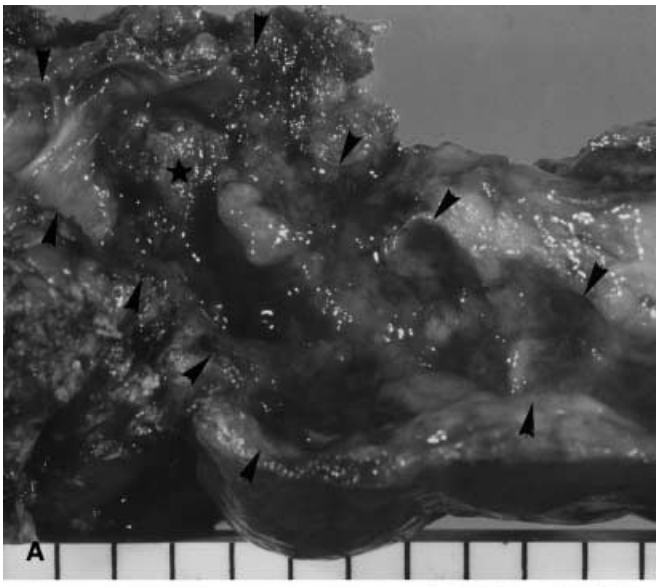
Table 2 Histological findings in the invasive components and the factors concerned with cancer invasion and metastasis,[a] and patient outcome [*muc* mucinous carcinoma-like invasion, *tub* tubular adenocarcinoma, *muc>tub* mucinous carcinoma-like invasion with small tubular adenocarcinoma areas, *ly* lymphatic invasion, *v* venous invasion, *ne* invasion of intrapancreatic nerves, s invasion of anterior pancreatic capsule (serosa), *rp* invasion of retroperitoneal tissue, *du* invasion of duodenal wall, *ch* bile duct invasion, *n* lymph node metastases, *n.e.* not examined, *AW* alive and well, *mo* months, *DOD* death of disease, *DOC* died of other cause, *Rec*. recurrence]

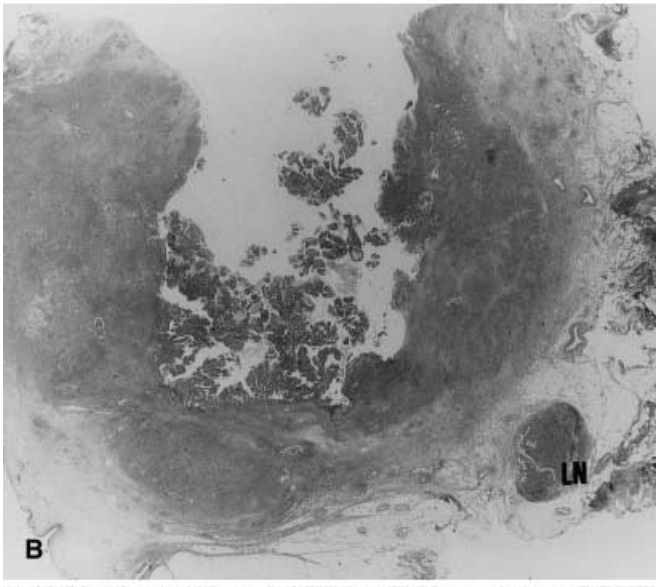
Case no.	Histology of the invasive components	ly	v	ne	s	rp	du	ch	n	Outcome
1	muc>tub	–	–	–	–	–	–	–	–	AW, 115 mo
2	muc	–	++	++	–	+	–	+++	+	DOD, 10 mo
3	muc, tub	–	+	++	–	+	–	+++	+	DOD, 9 mo
4	muc>tub	–	–	–	–	–	–	–	–	AW, 20 mo
5	tub	+	+++	+++	–	+	n.e.	n.e.	+	Rec.,[b] 10 mo
6	tub	+	++	++	++	++	++	–	+	DOC, 1 mo
7	tub	–	+	+	–	–	n.e.	n.e.	+	Rec.,[c] 21 mo
8	muc	+	–	+	–	–	+++	–	+	AW, 4 mo

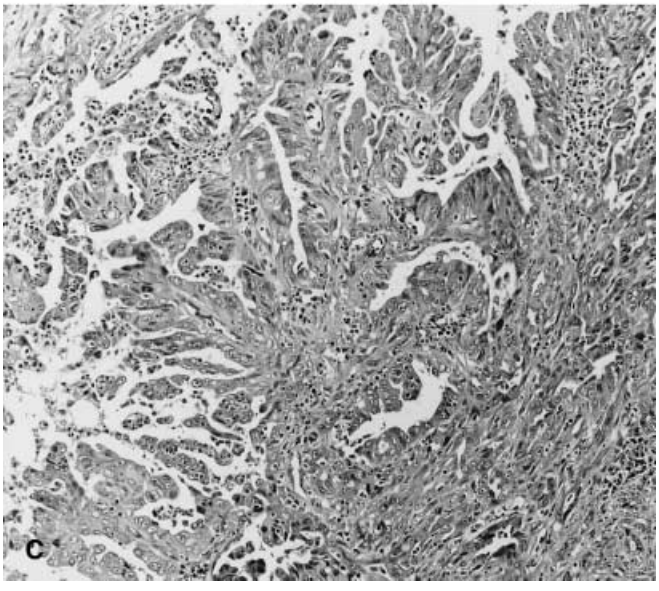
[a] Evaluation of each factor according to Japan Pancreas Society's Classification of Pancreatic Cancer: – negative; + slight; ++ moderate; +++ marked

[b] Liver and lymph node metastases

[c] Metastatic liver tumor was resected at the first surgery. After 21 months, metastatic liver tumor recurred and was resected again







mean of 66.6 years (Table 1). The presenting complaints were variable. Four patients presented with back and/or abdominal pain. Two presented with obstructive jaundice. In two cases the tumor was found on abdominal computed tomography (CT) scans performed for other chronic diseases. Pylorus-preserving pancreatoduodenectomy was performed in three patients, pancreatoduodenectomy in two, distal pancreatectomy in one, and total pancreatectomy in two.

Three patients were alive without recurrence 4–115 months after surgical resection (Table 2). One patient was alive, but tumor recurrence, including lymph node and liver metastasis, was confirmed 10 months after pancreatic resection. One patient underwent partial hepatectomy for tumor metastasis 21 months after the first surgical procedure. Two patients died of liver metastasis and carcinomatosa peritonei from the pancreatic tumor 10 and 11 months after surgery. One patient committed suicide.

Macroscopic characteristics

Of the original intraductal lesions, four were classified as main-duct type and three as combined or branch-duct type. We considered that the lesion in the remaining case (case 8) originated from a Santorini duct. The cystic components of all the tumors were connected to the pancreatic duct system. The longitudinal tumor size of the main-duct type ranged from 5.5–10.5 cm (mean 8.2 cm), and the greatest diameter of the other types ranged from 5.5 to 9.5 cm (mean 7.3 cm). Five lesions were located mainly in the head of the pancreas, and two lesions were located in the body and/or tail. In the remaining case the intraductal lesion involved the entire length of the pancreas from head to tail.

In the main-duct type there was diffuse ductal ectasia with a granular intraductal surface or papillary projections (Fig. 1A). The cut surface showed papillary growth of the intraductal epithelial component and periductal extension of the tumor (Figs. 1B, 2A). The surrounding pancreatic tissue was atrophic and fibrotic. In the branch-duct type, multiple cystic lesions are formed by bunches of ectatic ducts. In one case (case 7) partial hepatectomy was performed simultaneously for small liver metastases at the first operation. The resected liver contained two grayish-white nodules, measuring 1.8×1.2 cm and 0.7×0.5 cm. This patient underwent partial hepatectomy again, as described above. The new metastatic tumor was 2.0 cm in diameter.

Fig. 1A–C A case of main-duct-type IC-IPMC (case 5). **A** Specimen from distal pancreatectomy shows the dissected main pancreatic duct (*arrowheads*), which is markedly dilated, with intraductal papillary projections (*star*). **B** Cross section of the tumor, showing papillary growth in the dilated main pancreatic duct. Periductal invasion is prominent, and lymph node (*LN*) metastasis is visible. **C** The papillary tumor is accompanied by an invasive component of poorly differentiated adenocarcinoma

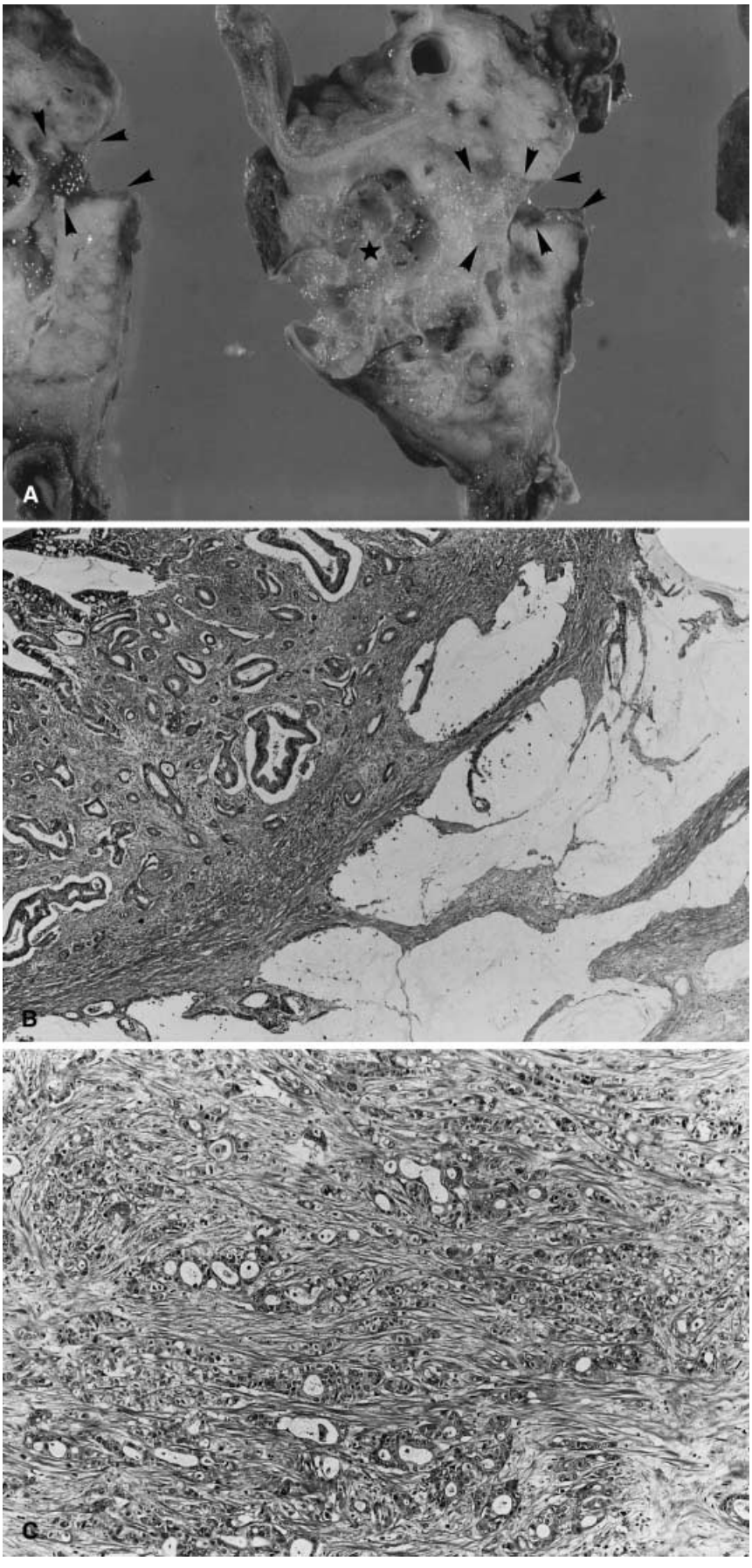


Fig. 2A–C A case of combined type IC-IPMC (case 3). **A** Cut surface shows the dilated main pancreatic duct (*arrowheads*) and an invasive area of mucinous carcinoma (*star*). **B** This lesion shows both tubular (*upper left*) and mucinous-carcinoma-like (*lower right*), invasive components. **C** Tubular adenocarcinoma invasion was accompanied by desmoplastic stromal change

Table 3 Immunohistochemical findings for invasive carcinoma derived from intraductal papillary-mucinous adenocarcinoma [carcinoembryonic antigen (*CEA*): - <10%, + apical, ++ both apical and cytoplasm; p53 nuclear staining (*p53*): – <10%, + >10%]

Case no.	CEA		p53	
	Intraductal component	Invasive component	Intraductal component	Invasive component
1	++	++	–	–
2	++	++	–	–
3	++	++	–	–
4	++	++	+	+
5	++	+	+	+
6	+	++	–	–
7	+	–	–	–
8	++	++	+	+

Table 4 Summary of immunohistochemical study (CEA: – <10%, + apical, ++ both apical and cytoplasm; p53 nuclear staining – <10%, + >10%)

No. of cases	CEA			p53	
	–	+	++	–	+
IPMC					
9	2 (22.2%)	6 (66.7%)	1 (11.1%)	6 (66.7%)	3 (33.4%)
IC-IPMC					
8	0	1 (12.5%)	7 (87.5%)	5 (62.5%)	3 (37.5%)
Ductal adenocarcinoma					
15	0	1 (6.7%)	14 (93.3%)	4 (26.7%)	11 (73.3%)

Microscopic characteristics

The epithelial intraductal growth observed corresponded to the macroscopic features in all cases. Different grades of cytological atypia were often seen in the same tumor. In at least five cases, adenomatous epithelium and carcinomatous epithelium were mixed in different ratios.

There were three major cell types in the IPMNs, as described previously [3]. The major cell type was “tall columnar cells with dense cytoplasm” in two cases, “tall columnar cells with clear cytoplasm” in four, and “cuboidal cells with eosinophilic cytoplasm” in two. In most cases, however, the cell types were mixed, or there was a transition from one type to the other. Adsay et al. reported IPMNs composed of oncocytic cells [1], which are identical to our third cell type. These cells are said to contain numerous mitochondria in the cytoplasm [1].

In the invasive area, tubular adenocarcinoma was the major component in three cases, mucinous carcinoma-like invasion in four, and both in one case (Fig. 2B). Other histological types were mixed with the major invasive component: papillary carcinoma, mucinous carcinoma with signet-ring cells, and poorly differentiated adenocarcinoma with desmoplastic stromal change (Figs. 1C, 2C).

Venous invasion and perineural invasion were each seen in five cases. Extrapancreatic invasion and/or metastasis were seen in six cases. In two tumors without extrapancreatic invasion, venous and lymphatic invasions were not detected. Four tumors had infiltrated to the peripancreatic connective tissue of the retroperitoneum. Serosal invasion was seen in one case. Two tumors located in the pancreatic head had penetrated to the common bile duct, and two other tumors had invaded as far as the duodenal wall. Lymph node metastasis was detected in six of the eight cases. In case 7, all the small liver tumors were confirmed to be histologically similar to pancreatic ductal adenocarcinoma with desmoplastic stromal change.

Immunohistochemistry

The results of the immunohistochemical study are summarized in Tables 3 and 4. In IC-IPMC we evaluated CEA immunoreactivity (Fig. 3A) in the intraductal component and invasive component separately: no clear difference was observed. Both cytoplasmic and apical staining for CEA was seen in seven cases of IC-IPMC (87.5%). Cytoplasmic staining for CEA was seen in one case of IPMC (11.1%). Most of the ductal adenocarcinoma cases showed cytoplasmic staining for CEA (93.3%). Within the same tumor, there was a tendency for the reduction of the staining intensity and/or the change of the staining patterns from cytoplasmic to apical staining in the areas of lower grade histological atypia.

We observed p53 immunoreactivity in the nuclei of the IC-IPMC tumor cells (Fig. 3B) Expression of p53 in more than 10% of the tumor cell nuclei (+) was detected in three of the eight IC-IPMC cases (37.5%). Expression of p53 in more than 10% of tumor cells (+) was detected in 3 of 9 IPMC cases (33.3%). Similar p53 immunoreactivity (+) was observed in 11 of 15 ductal adenocarcinoma cases (73.3%). We observed no differences in p53 expression between the invasive and intraductal components of IPMNs.

Pathologic findings and patient prognosis

We checked for any correlation between pathologic findings and patient outcome (Tables 1, 2). Two patients without extrapancreatic invasion showed neither venous nor lymphatic invasion, and survived for longer periods

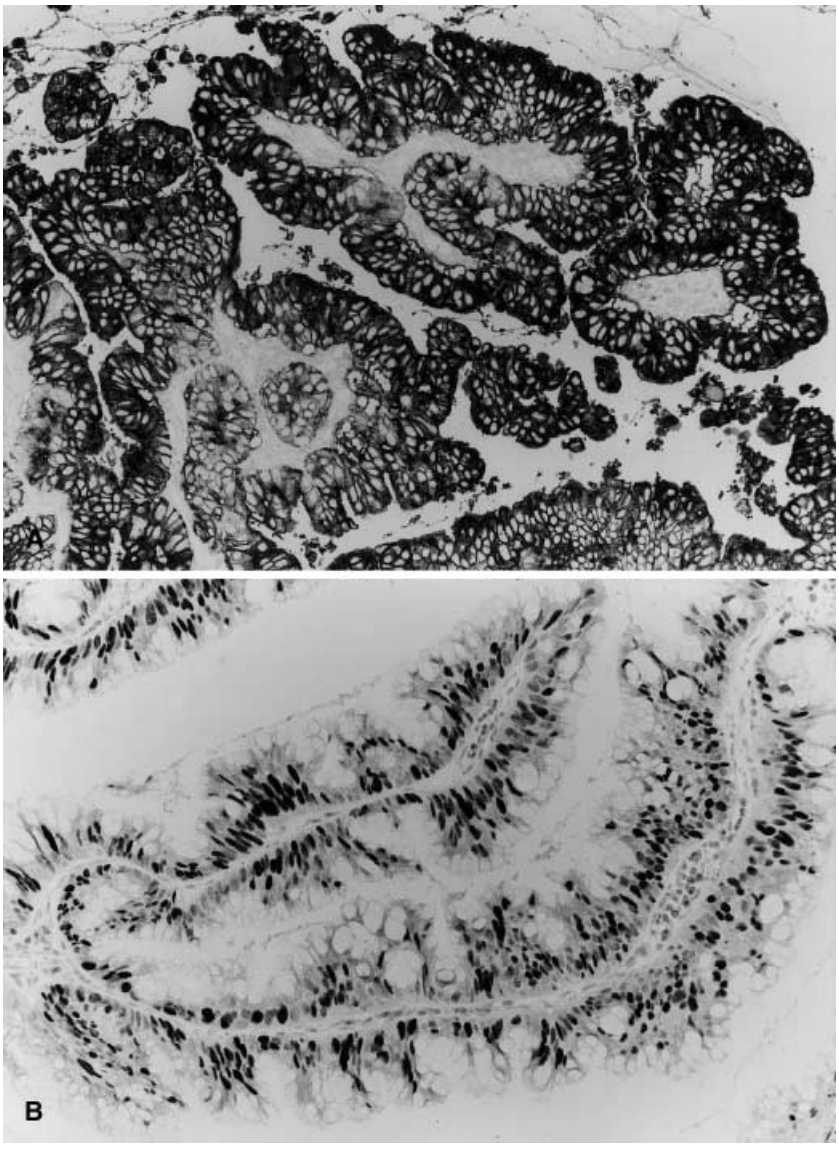


Fig. 3A, B Immunohistochemistry of IC-IPMC. **A** Both cytoplasmic and apical stainings for CEA (case 5). **B** Nuclear stainings for p53 (case 4)

(case 1, 115 months; case 4, 20 months). In contrast, three out of four patients with extrapancreatic invasion died or developed tumor recurrence within a year (cases 2, 3, and 5). One patient with liver and lymph node metastases at the time of surgery showed metastatic tumor in the liver again 21 months after first surgery, and this tumor was also resected (case 7). Neither chemotherapy nor radiation therapy had been performed in this patient.

There was no correlation between the histological features of the invasive components or the results of CEA and p53 immunostaining and patient outcomes (Tables 1, 2).

Discussion

Some invasive ductal carcinomas of the pancreas are considered to be derived from IPMC. However, the invasive features of the early invasive stage or of the development from IPMC to invasive carcinoma have not been well documented. Since most IPMTs are resectable and curable, it is important to define the characteristics of IC-IPMC.

Gender, age and tumor location were similar among IPMC, IC-IPMC and ductal adenocarcinoma. These tumors usually arise in the head of the pancreas of older male patients. IC-IPMCs tended to be larger than the other IPMNs, as we found in our previous study [4]. Both the largest diameter of the whole tumor and the size of the cystic or ductectatic lesions were larger in IC-IPMC than in the other tumors. In one case the tumor had spread over the entire length of the main pancreatic duct. These findings suggested that tumor invasiveness might have developed at a late stage of tumor progression. In other words, as the intraductal lesions became bigger, the histological grade may have become higher, leading eventually to invasive carcinoma. In our previous study [4] there were no IPMC tumors over 5 cm in

diameter, apart from the length of the main-duct type. However, in this study all the IC-IPMC primary tumors were greater than 5 cm at the largest diameter. Tumor size is an important indicator of aggressiveness when tumors are evaluated radiologically. The symptoms of IPMN are usually related to obstruction of the peripheral ducts by mucus, and detection of incidental IPMNs by ultrasonography or CT has been increasing in frequency [3, 4]. On the other hand, the patients with IC-IPMC were often found by symptoms similar to those of conventional invasive ductal adenocarcinoma, i.e., general fatigue, weight loss and jaundice.

We identified a high frequency of venous invasion, perineural invasion and lymph node metastasis by IC-IPMC, and this was an indicator of biological aggressiveness. Perineural invasion, a characteristic of pancreatobiliary carcinoma, was also prominent. Three-quarters of our cases showed extrapancreatic invasion or metastasis. This feature was also associated with short postoperative survival. In the literature, the first metastases from pancreatic cancer are said to occur in the regional lymph nodes, the peritoneum or the liver [10, 13, 16]. Two of our patients without lymph node metastasis showed neither venous nor lymphatic invasion, and survived for longer periods. In contrast, three patients with extrapancreatic invasion died from their tumors or developed tumor recurrence within a year. Adequate lymph node dissection and evaluation of the pancreatic resected margin are required to achieve complete resection. One patient had liver metastases at the time of the first operation, and had a partial hepatectomy for liver metastasis 21 months after the initial operation. Neither chemotherapy nor radiation therapy had been performed on this patient. Such cases are rare in pancreatic adenocarcinoma, and this may suggest the biological differences between IPMC and ductal adenocarcinoma.

The invasive component is usually either mucinous carcinoma-like or tubular adenocarcinoma [3, 7, 18]. In our cases, however, other minor components were also present. Although the scirrhous invasion in IC-IPMC was similar to that in ductal adenocarcinoma, its presence did not correlate with tumor extension or prognosis. Prognosis in IC-IPMC appears to be influenced mainly by the extrapancreatic tumor extension rather than the histological features of the invasive component.

On immunohistochemistry, CEA was positive in both the cytoplasm and the apical region of the tumor cells in almost all the invasive carcinomas (IC-IPMC and ductal adenocarcinoma). CEA was only weakly positive or negative in IPMC. Nagai et al. have reported that the staining pattern of CEA is correlated with the degree of cellular atypia of IPMNs [12]. In our series, the staining pattern of IC-IPMC was similar to that of ductal adenocarcinoma but different from that of IPMC. The most noticeable point was the strong staining of the cytoplasm of the tumor cells in the invasive tumors (IC-IPMC and ductal adenocarcinoma); IPMC showed only apical staining. These results may be useful for the identification of invasive cases by cytologic evaluation of pancreatic juice.

There was a clear difference in the frequency of p53 protein expression between IPMN (IC-IPMC and IPMC) and ductal adenocarcinoma. According to the literature [2, 12, 14, 15], the frequency of nuclear p53 immunostaining in ductal adenocarcinoma is 50–60%, and in IPMNs it is 30% or less. Our result showed a high p53 positivity in ductal adenocarcinoma (73.3%) and a low p53 positivity in IPMC and IC-IPMC (35.3%). These observations suggest that at least some IPMNs progress differently to ductal adenocarcinomas.

In conclusion, we studied eight cases of IC-IPMC and demonstrated that the primary tumors in these cases were larger than IPMCs and that the prognosis was dependent on the presence or absence of tumor extension rather than the morphology of the invasive component. IC-IPMC with extrapancreatic invasion or lymph node metastasis should be regarded as “invasive ductal carcinoma,” because it appears to have a poor prognosis similar to that of ordinary ductal adenocarcinoma. According to the results of our study, the size of the intraductal tumor and the presence of lymph node metastasis, as identified by CT, are important factors in the preoperative diagnostic process. Immunohistochemical p53 staining suggested that IPMNs and ductal adenocarcinoma at least partly follow different pathways of tumor development. Additional molecular characterization may help to define the relationship between IPMNs and ductal adenocarcinoma.

Acknowledgements This research was supported in part by a Grant-in-Aid for Second Term Comprehensive 10-year Strategy for Cancer Control from the Ministry of Health and Welfare, Japan.

References

1. Adsay NV, Adair CF, Heffess CS, Klimstra DS (1996) Intraductal oncocytic papillary neoplasms of the pancreas. Am J Surg Pathol 20:980–994
2. DiGiuseppe JA, Hruban RH, Goodman SN, Polak M, van den Berg FM, Allison DC, Cameron JL, Offerhaus GJA (1994) Overexpression of p53 protein in adenocarcinoma of the pancreas. Am J Clin Pathol 101:684–688
3. Fukushima N, Mukai K (1999) Pancreatic neoplasms with abundant mucus production: emphasis on intraductal papillary-mucinous tumors and mucinous cystic tumors. Adv Anat Pathol 6:65–77
4. Fukushima N, Mukai K, Kanai Y, Hasebe T, Shimada K, Ozaki H, Kinoshita T, Kosuge T (1997) Intraductal papillary tumors and mucinous cystic tumors of the pancreas. Clinicopathologic study of 38 cases. Hum Pathol 28:1010–1017
5. Japan Pancreas Society (1996) Classification of pancreatic cancer, 1st Engl edn. Kanehara, Tokyo, pp 27–38
6. Klöppel G (1998) Clinicopathologic view of intraductal papillary-mucinous tumor of the pancreas. Hepatogastroenterology 45:1981–1985
7. Klöppel G, Solcia E, Longnecker DS, Capella C, Sobin LH (1996) Histological typing of tumors of the exocrine pancreas. (WHO international histological classification of tumors, 2nd edn) Springer, Berlin Heidelberg New York, pp 11–21
8. Klöppel G, Hruban RH, Longnecker DS, Adler G, Kern SE, Partanen TJ (2000) Ductal adenocarcinoma of the pancreas. In: Hamilton SR, Aaltonen LA (eds) World Health Organization classification of tumors – pathology and genetics, tumors of the digestive system. IARC Press, Lyon, pp 221–230

9. Kuroda A (1988) Recent progress in clinicopathology of pancreatic tumors (in Japanese). Tan to Sui 9:1459–72
10. Loftus EV Jr, Olivares-Pakzad BA, Batts KP, Adkins MC, Stephens DH, Sarr MG, DiMagno EP (1996) Intraductal papillary-mucinous tumors of the pancreas: clinicopathologic features, outcome, and nomenclature. Gastroenterology 110:1909–1918
11. Longnecker DS, Adler G, Hruban RH, Klöppel G (2000) Intraductal papillary-mucinous neoplasms of the pancreas. In: Hamilton SR, Aaltonen LA (eds) World Health Organization classification of tumors – pathology and genetics, tumors of the digestive system. IARC Press, Lyon, pp 237–240
12. Mukawa K, Kawa S, Aoki Y, Zhai Y, Nikaido T (1999) Reduced expression of p53 and cyclin A in intraductal mucin-hypersecreting neoplasm of the pancreas compared with usual pancreatic ductal adenocarcinoma. Am J Gastroenterol 94:2263–2267
13. Nagai E, Ueki T, Chijiwa K, Tanaka M, Tsuneyoshi M (1995) Intraductal papillary mucinous neoplasms of the pancreas associated with so-called "Mucinous ductal ectasia." Histochemical and immunohistochemical analysis. Am J Surg Pathol 19:576–589
14. Satoh K, Shimosegawa T, Moriizumi S, Koizumi M, Toyota T (1996) K-ras mutation and p53 protein accumulation in intraductal mucin-hypersecreting neoplasms of the pancreas. Pancreas 12:362–368
15. Scarpa A, Capelli P, Mukai K, Zamboni G, Oda T, Iacono C, Hirohashi S (1993) Pancreatic adenocarcinomas frequently show p53 gene mutations. Am J Pathol 142:1534–1543
16. Sessa F, Solcia E, Capella C, Bonato M, Scarpa A, Zamboni G, Pellegata NS, Ranzani GN, Rickaert F, Klöppel G (1994) Intaductal papillary-mucinous tumors represent a distinct group of pancreatic neoplasms: an investigation of tumor cell differentiation and K-*ras*, p53 and c-*erb*B-2 abnormalities in 26 patients. Virchows Arch 425:357–367
17. Thompson LDR, Becker RC, Przygodzki RM, Adair CF, Heffess CS (1999) Mucinous cystic neoplasm (mucinous cystadenocarcinoma of low-grade malignant potential) of the pancreas. A clinicopathologic study of 130 cases. Am J Surg Pathol 23:1–16
18. Yamada M, Kozuka S, Yamao K, Nakazawa S, Naitoh Y, Tsukamoto Y (1991) Mucin-producing tumor of the pancreas. Cancer 68:159–168
19. Yamao K, Milchgrub S, Nakazawa S, Fujimoto M, Yamada M (1994) Intraductal papillary mucinous tumors, non-invasive and invasive. In: Pour PM, Konishi Y, Klöppel G, Longnecker DS (eds) Atlas of exocrine pancreatic tumors. Springer, Tokyo, pp 43–66
20. Zamboni G, Scarpa A, Bogina G, Iacono C, Bassi C, Talamini G, Sessa F, Capella C, Solcia E, Rickaert F, Mariuzzi GM, Klöppel G (1999) Mucinous cystic tumors of the pancreas – clinicopathological features, prognosis, and relationship to other mucinous cystic tumors. Am J Surg Pathol 23:410–422
21. Zamboni G, Klöppel G, Hruban RH, Longnecker DS, Adler G (2000) Mucinous cystic neoplasms of the pancreas. In: Hamilton SR, Aaltonen LA (eds) World Health Organization classification of tumors – pathology and genetics, tumors of the digestive system. IARC Press, Lyon, pp 234–236

Virchows Arch (2001) 439:14–20
DOI 10.1007/s004280000291

ORIGINAL ARTICLE

**Ken-ichi Inada · Harunari Tanaka · Hayao Nakanishi
Tetsuya Tsukamoto · Yuzuru Ikehara
Keiko Tatematsu · Shigeo Nakamura
Edith Martin Porter · Masae Tatematsu**

Identification of Paneth cells in pyloric glands associated with gastric and intestinal mixed-type intestinal metaplasia of the human stomach

Received: 1 November 2000 / Accepted: 4 July 2000 / Published online: 10 May 2001
© Springer-Verlag 2001

Abstract We have proposed that intestinal metaplasia (IM) of the human stomach be divided into two types on the basis of cell differentiation status: a gastric and intestinal (GI) mixed type and a solely intestinal (I) type. In the GI mixed type, gastric (foveolar epithelial and pyloric gland cells) and intestinal (goblet, intestinal absorptive, and Paneth cells) phenotype cells coexist in the same intestinalized gastric glands in various combinations and degrees. Consequently, intestinalized gastric glands are hybrids. Although we have described the rare appearance of Paneth-like cells in pyloric glands of GI mixed-type IM, the absence of an appropriate Paneth cell marker leaves room for doubt as to their true character. The purpose of this study was to clearly identify Paneth cells in pyloric glands in IM lesions using a new Paneth cell marker, a polyclonal antibody human defensin (HD)-5, raised against HD-5, which is included in granules of Paneth cells. A total of 105 gastric samples (4 biopsy and 101 surgical resected specimens) were examined. In only nine cases (8.6%), the antibody allowed demonstration of Paneth cells in pyloric glands in GI mixed-type IM, confirming our previous finding. Analysis of the proliferative cell (P) zone indicated that a common stem cell might generate both GI phenotype cells by upward and downward migration. No Paneth cells were found above the P zone. The results suggest that the stem cells show abnormal cell differentiation in IM lesions but preserve their normal direction of migration.

Keywords Paneth cell · Pyloric gland · Intestinal metaplasia · Cell differentiation marker · Defensin 5

K. Inada (✉) · H. Tanaka · H. Nakanishi · T. Tsukamoto
Y. Ikehara · M. Tatematsu
Laboratory of Pathology, Aichi Cancer Center Research Institute,
1–1 Kanokoden, Chikusa-ku, Nagoya 464-8681, Japan
e-mail: kinada@aichigw.aichi-cc.pref.aichi.jp
Tel.: +81-52-7626111, Fax: +81-52-7642972

K. Tatematsu
Internal medicine, Nagoya Memorial Hospital, Tempaku-ku,
Nagoya, Japan

S. Nakamura
Department of Pathology and Clinical Laboratory,
Aichi Cancer Center Hospital, Nagoya, Japan

E.M. Porter
Division of Pulmonary and Critical Care,
Department of Medicine, University of California, Los Angeles,
School of Medicine, Los Angeles, USA

Introduction

Intestinal metaplasia (IM) has been extensively studied as a possible premalignant condition in the human stomach [6, 30, 38]. However, the pathogenesis of IM development and its relationship to gastric cancers remain to be unequivocally confirmed. Recently, *Helicobacter pylori* (HP) infection has been established to be a major cause of gastroduodenal ulcers, chronic atrophic gastritis, and probably IM development [2, 4, 5]. Because IM is rather heterogeneous, a number of classifications have been proposed [6, 16, 30]. Most have focused on the similarities of IM to small or large intestinal epithelial cells morphologically, histochemically, or enzymatically [30].

We have proposed a unique classification based upon the cell differentiation status using both gastric and intestinal (GI) cell phenotypic markers [13]. With this classification, IM is divided into two major types; a GI mixed type and a solely intestinal (I) type. In the I type, three kinds of intestinal phenotype cells, goblet, intestinal absorptive, and Paneth cells, completely replace the gastric glands. In the GI mixed type, gastric phenotype cells are found sharing the same gastric gland with intestinal phenotype cells in various combinations. In many cases of the GI mixed type, atrophied pyloric glands are present under the intestinalized gastric pits. Although they are often diminished in size and decreased in cell number, they are apparently continuous to the upper intestinalized gastric pits across the proliferative cell (P) zone [13]. In very rare cases, we have found small numbers of Paneth-like cells, with prominent eosinophilic granules in their cytoplasm in such glands. Although

Paneth cells are frequent components of complete type IM [16], their presence in pyloric glands is controversial. Because no appropriate specific Paneth cell marker has hitherto been available, the question of the real identity of Paneth-like cells apparent on hematoxylin and eosin (H&E) staining has remained unanswered. Fortunately, we now have an antibody against human defensin-5 (HD-5) [22, 23, 25], which is one of the defensins – antibiotic peptides expressed in human and animal myeloid and some kinds of epithelial cells. The antibody almost exclusively reacts with HD-5 and allows clear detection of Paneth cells observed in the normal human small intestine and in the intestinal metaplastic glands [23].

The present study was aimed at demonstrating the presence of Paneth cells in pyloric glands associated with GI mixed-type IM using the antibody HD-5 in addition to class III mucin staining. Moreover, using MIB-1 immunohistochemistry, particular attention was paid to the distribution of both Paneth and pyloric gland cells relative to the P zone.

Materials and methods

All cases examined in this study were collected from the pathology file of Aichi Cancer Center Hospital and affiliated hospitals. A total of 105 gastric samples were studied. Four were biopsy specimens taken for diagnosis and 101 were from surgically resected carcinomas. The 78 male and 27 female patients ranged in age from 26 years to 77 years, with a mean of 59 years. The surgical material was separated into one or more specimens of carcinoma and surrounding non-neoplastic mucosa. Fifty-seven cases examined were fundic, and 48 were pyloric. As positive controls for Paneth cells, surgically resected human duodenal and jejunal samples were also examined. All materials were fixed in 0.1 M phosphate buffered 10% formalin, dehydrated through a graded alcohol series, cleared in xylene, and embedded in paraffin.

The generation of the HD-5 antibody was described previously [22, 23]. Briefly, recombinant human intestinal defensin-5 (rHD-5), biosynthesized by the baculovirus-insect cell expression system (Clontech, Palo Alto, Calif.), was coupled to ovalbumin as a carrier molecule and then injected mixed with physiological saline and Freund's adjuvant into female New Zealand White rabbits. Two boosts at 30-day intervals were similarly administered. The antibody titer of rabbit immune serum was determined using an enzyme-linked immunosorbent assay (ELISA). The specificity of the antibody was verified by means of dot blot and western blot assays [22, 23].

IM was evaluated and divided into two types, GI mixed type and I type, in H&E sections according to our previously described criteria [13]. The degree of IM was estimated as mild, moderate, and severe according to the proportion of the section occupied: less than one-third, over one-third to two-thirds, and over two-thirds, respectively. Serial sections of representative cases were then cut at 4 μm, mounted on APS-coated slides (Matsunami glass, Tokyo), and stained in the following order: first section, mucin histochemistry of paradoxical concanavalin-A (PCA) staining to identify pyloric gland cells; second, immunohistochemistry for HD-5 to identify Paneth cells; third, double staining of these two to demonstrate coexistence of Paneth and pyloric gland cells; and fourth, immunohistochemistry for Ki-67 antigen to analyze the P zone.

The precise staining procedures and the characteristics of PCA were as described previously [15, 33, 37]. Through PCA staining, mucins detected in the alimentary tract can be classified into two main types: (1) class III mucins in mucous neck cells, pyloric gland cells, and Brunner's gland cells; and (2) class II mucins in surface mucous cells, goblet cells, and the surface coat of intestinal absorptive cells. The class II mucins lose, whereas class III retain or increase their reactivity with a reduction step interposed between oxidation and concanavalin-A staining.

For HD-5 immunohistochemistry, the indirect immunoalkaline phosphatase method was employed [23, 26]. In brief, after deparaffinization and dehydration, sections were treated sequentially with normal goat serum to block nonspecific antibody binding, rabbit anti-HD-5 antibody (1:2000), and affinity-isolated alkaline phosphatase (ALP)-conjugated goat anti-rabbit immunoglobulins (Dako, Glostrup, Denmark). ALP-binding sites were visualized using a fuchsin substrate system (Dako, Carpinteria, Calif.) according to the manufacturer's instructions.

Double staining of PCA and HD-5 immunohistochemistry was achieved as follows: after PCA staining was performed using diaminobenzidine (DAB) as the chromogen, sections were thoroughly washed with phosphate buffered saline (PBS) and then incubated with the HD-5 antibody. The procedures after the primary antibody reaction were as described above. By this double staining, pyloric gland cells were stained brown and Paneth cells were stained blue.

For immunohistochemistry of the Ki-67 antigen as the proliferative marker, the avidin-biotin peroxidase complex (ABC) method was employed as described earlier [11, 17] with the mouse monoclonal antibody MIB-1 (Immunotech, Marseille, France) at a dilution of 1:100. Sections were lightly counterstained with hematoxylin for microscopic examination.

Results

Immunostaining of Paneth cells in the adult human small intestine

Although the specificity of the HD-5 antibody binding in histological sections has already been examined [23], it was again tested using adult human duodenal and jejunal tissue sections. Clear immunoreactivity limited to the cytoplasm of Paneth cells was evident at the bottom of the duodenal (Fig. 1a, b) and jejunal crypts (data not shown).

Identification of Paneth cells in IM lesions

First, evaluation of the IM type in H&E sections of all cases revealed that seven (6.7%) had no accompanying IM, while the other 98 (93.3%) demonstrated metaplasia to various degrees. Of the total, 51 (48.6%) were predominantly accompanied by the GI mixed type, 43 (41.0%) by the I type, and the other four (3.8%) were approximately equally with both types to the same degree. In only 9 out of 105 cases (8.6%), a few Paneth-like cells with intracytoplasmic eosinophilic granules appeared to be present among the mucous cells in pyloric glands (Fig. 2a). The mucous cells were PCA positive, while the Paneth-like cells showed immunoreactivity with the HD-5 antibody (Fig. 2b), confirming their true Paneth nature.

Double staining of pyloric gland cells and Paneth cells

Figure 2c illustrates the obvious coexistence of pyloric gland cells (brown) and Paneth cells (blue) in the same

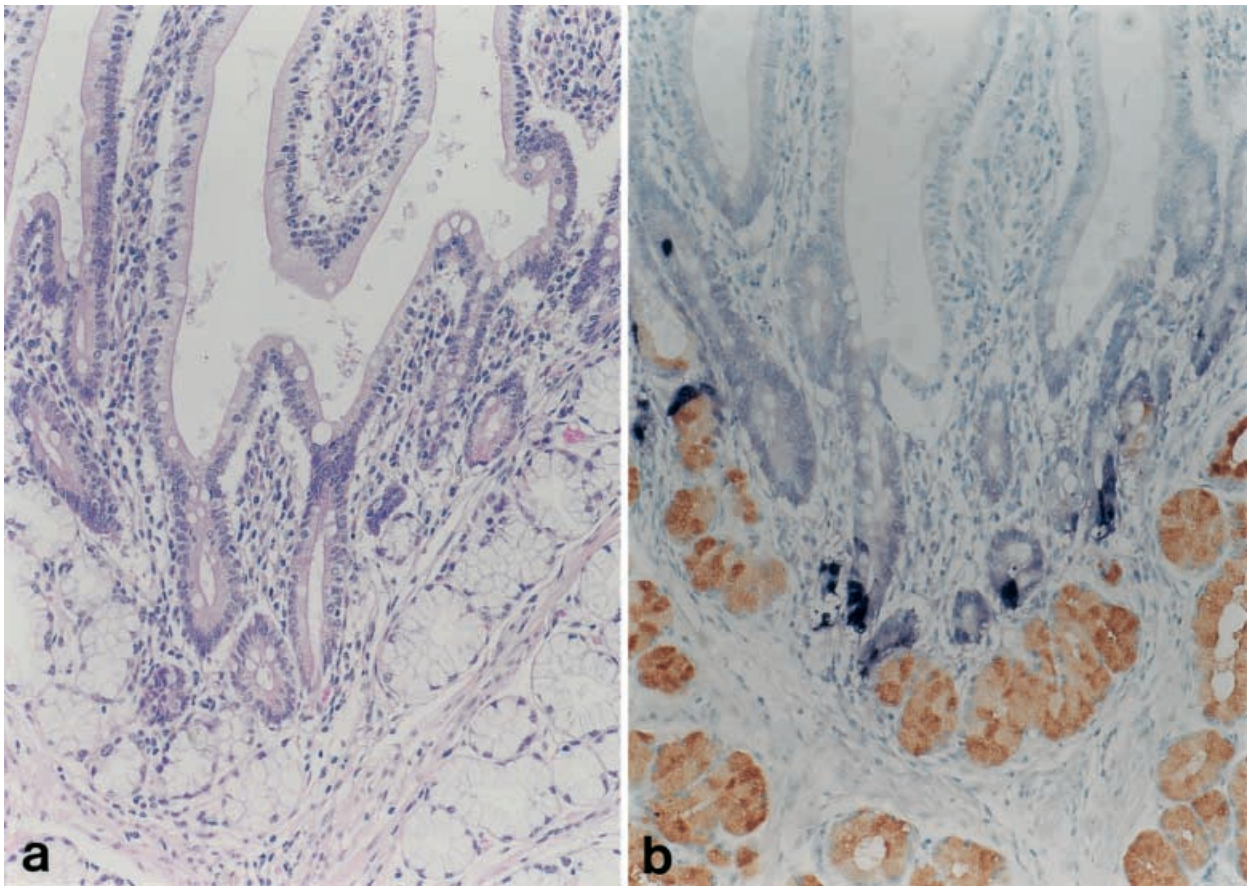


Fig. 1 Semi-serial sections through normal duodenal mucosa. **a** Paneth cells are present at the bottom of each crypt, while Brunner's gland cells are found both in the lamina propria and in the submucosa across the lamina muscularis mucosae. (hematoxylin and eosin, original magnification, ×40). **b** Paneth cells express immunoreactivity with the anti-human defensin (HD)-5 antibody, while Brunner's gland cells are positive for paradoxical concanavalin-A staining (double staining for HD-5 and class III mucins, original magnification, ×40)

Table 1 Clinicopathological data for cases with Paneth cells in pyloric glands. *P* pyloric, *F* fundic, *F with P* fundic gland with pseudopyloric gland, *IM* intestinal metaplasia, *GI* gastric and intestinal mixed-type IM, *I*, solely intestinal-type IM, *Pa* Paneth cells, *sig* signet-ring cell carcinoma, *well diff.* well differentiated adenocarcinoma, *mod. diff.* moderately differentiated adenocarcinoma, *por* poorly differentiated adenocarcinom, *N.D.* not determined because of the difficulty of correct estimation due to the small amount of sample

Case no.	Age (years)	Gender	Biopsy/operated	P/F	Degree of IM	Type of IM	Histology of cancer	Number of GI glands coexisting with pyloric gland cells and Pa cells/total number of GI glands (incidence) [number of Pa cells in each pyloric gland (average)]
1	69	Female	Biopsy	P	Moderate	GI>I	No cancer	N.D.
2	65	Male	Biopsy	P	Severe	GI≅I[a]	No cancer	N.D.
3	52	Female	Operated	F with P	Severe	GI>I	Well diff.	3/48 (6.3%) [3, 11, 15 (9.7)]
4	56	Male	Operated	P	Severe	GI≅I[a]	Well diff.	2/52 (3.8%) [5, 7 (6.0)]
5	52	Male	Operated	P	Moderate	GI>>I	Mod. diff.	3/48 (6.3%) [2, 3, 13 (6.0)]
6	54	Female	Operated	F with P	Severe	GI>I	Mod. diff.	6/65 (9.2%) [2, 6, 10,10, 12, 15 (9.2)]
7	52	Female	Operated	F with P	Severe	I>>GI	Well diff.	1/30 (3.3%) [6 (6.0)]
8	72	Male	Operated	P	Severe	GI>>I	Well diff.	6/110 (5.5%) [1, 2, 5, 6, 9, 10 (5.5)]
9	75	Female	Operated	P	Moderate	GI>>I	Por – sig	4/48 (8.3%) [1, 2, 5, 5 (3.3)]

[a] That is to say, nearly equal

pyloric gland of a GI mixed-type IM. Paneth cells were also observed at the bottom of I-type IM glands without pyloric glands (data not shown). Table 1 summarizes clinicopathological and histological data for the nine cases. There were no apparent common characteristics, although the degree of IM was severe in most, and there was a tendency for a link with GI mixed-type IM rather than the I type. The number of Paneth cells found in one

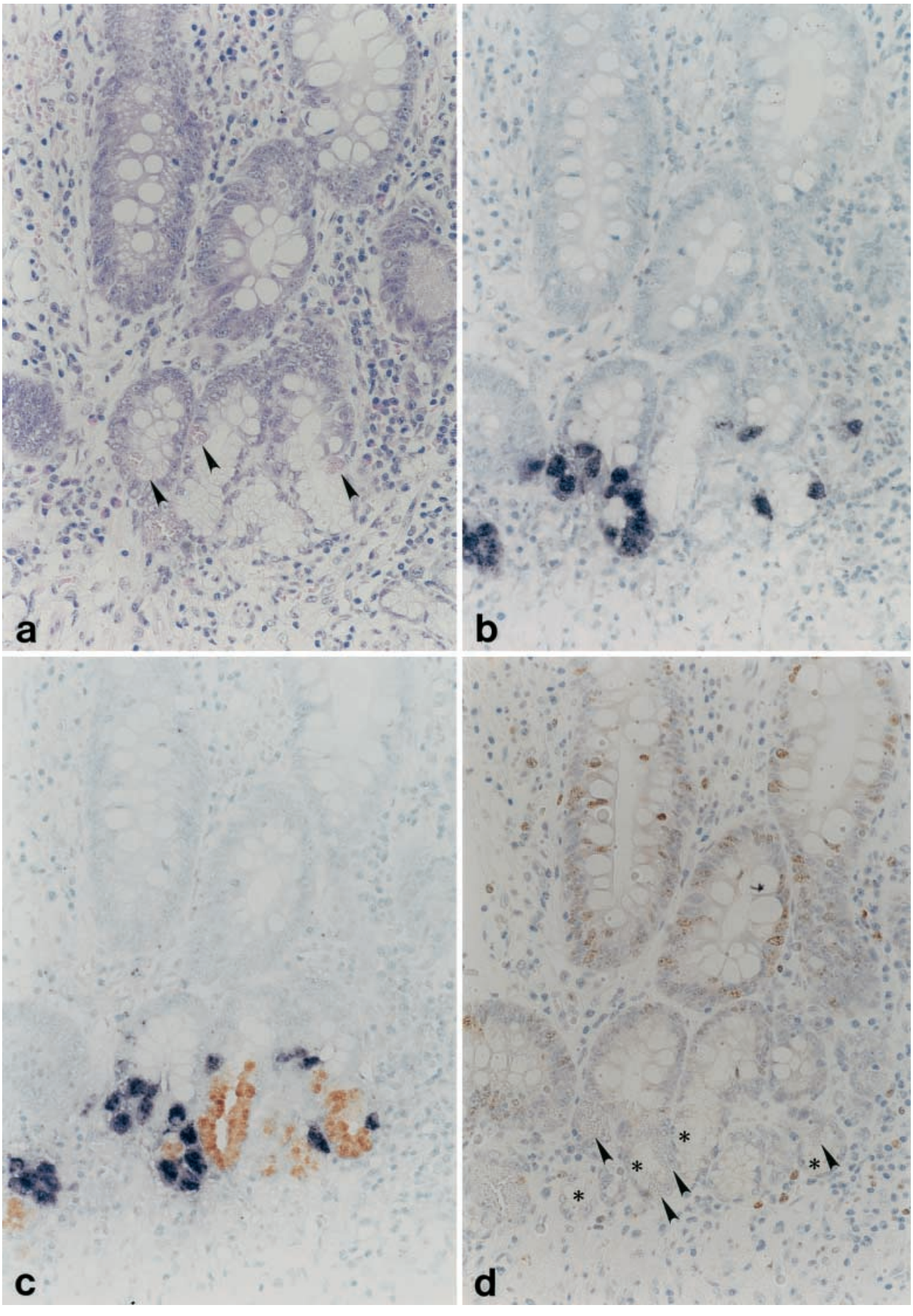


Fig. 2a–d Legend see page 18

pyloric gland was less than 15, with an average of 6.6. The numbers and incidences of GI mixed-type IM glands with coexistence of pyloric gland cells and Paneth cells were also estimated, confirming the rarity of this phenomenon (Table 1).

Detection of the P zone

The P zone was located in about the lower third of the I-type IM glands as in normal small intestine (Fig. 2d). Paneth cells were exclusively present underneath this region. In GI mixed-type IM glands with coexisting pyloric gland cells and Paneth cells, proliferating cells were perceived between the upper intestinalized gastric pits and the underlying pyloric glands in which Paneth cells were present.

Discussion

Our new classification of IM into GI mixed and I types is based upon the cellular differentiation status of IM glands using various cellular differentiation markers [13]. Hitherto, the IM classification has been mainly focused just on the appearance of intestinal phenotypic cells, but in our previous study, we first clearly demonstrated that a good many gastric phenotypic cells may remain, admixed with intestinal phenotypic cells in various combinations and degrees in the same IM glands, and we therefore termed this GI mixed-type IM. This allowed us not only to introduce the notion that IM might be due to an abnormal stem cell differentiation, but also to consider IM subtypes as not an independent entity but a sequence of pathological states, with gradual change from the stomach to the intestine. Moreover, this has made it possible to categorize lesions that did not fit well into the common Filipe's [6] or Kawachi's [16] classifications.

The present immunohistochemical study revealed that Paneth cells may indeed be present in pyloric glands in rare cases of GI mixed-type IM. Thus, the antibody against HD-5, a human homologue of alpha-defensin that was first cloned from murine small intestine and subsequently demonstrated to be localized in Paneth cells [22, 23], clearly showed positive staining in cells with eosinophilic granules. It is well known that Paneth cells possess lysozymal activity in their cytoplasmic granules [29]. Although such enzyme activity is not specific to Paneth cells, a histochemical method using substrates might be useful for demonstration of Paneth cells in some cases. However, pyloric gland cells also have lysozymal activity in their cytoplasm. Thus, the HD-5 antibody, which exclusively binds to HD-5 molecules included in Paneth cell granules [23], has major advantages for identification purpose.

Of the nine cases in which Paneth cells were observed in pyloric glands, seven had gastric carcinomas (Table 1). In one case (case 8), the GI mixed-type IM with Paneth cells in pyloric glands was located just beneath the carcinoma which was of well differentiated, intestinal type but without obvious Paneth cell differentiation (data not shown). Moreover, no correlation between carcinoma location and distribution of IM, including pyloric glands with Paneth cells, was demonstrated in the other six cases. Although it has been suggested that development of intestinal-type carcinomas could have a close interrelationship to IM, especially of incomplete type [6, 30, 38], our data do not support this hypothesis.

Paneth cells in an IM lesion were observed both in metaplastic pseudopyloric glands within the fundic mucosa and in the pyloric glands proper. We have proposed that the histological characteristics of IM shown in the fundic mucosa are similar to those of pyloric gland mucosa if fundic glands are accompanied by pseudopyloric gland metaplasia [13]. Our present results are compatible with our previous findings in this context.

It is believed that stem cells (multipotent progenitor cells) are present in the P zone in the isthmus region of the gastric glands, giving rise to all of the various cell types by differentiation so that consequently gastric glands are monoclonal in the adult stage [14, 18, 21, 34, 35]. In the environment of a normal gastric gland, undifferentiated stem cells undergo complex bipolar migration from the isthmus either upward or downward [24]. In fact, only the cells that are destined to be surface mucous cells move upward. Those cells that are committed to becoming pyloric, cardiac, or the three types of fundic gland cells and endocrine cells migrate downward. In the crypts of the small intestine, however, stem cells would be expected to be present in the P zone at the bottom of the crypts. In the normal intestinal gland, cells that will become absorptive, goblet, and endocrine cells move up, but only these differentiating into Paneth cells migrate lower than the P zone. The latter frequently appear in the intestinal metaplasia and are occasionally found in gastric adenomas or colorectal polyps [27, 28, 32, 36], while being exceedingly rare in gastric adenocarcinomas [3, 10, 19, 20]. The underlying mechanism remains to be clarified. In our cases, all Paneth cells were below the P zone, mimicking the normal small intestinal crypts. Sugihara et al. [31], Akamatsu et al. [1] and Fujimori et al. [7] revealed an organoid differentiation of intramu-

◀ **Fig. 2** Semi-serial sections through intestinalized gastric mucosa in which Paneth cells are apparent in pyloric glands (case 6). **a** A few Paneth-like cells with intracytoplasmic eosinophilic granules are observed within pyloric glands in a gastric and intestinal (GI) mixed type intestinal metaplasia (IM) gland (*arrowheads*; hematoxylin and eosin, original magnification, ×40). **b** Blue coarse granules, which are immunoreactive for anti-human defensin (HD)-5 antibody, are obvious in the cytoplasm of Paneth cells (immunostaining for anti-HD-5, original magnification, ×40). **c** Paneth cells (*blue*) and pyloric gland cells (*brown*) are admixed in the same intestinalized gastric gland (double staining for HD-5 and class III mucin, original magnification, ×40). **d** Both Paneth cells with granules (*arrowheads*) and pyloric gland cells (*asterisk*) are present under the proliferative cell zone composed of MIB-1 positive cells (MIB-1 immunohistochemistry, original magnification, ×40)

cosal signet ring cell or diffuse-type carcinomas, including Paneth cells, with disturbance of the tissue architecture once tumor cells undergo submucosal invasion. The available data would suggest that the appearance of a Paneth cell, in pyloric glands of mixed-type IM might be the consequence of abnormal differentiation of stem cells, while the normal cell migration pattern is preserved. Since epithelial cell differentiation and migration of gastric glands is thought to be closely linked, the reason why only the former is disturbed is not clear. Recently, epithelial-mesenchymal interactions have attracted attention due to an alteration in miscellaneous conditions and their role in organogenesis [8, 9, 12]. The question of whether the organization of an IM lesion might be influenced by interstitial cells clearly warrants further study.

Acknowledgements We gratefully acknowledge the assistance of Ms. Fukami, Ms. Yamamoto, Ms. Tominaga, and Mr. Wani of the Laboratory of Pathology, Aichi Cancer Center Research Institute, Nagoya, Japan.

References

1. Akamatsu T, Katsuyama T (1990) Histochemical demonstration of mucins in the intramucosal laminated structure of human gastric signet ring cell carcinoma and its relation to submucosal invasion. Histochemical J 22:416–425
2. Byrd JC, Yan P, Sternberg L, Yunker CK, Scheiman JM, Bresalier RS (1997) Aberrant expression of gland-type gastric mucin in the surface epithelium of *Helicobacter pylori*-infected patients. Gastroenterology 113:455–464
3. Capella C, Cornaggia M, Usellini L, Bordi C, Bondi A, Cook MG, Eusebi V (1984) Neoplastic cells containing lysozyme in gastric carcinomas. Pathology 16:87–92
4. Correa P (1992) Human gastric carcinogenesis:a multistep and multifactorial process-first American Cancer Society award lecture on cancer epidemiology and prevention. Cancer Res 52:6735–6740
5. Dixon MF (1995) Histological responses to *Helicobacter pylori* infection: gastritis, atrophy and preneoplasia. Bailliere's Clinical Gastroenterology 9:467–486
6. Filipe MI, MuÒoz N, Matko I, Kato I, Pompe-Kirn V, Jutersek A, Teuchmann S, Benz M, Prijon T (1994) Intestinal metaplasia types and the risk of gastric cancer: a cohort study in Slovenia. Int J Cancer 57:324–329
7. Fujimori Y, Akamatsu T, Ota H, Katsuyama T (1995) Proliferative markers in gastric carcinoma and organoid differentiation. Hum Pathol 26:725–734
8. Fukamachi H, Ichinose M, Ishihama S, Tsukada S, Yasugi S, Shiokawa K, Furihata C, Yonezawa S, Miki K (1994) Fetal rat glandular stomach epithelial cells differentiate into surface mucous cells which express cathepsin E in the absence of mesenchymal cells in primary culture. Differentiation 56:83–89
9. Fukamachi H, Ichinose M, Tsukada S, Kurokawa K, Shiokawa K, Miki K, Takeuchi S (1995) Growth of fetal rat gastro-intestinal epithelial cells is region-specifically controlled by growth factors and substrata in primary culture. Dev Growth Differ 37:11–19
10. Heitz PU, Wegmann W (1980) Identification of neoplastic Paneth cells in an adenocarcinoma of the stomach using lysozyme as a marker, and electron microscopy. Virchows Arch A 386:107–116
11. Hsu SM, Raine L, Fanger H (1981) Use of avidin-biotin-peroxidase complex (ABC) in immunoperoxidase techniques: a comparison between ABC and unlabeled antibody (PAP) procedures. J Histochem Cytochem 29:577–580
12. Ichinose M, Tsukada S, Fujimitsu Y, Tatematsu M, Matsubara Y, Yahagi N, Oka M, Suzuiki T, Shimizu Y, Yonezawa S, Kageyama T, Miki K, Fukamachi H (1997) Proliferation, differentiation and morphogenesis of fetal rat glandular stomach transplanted under the kidney capsule of syngeneic hosts. Dev Growth Differ 39:635–642
13. Inada K, Nakanishi H, Fujimitsu Y, Shimizu N, Ichinose M, Miki K, Nakamura S, Tatematsu M (1997) Gastric and intestinal mixed and solely intestinal types of intestinal metaplasia in the human stomach. Pathol Int 47:831–841
14. Karam SM, Leblond CP (1993) Dynamics of epithelial cells in the corpus of the mouse stomach I. identification of proliferative cell types and pinpointing of the stem cell. Anat Rec 236:259–279
15. Katsuyama T, Spicer SS (1978) Histochemical differentiation of complex carbohydrates with variants of the concanavalin A-horseradish peroxidase method. J Histochem Cytochem 26: 233–250
16. Kawachi T, Kogure K, Tanaka N, Tokunaga A, Sugimura T, Koyama Y, Kanasugi K, Hirota T, Sano R (1974) Studies of intestinal metaplasia in the gastric mucosa by detection of disaccharidases with Tes-Tape. J Natl Cancer Inst 53:19–30
17. Moriki T, Takahashi T, Kataoka H, Hiroi M, Yamane T, Hara H (1996) Proliferation marker MIB-1 correlates well with proliferative activity evaluated by BrdU in breast cancer: an immunohistochemical study including correlation with PCNA, p53, c-*erb*B-2 and estrogen receptor status. Pathol Int 46:953–961
18. Nomura S, Esumi H, Job C, Tan SS (1998) Lineage and clonal development of gastric glands. Dev Biol 204:124–135
19. Ohtani H, Sasano N (1988) Ultrastructural immunolocalization of lysozyme in Paneth-like cells in undifferentiated (gastric)-type carcinoma of the stomach. Acta Pathol Jpn 38:861–871
20. Ooi A, Nakanishi I, Itoh T, Ueda, H, Mai M (1991) Predominant Paneth cell differentiation in an intestinal types gastric cancer. Path Res Pract 187:220–225
21. Ponder BAJ, Schmidt GH, Wilkinson MM, Wood MJ, Monk M, Reid A (1985) Derivation of mouse intestinal crypts from single progenitor cells. Nature 313:689–691
22. Porter EM, Dam EV, Valore EV, Ganz T (1997) Broad-spectrum antimicrobial activity of human intestinal defensin 5. Infect Immun 65:2396–2401
23. Porter EM, Liu L, Oren A, Anton PA, Ganz T (1997) Localization of human intestinal defensin 5 in Paneth cell granules. Infect Immun 65:2389–2395
24. Potten CS (1998) Stem cells in gastrointestinal epithelium: numbers, characteristics and death. Phil Trans R Soc Lond B 353:821–830
25. Quayle AJ, Porter EM, Nussbaum AA, Wang YM, Brabec C, Yip KP, Mok SC (1998) Gene expression, immunolocalization, and secretion of human defensin-5 in human female reproductive tract. Am J Pathol 152:1247–1258
26. Rooijen NV, Kors N, Nieuwmegen RV (1984) Double immunocytochemical staining in the study of antibody-producing cells in vivo. J Histochem Cytochem 32:677–680
27. Rubio CA (1989) Paneth cell adenoma of the stomach. Am J Surg Pathol 13:325–328
28. Rubio CA, Kanter L, Bjôrk J, Poppen B, Bry L (1996) Paneth cell-rich flat adenoma of the rectum: report of a case. Jpn J Cancer Res 87:109–112
29. Sandow MJ, Whitehead R (1979) Progress report, the Paneth cell. Gut 20:420–431
30. Stemmermann GN (1994) Intestinal metaplasia of the stomach. A status report. Cancer 74:556–564
31. Sugihara H, Hattori T, Fukuda M, Fujita S (1987) Cell proliferation and differentiation in intramucosal and advanced signet ring cell carcinomas of the human stomach. Virchows Arch 411:117–127
32. Symonds DA (1974) Paneth cell metaplasia in diseases of the colon and rectum. Arch Pathol 97:343–347

33. Tatematsu M, Hasegawa R, Ogawa K, Kato T, Ichinose M, Miki K, Ito N (1992) Histogenesis of human stomach cancers based on assessment of differentiation. J Clin Gastroenterol 14 [Suppl 1]:1–7
34. Tatematsu M, Fukami H, Yamamoto M, Nakanishi H, Masui T, Kusakabe N, Sakakura T (1994) Clonal analysis of glandular stomach carcinogenesis in C3H/HeN↔BALB/c chimeric mice treated with *N*-methyl-*N*-nitrosourea. Cancer Lett 83:37–42
35. Tatematsu M, Masui T, Fukami H, Yamamoto M, Nakanishi H, Inada K, Kusakabe M, Sakakura T (1996) Primary monoclonal and secondary polyclonal growth of colon neoplastic lesions in C3H/HeN↔BALB/c chimeric mice treated with 1,2-dimethylhydrazine: immunohistochemical detection of C3H strain-specific antigen and simple sequence length polymorphism analysis of DNA. Int J Cancer 66:234–238
36. Xuan ZX, Ambe K, Enjoji M (1991) Depressed adenoma of the stomach, revisited histologic, histochemical, and immunohistochemical profiles. Cancer 67:2382–2389
37. Yamachika T, Inada K, Fujimitsu Y, Nakamura S, Yamamura Y, Kitou T, Itzkowitz S H, Werther J L, Miki K, Tatematsu M (1997) Intestinalization of gastric signet ring cell carcinomas with progression. Virchows Arch 431:103–110
38. You WC, Blot WJ, Li JY, Chang YS, Jin ML, Kneller R, Zhang L, Han ZX, Zeng XR, Liu WD, Zhao L, Correa P, Fraumeni Jr JF, Xu GW (1993) Precancerous gastric lesions in a population at high risk of stomach cancer. Cancer Res 53:1317–1321

Virchows Arch (2001) 439:21–26
DOI 10.1007/s004280100436

ORIGINAL ARTICLE

J.J. Bogers · P.A. Storey · G. Faile · E. Hewitt
L. Yelifari · A. Polderman · E.A. Van Marck

Human oesophagostomiasis: a histomorphometric study of 13 new cases in northern Ghana

Received: 8 November 2000 / Accepted: 6 February 2001 / Published online: 20 March 2001
© Springer-Verlag 2001

Abstract Oesophagostomiasis is an infrequently described and recognised parasitic infection in humans, caused by *Oesophagostomum bifurcum*. Although the disease is most often found in the northern part of Togo and the neighbouring part of Ghana, sporadic cases have been described in other parts of Africa and in Asia and South America: Uganda, Ivory Coast, Sudan, Kenya, Ethiopia, Indonesia, Malaysia and Brazil. Infection probably occurs by way of the ingestion of L3 larvae. These larvae penetrate the intestinal wall, especially that of the colon. Some of these larvae develop into young adult worms and return to the bowel lumen. Other larvae, however, develop into immature worms, which fail to settle in the lumen, forming abscesses in the bowel wall and causing pathology. In the literature 105 human cases have been described, many originating in the northern regions of Ghana and Togo. The present study was performed to evaluate 13 new cases originating in the northern part of Ghana (7 female and 6 male patients, aged between 2 and 60 years). Histopathologically, the patients could be divided into two groups: the first group showed multinodular disease, while patients in the second group presented with a single, nodular mass. In the first group, abscesses were seen throughout the colonic wall. The mean size of the cavities was 4.3±0.7 mm. There was no relation between the size and the localisation in the colonic wall. Abscesses were significantly larger in male patients than in female patients. There was no correlation with age. In the second group, histopathological examination showed a cyst of variable wall thickness with very limited inflammation. These cysts represented older lesions, often encapsulated in the mesentery. In conclusion, in this study we present 13 new cases of human oesophagostomiasis. The abscess formation was found to be organ specific, independent of age, and gender-related, producing a more intense tissue reaction in male patients.

Keywords Oesophagostomiasis · Intestinal · Helminthic infection

J.J. Bogers · E.A. Van Marck (✉)
Laboratory of Pathology, University Hospital Antwerp,
University of Antwerp, Wilrijkstraat 10, 2650 Edegem, Belgium
e-mail: eric.van.marck@uza.uia.ac.be
Tel.: +32-3-8213604, Fax: +32-3-8214753

P.A. Storey · A. Polderman
Department of Parasitology, Leiden University Medical Centre,
PO Box 9600, 2300 RC Leiden, The Netherlands

G. Faile · E. Hewitt
Baptist Medical Centre Nalerigu, Northern Region, Ghana

L. Yelifari
Ministry of Health, Bogatanga, Upper East Region, Ghana

Present address:
P.A. Storey, Edinburgh University Medical School,
United Kingdom

Introduction

Oesophagostomiasis is an helminthic infection that is infrequently described in humans. Although many species of *Oesophagostomum* have veterinary and economic importance, killing animal stock and causing tissue destruction in ruminants, in humans oesophagostomiasis is rarely recognised as an intestinal infection.

The disease was first described in 1905, and since then several human cases have been reported [19]. The taxonomy of the species important for human disease was studied by Chabaud and Lariviere and by Blotkamp, who recognized *Oesophagostomum bifurcum* as the most prevalent parasite in humans [4, 5]. Although the disease is most often found in West Africa, sporadic cases have been described in other parts of Africa, Asia and South America [1, 6, 11, 13, 15].

Infection probably occurs with the ingestion of L3 larvae. These larvae penetrate the intestinal wall, especially the colon. Some of the larvae develop and return to the bowel lumen. Other larvae, however, develop into immature worms, which fail to settle in the lumen, forming abscesses in the bowel wall and causing pathology. The adult worms live in the bowel lumen of their definitive host, where they mate and produce eggs, which are

passed with the faeces and hatch in soil producing L1 larvae. The L1 larvae moult twice in a period of 5–7 days to become infective L3 larvae: they can survive long periods of drought [17]. A definite diagnosis can be made on stool cultures using stool–charcoal mixtures cultured for periods of 6–10 days at local room temperature (25–35°C) [18]. Examination of stool for the detection of parasitic eggs is insufficient, because microscopically it is impossible to distinguish *Oesophagostomum* eggs from those of hookworms.

Recently two definite forms of disease presentation were described: the more classical, multinodular form and uninodular disease, which is also known as Dapaong tumour [17].

Diagnosis of the disease is suggested on the basis of characteristic clinical signs, often accompanied by epigastric or periumbilical masses. These masses are recognised by the native people themselves and are well known in the local culture [21]. They can cause localised abdominal pain and discomfort, commonly in the right lower quadrant. Often there is no accompanying nausea, vomiting, anorexia or diarrhoea.

Some of the cases need surgery. In the multinodular disease the colon is found to be studded with abscess-like pea-sized nodules. The bowel wall is diffusely hardened, and the surgical differential diagnosis is often against inflammatory bowel disease or even carcinoma. In the unilocular form a ligneous mass 30–60 mm in diameter is found [21]. In northern Ghana oesophagostomiasis accounts for approximately 1% of the annual major surgical procedures and 0.2% of patient contacts [20].

Judging from the literature and on the basis of resected specimens, however, human disease caused by *Oesophagostomum bifurcum* seems to be rare and very localised. In Table 1, a list of 105 endemic cases reported on the basis of surgical resection specimens and histology is given. Most of the cases were described in the northern region of Ghana and Togo, but the other major focus of reporting has been Uganda [1, 8].

The largest series of published cases backed up with surgical specimens and pathological analysis was published by Gigase et al. in 1987 and comprised of 51 cases with a male-to-female ratio of 1.1:1 [8]. The histology was characteristic for helminthoma. The lesions were described as spherical abscesses filled with material that was necrotically thickened or had a caseous appearance, material with collections of pycnotic leucocytes. Surrounding the abscess, fibrous tissue containing numerous eosinophils, macrophages and plasma cells was seen. The mucosa was always intact. In all cases a maximum of one worm per abscess was detected.

Systematic stool analysis in the endemic region in Togo and Ghana reveals a high prevalence of up to 70% stool positivity in some villages. The male-to-female ratio in this infected but apparently symptom-free population was reversed to 2:3 (14% infected in 1,525 men versus 20% infected in 1,717 women) [18]. On the basis of these data 250,000 people are presumed to be infected, with another 1 million at risk.

Table 1 Summary of human cases of oesophagostomiasis published in the literature

Country	No. of patients	Male	Female	Unknown	Reference
Uganda	36	19	17		[1, 7]
Ghana	10	3	7		[2, 10]
Togo	51	27	24		[8]
Ivory Coast	2		1	1	[3, 6]
Zimbabwe	1	1			[9]
Sudan	1	1			[11]
Kenya	1	1			[13]
Ethiopia	1	1			[15]
Indonesia	1	1			[12]
Malaysia	1	1			[14]
Brazil	1			1	[22]

Table 2 Morphological and morphometric data of 13 new cases of oesophagostomiasis, with diameters expressed as mean ± standard error of the mean (*M* multinodular disease, *U* unilocular disease; worm data: + present, – absent (in at least 10 abscesses/case), +–+++ semi-quantitative assessment of density, ranging from a few to abundant numbers of eosinophilic granulocytes in proportion to the number of plasma cells)

	Mean abscess diameter (mm)	Multi-nodular / unilocular	Worm present?	Eosinophilic granulocytes
1	3.6±0.5	M	+	+
2	8±0	U	–	++
3	6.1±0.7	M	+	+
4	2.4±0.6	M	+	+
5	6.6±0	U	–	+
6	5.5±0.4	M	+	+
7	8.1±3.9	M	–	++
8	4.5±0.4	M	+	++
9	1.7±0.5	M	–	++
10	7.2±0	U	–	+++
11	6.3±1.6	M	–	++
12	6.3±0.9	U	–	+
13	7.4±0	U	–	+

The present study was performed to evaluate 13 new cases of oesophagostomiasis in which surgical intervention was performed in northern Ghana and from which material was available (Table 2). The cases were investigated using routine histological techniques to evaluate the two distinct forms (unilocular and multinodular). Limited morphometric analysis was performed for objective quantification of tissue destruction and inflammation.

Materials and methods

Patients

Thirteen pathological specimens were collected from patients presenting at the Baptist Medical Centre in the Northern Region of Ghana and Dapaong Regional Hospital in northern Togo. The patients presented with the symptoms and signs of acute abdomen and needed surgery. They were 7 female and 6 male patients, ranging between 2 and 60 years of age.

The diagnosis of *Oesophagostomiasis* was suggested on clinical and epidemiological grounds and was confirmed by stool culture in all cases presented.

Histology

Resection specimens were formalin fixed and processed for routine histopathological examination. Paraffin sections were stained with haematoxylin–eosin, Masson's trichrome, periodic acid–Schiff and with the Dominici stain for the detection of eosinophilic granulocytes. In the multinodular disease, the presence of a worm was assessed in at least 10 abscesses/case.

Morphometry

To quantify the tissue destruction, the abscess diameters were measured. In multinodular disease at least 10 abscesses/case were measured. Morphometric analysis was performed using a computerised morphometry system (Fenestra, Kinetic Imaging, Liverpool, UK).

The number of eosinophilic granulocytes in the vicinity of the abscess was semi-quantitatively assessed and expressed as a density range in proportion to the plasma cells in the infiltrate from + eosinophilic granulocytes << plasma cells, ++ eosinophilic granulocytes = plasma cells to +++ eosinophilic granulocytes >> plasma cells.

Statistical analysis

All results were analysed using Graphpad Prism 3.0 (Graphpad Software, USA). For the evaluation of the abscess size in the various layers of the colonic wall a one-way analysis of variance (ANOVA) was used. For the comparison of two groups Student's *t*-test for unpaired values was used. *P*-values of less than 0.05 were considered significant. Results are expressed in millimetres and presented as mean ± standard error of the mean (SEM).

Results

Macroscopy

Multinodular disease

Each specimen was a large bowel segment with a thickened wall containing numerous cysts of varying sizes filled with necrotic material, either tissue fragments of fat or fibrous tissue from the mesentery, which on section also contained one or more cysts of varying dimensions. Figure 1a shows a cut section of a large bowel segment demonstrating numerous cavities. These cavities were often filled with necrotic material. In some of the cavities a worm was found.

Unilocular disease

The specimens each showed a hard nodule ranging from 3 to 5 cm in diameter, which was hard on palpation. On section the cyst wall ranged from 2 mm to 2 cm in thickness, consisting of grey-yellow fibrous tissue surrounding the pus-filled abscess cavity (Fig. 1b). No worms were found.

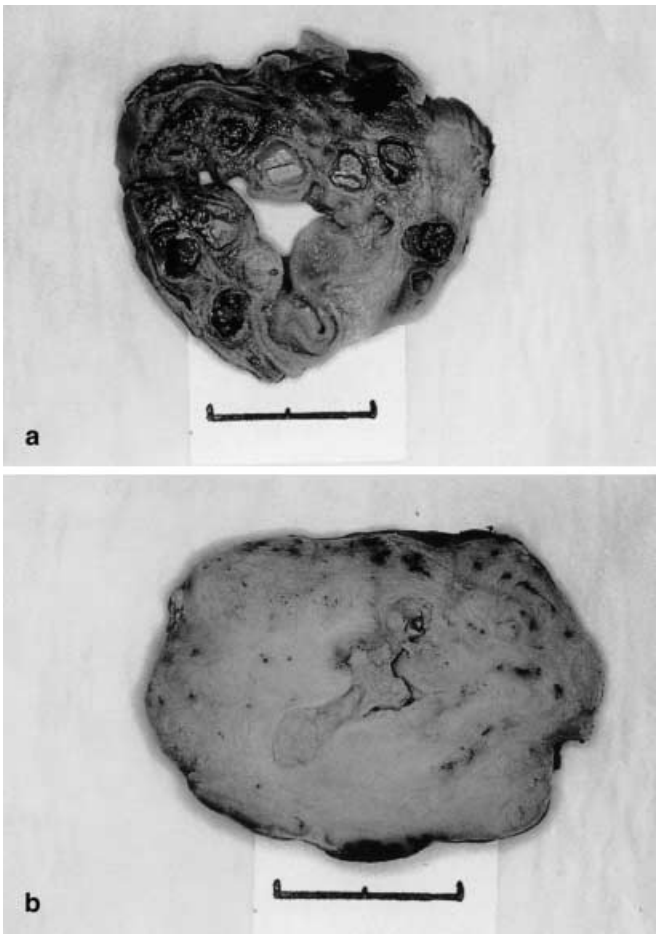


Fig. 1 Macrophotograph showing **a** the multinodular and **b** the unilocular disease. In multinodular disease there are numerous small abscesses filled with pus throughout the bowel wall. The unilocular disease consists of a fibrotic nodule with a central lumen surrounded by dense, whitish grey connective tissue. *Bar* 2×1cm

Microscopy

Multinodular disease

In the microscopic analysis the multinodular specimens could be divided into two groups on the basis of the cellular content of the abscesses. Both groups contained large abscess cavities, filled with necrotic material, pycnotic nuclei and fragmented granulocytes (Fig. 2a). In the necrotic material Charcot-Leyden crystals could be seen. In some of the cavities a transsection of a worm was seen (Fig. 2a). In the first group, the necrotic material was surrounded by fibrous tissue containing a large amount of eosinophilic granulocytes and neutrophilic granulocytes as well as histiocytes. There were moderate to low numbers of plasma cells. In the second group, the infiltrate consisted mainly of plasma cells, with a low number of eosinophilic granulocytes (Fig. 2b). The surrounding submucosa contained a variably intense, diffuse chronic inflammatory infiltrate containing plasma

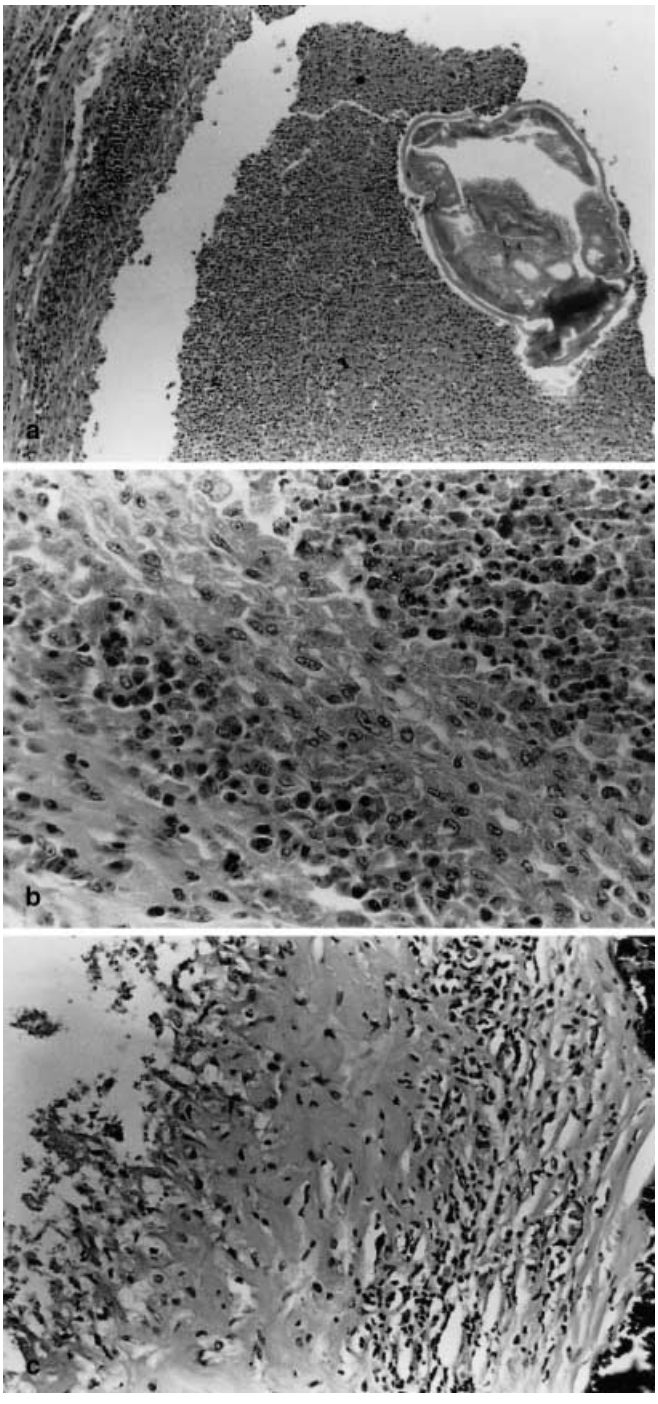


Fig. 2 Micrographs showing **a**, **b** the multinodular form versus **c** the wall of the nodule of unilocular disease. The abscess in the multinodular disease often shows a transsection through an *Oesophagostomum*. The rest of the lumen is filled with pus. The wall of some of the nodules consists of fibrous tissue with a mixture of inflammatory cells of variable intensity, with mainly eosinophilic granulocytes, plasma cells and histiocytes (**b**). In the unilocular form the wall is of variable thickness and is made up of fibrous tissue containing a mixture of inflammatory cells (eosinophilic granulocytes, histiocytes and plasma cells). In the wall of some of the nodules calcification was seen (**c**). **a** ×65; **b** ×300; **c** ×150

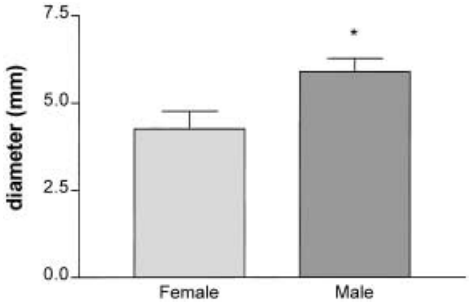


Fig. 3 Size of abscesses in the multinodular disease by gender. Abscesses in male patients are significantly larger than those in female patients. Whether this effect is biological or the result of differences in the social status (and accessibility of health care) remains to be elucidated. (Students *t*-test, **P*<0.05; *n*>10 abscesses/case; 7 female and 6 male patients; diameters (mm) expressed as mean ± standard error of mean)

cells, lymphocytes and neutrophilic granulocytes. The lamina propria contained a diffuse increased inflammatory infiltrate. In the surrounding connective tissue, both in the colon specimens and mainly in the mesenteric resections, numerous lymphocytic aggregates and follicles were detected. If the abscesses were seen in the muscularis propria the muscular fibres were dissected and pushed aside. In some of the specimens the abscess was partly replaced by connective tissue. In the vicinity of the cavity a proliferation of small blood vessels was seen. In each specimen all the abscesses looked similar and were apparently of the same stage and age.

Unilocular disease

In the unilocular form of the disease the abscess cavity was similar to the description above and surrounded by fibrous tissue containing a low number of plasma cells and eosinophilic granulocytes. The lumen was often rimmed with histiocytes. In the fibrous tissue calcification was often seen (Fig. 2c).

Morphometry

In multinodular disease, abscesses were seen in all layers of the colon wall. There was no statistically significant difference between the size of the abscesses in the various layers (ANOVA, at least 10 abscesses per group and per case, data not shown). When the diameters of the two groups of abscesses, surrounded by many (++ and +++) or a sparse number (+) of eosinophilic granulocytes, were compared, the first group were found to be significantly smaller than the second (3.7±0.8 mm versus 5.7±0.5 mm).

Abscesses in female patients were significantly smaller than those in male patients (Fig. 3).

There was no correlation between age and abscess size (data not shown).

Discussion

Oesophagostomiasis is generally thought to be a rare zoonosis in humans. However, systematic analysis of stool samples from an apparently healthy population in an endemic area of northern Ghana has shown differently: 30% of the population were shown to excrete eggs in the faeces [18]. One of the explanations for this surprising epidemiological result could be the morphological similarity between the eggs of *Oesophastomum bifurcum* and of hookworms (*Ancylostoma duodenale*). Only after culture can the difference be recognised. If this mix-up were found to be common, it would mean that the real prevalence of oesophagostomiasis in Africa is dramatically higher than that accepted so far, since the finding of hookworm eggs in faeces is common in some parts of the continent. While the usual clinical presentation of a hookworm infection is with anaemia and hypoproteinaemia, granulomatous inflammation caused by *Ancylostoma duodenale*, which is morphologically similar to the tissue reaction to *Oesophagostomum bifurcum*, has very rarely been described [16]. The internal granulomatous inflammation caused by *Ancylostoma* infection is extremely rare, and confusion with *Oesophagostomum* is not likely.

Pathological examination of the resected specimens in the present study revealed two groups of patients. The first group presented with a single nodular mass, often adherent to the abdominal wall or even the skin and consisting of a debris-filled, fibrous-tissue-walled cyst. These cysts probably represent older lesions, encapsulated in the mesentery or in the vicinity of the peritoneum. In the second group, laparotomy revealed multinodular disease with thousands of pea-sized nodules studding the intestinal wall of predominantly the colon and occasionally the terminal ileum. The finding that some of the cavities surrounded by a low number of eosinophilic granulocytes were significantly bigger than others could mean that these are older lesions.

In the epidemiological literature there is a discrepancy in the sex ratio, operated patients showing a slight male predominance while the results based on stool examination of apparently healthy individuals show a clear female predominance. This discrepancy could reflect different cultural attitudes towards health care, favouring male presentation at expensive hospitals, or it could be the result of a sociological priority setting. However, when evaluating the present series, we found that abscesses were significantly bigger in male patients than in female patients, although the threshold of access to the health care system could be expected to be lower for men than for women. Combining the epidemiological stool data with these histological findings suggests a higher rate of infection in female patients but a more pronounced tissue reaction in men when they do get infected. Whether this reflects a true gender-related difference or whether the less pronounced tissue reaction in female patients is the result of immunological down-regulation remains to be elucidated. The very slight, nonsignificant correlation between age and abscess size suggests a nonimmunological mechanism.

In conclusion, in the present paper we have described 13 new cases of oesophagostomiasis. The abscess formation was found to be organ specific, producing either a solitary confined nodule in the peritoneum or multinodular disease in the intestinal wall, independent of age, and gender related, producing a more intense tissue reaction in male patients. The abscesses found in each individual patient all proved to be at approximately the same stage, possibly suggesting a short window of infection. Whether this is the result of immunity or the effect of the known seasonal variation in infectivity remains to be elucidated.

Acknowledgment The authors acknowledge the help of Dr. E. Hauben in the macroscopic descriptions of some of the specimens. This study was supported by the Interuniversity Poles of Attraction Programme [grant P4/16) from the Services of the Prime Minister, Federal Agency for Scientific, Technical and Cultural Affairs (Belgium)]. The support of the technical staff of the Laboratory of Pathology at the University Hospital Antwerp has been much appreciated.

References

1. Anthony PP, McAdam IWJ (1972) Helminthic pseudotumors of the bowel: Thirty-four cases of helminthoma. Gut 13:8–16
2. Barrowclough H, Crome L (1979) Oesophagostomiasis in man, Trop Geogr Med 31:133–138
3. Baylet RJ, Paillet RJ (1959) Abcès musculaire par *Oesophagostomum* (Dakar). Bull Soc Pathol Exot 52:32–34
4. Blotkamp J, Krepel HP, Kumar V, Baeta S, Noordende JMv, Polderman AM (1993) Observations on the morphology of adults and larval stages of *Oesophagostomum* sp. isolated from man in northern Togo and Ghana. J Helminthol 67: 49–61
5. Chabaud G, Lariviere N (1958) Sur les oesophagostomes parasites de l'homme. Bull Soc Pathol Exot 51:386–387
6. Curan D (1975) Myositis caused by *Oesophagostomum*. Med Trop 35:333–335
7. Elmes BGT, McAdam IWJ (1951) Oesophagostome infection. East Afr Med J 28:333
8. Gigase P, Baeta S, Kumar V, Brandt J (1986) Frequency of symptomatic human oesophagostomiasis (helminthoma) in Northern Togo. In: Geerts S, et al (eds) Helminth zoonoses. Martinus Nijhoff, Amsterdam
9. Gordon JA, Ross CMD, Affleck H (1969) Abdominal emergency due to an oesophagostome. Ann Trop Med Parasitol 63:161–164
10. Haaf E, van Soest AH (1964) Oesophagostomiasis in man in North Ghana. Trop Geogr Med 16:49–53
11. Jacques JE, Lynch JB (1964) Massive oesophagostomiasis of the colon. Gut 5:80–82
12. Joe LK (1949) Helminthiasis of intestinal wall caused by *Oesophagostomum apiostomum*. Doc Neerl Indones Morb Trop 1:75–80
13. Kaminsky RG, Ndinya-Achola JO (1977) *Oesophagostomum* sp. from Kenya, identification through tissue sections. E Afr Med J 54:296–297
14. Karim N, Yang CO (1992) Oesophagostomiasis in Man: report of the first Malaysian case with emphasis on its pathology. Malays J Pathol 14:19–24
15. Leoutsakos B, Agnade N, Kolisiatis S (1977) Rectal bleeding due to *Oesophagostomum brumpti*. Report of a case. Dis Colon Rectum 20:632–634

16. Marcus LC (1982) Oesophagostomiasis. In: Schultz MG (ed) Handbook series in zoonoses. CRC Press, Boca Raton, pp 221–223
17. Polderman AM, Blotkamp J (1995) *Oesophagostomum* infection in humans. Parasitol Today 11:451–456
18. Polderman AM, Krepel HP, Baeta S, Blotkamp J, Gigase P (1991) Oesophagostomiasis, a common infection of man in northern Togo and Ghana. Am J Trop Med Hyg 44:336–344
19. Railliet A, Henry A (1905) Encore un nouveau sclerostomien (*Oesophagostomum brumpti* nov. sp.) Parasite de l'homme. C R Seances Soc Biol 53:643–645
20. Storey PA, Anemana S, van Oostayen JA, Polderman AM, Magnussen P (2000) Ultrasound diagnosis of oesophagostomiasis. Br J Radiol 73:328–332
21. Storey PA, Faile G, Hewitt E, Yelifari L, Polderman AM, Magnussen P (2000) Clinical epidemiology and classification of human oesophagostomiasis. Trans R Soc Trop Med Hyg 94:177–182
22. Thomas HW (1910) The pathological report of a case of oesophagostomiasis in man. Ann Trop Med Parasitol 4:57–88

Virchows Arch (2001) 439:27–34
DOI 10.1007/s004280100443

ORIGINAL ARTICLE

Pilar Arrizabalaga · Manuel Solé · Rosa Abellana
Carlos Ascaso · Antonio Cardesa

Renal expression of intercellular adhesion molecule-1 in immunoglobulin A nephropathy: tubulointerstitial injury and prognosis

Received: 16 October 2000 / Accepted: 20 February 2001 / Published online: 24 April 2001
© Springer-Verlag 2001

Abstract In immunoglobulin A nephropathy (IgAN), the abnormal expression of intercellular adhesion molecule-1 (ICAM-1) on proximal tubule epithelium is associated with the glomerular and interstitial infiltration of leucocytes, but its clinical significance remains uncertain. We analysed the relationship between the ICAM-1 (CD54) expression in tubular epithelial cells and interstitial leucocytes, macrophages (CD14) and T lymphocytes (CD3) with the histologic features, proteinuria and serum creatinine at the time of renal biopsy and after 2.42 years in 45 patients with IgAN and after 1.8±1.5 years in 29 patients with non-glomerulonephritis (non-GN). In IgAN, ICAM-1$^+$ tubule epithelium was 0.1±0.18 ($\bar{x}$±SD), and this was associated with extracapillary proliferation (up to 20% of Bowman's space), glomerular sclerosis involving less than 50% of glomerular area, interstitial cellular infiltration, tubular atrophy and proteinuria level. ICAM-1$^+$ interstitial leucocytes were correlated with glomerular sclerosis involving less than 50% of glomerular area, glomerular sclerosis involving more than 50% of glomerular area, tubular atrophy, interstitial fibrosis and serum creatinine level. In patients with an increase of 50% in serum creatinine, ICAM-1$^+$, CD14$^+$ and CD3$^+$, interstitial leucocytes were significantly outnumbered than in patients with stable serum creatinine. In non-GN, ICAM-1$^+$ tubule epithelium was 0.02±0.04 (U=344, P<0.05, vs IgAN), and this was inversely correlated with the percentage of the normal glomeruli and associated with glomerular sclerosis covering more than 50% of glomerular area, tubular atrophy and serum creatinine level. The association between tubular ICAM-1 and proteinuria and the association between interstitial ICAM-1$^+$, CD14$^+$ and CD3$^+$, leucocytes and renal failure at presentation and the deterioration in IgAN in contrast with non-GN suggest that tubular and interstitial expression of ICAM-1 may be a marker of tubulointerstitial disturbance in IgAN.

Keywords IgA nephropathy · Intercellular adhesion molecule-1 · Renal injury · Prognosis

P. Arrizabalaga (✉)
Services of Nephrology, Hospital Clínic, c/Villarroel, 170, 08036, Barcelona, Spain
e-mail: parrizabala@senefro.org
Tel.: +34-93-3598750, Fax: +34-93-3598750

M. Solé · A. Cardesa
Services of Pathology, Hospital Clínic, c/Villarroel, 170, 08036, Barcelona, Spain

R. Abellana · C. Ascaso
Department of Public Health, University of Barcelona, Institut d'Investigació Biomèdica August Pi i Sunyer, Barcelona, Spain

Introduction

Primary immunoglobulin A nephropathy (IgAN) is the most common form of glomerulonephritis (GN) in the developed world, and it progresses to end-stage renal failure in about one-third of patients within 10 years [11]. Nephrotic range proteinuria, renal function impairment and hypertension at presentation are strong predictors of an adverse clinical outcome [22, 41]. IgAN is characterised by predominantly mesangial IgA deposition, often in conjunction with C3 and IgG and/or IgM, and it appears with a highly variable degree of glomerular hypercellularity [20, 21]. Tubulointerstitial damage [12, 26], particularly the infiltration of mononuclear leucocytes [2, 18, 31, 37], plays a major role in this disease.

Renal entrapment and migration of leucocytes is mediated by interactions between adhesion molecules expressed on these cells and their ligands on renal cells. A major ligand in leucocyte trafficking is the intercellular adhesion molecule-1 (ICAM-1), a member of the Ig superfamily. ICAM-1 antigens are strongly expressed on monocytes and lymphocytes and up-regulated in vitro on epithelial and endothelial cells by several cytokines, such as interleukin (IL)-1, tumour necrosis factor (TNF)-α and interferon-γ [36]. In vivo, ICAM-1 expression is present on the normal renal vascular endothelium [29]. Induction of ICAM-1 expression has been reported on mesangium in focal segmental glomerulosclerosis [13] and parietal

Table 1 Glomerular pathology. Degrees of interstitial cellular infiltration, tubular atrophy and interstitial fibrosis in immunoglobulin A nephropathy (IgAN) and non-glomerulonephritis (non-GN)

Pathology	Interstitial cellular infiltration[b]					Tubular atrophy[c]				Interstitial fibrosis[c]				No.
	–	+	++	+++	++++	–	+	++	+++	–	+	++	+++	
IgAN[a]														
Minor	5	3	–	1	–	4	5	–	–	2	5	2	–	9
Focal GN	5	3	4	5	1	3	10	5	–	–	8	10	–	18
Diffuse GN	–	2	5	2	1	–	3	7	–	–	2	7	1	10
Sclerosis	–	2	–	5	1	–	–	4	4	–	–	–	8	8
No.	10	10	9	13	3	7	18	16	4	2	15	19	9	45
Non-GN														
Nephrosclerosis	–	11	1	1	2	–	5	7	2	–	2	7	5	15
Diabetes	–	1	2	2	–	–	–	3	2	–	–	3	2	5
Amyloidosis	4	1	1	–	1	2	1	4	–	1	1	1	4	7
Acute tubular necrosis	1	1	–	–	–	–	2	–	–	–	–	2	–	2
No.	5	14	4	3	3	2	8	15	4	1	3	14	11	29

[a] Minor glomerular abnormality when less than 20% of glomeruli showed proliferative lesions, focal GN when 20–80% of the glomeruli showed proliferative lesions, diffuse proliferative GN when more than 80% of the glomeruli showed proliferative lesions and advanced sclerosis when more than 80% of the glomeruli showed predominant sclerotic lesions rather than proliferation

[b] Interstitial cellular infiltration negative (–) when no cells were seen, + when cells were sparsely scattered, ++ when less than three infiltrate foci were detected, +++ when the number of foci was more than three and ++++ when the whole tissue was infiltrated

[c] Tubular atrophy and interstitial fibrosis negative (–) when when absent, + when less than 25% of the tubuli or interstitium were affected, ++ when the lesion was between 25% and 50% and +++ when the lesion affected more than 75% of the tubuli or interstitium

and tubular epithelium in proliferative GN [3, 7, 8], including IgAN [8, 29, 40]. In this disease, the tubular expression of ICAM-1 is associated with infiltration of leucocytes [29, 40], including the infiltration by CD18+ leucocytes that express the common beta chain of their counter ligands [4, 32], leucocyte function-associated antigen-1 (LFA-1; CD11a, CD18) and Mac-1 (CD11b, CD18), but its clinical significance remains uncertain. In order to examine the value of the renal expression of ICAM-1 as a marker of tubulointerstitial injury, we analysed the relationship between the abnormal tubular and the interstitial expression of ICAM-1 and renal impairment at the time of renal biopsy and the progression of the disease in a group of patients with IgAN in comparison with a group of patients with non-GN.

Materials and methods

Patients

Forty-five patients with primary IgAN [39 males and six females, 39±16 years ($\bar{x}$±SD) of age] and 29 patients with non-GN (17 males and 12 females, 50±13 years of age) were studied. All patients showed serum creatinine below 3 mg/dl. None of the patients with IgAN had clinical or biochemical evidence of Henoch–Schönlein purpura, liver disease or systemic lupus erythematosus. Serum creatinine was 1.6±0.7 mg/dl and proteinuria was 2±1.3 g/24 h. The patients with non-GN included benign nephrosclerosis [15], diabetes [5], amyloidosis [7] and acute tubular necrosis [2]. Their serum creatinine was 1.7±0.7 mg/dl and proteinuria was 2.8±1.6 g/24 h. The serum creatinine and the proteinuria were recorded 2.4±2 years after renal biopsy in the patients with IgAN and 1.8±1.5 years in the patients with non-GN. An increase of at least 50% in serum creatinine or proteinuria was considered as progression of the renal disease. Ten normal renal tissues originally obtained from patients undergoing biopsies for diagnostic purposes in the same unit were used as a control.

Tissue and histologic assessment

Diagnostic renal biopsies taken using needle aspiration under sonographic control were processed for routine conventional light microscopy using hematoxylin–eosin, periodic acid–Schiff (PAS), periodic acid–methenamine silver and Masson's trichrome and immunofluorescence microscopy for IgA, IgG, IgM, C3, C4, C1q and fibrinogen. In each biopsy, the following histopathologic glomerular features were evaluated in a blinded fashion: the number of glomeruli showing sclerosis involving less than 50% of glomerular surface area and the number of glomeruli showing sclerosis involving more than 50% of glomerular surface area. The number of glomeruli showing extracapillary proliferation when at least two layers of non-tubular cells occupied less than 20% of Bowman's space was assessed in the biopsy specimens stained prominently for mesangial IgA. The number of normal glomeruli was assessed in biopsies from non-GN patients. All biopsies were evaluated for the degree of interstitial cellular infiltration, tubular atrophy and interstitial fibrosis. The interstitial cellular infiltration was assessed as negative (–) when no cells were seen, + when cells were sparsely scattered, ++ when less than three infiltrate foci were detected, +++ when the number of foci was more than three and ++++ when the whole tissue was infiltrated. The tubular atrophy and the interstitial fibrosis were assessed as negative (–) when absent, + when less than 25% of the tubuli or interstitium were affected, ++ when the lesion was between 25% and 50% and +++ when the lesion affected more than 75% of tubuli or interstitium (Table 1).

Immunohistochemistry and immunohistochemical assessment

Renal biopsies selected on the basis of availability of material (at least four glomeruli) and ease of processing for immunohistochemistry were tested by means of avidin–biotin peroxidase [4], using monoclonal antibodies (mAbs) against ICAM-1 (CD54, RM-3-A5) [17], which was applied after incubation with the white of an egg to block the renal biotin, monocyte macrophages (CD14, Cris-6) [5] and all T lymphocytes (CD3, Leu-4; BectonDickinson, Mountain View, Calif.). Tonsil tissue and slides from each specimen incubated with ascites fluid of myeloma NS1 or phosphate-buffered saline (PBS) instead of the mAb were used as controls. A

Table 2 Spearman's correlation coefficients between the percentage of glomeruli with sclerosis involving less than 50% of the glomerular surface area and the percentage of glomeruli with sclerosis involving more than 50% of the glomerular surface area and the quantitative ICAM-1$^+$ expression on tubule and interstitium in immunoglobulin A nephropathy (IgAN) and non-glomerulonephritis (non-GN). *ICAM-1* intercellular adhesion molecule-1, *NS* not significant

ICAM-1$^+$	IgAN				non-GN			
	Tubule		Interstitium		Tubule		Interstitium	
	r value	*P* value	*r* value	*P* value	*r* value	*P* value	*r* value	*P* value
Percent glomeruli with sclerosis <50%	0.464	0.01	0.386	<0.05	–0.071	NS	0.201	NS
Percent glomeruli with sclerosis >50%	0.417	NS	0.549	0.01	0.558	<0.01	0.147	NS

Leitz microscope at magnification ×400 with an ocular grid (0.07 mm^2) was used. CD54-positive tubular epithelial cells were scored as present or absent. CD54 staining on proximal tubule epithelium was counted in 10–20 tubular cross sections. The ratio of the area of CD54$^+$ proximal tubule epithelium to total tubular area multiplied by a factor of ten was calculated. Interstitial leucocytes identified by any of the above mAbs were counted in 10–20 adjacent fields adjusted to avoid glomeruli and major vessels in an area of at least 0.2 mm^2 on sequential renal sections. The number of positive leucocytes per square millimetre of interstitium was calculated.

Statistics

SPSS version 8 Win 6.1.3 programs (SPSS Inc, Chicago, Ill.) were used. Results were not normally distributed and were thus analysed using the non-parametric Mann–Whitney *U* test for two-group comparisons and the Kruskal-Wallis test for comparisons among several groups. Spearman's correlation coefficient was used to identify the correlation of the quantitative value of the tubular expression of ICAM-1 and the interstitial ICAM-1$^+$ leucocytes with the histologic features, the proteinuria and the creatinine serum level at the time of renal biopsy. Differences were considered significant when $P<0.05$.

Results

Renal expression of ICAM-1 in normal kidney

ICAM-1 (CD54) antigens were strongly expressed on peritubular and glomerular capillaries and the endothelium of arterial vessels and veins. The tubular epithelium was negative (Fig. 1). We observed occasional staining for CD14 but no staining for CD3 within interstitium in normal renal tissue.

Renal expression of ICAM-1 in IgAN

Tubular ICAM-1

A common pattern of ICAM-1 antigens was unchanged with respect to that observed in the normal kidney in IgAN without interstitial cellular infiltration and with interstitial cellular infiltration of + (Fig. 2). In 25 (55%) of 45 biopsies of IgAN that showed interstitial cellular infiltration equal to or greater than ++, ICAM-1 antigens were seen on the proximal tubule epithelium (Fig. 3). In all biopsies, the ICAM-1$^+$ tubule epithelium was 0.1±0.18 ($\bar{x}$±SD), and this was associated with extracapillary proliferation (up to 20% of Bowman's space; $n=7$; $U=30$, $P<0.05$), glomerular sclerosis involving less than 50% of glomerular surface area ($U=41$, $P<0.005$), degree of interstitial cellular infiltration ($P<0.001$) and tubular atrophy ($U=31$, $P<0.001$), which was confirmed by analysing the quantitative ICAM-1$^+$ tubule staining. At the time of renal biopsy, proteinuria was 2.7±1.5 g/24 h in patients with tubular staining for ICAM-1 versus 1.5±1.8 ($U=44$, $P=0.005$) in patients without tubular staining for ICAM-1.

Interstitial ICAM-1

The number of ICAM-1$^+$ leucocytes was 234±307/mm^2 of interstitium, and these were correlated with glomerular sclerosis involving less than 50% of glomerular surface area, glomerular sclerosis involving more than 50% of glomerular surface area (Table 2), degree of tubular atrophy and interstitial fibrosis (Table 3). At the time of renal biopsy, a correlation was found between interstitial ICAM-1$^+$ ($r=0.6343$, $P<0.001$; Table 4) and CD14$^+$ leucocytes ($r=0.441$, $P<0.05$; Table 5) and serum creatinine. At the final follow-up period, the patients who presented an increase of more than 50% in serum creatinine showed 516±360/mm^2 of ICAM-1$^+$ interstitial leucocytes, 471.6±174.7/mm^2 of CD14$^+$ leucocytes and 836±295.5/mm^2 of CD3$^+$ leucocytes versus 66±87.8/mm^2 ICAM-1$^+$ leucocytes ($U=16$, $P<0.005$), 246.2±216.7/mm^2 of CD14$^+$ leucocytes ($U=36$, $P=0.01$) and 420.8±366.6/mm^2 of CD3$^+$ leucocytes ($U=22$, $P=0.01$) in the patients with stable serum creatinine.

Renal expression of ICAM-1 in non-GN

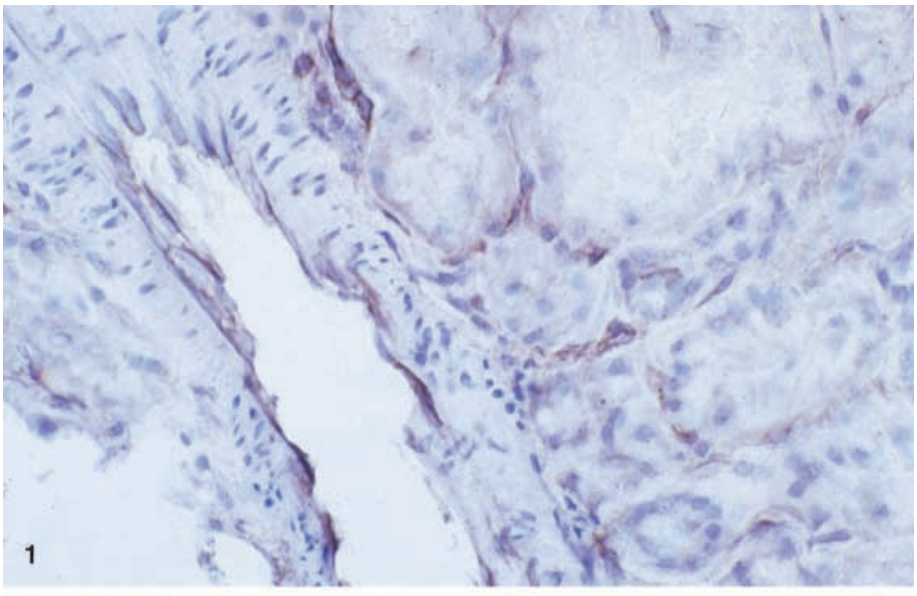
Tubular ICAM-1

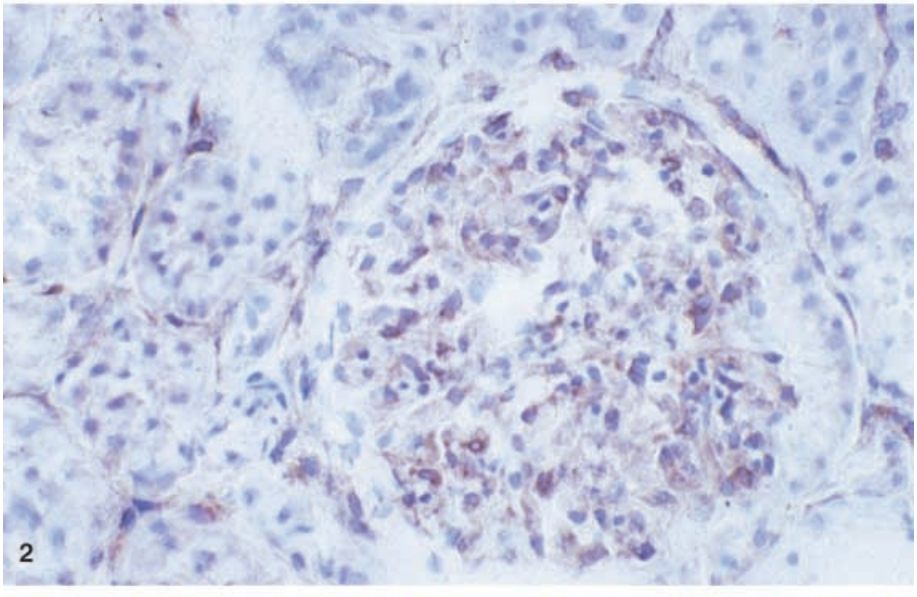
The distribution of ICAM-1 antigens was unchanged with respect to that observed in the IgAN, but ICAM-1 antigens on proximal tubule epithelium were detected only in seven (24%) of 29 biopsies with interstitial cellular infiltration. In all biopsies, the ICAM-1$^+$ tubule epithelium was 0.02±0.04 ($U=344$, $P<0.05$, versus IgAN), and this was inversely correlated with the percentage of normal

Fig. 1 Intercellular adhesion molecule (ICAM)-1 (CD54) antigens identified on the arterial endothelium and peritubular capillaries. The tubular epithelium is negative for this stain in normal renal tissue. Avidin–biotin–peroxidase (×250)

Fig. 2 Intercellular adhesion molecule (ICAM)-1 (CD54) antigens identified on the endothelial cells of glomerular and peritubular capillaries. The tubular epithelial cells were negative for this stain in a biopsy with immunoglobulin A nephropathy classified as focal glomerulonephritis. Avidin–biotin–peroxidase (×250)

Fig. 3 Intercellular adhesion molecule (ICAM)-1 (CD54) antigens identified on the proximal tubule epithelium in a biopsy with immunoglobulin A nephropathy classified as diffuse proliferative glomerulonephritis. Avidin–biotin–peroxidase (×250)





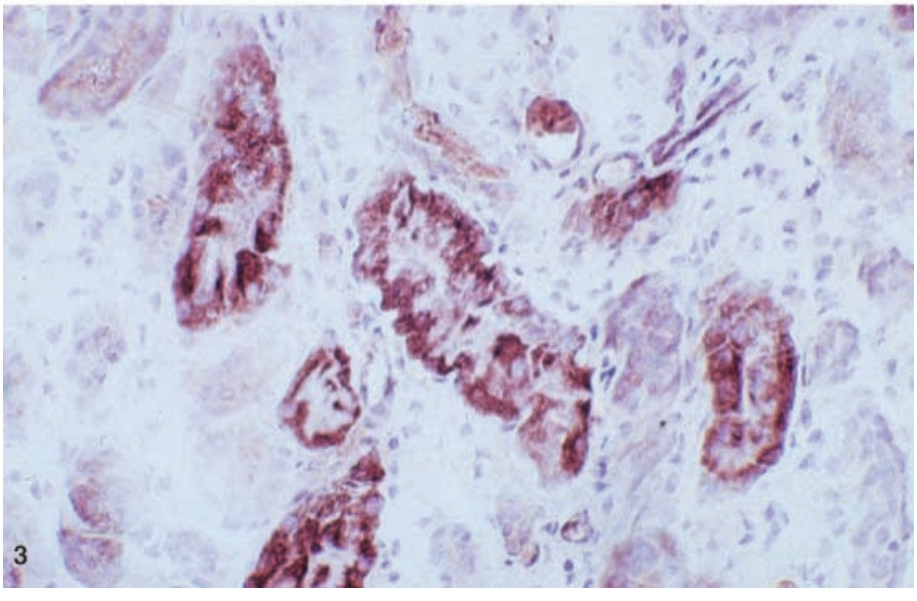


Table 3 Spearman's correlation coefficients between the degree of tubular atrophy and the degree of interstitial fibrosis and the quantitative intercellular adhesion molecule (ICAM)-1$^+$ expression on tubule and interstitium in IgA nephropathy (IgAN) and non-glomerulonephritis (non-GN). *NS* not significant

ICAM-1$^+$	IgAN				non-GN			
	Tubule		Interstitium		Tubule		Interstitium	
	r value	*P* value	*r* value	*P* value	*r* value	*P* value	*r* value	*P* value
Tubular atrophy	0.577	0.001	0.442	<0.05	0.430	<0.05	–0.135	NS
Interstitial fibrosis	0.372	<0.05	0.405	<0.05	0.304	NS	–0.169	NS

Table 4 Spearman's correlation coefficients between the clinical data at the time of renal biopsy and the quantitative ICAM-1$^+$ expression on tubule and interstitium. Significant Mann-Whitney *U* test of the follow-up clinical data according to ICAM-1$^+$ expression on tubule and interstitium in immunoglobulin A nephropathy (IgAN) and non-glomerulonephritis (non-GN). *NS* not significant

ICAM-1$^+$	IgAN				non-GN			
	Tubule		Interstitium		Tubule		Interstitium	
	r value	*P* value	*r* value	*P* value	*r* value	*P* value	*r* value	*P* value
At renal biopsy								
Proteinuria	0.4059	<0.05	0.2322	NS	0.063	NS	0.156	NS
Serum creatinine	0.282	NS	0.6343	<0.001	0.4356	<0.05	–0.203	NS
	U value	*P* value	*U* value	*P* value	*U* value	*P* value	*U* value	*P* value
Follow-up								
Proteinuria	19	NS	13	NS	48	NS	8	NS
Serum creatinine	41	NS	16	<0.005	42	NS	12	NS

Table 5 Spearman's correlation coefficients between the clinical data at the time of renal biopsy and significant Mann-Whitney *U* test of the follow-up clinical data according to interstitial CD14$^+$ and CD3$^+$ in immunoglobulin A nephropathy (IgAN) and non-glomerulonephritis (non-GN). *NS* not significant

	IgAN				non-GN			
	CD14$^+$		CD3$^+$		CD14$^+$		CD3$^+$	
	r value	*P* value	*r* value	*P* value	*r* value	*P* value	*r* value	*P* value
At renal biopsy								
Proteinuria	0.131	NS	0.132	NS	0.198	NS	0.091	NS
Serum creatinine	0.441	<0.05	0.208	NS	0.053	NS	0.085	NS
	U value	*P* value	*U* value	*P* value	*U* value	*P* value	*U* value	*P* value
Follow-up								
Proteinuria	51	NS	35	NS	8	NS	3	NS
Serum creatinine	36	0.01	22	0.01	2	NS	6	NS

glomeruli (r=–0.374, P<0.05). Tubular ICAM-1 was associated with the glomerular sclerosis involving more than 50% of glomerular surface area (U=19, P<0.005) and degree of tubular atrophy (U=55, P<0.05), which was confirmed by analysing the quantitative ICAM-1$^+$ tubule staining. In contrast with IgAN, no association between tubular ICAM-1 and the score of interstitial cellular infiltration was observed. At the time of renal biopsy, tubular ICAM-1 was correlated (r=0.4356, P<0.05) with the serum creatinine level.

Interstitial ICAM-1

The number of interstitial ICAM-1$^+$ leucocytes was 191±113/mm^2 (U=323, P value not significant, versus IgAN). No association between interstitial ICAM-1$^+$, CD14$^+$ or CD3$^+$ leucocytes and histologic features and clinical data was found in non-GN.

Discussion

The vascular renal expression of ICAM-1 is unchanged in the mild histologic forms of IgAN with respect to that observed in the normal kidney. In the severe forms of IgAN, there is an increase in glomerular ICAM-1 staining [40], which may be attributable to either infiltrating mononuclear leucocytes or up-regulated expression on endothelial [1, 30] and mesangial cells [1, 19]. In addition, ICAM-1 expression is induced on the proximal tubule epithelium, associated with glomerular [40] and interstitial cellular infiltration seen by means of light microscopy [29] and characterised using mAbs directed to leucocytes [4, 27]. The serum ICAM-1 level in histologic severe forms [28] and in both exacerbating clinical episodes and during quiescence [25, 27] is similar to that in healthy controls. Thus, the abnormal expression of ICAM-1 on tubule epithelium appears to be a specific local phenomenon rather than a reflection of the serum level, but its significance is uncertain. This study analyses the relationship between the abnormal tubular expression of ICAM-1 and the interstitial leucocyte expression of ICAM-1 with renal impairment at the time of renal biopsy and at the final follow-up period in a group of patients with IgAN in comparison with a group of patients with non-GN.

This work summarises a numerous group of patients with IgAN and control patients with non-GN and provides histologic and clinical information defining the disease that expands prior reports. The distribution of ICAM-1 antigens on vascular endothelium and interstitial leucocytes was similar in IgAN and in non-GN. However, the ICAM-1^+ tubule epithelium was significantly higher in IgAN than in non-GN. We found a significant association between the abnormal tubular expression of ICAM-1 and proteinuria in IgAN, whereas no association was noted in non-GN, which suggests that the expression of ICAM-1 antigens on the tubular epithelial cells may be a result of the renal damage in IgAN. Thus, tubular ICAM-1 expression may be a marker of tubular injury in IgAN.

Glomerular high-grade proteinuria itself may cause tubule epithelial cell injury through several mechanisms [15], as shown in experimental models of GN. Moreover, the association between the glomerular hypercellularity and the tubular expression of ICAM-1 observed in IgAN and the association between normal glomeruli and the lack of tubular stain for ICAM-1 observed in non-GN suggest that glomerular proliferation plays a role in the tubular expression of ICAM-1. Thus, the glomerular infiltration of macrophages [33, 38], showing TNF messenger (m)RNA signals in histologic studies of IgAN [23, 43], supports the hypothesis that glomerular inflammatory cytokines, such as TNF-α and IL-1, may reach the tubule interstitium via blood, urine or diffusion through extravascular tissue, which is a stimulus for the induction of ICAM-1 on tubule epithelium in this disease.

This study distinguished between glomerular sclerosis involving more than 50% of glomerular surface area and glomerular sclerosis involving less than 50% of glomerular surface area. An association between the abnormal tubular expression of ICAM-1 and the percentage of glomeruli showing sclerosis involving less than 50% of glomerular surface area in IgAN was found, which is in accordance with the adverse predictor factor of segmental hyalinosis and sclerosis in IgAN [24], even in patients with normal renal function at presentation [35]. This suggests that the tubular ICAM-1^+ staining provides reliable information on the progression of this disease.

The association between ICAM-1 on proximal tubule epithelium and the score of interstitial infiltrating leucocytes in IgAN [4, 27] and not in non-GN, as in our report, suggests that the tubular expression of ICAM-1 may be induced by interstitial cytokines and not simply as a by-product of extensive infiltration in IgAN. In support of this hypothesis, T cells cloned from renal cellular infiltrates in experimental nephritis demonstrate specific autoreactivity against renal tissue and induce ICAM-1 on cultured tubular epithelial cells; the induction is blocked by a mAb directed to interferon-γ [14]. Functional studies in different animal models of GN have demonstrated that cytokine-activated tubular epithelial cells can act as antigen-presenting cells and have revealed an improvement in both clinical and histologic manifestations of renal disease following the inhibition of ICAM-1 antigens [39, 42]. Alternatively, the correlation between the tubular expression of ICAM-1 and the tubular atrophy observed in IgAN and in non-GN [10] suggests that the proximal tubule epithelium expressing ICAM-1 antigens could reflect both the participation of the tubule epithelial cells in local cell-mediated immune interactions and the tubular injury.

The correlation between the number of interstitial ICAM-1^+ leucocytes and the histologic features, such as glomerular sclerosis, tubular atrophy and interstitial fibrosis and the creatinine serum level at the time of renal biopsy, are in accordance with the role of the interstitial T lymphocytes and macrophages [6, 34] in tubulointerstitial injury in IgAN. In contrast with a more heterogeneous histological report including less than 10% of biopsies with non-glomerular disease [9], we did not find these associations in non-GN, which indicates that the interstitial cell immunity could play a role in the renal impairment in IgAN as has been demonstrated in experimental [15, 16] GN.

Conclusions

The tubular and the interstitial expression of ICAM-1 may be a valuable marker of tubulointerstitial disturbance in IgAN for the following reasons: (1) the association between the abnormal tubular expression of ICAM-1 and proteinuria, (2) the association between the interstitial ICAM-1^+ leucocytes and renal failure at presentation and (3) the deterioration observed in IgAN. In spite of the association between ICAM-1^+ tubule and the adverse

factor of segmental hyalinosis and sclerosis in IgAN, interstitial ICAM-1 rather than tubular ICAM-1 could be used as a predictor of progressive deterioration in this disease.

Acknowledgements The authors thank Dr. R. Vilella and P. Engel for generous gifts of CD54 and CD14 mAbs and N. Babot for excellent immunohistochemistry work. This study was supported by the Fondo de Investigación de la Seguridad Social (no. 99/0187).

References

1. Adler S, Brady HR (1999) Cell adhesion molecules and the glomerulopathies. Am J Med 107:371–386
2. Alexopoulos E, Seron D, Hartley RB, Nolasco F, Cameron JS (1989) The role of interstitial infiltrates in IgA nephropathy: a study with monoclonal antibodies. Nephrol Dial Transplant 4: 187–195
3. Arrizabalaga P, Sans A, Torras A, Darnell A, Revert L (1998) Monoclonal antibody analysis of crescentic membranous glomerulonephropathy. Am J Nephrol 18:77–82
4. Arrizabalaga P, Solé M, Ascaso C, Quintó Ll, Engel P (1998) Leucocyte infiltration and ICAM-1 mediated cell interactions in Ig A nephropathy. Arch Pathol Lab Med 122:817–822
5. Bernstein ID, Self S (1986) Joint report of the myeloid section of the Second International Workshop on human leucocyte differentiation antigens. In: Reinherz EL, Haynes BF, Nadler LM, Bernstein ID (eds) Leucocyte typing II. Springer, Berlin Heidelberg New York, pp 1–25
6. Bohle A, Strutz F, Müller GA (1994) On the pathogenesis of chronic renal failure in primary glomerulonephritis: a view from the interstitium. Exp Nephrol 2:205–210
7. Brady HR (1994) Leucocyte adhesion molecules and kidney diseases. Kidney Int 45:1285–1300
8. Bruijn JA. Dinklo JCM (1993) Distinct patterns of expression of ICAM-1, VCAM-1 and ELAM-1 in renal disease. Lab Invest 69:329–335
9. Chaudry PR, Wu B, King G, Campbell M, MacLeod AM, Haites EN, Simpson JG, Power DA (1996) Adhesion molecule interactions in human glomerulonephritis: importance of the tubulointerstitium. Kidney Int 49:127–134
10. Chow J, Hartley RB, Jagger C, Dilly SA (1992) ICAM-1 expression in renal disease. J Clin Pathol 45:880–884
11. D'Amico G (1987) The commonest glomerulonephritis in the world: IgA nephropathy. Q J Med 64:709–727
12. D'Amico G, Ferrario F, Rastaldi MP (1995) Tubulointerstitial damage in glomerular diseases: its role in the progression of renal damage. Am J Kidney Dis 26:124–132
13. Dal Canton A (1995) Adhesion molecules in renal disease. Kidney Int 48:1687–1696
14. Díaz-Gallo C, Rubin-Kelley V (1993) Self-regulation of autoreactive kidney-infiltrating T cells in MRL-lp nephritis. Kidney Int 44:692–699
15. Eddy AA (1994) Experimental insights into the tubulointerstitial disease accompanying primary glomerular lesions. J Am Soc Nephrol 5:1273–1287
16. Eddy AA, Giachelli CM, McCulloch L, Liu E (1995) Renal expression of genes that promote interstitial inflammation and fibrosis in rats with protein-overload proteinuria. Kidney Int 47:1546–1557
17. Engel P, Serra C, Acevedo G, Vilella R, Gallart T (1992) Involvement of CD18 and CD54 in the mixed lymphocyte reaction to leukemic CD5+ B lymphocytes. Immunology 11: 21–31
18. Falk MC, Ng G, Zhang GY, Fanning GC, Roy P, Bannister KM, Thomas AC, Clarkson AR, Woodroffe AJ, Knight JF (1995) Infiltration of the kidney by αβ and γδ T cells: effect on progression in IgA nephropathy. Kidney Int 47:177–185
19. Gauer S, Yao J, Schoecklmann HO, Sterzel B (1997) Adhesion molecules in the glomerular mesangium. Kidney Int 51: 1447–1453
20. Haas M (1997) Histologic subclassification of IgA nephropathy: a clinicopathologic study of 244 cases. Am J Kidney Dis 29: 829–842
21. Habib R, Niaudet P, Levy M (1994) Schönlein-Henoch nephritis and IgA nephropathy. In: Tisher CC, Brenner BM (eds) Renal pathology. Lippincott, Philadelphia, pp 472–523
22. Ibels LS, Gyori AZ, Caterson RJ, Pollock CA, Mahony JF, Waugh DA, Roger SD, Coulshed S (1997) Primary IgA nephropathy: natural history and factors of importance in the progression of renal impairment. Kidney Int 61[Suppl]: S67–S70
23. Kashem A, Endoh M, Yano N, Yamauchi F, Nomoto Y, Sakai H, Kurokawa K (1997) Glomerular FcR expression and disease activity in IgA nephropathy. Am J Kidney Dis 30: 389–396
24. Katafuchi R, Oh Y, Hori K, Komota T, Yanase T, Ikeda K, Omura T, Fujimi S (1994) An important role of glomerular segmental lesions on progression of IgA nephropathy: a multivariate analysis. Clin Nephrol 41:191–198
25. Lai KN, Wong KC, Li PK, Lai CK, Chan CH, Lui SF, Chui YL, Haskard DO (1994) Circulating leucocyte-endothelial adhesion molecules in IgA nephropathy. Nephron 68: 294–300
26. Lee SMK, Rao VM, Franklin WA, Schiffer MS, Aronson AJ, Spargo BH, Katz AI (1982) IgA nephropathy: morphologic predictors of progressive renal disease. Hum Pathol 13: 314–322
27. Lhotta A, Schlögl A, Kronenberg F, Joannidis M, König P (1997) Soluble intercellular molecule-1 (ICAM-1) in serum and urine: correlation with renal expression of ICAM-1 in patients with kidney disease. Clin Nephrol 48:85–91
28. Mrowka C, Heintz B, Sieberth HG (1999) VCAM-1, ICAM-1, and E-Selectin in IgA nephropathy and Schönlein-Henoch syndrome: differences between tissue expression and serum concentration. Nephron 81:256–263
29. Müller GA, Markovic-Lipovski J, Müller CA (1991) Intercellular adhesion molecule-1 expression in human kidneys with glomerulonephritis. Clin Nephrol 36:203–208
30. Ogawa T, Yorioka N, Ito T, Ogata S, Kumagai J, Kawanishi H, Yamakido M (1997) Precise ultrastructural localization of endothelial leukocyte adhesion molecule-1, vascular cell adhesion molecule-1, and intercellular adhesion molecule-1 in patients with IgA nephropathy. Nephron 75:54–64
31. Ootaka T, Saito T, Yusa A, Munaketa T, Soma J, Abe K (1995) Contribution of cellular infiltration to the progression of IgA nephropathy: a longitudinal immunocytochemical study on repeated biopsy specimens. Nephrology 1:135–142
32. Ootaka T, Saito T, Soma J, Yusa A, Abe K (1996) Intercellular adhesion molecule-1/leucocyte function associated antigen-1 mediated and complement receptor type-4-mediated infiltration and activation of glomerular immune cells in immunoglobulin A nephropathy. Am J Kidney Dis 28:40–46
33. Ootaka T, Saito T, Soma J, Yusa A, Abe K (1997) Mechanism of infiltration and activation of glomerular monocytes/macrophages in IgA nephropathy. Am J Nephrol 17:137–145
34. Ootaka T, Saito T, Soma J, Sato H, Abe K (1997) Glomerulointerstitial interaction of adhesion molecules in IgA nephropathy and membranoproliferative glomerulonephritis. Am J Kidney Dis 29:843–850
35. Packham DK, Yan HD, Hewitson TD, Nicholls KM, Fairley KE, Kincaid-Smith P, Becker GJ (1996) The significance of focal sclerosis (FSHS) and nephrotic range proteinuria in IgA nephropathy. Clin Nephrol 46:225–229
36. Pober JS, Cotran RS (1991) Immunologic interactions of T lymphocytes with vascular endothelium, vol 50. In: Dixon FJ (ed) Advances in Immunology. Academic Press Inc, New York, pp 261–302
37. Sabadini E, Castiglione A, Colasanti G, Ferrario F, Civardi R, Fellin G, D'Amico G (1988) Characterization of interstitial

infiltrating cells in Berger's disease. Am J Kidney Dis 12: 307–315
38. Saito T, Ootaka T, Sato H, Furuta T, Sato T, Soma J, Abe K, Yoshinaga K (1993) Participation of macrophages in segmental proliferation preceding focal glomerular sclerosis. J Pathol 170:179–185
39. Schulz H, Karau A, Filsinger S, Schoels M, Kabelitz D, Richter R, Hansch GM (1998)Tubular epithelial cells as accessory cells for superantigen-induced T cell activation. Exp Nephrol 6:67–73
40. Tomino Y, Ohmuro H, Kuramoto T, Shirato I, Eguchi K, Sakai H, Okumura K, Koide H (1994) Expression of intercellular adhesion molecule-1 and infiltration of lymphocytes in glomeruli of patients with IgA nephropathy. Nephron 67:302–307
41. Van Es LA (1997) Immunoglobilin IgA nephropathy. In: Neilson EG, Couser WG (eds) Immunologic renal diseases. Lippincott, Philadelphia, pp 945–957
42. Van Kooten C, Langers AM, Bruijn JA, Daha MR (1999) Role of tubular cells in progressive renal disease. Kidney Blood Press Res 22:53–61
43. Yoshioka K, Takemura T, Murakami K, Okada M, Yagi K, Miyazato H, Matsushima K, Maki S (1993) In situ expression of cytokines in IgA nephritis. Kidney Int 44:825–833

Virchows Arch (2001) 439:35–45
DOI 10.1007/s004280100433

ORIGINAL ARTICLE

Yoshihide Fujigaki · Di Fei Sun · Taiki Fujimoto
Katsuhiko Yonemura · Tetsuo Morioka
Eishin Yaoita · Akira Hishida

Cytokines and cell cycle regulation in the fibrous progression of crescent formation in antiglomerular basement membrane nephritis of WKY rats

Received: 17 August 2000 / Accepted: 2 February 2001 / Published online: 24 April 2001
© Springer-Verlag 2001

Abstract Cytokines may regulate cell proliferation by cell-cycle-regulatory proteins, in which cyclin-dependent kinase inhibitors (CDKI) inhibit cell proliferation. We investigated whether CDKI p21 or p27, both of which are potentially regulated by transforming growth factor (TGF)-β, a key cytokine in fibrogenesis, are involved together with TGF-β and/or platelet-derived growth factor (PDGF) in the fibrous progression of glomerular crescent formation and examined the sequential change in the cell type and the cellular background of myofibroblasts in crescent formation. Crescentic glomerulonephritis (GN) was induced by i.v. injection of rabbit anti-rat glomerular basement membrane antiserum in WKY rats. Animals were killed 1, 2, 3 and 4 weeks after the induction of GN, and their kidneys were processed for immunohistochemical examination. After 1 week more than 85% of glomeruli showed cellular crescents, which became fibrocellular with decreased cellularity by 4 weeks. ED 1-positive macrophages were components of crescent cells in about 44% at 1–2 weeks, and this proportion declined markedly afterwards. Alpha smooth muscle actin (alpha SMA, a marker for myofibroblasts)-positive cells were found in Bowman's epithelial cells (BEP) and in some crescent cells at 1 week, becoming major components of crescent cells by 4 weeks (about 40%). It was 2 weeks before invasion of alpha SMA-positive interstitial cells into glomeruli was evident. PDGF-B and PDGF receptor β-positive cells, indicating possible targets for PDGF, were found in BEP adjoining crescent formation almost exclusively from 1 to 2 weeks. By contrast, both TGF-β receptor types I- and II-positive cells, indicating possible effectors for TGF-β, were found in BEP and crescent formation, and the percentage of these in the crescent formation did not change until 4 weeks (about 32%). Cells with positive immunostaining for proliferating cell nuclear antigen and cyclin A, markers for cell proliferation, in the crescent formation peaked in number and proportion at 1–2 weeks, then decreased. In contrast, cells with positive immunostaining for p21 and p27, CDKI, were sparse at 1 week, and then increased markedly in number and in proportion, peaking at 3 (39.6%) or 2–3 weeks (about 25–30%), respectively. The present study demonstrates that restrained expression or a transient increase in p21 and p27 may be associated with proliferation or with inhibited proliferation of crescent cells, most of which are macrophages and myofibroblasts. The action of PDGF and TGF-β may contribute to the recruitment of myofibroblasts into the crescent. The action of TGF-β on crescent cells might be linked to the expression of p21 and/or p27.

Keywords p21 · p27 · TGF-β · Glomerular crescent · Glomerulonephritis

Y. Fujigaki (✉) · D.F. Sun · T. Fujimoto · A. Hishida
First Department of Medicine,
Hamamatsu University School of Medicine, Handa-cho 3600,
Hamamatsu 431–3192, Japan
e-mail: yf0516@hama-med.ac.jp
Tel.: +81-53-4352261, Fax: +81-53-4349447

K. Yonemura
Hemodialysis Unit, Hamamatsu University School of Medicine,
Hamamatsu 431–3192, Japan

T. Morioka
Department of Cellular Physiology, Institute of Nephrology,
Niigata University School of Medicine, Niigata 951–8510, Japan

E. Yaoita
Department of Pathology, Institute of Nephrology,
Niigata University School of Medicine, Niigata 951–8510, Japan

Introduction

In crescentic glomerulonephritis (GN) the fibrous progression of cellular crescent is a crucial factor in the irreversible renal dysfunction. During the process of fibrogenesis, the discontinuation of cell proliferation is also observed. Cell proliferation is known to be controlled by cell-cycle-regulatory proteins [18], in which cyclin-dependent kinase inhibitors (CDKI) inhibit cell proliferation [26]. Recent reports indicate that the distribution

and function of these CDKI are not predictable or expected and are cell-type specific [24]. In the fibrous progression of crescent formation, the exact origin of the cell type that contributes to the fibrous progression and CDKI involved in the regression of proliferative cells is not clear.

Initial glomerular crescents are known to be formed by an accumulation of macrophages and proliferative Bowman's epithelial cells (BEP) [9, 31]. In the fibrous progression of crescent formation, periglomerular myofibroblasts may enter into the Bowman's space through a disrupted Bowman's capsule and contribute to the fibrogenesis [2, 6, 10]. Recently, BEP has been proposed as another candidate for the origin of fibroblast-type cell, as it was suggested that BEP transdifferentiate to myofibroblast [16]. Macrophages, which are reported to proliferate locally in the crescent formation [11], could also be a candidate, since macrophage–connective tissue cell transdifferentiation might be possible in in vitro conditions [29]. So far, the sequential changes in the ratio of the cell type involved in crescent formation and the cellular background of myofibroblasts in the fibrous progression of crescent formation have not been well described. In this process the cell cycles of macrophages and myofibroblasts, both of which are key cells in fibrogenesis, should be regulated by CDKI and also by profibrogenic cytokines, such as platelet-derived growth factor (PDGF) and transforming growth factor (TGF)-β. Indeed, TGF-β is reported to be involved in the fibrous progression of the crescent formation [13, 16].

The purposes of the present study are (1) to determine sequential changes in the ratio of macrophages or myofibroblasts and also changes in PDGF or TGF-β pathways in the crescent cells in respect to the key cells or major profibrogenic cytokines in fibrogenesis, respectively, (2) to examine cell proliferation in the crescent using proliferation markers, proliferating cell nuclear antigen (PCNA) which could be regulated by CDKI p21 [14] or cyclin A, which could be reduced by TGF-β1 [20, 23], and (3) to investigate whether CDKI p21 or p27, both of which are potentially regulated by TGF-β, a key cytokine in fibrogenesis [4, 12, 19, 20, 23], is involved in the fibrous progression of crescent formation. For these purposes we used an established model of crescentic GN, anti-glomerular basement membrane (GBM) GN in WKY rats, in which glomerular crescents are known to be simultaneously formed, with progression to the fibrous stage in a very high percentage [7].

Materials and methods

Induction of anti-GBM GN in WKY rats

Nineteen inbred male WKY rats (Charles River Japan, Kanagawa, Japan) each weighing 100 g were used for this study. Crescentic GN was induced in rats with a single injection of 50 µl of rabbit anti-rat GBM antiserum [7]. Groups of three or four rats were euthanized on days 7, 14, 21 and 28. As normal controls another group of four rats were also studied.

Tissue processing and renal morphology

Renal tissues were fixed in either 4% paraformaldehyde or methyl carnoy's solution and embedded in paraffin. To examine renal histology, 4-µm sections were stained with periodic acid and Schiff's reagent (PAS) or periodic acid–silver methenamine. Glomeruli were considered to exhibit crescent formation when at least two layers of cells were observed in the Bowman's space. The numbers of crescents or disruptions of Bowman's capsule were counted in at least 100 glomeruli per rat and expressed as mean percentages of each group.

Portions of renal tissue were snap frozen in *N*-hexane and stored at –70°C for immunofluorescence studies. To detect injected rabbit IgG direct immunofluorescence study was performed on 4-µm cryostat sections with FITC-conjugated goat anti-rabbit IgG (Cappel Laboratory, West Chester, Pa.).

Immunohistochemistry

For immunohistochemistry an indirect immunoperoxidase method was adopted. After deparaffinization and rehydration, endogenous peroxidase was blocked in 3% hydrogen peroxide for 30 min, and the sections were then incubated with normal serum corresponding to the species providing secondary antibodies for 20 min, followed by incubation with the primary antibodies including rabbit anti-mouse type IV collagen (LSL, Tokyo), mouse monoclonal anti-rat ED 1 (Serotec, Oxford, UK), a marker for macrophage, mouse monoclonal anti-human alpha smooth muscle actin (SMA) (DAKO, Glostrup, Denmark) a marker for myofibroblast phenotype, rabbit anti-PDGF receptor β (catalog no. K248, Santa Cruz, Calif.), mouse monoclonal anti-PDGF-B (PGF-007, Mochida, Tokyo) [22], rabbit anti-TGF-β receptor type I (T-19, catalog no. sc-402, Santa Cruz), rabbit anti-TGF-β receptor type II (L-21, catalog no. sc-400, Santa Cruz), mouse monoclonal anti-PCNA (Oncogene Science, Uniondale, N.Y.), rabbit anti-cyclin A (C-19, Santa Cruz), rabbit anti-p21 (H-164, Santa Cruz) and rabbit anti-p27 (M-197, Santa Cruz). Following washes in phosphate-buffered saline (PBS), the sections were incubated with biotinylated donkey anti-mouse IgG or donkey anti-rabbit IgG (Chemicon International, Calif.) for 60 min, washed in PBS, then incubated with streptavidin-conjugated peroxidase (Nichirei, Tokyo) for 30 min.

As histological controls the first antibodies were omitted or replaced by species-matched IgG.

Morphometric analysis

The number of total cell nuclei in PAS-stained sections or the number of PCNA-, cyclin A-, p21- or p27-positive cells (as identified by each immunostaining) was counted within a cross section of crescent formation. For assessment of ED 1-, PDGF-B-, PDGF receptor β (PDGFR)-, TGF-β receptor type I (TβRI)- and TGF-β receptor type II (TβRII)-positive cells, only those that had a visible nucleus were counted. Alpha SMA-positive cells were counted when a nucleus and at least one cytoplasmic process were present. The mean number of cells in the crescent formation was calculated from at least 50 glomeruli per rat and expressed as the mean number of each group. The percentage of each cell type per total number of cells in cross sections of the crescent formation in PAS-stained sections was also calculated and expressed as the mean percentage of each group. The glomerular cross sections that contained minor portions of the glomerular tuft were excluded from the analysis.

Statistical analysis

Data are expressed as mean±SD. Differences between data sets were determined by performing one-way analysis of variance followed by a Scheffe test. A level of $P<0.05$ was accepted as being statistically significant.

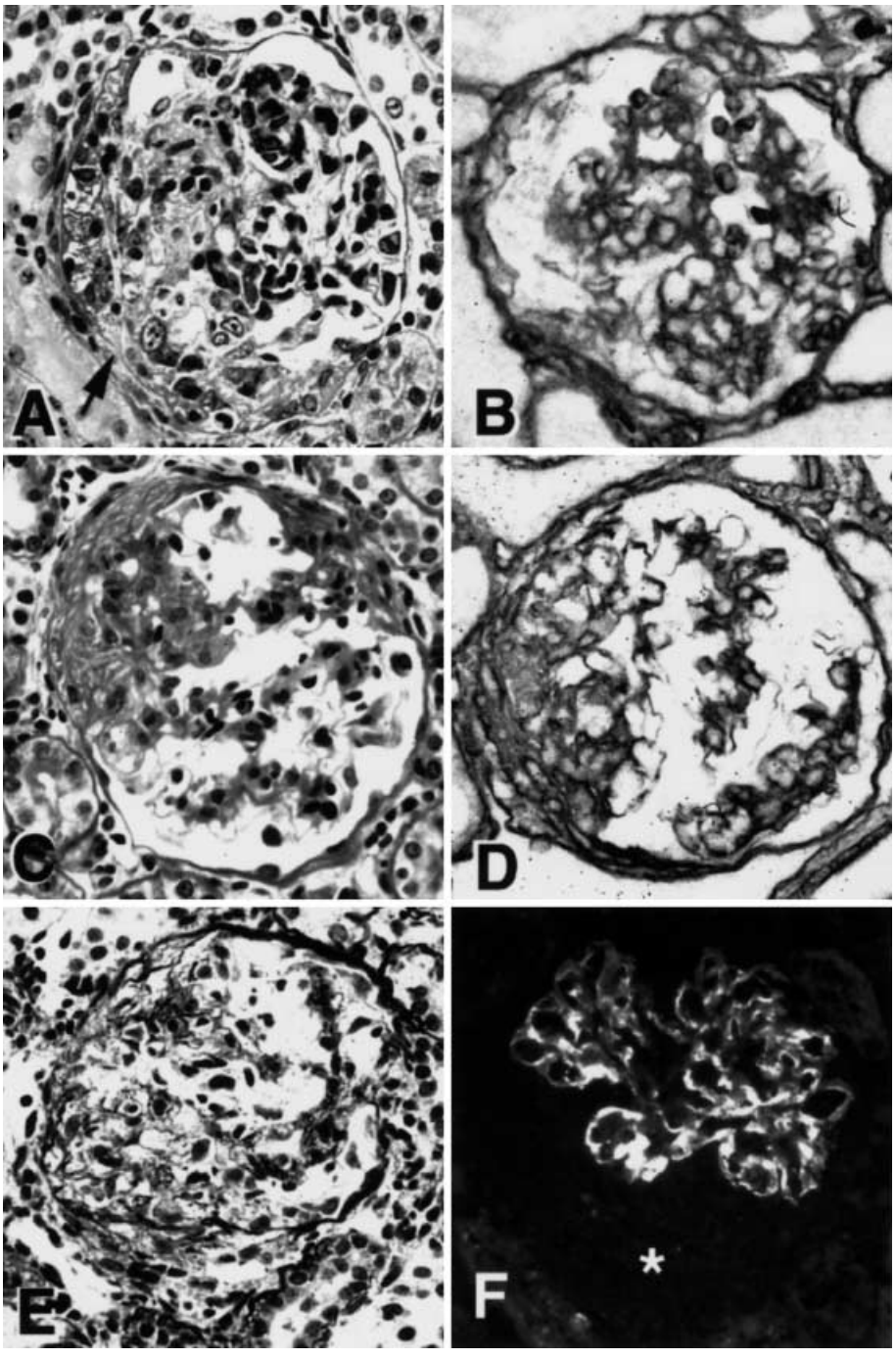


Fig. 1 Photomicrographs of glomeruli from antiglomerular basement membrane glomerulonephritis in WKY rats. **A** Periodic acid-Schiff (PAS) staining at 1 week (*arrow* small disruption of Bowman's capsule); **B** immunostaining for type IV collagen at 1 week; **C** PAS staining at 4 weeks; **D** immunostaining for type IV collagen at 4 weeks; **E** periodic acid silver-methenamine staining at 4 weeks; **F** immunofluorescence for rabbit IgG at 1 week (*asterisk*, crescent formation)

Results

Glomerular crescent formation and type IV collagen accumulation

More than 85% of glomeruli showed cellular crescent formation with necrotizing and mesangiolytic glomerular damage 1 week after disease induction (Fig. 1A, Table 1). Almost all cellular crescents (Fig. 1A, B) turned out to be fibrocellular ones with reduced cellularity (Fig. 1C, Table 2) and increased reticular fibers consist-

Table 1 The percentage of glomerulus with the crescent formation and the disruption of Bowman's capsule

Week	% Crescent formation	% Disruption of Bowman's capsule	*n*
1	85.5±3.4	20.5±3.1	4
2	86.5±3.1	83.2±4.2*[a,*b,*c]	4
3	89.3±3.0	96.6±1.5*[a,*c]	3
4	90.2±1.7	97.5±1.2*[a]	4

*[a]$P<0.01$ vs 1 week
*[b]$P<0.01$ vs 3 weeks
*[c]$P<0.01$ vs 4 weeks

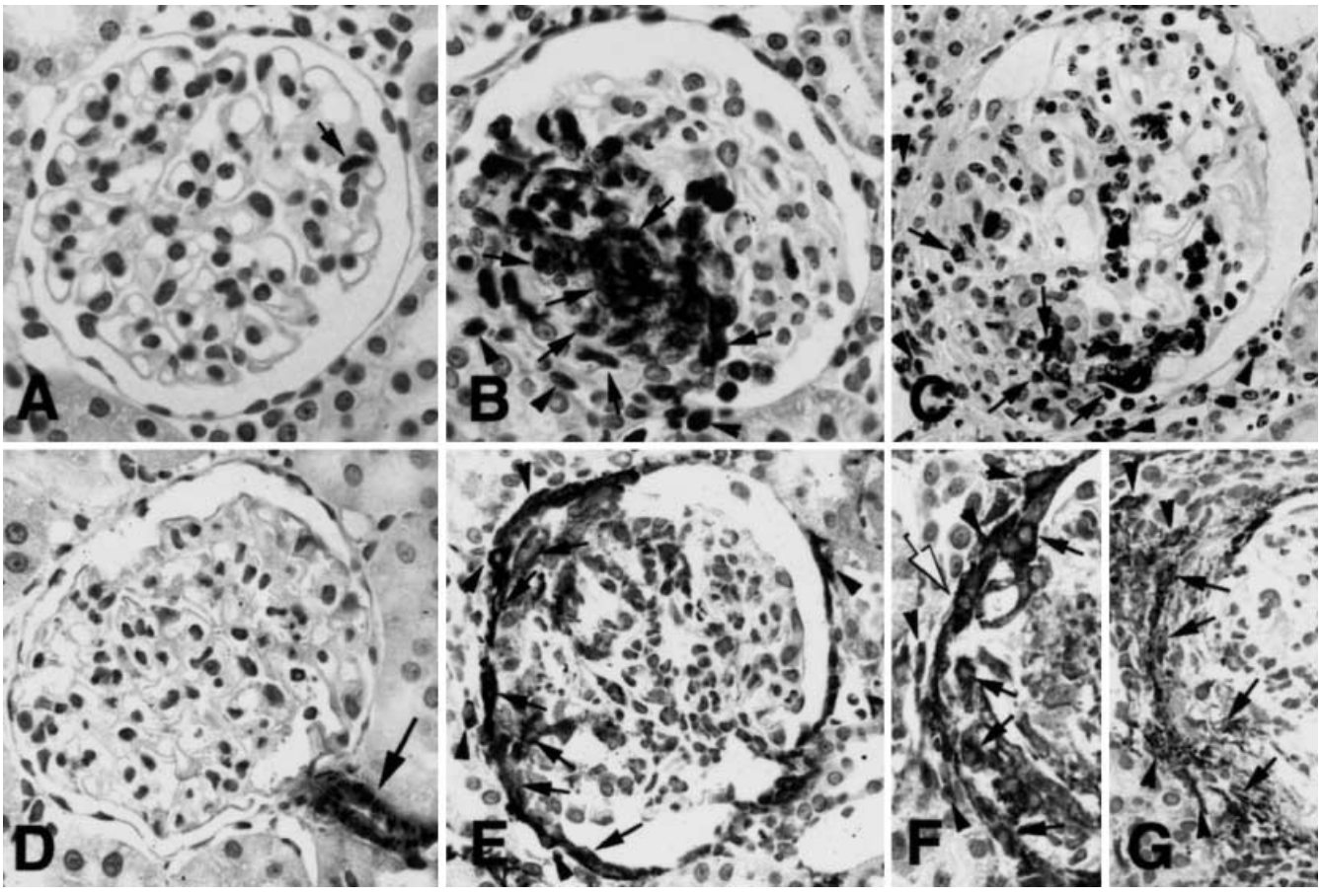


Fig. 2 Immunostaining for **A**–**C** ED 1-positive macrophages and **D**–**G** alpha-SMA-positive cells in the kidney. **A**–**C** ED 1-positive cells are stained with dark black and are seen in glomeruli (*arrows*) and in the periglomerular regions (*arrowheads*). **D**–**G** Cells with black-stained cytoplasm are positive for alpha-SMA. D *Arrow* indicates arteriole with alpha-SMA. **E- G** Periglomerular cells with alpha-SMA (*arrowheads*) and Bowman's epithelial cells or crescent cells with alpha-SMA (*arrows*). F *White arrow* indicates periglomerular alpha-SMA-positive cell invading glomerulus. **A**, **D** Normal control rat; **B**, **E** 1 week; **C** 3 weeks; **F** 2 weeks; **G** 4 weeks

ing with at least type IV collagen by 4 weeks (Fig. 1D). At 1 week, 20.5% of glomeruli showed very slight disruption of Bowman's capsule (Fig. 1A, Table 1), and most glomeruli had disruption of Bowman's capsules associated with thinning and lamellation by 4 weeks (Fig. 1E, Table 1). Immunofluorescence study showed the injected rabbit anti-rat GBM antibodies to be bound to capillary walls at all time points, but there was no deposition of rabbit IgG in Bowman's capsule, Bowman's space or areas of crescent formation (Fig. 1F). The last finding allows positive immunostaining with primary rabbit antibodies in these areas to be interpreted with no danger of artifacts.

ED 1-positive macrophages

In normal rats only a few ED 1-positive cells were detected in glomerulus and interstitium (Fig. 2A). There was an influx of ED 1-positive macrophages into segmental areas of glomeruli from 1 week onwards. About

Table 2 Total cells, ED 1+ cells, and alpha-SMA+ cells per crescentic cross section

Week	Total[a]	ED 1+[b]	Alpha-SMA+[c]	*n*
1	30.7±1.4	13.1±0.9	7.3±0.5	4
2	32.1±2.5**[d],**[e],**[f]	14.4±0.8**[d],**[e],**[f]	9.1±0.6**[e],*[h]	4
3	24.7±0.7**[d],**[f]	4.4±0.8**[d],*[g]	9.8±0.8	3
4	19.1±1.1	2.3±0.7	8.0±0.8	4

[a] Mean number of total cells per crescentic cross section
[b] Mean number of ED 1+ cells per crescentic cross section
[c] Mean number of alpha-SMA+ cells per crescentic cross section
**[d]P<0.01 vs 1 week **[e]P<0.01 vs 3 weeks **[f]P<0.01 vs 4 weeks
*[g]P<0.05 vs 4 weeks *[h]P<0.05 vs 1 week

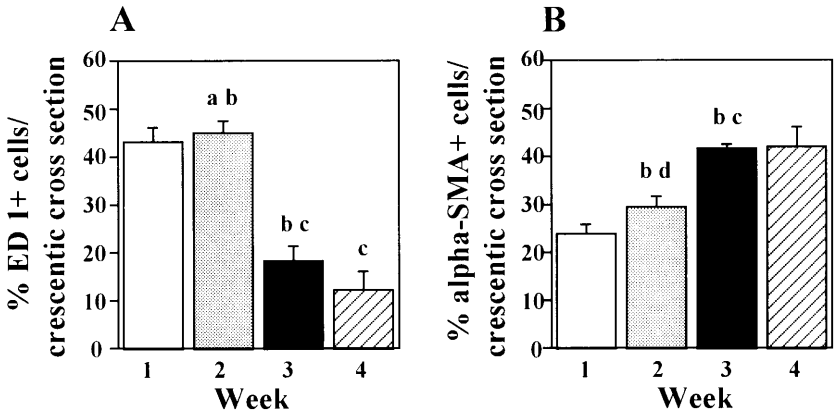


Fig. 3 Percentages of **A** ED 1-positive and **B** alpha-SMA-positive cells in crescent formation. *a* $P<0.01$ vs 3 weeks; *b* $P<0.01$ vs 4 weeks; *c* $P<0.01$ vs 1 week; *d* $P<0.05$ vs 3 weeks

Table 3 PDGF-B+ cells, PDGF receptor β+ cells, TGF-β receptor type I+ cells, and TGF-β receptor type II+ cells per crescentic cross section

Week	PDGF-B+[a]	PDGF-Rβ+[b]	TβRI+[c]	TβRII+[d]	*n*
1	5.7±0.5	4.9±0.8	10.1±0.6	9.4±0.8	4
2	5.7±0.6*[e,*f]	5.1±0.7*[e,*f]	11.1±0.5*[e,*f]	10.3±0.5*[e,*f]	4
3	2.1±0.2*[g]	0.7±0.1*[g]	9.2±0.6[f]	8.3±0.7*[f]	3
4	1.8±0.1*[g]	0.5±0.1*[g]	6.6±0.3*[g]	6.5±0.4*[g]	4

[a] Mean number of PDGF-B+ cells in crescentic cross section
[b] Mean number of PDGF receptor β+ cell in crescentic cross section
[c] Mean number of TGF-β receptor type I+ cells in crescentic cross section
[d] Mean number of TGF-β receptor type II+ cells in crescentic cross section
*[e] $P<0.01$ vs 3 weeks *[f] $P<0.01$ vs 4 weeks *[g] $P<0.01$ vs 1 week

44% of crescent cells consisted of ED 1-positive macrophages at 1 and 2 weeks (Fig. 2B), and ED 1-positive macrophages were markedly reduced in 12.0% by 4 weeks (Figs. 2C, 3, Table 2). Accumulation of ED 1-positive macrophages was found in the periglomerular regions at 1 week (Fig. 2B) and increased up to 4 weeks (Fig. 2C).

Expression of alpha SMA

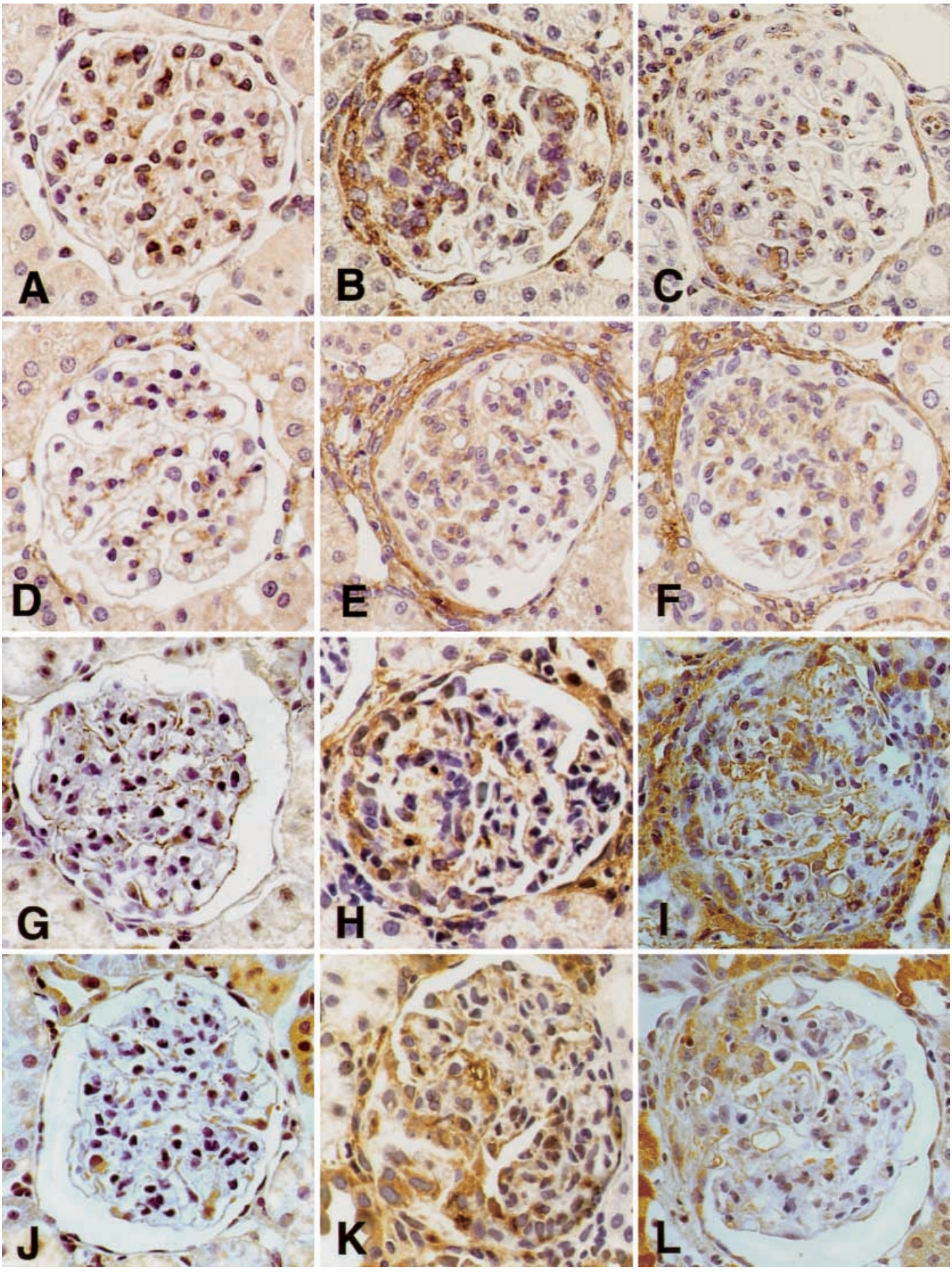
In normal rats no immunostaining of alpha SMA was detected in glomeruli, tubules or interstitial cells except vascular smooth muscle cells (Fig. 2D). At 1 week, alpha SMA-positive cells were found in the crescent formation (Fig. 2E), and BEP with or without facing crescent formation also expressed alpha SMA (Fig. 2E). The number of cells expressing alpha SMA in crescent formation was almost unchanged during the experimental period (Table 2), but the percentage of these cells in the crescent formation increased from about 23.7% at 1 week to about 40% by 3–4 weeks (Fig. 3). In periglomerular regions, alpha SMA-positive cells were found from 1 week onwards (Fig. 2E–G). No obvious invasion of alpha SMA-positive interstitial cells into glomeruli could be found at 1 week (Fig. 2E), but was evident after 2 weeks (Fig. 2F).

Expression of PDGF-B, PDGFR, TβRI and TβRII

There were minimal mesangial and BEP expression of PDGF-B in normal rats, but no significant expression in periglomerular cells (Fig. 4A). At 1 week strong immunostaining of PDGF-B in BEP and periglomerular cells was found, and some crescent cells also expressed PDGF-B with segmental accentuation (Fig. 4B). The number and percentage of PDGF-B-positive cells in the crescent formation were markedly decreased after 3 weeks (Figs. 4C, 5, Table 3). Periglomerular interstitial cells expressing PDGF-B persisted until 4 weeks.

There was minimal expression of PDGFR in the mesangial area, BEP, and periglomerular interstitial cells in normal rats (Fig. 4D). Expression of PDGFR, indicating a possible effector for PDGF, was found strongly in BEP facing crescent formation and in periglomerular cells at 1 week (Fig. 4E). Expression of those in the periglomerular regions persisted up to 4 weeks, but that of those in BEP or peripheral cells in the crescent formation was almost restricted at 1–2 weeks (Fig. 4E, F, 5, Table 3).

In normal rats, weak immunostaining of TβRI and TβRII could be seen in glomerulus, but no significant staining could be found in BEP and periglomerular interstitial cells (Fig. 4G, J). Immunostaining of both TβRI and TβRII, indicating possible effector for TGF-β, was found in the BEP, crescent cells as well as periglomerular interstitial cells from 1 week onwards (Fig. 4H, I, K, L). The number of TβRI and II-positive cells in the cres-


A
B
C
D
E
F
G
H
I
J
K
L

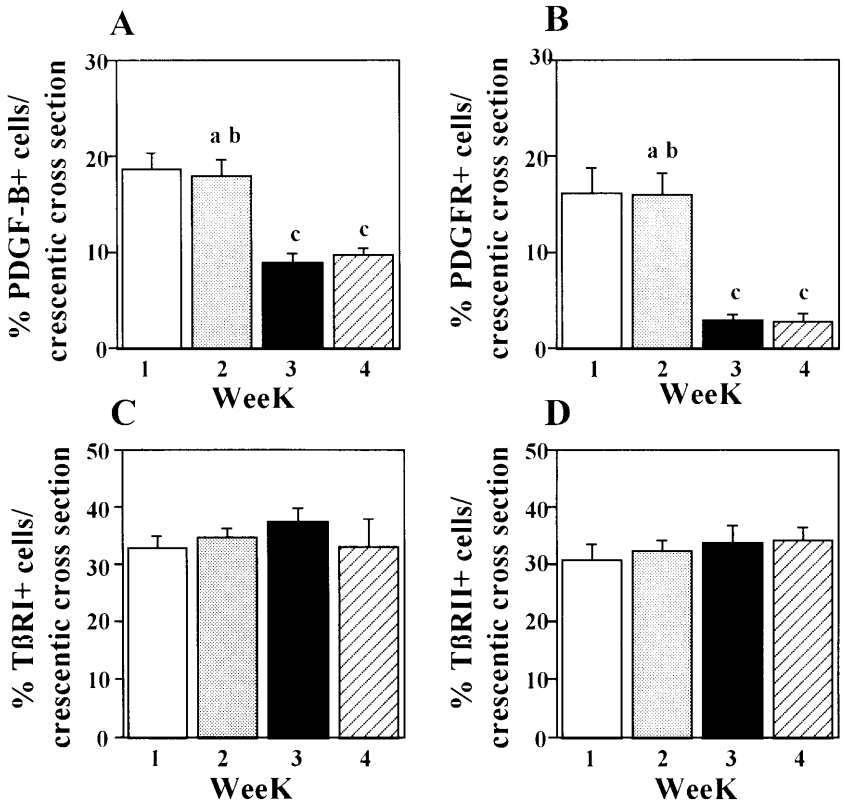


Fig. 5 The percentage of **A** PDGF-B, **B** PDGF receptor β, **C** TGF-β receptors types I (**C**)- and II (**D**)-positive cells in the crescent formation. *a* $P<0.01$ vs 3 weeks; *b* $P<0.01$ vs 4 weeks; *c* $P<0.01$ vs 1 week

Table 4 PCNA+ cells, cyclin A+ cells, p21+ cells, and p27+ cells per crescentic cross section

Week	PCNA+[a]	Cyclin A+[b]	p21+[c]	p27+[d]	*n*
1	15.0±1.4	11.4±1.3	0.8±0.2	1.0±0.1	4
2	14.4±1.3**[e],**[f]	10.5±1.0**[e],**[f]	7.9±1.0**[f],**[g],*[h]	9.7±1.4**[f],**[g]	4
3	8.8±0.7**[g]	5.4±1.3**[g]	9.8±2.0**[g],*[h]	6.1±2.2**[f],**[g]	3
4	6.5±1.1**[g]	4.2±1.2**[g]	2.6±0.4	3.5±0.7	4

[a] Mean number of PCNA+ cells in crescentic cross section
[b] Mean number of cyclin A+ cells in crescentic cross section
[c] Mean number of p21+ cells in crescentic cross section
[d] Mean number of p27+ cell in crescentic cross section
**[e]$P<0.01$ vs 3 weeks **[f]$P<0.01$ vs 4 weeks **[g]$P<0.01$ vs 1 week
*[h]$P<0.05$ vs 3 weeks

cent formation gradually decreased (Table 3), but the percentage of them was unchanged at about 32% up to 4 weeks (Fig. 5).

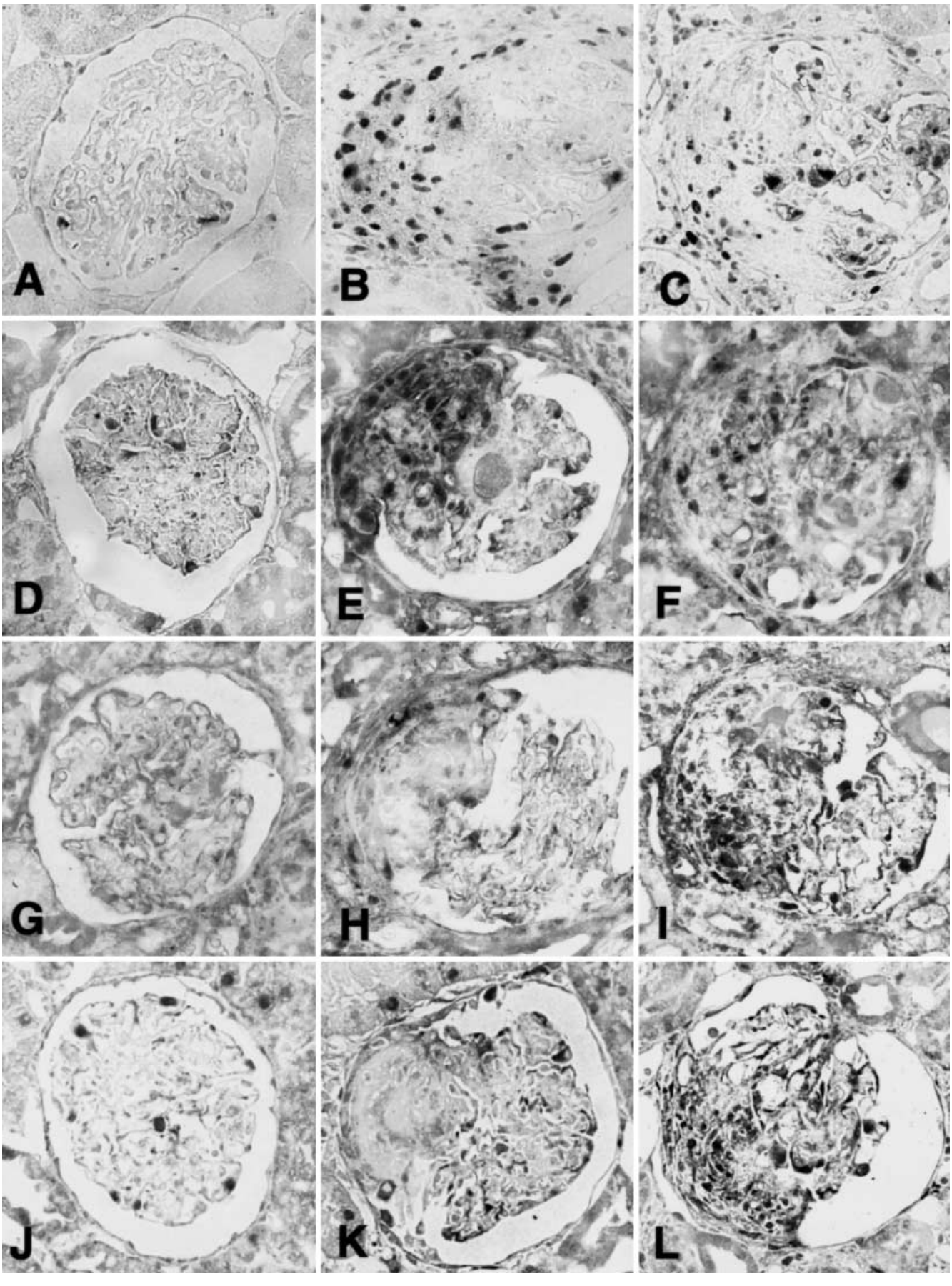
Expression of PCNA, cyclin A, p21 and p27

In normal rats, a small number of glomerular cells expressed PCNA and cyclin A (Fig. 6A, D). Immunostaining for p21 was absent in normal glomeruli, whereas p27 was constitutively expressed in some visceral glomerular epithelial cells (Fig. 6G, J). Cells with a nuclear pattern of immunostaining for PCNA and cyclin A were components of crescent cells in 46.8% and 37.1%, respectively, at 1 week (Fig. 6B, E), decreasing significantly after 3 weeks (Figs. 6C, F, 7, Table 4). The number and percentage of cells with nuclear pattern of immunostaining for p21 and p27 was low in crescents at 1 week (Fig. 6H, K), and then markedly increased with peaks of 39.6% at 3 weeks and 25–30% at 2–3 weeks (Figs. 6I, L, 7, Table 4).

◀ **Fig. 4** Immunostaining for **A**–**C** PDGF-B-, **D**–**F** PDGF receptor-β-, **G**–**L** TGF-β receptors **G**–**I** type I- and **J**–**L** type II-positive cells in the kidney. **A**, **D**, **G**, **J** Normal control rats; **B**, **E**, **H**, **K** 1 week; **C** **F** 3 weeks; **I**, **L** 4 weeks

Discussion

The current study on the ratio of macrophages or myofibroblasts in crescent cells has shown that crescent cells consist mainly of macrophages and myofibroblasts in more than 50% of crescent cells (66.3%, 73.1%, 57.4% and 53.8% in 1, 2, 3 and 4 weeks, respectively), confirm-


A
B
C
D
E
F
G
H
I
J
K
L

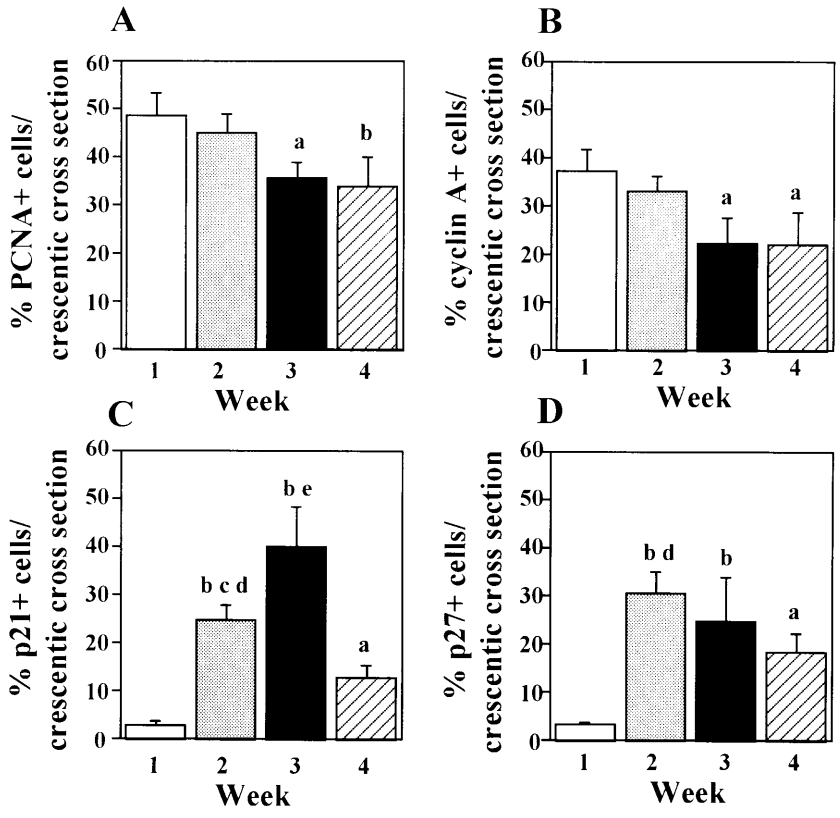


Fig. 7 Percentage of **A** PCNA-**B** cyclin A-, **C** p21-, and **D** p27-positive cells in crescent formation. *a* $P<0.05$ vs 1 week; *b* $P<0.01$ vs 1 week; *c* $P<0.01$ vs 3 weeks; *d* $P<0.05$ vs 4 weeks; *e* $P<0.05$ vs 4 weeks

ing that initial glomerular crescents are composed predominantly of macrophages and proliferative BEP [9, 31]. In our study, macrophages predominate initially and myofibroblasts later during the observation periods (Fig. 3). Apparent invasion of interstitial myofibroblasts into glomeruli could not be found at 1 week when BEP expressed alpha SMA, suggesting that BEP could transdifferentiate to myofibroblast as reported previously [16]. Invasion of interstitial myofibroblasts into glomeruli was evident after 2 weeks. Macrophage-connective tissue cells transdifferentiation was reported [29] in in vitro conditions, suggesting that macrophages infiltrated in the cellular crescent might contribute to produce collagen. Our findings suggest that accumulated myofibroblasts, which may lead to fibrosis in the crescent formation, originated from BEP, infiltrated macrophages, and interstitial myofibroblasts, though we cannot exclude the contribution of other cells.

As expected, immunostaining of PCNA and cyclin A, markers of cell proliferation, was found to be pronounced in the initial cellular crescents at 1 and 2 weeks, when at least macrophages and myofibroblasts would be expected to proliferate locally, and then decreased along with the reduction in cell numbers. Indeed, proliferation of macrophages in the crescent formation was reported [11]. On the other hand, immunostaining of CDKI p21 and p27 was low in cellular crescents at 1 week, then dramatically increased transiently, peaking at 3 or 2–3 weeks, respectively (Fig. 7C, D). As identification of cellular background of original cell type and cells after transdifferentiation was difficult, we did not clarify the specific cell type that is operated by p21 and/or p27; however, macrophages and myofibroblasts were consisted with major components in 73.1% at 2 weeks and 57.4% at 3 weeks, when p21 and p27 were increased dramatically. These findings suggest that p21 and/or p27 might control proliferation of macrophages and myofibroblasts in the crescent formation. In human crescentic GN, it is reported that the major component of the cellular crescents is made up of BEP in association with restrained expression of p27 [17]. However, it is not known that p27 is really required for inhibiting proliferation of crescent cells. Our findings have demonstrated for the first time that restrained expression and transient increase of p21 and p27 may be associated with proliferation and inhibiting proliferation of crescent cells, respectively in the fibrous progression of the crescent formation.

Immunostaining of PDGF-B was found in periglomerular cells, the BEP, and crescent cells in the segmental pattern at 1 week. The staining kinetics and staining pattern of PDGF-B-positive cells in the crescent formation may roughly parallel that of infiltrated ED 1-positive cells, suggesting that PDGF-B in an inflamed crescent lesion may be derived mainly from the macrophages. On

◀ **Fig. 6** Immunostaining for **A**–**C** PCNA-, **D**–**F** cyclin A-, **G**–**I** p21- and **J**–**L** p27-positive cells in glomeruli. Dark black-stained cell nuclei indicate corresponding antigens. **A**, **D**, **G**, **J** normal control rats; **B**, **E**, **H**, **K** 1 week; **C**, **F**, **I**, **L** 3 weeks

the other hand, PDGFR was expressed strongly in the BEP adjoining crescent formation only at 1 and 2 weeks, suggesting the contribution of PDGF to crescent formation. This is the first finding indicating that the PDGF pathway may function on BEP restrictively in the initial proliferative cellular crescent. PDGFR was also found in the periglomerular cells during experimental periods. PDGF is a potent mitogen and chemoattractant for fibroblasts [33], and even either direct or indirect profibrotic factor [21, 28]. In this model, PDGF might play a part in the activation and proliferation of BEP in paracrine and/or autocrine fashion, and also might transdifferentiate BEP to myofibroblasts in possible association with TGF-β action. In addition, it is also possible that PDGF derived from the BEP recruits periglomerular myofibroblasts, which may be activated by PDGF from interstitial macrophages and/or BEP, into the glomerulus.

In this study the expression of TGF-β could not be examined because appropriate antibodies for TGF-β were not available. However, immunostaining of both TβRI and TβRII was found in periglomerular cells, BEP and crescent cells at 1 week and was sustained there during observation periods. The percentages of both TβRI- and TβRII-positive cells in the crescent formation were not changed until 4 weeks. As both TβRI and TβRII cooperate for TGF-β signal transduction and they are both apparently required to be present on a particular cell type for TGF-β function to ensue [32], persistent expression of both TβRI and TβRII indicate that TGF-β may function on periglomerular cells, BEP and crescent cells during the observation periods. TGF-β has been known to play a part in renal fibrosis by accumulating extracellular matrix [1], inhibiting renal cell proliferation in vitro [25], renal cell apoptosis in vitro [3, 8] and phenotypic changes of renal tubular cells in vitro [5]. Therefore, in addition to possibly inducing the myofibroblast phenotype in BEP, it is also possible that the TGF-β pathway has a function in the inhibition of proliferation, reduction in cell number as well as deposition of extracellular matrix in the crescent formation, as observed in this study.

It has been reported that the TGF-β pathway regulates the cell cycle by arresting the cell cycle and inhibiting proliferation through p21 and p27 [4, 12, 19, 20, 23]. CDKI p57, which is the most recently identified, has also been documented in kidney. However, TGF-β-mediated arrest of cell cycle progression through p57 has not been determined. P21 can inhibit cell proliferation by inhibiting cyclin dependent kinase (CDK) or PCNA [14]. P27 binds to and inhibits both G1- and S-phase cyclin–CDK complexes and has been thought to function as a possible mediator of TGF-β-induced G1 arrest [12]. Cyclin A expression is decreased in certain circumstances, such as contact inhibition [34] and by TGF-β1 [20, 23]. Therefore, it is likely that the TGF-β pathway may induce, at least in part, cell cycle arrest and/or inhibition of crescent cell proliferation through p21 and/or p27 in the fibrous progression of crescent formation in this model. In addition, a role of p21 and p27 in apoptosis in vivo has been reported [15, 30]. Interestingly, Shimizu et al. report that apoptosis plays an essential role in the resolution of crescent cells within the scarring regions in the same model of crescentic GN [27].

In summary, PDGF and TGF-β might activate both periglomerular fibroblast and BEP to become myofibroblasts, which would presumably contribute to fibrous crescent formation. Restrained expression of or a transient increase in p21 and p27 may be associated with proliferation or inhibition of crescent cells (in which macrophages and myofibroblasts are major components), respectively. Action of TGF-β might induce inhibition of crescent cell proliferation through p21 and/or p27.

References

1. Border WA, Noble NA (1994) Mechanisms of disease. Transforming growth factor β in tissue fibrosis. N Engl J Med 331:1286–1292
2. Boucher A, Droz D, Adafer E, Noel LH (1987) Relationship between the integrity of Bowman's capsule and the composition of cellular crescents in human crescentic glomerulonephritis. Lab Invest 56:526–533
3. Choi ME, Ballermann BJ (1995) Inhibition of capillary morphogenesis and associated apoptosis by dominant negative mutant transforming growth factor-beta receptors. J Biol Chem 270:21144–21150
4. Datto MB, Panus JF, Howe DJ, Xiong Y, Wang X-F (1995) Transforming growth factor β induces the cyclin-dependent kinase inhibitor p21 through a p53-independent mechanism. Proc Natl Acad Sci USA 92:5545–5549
5. Fan JM, Ng YY, Hill PA, Nikolic-Paterson DJ, Mu W, Atkins RC, Lan HY (1999) Transforming growth factor-β regulates tubular epithelial-myofibroblast transdifferentiation in vitro. Kidney Int 56:1455–1467
6. Goumenos D, Tsomi K, Iatrou C, Oldroyd S, Sungur A, Papaioannides D, Moustakas G, Ziroyannis P, Mountokalakis T, El Nahas AM (1998) Myofibroblasts and the progression of crescentic glomerulonephritis. Nephrol Dial Transplant 13: 1652–1661
7. Kawasaki K, Yaoita E, Yamamoto T, Kihara I (1992) Depletion of CD8 positive cells in nephrotoxic serum nephritis of WKY rats. Kidney Int 41:1517–1526
8. Kitamura M, Suto TS (1997) TGF-β and glomerulonephritis. Anti-inflammatory versus prosclerotic actions. Nephrol Dial Transplant 12:669–679
9. Kondo Y, Shigematsu H, Kobayashi Y (1972) Cellular aspects of rabbit Masugi nephritis. II. Progressive glomerular injuries with crescent formation. Lab Invest 27:620–631
10. Lan HY, Nikolic-Paterson DJ, Atkins RC (1992) Involvement of activated periglomerular leukocytes in the rupture of Bowman's capsule and glomerular crescent progression in experimental glomerulonephritis. Lab Invest 67:743–751
11. Lan HY, Nikolic-Paterson DJ, Mu W, Atkins RC (1997) Local macrophage proliferation in the pathogenesis of glomerular crescent formation in rat anti-glomerular basement membrane (GBM) glomerulonephritis. Clin Exp Immunol 110:233–240
12. Li C-Y, Suardet L, Little JB (1995) Potential role of WAF1/Cip1/p21 as a mediator of TGF-β cytoinhibitory effect. J Biol Chem 270:4971–4974
13. Lianos EA, Liu J, Guglielmi K (1997) Quantification of changes in transforming growth factor-beta 1 gene expression in experimental crescentic glomerulonephritis. Proc Soc Exp Biol Med 214:180–186
14. Luo Y, Hurwitz J, Massague J (1995) Cell-cycle inhibition by independent CDK and PCNA binding domains in p21Cip1. Nature 375:159–161

15. Megyesi J, Safirstein RL, Price PM (1998) Induction of p21 (WAF1/Cip1/SDI1) in kidney tubule cells affects the course of cisplatin-induced acute renal failure. J Clin Invest 101:777–782
16. Ng YY, Fan JM, Mu W, Nikolic-Paterson DJ, Yang WC, Huang TP, Atkins RC, Lan HY (1999) Glomerular epithelial-myofibroblast transdifferentiation in the evolution of glomerular crescent formation. Nephrol Dial Transplant 14:2860–2872
17. Nitta K, Horita S, Honda K, Uchida K, Watanabe T, Nihei H, Nagata M (1999) Glomerular expression of cell-cycle-regulatory proteins in human crescentic glomerulonephritis. Virchows Arch 435:422–427
18. Pardee AB (1989) G1 events and regulation of cell proliferation. Science 246:603–608
19. Polyak K, Kato J, Solomon MJ, Sherr CJ, Massague J, Roberts JM, Koff A (1994) p27 kip1, a cyclin-Cdk inhibitor, links transforming growth factor-β and contact inhibition to cell cycle arrest. Genes Dev 8:9–22
20. Reddy KB, Hocevar BA, Howe PH (1994) Inhibition of G1 phase cyclin dependent kinases by transforming growth factor β1. J Cell Biochem 56:418–425
21. Sappino AP, Schürch W, Gabbiani G (1990) Differential repertoire of fibroblastic cells. Expression of cytoskeletal proteins as marker of phenotypic modulations. Lab Invest 63:144–161
22. Sasahara M, Sato H, Iihara K, Wang J, Chue CH, Takayama S, Hayase Y, Hazama F (1995) Expression of platelet-derived growth factor B-chain in the mature rat brain and pituitary gland. Mol Brain Res 32:63–74
23. Satterwhite DJ, Aakre ME, Gorska AE, Moses HL (1994) Inhibition of cell growth by TGFβ1 is associated with inhibition of B-myb and cyclin A in both ABl/MK and Mv1Lu cells. Cell Growth Differ 5:789–799
24. Shankland SJ (1999) Cell cycle regulatory proteins in glomerular disease. Kidney Int 56:1208–1215
25. Sharma K, Ziyadeh FN (1994) The emerging role of transforming growth factor-β in kidney diseases. Am J Physiol 266:F829-F842
26. Sherr CJ, Roberts JM (1995) Inhibitors of mammalian G1 cyclin-dependent kinases. Genes Dev 9:1149–1163
27. Shimizu A, Masuda Y, Kitamura H, Ishizaki M, Sugisaki Y, Yamanaka N (1996) Apoptosis in progressive crescentic glomerulonephritis. Lab Invest 74:941–951
28. Tang WW, Ulich TR, Lacey Dl, Hill DC, Qi M, Kaufman SA, Van GY, Tarpley JE, Yee JS (1996) Platelet-derived growth factor-BB induces renal tubulointerstitial myofibroblast formation and tubulointerstitial fibrosis. Am J Pathol 148:1169–1180
29. Vaage J, Lindblad WJ (1990) Production of collagen type I by mouse peritoneal macrophages. J Leukoc Biol 48:274–280
30. Wang X, Gorospe M, Huang Y, Holbrook NJ (1997) $p27^{Kip1}$ overexpression causes apoptotic death of mammalian cells. Oncogene 15:2991–2997
31. Wiggens RC, Holzman LB, Legault DJ (1997) Glomerular inflammation and crescent formation. In: Neilson EG, Couser WG (eds) Immunological renal diseases. Lippincott-Raven, Philadelphia, pp 669–682
32. Wrana JL, Attisano L, Wieser R, Ventura F, Massagué J (1994) Mechanism of activation of the TGF-β receptor. Nature 370:341–347
33. Xu J, Clark RA (1996) Extracellular matrix alters PDGF regulation of fibroblast integrins. J Cell Biol 132:239–249
34. Yoshizumi M, Hsieh C-M, Zhou F, Tsai J, Patterson C, Perrella MA, Lee M (1995) The ATF site mediates downregulation of the cyclin A gene during contact inhibition in vascular endothelial cells. Mol Cell Biol 15:3266–3272

Virchows Arch (2001) 439:46–54
DOI 10.1007/s004280100444

ORIGINAL ARTICLE

**Hiroyuki Kasajima · Shin-Ichiro Yamagishi
Satoshi Sugai · Norito Yagihashi · Soroku Yagihashi**

Enhanced in situ expression of aldose reductase in peripheral nerve and renal glomeruli in diabetic patients

Received: 10 January 2001 / Accepted: 20 February 2001 / Published online: 4 April 2001
© Springer-Verlag 2001

Abstract To explore the relationships between polyol pathway-related enzymes and pathologic features, we examined the immunohistochemical expression of aldose reductase (AR) and sorbitol dehydrogenase (SDH) in the peripheral nerve and kidney tissues collected postmortem from diabetic patients and compared it with those from non-diabetic patients. Tissue AR protein concentrations were also quantified. In non-diabetic patients, AR distributed in pericytes, smooth muscle cells of endo- and epi-neurial microvessels, Schwann cells in the sciatic nerve, and tubular cells of the renal medulla. By contrast, positive SDH reactions were observed in tubular cells of the renal cortex but were faint in the sciatic nerve. Diabetic patients frequently showed dense AR expressions in the sciatic nerve. In nephropathic diabetic patients, the glomerular mesangial area showed diffuse positive reactions for AR. The severity of structural changes in glomeruli correlated with the intensity of immunoreactive AR (r^2=0.626, P<0.01). AR contents in the renal cortex and sciatic nerve from diabetic patients were 1.5- and 1.8-fold greater than those from non-diabetic patients, respectively (P<0.05 for both). These findings are the first to demonstrate enhanced AR expressions in peripheral nerve and renal glomeruli in diabetic patients and its relevance to the characteristic pathology.

Keywords Aldose reductase · Sorbitol dehydrogenase · Diabetes · Nephropathy · Neuropathy

Introduction

The polyol pathway consists of two enzymes, aldose reductase (AR) and sorbitol dehydrogenase (SDH), which together convert glucose to fructose via sorbitol [10] (Fig. 1). During normoglycemia, most of the cellular glucose is phosphorylated into glucose 6-phosphate by hexokinase and glucokinase, and only a minor portion of cellular glucose enters the polyol pathway. Under hyperglycemia, where hexokinase and glucokinase appear to be saturated, there is an increased flux of glucose through the polyol pathway that, under these conditions, may account for as much as one-third of the total glucose turnover [14]. Experimental studies with AR inhibitors have implicated the accelerated flux of glucose through the polyol pathway in the pathogenesis of diabetic complications [10, 34, 39]. In diabetic patients, the incidence of chronic complications is associated with high AR activity or AR protein levels in erythrocytes [15, 16, 25,

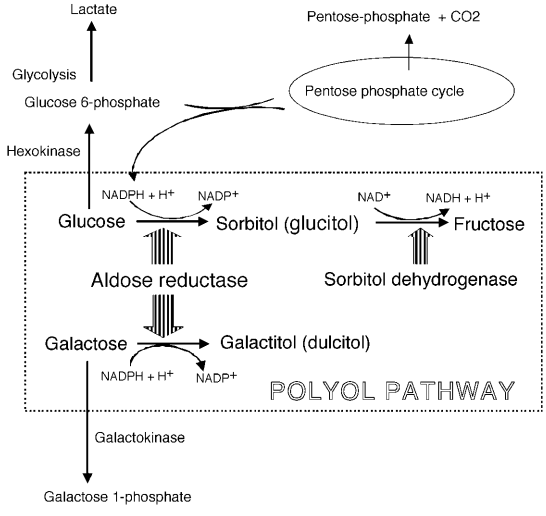


Fig. 1 Metabolic map of polyol pathway. Under a normoglycemic condition, glucose is converted into glucose-6-phosphate by hexokinase and, thereafter, incorporated into the tricarboxylic acid (TCA) cycle for the production of adenosine triphosphate (ATP). Once in a hyperglycemic condition, as much as one-third of the glucose will be converted to sorbitol, mediated by the enzyme aldose reductase. Sorbitol is then converted to fructose by sorbitol dehydrogenase. Galactose is also the substrate of aldose reductase and is converted to galactitol. Galactitol is not further metabolized

H.Kasajima · S. Yamagishi · S. Sugai · N. Yagihashi (✉)
S. Yagihashi
Department of Pathology,
Hirosaki University School of Medicine,
5 Zaifu-cho, Hirosaki, 036-8562 Japan
e-mail: yagihasi@cc.hirosaki-u.ac.jp
Tel.: +81-172-395024, Fax: +81-172-395026

Table 1 Clinical data of diabetic and non-diabetic subjects used in the present study. Diabetic patients used in this study were all type-2. Nephropathy was based on clinically overt proteinuria more than 0.5 g/day. Hypertension was defined by systolic blood pressure more than 150 mmHg and diastolic pressure more than 100 mmHg

	Cases	Age (years)/ gender	Major clinical diagnosis	Duration of diabetes (years)	HbA1C	Nephropathy	Hypertension
1	Diabetic	67/Male	Diabetes mellitus and hepatic cancer	17	10.6	+	+
2	Diabetic	64/Male	Diabetes mellitus and colon cancer	22	8.8	+	–
3	Diabetic	71/Male	Diabetes mellitus and hepatic cancer	18	6.9	+	+
4	Diabetic	46/Male	Diabetes mellitus and renal failure	13	11.7	+	+
5	Diabetic	73/Male	Diabetes mellitus and heart failure	4	7.0	+	–
6[a]	Diabetic	56/Male	Diabetes mellitus and renal failure	21	8.9	+	+
7[a]	Diabetic	68/Female	Diabetes mellitus and renal failure	26	6.1	+	+
		(63.7±8.8)		(17.3±6.6)	(8.6±2.1)		
8	Diabetic	69/Male	Diabetes mellitus and cerebral infarction	19	7.7	–	–
9	Diabetic	68/Male	Diabetes mellitus and hepatic cancer	12	5.5	–	–
10	Diabetic	58/Female	Diabetes mellitus and retroperitoneal tumor	4	6.4	–	–
11	Diabetic	45/Male	Diabetes mellitus and acute leukemia	4	7.9	–	–
12	Diabetic	60/Male	Diabetes mellitus and lung cancer	10	8.9	–	–
13[a]	Diabetic	62/Male	Diabetes mellitus and vesical cancer	12	11.0	–	+
14[a]	Diabetic	58/Female	Diabetes mellitus and ovarian cancer	13	9.2	–	–
15[a]	Diabetic	49/Male	Diabetes mellitus and colon cancer	8	6.1	–	–
		(60.9±8.6)		(10.3±4.7)	(7.8±1.8)		
1	Non-diabetic	53/Male	Renal cell carcinoma				+
2	Non-diabetic	59/Female	Renal cell carcinoma				–
3	Non-diabetic	59/Male	Amyotrophic lateral sclerosis				–
4	Non-diabetic	62/Male	Gastric cancer				–
5	Non-diabetic	44/Male	Colon cancer				–
6	Non-diabetic	52/Female	Cerebral infarction				+
7	Non-diabetic	51/Male	Colon cancer				–
8	Non-diabetic	74/Female	Fulminant hepatitis				–
9	Non-diabetic	75/Male	Esophageal cancer				+
10	Non-diabetic	79/Male	Lung cancer				–
11[a]	Non-diabetic	45/Female	Gastric cancer				–
12[a]	Non-diabetic	63/Female	Cardiac failure				+
13[a]	Non-diabetic	52/Male	Myocardial infarction				+
14[a]	Non-diabetic	61/Male	Colon cancer				–
15[a]	Non-diabetic	54/Female	Hepatic cancer				–
16[a]	Non-diabetic	59/Male	Lung cancer				+
	(58.9±9.9; mean±SD)						

[a] Cases used for determination of AR contents in tissues by means of an enzyme-linked immunosorbent assay (ELISA)

30, 36]. The transgenic expression of human AR has also been shown to elicit severe neuropathic changes under a galactosemic condition [40]. Despite this increasing evidence that AR plays a role in the etiology of diabetic complications, AR expression in human diabetic tissues and its relationship to pathological features has not been characterized.

With the recent production of monoclonal antibody specific for human AR, it has now become possible to perform a precise measurement of tissue AR protein levels [30, 36]. Here, we report the immunohistochemical localization of AR and SDH in human tissues of non-diabetic and diabetic patients. To explore the significance of AR expression in the development of diabetic nephropathy, we also examined the relationship between AR expression and the severity of pathological changes.

Materials and methods

For the evaluation of in situ expression of AR and SDH, we collected peripheral nerve (mostly sciatic nerve, but sometimes sural and tibial nerve) and renal tissue samples at autopsy from 15 type-2 diabetic patients, including seven cases with established nephropathy (Table 1) and 16 non-diabetic control subjects. The diagnosis of diabetes was based on the diagnostic criteria of the World Health Organization (WHO) [1], referring the record of the patients describing hyperglycemia and elevated glycated hemoglobin levels.

Established nephropathy was based on the previous history of continuous overt proteinuria of more than 0.5 g/day, elevated serum levels of urea nitrogen and creatinine, and by the characteristic pathology of renal glomeruli. Distribution and in situ expression of AR and SDH were studied immunohistochemically. For this purpose, tissue samples obtained within 2 h postmortem were used. From five patients of the diabetic group (three with and two without nephropathy) and six patients of the non-diabetic group, fresh tissues obtained at autopsy were used for the measurements of AR protein levels using an enzyme-linked immunosorbent assay (ELISA) [30, 36]. For reference, some liver and aortic tissues were also examined for the content of AR when the tissues were available.

Immunohistochemistry

All tissue specimens were fixed in a 10% formalin solution and embedded in paraffin. Immunostaining was started following deparaffinization of the tissue sections with xylene. The 4-μm-thick sections were pretreated with 0.3% methanolic H_2O_2 to eliminate endogenous peroxidase activity. A monoclonal anti-AR antibody (AR mAb25 and 55, Mitsubishi Gas Chem., Niigata, Japan) [30, 31, 36] or a polyclonal anti-SDH antibody (provided by Prof. N. Taniguchi, Osaka University, Japan) [20] was then applied to the sections overnight at 4°C. Subsequent development of antibody–bridge labeling was made using the streptavidin biotin–peroxidase method (Histofine SAB - PO Kit, Nichirei Co., Tokyo, Japan). Diaminobenzidine was used to visualize peroxidase deposition at the antigenic sites, and these sections were counterstained with hematoxylin.

Monoclonal antibody was used at a dilution of 1:100, and polyclonal antibody was used at a dilution. The intensity of immuno-positive reactions was evaluated with a four-step grading scheme: 0 negative; 1 weakly positive; 2 positive or, in glomerulus, only partial staining; and 3 strongly positive or, in glomerulus, diffusely positive staining. Immunoreactions were evaluated by two observers who were not aware of the identity of the samples. The specificity of immunostaining was confirmed by incubating the tissue sections with (1) the first antibodies (50 μl) following treatment with excessive antigens (50 μg/ml), (2) omission of the first antibody, or (3) replacement of the first antibody by normal swine sera during the immunostaining point in the process.

Quantitation of glomerular pathology

For the evaluation of glomerular changes, 4-μm-thick paraffin sections were stained with periodic acid–Schiff (PAS) and examined. Thirty glomeruli, selected at random, were evaluated in each sample. Pathological changes commonly found in diabetes were noted. These included (1) nodular lesion, (2) thickening of peripheral glomerular basement membranes, (3) hyalinous sclerosis of afferent and efferent arterioles, (4) fibrin cap, and (5) the expansion of the mesangial area with matrix deposition.

For the semi-quantitation of glomerular changes, each of the pathological changes listed above was evaluated in each glomerulus, and the tissue sample was assigned a value. If one glomerulus showed the presence of all five pathological findings, the score for that glomerulus was 5. Therefore, the index of glomerular pathology in one patient theoretically ranged from 0 to150. Glomeruli showing total hyalinosis were omitted for quantitation.

For objective analysis of mesangial expansion, quantitative measurement was performed on the PAS-stained glomeruli using National Institutes of Health (NIH) image analysis software to process data obtained with a light microscope equipped with a CCD video camera connected to a computer system (Power Macintosh G3, Apple Computer Inc., Cupertino, Calif.). Morphometric analysis of the glomerulus was based on the previously described method [35, 37]. Mesangial area was defined as the area of PAS-positive mesangial matrix along with the area of the mesangial cells. This morphometric evaluation was conducted by two observers in a double-masked manner.

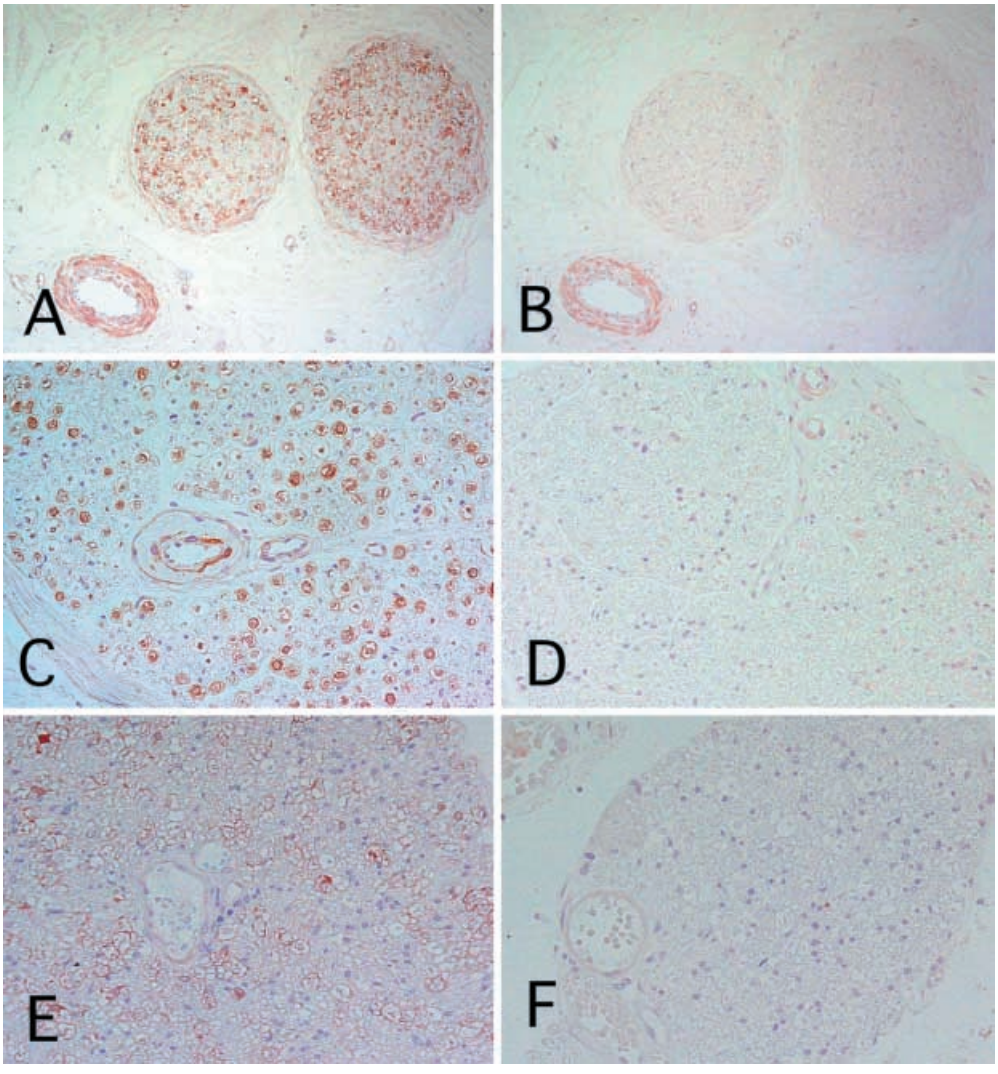


Fig. 2 Distribution of aldose reductase (AR) and sorbitol dehydrogenase (SDH) in the peripheral nerve of diabetic and non-diabetic patients. AR stained positively in endoneurial nerve fibers and smooth muscle cells of both epineurial arterial vascular walls (**A**, ×40). Smooth muscle cells of epineurial arteries were also positively stained with SDH, but the reactions of endoneurium were negative (**B**, ×40). The high-power view clearly depicts positive AR reactions in axolemma, Schwann cells of myelinated fibers, perineurial cells in the peripheral nerve, and pericytes of endoneurial vessels (**C**, ×480). Endoneurial microvessels also showed positivity for SDH in pericytes, although faint (**D**, ×400). The peripheral nerves of diabetic subjects frequently showed intensive positive reactions of nerve fibers and smooth muscle wall or pericytes of endoneurial microvessels (**C**) compared with those in non-diabetic subjects (**E**, ×420), while negative reactions of SDH were similar between diabetic and non-diabetic subjects (**F**, ×300)

Enzyme-linked immunosorbent assay

Homogenized tissues were assayed for protein levels of AR with an ELISA method, as previously described [30, 36]. For this assay, immunoplates were coated at 4°C overnight with purified AR antibody diluted in 150 µl of phosphate-buffered saline (PBS; 2 µg per well). All subsequent procedures were carried out at room temperature. The protein concentration was determined by the method of Bradford, calibrated with bovine albumin.

Statistaical analysis

Comparison was made on the difference in the mean values between two groups using an unpaired *t*-test. Comparative differences with *P* values less than 0.05 were considered statistically significant.

Results

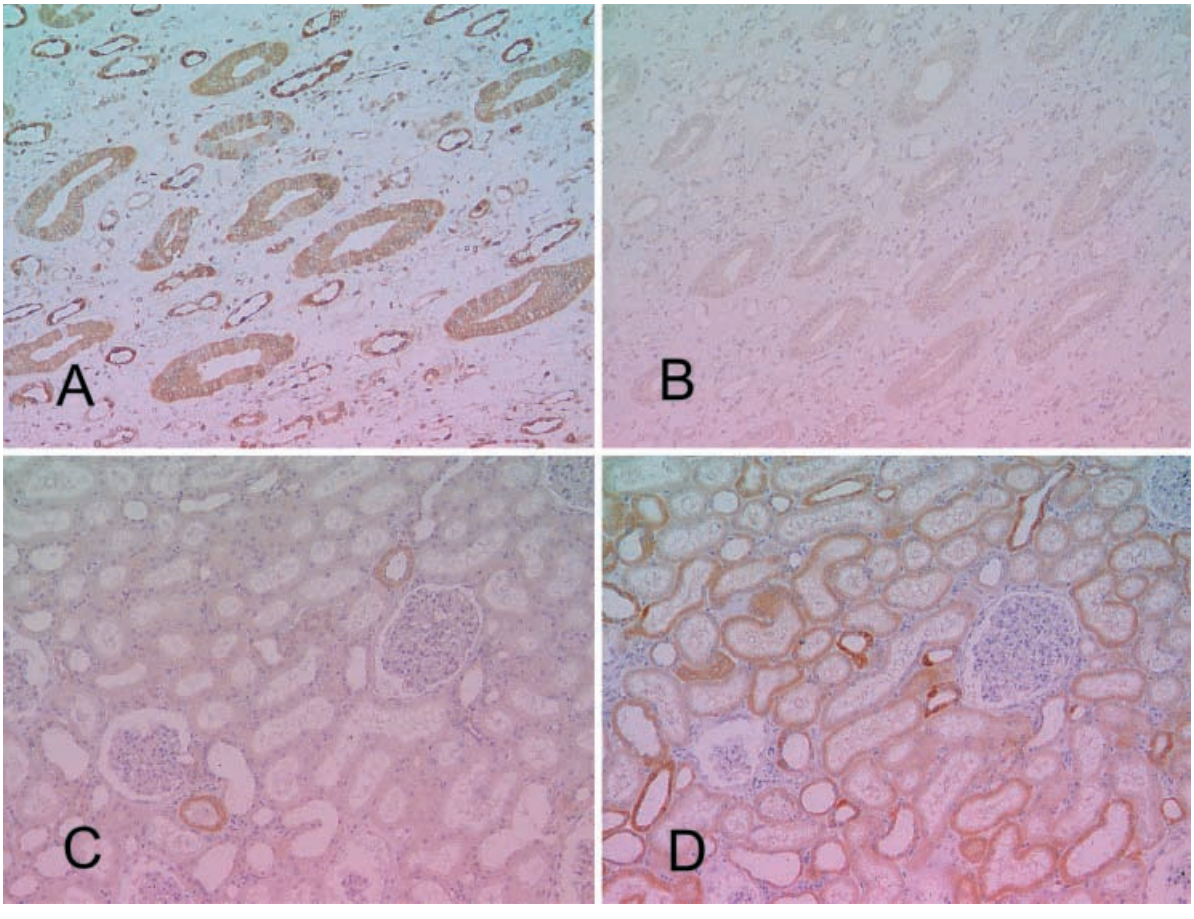
Clinical data

Clinical data for non-diabetic and diabetic patients are summarized in Table 1. The age of subjects in the non-diabetic and diabetic groups ranged from 44 years to 79 years old (58.9±9.9 years, mean±SD) and 45 years to 73 years old (60.9±8.6), respectively. In the diabetic patients without nephropathy, the duration of diabetes ranged between 4 years and 19 years (10.3±4.7 years). This was significantly shorter that the duration of diabetes in diabetic patients with nephropathy which ranged between 4 years and 26 years (17.3±6.6 years, $P<0.05$).

Immunohistochemical localization of AR and SDH

AR stained positively in endoneurial nerve fibers and smooth muscle cells of both epineurial venous and arterial vascular walls near nerve fasciculi (Fig. 2A). Smooth muscle cells of epineurial arteries were also positively stained with SDH, but the reactions of endoneurium were negative (Fig. 2B). Within the nerve fasciculi, Schwann cells of myelinated fibers and perineurial cells in the peripheral nerve were also positive for AR (Fig. 2C). Endoneurial microvessels showed positivity for both AR and SDH in capillary pericytes, although SDH reactions were faint (Fig. 2D). The peripheral nerves of diabetic subjects frequently showed intensive positive reactions of endoneurial Schwann cells and axon membrane areas and vascular pericytes compared with those in non-diabetic subjects (compare Fig. 2C with Fig. 2E), while negative reactions of SDH were

Fig. 3 Distribution of immunoreactive aldose reductase (AR)- and sorbitol dehydrogenase (SDH)-positive cells in the kidney of a non-diabetic patient. AR was detected in tubular cells of renal medulla (**A**, ×480), but SDH was equivocal (**B**, ×480). In the renal cortex, AR was faintly stained (**C**, ×240), whereas SDH was strongly positive for cortical tubular epithelial cells (**D**, ×240)



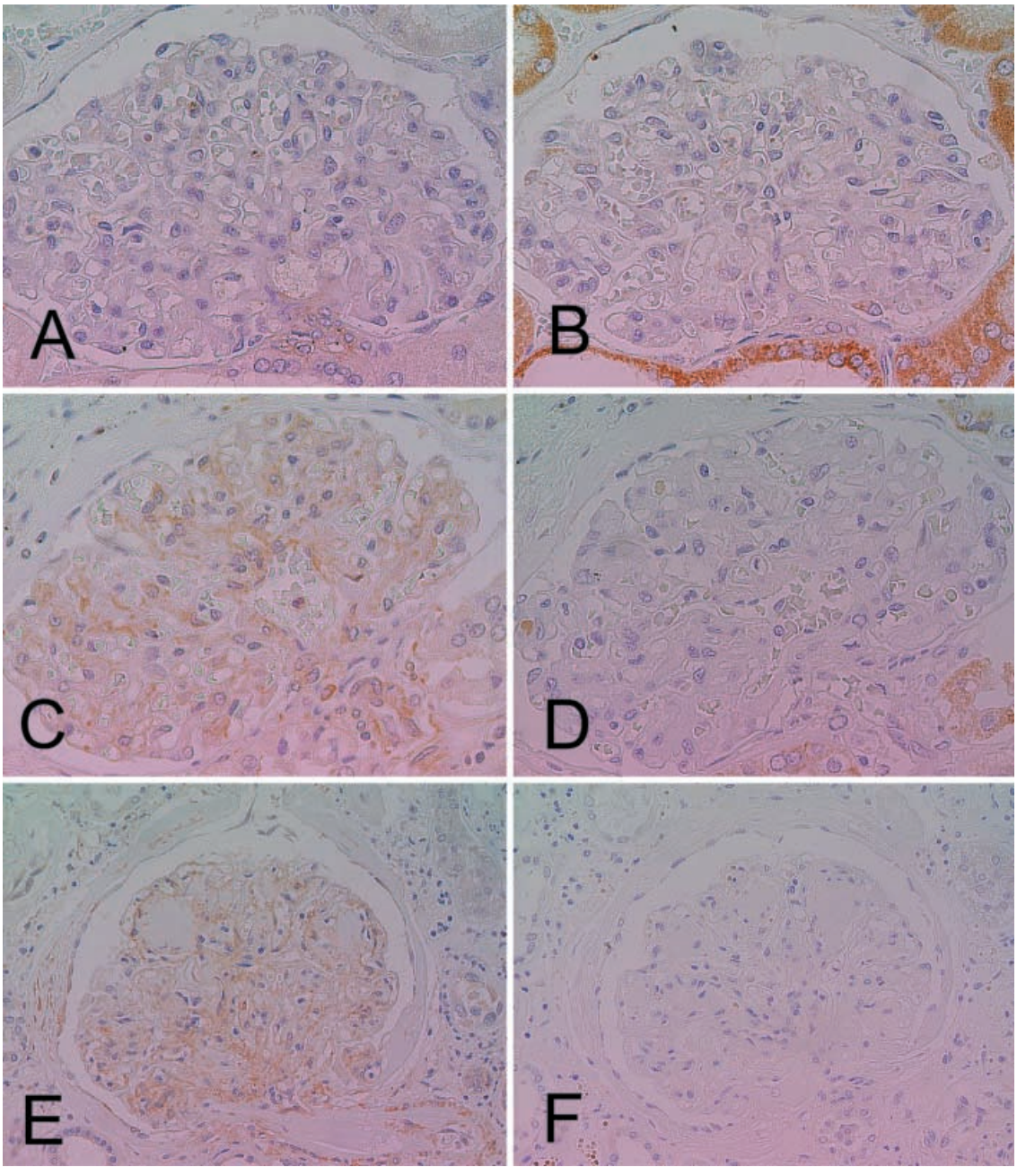


Fig. 4 Immunohistochemical detection of aldose reductase (AR) and sorbitol dehydrogenase (SDH) in glomeruli. In a non-diabetic patient, immunoreactive AR was hardly detectable in glomeruli (**A**, ×400), whereas SDH was strongly positive for cortical tubular cells but not for glomerular cells (**B**, ×400). In diabetic patients with nephropathy, immunohistochemistry shows diffusely positive AR (**C**, ×400) but negative for SDH (**D**, ×400) in the mesangial area in case 2. Reactions of SDH in atrophic tubular cells surrounded by thickened basement membrane and interstitial fibrosis were much reduced in a diabetic patient. In another diabetic patient with nephropathy (case 4), there was strong AR-positive depositions in mesangial area and around the nodular lesions (**E**, ×360), whereas SDH reactions were completely negative (**F**, ×360)

similar between diabetic and non-diabetic subjects (Fig. 2F).

In the kidney of non-diabetic patients, epithelial cells of collecting tubules and inner medulla and transitional cell layers of the papilla were strongly positive for AR (Fig. 3A), whereas they were negative for SDH (Fig. 3B). Renal cortical cells, including tubular cells, were only weakly stained with AR (Fig. 3C). SDH was strongly stained in tubular cells of the renal cortex in distal renal tubules (Fig. 3D). Vascular smooth muscle cells were positive for both AR and SDH, but glomeruli were all negative in non-diabetic patients**.**

There were no apparent differences in the intensity or distribution of AR expression between the non-diabetic and diabetic groups in the renal medulla and papilla. As

Table 2 Topographic expression of aldose reductase (AR) and sorbitol dehydrogenase (SDH) and its relationship to glomerular pathology. All values are expressed as mean±SD. *MSA* mesangial surface area, *TGSA* total glomerular surface area, *GTSA* glomerular tuft surface area

Group	*n*	Medulla[a]		Cortical tubule[a]		Glomeruli		Index of glomerular pathology[b]	MSA/TGSA	MSA/GTSA
		AR	SDH	AR	SDH	AR	SDH			
Diabetic with nephropathy	7	+++	0.3±0.5	0.7±0.7	+++	2.1±0.8[c]	0	88.3±10.6[c]	0.186±0.035[c]	0.327±0.064[c]
Diabetic without nephropathy	8	+++	0.1±0.3	0.2±0.4	+++	0.5±0.7	0	37.5± 7.1[d]	0.127±0.033[d]	0.190±0.028[d]
Non-diabetic	10	+++	0.2±0.4	0	+++	0	0	5.7±2.31	0.082±0.010	0.126±0.013

[a] Immunoreactions of AR in renal medulla and of SDH in cortical tubules were consistently positive in both diabetic and non-diabetic patients

[b] In each case, 30 glomeruli were examined as to nodule formation, fibrin cap, basement membrane thickening, arteriolosclerosis, and mesangial expansion, each of which scores as one point in a single glomerulus (see text)

[c] $P<0.001$ vs diabetic with nephropathy and non-diabetic

[d] $P<0.001$ vs non-diabetic

compared with negative reactions of AR and SDH in glomeruli in non-diabetic patients (Fig. 4A, B), diffuse positive reactions of AR were detected in the glomerular mesangial area (both matrix and mesangial cells) from diabetic subjects with nephropathy, showing expansion of the mesangial area (Fig. 4C). SDH reactions in diabetic renal cortex were much reduced and were associated with interstitial fibrosis and thickened basement membranes of tubules (Fig. 4C) compared with those in non-diabetic tissues (Fig. 3D and 4B). Patients with diabetes did not show SDH in mesangial cells (Fig. 4D). Positive reactions of AR were also strongly detected in the mesangial areas in glomeruli with nodular lesions (Fig. 4E), whereas SDH was still negative (Fig. 4F). Semi-quantitative analysis of AR immunoreactions in renal tissues demonstrated a significant increase in the scores of AR reactions in glomeruli of diabetic patients with nephropathy (Table 2).

Enzyme-linked immunosorbent assay

As shown in Table 3, the concentration of AR in the renal medulla was more than four times greater than in the renal cortex. There was a significant increase in AR protein contents in the renal cortex of diabetic patients (184±62 ng/mg protein; including two cases with nephropathy and three cases without nephropathy) compared with those in non-diabetic subjects (103±34 ng/mg protein; $P<0.05$). The AR levels in the sciatic nerve were more than twofold greater than the levels in the renal cortex in non-diabetic subjects. The average level in diabetic nerves (343±72 ng/mg protein) was significantly higher than that of non-diabetic subjects (228±56 ng/mg protein; $P<0.05$).

Quantitation of glomerular pathology

The index of pathology of diabetic patients with nephropathy was more than twofold greater compared with non-nephropathic patients (Table 2). Mean mesangial surface area per total glomerular surface area or per glomerular tuft surface area was also expanded in nephropathic patients compared with non-nephropathic patients. There was a significant correlation between the intensity of mesangial AR positivity and index of glomerular pathology ($r^2=0.626$, $P<0.01$) (Fig. 5).

Table 3 Contents of aldose reductase protein in various tissues and comparison between diabetic and non-diabetic subjects. Values are mean±SD (ng/mg protein) measured by means of an enzyme-linked immunosorbent assay (ELISA). *NE* not examined, *NS* not significant

Organs	Non-diabetic subjects		Diabetic subjects		
Liver	32±6	(*n*=6)	37±8	(*n*=5)	NS
Renal medulla	470±188	(*n*=6)	448±207	(*n*=5)	NS
Renal cortex	103±34	(*n*=6)	184±62	(*n*=5)	*P*<0.05
Aorta	178±62	(*n*=4)	NE		
Sciatic nerve	228±56	(*n*=5)	343±72	(*n*=4)	*P*<0.05

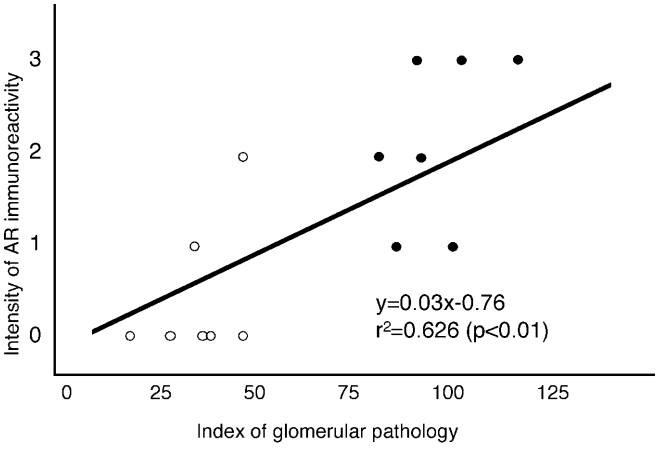


Fig. 5 Relationship between index of glomerular pathology and intensity of aldose reductase (AR) immunoreactivity. The index of pathology was defined in the text. Severe pathological changes were associated with intensified AR expressions. *Open circles* are non-diabetic patients and *closed circles* are diabetic patients

Discussion

This is the first report to characterize the distribution and expression of AR and SDH in tissues of peripheral nerve and kidney from diabetic and non-diabetic patients. AR contents in tissues as measured by means of ELISA showed 20 times higher concentrations in the nerve and ten times higher concentrations in the renal cortex than in erythrocytes [30, 36]. Immunohistochemistry demonstrated high AR expressions in the sciatic nerve (endoneurial vessel walls and myelinated fibers) and renal glomeruli in diabetic patients, and ELISA studies confirmed the increased AR contents in diabetic tissues compared with those in non-diabetic tissues. By contrast, the distribution of immunoreactive SDH did not correspond with that of AR in the nerve and renal cortex, but the smooth muscle layer of the vessels expressed both AR and SDH, indicating that the polyol pathway may operate differently in various tissues [7, 22].

Increased AR protein expression in renal tissues has been described in streptozotocin-induced diabetic rats and spontaneously diabetic Biobreeding (BB) rats [6, 11]. In these animal experiments, when hyperglycemia was treated with insulin, AR protein and its messenger (m)RNA expression were restored to non-diabetic control levels [12]. It is therefore likely that long-term metabolic abnormalities elicit augmented expression of AR in diabetic patients. In contrast to AR, there was no apparent alteration in the expression of SDH in the sciatic nerve and renal cortex in diabetic patients except for a reduction in atrophic tubules that were associated with interstitial fibrosis. The reduction of SDH in atrophic tubules may reflect the deteriorated physiological function of osmotic regulation.

The depletion of myo-inositol levels and the loss of Na^+, K^+-adenosine triphosphatase (ATPase) activity, abnormalities that occur after an increased flux of glucose through the polyol pathway, have been implicated in the etiology of the functional and structural impairments that characterize diabetic neuropathy and nephropathy [8, 13]. The co-localization of Na^+, K^+-ATPase with AR abundance at the nodal gap in nerve fibers detected in the diabetic rat model is also consistent with our immunohistochemical results and the hypothesis of polyol-related nerve dysfunction [32]. A redox imbalance, termed pseudohypoxia, produced by the consumption of nicotinamide adenine dinucleotide (NAD) during the conversion of sorbitol to fructose has also been proposed as major mechanisms of cell injury in diabetes [38]. This concept has recently been challenged by the study results from Ng et al. [29]. These investigators created a transgenic strain of mice that were SDH deficient. When these animals were made diabetic, the sciatic nerve conduction velocity (NCV) was decreased. This decrease in NCV was not different from that observed in normal mice under a comparable hyperglycemic condition [29]. Recent success in production of AR-knockout mice also demonstrated that diabetic hyperglycemia could not cause reduced NCV [19]. The predominance of AR protein expression over SDH in the sciatic endoneurium and renal glomeruli detected in this study may therefore reinforce the importance of the first half of the polyol pathway as a major culprit for the tissue damage in a diabetic condition.

The polyol pathway plays an important role in osmoregulation in renal medullary cells [3, 5]. Accumulation of sorbitol causes cellular hypertonicity, resulting in depletion of other osmoregulatory substances of betaine, taurine, and myo-inositol [3, 39]. Such a hyperosmotic condition after induction of the AR gene activates stress-related kinases to enhance signal transduction, activates protein kinase C, and synthesizes matrix proteins in human embryonic epithelial cells and renal tubular cells [27, 28, 41]. It is shown that the activation of the polyol pathway by osmotic stress and galactosemia elicits synthesis of matrix proteins, such as fibronectin and basement membrane collagen in microvessels [2, 27]. Consistent with these observations, hyperosmotic stress may induce enhanced AR expression in cultured mesangial cells and Schwann cells [23, 26]. These processes may be part of the mechanism that causes the characteristic microangiopathy seen in diabetes. Consistently, the AR inhibitor prevents thickening of basement membranes in retinal vessels of galactosemic animals [34].

There is growing evidence that genetic factors influence the onset and severity of diabetic complications. Gene polymorphism of angiotensin-converting enzyme, angiotensinogen, and AR is relevant to the onset of diabetic nephropathy [9, 17, 21, 25]. Erythrocyte AR protein levels or its enzyme activities correlate with the high incidence of diabetic neuropathy, retinopathy, and nephropathy [15, 16, 30, 31, 36]. Although our immunohistochemical studies showed a strong reaction of AR proteins in the mesangial area, because of ill-defined cell borders, we could not determine whether the cytoplasms or matrix of mesangial cells or both of these were the reactive sites. Immunoelectron microscopic examinations will further elucidate the precise localization of the AR-positive site. However, in diabetic glomeruli, mesangial cells are found to be elongated, with fine processes like myo-fibroblastic cells in the abundant matrix and may possibly manifest as the locations of AR protein [18]. Therefore, it is likely that the expression of AR protein, detected as constituents in the mesangial cells of our nephropathic patients, may serve as a determinant of the pathological changes. It may also be possible, however, that the augmented expression of AR in diabetic mesangial cells may be secondarily induced by osmotic stress or by excessive accumulation of oxidative stress-related aldehydes [4, 24]. AR mRNA was shown to be upregulated by the accumulation of aldehydes [4, 33]. Although the precise mechanisms of enhanced expression of AR in diabetic tissues with characteristic pathology are yet to be clear, early intervention to inhibit the expression of this enzyme might be crucial for interrupting the progressive development of diabetic complications in humans.

Acknowledgements We thank Dr. Tomokazu Tachikawa of Mitsubishi Gas Chemical Co. for the kind supply of monoclonal human AR antibody used in this study. We are indebted to Professor Naoyuki Taniguchi, Medical School Department of Biochemistry, Osaka University for providing us with the antibody to SDH. We also thank Dr. Thomas Hohman for his critical review of this manuscript. This study was supported by grant-in aids to SY from the Japanese Ministry of Education, Science, Culture and Sports (10470054), the Japanese Ministry of Health and Welfare (H11-Choju-018), the Japan Diabetes Foundation, and Juvenile Diabetes Foundation International (1-2000-263).

References

1. American Diabetes Association and 1980–1985 World Health Organization (1997). Diagnostic criteria. Diabetes Care 20: 1859–1862
2. Ayo SH, Radnik RA, Glass WF 2nd, Garoni JA, Rampt ER (1991) Increased extracellular matrix synthesis and mRNA in mesangial cells grown in high glucose medium. Am J Physiol 260:185–191
3. Bagnasco SM, Murphy HR, Bedford JJ, Burg MB (1988) Osmoregulation by slow changes in aldose reductase and rapid changes in sorbitol flux. Am J Physiol 254:788–792
4. Baynes JW, Thorpe SR (1999) Role of oxidative stress in diabetic complications. A new perspective on an old paradigm. Diabetes 48:1–9
5. Bondy C, Cowley BD Jr, Lightman SL, Kador PF (1990) Feedback inhibition of aldose reductase gene expression in rat renal medulla. Galactitol accumulation reduces enzyme mRNA levels and depletes cellular inositol content. J Clin Invest 86:1103–1108
6. Chakrabarti S, Sima AA, Nakajima T, Yagihashi S, Greene DA (1987) Aldose reductase in the BB rat: isolation, immunological identification and localization in the retina and peripheral nerve. Diabetologia 30:244–251
7. Corder CN, Collins JG, Brannan TS, Sharma J (1977) Aldose reductase and sorbitol dehydrogenase distribution in rat kidney. J Histochem Cytochem 25:1–8
8. Derylo B, Babazono T, Glogowski E, Kapor Drezgic J, Hohman T, Whiteside C (1988) High glucose induced mesangial cell altered contractility: role of the polyol pathway. Diabetologia 41:507–515
9. Freire MB, Ji L, Onuma T, Orban T, Warram JH, Krolewski AS (1998) Gender-specific association of M235T polymorphism in angiotensinogen gene and diabetic nephropathy in NIDDM. Hypertension 31:896–899
10. Gabbay KH (1975) Hyperglycemia, polyol metabolism, and complications of diabetes mellitus. Annu Rev Med 26:521–536
11. Ghahary A, Luo JM, Gong YW, Chakrabarti S, Sima AA, Murphy LJ (1989) Increased renal aldose reductase activity, immunoreactivity, and mRNA in streptozocin-induced diabetic rats. Diabetes 38:1067–1071
12. Ghahary A, Chakrabarti S, Sima AA, Murphy LJ (1991) Effect of insulin and statil on aldose reductase expression in diabetic rats. Diabetes 40:1391–1396
13. Goldfarb S, Ziyadeh FN, Kern EF, Simmons DA (1991) Effects of polyol pathway inhibition and dietary myo-inositol on glomerular hemodynamic function in experimental diabetes mellitus in rats. Diabetes 40:465–471
14. Gonzalez RG, Barnett P, Aguayo J, Cheng HM, Chylack LTJ (1984) Direct measurement of polyol pathway activity in the ocular lens. Diabetes 33:196–199
15. Hamada Y, Kitoh R, Raskin P (1991) Crucial role of aldose reductase activity and plasma glucose level in sorbitol accumulation in erythrocytes from diabetic patients. Diabetes 40: 1233–1240
16. Hamada Y, Odagaki Y, Sakakibara F, Naruse K, Koh N, Hotta N (1995) Effects of an aldose reductase inhibitor on erythrocyte fructose 3 phosphate and sorbitol 3 phosphate levels in diabetic patients. Life Sci 57:23–29
17. Heesom AE, Millward A, Demaine AG (1998) Susceptibility to diabetic neuropathy in patients with insulin dependent diabetes mellitus is associated with a polymorphism at the 5' end of the aldose reductase gene. J Neurol Neurosurg Psychiatry 64:213–216
18. Heptinstall RH (1983) Diabetes mellitus and gout. In: Heptinstall RH (ed) Pathology of kidney. Little Brown and Company, Boston, pp 1357–1453
19. Ho ECM, Lam KSL, Chung SSM, Chung SK (2000) Aldose reductase-deficient mice are protected from reduction of nerve conduction associated with diabetes (abstract). J Periph Nerv Syst 6:188
20. Hoshi A, Takahashi M, Fujii J, Myint T, Kaneko H, Suzuki K, Yamasaki Y, Kamada T, Taniguchi N (1996) Glycation and inactivation of sorbitol dehydrogenase in normal and diabetic rats. Biochem J 318:119–123
21. Jacobsen P, Rossing K, Rossing P, Tarnow L, Mallet C, Poirier O, Cambien F, Parving HH (1998) Angiotensin converting enzyme gene polymorphism and ACE inhibition in diabetic nephropathy. Kidney Int 53:1002–1006
22. Kicic E, Palmer TN (1994) Is sorbitol dehydrogenase gene expression affected by streptozotocin diabetes in the rat? Biochim Biophys Acta 1226:213–218
23. Ko BCB, Ruepp B, Bohren KM, Gabbay KH, Chung SS (1997) Identification and characterization of multiple osmotic response sequences in the human aldose reductase gene. J Biol Chem 272:16431–16447
24. Kolb NS, Hunsaker LA, Van der Jagt DL (1994) Aldose reductase-catalyzed reduction of acrolein: implications in cyclophosphamide toxicity. Mol Pharmacol 45:797–801
25. Maeda S, Haneda M, Yasuda H, Tachikawa T, Isshiki K, Koya D, Terada M, Hidaka H, Kashiwagi A, Kikkawa R (1999) Diabetic nephropathy is not associated with the dinucleotide repeat polymorphism upstream of the aldose reductase (ALR2) gene but with erythrocyte aldose reductase content in Japanese subjects with type 2 diabetes. Diabetes 48:420–422
26. Mizisin AP, Shelton GD, Wagner S, Rusbridge C, Powell HC (1996) Polyol pathway and osmoregulation in JS1 Schwann cells grown in hyperglycemic and hyperosmotic conditions. Am J Physiol 270:90–97
27. Morrisey, K, Steadman R, Williams JD, Phillips AO (1999) Renal proximal tubular cell fibronectin accumulation in response to glucose is polyol pathway dependent. Kidney Int 55:160–167
28. Nadkarni V, Gabbay KH, Bohren KM, Sheikh-Hamad D (1999) Osmotic response element enhancer activity. Regulation through p38 kinase and mitogen-activated extracellular signal-regulated kinase kinase. J Biol Chem 274:20185–20190
29. Ng TF, Lee FK, Song ZT, Calcutt NA, Lee AY, Chung SS, Chung SK, Ng DT (1998) Effects of sorbitol dehydrogenase deficiency on nerve conduction in experimental diabetic mice. Diabetes 47:961–966
30. Nishimura C, Hotta Y, Gui T, Seko A, Fujimaki T, Ishikawa T, Hayakawa M, Kanai A, Saito T (1997) The level of erythrocyte aldose reductase is associated with the severity of diabetic retinopathy. Diab Res Clin Pract 37:173–177
31. Nishimura C, Matsuura Y, Kokai Y, Akera T, Carper D, Morjana N, Lyons C, Flynn TG (1990) Cloning and expression of human aldose reductase. J Biol Chem 265:9788–9792
32. Powell HC, Garrett RS, Kador PF, Mizisin AP (1991) Fine-structural localization of aldose reductase and ouabain-sensitive, K^+-dependent p-nitro-phenylphosphatase in rat peripheral nerve. Acta Neuropathol 81:529–539
33. Rittner HL, Hafner V, Klimiuk PA, Szweda LI, Goronzy JJ, Weyand CM (1999) Aldose reductase functions as a detoxification system for lipid peroxidation products in vasculitis. J Clin Invest 103:1007–1013
34. Robison JrWG, Kador PF, Kinoshita JH (1983) Retinal capillaries: Basement membrane thickening by galactosemia prevented with aldose reductase inhibitor. Science 221:1177–1179
35. Sassy-Prigent C, Heudes D, Jouquey S, Auberval D, Belair MF, Michel O, Hamon G, Bariety J, Bruneval P (1995)

Morphometric detection of incipient glomerular lesions in diabetic nephropathy in rats. Protective effects of ACE inhibition. Lab Invest 73:64–71
36. Tanimoto T, Urakami T (1994) Enzyme immunoassay for erythrocyte aldose reductase. Clin Chem 40:889–894
37. Tateno S, Kobayashi Y (1987) Quantitative analysis of mesangial areas in serial biopsied patients with IgA nephropathy. Nephron 46:28–33
38. Tilton RG, Baier LD, Harlow JE, Smith SR, Ostrow E, Williamson JR (1992) Diabetes-induced glomerular dysfunction: links to a more reduced cytosolic ratio of NADH/NAD+. Kidney Int 41:778–788
39. Yabe-Nishimura C (1998) Aldose reductase in glucose toxicity: a potential target for the prevention of diabetic complications. Pharmacol Rev 50:21–33
40. Yagihashi S, Yamagishi S, Wada R, Sugimoto K, Baba M, Wong HG, Fujimoto J, Nishimura C, Kokai Y (1996) Galactosemic neuropathy in transgenic mice for human aldose reductase. Diabetes 45:56–59
41. Zhuang S, Hirai S, Ohno S (2000) Hyperosmolality induces activation of cPKC and nPKC; a requirement for ERK1/2 activation in NIH/3T3 cells. Am J Physiol Cell Physiol 278: C102–109

Virchows Arch (2001) 439:55–61
DOI 10.1007/s004280100439

ORIGINAL ARTICLE

**Karin Milde-Langosch · Sabine Riethdorf
Alexandra Kraus-Pöppinghaus · Lutz Riethdorf
Thomas Löning**

Expression of cyclin-dependent kinase inhibitors $p16^{MTS1}$, $p21^{WAF1}$, and $p27^{KIP1}$ in HPV-positive and HPV-negative cervical adenocarcinomas

Received: 4 December 2000 / Accepted: 12 February 2001 / Published online: 6 April 2001
© Springer-Verlag 2001

Abstract Inactivation or down-regulation of the cell-cycle inhibitors $p16^{MTS1}$, $p21^{WAF1}$, and $p27^{KIP1}$ is involved in the carcinogenesis of various human tumors. In cervical squamous cell carcinomas that are associated with human papillomavirus (HPV) infection, the expression or function of these proteins is impaired by the action of viral oncoproteins E6 and E7. Comparably less is known about the role of these cyclin-dependent kinase inhibitors in cervical adenocarcinomas, 15–40% of which are HPV negative. Therefore, we studied the expression of $p16^{MTS1}$, $p21^{WAF1}$, and $p27^{KIP1}$ by immunohistochemistry in 60 cervical adenocarcinomas. HPV infection was determined by PCR, and HPV 16 and 18 E6/E7 oncogene expression was analyzed by RNA-RNA in situ hybridization. We found significant correlations of strong p16 expression with HPV 16/18 infection and HPV 16/18 E6/E7 oncogene expression (P=0.001). Moderate or strong p16 expression was also observed in 41% of HPV-negative carcinomas, indicating that HPV-independent mechanisms might also lead to p16 overexpression. In addition, stronger p21 and p27 expression was significantly associated with the detection of HPV 16 or 18 E6/E7 transcripts (P=0.015 and 0.030, respectively). Obviously, the tumor suppressor action of these proteins can be overcome in HPV-positive lesions. In contrast, absent or low p16, p21, and p27 immunostaining was observed in most HPV-negative cervical adenocarcinomas and might contribute to carcinogenesis in these tumors.

Keywords Cervical adenocarcinoma · HPV · p16 · p21 · p27

K. Milde-Langosch (✉) · S. Riethdorf · A. Kraus-Pöppinghaus
L. Riethdorf · T. Löning
Institute of Pathology, Department of Gynecopathology,
University Hospital Eppendorf, Hamburg, Germany
e-mail: milde@uke.uni-hamburg.de
Tel.: +49-40-428033162, Fax: +49-40-428034961

K. Milde-Langosch
Institut für Pathologie, Universitäts-Krankenhaus Eppendorf,
Martinistrasse 52, 20246 Hamburg, Germany

Introduction

Our knowledge about the etiology of cervical cancer has dramatically increased during the last 20 years. It is now widely accepted that nearly 100% of cervical squamous cell carcinomas (SCC) are associated with certain high-risk human papillomavirus types, mainly HPV 16, 18, 31, 33, 35, 45 [34]. Malignant transformation of the cervical epithelial cells is associated with expression of the viral oncogenes E6 and E7 with dramatic implications for cell cycle regulation, differentiation, and genomic stability [32, 40].

Cervical adenocarcinomas represent 15–25% of all cervical carcinomas [10, 16]. In contrast to SCC, HPV18 is the most common HPV type in cervical adenocarcinomas, and 15–40% of these tumors are not associated with papillomavirus DNA [6, 21, 26]. The etiology of these HPV-negative cases is still unknown. Activation of oncogenes (i.e. K-ras) or inactivation of tumor-suppressor genes (i.e. p53) has only been detected in a small fraction of these carcinomas [11, 22].

Cyclin-dependent kinase (cdk) inhibitors are important negative regulators of cell cycle progression. After binding to cdk–cyclin complexes in the G1 phase of the cell cycle, they block the kinase activity of cdk's, preventing phosphorylation of members of the Rb gene family and transition to S phase [9, 37]. P16 (additional names: MTS1 for "multiple tumor suppressor 1" or CDK4I for "CDK4-inhibitor"), the product of the *ink4a* gene, specifically binds to cyclin D–cdk4/cdk6 complexes. Loss of this cell-cycle inhibitor by homozygous deletion of the gene, mutation or promoter hypermethylation is observed in several human tumors: many pancreatic carcinomas, bladder carcinomas, T-ALL, familial melanomas, etc. [27]. In contrast, strong p16 overexpression was observed in cervical squamous intraepithelial lesions (SIL) and squamous cell carcinomas which are associated with high-risk HPV types [28], indicating that the suppressor function of p16 can be overcome in the presence of viral oncogenes.

The cdk inhibitors p21/WAF1 and p27/KIP1 are able to bind in a less selective manner to various cdk–cyclin complexes [9]. Both cell-cycle inhibitors are bound and inactivated by HPV E7 proteins in experimental systems [39].

P21 is induced by p53 after DNA damage which leads to a delayed cell cycle progression and leaves some time for DNA repair processes [4]. In addition, activation of various intracellular signaling pathways, i.e. MAPK cascade or TGFß, can lead to enhanced p21 expression.

P27 expression is mainly regulated post-translationally by protein degradation via ubiquitin–proteasome complexes. Strong p27 expression is found in most normal epithelial cells, and p27 down-regulation is frequently observed in several human tumor types [3, 31].

The role of p16, p21, and p27 in the etiology of glandular cervical carcinomas has not been well analyzed. In a study without HPV analysis, Lu et al. [18] found enhanced expression of these cell-cycle inhibitors in most cervical adenocarcinomas relative to normal endocervical glands. However, to enhance our understanding of the role of these proteins in cervical cancer, the papillomavirus infections which influence their expression or function should be considered. To compare the expression of p16, p21, and p27 with the HPV status in cervical adenocarcinomas, we performed immunohistochemistry in 60 tumors. All cases were analyzed for HPV 16 and 18 infection by PCR, and HPV 16 and 18 E6/E7 oncogene expression was studied by RNA-RNA in situ hybridization.

Materials and methods

Tissue samples

We studied paraffin-embedded tissue samples from 60 patients (mean age 47 years; range 27–89 years) with cervical adenocarcinomas selected from the files of the Department of Gynecopathology, University Clinics Hamburg, and the Division of Women's and Perinatal Pathology at Brigham and Women's Hospital (Boston, Mass.). All cases were re-classified by two pathologists independently according to the most recent (1994) WHO criteria, and histological subtyping was performed. The pathologists classified 45 tumors as FIGO stage I (IA: 7 cases, stage IB: 38 cases), 8 cases as stage II, and 5 carcinomas as stage III or IV. In 2 cases, staging data were not available. The histological subtypes of the tumors included in the study are shown in Table 2. All tissues had been routinely fixed in 4% buffered formalin and paraffin embedded.

Detection of HPV infection and HPV 16/18 E6/E7 oncogene expression

HPV detection was performed by PCR after DNA extraction from paraffin sections as described with general primers MY09/MY11 [19] and type-specific primers for HPV 16, HPV 18, HPV 6/11 [26], and HPV 31 [20]. In order to analyze HPV 16 and 18 E6/E7 expression in the tumors, in situ hybridization with ^{35}S-labeled RNA probes was performed, and the results were evaluated as described before [25, 26]. For statistical analysis, all HPV 16 and 18 E6/E7 RNA-positive cases were combined and compared with those tumors without detectable HPV 16/18 oncogene expression.

Immunohistochemistry

P16 IHC was performed on paraffin-embedded tissue sections after microwave pretreatment with the monoclonal antibody G175-405 (Pharmingen, Hamburg, Germany; 1:100) in an automated immunohistochemistry system (Ventana Medical Systems, Strasbourg, France). Bound primary antibodies were detected using an amplification kit and a detection kit (both Ventana Medical Systems). Expression of p21 and p27 was investigated manually with the monoclonal antibodies NCL-p27 (Novocastra; 1:50), and SXM30 (Pharmingen, Hamburg, Germany; 1:150) after microwave pretreatment of the tissue sections.

Immunoreactivity was evaluated by examination of staining intensity (0: no staining; 1: weak staining; 2–3: intermediate and strong staining intensity) and percentage of positive tumor cells (0: no positive cells; 1: <10%; 2: 11–50%; 3: 51–80%; 4: >80% positive tumor cells) by two independent persons. After multiplication of both values, the IHC results were graded from 0 (no reactivity in tumor cells) to 12 (more than 80% positive tumor cells with strong staining intensity in the majority of the cells). For p16, both nuclear and cytoplasmic immunoreactivity was evaluated, whereas for p21 and p27, only nuclear staining was observed.

Statistics

Correlations of the data were examined by Chi-square statistics and Fisher's exact test using the SPSS 10.0 software. *P*-values of 0.05 or less were considered statistically significant.

Results

Sixty cases of cervical adenocarcinoma were included in the study. By PCR, 17 tumors (28%) were HPV-negative, 22 carcinomas (37%) harbored HPV 18 DNA, 15 cases (25%) were positive for HPV 16, whereas in 6 (10%) tumors, HPV 16 and 18 DNA could be detected. HPV 6/11 and HPV 31 DNA were detected in none of the tumors. In addition, none of the carcinomas was general primer-positive, but negative for HPV 16 and HPV 18.

RNA-RNA in situ hybridization with ^{35}S-labeled probes from the E6/E7 region of the HPV 16 and HPV 18 genomes was performed in 53 tumors. These results have partly been described before [26]. In 20 cases (38%), no E6/E7 mRNA could be detected. There were 24 carcinomas (45%) that were positive for HPV 18 mRNA, and 9 cases harboring HPV 16 mRNA (17%). In 4 tumors infected with both HPV 16 and HPV 18 only HPV 18 transcripts (*n*=4) could be detected. HPV infection and E6/E7 oncogene expression results are summarized in Table 1, and an example of HPV 16 E6/E7 ISH is shown in Fig. 1A.

Table 1 Comparison of human papillomavirus (*HPV*) infection as detected by PCR and HPV 16 or HPV 18 E6/E7 expression as detected by RNA-RNA in situ hybridization (*ISH*)

	HPV-DNA (PCR)			
	Negative	HPV 16	HPV 18	HPV 16+18
n	(17)	(15)	(22)	(6)
E6/E7-RNA (ISH)				
Negative	12	3	3	2
HPV 16	–	9	–	–
HPV 18	2	–	18	4
ISH not done	3	3	1	–

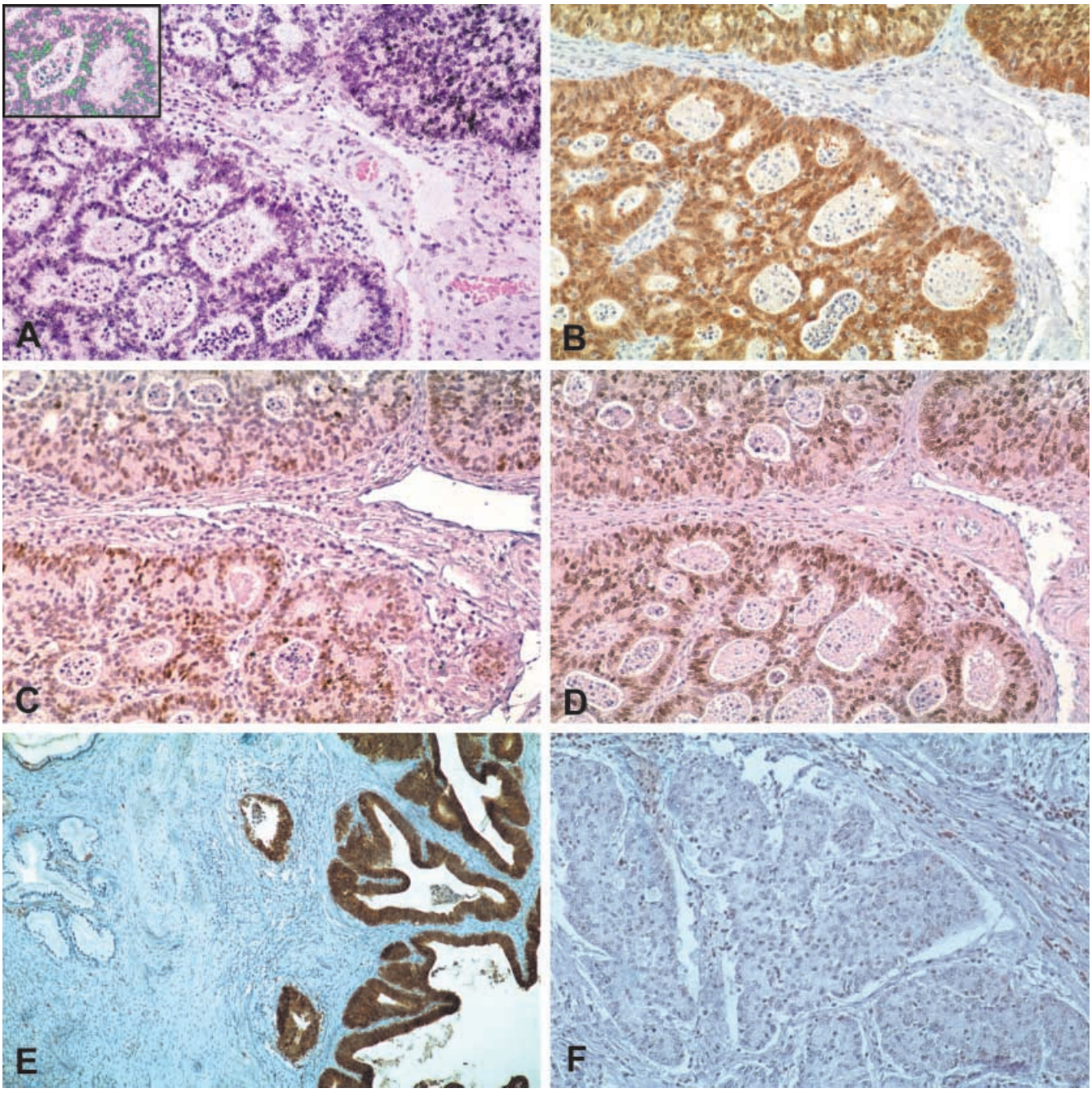


Fig. 1 **A** HPV E6/E7 expression and **B**, **E** p16, **C** p21, and **D**, **F** p27 immunostaining in cervical adenocarcinomas. **A**–**D** Well-differentiated adenocarcinoma. ×400 **A** HPV 16 E6/E7 oncogene expression shown by *black* grains over carcinoma cells. In the insert region, hybridization signals were labeled *green*. **B** Strong nuclear and cytoplasmic p16 expression in tumor cells, weak nuclear expression in single fibroblasts. **C** Moderate nuclear p21 expression in tumor cells. **D** Strong nuclear p27 expression in tumor cells and surrounding fibroblasts. **E** Well-differentiated cervical adenocarcinoma with strong nuclear and cytoplasmic p16 immunoreactivity in tumor cells. On the *left*, a normal endocervical gland without detectable p16 staining is surrounded by several weakly positive fibroblasts. ×200 **F** Adenosquamous cervical carcinoma showing very weak p27 expression in tumor cells and p27-positive nuclei in several fibroblasts. ×400

Evaluable p16 results were obtained in 58 cervical adenocarcinomas. In 50% of the cases (n=29), strong p16 immunoreactivity (IHC 8–12) in tumor cells was observed. In all p16-positive cases, both nuclear and cytoplasmic staining were present in varying proportions (Fig. 1B, E). Negative IHC results were obtained in only 8 cases (14%), among them mainly endometrioid and mucinous tumors (Table 2), whereas weak p16 staining was shown in 21 carcinomas (36%). Some carcinomas displayed strong heterogeneity with respect to staining intensity and the percentage of p16-positive tumor cells. Nuclear staining was observed in some stromal fibroblasts, whereas normal glandular or squamous epithelia were always p16 negative. In cases with positive p16 re-

Table 2 P16 expression in cervical adenocarcinomas: associations with HPV infection as detected by PCR, HPV 16/18 E6/E7 expression, and histological type

	n	p16 (IHC score)			
		0–2	3–7	8–12	
HPV-DNA (*n*=58)					
Negative	17	10	5	2	
HPV 16	13	1	4	8	
HPV 18	22	1	2	19	
HPV 16+18	6	1	5	–	*P*<0.001
E6/E7-mRNA (*n*=50)					
Negative	19	7	8	4	
Positive	31	2	6	23	*P*=0.001
Histological type					
Endometrioid	15	3	7	5	
Mucinous	21	8	3	10	
Clear cell	2	1	1	–	
Adenosquamous	9	1	5	3	
Serous-papillary	4	–	–	4	
Mixed differentiation	5	–	–	5	
Intestinal	1	–	–	1	
Undifferentiated	1	–	–	1	

Table 3 P21 and p27 expression in cervical adenocarcinomas: associations with HPV infection as detected by PCR, HPV 16/18 E6/E7 expression, and histological type

	n	p21 (IHC score)				p 27 (IHC score)		
		0	1–3	4–8		0–5	6–12	
HPV-DNA (*n*=58)								
Negative	17	8	6	3		8	9	
HPV 16	15	3	4	8		2	13	
HPV 18	22	9	7	6		4	18	
HPV 16+18	6	4	1	1	n.s.	3	3	n.s.
E6/E7-mRNA (*n*=52)								
Negative	20	11	7	2		10	10	
Positive	32	8	9	15	*P*=0.015	6	26	*P*=0.030
Histological type								
Endometrioid	16	5	3	8		2	14	
Mucinous	22	10	8	4		9	13	
Clear cell	2	2	–	–		1	1	
Adenosquamous	9	6	1	2		4	5	
Serous-papillary	4	–	3	1		–	4	
Mixed differentiation	5	1	2	2		–	5	
Intestinal	1	–	1	–		–	1	
Undifferentiated	1	–	–	1		1	–	

sults, normal glands and neoplastic cells were clearly distinguishable by their different p16 immunoreactivity (Fig. 1E).

P16 expression was significantly associated with both HPV 16/18 infection and HPV 16/18 oncogene expression (Table 2). Among the tumors with minimal or absent p16 staining, 10 of 13 were HPV negative according to PCR, and 7 of 9 had no detectable E6/E7 expression. In contrast, strong p16 expression was associated with HPV infection (mostly HPV 18) and HPV 16/18 E6/E7 oncogene expression. No correlations of p16 expression with age, stage, or histological subtype were found.

P21/WAF1 expression showed an exclusively nuclear pattern with 1–90% positive tumor cells in 60% (36/60) of the cases, whereas 24 tumors (40%) were p21 negative (Table 3, Fig. 1C). Interestingly, mucinous, clear-cell, and adenosquamous carcinomas were most often p21 negative, although the low numbers of cases in the histological subgroups do not allow statistical analysis. Normal glandular epithelia showed weak p21 staining in 10–30% of the cells. In squamous epithelia, moderate p21 immunoreactivity in the suprabasal epithelial layers was observed as described by others [38], and positive nuclei were only sporadically found in stromal cells.

For statistical analysis, p21-negative carcinomas, tumors with weak p21 expression (IHC score 1–3) and cases with higher p21 expression (IHC 4–12) were combined. No correlation of p21 expression with age, stage, histological subtype, or HPV infection as detected by PCR was observed. In contrast, strong p21 immunore-

activity was significantly associated with HPV 16 or 18 E6/E7 oncogene expression (P=0.015; Table 3).

Nuclear p27 expression was observed in all analyzed carcinomas with varying staining intensities and different proportions of positive tumor cells (Fig. 1D, F). Weak immunostaining was observed mainly in mucinous and adenosquamous carcinomas. Normal endocervical glandular epithelial cells and most stromal fibroblasts and endothelial cells were p27 positive. In squamous epithelia, negative or only weak p27 staining was found in basal cells and the first suprabasal cell layer, but strong p27 expression was detected in the outer epithelial layers as described [38].

For statistical analysis, carcinomas with p27 expression in less than 50% of tumor cells and an IHC score of <6 (n=17; 28%) were combined and compared with those with >50% positive tumor cells (n=43; 72%). No significant correlation of p27 expression with age, stage, histological subtype, or HPV DNA detection results was found (Table 3). However, in a similar way to p21, reduced p27 expression was significantly more often detected in carcinomas without detectable HPV oncogene expression (50%) than in HPV 16/18 E6/E7-positive tumors (19%).

Discussion

In contrast to cervical squamous cell carcinomas, only 60–85% of the cervical adenocarcinomas are associated with papillomavirus DNA [6, 21, 26], and the viral load is often very low in glandular lesions. The percentage of 72% HPV-positive cases detected in our study after PCR with general primers MY09/MY11 and primers for HPV 16, 18, 6/11, and 31 is lower than that of a recent study in which a highly sensitive short-fragment PCR was used, where 83% HPV-positive invasive carcinomas were found, among them 4% HPV45- and 1% HPV35-positive tumors [24]. These HPV types should have been detectable by general-primer PCR, but this method is not as sensitive as type-specific PCR protocols, resulting in smaller PCR products. Therefore, we cannot exclude the possibility that single carcinomas that are weakly positive for HPV 45, 35, 52, etc. may have escaped our approach, although HPV 45 is less prevalent in Europe than in North America [1].

The mechanisms of carcinogenesis in the HPV-negative cervical adenocarcinomas are still largely unknown. Cyclin-dependent kinase inhibitors (CDKIs) play an important part in the regulation of cell cycle progression and differentiation [9]. Inactivation of CDKIs is involved in the etiology of various malignant tumors, i.e. breast cancer, pancreatic carcinomas etc. [2, 3, 4, 5, 17, 27]. In cervical carcinoma cells, cell-cycle regulation is disrupted by viral oncoproteins in various ways, i.e. binding and inactivation of p53 by HPV E6 proteins and binding of Rb, p21, and p27 by E7 oncoproteins [32, 39, 40]. If this is a necessary condition for malignant transformation in HPV-associated tumors, inactivation of cell-cycle-regulatory proteins by HPV-independent mechanisms may be involved in the etiology of the HPV-negative group of cervical adenocarcinomas. Therefore, the aim of our present study was to compare the expression of CDKIs with the HPV status in cervical adenocarcinomas, and to ascertain whether CDKIs p16, p21, and p27 might be involved in carcinogenesis in HPV-negative cervical tumors.

Functional inactivation of p16/MTS1/Ink4a by homozygous deletion, somatic mutation, or promoter hypermethylation is involved in the etiology of many human tumors [27]. In cervical carcinomas (mostly SCC), p16 mutations have not been found [13, 36] and homozygous deletions were absent [13] or detected in only 5% of the carcinomas [36]. Instead, cervical squamous intraepithelial lesions (SIL) and carcinomas which are associated with high-risk HPV types show a striking overexpression of p16 [28]. A possible explanation of this phenomenon might be the functional inactivation of the retinoblastoma protein Rb which is able to act as a repressor of p16 transcription [27]. The release of p16 expression from Rb repression in HPV-infected cervical dysplastic cells might lead to strong p16 overexpression, but obviously displays no cell-cycle-inhibitory effect because Rb has already been blocked by HPV E7 oncoproteins. Therefore, additional inactivation of cdk4 by p16, which would normally keep the Rb protein in its active, hypophosphorylated form, probably has no influence on cell proliferation.

Detectable p16 expression has been described in 58% of cervical adenocarcinomas in a prior study [18]. The higher percentage of p16-positive tumors found by us is probably due to the highly sensitive immunohistochemistry protocol used in this study. P16 expression and HPV status in cervical adenocarcinomas have only been analyzed within the scope of larger studies on cervical carcinomas. In an immunohistochemical analysis of 44 cervical carcinomas, among them 5 adenocarcinomas, Kim et al. [14] found a positive association of p16 staining with HPV infection, but significantly weaker immunoreactivity in adenocarcinomas compared with squamous tumors. Similarly, Sano et al. studied 54 cervical carcinomas including 9 adenocarcinomas and 6 adenosquamous tumors and found negative p16 and HPV results in 4 adenocarcinomas and 1 adenosquamous carcinoma, but in none of the squamous cell carcinomas [28].

In our larger cohort of cervical adenocarcinomas, we found strong positive correlations of p16 expression and HPV infection status or HPV 16/18 E6/E7 expression, respectively. Interestingly, p16 expression was significantly associated with both HPV infection and HPV oncogene expression, even though in 20% of the HPV DNA-positive carcinomas, no E6/E7 mRNA was detected by in situ hybridization. This indicates that, in addition to the disruption of Rb control by E7 oncoproteins, other as yet unknown mechanisms might lead to p16 upregulation after HPV infection. In a model system with HPV-immortalized or transformed ectocervical and endocervical epithelial cells, Nakao et al. [23] found a

dramatic enhancement of p16 mRNA and protein expression after immortalization by HPV 16 or HPV 18. This overexpression was not further increased after malignant transformation of the cells. In in situ hybridization studies, strong E6/E7 expression was only observed in severe dysplasia or cervical carcinomas, but not in weak dysplasia [7], whereas p16 expression has already been shown in early stages of oncogenic progression [23]. Further studies will be necessary to elucidate the mechanism of p16 up-regulation after infection of cervical cells with high-risk HPV types.

In contrast to the tumors with strong p16 expression, which are associated with HPV infection in 93% of cases, 31% of the carcinomas showing moderate p16 immunostaining (IHC score 3–7) were negative for HPV DNA. In addition, moderate or strong immunostaining was observed in 41% of the HPV DNA-negative carcinomas. These results indicate that HPV-independent mechanisms can lead to p16 overexpression in these tumors, i.e. Rb inactivation or accumulation of the relatively stable p16 proteins in strongly proliferating cells.

In HPV-negative cervical carcinomas, the control of the G1 restriction point by the Rb protein is not influenced by viral oncoproteins. Therefore, weak or absent p16 expression in 10 out of 17 tumors may contribute to enhanced cell cycle progression in these cases.

Expression of p21/Waf1 was significantly associated with HPV oncogene expression but not with HPV infection, indicating that E6/E7 proteins may be involved in the regulation of this cell-cycle inhibitor. In cervical squamous carcinomas, Skomedal et al. [29] found p21 overexpression in 96% of the tumors, and in a study conducted in Sweden and Ireland on 40 cervical adenocarcinomas [30], p21 expression was detected in 85% of the tumors, in comparison with 60% p21 immunostaining found by us. These discrepancies might be explained by different IHC protocols or differences in evaluation of IHC results.

Mutations of the p21 gene are rare in human carcinomas and have not been described in cervical cancer. P21 protein expression is activated by the tumor suppressor protein p53, which is bound and blocked by HPV 16/18 E6 oncoproteins. Therefore, reduced p21 expression might be expected in tumors with E6/E7 expression. On the other hand, the HPV E7 oncoprotein leads to a stabilization and increased protein levels of p21/WAF1 in human fibroblasts or keratinocytes [12, 33]. The positive correlation of p21 and HPV oncogene expression found in our study is in accordance with this p53-independent p21 regulation. Zehbe et al. [38] reported that the cell-cycle-inhibitory function of p21 can be overcome in HPV-positive cervical carcinoma cells, probably through direct interaction of p21 with E7.

In contrast to the tumors with HPV 16/18 oncogene expression, which were p21-positive in 75% of cases, 55% of the HPV E6/E7-negative tumors had no detectable p21 protein. A possible reason might be p53 mutations, which are reported in 8% [22] to 32% [11] of cervical adenocarcinomas, mainly in HPV-negative tumors. Alternatively, p53-independent down-regulation of p21 may contribute to proliferation in these tumors. Werness et al. [35] reported that p21 expression in cervical carcinomas is influenced by various transactivators, such as TGFß, p73 and c/EBPß [8].

Similar to p21, p27/Kip1 expression was significantly associated with HPV E6/E7 expression, but not with HPV infection. P27 down-regulation was observed in 50% of the tumors without E6/E7 expression, but in only 19% of the E6/E7-positive carcinomas. The molecular mechanisms leading to these differences are still unknown. It was previously shown that HPV oncogenes can overrun the cell-cycle-inhibitory effects of p27, probably by direct interaction of E7 and p27 proteins [38]. In HPV-negative adenocarcinomas, down-regulation of p27 protein levels may be involved in enhanced cell-cycle progression and carcinogenesis.

In contrast to our results, Kim et al. [15] found lower p27 expression in HPV-positive than in HPV-negative tumors in a study on 45 cervical carcinomas including 4 adenocarcinomas. Yet, in this study HPV was only detected by HPV 16 and HPV 18 PCR, which resulted in 31% HPV-negative cases. Given the fact that nearly 100% of cervical SCC are associated with HPV according to various studies [34], the supposed HPV-negative cases probably harbored additional HPV types, such as HPV 31, 33, 35, 45, and 51, and the differences in p27 expression in this study may reflect variations in tumors with different HPV types.

In conclusion, our study has demonstrated high levels of the cdk inhibitors p16, p21, and p27 in cervical adenocarcinomas with detectable HPV E6/E7 protein expression. Obviously, the anti-proliferative effect of these proteins can be overcome by the viral oncogenes in these lesions. Interestingly, negative immunostaining or only low protein levels of p16, p21, and p27 were detected in most HPV E6/E7-negative carcinomas suggesting that down-regulation of these cell-cycle inhibitors may be involved in the etiology of this group of cervical adenocarcinomas.

Acknowledgments The authors would like to thank Prof. C.P. Crum, Prof. K.R. Lee, and Dr. J.T. O'Connell, Division of Women's and Perinatal Pathology at Brigham and Women's Hospital, Boston, Mass., for providing some cases. We are grateful to Ms. Sonja Petersen, Ms. Tanja Karstens, and Ms. Gabriele Rieck for excellent technical assistance, and to J. Koppelmeyer for photographic work.

References

1. Bosch FX, Manos MM, Munoz N, Sherman M, Jansen AM, Peto J, Schiffman MH, Moreno V, Kurman R, Shah KV (1995) Prevalence of human papillomavirus in cervical cancer: a worldwide perspective. J Natl Cancer Inst 87:796–802
2. Caffo O, Doglioni C, Veronese S, Bonzanini M, Marchetti A, Buttitta F, Fina P, Leek R, Morelli L, Dalla Palma P, Harris AL, Barbareschi M (1996) Prognostic value of $p21^{WAF1p}$ and p53 expression in breast carcinoma: an immunohistochemical study in 261 patients with long-term follow-up. Clin Cancer Res 2:1591–1599

3. Catzavelos C, Bhattacharya N, Ung YC, Wilson JA, Roncari L, Sandhu C, Shaw P, Yeger H, Morava-Protzner I, Kapusta L, Franssen E, Pritchard KI, Slingerland JM (1997) Decreased levels of cell-cycle inhibitor p27kip1 protein: prognostic implications in primary breast cancer. Nat Med 3:227–230
4. Chen YQ, Cipriano SC, Arenkiel JM, Miller FR (1995) Tumor suppression by $p21^{WAF1}$. Cancer Research 55:4536–4539
5. Clurman BE, Roberts JM (1996) Cell cycle and cancer. J Natl Cancer Inst 87:1499–1501
6. Duggan MA, McGregor SE, Benoit JL, Inoue M, Nation JG, Stuart GCE (1995) The human papillomavirus status of invasive cervical carcinoma: a clinicopathological and outcome analysis. Hum Pathol 26:319–325
7. Dürst M, Glitz D, Schneider A, zur Hausen H (1992) Human papillomavirus type 16 (HPV 16) gene expression and DNA replication in cervical neoplasia: analysis by in situ hybridization. Virology 189:132–140
8. Elbendary A, Berchuck A, Davis P, Havrilevsky L, Bast RC, Iglehart D, Marks JR (1994) Transforming growth factor β1 can induce CIP1/WAF1 expression independent of the p53 pathway in ovarian cancer cells. Cell Growth Differ 5:1301–1307
9. Elledge SJ, Winston J, Harper JW (1996) A question of balance: the role of cyclin-kinase inhibitors in development and tumorigenesis. Trends Cell Biol 6:388–392
10. Hopkins MP, Morley GW (1991) A comparison of adenocarcinoma and squamous cell carcinoma of the cervix. Obstet Gynecol 77:912–917
11. Jiko K, Tsuda H, Sato S, Hirohashi S (1994) Pathogenetic significance of p53 and c-Ki-ras gene mutations and human papillomavirus DNA integration in adenocarcinoma of the uterine cervix and uterine isthmus. Int J Cancer 59:601–606
12. Jones DL, Thompson DA, Suh-Burgmann E, Grace M, Munger K (1999) Expression of the HPV E7 oncoprotein mimics but does not evoke a p53-dependent cellular DNA damage response pathway. Virology 258:406–414
13. Kim JW, Namkoong SE, Ryu SW, Kim HS, Shin JW, Lee JM, Kim DH, Kim IK (1998) Absence of $p15^{INK4B}$ and $p16^{INK4A}$ gene alterations in primary cervical carcinoma tissues and cell lines with human papillomavirus infection. Gynecol Oncol 70:75–79
14. Kim YT, Cho NH, Park SW, Kim JW (1998) Underexpression of cyclin-dependent kinase (CDK) inhibitors in cervical carcinoma. Gynecol Oncol 71:38–45
15. Kim YT, Choi KE, Cho NH, Ko JH, Yang WI, Kim JW, Lee SH (2000) Expression of cyclin E and p27(KIP1) in cervical carcinoma. Cancer Lett 153:41–50
16. Kudo R (1992) Cervical adenocarcinoma. In: Sasano N (ed) Current topics in pathology, vol 85. Springer, Berlin Heidelberg New York, pp 81–111
17. Lloyd RV, Jin L, Qian X, Kulig E (1997) Aberrant p27 kip1 expression in endocrine and other tumors. Am J Pathol 150: 401–407
18. Lu X, Toki T, Konishi I, Nikaido T, Fujii S (1998) Expression of $p21^{WAF1/CIP1}$ in adenocarcinoma of the uterine cervix. Cancer 82:2409–2417
19. Manos MM, Ting Y, Wright DK, Lewis AJ, Broker TR, Wolinsky SM (1989) Use of polymerase chain reaction amplification for the detection of genital human papillomaviruses. Cancer Cells 7:209–213
20. Milde-Langosch K, Becker G, Löning T (1991) Human papillomavirus and c-myc/c-erbB2 in uterine and vulvar lesions. Virchows Arch [A] 419:479–485
21. Milde-Langosch K, Schreiber C, Becker G, Löning T, Stegner H-E (1993) Human papillomavirus detection in cervical adenocarcinomas by polymerase chain reaction. Hum Pathol 24:590–594
22. Milde-Langosch K, Albrecht K, Joram S, Schlechte H, Giessing M, Löning T (1995) Presence and persistence of HPV infection and p53 mutation in cancer of the cervix uteri and the vulva. Int J Cancer 63:639–645
23. Nakao Y, Yang X, Yokoyama M, Ferenczy A, Tang S-C, Pater MM, Pater A (1997) Induction of p16 during immortalization by HPV 16 and 18 and not during malignant transformation. Br J Cancer 75:1410–1416
24. Pirog EC, Kleter B, Olgac S, Bobkiewicz P, Lindeman J, Quint WGV, Richart RM, Isacson C (2000) Prevalence of human papillomavirus DNA in different histological subtypes of cervical adenocarcinoma. Am J Pathol157:1055–1062
25. Riethdorf L, Riethdorf S, Gützlaff K, Prall F, Löning T (1996) Differential expression of the monocyte chemoattractant protein-1 in human papillomavirus-16-infected squamous intraepithelial lesions and squamous cell carcinomas of the cervix uteri. Am J Pathol 149:1469–1475
26. Riethdorf S, Riethdorf L, Milde-Langosch K, Park TW, Löning T (2000) Differences in HPV 16 and HPV 18 E6/E7 oncogene expression between in situ and invasive adenocarcinoma of the cervix uteri. Virchows Arch 437: 491-500
27. Ruas M, Peters G (1998) The p16INK4a/CDKN2A tumor suppressor and its relatives. Biochim Biophys Acta 1378:F115-F177
28. Sano T, Oyama T, Kashiwabara K, Fukuda T, Nakajiama T (1998) Expression status of p16 protein is associated with human papillomavirus oncogenic potential in cervical and genital lesions. Am J Pathol 153:1741–1748
29. Skomedal H, Kristensen GB, Lie AK, Holm R (1999) Aberrant expression of the cell cycle associated proteins TP53, MDM2, p21, p27, cdk4, cyclin D1, RB, and EGFR in cervical carcinoma. Gynecol Oncol 73:223–228
30. Skyldberg BM, Murray E, Lambkin H, Kelehan P, Auer GU (1999) Adenocarcinoma of the uterine cervix in Ireland and Sweden: human papillomavirus infection and biologic alterations. Mod Pathol 12:675–682
31. Steeg PS, Abrams JS (1997) Cancer prognosis: past, present and p27. Nat Med 3:152–154
32. Stoler MH (2000) Human papillomavirus and cervical neoplasia: a model for carcinogenesis. Int J Gynecol Pathol 19: 16–28
33. Stoppler H, Stoppler MC, Johnson E, Simbulan-Rosenthal CM, Smulson ME, Iyer S, Rosenthal DS, Schlegel R (1998) The E7 protein of human papillomavirus type 16 sensitizes primary human keratinocytes to apoptosis. Oncogene 17: 1207–1214
34. Walboomers JMM, Jacobs MV, Manos MM, Bosch FX, Kummer JA, Shah KV, Snijders PJF, Peto J, Meijer CJLM, Munoz N (1999) Human papillomavirus is a necessary cause of invasive cervical cancer worldwide. J Pathol 189: 12–19
35. Werness BA, Wang H-Q, Chance J, Goldstein DJ (1997) P53-independent expression of $p21^{waf1/cip1}$ in preinvasive and invasive squamous neoplasms of the uterine cervix. Mod Pathol 10:578–584
36. Wong YF, Chung TKH, Cheung TH, Nobori T, Yim SF, Lai KWH, Yu AL, Diccianni MB, Li TZ, Chang AMZ (1997) $P16^{INK4}$ and p15INK4B alterations in primary gynecologic malignancies. Gynecol Oncol 65:319–324
37. Xiong Y (1996) Why are there so many CDK inhibitors? Biochim Biophys Acta 1288:O1-O5
38. Zehbe I, Rätsch A, Alunni-Fabbroni M, Burzlaff A, Bakos E, Dürst M, Wilander E, Tommasino M (1999) Overriding of cyclin-dependent kinase inhibitors by high and low risk human papillomavirus types: evidence for an in vivo role in cervical lesions. Oncogene 18:2201–2211
39. Zerfass-Thome K, Zwerschke W, Mannhardt B, Tindle R, Botz JW, Jansen-Dürr P (1996) Inactivation of the cdk inhibitor p27kip1 by the human papillomavirus type 16 E7 oncoprotein. Oncogene 13:2323–2330
40. Zur Hausen H (1994) Molecular pathogenesis of cancer of the cervix and its causation by specific human papillomavirus types. Curr Top Microbiol Immunol 186:131–156

Virchows Arch (2001) 439:62–69
DOI 10.1007/s004280000392

ORIGINAL ARTICLE

Zhenhe Suo · Heidi Siri Berner · Björn Risberg
Mats G. Karlsson · Jahn M. Nesland

Estrogen receptor-α and C-ERBB-4 expression in breast carcinomas

Received: 17 August 2000 / Accepted: 12 November 2000 / Published online: 15 February 2001
© Springer-Verlag 2001

Abstract The presence of estrogen receptors (ERs) in breast carcinomas is important for clinical response to endocrine therapy. However, the cellular mechanisms following ER activation are not fully understood. It has been indicated that expression of the ER is associated with the expression of c-erbB-4. To address this question, 103 breast carcinoma samples were studied using reverse transcriptase polymerase chain reaction (RT-PCR) analysis after application of a microselection method for RNA isolation. Total RNA for RT-PCR was isolated from 20-µm-thick frozen sections, which were made from microselected areas. Paraffin blocks from 98 of these 103 tumors were also immunohistochemically examined. Significant associations between ER-α and c-erbB-4 mRNA and protein expressions were found in the present study with both methods. One-fourth of the tumors did not express ER-α (22%, 24%, and 26% with chemical binding, immunohistochemistry, and RT-PCR, respectively). About one-half of the ER-α negative tumors did not express c-erbB-4 on both mRNA and protein levels (48% with RT-PCR and 46% with immunohistochemistry, P=0.001 for both methods). The endocrine therapy responsive breast cancer cell lines MCF-7 and T47-D were positive for both ER-α and c-erbB-4 expression, while the endocrine therapy non-responsive breast cancer cell lines MDA-MD-231 and SK-BR-3 were not. Thus, we confirm the association between the expression of ER-α and c-erbB-4 mRNA and protein in breast carcinomas, indicating a role for c-erbB-4 in estrogen signal transduction.

Keywords RT-PCR · Immunohistochemistry · ER · c-erbB-4

Z. Suo (✉) · H. Siri Berner · B. Risberg · J.M. Nesland
Department of Pathology,
The Norwegian Radium Hospital and Institute for Cancer Research,
University of Oslo, 0310 Oslo, Norway
e-mail: zhenhes@labmed.uio.no
Tel.: +47-22-060264, Fax: +47-22-730164

M.G. Karlsson
Department of Pathology, Örebro Medical Center Hospital,
Örebro, Sweden

Introduction

Estrogens play important roles in growth and development of normal human breast tissue and its tumors. By binding to the estrogen receptor (ER) [23], estrogens exert a growth-promoting effect on both benign and premalignant ductal epithelia [47]. Two different ERs, ER-α [21] and ER-β [35], have been characterized. The ER-α gene is located on chromosome 6 [45], while the ER-β gene is located on chromosome 14q [35, 55]. After ligand binding to the cytoplasmic ER-α, a conformational change takes place, and the complex is transported to the nucleus [57]. The translocated complex recognizes estrogen-responsive elements located upstream of target genes and alters the expression of the influenced genes [33].

Single or groups of ER-α positive cells are present in normal breast epithelium [48], comprising approximately 7% of the total epithelial cell population [40]. However, ER-α expression in breast carcinomas is dysregulated. Some tumors are lacking the receptor. In tumors expressing it, the majority of the tumor cells are positive [36, 37]. The ER-α negative tumors have lost the gene expression while most ER-α positive tumors have alterations in the ER gene or changes caused by alternative splicing of ER RNA and post-translational modification of the protein [13, 25, 43, 51].

ER-α status has been widely used as a predictor of response to endocrine therapy [1, 4, 5, 6, 8]. Most patients with ER-α positive tumors are likely to benefit from endocrine therapy [24, 38], while patients with ER-negative tumors usually have limited benefit of such a treatment [15]. Although a positive ER status has been correlated with favorable prognostic features, such as a lower rate of proliferation and better tumor histological differentiation [20, 38, 44] and favorable overall and disease-free survival in both newly diagnosed and relapsed breast carcinomas [56], 5–10% of patients with ER-α negative tumors do respond to this treatment [10].

Increased expression of ER-α in normal and benign breast epithelium has been associated with increased

breast cancer incidence [29, 32]. In the normal premenopausal breast, ER-α positive cells comprise the minority and are distributed singly, being surrounded by ER-α negative cells. ER-α positive cells show a statistically significant increase with age, reaching a plateau after menopause, and the increase is associated with a tendency for positive cells to become contiguous in patches of variable size. In contrast, all cases of atypical ductal hyperplasia, lobular in situ neoplasia and ductal carcinoma in situ show ER-α positivity of contiguous cells accounting for the majority in the lesions [48]. In a study of 1957 breast cancer patients from various parts of Croatia, the frequency of ER-α positive tumors and tumor mean ER concentration are shown to be higher in patients over 50 years of age, and the ER concentration in breast carcinomas is positively correlated with age [18]. It is also shown that ER-α positive tumors are more common in all age groups, steadily increasing from between 50% and 60% in premenopausal women to 70% or more in those aged over 80 years. In postmenopausal women, levels of ER-α in ER-α positive tumors are three times those in premenopausal women [39]. In addition, a number of breast carcinomas are ER-α negative, and these tumors are associated with a clinically aggressive behavior [7, 14, 16].

The c-erbB-4 gene belongs to the epidermal growth factor receptor (EGFR) family [41]. Its expression has been found to play a vital role in both cardiac muscle differentiation and axon guidance in the central nervous system (CNS). Mice lacking c-erbB4 die during mid-embryogenesis from the aborted development of myocardial trabeculae in the heart ventricle and display striking alterations in innervation of the hind brain in the CNS [19].

It is reported that inhibition of proliferation in breast cancer cells is proportional to a ribozyme-mediated downregulation of c-erbB-4 expression [53, 54], supporting the role of c-erbB-4 in promoting cell proliferation and tumor progression. However, in a previous clinical study, we reported reduced c-erbB-4 expression in malignant breast carcinomas compared with the expression in neighboring normal and benign breast tissues [52].

Since both ER-α and c-erbB-4 expression are present in normal breast epithelial cells associated with cell proliferation and tumor progression, and both are not expressed in a small number of breast carcinomas, we wanted to explore the possibility of an association between the expressions of these two factors in breast carcinomas.

To test this hypothesis, we isolated total RNA for semi-quantitative reverse transcriptase polymerase chain reaction (RT-PCR) analysis from a total of 103 breast carcinomas by applying a method of microselection of tumor cells from frozen materials to exclude the interference of normal breast epithelial cells in the material. In addition, immunohistochemistry on paraffin sections from 98 of the same 103 tumors was also performed, and we did find a strong association between the expression of ER-α and c-erbB-4 in breast carcinomas.

Materials and methods

Clinical information and material

Tumor tissues from 103 surgically removed breast carcinomas were frozen immediately in methylbutane cooled to –70°C in solid carbon dioxide and then stored at –70°C. Paraffin blocks from 98 of these tumors were also available for this study. The samples were collected at the Department of Pathology, Örebro Medical Center Hospital, Sweden. All of the tumors were from female patients from 32 years to 90 years old, giving a mean age of 64 years.

Light microscopy

Hematoxylin and eosin-stained sections from routinely formalin-fixed paraffin-embedded material (98 cases) and frozen sections were classified following the World Health Organization (WHO) criteria and graded according to the recommendation of Elston and Ellis [11]. Of the tumors, 85 were classified as infiltrating ductal carcinomas (grade I, six cases; grade II, 43 cases; and grade III, 36 cases) and 13 tumors were classified as infiltrating lobular carcinomas (grade I, one case; grade II, seven cases; and grade III, five cases). The remaining five tumors were classified as medullary carcinoma, three cases (grade III); adenoid cystic carcinoma, one case (grade I); and tubular carcinoma, one case (grade I).

Cell culture

Four commercially available breast carcinoma cell lines (MCF-7, T47-D, SK-BR-3, and MDA-MB-231) were routinely maintained in our laboratory with the suggested culture medium from American Type Culture Collection, ATCC.

Ligand-binding ER-α assay

Frozen tumor tissue from the surgical breast specimens was pulverized, and the standard dextran-coated charcoal (DCC) assay [34] was applied in this study.

Microselection of tumor cells from frozen materials

The principles used for microselection were: (1) to avoid any normal epithelial cells or normal glandular structures; (2) to select the most tumor cell concentrated areas; and (3) to avoid the areas with prominent infiltration of lymphoid cells.

Frozen sections (4 μm) were made and stained with hematoxylin and eosin. Both the frozen block and the corresponding 4-μm frozen section were orientated and marked. The morphology of the section was then analyzed with light microscopy, and an area fulfilling the above criteria was carefully selected. According to the selected tumor cell area on the section, the frozen block was trimmed to have only the corresponding area. The trimmed frozen block was then re-embedded with OCT compound, Tissue-Tek (Torrance, Calif.). Another 4-μm frozen section was made from this re-embedded block to control the morphology (no normal epithelial cells were identified inside the tumor area) before 20-μm frozen sections were made. The 20-μm sections were collected into liquid nitrogen-chilled Eppendorf tubes. To be sure that there were still no normal epithelial cells inside the last sections, one more 4-μm frozen section was made after the serial 20-μm sections, and the morphology was controlled. If normal glandular structures appeared, an additional area was selected, and the above-described procedure was followed until the morphology of the 4-μm frozen sections made before and after 20-μm sectioning was satisfactory.

RNA isolation

Total RNA was isolated from the sections made from the microselected material using a RNeasy total RNA isolation kit (Qiagen, West Sussex, UK), following the suppliers protocol. The same protocol was applied to isolate RNA from the cultured cells.

Reverse transcriptase polymerase chain reaction analysis

The Access RT-PCR system (Promega Corporation, Madison, Wis.) was used for one-step RT-PCR. β-Actin primers were used in each RT-PCR reaction as an RNA loading control. Forward (F) and reverse (R) primers used for c-erbB-4 and β-actin RT-PCR were: c-erbB-4F [27], 5'-CTC TGG TGG TCT TCC TTC TAC C-3' (nucleotides 4025–4046); c-erbB-4R [27], 5'-TGA TAG TAG GCA GCA TTG CC-3' (nucleotides 4237–4256); β-actinF, 5'-CTT TGA TTG CAC ATT GTT GT-3' (nucleotides 1325–1344); and β-actinR, 5'-GAA AGC AAT GCT ATC ACC TC-3' (nucleotides 1465–1484). The PCR product lengths of c-erbB-4 and β-actin in this reaction were 232 bp and 160 bp, respectively. Primers for ER-α and β-actin amplifications were: ERαF [42], 5'-AAG AGC TGC CAG GCC TGC C –3'19 (nucleotides 1063–1081); ERαR [42], 5'-TTG GCA GCT CTC ATGTCT CC –3'20 (nucleotides 1211–1230); β-actinF, 5'-CCC TGG AGA AGA GCT ACG AG-3' (nucleotides 685–704); and β-actinR, 5'-ATG CCA GGG TAC ATG GTG GT-3' (nucleotides 888–907). The PCR product lengths of ER-α and β-actin were 168 bp and 223 bp, respectively. cDNA synthesis was done at 48°C for 45 min and at 94°C for 2 min (to denature the cDNA and RNA duplex and inactivate the reverse transcriptase).

To ensure exponential phase amplification of ERα/β-actin and c-erbB-4/β-actin, the optimal number of PCR cycles was determined and found to be 30 cycles. Cycle conditions for c-erbB-4 and β-actin amplification were: 94°C for 45 s; 52°C for 1 min; and 68°C for 1 min. Cycle conditions for ER-α and β-actin were: 94°C for 45 s; 63°C for 1 min; and 68°C for 1 min. RT-PCR was performed in a final volume of 25 µl in the presence of 10 pM of each primer, 0.2 mM deoxynucleotid triphosphate (dNTP) mixture, 1 mM $MgSO_4$, 2.5 units of avian myeloblastosis virus (AMV) reverse transcriptase, and 2.5 U *Tfl* DNA polymerase. Both positive and negative controls were applied in each running. Negative controls were done either by omission of AMV reverse transcriptase or by omission of *Tfl* DNA polymerase. Cell lines MCF-7 and T47-D were used as positive controls for ER-α and c-erbB-4 mRNA expression. Both positive and negative controls were satisfactory.

Semi-quantitative analysis of PCR products

Photographs of the PCR results were analyzed by reading intensities of the amplified c-erbB-4 and ER-α bands. The housekeeping gene, β-actin, was used to control an equal loading of RNA for each sample. If the target band (c-erbB-4) was of an intensive illumination, it was scored as "+++". If the target band was of a weak illumination, it was scored as "+". "++" was given as the score if the target band was of a medium illumination. "0" was scored if the target band was not possible to identify.

Immunohistochemistry

A polyclonal c-erbB-4 (c-18, sc-283) antibody (Santa Cruz Biotechnology, Calif.) with a 1:300 dilution and a monoclonal ER antibody (NCL-ER-6F11, Novocastra Laboratories, Newcastle-upon-Tyne, UK) with a dilution at 1: 30 were used in this study. The biotin-streptavidin amplified (B-SA) system using the Optimax Automated Cell Staining System Plus (BioGenex, San Raman, Calif.) was applied. After mounting on silane-coated slides, the sections (5 µm) were dried in a 56°C incubator for 1 h and overnight at 37°C. Then, the sections were deparaffinized, rehydrated, and incubated with 0.3% hydrogen peroxide (H_2O_2) in methanol for 30 min to block the endogenous peroxidase activity. Sections were microwaved (2×5 min) in a citrate-buffer solution prior to immunohistochemistry. After incubation with primary antibody, the sections were incubated for 20 min with the multilink biotinylated anti-immunoglobulin (BioGenex; 1:30) and then 20 min with the streptavidin peroxidase (BioGenex; 1:30) using the automatic stainer. The sections were then stained for 5 min with 0.05% 3'3-diaminobenzidine tetrahydrochloride (DAB) freshly prepared in 0.05 M Tris-HCl buffer at pH 7.6, containing 0.01% H_2O_2. After counterstaining with hematoxylin, the sections were dehydrated and mounted. All series included known positive cases as controls. Negative controls included substitution of the primary antibodies with non-reacting antibodies of the same subclass. Peptide blocking of the c-erbB-4 antibody was done according to the manufacturer's (Santa Cruz Biotechnology) recommendation. All of the positive and negative controls gave satisfactory results.

The immunostaining results were analyzed semi-quantitatively. The number of the immunolabeled cells was graded as follows: less than 5% cells with positive staining was scored as (–); between 5% and 25% cells with positive staining was scored as (+); between 25% and 75% cells with positive staining was scored as (++); and more than 75% cells with positive staining was scored as (+++).

Statistical analysis

Comparative analysis of data was performed with the SPSS 8.0 for windows. All the data were analyzed using the χ^2 test.

Results

Microselection of frozen materials

All tumors were successfully trimmed using the microselection method before sections for RNA isolation were made. The smallest sections with this method were about 4 mm^2, but most sections were 25 mm^2. To get roughly an equal number of cells per sample, the numbers of sections collected in chilled tubes varied from two to eight sections, depending on the section size.

Estrogen receptor-α

The ER-α values with the chemical binding method varied from 0 to 16.8 units for 101 tumors. The examination of ER-α with the chemical binding estradiol assay was not done for two tumors. The variation of the intensity of the RT-PCR ER-α bands and immunohistochemical scoring was in line with the value variation with the chemical estradiol method in general. Of the 22 negative samples with the estradiol method, 18 were also negative with both RT-PCR and immunohistochemistry analyses. The remaining four chemical binding negative tumors were positive with both RT-PCR and immunohistochemistry methods (two cases), positive with immunohistochemistry but negative with RT-PCR analysis (one case), and negative with RT-PCR but not available for immunohistochemistry analysis (one case). Five tumors negative for both RT-PCR and immunohistochemistry methods were chemical binding positive, but their values were low, from 0.1 to 0.88 unit. One tumor was negative with

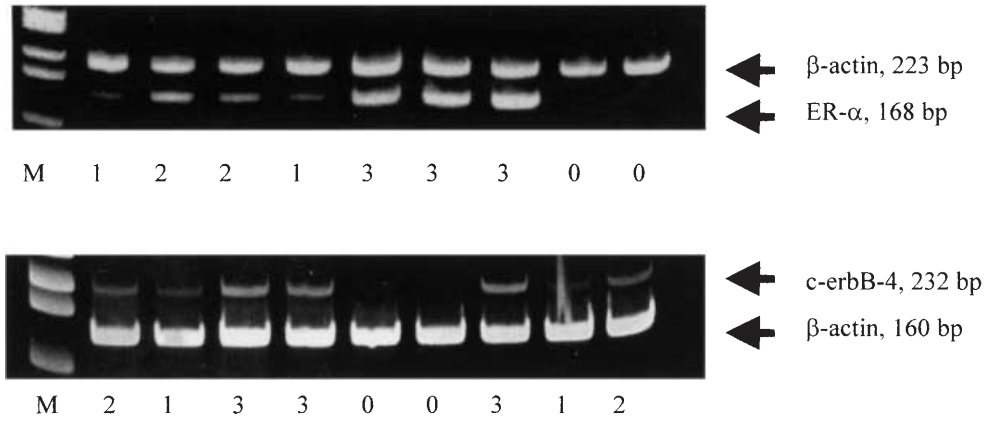


Fig. 1 Expression of c-erbB-4 (*low*) and estrogen receptor (ER)-α (*top*) mRNAs analyzed using reverse transcriptase polymerase chain reaction (RT-PCR) analysis in breast carcinomas. The gels were stained with SYBR green (Molecular Probes, Eugene, Ore.). The numbers under each lane show the semiquantitative scores. *M* DNA molecular marker ϕX174 DNA/*Hae*III

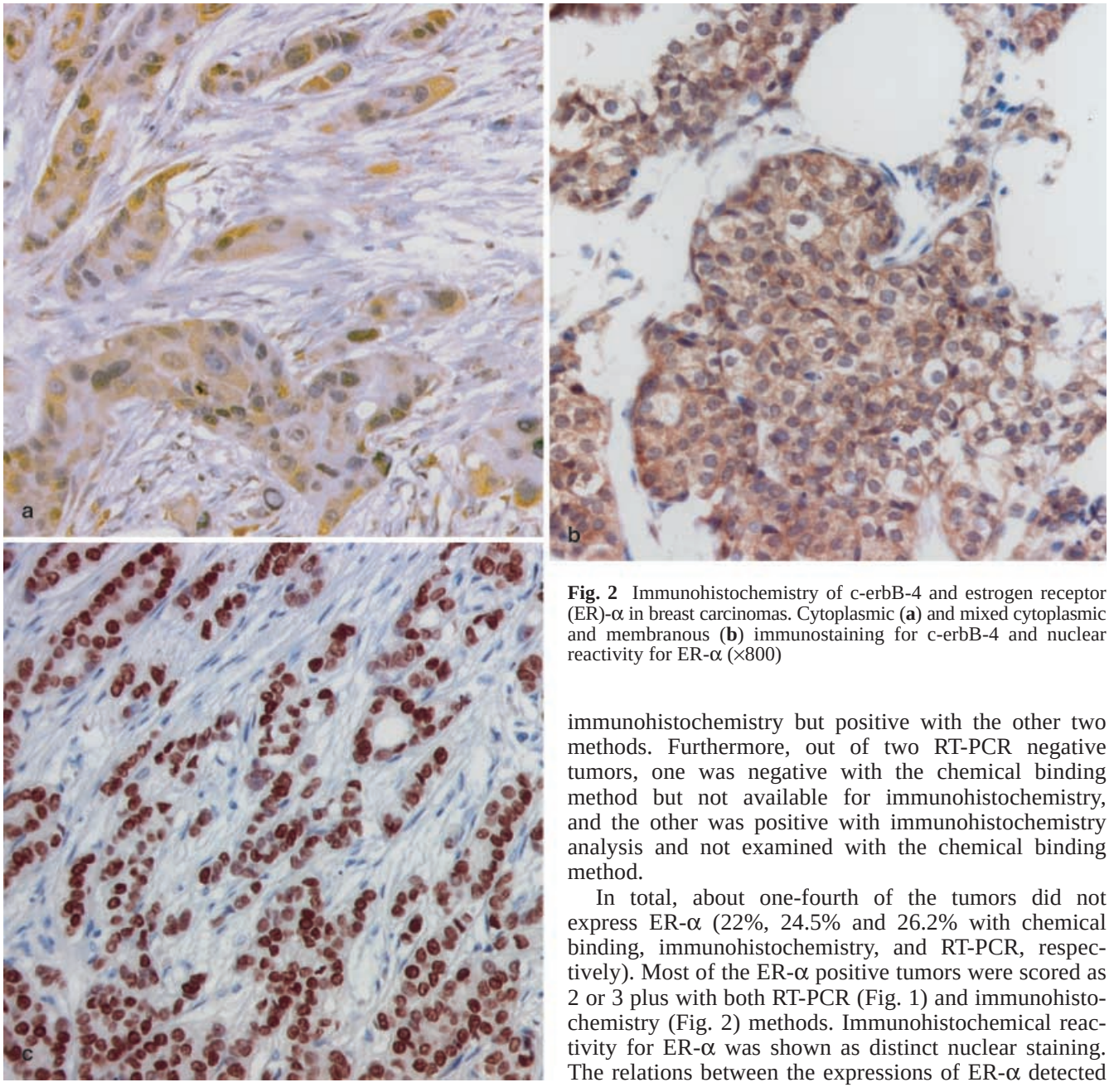


Fig. 2 Immunohistochemistry of c-erbB-4 and estrogen receptor (ER)-α in breast carcinomas. Cytoplasmic (**a**) and mixed cytoplasmic and membranous (**b**) immunostaining for c-erbB-4 and nuclear reactivity for ER-α (×800)

immunohistochemistry but positive with the other two methods. Furthermore, out of two RT-PCR negative tumors, one was negative with the chemical binding method but not available for immunohistochemistry, and the other was positive with immunohistochemistry analysis and not examined with the chemical binding method.

In total, about one-fourth of the tumors did not express ER-α (22%, 24.5% and 26.2% with chemical binding, immunohistochemistry, and RT-PCR, respectively). Most of the ER-α positive tumors were scored as 2 or 3 plus with both RT-PCR (Fig. 1) and immunohistochemistry (Fig. 2) methods. Immunohistochemical reactivity for ER-α was shown as distinct nuclear staining. The relations between the expressions of ER-α detected

Table 1 Relationships between expressions of estrogen receptor (ER)-α and c-erbB-4 detected using reverse transcriptase polymerase chain reaction (RT-PCR) analysis and immunohistochemistry and histological subtypes

	Infiltrating ductal carcinoma (grade)			Infiltrating lobular carcinoma (grade)			Medullary carcinoma	Adenoid cystic carcinoma	Tubular carcinoma
	I	II	III	I	II	III			
RT-PCR positivity for ER-α	6/6	36/42	21/37	1/1	6/7	4/5	1/3	1/1	0/1
Immunohistochemical positivity for ER-α	6/6	33/39	21/35	1/1	6/7	4/5	1/3	1/1	0/1
RT-PCR positivity for c-erbB-4	5/6	36/42	27/37	1/1	6/7	5/5	2/3	1/1	1/1
Immunohistochemical positivity for c-erbB-4	6/6	33/39	25/35	1/1	7/7	4/5	2/3	1/1	1/1

with the two different methods and histological subtypes are shown in Table 1. The breast cancer cell lines MCF-7 and T47-D were found positive, while SK-BR-3 and MDA-MB-231 were negative for ER-α mRNA expression using RT-PCR.

c-erbB-4

With RT-PCR, 18% (19/103) of these tumors were c-erB-4 mRNA negative. Among the remaining 78 c-erbB-4 mRNA positive tumors, 22% (23/103) were scored as "+", 6% (6/103) were scored as "++", and 54%(55/103) were scored as "+++" (Fig. 1).

Of the 98 immunoreactive tumors, 18 were immunohistochemically negative for the c-erbB-4 antibody. The remaining 80 immunoreactive tumors were semi-quantitatively scored; 6% (6/98) of the tumors were scored as "+", 21% (21/98) were scored as "++", and 54% (53/98) were scored as "+++". The c-erbB-4 positive tumors showed either cytoplasmic staining or mixed cytoplasmic and cell membranous staining (Fig. 2). No nuclear immunoreactivity with the c-erbB-4 antibody was observed. In most of the negatively stained tumor tissues, normal glandular structures next to tumors were immunoreactive with the c-erbB-4 antibody. Capillary endothelial cells and the number of stromal cells were also immunoreactive. Table 1 shows the relationships between the expressions of c-erbB-4 detected with the two different methods and histological subtypes. The breast cancer cell lines MCF-7 and T47-D were found positive, while SK-BR-3 and MDA-MB-231 were negative for c-erbB-4 mRNA expression using RT-PCR analysis.

Association between the expressions of ER-α and c-erbB-4

The expressions of ER-α and c-erbB-4 mRNAs examined using RT-PCR analysis and ER-α and c-erbB-4 proteins examined using immunohistochemistry are shown in cross tables (Table 2 and Table 3). The $\chi 2$ test showed a significant association between the expression of ER-α and c-erbB-4 mRNA (P=0.001) and protein (P=0.001). Histological grade of infiltrating ductal cell carcinomas was found inversely correlated with the expression of ER (P=0.013) and c-erbB-4 (P=0.019).

Table 2 Cross tabulation of expressions of estrogen receptor (ER)-α and c-erbB-4 mRNA using reverse transcriptase polymerase chain reaction (RT-PCR) analysis in the breast carcinomas

		c-erbB-4 Score				Total
		0	1	2	3	
ER-α score	0	13	5	1	8	27
	1	1	3	0	3	7
	2	1	2	2	7	12
	3	4	13	3	37	57
Total		19	23	6	55	103

Table 3 Cross tabulation of expressions of estrogen receptor (ER)-α and c-erbB-4 protein using immunohistochemistry in the breast carcinomas

		c-erbB-4 score				Total
		0	1	2	3	
ER-α score	0	11	1	3	9	24
	1	2	2	0	2	6
	2	0	0	3	5	8
	3	5	3	15	37	60
Total		18	6	21	53	98

Discussion

It is not uncommon to isolate RNA directly from larger tissue sections without any microselection for RT-PCR application. The specificity of RNA made in this way can be problematic for tumor studies when the target genes are expressed both in tumor and normal cells. Even a small number of unwanted cells appearing in the sections can make it difficult to interpret the PCR results. To overcome this problem, methods of microdissection either manually [22] or laser-controlled have been developed in the past few years [12]. The manual microdissection is laborious and not very convenient for studies of large sample numbers. Laser-controlled microdissection can be used to select even single cells and has great potential in molecular studies. However, special equipment is needed. The microselection method applied in our present study is a good alternative for controlling RNA quality made from frozen tumor tissues.

In our study, we used the housekeeping gene, β-actin, as a reference. It was our choice to apply this housekeeping

gene mainly because of its simplicity, and no competitor molecules were required as an internal standard. By testing the first 20 cases, we observed that the semi-quantitative values agreed largely with the values obtained with the chemical binding method for ER-α examination. We therefore continued with this semi-quantitative examination. It turned out, as reported in the Results, that the semi-quantitative RT-PCR results were, in general, in keeping with the values obtained with both the chemical binding method and immunohistochemistry for ER-α, with only a few exceptions. It shows that the housekeeping gene, β-actin, can be used as an internal control for semiquantitative RT-PCR in breast cancer studies, although some expression variation of this gene has been reported [46].

In total, 22 of the 101 breast carcinomas in our series were found to be negative for the ER-α protein with the chemical binding method, whereas 27 of the 103 tumors were identified as negative for ER-α mRNA expression with the RT-PCR method. In other words, 78% (with chemical method) or 74% (with RT-PCR) of the present tumors have been shown positive for ER-α in the present study. Theoretically, the RT-PCR should be much more sensitive than the chemical binding method and should demonstrate more positive cases. This low number of ER-α positive tumors identified with the RT-PCR method could be due to our introduction of the microselection of frozen materials in the isolation of RNA. Tumor cells are not evenly distributed in the tissue, and normal epithelial cells can also be positive for ER-α. Portions of involutionary lobules and hyperplastic epithelial cells, in particular, can be intensively positive for ER-α [48]. Thus, some positive tumors detected with the chemical method might be false positive. Indeed, the remaining five RT-PCR ER-α negative tumors had very low values detected with the chemical binding method (see Results), suggesting a normal epithelial cell origin of the detected ER-α. However, our study cannot exclude the possibility of an ER-α negative cell clone in an otherwise ER-α positive breast carcinoma. If this is the case, RT-PCR applied on small tumor cell areas might result in a false-negative result also. This possibility is to be confirmed. Meanwhile, we observed that six of the 22 ER-α negative tumors detected with the chemical binding method were positive with the RT-PCR method. Such a difference can be due to two factors. The high sensitivity of the RT-PCR method should be considered, and the microselection method applied guarantees a much higher tumor cell density.

We reported previously that the expression of c-erbB-4 was decreased in breast carcinomas relative to normal breast epithelium [52]. Although most of the tumors in that study were positive for c-erbB-4, both expression rate and expression intensity were lower in the malignant tumors than that in adjacent benign and normal epithelial structures. The present study of c-erbB-4 in a series of Swedish breast carcinomas also reveals that 18% of the tumors do not express c-erbB-4 mRNA/protein. c-erbB-4 expression is normally observed in differentiating tissue [49]. It has been found that c-erbB-4 signaling is necessary for mammary terminal differentiation during lactation [26]. Expression of c-erbB-4 in breast carcinomas is also associated with favorable prognostic factors [2, 3, 30]. Furthermore, Kew et al. [28] reported an inverse association between c-erbB-4 expression and histological grade, which was also confirmed in our present study of infiltrating ductal carcinomas. It seems from our results and others [2, 49], that decreased c-erbB-4 expression in breast carcinomas may be associated with tumor progression.

The expression of ER-α and c-erbB-4 mRNA/protein was statistically associated in our present study (P=0.001). To our knowledge, this is the first report about ER-α and c-erbB-4 expression in breast carcinomas on both the mRNA and protein level. The hormonal responsive breast cancer cell lines, MCF-7 and T47-D, were positive for both ER-α and c-erbB-4 mRNA, while the hormonal non-responsive breast cancer cell lines MDA-MD-231 and SK-BR-3 were negative. Differential expression of ER-α and c-erbB-4 protein/mRNA in these four cell lines has been reported [9, 17, 31], and this feature is still maintained although these cell lines have been passaged in our laboratory for more than 15 years.

The association of ER-α and c-erbB-4 in breast carcinomas has not been extensively studied, but such an association has been indicated in several publications in smaller series. With the same polyclonal c-erbB-4 antibody as we used in the present study, Bacus at al. [3] studied 72 breast carcinomas. They observed a positive association between c-erbB-4 and ER-α expression (P<0.01). Knowlden et al. [30], using RT-PCR analysis, examined 47 primary breast carcinomas for expression of both ER-α and c-erbB-4. In addition, immunostaining of ER-α protein was done. A direct association was observed on the mRNA level (P=0.02) and between mRNA expression of c-erbB-4 and protein expression of ER-α (P=0.01). By using a monoclonal c-erbB-4 antibody from NeoMarker, Tang et al. [54] immunohistochemically examined 50 primary breast carcinomas and found an association between the expression of c-erbB-4 and ER-protein (P=0.01). Furthermore, an examination of ten different breast carcinoma cell lines [54] has also revealed a similar result as we reported here. It should be noted that a recent immunohistochemical study by Kew et al. [28], with the HFR-1 c-erbB-4 monoclonal antibody, showed nuclear c-erbB-4 staining in 25% of the 127 breast carcinomas and no significant association between c-erbB-4 immunostaining (either cytoplasmic or membrane or nuclear), and ER-α expression was found. Similarly, Srinivasan et al. [50] also reported 49% nuclear c-erbB-4 immunostaining in a series of 178 breast carcinomas, and neither cytoplasmic nor nuclear c-erbB-4 immunoreactivity was associated with ER-α expression. Nevertheless, our results strongly support the previous observations of an association between c-erbB-4 and ER-α expression in invasive breast carcinomas.

Acknowledgements We are grateful to Elisabeth Emilsen for help with cell cultures and Ellen Hellesylt, Mette Ingrud, and Bruno Guggiana for the excellent immunohistochemical assistance.

References

1. Andersen J, Poulsen HS (1989) Immunohistochemical estrogen receptor determination in paraffin-embedded tissue. Prediction of response to hormonal treatment in advanced breast cancer. Cancer 64:1901–1908
2. Bacus SS, Zelnick CR, Chin DM, Yarden Y, Kaminsky DB, Bennington J, Wen D, Marcus JN, Page DL (1994) Medullary carcinoma is associated with expression of intercellular adhesion molecule-1. Implication to its morphology and its clinical behavior. Am J Pathol 145:1337–1348
3. Bacus SS, Chin D, Yarden Y, Zelnick CR, Stern DF (1996) Type 1 receptor tyrosine kinases are differentially phosphorylated in mammary carcinoma and differentially associated with steroid receptors. Am J Pathol 148:549–558
4. Bonadonna G, Valagussa P, Tancini G, Di Fronzo G (1980) Estrogen-receptor status and response to chemotherapy in early and advanced breast cancer. Cancer Chemother Pharmacol 4:37–41
5. Chang J, Powles TJ, Allred DC, Ashley SE, Clark GM, Makris A, Assersohn L, Gregory RK, Osborne CK, Dowsett M (1999) Biologic markers as predictors of clinical outcome from systemic therapy for primary operable breast cancer. J Clin Oncol 17:3058–3063
6. Chen PZ, Mei Z, Yao XY, Meng XG (1989) Selection of hormone-responsive advanced breast cancer with a cytoplasmic estrogen receptor assay. Analysis of 100 cases. Cancer 63: 139–142
7. Cooper LS, Gillett CE, Patel NK, Barnes DM, Fentiman IS (1999) Survival of premenopausal breast carcinoma patients in relation to menstrual cycle timing of surgery and estrogen receptor/progesterone receptor status of the primary tumor. Cancer 86:2053–2058
8. Crowe JP, Hubay CA, Pearson OH, Marshall JS, Rosenblatt J, Mansour EG, Hermann RE, Jones JC, Flynn WJ, McGuire WL (1982) Estrogen receptor status as a prognostic indicator for stage I breast cancer patients. Breast Cancer Res Treat 2:171–176
9. Eckert RL, Mullick A, Rorke EA, Katzenellenbogen BS (1984) Estrogen receptor synthesis and turnover in MCF-7 breast cancer cells measured by a density shift technique. Endocrinology 114:629–637
10. Edwards DP, Chamness GC, McGuire WL (1979) Estrogen and progesterone receptor proteins in breast cancer. Biochim Biophys Acta 560:457–486
11. Elston CW, Ellis IO (1991) Pathological prognostic factors in breast cancer. I. The value of histological grade in breast cancer: experience from a large study with long-term follow-up. Histopathology 19:403–410
12. Emmert-Buck MR, Bonner RF, Smith PD, Chuaqui RF, Zhuang Z, Goldstein SR, Weiss RA, Liotta LA (1996) Laser capture microdissection. Science 274:998–1001
13. Erenburg I, Schachter B, Mira y Lopez R, Ossowski L (1997) Loss of an estrogen receptor isoform (ER alpha delta 3) in breast cancer and the consequences of its reexpression: interference with estrogen-stimulated properties of malignant transformation. Mol Endocrinol 11:2004–2015
14. Esteban JM, Felder B, Ahn C, Simpson JF, Battifora H, Shively JE (1994) Prognostic relevance of carcinoembryonic antigen and estrogen receptor status in breast cancer patients. Cancer 74:1575–1583
15. Ferguson AT, Davidson NE (1997) Regulation of estrogen receptor alpha function in breast cancer. Crit Rev Oncog 8:29–46
16. Ferno M, Andersson C, Fallenius G, Idvall I (1996) Oestrogen receptor analysis of paraffin sections and cytosol samples of primary breast cancer in relation to outcome after adjuvant tamoxifen treatment. The South Sweden Breast Cancer Group. Acta Oncol 35:17–22
17. Friedl A, Jordan VC (1994) Oestradiol stimulates growth of oestrogen receptor-negative MDA-MB-231 breast cancer cells in immunodeficient mice by reducing cell loss. Eur J Cancer 10:1559–1564
18. Gamulin S, Romic-Stojkovic R (1991) Oestrogen and progesterone receptors in primary breast cancer: a population study. Eur J Cancer 27:491–495
19. Gassmann M, Casagranda F, Orioli D, Simon H, Lai C, Klein R, Lemke G (1995) Aberrant neural and cardiac development in mice lacking the ErbB4 neuregulin receptor (comments). Nature 378:390–394
20. Godolphin W, Elwood JM, Spinelli JJ (1981) Estrogen receptor quantitation and staging as complementary prognostic indicators in breast cancer: a study of 583 patients. Int J Cancer 28:677–683
21. Green S, Walter P, Kumar V, Krust A, Bornert JM, Argos P, Chambon P (1986) Human oestrogen receptor cDNA: sequence, expression and homology to v-erb-A. Nature 320: 134–139
22. Gupta SK, Douglas-Jones AG, Morgan JM (1997) Microdissection of stained archival tissue. Mol Pathol 50:218–220
23. Harlan LC, Coates RJ, Block G, Greenberg RS, Ershow A, Forman M, Austin DF, Chen V, Heymsfield SB (1993) Estrogen receptor status and dietary intakes in breast cancer patients. Epidemiology 4:25–31
24. Howell A, Anderson E, Blamey R, Clarke RB, Dixon JM, Dowsett M, Johnston SR, Miller WR, Nicholson R, Robertson JF (1998) The primary use of endocrine therapies. Recent Results Cancer Res 152:227–244
25. Iwase H, Greenman JM, Barnes DM, Hodgson S, Bobrow L, Mathew CG (1996) Sequence variants of the estrogen receptor (ER) gene found in breast cancer patients with ER negative and progesterone receptor positive tumors. Cancer Lett 108: 179–184
26. Jones FE, Welte T, Fu XY, Stern DF (1999) ErbB4 signaling in the mammary gland is required for lobuloalveolar development and Stat5 activation during lactation. J Cell Biol 147:77–88
27. Kataoka H, Joh T, Kasugai K, Okayama N, Moriyama A, Asai K, Kato T (1998) Expression of mRNA for heregulin and its receptor, ErbB-3 and ErbB-4, in human upper gastrointestinal mucosa. Life Sci 63:553–564
28. Kew TY, Bell JA, Pinder SE, Denley H, Srinivasan R, Gullick WJ, Nicholson RI, Blamey RW, Ellis IO (2000) c-erbB-4 protein expression in human breast cancer. Br J Cancer 82: 1163–1170
29. Khan SA, Rogers MA, Khurana KK, Meguid MM, Numann PJ (1998) Estrogen receptor expression in benign breast epithelium and breast cancer risk. J Natl Cancer Inst 90:37–42
30. Knowlden JM, Gee JM, Seery LT, Farrow L, Gullick WJ, Ellis IO, Blamey RW, Robertson JF, Nicholson RI (1998) c-erbB3 and c-erbB4 expression is a feature of the endocrine responsive phenotype in clinical breast cancer. Oncogene 17: 1949–1957
31. Kumar R, Mandal M, Ratzkin BJ, Liu N, Lipton A (1996) NDF induces expression of a novel 46 kD protein in estrogen receptor positive breast cancer cells. J Cell Biochem 62:102–112
32. Lawson JS, Field AS, Champion S, Tran D, Ishikura H, Trichopoulos D (1999) Low oestrogen receptor alpha expression in normal breast tissue underlies low breast cancer incidence in Japan (letter). Lancet 354:1787–1788
33. Leygue E, Dotzlaw H, Watson PH, Murphy LC (1999) Expression of estrogen receptor beta1, beta2, and beta5 messenger RNAs in human breast tissue. Cancer Res 59:1175–1179
34. McGuire WL, De La Garza M, Chamness GC (1977) Evaluation of estrogen receptor assays in human breast cancer tissue. Cancer Res 37:637–639
35. Mosselman S, Polman J, Dijkema R (1996) ER beta: identification and characterization of a novel human estrogen receptor. FEBS Lett 392:49–53
36. Murphy LC, Dotzlaw H (1989) Variant estrogen receptor mRNA species detected in human breast cancer biopsy samples. Mol Endocrinol 3:687–693
37. Murphy LC, Wang M, Coutt A, Dotzlaw H (1996) Novel mutations in the estrogen receptor messenger RNA in human breast cancers. J Clin Endocrinol Metab 81:1420–1427

38. Osborne CK (1998) Steroid hormone receptors in breast cancer management. Breast Cancer Res Treat 51:227–238
39. Pearce PT, Myles KM, Funder JW (1993) Oestrogen and progesterone receptor assays in breast tumours. The Prince Henry's hospital experience 1983–1990. Med J Aust 159:227–231
40. Petersen OW, Hoyer PE, van Deurs B (1987) Frequency and distribution of estrogen receptor-positive cells in normal, nonlactating human breast tissue. Cancer Res 47:5748–5751
41. Plowman GD, Culouscou JM, Whitney GS, Green JM, Carlton GW, Foy L, Neubauer MG, Shoyab M (1993) Ligand-specific activation of HER4/p180erbB4, a fourth member of the epidermal growth factor receptor family. Proc Natl Acad Sci U S A 90:1746–1750
42. Pujol P, Rey JM, Nirde P, Roger P, Gastaldi M, Laffargue F, Rochefort H, Maudelonde T (1998) Differential expression of estrogen receptor-alpha and -beta messenger RNAs as a potential marker of ovarian carcinogenesis. Cancer Res 58:5367–5373
43. Rea D, Parker MG (1996) Effects of an exon 5 variant of the estrogen receptor in MCF-7 breast cancer cells. Cancer Res 56:1556–1563
44. Rich MA, Furmanski P, Brooks SC (1978) Prognostic value of estrogen receptor determinations in patients with breast cancer. Cancer Res 38:4296–4298
45. Sauer T, Beraki K, Jebsen PW, Ormerod E, Naess O (1997) In situ hybridization of chromosome 6 on fine-needle aspirates from breast carcinomas: comparison of numerical abnormalities and ER/PgR status and staining pattern. Diagn Cytopathol 16:420–424
46. Serazin-Leroy V, Denis-Henriot D, Morot M, de Mazancourt P, Giudicelli Y (1998) Semi-quantitative RT-PCR for comparison of mRNAs in cells with different amounts of housekeeping gene transcripts. Mol Cell Probes 12:283–291
47. Shekhar MP, Nangia-Makker P, Wolman SR, Tait L, Heppner GH, Visscher DW (1998) Direct action of estrogen on sequence of progression of human preneoplastic breast disease. Am J Pathol 152:1129–1132
48. Shoker BS, Jarvis C, Sibson DR, Walker C, Sloane JP (1999) Oestrogen receptor expression in the normal and pre-cancerous breast. J Pathol 188:237–244
49. Srinivasan R, Poulsom R, Hurst HC, Gullick WJ (1998) Expression of the c-erbB-4/HER4 protein and mRNA in normal human fetal and adult tissues and in a survey of nine solid tumour types. J Pathol 185:236–245
50. Srinivasan R, Gillett CE, Barnes DM, Gullick WJ (2000) Nuclear expression of the c-erbB-4/HER-4 growth factor receptor in invasive breast cancers. Cancer Res 60:1483–1487
51. Sullivan JA, Cohn CS, Hill SM (1997) Identification of sequence alterations in the upstream regulatory region of the estrogen receptor gene in an ER-negative breast cancer cell line. Cancer Lett 113:131–139
52. Suo Z, Emilsen E, Tveit KM, Nesland JM (1998) Type 1 protein tyrosine kinases in benign and malignant breast lesions. Histopathology 33:514–521
53. Tang CK, Goldstein DJ, Payne J, Czubayko F, Alimandi M, Wang LM, Pierce JH, Lippman ME (1998) ErbB-4 ribozymes abolish neuregulin-induced mitogenesis. Cancer Res 58: 3415–3422
54. Tang CK, Concepcion XZ, Milan M, Gong X, Montgomery E, Lippman ME (1999) Ribozyme-mediated down-regulation of ErbB-4 in estrogen receptor-positive breast cancer cells inhibits proliferation both in vitro and in vivo. Cancer Res 59:5315–5322
55. Tsukamoto K, Inoue S, Hosoi T, Orimo H, Emi M (1998) Isolation and radiation hybrid mapping of dinucleotide repeat polymorphism at the human estrogen receptor beta locus. J Hum Genet 43:73–74
56. Valavaara R (1997) Reliability of estrogen receptors in predicting response to antiestrogens. Oncology (Huntingt) 11: 14–18
57. Vladusic EA, Hornby AE, Guerra-Vladusic FK, Lupu R (1998) Expression of estrogen receptor beta messenger RNA variant in breast cancer. Cancer Res 58:210–214

Virchows Arch (2001) 439:70–77
DOI 10.1007/s004280100446

ORIGINAL ARTICLE

**Gelareh Farshid · Farid Moinfar · David J. Meredith
Steve Peiterse · Fattaneh A. Tavassoli**

Spindle cell ductal carcinoma in situ

An unusual variant of ductal intra-epithelial neoplasia that simulates ductal hyperplasia or a myoepithelial proliferation

Received: 30 August 2000 / Accepted: 16 November 2000 / Published online: 11 May 2001
© Springer-Verlag 2001

Abstract Seventeen examples of a variant of ductal carcinoma in situ (DCIS) composed exclusively or predominantly of spindle cells arranged in fascicles, whorls, and solid sheets are described. The fascicular arrangement of the spindle cells simulates the "streaming" phenomenon associated with ordinary intraductal epithelial hyperplasia (IDH). This process also resembles the myoid, solid form of intraductal myoepithelial proliferation. The women ranged in age from 38 years to 79 years with a mean age of 59.3 years. Five patients presented with a palpable mass. The remaining tumors were discovered using mammography. The radiological appearances of the lesions raised concern for carcinoma, but there were no distinctive mammographic findings to suggest an unusual variant of DCIS. Cytological preparations were suspicious for malignancy in two patients and were reported as malignant in another case. Sixteen patients were treated with wide local excision, and one woman had a partial mastectomy. The tumors measured from 3 mm to 15 mm (mean 8.65 mm). In three cases, minute foci of stromal invasion were associated with the spindle cell DCIS. In another specimen, a 2.7-cm invasive ductal carcinoma of no special type was identified in an area away from the foci of the spindle cell DCIS. None of the patients has experienced recurrence or metastasis during the relatively short mean follow-up period of 16.2 months (range 4–77 months). Spindle cell DCIS is distinguished from the streaming pattern of ordinary IDH by its solid growth pattern, lack of secondary spaces or peripheral fenestrations, uniformity of appearance and distribution of nuclei, cytological atypia in the range of low to intermediate-grade DCIS, and negative immunoreaction with CK-34βE12 (HMW-CK903). When fenestrations are present, they are evident in areas of cribriform DCIS that merge with the solid, spindle cell areas in hybrid ducts harboring both patterns. This admixture, with conventional cribriform DCIS, and the association with foci of invasive ductal carcinoma in some cases further help recognition and confirmation of this lesion as in situ carcinoma. When there is no transition from the spindle cells to recognizable cribriform DCIS, distinction from intraductal myoepithelial hyperplasia (myoepitheliosis) requires immunostains for actin and S-100 protein. Recognition of this pattern of DCIS is important in order to avoid its frequent misclassification as a benign lesion.

Keywords Ductal carcinoma in situ · Spindle cell DCIS · Intraductal breast cancer · Mammary ductal intraepithelial neoplasia · Noninvasive breast cancer · Immunohistochemistry

G. Farshid
Department of Pathology, Adelaide, South Australia

G. Farshid · D.J. Meredith
University of Adelaide, Division of Tissue Pathology,
Institute of Medical and Veterinary Science, Frome Road,
Adelaide, South Australia

S. Peiterse
Clinpath Laboratories, Kent town, South Australia

G. Farshid · S. Peiterse
Breastscreen SA, Wayville, South Australia

F. Moinfar · F.A. Tavassoli (✉)
Department of Gynecologic and Breast Pathology,
Armed Forces Institute of Pathology, Washington, D.C. 20306, USA
e-mail: tavassol@afip.osd.mil
Fax: +1-202-7823939

Introduction

Intraductal proliferations in the breast seldom consist of a pure population of spindled cells. Azzopardi [1] has referred to parallel orientation of neighboring cells in an intraductal proliferative process as "streaming" [1], and Page and Anderson [7] consider the finding of swirling or streaming as "strong, impelling evidence of benignancy".

Most proliferations with partial spindling of cells fall into the category of ductal hyperplasia. Myoepithelial cells may also assume a myoid, spindle cell configuration and proliferate in a solid fashion within multiple ducts. This process has been named myoepitheliosis [12]. Both intraductal epithelial hyperplasia (IDH) and

myoepitheliosis are benign. Rarely, intraductal carcinomas composed predominantly or exclusively of solid proliferations of spindle cells develop in the breast. This uncommon variant of ductal carcinoma in situ (DCIS) is frequently mistaken for a benign process.

Little has been published on this diagnostically challenging lesion. The few reported cases are in the form of individual cases and in association with invasive carcinoma when in small groups [3, 4, 5, 8, 9, 10, 12, 13, 14]. The spindle cell variant of DCIS was probably first noted and illustrated in 1992 [13]; it was described as a most difficult pattern to recognize as DCIS [13]. Given the rarity of spindle cell DCIS and to prevent overdiagnosis of the common IDH with spindling as DCIS, it was suggested that spindle cell DCIS should only be diagnosed cautiously and generally when some other pattern of either unequivocal DCIS or an invasive carcinoma is present [13]. Assessing the immunoprofile of this lesion would obviate these precautions. Maluf et al. have reported two invasive ductal carcinomas of the breast which they designated spindle cell argyrophilic mucin-producing carcinoma because of the presence of abundant spindle cells and neuroendocrine differentiation [5]. In 1996, Ruffolo et al. [9] described three additional lesions that they interpreted as invasive spindle cell endocrine carcinoma, despite the rounded appearance of the nests, based on the large size of the nests and their irregular distribution. Judging from their illustrations and the presence of capillaries within the nests of spindle cells, the five tumors in these two reports had a large intraductal papillary component with prominent spindle cell differentiation. The five cases also contained either cells with intracytoplasmic lumens, signet-ring cells, and cuboidal cells that formed glands in addition to the spindle cells. Their presentation and discussion focuses on neuroendocrine differentiation in breast carcinomas in general, with or without mucin production, however [5, 9]. Only one paragraph is devoted to the diagnostic significance of this finding in terms of the largely benign differential diagnoses it evokes. A solid papillary carcinoma with endocrine differentiation with [4, 14] or without [3] mucin production has also been described. In some of these cases (exact number not specified by authors), spindle cells were dominant with marked streaming. Once again, the focus of at least some of these papers is the endocrine differentiation and frequent association with mucinous carcinoma. Aside from these few citations, our literature searches yielded no other specific articles on spindle cell DCIS. We report our experience with 17 examples of spindle cell DCIS, emphasizing their morphology and immunoprofile, particularly the value of CK-34βE12 as a diagnostic aid. The differential diagnosis is discussed in the hope of aiding pathologists' recognition of this rare variant of intraductal carcinoma that can be potentially mistaken for a benign proliferation.

Table 1 Sources and dilution of antibodies used

Antibody	Source	Dilution
Cam 5.2	Becton Dickinson	1/30
SMA	Sigma	1/30,000
S-100	Dako	1/30,000
Chromogranin	Lipshaw	1/5000
Synaptophysin	Dako	1/300
MIB-1	Zymed	1/500
ER	Dako	1/600
PGR	Abbott	1/40
NSE	Dako	1/1000
CK-34β12	Dako	1/500

Materials and methods

Two cases were routine, recent accessions to the division of tissue pathology at the Institute of Medical and Veterinary Science. The third was diagnosed at Clinpath Laboratories 6 years ago. Fourteen cases were retrieved from the files of the department of Gynecologic and Breast pathology at the Armed Forces Institute of Pathology. All cases were fixed in 10% buffered formalin and processed in the standard fashion. Sections were stained with hematoxylin and eosin (HE). Periodic acid–Schiff (PAS)-diastase, mucicarmine, and hyaluronidase stains were also performed in three cases.

Immunohistochemistry on paraffin-embedded tissue was performed with the following antisera: alpha smooth muscle actin, S-100 protein, CAM 5.2, CK-34βE12 (HMW-CK-903), chromogranin, neuron-specific enolase (NSE), synaptophysin, estrogen receptor protein, progestogen receptor protein, and MIB-1. Laminin and type-IV collagen were also used in one case. Table 1 lists the sources and dilutions of these antibodies. Reactions were revealed using the avidin–biotinylated peroxidase complex (ABC) method.

Results

Clinical and radiological features

Table 2 summarizes the case histories of the patients. The women ranged in age from 38 years to 79 years, with a mean age of 59.3 years. Five patients presented with breast masses. The remaining tumors were discovered using mammography, including screening mammograms. Mammograms revealed either stellate densities or suspicious calcifications. The radiological appearances of the lesions raised concern for carcinoma, but there were no distinctive mammographic findings. The palpable lesions ranged from 10 mm to 25 mm. Cytological preparations were suspicious for malignancy in two patients and were reported as malignant in another case.

Surgery

The surgical procedures ranged from excisional biopsy and wide local excision to partial mastectomy for a 15-mm clinically and cytologically suspicious mass detected in a woman who was debilitated by multiple sclerosis. Otherwise, wide local excision was performed for

Table 2 Patient summaries. *SBE* self breast examination, *NA* not available, *NED* no evidence of disease

Case	Ag (years)	Tumor size (mm)	Detection	Radiology	FNA	Procedure	Invasion	Follow-up (months)
1	71	15	Screening	Malignant	Suspicious	Lumpectomy	Foci of invasion	NED 6
2	79	15	SBE	Malignant	Positive	Mastectomy	None detected	NED 77
3	76	10	SBE	Not done	Suspicious	Lumpectomy	Ductal NOS, grade III	NED 7
4	46	11	Mammogram	Suspicious	NA	Lumpectomy	None detected	NED 11
5	57	4	Mammogram	Suspicious	NA	Lumpectomy	None detected	NED 30
6	50	10	Mammogram	Suspicious	NA	Lumpectomy	None detected	NED 18
7	50	8	Mammogram	Suspicious	NA	Lumpectomy	None detected	NED 25
8	46	5	Mammogram	Suspicious	NA	Lumpectomy	None detected	NED 8
9	55	10	Mass	Suspicious	NA	Lumpectomy	None detected	NED 11
10	38	3	Mammogram	Suspicious	NA	Lumpectomy	None detected	NED 10
11	73	6	Mammogram	Suspicious	NA	Lumpectomy	None detected	NED 10
12	70	5	Mammogram	Suspicious	NA	Lumpectomy	None detected	NED 9
13	64	4	Mammogram	Suspicious	NA	Lumpectomy	None detected	NED 12
14	62	6	Mammogram	Suspicious	NA	Lumpectomy	None detected	NED 16
15	76	15	Mass	Suspicious	NA	Lumpectomy	None detected	NED 4
16	46	15	Mass	Suspicious	NA	Lumpectomy	Ductal NOS, grade III	NED 11
17	49	5	Mammogram	Suspicious	NA	Lumpectomy	None detected	NED 7
Mean	59.3	8.65						16.2

the palpable lesions and for those with cytological confirmation of malignancy.

Pathologic findings

Gross features

In five cases, nodules or parenchymal densities ranging from 5 mm to 25 mm in maximum diameter were identified grossly. The consistency of these lesions was variously described as hard, firm, or gritty. No abnormal breast tissue was recognized grossly in the 12 remaining cases. In one case, the main lesion was a 2.7-cm high-grade infiltrating ductal carcinoma associated with high-grade (comedo) DCIS. The spindle cell DCIS was a 5-mm focus, discovered incidentally, 30 mm superior to the invasive tumor and was morphologically quite distinct from the infiltrating carcinoma or its comedo DCIS component. The other tumors were solitary lesions, where the spindle cell DCIS constituted the only abnormality.

Microscopic features

Of the 17 cases, 4 were composed exclusively of spindle cells. Five others were overwhelmingly spindled but also had a minor component of conventional solid or cribriform DCIS, amounting to no greater than 5% of the tumor area. In the mixed DCIS group, of which we had eight cases, conventional, low- to intermediate-grade DCIS with a solid or cribriform architecture formed between 5% and 40% of the proliferation, while the remainder of the lesion was composed of spindle cells.

The histological details were remarkably consistent in the spindled areas. Each lesion consisted of a haphazard scatter of distended ducts embedded in a fibrotic stroma. Irregular spokes emanating from a central area produced a stellate appearance in some cases. A monotonous population of spindle-shaped cells that formed sheets, whorls, and fascicles expanded the affected ducts (Fig. 1). In some of the lesions, small fibrovascular cores punctuated the sheets of spindled cells in some of the ducts, suggesting a papillary DCIS component. Some ducts were only partially replaced by the spindle cell proliferation, the remaining portions being sharply demarcated from the lesional areas.

In the spindle cell areas, the elongated nuclei of the spindle cells were spaced apart evenly, rather than overlapping. The spindle cell nuclei were at least twice the diameter of neighboring ductal epithelial cells. Their chromatin pattern was fine and grainy and one or two small nucleoli were visible (Fig. 2). Mitotic figures, including rare atypical mitoses were identified at a frequency of 2–14 per 10 HPF. The cytoplasm was pale and eosinophilic. Areas with the architectural features of conventional cribriform DCIS were identifiable in 13 cases (Fig. 3). These comprised less than 5% of the area of the tumor in five lesions. Larger proportions of generally cribriform DCIS, constituting up to 40% of the lesion, were documented in eight instances (mixed-type). The constituent cells in these areas were also spindled and identical to those forming the solid portion of the lesion.

Cytoplasmic vacuoles were focally noted in one case. H&E did not reveal any basophilic mucin either in the duct lumens or the cell cytoplasm in any of the 17 cases. The outermost cell layer of the ducts was distinctive in two cases due to its darker staining cytoplasm and flattening of the nuclei against the wall of the ducts. The overlapping nuclei or peripheral slit-like clefts associated with florid hyperplasia were absent. The DCIS was judged to be of low-grade in nine cases based on the absence of both nuclear pleomorphism and intraluminal necrosis [13]. The presence of moderate nuclear atypia and

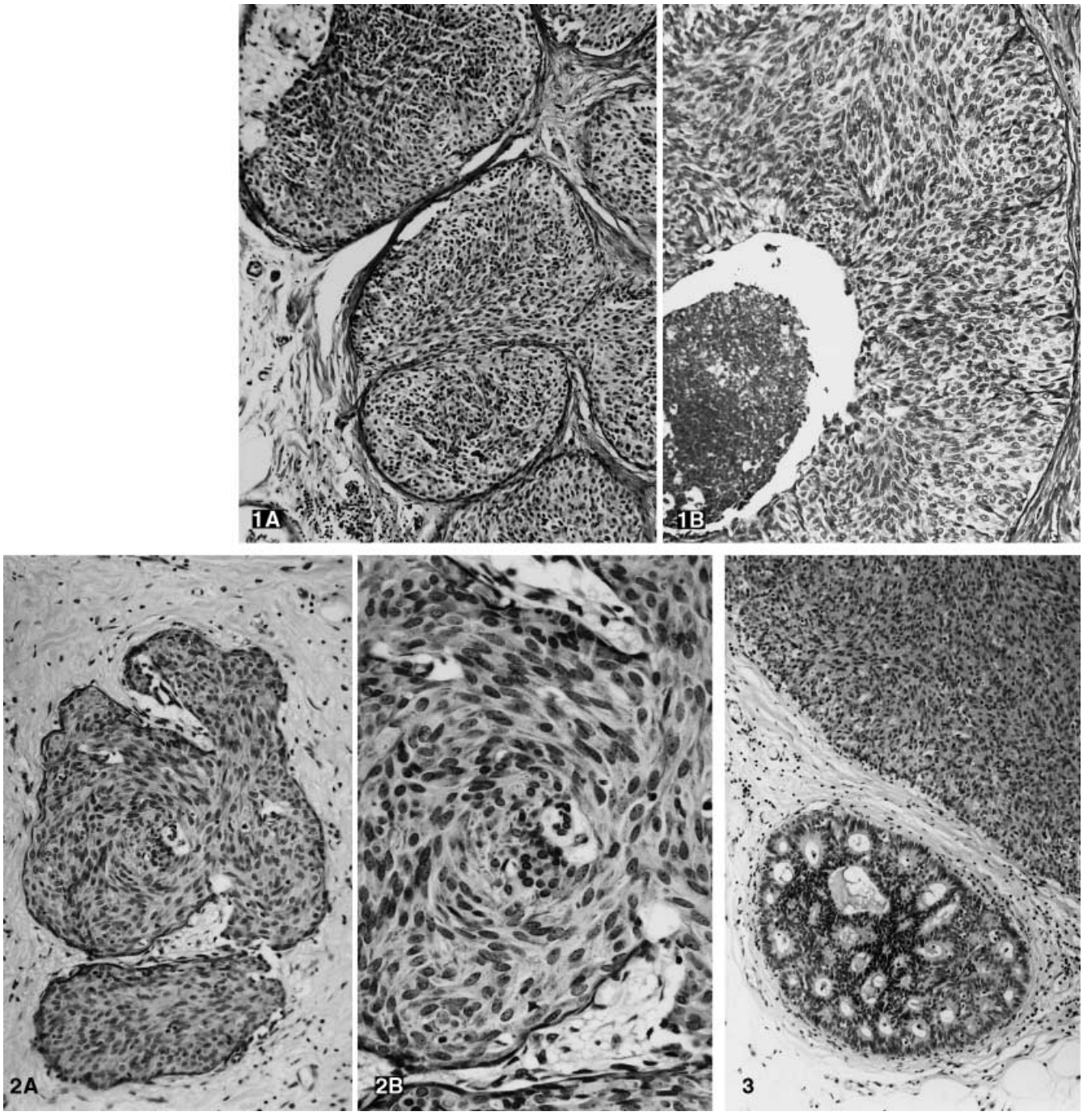


Fig. 1 Spindle ductal carcinoma in situ. **A** Most cases are characterized by a solid proliferation of spindle cells occluding the duct lumens. **B** In others, an occasional duct shows a small amount of intraluminal necrosis as well; the spindle cells display relatively bland nuclear features and lack notable mitotic activity

Fig. 2 **A** A duct distended by a monotonous population of spindle cells forming swirls and fascicles. **B** The spindle cells show little nuclear pleomorphism and have an even chromatin pattern and inconspicuous nucleoli

Fig. 3 A small duct with the punched out spaces, characteristic of cribriform ductal carcinoma in situ (DCIS) adjacent to a much larger duct distended by solid spindle cell DCIS. Note the somewhat elongated nuclear shape in both ducts

focal central necrosis in the remaining eight cases resulted in their classification as intermediate-grade tumors.

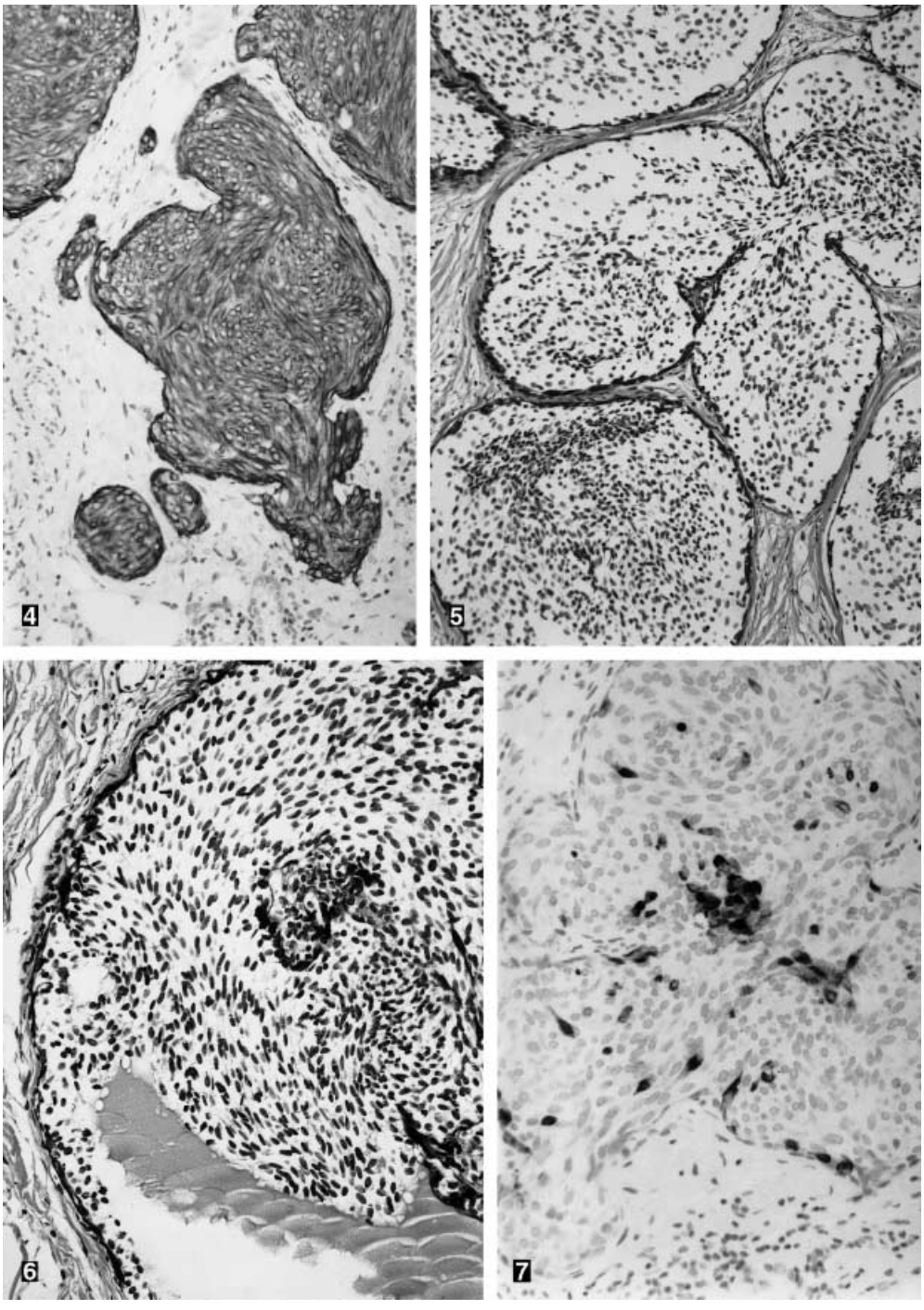
Small, irregular aggregates of atypical spindled cells, less than 3 mm in diameter, were scattered between the larger ducts of DCIS in two cases. No stromal reaction was identified, but these aggregates did not conform to the outline of a lobular unit. Only an incomplete layer of laminin and type-IV collagen was confirmed immunohistochemically in one case, such that it was impossible to exclude focal parenchymal invasion. No angiolymphatic space involvement was demonstrated. As already mentioned, a 2.7-cm, high-grade, invasive ductal carcinoma, accompanied by conventional, high-grade comedo

Fig. 4 Strong and uniform immunoreactivity with Cam 5.2 further highlights the fascicular arrangement of the intraductal proliferation

Fig. 5 Immunostain for actin shows a positive immunoreaction in the myoepithelial cell layer confirming the in situ nature of the lesion. The proliferating spindle cells fail to react with actin, excluding the possibility that the proliferating cells are myoepithelial in nature

Fig. 6 In a deeper level of the same region illustrated in Fig. 1A, the proliferating spindle cells fail to react with CK34BE12. In contrast, the myoepithelial cells around the duct and in the papillary processes show a positive immunoreaction

Fig. 7 Over 10% of the spindle tumor cells displayed a positive immunoreaction with chromogranin in four of seven tumors tested. All seven tumors tested were immunoreactive with synaptophysin and neuron-specific enolase



DCIS was found in one lumpectomy specimen that also contained foci of spindle cell DCIS in a different region. When invasion occurs, it is not necessarily spindle cell in nature but rather the appearances are that of an infiltrating duct carcinoma in most cases (clear-cut invasive cases were not included in this study).

It has been suggested that exclusion of an invasive process where multiple ducts are involved and very much enlarged by the proliferating spindle cells is difficult despite the rounded contour of the expanded ducts [9]. We agree that this feature can cause problems. As long as individual ductules within a terminal duct-lobular unit retain their configuration with the persistence of a basal laminar investiture, however, we would refrain from considering these invasive even when no myoepithelial cells or only rare remnants of myoepithelial cells persist. This is particularly true in cases with a papillary growth pattern where maximum distension is often associated with apparent disappearance of the myoepithelial cell layer but persistence of the basal lamina. Since desmoplasia is also seen around ducts with intraepithelial neoplasia, we do not consider this stromal feature diag-

Table 3 Summary of the results of immunohistochemical studies

Case	Cam 5.2	SMA	S-100	Chromogranin	Syn	NSE	ER	PR	MIB-1	CK-34βE12
1	+	–	<1%	<1%	+	+	+	+	21%	
2	+	–	<1%	+	+	+	+	+	4%	
3	+	–	<1%	–	+	+	+	+	4%	
4		–					+	+		–
5	+	–		–	+	+				–
6				+	+	+				–
7							+	+		<5% +
8										<20% +
9										
10	+	–								–
11		–								–
12	+	–	–							–
13		–		+	+	+	+	+	5%	<20% +
14		–		<1%	Focally +	+			80%	–
15										–
16		–		+	+	+	–	+	80%	–
17		–								50% +

nostic of an invasive process. Since invasion is more common in the setting of altered stroma, however, we do recommend a careful search to exclude the possibility of invasion.

Histochemistry

No mucin production was detected with PAS-D, mucicarmine, or hyaluronidase in the three cases tested.

Immunohistochemistry

The immunohistochemical features of the tumors are summarized in Table 3. In each of the six cases tested, the spindle cells showed strong and uniform expression of Cam 5.2, providing support for the epithelial nature of the spindle cells (Fig. 4). Thirteen cases were assessed for immunoreactivity with CK-34βE12. Nine (69%) were non-reactive with this marker (Fig. 5). CK-34βE12 highlighted isolated tumor cells (between 5% and 20% of the cells) in three lesions. In one case, however, approximately one-half of the tumor cells expressed CK-34βE12. Alpha smooth muscle actin decorated a myoepithelial cell layer around some of the ducts, but the spindle cells were uniformly negative for this antibody in each of the 12 tumors tested (Fig. 6). Sporadic tumor cells were immunoreactive for S-100 protein in one tumor. Immunostains for the neuroendocrine antibodies, chromogranin, synaptophysin, and NSE, were performed and evaluated in eight cases. All eight tumors expressed NSE and synaptophysin, although there was a high level of background staining for synaptophysin in one case. Over 10% of the tumor cells were intensely positive for chromogranin in four cases (Fig. 7). The remaining four tumors were either negative or expressed this antigen in <1% of their cells. The progestogen receptor was expressed by the spindle cells in all seven tumors tested. All but one also expressed the estrogen receptor. The proliferative index, as measured by the MIB-1 or Ki-67 counts, ranged from 4% to 80%.

Follow-up

A limited follow-up ranging from 8 months to 77 months with a mean of 16.2 months is available for these patients. Irrespective of the grade or the architectural patterns, none of the patients has experienced recurrence or metastasis during this relatively short time period.

Discussion

The clinical, morphologic, and immunohistochemical features of 17 examples of a spindle cell variant of intraductal carcinoma are reported. The main purpose of this report is to increase awareness and familiarity with this variant and prevent its frequent misinterpretation as intraductal hyperplasia or a myoepithelial lesion. Spindle cell DCIS is distinguishable from IDH on the basis of the equidistant spacing of its monotonous nuclei and its solid growth pattern, generally lacking the peripheral fenestrations of ordinary hyperplasia. Furthermore, ordinary IDH is composed of cells that display not only variation in the shape and size of their nuclei but also variation in cytoplasmic staining. The negative immunoreaction for CK-34βE12 further excludes IDH [6].

Areas with the architectural features of conventional cribriform DCIS were identifiable in 13 (76%) cases. The cribriform DCIS pattern comprised less than 5% of the area of the tumor in five lesions, but larger proportions of conventional DCIS were documented in eight other instances. These cases provide an important link between the pure form of spindle cell DCIS and well-recognized, conventional forms of low- and intermediate-grade DCIS. Stromal invasion was focally associated

with three of the tumors, attesting to the pre-malignant biological potential of this lesion.

The absence or only focal expression of the high molecular weight keratin CK-34βE12 in the great majority of these lesions is consistent with the expected immunoprofile of malignant ductal intraepithelial neoplasia as recently reported by Moinfar et al. [6]. There is sufficient morphologic overlap between spindle cell DCIS and myoepithelial proliferations that immunohistochemical studies are warranted to assess the differential diagnosis in each case of pure spindle cell DCIS. Immunohistochemically, myoepithelial cells express actin and S-100 protein, but only minimal expression of cytokeratin has been reported [12]. The negative immunoreaction of these cases with actin effectively rules out a myoepithelial process.

In addition to benign intraductal myoepitheliosis, Tamai has reported an intraductal form of malignant myoepithelioma that may be considered in the differential diagnosis [11]. This case report dealt with an intraductal proliferation of cells with atypical nuclei, clear cytoplasm, and strong expression of alpha smooth muscle actin and S-100. While it shares a spindled morphology with our cases, the cigar shaped cells, cytoplasmic clearing, central location of the nuclei and SMA expression distinguish it from the spindle cell DCIS.

The 17 cases of spindle cell DCIS reported here are morphologically similar to those previously described as occurring either as in situ or in association with spindle cell metaplastic carcinoma [13]. Our cases differ from the two carcinomas described by Maluf [5] under the title of spindle-cell argyrophilic mucin-producing carcinoma of the breast by the absence of either intracellular or extracellular mucin production.

Tsang and Chan have recently reported 34 cases of an endocrine DCIS (E-DCIS) [14]. Although all of their tumors exhibited endocrine differentiation by means of immunohistochemistry, there is considerable morphologic variation among their lesions. One-half of their cases were at least partially spindled. Interestingly, we observed reactivity with synaptophysin and NSE in all eight cases tested, while chromogranin was expressed by four of eight tumors tested. The ample, granular cytoplasm or polygonal nuclei that characterized thirty of their tumors were not observed among the 17 cases reported herein. Spindle cell DCIS most probably represents a subset of DCIS lesions that can show neuroendocrine differentiation by means of immunohistochemistry. However, the spindled appearance of the cells often associated with a palisading growth pattern is not particularly reminiscent of neuroendocrine differentiation. Yet it is the spindle cell aspect of this DCIS variant that is most likely to cause its misdiagnosis as a benign process.

In eight of our cases, fibrovascular cores supported the sheets of tumor cells in several of the involved ducts, indicating a papillary component. A papillary architecture has been noted for or is evident in the illustration of most previously reported cases of DCIS that had focal spindling and displayed neuroendocrine differentiation with [4, 5, 14] or without [9] mucin production.

Little information is available on the biologic potential of this subset of DCIS. Our patients have not experienced recurrence during the limited period of follow-up (mean 16.2 months). Maluf et al. [5] noted one local recurrence at 5 years, which was effectively treated by reexcision. Their other patient showed no recurrence in the 10 month period of follow-up. The follow-up of 12 patients by Tsang and Chan [14], including seven with an invasive component, revealed only one local recurrence at 5 years in a patient who had an in situ disease. The remaining four women with in situ endocrine papillary carcinoma were alive and well at 3–10 years post diagnosis (median follow-up of 6 years). Of the seven women with invasive carcinoma, one developed an invasive carcinoma, not otherwise specified (NOS), in the contralateral breast at 1 year, while another developed a colloid carcinoma with endocrine DCIS in the contralateral breast at 2 years post-diagnosis. The remaining four women had no problem related to their mammary carcinoma at 2–7 years post-diagnosis (median follow-up of 3 years).

There are overlaps between solid papillary DCIS, a subset of cases of endocrine DCIS, and spindle cell DCIS. A vast majority of solid papillary carcinomas are characterized by a compact (relatively solid) version of cribriform growth with a rosette-like arrangement of nuclei instead of true secondary lumens overlying the fibrovascular stalks. It is also reasonable to describe these spindled proliferations as solid DCIS. More frequently, however, solid DCIS manifests highly variable phenotypes, with some even composed of a mosaic of polyhedral cells that lack any suggestion of spindling. We note with interest that one of the photomicrographs of solid DCIS in Page and Anderson's textbook of breast pathology (their Fig. 12.4) has spindled areas [7], although the nuclear grade appears to be higher than the lesions we are describing.

When DCIS of any type, particularly the unusual types, involves a compact aggregate of ducts or ductules with or without periductal stromal fibrosis, distinction from an invasive process may be difficult. This is especially so when the myoepithelial cell layer has become attenuated and the basal lamina is not distinctively apparent. In such cases, immunostains for smooth muscle actin and/or laminin often helps resolve the issue [2, 13]. It is important to remember that even when the myoepithelial cell layer is absent, the persistence of basal lamina excludes an invasive process. While immunostain for laminin can beautifully enhance the basal lamina, a PAS stain can often accomplish the same at a lower cost.

It appears that several variants of DCIS may be composed of varying proportions of spindle cells. The distinction of spindle cell DCIS from other subsets of DCIS is probably unimportant, as we have no reason, at this point, to believe that the biological potential of the spindle cell variant of DCIS would be any different from any other DCIS of equivalent nuclear grade. The importance of highlighting the spindle cell variant of DCIS lies in aiding the recognition of the pure forms of this lesion, thus avoiding its misclassification as a benign process. This

label further alerts to the possibility that any associated or subsequent invasive carcinoma may assume a spindle cell configuration. Pure spindle cell invasive adenocarcinomas of the breast are rare. The in situ phase of this rare cancer may or may not be formed of spindle cells; likewise, the invasive carcinoma associated with spindle cell DCIS is not necessarily purely or even partially spindled.

Once recognized as a variant of in situ mammary carcinoma, until further data become available, the grade, extent of the lesion, and status of the margins should guide the management of patients with spindle cell DCIS. It is important to note that not all spindle cell DCIS lesions are mucin producing, as none of the 17 cases in this study had overt mucin production. Apparently, mucin production is a capability that many neoplastic cells may acquire. Whether or not the neuroendocrine differentiation of these tumors may prove of value in selection of specific therapeutic regimens has not been investigated and is worth exploring.

Acknowledgements We acknowledge the cooperation of all those pathologists and clinicians who have contributed specimens and follow-up information for this series. In particular, we thank Dr. G.M D'Onofrio of East Adelaide Medical Centre, Dr. D.Hurst of the Medical Clinic Milicent, and Dr. Erwin Foster-Smith of IMVS.

References

1. Azzopardi JG (1979) Problems in breast pathology. Saunders, Philadelphia
2. Damiani S, Ludvidova M, Tomasic G, Bianchi S, Gown AM, Eusebi V (1999) Myoepithelial cells and basal lamina in poorly differentiated in situ duct carcinoma of the breast. An immunocytochemical study. Virchows Arch 434:227–234
3. Lefort E, Groussard O, Bouguet de la Joliniere J, Degott C, Zafrani B (1999) Carcinome mammaire a cellules fusiformes et differenciation neuro-endocrine. Une Entite rare pouvant simuler une tumeur benigne. Ann Pathol 19:309–311
4. Maluf H, Koerner FC (1995) Solid papillary carcinoma of the breast: a form of intraductal carcinoma with endocrine differentiation frequently associated with mucinous carcinoma. Am J Surg Pathol 19:1237–1244
5. Maluf HM, Zukerberg LR, Dickersin GR, Koerner FC (1991) Spindle-cell argyrophilic mucin-producing carcinoma of the breast. Histological, ultrastructural, and immunohistochemical studies of two cases. Am J Surg Pathol 15:677–686
6. Moinfar F, Man YG, Lininger RA, Bodin C, Tavassoli FA (1999) Use of kerarin 34BE12 as an adjunct in the diagnosis of mammary intraepithelial neoplasia- ductal type- (benign and malignant intraductal proliferations of the breast). Am J Surg Pathol 23:1048–1058
7. Page DL, Anderson TJ (1987) Diagnostic histopathology of the breast. Churchill, Edinburgh
8. Paties C, Zangrandi A Taccagni GL, Kindl S, Vassallo G (1996) Spindle cell non-argyrophil carcinoma of the breast with neuroendocrine differentiation. Histopathology 29:471–473
9. Ruffolo EE, Maluf HM, Koerner FC (1996) Spindle cell endocrine carcinoma of the mammary gland. Virchows Arch 428: 319–324
10. Sapino A, Papotti M, Pietribiasi F, Bussolati G (1998) Diagnostic cytological features of neuroendocrine differentiated carcinoma of the breast. Virchows Arch 433:217–222
11. Tamai M (1992) Intraductal growth of malignant mammary myoepithelioma. Am J Surg Pathol 16:1116–1125 Issn: 0147–5185
12. Tavassoli F (1991) Myoepithelial lesions of the breast, myoepitheliosis, adenomyoepithelioma and myoepithelial carcinoma. Am J Surg Pathol 15:554–568
13. Tavassoli F (1992) Pathology of the breast. Appleton and Lange, Norwalk, Connecticut
14. Tsang W, Chan J (1996) Endocrine ductal carcinoma in situ (E-DCIS) of the breast. A form of low grade DCIS with distinctive clinicopathologic and biologic characteristics. Am J Surg Pathol 20:921–943

Virchows Arch (2001) 439:78–84
DOI 10.1007/s004280100402

ORIGINAL ARTICLE

N. Streichenberger · S. Peyrol · F. Philit · R. Loire
P. Sommer · J.F. Cordier

Constrictive bronchiolitis obliterans

Characterisation of fibrogenesis and lysyl oxidase expression patterns

Received: 26 May 2000 / Accepted: 29 November 2000 / Published online: 15 February 2001
© Springer-Verlag 2001

Abstract The process leading to irreversible fibrotic constriction of the bronchioles was studied in two cases of bronchiolitis obliterans (BO) after bone marrow transplantation. Because lysyl oxidase (LOX) is the main collagen cross-linking enzyme that might account for irreversible fibrosis, its expression was studied together with expression of extracellular matrix (ECM) proteins. Characteristic types of lesions could be distinguished on the basis of histological and immunohistological criteria. An inflammatory stage was characterised by infiltration restricted to the bronchioles by lymphocytes and dendritic cells. A fibro-inflammatory stage was characterised by the coexistence of a persistent immune cellular lesion pattern with further focal modelling of a sub-epithelial neo-synthesised connective matrix. LOX expression was observed at the tips of intra-luminal fibrotic protrusions, together with tenascin and cellular fibronectin. A fibrotic stage was characterised by dense ECM deposits spreading throughout the peri-bronchiolar connective tissue, resulting in bronchiole obliteration and final disappearance. In contrast to reversible cases of fibrosis, persistence of long-term LOX expression reflecting continuing fibrosing activity might account for the irreversible status of BO. Our two cases illustrated that, at inflammatory and fibro-inflammatory stages, BO may be stabilised by immunosuppressive treatment, while the persistence of LOX expression in the fibrotic stage might correspond to a disease that becomes irreversible and fatal.

Keywords Bronchiolitis obliterans · Lung fibrosis · Lysyl oxidase · Extracellular matrix · Allogenic bone marrow transplantation

N. Streichenberger (✉)
Service de Neuropathologie, Hôpital Neurologique,
BP Lyon-Montchat 69 394 Lyon cedex 03, France
e-mail: streiche@laennec.univ-lyon1.fr
Tel.: +33-4-72357630, Fax: +33-4-72357067

S. Peyrol
Centre Commun de Microscopie Electronique,
University Claude Bernard, Lyon, France

P. Sommer
Institut de Biologie et Chimie des Protéines,
CNRS UPR-UMR 5096, Lyon, France

F. Philit · J.F. Cordier
Service de Pneumologie,
Hôpital Cardiovasculaire et Pneumologique, Lyon, France

R. Loire
Service d'Anatomie Pathologique de l'Hôpital Cardiovasculaire
et Pneumologique, Lyon France

Introduction

The evolution of fibrosis depends on the balance between the neosynthesis of extracellular matrix (ECM) components and their degradation. The protective effect of a collagenised matrix might be determined by collagen cross-linking, which dictates fibrillar ECM proteins and basement membrane stability against metalloproteinases [25]. Because lysyl oxidase (LOX) is known to have a unique role in collagen and elastin cross-linking, its activity should be determinant. This extracellular enzyme catalyses the post-translational oxidative deamination of the ε-amino group of some lysines and hydroxylysines of collagen and of lysine in elastin [21]. This has raised the hypothesis that there might be a differential expression of the LOX gene as a function of fibrosis stabilisation [20], together with the expression of a tissue inhibitor of metalloproteinases [7].

The present study was undertaken to localise LOX in an irreversible fibrotic and lethal form of human constrictive bronchiolitis obliterans (BO). BO has been characterised as constrictive BO and BO-organising pneumonia (BOOP) [1]. BOOP, also termed "proliferative" BO, is characterised by endo-luminal fibrosis of distal airspace (bronchioles and alveoli). Pathological studies have analysed this type of fibrosis, which is reversible [17]. In contrast, the rare and severe inflammatory and fibrosing process of "constrictive" BO takes place within the bronchiolar wall, thus resulting in irreversible constriction and stenosis of the bronchiolar lumen [16, 20]. BO, developing after bone marrow graft or

lung transplantation, is in most cases of the constrictive type [6, 20]. Clinically, it is characterised by rapidly progressive dyspnea associated with marked airflow obstruction at lung function tests. The process is generally irreversible, and most patients die from ensuing respiratory failure. The cause of post-transplant constrictive BO is unknown, but several risk factors have been suspected, especially the chronic immune processes of rejection after lung transplantation or graft versus host (GVH) disease after bone marrow transplantation [2, 15, 20]. The present study was undertaken in order to analyse the changes leading to irreversible fibrotic constriction of the bronchioles in patients with constrictive BO after allogenic bone marrow transplantation, since understanding this dynamic process may allow an improved therapeutic management of the corresponding clinical syndrome. It was also undertaken to determine the pattern of expression of LOX as a marker of ECM cross-linking, leading to irreversible fibrosis and also as a marker of active sites of fibrogenesis [4, 5, 8, 23].

Materials and methods

Case report

Patient 1 was a 42-year-old man who developed an irreversible obstructive ventilatory defect 18.5 months after allogenic bone marrow transplantation for acute lymphocytic leukaemia. Patient 2 was a 34-year-old woman who had an irreversible obstructive ventilatory defect 10 months after a second allogenic bone marrow transplantation for acute myelogenous leukaemia. In both patients, GVH disease with severe skin manifestations developed before pulmonary manifestations. Neither had features suggesting initial responsibility of any infection in the development of the syndrome or criteria of ongoing infection, especially viral. A lung biopsy for diagnostic purposes was performed using video-thoracoscopic surgery at the time of diagnosis of the obstructive ventilatory defect. Treatment consisted of increased immunosuppression with corticosteroids and azathioprine. Patient 1 was in good general health, and his lung function tests were stabilised 46 months after lung biopsy. Patient 2 died 20 months after lung biopsy from progressive respiratory failure (autopsy was not allowed).

Histological evaluation

Lung biopsies were partly fixed in Bouin fixative, embedded in paraffin and partly snap-frozen in liquid nitrogen before storing at –80°C. In addition to conventional staining, 3-µm sections were stained with Gordon–Sweets impregnation for fibrosis evaluation. An indirect immuno-peroxidase method using streptavidin–biotin complex (Immu-Mark TM, ICN Biomedicals) was performed on 5-mm cryostat sections or 3-mm paraffin-embedded tissue sections for the detection of immunological markers, LOX and α-smooth muscle actin (α-SMA). An indirect immunofluorescence method using fluorescein isothiocyanate conjugates was performed on 5-mm cryostat sections of frozen tissue for matrix components and integrin staining.

Both biopsies were studied using immunological markers: monoclonal murine antibody against human leucocyte antigen (HLA)-A,-B,-C W632 (Novocastra, UK), HLA DP, CD4 (Leu 3a) and CD57 (Leu-7; Becton Dickinson, N.J.), CD1 (Immunotech, France), CD8 (Ortho-Diagnostic Systems, France), CD45 – panleucocyte – (Dako, Denmark). The ECM markers were analysed with polyclonal rabbit antiserum against human type-I collagen, bovine type-III procollagen, collagen type-V, human plasmatic (p-) fibronectin and murine laminin (Pasteur Institute, Lyon, France). The ECM markers were also analysed with monoclonal murine antibody against the human cellular (c-) fibronectin cell attachment site – clone II 3E3 A002 – and polyclonal rabbit antiserum against human tenascin, A107 (Telios pharmaceuticals, Calif.). Polyclonal rabbit antibody against murine LOX was obtained as described [23]. The integrin markers, monoclonal rat antibody against human integrin α6 (MAB 1972; Chemicon, Euromedex, France) and monoclonal murine antibody against human integrin β4 (clone 3E1 A054; Telios pharmaceuticals) and the cytoskeletal marker, monoclonal antibody against α-SMA (A254; Sigma Immunochemicals, France) were performed on the biopsies.

Results

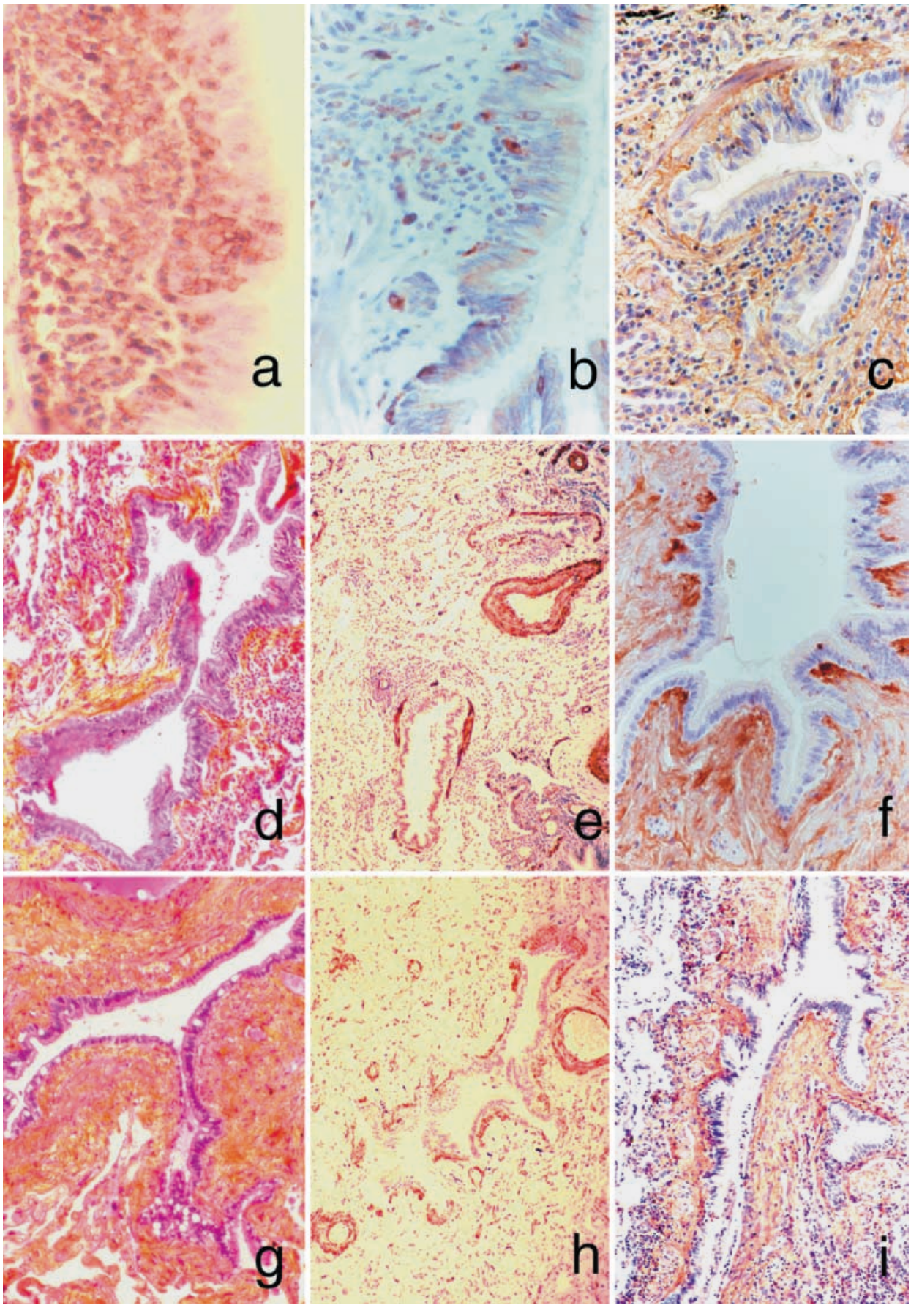
Histopathological characterisation of BO lesions

Constrictive BO are characterised by a progressive thickening of the bronchiolar wall, which initiates focal protrusions into the bronchiolar lumen until its complete obliteration. This occurred for patient 2, while patient 1 was rescued by treatment.

Histological analysis showed that the pathologic processes affected all of the terminal bronchioles without conspicuous involvement of the alveolar duct region. The structure of the adjacent arteriole remained unchanged, with only some contiguous peri-bronchiolar inflammation observed in the adventitial area. Venous and lymphatic vessels were not concerned by inflammation. Based on histological criteria, we were able to distinguish inflammatory and fibro-inflammatory lesions in patients 1 and 2, while only in patient 2, were additional fibrotic scar-like regions observed.

Inflammatory stage of BO lesions

The inflammatory stage was mainly observed in patient 1 (Fig. 1a–c). Inflammatory cell clusters were found in the enlarged sub-epithelial area, leading to deformation of the bronchiolar lumen and distortion of the smooth muscle cell bundles. Most of the inflammatory cells were lymphocytes (CD45+, Fig. 1a); T lymphocytes (CD3+) of the suppressor subtype (CD8+) predominate over the helper subtype (CD4+). There were occasional intraepithelial natural killer cells (CD57+, data not shown). Some dendritic cells (CD1+) were detected in the pseudo-stratified epithelium and in the sub-mucosa (Fig. 1b). Major histocompatibility complex (MHC) class-II antigens were expressed by most of the cells involved in the inflammatory process (including peri-bronchiolar and intraepithelial cells) and by the bronchiolar epithelial cells (data not shown). There was only faint LOX staining associated with this inflammatory response (Fig. 1c), while ECM protein deposition was not yet detectable.


a
b
c
d
e
f
g
h
i

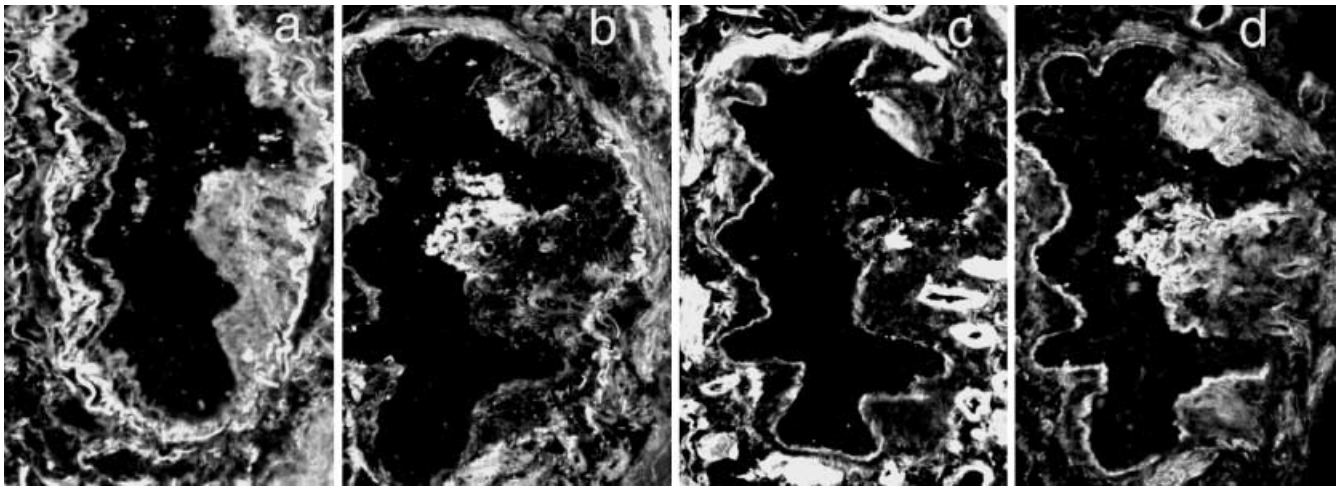


Fig. 2 Patient 1. Matrix pattern of the fibro-inflammatory-type lesions of bronchiolitis obliterans. Immunofluorescence staining of contiguous sections, (original magnification ×250). **a** Procollagen type-III staining of fibrillar matrix in bronchiole constrictions. **b** Tenascin expression in focal bronchiolar constriction. **c** Laminin staining indicating focal disruptions of basal lamina. **d** Plasmatic fibronectin neo-expression at the tip of bronchial constrictions

Fibro-inflammatory stage of BO lesions

Fibro-inflammatory regions were found in both patients (Fig. 1d–f and Fig. 2). Both inflammatory and fibrotic regions often affect the same bronchiole; focal lymphocyte infiltrates enclosed in a thin intercellular matrix network coexist with areas of fibro-cellular thickening of the bronchiolar wall, which initiate focal protrusions into the bronchiolar lumen (Fig. 1d). The bronchiolar epithelium appears well-preserved. The connective matrix shows a loose fascicular organisation and extends to the partially dissociated smooth muscle cell layer, positive for α-SMA (Fig. 1e). Alveolar septa and pleura remain unchanged.

◀ **Fig. 1** Patients 1 and 2. Inflammatory (**a**–**c**), fibro-inflammatory (**d**–**f**) and fibrotic-type (**g**–**i**) lesions in bronchiolitis obliterans. In inflammatory lesions, lymphocytes and dendritic cells are disseminated among the epithelium and the peri-bronchiolar infiltrates, while lysyl oxidase (LOX) is linked to the thin nascent fibrillar matrix associated with the inflammatory cells. **a** Anti-CD45 staining [original magnification (OM) ×400]; **b** anti B-cell antigen (OM ×400) and **c** anti-LOX staining (OM ×250). In fibro-inflammatory lesions, inflammatory cells are observed under the unaltered bronchiolar epithelial cell layer and are found inside the underlying connective tissue, while fibrillar deposits label nascent intra-luminal protrusions. Smooth muscle cells are labelled for α-smooth muscle actin (α-SMA), together with neo-differentiated myofibroblasts, while foci of LOX decorate the tip of the growing constrictive lesions. **d** Haematoxylin and eosin (HE; OM ×200); **e** anti-α-SMA staining (OM ×100) and **f** anti-LOX staining (OM ×100). In fibrotic lesions, dense concentric fibrosis leads to bronchiole collapse. The bronchiolar epithelium is still present. Staining for α-SMA is stronger and more widespread, indicating focal myofibroblast proliferation, while attenuated LOX staining diffusely covers the peri-bronchiolar fibrotic deposits. **g** HE (OM ×200); **h** anti-α-SMA staining (OM ×100) and **i** anti-LOX staining (OM ×100)

LOX is expressed in the nascent connective matrix associated with the inflammatory infiltrate (Fig. 1f). LOX is associated with collagen remodelling, and with the occurrence of type-III (Fig. 2a) and type-I collagen (data not shown). Together with LOX, tenascin forms plugs at the tip of intra-bronchiolar protrusions (Fig. 2b). Tenascin is found with LOX, as a sub-epithelial sheet extended between the sub-epithelial lamina and the proximal elastic layer. The distribution of laminin shows focal interruption and disorganisation (Fig. 2c). At these sites, p-fibronectin is also present at the tip of the lesion foci (Fig. 2d).

Fibrotic stage of BO lesions

Dense fibrotic regions with complete bronchiolar obstruction were only found in patient 2 (Fig. 1g–i and Fig. 3). The whole bronchiolar wall was invaded by dense concentric non-cellular fibrosis (Fig. 1g). The bronchiolar epithelium was preserved in the less severe parts of lesions, but complete bronchiolar obstruction consecutive to concentric fibrosis extension was found in the more severe parts with loss of bronchiole structure and even closure of these bronchioles. This network was prominent near the luminal edge where α-SM actin-positive cells were detected (Fig. 1h) and was thinner and related to microvessels at the bottom where the smooth muscle cell layer was sometimes interrupted.

LOX labelling emphasised the sub-epithelial basement membrane area and the fibrillar matrix at the tip of the constrictive lesion. It extended, with less intensity, to the peri-bronchiolar fibrotic deposits (Fig. 1i). The enzyme was not detected in the central large ECM deposit. Fibrillar collagens appeared co-distributed to form a fibrillar matrix stroma, whose density, at the tip of the lesion, contrasted with the loose network organisation at the site of connection with the residual peri-bronchiolar elastic belt (type-III collagen, Fig. 3a; type-V collagen, Fig. 3b). Laminin labelling indicated the continuity of the sub-epithelial basal lamina at the tip of the lesion (Fig. 3c). The fingerprint aspect of tenascin labelling

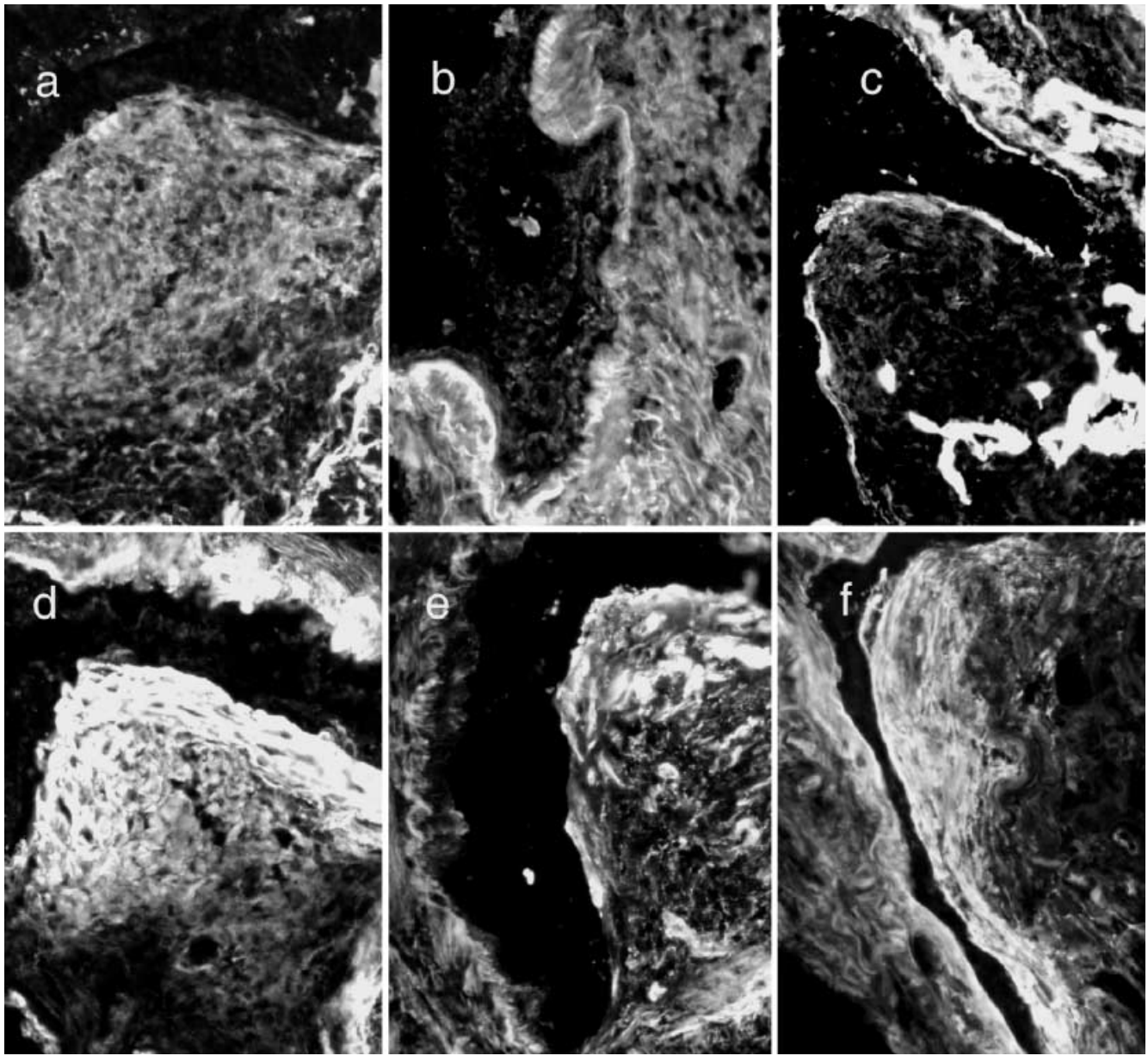


Fig. 3 Patient 2. Matrix pattern in bronchiolitis obliterans (BO) fibrotic lesions (immunofluorescence staining; original magnification ×250). **a** Procollagen type III is a major component of the fibrotic constriction. **b** Type-V collagen is present in the dense peribronchiolar fibrous assembly. **c** Laminin: continuous labelling of the sub-epithelial basal lamina is restored. **d** Tenascin is accumulated as a dense scaffold, stratified in parallel to the subjacent epithelium. **e** Plasmatic fibronectin is linked to the matrix framework of a large fibrotic bronchiolar constriction. **f** Cellular fibronectin remains intensely expressed around a collapsing bronchiole

(Fig. 3d) was coincident with LOX expression, while a massive p-fibronectin positive deposit was also observed beneath the bronchiolar epithelium (Fig. 3e). Likewise, c-fibronectin delineated the connective interface and outlined the matrix network (Fig. 3f).

In conclusion, in patient 1, the lesions corresponded to sub-acute inflammation, prior to extensive ECM remodelling, where LOX was strongly expressed at the tips of intra-bronchiolar protrusions without occlusion. The patient's disease was stabilised with treatment. In patient 2, a chronic stabilised fibrotic lesion was observed, resulting in almost complete bronchiolar obstruction with ongoing LOX expression, suggesting an ongoing active fibrogenetic process. The patient died from progressive respiratory failure despite treatment.

Discussion

In both cases of severe obstructive ventilatory disease associated with allogenic bone marrow transplantation (BMT), the main histological lesion of the airways consisted of constrictive BO. The terminal bronchioles were the specific target of a lesional process with a spectrum of lesions ranging from mural immune cellular infiltration to concentric fibrosis with further complete bronchiole loss.

Such a process is not specifically related to transplantation pathology and was previously described in a wide range of pulmonary disorders [3]. Nevertheless, BO has emerged as a major complication of BMT, which is now generally considered as a manifestation of chronic GVH disease [27], initiated by donor lymphocytes. CD4+ and CD8+ T-lymphocyte subtypes were indeed observed during both inflammatory and fibro-inflammatory stages of BO. These lymphocytes might initiate the GVH process induced by the histo-incompatibility between donor and recipient, as suggested by the transient expression of MHC type-II antigens in the bronchiolar wall, which suggests an immune reaction directed against the recipient bronchiolar epithelium by the donor T lymphocytes and the increased number of dendritic cells.

The luminal tip of the lesion was clearly the main site of expression of the earliest markers of fibro-inflammatory lesions. The α-SM actin revealed the presence of myofibroblasts. This cytoskeleton marker identified the phenotypic modulation of fibroblasts into myofibroblasts, known to occur in a wide range of pathological settings characterised by tissue remodelling and fibrosis [19]. LOX reached its major level of expression at the bronchial tips of the multifocal lesions. The accumulation of tenascin in the sub-epithelial inflammatory infiltrate was combined with the focal neo-expression of c-fibronectin at the tip of the constrictive lesion.

In all of the situations where tenascin over-expression has been reported (lung development [11], desmoplastic stroma reaction [10, 22, 24, 26], granulation tissue [12], wound healing [14]), tenascin has been mainly found at the epithelio–mesenchymal interface, where it takes part in the connective tissue activity supporting epithelial growth, migration, spreading or invasiveness and differentiation. Taken together, myofibroblast differentiation, LOX and tenascin expression indicate the active site of fibrogenesis [23], where they might be responsible for the remodelling of a neo-formed extracellular fibrillar matrix, revealed by the regular packing of matrix fibrillar polymers of type-I, -III, and -V collagen.

In more fibrotic BO constrictive lesions, the co-distribution pattern of LOX, tenascin and c-fibronectin partially diverges from the previously described pathological models. LOX was always expressed in BO, in contrast to reversible fibrosis [23] where it quickly disappears. In these models, LOX was synthesised by myofibroblasts very early during ECM remodelling and preceded myofibroblast differentiation [5]. In late granulomas, LOX disappeared. In contrast, for BO, LOX expression continues to label the ongoing cross-linking maturation of the collagen deposits into an irreversible peri-bronchiolar fibrotic scar. Persistence of tenascin, throughout the entire thickness of peri-bronchiolar fibrosis, differs both from healed wounds [14] and sclerotic portions of achieved fibrosis [9, 12], where tenascin is quite absent and from desmoplastic stroma, where tenascin is brightly stained [18]. However, the enhanced and extensive expression of c-fibronectin underlining collapsed bronchiolar segments is consistent with a sustained fibrogenic and organising activity of fibro-competent cells over the continuous tenascin scaffold.

This study highlights the complexity of events occurring at the level of ECM remodelling in cases of irreversible fibrosis. Animal models treated with β-aminoproprionitrile (β-APN), a LOX-specific inhibitor, presented almost total reversion of lung fibrosis [13, 21]. Upon patient biopsy, we found one main difference between fibro-inflammatory and fibrotic stage of BO. For fibrotic stage, a constant level of LOX was expressed at the edge of the scar-like ECM deposit. Such a pattern of distribution of LOX and other matrix proteins in the fibrotic lesions of constrictive BO may represent the long-term matrix frame leading to end-stage bronchiolar and peri-bronchiolar fibrosis with complete disappearance of distal bronchioles. Our two cases, which underwent biopsy at different stages of their development, illustrate that BO may be stabilised by immunosuppressive treatment in the inflammatory and fibro-inflammatory stages (patient 1). In contrast, more fibrotic stages with uninterrupted LOX expression in BO lung biopsies may lead to irreversible and fatal disease (patient 2). Though further studies are needed to confirm our findings, we propose LOX expression as a valuable marker for the evaluation of responsiveness to immunosuppressive treatment.

Acknowledgements The authors are very grateful to Liliane Loncke for reliable daily assistance in patient sample collection, to Mireille Raccurt and Marie Tedone for carrying out immunohistochemical staining, to Sylviane Guerret and Daniel Hartmann for the matrix protein antibodies, to G. Joly for photographic technical expertise, and to Susan Gamon for revising the English text. This work was supported by the Centre National de la Recherche Scientifique, the Hospices Civils de Lyon and by the Association pour la Recherche sur le Cancer.

References

1. Abernathy EC, Hruban RH, Baumgartner WA, Reitz BA, Hutchins GM (1991) The two forms of bronchiolitis obliterans in heart-lung transplant recipients. Hum Pathol 22:1102–1110
2. Chan CK (1994) Bone marrow transplantation bronchiolitis obliterans. In: Epler GR (ed) Diseases of the bronchioles. Raven, New York, pp 247–257
3. Colby TV, Myers JL (1992) Clinical and histologic spectrum of bronchiolitis obliterans, including bronchiolitis obliterans organizing pneumonia. Semin Respir Med 13:119–133
4. Decitre M, Gleyzal C, Raccurt M, Aubert-Foucher E, Csiszar K, Sommer P (1998) Lysyl oxidase-like protein localizes to sites of de novo fibronogenesis in fibrosis and in the early stromal reaction of ductam breast carcinomas. Lab Invest 78:143–151
5. Desmoulière A, Darby I, Monte Alto Costa A, Raccurt M, Tuchweber B, Sommer P, Gabbiani G (1997) Extracellular matrix deposition, lysyl oxidase expression, and myofibroblastic differentiation during the initial stages of cholestatic fibrosis in the rat. Lab Invest 76:765–778
6. Epler GR (1988) Bronchiolitis obliterans and airways obstruction associated with graft-versus-host disease. Clin Chest Med 9:551–556
7. Fukuda Y, Ishizaki M, Kudoh S, Kitaichi M, Yamanaka N (1998) Localization of matrix metalloproteinases-1, -2, and -9 and tissue inhibitor of metalloproteinase-2 in interstitial lung diseases. Lab Invest 78:687–698

8. Gindre D, Peyrol S, Raccurt M, Sommer P, Loire R, Grimaud JA, Cordier JF (1995) Fibrosing vasculitis in Wegener's granulomatosis: ultrastructural and immunohistochemical analysis of the vascular lesions. Virch Arch 427:385–394
9. Gould VE, Martinez-Lacabe V, Virtanen I, Sahlin KM, Schwartz MM (1992) Differential distribution of tenascin and cellular fibronectins in acute and chronic renal allograft rejection. Lab Invest 67:71–79
10. Howeedy AA, Virtanen I, Laitinen L, Gould NS, Koukoulis GK, Gould VE (1990) Differential distribution of tenascin in the normal, hyperplastic and neoplastic breast. Lab Invest 63: 798–806
11. Koch M, Wehrle-Haller B, Baumgartner S, Spring J, Brubacher D, Chiquet M (1991) Epithelial synthesis of tenascin at tips of growing bronchi and graded accumulation in basement membrane and mesenchyme. Exp Cell Res 194:297–300
12. Koukoulis GK, Gould VE, Bhattacharyya A, Gould JE, Howeedy AA, Virtanen I (1991) Tenascin in normal, reactive, hyperplastic and neoplastic tissues: biologic and pathologic implications. Human Pathol 22:636–643
13. Ledwozyw A (1995) The effect of beta-aminopropionitrile on bleomycin-induced lung injury in rats. Acta Physiol Hung 83: 91–99
14. Mackie EJ, Halfter W, Liverani D (1988) Induction of tenascin in healing wounds. J Cell Biol 107:2757–2767
15. Maurer JR (1994) Lung transplantation bronchiolitis obliterans. In: Epler GR (ed) Diseases of the bronchioles. Raven, New York, pp 275–289
16. Myers JL, Colby TV (1992) Bronchiolitis obliterans organizing pneumonia and constrictive bronchiolitis: comparative analysis of two distinct entities. In: Fenoglio-Preiser CM, Wolff M, Rilke F (eds) Progress in surgical pathology. Springer, Berlin Heidelberg New York, pp 167–179
17. Peyrol S, Cordier JF, Grimaud JA (1990) Intra-alveolar fibrosis of idiopathic bronchiolitis obliterans organizing pneumonia: cell-matrix patterns. Am J Pathol 137:155–170
18. Ramadori G, Schwögler S, Weit T, Rieder H, Chiquet-Ehrismann R, Mackie EJ, Meyer zum Büschenfelde KH (1991) Tenascin gene expression in rat liver and in rat liver cells. In vivo and in vitro studies. Virchows Arch 60:145–153
19. Sappino AP, Schurch W, Gabbiani G (1990) Differentiation repertoire of fibroblastic cells: expression of cytoskeletal proteins as marker of phenotypic modulations. Lab Invest 63: 144–161
20. Schlesinger C, Meyer CA, Veeraraghavan S, Koss MN (1998) Constricitive (obliterative) bronchiolitis: diagnosis, etiology, and a critical review of the literature. Ann Diagn Pathol 2: 321–334
21. Smith-Mungo LI, Kagan HM (1998) Lysyl oxidase: properties, regulation and multiple function in biology. Matrix Biol 16:387–398
22. Soini Y, Pääkkö P, Virtanen I, Lehto VP (1992) Tenascin in salivary gland tumors. Virchows Arch 421:217–222
23. Sommer P, Gleyzal C, Raccurt M et al. (1993) Transient expression of lysyl oxidase by liver myofibroblasts in murine schistosomiasis. Lab Invest 69:460–470
24. Stamp GWH (1989) Tenascin distribution in basal cell carcinomas. J Pathol 159:225–229
25. Vater CA, Harris ED, Siegel R (1979) Native cross-links in collagen fibrils induce resistance to human synovial collagenase. Biochem J 181:639–645
26. Vollmer G, Deerberg F, Siegal GP, Knuppen R (1991) Altered tenascin expression during spontaneous endometrial carcinogenesis in the BD II/Han rat. Virchows Arch 60:83–89
27. Yousem SA, Ray L, Paradis IL, Dauber J, Griffith BP (1990) Potential role of dendritic cells in bronchiolitis obliterans in heart-lung transplantation. Ann Thorac Surg 49:424–428

Virchows Arch (2001) 439:85–89
DOI 10.1007/s004280100405

ORIGINAL ARTICLE

Bastian Gunawan · Masoud Mirzaie
Hans-Jürgen Schulten · Bärbel Heidrich · László Füzesi

Molecular cytogenetic analysis of two primary squamous cell carcinomas of the lung using multicolor fluorescence in situ hybridization

Received: 22 August 2000 / Accepted: 7 December 2000 / Published online: 21 March 2001
© Springer-Verlag 2001

Abstract To fully characterize the numerous chromosomal aberrations in two human squamous cell carcinomas (SCCs) of the lung, molecular cytogenetic characterization was carried out utilizing conventional banding analysis and multicolor fluorescence in situ hybridization (mFISH), providing simultaneous color discrimination of all 24 human chromosomes. Both tumors displayed complex aneuploid karyotypes with a host of numerical and structural chromosome abnormalities. Structural aberrations common to both SCCs included rearrangements of chromosomes 1, 3p, 7q, and 8q, contributing to net loss of chromosomal sequences on 1p, 3p, and 8p, and a net gain of 8q. The recently introduced mFISH technique enabled the disclosure of cryptic translocations and the chromosomal composition of previously unrecognized marker chromosomes. Furthermore, mFISH greatly enhanced the ability to delineate chromosomal breakpoints when integrating banding information from conventional banding analysis. Eventually, the application of mFISH as a powerful approach to refine complex tumor karyotypes is expected to result in a more detailed and complete picture of cytogenetic events associated with the development and progression of solid tumors.

Keywords Lung cancer · Cytogenetic analysis · Karyotyping · Chromosome painting · M-FISH

B. Gunawan (✉) · H-J. Schulten · L. Füzesi
Institute of Pathology, University of Goettingen,
Robert-Koch-Str. 40, 37075 Göttingen, Germany
e-mail: bastian.gunawan@med.uni-goettingen.de
Tel.: +49-551-396858, Fax: +49-551-398627

M. Mirzaie
Department of Thoracic and Cardiovascular Surgery,
University of Goettingen, Germany

B. Heidrich
Department of Surgery, University of Goettingen, Germany

Introduction

For detailed karyotypic assessment of structural chromosome aberrations, fluorescence in situ hybridization (FISH) using whole chromosome painting (WCP) probes has become the method of choice [11]. Until recently, however, this technique was confined to a limited number of chromosomes, which could be tested simultaneously. With recent improvements in detection technology, two 24-color karyotyping techniques have been developed, now allowing genome-wide screening of any structural aberration involving non-homologous chromosomes in a single FISH experiment: interferometer-based spectral karyotyping (SKY) [4, 13] and the filter-based multiplex or multicolor fluorescence in situ hybridization (mFISH) [15]. More specifically, mFISH refers to hybridization of an optimized formulation of 52 directly labeled WCP probes mixed in combinations using a set of five different fluorophores, resulting in distinct color discrimination of all 24 human chromosomes. SKY has proven to be a powerful technique, complementing existing cytogenetic methods, particularly in characterizing complex karyotypes. The SKY technology has been applied successfully to the analysis of constitutional chromosomal abnormalities [14], cytogenetic alterations in hematological malignancies [12, 17], and tumor cell lines [10]. More recently, mFISH has been used to analyze radiation-induced chromosomal aberrations in lymphocytes and hematopoietic progenitor cells [5]. Herein, we evaluated the filter-based mFISH technique with regard to practical advantages and technical limitations in characterizing complex tumor karyotypes, exemplified by two primary squamous cell carcinomas (SCCs) of the lung with multiple chromosomal aberrations.

Materials and methods

Tissue samples were obtained from pneumectomy specimens of two male patients who had undergone surgery for primary lung tumors. Histopathological diagnoses were moderately to poorly dif-

ferentiated, partially keratinizing SCC (pT2, pN2, G2–3; case 1), and moderately differentiated non-keratinizing SCC (pT2, pN1, G2; case 2), respectively. For cytogenetic analyses, fresh tumor tissue samples were disaggregated mechanically and enzymatically and grown in culture flasks before harvest using standard cytogenetic techniques. Successful chromosome preparations were obtained within the first three culture passages. Chromosome banding was performed with 4′-6′-diamidino-2-phenylindole (DAPI) and actinomycin (Sigma, Deisenhofen, Germany).

In order to analyze the numerous chromosomal abnormalities more completely, mFISH was applied to metaphase spreads freshly prepared from short-term cultures of both tumors using the Vysis Spectra Vysion Assay (Vysis, Bergisch-Gladbach, Germany). Hybridization was performed according to the manufacturer's protocol. Visualization of painted chromosomes was achieved using filter-based fluorescence microscopy using a set of fluorophores and corresponding SpectraVysion optical filters, including DAPI (DAPI bandpass), SpectrumRed (Red single bandpass), SpectrumGold (Gold single bandpass), SpectrumGreen (Green single bandpass), SpectrumAqua (Aqua single bandpass) and SpectrumFRed (FRed single bandpass). Image acquisition and analysis of metaphase spreads were performed on a Vysis Quips Genetics Workstation, consisting of an epifluorescence microscope (Axioskop, Zeiss, Göttingen, Germany) and a CCD camera (Photometrics, Tuscon, Ariz.) using the Quips Karyotyping and the Quips Spectra Vysion software (Vysis, now distributed through Applied Imaging). For each tumor, more than ten metaphases were fully karyotyped according to the International System for Human Cytogenetic Nomenclature [8].

Results

The tumor karyotype descriptions of both SCCs, determined using combined cytogenetic analysis and mFISH, are given in Table 1. In case 1, the complementary use of DAPI banding and mFISH identified 30 structural rearrangements, including 26 unbalanced translocations, one dicentric chromosome, two isochromosomes, and one isoderivative chromosome (Fig. 1). Several structural aberrations were present in two copies, including der(1)t(1;16), der(3)t(3;9)t(3;3), der(7)t(7;7), der(9)t(2;9), dic(15;22), der(17)t(1;17), der(19)t(15;19)t(7;19), der(19)t(3,19), and der(22)t(8;22), contributing to a net gain of chromosome material on 2q, 3q, 7p, 8q, 15q, and 16p and a loss of sequences on 3p, 15p, 17p, 19p, 19q, and 22p. One small metacentric marker chromosome could not be clarified.

In case 2, combined DAPI banding and mFISH identified 20 chromosomal rearrangements, including ten unbalanced translocations, seven deletions, one duplication, one inversion, and one isodicentric chromosome (Fig. 2). Aberrations present in two or more copies were der(1)t(1;13), del(3), der(4)t(4;8), der(5)t(5;14), del(7), der(11)t(10;11), der(12)del(12)del(12)del(12), der(12)t(12;12), inv(12), der(13)dup(13)del(13), der(14)t(5;14), and der(21)t(6;21), contributing to a net gain of sequences on 8q and 13q and a loss of chromosomal regions on 1p, 3p, 4q, 7q, 11p, 12p, 14p, and 21p.

Table 1 Karyotypes of two squamous cell carcinomas (SCCs) of the lung

Case 1	60–66, X, -X, -Y, der(1)t(1;16)(q11;p12)x2, der(2)t(2;5)(p21;?)t(5;13)(?;q11), der(3)t(3;6)(p12;p21), der(3)t(3;9)(p11;p11)t(3;3)(q26;?), +der(3)t(3;9)(p11;p11)del(9)(p1?3)t(3;3)(q26;?), -4, -5, dup(5)(q31q35), der(5)t(5;6)(q33;q12), -6, ider(6)t(3;6)(p21;p21), +7, der(7)t(7;7)(q11;p13)x2, -8, der(9)t(2;9)(p21;p2?1)x2, der(9)t(9;9)(p22;q12), der(11)t(5;11)(q31;p15), der(12)t(12;21)(p11;q21), i(12)(p10), i(12)(q10), der(13)t(5;13)(p11;p11), -15, dic(15;22)(p11;p11)x2, der(16)t(12;16)(?;p13), der(17)t(1;17)(q12;p11)x2, +der(17)t(6;17)(q15;q11), der(18)t(14;18)(?;p21)t(14;18)(?;q11), der(19)t(15;19)(q11–13;?p13)t(7;19)(q11;?q13)x2, der(19)t(3;19)(?;?p13), +der(19)t(3;19)(?;?p13)add(19)(?q13), +der(20)t(6;20)(q13;p12), -21, -21, der(21)t(1;21)(q12;p11), -22, der(22)t(8;22)(q11;p11)x2, +mar1[cp12]
Case 2	92–109<5n>, XX, -X, -Y, -Y, der(1)t(1;13)(p13;q12)x2, del(2)(q22), +3, del(3)(p12p21)x3, +4, der(4)t(4;8)(q12;q11)x3, -5, der(5)t(5;14)(p14;q21)x2, der(6)t(3;6)(q26;q12), +7, del(7)(q11)x2, -8, -10, -10, +11, der(11)t(10;11)(q22;p11)x3, der(12)del(12)(p11)del(12)(q11q13)del(12)(q24)x2, der(12)t(12;12)(p12;q?24)x3, +der(12)t(12;12)(p12;q?24)t(8;12)(q22;q12), +inv(12)(q13q24)x4, der(13)dup(13)(q14q14)del(13)(q22)x2, -14, -14, der(14)t(5;14)(p11;p11)x3, -16, der(17)t(17;21)(p12;q11), -18, -18, -18, -19, +20, -21, -21, -21, der(21)t(6;21)(?;p11)x2, -22, -22, idic(22)(p1?1)[cp16]

Discussion

The present study was initiated to evaluate the practical advantages and technical limitations of the filter-based mFISH technique for the detection and identification of the numerous chromosomal rearrangements in two human SCCs of the lung. mFISH uncovered 31 structural aberrations in case 1 and 20 chromosomal rearrangements in case 2. Although none of the two SCCs had the same structural abnormality, several aberrations involving chromosomes 1, 3p, 7q, and 8q, contributing to a net loss of sequences on 1p, 3p, 7q, and 8p and a gain of chomosome regions on 8q, were present in multiple copies in both tumors, suggesting that these aberrations are likely to have occurred prior to polyploidization and probably represent earlier cytogenetic events. Previous cytogenetic studies on non-small-cell lung carcinomas have likewise demonstrated massive karyotypic changes with a host of structural and numerical aberrations, including rearrangements affecting chromosomes 1, 3, 6, 7, 8, 9, and 11, losses of 3p, 6q, 8p, 11p, 13, 14p, and 15p, and gains of 1q and 7 [1, 2, 3, 6, 7, 9, 16, 18]. However, the lack of quality and quantity of metaphase spreads and karyotypic complexity have often made it difficult to obtain complete cytogenetic data and to discern primary and secondary abnormalities.

The application of the filter-based mFISH technique enabled us to uncover and identify structural aberrations with more confidence. Simultaneous, inverted-DAPI counterstain helped to check the suggested mFISH results by allowing the identification of centromeres or satellites. The value of mFISH analysis is further enhanced by integrating banding information derived from additional conventional cytogenetic banding analysis. In order to assess and thoroughly delineate chromosomal breakpoints, simultaneous, inverted-DAPI chromosomes were aligned

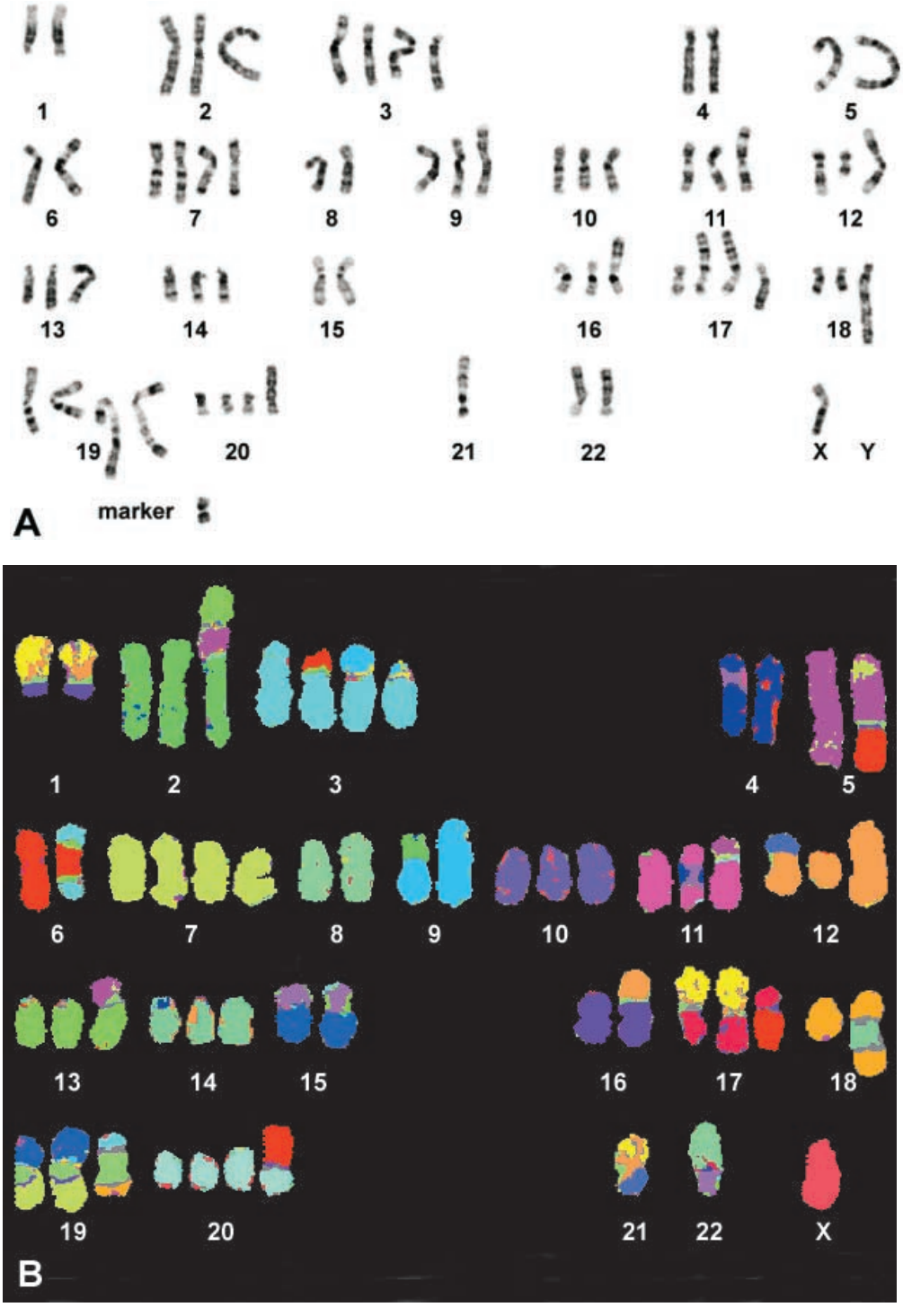


Fig. 1 Karyotypic analysis of case 1. Chromosomes are classified according to suggested multicolor fluorescence in situ hybridization (mFISH) results and inverse 4′-6′-diamidino-2-phenylindole (DAPI) banding pattern. **A** Representative hypotriploid karyogram of a previously DAPI-banded metaphase spread; the inverted DAPI-banded image has a banding pattern nearly identical to G-banding, except that DAPI stains the heterochromatic regions more intensely. **B** The pseudo-colored mFISH image of another metaphase spread from the same tumor; pseudocolors are assigned by the computer according to the chromosome-specific combinations of the individual hybridization signals

next to their respective mFISH image and compared with their counterparts derived from previous DAPI banding. With this approach chromosomal breakpoints could be determined with greater confidence. Nevertheless, mFISH does not detect all chromosome aberrations. Due to limited resolution, small marker chromosomes (as in case 1 of the present study) might not be identified unambiguously, and structural rearrangements below the detection limit of mFISH might be missed completely. Furthermore, in metaphases with condensed chromosomes, domain overlap, caused by blending of colors by fluorescence flaring at chromosomal junctions, may result in assignment of false pseudocolors at the sites of translocation breakpoints. In these instances, cytogenetic expertise and operator intervention is required to exclude a three-break rearrangement.

The present study has shown that mFISH is suitable for rapidly detecting structural aberrations involving

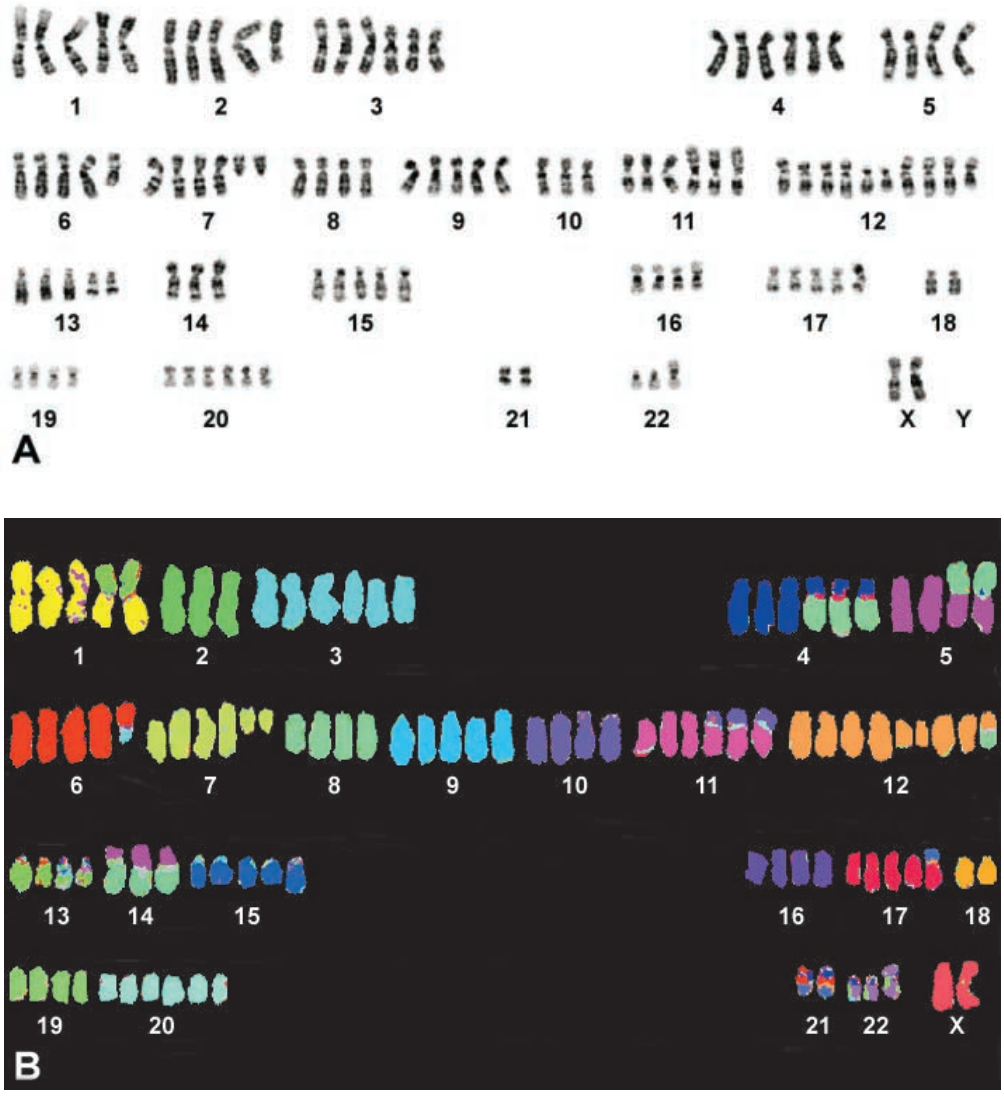


Fig. 2 Karyotypic analysis of case 2. Chromosomes are classified according to suggested multicolor fluorescence in situ hybridization (mFISH) results and inverted 4′-6′-diamidino-2-phenylindole (DAPI) banding pattern. **A** Representative hypopentaploid karyogram of a previously DAPI-banded metaphase spread. **B** The pseudocolored mFISH image of another metaphase spread from the same tumor

non-homologous chromosomes. This technique not only revealed previously unrecognized chromosomal rearrangements but also significantly enhanced the ability to map chromosomal breakpoints when integrating banding information derived from conventional banding analysis to maximize the cytogenetic information obtainable. The approach of combining classical cytogenetics with mFISH is expected to allow the identification of hidden translocations and complex rearrangements and to result in a more detailed and complete picture of cytogenetic events in tumorigenesis and tumor progression. Eventually, mFISH, as a rapid and powerful tool in tumor cytogenetics, will help researchers to discern primary and secondary abnormalities and facilitate the identification of genes involved in tumor development and progression.

Acknowledgements The authors thank Judit Wolf-Salgo for technical support and are especially grateful to Karin M. Greulich for valuable advice and technical assistance with mFISH analysis.

References

1. Berker-Karaüzüm S, Lüleci G, Özbilim G, Erdogan A, Kuzucu A, Demircan A (1998) Cytogenetic findings in thirty lung carcinoma patients. Cancer Genet Cytogenet 100:114–123
2. Feder M, Siegfried JM, Balshem A, Litwin S, Keller SM, Liu Z, Testa JR (1998) Clinical relevance of chromosome abnormalities in non-small cell lung cancer. Cancer Genet Cytogenet 102:25–31
3. Fu SB, Li P (1997) Cytogenetic study of twenty-three primary squamous cell carcinomas of the lung. Cancer Genet Cytogenet 99:54–58
4. Garini Y, Macville M, du Manoir S, Buckwald RA, Lavi M, Katzir N, Wine D, Bar-Am I, Schröck E, Cabib D, Ried T (1996) Spectral karyotyping. Bioimaging 4:65–72
5. Greulich KM, Kreja L, Heinze B, Rhein AP, Weier HUG, Brückner M, Fuchs P, Molls M (2001) Rapid detection of radiation-induced chromosomal aberrations in lymphocytes and hematopoietic progenitor cells by mFISH. Mutation Res 452: 73–81
6. Johansson M, Jin Y, Mandahl N, Hambraeus G, Johansson L, Mitelman F, Heim S (1995) Cytogenetic analysis of short-term cultured squamous cell carcinomas of the lung. Cancer Genet Cytogenet 81:46–55

7. Lukeis R, Irving L, Garson M, Hasthorpe S (1990) Cytogenetics of non-small cell lung cancer: analysis of consistent nonrandom abnormalities. Genes Chromosomes Cancer 2:116–124
8. Mitelman F (ed) (1995) ISCN. An international system for human cytogenetic nomenclature. Karger, Basel, 1995
9. Miura I, Siegfried JM, Resau J, Keller SM, Zhou JY, Testa JR (1990) Chromosome alterations in 21 non-small cell lung carcinomas. Genes Chromosomes Cancer 2:328–338
10. Padilla-Nash HM, Nash WG, Padilla GM, Roberson KM, Robertson CN, Macville M, Schröck E, Ried T (1999) Molecular cytogenetic analysis of the bladder carcinoma cell line BK-10 by spectral karyotyping. Genes Chromosomes Cancer 25:53–59
11. Pinkel D, Straume T, Gray JW (1986) Cytogenetic analysis using quantitative, high-sensitivity, fluorescence hybridization. Proc Natl Acad Sci U S A 83:2934–2938
12. Sawyer JR, Lukacs JL, Munshi N, Desikan KR, Singhal S, Mehta J, Siegel D, Shaughnessy J, Barlogie B (1998) Identification of new nonrandom translocations in multiple myeloma with multicolor spectral karyotyping. Blood 92:4269–4278
13. Schröck E, du Manoir S, Veldman T, Schoell B, Wienberg J, Ferguson-Smith MA, Ning Y, Ledbetter DH, Bar-Am I, Soenksen D, Garini Y, Ried T (1996) Multicolour spectral karyotyping of human chromosomes. Science 273:494–497
14. Schröck E, Veldman T, Padilla-Nash H, Ning Y, Spurbeck J, Jalal S, Shaffer LG, Papenhausen P, Kozma C, Phelan MC, Kjeldsen E, Schonberg SA, O´Brien P, Biesecker L, du Manoir S, Ried T (1997) Spectral karyotyping refines cytogenetic diagnosis of constitutional chromosomal abnormalities. Hum Genet 101:255–262
15. Speicher MR, Ballard SG, Ward DC (1996) Karyotyping human chromosomes by combinatorial multi-fluor FISH. Nature Genet 12:368–375
16. Testa JR, Siegfried JM, Liu Z, Hunt JD, Feder MM, Litwin S, Zhou JY, Taguchi T, Keller SM (1994) Cytogenetic analysis of 63 non-small cell lung carcinomas: recurrent chromosome alterations amid frequent and widespread genomic upheaval. Genes Chromosomes Cancer 11:178–194
17. Veldman T, Vignon C, Schröck E, Rowley JD, Ried T (1997) Hidden chromosome abnormalities in haematological malignancies detected by multicolour spectral karyotyping. Nat Genet 15:406–410
18. Viegas-Pequignot E, Flury-Herard A, De Cremoux H, Chlecq C, Bignon J, Dutrillaux B (1990) Recurrent chromosome aberrations in human lung squamous cell carcinomas. Cancer Genet Cytogenet 49:37–49

Virchows Arch (2001) 439:90–96
DOI 10.1007/s004280000360

ORIGINAL ARTICLE

I. Schott · D. Hartmann · V. Gieselmann
R. Lüllmann-Rauch

Sulfatide storage in visceral organs of arylsulfatase A-deficient mice

Received: 6 July 2000 / Accepted: 13 October 2000 / Published online: 6 February 2001
© Springer-Verlag 2001

Abstract The inherited deficiency of arylsulfatase A (ASA) in humans causes lysosomal accumulation of sulfatides in visceral organs and in the nervous system and leads to wide-spread demyelination (metachromatic leukodystrophy, MLD). ASA-deficient mice have previously been generated by means of targeted gene disruption. In the present study, visceral organs of ASA-deficient mice were investigated. A simple technique for the histochemical detection of accumulated sulfatides was elaborated using pre-embedding staining with alcian blue. The gall bladder, intrahepatic bile ducts, exocrine pancreatic ducts, respiratory epithelium and, with low degree, testicular Sertoli cells, showed sulfolipid storage. The storage pattern in the kidney will be described in a separate publication. Hepatocytes, pancreatic islets, adrenal glands, and gastric epithelium were unaffected. Ultrastructurally, the intralysosomal storage material displayed parallel and concentric lamellar patterns. Apart from some differences, the topographic distribution of the sulfatide storage resembled that in human MLD. In addition to being an animal model of the human disease, the ASA-deficient mouse may be useful for investigating the cell biology of sulfolipids in visceral organs.

Keywords Arysulfatase A deficiency · Metachromatic leukodystrophy · Lysosomal storage disease · Sulfatide · Gall bladder

Introduction

Metachromatic leukodystrophy (MLD) is an inherited lysosomal storage disease resulting from the deficiency for arylsulfatase A (ASA; E.C.3.1.6.8) [13]. The physiological substrates of this lysosomal enzyme are sulfolipids, mainly sulfogalactosyl ceramides (sulfatides), which become accumulated in cells of MLD patients. Clinically, the disease is heterogeneous with respect to the age of onset and the rate of progression. The late infantile type of MLD starts around the age of 2 years, the juvenile type starts between 3 years and 16 years, and the adult type starts at ages older than 16 years. The clinical course is influenced by the patient's genotype at the ASA locus: homozygosity for null alleles always causes the late infantile, rapidly progressing MLD. Heterozygosity for a null allele and an allele that still allows expression of low amounts of residual enzyme activity mitigates the course to the juvenile form of MLD. Homozygosity for two alleles with residual activity usually leads to the mild adult form of MLD. The ultimate fate of MLD patients is determined mainly by the sulfatide storage in neural tissues, the progressive demyelination, and the resulting neurological dysfunctions. Yet, the lysosomal sulfatide storage is not confined to the nervous system but occurs also in visceral organs. As an animal model for the human MLD, ASA-deficient mice have previously been generated by targeted disruption of the murine ASA gene [10]. ASA mRNA and the catabolism of sulfatide were shown to be totally deficient, thus the mice biochemically resemble the late infantile type of MLD.

The purpose of the present study was twofold:

1. A histochemical technique for detecting the accumulated sulfatides was elaborated, which is easy and more convenient for systematic investigations than the hitherto described methods. The usual procedure is staining with cationic dyes such as cresyl violet [11], toluidine blue [20], or pseudoisocyanine [1] at acid pH. These techniques make use of the metachromasia exhibited by these dyes when they are bound to densely arranged anionic sites as present in the sulfatide aggregates. Because of the lipid nature of the storage material, the usual techniques work with frozen sections. In the present study, pre-embedding

I. Schott · D. Hartmann · R. Lüllmann-Rauch (✉)
Department of Anatomy, University of Kiel, Olshausenstraße 40, 24098 Kiel, Germany
e-mail: r.lullmann@anat.uni-kiel.de
Tel.: +49-431-8802427, Fax:. +49-431-8801557

V. Gieselmann
Department of Physiological Chemistry, University of Bonn, Germany

block staining with the tetracationic dye alcian blue, post-fixation with osmium tetroxide, and embedding in paraffin or araldite was performed.

2. The sulfatide storage in selected visceral organs of ASA(–/–) mice was investigated using histochemistry and electron microscopy. Several organs, which are known to be affected in MLD patients, were examined, such as gall bladder, liver, pancreas and adrenal glands. Additionally, some organs, which are known to contain significant amounts of sulfolipids, were included. Tissue samples from two autopsy cases of human MLD served as reference. The alterations in the kidney, which is among the most severely affected visceral organs both in MLD-patients and in ASA (–/–) mice, will be described in detail in a separate report.

Materials and methods

ASA(–/–) mice were generated as described [10]. A total of 30 ASA-deficient mice between 1 month and 24 months of age were used to examine the liver. The other organs under investigation were taken mainly from aged mice (11–24 months). Age-matched ASA(+/+) and (+/–) mice served as controls. ASA(+/+) and ASA(+/–) mice gave identical results and are therefore summarized as "controls" throughout this paper. The animals were kept under conditions in accordance with the current German law on the protection of animals. The mice were deeply anaesthetized with an intraperitoneal injection of tribromoethanol and killed by means of transcardial perfusion fixation. For paraffin preparations, tissues were fixed with Bouin solution diluted 1:3 with phosphate-buffered saline (PBS) or occasionally with 4% paraformaldehyde in PBS. For araldite preparations and electron microscopic examination, fixation was performed with 6% glutaraldehyde in 0.1 M phosphate buffer. The tissues were stored for periods of days to months in 1% paraformaldehyde (in PBS) and 3% glutaraldehyde, respectively, until further processing.

Histochemical staining with alcian blue was performed under conditions which warrant selective demonstration of polysulfated material. Paraffin sections were obtained from tissue blocks which had been incubated with alcian blue (Alcec Blue, Aldrich, Deisenhofen, Germany) prior to embedding (0.05% dye in 0.025 M Na-acetate buffer, pH 5.7, containing 0.3 M $MgCl_2$ and 1% paraformaldehyde). Small blocks of Bouin-fixed tissues were equilibrated with the dye-free vehicle for 48 h, incubated with the complete dye solution under continuous shaking for 2–3 weeks, and rinsed in the vehicle for 48 h. After post-fixation with 2% OsO_4 for 3 h, the tissue blocks were dehydrated and embedded in paraffin. Sections (7 µm) were mounted with DePeX (Serva, Heidelberg) and viewed usually without counterstaining or after staining with nuclear fast red. Additionally, frozen sections were stained with alcian blue at pH 1 (1% dye in 0.1 M HCl) [16], rinsed in 0.1 M HCl, postfixed with a drop of 2% OsO_4 for 30 s, and mounted with DePeX.

The histochemical methods employing alcian blue at low pH or in the presence of high Mg^{++} concentrations have originally been devised for the detection of sulfated glycosaminoglycans [16, 22]. In the present context, the lipid nature of the alcian blue stainable material was verified by testing its extractability. Frozen sections of fresh tissues were incubated in chloroform/methanol (2:1) for 2 h at room temperature prior to staining. Sulfated glycosaminoglycans are known to be precipitated by organic solvents rather than being extracted. Since alcian blue does not permit the observation of metachromasia under the applied conditions [21], cuprolinic blue [23] (BDH Chemicals, Poole, England) was used instead of alcian blue to test whether the abnormal storage material gave a metachromatic staining reaction.

Electron microscopic examination served to check whether the storage material displayed patterns typical of polar lipids and whether the absence of alcian blue-stainable inclusions from a given cell type was paralleled by ultrastructurally normal lysosomes. For electron microscopy, tissue blocks were postfixed with 2% OsO_4 and embedded in araldite or epon. Ultrathin sections were processed according to standard methods and viewed with a Zeiss EM 900.

As a reference for the histochemical method, formalin-fixed samples of liver, pancreas, adrenal glands, and lung from autopsies of two human cases of MLD (a late infantile and a juvenile type) were subjected to the same pre-embedding staining with alcian blue as described above. The samples were made available through the kind help of Drs. F. Gullotta (Münster) and H. Harzer (Tübingen).

Results

In control mice, the organs were free of alcian blue-positive cells (Fig. 1a–c), except for mast cells encountered in various locations. In contrast, most organs of the aged ASA-deficient mice contained cells with strongly alcianophilic cytoplasmic inclusions (Fig. 1d–g), which gave a metachromatic purple staining reaction with cuprolinic blue. After incubation of cryostate sections with chloroform/methanol, the alcianophilia was abolished, indicating the lipid character of the storage material.

Gall bladder

While the gross appearance and general histoarchitecture of the gall bladder of ASA(–/–) mice was identical to that of controls, the epithelium and mucosal macrophages were stuffed with abnormal alcianophilic material (Fig. 1d). Ultrastructurally (Fig. 2a), the epithelium and macrophages displayed membrane-limited inclusions up to 10 µm in diameter, consisting of lamellar material of varying patterns similar to those shown in Fig. 2c (i.e., compact parallel stacks with a periodicity of approximately 5 nm or small concentric arrays). The histochemical and ultrastructural features of the epithelium were rather variable in gall bladders that had been stored in fixative for various periods of time (months) with the bile still enclosed in the lumen. In such cases, the alcianophilia of the epithelial cells was rather heterogeneous or missing, and the cells had a foamy appearance. Ultrastructurally, such cells displayed vacuoles with loosely arranged lamellae in contrast to the compact lamellae mentioned above. The most likely explanation is that sulfatides were leached to varying degrees during prolonged exposure to the lipid-solubilizing bile salts present in the lumen. A similar variability was observed in the epithelia of the large intra- and extrahepatic bile ducts.

Liver

In aged ASA(–/–) mice, the epithelium of small bile ducts was filled with alcian blue-positive inclusions

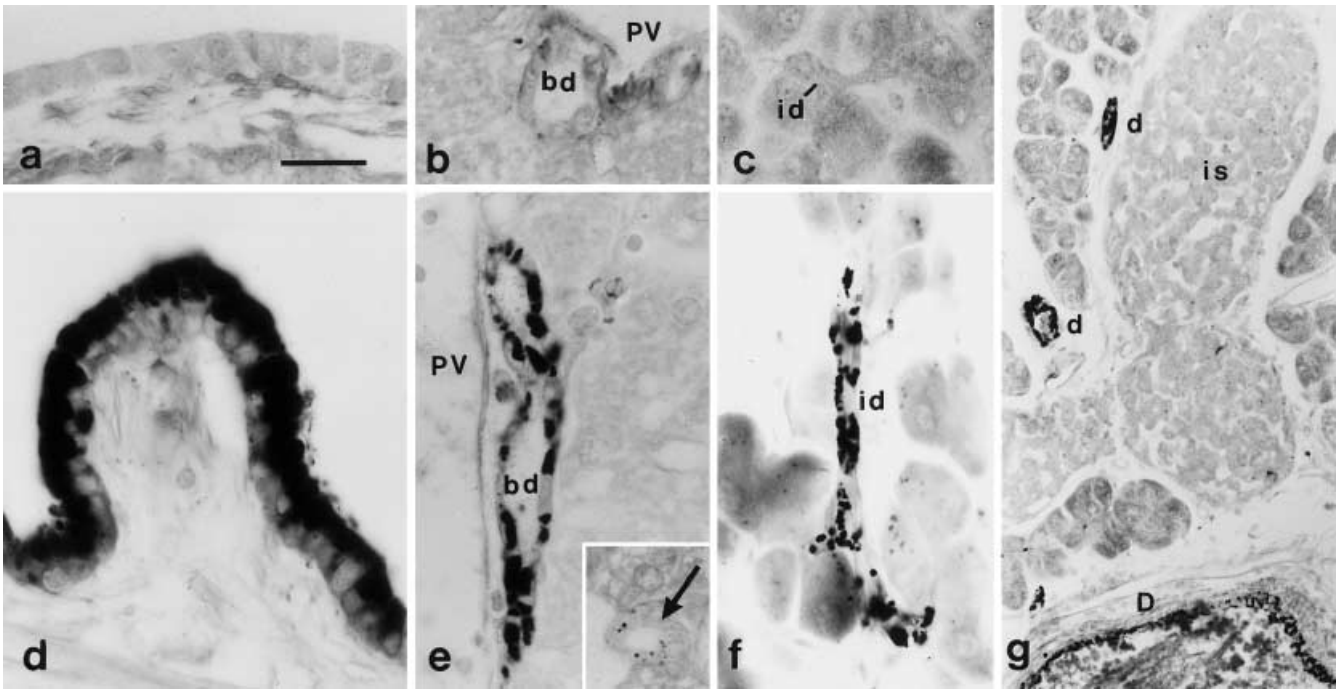


Fig. 1 Histochemical demonstration of sulfatide storage by preembedding incubation with alcian blue in the presence of 0.3 M $MgCl_2$. **a–c** Gall bladder, liver, and pancreas of a control mouse (26 months). **d–g** Gall bladder, liver, exocrine, and endocrine pancreas of arylsulfatase A (ASA; –/–) mice (23–24 months). Alcianophilic material was seen in the epithelia of the gall bladder. An intrahepatic bile duct (*bd*), a pancreatic intercalated duct (*id*), and two intralobular (*d*) and a large interlobular duct (*D*) of the exocrine pancreas are shown. The hepatocytes, exocrine pancreatic gland cells, and the islet cells (*is*) were devoid of alcianophilic inclusions. The *inset* in **e** shows a small bile duct *(arrow)* of a 4-week-old ASA(–/–) mouse with several small alcianophilic inclusions. In the organs of the control animal, all epithelia were unstained. *PV* branch of the portal vein. *Bar* is equivalent to 20 µm (**a–f)** and to 63 µm (g), respectively

(Fig. 1e). In young ASA-deficient mice (1–3 months), the epithelium of some small bile ducts displayed a few tiny granules (Fig. 1e, inset). The frequency and size of such alcianophilic granules increased with age. Ultrastructurally, the inclusions were membrane-limited and filled with multilamellated material as described for gall bladder and pancreatic ducts. Hepatocytes and the cells of the sinus wall were free of alcianophilic material, and under the electron microscope, the lysosomes resembled those in controls.

Pancreas

In the exocrine pancreas, the epithelia of intercalated, intralobular, and interlobular ducts contained alcian blue-positive inclusions (Fig. 1f, g). The acinar gland cells were always free of stainable material. The cells of the Langerhans islets were usually negative; very occasionally single cells at the periphery of an islet displayed small alcianophilic inclusions. Ultrastructurally (Fig. 2b, c), the duct epithelia contained inclusions with compact lamellated material. In the acinar cells and in the islet cells lamellated inclusions were not observed. Instead, the lysosomes were converted into lipofuscin organelles resembling those in age-matched controls (not shown). An ultrastructural equivalent of the few islet cells with alcianophilic inclusions could not be detected.

Lung

In the respiratory epithelium, the ciliated cells showed alcianophilic inclusions, while Clara cells were free of stainable material (Fig. 3). The alveolar epithelial cells and macrophages remained unstained. The ultrastructural observations confirmed that the ciliated cells in bronchioli, bronchi, and trachea contained lamellated inclusions (Fig. 3c), whereas the Clara cells and mucus-producing cells were unaltered.

Testis

In ASA-deficient mice (11 months and 24 months), the Sertoli cells contained some osmiophilic inclusions (Fig. 4) and occasionally an alcianophilic inclusion. In some atrophic seminiferous tubules, the Sertoli cells showed inclusions consisting of both osmiophilic and alcianophilic material. Systematic ultrastructural examination was not performed.

Adrenal glands and stomach

The adrenal cortex and medulla failed to show any histochemical features of sulfatide storage. In the gastric mu-

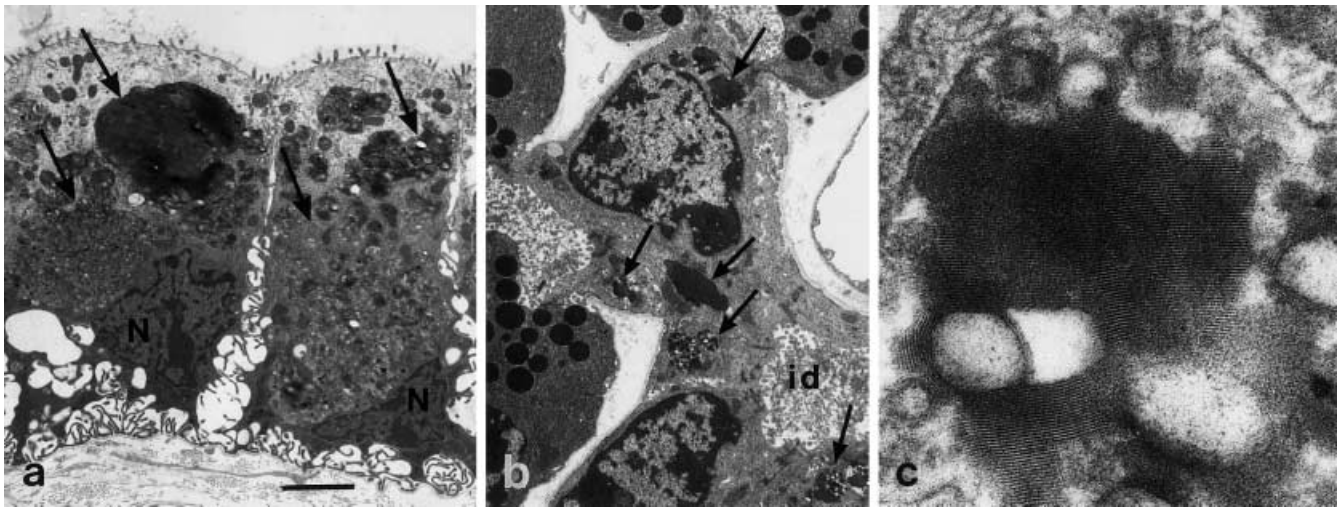


Fig. 2 Ultrastructure of sulfatide storing cells in arylsulfatase A (ASA; –/–) mice (23 months). **a** Gall bladder epithelium containing large inclusions (*arrows*). *N* nucleus. **b** Intercalated duct (*id*) of the exocrine pancreas. The *arrows* point to abnormal inclusions. **c** Storage material in pancreatic intercalated duct epithelium shown at higher resolution. Compact arrays of parallel or concentric lamellae are seen. **a**, **b** *Bars* 3 µm and 0.1 µm (**c**)

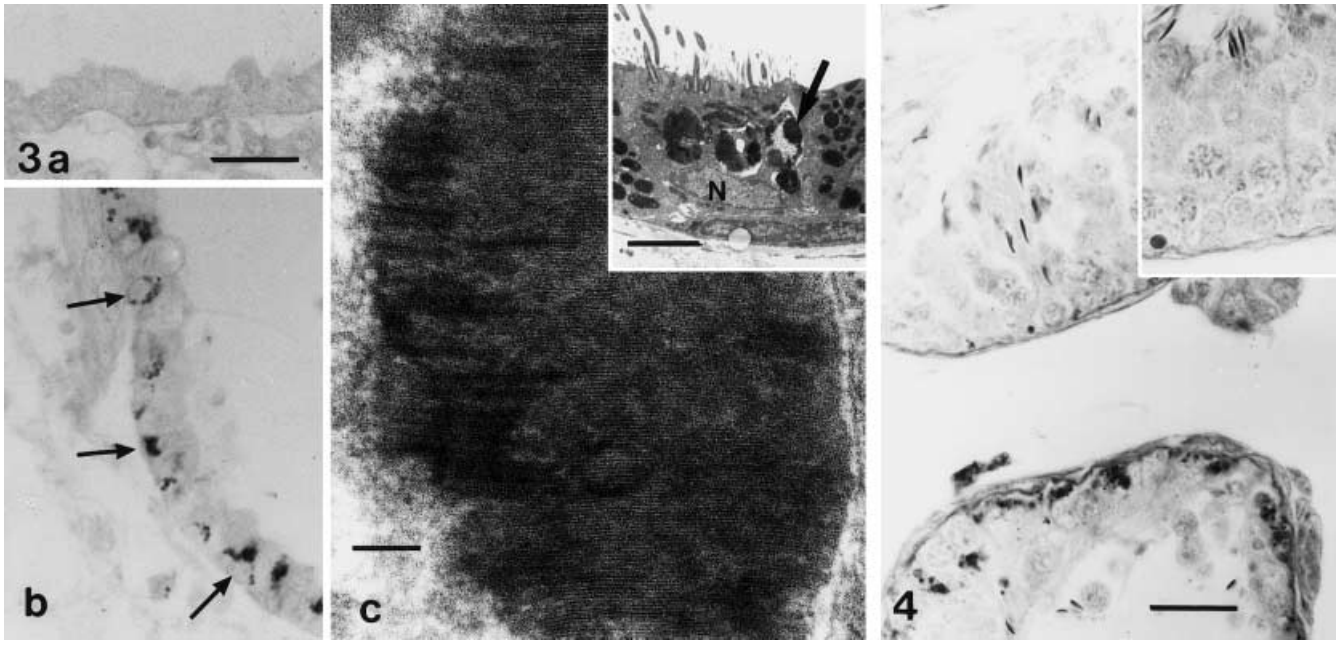


Fig. 3 Sulfatide storage in the respiratory epithelium. **a**, **b** Histochemical staining of sulfatide in the bronchiolar epithelium of a control mouse and an arylsulfatase A (ASA; –/–) mouse (both 26 months). In the latter, several cells contained alcianophilic material (*arrows*). Staining as in Fig. 1. **c** An abnormal inclusion (*arrow* in the *inset*) in a ciliated cell of the bronchiolar epithelium of an ASA(–/–) mouse (24 months) is shown at high resolution to demonstrate the lamellated pattern. *N* nucleus. *Bars* **a**, **b** 20 µm, **c** 0.1 µm, and *inset* 3 µm

Fig. 4 Seminiferous tubules from the testes of an arylsulfatase A (ASA)-deficient mouse and a control mouse (*inset*), both 24 months old. The upper tubule shows spermatogenesis and is representative for the majority of tubules in old ASA-deficient mice. Alcianophilic incusions were hardly detected. The lower tubule was atrophic, and the Sertoli cells contained several inclusions, several of which were, however, osmiophilic rather than alcianophilic. *Bar* 20 µm

cosa, the surface epithelium and the glandular cells were devoid of abnormal alcianophilic inclusions. In the subepithelial connective tissue, alcianophilic macrophages were seen, which were absent in controls. Ultrastructural examination of the two organs was not performed.

Human tissues

In the juvenile case of MLD, the hepatocytes throughout the lobule contained small alcianophilic inclusions while, in the late infantile case, only the periportal hepatocytes were affected. The small bile ducts contained a few abnormal inclusions. The gall bladders were not available, but large intrahepatic bile ducts were inspect-

ed. The supranuclear cytoplasm of the columnar epithelial cells was stuffed with alcian blue-positive inclusions. In the pancreas of both cases, the islets stained strongly positive. The ducts of the exocrine gland showed sulfatide storage similar to that seen in mice. In the lungs, the epithelia, in particular the ciliated cells of bronchi and bronchioli, were free of alcianophilic material.

Discussion

The histochemical method

Due to the polyanionic character of sulfatide aggregates, staining with cationic dyes is most appropriate for their histochemical detection. The present staining technique was borrowed from the histochemical methodology for sulfated glycosaminoglycans as elaborated by Scott and coworkers [21, 22, 23]. When applied under the present conditions (pH 5.7 with 0.3 M Mg^{++}), the staining is specific for polysulfated material, because sulfate residues remain the only partners available for the binding of the tetracationic dye. Lampert and Lewis [15] recommended the staining of frozen sections of MLD tissues with alcian blue at even more stringent conditions (0.8 M Mg^{++}) in order to eliminate most of the staining of sulfated proteoglycans in the extracellular matrix. In the present study, this appeared unnecessary, since the paraffin sections provided better structural preservation and resolution than the frozen sections; therefore, the faint diffuse staining of connective tissue fibers and the alcianophilic intracellular inclusions could easily be discriminated from each other. The present histochemical method produces brilliant and permanent staining of the storage material against a clear background, which is due to the osmication and is easily recognizable for histological analysis. The technique is recommended particularly for systematic investigations of the distribution pattern of sulfatide storage in autoptic samples of human MLD and in ASA-deficient mice. It should be mentioned that post-embedding staining of osmicated paraffin sections with alcian blue gave less satisfactory results; the preparations displayed unspecific background staining all over the tissues such that the sulfatide inclusions did not show up as brilliantly as with the recommended method.

Comparison of sulfatide storage in mice and humans

The pattern of sulfatide storage in the human reference samples was in accordance with the reports in the literature [13]. The topographic distribution of sulfatide accumulations in ASA-deficient mice shows several similarities with and some differences from the pattern of the human MLD. Apart from the kidney to be described elsewhere, the most severe storage in mice was presently found in the gall bladder epithelium. This is reminiscent of the human pathology, although the gall bladder of MLD patients is known to develop secondary alterations, such as shrinkage of the organ and papillomatosis of the mucosa [5, 24, 28]. The variability of the alcianophilia in the epithelium of the murine gall bladder is assumed to be an artifact as explained above. As a practical consequence, the gall bladder epithelium appears unfavorable for histochemical monitoring of the effects of therapeutic approaches, such as gene therapy.

In the murine liver, the epithelia of small bile ducts usually displayed sulfatide storage, whereas the hepatocytes were unaffected. The reports on human cases are heterogeneous. Bile ducts are described as storing or weakly storing or are not mentioned. Hepatocytes at the periphery of the lobules are reported to show some storage, as seen also in the present reference samples of late infantile MLD, or to show massive storage, whereas the remaining hepatocytes are usually unaffected or not mentioned [2, 4, 5, 9, 15, 20, 26, 28].

In the murine pancreas, only the ducts of the exocrine gland showed significant storage. In the reports on human MLD, pancreatic ducts are occasionally mentioned, but the islets are usually more prominently affected [2, 4, 9, 28] as observed also in the reference samples available to us. In the lung of ASA-deficient mice, the ciliated cells of the airways showed sulfatide storage. In human MLD, the lung, if mentioned at all, is reported to be unaltered [28], as it was also in the present reference samples. The murine adrenal glands were unaltered. In human cases of MLD, the adrenals are reported either as being unaffected [9], or the innermost cells of the reticular zone are described to store sulfatide [2, 28]. This was observed also in the present human samples.

Biological factors determining the distribution of sulfatide storage

Both in human MLD and in ASA(–/–) mice, the intensity of sulfatide storage varies greatly from one cell type to the other. Obviously, the degree of sulfatide accumulation in ASA-deficient cells is dependent, among other factors, on the sulfatide load normally to be coped with by the lysosomes. Thus, cells which endocytose sulfatide or which have high sulfatide contents and therefore presumably have a high sulfatide turnover, should be expected to be particularly affected. In the case of the epithelia of gall bladder, bile ducts and pancreatic ducts the basis for the high degree of sulfatide storage is unknown, since data on the contents or turnover of sulfatides in these cells are, to our knowledge, not available. Sulfatide accumulation in the ciliated cells of the airways of ASA(–/–) mice is in line with considerably high sulfatide contents in the respiratory epithelium and particularly in the ciliated cells as reported for human and porcine lung [14, 29]. It is all the more surprising that in the human MLD, the respiratory epithelium is free of sulfatide storage.

Some cell types of ASA-deficient mice were only weakly or not affected, although they are known to be rich in sulfolipids. Pancreatic islets of several species, including mice, have been described immunohistochemically to contain sulfatides [3, 6]. Therefore, the negative results on murine islets were unexpected, particularly in view of the pronounced sulfatide accumulation in islets of human MLD cases. Either there are quantitative species differences in the sulfatide contents and turnover, or the murine islet cells have an alternative pathway for the degradation of sulfatide. Similarly, the low sulfatide storage in testis was unexpected. Testicular tissue is known to be rich in sulfogalactosyl glycerides (seminolipids), which are also natural substrates of the ASA [7]. Seminolipids are constituents of the plasma membrane of the spermatozoa and their precursors, beginning with the primary spermatocytes [8, 27]. Thus, ASA-deficient Sertoli cells which have to endocytose and digest the residual bodies shed from the spermatides during maturation [12, 17, 18] might be expected to store larger quantities of sulfolipid than presently found. In the gastric mucosa, both the surface epithelium and the glandular cells are rich in sulfatides, at least so in man, rabbit, and rat [19, 25]. The absence of sulfatide storage from gastric epithelia of ASA(–/–) mice may be due, apart from species differences, to the relatively short life span of the cells. The present unexpected results suggest that the sum of factors determining the degree of sulfatide accumulation in ASA-deficient cells is more complicated than considered above.

In conclusion, the present study provides an easy histochemical method for the detection of intracellular aggregates of sulfatides and describes the pattern of sulfatide storage in visceral organs of ASA(–/–) mice. Apart from some differences, the essentials of the pattern resemble that seen in human MLD. In addition to offering an animal model for the human disease, ASA(–/–) mice may be useful for further investigations on the cell biology of sulfatides not only in nervous tissues but also in visceral organs.

Acknowledgements The excellent technical assistance of Dagmar Niemeier is gratefully acknowledged. We thank Drs. F. Gullotta (Münster), K. Harzer (Tübingen), H.U. Benz (Wildbad), and E. Mäusle (Trier) for making available to us tissue samples of human MLD cases. This work was financially supported by the Deutsche Forschungsgemeinschaft (Lu 172/8–1).

References

1. Benz HU, Harzer K (1974) Metachromatic reaction of pseudoisocyanine with sulfatides in metachromatic leukodystrophy (MLD). Acta Neuropathol 27:177–180
2. Burgess JH, Kalfayan B, Slungaard RK, Gilbert E (1985) Papillomatosis of the gallbladder associated with metachromatic leukodystrophy. Arch Pathol Lab Med 109:79–81
3. Buschard K, Josefsen K, Hansen SV, Horn T, Marshall MO, Persson H, Månsson JE, Fredman P (1994) Sulphatide in islets of Langerhans and in organs affected in diabetic late complications: a study in human and animal tissue. Diabetologica 37: 1000–1006
4. Castleman B, Kibbee BU (1962) Case records of the Massachusetts General Hospital. N Engl J Med 267:1198–1204
5. Dische MR (1996) Metachromatic leukodytrophic polyposis of the gall bladder. J Pathol 97:388–390
6. Fredman P, Mansson JE, Rynmark BM, Josefsen K, Ekblond A, Halldner L, Osterbye T, Horn T, Buschard K (2000) The glycosphingolipid sulfatide in the islets of Langerhans in rat pancreas is processed through recycling: possible involvement in insulin trafficking. Glycobiology 10:39–50
7. Gadella BM, Colenbrander B, van Golde LM, Lopes-Cardozo M (1992) Characterization of three arylsulfatases in semen: seminolipid sulfohydrolase activity is present in seminal plasma. Biochim Biophys Acta 1128:155–162
8. Gadella BM, Gadella TW, Colenbrander B, van Golde LM, Lopes-Cardozo M (1994) Visualization and quantification of glycolipid polarity dynamics in the plasma membrane of mammalian spermatozoon. J Cell Sci 107:2151–2163
9. Hagberg B, Sourander P, Svennerholm L (1962) Sulfatid lipidosis in childhood. Am J Dis Child 104:644–656
10. Hess B, Saftig, P, Hartmann D, Coenen R, Lüllmann-Rauch R, Goebel HH, Evers M, von Figura K, D'Hooge R, Nagels G, DeDeyn P, Peters C, Gieselmann V (1996) Phenotype of arylsulfatase A-deficient mice: relationship to human metachromatic leukodystrophy. Proc Natl Acad Sci USA 93:14821–14826
11. Hirsch T von, Peiffer J (1955) Über histologische Methoden in der Differentialdiagnose von Leukodystrophien und Lipidosen. Arch Psychiatr Z Neurol 194:88–104
12. Kerr JB, DeKretser DM (1975) Cyclic variations in Sertoli cell lipid content throughout the spermatogenic cycle in the rat. J Reprod Fertil 43:1–8
13. Kolodny EH, Fluharty AL (1995) Metachromatic leukodystrophy and multiple sulfatase deficiency: sulfatide lipidosis. In: Scriver CR, Beaudet AL, Sly WS, Valle D (eds) The metabolic and molecular bases of inherited disease, 6th edn. McGraw-Hill, New York, pp 2693–2739
14. Krivan HC, Olson LD, Barile MF, Ginsburg V, Roberts DD (1989) Adhesion of mycoplasma pneumoniae to sulfated glycolipids and inhibition by dextran. J Biol Chem 264: 9283–9288
15. Lampert IA, Lewis PD (1975) Staining of sulphatides in metachromatic leukodystrophy with alcian blue at high salt concentrations. Histochemistry 43:269–273
16. Lev R, Spice SS (1964) Specific staining of sulphate groups with alcian blue at low pH. J Histochem Cytochem 12:309
17. Morales C, Clermont Y, Nadler NJ (1986) Cyclic endocytic activity and kinetics of lysosomes in Sertoli cells of the rat: a morphometric analysis. Biol Reprod 34:207–218
18. Morales CR, Hay N, El-Alfy M, Zhao Q (1998) Distribution of mouse sulfated glycoprotein-1 (prosaposin) in the testis and other tissues. J Androl 19:156–164
19. Natomi H, Sugano K, Takaku F, Iwamori M (1990) Glycosphingolipid composition of the gastric mucosa. A role of sulfatides in gastrointestinal defense? J Clin Gastroenterol 12[Suppl 1]:52–57
20. Résibois A (1971) Electron microscopic studies of metachromatic leukodystrophy. IV. Liver and kidney alterations. Path Europ 6:278–298
21. Scott JE (1970) Histochemistry of alcian blue. I. Metachromasia of alcian blue, astrablau and other cationic phthalocyanin dyes. Histochemie 21:277–285
22. Scott JE, Dorling J (1965) Differential staining of acid glycosaminoglycans (mucopolysaccharides) by alcian blue in salt solutions. Histochemie 5:221–233
23. Scott JE, Orford, CR, Hughes EW (1981) Proteoglycan-collagen arrangements in developing rat tail tendon. Biochem J 195:573–581
24. Siegel EG, Lücke H, Schauer W, Creutzfeldt W (1992) Repeated upper gastrointestinal hemorrhage caused by metachromatic leukodystrophy of the gall bladder. Digestion 51:121–124

25. Sugano K, Tai T, Kawashima I, Kotani M, Natomi H, Kamisago S, Fukushima Y, Yazaki Y, Iwamori M (1995) Localization of sulfatides in the epithelial lining cells of gastric mucosa: studies with a monoclonal antibody to sulfatides. J Clin Gastroenterol 21[Suppl 1]:S98–S103
26. Toga M, Berard-Badier M, Pinsard N, Gambarelli D, Hassoun J, Tripier MF (1972) Étude clinique, histolgique et ultrastructurale de quatre cas de leucodystrophie métachromatique infantile et juvenile. Acta Neuropath 21:23–38
27. Vos JP, Lopes-Cardozo M, Gadella BM (1994) Metabolic and functional aspects of sulfogalactolipis. Biochim Biophys Acta 1211:125–149
28. Wolfe HJ, Pietra GG (1964) The visceral lesions of metachromatic leukodystrophy. Am J Pathol 44:921–929
29. Zhang Q, Young TF, Ross RF (1994) Glycolipid receptor for attachment of Mycoplasma hypopneumoniae to porcine respiratory ciliated cells. Infect Immunol 62:4367–4373

Virchows Arch (2001) 439:97–101
DOI 10.1007/s004280100455

CASE REPORT

Steffen Hauptmann · Bahram Nadjari
Joachim Kraus · Wolfram Turnwald · Manfred Dietel

Uterine tumor resembling ovarian sex-cord tumor – a case report and review of the literature

Received: 22 January 2001 / Accepted: 28 March 2001 / Published online: 15 May 2001
© Springer-Verlag 2001

Abstract A uterine tumor resembling an ovarian sex-cord tumor (UTROSCT) is a very rare lesion with only 38 cases reported in the literature so far. Here, we show an additional case of a pure UTROSCT with a DNA stemline at 1c in a 49-year-old woman presenting with abnormal vaginal bleeding. Problems in differential diagnosis arise mainly due to the variable histological picture of UTROSCT. Immunohistochemically, these tumors express cytokeratin, epithelial membrane antigen, vimentin, and smooth muscle actin. Moreover, in some cases, CD99 and α-inhibin are detectable. Although 36% of UTROSCT have infiltrative margins, almost all of them behave benignly. It is thus questionable whether the same prognostic criteria apply for these tumors as for endometrial stromal sarcomas. However, in the so-called mixed UTROSCT, the endometrial stromal sarcoma component determines the outcome.

Keywords Uterus · Myometrium · Tumors · UTROSCT · DNA cytometry

Introduction

An ovarian sex-cord-like differentiation within a mesenchymal neoplasm of the uterus can be found either focally within an otherwise typical endometrial stromal sarcoma (the so-called group-I tumors with <50% of sex-cord elements, according to Clement and Scully) [6] or forming lesions designated as uterine tumors resembling ovarian sex-cord tumors (UTROSCTs), which are composed almost completely of sex-cord-like structures (designated group-II tumors). The rarity and the variable histological picture of the latter and their less mature sex-cord differentiation compared with the correspondent ovarian tumors cause problems in the differential diagnosis. Here we describe one case of this peculiar lesion and summarize the reports in the literature.

S. Hauptmann (✉) · B. Nadjari · M. Dietel
Institute of Pathology, Charité Hospital Berlin,
Schumannstr. 20/21, 10117 Berlin, Germany
e-mail: steffen.hauptmann@charite.de
Tel.: +49-30-28028160, Fax: +49-30-28021296

J. Kraus
Institue of Pathology Traunstein, Cuno-Niggl-Straße 3,
83276 Traunstein, Germany

W. Turnwald
Department of Gynecology, Municipal Hospital Bad Reichenhall,
Riedelstr. 5, 83435 Bad Reichenhall, Germany

Methods

Morphology

Sections of 5-µm thickness were cut from paraffin-embedded material and stained with hematoxylin and eosin, periodic acid–Schiff (PAS), and Gomori. Immunohistochemical stainings were performed for pan-cytokeratin (Dako, Hamburg, Germany; prediluted), epithelial membrane antigen (EMA; M613; Dako; 1:100), melan A (M7196; Dako; 1:100), vimentin (M7020; Dako; 1:50), desmin (M760; Dako; 1:50), muscle-specific actin (MU090UC; BioGenex, San Ramon, Calif.; 1:60), smooth muscle actin (M851; Dako; 1:25), S100-protein (MU058UC; BioGenex; 1:1000), CD15 (M733; Dako; 1:25), CD30 (M751; Dako; 1:50), CD99 (M3601; Dako; 1:100), α-inhibin (MCA951S; Serotec, Oxford, UK; 1:100), α-fetoprotein (18–0003; Zymed, San Francisco, Calif.; 1:500), placental alkaline phosphatase (MU228UC; BioGenex; 2:250), estrogen receptor (NCL-ER-6F11; Loxo/Novocastra, Newcastle upon Tyne, UK; 1:50), progesterone receptor (M3569; Dako; 1:500), and MIB-1 (DIA505; Dianova, Hamburg, Germany; 1:50). The detection system used was alkaline phosphatase–antialkaline phosphatase (APAAP).

DNA cytometry

A 50-µm-thick section was cut from the formalin-fixed, paraffin-embedded material which had been dewaxed and enzymatically digested to prepare a single-cell suspension. A monolayer smear from this suspension was stained according to Feulgen, using acid hydrolysis with 5 mol/l HCl (27.5°C; 45 min) followed by incubation with Schiff's reagent (room temperature; 60 min). DNA measurement was performed using a TV-based image analysis system combined with an automated microscope. The DNA content of 330 randomly chosen tumor cell nuclei was analyzed. Thirty normal cells (myocytes) served as internal standards to determine the normal 2c value. The variation coefficient of the G0/1 phase fraction of reference cells was below 5%.

Case report

A 49-year-old woman was admitted with abnormal vaginal bleeding and multiple uterine leiomyomas. Therefore, an abdominal hysterectomy was performed. The patient is now without evidence of disease, 7 months after resection.

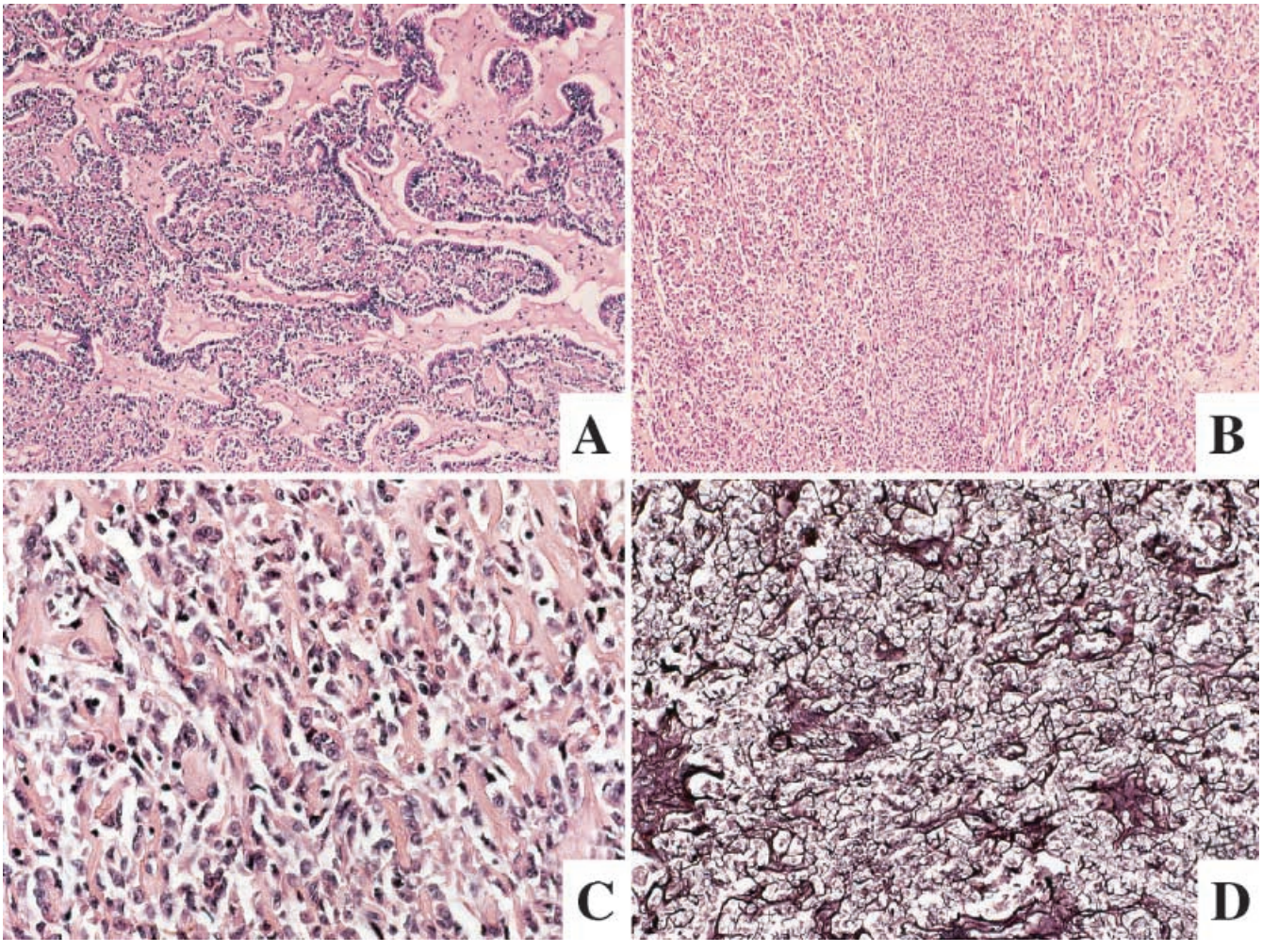


Fig. 1 Cut surface showing a sharply circumscribed, homogenous yellow tumor

The removed uterus had a weight of 440 g and contained multiple grayish-white intramural nodules with the typical aspect of a leiomyoma. Another nodule, which was also sharply demarcated, had a diameter of 4.5 cm and a homogenous yellow cut surface without the whirling pattern of the other nodules (Fig. 1). Whereas the grayish-white nodules were typical leiomyomas histologically, the appearance of the yellow lesion was completely different. This tumor was composed of solid and trabecular sheets (Fig. 2A) of small, isomorphic cells interspersed by broad hyalinized stromal bands (Fig. 2B). Cells lying on these stromal bands were cylinder-shaped, and their cytoplasmic edges were in contact with the connective tissue. Within the solid portion of the tumor, fine osteoid-like collagenous strands were visible, and sometimes cells formed a pseudoangiomatous pattern. The cytoplasm of the tumor cells was poorly developed; the nuclei were not atypical, containing indistinct nucleoli if any (Fig. 2C). Mitoses were not found. A delicate reticuline fiber network was found surrounding individual cells and small cell groups (Fig. 2D).

Immunohistochemistry revealed a positivity for vimentin and, with lower intensity, for pan-cytokeratin (Fig. 3). EMA was ex-

Fig. 2 Solid and trabecular sheets of small, isomorphic cells interspersed by broad hyalinized stromal bands (**A**). Cells lying on these stromal bands were cylinder-shaped (**B**), and their cytoplasmic edges were in contact with the connective tissue. Within the solid portion of the tumor, fine osteoid-like collagenous strands were visible. The cytoplasm of the tumor cells was poorly developed; the nuclei were not atypical; sometimes they contain an indistinct nucleolus (**C**). A delicate reticuline fiber network was found surrounding individual cells and small cell groups (**D**)



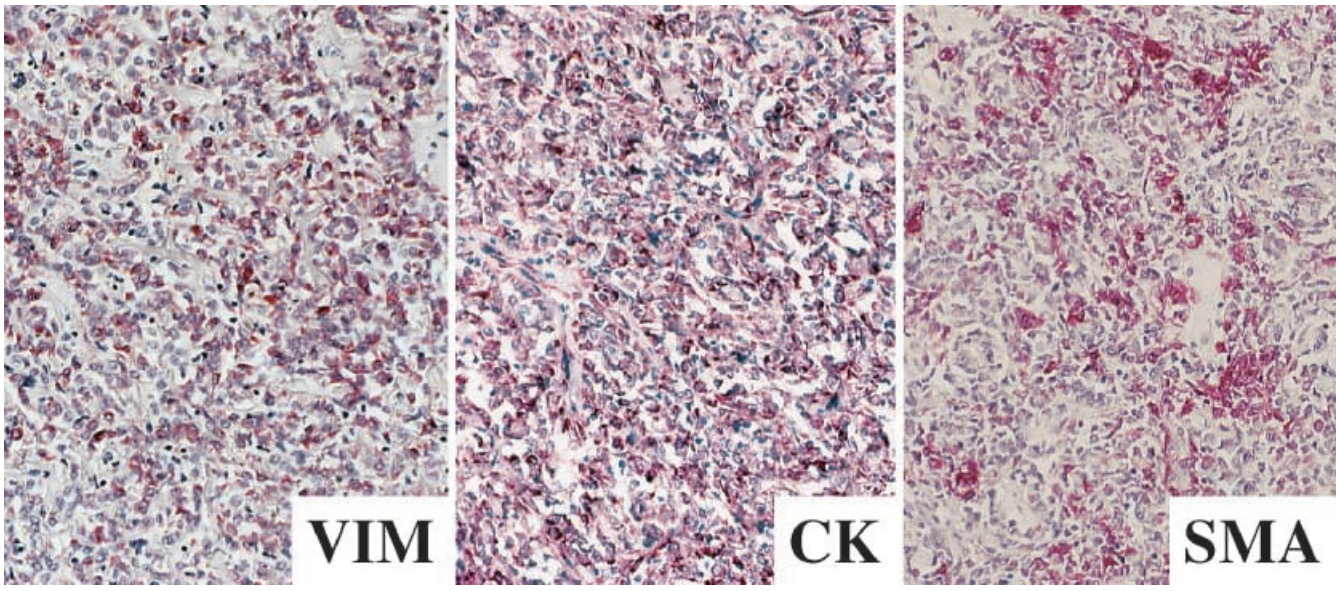


Fig. 3 Tumor cells express vimentin and, with low intensity, cytokeratin. An intense reactivity with smooth muscle actin is shown focally

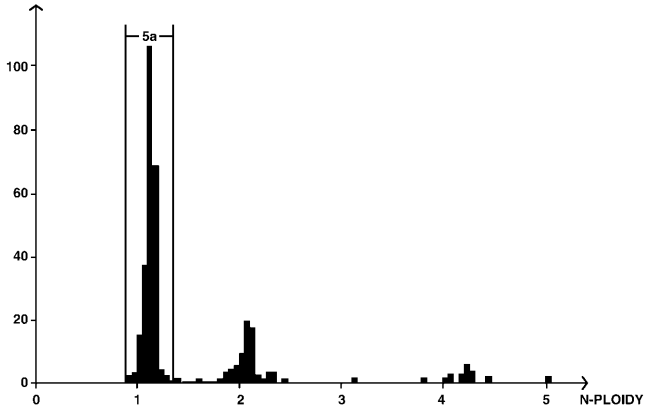


Fig. 4 DNA histogram showing a hypodiploid stemline at 1.14c and signs of polyploidization with peaks around 2c and 4c

pressed focally. The reactivity for CD99 was diffuse but weak. Large areas expressed smooth muscle actin with high intensity (Fig. 2). Only in some areas, a weak reactivity for muscle specific actin was found. A nuclear expression of progesterone receptors was found in one-half of the cells. Only few cells were MIB-1 positive. All of the other immunoreactivities were negative.

DNA cytometry showed the pattern of aneuploid polyploidization with a hypodiploid stemline and two doubling peaks around 2c and 4c (Fig. 4).

Discussion

In the literature, only 38 patients with UTROSCT have been described [1, 4, 6, 9, 10, 11, 13, 17, 20, 21, 26, 27, 28, 30, 34, 37, 38]. Their mean age was 48 years (range 16–86 years). Macroscopically, these tumors resemble leiomyomas but lack their whorled pattern, being more lobulated and are yellow. In one case, a microcystic pattern has been described [17]. The mean size of the tumors was 4.4 cm; their localization was myometrial in 14 cases, submucous in 11 cases, and subserous in 4 cases. The lesions were multiple in only two patients.

The microscopical picture is variable, with five basic patterns described: (1) anastomosing trabeculae, (1) plexiform cords one cell in width, (1) small solid cell groups (1) well-formed tubules, and (5) diffuse growth [6]. True Call–Exner bodies, however, were never described, which is important because the majority of these tumors have been initially misinterpreted as granulosa cell tumors. Rarely, a hemangioma-like pattern and papillary structures occur [37, 38]. The neoplastic cells are usually small with scant, indistinct eosinophilic (sometimes vacuolated) cytoplasm. Their nuclei are round to oval with little pleomorphism, slightly hyperchromatic, and have generally indistinct nucleoli. Nuclear grooves are absent. Sometimes, spindle-shaped cells are present, suggesting a mixture of epithelial and mesenchymal elements [31]. The stroma is generally sparse with some hyaline strands which, as in the present case, may resemble osteoid, little lymphocytic infiltration, foam cells, hemosiderin deposits, some giant cells, or cholesterol crystals [33]. Necrosis is absent, and mitoses are usually not found. The reticuline fibers surround cords or nests and single cells [11]. Therefore, according to the dominating architectural pattern, UTROSCT can exhibit a granulosa-like or Sertoli-like pattern [3]. Moreover, the presence of Charcot–Böttcher crystals in the cells of a UTROSCT [20] suggest that some of these lesions have a true Sertoli differentiation.

Immunohistochemically, most UTROSCT express vimentin, α-inhibin, and CD99 [1, 25]. Up to one-third express desmin, and some tumors even express myoglobin and smooth muscle antigen. A coexpression of cytokeratin has been described in up to 50% of cases, and around 10% express EMA. Receptors for estrogen, progesterone, and Melan-A were also found [1, 21].

This is the first UTROSCT which has been analyzed using DNA cytometry. We found an aneuploid stemline

Table 1 Differential diagnosis of uterine tumors resembling ovarian sex-cord tumors (UTROSCTs)

Lesion	Criteria
Low-grade endometrial stromal sarcoma	Infiltrative growth; only a few small and scattered glands or tubules that are below 10% of the area under inspection
Adenosarcoma	Contains numerous cystically dilated glands, evenly distributed throughout the lesion and has a condensed periglandular rim of stromal cells (so-called "cambium-layer")
Carcinosarcoma	High-grade stromal component; heterologous differentiation
Sertoliform endometrial adenocarcinoma	Usually contains areas with typical architecture
Plexiform tumorlet	>20 mm; 25% multiple; usually associated with myomas; homogenous histological picture [pattern (ii) or (iii)]; smooth muscle differentiation more pronounced
Metastatic ovarian sex-cord stromal tumor	Clinical picture

around 1c, indicating that the tumor cells had a marked loss of DNA reaching near haploid values. Obviously, this loss of DNA was followed by a polyploidization. Whether other tumors of this type show comparable alterations and this aneuploid DNA distribution indicates a more virulent behavior of the lesion remains to be clarified.

The histogenesis of these tumors remains controversial. It is perplexing that UTROSCT obviously have the capability of representing all tissues occurring in the Muellerian system. The epithelial differentiation is represented by the expression of cytokeratin and EMA and by epithelial features found ultrastructurally [11, 24]. There is resemblance of UTROSCT cells to both endometrial stromal cells and myofibroblastic cells. Such an intermediate cell type is similar to what is seen at the fusion area of endometrial stroma and myometrium at the base of normal endometrium, as described by Park [31]. Such intermediate cell types are also known from the embryological development when the features of endometrial stromal and muscle cells are difficult to distinguish [36]. Moreover, the capacity of the endometrial stroma to undergo smooth muscle differentiation is well known [2]. Consequently, Tang et al. [34] conclude that these tumors are actually "stromomyomas", whereas others had described UTROSCT under the designation "stromatosis" [8, 15, 32, 37] or stromal endometriosis [18].

It has been assumed by Goodall [12] that a uterine mesenchyme with the inherent capacity for differentiation into any uterine component extends as a diffuse network through the uterine wall. Adenomyosis may represent the most common non-neoplastic manifestation of this potential [24], and we think that a myoma represents the myogenic, a stromal nodule the "stromatous", and an UTROSCT the "sex-cord-like" end of the spectrum. Therefore, we are in agreement with Mazur and Kraus [24] that some uterine wall tumors with different histological patterns actually may share a common histogenetic origin, representing the capacity for differentiation of uterine mesenchymal blastema. In other words, even a differentiation, such as the ovarian sex-cord stroma or an epithelial differentiation is not surprising because it lies within the Muellerian potential [24]. Although purely speculative also, adenomatoid tumors localized within the uterine wall may belong in this category, representing the mesothelial differentiation of Muellerian epithelium. The relationships between UTROSCT, vascular leiomyomas, and glomus tumors of the uterine wall that have been suggested early in the literature indicate that differentiation toward really all parts of the uterine wall can be found in these tumors [3, 30].

The differential diagnoses of these tumors mentioned in the literature are summarized in Table 1 [14, 16, 22, 29]. Regarding the so-called plexiform tumorlet, we are in agreement with Fekete et al. [11] that they have more in common with UTROSCT than they do differences. The similarities are the mean age (45 years for plexiform tumorlets), the cytological and ultrastructural features, the immunoreactivity, and the benign nature [7, 19]. Whenever the tumor is in contact with the endometrium, a careful search for the presence of endometrial stromal sarcoma elements is particularly important.

The majority of patients with UTROSCT had a total abdominal hysterectomy with bilateral salpingo-oophorectomy, and it is evident that the pure form of UTROSCT behaves like a benign neoplasm. In none of the 18 patients, for which follow-up data were available (mean follow-up time of 32 months; range 4–84 months) has a recurrence been observed. It has been suggested that the aggressive potential of UTROSCT can be evaluated by using the criteria for endometrial stromal sarcomas, e.g., pushing versus infiltrative border, vascular invasion, and mitotic count [16]. However, it is remarkable that one-half of the 18 patients had tumors with infiltrative margins. Therefore, the pure form of UTROSCT seems not to have the same risk as low-grade endometrial sarcoma, but the mean follow-up time of these cases was only 25 months. Nevertheless, there are reports on distant metastases and recurrences. Kantelip et al. [20] described an UTROSCT with two omental metastases showing the same histology as the uterine tumor but, unfortunately, no follow-up information was given. The case described by Malfetano and Hussein [23] as recurrent UTROSCT [5] probably was not of the pure type.

References

1. Baker RJ, Hildebrandt RH, Rouse RV, Hendrickson MR, Longacre TA (1999) Inhibin and CD99 (MIC2) expression in uterine stromal neoplasms with sex-cord-like elements. Hum Pathol 30:671–679
2. Bird CC, Willis RA (1965) The production of smooth muscle by the endometrial stroma of the adult human uterus. J Pathol Bacteriol 90:75–81
3. Bogard-Erdle AM, Hirsch EF (1958) Glomus tumor of the uterus. Arch Path Lab Med 65:244–246
4. Caglar H, Traub B, Jenis EH, Gaeta J, Nezhat C, Hreshchyshyn MM (1983) Plexiform sex cord tumors resembling tumor of the uterus. Am J Obstet Gynecol 145:639–640
5. Chang KL, Crabtree GS, Lim-Tan SK, Kempson RL, Hendrickson MR (1990) Primary uterine endometrial stromal neoplasms. A clinicopathologic study of 117 cases. Am J Surg Pathol 14:415–438
6. Clement PB, Scully RE (1976) Uterine tumors resembling ovarian sex-cord tumors. Am J Clin Pathol 66:512–525
7. Devaney K, Tavassoli FA (1991) Immunohistochemistry as a diagnostic aid in the interpretation of unusual mesenchymal tumors of the uterus. Mod Pathol 4:225–231
8. Doran AHG, Lockyer C (1908) Two cases of uterine fibroids showing peritheliomatous change: long immunity from recurrence after operation. Proc R Soc Med 2:25–29
9. Eltabbakh GH, Samter GT (1995) Sex cord tumors of the uterus. Int J Gyn Obstet 48:113–114
10. Erhan Y, Baygün M, Özdemir N (1992) The coexistence of stromomyoma and uterine tumor resembling ovarian sex-cord tumors. Acta Obstet Gyn Scand 71:390–393
11. Fekete PS, Vellios F, Patterson BD (1985) Uterine tumor resembling an ovarian sex-cord tumor: report of a case of an endometrial stromal tumor with foam cells and ultrastructural evidence of epithelial differentiation. Int J Gyn Path 4:378–387
12. Goodall JR (1944) A study of endometriosis, endosalpingiosis, endocervicosis and peritoneo-cutaneo-ovarian sclerosis. A clinical and pathological study. 2nd edn. Lippincott, Philadelphia
13. Goodhue WW, Susin M, Kramer EE (1974) Smooth muscle origin of uterine plexiform tumors. Arch Pathol 97:263–268
14. Hart WR, Yoonessi M (1977) Endometrial stromatosis of the uterus. Obstet Gynecol 49:393–403
15. Henderson DN (1946) Endolymphatic stromal myosis. Am J Obstet Gynecol 152:1000–1012
16. Hendrickson MR, Kempson RL (1991) The uterine corpus. In: Sternberg SS, Mills SE (eds) Surgical pathology of the female reproductive system and peritoneum. Raven Press, New York
17. Horn LC, Stegner HE (1995) Uteriner Stromatumor mit ovarieller Keimstrang-differenzierung. Pathologe 16:421–425
18. Hunter WC (1962) Uterine stromal endometriosis (stromatosis). Am J Obstet Gynecol 83:1564–1573
19. Kaminski PF, Tavassoli FA (1984) Plexiform tumorlet: a clinical and pathological study of 15 cases with ultrastructural observations. Int J Gyn Pathol 3:124–134
20. Kantelip B, Cloup N, Dechelotte P (1986) Uterine tumors resembling sex cord tumors: report of a case with ultrastructural study. Hum Pathol 17: 91–94
21. Krishnamurthy S, Jungbluth AA, Busam KJ, Rosai J (1998) Uterine tumors resembling ovarian sex-cord tumors have an immunophenotype consistent with true sex-cord differentiation. Am J Surg Pathol 22:1078–1082
22. Löning T (2000) Mesenchymale Tumoren und verwandte Läsionen. In: Löning T, Riehtdorf L. Pathologie der weiblichen Genitalorgane III. Springer, Berlin Heidelberg New York
23. Malfetano JH, Hussain M (1989) A uterine tumor that resembled ovarian sex-cord tumors: a low-grade sarcoma. Obstet Gynecol 74:489–491
24. Mazur MT, Kraus FT (1980) Histogenesis of morphologic variations in tumors of the uterine wall. Am J Surg Pathol 4:59–74
25. McCluggage WG, Shah V, Walsh MY, Toner PG (1993) Uterine tumor resembling ovarian sex cord tumour: evidence for smooth muscle differentiation. Histopathol 23:83–85
26. McCluggage WG (1999) Uterine tumors resembling sex cord tumours: immunohistochemical evidence for true sex cord differentiation. Histopathology 34:374–375
27. Miliaris D, Bontis J (1997) Uterine tumor resembling sex-cord ovarian tumors: one more case of the pure type suggests a neoplasm with benign behaviour. Eur J Gynecol Oncol 18:133–135
28. Morehead RP, Bowman MC (1945) Heterologues mesodermal tumors of the uterus; report of a neoplasm resembling a granulosa cell tumor. Am J Pathol 21:53–61
29. Norris HJ, Taylor HB (1966) Mesenchymal tumors of the uterus. I. A clinical and pathologic study of 53 endometrial stromal tumors. Cancer 19:755–766
30. Nunez-Alonso C, Battifora HA (1979) Plexiform tumors of the uterus. Cancer 44:1707–1714
31. Park WW (1949) The nature of stromatous endometriosis. J Obstet Gynecol 56:759–776
32. Pellilo D (1968) Proliferative stromatosis of the uterus with pulmonary metastasis. Remission following treatment with a long-acting progestin: a case report. Obstet Gynecol 31:33–39
33. Symmonds RE, Dockerty MB, Pratt JH (1957) Sarcoma and sarcoma-like proliferations of the endometrial stroma. III. Stromal hyperplasia and stromatosis (stromal endometriosis). Am J Obstet Gynecol 73:1054–1070
34. Tang CK, Toker C, Ances IG (1979) Stromomyoma of the uterus. Cancer 43:308–316
35. TeLinde RW (1946) Discussion of Henderson: endolymphatic stroma myosis. Am J Obstet Gynecol 52:1013
36. Thatcher SS, Woodruff JD (1982) Uterine stromatosis: a report of 33 cases. Obstet Gynecol 59:428–434
37. Yu TJ, Iwasaki I, Teratani T, Tanaka T, Aoki M (1986) Circumscribed endometrial stromatosis of the uterus with marked epitheliogenesis. Gynecol Oncol 24:367–372
38. Zámecnik M, Michal M (1998) Endometrial stromal nodule with retiform sex-cord-like differentiation. Pathol Res Pract 194:449–453

Virchows Arch (2001) 439:109–117
DOI 10.1007/s004280100476

REVIEW ARTICLE

Ilka Vogel · Holger Kalthoff

Disseminated tumour cells

Their detection and significance for prognosis of gastrointestinal and pancreatic carcinomas

Received: 9 May 2001 / Accepted: 9 May 2001 / Published online: 7 July 2001
© Springer-Verlag 2001

Abstract Metastatic spread is a major factor in the prognosis of cancer patients. Early detection and eradication of circulating tumour cells prior to the development of metastases could help to improve the outcome of patients after tumour resection. Disseminated tumour cells have been detected in different compartments of the body using cytological and immunostaining methods and, more recently, using different molecular biological techniques. The most frequently studied body compartments are the bone marrow, peritoneal cavity, blood and lymph nodes, but other body fluids such as urine, bile, pancreatic juice and sputum have also been analysed. At all of these sites, tumour cells have been detected. However, the specificity and sensitivity of the methods and their prognostic impact are still being debated. This review discusses the accuracy of the detection methods and the prognostic value of detecting disseminated tumour cells in the bone marrow, blood and peritoneal lavage of patients with colorectal, gastric and pancreatic carcinomas.

Keywords Disseminated tumour cells · Immunocytochemical detection · Molecular detection · Prognosis · Gastrointestinal carcinoma · Pancreatic carcinoma

Introduction

Early tumour diagnosis, improved surgical treatment and multimodal therapeutic concepts have helped to reduce the mortality of patients with gastrointestinal and pancreatic carcinoma. Nevertheless, the survival rates of these patients are still highly unsatisfactory. The prognosis depends on local tumour recurrence and/or the occurrence of distant metastases. Staging systems, such as the TNM classification, have been developed to help estimate the probability of further tumour progression after treatment. Detection of disseminated tumour cells at a distance from the primary tumour before the development of metastases or local tumour recurrence may help to refine the TNM system [22].

In recent years, numerous immunocytochemical and molecular studies have shown that micrometastases and disseminated tumour cells can be demonstrated not only in lymph nodes that had appeared tumour free on conventional histology [37], but also in such body compartments as the bone marrow, peritoneal cavity and blood [15, 16, 25, 54, 55, 59]. Not only have increasing numbers of compartments been analysed; studies have been extended to other malignancies that seldom demonstrate metastatic spread to the bone, such as oesophageal, pancreas or primary hepatic tumours [32]. From these data, it has been concluded that conventional staging most likely underestimates the true tumour stage. However, because the techniques used to identify disseminated tumour cells have not yet been standardised, the detection of disseminated tumour cells was not included in the most recent TNM classification. It does, however, recommend documenting any relevant findings. If isolated tumour cells are detected immunocytochemically in lymph nodes, the UICC suggests adding an "i+" in parentheses along with the N stage. If molecular findings indicate the presence of tumour cells, a "mol+" should be added [23].

Disseminated tumour cells are detected by means of immunocytochemical or molecular methods designed to recognise certain tumour-associated antigens and/or cell lineage-specific markers, such as cytokeratins (CKs) [15, 16, 43, 54]. These markers are not tumour specific, however, but may also be expressed by non-neoplastic cells. If both the immunocytochemical and the molecular analyses are to be valid, it is therefore of the utmost importance to avoid generating "false-positive" data, i.e. recognising non-neoplastic cells instead of tumour cells. However, a high degree of sensitivity must be reached to reduce "false-negative" results.

Another crucial issue is the biological significance of the disseminated tumour cells that are detected. Are these

I. Vogel (✉) · H. Kalthoff
Molecular Oncology Research Laboratory,
Department of General and Thoracic Surgery, University of Kiel,
Arnold-Heller-Strasse 7, 24105 Kiel, Germany
e-mail: ivogel@surgery.uni-kiel.de
Tel.: +49-431-5974481, Fax: +49-431-597-1939

cells able to proliferate and give rise to metastases by interacting with the environment, or are they in a state of dormancy, arrested in the G0 phase [58] and waiting to proliferate at a later point in time? An important answer to these questions will probably come from studies on the prognostic relevance of disseminated tumour cells detected in the bone marrow, peritoneal cavity and blood. This article reviews these issues by discussing the various detection methods used so far and the prognostic relevance of the results gained from these studies.

Detection methods

Sensitivity and specificity

The detection rate of disseminated tumour cells is affected by various factors, including number of analysed cells, collection and treatment of the sample, cell separation protocol, selection of antibodies and primers, and evaluation techniques.

The number of cells investigated clearly determines the detection rate in a given patient, although the sensitivity of the various assays is high, ranging from one tumour cell in 10^6 to one in 10^7 mononuclear cells [27, 52, 66]. It has also been demonstrated that multiple samples taken from different sites result in higher detection rates than single samples [53].

All methods rely on the recognition of antigens or gene transcripts that are expressed only by tumour cells and not by the surrounding cells. It is often difficult to find such a specific antigen, but, even if there is a marker supposed to be expressed by the tumour cells, antigen expression in the disseminated tumour cells can vary greatly [33], because antigens expressed by the primary tumour may have been downregulated or lost. For some markers [prostate-specific antigen (PSA), mucins], modulation due to hormonal influence has been demonstrated [28]. This problem might be overcome by the parallel use of multiple markers.

False-positive results can also occur regardless of the methods applied [immunostaining or reverse-transcription polymerase chain reaction (RT-PCR)], if epithelial markers are used, due to contamination with skin cells or release of epithelial cells in benign proliferative diseases [24, 52, 72]. The isolation of mononuclear cells [34] may lead to loss of tumour cells and result in false-negative data due to small sample volumes.

Immunostaining approaches

Several studies have clearly demonstrated that immunocytochemistry is superior to conventional cytology at detecting isolated tumour cells in the bone marrow [42, 61]. Immunostaining methods for detecting disseminated epithelial tumour cells in mesenchymal compartments, such as the bone marrow, employ antibodies directed against a variety of epithelial cell markers. Pan-specific antibodies against CK seem to have a higher specificity than antibodies directed against the epithelial mucin family [14, 61] (Fig. 1). However, in addition to increased sensitivity, a higher number of false-positive results due to non-specific labelling have been observed. The main reasons were (i) expression of some epithelial antigens by a few haematological cells [5], (ii) endogenous alkaline phosphatase in cases where anti-alkaline phosphatase (APAAP) complexes were used [3] and (iii) phagocytosed stainable material in granulocytes [48].

Molecular biological approaches

Chromosomal abnormalities can be detected in haematological malignancies using breakpoint-specific PCR tests. In solid tumours, this molecular approach is not applicable, because the chromosomal abnormalities are much more heterogeneous and complex. However, in solid tumours, it is possible to identify disseminated tumour cells by detecting RNA specific to the tissue of origin of these cells [6]. The method of choice is the RT-PCR, which has been further refined by many investigators so that it is applicable to the detection of disseminated tumour cells.

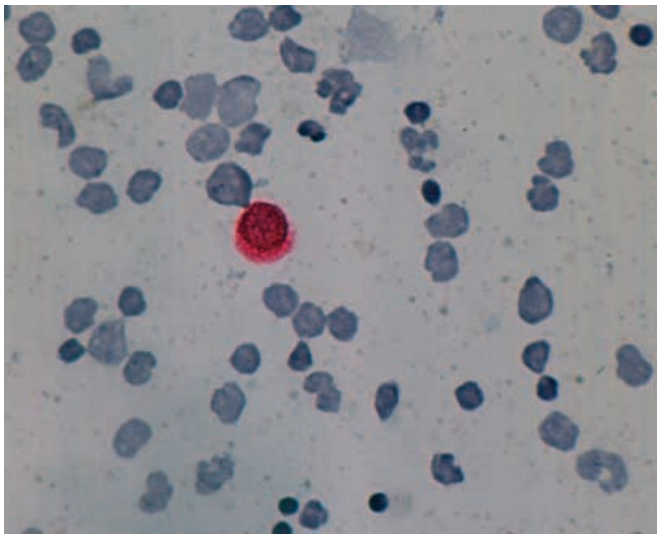


Fig. 1 Disseminated tumour cell in the bone marrow of a patient with colorectal carcinoma. Using the alkaline phosphatase with anti-alkaline phosphatase (APAAP) technique, staining was performed with a cocktail of the following antibodies: C1-P83 [carcinoembryonic (CEA)], Ca 19–9, KL-1 (cytokeratin); counterstaining with haemalum

When disseminated tumour cells are analysed using RNA-based assays for epithelial cells, it has to be assumed that cells of non-haematopoietic origin normally do not circulate in the peripheral blood or bone marrow. The target RNA should not be expressed by haematopoietic cells, but exclusively by the disseminated tumour cells that are to be identified. Alternatively, a two-step procedure of enrichment and/or derichment methods needs to be included. Studies of target RNAs for tumours of gastrointestinal origin have mainly focused on tissue-specific markers, such as CKs (CK19, CK20; Fig. 2) and mucins, or on tumour-associated antigens such as carcinoembryonic antigen (CEA) [15, 16, 25, 56, 59]. The PCR assays can detect a single target cell in up to 100 million irrelevant cells in spiking experiments [10, 66]. Direct comparison of molecular methods using immunostaining approaches showed that the PCR method is potentially 100 times more sensitive [64]. Moreover, by means of the PCR technique, target nucleic acids can be amplified by a factor of 10^6–10^9 within less than 1 h. The high sensitivity and specificity of these assays can be limited, however, by DNA contamination [35], "illegitimate" expression (transcription of any gene in any cell type) of epithelial or tumour-specific antigens in haematopoietic cells [5, 11, 29], upregulation of target mRNA expression by inflammation or hormonal induction of gene expression [28], the existence of pseudogenes, which can lead to false-positive results in healthy individuals [28, 29, 47] or in patients with benign diseases [16], or the degradation of RNA during the various steps of the assay protocol [31].

The detection rates achieved for venous blood samples using RT-PCR are lower than corresponding analyses in bone marrow samples. Possible explanations for this phenomenon are (i) qualitative and quantitative differences between cells in the bone marrow and venous blood, (ii) differences in survival or immune escape possibilities in different compartments and (iii) methodological aspects, such as loss of tumour cells due to masking with thrombocytes or clotting problems.

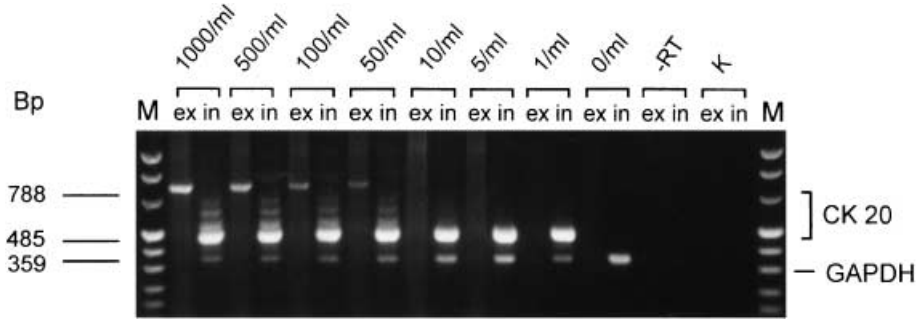


Fig. 2 Cytokeratin 20 (CK20)-specific nested reverse-transcription polymerase chain reaction (RT-PCR) after serial dilution of RNA from the pancreatic tumour cell line A818–4 (cells per millilitre). Separation of samples was done by agarose-gel electrophoresis and staining with ethidium bromide. The corresponding control reaction was performed as GAPDH RT-PCR (359-bp product) using a duplex approach. *ex* RT-PCR product (788 bp) using the external primers, *in* nested PCR product (485 bp), *–RT* amplification without reverse transcription, *K* water control, *M* molecular weight marker

Characterisation of disseminated tumour cells

In addition to detecting disseminated tumour cells, it is necessary to characterise them in more detail, especially because of therapeutic implications. Features that are of interest in this respect are the immunogenic potential of the cells, their proliferation activity, and their expression of growth factors and adhesion molecules. The identification of these features on disseminated tumour cells requires double labelling of the cells, which has been performed using various techniques. Studies using these methods revealed downregulation of major histocompatibility complex (MHC) class-I antigen in colorectal and gastric carcinomas [51, 62], neoexpression of intercellular adhesion molecule (ICAM)-1 and melanoma cell adhesion molecule (MUC-18) and downregulation of desmosomal protein [53], reduced expression of Ki67 (proliferation-associated antigen) in gastrointestinal carcinoma [51], reduced expression of PCNA (proliferating cell nuclear antigen) in prostatic cancer [45], expression of growth factor receptors (transferrin, c-erbB2) in metastatic breast cancer [51], expression of E-cadherin (adhesion molecule) in breast and gastric cancer [13] and expression of the urokinase plasminogen activator (uPA) receptor [1].

New methods have been developed in recent years by combining either immunostaining methods or immunofluorescence with in situ hybridisation (FISH) [30, 39, 44] or single-cell PCR techniques [33]. With these techniques, it was possible to prove the malignancy of cells by detecting identical chromosomal abnormalities to those in the primary tumour [45]. These techniques have also been used to demonstrate the heterogeneity of disseminated tumour cells found at different sites in a single patient [33]. Cultures of disseminated cells have been successfully established in vitro, increasing the cell number available for further phenotypic and genotypic analysis [49, 58].

Results of the clinical studies and prognostic impact

Colorectal carcinoma

Immunocytochemical analyses of bone marrow samples from patients with colorectal carcinoma were initially performed by Schlimok et al. [61] with a monoclonal antibody called CK2, which specifically reacts with CK18 [9]. Further studies with the same antibody revealed detection rates in the bone marrow between 16% and 32%. Other studies using combinations of antibodies found disseminated cells in the bone marrow in up to 74% of the cases [4], whereas PCR tests yielded positive results in 31–84% of the patients [26]. Specificity was evaluated in all studies by analysing samples from patients without any evidence of carcinoma or from healthy subjects. Most of the studies had a false-positive rate of below 10% [27, 52, 65, 78]. Using multivariate analysis, Lindemann [38] showed that detection of disseminated tumour cells in the bone marrow with the monoclonal antibody CK2 is an independent prognostic factor for survival (Table 1). Leinung et al. [36] used the pan-specific CK antibody A45-B/B3, which detects a common epitope on a variety of CK types, including CK8, CK18 and CK19 [68], and also found that the detection of disseminated tumour cells had a significant influence on survival. Other authors combined different antibodies directed against CKs and/or tumour-associated antigens, but none of them performed multivariate analyses to demonstrate prognostic relevance [4, 27, 65]. To date, none of the studies analysing peritoneal washings has demonstrated that the detection of disseminated tumour cells in patients with colorectal carcinoma is an independent prognostic marker [4, 27, 65] (Table 1).

Most molecular biological studies have been performed on bone marrow and/or venous blood from patients with colorectal carcinoma. CK genes, especially the CK19 and CK20 genes, have been used as marker genes [7, 10, 12, 17, 59, 66, 75, 77, 78]. The gene of the CEA was also tested in several studies [26, 59, 69]. Since haematopoietic cells can “illegitimately” express tumour-associated antigens or epithelial cell-specific antigens [17, 79] and pseudogenes may give rise to PCR products identical to those of marker genes, the RT-PCR assays resulted in a large number of false-positive signals [17]. So far, the CK20 gene seems to be the best marker, although some false-positive results have been observed with this also [75, 76]. Our analyses of 295 patients with curative resections showed for the first time that the detection of disseminated tumour cells in the bone marrow and/or venous blood is an independent prognostic factor for overall survival in patients with colorectal carcinoma [75] (Table 2). It was clearly demonstrated that tumour cells are present in the bone marrow and blood in colorectal carcinoma patients. Detection

Table 1 Prognostic relevance of immunocytochemical studies on bone marrow (*BM*) and/or peritoneal lavage (*PL*) obtained from patients with colorectal carcinoma prior to tumour resection

Marker	Pat. no.	No. of controls (pat. without carcinoma)	Bone marrow positivity	Prognostic relevance univar. analysis	Prognostic relevance multivar. analysis	Peritoneal lavage positivity	Prognostic relevance univar. analysis	Prognostic relevance multivar. analysis	Author
CK18 (MAb: CK2)	156	102 BM negative	42/156 (27%)	+	Ø				[62]
CK18 (MAb: CK2)	88	102 BM negative	28/88 (32%)	+	+				[38]
A33, AE1, CK18, CAM5	80	20 BM negative	4/42 (9%) resected pat. 13/38 (34%) non-res. pat.	-	Ø				[8]
CK (A45-B/B3)	145	51 BM negative	36/145 (24%)	+	+				[36]
CEA, Ca 19-9, 17-1-A, C 54-0, Ra 96, KL-1	109	45 pat. 2 pos. (BM) pancreatitis 3 pos. (PL) pancreatitis, hep. C	35/105 (33%)	-	Ø	34/109 (31%)	+	Ø	[65]

+: relevant to prognosis, –: not relevant to prognosis, ∅: not done; univar.: univariate analysis; multivar.: multivariate analysis

Table 2 Prognostic relevance of molecular biological studies (PCR) on bone marrow (*BM*) and/or peripheral blood (*BL*) obtained from patients with colorectal carcinoma prior to tumour resection

Marker	Pat. no.	No. of controls (pat. without carcinoma)	Bone marrow positivity	Prognostic relevance univar. analysis	Prognostic relevance multivar. Analysis	Blood positivity	Prognostic relevance univar. analysis	Prognostic relevance multivar. analysis	Author
CEA	53	32 healthy controls, 14 benign diseases all negative				18/53 (34%) peripheral blood 36/53 (68%) tumour-drainage blood	+ (dis. free)	Ø	[69]
K-ras	27	no details				9/27 (33%)	+ (dis. free)	Ø	[18]
CK20	65 (BM) 52 (BL)	22 patients 2/22 pos (BM) 58 pat. 2/58 positive (BL)	20/65 (31%)	+	Ø	9/52 (17%)	+	Ø	[67]
CK20	25	6 healthy pat. (BM) all negative, 12 healthy pat.(BL) 1 positive				12/25 (48%)	-	Ø	[77]
CK19, CK20, MUC1, MUC2	94	64 benign dis. 3/30 adenomas 4/34 inflammatory 0/20 normal				for all markers: 19/94 (20%)	+	+	[19]
CK20, CEA	52	10 pat. benign diseases, 10 healthy volunteers all negative				combination CEA/CK20 23/52 (44%) mesenteric; 8/52 (15%) peripheral	-	-	[78]
CK20	295	22 pat. 2/22 pos (BM) 58 pat. 2/58 positive (BL)	71/226 (31%)	+	+ (BM and/or BL)	82/243 (38%)	+	+ (BM and/or BL)	[75]

+: relevant to prognosis, –: not relevant to prognosis, ∅: not done; univar.: univariate analysis; multivar.: multivariate analysis

rates were higher in patients whose tumours were in an advanced stage than in those with early tumour stages, although disseminated tumour cells were already detectable in up to 20% of patients with early tumour stages [75]. Only a few other studies have also focused on the prognostic relevance of tumour cell detection (Table 2). They confirmed that disseminated cells are of prognostic value for these patients, but the results need to be established by multicenter clinical trials under standardised conditions.

Table 3 Prognostic relevance of immunocytochemical studies on bone marrow (*BM*) and/or peritoneal lavage (*PL*) obtained from patients with gastric carcinoma prior to tumour resection

Marker	Pat. no.	No. of controls (pat. without carcinoma)	Bone marrow positivity	Prognostic relevance univar. analysis	Prognostic relevance multivar. analysis	Peritoneal lavage positivity	Prognostic relevance univar. analysis	Prognostic relevance multivar. analysis	Author
CK18 (MAb: CK2)	97	75 pat. (BM) all negative	34/97 (35%)	+	∅				[63]
CK18 (uPA-R)	78	no details	47/78 (60%)	-	∅				[20]
CK18 (MAb: CK2)	180	64 pat. (BM) all negative	95/180 (53%)	+	significant for T1/T2 tumours, N0 and intest. type				[24]
CK18 (Mab: CK2)	219	no details	95/180 (53%)	+	Additional prognostic factor for T1/T2 N0 patients				[21]
CEA, Ca 19-9, 17-1-A, C 54-0, Ra 96, KL-1	84	45 pat. 2 pos. (BM) pancreatitis 3 pos.(PL) pancreat., hep. C	30/60 (48%)	-	∅	33/62 (53%)	+	∅	[65]

+: relevant to prognosis, –: not relevant to prognosis, ∅: not done; univar.: univariate analysis; multivar.: multivariate analysis

Table 4 Prognostic relevance of molecular biological studies (PCR) on bone marrow (*BM*) and/or peripheral blood (*BL*) obtained from patients with gastric carcinoma prior to tumour resection

Marker	Pat. no.	No. of controls (pat. without carcinoma)	Bone marrow positivity	Prognostic relevance univar. analysis	Prognostic relevance multivar analysis	Blood positivity	Prognostic relevance univar. analysis	Prognostic relevance multivar. analysis	Author
CK20	49 (BM) 30 (BL)	22 pat. (BM) 2/22 pos 58 pat. (BL) 2/58 pos.	11/49 (22%)	+	∅	3/30 (17%)	+	∅	[67]

+: relevant to prognosis, –: not relevant to prognosis, ∅: not done; univar.: univariate analysis; multivar.: multivariate analysis

Gastric carcinoma

In immunocytological studies of patients with gastric carcinoma, the same monoclonal antibodies have generally been used to detect disseminated tumour cells in the bone marrow and the peritoneal cavity as in colorectal carcinoma patients. Detection rates in the bone marrow ranged between 25% and 82% [1, 4, 27]. Overall, this seems to be slightly higher than in colorectal carcinoma. Even higher detection rates (32–72%) were observed in the peritoneal cavity [4, 27, 65]. The explanation for this might be the higher rate of peritoneal carcinomatosis at the time of the primary operation in gastric carcinoma compared with colorectal carcinoma.

One study, published by Jauch in 1996 [24], included a multivariate analysis. It demonstrated that the presence of three or more cells in the bone marrow was of prognostic significance for disease-free survival, but only in patients with T1/2 tumours (UICC classification; Table 3). Heiss et al. [21] showed that tumour cell dissemination in the bone marrow was an additional prognostic factor in patients who are in early tumour stages (UICC I/II), are lymph node-negative (N0) and express PAI-1 (plasminogen activator inhibitor type 1).

Molecular analyses have been performed with CEA, CK19 and CK20 as markers [7, 25, 59, 67]. To date, the only studies to demonstrate in univariate analyses a significant difference in overall survival for patients with tumour cells in the bone marrow and blood were done by our group (Table 4). These studies included 22 bone marrow samples and 58 venous blood samples [67]. It is rather striking that the detection rate in the bone marrow was low relative to immunocytochemical studies, although advanced stages were included [67]. The likely explanation for this is that CK20 is not expressed at the protein level in every gastric carcinoma [43]. It is therefore necessary to evaluate other markers that might be more consistently expressed in gastric carcinomas.

Pancreatic carcinoma

Still fewer studies have dealt with patients with pancreatic ductal carcinoma. This may be a reflection of the poor

Table 5 Prognostic relevance of immunocytochemical studies on bone marrow (*BM*) and/or peritoneal lavage (*PL*) obtained from patients with ductal pancreatic carcinoma prior to tumour resection

Marker	Pat. no.	No. of controls (pat. without carcinoma)	Bone marrow positivity	Prognostic relevance univar. analysis	Prognostic relevance multivar. analysis	Peritoneal lavage positivity	Prognostic relevance univar. analysis	Prognostic relevance multivar. analysis	Author
CK2, KL-1, A45-B/B3	42	25 pat. (BM) all negative	24/42 (57%)	+ (R0)	∅				[70]
CK2, KL-1, A45-B/B3	48	33 pat. (BM) all negative	14/31 (48%) resected pat. 10/18 (59%) not res. pat.	+	∅				[60]
CK2, KL-1, A45-B/B3	48	33 pat. (BM) all negative	25/48 (52%)	+	∅				[71]
CEA, Ca 19-9, 17-1-A, C 54-0, Ra 96, KL-1	80	45. 2 pos. (BM) pancreatitis 3 pos. (PL) pancreatitis, hepatitis. C	27/71 (38%)	(trend)	∅	24/62 (39%)	+	∅	[74]

+: relevant to prognosis, –: not relevant to prognosis, ∅: not done; univar.: univariate analysis; multivar.: multivariate analysis

prognosis for these patients and the lower incidence of the disease than with colorectal carcinoma. Immunocytochemical analyses of bone marrow samples have been performed using cocktails of antibodies, mostly including Ca 19–9 as a tumour-associated antigen [60, 70, 71, 74]. In view of the higher number of advanced-stage patients in the respective series, detection rates of disseminated cells of almost 40–60% have been found [60]. In univariate analyses, most of the studies demonstrated shorter survival in patients in whom tumour cells were detected in the bone marrow, while our investigations were the only ones to demonstrate that detection of cells in the peritoneal lavage has an impact on patient prognosis [74] (Table 5).

Molecular analyses have been performed in only a small number of cases [2, 50, 57, 66, 67]. Neither detection in the bone marrow nor detection in the blood has been evaluated for prognostic impact. The only study so far to test mutant- Ki-ras (that is known to occur frequently in ductal carcinomas but also in hyperplastic duct lesions of the pancreas [40]) as a marker in the blood was on a series of ten patients [50]. Bilchik et al. [2] reported a PCR combination of three markers: MET (hepatocyte growth factor receptor gene c-met), GalNAc-T (β1,4-*N*-acetyl-galactosaminyl-transferase) and β-hCG (β-human chorionic gonadotropin) in an analysis of 33 patients. Their detection rate was 100% in stage-IV patients and 87.5% in stage-II and -III patients, if all three markers were combined. Obviously, these markers will need to be evaluated in a larger series.

Conclusion and perspectives

Our evaluation of the studies on colorectal, gastric and pancreatic ductal carcinomas indicates that detection of disseminated tumour cells in different compartments may lead to more accurate tumour staging. Further studies will be required, however, to verify the independent prognostic impact in each of the compartments analysed so far. Such studies should try to evaluate methodological aspects, such as methods for enriching mononuclear or tumour cells, and develop highly specific and sensitive detection systems (including methods, marker and primer choices). Before these methods can be incorporated into clinical routine, they need to be standardised.

Further studies should focus, in particular, on (semi)-quantitative RT-PCR, which additionally allows the amplification rate to be standardised. PCR reactions using multiple markers may overcome tumour cell heterogeneity and false-positive results and would therefore increase the sensitivity and specificity. The enrichment of tumour cells, e.g. by magnetic beads, could solve the problem of false-positive results by reducing the background noise. Initial analyses using this method have been very promising [10, 46].

If future studies confirm the results published so far, patients with proven disseminated tumour cells who have no other clinical or radiological evidence of disease after resection of the primary tumour should receive adjuvant therapy, because conventional staging underestimates the lymphatic and haematogenous spread of the tumour. As recurrences are sometimes seen after a period of years, it is likely that disseminated cells can persist in a dormant state for prolonged periods. There is some evidence that these cells cannot be reached by means of conventional chemotherapy but might be better targeted by antibody-based adjuvant cancer therapies [41, 73].

One problem that has to be considered is the heterogeneity of solid tumours, since it reduces the likelihood that all disseminated cells will be removed. An individualised characterisation of the tumour cells might be one solution, but this does not appear practicable in daily routine. The use of a cocktail of antibodies is more promising. Further analyses that consider methodological aspects, cell characterisation, the prognostic impact and new adjuvant

therapeutic approaches are necessary and will certainly lead to improvements in the treatment of gastrointestinal and pancreatic carcinoma in the near future.

Acknowledgements The authors thank Prof. Klöppel for critical reading the manuscript. They are also thankful to Mrs. Kay Dege and Heinke Brütting for English editing and typing the manuscript.

References

1. Allgayer H, Heiss MM, Riesenberg R, Grutzner KU, Tarabichi A, Babic R, Schildberg FW (1997) Urokinase plasminogen activator receptor (uPA-R): one potential characteristic of metastatic phenotypes in minimal residual disease. Cancer Res 57: 1394–1399
2. Bilchik A, Miyashiro M, Kelly M, Kuo C, Fujiwara Y, Nakamori S, Monden M, Hoon DS (2000) Molecular detection of metastatic pancreatic carcinoma cells using a multimarker reverse transcriptase-polymerase chain reaction assay. Cancer 88: 103–104
3. Borgen E, Beiske K, Trachsel S, Nesland JM, Kvalheim G, Herstad TK, Schlichting E, Quist H, Naume B (1998) Immunocytochemical detection of isolated epithelial cells in bone marrow: non-specific staining and contribution by plasma cells directly reactive to alkaline phosphatase. J Pathol 185:427–434
4. Broll R, Lembcke K, Stock C, Zingler M, Duchrow M, Schimmelpenning H, Strik M, Müller G, Kujath P, Bruch HP (1996) Tumorzelldissemination in das Knochenmark und in die Peritonealhöhle. Langenbecks Arch Chir 381: 51–58
5. Brugger W, Bühring HJ, Grünebach F, Vogel W, Kraul S, Müller R, Brümmendorf TH, Ziegler BL, Rappold I, Brossart P, Scheding S, Kranz L (1999) Expression of MUC-1 epitopes on normal bone marrow: implications for the detection of micrometastatic tumour cells. J Clin Oncol 17:1535–1544
6. Burchill SA, Bradbury MF, Pittman K, Southgate J, Smith B, Selby P (1995) Detection of epithelial cancer cells in peripheral blood by reverse transcriptase-polymerase chain reaction. Br J Cancer 71:278–281
7. Burchill SA, Lewis IJ, Selby P (1999) Improved methods using the reverse transcriptase-polymerase chain reaction to detect tumour cells. Br J Cancer 79:971–977
8. Cohen AM, Garin-Chesa P, Hanson M, Weyhrauch K, Kemeny N, Fong Y, Paty P, Welt S, Old L (1998) In vitro detection of occult bone marrow metastases in patients with colorectal cancer hepatic metastases. Dis Colon Rectum 41:1112–1115
9. Debus E, Weber K, Osborn M (1982) Monoclonal cytokeratin antibodies that distinguish simple from stratified squamous epithelia: characterization on human tissue. EMBO J 1:1641–1647
10. Denis MG, Lipart C, Leborgne J, LeHur PA, Galmiche JP, Denis M, Ruud E, Truchaud A, Lustenberger P (1997) Detection of disseminated tumor cells in peripheral blood of colorectal cancer patients. Int J Cancer 74:540–544
11. Desol G, Gatter KC, Stein H, Erber WN, Pulford KAF, Zinnek B, Mason DY (1984) Human lymphoid cells express epithelial membrane antigen. Implications for diagnosis of human neoplasms. Lancet 11:1123–1129
12. Funaki NO, Tanaka J, Sugiyama T, Ohshio G, Nonaka A, Yotsumoto F, Furutani M, Imamura M (2000) Perioperative quantitative analysis of cytokeratin 20 mRNA in peripheral venous blood of patients with colorectal adenocarcinoma. Oncol Rep 7:21–76
13. Funke I, Fries S, Rolle M, Heiss MM, Untch M, Bohmert H, Schildberg W, Jauch KW (1996) Comparative analyses of bone marrow micrometastases in breast and gastric cancer. Int J Cancer 65:755–761
14. Gendler SJ, Lancaster CA, Taylor-Papadimitriou J, Duhig T, Peat N, Burchell J, Pemberton L, Lalini EN, Wuilson D (1996) Molecular cloning and expression of human tumor-associated polymorphic epithelial mucin. J Biol Chem 265:15286–15293
15. Ghossein RA, Bhattacharya S, Rosain J (1999) Molecular detection of micrometastases and circulating tumor cells in solid tumors. Clin Cancer Res 5:1950–1960
16. Goeminne JC, Guillaume T, Symann M (2000) Pitfalls in the detection of disseminated non-hematological tumor cells. Ann Oncol 11:785–792
17. Gunn J, McCall JL, Yun K, Wright PA (1996) Detection of micrometastases in colorectal cancer patients by K19 and K20 reverse-transcription polymerase chain reaction. Lab Invest 75: 611–616
18. Hardingham JE, Kotasek D, Sage RE, Eaton MC, Pascoe VH, Dobrovic A (1995) Detection of circulating tumor cells in colorectal cancer by immunobead-PCR is a sensitive prognostic marker for relapse of disease. Mol Med 1:789–794
19. Hardingham JE, Hewett PJ, Sage RE, Finch JL, Nuttall JD, Kotasek D, Dobrovic A (2000) Molecular detection of blood-borne epithelial cells in colorectal cancer patients and in patients with benign bowel disease. Int J Cancer 89:8–13
20. Heiss MM, Allgayer H, Gruetzner KU, Funke I, Babic R, Jauch KW, Schildberg FW (1995) Individual development and uPA-receptor expression of disseminated tumor cells in bone marrow: a reference to early systemic disease in solid cancer. Nat Med 1:1035–1039
21. Heiss MM, Allgayer H, Gruetzner KU, Babic R, Jauch KW, Schildberg FW (1997) Clinical value of extended biologic staging by bone marrow micrometastases and tumor-associated proteases in gastric cancer. Ann Surg 226:736–745
22. Hermanek P, Sobin LH (eds) (1998) UICC TNM Classification of malignant tumors, 5th edn. Springer, Berlin Heidelberg New York
23. Hermanek P, Hutter RVP, Sobin LH, Wittekind C (1999) Classification of isolated tumor cells and micrometastasis. Cancer 86:2668–2673
24. Jauch KW, Heiss MM, Gruetzner U, Funke I, Pantel K, Babic R, Eissner HJ, Riethmüller G, Schildberg FW (1996) Prognostic significance of bone marrow micrometastases in patients with gastric cancer. J Clin Oncol 14:1810–1817
25. Johnson PW, Burchill SA, Selby PJ (1995) The molecular detection of circulating tumor cells. Br J Cancer 72:268–276
26. Jonas S, Windeatt S, O-Boateng A, Fordy C, Allen-Mersh TG (1996) Identification of carcinoembryonic antigen-producing cells circulating in the blood of patients with colorectal carcinoma by reverse transcriptase polymerase chain reaction. Gut 39:717–721
27. Juhl H, Stritzel M, Wroblewski A, Henne-Bruns D, Kremer B, Schmiegel W, Neumaier M, Wagener C, Schreiber HW, Kalthoff H (1994) Immunocytological detection of micrometastatic cells: comparative evaluation of findings in the peritoneal cavity and the bone marrow of gastric, colorectal and pancreatic cancer patients. Int J Cancer 57:330–335
28. Jung R, Krüger W, Hosch S, Holweg M, Kröger N, Gutensohn K, Wagener C, Neumaier M, Zander AR (1998) Specificity of reverse transcriptase polymerase chain reaction assays designed for the detection of circulating cancer cells is influenced by cytokines in vivo and in vitro. Br J Cancer 78:1194–1198
29. Jung R, Petersen K, Krüger W, Wolf M, Wagener C, Zander A, Neumaier M (1999) Detection of micrometastasis by cytokeratin 20 RT-PCR is limited due to stable background transcription in granulocytes. Br J Cancer 81:870–873
30. Kell MR, Winter DC, O´Sullivan GC, Shanahan F, Redmond HP (2000) Biological behaviour and clinical implications on micrometastases. Br J Surg 87:1629–1639
31. Keilholz U, Willhauck M, Rimoldi D, Brasseur F, Dummer W, Rass K, de Vries T, Blaheta J, Voit C, Lethe B, Burchill S (1998) Reliability of reverse transcription-polymerase chain reaction (RT-PCR)-based assays for the detection of circulating tumour cells: a quality-assurance initiative of the EORTC Melanoma Cooperative Group. Eur J Cancer 34:750–753
32. Kienle P, Weitz J, Klaes R, Koch M, Brenner A, Lehnert T, Herfarth C, von Knebel Doeberitz M (2000) Detection of isolated disseminated tumor cells in bone marrow and blood samples of patients with hepatocellular carcinoma. Arch Surg 135: 213–218

33. Klein CA, Schmidt-Kittler O, Sachardt JA, Pantel K, Speicher MR, Riethmüller G (1999) Comparative genomic hybridization, loss of heterozygosity, and DNA sequence analysis of single cells. Proc Natl Acad Sci U S A 96:4494–4499
34. Krüger W, Jung R, Kröger N, Gutensohn K, Fiedler W, Neumaier M, Jänicke F, Wagener C, Zander AR (2000) Sensitivity of assays designed for the detection of disseminated epithelial tumor cells is influenced by cell separation methods. Clin Chemistry 46:435–436
35. Kwok S, Higuchi R (1989) Avoiding false positives with PCR. Nature 339:237–238
36. Leinung S, Würl P, Weiss CL, Röder I, Schönfelder M (2000) Cytokeratin-positive cells in bone marrow in comparison with other prognostic factors in colon carcinoma. Langenbecks Arch Surg 385:337–343
37. Liefers GJ, Cleton-Jansen AM, van der Velde CJ, Hermans J, van Krieken JH, Cornelisse CJ, Tollenaar RA (1998) Micrometastases and survival in stage II colorectal cancer. New Engl J Med 339:223–228
38. Lindemann F, Schlimok G, Dirschedl P, Witte J, Riethmüller G (1992) Prognostic significance of micrometastatic tumor cells in bone marrow of colorectal cancer patients. Lancet 340: 685–689
39. Litle VR, Warren RS, Moore D II, Pallavicini MG (1997) Molecular cytogenetic analysis of cytokeratin 20-labeled cells in primary tumors and bone marrow aspirates from colorectal carcinoma patients. Cancer 79:1664–1670
40. Lüttges J, Reinecke-Lüthge A, Möllmann B, Menke MAOH, Clemens A, Klimpfinger M, Sipos B, Klöppel G (1999) Duct changes and K-ras mutations in the disease free pancreas: analysis of type, age relation and spatial distribution. Virchows Arch 435:461–468
41. Maxwell-Amstrong CA, Durrant LG, Scholefield JH (1999) Immunotherapy for colorectal cancer. Am J Surg 177:344–348
42. Molino A, Colombatti M, Bonetti F, Zaradini M, Pasini F, Perini A, Pelosi G, Tridente G, Veneri D, Cetto GL (1991) A comparative analysis of three different techniques for the detection of breast cancer cells in bone marrow. Cancer 67: 1032–1036
43. Moll R, Löwe A, Laufer J, Franke WW (1992) Cytokeratin 20 in human carcinomas. A new histodiagnostic marker detected by monoclonal antibodies. Am J Pathol 140:427–447
44. Müller P, Weckermann D, Riethmüller G, Schlimock G (1996) Detection of genetic alterations in micometastatic cells in bone marrow of cancer patients by fluorescence in situ hybridization. Cancer Genet Cytogenet 88:8–16
45. Müller P, Caroll P, Bowers E, Moore D II, Cher M, Presti J, Wessman M, Pallavincini M (1998) Low frequency epithelial cells in marrow aspirates from prostate cancer patients are cytogenetically aberrant. Cancer 83:538–546
46. Naume B, Borgen E, Nesland JM, Beiske K, Gilen E, Renolen A, Ravnas G, Quist H, Karesen R, Kvalheim G (1998) Increased sensitivity for detection of micrometastatases in bone marrow/peripheral blood stem-cell products from breast-cancer patients by negative immunomagnetic separation. Int J Cancer 78:556–560
47. Neumaier M, Gerhard M, Wagener C (1995) Diagnosis of micrometastases by the amplification of tissue-specific genes. Gene 159:43–47
48. Nicholson AG, Graham AN, Pezzella F, Agneta G, Goldstraw P, Pastorino U (1997) Does the use of immunohistochemistry to identify micrometastases provide useful information in the staging of node-negative non-small cell lung carcinomas? Lung Cancer 18:231–240
49. Noack F, Schmitt M, Bauer J, Helmecke D, Kruger W, Thorban S, Sandherr M, Kuhn W, Graeff H, Harbeck N (2000) A new approach to phenotyping disseminated tumor cells: methodological advances and clinical implications. Int J Biol Markers 15:100–104
50. Nomoto S, Nakao A, Kasai Y, Harada A, Nonami T, Takagi H (1996) Detection of ras gene mutations in perioperative peripheral blood with pancreatic adenocarcinoma. Jpn J Cancer Res 87:793–797
51. Pantel K, Schlimok G, Kutter D, Schaller G, Genz T, Wiebecke B, Backmann R, Funke I, Riethmüller G (1991) Frequent down-regulation of major histocompatibility class I antigen expression on individual micrometastatic carcinoma cells. Cancer Res 51:4712–4715
52. Pantel K, Schlimok G, Angstwurm M, Weckermann D, Schmaus W, Gath H, Passlick B, Izbicki JR, Riethmüller G (1994) Methodological analysis of immunocytochemical screening for disseminated epithelial tumor cells in bone marrow. J Hematother 3:165–173
53. Pantel K, Schlimock G, Angstwurm M, Passlick B, Izbicki JR, Johnson JP, Riethmüller G (1995) Early metastasis of human solid tumors: expression of cell adhesion molecules. Ciba Found Symp 189:157–170
54. Pantel K, Cote RJ, Fodstad Ø (1999) Detection and clinical importance of micrometastatic disease. J Natl Cancer Inst 91: 1113–1124
55. Passlick B, Thetter O, Pantel K, Kubuschok B, Pichlmeier U, Schweiberer L, Izbicki JR (1995) Bedeutung der regionalen lymphatischen Tumorzelldisseminierung bei Patienten mit resektablem nicht-kleinzelligem Bronchialcarcinom. Chirurg 66: 780–786
56. Pelkey TJ, Frierson HF Jr, Bruns DE (1996) Molecular and immunological detection of circulating tumor cells and micrometastases from solid tumors. Clin Chem 42:1369–1381
57. Piva MG, Navaglia F, Basso D, Fogar P, Roveroni G, Gallo N, Zambon C-F, Pedrazzoli S, Plebani M (2000) CEA mRNA identification in peripheral blood is feasible for colorectal, but not for gastric or pancreatic cancer staging. Oncology 59:323–328
58. Putz E, Witter K, Offner S, Stosiek P, Zippelius A, Johnson J, Zahn R, Riethmüller G, Pantel K (1999) Phenotypic characteristics of cell lines derived from disseminated cancer cells in bone marrow of patients with solid epithelial tumors: establishment of working models for human micrometastases. Cancer Res 59:241–248
59. Raj GV, Moreno JG, Gomella LG (1998) Utilization of polymerase chain reaction technology in the detection of solid tumors. Cancer 82:1419–1442
60. Roder JD, Thorban S, Pantel K, Siewert JR (1999) Micrometastases in bone marrow: prognostic indicators for pancreatic cancer. World J Surg 23:888–891
61. Schlimok G, Funke I, Holzmann B, Göttlinger G, Schmidt G, Häuser H, Swierkot S, Warnecke HH, Schneider B, Koprowski H, Riethmüller G (1987) Micrometastatic cells in bone marrow: in vitro detection with anitcytokeratin and in vivo labeling with anti-17-1A monoclonal antibodies. Proc Natl Acad Sci U S A 84:8672–8676
62. Schlimok G, Funke I, Bock B, Schweiberer B, Witte J, Riethmüller G (1990) Epithelial tumor cells in bone marrow of patients with colorectal cancer: immunocytochemical detection, phenotypic characterization, and prognostic significance. J Clin Oncol 8:831–837
63. Schlimok G, Funke I, Pantel K, Strobel F, Lindemann F, Witte J, Riethmüller G (1991) Micrometastatic tumor cells in bone marrow of patients with gastric cancer: methodological aspects of detection and prognostic significance. Eur J Cancer 27:1461–1465
64. Schoenfeld A, Kruger KH, Gomm J, Sinnett HD, Gazet JC, Sacks N, Bender HG, Luqmani Y, Coombes RC (1997) The detection of micrometastases in the peripheral blood and bone marrow of patients with breast cancer using immunohistochemistry and reverse transcriptase polymerase chain reaction for keratin 19. Eur J Cancer 33:845–861
65. Schott A, Vogel I, Krueger U, Kalthoff H, Schreiber HW, Schmiegel W, Henne-Bruns D, Kremer B, Juhl H (1998) Isolated tumor cells are frequently detectable in the peritoneal cavity of gastric and colorectal cancer patients and serve as a new prognostic marker. Ann Surg 227:372–379
66. Soeth E, Röder C, Juhl H, Krüger U, Kremer B, Kalthoff H (1996) The detection of disseminated tumor cells in bone marrow from colorectal-cancer patients by a cytokeratin-20-specific nested reverse-transcriptase-polymerase-chain reaction is related to the stage of disease. Int J Cancer 69:278–282

67. Soeth E, Vogel I, Röder C, Juhl H, Marxsen J, Krüger U, Henne-Bruns D, Kremer B, Kalthoff H (1997) Comparative analysis of bone marrow and venous blood isolates from gastrointestinal cancer patients for the detection of disseminated tumor cells using reverse transcription PCR. Cancer Res 57:3106–3110
68. Stosiek P, Kasper M, Karsten U, Goertchen R (1991) Detection of cancer metastasis in regional lymph nodes: comparative histological and immunohistological investigations with the broad-range anticytokeratin monoclonal antibody A45-B/B3. Neoplasma 38:43–47
69. Taniguchi T, Makino M, Suzuki K, Kaibara N (2000) Prognostic significance of reverse transcriptase-polymerase chain reaction measurement of carcinoembryonic antigen mRNA levels in tumor drainage blood and peripheral blood of patients with colorectal carcinoma. Cancer 89:970–976
70. Thorban S, Roder JD, Pantel K, Siewert JR (1996) Epithelial tumor cells in bone marrow of patients with pancreatic carcinoma detected by immunocytochemical staining. Eur J Cancer 32A:363–365
71. Thorban S, Roder JD, Siewert JR (1999) Detection of micrometastasis in bone marrow of pancreatic cancer patients. Ann Oncol 10[Suppl 4]:111–113
72. Traweek ST, Liu J, Battifora H (1993) Keratine gene expression in non-epithelial tissues. Detection with polymerase chain reaction. Am J Pathol 142:1111–1118
73. Vermorken JB, Claessen AM, van Tinteren H, Gall HE, Ezinga R, Meijer S, Scheper RJ, Meijer CJ, Bloemena E, Ransom JH, Hanna MG Jr, Pinedo HM (1999) Active specific immunotherapy for stage II and stage III human colon cancer: a randomised trial. Lancet 353:345–350
74. Vogel I, Krüger U, Marxsen J, Soeth E, Kalthoff H, Henne-Bruns D, Kremer B, Juhl H (1999) Disseminated tumor cells in pancreatic cancer patients detected by immunocytology: a new prognostic factor. Clin Cancer Res 5:593–599
75. Vogel I, Soeth E, Röder C, Kremer B, Henne-Bruns D, Kalthoff H (2000) Multivariate analysis reveals RT-PCR-detected tumour cells in the blood and/or bone marrow of patients with colorectal carcinoma as an independent prognostic factor. Eur J Clin Oncol 26:281
76. Wharton RQ, Jonas SK, Glover C, Khan ZA, Klokouzas A, Quinn H, Henry M, Allen-Mersh TG (1999) Increased detection of circulating tumor cells in the blood of colorectal carcinoma patients using two reverse transcription assays and multiple blood samples. Clin Cancer Res 5:4158–4163
77. Wyld DK, Selby P, Perren TJ, Jonas SK, Allen-Mersh TG, Wheeldon J, Burchill SA (1998) Detection of colorectal cancer cells in peripheral blood by reverse-transcriptase polymerase chain reaction for cytokeratin 20. Int J Cancer 79: 288–293
78. Yamaguchi K, Takagi Y, Aoki S, Futamura M, Saji S (2000) Significant detection of circulating cancer cells in the blood by reverse transcriptase-polymerase chain reaction during colorectal cancer resection. Ann Surg 232:58–65
79. Zippelius A, Kufer P, Honold G, Köllermann MW, Oberneder R, Schlimok G, Riethmüller G, Pantel K (1997) Limitations of reverse transcriptase-polymerase chain reaction analyses for detection of micrometastatic epithelial cancer cells in bone marrow. J Clin Oncol 15:2701–2708

Virchows Arch (2001) 439:118–126
DOI 10.1007/s004280100418

ORIGINAL ARTICLE

Efthimios Sivridis · Alexandra Giatromanolaki

Prognostic aspects on endometrial hyperplasia and neoplasia

Received: 16 November 2000 / Accepted: 14 January 2001 / Published online: 17 March 2001
© Springer-Verlag 2001

Abstract There are various forms of endometrial hyperplasia which, in terms of prognosis and therapy, can be subdivided into those having cytological atypia and those lacking this feature. The former may progress into invasive endometrial malignancy through a transitional non-invasive stage. This is a continuous process and, as a result, the distinction between an atypical hyperplasia and an intraepithelial adenocarcinoma (IEA) or an adenocarcinoma with stromal invasion is not histologically reproducible. The concept of endometrioid neoplasia, which includes the entire spectrum of the aforementioned proliferating endometrial lesions, was introduced. Adenocarcinomas arising from an atypical hyperplasia are invariably of the endometrioid cell type, whereas those developing from an atrophic endometrium may be either of the endometrioid or of the non-endometrioid cell type. Endometrioid adenocarcinomas arising through the hyperplasia–neoplasia sequence are oestrogen induced and tend to be well differentiated and less invasive of the myometrium, lack lymphatic and metastatic involvement and have an excellent prognosis. Oestrogen-induced adenocarcinomas are also endometrioid, arising from an atrophic or a rather weakly proliferating endometrium, but these neoplasms are frequently of higher histological grade and have a somewhat less favourable prognosis. Finally, endometrial carcinomas of the non-endometrioid cell type, mainly serous papillary and clear cell carcinomas, are non-oestrogen induced, non-hyperplasia associated and show adverse aggressive histological features and an extremely poor prognosis. The antigenic characteristics and the molecular events associated with the development of these forms of endometrial malignancy are distinct and allow the description of, at least, two pathogenetic types of endometrial carcinoma.

E. Sivridis (✉) · A. Giatromanolaki
Department of Pathology, Democritus University of Thrace, Alexandroupolis, 68100, PO Box 128, Greece
e-mail: esivrid@med.duth.gr
Tel.: +30-551-22212, Fax: +30-551-37833

Keywords Hyperplasia · Neoplasia · Carcinoma · Endometrioid · Non-endometrioid

Introduction

The endometrial hyperplasias are common gynaecological disorders. These are, in terms of histology, of three forms: simple, complex and atypical [12, 95]. The latter is frequently progressed to a well-differentiated endometrioid adenocarcinoma with stromal invasion, probably through the transitional stage of an intraepithelial adenocarcinoma (IEA) [3, 20, 25, 28, 54]. The question is, how reproducible can a distinction be within the continuous spectrum of atypical hyperplasia, IEA and well-differentiated invasive endometrioid adenocarcinoma?

The endometrial carcinoma is the most common gynaecological malignancy in many parts of the world, including North America and Northern Europe [22, 38, 78, 115]. These tumours are associated either with a hyperplastic or, more frequently, with an atrophic endometrium. Adenocarcinomas arising from hyperplasias are invariably of the endometrioid cell type, whereas those developing from an atrophic or a rather weakly proliferating endometrium may be either of the endometrioid or of the non-endometriod cell type [13, 98]. These observations raise two questions [98]: (1) whether endometrioid adenocarcinomas arising from an atrophic endometrium are different in terms of hormonal stimulation, histological features and prognosis than those of similar histological type and grade, which are associated with a hyperplastic endometrium and (2) whether endometrioid adenocarcinomas arising from an atrophic endometrium are in some way similar with those carcinomas of the non-endometrioid cell type, arising from a similar type endometrium.

We present here a review of the silent features of the endometrial hyperplasias and their relationship to endometrial adenocarcinoma. We further discuss recent advances in histopathology, immunohistochemistry and molecular pathology of endometrial malignancy, with

special reference to the different pathogenetic types of endometrial carcinoma.

The endometrial hyperplasias

Hyperplasia is, in general terms, the increase in size of an organ or a tissue as a result of an increase in the number of its constituent cells. The hyperplastic cells are, in many ways, similar to normal or may appear slightly enlarged (hypertrophic). In the endometrium, there is the paradox that a distinction should be made whether the increased number of glandular endometrial cells are truly hyperplastic or whether they are "atypical". This has a tremendous impact on the subsequent biological course, since endometrial hyperplasias with cytological atypia are associated with a significant risk of evolving into an endometrial adenocarcinoma [3, 20, 25, 27, 54]. The other peculiarity of the hyperplastic process in the endometrial tissues is that this may affect, as indeed it should, both endometrial glands and stroma or may involve only the endometrial glands.

On the basis of these observations, the endometrial hyperplasias are classified into hyperplasias with and without cytological atypia, the latter being further subdivided into simple and complex forms [12]. In this classification, simple endometrial hyperplasia represents a true hyperplastic process involving both glands and stroma [12, 28]. It is invariably diffuse, and the cells resemble those of the normal proliferative endometrium. The complex and atypical endometrial hyperplasias involve only glands and are usually focal rather than diffuse. The glandular endometrial cells are hyperplastic in the first case, but show features of atypia in the latter. The common denominator for all forms of endometrial hyperplasia is prolonged oestrogenic stimulation of the endometrium, unopposed by progesterone action. These forms of hyperplasia commonly occur in pure forms, but it is by no means unusual to exist in any possible combination.

Endometrial hyperplasia without cytological atypia: simple and complex

Simple endometrial hyperplasia is by far the most common form of endometrial hyperplasia [12, 27, 28]. The main diagnostic features of this form of endometrial hyperplasia are: an increase in endometrial volume – bulky curettings, frequently misinterpreted as carcinomatous by clinicians; the patients' age, this usually being between 40 years and 50 years; the presence of a number of large cystically dilated glands, although many are of normal size or even smaller; the presence of an abundant cellular endometrial stroma; and the presence of mitotic activity in both glands and stroma. There is also some multilayering of epithelial cells, and there may be some epithelial budding into the surrounding stroma, but no intraluminal tufting or cytological atypia is seen. An equally characteristic and frequent feature, although less important in establishing the diagnosis, is the presence of large ectatic vascular channels. There is no appreciable risk of progression to endometrial adenocarcinoma (approximately 1%) [12, 25, 27, 28, 40, 54].

Complex endometrial hyperplasia is restricted to the glands of the endometrium, and it is usually focal rather than diffuse [12, 27, 28]. It is characterised by crowding of endometrial glands and a complex outline, often with outpouchings and infoldings, giving a characteristic "fingers-in-glove" appearance. There is a loss of endometrial stroma which appears inactive. There may be multilayering of the epithelium, but there is no evidence of cytological atypia and the risk of progression is only 3% [39, 54]. For reasons related to reproducibility and to the common clinical outcome, simple and complex hyperplasia were combined in one category called "hyperplasia" by Bergeron et al. in a recent multicentric study [7].

Endometrial hyperplasia with cytological atypia: atypical hyperplasia

The concept of endometrioid neoplasia

Atypical endometrial hyperplasia is also restricted to the glandular component of the endometrium, and it is usually focal, although it may be multifocal or diffuse [12, 28]. It is characterised by crowding and architectural complexity of the glands but, in addition, it shows features of nuclear and cytological atypia: round and, often, enlarged nuclei, prominent nucleoli, chromatin clearing, hyperchromatism and a tendency for epithelial stratification with a loss of nuclear polarity. The amount of the supportive endometrial stroma is considerably reduced, often producing a "back-to-back" arrangement. The risk of progression to endometrial adenocarcinoma has been estimated as being between 25% [4, 20, 25, 39, 40, 44, 54] and 100% [26, 112].

With so many cases committed to invasion, it is uncertain whether atypical hyperplasia is, indeed, a form of endometrial hyperplasia [96], or whether it is a truly neoplastic, yet not invasive, lesion from its conception. Harold Fox maintains that atypical hyperplasia is, in essence, a form of intraendometrial neoplasia (adenocarcinoma in situ) in which the glands have undergone neoplastic change, but in which there is no invasion of the endometrial stroma [12, 27, 28]. In his view, it is doubtful whether an adenocarcinoma of this type exists, or if it could be recognised even if it did [12, 27, 28]. Furthermore, there is the problem of differentiating such a lesion(s) from a well-differentiated endometrioid adenocarcinoma that is confined to the endometrium and is not invading the myometrium. This is thought to be distinguished from atypical hyperplasia and from endometrial intraepithelial carcinoma on the evidence of stromal invasion, i.e. stromal fibrosis, stromal necrosis or stromal polymorphonuclear leucocytic infiltration [27, 94]. However, in most cases these features are absent, and no objective distinction between these conditions can be

Table 1 The endometrial hyperplasias: progression from atypical hyperplasia through intraepithelial adenocarcinoma (IEA) to invasive endometrioid adenocarcinoma

Simple hyperplasia Complex hyperplasia		Simple hyperplasia
Atypical hyperplasia	→IEA ⇓⇑ Adenocarcinoma with stromal invasion	Endometrioid neoplasia
	⇓ Adenocarcinoma with myometrial invasion	Endometrioid adenocarcinoma
Morphological and biological continuum of hyperplasia – neoplasia		

achieved. Indeed, the uncertainty to define invasion in a stroma which normally contains glands may lead to erroneous diagnosis up to 39% (15–39%) [8, 113]. It is, therefore, more appropriate to consider these, histologically indistinguishable, endometrial lesions, i.e. atypical hyperplasia, IEA and endometrioid adenocarcinoma, with stromal invasion, under the unifying "umbrella" term of endometrioid neoplasia, as suggested by the study group of Bergeron et al. [7] (Table 1). This idea, first proposed by Sherman and Brown [90] and subsequently by Fox and Buckley [27], is both theoretically and practically justifiable.

The endometrioid adenocarcinomas

Endometrioid adenocarcinomas arising from atypical hyperplasia

All endometrial adenocarcinomas arising from a hyperplastic endometrium are of the endometrioid cell type. These tumours are oestrogen-induced and have been reported to occur with a frequency of 15–65% [9, 45, 56, 98]. The endometrioid adenocarcinomas are composed, in whole or in part, of complex glandular structures, reminiscent of normal proliferative glands [60]. They are lined by columnar cells showing a variable degree of nuclear atypia and mitotic activity. The glandular structures are closely packed, often assuming a true back-to-back pattern but, most importantly, they show myometrial or stromal invasion. This neoplasm occurs, for the most part, in young women, is diagnosed at an early stage, tends to be well-differentiated and less invasive of the myometrium, lack lymphatic involvement and has a most favourable prognosis: the 10-year survival rate is 92% [98]. Some G1 endometrioid carcinomas developing from a hyperplastic background can regress when treated with progestins [10, 59, 71], and it is therefore possible that they arise from cells which have undergone a relatively simple genetic change. The several histological variants of endometrioid adenocarcinomas, as categorised by Fox and Buckley, are shown in Table 2 [12]. This classification differs from that recommended by the World Health Organization (WHO) [95] only in its recognition of the adenosquamous carcinoma as a discrete entity.

Table 2 Endometrial carcinoma: pathogenetic types and histological variants

(1) Endometrioid adenocarcinoma associated with a hyperplastic endometrium

Usual type
Variants
- With squamous metaplasia
- Papillary
- Secretory
- Ciliated
- Sertoliform

(2) Endometrioid adenocarcinoma associated with an atrophic endometrium

Usual type
Variants
- (As above)

(3) Non-endometrioid carcinoma associated with an atrophic endometrium

Adenosquamous carcinoma[a]
Serous papillary adenocarcinoma
Clear cell adenocarcinoma
Mucinous adenocarcinoma
Squamous cell carcinoma
Mixed carcinoma
Undifferentiated carcinoma

[a] According to Fox and Buckley [12], adenosquamous carcinoma is a discrete entity

Endometrioid adenocarcinomas arising from an atrophic endometrium

The great majority of endometrioid adenocarcinomas, however, are unrelated to endometrial hyperplasia and develop from an atrophic, a weakly proliferating, or a normally cycling endometrium [98]. The role of oestrogens in the pathogenesis of this tumour type is less obvious, but it has not been eliminated. These women are somewhat older but have a more or less similar clinical and endocrine profile to those whose tumours arise from a hyperplastic endometrium and must, therefore, share a similar aetiology. However, oestrogenic stimulation has been shown to be relatively minor, albeit longer standing and, therefore, this neoplasm must arise from cells which are sensitive to low oestrogen levels and should, therefore, have a more complex genetic instability. Endometrioid adenocarcinomas arising from a non-hyperplastic endometrium tend, in general terms, to be of higher grade and stage, more deeply invasive of the myometrium and more commonly invasive of lymphatic spaces

than the endometrioid carcinomas arising from a hyperplastic background. The 10-year survival rate for women with endometrioid adenocarcinomas associated with an atrophic endometrium is 76% [98]. This difference in prognosis between the two groups of endometrioid adenocarcinomas is almost entirely due to the higher incidence of G2 and G3 carcinomas among those arising from an atrophic endometrium.

The non-endometrioid carcinomas

The non-endometrioid carcinomas occur with a frequency of less than 20% and develop from an atrophic endometrium [57, 98]. Typically, they occur in elderly women and are non-oestrogen-dependent. The non-endometrioid carcinomas show a higher incidence of the adverse prognostic factors of deep myometrial invasion, lymphatic space invasion and high stage than do either of the two subgroups of endometrioid adenocarcinomas. Serous papillary and clear cell carcinomas are the paradigms of this pathogenetic type.

Serous papillary carcinomas of the endometrium resemble ovarian serous carcinomas [15, 21, 34, 36]. The tumours comprise approximately 5% of all endometrial carcinomas. Characteristic histological features include complex papillae, with broad fibrovascular cores, lined by highly anaplastic tumour cells. Mitoses are numerous and often of abnormal forms. The neoplastic cells are of serous and of hobnail cell type and have the tendency to form intraluminal tufting and secondary papillae. There is a hyalinized or oedematous stroma. Psammoma bodies are frequently seen. In most cases (98%), these neoplasms appear to originate from an endometrial intraepithelial carcinoma [3, 105]. A serous papillary carcinoma may occasionally be confined to an endometrial polyp [92].

Clear cell carcinomas account for almost 5% of all endometrial carcinomas and are indistinguishable histologically from the clear cell carcinomas of ovarian, vaginal and cervical origin, also overlapping to some extent, with the serous papillary carcinoma of the endometrium [1, 12, 57, 61]. Clear cell carcinomas are composed of large tumour cells with clear or granular cytoplasm containing large pleomorphic, often bulging, nuclei. These hobnail cells are arranged in solid, papillary, tubulocystic or mixed patterns. The tumour cells contain abundant cytoplasmic glycogen but only rarely mucin. Hyalinisation may be prominent within the papillary cores, but psammoma bodies are infrequently identified. The tumours may involve, or occasionally be confined to, an endometrial polyp. Other, less common, variants of non-endometrioid carcinoma are shown in Table 2.

The non-endometrioid carcinomas are more aggressive (stage for stage) than their endometrioid counterparts and have an extremely poor prognosis: the 10-year survival rate is approximately 40% [1, 98].

Immunohistochemical and molecular characteristics of endometrial carcinomas: endometrioid versus non-endometrioid carcinomas

The notion of an endometrial carcinoma with at least two distinct pathogenetic types, i.e. endometrioid and non-endometrioid, is nowadays gaining considerable support by a number of immunohistochemical and molecular studies.

Oestrogen and progesterone receptor status

Oestrogen receptor (ER) and progesterone receptor (PR)-rich endometrial adenocarcinomas are usually well differentiated [14, 18, 97] and show superficial myometrial invasion [102] and low International Federation of Gynecology and Obstetrics (FIGO) stage [14, 18, 114]. These tumours are associated with the presence of bcl-2 [102], the absence of mutant p53 [68, 114] and with low intratumoural angiogenesis [102]. They are frequently of good prognosis [18, 56]. It is not surprising, therefore, that ER- and PR-loss is significantly associated with the non-endometrioid-type carcinomas [14, 102], including the adenosquamous variant [56] (Table 2).

Cell proliferation markers: proliferating cell nuclear antigen and Ki-67

Proliferating cell nuclear antigen (PCNA) expression in stage-I endometrial adenocarcinomas was found to correlate with tumour grade, depth of myometrial invasion and risk of recurrence [30]. Similar observations have been reported for the Ki-67 proliferation index [31, 67]. Most endometrioid carcinomas express low Ki-67 and have good prognosis, while most carcinomas of the serous papillary, clear cell and adenosquamous-type show high Ki-67 proliferation index and have poor prognosis [55, 56, 57].

p53

The mutant p53 oncoprotein is more commonly expressed in non-endometrioid tumours of the serous papillary and clear cell types than in endometrioid carcinomas [4, 41, 55, 56, 58, 62, 70, 92, 104, 106, 116]. p53 immunoreactivity is not a feature of endometrial hyperplasia [49, 92], but it occurs in approximately 85% of IEAs [89, 92, 104, 107, 116]. Most of the p53-positive cases were receptor negative (ER- and PR-negative) [52, 68] and observed in advanced stages and high histological-grade carcinomas [5, 50, 70, 75, 93, 104, 107]. Furthermore, p53 positivity is associated with poor prognosis [41, 50, 68, 84, 93, 103], the 5-year survival rate being 12% for patients overexpressing nuclear p53 compared with 90% for those who lack nuclear positivity [72]. These observations, though not unchallenged [32, 42, 43,

73], seem to indicate that endometrioid and non-endometrioid carcinomas are two distinct pathogenetic types of endometrial carcinoma.

bcl-2

The anti-apoptotic protein, bcl-2, is expressed cyclically in the normal endometrium, but it is also expressed in endometrial carcinomas with a frequency of 10–30% [32, 102]. The bcl-2 expression is not related to histopathological features or the surgical stage of disease [32, 63] and is, probably, of no prognostic value in endometrial carcinomas [32, 102]. bcl-2 is more frequently expressed in endometrioid carcinomas than in serous papillary tumours [116]. It is interesting that the staining intensity of bcl-2 diminished progressively from proliferative phase and hyperplastic endometrium to endometrioid carcinomas and then to serous papillary carcinomas [116].

Epidermal growth factor receptor

The epidermal growth factor receptor (EGFR) is expressed in 50% of endometrial carcinomas, particularly of the non-endometrioid cell type [47]. Its expression is related to the presence of metastatic disease at the time of diagnosis and to a decreased patient survival. However, other investigators failed to confirm these findings [75, 83].

c-erbB-2

The c-erbB-2 protein is a membrane glycoprotein growth factor receptor showing molecular homology with the EGFR. c-erbB-2 overexpression is detected in 10–85% of endometrial carcinomas [19, 47, 64, 76, 79, 111]. Overexpression of c-erbB-2 appears to be associated with high histological grade, deep myometrial invasion and lymph-vascular space invasion [47], emerging as an indicator of poor survival [37, 76, 79]. Both protein overexpression and gene amplification were associated with higher grade endometrial tumours and with serous papillary and clear cell types [74, 77].

Angiogenesis

Neo-angiogenesis is much more frequent in endometrial carcinomas than in endometrial hyperplasias [2] and may be connected with the state of the non-malignant endometrium adjacent to a carcinoma. In fact, endometrial tumours developing against a background of endometrial atrophy usually have higher microvessel density (MVD) compared with those arising from a hyperplastic endometrium [45, 65]. This is consistent with the view that endometrial carcinomas associated with endometrial atrophy have an unfavourable prognosis [98]. In some studies, angiogenesis was directly related with tumour grade [2, 46, 110], depth of myometrial invasion [2, 46, 85], lymph–vascular space invasion [46], lymph-node involvement [110] and stage of disease [85, 110]. Interestingly, Cheng et al. [17] reported comparable results in patients with endometrial carcinoma assessed for MVD pre-operatively using colour Doppler ultrasound. Yet other studies failed to establish any significant association between high MVD and histopathological parameters [6, 33].

There is, however, a clear relationship between high angiogenesis and poor prognosis. Indeed, patients bearing tumours with a high MVD have a significantly lower 5-year survival rate compared to those with a low MVD [33, 46, 48, 69, 80, 82, 85, 110]. Angiogenesis is unrelated to mutant p53 protein, but it is frequently connected with a loss of bcl-2 expression [33], an oncoprotein with a possible suppressive effect on new blood vessel formation [33, 53].

Vascular endothelial growth factor

Vascular endothelial growth factor (VEGF) and its receptors, mainly the VEGFR-2/Flk-1/KDR system, have been repeatedly implicated in the angiogenesis of many human tumours, including endometrial carcinoma [29, 35, 81, 86]. Thus, on many occasions, a high VEGF expression by endometrial tumour cells was connected with high MVD and with the adverse prognostic factors of aneuploidy [81], lymph vascular space involvement [86] and the non-endometrioid carcinomas of the serous papillary and clear cell type [81, 86]. In addition, there is a clear association between high VEGF expression and an unfavourable clinical outcome in patients with endometrial carcinomas.

Thymidine phosphorylase

Thymidine phosphorylase (TP) is another angiogenic factor which is invariably expressed in the normal, hyperplastic and malignant endometrium [99, 100]. In the normal endometrium, TP expression has well-defined cellular and tissue patterns which are dependent on the phase of the menstrual cycle. By contrast, TP expression in endometrial hyperplasias and carcinomas is at random. A high TP activity at the invading tumour front was associated with the non-endometrioid carcinomas and the adverse prognostic factors of high tumour grade, deep myometrial invasion and advanced stage of disease [99]. Furthermore, a high TP reactivity in the stromal cells was significantly related with poorly differentiated carcinomas and high MVD [85].

Concanavalin A

Canavalia ensiformis agglutinin (Con A) reacts strongly with the luminal borders and the cytoplasm of epithelial

cells. However, whilst in normal and benign endometrial tissues, the cytoplasmic staining was confined to the apical and the basal aspect of the cells in endometrial carcinomas and, in some atypical hyperplasias, lectin binding also occurred in the lateral cytoplasm (Con-A-lat), although in differing proportions of cells. Interestingly, extensive Con-A-lat in the tumour cells was much more frequent in non-endometrioid carcinomas than in endometriod neoplasms and was significantly associated with poor histological differentiation, low ER and PR content and an unfavourable survival [101].

Microsatellite instability, loss of heterozygosity and K-ras mutations

Microsatellites are simple repetitive DNA sequences that range in length from 100 bp to 300 bp [105]. There are approximately 100,000 such sequences scattered throughout the human genome [51]. Microsatellite instability (MI) is a common genetic abnormality in endometrial carcinomas, occurring with a frequency of 25–30% and appears to be an almost exclusive finding of the endometrioid carcinomas [16, 55, 58, 105]. K-ras gene mutations at codon 12 occur in 15–30% of endometrial carcinomas [23, 58, 87, 88, 109] and are also significantly more frequent in endometrioid carcinomas (26%) compared with serous papillary tumours (only 2%) [58].

By contrast, loss of heterozygosity (LOH) occurs more commonly in non-endometrioid carcinomas [108]; it is often on chromosome 10q25–10q26 [66]. Little information is, at present, available with regard to the prognostic significance of LOH and K-ras gene mutations in the various pathogenetic types of endometrial carcinoma.

DNA ploidy

DNA non-diploid patterns have been found in 13% of patients with endometrioid adenocarcinomas compared with 55% of patients with non-endometrioid carcinomas of the serous papillary, clear cell or undifferentiated types [24]. Aneuploidy is a significant objective indicator of poor survival [11, 24].

Conclusions

Atypical endometrial hyperplasias progress to endometrial carcinoma with a frequency of not less than 25%. Atypical hyperplasias are histologically indistinguishable from IEAs and from adenocarcinomas with stromal invasion, particularly in curettage specimens. It is suggested that the entire spectrum of these proliferating endometrial lesions should be considered under the unifying term of endometrioid neoplasia. Endometrial adenocarcinomas with myometrial invasion associated with atypical hyperplasia are invariably of the endometrioid cell type and have a favourable prognosis. Endometrial adenocarcinomas associated with an atrophic endometrium are either of the endometrioid cell type and have a relatively good prognosis or they are non-endometrioid carcinomas and have a grave prognosis. The antigenic and molecular profile of the malignant endometrium tends to favour the existence of these various pathogenetic types of endometrial carcinoma. Thus, most endometrioid carcinomas are ER/PR-positive, p53- and c-erbB-2-negative and express low Ki-67. In contrast, non-endometrioid tumours are ER/PR-negative, overexpress p53 and c-erbB-2 and show a high Ki-67 proliferative index. On the molecular genetic level, up to 30% of endometrioid carcinomas show MI and harbour mutant K-ras, whilst none of the serous papillary carcinomas show MI, and only 2% of them show K-ras mutations. With reference to DNA patterns, endometrioid carcinomas are usually diploid, whereas most serous papillary, clear cell and undifferentiated endometrial carcinomas are non-diploid.

References

1. Abeler VM, Kjorstad KE (1991) Clear cell carcinoma of the endometrium: a histopathological and clinical study of 97 cases. Gynecol Oncol 40:207–217
2. Abulafia O, Triest WE, Sherer MD, Hansen CC, Ghezzi F (1995) Angiogenesis in endometrial hyperplasia and stage I endometrial carcinoma. Obstet Gynecol 86:479–485
3. Ambros RA, Sherman ME, Zahn CM, Bitterman P, Kurman RJ (1995) Endometrial intraepithelial carcinoma: a distinctive lesion specifically associated with tumours displaying serous differentiation. Hum Pathol 26:1260–1267
4. Ambros RA, Sheehan CE, Kallakury BV, Ross JS, Malfetano J, Paunovich E, Figge J (1996) MDM2 and p53 protein expression in the histologic subtypes of endometrial carcinoma. Mod Pathol 9:1165–1169
5. Ayhan A, Tuncer ZS, Ruacan S, Ayhan A, Yasui W, Tahara E (1998) Abnormal expression of cripto and p53 protein in endometrial carcinoma and its precursor lesions. Eur J Gynaecol Oncol 19:316–318
6. Battifora H (1994) p53 immunohistochemistry: a word of caution. Hum Pathol 25:435–437
7. Bergeron C, Nogales FF, Masseroli M, Abeler V, Duvillard P, Muller-Holzner E, Pickartz H, Wells M (1999) A multicentric European study testing the reproducibility of the WHO classification of endometrial hyperplasia with a proposal simplified working classification for biopsy and curettage specimens. Am J Surg Pathol 23:1102–1108
8. Bhagavan BS, Parmley TH, Rosenshein NB, Jefferys JL, Grisso J-A, Stolley PD (1984) Comparison of estrogen-induced hyperplasia to endometrial carcinoma. Obstet Gynecol 64:12–15
9. Bokhman JV (1983) Two pathogenetic types of endometrial carcinoma. Gynecol Oncol 15:10–17
10. Bokhman JV, Chepick DF, Volkova AT, Vishnevsky AS (1985) Can primary endometrial carcinoma stage I be cured without surgery and radiation therapy? Gynecol Oncol 20:139–156
11. Britton LC, Wilson TO, Gaffey TA, Cha SS, Wieand HS, Podratz KC (1990) DNA ploidy in endometrial carcinoma: major objective prognostic factor. Mayo Clin Proc 65:643–650
12. Buckley CH, Fox H (1989) Biopsy pathology of the endometrium. Raven Press, New York, pp 149–165
13. Burton JL, Wells M (1998) Recent advances in the histopathology and molecular pathology of carcinoma of the endometrium. Histopathology 33:297–303

14. Carcangiu ML, Chambers JT, Voynick IM, Pirro M, Schwartz PE (1990) Immunohistochemical evaluation of estrogen and progesterone receptor content in 183 patients with endometrial carcinoma. Part I: clinical and histologic correlations. Am J Clin Pathol 94:247–254
15. Carcangiu ML, Tan LK, Chambers JT (1997) Stage 1A uterine serous carcinoma: a study of 13 cases. Am J Surg Pathol 21:1507–1514
16. Catasus L, Machin P, Matias-Guiu X, Prat J (1998) Microsatellite instability in endometrial carcinomas: clinicopathologic correlations in a series of 42 cases. Human Pathol 291160–1164
17. Cheng WF, Chen TM, Chen CA, Wu CC, Huang KT, Hsieh CY, Hsieh FJ (1998) Clinical application of intratumoral blood flow study in patients with endometrial carcinoma. Cancer 82:1881–1886
18. Creasman WT (1993) Prognostic significance of hormone receptors in endometrial cancer. Cancer 71:1467–1470
19. Czerwenka K, Lu Y, Heuss F (1995) Amplification and expression of the c-erbB-2 oncogene in normal, hyperplastic and malignant endometria. Int J Gynecol Pathol 14:98–106
20. Deligdisch L, Cohen CJ (1985) Histologic correlation and virulence implications of endometrial carcinoma associated with adenomatous hyperplasia. Cancer 56:1452–1455
21. Demopoulos RI, Genega E, Vamvakas E, Carlson E, Mittal K (1996) Papillary carcinoma of the endometrium: morphometric predictors of survival. Int J Gynecol Pathol 15:110–118
22. Dos Santos Silva I, Swerdlow AJ (1995) Recent trends in incidence of and mortality from breast, ovarian and endometrial cancers in England and Wales and their relation to changing fertility and oral contraceptive use. Br J Cancer 72:485–492
23. Esteller M, Garcia A, Martinez-Palones JM, Xercavins J, Reventos J (1997) The clinicopathological significance of K-RAS point mutation and gene amplification in endometrial cancer. Eur J Cancer 33:1572–1577
24. Evans MP, Podratz KC (1996) Endometrial neoplasia: prognostic significance of ploidy status. Clin Obstet Gynecol 39:696–706
25. Ferenczy A, Gelfand M (1989) The biologic significance of cytologic atypia in progestogen-treated endometrial hyperplasia. Am J Obstet Gynecol 160:126–131
26. Fox H (1984) The endometrial hyperplasias. Obstet Gynecol Annu 13:197–209
27. Fox H, Buckley CH (1982) The endometrial hyperplasias and their relationship to endometrial neoplasia. Histopathology 6:493–510
28. Fox H, Buckley CH (1991) Pathology for gynaecologists. 2nd edn. Edward Arnold, London, pp 118–160
29. Fujiwaki R, Hata K, Iida K, Maede Y, Watanabe Y, Koike M, Miyazaki K (1999) Co-expression of vascular endothelial growth factor and thymidine phosphorylase in endometrial cancer. Acta Obstet Gynecol Scand 78:728–734
30. Garzetti GG, Ciavattini A, Goteri G, De Nictolis M, Romanini C (1996) Proliferating cell nuclear antigen (PCNA) immunoreactivity in stage I endometrial cancer. A new prognostic factor. Int J Gynecol Cancer 6:186–192
31. Geisler JP, Wiemann MC, Zhou Z, Miller CA, Geisler HE (1996) Proliferation index determined by MIB-1 and re-currence of endometrial carcinoma. Gynecol Oncol 61:373–377
32. Giatromanolaki A, Sivridis E, Koukourakis M, Harris A.L, Gatter KC (1998) Bcl-2 and p53 expression in stage I endometrial carcinoma. Anticancer Research 18:3689–3694
33. Giatromanolaki A., Sivridis E, Koukourakis MI, Gatter KC, Harris AL (1999) Intratumoral angiogenesis: a new prognostic indicator for stage I endometrial adenocarcinomas? Oncol Res 11:205–212
34. Gitsch G, Friedlander ML, Wain GV, Hacher NF (1995) Uterine papillary serous carcinoma: a clinical study. Cancer 75:2239–2243
35. Guidi AJ, Abu-Jawdeh G, Tognazzi K, Dvorak HF, Brown LF (1996) Expression of vascular permeability factor (vascular endothelial growth factor) and its receptors in endometrial carcinoma. Cancer 78:454–460
36. Hendrickson M, Ross J, Eifel P, Martinez A, Kempson R (1982) Uterine papillary serous carcinoma. A highly malignant form of endometrial adenocarcinoma. Am J Surg Pathol 6:93–108
37. Hetzel DJ, Wilson TO, Keeney GL, et al (1992) HER-2/neu expression: a major prognostic factor in endometrial cancer. Gynecol Oncol 47:179–185
38. Hoffman K, Nekhlyudar L, Deligdisch L (1995) Endometrial carcinoma in elderly women. Gynecol Oncol 58:198–201
39. Ho SP, Tan KT, Pang MW, Ho TH (1997) Endometrial hyperplasia and the risk of endometrial carcinoma. Singapore Med 38:11–15
40. Horn LC, Bilek K, Schnurrbusch U (1997) Endometrial hyperplasias: histology, classification, prognostic significance and therapy. Zentralbl Gynakol 119:251–259
41. Inoue M, Fujita M, Enomoto T, Morimoto H, Monden T, Shimano T, Tanizawa O (1994) Immunohistochemical analysis of p53 in gynecologic tumors. Am J Clin Pathol 102:665–670
42. Ito K, Watanabe K, Nasim S, Sasano H, Sato S, Yajima A, Silverberg SG, Garrett CT (1994) Prognostic significance of p53 overexpression in endometrial cancer. Cancer Res 54:4667–4670
43. Ito K, Sasano H, Matsunaga G, Sato S, Yajima A, Nasim S, Garret CT (1997) Correlations between p21 expression and clinicopathological findings. p53 gene and protein alterations and survival in patients with endometrial carcinoma. J Pathol 183:318–324
44. Janicek MF, Rosenshein NB (1994) Invasive endometrial cancer in uteri resected for atypical endometrial hyperplasia. Gynecol Oncol 52:373–378
45. Kaku T, Kamura T, Hirakawa T, Sakai K, Amada S, Kobayashi H, Nakano H (1999) Endometrial carcinoma associated with hyperplasia – immunohistochemical study of angiogenesis and p53 expression. Gynecol Oncol 72:51–55
46. Kaku T, Kamura T, Kinukawa N, Kobayashi H, Sakai K, Tsuruchi N, Saito T, Kawauchi S, Tsuneyoshi M, Nakano H (1997) Angiogenesis in endometrial carcinoma. Cancer 80:741–747
47. Khalifa MA, Mannel RS, Haraway SD, Walker J, Min KW (1994) Expression of EGFR, HER-2/neu, p53, and PCNA in endometrioid, serous papillary, and clear cell endometrial adenocarcinomas. Gynecol Oncol 53:84–92
48. Kirschner CV, Alanis-Amezcua JM, Martin VG, Luna N, Morgan E, Yang IJ, Jordan EL (1996) Angiogenesis factor in endometrial carcinoma: a new prognostic indicator? Am J Obstet Gynecol 174:1879–1882
49. Kohler MF, Nishii H, Humphrey PA, Saski H, Marks J, Bast RC, Clarke-Pearson DL, Boyd J, Berchuck A (1993) Mutation of the p53 tumor-suppressor gene is not a feature of endometrial hyperplasias. Am J Obstet Gynecol 169:690–694
50. Kohler MF, Carney P, Dodge R, Soper JT, Clarke-Pearson DL, Marks J, Berchuck A (1996) p53 overexpression in advanced-stage endometrial adenocarcinoma. Am J Obstet Gynecol 175:1246–1252
51. Koreth J, O'Leary JJ, McGee J O'D (1996) Microsatellites and PCR genomic analysis. J Pathol 178:239–248
52. Koshiyama M, Konishi I, Wang DP, Mandai M, Komatsu T, Yamamoto S, Nanbu K, Naito MF, Mori T (1993) Immunohistochemical analysis of p53 protein over-expression in endometrial carcinomas: inverse correlation with sex steroid receptor status. Virchow Arch 423:265–271
53. Koukourakis M, Giatromanolaki A, O'Byrne K, Whitehouse R, Talbot DC, Gatter KC, Harris AL (1997) Potential role of bcl-2 as a suppressor of tumor angiogenesis in non small cell lung cancer. Int J Cancer 74:565–570
54. Kurman RJ, Kaminski PF, Norris HJ (1985) The behaviour of endometrial hyperplasia. A long-term study of “untreated” hyperplasia in 170 patients. Cancer 56:403–412
55. Lax SF, Kurman RJ (1997) A dualistic model for endometrial carcinogenesis based on immunohistochemical and molecular genetic analyses. Verh Dtsch Ges Pathol 81:228–232
56. Lax SF, Pizer ES, Ronnett BM, Kurman RJ (1998) Comparison of estrogen and progesterone receptor, Ki-67, and p53 immunoreactivity in uterine endometrioid carcinoma and endo-

metrioid carcinoma with squamous, mucinous, secretory, and ciliated cell differentiation. Hum Pathol 29:924–931
57. Lax SF, Pizer ES, Ronnett BM, Kurman RJ (1998) Clear cell carcinoma of the endometrium is characterized by a distinctive profile of p53, Ki-67, estrogen, and progesterone receptor expression. Hum Pathol 29:551–558
58. Lax SF, Kendall B, Tashiro H, Slebos RJ, Hedrick L (2000) The frequency of p53, K-ras mutations, and microsatellite instability differs in uterine endometrioid and serous carcinoma: evidence of distinct molecular genetic pathways. Cancer 88:814–824
59. Lee KR, Scully RE (1989) Complex endometrial hyperplasia and carcinoma in adolescents and young women 15–20 years of age: a report of 10 cases. Int J Gynecol Pathol 8:201–213
60. Longacre TA, Kempson RL, Hendrickson MR (1995) Endometrial hyperplasia, metaplasia and carcinoma. In: Fox H, Wells M (eds) Obstetrical and Gynaecological Pathology, 4th edn. Churchill Livingstone, Edinburgh, pp 421–510
61. Malpica A, Tornos C, Burke TW, Silva EG (1995) Low stage clear-cell carcinoma of the endometrium. Am J Surg Pathol 19:769–774
62. Manek S, Wells M (1996) The significance of alterations in p53 expression in gynaecological neoplasms. Curr Opin Obstet Gynecol 8:52–55
63. Miturski R, Semczuk A, Tomaszewski J, Jakowicki J (1998) bcl-2 protein expression in endometrial carcinoma: the lack of correlation with p53. Cancer Lett 133:63–69
64. Monk BJ, Chapman JA, Johnson GA, et al (1994) Correlation of c-myc and HER-2/neu amplification and expression with histopathologic variables in uterine corpus cancer. Am J Obstet Gynecol 171:1193–1198
65. Morgan KG, Wilkinson N, Buckley CH (1996) Angiogenesis in endometrial carcinoma. Int J Cancer 6:385–388
66. Nagase S, Sato S, Tezuka F, Wada Y, Yajima A, Horii A (1996) Deletion mapping on chromosome 10q25-q26 in human endometrial cancer. Br J Cancer 74:1979–1983
67. Nielsen AL, Nyholm HCJ, Engel P (1994) Expression of MIB-1 (paraffin ki-67) and AgNOR morphology in endometrial adenocarcinomas of endometrioid type. Int J Gynecol Pathol 13:37–44
68. Niwa K, Murase T, Morishita S, Hashimoto M, Itoh N, Tamaya T (1999) p53 overexpression and mutation in endometrial carcinoma: inverted relation with estrogen and progesterone receptor status. Cancer Detect Prev 23:147–154
69. Obermair A, Tempfer C, Wasicky R, Kaider A, Hefler L, Kainz C (1999) Prognostic significance of tumor angiogenesis in endometrial cancer. Obstet Gynecol 93:367–371
70. Ozsaran AA, Turker S, Dikmen Y, Erhan Y, Itil I, Terek C, Ozdemir N (1999) p53 staining as a prognostic indicator in endometrial carcinoma. Eur J Gynaecol Oncol 20:156–159
71. Paulsen RJ, Saure MV, Lobo PA (1990) Pregnancy after in-vitro fertilization in a patient with Stage I endometrial carcinoma treated with progestins. Fertil Steril 54:735–738
72. Pisani AL, Barbuto DA, Chen D, Ramos L, Lagasse LD, Karlan BY (1995) HER-2/neu, p53, and DNA analyses are prognosticators for survival in endometrial carcinoma. Obstet Gynecol 85:729–734
73. Porter PL, Gown AM, Kramp SG, Coltrera MD (1992) Widespread p53 overexpression in human malignant tumours: an immunohistochemical study using methacarn-fixed, embedded tissue. Am J Pathol 140:145–153
74. Prat J, Oliva E, Lerma E, Vaquero M, Matias Guiu X (1994) Uterine papillary serous adenocarcinoma: a 10-case study of 53 and c-erbB-2 expression and DNA content. Cancer 74:1778–1783
75. Reinartz JJ, George E, Lindgren BR, Niehans GA (1994) Expression of p53, transforming growth alpha, epidermal growth factor receptor and c-erbB-2 in endometrial carcinoma and correlation with survival and known predictors of survival. Hum Pathol 25:1075–1083
76. Riben MW, Malfetano JH, Nazeer T, Muraca PJ, Ambros RA, Ross JS (1997) Identification of HER-2/neu oncogene amplification by fluorescence in situ hybridization in stage I endometrial carcinoma. Mod Pathol 10:823–831
77. Rolitsky CD, Theil KS, McGaughy VR, Copeland LJ, Niemann TH (1999) HER-2/neu amplification and overexpression in endometrial carcinoma. Int J Gynecol Pathol 18:138–143
78. Rose PG (1996) Endometrial carcinoma. N Engl J Med 335:640–649
79. Saffari B, Jones LA, el-Naggar A, Felix JC, George J, Press MF (1995) Amplification and overexpression of HER-2/neu (c-erbB-2) in endometrial cancers: correlation with overall survival. Cancer Res 55:5693–5698
80. Salvesen HB, Iversen OE, Akslen LA (1998) Independent prognostic importance of microvessel density in endometrial carcinoma. Br J Cancer 77:1140–1144
81. Salvesen HB, Akslen LA (1999) Significance of tumour-associated macrophages, vascular endothelial growth factor and thrombospondin-1 expression for tumour angiogenesis and prognosis in endometrial carcinomas. Int J Cancer 84:538–543
82. Salvesen HB, Iversen OE, Akslen LA (1999) Prognostic significance of angiogenesis and Ki-67, p53, and p21 expression: a population-based endometrial carcinoma study. J Clin Oncol 17:1382–1390
83. Santini D, Ceccarelli C, Martinelli GN, et al (1994) Immunocytochemical study of epidermal growth factor receptor, transforming growth factor alpha, and “squamous differentiation” in human endometrial carcinoma. Hum Pathol 25:1319–1323
84. Save V, Sylander K, Hall PA (1998) Why is p53 protein stabilized in neoplasia? Some answers but many more questions! J Pathol 184:348–350
85. Seki N, Kodama J, Hongo A, Miyagi Y, Yoshinouchi M, Kudo T (1999) Angiogenesis and platelet-derived endothelial cell growth factor/thymidine phosphorylase expression in endometrial cancer. Int J Oncol 15:781–786
86. Seki N, Kodama J, Hongo A, Miyagi Y, Yoshinouchi M, Kudo T (2000) Vascular endothelial growth factor and platelet-derived endothelial cell growth factor expression are implicated in the angiogenesis of endometrial cancer. Eur J Cancer 36:68–73
87. Semczuk A, Berbec H, Kostuch M, Kotarski J, Wojcierowski J (1997) Detection of K-ras mutations in cancerous lesions of human endometrium. Eur J Gynaecol Oncol 18:80–83
88. Semczuk A, Berbec H, Kostuch M, Cybulski M, Wojcierowski J, Baranowski W (1998) K-ras gene point mutations in human endometrial carcinomas: correlation with clinicopathological features and patients' outcome. J Cancer Res Clin Oncol 124:695–700
89. Sherman ME (2000) Theories of endometrial carcinogenesis: a multidisciplinary approach. Mod Pathol 13:295–308
90. Sherman AI, Brown S (1979) The precursors of endometrial carcinoma. Am J Obstet Gynecol 135:947–956
91. Sherman ME, Bitterman P, Rosenshein NB, Delgado G, Kurman RJ. Uterine serous carcinoma (1992) A morphologically diverse neoplasm with unifying clinicopathologic features. Am J Surg Pathol 16:600–610
92. Sherman ME, Bur ME, Kurman RJ (1995) P53 in endometrial cancer and its putative precursors: evidence for diverse pathways of tumorigenesis. Hum Pathol 26:1268–1274
93. Shiozawa T, Xin L, Nikaido T, Fulii S (1997) Immunohistochemical detection of cyclin A with reference to p53 expression in endometrial endometrioid carcinomas. Int J Gynecol Pathol 16:348–353
94. Silverberg SG (2000) Problems in the differential diagnosis of endometrial hyperplasia and carcinoma. Mod Pathol 13:309–327
95. Silverberg SG, Kurman RJ (1992) Tumors of the uterine corpus and gestational trophoblastic disease. Atlas of tumour pathology. 3rd series, fascicle 3:47–89
96. Sivridis E (1996) Histological evaluation of the endometrium: from hyperplasia to cancer. Eur J Gynaecol Oncol 5:440–442

97. Sivridis E, Buckley CH, Fox H (1993) Type I and type II estrogen and progesterone binding sites in endometrial carcinomas: their value in predicting survival. Int J Gynecol Cancer 3:80–88
98. Sivridis E, Fox H, Buckley CH (1998) Endometrial carcinoma: two or three entities? Int J Gynecol Cancer 8:183–188
99. Sivridis E, Giatromanolaki A, Koukourakis M, Bicknell R, Harris A, Gatter KC (1999) Thymidine phosphorylase expression in endometrial carcinomas. Clin Exp Metast 17:445–450
100. Sivridis E, Giatromanolaki A, Koukourakis M, Bicknell R, Harris AL, Gatter KC (2000) Thymidine phosphorylase expression in normal and hyperplastic endometrium. J Clin Pathol 53:704–708
101. Sivridis E, Giatromanolaki A, Koukourakis M, Agnantis N (2000) Lectin-binding patterns in normal, hyperplastic and neoplastic endometrium: the prognostic value of concanavalin A. Virchows Arch 436:52–58
102. Sivridis E, Giatromanolaki A, Koukourakis M, Anastasiadis P (2001) Endometrial carcinoma: association of steroid hormone receptor expression with low angiogenesis and bcl-2 expression. Virchows Arch 438:(in press)
103. Strang P, Nordstom B, Nilsson S, Bergstrom R, Tribukait B (1996) Mutant p53 protein as apredictor of survival in endometrial carcinoma (abstract). Eur J Cancer 32:598–602
104. Tashiro H, Isacson I, Levine R, Kurman RJ, Cho KR, Hedrick L (1997) p53 gene mutations are common in uterine serous carcinoma and occur early in their pathogenesis. Am J Pathol 150:177–185
105. Tashiro H, Lax SF, Gaudin PB, Isacson C, Cho KR, Hedrick L (1997) Microsatellite instability is uncommon in uterine serous carcinoma. Am J Pathol 150:75–79
106. Taskin M, Lallas TA, Barber HRK, Shevchuk MM (1997) bcl-2 and p53 in endometrial adenocarcinoma. Mod Pathol 10:728–734
107. Teleman S, Mihailovici MS, Hilgarth M, Freudenberg N, Bettendorf H (1999) p53 and steroid receptors support double endometrial carcinogenesis. Rev Med Chir Soc Med Nat Iasi 103:131–135
108. Tritz D, Pieretti M, Turner S, Powell D (1997) Loss of heterozygosity in usual and special variant carcinomas of the endometrium. Hum Pathol 28:607–612
109. Varras MN, Koffa M, Koumantakis E, Ergazaki M, Protopapa E, Michalas S, Spandidos DA (1999) ras gene mutations in human endometrial carcinoma. Oncology 53:505–510
110. Wagatsuma S, Konno R, Sato S, Yajima A (1998) Tumor angiogenesis, hepatocyte growth factor, and c-Met expression in endometrial carcinoma. Cancer 82:520–530
111. Wang D, Konishi J, Koshiyama M, et al (1993) Expression of c-erbB-2 protein and epidermal growth factor receptor in endometrial carcinomas: correlation with clinicopathologic and sex steroid receptor status. Cancer 72:2628–2637
112. Wentz WB. Progestin therapy in endometrial hyperplasia (1974) Gynecol Oncol 2:362–367
113. Winkler B, Alvarez S, Richart RM, Crum CP (1984) Pifalls in the diagnosis of endometrial neoplasia. Obstet Gynecol 64:185–194
114. Yamauchi N, Sakamoto A, Uozaki H, Iihara K, Machinami R (1996) Immunohistochemical analysis of endometrial adenocarcinoma for bcl-2 and p53 in relation to expression of sex steroid receptor and proliferative activity. Int J Gynecol Pathol 15:202–208
115. Zaino RJ (1996) Taking another look at endometrial adenocarcinoma. Int J Gynecol Pathol 15:187–190
116. Zheng W, Cao P, Zheng M, Kramer EE, Godwin TA (1996) p53 overexpression and bcl-2 persistence in endometrial carcinoma: comparison of papillary serous and endometrial subtypes. Gynecol Oncol 61:167–174

Virchows Arch (2001) 439:127–131
DOI 10.1007/s004280100421

ORIGINAL ARTICLE

R. Kavalar · B. Sarcevic · G.C. Spagnoli
V. Separovic · M. Samija · L. Terracciano
M. Heberer · A. Juretic

Expression of MAGE tumour-associated antigens is inversely correlated with tumour differentiation in invasive ductal breast cancers: an immunohistochemical study

Received: 13 October 2000 / Accepted: 28 December 2001 / Published online: 31 March 2001
© Springer-Verlag 2001

Abstract MAGE (Melanoma antigen E) family gene products encompass tumour-associated antigens (TAAs) recognised by human leukocyte antigen (HLA)-restricted specific T-cells. Agents inducing DNA demethylation, an event typically detectable in cellular de-differentiation processes, were shown to induce the expression of MAGE genes. By using a monoclonal antibody specific for MAGE family gene products, we have studied the expression of these TAAs in a group of 144 patients with invasive ductal breast cancers. Immunohistochemical data were correlated with tumour differentiation, lymphatic vessel invasion, oestrogen receptor expression, intratumoural necrosis, lymphocytic infiltration, perineural invasion, tumour microcalcifications and axillary lymph node metastases. MAGE immunoreactivity was undetectable in non-neoplastic cells. In poorly differentiated cancers positive staining was observed in 30/63 cases (47.6%) as compared with 13/51 (25.4%) and 5/30 (16.6%) in moderately and well-differentiated tumours, respectively ($P<0.05$). In addition, MAGE immunoreactivity was significantly correlated with lymphatic vessel invasion and intratumoural necrosis. Moreover, a significant inverse relationship with oestrogen receptor expression was also observed. However, no significant correlation could be established between MAGE immunoreactivity and defined phenotypic characteristics of tumour infiltrating lymphocytes, including expression of CD3, CD4, CD8, CD20 or granzyme B. Thus, expression of MAGE family gene products in invasive ductal breast cancers appears to be associated with poorly differentiated histological phenotypes. These data support the concept of specific immunotherapy in highly aggressive forms of breast neoplasms. Furthermore, they suggest that MAGE immunoreactivity could represent a tumour marker of potential prognostic relevance.

Keywords Breast cancer · MAGE immunoreactivity · Tumour-associated antigens

R. Kavalar
Maribor General Hospital, Maribor, Slovenia

B. Sarcevic · V. Separovic · M. Samija · A. Juretic (✉)
University Hospital for Tumours, Zagreb, Croatia
e-mail: antonio.juretic@zg.hinet.hr
Fax: +41-61-2653990

G.C. Spagnoli · M. Heberer · A. Juretic
Department of Surgery, Division of Research,
University Hospital Basel, Switzerland

L. Terracciano
Department of Pathology, University of Basel, Switzerland

Introduction

Melanoma antigen E (MAGE) tumour-associated antigens (TAAs) were the first described in humans [24]. They belong to the so called cancer/testis (CT) TAA family characterised by expression in tumours of unrelated histological origin and in a restricted number of healthy tissues [3, 19]. Expression of MAGE genes has previously been studied in breast cancers [2, 9, 13, 18, 19]. MAGE 1-, 2-, 3- and 4-specific transcripts were indeed identified, but relatively low numbers of cases were studied and no histological or clinico-pathological correlation could be postulated.

The murine monoclonal antibody 57B (57B Mab) was produced upon immunisation of mice with recombinant MAGE-3 protein, as described elsewhere [14, 12]. Recently, however, detailed studies on transfected cells have established that it recognises different members of the MAGE family in "western" blot assays whereas in immunohistochemistry on tissue sections MAGE-4 TAA appears to be predominantly detected [15, 23]. However, no additional target molecules have been identified beyond the MAGE family gene products. Since it efficiently stains paraffin-embedded sections, this reagent appears to be suitable for the detection of MAGE family gene products in large numbers of archival tissues.

In this study Mab 57B immunoreactivity was analysed in 144 invasive ductal breast carcinomas in correla-

tion with a number of clinico-pathological parameters, including tumour differentiation, oestrogen receptor expression, lymphatic vessel invasion, intratumoural necrosis, lymphocyte infiltration, perineural invasion, tumour microcalcifications and lymph node metastases.

Materials and methods

Patients

Samples were obtained from female patients undergoing surgery at Maribor General Hospital (Maribor, Slovenia), over a 2-year period (1996–1997). Pathological examination of primary tumours and axillary lymph nodes was performed in the same hospital in the Department of Pathology. For routine histological analysis, resected material was fixed in 10% buffered formalin, embedded in paraffin and stained with haematoxylin and eosin.

Immunohistochemistry

Expression of MAGE TAA in primary breast cancer tissue was studied using 57B Mab. Briefly, tissue sections from paraffin-embedded breast tumour samples (0.5 mm thick) were placed on Silane- (3-aminopropyltriethoxysilane, Sigma, St. Louis, Mo.) treated glass microscope slides. Following deparaffinisation, sections were heated in a 800-W household microwave oven at maximal power for 8.5 min and 5 min in 10 mmol/l citric buffer (pH 6.0) and washed with phosphate-buffered saline (PBS, pH 7.2). The sections were then H_2O_2 treated in order to suppress endogenous peroxidase activity. After an additional PBS wash, sections were also incubated for 20 min with 1:10 diluted normal rabbit sera (DAKO A/S) at room temperature in a humidified chamber to prevent non-specific immunoglobulin binding. Mab 57B, in the form of undiluted hybridoma supernatant, was then applied for 90 min at room temperature [11]. Specific binding was revealed using a streptoavidin–biotinylated horseradish peroxidase-based detection system (DAKO A/S).

Immunoreactivity was scored as: 0, no positive tumour cells; +, up to 20% positive cells (“mild reaction”); ++, 20–50% positive cells (“middle strong reaction”); or +++, over 50% positive tumour cells (strong reaction). In all specimens, non-neoplastic cells, such as normal ductal epithelial cells, fibroblasts, etc., were indeed present but were not stained, and thus served as internal negative controls. Tumour differentiation was evaluated according to the Bloom-Richardson-Elston index [8]. Oestrogen receptor expression was evaluated by immunohistochemistry using a specific Mab (M 7047, DAKO A/S, dilution 1:75). Lymph vessel invasion was confirmed, when necessary, using anti-CD31, anti-CD34 and anti-factor VIII staining. Intratumoural necrosis and lymphocyte infiltration were estimated according to previously described criteria [10, 26].

Immunophenotypic characteristics of the tumour-infiltrating lymphocytes (TIL) were investigated with Mabs specific for CD3 (DAKO, Glostrup, Denmark), CD4 (Novocastra, Newcastle u.T., UK), CD8 (DAKO, Glostrup, Denmark), CD20 (DAKO, Glostrup, Denmark) recognising B lymphocytes and Granzyme B (Monosan, Sanbio, The Netherlands), identifying activated cytotoxic T-lymphocytes [17]. The avidin–biotin complex method (Vectastain, Burlingame, CA) was used as detection technique according to the manufacturer's recommendations.

The immunoreactivity for CD3, CD4, CD8 and CD20 was graded as mild (+) when involving more than 10% but less than 25% of TIL, moderate (++) and severe (+++) when 26%–50% or more than 50% of TIL, respectively, were reactive with the marker of interest. Focal reactivity of less than 10% cellular infiltrate was considered negative. The results were scored as such when two of the investigators (L.T. and G.C.S.) agreed on the presence of defined reactivity.

For granzyme B we counted cells positive with a sparsely granulated pattern as activated cytotoxic T-cells [17] in three neoplastic areas of maximal lymphocytic infiltration (400×, Zeiss Axioplan). The immunoreactivity was graded as mild (+) when greater than 1 but less than 5, moderate (++) when 6–10 and severe (+++) when greater than 10 Granzyme B+ lymphocytes were detected. Each case was scored blindly with respect to histological grading as well as 57B immunoreactivity. The statistical significance of the correlation of the parameters under investigation was evaluated by χ^2 tests.

Results

The invasive ductal breast cancers under investigation could be classified according to well-established histological criteria as well-differentiated (grade 1, n=30), moderately differentiated (grade 2, n=51) and poorly differentiated (grade 3, n=63) neoplasms [8]. As expected, well-differentiated cancers were characterised by a smaller tumour size, a lower frequency of lymphatic vessel invasion, a highly frequent intense reactivity upon staining with anti-oestrogen receptor Mab and a lower number of axillary node metastases, as compared with moderately or poorly differentiated neoplasms (data not shown).

57B Immunoreactivity, resulting in a moderate to strong, prevailingly cytoplasmic staining, could only be observed in neoplastic cells (Fig. 1A). Overall positivity was only detectable in 16.6% of well-differentiated cases, whereas 47.6% of the poorly differentiated breast cancers appeared to express to some extent MAGE gene products (P<0.05). Intermediate values (25.4%) were observed in the moderately differentiated tumours. Interestingly, in nine of the poorly differentiated cases (14.3%), 57B positivity apparently involved over 50% of tumour cells, as compared with four cases (7.8%) of moderately differentiated neoplasms. A similar picture was never observed in well-differentiated breast cancers (Table 1). Representative examples of 57B-stained sections from moderately differentiated and poorly differentiated tumours are reported in Fig. 1B,C, respectively).

57B Immunoreactivity was also significantly correlated with lymphatic vessel invasion and intratumoural necrosis (P<0.05) whereas a significant inverse correlation with oestrogen receptor expression could be detected (Table 2). In contrast, no correlation with lymphocytic infiltration, perineural invasion, tumour microcalcifications or the number of axillary lymph node metastases was observed.

Since MAGE gene products encompass well-defined class I and II restricted TAA [3, 4, 5, 7, 16, 27], we attempted a more detailed characterisation of the lymphocytic infiltrates in 57B positive (n=10) and negative (n=17) tumours. Staining with reagents specific for CD3, CD4 and CD8 revealed infiltration to different extents in virtually all cases. Limited CD20+ lymphocyte infiltration was also frequently detectable. However, no correlation with 57B expression could be established (data not shown). Furthermore, infiltration by lymphocytes positive for granzyme B, a marker of activated CD8+ cells

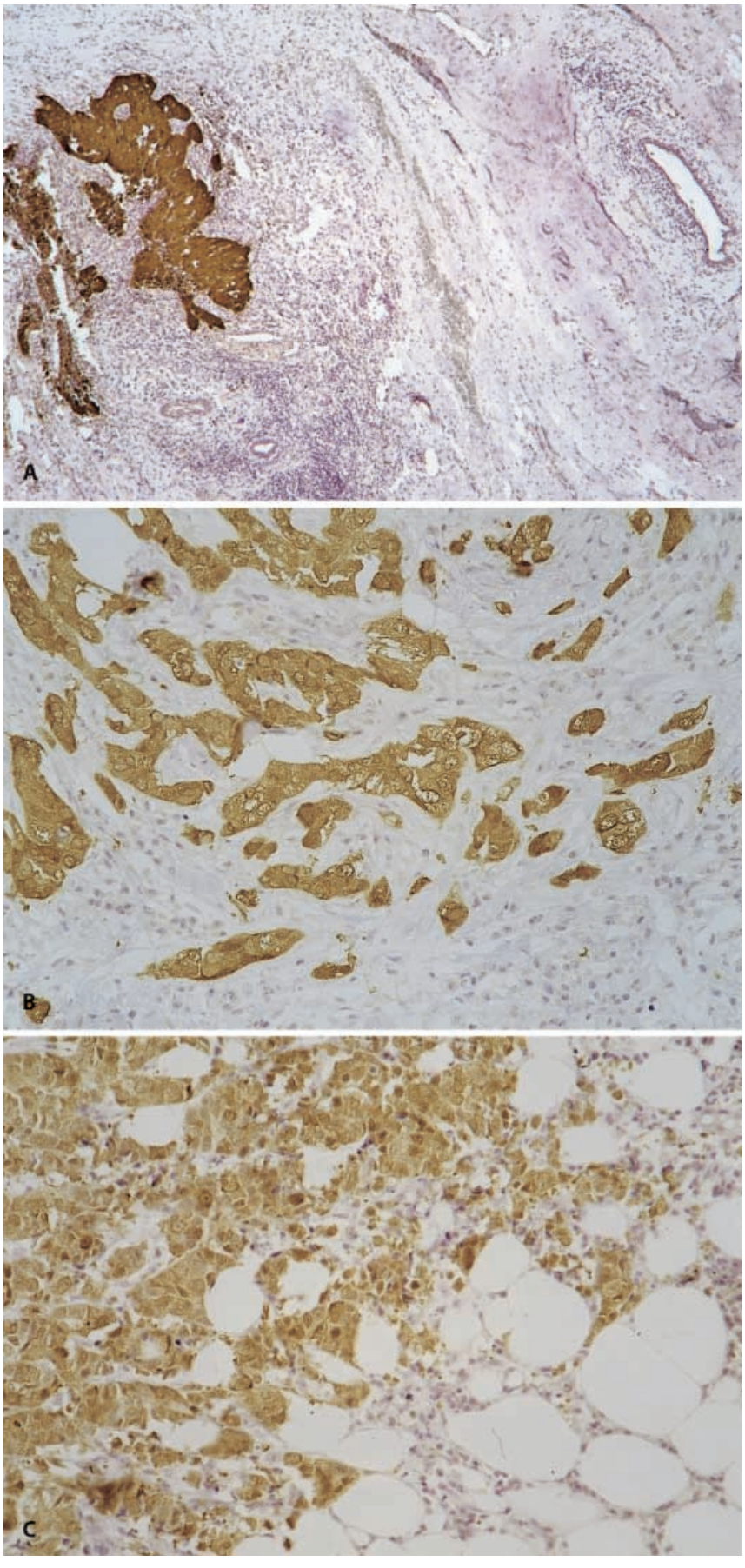


Fig. 1A–C 57B Staining in invasive ductal breast carcinoma. Tissue sections were incubated in the presence of 57B Mab and specific binding was revealed using the alkaline phosphatase–antialkaline phosphatase (APAAP) method. **A** A strong positivity of neoplastic cells (left) can be observed in the absence of staining of normal ducts (×100). **B** Intense, prevailingly cytoplasmic, staining in a case of moderately differentiated ductal carcinoma (×250). **C** Intense, predominantly cytoplasmic staining in a poorly differentiated ductal carcinoma (×200)

Table 1 57B Immunoreactivity in 144 cases of invasive ductal breast carcinoma as classified according to the grade of differentiation. – negative, + <20%, ++ 20–50%, +++ >50%, *NS* not significant

Tumor grade[a]	57B Immunoreactivity (% of positive cells)	57B Immunoreactivity [number of tumors (%)]
Grade 1 (well differentiated, *n*=30)	–	25 (83.3%)
	+	2 (6.6%)
	++	3 (10.0%)
	+++	0 (0%)
		Total 5/30 (16.6%)
Grade 2 (mod. differentiated, *n*=51)	–	38 (74.5%)
	+	3 (5.8%)
	++	6 (11.7%)
	+++	4 (7.8%)
		Total 13/51 (25.4%) NS
Grade 3 (poorly differentiated, *n*=63)	–	33 (52.3%)
	+	13 (20.6%)
	++	8 (12.6%)
	+++	9 (14.2%)
		Total 30/63 (47.6%) $P<0.05$

[a] Histological differentiation grade was evaluated according to the Bloom-Richardson-Elston index [8].

Table 2 57B Immunoreactivity in 144 cases of invasive ductal breast carcinoma: clinico-pathological correlations. *NS* not significant

	57B immunoreactivity		%		*P*-value
	+	–	+	–	
Oestrogen receptor expression[a]					
Positive (*n*=104)	29	75	27.8	72.2	<0.05
Negative (*n*=40)	19	21	47.5	52.5	
Lymphatic vessel invasion					
Positive (*n*=35)	19	16	54.3	45.7	<0.05
Negative (*n*=109)	29	80	26.6	73.4	
Intratumoural necrosis[b]					
Positive (*n*=71)	31	40	43.7	56.3	<0.05
Negative (*n*=73)	18	55	24.6	75.4	
Lymphocytic infiltration[b]					
Positive (*n*=110)	39	71	35.4	64.6	NS
Negative (*n*=34)	8	26	23.5	76.5	
Perineural invasion					
Positive (*n*=23)	7	16	30.4	69.6	NS
Negative (*n*=121)	40	81	33	67	
Tumour microcalcifications					
Positive (*n*=40)	17	23	42.5	67.5	NS
Negative (*n*=104)	32	72	30.7	69.3	
Axillary node metastases[c]					
None (*n*=19)	6	13	31.5	68.5	NS
1–3 (*n*=24)	7	17	29.1	70.9	
>3 (*n*=22)	9	13	40.9	59.1	

[a] Oestrogen receptor expression was detected upon staining with a specific Mab
[b] Intratumoural necrosis and lymphocyte infiltration were evaluated according to established criteria [10, 24]
[c] Surgical inspection of the axillary cavity was performed in 65/144 cases

[17], was also investigated. Indeed, granzyme B-positive lymphocytes were found to infiltrate breast cancer tissues in low numbers, but again, no correlation with 57B Mab staining was evident (data not shown).

Discussion

MAGE family gene products are of particular interest in tumour immunology since they encompass HLA class I- and class II-restricted epitopes, recognised by specific T-cells [4, 16, 24]. In particular, naturally processed peptides derived from MAGE-1, -2, -3, -4 and -6 targeted by tumouricidal cytotoxic T-lymphocytes (CTL) have been identified [5, 7, 20, 21, 27]. A number of them are presently being evaluated in the context of dedicated clinical trials.

No data are currently available on the physiological role of MAGE gene products. Several studies, however, have demonstrated that DNA-demethylating agents induce the expression of MAGE genes [6, 25]. Indeed, DNA demethylation is known to be typically associated with de-differentiation processes, which are likely to include events observed in advanced stages of cancer development [1]. Clearly, the availability of specific Mabs makes it possible, on the one hand, to enumerate neoplastic cells expressing CTL target molecules in clonally heterogeneous clinical samples and, on the other, to test the potential role of MAGE proteins as markers of defined tumour stages.

The data reported here document that expression of MAGE gene products is typically detectable in poorly differentiated invasive ductal breast cancer whereas it is rarely observed in well-differentiated cases. In keeping with this observation, MAGE immunoreactivity appears to correlate with lymphatic vessel invasion and intratumoural necrosis, whereas an inverse correlation with oestrogen receptor expression emerges. However, no obvious correlation with the infiltration of tumours by de-

fined lymphocyte subpopulations (CD3+, CD4+, CD8+, CD20+ or granzyme B+), suggestive of discrete specific immune responses, was detected. Remarkably, though, MAGE TAA-specific CTL have been derived from TIL-infiltrating breast cancers upon “in vitro” stimulation [22].

Our results suggest that the expression of MAGE gene products, as detectable using routine techniques on paraffin-embedded sections, could represent an important marker of de-differentiation in breast cancers. Further studies are warranted to clarify the prognostic relevance, if any, of MAGE TAA immunoreactivity. Most importantly, the data presented here support the concept of specific immunotherapy procedures targeting MAGE family TAA in highly aggressive forms of breast cancer.

Acknowledgements This study was partially funded by the Swiss National Fund (grant no. 31–57'473.99 to GCS) and by the Ministry of Science and Technology of the Republic of Croatia (grant no. 074001 to AJ).

References

1. Bernardino J, Roux C, Almeida A, Vogt N, Gibaud A, Gerbault-Seureau M, Magdelenat H, Bourgeois CA, Malfoy B, Dutrillaux B (1997) DNA hypomethylation in breast cancer: an independent parameter of tumor progression? Cancer Genet Cytogenet 97:83–89
2. Brasseur F, Marchand M, Vanwijck R, Herin M, Lethe B, Chomez P, Boon T (1992) Human gene MAGE-1, which codes for a tumor rejection antigen, is expressed by some breast tumors. Int J Cancer 52:839–841
3. Coulie PG, Weynants P, Lehmann F, Herman J, Brichard V, Wolfel T, Van Pel A, De Plaen E, Brasseur F, Boon T (1993) Genes coding for tumor antigens recognized by human cytolytic T lymphocytes. J Immunother 14:104–109
4. Chaux P, Vantomme V, Stroobant V, Thielemans K, Corthals J, Luiten R, Eggermont AMM, Boon T, van der Bruggen P (1999) Identification of MAGE-3 epitopes presented by HLA-DR molecules to CD4(+) T lymphocytes. J Exp Med 189:767–778
5. Chaux P, Luiten R, Demotte N, Vantomme V, Stroobant V, Traversari C, Russo V, Schultz E, Cornelis GR, Boon T, van der Bruggen P (1999) Identification of five MAGE-A1 epitopes recognized by cytolytic T lymphocytes obtained by in vitro stimulation with dendritic cells transduced with MAGE-A1. J Immunol 163:2928–2936
6. De Smet C, Lurquin C, Lethe B, Martelange V, Boon T (1999) DNA methylation is the primary silencing mechanism for a set of germ line- and tumor-specific genes with a CpG-rich promoter. Mol Cell Biol 19:7327–7335
7. Duffour MT, Chaux P, Lurquin C, Cornelis G, Boon T, van der Bruggen P (1999) A MAGE-A4 peptide presented by HLA-A2 is recognized by cytolytic T lymphocytes. Eur J Immunol 29:3329–3337
8. Elston CW (1987) Grading of invasive carcinoma of the breast. In: Page DL, Anderson TJ (eds) Diagnostic hystopathology of the breast. Churchill Livingston, Edinburgh, pp 300–311
9. Fujie T, Mori M, Ueo H, Sugimachi K, Akiyoshi T (1997) Expression of MAGE and BAGE genes in Japanese breast cancers. Ann Oncol 8:369–372
10. Gilchrist KW, Gray R, Fowble B, Tormey DC, Taylor SG (1993) Tumor necrosis is a prognostic predictor for early recurrence and death in lymph node-positive breast cancer: a 10-year follow-up study of 728 Eastern Cooperative Oncology Group patients. J Clin Oncol 11:1929–1935
11. Gudat F, Zuber M, Dürmüller U, Kocher T, Schaefer C, Noppen C, Spagnoli GC (1996) The tumour associated antigen MAGE-1 is detectable in formalin-fixed paraffin sections of malignant melanoma. Virchows Arch 429:77–81
12. Hofbauer GFL, Schaefer C, Noppen C, Böni R, Kamarashev J, Nestle FO, Spagnoli GC, Dummer R (1997) MAGE-3 immunoreactivity in formalin-fixed, paraffin-embedded primary and metastatic melanoma. Frequency and distribution. Am J Pathol 151:1549–1553
13. Kawamoto M, Shichijo S, Imai Y, Imaizumi T, Koga T, Yanaga H, Itoh K (1999) Expression of the SART-1 tumor rejection antigen in breast cancer. Int J Cancer 80:64–67
14. Kocher T, Schultz-Thater E, Gudat F, Schaefer C, Casorati G, Juretic A, Willimann T, Harder F, Heberer M, Spagnoli GC (1995) Identification and intracellular location of MAGE-3 gene product. Cancer Res 55:2236–2239
15. Landry C, Brasseur F, Spagnoli GC, Marbaix E, Boon T, Coulie P, Godelaine D (2000) Monoclonal antibody 57B stains tumor tissues that express gene MAGE-A4. Int J Cancer 86: 835–841
16. Manici S, Sturniolo T, Imro MA, Hammer J, Sinigaglia F, Noppen C, Spagnoli G, Mazzi B, Bellone M, Dellabona P, Protti MP (1999) Melanoma cells present a MAGE-3 epitope to CD4+ cytotoxic T cells in association with HLA-DR11. J Exp Med 189:871–876
17. Oberhuber G, Bodingbauer M, Mosberger I, Stolte M, Vogelsang H (1998) High proportion of granzyme B-positive (activated) intraepithelial and lamina propria lymphocytes in lymphocytic gastritis. Am J Surg Pathol 22:450–458
18. Russo V, Traversari C, Verrecchia A, Mottolese M, Natali PG, Bordignon C (1995) Expression of the MAGE gene family in primary and metastatic breast cancer: implication for tumor antigen-specific immunotherapy. Int J Cancer 64:216–221
19. Sahin U, Türeci O, Chen Y-T, Seitz G, Villena-Heinsen C, Old LJ, Pfreundschuh M (1998) Expression of multiple cancer/testis (CT) antigens in breast cancer and melanoma: basis for polyvalent CT vaccine strategies. Int J Cancer 78:387–389
20. Tahara K, Takesako K, Sette A, Celis E, Kitano S, Akiyoshi T (1999) Identification of a MAGE-2 encoded human leukocyte antigen-A24-binding synthetic peptide that induces specific antitumor cytotoxic T lymphocytes. Clin Cancer Res 5:2236–2241
21. Tanzarella S, Russo V, Lionello I, Dalerba P, Rigatti D, Bordignon C, Traversari C (1999) Identification of a promiscuous T-cell epitope encoded by multiple members of the MAGE family. Cancer Res 59:2668–2674
22. Toso JF, Oei C, Oshidari F, Tartaglia J, Paoletti E, Lyerly HK, Talib S, Weinhold KJ (1996) MAGE-1-specific precursor cytotoxic T-lymphocytes present among tumor-infiltrating lymphocytes from a patient with breast cancer: characterization and antigen-specific activation. Cancer Res 56:16–20
23. Van Baren N, Brasseur F, Godelaine D, Hames G, Ferrant A, Lehmann F, André F, Ravoet C, Doyen C, Spagnoli GC, Bakkus M, Thielemans K, Boon T (1999) Genes encoding tumor-specific antigens are expressed in human myeloma cells. Blood 94:1156–1164
24. van der Bruggen P, Traversari C, Chomez P, Lurquin C, De Plaen E, Van den Eynde B, Knuth A, Boon T (1991) A gene encoding an antigen recognized by cytolytic T lymphocytes on a human melanoma. Science 254:1643–1647
25. Weber J, Salgaller M, Samid D, Johnson B, Herlyn M, Lassam N, Treisman J, Rosenberg SA (1995) Expression of the MAGE-1 tumor antigen is up-regulated by the demethylating agent 5-aza-2'-deoxycytidine. Cancer Res 54:1766–1771
26. Whitwell HL, Hughes HP, Moore M, Ahmed A (1984) Expression of major histocompatibility antigens and leucocyte infiltration in benign and malignant human breast disease. Br J Cancer 49:161–172
27. Zorn E, Hercend T (1999) A MAGE-6-encoded peptide is recognized by expanded lymphocytes infiltrating a spontaneously regressing human primary melanoma lesion. Eur J Immunol 29:602–607

Virchows Arch (2001) 439:132–140
DOI 10.1007/s004280100410

ORIGINAL ARTICLE

**Wenancjusz Domagala · Markus Welcker
Maria Chosia · Magdalena Karbowniczek
Barbara Harezga · Jirina Bartkova · Jiri Bartek
Mary Osborn**

p21/WAF1/Cip1 expression in invasive ductal breast carcinoma: relationship to p53, proliferation rate, and survival at 5 years

Received: 15 September 2000 / Accepted: 28 December 2000 / Published online: 31 March 2001
© Springer-Verlag 2001

Abstract The p21/WAF1/Cip1 antibody, DCS-60, was characterized by means of immunoblotting and immunofluorescence on a variety of human breast cancer cell lines. Heterogeneous staining of nuclei was observed with strong staining of cells in early G_1. p21/WAF1/Cip1 expression in invasive ductal, not otherwise specified breast carcinomas was determined using immunohistochemistry with this antibody and computerized image analysis. Two hundred and twenty-two tumors, including 130 from patients with no axillary node involvement, were examined. p21-positive tumor cell nuclei were found in 30% of the breast carcinomas. The percentage of tumor cell nuclei that were positive ranged from less than 1% to greater than 10%. In the whole cohort of patients, p21 expression was significantly associated with a low histological grade. In the node-negative group, there was a significant negative correlation between p21 positivity and a high (>10%) MIB-1 score. The mean MIB-1 score was significantly lower in p21-positive tumors in the whole cohort of patients (P=0.03) and in the node-negative group (P=0.02). No association was found between p21 expression and overall survival at 5 years. With respect to p21/p53 phenotype, the significant difference in survival was noted only for the group of patients treated with adjuvant chemotherapy. The p21– p53+ phenotype had the worst survival (58% surviving 5 years), while the p21+ p53– phenotype had good survival (83% surviving 5 years; P<0.05). The results seem to suggest a correlation between p21/p53 phenotype and response to adjuvant chemotherapy.

Keywords p21/WAF1/Cip1 · Breast carcinoma · p53 · Prognosis

W. Domagala · M. Chosia · M. Karbowniczek
Department of Pathology, Faculty of Medicine,
Pomeranian Medical Academy, Szczecin, Poland

M. Welcker · J. Bartkova · J. Bartek
Institute of Cancer Biology, Strandboulevarden 49,
2100 Copenhagen, Denmark

B. Harezga
Department of Oncology, Medical Academy, Lodz, Poland

M. Osborn (✉)
Max Planck Institute for Biophysical Chemistry, Am Fassberg 11,
37077 Goettingen, Germany
e-mail: mosborn@gwdg.de
Tel.: +49-551-2011486, Fax: +49-551-2011578

Introduction

Poor prognosis in invasive breast cancer has been associated with both a high proliferation index of tumor cells [13] and with immunohistochemical p53 positivity [38]. The issue of p53 and prognosis in breast carcinoma is still controversial [3]. p53 mutations are found in 17–33% of breast carcinomas by DNA sequencing [2, 9, 26, 33, 37], and an accumulation of p53 is noted in 23–52% using histochemistry [1, 12, 20, 35, 38]. Such tumors also have a high growth fraction, presumably because tumor cells with p53 mutations that result in p53 accumulation are released from p53-mediated growth arrest. p53 can block the cell cycle by stimulating the *WAF1/Cip1* gene, which codes for a p21 protein that associates with and inhibits the cyclin-dependent kinases, the principal enzymes needed for cell cycle progression [17, 18, 41]. p21 is an important posttranscriptional effector in the p53-specific pathway of cell cycle control (reviewed in [10, 14, 15, 19]) and, therefore, it is reasonable to suppose that it may have prognostic significance in breast cancer. It seems, however, that p21 can be induced in cells by p53-dependent and p53-independent pathways [24, 27, 34, 36], and it is not clear whether this is also true for clinical specimens.

The clinical significance of p21 expression in breast cancer is still unknown. The few studies published to date on p21 expression in breast carcinomas reach different conclusions. Wakasugi et al. [40] and Jiang et al. [22] found a significant association of p21 expression with low histological grade, negative axillary lymph nodes, and better relapse-free survival, whereas Barbereschi et al. [4] and Caffo et al. [7] reported opposite results. Diab et al., [11] found no correlation between p21 expression

and survival in node-negative breast cancers. In two studies [22, 40], proliferation rate was not studied. Barbereschi et al. [4] and Caffo et al. [7] did not find a correlation between MIB-1 score and p21 expression, nor did Diab et al. [11] find a correlation between S-phase fraction and p21 expression. Finally, Rey et al. [32] reported a significant association of p21 positivity with an increased percentage of cells in S phase. The association of p53 accumulation with p21 expression in clinical specimens of breast cancer remains controversial. Positive [11], inverse [6, 22, 40], and no association [4, 7] have been reported in different studies.

One reason why p21 expression might be expected to have prognostic significance is its antiproliferative effect. In view of the controversies mentioned above and because the influence of the p53/p21 phenotype on proliferative activity of breast cancer cells has not yet been reported, the purpose of this study was threefold: (1) to explore the relationship between p21 expression, p53 accumulation, and tumor cell proliferation rate in invasive ductal not otherwise specified (NOS) breast carcinomas; (2) to look for correlations between p21 expression and clinicopathological prognostic factors, such as axillary lymph node status and tumor size; and (3) to assess the influence of p21 expression in tumor cells on the overall 5-year survival of patients with invasive ductal NOS breast cancer. To do so, we have used the largest cohort of invasive ductal carcinomas examined with p21 antibodies to date and a novel p21 antibody, DCS-60.

Materials and methods

Cell culture

The human diploid fibroblast cell line WI38, the simian virus (SV)40-transformed breast epithelial cell line HBL-100, and the human breast cancer cell lines MCF-7, BT-549, MDA-MB-134, MDA-MB-157, MDA-MB-231, MDA-MB-453, MDA-MB-468, ZR-75, BT-20, SK-BR-3, and T-47D were cultured in Dulbecco's modified Eagles' medium, supplemented with 10% fetal calf serum, 2 mM glutamine, 10 U/ml penicillin, and 10 U/ml streptomycin.

Immunoblotting

Total cell extracts were prepared through direct lysis of exponentially growing cells with hot Laemmli sample buffer, and loading was adjusted according to Coomassie staining of control gels. Extracted proteins were separated on 12% polyacrylamide gels in the presence of sodium dodecyl sulfate (SDS), blotted onto nitrocellulose using a semi-dry method and probed for p21 using the enhanced chemiluminescence system (Amersham, Aylesbury, UK) according to the manufacturer's instructions. Immunofluorescence staining was performed as described [23], using biotinylated anti-mouse immunoglobulin antisera as the secondary reagent, followed by Texas red-conjugated Streptavidin (Vector Laboratories). Hoechst dye was used to counterstain the DNA.

Patients and tumor material

Formalin-fixed and paraffin-embedded tumor tissues from 222 unselected female patients with primary invasive ductal NOS breast carcinoma were retrieved from the files of the Department of Oncology, Medical Academy, Lodz, Poland. All patients underwent mastectomy with axillary lymph node dissection, and clinical follow-up was available for at least 60 months. Histological typing was performed according to the procedure of Millis and Girling [28], and histological grading was performed according to the procedure of Bloom and Richardson [5]. The computerized database contained the age of the patient, the number of positive lymph nodes, the size of the tumor, the histological type and grade, the stage of the disease at diagnosis, the treatment protocol, the date of operation, and the date of the last checkup or of death. Twenty-nine (32%) of the node-positive patients received adjuvant systemic chemotherapy (CMF) (cyclophosphamide, methotrexate, 5-fluorouracil), five (5%) received adjuvant hormonotherapy (tamoxifen), and 19 (21%) received adjuvant chemo- and hormonotherapy. In the node-negative group of patients, 36 (28%) received adjuvant chemotherapy (CMF), 12 (9%) received adjuvant hormonotherapy (tamoxifen), and eight (6%) received adjuvant chemo- and hormonotherapy. In addition, p53 status was available for 221 tumors tested with the monoclonal p53 antibody, DO1, from results published previously [12], while the MIB-1 score was known for 192 tumors from results also published previously [13].

Immunohistochemistry for p21

Sections were deparaffinized, immersed in citrate buffer (pH 6.0), and subjected to four microwave cycles according to Catoretti et al. [8]. The sections were incubated with the monoclonal p21 antibody DCS-60 used as an undiluted supernatant for 60 min at room temperature, washed, and reacted with biotinylated rabbit anti-mouse antibody and streptavidin peroxidase (Histostain-SP kit: Zymed Laboratories, Inc., San Francisco, Calif.). The sections were washed and then lightly counterstained with hematoxylin. Areas with the highest numbers of p21-positive cells were identified by scanning sections at low magnification. One such area was selected to start the counting and then additional contiguous fields were selected at random until at least 1000 tumor cells had been counted. Counts were made using the Leica Quantimet 600 S computerized image analysis system connected to an Axiophot microscope (Zeiss, Germany) and a 40× objective. The results were scored as the percentage of tumor cell nuclei that were p21-positive.

Statistical analysis

The association between p21 status and clinicopathological factors was assessed using the χ^2 test. The association between MIB-1 score and p21 and p53 statuses was assessed using the Student's *t* test. Differences between Kaplan–Meier survival curves were tested using the Wilcoxon test, as modified by Peto. All data were analyzed with the Statistica computer program.

Results

Characterization of the p21 antibody on cell lines

The isolation of the DCS-60 monoclonal antibody specific for human p21 protein has been described [39]. The specificity of the DCS-60 antibody for p21 was verified by means of immunoblotting and immunoprecipitation on a series of cell lines with known p53 status (Fig. 1). Immunoblotting of p21 in total cell extracts revealed a good overall correlation with the presence of wildtype p53 (Fig. 1). Relatively high levels of the p21 protein were found in the MCF-7 and ZR-75 cell lines, which both contain wildtype p53. An intermediate level of p21

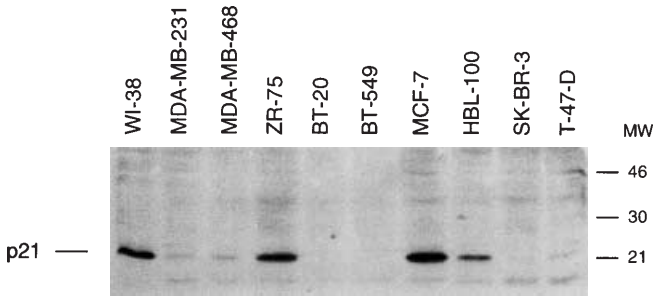


Fig. 1 Abundance of p21 correlates with p53 status in human breast cancer cell lines. Immunoblotting analysis of p21 in total cell extracts prepared from exponentially growing cells, using antibody DCS-60. Note that the highest levels of p21, comparable with that in control diploid fibroblasts (WI-38), are found in ZR-75 and MCF-7 breast cancer cell lines, which harbor wild-type p53. In contrast, a lower abundance of p21 is found in simian virus (SV)40-transformed HBL-100 cells, with very low or undetectable levels in the remaining six cell lines, which have different point missense mutations in the p53 gene. The cell lines are shown at the *top*, and the molecular weight of the markers on the *right* is given in kilodaltons

was found in the SV40-transformed HBL-100 cell line. Low or undetectable levels of p21 protein were found in the nine breast cancer cell lines which contain mutant p53, i.e., in MDA-MB-134, MDA-MB-157, MDA-MB-231, MDA-MB-453, MDA-MB-468, BT-20, BT-549, SK-BR-3, and T47D. It also recognizes p21 in mouse cells overexpressing exogenous human p21 (Welcker and Bartek, unpublished data). Immunoblotting with the mouse monoclonal antibody MO-1 against CDK7, a ubiquitously expressed nucleoprotein, showed that approximately equal amounts of extract had been loaded in all lanes in Fig. 1 (data not shown).

Immunofluorescence staining and evaluation of p21 at the single cell level showed that the p21 protein localized exclusively to cell nuclei. The abundance of p21 varied widely among individual cells in the MCF-7 or ZR-75 cell lines, with only a minor subpopulation of cells showing strong positivity. It was striking that the strongly stained cells were found often in pairs (Fig. 2), and their arrangements resembled cells in late telophase or early G1. In several breast cancer cell lines known to have mutant p53, there was a small subset of cells showing weak p21-specific staining (data not shown). In contrast, all nuclei were stained with the MO-1 antibody.

p21 positivity in histological specimens

Tumor cells were scored as positive for p21 if there was red nuclear staining (Fig. 3). Examination of normal breast tissue showed occasional p21-positive nuclei. The percentage of tumor cells that were p21-positive ranged from 0 to 16%. In 156 tumors, no tumor cells were stained. In 20 tumors, 0.1–1%, in 22 tumors 1–3%, in 20 tumors 3–10%, and in 4 tumors more than 10% of tumor cell nuclei were p21-positive. These 66 tumors constitut-

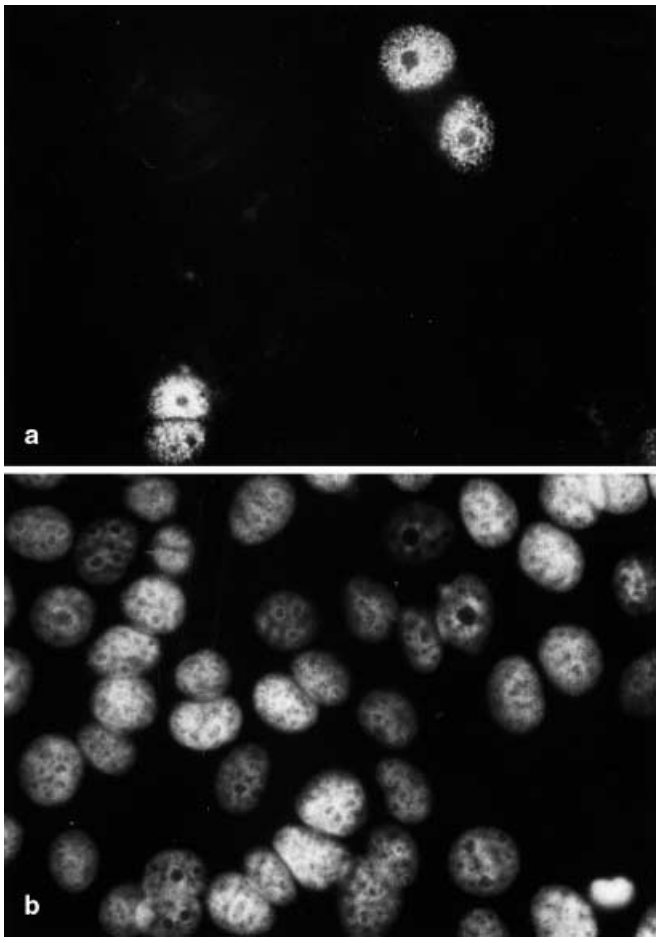


Fig. 2a,b Immunofluorescence visualization of p21 in the exponentially growing MCF-7 breast cancer cell line. **a** Strong nuclear positivity for p21 in a small subset of cells, as detected with the antibody DCS-60. Positive cells are usually found in pairs and are probably 'daughter cells' in late telophase or early G1. **b** Hoechst nuclear staining of the same cells as in (**a**). Magnification **a**, **b** ×800

ed the p21-positive group. The distribution of p21 tumor cells was heterogeneous, with p21 tumor cells often appearing in clusters (Fig. 3a, b), and sometimes in the tumor material it was easy to distinguish pairs of cells that were strongly stained with p21 antibody (Fig. 1b). The staining intensity of p21-positive tumor nuclei was heterogeneous. In some grade-III carcinomas, p21 expression was seen in very large nuclei (Fig. 3c) and in nuclei of multinucleated tumor cells (Fig. 3d). Tumor cells in 30% (66 of 222) of the invasive ductal NOS breast carcinomas expressed p21. In the node-negative subset, p21 was present in 32% (41 of 130), while in the node-positive subset, 27% (25 of 92) were p21-positive (Table 1).

Comparison of p21 status to other clinicopathological characteristics

The results in Table 1 show that p21 expression in the whole cohort of patients was associated with low histo-

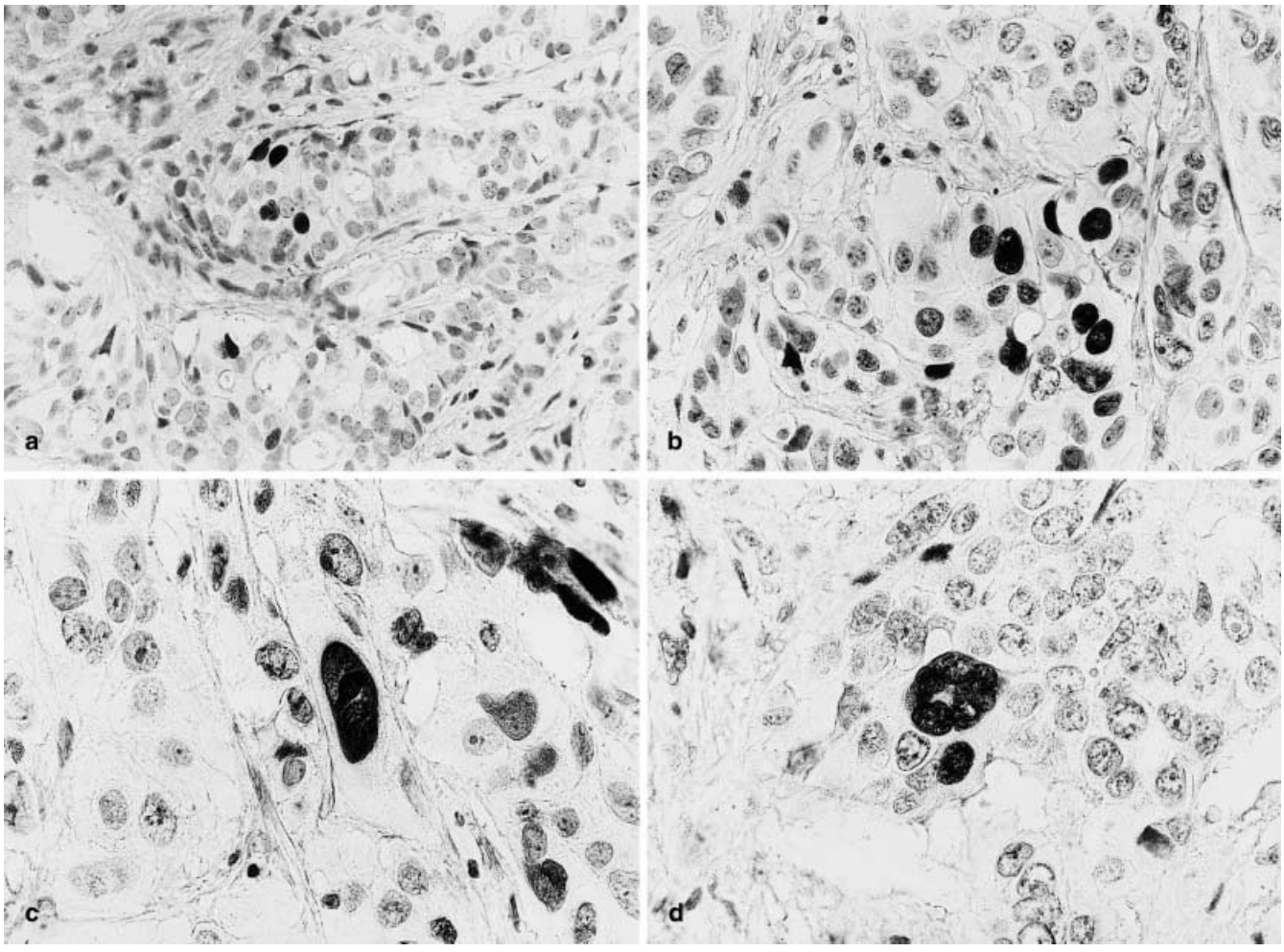


Fig. 3a–d p21 expression in invasive ductal not otherwise specified (NOS) breast carcinomas. **a** Grade-2 carcinoma with single p21-positive tumor cell nuclei. **b** Grade-3 carcinoma, with strong p21 reactivity in a group of tumor cell nuclei. **c** Huge p21-positive nucleus in a grade-3 carcinoma. **d** Multinucleated tumor cell with strong p21 expression. Streptavidin peroxidase method with 3-amino-9-ethylcarbazol (AEC) as the chromogen and light hematoxylin counterstain. Magnification: **a**, **b** ×250; **c**, **d** ×400

Table 1 p21 expression related to other clinicopathological factors. *NS* not significant

	All patients p21-positive		Node-negative p21-positive		Node-positive p21-positive	
	n (%)	*P*	*n* (%)	*P*	*n* (%)	*P*
Grade						
I+II	43/116 (37)	0.01	25/67 (37)	NS	18/49 (37)	0.03
III	23/106 (22)		16/63 (25)		7/43 (16)	
Size (mm)						
≤30	24/75 (32)	NS	12/49 (25)	NS	12/26 (46)	0.01
>30	42/147 (29)		29/81 (36)		13/66 (20)	
MIB-1						
≤10%	26/78 (33)	NS	17/41 (42)	0.01	9/37 (24)	NS
>10%	24/110 (22)		14/70 (20)		10/40 (25)	
p53						
Negative	53/158 (34)	(NS) 0.058	32/89 (36)	NS	21/69 (30)	NS
Positive	13/63 (21)		9/41 (22)		4/22 (18)	
Nodes						
Negative	41/130 (32)	NS				
Positive	25/92 (27)					

logical grade (grades I plus II vs grade III). p21 positivity showed a trend for an inverse correlation with p53 expression that, however, did not reach statistical significance ($P<0.058$). In node-negative patients, there was a significant negative correlation between p21 expression and a MIB-1 score greater than 10% ($P<0.01$). In node-positive patients, a significant correlation was found only between p21 expression and tumor size less than 30 mm ($P=0.01$) and between p21 expression and histological grade I plus II ($P=0.03$; Table 1).

p21 and proliferation rate of tumor cells

The mean MIB-1 score was significantly lower in p21-positive than in p21-negative tumors ($P=0.03$ for all and $P=0.02$ for axillary node-negative patients). In tumors from node-positive patients a similar trend was seen but it was not significant (Table 2). When tumors were divided into four groups according to p21 and p53 status, statistically significant differences in the MIB-1 score between the p21+ p53– group vs the p21– p53+ tumor group were found. This was true for all patients, for node-positive patients, and for node-negative patients (Table 3).

Prognostic significance of p21

One hundred and forty-two (64%) patients survived 5 years. The mean follow-up time for these patients was 69 months. When a cutoff level of less than 0.1% was used for p21 expression, Kaplan–Meier survival curves showed no statistically significant association between p21 expression in tumor cells and 5-year survival either in the whole cohort of patients or in the node-negative or node-positive subsets (data not shown).

When the p21 cutoff level was raised to more than 3%, and patients were stratified into four groups according to the p21/p53 status and further subdivided according to node status and therapy modality, five subsets could be analyzed, i.e., all, node-negative, node-positive, not treated with adjuvant therapy, and treated with adjuvant therapy. A significant ($P<0.035$) difference in Kaplan–Meier 5-year survival curves between patients with p21–/p53+ vs p21+/p53– tumors was found only in the group of patients treated with adjuvant therapy. In this group, only 58% of patients with p21–/p53+ tumors survived 5 years, whereas 83% of patients with p21+/p53– tumors survived 5 years. Thus, in patients treated with adjuvant therapy, the p21–/p53+ tumor phenotype was associated with the worst prognosis.

Table 2 p21 expression and proliferation rate of tumor cells in invasive ductal not otherwise specified (NOS) breast carcinomas

p21 status	*n*	MIB-1 (%)±SD	*P*
All patients	192		
p21-negative	140	18.3±14.6	
p21-positive	52	13.3±11.7	0.03
Node-negative	114		
p21-negative	82	19.5±14.1	
p21-positive	32	12.9±10.6	0.02
Node-positive	78		
p21-negative	58	16.2±15.1	
p21-positive	20	13.9±13.6	NS

Discussion

p21 expression in ductal carcinomas

In this report, we present immunohistochemical results on p21 expression in a homogeneous group of 222 invasive ductal NOS breast carcinomas. Previous studies have been concerned with p21 expression in histologically heterogeneous breast carcinomas and have usually not distinguished between the different histological types of breast carcinomas [4, 6, 7, 16, 22, 32, 40].

We found, using the DCS-60 antibody and a cut off level of 0.1%, that 30% of invasive ductal breast cancers expressed p21. p21 expression was heterogeneous both in terms of its distribution in the tumor tissue and intensity of expression, i.e., different percentages of p21-positive tumor cell nuclei were found in different tumors, and positive nuclei differed in staining intensity. In general, the level of expression of p21 was low. Only four tumors (6%) in our study expressed p21 in more then 10% of tumor cells. The highest percentage of p21-positive cells seen in a tumor was 16%.

Table 4 summarizes studies that have investigated p21 expression in breast carcinomas. Significant variation is

Table 3 The influence of p21 and p53 status on MIB-1 score in invasive ductal not otherwise specified (NOS) breast carcinomas

	p21	p53	All		Node negative		Node positive	
			n	MIB-1[a] (%±SD)	*n*	MIB-1[b] (%±SD)	*n*	MIB-1[c] (%±SD)
1	–	–	95	13.3±11	54	14.8±12	41	11.2±10
2	–	+	44	30.0±15	28	28.6±14	16	29.6±18
3	+	–	42	10.7±8	25	11.3±9	17	9.7±7
4	+	+	10	24.5±17	7	18.7±14	3	38.0±18

[a] 1 vs 2 $P<0.001$; 1 vs 4 $P>0.001$; 2 vs 3 $P<0.001$; 3 vs 4 $P<0.001$
[b] 2 vs 3 $P<0.001$; 1 vs 2 $P<0.001$
[c] 1 vs 2 $P<0.001$; 1 vs 4 $P>0.001$; 2 vs 3 $P>0.001$; 3 vs 4 $P>0.001$

Table 4 p21 expression in breast carcinomas. *F* formaldehyde; *Mw* microwave irradiation

	Series	Year	*n*	Histological type		Cutoff level p21+	p21+ MCF-7 cells	Antibody	p21+ nuclei (range)	p21+ Tumors	Fixation	Method of counting of p21+ cells
				Invasive ductal	Others							
1.	Barbareschi et al. [4]	1996	91	74	17	>10%		Oncogene EA10	0–50%	26%	F	Semi-quantitative[d]
2.	Caffo et al.[a] [7]	1996	261	164	34	>10%		Oncogene EA10	0–90%	32%	F	Semi-quantitative[d]
3.	Diab et al.[b] [11]	1997	115	?	?	>0%		Oncogene Ab3	0–60%	43%[c]	F	Not described
4.	Giannikaki et al. [16]	1997	102	88	14	>1%		Oncogene	0–25%	37%	F	Not described
5.	Jiang et al. [21]	1997	106	84	22	>25%		Santa Cruz clone 187	0–62%	32%	F?	Semi-quantitative[e]
6.	Wakasugi et al.[40]	1997	104	93	11	>10%	All[i]	Oncogene	?	49%	Mw	Semi-quantitative[g]
7.	Rey et al. [32]	1998	77	62	15	>5%		Oncogene EA10	?	57%	F	Semi-quantitative[f]
8.	Reed et al. [31]	1999	77	62	15	>0%		Oncog. Res. Prod. CC12	0–75%	68%	F	
9.	Mathoulin-Portier [25]	2000	162	162	–	≥1%		France Biochem. AB1	0–60%	53%	F?	Not described
10.	This study		222	222	0	>0.1%	Some[k]	DCS-60	0–16%	30%	F	Computerized image analysis[h]

[a] 91 cases from no. 1 included
[b] Node-negative only
[c] In 90% of positive tumors, the percentage of p21+ cells was low (>10%)
[d] At least 500 cells in the most densely stained areas
[e] 500 cells in five most representative areas
[f] In ten random high-power fields within the most stained areas
[g] In five different fields
[h] Count started in the most stained area and then additional contiguous fields were selected randomly until at least 1000 cells were counted
[i] All tumor cells p21-positive
[k] Only a fraction of tumor cells p21-positive

seen both in the percentage of p21-positive tumors, which varied from 26% [4] and 30% (this study) to 57% [6], and in the percentage of p21 nuclei that are positive in the different studies. In all studies, except one which used microwave fixation [40], formalin-fixed paraffin-embedded tissue was used and, therefore, the method of fixation is unlikely to be responsible for the differences. Factors that may explain the differences apparent in Table 4 include (1) the different histological material used in the different studies; (2) the different cutoff levels which ranged from 0% [11], to greater than 25% [22] (Table 4); (3) the different counting procedures. We started counts in a "hot spot" area and then additional contiguous fields were selected randomly until at least 1000 cells had been counted. Others counted p21-positive cells in "the most densely stained areas" [4, 7], in the "five most representative areas" [22], "in ten random high-power fields within the most stained areas" [32], or "in five different fields" [40]. We made counts using computerized image analysis, whereas others used semi-quantitative estimates; and (4) the different p21 antibodies. In this study, using the DCS-60 antibody, 0–16% of tumor cells were p21-positive. Diab et al. [11], using the Oncogene Ab3, found in almost all of their positive tumors (90%) that only a low proportion of cells (<10%) were stained for p21. However, in the other studies listed in Table 4, most of which used the EA10 antibody, the percentage of tumor cell nuclei showing p21 expression was higher. Thus, more than 10% of p21-reactive tumor cells were found in 26% [4], 32% [7], and 49% [40] of tumors, respectively. The highest percentage of p21+ nuclei in positive cases reached 90% in one study [7] and 62% in a second [22] (Table 4). Of the factors we list, probably the most important is the different p21 antibodies.

The DCS-60 antibody primarily detects cells in early G_1

Immunostaining of both cells in culture (Fig. 1) and of histological material (Fig. 3) suggests that cells in early G_1 are preferentially stained by the DCS-60 antibody. p21 has separate binding sites for the cyclins and cyclin-dependent kinase (CDK) and uses both of these contacts to bind the cyclin/CDK complexes with high affinity. The target epitope of the DCS-60 antibody has been located within the N-terminal domain of the p21 polypeptide, within the short region that physically interacts with the cyclins (Bartek et al., unpublished data). As a consequence, the DCS-60 antibody can immunoprecipitate free p21 or the transient complex of p21 with CDK but not the usually most abundant trimeric complex of

p21+cyclin/CDK, since the antibody competes for p21 with the cyclin. Thus, we speculate that the reason that immunostaining with DCS-60 reveals early G_1 cells is that this is the point in the cell cycle when the cyclins are still expressed at low levels, and p21 (if significantly expressed in a cell) is present in one of the two forms recognized by DCS-60. During other stages of the cell cycle, p21 is mainly found in a complex with cyclin/CDKs (and is lower in abundance as well).Therefore, the DCS-60 epitope is not accessible unless there is such a high level of p21 in the cell that some of it is in excess and thus in a free form which again is recognized by DCS-60. This latter scenario almost certainly explains the strongly p21-positive bizarre cells seen, for instance, in Fig. 3c. These may be damaged cells responding to a checkpoint with high levels of p21 or may be revealing a "senescence-like phenotype" in which p21 again plays a role and is expressed at high levels. A senescence-like phenotype has been shown to occur in tumor cells or diploid cells exposed to prolonged mitotic overload, and such a phenotype may represent one of the critical defense mechanisms against tumor development or progression. Such a mechanism may be able to stop or eliminate even tumor cells as long as they are able to respond by elevating p21.

p21 expression in p53-negative and in p53-positive breast carcinomas

Our results suggest a trend for an inverse relation between p21 expression and p53 accumulation in invasive ductal breast carcinomas, in keeping with previous findings showing a significant inverse relationship between p53 accumulation and p21 expression [22, 40] in breast cancer and a strong negative correlation between the presence of p53 mutations and p21 expression both in breast carcinoma [30] and in breast cancer cell lines [29, 30] on the messenger (m)RNA level. However, our results suggest that p21 could still be induced in tumors with mutant p53 since among p53-positive tumors those that were p21-positive had a lower mean MIB-1 score (24.5%) than did those that were p21-negative (30.0%). Although this difference was not statistically significant, it suggests a p53-independent pathway of p21-induced inhibition of tumor cell proliferation. These results are consistent with reports suggesting that p21, in breast cancer cell lines, may be induced by p53-dependent or p53-independent mechanisms. Thus, a few p53 mutant cell lines showed low levels of p21 expression [15], while some breast cancer cells expressed both p21 and (mutant) p53 [4, 32].

p21 expression and growth control in breast cancer

We found a significant association between p21 expression and a low MIB-1 score in all, and in node-negative invasive ductal NOS breast carcinomas (Table 2), which suggests p21-mediated growth control in breast cancer. This finding is consistent with data indicating that p21 suppresses tumor cell growth in vivo and in vitro [15]. Furthermore, we found striking differences in MIB-1 scores with p21+/p53– tumors having lower values than p21–/p53+ tumors. Barbareschi et al. [4] did not find a relationship between p21 expression and MIB-1 score, probably because they tested only 32 cases. However, using double staining, they documented that at a single cell level, p21 and MIB-1 were mutually exclusive. Also, Caffo et al. [7] saw no inverse association between p21 expression and MIB-1 score which, as they state, is difficult to explain. Rey et al. [32] and Mathoulin-Portier et al. [25] reported paradoxical results, i.e., a positive association between p21 expression and increased percentage of proliferating cells.

p21 expression and survival

High immunohistochemical p21 expression has been associated with short [4] and longer [22, 40] relapse-free and overall survival in breast carcinomas. However, in the studies, tubular, medullary, and mucinous carcinomas (which a priori have better prognosis) were included, and this may influence the results. Diab et al. [11], Reed et al. [31], and Mathoulin-Portier et al. [25] found no correlation with survival. In our series of breast carcinomas as well no statistically significant association was seen between immunohistochemical p21 expression or p21/p53 phenotype and overall survival at 5 years either in the whole cohort of patients or in the node-negative or node-positive subgroups. However, with respect to patients treated with adjuvant therapy, the p21–/p53+ phenotype was associated with the worst survival (only 58% surviving 5 years), while the p21+/p53– phenotype was associated with good survival (83% surviving 5 years). Caffo et al. [7] and Mathoulin-Portier et al. [25] also showed that a combined evaluation of p53 and p21 expression provides prognostic information in the group of patients given adjuvant therapy. However, they did not find an inverse association between p21 and the MIB-1 score, which would theoretically be expected and the lack of which is difficult to explain. We have significant (and theoretically expected) associations between p21 and MIB-1, but they do not seem to translate to differences in survival for node-negative, node-positive patients or for patients not given adjuvant therapy. A difference in survival is noted only for the group who received adjuvant therapy. Tumors with the p21–/p53+ phenotype presumably express mutated but not functional p53. Hence, they may not be able to activate apoptosis in response to chemotherapeutic DNA-damaging drugs. They also have a very high MIB-1 score of tumor cells, which may facilitate the emergence of clones of tumor cells resistant to chemotherapy. Since p21 is a key component of the DNA damage checkpoint, our results suggest a correlation between the p21/p53 phenotype and response to adjuvant chemotherapy. The results of Mathoulin-

Portier et al. [25] also suggest a correlation between the p53/p21/mdm2 phenotype and survival of patients with breast carcinomas treated by chemotherapy. These correlations are intriguing and suggest that in order to delineate better the group of breast cancer patients who may benefit from adjuvant chemotherapy, further studies are required of the relationship between the expression of p53 and some of its downstream effectors and chemotherapy and survival.

References

1. Allred DC, Clark GM, Elledge R, Fuqua SA, Brown RW, Chamness GC, Osborne CK, McGuire WL (1993) Association of p53 protein expression with tumor cell proliferation rate and clinical outcome in node-negative breast cancer. J. Natl Cancer Inst 85:200–206
2. Andersen TI, Holm R, Nesland JM, Heimdal KR, Ottestad R, Borresen AL (1993) Prognostic significance of TP53 alterations in breast carcinoma. Br J Cancer 68:540–548
3. Barbareschi M (1996) Prognostic value of the immunohistochemical expression of p53 in breast carcinomas. Appl Immunohistochem 4:106–116
4. Barbareschi M, Caffo O, Doglioni C, Fina P, Marchetti A, Buttitta F, Leek R, Morelli L, Leonardi E, Bevilacqua G, Dalla Palma P, Harris AL (1996) p21WAF1 immunohistochemical expression in breast carcinoma: correlations with clinicopathological data, oestrogen receptor status, MIB1 expression, p53 gene and protein alterations and relapse-free survival. Br J Cancer 74:208–215
5. Bloom HJG, Richardson WW (1957) Histologic grading and prognosis in breast cancer. Br. J. Cancer 11:359–377
6. Bukholm IK, Nesland JM, Karesen R, Jacobsen U, Borresen AL (1997) Relationship between abnormal p53 protein and failure to express p21 protein in human breast carcinomas. J Pathol 181:140–145
7. Caffo O, Doglioni C, Veronese S, Bonzanini M, Marchetti A, Buttitta F, Fina P, Leek R, Morelli L, Palma PD, Harris AL, Barbareschi M (1996) Prognostic value of p21(WAF1) and p53 expression in breast carcinoma: an immunohistochemical study in 261 patients with long-term follow-up. Clin Cancer Res 2:1591–599
8. Cattoretti G, Becker MHG, Key G, Duchrow M, Schlüter C, Galle J, Gerdes J (1992) Monoclonal antibodies against recombinant parts of the Ki-67 antigen (MIB1 and MIB3) detect proliferating cells in microwave-processed formalin-fixed paraffin sections. J Pathol 168:357–363
9. Coles C, Condie A, Chetty U, Steel CM, Evans HJ, Prosser J (1992) p53 mutations in breast cancer. Cancer Res. 52:5291–5298
10. Cordon-Cardo C (1995) Mutations of cell cycle regulators. Biological and clinical implications for human neoplasia. Am J Pathol 147:545–560
11. Diab SG, Yu YY, Hilsenbeck SG, Allred DC, Elledge RM (1997) WAF1/CIP1 protein expression in human breast tumors. Breast Cancer Res Treat 43:99–103
12. Domagala W, Striker G, Szadowska A, Dukowicz A, Harezga B, Osborn M (1994) p53 protein and vimentin in invasive ductal NOS breast carcinoma – relationship with survival and sites of metastases. Eur J Cancer 30A:1527–1534
13. Domagala W, Markiewski M, Harezga B, Dukowicz A, Osborn M (1996) Prognostic significance of tumor cell proliferation rate as determined by the MIB-1 antibody in breast carcinoma: Its relationship with vimentin and p53 protein. Clin Cancer Res 2:147–154
14. El-Deiry WS (1998) p21/p53, cellular growth control and genomic integrity. Curr Top Microbiol Immunol 227:121–137
15. Gartel AL, Serfas MS, Tyner AL (1996) p21-negative regulator of the cell cycle. Proc Soc Exp. Biol Med 213:138–149
16. Giannikaki E, Kouvidou C, Tzardi M, Stefanaki K, Koutsoubi K, Gregoriou M, Zois E, Kakolyris S, Mavroudi C, Delides G, Georgoulias V, Kanavaros P (1997) p53 protein expression in breast carcinomas. Comparative study with the wild type p53 induced proteins mdm2 and p21/waf1. Anticancer Res 17: 2123–2127
17. Harper JW, Adami GR, Wei N, Keyomarsi K, Elledge SJ (1993) The p21 Cdk-interacting protein Cip1 is a potent inhibitor of G1 cyclin-dependent kinases. Cell 75:805–816
18. Hunter T (1993) Braking the cycle. Cell 75:839–841
19. Hunter T, Pines J (1994) Cyclins and cancer. II: cyclin D and CDK inhibitors come of age. Cell 79:573–582
20. Isola J, Visakorpi T, Holli K, Kallioniemi OP (1992) Association of overexpression of tumor suppressor protein p53 with rapid cell proliferation and poor prognosis in node-negative breast cancer patients. J Natl Cancer Inst 84:1109–1114
21. Jiang H, Lin J, Su ZZ, Collart FR, Huberman E, Fisher PB (1994) Induction of differentiation in human promyelocytic HL-60 leukemia cells activates p21, WAF1/CIP1, expression in the absence of p53. Oncogene 9:3397–3406
22. Jiang M, Shao ZM, Wu J, Lu JS, Yu LM, Yuan JD, Han QX, Shen ZZ, Fontana JA (1997) p21/waf1/cip1 and mdm-2 expression in breast carcinoma patients as related to prognosis. Int J Cancer 74:529–534
23. Lukas J, Pagano M, Staskova Z, Draetta G, Bartek J (1994) Cyclin D1 oscillates and is essential for cell cycle progression in human tumour cell lines. Oncogene 4:707–718
24. Marchetti A, Doglioni C, Barbareschi M, Buttitta F, Pellegrini S, Bertacca G, Chella A, Merlo G, Angeletti CA, Palma PD, Bevilacqua G (1996) p21 RNA and protein expression in non-small cell lung carcinomas: evidence of p53-independent expression and association with tumoral differentiation. Oncogene 12:1319–1324
25. Mathoulin-Portier M-P, Viens P, Cowen D, Bertucci F, Houvenaeghel G, Geneix J, Puig B, Bardou VJ, Jacqumier J (2000) Prognostic value of simultaneous expression of p21 and mdm2 in breast carcinomas treated by adjuvant chemotherapy with antracyclin Oncology Reports 7:675–680
26. Mazars R, Spinardi L, BenCheikh M, Simony-Lafontaine J, Jeanteur P, Theillet C (1992) p53 mutations occur in aggressive breast cancer. Cancer Res. 52:3918–3923
27. Michieli P, Chedid M, Lin D, Pierce JH, Mercer WE, Givol D (1994) Induction of WAF1/CIP1 by a p53-independent pathway. Cancer Res 54:3391–3395
28. Millis R, Girling A (1989) The breast. In: Sternberg SS (ed) Diagnostic surgical pathology. Raven, New York, pp 253–313
29. Musgrove EA, Lilischkis R, Cornish AL, Lee CS, Setlur V, Seshadri R, Sutherland RL (1995) Expression of the cyclin-dependent kinase inhibitors p16INK4, p15INK4B and p21WAF1/CIP1 in human breast cancer. Int J Cancer 63: 584–391
30. Özcelik H, Mousses S, Andrulis IL (1995) Low levels of expression of an inhibitor of cyclin-dependent kinases (CIP1/WAF1) in primary breast carcinomas with p53 mutations. Clin Cancer Res 1:907–912
31. Reed W, Fllrenes VA, Holm R, Hannisdal E, Nesland JM (1999) Elevated levels of p27, p21 and cyclin D1 correlate with positive oestrogen and progesterone receptor status in node-negative breast carcinoma patients. Virchows Arch 435:116–124
32. Rey MJ, Fernandez PL, Jares P, Munoz M, Nadal A, Peiro N, Nayach I, Mallofre C, Muntane J, Campo E, Estape J, Cardesa A (1998) p21WAF1/Cip1 is associated with cyclin D1CCND1 expression and tubular differentiation but is independent of p53 overexpression in human breast carcinoma. J Pathol 184:265–271
33. Runnenbaum IB, Nagarajan M, Bowman M, Soto D, Sukumar S (1991) Mutations in p53 as potential molecular markers for human breast cancer. Proc Natl Acad Sci USA 88:10657–10661

34. Sheikh MS, Li XS, Chen JC, Shao ZM, Ordonez JV, Fontana JA (1994) Mechanisms of regulation of WAF1/Cip1 gene expression in human breast carcinoma: role of p53-dependent and independent signal transduction pathways. Oncogene 9:3407–3415
35. Silvestrini R, Benini E, Daidone MG, Veneroni S, Boracchi P, Cappelletti V, Di Fronzo G, Veronesi U (1993) p53 as an independent prognostic marker in lymph node-negative breast cancer patients. J Natl Cancer Inst 85:965–970
36. Steinman RA, Hoffman B, Iro A, Guillouf C, Liebermann DA, el-Houseini ME (1994) Induction of p21 (WAF-1/CIP1) during differentiation. Oncogene 9:3389–3396
37. Thompson AM, Anderson TJ, Condie A, Prosser J, Chetty U, Carter DC, Evans HJ, Steel CM (1992) p53 allele losses, mutations and expression in breast cancer and their relationship to clinico-pathological parameters. Int J Cancer 50:528–532
38. Thor AD, Moore DH, II, Edgerton SM, Kawasaki ES, Reihsaus E, Lynch HT, Marcus JN, Schwartz L, Chen LC, Mayall BH (1992) Accumulation of p53 tumor suppressor gene protein: an independent marker of prognosis in breast cancers. J Natl Cancer Inst 84:845–855
39. Thullberg M, Welcker M, Bartkova J, Kjerulff AA, Lukas J, Högberg J, Bartek J (2000) Monoclonal antibody probes for p21 WAF1/CIP1 and the INK4 family of cyclin-dependent kinase inhibitors. Hybridoma 19:63–72
40. Wakasugi E, Kobayashi T, Tamaki Y, Ito Y, Miyashiro I, Komoike Y, Takeda T, Shin E, Takatsuka Y, Kikkawa N, Monden T, Monden M (1997) p21(Waf1/Cip1) and p53 protein expression in breast cancer. Am J Clin Pathol 107:684–691
41. Xiong Y, Hannon GJ, Zhang H, Casso D, Kobayashi R (1993) p21 is a universal inhibitor of cyclin kinases. Nature 366: 701–704

Virchows Arch (2001) 439:141–151
DOI 10.1007/s004280100423

ORIGINAL ARTICLE

**Jeanne Marie Meis-Kindblom · Helene Sjögren
Lars-Gunnar Kindblom · Anabel Peydró-Mellquist
Eva Röijer · Pierre Åman · Göran Stenman**

Cytogenetic and molecular genetic analyses of liposarcoma and its soft tissue simulators: recognition of new variants and differential diagnosis

Received: 17 November 2000 / Accepted: 5 January 2001 / Published online: 31 March 2001
© Springer-Verlag 2001

Abstract Liposarcoma is one of the most common sarcomas of adults. Its differential diagnosis and accurate subclassification are often problematic; the latter is also important with regard to appropriate treatment and prognosis. We studied a series of 23 liposarcomas that had unusual or previously undescribed features and 10 liposarcoma simulators and correlated the morphologic, cytogenetic, and molecular genetic findings. We found that use of cytogenetic–molecular genetic techniques aids in the distinction between myxoid-round cell liposarcoma and their simulators, chondroid lipoma, myxoid spindle cell-pleomorphic lipoma, cellular intramuscular myxoma, and myxofibrosarcoma. Poorly differentiated forms of round cell liposarcoma lacking morphologic evidence of lipogenesis can also be diagnosed using these techniques; however, the techniques do not aid in distinguishing low-grade myxoid from high-grade round cell liposarcomas. This study also shows that retroperitoneal liposarcomas with myxoid liposarcoma-like zones are part of the morphologic spectrum of well-differentiated–dedifferentiated liposarcoma rather than true myxoid liposarcomas. Perhaps most importantly, our results provide the first molecular genetic evidence that true mixed liposarcomas (mixed well-differentiated and myxoid liposarcoma) do indeed exist. They also unequivocally demonstrate the existence of small, round cell variants of pleomorphic liposarcoma that closely simulate myxoid-round cell liposarcoma.

Keywords Liposarcoma · RT-PCR · Cytogenetics · FISH · Differential diagnosis

J.M. Meis-Kindblom (✉) · H. Sjögren · L.-G. Kindblom
A. Peydró-Mellquist · E. Röijer · P. Åman · G. Stenman
Lundberg Laboratory for Cancer Research,
Department of Pathology and the Musculoskeletal Tumor Center,
Göteborg University, Sahlgrenska University Hospital,
41345 Göteborg, Sweden
e-mail: jeanne.meis-kindblom@llcr.med.gu.se
Tel.: +46-31-3423869, Fax: +46-31-827194

Introduction

Lipomatous tumors are common human neoplasms that exhibit a broad morphologic and clinical spectrum, ranging from harmless lipomas to high-grade sarcomas. Liposarcoma, one of the more common soft tissue sarcomas of adults, is currently subclassified into four main groups, including well-differentiated (lipoma-like and sclerosing types), myxoid-round cell, pleomorphic, and dedifferentiated types. There are, however, liposarcomas that do not readily fit into this traditional morphologic classification scheme. Moreover, the histologic differential diagnosis of liposarcoma is wide and may be problematic; it includes benign lipomatous tumors and benign and malignant simulators without true lipogenesis.

Recent cytogenetic and molecular genetic studies have provided insight into the pathogenesis of various benign and malignant lipomatous tumors. These techniques have also been successfully applied to their diagnosis. Several lipogenic tumors have specific chromosomal abnormalities, the best known example being the t(12;16)(q13;p11) of myxoid-round cell liposarcoma [48]. This translocation results in a fusion gene consisting of the 5′ part of the *TLS* gene and the complete coding region of the *CHOP* gene [7, 39]. Well-differentiated liposarcoma and atypical lipoma are characterized by supernumerary ring chromosomes and giant marker chromosomes containing amplified sequences derived from different chromosomes, particularly chromosome 12 [11, 37, 38, 41]. Pleomorphic liposarcomas lack consistent abnormalities and often have multiple, complex structural rearrangements and occasional ring chromosomes, large markers, and double minute (dmin) chromosomes [26, 43]. Ordinary lipomas frequently show rearrangements of 12q13–15, 6p and 13q, or both [18], whereas spindle cell-pleomorphic lipomas have recurrent abnormalities of 13q and/or deletions of 16q [8]. Two cases of chondroid lipoma with seemingly identical

t(11;16)(q13;p13) have also been described [12, 47], suggesting that this abnormality may be specific for this recently described pseudosarcomatous tumor [14, 29]. Finally, structural rearrangements involving 11q13–21 and 8q11–13 are nonrandom changes in hibernomas [21, 25, 28] and lipoblastomas [36], respectively.

The purpose of our study was to correlate clinical, morphologic, cytogenetic, and molecular genetic features in lipomatous tumors that were problematic because they had either unusual or previously undescribed light microscopic features and to compare these findings to the relatively few detailed cytogenetic and molecular genetic studies reported in the literature. Similar studies were performed in benign and malignant non-lipogenic tumors that simulate liposarcoma, and the findings were compared with those of lipogenic tumors.

Materials and methods

Tumor material

Thirty-three tumors with unusual morphologic features were selected for this study, including 23 liposarcomas (from 20 patients), five myxofibrosarcomas [or myxoid variant of malignant fibrous histiocytoma (MFH)], two spindle cell-pleomorphic lipomas, one chondroid lipoma, and two cellular variants of intramuscular myxoma. Clinical records and hematoxylin and eosin-stained histologic sections were reviewed in all cases. In 28 cases, ultrastructural studies were also performed.

Cytogenetic and fluorescent in situ hybridization analyses

Fresh surgical specimens were obtained. Primary cultures were established as previously described [31]. Chromosome preparations were made from exponentially growing primary cultures. Cells were harvested after colcemide exposure followed by hypotonic treatment and fixation in methanol/acetic acid. Slides were subsequently G-banded and analyzed according to the recommendations of the International System for Cytogenetic Nomenclature (ISCN) [27].

Slides for fluorescent in situ hybridization (FISH) were aged for 2–10 days or were treated with 2×SSC (sodium saline citrate; pH 7.0) at 37°C for 30 min and subsequently denatured in 70% formamide in 2×SSC (pH 7.0), at 75°C for 2–6 min. Whole chromosome painting probes (Vysis) for chromosomes 12 and 16 were used. The conditions for hybridization and washes were as recommended by the manufacturer. Chromosomes were counterstained with 4′,6′-diamidino-2′-phenylindole dihydrochloride (DAPI) containing an antifade solution. Fluorescence signals were digitalized, processed, and analyzed using the PowerGene Image Analysis System (Perceptive Scientific Instruments).

Reverse transcriptase polymerase chain reaction analysis

Total RNA was extracted from tissue samples using TRIZOL (GIBCO/BRL) according to the supplier's protocol. RNA (5 µg) was reverse-transcribed using Superscript II reverse transcriptase (GIBCO/BRL) and oligo d(T) primers according to recommended conditions. A 0.25-µg aliquot of the resulting cDNA was amplified using the following *TLS-CHOP*-specific primers: 5′-CAGAGCTCCCAATCGTCTTACGG-3′ and 5′-GAGAAAGGCAATGACTCAGCTGCC-3′ corresponding to positions 331–353 and 960–983 of the *TLS-CHOP* cDNA sequence, respectively [32]. The conditions for amplification were essentially as described [32].

Southern blot analysis

High molecular weight DNA was isolated from tumors and control blood samples [42]. DNA was digested with the restriction endonucleases *Eco*RI, *Hin*dIII, and *Bam*HI under conditions recommended by the manufacturer. Digested DNA was electrophoresed in 0.8% agarose gels in 0.5×TBE buffer (45 mM Tris, 45 mM boric acid, and 1.25 mM EDTA) and transferred to nylon filters according to the method of Southern [44]. The filters were hybridized to a radiolabeled 550-bp *CHOP* cDNA probe (CHOP10; kindly provided by D. Ron) corresponding to the *CHOP* coding region [40].

Results

The clinical data, cytogenetic and molecular genetic findings, and histologic features are detailed in Table 1 and Table 2.

Spindle cell-pleomorphic lipoma and chondroid lipoma

Both spindle cell-pleomorphic lipomas had mature adipose tissue, abundant haphazardly arranged collagen fibers, bland spindle cells, and large cells with hyperchromatic multilobated nuclei (so-called floret cells). In both cases, there were rare lipoblasts and highly vascular, paucicellular myxoid zones resembling myxoid liposarcoma.

The chondroid lipoma contained an admixture of mature fat and myxohyaline to chondroid zones with nests and cords of small brown fat-like multivacuolated lipoblasts (Fig. 1A). This lesion closely resembled two myxoid liposarcomas in this series (Fig. 1B). Southern blot analysis revealed no rearrangements of the *CHOP* gene in either of the two spindle cell-pleomorphic lipomas or the chondroid lipoma, indicating that they lacked t(12;16)(q13;p11).

Well-differentiated liposarcoma variants

The two large retroperitoneal tumors were predominantly well-differentiated, lipoma-like liposarcomas, with focal sclerotic zones containing atypical non-lipogenic floret-like cells, scattered atypical univacuolated fat cells, and a few multivacuolated lipoblasts. In one of them (case 4), there were areas containing small lipoblasts in a richly vascularized myxoid matrix, resulting in an appearance indistinguishable from myxoid liposarcoma. The other case of well-differentiated liposarcoma (case 5) contained diffuse infiltrates of mature lymphocytes with occasional germinal centers (referred to as lymphocyte-rich well-differentiated liposarcoma) [5]. Neither of these cases showed rearrangements of the *CHOP* gene.

Dedifferentiated liposarcoma variants

One of the three tumors (case 7) consisted of a well-differentiated lipomatous tumor juxtaposed to a predomi-

Table 1 Clinical data, cytogenetic, fluorescent in situ hybridization (FISH), reverse transcriptase polymerase chain reaction (RT-PCR), and Southern blot analyses and histologic diagnoses in 23 lipogenic and 10 non-lipogenic tumors from 30 patients. *dmin* double minute chromosome; *MFH* malignant fibrous histiocytoma; *IM* intramuscular; *L* left; *R* right; *SQ* subcutaneous

Case no.	Age (years) and gender	Location	Size (cm)	t(12;16)	Rings, giant markers, dmin	TLS-CHOP fusion transcript	CHOP rearrangement	Histologic diagnosis
1	47, Male	L shoulder, SQ	8				–	Pleomorphic lipoma
2	71, Male	L upper arm, SQ/deep	8				–	Pleomorphic lipoma
3	40, Male	R lower leg, IM	4				–	Chondroid lipoma
4	48, Female	Retroperitoneum	10				–	Well-differentiated liposarcoma (myxoid liposarcoma-like foci)
5	31, Male	Retroperitoneum	20				–	Well-differentiated liposarcoma
6	71, Male	Retroperitoneum	29	–	+			Dedifferentiated liposarcoma (lipoma-like + MFH-like + myxoid liposarcoma-like foci)
7	53, Female	Abdomen	23	–	+			Dedifferentiated liposarcoma (lipoma-like + spindled-pleomorphic sarcoma + myxoid liposarcoma-like areas)
8	74, Male	Chest wall, IM	8	–	+			Recurrence of dedifferentiated liposarcoma (only MFH-like areas, no lipogenic differentiation)
9 A	29, Male	R thigh, SQ	13	+	+	+		Mixed myxoid + well-differentiated lipoma-like liposarcoma
9B		Supraclavicular region	10			+		Mixed myxoid + well-differentiated lipoma-like liposarcoma
10	34, Female	R thigh, IM	8				+	Myxoid liposarcoma (myxofibrosarcoma-like)
11	47, Female	R thigh, IM	4			+	+	Myxoid liposarcoma (cellular round cell component)
12	36, Female	L thigh, IM	8			+	+	Myxoid liposarcoma cellularity, well-differentiated (variable lipoma-like areas, chondroid lipoma-like areas)
13	48, Female	R thigh, IM	14	+	–	+	+	Myxoid liposarcoma (paucicellular–cellular round cell type, chondroid lipoma-like areas, well-differentiated lipoma-like areas)
14 A	33, Female	Abdomen	5	+	–	+	+	Myxoid liposarcoma (cellular type, transition to round cell)
14B		Retroperitoneum	4	+	–			Myxoid liposarcoma (cellular type, transition to round cell)
15	78, Male	L thigh, IM	9	+	–	+		Round cell liposarcoma (poorly differentiated, trabecular and adenoid growth pattern)
16	70, Female	L lower arm, deep	4			+		Round cell liposarcoma (poorly differentiated, no lipoblasts)
17	81, Male	Trunk, SQ	6	+	–	+		Round cell liposarcoma (poorly differentiated, no lipoblasts)
18	78, Male	R thigh, IM	6			+	+	Round cell liposarcoma (poorly differentiated)

Tab. 1 (continued)

Case no.	Age (years) and gender	Location	Size (cm)	t(12;16)	Rings, giant markers, dmin	TLS-CHOP fusion transcript	CHOP rearrangement	Histologic diagnosis
19	40, Female	R thigh, IM	4			+	+	Round cell liposarcoma (poorly differentiated, no lipoblasts)
20	51, Male	Retroperitoneum	25			–	–	Pleomorphic liposarcoma (predominantly poorly differentiated small round cell type)
21 A	76, Male	Chest wall, IM	8			–	–	Pleomorphic liposarcoma (predominantly high-grade spindled, few pleomorphic lipoblasts)
21 B	79, Male	Recurrence, chest wall	7			–	–	Pleomorphic liposarcoma (focal round cell-like areas)
22	73, Female	L upper arm, IM	7			–	–	Pleomorphic liposarcoma (predominantly small round cell type)
23	80, Male	R lower arm, SQ	10			–	–	Pleomorphic liposarcoma (predominantly MFH-like)
24	59, Male	R thigh, IM	6	–	–			Intramuscular myxoma, cellular variant
25	45, Male	Back, IM	6	–	–			Intramuscular myxoma, cellular variant
26	80, Male	L thigh, SQ	8				–	Myxofibrosarcoma, grade-III
27	73, Female	R lower arm, SQ	8				–	Myxofibrosarcoma. grade-III
28	57, Male	Trunk, SQ	11	–	–		–	Myxofibrosarcoma, grade-III
29	53, Male	Buttock, IM	10	–	–		–	Myxofibrosarcoma, grade-III
30	69, Male	R thigh, SQ	6	–	–			Myxofibrosarcoma, grade-II

nantly high-grade spindled and pleomorphic sarcoma. The high-grade component focally contained myxoid areas with a delicate, branching vasculature lined by small lipoblasts similar to myxoid liposarcoma (Fig. 1C). Four different areas of the pleomorphic myxoid sarcomatous component were analyzed cytogenetically (Table 2). Three of four areas had 1q- and 19q+ markers in common. In addition, giant markers were present in all four areas, and 1–3 ring chromosomes and dmin chromosomes were found in three areas (Fig. 2A). FISH analysis of metaphases from one area showed that the ring chromosomes and giant markers mainly contained chromosome 12 material (Fig. 2B).

Another case (case 6) showed transitions between well-differentiated lipoma-like liposarcoma, myxofibrosarcoma-like zones and high-grade fibrosarcomatous areas. In addition, there were myxoid, vascular areas resembling myxoid liposarcoma (Fig. 1D). This case also had extensive lymphocytic infiltrates. Cytogenetically, this tumor was mainly hyperdiploid with 1–2 markers of unknown origin. One ring chromosome was found in two cells. FISH analysis revealed that the rings were derived from chromosome 12 and that the dmin chromosomes found in two cells also contained chromosome 12 sequences.

The third case (case 8), which was a local recurrence of a classical dedifferentiated liposarcoma, consisted of a

Fig. 1 **A** A chondroid lipoma with small granular cells and multivacuolated lipoblasts (*insert*) in a myxohyaline to chondroid matrix. The lesion closely resembles myxoid liposarcoma (case 3). **B** Myxoid liposarcoma with chondrohyaline foci containing small lipoblasts. Note resemblance to chondroid lipoma (**A**, case 13). **C** Dedifferentiated liposarcoma with myxoid foci closely resembling myxoid liposarcoma (case 7). **D** Dedifferentiated liposarcoma with a high-grade spindle cell/pleomorphic component (*bottom*) adjacent to a myxoid liposarcoma-like area (*top*, case 6). **E**, **F** Predominantly well-differentiated, lipoma-like liposarcoma (**E**) with only focal paucicellular myxoid areas (**F**, case 9; compare with Fig. 2C). **G** Myxoid liposarcoma with areas lacking lipogenic differentiation closely simulating a myxofibrosarcoma (compare with **M**, case 10). **H** Myxoid liposarcoma with well-differentiated lipoma-like areas (case 13). **I** Poorly differentiated round cell liposarcoma without morphologic evidence of lipogenesis (case 17; compare with Fig. 3, lane 8). **J** Liposarcoma with predominantly small, rounded lipoblasts and only minimal foci with pleomorphic lipoblasts (*insert*). Although the tumor closely resembles a round cell liposarcoma, the absence of t(12;16) and the focal pleomorphism suggest it represents a small cell variant of pleomorphic liposarcoma (case 22). **K** Pleomorphic liposarcoma with large multivacuolated lipoblasts and small univacuolated lipoblasts; the latter are similar to those seen in round cell liposarcoma (case 21B). **L** Cellular variant of intramuscular myxoma; the bubbly matrix around the lesional cells (*insert*) may be misinterpreted as lipoblastic differentiation (case 24). **M** Myxofibrosarcoma resembling myxoid liposarcomas that lack obvious lipogenesis (compare with **G**); the cytoplasmic vacuoles and bubbly matrix simulate lipoblasts (*insert*, case 30). **A–M**, hematoxylin and eosin; **B**, **D**, **E**, **F**, **H**, **L**, **M** ×90; **A**, **C**, **G**, **I**, **J** ×120; **K** and *inserts* in **L** and **M** ×180

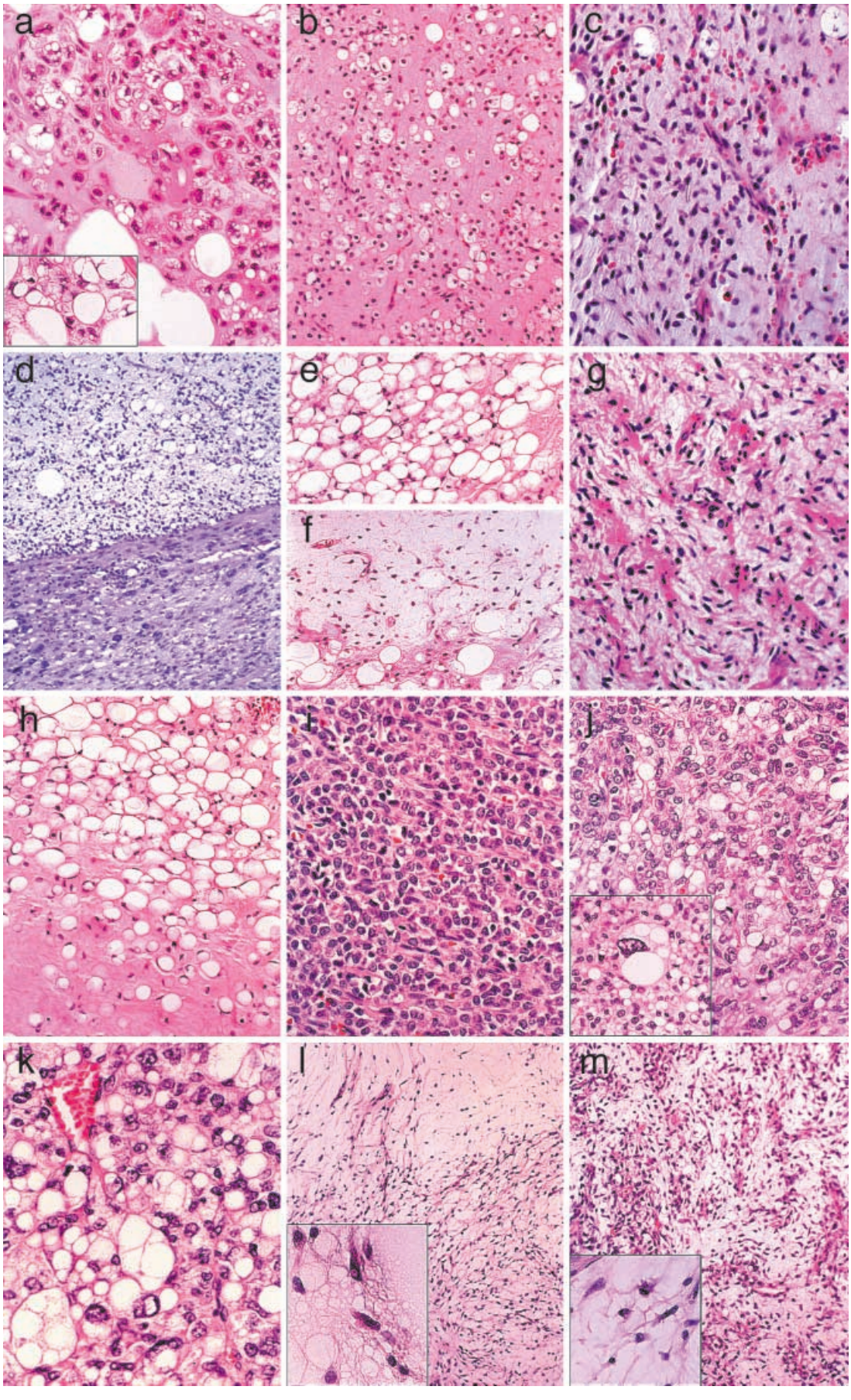

a
b
c
d
e
f
g
h
i
j
k
l
m

Table 2 Summary of cytogenetic and fluorescent in situ hybridization (FISH) observations in eight lipogenic and four non-lipogenic tumors

Case no.	Cytogenetic and FISH observations	Comments
6	44~49, XY, –19[3], –20[2], +1r[2], +1~2 mar[5] [cp8]. ish r(12)(wcp12+, wcp16–), ish dmin(wcp12+, wcp16–)	No evidence of t(12;16) by FISH
7	Area 1: 43~48, XX, del(1)(q23)[8], add(19)(q13.2–.3)[11], +4~5mar[14], 1~3dmin[2] [cp14]	No evidence of t(12;16) by FISH
	Area 2: 46~50, XX, +2~3r[6], +2~5mar[6], 2~4dmin[3] [cp6]	Giant marker chromosomes present in areas 1, 2, 3, and 4
	Area 3: 43~65, XX, del(1)(q23)[1], add(19)(q13.2-.3)[1], +1~3r[16], +2~6mar[13], 1~4dmin[5] [cp19]. ish r(12)(wcp12+,wcp16–)	
	Area 4: 44~50, XX, del(1)(q23)[3], add(19)(q13.2–.3)[3], +1r[1], +4~8mar[5] [cp5]	
8	65~75, XXX, +20~30mar[11], 1~2dmin[7] [cp23]	No evidence of t(12;16) by FISH
9A	41~49, XY, +1r[4], +5~20mar[17], 1~6dmin[13] [cp17]. ish t(12;16)(wcp12+, wcp16+), ish dmin(wcp12+, wcp16–)	Giant markers present in three cells
13	47, XX, +der(1)t(1;16)(p11;p11), t(12;16)(q13;p11), –16, +19	
14A	47, XX, +8, t(12;16)(q13;p11)	
14B	45~47, XX, add(2)(p15–16) [3], del(5)(q12) [2], add(6)(p25) [3], del(6)(q21) [3], t(12;16)(q13;p11) [3], add(17)(p12) [2] [cp3]. ish t(12;16)(wcp12+, wcp16+)	
15	46, XY, t(12;16)(q13;p11)	
17	45~48, XY, +7[3], der(12)t(12;16)(q13;p11)[4], +14[5],der(16) (16qter→16p11::12q13→12q24::?)[3], +mar[5] [cp5]. ish der(12)t(12;16) (wcp12+, wcp16+), ish der(16)(16qter→16p11::12q13→12q24::16?) (wcp12+, wcp16+)	
24	46, XX / 47, XX, +18[2]	
25	46, XX	Variant cell with 2 markers
28	46, XY	
29	46, XY	
30	44~46, XX, -16[3] [cp9]	Variant cell with t(13;17)(q10;q10)

high-grade MFH-like component without lipogenesis. This tumor had a near triploid chromosome count. The karyotype was very complex with 20–30 markers. The quality of the preparation did not allow detailed characterization of these markers. One to three giant marker chromosomes were present in four cells, and one to two dmin chromosomes were present in seven cells. There was no evidence of t(12;16) in any of the three dedifferentiated liposarcomas, including the ones with foci indistinguishable from myxoid liposarcoma.

Myxoid liposarcoma variants

One of the tumors (case 9A) demonstrated primarily lipoma-like areas (Fig. 1E). Rare small microscopic foci characteristic of myxoid liposarcoma with a richly vascularized matrix containing bland spindled and stellate cells and a few multivacuolated small lipoblasts were seen (Fig. 1F). In addition to the rings, giant markers and dmin chromosomes characteristic of atypical lipomatous tumors–well-differentiated liposarcomas, this case also had the specific t(12;16) of myxoid liposarcoma (Fig. 2C). FISH analysis in this case revealed the presence of t(12;16) and showed that the dmin chromosomes contained chromosome 12-specific sequences. Reverse transcriptase polymerase chain reaction (RT-PCR) analysis of this tumor and its metastases (case 9B) showed that they both contained the *TLS-CHOP* fusion transcript (Fig. 3).

The remaining six tumors displayed a wide spectrum of cellularity and lipoblastic differentiation. All six tumors had both paucicellular and moderately cellular areas with a predominantly myxoid matrix, containing an abundant capillary-like vasculature that was occasionally coarse. Lipogenic differentiation ranged from minimal, with mostly stellate or spindle-shaped tumor cells resembling myxofibrosarcoma (Fig. 1G), to prominent, with extensive lipogenic maturation and numerous univacuolated lipoblasts (Fig. 1H). Three of the tumors (cases 11, 13, and 14) contained foci of round cell liposarcoma, and two cases (cases 12 and 13) had well-differentiated lipoma-like areas (similar to case 9) and foci resembling chondroid lipoma (Fig. 1B). All four myxoid liposarcomas analyzed cytogenetically showed the characteristic t(12;16; Fig. 2D, E). The karyotypes of these tumors are described in Table 2. The remaining three myxoid liposarcoma variants expressed the *TLS-CHOP* fusion transcript and/or had rearrangements of the *CHOP* gene, indicating the presence of t(12;16).

Round cell liposarcoma variants

All five tumors were highly cellular and without myxoid zones; lipoblasts were seen in only two cases (cases 15 and 18). Three tumors (cases 16, 17, and 19) had no lipogenesis either light microscopically or ultrastructurally. Thus, a definite diagnosis of round cell liposarcoma could not be made (Fig. 1I). Ewing's sarcoma–primitive

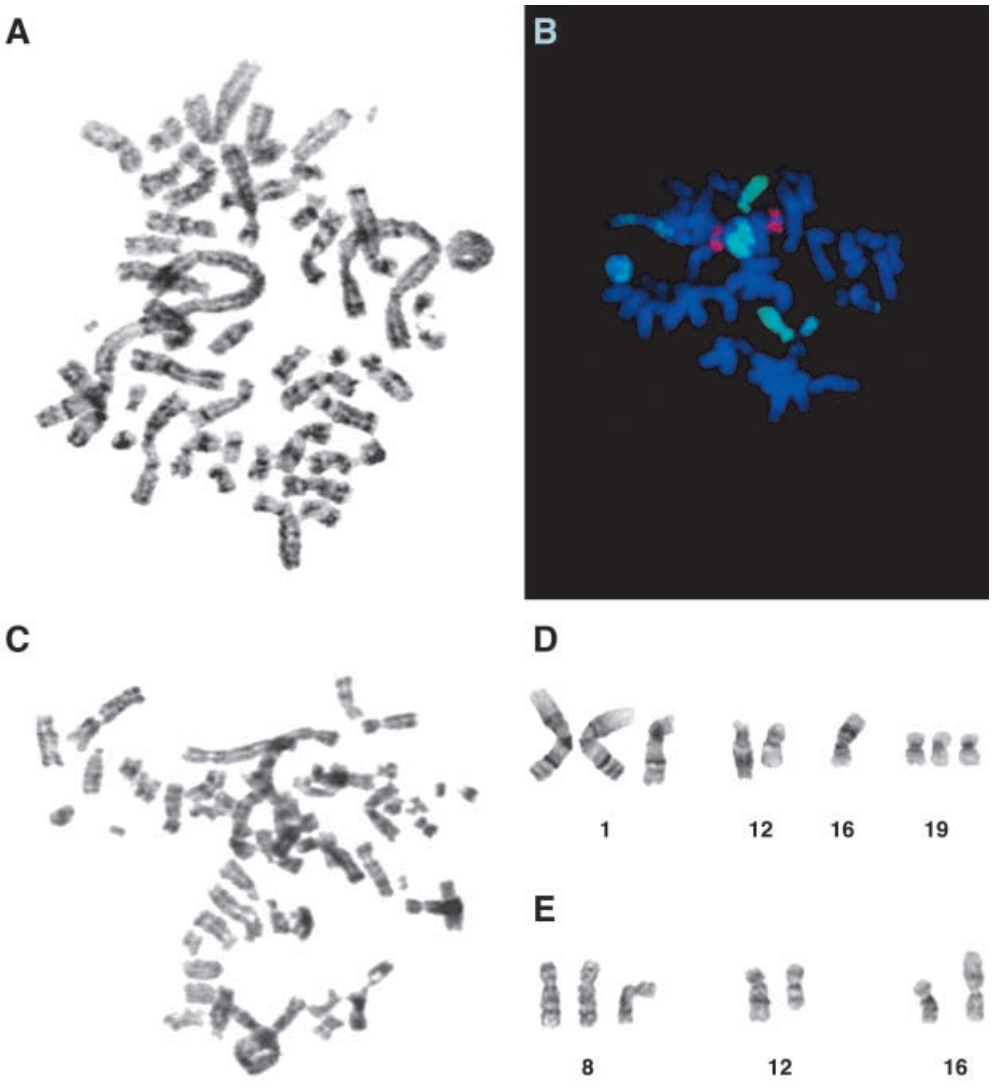


Fig. 2 Cytogenetic and fluorescent in situ hybridization (FISH) observations in four cases of liposarcoma. **A** G-banded metaphase from case 7 (dedifferentiated liposarcoma) with two long markers, one ring chromosome, and two double minute (dmin) chromosomes. **B** FISH analysis of a metaphase spread from case 7 using wcp 12 (*green*) and wcp 16 (*red*) probes. The two chromosome 12 homologues and the two ring chromosomes and three markers are painted by the wcp 12 probe. The wcp 16 probe paints only the two normal chromosomes 16. **C** G-banded metaphase from case 9A (mixed well-differentiated and myxoid liposarcoma) containing several long marker chromosomes and dmin chromosomes. **D** Partial karyotype from case 13 (myxoid-round cell liposarcoma) showing +der(1)t(1;6), t(12;16), –16 and +19. **E** Partial karyotype from case 14A (myxoid-round cell liposarcoma) showing +8 and t(12;16) as the only abnormalities

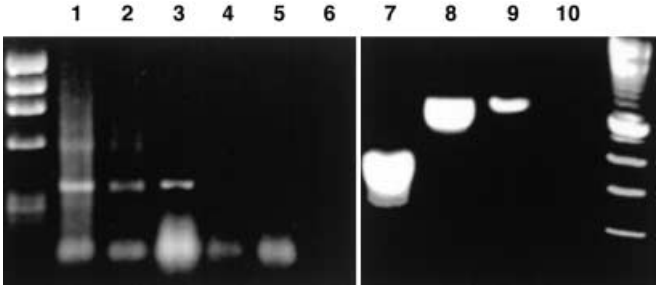


Fig. 3 Identification of TLS/CHOP fusion transcripts using reverse transcriptase polymerase chain reaction (RT-PCR) analysis in six myxoid-round cell liposarcomas (*lane 1*, case 14; *lane 2*, case 13; *lane 3*, case 19; *lane 7*, case 15; *lane 8*, case 17; and *lane 9*, case 9A). Four of the tumors expressed the type-II fusion transcript (~380 bp), and two tumors expressed the type-I fusion transcript (~650 bp). These transcripts were not detected in three pleomorphic liposarcomas (*lane 4*, case 22; *lane 5*, case 23; and *lane 6*, case 21B) or in a control sample without complimentary (c)DNA template (*lane 10*). Two of these three pleomorphic liposarcomas had predominantly (case 22) or focally (case 21B) round cell phenotypes and were virtually indistinguishable from true round cell liposarcoma histologically (compare with Fig. 1J and Fig. 1K)

neuroectodermal tumor (PNET), lymphoma, and a cellular monomorphic variant of tenosynovitis were considered in the differential diagnosis. All five tumors had t(12;16) using either cytogenetics, RT-PCR, and/or Southern blot analysis. Of the two cases analyzed cytogenetically, one showed t(12;16) as the sole abnormality (case 15) while the other, in addition to a complex 12;16-translocation, showed clonal gains of chromosomes 7 and 14 and a supernumerary marker chromosome (Table 2).

Pleomorphic liposarcoma variants

Two of the five tumors were predominantly high-grade, spindled, or pleomorphic sarcomas resembling fibrosarcoma and MFH. However, there were small foci with pleomorphic, bizarre, and multivacuolated lipoblasts. Two other tumors consisted predominantly of small round cells and were virtually indistinguishable from a round cell liposarcoma (Fig. 1J). However, rare microscopic foci containing slightly pleomorphic multivacuo-

lated lipoblasts were seen (Fig. 1J, insert). Another case with predominantly large cell pleomorphic liposarcoma features also contained foci of small round cells identical to round cell liposarcoma (Fig. 1K). None of these liposarcomas, including those with predominantly or partially round cell liposarcoma-like features, expressed the *TLS-CHOP* fusion transcript or showed any rearrangements of the *CHOP* gene.

Intramuscular myxoma

These two tumors were examples of the recently described cellular variant of intramuscular myxoma (Fig. 1L) [30]. The tumors were well-delineated and contained bland spindled to stellate cells in an abundant, hypovascular myxoid matrix. Scattered cells with bubbly or vacuolated cytoplasm simulated lipoblasts (Fig. 1L, insert). Cytogenetic analysis of one of these cases revealed a small clone with trisomy 18. The other case had a normal karyotype. One variant cell had two markers of unknown origin. There was no evidence of t(12;16) in any of the tumors.

Myxofibrosarcoma (myxoid variant of MFH)

All five tumors had features typical of myxofibrosarcoma, including multinodular, myxoid foci with variably pleomorphic, fusiform, stellate, or plump polygonal tumor cells diffusely infiltrating along subcutaneous fibrous septa and the characteristic abundant, interanastomosing coarse capillary-like vasculature (Fig. 1M) [23, 24]. Scattered multinucleated giant cells were also seen. Some tumor cells had bubbly or vacuolated cytoplasm that simulated lipoblasts (Fig. 1M, insert). Based on cellularity, atypia and mitotic activity, four tumors were classified as grade-III and one as grade-II (using a four-tiered grading system). Cytogenetic and/or Southern blot analyses revealed that none of the five tumors had t(12;16). Two of the three tumors karyotyped had a normal chromosome content. The third tumor (case 30) showed clonal loss of one chromosome 16. One of these cells also had t(13;17)(q10;q10).

Discussion

The 23 liposarcomas and 10 liposarcoma simulators in our study were selected for detailed cytogenetic and molecular genetic analyses because they had unusual and, in some cases, previously undescribed histologic features. The morphologic spectrum of these tumors caused problems in differential diagnosis. The overlapping appearances of different types of liposarcoma also raised conceptual questions; specifically, whether different types of liposarcoma are always biologically and genetically distinct or whether truly mixed or hybrid forms of liposarcoma exist.

Since the first description of t(12;16)(q13;p11) in myxoid liposarcoma [48] and the identification of the genes affected by this translocation [7, 39], several studies have demonstrated the translocation's specificity for myxoid-round cell liposarcoma and the diagnostic utility of cytogenetics, RT-PCR, and Southern blot analysis in documenting its presence [1, 10, 15]. The *TLS-CHOP* fusion is found in approximately 90% of all myxoid-round cell liposarcomas [35]. The majority of the remaining cases show a variant translocation t(12;22)(q13;q12) in which *TLS* is replaced by *EWS* in the *TLS-CHOP* fusion [9, 34]. To date, no clinicopathologic differences between these molecular genetic subtypes have been identified [9].

The *TLS-CHOP* fusion genes consist of the 5′ promoter region and exons 1–5 or, more rarely, 1–7 or 1–8 of *TLS* [16, 32] fused to the complete coding region, including exons 1–4 or 2–4, of *CHOP* [32, 33]. Transcriptional control of the fusion gene is dominated by the *TLS* housekeeping type of regulatory region, leading to stable expression of the fusion protein in tumor cells [2]. The transforming properties of the *TLS-CHOP* fusion protein have been demonstrated in NIH 3T3 cells in vitro [49]. The protein most likely functions as an abnormal transcription factor acting on a number of downstream target genes [46].

It is noteworthy that all 13 myxoid-round cell liposarcoma variants in this study revealed the characteristic t(12;16) and/or *TLS-CHOP* fusion, including those cases that closely resembled mature lipoma, intramuscular myxoma, and myxofibrosarcoma, and those cases composed of primitive round cells without clear lipogenic differentiation. An unequivocal subclassification of round cell liposarcoma would not have been possible in the latter group based on morphology alone. The morphologic variation observed in these cases could be caused by a number of factors, including secondary genetic changes, the stage of cell differentiation at the time of the translocation event, and the microenvironment of the tumor.

Six myxoid liposarcoma-specific transcripts (MLATs) strongly expressed in myxoid-round cell liposarcomas but not in normal adipocyte tissue have recently been identified [46]. Three of the MLATs are identified as transcripts from the glia-associated nexin (*PN1*), neuronatin (*NNAT*), and *RET* genes. These three genes are all involved and expressed in the developing nervous system, suggesting possible involvement of a neuroectodermal lineage differentiation program in the development of myxoid-round cell liposarcoma.

The clinical and morphologic spectrum of myxoid-round cell liposarcoma is broad, ranging from paucicellular myxoid tumors with a very low-grade behavior, to extremely cellular, primitive tumors with an aggressive, rapid, and fatal course. Whether the transition of myxoid liposarcoma to round cell liposarcoma is associated with specific chromosome abnormalities is unclear. Several nonrandom, secondary abnormalities have been identified in myxoid-round cell liposarcoma, including, +8,

i(7)(q10) and der(1)t(1;16) [19, 29]; trisomy has been suggested to correlate with more advanced disease [19]. One of the poorly differentiated round cell liposarcomas in our study had t(12;16) as the sole anomaly, suggesting that transition of myxoid to round cell liposarcoma is not always associated with secondary chromosome abnormalities.

In case 14 (A and B), two separate myxoid liposarcomas arising in the soft tissues of a 39-year-old woman were studied in detail. The development of ten myxoid round cell liposarcomas in the trunk, extremities, and abdomen/retroperitoneum over a 6-year period in this patient raised the possibility of multicentric lesions rather than metastases. Several malignancies had been reported on the maternal side of the patient's family as well, raising the possibility of Li-Fraumeni syndrome [17]. However, sequencing of exons 4–9 of the p53 gene in both the patient and her mother revealed only wild-type sequences (unpublished observations), indicating that a gene other than p53 is responsible for the patient's predisposition to develop multiple myxoid liposarcomas. The fact that both myxoid liposarcomas analyzed in this patient had t(12;16) indicates that both sporadic myxoid liposarcomas and liposarcomas developing in individuals with a genetic predisposition may develop along the same karyotypic pathways. A recent study has claimed that multiple myxoid liposarcomas of soft tissues are metastatic rather than multicentric and that the clinical outcome of these patients is poor regardless of low-grade histologic features [4]. The prolonged clinical course in case 14 of this series seems to contradict their conclusions.

The presence of mature fat in myxoid liposarcoma is well recognized. Case 9 (A and B) in our series was unusual in that it essentially had features of a mature lipomatous tumor with minimal myxoid change. Rare foci compatible with myxoid liposarcoma were identified only after extensive sampling. Interestingly, this tumor showed ring chromosomes, giant markers, and dmin chromosomes, i.e., abnormalities that are typically found in atypical lipoma/well-differentiated liposarcoma [11, 37, 38] in addition to the characteristic t(12;16) of myxoid liposarcoma. Moreover, FISH analysis revealed that the dmin chromosomes contained amplified sequences derived from chromosome 12, another finding that is characteristic of atypical lipoma/well-differentiated liposarcoma. To our knowledge, this case is unique, representing the first documented example of a liposarcoma with a mixed genotype corresponding histologically to a mixed well-differentiated and myxoid liposarcoma.

Four of the liposarcomas (three dedifferentiated and one myxoid with predominantly well-differentiated foci, case 9) showed evidence of gene amplification as demonstrated by the presence of ring chromosomes, giant markers, and/or dmin chromosomes. There was considerable intercellular heterogeneity in the number of markers containing amplified sequences. In three cases, we demonstrated that the markers contained amplified chromosome 12 sequences. In one of two well-differentiated liposarcomas (case 4), we could also show using Southern blot analysis that the *MDM2* gene (located at 12q15) was amplified (data not shown). These observations are in agreement with previous findings in which sequences preferentially derived from 12q13–15, including the *MDM2*, *HMGIC*, *SAS*, and *CDK4* genes, have been shown to be amplified in atypical lipomas/well-differentiated liposarcomas [6, 11, 45]. Thus far, no clear correlation between gene amplification and clinical outcome has been found. Our finding of gene amplification in a myxoid liposarcoma (case 9) demonstrates that amplification of genes in 12q14–15 may occur in liposarcomas other than the atypical lipoma/well-differentiated subtype.

The occurrence of low and high-grade myxoid areas in well-differentiated and dedifferentiated liposarcomas of the retroperitoneum is well recognized but has, nonetheless, generated speculation regarding the existence of true mixed types of liposarcoma in this location. Rarely, myxoid-round cell liposarcomas of the retroperitoneum–abdomen have also been reported to show dedifferentiation [22]. One well-differentiated and two dedifferentiated liposarcomas that occurred in the retroperitoneum in this series had myxoid areas that were indistinguishable from myxoid liposarcoma. None of these tumors, however, revealed any evidence of t(12;16), indicating that well-differentiated and dedifferentiated liposarcomas of the retroperitoneum with myxoid foci are genetically distinct from myxoid liposarcoma and that these myxoid areas are part of their histologic spectrum. Our findings are in agreement with two recent studies that utilized nested PCR [13] or only Southern blotting techniques [3] in retroperitoneal liposarcomas harboring myxoid foci. The myxoid foci of our three cases were indistinguishable from classical myxoid liposarcoma, whereas the myxoid areas described in the studies of Antonescu et al. [3] and Hisaoka et al. [13] had features of myxofibrosarcoma.

The morphologic distinction between myxoid liposarcoma, cellular myxoma, and myxofibrosarcoma with vacuolated, pseudolipoblastic cells and myxoid spindle cell-pleomorphic lipomas with a pronounced plexiform vasculature may be difficult at times. All of the latter lesions were clearly cytogenetically and molecularly distinct from myxoid liposarcoma, confirming the diagnostic utility of these techniques.

The problem of distinguishing certain benign entities, such as chondroid lipoma [14, 20], from myxoid-round cell liposarcoma is also illustrated in our series. Case 3 had originally been diagnosed as a myxoid liposarcoma prior to the first description of chondroid lipoma in the literature [20]. Our study further supports the contention that chondroid lipoma is genetically distinct from myxoid-round cell liposarcoma. Recent descriptions of t(11;16)(q13;p13) in chondroid lipoma confirm that it is yet another example of a unique lipogenic tumor with a characteristic chromosomal abnormality [12, 47].

Three of five pleomorphic liposarcomas in our series had predominantly small round cell areas indistinguish-

able from poorly differentiated round cell liposarcoma. The observation of focal cellular pleomorphism in two cases and very rare, large bizarre lipoblasts in another case suggested that they could be pleomorphic rather than round cell liposarcomas. This histologic interpretation was supported by the lack of t(12;16) in these tumors. Thus, the cytogenetic and morphologic findings in these three cases indicate the existence of a previously unrecognized small round cell variant of pleomorphic liposarcoma that is histologically quite similar to round cell liposarcoma.

In summary, this study illustrates the diagnostic utility of cytogenetic and molecular genetic techniques in certain lipomatous tumors and their simulators. Moreover, these techniques allow identification of new variants and hybrid forms of lipomatous tumors and enhance our understanding of complex genotypic–phenotypic relationships.

Acknowledgements This research was sponsored by the Swedish Cancer Society, the Inga Britt and Arne Lundberg Research Foundation, the Assar Gabrielssons Research Foundation, and the Johan Jansson Foundation.

References

1. Åman P, Ron D, Mandahl N, Fioretos T, Heim S, Arheden K, Willén H, Rydholm A, Mitelman F (1992) Rearrangement of the transcription factor gene CHOP in myxoid liposarcomas with t(12;16)(q13;p11). Genes Chromosomes Cancer 5:278–285
2. Åman P, Panagopoulos I, Lassen C, Fioretos T, Mencinger M, Toresson H, Hoglund M, Forster A, Rabbitts TH, Ron D, Mandahl N, Mitelman F (1996) Expression patterns of the human sarcoma-associated genes FUS and EWS and the genomic structure of FUS. Genomics 37:1–8
3. Antonescu CR, Elahi A, Humphrey M, Lui MY, Healey JH, Brennan MF, Woodruff JM, Jhanwar SC, Ladanyi M, Woodruff JM (2000) Specificity of TLS-CHOP rearrangement for classic myxoid/round cell liposarcoma. Absence in predominantly myxoid well-differentiated liposarcomas. J Molec Diagn 2:132–138
4. Antonescu CR, Elahi A, Healey JH, Brennan MF, Lui MY, Lewis J, Jhanwar SC, Woodruff JM, Ladanyi M (2000) Monoclonality of multifocal myxoid liposarcoma: confirmation by analysis of TLS-CHOP rearrangements. Clin Cancer Res 6: 2788–2793
5. Argani P, Facchetti F, Inghirami G, Rosai J (1997) Lymphocyte-rich well differentiated liposarcoma: report of nine cases. Am J Surg Pathol 21:884–895
6. Berner JM, Mesa-Zepeda LA, Kools PF, Forus A, Schoenmakers EF, Van de Ven WJ, Fodstad O, Myklebost O (1997) HMGIC, the gene for an architectural transcription factor, is amplified and rearranged in a subset of human sarcomas. Oncogene 14:2935–2941
7. Crozat A, Åman P, Mandahl N, Ron D (1993) Fusion of CHOP to a novel RNA-binding protein in human myxoid liposarcoma. Nature 363:640–644
8. Dal Cin P, Sciot R, Polito P, Stas M, de Wever I, Cornelis A, Van den Berghe H (1997) Lesions of 13q may occur independently of deletion of 16q in spindle cell/pleomorphic lipomas. Histopathology 31:222–225
9. Dal Cin P, Sciot R, Panagopoulos I, Åman P, Samson I, Mandahl N, Mitelman F, Van den Berghe H, Fletcher CD (1997) Additional evidence of a variant translocation t(12;22) with EWS/CHOP fusion in myxoid liposarcoma: clinicopathological features. J Pathol 182:437–441
10. Fletcher CD, Åkerman M, Dal Cin P, de Wever I, Mandahl N, Mertens F, Mitelman F, Rosai J, Rydholm A, Sciot R, Tallini G, van den Berghe H, van de Ven W, Vanni R, Willén H (1996) Correlation between clinicopathological features and karyotype in lipomatous tumors. A report of 178 cases from the Chromosomes and Morphology (CHAMP) Collaborative Study Group. Am J Pathol 148:623–630
11. Gisselsson D, Hoglund M, Mertens F, Mitelman F, Mandahl N (1998) Chromosomal organization of amplified chromosome 12 sequences in mesenchymal tumors detected by fluorescence in situ hybridization. Genes Chromosomes Cancer 23: 203–212
12. Gisselsson D, Domanski HA, Hoglund M, Carlén B, Mertens F, Willén H, Mandahl N (1999) Unique cytological features and chromosome aberrations in chondroid lipoma: a case report based on fine-needle aspiration cytology, histopathology, electron microscopy, chromosome banding, and molecular cytogenetics. Am J Surg Pathol 23:1300–1304
13. Hisaoka M, Morimitsu Y, Hashimoto H, Ishida T, Mukai H, Satoh H, Motoi T, Machinami R (1999) Retroperitoneal liposarcoma with combined well-differentiated and myxoid malignant fibrous histiocytoma-like myxoid areas. Am J Surg Pathol 23:1480–1492
14. Kindblom L-G, Meis-Kindblom JM (1995) Chondroid lipoma: an ultrastructural and immunohistochemical analysis with further observations regarding its differentiation. Hum Pathol 26:706–715
15. Knight JC, Renwick P, Dal Cin P, Van den Berghe H, Fletcher CDM (1995) Translocation t(12;16)(q13;p11) in myxoid liposarcoma and round cell liposarcoma: molecular and cytogenetic analysis. Cancer Res 55:24–27
16. Kuroda M, Ishida T, Horiuchi H, Kida N, Uozaki H, Takeuchi H, Tsuji K, Imamura T, Mori S, Machinami R, et al (1995) Chimeric TLS/FUS-CHOP gene expression and the heterogeneity of its junction in human myxoid and round cell liposarcoma. Am J Pathol 147:1221–1227
17. Malkin D, Li FP, Strong LC, Fraumeni JF Jr, Nelson DE, Kim DH, Kassel J, Gryka MA, Bischoff FZ, Tainsky MA, et al (1990) Germ line p53 mutations in a familial syndrome of breast cancer, sarcomas, and other neoplasms. Science 250:1233–1238
18. Mandahl N, Hoglund M, Mertens F, Rydholm A, Willén H, Brosjö O, Mitelman F (1994) Cytogenetic aberrations in 188 benign and borderline adipose tissue tumors. Genes Chromosomes Cancer 9:207–215
19. Mandahl N, Mertens F, Åman P, Rydholm A, Brosjö O, Willén H, Mitelman F (1994) Nonrandom secondary chromosome aberrations in liposarcomas with t(12;16). Int J Oncol 4:307–310
20. Meis JM, Enzinger FM (1993) Chondroid lipoma: a unique tumor simulating liposarcoma and myxoid chondrosarcoma. Am J Surg Pathol 17:1103–1112
21. Meloni AM, Spanier SS, Bush CH, Stone JF, Sandberg AA (1994) Involvement of 19q22 and 11q13 in hibernoma. Cancer Genet Cytogenet 72:59–64
22. Mentzel T, Fletcher CD (1997) Dedifferentiated myxoid liposarcoma: a clinicopathological study suggesting a closer relationship between myxoid and well-differentiated liposarcoma. Histopathology 30:457–463
23. Mentzel T, Calonje E, Wadden C, Camplejohn RS, Beham A, Smith MA, Fletcher CD (1996) Myxofibrosarcoma. Clinicopathologic analysis of 75 cases with emphasis on the low-grade variant. Am J Surg Pathol 20:391–405
24. Merck C, Angervall L, Kindblom LG, Odén A (1983) Myxofibrosarcoma. A malignant soft tissue tumor of fibroblastic-histiocytic origin. A clinicopathologic and prognostic study of 110 cases using multivariate analysis. Acta Pathol Microbiol Immunol Scand (Suppl) 282:1–40
25. Mertens F, Rydholm A, Brosjö O, Willén H, Mitelman F, Mandahl N (1994) Hibernomas are characterized by rearrangements of chromosome bands 11q13–21. Int J Cancer 58:503–505

26. Mertens F, Fletcher CD, Dal Cin P, De Wever I, Mandahl N, Mitelman F, Rosai J, Rydholm A, Sciot R, Tallini G, Van den Berghe H, Vanni R, Willén H (1998) Cytogenetic analysis of 46 pleomorphic soft tissue sarcomas and correlation with morphologic and clinical features: a report of the CHAMP Study Group. Chromosomes and Morphology. Genes Chromosomes Cancer 22:16–25
27. Mitelman F (ed) (1995) ISCN: an international system for human cytogenetic nomenclature. Karger, Basel
28. Mrózek K, Karakousis CP, Bloomfield CD (1994) Band 11q13 is nonrandomly rearranged in hibernomas. Genes Chromosomes Cancer 9:145–147
29. Mrózek K, Arthur D, Karakousis C, Koduru PRK, Le Beau M, Pettenati MJ, Tantravahi R, Mrózek E, Perez-Mesa C, Rao UNM, Frankel SR, Davey FR, Bloomfield CD (1995) Der(16)t(1;16) is a nonrandom secondary chromosome aberration in many types of human neoplasia, including myxoid liposarcoma, rhabdomyosarcoma and Philadelphia chromosome-positive acute lymphoblastic leukemia. Int J Oncol 6:531–538
30. Nielsen GP, O'Connell JX, Rosenberg AE (1998) Intramuscular myxoma: a clinicopathologic study of 51 cases with emphasis on hypercellular and hypervascular variants. Am J Surg Pathol 22:1222–1227
31. Nordkvist A, Mark J, Gustafsson H, Bang G, Stenman G (1994) Non-random chromosome rearrangements in adenoid cystic carcinoma of the salivary glands. Genes Chromosomes Cancer 10:115–121
32. Panagopoulos I, Mandahl N, Ron D, Hoglund M, Nilbert M, Mertens F, Mitelman F, Åman P (1994) Characterization of the CHOP breakpoints and fusion transcripts in myxoid liposarcomas with the 12;16 translocation. Cancer Res 54:6500–6503
33. Panagopoulos I, Mandahl N, Mitelman F, Åman P (1995) Two distinct FUS breakpoint clusters in myxoid liposarcoma and acute myeloid leukemia and the translocations t(12;16) and t(16;21). Oncogene 11:1133–1137
34. Panagopoulos I, Hoglund M, Mertens F, Mandahl N, Mitelman F, Åman P (1996) Fusion of the EWS and CHOP genes in myxoid liposarcoma. Oncogene 12:489–494
35. Panagopoulos I, Lassen C, Isaksson M, Mitelman F, Mandahl N, Åman P (1997) Characteristic sequence motifs at the breakpoints of the hybrid genes FUS/CHOP, EWS/CHOP and FUS/ERG in myxoid liposarcoma and acute myeloid leukemia. Oncogene 15:1357–1362
36. Panarello C, Rosanda C, Morerio C, Russo I, Dallorso S, Gambini C, Ricco AS, Storlazzi T, Archidiacono N, Rocci M (1998) Lipoblastoma: a case with t(7;8)(q31;q13). Cancer Genet Cytogenet 102:12–14
37. Pedeutour F, Suijkerbuijk RF, Forus A, Van Gaal J, Van de Klundert W, Coindre JM, Nicolo G, Collin F, Van Haelst U, Huffermann K, et al (1994) Complex composition and coamplification of SAS and MDM 2 in ring and giant rod marker chromosomes in well-differentiated liposarcoma. Genes Chromosomes Cancer 10:85–94
38. Pedeutour F, Forus A, Coindre JM, Berner JM, Nicolo G, Michiels JF, Terrier P, Ranchere-Vince D, Collin F, Myklebost O, Turc Carel C (1999) Structure of the supernumerary ring and giant rod chromosomes in adipose tissue tumors. Genes Chromosomes Cancer 24:30–41
39. Rabbitts TH, Forster A, Larson R, Nathan P (1993) Fusion of the dominant negative transcription regulator CHOP with a novel gene FUS by translocation t(12;16) in malignant liposarcoma. Nat Genet 4:175–180
40. Ron D, Habener JF (1992) CHOP, a novel developmentally regulated nuclear protein that dimerizes with transcription factors C/EBP and LAP and functions as a dominant-negative inhibitor of gene transcription. Genes Dev 6:439–453
41. Rosai J, Åkerman M, Dal Cin P, DeWever I, Fletcher CD, Mandahl N, Mertens F, Mitelman F, Rydholm A, Sciot R, Tallini G, Van den Berghe H, Van de Ven W, Vanni R, Willén H (1996) Combined morphologic and karyotypic study of 59 atypical lipomatous tumors. Evaluation of their relationship and differential diagnosis with other adipose tissue tumors (a report of the CHAMP Study Group). Am J Surg Pathol 20:1182–1189
42. Sambrook I, Fritsch EF, Maniatis T (1989) Molecular cloning: a laboratory manual, 2nd edn. Cold Spring Harbor Laboratory Press, Cold Spring Harbor, NY, pp 1.1–18.88
43. Sandberg AA, Bridge JA (1994) Tumors of fat. In: Sandberg AA, Bridge JA (eds) The cytogenetics of bone and soft tissue tumors. R.G. Landes Company, Austin, pp 193–216
44. Southern EM (1975) Detection of specific sequences among DNA fragments separated by gel electrophoresis. J Mol Biol 98:503–517
45. Tallini G, Dal Cin P, Rhoden KJ, Chiapetta G, Manfioletti G, Giancotti V, Fusco A, Van den Berghe H, Sciot R (1997) Expression of HMGI-C and HMGI(Y) in ordinary lipoma and atypical lipomatous tumors: immunohistochemical reactivity correlates with karyotypic alterations. Am J Pathol 151:37–43
46. Thelin-Jarnum S, Lassen C, Panagopoulos I, Mandahl N, Åman P (1999) Identification of genes differentially expressed in TLS-CHOP carrying myxoid liposarcomas. Int J Cancer 83:30–33
47. Thomson TA, Horsman D, Bainbridge TC (1999) Cytogenetic and cytologic features of chondroid lipoma of soft tissue. Mod Pathol 12:88–91
48. Turc-Carel C, Limon J, Dal Cin P, Rao U, Karakousis C, Sandberg AA (1986) Cytogenetic studies of adipose tissue tumors. II. Recurrent reciprocal translocation t(12;16)(q13;p11) in myxoid liposarcomas. Cancer Genet Cytogenet 23:291–299
49. Zinszner H, Albalat R, Ron D (1994) A novel effector domain from the RNA-binding protein TLS or EWS is required for oncogenic transformation by CHOP. Genes Dev 8:2513–2526

Virchows Arch (2001) 439:152–157
DOI 10.1007/s004280100428

ORIGINAL ARTICLE

**Jun Nishio · Hiroshi Iwasaki · Masako Ishiguro
Yuko Ohjimi · Teruto Isayama · Masatoshi Naito
Masahiro Kikuchi**

Identification of syt-ssx fusion transcripts in both epithelial and spindle cell components of biphasic synovial sarcoma in small tissue samples isolated by membrane-based laser microdissection

Received: 5 October 2000 / Accepted: 29 January 2001 / Published online: 30 June 2001
© Springer-Verlag 2001

Abstract In order to confirm the presence of SYT-SSX fusion gene in epithelial and spindle cell components of synovial sarcoma, we performed a nested reverse transcriptase-polymerase chain reaction (RT-PCR) using microbeam microdissection of membrane-mounted native tissue (MOMeNT) technique applied on formalin-fixed, paraffin-embedded tumor specimens from two biphasic synovial sarcomas and a control tissue of adamantinoma. Small targeted portions of either an epithelial or spindle cell component of the tumor tissue were microdissected together with the supporter membrane, by using an ultraviolet (337-nm) pulsed laser microbeam coupled into a robot-stage microscope with infinity optics. The SYT-SSX fusion transcript was detected in epithelial and spindle cell components of both biphasic synovial sarcomas, but not in the control tissue. Southern blot analysis also confirmed that the detected messages were derived from the SYT-SSX fusion gene. In conclusion, the microbeam MOMeNT is a useful method for isolating selected small portions from tissue sections. The SYT-SSX fusion gene is present in both cellular components of biphasic synovial sarcoma and is involved in oncogenesis of the synovial sarcoma rather than in morphologic epithelial differentiation. Therefore, in spite of the variable proportions of each component, our results confirm that the synovial sarcoma is of monoclonal origin.

Keywords Biphasic synovial sarcoma · SYT-SSX fusion transcript · Microbeam microdissection of membrane-mounted native tissue (MOMeNT) · Cold photolysis

J. Nishio (✉) · H. Iwasaki · M. Ishiguro · Y. Ohjimi · M. Kikuchi
Department of Pathology, School of Medicine,
Fukuoka University, 7-45-1 Nanakuma, Jonan-ku,
Fukuoka 814-0180, Japan
Tel.: +81-92-8011011, Fax: +81-92-8011011

T. Isayama · M. Naito
Department of Orthopedic Surgery, School of Medicine,
Fukuoka University, Fukuoka, Japan

Introduction

A specific chromosomal translocation, t(X;18)(p11.2, q11.2), has been demonstrated in synovial sarcoma [21], which results in the fusion of the SYT gene on chromosome 18 and SSX1 or SSX2 gene on chromosome X [5, 6]. The chimeric gene transcripts have been detected by reverse transcriptase-polymerase chain reaction (RT-PCR) in more than 90% of cases [6, 8, 9, 14]. Therefore, detection of this specific translocation by chromosome analysis and of SYT-SSX transcripts by RT-PCR are helpful in the diagnosis of synovial sarcoma [6, 8, 9, 20, 22, 24].

Recently, Hiraga et al. detected SYT-SSX fusion probe bound to the nuclei in both epithelial and spindle cell components of biphasic synovial sarcoma by in situ hybridization [10]. Birdsall et al. confirmed that the rearrangement was present in both cellular components using a two-color fluorescence in situ hybridization [1]. In the present study, to confirm and complement these findings, we performed a nested RT-PCR using microbeam microdissection of membrane-mounted native tissue (MOMeNT) technique applied on formalin-fixed, paraffin-embedded tumor specimens. Microbeam MOMeNT is a novel technique that utilizes membrane-based microdissection by using an ultraviolet laser microbeam, thus providing a flexible, easy-to-use, high-performance tool [2, 3]. Here, the feasibility of microbeam MOMeNT for RNA analysis is also demonstrated.

Materials and methods

Tumor samples

Formalin-fixed, paraffin-embedded samples of two histologically and immunohistochemically verified synovial sarcomas were obtained from the archives of the Department of Pathology, Fukuoka University. As a negative control, a paraffin-embedded tissue sample of adamantinoma of long bone (tibia) was used. All tumor samples were diagnosed according to internationally accepted cri-

Table 1 Clinicopathological and molecular features (*F* female, *M* male, *E* epithelial, *S* spindle, *RT-PCR* reverse transcriptase-polymerase chain reaction)

Case number	Sex	Age (years)	Site	Histology	Epithelial/spindle cell composed analyzed	RT-PCR	
						β-actin	SYT-SSX
1	F	60	Foot	Biphasic synovial sarcoma	E	+	+
					S	+	+
2	F	25	Thigh	Biphasic synovial sarcoma	E	+	+
					S	+	+
3	M	69	Tibia	Adamantinoma	E	+	–
					S	+	–

teria. The tissue sections were stained with hematoxylin and eosin and immunohistochemically labeled with cytokeratin (polyclonal, 1:500; DAKO JAPAN, Kyoto, Japan), epithelial membrane antigen (EMA, monoclonal, 1:50; DAKO), and vimentin (monoclonal, 1:50; DAKO) using a labeled streptavidin biotin and an alkaline phosphatase technique described earlier [11]. The clinical data are summarized in Table 1.

Microbeam microdissection of membrane-mounted native tissue

Microbeam microdissection of membrane-mounted native tissue (MOMeNT) allows a rapid, selective, and low-contamination procurement of tumor or other cells from histological sections by non-thermic, non-contact laser microdissection [2]. Tissue sections (4 µm thick) of formalin-fixed, paraffin-embedded tumor specimens were mounted on a specifically designed 1.5-µm-thick transparent supporter membrane. The membrane-covered glass slides were handled as ordinary glass slides, and hematoxylin and eosin staining was performed. Then, small targeted portions of epithelial or spindle cell component of the tumor tissue were microdissected together with the supporter membrane by an ultraviolet (337 nm) pulsed laser microbeam coupled into a robot-stage microscope with infinity optics (SL Microtest, Jena, Germany). The ultraviolet laser dissects by cold photolysis due to the high photon density of the microbeam rather than by local heating. The track of the laser microbeam can be preselected easily on a video screen, and the size and form of the dissectates can thus be adapted to the histological features of the section with a delineation accuracy in the micrometer range. The dissectates containing approximately 50–100 cells were removed on the tip of a 30-gauge needle and transferred into a PCR tube. These samples were utilized for RT-PCR and Southern blot analysis.

Reverse transcriptase-polymerase chain reaction

The microdissected tissue samples were homogenized and RNA was isolated according to the protocol described by Tsuji et al. [23], using a Trizol reagent (Life Technologies, Gaithersburg, Md.). Whole volume of total RNA was reverse transcribed using the T-Primed First-Strand kit: Ready-To-Go (Amersham Pharmacia Biotech, England). The resulting samples of complementary DNA (cDNA) were amplified by the nested PCR (RoboCycler). Two-microliter cDNA templates were initially amplified for 40 cycles with sytp3 (5′-GGATATAGACCA-ACACAGCC-3′) and ssxp2 (5′-CCAGATGCTTCTG[A/G]CACT-3′) primers. Then, aliquots of approximately 2 µl from the first PCR were reamplified for 30 cycles with sytp4 (5′-CAGCAGAGGCCTTATGGATA-3′) and ssxp1 (5′-C[G/T]TCCTCTGCTG-GCTTCT [T/C]G-3′) for the nested reaction [15]. Annealing temperature for all reactions was 55°C. The molecular size of the final PCR products was 55 bp for the nested PCR amplification of SYT-SSX. The PCR products were fractionated on 4.0% agarose gels and visualized by ethidium bromide staining and ultraviolet illumination. As positive controls for the integrity of cDNA in each case, a seminested PCR for ubiquitously expressed β-actin gene transcripts was performed with the following primers: act1 (5′-CCTTCTGACCCATGCCCACCA-3′), act2 (5′-TGATGATATCGCCGCGCTCGT-3′), and act3 (5′-ATGTGCA-AGGCCGGCTTCG-3′). This primer amplifies a 106-bp fragment of β-actin gene. As a negative control, an adamantinoma of long bone was analyzed by the same procedure. A positive control was a known case of previously detected chimeric product [11].

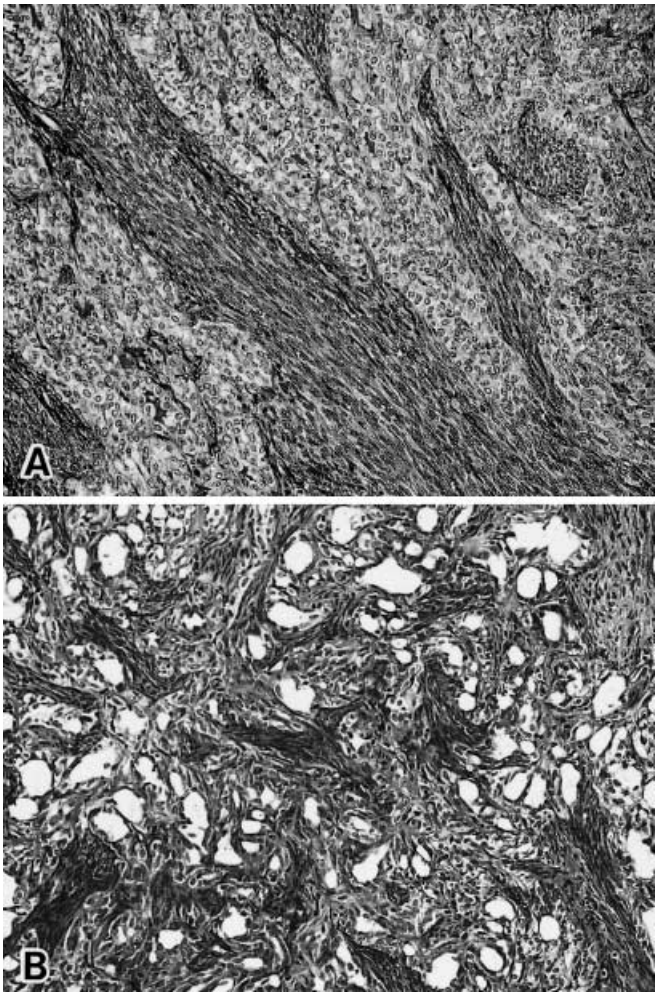


Fig. 1 Histologic features of synovial sarcoma. **A** Case 1. Typical biphasic synovial sarcoma with epithelial cells arranged into sheets separated by bundles of fibroblast-like spindle cells. **B** Case 2. Typical biphasic synovial sarcoma with epithelial cells forming gland-like structures admixed with fibroblast-like spindle cells. H&E, ×150

Southern blot analysis

The RT-PCR products were transferred onto nylon membranes (Oncor, Gaithersburg,Md.) for subsequent hybridization and de-

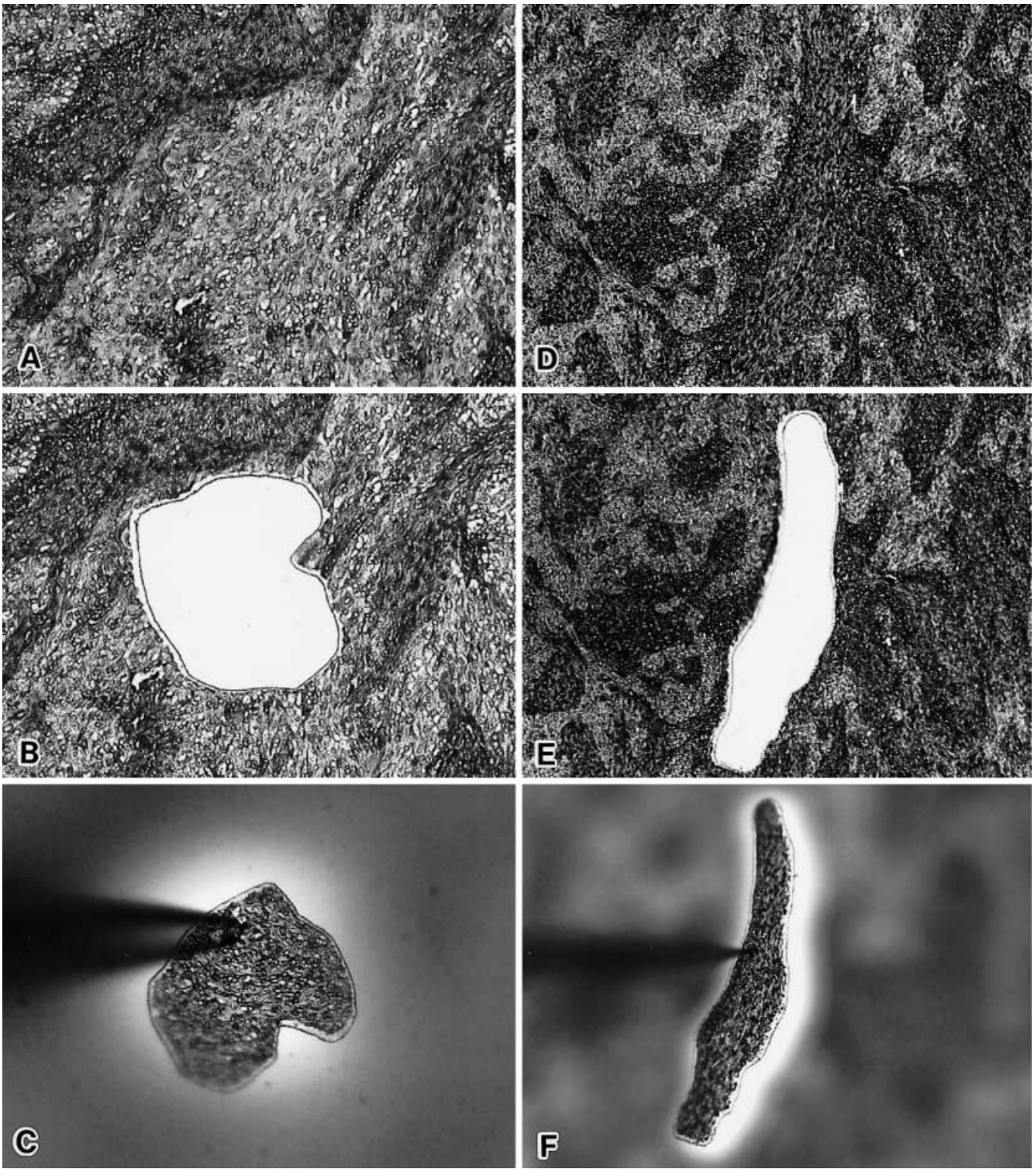


Fig. 2A–F Membrane-based laser microdissection (microbeam MOMeNT) of biphasic synovial sarcoma (Case 1). Hematoxylin and eosin stained 4 µm-formalin-fixed, paraffin-embedded sections are shown at original magnification ×260 (**A–C**), and ×130 (**D–F**). **A** Before microdissection of the epithelial cell component. **B** After removal of the dissectate. **C** Dissected sample from the epithelial cell component. **D** Before microdissection of the spindle cell component. **E** After removal of the dissectate. **F** Dissected sample from the spindle cell component

tection using ECL 3′-oligolabeling and detection systems (Amersham Life Science, UK). We used the oligonucleotide probe spanning the chimeric junction, SYT-SSX (5′-GGATATGACCAGATCATC-ATGCCCAAG-3′) [9].

Fluorescence in situ hybridization

In order to characterize the tumors in more detail, we employed fluorescence in situ hybridization (FISH). Fifty-micrometer thick

sections of paraffin-embedded tumor samples were disaggregated [13]. Isolated nuclei were spun onto silanized glass slides, fixated in 4% paraformaldehyde in PBS, and dried. Pretreatment consisted of 1 M sodium thiocyanate (NaSCN, Sigma, Munich, Germany) at 80°C for 3 min followed by digestion with 0.2% Proteinase K (Boehringer Mannheim, Germany) in PBS for up to 10 min. Two probes used in the analysis included the chromosome 18q11 region-specific probe (Human Band Specific Probes, Research Genetics, U.S.A. and Canada) and the chromosome Xp11.2–4 region-specific probe (Human Band Specific Probes, Research Genetics). Double-target in situ hybridizations were performed according to protocols described by Krams et al. [13]. Briefly, DNA probes were labeled with digoxigenin-dUTP or biotin-dUTP (both Boehringer Mannheim) with nick translation (Gibco BRL, Karlsruhe, Germany). Labeled probes were precipitated with human Cot-1 DNA (Gibco BRL) and sonicated salmon sperm DNA (Sigma).

The DNA pellet was dissolved in 10 µl hybridization mixture containing 5 µl deionized formamide, 1×SSC, and 10% dextran sulphate. The specimens were denatured in 70% foramide/2×SSC for 4 min at 75°C and dehydrated in cold ethanol. The hybridization mixture with the probe was denatured for 5 min at 75°C and pre-annealed for 10 min at 37°C. Hybridization, probe detection, and counterstaining were performed as described by Iwasaki et al. [11]. Hybridization signals were visualized by an in situ imaging system (Isis, Carl Zeiss Vision, Oberkochen, Germany).

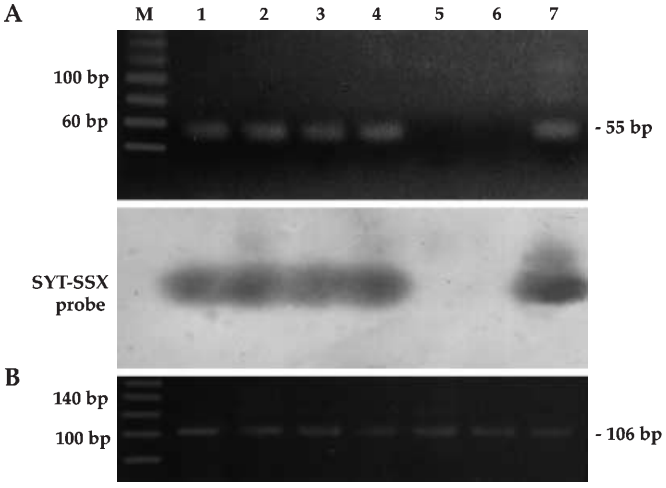


Fig. 3 RT-PCR amplification of (**A**, top) 55 bp SYT-SSX fusion gene transcripts and (**B**) 106 bp β-actin gene transcripts from formalin-fixed, paraffin-embedded microdissected samples. The specificity of the products was confirmed by transfer and hybridization with an oligonucleotide probe spanning the chimeric function, SYT-SSX (**A,** bottom). *M*, molecular weight marker. *Lane 1*, epithelial cell component from Case 1; *lane 2*, spindle cell component from Case 1; *lane 3*, epithelial cell component from Case 2; *lane 4*, spindle cell component from Case 2; *lane 5*, epithelial cell component from Case 3 (negative control); *lane 6*, spindle cell component from Case 3 (negative control); *lane 7*, positive control of synovial sarcoma

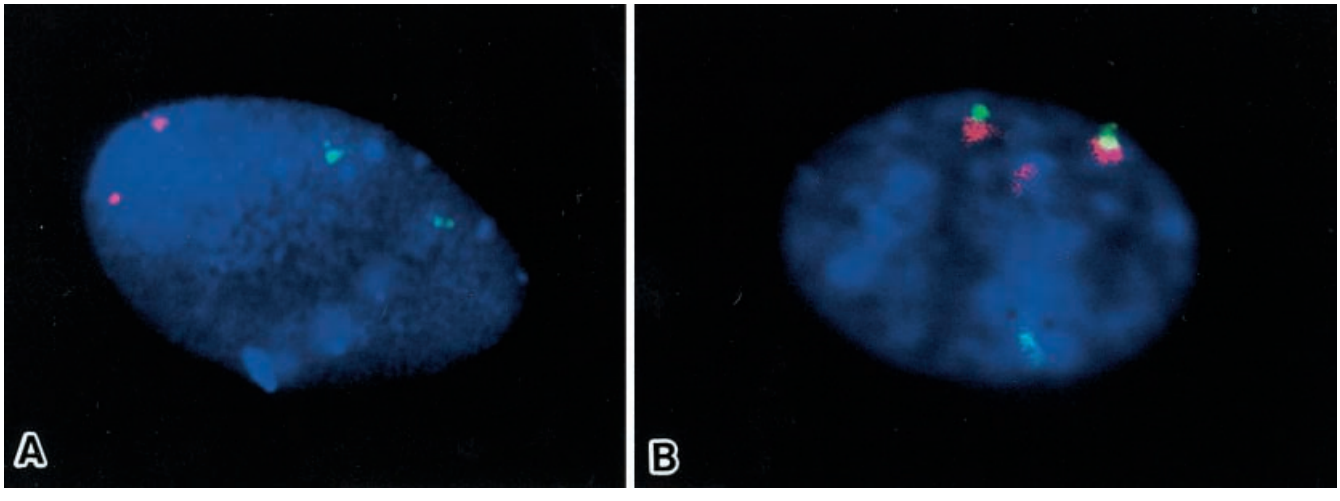
Fig. 4 Fluorescence in situ hybridization (FISH) analysis on isolated nuclei from a case of biphasic synovial sarcoma, Case 1, with human band specific probes for chromosome 18q11 (*green*) and chromosome Xp11.2–4 (*red*). **A** One normal nucleus showing two chromosome 18q11 region and two chromosome Xq11.2–4 region-specific probe signals that are separate from each other. **B** One tumor nucleus showing two areas with closely adjoining signals of chromosomes 18q11 and Xq11.2–4, corresponding to derivative chromosome 18 and derivative chromosome X. These findings confirmed the presence of the translocation t(X;18)

Results

Histologically, the two synovial sarcomas consisted of epithelial cells, resembling those of carcinoma arranged into pseudoglandular structures or sheets, and fibroblast-like spindle cells (Fig. 1). Immunohistochemically, epithelial cell components were positive for cytokeratin and EMA, while spindle cell components were positive for vimentin.

The precision for cutting out irregular lesions and specifically ablating undesired cells was probably the outstanding feature of microbeam MOMeNT (Fig. 2). In each sample, the test lesion was dissected accurately and immediately by the laser microbeam, followed by transfer of the dissectates to the PCR tube. The transfer process was enhanced by electrostatic attraction between the polyester supporter membrane and the transfer needle and PCR tube, respectively. The size of most dissectates was 0.5–1.0 mm and each of the obtained samples contained about 50–100 tumor cells.

Both the predicted 55-bp product of the SYT-SSX fusion transcript and the transcript of β-actin gene were identified in all four microdissected samples from each



of epithelial and spindle cell component of the two biphasic synovial sarcomas (Fig. 3 A, top panel and B). The specificity of the RT-PCR product was confirmed by hybridization with the SYT-SSX oligonucleotide (Fig. 3A, bottom panel), which spans the common junction point of both chimeric mRNAs. The adamantinoma of long bone showed no PCR product of the SYT-SSX fusion transcript, although the transcript of the β-actin gene could be detected (Fig. 3A, top panel and B). The results of analyses of synovial sarcomas and control are summarized in Table 1.

Interphase FISH on isolated nuclei demonstrated two areas with closely adjoining signals of chromosome 18q11 and chromosome Xq11.2–4, corresponding to derivative chromosome 18 and derivative chromosome X, in both samples. Figure 4 shows the FISH analysis of case 1, revealing one normal nucleus and one tumor nucleus.

Discussion

Nonrandom occurrence of t(X;18)(p11.2,q11.2) has been consistently found in synovial sarcoma. Clark et al. suggested that the formation of SYT-SSX fusion transcript represents the key event in tumor development [5]. Therefore, the SYT-SSX fusion transcript is considered as a highly sensitive diagnostic marker for synovial sarcoma and we previously reported a primary prostatic synovial sarcoma diagnosed by cytogenetic analysis [11].

The histogenesis of synovial sarcoma is unclear, although most investigators currently regard the cell of origin to be a primitive mesenchymal precursor stem cell, unrelated to synovial lining cell [4, 17,19]. On the other hand, other investigators have suggested that the histogenesis of biphasic synovial sarcoma involves epithelial differentiation of mesenchymal cells [7, 16,18].

Reporting the results of in situ hybridization analysis of a single case of biphasic synovial sarcoma using an antisense probe, Hiraga et al. suggested that SYT-SSX fusion gene was expressed in both cellular components [10]. Birdsall et al. used a two-color fluorescence in situ hybridization and demonstrated the presence of a specific genetic rearrangement in both cellular components of biphasic synovial sarcoma [1]. More recently, Kasai et al. reported that SYT-SSX fusion transcripts were detected in both cellular areas of biphasic synovial sarcoma using laser capture microdissection and RT-DOP-PCR-PCR [12]. In addition, they tried ordinary PCR and nested PCR, but failed to detect SYT-SSX fusion transcripts and porphobilinogen deaminase gene transcripts in the microdissected samples. We, on the other hand, were able to detect the SYT-SSX fusion gene transcripts and the β-actin gene transcripts in microdissected samples by the nested RT-PCR. The photographs in the former study (Kasai et al.) illustrated only dissection of the spindle cell component, while the separation of the epithelial cell component was unclear. In the present study, we clearly demonstrated the isolation of both epithelial and spindle cell components using the microbeam MOMeNT technique. The reliability of our results was further supported by data gained by means of FISH analysis.

Using the FISH technique on interphase nuclei, we could confirm the specific translocation t(X;18) in both biphasic synovial sarcomas.

Microbeam MOMeNT is a reliable method for the detection of tumor-specific alterations when using PCR assays and allows a rapid, selective, and low-contamination procurement of tumor cells from membrane-mounted tissue sections. Using this method, it is possible to accurately microdissect the tissue using a computer pointing device (e.g., mouse) and the procedure can be clearly seen on the monitor screen. Böhm et al. suggested that microbeam MOMeNT provides the flexibility and accuracy that may be critical in many irregular or infiltrated neoplastic lesions or in the procurement of specific cell clusters in development biology [2,3]. In the present study, we have demonstrated that efficient analysis of RNA from small tissue samples is feasible using the above procedure. To our knowledge, this is the first report of RNA analysis using formalin-fixed paraffin-embedded samples isolated by microbeam MOMeNT.

In conclusion, the microbeam MOMeNT is a useful method for isolating selected small portions from tissue sections. Our findings of the presence of the SYT-SSX fusion gene in both cellular components of biphasic synovial sarcoma confirmed that the synovial sarcoma is of monoclonal origin.

Acknowledgements The authors thank Dr. K. Anzai and Miss M. Sugihara for preparing the membrane-mounted tissue sections.

References

1. Birdsall S, Osin P, Lu YJ, Fisher C, Shipley J (1999) Synovial sarcoma specific translocation associated with both epithelial and spindle cell components. Int J Cancer 82:605–608
2. Böhm M, Wieland I, Schütze K, Rübben H (1997) Microbeam MOMeNT. Non-contact laser microdissection of membrane-mounted native tissue. Am J Pathol 151:63–67
3. Böhm M, Schmidt C, Wieland I, Leclerc N, Allhoff EP (1999) Membrane-based laser microdissection in molecular oncology. Onkologie 22:296–301
4. Bridge JA, Bridge RS, Borek DA, Shaffer B, Norris CW (1988) Translocation t(X;18) in orofacial synovial sarcoma. Cancer 62:935–937
5. Clark J, Rocques PJ, Crew AJ, Gill S, Shipley J, Chan AM, Gusterson BA, Cooper CS (1994) Identification of novel genes, SYT and SSX, involved in the t(X;18)(p11.2;q11.2) translocation found in synovial sarcoma. Nat Genet 7:502–508
6. Crew AJ, Clark J, Fisher C, Gill S, Grimer R, Chand A, Shipley BA, Gusterson BA, Cooper CS (1995) Fusion of SYT to two genes, SSX1 and SSX2, encoding proteins with homology to the Kruppel-associated box in human synovial sarcoma. EMBO J 14:2333–2340
7. Dardick I, Ramjohn S, Thomas MJ, Jeans D, Hammar SP (1991) Synovial sarcoma. Inter-relationship of the biphasic and monophasic subtypes. Pathol Res Pract 187:871–885
8. De Leeuw B, Suijkerbuijk R, Olde Weghuis A, Meloni A, Stenman G, Kindblom L, Balemans M, van den Berg E, Molenaar W, Sandberg AA, geurts van Kessel A (1994) Distinct Xp11.2 breakpoint regions in synovial sarcoma revealed by metaphase and interphase FISH: relationship to histologic subtypes. Cancer Genet Cytogenet 73:89–94

9. Fligman I, Lonardo F, Jhanwar SC, Gerald WL, Woodruff J, Ladanyi M (1995) Molecular diagnosis of synovial sarcoma and characterization of a variant SYT-SSX2 fusion transcript. Am J Pathol 147:1592–1599
10. Hiraga H, Nojima T, Abe S, Sawa H, Yamashiro K, Yamawaki S, Kaneda K, Nagashima K (1998) Diagnosis of synovial sarcoma with reverse transcriptase-polymerase chain reaction: analysis of 84 soft tissue and bone tumors. Diagn Mol Pathol 7:102–110
11. Iwasaki H, Ishiguro M, Ohjimi Y, Ikegami H, Takeuchi T, Kikuchi M, Kaneko Y, Ariyoshi A (1999) Synovial sarcoma of the prostate with t(X;18)(p11.2;q11.2). Am J Surg Pathol 23:220–226
12. Kasai T, Shimajiri S, Hashimoto H (2000) Detection of SYT-SSX fusion transcripts in both epithelial and spindle cell areas of biphasic synovial sarcoma using laser capture microdissection. J Clin Pathol 53:107–110
13. Krams M, Peters J, Boeckel F, Raether A, Ambros PF, Parwaresch R, Harms D (2000) In situ reverse-transcriptase polymerase chain reaction demonstration of the EWS/FLI-1 fusion transcript in Ewing's sarcomas and peripheral primitive neuroectodermal tumors. Virchows Arch 437:234–240
14. Ladanyi M (1995) The emerging molecular genetics of sarcoma translocations. Diagn Mol Pathol 4:162–173
15. Lasota J, Jasinski M, Debiec-Rychter M, Szadowska A, Limon J, Miettinen M (1998) Detection of the SYT-SSX fusion transcripts in formaldehyde-fixed, paraffin-embedded tissue: a reverse transcription polymerase chain reaction amplification assay useful in the diagnosis of synovial sarcoma. Mod Pathol 11:626–633
16. Miettinen M, Virtanen I (1984) Synovial sarcoma. A misnomer. Am J Pathol 117:18–25
17. Miettinen M, Santavirta S, Slatis P (1987) Intravascular synovial sarcoma. Hum Pathol 18:1075–1077
18. Motoi T, Ishida T, Kuroda M, Horiuchi H, Oka T, Matsumoto K, Nakamura T, Machinami R (1998) Coexpression of hepatocyte growth factor and c-Met proto-oncogene product in synovial sarcoma. Pathol Int 48:769–775
19. O'Keeffe LJ, Ramsden RT, Birzgalis AR (1993) Primary synovial sarcoma of the middle ear. J Laryngol Otol 107:1070–1072
20. Renwick P, Reeves B, Dal Cin P, Fletcher C, Hempski H, Sciot R, Kazmierczak B, Jani K, Sonobe H, Knight J (1995) Two categories of synovial sarcoma defined by divergent chromosome translocation breakpoints in Xp11.2, with implications for the histologic sub-classification of synovial sarcoma. Cytogenet Cell Genet 70:58–63
21. Sandberg AA, Bridge JA (1994) Synovial sarcoma. In: Sandberg AA (ed) The cytogenetics of bone and soft tissue tumors. RG Landes, Austin, Texas, pp 430–441
22. Shipley J, Crew J, Birdsall S, Gill S, Clark J, Fisher C, Kelsey A, Nojima T, Sonobe H, Cooper C, Gusterson B (1996) Interphase fluorescence in site hybridization and reverse transcription polymerase chain reaction as a diagnostic aid for synovial sarcoma. Am J Pathol 148:559–567
23. Tsuji S, Hisaoka M, Morimitsu Y, Hashimoto H, Shimajiri S, Komiya S, Ushijima M, Nakamura T (1998) Detection of SYT-SSX fusion transcripts in synovial sarcoma by reverse transcription-polymerase chain reaction using archival paraffin-embedded tissues. Am J Pathol 153:1807–1812
24. Turc-Carel C, Dal Cin P, Limon J, Li F, Sandberg AA (1986) Translocation X;18 in synovial sarcoma [letter]. Cancer Genet Cytogenet 23:93

Virchows Arch (2001) 439:158–169
DOI 10.1007/s004280100441

ORIGINAL ARTICLE

**Anna Maria Chiaravalli · Matteo Cornaggia
Daniela Furlan · Carlo Capella · Roberto Fiocca
Giovanna Tagliabue · Catherine Klersy · Enrico Solcia**

The role of histological investigation in prognostic evaluation of advanced gastric cancer

Analysis of histological structure and molecular changes compared with invasive pattern and stage

Received: 9 November 2000 / Accepted: 15 February 2001 / Published online: 6 April 2001
© Springer-Verlag 2001

Abstract The relative contribution of tumour histology or molecular changes, compared with invasion pattern or stage, to prognostic assessment of gastric cancer was investigated in a series of 185 advanced (T2 to T4, stage IB to IV) cancers that had undergone intentionally curative surgery at Varese General Hospital. Survival analysis of the histological types considered in commonly used classifications, such as Lauren, Kubo, the World Health Organization (WHO) and related classifications, allowed separation of a small high-grade (Hg, 12 cases) group of adenosquamous, anaplastic and small cell endocrine carcinomas from a large cohesive group (C, 86 glandular or solid cancers) and from another large (87 cases) group of tumours with dissociated cells [29 diffuse (D) and 58 mixed (M) tumours]. Univariate and multivariate analysis showed the independent prognostic value of this C/M+D/Hg classification approach, which proved superior to other classifications and to cell dissociation at the growing front or angio, lympho and neuroinvasion. Expression of sialyl Lewis^c, the DUPAN-2 antigen, proved to be an independent predictor of worse survival among tumours beyond stage I, showing an exclusively or predominantly cohesive structure. Microsatellite instability (MSI) predicted favourable survival in purely cohesive tumours of intermediate (II) stage, especially of solid/medullary and lymphoid stroma/lymphoepithelioma-like structure, among which two distinct tumour subsets were characterised, one MSI-positive and the other Epstein-Barr virus positive. T2N0M0 (stage IB) tumours showed mostly favourable survival independently from histological type, invasive pattern, DUPAN-2 or MSI status. It is concluded that an appropriate histological evaluation, coupled with sialylated glycoproteins histochemistry and, for stage-II tumours, MSI tests may contribute significantly to prognostic assessment of tumours beyond stage I. However, the stage itself, with special reference to lymph-node metastases and invasion level beyond subserosa, remains the most important prognostic clue for gastric cancer.

Keywords Advanced gastric cancer · Histological classification · DUPAN-2 · Microsatellite instability · Epstein-Barr virus · Stage

C. Capella (✉)
Department of Pathology, Ospedale di Circolo, viale Borri 57, 21100 Varese, Italy
e-mail: Carlo.Capella@ospedale.varese.it
Tel.: +39-332-278231, Fax: +39-332-278599

A.M. Chiaravalli · M. Cornaggia · D. Furlan · C. Capella
Department of Pathology, University of Insubria, Varese, Italy

R. Fiocca
Department of Pathology, University of Genova, Italy

G. Tagliabue
U.O. Registro Tumori, Istituto Nazionale Tumori, Milano, Italy

C. Klersy
Medical Statistics Unit, IRCCS Policlinico San Matteo, Pavia, Italy

E. Solcia
Department of Pathology,
University of Pavia and IRCCS Policlinico San Matteo, Pavia, Italy

Introduction

Histological findings relevant to the prognostic evaluation of gastric cancer have been investigated extensively [12, 20, 31, 35, 38, 42, 48, 55]. In general, factors such as local lymph-node or distant metastases, level of gastric wall invasion or angioinvasion have been found to be more important than histological classification of histochemically assessed tumour cell phenotype [8, 20, 49]. However, in some studies, gland-forming "intestinal" cancers, somewhat mimicking colorectal tumours, showed better survival than "diffuse" cancers made up of dispersed cells, minute cellular aggregates or microglands [48, 55]. Among minor tumour subsets, solid (medullary)

cancer with cohesive cells, forming well-defined cellular aggregates devoid of gland lumina [34, 54], indolent mucoid cancer with well-formed glandular structures sitting in lakes of extracellular mucous [9] or cancers with lymphoid stroma with or without lymphoepithelial-type histology [11, 37, 60] have been associated with better survival, whereas adenosquamous cancer [39, 42], hepatoid carcinoma [40], choriocarcinoma [28] or poorly differentiated small cell (neuroendocrine) carcinoma [36, 50] showed a more ominous outcome. In addition, tumours with an expanding type of growth, partly overlapping with Lauren's intestinal cancers, showed more favourable behaviour than those with infiltrative type, which include most of the diffuse cancers [38, 48]. More recently, the study of tumour cell dissociation at the invasion front of the neoplasia proved predictive of patient outcome [21].

To our knowledge, no study investigated systematically the predictive potential of all the different histological types, subtypes or growth patterns incorporated in the various classification systems so far developed. However, basic information on histology seems now necessary not only for prognostic assessment of the tumour disease but also as a prerequisite for correct interpretation of the role of genetic lesions and other molecular changes in its development and progression, an issue to which many studies are presently devoted. Indeed, different genetic changes, with special reference to microsatellite instability (MSI) and p53 or cadherin E gene mutations, have been detected between intestinal and diffuse cancers [5, 10, 33, 44, 47, 58], which may have epidemiological, pathogenetic and prognostic relevance [53]. However, the precise interplay of genetic factors with the wide spectrum of histological patterns displayed by gastric cancer deserves further investigation.

Sialyl-glucoconjugates, such as sialyl-Lewis^a (detected by the CA-19–9 antibody) and sialyl- Lewis^x have been associated with poor prognosis [3, 26, 41]. The DUPAN-2 antibody is known to react with the sialyl-Lewis^c epitope (a non-fucosylated biosynthetic precursor of sialyl-Lewis^a epitope), which is mostly expressed on MUC1, a large transmembrane mucin also bearing sialyl-Lewis *a* and *b* [24, 27, 30]. The antibody reacts with normal pancreatobiliary ducts, while showing scarce or no reactivity for normal uninflamed gastric mucosa [7, 51]. DUPAN-2 has been found to be a selective marker for pancreatic tumours of ductal origin, but it has never been investigated systematically in gastric cancer.

In this paper, the main histological criteria commonly used in gastric cancer classification and a few histology-related molecular factors have been extensively investigated using univariate and multivariate analysis as predictors of patient outcome against a background of gastric wall invasion and local or distant metastases.

Materials and methods

A series of invasive (T2–T4) gastric cancers operated on at Varese General Hospital from January 1980 to April 1987 were taken from the files of the Anatomic Pathology Service. All cases had been operated in the two surgical units of the hospital, using comparable guidelines and procedures. No chemotherapy was given. Stained sections and paraffin blocks of primary tumour tissue (three specimens as a mean), peritumour gastric wall, resection margins, lymph nodes and the original macroscopic and microscopic reports were available for all cases. All documents pertaining to the clinical history of the patient, including endoscopic and radiological examinations, description of surgical intervention, periodic ambulatory or distant follow-up, family doctor and home care and Varese Province Tumor Registry data were consulted and carefully evaluated. Special attention was paid to the stage of tumour disease at the time of surgery. The assessment of metastases was based on extensive clinical, X-ray and ultrasonography investigation, in addition to intraoperative exploration and histological sampling. In particular, negative liver ultrasonography and X-ray lung examinations were necessary requirements to include the patients among those lacking evidence of metastases. Patients who had undergone palliative surgery were excluded from the study. A total of 185 patients who had undergone potentially curative surgery entered the study. For most surviving persons, the follow-up was prolonged up to 4 April 2000. The cause of death was reconstructed from clinical and anatomical pathology records for those who died during hospitalisation. Tumour registry records and a family doctor interview were added for those who died at home.

Paraffin sections were stained with haematoxylin and eosin and with the alcian blue–periodic acid-Schiff method. For each case, archival and newly stained histological sections were reassessed independently by at least two of us (M.C. and A.M.C.) and than revised under the supervision of a third pathologist (C.C.), whose final judgement was taken in the few cases where the original two pathologists failed to agree. The histological classifications of Lauren [31], Kubo [29], Ming [38], Watanabe et al. [61] and Gabbert et al. [21] were applied. In addition, a classification of tumours into purely or predominantly glandular, purely or predominantly diffuse, heavily mixed (glandular and diffuse with at least 40% of each component) and mucinous (with at least 50% of extracellular mucinous component) was applied [19], with solid and adenosquamous tumours forming minor separate subtypes. A simplified classification scheme already adopted for molecular studies [32] was also tested; it considered glandular (Fig. 1), diffuse (Fig. 2) and mixed (Fig. 3) cancers, with the last group showing both glandular and diffuse components in excess of 10%, solid tumours being grouped with glandular and adenosquamous tumours being grouped with mixed cancers. Cancers with lymphoid stroma (CLS) [60], with or without a lymphoepithelioma-like pattern [11], and poorly differentiated small cell (neuroendocrine) carcinomas [50] were characterised as previously reported. Tumour stage was assessed using the tumour node metastasis (TNM) system according to the International Union Against Cancer (UICC) [52]. Tumours with invasion limited to muscularis propria (T2m) or subserosa (T2) were separated from those involving the serosa (T3) or adjacent organs (T4).

Tumour sections were stained with the avidin–biotin immunoperoxidase technique using monoclonal (Biogenex, San Ramon, Calif.) directed against the DUPAN-2 antigen [51]. Endocrine differentiation was searched in tumours showing solid medullary or mixed solid-diffuse histology using chromogranin A, synaptophysin, PGP 9.5 or neuron-specific enolase antibodies in immunohistochemical tests or with Grimelius silver, as previously reported [50]. Human leukocyte antigen (HLA)-DR expression was tested in lymphoepithelioma-like and medullary tumours using LN3 antibodies (Biotest, Dreich, Germany) while CD31 antigen immunostaining (M823 antibody, Dako, Glostrup, Denmark) of endothelial cells was applied whenever conventional histology was insufficient to confidently assess vessel invasion. In addition, nuclear accumulation of the P53 oncoprotein was investigated with D07 monoclonal antibodies (Dako), recognising both wild and mutated molecular forms, and the expression of hMLH-1 (G168–15 antibody, Pharmingen, San Diego, Calif.) and hMSH-2 (FE11 antibody, Oncogene, Cambridge, Mass.) mismatch repair genes was tested on tumour specimens using adjacent non-tumour mucosa as control tissue. All tumours showing frank (unreactivity of all tumour nuclei coupled with reactivity of non-tumour cells) or

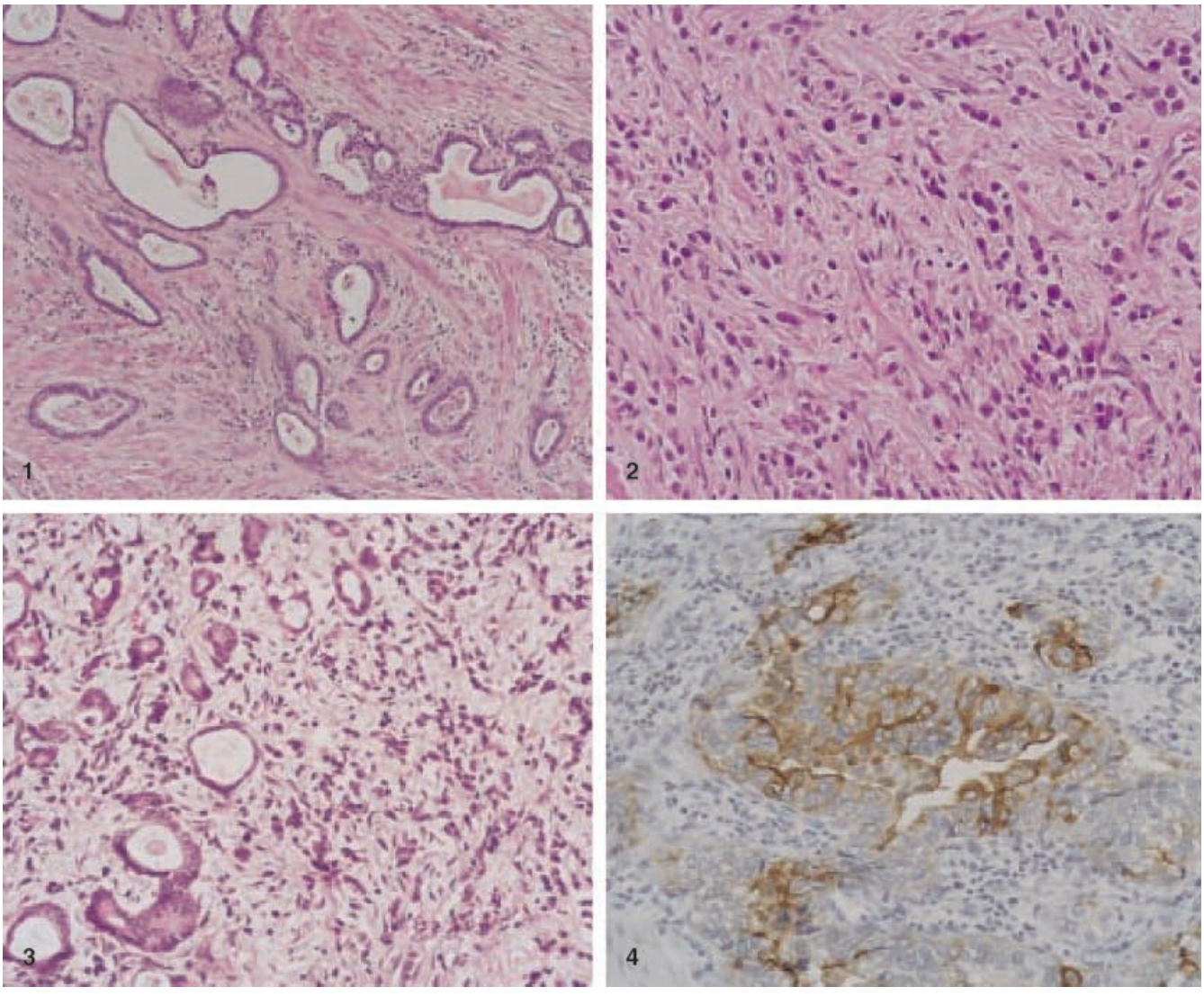


Fig. 1 Gastric carcinoma of glandular (cohesive) type (haematoxylin–eosin; original magnification ×100)

Fig. 2 Gastric carcinoma of diffuse type (haematoxylin–eosin; original magnification ×200)

Fig. 3 Gastric carcinoma of mixed type (haematoxylin–eosin; original magnification ×200)

Fig. 4 Cohesive gastric carcinoma (glandular) with intense cytoplasmic immunostaining for DUPAN-2 (immunoperoxidase; original magnification ×200)

questionable (reduced reactivity of tumour cells) loss of nuclear immunostaining for the latter gene products were tested for MSI at the molecular level [13].

For the identification of MSI, tumour and non-tumour tissue was carefully dissected out from haematoxylin–eosin-stained and consecutive unstained sections under direct microscopic control. Polymerase chain reaction (PCR) products of DNA extracted from tumour and non-tumour tissue were obtained using specific primers (BAT 26, BAT 25, BAT 40) which were end labelled with 6-FAM phosphoramidites [64]. The PCR product was analysed in an Applied Biosystems 310 automated DNA sequencer, using the Gene Scan 672 (version 1.2) software for fragment sizing analysis. According to Zhou et al. [64], MSI was present when Bat26 or, alternatively, Bat 25 and Bat40 were unstable.

The Epstein-Barr viral (EBV) genome was sought in tumour sections with a nonradioisotopic in situ hybridisation assay [46] using the digoxigenin-labelled 19-base synthetic oligonucleotide GAC AAC CAC AGA CAC CGTC [complementary to a portion of messenger (m)RNA expressed by the EBER-1 gene, known to be actively transcribed in latently infected cells] on deparaffinised sections treated with 0.25 mg/ml proteinase K and predenatured at 95°C for 5 min. After overnight hybridisation at 37°C and careful washing, the sections were incubated with 1:500 diluted sheep anti-digoxigenin antibody conjugated with calf intestine phosphatase (Boehringer, Mannheim, Germany) and developed with nitroblue tetrazolium salt. EBV-transfected B95.8 cells (Enzo Diagnostics) were used as a positive control and, when hybridised with a non-correlated probe, as a negative control.

Statistics

Data were described as mean and standard deviation (SD) or median and quantiles if skewed and absolute and relative frequencies for continuous and categorial variables, respectively. The considered outcome was death from disease. All other cases were censored at time of last observation or at time of death from other causes (including perioperative death, up to 2 months after surgery). Death rates were calculated as events per 1000 person months and reported together with their 95% confidence interval (95% CI). Cox survival models were fitted in order to compute the

relative hazard (and its 95% CI) for a series of candidate prognostic factors. Cox model assumptions were assessed graphically by comparing the observed survival with survival predicted by the model. A series of tumour variables of physiopathological relevance (histological classification, lympho, neuro and angioinvasion, DUPAN-2 antigen expression, MSI, diameter, level of gastric wall invasion, lymph-node involvement and distant metastases) were included in a multivariate model after checking for colinearity. To evaluate the role of different histological classifications, separate models were fitted. For model validation, we computed the likelihood-based explained variation and the LeCessie–van Houwelingen shrinkage (noise) coefficient. Discriminative capacity was assessed graphically by comparing quartiles of the predictor indexes. Variables were included in a logical physiopathological sequence. Hierarchical models were compared by means of a likelihood ratio test. Some subgroup analysis was performed. In these cases, both the 95% CIs and the *P* values are to be considered in the framework of an exploratory analysis. Stata 6.0 (College Station, Tex.) was used for computation. A *P* value less than 0.05 was retained for statistical significance.

Results

Histological classification

With the Lauren system, the 185 tumours investigated were classified as reported in Table 1. At univariate Cox regression analysis, the classification as a whole gave no significant prognostic information, although intestinal tumours showed a slight trend toward more favourable survival than diffuse cancers. The World Health Organization (WHO) classification showed no significant difference among its numerous types and subtypes (univariate Cox for the model: $P=0.061$). However, trends were found for the "undifferentiated" (mostly solid) carcinomas to show a better outcome and for the adenosquamous and mixed signet ring/tubular cancers to show a worse prognosis. There was no substantial difference in survival between well and poorly differentiated tumours among tubular cancers, while papillary and mixed signet ring/tubular tumours showed a trend for more severe behaviour than tubular cases as a whole. Kubo's classification showed a significant prognostic value, with more favourable survival of medullary tumours and well-differentiated adenocarcinomas, 34 cases in all, compared with the remaining 151 tumours ($P=0.013$). There was no substantial difference between moderately and poorly differentiated adenocarcinomas or between these and mucoid tumours showing large, overwhelming extracellular deposits of mucin. Among diffuse cancers, the signet ring subtype was slightly more favourable than the desmoplastic one, whereas the anaplastic subtype was more ominous (Table 2).

To simplify Kubo's diagnostic approach, while keeping as much as possible of its prognostic value, we added medullary to well-differentiated adenocarcinomas, poorly to moderately differentiated adenocarcinomas, signet ring to desmoplastic diffuse cancers and anaplastic to adenosquamous and poorly differentiated endocrine carcinomas. As extracellular mucin was found to be largely irrelevant in terms of survival, mucoid tumours were classified according to the pattern of their epithelial component. The resulting "simplified" Kubo classification is reported in Table 3. Univariate Cox analysis showed improved survival predictive power compared with the original classification, especially due to the significantly worse prognosis of high-grade (Hg) tumours. However, the difference between the two largest groups, namely moderately to poorly differentiated adenocarcinomas and diffuse cancers and between the former and well-differentiated tumours, remained non-significant.

Previous histopathological, histochemical and molecular findings [12, 19, 32] suggested the opportunity to test whether mixed glandular/diffuse tumours might have a worse prognosis than purely glandular cancers. Indeed, the 60 mixed (M, Fig. 3) tumours with 10–90% dissociated, diffusely growing cells (death rate 14.95, 10.97–20.38) showed significantly worse prognosis ($P=0.005$) than the 86 glandular (Fig. 1) to solid (cohesive, C) can-

Table 1 Lauren classification of 185 gastric cancers. Univariate Cox regression analysis: model $P=0.1085$. *C.I.* confidence interval

[a] Per thousand person months

Histologic type	No.	Cancer deaths [no. (%)]	Death rate[a]	95%C.I.
1. Intestinal	108	58 (54)	9.27	7.17–11.99
2. Diffuse	44	30 (68)	18.47	12.92–26.42
3. Unclassified	33	22 (67)	11.07	7.25–16.72

Table 2 Kubo classification. Univariate Cox: model $P=0.0026$; 9+10, $P<0.001$ vs all other groups apart from group 6 ($P=0.043$); group 6, $P<0.05$ vs, 1, 2 and 5. *C.I.* confidence interval, *w.d.* well-differentiated, *m.d.* moderately differentiated, *p.d.* poorly differentiated

Histological type	No.	Cancer deaths	Death rate	95%C.I.
1. Medullary[b]	17	7 (41)	5.81	2.77–12.19
2. Adenocarcinoma, w.d.	17	8 (47)	6.02	3.01–12.04
3. Adenocarcinoma, m.d.	54	30 (56)	10.25	7.17–14.66
4. Adenocarcinoma,p.d.	37	23 (62)	11.45	7.61–17.24
5. Mucoid	7	4 (57)	8.17	3.07–21.78
6. Adenosquamous	5	4 (80)	33.23	12.49–88.69
7. Signet ring	10	7 (70)	13.47	6.42–28.25
8. Diffuse desmoplastic	31	21 (68)	16.91	11.03–25.94
9. Diffuse anaplastic	5	4 (80)	161.82	60.73–431.14
10. Small cell (p.d. endocrine)	2	2 (100)	140.93	35.25–563.50

Table 3 Simplified version of the Kubo classification. Univariate Cox: model P=0.0001. Group 1: P=0.084 vs group 2, P=0.007 vs group 3 and P<0.001 vs group 4; group 2: P=0.129 vs group 3, P<0.001 vs group 4; group 3, P=0.002 vs group 4. *C.I.* confidence interval, *w.d.* well-differentiated, *m.d.* moderately differentiated, *p.d.* poorly differentiated

Histological type	No.	Cancer deaths	Death rate	95%C.I.
1. Adenocarcinoma, w.d. (1+2+w.d.5)[a]	35	15 (43)	5.58	3.36–9.25
2. Adenocarcinoma, m.d.+p.d. (3+4+m.d5)[a]	92	53 (58)	10.33	7.89–13.51
3. Diffuse (7+8+p.d.5)[a]	46	32 (70)	16.87	11.93–23.86
4. High-grade (6+9+10)[a]	12	10 (83)	62.86	33.82–116.83

[a] Corresponding groups of the original classification

cers, while resembling that of the 34 diffuse (D, Fig. 2) cancers. The resulting CMD classification is shown in Table 4, where five adenosquamous tumours were included in the mixed group.

To assess whether the extent of tumour cell dissociation among the 60 mixed (D/C) cancers was prognostically relevant, 22 tumours with more extensive tumour cell dissociation (>40%; MD tumours) were separated from 38 tumours showing frank predominance of the cohesive component (MC tumours). Only a slight non-significant trend for more severe prognosis was observed in the former group (death rate 18.57, 11.20–30.81 vs 13.38, 9.04–19.81), whose behaviour proved essentially identical to that of purely diffuse cancers (death rate 19.27, 12.81–29.00). Addition of all mixed tumours showing at least 10% of the dissociated component to the diffuse cancers of CMD classification gave a large group of 99 cases (death rate 17.24, 13.61–21.82) showing obviously worse prognosis (P<0.001) than that of the 86 cohesive tumours. When 12 Hg tumours (corresponding to group 4 of Table 3, simplified Kubo classification: five adenosquamous, five anaplastic and two poorly differentiated, small cell endocrine carcinomas) were separated from the remaining 87 M+D cases, the highly predictive C/M+D/Hg classification of Table 5 was obtained. Univariate Cox analysis of the remaining 173 tumours showed that both CMD (model P=0.0073, explained variation 0.0552) and C/M+D (model P=0.0019, explained variation 0.0542) classifications maintained predictive ability, although reduced in respect to that of the whole series.

Attempts to identify a low-grade group gave only non-significant trends for better survival of seven cytologically grade-1 well-differentiated adenocarcinomas, eight solid cancers and ten cohesive CLS than the remaining cohesive cancers.

The pattern of invasive growth investigated according to Ming [38] showed only a non-significant trend for better survival of the 51 expanding than 134 infiltrative cancers (model, P=0.1812). An investigation of tumour cell dissociation at the invasion front according to Gabbert and co-workers [21] gave more informative prognostic indications (model, P=0.040), with significant differences between 78 grade-3 (predominantly dissociated) tumours and 46 grade-0 (compact, 12 cases) or grade-1 (with single dissociated cells, 34 cases) tumours (P=0.030) or 61 grade-2 (with partial dissociation of tumours glands or cell complexes) tumours (P=0.044). However, no significant differences were found among grade-0, -1 or -2 tumours in our series, where the prognostic value of the Gabbert classification was essentially due to the significant difference (P=0.012) of grade-3 cases compared with the remaining cases. The Gabbert system correlated with CMD-based classifications (Pearson $\chi 2$>100, P<0.001). In particular, 31 of 34 (91%) diffuse and 44 of 65 (68%) mixed cancers of CMD classification fit in the Gabbert grade-3 group, compared with only 3 of 86 (3%) of cohesive tumours. This suggests that cell dissociation of cancer as a whole does not differ substantially from that occurring at its invasion front.

Table 4 Cohesive, mixed, diffuse (CMD) classification. Univariate Cox: model P=0.001; explained variation=0.072. 1 vs 2, P=0.002; 1 vs 3, P=0.001; 2 vs 3, P=0.5341; 1 vs 2+3, P<0.001. C, 77 glandular and nine solid; M, five adenosquamous and two anaplastic; D, three anaplastic and two small cell endocrine carcinoma. *CI* confidence interval

Histological type	No.	Cancer deaths	Death	95% C.I.
1. C	86	41 (48)	6.98	5.14–9.48
2. M	65	44 (68)	15.74	11.71–21.15
3. D	34	25 (74)	20.70	13.99–30.64

Table 5 Cohesive (C)/mixed (M)+diffuse (D)/high-grade (Hg) classification. Univariate Cox: model P<0.0001; explained variation =0.1143. 1 vs 2, P=0.003; 1 vs 3, P<0.001; 2 vs 3, P=0.001. *C.I.* Confidence interval

Histological type	No.	Cancer deaths	Death rate	95% C.I.
1. C	86	41 (48)	6.98	5.14–9.48
2. M+D	87	59 (68)	15.35	11.89–19.81
3. Hg	12	10 (83)	62.86	33.82–116.83

DUPAN-2 antigen expression

DUPAN-2 antigen was expressed by at least 1% of cells in 122 of 185 (65.9%) tumours and by more than 5% in 72 (38.9%) tumours (Fig. 4). Using univariate Cox analysis, the antigen was found to predict a worse survival, with more significant results when expressed by more than 5% of tumour cells, either in the whole series or

Table 6 Stratification of DUPAN-2 expression by histological type. *C* cohesive, *M* mixed, *D* diffuse, *C.I.* confidence interval. Bivariate Cox: model $P<0.0001$. C, positive vs negative, $P=0.001$; MC, positive vs negative, $P<0.001$; C vs MC, $P=0.012$

Type	DUPAN-2	No.	Ca-deaths	Death rate	95% C.I.
C		86	41(48)	6.98	5.14–9.48
	Negative	57	24(42)	4.88	3.27–7.29
	Positive	29	17(59)	17.69	11.00–28.45
Mixed, C>D(MC)		43	29(67)	14.59	10.14–20.99
	Negative	24	12(50)	7.44	4.23–13.10
	Positive	19	17(89)	45.28	28.15–72.84
Mixed, D≥C(MD)		22	15(68)	18.57	11.20–30.81
	Negative	13	9(69)	22.50	11.71–43.25
	Positive	9	6(67)	14.72	6.61–32.76
D		34	25(74)	20.70	13.99–30.63
	Negative	19	14(74)	19.69	11.66–33.24
	Positive	15	11(73)	22.15	12.27–39.99

Table 7 Interplay of histology, microsatellite instability (MSI) and DUPAN-2 expression in outcome prediction. Cohesive: MSI+ vs MSI–, $P=0.007$. MC: DUPAN + vs –, $P<0.001$. Cohesive vs MC, $P=0.043$, vs MD+D, $P=0.002$. *C.I.* confidence interval

Type	No.	Ca-deaths	Death rate	95% C.I.
Cohesive	86[a]	41(48)	6.98	5.14–9.48
MSI+	29	9(31)	3.14	1.64–6.04
MSI–	56	31(55)	10.52	7.40–14.96
DUPAN–	31	15(48)	6.85	4.12–11.36
DUPAN+	25	16(64)	21.17	12.97–34.56
MC	37	24(65)	12.86	8.62–19.19
DUPAN–	20	9(45)	6.00	3.12–11.53
DUPAN+	17	15(88)	41.06	24.76–68.12
MD+D	50	35(70)	17.69	12.70–24.64
High grade	12	10(83)	62.86	33.82–116.86

[a] One case missed MSI status assessment.

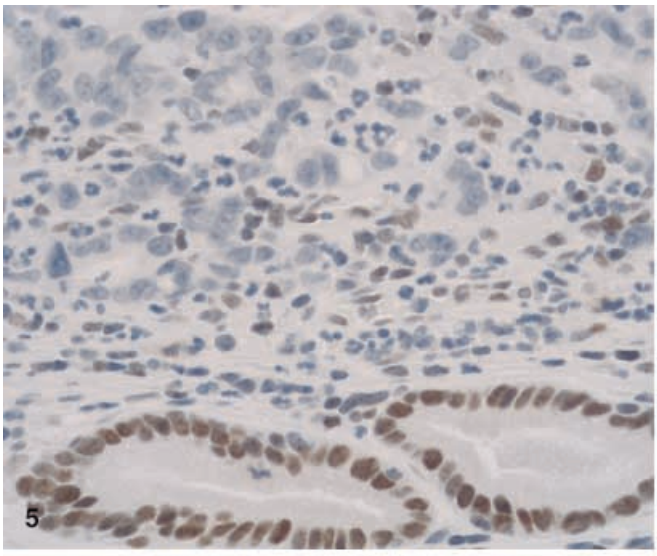
among cohesive cancers and mixed cancers with predominance of the cohesive component (MC tumours) but not among diffuse or mixed cancers with more than 40% dissociated tumour cells (MD tumours) (Table 6). In a parallel analysis, expression of P53 protein by more than 10% of cells (64 of 185 tumours, 34.6%) showed no significant influence on survival, even when analysis was restricted to histological types (glandular and mixed) of higher expression.

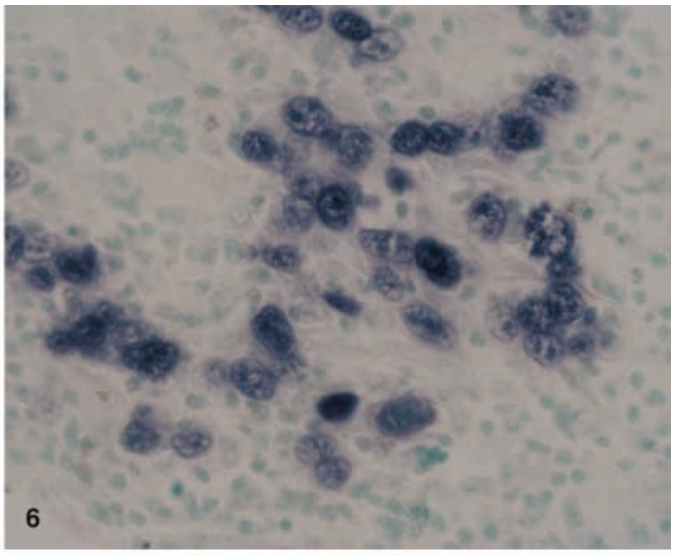
The lack of DUPAN-2 effect among both MD and D tumours suggests a need to group together all tumours showing more than 40% diffuse cells, irrespective of the presence or absence of a cohesive component, while keeping MC tumours as a separate group with prognosis significantly different from that of purely cohesive cancers ($P=0.016$). This would offer the possibility of identifying the particularly ominous subgroup of DUPAN-2-positive MC cancers significantly worse than their DUPAN-2-negative counterpart ($P<0.001$) and diffuse, MD or DUPAN-2-positive cohesive cancers ($P<0.05$), a behaviour mostly confirmed also after separation of the Hg group (Table 7).

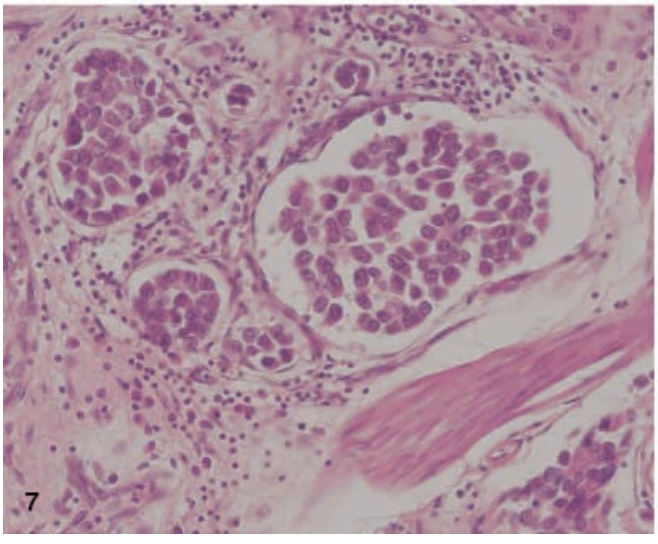
Microsatellite instability

Immunostaining for MLH-1 and MSH-2 of the 185 cases identified 143 cases whose tumour cells retained normal nuclear reactivity for both factors, 30 cases with obvious loss of MLH-1 (Fig. 5) and two cases with loss of MSH-2. In ten tumours, immunohistochemical tests for one (MLH-1 in four cases and MSH-2 in one case) or both (five cases) factors failed for technical reasons or gave inconclusive results. A search for MSI at the molecular level in 86 cases, including all immunohistochemical tests failures, gave instability in all 32 cases showing frank loss of MLH-1 or MSH-2 immunostaining, in 2 of 43 cases (4.7%) retaining immunostaining of both factors and in 2 cases w ith inconclusive MLH-1 coupled with positive MSH-2. Three of the five cases lacking reactivity for both factors and one lacking only MLH-1 also failed to react with the molecular test and were dropped out of MSI analysis. The other four cases with immunohistochemical failure of one or both factors proved stable by means of molecular analysis. The remaining 99 cases showing normal nuclear immunostaining for both MLH-1 and MSH-2 products, which should imply less than 5% probability of MSI (as shown using molecular analysis of the 86 cases), were assumed to be stable. Thus, proven MSI-positive cases turned out to be 36 out of 181 (20%) successfully tested.

MSI-positive cases were preferentially concentrated among solid tumours (six of eight cases, 76%) and glandular to solid CLS (four of ten, 40%) tumours (often showing a prominent, partly Crohn-like lymphoid cell infiltration), compared with the remaining glandular (19 of 67, 28%), mixed (5/55, 9%) or diffuse (0) tumours of CMD classification (Fisher exact test for MSI+ distribu-







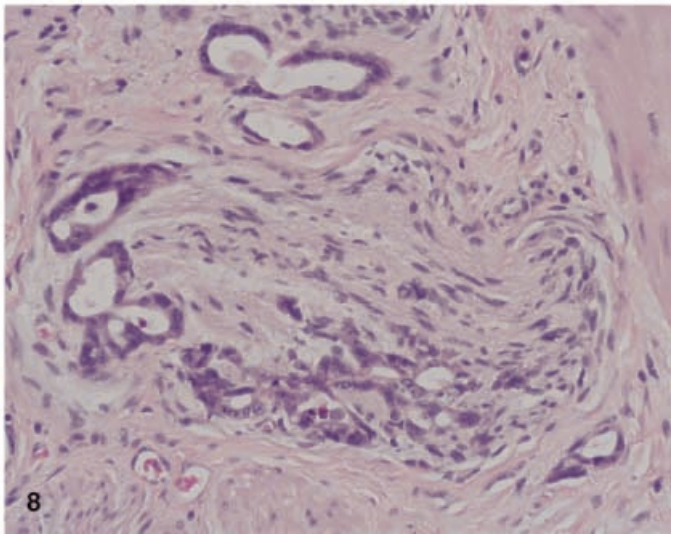


Fig. 5 Microsatellite-instable gastric carcinoma negative for MLH-1. Normal glandular and stromal cells are positive (immunoperoxidase; original magnification ×400)

Fig. 6 In situ hybridisation for Epstein-Barr virus RNA (EBER-1) in a gastric carcinoma with lymphoid stroma. Intense nuclear stain is present in neoplastic epithelial cells (nitroblue tetrazolium salt–methyl green, original magnification ×400)

Fig. 7 Lymphoinvasion in a gastric carcinoma of diffuse type (haematoxylin–eosin; original magnification ×200)

Fig. 8 Neuroinvasion in a gastric carcinoma of mixed-type (haematoxylin–eosin; original magnification ×200)

tion among subtypes of CMD classification: $P<0.001$). Among subgroups of Kubo classification, MSI-positive cases were more represented among medullary tumours (12 of 17, 71%) than adenosquamous cancers (2 of 5, 40%), well- (2 of 15, 13%), moderately (12 of 52, 23%) or poorly (8 of 37, 22%) differentiated adenocarcinomas or mucoid (0/5) cancers.

Univariate Cox analysis showed a significant improvement of survival in 36 patients with MSI-positive tumours versus 145 patients with MSI-negative tumours ($P=0.003$). The improvement, however, was restricted to cohesive tumours ($P=0.007$ compared with corresponding MSI negative tumours). A trend for negative association (Fisher exact test, $P<0.001$) found between MSI and DUPAN-2 positives and their opposite effects on survival suggested their combined use in a tentative diagnostic algorithm. As shown in Table 7, MSI-positive cohesive cases differ sharply from MSI-negative/DUPAN-2-positive cases ($P<0.001$); however, they do not differ significantly from MSI-negative/DUPAN-2-negative cases ($P=0.112$). Among MSI-negative tumours, the difference between DUPAN-2-positive and -negative cases remains significant ($P=0.012$).

EBV detection

EBV in situ hybridisation was performed on 66 tumours, inclusive of all CLS, all MSI-positive and 24 non-CLS MSI-negative cases. Eight cases were shown to be EBV-positive (Fig. 6), of which seven were among the 13 CLS tumours (54%) and one (an MSI positive case) was among

Table 8 Relationship of invasion level, lymph node metastases and tumour node metastasis (TNM) stage with survival. T2a vs T2b, P=0.031; T2b vs T3/4, P<0.001. LR x^2 (3)= likelihood ratio test. N0 vs N1 to 7, P<0.001; N1 to 7 vs N8 to 15, P=0.016; N8 to 15 vs N>15, P=0.054. N0 vs N1 to 3, P<0.001; N1 to 3 vs N4 to 8, P=0.020; N4 to 8 vs N>8, P=0.003. IB vs II, P<0.001; II vs III, P=0.103; III vs IV, P<0.002. *C.I.* confidence interval

[a] Univariate Cox models; [+] for models with A or B in addition to N0

	No.	Cancer deaths	Death rate	95%C.I.	*P* value[a]
Invasion level					<0.001
T2a	25	8 (32)	3.34	1.67–6.67	
T2b	80	44 (55)	8.92	6.63–11.98	
T3/4	80	58 (72.5)	22.76	17.61–29.47	
LN status					<0.001[+]
N0	51	14 (27)	2.81	1.67–4.75	
A:					
N1 to 7	94	63 (67)	15.69	12.25–20.08	
N8 to 15	25	20 (80)	27.38	17.67–42.44	
N>15	15	13 (87)	84.91	49.30–146.23	LR x^2 (3)=56.06
B:					
N1 to 3	57	35 (61)	11.30	8.11–15.74	
N4 to 8	43	31 (72)	24.20	17.02–34.41	
N>8	34	30 (88)	57.55	40.24–82.30	LR x^2 (3)=64.81
TNM stage					<0.001
IB(T2N0M0)	38	6 (16)	1.43	0.64–3.18	
II	57	37 (65)	11.41	8.26–15.74	
III	49	33 (67)	19.05	13.54–26.79	
IV	41	34 (83)	47.92	34.24–67.07	

53 (2%) non-CLS tumours (Fisher exact test, P<0.001), i.e. 1 of 31 MSI-positive and 0 of 24 MSI negative. Interestingly, among the CLS tumours, five of the six EBV-negative (83%) and none of the seven EBV-positive (Fisher exact test, P=0.005) proved to be MSI positive. HLA-DR antigen was found to be widely expressed in all CLS tumours, with or without lymphoepithelioma-like pattern and irrespective of their EBV or MSI status. None of the EBV-positive cases and only four of 36 (11%) MSI-positive cases showed P53 protein immunostaining in more than 10% tumour cells, against 60 of the remaining 139 tumours (43%; Fisher, P<0.001 vs MSI-positive cases).

Tumour stage

Tumour diameter less than 4 cm was found to significantly improve survival (death rate 5.14, 3.35–7.89) compared with those of 4–10 cm (death rate 14.82, 11.98–18.33; P=0.002 vs <4 cm), while tumours of more than 10 cm significantly worsened survival (death rate 66.48, 24.95–177.14; P=0.035 vs 4–10 cm).

The influence of the level of gastric wall invasion or lymph-node involvement on survival is reported in Table 8. Stratification of lymph-node involvement as 1–3, 4–8 and above 8 proved superior to the classical TNM system (1–7, 8–15, >15) both in terms of comparable numerosity of groups and of improved separation of prognostic classes. MSI was found to be negatively associated (Fisher exact test, P=0.006) and DUPAN-2 expression positively associated with lymph-node (Fisher, P=0.030) metastases, while both showed only marginal, non-significant association with the level of wall invasion. On the contrary, high histological grade was significantly associated with both lymph-node involvement (Fisher, P=0.002) and level of wall invasion (Fisher, P=0.004).

Lymphoinvasion (Fig. 7; P<0.001), perineural space invasion (Fig. 8; P<0.001) and blood vessel invasion (P=0.042) all proved predictive of worse survival at univariated Cox analysis. In addition, a correlation was found of lymphoinvasion and neuroinvasion with both level of wall invasion and lymph-node metastases (Fisher, P<0.001 in all cases), while angioinvasion correlated only with lymph-node metastases (P=0.002). Neuroinvasion was also related with extranodal metastases found at the time of surgery (P=0.006).

Intrabdominal extranodal metastases were detected at the time of surgery in 37 of the 185 patients (20%). They carried highly significant (P<0.001) worsening of survival (death rate 42.48, 29.33–61.53, vs 8.89, 7.16–11.04 of patients without metastases). DUPAN-2 expression correlated positively (Fisher, P=0.008) and MSI negatively, if any (Fisher, P=0.062), with metastases. A significant association was also found between metastases and M+D histology of CMD classification (Fisher, P<0.05) or Hg histology of C/M+D/Hg classification (Fisher, P<0.001).

The relationship between TNM stage and survival is shown in Table 8. It should be outlined that the prognostic influence of DUPAN-2 expression, MSI, lymphoinvasion, neuroinvasion (but not angioinvasion) and histological type (CMD or C/M+D/Hg) lost significance among 38 advanced tumours of stage-IB (T2N0M0). The favourable prognostic effect of MSI reached statistical significance only among stage-II tumours (death rate 3.26, 1.55–6.84, vs 12.96, 9.35–17.96), while the worsening effect of DUPAN-2 expression, lymphoinvasion, neuroinvasion and M/D or Hg histology retained significance among stage-II, -III and -IV tumours.

Multivariate analysis

Diameter: less than 4, 4–10 or greater than 10; level of wall invasion: T2a, T2b or T3/4; lymph-node status: N0, N1 to N7, N greater than 7; lymphoinvasion, neuroinvasion and angioinvasion; Kubo, simplified Kubo, CMD,

Table 9 Multivariate analysis with the cohesive (C)/mixed (M)+diffuse (D)/high-grade (Hg) classification (181 tumours). Model, $P<0.0001$ (with C/M+D classification: $P<0.0001$;M+D vs C: Hazard ratio 1.66, $P=0.048$, 95% C.I. 1.00–2.75). Model explained variation =0.458 (0.395 with C/M+D); noise in model=0.126 (0.143 with C/M+D). *C.I.* confidence interval; *MSI* microsatellite instability

	Hazard ratio	*P* value	95% C.I.
Histology	–	<0.001	–
M+D vs C	1.33	0.277	0.80–2.20
Hg vs C	10.87	0.000	4.72–25.04
Angioinvasion	0.98	0.940	0.61–1.58
Lymphoinvasion	1.82	0.073	0.95–3.50
Neuroinvasion	0.87	0.650	0.47–1.61
MSI	0.64	0.189	0.32–1.25
DUPAN, >5%	1.72	0.013	1.12–2.64
Diameter	–	0.772	–
4–10 cm vs <4 cm	1.20	0.521	0.69–2.08
>10 cm vs <4 cm	1.40	0.587	0.42–4.72
Invasion	–	0.018	–
T2b vs T2a	2.19	0.095	0.87–5.49
T3 vs T2a	3.43	0.011	1.33–8.84
Lymph-node involvement	–	0.001	–
N1–7 vs N0	2.73	0.003	1.41–5.28
N>7 vs N0	4.22	0.000	1.93–9.20
Metastases	1.74	0.028	1.06–2.87

C/M+D, C/M+D/Hg and Gabbert histological classifications; greater than 5% DUPAN-2 expression; MSI and extranodal metastases were included in the multivariate model. Colinearity was observed between each of the histological classifications. Thus, several models of multivariate analysis were developed, where one of the histological classifications was combined with the remaining factors. Lymph-node involvement, T3/4 invasion level, metastases, Hg histology of C/M+D/Hg or simplified Kubo classification and adenosquamous and anaplastic tumours of original Kubo classification and DUPAN-2 antigen expression proved to be independent predictors of poor survival (Table 9) in all models. M or M+D histology of CMD or C/M+D classifications and poorly differentiated adenocarcinoma of the original Kubo system also retained independent predictive power; however, these parameters lost independent predictive power when the 12 Hg cases were excluded from the analysis. The model with C/M+D/Hg classification proved superior to all other systems for its high-explained variation with lowest noise and equal only to that with original Kubo classification in providing the best quartile discrimination by graphical check (data not shown). The latter, however, was found to be unpractical because of undue complexity (ten or more subtypes considered).

At bivariate and stepwise-multivaried analysis of factors included in the multivaried model with the C/M+D/Hg classification, it was found that angioinvasion and neuroinvasion retained significance only in combination with diameter, while M+D histology lost significance with further addition of MSI and a diameter greater than 10 cm with the addition of invasion level. Diameter from 4 cm to 10 cm, lymphoinvasion, MSI and T2 invasion level lost significance only in the presence of lymph-node metastases. Omission of DUPAN-2 or metastases, though reducing significantly the information given by the model as a whole, did not change substantially the contribution of the remaining variables.

Discussion

Understanding the role of a plethora of new molecular factors in the progression of gastric cancer requires a precise knowledge of the natural history of this complex nepotistic disease, with special reference to the impact of histological patterns, invasion pathways and tumour stage on patient outcome. In this study, many efforts have been dedicated to a careful dissection of the various histological types and subtypes of gastric cancer considered in commonly used classifications and to their univariate and multivariate analysis from the point of view of patient outcome, in an attempt to clarify which histological structure (e.g. glandular vs solid/medullary or diffuse) or cellular factor (cell grade, cohesion vs dissociation, functional differentiation) might provide a clue to prognostic evaluation. For this purpose, Kubo's classification proved superior to the essentially descriptive WHO scheme [61] or to the popular Lauren's classification.

By dismissing the mucoid type from a previous four-group scheme we had modulated from Kubo's classification [19] and by classifying all tumours as gland-forming to solid (cohesive), diffuse or mixed [12, 32] based on the cohesive or dissociated pattern of tumour cells, we found that the cohesive-type was significantly predictive of a more favourable prognosis than both diffuse and mixed cancers. The resulting CMD (or C/M+D) classification proved superior to Lauren and Kubo classifications at both uni- and multivariate analysis and provided information independent from classical stage parameters. Concerning the mechanism through which the above histological patterns influence prognosis, it seems likely that tumour cell dissociation, as found in diffuse or mixed cohesive/diffuse cancers, favours local and lymph-node invasion [21] and peritoneal involvement [17], while the degree of differentiation of glandular structure is, by itself, devoid of significant prognostic value, provided cohesivity of tumour cells is retained.

Attempts to separate histologically low-grade (solid, CLS or grade-1) tumours were not successful as their relatively low death rate did not differ significantly from that of the remaining cohesive cancers. Staging, with specific reference to stage IB (T2N0M0), proved to be much more effective in identifying cases with favourable prognosis among advanced gastric cancers. A small group of histologically Hg tumours (6.5% of our series), formed by adenosquamous, anaplastic and poorly differentiated endocrine (small cell) carcinomas, proved to be prognostically worse than all other histological groups. The worse prognosis of adenosquamous [39, 42] or poorly differentiated endocrine (small cell) carcinomas

[36, 50] have been repeatedly documented. In addition, the poor outcome of "anaplastic medullary" cancers partly mimicking embryonal carcinoma [45] or choriocarcinoma [28] and of solid hepatoid carcinoma [40], which may also fit in our Hg group, has been outlined. Careful identification and separation of these rare tumour species from ordinary cancers is mandatory, because their Hg histology seems to represent a strong, independent predictor of poor outcome and to account for a substantial part of (though not all) the prognostic value of mixed, diffuse and related histological types of common classifications.

Improved separation of high and low survival tumours came from the study of DUPAN-2 expression and MSI or mismatch repair gene products, whose effect on patient survival proved, however, to be, at least in part, histology dependent. DUPAN-2 expression, which was well represented in all histological groups (with the exception of solid, CLS and anaplastic tumours) significantly worsened survival of cohesive tumours and of mixed cancers with predominance of the cohesive component, while showing no influence on mixed tumours with prominence of the diffuse component or on purely diffuse cancers. MSI and/or lack of repair gene expression, which were more frequently found in solid/medullary or glandular tumours compared with mixed cancers, while lacking in purely diffuse cancers, showed a favourable prognostic influence on cohesive but not on mixed tumours. Thus, selective addition of DUPAN-2 expression and/or MSI pattern to histological groups allowed significantly improved prediction of their behaviour.

Analysis of the stage dependence of prognostic factors showed that the influence of histological type, DUPAN-2 expression, MSI, lymphoinvasion and neuroinvasion was substantially negligible among T2N0M0 tumours, which formed a low malignancy group, accounting for about 20% of the whole series. The favourable outcome of N0 cancers with invasion limited to muscularis propria [23] or subserosa [1] has already been outlined. The prominent role of lymph-node involvement in determining the prognosis of advanced gastric cancer has been stressed by several investigators [4, 8, 42, 49]. Of interest is also our confirmation of previous findings suggesting separation of cases with a limited number (up to three according to Ichickura et al. [25]; Adachi et al. [2] and present study and up to four according to Wu et al. [62]) of metastatic lymph nodes from those with more extensive involvement. This is an important difference with respect to the one to seven involved lymph nodes fitting in the N1 group according to the TNM system [52], especially considering that a 0/1 to 3 (or 4)/4 (or 5) to 8/≥9 categorisation has been found to be prognostically more informative than the TNM or Japanese Rules staging systems [2, 25, 62].

The prominent negative influence of DUPAN-2 expression on survival that we have observed in this study may be accounted for in part by its correlation with lymph-node and extranodal metastases. However, DUPAN-2 antigen expression emerged as an independent prognostic factor in multivariate analysis also when both kinds of metastatic spread were part of the model. Thus, a more specific effect of the DUPAN-2 epitope is likely to operate. Indeed, sialylated surface carbohydrates of cancer cells have been shown to favour cancer invasiveness by (1) inhibiting homotypic cellular aggregation and adhesion to extracellular matrix, thus favouring local invasion, lymphatic channel permeation and lymph-node involvement [41, 56], (2) acting as ligands of E- and P-selectins in the vascular endothelium, thus favouring tumour extravasation [59] or (3) promoting angiogenesis and haematogenous metastases [3, 43, 57]. It seems likely that the biochemically related DUPAN-2 epitope may act through similar mechanisms and that its detection in a primary cancer of purely or prevalently glandular structure may signal a high potential for tumour invasion and metastatic spread.

Altered expression of cadherin E, another factor playing a role in intercellular adhesion, has also been shown in gastric cancer to correlate with shortened survival, independently from invasion level, lymph-node involvement and blood or lymphatic vessel invasion [22]. Preliminary investigation in our patient series (data not reported) showed no correlation between DUPAN-2 expression and cadherin E loss, the latter being mostly concentrated in diffuse cancers or the diffuse component of mixed cancers, two types of tumour where, as shown in this study, DUPAN-2 expression did not influence survival. Thus, these two prognostically unfavourable changes impairing cell adhesion seem to be unrelated to each other.

The better prognosis shown by cancers with MSI confirms previous investigations [16, 63]. However, its favourable effect on prognosis seems mostly restricted to solid and glandular tumours of intermediate (II) stage, being overcome by the strongly favourable effect of low stage (IB) and by the strongly unfavourable effect of highly advanced stage (III and IV). This stage-restrained and histology-related pattern, in addition to its lack of independent power in multivariate models inclusive of lymph-node involvement, limits the prognostic value of MSI, despite its obvious pathogenetic relevance [32, 44, 63]. MSI may have a role in preventing lymph-node (and distant) metastases during tumour progression. Its higher frequency in purely cohesive and, especially, in solid/medullary tumours, scarce occurrence in mixed and lack in purely diffuse tumours suggest some negative correlation with factors (mutation or suppressed expression of cadherin E and other adhesins) known to favour cell dissociation and a positive correlation with factors promoting cell cohesion without necessarily forming glands.

Our study confirms the occurrence of a prominent, partly Crohn-like lymphoid cell infiltration in MSI-positive tumours [15], which has been attributed to the expression, due to genetic instability, of a number of mutated proteins with antigenic potential, causing a specific cytotoxic immune response directed against neoplastic cells. The widespread expression by tumour cells of cathepsin E, which may have a crucial role in antigen processing [6, 18] and of class II HLA molecules, with a known role in antigen presentation, may support this in-

terpretation. A distinct subset of lymphoid cell-rich gastric cancer showed EBV genetic material, in addition to extensive expression of cathepsin E and HLA-DR antigen. This subset resembled more closely classic oropharyngeal lymphoepithelioma in its histological pattern, arose preferentially in proximal stomach or gastric stump (against the preferential antral origin of MSI positive tumours), and showed a negative correlation with MSI. A negative association between EBV and MSI was also observed by Chong et al. [14] in a Japanese series of gastric cancers. It seems likely that the two kinds of lymphoid cell-rich tumours, both of which are negatively correlated with P53 protein expression, represent two aetiologically separate types of cancer causing cellular immune response. The latter may possibly contribute to their relatively favourable prognosis.

In conclusion, the classification of a series of advanced gastric cancers on the basis of their cohesive (glandular to solid) or dispersed (diffuse) pattern of cellular aggregation, identification of mixed tumours (showing both cohesive and diffuse components) prognostically more akin with purely diffuse cancers and separation of a small group of histologically Hg tumours led to substantial improvement of the outcome predictive power of histology, which acquired an independent prognostic value. Careful comparison with previous investigations from the literature gave support to our findings and to the proposed classification criteria. Addition of DUPAN-2 antigen expression and, for stage-II tumours, of MSI, further improved the outcome predictive power of histology. Precise stage assessment remains the main factor in prognostic evaluation of most gastric cancers. In particular, lymph node-negative tumours strictly confined to the gastric wall have a mostly favourable outcome, which is largely independent of histology, invasive pattern, DUPAN-2 expression or MSI.

References

1. Abe S, Yoshimura H, Nagaoka S, Monden N, Kinugasa S, Nagasue N, Nakamura T (1995) Long-term results of operation for carcinoma of the stomach in T1/T2 stages: critical evaluation of the concept of early carcinoma of the stomach. J Am Coll Surg 181:389–396
2. Adachi Y, Kamakura T, Mori M, Baba H, Maehara Y, Sugimachi K (1994) Prognostic significance of the number of positive lymph nodes in gastric carcinoma. Br J Surg 81:414–416
3. Amado M, Carneiro F, Seixas M, Clausen H, Sobrinho-Simoes M (1998) Dimeric Sialyl-Le^x expression in gastric carcinoma correlates with venous invasion and poor outcome. Gastroenterology 114:462–470
4. Baba H, Korenaga D, Okamura T, Saito A, Sugimachi K (1989) Prognostic factors in gastric cancer with serosal invasion – univariate and multivariate analyses. Arch Surg 124:1061–1064
5. Becker KF, Atkinson MJ, Reich U, Becker I, Nekarda H, Siewert JR, Hofler H (1994) E-cadherin gene mutations provide clues to diffuse type gastric carcinomas. Cancer Res 54: 3845–3852
6. Bennett K, Levine T, Ellis JS, Peanasky RJ, Samloff IM, Kay J, Chain BM (1992) Antigen processing for presentation by class II major histocompatibility complex requires cleavage by cathepsin E. Eur J Immunol 22:1519–1524
7. Borowitz MJ, Tuck FL, Sindelar WF, Fernsten PD, Metzgar RS (1984) Monoclonal antibodies against human pancreatic adenocarcinoma: distribution of DU-PAN-2 antigen on glandular epithelia and adenocarcinomas. JNCI 72:999–1005
8. Bozzetti F, Bonfanti G, Morabito A, Bufalino R, Menotti V, Andreola S, Doci R, Gennari L (1986) A multifactorial approach for the prognosis of patients with carcinoma of the stomach after curative resection. Surg Gynecol Obstet 162: 229–234
9. Brander WR, Needham PRG, Morgan AD (1974) Indolent mucoid carcinoma of stomach. J Clin Pathol 27:536–541
10. Buonsanti G, Calistri D, Padovan L, Luinetti O, Fiocca R, Solcia E, Ranzani GN (1997) Microsatellite instability in intestinal- and diffuse-type gastric carcinoma. J Pathol 182:167–173
11. Burke AP, Benedict Yen TS, Shekitka KM, Sobin LH (1990) Lymphoepithelial carcinoma of the stomach with Epstein-Barr virus demonstrated by polymerase chain reaction. Mod Pathol 3:377–380
12. Carneiro F, Seixas M, Sobrinho-Simoes M (1995) New elements for an updated classification of the carcinomas of the stomach. Path Res Pract 191:571–584
13. Chiaravalli AM, Furlan D, Facco C, Tibiletti MG, Dionigi A, Casati B, Albarello L, Riva C, Capella C (2001) Immunohistochemical pattern of MSH2/MLH1 in familial and sporadic colorectal, gastric, endometrial and ovarian carcinomas with instability in microsatellite sequences. Virchows Arch 438:39–48
14. Chong JM, Fukayama M, Hayashi Y, Takizawa T, Koike M, Konishi M, Kikuchi-Yanoshita R, Miyaki M (1994) Microsatellite instability in the progression of gastric carcinoma. Cancer Res 54:4595–5497
15. Dolcetti R, Viel A, Doglioni C, Russo A, Guidoboni M, Capozzi E, Vecchiato N, Macrì E, Fornasarig M, Boiocchi M (1999) High prevalence of activated intraepithelial cytotoxic T lymphocytes and increased neoplastic cell apoptosis in colorectal carcinomas with microsatellite instability. Am J Pathol 154:1805–1813
16. Dos Santos NR, Seruca R, Constancia M, Seixas M, Sobrinho-Simoes M (1996) Microsatellite instability at multiple loci in gastric carcinoma: clinicopathologic implications and prognosis. Gastroenterology 110:38–44
17. Esaki Y, Hirayama R, Hirokawa K (1990) A comparison of patterns of metastasis in gastric cancer by histologic type and age. Cancer 65:2086–2090
18. Finzi G, Cornaggia M, Capella C, Fiocca R, Bosi F, Solcia E, Samloff IM (1993) Cathepsin E in follicle associated epithelium of intestine and tonsils: localization to M cells and possible role in antigen processing. Histochemistry 99:201–211
19. Fiocca R, Villani L, Tenti P, Cornaggia M, Finzi G, Riva C, Capella C, Bara J, Samloff im, Solcia E (1990) The foveolar cell component of gastric cancer. Hum Pathol 21:260–270
20. Gabbert HE, Meier S, Gerharz CD, Hommel G (1991) Incidence and prognostic significance of vascular invasion in 529 gastric-cancer patients. Int J Cancer 49:203–207
21. Gabbert HE, Meier S, Gerharz CD, Hommel G (1992) Tumorcell dissociation at the invasion front: a new prognostic parameter in gastric cancer patients. Int J Cancer 50:202–207
22. Gabbert HE, Muller W, Schneiders A, Meier S, Moll R, Birchmeier W, Hommel G (1996) Prognostic value of E-cadherin expression in 413 gastric carcinomas. Int J Cancer 69: 184–189
23. Harrison JC, Dean PJ, Vander Z, Waag R, El-Zeky F, Wruble LD (1991) Adenocarcinoma of the stomach with invasion limited to the muscolaris propria. Hum Pathol 22:111–117
24. Ho JJL, Siddiki B, Kim YS (1995) Association of Sialyl-Lewis^a and Sialyl-Lewis^x with MUC-1 apomucin in a pancreatic cancer cell line. Cancer Res 55:3659–3663
25. Ichikura T, Tomimatsu S, Okusa Y, Uefuji K, Tamakuma S (1993) Comparison of the prognostic significance between the number of metastatic lymph nodes and nodal stage based on their location with gastric cancer. J Clin Oncol 11:1894–1900

26. Ikeda Y, Mori M, Kido A, Shimono R, Matsushima T, Sugimachi K, Saku M (1991) Immunohistochemical expression of carbohydrate antigen 19–9 in gastric carcinoma. Am J Gastroenterol 86:1163–1166
27. Kawa S, Tokoo M, Oguchi H, Furuta S, Homma T, Hasegawa Y, Ogata H, Sakata K (1994) Epitope analysis of Span-1 and DUPAN-2 using synthetized glycoconjugates sialyllact-N-fucopentaose II and sialyllact-N-tetraose. Pancreas 9:692–697
28. Krulewski T, Cohen LB (1988) Choriocarcinoma of the stomach: pathogenesis and clinical characteristics. Am J Gastroenterol 83:1172–1175
29. Kubo T (1971) Histologic appearance of gastric carcinoma in high and low mortality countries: comparison between Kyushu, Japan and Minnesota, USA. Cancer 28:726–734
30. Lan MS, Korrami A, Kaufman B, Metzgar RS (1987) Molecular characterization of mucin-type antigen associated with human pancreatic cancer – the DUPAN-2 antigen. J Biol Chem 262:12863–12870
31. Laurén P (1965) The two histological main types of gastric carcinoma: diffuse and so-called intestinal-type carcinoma. An attempt at a histoclinical classification. Acta Pathol Microbiol Scand 64:31–49
32. Luinetti O, Fiocca R, Villani L, Alberizzi P, Ranzani GN, Solcia E (1998) Genetic pattern, histological structure, and cellular phenotype in early and advanced gastric cancers: evidence for structure-related genetic subsets and for loss of glandular structure during progression of some tumors. Hum Pathol 29:702–709
33. Machado JC, Soares P, Carneiro F, Rocha A, Beck S, Blin N, Berx G, Sobrinho-Simoes M (1999) E-cadherin gene mutations provide a genetic basis for phenotypic divergence of mixed gastric carcinomas. Lab Invest 79:459–465
34. Martin C, Kay S (1964) The prognosis of gastric carcinoma as related to its morphologic characteristics. Surg Gynecol Obstet 119:319–322
35. Martin IG, Dixon MF, Sue-Ling H, Axon ATR, Johnston D (1994) Goseki histological grading of gastric cancer is an important predictor of outcome. Gut 35:758–763
36. Matsui K, Kitagawa M, Miwa A, Kuroda Y, Tsuji M (1991) Small cell carcinoma of the stomach: a clinicopathological study of 17 cases. Am J Gastroenterol 86:1167–1175
37. Min KW, Holmquist S, Peiper SC, O'Learry TJ (1991) Poorly differentiated adenocarcinoma with lymphoid stroma (lymphoepithelioma-like carcinomas) of the stomach. Am J Clin Pathol 96:219–227
38. Ming SC (1977) Gastric carcinoma – a pathological classification. Cancer 39:2475–2485
39. Mori M, Iwashita A, Enjoji M (1986) Adenosquamous carcinoma of the stomach – a clinicopathologic analysis of 28 cases. Cancer 57:333–339
40. Nagai E, Ueyama T, Yao T, Tsuneyoshi M (1993) Hepatoid adenocarcinoma of the stomach. Cancer 72:1827–1835
41. Nakamori S, Furukawa H, Hiratsuka M, Iwanaga T, Imaoka S, Ishikawa O, Kabuto T, Sasaki Y, Kameyama M, Ishiguro S, Irimura T (1997) Expression of carbohydrate antigen Sialyl Le^a: a new functional prognostic factor in gastric cancer. J Clin Oncol 15:816–825
42. Nakamura K, Ueyama T, Yao T, Xin Xuan Z, Kenji A, Adachi Y, yakeishi Y, Matsukuma A, Enjoji M (1992) Pathology and prognosis of gastric carcinoma. Findings in 10,000 patients who underwent primary gastrectomy. Cancer 70:1030–1037
43. Nguyen M, Eilber F, Defrees S (1996) Novel synthetic analogs of sialyl $Lewis^x$ can inhibit angiogenesis in vitro and in vivo. Biochem Biophys Res Commun 228:716–723
44. Oliveira C, Seruca R, Seixas M, Sobrinho-Simoes M (1998) The clinicopathological features of gastric carcinomas with microsatellite instability may be mediated by mutations of different "Target Genes" – a study of the TGFβ RII, IGFII R, and BAX genes. Am J Pathol 153:1211–1219
45. Ooi A, Nakanishi I, Sakamoto N, Tsukada Y, Takahashi Y, Minamoto T, Mai M (1990) Alpha-fetoprotein (AFP)-producing gastric carcinoma. Is it hepatoid differentiation? Cancer 65:1741–1747
46. Pacchioni D, Negro F, Valente G, Bussolati G (1994) Epstein-Barr virus detection by in situ hybridization in fine-needle aspiration biopsies. Diagn Mol Pathol 3:100–104
47. Ranzani GN, Luinetti O, Padovan LS, Calistri D, Renault B, Burrel M, Amadori D, Fiocca R, Solcia E (1995) p53 gene mutations and protein nuclear accumulation are early events in intestinal type gastric cancer but late events in diffuse type. Cancer Epidemiol Biomarkers Prev 4:223–231
48. Ribeiro MM, Sarmento A, Sobrinho-Simoes M, Bastos J (1981) Prognostic significance of Lauren and Ming classifications and other pathologic parameters in gastric carcinoma. Cancer 47:780–784
49. Ribeiro MM, Seixas M, Sobrinho-Simoes M (1988) Prognosis in gastric carcinoma. The preeminence of staging and futility of histological classification. Dig Dis Pathol 1:51–68
50. Rindi G, Azzoni C, La Rosa S, Klersy K, Paolotti D, RAPPEL S, Stolte M, Capella C, Bordi C, Solcia E (1999) ECL cell tumor and poorly differentiated endocrine carcinoma of the stomach: prognostic evaluation by pathological analysis. Gastroenterology 116:532–542
51. Sessa F, Bonato M, Frigerio B, Capella C, Solcia E, Prat M, Bara J, Samloff IM (1990) Ductal cancers of the pancreas frequently express markers of gastrointestinal epithelial cells. Gastroenterology 98:1655–1665
52. Sobin LH, Wittekind C (1997) TNM classification of malignant tumors, 5th edn. Wiley-Liss, New York, pp 59–62
53. Solcia E, Fiocca R, Luinetti O, Villani L, Padovan L, Calistri D, Ranzani GN, Chiaravalli A, Capella C (1996) Intestinal and diffuse gastric cancers arise in a different background of *Helicobacter pylori* gastritis through different gene involvement. Am J Surg Pathol 20[Suppl 1]:S8–S22
54. Steiner PD, Maimon SN, Palmer WL, Kirsner JB (1948) Gastric cancer – morphological factors in five-year survival after gastrectomy. Am J Pathol 24:947–961
55. Stemmermann GN, Brown C (1974) A survival study of intestinal and diffuse types of gastric carcinoma. Cancer 33:1190–1195
56. Tabuchi Y, Deguchi H, Imanishi K, Saitoh Y (1990) Immunohistochemical studies on the main entrance-route of CA19–9 into peripheral venous blood of gastric cancer patients. Cancer 66:1529–1533
57. Tanigawa N, Amaya H, Matsumura M, Shimomatsuya T, Horiuchi T, Moraoka R, Iki M (1996) Extent of tumor vascularization correlates with prognosis and hematogenous metastasis in gastric carcinoma. Cancer Res 56:2671–2676
58. Uchino S, Noguchi M, Ochiai A, Saito T, Kobayashi M, Hirohashi S (1993) p53 mutation in gastric cancer: a genetic model for carcinogenesis is common to gastric and colorectal cancer. Int J Cancer 54:759–764
59. Varki A (1994) Selectin ligands. Proc Natl Acad Sci USA 91:7390–7397
60. Watanabe H, Enjoji M, Imai T (1976) Gastric carcinoma with lymphoid stroma. Its morphologic characteristics and prognostic correlations. Cancer 38:232–243
61. Watanabe H, Jass JR, Sobin LH (1990) Histological typing of oesophageal and gastric tumors. Springer, Berlin Heidelberg New York, pp 20–26
62. Wu CW, Hsieh MC, Lo SS, Tsay SH, Lui WY, P'eng FK (1996) Relation of number of positive lymph nodes to the prognosis of patients with primary gastric adenocarcinoma. Gut 38:527–527
63. Yamamoto H, Perez-Piteira J, Yoshida T, Terada M, Itoh F, Imai K, Perucho M (1999) Gastric cancers of the microsatellite mutator phenotype display characteristic genetic and clinical features. Gastroenterology 116:1348–1357
64. Zhou XP, Hoang JM, Li YJ, Seruca R, Carneiro F, Sobrinho-Simoes M, Lothe RA, Gleeson CM, Russel SE, Muzeau F, Flejou JF, Hoang-Xuan K, Liderau R, Thomas G, Hamelin R (1998) Determination of the replication error phenotype in human tumors without the requirement for matching normal DNA by analysis of mononucleotide repeat microsatellites. Genes Chromosomes Cancer 21:101–107

Virchows Arch (2001) 439:170–175
DOI 10.1007/s004280100453

ORIGINAL ARTICLE

K. Pollandt · C. Engels · E. Kaiser · M. Werner
G. Delling

Gsα gene mutations in monostotic fibrous dysplasia of bone and fibrous dysplasia-like low-grade central osteosarcoma

Received: 27 December 2000 / Accepted: 20 March 2001 / Published online: 31 May 2001
© Springer-Verlag 2001

Abstract A series of nine cases with monostotic fibrous dysplasia (FD) and five cases of fibrous dysplasia-like low-grade central osteosarcoma (fd-like lgcOSA) were applied in a mutational analysis. Restriction digestion analysis, single-stranded conformational polymorphism (SSCP) analysis, and repeated sequencing demonstrated a R201H mutation in six cases and a R201C mutation in three cases of patients with monostotic FD. These results demonstrate that the presence of Gsα gene mutations is a constant finding in monostotic FD. To our knowledge, this is the first report in the literature investigating Gsα gene mutations in lgcOSA, which is one of the most important differential diagnoses of FD because of its low-grade malignant behavior. In four of five cases of fd-like lgcOSA, no mutation has been detected. In one case of this tumor, a R201C mutation could be demonstrated. Because our results demonstrate a low prevalence of Gsα gene mutations in this tumor in contrast to monostotic FD, mutational analysis may be an additional helpful parameter in individual cases for the differential diagnosis of FD and fd-like lgcOSA.

Keywords Fibrous dysplasia · Mutational analysis · Gsα · Low-grade central osteosarcoma

Introduction

Fibrous dysplasia (FD) of bone is not an inherited congenital skeletal disorder. FD comprises nearly 1% of primary bone tumors [12]. Most commonly, it appears in a monostotic form with an isolated bone lesion, but also several bones can be affected in the polyostotic form [9]. The triad of polyostotic fibrous dysplasia, café au lait spots and precocious puberty has been termed McCune-Albright syndrome (MAS) [1, 11]. It has been suggested that the anatomical distribution of the cutaneous lesions reflects an underlying mosaic state, resulting from a postzygotic somatic mutation [7].

The discovery of activating point mutations of the Gsα gene, resulting in a substitution of arginine at position 201 by either cysteine or histidine in tissues of patients with MAS [21] has clarified the pathogenesis of the disease. These mutations lead to an increased activation of the adenylyl cyclase [8] and constitutively elevated intracellular cyclic adenosine monophosphate (cAMP) [19]. It has been postulated that the high concentrations of cAMP lead to increased proliferation and inappropriate differentiation of the mutated cells, resulting in the formation of a disorganized immature fibrotic matrix [10].

In subsequent studies, these mutations have been also identified in lesions of patients with non-MAS-related FD of bone [2, 4, 15, 17]. Since the seminal description of Gsα mutations in MAS by Weinstein et al. in 1991, mutational data of this relatively rare disease have been published quite frequently [3, 5, 10, 13, 14, 15, 16, 18, 24]. Only individual reports of Gsα gene mutations in monostotic and polyostotic FD are present in the literature [2, 4, 15, 17]. As the monostotic form is estimated to be at least six times more common than the polyostotic form [12], exact knowledge about the prevalence of Gsα mutations, especially of monostotic FD, is desirable. Therefore, one purpose of this study was to determine activating Gsα gene mutations in nine patients with monostotic FD from the Hamburg Bone Tumor Registry.

One of the most important differential diagnoses of FD is fibrous-dysplasia-like low-grade central osteosarcoma (fd-like lgcOSA), which shares substantial histological and radiological attributes with FD. Initially, correct diagnosis of this tumor entity is extremely difficult, also for the specialists [12]. Sometimes, only the clinical course can reveal the true nature of the lesion [22]. Recognition of fd-like lgcOSA is important, be-

K. Pollandt · C. Engels · E. Kaiser · M. Werner · G. Delling (✉)
Department of Bone Pathology/Center of Biomechanics,
University-Hospital Hamburg-Eppendorf,
Martinistr. 52, 20246 Hamburg, Germany
e-mail: delling@uke.uni-hamburg.de
Tel.: +49-40-428032171, Fax: +49-40-428032164

cause incorrect diagnosis will lead to inadequate therapy; initial surgery will be followed by local recurrence with consecutive increase of the risk of transformation in a tumor of higher grade malignancy with the potential of lung metastasis [23]. Histologically, fd-like lgcOSA consists of an immature fibrous stroma with only subtle anaplasia [12, 20] and, like FD, it also produces haphazardly distributed trabeculae consisting of woven bone [6]. Because the similar histological appearance of FD has been directly linked to the intracellular excess of cAMP caused by Gsα gene mutations [10], it is of interest whether these mutations are present in fd-like lgcOSA and whether the development of this tumor is based on the same pathogenetic pathway. To our knowledge, there are no mutational data in the literature concerning Gsα mutations in this tumor. In this study, we also analyzed Gsα mutations in five cases of fd-like lgcOSA.

Materials and methods

Patients

We examined the specimens of nine patients with monostotic FD of bone and five patients with the diagnosis of fd-like lgcOSA. A synopsis of the clinical data is given in Table 1. For all cases, X-rays and clinical and histological data were available for review. In five cases, the samples were obtained in the orthopedic department of our hospital. The specimens of the remaining cases were obtained from consultation files of the Hamburg Bone Tumor Registry.

Samples

In all cases, actual or archival paraffin-embedded specimens suitable for mutational analysis were selected after review of the histological slides. In patients 10 and 14, we additionally examined frozen tissue stored at –80°C under liquid nitrogen. In patient 10, we examined material from the second local recurrence and from a lung metastasis which occurred 7 years after primary diagnosis. In patient 11, material at initial surgery and at revisional surgery after a relapse 5 years later was available. In patient 14, only material from the relapse 3 years after initial surgery was investigated.

We excluded samples with extralesional tissue (i.e., bone marrow) to avoid decreasing the relative amount of possibly mutated cells. A negative control of a patient with no evidence of FD or fd-like lgcOSA was included in the analyses.

DNA extraction

We obtained three to five 11-µm-thick sections of the paraffin blocks, depending on the amount of embedded tissue and placed them in a 1.5-ml Eppendorf tube. The sample was incubated with 1000 µl xylene at 37°C and then centrifuged at 14000 rpm for 5 min. The supernatant was removed, and the process was repeated. The frozen material was washed twice with 1 mM ethylene diamine tetraacetic acid (EDTA) and centrifuged, and the supernatant was then removed.

The sample was washed with 500 µl absolute ethanol and incubated for 5 min on ice before centrifuging at 14000 rpm for 5 min. Again, the supernatant was removed and we repeated the process. The pellet was then allowed to air dry. After addition of proteinase K and extraction buffer, we incubated the sample at 37°C in a thermomixer overnight. Then, the sample was centrifuged at room temperature for 5 min at 14000 rpm, followed by incubation in a thermomixer at 95°C for 12 min to block the activity of the proteinase K. We then centrifuged the sample at 4°C for 10 min at 14000 rpm, and the supernatant was used as the template for polymerase chain reaction (PCR) analysis. The amount of obtained DNA was determined photometrically. The resulting probe was stored at 4°C.

Amplification of genomic DNA

We performed a PCR amplification using primers flanking the mutation site. We used 2.5 U of Ampli *Taq* Gold polymerase, Perkin Elmer (Foster City, Calif.) reagents and 1 µg each of forward primer (5′-TGACTATGTGCCGAGCGA-3′) and reverse primer (5′-CCACGTCAAACATGCTGGTG-3′) and 200–400 ng DNA in a 100-µl reaction, as described elsewhere [3]. For PCR analysis, the samples were hot started in the PE Applied Biosystems Gene AMP PCR system 9700 at 94°C for 15 min and cycled 35 times (94°C for 60 s, 55°C for 30 s, and 72°C for 60 s). The PCR was terminated at 72°C for 7 min [4]. Negative controls were included

Table 1 Synopsis of clinical data and results of mutational analysis. *Mon FD* monostotic fibrous dysplasia, *Fd-like lgcOSA* fibrous dysplasia-like low-grade central osteosarcoma, *Pt* paraffin-embedded tissue, *Fs* frozen specimen, *R201H* Arg to His, *R201C* Arg to Cys

Patient	Age (years)	Gender	Disease	Site of lesion	Sample	Mutation
1	50	Male	Mon FD	Tibia	Pt	R201H
2	55	Female	Mon FD	Os pubis	Pt	R201C
3	41	Male	Mon FD	Tibia	Pt	R201H
4	32	Male	Mon FD	Femur	Pt	R201H
5	63	Female	Mon FD	Femur	Pt	R201C
6	25	Male	Mon FD	Femur	Pt	R201H
7	22	Female	Mon FD	Femur	Pt	R201H
8	59	Male	Mon FD	Os ileum	Pt	R201C
9	51	Female	Mon FD	Tibia	Pt	R201H
10	17	Female	Fd-like lgcOSA	Humerus	Pt: first relapse after 1 year Pt; Fs: lung metastasis after 7 years	None None
11	18	Male	Fd-like lgcOSA	Lumbar spine	Pt: primary lesion Pt. Relapse after 5 years	None None
12	46	Female	Fd-like lgcOSA	Femur	Pt	R201C
13	44	Male	Fd-like lgcOSA	Cervical spine	Pt	None
14	26	Female	Fd-like lgcOSA	Fibula	Pt; Fs: relapse after 3 years	None

in every PCR analysis. The products were purified using the Qiagen (Hilden, Germany) QIAquick PCR purification kit according to the manufacturer's instructions.

The appropriate base pair length of the amplification product was analyzed using electrophoresis through 2% agarose gels and visualized with ultraviolet (UV) light after staining with ethidium bromide.

We performed at least two PCR analyses of every sample to exclude artifacts. We applied three independent methods to investigate the presence of Gsα gene mutations; a restriction digestion analysis, single-stranded conformational polymorphism (SSCP) analysis, and DNA sequence analysis were performed.

Restriction digestion analysis

The amplification products were digested with *Nla*III (New England Biolabs, Beverly Mass.) and analyzed using electrophoresis through 4% metaphore agarose gels. The restriction fragments were stained with ethidium bromide and visualized under UV light. The Arg→His missense point mutation at position 201 introduces a new *Nla*III restriction site into the DNA. Therefore, this method is only capable of ascertaining cases with this mutation.

Single-strand conformational polymorphism

SSCP analysis was performed to analyze the PCR products. The PCR products (5 µl) were mixed with 2 µl loading buffer (99.8% formamide, 0.1% 0.5 M EDTA, 0.05% xylene cyanol and bromophenol blue) and 5 µl of bidest H_2O. The samples were heated for 5 min at 95°C, quenched on ice, and electrophoresed on a 15% acrylamide gel at 30°C under nondenaturing conditions at 16 W for 18 h. DNA was detected by means of silver staining using a standard method. The resulting bands were extracted and subjected to reamplification to evaluate their sequence.

DNA sequence analysis

To investigate the described Arg→Cys [21], Arg→Gly [13], and Arg→Ser [5] substitutions at position 201, we sequenced the PCR products in all cases. The amplicons were analyzed using the Qiagen DyeEx Spin Kit according to the manufacturer's instructions. Sequencing was performed by means of automatic sequencing with the ABI sequencer 377 based on standard technique.

Results

Review of X-ray and clinical data

Nine of our patients clearly had monostotic FD with one single lesion in a single bone. The lesion was in the femur in four cases (Fig. 1a), in the tibia in three cases, and in the pelvis in two cases. One patient (no. 5) had three separate lesions in the femur and was considered to be monostotic with multifocal involvement. In all cases, there was no evidence of endocrinopathy or skin hyperpigmentation. All FD lesions were located in the axial–appendicular skeleton.

From the five patients with fd-like lgcOSA, two were located in the spine, one in the humerus (Fig. 1d), one in the fibula, and one in the femur. Patient 10 (fd-like lgcOSA) had a history of four local recurrences and three consecutive lung metastases [23]. Patient 11 and 14 have had local recurrence only once.

Histology

All FD cases showed the typical pattern of FD with a fibrous stroma and thin curved trabeculae composed of woven bone. Collagen fibers emerging perpendicular from the trabecular surface were regularly observed, which is a typical finding in FD [14] (Fig. 1b, c). The fibrotic tissue appeared to be homogen; regular mitoses were rarely detected. In the cases with fd-like lgcOSA, there was a subtle anaplasia of the fibroblastic stroma (Fig. 1e, f). The lesions showed irregular, disorganized seams of osteoid of variable amount, which were mostly not surrounded by osteoblasts. In one case (patient 12), there was an infiltrating growth pattern in the periphery of the tumor.

Mutation analysis of FD of bone

We were able to extract sufficient quantities of genomic DNA to perform mutational analyses using restriction digestion analysis, SSCP, and sequencing in all cases. We performed a PCR, which resulted in the amplification of an ~320-bp product. By restriction digestion analysis, we identified R201H mutations in six patients (patients 1, 3, 4, 6, 7, and 9). Sequencing revealed R201C mutations in three patients (patients 2, 5, and 8). The results of the restriction digestion analysis could be confirmed in all cases (Fig. 2).

SSCP also confirmed these results. Examination of the control sample showed four bands. Sequencing, following extraction and reamplification of these bands, confirmed the wild-type sequence. The samples with either mutation showed a characteristic migration pattern with the occurrence of two additional bands compared with the negative control. These bands were extracted and reamplified, resulting in the amplification of only the mutated allele as demonstrated by sequencing (Fig. 3). Varying proportions of the wild-type and mutated alleles of the Gsα gene were detected in all samples examined. These results provide further evidence of the presence of an activating mutation of the Gsα gene in monostotic FD.

Mutation analysis of fd-like lgcOSA

In eight different samples of four cases, neither restriction digestion analysis, SSCP, nor repeated sequencing could detect a mutation at position 201. However, in patient 12, we were able to demonstrate an Arg→Cys missense point mutation (Fig. 4). This patient did not have a history of a proceeding FD at the same or a different location.

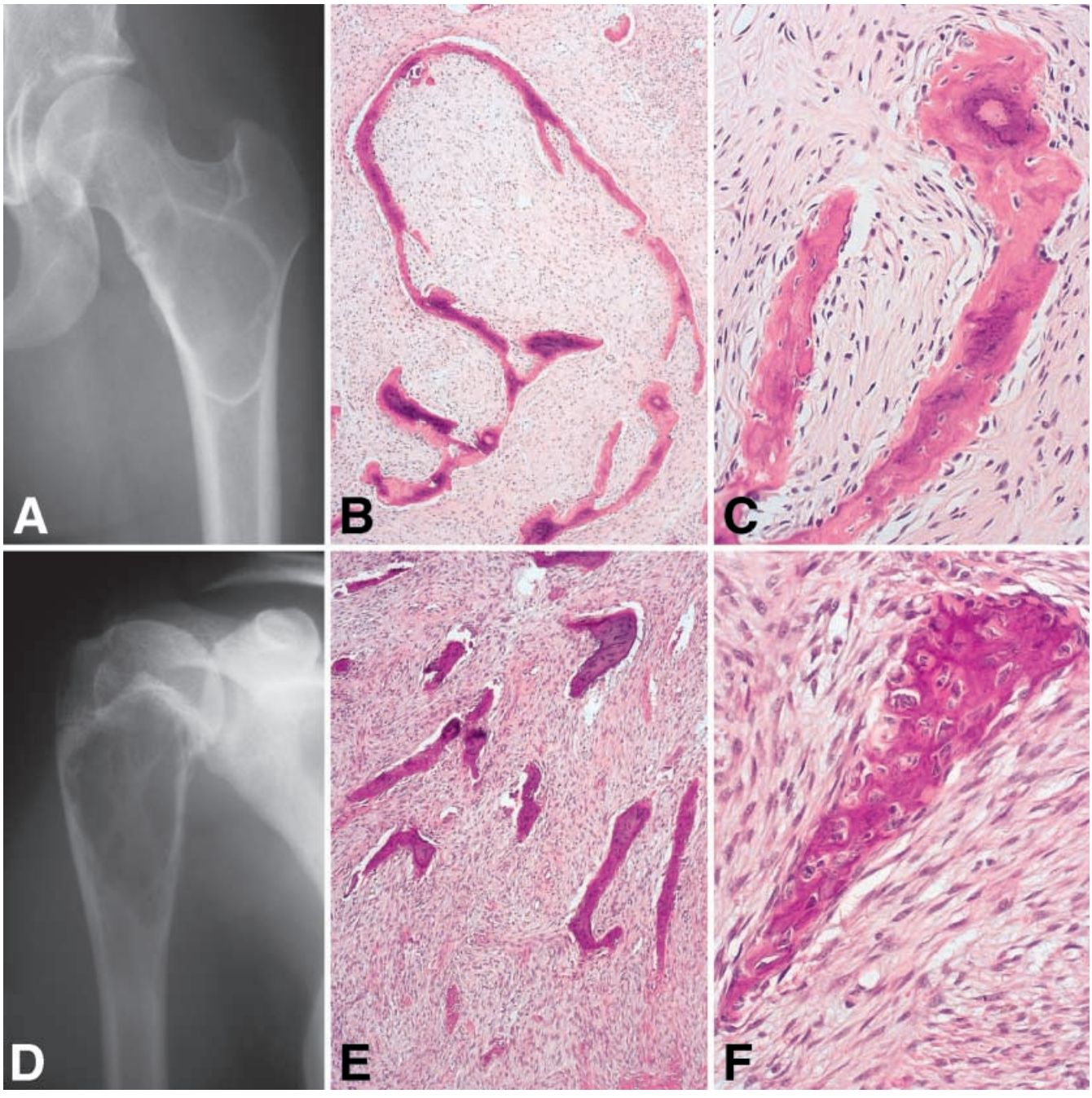


Fig. 1 **A**, **B**, **C** Fibrous dysplasia, patient 7. Typical X-ray showing a well-circumscribed lesion with ground glass appearance bordered by a sclerotic rim. Histologically, there are irregular trabeculae of woven bone separated by fibroblastic tissue with monotonous nuclei (hematoxylin and eosin staining; **B** ×50, **C** ×190). **D**, **E**, **F** Fibrous dysplasia-like low-grade central osteosarcoma: patient 10. X-ray reveals a purely lytic lesion without sclerotic margins and thinning of the corticalis. Light microscopy shows fibroblastic cells with minimally hyperchromatic and irregular nuclei between fibrous trabeculae (hematoxylin and eosin staining; **E** ×50, **F** ×190)

Discussion

Previous studies have shown that bone lesions in MAS and in polyostotic and monostotic FD present an activating missense mutation in the gene coding for the α subunit of the Gs protein. Monostotic FD is estimated to be at least six times more common than the polyostotic form, and there are only a few reports of Gsα mutation of monostotic FD. Therefore, we have investigated nine cases of the Hamburg Bone Tumor Registry with monostotic FD to evaluate the prevalence of the Gsα mutation, especially in this type. For this mutational study, we mainly chose paraffin embedded samples which included almost only tumorous tissue. We excluded samples with

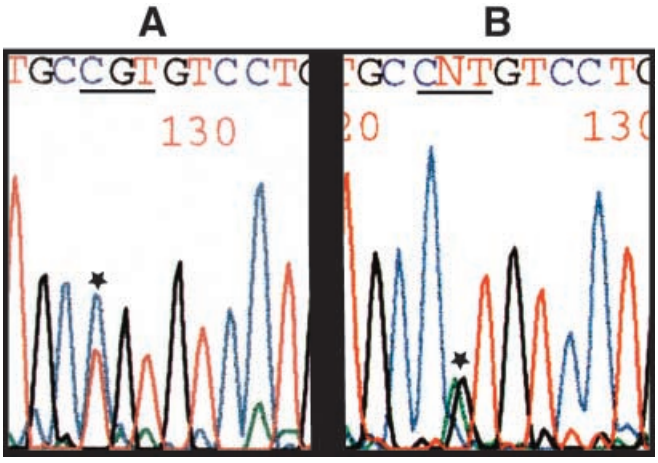


Fig. 2 Representative examples of sequences of polymerase chain reaction-amplified DNA extracted from paraffin embedded tumor tissue. Heterozygous C to T mutation (**A**) and G to A mutation (**B**) marked by *

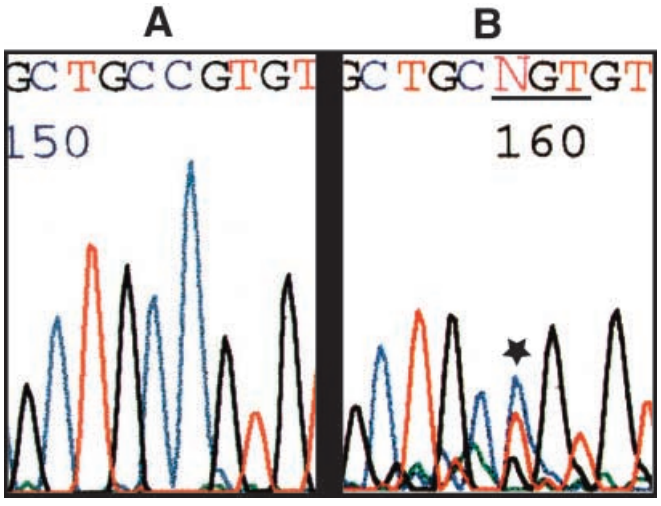


Fig. 4 Sequences of polymerase chain reaction-amplified DNA from two patients with fibrous dysplasia-like low-grade central osteosarcoma. Normal sequence in **A** (patient 14) and C to T mutation marked by * in **B** (patient 12)

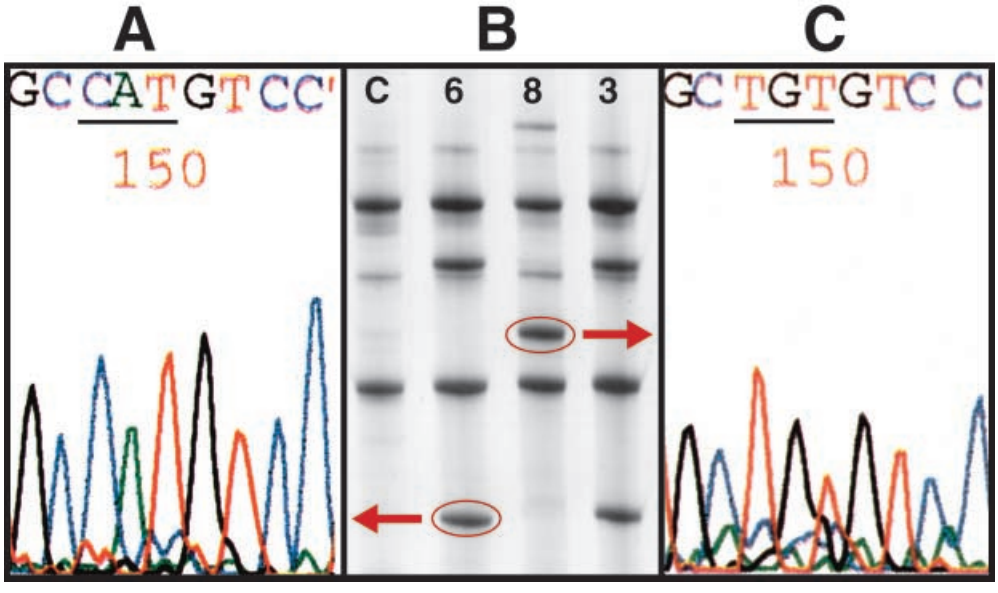


Fig. 3A–C Sequences of polymerase chain reaction-amplified DNA (A→ underlined G to A mutation encoding His201, C→ underlined C to T mutation encoding Cys201) extracted from the red marked aberrant bands in patients 6 and 8 of the single-strand conformation polymorphism analysis (*B→ C* control sample; *6*, *8*, *3* patient number)

extralesional tissue (i.e., bone marrow) to avoid decreasing the relative amount of possibly mutated cells. We have identified the most commonly described mutations R201H, in six cases, and R201C, in three cases, of monostotic FD. The analyses demonstrated a mixture of mutated and normal Gsα DNA in various proportions due to the heterozygous mutation, which is concordant with reports in the literature [17].

Mutational data of the common differential diagnoses of FD, i.e., desmoplastic fibroma or osteofibrous dysplasia, are rare. There is only a single study in the literature reporting the lack of mutations of the Gsα gene at position 201 in four cases of desmoplastic fibroma and one case of osteofibrous dysplasia [2]. Another very important differential diagnosis of FD is the fd-like subtype of lgcOSA, which shares substantial histological and radiological attributes with FD. Because of the apparently bland histology, fd-like lgcOSA may be misinterpreted as a benign lesion despite its primary low malignant behavior and late metastatic potential, including the capability of transforming into a highly malignant sarcoma [23]. Sometimes, only the clinical course can reveal the true nature of the lesion. As the histological appearance of FD has been directly linked to the intracellular excess of cAMP caused by Gsα gene mutations [10], it is worthwhile to find out whether this gene is mutated in patients with fd-like lgcOSA. To our knowledge, this is the first report in the literature investigating Gsα mutations in fd-like lgcOSA. We could demonstrate a lack of mutations in eight samples of four cases. In one patient, we identified a R201C mutation. This patient did not have a history of a preceding FD at the same or a differ-

ent location. As our results demonstrate a low prevalence of Gsα gene mutations in this tumor in contrast to monostotic FD, mutational analysis may be an additional helpful parameter in individual cases for the differential diagnosis of FD and fd-like lgcOSA. In addition, we demonstrated that from small amounts of paraffin-embedded tissue, a sufficient quantity of genomic DNA can be extracted for mutational analysis. This is important, because many cases of the Hamburg Bone Tumor Registry are from consultation files supplied as paraffin-embedded tissue and, therefore, fresh material for mutational analysis is rarely available.

This study was restricted to the analysis of DNA extracted from paraffin-embedded and frozen tissue. We are not able to give evidence concerning function of the altered G protein. Detailed investigations of corresponding mRNA and of protein function are needed, especially in the light of developing a new treatment of FD based on regulation of adenylylcyclase and intracellular cAMP or manipulation of G proteins.

Acknowledgements This work was supported by the Deutsche Forschungsgemeinschaft, Graduiertenkolleg 476 and the Deutsche Krebshilfe. The SSCP analyses were performed in the Institute of Hormone and Fertility Research (Head: Prof. Dr. W. Hoeppner) in Hamburg under the supervision of Dr. D. Ahrlt and K. Siebke, which is gratefully acknowledged. The authors would like to thank C. Mueldner for her assistance.

References

1. Albright F, Butler AM, Hampton AO, Smith P (1937) Syndrome characterized by osteitis fibrosa disseminata, areas of pigmentation and endocrine dysfunction, with precocious puberty in females. N Engl J Med 216:727–746
2. Alman BA, Greel DA, Wolfe HJ (1996) Activating mutations of Gs protein in monostotic fibrous lesions of bone. J Orthop Res 14:311–315
3. Bianco P, Kuznetsov SA, Riminucci M, Fisher LW, Spiegel AM, Robey PG (1998) Reproduction of human fibrous dysplasia of bone in immunocompromised mice by transplanted mosaics of normal and Gs alpha-mutated skeletal progenitor cells. J Clin Invest 101:1737–1744
4. Bianco P, Riminucci M, Majolagbe A, Kuznetsov SA, Collins MT, Mankani MH, Corsi A, Bone HG, Wientroub S, Spiegel AM, Fisher LW, Robey PG (2000) Mutations of the GNAS1 gene, stromal cell dysfunction, and osteomalacic changes in non-McCune-Albright fibrous dysplasia of bone. J Bone Miner Res 15:120–128
5. Candeliere GA, Roughley PJ, Glorieux FH (1997) Polymerase chain reaction-based technique for the selective enrichment and analysis of mosaic arg201 mutations in G alpha s from patients with fibrous dysplasia of bone. Bone 21:201–206
6. Fechner RE, Mills S (1993) Atlas of tumor pathology. Armed Forces Institute of Pathology, Washington D.C.
7. Happle R (1986) The McCune-Albright syndrome: a lethal gene surviving by mosaicism. Clin Genet 29:321–324
8. Landis CA, Masters SB, Spada A, Pace AM, Bourne HR, Vallar L (1989) GTPase inhibiting mutations activate the alpha chain of Gs and stimulate adenylyl cyclase in human pituitary tumours. Nature 340:692–696
9. Lichtenstein L, Jaffe HL (1942) Fibrous dysplasia of bone. Arch Pathol 33:777–816
10. Marie PJ, de Pollak C, Chanson P, Lomri A (1997) Increased proliferation of osteoblastic cells expressing the activating Gs alpha mutation in monostotic and polyostotic fibrous dysplasia. Am J Pathol 150:1059–1069
11. McCune DJ (1936) Osteitis fibrosa cystica: the case of a nine year old girl who also exhibits precocious puberty, multiple pigmentation of the skin and hyperthyroidism. Am J Dis Child 52:743–747
12. Mirra JM (1989) Bone tumors. Clinical, radiological and pathological correlations. Lea and Febiger, Philadelphia
13. Riminucci M, Fisher LW, Shenker A, Spiegel AM, Bianco P, Gehron RP (1997) Fibrous dysplasia of bone in the McCune-Albright syndrome: abnormalities in bone formation. Am J Pathol 151:1587–1600
14. Riminucci M, Fisher LW, Majolagbe A, Corsi A, Lala R, De Sanctis C, Robey PG, Bianco P (1999) A novel GNAS1 mutation, R201G, in McCune-albright syndrome. J Bone Miner Res 14:1987–1989
15. Riminucci M, Liu B, Corsi A, Shenker A, Spiegel AM, Robey PG, Bianco P (1999) The histopathology of fibrous dysplasia of bone in patients with activating mutations of the Gs alpha gene: site-specific patterns and recurrent histological hallmarks. J Pathol 187:249–258
16. Schwindinger WF, Francomano CA, Levine MA (1992) Identification of a mutation in the gene encoding the alpha subunit of the stimulatory G protein of adenylyl cyclase in McCune-Albright syndrome. Proc Natl Acad Sci U S A 89:5152–5156
17. Shenker A, Weinstein LS, Sweet DE, Spiegel AM (1994) An activating Gs alpha mutation is present in fibrous dysplasia of bone in the McCune-Albright syndrome. J Clin Endocrinol Metab 79:750–755
18. Shenker A, Chanson P, Weinstein LS, Chi P, Spiegel AM, Lomri A, Marie PJ (1995) Osteoblastic cells derived from isolated lesions of fibrous dysplasia contain activating somatic mutations of the Gs alpha gene. Hum Mol Genet 4:1675–1676
19. Spiegel AM (1997) The molecular basis of disorders caused by defects in G proteins. Horm Res 47:89–96
20. Unni KK, Dahlin DC, McLeod RA, Pritchard DJ (1977) Intraosseous well-differentiated osteosarcoma. Cancer 40:1337–1347
21. Weinstein LS, Shenker A, Gejman PV, Merino MJ, Friedman E, Spiegel AM (1991) Activating mutations of the stimulatory G protein in the McCune-Albright syndrome. N Engl J Med 325:1688–1695
22. Werner M, Delling G (2000) Pathohistologie maligner Knochentumoren. Erfahrungen des Hamburger Knochentumor-Registers an 8879 Fällen. Onkologe 6:709–722
23. Werner M, Rieck J, Delling G (1998) Zytogenetische Veränderungen bei niedrig malignen zentralen Osteosarkomen. Verh Dtsch Ges Pathol 82:189–194
24. Yamamoto T, Ozono K, Kasayama S, Yoh K, Hiroshima K, Takagi M, Matsumoto S, Michigami T, Yamaoka K, Kishimoto T, Okada S (1996) Increased IL-6-production by cells isolated from the fibrous bone dysplasia tissues in patients with McCune-Albright syndrome. J Clin Invest 98:30–35

Virchows Arch (2001) 439:176–184
DOI 10.1007/s004280100466

ORIGINAL ARTICLE

Erik Cabuy · Leo de Ridder

Telomerase activity and expression of telomerase reverse transcriptase correlated with cell proliferation in meningiomas and malignant brain tumors in vivo

Received: 12 March 2001 / Accepted: 20 April 2001 / Published online: 13 June 2001
© Springer-Verlag 2001

Abstract Telomerase activity was examined in intracranial tumors and compared with gene expression of the two core components of telomerase – the reverse transcriptase subunit (hTERT) and the RNA subunit (hTR) – and the proliferative index. We investigated 32 tumors across three to five sampled regions (20 meningiomas, 1 acoustic schwannoma, 1 pituitary adenoma, 8 gliomas, and 2 medulloblastomas). Telomerase activity was demonstrated by the telomeric repeat amplification protocol (TRAP) assay in seven (22%) intracranial tumors (four malignant brain tumors, two atypical meningiomas and one ependymoma) but could not be detected in the 18 (100%) benign meningiomas. hTERT and hTR mRNA were detected using reverse-transcription polymerase chain reaction (RT-PCR). hTERT mRNA was present in 20 (63%) intracranial tumors. Whereas hTERT mRNA transcripts were consistently low or absent in meningiomas, malignant brain tumors exhibited elevated hTERT mRNAs. Multiple regions of glioblastomas showed differences in telomerase activity and in the presence of hTERT mRNA. RT-PCR analysis revealed, for the first time in intracranial tumors, the presence of hTERT mRNA spliced products, corresponding to full-length mRNA as well as spliced mRNAs with critical reverse transcriptase motifs deleted. Only tumors with marked telomerase activity showed all hTERT spliced messages simultaneously. The absence of a positive correlation between telomerase activity and hTERT mRNA could not be attributed to the presence of hTERT spliced variants. We found a significant correlation between telomerase activity scores and Ki-67 proliferation index. A positive association is also seen between Ki-67 staining and the degree of hTERT mRNA expression. This shows that there seems to be a relationship between telomerase activity or the degree of hTERT expression and proliferation rate in intracranial tumors.

E. Cabuy (✉) · L. de Ridder
Department of Anatomy, Embryology and Histology,
Section Histology, University of Ghent, Louis Pasteurlaan 2,
B-9000 Ghent, Belgium
e-mail: erik.cabuy@rug.ac.be
Tel.: +32-9-2649247, Fax: +32-9-2649498

Keywords Meningioma · Glioma · Telomerase · Alternate splicing · Ki-67

Introduction

Telomeres are long repetitive nucleotide sequences at both ends of chromosomes. Their primary role is to protect chromosome ends from recombination, fusion, and DNA degradation [3]. Telomeres shorten progressively with each round of cell division as a result of the inability of DNA polymerases to replicate the 5' end of linear DNA, and erosion of these sequences beyond a critical point is thought to signal cell cycle arrest and entry into cellular senescence [9]. It is hypothesized that cell senescence can be overcome by reactivation of telomerase [3, 14, 20]. Telomerase is a ribonucleoprotein polymerase composed of an integral RNA component (hTR) [14] and several protein components, including the reverse transcriptase subunit hTERT [18, 32]. hTR contains the template for the reverse transcription of telomeres, and hTERT is the reverse transcriptase that catalyses this reaction. hTR and hTERT are indispensable for telomerase activity, and expression of these subunits in vitro leads to the formation of a functional telomerase enzyme [10, 32, 45]. Telomerase activity is thought to be essential in maintaining normal telomere length in proliferating cells. There is good evidence that telomerase is also involved in the healing of chromosome breaks [40] and it is possible that it has other functions as well. hTERT mRNA has been shown to undergo alternate splicing in several tissues and cell lines [18, 43, 44, 46]. The function of the alternate transcripts is unknown, although the positions of the splice sites suggest that the alternate transcripts do not code for functional reverse transcriptase and may play a role in the regulation of telomerase activity [43, 44]. In humans, telomerase has been detected in most cancers [20, 28], suggesting a role for telomerase in providing a proliferative capacity to cells, which is a requirement for progression towards malignancy. It is usually not detected in

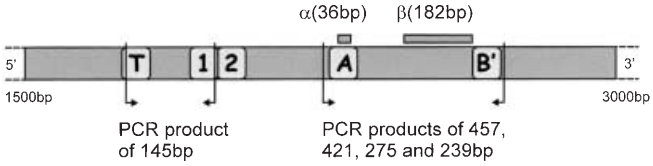


Fig. 1 Schematic detail of hTERT mRNA with telomerase-specific T-motif and 1, 2, A and B' conserved reverse transcriptase motifs *highlighted*. Deletion α, which occurs within the A motif, and deletion β, situated between motifs A and B', of hTERT cause four spliced products. First set of polymerase chain reaction (PCR) primers (hTERT-1784S and hTERT-1928A) amplifies a 145-base region upstream of the reverse transcriptase domain. Second set of PCR primers (hTERT-2164S and hTERT-2620A) amplifies a region within the reverse transcriptase domain, which includes both α and β splice sites

normal somatic cells, except for proliferating stem cells, during embryonic development [42, 43], and in adult germ-line tissues [48].

Meningiomas are estimated to constitute up to 23% of primary intracranial tumors [21]. They are typically benign tumors, but the incidence of growth at inoperable sites and recurrence complicate surgical management. The limited understanding of etiology and growth of these tumors has hindered the development of an adjuvant therapy. The hypotheses that reactivation of telomerase is required to maintain tumor growth [20] or may play a critical role in the progression or maintenance of the malignant phenotype [36] are in conflict with findings in benign meningiomas. Several previous studies performed on single specimens of intracranial tumors have reported that telomerase activity is present in the vast majority of malignant brain tumors while enzyme activity could not be detected in benign meningiomas [6, 11, 12, 17, 37]. However, some studies reported that up to 21% of single specimens of benign meningiomas had telomerase activity [25, 39]. These findings prompted us to investigate whether undetectable telomerase activity in benign meningiomas is also reflected in the absence of hTERT mRNA expression. Second, intratumoral differences in tumor tissues may have resulted in a falsely high proportion of telomerase-negative tumors. We therefore evaluated benign meningiomas for telomerase activity and telomerase gene expression in multiple specimens of a single tumor. Third, because hTERT spliced variants are believed to be a limiting factor for the expression of telomerase activity [43], we examined whether these were limiting components for the expression of telomerase activity in benign meningiomas. We therefore used primers to amplify a sequence located upstream and a sequence within the reverse transcriptase domains A and B', including two potential splice sites (Fig. 1), to determine hTERT mRNA expression. Hence, we amplified both functional and non-functional spliced variants. Finally, we investigated the tumor growth rate because a correlation was found between telomerase activity and proliferation index in other cancers [15, 30].

Materials and methods

Tissue samples and handling

Multiple tumor fragments were collected, when possible from different locations in tumors, during open surgery of 32 patients. Table 1 shows the clinical data and histopathological diagnosis. There were 21 female and 11 male patients, with ages ranging from 1.5 years to 88 years. All cases under study came from total surgical removal over the past year. No chemotherapy or radiotherapy was administered before surgery. Prior therapeutic embolization, which can cause extensive necrosis, was carried out on the tumors of two patients (cases no. 25 and no. 28). The tumors were classified according to World Health Organization (WHO) criteria [21] by neuropathologists at the University Hospital and the St Lucas Hospital (Ghent, Belgium). The tumors comprised 20 meningiomas, 18 of which were benign and two atypical, one acoustic schwannoma, one pituitary adenoma, eight gliomas, and two medulloblastomas. All biopsies were divided into approximately 125-mm^3 pieces, and a total of 121 samples were immediately frozen and stored separately in liquid nitrogen under RNase-free conditions. This procedure was carried out within 0.5 h after surgery, except for six samples (cases no. 3, 14–16, 23, and 29) which were frozen in liquid nitrogen 2–4 h after surgery. Dura mater and arachnoidal tissue could also be obtained from case 2 for in vitro cell culture. The histological identity of multiple formalin-fixed specimens of each tumor was checked by microscopy of serial sections stained with hematoxylin-eosin (H-E) and Masson trichrome.

Telomerase activity using telomeric repeat amplification protocol assay

Frozen samples were homogenized in 200–600 µl ice-cold extraction buffer [10 mM Tris-HCl (pH 7.5), 1 mM $MgCl_2$, 1 mM ethyleneglycol tetraacetic acid (EGTA), 0.1 mM benzamidine, 0.5% CHAPS, 5 mM β-mercaptoethanol, 10% glycerol], depending on the size of tumor sample. After 30 min incubation on ice, lysates were centrifuged at 12,000 *g* for 20 min at 4°C, and 40–200 µl each supernatant was collected. Protein content in each lysate was measured using the Bradford assay (Bio-Rad laboratories) and adjusted to 2 µg/µl. Aliquots of 40 µl protein extracts were frozen in liquid nitrogen and were used only once.

Telomerase enzymatic activity was determined in 49 samples using the telomeric repeat amplification protocol (TRAP) of the TRAPeze Telomerase Detection Kit (Intergen) with minor modifications. Briefly, 0.7 µg protein extract was incubated in 20 µl reaction mixture containing 1× TRAP reaction buffer, 50 µM dNTPs, 0.45 µl TS primer (5'-AATCCGTCGAGCAGAGTT-3'), 0.45 µl primer mix (RP primer 5'-GCGCGG $[CTTACC]_3$ CTA-ACC-3' (manufacturer's communication), K1 primer and TSK1 template for internal control), and 1 U *Taq* DNA polymerase at 30°C for 30 min for telomerase-mediated extension of the TS primers. Reaction mixtures were subjected to 33 cycles using the following conditions: 94°C for 40 s, 59°C for 30 s, and 72°C for 30 s. Ten microlitres of each polymerase chain reaction (PCR) sample was analyzed by electrophoresis on 10% polyacrylamide–urea gels (Novex) and visualized with SYBR-Green I nucleic acid gel stain by means of an ultraviolet (UV) transilluminator. High telomerase activity is defined as more than six incremental TRAP products. All samples were repeated twice to validate our findings. The inclusion of an internal control, a synthetic DNA construct added to all samples and which is amplified with the TS and RP primers to generate a 36-bp product, aided the detection of false negatives which can result from the presence of PCR inhibitors in the extracts. The immortal cell lines Hela (human cervix carcinoma), U251 (human glioblastoma), and Molt-4 (human T lymphoblastic leukaemia) showed telomerase activity and expressed all the alternately spliced products of hTERT mRNA. In all further experiments, Molt-4 was ultimately used as a positive control because of ease of production. As a negative control, cDNA was replaced by lysis buffer.

Table 1 Relationships of intracranial tumor type with KI-67 labeling index (LI), telomerase activity, and telomerase mRNA expression. All samples were frozen immediately except for those marked *, which were frozen 2–4 h after tumor resection

Case no.	Age	Sex	Diagnosis[a]	Recurrence	Ki-67 mean LI	Telomerase activity[b]	hTERT[c] 145 bp	hTERT rlu	hTERT spliced products[c]			
									457 bp	421 bp	275 bp	239 bp
1	72	Female	Meningothelial meningioma		0	–	–/–	0	–/–	–/–	–/–	–/–
2	28	Female	Meningothelial meningioma		1.7	–	–/–	0	–/–	–/–	–/–	–/–
3*	88	Female	Transitional meningioma		3.5	–/–	+/+	66	+/–	–/–	+/+	–/–
4	75	Female	Transitional meningioma		1.4	–	–/–	0	–/–	–/–	–/–	–/–
5	62	Female	Angiomatous meningioma		2	–	+/–	0	+/–	–/–	+/–	–/–
6	64	Female	Meningothelial meningioma		1.6	–	+/–	35	–/–	–/–	+/–	+/–
7	44	Female	Meningothelial meningioma		2.3	–	–/–	0	–/–	–/–	–/–	–/–
8	74	Male	Meningothelial meningioma		1.5	–/–	+/–	34	–/–	–/–	+/–	–/–
9	34	Male	Acoustic schwannoma		2.2	–	–/+	0	–/–	–/–	–/+	–/–
10	37	Female	Pituitary adenoma		1.8	–/–	+/+	53	+/+	–/–	+/–	–/–
11	3	Female	Medulloblastoma		12.1	++/++	+/+	100	+/+	+/+	+/+	+/+
12	33	Female	Astrocytoma	2nd	7.7	-/–	+/–	43	+/–	–/–	+/–	–/–
13	52	Female	Glioblastoma multiforme		13.7	++/+	+/+	92	+/+	+/–	+/+	+/+
14*	1.5	Male	Ependymoma		11.5	+/–	+/+	66	+/–	+/–	+/+	–/–
15*	41	Female	Glioblastoma multiforme*		1.2	–/–	+/+	23	–/–	–/–	–/+	–/–
16*	30	Female	Astrocytoma*		0	–	+/+	50	–/–	–/–	+/+	+/–
17	69	Male	Atypical meningioma		3.7	+/–	+/+	29	–/–	–/–	+/+	+/–
18	77	Male	Meningothelial meningioma		2.6	–/–	–/–	0	–/–	–/–	+/–	–/–
19	70	Female	Meningothelial meningioma		0.8	–	–/–	0	–/–	–/–	–/+	–/+
20	73	Female	Meningothelial meningioma		0.7	–	–/–	0	–/–	–/–	+/–	–/–
21	56	Female	Meningothelial meningioma		0.6	–/–	–/–	0	–/–	–/–	–/–	–/–
22	69	Female	Meningothelial meningioma		0.8	–	–/–	0	–/–	–/–	–/–	–/–
23*	9	Female	Medulloblastoma*	2nd	0	–/–	–/–	0	–/–	–/–	–/–	–/–
24	58	Male	Glioblastoma multiforme		11	++/–	+/–	100	+/–	+/–	+/–	+/–
25	70	Male	Transitional meningioma		0.2	–/–	–/+	0	–/–	–/–	+/–	–/–
26	64	Female	Fibrous meningioma		0	–	+/+	26	–/–	–/–	–/–	–/–
27	80	Female	Atypical mengioma	3rd	3.1	+/–	+/+	58	+/+	–/–	+/+	–/–
28	46	Female	Transitional meningioma		1.9	–	+/+	19	–/–	–/–	–/–	–/–
29*	64	Male	Glioblastoma multiforme		6	–	+/+	81	+/+	–/–	+/+	–/+
30	46	Male	Psammomatous meningioma		0.6	–/–	–/–	0	–/–	–/–	–/–	–/–
31	40	Male	Transitional meningioma		0.2	–	–/–	0	–/–	–/–	–/+	–/–
32	75	Male	Glioblastoma multiforme		33.3	++/+	+/+	96	+/+	+/–	+/+	+/+
						7/32 (22%)	20/32 (63%)					

[a] Edematous brain tissue present in samples from *

[b] – No telomerase activity, + low telomerase activity, ++ high telomerase activity detected in one or two samples

[c] + Transcript present, – transcript absent in two different samples

Reverse transcription-PCR analysis of hTERT and hTR

Total RNA was obtained from 72 previously frozen tissue samples using Tri-reagent (Sigma-Aldrich), in accordance with the manufacturer's protocol. RNA integrity was initially checked on a 1% agarose gel by judging the presence of the 18S and 28S ribosomal RNA bands. cDNA was synthesized from 1 µg total RNA in a volume of 20 µl at 37°C for 1 h with Moloney murine leukemia virus (MMLV)-reverse transcriptase using random hexamers, followed by inactivation of the MMLV enzyme by incubation at 95°C for 5 min. The cDNA samples were amplified in a 20-µl reaction mixture containing 50 µM dNTPs, 1 U *Taq* polymerase, and 0.2 µM primers. A nested PCR approach used primers according to the cDNA sequences as reported by Kilian et al. [18] and Ulaner and colleagues [43, 44] (Fig. 1). Primers hTERT-1784S (5'-CGGAAGAGTGTCTGGAGCAA-3') and hTERT-1928A (5'-GGATGAAGCGGAGTCTGGA-3') were used to amplify a region including the specific T-motif of hTERT to generate a 145-bp fragment. The reaction mixtures were heated at 94°C for 30 s, followed by 33 cycles of 94°C for 20 s, 68°C for 40 s and 72°C for 30 s. Primers 774 (5'-GGGAATTCAAAACTGGAACGGTGAAGG-3') and 775 (5'-GGAAGCTTATCAAAGTCCTCGGCCACA-3') were added at 72°C of cycle 13 for β-actin internal control. Primers hTERT-2164S (5'-GCCTGAGCTGTACTTTGTCAA-3') and hTERT-2620A (5'-CGCAAACAGCTTGTTCTCCATGTC-3') were used to amplify a sequence between the two reverse transcriptase motifs A and B' of hTERT to generate a 457-bp fragment. The reaction mixtures were heated at 94°C for 30 s, followed by 35 cycles of 94°C for 25 s, 68°C for 50 s and 72°C for 50 s. Primers 774 and 775 were added at 72°C of cycle 15 for β-actin internal control. Primers hTR-46S (5'-CTAACCCTAACTGAGAAGGGCGTAG-3') and hTR-148A (5'-GAAGGCGGCAGGCCGAGGCTTTTCC-3') were used to amplify a hTR region to generate a 103-bp fragment. The reaction mixtures were heated at 94°C for 30 s, followed by 28 cycles of 94°C for 20 s, 68°C for 40 s and 72°C for 30 s. Primers 5899 (5'-CAGGTCATCACCATTGGCAATGAGC-3') and 5900 (5'-CGGATGTCCACGTCACACTTCATGA-3') were added at 72°C of cycle 9 for β-actin internal control. Amplified products were electrophoresed on 4–20% polyacrylamide gels (Novex) and visualized with SYBR-Green I nucleic acid gel stain by use of an UV transilluminator. Double-checks were performed on most samples. Amplification of β-actin cDNA was used to conform cDNA synthesis and integrity in each sample and the leukemia cell line Molt-4 was used as a positive control. Some confluent, slow-growing cell cultures of meningiomas (cases 5, 7, 9, 17, and 20) were also tested for telomerase expression.

Proliferation activity

Eighty-five paraffin-embedded tissues of 32 intracranial tumors were used for the cell proliferation assessment. Sections of 3-µm

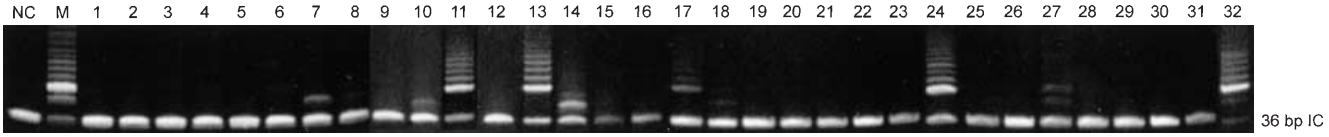


Fig. 2 Telomerase activity in intracranial tumors, as measured using telomeric repeat amplification protocol assay. The presence of a 6-base incremental ladder is evidence for telomerase activity in a given sample. *NC* cDNA was replaced by lysis buffer as negative control, *M* Molt-4-positive control, *IC* 36-bp internal control

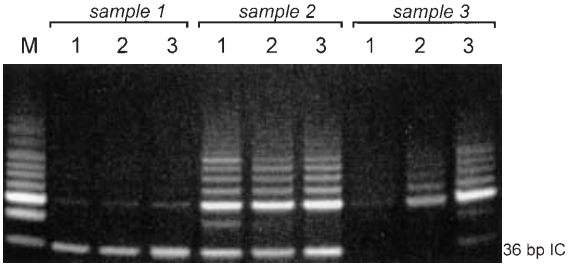


Fig. 3 Telomerase activity in three different samples of a glioblastoma (case 24). Polymerase chain reaction (PCR) cycles were 27, 30, and 33 in lanes 1, 2, and 3, respectively. *M* Molt-4 with 33 PCR cycles, *IC* 36-bp internal control

thickness, adjacent to H-E and Masson trichrome sections, were heated in sodium citrate buffer (10 mM, pH 6.0) for 10 min in a microwave oven for high-temperature antigen unmasking. The endogenous peroxidase activity was blocked by 3% H_2O_2 in Trisbuffered saline (TBS) buffer, pH 7.6, for 5 min. The standard streptavidin–biotin–peroxidase complex method was performed. Sections were first incubated with the monoclonal antibody Ki-67 (Novocastra NCL-Ki-67-MM1) at a dilution of 1:100. Subsequently, sections were incubated with biotinylated rabbit anti-mouse, 1:200 in TBS for 30 min, followed by the third incubation step with streptavidin-biotin-peroxidase complex, 1:200, for 30 min. Visualization of the complex was realized with diaminobenzidine (DAB) and sections were counterstained with H-E. Epidermis tissue and Molt-4 cells were applied as positive controls, whereas brain tissue was used as negative control. Ki-67 labeling indices (LI) were calculated as mean percentage values by counting nuclei of tumor cells in three 0.22-mm^2 areas of a single tumor, each area consisting of 500–1800 neoplastic cells, depending on the tumor type. Semi-quantitative analysis was performed using commercially available software that allows densitometric evaluation of the Ki-67 positive nuclei of the digitized image. The intensity of the 145-bp hTERT bands was quantified as a percentage relative to the signal in the M-lane, which was defined as 100%, in relation to the Ki-67 LI. Correlation was analyzed using the Spearman rank correlation coefficient.

Results

Telomerase activity in intracranial tumor samples

Telomerase activity was examined in 49 specimens of intracranial tumors from 32 patients (Fig. 2, Table 1). The presence of telomerase activity was tested only once in a previously frozen protein lysate in liquid nitrogen because rapid degradation occurs after two or more unfreezing cycles. Of all tumors examined, 7 of 32 (22%) contained detectable telomerase activity. The glioblastomas in lanes 13, 24, 32 and the medulloblastoma in lane 11 expressed high telomerase activity. The atypical meningiomas in lanes 17 and 27, and the ependymoma in lane 14 displayed reduced telomerase activity. Telomerase activity was undetectable in all (18) benign meningiomas at both 0.7 µl and 2.0 µl protein content per PCR reaction mixture. Two of the three locally recurring tumors (cases 12, 23, and 27) failed to display telomerase activity. The glioblastomas demonstrated focal differences for telomerase activity in that a TRAP-positive cancer region and a TRAP-negative cancer region were found within a given tumor. Individual variation in the amount of the protein was found in multiple samples of the glioblastomas (Fig. 3). Brain tissue, dura mater, and arachnoid tissue did not reveal telomerase activity. Telomerase activity could be assigned to a higher cellular density as a histomorphological feature in histological sections adjacent to telomerase-positive samples. To rule out false-negative results due to the presence of tissue-specific inhibitors, all extracts with no detectable telomerase activity were re-evaluated. Small amounts of protein extracts of Molt-4 cells with known telomerase activity were mixed with telomerase-negative extracts (1:4) and the TRAP assay was repeated. In all-re-evaluated cases, a telomerase-specific 6-nucleotide repeat ladder was obtained, indicating that these tissues did not contain telomerase inhibitors.

Expression of hTERT and hTR in intracranial tumors

hTERT transcripts were initially detected by means of reverse-transcription (RT)-PCR using a set of primers (hTERT-1784S and hTERT-1928A) that amplifies a region within the T-motif of hTERT mRNA and gave a product of 145 bp (Fig. 4A). 145-bp hTERT cDNA was present in 20 of 32 (63%) intracranial tumors (Table 1). Whereas hTERT mRNA was consistently low or absent in meningiomas, brain tumors with telomerase activity exhibited elevated levels. In 13 cases, detectable hTERT mRNA was demonstrated in the absence of telomerase activity (Table 1). Different samples from the same tumor showed individual variation in hTERT mRNA expression, e.g., in case 24. All tissues expressed hTR mRNA (Fig. 4B).

Alternate splicing of hTERT in intracranial tumors

RT-PCR using primers within the reverse transcriptase domain A and B' of hTERT amplified a region including two potential splice sites. The α splice site causes a 36-bp deletion in the conserved reverse transcriptase

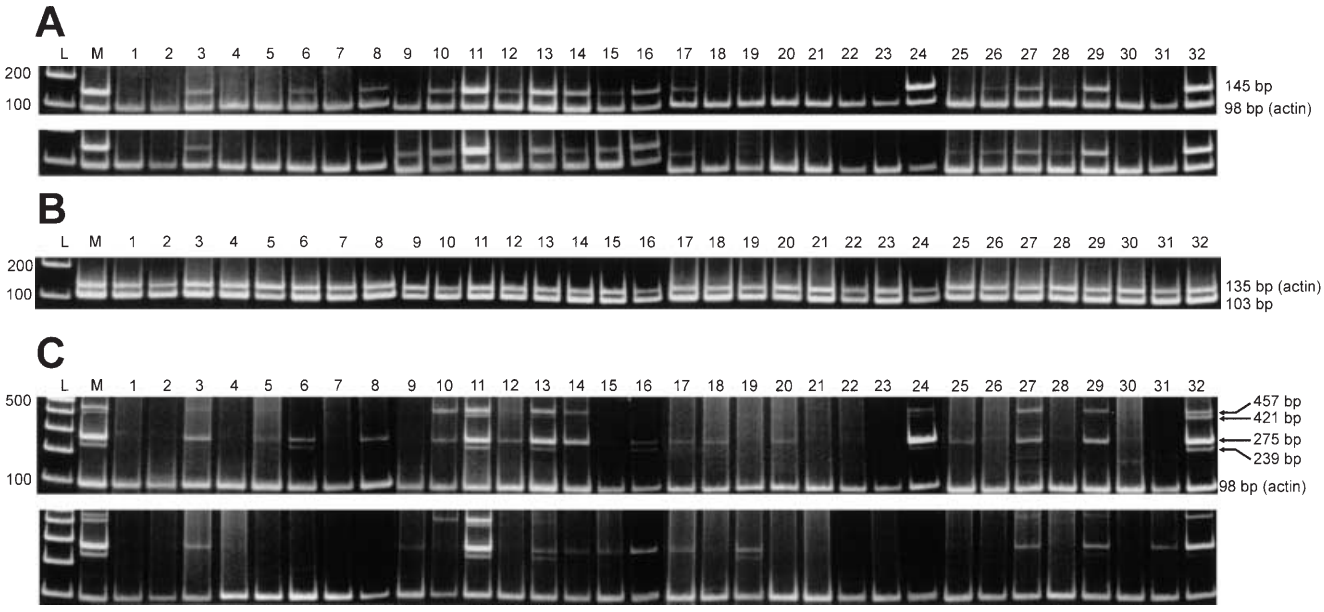


Fig. 4 Reverse-transcription polymerase chain reaction (RT-PCR) detection of hTERT and hTR in intracranial tumors. hTERT and alternate splicing of hTERT measured in two different samples of each tumor (*upper* and *lower* lanes in A and C). **A** Expression of hTERT with first set of primers. **B** Expression of hTR. **C** Expression of hTERT spliced products with second set of primers. Amplification of β-actin was used to conform synthesis and integrity of cDNA templates in all samples. *L* 100-bp DNA molecular marker, *M* Molt-4 positive control

motif A, which is required for an active reverse transcriptase. The β splice site results in a 182-bp deletion causing a non-sense mutation that truncates the protein, which also results in a non-functional reverse transcriptase. PCR performed using primers hTERT-2164S and hTERT-2620A revealed the presence of four spliced messages (Fig. 4C, Table 1). These four transcripts represent the full-length hTERT transcript (457 bp), the α deletion transcript (421 bp), the β deletion transcript (275 bp), and the α and β deletion transcripts (239 bp). Every tumor sample that expressed the 457-bp hTERT transcript with complete A and B' motif also expressed one or more spliced variants of hTERT mRNA. However, all four spliced transcripts were detected simultaneously only in tumors with marked telomerase activity and in Molt-4 cells. The two different sets of primers could not detect any of the hTERT PCR fragments in 7 of 18 benign meningiomas. Among the intracranial tumors, the full-length hTERT message was found also in the TRAP-negative tissues (3, 5, 10, 12, and 29), although some of them only showed low levels. Telomerase activity was observed in the absence of detectable 457-bp hTERT transcript in only one tumor (case 17). Of 13 TRAP-negative tumors with no detectable 457-bp hTERT transcript, but positive for 145-bp hTERT, 8 (cases 6, 8, 9, 15, 16, 25, 26, and 28) showed spliced hTERT transcripts. The frequency of the 275-bp cDNA product was highest (21 of 32, 66%). The 457-, 421-, and 239-bp transcripts occurred significantly less frequently. The presence of only the 457-bp DNA band was never detected, although, in case 10, a pituitary adenoma, its intensity was greater than the 275-bp band. The relative amount, deduced from the band intensity in the gel, of each of the four spliced fragments was not the same between tumor samples, e.g., the 275-bp DNA was relatively more or less present in comparison with the 457-bp DNA.

We were unable to detect hTERT mRNA expression in the confluent cell cultures of meningiomas (cases 5, 7, 9, 17, and 20), but all expressed the hTR mRNA. Neither could hTERT be detected in a nearly confluent cell culture derived from the arachnoid or from the dura mater. Meningiomas are considered to be derived from arachnoid cap cells. However, analysis of a rapidly growing cell culture from a glioblastoma, not being part of the brain tumors under study, all showed hTERT spliced products.

Immunohistochemical analysis of tumor proliferation

Immunohistochemical analysis of tumor proliferation has been accomplished with the Ki-67 monoclonal antibody which recognizes a nuclear antigen expressed during late G_1, S, G_2, and M phases of the cell cycle. The mean percentage of proliferating cells in the 32 intracranial tumors is given in Table 1. Most samples revealed relatively homogeneous staining, but in some malignant tumors a heterogeneous distribution was observed. Cases 15, 16, and 23 were excluded because most of the paraffin blocks contained partly or complete edematous brain tissue. In benign meningiomas, the mean proliferation index is 1.2% (SD=1.0), in atypical meningiomas 3.4% (SD=0.4), and in the remaining malignant brain tumors 13.6% (SD=9.0), revealing a highly significant difference between benign and malignant tumors. The mean proliferation index is 1.9% (SD=1.8) for TRAP-negative

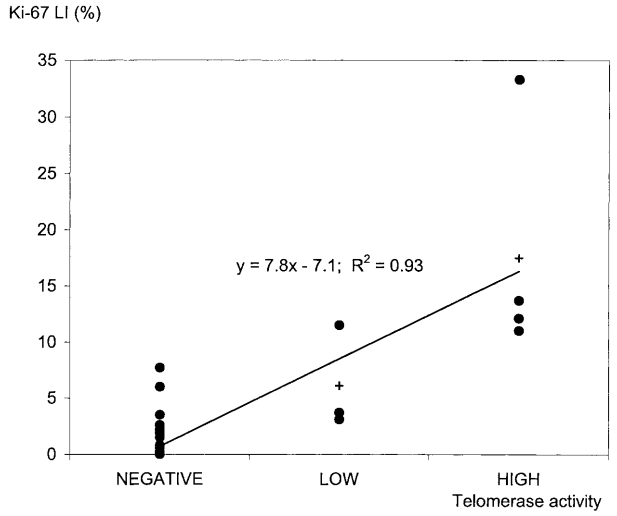


Fig. 5 Relationship between Ki-67 labeling index (%) and negative, low, and high telomerase activity in intracranial tumors

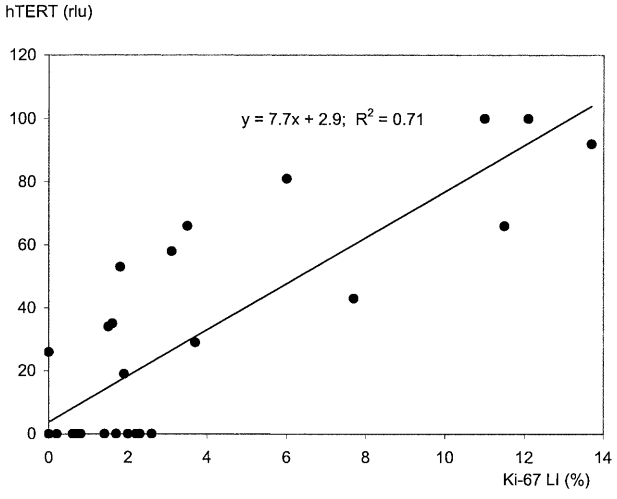


Fig. 6 Relationship between Ki-67 labeling index (%) and relative luminosity (*rlu*) of 145-bp hTERT transcripts in intracranial tumors

tumors, 6.1% (SD=4.7) for low telomerase activity, and 17.5% (SD=10.5) for high telomerase activity. A significant correlation between telomerase activity scores and mean Ki-67 LI was found in intracranial tumors ($y=7.8x–7.1$, $r_p=0.71$ Spearman rank correlation, Fig. 5), as well as between Ki-67 LI and the degree of the 145-bp hTERT expression ($y=7.7x+2.9$, $r_p=0.74$ Spearman rank correlation, Fig. 6).

Discussion

Telomerase activity

Telomerase activity was undetectable in benign intracranial tumors (20), the majority of which were meningiomas (18). It is important to determine whether these results of the TRAP assay on a given specimen are truly negative or positive, since the presence of inhibitors of either the polymerase used in PCR or the telomerase enzyme has been reported to be a potential problem in the analysis of a total protein extract [41, 47]. All meningiomas in our study were attached to the dura, and their histological sections, stained with Masson trichrome, mostly showed the presence of connective tissue. Proteins may be present in this connective tissue that inhibit *Taq* polymerase activity and prevent amplification of telomerase products [2]. However, we do not believe that telomerase activity in the specimens of meningiomas was suppressed by inhibitors. The amplified 36-bp internal control in each TRAP assay was always present in acknowledging the absence of PCR inhibitors. In addition, telomerase activity of Molt-4 cells was not inhibited when mixed with the TRAP-negative sample extracts.

Although the TRAP assay has internal controls to detect PCR inhibitors and spurious telomerase activity, it cannot assess the enzyme inactivation with time. We found that tissue preservation was important for the detection of telomerase activity. Some malignant tumors with a negative or reduced telomerase activity were frozen in liquid nitrogen 2–4 h after tumor resection. Protein degradation might have occurred in these tissues. We tested this assumption on other tissue samples that had previously been shown to have telomerase activity. We found that telomerase activity was undetectable or showed decreased TRAP products in tissues that had not been frozen immediately. Time that elapsed between tumor resection and freezing is apparently important. Although telomerase is thought to be detectable even when 10^2 cells are present, small biopsy sizes were excluded because they are far more susceptible to degradation.

Benign meningiomas which lacked telomerase activity in multiple regions showed uniformity of tissue samples in terms of tumor density and cell type. However, histological sections of malignant tumors invariably consisted of mixtures of tumor cells, necrotic tissues, and remnants of brain tissues. Multiple regions of glioblastomas showed variation in telomerase activity. This finding is supported by in situ hybridization of hTERT, which showed a focal pattern in both TRAP-positive and TRAP-negative glioblastomas [13]. Thus, the classification of a glioblastoma as telomerase positive, however, seems limited by the markedly intratumoral variation in telomerase activity we could demonstrate for this tumor type. This means that a single tumor sample which was assayed for telomerase activity can hardly be regarded as representative for a given glioblastoma, limiting the diagnostic value of the telomerase activity assays on glioblastoma cancer biopsies. Intratumoral variations in telomerase activity have also been documented in high-grade astrocytomas [22] and in prostate cancer [50]. In other studies on telomerase activity, tissue heterogeneity was often not taken into account. Histological sections of cases 15, 16, and 23 contained considerable amounts of edematous brain tissue, which might explain why these malignant tumors were telomerase negative in the specimens used for the TRAP assay.

The absence of telomerase activity suggests that telomerase activity is not an essential prerequisite for meningioma development. Similar observations were made for retinoblastoma [16], renal cell carcinoma [29], pheochromocytoma [23], as well as for soft tissue tumor [51]. Finding telomerase negativity in benign meningiomas might correspond with the short telomere lengths found in these tumors [7]. Also, the presence of dicentric chromosomes in telomerase-negative meningiomas [6], which are absent in glioblastomas [27], might represent abnormal telomere functioning due to absence of telomerase. Langford et al. [25] and Simon and colleagues [39] observed, however, telomerase activity in 5 of 30 and 7 of 34 benign meningiomas, respectively. These authors have used the downstream primer CX in the TRAP assay, which can form primer–dimer products and thus false-positive generations. We used the alternative downstream primer ACX, which results in a significant reduction of primer–dimer PCR artifact formation [19].

Telomerase mRNA expression

Messenger RNA, encoding the reverse transcriptase of telomerase, was present in 20 of 32 (63%) intracranial tumors, whereas in only 7 (22%) intracranial tumors could telomerase be detected. The detection of hTERT mRNA may be more sensitive than telomerase activity measurement due to its insensitivity to proteases or protein inhibitors. RT-PCR has the added advantage of being far more tolerant in amplifying fragments of partially degraded RNA than the TRAP assay in detecting enzyme activity. This may be seen in case 29, a glioblastoma which was frozen in liquid nitrogen exceptionally 2.5 h after surgery, where hTERT mRNA is expressed in the absence of an expected telomerase activity.

Previous studies have shown that the expression of hTERT mRNA determines telomerase activity [8, 18, 31, 32, 43, 44, 52] and may be used as an alternative tumor marker [24, 34, 49]. However, hTERT mRNA expression did not coincide perfectly with telomerase activity in cancers of various tissues (e.g., glioblastomas [13], endometrial cancers [24], lymphocytes [26], meningiomas [39], leiomyomas [44], skin tumors [49], sarcomas [51]). Intracranial tumors in our series express hTERT independently of the presence or absence of detectable telomerase activity. We found 13 cases with hTERT mRNA expression lacking telomerase activity, but with mostly lower levels of hTERT mRNA expression than those in TRAP-positive cases. We do not find a positive correlation between hTERT mRNA expression and measurable telomerase activity. Although the extracts used for TRAP assay and RT-PCR were obtained from different portions of the same tumor, these discordances cannot be fully explained by heterogeneity of the tumor cells contained in the specimens or by poor sample preparation for the TRAP assay. Indeed, if telomerase was present in an active or inactive form in our TRAP-negative tumors, we would expect to see a marked expression of hTERT mRNA as in the TRAP-positive tumors. The lack of telomerase activity in 13 hTERT mRNA-positive meningiomas could indicate that in addition to upregulation of hTERT expression, further events are required for the expression of functional telomerase, which might lead to proliferation.

Many of the intracranial tumors had spliced variants of the two conserved hTERT motifs: motif A contained a 36-bp deletion, resulting in the 421-bp band, whereas the 275-bp PCR product contained a 182-bp deletion between motif A and motif B of telomerase RT protein. Certain tumors, cell lines, fetal tissues, and normal tissues show similar spliced variants [4, 18, 43, 44]. Only the full-length hTERT transcript would be expected to code for an active reverse transcriptase. The other spliced products of hTERT encode for non-functional telomerase, resulting in a lack of telomerase activity. It is unclear whether these spliced variants are important for the regulation of telomerase activity or whether they give rise to proteins with different biochemical functions. We could detect all four spliced products only in samples with marked telomerase activity. Thirteen hTERT-positive tumors failed to express detectable enzyme activity. This cannot be explained by the fact that the presence of alternately spliced hTERT transcripts would account for enzyme inactivity in the absence of hTERT full-length transcripts. However, it might be the case in some of these tumors (cases 6, 8, 9, 15, 16, 25, 26, and 28).

To explain the absence of telomerase activity in tumors despite absence of telomerase inhibitors and optimal tissue preservation, the existence of an alternative lengthening of telomeres (ALT) mechanism has been suggested [5, 20, 35]. However, the occurrence of these mechanisms may be ruled out in benign meningiomas because reduced telomere lengths were detected in these tumors [7], suggesting that telomere elongation did not occur. Interestingly, seven benign meningiomas lacked any detectable hTERT spliced products, indicating that hTERT splicing may not contribute to the ALT mechanism in meningiomas. For the moment, undetectable hTERT mRNA in meningiomas cannot be explained by genetic alterations. The hTERT gene is located on chromosome 5p, and deletions in this region of meningiomas have not yet been reported in the literature [38].

Cancer cell proliferation

Telomerase activity was demonstrated in proliferating stem cells and in tissues during embryonic development [42, 43, 48]. Notably, all telomerase-positive tissues are permanently renewing epithelia or tissues that proliferate in regular cycles. It seems that telomerase activity can be detected also in brain tumors with a high proliferation index. Falchetti et al. [13] demonstrated that TRAP-positive glioblastomas have a much higher proliferation index than TRAP-negative glioblastomas. In our study, benign meningiomas showed no or very low numbers of

Ki-67 positive nuclei at the moment of observation, whereas malignant brain tumors with telomerase revealed high Ki-67 LI. Apparently, a slowly growing benign meningioma in which most of the cells are quiescent has no or maybe very low levels of telomerase, whereas a rapidly dividing tumor such as a glioblastoma and medulloblastoma has high levels of telomerase. Although the number of TRAP-positive tumors in our series was low, it seems that we found a significant correlation between telomerase activity scores and Ki-67 proliferation index. A positive association was also found between Ki-67 proliferation index and the degree of hTERT mRNA expression. The correlation that we found between telomerase and in vivo cell proliferation is in line with data for lung cancer [1, 15], melanoma [30], colorectal adenocarcinomas [33], and meningiomas [39].

In summary, we demonstrated that multiple specimens of benign meningiomas have no detectable telomerase activity and express no or low levels of hTERT mRNA. hTERT expression may therefore not be a marker for tumor diagnosis as such. Further experiments are needed to clarify whether hTERT splicing is a limiting factor for the expression of telomerase activity in meningiomas. High telomerase activity and hTERT mRNA expression were detected solely in glioblastoma and medulloblastoma, tumors with a high proliferation rate.

Acknowledgements We thank the neurosurgeons Dr. Jacques Caemaert, Dr. Jean-Pierre Kalala Okito, and Dr. Tom Vandekerckhove of the University Hospital and Dr. Dirk de Ridder and Dr. Luc De Waele of the St. Lucas Hospital in Ghent, who kindly provided us with tumor samples for this study.

References

1. Albanell J, Lonardo F, Rusch V, Engelhardt M, Langenfeld J, Han W, Klimstra D, Venkatraman E, Moore MAS, Dmitrovsky E (1997) High telomerase activity in primary lung cancers: association with increased cell proliferation rates and advanced pathologic stage. J Natl Cancer Inst 89:1609–1615
2. Bachor C, Bachor OA, Boukamp P (1999) Telomerase is active in normal gastrointestinal mucosa and not up-regulated in precancerous lesions. J Cancer Res Clin Oncol 125:453–460
3. Blackburn EH: Structure and function of telomeres. (1991) Nature 350:569–573
4. Brenner CA, Wolny YM, Adler RR, Cohen J (1999) Alternate splicing of the telomerase catalytic subunit in human oocytes and embryos. Mol Hum Reprod 5:845–850
5. Bryan TM, Englezou A, Dalla-Pozza L, Dunham MA, Reddel RR (1997) Evidence for an alternative mechanism for maintaining telomere length in human tumours and tumor-derived cell lines. Nat Med 3:1271–1274
6. Carroll T, Maltby E, Royds J, Timperley W, Jellinek D (1999) Meningiomas, dicentric chromosomes, gliomas, and telomerase activity. J Pathol 188:395–399
7. Chen H-J, Liang C-L, Lu K, Lin J-W, Cho C-L (2000) Implication of telomerase activity and alterations of telomere length in the histologic characteristics of intracranial meningiomas. Cancer 89:2092–2098
8. Chong EYY, Pang JCS, Ko C-W, Poon W-S, Ng H-K (2000) Telomere length and telomerase catalytic subunit expression in non-astrocytic gliomas. Pathol Res Pract 196:691–699
9. Counter CM, Avilion AA, LeFeuvre CE, Stewart NG, Greider CW, Harley CB, Bacchetti S (1992) Telomere shortening associated with chromosome instability is arrested in immortal cells which express telomerase activity. EMBO 11:1921–1929
10. Counter CM, Hahn WC, Wei W, Caddle SD, Beijersbergen RL, Lansdorp PM, Sedivy JM, Weinberg RA (1998) Dissociation among in vitro telomerase activity, telomere maintenance, and cellular immortalization. Proc Natl Acad Sci 95:14723–14728
11. DeMasters BKK, Markham N, Lillehei KO, Shroyer KR (1996) Differential telomerase expression in human primary intracranial tumors. AJCP 107:548–554
12. Falchetti ML, Pallini R, Larocca LM, D'Ambrosio E (1999) Telomerase expression in intracranial tumours: prognostic potential for malignant gliomas and meningiomas. J Clin Pathol 52:234–236
13. Falchetti ML, Pallini R, D'Ambrosio E, Pierconti F, Martini M, Cimino-Reale G, Verna R, Maira G, Larocca LM (2000) In situ detection of telomerase catalytic subunit mRNA in glioblastoma multiforme. Int J Cancer 88:895–901
14. Feng J, Funk WD, Wang S-S, Weinrich SL, Avilion AA, Chiu C-P, Adams RR, Chang E, Allsopp RC, Yu J, Le S, Wast MD, Harley CB, Andrews WH, Greider CW, Villeponteau B (1995) The RNA component of human telomerase. Science 269: 1236–1241
15. Fujiwara M, Okayasu I, Takemura T, Tanaka I, Masuda R, Furuhata Y, Noji M, Oritsu M, Kato M, Oshimura M (2000) Telomerase activity significantly correlates with chromosome alterations, cell differentiation, and proliferation in lung adenocarcinomas. Mod Pathol 13:723–729
16. Gupta J, Han L-P, Wang P, Gallie BL, Bacchetti S (1996) Development of retinoblastoma in the absence of telomerase activity. J Natl Cancer Inst 88:1152–1157
17. Hiraga S, Ohnishi T, Izumoto S, Miyahara E, Kanemura Y, Matsumura H, Arita N (1998) Telomerase activity and alterations in telomere length in human brain tumors. Cancer Res 58:2117–2125
18. Kilian A, Bowtell DDL, Abud HE, Hime GR, Venter DJ, Keese PK, Duncan EL, Reddel RR, Jefferson RA (1997) Isolation of a candidate human telomerase catalytic subunit gene, which reveals complex splicing patterns in different cell types. Hum Mol Genet 6:2011–2019
19. Kim NW, Wu F (1997) Advances in quantification and characterization of telomerase activity by the telomeric repeat amplification protocol (TRAP). Nucleic Acids Res 25: 2595–2597
20. Kim NW, Piatyszek MA, Prowse KR, Harley CB, West MD, Ho PLC, Coviello GM, Wright WE, Weinrich SL, Shay JW (1994) Specific association of human telomerase activity with immortal cells and cancer. Science 266:2011–2015
21. Kleihues P, Cavenee WK (ed) (2000) WHO Classification of tumours. Pathology and genetics. Tumours of the Nervous System. IARCPress, Lyon
22. Kleinschmidt-DeMasters BK, Hashizumi TL, Lillehei KO, Shroyer AL, Shroyer KR (1998) Telomerase expression shows differences across multiple regions of oligodendroglioma versus high grade astrocytomas but shows correlation with Mib-1 labeling. J Clin Pathol 51:284–293
23. Kubota Y, Nakada T, Sasagawa I, Yanai H, Itoh K (1998) Elevated levels of telomerase activity in malignant pheochromocytoma. Cancer 82:176–179
24. Kyo S, Kanaya T, Takakura M, Tanaka M, Yamashita A, Inoue H, Inoue M (1999) Expression of human telomerase subunits in ovarian malignant, borderline and benign tumors. Int J Cancer 80:804–809
25. Langford LA, Piatyszek MA, Xu R, Schold SC, Wright WE, Shay JW (1997) Telomerase activity in ordinary meningiomas predicts pour outcome. Hum Pathol 28:416–420
26. Liu K, Schoonmaker MM, Levine BL, June CH, Hodes RJ, Weng N-P (1999) Constitutive and regulated expression of telomerase reverse transcriptase (hTERT) in human lymphocytes. Proc Natl Acad Sci 96:5147–5152

27. Magnani I, Guerneri S, Pollo B, Cirenei N, Colombo BM, Broggi G, Galli C, Bugiani O, Didonato S, Finocchiaro G, Conti AMF (1994) Increasing complexity of the karyotype in 50 human gliomas. Progressive evolution and de novo occurrence of cytogenetic alterations. Cancer Genet Cytogenet 75:77–89
28. Meeker AK, Coffey DS (1997) Telomerase: a promising marker of biological immortality of germ, stem, and cancer cells. A review. Biochemistry 62:1323–1331
29. Mehle C, Piatyszek MA, Ljungberg B, Shay JW, Roos G (1996) Telomerase activity in human renal cell carcinoma. Oncogene 13:161–166
30. Miracco C, Pacenti L, Santopietro R, Biagioli M, Fimiani M, Perotti R, Rubegni P, Pirtoli L, Luzi P (2000) Detection of telomerase activity and correlation with mitotic and apoptotic indices, Ki-67 and expression of cyclins D1 and A in cutaneous melanoma. Int J Cancer 88:411–416
31. Nakamura Y, Hirose M, Matsuo H, Tsuyama N, Kamisango K, Ide T (1999) Simple, rapid, quantitative, and sensitive detection of telomere repeats in cell lysate by a hybridization protection assay. Clin Chem 45:1718–1724
32. Nakayama J-I, Tahara H, Tahara E, Saito M, Ito K, Nakamura H, Nakanishi T, Thara E, Ide T, Ishikawa F (1998) Telomerase activation by hTRT in human normal fibroblasts and hepatocellular carcinomas. Nat Genet 18:65–68
33. Okayasu I, Mitomi H, Yamashita K, Mikami T, Fujiwara M, Kato M, Oshimura M (1998) Telomerase activity significantly correlates with cell differentiation, proliferation and lymph node metastasis in colorectal carcinomas. J Cancer Res Clin Oncol 124:444–449
34. Park T-W, Riethdorf S, Riethdorf L, Löning T, Jänicke F (1999) Differential telomerase activity, expression of the telomerase catalytic sub-unit and telomerase-RNA in ovarian tumors. Int J Cancer 84:426–431
35. Reddel RR, Bryan TM, Murnane JP (1997) Immortalized cells with no detectable telomerase activity. A review. Biochemistry (Moscow) 62:1254–1262
36. Rhyu MS (1995) Telomeres, Telomerase, and Immortality. J Natl Cancer Inst 87:884–894
37. Sano T, Asai A, Mishima K, Fujimaki T, Kirino T (1998) Telomerase activity in 144 brain tumours. Br J Cancer 77: 1633–1637
38. Sanson M, Cornu P (2000) Biology of meningiomas. Acta Neurochir (Wien) 142:493–505
39. Simon M, Park T-W, Leuenroth S, Hans VHJ, Löning T, Schramm J (2000) Telomerase activity and expression of the telomerase catalytic subunit, hTERT, in meningioma progression. J Neurosurg 92:832–840
40. Slijepcevic P, Bryant PE (1998) Chromosome healing, telomere capture and mechanisms of radiation-induced chromosome breakage. Int J Radiat Biol 73:1–13
41. Sugino T, Yoshida K, Bolodeoku J, Tarin D, Goodison S (1997) Telomerase activity and its inhibition in benign and malignant breast lesions. J Pathol 183:57–61
42. Ulaner GA, Guidice L (1997) Developmental regulation of telomerase activity in human fetal tissues during gestation. Mol Hum Reprod 3:769–773
43. Ulaner GA, Hu J-F, Vu TH, Oruganti H, Giudice LC, Hoffman AR (1998) Telomerase activity in human development is regulated by human telomerase reverse transcriptase (hTERT) transcription and by alternate splicing of hTERT transcripts. Cancer Res 58:4168–4172
44. Ulaner GA, Hu J-F, Vu TH, Oruganti H, Giudice LC, Hoffman AR (2000) Regulation of telomerase by alternate splicing of human telomerase reverse transcriptase (hTERT) in normal and neoplastic ovary, endometrium and myometrium. Int J Cancer 85:330–335
45. Weinrich SL, Pruzan R, Ma LB, Ouellette M, Tesmer VM, Holt SE, Bodnar AG, Lichsteiner S, Kim NW, Trager JB, Taylor RD, Carlos R, Andrews WH, Wright WE, Shay JW, Harley CB, Morin GB (1997) Reconstitution of human telomerase with the template RNA component hTR and the catalytic protein subunit hTRT. Nat Genet 17:498–502
46. Wick M, Zubov D, Hagen G (1999) Genomic organization and promoter characterization of the gene encoding the human telomerase reverse transcriptase (hTERT). Gene 232: 97–106
47. Wright WE, Shay JW, Piatyszek MA (1995) Modifications of a telomeric repeat amplification protocol (TRAP) result in increased reliability, linearity and sensitivity. Nucleic Acids Res 23:3794–3795
48. Wright WE, Piatyszek MA, Rainey WE, Byrd W, Shay JW (1996) Telomerase activity in human germline and embryonic tissues and cells. Dev Genet 18:173–179
49. Wu A, Ichihashi M, Ueda M (1999) Correlation of the expression of human telomerase subunits with telomerase activity in normal skin and skin tumors. Cancer 86:2038–2044
50. Wullich B, Rohde V, Oehlenschläger B, Bonkhoff H, Ketter R, Zwergel T, Sattler H-P (1997) Focal intratumoral heterogeneity for telomerase activity in human prostate cancer. J Urol 161: 1997–2001
51. Yan P, Coindre J-M, Benhattar J, Bosman FT, Guillou L (1999) Telomerase activity and human telomerase reverse transcriptase mRNA expression in soft tissue tumors: correlation with grade, histology, and proliferative activity. Cancer Res 59:3166–3170
52. Yan P, Saraga EP, Bouzourene H, Bosman FT, Benhattar J (2001) Expression of telomerase genes correlates with telomerase activity in human colorectal carcinogenesis. J Pathol 193:21–26

Virchows Arch (2001) 439:185–190
DOI 10.1007/s004280000390

ORIGINAL ARTICLE

**Kyoko Imanaka-Yoshida · Ritsuko Matsuura
Naoki Isaka · Takeshi Nakano · Teruyo Sakakura
Toshimichi Yoshida**

Serial extracellular matrix changes in neointimal lesions of human coronary artery after percutaneous transluminal coronary angioplasty: clinical significance of early tenascin-C expression

Received: 16 August 2000 / Accepted: 15 November 2000 / Published online: 9 February 2001
© Springer-Verlag 2001

Abstract It has become clear that deposition of extracellular matrix(ECM) proteins is a major cause of human restenosis after percutaneous coronary angioplasty (PTCA). To define the composition and organization of the involved ECM in human restenotic tissue, we morphologically and semiquantitatively analyzed specimens obtained by means of directional coronary atherectomy at various stages after PTCA with anti-fibronectin, tenascin-C, collagens I and III, and PG-M/versican antibodies. Tenascin-C deposition transiently increased within 1 month after PTCA, when smooth muscle cell migration and proliferation was active. Following the disappearance of tenascin-C, PG-M/versican accumulation increased and peaked between 1 month and 3 months when clinical restenosis was most actively progressing. At later stages, the PG-M/versican was replaced by a more mature ECM consisting of collagens I and III. The volume ratio of elastin remained at a low level throughout. Our results demonstrate that the matrix proteins of human restenotic lesions sequentially change after angioplasty and that tenascin-C could be a key molecule in the early stages.

Keywords Angioplasty · Restenosis · Extracellular matrix · Tenascin · Proteoglycan

Introduction

Interventional revascularization is universally accepted as a therapeutic procedure for coronary vascular disease. However, it also initiates a healing response of intima that can result in a chronic renarrowing of the dilated vessels. A number of reports have suggested that restenotic lesions are formed by smooth muscle cell migration, proliferation, and extracellular matrix (ECM) deposition [8, 16, 18, 27, 36].

Recently, by analysis of human restenotic tissue obtained by means of directional coronary atherectomy (DCA), we found that proliferation of smooth muscle cells precedes clinical restenosis and that the mass effect of deposited ECM, especially PG-M/versican, can be a major cause of restenosis after percutaneous coronary angioplasty (PTCA) [26]. As we demonstrated, it is evident that restenotic lesions feature an abundant myxoid ECM surrounding smooth muscle cells. The deposition of ECM in neointima could be a result of a series of sequential changes. Several reports have documented distinct spatial patterns of expression of different ECM components in restenotic tissue [7, 12, 25, 28, 30, 31, 35]. However, the nature of the ECM in human lesions has not been fully characterized.

In order to define the composition and process of organization of the ECM in human restenotic tissue, we immunohistologically semiquantified the major components, fibronectin, tenascin-C, collagen I and III, and PG-M/versican in human neointima obtained with DCA at various stages after PTCA.

Materials and methods

Patients and histological specimens

Human coronary artery specimens were collected by means of directional coronary atherectomy from 43 patients (36 men and 7 women; mean age 61.4±11.2 years), as previously reported [26]. Atherectomy specimens included eight primary stenotic lesions without PTCA and 35 restenotic lesions after PTCA. Samples were classified into five groups according to the period after PTCA: group 0, de novo lesions (n=8); group 1, 0–1 month (n=6); group 2, 1–3 months (n=12); group 3, 3–6 months (n=11); and group 4, more than 6 months (n=6). The specimens obtained were routinely formalin fixed and paraffin embedded.

K. Imanaka-Yoshida (✉) · Teruyo Sakakura · Toshimichi Yoshida
The Department of Pathology, Mie University School of Medicine,
2-174 Edobashi, Tsu, Mie 514-8507, Japan
e-mail: imanaka@doc.medic.mie-u.ac.jp
Tel.: +81-59-2315009, Fax: +81-59-2315210

R. Matsuura · N. Isaka · T. Nakano
The Division of Cardiology of the First Department
of Internal Medicine, Mie University School of Medicine,
Tsu, Mie 514-8507, Japan

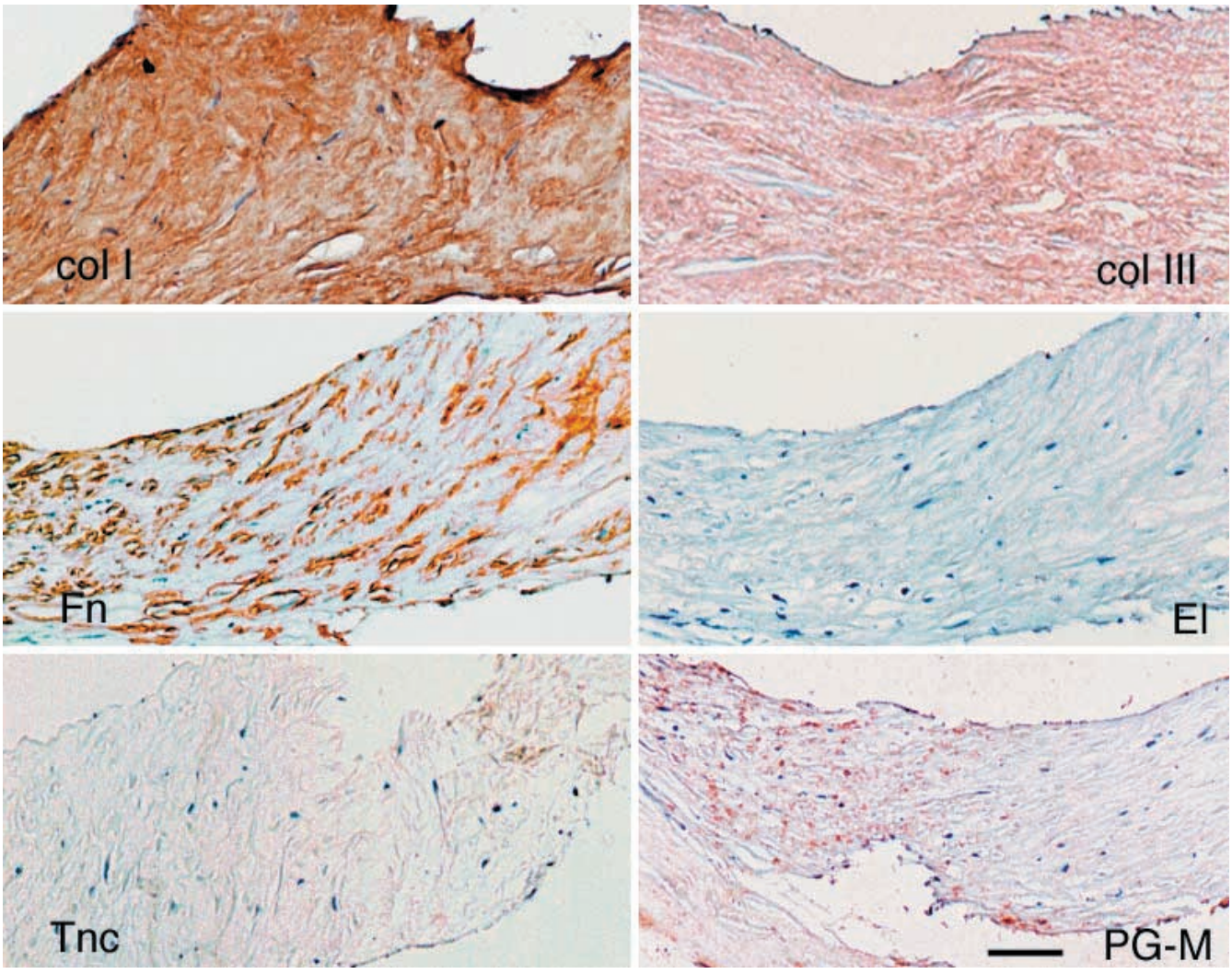


Fig. 1 Immunostaining for collagen I, collagen III, fibronectin, elastin, tenascin-C, and PG-M/versican in de novo primary lesions. Diffuse staining for collagen I and collagen III and patchy deposition of fibronectin are apparent. Anti-tenascin-C, anti-PG-M/versican, and anti-elastin staining are almost negative. ×130. *col I* collagen I; *col III* collagen III; *Fn* fibronectin; *El* elastin; *Tnc* tenascin-C; *PG-M* PG-M/versican

Immunohistochemical staining and histological analysis of restenotic specimens

We prepared 4-μm sections of all specimens. After dewaxing and rehydration, the sections were treated with 0.5% hydrogen peroxide in methanol for 30 min to inactivate the intrinsic peroxidase activity. They were then incubated with rat monoclonal anti-tenascin-C (1000-fold dilution, clone RCB1) [17], rabbit polyclonal anti-fibronectin (400-fold dilution, Sigma, St. Louis, Mo.), anti-collagen I (20-fold dilution, Sanbio, Udem, The Netherlands), or anti-collagen III (20-fold dilution, Sanbio) antibodies at 4°C overnight. All sections were then processed using an LSAB kit (Dako Japan, Kyoto, Japan).

Color reactions were developed in 0.03% diaminobenzidine solution, containing 0.01% hydrogen peroxide, and the sections were counterstained with hematoxylin solution for light microscopic examination. Negative controls consisted of serial sections incubated with buffer alone instead of primary antibody. Each run also included a positive control slide of tissue previously demonstrated to be strongly positive for the above proteins.

For quantification of each ECM component, the percentages of 500 points positively stained in neointimal areas were counted, employing a point counting method (positive points/total number of points counted). All data are presented as mean±SD. Differences in averages for cell numbers and percentages of positive cells and areas among the groups were analyzed with the Student's *t*-test.

Results

Histological characteristics of atherectomy specimens at various stages after PTCA

Atherectomy specimens from patients with de novo primary lesions (group 0, Fig. 1) were composed of collagen I- and collagen III-rich dense fibrous connective tissue. Deposition of fibronectin was also seen. Anti-tenascin-C, anti-PG-M/versican, and anti-elastin staining were almost negative. Less than 1 month after PTCA (group 1), specimens contained many spindle-shaped cells and showed intense diffuse staining of anti-tenascin-C. PG-M/versican was not deposited in the neointima at this stage (Fig. 2). In group 2 (1–3 months after PTCA, Fig. 3), the neointima contained fewer cells but,

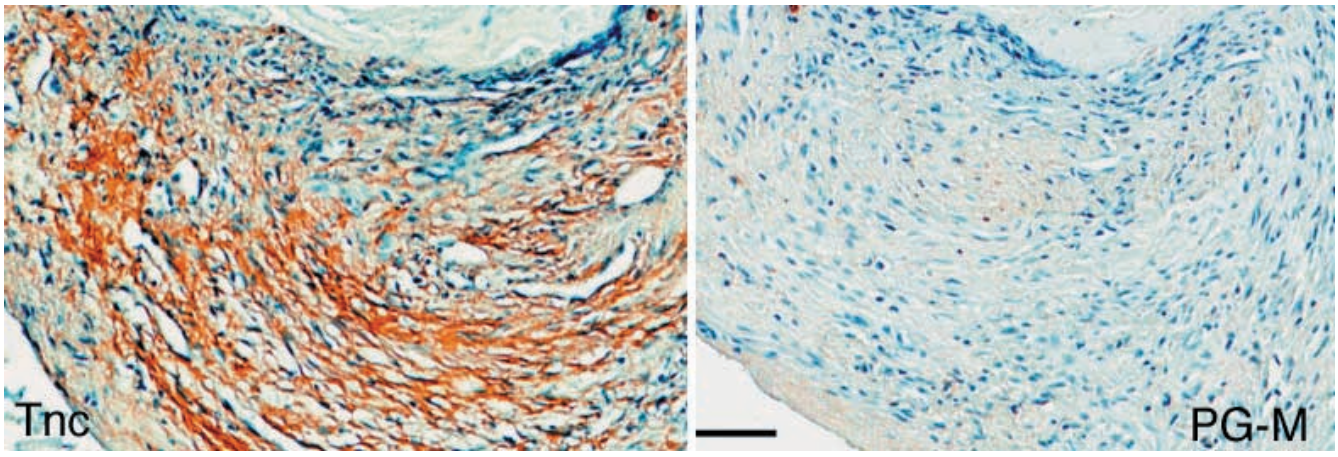


Fig. 2 Immunostaining for tenascin-C and PG-M/versican in an atherectomy restenotic specimen within 1 month after percutaneous coronary angioplasty. The tissue contains many cells and shows intense staining of anti-tenascin-C. No accumulation of PG-M/versican is evident at this stage. ×130. *Tnc* tenascin-C; *PG-M* PG-M/versican

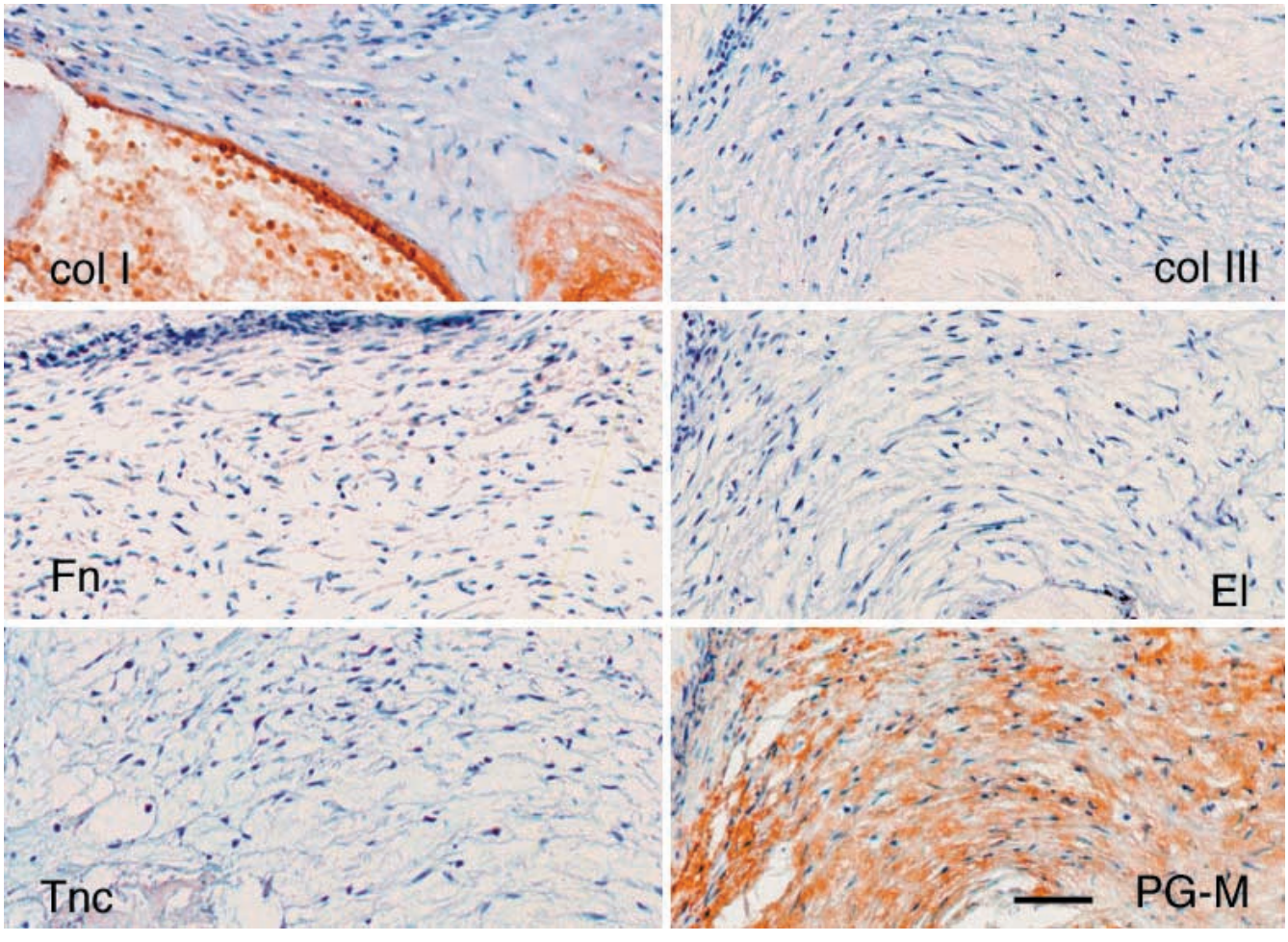


Fig. 3 Immunostaining for collagen I, collagen III, fibronectin, elastin, tenascin-C, and PG-M/versican in the atherectomy specimens 2 months after percutaneous coronary angioplasty. The neointima contains fewer cells and an abundant loose extracellular matrix. Anti-tenascin-C staining has almost disappeared. Instead, diffuse deposition of PG-M/versican is evident. ×130. *col I* collagen I; *col III* collagen III; *Fn* fibronectin; *El* elastin; *Tnc* tenascin-C; *PG-M* PG-M/versican

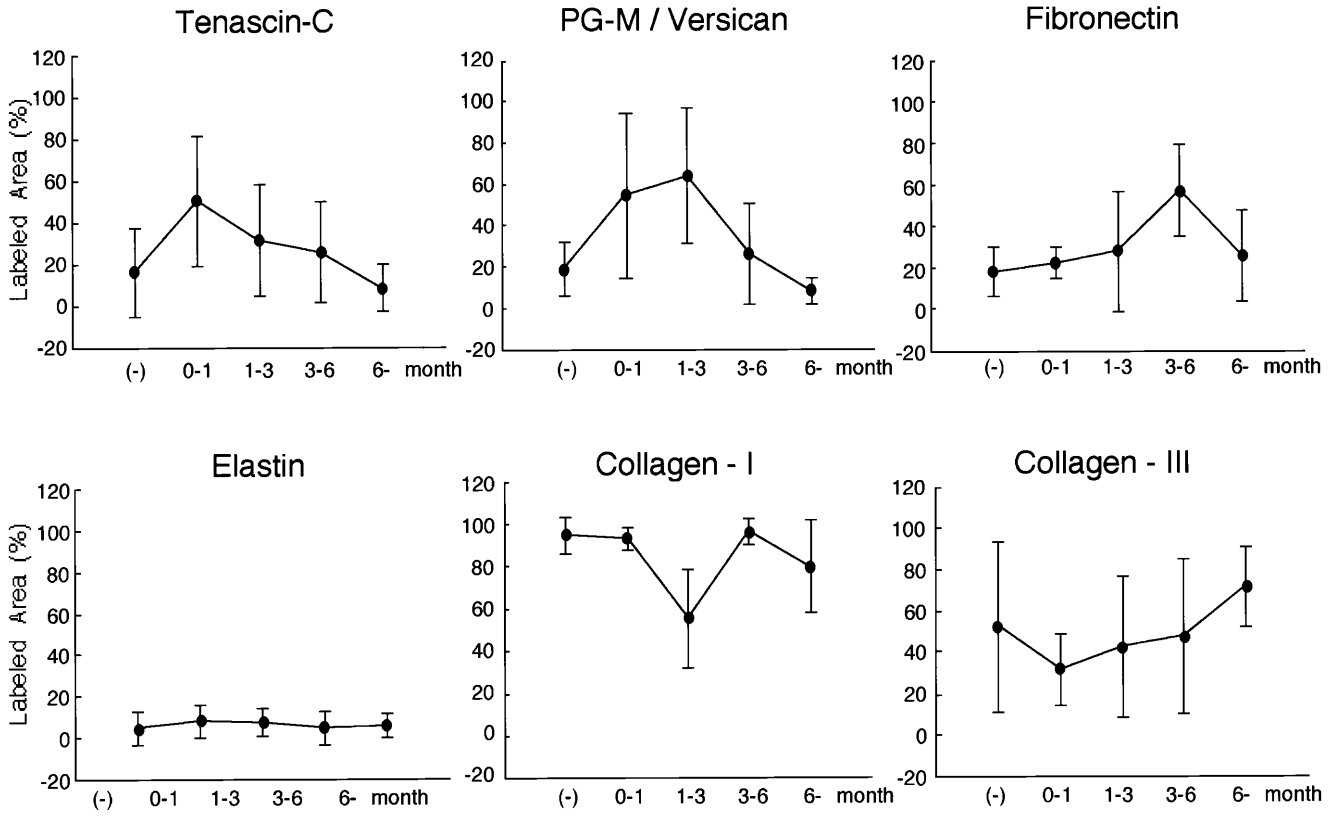


Fig. 4 Percentage positive areas of neointima stained for collagen I, collagen III, fibronectin, elastin, tenascin-C, and PG-M/versican. The area positive for anti-tenascin-C staining significantly increased within 1 month after percutaneous coronary angioplasty. PG-M/versican-positive areas increased and peaked in group 2 (1–3 months). Collagen I, collagen III, and fibronectin-positive areas increased at a later stage, while the elastin-positive area remained at a low level, below 10% throughout

instead, an abundant loose ECM, which was enriched with PG-M/versican. Anti-tenascin-C staining had almost disappeared. The specimens obtained from patients more than 6 months after PTCA (group 4) demonstrated similar characteristics to those of the de novo group 0 (data not shown).

Labeled percentage areas for individual ECM components of neointima

After PTCA, initially, the area of neointima positive for anti-tenascin-C staining significantly increased within 1 month after PTCA (50.5±30.9% vs 16.6±21.2% in primary lesions, $P<0.05$) (Fig. 4). Next, the PG-M/versican-positive area increased and peaked in group 2 (63.9±33.0% vs 18.6±13.1% in primary lesions, $P<0.01$), then decreased after 3 months (in group 3, 26.1±24.5%, $P<0.05$). In contrast, collagen I- and collagen III-positive areas increased at later stages. That for collagen I showed a gradual increment after 3 months (55.7±23.3% of neointima in group 2 vs 96.5±6.5% in group 3, $P<0.01$). The fibronectin-positive area also increased at later stages and peaked in group 3 (57.1±22.5% vs 27.8±28.6% in group 2 and 25.6±22.1% in group 4, $P<0.01$). Elastin-positive areas remained below 10% with no marked changes throughout.

Discussion

To our knowledge, this is the first paper documenting the sequential changes of the components of the ECM after PTCA in human restenotic neointima. At an early stage after PTCA, tenascin-C was transiently upregulated. Then, PG-M/versican markedly accumulated when the clinical restenosis was most actively progressing. The PG-M/versican-rich myxoid matrix was subsequently replaced by a more mature ECM consisting of collagen I and III.

Similar compositional changes have been observed in an experimental animal model after intimal balloon injury [7, 10]. In human tissue, previous reports suggested differences in the ECM in newly formed human neointima and advanced primary atherosclerotic plaques. The former was found to be enriched with proteoglycans [25], whereas the latter contained dense ECM composed primarily of type-I collagen [35]. Our immunohistological semi-quantitative analysis clearly showed a process of accumulation of various ECM proteins during neointimal hyperplasia, which is analogous to that during wound healing in various tissues.

The sequential change in ECM composition suggests that different components could play distinct roles in a cascade of biological events during the progression of

neointimal lesions. The ECM evidently constitutes most of the volume of the restenotic intima. As we reported previously, the coincidence of the timing of progression of angiographic restenosis and the increment of PG-M/versican suggests that a mass effect of the deposits is largely responsible for restenosis [26]. PG-M/versican is a chondroitin sulfate proteoglycan that entraps water itself and through its interaction with hyaluronan [34], the later also being deposited in the neointima [31]. This would be expected to cause the myxoid ECM to swell, consequently narrowing the vascular lumen.

Within 1 month after PTCA, before the extensive accumulation of PG-M/versican occurred, expression of tenascin-C in neointima was transiently upregulated. It is during this stage when cell proliferation in neointima occurs [26]. Smooth muscle cells also migrate from media during the very early stage after angioplasty [18]. The coincidence of timing suggests that tenascin-C may be closely linked to smooth muscle cell migration and proliferation during restenotic neointimal formation.

Indeed, it is well known that some ECM components can regulate cell migration, proliferation, differentiation, or synthesis of other ECM proteins [22, 23, 39]. Tenascin-C is one of the extracellular glycoproteins that is expressed in tissue remodeling sites, such as during embryogenesis or cancer invasion [5]. Tenascin-C is not expressed in most adult normal tissues but transiently reappears after injury and regulates cell behavior by modulating cell adhesion [15, 23, 24, 33, 38].

Generally, tenascin-C promotes cell migration [6, 13, 37]. It is also reported to stimulate proliferation of certain types of cells. For example, tenascin-C promotes the growth of pulmonary vascular smooth muscle cells, which is considered to be a mechanism of neointimal formation in pulmonary vascular disease [19, 20, 21].

Furthermore, ECM molecules can interact with one another [3]. There have been several reports showing that chondroitin sulfate proteoglycans bind to members of the tenascin family [1, 2, 4, 9, 11, 29]. The early deposition of tenascin-C may thus provide a scaffold for subsequent accumulation of PG-M/versican. Although the biological roles of tenascin-C remain to be elucidated, it could be a key contributor to early events during restenosis. Thus, tenascin-C inhibitors may be of therapeutic benefit for prevention.

It is also noteworthy that tenascin-C appears to be transiently upregulated only in the acute phase after PTCA. In various tissues, tenascin-C appears transiently at early stages after injury and disappears with healing [14, 24, 33, 38]. This restricted expression during the active phase of tissue remodeling might suggest that its appearance in neointimal tissue specimens reflects active progression of restenosis, which may be useful in evaluating the prognosis of restenosis in individual patients, especially in cases of late onset in-stent restenosis. Recently, Wallner et al. reported that tenascin-C is expressed in human coronary atherosclerotic plaques, correlating with the degree of inflammation [32]. In conclusion, our study demonstrated that the matrix composition in human restenotic lesions sequentially changes during the time course after angioplasty and that tenascin-C could be a key molecule in the early stage. Inhibition of tenascin-C may block the subsequent biological events causing neotinimal formation and be a new approach for prevention of the restenosis.

Acknowledgements We thank S. Naota for her technical assistance. This research was supported by a Grant-in-Aid (1998) from the Mie Medical Research Foundation and by Grants-in-Aid from the Ministry of Education, Science, Sports, and Culture of Japan to K. I.-Y.

References

1. Aspberg A, Binkert C, Ruoslahti E (1995) The versican C-type lectin domain recognizes the adhesion protein tenascin-R. Proc Natl Acad Sci U S A 92:10590–10594
2. Aspberg A, Miura R, Bourdoulous S, Shimonaka M, Heinegard D, Schachner M, Ruoslahti E, Yamaguchi Y (1997) The C-type lectin domains of lecticans, a family of aggregating chondroitin sulfate proteoglycans, bind tenascin-R by protein-protein interactions independent of carbohydrate moiety. Proc Natl Acad Sci U S A 94:10116–10121
3. Bost F, Diarra-Mehrpour M, Martin JP (1998) Inter-alpha-trypsin inhibitor proteoglycan family – a group of proteins binding and stabilizing the extracellular matrix. Eur J Biochem 252:339–346
4. Chiquet M, Fambrough DM (1984) Chick myotendinous antigen. II. A novel extracellular glycoprotein complex consisting of large disulfide-linked subunits. J Cell Biol 98:1937–1946
5. Chiquet-Ehrismann R, Kalla P, Pearson CA, Sakakura T (1986) Tenascin interferes with fibronectin action. Cell 53: 383–390
6. Chung CY, Murphy-Ullrich JE, Erickson HP (1996) Mitogenesis, cell migration, and loss of focal adhesions induced by tenascin-C interacting with its cell surface receptor, annexin II. Mol Biol Cell 7:883–892
7. Evanko SP, Raines EW, Ross R, Gold LI, Wight TN (1998) Proteoglycan distribution in lesions of atherosclerosis depends on lesion severity, structural characteristics, and the proximity of platelet-derived growth factor and transforming growth factor-beta. Am J Pathol 152:533–546
8. Forrester JS, Fishbein M, Helfand R, Fagin J (1991) A paradigm for restenosis based on cell biology: clues for the development of new preventive therapies. J Am Coll Cardiol 17: 758–769
9. Gates MA, Fillmore H, Steindler DA (1996) Chondroitin sulfate proteoglycan and tenascin in the wounded adult mouse neostriatum in vitro: dopamine neuron attachment and process outgrowth. J Neuroscience 16:8005–8018
10. Geary RL, Nikkari ST, Wagner WD, Williams JK, Adams MR, Dean RH (1998) Wound healing: a paradigm for lumen narrowing after arterial reconstruction. J Vasc Surg 27:96–106
11. Grumet M, Friedlander DR, Sakurai T (1996) Functions of brain chondroitin sulfate proteoglycans during developments: interactions with adhesion molecules. Perspect Dev Neurobiol 3:319–330
12. Gutierrez P, O'Brien KD, Ferguson M, Nikkari ST, Alpers CE, Wight TN (1997) Differences in the distribution of versican, decorin, and biglycan in atherosclerotic human coronary arteries. Cardiovasc Pathol 6:271–278
13. Halfter W, Chiquet-Ehrismann R, Tucker RP (1989) The effect of tenascin and embryonic basal lamina on the behavior and morphology of neural crest cells in vitro. Dev Biol 132:14–25
14. Imanaka-Yoshida K, Ishiyama S, Toyozaki T, Nishikawa T, Yoshida T, Sakakura T, Hiroe M (1998) Tenascin-C is expressed in myocardium during active stage of myocarditis (abstract). J Mol Cell Cardiol 30:317

15. Imanaka-Yoshida K, Yokoyama K, Sakakura T. (2000) Possible role of the tenascin family during heart development and myocardial tissue remodeling. In: Takeda N, Nagano M, Dhalla NS (eds) The hypertrophied Heart. Kluwer Academic publisher, Boston, pp 123–129
16. Ip JH, Fuster V, Badimon L, Badimon J, Taubman MB, Chesebro JH (1990) Syndromes of accelerated atherosclerosis: role of vascular injury and smooth muscle cell proliferation. J Am Coll Cardiol 15:1667–1687
17. Ishihara A, Yoshida T, Tamaki H, Sakakura T (1995) Tenascin expression in cancer cells and stroma of human breast cancer and its prognostic significance. Clin Cancer Res 1:1035–1041
18. Jackson CL (1994) Animal models of restenosis. Trends Cardiovasc Med 4:122–130
19. Jones PL, Rabinovitch M (1996) Tenascin-C is induced with progressive pulmonary vascular disease in rats and is functionally related to increased smooth muscle cell proliferation. Circ Res 79:1131–1142
20. Jones PL, Cowan KN, Rabinovitch M (1997) Tenascin-C, proliferation and subendothelial fibronectin in progressive pulmonary vascular disease. Am J Pathol 150:1349–1360
21. Jones PL, Crack J, Rabinovitch M (1997) Regulation of tenascin-C, a vascular smooth muscle cell survival factor that interacts with the alpha v beta 3 integrin to promote epidermal growth factor receptor phosphorylation and growth. J Cell Biol 139:279–293
22. Koyama N, Kinsella MG, Wight TN, Hedin U, Clowes AW (1998) Heparan sulfate proteoglycans mediate a potent inhibitory signal for migration of vascular smooth muscle cells. Circ Res 83:305–313
23. LaFleur DW, Chiang J, Fagin JA, Schwartz SM, Shah PK, Wallner K, Forrester JS, Sharifi BG (1997) Aortic smooth muscle cells interact with tenascin-C through its fibrinogen-like domain. J Biol Chem 272:32798–32803
24. Latijnhowwers MA, Bergers M, Van Bergen BH, Spruijt KI, Andriessen MP, Schalkwijk J (1996) Tenascin expression during wound healing in human skin. J Pathol 178:30–35
25. Lin H, Kanda T, Hoshino Y, Takase S, Kobayashi I, Nagai R, McManus BM (1998) Versican, biglycan, and decorin expression patterns in coronary arteries: analysis of primary and restenotic lesions. Cardiovasc Pathol 7:31–37
26. Matsuura R, Isaka N, Imanaka-Yoshida K, Yoshida T, Sakakura T, Nakano T (1996) Deposition of G-M/versican is a major cause of human coronary restenosis after percutaneous transluminal coronary angioplasty. J Pathol 180:311–316
27. O'Brien E, Schwartz SM (1994) Update on the biology and clinical study of restenosis. Trends Cardiovasc Med 4:169–178
28. O'Brien KD, Olin KL, Alpers CE, Chiu W, Ferguson M, Hudkins K, Wight TN, Chait A (1998) Comparison of apolipoprotein and proteoglycan deposits in human coronary atherosclerotic plaques: colocalization of biglycan with apolipoproteins. Circulation 98:519–527
29. Rauch U, Clement A, Retzler C, Frohlich L, Fassler R, Gohring W, Faissner A (1997) Mapping of a defined neurocan binding site to distinct domains of tenascin-C. J Biol Chem 272:26905–26912
30. Riessen R, Isner JM, Blessing E, Loushin C, S. N, Wight TN (1994) Regional differences in the distribution of the proteoglycans biglycan and decorin in the extracellular matrix of atherosclerotic and restenotic human coronary arteries. Am J Pathol 144:962–974
31. Riessen R, Wight TN, Pastore C, Henley C, Isner JM (1996) Distribution of hyaluronan during extracellular matrix remodeling in human restenotic arteries and balloon-injured rat carotid arteries. Circulation 93:1141–1147
32. Wallner K, Li C, Shah PK, Fishbein M, Forrester JS, Kaul S, Sharifi B (1999) Tenascin-C is expressed in macrophage-rich human coronary atherosclerotic plaque. Circulation 99:1284–1289
33. Whitby D, Ferguson MW (1991) The extracellular matrix of lip wounds in fetal, neonatal and adult mice. Development 112:651–668
34. Wight TN, Heinegard D, Hascall VC (1991) Proteoglycans: structures and function. In: Hay ED (ed) Cell biology of extracellular matrix. Plenum Press, New York, pp 45–78
35. Wight TN, Lara S, Riessen R, Le Baron R, Isner J (1997) Selective deposits of versican in the extracellular matrix of restenotic lesions from human peripheral arteries. Am J Pathol 151:963–973
36. Wilcox JN (1993) Molecular biology: insight into the causes and prevention of restenosis after arterial intervention. Am J Cardiol 72:88–95
37. Yoshida T, Yoshimura E, Numata H, Sakakura Y, Sakakura T (1999) Involvement of tenascin-C in proliferation and migration of laryngeal carcinoma cells. Virchows Arch 435:496–500
38. Yoshimura E, Majima A, Sakakura Y, Sakakura T, Yoshida T (1999) Expression of tenascin-C and integrin α9 subunit in regeneration of rat nasal mucosa after chemical injury: involvement of migration and proliferation of epithelial cells. Histochem Cell Biol 111:129–136
39. Zhang Y, Cao L, Yang BL, Yang BB (1998) The G3 domain of versican enhances cell proliferation via epidermal growth factor-like motifs. J Biol Chem 273:21342–21351

Virchows Arch (2001) 439:191–195
DOI 10.1007/s004280100413

ORIGINAL ARTICLE

A. Müller · K. Beyser · H. Arps · S. Bolander
H. Becker · J. Rüschhoff

Genotype and phenotype of a new 2-bp deletion of hMSH2 at codon 233

Received: 21 September 2000 / Accepted: 5 January 2001 / Published online: 22 March 2001
© Springer-Verlag 2001

Abstract Germline mutations within mismatch repair genes, such as hMSH2, hMLH1, and hMSH6, have been shown to be the hallmark of the hereditary nonpolyposis colorectal cancer (HNPCC) syndrome. The spectrum of tumors associated with mismatch repair gene defects and the possible relationship between genotype and phenotype are still unclear. Therefore, the spectrum of tumors and the possible genotype–phenotype relationship are still under discussion. Here, we report on a family with a new germline mutation in the hMSH2 gene with a 2-bp deletion at codons 232 and 233 leading to a frame shift and a stop at codon 254. Accordingly, immunohistochemistry revealed loss of hMSH2 expression in colorectal carcinomas of three affected family members. In this one family, there was a high penetrance. Interestingly, mutational screening of the family revealed a high penetrance of the mutation affecting four of five tested people at risk, with a high mortality rate and a trend toward lower age of onset in subsequent generations. Finally, a metachronous breast cancer in one patient turned out to be a tumor unrelated to microsatellite instability phenocopy, i.e., a sporadic tumor unrelated to HNPCC that expressed the hMSH2 gene and did not show any microsatellite instability.

Keywords Hereditary nonpolyposis colorectal cancer (HNPCC) · Genotype–phenotype correlation · Breast cancer

A. Müller (✉) · S. Bolander · H. Becker
Department of General Surgery and Human Genetics,
University of Göttingen, Robert-Koch-Strasse 40,
37075 Göttingen, Germany
e-mail: dramueller@aol.com
Tel.: +49-551-396132, Fax: +49-551-396106

K. Beyser · J. Rüschhoff
Department of Pathology, Klinikum Kassel, Kassel, Germany

H. Arps
Department of Pathology, Klinikum Fulda, Germany

Introduction

Hereditary nonpolyposis colorectal cancer syndrome (HNPCC) is currently one of the most common forms of hereditary colorectal cancers and accounts for about 2–13% of the total colorectal cancer burden [13, 19]. Since there are no single clinical features specific for HNPCC, the diagnosis is based on family history (Amsterdam or Bethesda criteria) [21] and is confirmed by the detection of a germline mutation in one of the responsible mismatch repair (MMR) genes. The identification of the human homologues of the yeast MMR genes, hMSH2, hMLH1, hMSH6, hPMS1, and hPMS2, offered the prospect of genetic screening, leading to an extensive search for mutations in HNPCC families [4, 6, 16]. The majority of the defects have been detected in hMSH2 (50%) and hMLH1 (30%) genes, with the other genes being only seldom affected [24].

Until now, several hundreds of germline mutations have been described in hMSH2 and hMLH1 genes. In contrast to FAP (familiar polyposis), however, the relationship between the type of mutation and the severity of the cancer predisposition [15, 17], its penetrance [18], and tumor spectrum is still under debate [11, 12, 13]. Here, we describe for the first time a HNPCC family presenting with some extraordinary, unusual features.

First, germline mutation analysis revealed a new, previously undescribed mutation site in the hMSH2 gene. Second, we could not detect a mutational loss of hMSH2 expression in a case of metachronous breast cancer in an affected family member that may exclude breast cancer from the HNPCC tumor spectrum. Finally, a high incidence of the mutation was found with a tendency to early cancer onset in subsequent generations, suggestive of anticipation.

Materials and methods

Identification and molecular analysis of the family were done in accordance with the guidelines of the German cooperative multi-

center study funded by the "Deutsche Krebsgessellschaft" German Cancer Aid. After taking the family history and obtaining informed consent, paraffin-embedded tumor specimens of the three patients were tested for microsatellite instability (MSI) and MMR. Thereafter, blood was taken for mutational analysis.

Screening for MSI

To carry out the MSI analysis first, DNA was extracted from a paraffin-embedded tumor and corresponding normal tissue. Adjacent sections were mounted on glass slides and stained with hematoxylin and eosin for histological examination to ensure that the DNA extracted originated from tumor and normal cells only. The extracted DNA was then amplified using the polymerase chain reaction (PCR). In accordance with the Bethesda recommendations [3], five microsatellite loci were used to detect MSI for which we could recently demonstrate the specific diagnostic value [5]. The PCR products were run on an ABI 310 using fragment analysis software. Extra peaks, indicating the presence of MSI in tumor DNA compared with the corresponding normal DNA, were used for MSI detection. Shifts at more than one microsatellite locus were indicative of a tumor with a high rate of MSI.

MMR gene expression

To determine the mismatch protein status, the tumors were subjected to immunohistochemical staining using the streptavidin-biotin peroxidase complex method with 3,5′ diaminobenzidine as the chromogen. Briefly, after deparaffinization, the sections were pre-treated by microwaving, and endogenous peroxidase activity was quenched by incubation with 3% of H_2O_2 followed by rinsing in phosphate-buffered saline (PBS). Non-specific binding was blocked by incubation with goat serum for 30 min. Primary hMSH2 (clone FE11 0.5 µg/ml; Oncogene Research Products, Cambridge, Mass.), hMLH1 (clone G168–728; 1 µg/ml; Pharmingen, San Diego, Calif.), or hMSH6 (AB-1, 0.5°mg/ml Oncogene Research Products, Cambridge, Mass) antibody was then incubated overnight at 4°C. The next day, the sections were washed with PBS, followed with the incubation of the secondary biotinylated antibody. After rinsing with PBS, the sections were incubated with streptavidin-conjugated horseradish peroxidase and then incubated with the chromogen 3-amino-5-ethylcarbazole for detection. A counterstaining was done with hematoxylin.

Mutation analysis

In the autosomal sequencing, we used a DNA primer label with four different fluorescent dyes. Each fluorescent primer hybridized to the template DNA and underwent the same synthesis reactions as in the case of manual sequencing. After elongation of the primer, samples containing the four kinds of newly synthesized fragments were cooled and subjected to direct laser beam analysis using an ABI sequencer.

Results

Family history

The pedigree disclosed a clear hereditary cancer predisposition with six affected family members spanning over four generations (Fig. 1). There were ten people at risk, with six being less than 10 years old. Interestingly, a tendency toward lower age of cancer manifestation was evident throughout the different generations. The oldest patient died of cancer with unknown primary at the age of 51 years, and the youngest died at the age of 33 years. One affected member is still alive. The genetic and molecular analysis was started with this individual. This patient suffered from two synchronous colorectal adenocarcinomas located in the colon ascendens (pT3, No, and Mo) and the sigmoid colon (pT1, No, and Mo).

Immunohistology and MSI testing

Tumor specimens of three patients were available from pathological files (provided by H.A.), comprising three colorectal carcinomas and one breast cancer specimen (of the 48, 49, and 33-year-old patients). All colorectal cancers showed loss of hMSH2 expression (Fig. 2a, b), which was not the case in the breast cancer specimen tested in one patient (Fig. 2c). The other two MMR genes (hMLH1, hMSH6) were highly expressed in all four tumors. Accordingly, only those carcinomas pre-

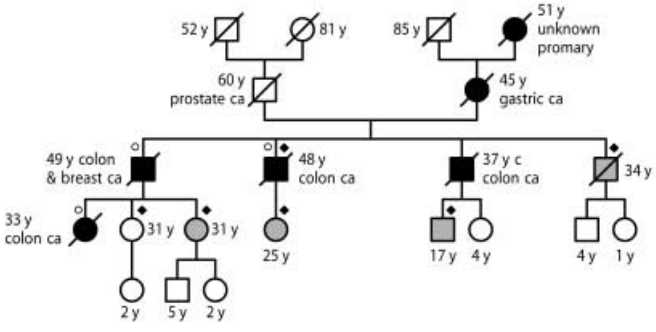


Fig. 1 Hereditary nonpolyposis colorectal cancer (HNPCC) family with six affected members, of which three were tested for microsatellite instability and mismatch repair gene expression. Mutational analysis was done in one patient and five people at risk, of which four exhibited the hMSH2 mutation

Table 1 Microsatellite instability (MSI) results in four carcinomas of three family members

Patient/age (years)	Tumor localization	BAT 26 (2p)	BAT25 (4q12)	APC/D5S346 (D5S346)	D2S123 (2p16)	Mfd15/D17S250 (17q11.2)
1/49	Colon	+	+	–	+	–
1/49	Breast	–	–	–	–	–
2/37	Colon	+	+	+	+	–
3/33	Colon	–	+	+	–	+

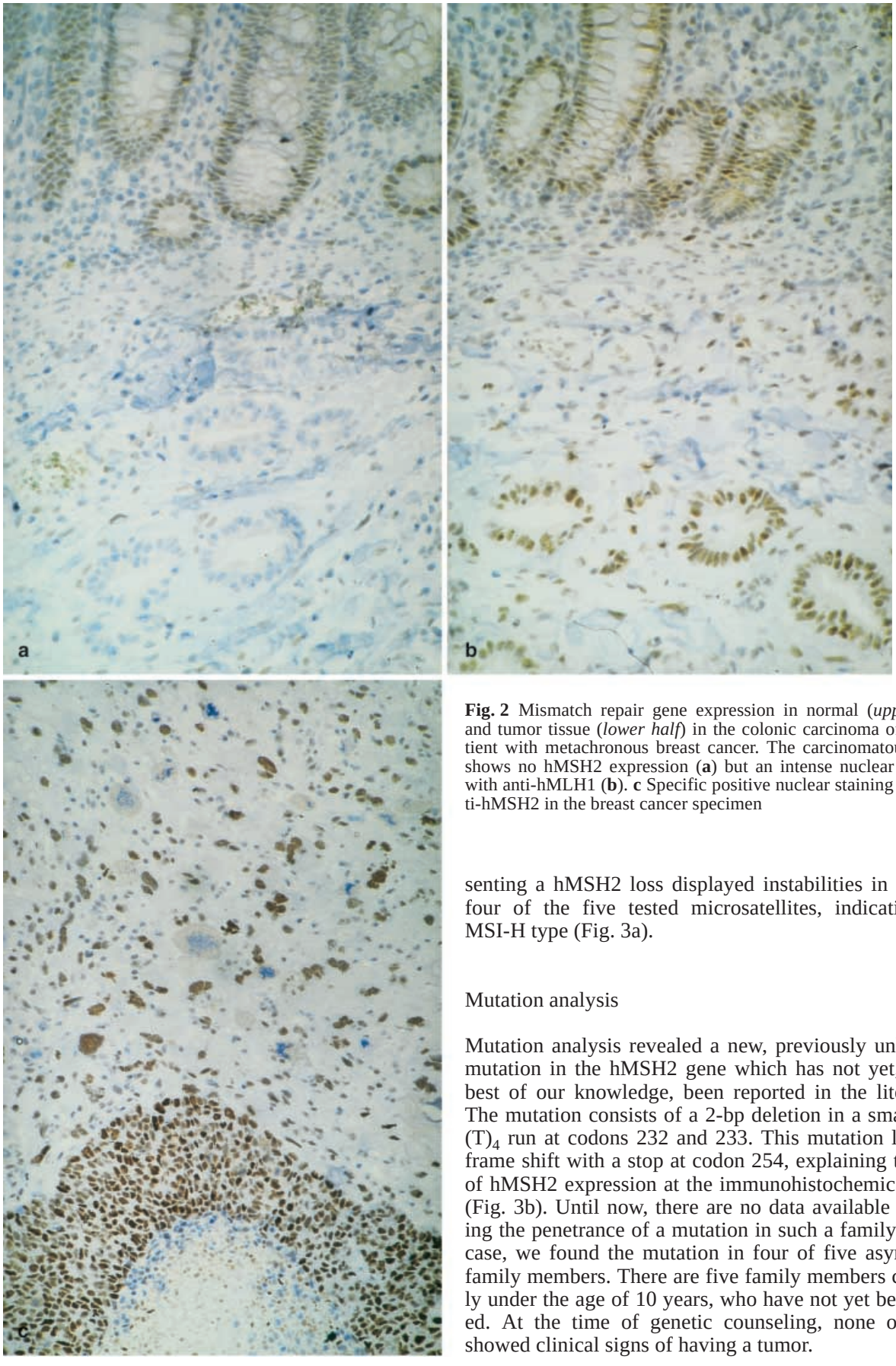
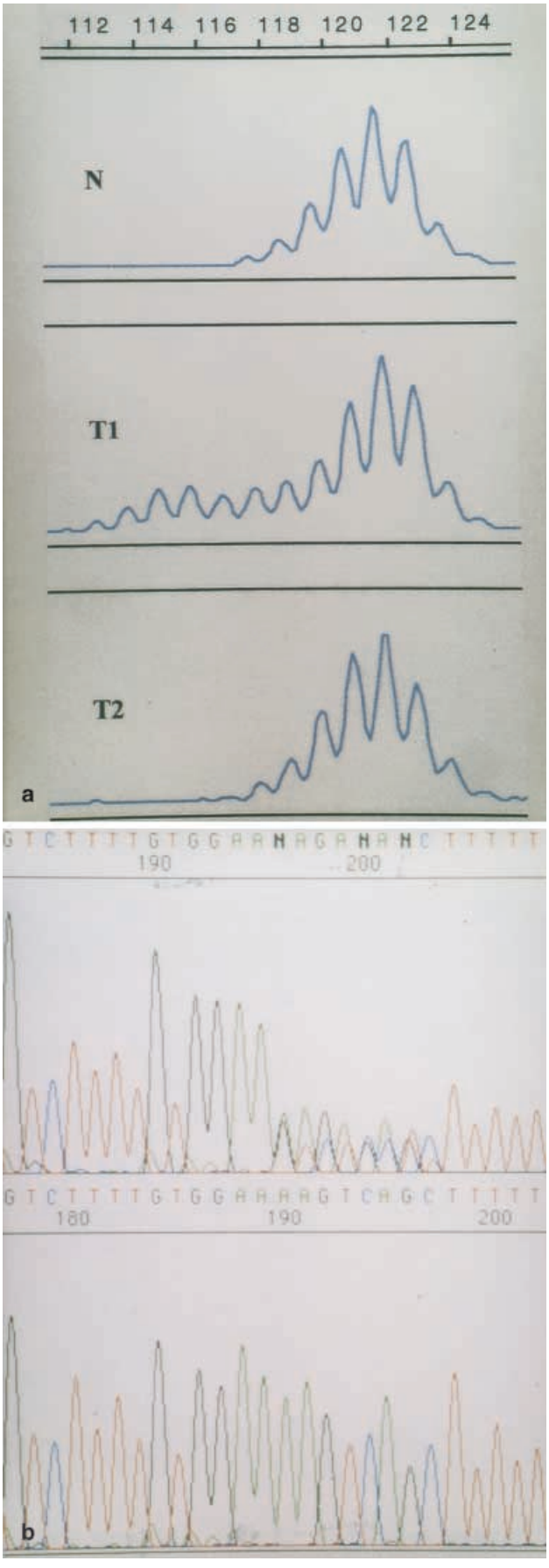


Fig. 2 Mismatch repair gene expression in normal (*upper half*) and tumor tissue (*lower half*) in the colonic carcinoma of the patient with metachronous breast cancer. The carcinomatous tissue shows no hMSH2 expression (**a**) but an intense nuclear staining with anti-hMLH1 (**b**). **c** Specific positive nuclear staining with anti-hMSH2 in the breast cancer specimen

senting a hMSH2 loss displayed instabilities in at least four of the five tested microsatellites, indicating the MSI-H type (Fig. 3a).

Mutation analysis

Mutation analysis revealed a new, previously unknown, mutation in the hMSH2 gene which has not yet, to the best of our knowledge, been reported in the literature. The mutation consists of a 2-bp deletion in a small poly $(T)_4$ run at codons 232 and 233. This mutation led to a frame shift with a stop at codon 254, explaining the loss of hMSH2 expression at the immunohistochemical level (Fig. 3b). Until now, there are no data available regarding the penetrance of a mutation in such a family. In our case, we found the mutation in four of five asymptotic family members. There are five family members currently under the age of 10 years, who have not yet been tested. At the time of genetic counseling, none of these showed clinical signs of having a tumor.



Discussion

Colorectal cancer is one of the common neoplasms in humans and perhaps the most frequent form of hereditary neoplasia. HNPCC is the most common form and accounts for approximately 2–13% of the colorectal cancers annually [1, 13]. The syndrome is clinically characterized with an early age of onset, a proclivity to the proximal colon, a frequency of mucinous and signet ring cells, and an increase in metachronous and synchronous colon cancers [7, 10]. These features compose the HNPCC I syndrome. Another subset of HNPCC is designated as type II. Families with type-II HNPCC have all of the features of type I but also harbor extracolonic cancers [14]. The most common extracolonic tumors are endometrial and gastric carcinomas.

The mode of transmission is compatible with autosomal dominant inheritance, but the location and characteristics of the putative susceptibility gene are unknown. A study by Ponz de Leon et al. [19] demonstrated in a classical segregation analysis of 605 families that cancer risk in families with one affected parent equals that in families where both parents are healthy. They formed a model of dominant transmission through a major gene with greatly reduced penetrance in heterozygotes. Herein, we show a family with a high penetration mutation in the hMSH2 MMR gene that has, to the best of our knowledge, not yet been reported. This mutation led to colorectal cancers in most affected family members with a double synchronous cancer in one patient and an unusually high mortality rate, which contrast the recent findings of Gryfe et al. [8]. In the parental generation, only one member in each family was affected. Therefore, we expected to find the mutation in the asymptotic family members in less than 50% of cases.

To our surprise, we found the germline mutation in the hMSH2 gene in four of five members tested. The children of the mutation carriers have not been tested yet, but one may expect that they also will have a high risk of carrying the mutation. All carriers of the germline mutation are admitted to a pre-screening program and, at present, they are asymptomatic. These findings may suggest that there are differences in the locus of mutation and the frequency of segregation, resulting in high and low penetrance mutations. More studies are, however, needed to evaluate the penetration of different mutations.

Interestingly, there was one case of breast cancer in this family that did not show any MSI (whereas all of the colorectal cancers showed MSI; Table 1) and no loss of MMR gene expression [22, 23]. Currently, the inclusion of breast cancer as an integral tumor of the HNPCC syn-

Fig 3 **a** Microsatellite analysis with mononucleotide repeat marker (BAT 25) shows distinct instability in the colon carcinoma (T1) but not in the metachronous breast tumor (T2). **b** Heterozygous mutation at codon 232 and codon 233 in the hMSH2 gene. The mutation consists of a 2-bp deletion in a small poly(t)$_4$ run. *Lower half* wild-type control

drome is controversial. Most studies [2] indicate that MMR errors are uncommon in human breast cancer and, therefore, breast cancer should not be included as part of the HNPCC syndrome. In contrast, a study by Risinger et al. [20] showed in a HNPCC family a case of breast cancer that exhibited widespread MSI and the expression of the mutant gene. Our findings clearly indicate that breast cancer appears not to be a part of the HNPCC tumor spectrum, although it should be mentioned that the histologic tumor type showed some peculiar features with an undifferentiated pseudosarcomatous portion beneath a usual ductal-type cancer.

In summary, we found a new mutation in the hMSH2 gene with a high mutation penetration and poor prognosis in affected patients. Because the breast tumor did not show the mutation or any MSI, we conclude that the particular case of breast cancer in the patient of this family was not related to HNPCC.

Acknowledgement We thank R. Fishel (Kimmel Cancer Center, Thomas Jefferson University, Philadelphia, PA) for revising the manuscript. Supported by the Deutsche Krebshilfe (70–2401-Rü 1)n Krebsgesellschaft.

References

1. Aaltonen LA, Peltomäki P, Leach FS, Sistonen P, Mecklin JP, Järvinen H, Powell SM, Jen J, Hamilton SR (1993) Clues to the pathogenesis of familial colorectal cancer. Science 260: 812–815
2. Anbazhagan R, Fujii H, Gabrielson E (1999) Microsatellite instability is uncommon in breast cancer. Clin Cancer Res 5:839–844
3. Boland CR, Thibodeau SN, Hamilton SR, Sidransky D, Eshleman JR, Burt RW, Meltzer SJ, Rodriguez-Bigas MA, Fodde R, Ranzani GN, et al (1998) A national cancer institute workshop on microsatellite instability for cancer detection and familial predisposition: development of international criteria for the determination of microsatellite instability in colon cancer. Cancer Res 56:5248–5257
4. Bronner CE, Baker SM, Morrison PT, Warren G, Smith LG, Lescoe MK, Kane M, Earabino C, Lipford J, Lindblomm A (1994) Mutation in the DNA mismatch repair gene homologue hMLH1 is associated with hereditary nonpolyposis colorectal cancer. Nature 368:258–261
5. Dietmaier W, Wallinger S, Bocker T, Kullmann F, Fishel R, Rueschoff J (1997) Diagnostic microsatellite instability: definition and correlation with mismatch repair protein expression. Cancer Res 57:4749–4756
6. Fishel R, Lescoe MK, Rao MR, Copeland NG, Jenkins NA, Garber J, Kane M, Kolonder R (1993) The human mutator gene homologue MSH2 and its association with hereditary nonpolyposis colorectal cancer. Cell 75:1027–1038
7. Fitzgibbons RJ, Lynch HT (1987) Recognition and treatment of patients with hereditary non-polyposis colorectal cancer. Ann Surg 206:289–295
8. Gryfe R, Kim H, Hsieh ET, Aronson MD, Holowaty EJ, Bull SB, Gallinger T (2000) Tumor microsatellite instability and clinical outcome in young patients with colorectal cancer. N Engl J Med 342:69–77
9. Jonsson M, Johannsson O, Borg A (1995) Infrequent occurrence of microsatellite instability in sporadic and familial breast cancer. Eur J Cancer 31:813–814, 2330–2334
10. Lynch HT, Lynch PM (1979) Tumor variation in the cancer family syndrome: ovarian cancer. Am J Surg 138:439–442
11. Lynch HT, Kriegler M, Christiansen TA, Smyrk T, Lynch JF, Watson P (1988a) Laryngeal carcinoma in a Lynch syndrome 2 kindred. Cancer 62:1007–1013
12. Lynch HT, Ens JA, Lynch JF, Watson P (1988b) Tumor variation in three extended Lynch syndrome 2 kindreds. Am J Gastroenterol 83:741–747
13. Lynch HT, Smyrk TC, Watson P, Lanspa SJ, Lynch JF, Lynch PM, Cavalieri RJ, Boland CR (1993) Genetics, natural history, tumor spectrum and pathology of hereditary nonpolyposis colorectal cancer: an updated review. Gastroenterology 104: 1535–1549
14. Lynch HT, Lynch JF (1993) The Lynch syndromes. Curr Opin Oncol 5:687–696
15. Lynch HT, Smyrk T (1996) Colorectal cancer, survival advantage, and hereditary nonpolyposis colorectal carcinoma. Gastroenterology 110:682–687
16. Nikolaides NC, Papadopoulos N, Liu B, Wie YF, Carter KC, Ruben SM, Rosen CA, Haseltine WA, Fleischmann RD, Fraser CM (1994) Mutations of two PMS homologues in hereditary nonpolyposis colorectal cancer. Nature 371:75–80
17. Percesepe A, Benatti P, Roncucci L, Sassatelli R, Fante R, Ganazzi D, Bellacosa A, Genuardi M, Neri G, Viel A, Ponz de Leon M (1997) Survival analysis in families affected by hereditary non-polyposis colorectal cancer. Int J Cancer 71:373–376
18. Ponz de Leon M, Scapoli C, Zanghieri G, Sassatelli R, Sacchetti C, Barrai I (1992) Genetic transmission of colorectal cancer: exploratory data analysis from a population based registry. J Med Genet 29:531–538
19. Ponz de Leon M (1994) Prevalence of hereditary nonpolyposis colorectal carcinoma (HNPCC). Ann Med 26:209–214
20. Risinger JI, Barrett JC, Watson P, Lynch HT, Boyd J (1996) Molecular genetic evidence of the occurrence of breast cancer as an integral tumor in patients with the hereditary nonpolyposis colorectal carcinoma syndrome. Cancer 1:1836–1843
21. Rodrigues-Bigas MA, Boland CR, Hamilton SR, Henson DE, Jass JR, Khan PM, Lynch H, Perucho M, Smyrk T, Sobin L, Srivastava S (1997) A national cancer institute workshop on hereditary nonpolyposis colorectal cancer syndrome: meeting highlights and Bethesda Guideline. J Cancer Inst 89:1758–1762
22. Ruschoff J, Bocker T, Schlegel J, Stumm G, Hofstaedter F (1995) Microsatellite instability: new aspects in the carcinogenesis of colorectal carcinomas. Virchows Arch 426:215–222
23. Thibodeau SN, Bren G, Schaid D (1993) Microsatellite instability in cancer of the proximal colon. Science 260:816–819
24. Thibodeau SN, French AJ, Roche P, Cunnigham JM, Tester DJ (1996) Altered expression of hMSH2 and hMLH1 in tumors with microsatellite instability and genetic alterations in mismatch repair genes. Cancer Res 56:4836–4840

Virchows Arch (2001) 439:196–200
DOI 10.1007/s004280000387

CASE REPORT

**Monica Falleni · Elena Roz · Enrico Dessy
Barbara Del Curto · Paola Braidotti
Umberto Gianelli · Giuseppe G. Pietra**

Primary intrathoracic meningioma: histopathological, immunohistochemical and ultrastructural study of two cases

Received: 17 August 2000 / Accepted: 8 December 2000 / Published online: 7 June 2001
© Springer-Verlag 2001

Abstract Meningiomas are common, usually benign slow-growing neoplasms of the central nervous system thought to arise from meningocytes capping arachnoid villi. Primary ectopic meningiomas are exceedingly rare extracranial and extraspinal tumors of controversial origin; they are usually limited to the head and neck region or to the paravertebral soft tissues. Only one mediastinal ectopic meningioma and few pulmonary ectopic meningiomas have been described in the literature until now. Because of their rarity and their intriguing pathogenesis, we report here a second case of primary mediastinal meningioma and an additional case of primary pulmonary meningioma. Their possible origin and differential diagnosis are discussed.

Keywords Ectopic meningioma · Unusual lung tumors · Immunohistochemistry · Electron microscopy

Introduction

Meningioma is one of the most common neoplasms of the central nervous system, presumed to arise from meningothelial cells capping arachnoid villi. It usually arises in the cranial cavity and less frequently in the intraspinal region. It commonly has an indolent clinical behavior and is characterized by morphological heterogeneity.

Primary ectopic meningiomas are well-known, exceedingly rare neoplasms arising outside the central neural axis for which a direct extension or a metastatic process from a mass in this site can be clinically excluded. They have been usually found in the head and neck region (orbit of the eye, temporal bone, nose, paranasal sinuses, mandible and ear) or paraspinal soft tissues [1, 2, 5, 6, 10, 11, 19]. Their etiology is still uncertain, and several mechanisms have been described [1, 5, 7, 9, 10, 11, 19].

A Medline search revealed only one case of primary mediastinal meningioma [19] and 17 cases of primary pulmonary meningiomas [7, 8, 12, 13, 15, 17] published up to now. In this report, we present the light microscopic, immunohistochemical and ultrastructural features of two new cases of primary intrathoracic meningiomas.

The tumors were discovered during routine chest X-ray examinations. In case 1, the lesion was located in the posterior mediastinum of an asymptomatic 45-year-old woman. In case 2, an intrapulmonary mass was detected in a 58-year-old man admitted to the hospital for adenocarcinoma and multiple adenomas of the colon. At the time of diagnosis, in both cases, there was no evidence of intracranial or intraspinal mass; the classification as meningioma was based on the histological, immunohistochemical and ultrastructural similarity to the homonymous neoplasm of the central nervous system. Both patients are still well and free of disease, 11 years and 30 months after diagnosis, respectively.

Clinical history

Case 1

A 45-year-old white woman was admitted to a hospital for varicose veins of lower extremities and absent left radial pulse. Her past medical history was unremarkable. Digital angiography showed a stenosis of the left subclavian artery involving the vertebral artery ostium and an asymmetry in the vertebral arterial caliber. Routine laboratory tests were within normal values, but both

M. Falleni (✉) · E. Roz · B. Del Curto · P. Braidotti · U. Gianelli
Department of Pathology, School of Medicine,
University of Milan, San Paolo Hospital, via di Rudinì 8,
20142 Milan, Italy
e-mail: monica.falleni@unimi.it
Tel.: +39-02-8135366, Fax: +39-02-89122032

E. Dessy
Department of Toxicology,
Section of Oncology and Molecular Pathology,
University of Cagliari, School of Medicine;
Interuniversity Centre of Oncologic Researches,
University of Milan, Italy

G.G. Pietra
Department of Pathology and Laboratory Medicine,
University of Pennsylvania, Medical School,
Philadelphia, PA 19104, USA

chest X-ray and computed tomography (CT) scan revealed an ovoid mass about 4 cm in its greatest dimension in the right mediastinal paravertebral region (D6), with densitometric characteristics suggestive of a neoplasm of neural origin. The mass was unrelated to her presenting symptoms; it was removed through a right lateral thoracotomy. On the basis of its pathologic features and the absence of any other intracranial or intraspinal primary tumor, it was classified as mediastinal ectopic meningioma. The patient is well and disease free 11 years after surgery.

Case 2

A 59-year-old white man was admitted to the Thoracic Surgery Division of our hospital for evaluation of a well-circumscribed and homogeneous mass, 2 cm in diameter, in the upper superior segment of the left upper pulmonary lobe of 7-months duration. His past medical history was remarkable for retinitis pigmentosa and total colectomy for left colonic adenocarcinoma (Dukes: B2; pT3, N0) and multiple villous adenomas.

The mass was discovered 2 months after surgery, and it was thought to be a solitary metastatic nodule. The patient was started on chemotherapy and, since the mass was unchanged upon chest X-ray and CT scan performed 5 months later, he was readmitted, and the lesion was resected through a left upper lobectomy. On the basis of the microscopic and ultrastructural features and the absence of any intracranial or intraspinal mass, the diagnosis of meningioma was made. The patient is well and disease free after 30 months follow-up.

Materials and methods

Representative specimens of the tumors were routinely fixed in 10% buffered neutral formalin and embedded in paraffin. Tissue sections (5-μm thick) were cut and stained with haematoxylin and eosin (HE), periodic acid–Schiff (PAS) with and without diastase digestion and reticulin stain (Gomori). For immunohistochemical studies, tissue sections were incubated using the standard avidin-biotin peroxidase complex (ABC) method with the following antibodies: cytokeratin pool (AE1/AE3), epithelial membrane antigen (EMA; E29), glial fibrillary acidic protein (GFAP), melanocytic antigen HMB45, S-100, vimentin (V9) and ki67 (MIB 1). Appropriate positive controls were run concurrently for each antibody tested. Ultrastructural investigation was carried out from paraffin-embedded material in case 1 and from formalin-fixed tissue in case 2. For the clinical follow-up, the referring physicians were contacted.

Pathology

Gross pathological findings

Case 1

The tumor was an ovoid, well-circumscribed, brown–gray, firm mass, 4.5 cm in greatest dimension and attached to a 1 cm in length filamentous structure resembling a small nerve. On the cut surface, it was brown to red in color, with diffuse microcalcifications and a cystic hemorrhagic area of about 2 cm in diameter.

Case 2

The lesion was an ovoid, smooth, lobulated mass, 2.5 cm in its greatest dimension, with no relation to the pleural surface or to the large airways. On the cut surface, it was soft, brown–red, with a gelatinous appearance and a central small cystic hemorrhagic area.

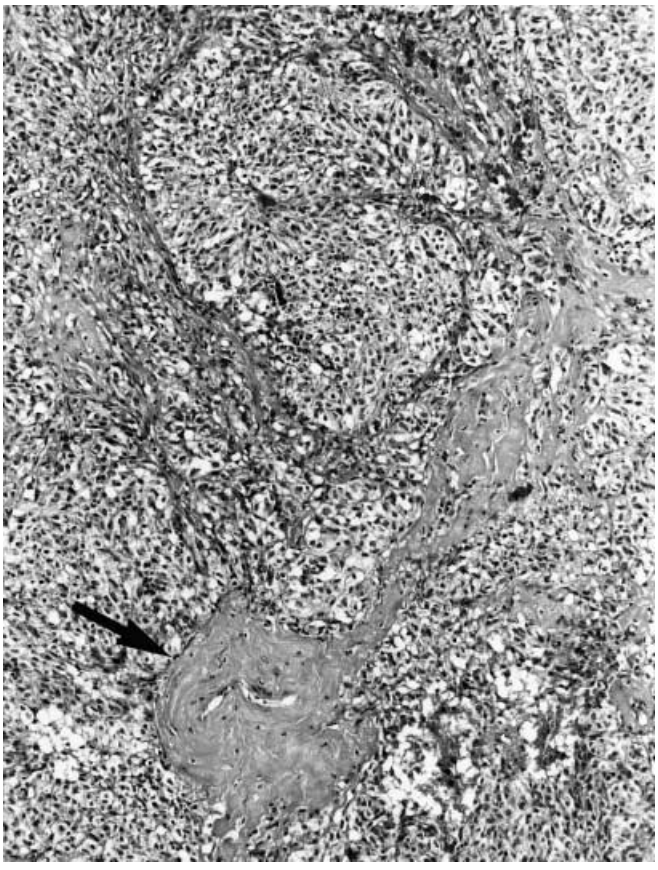


Fig. 1 Case 1. Lobules of clear cells with indistinct cell borders and prominent fibrovascular septa containing vessels with thick hyalinized walls (*arrow*) Hematoxylin and eosin; ×200

Microscopic findings

Case 1

The tumor was encapsulated and composed of nests of larger plump clear cells (Fig. 1) and of bundles of spindle cells often arranged in whorls (Fig. 2). The tumor cells had indistinct cytoplasmic cell borders and weakly eosinophilic or clear cytoplasms with uniformly dispersed finely granular PAS-positive, PAS diastase-resistant material.

The nuclei were large, round to oval and pale, with delicate chromatin distribution, inconspicuous nucleoli and frequent nuclear pseudoinclusions (Fig. 2, *inset*). Mitotic figures were absent. The interstitial stromal tissue was organized in prominent fibrous bands with vessels characterized by thick hyalinized walls (Fig. 1). Reticulin-bearing septa and reticulin-free parenchyma were appreciable (Fig. 2). Few hemorrhagic areas and microcalcifications were dispersed into the neoplasm, and

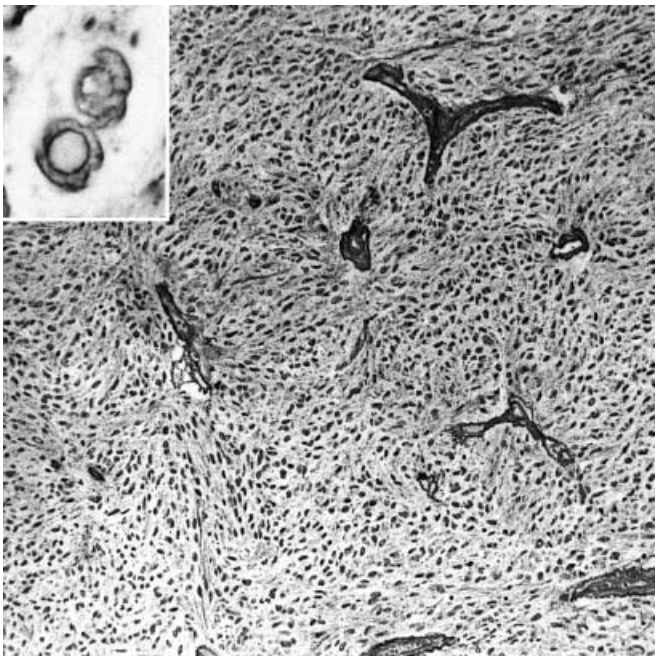


Fig. 2 Case 1. Absent reticulin fibers in between bundles of elongated cells arranged in a whorl-like fashion with frequent nuclear pseudoinclusions (*inset*; ×1000). Gomori's stain; ×250

structures resembling psammoma bodies were seldom seen. No cytologic atypia, necrosis or invasion of surrounding structures was observed.

The neoplastic cells were focally and weakly positive for vimentin, S-100 and EMA. They were negative for cytokeratin AE1/AE3, GFAP, HMB45 (Table 1). There were no Ki67 immunoreactive cells. The small nerve attached to the mass showed strong S-100 immunoreactivity.

Ultrastructural studies showed neoplastic cells with deep nuclear indentations and/or pseudoinclusions, desmosome-like cell junctions and some fibrous long-spacing collagen intermingled with the extracellular matrix. In light of the clinical and pathological data, a diagnosis of primary mediastinal transitional meningioma was made.

Case 2

The tumor compressed the surrounding pulmonary parenchyma and was unencapsulated (Fig. 3A). It was composed of monomorphous bundles of spindle or stellate cells, often organized in whorls, with indistinct cytoplasmic cell borders, long cytoplasmic cell processes,

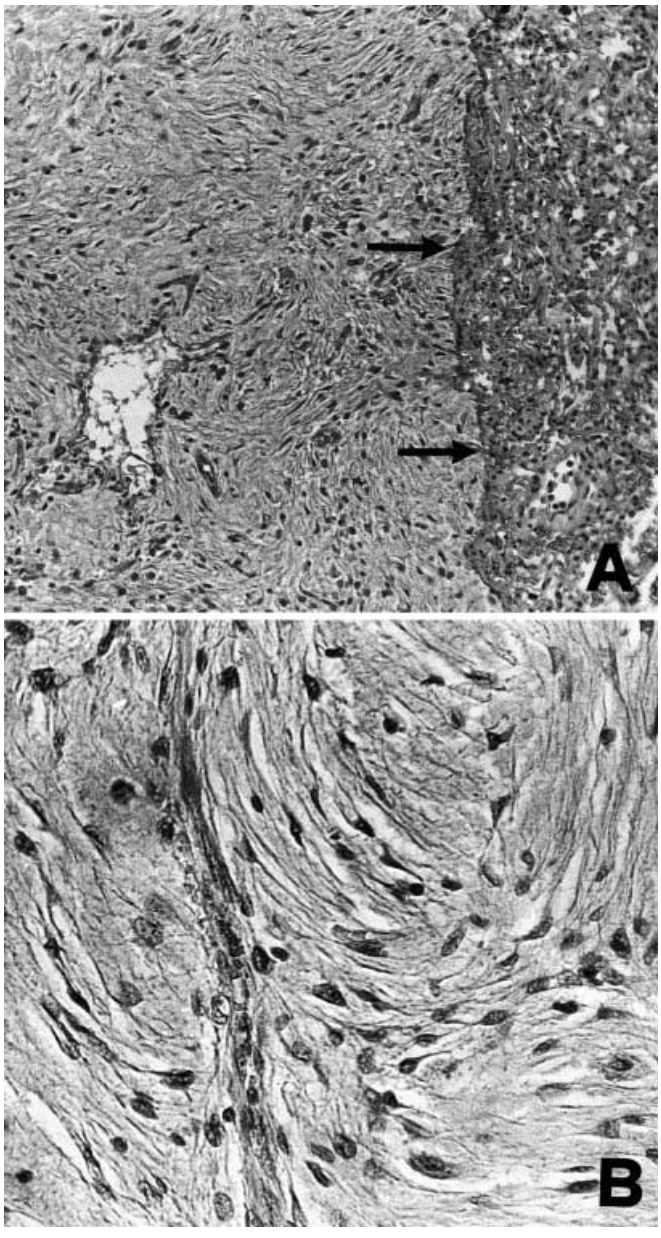


Fig. 3 Case 2. **A** The neoplasm, unencapsulated and compressing the surrounding parenchyma (*arrows*), was composed of bundles of elongated cells immersed in an abundant myxoid extracellular matrix. **B** Spindle-shaped neoplastic cells, often organized in whorls, were dispersed in abundant myxoid basophilic matrix. They showed indistinct cytoplasmic borders, scant weakly eosinophylic cytoplasm, ovoidal nuclei with inconspicuous nucleoli and occasional pseudoinclusion. Hematoxylin and eosin. **A** ×340; **B** ×600

Table 1 Immunohistochemical and ultrastructural features of cases 1 and 2. *EMA* epithelial membrane antigen; *CK* cytokeratin; *Vim* vimentin; *GFAP* glial fibrillary acidic protein. For other immunohistochemical results, see text

	S-100	EMA	CK	Vim	GFAP	Ultrastructural features
Case 1	+/–	+/–	–	+/–	–	Desmosome-like junctions, intranuclear inclusions, and fibrous long-spacing collagen in the extracellular matrix
Case 2	+/–	–	–	+	–	Complex interdigitating cell processes with desmosomes

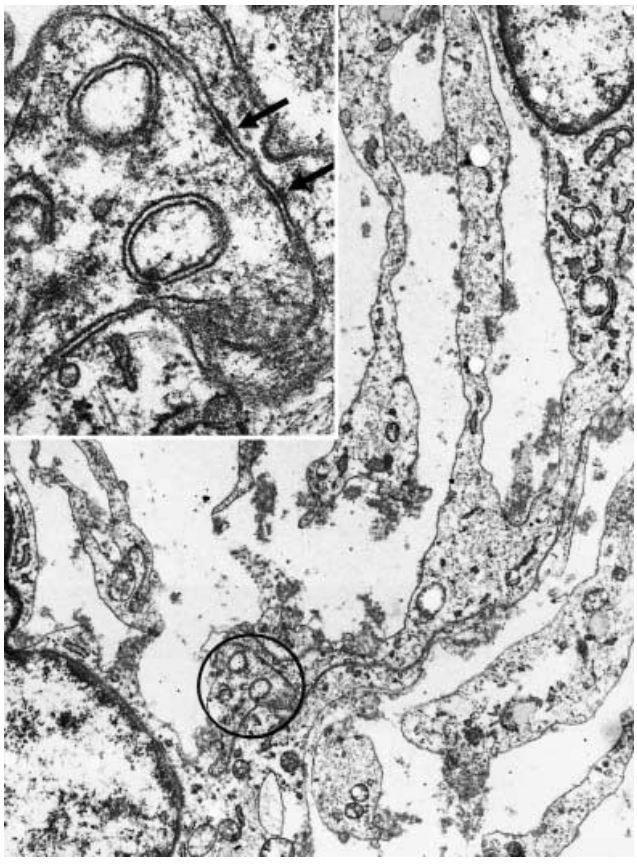


Fig. 4 Ultrastructural features of neoplastic cells showing very long complex interdigitating cytoplasmic processes with desmosome-like junctions (*arrows*; ×9000; *inset* ×37,500)

scant weakly eosinophilic cytoplasm (Fig. 3B) containing finely granular PAS-positive material. The neoplastic cells had ovoidal nuclei with delicate chromatin distribution, inconspicuous nucleoli and occasional nuclear pseudoinclusions. They were separated by abundant myxoid basophilic extracellular matrix (Fig. 3A, B) with scant reticulin and collagen fibers and a mild lymphoplasmacytic infiltrate. Necrosis and vascular invasion were never seen. The surrounding lung parenchyma was unremarkable.

The neoplastic cells were strongly immunoreactive for vimentin and focally for S-100, negative for EMA, cytokeratin AE1/AE3, GFAP, neurofilaments, chromogranin A, desmin, smooth muscle actin, CD31, CD34 and CD68 (Table 1). There were no immunoreactive Ki67 cycling cells.

Ultrastructural findings showed neoplastic cells with very long, bipolar or branched cytoplasmic interdigitating processes with desmosomes (Fig. 4 and *inset*), containing abundant cytoplasmic intermediate filaments. In the extracellular compartment, numerous elastic fibers and some collagen fibers were observed. The neoplasm was classified as metaplastic myxoid pulmonary meningioma [18].

Discussion

Primary ectopic meningiomas are exceedingly rare pathological entities. They have usually been found to arise in cephalic and paravertebral soft tissues and skin but also in the lung and mediastinum [1, 2, 5, 6, 7, 8, 10, 11, 12, 13, 15, 17, 20]. Different theories have been proposed on their pathogenesis and cell of origin [1, 7, 9, 20]. Meningiomas occurring distant from skull and vertebral fusion lines and without association with peripheral nerves have been thought to arise from ectopic meningothelial cells abnormally displaced during embryonal development [1, 5, 6, 10, 11].

Meningiomas with a close relationship to cranial or peripheral nerves are thought to arise from meningothelial cells sited near their appropriate foramina [1], in nervous sheaths carried out along peripheral nerves during fetal development [6] or from perineural cells (or their progenitor cell) morphologically, functionally and immunohistochemically similar to meningothelial cells [6, 11]. Both the mediastinal meningioma reported by Wilson et al. [20] and our case are consistent with this latter hypothesis. Both were encapsulated masses with fibrillary structures resembling nerves entering at one end. The case of Wilson et al. was connected to the stellate ganglion, and our case was connected with the intercostal nerve merging at D6.

As for intrapulmonary meningiomas, the pathogenesis is even more intriguing. They may derive from ectopic intrapulmonary arachnoidal cells [13, 15], from the pluripotential subpleural mesenchyme [15] or from the pulmonary meningothelial nodules described by Gaffey in 1988 [3] and now recognized in the new WHO/IASLC classification of pleural and lung tumors [19].

Despite their unusual site of origin, all ectopic meningiomas described in the literature show morphological, immunohistochemical and ultrastructural features similar to their nervous system counterparts. Most ectopic meningiomas show fibroblastic, meningothelial or transitional morphological features and an immunohistochemical profile with variable immunoreactivity for vimentin, EMA, cytokeratins, S-100, desmoplakins and desmin [15]. Ultrastructurally, they show abundant intermediate cytoplasmic filaments, complex interdigitating cell processes and desmosome-like cell junctions.

Our cases exhibited morphological features not previously described in the literature of ectopic meningiomas. The mediastinal meningioma showed areas of typical transitional meningioma mixed with nests of plump clear cells resembling the rare and more aggressive clear-cell variant of meningioma.

A feature not previously described was the presence of widespread myxoid changes we found in our case of pulmonary meningioma. Myxoid changes, sometimes associated with other mesenchymal metaplastic changes in meningiomas, are very rare in intracranial meningiomas and have been briefly reported in the literature either as regressive changes or features of tumor remodeling or

mesenchymal differentiation, a well-known characteristic potential of arachnoidal cells.

The histologic differential diagnosis of the two cases described here included tumors with similar morphological features, including benign peripheral nerve tumors, metastatic malignant melanoma, inflammatory myofibroblastoma and other mesenchymal pulmonary tumors. The immunohistochemistry ruled out epithelial or mesenchymal neoplasms, either benign or malignant.

However, the contribution of immunohistochemistry in the diagnosis of meningioma is notoriously limited since this neoplasm does not have a specific immunoprofile. The coexpression of epithelial and mesenchymal markers occurs in only 10% of neoplasms [14]. Immunoreactivity for both epithelial and mesenchymal markers is variable. Meis found that EMA and vimentin were present in at least 50% and 18% of cases, respectively [14]. More useful and crucial for diagnosis was the ultrastructural examination with the demonstration of desmosome-like structures linking neoplastic cells. The immunohistochemical and ultrastructural features of the mediastinal and the pulmonary neoplasms described here are summarized in Table 1.

As for clinical course, surgical excision was curative in both cases, in keeping with the lack of morphological features of aggressive behavior, as reported in the recent literature [16]. Both patients are alive and disease free after 11 years in case 1 and 30 months in case 2.

In case 2, the association of intrapulmonary meningioma with retinitis pigmentosa, colonic carcinoma and adenomatous polyps is intriguing. An association between primary meningioma of the lung and colonic carcinoma has been previously reported by Gluck et al. in 1993 [4] in a patient with dermatomyositis, carcinoma of the colon and meningioma of the lung. We have not found cases in which primary lung meningioma was associated with hereditary disorders, such as retinitis pigmentosa or adenomatous polyposis coli (APC) gene abnormalities. However, a longer follow-up and biomolecular studies might shed some light on the pathogenesis of ectopic meningiomas.

In summary, although intrathoracic meningiomas are exceedingly rare, they must be considered in the differential diagnosis of mediastinal and pulmonary neoplasms. At the present time, electron microscopic examination remains the gold standard for an unequivocal pathological diagnosis.

References

1. Coons SW, Johnson PC (1989) Brachial plexus meningioma, report of a case with immunohistochemical and ultrastructural examination. Acta Neuropathol 77:445–448
2. Farr HW, Gray GF Jr, Vrana M, Panio M (1973) Extracranial meningioma. J Surg Oncol 5:411–420
3. Gaffey JJ, Mills SE, Askin FB (1988) Minute pulmonary meningothelial-like nodules. A clinicopathologic study of so-called minute pulmonary chemodectoma. Am J Surg Pathol 12:167–175
4. Gluck Z, Kutsherwsky M, Abraham Z, Galper I (1993) Dermatomyositis, carcinoma of the colon and meningioma of the lung. J Dermatol 20:719–722
5. Ho K (1980) Primary meningioma of the nasal cavity and paranasal sinuses. Cancer 46:1442–1447
6. Husnar M, Fanburg JC, Dickersin RG, Kirshner JJ, Rosenberg A (1996) Retroperitoneal malignant meningioma. A light microscopic, immunohistochemical and ultrastructural study. Am J Surg Pathol 20:492–499
7. Kaleem Z, Fitzpatrick MM, Ritter JH (1997) Primary pulmonary meningioma. Report of a case and a review of the literature. Arch Path Lab Med 121:631–636
8. Kemnitz P, Spormann H, Heinrich P (1982) Meningioma of lung: first report with light and electron microscopic findings. Ultrastruct Pathol 3:359–365
9. Kepes JJ (1986) Presidential address: the histopathology of meningioma. A reflection of origins and expected behaviour. J Neuropathol Exp Neurol 45:95–107
10. Kershisnik M, Callender DL, Batsakis JG (1993) Extracranial, extraspinal meningiomas of the head and neck. Ann Otol Rhinol Laryngol 102:967–970
11. Landini G, Kitano M (1992) Meningioma of the mandible. Cancer 69:2917–2920
12. Lockett L, Chiang V, Scully N (1997) Primary pulmonary meningioma: report of a case and a review of the literature. Am J Surg Pathol 21:453–460
13. Marchevsky AM (1995) Lung tumors derived from ectopic tissues. Seminars in diagnostic pathology 12:172–184
14. Meis JM, Ordonez NG, Bruner JM (1986) Meningiomas. An immunohistochemical study of 50 cases. Arch Pathol Lab Med 110:934–937
15. Moran CA, Hochholzer L, Rush W, Koss MN (1996) Primary intrapulmonary meningiomas. A clinicopathologic and immunohistochemical study of ten cases. Cancer 78:2328–2333
16. Prayson RA (1996) Malignant meningioma: a clinicopathologic study of 23 patients including MIB1 and p53 immunohistochemistry. Am J Clin Pathol 105:719–726
17. Prayson A, Farver CF (1999) Primary pulmonary malignant meningioma. Am J Surg Pathol 23:722–726
18. Rubinstein LJ (1972) Tumours of the central nervous system. In: Atlas of tumor Pathology, 2nd series, fasc. 6. Armed Forces Institute of Pathology, Washington DC, pp 169–190
19. Travis WD, Colby TV, Corrin B, Shimosato Y, Brambilla E (1999) Histological classification of lung and pleural tumours. WHO, 3rd edn. Springer, Berlin Heidelberg New York
20. Wilson AJ, Ratliff JL, Lagios MD, Aguilar MJ (1979) Mediastinal meningioma. Am J Surg Pathol 3:557–562

Virchows Arch (2001) 439:201–205
DOI 10.1007/s004280100448

CASE REPORT

Janez Lamovec · Ana Pogaènik

Metastatic medulloblastoma to the breast

Received: 27 November 2000 / Accepted: 17 February 2001 / Published online: 16 May 2001
© Springer-Verlag 2001

Abstract We present a case of metastatic medulloblastoma to the breast in a 33-year-old woman who had a cerebellar medulloblastoma excised 2 years previously. Upon presentation, she had a bilateral breast tumor, which was diagnosed as a malignant small cell tumor by means of fine needle aspiration biopsy. An excisional biopsy of the tumor was performed, showing metastatic medulloblastoma, morphologically identical with a cerebellar primary. Eighteen months following breast surgery, the patient developed unilateral ovarian and peritoneal metastases and died of the disease 57 months after the cerebellar tumor was excised. Metastatic medulloblastoma to the breast is an extremely rare form of a secondary breast tumor, which may be easily diagnosed when both primary and secondary tumors are cytologically or histologically compared. If this is not possible, considerable problems may be encountered to get to the correct diagnosis.

Keywords Metastatic medulloblastoma · Breast

Introduction

Metastatic tumors to the breast are rare. They account for 0.5–1.3% of all breast malignancies [1, 11, 20]. If secondary lymphomas are excluded, the most common tumors to metastasize to the breast are malignant melanomas followed by lung carcinomas [1, 11, 20].

In this report, an extremely rare occurrence of metastatic medulloblastoma to the breast is presented. The metastases appeared 2 years after the primary tumor of the cerebellum was excised. To the best of our knowledge, this is the fifth case of metastatic medulloblastoma to the breast to be reported [2, 3, 4, 14].

J. Lamovec
Department of Pathology, Institute of Oncology,
Ljubljana, Slovenia

A. Pogaènik (✉)
Department of Cytology, Institute of Oncology, Zaloška 2,
1000 Ljubljana, Slovenia
e-mail: jlamovec@onko-i.si
Tel.: +386-61-1314180

Clinical history

A 33-year-old woman presented with a tumor in the right breast. Upon physical examination, two separate tumors were palpated in the upper outer quadrant of the right breast; in the contralateral breast, a lump was also found. A fine needle aspiration biopsy of the tumor in the right breast showed a highly malignant small cell tumor with predominantly necrotic and degenerated cells; no definitive diagnosis as to its nature was given. An excisional biopsy was performed. Following diagnosis, the patient was given chemotherapy.

The patient was operated upon 2 years previously in another institution for the tumor in the right cerebellar hemisphere. The tumor was excised and diagnosed as medulloblastoma; the patient was postoperatively irradiated.

One and a half years after breast surgery, the patient was admitted again to our institution because of an abdominal tumor and ascites. Upon laparotomy, an 830-g and 15×11×8-cm right ovarian tumor was resected; small peritoneal metastases were also excised. Postoperatively, she was given chemotherapy again. The patient died 15 months after the last surgery and 57 months after the brain operation. No autopsy was performed.

Materials and methods

The surgical specimen of the breast was fixed in a 4% buffered neutral formalin solution. All sections were stained with hematoxylin and eosin (HE). On selected paraffin sections, immunohistochemical reactions were performed using a standard peroxidase-labelled streptavidin–biotin complex method with diaminobenzidine as a chromogen. The antibodies against the following antigens were used: epithelial membrane antigen, dilution 1:500; CK MNF 116, dilution 1:100; CAM 5.2, dilution 1:20; neuron-specific enolase (NSE), dilution 1:1000; chromogranin A, dilution 1:1500; synaptophysin, dilution 1:100; glial fibrillary acid protein, dilution 1:4000; vimentin V9, dilution 1:500; neurofilament, dilution 1:2000; S-100 protein, dilution 1:750; desmin 33, dilution 1:50; smooth muscle actin, dilution 1:750; and CD99 (Mic 2), dilution 1:75.

In all cases except for CK MNF 116, microwave heating pretreatment was used. For CK MNF 116, protease pretreatment was employed. The immunostaining was performed automatically with Techmate 500 Immunostainer (BioTek, Santa Barbara, Calif.). All

antibodies were from Dako, Copenhagen, Denmark, except for CAM 5.2, which was a product of Becton Dickinson (San Jose, Calif.). We also obtained unstained slides of a cerebellar tumor from another institution while paraffin blocks were not available. HE-stained slides of cerebellar tumor, breast tumor, and ovarian tumor were compared.

Pathological findings

The gross specimen was represented by a 20-g segment of breast tissue, which contained two nodules measuring 4.0×3.2×2.0 cm and 1.5×1.5×1.2 cm, respectively. On the cut surface, the large nodule was composed of several matted nodules; the neoplastic tissue was white to yellow in color, and some of the nodules were hemorrhagic.

Microscopically, many of the nodules were hemorrhagic and necrotic, with sparse vital tissue. They were clearly circumscribed from the surrounding breast tissue. Nodules were composed of dense, dark, small neoplastic cells (Fig. 1). Focally, the cells were in relatively compact nests. Elsewhere there were less cellular foci with blood and floating tumor cells. Some nests of tumor cells were surrounded by dense collagen fibers, imparting alveolar features to the tumor (Fig. 2). Nuclei of tumor cells were oval, focally more spindle or irregular, with finely granular dense or coarser chromatin and indistinct nucleoli. Mitoses were numerous. The individual cell necroses were numerous and pyknotic, and karyorrhectic nuclei were in abundance. The cytoplasm of neoplastic cells was indistinct in many cells, focally moderately abundant, and intensively eosinophilic with pushed-aside nuclei giving cells an rhabdoid appearance. In rare foci, tumor cells were arranged around small vessels. They were taller and wedge-shaped; cytoplasmic prolongations of such cells produced a faint fibrillary background in a few foci. Some of these foci appeared as relatively clearly circumscribed nodules (Fig. 3).

Immunohistochemically, practically all tumor cells were strongly positive for NSE, and many were positive for vimentin; some cells and fibrillary matrix were positive for synaptophysin, particularly in and around nodules (Fig. 4), and only rare cells were positive for chromogranin. Neoplastic cells were invariably negative for cytokeratins, epithelial membrane antigen, desmin, smooth muscle actin, muscle-specific actin, S-100 pro-



Fig. 1 Low-power view of a clearly circumscribed metastatic nodule composed of small dark neoplastic cells. Hematoxylin and eosin

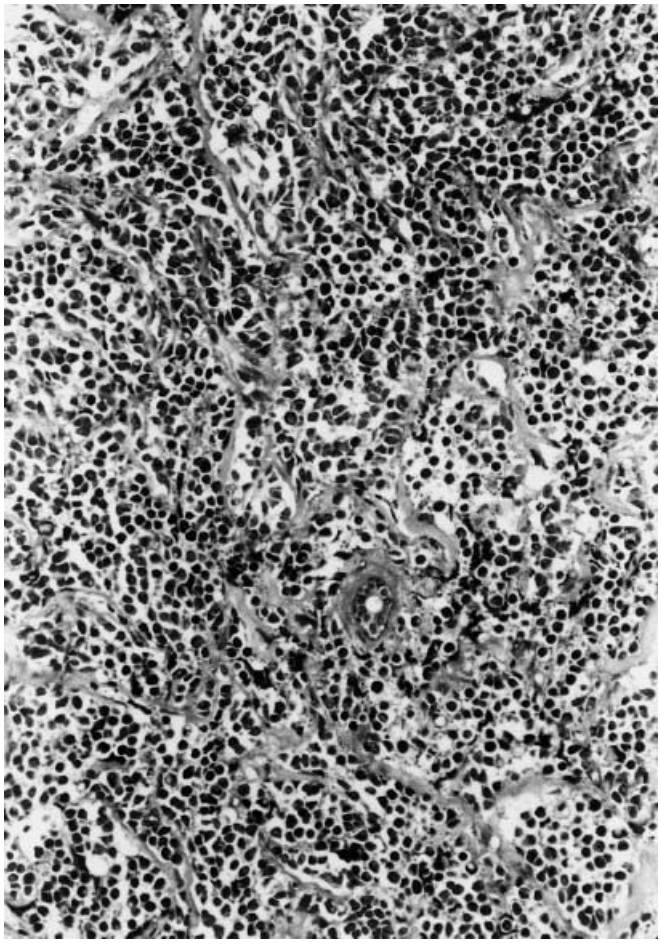


Fig. 2 Vague alveolar arrangement of dissociated neoplastic cells; a preexistent ductal structure is seen near the center of the figure. Hematoxylin and eosin

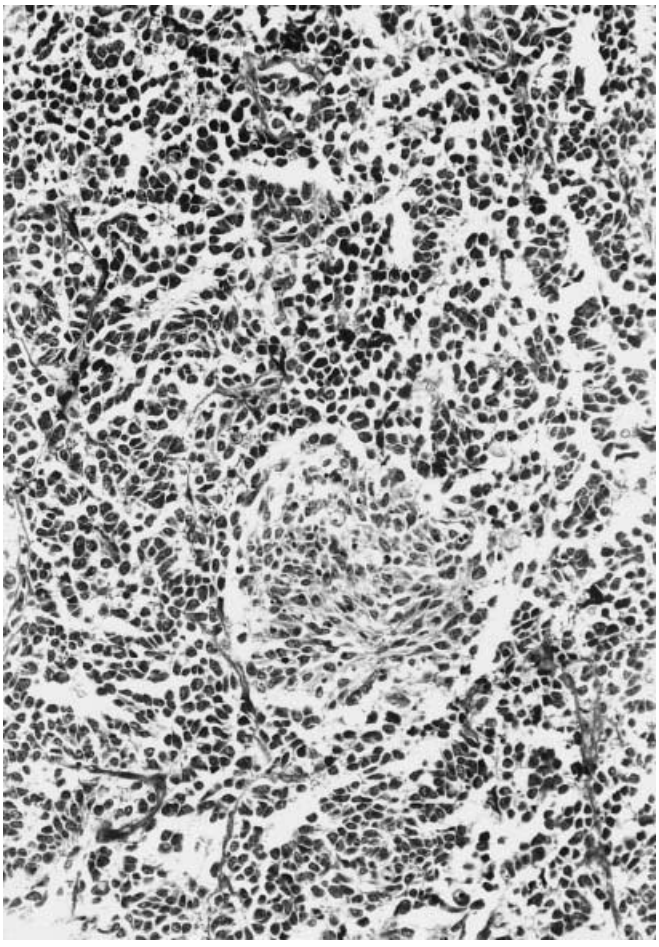


Fig. 3 Higher power view of the tumor to show oval, round, or slightly spindled cells with scant cytoplasm and dark nuclei. Centrally, a nest of more elongated cells with fibrillary extensions is shown, forming relatively clearly circumscribed nodule. Hematoxylin and eosin



Fig. 5 Primary tumor in the cerebellum showing infiltration of the brain substance and more pronounced nesting/nodular pattern of growth. Hematoxylin and eosin

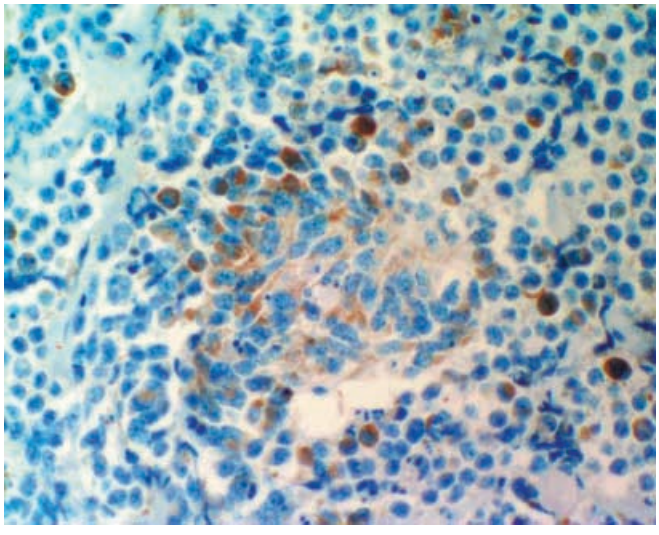


Fig. 4 Neoplastic cells of the nodule in the breast metastases show a positive reaction for synaptophysin

tein, neurofilament, glial fibrillary acid protein, and CD99.

The histological appearance of the breast tumor was identical to that of the cerebellar tumor except for less necrotic, hemorrhagic, and degenerative changes in the latter. The nodules seen in the breast tumor were even more pronounced in the cerebellar tumor (Fig. 5). The ovarian tumor also exhibited the same morphology as both previous tumors.

Discussion

Metastatic tumors to the breast are rare; apart from leukemia, lymphoma, and contralateral breast carcinoma, malignant melanoma, lung carcinoma, and carcinoid tumors are the most commonly reported primary tumors [11, 21]. In the vast majority of cases, metastases to the breast develop in the context of a known primary, and the diagnosis is not difficult if the cytology/histology of both tumors are compared. Fine needle aspiration biopsy

Table 1 Metastatic medulloblastoma to the breast. *H* histological, *C* cytological

Author/year	Age (years)/gender	Operation	Time to breast metastasis (months)	Diagnosis of breast metastasis	Other metastatic sites	Follow-up (months)
Brutschin and Culver, 1973 [3]	18/Female	Excision	14	H	Bones, lung	DOD – 31
Brydon and Carey 1991 [4]	17/Female	Excision	15[a]	H	? Bone marrow	DOD – 16
Baliga et al. 1993 [2]	35/Female	Lobectomy	16	C, H	Pleura, bones	No data
Kapila et al. 1996 [14]	9/Male	Decompression	36	C	None	Lost at 18
Lamovec and Pogačnik 2001[b]	33/Female	Excision	24	C, H	Ovary, peritoneum	DOD – 39

[a] Metastasis to fibroadenoma [b] Present report

of a breast tumor in such cases is a method of choice, obviating surgical procedure [7, 9]. However, in cases when a breast tumor is the first to appear and another primary is unknown, the diagnostic problems may be formidable, particularly in a frozen section setting [8, 11, 19, 21].

Metastases of medulloblastoma to the breast are extremely rare though not unheard of [2, 3, 4, 14]. Four previous cases are on the record. In three of them, the breast was the first metastatic site (Table 1). In one of the cases, medulloblastoma metastasized to the pre-existing fibroadenoma [4]. Medulloblastoma, a primitive, undifferentiated tumor of the cerebellum, frequently metastasizes along the cerebrospinal fluid pathways [5]. Moreover, approximately 5% of patients with medulloblastoma may expect to develop systemic metastases, most commonly to the skeleton [15].

In one pediatric series of 917 primary intracranial tumors, medulloblastoma accounted for 16.5% of all tumors but contributed 71% to all extracranial metastases [6]. In around 10% of cases, extracranial metastases develop in patients with a ventricular shunt [15]. In such patients, metastases appear approximately 1.3 years after diagnosis of the primary cerebellar tumor, while in patients without shunts, they present somewhat later, 2 years after diagnosis on average [15].

In the breast, metastatic medulloblastoma may not be that easy to diagnose, particularly using fine needle aspiration cytology. Comparison of imprints of the brain tumor with cytology smears of the breast lump is particularly helpful [2]; it was not possible in our case, however, and this may have contributed to the uncertainty to decide between metastasis or another primary.

Histologically, the differential diagnosis may include infiltrating duct carcinoma with neuroendocrine features, particularly rare oat cell types [17], a solid variant of lobular carcinoma [10], malignant lymphoma or hematopoetic malignancies [16], and, in childhood, metastasic neuroblastoma [18] and rhabdomyosarcoma. The latter is known to occur in the breast either as a primary tumor [12] or metastasis [12, 13]. If carefully analyzed clinically and histologically, all of these tumors may be correctly differentiated from medulloblastoma. In problematic cases, immunohistochemical examinations resolve the possible dilemmas. Moreover, second primary tumors in medulloblastoma occur but extraordinarily rarely. Therefore, the appearance of an extracranial tumor in a patient with a known medulloblastoma is much more likely to be a metastasis than another primary [15].

It is of interest to note that nodularity apparent in a cerebellar tumor that appeared to be a desmoplastic subtype of medulloblastoma was also, but to a lesser extent, evident in breast metastases. Furthermore, neoplastic cells in such nodules showed a positive reaction for synaptophysin which is also one of the characteristics of desmoplastic medulloblastoma [5].

In our case, the second metastatic location, 1.5 years following the appearance of the breast metastases, was that in the ovary accompanied by peritoneal spread. The ovarian tumor was unilateral, bulky, and grossly simulating an ovarian primary. Histologically, it was identical to the cerebellar and breast tumor. We are unaware of a report or a review of metastatic medulloblastoma listing the ovary as one of the metastatic locations for medulloblastoma; peritoneal metastases were previously reported, however [6].

In conclusion, the occurrence of metastatic medulloblastoma to the breast is a possible event. The diagnosis is easy if clinical data are known and if imprints of the brain tumor and cytological smears of the breast tumors are compared. When only surgical biopsy is performed, the diagnosis is straightforward if a comparison of histological slides of both tumors is possible. Otherwise, it may be difficult. Fine needle aspiration cytology is the preferred diagnostic procedure in the majority of cases when clinico-pathological correlations are at hand.

References

1. Abrams HL, Spiro R, Goldstein N (1950) Metastases in carcinoma: analysis of 1000 autopsied cases. Cancer 3:74–84
2. Baliga M, Holmquist ND, Espinoza CG (1993) Medulloblastoma metastatic to breast, diagnosed by fine needle aspiration biopsy. Diagn Cytopathol 10:33–36

3. Brutschin P, Culver GJ (1973) Extracranial metastases from medulloblastoma. Radiology 107:359–362
4. Brydon HL, Carey MP (1991) Medulloblastoma metastasizing to a breast fibroadenoma: a case report. Br J Neurosurg 5:73–75
5. Burger PC, Scheithauer BW (1994) Tumors of the central nervous system. Atlas of tumor pathology, 3rd series. Fascicle 10. Armed Forces Institute of Pathology, Washington D.C.
6. Campbell AN, Chan HSL, Becker LE, Daneman A, Park TS, Hoffman HJ (1984) Extracranial metastases in childhood primary intracranial tumors. Report of 21 cases and review of literature. Cancer 53:984–981
7. Deshpande ALH, Munshi MM, Lele VR, Bobhate SK (1999) Aspiration cytology of extramammary tumors metastatic to the breast. Diagn Cytopathol 21:319–323
8. Di Bonito L, Luchi M, Giarelli L, Falconieri G, Viehl P (1989) Metastatic tumors to the female breast: a study of 12 cases. Pathol Res Pract 187:432–436
9. Domanski HA (1996) Metastases to the breast from extramammary neoplasms. A report of six cases with diagnosis by fine needle aspiration cytology. Acta Cytol 40:1293–1300
10. Fechner RE (1975) Histologic variants of infiltrating lobular carcinoma of the breast. Hum Pathol 6:373–378
11. Hajdu SI, Urban JA (1972) Cancer metastatic to the breast. Cancer 29:1691–1696
12. Hays DM, Donaldson SS, Shimada H, Crist WM, Newton WA, Andrassy RJ, Wiener E, Green J, Triche T, Maurer HM (1997) Primary and metastatic rhabdomyosarcoma in the breast: neoplasms of adolescent females, a report of the Intergroup Rhabdomyosarcoma Study. Med Padiatr Oncol 29:181–191
13. Howarth CB, Caces JN, Pratt CB (1980) Breast metastases in children with rhabdomyosarcoma. Cancer 46:2520–2524
14. Kapila K, Sarkat C, Verma K (1996) Detection of metastatic medulloblastoma in a fine needle breast aspirate. Acta Cytol 40:384–385
15. Kleinman GM, Hochberg FH, Richardson EP (1981) Systemic metastases from medulloblastoma. Report of two cases and review of literature. Cancer 48:2296–2309
16. Lin Y, Govidan R, Hess JL (1997) Malignant hematopoietic breast tumors. Am J Clin Pathol 107:177–186
17. Papotti M, Gherardi G, Eusebi V, Pagani A, Bussolati G (1991) Primary oat-cell (neuroendocrine) carcinoma of the breast. Virchows Arch 420:103–108
18. Rogers DA, Lobe TE, Rao BN, Fleming ID,Schropp KP, Prat AS, Pappo AS (1994) Breast malignancy in children. J Pediatr Surg 29:48–51
19. Silverman EM, Oberman HA (1974) Metastatic neoplasms in the breast. Surg Gynecol Obstet 138:26–28
20. Toombs BD, Lester L (1977) Metastatic disease to the breast: clinical, pathological, and radiographic features. Am J Roentgenol 129:673–676
21. Vergier B, Trojani M, de Mascarel I, Coindre J-M, le Treut A (1991) Metastases to the breast: differential diagnosis from primary breast carcinoma. J Surg Oncol 48:112–116

Virchows Arch (2001) 439:206–211
DOI 10.1007/s004280100407

CASE REPORT

M. Elleder · H. Houštková · J. Zeman · J. Ledvinová
H. Poupětová

Pulmonary storage with emphysema as a sign of Niemann–Pick type C2 disease (second complementation group). Report of a case

Received: 30 August 2000 / Accepted: 11 December 2000 / Published online: 28 March 2001
© Springer-Verlag 2001

Abstract A case is described of Niemann–Pick type C2 disease presenting an infantile pneumopathic phenotype known to occur in this recently established, second, minor complementation group of Niemann–Pick type C (NPC) disease. However, the pulmonary involvement was unique, being dominated, in addition to the usual storage macrophage infiltration of the alveolar and septal compartments, by irregular emphysema attributed to storage cell migration into the bronchiolar lumen. The latter modified considerably the X-ray findings and hindered the initial clinical diagnosis. Otherwise, the storage phenotype, including the range of stored lipids, storage distribution, and cell and organ pathology, was found to be identical to that in the whole Niemann–Pick type C disease group dominated by NPC1. The biochemical findings (cholesterol esterification level) corresponded to the classical biochemical phenotype. Emphysema should thus be considered as a variant of the pulmonary NPC2 storage process, governed most probably by an epigenetic mechanism responsible for storage macrophage migration into the bronchiolar compartment.

Keywords Niemann–Pick type C2 · Pulmonary infiltration · Emphysema · Bronchiolar obstruction · Storage pattern

Introduction

The Niemann–Pick disease complex (types A–D) has proved to be remarkably heterogeneous. Sphingomyelinase (SMase) deficiency is represented by former types A and B, while the rest of the complex (types C and D) has been shown to be associated with defective intracellular cholesterol transport, recently specified as defective retroendocytotic transport of lysosomal cargo [17]. Types C and D were unified under one label as Niemann–Pick type-C disease, because both types proved to be allelic [11]. However, complementation tests [24, 28] have unraveled the genetic heterogeneity of Niemann–Pick type-C (NPC), proving the existence of a major complementation group (NPC1), the gene of which, assigned to locus 18q11-12, codes for a protein reputed to function as a sensor of cholesterol concentration in the endosomal system [1, 4, 30]. First, NPC1 gene mutations were reported [15], mutation detection being considered as an integral part of NPC diagnosis today. In the second, minor complementation group, both the underlying gene and the protein code are still missing. So far, six cases have been described in five families (see Table 1). In four of them a unique life-limiting pulmonary condition was present, caused by massive infil-

M Elleder (✉) · J. Ledvinová · H. Poupětová
Institute of Inherited Metabolic Disorders, Ke Karlovu 2, Div. B, Building. D, 128 08, Prague 2, Czech Republic
e-mail: melleder@beba.cesnet.cz
Tel.: +420-2-24918283, Fax: +420-2-24919392

H. Houštková · J. Zeman
Pediatric Clinic, Charles University,
First Faculty of Medicine and University Hospital, Prague, Czech Republic

Table 1 Niemann–Pick type-C2 survey of the published cases

	Age (years)	Pulmonary involvement	Reference
1. Infantile, neurological onset	1.66[a]	No	[4]
2. Juvenile, neurological onset[c]	20[b]	No	[4]
3. Infantile, hepatosplenomegaly[d]	0.583[a]	Severe fatal	[10]
4. Infantile hepatopathic	<1[a]	Severe fatal	[3]
5. Congenital (hepatomegaly, ascites)	0.6[a]	Severe fatal	[6]

[a] Age at death.
[b] Age of living patient.
[c] The patient's sibling suffered from the same disease (identical phenotype)
[d] The patient's sibling, with storage-based neonatal hepatitis, died at 6 weeks with severe fatal pulmonary involvement.

tration of the lung with storage macrophages [19, 23, 24]. This has never been described in the NPC group before, with the exception of one similar case [12], which, however, has not been subjected to complementation tests yet. The pulmonary process has been uniformly described clinically as “interstitial pneumonia” [19, 23] with subsequent “diffuse ground glass lung density” [23]. Recently, the NPC2 phenotype has been extended by the common infantile and juvenile phenotypes with neurological onset (free of overt lung involvement), which is well known in the NPC1 group [28]. The subject of this communication is to report the case of a peculiar pneumopathic NPC2 variant caused by storage-cell infiltration of the alveolar, septal, and bronchiolar compartments, leading to the combination of lung infiltration and irregular emphysema, the latter dominating the X-ray picture and thus hindering the initial clinical diagnosis.

Case report

Clinical history

The girl was born at term from the first uneventful pregnancy of healthy, young, unrelated parents. The birth weight and length were 2850 g and 49 cm, respectively. Oxygen support was necessary for a short time after delivery because of mild asphyxia with an Apgar score of 3-6-9 in the first, fifth, and tenth minute, respectively. The first clinical symptom of the disease was tachypnea, noticed by the mother from birth. Failure to thrive and poor feeding were observed during the first months of life but dyspnea was not present. No other pathological symptoms were observed during repeated physical examinations by the GP (including normal breathing sounds and absence of cough). Muscle hypotonia, moderate hepatosplenomegaly, and a mild delay in developmental milestones were observed at the age of 1 year, when the child was admitted to our department for the first time. Despite normal breathing sounds, the X-ray findings suggested pronounced pathology – multiple bilateral areas of patchy consolidation mixed with areas of increased irregular aeration (Fig. 1). Progressive dystrophy, marked hepatosplenomegaly, quadruspasticity, and clubbing of fingers developed during the second year of life. The lung disease progressed markedly, and the girl became oxygen-dependent from 20 months of age onward. She died at 4 years as a result of global respiratory insufficiency despite permanent oxygen therapy.

The first laboratory investigations were conducted at the age of 1 year. Standard biochemical parameters and findings from several tests for intestinal resorption were normal, except for aminotrans-



Fig. 1 X-ray of the chest. Multiple bilateral areas of patchy consolidation mixed with areas with increased irregular areation

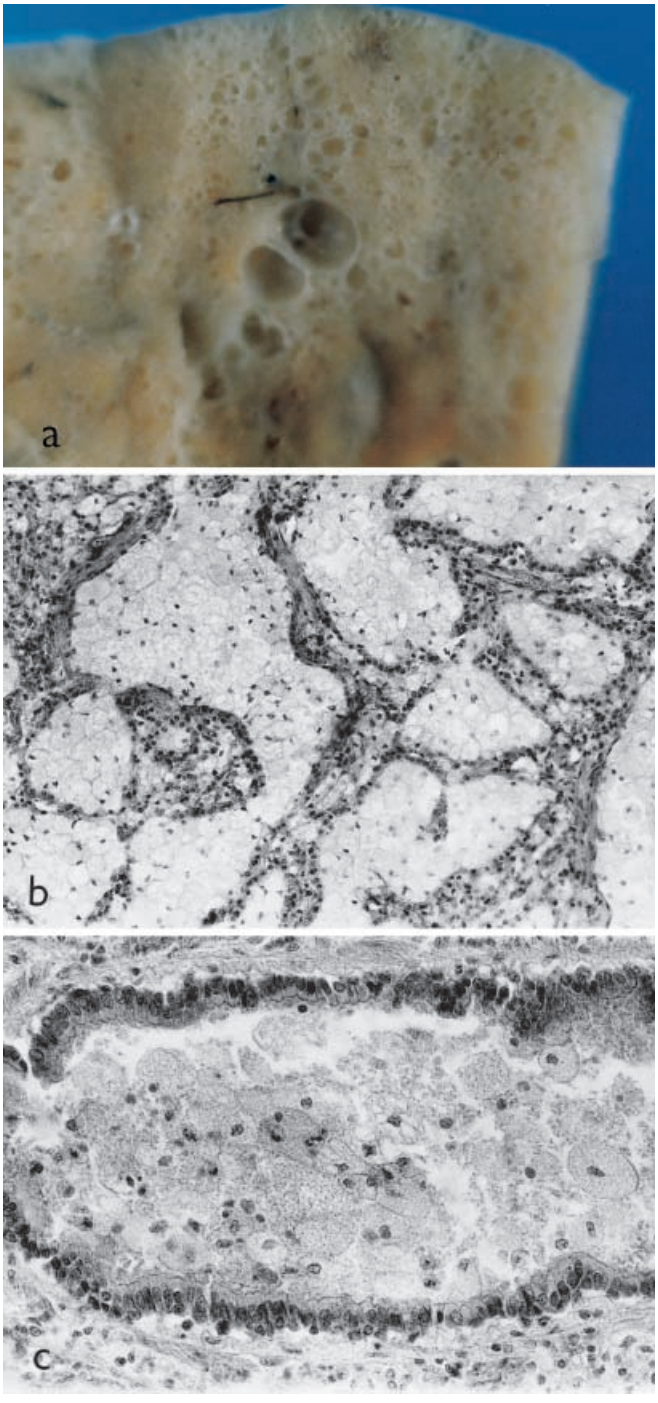


Fig. 2 **a** Section of the lung with pronounced irregular emphysema. **b** Massive infiltration of the lung with storage histiocytes in both alveolar and septal compartments. Hematoxylin and eosin (HE); ×190. **c** Abundant storage macrophages filling the distended bronchiolar lumen. HE; ×375

ferase levels (AST 0.93 μkat/l; controls <0.8) and sideropenic anemia [hemoglobin (Hb) 81 g/l; controls 120–135; mean corpuscular volume (MCV) 68 fl; controls over 80 fl]. X-ray of the chest at the age of 12 months revealed severe bilateral bullous-like changes in the lung parenchyma, suggestive of congenital cystic lung disease (Fig. 1). The blood or urinary levels of amino acids, organic acids, lactate, pyruvate, glycosaminoglycans, and oligosaccharides were normal. Foam cells with a lysosomal phospholipid storage pattern compatible with Niemann–Pick disease type C [7] were found in the bone marrow smear.

Sphingomyelinase activity in the peripheral leukocytes [26] was in the reference range (5.4 nmol/mg per hour; controls 3.3–6.41 nmol/mg per hour). Both the results of filipin testing and intracellular cholesterol esterification of exogenous lipoprotein-derived cholesterol measured in cultivated fibroblasts were highly abnormal, establishing the diagnosis of Niemann–Pick type C, classical biochemical phenotype. A complementation test showed participation of the second, minor complementation group (M.T. Vanier, Lyon).

Autopsy

Macroscopically, moderate hepatosplenomegaly (the spleen weight was 70 g versus 39 g in controls), enlarged lymphatic nodes, and pronounced pulmonary involvement;see below) were observed. The lungs displayed irregular emphysema, partly bullous in character (Fig. 2a), the intervening parenchyma being infiltrated and dense. The weight of each lung was 195 g (only 85–90 g in controls). The adrenal cortex, cerebral hemispheres, cerebellum, and brain stem were macroscopically normal.

Materials and methods

The postmortem tissues were examined after fixation with 10% formaldehyde and paraffin embedding. The sections were stained with hematoxylin and eosin (HE). Brain samples were also stained with Kluver–Barrera stain. Ultrastructural examination was performed after postfixation with buffered 1% OsO_4, dehydration, and embedding into an Epon–Araldite mixture. The thin sections were double-contrasted with uranyl acetate and lead citrate. Lipid biochemical examination was performed as described elsewhere [3, 8].

Structural and biochemical examinations

Microscopy revealed massive storage in macrophages which, in addition to the usual large pool in the lymphatic organs, were also abundant in the liver sinusoids. There was moderate deposition of ceroid in a small fraction of them. Storage was moderate in hepatocytes and relatively strong in the spleen sinus endothelium. Extensive histological examination of both lungs showed deep infiltration with storage of histiocytes, which occupied the alveolar and septal compartments and frequently penetrated massively into the non-cartilage-containing bronchioles (Fig. 2b, c).

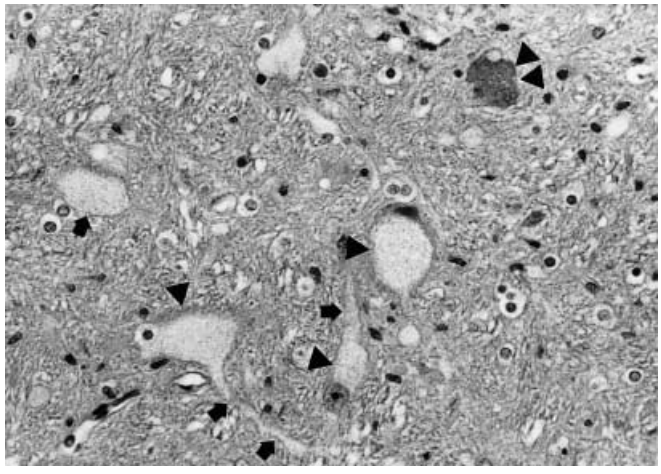


Fig. 3 Neuropathology showing storage distension of brain stem neurons in both the pericaryal (*arrowhead*) and neurite (*arrow*) location, together with neuroaxonal granular type spheroids (*double arrowhead*). Hematoxylin and eosin; ×375

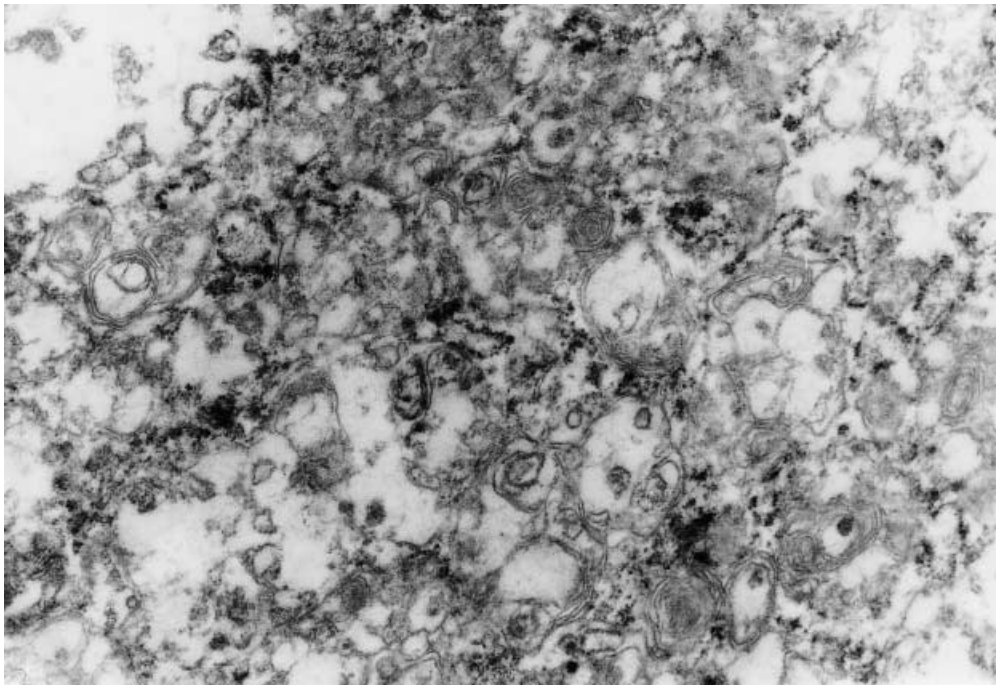


Fig. 4 Ultrastructure of spleen storage histiocyte. Note oligolamellar membranous structures in relatively lucent lysosomes. ×24,000

Table 2 Cholesterol and phospholipids in tissues of Niemann–Pick type C (NPC)2 patient, in previous NPC cases and in controls (in µmol/g wet weight). Concentration of individual phospholipids is expressed in µmolP/g wet weight. Determination has been made according to Bradová et al. [15]. *tr* <0.02 µmolP/g wet weight, *Controls* age-matched controls, (*n*=5), *NPC* previous cases of the NPC disease, age matched [14]. These cases reflect most probably values in NPC1, because it is the dominant type (95%) in this group [18], *LPC* lysophosphatidylcholine, *SM* sphingomyelin, *PC* phosphatidylcholine, *PS* phosphatidylserine, *PI* phosphatidylinositol, *DPG+PG+PA* sum of diphosphatidylglycerol, phosphatidylglycerol, and phosphatidic acid, *PE* phosphatidylethanolamine, *BMP* bis-monoacylglycerolphosphate, *ND* not detected

	Cholesterol	LPC	SM	PC	PS	PI	DPG+PG +PA	PE	BMP
Liver									
NPC2	32.8	1.35	3.56	5.45	1.74	3.14	0.25	3.66	1.67
NPC (*n*=4)									
Mean	22.5±8.4	1.56±1.28	5.52±1.67	11.07±3.23	1.61±1.53	2.59±0.85	0.63±0.36	4.46±2.71	1.86±1.57
Range	15.1–34.5	0.20–2.85	3.25–6.97	7.56–15.4	0.64–3.90	1.39–3.40	0.02–1.70	1.75–8.10	0.06–1.86
Controls (*n*=5)									
Mean	11.8±1.6	0.76±0.50	2.35±0.96	12.76±0.99	1.54±1,17	1.59±0.55	0.88±0.60	5.98±0.68	tr.
Range	10.0–14.3	0.17–1.23	1.00–3.29	11.30–13.88	0.48–3.30	0.8–2.28	0.1–1.58	5.2–6.7	
Spleen									
NPC2	51.9	0.95	10.69	7.20	1.24	1.44	0.13	5.60	1.72
NPC (*n*=4)									
Mean	29.8±7.1	1.39±0.98	12.6±2.27	8.30±3.90	1.45±1.25	1.46±1.17	0.19±0.14	2.46±1.78	1.93±1.09
Range	23.9–39.4	1.28–4.34	10.47–15.54	4.00–13.50	0.66–3.32	0.70–3.22	0.02–0.34	1.10–5.08	1.17–3.53
Controls (*n*=3)									
Mean	10.5±2.4	0.39±0.12	1.64±0.13	4.17±0.81	0.81±0.26	0.33±0.15	0.16±0.12	1.49±0.72	ND
Range	7.3–13.3	0.25–0.50	1.50–1.76	3.59–5.10	0.65–1.12	0.28–0.50	0.02–0.20	0.69–2.10	
Lung									
NPC2	71.4	4.52	6.60	23.55	4.41	3.01	tr	2.29	1.51
Control	4.6	0.35	0.68	2.16	0.77	0.27	tr	1.29	ND

Table 3 Glycolipids in tissues of Niemann–Pick type-C (NPC)2 patient and in controls (in nmol/g wet weight). Determination of individual glycosphingolipids was performed using high-pressure thin-layer chromatography of lipid samples and densitometry of spots, as described [14]. The CAMAG II TLC Scanner (Camag Scientific, Muttenz, Switzerland) was used for measurement in reflectance mode at 546 nm. *GlcCer* glucosylceramide, *LacCer* lactosylceramide, *Gb_3Cer* globotriaosylceramide, *Gb_4Cer* globotetraosylceramide (globoside), *GM3* ganglioside GM3

	GM3	Gb4Cer	Gb3Cer	LacCer	GlcCer
NPC2 spleen	1008	168	400	920	2000
NPC2 lung	948	20	92	430	784
NPC2 liver	488	48	124	374	540
Control spleen	210	36	60	210	68
Control lung	116	40	44	164	60
Control liver	190	16	56	134	20

Exceptionally, there were rudimentary signs of alveolar proteinosis. The alveoles were lined with hypertrophic alveolar type-II cells, rich in secretory lamellar bodies in the apical part but without discernible storage on electron microscopy. The large emphysematous parts were only partly filled with storage macrophages. There was discrete interlobular fibrosis with admixture of elastic fibers and rudimentary inflammatory exudate in several bronchioles without admixture of storage cells. Neuropathological examination was limited by the number of samples (cerebral and cerebellar cortex and brain stem) available as paraffin-embedded blocks.

Cortical and, especially, the brain stem neurons were ballooned because of storage. There was focal neurite storage distension and signs of neuroaxonal dystrophy abundantly expressed in the latter location (Fig. 3). The cerebellar cortex was relatively spared with an occasional drop out of the Purkinje cells, which displayed moderate storage in the dendrites. The ultrastructure of the lysosomal storage (spleen, liver, and lung) was oligomembranous (Fig. 4). The range of lipids stored in the spleen, liver, and lung are shown in Table 2 and Table 3.

Discussion

The overall parameters of the storage process of the presented case, encompassing organ distribution, the range of lipids stored, cell pathology, and neuropathology, corresponded well with the features of the NPC group [5, 6, 25, 27], dominated by NPC1 [28]. The sphingomyelin was clearly concentrated in organs abundantly infiltrated by storage histiocytes, which are the only cells with histochemically detectable sphingomyelin storage in NPC [5]. The disproportional increase in phosphatidylcholine in the lung specimen (Table 2) can easily be explained by hypertrophy of alveolar type-II cells stuffed with secretory granules rich in this phospholipid [29]. The lipid findings corroborate and extend the briefly reported results of the previously described NPC2 cases [7, 12]. The massive pulmonary involvement in our patient

strengthens its significance in the NPC2 phenotype and shifts the currently described ratio for pneumopathic and non-pneumopathic involvement to three out of five (see Table 1). However, the type of the herein reported lung involvement is unique even among the pneumopathic NPC2 variants, owing to the combination of storage infiltration with development of emphysema. The emphysema is undoubtedly directly related to the storage process itself, because there were no other changes known to be pathogenetically significant in this sense (chronic inflammation, loss of elastic fibers, and obstructive airway disease). Bronchiolar invasion (see Fig. 2c) was apparently absent in the cases of NPC2 for which an autopsy has been conducted so far [7, 12]. We, therefore, feel justified enough to conclude that an important, if not exclusive, causal factor is the notable migration of the storage histiocytes into the bronchiolar compartment, meeting thus the criteria of "small airway disease" and emphysema of the centrolobular type [20]. However, the migration pattern of the storage histiocytes is unusual and is most probably governed by epigenetic mechanisms of an unknown nature. It has never been reported in detailed histological studies of the lung tissue carried out in lysosomal enzymopathies affecting the lung, owing to their tendency to express histiocytic storage, such as Gaucher disease [2, 14, 16, 21, 22]. Sphingomyelinase deficiency tends to display recognizable pulmonary infiltration [10, 13, 18], probably frequently in the mild form [18], but severe involvement is extremely rare. There was only one case of variant type A of Niemann–Pick disease in our series of 24 cases of sphingomyelinase deficiencies (unpublished data) with massive pulmonary involvement [9]. A review of these showed that the bronchiolar compartment was only invaded rudimentarily.

Addendum: In the meantime, the gene defective in NPC2 has been identified [Naureckiene S, Sleat DE, Lackland H, et al. (2000) Identification of HE1 as the second gene of Niemann-Pick C disease. Science 290:2298–2301] coding for cholesterol-binding protein HE1. It was found to be mutated in the presented case (M.T. Vanier, personal communication).

Acknowledgements The authors would like to express their gratitude to Dr. L. Neubauer (pathology division, district hospital Strakonice, Czech Republic) for providing the autopsy samples. Dr. M.T. Vanier (Lyon) conducted the cholesterol esterification tests and the complementation assays. We are thankful to Dr. F. Šmíd and V. Bradová for assistance in phosphorus and cholesterol determination. The work was supported by project VS 96 127 of the Ministry of Education of the Czech Republic and partly by grant no. 37/2000/C from the Grant Agency of Charles University

References

1. Abstract Proceeding of the International Workshop on "The Niemann-Pick C. Lesion and the role of intracellular lipid sorting in human disease". October 14–17, 1999, National Institute of Health, Bethesda, MD
2. Amir G, Ron N (1999) Pulmonary pathology in Gaucher's disease. Hum Pathol 30:666–670
3. Bradova V, Šmíd F, Ledvinová J, Michalec (1990) Improved one-dimensional thin-layer chromatography for the separation of phospholipids in biological material (letter). J Chromatogr 533:297–299
4. Carstea ED, Morris JA, Coleman KG, et al (1997) Niemann-Pick C1 disease gene: homology to mediators of cholesterol homeostasis. Science 277:228–231
5. Elleder M (1989) Niemann-Pick disease. Path. Res Pract 185:293–328
6. Elleder M. (1994) The spleen and storage disorders. In: Cuschieri A, Forbes CD, (eds) Disorders of the spleen. Blackwell, Oxford, pp 151–190
7. Elleder M, Hrodek J, Èihula J (1983) Niemann-Pick disease: lipid storage in bone marrow macrophages. Histochem J 15:1065–1077
8. Elleder M, Šmíd F, Hyniová H, et al (1984) Liver findings in Niemann-Pick disease type C. Histochem J 16:1147–1170
9. Elleder M, Cihula J, Sverak J, Vanier MT (1988) Family with profound sphingomyelinase deficiency resisting closer subclassification. In: Salvayre R, Douste-Blazy L, Gatt S (eds) Lipid storage disorders. Plenum, New York, pp 153–161
10. Ferretti GR, Lantuejoul S, Brambilla E, Coulomb M (1996) Case report. Pulmonary involvement in Niemann-Pick disease subtype B: CT findings. J Comput Assist Tomogr 20:990–992
11. Greer WL, Riddell DC, Gillan TL, et al (1998) The Nova Scotia (type D) form of Niemann-Pick disease is caused by a G3097 T transversion in NPC1. Am J Hum Genet 63:52–54
12. Kovesi TA, Lee J, Shuckett E, et al (1996) Pulmonary infiltration in Niemann-Pick disease type C. J Inher Metab Dis 19:792–793
13. Lachman R, Crocker A, Schulman J, Strand R (1973) Radiological findings in Niemann-Pick disease. Radiology 108:659–664
14. Lee RE (1982) The pathology of Gaucher disease. In: Desnick RS, Gatt S, Grabowski GA (eds) Gaucher disease: a century of delineation and research. Liss, New York, pp 177–217
15. Millat G, Marcais C, Raffi MA, et al (1999) Niemann-Pick C1 disease: the I1061T substitution is a frequent mutant allele in patients of western European descent and correlates with a classic juvenile phenotype. Am J Hum Genet 65:1321–1329
16. Morimura Y, Hojo H, Abe M, Wakasa H (1994) Gaucher's disease, type I (adult type), with massive involvement of the kidneys and lungs. Virchows Arch 425:537–540
17. Neufeld EB, Wastney M, Patel S, et al (1999) The Niemann-Pick C1 protein resides in a vesicular compartment linked to retrograde transport of multiple lysosomal cargo. J Biol Chem 274:9627–9635
18. Niggemann B, Rebien W, Rahn W, Wahn U (1994) Asymptomatic pulmonary involvement in 2 children with Niemann-Pick disease type B. Respiration 61:55–57
19. Pin I, Pradines S, Pincemaille O, et al (1990) Forme respiratoire mortelle de maladie de Niemann-Pick type C. Arch Fr Pediatr 47:373–375
20. Pratt PC (1994) Emphysema and chronic airways disease. In: Dail DH, Hammar SP (eds) Pulmonary pathology, 2nd edn. Springer, Berlin Heidelberg New York, pp 847–866.
21. Santamaria F, Parenti G, Guidi G, et al (1998) Pulmonary manifestations of Gaucher disease: an increased risk for L444P homozygotes? Am J Respir Crit Care Med 157:985–989
22. Schneider EL, Epstein CJ, Kaback MJ, Brandes D (1977) Severe pulmonary involvement in adult Gaucher's disease. Am J Med 63:475–480
23. Schofer O, Mischo B, Püschel W, et al (1998) Early-lethal pulmonary form of Niemann-Pick type C disease belonging to a second, rare genetic complementation group. Eur J Pediatr 157:45–49
24. Steinberg SJ, Ward CP, Fensom AH (1994) Complementation studies in Niemann-Pick disease type C indicate the existence of a second group. J Med Genet 31:317–320

25. Vanier MT (1983) Biochemical studies in Niemann-Pick disease. I. Major sphingolipids of liver and spleen. BBA 750:178–184
26. Vanier MT, Revol A, Fichet M (1980) Sphingomyelinase activities of various human tissues in control subjects and in Niemann-Pick disease – development and evaluation of a microprocedure. Clinica Chimica Acta 106:257–267
27. Vanier MT, Suzuki K (1996) Niemann-Pick diseases. In: Moser HW (ed) Handbook of clinical neurology: leukodystrophies and neurolipidoses, vol 66. Elsevier, Amsterdam pp 133–162
28. Vanier, MT, Duthel S, Rodriguez-Lafrasse CP, et al (1996) Genetic heterogeneity in Niemann-Pick C disease: a study using somatic cell hybridization and linkage analysis. Am J Hum Genet 58:118–125
29. Veldhuizen R, Nag K, Orgeig S, Possmayer F (1998) The role of lipids in pulmonary surfactant. Biochim Biophys Acta 1408:90–108
30. Watari H, Blanchette-Mackie EJ, Dwyer NK, et al (1999) Niemann-Pick C1 protein: obligatory roles for N-terminal domains and lysosomal targeting in cholesterol mobilization. Proc Natl Acad Sci U S A 96:805–810

Virchows Arch (2001) 439:235–483
© Springer-Verlag 2001

To all contributors

a congress without free papers is like "a soup without salt." Often the most exciting results and most current developments are presented in selected oral presentations and poster sessions. Thus the related abstracts are especially welcome, and the current issue of *Virchow's Archive* is dedicated in particular to these contributions at the 18th European Congress of Pathology, Berlin 2001.

The enormous number – more than 800 – and extraordinary quality of the abstracts reflect the vitality and attractiveness of pathology, both from a scientific and diagnostic point of view. The content varies from high-tech molecular methods to clinical diagnostic work and again underlines the key function of our specialty as a bridge between laboratory research and clinical applications. It further shows that there are many unsolved problems and that the young generation of scientists still has a lot to do at the bench and at the microscope to further improve our insight into many pathophysiological pathways and increase the accuracy of pathohistological diagnosis, including prognosis and prediction of treatment response.

Rudolph Virchow, the patron of this journal, once wrote "medicine will be a science or it will not be" – let us keep this in mind when we enhance the relevance of experimental and surgical pathology step by step as an indispensable part of human medicine.

Manfred Dietel
President of the 18th European Congress of Pathology

O-001

High resolution analysis of chromosome 18 alterations in ulcerative colitis-related colorectal cancer

Daniela E. Aust**, Jonathan P. Terdiman*, Cornell G. Chang*, Robert F. Willenbucher*, and Frederic M. Waldman*
*Cancer Center, University of California San Francisco, **Pathologisches Institut der Ludwig-Maximilians-Universität, München

We previously have demonstrated that most ulcerative colitis-related cancers show loss of all or part of chromosome 18 by comparative genomic hybridization (CGH). Chromosome 18q is the site of at least three candidate tumor suppressor genes: *DCC*, *SMAD2* and *SMAD4*. One or more of these genes may be involved in the development of sporadic colorectal cancer. The goal of this study was to determine whether these genes are targeted in colitis-related carcinogenesis.
We performed a high-resolution analysis of chromosome 18 alterations in thirty-two colitis-related colorectal cancers by assessing allelic imbalance at 11 microsatellite markers and determining the relative copy number of five genes on chromosome 18 (*PACAP*, *DCC*, *SMAD2*, *SMAD4*, *GALNR*) using the TaqMan method. The results were compared with our previous CGH data.
Allelic imbalance was assessed successfully in 29 of 31 tumors. Allelic imbalance was detected in at least one marker on chromosome 18 in 25 tumors (86%). Allelic imbalance was most commonly detected at *D18S363* (78% of informative cases). This marker is in closest proximity to *SMAD4*. By TaqMan analysis, a relative loss of copy number of *SMAD2*, *SMAD4*, and *DCC* were detected in 40%, 57% and 53% respectively.
Loss of all or part of the long arm of chromosome 18 was detected by LOH or CGH in approximately 80% of colitis-related cancers. Allelic imbalance and gene copy number analysis indicated that loss of one or more of the candidate tumor suppressor genes on 18q (*SMAD2*, *SMAD4*, and *DCC*) occurred in most of the tumors with 18q losses. *SMAD4* appears to be the most frequent target of loss on 18q in colitis-related cancer.
Grant Support: NIH CA 74826 and Deutsche Forschungsgemeinschaft Au 141/1-1.

O-002

Gastrointestinal stromal tumours with skeinoid fibers. Clinical, morphological and immunohistochemical study of 12 cases

Handra-Luca A (1), Terris B (1), Fléjou JF (2), Couvelard A (1), Molas G (1), Duchatelle V (1), Belghiti J (3), Degott C (1)
Departments of Pathology (1) and Department of Digestive Surgery (3) Beaujon Hospital, Clichy; Department of Pathology, St. Antoine Hospital (2), Paris, France

New immunohistochemical and molecular data favor the hypothesis of the undifferentiated mesenchymal origin of gastrointestinal stromal tumours (GIST) in relation with the interstitial cells of Cajal. Skeinoid fibers (SF) in GIST are rare and suggestive for a neurogenic origin. We have studied the characteristics of 12 cases of GIST with SF.
Methods: Among the 25 GIST of the small intestine diagnosed between 1988–2001, 12 tumours contained SF. They were analysed for clinical (age, sex, clinical complaint, type of surgery, size, follow-up), histological, immunohistochemical (CD117, CD34, SMA, desmin, S100protein) and ultrastructural features (5 cases).
Results: All the GIST with SF were located in the small intestine: duodenum (6 cases), ileum (4 cases) and multiple tumours in duodenum and jejunum (2 cases). They represented 50% of GIST of the small intestine diagnosed between 1988–2001. The mean age of the patients was 54 years and the sex ratio was one male for 3 females. The surgical treatment consisted in a tumour resection (9 cases) and in a pancreaticoduodenectomy (3 cases). Tumour size was ranged between 1 and 8 cm. In all cases, SF were numerous and no histological features of malignancy were noted. All patients were alive.
The tumour cells expressed CD117 (83%), CD34 (83%) and SMA (75%). SF did not express any of antibodies used.
Electron microscopy showed inter- (all cases) and intra-cellular SF (1 case).
Conclusions: In our series, GIST with SK were exclusively located in the small intestine and had a benign evolution. As the other GIST without SF, a frequent expression of CD117 and CD34 was observed in these tumours.

O-003

Gastrointestinal stromal tumors with skeinoid fibers. Immunohistochemical study of 12 tumors

Julié C, Petit T, Régnier A, Malafosse R*, Penna C*, Nordlinger B*, Franc B.
Departments of Pathology and Digestive Surgery (*), Ambroise Paré Hospital, Boulogne, France

Introduction: Stromal tumors with skeinoid fibers (STSF) are usually described in the small bowel. These spindle cell tumors contain characteristic extracellular globules. Their place among the group of gastrointestinal stromal tumor (GIST) is not well-defined. The prognostic significance of skeinoid fibers is uncertain. Our aim was to test in a pure series of STFS whether these tumors present the GIST characteristic immnunohistochemical profile.
Methods: 12 STSF from 4 patients (one of them had multiple STSF in association with von Recklinghausen's disease) were stained with the following antibodies:
c-kit (CD-117), CD34, Smooth Muscle Actin (SMA), Desmin, S-100 protein, Mib1 (Ki67).
Results: Immunostaining of the tumoral cells

Case	Nb of tumors	c-kit	CD34	SMA	Desmin	S100-P	Mib1 (%)
1	1	+++	+++	+	-	-	1,4
2	1	+++	+++	+	-	-	0,1
3	1	+++	+++	+++	-	+	2,5
4	9	+++	6+++/ 3++	7+/ 2++	8–/ 1+	7+/ 2–	0,8–3

Staining +++: *>70%*, ++: *20–70%*, +: *<20%*, –: *no staining*
Skeinoid fibers were not stained by the used antibodies.
In case 3, the ultrastructural study confirmed the presence of skeinoid fibers as well as a smooth muscle differentiation.
Conclusions: All our STSF expressed both c-kit and CD34 GIST markers. Our results confirm that STSF represent a subset of GIST, having a similar possibility of predominant smooth muscle differentiation. In our study, the proliferative index was low, and was as-

sociated with other prognostic factors (small size and low mitotic count), all in favor of a benign behavior.

O-004

Gastrointestinal stromal tumors: Size, metastasis and BCL-2 expression as prognostic factors for survival in a mathematical model

Kontogianni E.[3], Demonakou M.[3], Dallas L.[1], Lariou K.[2], Vourlakou C.[2], Kavatzas N.[1], Davaris P.[1]
Departments of Pathology Medical School University of Athens[1], "Evagelismos" GH; "Sismanoglion" G H,[3] Athens, Greece

We examined 102 gastrointestinal stromal tumors (GISTs) by conventional light microscopy, immunohistochemistry and image analysis, [66 males, 36 females; their age ranged from 22 to 99 years (mean: 63.33)] to determine the prognostic factors for survival. The tumor's location and size, immunophenotype, histologic grade, proliferation activity index by PCNA and Ki-67, apoptotic markers BCL-2 and BAX, were considered as prognostic factors and were correlated with patient survival [0-82 months (mean: 33 months)]. Multivariate analysis selected: **a) Tumor size >8 cm, b) PCNA >10%, c) mitoses >5/10HPF, d) necrosis, e) metastasis**, as negative prognostic markers. **BCL-2 protein expression >37.42%** was associated with better survival. The **Linear Regression Technique** can predict lifetime expectation for patients with GISTs, if these tumors are considered as borderline malignancies. The mathematical model for survival is: **$Y=c-0.68\cdot X_1+0.25\cdot X_2-22.9\cdot I_3$, (Y=lifetime, c=49.6 months, X_1=size, X_2=% BCL-2, I_3=metastasis)** (r^2 =0.67, Prob >F=0.0001).
CONCLUSIONS: Tumor size (>8 cm), mitoses, PCNA, necrosis and metastasis are associated with poor prognosis, whereas BCL-2 protein expression is associated with better prognosis. The Linear Regression Technique can predict lifetime expectation in the 70% of patients with GISTs.

O-005

Detection of lymph node metastases in rectal carcinoma

P. Noelp, O. Dworak
Institut für Pathologie, Klinikum Fürth

Introduction: Lymph node metastases are one of the most important prognostic factor in rectal carcinoma. The significance of micrometastases is not solved. The detection of small metastases is difficult and different methods were applied. We compared classical histological with immunohistological methods for the detection of micrometastases.
Methods: 44 cases of rectal carcinomas were examined. All lymph nodes were cut on three step sections. The number of lymph nodes and metastases were counted on every step section. Immunohistological stain for pan-cytokeratin (Lu-5, BMA Biomedical AG) was applied on 21 cases without metastases.
Results: 32 cases showed no metastases after step sections. Comparing step sections 111 additional nodes could be detected (572 nodes on one section vs. 683 nodes on three sections). Immunohistological examination revealed only one case with micrometastasis classified as tumorfree previously. After reexamining of the HE slide this metastasis could be revealed. Twelve cases with metastases showed additional 55 nodes after step sections (212 vs. 267 lymph nodes). Applying step sections 13 new metastases could be detected (34 vs. 47).
Conclusion: Using step sections we found a higher number of lymph nodes and lymph node metastases. Immunohistological examination of cases without lymph node metastases revealed an only case with small metastasis which could be demonstrated after reexamination of the original slide. We think step sections are more useful for the detection of nodal metastasis than immunohistochemisty.
Corresponding author: Prof. Dr. (H) Otto Dworak, Institut für Pathologie, Klinikum Fürth, Jakob-Henle-Str. 1, 90766 Fürth, Tel.: 0911 7580380, Fax: 0911 7580892, e-mail: dworak@pathologie-fuerth.de

O-006

Gastrointestinal tumors: Clinicopathological study of a series of 24 cases

R. Orellana, I. Méndez, E. Musulén, M.R. Bella, J. Lloreta*, Ll. Pons, N. Combalia, M. Rey
Dept. of Pathology. UDIAT-CD, Corporació Parc Taulí, Sabadell, *Hospital del Mar. Barcelona, Spain

INTRODUCTION: Gastrointestinal stromal tumors (GIST) represent a heterogeneous group whose classification frequently requires ultrastructural and immunohistochemical studies although parameters for behavior are not definitively established. We studied various clinicopathological features of a series of GIST to try to find some prognostic factors.
METHOD: Twenty-four resected cases of GIST were revised. Collected date were: sex (F/M), location (gastric=G, small bowel=SB), size, necrosis, atipia, mitosis, follow-up, expression of actin, desmin, S-100 protein, NSE, CD-34 and c-kit (CD-117). Ultrastructural study (EM) was performed. Tumors were divided into benign (B), borderline (BL) and malignant (M) according to mitosis and size. Results were compared with the French Federation of Cancer Centers (FFCC) grading system.
RESULTS: Sex: 14F/10M; location: 15G, 9SB; size: 9<5 cm, 15>5 cm; 10 without and 14 with necrosis; 17 without and 7 with atipia; mitosis (×50HPF): 21<5 M and 3>5 M; follow-up: 18 alive and 6 dead. Any case was positive for muscular and neural markers and 18 cases were CD-34 diffusely positive. EM: 10 tumors were considered GANT. Nine cases were B, 12 BL and 3 M; with the FFCC system 1=grade 0, 16=1, 7=2, 0=3. Only location and mitosis (5×50HPF) of all the clinicopathological date studied were statistically significative in relation to follow-up (p=0.046 and p=0.075).
CONCLUSIONS: Grading according size and mitosis as well as the FFCC systems are not good predictors of outcome. Only location (small bowel) and more than 5 mitosis per 50HPF could be used as indicative of malignant behavior.

O-007

c-kit Deletion mutations, cell proliferation, and prognosis in subtypes of gastrointestinal stromal tumors (GIST)

Pauser, U., Oschlies, I., Capella, C., Heidorn, K., Höfler, H., Klöppel, G., Rudolph, P.
Departments of Pathology of the Universities of Kiel and München, Germany, and Varese, Italy

Introduction: Recently, we have shown that stromal tumors of the gastrointestinal tract may be classified in six categories (GI-PACT I [CD117+], GI-PACT II [CD34+], muscular, schwannian/glial, glial/neuronal, and fibrous) based on antigen expression patterns. Mutations of the c-kit gene, which confer a gain-of-function on the protein product, have been described in a portion of CD117-positive GIST.
Methods: Since in frame deletions in exon 11 are the most common c-kit mutations in GIST, 211 tumors comprising all above defined subtypes were screened by means of PCR amplification and capillary electrophoresis (CE). The proliferative activity (PA) was assessed using monoclonal antibody Ki-S5, and disease-specific survival was computed by Kaplan-Meier analysis.
Results: Molecular anylsis of the c-kit gene was sucessful in 128 cases. Deletion mutations were detected in 23 out of 57 GI-PACT I (40.4%), 2/17 GI-PACT II (11.8%), and 3/6 fibrous tumors (50%), but none of the other subtypes. Mutations were associated with a significantly increased average PA (p=0.004) and showed a weak trend towards an adverse out come (p=0.18). By contrast, tumor location (p=0.022), necrosis (p=0.001), tumor size (p=0.009), and PA (p=0.0006) were significant predictors of prognosis.
Conclusions: The occurrence of in frame deletions in exon 11 of the c-kit gene is predominantly - but not necessarily – associated with CD117 expression. Gain-of-function of the c-kit tyrosine kinase appears to stimulate the PA in GIST. However, the weak correlation of c-kit mutation with the clinical outcome suggests that additional genetic aberrations are required to enhance the malignant potential of GIST.

O-008

Gastrointestinal stromal tumors and KIT-positive mesenchymal cells in the omentum

Sakurai, S.
Jichi Medical School, Tochigi, Japan

INTRODUCTION: Gastrointestinal stromal tumor (GIST) is currently considered to be derived from interstitial cells of Cajal (ICC). To test the hypothesis that omental mesenchymal tumor is also a type of GIST, we evaluated the expression of specific molecules in GIST and c-*kit* gene mutation in omental mesenchymal tumors, and identified a possible counterpart of (ICC) in the omentum. **METHODS:** Immunohistochemical phenotypes were analyzed in five ometal mesenchymal tumors, which were morphologically consistent with GIST in tubular GI tract. Moreover, mutations in c-kit gene exons 9, 11 and 13, which were mutational hot spots of GIST, were examined by polymerase chain reaction-single strand conformational polymorphism (PCR-SSCP) analysis and direct sequencing
RESULTS: All of the omental mesenchymal tumors were positive for both KIT and CD34, and three of the five tumors were also positive for an embryonic form of smooth muscle myosin heavy chain (SMemb). Mutations in *c-kit* gene exon 11 were found in all five tumors. As for the ICC-counterpart, there were some KIT-positive mesenchymal cells resembling ICC at the surface of the omentum. Fluorescence double-immunostaining, using anti-KIT polyclonal antibodies and monoclonal antibodies against other molecules, demonstrated that KIT(+) CD34(+) SMemb(+) cells were present just beneath the mesothelial cells of the omentum.
CONCLUSION: These results indicate that omental mesenchymal tumor correspond to GIST of the omentum and that KIT-positive bipolar mesenchymal cells may be a counterpart of interstitial cells of Cajal in the GI tract.

O-009

Immunohistochemical investigation of drug resistance in recurrent colon carcinomas

H.S. Zorzos, N. Kavantzas, A.Ch. Lazaris, S. Tseleni, N. Tsavaris, P. Davaris
Dept. of Pathology, Medical School, University of Athens, Greece

Introduction/Aim: The resistance of cancerous cells to cytotoxic drugs is thought to be a major cause of the failure of chemotherapeutic treatments. The aim of this study is to detect changes of the expression of P-glycoprotein (P-gp), multi-drug-resistance protein (MRP), lung-resistance protein (LRP) and topoisomerase IIa (topoIIa) in recurrent colon carcinomas after chemotherapy and to evaluate the possible role of the above markers in the induction of multidrug resistance (MDR).
Material and Methods: Samples of 20 patients suffering from rapidly recurring stage C_2 colon carcinoma were used. Patients were treated with 5-fluorouracil (5-Fu) and leukovorin. The immunohistochemical expression of P-gp, MRP, LRP and topoIIa was evaluated by image analysis before and after chemotherapy. Statistical analysis was based on Wilcoxon signed rank test and Spearman test.
Results: Malignant cells from tumour recurrences were characterized by a statistically significant increase only in topoIIa immunolabeling by comparison to the primary tumours. As concerns the MDR-related proteins, the quantitative changes of LRP and MRP after chemotherapy though statistically insignificant, were positively interrelated.
Conclusion: Increased topoIIa immunohistochemical expression appears to be part of the relapsing tumours' phenotype. Therapeutic options after failure of 5-FU-based treatment could therefore include appropriate topoIIa targeted drugs. However, most of the topoIIa inhibiting agents are substrates for P-gp or for MRP; so P-gp or MRP positive tumors may be less effectively treated with topoIIa inhibitors. Therefore, before the selection of a topoIIa inhibiting agent, the expression of the MDR-related proteins should be estimated.

O-010

Pilot european protocol for adenocarcinoma of large bowel (EPPALB).
The greek experience

Hellenic Gastrointestinal Pathology Group: Working Team: P Arapadoni, C Barbatis, M Demonakou, I Delladestima, Z Kafiri, Z Manika, F Patakiouta, C Patsiaoura, C Petraki, C Skopa, A Skopelitou, C Spiliadis, T Toliou , I Venizelos, H Vretou
Sismanoglion General Hospital, Athens, Greece

AIM: The feasibility of using the EPPALB in Hellenic Pathology departments, by experts and non-experts pathologists throughout the country.
MATERIALS AND METHODS: The protocol was used in 12 hospitals (3 University hospitals, 7 regional, one Cancer Institute and 1 district hospital). Overall 34 Pathologists participated in the study. The applicability of the protocol was examined in 324 surgical specimens of colorectal adenocarcinoma and 28 parameters were assessed.
RESULTS: In 25 out of 28 parameters high applicability rate was achieved by 95-100%. Discordance was found for the recognition of the apical lymph node and for the assessment of the distance of the tumor from the deep (lateral) margins for all colorectal carcinomas. For rectal cancers there was difficulty in identification of the peritoneal reflection (54%) and in measuring the distance from the pectate line (58%).
CONCLUSIONS: EPPALB is an applicable protocol for most Pathology departments. Better use can be achieved after further discussion among pathologists and collaboration with the clinicians

O-011

Preneoplastic lesions of the gastric cardia in patients with Barrett's esophagus and patients with atrophic chronic gastritis associated with intestinal metaplasia

Armando Gamboa Domínguez[1], Ramón Carmona[2,3], **Alberto Rubio Tapia**[1], Arturo Angeles Angeles[1], Javier Elizondo[2], David Kershenobitch Stalnikowitz[3]
Departments of Pathology[1], Endoscopy[2] and Gastroenterology[3]; Instituto Nacional de Ciencias Medicas y Nutricion Salvador Zubirán, México City

Background: A rising incidence of adenocarcinoma in the EG junction has been reported. A great unknowledge of the preneoplastic lesions in this area exists.
Aim: To describe the morphologic changes in cardia of patients with Barrett's esophagus >3cm (BE >3cm), and in patients with chronic gastritis associated with intestinal metaplasia (CGMI).
Design: Prospective study of patients with endoscopic diagnosis of BE and CGMI who accepted expanded sampling of esophagus, EG-junction, cardias, fundus, body and antrum. A questionnary evaluating reflux and gastritis was applyed. Patiens with morphologic diagnosis of BE, CGMI and adecuated samplig were included. Sections stained with HE, PAS-D/AA were evaluated blindly by two pathologists using the actualized Sydney system. Numeric values were assesst to esophagic lesions. Differences were identified using t, X^2 and U-Mann-Whitney. Odds ratios were obtained using logistic regression.
Results: 120 patients were invited to participate, 94 were included (47 by group). No differences in age, gender, alcoholism nor tabaquism were observed. Hiatal hernia ($p<0.0006$) and regurgitation ($p=0.02$) were more frequent in BE. Abdominal pain ($p=0.005$) and painful hunger ($p=0.000$) with GCMI. Cardiac atrophy was observed more frequently in GCMI ($p=0.05$), and intestinal metaplasia with BE ($p=0.01$). More extensive and incomplete metaplasia was observed in the cardia of patients with BE ($p=0.04$) and 3.5 times higher risk of cardia lesion.
Conclusions: The risk of preneoplastic lesions in cardia mucosa of patients with BE >3cm is 3.5 times higher than that of patients with GCMI. The extension and severity of the metaplastic changes in cardia are higher in patients with BE.

O-012

Histopathologic profile of gastric carcinoma in southern western Turkey and northern Germany: A comparison

Y. Gürbüz [1,4], V. Kahlke[2], H. Öztürk[3], Z. Yumbul[1], G. Klöppel[4]
1. Dept. of Pathology, U.K. Kocaeli Turkey; 2. Dept. of Surgery, U.K. Kiel Germany; 3. Dept. of Pathology, Gen. Hosp. Antalya Turkey; 4. Dept. of Pathology, U.K. Kiel Germany

INTRODUCTION: Environmental factors play an important role in gastric carcinogenesis. The incidence of gastric carcinoma, age and gender distribution, localisation in the stomach and histopathological type are changing with rising living standards. The aim of this study is to investigate whether gastric carcinoma cases from Turkey and Germany differ in their histopathologic profiles, because of the differing lifestyle in the two countries.
MATERIAL and METHOD: The study is based on paraffin embedded tissue from 160 gastrectomy specimens (80 from Germany and 80 from Turkey). Data on age, gender and site were obtained from the protocols. All tumors were classified according to Lauren's or Carneiro's classification.
RESULTS: On average German patients are 8.47 years older than in the Turkish series (67.92 vs 61.11). Cardia localisation is nearly two times more common in the German gastric carcinoma series than the Turkish series (26.25% vs 11.25%). In the Turkish series the intestinal type according to Lauren's classification accounts for 55%. In contrast, there is no significant difference in frequency between the diffuse and the intestinal type in the German series (diffuse type 36.25% and intestinal type 38.75%). Adenoid type according to Carneiro's classification is most frequent in the Turkish series (45%), which it is the second most frequent in the German series.
CONCLUSION: There are significant differences between the clinical and phenotypic data of the two series. It appears that the intestinal type and an antral localisation characterize Turkish gastric carcinomas. This pattern of gastric carcinoma might be a result of chronic exposure to exogenous carcinogens that are more prevalent in Turkey than in Germany.

O-013

Disruption of the pericryptal myofibroblastic cell layer in colorectal adenocarcinoma

Yve Huttenbach, M.D., Candice Hamilton, Mamoun Younes, M.D.
Department of Pathology, Baylor college of Medicine and The Methodist Hospital, Houston, TX, USA

Introduction: A pericryptal myofibroblastic cell layer (PMCL) has been described in the normal colon and rectal mucoasa. The aim of this study is to determine whether PMCL is affected by the neoplastic process in the colon and rectum.
Methods: Sections of formalin-fixed and parafffin-embedded endoscopic biopsy tissues from 6 colorectal adenomas and 5 colorectal adenocarcinomas were immunostained for alpha smooth muscle actin (SMA) using standard immunoperoxidase method. Some of the sections contained pieces of normal mucosa. The immunosatining pattern was then recorded and compared with the morphologic findings.
Results: All pieces of tissue showing normal colonic mucosa or adenoma showed a thin PMCL intimately associated with the nor-

mal or dysplastic crypts, rspectively. By contrast, significant disruption or absence of PMCL was seen in all carcinomas.
Conclusion: Like the basal cell layer in the prostate and the myoepithelial cell layer in the breast, absence of PMCL in biopsies of colorectal tumors may help differentiate carcinoma in situ/high grade dysplasia from invasive adenocarcinoma. Prospective studies are needed to confirm these findings.

O-014

Tenascin expression in microscopic colitis

Salas A, Fernández-Bañares F, Casalots J, Forcada P, González C, González G, Tarroch X
Departments of Pathology and Gastroenterology,
Hospital Mutua de Terrassa, Terrassa, Barcelona, Spain

INTRODUCTION: Tenascin (TN) is an extracellular matrix glycoprotein, expressed during morphogenesis and tissue remodelling, that has an active role in epithelial-mesenchymal interactions. Immunohistochemical detection of TN has been considered of great utility in the diagnosis of collagenous colitis (CC). The aim of this study was to evaluate the expression of TN in CC and lymphocytic colitis (LC), two forms of microscopic colitis both characterised by lesions at the epithelial-stromal interface in colorectal mucosa.
METHODS: Immunohistochemistry for TN was performed in colorectal biopsies from patients with histological diagnosis of CC (n=24) and LC (n=10). We also included in the study two patients not fulfilling the standard diagnostic criteria of CC (mean subepithelial band thickness <10 μm in the trichrome stain). Biopsies from 10 patients with watery diarrhoea, and 5 asymptomatic patients, all of them without histological lesions, served as control groups.
RESULTS: All specimens from CC cases expressed strong subepithelial TN positivity. In general, the thickness of the TN-positive bands were greater than those measured by means of trichrome stain, and the inferior limits were more irregular and frayed. In the two patients with suspected CC by trichrome stain, the TN band thickness was 18 and 20 μm. All LC cases, as well as the cases of the two control groups, expressed only a slight and discontinuous subepithelial TN positivity, without differences between the groups.
CONCLUSIONS: Immunohistochemical detection of Tenascin in colorectal biopsies simplifies the diagnosis of microscopic colitis and allows correct classification of doubtful cases.

O-015

NADPH quinone oxidoreductase 1 (NQO1) inactivating codon 609 polymorphism predisposes towards adenocarcinoma in Barrett's esophagus

M. Bitzer[1], W. A. Schulz[2], M.Stahl[3], J. Szumilo[4], A. Dabrowski[5], H. Geddert[1], H. E. Gabbert[1], M. Sarbia[1]
Institute of Pathology[1], Department of Urology[2], University Düsseldorf; Internal Medicine, University Essen[3], Germany; Department of Pathomorphology[4], Department of General Surgery[5], University Lublin, Poland

Background: NQO1 is an antioxidant enzyme, important in the detoxification of environmental carcinogens and mutagens that could be involved in carcinogenesis. A single nucleotide polymorphism at codon 609 (null-allele) has been associated with decreased enzyme activity and with increased risk for various chemically induced tumors such as lung cancer and bladder cancer. Additionally, reduced NQO1 activity has been associated with resistance to chemotherapeutic agents such as mitomycin C. In the current study, the prevalence of the NQO1 null-allele was determined in patients with adenocarcinoma (ADC) or squamous cell carcinoma (SCC) of the esophagus. Additionally, it was investigated whether the presence of NQO1 null-allele in tumor tissue influences the outcome of patients with chemotherapeutically treated esophageal SCC.
Methods: DNA was extracted from normal tissues derived from 150 patients with esophageal SCC and from 50 patients with Barrett's esophagus-associated ADC. Additionally, DNA from tumor tissue of SCC that were treated either by polychemotherapy and surgery (n=21) or by radiochemotherapy and surgery (n=48) was studied. The prevalence of NQO1 null-allele was determined following PCR-based amplification of a codon 609-containing fragment of the NQO1 gene and subsequent restriction fragment analysis.
Results: Among 150 patients with SCC, 9 were homozygous for the null-allele and 28 were heterozygous. The null-allele overall frequency (0.153) was slightly higher than the previously published frequency in a normal population in the Düsseldorf area (0.135; p=0.0219). Among 50 patients with ADC, 2 were homozygous for the null-allele and 28 were heterozygous. The null-allele overall frequency (0.320) was significantly higher than among patients with SCC (p<0.0001) and than among the normal population (p<0.0001). Among chemotherapeutically treated SCC, the presence of NQO1 null-allele was neither correlated with response to chemotherapy nor with overall survival.
Conclusion: The high prevalence of the NQO1 null-allele in the patients with esophageal ADC indicates that it is a predisposing factor for this tumor type. The lower prevalence among patients with esophageal SCC probably reflects the profound differences in the etiology of both tumor types, i.e. nicotine and alcohol abuse in SCC and acid and bile reflux in ADC. Early determination of the codon 609 polymorphism in patients with Barrett's esophagus without cancer may allow the identification of patients with a high risk for the subsequent development of Barrett's ADC.

O-016

On the origin and location of cardiac mucosa - An autopsy study in fetuses

G. De Hertogh, P. Van Eyken, K. Geboes
Dept Pathol, KU Leuven, Belgium

INTRODUCTION: The cardia is described as the zone lined by mucus secreting glands just distal to the lower end of the esophagus. Recently, it has been proposed that such a zone is not present at birth but develops as a result of metaplasia.
The aim of our study was to examine the entire gastroesophageal (GE) junction – defined by the peritoneal reflexion – in fetuses to see if a cardia is present at birth.
METHODS: The entire GE junction of 21 fetal or perinatal autopsy specimens (range 11 weeks postmenstrual age – 7 months after timely birth) was examined. Sections stained with H&E and mucin stains (PAS, Alcian blue) were evaluated by 3 pathologists for the location and nature of the squamocolumnar junction and transition to the GE junction.

RESULTS: The squamocolumnar junction was always located above the GE junction. Mucus-secreting glands without parietal cells were present between the squamocolumnar junction and the GE junction. This zone seemed to shorten gradually with increasing postmenstrual age (range 5 crypts at 20 weeks – 2 crypts at 40 weeks). These findings were in conjunction with the results of the mucin stains.
CONCLUSIONS: A short segment of mucus-secreting columnar epithelium is present below the squamocolumnar junction in the distal esophagus from 11 weeks postmenstrual age to 7 months after birth. These findings confirm the existence of a genuine cardia.

O-017

Sporadic and syndromic fundic gland polyps with and without dysplasia: An immunohistochemical study

Paolo Declich (1), Fátima Carneiro (4), Matteo Cornaggia (4), Aldo Ferrara (3), Stefano Caruso (3), Monica Porcellani (1), Luciana Ambrosiani (1), Roberta Grassini (1), Aurora Bortoli (2), Alberto Prada (2), Stefano Bellone (1), Enrico Tavani (1), Claudio Gozzini (2)
(1) Service of Pathology, (2) Division of Gastrointestinal Endoscopy, Rho Hospital, Italy; (3) Division of Gastrointestinal Endoscopy, Legnano Hospital, Italy; (4) Service of Pathology, S. Carlo Hospital, Paderno Dugnano, IPATIMUP, Porto, Portugal

Introduction: Fundic gland polyps (FGPs) are small sessile (2–5 mm) usually multiple polyps arising in the gastric acid-secreting mucosa. They have been described, with identical histology, in a sporadic form, prevalently in middle-aged females, or associated with familial adenomatosis coli (FAP)-Gardner's syndrome and their genetic variants (syndromic FGPs). We performed an immunohistochemical study on 28 sporadic and 5 syndromic FGPs (4 without, 1 with dysplasia) in order to find any possible difference in their immunophenotype.
Methods: We stained our cases and 4 normal controls with a panel of monoclonal antibodies (MoAbs) against Ck20, M1, EMA, chromogranin A, Ck 7, oncofetal and proliferation antigens, using a standard ABC method.
Results: Ck20 and M1 were positive on surface and foveolar epithelium of controls, whereas sporadic and syndromic FGPs showed an enhanced deep positivity below foveolar necks ("foveolar metaplasia"); EMA (parietal cells) and chromogranin A on FGPs was like controls. Ck7, as expected, was negative in controls, whereas all 5 syndromic FGPs and 25 of 28 sporadic FGPs showed a diffuse superficial and deep expression. All FGPs showed a neoexpression of CEA and mucin oncofetal epitopes (ranging from occasional to almost universal). MIB1-labelling index of surface and deep compartments of FGPs showed a statistically steady increase from controls (16.9% superficial stain only), sporadic FGPs (15.8% and 19.5%), syndromic without (30.5% and 37.1%) and syndromic FGPs with dysplasia (60.8% surface, 56.6%).
Conclusions: Both sporadic and syndromic FGPs showed a neoexpression of CK7, CEA, and mucin epitopes. As CK7 and mucin epitopes are normally expressed by fetal stomach, FGPs showed an "immature" immunophenotype. The MIB1-labelling index showed a significantly different proliferation between sporadic FGPs, syndromic FGPs without dysplasia and syndromic FGP with dysplasia.

O-018

Histology of the gastroesophageal junction: A detailed study on 36 operation specimens

A. Donner[1], F. Borchard[2], H.E. Gabbert[1], M. Sarbia[1]
Institutes of Pathology, University Düsseldorf[1]; Klinikum Aschaffenburg[2], Germany

Background: It is currently under discussion whether the gastric cardiac mucosa represents a metaplastic change of the distal esophageal squamous epithelium resulting from gastroesophageal reflux disease (GERD). Furthermore, controversy exists whether intestinal metaplasia in the cardia develops as a result of GERD or as a result of HP-associated pangastritis.
Methods: The entire esophagogastric junction of 36 patients who had been operated for squamous cell carcinoma of the upper or middle esophagus was examined. H&E-stained slides were evaluated by two pathologists for the following histological details: minimal and maximal length of cardiac mucosa (CM) and oxyntocardiac mucosa (OCM – mixture of cardiac and fundic glands), degree of inflammation in CM and OCM as well as presence of intestinal metaplasia (IM) or pancreatic metaplasia (PM). Sections of gastric corpus mucosa were evaluated for the presence of gastritis and sections of esophageal squamous epithelium for the presence of GERD.
Results: CM was present in all cases but one (median length: 5 mm; range: 0–15 mm). The presence of OCM was verified in all cases (median length: 7 mm; range: 2–23 mm). The total length of junctional mucosa (CM+OCM) ranged between 5 mm and 28 mm (median: 12 mm). In 8 cases (22%), junctional mucosa was situated over submucosal esophageal glands, indicating a location in the esophagus. In 18 cases (50%), IM was present in the junctional mucosa; PM was found in 22 cases (61%). A not statistically significant tendency for increase of minimal length of CM, OCM and total junctional mucosa was found in the presence of GERD and in the presence of severe gastritis. Neither the presence of IM nor of PM in junctional mucosa was correlated with GERD or with severity of gastritis.
Conclusion: The mucosa at the gastroesophageal junction is characterized by high variability in length and a frequent occurrence of IM and PM. The finding of CM and/or OCM within the esophagus in a subset of cases indicates that junctional mucosa may be of metaplastic origin. The positive correlation between the length of CM and OCM and histological evidence of GERD suggests that gastroesophageal reflux may influence the length of junctional mucosa.

O-019

Rapid arrest of metastasizing melanoma cells under flow conditions

Robert H. Eibl*
C/o Weissman Lab, Department of Pathology, Stanford University School of Medicine, Stanford, CA 94305-5323, USA
*Present address: Institut für Allgemeine Pathologie und Pathologische Anatomie der Technischen Universität München, Trogerstraße 18, D-81675 München,
E-Mail: Robert.Eibl@LRZ.tu-muenchen.de

Integrins and other cell adhesion molecules play a critical role in migration and homing of leukocytes. We compare rolling and stick-

ing of leukocytes to the adhesive steps potentially involved in arrest of melanoma cells within the circulation. The parallel-plate flow chamber provides a well established model for analyzing these mechanisms under flow conditions. In this study B16 melanoma cells arrest spontaneously on bEnd3 endothelial monolayers. Antibodies against α4 integrin and VCAM-1, respectively, but not control antibodies, completely block this rapid arrest under flow. Similar results were obtained with immobilized VCAM-1 protein instead of stimulated endothelial monolayers, indicating that α4 integrin and its ligand VCAM-1 alone are sufficient for mediating spontaneous and rapid arrest of metastasizing B16 cells. Additionally, within seconds after arrest, B16 cells become resistant to higher shear stress, which indicates a rapid strengthening of the adhesion. We conclude, α4 integrin expressed on metastasizing B16 melanoma cells is sufficient for both, rapid arrest and induction of firm adhesion to endothelial VCAM-1. α4 integrins and other cell adhesion receptors are likely to contribute in directing metastasizing cells to secondary sites, where the respective ligands are expressed. This model provides new insights for an underestimated mechanism in metastasis formation and can be used for the development of new strategies in prevention of metastasis formation, mainly the identification and characterization of "metastasis inhibitors". It might also contribute to a better understanding of organ-specific metastasis mediated at least in part by cell adhesion molecules and homing events.

Supported by the Deutsche Forschungsgemeinschaft (Ei 378/1-1), Bonn, a Dean's Fellowship from Stanford University, and a tuition stipend from Irving L. Weissman

O-020

Differential and mutually exclusive expression of CD95 and CD95 ligand in epithelia of normal pancreas and chronic pancreatitis

Hasel, C.
Institut für Pathologie, Universität of Ulm, Germany

Introduction: Acinar regression in chronic pancreatitis may be due to immune attack in parenchymal areas neo-expressing HLA-DR molecules. CD4+Th1 cytotoxic T cells induce apoptosis of their targets via oligomerizing CD95 (APO-1/Fas) death receptors on target cells by their CD95 ligand (CD95L). We determined the expression of CD95 and CD95L in epithelia of normal and chronically inflamed pancreatic tissues.

Methods: We applied RT-PCR and Western blotting for CD95L expression profiles, serial frozen section immunohistochemistry to detect CD95, CD95L and HLA-DR molecules, CD3, CD4, CD11c and S100protein.

Results: Normal pancreas and chronic pancreatitis contain CD95L message and protein. Immunohistochemistry revealed a mutually exclusive expression of CD95 and CD95L. Physiologically, acini were $CD95^-/CD95L^+$, ducts were $CD95^-/CD95L^-$, and islets were $CD95^-/CD95L^+$. In areas of lymphohistiocytic infiltration, mainly consisting of $CD3^+CD4^+$ T cells and $CD11c^+$, $CD4^{+/-}$, S100protein$^+$ interstitial dendritic cells, and in areas of initial fibrosis, acini and ducts were $HLA\text{-}DR^+$, acini $CD95^+/CD95L^-$, and ducts $CD95^+/CD95L^-$. Islet cells were $CD95^-/CD95L^+$ in both conditions. IFNγ levels in protein lysates as measured by an immunoassay were significantly higher in chronic pancreatitis than in normal pancreas ($p<0.0003$). *In vitro*, IFNγ down-modulated CD95L message and protein in ASPC1 and BxPc3 pancreatic carcinoma cells.

Conclusion: Pancreatic epithelia differentially express CD95 and CD95L in a mutually exclusive manner. In chronic pancreatitis the $CD95^-/CD95L^+$ status is conserved in islet cells even in the close vicinity of lymphohistiocytic infiltrates while it is lost in acini co-expressing HLA-DR. As a potential consequence, and possibly triggered by local release of IFNγ, CD4+Th1 cells may cognately interact with and successfully attack exocrine cells by triggering CD95 on their target without being killed by epithelial, CD95L-mediated, counterattack.

O-021

Alterations in gene expression during pre-neoplastic stages of murine colon carcinogenesis: a microarray analysis

Serge Jothy, Noreen Mir
Department of Laboratory Medicine and Pathobiology, Faculty of Medicine, University of Toronto and Sunnybrook; Women's College Health Sciences Centre, Toronto, Ontario, Canada, M4N 3M5

Sporadic colon cancer is the second leading cause of cancer related deaths in the Western world, although the disease is thought to be largely preventable. The molecular alterations that occur during the pre-neoplastic stages of colon cancer are poorly understood, indicating a need to further identify and understand molecular and cellular alterations during this stage of colonic transformation. We hypothesize that alterations in the expression of critical genes occur during the pre-neoplastic stages of colonic neoplasia, before polyp formation and can thus identify surrogate markers of colon cancer risk. Using a murine model of colonic carcinogenesis induced by the carcinogen azoxymethane (AOM), we are investigating changes in gene expression in the colon. CF1 male mice received intraperitoneal injections of AOM 5 mg/kg or PBS only, once a week for 4 weeks. Colons were collected at varying time points after the last injection. Differential gene expression of 1176 gene products was investigated during the pre-neoplastic stages of colonic transformation by microarray hybridization analysis. Results from a pair of samples, control versus an AOM injected mouse (sacrificed 15 weeks after the last injection) showed upregulation of gene expression for nine genes and downregulation of seven genes. These observations are currently being confirmed by RT-PCR, northern blot analysis, immunoblotting and immunohistochemistry. The identification and evaluation of novel early biomarkers of colon carcinogenesis will be a useful tool for future clinical cancer chemoprevention trials and in identifying patients at risk of developing colon cancer.

(supported by the Canadian Institutes of Health Research)

O-022

Immunohistochemical studies of G and D cells in the mucosa of prepyloric part of the stomach in various types of inflammation

W. Kozlowski, A. Dobek, J. Trawiński, S. Wojtuñ, J. Gil, L. Wrzesiński, J. Patera
Division of Clinical Pathomorphology, Central Clinical Hospital, Military University School of Medicine in Warsaw

Endoscopy Centre, Central Clinical Hospital, Military University School of Medicine in Warsaw Polytechnical University in Warsaw

Colonization by Helicobacter pylori is accompanied by secretion disturbances of HCl, gastrin and also pepsinogen. The underlying causes of these disturbances include changes in the enterohormonal cell system of gastric mucosa, the pathological mechanism of which is not fully elucidated. In H.pylori infection gastrin concentration in blood is usually increased with simultaneous decrease of somatostatin level. The studies by other authors demonstrated an increase of G cell number with simultaneous reduction of D cell amount in gastric mucosa during H.pylori colonization. However, until presently, significant divergencies of opinions have been expressed concerning the participation of G and D cells in the pathological mechanism of gastritis in the presence of H. pylori.
The aim of the study was an assessment of the rate of changes of G and D cells in the prepyloric part of gastric mucosa in various types of gastritis taking into account also the dependence of these changes on the degree of H.pylori colonization.**Material and method:** The study was performed on gastric mucosa oligobiopsy specimens, taken from the prepyloric part of the stomach of 144 patients (106 men and 38 women) aged 10–79 years, with histologically confirmed H. pylori infection. The control group included biopsy specimens taken from 137 patients (106 men and 31 women) aged from 10 to 79 years, without H. pylori infection and cases of reflux gastritis. H. pylori was identified by Giemsa method. The sections embedded in paraffin were stained with HE and PAS reaction with alcian blue was carried out.The degree of H. pylori colonization was assessed according to the Sydney System. Gastritis was classified according to the modified Whitehead system. In the sections in which cross-section perpendicular to mucosal surface was obtained, G and D cells were identified by immunohistochemistry according to LSAB+DAKO System method and then these cells were counted, determining the G/D index.**Results and conclusions:** Inflammatory lesions in the mucosa of the prepyloric region in predominant number of cases were of severe character with high intensity of the inflammatory process and 2nd degree of H. pylori colonization intensity. In the course of chronic gastritis in the prepyloric part, with the presence of H. pylori infection, a significant decrease was observed of D cell count as compared to the same gastric mucosa lesions without H. pylori presence. Despite simultaneous decrease of G cell count, the G/D index slightly increased which, in final effect, was an evidence of relative increase of G cell number in these pathological conditions. In prepyloric chronic superficial gastritis with H. pylori infection, G and D cell counts increased significantly with maintained proper G/D ratio as compared to lesions of this type without the presence of H. pylori. Together with increasing intensity of prepyloric gastritis manifestations, in the presence of H. pylori the number of G and D cells decreased, with lower G/D index, while in the absence of H. pylori, this process was characterized by an increase of G and D cell counts with decreased G/D ratio.

O-023

Standardized approach for microsatellite instability detection in gastric carcinomas

E. Musulén, MR. Bella, V. Moreno*, FJ. Sancho+, MA. Peinado#, N. Combalia, G. Capellà&
Dept. of Pathology. UDIAT-CD, Corporació Parc Taulí, Sabadell, Barcelona; *Laboratori de Bioestadística i Epidemiologia.UAB. +Dept. of Pathology. HSCSP. Barcelona; #IRO. &ICO. Barcelona, Spain

Introduction: Microsatellite instability (MSI) definition is already a controversial issue due to is accepted that tumors with low MSI (MSI-L) could become high MSI (MSI-H) if more markers are analyzed. Also, these criteria could only be applied to colorectal carcinomas. Previously we have developed a mathematical model for MSI definition in colorectal cancer and we evaluate their utility to define MSI in gastric adenocarcinomas (GA).
Material and methods: Patients: Thirty-five fresh paired normal mucosa-tumor samples from primary GA surgically resected at the HSPSC.
Microsatellite Analysis: Seven microsatellite DNA regions (D18S58, D18S69, D18S51, DCC VNTR, TP53, BAT26 and D12S95) were amplified. The stability of each microsatellite was scored according to the absence (stable) or presence (unstable) of mobility-shifted bands or additional bands in tumor DNA compared with normal DNA. IHQ: p53 (D07). Mathematical model: We designed an algorithm for the efficient characterization of MSI. Theoretical models considering one, two (stable vs unestable), or three populations (stable vs MSI-L vs MSI-H) were tested against the data collected.
Results: MSI was observed in 25.7% (10) of the tumors. The misclassification rate was less than 5% when any seven loci were analyzed. Tumors with MSI were inversely associated with p53 protein overexpression. The observed frequencies of MSI in our series of samples best fit a two-population model, stable and unstable.
Conclusion: MSI in gastric tumors is defined by instability in two or more of seven markers analyzed. Its application demonstrates that the presence of MSI characterizes a subset of predominantly p53 (–) tumors.

O-024

Clinical and prognostic significance of the expression of egf-Receptor, cd44, Cyclin d1, bcl2 in squamous cell carcinoma of the oral cavity

Blotta, P., Cannatelli, G.*, Pitino, A.*, Pagliari,A., Freschi L.*, Caputo, V.*, Fontanella W., Bonelli A., Marcarini L., Passerini S., Failla C**Botticelli, A.R**
Unità Operativa di Otorinolarigoiatria Ospedale Maggiore di Crema, Istituto di Anatomia ed Istologia Patologica; *Ospedale Maggiore di Crema; **Ospedale Umberto I di Siracusa (SR);***Dipartimento di Patologia Umana ed Ereditaria, Università di Pavia (Italia)

The **Aim** of this study was the immunohistochemical expression of genetic alterations in the cell-cycle regulation, cell-cycle proliferation, angiogenesis and neoplastic progression in the oral squamous cell carcinoma (OSCC).
Methods: Ten cases of formalin fixed and paraffin embedded archival OSCC sections in various regions of the oral cavity were examined by immunohistochemical stains. Histologically three cases were well differentiated (G1), three moderately differentiated (G2) and four indifferentiated (G3). Immunihistochemistry was executed using the following antibodies: Epithelial Grow Factor Receptor (EGFR), p53, Cyclin D1, bcl2 (nuclear oncogenes), CD44 (cell adhesion) and CD34 (angiogenesis). The histological slides were incubated vith Streptavidin-Biotin Complex (Kit-Dako) and stained with diamminobenzidin (DAB Dako).
Results: The increase of wild-type p53, Cyclin D1, bcl2, EGFR and CD 34 immunocytological detection seemed to be related to the histological grade of the tumor. Reduced Cd44 expression was related to positive cervical lymph nodes metastasis and was a predictive factor of shorter survival time. The bcl2 immunoreactivity

was strongest in poorly differentiated carcinoma and dysplastic epithelium adjacent invasive tumor.
Conclusions: The results indicate that the markers used are useful in the clinical-pathological predictive identification of cancer progression in patients with OSCC.

O-025

Characterization of telomerase activity in squamous cell carcinomas of the head-neck region and in tumour margin samples

Eva-Maria Fabricius, Ulrike Gurr, Gustav-Paul Wildner, Berthold Hell, Angelika Langford, Jürgen Bier
Medical Faculty – Charité, Campus Virchow Hospital,
Clinic of Maxillofacial Surgery, Berlin, Germany

Introduction: The 5-year survival time of head-and-neck tumour patients is often determined by a recurrence and/or secondary tumours. For several years, researchers have been investigating whether proof of telomerase activity in these tumours can be used for the prognostic assessment of the postoperative course.
Methods: We examined the telomerase activity in 73 cryo-conserved tissue samples from 40 patients with a squamous cell carcinoma of the head-neck region. In 20 carcinoma tissue samples, in 33 specimens from tissue in the immediate vicinity and in 20 specimens from tissue in more distance, we carried out the TRAP assay with an easily reproducible PCR-ELISA Kit (La Roche) to demonstrate telomerase, and applied an internal standard from a PCR-ELISA-Plus-Kit (La Roche) to check taq-polymerase inhibition.
Results: The increase of telomerase in 9 of the 20 carcinoma tissues (45%) and 16 of the 53 carinoma-free tissues (30%) showed no statistically significant difference (Fisher Exact Test: $p>0.05$). However, a comparison of the ELISA absorbance values showed a highly significant difference between the high telomerase level in the carcinoma tissues and much lower level in the carcinoma-free margin tissues (U-Test: $p=0.001$).
Conclusion: Further studies should elucidate whether telomerase activity is a suitable molecular marker to supplement histopathological diagnosis to determine sufficient radical tumour extirpation in the head-neck region.

O-026

Importance of histopathological evaluation of pattern of invasion in laryngeal squamous cell carcinomas

M. Gryczynski*, W. Pietruszewska*, J. Kobos**
*Department of Otolaryngology, Medical University of Lodz;
**Department of Pathology and Laboratory of Pathology Institute of Pediatry, Medical University of Lodz

151 cases of Laryngeal Squamous Cell Carcinoma (LSCC) were selected from the files of the Department of Laryngology and the Department of Pathology Medical University f Lodz. Modified Anneroth, Luna & Batsakis classification was applied to evaluate the pattern of invasion as well as the degree of keratinisation, nuclear pleomorphism, the number of mitosis, the stage of invasion and lymphocytic infiltration. All characteristics were scored from 1 to 4 points. The pattern of invasion (PI) was scored as following: well delineated margins – 1, infiltrating solid cords and bands – 2, infiltrating thin strands etc>15 cells – 3, diffuse infiltration cell groups<15 – 4. The antibodies against Ki-67, NM23, CD44, CD34 and FVIII (Novocastra Ltd.) were used in our research. The pattern of invasion scored as 4 was seen in about a half LSCCs (42%) with numerous mitoses and in cases with high Ki-67 indices. 54% of cases with no keratinization belong to the "invasive" group (PI scored as 3 and 4). Invasive LSCCs were also characterised by minor or lack of lymphocytic infiltration. 85% of higly pleomorphic tumors represent extremely "invasive" (PI=4) character. Also 38% of grade 3 LSCCs belong to the most invasive cathegory. The presence of nodal metastases (N1, N2 and N3 tumors) and size of the tumor were positively correlated with invasive profile of the tumors. 46% of LSCCs with the highest NM23 expression represents the extremely "invasive" morphologic pattern but the results were not statistically signficant. Only 11,5% of LSCCs with "invasive" (PI=4) showed the highest CD44 expression but the results were not statistically significant. Invasive LSCC pattern was also reversely correlatd with an intensity of angiogenesis (measured with use of CD34 and FVIII antibodies). In conclusion we postulate that a pattern of invasion is an important morhologic feature really reflecting LSCC biology.

O-027

Comperative quantitative evaluation of epithelial adhesion complex proteins in normal, hyperplastic and malignant oral mucosa – A new application of confocal laser-scanning-microscopy

K.M. Haas, A. Berndt, P. Hyckel*, H. Kosmehl
Institute of Pathology and * Dept. of Maxillofacial Surgery,
Friedrich Schiller University, D-07740 Jena, Germany

Introduction: Laminin-5 (Ln-5) is a heterotrimeric basement membrane (BM) molecule ($\alpha3\beta3\gamma2$). It connects the BM with the hemidesmosomes via $\alpha6\beta4$-integrin. Ln-5 and $\alpha6\beta4$ represent major proteins of the epithelial adhesions complex (EAC) and are quantitatively analysed in normal and transformed oral mucosa.
Methods: Shock frozen samples of oral sqamous cell carcinoma (OSCC) of different histological grade (15×), normal (5×) and hyperplastic (5×) oral mucosa were examined. For quantitative analysis sections of the sample and of the reference mucosa placed on one slide were subjected to FITC immunolabelling with monoclonal antibody GB3 against Ln-5 γ^2 chain and to GoH3 against integrin $\alpha6$ chain. LSM images were scanned and quantified using a standardised procedure.
Results: The BM of normal oral mucosa showed a nearly uniform Ln-5 immunofluorescence intensity (99.28% to 100.48%). In all hyperplastic lesions of oral mucosa the Ln-5 immunofluorescence intensity was raised (106.67% to 140.97%). In contrast, in OSCC invasive front the retained BM segments were characterised by a decrease of Ln-5 immunofluorescence intensity (34.62% to 73.86%) correlating to malignacy grade and loss of hemidesmosomes ($\alpha6$ integrin chain).
Conclusion: The increased Ln-5 content in the BM of hyperplastic lesions suggests an increased keratinocyte-BM adhesion possibly resulting in a higher stability of the oral mucosa. In contrast, a loss of Ln-5 from BM indicates malignancy and correlates to malignancy grade in oral carcinoma. The loss of the major proteins of the EAC is an invasion associated phenomenon because in the tumour center up to normal level of Ln-5 could demonstrated.

O-028

Minimum dataset for histopathology reports of head and neck carcinomas; a review and audit

T.R. Helliwell, J.A. Woolgar*
Departments of Pathology and *Oral Pathology;
University of Liverpool, Liverpool, U.K.

Introduction and Methods: The Royal College of Pathologists sponsored the publication in 1998 of a minimum dataset for histopathology reports of head and neck squamous carcinomas. The dataset was produced following detailed discussion between pathologists, surgeons and oncologists, and defined those features of primary squamous carcinomas (site, size, grade, pattern of invasion, vascular invasion, status of margins) and their metastases (number of nodes involved, node levels, size of metastases, extracapsular spread) that were agreed to be important for patient management and prognosis on the basis of published evidence. Guidance was provided on how particular features should be assessed. The contents of the dataset and its use within the United Kingdom have been reviewed and audited by a postal questionnaire of pathologists, surgeons and oncologists.
Results and Conclusions: The minimum dataset is used by most centres that treat patients with head and neck squamous carcinomas, and many surgeons and oncologists have welcomed the improvement in the quality of histopathology reports that has followed its introduction. The criteria specified are regarded as being both clearly defined and useful. The evidence base for the inclusion of additional data items is being considered.
The definition of a minimum dataset will improved the standard and consistency of histopathology reporting for head and neck squamous carcinomas. The dataset will be extended to provide guidance on salivary neoplasms.

O-029

***int-2* and *hst-1* amplification detected by fish in correlation to clinicopathological characteristics in head and neck squamous cell carcinomas**

B. Kleist*, G. Lorenz* and M. Poetsch**
* Institute of Pathology and ** Institute of Forensic Medicine,
University of Greifswald

Introduction: Accumulation of genetic abnormalities is associated with development and progression in cancer. In this context we investigated squamous cell carcinomas of different head and neck sites for a possible correlation between clinicopathological characteristics and oncogene amplification.
Methods: Isolated interphase cells from paraffin sections of 47 squamous cell carcinomas of the oropharynx, hypopharynx and larynx were investigated by fluorescence *in situ* hybridization techniques (FISH) with digoxigenin-labeled DNA probes INT-2 and HST-1. The FISH results were compared with pTNM status, grade of differentiation and clinical outcome of the patients.
Results: *Int-2* and *Hst-1* amplification were most frequently seen in G2 tumors (85% and 67%, respectively). Furthermore, the *Int-2* alteration occurred with higher incidence in tumors of advanced local size (pT4=69%) and in lymph node negative carcinomas (62%). In tumors with *Hst-1* amplification the differences between the different pT and pN stages were not so obvious. An association between tumor-related death and gene amplification could not be demonstrated.
Conclusion: Since *Int-2* amplification seems to correlate with favorable as well as with unfavorable clinicopathological parameters, this genetic alteration may characterize a special group within HNSCC. Here, a study of a larger number of patients with HNSCC and long-term follow up may yield further information about prognostic value of *Int-2* amplification in these tumors.

O-030

Telomerase catalytic subunit in laryngeal carcinogenesis

Boštjan Luzar, Mario Poljak[1], Irena J Marin[1], Nina Gale,
Vinko Kambič[2]
Institute of Pathology, Microbiology and Immunology[1], Medical Faculty University of Ljubljana, Slovenia; Slovenian Academy of Sciences and Arts[2], Ljubljana, Slovenia

Introduction: The acquisition of telomerase catalytic subunit (hTERT) expression, a key determinant and rate limiting step for telomerase activity, has been described as an essential step in the development of a majority of human tumours including laryngeal squamous cell carcinoma (LSSC). The aim of the present study was to assess the role of hTERT in laryngeal carcinogenesis.
Methods: Thirty-two frozen laryngeal tissue samples, 18 cancerous and 14 non-cancerous mostly hyperplastic laryngeal lesions surrounding LSSC, were obtained after macro-microdissection from 18 patients with LSSC. Total RNA isolation by High Pure RNA tissue kit was followed by one-step RT-PCR kit for the quantitative detection of mRNA encoding for human telomerase catalytic subunit hTERT, using the LightCycler instrument (Roche Biochemicals). mRNA for a housekeeping gene porphobilinogen deaminase (PBGD) served for the control of RT-PCR performance as well as a basis for relative quantification of hTERT mRNA. For each sample, normalised hTERT index was calculated by dividing the amount of hTERT mRNA by the amount of PBGD mRNA, multiplying by 100.
Results: Total RNA was successfully isolated from all 32 frozen tissue specimens. hTERT mRNA was detected in 14 out of 18 LSSC (78%) and 5 out of 14 (35%) surrounding non-cancerous lesions. In addition, normalised hTERT index was significantly higher in LSSCs. Index above 0.71 was calculated in 13 out of 14 LSSC and in 0 out of 14 surrounding lesions.
Conclusion: hTERT re-activation appears to be an important, most probably late event in laryngeal carcinogenesis. Laryngeal epithelial hyperplastic lesions can also express hTERT mRNA, albeit at lower relative levels as in carcinomas. hTERT mRNA relative quantification in laryngeal specimens above certain level (0.71 in our study) is strongly suggestive of malignant transformation and invasive growth.

O-031

p53 and its homologues p63 and p73 in primary and secondary squamous cell carcinomas of the head and neck

Anette Weber[1], A. Tannapfel[2], U. Bellmann[2], F. Bootz[1],
Ch. Wittekind[2]
[1] Dept. of Otorhinolaryngology and Head and Neck Surgery and
[2] Institute of Pathology, University of Leipzig

Objectives: The tumour-suppressor protein p53 has recently been shown to belong to a family that includes two structurally related proteins, p63 and p73. This study investigated the status of p53 and its both homologues, p73 and p63, in primary and recurrent squamous cell carcinomas of the head and neck and corresponding non-neoplastic mucosa.
Materials and Methods: Expression and mutation of p53 and its homologues p63 (including the two major isotypes TAp63 and ?Np63) and p73 were examined by direct DNA-sequencing and immunohistochemistry in 68 squamous cell carcinomas of the head and neck of 29 patients. The results obtained were correlated with pathohistological stage (according to UICC [1997]) and grade.
Results: p53 mutations were detected in 32/68 (47%) carcinomas of 17 patients. All of them showed either a discordant mutation pattern of the p53 gene (12 patients) or wild type p53 (5 patients) either of the primary or the secondary carcinomas with mutations of the corresponding tumour. p63 positivity was found in 55/68 (81%) carcinomas of 29 patients. Immunohistochemistry revealed a positive expression of p73 in 32/68 (47%) tumours. p53 mutations of normal mucosa were found in 3/29 (10%) patients. We failed to detect specific mutations of the p73 or p63 gene.
Conclusions: p73 as well as p63 have rarely been found to be mutated in squamous cell carcinoma of the head and neck, but both proteins were found to be expressed in a subset of tumours. The status of p53 and its homologues p63 and p73 were discordant in all patients with recurrent squamous cell carcinoma of the head

O-032

Expression of Cyclooxygenase 2 (COX-2) in human ovarian carcinoma

Carsten Denkert, Stefan Berger, Sören Pest, Ines Koch, Martin Köbel, Michael Schwabe, Antje Siegert, Steffen Hauptmann
Institute of Pathology, Charité Hospital; Institute of Public Health, TU Berlin, Berlin, Germany (S.P.)

Introduction: Cyclooxygenase-2 (COX-2) is a rate-limiting enzyme in prostanoid biosynthesis and is involved in tumor progression. We investigated expression of COX-2 in cell lines and in 119 ovarian lesions (86 carcinomas, 19 LMP-tumors, 12 benign cystadenomas, 2 normal ovaries).
Methods: RT-PCR, Western Blot, ELISA, immunohistochemistry.
Results: Expression of COX-2 mRNA and protein was detected in OVCAR-3, CAOV-3 and ES-2 while OAW-42 and SKOV-3 were negative. PGE_2 production was strongly induced by IL-1β in OVCAR-3 and by TPA in CAOV-3 and could be inhibited by the selective COX-2 inhibitor NS-398. We found an expression of COX-2 mRNA in 6 of 8 samples of primary ovarian carcinomas. COX-2 immunoreactivity was detected in 42% of ovarian carcinomas and 37% of LMP-tumors, but not in cystadenomas or normal surface epithelium. In univariate analysis, patients with carcinomas positive for COX-2 had a significantly reduced median survival time (30.4 months) compared to patients with carcinomas negative for COX-2 (52.5 months, p=0.04). In multivariate regression analysis expression of COX-2 was an independent prognostic factor for poor survival (relative risk 2.74, 95% CI 1.38-5.47).
Conclusions: Based on the results of this study, it would be interesting to investigate whether ovarian carcinoma patients with tumors positive for COX-2 would benefit from treatment with selective COX-2 inhibitors.

O-033

Endometriosis-associated ovarian carcinoma is distinct from other ovarian carcinomas as suggested by a nested case-control study

[1]Eržen M, [1]Kopač D, [2]Rakar S, [3]Klančnik B, [4]Syrjänen K
[1] Unit of Gynaecological Pathology and Cytology, [2] Division of Operative Gynaecology, Dept. of Obstetrics and Gynecology, University Medical Centre, Ljubljana, Slovenia; [3] General Hospital Celje, Unit of Obstetrics and Gynecology, Celje, Slovenia; [4] Department of Pathology, University of Siena, Italy

Objectives: Endometriosis-associated ovarian carcinoma (EAOC) has recently received increasing attention due to its suggested peculiarities in biological behaviour, distinctive from those of usual epithelial ovarian cancer. A series of patients with EAOC were compared to women who had ovarian carcinoma without concomitant endometriosis.
Methods: To control the confounding effect of age a nested case-control study was designed, where all 58 EAOC patients (mean age 54.5±11.5 years) were nested with four perfectly age-matched non-EAOC patients (n=232; mean age 54.7±11.7). Pertinent clinical data and characteristics of the tumours were subjected to statistical analyses using life-table, univariate (Kaplan-Meier) and multivariate (Cox) survival techniques.
Results: When compared with age-matched non-EAOC patients nested to each EAOC case, the patients with EAOC proved to: have a lower stage (p=0.000), show a completely different distribution of histological subtypes (over-presentation of endometrioid- and clear cell carcinomas)(p=0.000), have predominantly lower grade lesions (p=0.029), be devoid of any primary residual tumour (p=0.000), and, most importantly demonstrated a significantly better overall survival (47/58 versus 126/232; OR 2.89, 95% CI 1.56-5.34, p=0.000). This better survival was evident in all age groups, and for all histological subtypes, but not explained by a better stage-specific survival. In EAOC group, the most significant (p=0.0000) predictors of OS in univariate analysis were age, histological type, observation time for endometriosis and distribution of endometriosis. In non-EAOC group, such significant predictors were age, residual tumour and type of therapy. In the multivariate model, age and FIGO stage were the only two significant independent prognostic factors shared by these two series. In addition, histological type and type of therapy proved to be significant independent predictors in the non-EAOC series.
Conclusions: EAOC seems to be an entity distinct from the usual ovarian carcinomas, and should deserve a proper attention in clinical management and prognostication.

O-034

Expression of αV integrin mRNA expression is a novel marker of poor prognosis in advanced-stage ovarian carcinoma

Iris Goldberg, PhD[1], Ben Davidson, MD[2], Reuven Reich, PhD[3], Walter H. Gotlieb, MD PhD[4], Gilad Ben-Baruch, MD[4], Magne Bryne, DDS PhD[2], Aasmund Berner, MD PhD[2], Jahn M. Nesland, MD PhD[2], Juri Kopolovic, MD[1]
Department of Pathology[1] and Gynecology[4], Sheba Medical Center, Tel-Hashomer, Israel; Department of Pathology[2], The Norwegian Radium Hospital, Oslo, Norway; Department of Pharmacology[3], Faculty of Medicine, Hebrew University, Jerusalem, Israel

Integrins are heterodimeric adhesion molecules with a role in mediating both cell- cell adhesion and binding to basement membranes and the extracellular matrix. Altered expression of integrins has been reported in various malignant tumors. The objective of this study was to analyze the possible correlation between mRNA expression of the αV and β1 integrin chains and survival in advanced-stage ovarian carcinomas, studying two patient groups with extremely different disease outcome. Sections from 56 primary ovarian carcinomas and metastatic lesions from 34 patients diagnosed with advanced stage ovarian carcinoma (FIGO stages III-IV) were evaluated for expression of αV and β1 integrin chains using mRNA In Situ Hybridization (ISH). Patients were divided into long-term (=16) and short-term (=18) survivors. The mean values for disease-free survival and overall survival were 115 and 132 months for long-term survivors, as compared to 4 and 23 months for short-term survivors, respectively. Expression of αV integrin mRNA was detected in carcinoma cells and stromal cells in 18/56 (32%) and 17/56 (30%) of the lesions, respectively. β1 integrin mRNA expression was detected in carcinoma cells and stromal cells in 25/56 (47%) and 19/56 (34%) of the lesions, respectively. αV integrin mRNA was detected more often in carcinoma cells in tumors of short-term survivors (p=0.018 for carcinoma cells). In univariate survival analysis for all cases, αV integrin expression in tumor cells correlated with poor survival (p=0.012). This finding retained its predictive power in a multivariate survival analysis, in which all molecules previously studied in this patient cohort were included (p=0.003). To our best knowledge this is the first evidence associating integrin mRNA expression and poor survival in ovarian carcinoma. αV integrin is thus a novel prognostic marker in advanced-stage ovarian carcinoma.

O-035

Molecular genetic analysis of endometrial carcinoma with clear cell changes: Evidence for 2 genetically distinctive entities

Sigurd F. Lax, Vera Abeler*, Peter Regitnig
Departments of Pathology, University of Graz, Austria;
*The Norwegian Radium Hospital, Oslo, Norway

Introduction: Clear cell changes are found both in clear cell (CCC) and secretory endometrioid carcinoma (SEC) of the endometrium, which show different prognosis. CCC and SEC are histologically distinctive but there may be similarities, in particular, if SEC is solid. The aim of this study was to compare molecular genetic changes between CCC and SEC.
Methods: 37 endometrial carcinomas, diagnosed as CCC and 6 SEC were included in this study. DNA was extracted from formalin-fixed, paraffin-embedded tumor and corresponding normal tissue after microdissection. 14 microsatellite loci on 9 chromosome arms were amplified by PCR using fluorescent labeled primers and detected on an automated sequencing device. A tumor was defined positive for microsatellite instability (MSI+) if an electrophoretic shift of the tumor compared to the normal DNA was found in at least 2 loci. Loss of heterozygosity (LOH) was defined as decrease of one allele in tumor DNA of at least 50% compared to normal DNA.
Results: 9 CCC (22%) were MSI+ whereas LOH >1 locus was found in 21 CCC (57%). Among these 21 CCC with >1 LOH, LOH for TP53 was found in 12 of 16 (75%) informative tumors. In contrast, 4 of the 6 SEC (67%) were MSI+ and >1 LOH was only found in 1 SEC (17%) combined with LOH for TP53.
Conclusion: CCC seems to be a genetically heterogeneous group of tumors that is more frequently associated with LOH than with MSI+. A subset of CCC seems to show genetic similarities to SEC, which are frequently MSI+. A histopathological reevaluation of the CCC group by independent observers and a subsequent comparison of geno- and phenotype are in progress.
Corresponding author: Prof. Dr. Sigurd Lax, Department of Pathology, University of Graz, Auenbruggerplatz 25, A-8036 Graz, Austria, Tel.: 0043-316-380-4445, Fax: 0043-316-384329, e-mail: sigurd.lax@kfunigraz.ac.at

O-036

MUC1 expression correlates with poor prognosis in endometrial carcinomas

E. Sivridis[1], A. Giatromanolaki[1], M.I. Koukourakis[2], L. Georgiou[1], G. Galazios[3] and P. Anastasiadis[3]
[1]Departments of Pathology, [2]Radiotherapy/Oncology and [3]Obstetrics and Gynaecology, Democritus Univerity of Thrace, Alexandroupolis, Greece

Aims: To investigate MUC-1 expression in the normal, hyperplastic and neoplastic endometrium, and relate patterns of tumour MUC-1 reactivity with histological characteristics, oestrogen and progesterone receptors, bcl-2 and p53 oncoproteins and, most importantly, with clinical behaviour.
Material and Methods: The material used comprised 42 normally cycling endometria, 45 endometrial hyperplasias of various forms, and 111 endometrial carcinomas of the endometrioid and non endometrioid cell type. The antigens in question were exposed with specific monoclonal antibodies employing standard immunohistochemical techniques. The follow up period ranged from 34–182 months with a median of 86 months.
Results: MUC1 was consistently expressed in the normal endometrium, following a cyclical pattern: "apical membrane staining"/early and mid proliferative endometrium, "purely cytoplasmic staining"/late proliferative endometrium, "cytoplasmic staining with intraluminal secretions"/secretory endometrium. Immunostaining patterns in simple and complex hyperplasia were similar to late proliferative endometrium, while atypical hyperplasias and endometrial carcinomas either simulated patterns of proliferative endometrium or were devoid of MUC1 reactivity. A membranous MUC1 positivity was statistically more frequent in endometrioid carcinomas compared with carcinomas of the non endometrioid type. Interestingly, a cytoplasmic MUC1 positivity was significantly associated with poor prognosis, while MUC1 negative carcinomas were related with PR expression and an improved survival. There was no association of MUC1 patterns with bcl-2 and p53 immunoreactivity or with other histopathological variables.
Conclusions: MUC1 is an integral component of the normal premenopausal endometrium and is probably hormonally regulated. It is frequently expressed in endometrial hyperplasias and carcinomas. The loss of MUC1 expression from endometrial carcinomas is connected with a favourable prognosis.

O-037

Expression of vascular endothelial growth factor by human peritoneal mesothelial cells is regulated by interleukin-1ß

Stadlmann, S.*, Günther Gastl G.**, Abendstein B.***, Zeimet A.G.***, Mikuz G*. Offner, F.A.****
Depts. of Pathology*, Urology**, Obstetrics and Gynecology***, University of Innsbruck; Dept. of Pathology****, Hospital Feldkirch, Austria

Introduction: Human peritoneal mesothelial cells (HPMC) act a bioactive cellular membrane which is involved in the regulation of peritoneal inflammation and ascites formation. We have recently shown that HPMC produce transforming growth factor-beta (TGF-ß) and basic fibroblast growth factor (bFGF), two key players in peritoneal fibrosis. In the present study we defined the production of vascular endothelial growth factor (vEGF) by HPMC.
Methods: vEGF was detected in situ by immunohistochemistry in normal and inflamed omental tissue. HPMC were isolated from human omentum majus and vEGF production was analyzed by specific immuno-assay and Northern Blot analysis.
Results: Immunohistochemical analysis of peritoneal tissue revealed expression of vEGF by HPMC that was markedly increased in serosal inflammation. Within 96 hours cultured HPMC constitutively released appreciable amounts of vEGF (53.6±6.6 pg/10^5 cells). Treatment of HPMC with IL-1ß resulted in an up to 36.8 fold increase of vEGF secretion which was time- and dose dependent. Stimulation of HPMC with IL-1ß also increased steady state levels of vEGF-specific mRNA.
Conclusion: vEGF, bFGF, and TGF-ß are regarded as key players in the regulation of wound healing and tissue repair. Our data suggest that HPMC by the release of these cytokines are crucially involved in peritoneal inflammation which may result in peritoneal fibrosis and ascites formation.

O-038

Gene expression profiling in human ovarian cancer

Kai Wiechen, *Luda Diatchenko, #Alexander Agoulnik, *Bakhyt Zhumabayeva, *Sejal Desai, *Sai Htun, #K. Michael Scharff, *Karim Hyder, *Paul D. Siebert, Manfred Dietel, Reinhold Schäfer and Christine Sers
Institute of Pathology, Charité, Humboldt University Berlin, Schumannstr. 20/21, D-10117 Berlin Germany, * Clontech Laboratories, Palo Alto; # Baylor College of Medicine, Houston Texas, USA

Differential gene expression in human ovarian carcinoma was investigated using a cDNA array of 437 genes recovered after subtracting cDNAs from human tumor versus normal tissues. 15 genes were found up-regulated and 33 genes down-regulated in 2 independent tumors by more than 2 fold. Eight genes were further characterized by hybridizing specific probes to an array containing 68 cDNA pairs derived from matched tumor and normal tissues. This analysis allowed confirmation of differential expression in threeindependent ovarian samples and provided a broad expression profile of individual genes in human solid tumors. Among the down-regulated genes we detected *Caveolin-1* (*CAV1*) which was consistently repressed in ovarian carcinomas. The CAV1 protein showed a strong, membrane-bound expression in normal and benign ovarian epithelium, but was down-regulated in high grade carcinomas. In low grade carcinomas, CAV1 was localized in the cytoplasm and phosphorylation of CAV1 was observed in tumor cell lines but not innormal ovarian epithelial cells. Ectopic expression of CAV1 in OVCAR-3 cells resulted in tumor cell growth inhibition in vitro. In addition, treatment of ovarian cancer cells with the inhibitor of DNA methylation 5-aza-2′-deoxycytidine resulted in an up-regulation of CAV1, suggesting that CAV1 acts as a class II tumor suppressor in human ovarian epithelium.

O-039

Primary myxofibrosarcoma of male breast

L. Di Filippo°, F. Calabrese°, M. Zanin°°, P. Paolucci°°, M. Valente°
° Department of Pathology, University of Padua Medical School, Padua, Italy; °°General Hospital of Padua, Italy

Background: Primary mammary sarcomas are rare entity and usually consiste of angiosarcomas.
Case report: A 53 year old man was admitted to the hospital because of a painless mammary nodule that was growing for 2 months. Mammary echography showed a circumscribed mass of the left breast, measuring 4 cm. Limphoadenopathy was absent. The tumor, that penetrated deeply, was surgically excised. At gross examination, the mass appeared gelatinous with white cut surface. At histology a neoplastic tissue was found consisting of abundant Alcian blue positive substance in which eosinophilic, PAS negative spindle or round-shaped cells, as well as pleomorphic and giant cells were enmeshed. Numerous mitoses, curvilinear capillaries with perivascular tumor cell condensation, and hemangiopericytoma-like areas were present. Hemorrhages and necrosis were also observed. At immunohistochemestry the cells stained for vimentine and, focally, for alpha smooth-muscle actin; MIB 1 was positive in more than 70% of the cells. At transmission electron microscopy fibroblast-like cells were found embedded in an abundant radiolucent matrix.. Thus diagnosis of mammary high-grade myxoid malignant fibrous histiocytoma (MFH) was put forward.
Conclusions: Mammary MFH is a very rare entity and often misdiagnosed as fibrosarcoma. The relative frequency of different types of breast sarcomas is difficult to determine from the literature because these lesions have sometimes been referred to by general term "stromal sarcomas." Moreover, mammary spindle cell sarcomashave not always clearly distinguished between fibrosarcoma and MFH.

O-040

Rapid evaluation of cell viability and apoptosis in cartilage via confocal microscopy

Shawn Grogan+, Balz Aklin+, Martin Frenz*, Thomas Schaffner+ and Pierre Mainil-Varlet+
+Institute of Pathology, University of Bern, Switzerland;
*Institute of Applied Physics, University of Bern, Switzerland

Increased interest in the field of apoptosis and the rising incidence of joint disease (e.g. rheumatoid arthritis and osteoarthritis) has prompted us to develop a range of rapid protocols for the assessment of cartilage specimens. A combination of commercially existing fluorescence markers were adapted for use in intact tissue slices to monitor live cells (calcein-AM) or dead cells (ethidium ho-

modimer-1), caspase-3 activity (Phiphilux; DEVD substrate), changes in mitochondrial membrane potential (CMXRos), and the degree of DNA fragmentation (TUNEL). All of which were visualised using a laser scanning confocal microscope. To investigate the usefulness of these markers, we employed an *ex vivo* Holmium:YAG laser débridement model. Bovine cartilage was exposed to a Ho:YAG laser (780mJ) and maintained in cell culture conditions for 1, 3 and 6 days. Active caspase signals were detected by day 1, which became TUNEL positive by day 6. The progression of the TUNEL signal significantly ($P<0.05$) increased between day 1 and 6 days. Therefore, the detection of caspase-3 activity may be a means of predicting an ongoing pathology and may even provide a window of therapeutic control. The mitochondrial membrane potential marker, CMXRos, revealed an identical signal pattern like calcein-AM and thus provides an alternative means of assessing cell viability. Ethidium homodimer-1 was perhaps the most useful in the prediction of the total damage caused by the laser exposure, as the measured area of ethidium positive cells (in terms of depth) coincided with the active caspase signal. Although both caspase and ethidium positive cells co-stained (by day 1), the ethidium homodimer was much easier to visualise and assess than was the caspase-3 positive signal due to unspecific staining of the cartilage matrix. The adapted methods described here are rapid (1 to 1.5 hours), allow spatial visualisation of various apoptotic processes in whole tissue sections and may be useful in the assessment and research of a variety of cartilage pathologies.

O-041

Bizarre parosteal osteochondromatous proliferation (Nora's lesion). A clinicopathological analysis of four cases

Maggy Grossin*, Christian Couture**, Valère Claude*, Régine Battin-Bertho*, Dominique Hénin*, Réal Lagacé**
*Department of Pathology, Bichat Hospital, Paris, France;
*Department of Pathology-University Hospital - Québec Canada

The clinical and pathological findings of four cases of Nora's lesion are presented. This entity, also known as bizarre parosteal osteochondromatous proliferation,has been described in 1983 and involves mostly the small tubular bones of the hands and feet. The patients were four males, aged 12,33,35 and 36. Two lesions were localized on the digits whereas one affected the toe and one the ulna. Grossly,they were firm, pedonculated,attached to the underlying bone and measured from 1 cm in diameter to 2×1.5 cm. Radiographically, lesions presented as well-delineated, cap-shaped lesions attached to the bone surface. Plain radiographs showed typical well-developed patchy or linear mineralization pattern. Histologically,they were characterized by a proliferation of bony,chondroid and fibrous tissues, sometimes with a high cellular density but were devoid of cellular atypia and necrosis.Areas of enchondral ossification were frequently seen within the cartilaginous component.The most important lesions that present differential diagnostic problems are chondrosarcoma, parosteal osteosarcoma,soft tissue chondroma,callus and florid reactive periostitis.
Nora's lesion belongs to a spectrum of reactive processes of the bone surface and represents an intermediate stage between florid reactive periostitis and acquired osteochondroma (turret exostosis).The lesion is probably initiated by a trauma, followed by a subperiosteal hemorrage giving rise to the reactive process. Local excision is the treatment of choice although recurrences are frequent.
M.F. Meneses, K.K. Unni, R.G. Swee. Bizarre parosteal osteochondromatous proliferation of bone (Nora's lesion). Am J. Surg. Pathol. 1993; 17 (7):691–7

O-042

Detection of CD137 (ILA/4-1BB) in human blood vessel walls

G. Richter, K. Broll, F. Hofstädter, H. Schwarz
Institute of Pathology, Regensburg, Germany

Aims: CD137 (ILA/4-1BB) is a member of the tumor-necrosis-factor receptor family. Members of this receptor family and their ligands are important regulators of a wide variety of physiological processes and play an important role in the regulation of immune responses. Via bidirectional signalling the CD137 receptor/ligand system costimulates the activity of T cells and antigen presenting cells. For example administration of anti-CD137 monoclonal antibodies can eradicate established tumors in mice. In this study, immunohistochemical techniques are used to evaluate the expression of CD137 in several human tissues.
Methods: 100 fresh-frozen specimens from different organs and tumor regions were investigated by immunohistochemistry for the expression of CD137 using the monoclonal antibody BBK-2 (Biosource, Germany). The monoclonal antibody MOP C21 (Sigma, Germany) was used as an isotype control.
Results: No CD137 was detected in normal specimens from different organs (surgical resection margin). In inflammatory, benign and malignant epithelial diseases CD137 was detected in blood vessel walls at a low frequency. In contrast, in several lymphomas and malignant soft tissue tumors CD137 is expressed at a high frequency in blood vessel walls.
Conclusions: Expression of CD137 in the blood vessel wall is accentuated in malignant mesenchymal diseases such as lymphomas and malignant soft tissue tumors. More studies are needed to elucidate the biological role of CD137 in malignant diseases. The negative reaction in normal tissue may allow the use of anti-CD137 antibodies in immunotherapy of human cancer.

O-043

Giant cell tumor of the occipital bone: Case report and literature review

Santos-Briz A, *Villarejo A, **Ramos A, **Millán JM, Ricoy JR, Martínez-Tello FJ
Departamentos de Anatomía Patológica, y Servicios de *Neurología y **Radiodiagnóstico. Hospital Universitario "12 de Octubre", Madrid, Spain

Introduction: Giant cell tumor (GCT) occurs mainly at the ends of long bones of patients with mature skeleton. However, it may appear in other rare locations such as the skull, mainly in the sphenoid and temporal bones. Its presence in the occipital bone is extremely rare, with only 8 cases reported up to date.
Case report: A 49-year-old male patient presented with clinical signs of twelfth-nerve palsy. Radiological studies discovered a lytic destructive lesion involving the right occipital condylus and extending into the clivus. Histologically, the lesion was composed of oval to spindle mononuclear cells, and multinucleated giant cells distributed uniformly throughout the lesion. The former lacked atypia and showed scattered mitotic figures. Foci of new bone formation were present around the periphery of the tumor.
Comments: GCT is extremely rare in the occipital bone with only eight cases described up to date. The patients showed a slight fe-

male predominance (5:4) with ages ranging from 8 to 61 years (mean 33,5). As in other skull bones, GCT of the occipital bone shows a tendency for progression and a more aggressive behavior than in other locations. Surgical ablation and radiation therapy seem to be the treatment of choice. Differential diagnosis include hyperparathyroidism and aneurismal bone cyst, which may appear secondarily in a GCT.

O-044

Platelet-derived growth factor-α receptor supports the growth of conventional chondrosarcoma and is associated with shorter overall survival.

Irene Sulzbacher*, M.D., Peter Birner*, M.D., Klemens Trieb•, M.D., Michaela Mühlbauer°, M.D., Susanna Lang*, M.D., Andreas Chott*, M.D.
Department of Clinical Pathology* and University Clinic of Orthopedics•,University of Vienna Medical School; Orthopedic Hospital Gersthof°, Vienna, Austria

Introduction: Platelet-derived growth factors (PDGFs) exert their biological function by binding to their tyrosine kinase receptors. They are secreted by a variety of mesenchymal cells. Bone cells are important targets of PDGFs as they stimulate proliferation of osteoblasts and chondrocytes. In this study we wanted to determine the expression of PDGF-AA and PDGF-α receptor in conventional chondrosarcomas and compare these results with the expression of the growth factor and its receptor in benign enchondromas.
Methods: Sixty-seven chondrosarcomas and 20 enchondromas were immunohistochemically analysed for expression of PDGF-AA and PDGF-α receptor. Additionally, the proliferation activity was examined with the MIB-1 antibody. In 53 cases complete follow- up data were available.
Results: Our results document a significant overepression of receptor and factor in chondrosarcomas compared to enchondromas (PDGF-AA P=0.013, PDGF-α receptor P<0.001). MIB-1 values were significantly higher in chondrosarcomas (P<0.001). Moreover PDGF-α receptor showed significant differences between Grade1/Grade3 (P=0.002) and Grade2/Grade3 chondrosarcomas (P=0.022). Spearmen rank correlation test showed a significant correlation between PDGF-α receptor expression and tumor grading (r=0.431, P=0.001). Survival analysis documented a significantly shorter overall survival for patients with high PDGF-α receptor expression (P=0.0147, log-rank test).
Conclusion: These data suggest that PDGF-α receptor is overexpressed in conventional chondrosarcomas. Additionally, PDGF-α receptor expression is associated with a less favorable outcome of chondrosarcoma patients. Therefore, the receptor may help to identify a group of clinically very aggressive chondrosarcomas.
Cardiovascular Pathology

O-045

Autoimmunoinflammation: Cell kinetics in the arterial wall and atherosclerosis

V. Anestiadi, I. Tsiple, V. Nagornev*, E. Zota
Centre of Pathobiology and Pathology, Academy of Sciences, Chisinau, Moldova; *Research Institute of Experimental Medicine, Academy of Medical Sciences, Saint-Petersbourg, Russia

We have studied the role of the immune inflammation (IINF) in the set-up and development of atherosclerosis, both in experimental material and in samples of human coronary arteries, obtained during surgical operations, from 250 patients. The material has been studied by ultrastructural and immunohistochemical methods. The role of the lymphocytes in the atherogenesis (AG) is viewed from the standpoint of their input into the expression of the lymphocytes and monokines, into the regulation of the production of chemokines and in situ antibody synthesis. The input of the smooth muscle cells (SMC) into the AG is analyzed not only from the standpoint of the proliferation of the synthetic phenotype of the SMC and the synthesis of connective tissue matrix proteins, but also taking into account their involvement into the IINF reactions, expression of cytokines and class II antigens. During initial AG the depositing and/or formation into the subendothelial intima layer of modified LDL, which acquire autoantigenic properties, is the triggering factor, that stimulates the expression by endothelial cells of chemoadhesive molecules, which connect with the ligands of non-granular leukocytes. Activated monocytes/macrophages and T-cells, which penetrate into intima, even during the most early stages of the AG, start a cascade of reactions, that make sure the development of the "early phase" of the inflammation. The involvement of the intimal cells into the inflammatory reaction (macrophages, SMC and endothelial cells begin to produce class II antigens) transfers the acute phase of the inflammation into a chronic one, like the delayed hypersensitivity reaction.

O-046

Typical and atypical bronchopulmonary carcinoids A clinicmorphological and immunhistochemical study of potentially prognostic parameters in 76 neuroendocrine lung tumors

Ch. Beres[1], Klaus, C.[1], Kaiser, D.[2], Fisseler-Eckhoff A.[1]
(1) Institute of Pathology; (2) Department Lungenklinik Heckeshorn, Zentralklinik Emil von Behring, Berlin

Background: The neuroendocrine tumors of the lung (NET) include a spectrum from the low-grade typical carcinoid (TC), intermediate-grade atypical carcinoid (AC) and high-grade categories of large cell neuroendocrine tumors and small cell carcinoma.Their histopathologic diagnosis, which carries therapeutic and prognostic significance, may sometimes be difficult because of their overlapping features.
Methods: A series of 76 surgically resected bronchopulmonary carcinoids, of which 48 were diagnosed as typical and 28 as atypical carcinoids accordingly to Capellas classification. All tumors were immunhistochemically analyzed for the p53 mutation, bcl-2 overexpression and TTF-1 expression by the Avidin-Biotin-enzyme-complex-method.
Results: Comparing both histological subgroups there were statistically significant differences referring tumorsize, localization, metastases and likelihood of tumor-recurrence P53 mutation and the oncogen bcl-2 were associated with a more aggressive, i.e. worse course within the group of the atypical carcinoids. The thyroid transcription factor 1(TTF-1) was found more often in the group of the atypical carcinoids than in typical carcinoids.
Conclusion: The expression of p53 and bcl-2 is strongly correlated with the patients outcome, respectively a reduced survival time. The TTF-1 expression also tends to be associated with a worse outcome, but the statistics were limited by the small number of atypical carcinoids.

O-047

The frequency of p16 promoter hypermethylation in atypical adenomatous hyperplasia of the lung

Mitsugu Hironaka, Shinji Sakurai, Sachiko Oguni, Shojiroh Morinaga, Ken Saito
Department of Pathology, Jichi Medical School, Yakushiji, Minamikawachimachi, Kawachigun, Tochigi, Japan

Introduction: Recently, atypical adenomatous hyperplasia of the lung (AAH) has been recognized as a precursor lesion of bronchioloalveolar carcinoma of the lung (BAC). Some authors reported that the p16 promotor hypermethylation was one of the epigenetic early events developing lung cancer. But, there has not been reported with regard to the frequency of p16 hypermethylation of AAH.
Methods and Materials: We performed microdissection of a AAH lesion under the laser capture microscopy and p16 methylation specific PCR. Sixty-one lesions of AAH consisted of both 35 lesions of solitary case and 26 lesions of 9 multiple case. Thirty-five cases involved adenocarcinoma of the lung including BAC.
Results:We obtained the result of p16 hypermethylation as follows: Solitary AAH (23%), Multiple AAH (31%), Adenocarcinoma with AAH (53%).
Conclusion: These results indicate that AAH is a precancerous lesion of adenocarcinoma of the lung.

O-048

Infection of restenotic coronary bypass grafts by Chlamydia pneumoniae and anti-cholesterol antibodies (ACHA) in the serum of patients with severe coronary artery disease

Horváth A°, Glasz T°°, Hortoványi E°°, Füst G°, Karádi I°, Kádár A°°, Horkay F*, Mózes G°°, Szik A°°, Sziller I**, Nagy B**, Bán Z**, Toth A***, Kassai I*, Dudás G*
°3rd Dept. of Medicine, °°2nd Dept. of Pathology, * Dept. of Cardiovascular Surgery, **1st Dept. of Gynecology, 2nd Dept. of Pathophysiology; Semmelweis University, Budapest, Hungary

The protective role of anti-cholesterol antibodies (ACHA) has been demonstrated in experimental atherosclerosis. Human serum ACHA levels were found to be considerably lower in patients with peripherial occlusive atherosclerosis compared to healthly counterparts. Also, Chlamydia pneumoniae (Cpn) infection in vascular structures have been proposed as a potential atherogenetic co-factor. In this study we examined the presence of Cpn infection in restenotic coronary artery bypass graft tissue along with serum ACHA levels of patients with severe coronary artery disease.
Twenty-one adult patients with restenotic coronary bypass grafts undergoing re-operations were involved in this study. Their ages ranged 36-70 years (average 62,1 years). Total number of grafts examined was 34 (1,61 grafts/patient), ages of grafts ranged 1–18 years (mean 10.5 years). Cpn was detected in graft tissue immunohistochemically and by PCR. Sera collected were determined for concentrations of IgG type ACHA by a solid-phase enzyme-immunoassay. Control sera were collected from healthy subjects.
Cpn infection was detectable immunohistochemically in graft tissues of 20 patients (95%). Six patients (29%) showed positivity by the PCR method. This shows that Cpn infection is detectable in an overwhelming majority of patients with restenotic bypass grafts. A direct relationship of Cpn infection with graft restenosis remains however to be cleared. ACHA were present in the sera of all persons examined. The ACHA levels were slightly lower in the serum of re-operated patients than in control sera. Although this difference did not reach statistical significance (Mann-Whitney test p=0,077), we have the opinion that this phenomenon would be more prominent when evaluating more cases.

O-049

Evaluation of 1593 frozen sections from thorax lesions: Diagnostic pitfalls

Kaygusuz G[1], Kutlay H[2], Sak SD[1], Akal M[2]
Departments of Pathology[1] and Thoracic Surgery[2], Ankara University Faculty of Medicine, Ankara, Turkey

Introduction: A retrospective evaluation of frozen sections from thorax lesions over 10-year period in Ankara University, Faculty of Medicine, Ibn-i Sina Hospital has been carried out and diagnostic pitfalls in frozen section examination has been noted.
Methods: A total of 1593 consecutive frozen sections performed from 1990 to 2000 on thorax lesions, from 1198 patients were re-evaluated retrospectively.
Results: 747 (46.8%) of the sections were performed for suspected pulmonary malignancy, 280 (17.5%) were from mediastinal lymph nodes, 107 (6.7%) were from resection margins. Pleural lesions and chest wall tumors constituted 14.8 and 5.4% of the sections respectively. The remaining sections were from esophagus, thyroid, pericardium, liver, colon and parathyroid in a descending order. There was diagnostic discordance in 34 (2.1%) sections, 26 (1.6%) were false negative and 8 (0.5%) were false positive. In a relatively high number of cases (190 cases, 11.9%) diagnosis was deferred.
Conclusions: False positive diagnoses were due to hyperplastic pneumocytes misdiagnosed for adenocarcinoma in lung, sinus histiocytosis in lymph nodes misinterpreted as metastasis and one case of sclerosing hemangioma misdiagnosed as adenocarcinoma.
False negative diagnoses were mainly due to micrometastases in mediastinal lymph nodes, small and particularly peribronchial tumor extension in bronchial resection margins, bronchioalveolar carcinoma misinterpreted as hyperplastic pneumocytes, low-grade sarcomas, and mesotheliomas.
High deferral rate at least in part may be attributed to the difficulty of consultation on frozen sections in our institute since frozen section room and pathology department are located in separate buildings with a considerable distance in between.

O-050

PROGNOSTIC VALUE OF HYALURONAN EXPRESSION IN NON-SMALL-CELL LUNG CANCER

Pirinen R[1] ,Tammi R[3] , Tammi M [3] , Hirvikoski P[4] , Parkkinen J[1] , Johansson R[2] , Böhm J[1], Hollmén S[5] , Kosma V-M [1]
Department of Pathology and Forensic Medicine[1], Oncology[2], and Anatomy[3], University of Kuopio and Kuopio University Hospital, Kuopio; Department of Pathology[4], Centre for Laboratory Medicine, Tampere University Hospital, Tampere; Department of Pathology[5], Satakunta Central Hospital, Pori, Finland

Introduction: The aim of this study was to examine the prognostic value of hyaluronan (HA) in a large number of patients (n = 261) with non-small-cell lung cancer (NSCLC).

Methods: A biotinylated affinity probe specific for HA was prepared and applied to paraffin-embedded tumour samples. The level of HA in the tumour cells and surrounding stroma was scored and compared with CD44 stainings, clinicopathological factors and survival data.
Results: Adenocarcinomas were characterized by a low percentage of HA-positive cells compared with squamous-cell and large-cell/anaplastic carcinomas. CD44 and cell-associated HA showed a strong positive correlation with each other. In the whole tumour material, recurrences were more often found in cases showing a low percentage of cancer cell-associated HA. However, within the adenocarcinoma subgroup (n=68), a high percentage of cell-associated HA was correlated with poor tumour differentiation, and a strong stromal HA signal with the increased number of recurrences. In survival analysis of the whole material (n=189), low percentage of HA-positive cells was associated with a shortened disease-free survival (DFS) together with stage and tumour type. However, in the subgroup of patients with adenocarcinoma (n=49), a strong stromal signal for HA predicted poor DFS. The level of HA in the stroma of adenocarcinomas retained its prognostic value in Cox's multivariate analysis.
Conclusion: The level of HA signal is associated with the progression of NSCLC. A strong stromal HA level predicts unfavourable disease outcome in patients with lung adenocarcinoma.

O-051

Large cell neuroendocrine carcinoma of the lung: a retrospective clinical and histopathological analysis of a series of 12 cases

Françoise Thivolet-Béjui, Isabelle Arnaud, Lara Chalabreysse, Sylvie Isaac, Janique Godenèche, Pierre Jean Souquet
Department of Pathology, Louis Pradel Hospital, Lyon;
Department of Chest Medicine Lyon Sud Hospital, Pierre Bénite France

This retrospective study was designed to evaluate the pronostic of large cell neuroendocrine carcinoma (LCNC) of the lung.
Methods: 18 peripheral neuroendocrine carcinomas were treated by curative surgery in Lyon University Hospital between 1985 and 1999. After histological and immunohistochemical study, the tumors were reclassified by 4 independent observers in 12 LCNC, 2 atypical carcinoid and 4 large cell carcinoma with neuroendocrine morphology according to the WHO classification (1999). **Results:** the series included 11 men and one woman of mean age 68 years. The diagnosis of LCNC was never established before surgery. All LCNC expressed 3 (8/12) or 2 (4/12) neuroendocrine markers as chromogranin A, synaptophtysin or NSE. Clinical classification identified 6 stage I, 3 stage II and 3 stage III. Two patients received adjuvant chemotherapy. The median overall survival was 12,73 months. The survival at 1 year and at 5 years was 50% and 8,3% respectivelly. The median disease-free survival was 6,8 months.
Discussion: Histological diagnosis of LCNC is difficult to establish on small specimens of fine needle aspiration biopsy or cytology without complete immunohistochemical study. Clinical prognosis of LCNC is very poor.
Conclusion: LCNC, even if their are recently classified with large cell carcinoma, should be treated more like SCC.

O-052

Chlamydia pneumoniae in arteries from the heart up to the brain: A PCR analysis

Wohlschläger J[1], Wimmer MLJ[2], Nägler DK[3], Nathrath W[1], Haberl R[2], Weis S[4]
Depts. of Pathology[1] and Neurology[2], Municipal Hospital Munich-Harlaching;

Depts. of Pathology[3] and Neuropathology[4], Otto-von-Guericke-University, Magdeburg, Germany
Background: Many papers report on an association of *Chlamydia pneumoniae* with coronary heart disease (CAD), myocardial infarction (MI) and general arteriosclerosis. Serological markers of *Ch. pneumoniae* infection have been found to be associated with CAD, MI and stroke. The organism could be demonstrated in vascular tissue of both surgical and post mortem specimens (carotid arteries, coronary arteries, aorta) by immunohistochemistry, electronmicroscopy and polymerase chain reaction.
Material and Methods: Purpose of this study was to determine the frequency of *Ch. pneumoniae* in post mortem specimens of different arteries including intracerebral vessels. We investigated 114 various samples obtained upon autopsy (coronary (CA) and carotid (ACC) arteries, basilar artery (BA) and middle cerebral arteries (MCA) from both sides) of 19 patients, 5 with ischemic brain infarction and 14 controls, who died of non-cerebral causes (4 males, 15 females, mean age 74.2 years, no statistical differences between cases and controls). PCR was performed to demonstrate specific *Ch. pneumoniae*-DNA in these specimens.
Results: Arteriosclerosis was macroscopically evident in all of the examined vessels. The overall prevalence of *Ch. pneumoniae* was 32% (6/19). The agent could be detected in all types of analyzed arteries: CA 16% (3/19), ACC 11% (2/19), BA 16% (3/19) and MCA 21% (4/19, both sides in 3 patients). PCR for *Ch. pneumoniae* was positive in one of the five patients (20%) with a history of stroke and in 5 of 14 (36%) control subjects without a history of cerebrovascular disease (chi^2-test, p=0.480).
Conclusion: To our knowledge, this is the first investigation demonstrating *Ch. pneumoniae* in intracerebral arteries. Despite the reported serological association of *Ch. pneumoniae* and cerebrovascular disease there is no correlation between positive PCR results and stroke in this preliminary analysis and a causative role of chlamydial infection in stroke cannot be supported by these data. The results show, however, an association of arteriosclerosis and the prevalence of *Ch. pneumoniae*. We continue to collect prospective data for this study and additionally perform immunohistochemical analysis, which will be presented at the congress.

O-053

Evaluation of video and digital image compression systems: Aplications in telepathology through internet

Luis Alfaro, Mª José Roca, Enrique Poblet
Department of Pathology, Hospital de la Marina Baixa-Villajoyosa (Alicante), Spain

Telepathology has acquired an increasing interest and development thanks to the immense possibilities of communication that offers Internet. The limitation of the bandwidth that affects most connections to this network, forces to use advanced methods of digital im-

age and video compression. Although video transmission in Internet has become something widely employed, generally sequences of very small size, and with appreciable lost of quality are used, so that are not applicable to systems of telepathology with diagnostic purpose.
We have selected the two most widely used systems in Internet for compression of video and sequences of images, RealNetwoks and Microsoft Windows Media, applying them to microscopic images, to evaluate the diagnostic possibilities of these methods under the conditions of speed that offers Internet with conventional lines. Rates of compression have been adapted for 28.8 and 56 kbps, as well as 64 and 128 kbps ISDN lines.
With this range of resolutions, files of compressed video have been generated, some of them with incorporated sound, and were inserted in web pages, so that any potential user of the network could be receptor of the telepathology system. Sequences of images and video were generated both for real time transmission, and for locally recorded in receptor's PC.
In conclusion, actual systems of compression video are insufficient to generate files of enough quality to allow microscopic diagnosis on modem connections. ISDN lines especially employing a double channel at 128 kbps, ADSL lines, and cable connection systems, are much more appropriate for real time telepathology.

O-054

Digital quality control in cytology: Advantages and technical approach

Della Mea V, Demichelis F*, Barbareschi M#, Dalla Palma P#, Beltrami CA, Forti S*
Inst. of Pathology, University of Udine, Italy; * Istituto Trentino di Cultura – Istituto per la Ricerca Scientifica e Tecnologica, Trento, Italy; # Inst. of Pathology, City Hospital of Trento, Italy

INTRODUCTION: Quality control for pathologists and cytotechnicians is an urgent need, but it is delayed by the difficulties in the specimen management: the usual way for carrying out a quality control programme is to circulate specimens among participating individuals or institutions, collecting their diagnostic answers. Because cytologic specimens are not duplicable, sequential delivery of the same material is mandatory, with obvious temporal applications.
METHODS: The digitisation of selected images, although proven useful in other fields, is not suitable for quality control, because screening capabilities on full specimens are also to be tested. Cytological Virtual Cases, i.e., collections of digital images entirely representing histological/cytological slides, could be the basis for digital quality control. Particular care should be taken in constructing such cases, in order to provide adequate information: more focal planes should be considered, and high magnification images are necessary.
A set of specific features have been introduced in the conventional virtual case visualization interface, including QUATE-like test forms, spot and screening test timer, and multiple focal planes navigation.
RESULTS: A preliminary test phase among eight cytotechnicians of the Institutes of Pathology of Trento and Udine allowed to improve the system, that is now on test by four Pathology Institutes with cytological screening activity. The digitised slides – 20 screening slides and 20 spot ones – are part of a material set used in a previous conventional aptitude test (Istituto Superiore della Sanità, 1993).
CONCLUSION: Cytological Virtual Cases may be useful for implementing quality control programmes based on aptitude tests.

O-055

Clinical interoperability: Taking telepathology to the next level

Ganslandt T[1,3], Korsching E[2], Prokosch HU[3], Herbst H[2], Böcker W[2], Senninger N[1], Spiegel HU[4]
[1] Klinik und Poliklinik für Allgemeine Chirurgie; [2] Gerhard-Domagk-Institut für Pathologie; [3] Institut für Medizinische Informatik und Biomathematik; [4] Abteilung für Chirurgische Forschung, Westfälische-Wilhelms-Universität Münster, Germany

Introduction: Telepathology today has matured to a point where its basic functionality is available in the form of integrated commercial systems. Further development aims at extending the simple transmission of images and video streams to a virtual slide approach. Integration of telepathology systems into clinical information networks enables additional uses including the digital exchange of findings, demographic or billing data, scientific telemicroscopy and computer based training. Support for standardized interfaces by telepathology systems is a crucial prerequisite for this kind of integration.
Methods. Over a period of 8 months 4 commercially available telepathology systems were evaluated with regard to support of standardized interfaces. Four levels of interoperability were noted:
• system-independent standardized interface (e.g. HL7, DICOM)
• platform-independent structured interface (e.g. XML/HTTP)
• vendor-dependent database-level interface (e.g. ODBC)
• vendor-dependent system-level interface (specific API-calls)
Results. None of the systems provided standardized or structured interfaces, only one system (Nikon/ZEM) offered a database-level interface using ODBC. While relying on the TCP/IP network standard all systems implemented proprietary protocols for client/server communication as well as microscope control. No system made use of a published encryption algorithm. All systems were mutually incompatible.
Conclusions. Implementation of standards is restricted to low-level interfaces like TCP/IP or ODBC effectively rendering the products evaluated as standalone systems. In order to realize the full potential of telepathology for broad-scale integration into clinical information networks, existing standards for information interchange must be embraced by vendors. Research efforts should be directed towards creation of vendor-independent protocols for client/server communication.
Corresponding Author: Thomas Ganslandt, Klinik und Poliklinik für Allgemeine Chirurgie, Waldeyerstr. 1, 48149 Münster (ganslan@uni-muenster.de), Tel.: 0251-83-56301

O-056

The UICC Telepathology Consultation Center: Internet-based Second Opinion for Pathologists

Stefan Gardziella, Peter Hufnagl, Manfred Dietel

Introduction. The UICC has created in July 2000 a Telepathology Consultation Center located in Berlin at the Charité Hospital which works – free of charge – via the Internet. Pathologists can get a second opinion for difficult tumor cases to provide better health care all over the word.

Methods. The software for the UICC-TPCC was developed in cooperation between the Institute of Pathology Charité and Siemens AG Erlangen, Germany and is based on the Siemens MedStage technology. The requesting pathologist needs an internet access with an actual web browser, a valid E-mail address and a video or digital camera to digitise histological images.
Results. About 50 well-experienced international pathologists selected by the UICC offer their services online. More than 80 case requests arrived in the first 6 months with an average turn-around-time between 2 and 3 days.
Due to the interest of other pathological institutes worldwide stable connections between different institutions (e.g. from India or Nepal) using this service have been established more and more.
Conclusion. The UICC service presents a new, cost-effective way of consultation the Internet – free of charge for the user – to improve and check the quality of histological diagnosis in tumour pathology and offer a simple way for discussions on difficult cases between pathologists worldwide.

O-057

Degre of bias in static telepathology: Aspects of image pyramid

Gombas, P
MI Central Hospital, Division of Pathology, Budapest, Hungary

AIMS: Although static telepathology (ST) have been generally recognised, cyber age methods are hardly used in routine surgical pathology. ST via Internet is inexpensive and accessible for routine practice, but many pathologists seem to feel aversion to biased store-and-forward image transfer. Determination of degree of bias may help to apply less biased image pyramid system.
METHODS: Images of various histopathological sections have been digitised with a bright field transmitted light microscope. Images were captured in size of 800×800 pixels using an Olympus BH2 microscope equipped with objective lenses with numerical apertures of 0.13, 0.3, 0.46 and 0.7, respectively. Degree of bias /DB/ was determined as a percentage: (explicit information÷implicit information) ×100. DB has been calculated on various samples using 50 bladder map biopsies and 50 liver biopsies.
RESULTS: The value of DB depends on four main factors such as (1) on size of the microscopic sample; (2) on magnification of the objective lens; (3) on size of captured image and (4) on number of analysed samples of the teleconsultation case. Values are presented on the next table:

objective lens magnification	DB at bladder biopsies	DB at liver biopsies
4×	62,6	31,2
10×	10	5
20×	2,25	1,12
40×	0,63	0,31

Images of small biopsies captured even at lowest objective magnification are biased in store-and-foreward transfer. Increasing the magnification and/or using larger biopsies increased the DB significantly.
CONCLUSION: Image pyramid architecture offer unbiased way of ST. This method seems to be specially able for consultation, expert discussions, archiving and remote education of various biopsy samples in daily routine practice.

O-058

No need for standards? Telepathology in the view of Nikon, Zeiss, Olympus and Leica

Korsching E[1], Ganslandt T[2,3], Prokosch HU[3], Herbst H[1], Böcker W[1], Senninger N[2], Spiegel HU[4]
[1] Gerhard-Domagk-Institut für Pathologie; [2] Klinik und Poliklinik für Allgemeine Chirurgie; [3] Institut für Medizinische Informatik und Biomathematik; [4] Abteilung für Chirurgische Forschung, Westfälische-Wilhelms-Universität Münster, Germany

Introduction: Faced with demands to raise quality standards and to bridge the distance in space and time between different medical institutions, telepathology is a solution to rejoin diagnostics with operational institutions like surgery. We have made a blueprint of the informatics and medical demands necessary to join pathology and surgery and invited 4 companies with their existing telepathology systems – each for 2 months.
Methods: Our analysis was based on a broad spectrum of technical and non-technical properties: 1) Medical workflow 2) Extracting relevant information for decision support and documentation 3) User interface and ease of use for physicians 4) System management 5) Hardware demands 6) Network demands 7) IT-Integration in existing structures and databases 8) Transmission and database security 9) Conformity with standards 10) Interoperability between different systems 11) Future developments.
Results: The medical documentation was very poor and in the light of unsolved legal questions insufficient. At the moment Nikon is the advanced competitor with the most challenging virtual slide model. The modern hardware and net resources on our campus are absolutely sufficient (10 to 100 MBit/s). The integration in existing IT-structures and the interoperability between different telepathology systems is not possible – no support for standardized interfaces.
Conclusion: All systems are currently run as stand alone applications. It appeared that all vendors have a primarily technical background. Therefore close cooperation with clinical users in further development is necessary. IT-standards and security questions must be forced in future developments.
Corresponding author: Dr. Eberhard Korsching, Gerhard-Domagk-Institut für Pathologie, Domagkstr. 17, 48149 Münster (korschi@uni-muenster.de), Tel.: 0251-83-56920

O-059

The International Group for Standardisation of Immunohistochemistry (IGSI) presents an Internet/image based knowledge exchange system for quality control and education in immunohistochemistry

Marius Nap, (NL), André Balaton (Fra), Tibor Krenacs (qualicont, Hung), Jacques Hassoun (AFAQAP, Fra), Hector Battifora (USA), Kiyoshi Mukai (Japan),), Allen Gown (chairman IGSI, USA)

Introduction: An internet based platform, free of charge, for the collection and retrieval of digitized microscopical images from immunohisto- and cytochemical stains would serve knowledge exchange beyond existing geographical borders. Images should have a systematic description covering essentials of tissues, preservation and reagents used. A ballot precedes final admission in the database. Electronic discussion platforms will enhance knowledge exchange.
Methods: Regular available internet software was used, integrated with a specific database structure from MedQix®. Supported by

comments from members of the IGSI, a webserver application was developped.
Results: Jpeg's or Tiff's can be uploaded and retrieved at www.ihcqc.com without local dedicated software. Image categories are: quality control, unexpected positives, artefacts and educational. A database manager can request additional information before transfer to the voting list. Several members of IGSI function as board member. Acceptance of the image by at least one board member transfers the image to the official database where it can be searched and discussed by end users. Ballot outcome is shown in search results.
Over 100 Images have been uploaded from three different countries, with various markers and organs. Images mainly belong to the QC category but also other categories have been addressed. Searches can be carried out on single and combined items and results can be narrowed on line.
Conclusion: Depending upon the quality of the images accepted by the board and the variety of contributing parties, this database can become a successful support tool for those having questions regarding technique, choice of antibody and interpretation.

O-060

Telepathology consultation centers in the internet
V. Renz, P. Hufnagl, S. Gardziella, H. Guski, S. Hauptmann, M. Dietel

Introduction. Telepathology Consultation Centers are a new kind of institution established by a group of pathologists offering a wide range of diagnostic services to other pathologists via Internet for different reasons. We tried to get an answer on the question: Are telepathology consultation centers in the Internet a valid alternative to get a second opinion in diagnostic pathology?
Methods. Currently several consultation centers are available e.g. AFIP, UICC-TPCC, TPC.P.C, ITPG. The conditions of the service of these centers are quite different (way of case submission, user identification, costs, experts). We submitted a set of 5 cases simultaneously to 3 telepathology consultation centers and tested the service: quality of diagnoses, turn around time, contact to consultants, convenience of the service.
Results. We found the quality of the diagnostic acceptable. There was no wrong evaluation. The turn around time ranged between 2 ours (AFIP) and 8 days (TPC.P.C). There have been no costs so far. The convenience of the services was different and sometimes difficult. All centers offered second opinion via simple email. To guarantee for the diagnoses the centers wanted to see the microscopic glass slides.
Conclusions. Pathologists will use telepathology to get a second opinion on difficult cases. Telepathology consultation centers will play an increasing role in future development of diagnostic pathology. Pathologists are encouraged to use existing free of charge services to get a personal impression.

O-061

From telepathology to teleradiology network in Croatia
Sven Seiwerth
Institute of Pathology, Medical Faculty University of Zagreb, Croatia

Telepathology as a very demanding branch of telemedicine poses real challenge to experts. Introduction of telepathology in underprivileged countries with poor infrastructure and low health-care budget represents a special task. On the other hand these countries would mostly benefit by introducing telemedicine/telepathology. In our experience it is possible to build an efficient telepathology/teleradiology network using simple POTS and still image transmission, as well as store and forward mode of operation. Also it is important that the applied system has a maximal scalability and support future introduction of faster infrastructure (such as ISDN or ATM). Our experience is based on 7 years of telepathology in Croatia leading to a national teleradiology network. The system used in this development was the ISSA/PHAROS system (Vamstec, Zagreb) integrating patient database with telepathology system. In this paper the ideas, development and software solutions in the process of establishing a national telepathology and teleradiology network are highlighted.

O-062

Endocrine tumors of the pancreas: Benign or malignant?
Borka, K[1]., Horányi, J[2]., Sipos, B[3]., Klöppel, G. [3]
12nd Department of Pathology, [2]1st Department of Surgery, Semmelweis University, Faculty of Medicine, Budapest, Hungary; [3]Department of Pathology, Christian Albrechts University, Kiel, Germany

Introduction: The biological behavior of pancreatic endocrine tumors and their morphological features show no equivocal correlation. According to the latest WHO classification the endocrine tumors are divided into two groups: well and poorly differentiated. Tumors belonging to the first category are either benign or of uncertain dignity.
The biological behavior of well differentiated tumors of uncertain dignity can be predicted using the following factors: hormone-production, tumor size, the proportion of AgNOR-rich cells and Ki-67 expression.
Methods: The diagnoses of 22 endocrine pancreatic tumors diagnosed in the past 5 years were reevaluated based on the new WHO classification. The first diagnosis of 15 cases was tumors with uncertain behavior and 7 cases were diagnosed as malignant. After reevaluation 9 of the cases proved to be benign whereas based on the presence of metastases, 9 were found to be malignant. Six tumors remained to be of uncertain behavior. In 16 cases immunohistochemistry was performed (insulin, glucagon, pancreatic polypeptide, somatostatin, VIP, gastrin, Ki-67), and AgNOR density, nucleus/cytoplasm ratio as well as pleomorphism were also evaluated. Direct counting and morphometric methods were used.
Results: The proportion of the AgNOR-rich cells had the greatest prognostic significance. The determination of the percentage of AgNOR positive cells in tumors of uncertain dignity helps to predict their behavior. The high percentage of AgNOR-rich cells correlates with the possibility of metastases, recurrence or local invasion.
Conclusion: In the evaluation of individual cases, a multiparametric pathological analysis is effective in the identification of tumors with higher risk of recurrence or metastasis.

O-063

Diagnostic value of AgNORs in endocrine tumours: A study in a series of thyroid and adrenal cortical tumours

Bukaeva I., Smirnova E., Probatova N., Pavlovskaya A.,. Baronin A., Makanin M., Raikhlin N.
Cancer Research Center of RAMS, Moscow, Russia

Introduction: The diagnostic value of silver staining of nucleolar organizer regions (AgNORs) in endocrine tumours is a matter a debate. The value of AgNORs as markers of malignancy was investigated in 39 follicular cell thyroid tumours (24 of benign adenomas and 15 of papillary and follicular carcinomas) as well as in 15 adrenal cortical tumours (5 of benign adenomas and 10 of malignant tumours).
Methods: The AgNOR staining was performed according Ploton et al. (1986). The AgNOR parameters studied were mean AgNORs number per cell and quantification of the number of AgNORs per tumour cell nucleolus (AgNOR distribution score).
Results: In comparison with adenomas mean AgNOR number per cell in papillary and follicular thyroid carcinomas was increased 2,7-fold and 2,3-fold, respectively (P<0,001). Benign and malignant thyroid tumours were also discriminated by AgNOR distribution score. In benign adenomas only 3,2% of cells had nucleoli with at least five AgNORs. The number of those cells from papillary and follicular carcinomas estimated at 22,8% and 16,8%, respectively. In addition, thyroid carcinomas had several cells with 10–15 AgNORs per cell nucleolus that not seen in adenomatous suamples. Assessment of AgNOR parameters in adrenal cortical tumours revealed that mean AgNOR count in malignant tumours was increased 4,2-fold (P<0,001) and malignant cells had the higher AgNOR score than their benign counterparts.
Conclusion: Thus, investigation of AgNORs may be helpful in discriminating malignant and benign thyroid and adrenal cortical tumours.
This work was supported by grant from Russian (99-04-50026) Fund Basic Research.

O-064

INCREASED INCIDENCE OF POINT MUTATIONS IN THE VON HIPPEL-LINDAU DISEASE TUMOR SUPPRESSOR GENE IN MALIGNANT SPORADIC PHEOCHROMOCYTOMAS

R.R. de Krijger, H. Dannenberg, E. van der Harst‡, W.J. Mooi¶, J.W. Oosterhuis, P.U. Heitz*, P. Komminoth*, W.N.M. Dinjens
Departments of Pathology, Josephine Nefkens Institute, and Surgery‡, Erasmus University Medical Centre Rotterdam, The Netherlands; Departments of Pathology, Netherlands Cancer Institute¶, Amsterdam, The Netherlands; University of Zürich*, Switzerland

Introduction: Somatic mutations of the Von Hippel-Lindau (VHL) tumor suppressor gene have been shown to be infrequent in sporadic pheochromocytomas (PCCs). It is well known that the VHL gene product has a wide spectrum of tissue-specific functions and that specific mutations in this gene are associated with clinical phenotypes in VHL disease. Particularly the susceptibility to PCCs is strongly correlated with missense mutations in the VHL gene. However, it remains unclear whether the spectrum and frequency of VHL mutations differ between benign and malignant PCCs.
Methods: We investigated sporadic PCCs in 80 patients, including 56 patients with a clinically benign and 24 patients with a malignant PCC. We used PCR-based SSCP analysis of the entire coding sequence and the intron-exon boundaries of the VHL gene. SSC variants were defined by DNA sequencing and normal DNA of these patients was examined for the presence of a germ line mutation.
Results: Eight different somatic mutations were identified in 3 (5,4%) of 56 benign tumors compared to 6 (25%) of 24 malignant lesions. We characterized 5 missense mutations and 3 nonsense mutations. No clear distinction in the nature of VHL mutations in benign and malignant PCCs was observed.
Conclusion: Somatic mutations of the VHL gene are more frequent in malignant PCCs compared to benign tumors (5,4% versus 25%). This may imply that PCCs carrying VHL mutations might be more prone to malignant degeneration and/ or aggressive tumor behaviour.

O-065

Identification of g protein alpha subunit mutations in pituitary adenomas by single-strand conformation polymorphism (SSCP) analysis. Morphological correlation in 22 cases

Niveiro M, Aranda FI, Boix E (*), Payá A, Ortega E, Alenda C, Pico A (*)
Service of Pathology and Endocrinology (*),
Hospital General Universitario de Alicante. Spain

Aims: To evaluate the presence of mutation in gsp gene in a series of pituitary adenomas and correlated with radiological, morphological and hormonal findings.
Methods: 22 cases of pituitary adenoma from patients treated by transesphenoidal surgery. Screening of gsp mutations in DNA extracted from paraffin embedded tissue, using PCR-SSCP method was performed. Cases were classified according clinical and immunohistochemical findings using antibodies to GH, PRL, ACTH, LH, FSH and alfa-subunit. Proliferative activity was obtained counting Ki67 expression in 1000 cells.
Results: Age of patients ranged 15-73 year-old, 9 male and 13 female. According clinico-pathological classification , 14 cases were GH adenomas (13 with acromegalic syndrome and 1 case of gigantism), 1 ACTH-secreting adenoma, 1 PRL-secreting adenoma and 6 cases of gonadotrophic adenoma (clinically silent adenoma). Of 14 GH-adenomas, 10 were sparse granulated and 4 dense granulated, according the density with immunohistochemical staining. Gsp-mutation was observed in 6 cases (2 in exon 8 and 4 in exon 9), 5 GH-adenomas (36%), and 1 gonadotrophic adenoma (17%). In GH adenomas with gsp mutation, only 1 case (20%) showed extrasellar extension versus 6/9 (67%) gsp negatives (p=0,09), and 2/4 were GHDG adenomas and 3/10 were GHPG (p=n.s). In relations with proliferative activity, 2/5 (40%) gsp (+) GH-adenomas and 2/9 (22%) gsp (–) GH-adenomas showed more than 5 per 1000 Ki67 positive cells (p=n.s.).
Conclusions. Gsp mutation was observed in 36% of GH-adenomas and in 1 case of gonadotrophic adenoma. GH-adenomas gsp (–) presented tendency to the extrasellar extension. No association between gsp mutation, granular density or proliferative activity measured with Ki67 was observed.

O-066

Oncocytic transformation in pituitary adenomas. Study of 42 cases with anti-mitochondrial antibody

Ortega E, Niveiro M, Aranda FI, Boix E (*), Perez-Berenguer H, Seguí J, Pico A (*)
Service of Pathology and Endocrinology (*),
Hospital General Universitario de Alicante. Spain

Aims. Oncocytic transformation in pituitary tumors is specially frequent in nonfunctioning adenomas. Recent studies have demonstrated that immunocytochemistry with antibodies specific for mitochondria are useful for the identification of oncocytes. The aim of our study is to evaluate the oncocytic transformation in a serie of pituitary adenomas with immunocytochemistry

Patients and methods. Study of 42 pituitary adenomas with anti-mitochondrial inmunocytochemistry using the monoclonal antibody 113-1 (Biogenex). The positive cells with a dense granular cytoplasmatic pattern were evaluated as oncocytic cells. In each adenoma we have evaluated the percentage of this oncocytic cells. Oncocytic adenoma were defined by the presence of more than 50% of oncocytic cells.

Results. The adenomas were classificated in: 17 GH adenomas, 2 prolactinomas, 3 ACTH adenomas (2 clinically nonfunctioning), 2 TSH adenomas, 16 gonadotrophic adenomas and 2 null adenomas (both, with inmunocytochemistry negative for all of the pituitary hormones and alpha-subunit). Five cases showed oncocytic change (positive with antimitochondrial antibody) in more of 50% of the cells (oncocytic adenomas), four of them were gonadotrophic adenomas and one a null adenoma. Five GH adenomas (30%), one TSH adenoma, one ACTH adenoma and seven gonadotrophic adenomas showed focal oncocytic change.

Conclusions. A 48% of the pituitary adenomas studied showed oncocytic change in more of 1% of the cells. 12% of the pituitary adenomas were evaluated as oncocytic adenomas and all of them were gonadotrophic or null adenomas. The anti-mitocondrial antibody is useful to evaluate the mitochondrial density and the oncocityc transformation in pituitary adenomas, without necessity of ultrastructural methods.

O-067

Adrenal lesions in biopsies: Report of 231 cases

W. Saeger, M.C. Fassnacht, F. Beuschlein, G. Prager, C. Nies, K. Lorenz, E.Bärlehner, D.Simon, B.Nierderle, B.Allolio, M.Reincke
Hamburg, Würzburg, Wien, Marburg, Halle, Berlin Buch, Düsseldorf

Introduction: Fine needle aspiration biopsies of adrenal lesions require a correct diagnosis for therapeutical decisions. To investigate the correctness of diagnoses, the results should be compared with the histopathology of the surgical specimens.

Material and methods: Using an "ex-vivo" approach of surgical specimens, 231 cut biopsies of adrenal lesions were investigated without knowledge of patient's age, clinical and intraoperative findings by conventional histology and by immunohistochemistry with a panel of antibodies (Keratin KL1, Vimentin, S100Protein, Synaptophysin, NSE, Chromogranin A, D11, Ki67 (Mib1), p53).

Results: 122 lesions (44.8%) were cortical tumors: 19 hyperplasias (8.2%), 78 adenomas (33.8%), and 25 carcinomas (10.8%). 55 lesions were medullary tumors: 50 presumably benign pheochromocytomas (21.7%) and 5 malignant pheochromocytomas (2.2%). Cortical and medullary tumors could mostly be differentiated by simple light microscopy but in 15% of cases immunohistochemistry was necessary presenting expression of D11 and negativity for Chromogranin A in cortical tumors and contrary results in medullary lesions. For differentiating benign from malignant cortical tumors a catalogue of criteria (necroses, fibroses, diffuse growth pattern, lipid content, nucleoli, nuclear pleomorphism, mitoses, Ki67 index, p53 expression) was used. 22 lesions represented metastases from extraadrenal carcinomas, mainly from bronchus but also from kidneys or gastrointestinal tract. In 50% of these immunohistochemistry was necessary for differentiating them from adrenal carcinomas showing mostly strong keratin positivity and mostly negative staining for D 11 in the metastases. Other lesions were: 3 ganglioneuromas, 1 neuroma, 2 neurofibromas, 4 myelolipomas, 4 retroperitoneal sarcomas, 1 angioma, 2 pseudocysts, 3 inflammatory processes and 1 scar. Due to extensive necroses (n=5) or bleedings (n=1) in 6 cases a diagnosis was not possible. Four biopsies contained normal adrenal tissue. 150 cases enabled a good comparison of diagnoses between biopsies und surgical specimens. Biopsy diagnoses were exact in 65%, sufficient in 22% and poor in 13%. For metastases the diagnoses were correct or nearly exact in 85%, for adenomas in 90%, for carcinomas in 74% and for pheochromocytomas in 96%. For assessment of malignancy the sensitivity was 92%, the specificity 94%.

Conclusions: Cortical lesions can be clearly distinguished from medullary and extraadrenal lesions in far most cases. A correct decision of dignity is possible in more than 90% of cases.

O-068

Pathomorphosis of thyroid diseases in Precarpathian endemic goiter region

Vovk V.I., Skaletska N., Chekan M.
Department of Pathology, Medical University, Lviv, Ukraine

Introduction: Precarpathian is one of the oldest endemic goiter regions in Europe. Since 1923 surgeons in the Lviv Medical University made operations on thyroid with further histological examinations of thyroid gland.

Methods: The retrospective analisys of histological examinations of thyroid from 10016 patients operated in Lviv Regional Hospital at the period 1923–1996 was performed.

Results: In 1923–1950 multinodular goiter was noted in 33.0–36.5% and Graves disease – in 6.7–8.6% of patients. Respectively in 1991-1996 multinodular goiter was noted in 40.0% and Graves disease – in 12.2%. In 1923–1960 autoimmune lesions of thyroid was found only in 1–3% of patients. In 1991-1996 autoimmune thyroiditis was found in 12.2%, focal thyroiditis – in 15.2%. Benign thyroid tumours in 1923–1940 was revealed only in individual cases, in 1991–1996 thyroid adenoma was noted in 37.7%, atypical adenoma – in 3.0% of patients. Thyroid cancer (TC) in 1923–1930 was found in 14.9%, in 1931–1970 – in 2.9–5.6%, in 1991–1996 – in 12.3% among all patients. In 1923–1930 among the total number of TC papillary carcinoma was found in 28.5%, follicular carcinoma – 7.1%, undifferentiated carcinoma – 57.1%. In 1991–1996 papillary carcinoma was found in 69.0%, follicular carcinoma - 14.6%, undifferentiated carcinoma – 2.9%. Medullary carcinoma was found at the first time in 1971–1980, in 1991–1996 – in 7.0% among total number of TC.

Conclusions: The increase of number of multinodular goiter, Graves disease, autoimmune thyroiditis, adenomas, TC among all operated patients and the increase of number of papillary carcinoma among all number of TC were found at the analysing period.
Cyto Pathology

O-069

Fine needle aspiration of ovarian cysts. A prospective study.

Granados R, Joste NE*, Santonja C.
Hospital Universitario de Getafe, Getafe, Madrid, Spain;
*Brigham and Women's Hospital; Harvard Medical School, Boston, MA, USA

Introduction: The clinical use of fine-needle aspiration biopsy (FNAB) of ovarian cysts has been controversial due to large variations in sensitivity and to fear of cyst rupture during the procedure. Therefore, the experience of most laboratories in this field is limited.
Methods: We prospectively evaluated 192 ovarian cystic masses by performing FNAB of surgically resected specimens.
Results: Twenty samples (10.4%) were considered insufficient for diagnosis. While 97.5% of benign cysts were correctly classified, there were three false positive diagnoses (either malignant or suspicious for malignancy), corresponding to a mature cystic teratoma and 2 serous cystadenomas that contained abundant papillary cell clusters. Only 20 of 33 malignant cysts were cytologically diagnosed, rendering a sensitivity of 60.6%. There were 12 false negative diagnoses. Nine of these cases (27.3% of all malignancies and 75% of false negatives) were very hypocellular. Among the 18 proliferating (borderline) tumors in this series, 12 had features of a benign cyst, 3 were classified as malignant or suspicious for malignancy, and 3 had only a few atypical cells admixed with benign-appearing cyst contents.
Conclusion: FNAB of ovarian cysts shows a high specificity but a low sensitivity, probably due to a large number of hypocellular specimens. Therefore, a definitive benign diagnosis of an ovarian cyst aspirate should only be rendered when an adequate number of cells is available for examination. Even with cellular specimens, FNAB cannot discriminate between benign neoplastic and borderline ovarian tumors. Clinical and radiological correlation is essential for adequate evaluation.

O-070

Determining Primary Site From Metastatic Adenocarcinoma In Serous Fluids

E. Inglis, O.J. Cooper, D.M. Bailey
Department of Cellular Pathology, High Wycombe, UK

Introduction: Metastatic adenocarcinoma commonly presents as pleural effusion or ascites. Determining site of origin can be difficult and is important in cases of occult primary tumour.
Methods: We examined 22 patients' serous fluids (12 pleural, 10 ascitic) which contained adenocarcinoma; histology from each patient was available. Air-dried and fixed smears were prepared; cell blocks were available in 19 cases, ThinPrep® smears in the remaining 3. Cytomorphology was recorded, together with results of immunocytochemistry for BerEP4, cytokeratins (CK) 7 and 20, CA-125 and CEA.
Results: 10 ovarian (7 serous, 2 mucinous and 1 mixed Mullerian), 4 breast (3 ductal, 1 lobular), 3 gastrointestinal tract (2 gastric, 1 rectal), 3 lung, one pancreatic and one peritoneal serous carcinomas were included. 70% of ascitic metastases were from ovarian primaries. 70% of ovarian metastases were to ascitic fluid. All breast and lung metastases were to pleural fluid. All ovarian primaries were CK7+, CA-125+ (sensitivity 100%, PPV 83.3%, NPV 100%). All gastrointestinal primaries were CK20+, CEA+ (sensitivity 100%, PPV 75%, NPV 100%). All lung and breast primaries were CK7+ (sensitivity 100%, PPV 35%, NPV 100%). Cytomorphology was non-specific, apart from true papillae being limited to ovarian tumours.
Conclusion: A panel of epithelial immunocytochemical markers may be used to exclude common primary sites of adenocarcinoma in cases of malignant serous effusions. This may focus clinical investigation, avoiding procedures that are often expensive and uncomfortable for the patient. Ovarian primary tumours may be predicted with a high degree of specificity.

O-071

Imprint Cytologic diagnosis of CNS Tumours. An old method in a new fashion. Itraoperative diagnostic accuracy of imprint cytology combined with frozen section. A report of 133 patients.

Lindal S, Dahl, IL, Hennig R
Departments of Neuropathology and Cytology,
University Hospital of Tromsø, Norway

Objective: To compare the diagnostic accuracy of intraoperative imprint smear from brain tumours to frozen sections from the same material.
Background of Study: Due to new stereotactic neurosurgical methods for diagnosis and excision of brain tumours, less brain tissue is available for for intraoperative examination. In order to have two different visual criteria for intraoperative diagnosis, we started up with cytological touch imprint examination of the brain tissue immediately before initiation of frozen sections.
Material and Methods: We evaluated all together imprints and frozen sections from 133 patients undergoing intracraneal surgery. Imprints were made from small pieces of stereotactic material or from larger pieces of tissue sent from the operating room for a rapid diagnosis. Hematoxilin & eosin (HE) and Papanicolaou staining was performed on alcoholfixed smear, immediately before preparation and cutting the same material for frozen section.
Results: Our imprint material included: 59 gliomas, 9 meningiomas, 11 pituitary tumours, 9 CNS lymphomas, 23 metastatic tumors and 22 others, including unspecific changes, infections etc.
Conclusions:
1. Imprint is diagnostically more accurate than frozen section in grading of astrocytomas and classifying metastatic carcinomas.
2. Advantages of the imprint method are excellent preservation of cellular details, speed and simplicity of the procedure, and possibility of high diagnostic accuracy from small pieces of brain tissue.

O-072

Cytopathological approach to sarcomas in serous effusions

Adhemar Longatto Filho, Hélio Bisi, Jeni Bortolan, Valéria Lombardo
Adolfo Lutz Institute, AC Camargo Hospital, Oncocenter Foundation, São Paulo, Brazil

Objective: To study the cytopathology of sarcomatous lesions found in serous effusions in a Cancer Hospital during 25 years, focusing the relevance of cytopathology in these lesions.
Materials and Methods: All records and available cytological specimens from patients with known primary sites, from 1966 to 1990, were reviewed according to each serous cavity. Cytological diagnosis originally classified with the Papanicolaou system were reported as negative, suspicious, positive and inadequate. All cases were prepared with cytospin and stained with both Papanicolaou and Leishmann methods. The performance of cytological method was correlated with histopatological analysis.
Results: A total of 4297 cases were reviewed: 3785 cases (88,1%) from patients with malignancy. Positive cytology was found in 1609 cases (37,45%). Definitive diagnosis of primary sarcomatous lesions was available in 158 cases causing serous effusions: 138 (87,4%) in pleura, 18 (11,4%) ascitic and 2 (1,2%) in pericardium. The frequencies of cytological diagnosis were: 120 (76%) cases negative for malignancy, 6 (3,8%) suspicious cases, 28 (17,7%) positive cases and 4 (2,5%) inadequate. No false positive case was found. Major histogenetic types were osteogenic sarcoma, fibrosarcoma and rhabdomiosarcoma.
Conclusions: Cytological examination is a very specific method to recognise malignancy arising from the sarcomatous lesions, in spite its low frequency in serous effusions.

O-073

Immunocytochemical determination of E-cadherin expression on FNAC from breast carcinomas. Reduced expression correlate with the degree of cohesion as reflected in the cell dissociation pattern on the smears

Torill Sauer*, Ghania Boudjema*, Peter W. Jebsen¤, Oddvar Næss*
Departments of Pathology, Ullevaal* University Hospital and Rikshospitalet¤, Oslo, Norway

Introduction: E-Cadherin mediates intercellular adhesion between epithelial cells. Altered expression has been suggested to be of prognostic significance in breast cancers. A dysfunctional, intercellular adhesion system may be responsible for the tumor cell dispersion pattern seen on fine-needle aspirates (FNAC).
Methods: The material consisted of fine-needle aspirates from 55 breast carcinomas. Slides were stored at –20ºC until immunocytochemical assessment. Three fibroadenomas and one benign, intraductal papilloma were used as benign controls.The degree of cellular cohesion was estimated semiquantitatively. E-cadherin expression was determined immunocytochemically. The following features were evaluated: membrane- and cytoplasmic as well as nuclear type of staining, percentage of positive cells and a semiquantitative estimate of membrane staining intensity (weak – moderate – strong). Full expression of E-cadherin was defined as a complete and strong membrane staining of virtually all tumor cells, in accordance with the staining pattern of the benign smears.
Results: None of the non-ductal subtypes revealed full expression of E-cadherin. 17% of G1 and G2 ductal carcinomas revealed full E-cadherin expression, in contrast to 5.6% of G3 tumors. Totally, 30% (14) of invasive, ductal carcinomas were negative, 15% (7) showed full expression, whereas 55% (26) had reduced expression. 25% of carcinomas with cohesion grade 1 (mainly in gruops) revealed full expression of E-cadherin, in contrast to 12.5% of tumors with cohesion grade 3 (mainly dispersed cells).
Conclusion: All non-ductal carcinomas showed reduced or negative E-cadherin expression. Reduced expression correlated both with cytologic grade and the degree of cohesion as reflected in the cell dissociation pattern in direct FNAC smears.

O-074

Cyclin D1 gene amplification assessed on breast cancer cytological specimens

Ph. Vielh, J. Couturier, S. Chevillard, F. Viard, J. Klijanienko, A. El-Naggar
Institut CURIE, Paris and CEA, Fontenay aux Roses, France

Introduction: Cyclin D1 is strongly implicated in cell cycle and its gene amplification, observed in less than 20% of primary breast cancer, has been associated with a poor outcome.
Methods: Cytological specimens obtained at the time of diagnosis from fine needle samplings without aspiration of 146 consecutive patients with breast cancer were used for detection of gene amplification by fluorescent in situ hybridisation (FISH) and quantitated by means of real time polymerase chain reaction (PCR).
Results: Of the 146 cytological specimens, 130 (89%) were suitable for both techniques. Twenty four (18%) cases were found amplified by FISH and 10 (8%) using real time PCR. Comparisons of the results obtained using both techniques showed concordance in 114 (88%) cases. The 16 discordant cases corresponded to 15 and 1 cases which were found amplified and non amplified by FISH, respectively.
Conclusion: Both techniques may be applied to cytological specimens of breast cancer obtained by fine needle sampling and give results that will be compared with prognosis before definitive validation.

O-075

Is grading of urothelial papillary bladder carcinoma the final result of the underlying molecular alterations?

T. Amaro, L. Santos, S. Pereira, M.J.Bento, P. Lopes, J. Oliveira, B. Criado, C. Lopes
Instituto Portugujs de Oncologia (UCI-B), Porto, Portugal

Introduction: The bladder cancer classification with prognostic intention defines two major groups: the low-grade papillary carcinoma and high-grade papillary carcinoma (WHO/ISUP 1998). Is this classification related to molecular alterations?
Material and Methods: Our sample consisted in 80 urothelial papillary bladder carcinomas treated at Instituto Português de Oncologia – Porto, Portugal. Twenty-three of them were low-grade and 57 were high-grade tumours. We performed an immunohistochemical study with specific monoclonal antibodies against the protein p16, p53 and Ki-67 (MIB1). In 55 cases of this sample we

also performed a FISH study with centromeric probes for chromosomes 7 and 17. For the analysis of TP53 gene we used a specific unique sequence probe. In the later sub-group 17 cases were low-grade and 38 cases were high-grade tumours.
Results: We observed a high frequency of p16 negative immunostaining in both groups. The p53 nuclear accumulation was suggestively higher in high-grade tumours (p=0.08). The frequency of cases with MIB1 positive in ≥20% of cells was higher in high-grade tumours but the difference was not statistically significant. The analysis of the numerical alterations of chromosomes 7, 17 and TP53 gene revealed that trisomy of chromosome 17 and trisomy of TP53 gene were more frequent in high-grade tumours but without statistical significance. The trisomy of chromosome 7 was statistically higher in high-grade tumours (p=0.01).
Conclusion: The molecular alterations were more prevalent in high-grade tumours. The classification of bladder carcinoma in low and high grade seems to be related with the molecular alterations.

O-076

Microdissection and quantitative "real-time" PCR as new tools in the analysis of paraffinized human renal biopsies

J.W. U. Fries, T. Roth, H.P.Dienes, M. Odenthal
Institute of Pathology, University hospital, Köln, Germany

Introduction: Activation of inflammatory signal pathways in the kidney may lead to a progression of existing mesangial lesions in immunological (i.e. lupus nephritis) or non-immunological (i.e. diabetic nephropathy) glomerular diseases. Their evaluation on biopsies requires a reliable quantitative analysis, for which established morphologic and immunhistologic techniques on limited material are not suited. Thus, we developed a quantitative PCR analysis from isolated glomeruli of paraffinized human biopsies.
Methods: After laser-guided microdissection (one 5 µm section/case) RNA was extracted from glomeruli with etiologically different mesangial proliferations. A quantitative "real-time"PCR was performed using specific probes and primers for the "vascular cell adhesion molecule-1 (VCAM; inflammatory marker) and for the "platelet-derived growth factor beta receptor (PDGF-ßR; proliferation marker). ß-actin served as housekeeping gene. A qualitative RT-PCR of the same RNA-extraction and an immunhistologic analysis of a parallel section served as comparison. **Results:** 1. Quantitative PCR allows a reliable detection of VCAM-1 and PDGF-ßR with different levels detectable in proliferative mesangial disease entities. 2. As little as 3 glomeruli of a single section/biopsy (one for each gene to be detected) are needed. 3. The procedure requires about 2 working days.
Conclusions: Detection of variable levels of inflammatory signals in mesangial proliferation suggest the necessity of
1.) a quantitative PCR as part of renal biopsy analysis; and
2.) a combined antiproliferative and anti-inflammatory therapy.

O-077

Loss of laminin 5 from basement membrane indicates invasive transitional cell carcinoma phenotype and poor prognosis

W. Hindermann, A. Berndt, H. Wunderlich*, D. Katenkamp, H. Kosmehl
Institute of Pathology and Department of Urology*, Friedrich Schiller University, Jena, Germany

Introduction: The heterotrimeric molecule laminin-5 (Ln-5) consists of the α3, β3 and γ2 chain. It represents a main protein of the anchoring filaments and links the basement membrane (BM) with the hemidesmosomes (epithelial adhesion complex). The study monitors the disintegration of epithelial adhesions complex via immunohistochemical Ln-5 demonstration in relation to expression of invasive TCC phenotype and prognosis.
Methods: Retrospective semiquantitative immunohistochemical analysis of 96 buffered formalin fixed, paraffin embedded samples of non-invasive and invasive TTC (follow up period of 36 month). Primary antibodies: D4B5 against the γ2 chain of Ln-5, CIV22 against collagen type IV, APAAP-technique. Statistical analysis using χ^2 test and Kaplan Meyer curves.
Results: In contrast to normal urothelium, three TCC associated Ln-5 γ2 chain pattern occur: cellular retention, stromal deposition and loss from the BM. Whereas cellular retention and stromal deposition could also be demonstrated in non-invasive TCC, the loss of Ln-5 from BM is strictly correlated to the invasive TCC phenotype. As shown by collagen type IV immunostaining, the loss of Ln-5 BM is not regular accompanied with a complete BM degradation. Moreover, stromal deposition and particularly the loss of Ln-5 from BM is statistically associated with a poor prognosis.
Conclusion: (**1**) Malignant transformation of the urothelium is constantly associated with a modulation of Ln-5 distribution. (**2**) The disintegration of the epithelial adhesion complex, visualised via the loss of Ln-5 from epithelial BM region, is a prerequisite for invasive behaviour of TCC. (**3**) Loss of Ln-5 is recommended as diagnostic marker of invasive TCC.

O-078

Nuclear penetrating antibodies in lupus nephritis

Jera Jeruc, Alenka Vizjak, Dušan Ferluga
Institute of Pathology, Medical Faculty, University of Ljubljana, Ljubljana, Slovenia

Certain autoantibodies can penetrate living cells and affect cellular functions; some have been shown to translocate into the cell nucleus and induce apoptosis. Although a nuclear localization of immunoglobulins is a frequent finding in lupus nephritis, its relevance to histomorphologic changes has not been systematically studied. Apoptosis was found to be decreased in proliferative lupus nephritis. We studied whether nuclear penetrating antibodies have influence on apoptosis and histomorphologic changes in lupus nephritis.
Kidney tissue samples of 301 SLE patients were examined by traditional light, immunofluorescence and electron microscopy. Additionally, 19 samples (13 with diffuse positive, 6 with negative nuclear reaction in tubular epithelial cells) were stained for the presence of apoptotic cells by TUNEL assay.
Nuclear localizing antibodies were demonstrated in 29.6% of patients. Immunoglobulins were most frequently found in nuclei of tubular epithelium (76.3%), followed by interstitium (46.2%) and glomeruli (33.3%). There was no correlation between the incidence of penetrating antibodies and the severity of glomerular inflammatory lesions according to the WHO classification or activity index. However, a negative correlation was obtained with the chronicity index ($p<0.01$) and tubulo-interstitial lesions ($p<0.05$). Apoptotic rate in tubular epithelium of patients with nuclear penetrating antibodies was higher as in patients without them, although the difference was not statistically significant.

Penetrating antibodies represent just one segment in complex pathology of SLE. Although our study did not confirm their pathogenic role inflammatory lesions lupus nephritis, their influence on apoptosis should be further investigated since defects in the apoptotic pathways have been shown to play an important role in autoimmunity.

O-079

Evaluation of a multi-color fluorescence in situ hybridization assay for the detection of bladder cancer – A continuing study in three european laboratories

E.C. Obermann[1], K. Junker[2], S. Schubert[2], H. Tanke[3], J. Wiegant[3], M. van der Burg[3], R. Pelger[4], L. Morrison[5], S. Seelig[5], C. Gamper[6], C. Blueml[1], A. Hartmann[1]
Institute of Pathology, University Regensburg[1]; Dept. of Urology, University Jena[2]; Dept. of Molecular Cell Biology[3] and Dept. of Urology, Leiden University Medical Center[4]; Vysis Inc., Downers Grove, IL, USA[5]; Dept. of Urology, St. Josef Hospital, Regensburg[6]

The analysis of urine sediments by conventional cytology provides good specificity but suffers from relatively low sensitivity. This problem was addressed using fluorescence in situ hybridization (FISH), and a commercial multi-color probe set has been developed (Vysis). The probe set was designed on the basis of existing data and additional testing, and was validated in a preliminary pilot study (Halling et al., J. Urol. 164:1768, 2000). The set includes centromeric probes for chromosomes 3, 7, and 17, and a unique sequence probe for the chromosome 9p21 locus. The purpose of this study is to assess the performance of the FISH assay in 3 European laboratories. Cells from urine were applied to slides either by cytocentrifugation or by pipetting and drying a cell suspension. The 25 morphologically most abnormal nuclei in each specimen were identified, based upon DAPI counterstaining, and each of the 4 targets enumerated. Specimens were considered positive by FISH if they contained cells with multiple chromosome gains (>4 cells), single chromosome gains (>9 cells) or homozygous loss of 9p21 (>9 cells). At present the three laboratories have tested over 200 specimens, and collectively have found higher sensitivity for FISH compared to cytology, with the specificity being similar for the two methods. The FISH assay was positive for 13 of the 41 specimens that were falsely negative by cytology. 15 of 30 equivocal cytology specimens with biopsy-proven cancer were identified correctly as positive by FISH. These findings indicate that FISH can enhance conventional cytology, and provide clarification of ambiguous cytology results.

O-080

Morphologic and Genetic Heterogeneity of Collecting Duct Tumors

Schierbrock S, Schmahl G, Rakozy C, Störkel S
Department of Pathology of the University Witten/Herdecke, Wuppertal, Germany

Introduction: The WHO classification of kidney tumors is based on morphological phenotypes. A small group of tumors (in total 10%) are thought to derive from the collecting duct system. These tumors can be subdivided into oncocytic adenomas, chromophobic carcinomas (including hybrid tumors), collecting duct carcinoma of high malignant potential and a recently described entity of collecting duct carcinomas of low malignant potential.
Methods: Out of 3332 tumors from the files of our kidney tumor registry we analyzed these 4 tumor entities morphologically (lightmicroscopy, immunohistochemistry) and in part genetically by using karyotyping, CGH and FISH techniques.
Results: Morphological diagnosis resulted in 261 oncocytomas with a unique phenotype, 144 chromophobic carcinomas (clear and eosinophil variant), 36 classical duct Bellini carcinomas and 5 mucinous collecting duct carcinomas of low malignant potential.
The analysed oncocytomas presented monosomy 1 and loss of Y or translocations t(5;11)(q35;q13). Extensive monosomies were typical for the chromophobe carcinoma (1, 2, 6, 10, 13, 17 and 21) and the collecting duct carcinomas of low malignant potential (1, 4, 6, 8, 9, 13, 14, 15 and 22). In contrast the duct Bellini carcinoma exhibited a more heterogenous and inconstant genotype.
Conclusion: There are 4 different types of kidney tumors that share morphological characteristics of the collecting duct. Presenting distinct genotypes the adenomas/carcinomas of rather low malignant potential share a loss of chromosomes whereas the more aggressive type of the duct Bellini carcinoma exhibits a more complex rearranged and heterogenous genome.

O-081

TIMP-1 protein and mRNA expression analysis in renal cell carcinoma using tissue microarrays and the LightCycler system

K. Struckmann, H. Moch, Th. Gasser, G. Sauter, M.J. Mihatsch, P. Schraml
Institute of Pathology, University of Basel, Basel, Switzerland

Identification and evaluation of molecular parameters is of utmost importance in cancer research and cancer treatment. To identify genes relevant for renal cell carcinoma (RCC) progression, the expression status of 1176 genes was assessed in 4 RCC cell lines, 2 renal carcinoma tissues and normal kidney.
Tissue using Human Atlas Cancer 1.2 cDNA microarrays (Clontech). 85 differentially expressed genes were identified. The gene of *TIMP-1*, a matrix-metalloproteinase inhibitor, was strongly expressed in all 6 tumors but only weakly detectable in normal kidney tissue. A renal cancer tissue microarray was immunohistochemically analyzed with a TIMP-1 antibody (clone 147-6D11, OncogeneResearch products) to study the prevalence of TIMP-1 protein expression. TIMP-1 protein was present in 373 of 383 clear cell RCC (97.8%), all papillary RCC (n=57), chromophobe RCC (n=23), oncocytoma (n=17) and collecting duct RCC (n=3), but also in all normal kidney tissues (n=6). As real-time PCR allows precise quantification of gene expression, *TIMP-1* expression was further determined in 45 fresh frozen CRCC with clinical follow-up information and 9 normal renal tissues using the LightCycler system. Compared to normal tissue *TIMP-1* was significantly higher expressed in renal tumors ($p<0.05$). 41 CRCC (91.1%) showed a 2 to 16 fold increased expression level of *TIMP-1*. Elevated expression levels of *TIMP-1* in CRCC were not correlated with patient prognosis, tumor stage and grade. It is concluded that elevated *TIMP-1* expression levels play an important role in the initiation of renal tumors (Supported by the Swiss National Science Foundation).

O-082

Leiomyomatosis of regional lymphnodes associated t o leiomyomatosis of tumoural capsule in patient with renal cell tumour; a possibly related condition

G.L. Taccagni; M. Ponzoni
Department of Pathology, Scientific Institute H San Raffaele, Milano, Italy

Introduction: We studied 8 cases of leiomyomatosis (L) of regional (hilar, paraaortic, paracaval) lymphnodes in patients with various histotypes of renal cell tumours, in which tumoural capsule was evaluated for the presence of a smooth muscle cells component (smcC).

Methods: The patients were six males and two females. The histotypes were as follows: clear cell carcinoma (4 patients), oncocytoma (2 patients), chromophilic cell (papillary) carcinoma (1 patient) and urothelial cell carcinoma of renal pelvis (1 patient). Both L of lymph nodes and smcC of tumoural capsule were graded in a semiquantitative method (from + to +++; mild, moderate, intense) and tested with a panel of antibodies (smooth-muscle actin, desmin, cytokeratins, vimentin, fibronectin, c-kit, HMB 45, bcl-2, S.100 protein, CD21,CD23 and CD34).

Results: In each patient the tumoural capsule had a significant smcC (identified cyto-morphologically and from desmin positive cells), although never complete nor circumferential, but focal with both diffusion and intensity ranging from moderate to intense. Four patterns of organization of smooth muscle cells were observed: small bundles, large bundles, nodules (small and/or large) and intratumoural extension, mainly in proximity to the capsule and in nodules. In four cases a mild degree of cytologic atypia was present; in one of them an epitheliod clear cell component was observed. In all cases an association of smcC organized in bundles with the wall of small vascular channels of venular type was evident; in one case a pseudo-infiltration of nerve trunks was reported. All the lymphnodes had a significate thickening of the capsule, with a smcC judged moderate or mild in 4/7 and 3/7 cases, respectively. The extension of L was partial in all cases from mild and/or initial to intense with severe effacement of nodal architecture. The small bundles pattern was always present, associated to large bundles in 4 patients. All cases were characterised by lack of cytologic atypia but one, in which an epitheliod clear cell component was also present. By immunohistochemistry, L of lymph nodes and smcC of renal tumoural capsule were strongly positive for smooth-muscle actin, desmin and vimentin; some cases were mildly reactive for bcl-2 protein; one case was focally positive for HMB45.

Conclusion: Leiomyomatosis of lymphnodes is a rare phenomenon observed mainly in pelvic region and in women with cervical cancer; the criteria we used to accept this condition were to find al least 3 small intraparenchimal bundles of smc. Control cases (25) constituted by lymphnodes of the same region but associated to others neoplastic condition (prostatic and cervical cancers) never had L. The presence of smcC in renal tumoural capsule has never been reported; also for this new condition we suggest the definition of leiomyomatosis. Control cases (8) constituted by renal tumours without L of lymphnodes, never had a significative smcC in tumoural capsule. The association of leiomyomatosis of regional lymphnodes and of renal tumoural capsule is striking; in our opinion these are possibly related conditions, with a common pathogenesis and strictly associated to renal tumour.

O-083

Studies into a possible relationship between interstitial fibrosis and early glomerular sclerosis – results of light and electron microscopic morphometric investigations

Aldona Woźniak[1], Wiesława Salwa-Żurawska[1], Elżbieta Kaczmarek[2]
Department of Clinical Pathomorphology[1], Department of Medical Statistics and Informatics[2], Karol Marcinkowski University School of Medical Sciences, Poznań, Poland

INTRODUCTION: According to current opinions as expressed in the literature, foci of interstitial cortical fibrosis are related to the level of glomerular damage. Enlargement of glomeruli also indicates early sclerosis.

THE AIM of the present study was to determine whether there is any correlation between the extent of interstitial fibrosis, the size of glomeruli, as estimated by light microscopy, and the ratio of mesangial matrix volume to the volume of mesangial cells (MAT/CELL) observed under electron microscopy.

MATERIAL AND METHODS: The analysis was performed on 40 renal biopsies: 10 with minimal change disease (MCD, the control group), 10 with focal segmental glomerulosclerosis (FSGS) and two other groups consisting of 10 cases with MCD and 10 with mesangioproliferative glomerulonephritis suspected of progressing into FSGS (MCD→FSGS, GN MES→FSGS).

RESULTS: The extent of fibrosis was related to the surface of the whole section (the area of glomeruli was not included). The results obtained were then correlated with the results of previous electron-microscopic morphometric studies (in press). The results achieved indicated a relation between glomerular area and the extent of sclerosis (MAT/CELL) in the FSGS. Significant differences in the extent of interstitial fibrosis were detected between the control group and the other examined groups (MCD→FSGS, GN MES→FSGS, FSGS). A linear correlation (k=0.9) was found between the amount of fibrous tissue and the MAT/CELL in the MCD group only. Similar correlations did not appear in the other groups. **CONCLUSION:** It is therefore probable that interstitial fibrosis is related to other factors, besides glomerular changes (sclerosis).

O-084

RNA in situ hybridisation of the large tenascin-c isoform indicates prostatic adenocarcinoma

Kathrin Katenkamp, A. Berndt, Laura Borsi*, H. Kosmehl
Institute of Pathology, Friedrich Schiller University Jena, Germany and Istituto Nazionale per la Ricerca sul Cancro, Genova, Italy

Introduction: Tenascin-C (Tn-C) and particular the (unspliced) large isoform (Tn-C_L) is considered as modulator of adhesion and is abundantly expressed in structure alterating processes like wound healing and cancer. Therefore, protein distribution and synthesis of Tn-C_L is analysed to reveal adenocarcinoma.

Methods: Shock frozen and formalin fixed, paraffin embedded tissue of 43 radical prostatectomy specimen. Immunohisto-chemistry: clone BC-2 against Tn-C_L and clone BC-4 against all Tn-C isoforms, APAAP technique. RNA/RNA in situ hybridisation: DIG-labelled cRNA probe against splicing domains A3-B (bp 4211-4779 of embl:HSTENAS3), proteinase K pretreatment, overnight

hybridisation, visualisation with DIG nucleic acid detection system (Roche).

Results: Tn-C (clone BC-4) was demonstrated within pre-existing myomatous stroma and strongly between carcinoma complexes. In contrast, Tn-C_L (clone BC-2) is restricted to the carcinoma, but the immunohistochemical distinction between the Tn-C isoforms requires native tissue. In 38 out of 43 routinely processed prostatectomy specimen, a synthesis of Tn-C_L could be demonstrated by the carcinoma cells. The hybridisation signal was particularly strong in invasive edges of the carcinoma. Hyperplasia or low grade PIN were distinguished from carcinoma by their stained basal and negative luminal cells, whereas in normal prostate no Tn-C_L synthesis was found.

Conclusions: (**1**) A prostate adenocarcinoma associated tissue distribution and synthesis of the large Tn-C isoform is demonstrated for the first time. (**2**) The strong synthesis in invasive front points to an invasion modulating function of the large Tn-C isoform. (**3**) Because of prostatic adenocarcinoma identification in 88% of our prostatectomy specimen, Tn-C_L in situ hybridisation is recommended for diagnosis.

O-085

Identification and Validation of Differentially Expressed Genes in Prostate Cancer

Glen Kristiansen, Christian Pilarsky; Edgar Dahl, Simone Kaiser, Christoph Wissmann, Yu Wongwei, Stefan Loening, Iver Petersen, André Rosenthal, Manfred Dietel

Introduction: Adenocarcinoma of the prostate is the most common malignant neoplasia of men in the western world. Despite its high incidence little is known about the genetic events in carcinogenesis. One approach to identify possible target genes for pharmaceutical intervention is to focus on genes which are differentially expressed, that is they are either over- or underexpressed in the tumor.

Methods: To screen these genes we have designed a proprietary cancer microarray (Affimetrix) containing 4000 genes. We hybridized matched pairs of RNA isolated from cancerous and normal prostate tissue, which was morphologically characterized and harvested by microdissection from 58 prostatectomy specimens. To validate the resultant candidate genes, conventional immunohistochemistry on frozen wholemount sections and mRNA in-situ-hybridization using arrayed (7 cases per slide) paraffin embedded material was employed.

Results: Using microarray hybridization we isolated a variety of differentially expressed genes in prostate cancer, some of these not associated with this disease before. Among the genes we subsequently validated morphologically by immunohistochemistry or in-situ-hybridization are CD166/ALCAM and CPGK-1, a small mucin-like molecule.

Conclusion. Microarray hybridization is a valid method to investigate gene expression patterns, which lead us to the discovery of genes differentially expressed in prostate cancer. These genes might be the basis for new therapeutic strategies to combat this disease.

O-086

Correlation of inflammatory cells (T-and B-lymphocytes; macrophages) in prostate biopsies to elevated PSA levels in a screening population

Patrizia L. Moser, M.D.[1]; Andrea Brunner, M.D.[1]; Georg Bartsch, M.D.[2], Gregor Mikuz, M.D.[1]
Department of Pathology[1], Department of Urology[2]

Introduction and Objectives: The relationship of inflammatory cells in prostate biopsies to total serum PSA levels in a screening population was investigated.

Methods: The study included TRUS-guided prostate biopsy specimens from 49 patients. All patients who underwent biopsy had elevated serum PSA and/or abnormal digital rectal examination. Immunohistological characterization of the inflammatory cells was performed using CD3, CD4 and CD8 antibodies to detect T-lymphocytes, CD20 antibodies for B-lymphocytes and CD68 antibodies to detect macrophages. The percentage of inflammatory cells and their distribution in stromal and glandular tissue was estimated by employing morphometric methods.

Results: The inflammatory cells of the stroma consisted of significantly more T-lymphocytes than of B-lymphocytes and macrophages. The T-lymphocytes also dominated the glandular region. A significant positive correlation was found between the percentage of macrophages and total PSA ($p<0.05$), and a significant negative correlation between percent free PSA and the percentage of T-lymphocytes as well as the percentage of B-lymphocytes.

Conclusions: The results indicate a significant positive correlation between macrophages and total PSA, and a significant negative correlation between T- and B-lymphocytes and percent free PSA levels. Further studies need to be performed regarding stage and grade of prostate cancer in positive biopsies and in radical prostatectomy specimens.

O-087

Post-mortem study of the prevalence of high grade prostatic intraepithelial neoplasia in the spanish population: Comparative assessment with post-mortem data from other ethnic groups and geographical areas

Olmedilla-Arregui G, Ruiz-Villaespesa A, Sanchez-Chapado M, Angulo Jc, Ramos P.
Servicios De Anatomia Patologica Y Urologia.Hospital Universitario. Principe De Asturias. Alcala De Henares. Spain

INTRODUCTION: Study of the prevalence and histological features of high grade PIN (HGPIN) in post-mortem specimens of a sample of the Spanish population, (Mediterranean Caucasian) comparing with Afro-Americans (AA) and American Caucasian individuals (AC).

METHODS: We studied prostatic glands from post-mortem examinations of 162 male patients born and living in Spain, aged >20 years. The glands were fixed on formaline , sectioned every 3–4 mm and studied after H-E staining. Criteria from the last Consensus Conference were applied. Only HGPIN cases were analyzed. All areas showing HGPIN from every block were mapped on individual plots. Extension of HGPIN was classified as focal and multifocal.

RESULTS: Of the total 162 prostatic glands examined, 16 were considered unsuitable. The final study was performed on 146

glands obtained from patients with a mean age of 48.5 years (20–81) Forty-two cases of HGPIN were found (28.26%), 20 of these being focal and 22 being multifocal. All focal HGPIN were located at the peripheral area (PA) and all multifocal HGPIN showed at least a peripheral growth. Prevalence by age was distributed as follows: 7.1%, 14.7%, 28.5%, 33.3%, 45.4%, 51.8% in the 3th–8th decades.

CONCLUSION. The development HGPIN in the Mediterranean Caucasian population starts in the 3rd decade, is usually unifocal and peripheral and its frequency and multifocality increase with age. The prevalence was lower in all MC age groups, compared with the AA and AC ethnic groups.

O-088

Oestrogen and androgen receptors in cultured human prostatic stromal cells upregulated by high doses of estradiol

Smith, P.*, Rhodes, N.P.**, Ke, Y.*, Foster, C.S.*
Department of Pathology* and Clinical Engineering**,
University of Liverpool, England

Aims. To develop and validate a new experimental model by which expression of oestrogen receptors (ER) in prostatic stromal cells can be reliably enhanced relative to similar cells with a low ER expression. Validation was confirmed by determining changes in expression of ER, AR, FGF-2 and FGF-7 in stromal cells exposed to high and low concentrations of estradiol and testosterone mimicking the different sex hormone levels between young and elderly men.

Methods. Human prostatic stromal cells, isolated from BPH resections, were grown in steroid-free medium plus 1μM β-estradiol. After 10 days cells were passaged and grown without estradiol until confluent. In another study cells were exposed to high and low concentrations of estradiol (500 nM or 0.075 nM) and testosterone (2000 nM or 1nM) in all combinations for 10 days. Cells were labelled with fluorescent antibodies to ER, AR, FGF-2 and FGF-7 and the fluorescence intensity measured by flow cytometry.

Results. Following exposure to 1 μM estradiol, stromal cells showed reduced expression of AR and ER but after passage without estradiol they showed a 20-60% increase in both receptors over controls. Different combinations of sex hormones induced inconsistent changes in expression of ER, AR and FGFs. However, there was a highly significant correlation between AR, ER and expression of both FGF-2 and FGF-7, largely related to cell strains.

Conclusions. We have devised a reliable, *in vitro* model to upregulate stromal ER. This model was validated by a study of the rôle of ER in stromal cell metabolism. Expression of ER is correlated with the synthesis of growth factors which may stimulate division of stroma and epithelium in BPH.

O-089

The sentinel lymph node concept in prostate cancer – Histopathological results of the „First 100 Patients"

Th.Wagner[1], B.Märkl[1], F.Wawroschek[2], H.Vogt[3], H.Arnholdt[1]
Departments of [1]Pathology, [2]Urology and [3]Nuclear Medicine,
Klinikum Augsburg, Germany

Introduction: The sentinel lymph node (SLN) hypothesis introduced by *Cabanas* in 1977 for the penile carcinoma has been modified successfully for an increasing number of malignancies. At Augsburg Klinikum the sentinel lymph node concept was transferred to prostate cancer for the first time.

Methods: 107 patients with prostate cancer underwent transrectal intraprostatic administration of ^{99m}Tc-Nanocoll® and dynamic lymphoscintigraphy one day prior to pelvic lymphadenectomy. SLN were identified during surgery by gamma probe and removed. Then standard pelvic lymphadenectomy was performed. SLN were examined by step-and-serial H.E.-sectioning and additional immunohistology with cytokeratine antibody. Remaining „nonsentinel lymph nodes" (NSLN) were examined in routine manner by at least one H.E.- section. Depending on histological results and clinical data part of NSLN were submitted to SLN-procedure as well.

Results: 5 out of 6 patients with negative lymphoscintigraphy had a history of transurethral prostatectomy. In 100 of the 101 patients with positive lymphoscintigraphy 4 SLN per patient were removed on average during surgery. 26 patients had positive SLN-metastasis,10 had additional NSLN-metastasis. One patient had a skip-metastasis in NSLN while SLN was negative and only one ‚occult' micrometastasis could be revealed from primarily nodal negative patients by additional immunohistochemistry of NSLN.

Conclusion: Results confirm feasibility and validity of sentinel lymph node concept in prostate cancer. Compared with conventional pelvic lymphadenectomy not only a significant increase of micrometastasis detection in SLN was observed but also detection of positive SLN beeing located outside the standard lymphadenectomy area. In future, pelvic staging lymphadenectomy might be restricted to SLN.

O-090

Analysis of the genome in normal and in cancer mammary tissues using proteomics technologies

Walter B. Battistutti 1, Kerstin Pischinger 1, Mahmood Manavi 2,
Mark Behnam 1, Klaus Czerwenka 1
1 Department of Gyneco-Pathology and 2 Special Gynecology,
University Hospital, Vienna, Austria

Introduction: Now that we have completed mapping the human genome, the logical next step is to determine the products of the individual genes. The expanding knowledge of the genome (DNA) and its macromolecular products (RNA, protein) is beginning to reveal that cancers can be linked to specific alterations in the molecular process of affected cells and tissues. Knowledge of the proteome has been greatly enhanced thanks to microdissection in association with the following techniques: Micro-array, 2-D and MALDI. A major advantage of proteomics over genomics is the ability to analyze post-translational modification. Areas where proteomics can make an impact in functional genomics are now becoming clear.

Method: Some of these areas were demonstrated with samples of normal and cancerous mammary tissues analyzed using the following high-tech methods: 1.) gene discovery (micro-array techniques), 2.) annotation of the through protein data and 3-protein-protein ineraction studies (2D/Maldi). teraction studies (2D/Maldi).

Results: To date we have identified increased expression (up-regulation) of cell cycle genes (Cyclin D1, CDK4, E2F and DP2) in mammary cancer in comparison to a low expression (down-regulation) fore, in malignant tissue thein normal mammary tissue. Therefore, in malignant tissue the proteins will make the cell dependent on growth stimuli (growth factors) and also dependent on

the protein-pathogen protein interacts) and also dependent on the protein-pathogen protein interaction.
Conclusion: In this presentation we demonstrate that the combination of DNA micro-array and 2D/MALDI are an emerging area in functional genomics and proteomics.

O-091

The sequential loss of Laminin-2 and Laminin-5 and their receptors indicates DCIS and invasive breast cancer

A. Berndt, J. Jagemann, D. Katenkamp, H. Kosmehl
Institute of Pathology, Friedrich Schiller University Jena, Germany

Introduction: Laminins (Ln) are differentially expressed and use different receptors. Therefore, we investigate the modulation of Ln-2 and Ln-5 and their receptors in relation to tissue organisation in normal breast, DCIS and invasive ductal carcinomas (IDC).
Methods: Shock frozen samples of normal breast (3), DCIS of different grade (10) and IDC (6), APAAP and ABC immuno-(double) labelling. Primary antibodies to BM antigens: collagen IV, Ln-2 and Ln-5; matrix receptors and associated proteins: integrin chains α_3 , α_6, β_1, and β_4; α-, β-dystroglycan, α-, β-, γ-, δ-sarcoglycans, dystrophin 1, 2 and 3; utrophin; ductal differentiation antigens as CK5/6, CK14, ASMA, caldesmon, calponin. Western blot. Statistics: cluster analysis.
Results: All normal breast ducts possess Ln-2 and -5 as well as its receptors of integrin and dystroglycan type. As demonstrated by double labelling, the myoepithelial cell expresses the dystroglycan receptor. In all DCIS Ln-2 and dystroglycan receptor proteins are at least focally vanished. Semiquantitative analysis demonstrates the loss of Ln-2 and utrophin as the quantitative most extensive marker of transformation in DCIS. Ln-5 and its $\alpha_6\beta_4$ receptor is only focally lost in 5 out of 10 DCIS, whereas in all IDC the epithelial adhesion complex (Ln-5/$\alpha_6\beta_4$) is mostly complete vanished.
Conclusions: (1) This is the first report demonstrating the dystroglycan receptor in breast myoepithelial cells. (2) There is transformation associated sequential modulation of BM-ductal cell adhesion: Whereas the loss of the Ln-2-dystroglycan adhesion is an early indicator of transformation the loss of Ln-5 is associated with the acquisition of invasive behaviour.

O-092

Genetic analysis of synchronous, bilateral breast carcinomas.

H. Buerger[1], C. Agelopoulos[2], B. Hinrichs[3], Burkhard Brandt[1], Werner Boecker[1]
[1]Gerhard-Domagk-Institute of Pathology, [2]Institute of Clinical Chemistry and Laboratory Medicine, Westfälische Wilhelms Universität Münster, Institute of Pathology Köln, Germany

Introduction: Clinical and immunohistochemical data characterize bilateral breast cancer cases as independent tumours. Only few cytogenetic studies exist, some of which supporting the idea of a breast-to-breast-metastasis sequence, especially in highly differentiated tumours.
Methods: In order to give an overview about the genetic changes in bilateral breast cancer and to answer the question of a clonal relationship between these tumours, we investigated 27 invasive and *in situ* carcinomas of 11 pairs of simultaneously detected, bilateral breast cancer cases. Comparative Genomic Hybridization (CGH) was used to give an overview about all unbalanced chromosomal alterations within these tumours. PCR-based multiplex microsatellite analysis, using 11 markers for 7p12-13, 7q31, 8p22, 8p12, 10q23, 13q14, 16q22-24, p53 and 17q21 determined the clonal relationship of these tumours.
Results: Morphologically all except one tumor pairs revealed a different histological pattern. This was confirmed by CGH, with bilateral breast cancer cases revealed a high intraindividual cytogenetic difference except of one patient. In this single case CGH and morphology (tubular carcinoma) displayed highly concordant features with gain of 1q and loss of 16q as the only cytogenetic alterations in both breasts. In multiplex analyis both carcinomas displayed a loss of different allels on 16q22-24 in multiplex PCR-analysis. No significant cytogenetic differences compared to unilateral, sporadic breast cancer were seen.
Conclusion: The combination of CGH and PCR-based multiplex microsatellite analysis clearly demonstrates that bilateral breast cancers are independent tumours without genetic evidence of a breast-to-breast metastasis sequence.

O-093

Chromogenic *in situ* hybridization for HER2 amplification in human breast carcinomas: A powerful alternative to FISH and IHC

N. Dandachi, C. Hauser-Kronberger, G. Vogl, H. Bartel, B. Mlineritsch, O. Dietze
Institute of Pathology, 3rd Department of Internal Medicine, Landeskliniken Salzburg, and University of Salzburg, Austria

Background: The high incidence of HER2 overexpression in breast cancers, and the recognized prognostic and potentially predictive value of HER2 render the HER2 receptor a novel and important therapeutic target. A prerequisite for successful Herceptin™ therapy in HER2-positive patients is the accurate and reliable detection of HER2 overexpression/amplification. Currently, the two most frequently used and FDA approved approaches to determine HER2 status are immunohistochemistry (IHC, HercepTest™) and fluorescence *in situ* hybridization (FISH, Vysis, Ventana). However, both methods have technical and interpretative limitations. Hence, the aim of this study was the development of a chromogenic *in situ* hybridization (CISH), which enables detection of HER2 gene copies with conventional peroxidase reaction.
Materials and Methods: We investigated and compared the HER2 status in 160 archival, invasive breast carcinomas by means of IHC, FISH and CISH. Furthermore, patient survival was analyzed in relation to HER2 status assessed by all three methodologies.
Results: Concordance was high overall (94%, 148 of 158 cases) and the level of agreement between IHC and CISH was excellent (kappa=0,83, $p<0.0001$). In the presence of HER2 amplification two (1.7%) cases showed no protein overexpression. Conversely, HER2 overexpression was found in four cases (3.3%) without gene amplification. Survival correlated with IHC results in strongly positive cases ($p=0.0001$) and strongly amplified CISH cases ($p=0.001$), but not in weakly positive IHC or CISH cases.
Conclusion: In terms of feasibility, specificity and reliability CISH provides a promising alternative to IHC and FISH, capable of overcoming many of the inherent technical and interpretative limitations of these techniques.

O-094

OESTROGEN RECEPTOR ALPHA AND HEAT SHOCK PROTEIN 27, TWO QUANTIFIABLE MARKERS DEFINING BREAST CANCER RISK

Abeer M. Shaaban, Christopher S. Foster
Dept. of Pathology, Royal Liverpool University Hospital, Liverpool, UK

Aims: Search is continuing for new markers by which breast cancer can be predicted early in patients' life history. Early dysregulation of oestrogen receptor (ERα) and heat shock protein 27 (hsp27) may represent an early event in mammary carcinogenesis.
Methods: Through a case-control study, foci of hyperplasia of the usual type (HUT) were identified in tissues from cases who subsequently developed breast cancer (n=120) and matched controls (n=385). HUT foci (n=161) and normal lobules (n=91) from cases (n=21) and controls (n=28) were stained using monoclonal antibodies for hsp27 and ERα and % of positively stained cells was quantified using morphometric image analysis.
Results: hsp27 and ERα expression was significantly higher in HUT foci from cases compared with controls (P<0.0001 and 0.015 respectively). In cases, % of hsp27 positivity was 29.32% compared with 13.92% in controls. The mean ERα+ cells in HUT was 57% in cases and 30.27% in controls. Among cases, a significant overexpression of hsp27 was found in HUT foci compared with normal lobules (P<0.001). A strong positive correlation was found between HSP27 and ERα expression r=0.836, P<0.0001).
Conclusions: Our data highlights a novel hormone dependent role mediated by hsp27 during mammary carcinogenesis and suggests that overexpression of both ERα and hsp27 may define a subset of phenotypically benign but high-risk lesions. This might improvebreast cancer risk assessment and management strategies.

O-095

Demonstration of clonality in FNAB material of lymph nodes with NHL

F.J. Bot, M. Lentjes, Y. Peeters, E. Meulemans
Dept. of Pathology, University Hospital Maastricht, The Netherlands

Introduction: When a malignant lymphoma (NHL) is suspected in Fine Needle Aspiration Biopsy (FNAB) material of a lymph node, determination of clonality may be helpful. We have examined the sensitivity and specificity of PCR based clonality assessment on archival FNAB material. We were especially interested in conditions that might cause false positive or false negative results.
Methods: 44 consecutive cases of NHL of which at least one unstained FNAB slide was available where used. As controls we have used 33 cases which carcinoma metastases and 15 cases with reactive changes. PCR of the VH-gene was done according to a standard method.
Results: Of the NHL cases 64% was monoclonal, 16% polyclonal and 20% inconclusive; of the metastatic cases, 43% was inconclusive, 39% polyclonal and 18% monoclonal; of the reactive cases 47% was polyclonal 20% inconclusive and 33% monoclonal.
Discussion: The results in the NHL cases were as expected. The NHL=s that did not show monoclonality were mainly follicular and large cell lymphoma=s which are known to have a lower yield with this technique. Addition of a PCR against the translocation t(14;18) may solve part of this problem. The high number of inconclusives in the metastatic cases is caused by necrosis and by the very low numbers of B-lymphocytes in nodes that are completely destroyed by tumor. Worrisome however is the high number of monoclonals (i.e. false-positives) in the reactive and metastatic cases. This may be caused by Apseudo-monoclonality≅due to sampling of low numbers of B-lymphocytes and in part by very specific immune reactions. In part however it remains unexplained. In conclusion we may say that with this PCR technique clonality can be satisfactorily demonstrated in FNAB material of NHL. The high number of falspositives however makes it an absolute requirement that the molecular results are viewed in conjunction withe the cytomorphology and that a Amolecular diagnosis≅ in itself should never be given.

O-096

Thymic neuroendocrine carcinoma: A clinicopathologic study of 5 cases

Carole Gengler, Lara Chalabreysse, Sana Sefiani, Françoise Thivolet-Béjui
Department of pathology, Louis Pradel Hospital, Lyon, France

Thymic neuroendocrine carcinomas (TNC) are rare neoplasms.
Methods: we report 5 new cases out of a series of 100 thymic tumours, registrated from 1970 to 2000 at the Louis Pradel Hospital in Lyon. After a clinical, histopathological and immunohistochemical (keratin, epithelial membrane antigen, chromogranin, synaptophysine, CD1a, CD5, CD99) study, we reclassified the 5 cases in 3 atypical carcinoid (AC) and 2 small cell carcinoma (SCC), according to the WHO classification (1999).
Results: AC occured in older patients (65 years versus 56 in SCC). Tumor size was smaller in AC (8,3 cm versus 9 in SCC). Pulmonary extension was observed in one case of AC, whereas 1 SCC developed cerebral metastasis. Histologically, mitotic activity was higher in SCC (13 mitoses for 10 high power field versus 5 in AC). Necrosis was more frequent and extensive in SCC. Keratin was expressed in all cases. All tumors were positive for chromogranin, with a higher expression in AC than in SCC. On the other hand CD5 expression remained negative in all cases, in opposition to non TNC. The expression pattern of EMA was higher and more intense in SCC than in AC. Staining with CD1a and CD99 antibodies remained negative, correlated with the absence of immature lymphocytes in malignant thymic neoplasm.
Conclusion: clinical and immunohistochemical features justify to apply the same classification to TNC as to pulmonary neuroendocrine tumors. The lack of CD5 expression is of great value for neuroendocrine differenciation.

O-097

Analysis of gene expression in lymphoma derived cell lines and malignant lymphoma using cDNA microarrays. Effects of CD30 stimulation

Kenner L.[1], Dürkop H.[2], Nöhammer Ch.[1], Beham-Schmid Ch.[1], Höfler G.[1]
[1]Institute for Pathology, University of Graz, Austria and [2]Institute for Pathology, Free University Berlin, FRG

Introduction: Analysis of gene expression using cDNA microarrays is a valuable tool for the rapid simultaneous analysis of thou-

sands of genes. The cytokine receptor CD30 induces apoptosis in anaplastic large cell (ALCL)- but not in Hodgkin's lymphoma (HL)-derived cell lines.
Methods: cDNA microarrays containing 1400 cancer-related genes involved in cell proliferation, signal transduction and apoptosis were used to study gene expression in lymphoma derived cell lines. Protein expression was studied in fixed, paraffin-embedded specimens from patients with malignant lymphoma using multiple tissue arrays. To analyse effects of CD30 stimulation, cells were incubated with a murine Ki-1 antibody.
Results: The most pronounced differences between the various lymphoma derived cell lines were observed in genes playing a role in apoptosis or signal transduction. Immunohistochemical studies on cell lines showed a good correlation to RNA expression in 6/7 antibodies. However, a much higher heterogeneity was detected in specimens from patients with corresponding malignant lymphoma. After anti-CD30 incubation, the ALCL-cell line Karpas299 showed an increased expression of the anti-apoptotic proteins A20 and cIAP1 (inhibitor of apoptosis protein) as well as TANK (TRAF-associated NF-kappaB activator), whereas stimulation of the ALCL-cell line JB6 and the HL-cell line KMH2 did not elicit significant differences in the CD30 pathway. Interestingly, CD30 expression was reduced only in JB6.
Conclusions: RNA expression profiling using cDNA microarrays is a useful tool for fast analysis and identification of differentially expressed genes in cell lines. Reliable results can be obtained when used in conjunction with immunohistochemical analysis using multiple tissue arrays.

O-098

Lymphocytes expressing recombination activating genes are present in human tonsils but not in germinal centre reactions
Nadine Meru, Andreas Jung, Irith Baumann, Gerald Niedobitek
Pathologisches Institut, Friedrich-Alexander-Universität, Erlangen, Germany

Introduction: V(D)J rearrangement is mediated by two recombination activating genes, RAG1 and RAG2, which are transiently expressed during B- and T-cell ontogeny. Upon completion of V(D)J rearrangement, RAG expression is shut down. Mature lymphocytes are believed to be RAG-negative thus maintaining allelic exclusion. This concept has been challenged by reports demonstrating RAG expression in germinal centre B cells. It has been suggested that re-induction of RAG expression may occur as a result of diminished or abolished antigen binding thus rescuing B-cells from apoptosis.
Methods: 25 hyperplastic tonsils were examined for RAG expression by in situ hybridisation. Microdissected germinal centres and extrafollicular areas were subjected to RT-PCR with primers specific for RAG1 and RAG2.
Results: Using in situ hybridisation, RAG expression was detected in immature lymphocytes in bone marrow and thymus. Germinal centres in all tonsils were uniformly RAG-negative. RAG-positive lymphocytes were detected outside germinal centres in 12 tonsils. These cells were mainly localised at the border between lymphoid tissue and fibrous connective tissue. By RT-PCR, RAG1 and RAG2 transcripts were identified in microdissected extrafollicular areas but not in germinal centres.
Conclusions: We conclude that RAG expression is not reinduced in germinal centre reactions. However, RAG-positive cells were detected in a poorly defined compartment at the interface between lymphoid tissue and fibrous connective tissue of the tonsils. It is uncertain if these are mature lymphocytes which have reacquired immature features or genuinely immature lymphocytes which have left the bone marrow prematurely or were generated locally.

O-099

Typing the clonal composition of T cell subsets in T cell lymphoma of AILD type by single cell PCR
K. Willenbrock, A. Roers, H.H. Wacker, R. Küppers, M.L. Hansmann
Senckenbergisches Institut für Pathologie, Johann Wolfgang Goethe Universität, Frankfurt am Main, Germany

Angioimmunoblastic lymphadenopathy with dysproteinaemia (AILD) has been recognized as a T cell non-Hodgkin`s lymphoma. The lack of conal T cell expansions in approximately one third of all cases has been explained by minor tumor cell expansions which cannot be detected by conventional techniques. We investigated eighteen lymph nodes with the characteristic histology of AILD by PCR amplification of T cell receptor (TCR) gene rearrangements from DNA extracted from whole tissue sections. Dominant T cell clones were found in twelve cases. In seven of these cases, four of which with a dominant clone, single $CD4^+$, $CD8^+$ and proliferating $Ki67^+$ cells were isolated by micromanipulation from frozen tissue sections. TCRβ gene rearrangements were amplified from these cells and sequenced. In the four cases with dominant T cell expansions, clonal gene rearrangements were only obtained from $CD4^+$ and $Ki67^+$ cells and not from $CD8^+$ cells, indicating that T cell lymphoma of AILD type derives from T helper cells. Minor clonal T cell expansions in those cases with no clonal gene rearrangement in the whole tissue DNA analysis were not detectable even at single cell resolution, suggesting that AILD without clonal T cell expansions exists. TCRβ gene rearrangements of four out of ten informative cases displayed similarities, indicating a potential role of (super-) antigen triggering in at least some cases of AILD.
Hepatopathology

O-100

Microarray-based expression-analysis of hepatic angiosarcomas
Markus Benicke, A. Tannapfel, A. Markwarth, Ch. Wittekind
Institute of Pathology, University of Leipzig

Aims: Microarray-based expression analysis enables users to simultaneously detect changes in expression of over 1,000 different genes in one experimental set-up. The aim of this study was to identify specific genes or expression-patterns representing the entity of hepatic angiosarcomas and to compare them with already known patterns of other liver diseases.
Methods: Tissue samples were obtained from 16 patients with hepatic angiosarcoma undergoing partial liver resection. Tumour surrounding, non-neoplastic liver tissue from the same patients as well as hepatocellular carcinomas (10 pts.), cholangiocarcinomas (5 pts.) and hemangiomas (5 pts.) served as controls. After microdissection the differential gene expression of the tissues was analysed by microarray-based expression profiling. Immunohistochemistry was performed in order to localise the corresponding proteins.

Results: By Microarray analysis, the expression of numerous known genes was detected. A distinct expression pattern for angiosarcomas consisting of constant overexpression of vascular endothelial growth factor receptor 1, 2 and 3 (VEGFR-1,-2,-3) and p53-binding mouse double minute 2 homologue (MDM2) was observed. VEGF was also found to be overexpressed in angiosarcomas. Immunohistochemically VEGF- and MDM2-protein were localised within the angiosarcoma cells.
Performing a computer-based comparison of mathematical equivalents to the achieved greyscaled gene expression levels, a similar expression pattern was neither seen in hemangiomas nor in the malignant liver tumours serving as controls.
Conclusions: Our results indicate, that the appearance of certain otherwise not seen expression patterns may represent key events in the pathogenesis of human angiosarcomas. VEGF and VEGFR subtypes as well as MDM2 could be useful in the differential diagnosis of angiosarcoma of the liver.

O-101

Vanishing small bile ducts as a cause of persistent hypertransaminasemia

R. Miquel, Z. Lozano, C. Iglesias, M. Bruguera
Pathology Dept. and Liver Unit, Hospital Clinic, Barcelona

A proportion of asymptomatic patients with persistently raised serum hepatic enzymes remain undiagnosed after a complete biochemical, serological and histological evaluation. In some of these cases liver disfunction could be related to subtle histologic changes, such a mild ductopenia.
Aim: To investigate if a reduction in the number of small bile ducts may be related to persistent hypertransaminasemia.
M & M: H&E and trichrome stained sections of liver from 52 patients were reviewed to assess the number of the interlobular portal tracts (ILPT) and terminal portal tracts (TPT) devoided of bile ducts. Ten patients with non-hepatic lymphoma with normal liver tests and normal hepatic histology were used as a control. Results were correlated with AST, ALT , GGT and AP determinations and age and sex.
Results: Bile ducts were present in ILPT of all liver biopsies from patients and controls. However, they were absent in >50% of TPT from 24 of 52 (46%) patients and between 25–50% of TPT from 14 of 52 (27%) patients. In the remaining 14 patients and in the 10 controls bile ducts were present in most TPT. The degree of small bile duct ductopenia, either severe or mild, did not correlate with age or sex.
Conclusions: Vanishing of small bile ducts is an overlooked finding in about 75% of patients with persistent hypertransaminasemia of unknown etiology. It seems to be a benign and non-progressive disorder because it is not associated with fibrosis. The accurate examination of TPT to assess the presence or absence of bile ducts is required to identify a morphologic change that correlates with biochemical abnormalities.

O-102

Fractal quantitative evaluation of collagen matrix in liver biopsy specimens during chronic disease

G. Soda[1], F.Grizzi[2,3], S. Nardone[1], N. Dioguardi[2,3], M. Melis[1]
[1]Dipartimento Medicina Sperimentale e Patologia, University "La Sapienza", Rome, Italy; [2]Scientific Direction, Istituto Clinico Humanitas, Rozzano, Milan; [3]Fondazione "Michele Rodriguez", Istituto Scientifico per le Misure Quantitative in Medicina, Milan, Italy

Introduction. Liver fibrosis is characterised by a *complex* three-dimensional ramified structure that can be detected in bioptical sections as two-dimensional irregular and sometime fragmented forms. Irregularity and complexity are the main features of every biological system, including human tissues, cells and sub-cellular components. These two properties of the *organised biological matter* cannot be quantified by means of the classical Euclidean geometry, which is able to measure regular objects, practically unknown in Nature. This study depicts the use of Fractal geometry to quantify the complex collagen deposition during chronic liver disease.
Methods. Thirty standard needle liver biopsy specimens were obtained from patients with chronic HCV-related disease. Three μm-thick sections were cut and stained by means of Picrosirius stain, in order to visualise collagen matrix. The degree of fibrosis was measured using a quantitative scoring system based on the computer-assisted evaluation of the *fractal dimension* of the deposited collagen surface.
Results. The obtained results by both study groups, show that the proposed method is reproducible, rapid and inexpensive. The mean fractal dimension was 1.35 (1.75–1.07). The fractal dimension that measure the space-filling property of the irregular collagen area, does not depend by the amount of the collagen deposited in the slide. The fractional dimension of its irregular shape defines fibrosis as a natural fractal structure.
Conclusion. The complex distribution of its collagenous components can be quantified using a single numerical score that seems to be a better alternative to the methods adopted so far. This study demonstrated that it is possible to quantify the collagen's irregularity in an objective manner, and that the study of the fractal properties of the collagen shapes is likely to reveal more about its structure and the complex behaviour of its development.

O-103

Multicentric or metastatic origin of hepatocellular carcinoma?

Andrea Tannapfel, M. Benicke, A. Markwarth, A. Katalinic 2, Ch. Wittekind1
Institute of Pathology, University of Leipzig, Institute of Cancer Epidemiology, University of Lübeck

Aims: The occurrence of multiple tumour nodules in hepatocellular carcinoma has not been clearly attributed to either the spread of one initial clone (intrahepatic metastasis) or to the independent origin of the cancer cells (multicentric carcinogenesis). This study em-ploys different markers in to answer the question of clonal (identical mutational or expression status) or independent (distinct genetic mutation or expression pattern) origin of these lesions.
Methods: Fresh frozen tissue from 25 patients with hepatocellular carcinoma having a total 56 tumour nodules was analysed. 15 pa-ti-

ents with 35 nodules had concomitant liver cirrhosis, 21 nodules from 10 patients arised in a non-cirrhotic liver. Microarray-technology was performed to identify up- and downregulation of over 1200 different genes (Clonetech Cancer Array1.2). For mi-croarry data analysis, a coupled two-way clustering approach was used. As controls, immunohistochemistry and in-situ-hybridisation were performed for in-situ localisation of the corresponding proteins and mRNA.

Results: We could recognise a distinct expression pattern for every hepatocellular carcinoma as well as for every tissue that served as control. Samples from the same patient were more similar to each other than samples from different patients. The identification of subsets of the genes revealed stable and significant partitions. We found nearly identical expression patterns within multiple tumours in non-cirrhotic livers. However, multiple tumours in cirrhotic livers ap-peared with different expression patterns.

Conclusions: Despite tumour heterogeneity, computer-based cluster analysis of microarray data suggest, that the appearance of multiple hepatocellular tumours in non-cirrhotic livers occurs due to intrahepatic metastasis, whereas the different patterns in cirrhotic livers revealed an independent tumour origin.

Transplantation Pathology

O-104

TTV in OLT.

A.Cecchetto, G Altavilla, D Tormen, P. Burra*, C. Cecchetto*, P.Angeli**, G. Guariso***
Istituto di Anatomia patologica, Dipartimento di scienze chirurgiche e gastro enterologiche*, Dipartimento di medicina clinica e sperimentale**, Dipartimento di Pediatria***, Università di Padova

The Orthotopic Liver Transplantation (OLT) is at risk of being infected by virus, a condition which may trigger rejection episodes. The risk is considered high with HCV in patient affected by HCV-Cirrhosis or by others liver disease unrelated with HCV infection.87–100% of transplanted liver patients is reported to be affected by acute or chronic hepatitis in long staging follow up with variable serologic and immunologic changes more frequently by HCV hepatitis.Lesions in OLT may be found without serologic markers because of the immunosoppressive therapy, however HCV DNA can be detected by PCR analysis in the liver and in other tissues. This high frequency also reported in HCV negative recipients may be caused by the large amount of blood transfusion during transplantation or by the presence of HCV in the donor tissues.HCV hepatitis recurrence in OLT have to be differentiated from HBV-HDV hepatitis, cellular rejection, Primary Biliary Cirrhosis (PBC) and from other opportunistic infection by immunologic, serologic and morphologic comparative assessment.We have examined in Padua Hospital by a continuous follow up and by sequential liver biopsies 450 liver grafts, 8 patients presented liver lesion suggestive of virus infection and grouped by us as "HCV-like alterations" characterised by: 1) mild and inconstant lymphoid inflammatory infiltrate in the portal tracts 2) mild or severe damage of the biliary ducts, 3) peace-meal necrosis 4) intra-sinusoidal lymphocytes.These patients lacked any immunologic HCV markers and even the molecular analysis gave negative results. Three of them were paediatric patients presenting the characteristic hepatitis HCV-like lesions. A new human virus: TTV ha been found by PCR in the grafted liver. TTV is retained to be able to infect liver cells and to cause liver disease in OLT patients.

O-105

Majority of long-term liver transplant patients with normal hepatitis tests present graft histological lesions

V. Costes[1], T. Rousset[1], G.P. Pageaux[1], M. Bismuth[1], C. Duvoux[2], D. Cherqui[2], P. Baldet[1], E.S. Zafrani[2]
1 Department of liver transplantation, Hopital Saint Eloi, 34295 Montpellier, France; 2 Department of liver transplantation, Hopital Henri Mondor, Créteil, France

Long-term follow up of liver transplant patients is based on clinico-biological data and liver biopsies are usually performed when liver tests are abnormal. The aim of our study was to evaluate graft histology in patients with normal liver tests.

Thirty-one patients transplanted for at least three years were included. The indications were: alcoholic cirrhosis (17), chronic active hepatitis B (5) or C (3), primary biliary cirrhosis (2), cryptogenetic cirrhosis (2), viral A fulminant hepatitis (1) and Budd-Chiari syndrome (1). Eighteen (58%) biopsies were considered abnormal. In 4 cases (22%), biopsies showed bile duct alterations suggestive of: biliary obstruction in 2 cases, sclerosant cholangitis in 1 case and recurrent PBC in 1 case. Six cases (33%) showed mild chronic active hepatitis. Isolated lymphocytic portitis was present in 8 cases (44%). The thirteen other biopsies (42%) showed only minimal nonspecific changes and were considered normal. We did not establish any correlation between abnormal histological status and sex, the indication for transplantation, the biopsy-transplantation delay, acute rejection history or CMV infection. Interestingly, we observed a significant correlation between the presence of PL and acute rejection episodes: 87.5% versus 30.7% (p=0.02) suggesting it is probably closely connected with the liver graft tolerance.

O-106

Acute renal allograft rejection: Prognostic signifiance of morphometric analysis and renal allograft pathology classifications

Régnier A *, François A **, Guerrier V ***, Etienne I ***, Helot MF ****, Godin M ***, Métayer J **
* Dpt of Pathology, CHU Ambroise Paré, Boulogne; Dpts of ** Pathology, *** Nephrology and **** Biostatistics, CHU Charles Nicolle, Rouen, France

Aim : As histological analysis occasionally fails to classify acute renal allograft rejection (ARAR), we tested the interest of a complementary concomitant morphological study. We determined both histological and morphometric criteria in ARAR and established their correlation with both survival graft as well as postrejection creatinine (18 months after rejection).

Methods: Hundred and twenty-one biopsies from 268 patients were re-evaluated and classified according to ARAR classifications (Banff 97 and Colvin). Sixty-three biopsies with acute rejection from a total of 51 patients were retained for our study. The interstitial area was measured with an "interstitial area/total area" ratio through morphometric automated analysis (software: *Leica Qwin*).

Results: During the study 5 grafts failed and 3 patients died. The interstitial area was significantly higher for patients with an elevated postrejection creatinine versus patients with a decreased postrejection creatinine (p=0,05), but did not correlate with the graft survival (p=NS). There was a correlation between the measured area

and tubulitis, interstitial oedema and classifications of renal allograft pathology ($p<0,05$) but not between this area and interstitial fibrosis (p=NS). Vascular rejection was frequently observed in the group "graft failure" (p=0,07), but did not correlate with postrejection creatinine (p=NS).
Conclusion: The interstitial area measured by morphometric analysis was correlated with the postrejection creatinine (18 months after rejection) and could therefore be considered as a new prognostic factor in renal allograft pathology, together in association with histological grading.
Neuropathology

O-107

Receptor tyrosine kinase expression ($p75^{NGFR}$, APO-1/Fas, c-kit) in human astrocytic neoplasms

Batistatou A, Zolota V, Melachrinou M, Bonikos DS
Department of Pathology, University of Patras Medical School, Greece

Introduction: The $p75^{NGFR}$ receptor protein and the Apo-1/Fas antigen are members of the Nerve Growth Factor (NGF)/tumor necrosis factor (TNF) superfamily of receptors. The protooncogene c-kit encodes a tyrosine kinase receptor which is structurally similar to the platelet derived growth factor (PDGF) and the colony stimulating factor (CSF) receptors. Studies have shown that all three receptors may regulate tumor growth and can function as mediators of apoptosis. The aim of the present study has been to to determine whether overexpression of $p75^{NGFR}$, APO-1/Fas and c-kit correlates with progression of human gliomas.
Materials and Method: We examined formalin-fixed, paraffin-embedded sections of 28 astrocytic neoplasms (5 grade I, 6 grade II, 4 grade III and 13 grade IV, WHO Classification), using LSAB immunohistochemical method, and the antibodies NGFR ($p75^{NGFR}$, monoclonal, DAKO), APO-1 (CD95, monoclonal) and c-kit (CD117, polyclonal). Membranous immunostaining of >5% of neoplastic cells was considered positive.
Results: Positive staining for $p75^{NGFR}$, APO-1/Fas, c-kit was detected in 20% (1/5), 0%and 0% of grade I, 17% (1/6), 0 and 33% (2/6) of grade II, 50% (2/4), 25% (1/4) and 75% (3/4) of grade III and 54% (7/13), 62% (8/13) and 77% (10/13) of grade IV astrocytomas respectively.
Conclusion: All three receptor tyrosine kinases examined are expressed in human astrocytic tumors. Their increased expression during malignant progression from low to high-grade neoplasms, could be reflecting their role in tumor growth or the increased apoptosis occuring in these tumors. If the latter holds true, then they could be potential targets for apoptosis-inducing therapy.

O-108

Morphological heterogeneity in Glioblastomas. Clinical, morphological, immunohistochemical and genetical (FISH and molecular biology) study

Cerdá-Nicolás M, López-Ginés C, Gil-Benso R, Pérez-Bacete M, López-Guerrero JA, Ruiz A , Talamantes F, Pellín A, Llombart-Bosch A
Department of Pathology. Medical School. University of Valencia. Spain

Glioblastoma Multiforme (GB) is a malignant neuroectodermal tumor of the CNS with rapid biological progression, high aggressivity and fatal outcome. Tumor cell heterogeneity and cellular anaplasia are the main morphological features and cause of different nosologic and histogenetic interpretations. A variety of genetic alterations are observed, among which trisomy 7, mutation of p53 and amplification of EGFR are considered implicated in the progression of these tumors.
Clinical, morphological, immunohistochemical (GFAP, S-100, EGFR expression, Ki67 and p53 labelled nuclear cells, and nuclear density) and genetical characteristics (FISH-D7Z1-α-satellite, p53 mutation and EGFR amplification) have been evaluated in 20 GB according to WHO classification.
In our results trisomy 7 has been observed in 18/20 tumors. In 10/20 of cases (50%) were more than 50 years of age, EGFR amplification and no p53 mutation were seen. In 2/20 of cases (10%) under of 50 years age, mutation of p53 but no amplification of EGFR was observed. No p53 mutation and no EGFR amplification were observed in 6/20 cases (30%). In one case p53 mutation and EGFR amplification were observed. No correlation was seen with immunohistochemical expression of p53, EGFR, Ki67 and nuclear density.
GB is a heterogeneous group of neoplasms with two different genetic pathways considered as primary and secundary Glioblastomas (GB1, GB2). In our cases, EGFR amplification (GB1) or p53 mutation (GB2), are the most common genetic anomalies (more than 60%). All these tumors showed trisomy 7. Another group of clinical/morphological GB with trisomy 7 did not show p53 mutation or EGFR amplification.
Supported by Grant :GV00-159-12

O-109

Brain cell dysfunction in sepsis. Is there a role for apoptosis ?

E Chatzigianni, E Messaris, P Christodoulou, N Memos, M.M Konstadoulakis, S Katsaragakis, E Menenakos, H Mahera, G Androulakis
Laboratory of Surgical Research, A' Department of Propaedeutic Surgery, Athens University, Greece

The role of apoptosis in sepsis has been focused in many organs undergoing obvious failure,but not in the brain,which seems to be drawn away by the effects of sepsis in other organs.This study investigates whether apoptosis is a possible mechanism of brain dysfunction occurring in septic syndrome.
Fifty-three rats were subjected to sepsis by cecal ligation and puncture.Sham-operated animals (n=10) underwent the same procedure but without ligation or puncture.Septic animals were randomly divided in five groups (n=10) and studied in 12 h, 24 h, 36 h, 48 h and 60 h after the operation.Brain and cecum were removed and post-fixed in paraffin sections, in which morphological criteria of apoptosis and expression of bax and bcl-2 proteins were investigated.
In septic rats apoptosis was detected in neurons of the choroid plexus and in Purkinje cells of the cerebellum.A high linear relationship of bax immunoreactivity and time of death was observed characterized by upregulation of bax in early stage of septic syndrome (12 h) and progressively decrease in the late phases ($p=0.001$).Bcl-2 remained in basal levels in all the time evaluated. However, bcl-2 was overexpressed in brain of rats whose cecum exhibit moderate inflammation ($p=0.03$).
There is evidence that neurons undergo apoptosis during the septic syndrome, leading progressively to their dysfunction.The pro-apo-

ptotic gene bax seems to play an important role in this process during the early hyperdynamic phase of sepsis, while bcl-2 tends to be expressed only in rats with moderate sepsis.

O-110

Expression of the CB2 cannabinoid receptor in human malignant gliomas

C. Corbacho*, C. Sánchez**, M. Ceballos***, T. Gómez del Pulgar**, M. Guzmán**, S. Ramón y Cajal*
*Departamento de Anatomía Patológica, Clínica Puerta de Hierro, Madrid; ** Departamento de Bioquímica y Biología Molecular, Universidad Complutense, Madrid; ***Grupo de Enfermedades Neurodegenerativas, Instituto Cajal, CSIC, Madrid

Cannabinoids, the active components of marijuana and their derivatives, act on the brain and some organs through the widely expressed CB1 receptor. By contrast, the other cannabinoid receptor subtype – the CB2 receptor – shows a much more restricted distribution and is absent in normal brain.
We have studied 37 human astrocytomas, 12 of them of low grade and 25 ones of high grade of malignancy. Expression of both receptors was studied immunohistochemically with CB1 and CB2 receptors antibodies using the avidin/biotin peroxidase technique. Moreover, the cell line C6 and malignant cells obtained from a human glioblastoma were injected in nude mice and treated with local administration of the selective CB2 agonist JWH-133.
Cannabinoid receptor immunoreactivity was detected in the 70% (26 out of 37) of the tumors analyzed, and the CB2 expression was related with tumor malignancy. Over 50% of high grade gliomas showed moderate or strong staining, while only about 25% of low grade gliomas showed clear positivity. *In vivo,* the C6 glioma and the human glioblastoma showed a significant decrease of tumor growth after injection of the CB2 agonist.
With these results we show that cannabinoids may induce regression of gliomas *in vivo* and that a significant number of high grade astrocytomas display a moderate or strong expression of CB2 receptors. These results support a therapeutic approach for the treatment of malignant gliomas with CB2 agonists devoid of psychotropic-side effects.

O-111

Influence of steroid hormone receptors on apoptosis, cell proliferation and prognosis in intracranial meningiomas

A-E. Konstantinidou, P. Korkolopoulou, H. Zorzos, E. Patsouris, H. Mahera, P. Davaris
Department of Pathology, National and Kapodistrian University of Athens, Athens, Greece

Introduction: Meningiomas often contain steroid hormone receptors, still their role in tumourigenesis, biological behaviour and tumour recurrence remains unclear. This study aims to investigate the correlation of receptor presence with the tumour proliferative potential, apoptosis and recurrence-free survival in patients harbouring meningiomas.
Material and Methods: Paraffin sections from 57 primary intracranial benign and atypical meningiomas were evaluated immunohistochemically for steroid hormone receptors, apoptotic rate, bcl-2, p53 and Ki-67 expression, using specific monoclonal antibodies. Six tumours recurred (10.5%), following complete surgical resection, within a follow-up period ranging from 21 to 108 months (median 60 months). Prognostic correlations were determined using statistical analyses that included clinical and histological variables.
Results: Nuclear staining for progesterone (PR), estrogen (ER) and androgen (AR) receptors was found in 77.2%, 33.3% and 29.5% of the tumours respectively. ER expression was mostly limited to a small number of nuclei (<1%). There was an inverse correlation between the mitotic index and PR counts (p=0.01). Meningiomas from older patients had higher ER counts (p=0.01). A high level of apoptotic cell death was associated with loss of PR expression by logistic regression analysis (p=0.042) and high Ki-67 values correlated with increased ARs (p=0.041). Among histological subtypes, meningothelial tumours displayed more PR and ER positive nuclei. Atypical meningiomas had a lower ER staining score (p=0.036). Multivariate analysis indicated that the absence of PR and large tumour size were significant factors for shorter disease-free intervals.
Conclusions: These data suggest that PRs and ARs may influence tumour cell proliferation, whereas the loss of PR expression is an indicator of increased apoptosis and early recurrence of meningiomas.

O-112

SKELETAL MUSCLE PARANEOPLASTIC PHENOMENON ASSOCIATED WITH HODGKIN AND NON-HODGKIN LYMPHOMAS

Pulido-Méndez, M.*, Finol, H.J.**, Márquez, A.*, Müller B.**, Montes de Oca, I.**
Institute of Experimental Medicine, Medicine Faculty*; Center for Electron Microscopy, Sciences Faculty**, Central University of Venezuela, Caracas, Venezuela

Introduction: Skeletal muscle is a target organ in the paraneoplastic phenomenon. Muscle ultrastructural pathology has been studied nearby the primary tumour (1) and at distant places of primary and metastatic tumours (2). In this work we describe the ultrastructural characteristics of this phenomenon in non-invaded muscles from lymphoma patients.
Methods: Needle biopsies from *quadriceps femoris* muscle were obtained from 17 patients with Hodgkin and non -Hodgkin lymphomas in stages II or III exhibiting muscle weakness. Biopsies were processed by routine techniques for transmission electron microscopy and observed in Hitachi H-500 and H-7100 electron microscopes.
Results: The patients had muscle damage characterized by different degrees of fibre atrophy, disorganization of contractile and sarcotubular systems, and sarcolemmal foldings. The capillaries exhibited two kinds of changes; most of them had proliferative appearance, with thickening of capillary wall and basement membrane, endothelial cell cytoplasmic infoldings to the capillary lumen, augmented number of pinocytotic vesicles and in some instances lumen occlusion. The other changes included capillary degeneration and necrosis. The degenerated endothelial cells showed cytoplasmic vacuoles, myelin-like figures, and widening of intercellular junctions. In some cases, a mononuclear cell infiltrate formed by macrophages and lymphocytes was found.
Conclusions: In all studied patients, non-invaded muscles showed the paraneoplastic phenomenon expressed as different degrees of

fiber aggression and microvascular compromise. The capillary alterations are mainly endothelial cell hypertrophy, degeneration and necrosis, which are in close similarity with changes observed in several autoimmune myopathies. It has been proposed the existence of an autoimmune process affecting the microvasculature and neural tissue in the ethiopatogenesis of paraneoplastic syndromes. This process could be an important factor in the subsequent muscle damage.

1) Finol, H.J. et al., *J. Exp. Clin. Cancer Res.* In press. 2001.
2) Finol, H.J. et al., *J. Submicrosc. Cytol. Pathol.,* 29:329-34, 1997.
Supported by CDCH of UCV (Nr. O3-10-4169-2000).

O-113

Rationales for Teleconsultation quality in pathology and cytology

G. Stauch[1], T. Kuakpaetoon[2], Y. Settakorn[3], Th. Bonthome[4]
[1] Aurich/Germany, [2] Bangkok/Thailand, [3] Chiang-Mai/Thailand, [4] Vientiane/Laos

Introduction: Several telepathology consultation centres have been established in the past and expert consultation service via electronic media is integrated into routine work. The limitation of consultation and the cost benefit analysis still has not been evaluated until now. Therefor some principle considerations should be pointed out.

Method and results: Following statements can be made: 1.Diagnostic quality is a function of diagnostic accuracy diagnostic probability. 2. Diagnostic information is a function of image quality and representatively. 3. Image quality is factor of colour truth, detail discrimination by soft- and hardware and slide quality, specimen preparation and staining technique. 4. Representatively is a function of heterogeneity of lesions. number of images. 5.Representatively of a lesion is influenced by the experience of periphere user. 6. Diagnostic quality depended on experts experience with electronic media. 7. Diagnostic accuracy is depended on experts use of special staining technique which cannot be offered via electronic media. 8. The technical demands for cytology diagnosis seams to be lower compared with histology one.

Conclusions: Today's technical standards of limited data transfer allows only a limited diagnostic accuracy even for experts. However diagnostic suggestions given by experts can guide inexperienced pathologists.

P-001

Primary malignant melanoma of the colon

Admella C, Muns R, Soler T, Fantova MJ, Bianchi A*,
Diloy R**, Sais G***
Department of Pathology, Surgery*, Gastroenterology**
and Dermatology***, Hospital de Mataró, Barcelona, Spain

Introduction: Malignant melanoma (MM) is the most common metastasic tumor to the gastrointestinal tract. Contrarily, primary MM involving the intestine is rare. Most of these are found in esophagus and anorectum and only few cases have been detected in small bowel. To our knowledge, no case of primary MM in the colon has been described.
Case Report: A-84-year old man was admitted to the hospital for evaluation of anemia. Colonoscopic examination identified a tumor in the right colon. Biopsy and brushing cytology allowed diagnosis of MM. Ophthalmologic and total body skin/mucosal examination showed no evidence of melanoma nor dysplastic/regressed nevus. Patient underwent ileocolectomy. Macroscopic examination showed a 11 cm polypoid mass involving mucosal epithelium, submucosa and muscular layer. Histologic and immunohistochemical features were diagnostic of MM. Metastasis in 2 regional lymph nodes were observed. Eighteen months later the patient developed mesenteric lymph node metastasis.
Discussion: Distinction between primary and metastasic intestinal melanoma is debatable. In 1999 Sachs et al proposed criteria for diagnosis of primary MM in the intestine. According to these, we believe that our case represents a primary colonic MM. First, we have found MM at a single focus. Second, there is no evidence of disease in other organs outside the regional drainage. Third, the patient has been free of disease for more than 12 months. Finally, only regional disease was detected at recidive.
The pathogenesis of primary intestinal MM is unknown. The rare presence of melanocytes within the mucosa could serve as potential sources for malignancy.

P-002

Expression of MUC1 and MUC2 mucins in gastric carcinomas: Its relationship with the clinicopathological parameters and prognosis

Akyürek Nalan*, Akyol Gülen*, Dursun Ayşe*,
Yamaç Deniz**, Günel Nazan**
Departments of Pathology* and Medical Oncology**,
Gazi University Medical School, Ankara, Turkey

Introduction: The aim of this study was to investigate whether there was a correlation between MUC1 and MUC2 mucins expression and well known prognostic impact such as TNM stage, angiolymphatic invasion and histopathologic type of gastric carcinomas as well as survival times.
Methods: Expression of MUC1 and MUC2 in 143 gastric carcinomas was investigated by immunohistochemically using monoclonal DF3 and CCP58 antibodies. Fourty-five patients were followed-up either until time of death or median survival time of 31 months, ranging from 29 to 80 months. Staining patterns were assessed semiquantitavely and correlated with the clinicopathological variables and overall survival.
Results: The MUC1 was detected in 83 (58%) and the MUC2 in 60 (42%) of 143 cases. Papillary adenocarcinomas showed significantly higher MUC1 and MUC2 immunoreactivity compared to tubular, signet-ring cell and mucinous tumors (p=0.02, p=0.04). MUC1 was highly expressed in intestinal-type carcinomas (p=0.006), but MUC2 expression did not differ between intestinal and diffuse carcinomas. There was a positive correlation between tumor differentiation and MUC1 expression. But, no correlation was found between MUC1 and MUC2 expression and angiolymphatic invasion. According to the TNM classification, stage IA tumors have significantly lower rates of MUC1 reactivity compared to the higher stage (p=0.04). The patients with gastric carcinomas expressing MUC1 showed significantly poorer survival than those without MUC1 expression (p=0.04). Although MUC2 reactivity was not statistically significant, the positive patients showed a trend toward longer survival.
Conclusion: The present study indicates that MUC1 expression might be a useful prognostic factor for poor outcome in patients with gastric carcinomas, however the role of MUC2 expression is still unclear.

P-003

CD 117 expression in GIST- a possible marker for future therapeutical concepts?

A. Ammon([1]), W. Höfer ([1]), F. Ernst ([2]), A. Fisseler-Eckhoff ([1])
([1]) Institut für Pathologie der Zentralklinik Emil von Behring, Berlin-Zehlendorf; ([2]) Chirurgische Klinik der Zentralklinik Emil von Behring, Berlin-Zehlendorf

Gastrointestinal stromal tumors (GIST), defined as KIT (CD 117)-positive spindle cell or epithelial mesenchymal neoplasm of the gastrointestinal tract, represent the most common group of mesenchymal tumors of the gastrointestinal tract. GIST`s occur typically in older individuals, most often in the stomach (60–70%), usually GIST`s are positive for CD 34 (70%), less often SMA (10%) and S 100 (<5%). They present a wide clinical spectrum, from benign, small to frankly malignant metastasing tumors.
GIST's commonly have activating mutations in exon 11, (rarely in 9 and 13), of the KIT gene that encodes a thyrosine kinase receptor for a growth factor named mast cell or stem cell growth factor. Beside surgical treatment there is yet no further therapeutic option avaliable. The thyrosine kinase receptor might be a target for future therapeutic concepts.
In a retrospestive analysis 16 cases of GIST`s were examined. Five of the tumors were estimated as certain benign, 3 as uncertain and 6 as malignant. Mean age was 65, range 41 to 82. The histopathologic findings, including histomorphology and immunhistology (CD 117, CD 34, Ki 67, S100, Desmin, Aktin1, Aktin2) were compared with the clinical findings and outcome.
Our investigations revealed a strong relationship between the histopathologic findings and the clinical outcome.

P-004

Carcinoid tumors of the stomach. Analysis of 11 cases

Arturo Angeles Angeles, Leticia Bornstein Quevedo
Department of Pathology. Instituto Nacional de Ciencias Médicas y Nutricion Salvador Zubirán, México, D.F. México

Background. Carcinoid tumors of the stomach (GC) are rare neoplasms. The distinction of antral carcinoids from tumors of the body and fundus is important.

Methods. A retrospective search for GC was made between 1990 and 1995. Clinical data data, location, histologic pattern, hormone production and size were assessed. Immunohistochemistry for p53 and bcl-2 was performed in 6 cases.
Results. Eleven cases were identified in 5 males and 6 females with a mean age of 49 years (33–77). Five tumors were located in the antrum, four were single and one multiple. From the four GC located in the gastric body, only one was munticentric. One case was found in the fundus and was multicentric. Also, one case was disseminated in body and antrum. In four multicentric GC the adjacent mucosa showed atrophic gastritis, intestinal metaplasia, G cell hyperplasia in the antrum and ECL cell hyperplasia in gastric body and fundus. None of the single tumors demonstrated this association. Solid and tubular patterns of growth were the most frequent. All cases were positive for chromogranin and antral tumors also expressed gastrin. Immunoreactivity for p53 was found in 1/5 antral GC, bcl-2 was negative in all GC. Metastases were demonstrated in 4 antral and 2 body GC.
Conclusions. Endocrine tumors of the stomach are gastrinomas, when located in the antrum and carcinoid tumors when placed in the body and fundus. Multicentric neoplasias are usually associated to atrophic gastritis, intestinal metaplasia and endocrine cell hyperplasia.

P-005

Detection of *Helicobacter pylori* in Gastric Biopsy and Resection Specimens

T. Babic[1], H. Basic[2], V. Katic[2], M. Otasevic[1]
[1] Institute of Microbiology and Immunology,
[2] Institute of Pathology, Faculty of Medicine of Nis University, Yugoslavia

Introduction: *H.pylori* infection is highly associated with gastritis and peptic ulcer, gastric adenocarcinoma, and gastric mucosa-associated lymphoid tissue-MALToma. A number of methods are currently available for the detection of *H.pylori*, but histological detection in a gastric biopsy is the commonest and among the most sensitive.
Aim: To compare the sensitivity of detecting H. pylori in gastric biopsy and resection specimens using haematoxylin and eosin (HE) stain, Giemsa stain and modified Giemsa stain.
Methods: Gastric antral biopsy specimens showing chronic gastritis (28 cases) together with tissue blocks from gastrectomy specimens for duodenal ulcer were histology reviewed. The paraffin sections were stained with classical histological HE method, for diagnosis of the antral mucosa and with histological methods for the identification of *H. pylori*: Classic Giemsa and modified Giemsa.
Results: The presence of chronic gastritis was confirmed in the 28 gastric biopsy specimens. A diagnosis of duodenal ulcer was confirmed in the mucosa from the gastrectomy specimens. The HE, Giemsa, and modified Giemsa treated sections were carefully examined for the presence of *H. pylori*. HE-stained H.pylori appeared as slightly basophilic, spiral-shaped organisms attached to the apical surface of the surface mucous cells. However, curved bacteria were only detected when found in great numbers. In some cases masked bacteria hidden within mucous were obvious only in modified Giemsa preparations. Using a modified Giemsa stain, the spiral shaped bacteria of *H. pylori* stained blue, were attached to the brush border of the gastric foveolar epithelial cells and inside gastric pits. *H. pylori* was identified in 36.6% sections stained with HE, but it could be identified with greater frequency in sections stained with classical Giemsa (60%). It could be detected at a still greater frequency in staining with modified Giemsa in 78.3%. In all cases the bacteria were more prominent and easier to detect in the modified Giemsa sections.
Conclusion: Giemsa modified technique is superior method, compared to the mentioned methods. It is a highly sensitive, economical and easy to use method for detecting *H. pylori* in gastric biopsy and resection specimens.

P-006

Occurrence of helicobacter pylori in dyspeptic patients with different degrees of renal function

Hala Badawi, Hoda Helimi, Maisa Omar, Mona Nosseir, Maged El-Ghannam and Azza El-Shamaa

The objective of the study was to evaluate the prevalence of Helicobacter pylori (Hp) in patients with different degrees of renal function and it_s relation with gastritis. Also, we aimed to evaluate the performance of ELISA test for detection of IgG antibodies to Hp as compared with conventional biopsy-based tests. Eighty patients requiring gastroscopy for upper intestinal symptoms were enrolled in this study: Group I, 30 chronic renal failure (CRF) patients, not undergoing haemodialysis (HD) before and serum creatinine concentration <884 mol/L. Group II, 20 patients who had been receiving HD treatment for at least one year prior to the study and serum creatinine concentration >884 mol/L. Group III, 30 dyspeptic non-renal disease (NRD) patients as controls. On endoscopy, three biopsy specimen were taken for analysis of Hp infection by histology (Hx. & E. and Giemsa stains), culture and rapid urea test. Serum samples were collected form all patients tested by ELISA for detection of IgG antibodies. In the whole series under study, Hp positivity was 73.33%. It was rather high in HD patients (75%) than CRF which was similar to NRD (73.33%) (P>0.05). ELISA test results showed an absolute sensitivity and NPV and a specificity of 90.47% and PPV of 96.72% as compared with biopsy-based tests. The test was quick, easy and especially recommended for screening dyspeptic patients to eliminate unnecessary endoscopies and also in diagnosis of atrophic gastritis commonly associated with Hp in uraemic patients where biopsy-based tests may be otherwise negative. Active chronic antral gastritis was highly associated with Hp in renal impairment groups (P<0.01) while chronic gastritis in NRD (P<0.01). Follicular and atrophic gastritis and gastric metaplasia were more frequently found in HD (P<0.01) in whom the prevalence of Hp infection was highly correlated with HD duration (P<0.01). In common with non-uraemic patients, our subjects showed an increased prevalence of Hp gastritis with age (P<0.05). Severe dyspepsia was more frequently associated with Hp (P<0.01). Haematemesis was significantly associated with Hp in all groups (P<0.001). In conclusion; gastric colonization of Hp in chronic renal failure is not more frequent than usual as the Hp prevalences are high as that for NRD group. The increased dyspeptic complaints may be partly related to Hp infection. But patients with renal impairment were found to be susceptible to more GIT complications as bleeding, atrophic gastritis and gastric metaplasia. Pre transplantation risk factors for subsequent development of peptic ulcer remain to be identified should be managed properly. We recommended Hp treatment before renal transplantation.

P-007

Primary tumor or metastasis? Signet-ring cells in abdominal speciments

Axel Bader[1], Karin Sorger[1], Roland Eisele[2], Albrecht Hettenbach[3], Egon Jetter[4], Edgar Plank[5], Theodor Karl Dinkelacker[6]
Institut für Pathologie[1], Abteilungen für Chirurgie[2], Gynäkologie[3] und Innere Medizin II[4] der Klinik am Eichert sowie den Chirurgischen[5] und Gynäkologischen[6] Abteilungen der Helfenstein-Klinik Geislingen/Steige

Introduction: Signet-ring cells are a common histomorphological characteristic of cancer in the upper gastrointestinal tract. Although signet-ring-like cells are found in invasive lobular breast carcinoma there is no such subtype mentioned by the latest WHO's tumor classification (1995). It is difficult – for both pathologists and clinicians – to distinguish between abdominal metastasis of that kind of breast cancer and primary abdominal carcinoma with or without metastasis.
Methods: In the last few years we received several abdominal biopsies or surgical specimens of five female patients between 62 and 77 years of age from different anatomical origin (stomach, colon, liver, omentum majus, mesenterium, fallopian tube, ovar) with so-called "signet-ring cell carcinoma." To determine definite tumor origin we used several markers (e.g. estrogene and progesterone receptor, gross cystic disease fluid protein-15, HER-2/neu) by running standardised automatic immunohistochemistry.
Results: All these patients have extensive abdominal metastasis within 5–15 years of a previously or recently diagnosed nodal positive invasive breast carcinoma (pT1–T3) with more or less distinct component of signet-ring cells. We find GCDFP-15 helpful to distinguish particularly hormone receptor negative metastasis of signet-ring cell breast carcinoma from cancer of other abdominal primary.
Conclusion: Our results show that abdominal metastasis of invasive breast carcinoma with component of signet-ring cells appear more often than one might expect. According to F. Tavassoli the appearance of signet-ring cells in breast carcinoma appears to predict an unfavourable outcome.

P-008

Origin of COX-2- interstitial cells in colorectal adenomas and Crohn's disease

S. Bellefqih[1], R. Benamouzig[1], C. Lagorce[1], M. Hourseau[1], S. Chaussade[2], A. Martin[1] and APCC group
Hôpital Avicenne[1]-Bobigny; Hôpital Cochin[2]-Paris, France

Cyclo-oxygenase-2 (COX-2) is an inducible enzyme that catalyses the conversion of arachidonic acid to prostaglandins and thromboxanes. COX-2 protein expression is observed in colorectal neoplasms and may be a target for the anticolorectal cancer activity of NSAIDs and aspirin in humans. Like other investigators, we have previously shown a strong expression in interstitial cells in a series of colorectal adenomas and in Crohn's disease. The origin and the role of these cells are uncertain. Certain authors have suggested a probable histiocytic origin in colorectal adenomas, but a myofibroblastic origin is not excluded.
In order to precisely ascertain the origin of these reactive cells, we used a dual-labelling indirect immunofluorescence for COX-2-CD68 or COX-2-smooth muscle actin (SMA) expression in colorectal adenomas (n=10) and Crohn's disease (n=10).
In the colorectal adenomas there was a coexpression in several interstitial cells for COX-2-SMA, but not for COX-2-CD68. Inversely, in Crohn's disease, in fissures and ulcerations, the interstitial cells were positive for COX-2-CD68 but negative for COX-2-SMA.
These results indicate that interstitial cells expressing COX-2 in colorectal adenomas and in Crohn's disease are of different types, respectively, myofibroblasts and macrophages. At the level of adenomas they probably intervene in tumoral growth favouring the proliferation of epithelial cells and angiogenesis, inhibiting apoptosis and controlling local immunity via paracrine signalling. They can support one of the target for the chemoprotective effects of NSAIDs. In Crohn's disease, these cells may similarly play a role in regeneration and repair as part of wound healing.

P-009

Cytokeratin 20 expression in pancreatic and colorectal cancer

Paola Billo, Luca Albarello, Carlo Capella, Fausto Sessa
Dept. of Clinical and Biological Sciences, University of Insubria, Varese, Italy

Introduction: Cytokeratin 20 (CK 20) has a restricted range of expression in human tissues. Because it lacks immunological cross-reactivity with other CKs, it could represent an important tool in detecting and identifying metastatic cells. Liver metastases from pancreatic cancers (PCs) are difficult to differentiate from those of colorectal cancers (CRCs) due to the overlapping histological and histochemical features. In the present study we compared the expression of CK 20 between PCs and CRCs and their related liver metastases.
Methods: We studied 68 PCs, 23 CRCs and 8 liver metastases (3 from pancreas and 5 from colon), by immunohistochemistry using an anti-cytokeratin 20.8 mAb (Dako) at 1:100 dilution, after antigen retrieval with citrate buffer pH 6 in microwave oven treatment.
Results: 20 out 23 cases (86%) of CRCs showed several CK 20 immunoreactive (IR) cells (mean % of positive cells: 55%). 14 out 68 (20%) PCs showed few CK 20 IR cells (mean 5%). The 5 liver metastases from CRCs were largely CK 20 IR, while only 1 metastasis from PCs (a case showing CK 20 IR in a primary cancer) showed a few CK 20 IR cells.
Conclusion: Our results show a high expression of CK 20 in CRCs and a faint CK 20 expression in PCs. It may be concluded that CK 20 is an excellent marker to differentiate colorectal from pancreatic liver metastases. We conclude that metastatic cells of PCs and CRCs retain the immunohistochemical profile of their primary cancers.

P-010

Detection of tumor cells in lymph nodes of colonic carcinomas (Dukes' B): step sectioning and immunohistochemistry

Roger Bjugn, Christian Lycke Ellingsen and Ivar Skaland
Department of Pathology, Central Hospital of Rogaland, Stavanger, Norway

Introduction: After curative resection of colonic carcinomas, lymph node status is the most important prognostic factor . Several

studies have been undertaken in order to investigate whether the presence of "micrometastasis" influence patient survival, but results are conflicting . As part of an ongoing study on colorectal cancer, we wanted to make a preliminary investigation on the occurrence of occult tumour cells in lymph nodes of patients with colonic carcinomas – Dukes' B.

Methods: Twenty-three patients were included. From paraffin blocks containing altogether 179 lymph nodes, two consecutive 2-µm-thick sections were cut at 2 levels separated by fifty µm. One section in each series was stained with hematoxylin-eosin-safranin and the other section stained by an anti-cytokeratin antibody (Pan-CK, Novocastra, Great Britain).

Results: Immunopositive cells were located in lymph nodes from 11 patients (48%). In five cases (22%), the cells were unequivocally identified as tumour cells in the adjoining routine sections, while the true nature of the immunopositive cells were uncertain in the other six cases (23%).

Discussion: Step sectioning identified five patients which now would have been staged as Dukes' C. Although the cells could be positively identified in the routine sections, immunohistochemical staining on an adjoining section greatly facilitated their identification. Whether the immunopositive cells in the other six cases represent tumor cells or not, is uncertain. As patients staged as Dukes' C will benefit from chemotherapy, larger studies on "occult" tumour cells in lymph nodes from "node negative" patients should be conducted.

References: 1. Fielding LP, Phillips RK, Fry JS, Hittinger R. Prediction of outcome after curative resection for large bowel cancer. Lancet 1986; 2:904–907

2. Calaluce R, Miedema BW, Yesus YW. Micrometastasis in colorectal carcinoma: a review. J Surg Oncol 1998; 67:194–202

3. Clarke G, Ryan E, O'Keane JC, Crowe J, MacMathuna P. The detection of cytokeratins in lymph nodes of Duke's B colorectal cancer subjects predicts a poor outcome. Eur J Gastroenterol Hepatol 2000; 12:549–552.

P-011

Cell kinetic of carcinoid tumors of the ampulla of Vater is different from duodenal carcinoid tumors

Leticia Bornstein-Quevedo, Armando Gamboa-Dominguez
Department of Pathology. Instituto Nacional de Ciencias Médicas y Nutricion Salvador Zubirán. México, D.F. México

Background: Carcinoids of the ampulla of Vater differ clinically and morphologically from duodenal carcinoids (DC)

Objective: Compare the proliferative index (PI) of primary ampullary carcinoids (AC) with DC.

Methods: Retrospective search for AC and DC was made between 1989–1999. Immunohistochemistry was performed for PCNA, Ki-67, p53, generic endocrine markers(GEM), hormone products (Dako) and for p21 and p27 (Santa Cruz). The nuclear signal for PCNA and Ki-67 was blindly counted in 500 neoplastic cells with a Leica Q 532 image analyzer. Clinical data and follow-up was obtained from charts. Fisher's test was used.

Results: Five AC and eight DC were identified in 9/F and 4/M with a median age of 59 for AC and 64 years for DC. Mean tumor size was 1.6cm and 1.85 cm respectively. All patients with AC presented with jaundice while most patients with DC were asymptomatic (p=0.047). Solid pattern was the most common in both and metastases were present in 4/AC and 1/DC (p=0.03). GEM were similar in both and 56% of DC expressed gastrin vs 20% of AC (p>0.05). Mean value for PCNA index was 4.0% for AC and 3.2% for DC while mean values for Ki-67 were 12.2 and 10.2% respectively; p21 and p27 expression was observed in 40–40% AC vs 37.5–12.5% of DC.

Conclusions: The more aggressive behavior of Ampullary carcinoids neither associated to high proloferative indeces nor different cell cycle inhibitors expression, but possibly to specific morphologic characteristics of the ampullary zone, i.e. a rich and superficial vascular network.

P-012

Dysplasia and hyperplasia – dangerous lesions in heliobacter pylori gastritis

Irina-Draga Caruntu*, Giaconda Dobrescu*, Alina Floarea-Strat*, T. Axinia**
* Department of Histology, "Gr.T.Popa" University of Medecine and Pharmacy, Iasi, Romania; ** Department of Internal Medicine, Municipal Hospital, Targu Neamt, Romania

Introduction: Most epidemiological studies associate Helicobacter pylori infection with gastric cancer. The preinvasive lesions contributing to the multistep gastric carcinogenesis are well known and certified as such. Thus, the hyperplasia and dysplasia of the gastric mucosa represent the final common pathway by which intestinal-type gastric cancers arise. The occurrence of this type of dangerous lesions is therefore regarded as a major risk factor.

Material and method: There were investigated 40 cases, 24 men and 16 women, aged between 30 and 80 years. The selected cases were previously examined using endoscopy techniques. There were also performed microbiological (urease test) and histological (routine and special stainings) exams on gastric mucosa fragments, obtained by endoscope guided biopsy. The aim was to identify the presence of the bacteria, to classify the lesions and to assess the degree of the damages.

Results: The diagnosis of Helicobacter pylori gastritis was confirmed and the following related aspects were approached: (*i*) *form* (acute or chronic; minor, moderate or severe; atrophic or hyperplasic; accompanied or not by intestinal metaplasia), (*ii*) *topography* (fundus, antrum, pangastritis) and (*iii*) *degree of spread* (superficial or diffuse). Additional morphological features accompanied the tipical lesions upon which the diagnosis was based, as follows: hyperplasia (2 cases), dysplasia (5 cases), intestinal metaplasia (15 cases), pyloric metaplasia (1 case), lymphoid follicles (4 cases), peptic ulcer (1 case) and polyps (4 cases). The hyperplasia (located in the pyloric antrum) affected either the gastric pits, which were enlarged, or the gastric glands. The latter appeared increased in number and size, displaying intraluminal proliferations or constituting microcysts; the epithelial cells were anizokaryotic and hyperchromatic. The dysplasia (extremely widely spread, located both in the antrum and fundus) was proved by the presence of atypical cells with hyperchromatic and anizokaryotic nuclei, as well as by frequent mitoses. In some cases, the whole histoarchitecture of the gastric mucosa was completely destroyed.

Conclusions: We can assert that this study emphasizes the relationship between Helicobacter pylori and a wide range of gastric lesions (chronic gastritis, hyperplasia, dysplasia, intestinal metaplasia, and cancer). For the clinician it is mandatory the follow-up of the cases with increased risk. Thus, it may be possible to identify, by endoscopy and histology, the potential premalignant transforma-

tions or the early stages of gastric cancer. The diagnostic and therapeutic issues are currently solved and, consequently, the next important step to be taken would be the preventive management of Helicobacter pylori infection, in order to avoid the development of more dangerous lesions, like dysplasia and hyperplasia.

P-013

Neuroendocrine differentiation in gastric adenocarcinomas: relation to TGF- alpha and EGFR expression

Celikel CA, Eren F, Sezgin S
Marmara University School of Medicine, Department of Pathology, Turkey

Introduction: We analyzed gastric adenocarcinomas in order to assess the effect of neuroendocrine differentiation (NED) on the expression of transforming growth factor-alpha (TGF-alpha) and epidermal growth factor receptor, that are known to be involved in autonomic tumor growth.
Methods: Paraffin embedded archival tissues of 30 subtotal-total gastrectomy specimens were included in the study. There were 15 diffuse and 15 intestinal type of gastric adenocarcinomas (GCA). Chromogranin-A (Chr A) immunohistochemistry was performed in the sections prepared from all the paraffin blocks that have areas of adenocarcinoma. NED was evaluated semiquantitatively. For each case TGF-alpha and EGFR immunohistochemistry was performed in sequential sections of a representative block selected based on neuroendocrine differentiation. Semiquantitative evaluation (0, 1, 2, 3) was made for TGF-alpha and EGFR immunexpression. Chi-square and Fisher test were used to compare EGFR and TGF-alpha expression of the two groups.
Results: Chr A expression was (+) in 30% and (++) in 33.3% of the cases. The percentage of cases expressing Chr-A was higher in diffuse type gastric adenocarcinomas, but the difference was statistically insignificant. In intestinal type GCA's, EGFR and TGF-alpha immunoreactivity were more prominent in higher stage tumors but in diffuse type GCA's especially TGF-alpha expression was more diffuse in low stage tumors. No difference could be established in both the TGF-alpha and EGFR expressions in respect to NED in intestinal type GACs. But TGF-alpha and EGFR expression were significantly higher in D-GACs with NED than without NED.
Conclusion: Our findings suggests that NED leads to growth autonomy by increasing the expressions of TGF-alpha and EGFR in diffuse type GCA's.

P-014

Association of *Helicobacter pylori* and the occurence of aneuploidy of chromossomes 3, 7, 8 and 9 in gastric benign and malignant lesions

Patricia Maluf Cury*, Ana Cristina Gobbo Cèsar**,
Aldenis Albanese Borin*, Alaor Caetano*, Ana Elizabete Silva**
* Faculdade de Medicina de São José do Rio Preto, São Paulo, Brazil, ** Departamento de Biologia, UNESP São José do Rio Preto, São Paulo, Brazil

Introduction: Gastric cancer has been associated with some histological benign lesions like chronic atrofic gastritis and intestinal metaplasia, and also with the presence of *Helicobacter pylori.* The purpose of this study was to evaluate aneuploydy in gastric precancerous lesions, associated with the presence or not of *H. pylori.*
Methods: FISH technique was performed using chromosome-specific centromeric probes for chromossomes 3, 7, 8 and 9 in interphase nuclei of fresh 82 gastric samples, and correlated with the histological diagnosis.
Results: The findings are summarised in the table, with the percentage of cases with aneuploidy:
Percentage (and number of cases) with aneuploidy

	Mild gastritis	Moderate /severe gastritis	Atrophic Gastritis	Gastritis with metaplasia	Gastric ulcer	Gastric Adenocarcinoma	Total
H. pylor positive	23.1% (3/13)	66.7% (4/6)	0% (0/1)	75.0% (6/8)	60% (6/10)	100% (6/6)	**56.8% (25/44)**
H. pylori negative	0% (0/1)	42.8% (6/14)	100% (2/2)	42.8% (3/7)	83.3% (10/12)	50% (1/2)	**57.9% (22/38)**
Total	**21.4% (3/14)**	**50% (10/20)**	**66.7% (2/3)**	**60.0% (9/15)**	**72.7% (16/22)**	**87.5% (7/8)**	**57.3% (47/82)**

Conclusions: The results suggest that the occurence of aneuploidy in benign gastric lesions may be a useful marker for monitoring the progression of precancerous lesions, but it is not associated with the presence of *H. pylori.*

P-015

Globular amyloid deposits in the wall of the gastrointestinal tract: Report of six cases

Demirhan B[1], Bilezikçi B[1], Kıyıcı H[1], Boyacıoğlu S[2]
Başkent University Faculty of Medicine,
Departments of Pathology[1] and Gastroenterology[2],
Ankara, Turkey

Amyloid deposition in the gastrointestinal tract basement membrane, lamina propria, and blood vessel walls has been well documented. This article describes six cases that exhibited the unusual globular pattern of deposition on light microscopy, yet exhibited the classic histochemical and immunohistochemical properties of deposited amyloid. This deposition pattern is a novel finding in the gastrointestinal system.
Endoscopic examination of five patients revealed mild nodularity of the gastric mucosa and diffuse gastritis. In the other case, macroscopic examination of resected small intestine showed focal mucosal depressions. In all six cases, light microscopy study revealed round- to oval-shaped globules in the lamina propria, with globule diameters of 3 to 40 μm. When stained with Congo red, the deposited material refracted polarized light, and immunohistochemical testing showed a positive reaction to Amyloid A primary antibody. The deposits did not react with antibodies to ß2 microglobulin, transthyretin, or lambda and kappa light-chain immunoglobulins. None of the patients' laboratory or clinical findings were compatible with monoclonal gammopathy or multiple myeloma.
The literature contains a few case reports of globular amyloid deposition in the liver, but this is the first description of a globular pattern in the gastrointestinal tract. The pathogenesis and significance of this finding are not clear, and will require further study.
KEY WORDS: Globular, amyloid, deposition.

P-016

CD44, Cathepsin D and c-erb- B2 expressions in gastric carcinomas

Gulen Dogusoy*; MD, Gokhan Ersoy*; MD, Suha Goksel*; MD, Selda Gocener*, Alper Doventas, MD**
* Department of Pathology, Cerrahpasa Medical Faculty;
** Department of Internal Medicine, Cerrahpasa Medical Faculty; Istanbul, Turkey

The aim of this study is to investigate the relationship between histopathologic parameters and immunohistochemical expressions of CD44, Cathepsin D and c-erb-B2 in gastric carcinomas.
55cases of gastric carcinomas were stained immunohistochemically for CD44, Cathepsin D and 46 of them were stained for c-erb-B2. None of the tumours were demonsrated to be positive for Cathepsin D whereas nonneoplastic gastric mucosa showed positivity especially in the neck region of foveolas in 18 cases. Tumor cells were positive for CD44 in 18 of 55 cases and for c-erb-B2 in 18 of 46 cases. In all cases, mucosal lymphocytes were strongly positive for CD44 and all glands and neck regions were positive for c-erb-B2. In respect to CD44 and c-erb-B2 expression, there is no correlation with histopathologic parameters like histologic type, histologic grade, depth of invasion, lymph node metastases.
In conclusion, we suggest that CD44 and c-erb-B2 expressions are not correlated with biologic behavior of gastric carcinomas and Cathepsin D negativity may be due to increased releasing and consuming of this extracelluler matrix proteolitic enzyme from cytoplasms of tumour cells as the invasing mechanism proceeds.

P-017

Goblet cell carcinoid

Dolenc-Stražar, Z.
Institute of Pathology, Medical Faculty University of Ljubljana, Slovenija

BACKGROUND: Goblet cell carcinoids, also called adenocarcinoids, crypt cell carcinomas or mucinous carcinoids, probably arise from an undifferentiated stem cell, and have features intermediate between adenocarcinoma and insular carcinoid. They may arise in duodenum, colon and rectum, but most frequently in appendix.
PATIENTS AND METHODS: We present two patients, with clinical signs of appendicitis in first, and ileus in second. Three years after appendectomy, hemicolectomy was performed because of ileus in first patient, and hemicolectomy was performed as a first procedure in second. In addition to Kreyberg staining, immunohistochemical stainings, PAS and grimelius were performed.
RESULTS: In both appendices only the thickening of the wall was shown macroscopically. Microscopically there were small uniform nests and strands of cells, or single tumor cells infiltrating all layers of the wall. In part of the tumor there were mostly goblet cells, with Kreyberg and PAS positive mucin, in other part carcinoid like pattern. Rare Paneth's cells were also found. Endocrine cells in the nests, positive with chromogranin, serotonin and grimelius, were in small numbers. Evidence of endocrine and mucinous differentiation was found in same cells.
CONLUSIONS: Goblet cell carcinoids with inconspicuous endocrine differentiation may be easily overdiagnosed as a signet ring carcinoma therefore special immunohistochemical stainings should be used to detect endocrine cell differentiation. They have different clinical behavior, with 5-year survival rate around 80%. Patients with extraappendiceal spread, and metastases, could die within a year of diagnosis.

P-018

Prognostic Implication of nm23-H1 Expression in Colorectal Carcinomas

Dursun Ayşe*, Akyürek Nalan*, Günel Nazan**, Yamaç Deniz**
Departments of Pathology* and Medical Oncology**, Gazi University Medical School, Ankara, Turkey

Introduction: Expression of nm23-H1 has been identified as a potential metastatic suppressor. This study aimed to investigate whether nm23-H1 expression is related to clinopathological parameters and overall survival in colorectal carcinomas.
Methods: The immunostaining was performed on 185 colorectal carcinomas using a polyclonal anti-nm23-H1 antibody. Ninety patients were followed-up either until time of death or median survival time of 36 months, ranging from 30 to 95 months. Staining patterns were assessed semiquantitatively and correlated with tumor histologic type, differentiation, Dukes' stage, angiolymphatic invasion and prognosis. Chi-square, multiple logistic regression model, Kaplan-Meier survival and multiple Cox regression analysis was performed.
Results: The nm23-H1 immunoreactivity was weak in 31 (17%), moderate in 48 (26%) and strong in 106 (57%) cases. Advanced Dukes' stage associated with reduced nm23-H1 expression ($p<0.001$). Well differentiated adenocarcinomas expressed significantly higher nm23-H1 than moderate / poorly differentiated, including signet-ring carcinomas ($p<0.001$). There was an inverse correlation between angiolymphatic invasion and nodal metastasis with nm23-H1 expression ($p=0.0002$, $p=0.0001$, respectively). Additionally survival times were found to be longer with strong nm23-H1 expression ($p=0.0002$). However, multivariate analysis indicated that distant metastasis at any time was an independent predictor of prognosis ($p<0.0001$).
Conclusion: The study indicated that nm23-H1 might have a role in progression of colorectal carcinomas and it may be a useful parameter in predicting prognosis.

P-019

Rapid non-invasive diagnosis of helicobacter pylori in dyspeptic patients

Inas El-Defrawi, Manal Diab, Mona Moussa, Ahmed El-Ray and Effat El-Sherbini

Different invasive and non-invasive tests are available for the diagnosis of Helicobacter pylori (H. pylori) infection. The aim of the current study was to assess the reliability of non-invasive techniques in diagnosing H. pylori infection, in comparison with histopathology, also to study the relevance of CagA and VacA as markers of virulence. Forty six dyspeptic patients were exposed to the invasive endoscopic procedure. Three antral biopsies were obtained for the analysis of H. pylori infection by histopathological examination {Hematoxylin and eosin (H & E), Giemsa and Diff-3}, culture and rapid urease test. Three non-invasive techniques were performed for detection of H. pylori antigen in stool (HpSA), quantitation of IgG antibodies and qualitative identification of anti-CagA and VacA antibodies. From the above tests it was found that 78.3%

(36/46) of dyspeptic patients were considered positive for H. pylori (group I) and 21.7 (10/46) were negative (group II) by histopathological and endoscopic examination. Histopathological examination revealed best sensitivity and specificity of 97.2% and 100% respectively with Giemsa stain. Non-invasive techniques revealed that detection of H. pylori antigen in stool (HpSA) had the best sensitivity (specificity) of 91.7% (100%) followed by anti-CagA and VacA antibodies and IgG serology of 80.6% (76.9%) and 75% (62%) respectively. From the above results, it was concluded that HpSA is a rapid non-invasive and non-expensive test that can be used successfully for pre-endoscopic screening of dyspeptic patients, an indicator of active infection and subsequently is an early predictor of efficient treatment. Also, the presence of CagA and VacA H. pylori positive strains denote severe histopathological damage that would sooner or later manifest itself clinically, if left untreated.

P-020

Quantitative morphometric analysis of interface of esophageal squamous cell carcinoma (Stage T1b and T2), using a computer-assisted fractal analysis

Endoh, M.*, Abe, S.*, Chiba, R.**, Watanabe, M.*, Moriya, T.* , Sasano, H.*
* Dept. of Pathol., Tohoku University Hospital, Sendai, Japan;
** Dept. of Pathol., Saka General Hospital, Shiogama, Japan

Introduction: Fractal dimension (FD) can examine complicated morphological structure such as an irregularity of invasive front of malignant tumor in a quantitative fashion. Therefore, in this study, we measured FD of invasive front of esophageal squamous cell carcinoma (SCC) and correlated the findings with clinicopathlogical factors of the cases.
Materials and Methods: The cases examined were 35 cases (18 cases with invasion limited in submucosa (T1b) and 17 with invasion into muscularis propria (T2)). Profile of the deepest margin of invasive front of the carcinoma was strictly traced at ×100 magnification in hematoxylin and eosin stained tissue sections. The traced line images were subsequently converted to digital data with a digitizer in order to incorporate the data into a computer-assisted fractal analysis system(Rise co. Sendai, Japan). FD of these findings were then calculated with the system applied of box-counting method. Correlation between the obtained FDs and clinicopathological factors of the cases were also examined.
Results: All of the analyzed data were considered to have fractal structure . FD was higher in T2 cases (mean FD=1.220) than in T1b cases(mean FD=1.183), although the difference did not reach statistical significance. FD of lymph nodes positive cases (n=21, mean FD=1.241) were significantly higher than that of node negative cases (n=14, mean FD=1.174) (p=0.0095) but its significance needs to be clarified by further studies.
Conclusion: Fractal dimension of the invasive front of carcinoma cells was considered a valuable indication of biological aggressiveness of esophageal SCC.

P-021

Analysis of p27 and TGF-beta expressions in kolorectal cancer associated with inflamatory bowel disease and/or poliposis coli

S. Erdamar, H. Aki, G. Dogusoy, S. Goksel, S. Gocener, N. Buyukpinarbasioglu
Cerrahpasa Medical Faculty, Pathology Department, Istanbul, Turkey

Introduction: The TGF-ß family is a collection of polypeptide proteins that are important in the modulation of cell growth, development and differentiation. TGF-beta1 is commonly overexpressed in solid malignancies. Down regulation of p27, a cyclin dependent kinase inhibitor, is associated with agressive behaviour in some tumors. We analysed immunohistochemically TGF-beta and p27 expression levels in human colorectal carcinomas associated with inflamatory bowel diseases e.g.colitis ulserosa (CU) and poliposis coli.
Methods: Formalin fixed-paraffin embedded sections from randomly selected 15 CU cases with epithelia displasia in various degrees, 25 colorectal adenocarcinoma (Cca) arised in polyposis coli (PC) were immunostained with a monoclonal antibody against TGF-beta and p27 proteins Immunoactivity was evaluated without any clinicopathologic knowledge. p27 analysis was recorded as p27 labeling index. TGF-beta analysis was revealed as intensity of staining, (+/+++).
Results: There was not any significant differences inTGF-beta levels in normal epithelia and CU group. It's found significant TGF-beta overexpression in Cca group ($p<0.05$). The p27 labeling index in normal colorectal mucosal epithelia. was 94.3%±3.2% (mean±SD), and in UC was 68.3%±5.4% ($p<0.05$). It was also found significantly reduced p27 expression in Cca group (25.05%±8.5%) and PC group (41.07%±2.6%) ($p<0.05$). Reduced p27 expression and TGF-beta overexpressions were associated with invasion level and histological grade in Cca group.
Conclusion: This study showed that the posttranslational reduction of levels the of p27kip1 which mediates TGF-beta growth inhibition, provides an additional means for colorectal adenocarcinoma cells to escape negative growth regulation by TGF-beta.

P-022

Neuroendocrine differentiation in gastric adenocarcinomas and its correlation with tumor stage, P-53 and vascular endothelial growth factor (VEGF) expression

Eren Funda, Celikel Cigdem
Marmara University School of Medicine, Department of Pathology, Istanbul, Turkey

Presence of neuroendocrine cells in normal gastric mucosa and tumors arising from these cells have been known for many decades. However studies on neuroendocrine differentiation in conventional gastric adenocarcinomas and its significance in tumor behaviour is limited. Our aim in this study is to search for the presence of neuroendocrine differentiation in gastric adenocarcinomas and to determine if it has any correlation with the important prognostic factors, like tumor stage, grade and expression of P-53 and VEGF. 40 gastrectomy specimens with gastric adenocarcinoma are included in our study.Tumors are classified as diffuse (n:17) and intestinal (n:23)according to Lauren classification. Immunreactivity for chromogranin A is used to detect neuroendocrine differentiation in

tumor cells. Expression of P-53 and VEGF is also analyzed by using immunhistochemistry. Neuroendocrine differentiation is detected in 42.5% (n:17) of the cases with 30% (n:5)showing diffuse immunreactivity. No statistically significant correlation is found between neuroendocrine differentiation and tumor histologic type. Also there was no significant difference in tumor grade, stage , p53 and VEGF expression between tumors showing neuroendocrine differentiation and the ones that do not. In conclusion our study suggest that although neuroendocrine differentiation is common in conventional gastric adenocarcinomas it does not seem to have a major affect on tumor behaviour.

P-023

Bcl-2 oncoprotein expression in colorectal polyps and adenocarcinomas

Famulski W., Sulkowska M., Miller-Famulska D., Sulkowski S.
Department of Pathological Anatomy, Medical Academy of Białystok

The Bcl-2 proto-oncogene is a known inhibitor of apoptosis and may therefore allow an accumulation of genetic alterations that become propagated by cell division and potentially contribute to neoplastic development. The aim of our study was to assess the possible role of Bcl-2 in colorectal tumorigenesis.
The immunohistochemical staining for Bcl-2 (Dako no M0 887) was performed on archival material from 20 hyperplastic polyps, 42 adenomatous polyps, 15 combined polyps contained both hyperplastic and adenomatous elements and 85 adenocarcinomas (pT_2 and pT_3, pN0, M0 acc. to pTNM). Histologically normal mucosa was analyzed from the proximal or distal margins of these cases.
In histologically normal mucosa Bcl-2 staining was observed in basal epithelial cells of the colonic crypts. As in normal mucasa, in the hyperplastic polyps Bcl-2 immunostaining was restricted to the lower portion of the colorectal crypts. Dysplastic cells of adenomatous and combined polyps stained positively for Bcl-2 in 43 of 57 (75%) cases. Forty seven of the 85 colorectal adenocarcinomas (55%) showed a positive cytoplasmic immunoreactivity for analysed oncoprotein. Bcl-2 expression was detected in parabasal and superficial regions in adenomas and adenocarcinomas whereas in normal mucosa and hyperplastic polyps it was restricted to basal epithelial cells of the colorectal crypts.
Our data indicate that Bcl-2 expression is characteristic for early phase of colorectal tumorigenesis and may facilitate tumor progression.

P-024

Ultrastructural study of capillaries in colon adenocarcinoma liver metastases

Finol, H.J.*, Márquez, A.**, Pulido-Méndez, M.**, Boada-Sucre A.***, Sosa L.****
Center for Electron Microscopy, Sciences Faculty*, Institute of Experimental Medicine, Medicine Faculty**. IDECYT, U.N.E.S.R.***, Department of Anatomy ****; Central University of Venezuela, Caracas, Venezuela

Introduction: Angiogenesis during neoplastic growth involves endothelial mitogenic and migration stimuli produced by tumor cells. It is known that angiogenesis takes place mainly in the tumor periphery, nevertheless the process of vessel growth in inner areas and its clinical role remain largely unexplored. In liver metastases this aspect is particularly important due to the existence of two sources for tumor vessels, portal vein sinusoids and hepatic artery capillaries. Development of effective treatments for hepatic metastases can be initiated by better understanding the tumor vasculature and its blood supply. A study of the ultrastructural characteristics of capillaries in liver metastases from colon adenocarcinomas was performed in order to ascertain the contribution of portal sinusoids and arterial capillaries in this angiogenic process.
Methods: Surgical biopsies were obtained of liver metastases from colon adenocarcinomas in ten patients, they were processed with routine techniques for transmisssion electron microscopy and observed in Hitachi H-500 and H-7100 electron microscopes.
Results: Only abnormal arterial capillaries were observed in the metastasis center exhibiting endothelial hypertrophy with mitochondrial swelling, RER proliferation, abundant free polysomes, and intraluminal infoldings. Heterochromatin amount was variable. Basement membrane was widened and laminated. Pericytes were also altered. Abnormal sinusoids were observed in metastasis periphery. They showed a variable wall thickness, swollen mitochondria, and abundant RER and lysosomal structures. Dilated fenestrae and widened basement membrane were also seen.
Conclusions: This ultrastructural study confirms that colon adenocarcinoma metastases induce angiogenesis in both liver capillary beds. This angiogenic activity produces abnormal or defective capillaries that are selectively located. These results are important for selecting a vascular way for local chemoterapy.

P-025

The presence and significence of stainable iron in byopsy spacements of some neoplasmas

Gligorijevic Jasmina, Tasic Desanka,
Zivkovic Vesna i Dimov Dragan
Institute of Pathology, Medical faculty of Nis, Yugoslavia

Introduction: Experimental and human data support the hypothesis that iron may be a carcinogenic factor involved in both cancer initiation (through activation of free radicals and reactive oxygen species) and promotion (by facilitating cancer growth and modifying immune equilibrium). A significant association between high serum feritin levels and neoplasia was found in several case-controlled studies, especially in patients with either liver carcinoma or colon adenoma. There are a very few data on distribution of tissue iron in liver carcinoma and colon adenomas with different grade of dysplasia.
Aim: The aim of this study is to demonstrate the presence of tissue iron in colonic biopsy specimens at the time of "adenoma cum dysplasia" (of grade I-III) as patohystological diagnosis is made. The presence of stainable iron in primary hepatocellular carcinoma (HCC) was also done.
Methods: Thirty five biopsies of colon adenomas and twenty surgical biopsies of HCC were rutinly prepared for light microscopy analysis and were stained by: HE,PAS,Van Gieson and Pearls stain.
Results: There was no demonstrable iron in colonic adenomas with dysplastic changes grade I and II. Adenomas cum dysplasia grade III and all five cases of adenomas and adenocarcinoma were positive to iron stored in mesenchymal cells in the stroma and various types of inflammatory cells. There was no iron stored in malignant

cells of HCC, but surrounding cells and macrophages, usually had strong positivity to iron.
Conclusion: This results suggest association of iron presence in environment of neoplastic cells possibly facilitating tumor growth and modulating local immune milley.

P-026

Cytokeratin 7 and 20 expression in benign mucinous tumours of the pancreas

Handra-Luca A (1), Couvelard A (1), Fléjou J-F (2), Terris B (1), Degott C (1)
Department of Pathology, (1) Beaujon Hospital, Clichy; (2) Saint-Antoine Hospital, Paris, France

The aim of this study was to compare the immunohistochemical expression of cytokeratin (CK) 7 and CK20 in mucinous cystadenomas (MCA) and intra-ductal papillary mucinous adenomas (IPMA) of the pancreas.
Methods: Benign mucinous tumours (9 cases of MCA, 8 cases of IPMA) were studied for clinical (age, sex, type of surgery), morphological and immunohistochemical (CK7 and CK20 expression) features. Normal pancreatic tissue at distance of the tumours was also studied for CK7 and CK20 expression.
Results: The patients with MCA were younger (mean 37 years) than patients with IPMA (mean 63 years). All the patients with MCA were female; patients with IPMA showed a sex ratio of m:f=1:2. MCA was located in the body or tail of the pancreas whereas IPMA were located in the head of the pancreas.
CK7 was strongly and diffusely expressed by the normal duct system and in all cases of MCA and IPMA. CK20 was not expressed by the normal duct system and neither by IPMA. In contrast it was expressed in most cases of MCA (6/9 cases) by numerous cells either scattered or forming small foci.
Conclusions: IPMA show identical immunohistochemical characteristics (CK7+ / CK20-) with the epithelia of the normal pancreatic duct system.
The phenotype of MCA (CK7+/CK20+) differentiate them from IPMA and account for a different histogenesis of these lesions.

P-027

Loss of heterozygosity and microsatellite instability in small colorectal carcinoma

Seiji Haraoka[1], Shingo Yoshioka[1], Kouichi Ohshima[1], Akinori Iwashita[2], Masahiro Kikuchi[1]
Department of Pathology, [1] School of Medicine;
[2] Chikushi Hospital, Fukuoka University, Fukuoka, Japan

INTRODUCTION: Multistep process of genetic alterations for the colorectal tumorigenesis has been proposed. In this series, we have investigated whatever the genetic disorders have affected the carcinogenesis of small colorectal adenocarcinoma, flat-elevated (nonpolypoid) type, with invasion into or beyond submucosa, less than 2 cm in diameter.
METHODS: Using DNA extracted from microdissected areas in 12 adenocarcinomas with an average diameter of 1.2 cm (range, 0.7–1.7), PCR-based direct sequencing of *K-ras* and *p53* genes, and analysis of the microsatellite instability (MSI) and loss of heterozygosity (LOH) at 10 microsatellite loci correlated with colorectal carcinogenesis, were performed. p53 protein overexpression was assessed by immunohistochemical stain.
RESULTS: 3 out of 12 (25%) tumors showed *p53* gene mutation simultaneously associated with LOH at *p53* locus. No correlation between *p53* gene mutation and p53 protein overexpression was defined. *K-ras* gene mutation didn't recognized in any tumors. High-grade MSI exhibiting replication errors at least 40% or more of informative loci was shown in all tumors. LOH was frequently detected at the *p53* (75%), *APC* (90%), *DCC* (83.3%), 8p22 (80%), *MSH2* (80%), and *MLH1* (50%) locus. In addition, different patterns of genetic change within the tumor, indicative intratumoral heterogeneity, were detected.
CONCLUSION: The small adenocarcinoma of the colorectum shows a high level MSI and a high frequency of LOH at the microsatellite loci known to be important for colorectal carcinogenesis. These results support the concept that small adenocarcinoma with aggressive invasion including *de novo* carcinoma can develop via unique carcinogenetic pathway.

P-028

Detection of Polyomavirus sequences in colon adenocarcinomas

J. Hernández-Losa, C. Corbacho, O. Rodríguez, C. Salas, S. Ramón y Cajal
Departamento de Anatomía Patológica, Clínica Puerta de Hierro, Madrid, Spain

Polyomaviruses (PMV) are widespread among animal species. In humans, the most extensively studied are JC (JCV), SV40 and the BK viruses, whose human cell transforming properties have been studied. Recently, it has been found T antigen DNA sequences of JC virus in the mucosa of normal human colons and in a large number of colorectal cancers.
We have studied 52 patients with colorectal carcinoma and we have analyzed the presence of PMV and JC sequences in tumors and in adjacent normal mucosa. The results were correlated, in every case, with microsatellite instability, p53 mutations, p53 expression, location and size of the tumor, depth of infiltration and presence of lymph node metastases. PMV and JC sequences were studied by PCR techniques. DNA was treated with topoisomerase and several combinations of primers were used. Microsatellite instability was detected studying at least 5 microsatellites by PCR-SSCP and the p53 status by using PCR-SSCP techniques and immunohistochemistry.
In 36.5% of colon tumors PMV sequences were detected by PCR, and about 50% of them had also PMV sequences in normal mucosa. We have found no correlation betwen the presence of JC sequences in tumoral tissue and the status of p53, microsatellite instability, the size or clinical stage of the tumors. The tumoral location was similar in positive and negative PMV cases. Depth of infiltration (86.95% of T3 level in PMV positive cases and 80.76% of T3 level in negative ones) and lymph nodes metastases presence (47.46% in polyomavirus positive cases and 38.46% in negative ones) were also similar in both groups. Moreover, a significant number of PMV was detected in normal mucosa but not in tumor samples of some patients (9.6% of the cases studied).
With these results we conclude that there is not significant correlation between the presence of JC sequences and most histological, molecular and clinical features studied in colon adenocarcinoma.

P-029

Defect of the DNA mismatch repair genes MSH2 and MLH1 is infrequent in esophageal adenocarcinoma

Nirag Jhala, M.D., Juan Lechago, M.D., Ph.D.,
Mamoun Younes, M.D.
Departments of Pathology, Baylor college of Medicine, Houston; University of Alabama at Birmingham (N.J.), USA

Introduction: Microsatellite instability (MSI), and defect in the DNA mismatch repair genes MSH2 and MLH1, have been detected in a significant number of squamous cell carcinoma (SCC) of the esophagus and adenocarcinoma of the stomach, and was suggested to play a significant role in the carcinogenesis of these tumors. The aim of this study was to determine whether defect in MSH2 and/or MLH1 play a role in malignant progression in Barrett's esophagus.
Methods: Formalin-fixed and parafffin-embedded tissue sections from 12 esophageal adenocarcinomas, arising in Barrett's esophagus, were studiesd for MSH2 and MLH1 using the immunoperoxidase technique. Sections of normal colon were used as positive control. The percent of positive nuclei was recorded by two observers.
Results: Of the 12 carcinomas, only one (8%) showed loss of MLH1 expression and none (0%) lacked MSH2 expression. Barrett's metaplasia without dysplasia showed a staining pattern similar to that of normal colon, with predominant staining of the epithelium in the bottom third of the mucosa.
Conclusion: Unlike esophageal SCC or gastric adenocarcinoma, MSI does not appear to play a significant role in the carcinogenesis of Barrett's-associated adenocarcinoma. Studies to determine whether MSI can differentiate esophageal from cardia adenocarcinoma are in progress.

P-030

$p16^{INK4A}$ is a target gene for β-catenin

Andreas Jung, Stella Wassermann, Michael Schrauder, Elke Hiendlmeyer, Angela Haynl, Marc Porzner, Per Berglund[2], Richard Palmqvist[2], Thomas Kirchner, Thomas Brabletz
Pathologisches Instituts der Universität Erlangen-Nürnberg, Germany; [2] Dep. of. Medical Biosciences Pathology, Umeål Universitet, Sweden

Introduction: Well differentiated colorectal adenocarcinomas show a strong nuclear localisation of β-catenin at their invasion front. Consequently, they co-express β-catenin target genes like cyclin D_1, c-myc, uPA or MMP-7. Though expression of cyclin D_1 and c-myc is found at the invasion front it is a zone with low proliferation. Here, we show that $p16^{INK4A}$ is a target gene of β-catenin transactivation . Thus β-catenin upregulates the expression of both cyclin D_1 and $p16^{INK4a}$ at the invasive front but the effect of $p16^{INK4A}$ overcomes the proliferative stimulus of cyclin D_1.
Methods and Results: Using immunohistochemistry using antibodies directed against $p16^{INK4A}$ and β-catenin we found a co-expression of these two antigens at the invasion front of well differentiated human colorectal adenocarcinomas. In the promoter/enhancer of the human $p16^{INK4A}$ a single TCF-4 binding element (ATCAAAG – Wnt responsive element: WRE) was found. This WRE binds specific to recombinant TCF-4 in Electric Mobility Shift Assays (EMSA). Transient transfection studies with the WT-WRE and MUT-WRE $p16^{INK4A}$ promoter/enhancer luciferase constructs in human colorectal cancer SW480 cells showed a dependency of expression on the WT-WRE element. Moreover, tetramers of WT-WRE but not MUT-WRE in front of a minimal thymidine-kinase promoter luciferase construct showed a strong transactivation in the presence of β-catenin in HEK 293T cells.
Conclusion: The paradox co-expression of cyclin D_1 and $p16^{INK4A}$ could enable tumor cells to react quickly on proliferative enviromental stimuli as they would just have to feed $p16^{INK4A}$ into a degradation machinery. Moreover, cyclin D_1 could play important roles in differentiation processes.

P-031

Immunohistochemical evaluation of cathepsin D expression in colorectal tumours and adenomas

Kanber Y. Demirbağ N., Demir Şam A., Aydin N., Akalin G.
Pathology and General Surgery Departments,
Haseki Hospital-Istanbul, Turkey

Introduction: The immunohistochemical expression of cathepsin D (CD) was evaluated in colorectal adenocarcinomas and adenomas. Its role in metastasis and correlation with other prognostic parameters were investigated.
Method: Thirty one colorectal adenocarcinomas and nine colorectal adenomas were studied. CD immunostaining cytoplasmic in both the cancer and stromal cells was evaluated separately. Both the stromal and tumoral CD staining were correlated with each other and with the tumor stage, histological grade, lymphovascular invasion and lymph node involvement separately. And the correlation was made between the staining properties of adenoma and carcinoma cases. Fisher exact chi-square and chi-square tests were used for statistical analysis.
Results: In both carcinoma and adenoma cases CD expression was present in all the stromal cells in variable degrees. Immunoreactivity in neoplastic cells was found in 90,3% of the carcinomas and 77,7% of the adenomas. There was a statistically significant correlation between the stromal CD staining in carcinomas and the tumor stage ($p<0,05$). Also there was statistically significant difference between the stromal CD staining of adenomas and carcinomas ($p=0,005$). No statistically significant correlation was found with the other parameters.
Conclusions: In this study CD was highly expressed in both neoplastic and stromal cells. The CD expression in colon cancer was higher than the expression in stromal cells of the colorectal adenomas. Also the statistically significant correlation between the stromal cell CD expression in colon cancer and tumor stage may show that stromal cell CD positivity may be a factor in predicting the outcome of the colon cancer patient.

P-032

Small intestinal and rectal mucosae in coeliac disease: An immunemorhometric study

Kansu A[1], Kuloglu Z[1], Ensari A[2], Kalayci AG[1], Girgin N[1], Erekul S[2]
University of Ankara Medical School Departments of Paediatric Gastroenterology[1] and Pathology[2], Sihhiye, Ankara, Turkey

Introduction: Paediatric patients with coeliac disease frequently present with atypical symptoms causing diagnostic difficulty. We therefore decided to analyze small intestinal and rectal mucosae of coeliac children by means of immunemorphometry.
Methods: A total of 40 patients comprising 10 children with coeliac disease (group 1), 10 with atypical symptoms, positive serology and normal biopsy (group 2) and 20 disease-controls with dyspeptic symptoms (group 3). AGA and EMA antibody tests and mucosal biopsies were performed on all subjects included in the study. Paraffin sections of 5 μm thick were stained with anti-CD3 and anti-CD8 antibodies using a streptavidin-biotine peroxidase technique. Positive cells were counted with reference to a test square of 10^4 μm^2 of muscularis mucosae. Villus height and crypt depth were also measured via a Zeiss Image Analysis System on KS400 software. Discriminant Analysis was performed using SPSS package.
Results: CD3+ lymphocytes were significantly higher ($p<0.01$) in the lamina propria in group 1 compared with groups 2 and 3 while epithelial and lamina propria CD8+ lymphocytes were significantly higher in group 1 patients compared with group 3 ($p<0.01$). Similarly lamina propria CD8/CD3+ lymphocytes were significantly increased ($p<0.01$) in both group 1 and group 2 compared with controls. Sensitivities of CD3+ and CD8+ lymphocyte counts were 85.7% and 100%, respectively, while specificities were 100% for both.
Conclusion: Our results suggest that, when used together, CD3+ and CD8+ lymphocyte counts could be highly discriminatory for coeliac disease. However, more detailed evaluations seem to be necessary for defining "potential coeliac" group.

P-033

Esophageal squamous cell carcinomas; histological subtypes and relation with bcl-2, bax, nm-23 protein expressions

Karayel, F; Goksel S; Gocener S
Department of Pathology, Ministry of Justice, Forensic Medicine Council; Department of Pathology, Istanbul University, Cerrahpaşa Medical Faculty, Istanbul, Turkey

Esophageal squamous cell carcinomas are aggressive neoplasms with a wide spectrum of morphology and generally poor prognosis. At one end of this spectrum , exists, Basaloid squamous cell carcinoma (BSCC) which has been a recently described rare and poorly differentiated variant of squamous cell carcinomas (SCC).
In our study, clinical, pathologic and immunohistochemical parameters (bcl-2,bax,nm-23) of BSCCs (non-keratinizing small cell type) of SCCs (keratinizing large cell type) of the esophagus were compared. In addition, the relations between histopathologic parameters which have different prognostic significance were assessed.
In conclusion, the prognosis of patients whit BSCC and mixed group (Keratinizing large cell and non-keratinizing small cell type) of the esophagus does not differ from that of patients with typical SCC.
Besides, Bcl-2 protein is often expressed in esophageal carcinomas and particularly in non-keratinizing, whereas Bax protein is often expressed in keratinizing types all of which are in accordance with the litteratüre.With regard to overall survival and prognosis, we failed to demonstrate any correlation with bcl-2 and bax protein expression, whereas nm-23 expression was correlated with metastasis and prognosis. However , evaluation of immünohistochemical parameters revealed no correlation with histologic type, depth of invasion of the tumor and lymph node metastasis.

P-034

Diversity of hemodynamic disorders in gastric ulcer affected stomach wall in correlation with endocrine cells population

Regina Kleina*, Velta Ose**
* Dept.of Pathological Anatomy, Medical Academy of Latvia;
** Faculty of Medicine, University of Latvia, Riga

Introduction: The aim is to evaluate circulation disturbances in sub-epithelial, submucosal and muscular layer of gastric wall and to test their possible correlations with endocrine cells /EC/ population.
Methods: 125 patients with pyloric peptic ulcer (58-diagnosed with gastrobiopsies and 67 operated cases) were analysed on different stages of disease. Concomitant pathology of cardiovascular system from case records were taken into consideration. Serial slides were stained with H&E,toluidine blue and immunohistochemistry with antibodies against vimentin, S-100 protein, synaptophysin, chromogranin A, gastrin was used in 48 patients, but 14 biopsies were examed by electron microscopy. Density, diameter of vessels and amount of EC were evaluated in $1mm^2$.
Results: In the subepithelial area there are hemorrhages,capillaries engorged with erythrocytes and margination of platlets.During exacerbation and partly healed ulcer density of capillaries in the edges of ulcer in comparison with resection lines is increased significantly ($p<0,005$). In the submucosal and muscular layers there are dilateted venules and thichening of their wall, but in the area of ulcer there are phlebofibrosis,arteriolofibrosis with inflammatory infiltrares in them. Statistically more common these lesions ($p<0,005$) are in the patients older than 60 years with concomitant atherosclerosis. The analysis of EC distribution has proved that only 12,6% of them are localised near by vessels.
Conclusion: Alterations in vascular caliber, type of circulation disturbances and their ultrastructural lesions are influenced by the duration of peptic ulcer and concomitant generalized vascular pathology. There is no possitive correlation between the hemodynamic disorders and characteristics of gastric EC.

P-035

Chromosomal changes in organ-specific metastasis in colorectal carcinomas

T. Knösel, K. Schlüns, H. Schwabe, U. Stein, S. Petersen, P.M. Schlag, M. Dietel, I. Petersen
Institute of Pathology, University Hospital Charité, 10098 Berlin, Germany; Department of Surgery and Oncology, RRC, Charité Campus Buch, Berlin, Germany

Comparative genomic hybridization was used to screen advanced colorectal carcinomas for chromosomal aberrations that are associated with the metastatic phenotype. In total, 70 tumor specimens from 45 patients were investigated comprising 29 primary tumors, 26 systemic metastases (12 liver, 6 brain, 8 lung), 11 lymph node tumors and 4 abdominal wall metastases. Using statistical analysis and histograms to evaluate the chromosomal imbalances overrepresentations were detected most frequently at 20q11.2-20q13.2,

7q12-7q11.2, 16p11-16p12, 19p13, 9q34, 19q13, 13q34, 13q13, 17q21, 22q11, 8q24 and 1q21. Deletions were prominent at 18q21-18q23, 4q27-4q28, 4p14, 5q21, 1p21-1p22, 21q21, 6q16, 3p12, 8p24-8p21, 9p21, 11q22 and 14q13-14q21. Comparing liver metastases with their corresponding primary tumors particularly deletions at 2q, 5q, 9p, 10q and 21q and gains of 1q, 12qter, 17q12-q21, 19, and 22q were more often observed. Hematogenous metastases showed more alterations than lymph nodes tumors, particularly more deletions on several chromosomes and gains on 7, 12qter, 13, 16 and 22q. The analysis suggest that the different pathways of tumor dissemination are reflected by a non-random accumulation of chromosomal alterations with specific changes being responsible for the different characteristics of the metastastic phenotype.

P-036

Adhesion and migration of human colon cancer cells with different CD44 profile on HA-containing ECM components

M. Köbel, K. Crüwell, C. Denkert, S. Hauptmann
Charité, Institute of Pathology, Humboldt-University, Berlin, Germany

Introduction: The hyaluronic acid (HA) receptor CD44 and its splicing variants (in particular CD44v6) has been shown to be a prognostic factor in some studies, but contradictory reports also exist. This inconsistency could be related to the matrix composition of the stroma, and particularly to its HA content. Therefore, we performed a study investigating the relationship between CD44 expression and matrix composition using *in vitro assays* for adhesion, migration and invasion.
Methods: Three cell lines of colorectal adenocarcinomas with different CD44 expression (HT-29: CD44s+ and CD44v6+; HRT-18: CD44s+, CD44v6-; CX-2: CD44s-, CD44v6-) were used. We'd studied adhesion and migration on collagen type I, III, and V, and fibronectin alone or in mixture with HA. Moreover, we had investigated whether the invasion through matrigel can be modified by HA.
Results: HA was shown to stimulate invasion of CD44v6 expressing cells. These cells were also strongly adhesive to HA. On the other hand, HA had no significant effect on adhesion and migration of tumor cells on other matrixes, regardless of CD44s expression.
Conclusion: Our data suggest that a high stromal content of HA may have an adverse prognostic effect in patients with CD44v6-positive colorectal carcinomas.

P-037

Inflammatory pseudotumor of colon. A case report

Kocmanovska Petreska S., Petrusevska G., Bogoeva B., Spasevska L., Banev S. (1) Stojanoski S.
Institute of Pathology, Medical Faculty, Skopje; (2) Center for Military Health Services, Skopje

Initially described in 1937, inflammatory pseudotumor inflammatory myofibroblastic tumor plasma cell granolomas are synonymous for an inflammatory solid tumor that contains spindle cells, myofibroblasts, plasma cells and histocytes. Common sites of presentation include lung, mesentery, liver and spleen; intestinal presentation are rare and the etiology remains obscure.

CASE REPORT: A case of 52-years-old woman was admitted at the Military Hospital for the symptoms of abdominal pain and vomiting. Cytology was done and verified as first classification group. Polypoid lesion in the area of column ascendens was found during the rectoscopic examination. Chemicolectomy was made and clearlylimited polypoid tumor formation with dimension of (6×4×3.5sm) was found.
On histologically examination we found a tumor consisted of spindle- shaped cells with tapering eosinophilic cytoplasm which were typically widely separated in a vascular myxoid matrix with acute and chronic inflammatory cells.
Immunohistohemical staining revealed positivity for LCA in the inflammatory cells. Staining for desmin was weakly positive in the spindle ovoid cells. The other immunohistochemical markers (Actin, HLAdr, MAC387, cytoceratin wide range spectrum, neurofilament protein) were negative.
The final diagnosis was inflammatory pseudotumor.
We consider that this condition should be differentiated from other malignant condition of the large intestine because of benign prognosis for the patient. Immunohistochemical staining helps to make a proper diagnosis.

P-038

Characteristics of "Russell body gastritis"

* Kostov M, ** Katic K, ** Lazarevic V, * Pecanac R, ** Katic V.
* Military Hospital Nis, ** Institute of Pathology, in Nis University, Yugoslavia

AIM: Reported data on "Russell body gastritis" are rare.
MATERIALS AND METHODS: Gastric biopsy specimens, taken during endoscopy and from ressected stomach antral carcinoma were routinelly fixed and processed. Paraffine sections were stained by: H@E, PAS, HID-AB, pH=2,5, Giemsa and Masson's trichrome methods.
RESULTS: The biopsy specimens from two patients with gastric ulcer and from one patient with antral gastric carcinoma showed marked and localized accumulation of plazma cells filled with Russell bodies in the cytoplasm in close association with Helicobacter pylori infection and in early gastric carcinoma: localized accumulation of numerous "histiocytoid cells" in the superficial lamina propria mucosae were filled with eosinophilic globules in the plump cytoplasm and possessed eccentrically located round nuclei. Helicobacter pylori infection was observed on the surface of the regenerative foveolar cells in Giemsa stained preparations. The histiocytoid cells were proven histochemically to be plasma cells and, hence, the eosinophilic globules should be called Russell bodies. The Russell bodies stained red by Masson's trichrome and by PAS. Plasma cells with Russell bodies have been called "Motts" cells.
CONCLUSION: Empirically, a smoll number of Motts cells are commonly identified in the gastric mucosa with heavy infiltration of mononuclear cells, but dense and localized accumulation of Motts cells in gastric mucosa with the presence of gastric carcinoma, was reported only once (Johansen A, et al. Acta Pathol Microbiol Scand Sect. A 1977; 85:245–250). The immunological role of "Russell body gastritis" in the slow evolution of gastric carcinoma was discussed.

Kostov Milos, MD, Department of Pathology, Vojna bolnica NIS, B. Taskovica bb, 18000 NIS, Yugoslavia, Fax: (+381) 018 338 191, e-mail: kolepath@bankerinter.net

P-039

Gastrointestinal stromal tumors – A prognostic study

D. Kovač[1], M. Jašić[1], M. Petrovečki[2], Z Iternička[1], M. Rubinić[3], N. Ivaniš[3], Š. Križanac[4], N. Jonjić[1], M. Melato[5]
1. Dpt. of Pathology, University of Rijeka; 2. Dpt. of Clinical Immunology, University of Zagreb; 3. Dpt. of Gastroenterology, University of Rijeka; 4. Dpt. of Pathology, University of Zagreb, CROATIA; 5. Dpt. of Pathology, University of Trieste, ITALY

Gastrointestinal stromal tumors (GIST) are rare neoplasms of unknown etiology and pathogenesis. Clinical behavior is very unpredictable and a reliable prognostic factor is lacking. The aim of this study is to analize some prognostic factors and estimate which one is the most reliable.
38 biopsy specimens of GIST were immunolabeled with PC-10 for PCNA, for CD-34, vimentin, NSE and actin. Greatest diameter, histological grading and mitotic count were estimated for each case. All patients were followed up for at least 24 months or to death. All data were analysed by univariate and multivariate statistical analysis using computer program. Results showed that greatest diameter, mitotic count and PCNA-index are useful prognostic factors and it may be also helpful for planning further therapy.

P-040

Studies of the histological and histochemical indices of mucosal lesions in the cardia, corpus and prepyloric part of the stomach depending on the degree of Helicobacter pylori colonization

W. Kozlowski, A. Dibek, J. Trawiński, S. Wojtuñ, J. Gil, L. Wrzesiński, J. Patera
Division of Clinical Pathomorphology, Central Clinical Hospital, Military University School of Medicine in Warsaw; Endoscopy Centre, Central Clinical Hospital, Military University School of Medicine in Warsaw; Polytechnical University in Warsaw

Helicobacter pylori infection accompanies gastritis in about 90% and the process of development of the lesions lasts usually from 20 to 40 years. It has been generally accepted that the intensity of H.pylori colonization increases with patients' age which is also true of the degree of gastritis progression.In this context, the fact of H. pylori presence in about 50% of healthy population without any complaints, and in 30% also without any morphological changes in gastric mucosa, requires further research, both clinical and experimental.The aim of the study was to assess the degree of H.pylori colonization in the prepyloric part, corpus and cardia with simultaneous classification of the accompanying inflammatory changes of gastric mucosa in these regions and to determine the effect on dysplasia, metaplasia, foveolar layer hyperplasia and also on lymphoplasia coexisting with gastritis.The study material included gastric mucosa oligobiopsy specimens, taken simultaneously from the cardia, corpus and prepyloric part of the stomach of 144 patients (106 men and 38 women) aged 10–79 years, with histologically confirmed H. pylori infection. The control group included biopsy specimens selected according to the same criteria, taken from 137 patients (106 men and 31 women) aged from 10 to 79 years, without H. pylori infection. Cases of reflux gastritis were excluded from the control group. H. pylori was identified by Giemsa method. The sections embedded in paraffin were stained with HE and PAS reaction with alcian blue was carried out. The degree of H.pylori colonization was assessed according to the Sydney System. Gastritis was classified according to the modified Whitehead system.
Results and conclusions: The incidence of H. pylori infection of the stomach increases with age up to 69 years of age with a significant decrease thereafter. The peak incidence is found in the age group of 60–69 years. In the cases assessed, 2nd degree of H. pylori colonization intensity predominated and the colonization itself involved simultaneously all studied regions of the gastric mucosa. The degree of H. pylori colonization is inversely proportional to the degree of progression of gastritis lesions. The most pronounced inflammatory changes were found in the prepyloric part. In the cardia region, H. pylori colonization (most frequently 2nd degree) was usually accompanied by superficial gastritis. Glandular epithelial cell dysplasia developed significantly more frequently in the group with H. pylori infection and this was true particularly of the cardia and prepyloric part in women and only the prepyloric part in men. Foveolar layer hyperplasia coexisted more frequently with H. pylori colonization and in men this was found in all studied regions of the stomach while in women this was true only of the prepyloric part. No significant differences were found between the studied groups in the incidence of intestinal metaplasia and lymphoplasia in gastric mucosa.

P-041

Morphological indices of cholecystic and gastroduodenal lesions and Helicobacter pylori colonization in patients surgically treated for cholelithiasis

W. Kozlowski, Z. Hebzda, I. Grys, J. Friediger, L. Goñczowski

Division of Clinical Pathomorphology, Central Clinical Hospital, Military University School of Medicine in Warsaw; Department of Internal Diseases, V Military Clinical Hospital in Cracow; Division of General Surgery, Bonifratres Hospital in Cracow; Division of General Surgery, Railway Health Service Hospital in CracowThe aetiological and pathogenetic relationship is generally recognised between the diseases of the oesophagus, stomach and duodenum. Dyspeptic manifestations accompanying cholelithiasis seem to point to the fact that similar pathological relations could be found between changes in the upper gastrointestinal tract and lesions in the bile ducts. Chronic cholecystitis coexists in 95% with choletithiasis. In the morphological picture of this type inflammatory process, pyloric metaplasia also develops, the incidence of which being estimated variously by various authors. In cholelithiasis, H.pylori is found in bile, beside other microorganisms.The aim of the study was the determination of the nature and degree of progression of morphological changes in the gastroduodenal and cholecystic mucosa in patients subjected to cholecystectomy. Besides that, the incidence was assessed of pyloric metaplasia in cholecystic and duodenal mucosa in the same patients.The study material included 52 patients after cholecystectomy. These were patients aged 36-76 years, including 37 women (71.15%) and 15 men (28.85%). The operation in these patients was preceded by gastroscopy during which oligobiopsy specimens were taken from the stomach and duodenum. The sections embedded in paraffin were stained with HE and PAS reaction with alcian blue was carried out. H.pylori was identified by Giemsa method. Gastritis was classified according to the modified Whitehead classification, while in the case of the duodenal changes, the three-grade scale was used (chronic superficial duodenitis, chronic duodenitis, chronic atrophic duedenitis).

Results and conclusions: Calculous cholecystitis was usually accompanied by chronic prepyloritis, mainly advanced and active (100%), and less frequently by duodenitis (86.54%) and inflammation of the stomach corpus (82.7%). The inflammation of the stomach corpus most frequently was superficial and non-active (32.7%). Relatively frequently the morphological indices were found of reflux prepyloritis (46.15%) and inflammation of stomach corpus (23.1%). Duodenitis in these cases was superficial (34.62%) or chronic, involving full thickness of the mucosa (44.23%), and atrophic changes were observed only in 5.77%. Pyloric metaplasia was found in 19 gall bladders (36.54%) and in 12 oligobiopsy specimens from the duodenum (23.08%). Among morphological lesions in the gall bladder chronic cholecystitis predominated (69.23%) which was most frequently accompanied by decubital ulcer (57.69%). Less frequently atrophic cholecystitis (13.46%) and xanthogranulomatous cholecystitis (7.7%) were observed. H.pylori was found most frequently in the prepyloric part (54.9%), slightly less frequently in the stomach corpus (42.86%) while in the duodenum H.pylori was found within the foci of pyloric metaplasia only in two cases.

P-042

Expression of vascular endothelial growth factor (VEGF) and its receptors in endocrine tumors of the gut

*S. La Rosa, L. Albarello, S. Uccella, *G. Finzi, F. Sessa, C. Capella
* Dept. of Pathology, Ospedale di Circolo and Dept. of Clinical and Biological Sciences, University of Insubria, Varese, Italy

Introduction: Angiogenesis is known to be related to tumor growth and malignancy and is mainly stimulated by VEGF, which acts on endothelial cells by binding with its two specific receptors (VEGFR1 and VEGFR2). Gut endocrine tumors (GETs) show different biological aggressiveness and behavior, which are not easily predictable on a morphological ground alone. The aim of this study was to evaluate the expression of VEGF, VEGFR1, and VEGFR2 and to correlate it with microvessel density (MVD) and malignancy of GETs.
Methods: endocrine cells of the normal gut and of 50 GETs of different types were immunostained with antibodies directed against VEGF, VEGFR1, VEGFR2, and various gut hormones. Immunoelectron microscopy was performed for the ultrastructural localization of VEGF. MVD was evaluated by counting the number of CD31 positive microvessels.
Results: VEGF-immunoreactivity (IR) was found in normal gut G-cells and it was ultrastructurally localized in secretory granules. VEGFRs-IR was lacking in endocrine cells of the gut mucosa. VEGF-IR was found in 25/49 GETs mainly represented by G-cell and EC-cell tumors, while IR for VEGFR1 was found in 27/48 GETs and for VEGFR2 in 30/48 GETs, with no predilection for a specific tumor type. 22 GETs displayed a VEGF/VEGFR coexpression. VEGF expression did not correlate with MVD and malignancy, but MVD correlated with malignancy in EC-cell tumors.
Conclusions: 1) VEGF is expressed in normal G-cells; 2) MVD correlates with malignancy of EC-cell tumors, independently from VEGF expression; 3) VEGF may be involved in tumor growth of G-cell and EC-cell tumors through an autocrine/paracrine fashion, because VEGFRs are widely expressed in these neoplasms.

P-043

Immunohistochemical analysis of insulin-like growth factor (IGF-I and IGF-II) and insulin-like growth factor I receptor (IGF-IR) expression in gastric carcinoma

C. Langner[1, 2], R. von Wasielewski[3], K. Beyser[1], J. Rüschoff[1]
Departments of Pathology, [1] Klinikum Kassel, Germany,
[2] University of Graz, Austria; [3] Medical School Hanover, Germany

Introduction: Tumour growth is controlled by various peptides and/or hormones, acting in a systemic, paracrine, or autocrine fashion. Among them, IGF-I and IGF-II as well as their receptor (IGF-IR) have recently been described in several epithelial neoplasms, but not yet in gastric carcinoma. The aim of this study was to evaluate the expression of IGF-I, IGF-II, and IGF-IR in a series of gastric carcinomas.
Material and Methods: Slides containing sections of 60 different gastric carcinomas (multiblock system, as commercially available) were evaluated by immunohistochemistry (En-Vision) using antibodies against IGF-I, IGF-II, and IGF-IR.
Results: 20/60 (33%) carcinomas were positive for IGF I, 17/60 (28%) for IGF II. In general, concomitant expression of both peptides was found more frequently than expression of a single peptide. IGF-IR immunoreactivity was found in 44/60 (73%) carcinomas. The staining pattern varied remarkably: A strong diffuse granular reaction was present in only 16 (27%) of the tumours, whereas in the remaining 28 (46%) tumours only a faint positivity was found. Immunoreactivity for all three antibodies was independent of Laurén's type and histological grade.
Conclusion: Expression of IGF-I, IGF-II, and IGF-IR seems to be frequent in gastric carcinoma. The simultaneous presence of growth factors and growth factor receptor is consistent with an autocrine control of tumour growth.

P-044

Malignant potential of colorectal serrated polyps

Mäkinen MJ, Kukathasan R, Junttila O, Karttunen TJ
Department of Pathology. University of Oulu, Oulu Finland

Introduction: Colorectal serrated lesions (hyperplastic polyps and serrated adenomas) likely form a morphological continuum, but malignant potential of different lesions is unknown. Recently we reported that 6% of colorectal cancers associate with serrated adenoma, indicating the significant malignant potential of serrated lesions.
Aim: To compare the malignant potential of colorectal serrated lesions and conventional (non-serrated) adenomas.
Methods: A consecutive series of colorectal polyps diagnosed in years 1978–1982 was re-classified as follows: serrated adenoma, atypical hyperplastic polyp, hyperplastic polyp, mixed lesions (serrated polyp and conventional adenoma), and conventional adenoma. Initial polyp of each patient was included as index polyp. Follow-up biopsies and surgical specimens up to year 1999 were evaluated for the number of subsequent lesions.
Results: Initial polyps: After re-classification there were 34 serrated adenomas, 24 atypical hyperplastic polyps, 35 hyperplastic polyps, 21 mixed polyps, and 66 conventional adenomas. In the follow-up, colorectal cancer was found in 6.1% of patients with serrated lesions (7/114): 3 (8.8%) patients with serrated adenoma, 0 with atypical hyperplastic polyp, 1 (2.9%) with hyperplastic polyp,

3 (14.2%) with mixed lesion. In conventional adenomas cancer was found in 4.5% (3/66; p=NS). Polyps were more common in patients with serrated adenoma (75%) than with hyperplastic polyp (48%).
Conclusion: Our study adds evidence for the malignant potential of serrated lesions. Serrated adenoma was associated with the highest incidence of malignancy, although the difference between the other types of polyp was not significant. Prospective follow-up studies are necessary to further evaluate the malignant potential of serrated lesions.

P-045

The prognostic significance of the expression of the deleted in colorectal cancer (DCC) gene protein in high risk resected gastric carcinoma

M. Michael[1], M. Bai[1], A.T. Bamias[2], N.A. Pavlidis[2], and N.J. Agnantis[1]
Depts of Pathology[1] and Oncology[2], Medical School, Univercity of Ioannina, Ioannina, Greece

Background: DCC gene is a candidate tumor suppressor gene, which may be associated with differentiation and proliferation of normal cells. Loss of heterozygosity (LOH) of 18q, where the gene is located, and absence of DCC protein expression have been associated with worse prognosis in certain subgroups of patients with colorectal adenocarcinoma. We studied the prognostic significance of loss of protein expression in patients with resected gastric cancer with a high probability of relapse (T3, T4, N+).
Patients and methods: Sixty six patients were included in the study. DCC protein was detected with immunohistochemistry using an anti-DCC monoclonal antibody on paraffin embedded sections.
Results: DCC protein expression was present in 51 cases (77.3%) and absent in 16 cases (22.7%). Poorly differentiated and signet ring carcinomas had significantly lower expression than more differentiated tumors ($p<0.05$) as did diffuse type tumors compared to intestinal and mixed ($p<0.01$). Absence of DCC protein was an independent prognostic factor assosiated with better median survival (57 months vs 18 months, p=0.0176). There was a significant correlation between DCC protein expression and relapse site: all patients with distant metastases were positive for DCC staining, while almost one third of patients with local/peritoneal relapse were negative ($p<0.01$).
Conclusion: DCC protein expression seems to be a significant prognostic factor and a predictor of relapse site in high risk resected gastric carcinomas.

P-046

Retrospective study concerning early gastric cancer

Milutin D.1, Coros MF2, Mocan S.1, Jung J.1
1. Dept. of Pathology, University of Medicine and Pharmacy Tg-Mures; 2. First Surgical Clinique, Tg-Mures, Romania

Aims: Early gastric cancer is a pathological entity, which represents a primary neoplastic growth confined to the mucosa or submucosa of the stomach with or without local lymphnode metastases. For this diagnostic it is necessarily to correlate the microscopic appearance with the endoscopic and radiological findings. The value of recognizing an early gastric cancer lies in the excellent results of the surgical treatment, with a cure rate of 95%.
Methods: We studied the incidence of early gastric cancer in the Department of Pathology of Clinical County Hospital Tg-Mures between 1997 and 2000. The operational fragments were processed through paraffin technique and stained with HE.
Results: The early gastric cancer was macro- and microscopically diagnosed. We found 310 cases operated for gastric cancer, from witch 6 (1,93%) were diagnosed with early cancer. Five (83,33%) of the six patients were men and 1 (16,67%) was women. Four patients were aged between 38 and 48 years old, and 2 between 65 and 77. The gross appearance of the lesions was superficial-depressed (in 5 cases) and nodular (in 1 case). The histopathological appearance was signet-ring type carcinoma (3 cases), papillary adenocarcinoma (2 cases) and mixed type carcinoma (adenocarcinoma with signet-ring type carcinoma). Just in 5 cases endoscopic examinations were performed, and in all cases the diagnostic were similar.
Conclusions: The incidence of the early gastric carcinoma is very low, because most of the lesions are discovered in advance stage. However, this percentage is rising, since endoscopy is being performed more frequently and endoscopists are becoming more skilled at the recognition of these early mucosal lesions.

P-047

GASTRIC TUMORS IN CARNEY'S TRIAD ARE AUTONOMIC NERVE TUMORS

Kyung-Whan Min, M.D., J. Aidan Carney, M.D., Ph.D., In Sook Seo, M.D., Patrice Abell-Aleff
Department of Pathology, Deaconess Hospital, Oklahoma City; Mayo Clinic, Rochester; Wishard Memorial Hospital-IU Medical Center, Indianapolis, USA

INTRODUCTION: Carney's triad of gastric leiomyosarcoma (GT), functioning extra-adrenal paraganglioma and pulmonary chondroma is a multitumor syndrome. We are aware of a total of 83 affected patients since its original report by Carney et al (N ENG J Med 296:1517–1518, 1977). The histogenesis of GT in this syndrome is controversial and remains unknown.
MATERIALS AND METHODS: To investigate this, we have analyzed electron microscopic characteristics of GT from seven patients and immunohistochemical phenotypic expressions of tumor cells in four cases with the disorder in light of current understanding of non-epithelial tumors of the stomach. All patients were female and their ages ranged from 9 to 28 years.
RESULTS: With hematoxylin and eosin staining, an organoid pattern was prominent in four tumors and was indistinct in the three others. Immunohistochemically, tumor cells exhibited positivity for neuron specific enolase in 4/4 and weak positivity for synaptophysin and cytokeratin in 2/4. Stains for S-100 protein and smooth muscle actin were negative. CD117 staining revealed diffuse cytoplasmic stain in 4/4. Ultrastructurally, the tumor cells were polygonal and epithelioid or elongated spindly cells. The epithelioid tumor cells usually formed closely apposed cell clusters without intervention of stromal elements. The cell membranes were closely apposed together with occasional desmosomal junctions. The cytoplasm contained a prominent number of mitochondria, profiles of rough surfaced endoplasmic reticulum and scattered lipolysosomes. Peculiar filopodal projections of neighboring cells merged together to form a zebra skin-like pattern. Incomplete basal lamina was present in two. In spindly areas, tumor cells were embedded in the stroma in a longitudinal fashion and cytoplasmic borders were sim-

ple with no external lamina. Aggregates of skenoid fibers were frequently seen in one. Extra-long spaced crystallized collagen was present in another. Dense core granules (120–150 nm) were present in three. Larger granules (300–500 nm) were present in all. Axonic processes containing longitudinal microtubules were found in one.
CONCLUSION: Our findings indicate that GT in Carney's triad exhibit ganglion cell features and their ultrastructural and immunohistochemical characteristics are quite similar to those of gastrointestinal autonomic nerve tumors. This syndrome appears to belong to a spectrum of neurocristopathy.

P-048

The histopathological chaenges of corn oil (C.O.) on the Liberkuhn glands of rabbit

B. Minaii, M.H. Noori
Department of Histology, Faculty of Medicine,
Tehran University of Medical Sciences (TUMS), Tehran, Iran

Recent investigations have shown that not only oils stimulate the cancer promotion but also interact with some drugs. This study was to identify the effects of regimens containing 10% (C.O) on the Liberkuhn glands of rabbit colon that may have an interaction with drugs. Twenty-four rabbits were divided in to 4 groups. The 1st group for 1, the 2nd for 2 and the 3rd for 3 months took test regimen. The 4th group was considered as match controls and took normal diet. Then colon samples were examined, using PAS and H&E methods and compared the cases with their controls (group 4). We found that Liberkuhn glands, in 1 and 2-month regimen groups, were shorter than controls. However, in 3-month regimen group, the glands have the same size as those of control. We concluded that consumption of (C.O) might induce some changes on the Liberkuhn glands, which will be ceased by some adaptation mechanisms in long term diet. Also recognition of histopathogenesis may help us to understand the role of drugs and nutrients interactions in the management of eating disorders. Therefore, more notification about nutrients and drugs interaction is very important.

P-049

Expression of COUP-TFI and II in colon carcinogenesis

Moré, C. Hauser-Kronberger*, Ch. Datz, H. Doppelmayr,
F. Sandhofer, B. Paulweber
1st Department of Medicine, St. Johann Spital, Salzburg, Austria;
Institute of Pathology, St. Johann Spital, Salzburg, Austria*

Chicken Ovalbumin Upstream Promoter Transcription Factors (COUP-TF) I and II are members of the nuclear receptor superfamily. Since no ligand for these receptors has been identified so far, they are considered as "orphan receptors". COUP-TF expression is high in developing tissues and organs and is repressed in terminally differentiated cells. This led us to suggest, that these proteins may also be upregulated in malignancies, when cells become dedifferentiated. To test this hypothesis we studied COUP-TF expression in human malignancies.
Colorectal carcinomas, which arise from benign adenomas, provide an excellent system to study the sequence of genetic alterations, which are responsible for cancerogenesis. Our data show that in normal colon mucosa, expression of COUP-TF mRNA and protein is very low, while in hyperplastic polyps, tubular and villous adenomas and carcinomas, expression is dramatically increased. The highest expression of COUP-TF is seen in hyperplastic polyps. Colon cancer cells with mutant APC contain high levels of free ß-catenin, which accumulates in the nucleus and causes changes in gene transcription. In cell culture experiments we will analyse the effect of restoration of the APC gene on COUP-TF expression in HT-29 cells, a colon carcinoma cell line, which harbours a mutant form of this gene. We will present results of this experiment.
In gastric carcinomas, overexpression of EGF and EGFR was found to correlate with the extent of tumour invasion with tumour stage and prognosis. Based on recently published observations, svp, the homolog of COUP-TF in Drosophila is induced by stimulation of the EGFR signal transduction cascade, we investigated whether EGFR expression is correlated with COUP-TF expression in colon malignancies. Expression of EGFR correlates with high COUP-TF expression in tubular and villous adenomas and carcinomas, but not in hyperplastic polyps.
COUP-TF is considered as a potent repressor of multiple genes. We observed that expression of $p21^{WAF1/CIP1}$, a potential target of COUP-TF is high in normal colon mucosa, but low in colon tumours.
These results represent that expression of COUP-TF is induced in the process of tumorigenesis but reasons for this induction remains to be elucidated.

P-050

Microsatellite instability in colorectal carcinomas : a prospective immunohistochemical study

Najat Mourra, Denis Chatelain, Valérie Rigau, Rolland Parc,
Jean-François Flejou
Service d'Anatomie Pathologique et de Chirurgie Digestive.
Hôpital St-Antoine, AP-HP, Paris-France

Introduction: Colorectal carcinomas (CRC) can be classified according to their microsatellite instability (MSI) phenotype. MSI cancers represent a subgroup of tumours with a better prognosis. Immunohistochemistry for the mismatch repair proteins (MMR) hMLH1 and hMSH2 has been proposed as an indirect method to assess the MSI phenotype, mostly in retrospective studies. The aim of this study was to estimate in a prospective series of CRC the prevalence and pathological association of MSI phenotype assessed by immunohistochemistry.
Methods: 133 consecutive cases of CRC were analyzed for the expression of MMR proteins with antibodies directed against hMLH1 (clone G168-728, PharMingen) and hMSH2 (FE11, Calbiochem). Tumours were localized in the right colon (32), left colon (43), and rectum (58).
Results: Loss of expression of one MMR protein was present in 10 cases (7%) (loss of hMLH1: 2 cases; hMSH2: 8 cases). Those 10 tumours were localized in the right colon (n=7/32=22% of cases), left colon (n=2/43=5% of cases) and rectum (n=1/58=1,7% of cases).
Tumours with loss of expression did not differ from those without regarding the age of the patients, the frequency of lymph node metastasis, the percentage of mucinous tumours. Among 20 tumors occuring in patients aged under 50 years, only one showed loss of expression of hMSH2.
Conclusion: The frequency of loss of expression of MMR proteins is lower in our prospective series (7%) as reported previously in re-

trospective studies. Although these results may be due partially to the large number of rectal cancers in our series, they suggest that MSI may be rarer in daily practice as previously reported, specially in young patients. However, we confirm that most MSI+ cancers are localized in the right colon.

P-051

Some characteristics of synchronous advanced colorectal adenomas

Nagorni A., Katic V., Zivkovic V., Stamenkovic I
Clinic for Gastroenterology and Hepatology; Clinic for Pathology, Clinical Center Nis, Nis, Yugoslavia

The term advanced colorectal adenoma (ACA) is introduced to describe colorectal polyps greater than 1 cm in diameter and/or villous component and/or severe dysplasia, features predicting an increased likelihood of malignant transformation. The aim of our study was to analyze characteristics of ACA in patients with synchronous ACA. There were 34 patients with 72 synchronous ACA. Complete colonoscopy with endoscopic polypectomy was done in all patients. HE and histochemic staining were done, too. Single criteria for ACA was found in 44 (61.11%) patients, two criteria in 22 (30.55%), but three criteria in 6 (8.34%). Among synchronous ACA with one criteria prevailed diameter (in 30 of 44 cases), while in ACA with two criteria in 18 of 22 cases prevailed severe dysplasia and diameter as the including criteria. There were 12 tubular (16.67%), 48 (66.66%) tubulo-villous, and 12 (16.67%) villous ACA. ACA were localized in all large bowel segments, but mainly in rectum and sigmoid. Conclusion: ACA are frequent finding during colonoscopy. ACA is link in a chain from benign adenoma to malignant alterated adenoma. Complete colonoscopy to cecum has to perform in all patients with distal ACA.

P-052

Histopathological and immunohistochemical factors in rectal cancer after preoperative radiochemotherapy

A. Nasierowska-Guttmejer
Cancer Centre, Warsaw, Poland

Aim: 1. To detremine the microscopic pattern of rectal cancer response to preoperative radiochemotherapy and 2. to evaluate the relationship between the tumor response and immunohistochemical factors as p53, MIB1, bcl-2, Bax.
Material and methods. The operative material of 37 pts after preoperative radiotherapy (2500 cGy in 5 fractions for 5 days) (I group) and 54 pts after radiochemotherapy (5000 cGy in 25 fractions for 33 days and 3 courses of chemotherapy 5Fu and Leucovorin) (II group) was evaluated. The following antibodies were used for immunohistochemistry: p53 (DO-7, Dako), Ki-67 (MIB1, Immunotech), Bax (Dako) and bcl-2 (Oncoprotein). All slides were scored to 1000 cells; none (–), weak (+,<30%), moderate (++, 31–70%), intense (+++, >71%). The tumor response was evaluated according to qualitative method based on following microscopic features:degree of degeneration of cancer cells, acellular mucin pools and necrotic mass. The semiquantitative method was used for analysis of regression of tumor mass: CR-100%, PR1>=90%, PR2<90–10%, SD>=10%.
Results: 1. The relationship between tumor response and microscopic features. CR was found in 8 cases of II group pts, PR1 in 1 case of I group and 24 cases of II group of pts, PR2 in 35 cases of I group and 22 cases of II group pts and SD in 1 case of I group pts. The accelular mucin polls were found in all CR cases. The high degree of degeneration of cancer cells (24/25) correlated with accelular mucin pools (17/25) and lack of necrosis (20/25) in PR1 cases. The low degree of degeneration of cancer cells (50/57), lack of mucin polls (35/57) and necrosis >50% of tumor mass (24/57) were observed in PR2 cases. 2. PR2 tumor response correlated with low expression of MIB1, Bax, p53 and Bcl-2 (p<0,00001).
Conclusions. 1. CR or PR1 tumor response correlated with high degree of degeneration of cancer cells, accelular mucin pools and lack of necrosis. 2. Low expression of proliferation and apoptosis markers were found in PR2 cases after preoperative radiochemotherapy.

P-053

Relation between genetic polymorphism of cytochrome P450 2E1; drinking habits; histological subtypes and p53 gene point mutations in Japanese patients with gastric cancer

Yoshio Oda, Isao Nakanishi
First Department of Pathology, School of Medicine, Kanazawa University, Kanazawa, Japan

Introduction: Genetic polymorphism of drug-metabolizing enzymes affect the susceptibility to cancer. In order to understand the molecular mechanism of individual susceptibility to gastric cancer, we studied the relation between genetic polymorphism of ethanol-inducible cytochrome P450 2E1 (CYP2E1), drinking habits, histological subtypes and p53 gene point mutations in Japanese patients with gastric cancer.
Methods: We examined genotypes of CYP2E1 by restriction fragment length polymorphisms following PCR in146 Japanese patients with gastric cancer (67 intestinal-type and 79 diffuse-type carcinomas) and 177 age-matched Japanese controls, and determined the point mutations of p53 gene in gastric cancer tissues by direct sequencing.
Results: The frequency of CYP2E1 c1/c1 genotype was significantly higher in patients with intestinal-type gastric cancer (52/67, 77.6%) than in control subjects (112/177, 63.3%) (p<0.05; OR, 2.01). In particular, habitual drinkers with CYP2E1 c1/c1 genotype had a risk for intestinal-type gastric cancer and the controls. Among intestinal-type cancer compared with non-drinkers with CYP2E1 c2 allele (p<0.05; OR, 3.79). These differences were not observed between patients with diffuse-type gastric cancer and the controls. Among intestinal-type cancer patients with CYP2E1 c1/c1 genotype, p53 point mutations were significantly more frequent in the group of habitual drinkers (13/25, 52.0) than in the combined group of occasional drinkers and non-drinkers (6/27, 22.2%) (p<0.05; OR, 3.79).
Conclusion: These findings suggest that individuals with both CYP2E1 c1/c1 genotype and habitual drinking have an increased risk of intestinal-type gastric cancer with a high frequency of p53 gene point mutations.

P-054

An unusual presentation of Helicobacter pylori infection: "Russell body gastritis"

Okçu Heper A[1], Serinsöz E[1], Ensari A[1], Kuzu I[1], Idilman R[2]
University of Ankara Medical School, Departments of Pathology[1] and Gastroenterology[2], Ankara, Turkey

Helicobacter pylori (H. pylori) is a major aetiological agent in a variety of gastroduodenal disease including chronic gastritis, peptic ulceration, gastric cancer and lymphoma. Varying degrees of mucosal inflammation and atrophy could be present in gastric biopsies infected with this microorganism. Here, a very unusual presentation of H. pylori gastritis is reported.
A 70 year-old male patient suffering from dyspepsia and nausea was seen in the outpatient clinics of Department of Gastroenterology. His physical examination was normal except for slight tenderness in the epigastric area. An upper gastrointestinal endoscopy was performed which revealed a pangastritis and multiple biopsies were taken. Gastric biopsy specimens demonstrated a diffuse infiltration of the lamina propria by plasma cells with extensive Russell body formation. These cells reacted strongly with MGP stain and also were positive with CD45, CD79a, Plasma cell antigen, lambda and kappa light chains. H. pylori infection was identified on the surface of the foveolar cells in slides stained with Giemsa.
In reviewing the literature there seems to be only one case of H. pylori gastritis with localized accumulation of Russell body containing plasma cells. Chronic bacterial stimulation by H. pylori might lead to the hyperactivation of plasma cells and the consequent hyperproduction of immunoglobulins. Our case seems to be the first demonstration of extensive Russell body containing plasma cell infiltration in H. pylori gastritis, hence deserving the name "Russell body gastritis."

P-055

Normogastrinemic mucinous carcinoid tumour of the stomach: Report of a case

Oz Puyan, F.*, Ozyılmaz, F.*, Kutlu, K.*, Tezel, A.**, Hoscoskun, Z.***
Dept. of Pathology*, Dept. of Gastroenterology**, Dept. of General Surgery***, Medical School, University of Trakya, Edirne, Turkey

INTRODUCTION: Carcinoid tumours of the stomach are rare and account for 4–5% of all gastrointestinal tract carcinoids. They usually appear as multiple polypoid lessions in the nonantral mucosa of the stomach and arise from enterochromaffin-like (ECL) cells, which have been shown to proliferate in patients with pernicious anaemia, chronic atrophic gastritis accompanied by achlorhydria and hypergastrinemia.Mucinous carcinoid (goblet cell carcinoid) which is mainly described in the appendix is a variant of mixed endocrine-exocrine tumours. They are described as mixed adenocarcinoid tumour in the stomach.We report a case of gastric carcinoid tumour with prominent mucin production and normal serum gastrin level.
CASE REPORT: A 51-year-old female presented with pernicious anaemia and intermittent rectal bleeding. Gastroscopic evaluation demonstrated two polypoid lesions (0,5-1cm in diameter) in the fundus-corpus passage on the anterior and posterior walls. The histological diagnosis of the biopsy from the anterior wall lesion was mucinous adenocarcinoma. Because of the inappropriateness between endoscopic appearance and histological diagnosis a second biopsy was taken from the other lesion. It revealed typical carcinoid tumour features with prominent mucin production. Serum gastrin level was normal.Total radical gastrectomi was performed. Histologically, we determined multifocal mucinous carcinoid tumour with submucosal invasion. There was no lymph node metastasis. In the surrounding mucosa, there were ECL hyperplasia-dysplasia, chronic atrophic gastritis, epithelial dysplasia and widespread intestinal metaplasia.
CONCLUSION: Because of its rarity in the stomach and the confusing terminology we report a case of a tumour which had pure mucinous carcinoid features without an area of adenocarcinoma. One must kept in mind that mucin production in a carcinoid could provide a misdiagnosis of mucinous adenocarcinoma.

P-056

Evaluation of gastric biopsies for dysplasia

K. Patsiaoura, F. Patakiouta, V. Tzarou, A. Asimaki, I. Venizelos, E. Vrettou, H. Kalekou, G. Karayiannopoulou, A. Kriaka, E. Nenopoulou, V. Tzioufa, T. Toliou, D. Koufogiannis
GI Pathology Group of Thessaloniki, Greece

Epithelial dysplasia is an unequivocal neoplastic transformation, which can be recognized on routing histologic examination. Because of the therapeutical consequences it is extremely important to use strict criteria for the diagnosis of dysplasia in the gastrointestinal tract. Dysplasia should be clearly separated from regenerative atypia. In practice there is often considerable disagreement for the diagnosis of dysplasia among pathologists.
The purpose of this study was to assess the interobserver agreement of twelve pathologists on the histologic diagnosis of regenerative atypia and dysplasia, to reach a consensus diagnosis and compare it with the previously issued histological report. Thus, 85 gastric biopsies were retrieved from the files of 6 hospitals of Thessaloniki and reevaluated (WHO classification). Consensus diagnosis on each biopsy was accepted as the opinion of the majority.
Results: 1) Interobserver agreement for the diagnosis of regenerative atypia and severe dysplasia was excellent, 93% and 100% respectively.
2) Interobserver agreement for the diagnosis of mild, moderate dysplasia and "indefinite" for dysplasia was 63%, 62% and 28% respectively.
3) The pairewise agreement between the consensus diagnosis and the original report was very low (k=0,01).
4) The original diagnosis of mild and moderate dysplasia was very often revised either to regenerative atypia or to lower grade upon reevaluation.
5) "Indefinite" for dysplasia was used as a consensus diagnosis more often than in the original report.
6) With careful observation the term moderate dysplasia can be eliminated in favor of a two grade system (mild and severe dysplasia) if also the terms "indefinite for dysplasia" and "regenerative atypia" are widely adopted, as has been previously proposed.

P-057

About some pecularities of oxidative and antioxidative system of E.coli strains from human intestinal microflora

Pepoyan A.Z.
Institute of Molecular Biology of NASRA, Yerevan, Armenia

It is known that the human pre-cancer state is related to the development of intestine disbacteriosis characterized by qualitative and quantitative changes in the intestine microflora. It was investigated the lipid peroxidation processes (LPP) of E.coli G35 strains from human intestinal microflora (Pepoyan A.Z., 1991). It was shown that the E.coli G35 strains from intestinal microflora of healthy persons and patients with some diseases are different by their growth and reproduction processes. It was established the same level of both ascorbat and NADP.H depending systems of peroxidation for investigated cells of E. coli. The presence of LPP and peroxidase activity in bacterial cell extracts and suspensions as well as in cells growth liquid mediums (after incubational period) was found. By the way it was shown if the level of LPP does not change in cell extracts of all studied E. coli strains, it is differed in cell suspensions and cultural liquids.In contrast, the peroxidase activity of studed E.coli strains were different in bacterial cell suspensions and cell extracts, when in cell growth liquid mediums there were similar. The comparative high level of peroxidase activity in bacterial exracts with the same level of LPP in E.coli strains dominanting in normal intestinal microflora apparently support the normal metabolic processes of this cells. When the changes of LPP and peroxidase activity in both cell suspensions and cultural liquids can be impotant for human metabilic processes.

P-058

p73 gene mutations in gastric and esophageal adenocarcinomas.

Emanuela Pilozzi*, Andrew Platt°, Caterina Talerico*,
Carrie Fidler°, James S Wainscoat, Luigi Ruco*
* Dpt of Experimental Medicine and Pathology, University "La Sapienza", Rome, Italy; ° University Dpt of Cellular Science, J Radcliffe Hospital, Oxford, United Kingdom

Introduction: The gene p73 maps on chromosome 1p. It encodes for a protein that shares considerably homology with the DNA binding, transactivation and oligomerizations domains of the tumour suppressor gene p53. Moreover when overexpressed p73 is able to induce apoptosis and activation of p53 responsive genes such as p21 WAF. Despite the similarity with p53 the inactivation mechanism seems somehow different for p53. Biallelic overexpression has been observed in lung, prostate and kidney cancer, whilst mutation have been found rare in human cancer. We performed the mutational analysis of p73 in 10 cases of gastric and esophageal adenocarcinoma to better understand to better understand its role in the pathogenesis of adenocarcinoma of the upper alimentary tract.
Methods: Nine cases adenocarcinomas of the stomach and one adenocarcinoma of esophagus were collected. PCR-SSCP of the 13 exons was performed on DNA extracted form the tumour and the matched normal mucosa. The exons that gave aberrant band of migration were cloned and sequenced.
Results: We identified a polymorphism and a mutation (A▶G) in exon five of esophageal adenocarcinoma case.
Conclusions: Our results suggest that p73 is not involved in gastric adenocarcinoma but it may have a role in the pathogenesis of esophageal adenocarcinoma. We are looking at more cases of esophageal adenocarcinoma to confirm it.

P-059

Classification of low-grade neuroendocrine tumors of gut and unknown origin

Pascal Quaedvlieg, Babs Taal, Henk Boot and Marie-Louise van Velthuysen*
Departments of Medical oncology, and *Pathology of the Netherlands Cancer Institute, Amsterdam, The Netherlands

Background and aims: Malignant neuroendocrine tumors are classified in two grades (low- or high-grade) according to the revised classification proposed by Capella et al. In contrast neuroendocrine lung tumors are classified in three grades. Many patients with neuroendocrine tumors present with metastasized disease. Often the primary site of the tumor remains unknown. This study was performed to investigate if the two classification methods, or other factors could predict survival in case of a malignant neuroendocrine tumor.
Methods: All patients with liver metastases from neuroendocrine tumors of midgut, or of unknown primary site, diagnosed between 1983 and 1999, were included (n=55). They were compared with patients with metastasized neuroendocrine tumors of the lung (n=10). Immunohistochemical staining for neuroendocrine markers, Ki-67, p53 and Bcl-2 was performed additionally. Clinical, histologic and immunohistochemical parameters were evaluated and correlated with survival.
Results: Both patient groups were comparable with regard to age, gender, follow-up time and the number of events (deaths). Both methods of classification revealed equal numbers of patients classified in each category. However lung tumors showed more often staining with Bcl-2 and p53. High-grade tumors in both groups had a significantly worse prognosis than low-grade tumors. Within the group of patients with low-grade neuroendocrine tumors of the gut or of unknown origin parameters predicting survival were not found. P53 nor Bcl-2 immunoreactivity, mitotic activity, nor the presence of elevated urinary 5-HIAA or the clinical carcinoid syndrome were useful in predicting survival.
Conclusions: Classification of malignant neuroendocrine tumors of the gut and of unknown primary site as high- or low-grade, according to the Capella classification is useful in predicting survival. Adding an intermediate category to this calssification, as used for neuroendocrine tumors of the lung seems to have no additive value in this group of tumors.

P-060

Prevalence of helicobacter pylori in chronic gastritis and in gastric carcinoma

D. Radulescu, G. Dobrescu, I. D. Caruntu, C. Amalinei,
A. Badescu, T. Axinia
Department of Pathology, University of Medicine and Pharmacy, Iasi, Romania

The **aim** of this study was to evaluate the prevalence and distribution of H. pylori in chronic gastritis and in gastric carcinoma.

Materials and methods: Gastric biopsies were obtained from 133 patients with dyspepsia. Four tissue specimens were taken for each case from antrum, corpus and eso-cardial regions. Specimens were examined for urease test. Infection was confirmed by finding H. pylori on Giemsa-stainings.
Results: We diagnosed 85 cases of chronic gastritis. They were classified according to the updated Sydney system. 61.17% presented atrophic changes. 71.76% gastritis were positive for H. pylori infection. 48 cases were diagnosed with gastric carcinomas. Intestinal metaplasia was observed in 68.75% of cases. 31.25% of carcinomas were positive for H. pylori infection.
Conclusions: The association between atrophic gastritis and H. pylori infection was highly significant. The high incidence of intestinal metaplasia in gastric carcinoma suggests that the ability to generate intestinal metaplasia in atrophic mucosa represents a preneoplastic change.

P-061

Microsatellite instability in colorectal cancer: Comparison of immunohistochemistry and molecular biology in a series of 212 cases

Valérie Rigau (1, 2), Nicole Sebbagh (1), Sylviane Olschwang (2), François Paraf (3), Yann Parc (4), Jean-François Flejou (1, 2)
Anatomie Pathologique (1), Chirurgie (4), Hôpital Saint-Antoine; Ceph Et Inserm U434 (2), Paris; Anatomie Pathologique, Hôpital Dupuytren (3), Limoges, France

Microsatellite instability (MSI) due to defective mismatch repair genes has been reported in the majority of tumours from patients with hereditary non polyposis colorectal cancer syndrome (HNPCC) and in 15% of sporadic colorectal cancer. The identification of MSI+ cancers requires molecular testing. Immunohistochemistry of mismatch repair (MMR) proteins has been proposed as a new screening tool for MMR deficient tumours.
Methods: In this retrospective study, 212 formalin-fixed, paraffin-embedded colorectal carcinomas were examined for protein expression (hMLH1, hMSH2, hMSH6, hPMS2), and analysed for MSI+ (at least 2 of 4 markers affected). These results were correlated with morphological parameters.
Results: Immunohistochemical analysis revealed that loss of expression of at least one protein was present in 19,3% of cases, with 66% of those cases loosing 2 proteins (only 2 combinations: hMLH1/hPMS2, hMSH2/hMSH6). 86,2% of MSI+ tumours had associated loss of expression of hMLH1, hMSH2, hMSH6, or hPMS2. In 6 cases, isolated loss of hMSH6 (n=2) or hPMS2 (n=4) expression was present. The immunohistochemical results were correlated with anatomical site (right colon) for the 4 MMR proteins, and with tumour type (mucinous carcinoma, undifferentiated carcinoma), expansive growth pattern and Astler Coller's stage for hMLH1 and hPMS2.
Conclusion: These findings confirm that immunohistochemistry looking for the loss of expression of MMR proteins is a simple method for screening tumours for MSI and mutation in the MMR genes. They suggest that the study of hMSH6 and hPMS2 expression may be useful, in complement to hMLH1 and hMSH2.

P-062

Hyperplastic polyps, colonic adenomas and serrated adenomas

B.H. Ruebner, R. Saroufeem, B.H. Min, H. Tesluk and M. Lawson
University of California Davis Medical Center & Kaiser Health Systems, Sacramento, CA USA

Background: The great majority of colonic polyps are easily classified as adenomas (AP) or hyperplastic polyps (HP). If identified at colonoscopy, follow-up of these lesions is relatively standardized. Polyps combining features of these lesions are difficult to classify. Terms for such lesions include mixed AP/HP and serrated adenomas (SA). We have reviewed polyps of this type seen in our department during the past three years and have attempted to identify immunohistologic criteria which might assist in defining these lesions more definitively.
Results: The proliferation antigen Ki 67 in AP, instead of being localized at the base of the crypts, was seen at all levels, particularly in the upper part of the crypts. HP showed increased intensity of the normal basal staining. SA maintained the basic pattern of hyperplastic polyps but with extension into the upper half of the crypts. Cytokeratin 20 is a marker of mature intestinal epithelium. It clearly distinguishes HP and AP which show staining of the upper and lower parts of the crypts respectively. SA show a pattern resembling more closely that of HP than AP. The tumor suppressor antigen P53 stained about half the foci of high grade dysplasia in all types of polyps. Small groups of positive cells were seen at the luminal surface in some AP and at the base of the crypts in some HP and SA without high grade dysplasia.
Conclusion: Ki 67 and cytokeratin 20 are useful in the definition of SA and its differentiated from HP and AP. P53 is correlated with dysplasia. P21, P27, Bcl 2 and ß catenin, so far, do not appear to be useful in this distinction.

P-063

Adjacent mucosal changes in EBV associated gastric adenocarcinoma

Milena Saqui-Salces, Armando Gamboa-Domínguez
Department of Pathology, Instituto Nacional de Ciencias Médicas y Nutrición Salvador Zubirán, Mexico City, Mexico

Background: Few data exists of the mucosal changes adjacent to EBV associated gastric adenocarcinoma. **Aim**: describe the morphological, immunohistochemical and EBV expression in remnant stomach mucosa of EBV associated gastric adenocarcinoma.
Methods: in situ hibridization for EBV-encoded small non-polyadenylated RNA (EBER) was made in 40 gastric adenocarcinomas (Discovery, Ventana. Tuczon AZ). In positive cases, sections were obtained from the adjacent mucosa to identify preneoplastic changes, presence of EBER, LMP-1 and type of inflammatory infiltrate. Clinical and demographic data were obtained from the charts.
Results: Four adenocarcinomas were highly associated to EBV (10%) in three female and a male with a median age of 54 years. All but one case had conventional poorly differentiated adenocarcinoma in stages II and III. Hyperplasia of the foveolar epithelium, incomplete intestinal metaplasia and epithelial dysplasia were observed in all cases in antrum and body (mean of 10 different mucosal sites). A few cells in metaplastic lesions were EBER positive in a case while all dysplastic lesions had a strong signal in nucleus of glandular and superficial epithelium. LMP-1 expression was ob-

served in a case. The dense inflammatory infiltrate was mainly composed of T-CD8 positive lymphocytes and NK cells. Bacteria consistent with H. pylori were observed in three cases.
Conclusions: Remnant mucosa in EBV associated gastric adenocarcinoma shows all the preneoplastic lesions observed in non-EBV associated carcinomas. No significant association was observed for EBER expression in early preneoplastic lesions.

P-064

C-myc gene amplification in different stages of esophageal squamous cell carcinoma: Prognostic value in relation to treatment modality

M. Sarbia[1], J. Szumilo[3], A. Dabrowski[3], J. Arjumand[1], M.Stahl[2], M. Rees[1], H.E. Gabbert[1]
Institute of Pathology, University Düsseldorf[1]; Internal Medicine, University Essen[2], Germany; Department of Pathomorphology, University Lublin[3], Poland

Introduction: The proto-oncogene *c-myc* is known to be involved in the regulation of proliferation, apoptosis and cell differentiation. *C-myc* activation in tumor cells may therefore influence survival of cancer patients, especially those treated by radio- and/or chemotherapy.
Methods: DNA was extracted from resection specimen of 77 superficial esophageal squamous cell carcinoma (ESCC) (pT1-2, pN0-1, cM0) as well as from pretherapeutic biopsies of 57 locally advanced ESCC (cT2-4 cN0-1 cM0). Superficial ESCC had been treated by surgery alone whereas locally advanced ESCC received a treatment that consisted of either polychemotherapy and surgery (n=14) or of radiochemotherapy and facultatively surgery (n=43). Amplification of *c-myc* in tumor samples was determined by means of differential PCR and the findings were correlated to overall survival and to response to polychemo-therapy.
Results: *C-myc* gene amplification was present in 8 of 77 (10.4%) superficial ESCC and in 16 of 57 (28.1%) locally advanced ESCC. Among surgically treated tumors, the presence of *c-myc* amplification was correlated with high proliferative activity (p=0.0399) but not with overall survival. Among multimodally treated ESCC, *c-myc* amplification was neither correlated with response to chemotherapy nor with overall survival.
Conclusion: Amplification of *c-myc* is found more frequently in advanced stages of ESCC than in early stages. This indicates that it is a late event in the molecular carcinogenesis of this tumor type. *C-myc* gene amplification does not influence the outcome of ESCC patients treated either by surgery alone or by combined treatment modalities.

P-065

Expression of the p53 homologues p63 and p73 in multiple simultaneous gastric cancer

Susanne Schmelzer[1], A. Tannapfel1, M. Klimpfinger[2], Ch. Wittekind[1]
[1] Institute of Pathology University of Leipzig;
[2] Inst. of Pathology, Kaiser Franz-Josef-Spital Wien

Aims: The tumour-suppressor protein p53 has recently been shown to belong to a family that includes two structurally related proteins, p63 and p73. This study investigated the status of p53 and its both homologues, p73 and p63, in multiple simultaneous gastric carcinomas.
Methods: Expression and mutation of p53, p73 and p63 (including the two major isotypes TAp63 and ?Np63) were examined by direct DNA-sequencing, in-situ hybridisation, and by immunohistochemistry in 68 gastric carcinomas from 32 patients. The results obtained were correlated with pathohistological stage (according to UICC [1997]), and several other histopathological factors and finally with the patient survival.
Results: p53 mutations were detected in 23/68 carcinomas (34%) of 18 patients with a disconcordant mutation pattern. Independent of p53 mutation status, p73 transcripts and protein expression was found in 33/68 carcinomas of 24 patients. p63 positivity were found in 21 patients. The number of cells containing p63 and their distri-bution depends on the degree of tumour differentiation. High grade carcinomas of the diffuse type exhibited a significant higher p63 ex-pression. In intestinal metaplasia and atrophic gastritis, an increase of TAp63 and ?Np63 staining was also observed. We failed to identify specific mutations of p73 or p63 causing amino acid sub-stitutions. Neither p53 nor p73 or p63 were related to the prognosis of the patients.
Conclusions: p73 as well as p63 have not been found to be mu-tated in gastric carcinomas, but both proteins were found to be expressed only in a subset of tumours. The status of the p53 homo-logues p63 and p73 were disconcordant in all patients with multiple simultaneous gastric carcinomas. Our data with an increased expression of p63 (TAp63 and ?Np63) in less differentiated gastric carcinomas may indicate that p63 can act to promote neoplastic growth in the gastric epithelium.

P-066

Histoloigical and mucin immunohistochemical aspects of gastric glandular carcinoma(differentiated or intestinal type)

Tadakzu Shimoda
Pathology of Clinical Laboratory Division, National Cancer Center Hospital, Tokyo, Japan

Recently, immunohistochemical examinations have demonstrated that gastric carcinomas are composed of three phenotypes; gastric (MUC5 and/or MUC6 positive), intestinal (MUC2 and/or CD10 positive)and gastric-intestinal phenotype. We have examined the relation between histological type and mucin phenotype of 351 early gastric cancer. Histological type can be divided into three types; pure differentiated (D-ca) is 150 (42.7%), pure undifferenitated (UD-ca) 93 (26.5%) and mixed with both types(D/UD-ca)108(30.8%). The tumor less than 10mm is 64 lesions and are consisted of 76.5% of D-ca and UD or D/UD type is very low incidence. The tumor more than 10 mm (287 lesions) are consisted 35.2% of D-ca, 29.6% of UD-ca and 35.2% of D/UD-ca. Regardless of tumor size, the mucin phenotype expression of those cancer demonstrated that 60% is gastric-intestinal phenotype (GIM), each 20% gastric and intestinal type. The thirty five out of 47 (74.5%) cancer less than 10 mm with GI mucin phenotye or gastric mucin phenotype consisted of D-ca, and UD-ca, while 64of 224 (28.6%) with GI or G-mucin phenotype measuring more than 10mm consisted of D-ca, and 160 (71.4%) D/UD and UD-ca. The differences between these two groups were statistically significant (p<0.001).

Twelve of 15 (80%) cancers with intestinal mucin phenotype measuring less than 10mm consisted of D-ca and 35 of 50 (70%) cancers with Intestinal mucin phenotype more than 10mm are D-ca. The differences between these two groups were not significant. These data suggest that small D-ca with gastric mucin expression may play to transformation into UD-ca during the progression of early gastric cancer, and histological type of gastric cancer should be classified morphologically D, UD and mixed (D/UD),because Intestinal type by Lauren's classification includes gastric and intestinal mucin phenotype.

P-067

The diagnostic difficulties in the case of primary oesophageal melanoma

Skomra D., Siezieniewska-Skowrońska Z., Chibowski D., Misztal B.A.
Chair and Department of Patomorphology Medical University, Lublin, Poland

A case of primary malignant melanoma with mixed epithelioid and spindle cell pattern in a 59 year old women is reported.
Primary malignant non epithelial tumours of the oesophagus are very rare (less than 1% of all primary oesophageal malignant neoplasms). Majority of them are sarcomas and about a quarter are malignant melanomas.
Endoscopic specimen, obtained as the first to examination, consisted of amelanotic spindle cells and was diagnosed as spindle cell neoplasm probably benign. The second diagnosis from frozen section was malignant spindle cell neoplasm probably leyomiosarcoma. Diagnosis from paraffin sections was malignant melanoma and did not make problems owing to presence typical melanotic cells in other examined sections. We researched the first endoscopic specimen with panel antibodies: cytokeratin, S-100, desmin, smooth muscle actin, HMB 45 and with Masson-Fontana stain. Results: cytokeratin (–), S-100 (+), desmin (–), small muscle actin (+), HMB 45 (+) Masson-Fontana stain (–) would enable making correct precise diagnose from endoscopic specimen.
Amelanotic spindle cell melanoma is difficult to distinguish from other malignant tumours. In reviewed literature the misdiagnosis is not rare. In cases non epithelial tumours additional histochemical and immunohistochemical methods should be performed in endoscopic material.

P-068

Expression of trypsin and tumor-associated trypsin inhibitor (TATI) in gastrointestinal cancer

Solakidi S[1], Tiniakos D[2], Petrakis K[3], Kittas C[1], Sekeris CE[1]
Labs of [1] Biological Chemistry & [2] Histology-Embryology, Medical School, University of Athens; [3] Dept. of Pathology, "Ippokration" General Hospital, Athens, Greece

INTRODUCTION: Trypsin and its specific inhibitor, TATI, are expressed in normal human pancreas and in a variety of tumors. Proteases and their inhibitors are thought to be co-expressed in malignant neoplasms. We studied trypsin and TATI expression in gastrointestinal cancer. To our knowledge this is the first time that tumor expression of trypsin and TATI is co-evaluated.
MATERIAL & METHOD: Trypsin and TATI expression was studied by immunohistochemistry on paraffin-embedded tissue sections from patients with gastric (n=23, mean age 62y, M/F: 1/1.1) and colorectal cancer (n=93, mean age 69y, M/F 1/0.8). RT-PCR was performed on fresh tissues from 8 gastric and 55 colorectal carcinomas. Normal and non-malignant tissues adjacent to the tumors were also studied.
RESULTS: Cytoplasmic expression of trypsin was found in 15(65%) of gastric and 69 (73%) of colorectal carcinomas, while TATI was expressed in the cytoplasm of 9 (39%) gastric and 61 (65%) colorectal carcinomas. Statistical analysis using Spearman's test has shown a significant correlation between trypsin and TATI immunohistochemical expression in colorectal tumors ($p<0.01$). RT-PCR has shown co-expression of trypsin and TATI mRNA in all carcinomas studied. Adjacent, non-malignant tissues were negatively stained, but exhibited both trypsin and TATI mRNA. Normal tissues were negative by immunohistochemistry.
CONCLUSIONS: Our results indicate co-expression of trypsin and TATI in gastrointestinal malignant tumors both at the mRNA and protein level. We conclude that in gastrointestinal neoplasms, high levels of trypsin and TATI may be important for malignant tumor formation and/or metastatic process.

P-069

Gastric atrophy: New ligth by image analysis

Staibano S, Rocco A, Mezza E, De Rosa G, Budillon G, Nardone G.
Department of Biomorphological and Functional Sciences, Faculty of Medicine and Surgery, University Federico II of Naples, Italy

The risk of gastric cancer increases with the degree and extent of mucosal atrophy. Atrophy is generally defined as glandular loss but nothing is said as what replaces the missing glands or the outcome of lesion. Recent image analysis techniques have led to development of automatic quantification of the tissue component of histological sections.
AIM: to develop a sensitive and reliable method to diagnose gastric atrophy by quantifying interstitial fibers, a true marker of fibrosis.
POPULATION AND METHODS: The study was performed on the gastric biopsies of 40 controls, (20 children and 20 adults) and 111 patients with atrophic gastritis. The latter underwent a follow-up biopsy one year later. Each sample was examined by conventional histology and image analysis software based on the histochemical affinity of Sirius Red for collagen fibers and Fast Green for non collagen fibers.
RESULTS: Intra or inter-operator evaluations of collagen fibers in controls and patients were not significantly different. Average fiber content was 10% mm^2 in in controls and 14.17 and 20% mm2 in patients with mild, moderate and severe atrophic gastritis, respectively. However, despite the significant different amongst the studied groups, atrophy degree and collagen fiber content were in good agreement only when inflammatory infiltrate was mild. One year later the atrophy degree varied remarkably (improved in 42% and worsened in 10%) while collagen fiber content was roughly stable.CONCLUSION: The use of image analysis of gastic biopsies appears to be a reliable method to measure collagen fiber content, a true expression of fibrosis. The study sheds new light on the controversial diagnosis of mucosal atrophy.

P-070

Primary Small Cell Carcinoma of the Esophagus: Expression of p53, bcl-2 and Rb Oncoproteins

Kaiyo Takubo, MD, Naoko Honma, MD (1), Ken-Ichi Mafune, MD (2), Yoichi Tanaka, MD (3) And Koji Sasajima, MD (4)
(1) Department of Clinical Pathology, Tokyo Metropolitan Institute of Gerontology; (2) Department of Surgery, Graduate School of Medicine, The Tokyo University, Tokyo; (3) Department of Abdominal Surgery, Saitama Cancer Center, Saitama-ken; (4) First Department of Surgery, Nippon Medical School, Tokyo, Japan

We examined undifferentiated small cell carcinoma of the esophagus from 21 patients and used immunohistochemical methods for detection of chromogranin A and p53, bcl-2, and Rb oncoproteins. Nine (43%) of the 21 carcinomas consisted solely of undifferentiated cells, but heterogeneous components of in situ and/or invasive squamous cell carcinoma or mucoepidermoid carcinoma were observed in the other 12 (57%) tumors. Squamous cell carcinoma in situ was observed in the mucosa adjacent to the main tumor in 7 (50%) of the 14 resected esophageal specimens. An admixture of invasive squamous cell carcinoma and undifferentiated carcinoma was observed in 4 (19%) of the 21 tumors, and mucoepidermoid carcinoma was noted in one case. Chromogranin A staining yielded a positive reaction in two (10%) undifferentiated components but was negative in all heterogeneous components. Multiple sites of p53 positivity were seen in the undifferentiated component of 17 (81%) of the 21 tumors, as well as in the in situ and/or invasive squamous cell carcinoma or mucoepidermoid carcinoma components of 9 (75%) out of 12 tumors. Seven (33%) of the 21 tumors revealed positive bcl-2 reactivity in the small cell component, but all the heterogeneous components were negative, suggesting that the bcl-2 oncogene may have a role in the development of small cell carcinoma. Rb protein reactivity was observed in the small cell component of one (5%) case and in 9 (75%) of the 12 heterogeneous components and 6 (86%) of the 7 in situ squamous cell carcinoma components were positive for Rb protein, suggesting that abnormalities of the Rb gene may play a role in carcinogenesis.

References: 1. Takubo K, et al. Primary undifferentiated small cell carcinoma of the esophagus. Hum Pathol 1999; 30:216–221
2. Takubo K. Pathology of the Esophagus. Educa Inc. Tokyo, 2000; 194–203

P-071

Follow up study of patients with juvenile polyposis who had undergone total colectomy.

Tertytchnyi A.S.*, Sotnikov D.N.**, Lukin V.V.**
* Dept. of Pediatric Pathology, Russian State Medical University; ** Dept. of Surgery, Centre of Children's Health, Russian Academy of Medical Science, Moscow, Russia

INTRODUCTION: We studied 11 patients with juvenile polyposis underwent total colectomy. Their age ranged from 9 to 25 years, with a mean of 18.6 years. The male to female ratio was 2:3. The mean follow up was 87.5 months (range 25 months to fifteen years).
METHODS: All of our patients were carried out the careful endoscopic examination. The multiple biopsy specimens have been taken from the stomach and small intestine. In addition to hematoxylin and eosin we used van Gieson, an Alcian-blue (pH 2.5) and periodic acid Schiff (PAS) stains.
RESULTS: On follow up, five of the eleven patients (45.5%) had polyps in the stomach. There were sessile polyps, and their size varied from 3 mm to 20 mm. On histological examination all polyps were juvenile. One patient (9%) had juvenile polyps in the cardia and duodenum with focal and low grade adenomatous change.
To study process of ileal adaptation we had done pathological examination of ileal mucosa. All of our patients showed the mucosal changes with shortened and smoothed of villi and goblet cell hyperplasia. The morphologic data suggest colonic transformation (metaplasia) of terminal ileal mucosa.
CONCLUSION: Follow up study of patients with juvenile polyposis who had undergone total colectomy demonstrates possibility of increased incidence of juvenile polyps in the stomach and small intestine. The histologic features of polyps show their low malignant potential. Morphologic changes in terminal ileal mucosa represent a biological adaptation of small intestinal mucosa toward colonic phenotype.

P-072

Microvessel density in anal cancer: Prognostic value and relationship with cell proliferation

D. Tiniakos[1], Tzortzis P[1,2], D. Karandrea[1], J. Karaitianos[3], C. Kittas[1]
Depts of Histology-Embryology[1] & Clin.Therapeutics[2], Medical School, Univ. of Athens; [3]3rd Dept. of Surgery, St. Savvas Hospital, Athens, Greece

INTRODUCTION: Angiogenesis is reportedly correlated with patient prognosis in some types of tumors. We assessed microvessel density (MVD) in anal cancer for the first time and correlated this with clinicopathological variables, cell proliferation and patients' outcome.
MATERIAL & METHOD: We studied 58 anal carcinomas from 58 patients (mean age 65.2 y, M/F 1:1.6) with 2–11 years follow-up (mean 55 months). There were 41 squamous cell carcinomas (SCC) (grade I 13, II 19, III 9, stage 0 1, I 2, II 10, IIIA 15, IIIB 4, IV 2), 16 adenocarcinomas (AC) (grade I 1, II 13, III 2, stage 0 & I 0, II 2, IIIA 4, IIIB 2, IV 5) and one small cell carcinoma (stage IV). Anti-factor VIII and anti-Ki-67 antibodies were employed on routinely-processed tissues using the streptavidin-biotin immunohistochemical technique. MVD applied to the mean number of microvessels from 5 vascular "hot spots." Relationships between variables were tested using the Spearman rank correlation coefficient and survival was analysed by the Kaplan-Meier method and the Wilcoxon test.
RESULTS: There was no statistical difference in MVD between SCC (mean:14.4±9.5/mm^2) and AC (mean:15.1±9.4 mm^2). In SCC, MVD was positively correlated with grade (p=0.001) and inversely correlated with tumor size (p=0.028), depth of invasion (p=0.023) and relapse (p=0.003). There was no correlation with age, gender, histological subtype and stage, lymph node status, Ki-67 labeling index (LI) and patient overall survival. In AC, MVD was positively correlated with Ki-67 LI (p=0.013), but no relationship was found with the rest of the above mentioned factors.
CONCLUSIONS: In anal SCC, high MVD was most commonly observed in high grade tumours. SCC with low MVD were usually of larger size and more invasive than tumors with higher MVD. In-

creased cell proliferation characterized anal AC with high MVD. In anal carcinomas, MVD did not affect overall patient prognosis, however SCC with low MVD were more prone to relapse compared with SCC with high MVD.

P-073

bcl-2 and bax expression in lymph nodes with metastatic involvement from colon carcinoma

AC Tsamandas, P Aroukatos, CD Scopa
Department of Pathology, University of Patras, School of Medicine, Patras, Greece

Introduction: In a previous study, we have shown that a positive immunoreactivity for bcl-2 oncoprotein, is directly related with low grade and early stage colorectal carcinomas, while a trend for loss of bax protein expression towards tumor high grade and advanced stage was observed. The purpose of this study was to investigate whether bcl-2 and bax immunohistochemical profile is similarly expressed in metastatic sites.
Method: Archival material of regional (pericolic) lymph nodes with metastatic disease, resected from 72 surgical specimens with stage C (Astler-Coller classification) primary colorectal carcinoma, was evaluated immunohistochemically. Tumors were classified according to a modified WHO grading system, as low grade (n=47, well+moderate differentiated) and high grade (n=25, poorly differentiated). A standard streptavidin-biotin method was employed on paraffin sections (4 μm thick), using the monoclonal antibody to bcl-2 (DAKO) and polyclonal antibody to bax protein (SantaCruz). Cases were considered as positive if at least 5% of tumor cells displayed cytoplasmic staining for bcl-2 or bax.
Results: Positive stain for bcl-2 oncoprotein was detected in tumor cells in 7% (5/72) of the cases. All 5 tumors were well-differentiated carcinomas. The remaining 67 cases exhibited a positive immunostaining for bax oncoprotein in all metastatic foci. Metastases of these tumors were originated from 25 (37%) high grade and 42 (63%) low-grade carcinomas. No simultaneous expression of these antibodies was detected.
Conclusions: Preliminary results of this study show that in regional lymph nodes with metastatic involvement from colon carcinoma bax protein expression is frequent. These findings comparing with those on primary tumors might simply reflect an immunophenotypic alteration of tumor cells in metastatic sites or may indicate that bax oncogene plays an important role in late stages of colon carcinoma. Results on bcl-2 immunostaining show that this oncoprotein does not seem to be involved in the progress of colon carcinoma.

P-074

The role of helicobacter pylori infection on gastric epithelial cell proliferation

Turan A.A., Dogusoy G., Göcener S.
Department of Pathology, Ministry of Justice, Forensic Medicine Council; Department of Pathology, Istanbul University, Cerrahpasa Medical Faculty, Istanbul, Turkey

H. Pylori infection, as a risk factor for gastric cancer, is associated with proliferation of gastric epithelial cells in H. Pylori positive hosts. Increased proliferation of gastric epithelial cells in H. Pylori positive hosts. Increased proliferation of epithelial cell proliferation of epithelial cells is an important marker for increased risk of adenocarcinoma.
The aim of this study is to assess both gastric epithelial cell proliferation and the influence of H. Pylori infection on cell kinetics in the progression from normal mucosa to gastric carcinoma.
55 subjects were assigned to study groups based on histology diagnosis and H. Pylori status: Microscopically normal mucosa and negative (n:14), chronic active gastritis H. Pylori positive and negative (n:19), atrophic gastritis and intestinal metaplasia (n:16), gastric carcinoma (n:8). Gastric epithelial cell proliferation was assessed using gastritis, p53, ki-67 labeling index percentages. Subjects with chronic active gastritis, atrophic gastritis- intestinal metaplasia and gastric carcinoma have increased epithelial cell proliferation compared with normal mucosa (Ln % p53 mean (SEM): 17 (0,4), 22 (0,4), 27 (0,4); Ln % ki-67 mean (SEM): 16 (0,8), 27 (0,8), 29 (0,3) $p<0.001$). H. Pylori infection although associated with an increased epithelial cell proliferation in subjects with chronic gasrtitis, does not influence the increased proliferation in subjects with precancerous lesions and carcinoma. This is further evidence that H. Pylori may be the trigger of gastric carcinogenesis.

P-075

Evaluation of gastroesophageal cancer by genetic analyses and arraying technologies

H. van Dekken, K. Vissers, P. Riegman, J. Alers, A. de Pender, W. Dinjens, H. Tanke, C. Rosenberg, and the Rotterdam Esophageal Tumour Study Group
Department of Pathology (HvD, KV, PR, JA, AdP, WD), Erasmus University Rotterdam, Rotterdam; Department of Cytochemistry and Cytometry (HJT, CR), State University Leiden, Leiden, The Netherlands

Introduction: Analyses of cancer incidence data in the United States and Western Europe revealed steadily rising rates over the past decades of esophageal (Barrett's) adenocarcinomas and gastric cardia cancers.
Methods: A genome wide overview, based on comparative genomic hybridization (CGH), was constructed enabling comparison of premalignant lesions and their malignant counterpart. In addition, micro-array CGH of gastroesophageal adenocarcinomas was carried out employing both commercial and custom-made DNA chips.
Results: Genomic events during transformation in Barrett's esophagus were revealed and a model was generated ordering the genetic changes and candidate genes involved. The frequency of losses and gains significantly increased in the subsequent stages of malignant transformation. Recently, we have performed a similar survey of gastric cardia carcinoma and dysplasia revealing essentially the same genetic patterns found in Barrett's esophagus and adenocarcinoma. This provides further evidence of a shared etiology for the two types of cancer. Micro-array CGH revealed genomic losses at locations, which were also found frequently altered by conventional chromosomal CGH. In addition, deletions were disclosed that were not detected by other techniques, and amplifications could be assigned to known genes or specific DNA clones on the chips.
Conclusion: Esophageal (Barrett's) and gastric cardia adenocarcinomas develop along a similar histological and genetic metaplasia-dysplasia-carcinoma pathway. Characterization of chromosomal deletion and amplification patterns will increase our knowledge of these frequent and poorly understood cancers.

P-076

The lamina propria in non-inflamed gut from spondyloarthropathy patients contains increased numbers of lymphoid follicles

J. Van Huysse, P. Demetter, F. De Keyser[1], H. Mielants[1], E.M. Veys[1], M. De Vos[2], C.A. Cuvelier
Department of Pathology, [1]Rheumatology and [2]Gastroenterology, Ghent University Hospital, Ghent

Introduction: Lymphoid follicles are considered to be a reflection of antigen handling and presentation. Several data indicate the involvement of the gut in the etiopathogenesis and development of spondyloarthropathy (SpA). This study investigated the number of lymfoid follicles in ileal and colonic lamina propria from patients with SpA.
Methods: The number of follicles in the lamina propria was counted on haematoxylin-eosin stained sections. The paraffin embedded tissue was derived from biopsy specimens obtained during ileocolonoscopy. All the biopsies showed now signs of inflammation. The entire lamina propria was evaluated and values were expressed per 5 high power fields. The SpA colonic (n=11) and ileal (n=7) biopsies were compared with normal colonic (n=12) and ileal (n=13) tissue. The age distribution and the left/right distribution of the colonic biopsies are comparable for both groups.
Results: We found a significant increase in the number of follicles in both ileal ($p<0.01$) and colonic ($p<0.001$) tissue of SpA patients compared to control biopsies.
Conclusion: These results confirm the increased immune activity in the gut from SpA patients. The larger number of follicles may indicate more antigen uptake, handling and presentation. This finding supports the hypothesis that the gut is involved in the development of SpA.

P-077

Helicobacter pylori infection and hepatobiliary disease in inflammatory bowel disease

P.O. Väre, B. Heikius, S.E. Niemelä, R. Karttunen, S. Lähde, J.K. Lehtola, T.J. Karttunen
Departments of Pathology, Internal Medicine, Microbiology, Diagnostic Radiology, University of Oulu, Finland; Department of Internal Medicine, Vaasa Central Hospital, Vaasa, Finland

Background: Hepatobiliary diseases are the most common extraintestinal manifestations of inflammatory bowel disease (IBD). *H. pylori* infection is rare in IBD, but there is some evidence suggesting that the infection may modify intestinal inflammation in IBD. Here we have evaluated the relationship between seroprevalence of *H. pylori* and the occurrence of hepatobiliary disease in IBD.
Methods: We studied 214 unselected patients with IBD for *H. pylori* antibodies and liver function tests, including serum aminotransferases, alkaline phosphatase, bilirubin and albumin. Endoscopic cholangiopancreatography (ERCP) and liver biopsy were performed in patients with abnormal liver function tests.
Results: The prevalence of abnormality in liver function tests was similar in *H. pylori* seropositive (7/36; 19%) and negative patients (52/178;29%). However, among female patients with ulcerative colitis an increase of alanine transferase was less common in the *H. pylori* positive patients than in the negative ones ($p=0.014$). *H. pylori* seropositive subjects showed a trend for absence of abnormalities in liver biopsy ($p=0.079$). No difference in the prevalence of bile duct abnormalities was observed.
Conclusion: *H. pylori* seropositivity shows no positive association with the hepatobiliary complications of IBD suggesting that the infection is not important in their pathogenesis. However, the trend for a weak negative association suggests that *H. pylori* infection could have some protecting effect for hepatobiliary complications, in a way similar as the recently reported negative association between *H. pylori* infection and the severity of intestinal inflammation in IBD.

P-078

Hep Par 1 in gastric and bowel carcinomas: an immunohistochemical study

D. Villari, R. Caruso, M. Grosso, E. Vitarelli, M. Righi, G. Barresi
Dipartimento di Patologia Umana, Policlinico Universitario di Messina, Italy

Hep Par 1 has been described as a specific marker of hepatocellular differentiation and its immunohistochemical use has been suggested as an helpful tool for diagnostic purpose of hepatocellular carcinoma (HCC). Most of the metastatic liver tumours arise in the gastrointestinal tract and they cannot be diagnosed only on the basis of histologic features since pseudoglandular differentiation is very frequent in HCC. The aim of our study was to evaluate by immunohistochemistry the specificity of Hep Par 1 studying the presence of the epitope that reacts with Hep Par 1 in a series of 39 cases of primary gastric carcinomas and 18 cases of primary bowel carcinomas. Of the 39 gastric carcinomas, 26 were of the intestinal type, 5 of the diffuse type, 3 of the mixed type and 5 with hepatoid differentiation. Of the 18 intestinal tumours, 16 were large bowel adenocarcinomas and 2 small bowel adenocarcinomas. Two of them were well differentiated, 14 moderately differentiated, 1 poorly differentiated adenocarcinoma and 1 was of the mucinous type. Five micron sections were stained by immunohistochemistry using Hep Par 1 (Dako, Denmark) as primary antibody. Immunohistochemical staining was observed in 26 gastric carcinomas. Sixteen of them were intestinal type cases, 4 diffuse type and 1 mixed type. All of the 5 hepatoid type cases stained positively. Eight of the large bowel tumours and 1 of the small bowel tumours showed a positive immunohistochemical staining. Of the 9 positive cases 1 was a well differentiated adenocarcinoma, 7 were moderately differentiated adenocarcinomas and 1 was of the mucinous type. The staining pattern was cytoplasmic and granular as described in benign and malignant hepatocytes. The percentage of immunostained cells was graded as follows: 0 (no staining); 1 (>0 to 5%); 2 (>5 to 50%); 3 (>50%). Of the 26 positive gastric tumours 13 showed a percentage of staining of 1; 8 cases of 2 and 5 cases of 3. Of the 9 positive intestinal carcinomas 4 showed a percentage of staining of 1 and 5 of 2.
Our results showed that Hep Par 1 is not specific for the identification of HCC, however it is an useful marker of hepatoid differentiation since all of the hepatoid gastric carcinomas showed a positive immunostaining.

P-079

Aberrant cytokeratin patterns in poorly differentiated colorectal adenocarcinomas

Vyberg M, Vestergaard V
Institute of Pathology, Aalborg University Hospital, Aalborg, Denmark

Introduction: The large majority of colorectal adenocarcinomas reveal the distinct and diagnostically useful immunohistochemical cytokeratin profile CK20+/CK7–. Deviant profiles in metastatic poorly differentiated colorectal adenocarcinomas (PDCA) involve a danger of misclassification. We wished to determine the frequency of aberrant CK20/CK7 patterns in PDCA correlated to the degree of tubular growth pattern, tumour localisation, and neuroendocrine differentiation.
Methods: Fifty resected PDCA specimens (right hemicolon: 20, left hemicolon: 20, rectum: 10) were stained for CK20, CK7, and synaptophysin. The tumours were grouped according to the relative area of tubular differentiation: A: >50%, B: 25–50%, and C: <25%. Positive staining was defined as ≥10% positive cells.
Results: A 'typical' CK20+/CK7- profile was seen in 33 of the 50 tumours (66%). The number of tumours in each group and the profiles identified are summarized in the table.

CK profile	A (n=10)	B (n=17)	C (n=23)
CK20+/CK7-	9 (90%)	12 (71%)	12 (52%)
CK20+/CK7+	1 (10%)	3 (18%)	1 (4%)
CK20–/CK7-	0	1 (6%)	9 (39%)
CK20–/CK7+	0	1 (6%)	1 (4%)

In PDCA from right hemicolon a deviant profile was seen in 12/20 (60%), while PDCA from left hemicolon and rectum was deviant in 5/30 (17%). However, 13/20 right hemicolon tumours (65%) belonged to group C but only 10/30 left hemicolon and rectum tumours (33%). Focal SYP positivity was found in ten tumours without correlation to the CK profile.
Conclusion: Aberrant CK patterns frequently occur in PDCA, associated with a solid growth pattern and right hemicolon localisation but not with neuroendocrine differentiation.

P-080

Inflammatory pseudotumor of the small bowel mimicking an acute appendicitis in a 36-year-old woman

N. Weber, T. Petit, B. Fraleu, M. Grossin, D. Hénin
Department of Pathology, Hôpital Bichat, Paris, France

Case Report: A 36-year-old woman presented a 48-hours history of fever and abdominal pain in the right iliac fossa suggesting appendicitis or ileocolitis. An right abdominal mass was palpable, CTscan revealed a mass adjacent to the terminal ileum. At surgery, ileon intussusception with pediculated tumor obstructing the lumina was discovered. Segmental resection was performed. Grossly, the pedunculated tumor was 3cm large, whitish, firm. Paraffin sections were stained with hematoxylin-eosin, PAS, Grocott, Gram, Ziehl. Immunohistochemical study was performed using antibodies against vimentin, α smooth muscle actin, desmin, cytokeratin and CD34 antigenes.
Microscopically, the lesion ulcerated the mucosa and involved the submocosa. It was made of highly vascularized connective tissue with interlacing fascicles of elongated spindle cells admixed with plasma cells, histiocytes, lymphocytes and eosinophils. No pathogen was observed. Spindle cells were vimentin positive, actin negative. Vessels stained with actin and CD34. Ki67 stained less then 2% of the spindle cells. An inflammatory pseudotumor was diagnosed.
Discussion: Inflammatory pseudotumor is rare in the ileon and can mimick acute appendicitis or neoplastic small bowel obstruction. In most cases, etiology remains unknown and the pathogenesis is supposed to be a myofibroblastic reparative process subsequent to inflammatory reaction or infective agent. Another hypothesis emphasizes a true neoplastic myofibroblastic proliferation.
In our case, spindle cells were negative for actin and appeared to be originated from the fibroblastic lineage. This fact associated with a highly vascularized component favored the reactive nature and emphasized benign course. Whatever the pathogenic hypothesis, a complete excision is the adequate treatment.

P-081

Microsatellite instability in cancer of the colon: relation with microvessel density, VEGF and COX2 expression

Wendum D (1, 2), Rigau V (1), Boëlle P-Y (3), Sebbagh N (1), Masliah J (2), Fléjou J-F (1)
(1) Service d'Anatomie Pathologique, Hôpital Saint-Antoine, Saint-Antoine, Paris; (2) Unité INSERM U538 et (3) Unité INSERM U444, Faculté de Médecine Saint-Antoine, Paris, France

Introduction: Adenocarcinoma of the colon can be classified according to the presence of microsatellite instability (MSI). MSI+ cancers have a better prognosis. We investigated microvessel density (MVD), VEGF and COX2 expression in MSI+ and MSI– adenocarcinomas of the colon, and determined the association between COX2 expression and angiogenesis in vivo.
Methods: 56 cases were studied, 24 MSI+ and 32 MSI-. They were selected from a series of 174 cases with a MSI phenotype determined by PCR at 4 loci including TGFβRII, in order to have similar Astler-Coller stages between MSI+ and MSI– cases. MVD was assessed after CD31 staining in ten ×250 fields (3.9 mm^2). VEGF and COX2 expression was studied by immunohistochemistry. Association of variables was compared with the Maentel Haenszel procedure, stratified on the stage, and deviance tests after analysis of variance, where appropriate.
Results: MVD was lower in MSI+ cases (p=0.03), and in 14 cases with a mucinous histological pattern (12 MSI+ and 2 MSI-) (p=0.012). VEGF and COX2 expression was lower in MSI+ cases (p=0.03 and p=0.04, respectively). A high MVD was associated with a strong VEGF expression (p=0.01). There was no association between MVD and COX2 expression nor TGFβRII instability.
Conclusion: The lower MVD in MSI+ adenocarcinomas of the colon could participate to the better prognosis of this type of tumour. This low vascularisation of MSI+ tumours may be related to the low level of VEGF expression. Although COX2 overexpression was shown previously to regulate angiogenesis in vitro, we found no arguments for a similar mechanism occurring in vivo, as we did not observe any association between COX2 expression and VEGF expression nor MVD.

P-082

Overexpression of PTEN, cyclin D1, CDK4, and p53 in cholangiocarcinomas

Yoo, Seong-ho
Dept. of Pathology, Seoul National University College of Medicine

Introduction: Intrahepatic cholangiocarcinoma (ICC) is one of the most common fatal cancers. However, there have been few previous studies using immunohistochemistry to investigate the expression of cell cycle regulators. PTEN (*P*hosphatase and *ten*sin homolog), a tumor suppressor associated in a variety of human cancers, has been reported to be related to retinoblastoma protein, with which p53 mediates G1 cell cycle. In addition, Hashemolhosseini et al. Have insisted that PTEN was related to other cell cycle regulators including cyclin D1 and CDK4 through P70 S6 kinase. However, the immunostainings of PTEN, cyclin D1 and CDK4 have not been yet perfomed in ICC.
Methods: To evaluate the potential contribution of the PTEN, cyclin D1, CDK4, and p53 genes to intrahepatic cholangiocarcinoma, we correlated the expression of these cell cycle regulators with variable clinicopathologic factors in 38 cases of ICC using immunohistochemistry.
Results: PTEN, cyclin D1, CDK4, and p53 were found to be expressed 39.5%, 15.8%, 23.7%, and 39.5%, respectively. PTEN expression was statistically significant with CDK4 expression (p=0.006) and histologic grade (p=0.03). Cyclin D1 expression showed significant correlation with tumor stage (p=0.032) and tumor grade (p=0.024). The overexpression of p53 showed significant correlation with cyclin D1 expression and CDK4 expression (p=0.027 and p=0.016, respectively), whereas the relationship between p53 expression and PTEN expression was not statistically significant. The correlation between p53 expression and ICC tumor grade was not significant. Other ICC clinicopathologic features such as tumor stage and macroscopic classification also did not significantly correlate with p53 expression. The overexpression of p53 showed inverse correlation with the outcome of the patients, which is in disagreement with the previous reports. This result may trigger further study based on more data of patients with ICC. We observed cyclin D1 expression and CDK4 expression were related with the outcome of patients (p<0.05).
Conclusion: Our finding suggest that PTEN may modulate cell cycle regulators in ICC. In addition, cyclin D1 and CDK4 may be useful prognostic factors in ICC.

P-083

Expression of the vascular endothelial growth factor receptor-3 (VEGFR-3) and its ligand VEGF-C in human colorectal adenocarcinoma

Mamoun Younes, M.D., Abraham Thomas, M.D., Najeeba Ali, B.S., Nicole Carlson, Deborah Witte, M.D.
Department of Pathology, Baylor College of Medicine;
The Methodist Hospital, Houston, TX, USA

Introduction: Vascular endothelial growth factors (VEGF) are secreted by many tumor types, and are believed to affect tumor growth by promoting angiogenesis through binding to their receptors present on vascular endothelium. Recently, mRNA for VEGF-C mRNA, the ligand for VEGFR-3, was found to be upregulated in colorectal adenocarcinoma (CRC). The aim of this work was to determine 1) the distribution of VEGF-C and VEGFR-3 in CRC, and 2) the biologic significance of such expression.
Methods: Sections of formalin-fixed and paraffin-embedded tissues from 56 CRC were immunohistochemically stained for VEGF-C and VEGFR-3. The type and percent of positive cells was recorded. Survival analysis was performed using the Kaplan-Meier method.
Results: All CRC were positive for VEGF-C which was present in the cancer cells themselves, as well as in stromal cells. Normal colon epithelium was usually negative. Only ten (17%) of the 56 CRC completely lacked VEGFR-3 expression. VEGFR-3 immunoreactivity was detected in <25% of the cancer cells in 22 cases and in >25% of the cells in 34 cases. Expression of VEGFR-3 in >25% of the cancer cells was associated with significantly poorer overall survival (p<0.05), but not with lymph node metastasis or depth of tumor invasion.
Conclusion: Our results suggest that VEGFs promote cancer growth not only by stimulating angiogenesis, but also by acting on receptors present on the cancer cells themselves.

P-084

Expression of estrogen receptor beta in esophageal adenocarcinoma

Pamela S. Younes, MSH, Susan Plaza, HT, Mamoun Younes, M.D.
Department of Pathology, Baylor college of Medicine;
The Methodist Hospital, Houston, TX, USA

Introduction: A second type of estrogen receptor, estrogen receptor beta (ERB), has been described. mRNA for ERB was found in many human colon cancer cell lines, and its expression was found to be associated with response to treatment with tamoxifen in vitro. We recently reported that ERB positive breast cancers, as determined by immunohistochemically, are associated with better survival in women treated with adjuvant hormonal therapy with tamoxifen (Human Pathology 2000; 32:113-118). The aim of this study was to determine whether ERB is expressed in esophageal adenocarcinomas.
Methods: Sections of formalin-fixed and paraffin-embedded tissues from 13 esophageal adenocarcinomas were stained for ERB using the immunoperoxidase method. The percent, intensity (0-3), and localization of the immunoreactivity in cancer cells was recorderd.
Results: All 13 adenocarcinomas were ERB positive. Immunoreactivity was nuclear, but was associated with faint cytoplasmic staining in many cases. Nuclear ERB immunoreactivity was present in >75% of the cancer cells in 10 (78%) of the cases and in 51–75% of the cells in 3 (22%). Staining intensity was 3+ in 7 (54%) of the cases and 1 to 2+ in 6 (46%).
Conclusion: Our findings show that ERB is expressed in the majority of cancer cells in essentially all esophageal adenocarcinomas, and raise the possibility that these tumors may respond to adjuvant hormonal therapy with tamoxifen.

P-085

CEA and PNA – lectin expression in colorectal adenomas and early invasive cancers

Zivkovic V.*, Kutlecic*, Bacic H.*, Milentijevic M.*, Nagorni A.**, Velinkovic Lj. , Djordjevic B.*
Dpts. of Pathology*, Clinic of Gastroenterology**,
University of Nis, Yugoslavia

Aims: The adenoma – carcinomas sequence is currently accepted as the origin of most colorectal carcinomas. Therefore, we evaluated immunohistochemically the expression and prognostic impact of CEA and PNA lectin in 24 colorectal adenomas with different grades of dysplasia and 15 early invasive carcinomas and correlation between these markers and grades of tumor differentiation.
Methods: Formalin – fixed and paraffin embedded specimens from tumors were stained by APAAP and PAP techniques using monoclonal antibodies against CEA and PNA lectin (DAKO, Copenhagen).
Results: All adenomas with severe dysplasia revealed a strong positive reaction with both antibodies in the apical part of epithelial cells and in the glycocalix. In contrast, reaction were low in adenomas with mild dysplasia. In all carcinomas markers showed a stronger reaction.
Conclusion: The expression of CEA and PNA – lectin clearly shows differences between adenomas with different grades of dysplasia and early carcinomas and could give good information on biological potential of colorectal tumors.
Head and Neck Pathology

P-086

Adenosquamous carcinoma of the head and neck. Immunohistochemical and flow cytometric study of 12 cases

Alos L., Castillo M., Nadal A., Caballero M.*, Mallofré C., Palacin A., Blanch J.L.*, Cardesa A.
Departments of Pathology and ORL*, Hospital Clínic, IDIBAPS, University of Barcelona

INTRODUCTION: Adenosquamous carcinoma (ASC) is an infrequent neoplasm that can develope in the upper aerodigestive tract. Only few cases of ASC of the Head and Neck region have been reported in the literature.
METHODS:We have reviewed 12 ASC of the Head and Neck region. We have studied their clinicopathological features and the proliferative activity, assessed by MIB-1 antibody and flow cytometry. Also we have studied the p53 protein expression and c-erbB-2 oncogen by immunohistochemistry.
RESULTS: The 12 ASC occurred in males, with an average age of 58 years. Six patients (50%) died of disease with a mean survival time of 23 months.In all cases squamous cell carcinoma "in situ" in the overlying mucosa was seen. The mean value of MIB-1 immunoreaction was 28%. Ten cases were aneuploid (83%). The p53 protein expression was higher than 20% in 8 cases (66%). The c-erbB-2 oncogen resulted positive in 5 cases (42%). We couldn't find statistical significance with these studied parameters and the clinical outcome of the patients.
CONCLUSION: ASC of the Head and Neck region is a neoplasm that originate from the mucosa of the upper aerodigestive tract. It is an aggressive neoplasm that courses with an adverse outcome. Most of the patients with lymph node metastases have aneuploid tumours with a high expression of p53 protein (higher than 70%).

P-087

Chondromyxoid fibroma of frontal sinus

C. Ballestín; D. Azorín; A. Santos-Briz, F.J. Martínez Tello
Department of Pathology, Hospital 12 de Octubre, Madrid, Spain

INTRODUCTION: Chondromyxoid fibroma (CMF) is a rare benign tumor, meaning less than 1% of all bone tumors. It typically affects young adults with a predilection to involve the long bones. CMF of craniofacial bones is very rare, being exceptional the involvement of the frontal bone. There are only seven well-documented cases reported in that location, from which, only two involved the frontal sinus too. We present a case of CMF located in the frontal sinus, which showed destruction of the frontal bone cortex.
METHODS: A 46 years old man presented with a mass in the frontal region. He had been asymptomatic. Imaging studies revealed a radiolucent mass located in the frontal sinus showing destruction of the front and the posterior cortex of the frontal bone. The mass was excised.
RESULTS: Grossly, the tumor was a 2.5 cm diameter polilobulated mass with a fibrous appearance. Hystopathological examination revealed a polilobulated tumor, consisting of spindle and round cells immersed in a myxoid background. The cells were located at the periphery of the lobes, which showed an hypocellular center. Inmunohystochemical stains showed a chondral phenotype.
CONCLUSION: CMF is a rare benign tumor of bone with a predilection for the long bones. Involvement of craniofacial bones is very rare, being exceptional the location in the frontal bone and even more in the frontal sinus. The reported cases of CMF located in the frontal sinus showed destruction of bone, a feature that is not usual in other sites. For hystological differential diagnosis chondrosarcoma and chondroblastoma have to be considered.

P-088

Radicular cyst as the initial manifestation of adult-onset histiocytosis x

A. Benito, F. Lopez-Rios, R. Garcia, A. Serrano, M.A. Martinez and C. Ballestin
Hospital "12 de Octubre", Madrid

INTRODUCTION: Langerhans' cell histiocytosis is a clonal proliferation of Langerhans cells (LC) with a broad clinical spectrum of disease. Involvement of the jaws is rare (1–2%) and may resemble a periodontal problem, delaying thus the diagnosis.
CASE REPORT: A 22-year-old man, smoker with episodes of productive cough, was referred because of pain and swelling in right mandibular area. Oral radiographs showed a cystic lesion with bone loss. Histopathologic examination revealed a cyst wall lined with a nonkeratinized squamous epithelium in a chronically inflamed fibrous tissue. Aggregates of large epithelioid cells with clear cytoplasm and indented nuclei were present within the infiltrate, which stained positively for S-100 protein and CD1a. Birbeck granules were detected ultrastructurally. Further studies demonstrated diffuse reticulonodular lung involvement and bilateral cystic change, with variable number of LC.
DISCUSSION: LC have previously been described in the epithelial wall of odontogenic cysts. Only one study reports 4 cases with minute aggregates of LC in relation to caries, without bone erosion, making the authors consider LC aggregates a reactive process. No report has been found of a radicular cyst associated with eosinophi-

lic granuloma with systemic involvement. Systemic LC histiocytosis (stage D Histiocyte's Society) is a relatively rare disease in adults that needs a more aggressive management. We conclude that LC histiocytosis should always be considered in the differential diagnosis of destructive periodontal disease. Detailed medical history is essential to rule out a systemic disorder.

P-089

Intratumoral heterogenity of AgNOR staining in laryngeal SCC

Ćorić M., Aralica G., Pešut A., Bumber Ž., Đanić D., Manojlović S., Seiwerth S.
Institute of Pathology Medical Faculty Zagreb

Relatively few studies have investigated the expression of AgNOR in laryngeal SCC. Among these studies there are conflicting results concerning the potential prognostic utility of AgNOR parameters. Intratumoral heterogeneity in laryngeal SCC has previously been demonstrated for DNA content. As this is a potential source of highly variable results we decided to investigate AgNORs in different intratumoral locations in a population of SCC of the larynx.
PATIENTS AND METHODS: 33 total laryngectomy specimen have been investigated. After standard silver impregnation the slides were analyzed a PC based image analyzer system (SFORM, VAMSTEC Zagreb, Croatia). Two areas were analyzed: invasive tumor margin and tumor center. Assessed were the following parameters: mean AgNOR area (**A**), mean number of AgNOR/nucleus (**B**) and number of AgNOR/100 nuclei (**C**). 100 nuclei were analyzed per tumor per area.
RESULTS AND CONCLUSION: Significant difference was obtained between the values in tumor center and invasive tumor margin for all the investigated parameters (A – p=0.002; B – p=0.007; C – p=0.008). Our results strongly underline the fact that intratumoral heterogeneity is not to be neglected in studies and in diagnostic approach. Also it underlines the need for studies with consistent material sampling and analysis regarding the macroscopical as well as microscopical areas. In this we suggest that the problem of potential prognostic utility AgNOR and DNA parameters should be accessed in a large scale study using standardized approach.

P-090

Malignant epithelial neoplasms of the nasal cavities and paranasal sinuses: A clinicopathologic study of 134 cases

Franchi A., Moroni M., Santucci M.
Department of Human Pathology and Oncology,
University of Florence Medical School, Florence, Italy

Introduction: The aim of our study was to review a series of sinonasal malignant epithelial neoplasms observed at the Department of Human Pathology and Oncology of the University of Florence Medical School, in order to investigate the clinicopathologic correlation and to define parameters correlated with survival.
Methods: A total of 134 cases of malignant epithelial tumors of the nasal cavities and paranasal sinuses were collected between January 1966 and December 1995. Tumors arising in the nasal vestibule were excluded. All available histologic slides were reviewed, and tumors were re-classified and graded as low grade and high grade The clinical records of each patient were reviewed for age, sex, site of the tumor, presence of lymph node or distant metastases, professional exposure, type of treatment, and follow-up.
Results: The most frequent histologic subtypes were squamous cell carcinoma (SCC, 66 cases, 49.3%) and intestinal type adenocarcinoma (ITAC, 42 cases, 31.3%), followed by cylindrical cell carcinoma (CCC, 11 cases, 8.2%), salivary gland-type carcinomas (SGC, 8 cases, 6%), sinonasal undifferentiated carcinoma (SNUC, 6 cases, 4.5%) and adenocarcinoma (1 case, 0.7%). Survival analysis according to Kaplan Meier showed that 5-year cumulative survival was 25% for SNUC, 34% for ITAC, 43% for SCC, 64% for CCC and 85% for SGC (p=0.3, log rank test). In addition, patients affected by ITAC and SNUC showed a significantly higher frequency of professional exposure (p<0.001). Using Cox proportional hazards analysis of survival, high histologic grade and advanced tumor stage were identified as independent predictors of poorer clinical outcome (p<0.001 and p=0.02, respectively), while histologic type, presence of lymph node or distant metastases, professional exposure and type of therapy were not.
Conclusion: Our study identifies SNUC and ITAC as the most aggressive sinonasal malignant epithelial neoplasms. Histologic grade should be reported by pathologists as a relevant prognostic element for these tumors.

P-091

Evaluation of protein p53 mutation in the epithelium of the tumor surrounding tissue of laryngeal cancer patients

Gabriel A., *Morawski K., Radłowski P., Tomaszek K., *Namysłowski G.
Chair and Pathomorphology Unit of the Medical University of Silesia in Zabrze, Poland; *II Chair and Otolaryngology Clinical of the Medical University of Silesia in Zabrze, Poland

The aim was a correlation between p53 index values in the epithelium of tumor surrounding tissue in laryngeal cancer patients and a local recurrence on the one hand and epithelial dysplasia, the progress degree (T) and G differentiation of the neoplasm on the other. The analysis included 31 sections collected from postoperative specimens in patients of the average of 57 years.
Methods: The routine histopathological examination was complemented with TNM progress stage and Broders differentiation degree. The immunohistochemical analysis employed monoclonal antibody p53 (DAKO) and ABC method. The index of p53 was defined as a percentage of positive reactions per 1000 cells in large fields of vision.
Results: The mean p53 index value (IDX) in laryngeal cancer sections was 14.2%. Epithelial IDX p53 around the tumor was lower (3.6%). Lack of epithelial p53 was found in 9 cases, while no epithelial changes were discovered in 6 tumor surrounding tissues. Hyperplasia acanthotica was encountered in 8 sections collected from the neoplasm border. Epithelial dysplasia in tumor surrounding tissue was diagnosed in 17 (55%) specimens. No IDX p53 differences were demonstrated in epithelial growth without dysplasia and in the cases accompanying dysplasia. No differences were found in IDX p53 for particular degrees of dysplasia.
Conclusions: No IDX p53 correlation was demonstrated in the neoplasm and epithelium surrounding the tumor of G degree and T scope. Comparable IDX p53 in epithelial growth without dysplasia with dysplastic epithelium may indicate mutations and accumulation of p53 protein in some epithelial growth, which may account for recurrence.

P-092

Histological and immunohistochemical prognostic markers in head and neck mucosal melanomas

García-Martín R.M, Rodríguez-Pinilla S.M, Ballestín C, Serrano Egea A
Department of Pathology, "12 de Octubre" University Hospital, Madrid, Spain

INTRODUCTION: Primary malignant mucosal melanomas of head and neck (MMHN) are rare, difficult to treat and have aggressive biological behaviour. Our current work concerns the potencial role of immunohistochemical markers in prognosis of MMHN. It's based on studies previously done on skin melanomas.
MATERIAL and METHODS: 10 MMHN were identified in our files from 1985-00. Different subgroups were done according to: clinical behaviour, histological pattern
and amount of pigment. Immunohistochemical studies were done on paraffin embedded tissue sections. An avidin-biotin complex method were used to demostrate binding of following antibodies: P53, Ki67, bcl-2, nm-23, VEGF, p21-RAS, CD34, Rb, vimentin, HMB-45, S-100, melan-A and AE1-AE3.
RESULTS:
– There were 7 women and 3 men, whose ages ranged from 44 to 91 years (median age 76,8). Only 20% started in oral cavity.
– Tree cases (30%) metastasized. 2 fusocellular (very and little-pigment). 1 epithelioid (non-pigmented). Seven cases (70%) were focally aggressive. 5 epithelioid (3 very, 1 little, 1 non-pigmented).
– All cases expressed vimentin, S-100, HMB-45, melan-A and were negative to AE1–AE3.
– Non-diagnostic immunohistochemical findings:
Expression in % P53 Ki67 BCL-2 VEGF p-21RAS Rb Nm-23 CD34
Metastatic-group. 21,6% 37,3% 66,6% 66,6% 66,6% 31,6% 100% 9,6 vessels
Non-metastatic-group. 22,8% 34,2% 57,1% 28,6% 28,6% 28% 100% 37 vessels
CONCLUSIONS:
– Melan-A antibody had more sensibility and less intensity of expression than HMB-45 in detecting non-pigmented melanomas.
– 50% of non-pigmented cases were fusocellular, showing a higher tendency to metastasize than epithelioid ones.
– High levels of p-21RAS and VEGF expression seemed to be related to metastatic potential.

P-093

Neoangiogenesis vs p53 and mib-1 expression in laryngeal squamous cell carcinomas (LSCC)

Carmen Georgiu[1], T. Kerenyi[2], G. Iacob[3], A. Georgiu[4], Annamaria Tokes[2], Doinita Crisan[1], Renata Vasiu[1], C.D. Olinici[1]
[1] University of Medicine and Pharmacy, Aluliu Hatieganu≅ Department of Pathology B, Cluj Napoca, [2] Semmelweiss University of Medicine, Department of Pathology B Budapest; [3] County Hospital B, Department of Pathology B Cluj Napoca, [4] CMI 80-Cluj Napoca

Aims: The aim of the present investigation was the study of laryngeal squamous cell carcinomas from the point of view of tumour neoangiogenesis according to the histologic subtype of LSCCs (keratinizing, adenoid and basaloid), the presence of laterocervical lymph-node metastases and the expression of p53 and MIB-1 antigens in the tumour cells.
Methods: 40 cases of LSCCs (pT3-4 stage), 20 of them with metastases were stained immunohistochemically with CD31, p53 and MIB-1 antibodies. Tumour neoangiogenesis was assessed morphometrically by counting the vascular buds (CD31 positive endothelial cells without lumen formation) per mm^2 of stromal tissue and p53 and MIB-1 expression by counting the positive cells of 500 to 1000 tumour cells on each case.
Results: A positive statistical correlation (r=0.33295) was noted between the expression of CD31 and MIB-1 and no correlation between CD31 and p53. The LSCCs with metastases presented a significantly more intense neoangiogenesis than those without metastases (p=0.0022). No differences were observed between the primary tumours and the metastatic cell populations. The adenoid type LSCCs showed a significantly higher neoangiogenesis and tumour proliferation index (MIB-1) than the keratinizing ones and much lower than the basaloid ones.
Conclusions: The p53 antigen has no relationship with neoangiogenesis in LSCCs. In LSCCs (T3-4 stage) neoangiogenesis could be a prognostic indicator, suggesting by its intensity the presence of laterocervical lymph-node metastases. The angiogenic potential of a tumour is established early, the metastatic cellular population having the same expression of CD31 in the stroma like the primary tumour. Adenoid carcinomas have a marked proliferation and neoangiogenesis what classifies them as an average aggressiveness, superior to the keratinizing ones.

P-094

Cyclooxygenase 2 (COX-2) upregulates neoangiogenesis in laryngeal squamous cell carcinoma (LSCC)

Marco Gessi*, Libero Lauriola*, Nicola Maggiano*, Bianca Rocca**, Giovanni Almadori°, Franco Oreste Ranelletti°°
Inst. of * Pathology, ** Internal Medicine, ° Otolaryngology and °° Histology, Univ. Cattolica del S. Cuore, Roma, Italy

Introduction: COX-2, the inducible form of cyclooxygenase, affects carcinogenesis by several mechanisms. COX-2 can induce angiogenesis that is essential in tumor growth. Recently, we observed that COX-2 expression is higher in well differentiated LSCC as compared to normal neighbouring mucosa, while its expression is lost in anaplastic tumors. However, no data about relationhip between COX-2 and angiogenesis in LSCC are available and the role of vascular endothelial growth factor (VEGF) in this context is still unclear. Consequently, we studied the correlation among COX-2 expression, tumor angiogenesis and VEGF expression in 40 LSCC.
Methods: Expression of COX-2 and VEGF was studied by quantitative immunohistochemistry and the immunostained area of tumor was normalized on the total tumor area examined. Microvascular density was evaluated as the ratio between CD34 immunostained area and total tumor area examined.
Results: Using the mean COX-2 value as a cut-value, we found that 9/40 (22%) tumors were COX-2 positive. All COX-2 positive tumors expressed high levels of VEGF. However, also COX-2 negative tumors expressed VEGF, although at various levels. This suggests that VEGF expression is regulated by factors other than COX-2. We observed a strong positive correlation between COX-2 expression and tumor neoangiogenesis (Spearman rank correlation: z=3.13, p=0.0018).

Conclusion: We suggest that in LSCC, COX-2 upregulates tumor neoangiogenesis by a mechanism involving VEGF expression.

P-095

Extramedullary plasmacytoma of the head and neck

Iglesias C, Alos L, Martinez A, Caballero M*, Campo E, Palacin A, Cardesa A
Departments of Pathology and ENT*, Hospital Clinic, IDIBAPS, University of Barcelona, Spain

INTRODUCTION: Extramedullary plasmacytomas (EMP) are plasma cell tumours which involves soft tissues. The vast majority of these neoplasms develope in the upper aerodigestive tract.
METHODS: We have reviewed the clinicopathological characteristics of 5 EMP of the Head and Neck region. In 4 of these cases we have performed immunohistochemical and in situ hybridization techniques for EBER-1 RNA Epstein-Barr virus (EBV). We have studied the expression of Kappa, Lambda light chains to assess clonality. The proliferative index of the tumours has been studied with the MIB-1 antibody.
RESULTS: All the patients were men with an average age of 61 years old. The disease was located in the nasal cavity (four cases, 67%), and pharynx. Four EMP (67%) were well differentiated, and had a proliferative index of 5 to 20%. The EBV was negative. Two of these four cases presented tumor recurrence. The fifth EMP exhibited poorly differentiated areas. This tumour showed a proliferative index of 40%, and was positive for EBV. This patient developed a nodal immunoblastic lymphoma one year later.
CONCLUSIONS: EMP of the Head and Neck affects preferently men in the fifth to seventh decades of life. The well differentiated neoplasms have a favourable clinical course. The poorly differentiated EMP, with a high proliferative index and positivity for EBV, had an adverse outcome. It seems that these biological parameters could be useful in order to predict the clinical outcome of the patients with EMP.

P-096

Re-evaluation of malignant salivary gland. Diagnoses in Finland 1991–1995

Ilmo Leivo[1], Heikki Luukkaa[2], Reidar Grenman[2], Pekka Klemi [3]
[1] Department of Pathology, University of Helsinki, Helsinki;
[2] Department of Otorhinolaryngology, University of Turku, Turku;
[3] Department of Pathology, University of Turku, Turku, Finland

All malignant salivary gland diagnoses reported to the Finnish Cancer Registry in 1991-1995 were retrieved, and the cases were reclassified according to WHO 1991 classification by two experienced salivary gland pathologists. Tissue blocks and follow-up data were obtained from a total of 244 cases comprising a full population-based material in Finland. The most frequent malignancy was adenoid cystic carcinoma (AdCC) with 65 cases (27%), followed by mucoepidermoid carcinoma (MEC) with 46 cases (19,2%), and acinic cell adenocarcinoma (ACC) with 41 cases (17%). In major glands, these three malignancies occurred with almost equal frequencies (AdCC 41 cases, MEC 42 cases and ACC 38 cases). In minor glands, the most frequent malignancy was AdCC with 23 cases (51%), followed by polymorphous low-grade adenocarcinoma with 8 cases (16%). New adenocarcinoma categories of the WHO 1991 classification (polymorphous low-grade adenocarcinoma, epithelial-myoepithelial carcinoma, basal cell adenocarcinoma, papillary cystadenocarcinoma, oncocytic carcinoma, salivary duct carcinoma) were diagnosed in 40 cases compared to 13 primary diagnoses. Four cases (1.6%) with malignant primary diagnoses were reclassified as pleomorphic adenomas. Occurrence of the major diagnostic categories in Finland was comparable to previous European materials. MEC was more frequent than in British materials but less frequent than in most American materials. In minor glands, MEC was less frequent in Finland than in other materials. A total of 34.8% of primary diagnoses were changed. The most common reason for changing a primary diagnosis was an inadequate general formulation which did not meet the appropriate WHO 1991 category. Our observations emphasize the need for experienced salivary gland pathologists to profit by the advantages of the WHO 1991 classification.

P-097

Eosinophil and fibroblasts in nasal polyps: An immunohistochemical and electronmicroscopic study

* Ayper Kacar, ** Alp Usubutun, ** Turkan Kucukali
* SSK Ankara Training Hospital, Ankara,
** Hacettepe University, Faculty of Medicine, Ankara

There are some in vitro studies suggesting a possible role of eosinophils and mast cells on fibroblast plasticity in recent years. In this study we aimed to evaluate the myofibroblastic differentiation and to correlate the findings with eosinophil, mast cell content histochemically and degranulation electron microscopically (EM) in a tissue model.
We included 25 nasal polyps in the study. 9 cases were also sampled for EM. The cases were evaluated for the eosinophil and mast cell content in H-E and toluidine blue sections. Cases were graded for inflammation as low, moderate and high according to cell counts in 10 hpf. Paraffin embedded sections of each case were treated with α-sm muscle actin and desmin. Immunostaining was graded as +, ++, +++ for each case semiquantitatively. 9 cases were evaluated for myofibroblastic differentiation, degranulation (mild and dense) and intraeosinophylic granule content (the mean number of granules for 10 eosinophils in each case) electron microscopically.
18 patients expressed α-sm muscle actin (2 cases +, 10 cases ++, 6 cases +++). Only 4 cases showed weak positivity for desmin. Eosinophil and mast cell counts on H-E slides showed no significant relationship with actin and desmin positivity. Myofibroblastic differentiation and degranulation was observed in 2 and 4 cases respectively (EM). Cases presenting myofibroblastic differentiation had also dense degranulation. Furthermore myofibroblasts were not detected in 5 cases without degranulation.
In conclusion myofibroblasts were considerably observed in nasal polyps. The correlation of myofibroblastic differentiation and degranulation observed in EM encouraged us to suppose that eosinophils might secrete factors which induce actin expression in stromal cells and thus may play a role in development of the microenvironment leading myofibroblastic differentiation.
Key words: eosinophil, mast cell, fibroblast

P-098

Rhinoscleroma with Rosai - Dorfman reaction of the regional lymph nodes

H.U. Kasper [1,2], B. Freigang[3], P. Buhtz[1]
Department of Pathology[1] and Head and Neck-Surgery[3], University of Magdeburg; Department of Pathology[2], University of Cologne, Germany

Introduction: Rhinoscleroma, an uncommon chronic destructive infection of the respiratory mucosa, is caused by Klebsiella rhinoscleromatis. In the proliferating stage, a granulation tissue is found with sheets of foamy histiocytes (Mikulicz cells), and an accompanying lymphoplasmacytic infiltrate. Lymph node involvement is very rare.
Sinus histiocytosis with massive lymphadenopathy (Rosai-Dorfman disease; SHMA) is a histiocytic proliferative disorder of unknown cause. It presents commonly with massive bilateral cervical lymphadenopathy. Histologically, the sinuses of the lymph nodes show packing by S-100 positive histiocytes with viable lymphocytes within their cytoplasm, the so called emperipolesis.
We report a case of rhinoscleroma with lymph node involvement, showing the typical features of SHMA but with bacteria demonstrable within the sinus histiocytes.
Case Report: A now 62 year-old woman presented in 1984 with a longer history of breathing problems and rhinitis due to a nodular thickening of the nasal mucosa. A surgical resection was performed. Histologically, a chronic inflammation with infiltrates of biclonal plasma cells, lymphocytes, and large histiocytes was seen and the diagnosis of rhinoscleroma was made. After several recurrences involving the paranasal sinuses and the orbita, she presented in 1998 again with soft tissue swelling of the face and enlarged lymph nodes. The surgical specimen of the soft tissue showed typical rhinoscleroma. In the lymph nodes SMHA was seen. Intracellular bacteria was demonstrated in the histiocytes of the lymph nodes.
Conclusion: The cause of SHMA is still unknown; the present theories propose infectious, autoimmune, neoplastic, or a combination of factors. Most probably SHMA represents an exaggerated response to an pathogenic agent. EBV and Klebsiellae have been suggested to play a role. In this first case of a patient with rhinoscleroma with SHMA in the regional lymph nodes, we were able to demonstrate the microorganisms in the Miculicz cells. This proves the idea of the Klebsiella species being one of the etiological agents of SHMA. We conclude that SMHA is not a disease entity but a special lymph node reaction to certain offending agents, probably in patients with immune dysfunctions. Therefore it should better be called Rosai-Dorfman lymph node reaction.

P-099

A disintegrin and metalloproteinase (adam) – a new class of invasion relevant proteins: expression of adam 9 in oral squamous cell carcinoma (OSCC)

H. Kosmehl, A. Berndt, Diana Schnabel, P. Hyckel*, D. Katenkamp
Institute of Pathology & Dept. Maxillofacial Surgery*, Friedrich Schiller University, Jena, Germany

Introduction: The ADAM family embraces more than 30 members and play a crucial role in sperm egg fusion. Because of the combination of adhesive and proteolytic properties the expression of ADAM9 is examined in relation to invasive behaviour in oral squamous cell carcinoma.
Methods: Shock frozen samples of normal (3), hyperplastic (7) and malignant oral mucosa of different grade (48). OSCC lines PE/CA-PJ15, PE/CA-PJ34. Immunhistochemistry: ADAM 9 antibody AB19025 (Chemicon), APAAP-technique. Western Blot: ADAM 9 antibody AB19024 (Chemicon). RT-PCR: Primer: 5′-TGT GGT AAT AAG TTG GTG GAC-3′ und 5′-TAG GCG TTT GAA TRA TAG CWG-3′.
Results: In normal oral mucosa ADAM 9 is restricted to the basal cells with polarisation towards the BM. In hyperplasia an increase of stained cells was seen including parabasal cells without polarisation. In OSCC a partial loss of ADAM 9 was demonstrated at deep invasive edges. The semiquantitative evaluation of ADAM 9 showed a positive correlation to malignancy grade. Additionally, ADAM 9 expression was evidenced in normal and malignant squamous epithelium and in OSCC culture by RT-PCR and Western blot.
Conclusions: (**1**) The expression of ADAM molecules is not restricted to fertilisation related cells. (**2**) ADAM 9 shows a distinct distribution pattern in normal mucosa with an association to the BM as the adhesive structure. (**3**) The ADAM 9 distribution pattern in normal and malignant oral mucosa parallels to the laminin binding $\alpha_6\beta_1$ integrin demonstration suggesting a role in regulation of invasive behaviour via the assumed function of modulating the $\alpha_6\beta_1$ integrin.

P-100

Proposal for a revisited classification of oral squamous cell carcinoma precursors: Oral Intraepithelial Neoplasia (OIN)

Küffer R., Lombardi T.
Laboratory of Oral Histopathology, Division of Stomatology, Faculty of Medicine, Geneva, Switzerland

Background: Clinicians classify oral "preneoplastic lesions" as "*leukoplakia*", "*erythroplakia*" and "*erythro-leukloplakia*", all beeing clinical terms. However, malignant transformation should be approached from the histological, and not merely clinical standpoint.
The concept of *cervical intraepithelial neoplasia* (CIN) could be adapted to the oral mucosa (**OIN**), with the same grades: OIN1 and OIN2 replacing respectively mild and moderate dysplasia, OIN3 replacing both severe dysplasia and carcinoma in situ (CIS). The problem of subjectivity in distinguishing the different grades is better resolved when OIN3 and OIN2 are grouped as ***high grade*** (HOIN), and OIN1 is considered as ***low grade*** (LOIN).
Clinical correlations for LOIN and HOIN, the same as those for micro-invasive squamous cell carcinoma, feature 4 fundamental clinical patterns with a spectrum of intermediate variants: "mosaic", a collection of white dots on a red plaque, "keratotic", an irregular white plaque with red background, "erythematous", a velvety red plaque without keratosis, and "normal mucosa" aspect, in which inconspicuous changes may appear only after application of special tests.
Conclusion: This unifying concept already accepted but not yet universally in use for other organs -- larynx: LIN; vulva: VIN, etc. – might allow a simplification and a better understanding of these lesions by clinicians, providing a more adequate treatment as a consequence of more consistency of histological diagnosis.

P-101

Salivary duct carcinoma oncocytic-like with endocrine features

Juan Laforga, M.D.
Department of Pathology, Hospital Marina Alta, Denia

Introduction: Salivary duct carcinoma (SDC) is a highly aggressive neoplasm affecting older, male patients and arising in major salivary glands. Clinically, these tumors are characterized by aggressive behavior with early distant metastasis, local recurrence and high mortality.
Methods: We present a SDC of parotid gland in a 75-yr. old male. The fine-needle aspiration was consistent with high-grade carcinoma.
Results: Histologically the tumor showed predominantly a solid and apocrine pattern. 12 regional lymph node metastases were observed. Immunohistochemical study showed positivity for cytokeratins (AE1/AE3), cytokeratin 7, GCDP-15, C-erbB-2, Mib-1, Topoisomerase II alpha, p53 and androgen receptors, Grimelius and Chromogranin-A. Phosfotungstic acid hematoxilyne, progesterone and estrogen receptors, cytokeratin 20 and S-100 stains were negative.
Conclusion: The clinical, cytomorphological and immunohistochemical features are consistent with a SDC displaying oncocytic-like and endocrine differentiation. We draw attention to the oncocytic-like and endocrine differentiation in SDC similarly as observed in breast cancer. The striking resemblance with both tumors might not be surprising.

P-102

Structure of vessels in squamous cell carcinoma of the larynx and its precursors

Jaakko Laitakari, Veera Näyhä and Frej Stenbäck
Department of Pathology, University of Oulu, Oulu, Finland

Introduction: Altered angiogenesis has been reported to have prognostic significance in laryngeal carcinoma development and in tumor classification, the characteristics of vessels are, however, largely unknown.
Material and methods: Structure, size, shape and staining intensity of Factor VIII, CD31 and CD34-stained blood vessels were examined by computer-assisted morphometry in 1420 vessels in squamous cell carcinoma of the larynx and its precursors.
Results: Vessel characteristics depended upon type of laryngeal lesion. The size of individual vessels increased in dysplastic epithelium prior to the formation of tumors, as did the number of large sized vessels. Alterations in vessel shape increased significantly with increasing degree of malignancy. FVIII staining intensity was decreased significantly in undifferentiated neoplasms. Comparing the characteristics of individual vessels showed the intensity of staining of vessel wall components to increase with vessel size. The intensity of endothelial staining was higher in regularly shaped vessels, while vessel shape abnormalities increased with increasing vessel size. The specificity and usefulness of different markers was also compared using a method giving 99.9% reproducibility and 99.9% sensitivity.
Conclusions: The results showed altered vessel characteristics to be an early event in laryngeal tumor development. Specific vessel populations were associated with morphologically distinct epithelial lesions and specific types of neoplasms. The results however, depended upon method of study.

P-103

Papillary squamous cell carcinoma of the oral cavity

Lombardi T., Samson J., Küffer R.
Laboratory of Oral Histopathology, Division of Stomatology, Faculty of Medicine, Geneva, Switzerland

Introduction: Papillary squamous cell carcinoma (PSCC), an unusual variant of squamous cell carcinoma is rarely observed in the oral cavity.
Aim of presentation: to illustrate the clinico-pathological features of PSCC, stressing the diagnostic difficulties.

Observations	Case 1	Case 2	Case 3
Sex/age	M/54	M/68	F/62
Cigarettes/day	80	40	–
Alcohol	++++	+++	–
Other risk factors	–	atrophic lichen planus	
Tumour site	floor of mouth	retromolar pad	floor of mouth
Invasion	non invasive/ invasive	non invasive	non invasive/ invasive
Evolution	nodes metastases with capsular effraction	lost at follow-up	recurrence/ extension fatal outcome

Clinical aspect is a solitary red papillomatous growth, sometimes with an adjoining patch of erythroplakia. Biopsy shows exophytic papillae with high-grade intraepithelial neoplasia. An invasive component, sometimes difficult to assess, may be present. Patients have no past history of viral papillomatosis. HPV DNA is rarely found with in situ hybridisation, but more often with PCR. Prognosis is poor.
Differential diagnosis: *Squamous Papilloma*, smaller and usually keratinised, *Condyloma acuminatum*, multiple, fleshy or greyish, *Inflammatory Papillary Hyperplasia* under an ill-fitting denture are easily ruled out. The main diagnostic challenge is *Verrucous Carcinoma* (VC) and its precursor *Verrucous Hyperplasia*, that are mostly more or less keratinised and rarely erythematous, with a pushing border for VC. Histologically, in VC mitoses and mild atypias when present are localised in basal and parabasal layers.

P-104

A prospective study of human papillomavirus infection as a risk factor for head and neck squamous cell carcinomas

Jon Mork, A. Kathrine Lie., Eystein Glattre, Sarah Clark, Göran Hallmans, Egil Jellum, Pentti Koskela, Bjørn Møller, Eero Pukkala, John T. Schiller, Zhaohui Wang, Linda Youngman, Matti Lehtinen, Joakim Dillner
From Cancer Registry of Norway, Oslo, Norway (J.M., E.G., B.M.); Department of Otolaryngology, National Hospital, Oslo, Norway (J.M.); Department of Pathology, Norwegian Radium Hospital, Oslo, Norway (A.K.L.), Clinical Trial Service Unit & Epidemiological Studies Unit, University of Oxford, Oxford, United Kingdom (S.C., L.Y.); Northern Sweden Health and Disease Study, Umeå, Sweden (G.H.); Janus Committee, Norwegian Cancer Society, Oslo, Norway (E.J.); National Public

Health Institute, Department in Oulu, Oulu, Finland (P.K.); Finnish Cancer Registry, Helsinki, Finland (E.P.); Laboratory of Cellular Oncology, National Cancer Institute, Bethesda, Maryland, USA (J.T.S.); Microbiology & Tumor Biology Center, Karolinska Institute, Stockholm, Sweden (Z.W., J.D.); National Public Health Institute, Helsinki, Finland (M.L., J.D.).

Background: Oncogenic human papillomaviruses (HPVs), especially HPV 16, cause anogenital epithelial cancers, and are suspected as a cause of epithelial cancers in the head and neck region.
Methods: We performed a nested case-control study within a joint Nordic cohort containing serum samples from almost 900000 subjects. Enrollment samples from 292 persons who developed head and neck squamous cell carcinoma on average 9.4 years after enrollment, and from 1568 matched controls, were analyzed for antibodies against HPV types 16, 18, 33 and 73, and for cotinine levels as a marker of smoking habits. Polymerase chain reaction (PCR) analyses for HPV DNA were performed on tumor tissue from 160 of the study patients.
Results: Cotinine-adjusted odds ratio for head and neck squamous cell carcinoma in case of
HPV 16 seropositivity was 2.2 (95 percent confidence interval=1.4–3.4). No increased risks were observed for other HPV-types. By subsite, significantly increased risks were seen for cancer of the oropharynx (odds ratio=14.4; 95 percent confidence interval=3.6–58.1) and tongue (odds ratio=2.8; 95 percent confidence interval=1.2–6.6), in particular base of tongue (odds ratio=20.7; 95 percent confidence interval=2.7–160). Fifty percent of oropharyngeal and fourteen percent of tongue cancers were HPV 16 DNA positive.
Conclusions: Evidence from a nested case-control study with prediagnostic assessment of virus exposure implicates HPV 16 infection as a risk factor for a sub-set of head and neck squamous cell carcinomas, most notably for base of tongue and oropharyngeal cancers.
Running head: HPV infection in head and neck squamous cell carcinoma
Key words: Seroepidemiology; Cotinine; Human papillomavirus DNA; Squamous Cell Carcinoma; Head and Neck cancer; Oropharyngeal cancer; Nested case-control-study.

P-105

Expression of MMP-9, E-cadherin and tenascin in laryngeal squamous cell carcinoma

Bahar Müezzinoğlu M.D., Önder Akdeniz M.D.,
Haluk Özkarakaş M.D.
Kocaeli University, Medical School, Department of Pathology and Department of ENT Surgery, Kocaeli, Turkey

Introduction: Cellular adhesion molecules, extracellular matrix and matrix degrading enzymes are presumably involved in the complex mechanism of cancer progression. In the current study the expression of E-cadherin (E-C), MMP-9 and tenascin (TN) in laryngeal squamous cell carcinomas (SCC) were investigated.
Methods: The localisation and intensities of E-C, MMP-9 and TN were immunohistochemically analyzed in paraffin embedded specimens of 41 primary laryngeal SCC cases. The results were correlated with tumor differantiation and the presence of lymph node metastasis (chi square test).
Results: MMP-9 was present in benign squamous epithelium. In 15 out of 41 (%37.3) SCC cases, MMP-9 expression was same or stronger than the normal epithelium. MMP positivity was detected in 19% of well differantiated and 55% of moderately or poorly differantiated tumors and the difference was statistically significant ($p<0.05$).
E-C was present in non-neoplastic squamous epithelium. E-C expression was significantly decreased in cases with lymph node metastasis ($p<0.05$). There was no correlation with E-C expresion and tumor differantiation.
Tenascin was present as weak and focal stromal staining beneath the non-neoplastic epitelium. In tumor tissue increased stromal expression was correlated with loss of tumor differantiation and presence of lymph node metastasis ($p=0.021$ and $p=0.049$ respectively).
Conclusion: Decreased E-C, increased stromal TN and presence of MMP-9 are possible indicators of loss of differantiation and enhanced invasive properties of laryngeal tumors.

P-106

Expression of $p21^{waf1/cip1}$ in sinonasal inverted papillomas, cylindrical cell papillomas, and associated carcinomas

Michael J. Schwerer, Adrian Sailer, Heinz Maier, Klaus Kraft
Abteilung Pathologie und Abteilung Hals-Nasen-Ohrenheilkunde, Bundeswehrkrankenhaus Ulm, Germany

Introduction: The $p21^{waf1/cip1}$ protein is associated with terminal differentiation and apoptosis. The expression of $p21^{waf1/cip1}$ was investigated in sinonasal lesions.
Methods: Archived surgical specimens from 38 patients were studied employing immunohistochemistry. Assessment involved $p21^{waf1/cip1}$ expression as well as Human papillomavirus (HPV) infection and p53 protein overexpression.
Results: Non-papillomatous nasal mucosa was negative for $p21^{waf1/cip1}$ expression, HPV infection and p53 protein overexpression. Sixteen of 20 inverted papillomas showed $p21^{waf1/cip1}$ expression. HPV infection was seen in 16 cases, p53 protein overexpression was found in 13 specimens. Expression of $p21^{waf1/cip1}$ was restricted to surface cells in 5 cases, but involved basal/ parabasal cells in 11 specimens. Immunoreactivity for $p21^{waf1/cip1}$ in basal/parabasal cells was closely associated with p53 protein overexpression. In cylindrical cell papillomas immunoreactivity for $p21^{waf1/cip1}$ was restricted to surface cells. HPV infection and p53 protein overexpression were found in all specimens. One of 5 squamous cell carcinomas associated with sinonasal papillomas showed $p21^{waf1/cip1}$ expression. HPV infection was demonstrated in 2 cases, p53 protein overexpression involved all carcinomas.
Conclusions: Expression of $p21^{waf1/cip1}$ is associated with terminal differentiation in surface cells in inverted papillomas and cylindrical cell papillomas, but not in non-papillomatous nasal mucosa. Overexpression of p53 protein activates $p21^{waf1/cip1}$ expression in basal/ parabasal cells in inverted papillomas but not in cylindrical cell papillomas. Expression of $p21^{waf1/cip1}$ involves a subset of p53-positive squamous cell carcinomas associated with sinonasal papillomas.

P-107

Sclerosing polycystic adenosis of parotid gland with dysplasia and ductal carcinoma in situ

Skálová A[1], Michal M[1], Simpson RHW[2], Stárek I[3], Přádná J[4], Pfaltz M[5]
Departments of Pathology, Medical Faculty of Charles University, Plzeň, Czech Republic[1]; Postgraduate Medical School, University of Exeter, England[2]; Department of Otolaryngology, Medical Faculty, Palacký University, Olomouc, Czech Republic[3]; Department of Pathology, District Hospital České Budějovice, Czech Republic[4]; Institute of Pathology, University Hospital of Zurich, Switzerland[5]

Introduction: Sclerosing polycystic adenosis (SPA) was recently described as a distinctive lesion of major salivary glands that bears a strong resemblance to benign fibrocystic disease of the breast. We describe three cases of sclerosing polycystic adenosis (SPA) of parotid gland with focal epithelial dysplasia that ranged from mild to low grade ductal carcinoma in situ. This feature has not previously been reported in SPA.
Methods and Results: Immunohistochemically, for the first time, we demonstrate a staining for oestrogen and progesterone receptors in ductal and acinar epithelium of SPA. Electron microscopic examination confirmed secretory activity in most cells of the lesion.
Conclusions: SPA is a rare salivary gland lesion that may simulate tumours, both clinically and microscopically, and despite possibly alarming features, such as epithelial hyperplasia and dysplasia, SPA seems to have a favourable outcome.

P-108

Immunohistochemical localization of extra-cellular matrix components in pleomorphic adenomas of salivary glands.

D. Stefanou[1], A. Nonni[1], M. Michael[1], D. Assimakopoulos[2], N.J. Agnantis[1]
Depts of Pathology[1] and Otorhinolaryngology[2], Medical School, University of Ioannina, Greece

INTRODUCTION: The distribution pattern of extracellular matrix components, i.e. tenascin, fibronectin, type IV collagen and laminin was studied immunohistochemically in normal human salivary glands and in pleomorphic adenomas.
METHODS: Fifteen pleomorphic adenomas and eight normal salivary glands were examined performing the LSAB method and using the monoclonal antibodies: anti-tenascin (DAKO), anti-fibronectin (Novocastra) and anti-collagen IV (DAKO) and the polyclonal antibody anti-laminin (Menarini).
RESULTS: In the normal salivary glands, all the components were almost co-localized in a linear delicate band-like pattern in the basement membranes surrounding ducts, acini, blood vessels, peripheral nerves and some fat cells. In pleomorphic adenomas, tenascin was strongly detected around the solid cell clusters and the ductular and trabecular structures, as well as in the areas with a myxoid and chondroid matrix. In almost all the cases, some cells in the solid epithelial nests or in the chondro-myxoid matrices, showed an intense cell membrane-like positivity. The immunoreactivity for fibronectin was similar to that one for tenascin, slightly more intense in some cases, with the presence of cells displaying cell membrane-like staining. Type IV collagen was localized around solid epithelial nests and tubular, trabecular or alveolar structures. It was also expressed in the myxoid and chondroid matrices. Laminin immunoreactivity appeared as basement membrane-like linear staining around the epithelial nests or structures, while the chondro-myxoid matrix was negative.
CONCLUSION: Our findings suggest, that these extracellular matrix components of pleomorphic adenomas, are involved in epithelial-mesenchymal interactions, which may contribute to tumour growth, cell differentiation and production of myxoid and chondroid matrices.

P-109

Expresion of p53 and Ki 67 in inverted sinonasal papillomas

Vladika I., Bura M., Nagy P.*, Aralica G., Perović D., Bijelić L., Seiwerth S.
Institute of Pathology, Medical Faculty, University of Zagreb, Croatia; * Medical University of Budapest, Hungary

Inverted papilloma (IP) is a benign tumor of the nose and paranasal. Squamosus cell carcinoma (SCC) appear synchronously or metachronously to IP. Most authors report 3-32% of IPs to be associated with SCC. It is obvious that identification of potential markers for malignant alteration of IP would be of great importance.
p53 is a well-known tumor suppressor gene. Its product plays an important role in cell cycle control and apoptosis. Mutations of the p53 gene are documented in nearly 50% of all human cancers.
Ki67 is one of the most prominent proliferation markers showing influence on biologic behavior or being associated with other prognostic factors in different tumors.
Material and methods: We analyzed 50 cases of IP including 8 cases of synchronous and 2 cases of metachronous SCC. The patients had diagnosed IP in the period from 1982 to 1999 at the Departments of Pathology in Zagreb, Osijek and Budapest. An image analyzer was used to determine the rate of nuclear staining.
Results and conclusion: p53: 14 specimens stained positive on immunohistochemistry. Among them all cases of SCC arising in IP, except one. The IP preceding SCC stained weakly positive in multiple areas, contrasting the negative staining of overt IP. This confirms a role of p53 mutations in the development of head and neck cancer, including SCC arising in IP. Ki67: Immunostaining was positive in all cases except one. The expression rate ranged from 0.03 in an papilloma to 0.7 in a carcinoma.

P-110

Squamous cell carcinoma of the larynx and hypopharynx-Expression of p53, p21, Rb and cyclin D1

Metka Volavšek, Nina Gale
Institute of Pathology, Medical Faculty, Ljubljana, Slovenia

Introduction: Increased cell proliferation is one of major mechanisms in carcinogenesis. Progression through cell cycle dependens on different growth promoting and inhibitory factors. Most important among them are cyclin D1, p53, p21, and Rb genes and proteins.
The presence and interrelation of immunohistochemically detected products of p53, p21, Rb and cyclin D1 genes in 102 squamous cell carcinomas (SCC) of the larynx and hypopharynx were studied.
Methods: Tissue samples were stained immunohistochemically with antibodies against proteins p53, p21, Rb and cyclin D1. Immune reactions were scored according to % of nuclear positivity in

tumor cells.
Results: Positive correlations were present between cyclin D1 and p21 (p=0,004), cyclin D1 and Rb (p=0,001), and p21 and Rb expression (p=0,025). An inverse correlation was present between tumor grade and Rb expression (p=0,004). There were no correlations with p53 immune reactions.
Conclusions: Our results showed alterations in cell cycle control in almost all cases. In tumor cells, both derailment of the apoptotic pathway (through p53) and growth promoting pathway (through overexpression of cyclin D1) of the cell cycle were present. The correlation between cyclin D1 and p21 (independent of p53) indicates that in tumor cells p21 expression is not always influenced by gene p53. The correlation between tumor grade and Rb expression suggests involvement of possible Rb gene mutations in development of SCC.
Prognostic significance of different alterations of the cell cycle control remains to be determined.

P-111

Computer ploidometria in differential diagnosing cancerogenesis stages
Avtandilov G.G., Perov Yu.L., Grigorjeva S.G., Zajratiants O.V.
Russian Medical Academy of Postgraduate Education, Moscow

Background: Solving many problems in oncology and surgery deals with precision of histopathological conclusions, the part of which is damaged by subjectivism. Objectivity of diagnosing early cancerogenesis stages is of particular importance.
Aim: Ploidometria results were used for histological diagnosing (mammary gland, for example).
Methods: Computer ploidometria of 15000 cell nuclei of mammary gland lobules and ducts in various cancerogenesis stages were performed. Sections with thickness 8 mkm, Feulgen's staining, were investigated (standard histological structures and their hyperplasia, mild and moderate dysplasia – mild intraepithelial neoplasia–MIN-1, severe dysplasia and cancer "in situ" – severe intraepithelial neoplasia – MIN-11 and infiltrating lobule and duct carcinomas). Analysers of imaging, Zeiss firm, with "Video-Test" programme and "Imager-CH" with "Avtan-San" ploidometria version were used.
Results: At epithelial hyperplasia indexes of DNA average contents in interphase nuclei increase within three quadratic deviation limits compared with the norm. In lobule epithelium further growth of ploidity is noted: at MIN-1 norm index exceeds1,3 times, at MIN-11–1,5 times, at invasive lobule carcinomas –1,9 times. Similar regularity is detected, when examining ploidity of duct epithelium cell nuclei: 1,1 times, 1,8 times and 2,1 times correspondingly. Special features of the dynamic of proliferative cell activity increasing have been established (exceeding DNA contents in nuclei of the level 2c).
Conclusions: Extensive employment of computer ploidometria in practice of making diagnosis is an additional objective criteria for a pathologist in order to make a decision while differential diagnosing benign or malignant tumor process.

P-112

Computed tomography-guided fine-needle aspiration (ctfnab) of intracavitary tumors
Baquera, J.
American British Cowdray Medical Center, Mexico

We performed 54 CTFNAB in 52 patients in a three year-period (1997–2000). The study group was divided by topography as follows: lung (53%), mediastinal (9%), liver (9%), páncreas (9%), spleen (4%), abdominal tumors (6%) and miscellaneous (9%). Cases were calssified as POSITIVE: those that showed unequivocal cytologic evidence of malignancy or tissue fragments with neoplastic features. NEGATIVE: those whose cytologic/structural features were characteristic of a benign or reactive process. NON-SPECIFIC: those samples with cellular elements native to the biopsied organ, which cannot explain the image or clinical picture. INADEQUATE: those bloody or acellular samples. Accordingly, material was divided as follows; positive 70%, negative 17%, non-specific 2% and inadequate 11%. A correlation of cases was made with surgical/trucut biopsy, immunohistochemical profile, a previously known primary neoplasm and, in selected cases, a highly suggestive CT or NMR impression. There were no false positive cases. There were five false-negative results. Cytologic results were, in lung, 4 adenocarcinomas, one Hodgkin's disease and two metastatic tumors. Mediastinal, one non-Hodgkin's lymphoma, one thymic cyst, one germ cell tumor and one metastatic neoplasm. Liver, one carcinoid tumor, one hepatocellular carcinoma and two metastasis. Pancreas, two adenocarcinomas and one neuroendocrine VIP-producing tumor. Overall sensitivity was 80%, specificity 100% and accuracy 83%. Complications were observed in four procedures; three pneumothorax and one patient with haemopthysis. CONCLUSION: In experienced hands, CTFNAB is a safety, cost-effective procedure to get adequate samples for cytopathologic examination.

P-113

Fine needle aspiration biopsy of a malignant rhabdoid tumour of the kidney associated with a neuroectodermal tumour of the central nervous system: report of a case
Barroca H, Magalhães J, Melo Pires M
Hernani Monteiro Servico de Anatomia Pathologica, Porto, Portugal

Introduction: Rhabdoid tumour is a rare tumour of childhood with a mortality rate that exceeds 80%. More frequently it appears as a primary renal tumour but other locations have been described. Association with embryonal central nervous system tumours is well documented. Several cases of rhabdoid tumour of the kidney have been described in association essentially with neuroepihelial tumours, and more rarely with gliomas or ependymomas.
Material and methods: we report a case of a newborn boy who presented a supratentorial mass. Biopsy was done. Six months later a tumour in the right kidney was detected. Fine needle aspiration (FNA) was performed. Nephrectomy was done for therapeutic reason. Immunohistochemistry studies were done both in the central nervous tumour and in the kidney mass. Material was also collected for ultrastructural studies.
Results and discussion: In the supratentorial tumour a PNET tumour was diagnosed. Cytologic diagnosis in the material obtained by FNA of the renal tumour was of a malignant rhabdoid tumour, confirmed by histology. Immunocytochemistry and electron microscopy studies of the renal tumour showed features already described by other authors in this kind of tumours.
The present case emphasises the association of embryonal tumours originating in the brain and in the kidney. This finding raises a hypothesis of a potentially fruitful area for biological investigation.

P-114

Systemic (AA) Amyloidosis in Rheumatoid Arthritis – The influence of septic infection, tuberculosis or associated malignant tumours. A Retrospective Study

M Bély*, T Szentjóbi Szabó*, Ágnes Apáthy**
Policlinic of the Hospitaller Brothers of St.John of God in Budapest*; National Institute of Rheumatology and Physiotherapy, Budapest, Hungary**

The aim of this study was to determine the role of lethal, generalised septic infection, or associated diseases like tuberculosis, and malignant tumours on the development and course of amyloidosis.
Patients and Methods: A randomized autopsy population of 234 in-patients (female 175, average age: 66.1 years; male 59, average age of 67.3 years at death) with *rheumatoid arthritis (RA)* was studied. AA amyloidosis (AAa), lethal septic infection (SI), inactive post-primary tuberculosis (Tb), or active miliary tuberculosis (mTb), and malignant tumours (mTu) was post mortem diagnosed histologically. The AA amyloid was characterized histochemically. The links between AAa and coexisting complications (SI, Tb, mT, and mTu) were analysed by χ^2-test.
Results: AAa was observed in 48 (20.5%), SI in 30 (12.8%), Tb in 23 (9.8%), mTb in 6 (2.6%) and mTu in 26 (11.1%) of 234 RA patients. AAa was associated with SI in 2, with Tb in 2, with mTb in 2, with mTu in 5 of 48 cases. There was no significant correlation between AAa and SI (χ^2=3.3960, p<0.06), Tb (χ^2=1.4547, p<0.22), mTb (χ^2=0.0760, p<0.78), or mTu (χ^2=0.0294, p<0.86).
Discussion: AAa may be considered a direct consequence of RA. Coexistent inflammatory complications (SI, Tb, or mTb, mTu) did not influence statistically the frequency of AAa in our autopsied RA patients.

P-115

Mortality in rheumatoid arthritis

M Bély*, T Szentjóbi Szabó*, Ágnes Apáthy**
Policlinic of the Hospitaller Brothers of St. John of God in Budapest*; National Institute of Rheumatology and Physiotherapy, Budapest, Hungary**

The aim of this study was to determine: the proportion of *basic* and *accompanying diseases* at autopsy of RA patients, the incidence of major complications, e.g. systemic vasculitis *(SV)*, AA amyloidosis *(AAa)*, and generalised sepsitc infection *(GSI)*, the mortality due to *SV, AAa,* or *GSI*, furthermore the clinically missed major complications in RA.
Patients and Methods: A randomized autopsy population of 234 in-patients (female 175, average age: 66.1 years; male 59, average age of 67.3 years at death) with *RA* was studied. The basic disease, complication(s), and causes of death were determined histologically.
Results: RA was the underlying cause of death in 175 cases (75%), while in the remaining 59 (25%) cases some other basic disease. *SV* was found in 51 (21.8%), *AAa* in 48 (20.5%), *GSI* in 30 (12.8%) of 234 RA patients. *SV* led to death in 23 (9.8%) of 51, *AAa* in 20 (8.5%) of 48, *GSI* in 30 (12.8%) of 30 cases. *SV* was detected clinically in 13 of 51 patients (25 rel%), *AAa* in 15 of 48 (31.2 rel%), *GSI* in 16 of 30 (53.3 rel%). Of a total of 129 complications in 114 patients only 44 (34.1%) were recognized clinically.
Discussion: Major complications, e.g. *SV, AAa, GSI* were the main causes of death in our RA patients. Coexisting complications modify the basic disease of RA and their own clinical manifestation, which may lead to an incorrect diagnosis or late recognition of the complications. More than half of de facto lethal complications was not diagnosed clinically

P-116

Somatic Genetic Alteration Testing ("Molecular Pathology") in Europe

Björn Logi Björnsson, M.D.
Department of Pathology, Lund University Hospital, Lund, Sweden
bjorn.logi.bjornsson@skane.se

Background
Somatic genetic alteration testing (SGAT) applications are increasing, however slower than scientific data. Methodology varies, which causes interpretation problems and calls for harmonisation. External quality assurance may be lacking. The expansion of SGAT places stress on continuing education and laboratory financing. These issues were explored in a European survey.
Methods
Fourhundred sixty-eight medical professionals 31 countries of Europe were selected for a survey, comprising European Society of Pathology (ESP) e-mail list members, ESP Advisory Board members, and authors of of 500 recent SGAT papers whose e-mail addresses were published. Only those who had responsibility for planning clinical nucleic acid-based tests on material submitted for anatomic or cytologic pathology examination were asked to respond. A Microsoft Excel® attachment contained 30 multiple-choice questions about types of SGAT and methodologies offered, quality assurance and method standardisation, limitations to use of the tests, and ideal functions of a SGAT-oriented profesional organisation.
Results
Forty-one response from 14 countries was valid. Twenty-six (63%) respondents were anatomic pathologists/cytologists and 6 (15%) were non-pathologist/cytologist M.D.s, others Ph.D.s. The most frequently mentioned difficulty with SGAT was test financing. The most important task for a molecular pathology organisation was considered test application consensus, followed by external quality assurance and e-mail information exchange forum. Other priorities included method harmonisation and collaboration in multicentre studies.
Conclusions
European practitioners of SGAT share several concerns. A discussion forum for SGAT diagnosticians in Europe is desirable. A website and e-mail "club" might satisfy initial needs and should be attempted.

P-117

Adult Gaucher's disease-report of four cases

Bogoeva B., Petrusevska G.
Institute of Pathology, Faculty of Medicine, Skopje, R. Macedonia

Gaucher's disease is an autosomal recessive lysosomal storage disease resulting from glucocerebrosidase deficiency.
We report four patients with "adult" Gaucher's disease, aged 19 and 65 (female), 17 and 66 (male). We used clinical histories and standard histochemical (hemalaun-eosin, PAS, Pearl's blue) and immunohistochemical stainings (CD68, HLA-DR).

Clinically they had episodes of weakness, paleness, fever, epistaxis, diffuse hemorrhages and haematomas, lymph node enlargement and chronic abdominal pain. Further clinical examination showed: progressive diffuse aseptic necrosis in the large bones, so called Erlenmeyer flask deformity and hepatosplenomegaly. The liver and the spleen were palpable at 4 to 8 cm and at 8 to 16 cm below the costal margin, respectively.

In one case symptoms of hypersplenism appeared and splenectomy was performed. The spleen weighed 4320 g, showing multiple nodules 0,5–2,5 cm in size and areas of subcapsular infarcts. Histologically the spleen tissue was infiltrated by large polygonal hystiocytic cells.

The other 3 cases were diagnosed on bone marrow biopsy.Gaucher's cells were seen as large cells with granular or fibrillar distended cytoplasm, with the characteristic "wrinkled tissue paper", and eccentric nuclei. PAS staining showed strongly positive granular or fibrillar material in the distended cytoplasm of the typical Gaucher's cells. Immunohistochemical stain for CD68 and HLA-DR helped to identify isolated Gaucher's cells. There was a correlation between the degree of splenomegaly and the parameters of hypersplenism. Splenectomy was effective in correcting thrombocytopenia, anemia and eliminating the distress caused by the massively enlarged organ. The treatment in all 4 patients was symptomatic.

P-118

Evaluation of multiple carcinomas using comparative immunoprofiling

O.J. Cooper (presenting author), D.M. Bailey
Department of Cellular Pathology, High Wycombe, UK

Introduction: In patients with multiple carcinomas, it can be difficult to distinguish metastatic lesions from new primaries or to decide the origin of metastases. This study uses multiple markers to distinguish carcinomas in 5 patients with multiple tumours.

Methods: All five patients were female. Patient 1 underwent hysterectomy for endometrioid adenocarcinoma. She was later diagnosed with rectal adenocarcinoma with similar appearances. Patient 2 underwent a mastectomy for ductal carcinoma. She later had a skin nodule removed from the mastectomy scar: differential diagnosis included melanoma and metastatic carcinoma. Patient 3 presented with squamous carcinomas of tongue, pharynx and oesophagus. Patient 4 had a ductal carcinoma of the breast removed. She later underwent nephrectomy for transitional cell carcinoma. She then developed liver metastases. Patient 5 underwent mastectomy for ductal carcinoma. She later underwent colectomy for adenocarcinoma. No nodal metastases were found, but a liver metastasis was biopsied.

Results:

Patient	Site	Immunoprofile	Conclusion
1	Endometrium	CA-125+, CK7+, CK20–, p53–	Two separate primaries
	Rectum	CA-125–, CK7–, CK20+, p53+	
2	Breast	CK7+, EMA+, S100–, bcl-2+	Skin nodule a melanoma
	Skin	CK7–, EMA–, S100+, bcl-2–	
3	Tongue	CK7+, p53–, bcl-2–	Three separate primaries
	Pharynx	CK7–, p53+, bcl-2–	
	Oesophagus	CK7–, p53+, bcl-2+	
4	Breast	CK7–, CK20–, bcl-2+, p53–	Hepatic metastasis from renal primary
	Kidney	CK7+, CK20–, bcl-2–, focally p53+	
	Liver	CK7+, CK20–, bcl-2–, focally p53+	
5	Breast	CA-125+, CK7+, CEA+, p53+, bcl-2+, EREC+, CK20–	Hepatic metastasis from colonic primary
	Colon	CA-125–, CK7–, CEA+, p53+, bcl-2–, EREC–, CK20+	
	Liver	CA-125–, CK7–, CEA+, p53+, bcl-2–, EREC–, CK20+	

Conclusion: A combined panel of epithelial and molecular markers may help delineate the nature of carcinomas in patients with multiple lesions. This can have significant impact on further management.

P-119

Histopathologic characteristics of chemically-induced mammary adenocarcinomas in rats fed diets high in (n-6) polyunsaturated lipids

I. Costa[1], J. Esquius[1], M. Solanas[2], R. Moral[2]; E. Escrich[2]
(1) Dpt. of Pathology. Hospital General de Granollers. Barcelona,
(2) Dpt. of Physiology. Fac. of Medicine. Universitat Autònoma de Barcelona

INTRODUCTION: The polyunsaturated lipids of vegetable origin -rich in linoleic acid, 18:2n-6- enhance mammary carcinogenesis. In the present study, we have analysed the effect of dietary n-6 polyunsaturated lipids on several histopathologic parameters of mammary adenocarcinomas chemically induced in the rat with 7,12-dimethylbenz(α)anthracene (DMBA).

METHODS: Two different experimental series (A and B) consisting of 60 Sprague-Dawley female rats each one, were used. The animals were given a single dose of 5 mg of DMBA per rat at 53 days of age, and were distributed in 3 groups: CONTROL (C), fed, once weaned, a normal diet -N3-, INITIATION (I), fed a high-fat diet -HL20 (20% corn oil)- from weaning until sacrifice and PROMOTION (P), fed the N3 diet from weaning until induction and the HL20 diet from this time until the end of the study.

RESULTS: In both experimental series, the number of epithelial proliferative lesions and adenocarcinomas was higher in the groups I and P than in the control group, specially in A (ci: 34, 64,7% malignant; I: 89, 78,6% malignant and P: 69, 94,5% malignant) ($p<0,05$). 19 adenocarcinomas from C, 64 from I and 66 from P in series A and 32 from C, 47 from I and 36 from P in B were submitted to histopathologic analysis. Similar results were achieved in both series. Thus, animals fed the high-fat diets, and specially those from group P developed more often than animals from group C pattern and nuclear grade III adenocarcinomas ($p<0,05$). Although most adenocarcinomas displayed less than 10 mitosis per 10 HPF,

adenocarcinomas with a high mitotic count were seen mainly in groups I and P. Adenocarcinomas exhibiting a moderate or a prominent lymphoplasmacytic and mast cell reaction and a desmoplastic stromal response were more numerous in group P than in C. Furthermore, group P adenocarcinomas presented higher rates of tumoral necrosis than group C ones and contained features of lipid secretion ($p<0,05$ in A).
CONCLUSION: Dietary fats could exert an effect on histopathologic characteristics of mammary adenocarcinomas, specially when acting as promoters of carcinogenesis, which are compatible with a greater degree of malignancy.

P-120

Clinical and pathological disagreement upon the cause of death in a school hospital – Analysis of 68 autopsy cases

Fernando L.P. de Carvalho, Patricia Maluf Cury,
José Antonio Cordeiro
Faculdade de Medicina de São José do Rio Preto, São Paulo – Brazil

Introduction: The autopsy rate is decreasing around the world due to the improving in the clinical and radiological diagnosis. However, there is still a disagreement between clinical and pathological cause of death when the patient is submitted to autopsy. In order to analyse this difference, we decided to evaluate the clinical and pathological diagnosis from autopsies performed in our hospital.
Methods: We studied 68 patients submitted to autopsy from July, 2000 to January, 2001.In all cases, the physician gave the immediate and the basic cause of death, and the diagnosis was compared with the autopsy macroscopic diagnosis done by the pathologist. Kappa coefficient was calculated.
Results: 41 men and 27 woman were submitted to autopsy (mean age 53,8). 29 patients died due to cardiovascular disease, 10 due to infectious disease and 29 due to other disorders. The kappa coefficient was 0,46 (95% CI: 0,33–0,59) in the immediate cause of death and 0,42 (95% CI: 0,30–0,55) in the basic cause. The agreement was greater with septicemia (10 cases) and acute myocardial infarction (6 cases) as immediate cause of death, and arteriosclerosis (7 cases) and AIDS (6 cases) as basic cause.
Conclusion: This study shows that there is a great disagreement in the clinical diagnosis when compared with the pathological one, proving that the autopsy is still a very important procedure.

P-121

Severe Tungiasis in a Community in Northeast Brazil: a clinico-pathological Study

M. Eisele*, J. Heukelbach**, E. van Marck***, H. Feldmeier*
* Institute of Tropical Medicine, Humboldt University Berlin, Germany, ** School of Public Health, Fortaleza, Brazil,
*** Department of Pathology, University of Antwerp, Belgium

Introduction: Tungiasis (jigger) is an ectoparasitosis caused by the flea *Tunga penetrans*. The female flea burrows into the epidermis and after fertilisation enlarges to a diameter of up to 10 mm. The disease is widely distributed in Latin America and sub-Saharan Africa. It mainly affects poor communities.
Methods: Patients with tungiasis were recruited from a „favela" (slum) in Fotaleza, Northeast Brazil. Eighty-six patients aged 1 and 67 years with tungiasis were examined clinically and biopsies were taken for histopathological sectioning.
Results: The average number of lesions was 28 per patient. Ninety % of all patients had lesions in the peri-ungual area of the toes, 24% showed tungiasis of hand and fingers. Signs of severe inflammation were observed in 64%. In 50% the nail was deformed, in 6% it had been lost. Ulceration occurred in 23%, bacteriological superinfection of the lesion was detected in 13% of the patients.
All biopsies showed hyperkeratosis, parakeratosis and epidermal hyperplasia. Spongiosis was observed in a few cases only. In the epidermis and the dermis reactive inflammatory changes were a constant finding. Lymphocytes, plasma cells, eosinophils and mast cells were the predominant cell types. In the late stage of tungiasis massive infiltration of neutrophils occurred eventually leading to the formation of micro-abscesses.
The histopathological examination of penetrated fleas confirmed the assumed correlation between clinical staging and vitality of the ectoparasite.

P-122

Histopathological Changes of Rabbits' Retina Induced by Therapeutic Doses of Hypericin

El Shazli, Elham
Research Institute of Ophthalmology, Cairo, Egypt

Hypericin and pseudohypericin have potent antiretroviral activity; these substances occur in plants of the Hypericum family. Both compounds are highly effective in preventing viral-induced manifestations that allow infections with a variety of retroviruses in vivo and in vitro. the aim of this study is to assess the effect of hypericin with the eye phototherapy doses on the retina of the rabbit in the dark and the light conditions.
This study included 7 groups of 5 rabbits each. The 1st and 2nd groups received hypericin (2.5 μM, 5 μM) topically (2.5 μM) and exposed to He-Ne laser (632.8mm) for 3 and 5 minutes respectively. The 5th and 6th groups received hypericin topically (5 μM) and exposed to He-Ne laser for 3 and 5 minutes respectively. The 7th group was used as control. The eyes were enucleated and processed for histopathological study.
Obtained data has revealed that group 1&2 showed vacuolation of retinal pigment epithelium disorganization & fragmentation of photoreceptors. Severe changes in the photoreceptor layer in the form of coagulative necrosis were seen when the eyes were exposed to laser (groups 3, 4, 5, &6) with the high dose rupture of the inner limiting membrane was recognized.
Phototherapy using hypericin is recommended under certain conditions via minimization of the drug concentration and the light exposure. Also fractionation of the hypericin dose and eye protection for those receiving such medications from the sun and artificial light are needed.

P-123

Carcinogenicity of dimethylarsinic acid, an inorganic arsenic metabolite in rodents

S Fukushima, H Wanibuchi, M Wei, E I Salim and K. Morimura
Osaka City University Medical School, Osaka, Japan

Arsenic is environmental carcinogen in human. However, there have been no animal data on arsenic carcinogenicity. Dimethylar-

sinic acid (DMA) is a major metabolite of inorganic arsenics in most mammals. Promotion effects of DMA were investigated using a rat multi-organ bioassay. Significantly increased tumor induction due to promotion of carcinogenesis by DMA was observed in rat urinary bladder, kidney, liver, and thyroid gland. Further experiments with two-stage rat urinary bladder and liver model systems showed that DMA enhanced tumor development with dose-response manner in both organs. In a carcinogenicity study, male rats received DMA in the drinking water for 104 weeks induced urinary bladder carcinomas. PCR-SSCP analysis of the bladder tumors revealed mutations to be few in H-ras and lacking in p53, Ki-ras, and fÀ-catenin genes. Also no alterations were observed microsatellite loci in carcinomas. Immunohistochemical analysis of the bladder tumors revealed high expression of COX-2 and cyclin D1. Increase of 8 hydroxydeoxyguanosine formation in the bladder treated with DMA was observed. Thus, the results indicate that DMA is a complete carcinogen in rat urinary bladder. In addition, p53 heterozygous knockout and C57BL/6T wild type, male mice were given DMA in the drinking water for 80 weeks. Carcinogenicity of DMA was evident by significantly earlier induction of tumors in both mouse genotypes. The promotion effects of DMA on skin carcinogenesis in the K6/ODC transgenic mice were investigated. Induction of skin tumors was significantly accelerated in the DMA-treated mice, as well as in the TPA-treated mice, indicating that DMA exerts promoting effects on skin carcinogenesis in K6/ODC transgenic mice. In conclusion, DMA is a rodent carcinogen and promoter which may be related to the human carcinogenicity of arsenics.

P-124

Mast cells variations with histopathological staging and grading in specimens of hepatocellular carcinoma

F. Grizzi, B. Barbieri, B. Franceschini, N. Dioguardi
Scientific Direction, Istituto Clinico Humanitas, Rozzano, Milan, Italy; Fondazione Michele Rodriguez, Istituto Scientifico per le Misure Quantitative in Medicina, Milan, Italy

Introduction: Mature mast cells (MCs) are important effectors cells found throughout the body. Although, a number of studies have highlighted different roles played by MCs in several human cancer, whether the density of MCs varies with histopathological staging and grading in specimens of hepatocellular carcinoma (HCC) has still to be established.
Methods: Twenty-three patients with primary HCC were studied. Patient's ages ranged from 48 to 80 years (mean, 69.7 years). Formalin-fixed and paraffin-embedded tumor sections were cut and subsequently analyzed. The lesions were graded and staged independently by two pathologists. Parenchymal MCs were stained with 0,1% Toluidine blue whereas extracellular collagen matrix by means of PicroSirius stain. The density of MCs per section was evaluated at a magnification of 200× under light microscopy. The amount of extracellular collagen matrix was measured by means of an image-analysis system. The results were assessed using the Spearman correlation and the Student's *t*-test.
Results: MCs are found within and at the periphery of the tumor tissue. A not significant correlation was found among the density of MCs and grade and stage of the lesions, age and sex of the patients, and serum enzymes (ALT, AST) levels. A strictly association betwen the MCs and extracellular collagen matrix was found.
Conclusion: This study evidences the independence among the density of MCs and histopathological staging and grading in specimens of HCC. Instead we identify a direct correlation between MCs and liver fibrogenesis, suggesting a possible role of MCs in the activation of producing-collagen cells, such as the Ito or fat-storing cells.

P-125

Adenomyoma of the vaterian system. Clinical and morphological characteristics of 11 cases and discussion of histogenesis

Handra-Luca A. (1), Terris B. (1), Couvelard A. (1), Kharsa G. (1), Bonte H. (2), Degott C. (1), Fléjou J.-F. (2)
(1) Department of Pathology, Beaujon Hospital, Clichy and (2) Department of Pathology, St. Antoine Hospital, Paris

Adenomyoma of the vaterian system is an exceptional benign, tumor-like lesion. The clinical and morphological characteristics of a large series of this lesion are reported.
METHODS: Clinical, morphological, histochemical and immunohistochemical (Mib1, SMA) characteristics of 11 cases of adenomyoma surgically resected between 1989–2001 were analyzed.
RESULTS: The age of the patients was between 39 and 78 years and the sex ratio male:female=5:6. In 2 cases the tumour was an incidental finding on echoendoscopy, in the other cases the main clinical complaints were jaundice and abdominal pain. The preoperative diagnosis was of ampullary tumour and patients were treated by pancreaticoduodenal resection.
The size of adenomyomas ranged between 10 and 30 mm. Adenomyomas involved the ampullary region, stenosing the common bile duct. Congenital anomalies of the pancreas were observed: pancreatic heterotopy in the duodenal wall (2 cases), pancreas divisum (2 cases) and annular pancreas (1 case). The lesion consisted in multiple lobules composed of glands, sometimes dilated, surrounded by a myofibroblastic proliferation and resulting in a "pseudohypertrophy" of the vaterian system . The epithelial cells stained with PAS and Alcian blue and showed low proliferative activity (Mib1 index). The myofibroblasts expressed SMA.
CONCLUSION: The location in the vaterian system of adenomyoma, is important because, in spite of its benign nature and small size, it is associated with biliary obstruction and is usually confused with carcinoma, often leading to extensive surgery. Pre-operative diagnosis on biopsy or frozen section specimen could lead to a limited surgical resection instead of pancreaticoduodenal resection.

P-126

Tyramide Signal Amplification (TSA™) in situ hybridisation for detection of human papilloma virus in routinely processed specimens dramatically increases sensitivity

Hauser-Kronberger C., Dandachi N., Zipperer E., Hacker GW., Dietze O.
Institute of Pathology, Landeskliniken Salzburg, Austria

INTRODUCTION: Human papilloma virus (HPV) are DNA tumour viruses associated with formation of epithelial tumours. Over 80 types of HPV have now been described and are categorised as

low risk (e.g. HPV-6 and HPV-11), intermediate risk (e.g. HPV-31 and HPV-33) and high risk (e.g. HPV 16 and HPV 18), based on their potential for malignant transformation. Non-isotopic *in situ* hybridisation (ISH) is a useful technique broadly applied in histopathology for detection of HPV in routinely processed paraffin-embedded specimens. A main disadvantage of conventionally performed ISH is the limited sensitivity of about 20 virus copies per cell. Tyramide based signal amplification (TSA) increases sensitivity and allows the detection of a single copy or very few copies of DNA-viruses. The aim of the present study was to evaluate the sensitivity and the routine use of TSA in Histopathology
METHODS: Routinely-processed, paraffin-embedded specimens from the years 1997/98 (n=151) were performed with conventional ISH without TSA. Specimens from the years 1999/00/01 (n=423) were detected for HPV combined with TSA-technique. Probe-mixes of HPV 6/11, HPV 16/18 and HPV 31/33/51 from Enzo (Germany) have been combined with Genpointkit (Dako, DK). HPV-negative or weakly-positive scored sections tested with conventional ISH were redone with TSA. For validation of the overall sensitivity SiHa cells known to contain 1–2 copies per cell of HPV 16 embedded in paraffin were used.
RESULTS: Sections routinely stained with a conventional ISH evaluated as negative or slightly positive for HPV 6/11, 16/18 or 31/33/51 turned out to be clearly positive after performing TSA. An increase of 15 % positive specimens using TSA was detected, more cellular structures were stained and single copy sensitivity has been achieved.
CONCLUSIONS: TSA-ISH dramatically increases sensitivity of HPV detection in routinely processed paraffin-embedded specimens.

P-127

Molecular Genetic Analyses in Laser Microdissected Single or Few Cell Samples Applications and Pitfalls

E. Heinmöller[1], B. Renke[1], K. Beyser, Steve S Sommer[2], J. Rüschoff[1]
Institute of Pathology, [1]Klinikum Kassel, Germany and [2]Dept.of Molecular Genetics, City of Hope, Duarte, USA

Introduction: Laser microdissection has opened an avenue to precise molecular analysis of histologically defined subcompartments of normal or diseased tissues. This directly enables insights into the molecular basis of dynamic processes such as carcinogenesis. Thereby, PCR-based whole genome amplification (WGA) prior to specific PCR enables multiple genetic analyses from sample sizes as low as a single cell.
Methods: We present a tissue fixation technique using ethanol and EDTA which allows immunohistochemical staining of two proteins (p53 and PCNA) simultaneously. From these tissues, single stained cells can be analysed for *TP53* mutations.
Results: Our optimised WGA protocol enables successful multiple molecular genetic analyses of more than 50% of single cells dissected from paraffin-embedded tissues. Allele drop out (ADO) is an important pitfall in the molecular analysis of templates consisting of 10 cells or less if the presence of a heterozygote sequence change or loss of heterozygosity (LOH) is of diagnostic interest. In our experiments, we found ADO-rates up to 78% when single cells prone to oxidative damage were analysed for heterozygote base changes.
In formalin fixed tissue samples from pancreatic cancer or preneoplastic duct changes we demonstrate multiple molecular genetic analyses in genes like *p16INK4, TP53* and *DPC4* using WGA prior to specific multiplex PCR. From one microdissected sample, we demonstrate analysis of LOH and genomic sequence analysis of particular genes simultaneously.
Conclusions: WGA together with multiplex PCR will greatly facilitate future studies of neoplastic disease from single or few cells dissected from either ethanol- or formalin fixed tissues.

P-128

The value of the immunocytochemical staining in the cytodiagnosis of malignant pleural effusions in breast cancer

Jovicic Milentijevic M., Ilic R., Zivkovic V., Stefanovic M.*
Institute of Pathology, Gynecology Clinic*,
Medical School of Nis, Yugoslavia

Introduction: The diagnosis of serous effusions remains one of the most difficult tasks in diagnostic cytology. This study was carried out in order to determine the usefulness of immunocytochemical analysis of pleural effusions due to breast carcinomas in discriminating between reactive mesothelial and neoplastic cells.
Methods: All samples (40) came from patients who had been documented as having primary breast carcinoma. Immunocytochemistry was performed by the ABC method, using following markers: carcinoembryonic antigen (CEA), epithelial membran antigen (EMA), cytokeratin (CAM 5.2) and S-100 protein.
Results: Neoplastic cells of breast carcinoma in all cases demonstrated a strong peripheral membrane type staining with EMA and CEA, while mesothelial cells were negative. All effusions gave negative results with S-100 protein. In 16 cases neoplastic cells exhibited moderate or strong diffuse cytoplasmic staining with CAM 5.2, while mesothelial cells showed strong positive reaction for cytokeratin.
Conclusion: Immunocytochemistry is advocated as very helpful especially in solving doubtful cases. It could be recommended as a routine procedure for greatly increasing the diagnostic yield of cytology in pleural effusion due to breast cancer. EMA and CEA , in contrast to CAM 5.2 and S-100 protein, are specific markers proposed to identify carcinoma cells and to differentiate them from reactive mesothelial cells in pleural effusions due to breast carcinoma.

P-129

Correlation of histopathologic features and serologic tests in toxoplasmosis

S. Kabukcuoglu[1], N. Dogan[2], N.Tel[1], U. Oner[1],Y. Akgun[2], E. Vardareli[3]
Departments of Pathology[1], Microbiology[2] and Gastroenterology[3], Osmangazi University Medical Faculty, Eskisehir, Turkey

In this study, various biopsy and autopsy cases which have histopathologic features of *Toxoplasma gondii* infection were prospectively investigated between 1999 July and 2001 January in Osmangazi University Hospital. Correlation between histopathologic diagnosis and serologic tests were studied. Suspected tissues were stained by PAS, PAS diastase, Prussian blue and Toxoplasma ab-1

(NeoMarkers) stainings. Histopathologic differential diagnosis was made among immunglobulin deposits, whipple disease and other parasiter diseases. Toxoplasma infection was considered as a possible reason of disease in 19 cases: there were 4 cases of chronic hepatitis, 3 cases of cervical lymphadenitis, 1 case of intestinal lymphangiectasia (abdominal lymph node biopsy), 1 case in lymph node of gall-bladder, 1 case of spinal arachnoiditis with old chorioretinitis scar was observed in retina, 1 case of muscle biopsy, 1 case of simple bone cyst, 1 case of bone marrow biopsy diagnosed as idiopathic trombocytopenic purpura, 3 cases of lung and liver micronecropsies from the newborns, and 3 cases of perinatal autopsy. Serologic studies were performed with specific *Toxoplasma gondii* antibodies including Ig G, Ig M, Ig A, avidity by EIA. 13 of 19 cases were studied until today serologically and had found positivity at least in one of the tests in all cases. In the same period, 2459 serum samples were studied in our hospital. Ig G positivity was found in 589 samples, Ig M positivity was found in 25 samples.
This study and our previous study on congenital toxoplasmosis revealed that Toxoplasmosis is an important health problem in our city and its surrounding and, this necessiates community education for prevention.

P-130

Nipah virus the newly discovered paramyxovirus infection in Malaysia: pathological findings of 9 fatal cases from Ipoh.

Norain Karim , Sherif R Zaki *, Thomas G Ksiazek *
Pathology Dept.,Ipoh Hospital, Ipoh, Perak, Malaysia;
* Centre for Disease Control and Prevention (CDC), Atlanta, Georgia

Ipoh City is the first focus of the newly discovered Nipah virus, which affect pigs and human closely in contact with pigs. During the epidemic from December 1998 until April 1999, Ipoh reported 15 deaths and 27 cases out of total 105 deaths and 265 cases throughout Malaysia. This study is to report the pathological findings of the 9 post-mortem cases from Ipoh. The virus causes systemic manifestation affecting the lung, kidney, spleen, heart with predilection to the brain. This could be explained by vasculitis along with microinfarction seen microscopically. Other unique microscopical characteristic findings are syncytial cell formation and eosinophilic inclusion. The immunohistochemical studies show presence of antigens in neurons, epithelial, stromal and inflammatory cells. All the 9 postmortem cases died of encephalitis and lung infection. The fact that the virus consistently affects the endothelial cells, neurons and only some of the organs, indicates the presence of tissue tropism of Nipah virus. The pathological study may also help deduce the pathogenesis of the disease.

P-131

The effects of Electromagnetic Fields on the spermatogenesis of Rats

Kateby, Majid
Tehran, Iran

Electromagnetic fields (E.M.F) are integral part of modern life. The present study was undertaken to investigate the short-term morphological responses of seminiferous tubules to the E.M.F. Adult wistar rats (n=48;weighing 250–300) were exposed to 80 gause E.M.F for tow months. Animals were injected intra peritoneal with heparin to facilitate clearance of blood vessels of testis (Sprando 1990) and subsequently perfused through the heart. The vessels of testis were first cleared with 0.9% saline and then perfused with Bouin's solution as fixative. Tissues was dehydrated with increasing concentration of alcohol,dealcoholized with xylene and infiltrated with paraphin. Cross sections were cut at approximately 4μm, stained with Hematoxylin and Eosin. A stage related (Stages VII, XIII and XIV) analysis was performed by using the criteria to classify cell; developed by Leblond and Clermont (1952) as modified by Russel et al. (1990). In instances where degenerating cells were seen, they were identified by their morphological characteristics as compared with viable cell types remaining in that seminiferous tubule or with cell types at the same phase of development in control animals. The results revealed that seminiferous tubules were separated from each other and their epithelium showed a significant ($P<0.05$) reduction in the numbers of Spermatogonia, Primary spermatocytes and Spermatids. These changes were associate with necrotic cells and piknotic nuclei in the germinal epithelium especially in stage XIV. These finding suggest, the possible detrimental effects of E.M.F on spermatogenesis in man, should be taken in consideration.

P-132

DFNA5 is involved in acquired etoposide resistance in melanoma cells

Hermann Lage[1], Claudia Grottke[1], Heike Helmbach[2], Manfred Dietel[1], Dirk Schadendorf [2]
[1] Institute of Pathology, Charité, Berlin, Germany,
[2] Skin Cancer Unit at the DKFZ, Heidelberg, Germany

Resistance to drug treatment is a common observation in malignant melanoma. In order to analyze alterations in mRNA expression profiles associated with drug resistance in melanoma cells we previously established a panel of various drug-resistant cell variants derived from the human melanoma line MeWo and compared the mRNA expression profiles by a differential display technique. By that approach it could be demonstrated that the expression level of a mRNA encoded by a gene found to be mutated in nonsyndromic hearing impairment, DFNA5, was distinctly decreased in the 33-fold etoposide-resistant melanoma cell line MeWo ETO 1. To evaluate the hypothesis that a decrease in DFNA5 mRNA expression level contributes to the acquired etoposide-resistant phenotype exhibited by MeWo ETO 1 cells, this drug-resistant line was stable transfected with the DFNA5-encoding cDNA. Transfected clones showed a 30–35% reduced etoposide susceptibility by comparing the IC_{25}, IC_{50} and IC_{75} values of these clones with those displayed by the non-transfected, etoposide-resistant melanoma cell line MeWo ETO 1 and controls. Furthermore, etoposide exposure of stable DFNA5 transfectants resulted in an increase of caspase-3 mediated apoptotic events in DFNA5 transfected clones in comparison to MeWo ETO 1 cells and controls. The data therefore, demonstrate that a decrease in DNFA5 mRNA expression level is associated with reduced etoposide resistance in melanoma cells due to an increased cellular susceptibility to trigger a caspase-3-depending signal pathway leading to programmed cell death.

P-133

Effect of combined chemotherapy and anti-inflammatory drugs on murine schistosomiasis

Madiha R. Mahmoud, Mona M.K. Zoheiry and Mona M.F. Nosseir.

Schistosomiasis is an endemic disease in Egypt, leading to hepatic granuloma formation around ova deposited by living worms. Anti-inflammatory drugs, ibuprofen (IBP)or naproxen (NAP) (200 mg/kg b.w. daily for two weeks) either alone or in combination with anti-schistosomal drug, praziquantel (PZQ) (500 mg/kg b.w. for two consecutive days) were given to mice 7 weeks post-infection. Animals were sacrificed 9, 11 and 16 weeks post-infection. The use of non-steroidal anti-inflammatory drugs (NSAIDs) which are known to inhibit cyclo-oxygenase might be effective in inducing regression of preformed granulomas or in ameliorating the pathological consequences of schistosomiasis mansoni infection. Infection with S. mansoni increased the level of alanine aminotransferase (ALT), gamma glutamyl transferase (GGT), Prostaglandin E2 (PGE2), hepatic collagen deposition, antibody (Ab) titre and circulating schistosomal antigen (CSA). The last parameter was reduced significantly by progression of infection at 11th and 16th weeks with marked diminution in granuloma diameter and increased collagen content. Treatment with PZQ was found to reduce the number of worms (97%), with complete absence of immature ova and increase in the number of dead ova. Also it reduced all the elevated parameters except PGE2. NSAIDs were found to reduce significantly the level of PGE2 at 9 weeks but not at 11 and 16 weeks post-infection. ALT & GGT were not significantly decreased compared to their corresponding controls. Treatment with IBP or NAP either alone or in combination with PZQ or PZQ alone reduced significantly the seveity of infection, attenuate hepatic fibrosis & granuloma diameters but didn_t affect the Ab titre, circulating Ag levels or granuloma type from their corresponding controls. Combined therapy of PZQ with IBP or NAP improved most of the parameters estimated including fibrotic area percentage as detected by Image Analysis System and maintained the reducing effect on PGE2 at 11 and 16 weeks post-infection. So, we can conclude that, in S. mansoni infection treatment with IBP or NAP is not preferable without treatment of schistosomiasis by using PZQ.

P-134

Peripheral blood film technique for the preparation of fine needle aspiration (FNA) of lymph nodes

J.M.E. Martin, G. Al Rasheed
King Faisal Specialist Hospital and Research Centre, Riyadh, Saudi Arabia

INTRODUCTION: FNA of lymph nodes is well established but there is ongoing debate as to whether FNA is adequate for an initial diagnosis of lymphoma. Often there is cell distortion resulting from the smearing technique used in slide preparation. This can result in cell overlapping and disruption, which obscures cellular detail. Operator dependent variables may further compromise morphology and assessment. Finally, economic constraints may make it difficult to schedule lymph node excisions, thus putting more pressure on the pathologist to make a definitive diagnosis by FNA.
METHODS: Twenty-five lymph node FNAs were prepared using both smearing and peripheral blood film techniques. In the latter, a drop of aspirate is placed at one end of the slide. A second slide is placed in front of and at a 45° angle to the specimen which is then "dragged" along the length of the slide.
RESULTS: There were 14 patients with lymphoma, seven with Hodgkin's disease and four with lymphoid hyperplasia. The blood film technique resulted in less overlapping and fewer bare nuclei. Intact cells were present in monolayer sheets toward the feathered end of the slide.
CONCLUSION: Peripheral blood film technique for FNA of lymph nodes produces consistent morphology with greatly reduced cell distortion. When used in conjunction with surface marker studies the findings may be sufficient to render a definitive diagnosis of lymphoma, thus precluding the necessity for a surgical biopsy.

P-135

The UK National External Quality Assessment Scheme for Immunocytochemistry [UK NEQAS]: the development of a website[http://www.ukneqas.org.uk] to help participants

KD Miller, CA Rhodes & RJ Medcalf
Histopathology, Royal Free & University College London Medical School, University Street, London WC1E 6JJ, UK

Introduction: The UK NEQAS for Immunocytochemistry has been established for 16 years and now has participants from many parts of the world. Besides offering assessment of immunostained slides it provides, through the Journal of Cellular Pathology, a detailed analysis of the methodology employed. This includes photomicrographs of some of the immunostained sections and examples of best methods.
For many years this has helped participating laboratories keep up to date with the rapid improvements in the field. Nevertheless, the difficulty with reporting only through a journal is that much time is required to publish and distribute the journals around the world. With website technology rapidly improving, it is now possible to distribute the information much more quickly via the net.
Development of the Website
The website for the Immunocytochemistry Scheme can be reached via http://www.ukneqas.org.uk which is the main site for all UK NEQAS activities. The immunocytochemistry website provides examples of best methods and images for a whole range of antigens employed. This includes those used in general histopathology practice, breast cancer, lymphoma, neuropathology and non-gynae cytology.

P-136

The histopathology effect of regemen contains 10% corn oil (C.O) consumtion on the exocrine part of rabbit pancreatic

Dr Minaii, B. Ph.D
Department of Histology, Faculty of Medicine, Tehran University of Medical Sciences, Tehran, Iran

The recent investigation have shown that (C.O) stimulates the cancer promotion. This study aimed to evaluate the effects of three regimens contains 10% (C.O) on the rabbit pancreatic tissues. Twenty-four rabbits were divided into four groups. The first group took the regimen for one month, the second group for two months,

the third group for three months, the third group for three months, and the fourth group was considered as control group with regimen without (C.O). At the end of each period, autopsy from the pancreas of the subjects were examined by using H & E and P.A.S staining methods. The pancreas histological views of each group were compared with the control. In the first group, the pancreas weight was reduced. In the second group there was hypertrophy in the pancreas and vaculation plus infiltration of lipid to the acinar cells. In the third group, the pancreas weight was reduced while there was increases in zymogenic granules and infiltration of adipose tissues. Based on the results, we concluded that (C.O) regimen in short term (one month) induces changes to pancreas that will be compensated in long term perhaps by some adaptation mechanisms.

P-137

Primary limphoma of the male breast (case report)

Nebojca B Mitic, Dani Milicic, Dragutin Savjak, Voja Pavlovic
Institute of Pathology, Faculty of Medicine Pristina; General Hospital Trebinje; Institute of Pathology, Faculty of Medicine, Podgorica; Institute of Phisiology, Faculty of Medicine, Nis, Yogoslavia

Primary limphomas of the breast are extremely rare. Up to 1994 reported only 293 cases of the primary female breast lyphomas. This paper presents primary limphoma of the male breast. In the male patient, 59 years old, insulin dependent diabetic, a few yeas after myocardal infarct, in yhe upper medial qadrant of the left breast the tumor was appeared. The tumor was diagnosed with ultrasound as a hypoechogenic zone with unclear margins dimensions 19×16mm. Axilary lymph nodes were not enlarged.
Laboratory analyses of the blood were SE 18/47, He 167, Er 5,2, Le 4,5, Ly 38,3%, Mo 4,3%, Gr 56,9, Hct 46,3, Plt 84.
Quadrranttectomy was done without biopsy before.
Morphologically, oval shape, solid tumor, smooth white-redish surface with quite clear margins, larger diametar 3 cm, deep in the fat tissue, dosen't link with skin and pectoral muscle.
Histologically, nodular pattern with nodular agregates of follicular small cleaved cells, with rare mitotic figures and little cytologic atypia. Tumor cells express CD20 and CD79α.
Clinical examination, rendgenography of the lung, echoyomography of the abdomen and laborbiochemical analyses didn't detect any other location of the tumour.
Ten mounts later patiebt feels well.

P-138

Mitotic density appreciation using cytomorphometrical method on malignant melanoma of the choroid

Simona Mocan[1], Simona Stolnicu[1], Doina Radulescu[3], Doina Frincu[2], Modis Laszlo[4], Cristian Podoleanu[5], Jung Janos[1]
1. Department of Pathology, University of Medicine Târgu-Mure, România; 2. Department of Anatomy, University of Medicine, România; 3. Department of Pathology, University of Medicine, România; 4. Eye Clinic, University of Medicine Debrecen Hungary; 5. 3rd Medical Clinic, University of Medicine Târgu-Mure, România

Introduction: Proliferation activity represent one of the most important prognostic factors in malignant melanomas of the choroid. It can be appreciate using several methods, including mitotic activity. We tried to establish a correlation between mitotic activity and the microscopic cell type in order to determine the survive of these patients.
Methods: H-E stained slices were made of specimens from 56 patients. The microscopic tumor types, established according to Callenders classification, modified by the pathologists from AFIP were: 27 MM spindle type, 28 MM mixed type and 1 MM necrotic type. The presence of very pleomorphic spindle cells in some of these tumors made us subclassified each type (except the necrotic type) in classic (without spindle pleomorphic cells) and pleomorphic (with spindle pleomorphic cells). The mitotic index and mitotic density were performed on 16 of the 56 cases (8 spindle cell type and 8 mixed cell type), using the Prodit 5.2 program.
Results: Both parameters were higher in mixed type than in spindle type. The highest results were observed in spindle and mixed tumors containing pleomorphic spindle cells.
Conclusions: Thus, we believe that the pleomorphic subtype of spindle and mixed malignant melanomas of the choroid may have a worse prognostic.

P-139

Cytopathological changes in ependymal cell nuclei in next generation of pregnant rabbits that consumped hydroquinone (H.Q)

Mohammad H.Noori, Babak Behnam
Department of Histology, Faculty of Medicine, Tehran University of Medical Sciences (TUMS), Tehran, Iran

This study is to identify epandymal cell nucleus abnormalities in next generation under the effects of (H.Q) consumption by pregnant mother. We took 32 (n=8, N=32) pregnant Albino rabbits with 5–6 months age and 1.8–2 kg weight as control and following 3 stages; I or predifferentiation (1–7 days), II or embryonic (8–15 days) and III or fetal stage (16–32 days). Remaining 8 pregnant rabbits received no drug, considered as match controls. We used 2% (H.Q) cream on the back skin of pregnant rabbits in 3 above stages, topically. Then spinal cords of embryonic stages were taken. All samples stained by H&E, observed by light microscopy and compared together & control, too. As a result, we found that only a limited number of ependymal cells in stage I showed any pyknotic nuclei. Some inactive nuclei observed in stage II. However, many of the nuclei showed pyknosis and vacualation in stage III. Since CSF secretion by ependymal cells have so important role in normal physiologic function of CNS & PNS and to avoid cytopathological & moderate cytotoxic side effects during pregnancy period, further study in human is recommended.

P-140

Comparative effectiveness of *malva sylvestris* (M.S) and bromhexine hcl (B.H) on intraepithelial mucous glands (IMG) of trachae in chicken

Mohammad H.Noori, Babak Behnam, Bagher Minaee
Department of Histology, Faculty of Medicine, Tehran University of Medical Sciences (TUMS), Tehran, Iran

The purpose of this study was to determine the effectiveness of (M.S) extract on IMG. The chicken were divided in 5 groups (n=6,

N=30). They exposed to extract of (M.S) orally and in nebulizing form, then compared to oral (B.H) & nebulizing form of normal saline. In oral route, 5ml of the extract (10%) and 5ml of (B.H) used every 12 hours. In nebulize form, 1ml of the extract (5%) and 1ml of normal saline used. A group received no drugs as control. After a period of 12 days, all of the animals' middle tracheas were taken for histopathology study using PAS and H&E methods under light microscopy. Number and size of (IMG) & cilia assessed in each sample (based on 1–4 plus) to compare. Histopathologic analysis demonstrated that nebulizing of (M.S) increases the number and the size of (IMG), also the size of cilia, compare to other 3 groups, significantly ($P<0.05$). In addition, the use of oral (M.S) extract resulted in an increment in number of mocous glands but not in size, significantly ($P<0.05$). The data suggest that (M.S) extract in particular the nebulizing form of it, may have good prospects as a mucociliary function activator.

P-141

Evaluation of the effect of Ro 15-5458 and combined antischistosomal drugs on different strains of Schistosoma mansoni infected albino mice: Histopathological and Parasitiological study

Mona Nosseir, Aisha Metwally, George Kamel, Fatem Guirguis and Nevine Nessim

Ro15-5458 is an experimental chemotherapy for schistosomiasis. Praziquantel is the established drug of choice, but recently some reports of tolerance and perhaps resistance to praziquantel have been reported. This work is a trial to study the efficacy of Ro 15-5458 and possible additive or synergistic effect of both praziquantel and Ro15-5458 on one praziquantel susceptible strain (CD group) and three recently isolated praziquantel resistant strains in S. mansoni infected albino mice, labeled as So5, Mo3, and EE2 respectively. Treatment was administered six weeks post-infection including full dose of both PZQ and Ro15-5458, subcurative dose of the same drugs alone and combined third dose of both drugs. The efficacy of these therapeutics was assessed by: Histopathological examination of the liver specimens; oogram changes; hepatic and intestinal worm and egg load.

The hepatic histopathological changes revealed decrease in granuloma count and size particularly in the CD susceptible and Mo3 resistant strains receiving combination therapy (2–3 and 2–4 per 5 successive LPF respectively and 200m in both groups). In the control infected untreated mice this range reached 8–11and 5–8 in 5 successive LPF and 250 and 275m respectively. The granulomas were small, fibrocellular & lobular in location. More degenerative changes were seen in ova and dead worms lodged in portal blood vessels. Maximal parasite reduction (100%) was recorded in CD susceptible strain. Comparing treatment with PZQ alone in most strains, the percentage parasite reduction was increased from 65.2% to 81.7% using combined therapy with disappearance of couples especially in CD susceptible and Mo3 & EE2 resistant strains. There was disappearance of the immature stages in the oogram pattern and rise in the percent of dead ova. The number of ova per gram tissue (liver and intestine) was decreased especially in EE2 resistant strain.

The importance of this study is that an alternative to praziquantel therapy appears to be a possibility in the event of the appearance of more widespread resistance to praziquantel.

P-142

Changing public attitudes to organs or media hype? The controversy about retention of organs following autopsy

D.S. O'Briain
Histopathology Department, St James's Hospital and Trinity, College Medical School, Dublin, Ireland

Parents of dead children with congenital heart disease, who had given permission for autopsy, learned in 1999 that the hearts had been retained in a Dublin pathology department. Their distress and anger led to a public campaign and resulted in condemnation by the media and politicians of pathologists and of organ retention, and the setting up of a national judicial inquiry. Similar controversy has also recently occurred in other countries. Pathologists responded by introducing new guidelines for hospital autopsies to ensure informed consent, to tell relatives if any organs are retained, and to give them options for disposal.

Method: examine why a practice in line with current international autopsy practice is suddenly condemned by the public.

Results: Multiple factors are involved including evolving attitudes to completely informed consent, dominance of individual rights over public good, emotion of bereavement, absence of specific laws or regulations, pressure groups and media coverage. A major underlying factor is that pathologists, and clinicians who obtained autopsy permission, regarded organs with dignity but not equating with the body for purposes of burial and so did not consider it a sufficient issue to further distress bereaved relatives about their retention. The contrary attitude of some relatives has now informed public opinion.

Conclusion: It's difficult to determine if there has been a change in attitude to organs, if a real latent attitude has been revealed, or if this is a temporary accentuation by the media of primal objections to the autopsy. Pathology has been damaged, both by loss of public confidence, and by
limiting optimal use of the autopsy for advancing medical knowledge.

P-143

New autopsy organ retention regulations: distressed relatives, agitated doctors but fewer autopsies

D.S. O'Briain, E.F. Gaffney
St James's Hospital and Trinity College Medical School, Dublin, Ireland

New guidelines on autopsy practice were introduced in Ireland in February 2000 after complaints from parents of dead children that organs had been retained following autopsy without their knowledge and consent. The guidelines require, for both paediatric and adult hospital autopsies, that relatives be fully informed on the nature of the autopsy before giving consent and must specifically decide if organs may be retained. Consent is not required for coroner (medicolegal) autopsies. If organs are retained in hospital or coroner autopsies the relatives must be informed and given the options for their disposal by the hospital or privately.

Methods: Review of autopsies in a major Dublin adult teaching hospital since the new guidelines. Findings: The number of hospital autopsies fell by 50%. Clinicians describe the need for prolonged detailed and often distressing discussions with relative be-

fore consent is given; refusal of consent is more frequent and permission for organ retention is frequently declined. For coroner autopsies it has been extremely difficult to notify relatives that organs (such as a brain when a neurological cause of death is suspected) have been retained. It has been necessary to appointment professional social workers as bereavement councillors to inform relatives but the information often causes considerable distress. Organ disposal ranged from hospital-arranged cremation to large funeral services.

Conclusion: The area of organ retention is now a difficult and distressing one for relatives, pathologists, clinicians and social workers. Despite extra resources and large input of effort by hospital staff, the optimal procedures are still in evolution.

P-144

The scientific achievement of Rudolf Virchow in Polish medical magazines in 19th century

Panasiewicz Małgorzata, Sabat Daniel, Dziembała Anna
Department of Pathomorphology, Medical Faculty in Zabrze, Silesian Academy of Medicine in Katowice, Poland

Development of pathological anatomy in the second half of the 19th century was mainly associated with the scientific activity of Rudolf Virchow. This year we celebrate the 180th birth anniversary and next year the 100th death anniversary of this outstanding man. The paper presents the scientific achievements of Rudolf Virchow as it was presented in Polish medical magazines in the 19th century. In 1858, the theory of cellular pathology introduced by him, became a basis of understanding and fighting against pathologic processes in living organisms. The theory also contributed to an increased interest in pathologic anatomy, especially histopathology and Virchow himself. In 1859 an extensive summary of the issued a year before article entitled "Cellular pathology based on physiological and pathological theory of cells" appeared in the subsequent issues of "Tygodnik Lekarski" ("Medical Weekly"). Also a translation of the XI chapter of "Cellular pathology..." devoted to nerve tissue appeared in the same magazine. This is the only written in Polish treatise on the most important work in the history of pathological anatomy of the 19th century.

Three years later, in 1862, Włodzimierz Brodowski delivered to the students of Medical and Surgery Academy in Warsaw a lecture "Introduction to a lecture on pathological anatomy" which was later printed in "Pamiętnik Towarzystwa Lekarskiego Warszawskiego" ("Diary of Warsaw Medical Association"). He presented a development of pathological anatomy along with the achievements of Virchow. Brodowski was the first polish anatomopathologist who lectured to students on Virchow's theory. The date of his lecture 7 February 1862 has been acknowledged as the beginning of the modern polish pathological anatomy based on microscopic – histopathologic study.

In 1869, "Gazeta Lekarska" ("Medical Magazine"), in a Foreign News column, issued a translation of Professor Virchow's lecture, delivered on the 43rd meeting of German doctors and naturalists in Innsbruck, entitled "Present Standpoint of Pathology". Moreover, a paper "Scientific activity of Rudolf Virchow and its importance for medicine" by Edward Przewoski was published in the series "Clinical Lectures" issued by the editors of "Gazeta Lekarska" ("Medical Magazine") in 1892. The article included a detailed description of scientific activity of that outstanding scholar. Apart from the above mentioned examples, Virchow's opinions not only on pathological anatomy and medicine but also on, for example, anthropology were often presented.

P-145

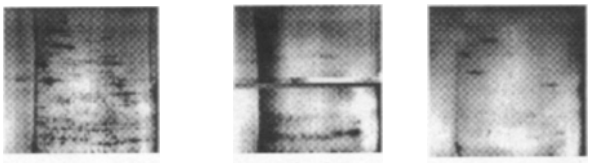
Utilization of cytology smears and manual micro-dissection for proteomic analysis

Panizo, D.Roberts, H. Al-Barazi, B. Bryant, M.C. Garcia-Macias, A. Chiesa, J. Pardo, M.J. Merino
National Cancer Institute, Bethesda, MD; University of Salamanca, and University of Navarra, Pamplona, Spain

Introduction: Proteomics-based studies contribute to our understanding of tumoral behavior and progression through identification and quantification of proteins. A major factor limiting the application of proteomics has been the difficulty in obtaining pure populations of cells, and the needed of fresh frozen tissue. These facts limit the utility of this technique on archival biopsy material. We performed manual microdissection (MM) and protein extraction for proteomic analysis from archival cytologic material.

Methods: 15 cytology specimens from thyroid, prostate and kidney (11 FNAC and 4 thinprep) were used in the study. All specimens were ethanol-fixed, and stained with either Diff-Quik (4), Papanicolaou (4), H&E (1), eosin (2), and unstained (4). Cytology smears were prepared from each case and manually microdissected (1–3 slides/case). A comparison of protein concentration and protein profiles between stains and type of cytologic material was performed. Microdissected cells were directly lysed in lysis buffer, and protein concentration was determined. First-dimensional electrophoresis was carried out on a Immobiline IPG DryStrip system using 3–10 pH nonlinear gradient. Second-dimensional electrophoresis was carried out using SDS-PAGE gels 1-mm thickness. Following electrophoresis, gels were fixed and stained using a silver staining kit and scanned. Scanned images were analyzed and compared.

Results: MM and protein extraction took 30 minutes in each case. MM from cytologic specimens permitted the detection of approximately 500 distinct proteins as visualized by silver staining. Cells from the ethanol-fixed and unstained cytologic slides gave the best results as compared with Papanicolau or Diff-Quik. Papanicolau and DQ showed either weakly detectable or undetectable spots in 2D gel. Thinprep specimens can not be used in proteomic analysis due to the very small amount of proteins extracted.



Conclusions: Proteomics is the most sensitive technique for detection of new proteins. Unstained ethanol-fixed cytologic smears provide a powerful tool for proteomic analysis, and therefore expand the range of archival materials available for retrospective proteomic study. MM from cytologic specimens may offer a viable, fast and cheap approach for the identification of new tumor-associated proteins important for the development of new markers that can be used in diagnosis, early detection and follow up.

P-146

Electromagnetic field - induced upregulation and expression of bone morphogenetic proteins 2, 4 and 7 in the kidney and lung of the rat embryo

Athina Pyrpasopoulou*, Vassiliki Kotoula*, Angeliki Heva*, Prodromos Hytiroglou*, Ioannis Magras**, Thomas Xenos***, Theodoros Tsiboukis***, George Karkavelas*
* Dept. of Pathology Medical School, ** Dept. of Anatomy, Histology and Embryology, School of Veterinary Medicine, *** Dept. of Electrical and Computer Engineering, Polytechnic School, Aristotle University of Thessaloniki, Greece

Introduction: Bone morphogenetic proteins (BMPs) are required for the patterning of most organ systems during vertebrate embryogenesis. In vitro irradiation of rat osteoblasts by pulsed electromagnetic fields (EF) has been shown to induce osteogenesis and transcription upregulation of BMPs 2 and 4. The aim of this study was to investigate possible effects of EF irradiation on the expression of BMPs in vivo.
Materials and Methods: We submitted rat embryos to pulsed modulation waves (9,35 GHz) during gastrulation or early organogenesis (days 1–3 or 4–8 pc respectively) at a power density of 5 $\mu W/cm^2$ and analyzed the expression of BMPs 2, 4 and 7 in the kidney and lung of day 1 newborns by immunohistochemistry and Western blotting. Tissues from the mother animals were also examined.
Results: In comparison to untreated matched control newborns, BMP 4 upregulation was observed in the kidneys (mesenchyme) of irradiated animals. Additionally, BMPs 2 and 4 were induced in the collective tubules. In the lung of control newborns, expression of the BMPs examined was restricted to the bronchial epithelium, while in EF irradiated animals it was also observed in the respiratory epithelial cells. These effects of EF irradiation were more prominent when applied during gastrulation. No differences in BMP expression were observed in the corresponding tissues of the mother animals.
Conclusion: These data suggest for the first time that EF irradiation influences BMP gene expression in vivo, preferentially affecting developing tissues. Because of the established roles of BMPs in epithelial-mesenchymal interactions, further investigation of the issue seems mandatory.

P-147

Amyloid accumulation in pituitary adenomas

Hakan Sayrak
Dr. Pakize I. Tarzi Laboratuvarlari, Patoloji Bölümü Sefi, Istanbul, Turkey

Introduction: To determine frequency of the amyloid deposits in pituitary adenomas, and it's relationship between histological types and stages, age and sex of the patients, retrogressive changes and lymphocytic inflammation.
Method: Study group consisted of 30 sequntial patients with pituitary adenomas ages between 20–70. The sections of the paraffin blocks of the surgical materials were stained with alkalen Kongo Red (with and without permanganate), Masson's trichrome, von Kossa, Prussian Blue and HE. A light microscope was used for examinations. Results were compared statistically with Spearman's correlation analysis.
Results: Permanganate resistant amyloid deposits of perivascular type were seen in 15 adenomas (50%). Amyloid deposits was found in 57. 14% of the nonfunctional adenomas and 47.8% of the functional adenomas. The proportion of the retrogressive changes in adenomas were as follow: fibrosis 90%, calcification 13.33%, infarction 43.33% and old hemorrhage 60%. Lymphocytic inflammation was seen in 11 cases, and 10 of them had amyloid deposits. There were no correlation between the amyloid deposits and either patient's age and sex, tumor stages-types, and retrogressive changes. There was a positive correlation between the amyloid deposits and lymphocytic inflammation in tumor tissue (p:0.022, r:0.4168).
Conclusion: Lymphocytic inflammation may play a role for amyloid accumulation in pituitary adenomas.

P-148

A test hierarchy to recognize mycobacterial infections by PCR

C. Schewe, M. Rizzello, M. Dietel and S. Hauptmann
University Clinics Charité, Institute of Pathology, Berlin, Germany

Background: In granulomatous inflammations an etiologically based diagnosis is mandatory. Unfortunately, conventional staining methods did not reach a satisfactory sensitivity, particularly for the diagnosis of mycobacterial infections. Therefore, PCR is the method of choice to ascertain a reliable diagnosis. In this study we summarize our experience in molecular diagnosis of mycobacterial infections with fixed material.
Materials and Methods: Mycobacterial DNA was detected in paraffin-embedded formaline-fixed tissue samples and cytological preparations. The tissue samples were subjected to enzymatic digestion and heat denaturation; DNA was purified by a Qiagen kit. Seven different primer sets were used: four were designed for genus-specific regions, one for *Mycobacterium tuberculosis* complex (MtbK), and two for specific detection of *M. tuberculosis*. The amplification products were detected by agarose gel electrophoresis and ELISA.
Results: Based on the experience with 400 cases within four years we have established a test hierarchy for reliable detection of mycobacteria. Sample digestion, purification and examination of DNA were optimised. For diagnostic purpose, the MtbK-PCR as well as a nested PCR were found to be reliable, but to establish an unequivocal diagnosis of *M. tuberculosis* infection positive results in two independent reactions are necessary.
Conclusions: Primers for MtbK are suitable for a primary screening for tuberculosis, but the nested PCR with *M. tuberculosis*-specific primers are necessary to ascertain the diagnosis. Positive results with genus-specific primers and negative results with primers for *M. tuberculosis* complex indicate atypical mycobacterial infections and necessitates further microbiological verification.

P-149

Upregulation of P-glycoprotein in the apical membranes of duodenal enterocytes after thyroxine administration

E. Schroeder[1], S. Vogelgesang[1], W. Meng[3], S. Altmannsberger[2], A. Paneitz[2], M. Knoke[3], B. Sperker[2], H.K. Kroemer[2], W. Siegmund[2], R. Warzok[1]
Dept. of Pathology[1], Dept. of Pharmacology[2], Dept. of Internal Medicine[3], University of Greifswald, Germany

Introduction: P-glycoprotein (P-gp), the MDR1-gene product, is a transmembrane protein that plays an important role in drug resistance. In patients with hyperthyroidism the effect of certain drugs such as digoxin is decreased. Since digoxin absorption is controlled by intestinal P-gp, we hypothesized that thyroid hormones might be inducers of P-gp expression in man.
Methods: Expression of intestinal P-gp was measured in 8 healthy volunteers by automated immunohistochemistry before and after treatment with thyroxine, as well as by quantitative RT-PCR. Protein expression of P-gp was evaluated semiquantitatively (Kontron, KS Release 3.0) and data are presented as the mean±S.D. Statistical analysis was carried out using the non-parametric Wilcoxon's signed rank test (SPSS software, SPSS Inc., Chicago, IL, U.S.A.).
Results: We found that MDR1-mRNA was localized in the cytoplasm of enterocytes and was up-regulated in six of eight volunteers after thyroxine (0,64±0,3 vs. 0,87±0,14; P>0,05). P-gp is mostly located in the apical membrane of enterocytes and to a lesser degree in the cytoplasm. Semiquantitative analysis of protein expression showed increased levels in all subjects after drug administration (5,2±5,8 vs. 16,4±13,6; P<0,05).
Conclusions: Thyroid hormones are endogenous inducers of P-glycoprotein. Up-regulation of P-glycoprotein in patients with hyperthyroidism might explain why higher doses of some drugs are required (eg. digoxin).

P-150

The role of FNAB in differential diagnosis between non functioning pan-creatic islet tumor and pancreatic adenocarcinoma. A case report

P. Sevastiadou[1], E. Athanassiou[1], I. Efstratiou[2], P. Xirou[2], Ch. Makridis[3], I. Tsitouridis[4]
1. Dep. of Cytopathology, 2. Dep. of Pathology, 3. 1st Dep. of Surgery, 4. Dep. of Radiology, G. Hospital "Papageorgiou" N.Efkarpia 56429, Thessaloniki, Greece

Non functioning pancreatic islet tumors are rare malignancies without association to a specific clinical syndrome. Either these tumors do not secrete enough hormones or the secreted hormone does not cause specific symptoms. Tumor behavior and prognosis are more favorable than in patients with exocrine pancreatic tumors. Since surgery as appropriate therapeutic option depends on diagnosis the tumors must be differentiated from pancreatic adenocarcinoma. Lack of circulated hormone peptides, except chromogranin, makes FNAB and immunocytochemistry necessary for preoperative diagnosis. SRS may contribute to diagnosis and detect small or distant metastases.
A 51 years old male was admitted in our hospital because of weight loss. Abdominal CT examination revealed multiple voluminous liver metastases and a tumor mass. The available checked circulating peptide levels were normal. SRS, 111-octreoscan, was strongly positive in all tumor localizations.
FNAB of a liver lesion was performed. Moderately cellular smears composed of a homogenous population of single cells or in loose clusters. Rare rosette-like clusters were also observed. The nuclei were round, uniform with finely granular chromatin and tiny nucleoli. Immunocytochemistry with available peptides was failed to express staining properties. The findings were not typical for an adenocarcinoma and suggested a probable malignant non functioning islet tu-mor. Though cytological findings could not be supported by immunocytochemistry the findings of SRS and CT imaging appreciated in addition to morphology advocated the diagnosis.
Distal pancreatectomy with dissection of lymph gland metastases was performed. Histopathology and immunohistochemistry expressed positive chromogranin staining and confirmed the diagnosis.

P-151

Morphology of brown adipose tissue in experimental fasting

Sidlo, J.*, Sidlová, H.**, Bukovská, E.***, Kvasnicka, P.****, Zaviacic, M.**
* Institute of Forensic Pathology, Slovak Postgraduate Academy of Medicine, Bratislava; ** Institute of Pathology, School of Medicine, Comenius University, Bratislava; *** Institute of Medical Biology, Jessenius School of Medicine, Comenius University, Martin; **** Faculty of Mathematics and Physics, Comenius University, Bratislava, Slovakia

Introduction: Fasting is considered to be a borderline state between physiology and pathology. Brown adipose tissue (BAT) is a very specialised tissue distributed only in certain portions of the body. Its metabolic activity is much higher than in white adipose tissue. The aim of the study was to investigate influence of fasting on rat intescapular BAT amount and morphology.
Methods: Male laboratory Wistar rats were divided in two groups. One group of animals was fasting for a period of seven days. Another group received standard chow diet ad libitum. Both groups had free access to water. After decapitation the interscapular BAT was removed and weighted. Samples were fixed in formalin, processed by routine methods and embedded in paraffin. Sections were stained with hematoxylin-eosin.
Results: Fasted rats showed significant reduction in body weight compared with ad libitum fed animals. Also the relative amount of interscapular BAT (calculated to 100 g of the body mass) decreased to 50% of control group. Microscopic appearance of interscapular BAT was as follows: in fasted animals was the structure composed of fat depleted D cells of BAT with addition of very rare cytoplasma rich (CR) cells of BAT containing only very small lipid droplets. In ad libitum fed group multilocular cells of BAT were present.
Conclusions: The occurrence of fat depleted D cells of BAT in animals was not up to now described. These cells are considered to be unable to produce heat. This fact may be partly responsible for arising of hypothermia ascertained by fasting.

P-152

Mast cells in the development of metha fibrosarcoma after i.t. rhTNF-α administration

Terlikowski S.J.*, Nowak H.F., Sulkowska M., Famulski W., Sulkowski S.
Depts. of Obstetrics and Gynecology* and Clinical Pathology, Medical Academy of Białystok, Poland

Aims: The aim of the study was the ultrastructural analysis of mast cells (MC) in the primary foci of methA fibrosarcoma after intratumor (i.t.) injections of the recombinant human tumor necrosis factor alpha (rhTNF-α).

Methods: The study used BDF_1 mice (n=40). The tumor was induced s.c. using methylcholantren (Sigma) in a dose of 100 μg/0.2 ml of sesame oil (Sigma). rhTNF-α (ZChB CBMiMPAN, Łódź, Poland; activity 4×10^7U/mg protein) was injected i.t. in a dose of 10 μg/24 h, in an 8-day cycle (n=25). Control group (n=15) received PBS i.t.
Results: MC constituted a constant compartment of all the tumor zones examined except for the hemorrhagic necrotic foci. On TEM the MC population after rhTNF-α administration was heterogenic. Two basic MC groups were distinguished: MMC (Mucosal Mast Cells) and CTMC (Connective Tissue Mast Cells). Numerous mitochondria, well-developed RER and Golgi apparatus, clusters of polyribosomes, a large number of lamellar and myelinic structures, and considerable polymorphism of granules were the exponent of MC activity after i.t. injections of rhTNF-α.
Conclusions: The criteria applied in the study allowed evaluation of maturity of the MC taking part in the local antitumor response induced by i.t. rhTNF-α injections.

P-153

The effects of corn oil on the Liberkuhn glands of rabbit
Thorabi [1*] G.A., Noori [2] M.H., Minaee [2] B.
Department of Histology, Faculty of Medicine [1] Tabriz University of Medical Sciences, Tabriz, Iran; [2] Department of Histology, Faculty of medicine, Tehran University of Medical Science, Tehran, Iran

The recent investigations have shown the oils such as corn oil stimulate the cancer promotion specially colon cancer. This study was under taken to evaluate the effects of three regimens containing 10% corn oil on the Liberkuhn glands of rabbit colon. Twenty-four rabbits were divided in to four groups. The first group took the regimen for one month, the second group for two months, the third group for three months and the fourth group were considered as control group with the regimen containing no corn oil. At the end of each regimen, biopsies from the colon of the subjects were examined using PAS and H&E staining methods. The results in each group were compared with the control. We observed that in the one-month and two-month regimen Liberkuhn glands were shorter than those of control were, but in the three-month regimen glands were the same as those of control were. We concluded that consumption of corn oil may induce some changes on the Liberkuhn glands and changes will be ceased by some adaptation mechanisms in long term diet (group3).
Key words: 1-rabbit, 2-corn oil, 3-Liberkuhn gland

P-154

Carcinosarcoma. A clinicopathological study of 39 cases
Tzaida O, Sotiropoulou G, Lekka I, Iakovidou I, Trichia H, Arapantoni-Dadioti P
Pathology Dpt , Metaxa's Cancer Hospital, Piraeus, Greece

Thirty nine cases of carcinosarcoma (CaSa), an unusual malignant neoplasm derived from a single totipotential stem cell that differentiates into separate epithelial and mesenchymal directions, are described.
In our material 15 cases (39,9%) were localized to the female genital tract in the form of the malignant mesodermal mixed tumors and 8 to the female breast (22,8%). The mean age of these two subgroups was 66,3 years. The rest of the tumors were localized to the lung (5), urinary tract (3), salivary glands (3), skin (3), gallbladder (1) and thyroid (1) in patients of both sexes with a mean age of 73,2 years and predominance of the males (M/F:14/3). The size of the tumors varied from 2 to 22 cm.
Histologically the tumors had the feature of biphasic neoplasms with sharp morphological appearance and discrete immuno-histochemical demarcation of the two components. In 23 cases the epithelial component was adenoCa (66,6%), in 6 squamous Ca (15,3%), in one mixed Ca and in 5 cases undifferentiated Ca. The mesenchymal component was mainly homologous in the type of fibro-, leiomyo- or stromal Sa. In 15 cases (38,4%) heterologous elements were diagnosed such as lipoSa (3), chondroSa (2), osteoSa (1), malignant fibrous histiocytoma (1) or a mixture of two or more of them (6). Regional LNs metastases were found in 7 cases (18%). In 11 patients (31,4%) we have observed infiltration of adjacent tissues or/and disseminated metastases to bones, liver and lung at or nearby the time of diagnosis. Despite the combined administration of radio- or chemotherapy 9 of them, all but one, with heterologous tumor element, died in a period varying from a few months to one year.
In conclusion CaSa are neoplasms of the elderly, have aggressive biological course and poor prognosis depending mainly on the clinical stage and the presence of heterologous tumor element.

P-155

Pitfalls in Fine-Needle-Aspiration (FNA) and Imprint – Cytology of skeletal and extraskeletal sarcomas
Liliana Vasile[1], Elena Lazar[2], Romanita Glaja[2], Marioara Cornianu[2], Alex. Prundeanu[3], O. Mazilu[3]
[1] Department of Histology, University of Medicine, Pharmacy Timisoara Romania, [2] Department of Pathology, University of Medicine, Pharmacy Timisoara Romania, [3] City Hospital, Deparment of Orthopaedics and Surgery Timisoara

Introduction: Cytodiagnosis of sarcomas represent an important step in the selection and therapy of bone and soft tissue tumors. Our study focused on the error sources which reduce the accuracy of cytological interpretation releated to clinical-radiological data.
Methods: Between 1998–2000 cytological samples were obtained from 35 selected cases via FNA and imprints of seriated biopsic specimens: bone malignant tumors (n=15), extraskeletal sarcomas (n=16), metastasis (n=4, of which primary lung tumors n=2, invasive melanomas n=2). The samples were air-dried or alcohol fixed before staining with Blue-Polichrom-Tanin-Dragan, MGG and Papanicolaou methods. The cytodiagnosis was correlated with the histodiagnosis by histochemical (Alcian-blue, PAS, silver impregnations) or immunohistochemical methods (CKs, S-100 protein, Vim, Desm, HMB45, lymphoid and neural markers).
Results: We have studied the chromatinian pattern, the cytological-architectural characteristics and tumoral matrix. The cytodiagnosis was based on the presence of 6 groups of predominant tumoral cells. Insuficience amount of aspirative material occured in 8% of cases. Reactive cell proliferation, small round cells, osteosarcoma cells were the most important source of error (fals-positive results, n=6; false-negative results, n=2). The main cause for false-negative results were extensive fibrosis, intratumoral calcifications, vascular ectasia, osteoblastic giant cells and atypical mezenchymal cells. The cytodiagnosis has a sensitivity=92% and specificity=83%.

Concordance of cyto-histopathological findings was 86% for imprints and 88% for aspirative pontions.
Conclusions: Source of error previously stated were found to reduce the accuracy of the cytodiagnosis for a quarter of cases.

P-156

P-glycoprotein (P-gp) and multidrug resistant related protein (MRP2) are up-regulated in duodenal enterocytes after carbamazepine administration

S. Vogelgesang[1], E. Schroeder[1], B. Sperker[2], I. Cascorbi[2], T. Giessmann[2], M. Knoke[3], U. Hecker[3], R. Warzok[1]
Dept. of Pathology[1], Dept. of Pharmacology[2], Dept. of Internal Medicine[3], University of Greifswald, Germany

Introduction: P-gp and MRP2 are transporter proteins that are involved in multidrug resistance, eg. in tumors and epilepsy. To test the hypothesis that carbamazepine is an inducer of P-gp and MRP2, we examined gene and protein expression in the apical membranes of duodenal enterocytes after drug administration.
Methods: Expression of intestinal P-gp and MRP2 was measured in 8 healthy volunteers before and after treatment with carbamazepine by automated immunohistochemistry and by quantitative RT-PCR. Protein expression of P-gp and MRP2 was evaluated semiquantitatively (Kontron, KS Release 3.0).
Results: In all cases the duodenal mucosa showed no histologic peculiarities. We found that P-gp was located in the apical membranes of enterocytes and to a lesser degree in the cytoplasm. Quantitative analysis of P-gp expression showed increased levels in seven of eight subjects after carbamazepine administration (P=0,07). mRNA-levels of duodenal P-gp were increased in seven out of eight volunteers too. Moreover, after carbamazepine administration we found increased levels of MRP2 expression in the apical membrane of enterocytes (P=0,008). and in the endothelium of capillaries in the lamina propria and submucosa.
Conclusions: Carbamazepine is an inducer of P-glycoprotein and MRP2. Up-regulation of transport proteins after carbamazepine administration might be responsible for the drug resistance in patients with epilepsy.

P-157

Histological Evaluation of Intraosseous Implantation of Silated Hydroxyethylcellulose Mixed with Hydroxyapatite or β-Tricalcium phosphate

Wierucka-Młynarczyk Beata*, Sabat Daniel**,
Książek-Bąk Halina*, Bulek-Juranek Grażyna*, Ilewicz Leszek*
* Department of Conservative Dentistry and Periodontology, Silesian Academy of Medicine in Katowice, Poland,
** Department of Pathomorphology, Medical Faculty in Zabrze, Silesian Academy of Medicine in Katowice, Poland

Silated hydroxyethylcellulose creates a network of hydroxyethylcellulose chains connecting by silane coupling agents, which are known as a useful means to form crosslinks between organic and inorganic materials. Such structure, enabling the penetration of newly formed bone into polymer, can help us treat bone defects (periodontal pockets, furcation defects). We predict the possibility of using polymer as a carrier, for such materials as hydroxyapatite, tricalcium phosphate or calcium hydroxide, in conservative dentistry, endodontics, periodontology etc.
Silated hydroxyethylcellulose was mixed with hydroxyapatite or β-tricalcium phosphate (βTCP) and implantated in jaws of 12 rabbits. The animals were put down after 8 or 12 weeks. The excised specimens (the implant sites) were demineralized in 10% EDTA, dehydrated and embedded in paraffin. They were then sectioned and stained with haematoxilin-eosin for light-microscopic observation. The tissue response was classified as minimal according to ISO standard, which means that there was no bone resorption around implants.

P-158

Histological, histochemical and immunohistochemical changes of benign prostatic hyperplasia (BPH) after the chernobyl accident in ukraine

Larisa Zabarko[1], Sergey Vozianov[1], Bela Szende[2], Alina Romanenko[1]
[1] Departments of Pathology and Endourology, Institute of Urology and Nephrology, Academy of Medical Sciences of Ukraine, Kiev, Ukraine, [2] First Institute of Pathology and Experimental Cancer Research, Semmelweis University of Medicine, Budapest, Hungary

After the Chernobyl accident during the last 14 years the incidence of prostate carcinoma in Ukraine increased from 5.1 to 18.3 per 100000 of the male population. It is known that a cancer risk at high doses of ionizing radiation implies a cancer risk at low doses. Morpholigical, histochemical (apoptosis) and immunohistochemical (expression of proteins p53, Ki-67 and PCNA) changes in prostatic tissues from patients with BPH were studied. Group I, the control group –45 patients who underwent surgery before the Chernobyl accident, group II –47 patients-inhabitans Kiev-City and group III –76 patients who are living in the radiocontaminated areas of Ukraine. The levels of the ^{137}Cs in the urine of 51 patients with BPH from group II, III have been measured.
The present study shows the significant increase of incidence of the prostatic intraepithelial neoplasia (PIN) in BPH from patients of groups II and III ($p<0.02$).The apoptotic indices, the indices of PCNA-, Ki-67-reactivity in BPH and PIN of groups II and III were significantly greater than of group I ($p<0.001$). The indices of p53 reactivity in groups II and III were significantly greater than in group I ($p<0.05$).
The radionuclide ^{137}Cs was detected in the urine in all cases of groups II and III. The difference between the levels of ^{137}Cs in those groups is not significant (1.14 ± 0.43 and 3.22 ± 1.90 correspondingly; $p>0.05$). Those changes could be a result of influence of the long-term low dose ionizing radiation.

P-159

Efficacy of cortisone as immuno-pharmacological therapy and schistosomicide in murine schistosomiasis mansoni

Nayera R. Zaki, Amal A. El-Shafei, Mona M. Moussa, Mona M.K. Zoheiry, Salwa H. Mohamed

The design of immunopharmacological therapy for regulating the granuloma formation and subsequent control of morbidity in schistosomiasis is a necessity. It would be of great value to get a maxi-

mum benefit from that therapy by proving in addition to its main action a schistosomicide effect. Cortisone which has been recently tried to relief inflammatory symptoms in cerebral schistosomiasis, was proved in this study to have both actions. This study pays an attention to the effect of cortisone on Schistosoma mansoni (S. mansoni) infection in mice. This was estimated by using different parameters which included parasitological, histopathological and immunohistochemical studies as well as the evaluation of the level of circulating egg antigen in addition to the trial of two different doses of the drug. Mice were sacrificed at eight weeks post infection. By analysis of the obtained results, cortisone induced in both treated groups reduction in number of liver and intestinal egg load, number of adult worms, granuloma size and cellularity and the level of circulating egg antigen. The immunoreaction intensity of schistosomal antigen in and around the entrapped eggs were also reduced. Moreover, there was an amelioration of hepatocytic histopathological changes in mice treated with low dose. However a hepatotoxicity in mice treated with high doses was noticed. Schistosomal kidney pathology improved in both groups. The promising results detected in this study may encourage further investigation of the positive findings of this drug taking into consideration the dose to be used.

P-160

Lipid-peroxidation (LP) of cellular membranes following PDT with photosensitizers: sulfoxaporphyrin, dithiaporphyrin and hematoporphyrin derivative (HpD)

P. Ziółkowski*, K. Symonowicz*, B.J. Osiecka**, P. Dzięgiel**, A. Bronowicz*, P. Chmielewski***, L. Latos-Grażyński***
* Dept Pathology, ** Dept Histology, Wrocław Medical University; *** Faculty of Chemistry, University of Wrocław, Poland

Photodynamic therapy (PDT) is known method of anticancer treatment involving application of photosensitizer and subsequent irradiation with light of appropriate wavelength. Mechanisms of PDT action are poorly understood. Aim of study was checking whether new compounds in terms of PDT impair cellular membranes, thus facilitating cell death.
Sulfoxaporphyrin(OXA) and dithiaporphyrin(DTP) were injected i.p. to BALB/c mice transplanted with fibrosarcoma in doses 2.5–5.0–7.5 mg/kg. After 24 hours tumors were irradiated at total doses 50 or 100 J/sq.cm. Following 30 minutes, 6, 24 and 48 hours observation mice were sacrified, tumors excised, and processed for LP. LP was spectrophotometrically measured using kits for malonaldehyde (MDA) and 4-hydroxyalkenals (4HNA). LP was given in μM MDA+4HNA/g of tissue.
Level of LP for particular photosensitizer did not vary significantly. LP showed to be photodynamic dose-dependent (photosensitizer×light doses). Highest levels of LP occurred after 6 hours from light application at 100 J/sq.cm (compound dose 7.5 mg/kg). OXA-PDT resulted in 998.15, DTP-PDT in 899.04 and HpD-PDT in 1137.36 μM/g, whereas in controls it did not exceed 73.0 μM/g. At later time points (48 hrs) these values were 10 times lower.
All chemicals impaired cellular membranes via lipid peroxidation. We presume that mechanism of action of new photosensitizers on cellular membranes in tumor is similar to that of HpD and increase in LP depends mainly on photodynamic doses used in study.

P-161

The pathomorphism of intrauterine generalized chlamidioses infection.

S.A. Zvorygin, V.Ya. Glumov, Ye.L. Bazhenov, A.B. Baschmakov, V.Z. Terekhov
Dpts.of Pathology, Medical Academy, Izhevsk, Russia

Intrauterine chlamydioses infection (ICI) has an substantial part in the structure of perinotal mortality. The fetus can be infected both antenatally and intranatally. In 50/60% of the cases under study ICI has a generalized nature.
The materials of the autopsy of 182 fetuses and neonates with generalized ICI have been studied by us. The diagnosis of chlamidiosis infection was made immunofluorescent method, besides histological treatment of the material sections were steined with Shiff-iodin and osmium acid, silver nitrate, the part of the material was invesyigated under the electronic microscope.
According to macroscopic examenation the greyish-white nodules, 0.5–3 mm in diameter, are registrated in pia mater encefaly (PME) of mortinatus and neonates. The internals of dead fetuses with ICI are changed little. The size and shape of parenchymal organs conform to the term of gestation.
Histologically the most severe structural changes are observed in PME. The tubercles, which were found by macroscopic examination are the granulomes locating in the under cobwebby space. The chlamidioses granuloma is formed by macrophages, lymphocytes, proliferating meningocytes and fibroblast. Block-fibrous protein masses and necrotic detritus are seen in its center. Marked structural changes in ICI are also observed in vascular plexuses of the first and lateral ventricles of cerebrum. Histological manifestations of ICI in the parenchymal organes are not especially specific. Frequently there is desquamative- interstitial pneumonia in lungs. The cytoplasm of desquamative alveolocytes isn't smooth, the nucleuses are located excentrically. The chlamidias are found in their cytoplasm perinuclear. Diffuse or focal, predominantly mononuclear infiltration is registrated in the interalveolar septums. Some signs are observed in placenta: delayed maturity of shaggy chorion and signs of denutrition of the compensator-adaptation reactions. The inflammatory changes in placenta and its membrane aren't registrated every time. This is a focal or diffuse chorionitis and choriodeciduitis predominantly in lymphocytes infiltrate.
Electronic Pathology

P-162

Renal donor evaluation by real time telepathology (TP)

David Brenner, M.D.*, Cinthia Drachenberg, Kim Gyure, M.D., Michael Henry, M.D., Olga Ioffe, M.D., Chen-Chih Sun, M.D. and John C. Papadimitriou, M.D., Ph.D
Department of Pathology, University of Maryland School of Medicine Baltimore, Maryland, USA. * Department of Pathology, Bayhealth Medical Center, Dover, Delaware, USA

Introduction: TP the process of making pathologic diagnosis by transmitting images via electronic means, is quickly emerging as a useful technology in general Surgical Pathology. *Dynamic* or *real-time* TP describes a format in which *live* pictures are continuously transmitted while a slide is moved either by a person at the primary location, or robotically by the observer at the remote location.

Evaluation of renal donor biopsies represents an ideal example for comparison of the traditional light microscopic analysis (TA) and real time TP since the morphologic criteria are well defined and can be expressed numerically and/or semiquantitatively

Materials and Methods: In 100 cases of donor graft evaluation performed after working hours we compared the percentage of glomerular sclerosis (GS) reported at the time of frozen section with that in the final report generated later from the permanent section (kappa value). 50 of them were performed by TP from a remote location (pathologists' residences) and 50 by TA within the pathology laboratory with the pathologist having to commute. The pathologists were not aware of this study at the time of performance of the frozen section. The 100 cases were selected randomly by a computer program. The real time needed to reach the diagnosis was also analysed.

We used the Illumea FiberPix software platform on a Dell Pentium III 500 MHZ internet server running Windows NT. The server was connected to an Olympus BX-40 microscope, equipped with a Panasonic high-resolution analog camera, which connects to the server through a digital capture card. The microscope was equipped with a motorized nosepiece, stage, and focus which were connected to the server via a controller card. Using this system, the slides were viewed by the pathologist at the remote locations via the internet using the Illumea FiberPix Client software platform.

Results: The kappa value between frozen and permanent section for TA was 0.687 (p=0.0000) (i.e. substantial agreement), versus 0.811 (p=0.0000) (i.e. almost perfect agreement) for TP. The average time needed for TA, which includes commuting plus reading the slide was 80 min. The average time required for the pathologist to complete the diagnosis via TP was 12.77 minutes (range 8 to 20 minutes).

Conclusions: The TP system used in this study leads to equal results to TA when applied to renal donor biopsies. The resulting reduction in overall time required is significant. Excellent quality of image, easy functioning and speed of transmission assure reliability and reproducibility.

P-163

Telemorphology: practical applications in scientific investigations

S.V. Buravkov, V.I. Sorokovoy and I.A. Kirpich
Faculty of Basic Medicine, Moscow State University, Moscow, Russia

Introduction: Wide spread introduction new telecommunication technologies in medicine especially remarkable in Russian Federation made conditions for distributed scientific work. The situation in scientific field is resembled to remote telemedicine consultations in clinical practice. The highest qualified scientific specialists are still located in large cities including high-tech equipment. At the same time experimental basis (especially in fields like geographic and ecological pathology) are remained in remote areas. In the last several years the system of expeditions was applied for gathering the experimental material. Unfortunately now it became time and money consuming things.

Methods: Experiments on investigation of alcohol influence on rats were performed as *per se* as on background of mixed application of protein and vitamin-B deficiency. Erythrocytes of peripheral blood were investigated by light and scanning electron microscopy. After double fixations with aldehyde + osmium tetroxide and dehydration the images have been captured by computer both from light and electron microscope.

Results: Just immediately after examination obtained images were transferred through Internet from Moscow to Archangelsk both using electronic mail or FTP (File Transfer Protocol). Results also have been discussed through e-mail. Light microscopy revealed deformations and allowed qualitatively estimating the presence of echinocytes and stomatocytes. More detailed observations of the same preparation have been made by scanning electron microscope.

Conclusion: One of recent tendency in clinical and scientific equipment is the development and growth of number apparatus with networking abilities. Therefore the approach used in our investigation seems to be very perspective not only for Russia but also for international scientific cooperation.

P-164

The use of IIP (Internet Imaging Protocol) for image visualization in educational pathologic multimedia cases

Della Mea V, Beltrami C.A.
Institute of Pathology, University of Udine, Italy

INTRODUCTION: Multimedia educational material aimed at self or distant learning in Pathology include histocytologic images coming from specimens, which are acquired in a variety of ways. Recent evolutions in acquisition devices allow now to obtain ver high resolution images,, as well as to fully digitize whole glass slides into so-called "virtual slides." In particular, resolutions above 1800×1200 are easily reachable with regular digital cameras. However, the availability of large images poses new problems in visualization, which may become troublesome, and in networking, due to the storage.

METHODS: Recently, a communication protocol (IIP, Internet Imaging Protocol) for the distribution of multi-resolution images through the Web has been developed, aimed at easily providing images suitable either for Web display (low resolution) and printing (high resolution). An analysis of such protocol made clear that it is also suited for histopathologic images, because of the features of the protocol itself (that allows the partial transmission of rectangular areas of an image) and of the clients, usually provided with pan and scroll tools for browsing the image, which are similar to the microscope movement. Thus, we added to an already implemented educational case archive an IIP server (the open source implementation of the Digital Imaging Group) for distributing the images, with the corresponding Java client.

RESULTS: Accessibility of large images (i.e., greater than the monitor' screen) has been enhanced, and the multi-resolution feature of IIP closely emulates the different magnifications available with a traditional microscope, giving a greater user-friendliness to the system interface. Furthermore, the visualization of images where only a small part is significant is faster, because just the interesting part is transmitted on the network.

CONCLUSION: IIP may be applied in the efficient distribution of histocytologic images, and the already available client tools are adequate for their exploration. Extensions may be studied for representing multiple focal planes of the same image.

P-165

The knife of the pathologist in the hands of the surgeon – Legal aspects of subdelegation in telepathology

Dierks, C.
Rechtsanwaltskanzlei Dierks & Bohle, Berlin, Germany

Many concepts of telepathology provide a subdelegation of intraoperative specimen preparation by a trusted surgeon under the supervision of a remote-controlled camera, laser-beam and/or remote-controlled microscope. This concept has been welcomed as a breakthrough by some as well as criticized as the end of pathology by others. In favor or not, the legal aspects of this provision should be well investigated. The following points need special attention:
1. Contractual law brings about the question if this form of sub-delegation is permissible. Special agreements in the doctor-patient-contract should prevent bad surprises.
2. Negligence is at hand when the standard of a qualified pathologist might not be ensured. The chances of sharing medical expertise will have to be weighed against a mere rationing to the disadvantage of quality or rationalization with the chance of raised efficacy, which could free resources in the allocation process.
3. Reimbursement is at stake, if the service rendered might be qualified imperfect due to unpermissible delegation. A definition of essential services is required that eventually needs alteration to meet new standards.
4. The necessity for a new outline of pathological/surgical cooperation will have to be evaluated. Already existing examples of rearranging borderlines between medical specialties provide possibilities to reconcile adequate medical standard, patient's security and the professional's cooperation on a high-end satisfactory level.

P-166

Remote microscopy as application of Telemedicine – Application of an emerging technology

B. Knoblauch (a.G.), A. Schulz, A. Battmann (a.G.)
Institute of Pathology, Justus Liebig University, Giessen, Germany

The development of modern telecommunication by means of high-speed data transfer either by normal telephone lines or the Internet opens up new possibilities and chances in pathology. Using a remote controlled microscope for telepathology, transfer times between hospital and pathologist can be eliminated and pathological expertise obtained independently of the geographic location of the hospital.
In cooperation with a community hospital located 100 km apart from the Institute of Pathology of the Justus Liebig University Giessen, telepathological intraoperative consultations have been performed. After preparation and staining of cryosections in the community hospital, slides were examined in our institute using a remote-controlled microscope (Leica DMRXA) and a special telepathological software (Leica TPS1.5). Data were transferred via two ISDN connections in parallel. For an interactive sampling, the pathologist can obtain additional information by using a supplementary macroscopic examination equipment. Areas of interest can be marked using an annotation instrument within the TPS software. Up to now more than 65 telepathological consultations have been done. Time required for the microscopical diagnosis ranged between 4 and 26 minutes. The amount of time saved, compared to the transfer to the next available pathologist, was approximately 45 minutes. The quality of the diagnoses was comparable to those specimens processed directly in our institute.
However, while using this technology storage and amount of images screened for diagnosis as well as the diagnosis transmitted require new forms of documentation.
Thus, protocols need to be developed assuring sufficient and reproducible image sampling. Additionally, a combined macroscopic/microscopic approach needs to be defined.

P-167

Non-robotic real-time web-based telepathology – a system for frozen section diagnosis and second opinion consultation

F.J.W.-M. Leong[1], J.O.'D. McGee[2]
[1] University of Oxford, Nuffield Department of Clinical Laboratory Sciences, John Radcliffe Hospital, Oxford,
[2] University of Oxford, Nuffield Department of Medicine, John Radcliffe Hospital, Headington, Oxford, UK

INTRODUCTION: The ability to view a regularly-updated image is the key requirement for a telepathology system used for live consultation. In the past this has been achieved with adapted video-conferencing methods, and termed 'dynamic telepathology' although most current commercial robotic systems now provide better image quality by creating montages of multiple still images.
The addition of microscope robotics to a telepathology contributes to most of the cost and may be unnecessary with a competent human operator. We describe a cost-effective web-based telepathology system for live consultation offering image quality superior to video-conferencing and comparable with commercial robotic systems.
METHODS: The system uses a microscope camera, video digitiser board and converts any existing microscope and internet-connected workstation into a limited telepathology webserver. Live images are broadcast to the Internet and accessed through a web-browser. The system can be modified for consultation over single ISDN or even standard V.90 modem, without degradation in image quality. One pathologist tested this system by viewing 109 sequentially-selected archival frozen section cases via local area network, and compared diagnoses with the original frozen section report.
RESULTS: There were only two discrepancies – an adrenal phaeochromocytoma was diagnosed as adenoma and a biopsy from a pancreatic adenocarcinoma was deferred. All other diagnoses concurred with the original report. The system performance was adequate and user accuracy within tolerable limits.
CONCLUSIONS: This system provides a small laboratory with an economical entry point to telepathology. It is adaptable, expandable and the underlying technique has applications in other areas of telemedicine.

P-168

Use of Wireless Application Protocol (WAP) to facilitate pathology education and interactive decision support systems

F.J.W.-M. Leong, K. Pal
Oxford University Nuffield Department of Clinical Laboratory Sciences, John Radcliffe Hospital, Oxford, United Kingdom

INTRODUCTION: Wireless Markup Language (WML) is the means by which information may be displayed on Wireless Appli-

cation Protocol (WAP) mobile phones. WAP-functionality is found on many new phones, allowing access to certain internet-based resources, albeit at low baud rates (<9600 kbps). While this medium has been used to provide news, information and financial services, it is underutilised in medical education.
The current Oxford University Laboratory Medicine course uses a combination of lectures, practicals, tutorials and web-based electronic teaching resources. We demonstrate how a WAP-enabled Internet site may facilitate and supplement existing medical teaching resources.
METHODS: Students were polled for mobile phone ownership. Pertinent aspects of our existing website (information, timetabling, assessment, contacts) were converted to WML format. A decision support system for microbial identification, infection management and antibiotic therapy was developed in WML. A more sophisticated version, supplemented with images was also developed for a conventional website.
RESULTS: A survey of the 2000/2001 1st year clinical students indicated that 83% have a phone and 81% plan to upgrade this phone in the next two years. Positive feedback from users indicates that WML can be an interactive learning aid.
CONCLUSIONS: The shortcomings of current WAP technology may be overcome through good design and strategic application. Although many medical schools have developed web-based educational resources, these are not compatible with WAP due to their formatting and size. We believe the benefits of such technology and its usage among our target audience warrant extension of our existing electronic education resources into this area.

P-169

Two years experiences in telecytology in Yugoslavia

I. Milosavljevic, M. Kostov, R. Bokun, Z. Tatomirovic, V. Tatic, P. Kostic
Institute of pathology and forensic medicine, Military Medical Academy, Belgrade, Military hospital, Nis; School of electrical engineering, University of Belgrade, Yugoslavia

Introduction: Digital imaging have many applications in cytopathology that encompass training and education, image analysis, diagnosis, report documentation and archiving, and telecommunications. Development of digital imaging applications in last few years was played an important place in pathology and cytopathology of Military Medical Academy.
Material and methods: They are two basic systems for telepathology or telecytology, dinamic and static. We are developed the static system for remote consultation based in relation between relational databases model and WWW, which we are using in manner to having us some real-time interpretabilities.
Results: Last two years, pathology division of Military Hospital in Nis, 250 km away from Belgrade, sending us, via POTS, multimedial documented requests for remote consultations in pathology and cytology. All of cases were imaged using the Pixera digital camera, at a resolution of 1024×768 pixels. Our first experiences based on 62 cases of telecytology, in period 1999–2000, are caracterized with high level of accuracy and quality assurance. 86% of all cases are definitive resolved in first remote consultation. 12,5% of cases are also definitive resolved after: repeat sampling procedure, accessary of clinical datas or images. Only in one case definitive diagnosis was glas slide diagnosis. Conclusion: The aim of this paper are directed toward assisting the profession to stay informed and in control of these applications in the laboratory. Telecytology is an area in particular need of studies of good quality to provide data on factors affecting accuracy. New technologic approaches to addressing the issue of selective sampling in static image consultation are needed.

P-170

Inexpensive gross and microscope digital image recording and analyzing

M. Ristovski, V. Janevska, L. Spasevska, S. Duganovska, S. Kostadinova
Institute of Pathology, Medical Faculty Skopje, Republic of Macedonia

Recent developments in digital image recording have brought rapid changes to photography and in consequence also to photomicrography. Advanced digital imaging techniques and equipment are still expensive for a small and modest laboratory.
The aim of this paper is to represent the use of amateur digital camera to record morphology of the gross and microscopic specimens. We practice with following digital camera: Nikon Coolpix 990, Canon Power Shot, Olympus C-3030, Sony Ciber Shot. As a rule, taking photography of gross specimens does not need any optical accessories. The images have high resolution (up to 2048×1536 pixels) and there is possibility to print them in A4 format with good quality.
Taking photography from microscope goes to the CCD through optical system of the camera. The cameras are fitting to microscopes across optical adapter or directly attaching to the eyepiece. You can use Leitz Periplan eyepieces (Model No 519 815) like optical adapter for Nikon Coolpix 990 or appropriate model of digital adapter from LMscope (www.LMscope.com). "Directly attaching" (camera to eyepiece of microscope) needs a few conditions: diameter of eyepiece more than 20 mm, focus of eyepiece minimum 10 mm and any type of improvised mechanical camera holder. The size of pixel in 3,3 megapixles 1/1,8″ CCD is about 7–8 microns. There is a possibility to standardize color and size of images. Standardized images are appropriate to import in any imaging analyzing program like Lucia M.
Now, all pathologists and morphologists over the world can collaborate more than ever.

P-171

The advantages and pitfalls for diagnose small biopsy specimens

Jongkolnee Settakorn, MD.[1], Thiti Kuakpaetoon, MD.[2], F. Joel W.-M. Leong, MB.BS.[3], Kamthorn Thamprasert, MD.[1], Kunio Ichijima, MD.[4]
1. Department of Pathology. Faculty of Medicine. Chiang Mai University. Chiang Mai, 50200 Thailand, 2. Department of Pathology. Rajavithi Hospital. Bangkok 10400 Thailand, 3. Nuffield Department of Pathology and Bacteriology. University of Oxford. John Redcliffe Hospital, Headington, Oxford, United Kingdom, 4. The First Department of Pathology. Nara Medical University. Kashihara City. Nara, Japan

Introduction: Diagnostic telepathology by electronic mail (e-mail) attachment is a relatively cost less and easy method. But "can it be really used in routine pathology work"?

Methods: Focusing on the tiny biopsy specimens, for evaluating diagnostic efficacy, advantage and limitation of this tool, 1488 images were digitally taken from the entire histological surface area of 100 specimens. They were orderly sent as e-mail attachment from Nara Medical University, Japan, to the remote pathologist at Rajavithi Hospital, Thailand.
Results: Setting the glass slide diagnosis as the gold standard, the diagnostic accuracy, sensitivity, specificity, and positive and negative predictive values of telepathologic diagnosis for malignant lesions were 98, 88.9, 98,9, 98.9, and 88.9% respectively. The average time using per case was only 3.58 hours.
Conclusions: We concluded that this method gave the acceptable efficacy, rapidly turn around time and can be use as routine work. The diagnostic pitfalls included the over diagnosed due to large image size and misdiagnosed of individual malignancy cells.
Keywords: Telemedicine, Telepathology, Internet, e-mail attachment

P-172

Controversial cases in a diagnostic consultative telepathology - Pulmonary and paediatric pathology (own experiences)
Janina Slodkowska, Klaus Kayser, Jadwiga Maldyk
Dept. Quantitative Pathology, Inst.TB&Lung Diseases and
** Dept. Pathology Medical Academy – Warsaw, Poland;
***Dept. Pathology, Thoraxklinik, Heidelberg, Germany

Implementation of static telepathology (sTP) enables professional international consultations. The critical factors influence this method like image quality and/or field selection can be eliminated by application of the high quality TP system in experts TP consultations. Even thought the diagnostic accuracy of some sTP cases necessitates a conventional microscopic examination.
The group of consultative sTP cases – controversial or difficult – finally re-assessed by using traditional microscopy, was analysed to determine the degree of diagnostic difficulties in our sTP consulted material. The selected cases from the TP-file of Dept. Quant. Path ITB&LD were referred to a several TP consulting Centres and represent 3 groups of disorders: I – lymphoidal tissue lesions: *pulmonary plasma cell granuloma with heavy lungs infiltrates LIP v. preleucemic infiltrates; *border line pulmonary infiltrates LIP v. B cell lymphoma – MALT-type; *peripheral T-cell lymphoma v. inf. mononucleosis; *abdominal plasma cell granuloma v. neoplastic process of accessory immune system cells. II – interstitial lung diseases especially non-specified interstitial inflammation "end-stage"; III – pulmonary neoplasms.
The diagnostic problems arising from the using sTP in our controversial cases, had a similar spectrum to those of the conventional microscopic examination. The list includes: *quality of microscopic slides influencing the high resolution cytological details, *limited spectrum of immunostainings, *a necessity to perform molecular biology studies, *scanty microscopic material, *the experience of pathologist, *confidence to a referring TP centre.

P-173

[abstract withdrawn]

P-174

Demands on the quality of macroscopic images for telepathology
K. Wehrstedt, P. Hufnagl, M. Dietel
Department of Pathology, Charité Hospital of the Humboldt University, Berlin, Germany

Introduction: Image quality is a crucial factor in diagnostic pathology. This applies for microscopic images as well as for macroscopic images espescially in telepathology. With respect to bandwidth and transmission time there has to be made a compromise between high image quality and fast image transmission. But until now there are no standardized demands for minimal requirement on image quality.
Aims: Within the study we analyzed the effect of decreasing resolution and increasing compression systematically. We want to determine limits for resolution reduction and image compression.
Material and Methods: We used a set of macroscopic images from a malformed fetal heart taken with different magnifications. Image pairs (reference vs. test image) were presented to 20 observers (pathologists and non-pathologists). The observers were asked to compare the image pairs presented by Power-Point-Presentations on 21″ monitor with a resolution of 1600×1200 pixel.
Results: The reduction of the image size is possible in several ways. Wr found, that decreasing the resolution and compressing the image with JPEG and WAVELET is not critical until a certain threshold. Below that threshold the image quality may be insufficient for a secure diagnosis. According to our results it would be recommendable to prevent compression rates higher than 1:50 with JPEG as well as Wavelet.
Conclusion: High image quality is an important prerequisite for diagnostic accuracy. In comparison to microscopic images there are higher compression rates possible for macroscopic images. Compression rates higher than 1:50 should not be enable for macroscopic images within telepathology solutions.

P-175

Adenocarcinoma of the uterine cervix. Incidence, prognosis and reproducibility of classification
Alfsen GC, Abeler VM, Reed W, Kristensen GB, Skovlund E, Pettersen E, Thoresen SØ
The Norwegian Radium Hospital, Oslo, Norway

Object of study: To evaluate incidence changes and prognostic factors of adenocarcinomas (AC) of the uterine cervix. **Material/methods:** 505 patients with non-squamous cell carcinomas from three 5-year periods (1966–70, 76–80, 86–90) were identified through the files of the population based Norwegian Cancer Registry, and reviewed. Results: Incidence rates of AC were increasing, but varied according to histological subgroup and age. Endometrioid tumours increased in all age groups. Endocervical tumours decreased after 1980 in women >55 years. Independent prognostic factors for non-squamous cell carcinomas were clinical stage, age, vascular invasion, lymph node metastases, histology of clear cell carcinoma or small cell carcinoma, tumour volume and tumour infiltration into isthmus uteri. Intra- and interobserver kappa values of the WHO classification as a whole were only moderate (0,53 and 0,44). Reproducibility of diagnosis of high risk subtypes was

somewhat better for the group of clear cell carcinomas (intra- and interobserver kappa: 0.64 and 0.65). However, reproducibility of small cell carcinomas was clearly more complicated, with intra- and interobserver kappa values of 0.73 and 0.50.
Conclusion: The prognostic impact of isthmus infiltration in AC favours a new staging system. Low levels of reproducibility and lack of prognostic impact of most subgroups of AC indicate the need for a simplified classification of AC of the cervix uteri.

P-176

Squamous intraepithelial lesions (SIL) and microinvasive carcinoma (MC) of the uterine cervix-immunohistochemical and virologic aspects

C. Amalinei, C. Stratone, D. Radulescu, C. Cotutiu, A. Badescu, G. Dobrescu
Departments of Pathology and Obstetrics and Gynecology, University of Medicine and Pharmacy, Iasi, Romania

The **aim** of our study was to evaluate the immunohistochemical and virologic markers in SIL and MC of the uterine cervix.
Material and methods: 79 biopsies and surgical specimens were analyzed and diagnosed as following: 36 cases of Low grade squamous intraepithelial lesion (LSIL), 25 High-grade squamous intraepithelial lesions (HSIL), and 18 cases of Microinvasive carcinoma (MC). Immunostaining for citokeratins, p53, PCNA, and Ki-67 was performed. Specimens were tested for the presence of human papillomavirus (HPV) infection by *in situ* hybridization.
Results: Citokeratins differentiated LSIL from HSIL and from MC. P53, Ki-67 and PCNA expression correlated strongly with the progression of lesions. Infection with low-risk HPV was infrequent (only16.66% of LSIL). Infection with high-risk HPV (16/18) was highly associated with HSIL and MC (93.2%).
Conclusions: Citokeratins are useful in differentiating HSIL from MC. P53, Ki-67 and PCNA expression are valuable parameters related to the severity of the lesions. Our results support the association of progression of premalignant cervical lesions with the continuous presence of high-risk HPV types and correlates with the aggressive cervical squamous lesions behavior in our region.

P-177

Expression of Bcl-2, Bax and CD-34 in normal pregnancy, spontaneous abortion and hydatidiform mole

Bairaktari-Kouri E., Kounelis S., Arvaniti I., Stylianidou A., Gratsia A., .Sfikas K., Karaiossifidi H.
Pathology Department, Hel Venizelou Gynecological Hosp., Athens, Greece

The regulatory of apoptosis genes Bcl-2 and Bax have been found to be expressed in trophoblastic lesions. Nevertheless the trophoblastic cells seem to play an important role in angiogenesis occurring in early gestation, mainly by releasing angiogenic growth factors. Usually the molar villi are avascular, however some investigators using the monoclonal antibody CD-34, raised against endothelial cells found in the stroma of complete moles a number of vessels corresponding to that of normal villus. In this study, we investigated the expression of Bcl-2 and Bax in order to determine the role of apoptosis and correlate it with the expression of CD-34 antibody reflecting angiogenesis. Formalin-fixed paraffin-embedded tissue of 9 normal placentas, 8 spontaneous abortions with hydropic degeneration, 21 partial moles and 12 complete moles, were examined. Expression of Bcl-2, Bax and CD34 were assessed immunohistochemically. Bcl-2 and Bax accumulation was observed predominantly in syncytiotrophoblast whereas cytotrophoblast did not express these markers in all cases. CD-34 highlighted vessels of villous stroma.. No difference in the expression of Bcl-2 and CD-34 between the four groups was confirmed. Extensive staining for Bax was observed in complete and partial moles without any correlation with Bcl-2 expression. Bcl-2 and CD-34 were inversely correlated in moles. This relation was not found in normal pregnancies and abortions. No correlation was observed between Bax and CD-34 expression. We conclude that Bcl-2, Bax and CD-34 are not useful as diagnostic markers but the differences in their expression if further investigated may prove usefull in the understanding of this entity

P-178

Expression pattern of the adhesion molecule CEACAM1 in benign extravillous trophoblast and in gestational trophoblastic disease

A.M. Bamberger, S. Sudahl, K. Milde-Langosch, T. Löning
Departement of Gynecopathology, Institute of Pathology and Dept. of University Hospital Eppendorf, Hamburg, Germany

The purpose of the present study was to investigate the expression pattern of the adhesion molecule CEACAM1 in gestational trophoblastic lesions and to compare this expression with the one in normal trophoblast. For this purpose, we used the 4D1/C2 monoclonal antibody, which specifically recognizes CEACAM1, to perform immunohistochemistry on a total of 20 cases of gestational trophoblastic lesions including complete hydatidiform moles, one placental site trophoblastic nodule (PSN), one placental site trophoblastic tumor (PSTT) and three choriocarcinomas, which were also characterized by cytokeratin, hPL and hCG and Ki-67 staining. Normal placental samples served as a control. CEACAM1 was absent from villous cyto- and syncytiotrophoblast in both normal placenta and hydatidiform molar samples. It was present in the benign extravillous trophoblast, with stronger expression in the proximal extravillous trophoblast of anchoring villi, but was also observed in interstitial and endovascular intermediate trophoblast and chorionic intermediate-like trophoblast. Partial expression was observed in the trophoblast proliferating from the surface of molar villi. In choriocarcinomas, areas of weak expression could be observed along with large areas without CEACAM1 expression. In the PSN and especially in the PSTT, CEACAM1 expression was stronger and in wider areas. The specific localization to extravillous trophoblast and its expression pattern in gestational trophoblastic lesions indicate that CEACAM1 can potentially be a helpful additional diagnostic marker in the differential diagnosis of such lesions.

P-179

Blood vessel invasion and inflammatory stromal at the invasion front as additional significant prognostic factors in surgically treadted patients with cervical carcinoma

Basheska, N.*, Yashar, G.*, Veljanovska, S.**, Kubelka, K.*, Prodanova I.*, Zografski, G.*, Stavric, G.*
* Department of Histopathology and Clinical Cytology,
** Institute of Radiotherapy and Oncology, Medical Faculty, Skopje, Macedonia

Introduction: The objective of this study was to evaluate the prognostic significance of 23 clinical and histopathological variables in relation to disease-free (DFS) and overall survival (OS) in patients with early stage cervical carcinomas.
Methods: A retrospective analysis of 237 patients with cervical carcinoma, undergoing radical hysterectomy and postoperative irradiation between 1988 and 1997 was conducted. The operative specimens were subjected to detailed and uniform histopathological work-up. The patients were staged according to the postoperative TNM classification of UICC (1997) guidelines. Mean follow-up time was 57 (18–124) months.
Results: The 5 and 10-year OS rate was 80.8%, while DFS rates at 5 and 10 years were 76.8% and 75.5%, respectively. In multivariate analysis, blood vessel invasion, pelvic lymph node metastases, tumor diameter, inflammatory stromal reaction at the invasion front, and minimum thickness of uninvolved cervical stroma/parametrial extension, were independent and significant variables. The prognostic index, as an indicator of the patient's place in the prognostic spectrum, defined by the Cox regression model, was able to categorize the patients into three distinct risk groups. The 5-year DFS and OS rates of the low-, intermediate-, and high-risk groups were 97.5%, 86.3%, and 43.8%, vs. 98.8%, 84.5%, and 45.3%, respectively ($P<0.0001$).
Conclusions: The prognostic index could be a sound basis for an appropriate planing of the following therapeutical strategy for the surgically treated patients with cervical carcinoma. The postoperative TNM classification should be modified, incorporating the blood vessel invasion and the inflammatory stromal reaction at the invasion front, as additional significant prognostic factors.

P-180

The correlation of apoptotic index with p53 and bcl-2 expressions in ovarian carcinoma

Berker B[1], S[2], Ensari A[2], Dünder I[1], Dinçer Cengiz S[1]
University of Ankara Medical School, Departments of Obstetrics and Gynaecology[1] and Pathology[2], Sihhiye, Ankara, Turkey

Introduction: It is well documented that programmed cell death (apoptosis) plays a critical role in tumor growth. We therefore aimed to study the apoptotic process by means of apoptotic index (AI), and apoptosis regulatory protein expressions.
Methods: Fifty ovarian carcinoma cases operated between 1990 and 1997 were included in the study. Clinical records were reviewed to obtain information about patients' age, surgical stage, and follow-up. Apoptotic cells were detected in paraffin sections with an in situ hybridization technique (Apopdetec®/Cell Death Assay System, Enzo). AI was calculated by counting positive cells among 1000 tumor cells. p53 and bcl-2 proteins were analyzed immunohystochemically using a streptavidin-biotin-peroxidase technique. Cox's regression analysis was used to build a multivariate model for survival to identify independent prognostic factors.
Results: Median value for AI was found as 2.48 and cases were classified accordingly as high AI (>2.48) or as low AI (<2.48) group. p53 protein expression was positive in 20 cases with low AI and 13 cases with high AI whereas bcl-2 expression was positive in 13 cases with low AI and 11 cases with high AI. Median survival was 71 months in the low AI group, and 72 months in the high AI group which was not statistically significant. Multivariate analysis showed that AI did not have prognostic value as an independent factor.
Conclusion: Although apoptosis plays an important role in ovarian cancer, it does not seem to act as an independent prognostic factor. The lack of statistically significant correlation between p53 and bcl-2 and apoptotic index suggests that other genes are involved in the molecular mechanisms underlying apoptosis.

P-181

Morphometric changes in the stromal and vulvar epithelium and the relation with ageing

Jane Lopes Bonilha , Reinaldo Azobel, Patricia Maluf Cury
Faculdade de Medicina de São José do Rio Preto, São Paulo, Brazil

Introduction: Senescence is a process that modifies the vulvar mucosa, with changes that varies from vulvar atrophy to carcinoma. The aim of this study was to verify the morphometric changes in the normal vulva of postmenopausal women.
Material and methods: five patients with menopause (age varying between 55 and 82 years old) were compared with the 5 premenopausal patients from the control group (age ranging from 18 to 46 years old). Biopsies from the vulvar epithelium were studied and by morphometric means it were measured the epithelium thickness, the pilo-sebaceus apparatus and the sweat glands. 40 measurements were obtained in each item, in a microscopic immersion view (1250×)
Results: we observed that: 1 – the thickness of the epithelium was about 50% less that in the control cases; 2 – the diminishing of the epithelium thickness was statistically greater in the stratum spinosum layer; 3 – the conjuntival fibres appear in greater number, but shorter and compacted; 4 – the blood capillaries are fewer and with a lesser diameter; 5 – the pilo-sebaceum apparatus are fewer and with a smaller volume; 6 – the sweat glands appear in a few number and with a greater diameter.
Conclusions: The morphometry showed that not only the vulvar epithelium suffers atrophy, but also all the adnexae and stromal fibres of the vulvar mucosa in the elderly patients.

P-182

Five cases of uterine (two intraligamentary) lipomatous tumours with immunohistochemical features

Leyla Cinel*, Duygu Düsmez*, S.H. Nabaei**, Dilara Taner***, Özlem Pata****
* Mersin University, Faculty of Medicine, Department of Pathology, Assistant Prof. MD, Mersin, Turkey, ** Kirikkale University, Faculty of Medicine, Department of Pathology,

Assistant Prof. MD, Kirikkale, Turkey, *** Ankara ZTB Woman's Hospital, Department of Pathology, MD, Ankara, Turkey, **** Mersin University, Faculty of Medicine, Department of Obsterics and Gynecology, Assistant Prof. MD, Mersin, Turkey

Introduction: The histogenesis and the origin of the lipocytes of rare lipomatous tumours of the uterus are controversial. There are two theories, one being the metaplastic theory and the other involving misplaced embryonic mesenchymal cells.
Methods: To investigate their possible origin, an immunohistochemical panel of S-100, desmin and SMA was performed on five patients, four with uterine lipoleiomyomas one with a pure lipoma.
Results: Three of the tumours were located in the uterine corpus (two intramural, one subserosal), and the remaining two were intraligamentary. The lipocytes showed a positive reaction for S-100 protein. Desmin and SMA were barely detectable in the cytoplasm of smooth muscle cells. Two of the cases differed from the others in that their lipocytes stained with desmin
and SMA.
Conclusion: The theory of metaplasia cannot fully explain the origin of the cells in all of the cases. We agree that these tumours might arise from misplaced embryonic mesenchymal cells or immature cells with differentiation potential.

P-183

Endometrial malignancy in tamoxifen treated patients (TAM-EM). A report of ten cases

Condom-Mundó E., Vidal A., Paúles M.J., Vidal N., Balagueró L.*
Depts of Pathology and Gynecology*, Hospital de Bellvitge – Institut Català d'Oncologia. L´Hospitalet de Llobregat, Barcelona, Spain

Introduction: Several studies have shown that Tamoxifen (TAM) may be associated with endometrial malignancies.
Methods: Slides and charts were reviewed on ten patients with TAM-EM diagnosed at a single institution (1993–2000).
Results: The patients ranged from 49 to 86 (mean 70) years of age. The interval between breast and endometrial cancer ranged from 10 to 230 months (mean 86), the length of TAM use from 10 to 144 months (mean 45). The dose of TAM was 20 mg. day in each case. The malignant endometrial lesions were: Three cases of carcinosarcoma (CS), two of them being multifocal and with diffuse intraepithelial carcinoma (EIC), and one with extensive neuroectodermal differentiation; one serous carcinoma, one clear cell carcinoma, one case of pure EIC and four cases of endometrioid carcinoma (one with a synchronous ovarian mixed endometrioid/mucinous/clear cell carcinoma). Additionally, in each uterus, one or more of the following changes were found: myohyperplasia (9 cases), adenomyosis (6), endometrial polyp (4), leiomyomata (4), hyperplasia (2).
Conclusions: Signs of an estrogenic-agonist effect have been found in all ten uteri bearing TAM-EM. A high number of aggressive neoplasms is seen among TAM-EM, with CS (3/10 cases, two with unusual features) as the second most common malignancy.

P-184

Primary peritoneal papillary serous carcinoma: report of three cases

Çulha E.N.[1], Savas B.[1], Kaygusuz G.[1], Ensari A.[1], Sertçelik A.[1], Ortaç F.[2], Demirci S.[3]
University of Ankara Medical School Departments of Pathology[1], Gynaecological Oncology[2] and Surgery[3], Ankara, Turkey

Primary peritoneal serous carcinoma (PPSC) arising from the peritoneal surface is a distinctive neoplasm with a histopathologic resemblance to serous ovarian papillary carcinoma (SOPC). It has been reported that both neoplasms have almost identical immunophenotypic properties. Here we report three cases of PPSC with their immunophenotypic properties.
Patients were 37, 65 and 73 years-old multiparous females admitted to gynaecology department with ascites and abdominal pain. Last two patients were in menopause for 14 and 20 years, respectively. Abdominal ultrasound confirmed the presence of ascites together with a cystic mass in one of the ovaries measuring between 20–75mm in diameter. Serum CA125 values ranged between 191–1938 U/ml. Cytological examination revealed Class V papillary adenocarcinoma of the ovary in all patients. Grossly ovaries were normal size or even atrophic while there was diffuse or nodular tumoral mass in the omentum. Microscopical evaluation revealed solid-papillary areas of tumoral involvement on the serosal surfaces of the ovaries not exceeding 1cm in diameter. All three cases also showed tumoral infiltration in the serosal surface of the uterus, uterine salpinx. Omental tumorous masses measured between 8–14 cm. Histologically all tumours expressed features of papillary adenocarcinoma of varying differentiation containing numerous psammoma bodies. Immunohistochemical examination revealed that tumour cells showed diffuse expression of LMW-cytokeratins, HMW-cytokeratins, and EMA together with focal positivity by S-100 and CA-125.
PPSC is an entity which may cause difficulties in the differential diagnosis especially from SOPC even in the presence of immunohistochemical findings. This seems to be due to the possible common origin of these tumours from the cells bearing Müllerian differentiation potential.

P-185

The value of estradiol localization in differentiating epithelial ovarian tumours and ovarian metastases of colonic origin

Samy A. Darwish. Ph.D.
Department of Pathology, Benha Faculty of Medicine, Zagazig University, Egypt

Introduction: The pathology of ovarian tumours constitutes the most complex area of gynaecologic pathology. The diagnosis by examination of a tissue section is often uncertain and opinions of experienced pathologists may differ critically. The current investigation aimed to find out the benefit of Estradiol localization in solving some diagnostic problems in ovarian tumours.
Methods: The distribution of Estradiol (ES) was investigated by the immunohistochemical method in 48 cases of formalin-fixed, paraffin-embedded ovarian tumour sections, representing 17 serous and 24 mucinous tumours, in addition to 7 cases of ovarian metastatic lesions from mucinous adenocarcinomas of colonic origin. Also, 6 cases of primary colonic carcinoma were examined.

Results: Estradiol was only confined to the stroma of all benign (BN), borderline (BL) and malignant (ML) serous tumours with no staining in the epithelium. In contrast, ES was found to be localized in the epithelial nuclei of BL and ML mucinous tumours in addition to the epithelial cytoplasm and stroma. On the other hand, the epithelial nuclei of metastatic tumours did not show any staining reaction for ES in all cases examined.
Conclusion: The differentiation between serous and mucinous malignant tumours could be accurately done by ES localization (cytoplasmic and nuclear) in mucinous tumour and its abscenes in serous tumours. The presence of intranuclear ES in BL and ML mucinous tumours could be taken as a sharp line of demarcation between BN and BL mucinous tumours. Also, intranuclear ES localization could be helpful in differentiating primary ovarian mucinous adenocarcinoma from metastatic mucinous tumours to the ovary specially those having a colonic origin.

P-186

The epithelia-vascular changes in condylomas and uterine cervix carcinoma under HPV infection

Derizhanova Irina, Gamaleeva T.
State Medical University, Rostov-on-Don, Russia

HPV infection plays the essential role in uterine cervix pathology, causing chronic non purulent ectocervix inflammation in some cases accompanied with papillomas (condilomas) growth, epithelia dysplasia and carcinoma. The epithelia-vascular changes are essential in their genesis. To study them there were taken 184 biopsies and 736 ectocervix smears from 184 patients with HPV infection proved by PCR. The cytological, histological, histochemical, ultrastructural and morphometric methods were used. The following uterine cervix pathology was obtained: cervicitis – 40%, pseudoerosion – 54%, condiloma accuminatum – 1%, carcinoma – 5%. CIN was distinguished in 55,43% cases, in particular – 1 stage – 19,03%, 2 stage – 28,8%, 3 stage – 7,6%. The cell nuclei and cytoplasm lytic changes by HPV action, apoptosis disturbances, proliferative processes in basal layer pending to dysplasia of various differentiation took place in squamous epithelium. Similar changes advanced in endothelial cells, especially in tunica mucosa capillaries. The dystrophic cytoplasm changes and nuclei dechromatisation were observed. Some cells were affected by lysis and apoptosis. Simultaneously neoangiogenesis took place in epithelium. Capillaries penetrated basal membrane from the mucosa lamina propria. They grew into epithelium as arcades, then endothelial cells propagation and protrusion inside vascular and outside basal membrane took place, following with narrow splits and ducts among them. These demonstrated the multitrunk capillar structure growth, surrounded with proliferative epitheliocytes , one can call them epithelia-vascular sockets. They can regress, progress or become atypical. Consequently, corresponding endothelial and epithelial proliferation is specific for HPV infection in endocervix and appears not only in manifesting carcinoma but in preceding stages, in condylomas, long before malignisation morphologic features.

P-187

Morphological changes suggestive of malignancy in ovarian epithelial tumors

Djordjevic, B., Dimov, D., Mihailovic, D., Zivkovic, V., Velickovic, Lj., Stanojevic, Z.*
Institute of Pathology, Medical Faculty Nis, Yuguslavia;
*Clinic of Oncology, Clinical center Nis, Yugoslavia

Epithelial tumors of the ovaries account tor about 60% of all ovarian neoplasms and 80–90% of primary ovarian malignancies. The spectrum of proliferative change these tumors exhibit is divided arbitrarily into benign borderline and malignant categories. The aim of this study is to analyse morphological changes suggestive of malignancy beside the well-known criteria. Histologic slides of the surgical specimens of 406 consecutive patients with ovarian epithelial tumors were reviewed. 259 of these tumors were benign, histologically 132 belonged to the serous group, 96 to the mucinous, 27 were mixed, and 4 Brenner tumors. The number of borderline tumors was 13 only, among them 8 serous and 5 micinous. 134 tumors were malignant, 67 of serous, 29 of mucinous, 18 of endometrioid, 9 of mixed, 7 of clear cell, 2 of transitiocellular and 2 of undifferentiated type. Benign tumors occur in younger age then the malignant counterpart of the same histological type. Definite signs of malignancy are destructive stromal invasion and the presence of the atypical mitotic figures in every histological type. In cases of serous tumors highly complex micropapillae arising directly from large, bulbous densely fibrotic pappilary structures with smooth epithelial-stromal interface are suspicious of malignancy. Epithelial stratification of more than 4 cells, high mitotic counts, and a cribriform gland pattern in mucinous tumors are indicative of invasive carcinomas even in the absence of stromal invasion. Cytologic atypia can be caused by degeneration. A great number of granulocytes with marked cytological atypia may be the result of torquation.

P-188

Granulocytic sarcoma of the vagina. A case report

M.J. Fantova, C. Admella, T. Soler, R. Muns, E.Genover*, M.S. Vicen*, J.L. Mate**
Department of Pathology and Ginecology*, Hospital de Mataró, Hospital Germans Trias i Pujol**, Barcelona, Spain

INTRODUCTION: Granulocytic sarcoma (GS) is a extramedullary myeloid tumour that tend to occur in young patients, presenting usually in the soft tissues, bone, skull, lymph nodes and skin. Genital tract is rarely involved, being the ovary the most commonly affected site. Only isolated cases of GS of the vagina have been reported. Most cases of GS occur simultaneously with or following the onset of acute myeloid leukaemia (AML) and other myeloproliferative and myelodisplastic syndromes. Rarely they are the first manifestation of AML and there are some cases in which sequential transformation doesn't happen.
CASE REPORT: A 47-year-old woman developed leucorrhea and pelvic pain. Gynaecologic examination revealed a 4-cm polypoid, ulcerated mass in the right lateral wall of the vagina that was excised. Histologically, a diffuse submucosal infiltration of intermediate-size undifferentiated cells was observed. Special studies with chloracetate esterase (Leder), CD68, lisozime, CD45 and CD43

disclosed the myeloid nature of the neoplastic cells. Peripheral blood and bone marrow aspiration were both normal.
DISCUSSION: The histologic diagnosis of GS may be extremely difficult when the myeloblastic cells are poorly differentiated, the tumour lacks the characteristic green colour and it develops without clinical evidence of leukaemia. When GS occurs as an isolated lesion, it is frequently misdiagnosed as malignant lymphoma or poorly differentiated carcinoma. Chloracetate esterase activity and immunohistochemical techniques help to the diagnosis. Radiation has been the treatment for isolated non-leukaemic cases, but recent studies suggest that chemotherapy for AML would prevent blastic transformation.

P-189

The quantification of vaginal reactivity while radiotherapy of cervical neoplasia

[1]I. L. Francu, [1]Dorelia Calin, [1]Anca Ciobanu, [3]E. Crauciuc, [4]Simona Stolnicu
Departments of [1] Anatomy and [3] Gynecology, University of Medicine, Iasi; Department of [4] Pathology, University of Medicine, Targu Mures, Romania

Introduction: The irradiant anticancerous therapy produces numerous complications in genital territory. This is the reason why we perform a qualitative and quantitative examination of the vagina, to evaluate its functionality after radiotherapy for uterine neoplasia.
Material and methodes: The vaginal fragments from patients diagnosed with neoplasm of the uterine cervix stage II, before or after radiotherapy has been bioptic processed and then compared with witness fragments from patients suffered by nonneoplasic diseases. These fragments were processed by paraffin technique, using current stained methods (H&E) and specials. Quantitative assessments of bioptic fragments have been done, using a video digital interactive system with a professional program. Because qualitative exam of histological section has shown lesions of lamina propria of mucosa and of muscular layer, we have done stereological measurements of procentual volumes of different components of vagina before and after radiotherapy.
Results: The semnficative changes, relieved by stereological measurement involve lamina propria, muscularis and vessels of two vaginal structures. In muscular layer the % volume of muscular fiber decreased (fom 81.34 to 70.31), but increased % volume of colagen stroma (from 14.22 to16.51), the last one suffering a hyalinization process. In lamina propria elastically fibres decreased, finally % volume of connective tissue increased (from 22.36 to 28.71). Vessels, especially the arterioles, present parietals changes with hyalinisation, resulting decreasing % volumes of vascular lumina, permeables in both investigate structures.
Conclusions: The objective vaginal changes, which were found out after radiotherapy, guide the treatment in order to conserve its functionality after radical surgical interventions in neoplasia of uterine cervix.

P-190

Hyperplastic processes of endometrium after cesarean section

Gabidullina R.I. (1), Saveliev E.V. (2)
(1) Department of Obstetrics and Gynecology of Kazan Medical University; (2) Department of Obstetrics and Gynecology, Iupatov.E., Kazan, Russia

Introduction: Hyperplastic processes of endometrium most often meet in the meno- and postmenopausal aged women and are contributing for development of endometrial cancer.
Goal: The goal of our research was the study of a condition of endometrium and revealing of frequency of hyperplastic processes in the fertil-aged women which has undergone the cesarean section.
Methods: The scrinning was perfomed in 82 fertil-aged women in 1–5 years after operation. All patients underwent endovaginal echoscopy with application of anechogenic contrast amplification on the HDI 1000 (USA) device every 12–14 day of menstrual cycle, hysteroscopy every 4–5 days with the usage of "Olympus" HCL-3 (Japan) hysteroscope.
Results: As a result of hysteroscopy 32 (39%) of women after cesarean section had hyperplastic processes of endometrium .Adenomatous hyperplasya was observed at 14 (44%), adenomatous endometrial polyps - at 18 (56%). All diagnoses were verified with subsequent hystologycal study. During ultrasonic research conducted before hysteroscopy, hyperplastic processes was not found. The application of method of contrast amplification allowed to reveal endometrial polyps in 12,5% of cases. The analysis of anamnesis has shown, that in group with hyperplastic processes of endometrium is reliably more often the menstrual cycle disoders like intermenstrual bleedings and spottings, hyperpolymenorrhea, abnormal uterine bleedings were observed .Neuro-endocrynological disoders were observed only at 9,4%.
Conclusion: Thus, hyperplastic processes of endometrium is being observed much more often in the fertil-aged women which underwent cesarean section. Hysteroscopy as most informative method of diagnostics should enter into the program of examination of such patients.

P-191

Serous papillary cystadenofibroma of fallopian tube: An incidental finding. Cystadenofibroma of fallopian tube

Yesim Gürbüz, Bahar Müezzinoğlu, Zuhal Yumbul
Kocaeli University Medical School, Department of Pathology, Kocaeli, Turkey

Cystadenofibromas of the fallopian tube are rare tumors of the female genital tract. These tumors are usually asymptomatic and found incidentally. In this article the authors present an incidentaly found fallopian serous cystadenofibroma in a 48 year old woman with leiomyoma uteri. The pathologic findings of Müllerian type epithelium suggested that the tumor was an embriyologic remnant originating from Müllerian duct. However origin may also be considered mesonephric because of the coexisting Walthard nest at the same fallopian tube.
Key words: Cystadenofibroma, Adenofibroma, Fallopian tube.
Introduction: Neoplasms of the fallopian tube are the rarest tumors of the female genital tract (1). Most of the benign tumors of fallopian tube are endometrioid polyps and occasionally papillomas (2). Se-

rous papillary cystadenofibroma is an unusual tumor of the fallopian tube. In this paper we present an incidental fallopian serous cystadenofibroma in a 48 year old woman with leiomyomatosis uteri and discuss the origin and clinical presentation of this rare neoplasm.

Case report: A 48 year old woman applied to our hospital complaining irregular vaginal bleeding. She was diagnosed as leiomyoma uteri and total abdominal histerectomy and bilateral salphingo-oophorectomy operation was performed.

In macroscopic examination of the operation material was 9×6×5 cm. A leiomyoma of 2 cm diameter was detected in corpus uteri. Endometrium, cervix and ovaries were unremarkable. Besides, a 0.4 cm cyst with intracystic papillary projections attached to the serosal surface of right fallopian tube was identified (Figure 1). There were also bilateral multiple paratubal cysts largest one measuring 0.5 cm in diameter.

Microscopically paratubal papillary cystic lesion had coarse papillary projections lined by simple slightly pseudostrafied cuboidal columnar epithelium some of which were ciliated . There was an acellular zone under the epithelium (Figure 2–3). The cyst wall and stroma of the papillary projections were supported by fibrous tissue. Depending on these features the cystic lesion at the right fallopian tube was diagnosed as serous papillary cystadenofibroma.

Additionally there were a cystic Walthard nest and an endomeriosis focus at the right paratubal region.

Discussion: Adenofibromatous tumors of the fallopian tube especially serous papillary cystadenofibromas are rare tumors. Cystadenofibroma of the fallopian tube was first described by Iwanow in 1909. He termed this lesion as 'Cystadenofibroma papilliferum' (3). Since then eight cases of papillary serous cystadenofibroma were reported (1–6) . Two cases were associated with pregnancy one of which was a borderline lesion (1, 5). All the tumors were incidental findings except the one misdiagnosed as ectopic pregnacy (5). Two cases were at fimbrial localization and one was intamural. Seven cases of papillary adenofibroma which is the solid variant of this neoplasm were reported. (2, 7, 8, 9) including a case of bilateral tumor (8).

The origin of this neoplasm has not been clearly described yet. There is a consensus that the origin of this tumor is embriyologic. However there is still controversy about Wolffian (3), Müllerian (1, 4, 8) or mesonefric (1) origin. Also it was considered as a benign counterpart of malignant mixed Müllerian duct tumor (7). As most of the cases were incidental it may be an embriyologic remnant is more likely than a proliferating neoplastic process.

In conclusion, adenofibromas and cystadenofibromas of the fallopian tube are mostly asymptomatic and diagnosed incidentally. The only reported clinical presentations of these tumors were, infertility in a bilateral case with fimbrial localisation, and the other was a paratubal mass in a pregnant woman diagnosed radiologically as ectopic pregnancy (5, 8). In our case the tumor was at paratubal region attached to the serozal surface and away from the fimbrial end. The epithelium of the tumor was similar to paramesonephric duct cysts derived from Müllerian tissue. Therefore, we suggest that this lesion was originated from Müllerian duct it may be an unusual form of paramesonephric duct cyst. On the other hand, presence of a cystic Walthard nest in the same fallopian tube may be interpreted as a clue for the mesonephric duct origin.

References: 1. Silverman AY, Artinian B, Sabin M. Serous cystadenofibroma of the fallopian tube: a case report. Am J Obstet Gynecol 1978; 130:593–595

2. Alvarado-Cabrero I, Navani SS, Young RH, Scully RE. Tumors of fimbriated end of fallopian tube: a clinicopathologic analysis of 20 cases. Int J Gynecol Pathol 1997; 16:189–196

3. Iwanow WM. Cystadenofibroma papilliferum tubae fallopie. Zentalbl Gyneakol 1909; 33:745

4. Küster I. Einen tumor der fimbria overica. Berl Klin Wochenschr 1914; 51:1486

5. Valerdiz Cassalo S, Pardo Mindan J. Cystadenofibroma of fallopian tube. Appl Pathol 1989; 7:256–259

6. Kanbour AI, Burgess F, Salazal H. Intramural adenofibroma of the fallopian tube. Light and electron microscopic study. Cancer 1973; 13:1433–1439

7. de la Fuente AA. Benign mixed Müllerian tumor-adenofibroma of the fallopian tube. Histopathology 1982; 6:661–666

8. Chen KT. Bilateral adenofibroma of the fallopian tube. Am J Clin Pathol 1981; 75:229–231

9. Vaja K, Halmos L. Adenofibroma of the fallopian tube. Morphol Igazsagugyi Orv Sz 1988; 28:81–84

Figure 1: Cysadenofibroma at the serosal surface of the fallopian tube with intracystic papillary projections.

Figure 2: Rough intacystic papillary projections supported by fibrous tissue. (H & E ×32)

Figure 3: Slightly pseudostrafied cuboidal columnar ciliated epithelial cells and acellular zone under the epithelium. (H & E ×500)

P-192

Detection of active human papilloma virus infection by immunohistochemistry

S . Habedank, C. Schewe, M. Rizzello, M. Dietel, S. Hauptmann
Institute of Pathology, Charité Hospital Berlin, Germany

Background: Human papilloma virus (HPV) infection is associated with a variety of epithelial proliferations in the female genital tract. Examples for virus-induced alterations are benign *Condyloma accuminata* (CA), squamous intraepithelial lesions (SIL), and invasive carcinomas (IC). The aim of the present study was to investigate whether there is an association between the type of the lesion and the activity of the viral infection.

Materials and Methods: Material from 30 patients with PCR-proven (MY09/MY11 primer set, Digene) HPV infection (13× CA; 15× SIL, 2× IC) was investigated by immunohistochemistry using monoclonal antibodies (from Virofem) against different epitopes of the capside protein L1 which is produced in active infection. The antibody T16 recognises epitopes of this protein on high-risk (B) types 16, 18, 33, 39, whereas T33 recognises all HPV types (with the exception of types 1, 40, and 63).

Results: CA were in 92% HPV-A (low risk) positive (+), but had HPV-B in one case. All but one CA with HPV-A were S33 (+) and T16 (–); both the other cases were S33 (+) and T16 (+). Low grade SIL were HPV(–) in 2 cases, were infected by HPV-A twice, and by HPV-B in 3 cases. They usually did not express either of the antigens but were S33 (+) and T16 (+) in one case and S33 (+)/T16 (–) in another one. High grade SIL were HPV-B infected in 7 cases and HPV (–) once. They were S33 (+)/T16 (+) in 6 cases and failed to express these antigens in two cases. One carcinoma was HPV-B (+) and the other were HPV (–); both were T16 (–)/S33 (–).

Conclusions: The viral infection in condylomas is usually active. Most cases of LGSIL are inactive whereas HGSIL is characterised by an active infection. Whether this activity is getting lost in invasive carcinomas remains to be clarified.

P-193

The role of p53 expression and agnor count in aggressive behaviour and malignity potential of trophoblasts

Fevzi Harorlu [1], M. Akif Çiftçioğlu[2]
[1] Bursa State Hospital, Bursa, [2] Akdeniz University, Antalya, Turkey

Introduction: It is difficult to predict aggressive behaviour and malignity potential of trophoblasts in persistent mole and choriocarcinoma cases. The aim of the present study is to investigate if there is a difference in p53 expression and AgNOR count in hydatid mole, persistent mole and choriocarcinoma
Methods: In this study, sections of 68 hydatiform mole, 15 persistent mole and 8 choriocarcinoma, totally 91 cases were stained by AgNOR method and p53 immunohistochemistry. Three hundred and 100 cells were counted for p53 and AgNOR respectively. Relation of these parameters with trophoblastic necrosis, degree of atypia, trophoblastic mitosis, and patient age were also investigated.
Results: Mean p53 indexes were 6.5%, 23.8%, and 48.4% in hydatiform mole, persistent mole and choriocarcinoma cases respectively. Corresponding AgNOR counts were 16.2, 24.1, and 33.3. There was a significant positive correlation between p53 index and AgNOR count ($p<0.05$). Both p53 index and AgNOR count were demonstrated significant positive correlation with degree of atypia, trophoblastic mitosis, and patient age ($p<0.05$). No correlation is observed between trophoblastic necrosis and stain parameters.
Conclusion: The results of this study suggests that, by determination of p53 index or AgNOR count, persistent mole may be recognised at an early stage and a by the help of a more aggressive therapy.

P-194

Case Report: Hepatoid carcinoma of the ovary coexisting with a dermoid cyst

Hatzianastassiou Dimitris[1], Moraitis N.[1], Vgenopoulou S.[1], Kyriakou V.[1], Drakos E.[1], Polyzos A.[2] and Androulaki Athina[1]
[1] Pathology Department, Laikon Hospital, Athens; [2] 1st Prop. Dept. of Medicine, Medical School, Univ. of Athens, Greece

Introduction: We report a case of *hepatoid carcinoma of the ovary (HCO)* coexisting with a dermoid cyst, presenting as a right adnexal tumor, with multiple peritoneal implants, in a 66 year-old female, with elevated serum AFP and CA125 levels.
Methods: Multiple slides were available for routine histology and immunohistochemistry.
Results: The main lesion appeared to develop within the wall of a dermoid cyst. Both the lesion and the implants showed features of a low-grade hepatocellular carcinoma (HC). Tumor cells were medium to large-sized, arranged in nodules, cords or sheets, had moderate to abundant eosinophilic cytoplasm, with focal clearing and few Mallory bodies. Nuclei were central, round-to-ovoid, with prominent intranuclear inclusions and low mitotic activity. The immunophenotype was: AFP, CK8 and CK18 positive, canalicular reactivity for polyclonal CEA, negative for CK7, CK20 and PLAP.
Conclusions: HC and hepatoid carcinoma metastatic to the ovary were excluded since multiple abdominal CT-scans revealed no other primary, the lesion was unilateral and both tumor marker levels dropped to normal following resection. Hepatoid yolk sac tumor (H-YST) was ruled out due to lacking evidence of additional YST patterns or other germ cell tumor component -besides the dermoid cyst-throughout the lesion. The diagnosis of HCO was based on overall histology and immunophenotype in association with age, unilateral location, clinical findings and course. Hepatoid carcinoma of the ovary is a rare tumor and its exact origin is still controversial. Our findings favor somatic lineage.

P-195

Toxicopathology of the antiestrogens

Hirsimäki, Pirkko
Turku University Central Hospital, Department of Pathology, Turku, Finland

1. Introduction. The objective of the present paper is to review the safety of some antiestrogens. Tamoxifen, toremifene, droloxifene and idoxifene are polyphenylethylene antiestrogens while the pure antiestrogen, ICI 182,780 or faslodex as well as raloxifene are of a different structure.
2. Preclinical studies. Genotoxicity. Tamoxifen has to been shown to be genotoxic in several studies. It induces unscheduled DNA synthesis in rat hepatocytes and micronuclei in MCL-5^a-cells *in vitro*. Tamoxifen also induces aneuploidy in rat liver *in vivo* and chromosome aberrations and micronuclei in mouse bone marrow. Toremifene has shown to be genotoxic to a far lower extent. *Carcinogenicity*: Tamoxifen has shown to be hepatocarcinogenic in the rat in at least four independent long-term studies. The initiation of tumors in the rat is the result of metabolic activation by cytochrome P-450 isoenzymes to an electrophile(s) that binds irreversibly to DNA. The other antiestrogens are not carcinogenic in rodents.
3. Clinical studies. In several independent clinical studies the risk of endometrial cancer has increased among tamoxifen treated women. Reviewing the available data the International Agency for Research on Cancer (IARC) concluded that there was sufficient evidence to show that tamoxifen is a class I human carcinogen. It is not clear if the uterine tumor formation is a result of genetic mechanisms, analogous to those seen in the rat liver or due to the estrogen agonist action of tamoxifen. However, the other antiestrogens with a more or less similar intrinsic estrogenic potential have not been shown to be carcinogenic in humans.

P-196

Chronic inflammatory disease of womb and adnexal organs: Immunomorphological and lectinohistochemical research

Kazachkov Eugenij, Kazachkova Ella
Medical Academy, Chelyabinsk, Russia

The clinical and laboratory examination of 430 women with chronic inflammatory diseases of womb and adnexa (PID) and complex morphological research of endometrial biopsy specimens were carried out. The last one included immunomorphological and lectinohistochemical study of womb mucous. It was established the secondary deficiency of secretory IgA (SigA) due to depression of synthesis of secretory component, increased level of IgG-producing cells and fixed immune complexes in walls of postcapillar-s venuls were registered in endometrial specimens at PID. Among Ò-cells the amount of suppressers was considerably increased, the

number of natural killers and helpers was reduced. At lectinohistochemical research the change of protective properties of slimy covering of endometrium as hyperproduction of neutral slime and reduction of sialic acids contents was revealed. It could promote stagnation of slime in a womb cavity, persistence of microorganisms in structures of its internal environment, cause development of inflammatory, dystrofic and dysregenerating processes in endometrium. Also it could matter in infringement of synthesis of SIgA and formation of local immunopathological reactions. After the base treatment and local immunocorrection therapy including 0,25 % a solution of derinat in 1 month it was registered amplification of production of secretory component and increased level of SigA in repeatedly taken of endometrial biopsy specimens. The parameter of a parity CD4/CD8 came nearer to norm, a level of IgG-producing cells and fixed immune complexes was considerably decreased. The revealed frustration in production and distribution of glycoproteins in epithelial structures of a mucous environment of womb allow to recommend measures on improvement of drainage of surplus neutral of womb-s slime from reproductive tract and to include preparations - immunomodulators in complex therapy of this suffering. Thus amplification synthesis of glycoproteins riched by syalic acids was marked. The proof clinical recovery was reached in 97,5% of the women. At 60 % fruitless women the pregnancy which has finished by sorts was developed.

P-197

Results of radiation therapy of andometrial adenocarcinoma according to tumour. Differentiation

Krikunova L., Shentereva N.
Department of Radiation Therapy of Gynecologycal Diseases, Medical Radiological Research Center of RAMS, Obninck, Russia

Mixed radiation therapy of endometrial adenocarcinoma was given to 68 patients. Among them 36 (52,9%) patients had Stage I – histologicalli provenhighly differentiated adenocarcinoma was revealed in 9 (13,2%), moderately differentiated – in 20 (29,4%), and poor differentiated – in 7 (10,3%); 22 (32,4%) – Stage II – histologicalli provenhighly differentiated adenocarcinoma was revealed in 4 (5,9%) , moderately differentiated – in 14 (20,6%), and poor differentiated – in 4 (5,9%) and 10 (14,7%) – Stage III disease – histologicalli provenhighly differentiated adenocarcinoma was revealed in 2 (2,9%), moderately differentiated – in 7 (10,3%), and poor differentiated -in 1 (1,5%). Total dose for mixed radiation therapy was 78–80 Gy to Point A and 50–60 Gy to Point B depending on the disease stage. 5-year survival of patients was 87,3% (I stage – 89,5±5,7%; II stage – 91,3±8,3%; III stage – 63,6±20,5%. In this case 5 (97,4%) died from relapses occurred regardless the stage of the disease, distant metastases to lymph nodes caused death of 1 (1,5%). Among them histologicalli provenhighly differentiated adenocarcinoma was revealed in 2, moderately differentiated – in 3, and poor differentiated – in 1 patient.

P-198

The morphological analysis of outcomes of CEA and ferritin determination in peritonel liquid of the patients with various gynecological pathology

Krylou Y.V., Malashenko S.V., Matveenko M.E.
Vitebsk State Medical University, Vitebsk, Republik of Belarus

There are publications about CEA and ferritin (F) determination in blood serum at cancer and non-cancer pathology and other pathology, including gynecological one. The datas on the CEA contents in blood serum at cancer and non-cancer ovarium pathology are useful to screening and differential diagnosis a little. It is easy to receive peritoneal liquid with a punction through back of vagina and at diagnostic laporoscopy, which has direct contact to a tumor tissue.

The purpose of a research was morphological analysis of the CEA and F contents in peritoneal liquid at various gynecological pathology for the differential diagnosis.

Peritoneal liquid was received with a punction through back of vagina, and at operating interferences concerning gynecological pathology, and at diagnostic laporoscopy. CEA (50 patients) and F (31) were determined with radioimmunological method.

For all 13 benign epitelial ovarial tumors (5 mucous and 8 serous cystadenomas) the CEA levels were uniformly low (54.4±31.3 ng/ml). At ovarial cancer the CEA levels were hardly variable (20-500 ng/ml). For serous carcinomas (9 cases) the average CEA level was 46.0±19.8 ng/ml. For mucous carcinomas (6 cases) it was much above (348,2±40,1 ng/ml). The CEA levels in 2 cases of borderline serous ovarial cystadenomas did not differ from an average level of the benigns. At inflammatory processes (14 cases: chronic adnexitis, pelvioperitonitis) the СEA level met average for benign tumors. In 6 cases оf uteral myoma СEA was not revealed. The low F levels were characteristic for benign epitelial ovarial tumors, both serous (5 cases), and mucous (3 cases) on the average 43,4±31,3 ng/ml and 52,3±22,7 ng/ml accordingly. On the contrary, in all 9 cases of ovarial cancer (3 mucous and 6 serous) the F contents was more than 200 ng/ml. In 11 cases of chronic adnexitis the F contents was also high, and did not differ from ovarial cancer group. In 2 of 3 researched cases of uteral myoma the F contents was lowest. Thus, the high F levels were detected at ovarial cancer of various histological structure, and at ovarial inflammations. The high СEA levels from all epitelial ovarial tumors were observed only at mucous cancers, that alongside with cytological diagnostics can help in cancer diagnostics after ultrasonic detection of mucous cysts.

P-199

Benign and malignant pigmented lesions of the female genital tract (FGT). Report of 15 cases.

Kubelka K., Basheska N., Yashar G., Prodanova I., Ivkovski L., Zografski G.
Department of Histopathology and Clinical Cytology, Institute of Radiotherapy and Oncology, Medical Faculty, Skopje, Macedonia

Introduction: Benign and malignant pigmented lesions (PL) of the FGT are uncommon, predominantly affecting the vulva.

Methods: We report the clinical and pathological features of the 15 PL of the FGT retrieved in a 12-year, retrospective analysis at our Department. Patient records and archival pathology specimens of 7 benign and 8 malignant PL of the FGT, were reviewed.

Results: The mean age of all patients was 47 (range, 28–67). Three patients had vulvar nevi (2 intradermal and 1 dysplastic), while blue nevi ranging 2–10 mm in diameter were accidentally discovered in the endocervix of the hysterectomy specimens in four other patients. Vulvar primary malignant melanomas (PMMs) were uncommon (4 cases), comprising 2.5% of female PMMs and 4.3% of all vulvar malignancies diagnosed between 1989 and 2000. Con-

trary to other studies, all vulvar PMM in our series were of nodular type, ranging 3–13 mm in depth according to Breslow and III-IV level according to Clark. Within the same period, two patients with malignant PL of the uterine cervix were detected, accounting for 0.13% of all females with malignant cervical neoplasms. One of them had a PMM diagnosed in advanced clinical stage (FIGO III), and the other patient had an unusual pigmented squamous cell carcinoma in IIB postoperative stage. There were also 2 cases of delayed unilateral ovarian metastases of cutaneous PMM. The diagnosis in all cases of non-vulvar pigmented lesions was confirmed by immunohistochemistry.

Conclusions: Although uncommon, PL especially those affecting rare localizations must be considered as diagnostic possibility in FGT.

P-200

Alteration of stromal-epithelial interaction in chronic endometritis associated with recurrent abortions

Kuznetsova A., Voloschuk I., Paukov V.
Dept. of Pathology, Moscow Medical Academy, Moscow, Russia

The chronic endometritis (CE) is considered to be one of the reasons of the recurrent pregnancy loss. Currently pathogenesis of the fetal wastages in CE remains unclear.

Aim: To study the stromal-epithelial interaction in CE from patients with recurrent pregnancy loss.

Methods: Biopsies of endometrium from 25 women with recurrent abortions in anamnesis combined with CE were investigated with antibodies against the extracellular matrix components (ECM) (collagen types I (CoI), III (CoIII), IV (CoIV), VII (CoVII), merosin, fibronectin, tenascin (TN)), CD4, CD8, CD56, CD68, IgG, Ki67, αSMA and cytokeratins 5/18 with streptavidin-biotin-peroxidase method.

Results: Expression of TN was decreased in the stroma of the functional region of the endometrium during the proliferative stage; distribution of TN was irregular. CoI and CoIII had a similar pattern of distribution in comparison with that of normal endometrium: CoI, CoIII were diffusely localized in the stroma and expression of CoIII was higher than that of CoI. However their density was increased around spiral arteries and glands. Expression of αSMA was increased in wall of spiral arteries. Ki67 expression was decreased in the stromal cells, luminal and glandular epithelium in CE. The accumulation of IgG was augmented on the surface luminal and glandular epithelium. The leukocyte infiltration was significantly increased, but CD8+ lymphocytes were present in greater numbers than CD4+ lymphocytes.

Conclusions: Thus the lack of expression of TN and proliferative activity of the epithelium may result in implantation failure in women with CE. The high accumulation of IgG and the increase of the leukocyte infiltration in the endometrium demonstrated that the disorder of the local immune response in CE was significant.

P-201

Histological findings on cone specimens related to the residual neoplasia on hysterectomy

Lilic, V., Djordjevic, B.*, Zivadinovic, R.
* Institute of Pathology, Medical Faculty Nis, Yugoslavia;
Clinic of Gynecology and Obstetrics, Clinical center Nis, Yugoslavia

Conisation may be one of the treatment options for cervical microinvasive carcinoma and may represent a good alternative for a group of women that would otherwise be submitted to hysterectomy.

The aim of the study is to evaluate which histological information should be obtained from the cervical cones that give the best possible assurance of presence of residual neoplasia in the hysterectomy specimens.

Nineteen patients with microinvasive carcinoma who underwent biopsy, conisation and hysterectomy were reviewed. The majority of the cases (N=13) were figo stage Ia1. The following histological features in cone specimens, relating them to the residual neoplasia in hysterectomes, were examined: depth of invasion, lateral extension, unifocal or multifocal lesion, vascular invasion, extension and grade of associated dysplasia (CIN, SIL), morphological signs of HPV infection, and free or involved surgical margins of cone.

Residual neoplasia on hysterectomy was more frequent when surgical margin on cone were involved and in cases with extensive and high grade dysplasia (CIN, SIL). However, these histological variables were not indipendent and the only important histological finding to predict residual neoplasia on hysterectomy was the presence of dysplastic epithelium in surgical margins of the cone.

The detailed study of the cone surgical margins supports a conservative conduct in microinvasive carcinoma of the uterine cervix.

P-202

Primary clear cell carcinoma of the broad ligament

Losito N.S., De Chiara A, Botti G, Pignata S.* and Greggi, S.*
Dpts. of Pathology, I.N.T. Pascale, Naples; Div. of Med. Onc. B* an Div. of Gynecology** I.N.T. Pascale, Naples, Italy

Introduction: Primary tumors of the broad ligament are very rare and, among them, carcinomas are exceptional. Hereby, we describe a case of clear cell carcinoma arising in an endometriotic cyst of the broad ligament.

Methods: A 79-year-old woman, was admitted to I.N.T. Pascale because of lower abdominal pain. A C.T. scan disclosed a 15×8 cm left paraovarian cystic mass, which displaced the bladder and the uterus on the right.

Additionally to routine methods, mucicarmine and PAS stains with diastase digestion were performed.

Results: At operation, because the resection en bloc of the tumor was unfeasable, two main fragments were removed. Both were composed of an hemorrhagic cystic wall, one covered by streched ovary and fallopian tube, the other adherent to the left outer uterine margin and deeply penetrating into the isthmic and cervical miometrium. Right oophorectomy and omentectomy were also performed.

Microscopic examination showed, in both specimens, a fibrotic an eroded cystic wall containing hemosiderin-laden histiocytes, consistent with endometriosis, in which a largely necrotic neoplasm had grown. The tumor was mainly composed of sheets of glycogen-rich clear cell with pleiomorphic nuclei; cells with abundant eosinophilic cytoplasm and some extracellular mucus were also found. The ipsilateral overary was scleroatrophic, with fibrous tissue separating it from the cystic wall; endometrium was atrophic; omentum contained extravasated eritrocytes and lymphocytic infiltrates.

Conclusions: Up to date, only fourteen cases of carcinomas of mullerian type of the broad ligament have been reported; at our

knowledge, this is the fifth case of clear cell carcinoma occurring in this paraovarian site.

P-203

Protein p53 and papillomavirus antigen expression in squamous cell carcinoma of the vulva

*Olejek Anita, **Ziółkowski Adam
* Chair and Clinical Department of the Obstetrics and Gynecology of the Medical University of Silesia in Bytom, Poland,
** Chair and Pathomorphology Unit of the Medical University of Silesia in Zabrze, Poland

Vulvar carcinoma is a fairly rare condition whose pathogenesis still remains to be fully explained.

Material and methods: The study included the cases of women who had vulvar cancer between 1997 and 2000. The patients underwent surgery at the Chair and Clinical Department of Obstetrics and Gyncology, Silesian Medical University in Bytom. Post-operative specimens were processed with routine histopathological techniques. The number of examined cases totalled 46 and all revealed the type of squamous cell carcinoma (41 cornifying and 5 of the non-cornifying type). The differentiation stage G was as follows: G1 – 12 patients, G2 – 17 and G3 – 10 patients.

There were 15 cases of T I clinical progress, 22 cases of T II and 2 cases of T III. In situ carcinoma was found in 7 patients. Immunohistochemical examination was carried out with ABS and LSAB methods, while the antibodies used were p53, Papillomavirus, DAKO. The statistical analysis employed Chi test – square.

Results: Antigen p53 stained in the total of 19 cases, which accounted for 41%. Analysis of the correlation between the p53 protein index and G feature revealed statistical dependence ($p<0,01$). Protein p53 index tended to increase with the degree of tumor malignancy Papillomavirus antigen stained in 21%, most frequently in the cases of low differentiation carcinomas. No correlation was found between the clinical progress stage T and the number of positive staining reactions of the antigens which had been examined immunohistochemically.

Conclusions: The examination of p53 protein is an essential supplement of the histopathological evaluation of vulvar cancer. Protein p53 expression is directly proportional to the degree of cancer malignancy. Papillomavirus antigen expression is low in squamous cell carcinoma of the vulva.

P-204

Ovarian sertoli cell tumors: A clinicopathologic study of 56 cases emphasizing their immunohistochemical profile

E. Oliva, RH.Young, RE Scully
Department of Pathology, Massachusetts General Hospital, Harvard Medical School, Boston

Introduction: Ovarian Sertoli cell tumors (SCT) may be mimicked by tumors of diverse other types. Immunohistochemistry (IHC) may aid in this differential, but its role has not been analyzed in a large series.

Methods: We studied 56 SCT, and performed IHC for AE1/3-CAM 5.2, EMA, Inhibin, CD99, Vimentin, SMA, Chromogranin, S-100, NSE, and Calretinin.

Results: The patients were 2 to 76 years old. 5 had Peutz-Jeghers syndrome. The tumors were 0.8 to 30 cm. The predominant microscopic pattern was tubular, other patterns were cord-like (27), diffuse (21), retiform (3), sarcomatoid (1), and pseudopapillary (4). Stroma was abundant in 14 tumors with marked sclerosis in 4. The cells usually had eosinophilic cytoplasm, but 5 tumors had prominent vacuolated cytoplasm. 44 tumors were stage I, and 8 stage III.

KERATIN		EMA		INHIBIN		CD99		VIM		SMA		CHROM		S-100		NSE		CALRE	
+	–	+	–	+	–	+	–	+	–	+	–	+	–	+	–	+	–	+	–
16	9	0	24	18	4	10	11	18	1	5	14	0	23	2	20	10	10	7	12

Conclusion: SCTs usually have a distinctive tubular pattern facilitating diagnosis, but other patterns may occasionally predominate causing confusion with other tumors. EMA, inhibin, and chromogranin are the most helpful markers. CD99 is frequently expressed in these tumors. Calretinin may be seen in them and accordingly does not distinguish them from mesothelioma.

P-205

Cytological diagnosis of dysplasia and cervical intraepithelial neoplasia

Zorica Pavlovic, Voja Pavlovic, Zoran Pavlovic
Medical Faculty of Nis, Yugoslavia

Early diagnosis of the endometrial carcinoma and the indentification of the morfological precursors in the natural history of the cancer of the endometrium constitute one of the main problems in the gynecological diagnostics.

In the last 10 years (1995 to 2000) 3000 Papanicolaou smears were examined in order of prevention of cervical cancer. The women were between 18–80 years old. The study gives a synopsis of the results in prevention of cervical cancer as well in view of detecting of the early stages of endometrial cancer. In the respect to the numbers of late stages of cervical cancer, we found less late stages of cervical cancer in the second half of the last decenium in correation to an increase of the numbers of early stages of cervical cancer and carcinima in situas well as to dyspastic tissues. Cancer prevention with Papanicolaou smears reveals a 95% succes rate. The security in early detection of endometrial cancer is very low.

It was observed that in the age between 30 to 40 years only 33% of the women had midl dysplasia, in contrary to the previous and subsequent ten year period, where the respective percentages were 80. This study show that mass scrining of the Papanicolaou smers is possible to use for early detection carcinoma from women after 4o yerars of age.

P-206

Dynamic's parameters of uterine leiomyoma's growth and proliferative activity of the tumor cells

Petrov S.B., Kiassov A.P., Borodin Y.I., Klyucharov I.V.
Kazan State Medical University, Kazan, Russia

Objective: to understand the cause of difference of the dynamic's parameters of leiomyoma growth we investigated proliferative activity of the tumor cells. Materials and methods: 96 cases of uterine leiomyoma were divided in to two groups: with clinically determined "rapid growth" and without it. Proliferative activity was determined by mitotic and immunohistochemically by PCNA indices by computer videomicroscopical complex. We have used binary-

zation by color specter and brightness. For leiomyomas with rapid growth was counted average speed of enlargement of the complex corpus of the uterus-leiomyoma (CUL). Results: all leiomyomas with rapid growth (32 cases) had subserosal-interstitial localization. Average PCNA index (I) was 21,25. There was find no direct interrelation between the speed of the CUL complex growth and proliferative activity of the tumor cells (by PCNA). The constructing of the polynomial trend lines have shown that maximum of speed of enlargement is accompanied with low or absent of proliferative activity, and increase in speed of enlargement is accompanied by decrease of proliferative activity. Leiomyomas without rapid growth had no preferential localization. Average PCNA index (II) of the subserosal – interstitial leiomyomas without rapid growth (41 case) was 11. Number of mitotic figures in all leiomyoma cases was minimal or absent. Comparison of the I and II PCNA indices by W- criterion (Mann, Whitney) show significant difference ($p<0,05$).

Conclusions: The received data show that the speed of enlargement linked with the level of proliferative activity. This interrelation has no direct but complex character. PCNA index can be used as a prognostic criterion for measuring dynamic of the CUL-complex enlargement.

P-207

T-cell clonality is a focal event in vulvar lichen sclerosus and squamous cell carcinoma arising in lichen sclerosus

Sigrid Regauer, Olaf Reich*, Christine Beham-Schmid
Institute of Pathology and *Department of Obstetrics and Gynecology, University of Graz, Austria

Background: The lymphoid infiltrate in lichen sclerosus (LS) shows a high percentage of gT-cell-receptor rearrangement (gTCR). Carcinoma arising in LS are usually highly differentiated, keratinized SCC in elderly women without HPV risk factors. We were interested if gTCR is required for development of SCC in LS.
Methods: Multiple biopsies of a single lesion of LS and SCC, as well as multiple lesions of LS in the same patient were evaluated in 15 patients each with vulvar LS, vulvar SCC arising in LS and vulvar SCC without LS by PCR for gTCR and immunohistochemically for the expression of CD3, CD4, CD8, CD20, CD57, fascin, granzyme, TIA and perforin. Results: gTCR was identified in 7/15 LS, 10/15 SCC with LS and in 0/15 SCC without LS. However, only one of three or four concomittant biopsies of a single lesion of LS showed gTCR, and multiple independent lesions of LS in the same patient were also heterogeneous. SCC arising in LS and adjacent lesions of LS were similarly heterogeneous. Recurrences of gTCR-positive SCC were also heterogeneous in regard to their gTCR. Immunophenotypical differences between gTCR-positive and gTCR-negative biopsies were only observed within submucosal lymphocytic aggregates (LA). In contrast to gTCR-negative cases, LA in gTCR-positive samples were predominantly positive for CD20 and TIA with numerous fascin-positive cells in the B-cell fraction, and individual CD8, CD57, granzyme and perforin-positive cells in the peripheral zones of the LA. gTCR-negative samples showed no B-cells and perforin staining. Conclusion: Development of T-cell clones in vulvar LS and SCC appears to be a focal event. We postulate that gTCR, although not a prerequisite, may facilitate the development of SCC in LS. The presence of B-cells, fascin and perforin-positive cells in gTCR-positive biospies of LS may represent an immunologic mechanism to exert cellular cytotoxicity to the proliferating T-cell clones.

P-208

Analysis of p16/MTS1, Ki67 and HPV 16/18 E6/E7 oncogene transcription in adenocarcinoma in situ and benign glandular lesions of the cervix uteri

S. Riethdorf, L. Riethdorf, K.R. Lee*, A. Cviko*, T. Löning, C.P. Crum*
Dept. of Gynecopathology, University of Hamburg, Germany; *Dept. of Pathology, Brigham & Women's Hospital, Boston, MA, USA

Introduction: Adenocarcinoma in situ (ACIS) of the cervix is an important preinvasive disease, and proper laboratory management requires that this lesion can be distinguished from benign but morphologically atypical glandular epithelium. Recently, host biomarkers expressed in response to HPV infection have been identified, including the tumor suppressor gene p16. P16 is expressed in cervical squamous cell carcinomas, their precursors and cervical adenocarcinomas. In the vast majority of these lesions HPV(Human Papillomavirus) 16 and/or 18 infections are detectable and a strong relationship between p16 expression and the presence of HPV encoded E6/E7 transcription exists. This study analyzed the relationship between HPV status and p16 expression in ACIS and compared it to that of benign glandular lesions.
Methods: 81 paraffin-embedded benign and premalignant glandular lesions were immunostained with monoclonal antibodies against p16 (PharMingen) and Ki67 (Immunotech). HPV E6/E7 transcription was detected by in situ hybridization.
Results: HPV 16 or 18 E6/E7 transcription as well as strong p16 expression with diffuse pattern could be detected only in ACIS. Atypical tubal metaplasia also showed strong p16-expression, but in contrast to ACIS, p16 expression was heterogeneous and percentage of Ki67-positive cells was low. In tubal and endometrial metaplasia as well as microglandular and mesonephric hyperplasia, p16 expression was either absent or weak to moderate and most of these cases were only weakly Ki67-positive.
Conclusions: Based on analysis of HPV E6/E7 transcription as the gold standard for HPV-related glandular neoplasia, the pattern of p16 and Ki67 expression appears to be helpful for the differentiation of ACIS from benign hyperplastic and metaplastic glandular epithelia.

P-209

Correlation between microsatellite instability, clinico-pathological and immunohistochemical features in endometrial carcinomas

C. Riva, C. Facco, D. Furlan, E. Dainese, A. Dionigi, M.G. Tibiletti, A.M. Chiaravalli, C. Capella
Department of Clinical and Biological Sciences, University of Insubria, Varese, Italy

Introduction: Microsatellite instability (MI) has been detected in approximately 20% of sporadic endometrioid carcinomas of the endometrium. Nevertheless the biological significance of MI in these tumors remains to be clarified. The aim of the study was to evaluate 1) the prevalence of MI in our series of endometrial cancers 2) the clinico-pathological and phenotypic profile of MI endometrioid carcinomas (ECs), 3) the reliability of mismatch repair (MMR) protein antibodies in predicting MI.

Methods: A series of 120 endometrial tumors (100 endometrioid, 11 serous, 2 clear cells, 1 mucinous, 2 undifferentiated carcinomas, 3 carcinosarcomas and 1 adenosarcoma) was evaluated for size, grade, stage, mitotic index and necrosis.
MI was investigated with mononucleotide loci (Bat-26, -25, -40) by PCR amplification. Immunohistochemistry was performed with antibodies against hMLH1, hMSH2, p53, estrogen receptor (ER) and progesteron receptor (PgR).
Results: MI was detected in 26/120 (22%) cases, including 24 (98%) endometrioid, one mixed mucinous-endometrioid and one undifferentiated carcinomas. No clinico-pathological differences were found between ECs with and without MI. MI was detected both in early and advanced stage ECs. In ECs with MI, PgR was abundantly expressed (100% vs 86%), whereas p53 was very scarce (8% vs 18%). Near absolute concordance was found between molecular MI and immunohistochemical data (63/64 cases, 98%).
Conclusion: Our results confirm the correlation between MI and ECs. In addition, these data suggest that the mutator phenotype could play a role also in early stages of a subset of PgR positive/p53 negative ECs. Finally, hMLH1 and hMSH2 immunohistochemistry seems to be a reliable method in predicting MMR system defects in endometrial carcinomas.

P-210

Expression and cytokine – Mediated regulation of MAPK – Phosphatases in ovarian cancer

W. D. Schmitt, C. Denkert, S. Hauptmann
Institute of Pathology, University Hospital Charité, Humboldt-University, Berlin, Germany

Introduction: MAPK-Pathways are involved in regulation of tumor proliferation and invasion. Their activity is controlled by a number of MAPK-Phosphatases and any defects influencing this complex regulatory network may lead to abnormal behavior of tumor cells.
Methods: Basal expression of MAPK-Phosphatases in ovarian cancer cell lines (SKOV-3, OVCAR-3, A27/80, PA-1, Mdah2774, OAW-42, ES-2 and CAOV-3) was investigated by RT-PCR. Regulation after cytokine-stimulation, namely Il-1ß or TNFα, in ovarian cancer cell lines and basal expression in human epithelial ovarian tumors was determined by Northern Blot.
Results: A basal expression of CL100, Pyst1, MKP-5, hVH-5 and MKP-4 was found in all cell lines, the latter three phosphatases with variable intensity, OVCAR-3 was negative for MKP-4. CL100 was highly inducible by Il-1ß and TNFα in SKOV-3 and OVCAR-3 cell lines with a maximal mRNA peak after 1 hour. In SKOV-3 this peak disappeared quickly when stimulated with Il-1β but remained increased for at least 3 hours after TNFα stimulation. The reaction of OVCAR-3 was similar with a prolonged stimulation by Il-1β.
Conclusions: Our results show that MAPK-Phosphatases are expressed in some ovarian carcinoma cell lines and can be induced by inflammatory cytokines. It remains to be determined whether dysregulations of the network of MAP-Kinases and MAPK-Phosphatases may be involved in ovarian carcinoma growth and metastasis.

P-211

Immunohistochemical characterization of extracellular matrix components of ovarian tumors

Michael Schwabe, Steffen Hauptmann
Institute of Pathology, Charité Hospital, Berlin, Germany

Introduction: Interactions between tumor cells and extracellular matrix (ECM) components and inflammatory cells as well are crucial determinants of tumor cell migration and invasion. Therefore, we have examined the expression of tenascin, fibronectin, collagen I, III, V, VI, and the inflammatory stromal reaction of ovarian tumors.
Methods: The extracellular matrix components were investigated immunohistochemically in samples of 71 patients with epithelial ovarian tumors. The tissue specimens included cystadenomas, borderline tumors, serous carcinomas, and non-serous carcinomas. Monoclonal antibodies were used against the above mentioned extracellular matrix components and against CD3, CD20, CD57, and CD68(PGM-1). A standard immunohistochemical APPAP technique was applied.
Results: The extracellular matrix proteins tenascin and fibronectin were overexpressed in borderline tumors and carcinomas but the amounts were variable in the latter. The collagens type I and VI were overexpressed in malignant tumors. Predominant components of the inflammatory reactions were CD3-positive T-cells and CD68-positive macrophages.
Conclusion: Our data indicate that the stromal expression of tenascin and fibronectin starts already in borderline tumors. Therefore, it is not helpful to distinguish invasive carcinomas and borderline tumors. Whether the amount of tenascin and fibronectin as well as the inflammatory stromal infiltrate are of prognostical importance, remains to be clarified.

P-212

Germ cells tumors in dysgenetic gonads

Jasna Šinkovec,Sreèko Kovaèiè
Dept. of Gynecology & Obstetrics,
University Medical Centre Ljubljana, Slovenia

In XY gonadal dysgenesis with kariotype 46,XY or 45,X/46,XY, female phenotype, there is a high risk of malignant transformation of the aberrant gonads. The most freguent tumor type is the gonadoblastomas (90%) mostly unilateral (80%) often overgrown by dysgerminoma (50%), endodermal sinus tumor, teratoma, embrional carcinoma, choriocarcinoma. (10%). In our two cases female had large right ovarian tumor, left ovary represents as a streak gonad. First female had 27 years, her kariotype is 46,XY. Serum tumor markers: AFP 9595 E/ml, Ca 125 197 KE/l, CEA 6,6 mg/l, FSH 79 IE/l, LH 105 IE/l. Tumor with median diameter of 16 cm had external surface smooth and glistening. On section tumor was solid and cystic with hemorage, calcifications necrosis honeycomb appeareance. Microscopically, tumor is a gonadoblastoma: nests of germ cells and sex cord derivates resembling immature Sertoli and granulosa cells, with Call-Exner bodies; overgrouth by a dysgerminoma, and yolk sac tumor: isolated papillary projections with a central blood vessel and peripherical sleeve of embryonic epithelial cells (Schiller-Duval bodies), hyaline globules, reticular areas. Second female had 26 years, with kariotype 45,X/46,XY. Serum tumor

markers: CA 125 376.9 KE/l, AFP 1530 E/ml. Tumor was 17 cm large microscopically the same as in first case, with embrional carcinoma and syncytiotrophblastic giant cells immunoreactive for hCG.

P-213

Retinoblastoma, p53,and bcl-2 protein expression in cervical carcinomas

Siti-Aishah M.A., Noraini M.D., Kwan S.H., Fatimah S., Nor-Salmah B., *Abd. Aziz Y.
Department of Pathology, Faculty of Medicine, Universiti Kebangsaan Malaysia; *Obs. and Gyn. Clinic, Gleneagles Intan Medical Centre, Kuala Lumpur, Malaysia

Retinoblastoma (pRb) and p53 proteins are products of tumour-suppressor genes that normally maintain cell proliferation and growth,while the oncoprotein bcl-2 inhibits apoptosis. In this study, the immunohistochemical expression of the retinoblastoma, p53 and bcl-2 proteins was evaluated with commercially available antibodies in formalin-fixed, paraffin-embedded surgical specimens from 58 patients with cervical carcinomas. Forty-eight cases were squamous cell carcinomas and ten were adenocarcinomas. Expression for pRb showed +3 positivity in twenty-one cases, +2 in twenty-four and negative in only one case. With p53 (DO-7) there was +3 positive nuclear staining in only three cases, +2 in twenty-eight cases and negative in nine cases. Bcl-2 positivity was seen in five cases showed +3 and eleven were +2 cytoplasmic staining. Thirty-nine cases were negative for bcl-2. Expression of pRb, p53 and bcl-2 among carcinomas were not correlated to histological type, grade of differentiation, and FIGO stage. pRb, p53 and bcl-2 proteins can be detected by immunohistochemistry in 98.3% (57/58), 84.5% (49/58) and only 32.8% (19/58) respectively of cervical cancers. There appears to be an inverse pattern of +3 staining between pRb (36.2%; 21/58) with p53 (5.2%; 3/58) and bcl-2 (8.6%; 5/58) in cervical carcinomas, which was not statistically significant.

P-214

Microvessel density in relation to the expression of vascular endothelial growth factor and transforming growth factor-β: prognostic significance in ovarian carcinoma

Sönmezer M[1], Savas B[2], Ensari A[2], Güngör M[1], Ortaç F[1]
University of Ankara Medical School, Departments of Obstetrics and Gynaecology[1] and Pathology[2], Ankara, Turkey

Introduction: There are many reports suggesting that quantification of tumor angiogenesis could serve as an independent prognostic factor. In the present study the prognostic significance of microvessel density (MVD) in relation to the expression of vascular endothelial growth factor (VEGF) and transforming growth factor β (TGF-β) in ovarian carcinoma has been evaluated.

Methods: Forty-seven cases of primary ovarian surface epithelial carcinoma were included in the study. Extended surgical staging, histopathological grading according to FIGO were performed in all cases. Paraffin sections of the tumors were stained with antibodies to factor VIII-related antigen (FVII-Rag), VEGF and TGF-β using a streptavidin-biotin peroxidase technique. Microvessel density (MVD) was measured using 200× magnification in three separate areas in slides stained with FVII-RAg. Expressions of VEGF and TGF-β were measured arbitrarily on a scale of (+–+++). Spearmen correlation analysis, Khi square test, Kaplan Meier survival analysis and log-rank test were used as appropriate for statistical analysis.

Results: MVD was not found to be correlated with stage, type or grade of the tumors studied. Similarly, neither MVD, nor VEGF or TGF-β expressions showed any correlation with the clinicopathologic factors studied (r=0.1646. p>0.05). However, a positive correlation was observed between VEGF expression and ascite volume ($p<0.05$). There was also no correlation between MVD and the expressions of VEGF or TGF-β.

Conclusion: In contrast to several other solid organ tumors, angiogenesis does not seem to be a prognostic factor in ovarian carcinoma. VEGF proves to be a potent factor for vascular permeability and may be responsible for the increased ascite volume in ovarian carcinoma.

P-215

Immunohistochemical expression of wilms tumor gene product (WT1) in malignant epithelial ovarian tumors

Waldstrøm Marianne, Grove Anni
Institute of Pathology, Aalborg Hospital, Denmark

Introduction: The purpose of the present study was to evaluate the expression of WT1 in different subtypes of malignant epithelial ovarian tumors.

Methods: Seventyeight malignant epitelial ovarian tumors were drawn from our files. One representative formalin-fixed paraffin-embedded section from each case was immunohistochemically stained for WT1 (clone 6F-H2, DAKO) using Envision+ (DAKO) as detection system. The immunoreactivity was graded. A tumor was considered negative if less than 1% of the cells were stained

Results:

Histologic subtype of carcinoma	Percentage of positive tumor cells			
	<1%	1–10%	10–50%	50–100%
Serous (n=28)	–	–	7%	93%
Mucinous (n=14)	100%	–	–	–
Endometrioid (n=16)	50%	–	–	50%
Clear cell (n=14)	100%	–	–	–
Undifferentiated (n=5)	60%	–	–	40%
Brenner (n=1)	100%	–	–	–

Conclusions: Our results suggest that WT1 seems to be a very sensitive marker for serous carcinoma of the ovary. Half of the endometrioid carcinomas and 40% of the undifferentiated tumors included in our study turned out to be positive, while mucinous, clear cell and brenner tumors were all negative.

P-216

Are metastasizing well differentiated uterine smooth muscle neoplasms endometrial stromal sarcomas effaced by smooth muscle metaplasia?

Yilmaz A., Antonescu C., Delgado R., Soslow R.A.
Memorial Sloan-Kettering Cancer Center, New York, NY USA

Introduction: Endometrial stromal sarcomas are defined by strict morphologic criteria, express CD10 and have specific ultrastructural attributes; however, they display a range of morphologic appearances, which can result in misdiagnosis. The distinction between well differentiated smooth muscle neoplasms, including leiomyoma, and low grade endometrial stromal sarcoma can be problematic when stromal sarcomas show prominent smooth muscle differentiation. Although the existence of mixed endometrial stromal/smooth muscle tumors is an accepted phenomenon, endometrial stromal tumors that are almost entirely effaced by smooth muscle differentiation (>95%), so-called "effaced stromal tumors (EST)" have not been described previously.
Methods: We studied the clinicopathologic characteristics of gynecologic mesenchymal neoplasms with striking smooth muscle differentiation that did not meet the histologic criteria for leiomyosarcoma, and were otherwise difficult to classify using current diagnostic criteria. CD10 reactivity in populations of primitive cells that did not resemble smooth muscle cells and cells lacking the ultrastructural characteristics of smooth muscle were considered support for endometrial stroma.
Results: Our study consisted of 4 ESTs and 3 mixed endometrial stromal/smooth muscle neoplasms. Six were uterine primaries or suspected uterine primaries and one was primary retroperitoneal. Two ESTs recurred in the pelvis and one metastasized to the lungs; one additional mixed tumor recurred in the retroperitoneum and involved both ovaries. All neoplasms expressed smooth muscle actin and desmin. CD10 was preferentially expressed in perivascular aggregates of dark, ovoid cells with scant cytoplasm and in nodular, sometimes swirling aggregates of small, ovoid and somewhat spindled cells, set in a myxoid or edematous stroma.
Conclusions: We conclude that ESTs are endometrial stromal sarcomas and that they are part of the spectrum of mixed endometrial stromal and smooth muscle tumors. Since these tumors have recurring and metastasizing potential, it is crucial to recognize stromal differentiation and to avoid misdiagnosis as leiomyoma. It is possible that a number of tumors previously designated "benign metastasizing leiomyomata" might indeed represent ESTs.

P-217

Morphological characterization and expression of estrogen and progesterone receptors in menopause endometrium

Zadorozhna T.D., Tatarchuk T.F., Bondarenko G.I.,
Zakharenko N.F., Burlaka O.V., Popova T.O.
Institute Pediatrics, Obstetrics and Gynecology of Academia of Medical Science of Ukraine, Kyiv, Ukraine

Introduction: Women in perimenopause with hyperplastic process in endometrium are in the risk group on development of malignization. Many invastigator have reported the dependence of endometrium hyperplasia from hormonal disorder (estrogen and progesterone). This hormones influence on endometrium through specific receptor – estrogen receptor (ER) and progesterone receptor (PR).
Methods: Paraffin-embeded sections of endometrium in 78 women (54 in perimenopause 38-52 years of age and 24 in postmenopause 50–69 years of age) were histological examination. Expression of ER and PR in cases of endometrial hyperplasia studied by indirect immunohistochemical (streptavidin/peroxidase) method.
Results: Simple and glandular-cystic hyperplasia of endometrium were found in 40,7% women in perimenopause and 8,3% in postmenopause. Adenomatous was found in 27,9% (grade I – 13%, grade II – 13%, grade III – 1,9%) women in perimenopause and 12,5% (grade I – 4,2%, grade II – 8,3%) women in postmenopause. Immunohistochemical reaction on ER and PR in simple and glandular-cystic hyperplasia in peri- and postmenopause was identical: expressive in nuclei and cytoplasm of stromal and epithelial cells on PR and negative or low expressive in the same structures on ER. In adenomatous endometrium grade I immunohistochemical reaction on ER and PR in nuclei and cytoplasm of stromal and epithelial cells was low expressive or negative in perimenopause and negative in the same structures in postmenopause. Adenomatous of endometrium grade II characterized by negative immunohistochemical reaction on ER and PR in nuclei and cytoplasm of stromal and epithelial cells.
Conclusion: Our findings show that expression of ER and PR in endometrium at the women in peri- and postmenopause decreases with the progression of hyperplastic changes.

P-218

Clinico-morphological characteristics of carcinosarcomas of the corpus uteri

Zakharova T., Smirnov A., Lazareva N., Petrovichev N.,
Kuznetsov V.
Cancer Research Center of RAMS, Moscow, Russia

Introduction: The aim was to study the clinical and morphological characteristics of carcinosarcomas of the corpus uteri.
Material and methods: Thirty five carcinocarcomas of the corpus uteri were studied in women 46 to 78 years of age. Paraffin embedded material was stained with hematoxylin and eosin, and picro fuchsin. Antibodies against EMA, cytokeratins, vimentin, desmin, neurofilaments, glial fibrillar protein, S100 protein, myoglobin, myosin of skeletal muscles, PCNA and Ki 67 were used. The size of tumor, depth of myometrial invasion, presence of vascular invasion, necroses, cellular atypia and differentiation, and mitotic activity was analyzed.
Results: All the tumors were characterized by the large size of tumor node. Morphological and immunohistochemical analysis proved biphasic structure of the tumors. Epithelial component of majority of cases was presented by various adenocarcinomas. In two cases epithelial component was presented by squamous cell carcinoma and in one case by adenosquamous carcinoma. Mesenchymal component in homologous tumors was presented by leiomyosarcoma, in heterologous by rhabdomyosarcoma and liposarcoma and in one observation by osteosarcoma. In poorly differentiated tumors mesenchymal tumor cells expressed the epithelial antigen markers. All the metastases in ovaries, lymph nodes, lungs and omentum consisted of adenocarcinoma.
Conclusion: The survival of the patients with carcinosarcoma correlated with the depth of myometrial infiltration, cellular atypia of the epithelial component and the presence of necrosis in the tumor. Expression of epithelial markers in the mesenchymal component of

carcinosarcomas suggests these tumors can arise from one pluripotent stem cell.

P-219

Diagnostic value of inhibin immunoreactivity in ovarian granulosa cell tumors and epithelial carcinomas

Zekioglu O., Erhan Y., Ciris M., Bayramoglu H., Ozdemir N.
Dept. of Pathology, Medical Faculty, Ege University, Bornova-Izmir, Turkey

Background and purpose: Inhibin is a glycoprotein hormone produced by normal ovarian granulosa cells and testicular sertoli cells. In the ovary, it inhibits the eccretion of follicle-stimulating hormone. Patients with granulosa cell tumors have elevated serum levels and these tumors show inhibin positivity. Recent studies have evaluated the expression of inhibin in granulosa cell tumors and in other ovarian neoplasms. Inhibin positivity in granulosa cell tumors was found in high levels but in epithelial tumors has been variable. The purposes of this study were to examine inhibin immunreactivity in granulosa cell tumors and to assess its value in the differential diagnosis of the other ovarian tumors.
Material and method: The study material consisted of 35 granulosa cell tumors, 27 primary ovarian carcinomas, and 3 metastatic ovarian carcinomas. A paraffin-embedded tissue block was selected from each ovarian tumor and they were immunohistochemically stained with anti-?-inhibin using streptavidin-biotin method.
Results: Inhibin immunostaining was expressed in 23 of 35 (65%) granulosa cell tumors. There was no staining in the neoplastic cells both of the primary and metastatic ovarian carcinomas. However, in some of these tumors, inhibin was detected in the reactive stromal cells.
Conclusions: Inhibin is a sensitive immunohistochemical marker for granulosa cell tumors and is of value in the differential diagnosis of epithelial ovarian neoplasms.

P-220

The presence of progesteron receptor and cerb-b2 immunreaktivity and their effect on prognosis in endometrial adenocarcinoma

Zergeroğlu S., Özdemir H.B, Özer M., Mocan G., Gökmen O.
Department of Pathology and Gynecology, Zekai Tahir Burak Hospital; Department of Pathology, Faculty of medicine in Hacettepe Univercity, Ankara, Turkey

Objective: The purpose of this study was to research the precence of progesteron receptor(PR) and cerb-b2 immunreactivity and their effects on prognosis in endometrioid type adenocarcinoma of endometrium.
Material and method: PR and cerb-b2 primary antibodies were used by immunhistochemical method in 42 endometrioid type endometrial adenocarcinoma. The results were compared wih,grade,stage,myometrial invasion,and metastasis to lymp node.
Results: Among 42 cases were 25 stained PR positive and 21 were stained cerb-b2 positive. Both primary antibodies were stained positively more in grade I cases, stage I cases,in cases with superficial myometrial invasion and in nonmetastatic cases ("Chi Squre test") ($p<0.05$).
Conclusions: PR and cerb-b2 can be used as a good prognostic marker in endometrial adenocarcinoma.
Keywords: Endometrium ,adenocancer, progesteron receptor, cerb-b2, immunohistochemistry

P-221

Bronchoalveolar lavage in aids patients

Homa Adle–Biassette, Nina Weber, Didier Trophilme,
Bruno Crestani, Valérie Andrieux, Raymond Ruimy,
Françoise Brun-Vésinet, Jean-Louis Vildé, Jean-Pierre Coulaud,
Bernard Régnier, Dominique Hénin
Department of Pathology, Hôpital Bichat, Paris, France

Aim: To assess cytological abnormalities and presence of pathogens in bronchoalveolar lavage (BAL) in AIDS patients.
Material: Preliminary data from 374 AIDS patients (1998-2000) are analyzed considering conventional stainings, cultures, lymphocyte typing.
Results: cellularity <250000/ml with normal formula was found in only 10% of BAL, 1 of these had mycobacterial and 4 PC infections. In the remaining BAL, either high cellularity >250000/ml and/or abnormal formula were present. High percentage of neutrophils (>5%) was found in 87% of BAL and high percentage of lymphocytes (>20%) was present in 15%. Pathogens were detected using conventional stainings in 49/160. Pneumocystis carinii (PC) was found in 189 (CD4=2–70/mm^3), only 20% of them had cellularity >250000/ml. The others had high percentage of neutrophils (5–70%), with lymphocytosis in few of them.
Fungal infections were found in 20 BAL (3 aspergillosis, 17 candidiasis) always with high cellularity (>450000/ml) and high percentage of neutrophils (>5%), but lymphocytosis was observed in only 3 cases. CMV (4) or mycobacterium (2) were rare. Multiple pathogens were found in few patients.
Conclusion: In AIDS patients the vast majority of BAL exhibit abnormal cellularity/formula. Normal cellularity or formula does not exclude the presence of pathogens. PC is the predominant pulmonary pathogen in AIDS, even under prophylactic treatment. Aspergillosis is rare. Cytomegalic cells are rarely detected, and immunohistochemistry does not improve their detection. Culture is more reliable in the diagnosis of bacterial, and CMV infections.

P-222

DNA copy number changes in malignant spindle cell tumours of the pleura

Sisko Anttila, Kowan J. Jee, Eero Taskinen, Henrik Wolff and Sakari Knuutila
Finnish Institute of Occupational Health, Helsinki;
Transplantation Laboratory and Department of Medical Genetics, Haartman Institute, University of Helsinki, Finland

The differential diagnosis of sarcomatous malignant mesothelioma, sarcomas of the pleura, and pleomorphic carcinoma of the lung with invasion to the pleura is often difficult on the basis of morphological and immunohistochemical criteria. The characteristic immunohistochemical finding of mesothelioma, the coexpression of cytokeratin and vimentin, may occur also in pleomorphic carcinoma. Furthermore, cytokeratin expression tends to decrease in poor-

ly differentiated epithelial tumours but may be detected in some sarcomas. Thirteen malignant spindle cell tumours of the pleura were drawn from the archives of the Finnish Mesothelioma Panel. Seven cases were classified as probable mesotheliomas and six cases as unlikely mesotheliomas by light microscopy and immunohistochemistry for cytokeratin, vimentin, calcretinin, CD34, CD31, S-100, and muscle antigen, among others. DNA copy number changes were investigated by a comparative genomic hybridization (CGH) technique. Two of the probable and one of the unlikely mesotheliomas had a normal karyotype by CGH. In mesotheliomas, on average more losses and less gains and high-level amplifications were observed as compared to unlikely mesotheliomas. The features most characteristic to mesotheliomas were losses in 4p11-p13-15 and 4q that were detected in four of the five mesotheliomas with abnormal karyotype but in none of the unlikely mesotheliomas. Identification of a CGH pattern characteristic to sarcomatous malignant mesotheliomas requires investigation of a larger number of tumours. Our results suggest that a typical CGH pattern may exist and it might provide additional confirmation of the diagnosis of sarcomatous mesothelioma.

P-223

Mediastinal neoplasmas – 5-years retrospective analysis

Banev S.[1], Jovanovic R.[1], Cvetkovski P.[1], Tolovska M.[1], Spirkovski Z.[2], Arsovski A.[2], Karagjozov M.[2]
[1)] Institute of Pathology, Faculty of Medicine, Skopje, R. Macedonia, [2)] Clinic for Thoraco-vascular Surgery, Clinical Center, Skopje, R. Macedonia

The aim of the study was to investigate the most frequent primary mediastinal neoplasmas, in a 5 years period, analysing the material obtained by biopsy and open mediastinotomy. The total number of samples counted 42. Six of them were metastatic lung tumors and one was a metastatic renal cell adenocarcinoma. There were 4 samples refered to as non-conclusive material. The rest of the cases (31) were primary mediastinal tumors distributed by origin as follows: thymic neoplasmas (n=8), primary neurogenic tumors (n=8), Hodgkin's disease (n=4), Non-Hodgkin lymphoma (n=5), hystiocytosis X (n=1), cases of mediastinal lymphadenitis (n=3), dysgerminoma (n=2). The group of thymomas covered type A thymoma (n=1), AB type (n=2), B1 type (n=2) and B3 type (n=2). Appearing in age group over 12 years.
The group of neurogenic neoplasmas covered the following: paraganglioma, schwanoma, ganglioneuroma, ganglioneuroblastoma, neuroblastoma (all represented by one case) and three neurofibromas. All of them appeared in children younger than 12 years, except for the paragaglioma and schwanoma, diagnosed in adults (42 and 41 years old respectively).
This shows that the most common primary mediastinal neoplasmas for the last 5 years in the pediatric group were neurogenic neoplasmas, while thymic neoplasmas were more commonly found in adults.
We also found 2 cases of dysgerminoma, despite the fact that they are extremely rare at this location.

P-224

Pleural mesothelioma following domestic exposure to asbestos

C. Bianchi, A. Brollo, L. Ramani, C. Zuch, T. Bianchi
Laboratory of Pathological Anatomy, Hospital of Monfalcone, Monfalcone, Italy

Introduction: The cleaning of work clothes polluted by asbestos may induce asbestos-related disease. In a series of 174 malignant pleural mesotheliomas, 17 cases had developed after domestic exposure to asbestos.
Methods: The group included 17 women, aged between 57 and 89 years (mean 75, median 80). The diagnosis of mesothelioma was made on (or confirmed by) necropsy findings in 14 cases, and on surgical material in 3. Routine lung sections were examined for asbestos bodies in 14 cases. Asbestos bodies were isolated after chemical digestion of the lung tissue in 7 cases. In 7 cases necropsy or surgery material obtained from the family members, occupationally exposed, was also examined.
Results: The patients had cleaned the work clothes of their family members (mostly the husband), employed in the shipyards. Asbestos bodies were found on lung sections in 6 cases. Asbestos body burdens ranged between 70 and 6000 bodies/gram of dried lung tissue (mean 1400, median 400). Pleural plaques were observed in 10 cases. Pathological studies performed in the family members of 7 patients showed pleural mesothelioma in 3 cases, lung adenocarcinoma and asbestosis in one case, asbestosis in one case, small pleural plaques in one case, renal lymphoma and asbestosis in one case. Lung asbestos bodies, isolated in 3 of such cases, were 18000, 110000, and 4 millions/gram respectively.
Conclusions: Apparently trivial exposures to asbestos are sufficient to induce asbestos-related cancer. This has relevant implications for the risks in the general population, exposed to low doses of asbestos.

P-225

The influence of exogenous surfactants (exosurf and survanta) on lung tissue of adult animals

Wiesława Biczysko*, Andrzej Marszałek*, Marcin Wąsowicz**, Dawid Murawa*, Ewa Florek#
* Chair of Clinical Pathomorphology and # Department of Toxicology Karol Marcinkowski University School of Medical Sciences Poznań, Poland, ** Chair of Anesthesiology and Intensive Care, Collegium Medicum Jagiellonian University, Kraków, Poland

Exogenous surfactants are widely used for treatment of newborn respiratory distress syndrome (RDS) as method for supplementation of natural surfactant deficiency caused by immaturity of type II pneumocytes. Surfactant therapy was applied also for treatment of respiratory disturbances of other aetiologies, but effects were poorer than expected. THE AIM of present studies was evaluation of interaction between lung tissue and the exogenous surfactants in animal model.
MATERIAL AND METHOD: Adult, pathogen free male Wistar strain rats were used. Under anaesthesia animals were intubated and in two boluses of Egzosurf or Survanta (in total equivalent of 100 mg lipids per kg of b.w.) were applied. Control animals received an equivalent volume of 0.9% NaCl. Animals were sacri-

ficed after 30 minutes, 6 and 24 hours. The whole lungs were processed for light and electron microscopy.
RESULTS: In the control lungs the only changes were found 30 min after treatment as a slight oedema within endothelium. In Egzosurf group destruction of air-blood barrier increasing with time, intraalveolar exudate rich in fibrin and erythrocytes, and increasing number of macrophages was observed. In Survanta group oedema of endothelia and epithelia with activation of pinocytotic transport was observed. Additionally fragments of Survanta were incorporated into cellular membranes. Some cells were desquamated. Within alveolar lumen a moderate amount of exudate with few erythrocytes and large amounts of surfactant particles were observed.
CONCLUSIONS: Both exogenous surfactants lead to destruction of air-blood barrier. Egzosurf therapy can be described as implemantation of excess of detergent. The changes caused by Survanta were milder.

P-226

Molecular Pathology of myocarditis and dilated cardiomyopathy in children

F. Calabrese, E. Rigo, A. Angelini M., Valente, G. Thiene
Department of Pathology, University of Padua, Medical School, Padua, Italy

Introduction: The aim was to investigate viral etiology of myocarditis/dilated cardiomyopathy (DCM) in children and to correlate molecular findings with hemodynamic and clinical data. Myocarditis is a most common cause of heart failure in children an and may evolve into DCM.
Methods: Polymerase chain reaction (PCR) or reverse transcription (RT)-PCR were used to analyze 59 endomyocardial biopsies from 48 consecutive young (<18 yrs) patients (pts) with clinical and histological diagnosis of myocarditis and DCM employing primers designed to amplify specific sequences of various DNA and RNA viruses.
Results: Nucleic acids were successfully extracted in 41 pts and viral genome was found in 20 of them (49%): 12 out of 26 pts (46%) with myocarditis and 6 out of 13 (46%) pts with DCM. Enteroviruses were more common in viral DCM (83%) whereas adenoviruses and enteroviruses shared the same rate (42%) in acute myocarditis. Mumps virus genome was detected in two pts with endocardial fibroelastosis (EFE). More diffuse inflammatory infiltration and myocyte damage were noted in viral positive cases. Left ventricular end diastolic volume and shortening fraction were more impaired in PCR positive myocarditis. PCR positive pts had worse outcome. Eleven follow-up biopsies were performed in 8 pts with myocarditis and persistence of viral infection was associated with clinical deterioration. Three out of 8 pts with viral myocarditis had recurrent graft viral infection after transplantation.
Conclusion: Viral myocarditis/DCM appear to be a more severe disease than non-viral forms. Enteroviruses were more common in DCM whereas adenoviruses were as frequent as enteroviruses in acute myocarditis. Persistence of viral infection was associated with disease deterioration. Viral myocarditis can recurr after transplantation.

P-227

Thymic carcinoma : a series of twenty cases

Lara Chalabreysse, Carole Gengler, Alain Tabib, Robert Loire, Françoise Thivolet-Béjui
Department of pathology, Louis Pradel Hospital, Lyon, France

Numerous types of thymic carcinomas (TC) are described.
Methods: twenty cases of primary TC were identified from 100 cases of primary thymic tumors. The tumors were reclassified by two independent observers according to the WHO classification (1999). Cytokeratin, EMA, chromogranin, synaptophysin, CD1a, CD3, CD5 and CD99 were determined by immunohistochemistry.
Results: histological study showed 8 cases of epidermoid TC (ETC), 5 cases of neuro-endocrine carcinoma (NEC) with 3 atypical carcinoid and 2 small cell carcinoma, 2 cases of lymphoepithelioma-like carcinoma (LELC), 2 cases of sarcomatoid carcinoma, 1 spindle cell TC, 1 mucoepidermoid carcinoma and 1 rhabdoid tumor. ETC was seen in the youngest patients (44.5 year), while LELC was seen in the oldest (70.5 year). All TC were more frequent in men. Tumor resection was incomplete in 95% of cases. Metastasis were seen in 62% of ETC, 40% of NEC and 50% of LELC. 40% of NEC died within 2.5 year, 62% of ETC within 4.9 year and 100% of LELC within 7.5 year. TC are characterized by similar immunohistochemical patterns: keratin (100%), EMA (85%). CD1a and CD99 were negative in all cases. Chromogranin was particularly positive in NEC (100%), and CD5 in non-neuroendocrine TC.
Conclusion: histopathologic variants of TC appeared to be histogenetically closely related and to present similar clinical features with bad prognosis.

P-228

Lung cancer frequency: morphology and biomolecular characteristics in patients engaged in radionuclide industry

Cherniaev A., Samsonova M., Ali-Risa A., Kogan E.*,Demura S., Chuchalin A.
Pulmonology Research Institute, *Setchenov Moscow Medical Academy, Moscow, Russia

Aim: To assess the frequency, histological and immunohistochemical speciality of lung cancer in patients which are employed in radiochemical industry in Krasnoyarsk region.
Material and methods: 1259 autopsy protocols were analyzed, 96 of them – those of dead workers involved in radionuclide industry. Cancer frequency was counted per 100 autopsies. Histologic and immunohistochemical examination of 24 cases were performed.
Results: Cancer frequency was twice higher among radionuclide workers as compared with patients living in the same region. Central carcinomas prevailed in both groups. Small cell lung carcinoma (SCLC) with positive chromogranin staining was the most often tumor in industrial workers, whereas in non-workers squamous carcinoma was of highest frequency. The most of peripheral tumors appeared to be adenocarcinomas. All the examined "radionuclide" tumors showed low or undetectable expression of bcl2 (1.6±0.7 points), high expression of p53 (39.4±11.7%) and c-myc (4.0±0.8) and high proliferation rate (ki67 9.5±3.2%).
Conclusion: These data prove that cancer frequency in patients exposed to low dose of radiation is twice higher. SCLC prevailed

among these tumors. Lung cancer in these patients has specific. immunohistichemical features.

P-229

The cytology of pulmonary well-differentiated fetal adenocarcinoma

Chin Aleong J, Calaminici M, Sheaff M
Department of Histopathology, St. Bartholomew's and the Royal London Hospitals, London, U.K.

Pulmonary well-differentiated fetal adenocarcinoma (WDFA) also known as pulmonary endodermal tumour was first described in 1982 by Kradin. It is composed solely of neoplastic glands which resemble fetal lung between 10 and 16 weeks gestation without any sarcomatous elements is currently regarded as a variant of bronchogenic adenocarcinoma.
The tumour presents most commonly in the fourth decade and with equal sex prevalence. Most of the cases have occurred in smokers. The tumour is usually a solitary well-demarcated peripheral lesion. Lymph node or pleural involvement is unusual.
The tumour is composed of branching tubules lined by nonciliated columnar cells with eosinophilic morules. The epithelial cells contain glycogen and express the usual epithelial markers. Evidence of neuroendocrine differentiation is often found in the morules.
We present a case of WDFA in a 26 year old male non-smoke who had initially presented with right sided chest pain, cough and night sweats. A large mass seen in the right lower lobe on CT scan was aspirated. The smears were cellular and predominantly composed of groups and individual monomorphic bare nuclei. Some of the nuclei showed the 'salt and pepper' appearance suggesting neuroendocrine differentiation while others had small, sometimes multiple nucleoli. Occasional cells retained cytoplasm to one side of the nucleus and appeared more columnar. Differential diagnosis included small cell carcinoma, carcinoid and lymphomatous infiltration. Immunocytochemistry showed positive staining for cytokeratin and negative staining for neuroendocrine and leukocyte markers.
The diagnosis of WDFA was confirmed at subsequent lobectomy.

References: Kradin R.L. et al. Pulmonary blastoma with argyrophil cells lacking sarcomatous features (pulmonary endodermal tumour resembling fetal lung). Am J Surg Path 1982; 6:165–172
Colby T.V. et al. Tumours of the Lower Respiratory Tract AFIP 1995
Nakatani Y. et al. Pulmonary Adenocarcinomas of the Fetal Lung Type. Am J Surg Path 1998 22(4):399–411

P-230

Sarcomatoid carcinoma of the lung: An immunohistochemical study of 20 cases, with histogenetic considerations

Chung, Jin-Haeng
Dept. of Anatomic Pathology, Korea Cancer Center Hospital, Seoul, South Korea

Twenty cases of sarcomatoid carcinomas of the lung were reviewed histologically and studied immunohistochemically. The two aims of immunohistochemical study were to analyze the histogenetic relationship between the carcinomatous and sarcomatous components and to make sure its validity in diagnosis and classification of these tumors. Nineteen patients were men, and one was woman; average age was 60.7 years (range, 47–77 years). Two, 6, 8, and 4 cases were stages I, II, III, and IV, respectively. Five morphologic patterns of sarcomatoid components were observed: rhabdomyosarcomatous (8 cases), malignant fibrous histiocytomatous (6 cases), fibrosarcomatous (2 cases), osteosarcomatous (1 case) and unclassified sarcomatoid (3 cases). Light microscopically definite carcinomatous areas were identified in 19 cases and one case showed epithelial differentiation only immunohistochemically. Associated carcinomas were squamous cell carcinomas (8 cases), adenocarcinomas (7 cases), adenosquamous carcinomas (2 cases), large cell undifferentiated carcinoma (1 case), and combined squamous and small cell carcinoma (1 case). Immunohistochemically epithelial differentiation (cytokeratin antigen expression) was confirmed in all carcinomatous component and 80% (16 cases) of the sarcomatous area. In the case without light microscopic carcinomatous area, it would be confused with true sarcomas diagnostically unless immunohistochemical study was performed. We also examined p53 immunostaining in 18 cases of sarcomatoid carcinomas and found positivity in 15 cases (83%). There was no disparity in immunostaining between the epithelial and the sarcomatous components in any of the 18 tumors. This concordance in every tumor supports the hypothesis that sarcomatoid carcinomas were monoclonal.

P-231

Myocardial cell injury and microvascular damage in sepsis: Morphometric analysis

[1]Anca Ciobanu, [2]Doina Lucia Frincu, [2]L. L. Francu, [3]Doina Radulescu, [1]D.L. Calin, [2]R. Crisan Dabija
Departments of [1] Infectious Disease, [2] Anatomy and [3] Pathology, University of Medicine, Iasi, Romania

Introduction: Previous experimental studies have shown an association between sepsis and microscopic evidence of parenchymal and microvascular injury, but the cause of sepsis-induced myocardial dysfunction is incompletely understood. The objective of the present study was to define the relationship between the morphometric myocardial parenchymal or microcirculatory alterations and the cardiac dysfunction in sepsis.
Material and methods: We have studied fourty-eight patients, who died of sepsis caused by abdominal infections sepsis and were been postmortem examination. The fragments from all cavities of the heart have been processed by paraffin technique and have been examined for qualitative diagnosis. The quantitative study has been done with a digital interactive program which utilized: standard measurement of cardiac muscle fibres and stereology of procentual volumes of myocardial components (muscles cells, vessels and connective tissue), all results being compared with hearts witness.
Results: Autopsy studies provide circumstantial evidence that histology changes are also a feature of myocardial injury in human sepsis. We noted alterations in the myocardium that consisted of interstitial miocarditis (29.16%), interstitial edema (25%), and muscle-fibres necrosis (10.41%). We remarked differences between heart cavities, ventricles being more affected by necrosis. Morfometry relieved the increased of interstitial space and decreased of vascular lumina.
Conclusions: The present study suggests that obiective myocardial cells injury and coronary microcirculatory damage may lead to reduction in myocardial contractility associated with sepsis.

P-232

Pulmonary glomangiosarcoma with large bowel metastasis. A case report

Ciupea A.#, Pernet P.H.##, Blaison D.###, Mehaut S.#, Hopfner C.#
Centre Hospitalier Troyes, # Service d'Anatomie Pathologique, ## Service de Pneumologie, ### Service de Chirurgie, Troyes, France

The glomus tumors with deep location and/or agressive outcome are rare lesions. After a literature review, we found only three previously reported primary pulmonary glomangiosarcoma.
The authors report the cas of a malignant glomus tumor of the lung associated, few months later, with a large bowel metastasis. They present the tumors macroscopic and histologic features and the immunohistochemical profile.
The goal of this work is to illustrate the criteria (including size, growth pattern, cytologic atypia and mitotic rate) who may indicate a local agressive evolution or a metastatic potential.

P-233

The use of epithelial membrane antigen (ema) in the differential diagnosis of reactive mesothelial hyperplasia from mesothelioma

Comin C.E., Novelli L., Paglierani M., Dini S.
Dipartimento di Patologia Umana ed Oncologia, Università degli Studi di Firenze, Firenze, Italia

Introduction: The separation of reactive mesothelial hyperplasia from epithelial mesothelioma has emerged as a major problem in the pathology of the serosal membranes, especially when dealing with small tissue samples. The aim of our study was to access the value of epithelial membrane antigen (EMA) in differentiating benign from malignant mesothelial proliferations.
Methods: Formalin-fixed, paraffin-embedded archival tissue from 25 reactive mesothelial hyperplasias and 42 epithelial mesotheliomas of the pleura was immunostained with the antibody anti-EMA. Sections were also stained with antibodies against cytokeratin CAM5.2, calretinin, thrombomodulin, CD44H, and the antibody HBME-1, using the avidin-biotin-peroxidase complex method. Immunoreactivity was scored as negative (no immunostaining) or positive. The percentage of immunostained cells was recorded as follows: 1+ (1–25%); 2+ (26–50%); 3+ (51–75%); 4+ (76–100%).
Results: Forty-one of the 42 mesotheliomas were immunoreactive for EMA but only 4 of the 25 mesothelial hyperplasias reacted quite equivocally. All mesothelioma cases showed strong positive membranous staining whereas benign cases demonstrated only faint, aspecific cytoplasmic staining. Immunoreactivity for cytokeratin, calretinin, thrombomodulin, CD44H and antibody HBME-1 showed similar results both in benign and malignant lesions.
Conclusions: This study suggests that the use of EMA as ancillary test in the differential diagnosis of difficult pleural biopsies may have a role in separating mesothelial hyperplasias from epithelial mesotheliomas.

P-234

Relationship between proliferative rate and p53 protein expression in neuroendocrine lung tumors

Marioara Cornianu[1], N. Tudose[1], Anca Ro}ian[1], Liliana Vasile[2]
[1] Department of Pathology, University of Medicine, Pharmacy Timisoara, [2] Deparment of Histology, University of Medicine, Pharmacy Timisoara, Romania

Background: Lung tumors with neuroendocrine morphologic features include low-grade typical carcinoid (TC), intermediate-grade atypical carcionoid (AC) and ligh-grade categories of large cell neuroendocrine carcinoma (LCNEC) and small cell carcinoma (SCLC).
Methods: This paper investigates the immunohistochemical expression of p53 protein together with proliferation (Ki-67 and PCNA) and neuroendocrine differentiation markers (Chr, Syn and NSE), in 7 TC, 5 AC, 2 borderline AC/SCLC and 12 SCLC.
Results: p53 protein was absent in all TC, focal (<10% isolated stained cells) in 2 AC, while it was abnormally expressed in 8 SCLC and one borderline case.
TC showed a Ki-67 Li of 3% (range 1-4%) SCLC had a much higher Li, with values higher of 75% (range 77–92%). PCNA - labelled cells were less than 5% in TC (Li PCNA <5%) about 37% in AC (Li PCNA 37%, range 20–42%) and over 81% in SCLC (Li PCNA 81%, range 70–95%); PCNA labelling index (Li) discriminates between TC and AC. Borderline neoplasms had a PCNA Li of 55% (range 31–62%).
Neuroendocrine differentiation was evaluated by a semi-quantitative method: a mean score value was obtained, which was hight in TC (MSV 4,5, range 3.0–6.0), intermediate in AC (MSV 2,75 range 1,0–4,5) and low in SCLC (MSV 1,94 range 0–4,5).
Conclusions: Our results show that the decrease in neuroendocrine features from TC to SCLC is paralleled by an increase in proliferative activity and by an altered expression of tumour suppressor gene products.

P-235

The role of bcl-2 oncoprotein family in the process of apoptosis and proliferation in neuroendocrine tumors of the lung

Demoura S., Kogan E., Jaques G., Szende B., Paltsev M.
The Setchenov Moscow Medical Academy, Moscow, Russia,; Institute of Pathology and Experimental Cancer Res. Semmelweis University of Medicine, Budapest, Hungary; Philipps University, D-35033, Marburg, Germany

Aims: to investigate the role of Bcl-2, Bax, Bak in the process of spontaneous apoptosis and proliferation in Small Cell Lung Cancer (SCLC) and carcinoid tumors of the lung.
Methods: 60 paraffin-fixed patterns of Neuroendocrine Tumors of the Lung (NETL) were examined with hematoxylin-eosin staining, immunohistochemical assay of chromogranin (Dako), pancytokeratin (Immunotech), p53 (Dako), Ki-67 (Dianova), bcl-2 (Dako), bak (Calbiochem), bax (Calbiochem) and ApopDetek Cell Death Assay System (Enzo Diagnostics, US). Index of apoptosis (AI) and p53 and Ki-67 oncoprotein expression were calculated in percent among 300–3000 tumor cells.
Results: SCLC distinguished from carcinoids by the higher level of AI (2–12.3%), p53 (30–97%), Ki-67 (20–70%), bcl-2 (2–6 sc.),

bak (1–6 sc.), as well as by the nuclei accumulation of bcl-2, bak and bax products. SCLC without metastasis differed from SCLC with metastasis by the higher rate of AI (4,2%<7.3%).
Conclusions: Obtained data showed that bcl-2, bak and bax oncoproteins are used to be co-expressed in NETL and participate in regulation of the NETL growth and apoptosis. The nuclei accumulation of Bcl-2 oncoprotein correlates with a high level of apoptosis in SCLC. Molecular-genetic rearrangements in SCLC with metastasis lead to the decrease of apoptotic level.

P-236

Myocarditis and Sudden infant death syndrome (SIDS)
R. Dettmeyer, A. Baasner, M. Schlamann, S. Winkelmann, M. Graebe, B. Madea
Institute of Forensic Medicine, University of Bonn, Germany

Introduction: The incidence of virus-induced lethal courses of myocarditis in cases of so called sudden infant death syndrome (SIDS) is still unclear. Although immunohistochemical and molecularpathological techniques have improved the diagnosis, there are ony single cases published concerning the phenomen SIDS.
Methods: Myocardial samples from 40 autopsy cases of children with unknown death were taken from different regions and investigated with conventional histological methods, immunohistochemical and molecularpathological techniques. Conventional stainings revealed no signs of myocarditis according to the Dallas criteria. Antibodies against enteroviral VP1-capsid protein, additionally specific markers against infiltrating leucocytes (LCD, CD68) and the major histocompatibility complex class II antigens (HLA-DP,DQ,DR and HLA-DR) known to be enhanced in cases of myocarditis were used. Also molecularpathological investigations with PCR and semi-nested Reverse transcription-polymerase chain reaction (RT-PCR).
Results: Within the cytoplasma of cardiomyocytes, enteroviral capsid protein VP1 was found immunohistchemically in more than 20 cases, PCR revealed single cases with myocardial infection due to parvovirus B 19, in the myocardial samples of one case, both enteroviruses and parvoviruses B 19 were found. In all myocardial samples, conventional stainings revealed no significant pathological findings and immunohistchemical techniques only a moderate increased number of LCA-positive leucocytes and CD68-positive macrophages.
Conclusion: The findings demonstrate that cases of sudden death in pediatrics without any pathological findings in routine histology should be investigated with immunohistochemical methods and molecularpathological techniques, especially cases of sudden infant death syndrome, to detect viral infection, especially due to cardiotropic enteroviruses and PVB 19.

P-237

Postintubation tracheal stenosis? Morphological and clinical studies
G. Dyduch, B. Papla, H. Olechnowicz
Department of Clinical Pathomorphology, Jagiellonian University Medical College, Ward of Thoracic Surgery, John Paul II Hospital, Kraków

From 1997 to 2000 the Ward of Thoracic Surgery, John Paul II Hospital in Krakow (ward head: dr. H. Olechnowicz) admitted 46 patients aged from 4 to 71 years for surgical operation due to postintubation tracheal stenosis. The narrow segment of the airways varying in length was removed and studied by microscopy. A number of characteristic changes were detected in correlation with the duration of intubation and time to patency restoration. They included ulcerations with granulomatous tissue with multiple fine capillary vessels and various migrating cells, mainly granulocytes, and in advanced cases epithelium-devoid decubital changes with proliferated connective tissue fibres and hyalinisation with foci of thin-walled dilated blood vessels resembling cavernous haemangiomas. The changes resulting in segmental stenosis of tracheal lumen involved mainly mucosa and submucosa, frequently fragments of tracheal cartilage and sometimes the inflammatory process penetrated outside the cartilage. In some young patients in the third decade (4 cases) we observed the signs of cartilage ossification. The morphological changes resembled those observed in the oesophagus and stomach due to accidental chemical injury and stenosis. Review of the available literature in the last 20 years shows only single reports describing postintubation tracheal stenosis, especially in older reports. This argues for the need of special emphasis on the management of patients admitted to intensive care units in Poland in order to avoid this severe complication.

P-238

Tumors or the arteriolar wall, a reality?
Enache Stelian Dănut*, Pleşea Iancu Emil**, Comănescu Violeta*, Zaharia Bogdan**
* Department of Pathology and Citology, Universitary Hospital, Craiova; ** Department of Pathology, University of Medicine and Pharmacy Craiova, Romania

Introduction: We observed six months ago, during the examination of a case with laryngeal papilloma, an arteriole in the neighbourhood of the tumor which presented a pedunculated proliferation of leiomyofibromatous type, protruding in the vascular lumen. From that moment we looked for this kind of peculiar feature more carefully in our daily examinations.
Aims: We intended to present the morphological features and to point out this peculiar kind of tumors we did't find anything about in the literature.
Material and methods: A group of 12 cases with endoluminal neoplastic proliferations were selected in the last six months from about 6000 examined samples in our laboratory. The material was represented by the surgical samples drawn during the surgical interventions for any kind of surgical pathology. The tissue fragments were fixed in formalin, included in paraffin wax and stained with hematoxilin Meyer-eosin, trichrome van Gieson and Gömöry technique.
Results: The primary lesion belonged to a variety of organs: laryngs, gallbladder, ovary, stomach, uterus, epiploon, prostate and was of different type itself, from inflammation to malignancy. The arteriolar tumors were observed both within the primary lesion and in its neighbourhood. The tumors exhibited two main aspects: a pedunculated, roud-shaped with intraluminal protrusion one and a sessile one also with the diminution of the arteriolar lumen. Histologically, they were in their majority of leiomyomatous type or of myxoid type.
Conclusion: The study of theese proliferations has to be continued for precising if they are a lesional entity in the vascular arteriolar pathology, if they are a true neoplastic proliferation and the possible patogenic factors.

P-239

Fluorescent in situ hybridization of c-erb-b2 in lung cancer: A comparative study with quantitative real time RT-PCR and immunohistochemistry

Falleni M.*, Cassani B.*, Miozzo M.*, Marchetti A.°, Roncalli M.*, Buttitta F.°, Bosari S.*, Coggi G.*
Department of Pathology, University of Milan* and Chieti°, Italy

Background: C-erb-B2 oncogene overexpression is a marker of poor prognosis in several human tumours. It is correlated with lymph node metastasis, high tumor grade, relapse free interval and survival and chemoresistence.
The evaluation of c-erb-B2 has now become crucial since it is now possible to target it with a humanized monoclonal antibody which inhibits cell proliferation.
In lung cancer c-erbB2 protein expression has been evaluated only by immunohistochemistry. C-erb-B2 immunoreactivity has been detected in 10–15% of non small cell carcinomas (NSCLC) and may be as high as 30% of adenocarcinomas where it appears to be correlated with advanced stage, short survival and chemoresistence.
Design: Dual color fluorescent in situ hybridization (FISH) for c-erb-B2 gene (17q21) and chromosome 17 α-satellite was used to evaluate gene amplification in a subset of 41 NSCLC from a series of 115 carcinomas previously investigated for c-erb-B2 mRNA levels by real time quantitative RT-PCR, and for protein expression by immunohistochemistry (IIC), using a policlonal antibody (DAKO, Glostrup, Denmark).
Results: C-erb-B2 gene amplification was found in 9/41 tumors. Our results are summarized in the following table:

FISH	Not amplificate 32	Polisomy 1	Low amplificate 5	High amplificate 3	Total 41
IIC					
IIC 0	13	0	0	0	13
IIC 1+	8	0	2	0	10
IIC 2+	11	1	2	0	14
IIC 3+	0	0	1	3	4
RT-PCR					
normal mRNA level	21	0	0	0	21
mRNA overexpression	11	1	5	3	20

Conclusions. FISH, immunohistochemistry and RT-PCR are complementary and useful techniques to evaluate c-erb-B2 activation in NSCLC. Gene amplification has been detected only in those cases with high levels of mRNA together with protein overexpression. Our results suggest that other mechanisms not related to gene amplification could be responsible for mRNA or protein overexpression of c-erb B gene product.

P-240

A multiarterial study of atherosclerotic lesions, myocardial damage and lipidograms

José E. Fernández-Britto[1], Roberto Wong[1], Rosa Campos[1], Leonel Falcon[1], Klaus Affeld[2] and Hans Guski[3]
[1] Center for Investigations and References of Atherosclerosis of Havana, Higher Institute of Medical Sciences of Havana, Cuba; [2] Laboratory of Biofluids Mechanics, Humboldt University of Berlin; [3] Institute of Pathology, Humboldt University of Berlin

Aims: To study the pattern of atherosclerotic lesions between differents arterial sectors, the impact of serum lipid disorders on the cardiac and arterial damage and the association between atherosclerotic lesions in different arterial sectors and the degree of myocardial damage.
Material and methods: 472 autopsy cases of patients were studied who had died at the Unit of Intensive Care (UIC) of the General Hospital "Dr. C.J. Finlay", Havana, Cuba. Immediately to the patient admitted at the UIC a lipidogram was performed. Total cholesterol, HDL-c, LDL-c, VLDL-c, and triglycerides were analyzed. Morphologically, the circle of Willis, common carotid arteries, three major epicardial branches of coronary arteries, aorta, renal, iliac, and femoral arteries were studied using the atherometric system for morphometric analysis.
Results: The most relevant findings were the following: 1. the lipid disorders show the greatest impact in the heart, coronary and femoral arteries and abdominal aorta; 2. the strongest correlations between the arterial sectors were found in those which have anatomical continuity, i.e., cerebral arteries with carotid arteries, coronary arteries with the aorta, etc.; 3. some specific features were found among different vascular sectors, such as associations between the right and left anterior descending coronary arteries on one hand and the femoral arteries and abdominal aorta on the other, while the cerebral and left circumflex cronary arteries were strongly associated with the thoracic aorta and iliac arteries.
Conclusions: In spite of the fact that atherosclerosis is a systemic process, different distributions are encountered that are characterized by particular correlations between some specific vascular sectors. Lipid disorders are correlated with myocardial damage and with atherosclerotic lesions of the coronary and femoral arteries and the abdominal aorta.

P-241

Coincidence of Adenocarcinoma with Necrotizing Sarcoid Granulomatosis (NSG) of the Lung. A case report

Galle J.[a], Kirsten D.[b], Branscheid D.[b], Goldmann T.[a], Vollmer E.[a]
[a] Research Center Borstel, Clin. & Exp. Pathology, Parkallee 3, Borstel; [b] Hospital of Großhansdorf, Center of Pneumology and Thoracic Surgery, Großhansdorf, Germany

Introduction: NSG of the lung is a rare disease and was originally described by Liebow in 1973. No coincidence of NSG and bronchialcarcinoma side by side was reported till now.
Case report: During a routine check of a 63 year old male, cigarette smoker with COPD, an irregular shaped mass was detected in the right upper lobe of the lung by x-ray.
Macro- and microscopy: After lobectomy a centrally located adenocarcinoma up to 3.4 cm in diameter of solid, bronchioloalveolar

and papillary histologic pattern was discovered (pT2, N1, MX). Furthermore in close neighborhood of the tumor an irregular gray-white, patchy infiltrate including the visceral pleura and histologically revealing necrosis and confluent sarcoid-like granulomas with involvement of blood vessels and bronchi typical for NSG.
Diagnostic supporting methods: Expression of surfactant-apoprotein-A (SP-A) and thyroid transcription factor-1 (TTF-1) in the tumor. In NSG no detection of infectious agents by different stainings and no disclosure of mycobacterial sequences by PCR. No detection of ACNA or elevated ACE in the serum.
Conclusion: Each of the diseases, adenocarcinoma and NSG of the lung, is so typically developed that there is no hint of an interdependence. This favors a mere collision of the two entities.

P-242

Patterns of expression of three hypoxia regulated proteins (Hypoxia Inducible Factors HIF1α/HIF1β and Carbonic Anhydrase CA9) in squamous cell carcinoma of the lung

A. Giatromanolaki[1], E. Sivridis [1], K.C.Gatter [4], A.L. Harris [4], G. Bougioukas[2], M.I. Koukourakis [3]
[1] Departments of Pathology, [2]Thoracic Surgery and [3]Radiotherapy/Oncology, Democritus University of Thrace, Alexandroupolis, Greece; [4] Departments of Cellular Science and ICRF Medical Oncology Unit, Oxford Radcliffe Hospital, Headington, Oxford, UK

Introduction: The hypoxia inducible factors HIF1α and HIF2α, have been recently identified as key molecules regulating the transcription of a variety of genes related to erythropoiesis, glycolysis and angiogenesis, following hypoxic stimulation. Carbonic anhydrase-9 (CA9), an enzyme involved in the reversible metabolism of carbon dioxide to carbonic acid, has been also shown to be regulated by hypoxia through the HIF pathway.
Materials and Methods: Using immunohistochemical methods, we evaluated the expression of HIF1a, HIF2a and CA9 proteins in normal lung tissues and in 74 sqamous cell carcinomas (SqCLC). The results were related with the extent of tumour necrosis.
Results: HIF1a and HIF2a proteins were expressed in 62% and 45% of cancer cases, respectively. They showed a mixed nuclear/cytoplasmic pattern of staining which was extended throughout the entire tumour. The adjacent normal lung tissue showed negative or very weak cytoplasmic staining. A significant co-expression of these proteins was observed, but there was no association with the extent of necrosis. By contrast, CA9 expression was distinctly membranous (with or without cyroplasmic expression) and was noted, almost exclusively, in cancer cells around areas of necrosis. A clear association of CA9 expression with the extent of necrosis was observed. CA9 was not expressed in normal lung tissues.
Conclusions: An up-regulation of the hypoxia regulated proteins HIF1α, HIF2α and CA9 is a common event in SqCLC. However, only HIFs are upregulated by low levels of hypoxia. The clinical relevance of these hypoxia related markers in response to radiotherapy, chemotherapy and in the prognosis of cancer patients is currently under investigation.

P-243

Generation of pulmonary granulomas in SCID mice upon BCG infection

T. Goldmann[1], G. Zissel[2], R. Sen Gupta[1,4], J. Galle[1], M. Schlaak[2], J. Müller-Quernheim[2] and E. Vollmer[1]
[1] Klin. & Exp. Pathologie, [2] Medizinische Klinik , Forschungszentrum Borstel, [3] Abteilung Pathologie, AKH Altona, Hamburg, Germany

Introduction: We studied the granuloma forming capacities of severe combined immunodeficient (SCID) mice upon infection with Bacillus Calmette-Guerin (BCG)
Methods: BCG was intravenously inoculated into SCID-mice. After a period of 30 days we performed histomorphological examinations and PCR-analyses.
Results: The spleens of BCG infected mice were significantly enlarged compared to control animals. We observed granulomas in spleen and liver reproducing previous results of an other group(1). Furthermore, we found granulomas also in the lungs, and as previously observed heavily infected alveolar macrophages. The mycobacteria inside these granulomas were positively Ziehl-Neelsen-stained and the results were verified by polymerase chain reaction.
Conclusion: We conclude that SCID-mice infected with BCG can generate granulomas in the lungs, which provides new insights into the process of pulmonary granuloma formation.
(1) North RJ, Izzo AA: Am J Pathol 1993;142:1959–1966

P-244

Morphological alterations of myocardial structure after heart transplantation

Nicola E. Hiemann, R. Meyer, R. Hetzer
Department of Cardiothoracic and Vascular Surgery, Deutsches Herzzentrum Berlin, Germany

Introduction: Ongoing conflict between graft and recipient occurs in all organ transplants in episodes of different degrees of acute and chronic rejection.
Methods: We studied 41 heart transplant patients: 15 with angiographic evidence of graft vessel disease (GVD) (four women, 11 men, mean survival 57 months) and 26 patients (five women, 21 men, mean survival 59 months) without any signs of GVD. Paraffin-embedded endomyocardial biopsies (n=272) were investigated immunohistochemically for smooth muscle cells (SMCs) (α-actin), endothelial cells (CD31, factor VIII) and connective tissue (collagen III and IV); histological staining was done with H&E and Domagk. Investigations were done at ×200–500. Structural, morphological changes of the myocardium were studied using morphometric methods.
Results: Postoperatively changes within the endomyocardial structure and the microvascular system occur in all transplanted hearts independently of presence or absence of acute rejection episodes and/or occurrence of macrovascular disease. These changes consist of: 1. a neomuscularization of intramyocardial blood vessels and a proliferation of SMCs in preexisting arterioles, 2. phenotypic changes of microvascular endothelial cells, which finally induct the development of microvascular GVD and may occur in association with macrovascular GVD and 3. chronic ischemia with its morphological characteristics of single cell death, myocyte hypertrophy

and myocardial architectural changes. Myocardial fibrosis and scars represent the result of persisting ischemia.
Conclusion: Morphological changes of endomyocardial structure and alterations of the terminal vascular system occur in all transplanted hearts. If these changes exceed the adaptive capability of the transplanted organ they result in acute or chronic graft failure.

P-245

The incidence of thymic epithelial tumors in Macedonia according to the new WHO classification

Jovanovich R., Petrusevska G., Bogoeva B., Banev S.
Institute of Pathology, Faculty of Medicine, Skopje, Macedonia

Classification of thymic neoplasms has been one of the most controversial fields in tumor pathology. The WHO histological classification of thymic epithelial tumors (TET) has given the opportunity to classify these tumors easier. The aim of this analysis was to determine the distribution of TET regarding the age, sex, and histological appearance according to the WHO classification as well as their biologic behavior.
We analyzed biopsic material as well as material obtained by open mediastinotomy, from the last 10 years. Sixteen cases of thymic neoplasms were found, appearing at the age from 26 to 73 years. Obtained specimens were processed by standard techniques, and additional histochemistry (Giemsa, reticulin, Alcian blue) and immunohistochemical (ESA, CEA, LCA, CD3, CD20, CD79, CD43, Bcl-2, CKWS, CK19, CD18, CD45RA, NSE) analyses were performed.
Reviewing the cases retrospectively with this combined approach, we found eight cases of type A thymoma, four cases of type B3, two cases of AB type, and one case of B1 type TET. One of the cases was revised and re-diagnosed as T-lymphoblastic lymphoma. The analysis of sex and age distribution showed that 83% of the patients were males aging from 26 to 69 years, and the rest of them females with similar age interval. Immunohistochemistry especially helped in differentiating the AB type thymoma, where among the lymphocytic population between thymoma cells, reactive B-cell germinal centers were found.
This analysis shows that the new WHO classification, makes the TET classification much more easier and uniform, providing solid basis for precise comparative studies.

P-246

Metastatic primary pulmonary rhabdomyosarcoma mimicing small cell lung cancer – A case report

J. Knolle[1], J. Schreiber[2], P. Hinze[3], R. Schön[4] and S. Hofmann[5]
Municipal Hospital Dessau, [1] Institute of Pathology, [2] Dept. of Pulmo-nology, [3] Dept. of Neurosurgery; Martin-Luther-University Halle-Wittenberg, [4] Institute of Pathology and [5]Dept. of Thoracic Surgery

Primary pulmonary rhabdomyosarcoma is a rarity. The histological differential diagnosis can be difficult.
In a 43-year old female patient, smoker (25 pack-years) a big solitary brain metastasis was diagnosed and enucleated. Histological examination (HE-stain) revealed a typical small cell carcinoma.
Chest X-ray showed a solitary nodule in the left upper lobe and tumor growth was verifiable in the left upper lobe bronchus during broncho-scopy. Histological examination of bronchial biopsies was compatible with a small cell carcinoma.
Thus chemotherapy (CEV) combined with neurocranial irradiation was performed. Nevertheless there was a progressive growth of the pulmo-nary tumor. That's why the patient was reexamined. Now bronchial biopsies showed the picture of a small cell tumor. Immunohisto-chemistry (Cytokeratin neg., Vimentin +, Desmin +, Aktin neg., CD56(N-CAM) +, Myoglobin focal +) proved a pleomorphic rhabdo-myosarcoma. Reexamination of the brain metastasis and of the initial bronchial biopsies confirmed this diagnosis.
Because no further metastasis were detectable and due to progressive tumor growth with poststenotic abscess-forming pneumonia lobectomy of the left upper lobe was performed. The operation was complicated by postoperative pleural empyema, which limited the possibilities of adjuvant radio- or chemotherapy. Early relapse occurred with pleural, chest wall and spinal metastases. Laminectomy and extirpation of the spinal metastases, local irradiation and chemotherapy with iphosphamide and doxorubicine led to partial remission and clinical improvement.
This rare tumor mimiced small cell lung cancer. Appraisal of the atypical clinical course and a close dialogue between pathologists and clinicians enabled the correct diagnosis.

P-247

Apoptosis and proliferation in human lung cancer

Kogan E.A., Demoura S.A., Sekamova S.M., Jaques G., Szende B.
The Setchenov Moscow Medical Academy, Russia; Philipps University, Marburg, Germany; Institute of Pathology and Experimental Cancer Res. Semmelweis University of Medicine, Budapest, Hungary

Aims: Of the study was to investigate the morphological particularities of spontaneous apoptosis of tumor cells in lung carcinomas.
Methods: Surgical material from 100 patients with non-small cell lung carcinomas and 60 neuroendocrine tumors was used. Paraffin-fixed patterns were examined with hematoxylin and eosin staining, immunohistochemical assay of chromogranin (Dako), pancytokeratin (Immunotech), p53 (Dako), Ki-67 (Dianova), bcl-2 (Dako), bak (Calbiochem), bax (Calbiochem) and ApopDetek Cell Death Assay System (Enzo Diagnostics, US). Index of apoptosis (AI) and p53 and Ki-67 oncoprotein expression were calculated in percent among 3000 tumor cells. Electron microscopy with semithin sections was performed in 17 cases.
Results: Peculiarities of apoptosis in lung cancer are characterized by the following features: predominance of proliferation (5,1%–70%) in comparison with apoptosis (0,01%–15,6%) in lung cancer concerning the percentage of involved cells; absence of phagocytosis of apoptotic bodies in small cell lung cancer and their common localization in foci around so called necrotic detritus and often nearby mitotic cells. Apoptotic bodies accumulate different mitogenic substances (oncoproteins, growth factors) which can be released in the process of postapoptotic autolysis and stimulate cancer cell proliferation.
Conclusions: Dysregulation of apoptosis in cancer includes two major aspects: its inhibition in comparison with prolireration and absence of phagocytosis of apoptotic bodies that may undergo postapoptotic autolysis and stimulate mitosis.

P-248

Tumor angiogenesis in non-small cell lung carcinoma after preoperative chemotherapy - Association with survival time

Korobowicz E.[1], Zdunek M.[1], Jabłonka A.[2], Borowska B.[3], Chibowski D.[1]
[1] Chair and Department of Pathology, Medical School, Lublin;
[2] Chair and Department of Thoracic Surgery, Medical School, Lublin;
[3] Department of Chemotherapy, Cancer Center of Lublin Land

Angiogenesis is a crucial step in a tumor growth and progression and may be useful in predicting disease outcome. In the present study we evaluated the relationship between tumor angiogenesis, tumor size, histological type of carcinoma and survival time for 45 patients with non-small cell lung carcinoma. The study population consisted of 42 male and 3 female patients who were treated with preoperative chemotherapy and surgery from January 1997 through December 1999. Follow-up was obtained for all cases (median 14,068±8,09 months). Tissue sections of tumors were immunostained with vascular markers CD31 and CD34. In each case three microscopic fields (×250) with the highest number of microvessels were counted. The median microvessel count in the series was 40 for CD31 and 42 for CD34 and the counts were categorized as low versus high (≤40 versus >40 microvessels and ≤42 versus >42 microvessels consecutively). The mean age of patients was 57,56 (M±7,102) years. 30 patients (66,6%) died of lung cancer during the observation.
Statistically significant association was observed between microvessel count in more vascularized tumors and reduced overall survival ($p<0,018$, $chi^2=8,001$) when sections were stained with CD31. There was no significant difference in survival time between patients with different histological type of carcinoma and with different size of tumor.

P-249

Lung in long-term mitral stenosis

Z. Kosjerina, V. Kosjerina-Ostric
Institute of Lung Diseases , Sremska Kamenica, Yugoslavia

Objective of the study is to analyse the histologic lung changes in long-term mitral stenosis.

Material of the investigation includes the lung specimens obtained from 33 autopsied patients with long-term mitral stenosis for an underlying disease.
Results: Interalveolar septa were found to be mildly thickened in 60.6% of the autopsied, particularly in the surroundings of siderophages' collections. The septal thickening developed due to the connective multiplication. Siderophages were detected in the lumen of the alveoli in all patients, while siderotic nodules were evidented in 60% of the autopsied. Intraalveolar edema was present in 63% of the cases, while the chronic alveolar and interstitial edema were rare. Capillary congestion was found in 97% and aneurysmal dilatation in 36% of the autopsied patients. Hypertrophy of the muscle arteries' medium was registered in all cases, as well as a stricture of the artery lumen. Fibrosis of the intima was found in 40% of the patients. Pulmonary hypertension – stage I, was most frequently evidented histologically (57.6%). Hypertrophy of the smooth muscle in the bronchioli was found in 90.9% of the autopsied, while the alveolar cell cuboidization was evident in 63% of them.
Conclusions: In long-term mitral stenosis the lung finding is most often characterized by the presence of siderophages and hypertrophy of the media in the muscle arteries (100%), less frequently by capillary congestion (97%), intra-alveolar edema (67%), siderotic nodules (60%) and fibrosis of the intima in the muscle arteries (40%).

P-250

Chloroquine-induced cardiomyopathy : Ultrastructural study of two cases

Labrousse F. (1), Delage-Corre M. (1), Aldigier J.C. (2), Leboutet M.J. (1), Pommepuy I. (1), Paraf F. (1)
Services d'Anatomie Pathologique et de Néphrologie, Hôpital Universitaire Dupuytren, Limoges, France

Introduction: Chloroquine and its derivates are used in the treatment of systemic lupus erythematosus (SLE), rheumatoid arthritis, malaria and other diseases. This drug can induce various toxic effects including cardiotoxicity. We report the histological and ultrastructural findings in right endomyocardial biopsies performed in two patients having SLE and treated by chloroquine.
Patient and methods: A 56-year-old man, was hospitalised because of an atrioventricular block and a 43-year-old woman, because of severe heart and renal failures. Formalin fixed biopsies were embedded in paraffin and sections were stained with hematoxylin and eosin. For ultrastructural study, biopsies were fixed in buffered glutaraldehyde, postfixed in osmium tetroxide. Ultrathin sections were stained with lead citrate and uranyl acetate. Follow-up biopsies were not performed.
Results: At optical level, no morphological change was observed in the myocardial fibres. There was no inflammatory infiltrate or vasculitis. The ultrastructural analysis revealed an accumulation of concentric lamellae (myelinic bodies or myelinosomes) and of curvilinear bodies in the cytoplasm of cardiomyocytes. Curvilinear bodies consisted of short curve profiles surrounded by a single unit membrane. Concentric lamellae were abundant and the myocytes contained large amounts of glycogen.
Conclusion: Isolated myelinic bodies are not specific for chloroquine toxicity, as they have been reported in tumours or in lysosomal storage diseases. Although curvilinear profiles have been described in lipofuschinosis, these bodies are considered to be more helpful for the diagnosis of chloroquine toxicity. The potential of reversibility of these lesions is still unknown.

P-251

Complement activation in human myocarditis

Pekka Laurila, Antti Väkevä, Seppo Meri
Department of Pathology and Department of Bacteriology and Immunology, University of Helsinki, Finland

The role of complement system in the pathogenesis of human myocarditis is unknown. We investigated the expression of complement cell membrane -bound regulators (DAF, MCP, CD59) and the deposition of complement soluble regulators (vitronectin, clusterin) and complement components in human myocarditis lesions by in-

direct immunofluorescence microscopy. Endomyocardial biopsy and autopsy heart specimens obtained from patients with idiopathic (n=4) or granulomatous (n=3) myocarditis. CD59 expression was strong in normal myocardium, but it was lost in active myocarditis lesions. MCP and DAF were not at all or only faintly expressed on normal cardiomyocytes or cardiomyocytes of myocarditis lesions. Vitronectin was deposited in myocarditis lesions in association with components of complement terminal pathway (C5, C6, C9). On the contrary, the deposition of clusterin was observed only in the coronary arteries, no cardiomyocyte-associated deposition was seen. Components of the complement early (C1q, C3d, C4) and terminal (C5, C6, C9) pathways were selectively deposited into the myocarditis lesions. Complement deposits were mainly stronger in idiopathic than in granulomatous myocarditis. All the lesions containing complement deposits had also strong deposits of immunoglobulins.
Our results suggest that the complement system is activated in human myocarditis lesions. Complement activation is probably favored by a relatively weak expression of complement regulators in myocarditis lesions. Complement activation could possibly be involved in the post-injury clearance of injured cardiomyocytes

P-252

Changes of the lung periphery structure after administration of egzogenous surfactants in newborn rats

Andrzej Marszałek*, Marcin Wąsowicz**, Wiesława Biczysko*, Ewa Florek#
* Chair of Clinical Pathomorphology and # Department of Toxicology Karol Marcinkowski University School of Medical Sciences Poznań, Poland, ** Chair of Anesthesiology and Intensive Care, Collegium Medicum Jagiellonian University, Kraków, Poland

Treatment of respiratory distress syndrome in newborns (RDS) with exogenous surfactant preparations was introduced in 1980. It was a breakthrough in the therapy of RDS, but also a wide range of therapy complications was described.
THE AIM: of the present study is to describe morphological changes in the lungs after surfactant administration into the healthy newborn rats.
MATERIAL AND METHOD: pathogen free 1-day-old rats were used. Animals were given a single intratracheal dose of surfactant preparations (Survanta or Egzosurf; an equivalent of 100mg of lipids per kg of body weight) under general anesthesia. The controls received 0.9% NaCl in an equivalent volume. Animals were sacrificed after 15, 20, 25 or 30 minutes and isolated lungs were processed for light and electron microscopy.
RESULTS: In control group lungs had sacculo-alveolar structure and no damage was observed. Tissue specimens from Exosurf group revealed multiple foci of atelectasis, frank edema in the parenchyma, air-blood barriers were focally disrupted, hemorrhages in many alveoli, surfactant particles were found in many alveolar capillaries, and alveolar macrophages were strongly activated. Changes appeared as early as 15 minutes after surfactant administration and intensity of lung injury increased with time. Also, Survanta administration caused damage to the lung tissue. However, comparing to Exosurf group the changes were less intense and appeared later (20–25 minutes).
CONCLUSIONS: Administration of exogenous surfactant to healthy rat newborns caused lung damage. Exosurf leads to stronger and faster damage to lung alveoli when compared to Survanta.

P-253

Lack of apoptosis of cardiomyocytes in chronic chagasic myocarditis

Martin Metzger, Maria de Lourdes Higuchi, Thales de Britto
Heart Institute (InCor), University of São Paulo Medical School, Brazil

INTRODUCTION: Chagas disease, caused by the hemoflagellate protozoan *Trypanosoma cruzi*, is a widespread disease that affects millions of people in South and Central America. Chronic chagasic myocarditis (CCM) is the most devastating manifestation of Chagas disease, affecting about a third of the infected people. Despite this obvious clinical importance the pathogenesis of CCM is still poorly understood and several different mechanisms have been proposed including auto-immunity. Severe diffuse fibrosis and foci of myocardial cell loss associated with an inflammatory infiltrate are the most significant morphological characteristics of CCM. The aim of this study is to test the hypothesis that apoptosis of cardiomyocytes might contribute to the myocardial cell loss observed in CCM and whether it is associated with apoptosis of interstitial cells.
MATERIAL AND METHODS: Apoptosis was detected by a fluorescent TUNEL assay (Roche) in 2 cm long paraffin-embedded myocardial fragments from chagasic patients (n = 7) who underwent heart transplantation for treatment of heart failure. To clarify the exact nature of blood-derived apoptotic cells, sections were immunohistochemically stained after completion of the TUNEL assay either for the T-cell marker CD4 or the human macrophage marker CD68. Double-stained sections were subsequently analyzed by confocal laser scanning microscopy
RESULTS: Apoptotic nuclei were present in all fragments examined. The mean number of apoptotic nuclei in the analyzed fragments was 33.00±22.17 per fragment. However, all stained nuclei were confined to interstitial cells and no apoptotic cardiomyocyte at all could be detected. The majority of the TUNEL-stained interstitial cells showed morphological characteristics of inflammatory mononuclear cells. Double labeling experiments confirmed that about 30% of the inflammatory apoptotic cells stained positively for the human macrophage marker CD68. In contrast few, if any, of the apoptotic cells stained positively for CD4.
CONCLUSION: The absence of apotosis in cardiomyocytes indicates that necrosis rather than apoptosis should be considered as the mechanism of myocardial cell loss in chronic chagasic myocarditis. The results from the double-labeling study give evidence that a great percentage of apoptotic interstitial cells are macrophages and that apoptosis of CD4 T-cells is not an important event in this phase of the disease.
This work was supported by: CAPES-DAAD

P-254

The histopathological time dependent consumption chenges of corn oil (C.O.) on the rabbit artereis

B. Minaii, Ph.D.
Department of Histology, Faculty of Medicine, Tehran University of Medical Sciences (TUMS), Tehran, Iran

Several studies indicated the effects of oils and its histopathological effects on arteries and the relationship of the time longs consumption. In this study we try to find the effects of dietary corn oil (10%) on rabbits' arteries wall. Rabbits were female Albino and raised 4 to 7 months of age. A group of 24 rabbits were fed defined diets for 1, 2 and 3 months as test group. The control group was fed a standard laboratory diet while the test group received a diet containing 10% corn oil. Animals were killed in the end of 1, 2 and 3 months. The samples stained with H&E and Mallory's Trichorome. Aortic segments (Ascending, Horizontal. Thoracic and Abdominal Aorta) Carotid (External & Internal) and Subclavian arteries from the rabbits which fed corn oil were compared with those that fed standard diets. By study of Intima, Media and Advantitia in rabbit arteries raised on diets with corn oil we found that:
1) increases in the number of smooth muscle cells 2) decreases in number of elastic fibers 3) extracellular lipid accumulation.
These results demonstrated that diet with corn oil during the long of consumption my have a role to increases the deleing in histopathological changes in large arteries. These observed effects are more in 3 months than one or two months.

P-255

Multiple glomangioma of the lung

Mukenšnabl P., Michal M., Dvořáčková J.*
Department of Pathology, Faculty Hospital, Plzeň,
Czech Republic, Private Cytological and Bioptical Laboratory*,
Ostrava, Czech Republic

We report the case of a 36-year-old non-smoking man who presented with a lung tumor. The chest radiograph revealed three small nodules in the left upper lobe. There were three well circumscribed nodules 1.2 cm, 1.0 cm and 0.5 cm in diameter without connection to the visceral pleura in the resected lung specimen. Microscopic finding was the same in all three nodules. Tumors were composed of solid sheets of round uniform cells interrupted by vessels of varying size. The tumor cells had a pale eosinophilic cytoplasm and sharply punched-out rounded central nuclei. No cytologic pleomorphism, atypical mitoses or necroses were found in all tumors. Reticulin staining showed a delicate interstitial pattern of reticulin fibres. In addition to routine histologic stainings immunohistochemistry and electron microscopy were performed. Tumor cells were positive for vimentin, smooth muscle actin and muscle specific actin. Ultrastructurally individual cells were surrounded by basement membranes substance, the cytoplasm contained dense microfilamentous bodies and pinocytic vesicles were observed along the plasmalemma. We diagnosed the lesion as multiple benign glomangioma of the lung – an unusual site for such a lesion.

P-256

Expression of von Willebrand-factor in lungs of children and adults with and without pulmonary hypertension

Annette M. Müller[1], Carmen Skrzynski[1], Guido Skipka[2], Klaus-Michael Müller[1]
[1] Institute of Pathology, University-Clinic Bergmannsheil,
[2] Department of Biometry, Ruhr-University Bochum, Germany

Aims: Up until now little is known about the functional capacity of pulmonary endothelial cells (EC) in children with normal lungs or pulmonary hypertension (pH) compared to adults. Hence we studied the pattern of expression of the von Willebrand-factor (vWF), a coagulatory protein. VWF served as a marker for endothelial dysfunction and was contrasted to the ubiquitously expressed endothelial marker CD 31.
Material and Methods: The expressed patterns of vWF and CD 31 were compared by semiquantitative analyses of immunohistochemically stained lung specimens of 64 patients (age range: 6 weeks - 86 years) with and without pH.
Results: In contrast to the homogenous strong staining of CD 31 in both groups (normal lungs vs pH) the pattern of expression of vWF showed differences not only with regard to the type of vessel, but also with regard to the extent of disease affecting the vessels except in arteries. VWF was also expressed differently by arteriolar and capillary EC in different age groups.
Discussion: The expression pattern of vWF not only showed toporegional differences in normal lungs but also in different age groups and in diseased lung tissue. Hence 2 main questions arise: 1. Are these findings indicative to attempts by the EC to maintain the coagulatory balance within the lungs under different conditions resulting from blood pressure changes or age? 2. Can these findings serve to monitor improvement or deterioration in patients with pH or with advanced age?

P-257

Diagnostic difficulties in serous cavities tumors. A cytological and immunohistochemical study

Carmen Muntean[1], Elena Lazar[1], Liliana Vasile[2], Eugen Lazar[3], Codruta Lazureanu[1]
[1] Department of Pathology, [2] Deparment of Histology,
[3] Department of Anatomy – University of Medicine – Pharmacy Timiroara – Romania

Introduction: Numerous primary or metastatic tumors are seen in serous cavities, with a variety of cellular types, which require an accurate diagnosis. The association of cytological examination and immunohistochemistry permits to differentiate correctly the proliferated cellular type in over 80% of cases in biopsy specimens and in 50% of cases in serous effusions.
Materials and methods: We studied 38 primary and metastatic malignant tumors of serous cavities (peritoneum, pleura, pericardium): 2 mesotheliomas, 5 sarcomas, 31 metastatic tumors (18 adenocarcinomas, 10 squamous cell carcinomas, 2 malignant melanomas and 1 lymphoma). For the frozen sections and formalin-fixed and paraffin-embedded sections we used the conventional histochemical technique and immunostaining for CK8, 18, 19, 20, vimentin, EMA, CD 8, CD 20, CD 45, HMB 45, S100 protein, NSA, CD 34, actin and factor VIII. Cytological specimens were used for the

preparation of smears alcohol – fixed/air – dried, stained blue – polichrom – tanine (original method) and May – Grunwald – Giemsa.
Results: Mesothelial cells hyperplasia and the inflammatory reaction were common for all tumors. The malignant cellular and tissue pattern was diagnosed in 87% of cases, immunohistochemistry improving the accuracy of diagnose in 73% of cases. The histochemical investigation of hyaluronic acid and mucins was useful in 60% of cases for the differentiation of cellular type and tumor pattern. The reactive aspect of stroma and of mesothelial cells influenced the diagnose accuracy for carcinomas (5 false positive and 2 false negative results).
Conclusions: The diagnose of serous tumors is difficult and needs combined morphological techniques – cytological, histological and immunohistochemical – in over 2/3 of cases.

P-258

Atherosclerotic histopathologic changes to corn oil 10% (C.O.) in rabbits aorta segments

Mohammad H. Noori, Babak Behnam
Department of Histology, Faculty of Medicine, Tehran University of Medical Sciences (TUMS), Tehran, Iran

We investigated to identify the effects of dietary corn oil 10% on arteries wall. Rabbits were female Albino and raised 4 to 7 months of age. A group of 24 rabbits were fed defined diets for 1, 2 and 3 months as test groups. The control group was fed a standard laboratory diet while the test group received a diet containing 10% corn oil. Animals were killed in the end of 1, 2 and 3 months. The samples stained with H&E Aortic segment from the rabbits, which fed corn oil, were compared with those that fed standard diets. Study of intima, media and advantitia in rabbit Aorta segments raised on diets with corn oil, demonstrated that elastic lamella was less crowded while the smooth muscle cells were more in tunica intima. The other changes including calcification, foam cells and extracellular lipid observed. These results demonstrated that diet with corn oil increases the risk of developing atherosclerosis and luminal narrowing in large arteries. These observed changes are more noticeable in 3-month diet than one or two months. We concluded that the more the time of corn oil consumption, the more risk of atherosclerosis.

P-259

Cadherins and cell growth control in malignant mesothelioma

S. Orecchia, F. Schillaci, C. Porta*, R. Libener, P.G. Betta.
Pathology Unit. Dept. Oncology, A.S.O. Alessandria;
* Policlinico S. Matteo IRCCS, Pavia, Italy

Introduction: Cadherins and the related α-, β- and γ-catenins partecipate in the regulation of cell-cell adhesion as well as in embryo development, morphogenesis and maintenance of tissue integrity. Cadherins act also as tumour suppressors and changes in their expression induce a migratory and invasive phenotype. We previously reported (ASCO Proceedings 19, 663A, 2000) the heterogeneous expression of cadherins and catenins in human malignant mesothelioma (MM) with respect to the normal mesothelium lining the serosal cavities. The present study aims at assessing a possible relation of E- and N-cadherin expression in MM cells to cell kinetics.
Methods: The cadherin expression was evaluated in 8 human MM cell lines, established from pleural MM effusions, using immunohistochemistry and Western blotting. Cell cycle analysis at the DNA content level was performed by means of flow cytometry.
Results: All 4 N-cadherin +ve cell lines, when they reached confluency, continued to proliferate and their S-phase was similar to the S-phase of non-confluent still growing cells. On the other hand, MM cell lines expressing E-cadherin, either alone or partnered by N-cadherin, entered a state of quiescence following confluency with a reduced or absent S-phase
Conclusion: These findings suggest that N-cadherin expression occurs in MM cells featuring a higher proliferation rate with respect to E-cadherin +ve MM cells. These results are in keeping with the more aggressive behaviour of sarcomatoid MM with respect to epithelioid MM, the latter phenotype being related to E-cadherin expression.

P-260

Tobacco smoking factor in progression of pulmonary tuberculosis

Ougrioumov A.I.
The Setchenov Moscow Medical Academy, Moscow, Russia

Aims: To determine the particular structure of tuberculosis cavern in tobacco smoking men.
Methods: morphometric analysis was undertaken (pointcounting method) to determine expression of suppurative necrotic, granular and fibrosis layers (in conditional units (cond.un.)) in tuberculosis caverns, tissue specimens stained by hematoxylin and eosin of 13 tobacco smoking and 5 non-smoking patients (28–66 aged male), operated in connection with fibrocavernous tuberculosis. To evaluate tobacco smoking level it was proposed to calculate the summary toxicity of nicotine (N) and tobacco tars (TT) in the whole period of smoking. These indexes were taken from patient's questionnaires and expressed in grams as a product of each component divided on days of smoking. The Spirmen index of range correlation (R) was counted.
Results: The cavern suppurative necrotic layer increases in group of tobacco smokers (0,047±0,007 cond.un. in compare with 0,031±0,0011 cond.un. from control group, p=0,001). The granular layer increases as well (0,42±0,03 cond.un. in compare with 0,185±0,07 cond.un., p<0,05). The fibrosis layer decreases in tobacco smoking group (0,61±0,012 cond.un. in compare with 0,72±0,04 cond.un. control, p<0,05). There was a direct connection between N, TT and expression of suppurative necrotic layer (R=+0,30 and +0,41, consequently). The same relations were found between N, TT and granular layer (R=+0,28 and +0,33, consequently). The reverse relations were found between N, TT and fibrosis layer (R=–0,41 and –0,45, consequently).
Conclusions: tobacco smoke products promote progression of tuberculosis pulmonary inflammation.

P-261

Tumor markers in progression of non-small cell lung cancer

Ougrioumov D.A., Kogan E.A.
The Setchenov Moscow Medical Academy, Moscow, Russia

Aim: To investigate the relationship between different tumor markers and the processes of proliferation, differentiation and metastasis

in non-small cell lung cancer (NSCLC): squamous cell lung cancer (SqCLC), adenocarcinoma (AC), bronchioloalveolar cancer (BAC), large cell lung cancer and combined NSCLC.
Methods: Paraffin-embedded samples from 100 surgically treated patients with NSCLC were examined histologically with hematoxylin-eosin staining and immunohistochemically with pancytokeratines, chromogranin, p53, bcl-2, bax, bak, c-fos, c-myc, Ki-67, apoptosis (by TUNEL-test).
Results: Each type of NSCLC can be characterized by different patterns of tumor markers distribution and different levels of proliferation and cell death (by means of apoptosia or terminal differentiation through keratinization), which have been described in our investigation. This patterns have to be taken into account for correct prognosis of tumor behavior. In addition we have found a correlation between expression of pancytokeratines – Ki-67 (r=–0,609 p=0,002), p53 (r=–0,714 p=0,001) and metastases (r=–0,568 p=0,05) in SqCLC; c-myc – metastases (r=0,436 p=0,037) in SqCLC; level of apoptosis – p53 expression (r=0,847 p=0,008) in SqCLC; c-myc expression – bax (r=0,402 p=0,015), bak (r=0,460 p=0,012), bcl-2 (r=0,398 p=0,048) in AC; bcl-2 – bak (r=0,512 p=0,036) in AC; bax – bak (r=0,589 p=0,010), ki-67 (r=0,840 p=0,036) in AC; p53 – bax (r=–0,880 p=0,020) in BAC.
Conclusions: Dynamic balance between the processes of tumor cell death and growth is the most important factor, which determine the progress of NSCLC. Nevertheless it can not be taken into consideration separately. The prognosis of tumor behavior has to be based on the complex approach with use of different tumor markers.

P-262

Impact of neuroendocrine differentiation in non-small cell lung carcinoma

Özturk S.[1], Bircan S.[1], Kayı Cangır A.[2], Sertcelik A.[1], Sak S.D.[1], Kutlay H.[2], Akay H.[2]
Departments of Pathology[1] and Thoracic Surgery[2],
Ankara University Faculty of Medicine, Ankara, Turkey

Introduction: In the past 30 years it has been shown that some of the primary lung tumors reflecting the "grey area" between small cell lung carcinoma (SCLC) and non-small cell lung carcinoma (NSCLC) contained neurosecretory granules and produced specific peptide/amine hormones. Neuroendocrine (NE) differentiation shown by the studies including clinical trials, based on immunohistochemical techniques has been detected in 10%-30% of NSCLCs and evidence of such is observed mostly in adenocarcinomas. It has been hypothesized that NSCLC-NE tumors would carry a worse prognosis and moreover these tumors would be more responsive to chemotherapy. However many studies carried out to investigate this issue have shown conflicting results.
Methods: In a series of retrospective cases diagnosed as bronchial margin negative NSCLCs with clinical parameters, comprising 71 resection materials (31 squamous cell carcinomas, 31 adenocarcinomas, 9 large cell carcinomas), NE differentiation and prognostic significance of NE differentiation were investigated by immunohistochemistry using neuron specific enolase (NSE), chromogranin A (Chr A) and neurofilament (NF).
Results: While NSE expression was detected most often in large cell carcinomas (66.7%) that of Chr A was seen mostly in adenocarcinomas (25.8%) but none of the cases showed immunoreactivity with NF. Multivariate analysis showed that pneumonectomy versus lobectomy carried a poorer while NSE expression predicted for a better prognosis in NSCLC cases.
Conclusion: NE differentiation may be of prognostic significance in patients with resected NSCLC but the clinical significance of NE differentiation in this subpopulation deserves further analysis on larger series.

P-263

Non-ischemic and non-congenital cardiac death in young patients – A study of 45 autopsy cases

Fabio M.C. Palma , Donizete Scudeler, Veronica M.G. Furtado, Patricia Maluf Cury
Faculdade de Medicina de São José do Rio Preto,
São Paulo – Brazil

Introduction: Cardiac disorders are one of the commonest cause of death in adults. Acute myocardial infarction is the most frequent event, often found in patients over the 5th decade. The purpose of this study is to analyse any cardiac events resulting death, except ischemic and congenital diseases, in patients with less 40 years old.
Methods: We studied all patients under 40 years old from 1993 to 2000 who underwent autopsy and died due to cardiac disorder. Clinical, macroscopic and histological data were reviewed. Ischemic and congenital cases were discharged.
Results: There were 45 patients,32 men and 13 women (mean age: 30.1 years old). The main disorders are in the following table:

	Systemic Arterial Hypertension	Idiopathic Dilated Cardiomyopathy	Chagas Disease	Rheumatic Heart Disease	Other cardiac disorders*
Number of cases	16	9	7	7	6
Mean age (years)	36.5	19.0	38.6	28.4	27.8

*3 cases of lymphocytic myocarditis, 1 case of peripartum cardiomyopathy, 1 case of mitral valve infective endocarditis and 1 case of constrictive pericarditis.
Conclusions: Non-congenital cardiac disorders is a common cause of death even in young patients, thus more attention is required on the diagnosis of cardiac problems on the third and fourth decades in order to prevent it.

P-264

Pulmonary langerhans cell granulomatosis. A study of 11 cases

B. Papla, E. Malinowski, E. Nisankowska
1 Department of Pathomorphology, Jagiellonian University Medical College, Kraków, 2 Ward of Thoracic Surgery, Hospital of Lung Diseases, Bystra, Slovakia, 3 II Department of Internal Diseases, Jagiellonian Univeristy Medical College, Kraków

From 1994 to 2000 we diagnosed 11 cases of histiocytosis X in the lungs. There were 5 women and 6 men aged from 20 to 68, mean age 39 years. The symptoms had occurred usually several months earlier and consisted mainly of cough and dyspnoea. Chest X-rays revealed scattered nodular or infiltrative changes, sometimes with translucency in the medial segment in both lobes. Preliminary diagnosis was sarcoidosis, interstitial fibrosis and other disseminated

processes, only in two cases high-resolution computerised tomography suggested the presence of histiocytosis X. Small specimens of subpleural pulmonary tissue were obtained using a thoracocamera to establish the final diagnosis. Formalin-fixed and paraffin-embedded tissue was routinely processed for study by histopathology and immunohistochemistry. Pulmonary specimens contained scattered stellate or nodular changes located subpleurally or in the vicinity of bronchi, sometimes in the central part with an irregular cavernous space. The changes were separated by normal pulmonary parenchyma, where the alveoli were filled with relatively numerous phagocytes, frequently with a brown pigment in the cytoplasm. Infiltrates contained Langerhans cells with moderate pale pink cytoplasm and nucleus with visible nuclear membrane, lying mainly in the lung stroma, and sometimes in the lumen of aerial structures. In the infiltrates there were also eosinophils in various quantities, lymphocytes, plasmocytes and neutrophiles. The process was accompanied by fibrosis varying in intensity. Immunohistochemical staining for S-100 antigen confirmed that Langerhans cells were the main component of the infiltrate. High-resolution computerised tomography and sampling by using a thoracocamera help establish the diagnosis of this relatively rare entity requiring special.

P-265

Genetic analysis of 18 carcinoid lung tumors

Payá A., Ortega E., Aranda F.I., Seguí J., Niveiro M.
Servicio de Patología, Hospital General Universitario de Alicante, Spain

Purpose: To analyze genetic alterations in carcinoid lung tumors and its correlation with pathological, clinical and immunohistochemical variables.
Methods: 18 cases of carcinoid lung tumors (13 typical,TC; 4 atypical, AC; 1 metastasis of AC), classified according with Travis criteria. DNA was amplified by PCR with primers flanking seven polymorphic markers spanning at the following genes or chromosomal regions: D3S1514 and D3S1295 (3p21.1-14.2, FHIT gene region), D5S346 (5q21-22, APC gene region), D10S2435 (10q23.1-23.3, PTEN gene region) D6S304 (6q21-23), TP53CA (17p13.1, TP53 intragenic), PYGM (11q13.1, MEN-I gene region).
Results: Five cases showed LOH in some of the regions (3 atypical, 2 typical). Results of LOH analyses of the cases are shown in table. LOH at 3p21.1-14.2 were observed only in AC, (3 of 5 cases, p=0.03), and were associated with metastasic disease (p=0.01). LOH at 11q13 were observed in 4 of 16 cases (25 %). All the AC with LOH at 3p also showed LOH at 11q13. No 17p13.1 LOH were found, according with the very low p53 immunohistochemical expresion in all of them.

Case	Type	D3s1514	D3s1295	PYGM	D5s346	D6s304	D10s2435	p53CA
4	TC	N.I.	N.I.	+	N.I.	–	–	–
3	TC	–	–	–	+	–	–	–
15	AC	+	N.I.	+	–	–	N.I.	–
18	AC	+	+	+	–	–	–	–
14	AC	+	+	+	–	–	–	–

Conclusion: LOH at 3p is a frequent finding in AC and it is not present in TC. Furthermore, LOH at 3p21-14 in our serie, seems to be a prognostic factor because it is associated with an increased metastasic risk. On the other hand, p53 is not associated with the development of carcinoid lung tumors.

P-266

Comparison of vasoactive response of left and right internal thoracic arteries to isosorbide-dinitrate and nitroglycerin: An in-vitro study

Yosef Paz, Ina Frolkis, Itzhak Shapira, Menachem Matsa, Jacob Gurevitch, Amir Kramer, Dmitry Pevni, Chaim Locker, Oren Lev-Ran, Beatrix Lifschitz-Mercer, Rephael Mohr
Departments of Thoracic and Cardiovascular Surgery and Pathology, Tel Aviv Sourasky Medical Center; Sackler Faculty of Medicine, Tel Aviv University, Israel

Introduction: The internal thoracic artery (ITA) is the most important graft in coronary artery bypass grafting. Its distal region is, however, prone to vasospasm. We studied the effects of nitroglycerin (NTG) and isosorbide-dinitrate (DSDN) on distal segments of left versus right ITA.
Methods: Rings of distal segments (6–9 mm proximal to bifurcation) of the human left and right ITA were studied. After baseline contraction of the rings, achieved using 60 mmol/L of KCl, they were exposed to increasing doses of ISDN and NTG (10–100 μg/ml), and dose-response curves were recorded.
Results: The contractile response of left ITA rings to KCl were significantly lower than those of right ITA rings (1.87±0.25 g versus 3.5±0.61 g, $p<0.005$). Both nitrates inhibited the contractile response in a concentration-dependent manner, with relaxing effects of ISDN higher than those of NTG ($p<0.01$) in both left and right ITA rings.
Conclusions: The distal segment of the left ITA is less prone to vasospasm than that of the right. ISDN has a considerably higher relaxant effect on this segment than NTG. We therefore recommend favoring high doses of ISDN over NTG as an antispastic measure.

P-267

Pulmonary apoptosis in patients with ventilator-associated pneumonia

Ramirez J.[1], Arce Y.[1], Torres A.[2], Quintó L.l.[3], Ferrer M.[2], Pic O., Ferrer B.[1], Cardesa A.[1]
[1] Anatomia Patològica, [2] Pneumologia i [3] Epidemiologia i Bioestadística. Hospital Clínic, IDIBAPS, Universitat de Barcelona, Spain

Introduction: To assess the usefulness of apoptosis as a mechanism of cell death implicated in the physiopathology of pneumonia, we have studied the lung tissue of a series of patients with clinical criteria of acute lung injury (ALI) who were admitted to the respiratory intensive care unit and died due to pneumonia.
Methods: We obtained a total number of 222 lung specimens coming from 25 patients. We performed a routinely histopathological evaluation and assessment of apoptosis through the TUNEL (Terminal deoxynucleotidyl transferase (TdT) mediated dUTP Nick End Labelling)) technique. The evaluation of TUNEL is expressed by the Apoptotic Index (number of positive cells/total cells ×1000). The probability of having pneumonia in a given lung specimen evaluated for apoptosis was statistically calculated by an statistical model of logistic regression.
Results: Histopathologically we saw 109 over 222 slides with acute pneumonia. The remaining specimens ranged from normal parenchyma to non-specific changes related to ventilator and diffuse alveolar damage.

The results concerning the counting of cells is expressed in the table, as media of each counting.

	N	Apoptotic cells	Total # of cells	Apoptotic index
No pneumonia	113	22.450	1962.20	11.44
Pneumonia	109	39.234	2161.78	18.14

Conclusions: There is a significant correlation between apoptotic index (AI) and the probability of having pneumonia (OR:1.077, $p<0.001$). There is not a cut-off to make the diagnosis of pneumonia through the AI, but for each unit of AI, the probability of pneumonia increases in a 7.7%.

Supported by a grant from FIS 00/0329. Spain. Dr. Arce is a recipient of a grant from Fundació Pedro Pons. University of Barcelona. Spain.

P-268

Pulmonary Alveolar Proteinosis. Report of a case with an uncommon clinical presentation

Ramos S.*, Pinto H.**, Alfarroba E.**, Rebordão M.**, Sena Lino J.*, Martins A.P.*
Hospital de Stª Cruz* , Hospital Militar de Belém**, Lisboa, Portugal

Introduction: Pulmonary Alveolar Proteinosis (PAP), or pulmonary alveolar phospholipoproteinosis, is a rare pulmonary syndrome of variable etiology, characterized by the accumulation of amorphous, PAS positive lipoproteinaceous material in the distal air spaces. These finding results from impaired production and/or degradation of surfactant, related with macrophage dysfunction, either primary or acquired. The disease may occur either as an isolated finding, or associated to various conditions. Patients usually present with respiratory complaints and, radiographically, with bilateral, symmetric airspace opacities, especially in the hilar and basal regions.

Material and Methods: An assymptomatic 50 year-old army officer with no past medical history, and occasional exposure to muriatic acid, underwent a routine chest X-ray that showed several bilateral nodular opacities. The CAT scan disclosed peripheral infiltrates along segmental and sub segmental bronchi. Respiratory function tests and bronchoscopy were unremarkable as well bronchial wash material. The bronchoalveolar lavage (BAL) had few cells, mostly lymphocytes, but also macrophages and some multinucleated giant cells. A surgical lung biopsy (9×3×1.5 cm) was performed.

Results: Lung parenchyma had multiple white solid nodules, the largest one with 3.5 cm. On microscopic examination diagnosis of PAP was made.

Conclusions: PAP has several different clinical presentation and the diagnosis is usually suspected based on respiratory complaints, associated to a diffuse interstitial lung disease, with BAL being diagnostic. Our case is very uncommon, as clinical, radiological, laboratory findings, including BAL, as well as gross examination of the surgical specimen did not suggest this diagnosis.

P-269

Multiple pathologic changes in surgically resected lung specimens

[1]Tomaž Rott, [2]Janez Eržen, [2]Stane Vidmar
[1] Institute of Pathology, Faculty of Medicine, University of Ljubljana, [2] Clinical Department of Thoracic Surgery, University Medical Centre, 1000 Ljubljana

Introduction: Multiple pathologic changes in the lung are frequently found in surgically resected pulmonary tissue. They are not always clinically detected, moreover, visible multiple lesions may be misinterpreted. In patients (pts) with history of malignoma in the lung or elsewhere, they suggest the diagnosis of recurrent or metastatic malignoma. Beside tumours, histologic examination of surgical specimens in patients with multiple pulmonary lesions reveals a wide spectrum of other pathologic lesions. The object of our study was to determine the incidence and the true nature of multiple lesions in the lung.

Patients and the methods. Patients admitted to the hospital during years 1999-2000 were subject to various surgical procedures because of clinically suspected pathologic pulmonary changes. Surgical specimens were assessed by standard gross and light-microscopic examination. Available history data were included in the evaluation of pathologic lesions.

Results: Multiple pulmonary lesions were found in 58 of 409 pts (14%). They represented: malignoma and not tumourous lesions – aspergillosis, haemorrhagic infarction, etc. (26 pts, 45%), only not tumourous lesions, such as combinations of tuberculosis with actinomycosis or aspergillosis (11 pts, 19%), malignoma and benign tumour (6 pts), multiple primary lung tumours (5 pts), metastatic extrapulmonary tumours (3 pts), lung tumours metastazing to intrapulmonary lymph nodes (3), recurrent tumours (2 pts), and single cases of bifocal carcinoma and multinodular tumour.

Conclusions: In patient with multiple lung lesions, all possible combinations of multiple lesions should be considered in differential diagnosis. They should be histologically or at least citologically confirmed, especially in patients with history of a malignoma, who may have only not tumourous lesions, to choose a proper treatment.

P-270

Struma cordis in the right ventricle – A case report

Sabat Daniel*, Zajęcki Wojciech*, Myrcik Grażyna**, Ziółkowski Adam*
* Department of Pathomorphology, Medical Faculty in Zabrze, Silesian Academy of Medicine in Katowice, Poland, ** Department of Pathological Anatomy of the Specialist Hospital N° 1 in Bytom, Poland

A very rare case of the intracardiac heterotopic thyroid tissue in a 43-year old woman without clinical symptoms, was presented in the report. The woman died because of the diffuse neoplastic disease (SLL – small lymphocytic lymphoma). On autopsy a body-colour, soft, elastic tumour measuring 4×4×3 cm and growing towards the ventricle lumen was found in the right ventricle of the heart. The tumour was covered with the thin fibrous capsule separating it from the septomarginal trabeculae of the cardiac muscle. The structure of the thyroid tissue with the features of the colloidal

changes with macro- and microfollicular pattern was revealed on histopathological and immunohistochemical (TGB – thyroglobulin) examinations.

P-271

Immunohistochemistry of IGF family members in lung cancer in persons lived in the radioactive-polluted semipalatinsk territories of Kazakhstan

Sagindikova G., Kogan E., Jaques G*.
Dept. of Pathology, Moscow Medical Academy, Russia;
Phyllips University, Marburg, Germany*

Aim: of the study was to investigate the expression of IGF family members in cells of the lung carcinoma in persons who have been living in Kazakhstan regions with elevated radiation level.
Methods: 17 cases of patients with the lung carcinoma living in Kazakhstan regions with high radiation level (Sempalatinsk) (group I) were selected for study. 40 patients had been living in regions with normal level of radiation (30 in Moscow and 10 in Kazakhstan) (group II). The studied groups included 52 males and 5 females with the mean age of 60. Paraffin-embedded microwave pretreated sections were stained immunohistochemically to detect the presence of chromogranin A, IGFI, IGFII, IGFBP1-6.
Results: All the 17 cases of small cell (11) and nonsmall cell (6) lung cancer in group I were characterized by expression of chromogranin A, that proves neuroendocrine differentiation of the tumor cells in all histological types of lung carcinoma. In the group I the study showed high expression of IGFBP1,2 and low expression of IGFBP3,4,5 in lung cancer. In control group II high expression of IGFBP4,5,6 and low expression of IGFBP1,2,3 was a characteristic feature of lung cancer.
Conclusion: The IGF system plays an important role in morphogenesis of different types of lung carcinoma. The particular feature of radiation-induced lung cancer was neuroendocrine differentiation in all morphologic variants of this neoplasm with increasing accumulation in tumor cells of IGFBP 1,2.

P-272

Two cases of so called mesothelioma of atrioventricular node

Salamon, F., Magyar É.
Department of Pathology, Semmelweis University,
Faculty of Health Sciences, Budapest, Hungary

Introduction: So called mesothelioma of the atrioventricular node is a rare lesion. Clinically it is associated with heart blocks and sudden death. The definitive diagnosis is made usually at autopsy. The histogenesis of this condition is controversial, both mesothelial and endodermal origin are suggested.
Methods: The cases are two young women of 31 and 19 years are presented. They died suddenly, previous heart blocks, Adam-Stokes syndrome and pacemaker implantation are known from the clinical history. Postmortem examination included autopsy and histology of cardiac conduction system. Conventional histopathological and immunohistochemical examination were completed by ultrastructural study both transmission and scanning electronmicroscopy.
Results: Histology revealed a polycystic tumour with tubular structures and solid nests in the atrioventricular node region. Immunohistochemically the tumour cells expressed cytokeratines, EMA, CEA. Focal positivity for chromogranin A and calcitonin was observed. The mesothelial marker (HBME1) was negative. Ultrastructural investigation failed to prove the mesothelial origin, it favoured endodermal differentiation instead.
Conclusion: Both immunohistochemistry and electronmicroscopy confirmed the endodermic differentiation of the presented tumours. The lesion itself is benign but it can be dangerous because of its location. In cases of heart block in children and young adults the possibility of this tumour has to be taken into account.

P-273

Morphology and biomolecular markers of bronchial epithelium proliferation in decontaminators of the chernobyl accident

Samsonova M., Ali-Risa A., Demoura S., Cherniaev A., Chuchalin A.
Pulmonology Research Institute, Moscow, Russia

Aim of the study: Morphologic examination and immunohistochemical assessment of proliferative activity in bronchial epithelium of patients which have worked at Chernobyl station after the catasthrophe.
Material and methods: Tissue samples from 33 Chernobyl workers (males, mean age 43.20±1.35 yrs) were analyzed. The official mean dose of radiation which has been received by decontaminators was 19.2±4.8B. Morphologic examination of bronchial epithelium and immunohistochemical examination with Ki-67, p53, bcl-2, c-myc and chromogranin antibodies were performed on paraffin sections using standard procedure. Control tissue samples have been obtained from 20 patient with COPD. All chernobyl patients were re-examined after two years.
Results: In 60 per cent of patients basal cell hyperplasia was revealed, catarral changes in epithelium were found in 43%. Squamous metaplasia of bronchial epithelium was observed in 48% of patients, and in 12 patients – with cell dysplasia, athrophic changes were found only in 4 patients. Squamous methaplasia and severe displasia more often can be seen in the group of Chernobyl patients as compared to COPD group. Proliferating assotiated Ki67 antigen level was three times higher in chernobyl patinents. (28.15±4.25% and 8.2±2.2 correspondingly). The very high level of p53 were found in chernobyl patient (57.6±7.35 versus 10.6±3.8 in control group). The level of detection of chromogranin granules was higer in Chernobyl group. After two-year observation the progression of dysplasia, p53 level and basal membrane thickness were registered.
Conclusion: Our data confirmed that regenerative and disregenerative processes could be seen in epithelium of patients exposed to radiation. Marked proliferative level with high Ki67, p53 level with its progression during the period of observation as well as increased number of neuroendocrine-differentiated cells was registered in this group of patient.

P-274

Expression of γ-glutamyl cysteine synthase in non-small cell lung carcinoma

Y. Soini, U. Näpänkangas, K. Järvinen, R. Kaarteenaho-Wiik, P. Pääkkö, V.L. Kinnula
Departments of Pathology and Internal Medicine, University of Oulu, Oulu, Finland; Occupational Health Institute, Helsinki, Finland

Introduction: We investigated the expression of gamma glutamyl cysteine synthase (γGCS) in 85 cases of non small cell lung carcinomas (NSCLC).
Methods: For immunohistochemistry polyclonal rabbit antibodies against γGCS heavy and light chains were used.
Results: γGCSh positivity was found in 71% and γGCSl positivity in 67% of NSCLCs. There was a strong association between the expression of heavy (catalytic) and light (regulatory) subunits of γGCS in NSCLC (p=0.003). Squamous carcinomas expressed more often moderate or strong staining for γGCSh than adenocarcinomas (p=0.00013). Moreover, strong or moderate γGCSh expression was found significantly more often in grade I-II than in grade III tumors (p=0.008). A similar tendency was observed with γGCSl, but the association was not statistically significant (p=0.07). There was a significantly higher extent of apoptosis in tumors with a low γGCSh expression (p=0.016). A similar tendency was observed with γGCSl (p=0.073). There was no association between patient survival and high or low expression of γGCSl or γGCSh in NSCLCs (p=0.34 and p=0.47, respectively).
Conclusion: The results show that γGCS is strongly expressed in NSCLCs and probably takes part in the defense of the tumor cells against oxidative damage. This is reflected by the lower extent of apoptosis in tumors with a high γGCS expression. Since expression of γGCS has been connected with chemoresistance to some chemotherapeutics, downregulation of its activity by inhibitors in NSCLC might have putative therapeutic potential in the treatment of lung cancer.

P-275

Pathomorphological aspects of the classification of pulmonary tuberculosis

Soloveva I.P., Berestova A.V.
Dept. of Pathology, Moscow Medical Academy, Moscow, Russia

Introduction: Epidemiologic situation with tuberculosis (TB) is worsening in Russian Federation, all cases of TB must be analysed and classified. It is especially important for pulmonary TB, which is the most frequent variant of this disease. Death rate due to pulmonary TB increases every year.
Methods. We performed a retrospective study of about 2000 autopsy cases of TB revealed in different Moscow hospitals and examined 350 fragments of lungs, removed during surgical operation in Moscow Medical Academy and in Russian Research Institute of Phtisiopulmonology within 1995-1999. Macroscopic examination, histotopograms and microscopic sections, stained by routine methods were used.
Results: The obtained morphological characteristics differed greatly from presented in the International statistical classification of diseases (ICD). We found nodular or multinodular changes with pulmonary fibrosis and different rate of tubercular inflammation, tuberculomas, cavernous and fibrocavernous TB with large multiple cavernas and fibrocalcific scar, caseous pneumonia with different extent of involvement. Usually lesions were present in the apical or posterior segments of the upper lobes, in some cases they spread to the superior segments of the lower lobes. Most of this forms are presented in the classification adopted in Russia but they are not detailed in the ICD.
Conclusion. Different forms of pulmonary tuberculosis, revealed in the examined material, differed from those, suggested in the ICD. Classification of pulmonary tuberculosis into groups according to morphological characteristics will permit to improve statistical analysis and to develop differentiated treatment methods.

P-276

Pleomorphic carcinoma of the lung – immunohistochemical features

Florica Staniceanu[1], Carmen Ardeleanu[2], Sabina Zurac[1], Florin Chirculescu[3]
1. Department of Pathology, Colentina Hospital, 2. Department of Pathology, Victor Babes Institute, 3. Department of Surgery, Hospital of pneumoftiz.iology of Bucharest, Bucharest, Romania

The pleomorphic form of pulmonary carcinoma is a poorly differentiated non-small cell carcinoma with at least 10% of the tumor consisting in spindle cell and/or giant cell.
We report 15 cases of pleomorphic carcinoma of the lung, all of them including large areas of squamous cell carcinoma (WHO 1999). All the cases included areas of giant cells and 9 cases presented spindle cell and giant cell proliferation. We analyzed the expression of vimentin, cytokeratin 7 (CK7), epithelial membrane antigen (EMA) and carcinoembrionic antigen (CEA).

IHC	Squamous cell component				
	+++	++	+	+/–	–
CK 7	6	0	6	3	0
EMA	9	6	0	0	0
CEA	3	9	3	0	0
Vim	0	0	0	0	15

IHC	Giant cell component				
	+++	++	+	+/–	–
CK 7	3	0	0	0	12
EMA	0	9	6	0	0
CEA	3	6	6	0	0
Vim	0	0	3	6	6

IHC	Spindle cell component				
	+++	++	+	+/–	–
CK 7	0	0	0	3	6
EMA	0	0	0	6	3
CEA	0	3	3	3	0
Vim	3	3	0	0	3

The giant cell component is weak positive for vimentin; the epithelial markers are positive but less intense as in the squamous cell component. The spindle cell component is mostly negative for epithelial markers and positive for vimentin.

P-277

Importance of ultrastructural changes of myocardial capillaries in the development of heart failure following open-heart surgery

E.Stefanovic, M. Jakovljevic, P. Otasevic
Dedinje Cardiovascular Institute and Belgrade University School of Medicine, Belgrade, Yugoslavia

Aim: The reversibility of ischemic injury to cardiomyocite during open-heart surgery depends upon the condition of myocardial microcirculation following cross-clamp release. We designed the present study to assess the influence of intraoperative changes of myocardial capillaries on the severity of heart failure (HF) in the postoperative course.
Methods: Two groups were analyzed; group A, consisting of 13 patients with signs and symptoms of mild HF in the postoperative course; and group B, consisting of 7 patients who died from second to tenth postoperative day due to HF. The ischemic period was 77.6±4.2 min in group A, and 94.2±5.2 min in group B. Intraoperative biopsies from the right ventricle, taken during different time points during the ischemic period and reperfusion, were analyzed using quantitative stereological analyzes.
Results: Myocardial ultrastructural analysis showed increase in permeability of the capillary wall, edema and degenerative changes of cardiomyocites that were similar in both groups. Stereological analysis of endothelial cells organelles revealed decrease of 48% in volume fraction of basic pinocite vesicles in group II after release of the cross-clamp as compared to immediate preoperative level, suggesting that the elimination of metabolic products form interstitium to microcirculation is altered.
Conclusion: Ischemic changes of myocardial capillaries during the open-heart surgery, as assessed by stereological analysis, are more profound in patients who died due to HF, suggesting that the disturbance of transendothelial transport may play certain role in the development of HF.

P-278

Apoptosis in dilatated cardiomyopathy: an ultrastructural study

E. Stefanovic, M. Jakovljevic, P. Otasevic, S. Gradinac, M. Miric
Dedinje Cardiovascular Institute and Belgrade University School of Medicine, Belgrade, Yugoslavia

Aim: Apoptosis plays an important role in acute ischemia and hibernation of myocardium, yet its role in the development of heart failure in dilated cardiomyopathy (DCM) is still to be determined. The aim of the present study was to investigate the presence of apoptosis in patients with DCM.
Methods: Myocardial samples were taken using endomyocardial biopsy of the left ventricle and intropertively during partial left ventriculotomy (Batista procedure). The study enrolled seven patients (5 male and 2 females), who were in NYHA class II-IV. All samples were analyzed by electron microscope.
Results: Hypertrophied cardiomyiocites with large number of mitochondria were observed, as well as few cardiomyocites with signs of necrosis, including enlargement of cells with bright cytoplasm, reduced number of organelles and nuclear edema. Apoptosis, defined as reduction in cell size, dark cytoplasm and nuclear condensation, was seen only in capillary endothelium.
Conclusion: Qualitative electronmicroscopic study of myocardium in DCM showed the presence of necrosis in few cardiomyocites, whereas apoptosis was noted in myocardial capillary endothelial cells only.

P-279

Pathology of the heart conduction system in selected cases of sudden cardiac death

Suárez-Peñaranda J.M., Muñoz J.I., Rodrílguez-Calvo M.S., Concheiro Carro L.
Institute of Legal Medicine. University of Santiago de Compostela. Spain

Introduction: The study of the heart conduction system (HCS) is not routinely done, not only because it involves an expensive and time consuming methodology but also because the results are usually inconclusive and show poor clinical correlation. We have studied the HCS in selected cases of sudden death using a simplified technique to check the validity of these assumptions.
Methods: The HCS was investigated in selected cases of unexplained sudden (occurring in the first six hours from the onset of the symptoms) death. A complete autopsy was carried out in every case to rule-out non cardiac death, including toxicological screening. After overnight fixation, two blocks of tissue were excised from the heart, including the main structures of the HCS (sinoatrial and atrioventricular nodes, bundle of His and proximal portion of its terminal brunches).
Results: We found relevant pathology in the HCS to explain the death in five cases. In one case of a 72 year old man, there was a tumour in the AV node, responsible for an AV block. In two cases (a 4-year-old girl and a 42-year old man), estenosis of the atrioventriclar node artery was the most conspicuous finding. In the remaining two cases, persistent fetal dispersion of the conducting tissue in the atrioventricular node was the only finding at autopsy.
Conclusion: In our experience, we have found that systematic study of the HCS in cases of sudden death may be helpful in some cases and that good results can be achieved even by using a simple technique available for small laboratories.

P-280

Myocardial capillary in cor pulmonale development in experimental lung emphysema

M. Sulkowska, W. Famulski, S. Terlikowski, S. Sulkowski
Department of Pathological Anatomy, Medical Academy of Białystok, Poland

A morphometrical and ultrastructural analysis of changes in the heart of rats with experimental lung emphysema due to single intratracheal administration of proteolytic enzyme, papain, has been done. The research was carried out on 54 male Wistar rats, of initial body weight 180–220 g. Thirty three animals were given intratracheally papain in a dose of 20 mg/kg b.w./0.5 ml PBS. At the same time 21 animals were administrated intratracheally, a PBS solution. The animals were sacrificed after 1, 3 and 6 months of papain treatment.
It has been found that a single administration of papain caused emphysematous changes in the lungs, growing more intense until the third month of the experiment. The progression of these changes

correspondent to a capillary density increase in the right ventricle, interventricular septum and in the subendocardial layer of the left ventricle. After six months of the experiment, a reduction in capillary density in the heart regions mentioned above and a simultaneous increase in the cardiomyocyte transversal diameter were observed, being the exponents of evident myocardial hypertrophy.

P-281

Application of Scanning Microscopy and X-ray Microanalysis in Pulmonary Cancer Investigation. Preliminary report.

*Szczurek Zbigniew, *Ziółkowski Adam, **Grzybek Henryk, ***Łaskawiec Jan, ***Sozańska Maria, **Jasik Krzysztof
* Chair and Pathomorphology Unit of the Medical University of Silesia in Zabrze, Poland, ** Chair and Department of Histology and Embriology of the Medical University of Silesia in Zabrze, Poland, *** Chair of Material Science of the Silesian Technical Academy, Katowice, Poland

X-ray micronalysis enables quantitative assessment and linear distribution of chemical elements in tissue micro-areas. The presence and place of a given element may be linked with the pathogenesis of change in the examined tissue sample. The study included cases of original lung cancer in patients coming from regions of high ecological risk. The types of analysed cancer included squamous carcinoma, small cell carcinoma and adenocarcinoma, while the control group consisted of cancer free cases of lung tissue. Routine histopathologic procedures were followed by scanning microscopy and x-ray micro-analysis examination of the sample micro-areas. As regards squamous cell carcinoma group, the microexaminations revealed the presence of silicon (Si), coal (C) and oxygen (O). All the samples of all types of cancer showed peaks of x-ray radiation characteristic of coal (C) and oxygen (O). Prominent differences were encountered in the incidence of the x-ray radiation Kα1 characteristic of silicon (Si) in the micro-areas of different samples of squamous cell carcinoma. Differences were found in the content of the examined elements in the micro-areas of the samples of different histopathological types of lung cancer. The micro-areas of the control group samples showed coal and oxygen peaks only. The method of x-ray microanalysis failed to confirm the presence of other elements in any of the examined samples. Standard histopathologic examinations of lung squamous cell carcinoma samples revealed slightly intensified exponents of coal or silicon coniosis. The authors indicate the possibility of extending the histopathological diagnostics with micro-analytic examination. The incidence of peaks characteristic of silicon in squamous cell carcinoma samples may indicate the necessity of multi-factor analysis in the search for the cause of cancerogenesis, implying the necessity to include environmental and occupational factors.

P-282

Morphological analysis of saphenous vein segments taken in situ, after the surgical preparation as well as after the implantation as aortocoronary graft in cases with lethal outcome

Vujadin Tatić, Vladimir Kanjuh, Milomir Todorić
Institute of Pathology, Clinic for Cardiac and Chest Surgery of Military Medical Academy, Serbian Academy for Sciences and Arts, Belgrade, Yugoslavia

The aim of the study was to analyze morphological changes of saphenous veins: a) taken in situ, b) after the surgical preparation, before the implantation as the aortocoronary graft, and c) post mortem to comparate the changes before and after the implantation in patients with lethal outcome.
METHODS: In 175 patients (121 men and 54 women), aged 20 to 75, it was examined histologically, histochemically, imunohistochemically and ultrastructurally 175 segments of saphenous veins taken in situ and before the implantation as well as including in 25 patients after performed surgery and death.
RESULTS: Out of the total 175 saphenous veins segments, 87 showed in situ and before the implantation bigger or smaller morphological changes: the demage of endothelium, intimal hyperplasia and fibrosis of media and adventitia. Among them, 67 had changes in situ and only 20 after the surgical preparation before operation. It was found the significant increase of the number of smooth muscle cells and fibroblasts in the intima of the damaged veins. In 25 patients with lethal outcome, all with preoperative damages of saphenous veins, death occured in 19 patients after the surgery due to acute thrombosis of the vein graft. The morphological damages of these veins were greater than before the surgery.
CONCLUSION: Out of 175 saphenous veins 87 had morphological changes before the implantation as the aortocoronary graft (in 67 changes were already in situ,and in 20 occurred after the surgical preparation for graft) which could be the cause of postoperative complications. In the future, the histological ex tempore examination of saphenous vein may be necessary to avoid the implantatione of veins with morphological changes and to replace them by veins from vein banks taken from appropriate donors.

P-283

Myocardial fluorescence measurements as morphopathologic criteria for determining the duration of myocardial infarction

I.Tsiple, V.Anestiadi
Centre of Pathobiology and Pathology, Academy of Sciences, Chisinau, Moldova

In this study we attempted to find new morphopathologic criteria for the determination of the duration in time of the myocardial infarction (MI). We selected 52 hearts from persons deceased from MI, in which the beginning of MI was well documented clinically and by ECG. 30 hearts of persons deceased almost instantaneously from major traumas served as controls. In each case, there were performed 1000 measurements of the intensity of myocardial primary fluorescence (MPF) at the wavelength of 360 nm., both in the necrotic (ischaemic) zone (NZ) and in extrainfarctic zones (EZ). During the first 8–12 hrs from the beginning of MI, the MPF decreased concordantly in both zones, being 89.6±2.3% of the control values. At 24 hrs after MI onset the MPF in NZ was 78.8± 4.3%, while in EZ was 84.4±3.1% of the control data. The most prominent decrease of MPF in the NZ was noted at 4-5th and 9–10th days (66.3±2.5% and 62.6±2.1% of controls, $p<0.001$), with subsequent maintaining at this level during the resorbtion of necrotic tissues. The MPF in the EZ at 4–5th days was 77.4±3.5%, with an increase at 9–10th days up to 82.3±2.2% and at 14–15th days to 85.7±2.8%, remaining even up to 30–35th days of MI 7.3±0.8% below control limits. MPF variations in time could be approximated by spline functions. By solving a system of equations, which included formulae for EZ and NZ MPFs, it was possible to determine the time elapsed from the MI onset, with an accuracy of 9.6 hours.

P-284

Incidence of myocarditis: Correlation between clinical and pathohistological findings on endomyocardial biopsy

Vasiljevic J.D., Babic D., Jovic V., Popovic Z.V., Miric M., Tucakovic G., Oklopdžija M.
Institute of Pathology, Belgrade University Medical School and Dedinje Cardiovascular Institute, Belgrade, Yugoslavia

Since it's introduction in 60's, endomyocardial biopsy (EMB) has become a routine procedure for the diagnosis of myocarditis (MC). The aim of this study was to correlate the incidence of clinical diagnosis of MC (made on laboratory tests, non-invasive and invasive studies), and pathohistological (PH) diagnosis (made using standard technique and modified Dallas classification).
Among 1090 non-transplant, diagnostic EMBs, performed during last 15 years, only 303 patients (63.3% male and 36.7% female, mean age 38.4 years) had the following clinical diagnoses: suspected MC (59.1%), acute (18.8%), post-MC status (17.8%), and chronic MC (4.3%). The second clinical diagnosis was: none (71.3%), dilated cardiomyopathy-DCM (14.9%), pericarditis (8.3%), major dysrhytmias (4.0%), boreliosis (1.0%), and unexplained heart failure (0.7%).
PH diagnosis was made on first EMB in 86.1%, on first rebiopsy in 12.9%, and second rebiopsy in 1.0% of patients. The correlation between clinical and PH diagnoses was evaluated as: confirmed (67.7%), changed (25.1%), non-specific findings (4.0%), and inappropriate biopsy (3.3%). Confirmed clinical diagnosis on first EMB was made in 64.0%, on first rebiopsy in 92.3%, and on second rebiopsy in 66.7%, showing the best corelation on second biopsy, when diagnosis of MC was clinically already established.
PH findings on first EMB showed: active MC (29.9%), border-line (17.9%), focal (active, 19.8%), and healing (32.3%), out of 167 confirmed cases of MC. We found that even on the first EMB it is possible to make PH diagnosis of focal or healing MC, depending on appropriate histological appearance.The findings on second EMB were: on going MC (20.5%), healing (64.1%), and healed (15.4%).The change of clinical diagnosis occurred in 76 patients (25.1% of total) with DCM (90.8%), ischemic cardiomyopathy (7.9%), and haemochromatosis (1.3%) as new entities.
In conclusion, by adding the percentage of confirmed clinical diagnoses (67.7%) to changed ones (25.1%), the overall diagnostic value of EMB for the clinician (and the appropriate choice of treatment modalities of MC) is very high – 92.7%. The new diagnosis of DCM (90.9% of all changed diagnoses) indicates that the biopsy is often performed to late. Finally, we need more unification and consensus among pathologists in the field of diagnostic accuracy of MC.

P-285

Head-to head comparison of three different methods of myocardial histomorphometry in patients with heart muscle disease

Vasiljevic J.D., Popovic Z.B., Otasevic P., Popovic Z.V., Vidakovic M., Gradinac S., Neskovic A.N.
Dedinje Cardiovascular Institute, Belgrade, and Institue of Pathology, University Medical School, Belgrade, Yugoslavia

No study directly compared different histomorphometric methods of quantification of major myocardial components myocardial fibres and interstitial fibrosis. The aim of the study was to compare the results of semiquantitative, point-counting and computer-based methods in the assessement of interstitial myocardial fibrosis in a consecutive series of surgical biopsies and endomyocardial biopsy (EMB) samples from patients with different heart muscle disease.
Histological samples (at least 3 per patient) were obtained by EMB from 11 patients with focal myocarditis (control group), and from 24 ambulatory patients with idiopathic dilated cardiomyopathy, or during surgery in 10 patients that underwent partial left ventriculectomy (Batista procedure). Samples were cut and stained with Masson-trichrome for better contrast. From each sample, a representative field was chosen, then digitized, and the amount of fibrosis was assessed by semiquantitative scoring, by point-counting, and by computer-based software.
Semiquantitative scoring correlated with both point-counting (Spearman's $r=0.69$, $p<0.0001$) and computer-based (Spearman's $r=0.83$, $p<0.0001$) methods. There was also a good correlation between a point-counting and computer-based methods ($r=0.71$, $p<0.0001$). However, when compared with point-counting method, computer-based method overestimated percent fibrosis by $3.0\pm6.7\%$ ($p=0.004$). This over-estimation correlated with the mean percent fibrosis ($r=0.38$, $p=0.014$).
In conslusion, our data show good correlation between the three methods of myocardial fibrosis volume assessment. However, systematic differences between them point out that this should be taken into consideration when comparing results of the studies using different modalities of volume fibrosis assessment.

P-286

Laminin α2 chain (merosin m chain) and metastatic potential of microcitoma

D. Vitolo, L.Ciocci and C.D. Baroni
II Pathological Anatomy, University of Rome "La Sapienza", Italy

Introduction: Lamin α2 chain is expressed in basal membrane of about 20 % of vessels of head and neck, lung and breast carcinomas. These tumors express α6β4 integrin. Moreover β4 chain is up regulated by EGF and represents the ligand of lamin α2 chain and laminin. Therefore lamin α2 chain expression during angiogenesis in EGF producing tumors, might favour intravasation. We have evaluated the ability of lamin α2 chain and other basal membrane proteins to facilitate migration of lung carcinomas cell lines using an in vitro test migration assay.
Methods: 13 mm diameter, polyvinilpyrrolidone free polycarbonate filters, 12 μm pore size, were coated with merosin, laminin, type I collagen, type IV collagen, and fibronectin. 3×10^5 cells of microcitoma, adenocarcinoma and squamous cell carcinoma from A.A.T.C. were suspended in serum free media and added to the upper compartment of chemotaxis Boyden chambers for 24h at 37°C in 5% $C0_2$. 50 ng /ml EGF were used as chemoattractant in the lower compartment of the chambers. EGF was omitted in controls. After incubation, the cells of the upper surface of the filters were removed whereas those of the lower surface were stained and counted in 10 HPF, and their migration capacity was expressed as number of cell/mm^2+SD in triplicate experiments.
Results: Microcitoma cell line cells were significatively more numerours in lamin α2 chain coated filters after incubation with EGF (175+25) than in control assays without EGF(17+4). Moreover, this difference was more significant than that observed in laminin (250+9 v.s. 170+4) and fibronectin (25+1v.s. 20±9) coated filters.

Conclusions: In EGF producing tumors lamin α2 chain expression during angiogenesis may favour neoplastic vessels invasion more efficently than lamin and fibronectin.

P-287

Diagnostic value of Surfactant-Apoprotein-A in malignant tumors located in the lungs

Vollmer E.[a], Goldmann T.[a], Galle J.[a], Wiedorn K.H.[a], Deutschbein M.E.[a], Nakashima M.[b], Branscheid D.[b]
[a] Research Center Borstel, Clinical and Experimental Pathology, Germany, [b] Krankenhaus Großhansdorf, Department for Thoracic Surgery, Großhansdorf, Germany

Introduction: By presenting case reports of patients suffering from multiple tumors in the lungs with a questionable origin we show the detection of Surfactant-Apoprotein-A (SP-A) in tumor cells to be useful for diagnosis.
Methods: Formalin fixed, paraffin embedded specimen of different malignancies with pulmonary location were analyzed for the expression of SP-A by the use of PE-10 together with the Thyroid Transcription Factor-1 (TTF-1).
Results: In normal lung areas a distinct staining of the pneumocytes II has been observed, all the control sections of primary and metastatic non-lung-carcinoma-specimen in our study remained negative. The monoclonal antibody PE-10 used in this study provides high specificity when compared to the results obtained with polyclonal antibodies. There were cases with positivity for SP-A even when the tumors were negative for TTF-1.
Conclusion: SP-A detected by immunohistochemistry using PE-10 together with other parameters such as TTF-1 may be a useful tool for individual diagnoses of malignomas located in the lungs with a questionable primary origin.

P-288

Molecular and cellular mechanisms of human endothelium apoptosis in neurohumoral stress

A.F. Yakovtsova[1], I.K. Kondakov[2], I.I. Yakovtsova 1, N.I. Gorgol[1]
[1] State Medical University, [2] Institute of Therapy of AMS, Kharkov, Ukraine

We investigated ultrastructural and biochemical effects of natural and artificial agonists of - and -adrenoreceptors in the vascular endothelium for determination of mechanisms of focal reduce of endothelium (En) in neurohumoral stress in the conditions of isolated perfusion of the dead carotid artery (c.a.). The hour c.a. perfusion with adrenalin (10.6Ì) causes the En focal loss and desquamation. Ultrastructurally En apoptosis appears both in direct cells necrosis and in progressing of En hydrolytic degeneration.
Simultaneous activation of En - and  -adrenoceptors with isoproterenol (I) and phenilefrin (Ph) in equimolar concentrations also increases index of En damage. Addition in perfusion medium of -àntagonist phentolamin or  1 - àntagonist prazozinum, or àdrenoceptors  -àntagonist propranolol (10-6 Ì) completely protects En from damage with catecholamines. Selective  2-adrenoreceptor antagonist yohimbine did not render vasoprotective effects. The analysis of molecular mechanisms of receptor mediated En destruction has shown, that simultaneous activation of  1- and  -adrenoreceptors causes the increase of endocellular concentrations of inositol-3-phosphat, cÀÌP and Ñà2+ions, that results in En construction and development of progressing hydrolytic dystrophy, destruction and desquamation of endothelial cells. The carried out investigation shows, that the phenomenon of a synergy in action of adenilatcyclase system stimulators and phosphoinositide exchange underlines En catheholamine damages during neurohumoral stress, which results in focal apoptosis and destruction of endothelial cells and in increase of permeability of a vascular wall for LDL.

P-289

Pulmonary sarcoidosis with cor pulmonale. Post mortem case report

Yanin V.A., Shirokova N.A.
Mytishchy Clinical Hospital, Moscow Region, Russia

Introduction: Sarcoidosis (Boeck's) is a disorder of unknown etiology, characterized by granulomatous inflammation in the affected organs. The incidence of sarcoidosis in Russia is about 20 per 100,000 of the population. It occurs predominantly between ages 20 and 40.
Case report: 50-years-old female patient died with severe dyspnea. Patient did not call the physician during last years and no x-ray examinations performed. Pathological examination disclosed bilateral lesion in lungs and lymph nodes. Macroscopically there are lots of grayish-white nodules up to 57 mm in diameter scattered throughout the lungs together with fibrosis near periphery of the upper lobe of the lungs, resulting in a honeycomb of air spaces. Regional lymph nodes was a tumour-like. Microscopically lesions was presented by sarcoid non-caseating granulomatous process with lots of the giants cells. Sarcoid lesions are found throughout the interstitial perivascular and peribronchial tissues of the lungs. There was extensive fibrosis of the lungs. Examination of the heart has shown the cor pulmonale. In other organs there are chronic congestion due to right ventricle failure. No sarcoid lesions are found in other organs.
Conclusion: The case we described is quite rare. Diagnosed and treated sarcoidosis allows patients rather long life. There are spontaneous remissions that are sometimes permanent, and only a few instances do the patients run a rapidly progressive, usually to die of intercurrent infections or cor pulmonale due to diffuse lung fibrosis.

P-290

Diffuse pulmonary lymphangiomatosis (DPL)

Yılmazbayhan D, Bilgiç B, Vural S, Öneş Ü, Çelik A.
Medicine Faculty of Istanbul, Department of Pathology Capa, Istanbul, Turkey

Introduction: Angiomatous lesions of the lung are uncommon. Primary lymphatic lesions are very rare and difficult to classify among them. And so we would like to introduce histopathological findings of a case of DPL.
The case:Patient was an 8 years old girl admitted with a pericardial effusion three years ago. Then we lost the patient. In the first

month of the 2001 she came back with dyspnea . She had wheezing, cough and haeomopthysis few times in this period. Diffuse bilateral interstitial pattern in the lung and mediastinal enlargement were detected by CT. After detailed clinical examination, open lung and mediastinum biopsy were performed and haemorragy was noted.

Results: No specific gross features were noted. Histological examination of the lung, anastomosing variably sized endothelial lined spaces along pulmonary lymphatic routes, subpleural and interlobuler septal parts were seen. These spaces were lined by a layer of flattened endothelial cells. Collagen accumulation around the vessels were prominent by Masson-trichrom stain. Spindle cells with oval nuclei, indistinct cytoplasmic membranes were arranged fascicles around the vessels asymetrically. The surrounding pulmonary parenchyma contained intraalveoler haemosiderin laden macrophages and small numbers of interstitial lymphocytes. Immunohistochemically spindle cells were positive with CD 31 and Vimentin and negative with CD 34, Smooth muscle actin, ER, S-100 and HMB-45. In the mediastinum, collagen deposition near pleural surface, vascular channels with small foci of spindle cells were seen.

Conclusion: DPL is a very rare lesion, and must be differentiated from other vascular lesions. In this case mediastinal involvement was prominent and first presentation was pericardial effusion. Histological and immunohistochemical findings were contributed lymphatic origin.

P-291

Difficultites in diagnosis of neuroendocrine lung tumors

Zajęcki Wojciech, Sabat Daniel, Szczurek Zbigniew
Department of Pathomorphology, Medical Faculty in Zabrze, Silesian Academy of Medicine in Katowice, Poland

Introduction: The term neuroendocrine is applied to the group of tumors for which neuroendocrine differentiation is a constant feature seen on morphological ground and proved by ultrastructural and immunohistochemical investigations. Such group of tumors encompasses a broad spectrum of cancers from typical carcinoid to small cell lung carcinoma. The last morphological criteria for diagnosis of moderately differentiated form were established in 1998 by Travis.

Aim: The aim of the study was: retrospective verification of cases primarily diagnosed as typical or atypical carcinoid based on a latest morphological criteria and supported by a immnunostaining with a panel of antibodies for determination of neurosecretory activity; evaluation of differences in a neurosecretory activity of small cell lung carcinoma in various kind of specimens, estimation of p53 protein expression in different groups of lung cancers and determination of their diagnostic value.

Material and methods: The material consists of 25 tumors diagnosed in the years 1989-98 in the Department of Pathomorphology, Silesian Academy of Medicine as typical and atypical carcinoids. Revision of morphological diagnosis was performed on Travis criteria, based on mitotic activity and necrosis. Ultimately, diagnosis was changed in 14 cases. Typical carcinoid primarily diagnosed as atypical made up a half of such cases. To identify "atypical" features responsible for such a primary diagnosis, detailed morphological study with a use of semithin section was performed. Among next cases one case of large cell neuroendocrine carcinoma was diagnosed. Next two cases were reclassified as non neuroendocrine tumors (squamous cell carcinoma and adenoid cystic carcinoma). The materials from last three patients' tumors were too small for immunohistochemical investigations. The great diversity in a morphological structure of atypical carcinoid was found. Immunostainig for neuroendocrine differentiation was performed with antibodies for panneuroendocrine markers (synaptophysin, chromogranin) and for secretory products (calcitonin, bombesin). Reactivity to cytokeratin was also studied.

Results: The study confirmed a high sensitiveness of synaptophysin and chromogranian as neuroendocrine markers in the studied groups of carcinoid tumors. There were differences in immunoreactivity for chromogranin in the groups of small cell cancers depending on a kind of material. Positive reaction was found in 4 per 10 studied bronchoscopic materials and none in poostopertive and autopsy materials. The immunostainig performed with antibodies for calcitonin and bombesin gave only a few positive reactions. A specific form of cytoplasmatic reaction for cytokeratins (known as point or fibrous reaction) was stated in most neuroendocrine tumors. So the study confirmed usefulness of immunostaining for cytokeratin for a differential diagnosis of neuroendocrine tumors especially small cell cancers. Evaluation of p53 protein expression in the studied groups of tumors showed constant lack of activity in typical carcinoid and great diversity of activity in other kinds of tumors.

Conclusions: Detailed morphological diagnosis of neuroendocrine lung tumors is possible when based on postoperative materials, supplementary morphological techniques and immunohistochemical reactions. Cytokeratins, synaptophysin and chromogranin A are sensitive and specific indicators of neuroendocrine differentiation useful in the diagnosis of carcinoid and large cell carcinoma. The results of immunostainig with antibodies to chromogranin are depended on a kind of study material in small cell lung cancer. Evaluation of p53 protein can be useful in cases of carcinoid.

P-292

Neutrophils in human myocardial infarction with and without free wall rupture

Zidar Nina, Štajer Dušan
Institute of Pathology, Medical Faculty, and Centre for Intensive Internal Medicine, University Medical Centre, Ljubljana, Slovenia

Introduction: Experimental studies have shown that neutrophils might play an important role in the pathogenesis of ischemic and reperfusion injury of acute myocardial infarction (AMI). Our aim was to compare histologic characteristics of AMI with and AMI without free wall rupture (FWR), with particular emphasis on the density of interstitial neutrophilic infiltration.

Material and methods This study included autopsy samples of infarcted heart tissue from 60 patients with AMI (30 with and 30 without FWR). Samples from the rupture were not included. On the basis of histologic changes and clinical data, all cases were divided into 3 groups according to the duration of AMI (<1 day, 1–7 days, >7 days). Neutrophils were stained immunohistochemically with antibodies against CD15 and the percentage of the infiltrated myocardium was estimated using an image analysis system.

Results: In AMI which were less than one day or more than 7 days old, we didn't observe any differences in histologic characteristics between cases with and those without FWR. In AMI which were 1–7 days old, we observed a significantly more intensive interstitial neutrophilic infiltration in cases with FWR than in those without FWR. There was no significant difference in neutrophilic infiltra-

tion between patients who received reperfusion treatment and those who didn't.
Conclusion. Our results suggest that intensive interstitial neutrophilic infiltration in AMI might increase the risk of the FWR. We failed to confirm the hypothesis based on experimental studies that reperfusion treatment contributes significantly to the density of neutrophilic infiltration.

P-293

Immunohistochemical examination of p53 protein and the composition of inflammatory infiltrations in tumor front in patients with lung cancer

*Ziółkowski Adam, *Gabriel Andrzej, **Gawrychowski Jacek, *Sabat Daniel, *Gajewska Anna, *Gajda Tomasz
* Chair and Pathomorphology Unit of the Medical University of Silesia in Zabrze, Poland; ** Chair and Clinic of Thoracic Surgery of the Medical University of Silesia in Zabrze, Poland

Aims: The expression of p53 protein antigen and the evaluation of tumor microenvironment inclusive of tumor front grading form a valuable supplement of the classical morphological examination in lung cancer evaluation.
Material and methods: The study included 30 patients with original lung cancer. Postoperative specimens were subjected to standard procedure. Histopathologic types of cancer included squamous cell carcinoma, small cell carcinoma, adenocarcinoma and bronchioloalveolar carcinoma. Immunohistochemical examination was carried out with p53, CD3 and CD20 antibodies (DAKO). Immunohistochemical procedures were applied according to the producer's instructions.
Results: Small cell carcinoma yielded 100% of staining reactions (highest cellular index), squamous cell carcinoma accounted for 85%, while the remaining types for 50%. In adenocarcinoma cases CD 20 phenotype lymphocytes accounted for as much as 50% of the tumor front inflammatory infiltrations. CD20 lymphocytes in tumor front occurred partly in the form of lymphatic follicles. The lowest number of CD20 cells was found in squamous cell carcinoma. CD3 cell tumor front infiltrations were poor in most of the examined specimens. No correlation was found between the differentiation degree and progress stage on the one hand and the number of positive staining reactions on the other.
Conclusions: The examination of protein p53 antigen supplements the routine histopathological examination of lung cancer. More intensive expression of p53 was found in small cell and glandular carcinoma. The intensity of CD 20 cell tumor front infiltrations may prove to be an auxilliary prognostic factor in lung cancer.

P-294

Melanocytes in trichoepitheliomas - trichoblastomas. Are they simple bystanders?

Z. Aly, E.A. Husain, R. Cerio, L. Pozo, S.J. Diaz-Cano
Dept of Pathology, The Royal London Hospital, London (UK)

Background: Epithelial neoplasms with pilar differentiation are relatively rare and represent a heterogeneous group of tumors, which exceptionally reveal pigment. No systematic evaluation of histologic features is available, resulting in a low diagnostic reproducibility. In addition, the presence of melanocytes has not been studied.
Methods: We selected 46 cases of trichoepithelioma/trichoblastoma for which appropriate archival material was available. We systematically evaluated growth pattern (multifocal or not), type of squamous differentiation, cytological evidence of catagen, presence of dual cell population, epithelial and stromal pigment, epithelial and stromal calcification, stromal reaction (myxoid, lamellar fibrosis, hyalinization), nuclear features, and mitotic figure counting/10 high-power fields. The presence of melanocyte was investigated by immunohistochemistry (S100, HMB-45).
Results: A dual cell population was observed in all cases. On one hand, the epithelial cells characterized by bland nuclei and distinct nucleolus. The second cell type shows hyperchromatic spindle nuclei and reveals an irregular interstitial distribution within the epithelial nests. These cells were revealed positive for S-100 and HMB-45. Tumors revealing multifocal growth pattern did show mitotic figures (80%), while mitotic figures were less frequently present in non-multifocal neoplasms (49%). The presence of epithelial pigment also correlated with catagen cytological features (71%). The other histological variables were equally distributed and did not show any correlation.
Conclusions: Melanocyte colonization is a very common finding in trichoepitheliomas/trichoblastomas and can be used as an adjuvant tool to identify these neoplasms. Multifocal growth pattern should be investigated especially in mitotically active neoplasms. The reason of the melanocyte colonization needs further investigations.

P-295

Morphometrical analysis of pigmented skin lesions

Aralica G., Konjevoda P., Štambuk N., Mravunac M., Ćorić M., Seiwerth S.
Institute of Pathology Medical Faculty
and Institute Ruđer Bošković Zagreb, Croatia

Pigmented lesions are the most common skin lesions. Most frequent among them is the common acquired nevus, especially intradermal nevus. Dysplastic nevi are benign lesions, but many studies have shown that they are also very important precursors of malignant melanoma. Nowadays, this is even more significant since the incidence of melanoma is constantly increasing. For this reason, it is very important to develop new methods to recognise the malignant potential of precursor lesions.
PATIENTS AND METHODS: In this study, 20 intradermal nevi, 20 dysplastic nevi and 20 malignant melanoma were analysed. Three microscopical fields from the central part of each lesion were recorded (magnification 40×). Circumference and area of nuclei were measured and a computer net of 10×10 fields applied. The number of nuclei was counted in each net field (PC software ISSA – Vamstec, Zagreb, Croatia). Analysis of the obtained data was performed using Poisson's distribution, machine learning system Weka and neural net aiNet 1.25.
RESULTS: Nuclei of malignant melanoma are the biggest and they have the largest nuclear roundness factor. Dysplastic nevi have the largest number of net fields with high number of nuclei. Poisson's distribution showed that nuclei of examined groups have different way of distribution in space. Machine learning system Weka and neural net aiNet 1.25 gave very high level of accuracy of the classification by using measured parameters (app.95%).

CONCLUSION: Our results indicate that morphometrical parameters combined with complex statistical analysis systems can produce a potentially useful diagnostic help in the analysis of pigmented skin lesions.

P-296

Bénard L., Le Pelletier F., Charlotte F. (1), Becherel P.A., Chosidow O., Frances C. (2), Wechsler J. (3)
(1) Departments of Pathology and (2) Dermatology of Pitié-Salpêtrière Hospital, Paris; (3) Department of Pathology, Henri Mondor Hospital, Creteil, France

Introduction: Subcutaneous panniculitis-like-T-cell lymphoma (SPTCL) is an uncommun cutaneous lymphoma that has been proposed as a distinct clinicopathologic entity. We studied the immunophenotypic and genetic features of fives SPTCL.
Methods: Selected cases concerned lymphomas infiltrating the subcutis in a lobular panniculitis like pattern with hemophagocytosis. The immunohistochemistry studies by paraffin used antibodies against CD2, CD3, CD5, CD7, CD8, TIA-1, CD30, EBV-LMP1. In situ hybridation for EBV was performed in paraffin with probe to latent EBV-encoded RNAs (EBER-1) as well as T-cell receptor gene rearrangement analysis using a PCR with three sets of consensus primers for Vγ and Jγ.
Results: All cases expressed cytolytic granule-associated protein TIA-1 and T-cell-associated antigens with an aberrant expression of CD2, CD3 or CD5. One case was CD8+. None case was positive for EBER-1 latent EBV RNA. T-cell recptor gene was clonally rearranged in all cases.
Conclusion: SPTCL are clonal, EBV-, cytotoxic T-cell lymphomas. The demonstration of clonal TCR gene rearrangements and aberrant phenotype are additional criteria to differenciate SPTCL from other subcutaneous panniculitis etiologies.

P-297

PCNA and Ki67 proliferation markers are associated with prognosis in anorectal malignant melanoma

Ofer Ben-Izhak, Micha Bar-Chana, Louis Sussman, Victoria Dobiner, Judith Sandbank, Manuela Cagnano, Hector Cohen, Edmond Sabo
Departments of Pathology, Rambam Medical Center, Haifa; Hadassa Medical Center; Asaf Harofe Medical Center; Soroka Medical Center; Western Gallilee Hospital; Carmel Medical Center, Israel and the Israel Cancer Registry

Introduction: Anorectal Malignant Melanoma (ARMM) is a rare disease with a very poor prognosis. In an attempt to find clinical and histologic parameters for prediction of survival, 30 patients with ARMM were studied.
Methods: Percent of tumor cells stained for Ki67 and PCNA in paraffin sections was assessed. Mode of treatment (local excision or abdominoperineal resection), attempt for cure as defined by complete tumor excision and absence of distant metastases at presentation, depth of tumor invasion, blood vessel invasion, tumor necrosis, Ki67 and PCNA scores were all correlated with survival.
Results: By univariate analysis, PCNA ($p<0.0001$), Ki67 ($p<0.002$), attempt for cure ($p<0.014$), local excision ($p<0.019$) and depth of invasion ($p<0.028$) were all significantly associated with longer survival. By multivariate analysis only PCNA ($p<0.0003$) was significantly associated with survival, while Ki67 showed significant positive correlation with PCNA ($p<0.0001$). With cutoff point of 40%, patients with lower Ki67 scores showed survival advantage over those with higher Ki67 scores ($p<0.0004$). With cutoff point of 80%, patients with lower PCNA scores showed survival advantage over those with higher PCNA scores ($p<0.0001$).
Conclusions: Ki67 and PCNA immunostaining may be useful for survival prediction in patients with ARMM. The staining for proliferation markers was also associated with depth of tumor invasion. It should be stressed, however, that of the 6 long term survivors for over five year, 3 eventually died of disease, 1 died with recurrent disease and only 2 were disease free survivors (for over 8 years).

P-298

Age related differences in tumors and tumor-like lesions of the skin

Brasanac D., Mitrovic D., Boricic I.
Institute of Pathology, School of Medicine, University of Belgrade, Yugoslavia

Introduction: Analysis of age differences in male and female patients with skin tumors and tumor-like lesions.
Material and Methods: 3785 skin tumors and tumor-like lesions were classified according to their origin and histopathological diagnosis, and correlated with patients' age. Statistical measurements were performed with t-test.
Results: Average age of male patients was 53,2 years and 49,9 years of females ($p<0.00001$). Regarding biological behavior of skin lesions, significant differences in age distribution were noticed among benign lesions as a whole (male 43,2 years, female 41,5 years; $p<0.05$), benign pigmented (30,9 vs. 34,7 years; $p<0.01$) and malignant epidermal lesions (63,6 vs. 69,8 years; $p<0.0001$). Considering a particular histopathological diagnosis, age differences were found among squmous cell carcinomas (63,7 vs. 69,7 years; $p<0.001$), compound nevi (21,6 vs. 29,2 years; $p<0.05$) and molluscum contagiosum (19,5 vs. 47,3 years; $p<0.05$). Comparing the average age of male and female patients with skin tumors on various localizations, statistically important differences were observed in the temporal region (62,5 vs. 52,1 years; $p<0.01$), on ears (64,9 vs. 44,2; $p<0.01$), on the neck (51,1 vs. 45,2 years; $p<0.05$) and in the axillary region (51,9 vs. 38,5; $p<0.05$). In general, male patients were of older age as a group and among those with benign lesions, whereas females were older in cases that belong to benign pigmented (especially compound nevi) and malignant epidermal (particularly squamous cell carcinoma) lesions. Interestingly, male patients with molluscum contagiosum were much younger than females with the same diagnosis.
Conclusions: Statistically significant differences in age distribution related to the histopathological type of skin tumors and tumor-like lesions exist among male and female patients, some of them being caused, probably, by environmental and social factors.

P-299

Transforming growth factor α immunostaining in keratoacanthoma and squamous cell carcinoma of the skin

L. Čabrijan,[1] G. Zamolo,[2] S. Štifter,[2] M. Kaštelan,[1] M. Palle,[1] F.Gruber[1]
[1] Department of Dermatovenerology, Clinical Hospital Centre;
[2] Department of Pathology, Medical School, Rijeka, Croatia

Introduction: Keratoacanthomas may be difficult to distinguish clinically and histologically from squamous cell carcinoma. The aim of this study was investigate the possibility to differentiate the tumors analyzing the expression of tumor growth factor alpha with an immunohistochemical staining.
Method: Formaldehyd fixed and paraffin embedded sections of 20 keratoacanthomas and 20 squamous cell carcinomas were incubated with the TGFα (Ab-2) antibody against transforming growth factor alpha. The primary antibody was then visualized by a secondary IgG antibody and the use of the avidin-biotin-peroxydase complex. to determine if the pattern of transforming growth factor alpha in the tumors.
Results: 90% of the keratoacanthomas showed diffuse immunostaining of the lobules, while in the outermost one or two layers of tumor cells were not stained. Squamous cell carcinoma shows patchy immunostaining in 45% cases and diffuse immunostaining in 55% cases. The outermost one or two cell layers of the tumor lobules expressed the tumor growth factor in all the cases ($p<0.001$).
Conclusion: Our results suggest that transforming growth factor may be a marker for differentiation between keratoacanthoma and squamous cell carcinoma.

P-300

Mohs' micrographic surgery for the basal cell carcinoma treatment

Compañ A., Herrero J., Sancho-Moroder S.*, Sanmartín O.*, Illueca C., Almenar-Medina S.
Department of Pathology and Dermatology*,
Instituto Valenciano de Oncologìa, Valencia, Spain

Background: Mohs' micrographic surgery of facial basal cell carcinoma, recommended for tumors that are recurrent, large or aggressive, ensures a high cure rate with maximal preservation of healthy tissue. Horizontal frozen histologic sections of the excised tumor permit more complete microscopic examination of the surgical margin than traditional methods. Residual tumor is graphically mapped and malignant extensions are pursued with staged excisions until the tumor is removed.
Methods: We prospectively studied 850 patients with basal cell carcinoma using Mohs' micrographic technique.
Results/Conclusions: To achieve radical excision tumors needed and average of 2.8 excisions. The recurrence rate was *5%. Recurrent tumors, morphea-like or fibrosing basal cell carcinoma and long time evolution tumors required the highest number of excisions.

P-301

Chromoblastomycosis in São José do Rio Preto – São Paulo Brazil: clinical, mycology, histopathology and immunocytochemistry characteristics

*Solange Pires D'Avila, **Carla Pagliari,
**Elaine Raniero Fernandes, **Maria Irma Seixas Duarte
* Faculdade de Medicina de São José do Rio Preto – SP,
** Faculdade de Medicina da USP – São Paulo, Brazil

Introduction: Chromoblastomycosis is a fungal infection caused dematiaceous fungi. We purposed to characterise tissue reactions cells mediated in the skin in cases of Chromoblastomycosis, and to correlate clinical forms of Chromoblastomycosis with the tissue reaction.
Methods: We studied 19 patients with Chromoblastomycosis. The biopsy was stained with HE, Giemsa and immunohistochemically using CD45RO, CD20, CD4, CD8, CD68, CD1a, CD34, Il4, Il10, TNF-alfa and INF-gamma antibodies. A semi-quantitative estimative of the cell subsets was obtained by counting positive cells in ten high-power fields (400x) in the inflammatory infiltrates.
Results: The cutaneous lesion presented as verrucous plaque (n=15) and erythematous atrophic plaque (n=4). We observed two types of tissue reaction: **A**) granulomatous reaction with suppurative granuloma in cutaneous lesions presented as verrucous plaque; **B**) granulomatous reaction with tuberculoid granuloma in cutaneous lesions presented as atrophic plaque. The data obtained with the antibodies are described in the table below (mean of positive cells in both groups):

Cases	CD45RO	CD20	CD4	CD8	CD68	CD1a	Il-4	Il-10 alfa	TNF-gamma	IFN-cells	Mast
A	30.1	25.2	11.1	21.8	22.9	4.1	1	1	1	0	4.4
B	33.5	18.8	14.5	12.2	27.O	5.0	0	0	2	1	2.0

Legend: **A-** cases with suppurative granuloma **B**- cases with tuberculoid granulomas, 0=negative; 1=few positive cells; 2=moderated positive cells; 4=high positive cells
Conclusions: These data suggest that in the cases of **A** group there is a immunological response type Th2, while in the cases of **B** group there is a response type Th1

P-302

Cellular atypia in spitz tumors is mainly expression of apoptosis and regressive features

S.J. Diaz-Cano,1 E.A. Husain,1 Z. Aly,1 R. Cerio,1, A. Blanes2
Dept of Pathology, 1 The Royal London Hospital, London, UK;
2 University Hospital, Malaga, Spain

Background: Spitz tumors are atypical melanocytic lesions that show a prominent vascular pattern and variable lymphocytic infiltrate. The latter two features can be the histological expression of regression, but the kinetic evidence supporting this issue has not been reported to date.
Methods: We selected 42 Spitz tumors (including 6 with atypical features), diagnosed according to standard criteria. No lymph node metastasis or systemic disease was detected in any patient. The kinetic evaluation and expression of E-cadherin were performed by topographic compartments (junctional, and dermal superficial and deep to 0.76 mm), screening the whole compartment in each case. Proliferation was evaluated by Ki-67 index and apoptosis was studied by the in situ end labeling (ISEL) of fragmented DNA using bi-

otin-labeled dUTP and Escherichia coli DNA polymerase I (Klenow fragment). E-cadherin expression was also analyzed by immunohistochemistry. The results were expressed as percentage of positive cells. Variables were statistically compared in each compartment using analysis of variance and Student *t*-test, and considered significant if $P<0.05$.

Results: From the junctional to the deep demal compartment of Spitz tumors, a progressive decrease was observed for Ki-67 index (10.23%, 6.51%, 3.12%), whereas an opposite increasing pattern was revealed for ISEL index (4.38%, 4.73%, 8.35%). Both variables were demonstrated statistically significant.

In general, the E-cadherin membranous expression significantly decreased at the dermal compartments (junctional 53.0%, dermal 36.3%). A subset of Spitz tumor (18%, all non-atypical) revealed an inverted E-cadherin profile by topographic compartments and higher expression at the dermal compartment, however.

Conclusions: The inverted pattern for proliferation and apoptosis by topographic compartments and the up-regulation of apoptosis of Spitz tumors are consistent with an overall regressive lesion that shows a superficial expansive compartment. In this setting, the atypia described must be considered expression of apoptosis rather than evidence of malignant potential. This regressive kinetic profile and the maintained expression of E-cadherin also suggest a low probability of biologic progression for Spitz tumor.

P-303

Morphological aspects in cutaneous mastocytosis

Gioconda Dobrescu*, Irina-Draga Caruntu*, Doinita Radulescu**, Tatiana Tarantu***
*Department of Histology, **Department of Pathology, ***Department of Dermatology, "Gr. T. Popa" University of Medecine and Pharmacy, Iasi, Romania

Introduction: In literature four types of cutaneous mastocytosis have been identified: (*i*) *urticaria pigmentosa* arising in infancy or early childhood without systemic lesions; (*ii*) *urticaria pigmentosa* arising in youth or adulthood without significant systemic lesions; (*iii*) *systemic mast cell disease*; (*iiii*) *mast cell leukemia*. In all these forms the clinical features might be maculopapular, nodular (solitary or diffuse), erythrodermic, bullous or telangiectasic. Despite this diversity the histological picture is identical.

Material and method: There were examined 47 cases, 32 children (16 females, 16 males) and 15 adults (5 females and 10 males). From the clinical point of view, 32 cases – 12 adults and 20 children presented macular lesions, 13 cases of children exhibited papular and nodular lesions, and 2 cases of adults showed erythrodermic lesions. Skin specimens were stained by routine (hematoxylin-eosine, van Gieson, Szekelly) and special methods (PAS, Alcian blue at pH 3.5, Giemsa, Toluidine blue, Spicer). 11 cases were investigated with the electron microscopy.

Results: The granules of the mast cells were not visible in the specimens stained with hematoxylin-eosine. Moreover, their nuclei resemble those of fibroblasts or pericytes and, therefore, the diagnosis might be missed. Nevertheless, the increased amount of melanin (pigmentation) in the basal layer of epidermis offered a significant hint. In the specimens stained with special techniques, the mast cells had a large eosinophilic cytoplasm and a well-defined cell border; characteristic metachromatic granules filled the cytoplasm. Such granules were also present around the cells, due to the process of degranulation. The mast cells were located around capillaries, usually in dense aggregates. Additionally, small amounts of eosinophils could be distinguished. The electron microscopy rendered evident round or ovoid cells, with an abundant cytoplasm, containing double-bounded granules of different sizes and densities. Some granules appeared also in the ground substance from the extracellular space, resulting from the degranulation process. There could also be noticed some other aspects of this process: the mast cells had long, fine villi and the granules were concentrated at the outside surface of the cell. Some mast cells were in close association with lymphocytes and even with Langerhans' cells.

Conclusions: The morphological pattern of cutaneous mastocytosis is monomorphous in spite of the polymorphous clinical picture. The existence of an abundant infiltrate with mast cells (most of them degranulated) and the release of a wide range of chemical mediators in the degranulation process explain the diversity and complexity of the clinical symptoms.

P-304

The features of reparation of chronic cutaneous wounds

Fedorov D., Ivanov A., Ivashkin A., Shinin V.*, Paukov V.
Moscow Medical Academy, Institute of Development Biology*, Moscow, Russia

The chronic cutaneous wounds are characterized by chronic inflammation and disbalance of extracellular matrix's (ECM) components, which leads to the dysfunction of the basal membrane formation and prevents wound defect re-epithelialization.

Aim: The characterization of remodeling ECM in the chronic wounds after covering by cryopreserved allogeneic epidermis during different periods of healing.

Methods: Intraoperational biopsies were received from 25 patients with chronic cutaneous wounds before curing and at the 5th and 15th days after transplantation. Immunohistochemical investigation was performed at the cryostat sections with antibodies against collagen type I (CI), III (CIII), IV (CIV), VII (CVII), laminin (L), tenascin (Tn), aSMA, CD68, CD4, CD8.

Results: Before transplantation in the wound was found decreasing of the CIII in combination with few numbers of myofibroblasts and accumulation of Tn. Monocytes/macrophages cells prevailed in inflammatory infiltrate. On the 5th day after transplantation increasing of CIII was noted, moreover, decreasing of Tn's including into ECM was detected. On the 15th day the ratio of CI and CIII in ECM practically was normal. TN in the ECM was found in minimal quantities. Formation of normal basal membrane, including CIV, CVII and LN was revealed in most cases, but at the same time containing of myofibroblasts was still minimal.

Conclusions: The transplantation of cryopreserved allogeneic epidermis lead to reestablishment of normal deposition ECM components, basal membrane forming and re-epithelialization. ECM remodeling is going practically without wound contraction and scar tissue formation that probably is specific feature of the reparative processes in chronic cutaneous wounds.

P-305

AgNOR analysis of actinic keratosis, basal and squamous cell carcinomas of the skin

G. Giuffrè, M. Lentini, D. Batolo, G. Barresi, G. Tuccari
Department of Human Pathology, University of Messina, Italy

INTRODUCTION: The prognostic value of the quantity of silver-stained nucleolar organizer region (AgNOR) proteins as an independent variable in various kinds of malignancies as well as skin tumours is well known. In order to assess if the AgNOR quantity may represent a predictive tool of the biological behaviour of actinic keratosis (AK), a standardized AgNOR analysis has been performed on 51 cases of AK (12 Stage I, 14 Stage II, 15 Stage III and 10 Stage IV); two cases of AK (1 Stage I and 1 Stage II) were associated with squamous cell carcinomas. In addition, 10 cases of squamous cell (SCC) and 10 cases of basal cell (BCC) carcinomas as well as 10 normal skin fragments were also studied.
METHODS: On formalin-fixed and paraffin-embedded sections, AgNOR analysis was performed according to the guidelines of the Committee on AgNOR Quantification (1995), evaluating the mean area (μm^2) of AgNORs per nucleus (NORA). Differences among categories were assessed by analysis of variance and the Newman-Keuls' test.
RESULTS: A highly significant P value (<0.001) was found in the comparison among NORA values of normal skin (1869 μm^2; SD$\pm$0.332), AK (3.988 μm^2; SD$\pm$0.914), BCC (3.044 μm^2; SD $\pm$0.254) and SCC (5.286 μm^2; SD$\pm$0.920). In AK, a progressive increase of mean NORA values was observed moving from Stage I (3.161 μm^2; SD $\pm$0.600) to Stage II (3.455 μm^2; SD $\pm$0.562), Stage III (4360 μm^2; SD$\pm$0.295), and Stage IV (5168 μm^2; SD$\pm$0.694); highly significant differences (P<0.001) were noted when Stages I or II were compared with Stage III or Stage IV and between these latter. The two cases of AK associated with SCC showed the highest NORA value of corresponding Stage I (4550 μm^2) and Stage II (4960 μm^2).
CONCLUSION: We retain the AgNOR method may be suggested as an objective and inexpensive tool in the assessment of the rank of risk in AK, identifying cases with high proliferative activity that may develop malignant tumours.

P-306

Expression of the histiocytic marker pg-m1 in granuloma annulare and rheumatoid nodules of the skin

Gabriel M. Groisman, Mary Amar, Edmond Sabo[1], Ion Schafer[2]
Hillel-Yaffe Medical Center, Hadera, Carmel Medical Center[1], Haifa and Haemek Medical Center[2], Afula, Israel

Introduction: The expression of the histiocytic marker PG-M1 in granuloma annulare (GA) and other palisaded granulomas of the skin has not yet been studied. We evaluated the reactivity of PG-M1 with a series of GA and rheumatoid nodules (RN), to establish the sensitivity and potential usefulness of this marker in the diagnosis and characterization of these entities.
Methods: Formalin-fixed, paraffin-embedded sections from 30 GA and 15 RN were immunostained with PG-M1. For comparison, additional sections were stained with KP-1 and lysozyme. The stains were recorded as negative, weakly positive (1+), and strongly positive (2+) based upon the opinion of two independent experienced pathologists.
Results: PG-M1 stained mono and multinuclear histiocytes in all the cases of GA (100%) and RN (100%). The average intensity of staining was 1.8 for GA and 1.6 for RN. KP-1 stained 26 GA (86%) and 12 RN (80%). The average intensity of staining was 1.4 for GA and 1.2 for RN. Lysozyme stained 18 GA (60%); the average intensity of staining was 0.9. All RN were lysozyme negative.
Conclusion: PG-M1 is consistently and strongly expressed by the histiocytic population of GA and RN being more sensitive and reliable than other histiocytic markers. We recommend its use in difficult cases suspicious of GA or RN in which the histiocytic nature of the lesion needs to be confirmed.

P-307

The study of skin of human after local radiation influences.

G.I. Hubina-Vakulyck, T.V. Zvyagintseva, E.A. Broshe, V.P. Starenkyy
Department of Pathology, Medical state university, Kharkov, Ukraine

Radiation therapy of cancer of mammary gland is often complicated by development of dry or humid dermatitises, formation of hardly healing ulseres of skin in focus of radiation.
Skin of 14 byopsies is subjected to light microscopy research. Byopsies were got during operation on removing the cancer of mammary gland. Patients were conducted to radiation therapy before operation with variation the absorbed dose varying from 13 Gr. to 60 Gr.
Proliferation of epidermis, acanthosis and vacuolar degeneration of some epidermocytes are noted. Basal membrane of epidermis is thickened and loose. The capillaries of upper layers of derma are with hyperplastic or oppressed endothelium. There are poor perivascular macrophagic-lymphocytic infiltrations, edema and locuses of degeneration in the derma. The quantity of fibroblastes is increased. A dependency between degree of injure of epidermis, components of derma, degree of development of inflammatory reaction, on the one hand, and activities of melaninproduction in melanocyties, presence of melanosomas in epidermocyties and dermal melanophores, on the other hand, is observed. Weak reaction of melanocyties to radiation influence coincides with the non-active proliferation of epidermocyties and maximum injures of skin and minimum quantity of macrophages in infiltration.
It was suggested that the quick exhausting of adaptational hypermelaninproduction is a link located at the very beginning of morphogenesis of the radiation injure of skin.

P-308

Cell kinetic and adhesion features suggest progression at the junctional compartment of high-grade atypical melanocytic nevi

E.A. Husain, Z. Aly, R. Cerio, L. Pozo, S.J. Diaz-Cano
Dept of Pathology, The Royal London Hospital, London, UK

Background: Atypical (dysplastic) melanocytic nevi (AMN) are considered the precancerous lesion of malignant melanomas, but probably represent a heterogeneous condition. The grading system is controversial and the biological potential remains unpredictable. No cell kinetic evaluation by topographic compartments has been reported for these lesions to date.

Methods: We selected 123 lesions, classified into low-grade AMN (92) and high-grade AMN (31) according to standard criteria (junctional asymmetry, presence of suprabasilar melanocytes, and nuclear features such as hyperchromatism, pleomorphism, and prominent nucleolus). The kinetic evaluation and expression of E-

cadherin were performed by topographic compartments (junctional, and dermal superficial and deep to 0.76 mm), screening the whole compartment in each case. Proliferation was evaluated by Ki-67 index and apoptosis was studied by the in situ end labeling (ISEL) of fragmented DNA using biotin-labeled dUTP and Escherichia coli DNA polymerase I (Klenow fragment). E-cadherin expression was also analyzed by immunohistochemistry. The results were expressed as percentage of positive cells. Variables were statistically compared in each compartment using analysis of variance and Student *t*-test, and considered significant if $P<0.05$.

Results: Proliferation was mainly restricted to the junctional compartment in high-grade AMN (junctional 5.89%, dermal 0.1%), whereas no significant differences by compartments were detected in low-grade AMN (junctional 3.73%, dermal 5.28%). ISEL index was significantly lower at the junctional compartment of high-grade AMN (2.21%) than at the dermal one of high-grade AMN (4.01%). No significant differences were observed for ISEL index by compartments in low-grade AMN (junctional 4.39%, dermal 4.45%).

E-cadherin revealed membranous pattern and preferential expression at the junctional compartments (82.6% vs. 59.2% for dermal), especially for low-grade AMN (87.2% vs. 73.1% for high-grade AMN).

Conclusions: Both kinetic features (maintained proliferation and down-regulated apoptosis) and decrease expression of E-cadherin at the junctional compartment of high-grade AMN are consistent with tumor cell progression. In contrast, low-grade AMN reveals features of a regressive lesion with low progression potential.

P-309

The stromal-epidermal interaction in chronic wound healing

Ivanov A., Fedorov D., Shinin V.,* Vasiliev A., * Paltsev M.
Moscow Medical Academy, Institute of Development Biology*, Moscow, Russia

Impaired re-epithelialization is a hallmark of chronic wounds, which is seen in both clinical studies and in animal models of impaired healing

Aim. To investigate the role of stromal components and keratinocytes in chronic wounds healing.

Methods: We studied the effect of cryopreserved allogeneic epidermis for healing of skin ulcers in 23 patients and alkali burns of cornea in 24 rabbit eyes. The zone of injury in eye preliminary was filled with cultured fetal allogeneic fibroblasts into collagen (FAFC). The cellular markers and extracellular matrix components were detected by immunohistochemical method.

Results: The network rich in tenascin and monocyte/macrophage infiltration in derma and FAFC were found on day 5 of treatment. In zone of dermo-epidermal contact and in FAFC-epidermal contact appeared thin layer contained laminin and merosin. Strong expression of $\alpha_2\beta_1$ (VLA-2) and $\alpha_6\beta_1$ (VLA-6) was detected in keratinocytes. Separate basal keratinocytes, which expressed cytokeratins 10/13 migrated into derma and FAFC. The formation of basement membrane which contained collagen type IV and VII in skin and only collagen type IV in eye was observed on day 10 in skin and day 14 in eye accordingly. In the same time allogeneic keratinocytes disappeared in derma and FAFC, and the substitution of allogeneic epidermis by host keratinocytes and corneal epithelium began. Complete re-epithelialization without scar was detected on day 24 in skin and on day 30 in eye accordingly.

Conclusion: The formation of provisional basement membrane by dermal or cultured fibroblasts and allogeneic keratinocytes; remodeling of extracellular matrix are important factors for correct epithelialization during the process of wound healing.

P-310

Immune deposits in chronic urticaria

Izidor Kern[1], Mitja Košnik[1], Alenka Vizjak[2], Vesna Jurčrič[2]
[1]University Clinic of Respiratory and Allergic Diseases Golnik;
[2]Institute of Pathology, Medical Faculty Ljubljana, Slovenia

Introduction: Chronic urticaria is characterised by appearance of widespread pruritic, erythematous wheals that blanch with pressure for at least six weeks. Autoimmunity and immune complex mediated complement activation have been assumed to be involved in the pathogenetic mechanism. Aim of the study was to analyse immune deposits in skin biopsies in comparison to particular histopathologic categories.

Methods: The study included 47 consecutive biopsies of clinically involved skin in 41 patients with chronic urticaria. The formalin fixed and paraffin embedded specimens were stained by HE, acian blue and Giemsa for light microscopy examination. Deposits of IgA, IgG, IgM, C3 and C1q components of complement, and fibrin/fibrinogen were assesed in frozen samples by imunofluorescence microscopy.

Results: Granular and/or linear immune deposits were found in 37.5% in normal skin, in 69.2% in supeficial perivascular dermatitis, in 83.3% in suspicious vasculitis and in 100% in vasculitis. In all categories IgM and C3 were the predominant immune reactants. Full-house immunofluorescence was found associated with superficial perivascular dermatitis and vasculitis. The intensity of immune deposits in the blood vessels, at dermo-epidermal junction, and along connective tissue fibres increased from normal skin, to superficial perivascular dermatitits and vasculitis, being the most intense in vasculitis.

Conclusion: In this study, we cofirmed the association of frequency and intensity of immune deposits with histomorphologic lesions. The frequent occurrence of extracellular immune deposits in the skin of patients with chronic urticaria suggests deposition or in situ formation of immune complexes and possibility of binding of autoantibodies to still undefined autoantigens.

P-311

The role of basic fibroblast growth factor receptor (bFGFR) and c-kit receptor in progression of cutaneous melanocytic lesions

E. Kotiloğlu, H. Kaya, S. Sezgin, G. Ekicioğlu
Dept. of Pathology, Medical School, Marmara University, Istanbul, Turkey

There is an interaction between the cytoskeletal proteins and extracellular matrix through cellular membranous ligands. This interaction is supposed to be the most important factor in cell migration and its metastatic potential. The largest group of such cytoskeletal proteins are tyrosine kinases. In this study, we aimed to investigate

the role of two mreceptors related to this group, namely basic fibroblast growth factor receptor (bFGRF) and c-kit proto-oncogene receptor in progression to malignancy and the metastases of melanocytic lesions. The study group was composed of compound nevi, vertical growth phase malignant melanomas (MM) and metastatic MM with 12,12 and 15 cases respectively. Sections from representative paraffine blocks were stained by PAP method, using DAB as chromogene. The staining resuts were evaluated as absent, +1-faint and +2-strong reactivity. Immunreactivity of bFGFR was scored as none or +1 in compound nevi, +1 and/or +2 in primary and metastatic melanoma cases whereas c-kit immunreactivity was observed in none of the groups except +1 pozitivity in 2 cases of primary MM. Therefore, we concluded that bFGFR synthesis is important in progression to malignancy but its immunreactivity is not different in local extension or metastases.

P-312

Microsatellite analysis in cutaneous malignant malanoma

Massi D., Sardi I.*, Franchi A., Urso C.^, Borgognoni L.°, Salvadori A.^, Giannini A.^, Reali U.M.°, Santucci M.
Departments of Human Pathology and Oncology, and *Clinical Physiopathology; Medical Genetics Unit, University of Florence; ^Departments of Anatomic Pathology – Dermatopathology Section, and °Plastic and Reconstructive Surgery, S.M. Annunziata Hospital, Florence, Italy

Introduction: Alterations of the repetitive nucleotide sequences or microsatellites have been recently identified in a variety of human tumors but the frequency of microsatellite alterations in sporadic melanoma has not been investigated in depth.
Methods: Twenty-one consecutive patients with sporadic cutaneous melanoma were enrolled in the study. For molecular analysis, DNA was extracted from microdissected paraffin or frozen sections (12 μm thick) adjacent to those examined histopathologically obtained from the primary melanoma, its positive sentinel lymph nodes (1 case) and metastasis in transit (1 case). The following microsatellite markers were evaluated: D2S2182; D2S2291; BAT25; IFN-α; D9S156; D9S171; D16S260; D21S1245; D17S250; D17S261; TP53. Samples were scored for alterations (presence of new alleles [shifts] or loss of heterozygosity [LOH]).
Results: We found LOH or alterations by microsatellite analysis in the primary tumor DNA of 4 (19%) melanomas. Among these, 1 case showed alteration at marker D17S261 (at 17p12) whereas in another case alterations at three loci, i.e., D2S2182 (at 2p16), D2S2291 (at 2p16) and D9S171 (at 9p21) were found. The third patient demonstrated alteration at locus D9S171 (at 9p21) identical to the primary tumor DNA in the histologically positive SLN. The fourth case was characterized by alterations at D2S2182 and D17S261 (at 17p12) whereas the corresponding in transit metastasis showed the same alterations of the primary tumor and an additional alteration at IFN-α (9p21).
Conclusion: Our data suggest that microsatellite alterations occur in a proportion of sporadic melanoma and alterations at chromosome region 2p16 and 9p21, which encompasses the tumor suppressor gene $p16^{ink4}$, represent significant events in this setting. Genetic analysis of the corresponding metastatic lesions revealed that the same microsatellite alterations of the primary tumor occur but also additional genetic changes may develop during disease progression.

P-313

S100B positive macrophages in resistant fungal infection

McNutt N.S., Cuevas-Santos J., Contreras F.
Cornell Weill Medical Center, New York, NY; Hospital La Paz, Madrid, Spain

Introduction: S100B is the "S100 protein" commonly detected by commercial antibodies for diagnostic use. S100B+ (CD1a–) macrophages are in Rosai-Dorfman Disease, some xantho-granulomas, lepromatous leprosy, and mycobacterial infection in HIV+ patients. The positive macrophages are globular with abundant cytoplasm and single to multiple nuclei. We have examined cutaneous fungal infections.
Methods: Selected for study were one patient with recalcitrant chronic chromoblastomycosis (Fonsecaea pedrosoi), two patients with lobomycosis (Loboa loboi), and one patient on steroid therapy with Majocchi's granuloma. Routine paraffinized tissue sections were immunoreacted to detect S100B protein, CD68, and CD1a. The antibodies were localized by an alkaline phosphatase method using a red chromogen or by avidin-biotin-peroxidase methods using diaminobenzidine, including positive and negative controls.
Results: Granulomas containing F. pedrosoi were strongly S100B+ in mononucleated and multinucleated macrophages. These cells were strongly CD68+ (CD1a–). The Majocchi's granuloma had abundant S100B+ CD1a– multinucleated giant cells. In chronic lobomycosis, the granulomatous infiltrate contained a few S100B+ macrophages. In acute lobomycosis, the granulomas were negative for S100B. Control Langerhans cells were S100B+CD1a+. **Conclusion**: S100B+ (CD1a–) macrophages are found in certain chronic fungal infections, suggesting that they are associated with a partial immunodeficiency state.

P-314

Survival analysis of the patients with uveal malignant melanoma

Mihaela Mera, Mihai Calugaru*
Department of Pathology, * Department of Ophtalmology, University of Medicine and Pharmacy, "Iuliu Hatieganu", Cluj, Romania

Purpose: Survival rate estimate in patients with uveal malignant melanoma.
Methods: 100 cases of uveal malignant melanoma were retrospectively reviewied clinically and histopathologically. Survival rate assessment of the patients was carried out by means of uni and multivariate analysis. Univariate evaluation was performed using the Kaplan-Meier's method and multivariate analysis by means of the proportional hazards model of Cox. Results: Univariate analysis disclosed some significant factors predicting suxvival rates such as: the period of time elapsed between occurring the first disease symptoms and the objective appearance of uveal melanoma, personal history connected with melanoma, the size, shape and extrascleral extension of the tumor, the Callender's cell type, the reticulin and melanin amount existing within the tumor, the necrosis extension into the tumor and development or not of the metastases. Multivariate analysis succeeded in disclosing a hierarchy of factors predicting survival rates headed by the histopathologically necrosis cell type.

Conclusions: There are not significant differences between sexes, different groups and professions with regard to survival rates of the patients with uveal malignant melanoma. Multivariate analysis represents the main means of assessment of the part played by a combination of different prognostical factors in survival of uveal malignant melanoma patients.
Keywords: uveal malignant melanoma, survival rate, prognostical factors, uni and multivariate analysis.

P-315

Discriminant analysis of image karyometric variables in benign and malignant melanocytic skin lesions

Mijovic Z, Kutlesic C, Mihailovic D
Institute of Pathology, University of Nis, Serbia, Yugoslavia

Background: Making a morphologic distinction between malignant melanoma and benign nevi is frequently difficult. Because the differential diagnosis of melanocytic tumors is subjective, we performed a quantitative analysis with the aim to identify which of 7 nuclear morphometry-related variables are of diagnostic value in distinguishing benign from malignant melanocytic lesions of the skin.
Material and Methods: At Institute of Pathology, University of Nis formalin-fixed, paraffin-embedded skin biopsies from 23 cases of benign nevi and 25 cases of primary malignant melanomas were retrieved. Specimens were routinely stained with hematoxylin and eosin (HE), and analyzed using a computer-assisted interactive image analysis system Lucia M 3.51 ab (Nikon). Nuclear area, equivalent diameter, volumen of equivalent sphere, perimeter, mean chord, circularity and integrated optical density were estimated after editing of binary image.
Results: In univariate analysis, 6 features were found to be significantly different between benign and malignant groups ($p<0.0001$); all measured nuclear variables (except circularity) were higher in malignant melanomas. No significant differences were found among lesions with respect to nuclear shape. Using discriminant function analysis, a correct diagnosis was achieved in 95,8% of benign nevi cases and 84% of malignant melanoma cases. The best discriminant variable is nuclear area.
Conclusion: This study reveals that image analysis is diagnostically relevant to the evaluation of melanocytic lesions of the skin. The area of nucleus appeared to have potential for differentiating benign from malignant tumors and can be estimated in the course of routine histology.
Keywords: Image analysis; malignant melanoma; benign melanocytic nevi

P-316

Expression of fibronectin and tenascin in skin tumors: its meaning as a diagnostic and prognostic tool.

J.A. Ortiz-Rey, J.M. Suárez-Peñaranda*, C. Álvarez, I. Antón, P. San Miguel, I. Muñoz-Barús*, M.S. Rodríguez-Calvo*, A. De la Fuente
Department of Pathology, POVISA (Vigo); *Institute of Legal Medicine, Santiago, Spain

Introduction: Fibronectin (FN) and tenascin (TN) are glycoproteins of the extracellular matrix that mediate cell-matrix adhesion and modulate cell behaviour.
Methods: We analysed the expression of FN and TN in 35 skin tumors from the files of Povisa: basal cell carcinomas (BCC) (circumscribed and infiltrative subtypes); actinic keratoses (AK) and squamous cell carcinomas (SCC); and mesenchimal tumors (MT) (dermatofibromas, leiomyomas, neurofibromas). Formalin-fixed paraffin-embedded sections were stained with monoclonal antibodies (Dako) with the streptABC method.
Results: A more intense dermal staining for FN and TN was observed in SCC than AK, and in infiltrative (85%) than circumscribed BCC. MT showed a positive reaction in all of the cases except 80% of neurofibromas, negative for TN.
Conclusion: The differences in staining in SCC versus AK reflects the implication of matrix molecules, like FN and TN, in tumor cell spreading. In BCC the overexpression of FN and TN could be a marker for predicting an aggressive behaviour. With regard to MT, immunohistochemical detection of these molecules cannot help in the differential diagnosis of spindle cell lesions: overexpression of FN and TN occurs as an unespecific reaction of the stroma against a variety of tumors.

P-317

Photodynamic therapy of dermatological lesions

Osiecka B.J.*, Ziółkowski P.**, Woźniak Z.**
Departments of *Histology and Embryology, and **Pathology, Medical University of Wrocław, Poland

Introduction: The main disadvantage of systemic PDT is skin photosensitivity. Therefore,in the last years topical application of photosensitizers, e.g. ALA, gained interest. In present study, we treated 8 patients: 7 with BCC (total – 10 lesions) and 1 with SCC (single lesion). All lesions were located on face. A 20% ALA ointment was applied under occlusion for 5–6 h and then skin was exposed to 630 nm from halogen lamp (total light dose from 80 to 100 J/sq.cm). Treatments were delivered once or 2–3 times until complete clinical disappearance of lesions was observed.
Results: All lesions clinically disappeared following single or after 2–3 treatments within 7–10 months. All cases were followed-up for another 12 months and no tumor recurrence has been observed during this time period. No side-effects has been noticed at time of light irradiation and later, except for slight edema, erythema and pain around the treated lesions.
Discussion: Our results suggest that ALA-PDT is very effective method of treatment of malignant skin tumors with very good cosmetic outcome. The results of our treatment stay in agreement with other investigators data.

P-318

Cytoplasmic accumulation of PNA-binding glycoconjugates in primary melanoma cells a rare finding without any correlation with tumor thickness and/or clinical outcome

E. Pasmatzi[1], C.D. Scopa[2], A. Monastirli[1], S. Georgiou[1], P. Spiridonos[3], G. Nikiforidis[3], J. Varakis[4], D. Tsambaos[1]
Departments of Dermatology[1], Pathology[2], Medical Physics[3] and Anatomy[4], University of Patras, Greece

Introduction: Lectins are proteins or glycoproteins of plant or animal origin which can specifically bind to particular carbohydrate

residues and are used for their biochemical and histochemical demonstration. Recently, it has been reported that cytoplasmic PNA-binding glycoconjugates represent an important tool for the differential diagnosis between melanocytic nevi (MN) and primary malignant melanoma (MM) and for the prognosis of MM, as well.
Methods: In the present paper we investigated the cytoplasmic PNA-binding pattern in formalin-fixed and paraffin-embedded 4μm sections of 76 MN and 68 MMs by employing the avidin-biotin-peroxidase complex and image analysis techniques.
Results: PNA-reactive melanocytes were not found in MN, whereas, cytoplasmic accumulation of PNA-reactive material was rarely observed in MMs even subsequent to incubation with neuraminidase. Neither the percentage of PNA-positive cells nor the quantity of the accumulated material revealed any statistically significant correlation with MM thickness and/or clinical outcome.
Conclusions: Our results indicate that cytoplasmic accumulation of PNA-binding glycoconjugates cannot be regarded as a reliable marker for the differentiation of MN from MM and for the prognosis of MM.

P-319

P21 $^{WAF1/CIP1/SDI1/PIC1}$ and bax expression in malignant melanomas: Correlation with histologic prognostic parameters

Poyraz, Aylar, Akyurek, Nalan, Işık, Ipek, Erdem, Ozlem
Department of Pathology, Gazi University Medical School, Ankara, Turkey

Introduction: The main objective of this study was to analyze the role of p21 and bax expression in the prediction of biological behavior of cutaneous malignant melanomas.
Methods: 48 primary cutaneous malignant melanomas were stained with p21 $^{Waf1/Cip1/Sdi1/Pic1}$ (DCS-60.2) and bax (2D2) immunohistochemically and cases were analyzed for the presence of a correlation between p21 and bax expression and following prognostic histological parameters: tumour type, depth of invasion according to Clark, tumour thickness according to Breslow, angiolymphatic invasion, mitotic index, growth phase, dermal lymphocytic infiltrate, superficial ulceration and stage according to American Joint Committee Cancer staging system.
Results: p21 expression was detected in 22 (46%) of 48 cases and found to be significantly correlated to the depth of invasion and mitotic index among other prognostic parameters. However, bax was expressed in 32 (67%)of them and showed significant correlation with tumour thickness, Clark level, growth phase and mitotic index. Clark level III, IV, V tumours expressed significantly higher bax positivity than Clark level I, II (p: 0.003). Similarly, vertical growth phase melanomas had higher bax activity than radial ones (p:0.004) its expression was low in lentigo maligna melanomas. But no significant correlation was found between bax expression and tumour type, angiolymphatic invasion and AJCC staging system.
Conclusion: Our study suggests that both bax and p21 might have a role in tumorogenesis and progression of cutenous malignant melanomas.

P-320

Neuroendocrine differentiation in infiltrating basal cell carcinoma

Sakız D., Sungun A., Arabalı A., Evren I.
Department of Pathology, Sisli Etfal Training and Research Hospital, Istanbul, Turkey

Introduction: Basal cell carcinoma (BCC) is one of the most common tumor of the skin. Many of them attempt to differentiate along adnexal structures. Up to date there are limited number of studies about neuroendocrine differantiation of BCC. In these studies, although the argyrophilia may seem to be a relatively common finding for identification of this condition, immunoreactivity for neuroendocrine markers is exceptionally rare. Infiltrating basal cell carcinomas are locally agressive tumors and tend to show local recurrence.
Methods: Paraffin sections of 32 randomly chosen infiltrative basal cell carcinomas were immunohistochemically evaluated for the expression of neuron-specific enolase (NSE), chromogranin-A and synaptophysin.
Results: The positive reaction was detected in 10 of 32 cases with NSE. Focal positive reaction was detected in 8 of 32 cases with NSE, 9 of 30 cases with chromogranin-A and 2 of 27 cases with synaptophysin.
Conclusion: Our results suggest that neuroendocrine differentiation is not rare in infiltrating BCCs. Further studies with larger series are needed to demonstrate the relationship between neuroendocrine differentiation and tumor recurrence.

P-321

Intraepidermal merkel cell carcinoma: A case report

Sakız D., Sungun A., Demirkesen C., Livaoglu A.
Department of Pathology, Sisli Etfal Training and Research Hospital, Cerrahpasa Medical School, Istanbul, Turkey

Introduction: Merkel cell carcinomas (MCC) are neuroendocrine tumors of the skin which rarely exhibits focal or extensive intraepidermal spread.
Case Report: We present a case of intraepidermal MCC with dermal involvement in a 70 years old female. The tumor was located on the leg. Incisional biopsy was interpreted as basosquamous carcinoma. The tumor shows marked epidermal hyperplasia, focal squamous cell atypia and intraepidermal and dermal involvement. In focal areas glandular differentiation was observed. Tumor cells were argyrophilic with Grimelius reaction. Immunohistochemically , positivity for cytokeratin (AE1/AE3), cytokeratin 20, epithelial membrane antigen and focal positivity for synaptophysin, chromogranin-A and neuron-specific enolase was obtained.
Conclusion: Although MCC could be diagnosed easily with the histopathological and immunohistochemical features, it should be kept in mind that intraepidermal tumor growth may lead to misinterpretation, especially in incisional biopsies.

P-322

Cutaneous osteogenic melanoma. Positivity of melanocytic markers in the osteocartilaginous component

Santonja C., Granados R., Rodríguez-Justo M., Aramburo J.A.
Department of Pathology, Hospital Universitario de Getafe, Madrid, Spain

Introduction: Osteocartilaginous differentiation in malignant melanoma of the skin is a very rare occurrence, with a total of 19 cases described in the english language medical literature. The pathogenesis of this component has been controversial since, in most reported cases, immunohistochemical data have not included specific melanocytic markers.
Methods: A 57-year-old man had an ulcerated, exophitic grayish 4.0×3.0 cm mass on the skin of his left calcaneal region, of one-year duration. The clinical diagnosis was a pyogenic granuloma or a squamous cell carcinoma. A punch-biopsy was followed by wide local excision.
Results: The lesion consisted of an acral lentiginous malignant melanoma, Clark level IV, Breslow index 8.0 mm. The invasive cellular component was spindle-shaped or epithelioid, and lightly pigmented. In the mid-dermis, there was a focally calcified osteocartilaginous and mixoid nodule, composed of spindled or polygonal atypical cells surrounding islands of osteoid, with areas of well-formed bony trabeculae. These atypical cells were immunoreactive for S-100 protein, HMB45 and Melan-A. Thirty-three months after diagnosis, the patient developed metastases to two left inguinal nodes, with epithelioid and spindle cell appeareance. He is currently alive with metastatic visceral involvement 45 months after presentation.
Conclusion: Our immunohistochemical findings further support the pathogenic hipothesis that the osteocartilaginous nodules in osteogenic melanoma are the consequence of mesenchymal differentiation by melanoma cells.

P-323

Morpho-ontogenetic data supporting the interpretation of fetal skin biopsy

Nadia Schmidt, Renata Vasiu*, Antonia Popescu**
Department of Anatomy and Embryology, *Department of Pathology, **Department of Neonatology, University of Medicine and Pharmacy, "Iuliu Hatieganu", Cluj, Romania

Fetal skin biopsy allows prenatal diagnosis of serious diseases: oculocutaneous albinism, epidermolysis bullosa (Herlitz disease) or the confirmation of mosaicism cases (trisomy 22). The embryological origin of the tegumental system is double: the ectoderm for the epiderm and the mesoderm for the derm and hypoderm. Between the two components of origin, a close inductive interaction is manifest, which regulates very accurately the quantity and quality of tegumental morphogenesis. Neural crests also play an important role in skin structuring. The morphological study of skin was performed on 5 human subjects (3 males and 2 females – abortions of maternal etiology) with gestational ages between 10 and 14 weeks. Skin flaps were taken from the lower facial, anterior antebrachial, anterior thigh regions as well as from the antero-lateral abdominal wall. Histological preparations were stained with hematoxylin-eosine, orcein, Sirius red. The sections were studied and photographed using a microscope Amplival Carl Zeiss-Jena. On the surface of fetal skin, at the level of all investigated areas, the periderm is covered with keratin. In the epiderm the granular and spinous layers are outlined. In the derm, the papillary layer is clear-cut, while the reticular layer shows blood vessels, nervous filaments and hair follicles in different evolution stages. Skin ontogenesis is a complex phenomenon, which is strictly staged. This phenomenon, initiated as early as the 3rd week of intrauterine life, is in full progress during the stage studied.

P-324

A series of cases with eosinophilic granuloma

Florica Staniceanu*, Carmen Ardeleanu**, Stefan Costinean*, Sabina Zurac*, Luminita Alexandra Oprisan*
* Colentina Hospital, U.M.F. "Carol Davila";
** "V. Babes Institute of Morphopathology", U.M.F. "Carol Davila", Bucharest, Romania

Introduction: We present 5 cases of skin tumours that, after a microscopic analysis, were diagnosed as eosinophilic granuloma, a rare form of Langerhans histiocytosis. For all four cases we used immunohistochemical confirmation, and all our diagnoses were correct.
Methods: Our patients were clinically investigated in Colentina hospital, the clinics of dermatology. The tumours were excised by surgical means and brought in the laboratory of pathology. Here they were fixed in 10% buffered formalin, embedded in paraphin, sectioned at a microtome and coloured in standard HE and Van Gieson colours. Thereafter, we performed immunohistochemical identification for S 100 protein, CD 1a and CD68. All immunohistochemical tests were done at the "V. Babes Institute".
Results: We discovered that, being given the rarity of the Langerhans histiocytoses, the clinician is frequently misled in his interpretation, considering these lesions as nevi or tumours. All our cases had quite characteristic microscopic features. Immunologically, all our microscopic diagnoses were confirmed. Immunohistochemistry was useful not only to rule out other possible diagnoses, but also to establish a link between the histological aspect and immune status of Langerhans histiocytosis cells.
Conclusions: We concluded that, for the clinician there is still place to deepen the knowledge of such lesions. Our microscopic study helped us in clarifying the histological criteria for diagnosing unifocal chronic Langerhans histiocytosis. Immunohistochemistry certified our diagnoses, and helped us identifying, in a more definite way, the microscopic features of Langerhans histiocytosis cell.

P-325

Cooccurence of a Merkel cell carcinoma of the thigh and well-differentiated squamous cell carcinoma of the anus – A case report

Florica Staniceanu[1], Sabina Zurac[1], Carmen Ardeleanu[2], Stefan Costinean[1], Alexandra Oprisan[1], Sorin Simion[3]
Department of Pathology, Colentina Hospital, 2 Department of Pathology, Victor Babes Institute, 3 Department of Surgery, Colentina Hospital, Bucharest, Romania

Merkel cell carcinoma (neuroendocrine carcinoma of the skin) is a rare malignant tumor primary in the skin. Very few cases of associ-

ation between Merkel cell carcinoma and other malignant tumors were reported.
We report the case of a 64 years old woman with an anal tumor (4/3/1.5 cm) and a thigh nodule (5/5/3 cm) that was considered, before surgery, as a soft tissue metastasis of the anal tumor. Because the patient refused any radical treatment, the surgical procedure consists in tumorectomy both of the anal and the thigh tumors.
The microscopic examination of the anal tumor revealed the presence of a well-differentiated squamous cell carcinoma with papillary architecture of the surface. The thigh nodule consists in a dermal and hypodermal proliferation with a diffuse or trabecular pattern of growth; the tumoral cells were small to medium sized with roundish nuclei with fine granular chromatin; many mitoses were identified. Immunohistochemical stains revealed diffuse positivity for cytokeratins 20, cam 5.2, neuron-specific enolase and chromogranin; dot-like positivity for neurofilaments was identified. Based on the morphologic and immunohistochemical features the thigh nodule was considered a Merkel cell carcinoma.

P-326

New molecular makers of the progression of melanoma
Tímár J., Döme B., Somlai B.,* Bánfalvy T., Gilde K.
National Institute of Oncology, Budapest; *Department of Dermato-Venerology, Semmelweis University, Budapest, Hungary

We have found that human melanoma express a unique splice variant of the CD44 molecule, the v3 heparan sulphate variant, both at mRNA and protein levels. Analysis of primary skin melanomas with various clinical outcome and 5 year survival, indicated that CD44v3 is expressed in organ metastatic tumors exclusively and the survival of positive tumors is significantly shortened, suggesting that CD44v3 expression can serve as a marker of organ metastasis.
We have also studied ectopic αIIb(β3) expression. The αvβ3 is constitutively expressed in melanoma, irrespective of the thickness of the tumor, unlike αIIb(β3). The ectopic αIIb is rare in thin tumors but with increased thickness the expression becomes equivalent with αvβ3 suggesting that the increased aggressiveness is associated to the expression of αIIb(β3) integrin.
The motility (and the corresponding metastatic potential) of murine and human melanoma was shown to be regulated by an autocrine cytokine, autocrine motility factor-AMF/phosphohexose isomerase/neuroleukin, the receptor of which is gp78, a new member of the chemokine receptor family. We have studied in clinical material the expression of the AMF receptor in primary skin melanoma. We have shown that AMFR expression is weak in thin tumors and is gradually increased with advanced stage suggesting that the acquisition of the metastatic phenotype frequently requires the expression of this motility factor receptor.

P-327

Merkell-cell carcinoma on the face (case report)
M. Tolovska, S. Duganovska, G. Petrusevska, M. Ristovski, V. Cadieva
Institute of Pathology, Medical faculty, Skopje, R. Macedonia

Merkel-cell carcinoma presents a cutaneous neuroendocrine carcinoma of the skin. It was first described by Toker in 1972 as a trabecular carcinoma and it derived from the cells described by Merkel, which are with neuroendocrine nature.
The aim of this study is to present a rare case of this type of tumor in the biopsy material of the Institute of pathology in Skopje. Specimens were obtained from the maxillofacial surgery clinic with clinical diagnosis of malignant melanoma. The material was formaline fixed, paraffin-embedded and stained by routine HeEo method, with Giemsa and reticulin.
Immunohistochemical studies were performed using avidin-biotin peroxidase complex method of Hsu with following primary monoclonal antibodies: CKWS, CK-19, LCA, CD-3, CD-43, CD-79, vimentin, S-100 protein, chromogranin, NSE, synaptophysin, NF and p53.
Results: The tumor was located in the dermis with extension into the subcutis. The majority of neoplastic cells had an intermediate size, arranged in clusters or with trabecular pattern. In some parts of carcinoma, the cells have a solid diffuse pattern with numerous mitotic figures, necrotic foci and apoptosis.
The tumor cells showed highest immunoreactivity with chromogranin, NSE and vimentin, as well as focal positivity with synaptophysin. This suggested the neuroendocrine origine of the tumor cells. Metastatic deposits were found in one salivary gland.

P-328

Incontinentia pigmenti: A case report
Valentí C., López A., Laplaza Y., Aseguinolaza B.*, Olaizola Y.*
Depts. of Pathology and *Dermatology; Hospital de Zumárraga, Gipuzkoa, Spain

BACKGROUND: Incontinentia pigmenti (IP; Bloch-Sulzberger syndrome) is an uncommon genodermatosis, inherited disorder of skin pigmentation that is associated with skin, dental, skeletal, central nervous and ocular abnormalities. The disease is usually seen in females, as it is an X-linked dominantly inherited disease which is lethal in males.
CASE REPORT: We present a girl with the classical signs of IP with typical histopathology and clinical photography. She presented, in her first month of life, inflammatory vesicular skin changes. Within some weeks, she also showed linear verrucous plaques which changed after into pigmented skin alterations. Pathologic evaluation of the skin lesions confirmed the clinically suspected diagnosis of incontinentia pigmenti. The vesicles seen during the first stage arise within the epidermis and are associated with spongiosis. There are numerous eosinophils within and around them. Results of subsequent neurologic, ophthalmologic, and pediatric evaluations have been normal. In our patient, the spontaneous mutation may have been caused, because her parents were healthy.
CONCLUSIONS: IP is characterized by swirling hyperpigmented skin lesions and associated with a high incidence of systemic defects. Nearly one third of patients present with neurologic complications. Consequently, pathologists, neurologists and dermatologists involved in the care of these patients must be able to identify the cutaneous markers and systemic findings of IP.

P-329

Brooke-Spiegler Syndrome

Sofia Vazquez Navarrete
Anatomia Patologica, Hospital SAS La Linea, Spain

Brooke-Spiegler Syndrome(BSS) is an autosomal dominantly inherited disease characterized by the development of multiple trichoepitheliomas and cylindromas. Sometimes others neoplasm may also occur in BSS as spiradenomas and basal cell carcinoma, parotid basal cell adenomas, milia and organoid nevi. The histogenesis of adnexal tumor is controversial. Spiradenomas and cylindromas have features in common, so they have been regarded as variants of the same neoplasm. In BSS the tumor appeared at puberty and afterwards develops many slow growing lesions which are benign, but they can became malignant. We report a case of BSS in 5 generations of a family. Most of the cases were in the female members. Of the multiple tumors excised we found tricoepitheliomas, cylindromas and spiradenomas. further study of patients with BSS could be helpful in the understanding of the origin of adnexal tumor. As well in these patient is important to explorer for malignant neoplasm and a family study is indicated.

P-330

Recovery of mycobacterium tuberculosis DNA in papulonecrotic tuberculids using the LCx M. Tuberculosis

Vieites B.[1], Rajo M.C.[2], Pérez del Molino M.L.[2], Vázquez-Veiga H.[3], Del Rio E.[3], Antúnez J.R.[1], Forteza J.[1], Suárez-Peñaranda J.M.[1]
Departments of Pathology (1), Microbiology (2) and Dermatology (3), University Hospital of Santiago de Compostela, Spain

Introduction: The identification of mycobacterial DNA, using the PCR technique, comes to support the concept of tuberculid as an immunologic reaction to degenerate dead bacilli. We have used the ligase chain reaction for direct detection of M. tuberculosis in cases of papulonecrotic tuberculids.
Material and Methods: Paraffin embedded tissue from seven biopsies from six patients was tested with the LCx M. tuberculosis test (Abbott). In every case three sections, 10 μm thick, were obtained. After deparaffination with xylene and buffered with sterile phosphate buffer (pH 7,2), the suspension was lysed with sonication for 10 min and 100 μl of supernatant were transferred to a tube containing the amplification mixture. Amplification was performed in a thermal cycler as follows: 94° for 1s, 64° for 1 s and 69° for 40s with a 25°C holding at the end of the last cycle. Positive and negative control cases were processed along with the problem cases. In the negative cases the presence of ligase chain reation inhibitors was ruled out.
Results: We have been able to recover DNA from M. tuberculosis in two out of the seven cases studied.
Comments: The demonstration of fragments of M. tuberculosis DNA in spite of the negativity of techniques for fast-acid bacilli comes to support the thinking of papulonecrotic tuberculid as a hypersensitivity reaction to fragments of bacilli. The negativity of some case could be explained by technical considerations (lack of sensibility) or by the fact that some bacilli proteins, not demonstrable with this procedure could trigger hypersensitivity reaction.

P-331

Atypical dermal nodules in nevi: Their phenotype and normal counterpart

Véronique Winnepenninckx and Joost J. van den Oord
Dept. Pathology, Lab. of Morphology and Molecular Pathology, University Hospitals, Katholieke Universiteit Leuven, Leuven, Belgium

Introduction: Atypical dermal nodules (ADN) or "proliferation centers" are sharply demarcated nodular aggregates of rather large, polygonal, often pigmented cells, that may occur in the dermal part of nevi and that have particularly been observed in congenital nevi. Their worrisome histology may result in a wrong diagnosis of malignancy.
The **aim of this study** was to analyze the phenotypical profile of the large polygonal cells in ADN and to find out whether these cells have a normal counterpart in early congenital nevi.
Materials and Methods: Eighteen nevocellular nevi with ADN and 29 congenital nevi, removed between the first day and the 11th month after birth, were reviewed histologically; semi-serial sections were subjected to immunohistochemistry using the following antibodies: anti-S100 protein, anti-gp100 (HMB-45), NKI-C3, anti-Tyrosinase Associated Protein (TAP), anti-Melan A, anti-c-KIT and the proliferation marker Mib-1.
Results: The large polygonal cells in ADN expressed gp100 (HMB-45), S100 protein and reacted with monoclonal antibody NKI-C3. In addition their was intense TAP and Melan-A expression but no reactivity for Mib-1. Immunoreactivity was usually more intense than that of adjacent small nevus cells. Unexpectedly, this approach allowed us to find cells with similar morphology and phenotype in 39% of congenital nevi without clinical features of ADN where these large polygonal cells formed small clusters or were present as scattered, single cells among small nevus cells.
Conclusions: Our data indicate that ADN have a normal counterpart in congenital nevi, and suggest that ADN represent an abnormal nodular hyperplasia of these cells. This study will allow us to speculate on the relationship of ADN-cells to other melanocytic cells and on the mechanism of ADN-development.

P-332

Hints for the participation of a novel tumor suppressor gene *TTC4*, located at 1p31, in the pathogenesis of malignant melanoma

Christian Woenckhaus[1], Micaela Poetsch[2], John K Cowell[3], Gerd Lorenz[1], Thomas Dittberner[4]
[1] Institute of Pathology, University of Greifswald, Germany; [2] Institute of Forensic Medicine, University of Greifswald, Germany; [3] Center for Molecular Genetics, Cleveland Clinic Foundation, Ohio, U.S.A; [4] Department of Dermatology, University of Greifswald, Germany

Introduction: Deletions of the short arm of chromosome 1 are among the most frequent aberrations in many solid tumors, especially malignant melanoma of the skin. We were able to demonstrate in recent fluorescence in situ hybridizations the loss of 1p31, were a novel tumor suppressor gene *TTC4* has been mapped. Therefore we investigated DNA of paraffin embedded naevi and primary melanomas for mutations in the region of *TTC4*.

Methods: DNA was isolated from paraffin sections comprising 16 typical naevi, 19 atypical naevi and 32 primary melanomas (15 superficial spreading melanomas, 17 nodular melanomas) including a wide range of tumor thickness, 25 metastases and DNA from four melanoma cell lines. Using PCR and direct sequencing analysis we screened for mutations in exons 1 through 10 of *TTC4*.
Results: No mutations could be detected in typical or atypical naevi, but we found *point mutations* in six of 25 metastases, in two of 15 superficial spreading melanomas and in two of 17 nodular melanomas. In two cell lines, a loss of a whole exon could be demonstrated and in one cell line we found a point mutation. In addition, three polymorphisms were found.
Conclusions: Mutations of *TTC4* were distributed over primary tumors and metastases in about the same manner as the deletions found in our previous FISH study. Although case numbers are relatively small we propose a participation of *TTC4* in the pathogenesis of malignant melanoma of the skin.

P-333

Mohs micrographic surgery experience in a french hospital

Zimmermann U.*, Deroide F.*, Clerici T.*, Sei JF.**, Saiag P.**, Franc B.*
* Dept of Pathology and ** Dept of Dermatology,
Centre Hospitalo-Universitaire Ambroise Paré, Boulogne, France

Aims: Mohs micrographic surgery (MMS), not frequently used in France, is a well established treatement of head and neck basal cell carcinoma (BCC). It permits microscopically controlled tumor removal with maximal conservation of normal tissues. We report a French team experience.
Methods: Tumor is removed, the underlying layer excised apart and submitted for frozen sections (FS) oriented on polystyren and cut in subsegments when needed. Different inks identified each margin. FS results represented on a map, permitted complementary resection. FS slides were conserved and compared with final histology.
Results: Since 1996, 95 MMS were performed: 82 BCC, 7 lentiginous melanoma (LM), 3 other skin carcinomas, 3 malignant soft tissues tumors. Excision was complete in one, 2 or 3 to 5 steps in 51, 33 and 11 cases respectively. Subsegments per layer ranged from 1 to 23 (mean 3.2), and 1 to 23 (mean 5.1) per patient. The FS lapse of time, per each step, was 15 to 95 minutes (mean 36.6) and 23 to 140 minutes (mean 60.3) per patient. Final histology showed tumor tissue in 15 cases (16%) due to small margins. MMS was incomplete in 2 cases: 1 patient didn't tolerate the technique ; 1 tumor was too extensive (dermatofibrosarcoma). Three recurrences were noted even with safe margins: 1 LM, 1 adnexial microcystic carcinoma, and 1 BCC.
Conclusion: Due to its time consuming, MMS use is limited to hospitals. Its use in indications others than BCC needs to be cautiously determined through multicentric studies.

P-334

Towards a new understanding and classification of chondrogenic neoplasias of the skeleton

T. Aigner
Cartilage Research-Department of Pathology,
University of Erlangen-Nürnberg, Germany

Despite substantial knowledge on clinical and radiological aspects of chondrogenic skeletal neoplasms, only limited insights into the cellular biology of the tumour variants are available. Established molecular markers for identification and classification of these neoplasms are missing. Our aim was to perform a systematic investigation on the biochemistry and cell biology of chondrogenic neoplasms of the bone.
The hallmark of all differentiated chondrogenic tumours is the presence of chondrocytic cells, expressing collagen type II and other cartilage matrix components. These cells can show the full differentiation potential of physiologic chondrocytes depending on the tumour entity investigated. The phenotypic diversity of neoplastic chondrocytes explains the so far poorly understood heterogeneity of these neoplasms.
Tumour classifications, so far based only on histomorphological criteria were either confirmed or corrected: mesenchymal chondrosarcomas represent the prototypic neoplasm of pre-chondrogenic undifferentiated cells undergoing multifocal chondrocytic differentiation. Enchondromas, osteochondromas and conventional chondrosarcomas are neoplasms of multiphenotypically differentiated chondrocytes. Clear cell chondrosarcomas appear to be neoplasms of hypertrophic chondrocytic cells. A peculiar biology is displayed by dedifferentiated chondrosarcomas, which at least in most cases show neither "anaplasia" nor "dedifferentiation", but most likely "transdifferentiation" of part of the neoplastic cells to a cellular phenotype of a different mesenchymal differentiation lineage. Chondroblastomas do not show any chondroblastic differentiation.
Our study provides molecular markers of chondrogenic neoplasms, which have the potential to be the basis of a new biology-orientated classification of skeletal neoplasms. The expression analysis of matrix genes, in particular of the collagen types, can play herein a leading role in classification and diagnosis, similar to the cytokeratin-subtypes or the CDs (cluster of differentiation) for the classification and diagnosis of neoplasms of the epithelia and the lymphatics.

P-335

Solitary fibrous tumour of the orbit

Andrulis M, Bendix K.
Dept. of Pathology, Kaunas University of Medicine Hospital,
Kaunas, Lithuania

INTRODUCTION: The solitary fibrous tumour (SFT) is a very rare neoplasm that arises most commonly in the pleura. Recent evidence indicated, that it is a tumour that originates from mesenchymal cells and is not restricted to the pleura. When SFT arises in the orbit, it may be misdiagnosed as fibrous histiocytoma, haemangiopericytoma, or other orbital neoplasm.
METHODS: A 50-year-old woman was referred to department of ophthalmology due to impaired vision and exophtalmus of the right eye. Magnetic resonance imaging showed a well-circumscribed lateral mass in the right orbit. Total excision of the tumour was followed by complete recovery.
RESULTS: Histologically, the tumour was a spindle cell neoplasm with alternating zones of hypocellularity and hypercellularity, prominent vascularity with thick-walled vessels, haemangiopericytoma-like pattern and fibrocollagenous stroma with thick and keloid-like collagen. The tumour cells where without atypia and no mitotic figures where seen.

The immunohistochemical profile (vimentin, CD34 positive; CK116, S100, smooth muscle actin, desmin and HMB45 negative) was consistent with those of previously reported cases. Staining with MIB-1 showed a low proliferation rate.
CONCLUSION: The positive immunostaining for vimentin and CD34 facilitates recognition of this tumour. The negativity for antibodies directed against epithelial, muscle and neurogenic tissue provides further support for mesenchymal origin of the SFT.

P-336

Vascular Tumors of the Bones (Clinicopathological study of 35 cases)

Gabriella Arató, Miklós Szendrői
Department of Pathology Faculty of Health Sciences and Orthopaedic Clinic, Semmelweis University, Budapest, Hungary

Primary vascular tumors of the bones are uncommon. The WHO classification of the bone tumors describes benign, intermediate and malignant categories. Benign tumors are the haemangioma, lymphangioma and the glomus tumor. Special rare condition of this group is the massive osteolysis too. Other terms for this lesion include phantom bone disease, disappearing bone disease or Gorham disease. The intermediate catagory includes the haemangioendothelioma and the haemangiopericytoma, while the highly malignant vascular tumor is the angiosacroma.
In our study we have investigated 35 vascular tumors which occurred in the Hungarian Bone Tumor Register in the last 15 years. The 35 vascular tumor represents 1% of all primary bone tumors. The research considered only the undoubted bone origin cases, the uncertain ones were not accepted.
25 cases of the tumors were benign: 23 haemangioma and 2 massive osteolysis. We are discussing these 2 cases in details because of the special radiological and histological appearance. Among the 23 haemangioma 18 developed in the vertebra, which is the typical localisation of the lesion.
6 haemangioendothelioma occurred in the examined period. 3 of the tumors were multicentric. The multiple foci were limited to only one extremity. 2 haemangiopericytoma and 2 angiosarcoma were found.
The clinicopathological study compares the clinical history, radiological features and the histology of the cases, and calls the attention to the diagnostic difficulties.

P-337

Morphological analysis of the healing processes of the defects of the hyaline cartilage of the larynx of the sheep, filled with the composite of carbon fibres with polysulphone

Bielecki Ireneusz**, Sabat Daniel*, Szczurek Zbigniew*, Gierek Tatiana**, Zajęcki Wojciech*, Pilch Jan**
* Department of Pathomorphology, Medical Faculty in Zabrze, Silesian Academy of Medicine in Katowice, Poland;
** Department of Laryngology, Silesian Academy of Medicine in Katowice, Poland

Introduction: The researches carried out for several years showed that carbon fibres have a positive influence on the healing processes of the defects of tissues. The fibres stimulate the proliferation of connective tissue in soft parts and stimulate the bone tissue repair. The combination of the carbon fibres and the polysulphone gives resilience and elasticity to the new material. Material prepared in such a way can be used as an implant in reconstructive surgery. Two new kinds of the carbon fibres with polysulphone were used in the researches: a material consisting of three layers of laminate (group I) and a material consisting of two layers of laminate (group II).
Aim: The aim of the research was a morphological analysis of the healing processes of experimentally made defects of the cartilage of the larynx filled with composite.
Methods and results: After acquiring the permission from the Regional Ethic Commission for Experiments on Animals, the researches were performed on 12 sheep. On surgical operation the piece of the lateral part of the thyroid cartilage of the larynx was removed and the defect was filled with the modeled experimental material and covered with perilaryngeal muscles, subcutaneous tissue and skin. The control group were the sheep of which the defect of the cartilage of the larynx was covered with the layer of perichondrium and perilaryngeal muscles. During the operation the material I was found to be thick, stiff and difficult to model. The material II was thin, resilient and elastic.
Conclusion: It was easy to model it to form a shape similar to the natural shape of the removed cartilage. The morphological analysis was done after 6, 12 and 24 weeks of the experiment. It was proved that the process of regeneration and creation of the connective capsule around the implant was the fastest and the most active in case of the material II. The beginning of the biodegradation of the carbon fibres was also observed in this case.

P-338

Malignant lymphoma initially presenting as a bone mass: Cytologic, histologic, and immunohistochemical study

Chung, Jin-Haeng
Dept. of Anatomic Pathology, Korea Cancer Center Hospital, Seoul, South Korea

Twelve cases of malignant lymphoma initially presenting as a bone mass were reviewed histologically and studied immunohistochemically. Cytologic features were also reviewed if fine needle aspiration(FNA) was done. Ten patients were men, and two women; average age was 33.8 years (range, 15–54). Ten cases were diffuse large B cell type, one was Burkitt's lymphoma and lymphoblastic lymphoma of T-cell lineage, respectively. Histologically, malignant lymphoma of bone seemed to be different from that of other organs to the points of marked squeezing artifact, fibrosis and cluster formations. Therefore, immunohistochemical study was inevitable for confirmative diagnosis. FNA of bone tumors is not only an important procedure of the preoperative diagnosis but also a difficult task for pathologist to interpret it. Ten aspirates from 9 patients were identified and reviewed. Ten cases received the following diagnoses; 4 positive for malignancy (2 malignant lymphoma and 2 malignant tumor, type indeterminate), 2 atypical cell and 4 negative or benign lesion. In the cases diagnosed as malignant lymphoma, abnormal lymphoid cells and identifiable lymphoglandular bodies were present which indicated malignant lymphoma. The other two cases diagnosed as "malignant tumor, type indeterminate" showed large clusters including tumor cells admixed with loose fibrous tissue which would mimic primary bone sarcoma or metastatic carcinoma. False negative (4 cases) diagnoses were attributable to inappropriate

sampling. Rather conservative diagnoses (2 atypical cells) would be made because of pathologist's tendency to avoid false positive results and low suspicion index of NHL of bone. In conclusion, the cytologic diagnosis of malignant lymphoma of bone is difficult compared to other bone tumors. It would be due to the facts that the cellularity of bone lymphoma is not so high and the tumor cells frequently appear as clustered form due to its fibrogenic tendency in bone. Moreover, low suspicion of index for malignant lymphoma of bone is another cause. FNA of NHL of bone represents their histologic features, however, knowledge of these results and appropriate use of immunocytochemistry will be a great help to diagnose malignant lymphoma of bone in cytologic examinations

P-339

Mature retroperitoneal teratoma in adult

El Attar Hicham[1], Azzousi Soufia[1], Benkirane Amal[1], Aboussaouira Touria[2], Sqalli Saida
1. Laboratoire d'Anatomie Pathologie, Centre Hospitalier Universitaire Ibnou Rochd, Casablanca, Maroc ; 2. Laboratoire d'Histologie-Embryologie, Faculté de Médecine et de Pharmacie, Casablanca, Maroc

Retroperitoneal teratomas are rare in adults. We report here a case of primitif mature retroperitoneal teratoma in adult. A 60-year-old woman was presented with general fatigue and being traited for acuate pyélonephrite. The initial diagnosis with sonography and computed tomography suspected an immature retroperitoneal teratoma or liposarcoma. The tumor was resected surgyally and dignosed histologically as a primitif mature retroperitoneal teratoma. The patiente alive since 16 months without adjuvant therapy and nor recurrence. We conclude that histological examination is useful for the retroperitoneal teratoma since it should orientate the adjuvant therapy.

P-340

Morphologic quantitative findings to assess the aggressiveness of giant cell tumors of bone

[1]Doina Lucia Frincu, [1]L. L. Francu, [2]Alice Chirana, [3]Doina Radulescu, [4]C. Ardelean
Departments of [1]Anatomy and [3]Pathology, University of Medicine; [2]Reabilitation Hospital, Iasi; [4]V. Babes Institute, Bucuresti, Romania

Introduction In practice, the giant cell tumors of bone are not homogenous group of tumors which lead to many problems in establishes the stage of tumor and the wright therapy. We undertook the present study for explore the more objective features of giant cell tumor of bone in relation to their aggressiveness.
Material and methods We have studied sixty-two patients with bone tumors that were operated and histopathologically diagnosed as giant cell tumors. The tissue fragments were evaluated following four groups of parameters: 1) the morphometric cells and tissues assessment, 2) the proliferative activity measurements, 3) the quantification of the argyrophilic nucleolar organizer regions (Ag-NORs) and 4) immunohistochimical study used cellular proliferative markers as PCNA and P53. The quantitative microscopic study was made on the representative sections, using an interactive video overlay system. Our results were compared with Jaffe and Lichtenstein's grading system.
Results The clinical and radiological criteria of malignancy and recurrence could not be identified on a histologic and morphometric data. The stereology and mitotic activity index are essential predictive indicators and may be used in early detection of aggressiveness and malignancy, having an independent prognostic value.
Conclusions Our criteria, based on the more objective and quantifiable features, might therefore be of practical value in the assessment of giant tumor of bone.

P-341

Immunohistochemical properties of peripheral nerve sheath tumors and tumor-like lesions

Hirose T., Tani T., Ishizawa K., Sano T.*
Dept of Pathology, Saitama Medical School; *First Dept of Pathology, University of Tokushima, School of Medicine, Irumagun, Saitama, Japan

In addition to epithelial membrane antigen (EMA), erythrocyte glucose transporter (Glut1) has recently been recognized as a specific marker for perineurial cells. Schwann cells are known to be positive for S-100 protein, while endoneurial fibroblasts lack specific markers. To elucidate the cellular constituents of peripheral nerve sheath tumors and tumor-like lesions, immunohistochemical studies were carried out on traumatic neuroma (5 lesions), schwannoma (10), neurofibroma (12), perineurioma (3), malignant peripheral nerve sheath tumor (MPNST) (7) and perineurial MPNST (3). Antigens studied included S-100 protein, EMA, Glut1 and CD34. All antigens were detected by ENVISION method and, in addition, EMA was by catalyzed signal amplification method. Cells constituting perineurium found in traumatic neuromas and neurofibromas were immunoreactive for Glut1 and EMA. Traumatic neuromas contained many CD34-positive spindle cells within the endoneurium of proliferated nerve bundles!
From the topographic location of the positive cells, they seemed to correspond to endoneurial fibroblasts. In Schwannomas predominantly composed of S-100 protein-positive Schwann cells, CD34-positive fibroblastic cells were also present in Antoni B areas. Furthermore, these cells occasionally coexpressed Glut1, suggesting the immunophenotypic transition between perineurial cells and endoneurial fibroblasts in neoplastic conditions. The present study revealed that the principal constituents of neurofibroma were Schwann cells and varied numbers of perineurial cells and fibroblasts were included as well. All tumors of perineurioma and perineurial MPNST were EMA/Glut1-positive and S-100 protein-negative. Lastly, conventional MPNST contained a few EMA/Glut1-positive cells and CD34-positive cells, indicating the heterogeneous cellular constituents of MPNST.

P-342

The accuracy of CT-guided core needle biopsy of bone and soft tissue tumors

[1] Issakov J.,[3] Flusser G., [2]Kollender Y., [4]Merimsky O., [1]Lifschitz-Mercer B., [2]Meller I.
[1] The Departments of Pathology, [3] Radiology, [4] Oncology; [2] The National Unit of Orthopedic Oncology; Sackler Faculty of Medicine; Tel-Aviv University; Tel-Aviv Sourasky Medical Center, Tel-Aviv, Israel

Background: Imaging guided core needle biopsy is today a well established technique for diagnosis of bone and soft tissue tumors

and tumor-like lesions in specialized orthopedic oncology centers. We present the results of CT-guided CNB with assessment of the accuracy of the technique.

Materials and Methods: From July 1998 till October 2000, 215 CT-guided CNB were performed and histologically examined in The Unit of Bone and Soft Tissue Pathology. There were 80 soft tissue and 135 bony lesions. All CNB were performed by one radiologist and the histologic examination was done by one pathologist. Usually, 1-10 cores of bone or soft tissue were sent fixed in formalin to the Department of Pathology. Quick decalcification of bone was performed. Immunohistochemical stains were done when necessary. To assess the accuracy of the procedure, we compared the diagnosis at biopsy with the diagnosis after definitive surgery.

Results: The bone CNB lesions showed in 85 cases malignancy (primary or recurrent bone sarcoma; lymphoma; myeloma; metastatic carcinoma or melanoma). In 30 CNB the histology revealed normal bone tissue. The benign lesions were: chronic osteomyelitis, fibrous dysplasia, epitheloid hemangioma, chondroblastroma, osteoid osteoma and others. In 9 cases the result was inconclusive, and an open biopsy was performed. On the soft tissue lesions, 35 were malignant (25 soft tissue sarcomas, 6 lymphomas, 4 metastatic carcinomas); the other were benign (myositis ossificans, neurofibroma, desmoid tumor, schwannoma, hematoma and others), and 6 were inconclusive and followed by an open biopsy. The CNB histologic diagnosis was compared with that of the open biopsy or the definitive surgery, and the diagnostic accuracy was 90% with only three CNB which were initially diagnosed as benign and turned out to be malignant.

Conclusions: CT-guided CNB of musculoskeletal leisons is a safe and effective procedure which can assure enough and proper material for histologic examination. Tumor sampling is extremely important, especially in soft tissue sarcomas and cores should be taken in different directions including areas of necrosis. The processing is quick, especially for bone CNB, and diagnosis can be achieved within 24 hours. The material undergoes excellent fixation and the immunostains are reliable. The accuracy of CNB is 90%, in our Center.

P-343

Immunohistochemical caracteristics of primary malignant bone tumors

V. Janevska[1], L. Spasevska[1], M. Ristovski[1], G. Zafirovski[2], M. Nikolovski[1], S. Kostadinova[1], J. Zivadinovic[1]
1. Institute of Pathology, 2. Clinic of orthopedic surgery, Skopje, Macedonia

Summary: A histological and immunohistochemical analisis of 73 primary malignant bone tumors was made in order to determinate the immunophenotype of these neoplasms.

Material and methods: The standard procedure of paraffin embedded tissue samples stained with Hemotixilin-Eosin was applied end immunohistochemical dyeing was made using avidin-biotin immunoperoxidase technique with the antibodies CKWS, vimentin, desmin, S-100 protein, NSE and LCA, for 20 osteosarcomas, 20 chondrosarcomas, 23 Ewing's sarcomas and 10 fibrosarcomas. Chromogranin and synaptophysin were added to the group of Ewing's sarcomas.

Results: The presence of CKWS was demonstrated in 3 osteosarcomas, 1 chondrosarcoma and 2 Ewing's sarcomas. Vimentin was present in 17 osteosarcomas, 17 chondrosarcomas, 13 Ewing's sarcomas and 10 fibrosarcomas. Desmin was present in 1 osteosarcoma and 1 Ewing's sarcoma, S-100 protein in 7 osteosarcomas, 17 chondrosarcomas, 10 Ewing s sarcomas and 1 fibrosarcoma, NSE in 12 osteosarcomas, 16 chondrosarcomas, 14 Ewing's sarcomas and 1 fibrosarcoma, osteocalcin only in 10 cases of osteosarcoma. PNET-s showed positivity with vimentin, NSE, S-100 protein and synaptophisin.

Conclusion: The antibody panel of immunohistochemical dyeing proved sucsessful in differentiation of particular types of PMBT within the histological pattern, but it did not provide an indication of strict specifity, except for osteocalcin antibody.

P-344

A case of psammous desmo-osteoblastoma of the skull

Gordana Jurić[1], Spomenka Manojlović[1], Pavle Miklić[2], Kamelija Žarković[1]
[1] Department of Pathology and [2] Department of Neurosurgery, Zagreb Clinical Hospital Center, Zagreb, Croatia

Introduction: Fibro-osteo-cemental lesions of the jaw and skull represent a very heterogeneous group of diseases. The variety of the clinical and histological features sometimes leads to confusion. The separation of these lesions into distinct pathological entities is justifiable on their differences in biological behavior. Psammous desmo-osteoblastoma (PDOB) is described as one of these lesions. PDOB presents as progressively enlarging, usually painless mass of the bone; radiologically exhibits a well-defined area of lytic bone.

Clinical details: A 16-year-old man patient presented with an incidentally detected painless and swelling lesion of the skull situated in the right parieto-occipital region. CT scan demonstrated a hypodense osteolytic area of 2,5-cm diameter with thinning of the outer and inner tables. The radiolucent area had a uniform appearance with focal osteosclerosis. There was no change in the subjacent dura. According to radiographic features suspected osteoid osteoma was diagnosed. Surgical therapy consisted of resection of the lytic area.

Pathologic features: The bone sample was formalin-fixed and decalcified. Paraffin-embedded material showed a tumor with fasciculi and whorls of varying cell density composed of a poorly vasculized fibrous tissue. In these fasciculi basophilic calcified structures were found, frequently spheroidal like, the so-called psammoma bodies. Most of them were concentrically surrounded by spindle cells. Furthermore, foci of osteoid and woven bone trabeculae were also found. Examination of the peripheral areas of the tumor showed no clear evidence of encapsulation, but rather, the new bone formation appeared to be simply reactive.

Conclusion: PDOB is extremely rare tumor and represents a distinct entity occurring in desmal performed craniofacial bones. Based on light microscopical and ultrastructural features PDOB supports the view of the osteogenic histogenesis.

P-345

Multifocal fibromatosis: A case report

Korobowicz E., Radwańska-Konarzewska U., Szumiło J.
Chair and Department of Patomorphology, Medical University, Lublin, Poland

In 1996 she was evaluated for the tumour of the right breast and extraabdominal fibromatosis was diagnosed on the basis histological examination of surgical specimen. Four years later, she was again evaluated for the tumour of the right lung and the right pulmonectomy was performed. Microscopic examination revealed histological pattern of the pulmonary tumour identical with earlier diagnosed breast lesion. This allowed to recognise multifocal fibromatosis. In the case presented herein the recurrent lesion was located proximally to the primary one. Histological features like high maturity, infiltrative growth pattern and sparse mitotic figures, as well as relatively abundant collagen fibres within the tumour permitted us to exclude fibrosarcoma.

P-346

Intraosseous neurilemoma of the fourth unguinal phalanx of the toe of the left foot

H. Mahera[1],E. Chatzigianni[1], J. Sfiniadakis[2], A. Politi[2], A. Skamagis[2]
[1] Pathology Department, District General Hospital of Athens "KAT"; [2]Athens Naval Hospital

Neurilemomas are benign neoplasms that are very rarely encountered in the skeletal system and constitute less than 0.2% of all primary bone tumors. The most common intraosseous location is in the mandible, followed by the sacrum, vertebrae and the tibia. A few cases have been reported in the maxilla or the rib or in other parts of the skeleton.
Our case concerns a 45 year old male who came to the surgeon with a painless tumor mass measuring 4X3X1cm. in the fourth unguinal phalanx of the toe, of about two years duration.At the beginning there was a slightly painful feeling which disappeard after a while as the tumor was progressively enlarging. The radiologic studies revealed a large circumscribed lesion with disappearence of the bone and without capsulation or ossification observed. On cut section the tumor had a whitish-yellow appearance and cystification. Histologically the tumor was composed of multinodular cellular aggregations surrounded by fibrous capsule ,and showed cellular Antoni A and myxoid Antoni B areas together with degenerative changes such as cyst formation and nuclear atypia and thickened hyalinized vessels. The immunohistochemical examination revealed S100 protein positivity. The diagnosis of an ancient neurilemoma was made. He was treated surgically and up to now there is no evidence of recurrence.

P-347

Karyometric differences between benign and malignant fibrous histiocytomas

Mihailovic D, Mijovic Z, Djordjevic B, Stojanovic D, Penev G
Institute of Pathology, University of Nis, Serbia, Yugoslavia

Introduction: Fibrohistiocytic tumors, both benign and malignant, share common light microscopic features characterized by the presence, in varying proportions, of cells with histiocytic and fibroblastic characteristics. Nuclear atypia may be found in benign cases.
Methods: At Institute of Pathology, University of Nis, five cases of benign fibrous histiocytoma and four cases of malignant fibrous histiocytoma were analyzed. After standard fixation, embedding and processing, 4 μm thick sections were stained with hematoxilin and eosin. Karyometric analysis was done by image analyzer MicroImage 4.0 (Olympus, Tokyo), using objective 40×. Nuclei were selected using a grid. After manual editing of image, eleven nuclear variables were estimated: area, mean density, major axis, minor axis, mean diameter, perimeter, roundness, integrated optical density (IOD), fractal dimension, mean feret and margination. In each case, a hundred nuclei were analyzed. Statistical significance of differences was estimated using Mann-Whitney test.
Results: Nuclear area, perimeter and IOD of malignant nuclei (46.27±7.23 μm^2, 29.82±1.12 μm, and 13.76±2.56) were significantly greater than in benign nuclei (32.71±1.25 μm^2, 22.53±0.29, and 5.37±0.39, respectively) ($p<0.05$). Other differences were not statistically significant.
Conclusion: Karyometric analysis revealed significant differences between benign and malignant histiocytomas, and this method may be used in decision making in doubtful cases.

P-348

The presence of propioceptive mechanoreceptors in the remnats of the ruptured anterior cruciate ligament (ACL) as a possible source of re-innervation of the ACL autograft

Pappa L., Georgoulis A.*, Malamou-Mitsi V., Papageorgiou C.*, Moebious U.*, Pappa S., Agnantis N.J., Soucacos P.*
Departments of Orthopaedic Surgery* and Pathology, Medical School, University of Ioannina, Greece

Introduction: Anterior cruciate ligament (ACL) rupture results in progressive instability in the human knee. Loss of propioceptive feedback of the ACL has been proposed as contributing to this decline. Re-innervation that occurs in the ACL graft is a critical factor for the fate of the ACL reconstruction. The aim of this stud was to examine the presence of neural mechanoreceptors in the remnants of the torn ACL, as a possible source of the ACL autologous graft re-innervation.
Material-Methods: The ACL remnants of 25 patients (mean age 15–45 years old) with torn ACL were harvested 3–42 months post injury during the ACL reconstruction. The specimens were immediately stained histochemicaly by using the gold chloride method, or were formalin fixed, paraffin embedded and stained immunohistochemicaly for S-100 and synaptophysin proteins.
Results: Two types of ACL remnant were identified. Torn ACL from the femoral insertion adapted to the posterior cruciate ligament (PCL) in 19 patients (group A), or small mushroom like remnants on the tibial insertion in 6 patients (group B). Large number of mechanoreceptors, especially types I, II and IV was found in all but one patients of group A (mean number: 50/cross section) and very sparse or no-one free neural ends were found in group B (Mean number: 10/cross section).
Conclusion: In young patients with ACL remnants adapted to the PCL, mechanoreceptors exist even 3 years post injury. However

preserving these mechanoreceptors a possible source of re-innervation in the ACL graft will be a benefit to the patient.

P-349

DNA ploidy as a prognostic factor in rhabdomyosarcoma: Analysis of 35 cases with image cytometry and review of literature.

Ziva Pohar-Marinsek, Matej Bracko, Jaka Lavrencak, Marija Us-Krasovec
Institute of Oncology, Depts. of Cytopatology and Pathology, Ljubljana, Slovenia

Introduction: Predictive value of DNA ploidy in rhabdomyosarcoma (RMS) has not been unequivocally confirmed. We correlated ploidy in RMS to other prognostic factors and to patient survival and compared similar studies.

Material and methods: Study included 35 patients, 23 children and 12 adults. We noted tumor size, location, histological subtype and stage of disease. Cell suspensions prepared from parafin embedded tissue of RMS, prior to therapy, were stained by modified Feulgen method. DNA analysis was performed by image cytometer. In statistical evaluation we used Kaplan-Meier procedure, log-rank test, Cox multivariate regession analysis and Chi ^{2} test.

Results: Significant correlation was found between ploidy and patients' sex, age and histological subtype of RMS. Hyperdiploid RMSs were mainly embryonal, among tetraploid and hypertetraploid tumors alveolar predominated. The highest five-year survival rate was among patients with hiperdiploid RMS, followed by those with diploid and tetraploid. The lowest survival rate was among patients with hypertetraploid RMS. For all 35 patients, age was the best prognostic parameter, while morphology was most significant in children. Ploidy was second, however, not statistically significant. We compared 12 articles reporting correlation between ploidy and survival in RMS: 6 found correlation and 6 did not. Main reasons for discrepancies could be: including chemotherapy- treated and non-treated patients, low patient number and differences in grouping DNA histograms.

Conclusions: Our study agrees with those who demonstrated significant correlation between ploidy and survival of RMS patients. Since studies show inconsistencies in precise correlation of ploidy to survival and to other prognostic factors, a cooperative study with large number of patients is needed.

P-350

Early osteoarthritis of the knee mechanically induced in adult lamb

V. Rona,* R. Ramon**, J. Faig,** B. Gerber***
*, **, University Hospital, Barcelona, Spain;
***Swiss Institute of Medical Applications of Laser

OBJECTIVE: The aim of our study was to obtain a convenient model by avoiding common drawbacks of induction of early osteoarthritis.

MATERIAL AND METHODS: In 8 lambs a partial joint cartilage defect of one femoral condyle was created under arthroscopy. Deambulation was allowed afterwards. 4 cases were sacrificed at 28 weeks, 4 cases at 48 weeks.

The condyles and controls obtained from the same animals were divided for histomorphometric and biochemical analysis. Histologic sections of paraffin-embedded safranin-stained cartilage were assessed for 8 morphologic features by a point counting method. The evolution of these features was analyzed in the upper and lower halves of joint cartilage. Fresh cartilage was used for biochemical and water content analysis.

RESULTS: At 28 weeks, both destructive features, such as necrosis or fissures, and clustering of chondrocytes, indicating regeneration, appeared in upper layers. At 48 weeks, former features were more markedly increased and fibrous tissue spanned the joint cartilage reduced in thickness. Vasculature proliferated in deep layers. Global cellularity increased from the beginning, predominantly in superficial layers, although chondrocytes decreased at the surface after an early peak but showed a steady increase in deep layers . Progressive reduction in cartilage matrix , mainly near the surface, was associated with increased dermatansulphat and water contents.

CONCLUSION: Our findings point to a failure of mechanisms involved in joint cartilage function and repair, resulting in progression of destructive lesions.

P-351

Histological evaluation of local polypoid fibroproliferation on anterior cruciate ligament as a cause of cyclops syndrom of knee

Rotter Aleksander*, Šačiri Valdet**, Veselko Matjaž***, Tonin Martin***
Institute of Pathology*, Medical faculty, University of Ljubljana, Slovenia, Departments of Orthoapedic Surgery** and Traumatology***, University Clinical Center, Ljubljana, Slovenia

Introduction: Cyclops syndrome is a limited extension of knee due to impingement of pedunculated fibrous tissue proliferation on anterior cruciate ligament (ACL). It usually arises after injury without or with ACL reconstruction at younger people.

Aim of the study: To evaluate the histomorphological characteristics of fibrous nodule with the emphasize on possible proliferation of atypical fibroblasts.

Material and methods: We checked up 133 patients operated due to the lack of knee extension, and only 12 had nodular fibroproliferation on ACL. Ten of 12 nodules removed from ACL were evaluated histologically. Biopsy specimens were stained with H&E, Acid Orcein Giemsa, Weighert van Gieson and trichrome. Immunostaining on callagen type I, III and IV was used. Semithin sections stained with Azur II for electron microscopy have been prepared.

Results: In all ten cases we found granulation tissue with angioproliferation and mild chronic inflammation in combination with compact fibrous proliferation resembling regular type of original ligament dense connective tissue mixed with different amount of fibroblasts proliferation. Collagens type I and III were found in all interstitial fibrous tissue, but collagen IV was present only in vascular walls and partially in fibrous proliferation of granulation tissue. The majority of fibroblast cells revealed plump nuclei, and approximately 15–20% of plump nuclei had nuclear membrane indentations, the characteristic figures of activated fibroblasts. But there were no cellular or nuclear atypia of fibroblasts or increased mitotic rate.

Conclusion: Fibronodular proliferation on ACL after injury is reactive by nature and there are no really atypical fibroblasts present.

P-352

Extraskeletal epithelioid myxoid chondrosarcoma

Renata Vasiu, C.D. Olinici, Nadia Schmidt*
Department of Pathology, *Department of Anatomy
and Embryology, University of Medicine and Pharmacy
"Iuliu Hatieganu", Cluj, Romania

Introduction: Generally, the majority of extraskeletal myxoid chondrosarcoma are slow-growing tumor capable of recurrence and metastasis sometimes many years after the initial diagnosis. Extraskeletal epithellioid myxoid chondrosarcoma (EEMC) behaving like a high grade sarcoma is a rare soft tissue tumor. The histological description of this rare form of EEMC is limited, so the authors report the clinical, pathological and immunohistochemical aspects of one case. Case report - a 66 years old woman presented with a two years history of a perirectal tumor previously resected, is addmited in the Municipal Hospital in the Chirurgery Department of Cluj with a recurrence in the ischiorectal fossa. Clinical informations were obtained from medical records and from the trating physicians.
Material and method: The tumoral tissue was sectioned, formalin-fixed and paraffin-embeded; the sections were stained with hematoxilin and eosin. Immunohistochemistry was performed on formalin-fixed and paraffin embe-ded tissue with S100 protein. The tumor was confined to six lymph nods of 0.5 to 3 cm in size, white and rather ferm.
Results: There are some caracteristical features of this tumor: the great cellularity, the epithelioid aspect of the cells and the paucity of myxoid matrix. The epithelioid cells are arranged in compact sheets without of matrix, in interanas-tomosing cords with some myxoid matrix and, in few areas, in a chondroid manner; the epithelioid feature was with abundant eosinophilic cytoplasm and with vesicular nuclei; in some areas the cells had a rhabdoid morphology with eccentric nuclei. The mitoses and the pleomorphic features were absent; hemorrage and necrosis were present but in a minor quantity. The tumor architecture was multilobular encased by fibrous septa with many lymphocytes, especially at the periphery where the tumor was encapsulated (and the lymph node structure is visible). Immunohistochemistry: the S100 protein was consistently positive.

P-353

Thyroid papillary carcinoma: Tumor cells release factors able to recruit dendritic cells and to induce dendritic cell differentiation from peripheral blood CD14+ monocytes

Francesca Ballarini, Stefania Scarpino, Maria Cristina Giustiniani,
Luigi Ruco, Stoppacciaro Antonella
Dpt. of Experimental Medicine and Pathology,
University La Sapienza, Rome, Italy

Introduction: In a recent paper we demonstrated that hepatocyte growth factor (HGF) stimulation of c-Met positive thyroid cells induces production of chemokines able to activate migration of immature dendritic cells (DC). Moreover we produced evidence that this molecular mechanism may be active in vivo in the thyroid papillary carcinoma. In the present study we have tested the possibility that thyroid papillary carcinoma cells produce factors capable of modulating DC maturation into efficient APC.
Methods: The factors produced were measured by RPA and ELISA. DC generation was achieved by adding supernatants from thyroid cells to CD14+ peripheral blood monocytes (PBM) cultures with or w/o GM-CSF+IL-4.
Results: Among the factors involved in Dc modulation, thyroid cells expressed IL-6, IL-1b, VEGF, GM-CSF and HGF but not IL-12p40 and IL-10. HGF stimulation increased the production of all the evaluated factors and induced IL-1a. Two of three supernatants were as efficient as GM-CSF+IL-4 in inducing DC differentiation from CD14+ PBM monocytes.
Conclusion: Our finding indicate that papillay carcinoma cells produce chemokines active on dendritic cells and release factors able to induce dendritic cell differentiation.

P-354

Adenovirus-mediated transfer of the thyroid sodium/iodide symporter gene into tumors for a targeted radiotherapy

A. Boland[1], M. Ricard[2], P. Opolon[1], J.M. Bidart[3], E. Connault,
P. Yeh[1], S. Filetti[4], M. Schlumberger[5], M. Perricaudet[1]
[1] UMR1582, CNRS-IGR-Rhône-Poulenc, PR2, 94805 Villejuif
France; [2] Service de Physique, [3] Département de Biologie Clinique
and [5] Service de Médecine Nucléaire, Institut Gustave Roussy,
Villejuif, France; [4] Dipartimento di Medicina Sperimentale
e Clinica, Università di Catanzaro, Catanzaro, Italy

The Na^+/I^- symporter (NIS) present in the membranes of thyroid cells is responsible for the capacity of the thyroid to concentrate iodide, allowing treatment of thyroid cancers with ^{131}I. We propose to extend this therapeutic strategy to non-thyroid tumors by using an adenoviral vector delivering the *NIS* gene into the tumor cells. We constructed a recombinant adenovirus encoding the rat *NIS* gene under the control of the CMV promoter (AdNIS). Infection of SiHa cells (human cervix tumor cells) with AdNIS resulted in perchlorate-sensitive ^{125}I uptake by these cells, at a level 125 to 225 times higher than non-infected cells. Similar results were obtained for other human tumor cell lines, including MCF7, T-47D (mammary gland), DU 145, PC-3 (prostate), A549 (lung) and HT-29 (colon), demonstrating that the AdNIS vector is efficient in tumor cell lines of various origins. In addition, AdNIS-infected tumor cells were selectively destroyed by exposure to ^{131}I, as revealed by clonogenic assays. To assess the efficiency of this cancer gene therapy strategy *in vivo*, we injected the AdNIS vector in human cervix (SiHa) or mammary (MCF7) tumors established subcutaneously in nude mice. Immunohistochemistry confirmed the expression of the NIS protein in the tumor. Three days after intratumoral injection, AdNIS-treated tumors could specifically accumulate ^{125}I or ^{123}I, as revealed by kinetics and imaging experiments. A quantitative analysis demonstrated that the uptake in AdNIS-injected tumors was 4 to 25 times higher than in non-treated tumors. On average, 11 % of the total amount of injected ^{125}I could be recovered per g of AdNIS-treated tumor tissue.
Altogether, these data indicate that AdNIS is very efficient in triggering significant iodide uptake by a tumor, outlining the potential of this novel cancer gene therapy approach for a targeted radiotherapy.

P-355

The antral mucosa as a new site for endocrine tumors in MEN-1/Zollinger-Ellison syndromes

C. Bordi, C. Azzoni, G. Ferraro, V. Corleto, F. Gibril, G. Delle Fave, R.T. Jensen
Universities of Parma, and Rome "La Sapienza", Italy and National Institutes of Health, Bethesda, MD

Background: In multiple endocrine neoplasia type 1 (MEN1) syndrome endocrine tumors were described in the pituitary, parathyroids, pancreatic islets, duodenum, gastric body-fundus, lung and thymus. No systematic investigation has been performed so far in the antral mucosa of the stomach.
Design: A systematic study of antral and gastric body endoscopic biopsies was performed in 124 consecutive patients with sporadic Zollinger-Ellison syndrome (ZES) and 46 patients with MEN-1/ZES from two reference clinical centers.
Results: Carcinoids were identified in the antral mucosa of 4 of 46 patients with MEN-1/ZES (8.7%) but in none of 124 cases of sporadic ZES ($p<0.001$). Immunohistochemically the tumors did express chromogranin A but not the hormones produced by antral endocrine cells (gastrin, somatostatin, serotonin). In contrast, two of them were diffusely immunoreactive for the isoform 2 of the vesicular monoamine transporter (VMAT-2), a marker specific for the gastric non-antral ECL cells. In one of these patients a second antral VMAT-2 positive carcinoid was seen 21 months after the first diagnosis. The other two an-tral carcinoids were unreactive for VMAT-2. Multiple ECL cell tumors were found in the gastric body-fundus mucosa of the two patients with VMAT-2 positive but not in those with VMAT-2 negative antral carcinoids. In one case the former tumors were diagnosed 22 months after the detection of the antral tumor. Body ECL cell carcinoids were found in 15 (32.6%) of 46 patients with MEN-1/ZES and in no patients with sporadic ZES.
Conclusions: The antral mucosa is an additional tissue that may harbor endocrine tumors in MEN-1 syndrome. These tumors did not express the phenotype of normal antral endocrine cells and, in at least two cases, were identified as ectopic ECL cell carcinoids. The absence of this tumors in sporadic ZES patients indicates a preminent role for MEN-1 gene defects in tumor development.

P-356

Spindle mesenchymal-like variant of papillary thyroid carcinoma

Cameselle-Teijeiro J., Woenckhaus C., Ruiz-Ponte C., Barros F.
Department of Pathology and Molecular Medicine Unit, Complexo HospitalarioUniversitario, Santiago de Compostela, Spain; Institute for Pathology, Ernst-Moritz-Arndt-University, Greifswald, Germany

Introduction: Focal spindle shaped cells have been reported in some papillary thyroid carcinomas (PTC), mainly in the cribriform-morular variant (including tumors related to familial adenomatous polyposis). We describe a peculiar case of PTC characterized by an overwhelming abundance of spindle cellular proliferation.
Methods: The patient was a 32-year-old woman admitted due to a mass in her neck. The transection of the thyroidectomy specimen showed an encapsulated mass measuring 27 mm in the right lobe. Immunohistochemical and molecular studies were performed on paraffin embedded tissues. The mutation cluster region as well as codons 313, 539, 848 and 1061 on the APC gene were amplified by PCR and analized by direct sequencing.
Results: Microscopically the tumor was composed of spindle cells admixed focally with a much lesser proportion of follicles. The pattern of growth was solid with spindle cells arranged in bundles having a mesenchymal-like appearance. The nuclear characteristics fit very well with those of the typical PTC. Throughout the nodule there is no significant atypia, mitosis, necrosis, or invasiveness. Immunostains showed reactivity for thyroglobulin, TTF-1, high-and low-molecular-weight cytokeratins, vimentin, S100 protein, and bcl-2. A normal pattern of E-cadherin expression was found in follicles but not in spindle cell areas. Calcitonin, chromogranin A, synaptophisin, actins, CD34, HMB45, and p53 were negative. No mutations were detected in the APC gene.
Conclusions: The recognition of this rare variant of PTC is necessary to avoid a misdiagnosis. Grants PM98-045 from DGESIC, Madrid, and PGIDE99PXI90201B from Xunta de Galicia, Spain.

P-357

Immunohistochemical expression of E-cadherin in normal and neoplastic follicular cells of the thyroid

Cameselle-Teijeiro J., Reyes-Santias R., Alfonsín N., Bernabeu I., Cabezas J.M.
Departments of Pathology and Endocrinology, Hospital Clínico Universitario, Santiago de Compostela; Department of Pathology, Hospital do Meixoeiro, Vigo, Spain

Introduction: Reduced expression of E-cadherin (E-cad), a transmembrane glycoprotein, is associated with loss of differentiation, acquisition of an invasive phenotype, and unfavorable prognosis in carcinomas from several sites. We used immunohistochemistry to study the expression of E-cad in normal and neoplastic follicular epithelium of the human thyroid gland.
Methods: The immunohistochemical studies were performed on paraffin-embedded tissue sections, using a monoclonal antibody anti-human E-cad (36, 1/2000, Transduction Laboratories, Lexington, KY, USA) with the reaction detected by an indirect, non-avidin-biotin detection system (EnVision System, Dako, Glostrup, Denmark). Normal thyroid (NT, n=10), multinodular goiter (MNG, n=11), follicular adenomas (FA, n=10), oxyphilic (Hürthle) cell adenomas (OA, n=7), follicular carcinomas (FC, n=10), oxyphilic carcinomas (OC, n=9), papillary carcinomas (PC, n=10), poorly differentiated carcinomas (PDC, n=7), and undifferentiated carcinomas (UC, n=8) were analyzed.
Results: A membranous pattern of E-cad stain was found in NT and MNG. Reduced and heterogeneous ("all-or-nothing") expression of E-cad was found in PC whereas FA, OA, FC and OC showed moderate to strong immunoreactivity. Focal cytoplasmic stain was also found in PC and OC. PDC and UC showed no or very faint immunostain.
Conclusions: Immunoexpression of E-cad is variably lost in thyroid carcinomas of different histotypes. A complete loss of E-cad, as detected by immunostaining, correlates with dedifferentiation. Supported by grants no PM98-045 from DGESIC, Madrid, and no PGIDE99PXI 0201B from Xunta de Galicia, Spain.

P-358

Endothelial cell recruitment in the vascularization of papillary carcinoma of the thyroid

Cancellario F, Scarpino S, Di Napoli A, Stoppacciaro A, Ruco LP
Department of Experimental Medicine and Pathology, University "La Sapienza", Rome, Italy

Introduction: The concept of vascular cooption was recently introduced to explain vascularization of solid tumours. It was proposed that in the early stages of tumour growth blood vessels of the host are actively recruited to provide the nutritional support. We have used tumour sections of 36 papillary carcinomas and primary cultures of 5 cases to investigate the pattern of vascularization of this tumour.
Methods: Tumour sections were immunostained for CD31/vWF to visualize blood vessels, for phosphorylated tyrosine and endothelial-specific nitrix-oxide-synthase (E-NOS) to determine endothelial cell activation, and for Ki-67. Primary cultures of papillary carcinoma cells were used as a source of factors active in the recruitment of SIEC microvascular endothelial cells.
Results: Two types of vessels were apparently involved in the tumour vascular support. Large-, medium vessels mainly located at the tumour periphery, and capillary vessels in tumour papillae. Neoangiogenesis occurred mainly in the medium- large vessels; in these latter endothelial cells were strongly E-NOS+, and occasionally Ki-67+. Capillary vessels of papillae were Ki-67-, and weakly E-NOS+. The in vitro study revealed that papillary carcinoma cells release large amounts of chemotactic factors for endothelial cells in the culture supernatants which resulted to be mostly VEGF. Moreover, HGF stimulation increased the amount of VEGF produced, and induced RNA synthesis for angiopoietin.
Conclusion: At least two steps can be recognized in tumour vascularization. Vascular recruitment, mediated by VEGF and/or by other chemotactic factors released by tumour cells, and vascular maturation in tumour papillae.

P-359

Expression of proliferative antigens (PCNA and Ki-67), bcl-2 and p53 in differentiated tumors of the thyroid gland

H. Čupić, B. Krušlin, Z. Kusić, M. Belicza
Ljudevit Jurak University Department of Pathology,
Sestre milosrdnice University Hospital, Zagreb, Croatia

Introduction: Differentiated thyroid carcinomas are usually associated with favorable prognosis. However, a subset of these tumors is showing more aggressive biologic behaviour. In this study we analysed the expression of PCNA, Ki-67, bcl-2 and p53 in differentiated thyroid carcinomas and follicular adenomas.
Material and methods: The study group consisted of 10 localised thyroid papillary carcinomas, 10 primary papillary carcinomas with metastatic involvement of regional lymph nodes and 10 associated metastatic tumors, 10 follicular carcinomas, 30 follicular adenomas and normal thyroid gland tissue. The study was carried out by immunohistochemistry on paraffin embedded material after microwave antigen retrieval procedure using APAAP, and PAP methods. The intensity of staining was graded semiquantitatively.
Results: Comparing the expression of PCNA, Ki-67, bcl-2 and p53 in these tumors we observed a statistically significant difference in the expression of bcl-2 and p53 in metastatic papillary tumors in lymph nodes ($p<0.001$ and $p<0.05$, respectively). We also observed a statistically significant difference in the expression of bcl-2 between localised papillary carcinomas and papillary carcinomas with metastatic involvement of regional lymph nodes ($p<0.05$), and finally in the expression of p53 and PCNA between follicular adenomas and follicular carcinomas of the thyroid gland ($p<0.01$ and $p<0.05$, respectively).
Conclusion: Our findings indicate a difference, particulary in the expression of bcl-2 and p53 between localised and metastatic papillary thyroid tumors. These results suggest that future studies on the expression of investigated and additional markers are needed to predict biologic behaviour of differentiated thyroid tumors.

P-360

A comparison between the lipid metabolism in alcoholics and diabetics

Lilan Engel & Jørgen L. Thomsen
University Institute of Forensic Medicine, Odense, Denmark

The fatty degeneration of the liver in alcoholics is well known. It was recently demonstrated that there is an accumulation of lipids in the proximal tubules of the kidneys in patients with diabetic coma. The metabolism of alcoholics and diabetics is very similar. For example, the development of ketoacidosis is common for both. Alcoholics, however, do not accumulate lipids in the kidneys. A theory is developed for the explanation of this difference.
The theory is based upon known structural changes in the diabetic kidney such as an increased permability of the glomerular endothelium. There is further a high serum level of fatty acids in diabetic coma. The fatty acids may pass the glomerular membrane into the tubules. They are there reabsorbed in the proximal tubules. In the mitochondria they are undergoing synthesis into tryglycerides.

P-361

p27 expression in tyroid neoplasms: Could be used as indicator of cancer?

S. Erdamar, F. Aksoy, M. Düren
Cerrahpasa College of Medicine, Istanbul, Turkey

Introduction: p27 is a member of the Kip Family of cyclin-dependent kinase inhibitors. Reduced expression of p27 has been shown to predict poor survival of patients with breast, colorectal, lung and prostate cancers. We studied the expression of p27 in tyroid carcinomas by immunohistochemistry to determine whether decrease of p27 has implications for diagnosis in follicular neoplasia e.g adenoma and carcinoma.
Methods: Formalin fixed-paraffin embedded sections from 68 randomly selected thyroid neoplasia cases with follicular adenoma (FA), Follicular carcinoma (FC) and papillary carcinoma (PC) were immunostained with a monoclonal antibody against p27 protein using avidin-biotin complex (ABC) immunohistochemical method. Immunoactivity was evaluated without any clinicopathologic knowledge and recorded as p27 labeling index (defined as percent of p27 positive cells among normal epithelia or cancer cells).
Results: The p27 labeling index in normal follicular epithelia was 98.01%±5.3% (mean±SD) , FA were 68.03%±6.6% ($p<0.05$). The

p27 immunoactivity was lower in FC (48.14%±11.23%) ($p<0.05$). It was also found significantly reduced p27 expression in PC group 39.12%±9.6% ($p<0.05$). There was no association of mean p27 labeling index with histologic grade and vascular invasion in FC and PC groups.

Conclusion: This immunohistochemical study demonstrated down-regulation of p27 would be helpful for pathologist to differantiate adenoma from carcinoma in follicular tyroid neoplasia.

P-362

Preliminary study of E-cadherin, β- and γ-catenin, and MMP-2 expression in morphological variants of differentiated thyroid cancer

Franco Fulciniti, M.D., Giulio Benincasa, M.D., Pio Zeppa, M.D., Antonio Vetrani, M.D., Lucio Palombini, M.D.
Dipartimento di Scienze Biomorfologiche e Funzionali dell' Università degli Studi di Napoli "Federico", Sezione di Anatomia Patologica e Citopatologia, Italy

Introduction: Concern still exists among pathologists on whether the identification of morphological variants of differentiated thyroid cancer may provide adjunctive prognostic implications. In an attempt to address this issue, we investigated E-cadherin, β- and γ-catenin, and MMP-2 immunoreactivity in a series of morphological variants of differentiated thyroid carcinomas, reporting a differential pattern of expression of these proteins between morphologically "aggressive" and "non aggressive" variants.

Material and methods: The study was carried out retrospectively (1994–2000) on archival cases of thyroid cancer from our Department. The following differentiated neoplasms were examined: a) three follicular variants of papillary carcinoma (FVPC); b) three cases of solid and cribriform papillary carcinoma (sporadic counterparts of familial adenomatous polyposis-associated papillary carcinoma) (FAPPC); c: six tall-cell variants of papillary carcinoma with Hashimoto's thyroiditis (TCVPC-HT); d: four tall-cell variants of papillary carcinoma without Hashimoto's thyroiditis (TCVPC) and: e) two Hurthle cell carcinoma (HCC). According with the reported aggressiveness for these histological types, these variants were divided as follows: group 1 (a, b, c) (non aggressive); and group 2 (d, e)(aggressive).

Results: Non aggressive variants revealed moderate-to-strong E-cadherin, β- and γ-catenin expression and absent-to-moderate cytoplasmatic (granular) MMP-2 immunoreactivity. In particular, in all FAPPC E-cadherin and β-catenin expression was de-localized in the nuclei of malignant thyroid epithelial cells. Conversely, aggressive variants revealed absent-to-moderate E-cadherin, β- and γ-catenin expression and moderate-to-strong cytoplasmatic (granular) MMP-2 immunoreactivity.

Discussion: In the present study we documented significant higher E-cadherin, β- and γ-catenin expression in nonaggressive morphological variants of differentiated thyroid cancer as compared with aggressive variants. Specifically, TCVPC-HT variants showed preserved expression of cadherin-catenin complex as compared with TCVPC variants, confirming that the presence of thyroiditis is *de facto* an histological marker of low aggressiveness. In addition, as previously reported, FAPPC variants showed an intranuclear de-localization of β-catenin, and more Interestingly, we observed for the first time an intranuclear de-localization of E-cadherin. However, the biological significance of this finding remains unclear. Finally, MMP-2 immunoreactivity appeared notably higher in aggressive morphological variants of differentiated thyroid cancer as compared with nonaggressive variants, and specifically expressed by epithelial cell. Taken together, the results of the present preliminary study suggest that aggressive morphological variants of differentiated thyroid cancer appear to have a higher risk for progression than nonaggressive variants, as indicated by the specific pattern of cadherin/catenin and MMP-2 expression. In conclusion, it may be important to provide the clinician with detailed morphological description of differentiated thyroid cancer.

P-363

Morphofunctional changes of thyroid in patients with bronchial asthma

Alexei Grigorenko, Boris Rabinovich
Amur State Medical Academy, Blagoveschensk, Russia

Endocrine system plays an important role in bronchial asthma (BA) pathogenesis. However data on morphofunctional state of thyroid regarding patient age and asthma duration are scarce and controversial.

These issues appear to be especially important in the regions reported to be deficient in iodine. Amur region and Far-Eastern part of Russia are among these regions.

We studied thyroid hormone level in 250 normal persons and 100 patients with BA using full automated chemiluminiscent system ACS-180, Chiron-Bayer. We also analysed iodine excreted with urine, using atom-adsorbing spectrophotometer.

Post-mortem examination was made in 45 patients aged 17–60 with BA of 1–20 year duration. Thyroid and segmentary bronchi were studied with the help of routine pathomorphological, histochemical and morphometric methods.

Studies suggested marked structural disturbances correlated with patient age and disease duration. Follicular epithelium height decreased with cubic epithelium changing into low prismatic epithelium.

BA exacerbation resulted in average follicular diameter decrease. Follicular index decreased due to sclerotic changes and stromal component predominance over colloid and follicular component.

Thus, BA progression leads to increasing morphofunctional thyroid disturbance, manifested in decreased thyroid TT4, TT3 and FT4 hormone synthesis, decreased compensation of iodine excretion, and elevated TSH level. Involutive pathomorphological changes in thyroid are correlated rather with BA duration than with patient age and they play significant role in disease pathogenesis especially under conditions of iodine deficiency.

P-364

Hyalinizing trabecular adenoma of thyroid associated with follicular carcinoma, papillary carcinoma and throiditis

Heper AO[1], Sak SD[1], Baskan S[2]
Departments of Pathology[1] and General Surgery[2],
Ankara University Faculty of Medicine, Ankara, Turkey

Hyalinizing Trabecular Adenoma (HTA) is an unusual neoplasia of follicular epithelium of the thyroid with a peculiar histologic pattern. Especially in FNAB and intraoperative frozen sections, it may

be confused with medullary carcinoma and papillary carcinoma. In the literature, there is an interesting argument based on the nature of this newly described lesion with regard of the histopathologic and immunohistochemical findings. We report here a new case associated with thyroiditis, minimally invasive follicular carcinoma adjacent to HTA and papillary carcinoma at the other lobe in a 63-year old female. Immunohistochemically, thyroglobulin was diffusely (+), calcitonin, CEA and synaptophysin were (–) and chromogranin-A showed focal staining in HTA. In previous studies, it was demonstrated that HTA could be associated with malignant and benign thyroid lesions. To our knowledge, this is the first case associated with follicular carcinoma in the literature. In the present case HTA was located adjacent to the capsule of follicular carcinoma but we did not observe any HTA-like organization in the follicular carcinoma or elsewhere in the thyroid.

P-365

Encapsulated papillary variant of medullary carcinoma of the thyroid gland with extensive cystic degeneration

Sevgiye Kaçar Özkara, Yeşim Gürbüz, Bahar Müezzinoğlu, Zuhal Yumbul
Kocaeli University, School of Medicine, Department of Pathology, Kocaeli, Turkey

Introduction: Papillary variant of medullary carcinoma of the thyroid (MCT) is an unusual histological pattern with some diagnostic difficulties. A case of encapsulated papillary variant of MCT with extensive cystic degeneration is reported.
Materials and methods : A euthyroid, 43-year-old woman with bone pain was incidentally found to have a 4.0 cm. cold nodule on her left thyroid lobe. Histopathological examination revealed an encapsulated tumor composed of a large cystic cavity with small papillary projections. The papillae were lined by multiple layers of neoplastic cells with small and regular nuclei containing condensed chromatin and lacking the characteristic "ground glass" appearance of the papillary carcinoma of the thyroid gland.
Results : Staining with Congo red disclosed amyloid deposits. Immunohistochemical studies revealed specific cytoplasmic staining of the tumor cells for calcitonin, chromogranin A, neuron specific enolase, carcinoembryogenic antigen and cytokeratin. Specific staining for thyroglobulin was not observed in any neoplastic cell. The case was diagnosed as papillary variant of medullary carcinoma of the thyroid gland.
Conclusions : Thyroid carcinomas should be classified according to their major immunoreactivity pattern rather than to their morphological pattern. Immunohistochemical and / or histochemical studies should be performed in all thyroid tumors that show unusual histological features.

P-366

Expression of dipeptidylpeptidase IV and thyroid peroxidase in thyroid tumors

[1]Kholová I., [1]Ryška A., [2]Čáp J., [3]Ludvíková M.
[1] The Fingerland Department of Pathology and [2]Internal Medicine, Charles University Faculty Hospital, Hradec Králové;
[3] Šikl's Department of Pathology, Charles University Faculty Hospital, Plzeň, Czech Republic

Introduction: The aim of the study was to evaluate dipeptidylpeptidase IV (DPP) and thyroid peroxidase (TPO) in differential diagnosis of thyroid tumors. DPP is a membrane protease not present in normal follicular cells, but aberrant expression was noticed in thyroid carcinoma. TPO is an essential enzyme in the biosynthesis of thyroid hormones. Its expression varies in different thyroid diseases with marked decrease in thyroid carcinoma.
Methods: We examined 16 thyroid carcinomas and 20 adenomas for DPP and TPO. There were 31 females and 5 males in this series and the mean age was 51 years. DPP was assessed both in frozen sections and in smears. In cytology, the threshold of 50% positive follicular cells was suggested as optimal. TPO was evaluated immunohistochemically.
Results: DPP sensitivity and specificity in frozen sections is 74%, and 88%, respectively. In cytology, using 50% threshold the sensitivity is 77% and the specificity is 96%. TPO sensitivity and specificity is 78%, and 92%, respectively. Using both markers sensitivity and specificity increased to 81%, and 96%, respectively.
Conclusions: These data suggest DPP and TPO to be helpful additional markers in differential diagnosis between benign and malignant thyroid tumors.
Supported by Charles University Grant Agency Grant No. 87/2000/C and IGA MZ CR No. 5306-3.

P-367

Focal sarcoid-like change of the thyroid gland. Possible consequence of aspiration cytology?

[1]Ludvíková M, [2]Ryška A, [3]Dvořáková E
Departments of Pathology and Internal Medicine, Charles University Medical Faculty, [1, 3] Plzeň and [2] Hradec Králové, Czech Republic

Introduction: The authors present a rare case of focal granulomatous reaction within the thyroid gland in a 43-years old female.
Material: The patient had a five years history of nodular goiter. Fine needle aspiration cytology from the largest this node was performed, however, the result was inconclusive due to inadequate amount of material. Four months after the aspiration, she was operated on because of slow progression; near total thyroidectomy was performed.
Results: Grossly, the thyroid lobes measured 35×20×18 mm (left) and 38×25×24 mm (right). Both showed nodular arrangement, with nodes up to 24 mm in greatest diameter. Histological examination showed features of nodular hyperplastic goiter with mild to moderate focal lymphocytic thyroiditis. Oncocytic differentiation was focally present. Surprisingly, in the area of previously performed aspiration, marked accumulation of granulomas composed of both epithelioid cells and multinucleated giant cells of Langhans type was seen. These granulomas did not show any relation to colloid within follicles. The overall appearance strongly resembled sarcoidosis, but the finding of granulomas was confined solely to the area of aspiration. Moreover, neither clinical examination nor the laboratory tests confirmed presence of any systemic granulomatous disease (such as sarcoidosis).
Conclusion: We interpret this finding as a possible uncommon reaction to the previously performed fine needle aspiration of the thyroid. Similar reaction was previously described in Warthin's tumor of the parotid gland. However, we are not aware of any report of a similar case in the thyroid gland.
Supported by a grant IGA MZ CR 5306/3

P-368

Evidence of fetal microchimerism in Hashimoto's thyroiditis

Sebastian Mannweiler1, Sigrid Regauer1, Patrizia Schwaiger2, Manfred Kleiber3, Michael Klintschar3*
1 Institute of Pathology, University Graz, Austria; 2 Department of Paediatrics and 3 Institute of Legal Medicine, Martin Luther University, Halle-Wittenberg, Germany

Introduction: Fetal microchimerism, the engraftment of fetal progenitor cells into maternal tissues, has been implicated in the etiology of autoimmune diseases such as systemic sclerosis. We examined the frequency of microchimerism in women suffering from Hashimoto´s disease, an autoimmune disease with a high prevalence in women.
Methods: We analyzed formalin-fixed, paraffin-embedded thyroid tissue of 17 patients with Hashimoto's thyreoiditis and 25 patients with nodular hyperplasia of the thyroid gland by polymerase chain reaction (PCR) for microchimerism. PCR amplification was performed using primers unique to a Y-chromosomal sequence (SRY gene) and primers for a sequence that is Y/X-chromosomal homologous except for a 6 base pair deletion in the X-chromosomal sequence (amelogenin).
Results: Microchimerism was detected in 8 of 17 patients with Hashimoto's thyreoiditis but in only 1 of 25 nodular hyperplasias using the SRY gene. Analysis for the amelogenin gene demonstrated Y-chromosomal DNA in only 4 of the 8 SRY-positive Hashimoto patients, but in none in the control group. Both patient groups were of similar age with comparable numbers of male pregnancies. All women with microchimerism had given birth to at least one son and a negative history for blood transfusions and organ transplantation. However, women with microchimerism had an overall higher number of pregnancies than women without michrochimerism.
Conclusions: Our results show that microchimerism is common in Hashimoto's thyreoiditis, but not present in nodular hyperplasia of the thyroid gland. Fetal microchimerism may play a significant role in the development of Hashimoto's disease, although we can not completely dismiss the theory that microchimerism is just an "innocent bystander" in a process triggered by other mechanisms.

P-369

Imunohistochemical study of poorly differentiated carcinomas of the thyroid

Martínez-Tello FJ, Santos-Briz A, Ballestín C, *Rigopoulou D
Departamento de Anatomía Patológica y
*Servicio de Endocrinología, Hospital Universitario
"12 de Octubre", Madrid, Spain

Introduction: Poorly differentiated carcinomas of the thyroid (PDCT) are tumors with an intermediate clinicopathologic position between well differentiated carcinomas (WDC) and undifferentiated carcinomas (UDC). However, no unanimous histological criteria have been used to define PDCT. Tall cell carcinomas (TCPC) and diffuse sclerosing carcinomas (DSC) are defined as variants of papillary carcinoma with a worse outcome. Immunohistochemical studies have been proved useful in distinguishing WDC from benign lesions as well as from UDC. The aim of this study is to investigate if PDCT shows a different immunohistochemical pattern from WDC, TCPC, DSC and UDC.
Material and methods: Immunostaining for keratins (CK-19, K-903, CK-20) and HBME-1 was performed in 51 thyroid lesions, including 15 PDTC, 19 TCPC, 3 DSTC, 5 follicular carcinomas, and 9 UDC.
Results: 80% of PDPC were positive for CK-19, 47% for HBME-1, 40% for K-903 and 20% for CK-20. TCPC and DSTC exhibited intense positivity for all antisera. Follicular carcinomas were positive for HBME-1 and negative for CK, with the exception of one case. Anaplastic carcinomas were negative for all antibodies.
Conclusions:
1. Our results confirm previous studies about the immunostaining features of WDC and UDC.
2. TCPC and DSPC show intense positivity for cytokeratins and HBME-1.
3. PDC show an intermediate immunophenotype between WDC and UDC, suggesting a loose of epitopes upon high-grade malignant transformation. The positivity for CK-19 is the most constant finding, and correlates with a posible papillary origin in many cases. HBME-1 seems to be preserved in cases with a possible follicular origin.

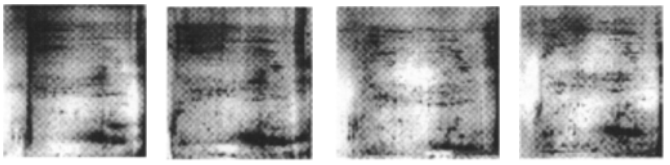
P-370

Proteomic analysis of microdissected benign and malignant thyroid tissues allow identification of new proteins with potential use in diagnosis and treatment

A. Panizo, D. Roberts, N. Sarlis, H. Al-Barazi, A. Chiesa,
B. Bryant, S.K. Libutti, M.J. Merino
National Cancer Institute, Bethesda, MD

Introduction: Thyroid cancer is the most common endocrine malignancy, accounting for 1300 deaths per year. Diagnosis of these neoplasms might be hampered due to similar morphologic characteristics and lack of specific tumor markers. Proteomic analysis is a technique capable of identifying known and unknown proteins, including those unique to different tumor types. Identification of specific proteins within the wide spectrum of thyroid neoplasms can not only provide understanding of disease progression, but may allow for the development of new and specific markers to be used in diagnosis and treatment. Our goal was to study by 2D-gel electrophoresis the differences in cellular proteins between normal and pathological thyroid tissues, which could aid in the differential diagnosis of thyroid cancer.
Methods: Thirty-three samples of thyroid lesions were studied (5 follicular adenomas, 3 follicular carcinomas, 12 papillary carcinomas, 3 goiters, and 10 normal thyroid). Frozen sections slides were prepared from each case and manually microdissected. In each case 5 to 10 slides were microdissected. Microdissected cells were directly lysed in lysis buffer, and protein concentration was determined. First-dimensional electrophoresis was carried out on a Immobiline IPG DryStrip system using 3–10 pH nonlinear gradient. For analytical 2D-gels, a sample corresponding to 30 μg of protein was applied to each strip. For the preparative 2D-gels, 0.5 g were applied. Second-dimensional electrophoresis was carried out using SDS-PAGE gels 1-mm thickness. Following electrophoresis, gels were fixed and stained using silver staining kit and Coomassie blue and scanned. Scanned images were analyzed and compared. Only spots that were present/completely absent between normal-tumor were defined as altered. Proteins of interest contained in 2D-gels were excised and analyzed by LC/MS to determine their identity.

Results: Approximately 300–500 silver stained polypeptides were detected over the pH range of 4.8 to 9 and molecular weight range of 4.1–40 kDa. The 2D-PAGE patterns of polypeptides from normal and malignant tissue were very similar, although both qualitative and quantitative polypeptide differences were noted. A general increase in polypeptide expression was noted in malignant tissues as compared to normal thyroid.



Normal Adenoma Follicular Ca. Papillary Ca.

Conclusion: Proteomic analysis of microdissected thyroid tissue is capable of providing specific protein profiling of normal and neoplastic tissues. This technique may allow for the identification of unique tumor-associated peptides that may be helpful in differentiating between thyroid neoplasms, as well as in developing tumor markers useful for early detection of malignancy and tumor progression.

P-371

Extensive DNA fragmentation in oxyphilic cell lesions of the thyroid

Mauro Papotti, Marco Volante, Patrizia Gugliotta, Antonio Migheli*, Gianni Bussolati
Dept. of Biomedical Sciences and Oncology, and of *Neurosciences, University of Turin, Torino, Italy

Introduction: The in situ end labeling (ISEL) method demonstrates DNA fragmentation, commonly regarded as a marker of apoptosis. No large investigations have been reported on apoptosis in oxyphilic cell lesions.
Methods: By the ISEL procedure we have investigated a series of 52 thyroid lesions, including 24 lesions of mitochondrion-rich oxyphilic cells, both benign and malignant, and 28 non-oxyphilic control tumors. Ten oxyphilic lesions of other organs were also included. Caspase activation was evaluated by immunohistochemistry.
Results: A high percentage of nuclear ISEL staining (approaching to 100% in most cases) was observed in the vast majority of oxyphilic cells from both adenomas and carcinomas, in the absence of morphological apoptotic changes and with no immunocytochemical evidence of caspase activation. This pattern of DNA fragmentation was not observed in non-oxyphilic lesions and was confirmed in total extracted DNA. Moreover, a peculiar cytoplasm staining was also observed in oxyphilic cells from both benign and malignant lesions, probably related to an abnormal fragmentation of mitochondrial DNA. Similar staining patterns were detected in oxyphilic cell tumors of other organs (parathyroids, salivary glands and kidney).
Conclusion: Our data are consistent with the presence of an extensive genomic and, possibly, mitochondrial DNA fragmentation peculiar to oxyphilic cells, which is not directly related to apoptosis and whose origin and biological significance are presently unclear.

P-372

The role of succinate-dehydrogenase-d (*SDHD*) tumor suppressor gene on 11q23 in endocrine tumors

Perren, A. Barghorn, S. Schmid, P. Saremaslani, J. Roth, Ph. U. Heitz, P. Komminoth
Department of Pathology, University Hospital Zurich, Zurich, Switzerland

Background: Sporadic endocrine pancreatic tumors (EPT), carcinoids pheochromocytomas, and parathyroid adenomas frequently display losses of 11q23 distally of the *MEN1* gene in comparative genomic hybridisation and loss of heterozygosity (LOH) studies. The recently cloned *SDHD* gene which is causative of familial paragangliomas is located in the region of the suspected tumor supressor. Therefore we analyzed a series of neuroendocrine tumors (NET) for mutations and allelic loss of the *SDHD* gene.
Design: We examined 21 EPTs, 14 carcinoids, 10 parathyroid adenomas, 9 pheochromocytomas and 7 paragangliomas using the flanking polymorphic markers D11S1893, D11S1347 and D11S900 for allelic loss of the *SDHD* gene. Mutation analysis was performed using PCR/SSCP and direct sequencing.
Results: Four of 13 EPTs, three of 6 carcinoids, one of two pheochromo-cytomas, one of 5 paragangliomas and none of 5 parathyroid adenomas showed allelic loss of the 11q23 region (75% of the tumors were informative for at least one marker). Mutation analysis revealed two amino acid variants present both in the tumor and germline DNA of three patients. The H50R variant in exon 2 was found in two patients and is located in a non-conserved region. Ongoing analysis will show if it represents a new polymorphism or a germline mutation. The G12S variant on the other handis most likely a new mutation: The affected patient exhibited the combination of extra-adrenal paraganglioma, C-cell hyperplasia and a pituary tumor.
Conclusion: We detected no sporadic *SDHD* mutations, therefore *SDHD* is unlikely to be an important tumor suppressor gene for NET on 11q23. As *SDHD* is an imprinted gene, LOH alone could lead to a complete loss of function in a subset of NET. Further expression analysis are needed to clarify this issue.

P-373

APUD-system tumours – ultrastructural diagnosis and prognosis

Raikhlin N., Smirnova E., Probatova N., Bebezov B., Badaljan X., Tschistjakova O., Bronstein M., Bukaeva I., Baronin A.
Cancer Research Center of RAMS, Moscow, Russia

Introduction: Histological criteria of malignancy and prognosis in common use are not informative enough, as far as endocrine cell tumours of APUD-system (ECTAS) is concerned. The aim of this study was to examine the influence of ultrastructural peculiarities of tumour cell phenotype on prognosis of ECTAS.
Methods: The 123 cases of endocrine tumours of different organs were investigated. Long-term follow-up data (15 years) were available in all cases. Histologic, cytologic and electron microscopic studies were performed.
Results: According to earlier elaborated ultrastructural classification of tumour cells, two groups of cells were detected in ECTAS: differentiated cells (with organo,- tissue,- and/or cell specific features) and undifferentiated cells (without these features). It was es-

tablished that clinical course of ECTAS, especially survival of patients, are associated with proportion of differentiated and undifferentiated cells: the more former cells and the higher degree their ultrastructural differentiation, the better prognosis. Eighteen percents to 27% of some type of ECTAS need of electron microscopic verification. On the basis of ultrastructural criteria it is also possible to establish differential diagnosis between ECTAS and tumours of other histogenesis, even when single cells with endocrine granules are present in ECTAS tissue, that is not always attainable by immunohistochemistry. Ultrastructural preoperative study of cytological material is highly representatively.

Conclusion: Electron microscopic peculiarities of ECTAS are reliable ultrastructural features of their malignancy degree, prognosis and differential diagnosis.

This work was supported by grant from Russian (99-04-50026) Fund Basic Research.

P-374

Immunohistochemical detection of MAGE-3 gene in thyroid papillary carcinoma

Šarčević Božena, Juretić Antonio, Spagnoli Giulio
University Hospital for Tumors, Zagreb, Croatia;
University of Basel, Basel, Switzerland

INTRODUCTION: Genes of MAGE family encode tumor-specific antigens recognized by cytotoxic T-lymphocytes in a variety of neoplasms. The human MAGE-gene family has been located to the X chromosome. The genes encoding the MAGE family TAA are expressed in tumors of different origin, but not in healthy tissues with the exception of testis and placenta.

METHODS: Only the limited number of histologically different neoplasms was examined for MAGE-3 protein expression. Therefore, we examined the frequency of MAGE-3 immunopositivity and the distribution of immunoreactivity within a group of 36 patients with primary papillary carcinoma of the thyroid gland. Paraffin blocks of 36 patients were examined immunohistochemically with monoclonal antibody 57 B.

RESULTS: 29 out of 36 papillar carcinoma were positive for MAGE-3 (25 cases of usual type, 3 cases of follicular type and 1 case of oxyphilic type). 18 out of 29 positive tumors showed diffuse cytoplasmic staining, and 11 out of 29 cases stained focally.

CONCLUSION: The results showed that MAGE-3 gene products could be identified by the 57mAb in the papillary carcinoma of the thyroid gland. Further, functional and histological studies are warrented to establish their potential value as tumor markers in the group of the thyroid carcinoma.

P-375

Diagnostic value of the morphologic, immunohistochemical and ultrastructural studies in adrenal gland tumours

Smirnova E., Probatova N., Raikhlin N., Bronstein M., Petrov S., Bukaeva I., Baronin A.
Cancer Research Center of RAMS, Moscow, Russia

Introduction: The tumours of adrenal gland may display different histogenesis and arise from the cells of adrenal cortex, endocrine cells of adrenal medulla and from neural cells. These tumours may be both separate entities and may show mixed type differentiation. In addition, the metastatic neoplasms are also observed in adrenal gland. Broad range of histopathological appearances of adrenal gland tumours introduce problems in establishing a differential diagnosis.

Methods: The 160 tumours of adrenal gland location were investigated by use histologic, immunohistochemical and electron microscopic methods. The antibodies used included vimentin, cytokeratin PAN, cytokeratin VIII, neurofilament proteins, chromogranin A, synaptophysin and neuronspecific enolase.

Results: The 137 cases (85,6%) of adrenal gland were verified by morphology alone. However, 17 tumours (10,6%) were further studied by electron microscopy and 6 tumours (3,8%) were verified only by immunohistochemistry. Positive staining for neuroendocrine markers and negative staining for cytokeratins are considered to result that these lesions should be regard as pheochromocytomas (4 cases). Negative staining for neuroendocrine markers and electron microscopic features of tumour cells permit diagnosis of adrenal cortical carcinomas (2 cases).

Conclusion: The combination of morphologic, immunohistochemical and ultrastructural studies may provide to improve differential diagnosis of adrenal gland tumours. Correct identification of these tumours is important for specific therapy.

This work was supported by grant from Russian (99-04-50026) Fund Basic Research.

P-376

Influence of local cryodestruction on experimental autoimmune thyroiditis

Sorokina I'., Karachenzov U[2]., Gargin V'.,Gopkalova I[2]
Department of Pathological Anatomy, Medical University, Kharkiv,Ukraine; 2. Research Institute of Endocrinology, Kharkiv, Ukraine

Autoimmune thyroiditis comprises about 46% of thyroid diseases in Ukraine. There are therapeutical and surgical methods of treatment of autoimmune thyroiditis but their results do not satisfy modern medicine.

The purpose of the present study was to investigate dynamics of morphofunctional structure of the thyroid gland in experimental autoimmune thyroiditis after local cryodestruction.

Our material included slices of the thyroid gland of 45 rabbits with experimental mercazolile autoimmune thyroiditis. The controls consisted of 22 intact rabbits. Under hexenal anesthesia local cryodestruction of the thyroid gland (exposure 1 minute, at –150–196°C) was performed in 23 animals. Thyroid tissues were analyzed using histological, histochemical and immunomorphological methods of investigation as well as morphometry.

Results: After local cryodestruction increased relative volume of the parenchyma, decreased relative volume of fat tissue and lympho-plasmocyte infiltration. The main characteristic was changing in the quality of lympho-plasmocyte infiltration. Decreased amount of CD22 and CD4 and increased amount of CDS were revealed. In addition pronounced reduction of the amount of HLA-Dr-cells was observed. It is known that deficiency of HLA-Dr-cells may stabilize CDS population. CDS-cells inhibit proliferative activity of the CD4 and they can decreased transformation and antibodiprodaction of CD22.

Conclusion: Local cryodestruction of the thyroid gland in rabbits in the experimental autoimmune thyroiditis causes marked positive

immunomorphological changes, activation of reparative regeneration and reduction of autoimmune agression.

P-377

Comparative genomic hybridization analysis of sporadic parathyroid adenomas

Tardío JC[1], García JL[3], Gutiérrez NC[3], González MB[3], Hernández JM[3], Menárguez J[2]
Departments of Pathology, [1]Hospital El Escorial; [2]Hospital General Universitario Gregorio Marañón de Madrid; [3]Department of Hematology, Hospital Universitario de Salamanca and Centro de Investigación del Cáncer, Universidad de Salamanca-CSIC, Spain

Introduction: Although cyclin D1 overexpression and MEN1 gene inactivation are known to be implicated in the pathogenesis of a subset of sporadic Parathyroid Adenomas (PAs), the genetic bases of the majority of PAs are unknown. Comparative genomic hybridization (CGH) provides, in a single experiment, a general view of genomic imbalances, including partial or complete trisomies, monosomies or amplifications within the tumour genome. We have applied CGH to identify genomic imbalances in 14 patients with sporadic PAs.
Methods: Tumour DNA was isolated from 14 PAs. Reference DNA was obtained from peripheral blood lymphocytes of healthy donors. The phenol-chloroform method was used for DNA extraction according to standard procedure. CGH analysis was performed by the method described by Lichter et al..
Results: Chromosomal gains were observed in all 14 cases and three cases (21%) presented also chromosomal losses. No cases of amplification were observed. The more frequent recurrent abnormality was located on chromosome 9: genetic gains at 9p22–24 and 9q34, each in six of 14 cases (43%). Other recurrent gains included: Xq26–27 in 5 adenomas (36%); 4q21–28 and 8p22–23, each in four of 14 cases (29%); and 1p32, 1q41–43, 4q34, 10q25–26, 12q24, 14q32, 18q22–23 and 20q13, each in three of 14 cases (21%). Regions of recurrent genetic loss included whole chromosome 11 and 20q12–13, each in two of 14 cases (14%).
Conclusion: Our findings show several candidate locations for genes implicated in pathogenesis of sporadic PAs, including previously not reported potential regions as 9p22–24 and 9q34.

P-378

Expression of Int-2 gene product in parathyroid lesions

G. Thomopoulou, S. Tseleni-Balafouta, P. Xirou, A.Ch Lazaris, H. Koutselini, P. Davaris
Department of Pathology, The Athens National University School of Medicine, Greece

Fibroblast growth factors (FGFs) comprise a family of polypeptides implicated in the control of proliferation of glandular tissues. FGF-3, which is encoded by the proto-oncogene int-2, stimulates mitosis of parathyroid cells in culture. The int-2 proto-oncogene is located on chromosome 11q13.3, a region identified as being susceptible to rearrangement/mutation in parathyroid diseases. The aim of this study was to determine whether int-2 protein is detectable in normal and abnormal parathyroid glands.
Samples from 37 patients with sporadic primary hyperparathyroidism due to either adenoma (12 cases) or primary parathyroid hyperplasia (25 cases) and from 30 patients with secondary hyperparathyroidism due to renal failure were immunostained using a sheep anti-human int-2 antibody (TCS Biologicals Ltd). As controls, 7 normal parathyroid glands were also examined.
The ratio of immunoreactive specimens was 7/37 in patients with primary hyperparathyroidism and 13/30 in uremic patients; the difference between the two groups was significant($p=0.029$). Int-2 immunolabelling was only occasionally detected at high levels irrespective of gland size; it mainly demonstrated a focal, distinctly granular pattern expressed on oxyphilic and transitional oxyphilic cells, often in nodular arrangement. None of normal parathyroid glands stained positively.
These findings imply that oxyphilic parathyroid cells are potentially responsive to FGF-3, which is likely to participate in the proliferation of this cell subpopulation. Since the number of such cells is expectantly higher in secondary hyperplasia, int-2 expression appears to be involved in the pathogenesis of parathyroid hyperplasia in chronic renal failure.

P-379

Tenascin tissue-immunoexpression in thyroid disorders

S. Tseleni-Balafouta, N. Kavantzas, H. Paraskevakou, M. Anapliotou, N. Mitsiades, P. Davaris
Department of Pathology, Medical School, University of Athens, Greece

Introduction/aim: Tenascin is a glycoprotein found re-expressed in the connective tissue adjacent to neoplastic tissues. The aim of our study was to investigate the distribution of tenascin in thyroid neoplasms in comparison to non-neoplastic conditions.
Material and methods: 48 thyroid specimens from non-neoplastic as well as neoplastic glands were studied by immunohistochemistry using a monoclonal antibody against tenascin (6 nodular goiters, 6 Hashimoto's thyroiditis, 2 Graves diseases, 15 papillary carcinomas, 3 invasive follicular neoplasms, 2 non-invasive follicular neoplasms, 3 invasive Huerthle-cell neoplasms, 6 medullary carcinomas, 2 anaplastic carcinomas and 3 normal autopsy-thyroids as control group).
Results: All the tissues from control group as well as the non-neoplastic tissues were negative for tenascin. Also, tenascin was negative for follicular neoplasms, Huerthle-cell and anaplastic carcinomas. Most of the papillary carcinomas (11/15) showed a focally intensive extracellular staining mainly located in the connective tissue, around vessels of the papillae and around the invasive edges. Microcarcinomas seemed to stain in a lesser degree. Also, most of the medullary carcinomas (4/6) showed a positive staining in the connective tissue as well as in intracellular location mainly in spindle-cell areas.
Conclusion: Tenascin re-expression has been found in papillary and medullary carcinomas of thyroid. The intracellular expression in medullary carcinomas suggests that tenascin is produced by the tumor cells and not by activated stromal cells.

P-380

Increased expression of vascular endothelial growth factor in recurrent papillary thyroid carcinoma

Nevzat Türe*, Yersu Kapran**, Alp Bozbora*, Neşe Özbey***, Selçuk Özarmağan* and Ferhunde Dizdaroğlu**
* Department of Surgery, İstanbul Faculty of Medicine;
** Department of Pathology, İstanbul Faculty of Medicine;
*** Department of Internal Medicine, Division of Endocrinology, İstanbul Faculty of Medicine, Istanbul, Turkey

Vascular endothelial growth factor (VEGF) is an angiogenic mitogen that induces proliferation, migration, fenestration of endothelial cells, and also it enhances endothelial and vascular permeability. It has been implicated in tumor growth and metastasis of various types of malignant tumors. The aim of this study is to determine whether immunohistochemical expression of VEGF is related to local or distant recurrence of papillary thyroid carcinoma. VEGF expression was searched immunohistochemically in 46 papillary carcinomas retrospectively on paraffin-embedded tissue sections. Ten normal thyroid tissues were used as controls. Patients were followed-up for 12–144 months (median 2 years), 15 of the patients had local or distant recurrences. The VEGF immunostaining was quantified as 0 (absent), 1 (slight), 2 (moderate-patchy), 3 (moderate-diffuse), 4 (intense-diffuse). Mann-Whitney U test was used for statistical analysis. VEGF expression was statistically significant (p=0.011) when recurrent carcinomas (n=15) were compared to cases that had not recurred (n=31). VEGF expression was greater in papillary thyroid carcinomas compared to normal thyroid tissues. These data indicate that VEGF may contribute to the aggressive behavior of papillary thyroid carcinomas and the immunohistochemical profile of the expression may be used as a helpful marker for predicting the cases that have metastatic potential.

P-381

Influence of the abolition mercazolile to morphometrical parametres of the thyroid gland.

V.B. Shadlinski, S.M. Rustamova
Human anatomy chair of AMU, Baku, Aazerbaijan

At constantly change condition external surroundings conservation the morpho-functional stabilization of biology systems is one of the main function in being organizm. Feasible this dynamic entirety and regulare stabilization of the functional processes of thyroid gland determine the state structure homeostasis. For the electron microscopic analize we are used from % 25 OsO_4. The aim of present work is consist of influence and abolition mercazolile to the some morphometrical parametres of rat thyroid gland. The investigation conveys on 60 rat with the weight 130–160 gr. I – Control group was composed from 20 rat, which receiving 10 mg. mercazolile for 100 gr. body weight. The morphologic picture of the cell elements thyreomorphocomplex of the rat thyroid gland, learning us until receive mercazolile and after abolition 7 day during discontinuance the remedy is enough diversity. During 7 day us was learned the morphologic picture of the thyroid gland after abolition mercazolile. After abolition mercazolile accumulation of the colloid essentoally increases, but the vessel reaction decreases. During receiving 7 day mercazolile accumulation the amount of picnotizirations nucleus of thyrosits at 1 mm^2 incision of thyroid gland was 823,0±78,0, P<0,0001. After abolition mercazolile during 7 day this index was 473,0±130,0, P<0,001. During this period also observed the distrofical changes, which showing the positive height of thyrosits with the picnotization nucleus. Our observing the distrofical changes at thyrosits, showes as their destruction and partial descvamation at chink follicles. We observed the insignificant inflation at stroma. After abolition 7 day of preparat also recoveries the tinktorial attributes of the collagen carcas capsul and stroma organ. The thyroidal-parathyroidal communications returnes to intact frame. At result electron microscopic investigation showes that the 7 day after receive mercazolile, the amount of mytochondries increases, the endoplazmatic reticulum inlargers, thyroid gland. Our notes the relative normalization of morpho-functional picture of throid gland, but showed the invaginates of follicles after abolition mercazolile 7 day. During abolition mercazolile observed the descvamation, also insignificant degranulation. Our observed the insignificant amountal increasing corpulent cells.

P-382

Expression of p16 and cyclin D1 in endometrial cancer

Yong hee, Lee, Jeongyeon, Shim, Jeeyong, Kim, Heejung, Ahn
Department of Pathology, College of Medicine, Pochon CHA University, Korea

The components of the p16-cyclinD/CDK-pRb pathway are frequently found to be altered in various types of cancer. Endometrial carcinoma is common malignant neoplasm of the female genital tract. However, there are few reports about the role of p16 and cyclin D in endometrial cancer. We performed the immunohistochemical staining for two G1 check point cell cycle proteins to study their expression pattern and roles in endometrial cancer. We studied 48 cases of paraffin block including 43 endometrioid type and 5 serous papillary type. 9 cases of complex hyperplasia are coexisting in specimens of endometrial cancer and also evaluated. Normal proliferative endometrium and complex hyperplasia show diffuse positive p16 reaction. We found that abnormal expression of p16(70%) increased with the increased tumor stage and tumor grade. Immunohistochemical results of cyclin D1 reveals negative or weak positive reaction in normal proliferative endometrium, diffuse positive reaction in complex hyperplasia. There is tendency to express high positive reaction for advanced stage of endometrial cancer in cyclin D1 immunostaining. In conclusion, loss of p16 and overexpression of cyclin D1 seem to play a significant role during the endometrial carcinogenesis.

Keyword: endometrial cancer, p16, cyclin D1

P-383

Moscow thyroid autopsy study: Thyroid pathology and death causes.

O.V. Zayratyants, T.G. Barsanova, V.V. Fadeyev,
* G.A. Melnichenko,* Y.L. Perov**
Moscow City Center of Pathological Anatomy,*Sechenov Moscow Medical Academy;**Russian Medical Academy for Postgraduate Education, Moscow, Russia

Mild iodine deficiency (ID) was revealed in Moscow region in 1994–1996. The median renal iodine excretion is 70–90 μg/l, the prevalence of goiter based on thyroid ultrasonography is 10–12%.

The aim of the study was to evaluate the prevalence of the thyroid pathology in Moscow region in autopsies in adults with the various causes of death.
Thyroid glands were studied macroscopically and histologycally in 1273 autopsies (age range – 19-95 years, mean – 72 years, M:F ratio – 1:1,3). Cardiovascular diseases (CD) were the death causes in 65% of cases (myocardial infarction in 25%, insults in 27%), gastric, pulmonary, breast and other carcinomas (Cr) in 10%, alcoholic leasions (AL) of hepar, heart, brain in 8%, and other diseases in 17% (typical mortality data for Moscow region in 1999–2000). Data was analyzed using software STATISTICA '99 (StatSoft Inc., USA).
The study revealed goiter in 44% (diffuse – 14%, nodular and mixed – 30%), autoimmune thyroiditis in 12% (hypertrophic form – 5%, atrophic form – 7%), thyroid carcinomas in 2%, adenomas in 4%, and other thyroid pathology in 6% of autopsies. The frequency of goiter and thyroiditis was considerably higher in female and in cases aged 66–85 years. In cases with CD goiter was diagnosed in 51% (with myocardial infarction – 56%, with insults– 40%), but in cases with AL only in 25% and with Cr in 20%.
The data demonstrates high frequency of the different thyroid pathological changes in Moscow region and some correlations between thyroid pathology and the diseases – causes of death.

P-384

Predictive value of Ki 67 expression in schistosomal associated bladder lesions versus non schistosomal ones in correlation to urothelial ploidy and morphometric paramters

Akl M.M.*, El-Hindawi A.F.**, Hamam O.A.*,
Abou-Shousha T.*, El-Baz A.G.***, Abdel-Hady A.H.*,
Badawy A.A.*
Pathology Department, * Urology Department,
*** Theodor Bilharz Research Institute; Pathology Department,
** Faculty of Medicine, Cairo University, Egypt

Schistosomal (Sch.) bladder cancer may biologically differ from non-schistosomal bladder cancer. The aim of this work was to evaluate the cytoproliferative marker; Ki67 in Sch. & non-Sch. neoplastic and non-neoplastic & comparison of the proliferative activity with urothelial nuclear ploidy and morphometrical parameters assessed by the computerized Kontron Image Analyzer (IA). This study included 100 cases; 95 patients & 5 control. Cases were classified into two groups according to their cystoscopic biopsy diagnosis: a) Sch. lesions; including cystitis (20%), Dysplasia (15%), in situ (CIS) transitional lesions (10%), TCC (19%), Sq. CC (10%) and b) Non-Sch. bladder lesions; including similar types as above, with the following incidence repectively (10%), (15%), (10%), (11%) and (5%). In all the cases we applied two techniques for predicting the prognostic behaviour of the mentioned lesions: a) Immunohistochemical assessmentof ki 67 as a labling index for proliferative activity (LI) and as integrated optical density (IOD) using the IA. b) Nuclear ploidy analysis and nuclear morphometric characterization of urothelial cells by the IA. The mean Ki-67 IOD value was 152.57+15.45, in cases of Sch. cystitis, progressively significantly increased in cases of Sch. dysplasia and Sch. CIS changes (176.34+35.36, & 176+88, respectively) and consequently increased in Sch. TCC and SqCC (213.47+68.30 and 184.639+40.54) . The mean Ki-67 IOD value in each Sch. bladder lesion was found significantly higher ($P<0.01$) than in its equivalent non-Schistosomal one. IOD and LI values of Ki-67 expression were significantly parallel and correlated the same way with the studied lesions. The following Image analyzed parameters for urothelial cells including – nuclear ploidy (NP) mean nuclear area (MNA), mean number (N0) of cells in S-phase, mean N0 of aneuploid cells and mean N0 of cells at 5c exceeding rate – showed significantly increased values ($p>0.01$) in all the studied sch.bladder lesions in comparison to the non sch. ones and positively correlated with the results of Ki-67 (IOD) expression values within the bladder urothelium. In conclusion, schistosomal lesions exhibit more aggressive biological behavior compared to non schistosomal lesions.

P-385

Human leukemia cell differentiation factor (HLDF) – new tool for apoptosis visualization at prostate

Babichenko, N. Shelastina, I. Kostanyan*, S. Dranicina*,
L. Gundorova**
Dpt. of Pathology, Peoples' Friendship University of Russia,
M.M.Shemyakin and U.A.Ovchinnikovs' Institute of bioorganic chemistry*; Hospital of wars veterans No 2 in Moscow**, Russia

Human leukemia cell differentiation factor (HLDF) with molecular mass 8,2 kd, having DNA/RNA hydrolyzing activity, was originally allocated from HL-60 cell line of promyelocyte leukemia medium, processed by retinoid acid. The HLDF caused differentiation and interrupted proliferation of initial cell line. It was possible to determined HLDF after hydrolyzing of nuclei in the cell cytoplasm.
The task of the study was to provide the comparative investigation of immunohistochemical features of bcl-2 and HLDF distribution in epithelial cells of prostate at various stages of oncogenesis (BPH, PIN and adenocarcinoma).
Immunohistohemical detection of HLDF antigens was performed at paraffin embedded biopsies from human prostate (21 cases) with LABS+ set of DAKO Corporation (Denmark). As primary we used the rabbit polyclonal antibodies to HLDF in dilution 1:800 and commercial monoclonal antibodies to the bcl-2 factor (DAKO Corporation Denmark).
The analysis of slices have shown, that in normal prostate glands, BPH and PIN LG bcl-2 and HLDF factors were not distributed in the same cells. Bcl-2 was found only in the cytoplasm of cells at the basal layer, while HLDF was obtained as "honeycomb-like" structures of died cells envelopes in the centres of glands. On the other hand, at the cases of PIN HG and adenocarcinoma the bcl-2 and HLDF were arranged in the same regions in secretory epithelial cells cytoplasm at anaplasia. There were no "honeycomb-like" structures in the centres of glands that show off the absence of apoptosis in them.
The results testified that the antibodies to HLDF allow carrying out differential diagnostics between benign and malignant processes in prostate and can be used as new marker for revealing early stages of anaplasia at biopsy specimens.

P-386

c-erbB-2 expression in human prostate hyperplasia, prostatic intraepithelial neoplasia and prostate adenocarcinoma

Kemal Bakir*, Ramazan Uçak*, Kemal Sarica**, Faruk Yağci**
* Medical Faculty of Gaziantep University, Pathology Department, ** Medical Faculty of Gaziantep University, Urology Department

The human proto-oncogen c-erbB-2/neu gene, which is structurally similar to the epidermal growth factor receptor gene, encodes a transmembrane protein of 185 kDa (p185) with tirosin kinase activity.
The results of previous studies investigating the correlation between c-erbB-2 expression and prognostic parameters in prostate cancer; and c-erbB-2 expression in BPH and PIN were controversial. In this study, we investigated, immunoreactivity of c-erbB-2 in -BPH (23 cases), PIN (12 cases) and CaP (66 cases) – total of 101 cases and its' relation with prognostic parameters in CaP.
In our study from the paraffin blocks of 101 cases, immunohistochemically with Avidin-Biotin Horse Radish Peroxidase method to searched for c-erbB-2 reaction. Results were evaluated semiquantitatively by means of (–) and 3 positive values (+, ++, +++). We determined tumor grade by using Gleason scor system from the H.E. stained preparations. The results of BPH, PIN and CaP were compared. Also, we investigated correlations between c-erbB-2 expression and tumor grade-clinical stage. Results were statistically analysed by using chi-square tests and Pearson Correlation Coefficient.
In our study we couldn't detect a significant relation between c-erbB-2 expression in BPH and PIN, tumor grade and CaP ($p>0.05$). But we found, statistically significant differences ($p<0.05$) between c-erbB-2 expression in BPH and CaP, PIN and CaP. Also, we couldn't detect a significant relation between c-erbB-2 expression and T status and M status ($p>0.05$) but we found statistically significant correlation between c-erbB-2 expression and metastases to lymph node ($p<0.01$).
Finally, according to us c-erbB-2 expression can be used as a differential diagnostic factor in BPH, PIN and CaP. Also, it seems that strong immunoreactivity of c-erbB-2 supports metastases of lymph node.

Keywords: c-erbB-2 expression, Prostate tissue, Immunohistochemistry
Abbreviations: BPH: Benign prostatic hyperplasia, PIN: Prostatic intraepithelial neoplasia, CaP: Prostate adenocarcinoma

P-387

NeuroEndocrine cell relationship with prostate carcinoma progression.

[1] Botticelli A.R., [3] Pitino A., [4] Botticelli L., [5] Failla C., [2] Zaffe D.
[1] Dept. of Human Pathology-Univ. of Pavia,
[2] Dept. of Morphological Sci. and Forensic Med.-Univ. of Modena; Reggio Emilia, Hospital Pathology Service of [3] Crema CR, [4] Carpi MO, [5] Siracusa SR, Italy

Introduction: The predictive significance of neuroendocrine (NE) cells in prostate carcinoma (PC) has not yet been clearly defined. The aim of this study is to analyze NE cells to establish the relationship between PC progression and vascular, cellular, oncogenic and nuclear cell-cycle proliferation indexes.
Methods: Immunocytochemisty was performed on formalin fixed and paraffin embedded archival PCa sections of 20 patients (m=66.8 y) undergoing radical prostatectomy (GHS<6=10 cases and GHS>7=10 cases). Slides were treated with the antigens of *Vascular endothelial growth* CD34, *extracellular matrix* CD44, *androgen receptors*, *somatostatin*, *chromogranin A*, *E-cadherin*, *interleukin-1 and -2* CD25, Ki67/MiB1 or bcl2 or P53 *oncogenes*, incubated with SBC and revealed with DAB. Double immunocytologic staining, using *MIB1/Ki67* or *E-cadherin* (DAB), and *chromogranin A* or *somatostatin* (PAP), were performed using the ABC System.
Results: Ki67/Mib1, p53, bcl2 and E-cadherin are scanty expressed by NE cells. The number of NE cells seems to have risen in the areas with low androgen receptor markers, high interleukin-1 expression and high microvessel density.
Conclusion: A low androgen receptor level suggests a possible immunomodulator production by NE cells (Deftos et al. 2000). Moreover, the angiogenesis inside PC and the increased detection of NE cell markers PC-associated seems to be an expression of a more aggressive phenotype cancer. The presence of active NE cells near new formed vessels can be related to a possible NE production of angiogenic factors (Borre et al. 2000). These observations may suggest the important role of NE cells on the development and progression of PC.

P-388

17β-estradiol increases levels of $p21^{Waf1/Cip1}$ and telomerase activity in prostate cancer cell line LNCaP

Bouchal J, Madarova J., Hlobilkova A, Kolar Z
Laboratory of Molecular Pathology, Palacky University, Olomouc, Czech Republic

Introduction: The effects of the 17β-estradiol (E), dihydrotestosterone (D) and estrogen/androgen antagonists tamoxifen (T) and bicalutamide (B) on telomerase activity and expression of different proteins in the androgen-sensitive prostatic cancer cell line LNCaP were studied.
Methods: LNCaP cells, cultivated in RPMI with 2.5% charcoal-stripped FBS, were tested for both IC_{50} of antagonists and optimal concentrations of E and D by the MTT cell-viability assay. Activity of telomerase in treated cells was measured by the TRAP protocol and the expression of proteins was determinated by Western blot analysis.
Results: 10 nM E stimulated cells more effectively then 1nM D and induced the expression of $p21^{Waf1/Cip1}$ and increased telomerase activity. 50 μM B down-regulated the levels both of the androgen receptor and PCNA, decreased telomerase activity and increased the level of $p27^{Kip1}$. 5 μM T produced cells with a similar morphology as those treated with B, but did not affect any of the studied proteins. The expression of estrogen receptors in LNCaP cells was not observed.
Conclusion: The results showed the unexpected relationship between the activity of telomerase and the expression of $p21^{Waf1/Cip1}$ after estradiol stimulation. The effect of estradiol and tamoxifen is probably not mediated by estrogen receptors. Possible explanations for this phenomenon will be discussed in our presentation.
This work was supported in part by MSM151100001 and NC6200-3.

P-389

Proliferative lesions of prostate – A multivariate approach for the differential diagnosis

Fernanda B.C. Cavalcanti; Venancio A.F. Alves;
Julio C.R. Pereira; Cristina Kanamura; Alda Wakamatsu ;
Luiz B. Saldanha
Divisão de Patologia, Instituto Adolfo Lutz, São Paulo, Brazil

INTRODUCTION: In the context of many "new entities," based on numerous criteria, this study aims at selecting sets of criteria to yield diagnosis of main proliferative lesions of prostate.
MATERIALS and METHODS: Casuistic: 142 biopsies, from well-defined usual prostatic hyperplasia (22), postatrophic hyperplasia (24), basal cell hyperplasia (15), atypical small acinar proliferation (ASAP) (19), high grade intra-epithelial neoplasia (PIN)(31) and adenocarcinoma (31: Gleason 2–6:19; Gleason 7–9:12)
Methods: 46 histologic criteria and 34be12 immunostaining were assessed. Spearman correlation at r>0.30 selected 16 criteria for Multiple Discriminant Analysis (MDA), thus yielding the definition of three mathematical functions.
RESULTS and CONCLUSIONS: The 16 histologic criteria statistically discriminant are: glandular fusion, prominent nucleoli, cristalloids, delicate chromatin in luminal cell, 34be12 immunoexpression, solid arrangement, eosinophilic secretion, stromal sclerosis, absence of luminal content, PMN, nerve invasion, papillary arrangement, 2 cell layers, basal cell visualization, n:c ratio and granular cytoplasm of luminal cell.
The three discriminant functions were: "1. Adenocarcinoma": glandular fusion, prominant nucleoli and cristalloid; "2.PIN": papillary arrangement; "3. ASAP": n:c ratio , basal cell evident. The 34be12 immunostaining was found most helpful for discrimination from ASAP to adenocarcinoma.
The validity of these simple sets of criteria will be tested a prospective cohort of needle biopsies, with clinical and surgical follow-up

P-390

Correlation of p53 expression with the clinicopathologic parameters and prognosis of renal cell carcinoma

Celik Betül MD*, Dursun Ayse MD**, Isik Ipek MD**,
Oguzulgen Ibrahim MD**, Aktas Serpil Phd***
* Kirikkale State Hospital, ** Gazi University Medical School,
*** Hacettepe University Dept. of Statistics

Objective: P53 gene expression has been demonstrated in several tumors. This study aimed to investigated whether p53 gene expression is related to clinicopathological parameters, including patient sex, age, tumor size, cell type, capsular invasion, nuclear grade, stage and overall survival in renal cell carcinoma (RCC).
Method: The immunstaining was performed on 55 RCC using an anti-p53 monoclonal antibody (DO7,Dako). 31 patients were followed-up either until time of died or median survival time of 44,0 months, ranging 3 to 104 months.
Results: The p53 positivity was demonstrated in 9 patients (16,3%). Statistical analysis showed that p53 immunreactivity correlated significantly with low (G1+G2) and high (G3+G4) nuclear grades but didn't correlated with patient age, sex, tumor size, cell type (papillary vs nonpapillary or clear vs nonclear), sarcomatoid area, capsular invasion and stage. Survival time was higher in p53 negative patients (81,51 months) than taht of p53 positive patients (31,88 months). However, no statistically significant relationship was found with survival data.
Conclusion: P5 gene expression might be seen within any of the histological subtypes of RCC. Since the expression of p53 gene was unrelated to the clinicopathological features of the tumor, it has no impact on prognosis of RCC. P53 gene expression could be expected in high nuclear grades but to make a conclusion needs further studies.

P-391

Somatic mutations and loss of heterozygosity of the vhl tumor supressor gene in unclassified renal cell carcinomas

Chiesa, M. Sobel, B. Brynat, A. Panizo, W.M. Lineham,
M.J. Merino
National Cancer Institute, Bethesda, MD

Introduction: The present classification of renal epithelial tumors (Heidelberg-1997) includes an unclassifiable category that accounts for 6% to 7% of renal malignancies. These neoplasms are difficult to classify because of their lack of specific morphologic characteristics or mixed histologic patterns. Although genetic studies of clear cell and papillary renal cell carcinomas have shown a correlation between chromosomal abnormalities and histologic features, genetic aberrations of the unclassified tumors remain unknown. We studied four cases of unclassified renal cell carcinoma (URCC) to investigate the presence / absence of the VHL mutation.
Methods: Four cases of URCC (3 men, 1 woman) were studied. One additional case of renal cell carcinoma, clear cell type, with a known mutation and loss of heterozygosity (LOH) at 3p was included as a positive control. Ages ranged from 42 to 65 years old. Three tumors were located in the right kidney and one in the left kidney. Tumor sizes ranged from 7 to 14 cm. Histologically the tumors showed a mixture of papillary and solid growths, high nuclear grade, and/or undifferentiated patterns. Tumor and morphologically normal cells were microdissected from paraffin-embedded tissue for PCR amplification to detect LOH at D3S1038 (3p26.1-3p25.2) and for direct DNA sequencing on both stands of all three exons of the VHL gene.
Results: Wild type sequence was detected in every case. LOH was detected in case 3. The control showed LOH and C>T at nucleotide 908.
Conclusion: In contrast to genetic alterations in clear cell carcinoma, inactivation of the VHL gene by somatic mutation in one allele and LOH of the other do not seem to occur in unclassified renal epithelial tumors. Correlation between VHL mutation and 3p LOH was found in three cases (cases 1, 2, and 4). However, LOH at 3p may occur occasionally in patients without mutations in the remaining allele (case 3).

P-392

Extracellular matrix proteins in glomerulonephritis

Čužić S., Šćukanec-Špoljar M., Jelaković B., Kuzmanić D.,
Laganović M.
University Hospital Zagreb, Zagreb, Croatia

Chronic renal insufficiency develops only in those cases of glomerulopathy in which the lumina of postglomerular capillaries in the

renal cortex are narrowed. The cortical interstitial edema and increase of the extracellular matrix (interstitial fibrosis) lead to obliteration of postglomerular capillaries. The composition of glomerular and interstitial extracellular matrix (ECM) proteins is changing in glomerulonephritis (GN). Their role is not only mechanical support of the cells, but also modification of cell phenotype and mediation of cellular response, like cell proliferation.
The aim of this study was to elucidate the distribution of extracellular matrix proteins in various forms of glomerulonephritis. We examined renal biopsies from 55 patients with various forms of primary GN: minimal change GN (9), IgA-GN (29), mesangioproliferative GN (10), membranoproliferative GN (2), focal glomerulosclerosis (4) and rapidoprogressive GN (1). Normal renal tissue (5) was obtained from nephrectomy due to small renal tumour. Specimens fixed in B5 and/or Dubosque fixative were analysed by immunohistochemistry (APPAP-method) using a monoclonal antibodies against tenascin (TN), fibronectin (FN), collagen I, III and IV (COI, COIII, COIV) (DAKO). The same fixatives were used for controle renal tissue.
In normal renal tissue glomerular mesangium is TN, FN and weakly COI positive. COI staining was observed along endothelial side of glomerular basement membrane. Glomerular and tubular basal membrane stained with COIV antibody. FN is found around TBM. There was a weak COI expression in interstitium. Intensive TN staining was found in medulla interstitium only. Epithelial cells of proximal tubules and medullary collecting ducts showed COI and COIII staining, while TN was detected only in proximal tubules. No matter which histological form of GN was examined, foci of glomerular sclerosis were TN, FN, COI, COIII and COIV positive. In focal glomerulosclerosis mesangium, apart from sclerotic foci, was FN negative. Fibrous crescents showed TN, FN, COI, COIII and COIV staining. Thickened Bowman's capsule expressed COI, COIV and TN. At sites of interstitial inflammation in renal cortex there was a *de novo* TN expression. Interstitial fibrosis is characterized by expansion of FN and COI staining, while a COIV is a novel ECM constituent.
Our results show that there is a marked change of mesangial and interstitial ECM in various forms of GN. TN is an essential constituent of ECM during inflammation, while COIV emerges at sites of sclerosis/scar.

P-393

Prostate adenocarcinoma (PC):
Quantitative immuno-expression of tumor markers as related to histologic grade and pathologic stage
Di Loreto, C., Alves, V.A.F., Kanamura, C.T., Cavalcanti, F.
Divisão de Patologia, Instituto Adolfo Lutz, São Paulo, Brazil

Introduction: Since most studies approach tumor markers individually, we now assessed quantitative immunoexpression of p53, HER-2, neuroendocrine (NE) differentiation, cellular proliferation and microvessel density (MVD) as related to Gleason score (GS) and pathological stage (PS).
Methods: Ninety-seven specimens were divided in five groups:
A – 20 low grade (GS 2–6), confined (pT2);
B – 20 high grade (GS 7–10), confined (pT2);
C – 8 low grade, non-confined (pT3);
D – 28 high grade, non-confined ;
E – 21 high grade, metastatic.
Primary antibodies: p53 (DO7, Dako); HER-2 (polyclonal, Dako); chromogranin A (LK2H10, Dako); Ki-67 antigen (MIB-1, Immunotech); CD34 (QB-End/10, Dako).
Antigen retrieval: Pressure cooker.
Amplification: Labelled Streptavidin-biotin-peroxidase (LSAB-2, Dako).
Results: Immunoreactivity for p53, chromogranin A and Ki-67 antigen was signficantly higher in high grade tumors ($p=0.02$, 0.01 and<0.01, respectively). No significant difference was found among the stages. MVD was higher in high grade tumors, and in higher stages ($p<0.01$). HER-2 imunoexpression was restricted to high grade non-confined tumors. The presence of three or more "altered" markers was related to high grade ($p<0.01$) and to metastasis, when compared to high grade non-confined cases ($p<0.01$).
Conclusion: All these markers are closer related to histological grade than to the stage. The presence of three or more positive markers is related to high histological grade and to metastasis, thus suggesting a possible cumulative effect in carcinogenesis.

P-394

Mast cells and fibrosis on testicular biopsies in the male infertility
Duygu Düsmez M.D., Selahittin Çlayan M.D.*. Ayse Polat M.D., Handan Çlamdeviren PhD**
University of Mersin, School of Medicine*,
Departments of Pathology, Urology*, and Biostatistics**

Introduction: Testicular dysfunction may correlate with an increase in the number of testicular mast cells. Mast cells can activate fibroblasts and promote collagen synthesis. The aim of the study was to examine the total number of mast cells contain tryptase, their location and relation with different stages of parenchymal and tubular fibrosis.
Methods: Testicular biopsies from adult men with fertility problems were assigned to two groups: normal spermatogenesis (n=10), and defective spermatogenesis (n=23). Total, interstitial and peritubular mast cells were examined with antihuman tryptase immunohistochemically. The fibrosis stage was evaluated with the help of two immunohistochemical antibodies, vimentin and alpha-smooth muscle actin. The ratio of tubules with sclerosis to total tubules was also calculated.
Results: Most mast cells in the specimens with normal and defective spermatogenesis were localized mainly in the interstitium. The number of total mast cells was statistically significantly higher in the cases with defective spermatogenesis. Both in the cases with defective and normal spermatogenesis, interstitial mast cells were higher than peritubular mast cell counts. Total, peritubular and interstitial mast cell counts were not different from each other in cases grouped according to the immunostaining results with vimentin and alpha-smooth muscle actin. Total and interstial mast cells were significantly higher in the cases with sclerosing seminiferous tubules.
Conclusion: Since mast cells have become evident in testicular biopsies when the last stage (tubular hyalinisation and sclerosis) takes place, the mast cells and the mast cell product tryptase could be involved in the etiology of these changes.

P-395

Squamous cell carcinoma (SCC) of the urinary bladder (UB). A clinicopathologic review of eighteen cases

J. Esquius[1] M. Alejo[2] I. Costa[1] J. Autonell[2] F. Algaba[3] and Ll. Cortadellas[4]
Dpts. of Pathology[1] and Urology [4] Hosp. Gral. Granollers; Dpts. of Pathology Hosp. Gral. Vic[2] and Fundació Puigvert of Barcelona[3], Barcelona, Spain

INTRODUCTION: SCC represents 5% of UB malignant tumors. We have conducted a retrospective study of our collected cases to describe clinicopathologic traits.
MATERIAL: Eighteen cases coded as SCC were retrieved from the files of two Institutions. Charts and pathologic reports were reviewed to get: age at diagnosis, sex, smoke intake history, clinical presentation, cistoscopic appearances, treatment, size, histology, pT and pN categories, clinical follow-up and presence or not of other urothelial lesions such as dysplasia and metaplasia. All was tabulated and a decriptive analysis was underwent.
RESULTS: The 18 cases – 16 men and 2 women- were aged 49–87 (mean, 71). Tobacco was recorded in 13 (72%) cases. Macroscopic hematuria compiled in 14 (78%) cases was the most frequent clinical complaint. Cistoscopic appearance almost always revealed huge masses filling the UB. Ten patients (55.5%) underwent with or without prior transuretral resection, radical cistectomy. Five patients (28%) presented with a pathologic stage IV with lymph node metastasis (4) and intraabdominal dissemination (1). In 6 out of 10 surgical specimens there was wide invasion of perivesical fat. Histologically, 11 cases (61%) were pure SCC, 6 had little component of transitional neoplasm and a last one had pseudosarcomatous areas. Tumor sizes were between 3 and 9 cm in greatest dimension. Urothelial dysplasia, "in situ" carcinoma and squamous metaplasia were recorded respectively in 5, 2 and 6 cases.
Follow-up was available in all except one case. This period ranged from 2 to 61 months (mean, 17.3 mo). Eight patients (44%) are alive without disease, 7 (39%) died of tumor and 2 are alive with local residual or new tumor. The pT categories were heterogeneous even in alive patients; 4 (50%) were pT2, 2 pT3, 1 pT4 with extension to the prostatic gland and the last one presented with lymph node metastasis.
CONCLUSIONS: SCC of UB are unusual tumors that in general present in elderly men with macoscopic hematuria. In our series mortality rate was 27.7% (5 cases) in the first year of follow up. Although stage IV at presentation is associated with the worse prognosis, other pathologic parameters such as pT 2 and 3 categories, necrosis, size and perivesical fat invasion yielded non conclusive results as prognostic factors. Large, multicentric and wider follow up series must be collected to achieve convincing parameters concerning prognosis.

P-396

Immunohistochemical study of high-grade intraurotelial neoplasia and early carcinoma of bladder

Frank G., Zavalishina L., Andreeva Ju.
Dpt. of Pathology, Herzen's Research Oncologycal Institute, Moscow, Russia

AIMS: Immunohistochemical analisis of 32 patients with high-grade intraurotelial neoplasia and early carcinoma of urinary bladder.
METHODS: 17 cases of high-grade intraurothelial neoplasia and 15 – early carcinoma of urinary bladder have been reviwed. Using formalin-fixed and parafin-embedded specimens, we examined bcl-2, bcl-x, CD 95, p53, PCNA, Ki-67, C-erbB-2, MMP-1, MMP-9, TIMP-1, TIMP-2 by immunohistochemistry. By in situ hybridisation HPV DNA have been detected in the same cases.
RESULTS: We reviwed the straight correlation of expression bcl-x and CD-95 both in high-grade dysplasia and early carcinoma. The expression of TIMP-2 was found in 67% of all cases. On the other hand, the expression of MMP-1 was found in the rare specimens and the expression of MMP-9 – in 33%. The overexpression of p53 was demonstrated in invasive forms of cancer and it correlated with high proliferative activity. We haven't positive reactions with antibodies for oncoprotein bcl-2.
HPV DNA 16/18 types were detected in 50% specimens predominantly of the premalignant lesions.
CONCLUSION: Our resultats confirm the role of cancerogenous types HPV in the malignancy of urothelium, destroy of intercellular junctions and apoptosis by early carcinoma of urinary bladder.

P-397

High expression of Epstein Barr virus in testicular germ cell tumors of immunodeficient patients

Gamboa-Domínguez A., Chavarri-Guerra Y., Saqui-Salces M., Pérez-Santos L.G., Gabilondo F.
Department of Pathology and Urology, Instituto Nacional de Ciencias Médicas y Nutrición Salvador Zubirán, México City, México

Background: Controversies exist in series exploring the association of Epstein Barr virus (EVB) and testicular tumors in general population, but a higher incidence of these tumors in immunosupressed patients (ISP) has been observed.
Objective: Identify EBV-encoded small non-polyadenylated RNA (EBER) and latent membrane protein-1 (LMP-1) in testicular germ cell tumors (TGCT) of ISP.
Methods: Retrospective search of cases with testicular tumors from files of patients with acquired immunodeficiency syndrome (AIDS), autoimmune/hemathologic diseases, and organ receptors was made. Representative tissue was obtained from blocks for EBER *in situ* hybridization and LMP-1 detection by immunohistochemistry. Both procedures were performed in automatic stainers (Ventana Nexes and Discovery, Tuczon, AZ). Clinical data was obtained from records.
Results: Five ISP with TGCT were identified. All but one showed EBER in the nucleus of neoplastic cells and two patients had signal in the nucleus of intratubular germ cell neoplasia adjacent to seminoma. LMP-1 was positive in two cases.

Age	Immunodeficiency	Tumor/stage	EBER	LMP-1	Follow up
35	AIDS A2	Seminoma/I	+	–	18 m DOC
27	AIDS A1	Embrionary ca/III	+	+++	15 m DOD
30	AIDS	MGCT/I	–	–	3 m DOC
20	Aplastic anemia	Seminoma/II	+	+	28 m ANED
30	Renal transplant	Seminoma/I	+		429 m ANED

Conclusion: High EBERs expression was observed in TGCT in ISP and in preneoplastic lesions. These results support the hypothesis of EBV as oncogenic in germinal epithelium.

P-398

Telomerase reverse transcriptase (hTERT) quantitation in transitional cell carcinoma biopsies

Gazzano G., Pellegrini C., Maggioni M., Carmignani L., Rocco F., Coggi G., Bosari S.
Departments of Pathology and Urology, University of Milan, Italy

Introduction: Telomerase is a ribonucleoprotein enzyme that uses its own integral RNA as a template for synthesis of telomeric repeats. In transitional cell carcinoma (TCC) elevated telomerase activity has been described suggesting its value as diagnostic marker. Most investigators have evaluated telomerase activity using the Telomeric Repeat Amplification Protocol (TRAP) assay. The purpose of our investigation was to quantify the catalytic subunit of telomerase, the telomerase reverse transcriptase (hTERT) using a recently described quantitative real time RT-PCR technique.
Methods: We tested 22 neoplastic and non neoplastic bladder biopsies. RNA was extracted using the Trizol kit (Life technologies). After reverse transcription 10 υl. of cDNA were used to analyse hTERT levels with the real-time quantitative PCR technique and the ABI Prism 7700 sequence detection system (Applied Biosystems). β-actin mRNA levels were used as controls.
Results: hTERT mRNA could be detected in all the specimens. Elevated levels of hTERT were present in 16 tumors (73%). In two cases of chronic cystis and in 4 TCC low levels of hTERT were demonstrated, comparable to the matching normal mucosa controls. hTERT levels were not correlated to tumor grade and stage.
Conclusions: Real time RT-PCR provides a quantitative evaluation of hTERT in endoscopic bladder biopsies. Most bladder tumors display elevated levels of hTERT. Further studies will be needed to assess the sensitivity and specificity of this technique and its clinical value.

P-399

Renal mesenchymal neoplasms in adults classical and challenging cases

Geethanjali Sathja Sukumar, Karuna Rameshkumar
St. Martha's Hospital, Bangalore, India

Introduction: To analyze renal mesenchymal tumours during twenty five years (1966 to 1992) for rarity and diagnostic difficulties.
Methods: Records of 239 nephrectomies (1966 to 1992) were reviewed which yielded 9 renal mesenchymal tumours compared to 92 renal carcinomas in adults. Slides were reviewed and in addition to Haemotoxylin and Eosin stain, Masson's Trichrome, reticulin and Oil red O stains were done for subtyping.
Results: Angimyolipoma accounted for 50%; Rest of the spectrum consisted of leiomyosarcoma presented with classic of them clinically presented with massive haemorrage, necessitating great effort in diagnosis and management. Subtyping of malignant tumours required additional studies and data. Clinical course was that of aggressive malignancy resulting in death of three of four patients, while one patient was lost to follow up after surgery. Sarcomatoid variant of renal cell carcinoma presented on histology a diagnostic challenge, which was resolved by immunohistochemistry.
Conclusions: Rena mesenchymal neoplasms are rare and accounted for 5% of total renal tumours in a 25 year period. A combination of clinical, radiographical, histological and special stains is critical in optimizing outcome in these tumours, especially in malignant tumours.

P-400

DNA-Based Detection of Prostate Cancer in Washings from Transrectal Biopsies

Carsten Goessl, Rüdiger Heicappell, Markus Müller, Kurt Miller
Department of Urology, Benjamin Franklin Medical School, Free University of Berlin, Germany

Background: The use of prostate biopsy samples for analysis of molecular changes indicating malignant transformation of prostate cells is limited by the demand for complete histologic examination. We therefore tested if promoter hypermethylation of the glutathione-S-transferase P1 gene (*GSTP1*), a near unique feature of prostate cancer including early stages (W.H. Lee et al., 1994, 1997), is detectable in washings of prostate biopsy samples.
Patients and Methods: We investigated *GSTP1* promoter hypermethylation in DNA isolated from saline washings of sextant transrectal prostate biopsies. *GSTP1* promoter hypermethylation was detected by bisulfite treatment of DNA followed by methylation specific polymerase chain reaction (MSP). *GSTP1* promoter methylation status was correlated to the pathohistological findings in 10 men diagnosed with pure benign prostatic hyperplasia (BPH; serum prostate specific antigen [PSA] 6.5 to 32.4 ng/mL), 6 men with prostatic intraepithelial neoplasia (PIN; PSA 4.5 to 13.9 ng/mL) without adenocarcinoma, and 10 men with adenocarcinoma of the prostate (PSA 3.4 to 49.0 ng/mL).
Results: Whereas *GSTP1* promoter hypermethylation in at least one of six washing samples was not detectable by MSP in all 10 patients diagnosed with pure BPH (0%), we found it in 4 patients with PIN (66%) and in all 10 patients with adenocarcinoma (100%).
Conclusion: We conclude that patients with prostate cancer including preinvasive stages are detectable by tissue-free, DNA-based analysis of prostate biopsy washings without compromising pathohistological examination of complete biopsy samples. Targeting at other tumor-specific methylation patterns this approach appears suitable for a broad variety of human cancer entities.

P-401

Wunderlich syndrome as first manifestation of renal neoplasms.

Dra. M. Gómez Dorronsoro, B. Larrínaga, I. Amat,
M.C. Caballero, J.A. Cuesta*
Dtp. of Pathology and Urology*, Hospital de Navarra, Spain

Introduction: Wunderlich syndrome or spontaneous perirenal haemorrhage is an uncommon condition consisting in the sudden formation of an haematic collection in the subcapsular and perirenal regions (retroperitoneum).
The etiology is varied: renal neoplasms, vascular lesions, haematologic diseases, anticoagulant therapy etc ...
Material: Excluding those patients with history of trauma, renal biopsy or haemodialysis, we have seen six cases in the last three years with spontaneous perirenal haemorrhage.

Results: Almost all our patients with Wunderlich syndrome respond to malignant renal neoplasms as were:
- Primitive neuroectodermical tumor (1)
- Clear cell renal carcinoma (1)
- Suprarenal metastases of melanoma (1)
- Chromophobe cell renal carcinoma (2)
- Acute pyelonephritis (1)

In all these patients, the therapeutical approach was radical nephrectomy.
Conclusions: In our cases, the rate of a malignant tumoral cause of Wunderlich syndrome is high, so treatment by nephrectomy or conservative surgery will depend on the hemodynamic status of the patient , on the surgical approach and on the intraoperative diagnosis of the etiology.

P-402

According to WHO/ISUP consensus classification: Reerrangement of none invasive papillary urothelial neoplasies and evaluation pf p 53 and Ki67 overexpression in these subgroups

Z. Gülçiftçi, A. Akyildiz İğdem, P. Tuzlali, R. Sari, C. Arat, N. Erdoğan
Taksim State Hospital Departments of Pathology and Urology

Objective: In 1998 WHO/ISUP consensus meeting, stage pTa urothelial cell neoplasms of the bladder were classified under the term "non-invasive papillary urothelial neoplasms" and four histomorphologic subgroups were defined. This study to evaluate whether p53 and Ki67 overexpression in these subgroups may be of value in estimating recurrences and prognosis.
Materials and Methods: A retrospective review was made of 50 cases who were diagnosed with papilloma, gradel-II (Mostofi) and stage pTa urothelial cell carcinoma between 1995–99 in Taksim State Hospital. All cases were classified into four subgroups according to the concensus. Samples were stained immunohistochemically for p53 and Ki67 and correlation was sought between overexpression of p53 and Ki67 and prognosis.
Result: 95% of the bladder cacinomas diagnosed in our laboratory were of urothelial cell origin and 32% of these were in stage pTa and papilloma grade I-II (Mostofi). 15% of the cases were urothelial papilloma (UP), 33% papillary urothelial neoplasm with low malignant potential (PIN-LMP), 29% low-grade papillary urothelial carcinoma (LG-PUC) and 23% high-grade papillary urothelial carcinoma (HG-PUC). Mean expression levels of p53 and Ki67 were 0.03 and 0.0380 in urothelial papilloma, 0.0660 and 0.080 in papillary urothelial neoplasm with low malignant potential, 0.1999 and 0.1969 in low.grade and 0.3517 and 0.3010 in high-grade papillary urothelial carcinoma, respectively.
Conclusion: The study results were consistent with WHO/ISUP concensus classification with respect to recurrence and progression of papillary urothelial neoplasms, with p53 and Ki67 overexpression levels being competible with the dignosis of the subgroups.
Keywords: urothelial cell carcinoma, non-invasive papillary urothelial neoplasms, 1998 WHO/ISUP consensus meeting, p53, Ki67, prognosis

P-403

P21, p27, and pRb as prognostic indicators in clear cell renal cell carcinoma

Andrea Haitel MD*, Helene G. Wiener MD**, Barbara Neudert*, Michael Marberger MD** Martin Susani MD*
Department of Pathology and ** Department of Urology, University of Vienna, Austria

Introduction: Cyclin-dependent kinase inhibitors like p21 and p27 prevent phosphorylation of cell cycle regulating proteins such as retinoblastoma gene protein.
Methods: The expression of three negative regulators of the cell cycle, the retinoblastoma gene product (pRb), the WAF1/Cip1gene product (p21), and the Kip1 gene product (p27) was investigated by immunohistochemistry on paraffin sections from 104 formalin fixed clear cell carcinomas and related to p53 overexpression, clinicopathological parameters, and survival.
Results: pRb expression was not associated with tumor stage, but correlated statistically significant with p27 and p21 positivity (r=0.26, p=0.008; r=0.3, p=0.002, respectively). Tumors representing p53 overexpression showed a higher pRb labeling index compared to p53 negative tumors (p=0.0004). p21 protein expression was significantly correlated with p27 positivity (r=0.2, p=0.04) and was associated with p53 overexpression (p=0.0005), but did not correlate with tumor stage or grade. No association could be found between p27 positivity and tumor grade, tumor stage or p53 overexpression. In univariate survival analysis an increased pRb positivity (p=0.002) and a low p27 expression (p=0.0001) predict poor outcome, especially if combined to p53 overexpression (p=0.001, p=0.0001, respectively). p21 did not give any prognostic information. In multivariate analysis pRb and p27 revealed statistically significant.
Conclusion: In clear cell renal cell carcinomas the cell cycle proteins p27 and pRb are powerful and independent prognostic factors whereas p21 has no predictive value.

P-404

HER2/neu oncogene in transitional cell carcinoma of the urinary bladder

Hauser-Kronberger C., Prokop E., Mack D., Esterbauer B., Schmeller. N., Dietze O.
Institute of Pathology and Department of Urology, Landeskliniken Salzburg, Austria

INTRODUCTION: The HER2/neu protooncogene encodes a cell surface receptor protein (p185, c-erbB2) which plays a role in growth factor-stimulated mitogenic signalling. HER2/neu gene was originally defined by its significant homology to the gene which encodes the epidermal growth factor receptor (EGF-R), also known as HER1. HER2/neu is amplified in about 30% of human breast carcinomas with up to more than 20 copies per nucleus. HER2/neu amplification is a strong predictor of risk for recurrence and overall survival independent of commonly used prognostic marker. HER2/neu overexpression has also been seen in a significant fraction of ovarian, lung, pancreatic tumours, but only few information exists on bladder cancer.
METHODS: In the present study we investigated 23 cases of urinary bladder cancer for the amplification of the Her2/neu gene and

the overexpression of its encoded protein c-erB2. Additionally p53, $p21^{Cip1/WAF1}$ and EGF-R expression were evaluated. Routinely processed paraffin-embedded tissue from bladder cancer were investigated for the HER2/neu gene-amplification using chromogenic *in situ* hybridisation (CISH) and fluorescence *in situ* hybridisation (FISH). Over-expression of the encoded protein c-erbB2, EGF-R, mutant p53 and $p21^{Cip1/WAF1}$, was detected using immunohistochemical methods (HercepTest™; Streptavidin-Biotin-Peroxidase).
RESULTS: 59% of the investigated carcinomas showed a weak expression of the c-erB2 protein, 29% showed a slightly overexpression and one was evaluated with a high overexpression. HER2/neu gene amplification detection using CISH and FISH correlated with overexpression of the protein c-erbB2. p53 mutant protein was highly expressed in one case and $p21^{Cip1/WAF1}$ was expressed in 40% of all cases investigated. No correlation could be found between HER-2/neu and EGF-R expression.
CONCLUSIONS: HER2/neu seem to be of prognostic and predictive value not only in breast cancer, but also in bladder cancer and patients may receive anti-HER2/neu treatment with the recently developed antibody Herceptin™.

P-405

Aminoterminal propeptide of type I procollagen is a useful marker in the clinical management of prostate cancer

R.K. Iles, *U. Otite, #K Jefferson, U. Jahnke, §M. Sheaff, *V.H. Nargund, *F. Chinegwundoh, #R. Persad, §S. Baithun
Williamson Laboratory and *Departments of Urology and §Histopathology, St Bartholomew's and The Royal London Hospitals, London; #Department of Urology, Bristol Royal Infirmary, Bristol, UK

Introduction: In prostate cancer, a major clinical consideration is whether the disease has spread to bone at diagnosis. We evaluated serum aminoterminal propeptide of type I procollagen (PINP), a marker of increased bone turnover, to determine whether it could discriminate between metastatic and non-metastatic prostate cancer.
Patients and Methods: 227 patients were included in this study of which 98 had benign prostate disease (control group) and 129 had newly diagnosed prostate cancer. All patients with cancer had bone scans at diagnosis of which 98 were negative (BS-ve), 21 positive (BS+ve) and 10 equivocal (Bseq). Serum specimens were obtained prior to treatment for measurements of PINP using radioimmunoassay (RIA). Other clinical information such as PSA and tumour grade was documented.
Results: The mean serum PINP level in the control population was 46.2 μg/L while levels in the BS-ve, BSeq, and BS+ve groups were 40.6 μg/L, 42.5 μg/L and 156.9 μg/L respectively. The BS+ve group had a statistically significant higher serum PINP level compared to all other groups ($p<0.0001$). ROC curve analysis revealed that at an optimum cut-off of 58.3 μg/L, the sensitivity and specificity of serum PINP for detecting bone metastases were 91% and 89% respectively (compared to sensitivity of 76% and specificity of 97% for PSA at a cut-off of 105 μg/L). Used in combination with PSA, the specificity increased to 100% but with reduced sensitivity to 71%.
Conclusion: This study confirms that serum PINP level is able to identify patients with prostate cancer who have bone metastases and suggests that it may have a role in the clinical management of prostate cancer.

P-406

Mast cells, testis volume and status of seminiferous tubules & spermatogenesis in patients with non-obstructive azoospermia

D. Ježek[1], A. Hittmair[2], Lj. Banek[1], I. Krhen[1], Ž. Vukelić[1], G. Mikuz[2]
[1] Medical School University of Zagreb, Zagreb, Croatia, [2] Institute of Pathology, University of Innsbruck, Innsbruck, Austria

Introduction: Within the human testis, mast cells are situated in the interstitial compartment. The aim of our study was to correlate the number of these cells with the testis volume and status of seminiferous tubules & spermatogenesis in patients with non-obstructive azoospermia.
Materials & methods: A total of 44 testicular biopsies from infertile patients with non-obstructive azoospermia and 8 control biopsies were analyzed. Mast cells were identified by immunohistochemistry (IHC). The testis volume was determined by an ultrasound examination and/or by orchidometer. The status of spermatogenesis was evaluated according to a modified Johnsen's score. The total number of mast cells, the length and curvature of seminiferous tubules were determined by stereology.
Results: The infertile group of patients displayed a significantly increased total number of mast cells, lower testis volume and score (status of spermatogenesis) when correlated to the control group ($p<0.001$). The length and curvature of seminiferous tubules per entire organ were significantly decreased in infertile group of patients ($p<0.01$). A significant negative correlation was found between the number of mast cells, testis volume, score, length and curvature of seminiferous tubules ($p<0.01$-0.001).
Conclusion. The increased number of mast cells within the testicular tissue has a negative impact on spermatogenesis, the length and curvature of seminiferous tubules.

P-407

Nitric oxide effects on gentamicine toxicity in the isolated perfused rat kidneys

Kadkhodaee M., Faghihi M., Ghaznavi R., Shams S.
Department of Physiology, Faculty of Medicine, Medical Sciences University,Tehran, Iran

There are many studies in recent years on the role of nitric oxide in acute renal failure (ARF). In this study, the effects of inhibition or induction of NO synthase (NOS) on renal toxicity of gentamicine was investigated using measurements of urinary lactate dehydrogenase (LDH) and alkaline phosphatase (ALP) activities. Kidneys from male albino rats were perfused in situ for 115 min and the urinary samples were collected at 70, 90 and 110 min of perfusion for 5 min. Six groups of rats were studied in which L-Name (0.1 mM) was used as a NOS inhibitor and L-Arginine (L-Arg, 2 mM) was used as a NOS inducer: group 1, control with no treatment; group 2, L-Arg; group 3, L-Name; group 4, gentamicine (0.5 mg/ml); group 5, gentamicine+L-Arg, group 6, gentamicine+L-Name. Perfusion with L-arginine before gentamicine significantly decreased toxicity compared with gentamicine group (ALP, 188 29 vs 310.3. 40.5 and LDH, 66.2  20 vs 158.8  20, $P<0.001$). Perfusion with L-Name before gentamicine increased toxicity significantly, compared with gentamicine group ($P<0.001$). This study suggests that renal gentamicine toxici-

ty may be as a result ofdecrease in NOS activity. nitric oxide, gentamicine, kidney.

P-408

Nuclear and nucleolar morphometry in addition to DNA image cytometry in prostatic carcinoma

N. Kavantzas, E. Agapitos, A.C. Lazaris, P.M. Pavlopoulos, C. Eftychiadis, P. Davaris
Department of Pathology, Medical School, University of Athens, Greece

Introduction/aim: In the present study we examined several nuclear and nucleolar morphometric parameters and DNA content status of prostatic carcinomas in an attempt to determine if these parameters can provide significant additional information to the Gleason grading.
Material and methods: Image cytometry, nuclear and nucleolar morphometry were carried out on paraffin tissue sections from 50 prostatic carcinomas. Using an image analysis system the following nuclear morphometric parameters were estimated: area, major and minor axis length, Feret diameter, shape factor and compactness. The mean number of nucleoli, the percentage of nuclei with visible nucleoli and the mean nucleolar area were also estimated. For DNA image cytometry the Feulgen method was used. At least 200 carcinoma nuclei were measured from each case and ploidy histograms were plotted.
Results: Tumors of grade I or II showed lower DI values compared to grade III and IV (t-test, p=0.014). Grade I tumors have a significantly higher percentage of nuclei with visible nucleoli (t-test, p=0.050). Although the relationships were dubious, it seems that the higher is the DI, the fewer are the nuclei with obvious nucleoli (p=0.100) and the higher is the mean value of nuclear area, the more obvious nucleoli the have (p=0.095). The nuclear size of hypodiploid tumors was larger than in the rest DI categories (t-test, area: p=0.041, Feret diameter: p=0.044, major axis: p=0.066).
Conclusion: In addition to conventional grading, our results suggest that nuclear and nucleolar morphometry combined with image cytometry determination of ploidy level can provide significant information, concerning the diagnosis and physical history of prostatic carcinoma.

P-409

CGH and microsatellite analysis of renal angiomyolipomas

K. Koch, G. Schmahl and S. Stoerkel
Institute of Pathology, University of Witten/Herdecke, Wuppertal, Germany

Introduction: Angiomyolipoma (AML) is the most common mesenchymal tumor of the kidney and, as the name indicating, consists of variable amounts of mature fat, smooth muscle and thick-walled blood vessels. Controversy exists whether it is a tumor entity with uncertain biological potential. AML has been considered a hamartomatous polyclonal proliferation which rarely undergoes malignant transformation (especially epitheloid AMLs). Recent investigations, however, demonstrated clonality, but so far only few genetic data are available emphasizing some genomic regions of interest.
Methods: Paraffin-embedded tissue was analysed from 30 tumors classified as renal AMLs. Whenever possible tumor areas of muscular or lipomatous cells were microdissected separately and the extracted DNA subjected to CGH and microsatellite analysis.
Results: In all tumors no obvious losses or gains of genetic material could be demonstrated by CGH analysis. Even separate analysis of solely muscular (25 cases) and lipomatous tissue (9 cases) did not reveal any detectable chromosomal imbalances. Applied LOH studies confirm these data.
Conclusions: Our results on genomic analysis of AMLs demonstrate no chromosomal numerical aberrations including losses and amplifications even in adipose and muscle tissue. These findings are in concordance with the benign appearance of these lesions. Our current clonality studies will provide further information on elucidating the tumor status of AML.

P-410

Vascular endothelial growth factor (VEGF) and its receptor Flk-1 in malignant and nonmalignant prostate tissue

J. Köllermann, B. Helpap
Institute of Pathology, Hegau-Klinikum Singen, Germany

Introduction: VEGF stimulates tumor angiogenesis. It acts via binding to specific receptors, primarily expressed by endothelial cells. Recently VEGF receptor Flk-1 was reported to be expressed also by prostate basal cells. Flk-1 expression in high grade prostatic intraepithelial neoplasia (HGPIN) indicates a close association with dedifferentiation. Surprisingly in prostatic carcinomas (PC) Flk-1 is reported to be downregulated with dedifferentiation. We tested the reproducibility of this contradiction.
Methods:VEGF and Flk-1 expression was immunohistochemically analyzed in 21 radical prostatectomy specimens, containing benign glands, HGPIN, and PC. Anti VEGF and FLK-1 immunoreactivity was graded semiquantitatively as light, moderate or strong staining.
Results: In benign glands VEGF and Flk-1 expression was almost exclusively confined to the basal cell layer. All HGPIN lesions were strongly positive for both markers. VEGF expression was seen in 19 of 21 PCs (90.5%), Flk-1 expression in 20 of 21 (95.2%). There was a trend for increasing marker expression with tumor grade. 9 of 11 Gleason score (GS) 7–9 PCs (81.8%) were strongly positive for Flk-1, whereas none of the GS 4 and 5 PCs (n=4) showed a strong marker expression. All GS 7–9 PCs (11/11) showed moderate to strong VEGF expression, whereas GS 4 (n=2) PCs were negative and GS 5 PCs showed only minor VEGF expression.
Conclusions: Tumor growth stimulated by the VEGF-Flk-1 system is not only promoted by neoangiogenesis but also by tumor autostimulation which may play an important role in the process of malignant transformation and tumor progression.

P-411

Leiomyosarcoma of the prostate: Report of two cases.

Larrinaga B., Gomez M.., Caballero C., Amat I., Grasa V.*
Department of patology and urology *. Hospital of Navarra, Pamplona, Spain

Leiomyosarcoma of the prostate is a rare neoplasm that account for 0.1% of prostate malignancies, is the most common sarcoma in

adults. We herein present two cases observed in our departaments since 15 years ago.
The first case was in a 62 years old man, CT scans showed a large (15 cm) cell prostatic tumor, microscopic and inmunochemical studies showed a low grade leiomyosarcoma, diploide with low proliferation index. Total prostatectomy were performed and all tumor were removed, no adyuvante therapy was done. 24 moths after were alive and without residual tumor.
The second case was in a 58 years old man with a large hipogastric tumor , to concern cell prostatic.The diagnosis was made with trucut biopsy. High grade leiomyosarcoma aneuploide with high proliferation index was diagnosed. Radiation therapy was treatment of choice. The patient died 6 moth after diagnosis.
Conclusions: Histologic grade of leiomyosarcoma of the prostate is a survival factor. Radical surgery was the treatment of choice. If the excision is complete, the size of tumor is not a factor to deal with, in order of prognostic.

P-412

A renal metastasis of an occult prostate carcinoma – A case report –

Elena Lazar[1], G. Feichter[2], Alis Dema[1], Codruta Lazureanu[1], S. Dema[3], M. Botoca[3], Daniela Lazar[1]
[1] Department of Pathology, University of Medicine , Pharmacy Timisoara, Romania, [2] Deparment of Patology, Institute of Patology, Basel, Elvetia; [3] City Hospital, Timisoara - Romania

Introduction: The occult prostate carcinomas, diagnosed because their metastases, are more often reported and the sites of metastases are more and more diverse, leading to both clinical and histopathological diagnostic difficulties.
Material and method: We present an unusual case of prostate carcinoma, in which the symptoms are produced by the renal and urinary bladder invasion/metastases. The case demonstrates that the possibility of an invasion/metastasis, although rare, should be considered for the differential diagnosis of a renal tumor, emphasizing, in the same time, the importance of immunohistochemistry for positive diagnosis.
A 51 years old patient is operated for left renal tuberculosis. Gross examination reveals an enlarged kidney, on cross section a pale cortex and medulla and, in the middle part, a zone with cystic cavities and necrosis. Tissue fragments, fixed in formalin 10%, paraffin embedded and stained with H&E, presented a tumoral proliferation developed beneath the transitional epithelium of pelvis and ureter, which are intact. The tumor invaded the muscular layer and surrounding adipose tissue consists of small tubular structures, lined by cuboidal cells with eosinophilic/clear scanty cytoplasm, slightly pleomorphic nuclei and reduce mitotic activity. In other parts the neoplastic cells are disposed in compact sheets and even as pseudopapillary structures. The stroma is poorly developed. The diagnosis is Wilms' tumor of adulthood, the tubular epithelial subtype with pelvis and ureteral invasion. The patient is directed to radiotherapy and chemotherapy. A CT procedure before the radiant therapy reveals a thickened urinary bladder. A diagnostic transurethral resection follows. The microscopic aspects show, beneath the normal urothelium, a malignant proliferation similar with the prior renal neoplasm.
The particularity of the case requires immunohistochemistry for further explanations. We use monoclonal antibodies for cytokeratin (Lu5) and for specific prostatic antigen, ABC method with DAB. On the ground of positive reaction for CK and PSA we conclude that prostate carcinoma is the primary tumor with secondary involvement of urinary bladder and kidney.
We consider this case as real diagnostic challenge, especially due to the unusual onset – a renal secondary tumor of an occult prostatic carcinoma – which is very rare communicated in literature.

P-413

Mitochondrial Mutations in Early Stage Prostate Cancer and Bodily Fluids

C. Lopes, C. Jerónimo, S. Nomoto, O.L. Caballero, H. Usadel, R. Henrique, G. Varzim, J. Oliveira, M.S. Fliss, D. Sidransky
Instituto Portugues de Oncologia, Centro Regional do Porto, Portugal, Unit of Molecular Pathology-Department of Pathology [C.L., R.H., G.V.,]and Department of Urology [J.O.], Instituto Portugues de Oncologia de Francisco Gentil – Centro Regional do Porto, Porto, Portugal; and Department of Otolaryngology-Head and Neck Surgery [C.J., S.N., O.L.C., H.U., M.F., D.S.], Head and Neck Cancer Research Division, The Johns Hopkins University School of Medicine, Baltimore, Maryland 21205-2195, USA

Introduction: The existence of specific patterns of somatic mitochondrial DNA (mtDNA) mutations was recently demonstrated in several cancers. Here we sought to identify the presence of mtDNA mutations in prostate cancer and their paired PIN lesions.

Material & Methods: The D-loop region, 163 rRNA, and the NADH subunits of complex I were sequenced to identify the presence of mtDNA mutations in 16 matched PIN lesions and primary prostate cancers. Peripheral blood lymphocytes were used as normal controls.
Results: Twenty mtDNA mutations were detected in the tumors tissue of three patients. Identical mutations were also identified in the PIN lesion from one patients. This patient with multiple point mutations also harboured a high frequency of micro satellite instability (MSI-H) in nuclear mononucleotide repeat markers. Remarkably, these mutations were also detected in all 3/3 matched urine and plasma samples obtained from these patients.
Conclusions: Although mitochondrial mutations are not common in prostate adenocarcinoma, they occur early in cancer progression and they can be detected in bodily fluids of early stage disease patients. The identification of mtDNA mutations may complement other early detection approaches for prostate cancer.
C.J. is supported by a glnt of the Fundacao para a Ciencia e Technologia, Portugal (Program PRAXIS XXI – BD 13398/97)

P-414

Importance of multiple testicular biopsies in severe oligozoospermia in view of assisted reproduction

Magyar, É.*, Erdei, E.**, Lellei, I.*
Depts of Pathology* and Andrology**, Semmelweis University, Faculty of Health Sciences, Budapest, Hungary

Introduction: According to the spermogram severe oligozoospermia (OATS) is a common reason of male infertility. In view of successful assisted fertilisation multiple testicular biopsy supposed to be of great help.
Methods: Testicular biopsies of 22 patients with OATS were examined histologically. The biopsies were performed by atraumatic mi-

crosurgery. Samples taken from the upper inner and lower outer quadrant were processed after Bouin fixation.
Results: Histology revealed maturation arrest in 15 cases, decreased spermatogenesis in one, atrophy also in one, while in 5 cases the spermatogenesis was normal. By 6 patients all samples showed similar picture. Inhomogeneous distribution of spermatogenetic activity appeared in 3. By 13 cases the spermatogenetic activity was inhomogeneous with or without maturation arrest. All of the cases showing maturation arrest histology was different in the four samples eighter in spermatogenetic activity or in the grade of the arrest. The only patient with hypospermatogenesis presented different spermatogenetic activity in the samples taken from different places, while the one with atrophy and the 5 cases of normal spermatogenesis showed homogenous histological appearances in all of the biopsies.
Conclusion: As spermatogenesis is not homogenous in the testes, the four biopsy samples give fairly realistic information. This method helps to show the optimal location of sperm extraction for assisted fertilisation.

P-415

Detection of telomerase activity by PCR -based trap technique in prostate cancer

Soleiman Mahjoub
Department of Biochemistry, Babol University of Medical Sciences, Babol, Iran

Telomerase, a ribonucleoprotein enzyme adds hexanucleotide repeat (TTAGGG)n to the end of chromosomes, forming telomers.In most eukarotic somatic cell, the absence of telomerase activity resalts in a loss of telomeric repeat with each round of chromosomal DNA replication. Activity of the enzyme is frequently up-regulated on cancer tissues and immortalized cell line when compared with normal tissues.
In this study, telomerase activity was detected by using very sensitive PCR-based TRAP technique in 65 prostate cancer and in tissues adjacent to tumor including 12 prostatic intraepithelial neoplasia (PIN), 23 benign prostatic hyperplasia (BPH), 9 atrophy and 11 normal samples.
Telomerase activity was present in 93.8% of prostate cancer, 75% of PIN, 74.8% of BPH , 22.2% of atrophy and 27.3% of normal samples. In contrast to the BPH tissue from cancer – bearing glands, all 21 BPH specimens from patients only diagnosed with BPH were telomerase activity negative. This results indicate that telomerase activity is present in most of prostate cancers.The high rate of telomerase activity in tissue adjacent to tumor may be attributed either to early molecular alterations of cancer that were histologically inapparent or to the presence of occult cancer cells.
Keywords: Telomerase, Prostate cancer,PCR, TRAP assay.

P-416

Cytokeratin 20 (CK20) expression in transitional cell carcinoma (TCC) of renal pelvis and ureter

C. Mallofré, M. Castillo, C. Romagosa, J. Muntané, A. Palacín, A.Cardesa
Dpt. Anatomia Patologica, Hospital Clínic, IDIBAPS, Facultat de Medicina, Barcelona

INTRODUCTION: CK20 inmunohistochemical expression has been considered in no-invasive TCC of the bladder as a factor of recurrence. We studied the expression of CK20 in TCC of renal pelvis and ureter to find out if it had a prognostic significance.
METHODS: We studied retrospectively 36 patients diagnosed of TCC of renal pelvis and/or ureter in our center for the last 5 years. Immunostaining for CK20 was performed both in normal urothelium and carcinomas. We evaluated the positivity for CK20 by two methods: First with a two categories classification (positive and negative) and secondly with a four categories classification as has been stated by other authors for bladder TCCn (diffuse, negative, superficial and diffuse with superficial accentuation). We divided the patients into three groups depending their evolution: Non-recurrent tumors, recurrent and presence of metastasis.
RESULTS: Of the 36 TCC, 5.5% were pTa, 30.5% were pT1, 11.2% were pT2, 30.5% were pT3 and 22.3% were pT4. Only 22 cases of cases (61%) were positive for CK20. When considering the 4 categories classification, we obtained that 41.6% were diffusely positive (D), 27.7% were negative (N), 11.1% presented positivity only in superficial cell (S), and 19.6% were diffuse with a superficial accentuation (DS). The patterns of CK20 expression (D, N, S, DS) were independent to TCC stage and grade, and did not have statistical significance when correlated with patient's evolution.
CONCLUSIONS: In our study, only 61% of the TCC were positive for CK20, and this factor was not related to grade nor stage. The different patterns of expression of CK20 proposed by some authors to be a prognostic marker for bladder cell carcinoma is not useful for upper tract TCC.

P-417

Frequency and morphology of prostate cancer in our material

S. Manxhuka-Kërliu, Xh. Kamberaj, B. Slamniku, A. Kërliu, H. Ahmetaj
Institute of Pathology, Faculty of Medicine, University of Prishtina, Kosovo

Prostate cancer is the malignant transformation of the epithelial cellular component most times at the expense of secretors cells. The aim of our study was to report our data about the incidence, morphology and prognosis of prostate cancer in our material as well as to apply major and minor criteria for the diagnosis of cancer in core needle biopsy determinate by the consensus. During our research we have found 25% of cases with prostate cancer out of 188 reviewed biopsies of prostate. We have represented the distribution of prostate cancer according to the age and grade of cancer. The highest incidence of prostate cancer was in 7th decade of life (57.44%), $p<0.01$.It was studied also the distribution of different morphological variants of prostate cancer. Glandular well differentiated were in 25.53% of cases, glandular poorly differentiated were in 27.65%, cribriform in 8.51%, solid-trabecular in 19.14% and mixed type in 12.76% of cases. The highest incidence belong to poorly differentiated variant. The most known grading system (Gleason system) was used as an important prognostic factor; 27.65% were low-grade carcinoma G2-G6) and 65.95% of cases were high grade carcinoma (G7-G10). High grade carcinoma was most frequent. $D=0.269$, $p<0.01$. In our study we have represented also the distribution of prostate cancer according to TNM staging system of 1992. The highest incidence belong to stage pT3 – 38.29%,which means that most of cases with cancer penetrated

capsular; stage pT2 was in 23.40% of cases, whereas stage pT1 was in 36.16% of cases with prostate cancer. We didn't have any case of stage pT4. X2=2.21,DF=2. The distribution of prostate cancer in core needle biopsy was 29.78%. It was necessary to combine biopsy findings with clinical data as well as new biomarkers to enhance prediction of the biological behavior of prostate cancer identified in core needle biopsy. Our results indicate that the percent of prostate cancer is lower than reported in literature; and as far as the grading of prostate cancer is concerned we have concluded that the grade of cancer increases with increased age of life.

P-418

Human α-defensins hnp1-3 are present in renal cell carcinomas and lead to their necrosis or proliferation

J. Marković-Lipkovski[1], G.A. Müller[2], T. Flad[3], T. Klatt[3], S. Widmann[3], C.A. Müller[3]
[1] Institute of Pathology, Medical Faculty, University of Belgrade, Yugoslavia, [2] Center of Internal Medicine, Georg-August University of Göttingen, Germany, [3] Medical University Clinic, Eberhard-Karls University of Tübingen, Germany

The α-defensins HNP1-3 are cytotoxic peptides with restricted expression in neutrophils. In this study we investigated the presence, the origin and the role of HNP1-3 defensins in renal cell carcinoma (RCC). HNP1-3 were detected in vivo in 31 tissues by immunohistological methods with specific antibodies. In the most of low grade RCC the focal staining of tumour cells grouped mainly around neutrophils was seen. In six tumours of high-grade malignancy all tumour cells were strongly and diffusely stained for HNP1-3 defensins. Neutrophils, labelled by antibody to neutrophil esterase, participating in the considerable number of tumour infiltrating cells, could release a great amount of defensins in RCC tissue. However, we further investigated possibility that RCC synthesised HNP1-3 defensins. All eight investigated RCC lines were found to express mRNA for HNP1-3 as well as the specific peptides detected by flow cytometry, confocal microscopy and mass spectrometric analysis. In vitro HNP1-3 stimulated cell proliferation in two out of five RCC lines at physiological concentrations. Thus, α-defensins could be expected to exert autocrine growth factor activity also in vivo on a subset of RCC. Cellular necrosis observed in RCC tissues associated with intensive and extensive stains of HNP1-3 appeared to be related to higher concentrations of α-defensins that were also cytotoxic for all cell lines tested. In addition, α-defensins were found to be bound to HLA-class II molecules with inhibitory effects on recognition of tumour cells by alloreactive T-cells. These findings suggest that α-defensins represent new effector molecules of RCC involved in tumour pathogenesis by regulatory influences on tumour cell survival and immune recognitio

P-419

Morphometrical study of ultrastructural changes in cavernosal tissue of diabetic men with erectile dysfunction

Matsionis A., Fomkin R., Kogan M., Povilaitite P.
Rostov Regional Bureau of Pathology, Rostov-on-Don, Russia

Introduction: Diabetes mellitus is on the first place among organic causes of problems with potency. At the same time issues of pathogenesis of erectile dysfunction (ED) with underlying diabetes mellitus (DM) are not yet completely studied. The work was aimed to morphometrical study of ultrastructure of nerve fiber and cavernosal tissue in case of ED accompanying DM.
Methods: The subjects of the study were bioptates of corpora cavernosa in case of ED on DM background (n=10), prepared according to the standard procedure for electron microscopy. Hardware and software AnalySys with electron microscope EM-208 (Philips) was used for morphometry. Material from patients with psychogenic ED (n=10) was used as control series.
Results: Morphometrical analysis of ultrastructural parameters of cavernosal nonmyelinated nerve fibers showed that in case of DM number of axons, included into the single nerve fiber, is reduced by 35%, and the number of axonal and Schwann cells mitochondria was three times reduced ($p \leq 0{,}001$). Extracellular matrix of nerve fibers (basal lamina) and Schwann cells membrane are definitely enlarged as compared to the control samples. Analysis of histograms of axon distribution according to the number of neurosecretory granules revealed nerve fibers, that are deprived of neurosecretory granules due to axoplasm dystrophic and degenerative changes. On the contrary, some axons contain excess of granules that may be considered as compensation reaction or the result of inadequate secretion of granule's content through the enlarged membranes. Analysis of cavernal lumina and walls revealed significant (more than twice) reduction of walls sinuosity ($p \leq 0{,}001$), thinning of basal membrane and endothelium by 50% and 30%, respectively ($p \leq 0{,}001$).
Conclusion: Development of diabetic ED is associated with quantitative changes in ultrastructure of cavernosal nerve fiber and vascular walls that may be one of the causes of disorders in neurogenic and vasculogenic component of control and regulation of erection process.

P-420

Prostate carcinomas with negative initial needle biopsies

Peter R. Mazal[a], Andrea Haitel[a], Christian Windischberger[b], Bob Djavan[c], Roland Sedivy[a], Ewald Moser[b], Martin Susani[a]
[a] Department of Clinical Pathology, [b] AG NMR of the Institute for Medical Physics, and [c] Department of Urology, University of Vienna, Austria

Objectives: The spatial distribution of cancer foci of prostate carcinomas with negative initial biopsies was compared to that of prostate carcinomas with positive initial biopsies to detect areas in which carcinomas were more frequently located when the initial biopsy was negative.
Methods: Twenty patients with prostate cancer and a negative initial biopsy trial were detected among 218 patients with preceding systematic biopsies (9.2%) in our hospital. Analysis of the prostatectomy specimens regarding cancer distribution, multifocality, tumour size, Gleason score, and stage was performed using pathohistological techniques and three-dimensional computer reconstruction.
Results: Prostatectomy specimens with negative initial biopsies showed more frequently cancer foci in apical ($p<0.0001$) and dorsal ($p<0.02$) prostatic compartments, higher incidence of multifocality ($p<0.01$), and smaller size of carcinoma foci ($p<0.00001$)

compared to carcinomas in 81 stage matched prostatectomy specimens with positive initial biopsies. Comparing both groups, no significant differences were noted in Gleason score of preoperative biopsies and prostatectomies, prostate weight, PSA level, digital rectal examination, and patients age.
Conclusion: Missing the cancer in clinically significant prostate carcinomas by current systematic biopsy techniques may also be due to an apico-dorsal cancer location, particularly in combination with multifocality and small size of carcinoma foci in large prostates. In case of reasonable clinical suspicion of prostate cancer and negative initial biopsy, an early repeat biopsy with special emphasis on the apico-dorsal peripheral zone should be envisaged.

P-421

Is methylation status of $p14^{ARF}$, $p15^{INK4B}$ and $p16^{INK4A}$ related to pathological type or cytogenetic findings in renal-cell carcinoma?

L. Morell-Quadreny, J.A.. López Guerrero, C. Mejía,
M.A. Gregori-Romero, A. Pellín, J. Rubio*, E. Solsona*,
A. Llombart-Bosch
Department of Pathology, Medical School, University of Valencia, Instituto Valenciano de Oncología (IVO), Spain

Adult renal tumors comprise various pathological subtypes with specific cytogenetic markers, as well as differences in prognosis. Abnormal behavior of cancer cells can be suspected by histological findings and can be explained by quantitative and/or qualitative changes in the active gene set. Enzymatic methylation of the C-5 position of citosine residues can affect epigenetic inheritance by altering the expression of genes and by transmission of DNA methylation patterns through cell division.
We studied the pathological and molecular status of $p14^{ARF}$, $p15^{INK4B}$ and $p16^{INK4A}$ in 21 RCCs and in peritumoral kidney from 11 cases. Molecular analysis included extraction of DNA from cryopreserved tissue, followed by PCR differential for homozygous deletions and methylation specific PCR for the status of methylation of the $p14^{ARF}$, $p15^{INK4B}$ and $p16^{INK4A}$ genes. Moreover, in 11 tumors (seven conventional, two papillary, one chromophobe and one collecting duct carcinoma) cytogenetic study was performed after short term culture, by means of standard method GTG staining banding. Karyotypes were described according to ISCN (1995). At diagnosis, 10 patients were stage I, 6 stage II, 3 stage III and 2 stage IV. Histological study of tumors revealed 16 conventional, 3 papillary, 1 chromophobe and one collecting duct carcinoma. There were 5 cases of grade 1, 7 grade 2 and 9 grade 3. Methylation in $p14^{ARF}$ was in 4 tumors as well as in 2 peritumoral kidneys, and $p15^{INK4B}$ was in 9 tumors and 4 peritumoral kidneys; only two high grade tumors showed methylation in both $p14^{ARF}$ and $p15^{INK4B}$. No cases were methylated in $p16^{INK4A}$. All conventional RCCs showed del 3(p) and/or loss of #3. Papillary neoplasms presented both alterations in #7, 9 and 17. Chromophobe and collecting duct cases were gain of #17 and alterations in 9. There was no statistical relation between methylation status and pathological and cytogenetic findings, but we observed a trend to show $p15^{INK4B}$ hypermethylation of high grade, non-conventional type tumors. Moreover, most cases which showed loss or gain of chromosomes 9 and/or 17 were also $p15^{INK4B}$ hypermethylated.
Supported by a grant of Instituto Valenciano de Oncología (IVO) and AECC nº C-211/97. Valencia. Spain

P-422

Serum PSA and free- to-total PSA ratio measured 0 to 7 years before the diagnosis of prostate cancer correlate with the histological differentiation

S. Nordling, H. Mäenpää, N. Malila, J. Virtamo, U.-H. Stenman, M. Virolainen, H. Alfthan, H. Joensuu
Departments of Pathology, Oncology and Clinical Chemistry, University of Helsinki; Helsinki University Central Hospital; National Public Health Institute, Helsinki, Finland

Objective: To assess whether serum PSA (S-PSA) levels and free-to-total PSA ratio (F/T)in sera taken years before the diagnosis of prostate cancer are associated with histological differentiation.
Methods: Prostate cancer was diagnosed in 246 men participating in the Alpha-Tocopherol, Beta-carotene Cancer prevention study. Paraffin-embedded tissue was available in 101 tumours. PSA and F/T were determined from sera taken 0.1 to 7.1 (median 4.0) years prior to diagnosis. The malignant potential estimated by Gleason score, DNA flow cytometry, and Ki-67 immunostaining.
Results: S-PSA and F/T associated with Gleason score, but not with DNA ploidy or Ki-67 staining. In 72 (71%) men S-PSA was4 ng/ml or less, and in 56 (55%) F/T was below10%. When sampled at least4 years prior to diagnosis, S-PSA increased with an increasing Gleason score from a median of 4.4 ng/ml (scores 2 to 4) to 10.7 ng/ml (5 to 7) and 30.8 ng/ml (8 to10, P=0.0047). This was not the case in samples collected less than4 years prior to diagnosis (P=0.11). In samples taken less than4.0 prior to diagnosis, the median F/T PSA ratio decreased with an increasing Gleason score from 12% (scores 2 to 4) to 9% (5 to 7) and 5% (8 to 10, P=0.04).There was a similar trend in samples taken at least 4 years prior to diagnosis, median ratios 15%, 9%, and 8%, (P=0.08).
Conclusions: A high serum PSA level and low F/T ratio determined years before the diagnosis of prostate cancer are associated with poor differentiation as assessed by the Gleason score.

P-423

Post-mortem study of the prevalence of high grade prostatic intraepithelial neoplasia in the spanish population: Comparative assessment with post-mortem data from other ethnic groups and geographical areas

Olmedilla-Arregui G., Ruiz-Villaespesa A., Sanchez-Chapado M., Angulo Jc., Ramos P.
Servicios De Anatomia Patologica Y Urologia. Hospital Universitario, Principe De Asturias, Alcala De Henares, Spain

INTRODUCTION: Study of the prevalence and histological features of high grade PIN (HGPIN) in post-mortem specimens of a sample of the Spanish population, (Mediterranean Caucasian) comparing with Afro-Americans (AA) and American Caucasian individuals (AC).
METHODS: We studied prostatic glands from post-mortem examinations of 162 male patients born and living in Spain, aged >20 years. The glands were fixed on formaline, sectioned every 3–4 mm and studied after H-E staining. Criteria from the last Consensus Conference were applied. Only HGPIN cases were analyzed. All areas showing HGPIN from every block were mapped on individual plots. Extension of HGPIN was classified as focal and multifocal.

RESULTS: Of the total 162 prostatic glands examined, 16 were considered unsuitable. The final study was performed on 146 glands obtained from patients with a mean age of 48.5 years (20–81) Forty-two cases of HGPIN were found (28.26%), 20 of these being focal and 22 being multifocal. All focal HGPIN were located at the peripheral area (PA) and all multifocal HGPIN showed at least a peripheral growth. Prevalence by age was distributed as follows: 7.1%, 14.7%, 28.5%, 33.3%, 45.4%, 51.8% in the 3rd–8th decades.
CONCLUSION. The development HGPIN in the Mediterranean Caucasian population starts in the 3rd decade, is usually unifocal and peripheral and its frequency and multifocality increase with age. The prevalence was lower in all MC age groups, compared with the AA and AC ethnic groups.

P-424

Immunohistochemical E-Cadherin expression as a prognostic parameter in bladder carcinoma classified according to the 1998 WHO/ISUP classification

Orhan D.*, Tulunay Ö., Canoglu V.A.**, Bedük Y.**
Departments of Pathology* and Urology**, Medical School of Ankara University, Ankara, Turkey

Introduction: We examined E-Cadherin expression in bladder cancer samples from patients with known clinical follow-up to assess its relationship to prognosis and response to therapy.
Methods: Histologic slides of 77 bladder carcinomas and 15 control cases (normal urothelium) were graded using the 1973 WHO and 1998 WHO/ISUP classifications. We classified strong membranous immunohistochemical E-Cadherin expression (like normal urothelium) as normal E-Cadherin expression and all other staining patterns (absent, cytoplasmic and heterogenous) were considered as abnormal E-Cadherin expression.
Results: All control biopsy specimens showed normal E-Cadherin expression. In cancer samples, normal E-Cadherin expression frequency was 51.9% and E-Cadherin expression showed significant difference between control and cancer cases ($p<0.001$). Abnormal E-Cadherin expression correlated with both increased stage, WHO and WHO/ISUP grades ($p<0.001$ for each parameter). In the superficial bladder cancer group (n=43), normal E-Cadherin expression was not found to be associated with the risk of clinical progression ($p>0.05$). In the invasive cancer group (n=34), normal E-cadherin expression correlated with a low risk of clinical progression ($p>0.001$). Normal E-cadherin expression frequency was found to be 77.8% in invasive cancer patients who didnot show recurrence after M-VEC chemoterapy. On the other hand, in patient group with recurrence after M-VEC chemoterapy none of the tumors showed normal E-Cadherin expression indicating that abnormal E-Cadherin expression correlated with poor response to M-VEC chemoterapy in invasive bladder cancers ($p<0.001$).
Conclusion: These data suggest that abnormal E-Cadherin expression may define a high risk group of patients and the use of this antigen may prove valuable in planning the treatment of patients with invasive bladder cancer.

P-425

Detection of serum and urinary beta human chorionic gonadotrophin (hCGβ) by immunoradiometric assay and enzyme-linked immunosorbent assay: Is this a useful marker for the clinical management of prostate cancer?

U. Otite, *R.K. Iles, *E. Jacoby, #M. Sheaff, F. Chinegwundoh, V.H. Nargund, #S. Baithun
* Williamson Laboratory and Departments of Urology and
# Histopathology, St Bartholomew's Hospital; The Royal London Hospital, London

Introduction: Immunhistochemical detection of hCGβ has been shown to be of prognostic value in prostate cancer (Sheaff et al J Clin Pathol 1996; 49:329-332). We evaluated the role of hCGβ and its breakdown product (hCGβ core fragment; hCGβcf) detected by immunoassay in the clinical management of prostate cancer.
Patients and Methods: 104 patients with newly diagnosed prostate cancers were included in this study. Serum and urine specimens were obtained prior to treatment for measurements of hCGβ using immunoradiometric assay (IRMA) and of hCGβcf using enzyme-linked immunosorbent assay (ELISA). A control group was introduced to determine the cut-off levels (95th centile) for normal. PSA, tumour grade and stage at diagnosis were documented.
Results: Of the 104 patients, 70 had early disease (T1-2N0M0), 17 had locally advanced disease T3-4N0/+M0) and 17 metastatic disease (T2-4n+M+). hCGβ levels were elevated in the serum of 4 patients and in the urine of 11 patients, while hCGβcf was elevated in the urine of 14 patients. There was no statistically significant correlation between serum hCGβ, urinary hCGβ or hCGβcf at diagnosis with tumour stage ($p=0.129$, $p=0.404$ and $p=0.622$ respectively), Gleason grade ($p=0.402$, $p=0.220$ and $p=0.933$ respectively) or PSA level ($p=0.692$, $p=0.827$ and $p=0.657$ respectively).
Conclusion: These initial results suggest that hCGβ and the hCGβcf detected by immunoassay has a limited role in the clinical management of prostate cancer. Follow up of these patients will determine whether elevated levels of these markers at diagnosis correlates with a poor prognosis as indicated in several other urogenital tumours.

P-426

Role of TGFβ and bFGF in extracellular matrix remodeling induced by immunosupressors

Paltseva E., Gladskikh O., Ivanov A.
Moscow Medical Academy, Moscow, Russia

Many investigations confirm the role of cytokines and growth factors in the glomerulosclerosis. The association between changes in the level of cytokines and extracellular matrix (ECM) components accumulation under immunosuppressive treatment is not clearly understood.
Aim: The study of correlation between levels of TGFβ and bFGF and ECM accumulation in accelerated nephrotoxic nephritis (NTN) and puromycin aminonucleoside nephrosis (PAN) under methylprednisolone (MP) and cyclosporine A (CsA) treatment.
Methods: Rats with NTN and PAN were treated with MP and CsA from day 21–35 (NTN), day 30-44 (PAN) after disease induction. The distribution of ECM components in cryostat sections and mesangial cell culture was studied by immunohistochemical methods. Levels of TGFβ and bFGF were detected by ELISA.
Results: MP decreased the accumulation of collagen type IV in NTN and increased the deposition of laminin in both models in vi-

vo and in vitro. CsA decreased the accumulation of collagen type IV and increased the deposition of fibronectin in both models. CsA and MP decreased the level of TGF-β in supernatant in both models but CsA was more effective in PAN than MP. The accumulation of latent forms of these growth factors increased in both models. CsA decreased the amount of active form of bFGF in NTN and PAN. MP induced the augmentation of bFGF in supernatant in PAN.

Conclusion: Thus the accumulation of fibronectin and laminin induced by CsA and MP accordingly was mediated another than the TGFβ and bFGF growth factors. TGF-β and bFGF regulated only collagen production in these models.

P-427

Molecular analysis of aggressive chromophobe renal cell carcinoma

Panizo, B. Bryant, A. Chiesa, M.M. Walther, W.M. Linehan, M.J. Merino
National Cancer Institute, Bethesda, MD

Introduction: Chromophobe renal cell carcinoma (CRCC) is a subtype of RCC, which appears to have a better prognosis than clear RCC. Only a few cases of CRCC have been reported to metastasize, and the proclivity for hepatic metastases may distinguish CRCC from other subtypes of RCC. The development of metastases depends on changes in a large number of genes. It is also connected with the interaction of tumor cells with the environment LOH studies in CRCC have supported losses of portions of chromosomes 1p, 2p, 6p, 10p, 13q, 17p, and 21q, providing evidence that CRCC represents a distinct genetic entity. We studied 6 cases of CRCR with metastases to investigate the pathological features and for LOH at the chromosomal regions 1q31, 2q, 2p25-22, 3p25 (VHL gene), and 14q32.

Methods: Six cases of aggressive CRCC (3 male, 3 female) were studied. Ages ranged from 34 to 51 years old. From two cases (#1 and #2), primary tumor, metastases, and normal cells were microdissected, and from other 2 cases (#3 and #4), only metastases and normal cells were microdissected from paraffin-embedded tissue for PCR amplification to detect LOH at 1q31, 2q, 2p25-22 (tumor metastases suppressor gene), 3p25 (VHL gene), and 14q32.

Results: Four CRCC were located in the right kidney and 2 in the left side. Tumor sizes ranged from 8 to 14 cm. Histologically the tumors were typical CRCC (2 patients), eosinophilic (2 patients) or mixed (CRCC-clear RCC and CRCC-sarcomatoid). Two cases were Fuhrman grade 2 and 4 were grade 3. Two patients had extensive necrosis. Metastases were found in the liver (3 cases), lymph nodes (2 cases), and supraclavicular soft tissue (1 case). Three patients had metastases at the time of diagnosis, one patient at 7 months, one at 3 years, and one at 15 years.

	1	2	3	4
LOH 1q31	INF/NF	INF/INF	INF	**LOH**
LOH 1q42	INF/INF	INF/INF	NINF	**LOH**
LOH 2p25 (T/MTS)	INF/INF	INF/INF	NINF	INF
LOH 2q (T/MTS)	INF/INF	INF/INF	**LOH**	LOH
LOH VHL gene (T/MTS)	INF/INF	**LOH/LOH**	INF	INF
LOH 14q32 (T/MTS)	INF/INF	**LOH/LOH**	INF	INF

INF: informative heterozygous; LOH: loss of heterozygosity; NINF: non-informative

Conclusions: Despite the overall favorable prognosis, identifying aggressive variants of CRCC is important in kidney surgical specimens. Large tumors and those with high Fuhrman grade tend to metastasize to liver and lymph nodes. The follow up of these patients must include the image study of the liver due to the proclivity for hepatic metastases of CRCC. It does not seem to be a specific molecular pattern of LOH in CRCC and its metastases that could aid in the diagnosis of this aggressive variant of CRCC.

P-428

Leiomyosarcoma of the renal pelvis. A case report and review of literature

S. Papadopoulos[1], C. Filintadji[1], C. Pascalidis[2], I. Chrisos[2]
Departments of Pathology[1] and Urology[2], General Hospital of Veria, Veria, Greece

We report a case of leiomyosarcoma arising from the renal pelvis in a 55-year-old woman presented with a mild abdominal pain. Retrograde pyelography showed obstruction of the ureteropelvic junction. A compressed left renal pelvis and a solid hilar mass without hydronephrosis were demonstrated by computed tomography (CT).

The clinical diagnosis was that of a renal tumor (hypernephroma).

A left radical nephrectomy was performed disclosing a well-circumscribed, lobulated, 5.0 cm pale gray, firm and fleshy nodular tumor, situated peripherally in the hilar fat without renal parenchymal involvement or extension into the renal vein. The tumor appeared to arise from the renal capsule or from the wall of the renal pelvis. There were no metastatic lymph nodes or hepatic metastases during the operation.

Histologic examination demonstrated features suggestive of leiomyosarcoma with high degree of pleomorphism and areas of necrosis. The mitotic index was high, more than 7 atypical mitotic figures per 10 high-power fields.

Immunohistochemical staining confirmed the diagnosis of leiomyosarcoma. The neoplastic cells showed intensely positive cytoplasmic staining for smooth muscle-specific actin and vimentin. Staining with CAM 5.2, EMA, S-100 protein and NSE was negative.

Differential diagnosis includes other sarcomas of the kidney, sarcomatoid renal cell carcinoma, peripheral nerve seath tumor and renal angiomyolipoma.

The postoperative course was uneventful. The patient was received adjunctive chemotherapy. One year later after surgery this patient remains disease-free without recurrence.

According to the reviewed literature, renal leiomyosarcomas are extremely rare neoplasms with aggressive behavior and a very poor prognosis.

P-429

Metanephric adenoma of the kidney

Passetchnik, Dmitri
Rostov on Don State Medical University, Russia

Metanephric adenoma of the kidney (íá) is a very rare insufficiently known renal tumour concerning the group of nephroblastic neoplasms. We have two case observations of such tumors. Case 1 involved a 36-year-old man having died of membranopro-

liferative glomerulonephritis. At autopsy the subcapsular well-circumscribed 1,5 cm tan-pink tumor was revealed in the right kidney. Case 2 involved a 66-year-old woman having been suffering from secondary pulmonary tuberculosis with secondary kidney amyloidosis. At autopsy the subcapsular 2,5 cm tumor similar to the one described above was revealed in the right kidney. Microscopally, the tumours were composed of small uniform round cells with scant dark cytoplasm and small nuclei with fine even chromatin. The cells formed very small acini and tubules, non anastomosing between each other. They resembled immature embryonal renal tubules. Sometimes there were found separate dilated tubules with abortive glomeruloid-like structures. The blastema patterns were absent. Outside the tumours in both cases on the background of nephrosclerosis multiple groups of tubules were revealed with the signs of epithelium dysplasia, sometimes with the formation of papillary microadenomas not more than 0,1–0,2 cm in size. It is known, that nephrosclerosis can be the background for the renal papillary adenomas (PA) origin. The detection of similar changes at íá can point to probable connection of these processes, and also to common mechanisms of the PA and íá origin. One of the confirmations is the description of similar cytogenetic changes (gain of 7 and 17 chromosomes, loss of Y chromosome) at these tumours (Brawn S.A. et al., 1997).

P-430

Glomerular diseases of childhood and cytomegaloviral infection in the south region of Russia (histologic, ultrastructural and immunomorphologic characteristics)

Povilaitite P., Matsionis A.
Rostov Regional Bureau of Pathology, Rostov-on-Don, Russia

Introduction: Attention of investigators during the last years in Russia is focused on study of infections, which often accompany different types of glomerular pathologies. We have summarized last 2 years materials obtained from renal biopsies of children in our region. The study was aimed to detection of diagnostic criteria of associated cytomegaloviral infection (CMVI) and peculiarities of the underlying pathological process.
Methods: Renal bioptates (n=25) were the subjects of the study. Children were from 2 to 14 years old. The material was prepared by the standard methods for light microscopic, immunofluorescence and electron microscopic (EM-208/Philips) examination. CMVI diagnosis was confirmed immunomorphologically (DAKO).
Results: 40% of renal biopsis showed ultrastructural signs of DNA-viral infection. Electron-dense material was distributed along inner nuclear membranes, formation of large chromatin blocks, intranuclear chromatin granules and numerous nuclear bodies are the most reliable electronmicroscopic criteria. In case of marked CMVI large nucleolus-like structures ("owl's eye") are visualized in nucleoplasm, laminate of inner and outer nuclear membranes and degeneration of cytoplasmic organelles is pronounced. Immunofluorescence examination reveals deposition of all types of immunoglobulins (IgA, IgG, IgM, C-3) in basal lamina of glomerules and nephrothelial cells of tubules. The most frequent forms of underlying pathology – chronic glomerulonephritis, dysembryogenesis and renal amyloidosis, are accompanied by tubulointerstitial alterations.
Conclusion: The results show that DNA-viral infections in our material accompany basic glomelural pathologies in 40% of cases. We have revealed ultrastructural criteria that allow suggesting the presence of concomitant infection.

P-431

The role of radical prostatectomy in the treatment of cancer of the prostate – histopathological evaluation of 49 cases –

Radoslav Radosavljevic, J. Hadzi-Djokic, S. Micic, C. Tulic, M. Acimovic
Clinic of Urology of Clinical Center of Serbia, Belgrade, Yugoslavia

Introduction: Radical prostatectomy is indicated in patients who have cancer localized to the prostate. The aime of the study is to make histopathological evaluation of this method.
Methods: We analyzed 49 cases of radical prostatectomy due to cancer localized to the prostate, in the period 1996-2000 in Clinic of Urology in Clinical Center of Serbia. We analyzed average age of the patients, Grade, Gleason score, staging of the tumors, and premalignant lesions. We used statistical analysis H test.
Results: In 49 cases average age of the patients was 65,6 yr. (range 44–76). We found Grade 1 in 9 (18%), Grade 2 in 11 (22%), and Grade 3 in 29 (60%) cases. Gleason score 3 was in 6,1%, 4 in 12,2%, 5 in 8,1%, 6 in 16,3%, 7 in 24,5%, 8 in 26,6% and 9 in 6,1%. Premalignant lesions – PIN in 28 (57,1%) – PIN I in 10, PIN II in 11 and PIN III in 6 cases, adenosis in 20 (40,8%) – mild in 10, moderate in 7 severe in 3 cases. Staging T1 of tumors in 1 case, T2 in 33 (67,3%) $p < 0,05$, T3 in 13 (26,5%), T4 in 2 cases.
Conclusion: Our results correlate with literature data and suggest that radical prostatectomy is adequate method in treatment cancer localized to the prostate.

P-432

Prognostic evaluation of 58 renal cell carcinomas

Ramos Guillen P*, Ruiz Villaespesa A*, Olmedilla Arregui G*, Tejido Sanchez A**, Sanchez Chapado M**
* Dpt. of Pathology and ** Dpt. of Urology, "Príncipe de Asturias" University Hospital, Alcalá de Henares, Madrid, Spain

Introduction and objetives: To investigate the prognostic usefulness of some histopathological and biological markers in renal cell carcinoma, and to analyze the relationship of these markers with patient survival.
Methods: 58 patients diagnosed of renal cell carcinoma stage pT1, pT2 and pT3a N0 M0 (TNM,1997), were treated by radical nephrectomy. The tissue was included in paraffine, and conventional and immunohistochemical techniques were performed to assess size, stage and multifocality of the tumor, histological type, growth pattern, grading (Fuhrman et al.,1982), expression of PCNA, Ki67, p21, bcl2 and cathepsin D. Quantitative and qualitative analysis and a study of the association between these variables and patient survival were also carried out.
Results: Tumor size, stage and nuclear grading were significantly related to a higher possibility of reccurrence, whereas multifocallity or growth pattern didn't show that relationship. Ki67 was significantly related to size, stage and tumoral grading, while PCNA expression was only associated with nuclear grade. Bcl2, p21 and cathepsin D were not related to any of the histopathological features studied. Survival was significantly lower in tumors with higher degrees and a higher stages. Pattern of growth was not related to survival. Both Ki-67 and PCNA showed a statistically significant relationship with patient survival in the univariate analysis, but when multivariate analysis was performed, only PCNA was identi-

fied as an independent factor related to prognosis. Bcl2, p21 and cathepsine D were not related to survival.
Conclusions: In our study, nuclear degree, tumor size and stage, as well as both PCNA and Ki67 expression, were related to patient survival, though only PCNA was found to be an independent prognostic factor.

P433

"Retrospective study of multiple prognostic factors in low grade papillary urothelial tumors of the urinary bladder"
Ramos D, Ruiz A, Morell L, Navarro S, Llombart-Bosch A
Department of Pathology. University of Valencia. Spain

We evaluate the predictive value of multiple clinicopathological, morphometric, cytometric and immunohistochemical factors in a series of 120 patients with low grade neoplasms of the urinary bladder: papillary neoplasms of low malignant potential (LMP) and low grade carcinomas (LG, WHO grade 1). Subjectively two different histological grades were considered in each case: a primary predominant grade and a secondary non-predominant grade. All cases were followed for a mean of 76.6 months (range 39 to 128), considering for prognostic purposes the time to first recurrence or free relapse interval (FRI), the number of recurrences, the recurrence rate (RR) and tumor progression in grade or stage. Also taken into consideration was a prognostic subdivision of cases into two different "real" groups in regard to clinicopathological evolution of patients. Therefore, those cases with an indolent outcome were defined as "real" LMP, whereas those other cases with recurrence at first cystoscopic examination, RR>1 or tumor progression were considered "real" LG carcinomas. Univariate statistical studies revealed that numerous factors, such as clinicopathologic (grade, stage, size, multiplicity and Parmar score), morphometric (nuclear area and perimeter from different tumor zones), cytometric (ploidy of ten largest nuclei by image analysis), and cell proliferation marker (MIB-1 score) showed a high predictive value ($p<0.001$) in regard to different prognostic functions. Nevertheless, multivariate analysis demonstrated that only two factors showed independent prognostic value in both the prediction of FRI and in the definition of "real" prognostic groups: mean nuclear area (MNA) of 10 largest nuclei ($\geq 52\mu m^2$) and MIB-1 score ($\geq 79‰$). However, only MNA of the 10 largest nuclei presented predictive value in relation to RR. In conclusion, according to our results subjective histological grade should be assessed in relation to the secondary most atypical grade, which is in close relation with the predictive value of MNA of the 10 largest nuclei (atypical clone of cells), as well as the proliferative rate of the tumor measured by means of MIB-1 score.

P-434

Differential expression of protooncogenes and tumor suppressor genes in human testicular tumors
Ravazoula P[1], Batistatou A[1], Tsamandas A[1], Kalofonos C[2], Bonikos DS[1]
Department of Pathology[1] and Internal Medicine[2], University Hospital of Patras, Rion, Greece

Introduction: Testicular carcinogenesis is a complex multistep process whose molecular mechanism has not been fully elucidaded.The aim of the present study has been to examine the roles of the protooncogenes c-erbB-2 and ret and tumor suppressor genes p53 and Rb in testicular tumorigenesis.
Materials and Method: We examined paraffin-embedded sections from 70 testicular neoplasms (27 seminomas, 13 embryonal carcinomas, 16 mixed tumors, 6 teratomas, 4 lymphomas, 2 sarcomas and 2 Leydig tumors), using standard immunohistochemical techniques. The antibodies ret (monoclonal, Novocastra), c-erbB-2 (monoclonal, Biogenex), p53 (monoclonal, Biogenex) and Rb (polyclonal, DAKO) were employed. For all antibodies staining of >5% of tumor cells was considered positive.
Results: The oncoprotein c-erb-B2 was not detected in any of the examined neoplasms. Positive immunoexpression of ret was noted in 11% (3/27) of seminomas, 23% (3/13) of embryonal carcinomas, 19% (3/16) of mixed tumors, 100% (6/6) of teratomas and 50% (1/2) of Leydig tumors. Positive staining for p53 and Rb was noted in 11% (3/27) and 26% (7/27) of seminomas, 92% (12/13) and 23% (3/13) of embryonal carcinomas, 63% (10/16) and 6% (1/16) of mixed tumors, 83% (5/6) and 17% (1/6) of teratomas, 0 and 100% (2/2) of Leydig tumors, 50% (1/2) and 0 of sarcomas and 0 and 75% (3/4) of lymphomas, respectively.
Conclusions: Testicular neoplasms differentially express the oncoprotein ret and the tumor suppressors p53 and Rb, depending on the histologic type. p53 is implicated in pathogenesis of more aggressive tumors such as the embryonal carcinomas. The high expression of ret in teratomas indicates that it may be utilized as a tumor marker for this neoplasm.

P-435

Immunohistochemical p53 expression don't correlate with prognosis of the upper urinary tract carcinomas. Experience of the hospital clinic of Barcelona
Cleofé Romagosa, Mireia Castillo, Carme Mallofré, Antonio Palacín, Juan B. Alcover*, Antonio Cardesa
Dpt. of Pathology and Urology *, Hospital Clínic, IDIBAPS, Universitat de Barcelona, Spain

Introduction: Immunohistochemical p53 nuclear over expression has been correlated with prognosis of transitional cell carcinoma (TCC) of the urinary bladder by many groups, including ourselves. This relation in the upper urinary tract has been less studied and defined. The objective of our study was to prove the same correlation we had previously seen in bladder urothelial carcinoma in uretheral and pelvic TCC.
Methods: 41 TCC of the upper urinary tract from the our files were reviewed for their expression of p-53 and correlated with histological grade, stage, and clinical evolution. The Envision method on paraffin sections were prepared using the monoclonal antibody (BP-nfl Novocastra). Cases were considered positive when at least 10% of neoplastic cells showed nuclear p-53 expression. Statistical analysis were performed with the SPSS statistical software.
Results: There were 4 grade I (9,7%), 18 grade II (43,9%) and 19 grade III (46,3%) cases. It was possible to establish the stage in 37 cases: 3 (8,1%) pTa, 12 (32 %) pT1, 5 (13,5%) pT2, 11 (29,7%) pT3 and 6 (16,2%) pT4. Clinical follow up was possible in 36 cases: 11 (30,5%) cases metastatized and 13 (36,1%) had local recurrence. p-53 was considered positive in 25 (62,5%) cases and negative in 15 (37,5%). We didn't find any statistical relationship between p-53 expression and clinical evolution, nor with grade or stage, although there was tendency of low grade tumors (I and II) to be more positive (72,7%) than high grade (III) cases (50%).

Conclusions: In our experience p-53 immunohistochemical expression is not a prognosis marker of upper urinary tract transitional cell carcinoma in contrast what is found with TCC from the bladder.

P-436

Molecular cytogenetic analysis of chromosome 7 and 17 and TP53 in bladder cancer: a comparative study between young and old patients

L. Santos, S. Pereira, B. Criado, T. Amaro, M.J. Bento,
R. Guedes-Carvalho, C. Lopes
Instituto Portugujs de Oncologia (UCI-B), Porto, Portugal

Introduction: Biological markers are being developed in an attend to identify and monitor those superficial urothelial papillary carcinomas (UPC) of the bladder that are likely to develop recurrent or progressive disease. Numerical alterations of chromosome 7, 17 and alteration of TP53 gene were defined as important alterations in UPCs but their significance was not well established in the superficial ones. On the other hand, bladder cancer is rare in the first 4 decades of life and the molecular characteristics of UPCs in young patients remains unclear.
Material and Methods: Our sample consisted in 46 superficial urothelial papillary bladder carcinomas treated at Instituto Português de Oncologia – Porto, Portugal with curative intention, divided in two groups: Serie A (n=22) patients with more than 45 years of age and Serie B (n=24) patients with ≤45 years. We performed a FISH study with centromeric probes for chromosomes 7 and 17. For the analysis of TP53 gene we used a specific unique sequence probe.
Results: In both series (A and B) we found that cases with monosomy of TP53 presented a poorer disease-free survival and this alteration is significantly related with UPCs recurrence (p=0.03 and p=0.02 respectively) With respect to chromosome 17 no differences was observed between both series. Trisomy of chromosome 7 was more frequent in serie B (p=0.056). Alterations of chromosome 7 did not reveal any associations with poor disease-free survival in both series.
Conclusion: We can conclude that loss of one allele of TP53 can be an early event in bladder carcinogenese and could be an important biological marker of recurrence in UPCs. Trisomy of chromosome 7 seems to be related with younger patients but further studies are needed.

P-437

Retinoblastoma gene product(pRb) and p53 expression in a series of schistosomias and non-schistomiasis related bladder cancer in Egypt

Laila Seada*,Nadia Galal**
* Pathology Department, Benha Faculty of Medicine, Egypt;
** Pathology Department Ain Shams Faculty of Medicine, Egypt

Background and Objectives: Schistosomiasis-related bladder cancer is a major oncogenic problem in Egypt, many parts of the Middle East and Africa. It differs from non-Schistosomiasis related bladder cancer in its squamous differentiation and occurrence at young age. In the present study, a series of bladder cancers, both Schistosomal and non-Schistosomsl related, is studied for the immunohistochemical expression of pRb and p53 on formalin-fixed paraffin embedded material. The results are correlated with the age ,gender,grade,stage and aggressive behavior of the tumors resulting in metastasis, recurrence and/or death.
Material and Methods: A series of 49 bladder cancer specimens comprising 33 transitional cell carcinomas(TCC), 10 squamous cell carcinomas (SCC), 3 adenocarcinomas (AC), and 3 poorly differentiated carcinomas (PC) were studied. Paraffin sections mounted on poly-L-lysin were immunohistochemically stained using the monoclonal mouse Anti-human antibodies against p53 (DO-7) and pRb (Rb1) from DAKO, Denmark. The StreptABComplex/HRP Duet kit (K0492) and DAB as chromogen and the DAKO two-step Envision System {AP.Rabbit/Mouse(fast red)}were used as visualization systems for pRb and p53 proteins respectively.
Results: Schistosomal ova were present in association with 7/33 of the TCC (4 cases having squamous differentiation), 7/10 of the SCC, 1/3 of AC and 2/3 of the PC. The mean age for Schistosoma-associated cancers (group 1) was 53.2 years, while in non-Schistosoma-associated cancers (group 2) it was 60.7 years. Loss of pRb expression was present in 6/18 (33.3%) of group1 and was statistically correlated to poor survival (p=0.035). P53 overexpression was found in 9/18(50%) of cases but had no statistically significant correlation with other parameters. In group 2, loss of pRb expression was found in 11/31(35.5%) of cases, while p53 was over expressed in 18/31 (58.1%) of cases. A statistically significant correlation could be found between loss of pRb expression and p53 overexpression (p=0.049). P53 overexpression also correlated with younger age of the patients (p=0.002), and had a borderline statistically significant correlation with poor survival (p=0.058).Conclusion:Our data indicate that alterations in pRb and p53 suppressor genes expression in Schistosomal and non-Schistosomal bladder cancer are comparable; nevertheless, loss of pRb in Schistosomal-related bladder cancer is indicative of aggressive behavior in these neoplasms.

P-438

Effect of cimetidine on male reproductive system

N.Takzaree
Tehran University of Medical Sciences, Faculty of Medicine,
Tehran. Iran

In the present study the effect of cimetidine on male reproductive system and sperm motility. 60 mature male rats divided in 3 groups.control group.received normal saline and test 1 group received cimetidine 100 mg/kg/day for one week test 11 group received cimetidine 100 mg/kg/day for five weeks. the result revealed that sperm count was decreased in the test compared to control groups and non motile sperms were increased in compared to control groups t-test was done and p value <0.05 showed significant decrease in sperm counts. then the testises were excised from body and after weighing we studied then microscopically results revealed lower testicular weights in test 2 group. atrophy of spermatic germ cells and hypoplasia of spermaticgerminal layer of seminiferous tubules were observed microscopically. we concluded that the above changes may be due to the direct effect of cimetidine on the seminiferous tubules which is reversible.

P-439

The fatty kidney in diabetics

Jørgen L.Thomsen, Ingrid Bayer Kristensen, Peter Ottosen
Institutes of Forensic Medicine, University of Southern Denmark and Aarhus, and Institute of Pathology, Odense, Denmark

INTRODUCTION: Luciano Armanni described in 1872 the characteristic vacuolisation of the cells in the proximal kidney tubules in diabetic coma. The vacuoles have hitherto been interpreted as glycogen deposits. It was the purpose of the present investigation to test the authors´ hypothesis that the deposits represent lipids rather than glycogen.
METHODS: A prospective examination of medico-legal autopsies was performed. The following categories were included: eight cases of death due to diabetic coma, seventeen diabetics who died from other causes, nine alcoholics without diabetes, and nine who were neither alcoholics nor diabetics. Frozen sections of the kidneys were stained for lipids. Formalin fixed tissue was examined in the electron microscope.
RESULTS: All of the coma patients showed strong positivity for lipids in the proximal tubules. There was only sparse positivity in the controls. The lipids are probably triglycerides.
CONCLUSION AND PERSPECTIVES: Diabetics are known to have an abnormal lipid metabolism. Our finding may help in the understanding of the metabolism in diabetics and of the late manifestations. It may further help in the diagnosis of diabetic coma post mortem. The fatty kidney may be a parallel to the fatty liver in alcoholics

P-440

Microvessel density as a prognostic marker in bladder carcinoma classified according to the 1998 WHO/ISUP classification

Özden Tulunay*, Diclehan Orhan*, V. Ali Canoğlu**, Yaşar Bedük**
Departments of Pathology* and Urology**, Medical School of Ankara University, Ankara, Turkey

Introduction: The angiogenetic activity of tumor tissue is considered to have prognostic value. Microvessel density (MVD), a measure of tumor angiogenesis, correlates with clinical outcome in many human tumors. To evaluate tumor angiogenesis as a prognostic marker of transitional cell carcinoma of the bladder and to asses its relationship to established variables for survival and response to therapy, MVD in 77 primary bladder cancers were assessed.
Methods: Histologic slides of 77 bladder cancer patients were reviewed according to the 1973 WHO and 1998 WHO/ISUP classifications. MVD in these tumors and in 15 normal urothelium (control) were assessed. Microvessels were identified by immunostaining of endothelial cells for CD34 antigen. Microvessels were scored in selected areas showing active neovascularization counting 10 different 200x fields, and mean microvessel count was considered as the MVD.
Results: MVD of cancers (91.15±6.72) were significantly higher than control cases (12.57±3.78) ($p<0.001$). There was a relationship between stage, WHO, WHO/ISUP grades and MVD. MVD in invasive tumors (94.02±6.55) was higher than the superficial cancers (88.88±6.01) ($p<0.05$). In superficial cancer group, the tumors which showed recurrence had higher MVD (92.67±3.65) than the tumors which showed no recurrence or progression (87.42±6.14) ($p<0.05$). In the invasive cancer group, MVD of tumors which showed recurrence after chemotherapy (97.43±1.42) was higher than the tumors without recurrence after chemotherapy (93.83±3.38) ($p<0.05$).
Conclusion: These data demonstrate that MVD in bladder carcinoma is a predictor of grade, stage and, presumably malignant potantial. Quantification of tumor angiogenesis may allow stratification of bladder cancer patients to type of treatment.

P-441

Metanephric "adenoma" of the kidney: Benign and malignant behaviour. Histologic, immunohistochemical and cytogenetic analyses

Vázquez Martul EV, Sacristán Lista F, Prada Puentes C, Busto Castañón L, Matheu G. Schmitt F*
Juan Canalejo Hospital (La Coruña-Spain) and (*)IPATIMUP, Porto, Portugal

Metanephric adenoma of the kidney is a very rare neoplasm, usually reported as a benign tumor; only no more than 90 well-documened cases have been reported to date. All the cases reported before have shown that these tumors consist of very small epithelial cells that form very small acini, without mitoses, in an almost acellular stroma. They are often misinterpreted as renal papillary carcinoma or epithelial Wilm´s tumor. In 1999, Pins M.R., Jones E.C., and ours, we reported the first metastatizant metanephric adenoma-like tumor (1), initially diagnosticated for us,in 1980,as an adult Wilm's tumor(2). This malignant case showed the same citogenetic anormalities described by Renshaw AA (2) in the benign metanephric adenomas using the fluorescence in situ hybridization technique (FISH) (disomic pattern of chromosomes 17). Recently, we have had the opportunity of to diagnose a new case of renal benign metanephric adenoma and to compare the histologic, immunohistochemical and cytogenetic analyses of the two cases: a benign and a malignant metanephric "adenoma-like" with revision of the literature.
REFERENCES: 1. Metanephric adenoma-like tumors of the kidney: report of 3 malignacies with emphasis on discriminating features. Pins MR, Jones EC, Martul EV, Kamat BR, Umlas J, Renshaw AA. Arch Pathol Lab Med 1999; 123:415–420
2. Tumor de Wilm's en adultos. Presentación de un caso y revisión de la literatura. Vazquez Martul E., Bustos Castañon L., Forteza Vila J. Patologia 1980; 13:267–275
3. Cytologic and fluorescence in situ hybridization (FISH) examination of metanephric adenoma. Renshaw A.A., Maurici D., Fletcher J.A. Diagnostic Cytopath. 1997; 16:107–111

P-442

Correlation of gleason score-grade in fnab of prostate and prostatectomy specimens

G. Vecchini, G. Sotiropoulou, V. Leodara, J. Lekka, P. Arapantoni-Dadioti
Pathology Dpt. METAXA'S Cancer Hospital, Piraeus, Greece

The aim of this study is to look at the correlation between prostate needle biopsy and radical prostatectomy grades according to the Gleason score system.

We analyzed 36 cases of radical prostatectomy or TUR specimens and compared them with the preoperative needle biopsy Gleason grade.
There was exact agreement for the grading between biopsy and prostatectomy or TUR in 20 cases (55,5%) and disagreement in 14 cases (39%) . For the remaining 2 cases (8%) the diagnosis in preoperative biopsy was malignancy whereas in TUR specimens (16 and 2,5 cm^3) we didn't find malignancy.
It is important to underline that 13 out of 14 cases (93%) with disagreement in grading were undergraded in the prostate needle biopsy and in only 1 (7%) the Ca was upgraded.
In conclusion from our experience in 55,5% of the cases there is exact agreement in score system between the needle biopsy and surgically excised specimens. According to our opinion the disagreement is the result of two reasons: a) the heterogeneity of the prostatic Ca it is very difficult to always be included in small biopsies and b) the small size of the sample in prostate needle biopsy. From our study is confirmed that the accuracy of Gleason score system in FNAB is very low except for the presence in the sample of a high grade component of Ca.

P-443

Morphological and histochemical analysis of prostatic intraepithelial neoplasia

Velickovic Lj1., Katic V1., Dimov D.1, Ilic R.1, Zivkovic V1, Djordjevic B1, Marjanovic V2.
1 Institute of Pathology, Faculty of Medicine; 2 Department of Childs Surgery Clinical Center Nis, Yugoslavia

Prostatic intraepithelial neoplasia (PIN) is clinically important because it has a high predictive value as a marker for adenocarcinoma. Having in mind that reports on mucin histochemistry in PIN lesions are rare, we have decided to investigate both qualitative type of mucin content and morphological characteristics. Paraffin sections were stained with HE, PAS and HID-AB, pH 2,5. This study includes 32 patients with diagnosed adenocarcinoma prostate, who had PIN low grade (8 patients), PIN high grade (13 cases), and 11 biopsy specimens of the prostate have had PIN low and high grade both at the same time. The most frequent Gleason score of adenocarcinoma prostate associated with PIN lesions was score 5–10, but in prostatic carcinoma with low score (2–4) these lesions were not found. Our findings confirm that mucinous secretion is present in PIN lesions. The most significant finding is hyper secretion of acid mucins in 8/24 focus of PIN high grade (33,33%). In 25% of them, only sialomucins were found; the other 8,33% had had mixed sialo-sulfomucins type secretions. Fucomucins (neutral) were detected in 20,83% of PIN high grade (5/24). Histochemicaly, the presence of neutralmucin was also conformed in PIN low grade in 52,63% (10/19), while the presence of acidmucin had been absent. The authors discuss the role of sialo- and sulfomucins in determination of potential malign characteristics of PIN high grade.

P-444

Nested variant of urothelial carcinoma of the urinary bladder(uc-nv). A report of five cases

Vidal-Bel A*, Condom-Mundó E, Muñoz J, Vigués F, Garcia del Muro X*
Depts of Pathology, Urology and Oncology, Hospital de Bellvitge-Institut Català d'Oncologia*, L'Hospitalet de Llobregat, Barcelona, Spain

Introduction: UC-NV is uncommon and poorly known by pathologists and clinicians.
Methods: Slides and charts were reviewed on five patients with UC-NV. Immunostains for p53, Mib1 (Ki67) and prostate specific antigen (PSA) were performed.
Results: All five patients were male, ranging from 59 to 69 (mean 64) years of age. Four patients had hydronephrosis. Grossly, 4/5 lesions were infiltrating and 1/5 was exophytic. Four patients underwent radical surgery. The remaining one was found to have peritoneal implants at surgery. All the tumors were pT3 and two were pN2. The nested pattern was retained in the nodal metastases. UC-NV made up 100% of the lesion in 2 cases and 90%, 40%,and 10% in the other three. In each case a "radial phase"-like growth of UC-NV was seen, with nests of bland urothelial cells growing laterally in the corion under a normal urothelium. This radial growth involved the prostatic urethra and the grossly healthy vesical mucosa in 3 and 2 cases respectively. p53 overexpression was absent. Proliferative index was <5%. PSA was negative in all cases.
Conclusions: Despite its histological blandness,UC-NV is an aggressive, deeply infiltrating and metastasizing neoplasm which is able to grow in a radial pattern under an apparently healthy vesical and urethral mucosa. Immunostains for p53 and ki67 are of no help in diagnosis.

P-445

Immunohistochemical expression of FAS and GLUT1 in malignant urothelial neoplasms

Paolo Visca*, Simona Monaco**, Valeria Sebastiani**, Tiziana Andreano**, Claudio Botti*, Piero De Carli*, Ugo Di Tondo**
* Departments of Cytopathology [P.V.], Surgery [C.B.] and Urology [P.D.C.], Regina Elena Cancer Institute of Rome;
** Department of Experimental Medicine and Pathology, University of Rome "La Sapienza", Italy

INTRODUCTION: In order to evaluate the role and the predictive strength of fatty acid synthase (FAS) and human erythrocyte glucose transporter 1 (GLUT1), human malignant urothelial neoplasms and their adjacent normal tissues were studied. FAS and GLUT1 are both involved in the cellular metabolic activities of many normal tissues and are overexpressed in non-neoplastic highly proliferative lesions and in aggressive carcinomas with poor outcome.
METHODS: Paraffin embedded retrieved material from 31 transitional cells carcinomas of the bladder including adjacent-to-tumour non neoplastic mucosa(ANNM) were studied, by means of immunohistochemistry, using monoclonal mouse purified antibodies specific to GLUT1 and FAS. FAS and GLUT1 expression was correlated to clinico-pathological features and overall survival(OS). Patients were followed-up for five years until July 2000.
RESULTS: Six carcinomas were G1, 6 were G2 and 19 were G3(sec. ISUP/WHO '98). PT1 stage was observed in 18 cases, pT2 in 6 and pT3 in 7 cases. All patients showed no nodal involvement(N0). FAS was considered positive in 16 and in 20 cases, GLUT1 was positive in 20 and in 9 cases of cancer or ANNM respectively. Controls, stained from bladder biopsies for non-neoplastic disease, were FAS and GLUT1 negative. Statistical analysis revealed relation of FAS expression to histological grade(p=0,004) and to pT stage(p=0.002). Multivariate analyses showed correlation between pT stage and OS(p=0,001). GLUT1 expression seemed to be related to OS(p=0,13).

CONCLUSIONS: Aim of this study was to find some new predictive markers of neoplastic behaviour and prognosis in urothelial carcinogenesis. An overexpression of GLUT1 and FAS in cytological samples or in normal tissue may suggest different therapeutic approaches or closer follow-ups.

P-446

Constitutive activation of hypoxia-inducible genes related to overexpression of hypoxia-inducible factor-1α in clear cell renal carcinomas

[1]MS Wiesener, [1]PM Münchenhagen, [4]I Berger, [2]J Roigas, [3]PH Maxwell, [2]SA Löning, [1]U Frei, [1]K-U Eckardt and [4]H-J Gröne
Departments of [1] Nephrology and Medical Intensive Care (M.W., P.M., J.S.J., U.F., K.-U.E.) and [2] Urology, Charité, Humboldt-University, Berlin, Germany; [3] Wellcome Trust Centre for Human Genetics, Oxford, UK and [4]German Cancer Research Centre, Heidelberg, Germany

The transcription factor hypoxia-inducible factor (HIF)-1 is an important mediator of hypoxic adaptation of tumor cells and controls several genes, which have been implicated in tumor growth. Oxygen-dependent degradation of HIF-1α, the regulatory subunit, requires binding to the von Hippel Lindau (VHL) protein. Since functional inactivation of the VHL tumor suppressor gene occurs in approximately 70% of clear cell renal carcinomas, we investigated whether this results in overexpression of HIF-1α and target genes. Increased expression of HIF-1α was found in 75% of clear cell renal carcinomas. Immunohistochemistry revealed distinct patterns of nuclear staining for HIF-1α, depending on histological type and overall abundance of HIF-1α. In those clear cell renal carcinomas, which showed increased expression on immunoblots, HIF-1α was expressed in almost all cells. In the remaining clear cell and in non-clear cell tumors, staining was focal; these different patterns thus being compatible with genetic stabilization in contrast to microenvironmental stimulation of HIF-1α as the primary mechanism. The mRNA expression of two known target genes of HIF-1α, VEGF and glucose transporter 1 (GLUT1) increased progressively with increasing amounts of HIF-1α in tumor extracts. In addition, GLUT1 protein levels correlated with HIF-1α abundance.
In conclusion, the data provide in vivo evidence for a constitutive upregulation of HIF-1α in the majority of clear cell renal carcinomas, that leads to more widespread accumulation of this transcription factor than hypoxic stimulation. Increased expression of HIF-1α is associated with alterations in gene expression patterns, that are likely to contribute to tumor phenotype and progression.

P-447

Expression of bcl-2 and p53 in transitional cell carcinoma of urinary bladder and their relationship with other prognostic factors

Zergeroğlu S., Özdemir H.B., Sertçelik A., Sertçelik N.
Department of Patology, Zekai Tahir Burak Hospital; Department of Pathology, Faculy of Medicine, Ankara Univercity; Department of Urology, Social Security Hospital, Ankara, Turkey

Objective: Comparison of tumor suppressor genes P53 and bcl-2 with grade,stage, necrosis, vascular involvement and inflamatory response in transitional cell carcinoma ofthe urinary bladder in order to determine their prognostic roles.

Material and metods: 53 patients who were diagnosed as transitional cell carcinoma of urinary bladder between years 1996 and 1999 were studied. Primary antibodies for tumor supressor gene p53 and protooncogene bcl-2 were determined by immunohistochemical method (conjugation with streptoavidine-biotine,alkalen phosphatase), and their relationships with other prognostic parameters were researced
Results: Among 53 tumor cases, 23 were stained positive with bcl-2 while 30 were stained positive with p53. Positive staining with p53 significantly increased with incrising grade but there was no relationship with stage and others parameters. In addition, no significant relationship was found between bcl-2 positivity and other prognostic parameters.
Conclusions: In transitional cell carcinoma of the urinary bladder, tumor supressor gene p53 is correlated only with grade of the tumor. And for the diagnosis and determination of the prognosis of urinary bladder cacinoma protooncogene bcl-2 is not more valuable than histological grade, stage and other prognostic parameters.
Keywords: Transitional cell carcinomaof the urinary bladder, immunohistochemistry, p53, bcl-2.

P-448

Estrogene receptor and cerb-b2 immunreactivity in adenocarcinoma of prostate gland

Zergeroğlu S., Özdemir H.B., Sertçelik A., Sertçelik N.
Department of Pathology in Zekai Tahir Burak Hospital, Faculty of medicine in Ankara Univercity; Department of Urology in Social Security Hospital, Ankara, Turkey

Objective: The purpose of this study was to determine the presence of estrogen receptor (ER) and cerb-b2 immunreactivity in adenocarcinoma of prostate, and to identify their relationships with histological grade, stage, and other progostic parameters
Material and metods: 64 prostate adenocarcinoma cases, which were diagnosed between years 1996 and 2000, were taken into study group. ER and cerb-b2 primay antibodies were used for immunhistochemical staining (DAB, and AEC chromogen conjugated with streptoavidine biotine peroxidase). "Chi Square" and "One Way Anova" test were used.
Results: Among 64 tumors, 34 were stained positive with ER while 41 were stained positive with cerb-b2. No significant relationship was observed between ER and grade and stage whereas cerb-b21 were positively stained in low grade tumor cases. An inverse relationship was found between cerb-b2 positive stainimg and grade and stage.
Conclusions: cerb-b2 can be used as a valuable marker in low grade and stage adenocarcinoma of prostate.
Keywords: Prostate,adenocarcinoma,estrogen receptor, cerb-b2, immunochemistry
Hematopathology

P-449

Pattern of Expression of BOB.1, MUM1 and Bmi in DLBCL

Howayda Abd El All*, Philippe Gaulard**
* Dept of Pathology, Faculty of Medicine, Suez Canal University, Ismailia, Egypt; ** Dept of Pathology, CHU Henri Mondor, Créteil, France

Background: BOB.1, MUM1 and Bmi proteins are strictly regulated during B cell development and maturation. **Objectives:** As diffuse large B cell lymphoma (DLBCL) as described in the WHO classification is an entity comprising different biologic entities that cannot be distinguished by morphologic or immunophenotypic analysis we investigated if the immunohistochemical (IHC) expression of BOB.1, MUM-1 and Bmi could identify new subsets. **Methods:** Paraffin sections of 76 cases were included: 9 reactive lymph nodes, 5 follicular lymphoma (FL) and 62 DLBCL. **Results:** In reactive node, the expression of BOB.1 [1], MUM1 [2] and Bmi [3] was similar to that described in the literature. Table 1 illustrate the expression of BOB.1, MUM-1 and Bmi in FL and DLBCL. Most of MUM1$^+$ cells in centroblastic lymphoma correspond to large pleomorphic, histiocytic or plasmacytic cells or immunoblasts. All immunoblastic lymphoma were MUM1$^+$. Bmi stained centroblasts, plasmacytic cells and immunoblasts. Nine cases were BOB.1+ MUM1$^+$ Bmi$^+$ cases.

Table 1

	BOB.1	MUM1	Bmi
FL (5)	5/5	0/5	0/5
DLBCL on top of			
– FL (12)	11/11	2/10	0/9
– nodal MZL (2)*	2/2	2/2	2/2
– lymphoplasmacytic lymphoma (3)	3/3	3/3	1/3
De novo DLBCL (33)	33/33	19/32	8/28
Extranodal DLBCL (13)	12/13**	6/12	4/13
Total DLBCL (63)	61/62	32/60	16/56

*plasmacytoid differentiation

**This BOB.1$^-$ case (CD79a$^+$) is also MUM1$^-$ and Bmi$^-$ (positive internal controls)

Conclusion: BOB.1 can be considered a pan-B marker, it's expression parallel CD79a. The IHC profile in DBCL on top of FL is almost similar to FL. MUM1$^+$ cells are more frequent in de novo and extranodal DLBCL. Bmi positivity is different between reactive and neoplastic conditions. BOB.1$^+$ MUM1$^+$, BOB1$^+$ Bmi$^+$ and BOB1$^+$ MUM1$^+$ Bmi$^+$ DLBCL may represent distinct pathologic subsets within the DLBCL necessitating further studies and correlation with patients' disease free and overall survival.

References: 1. Greiner et al. Am J Pathol 159:501–507, 2000
2. Falini et al . Blood 95:2084–2092, 2000
3. Raaphorst et al. J Immunol 164:1–4, 2000

P-450

In situ hybridization (ISH) with signal amplification reveals HIV infection at single-cell resolution in formalin-fixed and paraffin-embedded tissue

Cannone M°, Vago L*, Viale G*, Barberis M°
° Service of Pathology and Laboratory Medicine, Multimedica and
* Institute of Anatomic Pathology, University of Milan, Milan, Italy

In situ hybridization (ISH) has proven to be a powerful tool in the diagnosis of viral diseases. However its usefulness is limited by low detection sensitivity (10–50 viral copies per cell). To improve the threshold detection level of HIV-provirus in formalin-fixed and paraffin-embedded tissue, we describe a new protocol of ISH with a non radioactive probe and signal amplification.

Materials: 3 lymph nodes were surgically removed from 3 HIV+ patients with persistent lymphadenopathy. Coltures and histology excluded opportunistic infections and tumors. 3 lymph nodes from HIV negative patients were used as negative controls. We studied the sensitivity of our technique with 2 HIV-chronically infected cell lines (U1 and ACH2), respectively containing 2 and 1 viral copies per cell. Cell blocks and monolayered cytological specimens with 100, 50, 10 and 0% infected cells were obtained from the cell suspensions. A 42 bp , 5′ byotinilated sk 19 probe for the *gag* sequence was used for ISH. The signal was amplified with a catalyzed reporter deposition technique using byotinil tyramine. A 40 bp probe for the IS6110 insertion sequence of M.tuberculosis DNA was used to evaluate verify the specificity of ISH.

Results: In the lymph nodal sections, the signals consisted in small nuclear dots in lymphocytes and macrophages. In the cytoblocks, signals were found in 12% of the ACH2 cells and in 20% of the U1 cells. The positivity of the monolayers ranged from 54% of the 100% HIV-infected U1 cells to 18% of the 50% HIV-infected ACH2 cells. No signals were detected in the negative controls and after ISH with M. tuberculosis-probe.

Conclusions: This highly sensitive and accurate technique could represent a tool in the monitoring of the patients treated with the new antiretroviral therapies.

P-451

Composite follicular dendritic cell sarcoma and langerhans cell histiocytosis

Mireia Castillo, Antoni Martinez, Benet Nomdedeu, Antonio Cardesa, Elias Campo
Departments of Pathology and Hematology, Hospital Clínic, University of Barcelona, Barcelona, Spain

Introduction: Neoplasms of dendritic cell (DC) origin are uncommon and include follicular dendritic (FDCT), interdigitating (IDCT), and Langerhans (LCT) cell tumors/sarcomas. LC proliferations and IDCT have been occasionally identified in association with different lymphoproliferative disorders. However, composite tumors of different DC lineage have not been previously recognised.

Patient and Methods: A 69 years old woman presented with a four-year history of recurrent cervical lymph node enlargement. A submaxillary mass was interpreted as Hodgkin disease by fine needle aspiration and a biopsy was obtained. Two subsequent cervical node recurrences seven and nine months after diagnosis were also biopsied. Immunohisto-chemical studies and EBER in situ hybridization were performed.

Results: The initial biopsy showed a diffuse proliferation of FDC (CD21+/CD23+/CD35+/KIMP4+/CNA42+/S-100±/CD1a–) with multi- nucleated giant cells and occasionally intermingled eosinophils and Langerhans cells (CD1a+/S-100+). The recurrences showed areas of well differentiated FDCT and an increasing sarcomatous component displaying pleomorphic cells, atypical mitosis and necrosis, and lacked CD23 expression. In addition, CD57 and bcl-6 lymphocites were identified in the well differentiated FDCT areas but were absent in the sarcomatous component, suggesting a potential functional relationship between the degree of differentation of FDCT and the associated lymphocytes. Moreover, the LC population (CD21–/CD23–/CD1a+/S-100+) with intermingled eosinophils increased in the recurrences and tended to merge with the FDC component. EBV was negative in both FDC and LC components.

Conclusions: Similarly to different lymphoproliferative disorders, FDCT may be associated with Langerhans cell histiocytosis. Whether this LC proliferation represents a true neoplastic or a reactive process is uncertain.

P-452

Expression of p53, MDM-2, p21/waf-1, BCL-2 and retinoblastoma (rb) in relation to clinical behavior and patient survival in non-Hodgkin's lymphoma

Edison Catalano, M.D.
Univ. Med. Center, Cooper Hospital, Camden, United States

Introduction: Oncogene products are becoming important to the clinicians to facilitate the information and more refined methods for the treatment of choice.
Purpose: To evaluate the expression and effects of p53, MDM-2, p21/fas-1, BCL-2 and retinoblastoma gene protein products in all forms of non-Hodgkin's lymphoma.
Materials and Methods: 90 cases were studied with immunohistochemical techniques.
Results and Discussion: Expression of p53 was observed in 87% small cell lymphoma (SCL), large cell lymphoma (LCL) and mixed and small/large cell lymphoma (SLCL) 80% and 57%, respectively. Expression of MDM-2 was seen in 56% SCL, 60% LCL, 57% SLCL. WAF-1/p21 expression was detected in 26% SCL, LCL and SLCL 43 and 47%, respectively. The demonstration of BCL-2 was observed in 82% SCL, 81% LCL and 72% SLCL expressed BCL-2 oncoprotein. Loss of expression of retinoblastoma gene product was observed in 25% SCL, 30% LCL and 43% SLCL. In general, the studies showed that in the case of p53, there was more intense and higher positivity in the aggressive tumors in comparison with the indolent or intermediate type. The increase of MDM-2, as well as the increase of p21 was seen most commonly in the low grade lymphomas.
Conclusion: Our study demonstrates overexpression of p53, and the lack of others like, WAF-1/p21 and retinoblastoma, can help in predicting the response to treatment.

P-453

A comparative analysis of retinoblastoma gene product and cyclin-dependent kinase inhibitors p16 ^{ink4}, p21^{waf-1} and p27^{kip1} in non-Hodgkin's lymphoma

Edison Catalano, M.D.
Univ. Med. Center, Cooper Hospital, Camden, United States

Introduction: p16, p21 and p27 are cyclin-dependent kinase inhibitors acting in different areas of the cell cycle, interacting with rb.
Purpose: To investigate the regulatory effects of p16, p21 and p27 proteins on rb gene protein expression in non-Hodgkin's lymphoma.
Materials and Methods: 90 cases of non-Hodgkin's lymphoma were selected. Immunohistochemical techniques were employed against antibodies to rb, p21/waf-2 and p27.
Results: p16 expression was observed in 25% small cell lymphoma (SCL), 41% large cell lymphoma (LCL), 15% small/large cell lymphoma (SLCL), 20% immunoblastic (IB), 40% lymphoblastic (LB) and 100% Burkitt's lymphoma (BL). Expression of waf-1/p21 was seen in 26% SCL, 42% LCL, 37% SLCL, 60% IB, 60% LB and 50% BL. p27 expression was seen in 100% SCL, 49% LCL, 100% SLCL, 80% IB, 80% LB and absent in BL. Inactivation or loss of expression of rb was seen in 25% SCL, 30% LCL, 43% SLCL, 20% IB, 20% LB and 75% BL.
Discussion: We noted a reverse correlation between the expression of rb, p16 and p21. Of the 61 cases that expressed rb, 45 or 74% co-expressed p27 protein.
Conclusion: Our study showed that the alteration of rb gene plays a key role in regulating the cell cycle interacting with cyclin-dependent kinases, leading to deregulated cell growth which promoted a more aggressive behavior in aggressive forms of non-Hodgkin's lymphoma.

P-454

Human thymic epithelial cells and thymomas constitutively express high levels of the truncated isoform of p63, a member of the p53 family

Chilosi M, Brighenti A., Canal F, Montagna L, Piccoli P, Marinello A, Fazion M, Pecciarini L, Cangi MG, Macrì E, Zamò A, Santacatterina M, Lestani M, Menestrina F, Doglioni C
Departments of Pathology, University of Verona and Anatomia Patologica Ospedale di Belluno, Italy

p63 is a member of the p53 tumour suppressor gene family, exerting important physiological functions in the maintenance and function of reserve cells in specialised epithelia, including skin, lung and bladder. Transactivating isoforms of p63 (TA-p63) have functions similar to p53 in inducing cell-cycle arrest and apoptosis, whereas the ΔN-p63 N-terminal truncated proteins act as dominant-negative agents toward transactivation by p53 and p63 itself. We have used immunohistochemistry, flow cytometry and western blot techniques with antibodies recognising either all p63 molecular species (4A4), or specific for ΔN-p63 (rabbit anti p40), to investigate p63 expression in normal thymus and in 32 human thymomas classified following the W.H.O. criteria. All epithelial cell types in normal thymus, including subcapsular, cortical and medullary epithelia, expressed high levels of p63, strictly confined to the cell nuclei. Both antibodies provided the same level of immunoreactivity, thus providing evidence that ΔN-p63 is in fact the main isoform expressed by thymic cells, as observed in reserve (basal) cells in stratified epithelia. All types of thymic epithelial neoplasms, including the A, AB, B1, B2, B3, and also cases of thymic carcinoma (W.H.O. type C), showed consistent expression of the ΔN-p63 isoform. According to these results it is possible to argue that the constitutive expression of ΔN-p63, a potent p53 antagonist, in normal thymic epithelial cells is necessary for their renewal strategy, as recently demonstrated for stratified epithelia. In addition, the observed expression of ΔN-p63 in thymomas could be involved in cell transformation by impairing the tumour suppressor functions of p53.

P-455

Cytotoxic protein expression in Hodgkin's disease and HD-like ALCL

García-Cosío M., Santón A., Palmeiro A., *Martín C., Bellas C.
Departments of Pathology Ramón y Cajal Hospital and *Clínico San Carlos Hospital, Madrid, Spain

Several authors have suggested a cytotoxic T-cell or NK-cell origen for 10% to 20% of classic Hodgkin's disease (HD). In the past years , several groups drew attention to a group of nodal cytotoxic-cell lymphomas that appear to be distinct from anaplastic large cell lymphoma (ALCL) and HD morphologically, immunophenotypically and biologically. Their relationship with the relatively well defined entities of ALCL and HD requires clarification.
For these reasons we have investigated by immunohistochemistry 50 case of clasical HD and HD-like ALCL for the expression of the cytotoxic proteins TIA-1 and Granzyme-B.
The tumours of HD-like ALCL cases were composed of confluent sheets of large lymphoid cells with a cohesive patern similar to the classic ALCL. Reed-Stenberg (RS) and related cells, were cattered in the lesion. We detected expression of TIA in the great majority of these cases and more than 50% were positive for granzyme B. Both cytotoxic molecules were seen in large lymphoid cells, including RS cells. Many of the cases were positive for CD30, CD15 and EMA but negative for p80/ALK. Around 30% of cases were also EBERs positive.We found high frecuency of TIA-1 and/or Granzyme-B expression in HD-like ALCL cases than in HD cases.
These data confirm previous studies that suggested that a small proportion of HD is a cytotoxic cell origen. And also, these subgroup of HD could be part of the spectrum of the cytotoxic HD-like ALCLs.

P-456

Non-Hodgkin lymphomas in Zimbabwe

R. Hohle, R. Makunike, C. Muronda, T. Rüdiger, W. Kasiya, M. Bast, D. Weisenburger, B. Nathwani, J. Diebold, K. MacLennan, H. Müller-Hermelink, A Coutts, L. Levy, A. Cakana
Department of Histopathology, School of Medicine, University of Zimbabwe, Harare, Zimbabwe

Background: During the last twenty years lymphomas in Zimbabwe have been classified by means of conventional histology according to the working formulation and the Kiel classification. Current classifications, such as the REAL-Classification and the new WHO-Classification require additional techniques, as a minimum immunohistochemical investigations. Therefore we undertook a retrospective study of Non-Hodgkin lymphomas as part of the International Non Hodgkin lymphoma classification project.
Methods: 204 consecutive cases from 1992 to 1998 were reviewed according to the protocol of the International Lymphoma Study Group.
Results: Using the REAL-classification immunohistochemical studies revealed 164 B-cell lymphomas and 15 T-cell lymphomas, 24 cases were unclassifiable or cases other than lymphoma. B-cell lymphomas included: 75 diffuse large cell lymphomas, 34 high grade Burkitt like lymphomas, 12 unclassifiable high grade lymphomas, 12 cases of CLL, 5 Burkitt's lymphomas, 6 follicle center lymphomas 4 marginal zone lymphomas, 3 mantle cell lymphomas. 15 T-cell lymphomas included 8 precursor T lymphoblastic lymphomas and 4 peripheral T-cell mixed med. & Ig. cell. 124 cases were AIDS related: 60 diffuse large B-cell lymphomas and 34 high grade Burkitt-like lymphomas.
Conclusions: 60% of all lymphomas, most frequently diffuse large B-cell lymphomas and all cases of high grade Burkitt-like lymphomas were HIV related. This finding suggests that the group of Burkitt-like lymphomas might be an entity specifically linked to HIV/AIDS. Whether HIV positivity in 10 lymphoma cases other than large B-cell or Burkitt-like is a coincidental finding, has to be established by further studies.

P-457

Mantle cell lymphoma: Rare variants

Ida Ikonomou, Sverre Heim, Ruth Langholm, Jahn Nesland, Jan Delabie
The Norwegian Radium Hospital, Oslo, Norway

Mantle cell lymphoma is a B-cell lymphoma subtype with characteristic morphologic, phenotypic and cytogenetic findings. Mantle cell lymphomas consist of a proliferation of small to medium sized cells with irregular nuclei. The lymphoma cells express CD5 and overexpress cyclin D1. The typical cytogenetic finding is t(11;14)(q13;q32) with juxtaposition of the immunoglobulin heavy chain genes and the cyclin D1 gene.
Here we report two unique variants of mantle cell lymphoma. The first is the case of a 67-year old man presenting with a single enlarged lymph node of the neck. Morphology revealed a proliferation of large pleomorphic cells with the striking formation of rosettes. The lymphoma cells expressed CD5 and cyclin D1 and cytogenetics revealed the typical t(11;14)(q13;q32) translocation. Rosette formation in lymphoma is very rare. This is the first mantle cell lymphoma case with rosettes reported. The case stresses that the presence of rosettes does not exclude a lymphoma diagnosis and that rosettes can be observed in a variety of lymphoma subtypes.
The second case is that of a 52-year old man diagnosed with stage IVA lymphoma. A biopsy of a lymph node from the neck revealed the typical morphologic and phenotypic (CD5+, cyclin D1+) findings of mantle cell lymphoma. However, cytogenetics revealed a t(5;11)(p15;q13). Variant translocations in otherwise typical cases of mantle cell lymphoma are extremely rare. The present case represents a unique case. The rearranged genes involved in this case will be further investigated to shed more light on the molecular pathogenesis of mantle cell lymphoma.

P-458

Intravascular lymphomatosis (IVL) diagnosed by bone marrow histology

Masafumi Ito, Yong-Goo Kim, Masahiko Fujino
Department of Pathology, Nagoya University Hospital;
Department of Pathology, Nagoya University, School of Medicine

Introduction: Intravascular lymphomatosis (IVL) is a unique type of lymphoma, lymphoma cells distribute in vascular space and patients manifest skin and neurological symptoms and associate hemophagocytic syndrome. In contrast, lymphadenopathy is uncommon, so the correct diagnosis is difficult. In this study, we show that the histological examination of bone marrow clot sections with immunohistochemistry is very useful to diagnose IVL. We also present the characteristic clinicopathological features of IVL. Cases and Methods: Twelve cases diagnosis as IVL in our bone marrow case files were further studied. Smears and paraffin embedded clot samples of bone marrow aspiration were examined using immunohistochemistry.

Results: Eight male and 4 female cases were ranged 62-88 (median 74) years old. Eleven cases showed abnormal peripheral blood counts (pancytopenia of 8 cases, anemia of 2 and thrombocytopenia of 1). Atypical lymphoid cells were observed in smear at less than 1% of total marrow cells. In contrast, small clusters of large lymphoid cells were easily identified in clot sections of all cases. In clot sections, hemophagocytosis was detected in 10 cases with using CD68 immunostaining. Immunohistochemistry revealed the atypical lymphoid cells expression of CD20, 79a. CD5 and vimentin were expressed in 6 cases. All 12 cases were confirmed the diagnosis of IVL by clot section histology. Conclusion: Histological examination using immunohistochemistry of clot section is better method than smear with FACS analysis to confirm the diagnosis of IVL. Hemophagocytosis is characteristically associated with B-cell type IVL. CD5 and vimentin expression by lymphoma cells is unique marker of IVL.

P-459

Mantle cell lymphoma (MCL):
a combined immunohistochemical (IHC), fluorescence *in situ* hybridization (FISH) and PCR study

Kodet R.*, Mrhalová M.*, Krsková L.*, Soukup J.*, Szépe P.**
Department of Pathology, Charles University, 2nd School of Medicine, Prague*; Department of Pathology, Medical School, Komenský University, Martin**; Czech Republic and Slovak Republic

INTRODUCTION: Diagnosis of MCL belongs to a difficult one among the small cell lymphomas. To recognize MCL is important because of its poor prognosis. Lesions with suggestive morphology of MCL should be further analyzed. The results of IHC may not be always reliable. FISH and PCR are also of diagnostic significance.
METHODS: Fourteen patients with a tentative diagnosis of MCL were analyzed. The IHC included a panel of antibodies (CD5, CD10, CD20, CD23, cyclinD1). For FISH we used locus specific probes for IgH and CNND1 genes to detect t(11;14)(q13;q32); all patients were analyzed. PCR diagnostics was performed on DNA extracted from frozen material of primary tumors – 6 patients from the subset of FISH investigated patients.
RESULTS: The IHC showed positive results for CD5 and cyclinD1 in two thirds of the patients. FISH showed fusion signals indicating t(11;14) in 12 patients. In two, the diagnosis of MCL was not confirmed; one was reevaluated as atypical reactive hyperplasia, one as low grade follicular lymphoma. DNA diagnosis revealed t(11;14) in four of six cases; in two the DNA was fragmented and DNA analysis was not performed.
CONCLUSION: The diagnosis of MCL should be supported by ancillary methods. FISH on paraffin sections is a reliable method though tissue imprints are superior due to preservation of whole nuclei. IHC is capricious especially for tissues received for consultations. DNA diagnostics is dependent on fresh/frozen material and seems to be of a lesser utility than FISH.
The work was supported by grant IGA MZ ČR NC6296-3

P-460

A new combination of antibodies helps to distinguish between classical Hodgkin's disease and anaplastic large cell lymphomas

Korinna Leder, Hans-Dieter Foss, Ioannis Anagnostopoulos, Harald Stein
Institute of Pathology and Reference Center for Lymph node Pathology and Haematopathology, University Hospital Benjamin Franklin, Free University, Berlin, Germany

The tumour cells of classical Hodgkin's disease and anaplastic large cell lymphoma (ALCL) may resemble each other in terms of morphology and immunophenotype. These cases which exhibit features of Hodgkin's disease and ALCL were called – according to the REAL classification – ALCL Hodgkin-like. We present here a new combination of monoclonal antibodies which allow the classification of 90% of these cases as either being divergences of Hodgkin's disease (common), or divergences of ALCL (less common). Antibodies which are the most helpful are directed against ALK protein, PAX5, BOB.1, Oct2 and Clusterin. The discriminating power of the antibody panel will be demonstrated by the features obtained by the investigation of 10 ALK-positive ALCL, 10 ALK protein-negative ALCL, 15 ALCL Hodgkin-like and 15 classical Hodgkin disease cases. The data obtained suggests that ALCL-Hodgkin-like do not represent a biological disease entity, but include variant cases of Hodgkin's disease, ALCL and diffuse large B-cell lymphomas, anaplastic subtype.

P-461

Conjunctiva Associated Lymphoid Tissue (CALT) lymphoma associated with virus C chronic hepatitis. Report of one case

Lome-Maldonado C, Maldonado-Martínez H, Lazo-Langner A, Angeles A
Departamento de Patología, Instituto Nacional de Ciencias Médicas y Nutrición S.Z, Mexico City, Mexico

Background: Lymphomas originated from Mucosal Associated Lymphoid Tissue (MALT) were first described by Isaacson in 1983. About 60% of this lymphomas are of gastrointestinal origin, but primary extra gastrointestinal locations have been described in other sites. MALT type lymphoma generally occurs in adults in the fifth decade or older, as a result from prolonged antigen stimulation. CALT is acquired upon antigenic stimulation or certain viral infections. CALT type lymphomas account for 8% of non-gastrointestinal MALT type lymphomas. Several studies demonstrate a higher frequency of hepatitis C virus (HCV) infection in centrofollicular, marginal zone, large B-cell and MALT type lymphomas.
Methods and Results: We report the case of 63 years old woman with diagnosis of chronic active hepatitis related to VHC. She had been treated for blefaroconjunctivitis over 40 years achieving only temporal remissions. On physical examination little white nodules were evident in both conjunctivae. A biopsy showed lymphoid nodular hyperplasia. Two years latter a biopsy showed CALT type lymphoma. This lymphoid proliferation was positive to CD 45, CD 20 and CD43 in lymphoid neoplastic cells. Keratoconjunctivitis was excluded on physical examination. Bone marrow showed focal infiltration by the same lymphoid population. Local radiotherapy was administrated to the patient. The patient achieved remission and is free of disease 6 months after therapy.

Conclusions: VHC infection has been associated to sjögren syndrome, SICCA and large cell lymphoma of B origin. Reports on the association of MALT lymphoma and HCV are sparse. Luppi et al in a small series reported a 50% incidence of positive HCV in patients with MALT type lymphoma in different locations. On the contrary Tkoub et al didn't find any differences between MALT lymphoma patients and controls. Though it is still controversial, evidence suggests that HCV might be an infectious adjuvant in the pathogenesis of MALT type lymphoma.

P-462

Aggressive NK lymphoma/leukemia not associated to Epstein Barr virus. Fatal outcome in a Mexican patient

Lome-Maldonado C, Nuncio JF, Bornstein L, De la Peña R, Angeles A, Delfau-Larue MH, Gaulard Ph
Departamento de Patología, Instituto Nacional de Ciencias Médicas y Nutrición, Salvador Zubirán, México D.F: México ; Département de Pathologie, Hôpital Henri Mondor, Créteil, France

Background: Peripheral T-cell and NK-cell lymphomas are uncommon. They account for only 5% to 20% of al non-Hodgkin lymphomas. In initials descriptions, NK- cell neoplasms were limited to the sinonasal region and had a strong association to EBV infection. The conceptual view of natural killer (NK) cell malignancies has undergone a significant evolution along past years; actually, a group of nasal and nasal-type NK/T cell lymphoma, NK-cell leukemia and blastic forms have been describes.
Methods: We present an unusual case of aggressive NK-cell lymphoma/leukemia with systemic affection, occurring in a 37 years old male with significant weight loss and hepatosplenomegaly. No nasal tumor or peripheral lymphadenopathies were documented. Hepatic and bone marrow biopsies were performed. The patient received chemotherapy (MACOP-B) and no response was observed. He died 6 months after diagnosis with active disease. Postmortem study was not performed.
Results: Hepatic biopsy revealed a sinusoidal lymphoid infiltration with a mixture of medium to large cells with areas of necrosis. In the bone marrow the same population was observed with an interstitial infiltration pattern as well as in peripheral blood. Immunophenotype results, performed on paraffin sections, revealed that the abnormal cells expressed CD3ε+, CD2+, CD5–, CD7–, CD56+++, in this population a cytotoxic active phenotype was also documented: TiA-1+ and Granzyme B+. Molecular biology analysis with PCR technique demonstrated no rearrangement of gamma T-cell receptor. Immunohistochemistry (LMP-1) and in situ hybridization (EBER probe) for EBV were negative.
Conclusion: This peculiar case provides information concerning the clinical, morphological, immunophenotipic and genetic diversity of this group of NK-cell non-Hodgkin lymphomas.

P-463

Mantle cell lymphoma. Correlation of clinical and biological features in two histological variants

Carmen Lome-Maldonado, Leticia Bornstein-Quevedo, Héctor Maldonado, Danielle Canioni, Nicole Brousse
Departamento de Patología, Instituto Nacional de Ciencia Médicas y Nutrición, Salvador Zubirán, Mexico City, Mexico; Service d'Anatomie Pathologique, Hôpital Necker, Paris, France

Background: Mantle cell lymphomas (MCL) are B cell non Hodgkin lymphomas (NHL) developed form immature, CD5+ B cells. MCL comprise 2–10% of non-Hodgkin lymphomas. They are characterized by an aggressive clinical course, as well as specific and well established morfological, immunophenotipical, cytogenetical and genotipical features, which have been defined in recent years. Diferent isoforms of the CD 44 marker have been found to be associated to high grade NHL or with a more agresive behavior in low grade lymphomas. However expression of this marker in MCL has not been reported to date. Two morphologic variants have been described in MCL : classic and blastic. Previous reports have demonstrated a poor prognosis in blastic MCL.
Objective: Identify and characterize clinical, morphologic and immunohistochemical parameters in classic and blastic MCL.
Methods: Twenty-one MCL from the Hopital Necker (France) were retrospectively reviewed. Demographic and clinical data were assessed. Immunohistochemistry for bcl-2, Ki67, p53, CD44s CD44-9v, CD44 6v, cyclin D1 were performed. Counting positive cell in 500 neoplastic cells performed an index of positive cells. Mitosis was evaluated in 20 high power fields. In 16/21 cases bcl-1 was performed by PCR. Comparisons between groups were performed using T test.
Results: The median age of patients with MCL was 63 tears (46-76). Fifteen cases were classic and 6 were plastic MCL. Most of the cases were located in lymph nodes. In 12 cases a nodular pattern was observed, 7 were diffuse and 1 mixed. The number of mitosis and the proliferation index for ki67 were higher inn blastic MCL ($p<0.05$), The other antibodies, including cyclin D1 were non statistically different. Gene rearrangement of the bcl-1 gene was documented by PCR in 15/21 cases.
Conclusion: MCL are uncommon neoplasias with a poor prognosis. The blastic variant has a less favorable clinical course and is associated two the expression of cell proliferation antigens. We didn,t find any association of CD 44 with worse prognosis or its presence in blastic MCL.

P-464

Lack of HER2/neu-overexpression in malignant lymphoma – a confirmatory analysis

Lüftner D, Genvresse I, Geppert R, Kaufmann O[1], Dietel[1] M, Possinger K
Medizinische Klinik II, Charité, Campus Mitte, Humboldt-Universität Berlin; [1]Institut für Pathologie, Charité, Campus Mitte, Humboldt-Universität Berlin, Germany

Introduction: In case reports, overexpression of HER2/neu is suggested not only in solid tumors but also in malignant lymphoma [Mineshita et al. 1993; Cheung et al. 1999].
Methods: From a serum bank of an oncological department, we retrospectively retrieved serum samples of 105 patients with active lymphoma of any histology and tested for the shedded antigen of HER2/neu using the Oncogene Science® ELISA assay (Cambridge, MA, USA). Among those lymphoma patients were 27 cases with diffuse large-cell lymphoma. The paraffin-embedded lymph-node specimens of these 27 patients were stained with the HER2/neu DAKO HercepTest® as in the original report HER2/neu overexpression by immunohistochemistry was found in this lymphoma entity [Mineshita et al, 1993].
Results: In 105 lymphoma patients, the serum level of HER2/neu ranged from 3.6–244.1 ng/ml (median 8.0 ng/ml). Only 2 patients

showed a marginal or increased HER2/neu level with 15 ng/ml and 244.1 ng/ml, respectively, using an upper limit of normal of 15 ng/ml. No patient with diffuse large-cell lymphoma showed HER2/neu overexpression by immunohistochemistry. The paraffin block of the one patient with a very high HER2/neu level suffering from high-grade T-cell lymphoma of the skin is just being stained for HER2/neu overexpression.
Conclusions: HER2/neu is not overexpressed in (diffuse large-cell) lymphoma using a standardized immunohistochemistry technique with complementary serum testing.

P-465

LN2 immunostaining of acute myeloid leukemias and myelodysplastic syndromes in routinely processed bone marrow biopsy specimens. Comparison with CD34 immunostaining

M. Melachrinou, V. Zolota, A. Symeonidis*,
A. Kourakli-Symeonidou*, D.S. Bonikos
Department of Pathology and *Department of Internal Medicine
Division of Hematology, University of Patras Medical School,
Patras, Greece

Introduction: LN2(CD74) monoclonal antibody (MoAb) recognizes the 35 kD Class II invariant chain, expressed in the nuclear membrane and cytoplasm of B-lymphocytes, and reacts with B-lymphomas (80%), T-lymphomas (20%), R-S cells in Hodgkin's disease (60–70%), precursor B-ALLs (60–70%), AMLs (50%) and some epithelial tumors. The aim of the study was to investigate whether LN2 might be a useful marker as CD34 for the immunodetection of blasts in routinely processed bone marrow biopsy specimens from patients with MDS.
Methods: One hundred ten formalin fixed, paraffin embedded bone marrow biopsy specimens [54 AMLs, 46 MDS (11 RA, 20 RAEB, 9 RAEB-t, 6 CMML), 10 normal/reactive) were immunostained with LN2 and anti-CD34(QBEND10) monoclinal antibodies using LSAB method.
Results: 70.4% of AMLs showed positive immunostaining for LN2 and CD34 in >20% of leukemic cells. The results are summarized in the table.

	M0	M1	M2	M3	M4	M5	M6	TOTAL
LN2	4/4	8/12	10/16	1/3	12/14	3/4	0/1	38/54
CD34	4/4	11/12	11/16	0/3	11/14	0/4	1/1	38/54

In MDS cases the percentage of LN2- and CD34-positive blastoid cells was <5%/RA, <5–10%/RAEB, 5–25%/RAEB-t and <5%/RA, 5–15%/ RAEB, 10–25%/RAEB-t respectively. In CMMLs mono- and promonocytes immunostained with LN2; blastoid cells were positive for both antibodies. In normal/reactive cases LN2 immunoreacted with sparse small lymphocytes and anti-CD34 with endothelial cells.
Conclusion: LN2 might be included into the panel of antibodies that are used for the diagnosis of myelodysplastic syndromes.

P-466

Bcl-2 related proteins and proliferation in myelodysplastic syndromes and acute myeloid leukemia secondary to MDS

M. Melachrinou, V. Zolota, E. Fragopanagou*, P. Matsouka*,
D.S. Bonikos
Department of Pathology and * Department of Internal Medicine
Division of Hematology, University of Patras Medical School,
Patras, Greece

Introduction: Apoptosis and its dysregulation have been implicated in the pathogenesis of myelodysplastic syndromes (MDS) and their progression to acute myeloid leukemia (AML). To evaluate the alterations in the balance between cell growth and cell death we investigated the proliferation rate and the expression of a pro-apoptotic (Bak) and an anti-apoptotic (Bcl-2) protein in bone marrow specimens from patients with MDS and AML secondary to MDS.
Methods: Formalin-fixed, paraffin-embedded bone marrow biopsy specimens from 55 MDS (12 RA, 26 RAEB, 10 RAEB-t, 7 CMML) and 20 AMLs secondary to MDS were immunostained with antibodies to Bak (polyclonal, DAKO), Bcl-2 (monoclonal, DAKO) and Ki67 (polyclonal, DAKO) using LSAB method. Bak/Bcl-2 ratio was calculated by dividing the percentage of Bak (+) cells to the percentage of Bcl-2 (+) cells.
Results: Bak overexpression was observed in all disease subtypes (60.5/RA, 65.9/RAEB, 65.5/RAEB-t, 63.8/CMML, 66.3/AML). Bcl-2 expression was significantly increased in RAEB-t/AML [35.6 (1.5–75.6)] compared to RA/RAEB (<10% blasts) group [7.4 (1.2–30.3), P=0.000]. A significantly higher Bak/Bcl-2 ratio was detected in RA/RAEB [25.5 (2–90)] compared to advanced disease (RAEB-t/AML) [5.6 (0.93-65), P=0.0000]. The degree of proliferation was variable within the subtypes (16.4/RA, 21.4/RAEB, 18.5/RAEB-t, 9.8/CMML, 18.4/AML). A significant correlation between proliferation rate and disease progression was not found.
Conclusion: This study indicates that an increased Bcl-2 expression and a fall in Bak/Bcl-2 ratio are suggestive of disease progression in MDS.

P-467

Malignant mastocytosis with an agressive course

Moreno J., Bellas C*., Gordillo J., Novo O., Limón M.,
Jiménez-Almodóvar M.
Department of Pathology, Hospital de Mérida; *Hospital Ramón y Cajal de Madrid, Spain

Introduction: Systemic mastocytosis is a disorder characterized by abnormal growth and accumulation of mast cells that preferentially involves the bone marrow, skin, spleen, liver and lymph nodes.
Patient and method: A case of 53 year-old woman with unknown fever, loss weight, severe pancytopenia and eosinophilia is presented. The patient showed hepato-esplenomegaly without adenopathies. Cutaneous manifestations or history of anaphylactic episodes were not detected. The patient was treated with interferon alpha-2b, and died because of the disease nine months after the first symptoms.
Results: Histologycally the bone marrow lesion consisted of a diffuse involvement with predominance infiltration of spindle-shape cells accompanied by many eosinophils and fibrosis. Nucleoli were inconspicuous and mitotic figures were infrequent. Normal hema-

topoietic elements were markedly reduced. The spleen showed infiltration of the red and white pulp by the same cell population, forming aggregates of spindle-shape cells and fibrosis. These cells expressed positivity for Tryptase, CD45, CD15, CD117(c-KIT), CD68, alpha-1-antitrypsine, alpha-1-antichemotrypsine and MAC 387. Giemsa, blue toloudine, Leder (Choloroacetate esterase), PAS, S-100 protein, UCHL-1, L26 and myeloperoxidase were all negative.

Discussion: Malignant mastocytosis is a rare form of mastocytosis characterized by uncontrolled and progressive proliferation and infiltration of mast cells in diverse organs. These patients are often presented without cutaneous lesions and have a very unfavorable prognosis. Because of the immature morphology of the cells the basic dyes for mast cells such as Giemsa, blue toloudine and Leder can be negative, in such cases the histopathological diagnosis may be difficult to establish and the disease is often considered in the differential diagnosis of other lymphoreticular and hematopietic neoplasias. However, the use of antibodies to mast cells antigens such as tryptase together with CD117 and CD68, is unique to mast cell disease among hematopoietic tumors. In systemic mastocytosis, survival is significantly reduced in cases with tryptase +/Giemsa – or tryptase+/Leder–.

P-468

Possible immortalization of Hodgkin and Reed-Sternberg cells: Telomerase expression, lengthening of telomere, and inhibition of apoptosis by NF-kappaB expression

Koichi Ohshima, Seiji Haraoka, Junji Suzumiya, Chika Kawasaki, Masahiro Kikuchi
Dept. of Pathology, School of Medicine, Fukuoka University, Fukuoka, Japan

Telomerase, an enzyme associated with cellular immortality, is expressed on malignant tumor cells. Deregulation of telomerase is thought to facilitate tumorigenesis and cellular immortality by providing cancer cells with unlimited proliferation capacity. Hodgkin and Reed-Sternberg (H&RS) cells are generally considered as neoplastic cells in Hodgkin's disease (HD), however, such cells are only found in a minority of HD lesions. In addition, H&RS cells with mitotic features are rare and mummified forms are occasionally encountered. There are no available data on the relationship between telomerase activity and apoptosis in HD. We studied 14 cases with Hodgkin's disease (mixed cellularity type, nine cases; nodular sclerosis type, five cases) to clarify the relationship between telomerase activity and apoptosis using in situ hybridization of human telomerase reverse transcriptase (hTERT), reverse transcriptase-polymerase chain reaction (RT-PCR) of hTERT, using extracted RNA and immunohistochemistry of nuclear factor-κB (NF-κB), and TdT-mediated dUTP-digoxigenin nick end-labeling (TUNEL) technique for apoptosis. We also analyzed the telomere length, using sorted H&RS cells. TUNEL showed a few apoptotic H&RS cells, but the cells frequently expressed hTERT, as confirmed by ISH and RT-PCR. Lengthening of the telomere of H&RS cells was noted in ten cases. In addition, H&RS cells frequently expressed NF-κB, which is known as an inducible transcription factor and inhibitor of apoptosis. Our findings of telomerase activity in H&RS cells indicate that these cells are neoplastic and are potentially immortal. In addition, NF-κB expression on H&RS cells suggests its possibility in inhibition of apoptosis of these cells.

P-469

Proliferation in pediatric b-cell-lymphoma with respect to G1-phase of cell cycle

Oschlies I.*, Mordhorst C.*, Schirrmacher J.*, Reiter A.**, Parwaresch R.*
Dpt. of Hematopathology, University of Kiel* and Dept. of Pediatric Hemato-Oncology, University of Gießen**, Germany

Introduction: The proliferative activity, an important parameter in estimating the biology of malignant tumors, was investigated in the spectrum of pediatric Non-Hodgkin-B-cell-lymphoma (NHL-B) with special respect to the G1-phase of cell cycle.

Methods: Samples of 123 pediatric B-cell-lymphomas included in the German multicentric NHL-BFM-study-protocol selected from files of the lymphnode registery (LKR Kiel) were available. Histological diagnoses were Burkitt lymphoma (BL, n=64), Centroblastic lymphoma (CB, n=33), Immunoblastic lymphoma (IB, n=5), Mediastinal large B-cell lymphoma (MLBL, n=7) and Lymphoblastic lymphoma (LB, n=14).

We evaluated immunohistochemically 1. proliferation by KiS5 (Ki 67-antigen, expressed in G1, G2, S and M) 2. proliferation by KiS2 (p100-p86 antigen, expresssed in G2, S and M) 3. percentage of cells in G1 calculated by KiS5-KiS2 and 4. percentage of proliferating cells in G2, S, M by the ratio KiS2/KiS5.

Proliferation rates were obtained by counting 1000 tumor cells in at least 10 different high power fields.

Results: The mean proliferation of all lymphomas by KiS5 was 79%±17 (37-99), by KiS2 was 42% ±12 (13–74). The mean percentage of cells in G1 was 38%±12 (13–67) and the mean ratio KiS2/KiS5 was 0,52±0,1 (0,3–0,8). In BL, the mean of KIS5, KiS2 and KiS5-KiS2 was significantly higher than in the other lymphoma subtypes.

No significant difference could be seen when comparing the results for CB, IB, MLBL and LB. The ratio KiS2/KiS5 prooved to be highly stable in all investigated lymphoma types being 0,52 in BL, 0,52 in CB, 0,60 in IB, 0,52 in MSLB and 0,49 in LB.

Conclusion: Pediatric NHL-Bs are highly proliferating lymphomas. Only BL differs significantly from the other lymphoma subtypes by a higher percentage of cells in cycle (KiS5 and KiS2) and by a higher total amount of cells in G1. The ratio S2/S5 is constant in all lymphoma subtypes and higher than in adult lymphomas and other malignancies. Therefore G1-arrest does not seem to be a feature of pediatric B-cell-lymphoma.

P-470

Detection of Epstein Barr Virus in Hodgkin's disease in Thracian region of Turkey; by in situ hybridization

Özdil A.[1], Doganay L.[1], Demir M.[2], Oz Puyan F.[1], Bilgi S.[1]
[1] Trakya University Medical Faculty Dept.of Pathology; [2] Trakya University Medical Faculty Dept.of Haematology, Edirne, Turkey

Introduction: The relation of Epstein Barr Virus (EBV) and Hodgkin's disease (HD) has been suggested by serologic, epidemiologic and molecular biologic studies. Incidence of EBV in HD is high. In the present study, the EBV association with HD in Thracian region of Turkey was investigated.

Methods: We investigated the presence of EBV in 44 cases of HD. Fluorescein-labelled antisense EBV (EBER-RNA) was performed by in-situ hybridization from selected paraffin-embedded tissues.

Results: There were 28 males and 16 females, with a mean age of 40 years (range 4–80 years). Histologic subtypes included nodular sclerosis in 18 (40.9%), mixed cellularity in 16 (36.4%), lymphocyte predominance in 7 (15.9%), and lymphocyte depletion in 3 (6.8%). Overall, EBV was expressed in 30 cases (68.2%). High EBV association was found with mixed cellularity 75% and nodular sclerosis 72.2%. In lymphocyte predominance and in lymphocyte depletion cases the EBV positivity was 57.1% and 33.3%, respectively. 7 cases which were younger than 15 years old were all positive for EBV (100%).
Conclusion: HD in Thracian region showed a high association with EBV as other developing countries. Our findings suggest that EBV plays an important role in the pathogenesis of HD in Turkey.

P-471

The association of Epstein-Barr virus (EBV) with Burkitt's lymphoma in a multi-ethnic population

Peh SC, Tai YC, Kim LH, Shaminie J
Department of Pathology, University of Malaya, 50603 Kuala Lumpur, Malaysia

Introduction: The pattern of EBV association differs between endemic and sporadic Burkitt's lymphoma (BL). This study aims to investigate the disease pattern in a malaria endemic country, with multiethnic population.
Methods: Fifty-five cases of reconfirmed BL with available tissue blocks were retrieved for immunohistochemical stain for bcl-2, p53 and pRB expressions, EBER by in situ hybridization technique, EBV-subtype and t(14;18) by nested-PCR methods. The demographic data and site of presentation was retrieved from patients' records.
Results: There was a predominant of male patients (male:female ratio=3.6:1). Majority (67.3%) was less than 15-years old. Chinese constitutes the largest group (31/55). The disease presented in the lymph nodes (40%), followed by abdominal viscera (18.2%). Jaw presentation was seen only in 3 patients. Overall, 36% of these cases were EBV-associated, all were subtype A. EBER expression was more common in BL from Malay, and indigenous tribes from East Malaysia (50%), when compared to Chinese (25.8%). Bcl-2 expression was detected in 9 (16.4%), over-expression of p53 in 41 (85.4%) and loss of pRB in 3 (6%) of the cases tested. All the bcl-2 expressing tumours did not show t(14;18) by PCR technique.
Conclusion: BL is more commonly seen in the ethnic Chinese in Malaysian patients, and the disease follows sporadic pattern of EBV-association and clinical presentation.

P-472

CD30+ diffuse large b-cell lymphoma arising in malt-lymphoma within warthin tumor: case report with distant nodal and cutaneous dissemination

Plank L., Rešl M.[1], Szépe P., Kejmar A.[2], Voženílek J.[3], Cieslar P.[4]
Dept. of Pathol. in Martin, (Slovak Rep.), of Pathol. in Hradec Králové[1] and Mělník[3], of Medicine in Prague[4] and of Otorhinolaryngol. in Mělník [2] Czech Republic

Introduction: Malignant epithelial or lymphoid transformation of Warthin tumor (WT) is a rare event – its lymphoid stroma may transform into diverse lymphomas, but only 4 cases of diffuse large B-cell lymphoma (DLBCL) were reported.
Case report and biopsy results: a left parotidectomy performed in 51-year-old woman presenting with a painless 3-months growing mass showed lymphoma of the MALT-type (CD20+/CD30- with centrocytoid morphology, lymphoepithelial lesions and monotypic c-Ig positivity of κ light chain) with areas of CD20+/CD30+ DLBCL (with identical c-Ig). The staging procedure was negative with exception of bilateral inguinal lymphadenopathy, which showed by biopsy the nodal infiltration by DLBCL without MALT- or WT structures. Four months later, identical DLBCL dissemination appeared in a form of bilateral axillar lymphadenopathy and subcutaneous involvement of the low extremities. After the 2nd chemotherapy cyclus, there are no signs of neoplastic disease. Conclusion: While lymphomas arising in WT are rare and represent mostly follicular lymphomas and only rarely DLBCL, the presented case demonstrated in this localisation unique features of low grade MALT-lymphoma type with transformation to CD30+ DLBCL. The disease presented peculiar dissemination not only in the form of distant nodal involvement (observed also in 2/4 other reported WT-DLBCL cases), but a late distant cutaneous dissemination as well. The case seems to support indirectly the most accepted theory on development of WT from heterotopic salivary gland tissue components of intra- or periparotid nodal lymphoid tissue.

P-473

The Topoisomerase II alpha and Ki-67 expression correlates with survival in patients with Hodgkin lymphoma

M. Provencio*, C. Corbacho**, C. Salas**, S. Ramón y Cajal**
*Servicio de Oncología Médica, **Departamento de Anatomía Patológica, Clínica Puerta de Hierro, Madrid, Spain

Topoisomerase II isoenzymes are the targets for drugs, such as epidophyllotoxins and doxorubicin, usually used in treatment of Hodgkin lymphomas. Due to Topoisomerase IIα has been related with cell proliferation and has been considered as an indicator of chemosensitivity in non-Hodgkin lymphomas and other tumors, we analyzed the expression of Topo IIα in 42 patients with Hodgkin lymphomas stage III or IV with two or more risk factors.
Immunohistochemistry of paraffin-enbedded tissue sections of Hodgkin lymphomas was performed with anti-topoisomerase IIα, Ki-67, CD30, CD15, CD20 and CD3 antibodies. Percenteage of positive Reed-Sternberg cells was correlated with response to therapy and clinical outcome.
Positive nuclear staining for Topo IIα in RS, or RS variant cells, was seen in 90% of Hodgkin disease cases (and co-expression of Ki-67 and Topo IIα in 90% of HD). No significant difference in percenteage of Topo IIα positive cells was detected among histological HD subtypes. In the stadistic study (either using an univariant or multivariant analysis) for overall survival, only Topo IIα <30% was associated with shorter survival.
With these results, we show that the evaluation of Topo IIα expression in Hodgkin lymphoma provide independent prognostic information and correlates with overall survival.

P-474

Diagnostic value of bone marrow biopsy in the staging of low-grade b-cell malignant lymphoma.

Rodríguez-Pinilla S.M*.; Escalante F.**; Martinez-Gonzalez M.A.*
Departments of Pathology* and Haemathology**,
12 de Octubre University Hospital, Madrid, Spain

AIMS: To compare the sensitivity of the histologic study of bone marrow biopsy with cytological smear examination and flow cytometry of aspirate bone marrow in medullary involvement by low grade B-cell lymphomas.
MATERIALS and METHODS: We evaluated 81 bone marrow biopsies from 27 patients with low grade B-cell lymphomas. Flow cytometry (FC) and cytological smears studies were performed simultaneously in 51 cases. Histologic and cytologic diagnoses of positivity or negativity for lymphoma involvement were based on the generally established criteria. In this study, the mere suggestion of malignancy was considered as negative.
RESULTS: Histologically, marrow involvement by lymphoma was found in 23 cases (8 on trephine biopsy exclusively, 4 on clot sections of the aspirate and 11 on both specimens). Among these 23 histologically positive samples, 13 cases were also positive on cytologic studies, while flow immunophenotyping identified 15 cases as monoclonal B-cell processes. On the other hand, among the 28 histologically negative samples, three specimens proved to be positive on cytology and/or flow cytometry.
CONCLUSIONS: Histologic assessment of biopsy specimens remains as the most sensitive technique in staging patients with low-grade B-cell malignant lymphoma, being the rate of involvement in our study of 45% (23 from 51 cases). Nevertheless smear examination and FC detect an additional 6% (3 from 51 in our series) of cases that can not be identified on biopsy specimens.
Compared with exclusively trephine bone marrow biopsies, the evaluation of both trephine biopsy and clot sections from aspirates increases the rate of detection of lymphoma.
In our studies none of the different subtypes of low-grade B-cell lymphomas seemed to have an increased risk bone marrow involvement.

P-475

Inflammatory pseudotumor of the spleen : A proliferation of dendritic cells associated with epstein barr virus. A case report

T. Rousset (1), K. Costa (1), V. Costes (1), T.Lavabre Bertrand (2), P. Baldet (1)
(1) Service d'Anatomie Pathologique CHRU, Montpellier,
(2) Laboratoire de Biologie CHRU, Nîmes, France

Aims: Inflammatory pseudotumors (IP) of spleen are exceptional lesions. We report a new case with Epstein Barr virus (EBV) association.
Case report: A 61 year-old woman present purpura. After investigations diagnostic of idiopathic thrombocytopenic purpura (ITP) is made. Computed tomography scanning of spleen showed one superior pole nodule (4 cm). Corticotherapy was curative. Two years later, splenic nodule diameter was 8 cm: splenectomy was performed.
Results: At gross examination the spleen weight was 484 g. There was a circumscribed scleroelastic tumor with a yellowish color and extensive hemorrhagic areas. Microscopic analysis showed interlacing fibroblast-like spindle cells, plasma cells, lymphocytes and epithelioid granulomas. Plasma cells were polyclonal using immunohistochemistry and PCR analysis. Spindle cells exhibited follicular dendritic cell phenotype (CNA42+) and were EBV positive with EBER oligonucleotides in situ hybridization.
Comments: IP was rarely reported in spleen. Several cases were associated with EBV and a follicular dendritic cell origin was supported by phenotype. Association with ITP in few cases suggested autoimmun mechanism. Our case confirms these data: a follicular dendritic cell infection EBV seems to play a role in the pathogenis of some IP.
Splenectomy is diagnostic and curative.

P-476

Co-infection of different Epstein-Barr virus strains in Hodgkin's disease patients and normal controls

Santón A., García-Cosío M., *Pascual A., *Martín C., Bellas C.
Departments of Pathology Ramón y Cajal Hospital and *Clínico San Carlos Hospital, Madrid, Spain

The aim of the present work was to assess the presence of multiple Epstein-Barr virus (EBV) strains in three different Hodgkin's disease (HD) groups: adult ordinary, paediatric and HIV-associated, and in two healthy populations one made up of adults and another of children.
Material and Methods: Ninety three cases of HD were selected: 39 ordinary, 30 HIV-associated, and 24 paediatric, all of them expressing the EBV latent membrane protein-1 (LMP-1) in diagnostic HRS cells as probed by immunohistochemistry. Two control groups were also chosen: a) samples from 50 healthy adults consisting on reactive tonsills, reactive lymphadenitis and peripheral blood lymphocytes from infectious mononucleosis, and b) 39 cases of normal tonsillar tissue from healthy children.
Genomic DNA was amplified by PCR using primers for the following EBV genes: EBNA 2, EBNA 3C, LMP1 30 bp deletion and LMP-1 33 bp repeats. DNA extracted from the cell lines B95.8 and AG876 were used to control for EBV types 1 and 2, respectively. The latter was also used as control for the LMP-1 30-bp deletion.
Results: When performing EBV strain type assignment we found co-infections by EBV of type 1 and 2 in 6.7% of HIV-associated HD, 5.1% of ordinary HD and in 10% of adult controls. The study of the region containing 33 bp repeats within the LMP-1 gene showed the simultaneous presence of EBV strains carrying different number of repeats in 10% of ordinary HD and in 8.3% of paediatric HD patients.
The highest level of dual infections was observed when studying the occurrence of LMP-1 30 bp deletions. The simultaneous presence of LMP-1 deleted and non-deleted EBV strains was observed in 33.3% HIV-associated HD, 12.8% ordinary HD, 50% childhood HD, 26.5% adult controls, and 27.3% infantile controls. Noteworthy is the fact that in 30% of infectious mononucleosis cases dual infections of deleted and non-deleted strain were detected.
Conclusions: Co-infections with different EBV strains are much more frequent than previously thought. The high percentage of dual infections found in healthy controls could indicate that although the infection by EBV triggers an immune response, which in most cases seem to protect against additional infections by exogenous strains, this protection is not always complete in some individuals.

P-477

Morphologic, immunophenotypic and clinical characteristics of anaplastic large-cell lymphoma

Bahram Shahgoli[1], Tatjana Terzić[1], Vesna Jovanović[1], Karolina Smiljanić-Radotić, Zvezdana Tepavčević[2]
[1] Institute of Pathology, School of Medicine, Belgrade, Yugoslavia; [2] Institute of Pathology, University of Stomatology, Belgrade, Yugoslavia

INTRODUCTION: Anaplastic, CD30 positive, large-cell lymphoma (ALCL) is now a well recognized pathologic entity that accounts for 2% of all lymphomas. It is cytologically undifferentiated malignant lymphoma that need to be distinguished from a variety of other neoplasms using immunohistochemistry.
CASE: A previosly healthy 19-year-old female, 8 months after a normal pregnancy and delivery, presented with mediastinal bulky disease, involvement of retroperitoneal lymph nodes and hepatosplenomegaly revealed on computerized tomographic scan. The diagnosis was obtained on the review of the hematoxylin and eosin-stained slides and immunophenotype data.
RESULTS: The neoplastic infiltrate showed the typical appearance of common-type ALCL with diffuse involvement of a lymph node and cohesive growth pattern. The tumor was composed of large blastic cells with pleomorphic and eccentric nucleus with multiple or single prominent nucleoli. Multinucleated forms were rare. Mitoses were readily apparent. Immunohistochemical investigations of biopsy specimens revealed ALCL, null-cell lymphoma, positive to CD30 (Ki-1) antigen. Tumor cells also showed positive staining for vimentin and CD45 (LCA). Tumor cells were negative for B-cell marker (CD20), T-cell marker (CD3), epithelial membrane antigen, cytokeratin, S-100 and HMB-45. CONCLUSION: Immunophenotypic findings confirmed that ALCL should be considered in the differential diagnosis of anaplastic tumor, primary localized in mediastinum. The differential diagnosis may include anaplastic carcinoma, choriocarcinoma, malignant melanoma, sarcoma, Hodgkin's disease and histiocytic lymphoma.

P-478

Ethanol fixation of lymphoma samples as an alternative way to preserve nucleic acids (NA)

Jan Soukup, Lenka Krsková, Irena Hilská, Iva Veřmiřovská, Roman Kodet
Department of Pathology, Charles University, 2nd Medical School, Prague, Czech Republic

Introduction: A major problem in lymphoma diagnostics is an inappropriate preservation of samples. A portion of each sample should be frozen for special immunohistochemical and/or molecular investigation. Nevertheless, frozen samples are not available in many cases, especially consults. To avoid this problem we try NA isolation from ethanol-fixed paraffin-embedded samples.
Methods: Fresh lymphoma samples were separated, frozen, pieces were fixed in ethanol and formalin and then embedded in paraffin. From each sample we prepared histologic and basic immunohistochemical slides we isolated DNA and RNA for PCR and RT-PCR (detection of IGH rearrangements, translocation t(14;18), control genes: betaglobin, ABL).
Results: We investigated ten malignant lymphomas. Comparing PCR products with differently pre-treated samples we showed, that the quality of NA isolated from ethanol-fixed samples was close to that of frozen samples and considerably better than fragmented NA from formalin-fixed samples. Histologic and immunohistochemical slides were applicable in diagnostic process, but formalin-fixed sections were of a better quality.
Conclusion: Ethanol-fixed paraffin-embedded samples may be helpful for preservation of NA in lymphoma samples. The method is easy and inexpensive, therefore we recommend this procedure for hospitals without possibility to provide frozen material.
The work was supported by grant IGA MČR NC6296-3

P-479

Expression of Nerve Growth Factor Receptor in Reed Sternberg cells and variants

V. Stracca Pansa, A. Scapinello°, E. Bonoldi*, P.A. Bevilacqua*
Servizio di Anatomia Patologica di Venezia, Vicenza*, Castelfranco Veneto° , Italia

Several lines of evidence suggest that in most cases of classic Hodgkin's Disease (cHD) the Reed Sternberg cell and variants are derived from germinal centre B-cells. Recently , the hypothesis of an alternative origin of RS cells from follicular dendritic cells (FDRCs) has been proposed, based on the immunohistochemical detection of FDC markers such as CD21,CD35,fascin and CD83 in RS cells (1) (2). Moreover, other studies suggest that Epstein Barr virus is an important factor in the pathogenesis of HD and that the Latent Membrane Protein 1 (LMP1) is the most likely EBV encoded protein responsible for the EBV mediated pathogenic effect. Nerve Growth Factor Receptor (NGFr) is a member of TNF superfamily protein that is known to be consistently expressed in FDRc, but not in B or T cells of the lymphoid tissue. Aim of our study is to evaluate the expression of NGFr in RS cells of cHD and to investigate the possible correlation with the expression of LMP1 protein.
METHODS: A series of 49 consecutive cases of cHD were sub typed according to the WHO classification. into 29 NS, 17 MC, 2 LD and 1CLP . Paraffin sections were stained with anti NGFr (clone NGFr 5 DAKO) and with anti-LMP1 (Novocastra) using ABC method. Immunostaining was semi quantitatively evaluated from + (at least 5% of RS cells) to +++ (more than 50%).
RESULTS: In 21 cases neoplastic cells exhibited strong diffuse cytoplasmic staining for NGFr (1+7 cases, 2+8 cases and 3+6 cases) and frequently assumed dendritic shapes. In 5 cases only scattered RS cells were immunostained. The remaining 23 cases were negative. EBV-LMP1 was detected in 9 cases (1+1 case, 2+5 cases and 3+3 cases) with a prevalent expression in MC subtype (6 cases). In 4 out of the 9 positive cases we observed a coexpression of NGFr and LMP1.
CONCLUSION: Our data show, for the first time, that a consistent number of cHDs (43%) express NGFR in RS cells and that there is a wick correlation, if any, with EBV infection . These findings support the hypothesis that, at least in a subset of cHD, the RS cells and variants may exhibit a FDC phenotype. It should also be considered unlikely that NGFR expression in RS cells is induced by Epstein-Barr virus infection.
1. S. Nakamura et al. Am J Surg Pathol 23, 363–376, 1999
2. GS Pinkus et al. Am J Pathol 150, 543–562, 1997

P-480

Extranodal soft tissue lymphoma of the lower extremities

Tatjana Terzić, Vesna Jovanović, Mirjana Atanacković, Jelena Sopta, Aleksandar Đorđević*
Institute of Pathology, School of Medicine, University of Belgrade, *Institute of Orthopedic Surgery "Banjica", Belgrade, Yugoslavia

INTRODUCTION: Extranodal soft tissue lymphoma (ESTL) is rare and thus may be confused with the more common soft tissue tumors. We presented three cases of ESTL of the lower extremities with histologic appearance of small cell cancers.
CASES: Clinical presentation was the following: Case 1: a 91-years-old man, presented with an enlarging deep medial thigh soft tissue mass and ipsilateral edema, both of 6 months' duration. Case 2: a 52-years-old man presented with firm mass of the Achil tendon, that had increased in size during the last one month. Case 3: a 53-years-old man, presented with large deeply seated mass of gluteal region. The diagnosis was obtained on the review of the hematoxylin and eosin-stained slides and immunophenotypic data.
RESULTS: All patients had follicular lymphoma, with diffuse pattern of growth, grade 1 (REAL), except the third, who had grade 3. The tumor cells expressed LCA, pan B-antigens (CD20), immunoglobulins with light chain restriction and the bcl-2 protein. A large panel of monoclonal antibodies were applied in order to resolve the problem of differential diagnosis (cytokeratin, vimentin, desmin, synaptophysin, NSE, HMB-45, S-100, CD99).
CONCLUSION: ESTL of the extremities must be considered in the differential diagnosis with other small cell cancers: metastatic anaplastic carcinoma, metastatic oat cell carcinoma, rhabdomyosarcoma, extraskeletal Ewing's sarcoma, small cell osteosarcoma, mesenchymal chondrosarcoma, neuroblastoma, plasmacytoma, Merkel cell carcinoma.

P-481

Coexpression of tissue inhibitor of metalloproteinases-1 and EMMPRIN in anaplastic large cell lymphoma and Hodgkin's disease

C. Thorns, T. Gaiser, K. Lange, I. Latendorf, A.C. Feller, H. Merz
Institute of Pathology, Medical University Lübeck, Germany

Introduction: The role of tissue inhibitor of metalloproteinases (TIMP-1) in cancer biology is still a matter of debate. On the one hand TIMP-1 may be cancerogenic through its anti-apoptotic activity, on the other hand it may decrease lokal tumor growth and metastases through its inhibitory effect on metalloproteinases. EMMPRIN is an potential inductor of metalloproteinases. For our best knowledge nothing is known about the expression of EMMPRIN in lymphoid cells.
Methods: Using cDNA array technology (Human Cancer 1.2, Clontech) we studied the gene expression of 5 ALCL derived cell lines, 4 Hodgkin derived cell lines, and peripheral B- and T-lymphocytes.
Immunhistochemistry for TIMP-1 and EMMPRIN using the polyclonal goat antibody anti-hTIMP-1 (R&D systems) and the monoclonal goat antibody anti-hEMMPRIN (R&D systems) was performed on HD and ALCL samples.
Results: On the mRNA level TIMP-1 was over-expressed in all 5 ALCL derived cell lines in comparison to B-/T-lymphocytes and HD derived cell lines. Interestingly no significant difference between ALCL and HD was detected when HD and ALCL samples were stained for TIMP-1. EMMPRIN was over-expressed in 3 ALCL and 2 HD derived cell lines. The majority of HD and ALCL samples were positive for EMMPRIN and TIMP-1, indicating that TIMP-1 and EMMPRIN are indeed coexpressed in ALCL and HD.
Conclusion: TIMP-1 and EMMPRIN are coexpressed in Hodgkin's disease and anaplastic large cell lymphoma. We speculate that TIMP-1 may act mainly cancerogenic through its antiapoptotic potential. Its inhibitory effect on matrix metalloproteinases may be dominated by the expression of EMMPRIN.

P-482

Hemophagocytic syndrome associated with multiple myeloma

I. Venizelos[1], S. Pervana[1], E. Pazarli[1], G. Georgiou[1], V. Perifanis[2], V. Garipidou[2]
[1] Department of Histopathology, [2] B. Prop. Department of Medicine, Hippocration General Hospital, Thessaloniki, Greece

We report a case of a 54-year-old woman who admitted to our Hospital with a 5 months history of fever. On physical examination splenomegaly was found with no enlarged lymph nodes. Hematological examination revealed renal impairment with serum creatinin: 2 mg/dl. A renal biopsy was performed and features were consistent with IgA nephropathy. The patient was discharged with nutritional advices. One month later the patient readmitted and was found to have renal failure and pancytopenia. Bone marrow biopsy revealed proliferation of mature histiocytes with marked hemophagocytosis associated with multiple myeloma. Immunohistochemical examination showed monoclonality of the plasma cell population for k light chain. All laboratory tests for bacteria, viruses, fungi or parasites as well as complete immunological studies for autoimmune diseases were negative. After the diagnosis was made, the patient completed 6 courses of systemic chemotherapy with vinblastin, adriamycin and dexamethazone .Her renal failure was supported with extrarenal blood clearing. Two years after the onset of treatment the patient is in a good condition.
Hemophagocytic syndrom (HS) is an uncommon disorder characterized by proliferation of histiocytes that actively engulf other hematopoetic cells causing cytopenia. Pathophysiology is related to a deregulation of T-lymphocytes and excessive production of cytokines. Aquired HS has been found associated with non-Hodgkin's lymphomas usually T-cell type, Hodgkin's disease, gastric adenocarcinoma, acute leukemias, S.L.E., reumatoid arthritis, Henoch-Schönlein purpura and infections from bacteria, viruses, mycobacteria and parasites.
To the best of our knowledge only 1 case of HS associated with multiple myeloma has previously been reported.

P-483

Primary pulmonary hypertension (PPH): Report of two families and a clinicopathologic review

M. D'Armiento, G. Ciancia, R. Giannatiempo, C. Olla Atzeni, R. Vecchione
Dept. of Pathology, University "Federico II", Naples, Italy

PPH is a uncommon and poorly progressive disease characterized by increased pulmonary artery pressure and pulmonary vascular re-

sistance. A careful diagnostic evaluation is a requirement for appropriate management of this disease which leads to right ventricular failure and death of the patient.
We describe two couple of siblings (aged from 3 to 6 months) died by PPH unresponsive to nitric oxide inhalation therapy.
The autopsy tissue was examined histologically, immunohistochemistry and ultrastructurally. We observed a pattern characterized by medial thickening in small pulmonary arteries together with peripheral muscularization with plexiform pattern, but with deficient capillaries in thickened air space walls, anomalous small pulmonary veins in bronchiolar arterial rays, denying a clear distinction between pulmonary and bronchial veins small muscular pulmonary arteries extended to the precapillary level. This complex vascular abnormality has been termed alveolar capillary dysplasia related to a failure of fetal lung vascularization. In two cases we found double capillaries on both sides of alveolar walls and capillary invasion of vessels and airways ("capillary hemangiomatosis"). In the case of the sib dead at 6 months we observed nodular regenerative hyperplasia of liver (NRHL). For that we suppose that centroacinar veins may represent bronchial veins that do not normally develop beyond the ends of cartilaginous bronchi and arterial pulmonary occlusive changes reactive to obstructive at the level of pulmonary arterials.
But we argue that coexistent venous changes of systemic veno-occlusive disease in case of capillary hemangiomatosis are secondary and we see "a spectrum" of lesions related to length of disease.

P-484

Congenital Varicella Syndrome

Dhaene K*, Matthys B*, De Waele K**, Goossens L**,
De Praeter C**, Praet M*
* Institute of Pathology ; ** Department of Pediatrics, University Hospital Ghent, Belgium

Introduction: Early intrauterine infection with varicella zoster virus (VZV) results in the rare Congenital Varicella Syndrome (CVS). Clinical, molecular and autopsy findings of CVS, acquired at 12 wks, are reported.
Clinical findings: Sonography at 26 wks demonstrated polyhydramnion, impaired fetal growth, left limb hypoplasia and abdominal calcifications. VZV DNA was detected by PCR in amniotic fluid. Propositus, born at 37 wks, exhibited symmetrical growth retardation, segmental cutaneous scar and limb hypoplasia. Hypotonia and seizures were noticed. Brain MRI showed pachygyria and hemicerebellar hypoplasia. CT abdomen revealed meconium peritonitis, gut obstruction and pyeloureteral distension. The patient expired on day 4.
Autopsy findings: Multiple calcified atretic small bowel segments with preatretic dilatations were present. Microscopy showed destruction of ganglion cells in the mesenteric plexus and the periadrenal tissue. Dystrophic calcifications were present in the mesenteric plexus, lung and liver parenchym and the urinary bladder wall. Central liver veins were surrounded by an active lymphohistiocytic infiltrate. Brain inspection demonstrated right cerebellar hypoplasia. Nested PCR documented the presence of VZV DNA in brain tissue and paraffinised lung, adrenal and bladder tissue blocks.
Discussion: Central neurologic features, due to inflammatory, destructive effects and developmental derangements, are prominent. Destruction of peripheral nervous tissue resulted in severe bowel pathology. Though primo-infection occurred weeks before, active inflammation was still present both in neuronal and non-neuronal tissues.

P-485

Pathomorphological study of the pulmonary vascular tree in congenital heart disease

Duganovska S, Petrusevska G. Tolovska M, Kostadinova S, Ristovski M.
Institute of pathology, Medical faculty, Skopje, R. Macedonia

This study is made on autopsy material between 1992–1999. There were 220 cases with congenital heart disease (CHD). 26 of them were with pulmonary vascular disease (PVD): 4 had an atrioventricular (AV) septal defect; 5 a ventricular septal defect (VSD), 8 a complete transposition of the great arteries (TGA)+VSD, 3 an atrial septal defect, and 6 had other malformations. Lung specimens from 26 cases with PVD and 10 controls with sudden death syndrome were analysed. The age of children with PDA ranged from 3 weeks to 10 years. Sections were stained with He-Eo, Elastic-van Gieson, Trichrome, Reticulin. Changes in the perifferal vessels were graded according to the modification Heath – Edwards (H/E) grades: all the infants <6 months of age had changes graded al level I of the H/E. More severe changes were seen in patients older than 6 months. In patients >2 years of age only one had histological changes less severe than H/E gradus II. Out of the four patients with the most advanced PVD, (H/E grade III–IV), two had complete transposition and two had atrioventricular (AV) septal defect. In this group we found arteriolar muscularisation with cellular intimal proliferation. The elastic pulmonary arteries showed dilatation lesions.
We conclude, that the most severe morphological changes appear in the elastic pulmonary arteries of the patients with pulmonary hypertension, including thickening of the media and intima, dilatation of the lumen and atherosclerosis.
It probably means that the irreversibility of the changes happens in the group of older patients.

P-486

A detailed histopathological profile of hepatoblastoma

Vera Ferlan–Marolt, Lena Perger
Institute of Pathology, Medical Faculty, Ljubljana, Slovenia

Introduction: Hepatoblastoma (HB) is a childhood malignant tumor characterized by a variegated morphological picture due to the histopathological variants of the epithelial and mesenchymal components. The purpose of our study was to evaluate the most distinctive features of HB that should suggest the correct diagnosis.
Material, methods, results: Surgically treated patients enrolled in the study were 4 boys and 2 girls, 11–45 months old. After liver resection diagnostic material was obtained from the huge primary tumorous growths in this organ.
According to standard histopathological examination the tumors were classified as HB. Malignant liver cells that express the features of embryonal and fetal stage of maturation were accompanied by sparse connective and myxomatous tissue in 3 cases recognized as typical epithelial HB. Other variants of HB were detected in sin-

gle cases. Mixed HB was diagnosed when the mesenchymal component composed 50 % of the growth. The anaplastic variant was characterized by small, dark cells incorporated in loose mixomatous tissue with some immature muscle cells. In one case, the features of the anaplastic variant included a prominent area of the epithelial growth resembling hepatocellular carcinoma. According to the mesenchymal component the tumor was defined as HB with macrotrabecular growth pattern.

Immunohistochemical staining:

Immunohistochemical reaction Staining component of HB	+	++	+++
Fetal component	AAT	AFP, CEA	Hep Par 1, CK 18, CAM 5,2
Embryonal component	Hep Par 1, CK 7, CK 19, Ki-67, AAT	CK 18, CAM 5,2, AFP, EMA, CEA, VIM	
Anaplastic variant			Ki-67, AAT, VIM
Anaplastic and HCC differentiation		AAT, AFP, EMA, CEA	Hep Par 1, CK 18, CAM 5,2

Conclusions: In the study, all variants of HB were represented. αFP, CEA and Hep 1 were positive in the epithelial subtypes, vimentin in the less differentiated areas. Simultaneous expression of vimentin and cytokeratins in the cells suggested that the various components of HB might be metaplastic and of common origin.

P-487

Congenital diaphragmatic hernia and associated malformations

Gonda P.[1], Szabó M.[2], Illyés Gy.[1], Kovács M. [1]
2nd Dept. of Pathology[1], 1st Clinic of Pediatrics[2],
Faculty of Medicine, Semmelweis University, Budapest

The incidence of congenital diaphragmatic hernia is approximately 1:5000 per live births. In one third of cases the hernia is accompanied by various malformations. Mortality is quite high in these combined cases. Isolated diaphragmatic hernia, a closure defect with multifactorial, polygenous inheritance is mostly curable. Cases associated with malformations can be classified into known genetic syndromes, sequences with characteristic macroscopic features and inheritance patterns in 50%.
18 autopsy cases of diaphragmatic hernia in the period of 1993–2000 were reviewed. 6 of them were associated with multiple malformations. Two cases were suggestive of Fryns syndrome, a well documented autosomal recessive, lethal malformation. The rest of the cases were unclassified according to the above criteria.
Our study emphasizes the importance of detailed description and documentation of the major and minor anomalies of newborns with congenital diaphragmatic hernia. Even without the technical possibility of genetic analysis a suggested diagnosis based on macroscopic features can help and direct genetic counseling.

P-488

Morphology of chorion and decidua in spontaneous abortuses with normal and pathologic karyotypes

Gorbatcheva J., Voloschuk I., Dyscheva N.
Dept. of Pathology, Moscow Medical Academy, Moscow, Russia

Generally, about one half of clinically recognized first-trimester spontaneous abortions (SA) are chromosomally abnormal. There are different points of view on morphological features of chorion and decidua with pathologic karyotypes.
Aim: To compare morphology of chorion and decidua in А with normal and pathologic karyotypes.
Methods: SA with normal and abnormal karyotype (46 specimens of first trimester SA) was investigated morfologically. It included a histologic pattern and proliferative activity. The last one was determinate as the rate of Ki-67-positive cytotrophoblast cells. The karyotyping was made on chromosome preparations of chorion villi prepared by direct method with routine and G-staining.
Results: Identical morphological signs of the development retardation of villi were diagnosed among abortuses with normal karyotype and with aneuploidies. Changes in the decidua, which reflected mechanism of realization of abortion (hemorheologic disturbances, necrosis, etc.) also were the same. The diameter of villi was bigger in aneuploid SA than that in SA with normal karyotype ($p<0.05$). The trophoblast proliferative activity was high in SA with abnormal karyotype and it was low in SA with normal karyotype. The partial moles were diagnosed in triploidy, as it was expected. The erythrocytes in the intervillous space were detected in all specimens with chromosomal aberrations.
Conclusions: Changes in the decidua and chorion with pathologic karyotypes are not specific excluding triploidy. The disorders of placentation that cause blood flow in the intervillous space are probably associated with defects of the trophoblast invasion, but not the trophoblast proliferative activity.

P-489

Changes of the cytoskeleton in fetal development and pediatric heart disease

Guertl B.[1], Ratschek M.[1], Tessaro B.[1], Kratky D.[2], Hoefler G.[1]
Institutes of Pathology[1] and Biochemistry[2], University of Graz, Austria

Introduction: In a mouse model for metabolic cardiomyopathies, developed in our laboratory, male animals show a drastically reduced life span and in both genders a significantly lower left ventricular developed pressure was demonstrated. Differential display analysis revealed, among other genes, overexpression of α-tubulin. An overexpression of α-tubulin has already been described for hypertrophied and failing heart in animal models and human disease. We investigated the role of α-tubulin in development and different types of pediatric heart disease.
Methods: Samples of left ventricular anterior wall were taken during routine autopsies. In addition to different stages of fetal development, various metabolic and mechanical cardiomyopathies either developed before or after birth were included in the study. Total myocardial RNA was used for Northern blot analyses.
Results: Expression of α-tubulin was lower during intrauterine development, but immediately upregulated after birth. A significant

overexpression of α-tubulin was demonstrated in mechanically caused cardiomyopathies evolved before as well as after birth. In a metabolic cardiomyopathy no change was observed.
Conclusion: The upregulation of α-tubulin seems to be an important change in myocardial cytoskeleton after birth and in mechanical cardiomyopathies developed before and after birth, but seems not to be possible in some metabolic cardiomyopathies.

P-490

Childhood bone tumors. Analysis of 15 year period
Ilić I., Ćorić M., Čepulić M., Bijelić L., Orlić D., Seiwerth S., Manojlović S.
Institute of Pathology, Clinic for Childhood Diseases and Clinic of Orthopedics Medical Faculty University of Zagreb

The incidence of primary bone tumors in childhood, excluding tumors of bone marrow origin is low. Among this tumors the waste majority is reported to be benign, while malignant tumors account for 5 – 10% of cases depending on the source. In this retrospective study of biopsy records we investigated the incidence of these tumors in our material and their clinical outcome.
363 Primary childhood bone tumors from the Bone tumor registry of the Institute of Pathology were included in the study. The patients were treated at the Clinic for Childhood Diseases and Clinic of Orthopedics Zagreb and the specimen analyzed at the Institute of Pathology Zagreb. Histopathological findings revealed 289 benign (79,61%) and 74 (20,38%) malignant tumors. Among benign osteochondromas (61% of all/77% of benign) were the most frequent and among malignant osteosarcoma and Ewing's sarcoma (37 and 36 respectively) were equally distributed (10%).
Recurrences were histologically verified in 2 patients, and metastases in 16 patients. Twenty children (27% of malignant tumor patients) died in the investigated period with metastatic spread.

P-491

Explosion of neoplastic disease in infancy, childhood and young people in nis region of Serbia
V Katic, J Gligorijevic, Lj Velickovic, S Jovanovic, S Jancic
Institute of Pathology, Faculty of medicine in Nis University, Serbia

Aim: cancer (including leukemia) is the leading cause of death from disease in Serbia in children over the age 4 and to 14 years of age. The reason for this report is surprisingly increased frequency of uncommon malignant neoplasm of infancy, childhood and young people in Nis region of Serbia, from NATO bombing.
Material and Methods: material is consisted of 17 tumors, discovered during the operation. Diagnosis has been done from pathologists on surgical biopsies. The specimens were fixed, processed and embedded in paraffin. Laboratory sections were stained with histological, histochemical and immunohistochemical methods.
Results: during 22 months from March 1999., 17 malignant tumors were discovered (Table 1).
Conclusion: having in mind that reported tumors have been discovered during short time from NATO aggression, we suggest that mental stress (causing rapide increase of ACTH secretion and immunossupression) has important role in arising of these neoplastic lesions in our region.

Table 1 Uncommon neoplasms

Age	Sex	Type of neoplasm	Localisation
4 month	m	Hepatoblastoma	liver
2 years	m	Neuroblastoma	Adrenal gland
3 years	m	Mal. Schvannoma	Face
4 years	m	Large cell lymphoma	Periton cavity
8 years	f	Serotoninoma	Appendix
12 years	m	adenocarcinoma	Coecum
13 years	m	GANToma	Stomach
14 years	f	Dysgerminoma	Ovarii
21 years	m	Embrional carcinoma	Testis
23 years	m	Seminoma	Testis
25 years	m	adenocarcinoma	Rectum
28 years	f	FAP+carcinoma	Rectum
29 years	f	FAP+carcinoma	Rectum
*33 years	m	Lynch I-carcinoma	Colon
*35 years	m	Lynch I-carcinoma	Colon
23 years	m	Signet ring carc.	Stomach
33 years	f	Signet ring carc.	Stomach

male:female=12:5; *brothers

P-492

Application of modern immunohistochemistry in the diagnosis of solid tumors of childhood.
J. Kobos*,**, E. Salacinska-Los*, K. Taran*
* Laboratory of Pathology, Institute of Pediatry Medical University of Lodz; ** Department of Pathology Medical University of Lodz, Poland

Solid tumors belong to the diagnostically very difficult group of children's neoplasms. 136 formalin-fixed and paraffin-embedded tissue sections from cases diagnosed in the Laboratory of Pathology Institute of Pediatry, Medical University of Lodz (40 cases of nephroblastoma, 40 cases of neuroblastoma, 30 cases of rhabdomyosarcoma (RMS), 6 cases of pPNET, 10 cases of germinal tumors and 10 cases of Non-Hodgkin Lymphomas – comparative group) were selected for our study. For immunohistochemistry we applied antibodies against MyoD1 and Myf-3 gene products, against sarcomeric actin, desmin, myoglobin and SMA, against NSE, Neuroblastoma Marker (NB84), NF, MIC-2, CEA and anti-Human WT1, clone 6F-H2. We also used antibodies against LCA, CD3, CD5, CD20, CD23, CD15, CD30, CD68 and ALK1 in the differential diagnosis. Expression of NB84 was observed in 90% cases, expression of NSE in all cases and expression of NF in 65% cases of neuroblastoma. In all cases in the pPNET group we observed NSE and MIC-2 positivity, but there were not expression of NB84 and NF. Additionally, we noted NSE expression in singular tumor cells of some RMS cases. All RMSs showed an expression of products of both MyoD1 and Myf-3 genes. Immunopositivity for desmin was observed in most cases but only a small number of neoplastic cells. Expression of SMA was seen in some RMS cases and Myoglobin and sarcomeric Actin expression were found in a few highly differentiated RMSs. We also observed expression of both MyoD1 and Myf-3 genes in group of blastemal cells in a few cases of nephroblastomas in which we have seen myogenic transformation. No expression of MyoD1 and Myf-3 genes products in other investigated tumors was observed. We saw the expression of Wt1 gene product exclusively in nephroblastomas. The highest expression of

Wt1 protein was observed in anaplastic Wilms' tumors. Application of antibodies against NSE, NB84, MIC-2, MyoD1 and Myf-3 genes and Wt1 gene product might be helpful in the differential diagnosis of solid tumors of childhood.

P-493

Association of hypertrophic gastropathy and tetralogy of fallot in a newborn. Etiological considerations

A.-E. Konstantinidou, C. Eftychiadis, P. Korkolopoulou, H. Zorzos, E. Agapitos, P. Davaris
Dept.Pathology, Medical School of National University of Athens, Greece

Introduction: In newborns, an association of hypertrophic gastropathy (HG), similar to Ménétrier's disease in adults, and cyanotic congenital heart disease (CCHD) has been twice reported in the literature. Viral infection and prostaglandin E_1 (PgE_1) administration have been closely associated with diffuse and antral HG respectively, being also common denominators in both HG and CCHD. On the occasion of a case of HG and tetralogy of Fallot (tF) in a newborn, etiologic factors are considered.
Material and Methods: Autopsy was performed on a 21-days-old cyanotic infant with generalized oedema, who died by heart failure, after a progressively deteriorating course, having received antibiotics and intravenous PgE_1. Complete autopsy was followed by histological examination of organs and tissues and by immunoperoxidase stains for cytomegalovirus (CMV) and herpes simplex virus (HSV).
Results: The main pathological findings were a tF, pulmonary hemorrhage and oedema, marked cholestasis of the liver, a marked involution of the thymus, organized thrombi in visceral veins and brain hemorrhage. The stomach, with the exception of the antrum, presented macroscopical and microscopical findings consistent with Ménétrier's disease. Immunohistochemistry for CMV and HSV was negative.
Conclusions: Our data suggest that viral infection is not always the cause of diffuse HG in infants, whereas PgE_1 administration, closely associated with antral hypertrophy, might be responsible for HG in our case. However, the extensive involvement of the stomach noted in this infant suggests that other, as yet undetermined factors may contribute to the development of HG and CCHD in newborns.

P-494

Autoimmune reactions among children with bacterial and viral meningitis and meningoencephalitis

Kovaleva, Tatjana
Vitebsk Research Institute for Radiation Medicine and Endocrinology, Vitebsk, Belarus

Introduction: Importance of the study of neuroinfection is stated by the frequency of morbidity, mortality and serious reccurent change, poor study pathogenesis, special features of the clinic of certain forms of diseases.
Methods: Neurospecific enolase (NSE) was measured in spinal liquor and blood serum by enzyme immunoassay (Hoffmann-Roche). We investigated 12 children with septic meningitis, 5 with serous meningitis, 10 with viral meningoencephalitis, 8 – viral encephalitis, 8 patients with acute febrile encephalopathy and control group. Autoantibody to protein S-100 were measured by enzyme immunoassay. We investigated 50 children with septic meningitis, 20 with serous meningitis, 13 with viral meningoencephalitis, 10 – viral encephalitis and 220 healthy people.
Results: Rising level of NSE among the patients with meningitis and meningoencephalitis was found in spinal liquor and blood serum ($P<0.05$). In an acute period of meningitis and meningoencephalitis NSE in liquor was increased considerably as compared to the period of reconvalescence ($P<0.05$). NSE index in spinal liquor and blood serum is taken as diagnostics and prognostic criteria in the valuation of the severity of the damage of brain cells during meningitis and encephalitis. The high level of antibody to the protein S-100 was detected in blood serum in acute period and period of reconvalescence as compared to the donors group. The frequency of antibody to the protein S-100 depend on current of disease.
Conclusion: Autoimmune reactions take place among children with bacterial and viral meningitis and meningoencephalitis.
MS-DOS, if possible Word 97, otherwise Rich Text Format or ASCII-Text to CTW. Please note that abstracts sent by fax will not be reviewed.

P-495

Proliferative activity of neuroblastoma as a predictor of clinical outcome

Krams, M., Claviez, A.*, Berthold, F.#, Rudolph, P., Harms, D.
Institut für Pathologie und *Kinderklinik der Christian Albrechts Universität Kiel; #Universitäts-Kinderklinik Köln, Germany

Introduction: Biological criteria are believed to refine prognostic predictions in neuroblastoma. Various cytogenetic abnormalities have been described, and their usefulness has been proven in several studies. Herein, we have assessed the predictive power of cell proliferation (CP) in relation to the *MYCN* status and clinical data.
Methods: Paraffin-embedded neuroblastoma specimens from 161 patients (aged 0-191 months, mean 31.7±37.5 months) were investigated immunohistochemically for tumor cell proliferation by means of the monoclonal antibody Ki-S5 (Ki-67). *MYCN* amplification was analyzed by means of FISH and Southern blotting. Clinical data were recorded from the files of the German Neuroblastoma Study Group.
Results: Ki-S5 Expression ranged from 0 to 82% and correlated with Hughes' grade, tumor stage, and *MYCN* amplification. By univariate analysis, tumor stage and grade, the patients' age, the *MYCN* status, and CP were significant predictors of the disease-free interval (DFI) and tumor mortality (TM). Both *MYCN* status and the proliferative activity identified cases with poor prognosis in different stage groups. However, only stage ($p<0.0001$) and CP ($p=0.002$) emerged as independent predictors of DFI and TM ($p<0.0001$ and 0.005, respectively). The *MYCN* status achieved significance only when CP was excluded from the multivariate model.
Conclusions: Many molecular aberrations influence the growth rate of tumors, e.g. by virtue of cell cycle deregulation. CP therefore is likely to reflect the sum of all these effects, which may explain ist usefulness as a prognostic indicator in neuroblastoma.

P-496

DNA ploidy and cell proliferation in congenital malignant tumors

Krušlin B, Cizmic A, Tomicic I, Radotic V, Manojlovic S, Višnjic A, Stepan Giljevic J, Belicza M
Department of Pathology, School of Medicine, University of Zagreb, Ljudevit Jurak University; Department of Pathology, Sestre milosrdnice University Hospital; Department of Oncology, Children's Hospital, Zagreb, Croatia

Introduction: Congenital tumors are very uncommon, occurring in 1–4/100000 birth. They are predominantly benign but different malignant tumors may also appear. Numerous studies have shown a correlation between DNA ploidy and clinical outcome for various solid malignant tumors in adults. Therefore, in this study we analyzed DNA ploidy and DNA index and cell proliferation of congenital malignant tumors.
Material and Methods: We analyzed DNA ploidy of 8 congenital malignant tumors of different histologic types diagnosed in the period 1985-1999. DNA ploidy analysis was performed by flow cytometry on paraffin embedded tissue. The expression of proliferative antigens (Ki-67 and PCNA) was analyzed by immunohistochemistry after microwave antigen retrieval procedure.
Results: The study group consisted of four nephroblastomas, 3 neuroblastomas and 1 rhabdomyosarcoma. There were 4 male and 4 female children aging from 26 days- 3 months. Five tumors were diploid (3 nephroblastomas and 2 neuroblastomas) and 3 aneuploid (1 nephroblastoma, 1 neuroblastoma and 1 rhabdomyosarcoma). Positive nuclear staining for PCNA was observed in 7 cases. Ki-67 positivity was found in four cases (2 neuroblastoma and 2 nephroblastoma). The patients were followed from 1–162 months. Patient with aneuploid neuroblastoma survived for 5 months while other two died within 1 month after diagnosis. Two patients with diploid nephroblastoma are still alive at 126 and 162 months after diagnosis, respectively.
Conclusions: Our findings suggest that aneuploidy was associated with poor prognosis of malignant congenital tumors. It seems that PCNA may reflect the proliferative activity of these tumors, however, this should be further analyzed.

P-497

Interaction of interstitial trophoblast with placental bed capillaries and venules of normotensive and human pregnancies with anemia

I. Kuzmina
Department Obstetrics & Gynaecology, State Medical University, Kharkov, Ukraine

While endovascular trophoblast invasion of human placental bed spiral arteries has been extensively studied, no information is available on the interaction between interstitially invading trophoblast and uterine capillaries and venules.
Placental bed biopsies of 10 normotensive and 24 patients with anemic were fixed in buffered paraformaldehyde and embedded in paraffin. Sections were double-immunostained for cytokeratin and the endothelial marker CD34, to allow evaluation of different degrees of perivascular approach of non-arterial vascular structures by interstitially invading trophoblast.
Interstitial trophoblast tissue density did not differ between the two groups. A similar incidence of perivascular approach of non-arterial vascular structures by invading trophoblast was found in both groups. Differences in CD34 staining intensity were observed in different vascular cross sections within each biopsy, and lower staining intensities were found to be related to the presence of perivascular trophoblast.
Since the endothelial marker CD34 is identical to the platelet-endothelial cell adhesion molecule, the trophoblast-dependent downregulation of CD34 in maternal endothelia may play a role in the control ofleukocytic traffic within the placental bed. No difference was found between normotensive and patients wiht anemia, indicating that the phenomena described in this study are probably not related to the pathogenesis of anemia.

P-498

Alveolar and embryonary rhabdomyosarcoma: A correlation between histology and genetics

Llombart-Bosch, R. Gil-Benso, C. López-Ginés, C. Carda, J.A. López-Guerrero, J. Ferrer and A. Pellín-Pérez
Department of Pathology. Medical School. University of Valencia. Spain

Rhabdomyosarcoma (RMS) is a very common pediatric soft tissue sarcoma thought to be derived from muscle cell precursors. Histologically RMS have been subdivided into two main subtypes among others: embryonal (ERMS) and alveolar (ARMS) with distinct appearance and behavior. ARMS is associated with the specific chromosomal translocations t(2;13)(q35;q14) and t(1;13)(p36;q14). ERMS is characterized by loss of heterocygosity at chromosome region 11p15.5. Furthermore, a number of oncogenes, primarily MYCN and MDM2 has been found amplified in RMS.
Pathologic study was performed on 8 primary tumors, supported by ultrastructure and immunohistochemistry. Xenografts were established from 7 of 8 cases. RT-PCR was used to detect the expression of PAX3/PAX7-FKHR mRNA, MYCN and MDM2 oncogenes.
Histologically four tumors were alveolar and four embryonal. Cytogenetically one ARMS had normal karyotype and 3 were hypertetraploid. Two tumors had t(2;13)(q35;q14), and one a microchromosome of unknown origin. ERMS were two hyperdiploid with a gain of chromosomes 2, 7, 8, 19 and 20 in common, and two hypertetraploid. Four cases showed genomic amplification as dmin (3 cases) or hsr (1 case). RT-PCR demonstrated the expression of PAX3-FKHR mRNA in two ARMS according to the cytogenetic findings and PAX7-FKHR in one. Amplification of MYCN oncogene was found in two cases of ARMS. MDM2 was not amplified. Fluorescence in situ hybridization analysis using N-myc DNA probe identified multiple copies of MYCN gene on dmin of the alveolar cases. Analysis of p53, p14, p15 and p16 was made in order to better understand the biological behavior of RMS.
The fusion genes created by the characteristic translocations provide a unique marker for molecular and cytogenetic detection that can be used as an adjunct to classical histological diagnosis.
Supported by FISS 98/0600 Madrid. Spain.

P-499

Pathological, clinical and biological results in relapsed and refractory neuroblastoma

R. Noguera, S. Navarro, A. Cañete*, A Pellin, A. Ruiz, V. Castel*, A. Llombart-Bosch
Department of Pathology, University of Valencia and
* Pediatric Oncology Unit Hospital " La Fe " Valencia, Spain

The significance of histology, DNA index, MYCN amplification and deletion of short arm of chromosome 1 in relapsed and refractory neuroblastoma (NB) was evaluated. In 4 years, 35 heavily pretreated patients (median age: 1.96 years) were registered in N-III-95 study for NB non-responders or relapses. 25 were relapsed patients (14 metastatic, 5 local, 5 both) and 10 refractory. All were stage 4 at diagnosis except 2 (1 2 A, 1 3). Bone (74%) and bone marrow (51%) infiltration was predominant. Patients had continous infusion chemotherapy alternating with therapeutic MIBG. Probability of 5-year overall survival is 0.19, median survival 9 months. 27 patients died and 8 are alive. Tumor samples were obtained from 26 patients and were completely studied by image cytometry, FISH, Southern blot and PCR. Unfavorable Shimada histology was found in 19 out of 26 tumors assessed (7/7 undifferentiated NB, 11/11 poorly differentiated, 1/2 Ganglioneuroblastoma and 0/6 not classifiable). Image cytometric measurement was used for tumor cell ploidy assessment. and DNA index was diploid/tetraploid in 13 and aneuploid in 12. Southern blot, PCR and FISH were used for MYCN and chromosome 1p36.3 evaluation. MYCN was amplified in 10/25 cases (2/10 with HSR and dmins simultaneously, 2/10 with 10dmins: 2 and 6/10 >25 dmins: 2, 3, 4). Deletion of chromosome 1p36 (1:2) was observed in 15/25 cases (12/15 in >30% of tumor cells and 3/15 in 10% of tumor cells). Univariate and multivariate analysis were performed (Spss package) in 26/35 patients. There was statistical difference according to age ($p<0.0002$) and MYCN amplification ($p<0.04$). In multivariate analysis, when considering clinical and biological factors, age was the strongest factor in predicting survival. In conclusion, age and MYCN status are the powerful prognostic indicators in this cohort of patients.
Supported with Grant 99/1197 from FIS (Madrid)

P-500

The effects of histological parameters and scoring on prognosis in neonatal cholestasis

*Dr.Aylin Okçu Heper, *Dr. Esra Erden, **Dr. Tümay Doğanci, *Dr.Emre Çulha, ***Dr.Aydan Kansu
*University of Ankara, Medical School, Department of Pathology; **SSK Dışkapı Child Disease Hospital; ***University of Ankara, Medical School, Department of Pediatry, Ankara, Turkey

The diagnostic possibilities of Neonatal Cholestasis (NC), are focused on Biliary Atresia (BA), Neonatal Hepatitis (NH) and Intrahepatic Bile Duct Paucity (IBDP). We aimed to assess the prognostic value of scoring histological parameters for NC in this study. A total of 44 patients with BA (18), NH (12) and IBDP (14), who were followed for 4 months to 5 years, were studied. For scoring, portal inflammation (PI), portal and periportal fibrosis (PF), bridging necrosis with fibrosis (BN) and giant cell transformation (GCT) were evaluated as present (+) and absent (–) in liver biopsy. The (+) ones were scored as "1" and the (-) ones as "0."" By adding all scores, we get a "hepatic injury score" (HIS), for each case. According to follow-up data, we devided the cases into two prognostic groups as "good" and "poor" prognosis. The results were evaluated with ki-square, Kruskal-Wallis, Mann-whitney-U tests and ROC curve. We noted that in BA cases, PF (p:0.005) and BN (p:0.004) were the prominent histologic feature. Besides, GCT was dominant finding in NH cases (p:0.002).The mean HIS of BA cases was the highest and the mean HIS of IBDP cases was the lowest and the difference was statistically significant (p:0.015). There was a positive relation between prognosis and PF (p:0.01) and also BN (p:0.000). Furthermore a strong correlation between HIS and prognosis were noted with both Mann-Whitney U test (p:0.000) and ROC curve (AUC:0.875). Finally we think that the scoring of histological features will be usefull in predicting prognosis in NC.

P-501

Histopathology of gastroesophageal junction (GEJ) and distal esophagus in children and young adolescents and its relationship to *Hp*

Janina Orlowska*, Piotr Konieczny, Wlodzimierz Borowski, Ewa Michalowicz-Wojczynska
Histopathology Laboratory of Dept. of Gastroenterology, Med. Ctr. Postgrad. Educ., Warsaw; 2nd Dept. of Pediatrics, Children's Hospital, Dziekanow Lesny, POLAND

Gastroesophageal reflux disease (GERD) is a strong risk factor for esophageal carcinoma. The first step of GERD is reflux esophagitis (RE) going next to columnar lined esophagus (CLE), specialised intestinal metaplasia (SIM), dysplasia and carcinoma. The presence of cardiac mucosa (CM) at GEJ should be used to define GERD. There is still disagreement concerning the role of *Hp* in the development of RE.
The *Aim* of the study was to evaluate: 1. the prevalence of gastric mucosa at GEJ and CLE in distal esophagus in children, 2: its relationship to the age and Hp infection.
Methods: in a period of 1995–2000 gastroscopy with antral and corpus biopsy was performed in 392 pts (2.5–30.0y; mean:13.4). Endoscopical signs of RE were found in 110/392 (28.0%)pts (6.0–25.0y; mean:13.4; M/F=52/58) and then specimens from GEJ and/or distal esophagus were taken. *Hp* was evaluated by Giemsa stain on antral biopsies. Esophagitis and *Hp* were scored according to Sydney System: no positivity=0, mild=1, moderate=2, severe=3.
Results: Gastric mucosa at GEJ was found in 28/63 (44.5%)pts (6-19y, mean 12.0): 20 CM (71.4%), 4 fundic (FM), and 4 oxynto-cardiac (OCM). In the distal esophagus focal CLE was present in as many as 19/62 (30.7%)pts (8–25 y, mean 13.8): CM in 12 (63.2%), 4 FM, 2 OCM and one CM with SIM (22.0y). Histological signs of RE were confirmed in 85/110 (77.3%) pts (9.0–25.0 y), but there were no statistically significant correlations between the presence of gastric mucosa at GEJ or CLE in distal esophagus with esophagitis score, age and *Hp*.
Conclusions: 1.Gastric mucosa at GEJ and CLE in distal esophagus occur frequently in a childhood (44.5% & 30.7%), respectively, mostly as CM. 2. Barrett's esophagus was found in only one case. 3. *Hp* does not influence the development of RE.

P-502

Morfo-functional peculiarities of placenta and thyroid gland of the fetus with hipotyroidism

Pavlova, Tatiana
Belgorod University, Russia

In 1995–1999 years in Russia there was an abrupt increase of cases of pathology of thyroid gland, in particular on the territory of Belgorod region – from 7,4 to 14,2%, wham is connected with such peculiarities of the region as: increased content of magnesium salts, calcium, iron, tack of iodine as well as deterioration of social status of the population connected with the catastrophe at Chernobilskaya Atomic Power Station.
The most important thing is intrauterine formation of pathology. With the help of light and electronic microscopy were investigated placenta of women with hypothyroidism. The analyses of the data we managed to get proves, that in the formation of the pathology of a newborn child all the components pathology of a newborn child all the components of the chain mother- placenta- fetus take part. So the lack of iodine affects mothers placenta as well as the thyroid gland of the fetus and gladually the physiological adaptation is getting replaced by pathological changes.

P-503

A morphological study of Meckel's diverticulum in children

Pleşea Iancu Emil*, Enache Stelian Dănuţ**,
Stănescu Ligia***, Zaharia Bogdan*, Sabetay Cornel****
* Department of Pathology, University of Medicine and Pharmacy; ** Department of Pathology and Citology, Universitary Hospital; *** Department of Pediatrics, Municipal Hospital; ****Department of Pediatric Surgery, Universitary Hospital,

Craiova, Romania

Introduction Aims: We intended to do a morphological study of both macroscopic and microscopic features of either normal or affected Meckel's diverticulum. This study is a part from an national study on Meckel's diverticulum made by the Romanian National Society of Pediatrics Surgery.
Material and methods: There were selected 768 cases operated in the romanian Pediatrics Surgery Centers between 1979 and 1997. The material was represented by the surgical samples drawn during the surgical interventions. The tissue fragments were fixed in formalin, included in paraffin wax and stained with hematoxilin Meyer-eosin and trichrome van Gieson.
Results: There were 599 incidentally discovered and 209 symptomatic diverticula. DM was situated practically on the antimesostenic site of the ileal wall, at between 30 and 60 cm from the cecum, more frequently with a large base of implantation and a length more oftenly between 4 and 6 cm. In 19 cases other remnants of viteline duct were associated. Ectopic tissues were present in 91 cases, 56 in symptomatic group (26,8%) and 35 in incidentally discovered group (6,3%). Gastric mucosa was found in 73 cases, 42 in symptomatic group and 31 in asymptomatic group. Duodenal and colonic type mucosa and pancreatic inclusions were also found. Inflamatory processes were the most frequent lesions (150 cases) and were dominated by acute forms. Ulcerations were the second (46 cases) 33 associated with hemorrhage and 12 with perforation. Ischemic necrosis, due to either volvulus or invagination was present in 11 cases, 3 of which were associated with perforation. In 11 cases the DM, long and with a large base, was inverted, generating intestinal occlusion by invagination.
Conclusion: The dimensions, the base of implantation and the presence of the ectopic tissue (especially gastric mucosa) are the main risk factors in the DM pathology.

P-504

Liver histopathology in children and young adults with Turner's syndrome and abnormal liver function tests

Pronicki M., Rujner J., Czarnowska E., Iwanicka K.
Department of Pathology, Children's Memorial Health Institute, Warsaw, Poland

Introduction: Liver is not typically affected in Turner's syndrome (TS). However, both biochemical and morphological liver abnormalities have been reported in TS. Liver function tests may disclose cholestasis, hypertransaminasemia, portal hypertension. Morphological abnormalities rarely reported include cholestasis, portal fibrosis, cirrhosis, neonatal hepatitis, primary sclerosing cholangitis, nodular regenerative hyperplasia, fetal liver architecture, vascular abnormalities.
Aim: The aim of our study is to assess liver histopathology and ultrastructure in patients with TS in whom persistent abnormal liver tests have been observed for over 6 months.
Material and methods: Eight patients aged 7 to 19 years (med. age 15 yrs) underwent percutaneous liver biopsy. Material was studied by light and electron microscopy.
Results: Liver histopathology revealed only non-specific features such as portal fibrosis, in one case with delicate fibrous porto-portal bridges, early cholestasis, slight lymphoid infiltrations of portal spaces. Ultrastructural examination disclosed numerous collagen fibres in Disse spaces, increase of smooth endoplasmic reticulum profiles and polymorphic mitochondria.
Conclusions: We conclude that in some TS patients liver tends to be involved in certain pathological process not yet fully understood. The most frequent morphological abnormality is different degree of fibrosis. Its intensity may be age related so it was only mild in our patients. TS patients should be lifelong monitored for liver function.

P-505

Spinal muscular atrophy-like picture with lactic acidosis, cytochrome c oxidase deficiency and intact survival motor neurone gene

Pronicki M., Zaremba J., Karczmarewicz E., Taybert J., Iwanicka K.
Department of Pathology, Children's Memorial Health Institute, Warsaw, Poland

Spinal muscular atrophy (SMA) is defined as autosomal recessive symmetrical proximal muscle atrophy associated with degeneration of anterior horn cells of spinal cord. Three forms of the disease are recognized depending on the age of onset and the severity of clinical course. Almost all of them are caused by mutation (deletion) involving survival motor neurone (SMN) gene located on the 5q13 chromosome. Several pathological lesions and dysfunctions were

reported to be sometimes associated with SMA eg. cerebellar hypoplasia, arthrogryposis, congenital heart defects, long bone fractures and others. They probably consist separate syndromes associated with
anterior horn cell damage. We present a child aged 6 months with encephalopathy associated with lactic acidosis in whom muscle biopsy revealed features consistent with SMA type I (Werdnig Hoffmann disease). Biochemical studies disclosed decreased level of COX in muscle. Genetic mutations typical for SMA were excluded by molecular analysis. In our opinion the patient suffers from some mitochondrial disorder with anterior horn cells damage. Sporadic cases of COX deficiency associated with upper or lower motor neurone dysfuction were reported in literature earlier. We conclude that SMA-like muscle biopsy features coexistent with intact SMN gene should prompt diagnostic search for mitochondrial disease.

P-506

Intestinal/peritoneal tuberculosis in children. An analysis of autopsy cases

Cecilia Ridaura-Sanz, Eduardo López-Corella
Department of Pathology.National Institute of Pediatrics, Mexico City

Introduction: Intestinal involvement, considered infrequent, is often overlooked in the clinical approach to tuberculous infection in children. The purpose of this study is to determine the frequency and the clinical and pathologic features of intestinal involvement in autopsies of children dying with tuberculosis.
Material and Methods: Intestinal involvement was present in 35 of 110 autopsied patients dying with active tuberculosis; in 17 of them the abdominal disease was responsible for the dominant clinical expression. These 17 patients are analysed in the present report.
Results and Discussion: Twelve of our 17 patients were between 3 and 12 years of age with a mean of 7.4 years. Boys and girls were equally affected. The disease followed a prolonged course (mean 7 months) with fever, diarrhea and abdominal pain. Extraintestinal clinical manifestations were present in one half of our cases with respiratory disease in 30%, neurologic disease in 7% and lymph node involvement in 20%. The terminal ileum and colon were involved in 90% of the cases. The main complications were perforation, occlusion and hemorrhage. In practically all cases systemic visceral lymphohematogenous spread was present. Culture for *M. tuberculosis* grew *hominis* in 6 patients, *bovis* in 4 and were negative in 5. Two patients were not cultured.. The clinical diagnosis was of tuberculosis in 11 cases; lymphoma in 3 and inflammatory disease in 3.

P-507

Localisation of HLA-G in placentas infected by *Plasmodium falciparum*

Sartelet H, Schleiermacher D, LeBouteiller P, Graesslin O, Puijalon O, Le Hesran JY, Gaillard D
Laboratoire Pol Bouin and Department of Obstetrics CHU de Reims, Reims, France; Laboratory of Molecular Immunology of Parasite Institut Pasteur, Paris, France; Inserm U395 CHU Purpan Toulouse, IRD Dakar, Senegal

Introduction: During pregnancy, *Plasmodium falciparum* (*P. falciparum*) malaria is associated with a number of materno-fetal complications such as preterm delivery. The decrease of the immune maternal tolerance can partly explain prematurity. The absence of maternal immune response against the fetal semiallogenic graft was correlated with the expression of HLA-G in extravillous cytotrophoblast. This molecule interacts with a killing inhibitory receptors found on NK.
Methods: Placentas Infected by *P. falciparum* was collected in a malaria hypoendemic area (Dakar, Senegal). The distribution of HLA-G and the quantification of NK cells was analyzed by immunohistochemistry in 15 infected and 15 control fixed placentas at term into a prospective case-control study.
Results: In control placentas, HLA-G was constantly expressed in extravillous cytotrophoblat and inconstantly in fetal endothelial cells. In infected placentas, the expression decreased in extravillous cytotrophoblat with only a few cells immunostained, was not changed in endothelial cells and was also detected in macrophages present in intervillous spaces. The number of NK cells was higher in infected than in control placentas and these cells were localized not only in intervillous space but also in villi and in fetal capillaries.
Conclusion: These data suggest that maternal immune tolerance can decrease in placentas infected by *P. falciparum* with a low expression of HLA-G.

P-508

Crystal storing histiocytosis in a 3 year old girl with Fanconi's anaemia and plasmacytic proliferation expressing kappa light chain

Irene Scheimberg*, Paul Telfer+, Tim Diss#, Begonia Flores+ and Peter Isaacson#
Departments of Histopatholgy* and Haematology+, The Royal London Hospital and Department of Histopathology#, University College Hospital

Crystal storing histiocytosis is an uncommon finding associated with multiple myeloma and in other lymphoplasmacytic tumours. It has never been described in children.
A 3 year old girl with Fanconi's anaemia type D presented with persistent infection and lymphadenopathy. Investigations showed anaemia and lymphopenia. Her plasma viscosity was 3.5 mPa.s with a monoclonal IgM of 52 g/dl. A bone marrow trephine showed large number of histiocytes containing prominent eosinophilic inclusions. The inclusions in the majority of these cells were strongly positive for kappa light chain and a moderate number were also positive for IgM.
A lymph node biopsy performed a few days later showed an expansion of the interfollicular area occupied by large numbers of mature plasma cells and some histiocytes, both containing granular eosinophilic material similar to that found in the bone marrow. Plasma cells showed strong positivity for IgM and kappa. The plasma cells were monoclonal by immunophenotype and presumably clonally related to the nodal population.
Crystal storing histiocytosis has been previously reported in adults with hypergammaglobulinaemia, generally monoclonal, although a few cases showed polyclonal immunoglobulin activation.

P-509

Classification of morphological changes in placenta at herpes virus infection

Serov V.N., Muzukantova V.S., Kuzmin V.N.
Department of Obstetrics and Gynecology, Moscow Medical, Stomatological University, Russia

Interest of infection of fetus and newborn of virus herpes. However heading of defeats placenta by virus infections in the international classification of illnesses of X-reconsideration (Geneva, 1995ã.) in section 0.43 "Placenta of infringement" are absent. We carry out complex inspection 107 of placenta from the women with herpes virus infection. The verification of the diagnosis was carried out in view of the data clinical and special methods of researches – enzyme immune assay and polymerise of chain reaction and microscopic research were exposed all placenta and the electronic-microscopic research is carried out.

On the basis of the carried out(spent) work we offer the following definitions in section 0.43 "Placenta of infringement."

1. Defeat placenta at virus herpes infection
2. Defeat placenta at virus herpes infection in a combination to other viruses
3. Defeat placenta at virus herpes infection, complicated monomicrobiological bacteriological in a combination to other viruses
4. Defeat placenta at virus herpes infection complicated polymicrobiological bacteriological (chlamydia, mykoplasma, ureaplasma)
5. Defeat placenta at virus herpes infection with teratological by effect
6. Defeat placenta at virus herpes infection in a combination to others virus- bacteriological, fungus by associations and teratological by effect
7. Defeat placenta at virus herpes infection in a combination to other viruses, complicated infection-toxic by a shock. "Shock placenta."

Examination of structural changes placenta, resulting to insufficiency of placenta:

1. Inherent defects of development (regional and membrane an attachment cord, placenta surrounded by the platen, aplasia artery of cord)
2. Hypoplasia of placenta
3. Hyperplasia of placenta

In placenta, which weight corresponded gestation to norm, the attributes placental of insufficiency as dystrophic and necrosis of changes, productive inflammation and compensation vessel of reactions were found out. In a number of supervision came to light etiologically the factors of herpes virus. The results of complex inspection of the pregnant women and them placenta testify to a defeat placenta and placental of insufficiency developing during herpes infections and their combinations, and also virus-bacteriological associations and can be brought in to the International classification of illnesses of X-reconsideration – heading 0.43 "placenta of infringement."

P-510

Morphological and immunohistochemical findings of the placenta in maternal systemic lupus erytematosus with intra-uterine fetal death; case report

L. Spasevska, V. Janevska, B. Bogoeva, V. Cadieva, S. Kocmanovska, M. Ristovski
Institute of pathology, Medical faculty Skopje, Macedonia

Sistemic lupus erytematosus with or without antiphosholipid antibodies is associated with poor pregnancy outcome.

We report a case of pregnancy complicated by hypertension (190/130), intra-uterine growth retardation (500 gr.) and fetal loos at 25 ht week of gestation in patient with SLE (four 12 years) without antiphospholipid antibodies.

Material and methods: Pathological examination of the placenta was performed using the technige described by M. Vogel. Tissue blocks were routinely processed and slides were stained with H.E., PAS, trichrom and Weighert for fibrin. Immunoperoxidase staining for IgM, IgG and IgA were performed in sections from basal and parietal deciduas.

Results: Maternal decidual vessels showed a lesion termed acute atherosis and decidual thrombosis. The changes were so extensive as to result in complet vascular occlusion, decreased placental perfusion and resultant placental villous infarction. Extensive infarction involved about 57% of the parenchyma. Immunohistochemical examination showed massive intramural granular deposits of JgM and slight deposits of IgG and IgA in all vessels with acute atherosis. Deposits of IgG were also found in the vascular endothelial cells in the villi and to the trophoblast basement membrane. As a result of prolonged hypoxia placental villi showed obliterative endarteritis, fibrosis, hipovascularity and increased number of syncytial knots. These findings were associated with generalized villous immaturity and a failure of trophoblastic differentiation, wich showed a lack of vasculo-syncytial membranes. These abnormalities diminish the functional efficiency of the placenta.

Conclusion: Histopathological syudy of placenta has helped to elucidate the pathology that may contribute to IURG, fetal loss and other obstetric complations.

P-511

Expression of proliferative antigens (Ki-67 and PCNA), p53, bcl-2 and bax in neuroblastomas

Stepan Giljević J, Torlaković E, Pavlović E, Čizmić A, Ćepulić M, Jukić S, Belicza M, Krušlin B
Department of Oncology, Children's Hospital Zagreb, Croatia; Overlege, Patologi, Det Norske Radium Hospital, Oslo, Norway; Department of Pathology, School of Medicine; University of Zagreb, Croatia

Introduction: Neuroblastoma is the most common solid tumor of the childhood. Different prognostic factors were used, particularly histologic type and n-myc expression. In this study we analyzed the expression of proliferative antigens (Ki-67 and PCNA), p53, bcl-2 and bax in patients with neuroblastoma.

Patients and methods: There were 21 patients ranging in age from 2 months to 12 years (6 female and 15 male). The tumors were classified according to International Neuroblastoma Pathology Classification. The expression of analyzed antigens was analyzed by immunohistochemistry after microwave antigen retrieval procedure. The intensity of staining was denoted as (–) for no staining, (+) for up to 10% of positive cells, (++) for 10-25% of positive cells and (+++) for more than 25% of positive cells. Statistical analysis was performed by regression tree method using S2000 PLUS 1998 program.

Results: There were 9 undifferentiated, 6 differentiating neuroblastomas, 4 intermixed and 1 nodular ganglioneuroblastoma, and 1 maturing ganglioneuroma. Positive immunostaining for PCNA

and Ki-67 was found in 15 cases, for bcl-2 in 12 and for bax in 18 cases. p53 positivity was observed in four cases. N-myc expression was observed in 16 cases with strong positivity in four cases. Statistical analysis showed association of strong intensity PCNA and n-myc immunostaining with undifferentiated histology. There was no association between the intensity of immunostaining of other marker and histologic types of neuroblastoma.
Conclusion: Our findings indicate that immunohistochemical expression of PCNA as well as n-myc might be valuable in the prediction of the biologic behavior of neuroblastoma.

P-512

Correlation of modified shimada classification with prognosis and expression of Trk and bcl-2 in neuroblastoma

Vila-Torres J.*, Medina-Zurinaga M.*, Cusí-Sánchez V.*, Llombart-Bosch A.****, Farré-Pueyo X.***, Cruz O.**, Pascual P.**
Servicios de *Anatomia Patológica y **Oncología, Hospital Universitari Sant Joan de Déu; ***Departamento Anatomía Patológica, Hospital Clínic, Barcelona; ****Departamento de Patología, Hospital Clínico, Valencia, Spain

Introduction: A retrospective study of the clinical-pathological features and immunohistochemical markers was undertaken to assess their relationship with the outcome of 86 cases of neuroblastoma.
Method: Clinical and pathological findings were recorded for evaluation. Prognosis was analyzed according to the International Neuroblastoma Pathology Classification. Histologic grade was determined by the Joshi method (mitosis, calcification). Pediatric Oncology Group Neuroblastoma Staging System was used for assessment of clinical extension. NSE, S-100 and Trk were used as markers for neuroblastic differentiation. Expression of bcl-2 was checked for prognosis. The outcome was classified as disease-free, living with disease, and death from disease.
Results: Mean age was 2 years and 10 months, sex ratio was M/F, 1/1.2. Most cases were located in the adrenal gland (60.5%), and mediastinum (21.7%). When only the Shimada classification was used, 87% of the cases showed high correlation with the outcome, but when Trk and bcl-2 were also considered, that figure rose to 95%.
Conclusions: A high level of Trk expression is predictive of a favorable outcome, whereas bcl-2 expression was associated with a poor outcome. Therefore, both markers should be added to the Shimada classification to improve prognostic information in reporting neuroblastomas.

P-513

Chernobyl ionizing radiation pollution is the risk factor for infantile mortality rate due to herpesviral infections in Belarus

Evgenii Voropaev
Vitebsk Research Institute for Radiation Medicine and Endocrinology, Vitebsk, Republic of Belarus

Introduction: More than 20000 children are under the effects of Chernobyl ionizing radiation in Belarus. The demographic situation in Belarus is unfavorable, and the analysis of infantile mortality rate (IMR) reasons, especially reasons, connected with radiation, is extremely actual.
Methods: We investigated IMR in 3 Belarus regions, with were divided according to degree of ^{137}Cs density of pollution: 1 – less than 1 Cu/km^2, 2 – from 1 to 5 Cu/km^2, 3 – more than 5 Cu/km^2. The correlations between IMR reasons and level of ^{137}Cs pollution, such as the changes in IRM and relative risk of IMR during long period (1987–1999 yy.) have been analised. Last data were received from first year children autopsy protocols. The reasons of death were intrauterine herpesviral (Herpes Simplex virus 1–2, Cytomegalovirus, Epstein-Barr virus) infections, bacterial infections and congenital malformation. Risk coefficient was detected as ratio IMR indicators in groups, which were undergone risk factor in different degree.
Results: The average level and increase of IMR due to herpesviral infections mostly correlate with ^{137}Cs pollution ($r=+0.77$) in comparison with bacterial infection ($r=+0.25$) and congenital malformation ($r=+0.08$) significantly increase in Gomel region (density of pollution more than 5 Cu/km^2). Risk of IMR elevated with growth of ^{137}Cs pollution degree. The most risk coefficient (6.9) have been noted for herpesviral infections ($p<0.01$).
Conclusion: IMR due to herpesviral infections correlates with ionizing radiation pollution.

P-514

Expression microarray analysis of pediatric solid tumor cell lines

Daniel H. Wai, Karl-Ludwig Schaefer, Alexander Schramm, Werner Boecker, Barbara Dockhorn-Dworniczak, Christopher Poremba
Gerhard-Domagk-Institut of Pathology, Muenster, Germany

Introduction: The aim of this study was to identify patterns of differentially-expressed genes in cell lines derived from several pediatric solid tumors. This will aid in tumor diagnostics and in developing novel therapeutic strategies.
Methods: We applied Affymetrix Human Cancer G110 Arrays, containing 1700 cancer-associated genes, to a panel of 11 cell lines originating from Ewing tumors (ETs), neuroblastomas (NBs), and malignant melanoma of soft parts (MMSP).
Results: Hierarchical clustering clearly differentiated ET, NB, and MMSP cells, and we observed tumor-type specific up-regulation of 75, 102, and 36 genes, respectively. ET lines demonstrated high expression of cell-cycle genes including microtubule-associated protein tau (*MAPT*), protein phosphatase 1 regulatory subunit 1A (*PPP1R1A*), and NIMA (never in mitosis gene a)-related kinase 2 (*NEK2*). NB samples exhibited high transcript levels of wingless-type mouse mammary tumor virus integration site family member 11 (*WNT11*), *Drosophila* frizzled homolog 2 (*FZD2*), and adenomatous polyposis coli (*APC*) which are involved in regulating free β-catenin levels. Increased expression of related genes such as avian erythroblastic leukemia viral oncogene homolog 3 (*ERBB3*), neuregulin 1 (*NRG1*), fibroblast growth factor 9 (*FGF9*), and fibroblast growth factor receptor-1 (*FGFR1*) was observed in the MMSP cell line. Gene up-regulation could be correlated to genomic-DNA gains revealed by comparative genomic hybridization.
Conclusions: We identified clusters of differentially-expressed genes which permit the distinction of several small blue round cell tumors of childhood. These groups of up-regulated genes are likely

to be instrumental in maintaining tumor-specific characteristics and, therefore, participate in key signaling processes and downstream regulatory mechanisms.

P-515

P53 immunostainning is a predictive factor of the presence of metastasis in invasive ductal carcinoma of the breast

Martha I.A. Alba, Ana Regina F. Travolo, Eduardo H.F. Monteiro, Patricia M. Cury
Faculdade de Medicina de São José do Rio Preto, São Paulo, Brazil

Introduction: Immunohistochemistry has been done in order to study prognostic factors in breast carcinoma. Usually, a panel of antibodies is used, mainly Estrogens Receptor (ER), Progesterone Receptor (PR), p53 protein, and C-erbB-2. However, there is still a controversy in the literature about the value of these antibodies. The aim of this work is to study positivity of these markers in order to validate the use of the method and in the search of a good prognostic factor.
Methods: We analysed 134 patients with invasive breast ductal carcinoma that had the immunohistochemical prognostic panel (ER, PR, p53 and C-erb-B2) performed in our hospital. Clinical and pathological data such as age, menopausal status, histological and nuclear grade, size of the tumour and the presence of lymph node metastasis were collected.
Results: From the 134 patients, 45 patients were submitted to mastectomy where we could have the nodal status. In this group, the mean age was 54.2 years old (ranging from 30 to 83 years old). Fifteen patients did not have nodal metastasis, while 30 had metastasis. Using a logistic regression, we observed that p53 positivity is a predictive factor for the presence of nodal metastasis, with an Odds-ratio of 6.61 and a p=0.034 (95% confidence interval=1.2–37.8). The ER positivity had a trend to correlate with the absence of metastasis (p=0.0891).
Conclusion: p53 and ER are good prognostic markers and should be used to predict the presence of nodal metastasis before the surgical treatment.

P-516

Prognostic value of tissue inhibitor of matrix metalloproteinase-1 in breast cancer

P. Alexandrou[1], S. Katsarou[1], E. Panayotopoulou[1], I. Tsirmpa[1], I. Giannopoulou[1], K. Stefanaki[1], S. Markaki[3], A. Keramopoulos[2], L. Nakopoulou[1]
[1] Dept of Pathology and [2] First Dept of Gynaecology and Obstetrics, Medical School, The National and Kapodistrian University of Athens; [3] Dept of Pathology, "Alexandra Hospital", Athens, Greece

Tissue inhibitor of metalloproteinase-1 (TIMP-1) has emerged as a multifunctional protein with diverse biological effects.The clinical significance of TIMP-1 expression in carcinomas has not been fully determined yet.
For this purpose we examined the localization of TIMP-1 mRNA in 117 invasive breast carcinomas and correlated it with clinicopathological parameters (tumor size, histologic type, nuclear and histologic grade, stage and ER/PR status), the immunohistochemical expression of c-erbB-2, bcl-2, p53 and E-cadherin/catenin complex and patients' survival. mRNA in situ hybridization with a digoxigenin labeled probe was applied in order to localize transcripts corresponding to TIMP-1.
TIMP-1 mRNA was detected in stromal cells within the tumours and in the marginal portion of the tumours. High levels of TIMP-1 mRNA localized within the tumour correlated significantly with positive ERs (p=0.002). TIMP-1 mRNA localized in the marginal portion of the tumours correlated positively with the presence of lymph node metastasis (p=0.05), c-erbB-2 protein expression (p=0.05) and normal E-cadherin, α- and p-120-catenin expression (p=0.070, p=0.009 and p=0.055 respectively). Multivariate analysis demonstrated worse survival of patients with high levels of TIMP-1 mRNA localized in the marginal portion of the tumours. Among the patients in this group, those co-expressing high levels of TIMP-1 mRNA within the tumours as well, had even worse overall survival (p=0.034).
In conclusion our findings support the multifunctional hypostasis of TIMP-1, particularly its growth factor-like activity (due to the correlations to LN status, c-erbB-2 and poor overall survival) as well as a potential association with tumour cell differentiation (through the positive relation with the presence of ERs and normal expression of the E-cadherin/catenin complex).

P-517

Correlation between p53 immunostaining and p53 single-strand conformation polymorphism (SSCP) analysis in ductal infiltrating carcinoma of breast. Evaluation of prognostic value

Aranda F.I., Gil-Hervás P., Durán R., Picó C., Payá A., Sanchez-Payá J., Niveiro M.
Service of Pathology, Hospital General Universitario de Alicante, Spain

Purpose: Some studies have demonstrated the immunohistological evidence of the p53 protein in breast cancer to be of prognostic value. In this work we study the prognostic significance of the expression of p53 and the alterations in the gene of p53 in a series of ductal invasive carcinoma of breast NOS.
Methods: Tumor tissues from 90 patients with ductal invasive carcinoma NOS were analyzed immunohistochemically for the presence of p53 protein in paraffin-embedded material using DO7 antibody. In 52 cases a molecular study for exons 5–9 using PCR-SSCP was performed. Other morphological findings such as histological grade, tumor size, axillary status, proliferative activity (Ki67) and c-erbB2 overexpresion were evaluated. A 5-year follow-up and the recurrence-free survival (RSF) and overall survival (OS) were analyzed.
Results: With a 5-year follow-up, 30 relapses and 19 deaths were observed. 49 patients showed lymph node metastases (54%). P53 alterations using SSCP were identified in 17 of 52 tumors (32%), the majority localized in exons 7 (7 cases) and 8 (5 cases) . In 20/90 (22%) cases positivity for p53 protein in more of 20% of tumor cells was observed. P53 expression was significantly associated with molecular alteration in p53-SSCP. Univariate analysis showed that the number of lymph node metastases, histological grade (Nothingam) and proliferative activity measured with Ki67 (cut-off 15%) was significaly predictive of both RFS and OS. Cases with immunohistochemical positivity for p53 showed a ten-

dency to present worse prognoses, but without statistic significance. The optimum cut-off values for p53 immunohistochemistry in relationship with RFS and OS were more than 25% of positive cells. Non significance between p53-SSCP alteration both RFS and OS were observed.
Conclusion: P53 overexpression correlated with SSCP-p53 alterations. Cases with overexpression of p53 showed tendency to present worse prognosis. On the other hand, no significance between SSCP-p53 alterations and RFS or OS were observed.

P-518

The importance of assessment of expression of bcl-2: A new approach signifies a most favorable prognosis subgroup of operable breast cancer

M. Bai[1], N.J. Agnantis[1], P. Zagorianakou[1], N. Pavlidis[2], E Briasoulis[2]
Departments of Pathology[1] and Medical Oncology [2] Medical School, University of Ioannina, Greece

Backgaund: Bcl-2 is the prototype of the bcl-2 gene family that constitutes a rheostat-like system of pro-apoptotic (Bak, Bax, Bam, bcl-X_L) and anti-apoptotic cell proteins (bcl-2, bcl-X_s and MCL-1) in a state of dimerization. The aim was to correlate protein expression of these three apoptosis modulation genes of the bcl-2 family with several standard clinicopathological variables and treatment outcome.
Patients and methods: Fifty four cases of operable (early stages) breast cancer were analyzed by immunohistochemistry for the expression of bcl-2, bax and bcl-X proteins. Follow up was available in all patients for a median of 27 months (range: 3-144 months).
Results: Immunostaining for bcl-2 was negative or weak in 36.7% of the cases and involved the entire tumor cell population in 38.3%. No negative cases were identified for bax and bcl-X, while in the majority of the cases expression of both these proteins was absolute. Estrogen receptors were correlated positively to bcl-2 expression (p=0.01). An impressive positive impact of absolute bcl-2 expression on clinical outcome was identified. None of the patients in whom absolute expression of bcl-2 was detected on their primary cancer at early stage, died or even relapsed during follow up. This was not the case for the other two studied proteins.
Conclusion: We consider that this study provides evidence that assessment of bcl-2 at the level of absolute expression constitutes a new approach that provides important prognostic information in operable breast cancers.

P-519

Microvessel density and HER-2 status in invasive ductal breast carcinomas

Bartel H., Vogl G., Dandachi N., Mlneritsch C., Dietze O., Hauser-Kronberger C.
Institute of Pathology, 3rd Department of Internal Medicine, Landeskliniken Salzburg, Austria

Introduction: In breast carcinomas the density of intratumoral microvessels (MVD) has been reported to be a independent prognostic marker predicting poorer survival. Correlations between MVD, the expression of vascular growth factors (e.g. VEGF, PD-ECGF) and HER-2 and EGF-R have been reported. HER-2/neu overexpression in about 25–30% of invasive breast carcinomas is associated with tumor aggressiveness and poor prognosis. HER-2 gene amplification might contribute malignant transformation of breast carcinomas by promoting tumor angiogenesis by up-regulation of the expression of angiogenic factors. The present study has focused on the relationships of MVD histopathological parameters and the expression of VEGF, EGF-R and HER-2 in invasive ductal breast carcinomas.
Methods: MVD, VEGF, EGF-R and HER-2 were evaluated in 69 routinely processed, paraffin-embedded primary breast cancer specimens. Counting of CD31 antibody stained blood vessels was performed in three hot spots per section using an OPTIMAS image analysing system.
Results: Mean value of MVD was 128 (standard deviation 42, range 56-226) for vascular hot spots. Preliminary results did not show significant correlation between MVD and tumor grade, pT, pN, VEGF, EGF-R, HER-2, ER, PgR, Ki 67.
Conclusions: The additional prognostic value of tumor angiogenesis in invasive breast cancer might be useful for new therapeutic strategies.

P-520

Immunohistochemically detection of prostate specific antigen expression in invasive ductal carcinoma of the breast

Bayramoglu H., Zekioglu O., Duzcan E., Ozdemir N., Erhan Y.
Pamukkale University Medical Faculty, Turkey

Background and aims: Prostate specific antigen (PSA) is a glycoprotein produced by all non-neoplastic and nearly all neoplastic prostatic epithelial cells. It can be detected in most tissue samples of prostatic cancer by immunohistochemical methods. However, PSA has been found in various nonprostatic tissues and tumours, for instance in some breast carcinomas. Morever in some studies, has been suggested that in the breast carcinomas PSA could be used like a prognostic indicator. Our aim was to evaluate the prevalance and prognostic value of PSA immunohistochemically in the invasive ductal carcinoma of the breast.
Material and method: Fifty cases of invasive ductal carcinoma of the breast were evaluated immunohistochemically for PSA. Immunohistochemical staining for PSA was carried out on formalin-fixed, paraffin-embedded tissue using the avidin-biotin peroxidase complex method.
Result: Immunohistochemical staining for PSA was found in no one of our cases.
Conclusion: We concluded that, using PSA as a prognostic indicator in the invasive ductal carcinomas is not reliable yet and it should take much more studies.

P-521

Quantitative PCR is a powerful tool to assess HER2 positivity in breast cancer

K. Beyser[1], A. Reiser[2], C. Gross[1], J. Stiefken[1], K. Gloeckner-Hofmann[1], K. Tabiti[2], M. Pedrocchi[3], J. Rüschoff[1]
[1] Institute of Pathology, Klinikum Kassel, Germany;
[2] Roche Diagnostics GmbH, Penzberg, Germany;
[3] F. Hoffmann-La Roche LTD, Basel, Switzerland

Introduction: The tyrosine growth factor receptor HER2/neu is frequently overexpressed in breast cancer and other solid tumors, mostly due to gene amplification. This gene amplification/overexpression is currently detected by fluorescence in situ hybridization (FISH) and immunohistochemistry (IHC). We have evaluated a PCR method (Light Cycler HER2/neu Test, ROCHE; for research use) to quantify HER2/neu gene copies in several breast cancer samples.
Methods: DNA was extracted from formalin-fixed tissue in triplicates from 45 cases with an IHC-score of 0 or 1+, from five cases with an IHC-score of 2+ but non-amplified by FISH and from eight cases with amplification (IHC-score: 2+ or 3+). PCR was performed with the LightCycler Her2/neu test, which uses gastrin (also localized on chromosome 17) as reference gene and as control for polysomy. A positive result is defined by a ratio HER2/gastrin>2. In order to minimize the diluting effect on the signal by non-tumor/ non-amplified intraductal tumor cells, dissections were performed by scratching only invasive tumor areas from the slides in five representative cases.
Results: All fifty negative/non-amplified cases gave a negative PCR result. 5/8 amplified samples were positive by PCR when extracting DNA from the entire section, three were negative. After tumor dissection, the ratio of HER2/gastrin was generally increased in the positive cases resulting in a 100% concordance of PCR to the FISH results.
Conclusion: These preliminary results indicate that quantitative PCR may be a valid and sensitive alternative to determine HER2 positivity. By virtue of the rapid performance, a high level of reproducibility, fully objective results and moderate costs it may be particularly suited as a first line screening tool for HER2 in breast cancer.

P-522

The presence of HER2-antigen in recurrent breast cancer. An intra- and interobserver investigation

Birgitte Bruun Rasmussen, Eva Balslev
Department of Pathology, Roskilde County Hospital, Roskilde, Denmark

Recently a new treatment modality for recurrent breast cancer has been introduced. The patients are treated with a humanised monoclonal antibody (Herceptin®) against the growth factor HER2, if the carcinoma overexpress HER2 on the cell membrane. Overexpression of HER2 in breast cancer has been detected immunohistochemically for several years, but with inconsistent results. Some of the reasons for the discrepancies could be the use of different antibodies in different solutions and different definitions of a positive reaction. In relation to Herceptin treatment a new antibody kit, Herceptest®, has become available, standardizing not only the staining procedure, but also the interpretation of the reaction, with a grading system with 4 levels (0, 1, 2, 3) where grade 0 and 1 are negative, grade 2 and 3 positive. With regard to Herceptin treatment only patients with grade 3+ tumors are candidates for treatment.
The aim of the present study was to test the kit and investigate the intra- and interobservervariation of the semiquantitative grading system.
The material consisted of 97 carcinomas from patients with recurrent breast cancer. Fourtytwo per cent of the carcinomas were positive, 22,7% strongly positive (grade 3+).
The intraobserver accordance was 79,4% (kappa 0,68), for positive versus negative 91,8% (kappa 0,82). The interobserver accordance was 76% (kappa 0,67) and 89,2% (kappa 0,76), respectively.
The Herceptest and the recommended grading system has thus a high level of reproducibility, and may, in our opinion, safely be used in relation to deciding whether treatment with Herceptin is relevant.

P-523

Intraductal component of infiltration breast carcinoma and clinical outcome

Ewa Chmielik, Krystyna Wołoszyńska, Beata Maksymiuk, Anna Smok, Dariusz Lange
Centre of Oncology, Gliwice, Poland

This study assessed correlation in locoregionally advanced ductal breast carcinomas between occurrence as well as type of intraductal component of tumors and surrounding tissues and disease progression. Individuals included in this study underwent breast cancer surgery between 1994 and 1996 in the Clinic of Surgical Oncology at the Institute of Oncology in Gliwice, Poland. Cases analyzed were locoregionally advanced tumors in which no dimension exceeded 5 cm.
Material suitable for microscopic observation was obtained by slicing a 2-mm tissue section from the thickest cross-section of the tumor. From the obtained slice 4 tissue blocks were further cut from the tumor itself and 4 tissue blocks were cut from the 2- and 4-centimeter margins each. The blocks obtained from the tumor and both margins were serially sliced and examined under the microscope. Assessment of ductal carcinoma was based on criteria decided upon during the *Consensus Conference on the Classification of In Situ Ductal Carcinoma Philadelphia – 1997*. The presence of intraductal component (DCIS) was confirmed in 33 cases which make 39% of the examined tumors. In 22 cases (26%) the texture of the intraductal carcinoma was localized at a distance greater than 2 cm. High DCIS malignancy was concluded in 12 cases of 2-cm margin and in 7 cases of 2–4-cm margin. The analysis carried-out did not reveal relationship between the presence, type and degree of malignancy of the intraductal component accompanying the infiltrating breast carcinoma and the clinical outcome.

P-524

Primary angiosarcoma of the breast

Cingil, H.
Department of Pathology, Istanbul Naval Hospital, Istanbul, Turkey

Introduction: Primary angiosarcoma of hte breast is an uncommon tumor accounting for less than 0.05% of primary mammary cancers. It is highyl malignant neoplasm of vascular origin and mostly affects females in their fourth and fifth decades. My aim is to present the case of a 43-year-old woman with primary angiosarcoma of the left breast.
Methods: Tissues from the incisional biopsy and the mastectomy specimen were fixed in formalin and embedded in paraffin for routine histologic examination. Samples were stained with Haematox-

ylin-Eosin and immunohistochemical method for CD31, cytokeratin, vimentin and factor VIII.
Results: This woman complained of a four months history of palpable, painless mass on her breast. On mammograms there were signs of malignancy. On gross examination the measure of the tumor was 8.5×4.5×3 cm. and usually poorly defined, consisting of spongy hemorrhagic spaces. Microscopically anostomoses, irregular vascular channels lined by plump and flattened atypical endothelial cells. Reticular dermis was infiltrated by tumor cells. Immunohistochemically the tumor cells exhibit CD31, vimentin and factor VIII, cytokeratin negativity. After mastectomy, the patient had received 5100 cGy radiation therapy. The patient has been free of disease for 24 months.
Conclusion: Angiosarcoma is regarged as a highly aggressive tumor with a rapid growth and poor survival after diagnosis, but the low histologic grade and early diagnosis are the most importanat factors of good prognosis.

P-525

Fibrotic focus is a surrogate for quantifying angiogenesis and an independent predictor of early metastasis in lymph node negative breast cancer patients.

C. Colpaert, P. Vermeulen, P. van Beest, G. Goovaerts*, J. Weyler#, P. Van Dam*, L. Dirix*, E. Van Marck
Dept. of Pathology, University Hospital Antwerp; #Dept. of Epidemiology and Community Medicine, University of Antwerp; The *Angiogenesis Group, AZ Sint Augustinus, Antwerp, Belgium

Introduction: Fibrotic focus (FF)-defined as a scar-like area replacing necrosis in an infiltrating ductal carcinoma- was proposed in 1996 by Hasebe et al. as an indicator of tumour aggressiveness in breast cancer. Although FF is readily apparent in routine microscopical tissue sections, it is not widely used as a prognostic factor in daily practice.
Methods: 104 $T_{1-2}N_0M_0$ breast carcinoma patients were divided into two groups: group 1 (46 patients) showing early distant relapse (median disease free survival: 25 months) and group 2 (58 patients) showing no evidence of disease (median follow-up: 91.5 months). All tumours were evaluated for medial/lateral location, size, histological grade, mitotic activity, necrosis, FF, angiogenesis (Chalkley point counting), vascular permeation and growth pattern.
Results: A FF was present in 53% of the tumours. Multiple regression analysis showed that histological grade (p=0.004) and the presence of a FF (p=0.01) were the only independent predictors of early distant relapse. A relative size (FF/tumour ratio) >1/3 was most strongly associated with unfavourable outcome (p=0.01). The presence of a FF (p<0.0001), necrosis inside the FF (p<0.0001) and the absolute (p=0.01) and relative (p=0.0063) size of the FF were positively correlated with microvessel density. FF was significantly associated with large (p=0.018), expansively growing tumours (p<0.0001) with high histological grade (p<0.0001) and numerous mitoses (p<0.0001).
Conclusion: FF can be used as a surrogate for quantifying angiogenesis and as an independent predictor of early metastasis in node-negative breast cancer. It merits confirmation as a prognostic factor in randomised prospective clinical trials.

P-526

AgNOR analysis in invasive lobular carcinoma and particularly differentiated tumor types of the breast

A. Czerwinski1, H. Guski[1], P. Hufnagl1, K.-J. Winzer[2]
[1] Institut für Pathologie und [2] Klinik für Allgemein-, Visceral-, Gefäß- und Thoraxchirurgie, Universitätsklinikum Charité, Humboldt-Universität zu Berlin, Germany

Introduction: Several studies has been undergone in invasive ductal carcinoma in which the significance of nucleolus organizer regions for the prognostic evaluation of breast cancer was demonstrated. In contrast to these findings no results are available in breast carcinomas with special differentiation.
Material and methods: 101 patients with invasive lobular carcinoma (n=51) were examined and the results compared with particularly differentiated tumors (n=50). AgNOR structures were stained by using a standardized silver staining method and measured by means of microscopic image analysis. AgNOR features representing number, volume, area, size and the topology of the structures were compared with tumor grading, growth fraction, and the expression of estrogen and progesteron receptors. Selected AgNOR features were correlated with clinical data (follow up of 30–90 months).
Results: AgNOR number and area increased with the decrease of tumor differentiation. In invasive lobular carcinoma these AgNOR features were correlated with the survival time of the patients: AgNOR number <3=50 months, AgNOR number >6=29 months, AgNOR area <3μm2=44 months, AgNOR area >3 μm2=33 months. Statistically significant differences of the AgNOR area were found between 3 groups of tumors: 1. medullary carcinoma (2.48 μm^2), 2. lobular, mucinous, papillary, and adenoid cystic tumor type (1.34–1.97 μm^2) and 3. apocrine carcinoma (0.7 μm^2). AgNOR number of particularly differentiated tumor types was correlated with tumor size.
Conclusion: AgNOR analysis allows to distinguish two subgroups of invasive lobular carcinoma with different prognosis. No differences were found between well differentiated invasive lobular carcinoma and tumors with mucinous, tubular, papillary and adenoid cystic differentiation.

P-527

Overexpression of p53 proteine – retrospective study of survival in breast cancer

Victor Dabelea[2], Anca Ro}ianu[1], N. Tudose[1], Marioara Cornianu[1]
[1] Department of Pathology, [2] Clinic of Oncological Surgery, University of Medicine, Pharmacy Timisoara, Romania

Summary
Background: Overexpression of p53 oncogene is one of the most frequent genetic anomalies in breast cancer. We performed the p53 expression on 40 patients with breast cancer treated in Country Hospital from Timisoara during 1993–1994.
Methods: Immunohistochemical determination of p53 protein was performed on tissue samples formalin 10% fixed and paraffin embedded using mouse monoclonal antibody DAKO-p53 DO7 p53 human antiproteine.
Results: From the 40 breast carcinomas, 11 (27,5%) were p53 positive; the tumours ranging between 2–5 cm overexpressed the p53

protein in 29,2% of cases and the tumors over 5 cm in 25% of cases. The tumors with G3 differentiation degre was p53 positive in 42,9% of cases comparative to carcinomas with G1 (15,8%) or G2 (35,7%). The tumors with axillary lymph nodes metastates were significantly immunoreactive for p53 (27,2%) comparative to tumors with negative auxilliary lymph nodes 22,2%, but no significantly statistical difference was seen.
Conclusion: The five year survival rates was significantly greater for the patients with p53 negative tumors comared to patients with p53 positive tumors ($p < 0.001$).

P-528

Ductal carcinoma in situ (DCIS) – Assessment of residual tumor after excision for breast conserving therapy

Decker T., Obenaus R.*, Kettritz U.**, Ruhnke M., Schmidt D., Morack G.*, Schneider W.
Departments of Pathology, Gynecology* and Diagnostic Radiology**, The Breast Unit, Berlin-Buch Medical Center, Berlin, Germany

Introduction: Recurrence of DCIS after breast conserving therapy (BCT) means, in reality, a manifestation of the natural history of residual DCIS. We examined the impact of a standardised pathological work- up on the assessment of the risk and amount of residual DCIS.
Methods: In 205 out of 217 patients with DCIS (19.7% of 1096 breast cancers during a 5 year period) an excision was performed to attempt BCT. The specimens were examined pathologically according to the "Berlin-Buch practice protocol" In every case with DCIS within a distance of 5 mm to the resection lines (RL) a re-excision (RE) followed.
Results: There was no statistical relationship between the grade and size.

Grade\Size	A. 0–15 mm	B. 16–40 mm	C.>40 mm	Σ
Low grade	6	8	41	55
Intermediate	11	8	48	67
High grade	29	7	47	83
Σ	**46**	**23**	**136**	**205**

Free margins of more than 5 mm were found in 60 Excisions (29.3%, including all of group A). In the remaining 145, REs were performed. In all 136 DCIS >40 mm (C) free margins could not be reached: After mastectomy an involvement of more than one quadrant could be proofed.
Conclusions: The margin status of DCIS is useful for deciding on RE to reach an oncologically acceptable excision, whereas a size over 40mm represents a contraindication for BCT. The combination of both, the size of DCIS and the margin status, by the pathologist as a member of the breast team is a precondition for therapeutic decision making.

P-529

Distribution of immunal lymphocytes and Ig A in perivascular zones of breast cancer as criterion of radiotherapy effect

Dorosevich A.E., Golubev O.A., Shisterova O.A, Abrosimov S.U.
Smolensk Regional Inst. of Pathology, Smolensk, Russia

The study is aimed at finding out the radiotherapy (RT) efficiency in patiens with breast cancer (BC) by investigation of microvessels with their cell environment, as the place of tissue reactions of antitumoral immunity in oncological patiens is stroma of an injured organ, mostly the microvessels.
Material and methods: center and peripheral zones of BC before (80 cases) and after (131 cases) RT were investigated by histological and immunohystochemical (anti-T and B-cells, Ig A) methods.
Results: B-lymphocytes are found in minimal quantity in all zones. They are forming the structures similar to lymphoid folliculi. T-cell infiltration is often revealed. The concentration of T-cells is maximal around venules and capillaries in tissues of BC before RT. RT leads to the destruction of a third part of T-cells in peripheral zones. After RT around capillaries their number decreases in the center and increases twice as much in the peripheral zones. The number of T-cells and macrophages with revealed Ig A on their cellular membranes is maximal in the central zones around capillaries and venules before RT. But their number increases considerable after RT.
Conclusion: RT (intensive-concentrative method) causes the part of the tumoral cells to destruct. Thougt it doesn't lead to any changes in the tumoral stroma. This method of RT is probably not sufficiently effective in formation of the conditions for intercellular interaction desintegration.

P-530

P53-SSCP-LOH alterations and p53 overexpression in ductal infiltrating carcinoma of breast. Correlation with clinicopathological variables

Durán R., Ortega E., Gil-Hervas P., Payá A., Picó C., Laforga J.B., Aranda F.I.
Service of Pathology, Hospital General Universitario de Alicante, Spain

Purpose: To identify molecular alterations using SSCP in p53 gene in cases of ductal infiltrating carcinoma NOS and to correlate with immunohistochemical expression of p53 and other clinicopathological variables.
Methods: 90 cases of ductal infiltrating carcinoma excluding specific histological grade were evaluated. In all the cases variables such as tumor size, histological grade, axillary status, and immunohistochemical expression of p53 (DO7) and c-erbB2 (CB11) were evaluated. In 52 cases a molecular study using PCR-SSCP for exons 5–9 , and loss of heterozigocity (LOH) for exon 4 of p53 gene were performed. Results were analyzed using univariable analysis (chi-square test).
Results: Molecular techniques were used in 52 cases. 17 cases (32%) showed some mutation of p53 gene in exons 5–9 by SSCP. 29 cases (55,8) showed LOH in exon 4. In 14 tumors (27%) both abnormalities were identified.
20/90 cases (22%) showed p53 overexpression. Association between p53-SSCP alteration, p53-LOH and p53 overexpression was observed (p=0,007). Association between histological grade, p53 expression, p53-SSCP, and LOH-p53 alteration was found. Lack of association between tumor size, axillary status and the c-erbB2 expression with p53 abnormalities were detected.
Conclusions: P53 overexpression and the gene alteration using SSCP-LOH showed a similar level of significance with the clinicopathogical variables analyzed.

P-531

Breast carcinomas with neuroendocrine differentiation

Erhan Y., Zekioglu O., Bayramoglu H., Ozdemir N.
Ege University, Medical Faculty, Pathology Department, Bornova, Izmir, Turkey

Background and aims: Some primary carcinomas of the breast have classified as neuroendocrine. The frequent association of neuroendocrine differentiation and mucin production have been noted by several investigators. We reported 9 cases of neuroendocrine carcinoma of the breast displaying usual and unusual histologic features.
Material and method: In 9 cases the tissues had been fixed in formalin and routinly processed. In all cases, PAS, alcian blue and haematoxyline and eosin were performed. Immunohistochemical studies were carried out with the avidin-biotin method using the following antibodies: estrogen receptor protein (ER), chromogranin, neuron spesific enolase (NSE), and synaptophysin.
Results: All patients were aged from 43 to 79 years (median 66). The tumors were unilateral and ranged from 0,8 to 7 cm (median 2,3 cm). In all cases the prýminent histologic features were: extensive intraductal growth pattern, perivascular pseudorosettes, extracellular and intracellular mucin. Of 6 cases harboring a different invasive component, 4 tumors were associated with mucinous carcinoma and 2 tumors with invasive micropapillary carcinomas. Two cases showed signet ring cell differentiation. One case had Merkel-like, other one lobular carcinoma-like and another one spindle cell histologic subtype. The tumor cells of the all cases were stained positively for NSE. Synaptophysin positivity was detected in 8 cases, and chromogranin in 5 cases, respectively. Eight cases were stained positively for ER. ER negativity has been found in the case with signet ring cell differentiation.
Conclusion: In these cases the prominent clinical and histological features were: elderly age, extensive intraductal growth, perivascular pseudorosettes, low-grade cytologic atypia, intra and extracellular mucin.

P-532

Clinical, histological and immunological predictors of response to neoadjuvant chemotherapy (NAC) in patients with locally advanced breast cancer (BrCa)

S.S. Ghataura (presenting author), O.J. Cooper,
G.A.D. MacPherson, D.M. Bailey
Departments of Cellular Pathology and Surgery, High Wycombe, UK

Introduction: Use of NAC for locally advanced BrCa has increased since early reports in 1985. Clinical response consistently correlates with survival. No predictive factors have correlated reliably with response.
Methods: Since 1999, 24 patients at Wycombe Hospital have received NAC. Aims of treatment were reduction in tumour size, or elimination of palpable nodes or tumour fixity. Treatment consisted of 5-fluorouracil, epirubicin and cyclophosphamide, or adriamycin and cyclophosphamide. 17 patients have received definitive surgery; one patient died from metastatic disease before completing chemotherapy. Diagnostic biopsies and clinical notes were studied retrospectively. Histology and the following immunohistochemistry were analysed: oestrogen and progesterone receptors, Ki-67, cErbB2, E-cadherin, p53, p21, bcl-2, and cytokeratins 7 and 20. Good clinical response (GCR) was defined as stage reduction in tumour size, elimination of nodes or tumour fixity and negative resection margins. Poor clinical response (PCR) was defined as failure of any of these factors, or metastatic spread or death within 12 months.
Results: 10 patients achieved GCR, 8 showed PCR. Univariate analysis showed differences in bcl-2 ($p=0.03$) and cErbB2 ($p=0.04$) staining. The only significant clinical factor was age ($p=0.04$). GCR correlated with higher cErbB2 and lower bcl-2 staining, and lower mean age. Multivariate analysis showed persistent bcl-2 significance ($p<0.05$) with cErbB2 just failing to reach significance ($p=0.07$). An index using cErbB2 and bcl-2 staining, grade, vascular invasion and age, showed strong predictive value for response ($p=0.0001$).
Conclusion: Bcl-2 positivity correlates with poor response. A combination of factors predicts outcome, reflecting the multifactorial determination of treatment response. Patients with high index values may forego NAC and proceed directly to surgery.

P-533

Breast hamartomas: Clinico pathologyic and immunohistochemical study of 24 cases

M. Herbert , J. Sandbank , P. Liokumovich, M. Segal, G. Hermann, L. Habler
Pathology Department, Assaf-Harofeh Medical Center, Zerifin, Israel

Introduction: Breast hamartoma is a rare benign breast tumor-like nodule. The hamartomas are composed an overgrowth of mature cells and tissue that normally oceure in the affected part, often with one element predominating. This study presents clinical, pathological, and immunohistochemical analysis of 24 breast hamartomas. Four cases of fibrocystic changes are used as a control group.
Methods: The immunohistochemical panel included: Estrogen and progesteron receptors, Her2/neu protein, P53, Ki-67, CK MNF –116, Vimentin, Alpha SMA.
Results: The patients ranged in age between 30 and 78 years with a mean age of 48 years. All patients presented with a palpable unilateral mass. Three patients showed 2 hamartomas in the same breast. No recurrences were observed after local excision.Tumor size ranged from 2 to 5 cm in diameter. Typical macroscopical and microscopical features were noted. Immunohistochemical studies showed estrogen and progesteron receptors positivity in epithelial cells as well as in the stromal cells in all 24 hamartomas. No Her2/neu protein overexpression was noted. No. P-53 expression was not observed. Ki-67 showed a 2-3% positivity in epithelial cells in most cases.
Conclusion: There was no association with side, ethnic origin or dietery habits. The immunohistochemical profile of hamartomas is generally similar to normal breast or fibrocystic breast tissue. Ki-67 tagether with the receptor positivity may reflect some proliferative activity and may explain the observed faster growth of hamartomas during pregnancy or lactation.

P-534

Prognostic significance of tumor angiogenesis in breast cacinoma patients

Jasminka Jakic-Razumovic, Mladen Petrovecki [1],
Valerija Blazicevic [2]
Department of Pathology Clinical Hospital Center Zagreb;
[1] Department of Computer Science, Rijeka School of Medicine;
[2] Department of Pathology Clinical Hospital Osijek

Introduction: Breast carcinoma is a heterogenous disease, the prognosis of which correlates with various prognostic significance of tumor angiogenesis in breast carcinoma patients in association with other known prognostic factors.
Material and methods: In this study the relationship between immunohistochemicaly detected blood vessels/mm^2 (using anti-factor VIII monoclonal antibody) of 96 ductal invasive breast carcinoma patients and various establishment prognostic factors such as age, tumor size, histological grade, axillary lymph node metastases, estrogen (ER) and progesterone (PR) receptor expression, percentage of cells in S-phase of cell cycle, cell ploidy status is presented. The number of new blood vessels/mm^2 in the stained tumor tissue specimens was analysed using a light microscope with Weibel graticule on the eyepiece.
Results: There was no statistically significant correlation of number of blood vessels/mm^2 and age, axillary lymph node status, ploidy of tumor cells, size and tumor grade, but there is correlation with number of cells in S-phase of cell cycle (p=0,037). The cut of value of tumor blood vessels/mm^2 was 170. Univariate analysis shoved that overall survival correlated significantly with axillary lymph node involvement (p<0,001), ER (p=0,012) and PR (p=0,001) status, and number of blood vessels/mm^2 of tumor (p=0,033). IN multivariate analysis only axillary lymph node metastases (p=0,015) and progesterone receptors (p=o,026) were found to be independent and significant prognostic factors.
Conclusion: When patients were stratified according number of blood vessels/mm^2 of tumor it was shown that those with number of blood vessels/mm^2 of tumor greater that 170, younger than 50 years, number of cell in S-phase of cell cycle greater than 4%, diploid tumor cells, and negative PR had shorter survival than patients with tumors with less than 170 blood vessels/mm^2 of tumor. These patients might be considering as high-risk patients.

P-535

Cyclooxygenase-2 (COX-2) expression in breast cancer

Jeongyeon, Shim, Jonghee, Lee, Heejung, Ahn
Department of Pathology, College of Medicine, Pochon CHA University, Korea

Cyclooxygenase-2(COX-2) is known to be overexpressed in various human cancers. We evaluate COX-2 expression by immunostaining to determine the role of COX-2 in breast cancer and relationship with variable prognostic factors. 44 cases were chosen including 26 invasive ductal carcinoma, 5 DCIS, 4 mucinous carcinoma, 3 apocrine carcinoma, 2 mixed ductal and lobular carcinoma, each 1 case of variable carcinoma including medullary, atypical medullary, metaplastic and papillary carcinoma. Immunohistochemical results are followed: estrogen receptro(ER) positive in 16 cases, progesterone receptor(PR) positive in 14 cases, COX-2 positive in 26 cases. COX-2 was overexpressed in 11 of 16 cases showing positivity to ER as compared to 15 of 28 ER negative cases(p=0.118). Although COX-2 overexpression was observed in cases with larger size, nodal metastasis, higher stage and expression of PR, there was no statistically significant correlation. In invasive ductal carcinoma, COX-2 overexpression was statistically significantly different between cases of high and low nuclear grade(p=0.0280). COX-2 overexpression was also statistically significantly different between high and low histologic grade(p=0.034). COX-2 may be a feature of the aggressive, metastatic phenotype but further studies including more cases and survival data are indicated for confirming COX-2 expression as a prognostic indicator.

P-536

CGH analysis of ductal carcinoma of the breast with myoepithelial differentiation

Jones C1, Nonni A2, Fulford L1, Merrett S1, Chaggar R1, Eusebi V3 and Lakhani SR1
LICR/UCL Breast Group1, Dept of Histopathology, Royal Free & University College Medical School, UCL, London, UK; Dept of Histopathology2, Ioannina, Greece; Dept of Pathology3, Universita Di Bologna, Italy

Introduction: Pure myoepithelial carcinomas of breast are rare in clinical practice. We have demonstrated that these aggressive tumours are genetically different from ductal carcinoma-NOS in having very few but specific genetic alterations. 3–15% of ductal carcinoma-NOS are reported to express basal keratins. Tumours with a basal phenotype have been reported to have a different metastatic pattern and prognosis. We have therefore studied the molecular cytogenetic profile of ductal carcinomas exhibiting a basal/myoepithelial phenotype.
Methods: We performed immunohistochemistry for cytokeratin(Ck) 19 (luminal) and 14 (basal) on 100 ductal carcinoma-NOS. Those tumours (7%) showing a focal or diffuse Ck14 expression were analysed by comparative genomic hybridisation (CGH). Ck14 positive and negative areas were microdissected from formalin-fixed, paraffin-embedded sections using Laser Capture Microdissection.
Results: The 7 cases of ductal carcinoma-NOS exhibiting a basal phenotype were all Grade III tumours. They all showed a molecular cytogenetic profile similar to pure myoepithelial carcinomas. The mean number of DNA copy number change was 3.0 in Ck14+ areas (pure myoepithelial carcinoma-mean 2.1, ductal carcinoma grade III – mean 11.7) and the common alterations were losses at chromosomes 16, 17 and 19, similar to pure myoepithelial carcinomas.
Conclusion: Compared to invasive ductal carcinoma showing a luminal phenotype, ductal carcinomas with a basal/myoepithelial phenotype immuno-histochemically exhibit genetic alterations similar to pure myoepithelial carcinomas. Grade III ductal carcinomas contain a subset of tumours with different biological characteristics and hence prognosis for the patient.

P-537

An investigation of the clonal 'patch size' in the normal human breast

Jones C1, Rashid TG1, Davies S2, Chaggar R1, Easton D3, O'Hare MJ2, Lakhani SR1
LICR/UCL Breast Group, Departments of Histopathology1 and Surgery2, Royal Free & University College Medical School, University College London, UK; CRC Genetic Epidemiology Unit3, Cambridge, UK

Introduction: Using X-chromosome inactivation methodology, in situ and invasive breast carcinoma, as well a proportion of hyperplasias, have been demonstrated to be monoclonal. However, the clonal 'patch size' in the breast is unknown. The size of the 'patch' has implications for interpretation of data using X-linked analysis as well as the functional organisation of the breast.

Methods: Informative normal breast specimens from reduction mammoplasties were disaggregated to obtain epithelial fragments (organoids) of various sizes (acini, lobules, ducts, whole duct-lobular units). Clonality of the organoids was assessed using an RT-PCR-based method for X-linked inactivation patterns of the G6PD and IDS genes.

Results: 478 organoids from 9 informative patients were studied. Of 65 organoids less than 0.005 mm^2 in area, 41 (63%) were monoclonal. With increasing size, there was a trend towards polyclonality, however monoclonal patches were still seen. For example, using arbitrary cut-offs of between 0.1 and 0.2 mm^2, 26% of samples were monoclonal. The data did not reach formal statistical significance.

Conclusion: Unlike the colon where the clonal patch is well defined (a single crypt), these data suggests that although monoclonality is seen more frequently with smaller fragment size, the clonal organisation within the breast duct-lobular tree is variable. X-linked analysis may therefore not be an appropriate tool for studying proliferations within the breast. Further studies using a larger sample size and investigation of the influence of menstrual cycle and pregnancy on the clonal organisation are warranted.

P-538

Expression of Ki-67, PCNA, p53, nm23 and c-erbB-2 in axillary lymph nodes metastases of breast cancer.

Karmolinski A., Rzepko R., Kobierska G., Roszkiewicz A.
Department of Pathomorphology, Medical University of Gdańsk

Introduction: The main prognostic factor in breast cancer is axillary lymph nodes status. To find factors connected with lymph nodes metastases many investigations were performed, almost exclusively on the primary tumors. Some of these factors are: Ki-67, PCNA, p53, nm23 and c-erbB-2. We believe that assessment of their expression in neoplastic cells of lymph nodes metastases could be helpful in determining their role in metastatic process.
Aims: We tried to establish an immunomorphologic profile of neoplastic cells of breast cancer metastases in axillary lymph nodes by the expression of the following antigens: Ki-67, PCNA, p53, nm23 and c-erbB-2.
Material and methods: Metastatic axillary lymph nodes from 109 patients with breast cancer. 80 of them present ductal type, 24 – lobular type, 5 – other types of breast cancer. Number of metastatic lymph nodes was from 1 to 20. Expression of Ki-67, PCNA, p53, nm23 and c-erbB-2 was detected immunohistochemically (IHC) and then assessed quantitatively (Ki-67 and PCNA) or semiquantitatively (p53, nm23 and c-erbB-2).
Results and conclusions: Expression of proliferative antigens Ki-67 and PCNA in metastatic lymph nodes is similar and we found statistically significant correration between them. In great majority of cases we found expression of p53 protein and only weak or no expression of nm23 protein. Expression of c-erbB-2 protein we found in about half of cases. In metastases of ductal type of breast cancer expression of Ki-67 and p53 was higher then in lobular type. In cases with greater number of metastatic lymph nodes expression of p53 was higher. Higher proliferative activity of cells was accompanied by the higher expression of c-erbB-2 and p53.

P-539

HER-2/neu gene amplification compared with her-2/neu protein overexpression in breast carcinomas

H. Kaya, E. Arıbal, İ. Güney, E. Kotiloğlu
Dept. of Pathology, Medical School, Marmara University, Istanbul, Turkey

Her-2/neu status has been considered as a prognostic factor in breast carcinoma. The aim of our study is to search the correlation between Her-2/neu gene amplification and immunohistochemical overexpression in breast carcinomas. Twenty formalin fixed paraffin embedded breast carcinomas were investigated for gene amplification by florescent in situ hybridization technique and immunohistochemistry by using Dako and BioGenex antibodies. Immunostaining was classified as follows: 0=no staining, 1+=faint incomplete membranous pattern, 2+=moderate complete membranous pattern, 3+=strong membranous pattern. Gene amplification was evaluated in 100 tumor cell nuclei and ≤3 mean signals per nucleus was considered as nonamplified, >3 mean signals per nucleus as amplified. Gene amplification was observed in 5 of the 20 invasive tumors (25%). All tumors with 3+,2+ immunreactivity with both of the antibodies had gene amplification and all other cases with 1 or 0 staining were negative. There was a strong correlation between the immunoexpression of the 2 antibodies and complete perimembranous staining with the gene amplificaiton.

P-540

Frozen section examination of core needle biopsy in the breast carcinoma as the preoperative diagnostic method

Y.J. Kim, Y.K. Chun, H.S. Kim, S.R. Hong, H.S. Kim
Department of Pathology, Sungkyunkwan University School of Medicine, Samsung Cheil Hospital, Seoul, Korea

INTRODUCTION: Core needle biopsy(CNB) is widely used as the initial sampling method for breast cancer. Frozen section(FS) examination is rapid and reliable, so we studied the diagnostic agreement between the diagnoses of FS of CNB and final diagnoses after surgery to evaluate the diagnostic accuracy of the FS of CNB.

METHODS: Of 409 patients preoperatively diagnosed by FS of CNB and underwent final surgery from 1996 through 2000 at our institution, 385 cases were ductal carcinoma in situ (DCIS) and 24 were invasive carcinoma (IC). The diagnoses of FS of CNB were compared with final diagnoses.
RESULTS: The diagnostic rate of carcinoma is 63.6% in DCIS and 86.9% in invasive carcinoma. Five cases (1.2%) were insufficient for diagnosis. Of 22 cases (5.4%) were diagnosed as benignancy on FS, 20 (90.9%) were resulted from sampling error. Of 27 cases (6.7%) were deferred on FS, 4 cases were DCIS, 5 were invasive lobular carcinoma (ILC), the rest of them showed low nuclear grade or marked freezing artifact.
CONCLUSION: The diagnostic accuracy of FS of CNB is very high excluding ILC and low grade DCIS. Considering the advantage of rapid evaluation, more definitive diagnosis, familiarity with pathologists and availability of ancillary study, FS of CNB is very useful method as the preoperative evaluation.

P-541

Immuniohistochemical studies of the coexistence of HER-2, estrogen and progesterone receptor overexpression in breast cancer

W. Kozlowski, E. Szacikowska, P. Wiœniewski, M. Kowañski, E. Stanowski, M. Maruszyñski, C. Szczylik, R. Zablotna
Division of Clinical Pathomorphology, Central Clinical Hospital, Military University School of Medicine in Warsaw; I and II Departments of Surgery, Institute of Surgery, Central Clinical Hospital, Military University School of Medicine in Warsaw; Department of Oncology, Central Clinical Hospital, Military University School of Medicine in Warsaw, PolandIt is generally accepted that in about 60% of breast cancer cases overexpression of estrogen receptors (ER) is present. On the other hand, in 25-40% of cases of primary breast cancers, HER-2 receptor (p 185 protein) overexpression is observed. Usually, HER-2 receptor overexpression develops in cancers in women below 50 years of age, and the most frequent histological type is intraductal carcinoma. Less frequently observed coexpression of HER-2 and estrogen receptors is a phenomenon of not fully elucidated clinical importance. Relatively few authors think, however, that such coexpression has very poor prognosis, especially due to the fact of its occurrence in cancers in young women.

The aim of the study was an attempt at finding the relationship between the coexpression of HER-2 and estrogen receptors identified immunohistochemically and patients' age, degree of progression and histological type of breast cancer.
Material and method: The studies were performed on material from the archives of the Division of Clinical Pathomorphology, Central Clinical Hospital, Military University School of Medicine in Warsaw, from 150 women aged 31–79 years, with breast cancer, treated in the I and II Departments of Surgery and Department of Oncology, Central Clinical Hospital, Military University School of Medicine in Warsaw. The tumours were classified according to WHO system, degree of progression according to TNM system, and degree of differentiation according to Bloom-Richardson grading system. The HER-2, estrogen and progesterone receptors were identified by means of immunohistochemical reaction with appropriate monoclonal antibodies, according to DAKO EnVision+System, Peroxidase (DAB). Quantitative studies of the cells with overexpression were carried out using an OLYMPUS analySIS 3.0 computer-assisted microscopic image analyser.
Results and conclusions: HER-2 receptor overexpression was found most frequently in women below 50 years of age, 10 years earlier, on the average, as compared to cancers without these receptors. In 60% of cases, HER-2 receptor overexpression involved almost all malignant cells. Coexpression of HER-2 and estrogen receptors was observed in about 30% of breast cancer cases. In the group of patients with HER-2 receptor overexpression, intraductal carcinoma occurred in 37% of cases and in 53% of these patients metastases to lymph nodes were found (pN1a-pNbIV). Most frequently, metastases developed in HER-2-positive and ER-negative tumours, less frequently (50%) in tumours with HER-2 and ER receptor coexpression and least frequently (20%) in ER-positive and HER-2-negative patients.

P-542

Ductal Carcinoma In Situ (DCIS) in mammographically detected lesions of the breast

Lacerda M, Moniz AP, Pires I, Leão JE, Figueiredo P
Centro Regional de Oncologia de Coimbra (C.R.O.C.) do I.P.O.F.G., Portugal

Introduction: Mammography has became almost universally accepted for breast cancer screening and with its improvement the diagnosis of DCIS has became commonplace.
Aim: The aim of this study is to present the experience of the Histopathology Department of C.R.O.C. between 1991–1999.
Materials and Methods: We studied 777 guide wire breast biopsies provided from breast cancer screening program of the central region of Portugal. We followed the methodology proposed by the Quality Assurance Guidelines for Pathology produced by the E.C. Working Group on Breast Screening Pathology, either in the macroscopic examination, radio-histological correlation, sampling, histological classification and recording of prognostic data of DCIS.
Results: In 777 guide wire breast biopsies we diagnosed 398 malignant breast lesions (predictive value - 51%). Of these malignant lesions, 168 (42%) were DCIS and 230 (58%) were invasive breast cancers. The pathological classification of DCIS lesions according to the nuclear grade showed 74 high nuclear grade, 62 intermediate nuclear grade and 30 low nuclear grade DCIS. The histological extention of the lesions (cut-off at 2.5cm) was:
High nuclear grade: <2.5 cm: n=45; >2.5cm: n=28; non measurable: n=6
Intermediate nuclear grade: <2.5 cm: n=45; >2.5cm: n=8; non measurable: n=9
Low nuclear grade: <2.5 cm: n=22; >2.5cm: n=6; non measurable: n=2
Resection margins and Reexcision:
High nuclear grade: not assessable: n=13; adequate excision: n=13; with lesion: n=48 – after reexcision: 27 with DCIS, 18 without lesion and 3 with invasive carcinoma.
Intermediate nuclear grade: not assessable: n=17; adequate excision: n=14; with lesion: n=31 – after reexcision: 13 with DCIS, 11 without lesion and 3 with invasive carcinoma.
Low nuclear grade: not assessable: n=6; adequate excision: n=7; with lesion: n=17 – after reexcision: 4 with DCIS, 6 without lesion and 4 with invasive carcinoma.
Radio/Histological Correlation:

Microcalcifications were more frequent in high nuclear grade (n=70) and intermediate nuclear grade (n=55) than in low nuclear grade lesions (n=24).
Conclusions: Our predictive value (51%) is higher than in the USA but lower than in some European countries, namely Sweden and Norway, where stereotactic FNAC (fine needle aspiration cytology) is a standardised technique. Since the criteria used for gross examination, radio-histological correlation and sampling are different from other series, results concerning free margins could not be compared. Although there is a good working relationship between pathologists, surgeons and radiologists, we should improve our system in order to obtain surgical margins free of lesions and to achieve optimal conical excision.

P-543

Angiogenesis in breast cancer. Determination of histological grade and axillary status with recurrence-free survival

Laforga J.B., Aranda F.I., Sanchez-Payá J., Payá A., Seguí J., Picó C.
Service of Pathology, Hospital General Universitario de Alicante, Spain

Introduction: There is controversy regarding the assessment of intratumor microvessels (angiogenesis) as a prognostic factor in breast cancer.
Methods: The study was carried out by immunohistochemical method on formalin-fixed tissue sections from 88 cases of ductal infiltrating carcinoma NOS. The vessels were stained with F-VIII-RA. We analysed microvessels data in two ways: vessels/mm^2, counted in ten consecutive high power fields (400×) and angiogenic index (AI), number of vessels by 1000 tumor cells. The recurrence-free survival (RFS) in five years was estimated by Kaplan-Meier method.
Results: 1) vessels/mm2 (cut-off </=70) n.s 2) AI (cut-off </150) n.s. and into 3 groups 1) vessels/mm2 (<50; 51–75; >75) n.s 2) AI (<100; 101-200; >200) n.s
Axillary status: N0 (n: 41), 82% RFS; N1 (n: 23), 70% RFS; N2 (n: 24) 42% RFS (p=0.0006). Histological grade: I (n: 25), 84% RFS; II–III (n: 63), 61 % RFS (p=0.09)
Conclusion: Significative association between angiogenesis with axillary status and histological grade was observed. However, angiogenesis was not related with RFS, with independence of the method used.

P-544

Multiparameter flow cytometric (MP-FCM) Her-2/neu analysis in formalin fixed, paraffin embedded samples of human breast cancer, a comparison with immunohistochemistry

Mathie P.G. Leers and Marius Nap
Atrium Medical Center Heerlen, Dept. of Pathology, Heerlen, The Netherlands

Purpose: Determination of Her2/*neu* overexpression has become necessary for selection of breast cancer patients for Herceptin therapy. We compared the results from Her2/*neu* MP-FCM with immunohistochemistry (IHC) and ER status.
Materials & Methods: Single cell suspensions from 50 breast cancers were analysed on a DAKO Galaxy flow cytometer after simultaneous (immuno)staining for cytokeratin (MNF116, DAKO), Her2/*neu* (polyclonal, DAKO), and DNA (propidium iodide). Immunohistochemistry for Her2/*neu* was done on paraffin sections using the same polyclonal primary antibody in a SABC-peroxidase procedure after heat induced antigen retrieval. From all tumors MP-FCM results for ER and PR were available.
Results: Her2/*neu* overexpression as determined by IHC showed a score of 0 in 36%, 1 in 20%, 2 in 30% and 3 in 14% of the cases. IHC and MP-FCM showed a significant correlation (r=0.89, p<0.0001).
Comparing Her2/*neu* expression with ploidy and ER, three groups could be distinguished. *Group 1*: Diploid tumors (n=18) showed relative high ER (59%±17%) and moderate fraction of Her2/*neu*-positive cells (27%±16%). *Group 2*: Aneuploid primary tumors with less than 60% aneuploid epithelial cells (n=17) had an ER expression of 34%±19% and rather low fraction of Her2/*neu* positive cells (20%±7%). Finally *Group 3*: Aneuploid breast tumors with more than 60% aneuploid epithelial cells (n=15) had next to low expression of ER (26%±18%) an overexpression of Her2/*neu* oncogene product (51%±15%).
Conclusion: MP-FCM is a useful alternative for an objective Her2/*neu* quantification in breast cancer. Immunohistochemistry can not provide the additional DNA-ploidy information which allows more detailed classification.

P-545

HER2/neu-overexpression in breast cancer– non-automated vs. automated evaluation.

Lüftner D, Henschke P, Geppert R, Anagnostopoulos I[1], Possinger K, Stein H[1]
Medizinische Klinik II, Charité, Campus Mitte, Humboldt-Universität Berlin. [1]Institut für Pathologie, Klinikum Benjamin Franklin, Freie Universität Berlin, Germany

Introduction: Determination of HER2/neu overexpression by immunohistochemistry (IHC) is mandatory for Herceptin® therapy in breast cancer. We compared the results of a conventional IHC technique vs. an automated computerized IHC evaluation method by the ChromaVision ACIS® system (San Juan Capistrano, CA, USA) vs. fluorescence-*in situ*-hybridisation (FISH).
Methods: A total of 64 IHC slides of breast cancer specimens (primary tumor and/or metastatic lesions) of 30 patients with metastatic breast cancer were stained using the DAKO HercepTest® and scored manually by a highly experienced pathologist. The same slides were then re-run on the automated ACIS® system based on a colour-space transformation. In this technique, pixels of colour are counted with a threshold suppressing background staining.
Results: Of 64 results, the final scores differed in only 4 cases (6%) between conventional – and computerized evaluation. In 3 cases, conventional IHC diagnosed HER2/neu negativity while the computer scored for HER2/neu positivity, while in 1 case the conventional technique showed HER2/neu positivity while the computer scored for HER2/neu negativity. FISH results were always concordant to the computerized IHC result.
Conclusions: The concordance between conventional IHC evaluation and computerized testing of the same slide is excellent. Computerized determination should be taken into consideration in insti-

tutes with high through-put of slides. HER2/neu overamplification as diagnosed by FISH must be considered a complementary method of HER2/neu determination.

P-546

Invasive micropapillary carcinoma of the breast – are the pure forms more aggressive than the mixed forms?

João Magalhães, Isabel Amendoeira, Margarida Damasceno
Dept. of Pathological Anatomy, Hospital de Sao Joao, Porto, Portugal

Introduction: Invasive micropapillary carcinoma of the breast (IMC) is a rare variant of invasive carcinoma of the breast that has in most cases massive axillary lymph node metastization and other peculiar histological and biological characteristics that may have prognostic implications. IMC can occur as a pure form or associated with other types of invasive carcinoma.
Material and methods: We reviewed eight cases of IMC: four pure and four mixed forms. Analysis of histological grade, vascular invasion, number of metastasized lymph nodes and other clinical and pathological features was done. Nottingham Prognostic Index (NPI) was determined. Hormonal receptors, overexpression of c-erbB2 and P53 were evaluated by immunohistochemistry.
Results: Pure group – mean size 41,5 mm, two carcinomas grade 3 and two grade 2, lymph node metastasis in all cases, vascular invasion in all cases. Hormonal receptors positive in three cases, c-erbB2 and P53 positive in two cases. NPI- mean 6,07.
Mixed group – mean size 27,5 mm, one carcinoma grade 3, two grade 2, one grade 1. Two with lymph node metastases, one without metastases, one unknown; vascular invasion in three cases. Hormonal receptors positive in all cases, c-erbB2 negative in all cases, P53 positive in one case. NPI – mean 3,9.
Conclusion: Our data confirm that IMC has a metastasizing phenotype both in pure and mixed forms. Although our results point to the increased aggressiveness of pure forms, the follow-up period is too short and the size of the sample too small to allow a meaningful comparison between the clinical behaviour of the two groups.

P-547

Thymidine phosphorylase expression in breast cancer: A potential predictor of responsiveness to CMF chemotherapy

F. Mauri[3], M. Barbareschi[2], Q. Yang[1], I. Mori[1], M. Muscara'[3], O.Caffo[4], E. Galligioni, K. Kakudo[1], P. Dalla Palma
[1] Second Department of Pathology, Wakayama Medical University School of Medicine, Wakayama, Japan; [2] Department of Histopathology and [4] Medical Oncology, St. Chiara Hospital, Trento, Italy; [3] Department of Histopathology, SS. Trinità Hospital, Borgomanero, Italy

Objective: Thymidine phosphorylase (TP) catalyzes the reversible dephosphorylation of pyrimidine and plays a role in the metabolic activation of 5-fluorouracil (5-FU). TP has also has angiogenic properties.
Design and Methods: We examined TP expression using immunohistochemistry (654-1 Mab) in 182 invasive BC (67 N0 and 115 N1/2; median follow-up 78 months (range, 3-177); 51 patients treated with adjuvant CMF chemotherapy, and 82 with tamoxifen).
Results: High TP expression was found in 142 cases (78%) and was associated with lower histological grade and low p53 expression. No correlation was found with vascular density. TP-positive tumors had a significant increase in both relapse-free survival (RFS) (p=0.0025) and overall survival (OS) (p=0.0070). By subgrouping patients on the basis of post-surgical therapy (CMF, Tamoxifen, no therapy), these significant trends were observed only in patients treated with CMF. Bivariate analysis showed that TP+/ER+ tumors were associated with long DFS and OS, whereas TP-/ER-tumors had the worst prognosis.
Conclusions: Our findings show that the major prognostic role of TP is restricted to patients receiving adjuvant CMF chemotherapy and suggest that high TP expression could be a potential predictor of responsiveness to CMF.

P-548

Expression of FosB in breast cancer

K. Milde-Langosch, A.M. Bamberger, H. Kappes, S. Riethdorf, T. Löning
Department of Gynecopathology, Institute of Pathology, University Hospital Eppendorf, Hamburg, Germany

FosB is a member of the AP-1 family of transcripton factors which regulate expression of various target genes, many of which are involved in cell proliferation and invasion. In a prior Western blot study on mammary carcinomas, we observed an association of FosB expression with a well-differentiated, receptor-positive phenotype. In order to further analyze the role of fosB in breast cancer, we performed immunohistochemistry (IHC) and, partly, in-situ hybridization (ISH) and fosB sequence analysis on 68 mammary carcinomas and several normal breast tissue samples. Strong fosB expression was observed in normal mammary epithelial cells by IHC and ISH, with weaker expression in a part of the stromal cells. In mammary carcinomas, fosB expression varied from negative to strong. Negative or weak fosB immunostaining was significantly associated with high grading, a negative estrogen and progesterone receptor status, and younger age, but not with clinical stage or nodal involvement. In order to study the influence of fosB expression on cell cycle progression, we compared it with expression of 7 cell-cycle regulatory proteins which were analyzed by Western blot analysis: loss of fosB expression correlated significantly with p16 overexpression, which is a negative prognostic indicator, but not with cyclin D1, cyclin E, p21, p27, Rb, and Rb2. FosB sequence analysis in 4 mammary cell lines revealed a mutation of the transactivation domain in HBL-100 cells. These results indicate that FosB is involved in differentiation of normal mammary epithelial cells, and loss of fosB expression in breast cancer is associated with an undifferentiated, highly malignant phenotype.
Supported by the *Deutsche Krebshilfe* (No. 10-1522-BaI)

P-549

Paget's disease of the breast – copy numbers of c-*erb*B-2, CCND1 and TP53 genes (FISH), expression of their protein products (IHC)

Mrhalová M., Kodet R., Neradová M.
Department of Pathology, Charles University, 2nd School of Medicine, Prague, Czech Republic

INTRODUCTION: We investigated a group of eight patients with Paget's disease of the breast. The aim of the study was to evaluate copy numbers of c-*erb*B-2 gene, CCND1 gene and TP53 gene together with enumeration of chromosomes 17 and 11 to asses relations with Paget's disease. We compared the findings with the expression of erbB-2, cyclin D1 and TP53 proteins.
METHODS: We used fluorescence *in situ* hybridization (FISH) on interphasic nuclei to evaluate copy numbers of locus specific regions (LSI), and to enumerate chromosome 17 and 11 (CEP). Protein expression was detected by imunohistochemistry (IHC).
RESULTS: We found amplification of the c-*erb*B-2 oncogene in all cases. A strong overexpression of erbB-2 protein corresponded to this finding in all but one case. The signals for chromosome 17 suggested diploid status, occasional cells showed triploidy and tetraploidy. No amplification of the CCND1 gene was detected which correlated with a weak expression of the cyclin D1. TP53 gene gave two signals in most cells.
CONCLUSION: Archival paraffin embedded tissue was suitable for FISH detection of the copy numbers of the evaluated genes. The overexpression of erbB-2 protein was associated with amplification of the c-*erb*B-2 gene which is considered to contribute to the pathogenesis of the Paget´s disease. We did not find any significant pathology in the copy numbers of other genes studied in patients with Paget's disease. This suggests that amplification of the c-*erb*B-2 oncogene is an early and important pathogenetic event in Paget's disease.
The work was supported by grant GAUK 140/99

P-550

Micrometastases – A new prognostic factor?
J.M. Nesland, E. Borgen, G. Kvalheim, B. Naume
Dept. of Pathology, University Clinic, The Norwegian Radium Hospital, Oslo, Norway

Circulating tumor cells in bone marrow of patients with solid tumors are appearing early in tumor progression. Several methods have been applied to identify the cells, such as immunohistochemistry, PCR-based methods, use of immunomagnetic beads and others. In our studies of breast cancer we have examined 925 cases of early breast cancer and a series of cases with advanced breast cancer disease. Clinical data, characterization of primary tumor and identification of circulatiang tumor cells in bone marrow have been registered. The data show that presence of circulating tumor cells is an indication of an unfavourable prognosis, but that a longer follow-up period is needed to finally settle the prognostic impact.

P-551

Phyllodes tumor of the breast: Assesment of histology; proliferate activity and DNA values
A. Niezabitowski, B. Lackowska, J. Rys, A. Kruczak, J. Mitus, M. Reinfuss
Center of Oncology, Cracow, Poland

Introduction: The goal of the study was comparative assessment of histology, DNA values and proliferative activity for the prediction of clinical outcome among patients with breast phyllodes tumor. The study was performed on the biggest group of patients with long term of follow-up.
Methods: Among 119 patients with phyllodes tumor; overgrowth, cellularity, nuclear pleomorphism, mitotic rate, necrosis and secondary changes (sclerosis, myxoid edema) of the tumor stroma were assessed by histology. Expresion of p53 protein, MIB 1 antigen by immunohistochemistry and DNA values by flow cytometry, were evaluated from representative paraffin blocs.
Results: In 53, 24 and 42 cases-benign, borderline and malignant pyllodes tumors were found respectively. In 20 tumors of the last group, heterologous differentation (predominantly liposarcoma) occurred. Tumor relapsed in 17 patients and 13 of them died of the tumor. Clinical outcome was related with histological tumor type and overgrowth, cellularity, nuclear pleomorphism, mitotic rate and secondary changes of the tumor stroma as well as with values of MIB 1, p53 and S-phase. Independent prognostic indicators were only-tumor type, characteristics of tumor stroma (cellularity and secondary changes) and completeness of the surgery. Heterologous differentiation of the tumor stroma didn't influence clinical outcome in malignant phyllodes tumors.
Conclusions: Most important prognostic indicators in patients with phyllodes tumor of the breast comprise histological parameters predominantly tumor type, whereas other variables are of auxiliary value.

P-552

Redefining the cut-off point for determining oestrogen receptor (er) positivity in breast cancer.
P.A. O'Neill[1], D.R. Sibson[1], C.S. Foster[2]
[1] Clatterbridge Cancer Research Trust, Bebington, Wirral;
[2] Dept. of Pathology, University of Liverpool, U.K

Aims: Most U.K laboratories define ER positivity using a 10% cut-off point, however patients with <10% positive cells may also benefit from adjuvant hormone treatment.
Methods: The % of positive stained cells as a proportion of the total tumour cells present was recorded in a retrospective review of ER immunohistochemistry (n=311). Three groups were identified: group 1 (n=74) showed no positive staining for ER, Group 2 (n=39) had <10% positive cells and group 3 (n=198) had ≥10% positive cells.
Results: Relapse rates were highest for group 1 and group 2 at 34% and 48% respectively compared with 18% for group 3. Median time to relapse (TTR) did not differ significantly between the 3 groups showing ER is a weak prognostic indicator. For the patients who received only adjuvant hormone treatment (n=155) the median TTR was significantly longer for group 3 at 33.8 months compared to 16.5 months for group 1 and 22.3 months for group 2 (p=0.03).
Conclusion: Patients with <10% ER+ve cells may benefit from adjuvant hormone therapy but the behaviour of these cancers more closely simulates that of ER-ve tumours. Reclassifying these as ER+ve would inevitably result in under-treatment of these patients unless they were defined as a separate cohort of ER+ve patients with a higher risk of relapse.

P-553

Immunohistochemical localization of GST isoenzymes i n normal and neoplastic breast tissue: Correlation with prognostic factors

Oguztuzun S[1], Iscan M[2], Reed CJ[3] , Sak SD[4]
1: Department of Biology, Kirikkale University, Kirikkale,Turkey; 2: Department of Biology, Middle East Technical University, Ankara, Turkey; 3: The School of Biomolecular Science, Liverpool John Moores University Liverpool, UK; 4: Department of Pathology, Ankara University Medical School, Ankara, Turkey

Introduction: Glutathione S-transferases in breast tissue are important in susceptibility to the mutagenic effects of chemical carcinogens and in the response of breast tumors to chemotherapy.
Methods: In this study, the immunohistochemical staining characteristics of GST isoenzymes (alpha, mu, pi and theta) were investigated in intraductal, invasive carcinoma and normal breast tissue from the 43 patients. The relationships between expressions of the GST isoenzymes and some clinicopathological features were also examined.
Results: Diffuse cytoplasmic staining with varying intensities was observed for GST alpha, theta and pi in normal and tumoral breast tissue in 100% of the samples. Cytoplasmic staining for mu was weaker and patchy. In addition, for all isoenzymes, patchy nuclear staining was observed. In normal epithelium there was no difference between the staining scores of GST isoenzymes. However, in intraductal and invasive tumor tissues, staining scores of the GST isoenzymes showed statistical difference (for intraductal areas $p=0.0001$, for invasive areas $p=2.29\ 10^{-5}$). In addition, statistically it was proved that expressions of pi and theta isoenzymes were dependent on tissue type (normal, in situ or invasive tumor).
In this study, significant relationships were observed between patient's age and GST alpha; parity and GST pi; hormone therapy and GST theta expressions. No relationship between the expressions of the GST isoenzymes and oestrogen receptor status, stage, smoking or chemotherapy was observed
Conclusion: All four GST isoenzymes are expressed in normal and neoplastic human breast. Normal and neoplastic tissue shows some differences in staining scores. GST's may have important role in breast carcinogenesis.

P-554

BRCA1 expression is retained in the sporadic carcinoma *In Situ* irrespective to grade

PP Osin, C Wilson, BA Gusterson
University College London & Institute of Cancer Research, London, UK

Background: Mutations in BRCA1 gene are responsible for a significant proportion of familial breast and ovarian cancer. Molecular mechanism of its function is not entirely clear, however BRCA1 gene is considered as important regulator of cell cycle. Recent studies demonstrated that BRCA1 expression is often reduced in sporadic breast cancers. It is unknown on which stage of tumourigenesis the inactivation of BRCA1 occurs. In our study we attempted to answer this important question.
Methods: Immunohistochemical staining of 60 samples of sporadic carcinoma *in situ* (20 samples of lobular carcinoma *in situ*, 40 samples of ductal carcinoma *in situ*) has been performed using the antibody to BRCA1 protein (Ab1). Samples of invasive ductal carcinoma with wild type BRCA1 gene were used as a control.
Results: The normal breast tissue showed strong BRCA1 staining in the majority of cells of all types. All samples of both ductal and lobular carcinoma *in situ* also showed strong nuclear staining of tumour cells similar to the one of adjacent normal epithelium. Majority (64%) of invasive cancers showed weak or negative staining
Conclusion: These data suggest that inactivation of BRCA1 in sporadic breast cancer is relatively late event and could be responsible to development of an invasive tumour phenotype. It supports the view that BRCA1 plays a key role in development of sporadic breast cancer and is important diagnostic and prognostic marker and potential therapeutic target.

P-555

Significance of cell proliferation rate for the prognostic evaluation of breast cancer

E. Ozourma1, H. Guski1, P. Hufnagl1, K.-J. Winzer2
1Institut für Pathologie und 2Klinik für Allgemein-, Visceral-, Gefäß- und Thoraxchirurgie, Universitätsklinikum Charité, Humboldt Universität zu Berlin, Germany

Introduction: The importance of nucleolus organizer regions as a prognostic factor in breast cancer ist still controverse discussed in the literature. Therefore, these cell structures were measured by using a reproducable method and correlated with other prognostic markers and clinical data.
Material and Methods: 122 patients with invasive ductal carcinoma were examined with a follow up of 30-120 months. Sections of tumor tissue were stained by using a standardized silver staining method for argyrophilic nucleolus organizer regions (AgNORs). AgNORs were measured by means of microscopic image analysis. AgNOR features were calculated and correlated with histological tumor grading, tumor staging, perinodular tumor infiltration of axillary lymph node metastses, recurrence free period and survival time of the patients.
Results: A total of 48 features of number, volume, area , size and topology of AgNOR structures were determined characterizing cell proliferation activitity and proliferation rate. Tumor grading was correlated with several AgNOR features, e.g. AgNOR number, sum AgNOR area and areas of the largest AgNOR. The formation of AgNOR clusters increased with higher malignancy of the tumor. Strong correlation was found between AgNOR number and survival time of the patients ($p<0.0078$). No statistically significant relationship was found between AgNOR features, tumor staging, penetration of the axillary lymph node capsule, and the recurrence free period.
Conclusion: Selected AgNOR features representing tumor cell proliferation rate are correlated with tumor grading and survival time of the patients. Therefore, AgNOR analysis can be used for prognostic evaluation of breast cancer.

P-556

P-cadherin expression in breast carcinomas is associated with biological agressiveness

Paredes J[1]; Milanezi MF[1]; Athanazio D[2]; Cameselle J[3]; Schmitt FC[1]
[1]Institute of Pathology and Molecular Immunology of Porto University (IPATIMUP), Porto, Portugal; [2]Federal University of Bahia, Brazil; [3]General Hospital, Vigo, Spain

INTRODUCTION: P-cadherin is one of the Ca^{2+}-dependent cell-cell adhesion glycoproteins, that present a distinct adhesive specificity and distribution in human tissues. Recent studies showed that this molecule has an important role in many cellular events, including cell polarity, differentiation, growth and repair. In normal breast tissue, P-cadherin is expressed only in the membrane of myoepithelial cells, but its presence has also been reported in breast carcinomas, where it was associated with higher histological grade and proliferation. The aim of this work was to analyse the expression of P-cadherin in a series of 150 breast carcinomas and related it with expression of prognostic factors.
METHODS: P-cadherin expression was evaluated by immunohistochemistry using a specific monoclonal antibody. Only cells with membranous and/or cytoplasmic staining were scored as positive. For statistical analysis, contingency tables and chi-square tests were used, and two values were considered significantly different when $p<0.05$.
RESULTS: Positive P-cadherin expression in breast carcinomas showed a strong correlation with high histological grade (p=0.0011), high rate of proliferation (MIB-1) (p=0.0003), loss of estrogen receptors ($p<0.0001$), positive c-erbB-2 (p=0.0315) and p53 (p=0.0090) expression, and poor survival ($p=0.05$). No significative correlation was observed with the histological type, but the majority of positive P-cadherin tumours were invasive ductal carcinomas and medullar carcinomas. P-cadherin expression was independent of tumour size, lymph node metastasis and angiogenesis. CONCLUSIONS; P-cadherin expression is associated with more aggressive tumour parameters and survival, and seems a better indicator of clinical outcome than alterations in the expression of other cadherins.

P-557

Nm23 and vimentin expression in breast carcinoma: correlation with other clinicopathologic variables

Pestereli H.E, Erdogan O.*, Gulkesen K.H.**, Karaveli FS, Colak T.*, Akaydin M*
Akdeniz University, School of Medicine, Departments of Pathology, General Surgery* and Biostatistics**, Antalya, Turkey

Introduction: Nm23 is a putative metastasis suppressor gene in many malignancies including breast carcinoma. Vimentin is an intermediate filament, and co-expression with keratin in breast carcinomas is related to tumor invasion and metastasis.
Material-Method: We investigated the nm23 and vimentin expression in formalin fixed, paraffin embedded blocs of 98 breast carcinomas (68 invasive ductal, 17 invasive ductal+lobular, 2 invasive lobular, 4 mucinous, 2 apocrine, 2 intraductal, 2 papillary, 1 histiocytic) by using immunohistochemical method retrospectively and tried to find out their correlation with eachother and with known clinicopathologic findings (menopause, grade, stage, lymph node status, hormone receptors). Immunohistochemical results were assessed semiquantitatively. We also figured out their effect on disease free survival by Kaplan-Meier analysis. The follow-up time ranged between 12 and 160 months (mean 86 months).
Results: Nm23 expression was observed in 62 (63.3%) carcinomas where vimentin positivity was found in 21 (21.4%). Pearson chi-square and Spearman's correlation tests were used for statistical analysis. No association was seen neither between nm23 expression and other clinicopathologic parameters nor with vimentin immunopositivity. Vimentin immunopositivity was found significantly related to disease free survival (p=0.0049) as well as tumour diameter (0.0316) and lymph node positivity (p=0.0002).
Conclusion: We have concluded that vimentin immunopositivity affects disease free survival in breast carcinomas.

P-558

Diagnostic and prognostic markers in breast cancer (immunohistochemical trial)

S. Petrov, G. Moukhametshina, R. Minullina, N. Balatenko, F. Mazitova, R. Khasanov
Kazan Cancer Center, Kazan Medical University, Kazan, Russia

Material and methods: 288 patients with breast cancer were recruited between 1997 and 1999 into the trial. We have studied the expression of the estrogen and progesterone receptors, Ps2 antigen (connected with estrogen receptors), p53 gene-suppressor mutant protein, c-erb2 protein (HER2/neu oncogene product), as well as integrity of the blood vessels in tumors (antigenes CD31 and FVIII), myoepithelium (smooth muscle actin), basal membranes (collagen type IV), proliferation index (antigenes Ki-67, PCNA).
Results: The trial results have revealed that oncogene NEU was expressed in 40,6% of cases presumably among the young women independent on their histology. Reverse correlation was marked between the NEU expression and presence of the steroid hormones receptors. We have noted that tumor cells beyond the capsule of metastatic lymph nodes and cancer emboli in blood vessels are found in patients with the NEU positive status. Analysis of myoepithelium and basal membranes has allowed an objective evaluation of the lobular cancer in situ and microinvasive carcinomas.
The performed complex analysis of the breast cancer biomarkers makes possible to define the treatment modality taking into account the up-to-date clinical oncology requirements and to prognosticate the disease. Furthermore, during the study of the remote results in breast cancer we have found its more aggressive character in patients with the positive expression of the NEU. The early metastases were revealed in 28% of patients with the visceral and multiple metastases being the half of the cases. In patients with the negative expression of the NEU oncogene early metastases were found in 17% of patients with only 30% of them being visceral and multiple.

P-559

Practice and reliability of steroid hormone receptor immunohistochemistry in Austria

A. Reiner*, P. Regitnig**, H.P. Dinges***, G. Höfler**, S. Lax**, E. Müller-Holzner****, P. Obrist****, M. Rudas*****
Donauspital Wien*, Universität Graz**, Krankenhaus Klagenfurt***, Universität Innsbruck****, AKH Universität Wien****, Austria

Introduction: The aim of our study was to determine the practice and accuracy of steroid hormone receptor immunohistochemistry in austrian hospitals.
Methods: The trial consisted of two slide series. In the first series slides were stained for estrogen (ER) and progesterone (PgR) receptor in a reference laboratory and participants assessed them. In the second series participants were asked to stain and assess slides from the same cases.
Results: Participation rate was 97%. The results are given by kappa statistics. Slides stained by participants gave a moderate kappa when results were grouped (negative, weak, intermediate, high positivity; ER κ=0,53, PgR κ=0,47). Slides only assessed by participants showed a substantial kappa (ER κ=0,84, PgR κ=0,76). Most reliable results were achieved in highly positive and negative cases (ER-negative κ=0,95, ER-highly positive κ=0,75; PgR-negative κ=0,88, PgR-highly positive κ=0,87). Overall three different staining methods were used (manual, automated using Ventana, automated using Dako). Slightly better reproducibility was achieved with automated staining (manual ER κ=0,38, PgR κ=0,26; Ventana ER κ=0,42, PgR κ=0,36; Dako ER κ=0,45, PgR κ=0,31).
Conclusions: The participation rate in this trial was very high. Results are highly reliable regarding ER and PgR immunohistochemistry with respect to positivity or negativity. However variation occurs regarding the grade of positivity. Automated staining gives slightly better results.

P-560

Expression of angiotensin II type 1 receptor (AT1) in breast cancer

Resta L., Serio G.,* Marsigliante S., Vadrucci S., *Muscella A., Giardina C.
Department of Pathological Anatomy and Genetics, University of Bari, Italy; *Department of Biology, University of Lecce, Italy

The expression of Angiotensin II type 1 (AT1) receptor has been demonstrate in normal and neoplastic breast tissue and its correlation with the normal functions of the breast ducts has been verified. In this preliminary work we correlate the expression of AT1 in 29 invasive breast carcinomas and the common clinico-pathological findings in order to investigate the possible role of this receptor.
Two groups of 29 consecutive cases of breast cancer (group 1=15 cases and group 2=14 cases) with a low (<50% of positive neoplastic cells in group 1) and high (>50% of positive neoplastic cells in group 2) were compared with the following parameters: age, maximum tumor diameter, grading, nodal status, estrogen and progesterone receptors, proliferative index (Ki-67). The two groups show similar mean age (56,3 vs 59,3), maximum tumor diameter (cm 3,12 vs cm 2,9) and nodal status (8 vs 9 cases of nodal metastases). In the group of minimal AT1 expression positivity for ER and PgR was lower (respectively 6 and 8 cases in contrast to 11 e 12 cases of group 2). The proliferative index (Ki-67) was low in 4 patients of the group 1, whereas patients with low Ki-67 were 9 in the group 2. Our findings correlate the expression of AT1 in breast cancer with hormonal receptor status, as referred in other human neoplasms (endometrium and larynx) and with minor proliferative index of neoplastic cells.

P-561

Standardisation of immunohistochemistry for predictive and prognostic markers used in breast cancer

Rhodes A,[1] Jasani B,[2] Balaton AJ,[3] Miller KD.[1]
[1]Dept of Histopathology, UCL Medical School, London, UK; [2]University of Wales College of Medicine, UK; [3]Centre de Pathologie, Bievres, France

Introduction: Immunohistochemical assays for oestrogen receptors (ER), progesterone receptors (PR) and the HER-2/neu protein are unique in their role in the management of breast cancer. However, the results are interpreted semi-quantitatively and inappropriate assay sensitivity can affect their reliability. Multi-laboratory participation in External Quality Assessment (EQA) allows a laboratory to gauge its assay sensitivity against that achieved by a large number of other laboratories, some of which achieve optimal results using clinically validated methods. Subsequent analysis of methods associated with optimal results identifies parameters associated with reliable assays of appropriate sensitivity and thereby assists in their standardisation.
Methods: Over 100 European laboratories participating in EQA were sent sections of invasive breast carcinomas or cell lines, with differing levels of expression for hormonal receptors and HER-2/neu protein, respectively. Participants immuno-stained the slides and in house tumours for ER, PR and HER-2/neu and returned them for independent assessment of the sensitivity of the assays along with data on the antibodies and methods employed.
Results: Reliable ER and PR assays were found in 36% of laboratories participating in continual EQA over a 2-year period, including the majority of centres known to have clinically validated results. Inadequate assay sensitivity was the main cause of poor results for ER and PR by laboratories using microwave antigen retrieval, with too short a heating time identified as the principal contributory factor (1). The assessment run for HER-2/neu assisted in the validation of a new cell line control as a valuable standard against which assay sensitivity can be monitored, regardless of the antibody employed.
Conclusions: Multi-laboratory participation in EQA is an effective means by which to identify and ameliorate parameters influencing the reliability of assays for predictive and prognostic markers and thereby assists in their standardisation.
Reference: 1. Rhodes A, Jasani B, Balaton, et al. Study of interlaboratory reliability and reproducibility of estrogen and progesterone receptor assays in Europe. *Am J Clin Pathol* 2001; **115**:44–58

P-562

C-erbB2 oncoprotein and survival in breast cancer

Anca Rosianu[1], N. Tudose[1], Marioara Cornianu[1], Victor Dabelea[2], Liliana Vasile[1]
[1]Department of Pathology; [2]Clinic of Oncological Surgery, University of Medicine, Pharmacy Timisoara, Romania

Summary
Background: For this study we selected 56 patients with breast cancer with age ranging essays between 37 and 73 years during 1993–1994
Methods: Immunohistochemical determination of c-erbB2 oncoprotein was performed using the antibody DAKO-cerbB2 on tissue

samples 10% formalin fixed and paraffin embedded. For evaluation of immunostaing we considered the membrane staining of the cells; 18 (32,1%) of tumors overexpressed the c-erbB2 protein (3+ intensity of staining).
The c-erbB2 positivity was more frequent in G1 carcinomas comparative to carcinomas with G2 and G3 differentiation degrees (34,8% comparative to 25% and 23,1%). There was no correlation between c-erbB2 expression and axillary nodes invasion (6 from 26 patients with nodal positivity was c-erbB2 over expressed).
In our study we found a correlation between the size of the tumor and c-erbB2 protein: 16,7% from the tumors lees than 2 cm, 29% for the tumors between ranging 2–5 cm and 37,5% for the tumors over 5 cm in diameter.
Conclusion: The 5 years survival rates was significantly lower for the patients with tumors c-erbB2 (3+) compared to patients with c-erbB2 (1+) or c-erbB2 2+ ($p<0.001$).

P-563

Pathogenesis of Paget's disease: Epidermal heregulin-a, motility factor, and the HER receptor family

Vera R.J. Schelfhout, Elisabeth D. Coene, Bernard Delaey, Sofie Thys, David L. Page, Christian R. De Potter
Dept. of Pathology, University Hospital, Gent, Belgium

Introduction: In Paget's disease of the breast, the epidermis of the nipple is infiltrated by large neoplastic cells of glandular origin. It has been hypothesized that the spread of Paget cells through the nipple epidermis is induced by a motility factor that acts via the HER2/NEU receptor. To test this hypothesis, we characterized and purified a motility factor released by keratinocytes and identified its target receptors in specimens from patients with Paget's disease and in SK-BR-3 breast adenocarcinoma cells, which overexpress HER2/NEU.
Results: We isolated the motility factor from keratinocyte-conditioned medium and sequenced tryptic peptides. These sequences were used to identify the motility factor as heregulin-a, which is released by skin keratinocytes. Heregulin-a induces spreading, motility, and chemotaxis of SK-BR-3 cells, as does motility factor. Motility factor activities of heregulin-a are inhibited by monoclonal antibody AB2, directed against the extracellular domain of HER2/NEU, which blocks the binding of heregulin-a. We used in situ hybridization to show that normal epidermal cells produce heregulin-a mRNA and that heregulin receptors, HER3 and/or HER4, as well as their coreceptor HER2/NEU, are expressed by Paget cells.
Conclusions: Heregulin-a is a motility factor that is produced and released by normal epidermal keratinocytes and thus plays a key role in the pathogenesis of Paget's disease. Paget cells express heregulin receptors HER2/NEU, as well as HER3 and/or HER4, both of which function as a co-receptor of HER2/NEU. Binding of heregulin-a to the receptor complex on Paget cells results in the chemotaxis of these breast cancer cells, which eventually migrate into the overlying nipple epidermis.
V.R.J. Schelfhout et al. JNCI, 92, 622–628, 2000

P-564

Incidence of local recurrence of breast cancer depending on the pathologist after breast conserving therapy

J. Theuerl, H. Guski2, K.-J. Winzerl
1Klinik für Allgemein-, Visceral-, Gefäß- und Thoraxchirurgie und 2Institut für Pathologie, Universitätsklinikum Charité, Humboldt-Universität zu Berlin, Germany

Introduction: Although the principles of the resection technique in breast cancer surgery are established, the influence of diagnostic pathology using frozen section technique on the incidence of local recurrence after breast conserving therapy is unknown.
Material and methods: 578 patients with tumor stage I or II operated between 1984 and 1997 received lumpectomy combined with additional radiation (66.4%), application of tamoxifen (29.5%) or chemotherapy (13.5%), respectively. The adjuvant standardized treatment could not be applicated in all cases. Histologically, in 74.8% of the patients an invasive ductal carcinoma, in 6.4% an invasive lobular carcinoma and in 9.5% a DCIS was found. A subgroup of patients with DCIS refused mastectomy despite of the contraindication for breast conserving therapy because of an extensive intraductal component. The treatment for all DCIS cases was lumpectomy alone without radiation.
Results: The local recurrence rate for the DCIS group was 30.9%. The total local recurrence rate for all cases was 11.7% (n=69). The average postoperative observation time was 51.4 months. The average time to local recurrence was 36.5 months. Pathologists were divided into two groups: 22 pathologists with long time experience analyzed 452 cases while 11 pathologists with less experience examined 126 cases of breast cancer. Both groups used the same standardized technique of diagnostic pathology. Statistically, no correlation was found between the two groups of pathologists and the local recurrence rate ($p=0.59$).
Conclusion: Standardization of macroscopical and histological examination in intraoperative frozen section technique is essential for conserving breast cancer surgery. It seems to be possible that no differences between the two groups of pathologists were found because of the unsufficient number of patients.

P-565

Expression of HER2 and steroid receptors in comparison with proliferation index in breast carcinoma

T. Tuziak, W.P. Olszewski, W.T. Olszewski
Department of Pathology, Center of Oncolgy, Warsaw

Comparison of proliferation indexes of breast cancer cells in relation to expression of HER2 and steroid receptors was the main aim of our work.
Study was based on a group of 89 cases of infiltrating ductal breast carcinoma. According to histological grade (Bloom and Richardson) there were 12 cases (13%) of G1 cancers, 38 cases (43%) of G2 cancers, 39 cases (44%) of G3 cancers.
Immunohistochemical evaluation of estrogen receptor ER, progesteron receptor PGR, HER2 receptor and antigen MIB1 was performed on slides from paraffin embedded tissues. Semi-quatitative method was used to evaluated strength of the stains. Steroid receptors staines (ER positive, PGR positive or both positive stained nuclei) were found in 64% of cases. HER2 receptor was positive in

50% of cases. Proliferation index were low (<1% of nuclei) in 24% of cases, intermediate (>1% and <10% of nuclei) and high in 57% of cases.
Depending on expression of steroid receptors and HER2 receptor in all material, 4 groups of tumors were found (15 to 29 cases for one group). Those groups were subdivided according to mitotic index.
The highest precentage (80%) of high proliferative index cases were among steroid negative and HER2 positive cancers.
The highest precentage (31%) of low proliferative index cases were among steroid positive and HER2 positive cancers.

P-566

HER2/neu and angiogenic factors in breast carcinoma

Vogl G., Dandachi N., Bartel H., Doppelmayr H., Dietze O., Hauser-Kronberger C.
Institute of Pathology, Landeskliniken and University of Salzburg, Austria

INTRODUCTION: Solid tumours up to a size of 2 mm diameters are able to obtain the necessary oxygen and nutrient supplies needed for growth and survival by simple passive diffusion. However, every subsequent increase in tumour mass must be preceded by the proliferation of new capillary blood vessels. As a result autocrine stimulation of tumour cells becomes necessary and angiogenic factors like vascular endothelial growth factor (VEGF), platelet derived–endothelial cell growth factor/thymidine phosphorylase (PD-ECGF/TP) and other angiogenic factors are released. The antibody Herceptin™ blocks to extracellular binding domain of the HER2 receptor. Therefore, the aim of the present study was to investigate the effect of Herceptin™ treatment on the regulation of vascular growth factors.
METHODS: Paraffin-embedded specimens from 160 invasive ductal and lobular breast cancer have been tested immunohistochemically for the presence of HER2, HER1/EGF-R, VEGF and PD-ECGF/TP. Human breast cancer cells containing 13 copies of HER2/neu gene (BT474) have been treated with Herceptin™ (50 µg/ml for 72 h). After blocking of HER2-receptor with Herceptin™ the expression of VEGF and PD-ECGF/TP was studied using immunofluorescence techniques.
RESULTS: In human breast cancer tissue VEGF-expression correlated with high grade invasive ductal carcinomas. HER2/neu status was not significantly correlated with VEGF-, PD-ECGF- and EGF-R-protein expression. However, preliminary results of the cell culture experiments indicate a down-regulation of VEGF after HerceptinTM treatment.
CONCLUSIONS: Tumour angiogenesis in invasive breast cancer regulated via HER2 pathway might be of potential and therapeutic value.

P-567

Value of cytokeratin 5/6 immunostaining using D5/16B4 antibody in the spectrum of proliferative epithelial lesions in situ of the breast. A comparative study with 34βE12

Voigt J.J., Istier L., Mery E., Rochaix P.
Department of Pathology, Institut Claudius Regaud, Toulouse, France

Introduction: Previous studies have shown the interest of basal-type cytokeratin (CK) immunoprofile to distinguish between ductal hyperplasia (DH) and the spectrum of atypical ductal hyperplasia (ADH), ductal carcinoma in situ (DCIS) and lobular carcinoma in situ (LCIS). However, the practical value of D5/16B4 immunostaining versus 34βE12 has never been investigated.
Methods: Immunostaining of CK5/6 and CK1/5/10/14 was performed, using respec-tively D5/16B4 and 34βE12 antibodies on serial sections of 100 breast specimens. Lesions included DH (n=31), ADH (n=5), DCIS (n=54) and LCIS (n=10). The percentage of positive cells was evaluated using a four point score: 1+=0–25%; 2+=26–50%; 3+=51–75%; 4+=76–100%.
Results: Staining of most of the cells (3+ or 4+) was observed in all the 31 cases of DH using both antibodies. None of the ADH had 3+ or 4+ staining by D5/16B4, with a score 1+ in 4/5 cases. Scores with 34βE12 were 1+ in 3, 2+ in 1, 3+ in 1/5 cases. Using D5/16B4, none of the DCIS had a 3+ or 4+ score, with a 1+ score in 52/54 cases. Using 34βE12, 13/54 of the DCIS showed 3+ or 4+ labeled cells. All the 10 cases of LCIS showed D5/16B4 1+ positive cells whereas 34βE12 was scored 3+ in 2/10 cases and 4+ in 6/10 cases.
Conclusion: Anti-CK5/6 antibody D5/16B4 is useful to distinguish these immuno-profiled proliferative lesions in situ of the breast. This antibody appears more valuable in the differential diagnosis between DH and atypical- malignant lesions than the anti-CK1/5/10/14 antibody 34βE12.

P-568

Myoepithelial carcinoma of the breast arising in adenomyoepithelioma. A case report

Yashar G., Basheska N., Ivkovski Lj., Kubelka K., Zografski G.
Department of Histopathology and Clinical Cytology, Institute of Radiotherapy and Oncology, Medical Faculty, Skopje, Macedonia

Introduction: Adenomyoepithelioma (AME), and especially myoepithelial carcinoma (MC), the malignant variant of this tumor, is a rare breast neoplasm. This report comprises the pathological features of a breast MC arising in AME with an aggressive clinical course.
Case report: A 48-year old woman with a palpable mass in the right breast was admitted in November 1998. A month later following FNAB, surgical excision was performed. During the follow-up period of 17 months, until the patient's death, two local recurrences developed. Despite the aggressive chemotherapy, administrated after the first recurrence, subsequently bone, pulmonary and brain metastases appeared.
Results: The primary tumor was an ovoid, white-gray, encapsulated mass measuring 4×3.5×1.5 cm. Microscopically, this biphasic tumor was composed of rare tubules surrounded by interlacing bundles of spindle cells exhibiting mild atypia. It was initially classified as a benign phyllodes tumor. The immunohistochemical analyses performed after the second recurrence proved the myoepithelial origin of the neoplasm (S-100, cytokeratin and alpha-SMA positive cells), with a high mitotic index (11 MF/10 HPF), and an immunophenotype indicating aggressive biological potential (steroid receptor negative, 50% Ki-67 and 30% p53 positive cells). Therefore, it was reclassified as MC arising in spindle cell type of AME.
Conclusion: The histopathological diagnosis of AME could be very difficult, especially when a distinction from other spindle cell

breast neoplasms must be done. Immunohistochemistry is essential to confirm the diagnosis, having in mind the reported pathological characteristics and the immunohistochemical profile of recurrent and malignant tumors of this type.
Hepatopathology

P-569

Expression of MET-protein and of the EDB isoform of fibronectin in chronic HVC hepatitis.

Maria Addesso*, Anna Pasquini°, Emanuela Pilozzi°, Giorgio Antonucci* and Luigi P. Ruco*
*IRCCS "L. Spallanzani" and University "La Sapienza" Rome, Italy

Introduction: The c-MET proto-oncogene encodes a 190-kd transmembrane tyrosine kinase. This molecule is the receptor for the hepatocyte growth factor (HGF) which is a potent mitogen for hepatocytes in vivo as well in vitro. Serum levels of HGF vary in liver diseases, reflecting liver damage and dysfunction. Fibronectin is a major constituent of extracellular matrix and participates in adhesion processes and functions as substrate for cell migration, particularly during embryogenesis and wound healing. EDB is one of the cellular isoforms originated from alternative splicing patterns of the primary transcript of a single gene. EDB is absent in normal adult tissue, but is highly expressed in fetal and tumour tissue.
Methods: To clarify the potential clinical significance of c-met protein and EDB in HCV hepatitis, we have investigated their expression by immunohistochemistry in frozen sections of 38 liver biopsies, using DO-24 (Met protein) and BC-1 (ED-B) monoclonal antibody. The histology, activity and fibrosis were scored using the METAVIR system.
Results: The anti c-Met showed a typical membrane staining in all cases, and the signal was much stronger in biopsies with more elevated activity and/or fibrosis. The immunostaining for EDB was detected in sinusoids and in portal tracts. In these latter, EDB was correlated with the extent of fibrosis. In sinusoids, a positive correlation was noted between Met-protein staining of the hepatocytes and EDB expression in the basement membranes ($p<0,001$; R: 0,863).
Conclusions: Our findings suggest that expression of Met protein and EDB are upregulated during HCV-induced inflammation, and that EDB may represent an early marker of liver fibrosis.

P-570

Expression of schistosomiasis mansoni antigen could confirm the frequent coexitance of hepatic schistosomiasis with chronic hepatitis C. An immunohistochemical study including assessement of ICAM-1 and collagen IV among those cases in comparison to pure hepatic schistosomiasis

Akl M.M.*, Hamam OA*, El-Baz H.G.**, El-Demerdash Z.**, Ibrahim H.A.***
Pahology Department*,Immunology Department**of Theodor Bilharz Research

Institute; Tropical Medicine Research Institute***, Cairo, Egypt

Diagnosis of hepatic schistosomiasis (HS) in liver needle biopsies is sometimes difficult without the accidental detection of a schistosomal periovular granuloma, and especially when associated with chronic viral hepatitis.The purpose of the present study is to verify or confirm the coexistence of hepatic schistosomiasis in some cases of chronic hepatitis C, in liver needle biopsies when suspected in pathological diagnosis.to be treated as mixed lesions of viral and parasitic pathogenesis and to evaluate the role of both; the soluble intercellular adhesion molecule (sICAM-1 as expressed in hepatic tissue in relation to its serological levels and the expressed interstitial collagen IV, in relation to the severity of the disease as correlated with the different grades of chronic inflammation and stages of fibrosis in the examined livers. The material for this study comprised 36 patients suffering from chronic liver disease, diagnosed and classified as 31 (86%) cases of chronic hepatitis C (CHCof which 21 (about 58% of total) were proved mixed hepatic lesions (MH); and 5 (about 14%) cases as pure hepatic schistosomiasis, beside 4 control cases. Serological markers for HCV were performed for all the patients as well as serological levels for ICAM-I and for the schistosoma mansoni antigen (SMA). Liver needle biosy specimens were obtained from all patients and processed for the histopathological assessement of the hepatic lesions including grading & staging of the disease according to Desmet et al. (1994). Unstained sections were immunohistochemically treated for the expression of (SMA), sICAM-1 and the interstitial collagen IV within the hepatic tissue . Expression of SMA was strongly positive in all cases diagnosed as pure HS and was significantly positive in 10 (47.6%) of the examined CHC cases confirming the coexistence of HS in 5 (about 24%) of them which was only suggested. SMA expression was negative in all cases of CHC; 11 (52.4%) .It was maily localized within sinusoidal cells (kupffer & endothelial cells), diffused within hepatocytic cytoplasm and in macrophages in portal areas. sICAM was more significantly strongly positive in cases of CHC of grades II and III inflammation and stages II & III fibrosis as well as in hepatic schistosomiasis, stages II & III portal fibrosis more than in cases with established cirrhosis or with advanced schistosomal fibrotic stage. sICAM was mainly detected within sinusoidal cells, hepaocytes, focal areas of hepatic necrosis and within mononuclear inflammatory cells. There was a high significant correlation ($p<0.001$) between serum levels of sICAM-1 and the grades of inflammation in the groups of CHC & MH without cirrhosis. Collagen IV expression was strongly positive at periphery of schistosomal granulomas whenever detected and increased progressively with the increased stage of the disease in all the examined groups slightly more increased with the advanced schistosomal infection,wether pure or mixed and mainly found located in stroma of portal areas and fibrous septae ,in walls of blood vessels and basement membranes of bile ductules and along perisinusoidal walls. We concluded that we can use the immunohistochemical detection of schistosomal antigen to confirm the diagnosis of hepatic shistosomiasis in needle liver biopsies whenever in question. sICAM -1 and collagen IV can be used for monitoring the disease activity.

P-571

Changes of hepatic sinusoidal wall structure in chronic viral hepatitis: An electron microscopic and immunohistochemical study

Bahrom Aliev, Shabat Hodjaev
Institute of Virology, Tashkent, Uzbekistan

Change of the hepatic sinusoid is one of the principle manifestsations of chronic hepatitis. However, its structure in chronic viral

hepatitis has not been well defined. In present work we studied sinusoidal wall structure in chronic B and D hepatitis using histological,histochemical and electron
microscopic methods. Biopsy liver specimens of the patients with chronic hepatitis B (20 cases) and chronic hepatitis D (15 cases) for electron microscopy were fixed in 2,5% glutaraldehyde, postfixed with 1% OsO4 and embedded in Epon. For immunofluorescent examination liver biopsies were frozen in liquid nitrogen. In the serial cryostat sections distribution of the main extracellular matrix components: types I, III, IV, V collagen, fibronectin and laminin were detected. Electron microscopic study revealed besement membrane formation around the hepatic sinusoids and perisinusoidal fibrosis in chronic viral hepatitis. Immunohistochemical increasing amount of interstitial collagen and collagen types IV, V and fibronectin in the sinusoidal wall was detected Besides, we visualized the presence laminin – one of the basic components of the basement membrane around the sinusoids. Continuous linear deposition of type IV collagen and laminin clearly underlined enlarged sinusoidal borders. In several cases of chronic hepatitis D the changes described above were more aggressive.Our results collectively demonstrate the importance of electron microscopy and immunohistochemistry in the diagnostics of sinusoidal capillarization and perisinusoidal fibrosis.

P-572

Mast cells and liver sinusoidal capillarization

B. Barbieri[1,2], F. Grizzi[1,2], P. Colombo[3], B. Franceschini[1,2], M. Roncalli[3], N. Dioguardi[1,2]
[1]Scientific Direction and [3]Department of Pathology, Istituto Clinico Humanitas, Rozzano, Milan, Italy; [2]Fondazione Michele Rodriguez, Istituto Scientifico per le Misure Quantitative in Medicina, Milan, Italy

Introduction: Mast cells (MCs) are important effector cells providing cytoplasmic granules, cytokines and growth factors in inflammatory diseases. Although several studies have associated MCs hyperplasia with fibrosis development during chronic liver diseases, the mechanisms involved in the increase of the MCs density during liver neoplasies have still to be established.
Methods: We report two cases of 73-years-old and 72-years-old men, respectively case 1 and case 2, who presented a well differentiated trabecular primary hepatocellular carcinoma. Two serial sections of three-μm thick for each specimen were stained one with the basic dye Toluidine Blue, which metachromatically stains the glycosaminoglycans of MCs granules, and the other with Sirius Red to identify the extracellular matrix collagen.
Results: Histological examination demonstrated in both cases no foci of necrosis whereas diffuse intra- and perilesional vascular invasion in case 1. We observe in case 1 an high density of MCs both at periphery and in tumoral tissue and contemporarely strongly sinusoidal "capillarization", while in case 2 no MCs were recognized and simultaneously the absence of development of a basal lamina and defenestration of sinusoidal endothelial cells was observed.
Conclusion: The microscopical examination of both cases suggest a pivotal role of MCs in the development of extracellular matrix collagen. In addition, since capillarization proceeds concurrently with arterial blood supply during hepatocarcinogenesis, MCs may be considered as a key element in the process of transition from sinusoidal endothelial cells into capillary-type endothelial cells. Moreover, these data confirm that arterialization might be one of the biological events which induce sinusoidal capillarization in the development of hepatocellular carcinoma and its metastasis.

P-573

Computer morphometry for quantitative measurement of hepatic lesions in response to antituberculous-mediated hepatotoxicity

[1]Dorelia Calin, [1]L.L. Francu, [2]Anca Ciobanu, [3]Irina Chiselita
Departments of [1]Anatomy, [2]Infectious Disease and [3]Pneumology, University of Medicine, Iasi, Romania

Introduction: It is demonstrated organ damage after long-term administration of some drugs. Objectives of this study were to quantify liver microscopic change in-patients with chronic antibuberculous therapy.
Material and methods: We studied fourty-nine autopsies of patients who died of tuberculosis and presented liver lesions. A personal computer with a digital interactive system and a microscope equipped with a computer-controlled slide-driver was used for morphometry. The characteristics of the liver components were assessed on slides stained by Haematoxylin and Eosin, periodic acid-Schiff and Szekely's trichrome. Of these patients, 20.41% had granulovacuolar degeneration, 14.28 % had chronic aggressive hepatitis, and 24.45 had cirrhosis. Conventional description reports were obtained from reviews of patient charts.
Results. A significant correlation was observed between the area of fibrosis (the ratio of the area of fibrosis to that of the entire tissue specimen) and drug association. The results from computer morphometry were highly correlated with antituberculous treatment (duration, drug association, and alcohol abuse and hepatoprotector therapy).
Conclusions: Our computerized morphometry system is a reliable tool for the evaluation of the severity of liver changes and can be used as a tool for the objective quantification of hepatotoxicity.

P-574

Unilocular serous cystadenoma of the pancreas. Clinicopathologic and immunohistochemical study of 8 cases

Denis Chatelain (1), Pascal Hammel (2), Dermot O'toole (2), Benoît Terris (3), Valérie Vilgrain (4), Laurent Palazzo (2), Jacques Belghiti (2), Phillipe Levy (2), Philippe Ruszniewski (2), Jean-François Flejou (1)
(1) Service d'Anatomie Pathologique, Hôpital Saint-Antoine, Paris; (2) Fédération Médico-Chirurgicale d'Hépato-Gastro-entérologie, (3) Service d'Anatomie Pathologique, (4) Service de Radiologie, Hôpital Beaujon, Clichy, France

Among cystic lesions of the pancreas, unilocular large cysts raise difficult diagnostic issues. We aimed to describe morphological characteristics and cyst fluid analysis in a series of macrocystic unilocular serous cystadenomas of the pancreas.
Patients and methods: Eight patients underwent pancreatic resection for a unilocular cystic lesion of the pancreas that proved to be unilocular serous cystadenoma on examination of the surgical specimen. Endoscopic ultrasonography (EUS) and pre-operative fine-needle aspiration were performed in 7 patients. Immunohistochem-

ical analysis of the surgical specimen with antibodies to carcinoembryonic-antigen (CEA), CA19-9, estrogen receptor (ER) and progesterone receptor (PR) was performed in all cases.
Results: Patients included seven women and one man with a mean age of 48 years. Lesions were incidentally discovered on ultrasonography in six patients and had a mean size of 3 cm (range: 1.5 to 5 cm). EUS revealed millimetric cysts in the wall of the main cyst in three cases. In the seven aspirated cysts, cytological analysis was non contributive but biochemical analysis showed low levels of CEA (<5ng/ml) and CA72.4 (<40U/ml) in all but two. At histology cysts were lined by a clear cuboidal epithelium focally expressing CA19-9, negative for anti-CEA, anti-ER and anti-PR antibodies. In five cases microscopic cysts were demonstrated in the wall of the lesion.
Conclusion: Unilocular macrocystic serous cystadenomas appear as a particular form of serous microcystic cytadenoma. EUS may be useful in detecting peripherally located millimetric cysts in unilocular lesions. Low levels of enzymes and tumour markers on cyst fluid analysis support the diagnosis and may avoid surgical resection in asymptomatic patients.

P-575

The expression of cytokeratin 7 and cytokeratin 20 is correlated with the progression of dysplasia in papillary intra-ductal mucinous tumours of the pancreas

Couvelard A (1), Handra-Luca A (1), Terris B (1), Fléjou J-F (2), Degott C (1)
Department of Pathology, (1) Beaujon Hospital, Clichy, (2) Saint-Antoine Hospital, Paris, France

The aim of this study was to investigate the immunohistochemical expression of cytokeratin (CK)7 and CK20 in papillary intra-ductal mucinous tumours of the pancreas (PIMT) with different grade of dysplasia.
Methods: Immunohistochemical expression of CK7 and CK20 was studied in 20 cases of PIMT (adenoma-non dysplastic hyperplasia: 8 cases, borderline-moderate dysplasia: 7 cases, *in situ* carcinoma-severe dysplasia: 5 cases) and in the normal pancreas taken at distance of the tumours. Cytokeratin expression was scored semi-quantitavely: the score corresponding to the sum of staining intensity (0=no, 1=weak, 2=strong) for each 25% of the tumour cells, can be comprised between 0 and 8.
Results: Cytokeratin 7 was strongly and diffusely expressed by the normal duct system and in all cases of PIMT-adenoma (mean score 6,75). Its expression was moderate in PIMT-borderline (mean score 5) and weak in PIMT-*in situ* carcinoma (mean score 2,6).
Cytokeratin 20 was negative in the normal duct system and in PIMT-adenoma (mean score 0). In contrast, it was expressed in PIMT-borderline (mean score 3) and PIMT-in situ (mean score 2,6)
Conclusion: PIMT-adenoma and normal ducts have identical CK7+/CK20- immunophenotype.
The CK7/CK20 phenotype varies with the progression of dysplasia in PIMT, consisting in the acquisition of CK20 and in the decreasing of CK7 in borderline tumors and *in situ* carcinoma.

P-576

Detection of HCV-RNA by RT-PCR in formalin-fixed and paraffin embedded needle biopsies (NB) in liver transplant recipients

D'Amico M°, Cannone M°,Minola E*, Alberti A*, Belli L*, Barberis M°
° Dept of Pathology and Laboratory Medicine, Multimedica and Liver Transplant Unit, Ospedale Niguarda Ca'Granda, Milan, Italy

We used and compared 2 different methods of HCV-RNA extraction from NB of liver transplant recipients. 18 NB were obtained from 12 patients with histologically and serologically RT-PCR-confirmed HCV re-infection and from 6 patients without evidence of re-infection. 2 series (A and B) of unstained sections were obtained from the NB blocks. In the A series, RNA was extracted from sections previously dewaxed in xylene by a digestion buffer containing 400 µg/ml of proteinase K. In the B series, RNA was directly extracted from paraffin sections with TRIzol reagent in tubes incubated at 65°C to melt the paraffin. Primers were used to amplify the 5'non codifying region of the HCV-RNA genome. Positive controls consisted in sections obtained from blocks of liver explanted for HCV-related end-stage cirrhosis. Paraffin-embedded foetal tissues obtained from spontaneous abortions were used as negative controls.
Results: HCV-RNA was detected in 7 cases (38.8%) of the A group and in 12 cases (66.6%5) of the B group. All the NB from the 6 patients without re-infection were negative for HCV-RNA and the patients do not show evidence of recurrence 36 months after the biopsy. All the NB from the re-infected patients were positive. There were no false positive results. In conclusion ous study confirms that paraffin embedded liver tissue is appropriate for further molecular studies. In our hands, the technique based on the association of heath and TRIzol gave better results than the association of xylene with proteinase K.

P-577

Chronic hepatitis C and apoptosis in hemophilia patients with HCV/HIV co-infection

J. Delladetsima[1], O. Katsarou[2], S. Vgenopoulou[1], P. Touloumi[3], A. Hatzakis[3], A. Karafoulidou[2]
[1]Pathology Dept., [2]2nd Reg. B.T.C. – Comprehensive Haemophilia Care Center, Laiko General Hospital of Athens, [3]Dept. of Hygiene and Epidemiology, Athens University Medical School

Aim of this study was the correlation of apoptosis of the hepatocytes, histological activity index (HAI) and stage of chronic hepatitis (CH) with CD4 cell count in the peripheral blood and liver tissue as well as with HCV and HIV viremia levels in 21 hemophiliacs with HCV/HIV co-infection. CD4 lymphocytes in liver biopsies were assessed immunohistochemically and evaluated semiquantitatively and in relation to the total T cell population. DNA fragmentation was detected by TUNEL assay in 15 cases and was registered numerically per 10 high power fields. Peripheral CD4 were >200/µl in 7 (30%), 50–200/µl in 11 (48%) and <50/µl in 5 (22%) pts. CHC was minimal in 5 (24%), mild in 9 (43%) and moderate in 7 (33%) patients, while hepatitis stage was 0–2 in 7 (33%), 3-4 in 8 (38%) and 5–6 in 6 (29%) cases (Ishak et al. 1995). DNA fragmentation was observed in 0–1 hepatocytes in 8 (53%),

2–4 in 4 (27%) and in ≥5 in 3 (20%) cases. Statistically significant correlation was found between low CD4 count in the peripheral blood and liver tissue and minimal CH (P=0.003), as well as between high CD4 count and mild/moderate CH (P=0.012). There was no association of hepatitis activity with viremia levels. Apoptosis was significantly correlated with HCV RNA load (P=0.013), but did not show any association with hepatitis HAI or with CD4 count.

Conclusions: HCV/HIV co-infection seems to aggravate hepatitis course in the phase of immunocompetence suggesting an immune mediated process. There are strong indications of a direct pathogenetic relationship of high HCV load with apoptotic cell death.

P-578

Activated stellate cells in chronic hepatitis C(CHC): An immunochistocemical study

M. Demonakou, A. Kontogianni, D. Presvelos, A. Margariti, N. Tamvakis, C. Barbatis
Departments of Pathology, Sismanoglion GH, HRC "Korgialenion-Benakion", Athens, Greece

In CHC age and fibrosis are the main prognostic factors.The Activated Stellate Cells(ASCs) are the major source of extracellular matrix.

The presence and distribution of ASCs was correlated with the histological grade and stage of the disease in 60 untreated patients. ASCs were identified as α-SMA positive cells ,using Streptavidin-HRP techinque. A semiquantitive method was used to assess the presence of ASCs within the hepatic lobule and the portal tract and a score 0-3 were given. The mean values were correlate with the grade and stage of CHC(Ishak 1997) by t-test.The stage and grade of the CHC were: stage 0:13 (21%), 1&2:25 (42%), 3&4:11 (18.5%), 5&6:11 (18.5%). Grade: 0–3:12 (20%), 4–8:45 (75%), 9-12:3 (5%).

Mean Values were: stage 0:0.9, stage 1&2:2.1, stage 3&4:3.5, stage 5&6:4.3 grade 0–3:2.3, grade 4–8:2.5, grade 9–12:4.

Strong association was found between the density of ASCs and the stage ($p<0.005$) and grade ($p<0.005$). A different pattern was observed in cirrhosis where myofibroblastic activity was intense in the fibrous septa ($p<0.005$).

CONCLUSIONS: ASCs are increase in the lobule and portal tract in CHC and this phenomenon is associated with the necroinflammatory activity and fibrosis.

P-579

Carcinoma of the gallbladder; incidence and histopathologic features

Gokhan Ersoy*; MD, Nail Gungor**; MD, Gulen Dogusoy*; MD, Suha Goksel*; MD, Sibel Erdamar; MD, Selda Gocener; PhD*
* Cerrahpasa Medical Faculty, Department of Pathology,
** Istinye State Hospital, Department of Pathology, Istanbul, Turkey

The carcinoma of gallbladder is a rare and aggressive tumour of human body. We estimated the incidence of carcinomas in all surgically removed gallbladders which were examined in department of pathology of Cerrahpasa medical faculty from January 1987 to January 2000.

We've analyzed 6478 gallbladders and found 83 carcinomas among them. In the carcinoma cases, median age was 64 and male /female ratio was 2,2/1. 68 of the tumours were classical adenocarcinomas and there were 4 mucinous, 2 signet ring cell, 3 papillary and 3 undifferantiated carcinomas – which one of this is pleomorfic carcinoma, 1 adenosquamous, 1 squamous, 1 mixed neuroendocrin – exocrin carcinoma. The ratio of classical adenocarcinomas in all gallbladder carcinomas is 83% and the second most frequent tumour is mucinous carcinoma.

In conclusion, frequency of primary carcinoma among gall bladder resection materials is 1,2% in our series and our findings about gall bladder carcinoma exhibit similar results with other previously published series.

P-580

"Oval" cell activation in alcoholic and nonalcoholic steatohepatitis

Fotiadu A., Tzioufa V., Hytiroglou P.,Vrettou E., Koufogiannis D., Papadimitriou C.S.
Departments of Pathology and Medical Physics, Medical School of the Aristotle University of Thessaloniki, Greece

We investigated whether there is activation of "oval" cells in patients with alcoholic or nonalcoholic steatohe-patitis by evaluating possible correlations of their numbers with histologic features.

Thirty-one liver biopsy specimens were assessed by histochemical stains and by immunostains for cytokeratins 7, 8, 18, 19 and "hepatocyte specific antigen" (HepPar1). Oval cells were detected on the basis of morphological and immunohistochemical criteria.Oval cell counting was performed on sections stained for cytokeratin 7. Fibrosis was classified in 4 stages ranging from I (mild fibrosis) to IV (cirrhosis).

Oval cells were identified in all cases evaluated. The number of oval cells increased in parallel to the degree of fibrosis (stage of disease). This correlation was statistically significant($p<0.001$).In conclusion, oval cell activation does occur in alcoholic and nonalcoholic steatohepatitis, and appears to increase with disease progression.

P-581

TGF beta content analysis in liver biopsies of chronic hepatitis type C patients depending on fibrosis stage and progress pace

Gabriel A.,*Ziółkowski A., Dziambor A.,** Radłowski P., * Matysiakiewicz J.*
*Chair and Department of Pathomorhology, Silesian Medical Academy in Zabrze; ** Clinical Department of Contagious Diseases, Silesian Medical Academy in Bytom, Poland

Aim: TGF beta evaluation in lobes (LB) and portal spaces (PS) depending on the pace of fibrotic progress and its stage. The study included 21 advanced fibrosis patients, who had developed hepatitis type C less than five years before (group I), while group II consisted of 11 patients, who had been more than 5 years. The control group was formed from 17 patients who were diagnosed as having normal or portal fibrosis. Immunohistochemical analysis was caried out with ABC method and monoclonal antibody TGF beta (Novocastra). Inflammatory activity and fibrosis in biopsies were evaluated according to Scheuer's scoring system.

Results: TGF beta LB expression in group I amounted to 2.23%, 3.1% in group II and 0.75% in the control group. PS respective values were: 2.42%, 1.21% and 0.79%. Mean TGF beta values at the stage of septal fibrosis in fast fibrotic progress patients were: 3.4% in PS and 4.5% in LB. As regards slow fibrotic progress and equivalent stage group the values equalled 1.63 and 3.79 respectively. TGF beta content was low in cirrhotic biopsies and in both groups – ranged from 0.49 to 0.81 in PS while 1.25% to 1.68% in LB. The control group yielded low LB and PS TGF beta values. TGF beta PS value was higher in the fast fibrosis group and tended to rise with the degree of inflammatory activity (from 3.15 to 3.8 in group I, and from 0.85 to 1.6 in group II) with the exception of high inflammatory activity, where the TGF beta value was low (group I – 1.49, group II – 0.76%). TGF beta LB content was similar (from 1.6% to 4.8%) in particular degrees of inflammatory activity with the exception of high inflammatory activity, where the values were low (1.95%).TGF beta LB presence was more prominent in the slow fibrosis group as compared with its fast fibrosis counterpart, irrespective of the inflammatory activity degree.
Conclusion: TGF beta PS liver expression in fast fibrosis progress patients was 100% higher as compared with the values found in slow fibrosis patients. LB values were comparable in both groups. With cirrhosis found in both groups the percentage of TGF beta was four times lower in LB and PS as compared with septal fibrosis. In chronic hepatitis type C patients TGF beta liver expression appears to drop in the presence of high inflammatory activity as compared to fibrosis which continues to progress towards cirrhosis.

P-582

Telomerase activity in human hepatocellular carcinoma: parallel correlation with human telomerase reverse transcriptase (hTERT) mRNA isoform expression but not with cell cycle modulators or c-Myc expression

Horng-Jyh Harn*[3,7], Cheng-Jueng Chen,[1,2] Nu-Man Tsai,[3] Yao-Chi Liu,[2] Li Ing Ho,[4] Huan-Fa Hsieh,[5] Chung-Yang Yen[6]
[1]Graduate Institute of Medical Sciences, National Defense Medical Center, Taipei; [2]Division of General Surgery, [3]Department of Pathology, Tri-Service General Hospital, Taipei; [4]Section of Respiratory Care, Veterans General Hospital, Taipei; [5]Department of Surgery, Yee-Zen General Hospital, [6]Department of Surgery, [7]Department of Emergency Medicine, Armed Force Taoyuan Hospital, Taoyuan County, Taiwan

Introduction: To explore the possible regulatory mechanisms of telomerase, we examined the telomerase activity (TA), expression of human telomerase RNA (hTR), human telomerase reverse transcriptase (hTERT) mRNA isoforms and cell cycle modulators in human hepatocellular carcinoma (HCC) cell lines (J5, J7) and a normal human immortalized hepatic epithelial cell line (Chang-liver).
Methods: The cell lines were chemically synchronized in either G_1, G_1/S, G_2/M or M phases. TA was measured by PCR-based telomerase repeat amplification protocol assay. The hTR and hTERT mRNA levels were analyzed by reverse transcriptase-polymerase chain reaction. Western blotting and immunohistochemistry were used to assay the cell cycle modulators.
Results: The TA of J5, J7 and Chang-liver cell lines tested was highest in M phase. The expression level of hTERT mRNA associated with the highest TA detected in the M phase of HCC cell lines. Chang-liver expressed markedly less TA and hTERT mRNA than J5 or J7. The elevated TA and expression of hTERT mRNA in M phase of HCC cell lines did not significantly correlate with that of the cell cycle modulators and c-Myc.
Conclusion: The results implicate that regulation of TA is related to hTERT mRNA isoform expression, and that regulation is different between the cell immortalization and tumorigenesis.

P-583

Immunocytes and activated stellate cells in pancreatic fibrogenesis

K. Jaskiewicz, A. Nalecz, R. Rzepko
Department of Pathology, University Medical School of Gdansk, Poland

Chronic pancreatitis is a progressive chronic inflammatory disease characterised by irreversible destruction of exocrine pancreatic tissue and extensive fibrosis. Excessive alcohol consumption has ben identified as the main etiologic factor in the Western industrilised world. Idiopathic pancreatitis accounts for approximately 30%. Autoimmune mechanism may be involved in some patients, but this concept has not been accepted as new clinical entity.
The purpose of this work is to investigate the pathogenesis of pancreatic fibrosis and to establish the role of immunocytes and activated stellate cells in chronic panceatitis which is categorized into three groups: chronic alcoholic pancreatitis (AP), chronic idiopathic pancreatitis (IP) and chronic pancreatitis in the presence of pancreatic cancer (CA).
Methods: 51 pancreatic tissue samples were studied histopathologically and immunohistochemically (AP n=16, IP n=12, CA n=12 samples and 11 samples of tisssue with apparently normal pancreatic histology). The following immunohistochemical staining were used: SMA, desmin and synaptophisyn - as markers of activated stellate cells; laminin, fibronectin and colagen IV as markers of extracellular matrix proteins. Immunocytes were stained with LCA, CD68 antibody (macrophages), CD8 antibody (natural killer T-cell subset) and mast cells were examined using Giemsa method. Positively stained macrophages, lymphocytes and mast cells were counted in 3 high power fields of light microscope. The immunoreactivity of activated stellate cells and ECM proteins was assessed by semiquantitive method (0-lack of positive staining, 5-numerous cells with strong positive immunostaining). Results were assessed statistically.
Results: Immunocytes: We found no statistical differences between cases with AP, IP and CA in total count of lymphocytes (mean number in groups: 416, 418, 407 per 3 hpf respectively) The percentage of CD8 positive T-cells in IP was statistically higher in comparison with AP group. The count of macrophages was significantly higher in the IP group than in AP and CA. The count of mast cells was markedly higher in IP group, when compared to other investigated groups. Activated stellate cells: Stellate cells markers SMA and desmin showed slightly higher immunoreactivity in IP. Immunopositivity for synaptophysin was also higher in IP group. There was positive correlation between SMA, desmin and synaptophysin expression and degree of fibrosis. ECM protein markers showed no statistically significant differences between investigated groups (IP, AP, CA).
Conclusion: Results of this work showed, that significant number of IP cases might have autoimmune etiology. There is positive correlation between activated stellate cells markers expression and degree of fibrosis.

P-584

Endocrine differentiation in ductal carcinoma of the pancreas: reactive or neoplastic?

Jürgensen, U. Solterbeck, J. Lüttges , G. Klöppel
Department of Pathology, University of Kiel, Germany

Introduction: The immunohistochemical demonstration of neuroendocrine cells in ductal adenocarcinomas of the pancreas has lead to the hypothesis that many of these tumors may have a dual differentiation into exocrine and endocrine cells. The aim of our study was to analyse the occurence of endocrine cells in ductal carcinomas of the pancreas and their lymphnode metastases, in order to find out wether neuroendocrine cells are an integral neoplastic component of ductal carcinomas or are innocent bystanders.
Methods: Paraffin embedded and formalin fixed tissue of 19 ductal pancreatic adenocarcinomas as well as their lymphnode metastases were immunostained for synaptophysin, chromogranin A, insulin, glucagon, somatostatin, pancreatic polypeptide and the proliferation marker Ki-S5. The tumors were graded according to the WHO criteria.
Results: Eleven carcinomas (58%) showed foci where tumor cells and neuroendocrine cells were in intimate contact. This was observed in neoplastic duct structures which occasinally seemed to be integrated into preformed islets. All ductal carcinomas with integrated endocrine cells were well differentiated (G1 and G2).The endocrine cells lacked proliferative activity. No endocrine cells were found in the lymphnode metastases of the respective tumors.
Conclusion: In well differentiated ductal adenocarcinomas of the pancreas the integration of cells is a common phenomenon. It seems, however, that the neuroendocrine cells in these neoplasms are not a genuine part of the carcinoma because of their lack in metastases. It is hypothesized that ductal carcinoma cells may induce islet cell neogenesis.

P-585

Alcoholic ketoacidosis as the cause of death in chronic alcoholics

Peter Kadis*, Vera Ferlan-Marolt**
*General Hospital Slovenj Gradec, Slovenia; **Institute of Pathology, Medical Faculty, Ljubljana, Slovenia

Introduction: Sudden deaths of chronic alcoholics are commonly investigated by autopsies due to uncertain cause of death. However, this cause remains undetermined in many alcohol abusers despite of careful postmortem analysis comprising histological, toxicological, and microbiological examinations. We anticipated that alcoholic ketoacidosis proved by β hydroxybutyric acid (β-HBA) as a specific postmortem indicator could be the cause of death in some, otherwise unexplained cases.
Material and methods: In this prospective study we analyzed the cause of death, liver pathology and concentration of β-HBA in postmortem blood, urine, cerebrospinal fluid and vitreous humor of 50 suddenly deceased chronic alcoholics. The control group comprised 30 cases of suddenly deceased nonalcoholics.
Results: The main causes of death in chronic alcoholics were cardiovascular diseases, respiratory infections, gastrointestinal bleeding and acute ethanol intoxication. In 20% of cases where the cause of death remained unclear, the levels of β-HBA were pathologically increased in blood, vitreous humor and urine (over 2000 μmol/l). The measurements were significantly higher than in group of the known cause of death of chronic alcoholics and in the control group ($p<0,001$). The levels of β-HBA in cerebrospinal fluid were not statistically significant in the both groups of chronic alcoholics and in the control group. The main liver pathology represented fatty liver with variously pronounced fibrotic changes and inflammation. Liver cirrhosis was found in 14% of all cases of sudden deaths of chronic alcoholics.
Conclusions: According to our study we are convinced that the level of β-HBA in postmortem blood andvitreous humor over 2000 μmol/l is a specific postmortem indicator of fatal ketoacidosis, which could represent the cause of death up to 20% of all sudden natural deaths of chronic alcoholics. The level of β-HBA in cerebrospinal fluid proved not to be appropriate for postmortem investigations of alcoholic ketoacidosis. We suggest postmortal determination of β-HBA to become a routine examination in all cases of sudden deaths of chronic alcoholics.

P-586

Three dimensional reconstruction of the Langerhans' islets using paraffin sections*

Karayannopoulou G.[1], Parathyra A.[1], Tsakaloudi V.[1], Krinidis S.[2], Pitas I.[2], Papadimitriou C.S.[1]
Medical School, Department of Pathology, School of Informatics, Aristotle University of Thessaloniki, Greece

In the present study a three dimensional reconstruction of the Langerhans' islets was achieved, as well as of their capillary plexus, using material from five normal specimens, five cases of chronic pancreatitis and five of pancreatic carcinoma.
The three-dimensional reconstruction of Langerhans' islets included serial sections of the specimens that were immunohistochemically stained using chromogranin (DAKO). In order to reconstruct the capillary plexus inside the islet the sections were stained using the endothelial cell marker CD 34 (NCL). The slides were then acquired directly in digital format by means of a video camera connected to a PC-mounted frame grabber. The three-dimensional reconstructing procedure involved alignment and interpolation of the two-dimensional digital images, in order to increase the resolution in the vertical direction. Transparency of the volumes was achieved using certain algorithms. Our attention was focused in the three dimensional inner structure of the islets and more specifically in the distribution of their capillary plexus.
Three-dimensional transparent models were achieved that showed either the islets or the capillary plexus, with the main advantage of 3-D rotation.
The specific method gave us the opportunity of observing the islets and their capillaries and helped us to reach a clearer understanding of their three-dimensional structure. We think that a wider use of the method in a great range of cases could give the opportunity of comparative results between normal and different pathological conditions.
**This work has been supported by the research project 99ED 599 (PENED 99) funded by GSRT and the European Social Fund.*

P-857

Review of cystic lesions and neoplasms of the pancreas, including two previously unrecognized tumors: Mucinous cystic lesion (MCL) and cystic acinar transformation (CAT)

M. Kosmahl[1], N. Egawa[2], S. Schröder[3], G. Zamboni[4], G. Klöppel[1]
[1]Department of Pathology, University of Kiel, Germany;
[2]Department of Internal Medicine Tokyo Met. Komagone Hospital, Japan; [3] Department of Pathology, Hamburg, Germany;
[4]Department of Pathology, University of Verona, Italy

Introduction: Cystic neoplasms of the pancreas are important because of their special pathology and biology. We reviewed pancreatic tumor files for cystic tumors and lesions. This report describes a series of cystic lesions of the pancreas that could not be classified as one the known cystic neoplasms of the pancreas.
Methods: A series of pancreatic focal lesions and neoplasms (1723) were screened for macro- and microcystic lesions or neoplasms.
Results: We identified 343 pancreatic cystic lesions and neoplasms. Most common were solid-pseudopapillary neoplasms (76), intraductal papillary-mucinous neoplasms (56), serous cystic neoplasms (29) and mucinous cystic neoplasms (20). Among there were 37 ductal adenocarcinomas, 18 endocrine tumors and 4 acinar cell carcinomas with cystic changes. Nine lesions presented as unilocular or multilocular cysts with thin cyst walls and sizes, varying between 3 to 10 cm. Microscopically, the cysts were either lined by cuboidal to columnar mucin producing cells or by acinar cells. Immunocytochemical staining revealed a ductal phenotype in the MCL's and an acinar phenotype in the CAT's.
Conclusions: Among 343 pancreatic cystic lesions and neoplasms we found nine cases of a previously unrecognized type of pancreatic cystic lesion. For these lesions we propose the descriptive term mucinous cystic lesion (MCL) and cystic acinar transformation (CAT), respectively.

P-588

Von Meyenburg complexes associated with multiple benign and malignant tumors – a case report

S. Kostadinova, S. Banev, M. Tolovska, V. Janevska,
E. Trajkovska, J. Zivadinovic
Institute of Pathology, Medical faculty, Skopje, R. Macedonia

Von Meyenburg complexes (biliary microhamartomas) are dilated bile ducts enmeshed in collagenous stroma.
We report an autopsy case of a 68-year-old man previously treated operatively because of colorectal adenocarcinoma. The patient was hemodyalised due to chronic renal failure caused by chronic pyelonephritis and chronic glomerulonephritis, and died from dilatative heart failure. The liver analysis during the autopsy revealed small multiple nodes (interpreted as diffuse metastatic deposits), as well as a larger focus with gelatinous consistency. Numerous small cysts were found in both kidneys, and also a solitary node with a diameter of 1,5 mm in one of them. A tumorous formation on the left upper arm was also found.
The histological examination of the liver tissue specimens showed numerous foci of distorted and dilated bile ducts, some containing bile, lined by regular cuboidal epithelium surrounded with fibrous stroma. They were adjacent to or within portal tracts. Some of them were embedded in a metastatic focus of gelatinous adenocarcinoma. The cysts in the kidneys were acquired and associated with cortical adenoma with papillomatous appearance. The upper arm tumor was diagnosed as calcified fibrolipoma.
The clinical significance of the von Meyenburg complexes is that, despite its rare incidence, it could mimic metastases, microabscesses or microcysts. In our case, the coexistence of adenocarcinoma and von Meyenburg complexes could have been misinterpreted as a diffuse metastatic process in the liver and their coexistence with renal cysts and chronic renal failure could have misled to a polycystic kidney disease.

P-589

Liver iron storage in chronic hepatitis C

Ziyadulla Kushimov, Bahrom Aliev
Institute of Virology, Tashkent, Uzbekistan

Little is known about the pathogenesis of liver damage in hepatitis C. In the present work we studied whether hepatitis C virus-related damage in chronic hepatitis C might be mediated by iron accumalation.
Diagnosis was made on the basis of histological findings and clinical information. Iron storage was defined as the positive Prussian blue reaction in formalin-fixed paraffin-embedded liver sections from 14 patients with chronic hepatitis C.
Our results showed high liver tissue iron concentration in chronic hepatitis C. The staining pattern for iron was found to be finely granular in the sinusoidal lining cells and in scattered clusters of macrophages and in portal endothelial cells.
These findings suggest that liver damage in chronic hepatitis C is characterised by increased iron storage which elicits a lipid peroxidation, oxidative damage to proteins and nucleic acids. Such changes produce defects in organelle function , steatosis and chronic deposition of scar tissue.

P-590

Frequency and gross features of macronodules in cirrhosis liver

Mello ES; Alves VAF; Carrilho FJ; Vezozzo DP; Gayotto LCC
São Paulo University Medical School, Brasil

Introduction: Frequency , etiology and gross features of macronodules are reported.
Methods: Sixty three consecutive liver explants were serially sectioned at 0.5 to 1.0 cm searching for nodules distinct from the surrounding parenchyma in color or size. A digital picture from each nodule was studied for: *tonality*; *color*; *color variation inside the nodule*; *circumscription*; *capsule*. Histology followed IWP (1995): large regenerative nodule (LRN), low grade dysplastic nodule (LGDN), high grade dysplastic nodule (HGDN), well (WHCC) and moderately differentiated HCC (MHCC).
Results: Twenty nine (46%) cases had 95 macronodules. HCC was only found in HCV, alcoholic and cryptogenic cirrhosis. Average number of non-HCC nodules was 2.42 in HCC, and 0.8 in non-HCC cases. Most HGDN were associated to HCC. Average size was 7.47 mm (LRN); 10.95 (LGDN); 12.21 (HGDN); 14.07 (WHCC) and 24.27 (MHCC). Seventeen/22 HCC showed tonality different from surrounding parenchyma. Green color was almost

exclusive of HCC and HGDN (11/42). Color variation inside the nodule was marked in 4/8 MHCC, 2/14 WCHC, 1/21 HGDN, and 0/38 LGDN and LRN. Six/14 WHCC and 1/8 MHCC were ill circumscribed. Five/8 MHCC, 5/14 WHCC and only 8 non-HCC nodules had a thick capsule.
Conclusions: Macronodules are frequent in cirrhosis. The size increases with severity, suggesting multi-step progression. Gross features select the more suspicious nodules.

P-591

Pathological and clinical particularities of a case of pancreatic carcinoma

S. Neagu, A.C Dinulescu, R. Costea, V. Badea, V. Dinca, M. Vlase, M. Neagu
Second Department of Surgery, University Hospital Bucharest, Romania

Introduction: The pancreatic fistula it is one of the major and frequent complications after pancreatic resection for cancer. Multiple protective methods of the pancreaticointestinal anastomosis were developed.
Methods: We report the case of a 43 years-old male operated for carcinoma of the head of the pancreas, without jaundice, in which we performed, in order to protect the pancreaticojejunal anastomosis after radical pancreaticoduodenectomy, an external drainage of the duct of Wirsung with a polyten drainage tube externalized transjejunal according to Witzel's method. Another particularity of this case is the biliary intestinal anastomosis; because the bile duct was normal we performed a cholecystojejunostomy.
Results; conclusion: The postoperative evolution was excellent. We suppress the external drainage of the duct of Wirsung after ten days, and the patient was discharged after 14 days from surgery. The histopathologic analysis revealed ductal adenocarcinomas.

P-592

TEM analysis of endothelial cells in Morris hepatoma 5123 after i.t. rhTNF-α administration

Nowak H. F*., Terlikowski S.J.
Depts. of Clinical Pathology* and Gynecology and Obstetrics, Medical Academy of Białystok, Poland

Aims: The aim of the study was to evaluate the ultrastructure of endothelial cells (EC) in the early phase of angiogenesis in the growth of Morris hepatoma 5123 after intratumor (i.t.) administration of the recombinant human tumor necrosis factor alpha (rhTNF-α).
Methods: The study used 14 Buffalo rats, divided into 2 groups (n=7). Group I received 8× i.t. rhTNF-α (ZChB CBMiMPAN, Łódź, Poland; activity $4x10^7$U/mg protein) in a dose of 10 μg/24h/0.5 ml PBS. Group II rats were given 8× i.t. 0.5 ml PBS. Tissue fragments collected from the peripheral, intermediate and central zones of the tumors were analyzed using TEM OPTON EM900PC.
Results: In the examined zones young EC (single/dispersed) outnumbered the capillaries formed due to germination or budding. TEM analysis showed the presence of proliferating embryonic-type EC with a larger number of RER, Golgi fields and mitochondria compared to mature EC present within the non-infiltrated muscular tissue of the host and in the vicinity of growing capillaries. Numerous destructive changes were observed in the foci of hemorrhagic necrosis in the central zone induced by a direct action of rhTNF-α in EC.
Conclusions: Analyses in TEM seem to confirm that rhTNF-α has a cytotoxic effect both on the EC of tumor and host capillaries. The results suggest that rhTNF-α exerts a certain angiogenic action expressed by the stimulation of capillary formation from mature EC at the sites of post-necrotic foci cleared by cells of the monocyto-histiocytic system.

P-593

Does retinoic acid influence topoisomerase ii activity in human ductal adenocarcinoma cell lines?

K. Peters[1], M. Clark[2], F. Gieseler[2], G. Klöppel[1]
Dept. of Pathology[1] and Int. Medicine[2], University of Kiel, Germany

Introduction: Retinoic acid (RA) induces differentiation and growth inhibition of pancreatic carcinoma cell lines as indicated by morphologic criteria. mRNA of retinoic acid receptor (RAR)α and γ is up-regulated and RARβ expression reduced. Little is known about the possible influence of RA on topoisomerases (TOP), a major target for cytotoxic drugs.
Methods: 8 different pancreatic ductal adenocarcinoma cell lines were incubated with RA for 7 days; 4 cell-lines were additionally incubated for 2, 4, and 7 days. Nuclear extracts were prepared and the activity of TOP IIα and TOP IIβ was determined with a modified relaxation assay and compared with untreated cells. FISH analysis with a TOP IIα locus specific probe was carried out on treated and untreated cells.
Results: After incubation with RA, TOP IIα activity decreased in 4/8 cell lines with a concomitant increase in TOP IIβ activity in 3 of the cell lines. One cell line showed an increase in TOP IIα activity with a decrease in TOP IIβ activity. Two cell lines showed no TOP activity changes, another very low TOP activity. The gene copy number of TOP IIα was found to be identical in RA-treated and untreated cells.
Conclusion: RA does not necessarily induce a decrease in TOP IIα activity, as expected because of its antiproliferative effect. A complete differentiation of ductal adenocarcinoma cells in vitro cannot be induced by RA. No effective cytotoxic drug has yet been found for this devastating disease. Investigation for a predictor at the DNA level, which contributes to responsiveness to cytostatic drugs, still has to be carried out.

P-594

Cathepsin D partisipation in collagen degradation during the recovery from experimental hepatic fibrosis

Ryvnyak V., Baciu E.*
"Nicolae Testemitsanu" Medical University, Kishinev, Moldova; Centre of Pathology, Academy of Sciences*, Kishinev, Moldova

Introduction: Cathepsin D is one of the most important lysosomale aspartile proteinase, present in different cells and tissues and

indispensable for proteolitic processes. The enzyme is capable to degrade the main components of the intercellular matrix.
Methods: The activity of cathepsin D in fibrotic rat liver at the 7 and 14days after the CCl_4-treatment cancellation was investigated electron-histochemically. BZ-Arg-Gly-Phe-Phe-Pro-4MBNA (Bachem) served as the substratum for cathepsin D. The technique of Smith and Van Frank (1975) was used. Biochemically cathepsin D activity and hidroxyproline level was determined in normal, CCl_4-induced fibrotic rat liver and at 7, 14, 21, 30, 60 days after discontinuation of treatment.
Rezults: The reaction product was revealed in the phagolysosomes of Kupffer cell and fibroblaste containing the fragments of collagen fibrils and in the endotheliocyte lysosomes. The reaction product was found also extracellulary on the hepatocyte and Kupffer cell plasmalemma and on adjacent collagen fibrils. Biochemically in fibrotic liver was revealed an increase of cathepsin D activity as compared with normal liver. During the fibrosis regression the maximums of enzymatic activity were fixed at 14 days (125%) and 30 days (124%) after cessation of CCl_4-treatment. At the 21-th day of recovery was noted some diminution of cathepsin D activity. At 60 days after toxin abolition enzyme activity was close to control. A close correlation between cathepsin D activity and liver hidroxyproline level was found.
Conclusions: Cathepsin D is direct implicated in collagen resorbtion and participates both in extracellular and intracellular collagen degradation.

P-595

hMLH1 and hMSH2 expression in an osteoclast-like giant cell tumour of the pancreas associated with mucinous cystadenocarcinoma

R. Sedivy[a], R. Kurzbauer[c], F. Mühlbacher[b], L.A. Huber[c], F. Wrba[a]
[a] Department of Clinical Pathology, [b] Department of Surgery, University Hospital Vienna, [c] Research Institute of Molecular Pathology, Vienna, Austria

Osteoclast-like giant cell tumours (OCGT) are very rare neoplasms of the pancreas, first reported by Rosai in 1968. Since then this tumour entity was described 36 times in the published literature. Even less OCGTs were associated with mucinous cystic neoplasms.
OCGTs contain sheets of mononuclear tumour cells between scattered multinucleated giant cells. It was shown that the mononuclear tumour cells harbor K-*ras* mutations suggestive as to be of ductal origin. The multinucleated giant cells express the macrophage marker CD 68.
In this report we present such an unusal case of an OCGT associated with a mucinous cystadenocarcinoma. Using immunohistochemistry and Western Blot analysis we found an expression of the mismatch repair genes hMLH1 and hMSH2. While hMSH2 was expressed equally in both tumour components, OCGT displayed a reduced hMLH1 expression as compared to the cystadenocarcinoma.
As mismatch repair defects are related to a less favourable prognosis, this finding supports the notion OCGT as to be an undifferentiated carcinoma with osteoclast-like giant cells.

P-596

Correlation of hepatocyte proliferation and viral load with nuclear localization of HBcAG and p21 expression

E. Serinsöz[1], E. Erden[1], M. Varli[2], H. Çetinkaya[2], M. Bozdayi[2], C. Yurtaydin[2], Ö. Uzunalimoğlu[2], H. Bozkaya[2]
Departments of Pathology[1] and Gastroenterology[2], Ankara Medical School, Ankara

Introduction: The present study aimed to investigate the relationship between the subcellular localization of HBcAg in the hepatocyte, the liver inflammatory activity, the proliferative activity of hepatocytes and the role of p21 in the control of hepatocyte proliferation in chronic hepatitis B infection.
Methods: HBsAg (+) 98 cases were included in the study. HBV DNA levels were determined for each case. Liver histology was assesed according to Knodell's scoring system. Hepatic expressions of HbcAg, PCNA and p21 were studied immunohistochemically by counting 1000 cells.
Results: A total of 48 cases (48.9%) were positive for HBcAg staining. HBV DNA was positive in 80 (81.6%) cases. When HAI score 8 was determined as a cut-off value, 53 (54.08%) cases had HAI<8 and 45 (45.9%) cases ≥8. Patients with positive nuclear HBcAg staining had lower HAI (<8) than those with negative HBcAg staining ($p<0.05$).
ROC analysis determined 350 as a cut-off value for PCNA score. Sixty one (62.2%) patients had PCNA score <350 and 24 (24.4%) patients had PCNA score >350. Most of the patients with nuclear HBcAg staining had lower PCNA score ($p<0.05$).
P21 expression could be evaluated only in 35 of the cases. Twenty two cases (62.8%) had varying degrees of nuclear p21 staining. P21 positivity was detected to be in higher numbers in the group with HAI ≥8 than the group with HAI<8 ($p=0.598$).
Conclusion: The present study revealed a close relationship between the inflammatory activity in the liver and the HBV DNA level in the serum and p21 expression as well as the topographical distribution and quantitative expression of HBcAg in the liver.

P-597

Neogenesis of pancreatic islets in IDDM patients

E. Severgina*, L. Severgina*,T. Dyuzheva*
*Department of Pathological Anatomy, I.M. Sechenov Medical Academy, Moskow, Russia

Pancreatic islet neogenesis in IDDM patients is still unclear. That was the aim of our investigation. Pancreatic incision biopsies after IDDM surgical treatment were investigated by light and electron microscopy. B-cells insulin granules and A-cells glucagon granules were revealed with indirect immunoperoxidase method.
Investigation of biopsies from 65 IDDM patients with different age, time of manifestation and duration of the disease showed the groups of endocrine cells with morphological signs of A-, D-, C-, B-cells in acini and more frequently in ducts. These groups of endocrine cells formed the separate structures – newly formed islets (in 9,7% of all cases). These cells with high grade of functional activity contained a small amount of endocrine granules and organells, had an unusual elongate, ductal cell-like shape. Blood vessels were placed near these islets. It was remarcable that the presence of great number of acinar B-cells predisposed pancreatic islets neo-

genesis. The positive correlation between the number of newly formed islets and degree of Langerhans islet B-cells destruction was absent. Some of B-cells destruction was in 6,4% (C-peptide level in serum – 0,31±0,1 ng/ml) and of great bulk of B-cells – in 3,3% of all cases (C-peptide level in serum – 0,02±0,01 ng/ml). Immunohistochemical reaction with antiserum to insulin and glucagon confirmed the endocrine genesis of newly formed islet cells.
Our investigation revealed the possibility of pancreatic islet neogenesis non-correlated with B-cell destructive changes in IDDM patients.

P-598

Vascular endothelial growth factor-A plays a dominant role in the *in vitro* angiogenic activity of pancreatic carcinoma cell lines

B. Sipos*, D.Weber*, H.Ungefroren**, H. Kalthoff**, G. Klöppel*
*Department of Pathology and ** Molecular Oncology Division, Department of Surgery, Christian Albrechts University, D-24105 Kiel

Aims: To determine the angiogenic potential of ductal pancreatic carcinoma cell lines (PCCLs). In a first step, we examined the capability of PCCLs to produce and release the two most potent angiogenic growth factors, vascular endothelial growth factor (VEGF-A) and basic fibroblast growth factor (bFGF).
Methods: 11 well characterized PCCLs were grown under normoxic (5% CO_2, 95% air) and hypoxic (5% O_2, 10% CO_2, 85% N_2) and anoxic (18% CO_2, 82% N_2) conditions. Expression of VEGF-A and bFGF mRNA were quantified by RT-PCR, VEGF-A protein by immunoblot analysis. Conditioned media (CM) were analyzed by sandwich enzyme linked immunoadsorbent assay (ELISA) with anti-VEGF-A and anti-bFGF antibodies. *In vitro* angiogenic activity of CM of PCCLs was determined by a proliferation assay using dermal microvascular endothelial cells (DMVECs) with and without neutralizing antiVEGF-A-antibody.
Results: VEGF-A mRNA and protein expression were detected in all PCCLs. bFGF was detected by RT-PCR and ELISA in 3 of 11 PCCLs. Hypoxia was not able to induce VEGF expression, while anoxia stimulated VEGF-A mRNA and protein expression in 9/11 and in 7/11 of PCCLs, respectively. In 77% of 44 DMVEC proliferation assays (11 cell lines, 4 conditions) showed CM a significant stimulation, which could be specifically inhibited by neutralizing antiVEGF-A-antibodies in nearly all cases.
Conclusions: VEGF-A plays a dominant role in angiogenic activity of human pancreatic carcinomas *in vitro*. The overexpression of VEGF-A in a hypoxic/anoxic microenvironment may contribute to the vascularization of pancreatic carcinomas

P-599

Progressive chromosomal alterations in intra-ductal papillary mucinous tumors and putative precursor lesions of the pancreas

D. Soldini, E. Burckardt, M. Gugger, J.A. Laissue, L. Mazzucchelli
Institute of Pathology, University of Bern, Bern, Switzerland

Intraductal papillary mucinous tumors (IPMTs) of the pancreas are rare neoplasms characterized by a broad biological behavior. Their relationship with ductal papillary metaplasia (DPM) occurring in adjacent non-neoplastic pancreatic ducts is controversial. Numerical chromosome aberrations were analyzed by fluorescence in situ hybridization on tissue samples obtained from 9 patients with non-invasive IPMT and 5 patients with invasive carcinoma arising in IPMTs. DPM was analyzed in tissues obtained from 6 patients with IPMT, 7 patients with ductal adenocarcinoma and 11 patients with chronic pancreatitis. Monosomy for chromosomes 6 and 17 was found in all samples with IPMTs. Loss of chromosomes 6 and 17 was also detected in DPM from patients with IPMT (4/6 and 3/6, respectively), ductal adenocarcinoma (7/7 and 5/7) and chronic pancreatitis (4/11 and 3/11). Monosomy for chromosome 18 was detected in 4/9 patients with non-invasive IPMTs and in 5/5 patients with IPMTs and invasive carcinoma. Loss of chromosome 18 was found in DPM from 3/7 patients with ductal carcinomas but not in DPM from patients with IPMTs and chronic pancreatitis. None of the samples showed abnormalities for chromosome 1. We conclude that monosomies are a frequent finding in IPMTs and we suggest that chromosome 18 loss may be implicated in the progression of IPMTs to invasive carcinoma. The chromosomal aberrations detected in DPM adjacent to IPMTs and ductal carcinomas, and in chronic pancreatitis may represent field defects that increase the risk of subsequent neoplasia and suggest a hyperplasia to dysplasia to adenocarcinoma sequence in pancreatic ducts.

P-600

Helicobacter identified in the pancreas of patients with pancreatic carcinoma

U. Stenram[1], B. Carlén[1], I. Ihse[2], H.-O. Nilsson[3], T. Wadström[3]
Dept. of Pathology[1], Dept. of Surgery[2], Dept. of Medical Microbiology, Dermatology and Infection[3], Lund University, Sweden

Objectives: To analyze the benign part of pancreas for *Helicobacter* species from patients with pancreatic carcinoma by PCR, DNA-sequencing and electron microscopy (EM).
Methods: 10 paraffin-embedded and 3 fresh pancreas specimens from patients with pancreatic carcinoma were primarily analyzed. Samples were deparaffinized by xylene and ethanol washing and DNA extracted by heat and detergent lysis and ion-exchange resin purification. Samples were analyzed with PCR using *Helicobacter*-specific 16S rDNA primers and amplified products were purified and sequenced with an Applied Biosystems DNA sequencer by the protocols of the manufacturer (Perkin-Elmer) by using the ABI PRISM BigDye Kit. From the 3 patients, where fresh tissue was available for PCR, EM was performed on deparaffinized tissue.
Results: 1/10 paraffin-embedded and 3/3 fresh pancreas samples from patients with pancreatic tumours was positive for *Helicobacter* spp. by 16S rDNA PCR analysis. Two 400-bp PCR-products were analyzed by DNA sequencing and verified to be *Helicobacter* spp. by GeneBank database comparison. EM did not disclose *Helicobacter*-like structures, though so far only deparaffinized material has been used.
Conclusions: *Helicobacter* spp. were detected by PCR and DNA sequencing in the benign part of pancreas from patients with pancreatic carcinoma.

P-601

Fine needle aspiration diagnosis of rare pancreas neoplasms

E. Szekely, B. Jaray, T. Winternitz, G. Toth
2nd Dept. of Pathology, 1st Dept. of Surgery, Dept. of Radiology, Semmelweis University, Budapest

Aim: Fine needle aspiration biopsy of the pancreas has become a frequently applied method in the preoperative diagnosis of several pancreatic lesions. However, there are pathologists and there are surgeons, who question the usefulness and benefits of that sort of preoperative morphologic investigations. In this study we demonstrate the efficacy of this diagnostic approach, by showing some challenging, rare-occurring lesions that were diagnosed preoperatively.
Materials and methods: In the files of the 2nd Department of Pathology more than 2000 biopsies had been taken from the pancreas since the beginning of 1994. Most of the patients had been operated on, and after processing the surgical specimens, cytological diagnoses were compared with histological results. The smears were wet-fixed, and both smears and histological slides were stained with H&E.
Results: There were no false positive diagnoses given. The vast majority of cases proved to be either chronic pancreatitis with or without acute exacerbation, pseudocysts or conventional adenocarcinoma. In addition, we were able to diagnose lesions that occur more rarely, such as malignant pancreas tumor with osteoclast like giant cells, neuroendocrine tumor, malignant carcinoid, Gruber-Frantz tumor, acinic cell carcinoma, mucinous cystadenoma, and metastatic tumors as well preoperatively.
Conclusions: Fine needle aspiration cytology is a very useful, accurate and effective preoperative diagnostic tool, with which even rarely occurring lesions can be revealed in skilful hands. Of course, without good teamwork and communication among radiologist, surgeon, and cytologist only worse results can be obtained.

P-602

Giant mitochondria in routine liver biopsy specimens as observed by light microscopy

N. Tomanovic, I. Boricic, D. Brasanac, A. Begic-Janeva, B. Brmbolic
Institute of Pathology, School of Medicine, Dr Subotica 1, Belgrade, Yugoslavia

Introduction:This study evaluates the occurence and morfological features of giant mitochondria in routine liver biopsy specimens.
Methods: 1445 samples were stained with Masson trichrome (giant mitochondria stain bright red and are larger than nucleolus).We performed statistical analysis by using chi-square test.
Results: Study showed presence of giant mitochondria in 51 (3.6 %) liver biopsy sample. Presence of giant mitochondria is highly connected (38.5%) with alcoholic liver disease (ALD).Giant mitochondria are more frequent in liver cirrhosis (25%) than in any other form of ALD (13.5%). They are also frequent in chronic viral hepatitis (9.8%) and in liver cirrhosis connected with chronic viral hepatitis (15.4%). They are also visible in primary biliary cirrhosis (7.8 %), chronic autoimmune hepatitis (1.9%), genetic haemochromatosis (1.9%), but also in light, non-specific pathological changes (15.6%).
In 66% of samples were present round-shaped,in 16% spindle-like,and in 18% both round and spindle-like shaped giant mitochondria.79% of round, 85% of spindle-like and 75% of both round and spindle-like were distributed around portal areas.
There is no statistically significant connection between liver steatosis and presence of giant mitochondria, nor is their presence sex-related. They are much often visible in macrovesicular than in any other sort of liver steatosis.
Conclusions: Altough they are mostly visible in ALD, giant mitochondria are also present in various forms of liver disease.Because of that, their presence, shape, size and distribution cannot be of great importance in routine evaluation of liver biopsies.

P-603

CD44 isoforms expression in intraductal and invasive pancreatic cancer and its correlation to p53 gene mutations

Romana Tomaszewska, Krystyna Nowak , Jerzy Stachura
Department of Clinical and Experimental Pathomorphology, First Chair of General Surgery, Collegium Medicum, Jagiellonian University, Kraków, Poland

The expression of the CD44 antigen and its isoforms is found in many normal and malignant .tissues. Numerous studies indicate that the antigen affects the course of the disease, and its v6 isoform exerts a particularly negative effect on the prognosis. High CD44s (standard) and v6 isoform expression has been noted in pancreatic cancer. A similarly common genetic change in pancreatic cancer is the p53 gene mutation. The aim of the investigation was to study the expression of the CD44s and CD44v6 antigens in invasive and intraductal pancreatic cancer and its possible correlation to the p53 gene mutations. Immunohistochemical studies were carried out in 12 patients operated on for pancreatic cancer, in whom intraductal cancer had been detected in addition to neoplastic infiltration. The results indicate that pancreatic cancer is characterized by a high, yet independent expression of CD44s and the p53 protein. CD44s expression shows no correlation with the degree of tumor differentiation, while v6 expression is higher in cancers with higher histological malignancy grades. Intraductal pancreatic cancers show a similarity to invasive cancers with respect to CD44s and v6 expression, what indicates that already at the stage of its intraductal growth pancreatic cancer manifests the presence of properties affecting its invasiveness and tendencies to metastasizing.

P-604

Prognostic role of Cyclin E and p27 molecules in adenocarcinoma of the pancreas

V. Török, A. Keller, E. Paál
2nd Department of Pathology, Semmelweis University, Budapest

Aims: The regulation of the cell cycle plays an important role in the development prognosis of various tumors. Cyclin E and p27 are known as G1-S regulating proteins. Their independent prognostic significance has been proven in various tumors. The aim of this study to investigate the expression and prognostic role of these proteins in pancreatic adenocarcinoma.
Materials and methods: 14 cases of pancreatic adenocarcinoma with complete follow-up were retrieved from the archives from the period of 1995–1998. The cases were divided into 2 groups: patients with less then two years of survival (n=9) and patients who survived more than two years (n=5). We compered the clinical and histological data along with immunohistochemical Cyclin E and p27 protein expression. We used normal pancreas (n=10) and pan-

creas with microcystic adenomas (n=10) as controls. The results were evaluated semiquvantitatively.
Results: There was no significant difference in the demographic data and localisation between the 2 groups and the grades and stages of the 2 groups were comparable. The short surviving group showed a high Cyclin E expression as compared to the long surviving group and the controls. There was no significant difference among the four groups in p27 protein expression.
Conclusion: High Cyclin E protein expression alone or combined with p27 expression seems to have a prognostic significance in pancreatic adenocarcinomas.

P-605

Combined Hepatocellular and Cholangiocarcinoma: Clinicopathologic features and correlation with c-met and hepatocyte growth factor (HGF)

Heike Varnholt, M.D.1, Yoshiki Asayama, M.D.2, Shin-ichi Aishima, M.D.2, Ken-ichi Taguchi M.D.2, Keishi Sugimachi, M.D.2, Masazumi Tsuneyoshi, M.D., Ph.D.2
1Massachusetts General Hospital, Harvard Medical School, Molecular Pathology Unit, Boston; 2Kyushu University, Department of Anatomic Pathology, Fukuoka, Japan

Background: Both c-met, a membranous tyrosine kinase receptor protein, and hepatocyte growth factor (HGF), its natural ligand, have been postulated to have an important impact on development and spread of primary liver carcinomas, such as Combined Hepatocellular and Cholangiocarcinoma (cHCC-CC), which is very rare.
Methods: Immunohistochemical staining was performed on 30 cHCC-CC, including 4 double cancers (13,3%), 20 combined types (66,7%) and 6 mixed types (20,0%). The association of c-met and HGF expression with the following clinicopathologic parameters was examined: differentiation degree, liver cirrhosis, vascular invasion, perineural invasion, lymphatic permeation, intrahepatic metastasis, lymph node metastasis.
Results: Immunoreactivity for HGF was significantly correlated with the differentiation degree of cholangiocellular components, being highest in well and moderately differentiated and lowest in poorly differentiated components (p=0,0119). No significant association was observed between expression of c-met or HGF and the presence of liver cirrhosis, vascular invasion, perineural invasion, lymphatic permeation, intrahepatic metastasis or lymph node metastasis.
Conclusion: HGF may have an important impact on the differentiation of certain cHCC-CC. Other clinicopathologic factors related to tumor development and spread may not be influenced by c-met or HGF, at least not on the protein level.

P-606

Frequent k-ras-2 mutations and p16INK4A methylation in hepatocellular carcinomas in workers exposed to vinyl chloride

Markus Weihrauch1, Markus Benicke2 , Gerhard Lehnert3, Christian Wittekind2, Renate Wrbitzky1, Andrea Tannapfel2
1Institute of Occupational and Environmental Medicine, University of Hannover; 2Institute of Pathology, University of Leipzig; 3Institute of Occupational, Social and Environmental Medicine, University of Erlangen-Nuremberg, Germany

Vinyl chloride (VC) is a known animal and human carcinogen associated with liver angiosarcomas (LAS) and hepatocellular carcinomas (HCC). Recent data indicate K-ras-2 mutations induce p16 methylation accompanied by inactivation of the p16 gene. This study investigates mutations of the K-ras-2 oncogene and its possible association with p16 in VC induced human HCCs.
The presence of K-ras-2 mutations was analysed in tissue from 18 patients with VC associated HCCs. As a control group, 20 patients with hepatocellular carcinoma due to hepatitis B (n=7), hepatitis C (n=5) and alcoholic liver cirrhosis (n=8) was used. The specific mutations were determined by direct sequencing of codon 12 and 13 of the K-ras-2 gene after microdissection. The status of p16 was evaluated by methylation-specific PCR (MSP), microsatellite analysis, and DNA sequencing.
K-ras-2 mutations were found in six of 18 (33%) examined VC-associated HCCs and in three cases of adjacent non-neoplastic liver tissue. There were three G ® A point mutations in the tumour tissue. Hypermethylation of the 5´ CpG island of the p16 gene was found in 13 of 18 examined carcinomas (72%). Of six cancers with K-ras-2 mutations, five specimens also showed methylated p16. Within the control group, K-ras-2 mutation were found in three of 20 (15%) examined HCC. p16 methylation occurred in eleven out of 20 (55%) patients.
K-ras-2 mutations and p16 methylation are frequent events in VC associated HCCs. We observed a K-ras-2 mutation pattern characteristic of chloroethylene oxide, a carcinogenic metabolite of VC. Our results strongly suggest that K-ras-2 mutations play an important role in the pathogenesis of VC associated HCC.

P-607

DHPLC mutation screening of ATP7B in 5 families affected by Wilson's disease

G. Weirich*, A. Cabras*, S. Serra°, P.P. Coni°, A.M. Nurchi$, G. Faa°, H. Höfler*
Institutes of Pathology GSF&TUM Munich*, Germany; Cagliari°, Pediatric Clinic I$ University of Cagliari, Italy

Background: Wilson's disease (WD) is an autosomal recessive disorder characterized by decreased biliary copper excretion and reduced copper incorporation into ceruloplasmin. The WD gene, ATP7B, maps to chromosome 13q14.3 and contains 21 exons. ATP7B encodes a copper-transporting P-type ATPase which regulates copper transport across the cellular membrane. Screening for mutations of the ATP7B gene has yielded more than 100 mutations distributed over the entire coding sequence. In order to detect individuals at risk for WD, sensitive and reliable methods for mutation screening of the entire ATP7B gene are in demand. Using DHPLC, more than two hundred samples can be analyzed within 24 hours. In this study, we have tested DHPLC as a mutation detection method in WD patients.Material & Methods: Five Sardinian families were included in this study after informed consent was given. DNA was obtained from 20cc whole blood and subjected to PCR amplification of the 5′ UTR region and exons 2, 3, 8, 10, 11, 12, 13, 14, 15, 16, and 18 of the ATP7B gene, sites which were recently shown to predominantly harbor mutations in the Sardinian population including three hot spots mutations: -441/-427del (5′UTR), 2463delC (exon 10), V1146M (exon16). PCR-products were subjected to heat-denaturation (95°) followed by controlled cooling to 37°C over a period of 45 min. Samples were then injected into a chro-

matographic column in order to separate mismatched and matched double strands. PCR products giving rise to non-wild type chromatograms were further analyzed by direct sequencing.Results: 36 individuals were tested. We detected 13 individuals heterozygous for the 5'UTR mutation, as well as five WD patients homozygous for this change in three families. In one family, we detected the presence of 2463delC combined with the 5'UTR mutation in an affected individual. In another family, affected patients and one parent were heterozygous for 2463delC. Neither the -441/-427del nor the V1146M mutation were detected in this family. Screening of ATP7B exons 2, 3, 8, 11, 12 and 18 revealed several polymorphisms in this family including two novel mutations, 2732C>T (A911V, exon 11) and 2855 A>G (K952R, exon 12), none of them segregating with the disease. Screening of the remainder exons is progress. In this sample of five families, DHPLC showed a mutation detection rate of 100% as verified by direct sequencing.Conclusions: Our results demonstrate that DHPLC is a reliable tool for mutation screening of the ATP7B gene. Using this method, the carrier status of members in families affected by Wilson's disease can quickly be determined, especially in populations with endemic occurrence of hot spot mutations.

P-608

"Clinical and morphological characteristics of recidives and continued grow of brain neuroepithelial tumours"

Abildinov D.R., Mambetova G.K.
Kazakh State Postgraduate Institute, Almaty

Purpose: to revial to proposition of brain secondary tumours recidives and continued grow in general structure of all intracranial tumours.
Methods: a correlation between histological type and recidives of the tumours had been detected.
The peculiarityes of tumours clinical manifestation had been studied. 62 patients from aged from 20 to 50 years, who earlier underwent the surgery due to the brain tumours, had been followed up. Because of recidives of the tumours 52 patients underwent second surgery.
Conclusion: hystological secondary tumours of neuroepithelial origin had higher degree of anaplasy.

P-609

Stereotactic biopsy of brain. Practical remarks based on own experiences with protocol including routinely applied immunocytochemistry on cytological smears

Adamek D., Moskala M.*, Kaluza J., Goscinski I.*, Korzeniowska A.
Department of Neuropathology and *Department of Neurotraumathology, Jagiellonian University, Medical College. Kraków, Poland

Introduction: Stereotactic biopsy of brain (SBB) has been performed in our center since 5 years (112 SBBs so far). Our material includes only primarily diagnosed changes. Due to an extreme scarcity of material (10–15 mm^3) we tried to evaluate the role of simultaneously applied different techniques including immunocytochemistry and electron microscopy in the diagnosis.
Methods: The routinely applied panel includes: Ki-67, topoisomerase II alpha, p53, bcl-2, and GFAP. Others like cytokeratines, LCA, etc. are applied accordingly to particular needs of differential diagnosis. The smears stained with HE (usually 4 slides) play a decisive role for the diagnosis, enabling an excellent assessment of cellular morphology and however they take a little more time, they are preferred over single-component methods of staining. The rest of smears (usually 16 slides) are assigned for immunocytochemistry. Only minor part of material is processed into paraffin block and also for electron microscope.
Results: The proliferation "markers" and p53 help to evaluate the grade of glioma and, in some cases, to differentiate between reactive and neoplastic gliosis. The positive reaction for p53 was never noted in reactive gliosis but, on the contrary, it was noted in most cases of primary and secondary tumors. An immunolabeling with topoisomerase II alpha seems to be also noteworthy since this enzyme is a "target" for some antineoplastic drugs.
Conclusions: The use of protocol based on combined cytological and immunocytochemical methods is necessary in SBB. Acknowledgements: This study was supported by Polish Committee for Scientific Investigations, grant No. KBN 501/G/240

P-610

CT guided streotactic biopsy of brain lesions: Experience of 125 cases

Fügen Vardar Aker*, Tayfun Hakan**, Selhan Karadereler***, Neşe Karadağ*
Pathology Department*, Haydarpaşa Numune Hospital, İstanbul; Neurosurgery Department**, Kartal Research Hospital, İstanbul; Neurosurgery Department*** Haydarpaşa Numune Hospital, İstanbul; Pathology Department****, İnönü University, Malatya, Turkey

ABSTRACT: Treatment strategies for intracranial mass lesions are most effective when based upon histopathological diagnosis. Image-guided stereotaxy has provided the means to sample tissue from small or deeply located intraparencymal lesions with a relatively high degree of safety and accuracy. The stereotactic procedures was performed by using Lexell system on one hundred twenty five cases during 63 month period starting in 1995.
METHODS: One hundred twenty five procedures for intracranial lesions are performed on 125 patients. There were 81 men, 44 women whose ages ranged between 2 and 82 years. The lesions were located on deep (46 cases) and lober (46 cases). In 20 cases (% 16), resection of the lesion is performed after the stereotactic biopsy. The 86 patients (% 68.8) were followed for 5 years (68 months).
RESULT: Lesions were neoplastic (98 cases) non-neoplastic (17 cases). Glial tumors accounted for the majority (% 53.6) of biosied lesion; metastases (% 14.4) and lymphoma (% 5.7) were also relatively common. Diagnostic material were not obtained only in 10 cases. Two cases were evaluated false negative and false positive. Diagnostic accuracy was % 90.4. There was no mortality and no major complication was seen but only one intracerebral hematoma in a case of temporal lobe astrocytoma which required craniotomy and evacuation.
CONCLUSION: Sreteotactic biopsy is a widely available procedure for obtaining tissue from CNS masses. It is generally well-tolerated with minimal morbidity and offers a high diagnostic yield.

P-611

Immunohistochemical expression of cell cycle regulatory proteins (Cyclin D1, Cyclin E, p21 and p27) in retinal membranes

Aletra C[1], Batistatou A[1], Ravazoula P[1], Theodosiou A[2], Feretis E[2]
[1]Department of Pathology, University Hospital of Patras, Patras; [2]Department of Opthalmology, Red Cross Hospital, Athens, Greece

Introduction: The membranes, which develop in retina during several pathologic states (diabetic retinopathy, hyperplastic vitreoretinopathy, trauma and membranes of macula lutea) cause loss of its architectural integrity and function. The aim of the present study has been to investigate whether the cell cycle-regulatory proteins Cyclin D1, Cyclin E, p21 $^{WAF-1}$ and p27 $^{Kip-1}$ play a role in the development of retinal membranes in humans.
Materials and Methods: We examined immunohistochemically the expression of the above proteins using the following monoclonal antibodies: Cyclin D1 (Novocastra), Cyclin E (YLEM), WAF-1 (p21, YLEM), and p27 (Novocastra) in paraffin-embedded sections of formalin-fixed biopsies from 20 retinal membranes, using standard immunohistochemical technics. Of these, 12 cases were due to hyperplastic vitreoretinopathy, 3 to hyperplastic diabetic retinopathy, 4 to membranes of macula lutea και 1 to trauma.
Results: The proteins Cyclin D1, Cyclin E and p21 $^{WAF-1}$ were not detected in any of the 20 cases. Nuclear expression of protein p27^{Kip-1} was evident in 5 cases of hyperplastic vitreoretinopathy (42%) in membrane fibroblasts (spindle cells immunopositive for vimentin and negative for GFAP).
Conclusions: The results of the present study suggest that the mechanism of membrane development in hyperplastic vitreoretinopathy is different from that in diabetic retinopathy. In cases of hyperplastic vitreoretinopathy protein p27 $^{Kip-1}$ appears to play a role in development and maintainance of retinal membranes.

P-612

Comparative analysis of the proliferative activity and the grade of glial neoplasms of the brain with respect to the prognostic accuracy

Grazyna Bierzynska-Macyszyn, Piotr Karczewski, Bogdan Bialas, Wojtacha M.*, Bazowski Piotr*
Department of Pathomorphology, The Medical University of Silesia, Katowice-Ligota, Poland

The aim of the study was to correlate relapse-free survival after surgery with the tumor grade determined according to Kernohan, WHO, and Daumas-Duport Scale (DDS), and the proliferative activity assayed with immunohistochemical methods (PCNA, Ki-67, p53, Bcl-2). Diagnostic accuracy is important issue for planning therapy and prognosis especially in stereotactic biopsies.
Patients and Methods: One hundred adult patients with supratentorial astrocytomas, operated in the Department of Neurosurgery in Katowice, in 12 year period (1989–2000) were retrospectively reviewed to determine factors influencing outcome. All underwent subtotal (27) or total (23) tumorectomy and were observed for up to 7 years. Sex, age at diagnosis, first symptoms, preoperative Karnofsky perfomance status (KPS), tumor diameter, and location, radio-, and chemotherapy, macro- and microscopical appearance were analyzed. The histological type, and tumor grade were determined. Relapse curves were estimated by the Kaplan-Meier method, and tested for equality with the log-rank test. Proliferative activity (PCNA, Ki-67) and apoptotic index (p53, Bcl-2) were estimated, correlated with other parameters, and associated with improved or worsened survival.
Results: We have found the significant ($p<0.05$) negative correlation between DDS, and WHO grade, and relapse-free survival. The study reveals that the estimation of PCNA, Ki-67, p53, and Bcl-2 are good tools for determination of proliferative activity of astrocytomas and they correlate with tumor grade and aggressiveness.

P-613

Prognostic significance and relationship of p27, bcl-2 and Ki-67 immunohistochemical expression to tumor grade and survival in astrocytomas

Sezer Cem , Memiş Leyla , Işık İpek
Department of Pathology, Gazi University Medical School, Ankara , Turkey

Introduction: The aim of this study was to evaluate the Ki-67,bcl-2 and p27 label indices as prognostic indicators for patients with astrocytomas.
Methods: Ki-67, bcl-2 and p27 immunohistochemistries were performed on samples of tumor tissues of 62 patients with astrocytomas , anaplastic astrocytomas or glioblastoma multiforme and results statistically compared to tumor grade (according to both WHO and St. Anne-Mayo grading systems) and overall survival with Chi-square, Kaplan-Meier survival and multipl Cox regression analysis.
Results: bcl-2 and p27 label indices were higher in the group of low grade astrocytomas and showed significant decrease with the increasing grade according to both grading systems (for bcl-2:WHO; p: 0,002/St.Anne-Mayo; p<0,001- for p27: WHO; p<0.001/St.Anne-Mayo; p<0.001). However, there was a positive correlation between tumor grade and Ki-67 label index (WHO; p<0.001/St.Anne-Mayo; p<0.001). Using the Kaplan-Meier method, we found that survival times were significantly shorter with strong Ki-67 expression (p<0.001) and longer with strong p27 expression (p<0.01). Altough bcl-2 expression was not statistically significant, positive patients showed a prolonged survival time compared to negative ones. A Cox multivariate regression analysis indicated that WHO grading system was the independent , significant positive prognostic factor among other parameters investigated (p<0.0001).
Conclusion: This study indicates that Ki-67, p27 and bcl-2 label indices might be useful in predicting survival times of patients and grading of astrocytomas.

P-614

Angiotropic lymphoma of the central nervous system: biopsy findings in a case of 53-years old female

Cvetkovic-Dozic D, Dozic S, JovanovicV, Skender-Gazibara M, Govedarovic V and Grujicic D*
Institute of Pathology and Institute of Neurosurgery*, University School of Medicine, Belgrade, Yugoslavia

Introduction: Angiotropic lymphoma is a rare systemic neoplasm in which the central nervous system (CNS) and skin are most often involved.

Case: Our patient, 53-years old female, suffered from spastic quadriparesis and diverse neurological symptomathology with domination of progressive dementia. Clinical investigation, including bone marrow biopsy, failed to demonstrate any lesion outside the CNS. The patient was HIV and Epstein-Barr virus negative. Magnetic resonance imaging (MRI) revealed the multifocal lesions predominantly in the cerebral cortex.
Methods: The surgical cortical biopsy of the 1st frontal gyrus (the largest lesion) was performed. Tissue samples were prepared for light microscopy using routine histological and immunohistochemical methods with DAKO monoclonal antibodies (CD3, CD20, CD45RA, LCA, GFAP, cytokeratin, vimentin, desmin, neurofilament and Ki-67).
Results: The small and medium sized vessels of the leptomeninges, cortex and subcortical white matter were partially or totally occluded by large atypical lymphoid cell. In the majority of vessels the neoplastic cells were noncohesive, free floating in the lumina. The cells were large, oval with amphophilic cytoplasm, hypechromatic nuclei and visible nucleoli. Other findings included multiple cortical and subcortical small areas of subtotal and total necrosis, reactive gliosis and brain edema. The tumor cells expressed markers for LCA and B-cells. They showed the prominent proliferative activity with the expression of Ki-67 immunoreactivity in 35% of cell nuclei. The biopsy diagnosis was angiotropic large-cell B lymphoma of the CNS.
Conclusion: In the cerebral form of angiotropic lymphoma the exact intra vitam diagnosis can be made only by brain biopsy.

P-615

SDHD mutations in a population-based series of patients with parasympathetic paragangliomas.

Hilde Dannenberg, Winand N. M. Dinjens, Mustaffa Abbou, Hero van Urk‡, Diane Mouwen‡, Wolter J. Mooi¶, Ronald R. de Krijger
Departments of Pathology, Josephine Nefkens Institute, and Surgery‡, Erasmus University Medical Centre Rotterdam, The Netherlands; Department of Pathology, Netherlands Cancer Institute¶, Amsterdam, The Netherlands

Introduction: Inherited mutations in the *SDHD* (succinate dehydrogenase subunit D) gene are associated with a high risk of parasympathetic paraganglioma (PGL) in some families. However, little is known about the contribution of *SDHD* mutations to PGL in the general population. We conducted a population-based study to assess the spectrum and frequency of *SDHD* mutations in patients with parasympathetic PGL.
Methods: We analyzed 58 consecutive patients diagnosed with parasympathetic PGL (n=76) between 1987 and 1999 at the Erasmus university Medical Centre Rotterdam. Eightteen (31%) of 58 patients had a positive family history of parasympathetic PGL. We used PCR based SSCP analysis and DNA sequencing of germline and tumor DNA to identify *SDHD* mutations. In addition, more than 200 control alleles were examined for sequence variants of the *SDHD* gene.
Results: We found 3 *SDHD* germline mutations in 17 (94%) of 18 patients with familial PGL and in 10 (25%) of 40 patients with apparently sporadic PGL. No somatic mutations were found. All three mutations involved missense mutations in highly conserved regions (D92Y, L95P and L139P) and were not identified in the control alleles. The specific D92Y mutation was slightly associated with a positive family history and younger age of onset compared to L95P.
Conclusion: Alterations of *SDHD* were identified in 46 percent of this cohort of patients with parasympathetic PGL. The risk of harboring a germline mutation was not limited to patients with familial PGL. Genetic testing for *SDHD* germline mutations is an important diagnostic tool in the assessment of heredity in patients with parasympathetic PGL.

P-616

Atypical malignant teratoid/rhabdoid tumor in an adult – case report

Dozic S, Skender-Gazibara M, Cvetkovic-Dozic D, Govedarovic V, JovanovicV, Jovanovic I*
Institute of Pathology and Institute of Neurosurgery*, University School of Medicine, Belgrade, Yugoslavia

Introduction: Atypical malignant teratoid/rhabdoid tumour (AMTRT) is an extremely rare embryonal agressive central nervous system (CNS) neoplasm usually of early childhood. The histogenesis is undetermined. A few adult cases have been reported.
Case: Our patient, 67 years old male, suffered from a clinical symptomathology comparabile with Garcain syndrome in a duration of several months. Computed tomography (CT) and magnetic resonance imaging (MRI) revealed a great temporo-basal inhomogenous intradural, extracerebral tumour. It was surgically subtotally excised.
Results: Essential part of tumour was highly cellular, composed of rhabdoid cells. They were round or oval in shape, with abundant eosinophilic cytoplasm and rather prominent nucleolus in great majority of the cells. A number of cells contained cytoplasmic hyaline eosinophilic inclusions composed of whorled bundles of intermediale filaments at electron microscopic examination. The rhabdoid cells expressed positive vimentin and SMA and were negative for a buttery of antibodies including GFAP, desmin, NSE, alpha –fetoprotein, synaptophysin and EMA. The epithelial tissue was composed of nests of large, vacuolated keratin-positive cells. Between these nests was rhabdoid or mesenchimal tissue. There are several glial GFAP positive fields. Mesenchymal component was composed of small and larger spindle cells fascicularly or loosely arranged. In the mesenchymal fields there are small groups of GFAP-positive cells. Mitotic figures were numerous in the rhabdoid portion and less common in mesenchymal fields.
Conclusion: An extensive clinical and radiological investigation failed to reveal tumor deposits in the other parts of the body. We think that this tumor fulfills the histological, immunochistochemical and ultrastructural criteria for AMTRT of the CNS.

P-617

Intracranial extraskeletal myxoid chondrosarcoma: Report of a cellular case and review of the literature

Carmen González-Lois, Cristobal Cuevas, Osamah Abdullah, Miguel A. Martinez, Ana Cabello, José R. Ricoy
Department of Pathology, Complutense University School of Medicine, Hospital Universitario 12 de Octubre, Madrid, Spain

INTRODUCTION: We describe a patient with an intracranial extraskeletal myxoid chondrosarcoma (EMC), an unusual neoplasm

of the deep soft tissues of the extremities. Very rarely are they localized as an intracranial lesion, and we believe it is very important to accurately distinguish EMC from other intracranial tumors such as classical or "skeletal" chondrosarcomas, mesenchymal chondrosarcoma, enchondroma, and myxoid tumors (chordoma, and chondromyxoid fibroma) in order to determine their prognostic implications. Furthermore, this case present in the third local recurrence, higher-grade cellular areas, such event has never been reported in intracranial cases.
CASE REPORT: A 17 year-old female presented tonic and clonic seizures, episodic left hemiplegia and intense right-sided headaches. Computed tomography and magnetic resonance of the skull showed a right fronto-parietal cortical lesion.
Complete surgical excision of the lesion through a right parieto-temporal craniotomy was performed. The tumoral lesion recurred locally twice (16 and 19 months after the initial surgery respectively). First and second surgical specimens where diagnosed as extra-skeletal myxoid chondrosarcoma. Microscopically, the third local recurrence showed abrupt transition from areas of conventional myxoid chondrosarcoma to high-grade cellular areas with fusiform features.
CONCLUSION: Extraskeletal myxoid chondrosarcoma is very rarely described as an intracranial lesion. Reference on this topic is very confusing as there is no clear-cut distinction between skeletal chondrosarcomas with prominent myxoid matrix and extraskeletal myxoid chondrosarcoma which is a definite entity first defined by Enzinger and Shiraki in 1972 in deep soft tissues of the extremities. We review the cases reported in the literature with the diagnosis of myxoid chondrosarcoma either of extraskeletal origin or with skeletal attachment, and analyze their clinico-pathologic features.

P-618

"The recurrent Glioblastomas after radiotherapy-immunomorphological study of cellular populations and vasculature"

E. Iżycka-Świeszewska, R. Rzepko, J. Borowska- Lehman, A. Roszkiewicz

Introduction: Recurrent Glioblastomas (GBrec) after irradiation have two morphological fractions: radiotherapy-induced changes and regrowing neoplastic tissue. The examination of GBrec gives the information of final evolution of astrocytomas.
Methods: The study was performed on 15 cases of reoperated GBrec after irradiation. The interval between operations was from 2,5 to 25 months (mean 11,5), both tissue material was examined. Morphology of neoplastic cells and changes of vascular stroma were analized. Immunohistochemical examination was performed based on antibodies against p53, Ki-67 and ubiquitin.
Results: Neoplastic tissue consisted of four main populations: monstrous cells, gemistocytes, fibrillary astrocytes and small anaplastic cells. The vascular stroma components were: glomeruloid vessels, capillaries, and the vessels with degenerative changes- fibrosis, hyalinization, telangiectases, thrombosis.
In GBrec in contrast to the primary tumor: the monstrous cellls and gemistocytes were more abundant or appeared *de novo* (all cases), the population of small anaplastic cells was more pronounced or appeared *de novo* (most cases), the fibrillary astrocytes were less numerous (most cases).
All tumors showed fields of radionecrosis and gliomesenchymal scar was observed in longer cases. The postirradiated vascular alterations included degenerative changes and adventitial proliferation. In areas of regrowing GB features of complex angiogenesis were more intense than in primary tumor.
Immunophenotype of neoplastic cells populations in GBrec: monstrous cells- Ki-67- , p53-negative, ubiquitin- positive; gemistocytes- Ki-67+/–, p53+, ubiquitin- positive; fibrillary astrocytes Ki-67++, p53+/–, ubiquitin- negative; small anaplastic cells- Ki-67+++, p53++, ubiquitin- negative.
Conclusions: Regrowing GBrec present features of further dedifferentiation-proliferating small anaplastic cells, increasing expression of p53 and intense aberrant angiogenesis.

P-619

Immunomorphological study of the central and peripheral Schwannomas

M. Kamiński, E. Iżycka-Świeszewska, R. Rzepko, A. Karmoliński, A. Roszkiewicz
Dept. of Pathology, Medical University of Gdansk, Gdansk, Poland

Introduction: Schwannoma is a nerve sheath tumor composed of cellular component Antoni A (AA) and loose myxoid Antoni B (AB). Immunomorphological characteristic of components in central and peripheral tumors are presented.
Methods: 44 Schwannomas: 24 central (acoustic-21, spinal root-3) and 20 peripheral (mediastinal-5, subcutaneous-5, peripheral nerve-7, retroperitoneal-3) were analized. Immunohistochemical study was made with anty S-100, GFAP and CD34.
Results: 22 central neurinomas were classic type, one-cellular and one-ancient. Component AA was equally present with AB, Verrocay bodies were almost absent. The transition between patterns was delicate. Peripheral tumors were: 16 classic type, 3-cellular, 1-plexiform. AA pattern dominated, Verrocay bodies were often present. The transition between patterns was usually sharp. S-100 protein prominent expression was present in all tumors, less intense in AB areas. GFAP-positive cells were found usually in AA. Staining in central Schwannomas: scattered cells+ (4), focal+ (3), focal++ in 2cases; in peripheral tumors- focal+ (4), focal++ (3) and focal+++ (2). CD34-positive cells were spindle bipolar or had branching processes. Outside endothelium they were present in AB areas, they accumulated in borders with AA, some were perivascular. CD34 staining was stated in diverse quantity in 18 central and in 12 peripheral tumors.Vascular changes included: hyalinization, telangiectases, thrombosis, haemangiomas. In 5 peripheral and 10 central tumors microvascular glomeruloid proliferation was observed. Vascular density in all tumors was low.
Conclusions: CD34-positive cells are often present within Schwannoma. GFAP reactivity is more pronounced in peripheral tumors. There are some immunomorphological differences within Scwannomas depending on the site of their origin.

P-620

Hypothalamic lesions in mice treated with monosodium glutamate

K Katic, S Najman, S Cekic, V Bojanic, V Katic
Medical Faculty of Nis University, Serbia

Aim: In an earlier reports from this laboratory, neonatal treatment with monosodium glutamate (MSG) was shown to cause a disrup-

tion of the hypothalamic-pituitary-gonadal axis which induced Cushing's obesity, letargy, hypogonadism and sterility, as well as spleen atrophy. Having in mind the contradictory data on hypothalamic lesions in obese mice, the aim of the present work was thus to study the MSG-effect on hypothalamus.

Material and methods: Twenty newborn C57BL/6J mice were injected daily with MSG (4,4 mg/g body wt) sc, on days 1–10 of life, for the first 5 postnatal days. Another group of 10 mice, which were injected with saline solution, 0,02 ml/g body wt, every 24 h for the first 5 postnatal days, served as controls.

Mice were killed at 4 months of life. Their hypothalamic tissue was fixed in 10% Formalin for 24 h. After fixation, hypothalami were routinelly processed and embedded in paraffin. Each section (5 μm in thickness) was stained with HE, Van Gieson and Gomori, and observed microscopically.

Results: Treated animals were quite lethargic as adults, and they lacked the sleekness of body coat, seen in controls. Cushing-type of obesity was evident macroscopically. Basophyl cells of pituitary gland were hyperplastic of large size and with foamy aspect. Cortical cells of the adrenal gland, symetrically, were also hyperplastic.

Hypothalamic tissue

The arcuate nuclei were completely destroyed along with neuronal constituents in the median eminence. Instead these tissues, gliosis was found, the most important histopathologic indicator of CNS injury. So, astrocytes were hypertrophic and hyperplastic, their nuclei small and dark located in a dense net of processes (glial fibrils).

Multifocal small foci of microglial nodules, associated with neuronophagia, were also observed.

Conclusion: Brain lesions, obesity, endocrine gland dysfunction and hypothalamic multifocal lesions in mice treated with MSG suggest a complex hypothalamo-pituitary-adrenal-gonadal disturbance.

P-621

The patology changes puttern in brain induced by cryptococcosis

O.K. Khmelnitsky, R.A. Nasyrov, N.U. Vasilyeva
Mycology Institute of Medical Academy for postgraduate education. Scientific Research Institute of infectious diseases in children, S-Petersburg, Russia

Nowadays, the number of cryptococcosis cases is increasing both because of secondary immunodeficiency and AIDS.

Objective: To evaluate brain lesions in patients who died of generalized cryptococcosis following secondary immunodeficiency syndrome.

Methods: Paraffin slides of brain tissue were explored with routine and special staining technicues.

Results: Different types of pathohystologycal changes were determined in patients who died of cryptococcosis infection. Single us cryptococcoses in pia mater and lymphocyte-monocyte infiltrates were specific for the first type of changes. We also observed endothelium cells descguamation and microvessels wall necrosis in cortex and pia mater. Necrosis focuses in brain tissue were observed as a seguence of microcirculation disorders. Neuroglia remained intact.

Numerous cryptococcoses focuses and mild inflammatory infiltration of pia mater were registered as main characteristics of the second type changes. A large amount of cryptococcoses was found in microvessels lumen. Microvessels walls were destroyed. Cryptococcoses colonies were found in cortex and in white substance of brain. The colonies were surrounded with astrocytes proliferation zones. Colliguation necrosis and exsanguinations were observed in white substance.

The third type of changes was observed after the prolonged brain cryptococcosus infection. Inflammatory infiltration was found in pia mater. Cryptococcoses were observed in gigantic cells cytoplasma. Arteryolas wells necrosis and cortex necrosis focuses were determined. Simplast consists of proliferating astrocytes and vessels was observed in brain white substance.

P-622

Enhanced proteolysis of IκBα and IκBβ proteins in astrocytes by Moloney murine leukemia virus (MoMuLV)-*ts*1 infection: a potential mechanism of NF-κB activation

Hun-Taek Kim[a], Serban Tasca[a], Wenan Qiang[b], Paul K. Y. Wong[b], George Stoica[a]
[a] Department of Veterinary Pathobiology, Texas A&M University, College Station, USA; [b] Department of Carcinogenesis, The University of Texas, M.D. Anderson Cancer Center, Science Park-Research Division, Smithville, USA

We previously reported that Moloney murine leukemia virus (MoMuLV)-*ts*1-mediated neuronal degeneration in mice is likely due to loss of glial support and release of inflammatory cytokines and neurotoxins from surrounding *ts*1-infected glial cells. NF-κB is a transcription factor that participates in the transcriptional activation of a variety of immune and inflammatory genes such as tumor necrosis factor (TNF)-α. Here we show that infection of astrocytes by *ts*1 activates NF-κB *in vitro* and *in vivo* by enhanced proteolysis of the NF-κB inhibitors IκBα and IκBβ. We examined the pathways responsible for the degradation of IκBα and IκBβ. In *in vitro* studies using protease inhibitors IκBα proteolysis in astrocytes by *ts*1 infection was partially blocked by the specific calpain inhibitor calpeptin but not by several proteasome inhibitors, whereas rapid IκBβ proteolysis was blocked by proteasome inhibitors. Furthermore, treatment with MG-132, a specific proteasome inhibitor, significantly increased levels of multiubiquitinated IκBβ protein in *ts*1-infected cells, but was ineffective in building up multiubiquitinated IκBα protein. These results indicate that the calpain proteolysis is an alternate mechanism of IκBα proteolysis in *ts*1-infected astrocytes, even though the ubiquitin-proteasome pathway is a well-known IκBα degradation pathway. Additionally, we demonstrated that *ts*1 infection of astrocytes *in vitro* increased expression of inducible nitric oxide synthase (iNOS), a NF-κB-inducible gene product. Our results suggest that NF-κB activation in astrocytes by *ts*1 infection is mediated by enhanced proteolysis of IκBα and IBκ through two different proteolytic pathways, the calpain and ubiquitin-proteasome pathways, resulting in increased expression of iNOS.

P-623

Meningiomas associated with meningioangiomatosis; the largest collection of five cases

Na Rae Kim[1], Je G. Chi[2]
[1]Department of Pathology, Kangnam General Hospital,
[2]Department of Pathology, Seoul National University College of Medicine, Seoul, Korea

Aims: Meningioangiomatosis (MA) is a unique, rare hamartomatous lesion on its own. Rarely MA has coexisted with meningiomas, arteriovenous malformation, encephalocele, oligodendroglioma, meningeal hemangiopericytoma, and orbital erosion. Among these, meningiomas arising in the background of MA are rare conditions which pathologically and radiologically mimick invasive meningiomas, and take on a benign clinical course in children and young adults. We focused on meningiomas associated with MA, which are the most frequent combination. Herein we assess meningiomas associated with MA and discuss their pathogenesis.
Methods: The surgical pathology database was searched for patients of MA associated with meningioma. All the microscopic slides were reviewed in each case. Follow up duration ranged from 13 months to 10 years (mean 66 months). Meningiomas were assessed for the histologic type (meningothelial, fibroblastic, transitional, sclerosing, etc), cellularity, mitotic rate, cellular pleomorphism, macronucleoli, necrosis, and brain invasion. When neoplastic cells break through the pia mater to involve the underlying cortex and encircle islands of heavily gliotic tissue, we regarded them true brain invasion.
Results: Five such cases were found. The patients aged 3, 4, 6, 9, and 19 years. They had a history of longstanding intractable seizures. Radiologically intradural, extra-axial masses were detected and gross total resections were done except for one. Grossly the tumors were globular and tightly adhered to the dura mater. The types of meningiomas are as follows: sclerosing (n=2), transitional (n=1), and meningothelial type (n=1). The adjacent neural parenchyma showed prominent proliferation of vessels, which were cuffed by meningothelial cells, or fibroblasts with calcification and gliosis. These findings were compatible with MA. Four out of five meningiomas (80%) showed brain invasion and bland-looking histology without cellular pleomorphism, mitosis or necrosis. Except for one recurrence which was subtotally resected at first operation, all patients are free of recurrence and alive during the follow-up period.
Conclusion: The most frequent association of meningiomas with MA support that MA is primarily a meningothelial lesion with occasional marked proliferation to a solid mass of a meningioma.
We emphasize that the recognition of these rare coexistent conditions showing frequent brain invasion is important to avoid unnecessary postoperative radiation or additional treatments due to erroneous interpretation as aggressive meningiomas in children and young adults.

P-624

Detection of the SYT-SSX chimeric mrna in paraffin-embedded synovial sarcoma

Koković, I., Bračko, M. and Golouh, R.
Department of Pathology, Institute of Oncology, Ljubljana, Slovenia

Introduction: Synovial sarcoma is soft tissue tumor of young adults, characterised by the t(X;18)(p11.2;q11;2) chromosomal translocation in 90% of cases. Thus, identification of the t(X;18)(p11.2;q11.2) and detection of resulting SYT-SSX fusion transcript is useful diagnostic marker for this tumor. In this study we introduced reverse transcription-polymerase chain reaction (RT-PCR) assay to amplify SYT-SSX fusion transcripts from formalin-fixed, paraffin-embedded (FFPE) synovial sarcoma.
Methods: The FFPE tumor samples of 24 patients with synovial sarcoma were collected from the files of Department of Pathology, Institute of Oncology, Ljubljana. Total RNA was isolated from deparaffinized tissue sections by proteinase K digestion, phenol/guanidine isothiocyanate extraction and isopropanol precipitation. RT-PCR was performed using GeneAmp PCR kit (Perkin Elmer) according to the manufacturer's protocol. The SYT-SSX fusion transcripts were detected using forward primer SSA (for SYT gene) and reverse primers SSX1-rev and SSX2-rev (for SSX1 and SSX2 gene, respectively). The primers were chosen to specifically amplify junctional regions of the SYT-SSX1 and SYT-SSX2, thus enabling identification of either type of fusion transcript. Amplified fragments were analysed by polyacrylamide gel electrophoresis. Regardless the type of fusion transcript, SYT-SSX1 or SYT-SSX2, the length of amplified fragment is 110 bp.
Results: SYT-SSX fusion transcripts were detected in 21/24 (87,5%) analysed cases, while 3/24 (12,5%) cases were negative. Six cases were positive for SYT-SSX1 and 15 were positive for SYT-SSX2 transcript.
Conclusions: We introduced RT-PCR assay for detection of the t(X;18)(p11.2;q11;2) chromosomal translocation in paraffin-embedded synovial sarcoma. The specificity of described assay is in agreement with results published elsewhere. We suppose that this assay could be useful adjunct test for diagnostically difficult cases or in retrospective studies to refine the diagnosis of synovial sarcoma in archival material.

P-625

A morphometric study of angiogenesis i n diffuse astrocytic neoplasms

P. Korkolopoulou, N. Kavantzas, A.E. Konstantinidou,
E. Patsouris, P. Christodoulou, E. Thomas-Tsagli, C. Eftychiadis, P. Davaris
Department of Pathology, National and Kapodistrian University of Athens, Athens, Greece

Introduction: Astrocytic brain tumors, particularly malignant astrocytomas, are recognized to be highly vascular neoplasms with potent angiogenic activity. Recent research has shown that quantitation of microvessel density (MVD), as a measure of the degree of angiogenesis, constitutes a strong prognostic indicator in patients with astrocytomas. However, the significance of other morphometric aspects of microvessel network has not been tested so far.
Materials and Methods: In this report, histologic sections from 70 astrocytomas (grades II to IV), immunostained for CD34, were evaluated by image analysis for the quantitation of MVD, total vascular area (TVA), and microvascular branching as well as several morphometric parameters related to vessel size or shape. Patients were followed up till death (n=60) or for a median period of 32 months.
Results: Minor axis length increased with grade (p=0.045) but MVD and TVA presented a peak in grade III (p=0.033 and p<0.001 respectively). Size and shape related parameters affected survival in univariate analysis of grade IV and grades II/III respectively. In multivariate analysis, only branching counts, along with age and grade, were the independent predictors of survival. Although MVD, TVA and branching counts were adversely related to disease-free survival in grades II/III (univariate analysis), only TVA remained statistically significant in multivariate analysis
Conclusions: TVA and branching counts are prognostically more informative than MVD for patients with diffuse astrocytic tumors.

P-626

Quantitative and morphometric investigations of the expression of topoisomerase II alpha and Ki-67 in relation to type and grade of brain tumors diagnosed by means of stereotactic biopsy

Korzeniowska A., Adamek D., Moskala M.*, Kaluza J., Goscinski I.*
Department of Neuropathology and *Department of Neurotraumathology, Jagiellonian University, Medical College. Kraków, Poland

Introduction: There is no broadly accepted system of tumor grading (esp. gliomas) applicable specifically for stereotactic brain biopsy (SBB). To get maximum from minimal material (10–15 mm^3) we applied quantitative and morphometric analysis as an adjunct procedure for cytology and immunocytochemistry (performed on smears). The labeling indexes (LI) of: topoisomerase II alpha (TIIa) and Ki-67 were investigated in relation to semiquantitatively evaluated expression of p53, Bcl-2, GFAP, and to the WHO and Daumas-Duport (DD) grade of neoplasm. Special attention was paid to TIIa, an enzyme involved in DNA replication and regarded as a "target" for some antineoplastic drugs (a potential index of drug sensitivity).
Methods: 28 (20 gliomas) of all 112 SBBs performed in our center were included into analysis (quality of slides, suitable for morphometry). The LIs of TIIa and Ki-67 were calculated in smears with the immunocytochemical reaction. Morphometric calculations of nuclei (area, diameter) were performed by means of image analysis system (MultiScan).
Results: The LIs of TIIa and Ki-67 (both mutually positively correlating) were similar in WHO grade III and IV gliomas, whereas in grade IV gliomas, classified accordingly to DD, the LI of TIIa was 2 times higher as compared with grade III. Morphometry of nuclei in gliosis is not statistically significantly different from nuclei of astrocytoma II.
Conclusions: Immunocytochemistry for TIIa and Ki-67 together with DD system of grading are recommended for SBB. Acknowledgements: This study is supported by Polish Committee for Scientific Investigations, grant No. KBN 501/G/240

P-627

Splice variants of the catalytic subunit of human telomerase in high grade astrocytic tumors

Vassiliki Kotoula, Sotiris Barbanis, Martha Avramidou, Constantine S. Papadimitriou, George Karkavelas
Department of Pathology, Aristotle University – Medical School, Thessaloniki, Greece

Background-Aim: Telomerase activity and the expression of its reverse transcriptase subunit, hTERT, have been recently proposed as prognostic parameters in brain neoplasms. hTERT has been reported to undergo alternative splicing in other organ and tumor systems. In this study, we investigated hTERT expression in high grade astrocytic tumors by targeting multiple areas of the transcript, in correlation with telomerase activity.
Materials and methods: A total of 20 frozen high grade astrocytic tumor and 4 normal brain specimens were examined. hTERT expression was determined by multiple RT-PCR approaches and subsequent multiprobe blotting. Nested RT-PCR protocols to selectively demonstrate the expression of the full length transcript were also established. Telomerase activity was assessed by a non-radioactive TRAP assay.
Results: Seventeen out of the 20 tumor specimens demonstrated various levels of telomerase activity; interestingly, all tumors expressed hTERT. Both parameters were negative in normal samples. Splice variants lacking exons 7 and 8, and occasionally a region in exon 6, could be identified in all hTERT positive cases. The full length transcript was present only in 14 cases; its relative high expression, compared to this of the splice variants, correlated well with high levels of telomerase activity.
Conclusions: This study shows that hTERT splice variants are expressed in high grade astrocytic tumors; these variants do not seem to be related with telomerase activation, while the full length transcript does. Selective targeting of the full length transcript should be taken into account when designing protocols for the determination of hTERT expression in this tumor system.

P-628

Primary Epithelioid Sarcoma of Dura: Case Report

Kurtkaya-Yapıcıer Ö[1], Scheithauer BW[1], Dedrick DJ[2], Wascher TM[2]
Department of Laboratory Medicine and Pathology, Mayo Clinic, Rochester, Minnesota[1], and St. Elizabeth Hospital, Appleton, Wisconsin[2]

Epithelioid sarcomas are rare mesenchymal neoplasms most of which occur in the extremities of young adults. Despite isolated reports of epithelioid sarcomas arising in the head and neck region, to our knowledge it has not been described in the central nervous system (CNS). We present a unique dural example arising in the right temporal dura of an 18 year old female. Enhancing on MRI, the 4.5 cm tumor focally traversed the skull to penetrate galea, temporal muscle and subcutaneous tissue. No brain invasion was noted. Despite gross total removal and postoperative radiotherapy (59 Gy), a large recurrence was noted at 5 months. Histologically, the partly necrotic tumor consisted of epithelioid and spindle cells showing widespread vimentin and variable cytokeratin as well as epithelial membrane antigen immunoreactivity. Ultrastructurally, the cohesive cells featured various organelles, intermediate filaments, junctions and filopodia-containing intercellular spaces. With the inclusion of epithelioid sarcoma, the spectrum of CNS sarcomas continues to expand.

P-629

A von Hippel-Lindau disease in a patient without a family history – a case report

Codruta Lazureanu, Carmen Muntean, Elena Lazar, N. Tudose
Pathology Department, University of Medicine Timisoara

Histological differentiation between cerebellar capillary hemangioblastoma and a metastasis of a clear cell carcinoma with the same topography is impossible to resolve just on H&E stain. The complete clinical data and immunohistochemistry make the needed difference.
We present a case of a 65 years old women, who underwent left nephrectomy 20 years ago for a Grawitz tumor. In 1997 she had two

concomitant neoplasms: thyroidian and cerebellar. Only the cerebellar neoplasia was operated; the tissue fragments being stained with H & E, periodic acid- Schiff and silver impregnation for reticulin, the Gordon-Sweet method. The tumor was formed by clear cells (H&E stain), PAS-positive. It had an impressive capillary network and displayed an argyrophilic reticular fibers supporting frame. The border with normal cerebellar parenchyma was sharp and in the middle of the tumor there was an area of hemorrhage and necrosis. Immunohistochemistry was completely negative for surface membrane staining for RCC and for thyreoglobulin. The diagnosis of cerebellar capillary hemangioblastoma was established.

She died 3 years later with cardio-pulmonary failure. The autopsy revealed multiple tumoral masses in right parietal cerebral lobe beneath the meningeal convexity, around and within tracheal wall and within pancreatic parenchyma. All the fragments taken from these neoplasms presented on H&E stain a similar structure as the cerebellar hemangioblastoma did before. We concluded that this case respects the diagnostic criteria of von Hippel-Lindau disease in a patient without a family history.

P-630

The role of RB2/p130 tumor suppressor gene and HIV-1 infection in the pathogenesis of AIDS-related Lymphomas

Leoncini L., Cinti C., Bellan C., De Falco G., Lazzi S., Ferrari F., La Sala D., Vatti R., Tosi GM., Claudio PP., Nyongo A., Gloghini A., Carbone A., Tosi P., Giordano A.
Ist. di Anat. e Istol. Patologia, Univ. degli Studi Sienna, Siena, Italy

Mutations in the RB2/p130 nucleotide sequence have been detected in different human tumors, suggesting that RB2/p130 could act as a tumor suppressor gene. In addition to mutations of the gene, interaction with viral oncoproteins is another important mechanism of RB2/p130 inactivation. Few data are available in literature on the interaction between HIV-1 and cell cycle regulatory proteins, including the retinoblastoma (RB) family proteins. The aim of the present study was to investigate RB2/p130 gene expression in a series of 23 cases of AIDS-related lymphomas and its interaction with Tat protein of HIV-1 by an in vitro binding assay. We found no mutations in the RB2/p130 gene and unusually high levels of nuclear expression of pRb2/p130, p107 and other proliferation associated proteins. These findings might suggest that a molecular mechanism usually observed in viral-linked oncogenesis could be involved. Interestingly, the results of our in vitro binding assay revealed that the HIV-1 Tat protein binds specifically to the pocket region of pRb2/p130. This results in the inactivation of its oncosuppressive properties and the induction of genes needed to proceed through the cell cycle including p107, cyclin A and cyclin B. By using single cell PCR assay, we found HIV-1 DNA in the neoplastic cells of 2 cases of DLBCL. Alternatively, in the remaining cases where HIV was detected by PCR only on whole tissue, soluble Tat protein could function as a biologically active extra-cellular protein released by infected cells, readily taken up by uninfected B-cells. Our results suggest, and point out, that pRb2/p130 oncosuppressor protein may be a target in the interaction between the HIV-1 and host proteins. The reevaluation of HIV-1 itself as an oncogenic virus is thus warranted.

P-631

Vascular anomalies of the spinal cord

Matsko D.E., Ivanova N.E., Panuntsev G.K.
Russian Polenov Neurosurgical Institute, St.Petersburg

33 cases of vascular anomalies (VA) were analyzed. Pathologic diagnosis was made on surgical specimens in 30 cases, at autopsy in 2, and using both the studies in 1.

Histologically VA were classified as arteriovenous malformations (AVM) – 21 cases, cavernous (CM) – 4, venous (VM) – 2, capillary-venous – 2, capillary angioma – 1, non-classifiable – 3.

VAs first manifested at the age of 10 to 30 in 59%, were of 4 types as to their clinical course (apoplectic – 22%, progressive – 31%, intermittent – 12%, mixed – 35%) and resulted in marked motor disturbances, pelvic and different sensitivity disorders. Mean period of the proper diagnosis-making was 7.6 yrs, primary diagnosis was wrong in 71% of the cases, VMs were masking as over 10 nosologic entities, i.e. osteochondrosis, multiple sclerosis, "acute abdomen" etc. 25 accompanying congenital anomalies were found including heart disease (2), retinal angiodisplasia (2), cutaneous angiomatosis (4), renal hydronephrosis (5), spinal anomalies (6), Friedreich's foot (2), pontine telangioectasia (1), kidney doubling (1), Parks-Weber's syndrome (1), elephantiasis (1).

Macroscopically AVMs differed from their brain analogues by their elongated form first of all. AVM body (the knot of dysplastic vessels, proper) was of less volume, as referred to feeding and draining vessels, than that of intracranial AVMs. The feeding arteries usually paralleled the spinal roots. Afferent portion of the AVM consisted of several (2 to 4) arteries in 10 cases. The anomalous arteries could enter the spinal canal either at the level of AVM body or at some other one; sometimes, having entered the spinal canal at the level of vascular knot, the afferent vessel made a loop along a considerable portion of the spinal cord to come to AVM body consisting of a conglomerate of plexiform vessels. Several conglomerates of the kind were found in 2 patients. AVM bodies were usually localized at the surface of the spinal cord, sometimes compressing or pushing it aside, predominantly at the posterior surface or within the posterior spinal regions. In 1 case of cervical AVM the course and localization of the draining vein was atypical: situated at the anterior spinal fissure, it ran upwards to the cranial cavity. The draining vessels made venous lacunae in 9 patients, multiple in 3 cases. The lacuna was localized intramedullarly in 1 patient. The results of histologic study of all the three spinal AVM portions corresponded in general to those of brain AVMs.

CM were localized extramedullarly, intramedullarly, and extradurally. In 1 case the pathologic structure originated from the dorsal root. Thoracic CM was found in 3 cases, at C1-2 in 1. CM varied in size 1×0.5×1 cm to 2×6×2 cm. They were rounded or oval. Microscopic structure of the removed CMs did not differ from their extra-cord analogues.

Grossly VMs were conglomerates of plexiform veins. Both the VMs were adjacent to the dura, one underneath, the other above it. Both the capillary-venous malformations were localized without the spinal cord limits (one exradurally, the other intravertebrally).

Thus, VA of the spinal cord is a heterogenous group of pathologic structures of vascular origin, with no signs of blastomatous grouth, localized within the spinal cord, its roots, thecae, surrounding fat, and vertebrae, taking part in their feeding and venous outflow, and often combined with congenital anomalies of other systems and organs. VA of the spinal cord obtains certain specific signs, i.e. elongated form, frequent anatomic connection with the structures sur-

rounding the spinal cord, peculiar localization (within the limits of spinal-cord matter – 80%, at the posterior surface or posterior regions of the spinal cord – 73%).

P-632

Cytokeratin – staining pattern, hormone expression profile, and cell proliferation in pituitary adenomas of akromegalic patients

Peter R. Mazal, Thomas Czech, Roland Sedivy,
Martin Aichholzer, Julia Wanschitz, Herbert Budka
Institute of Clinical Pathology, Dep. of Neurosurgery, Institute of Neurology, University of Vienna, Austria

Object: To find out the prognostic relevance of the intracytoplasmic distribution of cytokeratins (CK), immunohistochemically defined hormone production profile, proliferative activity, and clinical presentation, 76 pituitary adenomas of akromegalic patients were investigated. *Methods*. CK distribution, growth fraction (MIB1 index) and hormone production profile were analyzed by means of immunohistochemistry. Apoptotic activity was investigated by the TUNEL method. *Results*. Two different CK distribution patterns were seen: a dot-like pattern in 29 cases (type 1 adenomas), and a perinuclear fibrillary pattern in 47 cases (type 2 adenomas). Type 2 adenomas showed more prominent co-expression of prolactin ($p<0.0001$), luteotrophic hormone ($p<0.002$), follicle stimulating hormone ($p<0.005$), thyroid stimulating hormone ($p<0.0001$), and α-subunit ($p<0.005$), as compared to type 1 adenomas. The mean MIB1 index was significantly higher in type 1 vs. type 2 tumors (4.23%, range: 1.93%–9.83% vs. 2.07%, range: 0.67%–4.87%, $p<0.0001$). Apoptotic activity was too low in both examined groups to be used for bilancing of tumor cell turnover. Clinical analysis of patients with type 1 adenomas revealed female predominance, younger age, larger tumor size, and more frequently aggressive growth with higher incidence of suprasellar extension ($p<0.0001$) and cavernous sinus infiltration ($p<0.0001$), as well as larger proportions of re-operations and incomplete resections (34.5% vs. 8.51%). Additionally, the interval of re-operation was shorter in group 1 adenomas (mean: 16 months, range: 9–21 months vs. mean: 57 months, range: 18-158 months).
Conclusions: We conclude that classification of adenomas of akromegalic patients based on intracytoplasmic CK distribution, combined with examination of proliferative activity, and immunohistochemically defined hormone production profile, provides important prognostic information for the management of akromegalic patients.

P-633

The epithelial differentiation of secretory meningiomas is associated with a strong expression of CK7 and CK18.

Meyronet D (1), Fotso Mj (2), Duthel R (2), Brunon J (2), Mosnier Jf (1)
(1) Pathology Department, (2) Neurosurgery Department, CHU de Saint Etienne, 42055 Saint Etienne cedex 2

Introduction: Meningiomas are particular tumours with both mesenchymal and epithelial differentiations. Secretory meningiomas are characterized by glandular structures strongly expressing cytokeratin and integrin subunits alpha6 beta4. The goal of this work was to study the expression of cytokeratin subtypes in order to highlight the mechanism of tumour epithelial differentiation in meningiomas.
Methods: Twelve secretory meningiomas were retrieved from the files of Hôpital de Bellevue, Saint-Etienne. They were classified according to the WHO brain tumours classification. Frozen sections were immunostained for vimentin (Dako), epithelial membrane antigen (EMA) (Dako), 34betaE12 (Dako), AE1/AE3 (Dako), KL1 (Immunotech), cytokeratin (CK) 7 (Dako), CK 18 (Dako), and CK20 (Dako), using a three step indirect immunoperoxydase technique
Results: Secretory meningiomas strongly and diffusely expressed vimentin and EMA. Glandular structures only strongly expressed 34betaE12, AE1/AE3 and KL1. They also strongly expressed CK 7 in all cases and CK 20 in 5 cases. CK 18 was constantly expressed in glandular structures and was absent from the extra glandular areas but in one case.
Conclusion: The morphological epithelial differentiation of meningiomas is associated with the expression of CK7 and CK 20 like in highly differentiated epithelia such as colon. The immunoreactivity of extraglandular tumour cells for CK 18 in meningiomas suggests its precessive expression during meningeal tumorogenesis.

P-634

Effect of crystal violet 0.05% on the corneal endothelium and trabecular meshwork of rabbits

Elham ElSayed, Ahmed Mohamed Reda Awadein,
Mohamed Hassan El-Hoshy
Research Institute of Ophthalmology, Cairo, Egypt

Introduction of substances in the anterior chamber of the eye, which stain the anterior lens capsule without staining the underlying lens cortex, offered a great help during capsulorhexis. Several Dyes have been tried to stain the anterior capsule. The aim of this study is to try crystal violet as a new stain and to study its possible effect on corneal endothelium and trabecular meshwork.
The study was performed on 24 adult pigment rabbits. The rabbits had one eye injected with 0.2 cc 0.05% crystal violet and the fellow eye injected with lactated Ringer's solution as a control. The specimens were examined at 1 day (Group A), 3 days (Group B) and 1 week (Group C) after injection, using light microscopy, scanning and transmission electron microscopy.
Group A revealed pigment deposition in the epithelial cells, stromal keratocytes, endothelium and trabecular meshwork in all eyes examined. SEM of the corneal endothelium revealed junctional seperation and decrease in microvilli. Group B revealed marked decrease in pigment deposition. Only one of the 8 eyes (12.5%) examined showed residual pigment deposition in the epithelium and endothelium. The stroma however retained its pigment in 6 of the 8 eyes (75%) examined. The corneal endothelium showed mild vacuolation in all eyes examined. Those vacuoles were seen by TEM to correspond to enlarged mitochondria. Group C (1 week after injection) revealed no pathological changes or pigment deposition in all layers of the cornea, as well as the trabecular meshwork, in all eyes examined. SEM of the corneal epithelium and endothelium appeared normal in all eyes examined. The corneal endothelium appeared normal by TEM. Only in 3 of the 8 eyes examined, parts of the corneal endothelium retained the picture of enlarged mitochondria.

The safety of intracameral crystal violet 0.05% has given encouraging results as regards effect on the corneal endothelium and trabecular meshwork.

P-635

Evaluation of proliferation, apoptosis and angiogenic factor in brain avernomas

Hiromichi Nakabayashi, Takaho Murata, *Mitsuhiro Hara
Department of Neurosurgery, Murata Hospital; *Department of Neurosurgery, Osaka City University Medical School, Japan

Introduction: The prevalence of brain cavernoma is about 0.5%. Although they seem to be stationary, some of them show dynamic changes characterized by repeat bleeding, growth, or de novo appearance. We analyzed the proliferation, the frequency of apoptosis and the expression of angiogenic factor in order to search the dynamic mechanism of brain cavernomas.
Methods: 22 surgically resected and histologically verified brain cavernomas were studied. These cases were divided into three groups. Group 1 consisted of cavernomas with tumor-like growth (n=4). Group 2 consisted of de novo cavernomas (n=2). Group 3 consisted of cavernomas without growth or de novo appearance (n=16). Proliferation was evaluated immunohistochemically using the Ki-67 (MIB-1) antibody. Apoptotic cells were visualized by staining with anti-single strand DNA antibody. The anti-thymidine phosphorylase (TP) antibody was used for the evaluation of angiogenic factor.
Results: The mean Ki-67 labeling index (LI) were 2.25% for group 1, 1.43% for group 2 and 0.12% for group 3. The Ki-67 LI showed good correlation with the growth pattern of cavernomas. The frequency of apoptosis (apoptotic rate) varied from 0% to 0.37%. There were no significant differences among the three groups. Immunopositivity of TP was recognized in all cases. Group 1 and 2 had higher TP positive rate than group 3.
Conclusions: The evaluation of Ki-67 suggests that brain cavernoma is a dynamic lesion. It is also suggested that angiogenic factor is involved in the growth of brain cavernomas.

P-636

Immunoexpresion of DNA topoisomerase I in a series of human gliomas

Michel Pluot[1,3], Lydie Ventéo[1,3], Igor Bronstein[2], Igor Nabiev[3], Alyona Sukhanova[3]
[1]University Hospital, Reims, [2]Department of Chemistry, University of York, [3]EA 2063, University of Reims Champagne-Ardenne

Introduction: DNA topoisomerases have a catalytic activity on DNA single-strand (top 1) or double-strand break (top 2). The principal role of top 1 is to relieve DNA supercoiling ahead of replication and transcription complexes. The goal was to determine the hitherto unknown top 1 reactivity in paraffin-embedded glial tumors.
Methods: 66 cases were collected: 44 astrocytomas (grade 2: 14, grade 3: 10, grade 4: 20, St-Anne Mayo system, 1988), 3 pilocytic astrocytomas, 13 oligodendrogliomas (low grade: 6, anaplastic: 7), 4 oligoastrocytomas (low grade: 1, anaplastic: 3), 1 pleomorphic xanthoastrocytoma, 1 ganglioglioma, (WHO system, 1993). The monoclonal antibody (a gift of I. Bronstein) was diluted (1/20); 1000 cells were counted. T98G cells from a human glioblastoma multiforme in spheroid cultures were examined with or without top 1 inhibitors.
Results: positive cells are less than 15% in pilocytic, less than 50% in grade 2, more than 70% in grades 3 and 4 astrocytomas. Differences between low and high grade are also observed in oligodendrogliomas (<10% vs 65%), and oligoastrocytomas (20% vs 75%). 98% of spheroid cells are positive; camptothecin lowers percentages to 10%.
Conclusion: in this study, the expression of top 1 correlates with the histological grade of gliomas. As top 1 inhibitors are among the effective anticancer drugs, the presence of top 1 should be checked in high grade gliomas, to determine whether binding of drugs in the top 1 – DNA complexes might be effective by converting them into a cellular poison.

P-637

Diffuse leptomeningeal gliomatosis

Saracibar N.; Caton B.; Lozano M.
Hospital Santiago Apostol, Vitoria, Spain

Leptomenigeal gliomatosis is a primary glioma residing mainly in the leptomeninges. It occurs in 20–25% of patients suffering from extensive recurrence of intracerebral gliomas. Primary L.G. without intraparenchymal tumor have been described only rarely. We present a case of diffuse leptomeningeal gliomatosis in a 28 year old boy in which the morphological features of the cellular infiltrates were those of oligodendrocytes.
CLINICAL HISTORY: A 28-year-old man developed progressive headache and backache vomiting, altred consciousness. A biopsy revealed a leptomenigeal gliomatosis. He died two years later. An autopsy was carried out. General examination revealed diffusely thickened leptomeniges throughout the brain surface, which was accentuated around the brain stem and cerebellar surface. Histological examination showed diffuse infiltration of the subarachnoidl space with tumor cells with round, regular nuclei, perinuclear haloes and focal positivity for GFAP. Interestingly, the ependymal surface was infiltrated.
Most cases of diffuse leptomenigeal gliomatosis have been astrocytomas of various histological grades. Only a few cases of "oligodendrogliomatosis" have been described.

P-638

[abstract withdrawn]

P639

Pleomorphic xanthoastrocytoma. Immunohistochemical analysis of five cases

Skender-Gazibara M, Dozic S, Cvetkovic-Dozic D, Jovanovic V, Govedarovic V, Grujicic D*
Institute of Pathology and Institute of Neurosurgery*, School of Medicine, University of Belgrade, Yugoslavia

Introduction: Owing to some different data in literature concerning on immunohisto-chemical reactions and histogenesis of Pleomorphic xanthoastrocytoma (PXA) we performed immunohistochemical analysis of our cases of PXA.
Material and methods: In our serie of 8386 primary tumors of central nervous system (CNS) we diagnosed five cases of PXA. In four cases tumor was typicaly located in temporal lobe and in one it was located in right parieto-occipital region. Tissue samples were prepared for light microscopy using routine and immunohistochemical methods. For immunohistochemistry we used the following DACO monoclonal antibodies: GFAP, vimentin, S-100 protein, neurofilaments, synaptophysin, EMA, LCA, alpha1-antitrypsin and CD68. Frozen section were used for oil red O and Ki67 for assessment of proliferative activity.
Results: Microscopically tumor was composed of markedly pleomorphic cells, which varied in shape from round to elongate, intermingled with mono or multinucleated giant cells sometimes of bizarre appearance. Although the nuclei showed great variation in size, shape and staining properties, mitotic figures were rare or absent. Lipidization of the neoplastic cells and the amount of reticulin fibers were variable from case to case. The large number of tumor cells in all cases expressed GFAP, vimentin and S-100 protein immunopositivity. Neurofilaments and synaptophysin reactivity of tumor cells was noted in two cases. Less than 1% of cell nuclei were positive with Ki67.
Conclusion: Although PXA is considered to be of astrocytic origin, the demonstration of neurofilaments and synaptophysin reactivity in two of our cases can suggests that histogenesis of PXA is more complex then it was thought previously.

P-640

Ultrastructure of microglial response to prolonged application of valproate and after its terminating in temporal lobe neocortex

Maria Sobaniec-Lotowska
Dept. of Pathological Anatomy, Medical Academy, Bialystok, Poland

The main **aim** of this study was describing the most revelant morphological features of microglia/macrophages in the temporal lobe neocortex in experimental valproate encephalopathy induced by chronic application of sodium valproate (VPA) to rats and after ceasing the administration of this antiepileptic.
Material and methods: Male Wistar rats received VPA once daily, before feeding, intragastrically at a dose of 200 mg/kg b.w. for 1, 3, 6, 9 and 12 months. After 12 months there was ceasing the long-term application of this drug for 1 and 3 months. After intracardiac perfusion with 2,5% glutaraldehyde the material was taken from the temporal lobe neocortex, processed in the routine way for ultrastructural studies and examined with on Opton 900 microscope.
Results: After 9 and 12 months of experiment the studies revealed markedly microglial response to prolonged valproate neurotoxicity which lasted for 1 and 3 months after terminating chronic applied VPA. The number of microglial cells and intensity of their phagocytic activity was increased. We have shown that microglia/macrophages were present in the close vicinity of altered neuronal somata as well as in injured elements of neuropil (especially nearly changed synapses). Phagocytic microglial cells contained rich lysosomal apparatus (with characteristic polymorphic frothy phagosomes) and numerous lipofuscin-like structures. Their nuclei were oval with distinct accumulation of hetrochromatin under nuclear envelope. The electron-dense perikaryal area contained an active Golgi zone.
Conclusion: The phagocytic activity of microglial cells observed in valproate encephalopathy may interfere with other functions of glial population and play a role in central nervous tissue recovery.

P-641

Rabies in Romania – epidemiology and two human cases: Autopsies report

Florica Staniceanu[1], Sabina Zurac[1], Adrian Streinu Cercel[2]
(1) Department of Pathology, Colentina Hospital; (2) Department of Infectious diseases, Matei Bals Institute, Bucharest, Romania

Rabies is an acute encephalitis with almost always fatal outcome (there are only six documented cases of human survival from clinical rabies, all of them with history of prophylaxis – pre- or postexposure); it is caused by rabies virus – a Rhabdovirus with nonsegmented, negative-stranded RNA genome; most of the cases of rabies occur in wild animals and, accidentally, may occur in humans bitted by a rabid animal.
A total of 69 cases of rabies were reported in Romania during 2000, most of them in animals (67 in animals and 2 human cases). 32 cases appeared in wild animals (43.37% – the vast majority in foxes: 90.62% of the wild cases) and 35 cases in domestic animals (50.72% – most of them in cats and dogs: each category representing 31.42% of the domestic cases).
We report the two cases of rabies in humans from Romania (25% of the human cases from Europe in 2000). Both were men, 32 and 48 years old, bitted by rabid foxes. None of them presented to a doctor, no prophylaxis pre or post exposure was performed. The diagnosis was establish before death using direct fluorescent antibody testing of the serum of the patients. The histopathologic picture of both of the cases was that of an encephalomyelitis with mononuclear infiltration and perivascular cuffing of polymorphonuclear cells, Babes nodules and numerous Negri bodies in the neuronal cells, especially in the pyramidal cells of the hippocampus and Purkinje cells of the cerebellum.
Abstract only for poster presentation; presenting author dr. Sabina Zurac, category Neuropathology.

P-642

Correlation between cell type and tumor vascularization using stereological method on malignant melanoma (MM) of the choroid

Simona Stolnicu[1], Simona Mocan[1], Doina Frincu[2], Doina Rădulescu[3], Modis Laszlo[4], Cristian Podoleanu[5], Jung Janos[1]
1. Department of Pathology, University of Medicine, Târgu-Mure, România; 2. Department of Anatomy, University of Medicine, România; 3. Department of Pathology, University of Medicine, România; 4. Eye Clinic, University of Medicine, Debrecen, Hungary; 5. 3rd Medical Clinic, University of Medicine, Târgu-Mure, România

Introduction: This study is aimed to find a correlation between the cell type and the vascularization in malignant melanoma of the choroid, using stereological method.

Methods: H-E stained slices were made of specimens from 56 patients. The microscopic tumor types, established according to Callenders classification, modified by the pathologists from AFIP were: 27 MM spindle type, 28 MM mixed type and 1 MM necrotic type. The presence of very pleomorphic spindle cells in some of these tumors made us subclassified each type (except the necrotic type) in classic (without spindle pleomorphic cells) and pleomorphic (with spindle pleomorphic cells). The stereologic measurements were made on 16 of the 56 cases (8 spindle cell type and 8 mixed tcell ype), using the Prodit 5.2 program.

Results: We observed that in spindle cell type, the vascularization of the tumor occupied a smaller volume than in mixed type. The tumor blood vessels occupied a larger volume in the pleomorphic spindle type and in pleomorphic mixed type.

Conclusion: Thus, we believe that malignant melanoma of the choroid containing spindle pleomorphic cells may have a worse prognostic.

P-643

The relationship of genetic aberrations detected by comparative genomic hybridization to DNA ploidy in pilocytic astrocytomas

Janusz Szymas[1], Iver Petersen[2], Karsten Schluens[2], Klaus Dietmar Kunze[3], Gunter Haroske[4], Wolfdietrich Meyer[3], Dorit Konrad[3]
[1] Department of Pathology, University of Medical Sciences, Poznan, Poland; [2] Institute of Pathology, University Hospital Charite,Berlin, Germany; [3] Institute of Pathology, University Hospital Carl Gustav Carus, Dresden, Germany; [4] Institute of Pathology, Dresden-Friedrichstadt General Hospital, Dresden, Germany

We have examined genetic alterations in 18 surgically removed pilocytic astrocytomas using comparative genomic hybridization (CGH) and DNA image cytometry, which allow quantitative analysis of chromosomal abnormalities. CGH analysis revealed gains and/or losses of DNA sequence copy number in all tumors. Gains in DNA sequence copy number were detected frequently for chromosome arms 5p12, 5q23, 5q31, and 6q23, and losses in chromosome arms 4q24, 5q14-21, 6q12, 9p21-2, and 13q21. Modern image cytometry allows assessing the total amount of nuclear DNA of studied cell population. Of the 18 pilocytic astrocytomas, image cytometry DNA ploidy were obtained in 14 cases. The ploidy distribution was as follows: four cases were euploid and ten cases were aneuploid. Two of four euploid tumors and three of ten aneuploid tumors were additionally polyploid. Average number of gains in euploid tumors was 5.75±4.03 whereas in aneuploid tumors14.57±6.93. These differences were statistically significant (p=0.0291). Average number of losses in euploid tumors was 20.00±3.37 and in aneuploid tumors15.64±7.53 (p=0.2847). Our results suggest that DNA aneuploidy, which indicates aggressive behavior, is also connected with multiple gains of chromosomal instability.

P-644

Alteration in pituitary macroadenomas by comparative genomic hybridization

Janusz Szymas [1], Karsten Schluens [2], Wlodzimierz Liebert [3], Iver Petersen [2]
[1]Department of Pathology, University of Medical Sciences, Poznan, Poland; [2] Institute of Pathology, University-Hospital Charite, Berlin, Germany; [3] Department of Neurosurgery, University of Medical Sciences, Poznan, Poland

Pituitary adenomas are slowly growing tumors located in the sella turicica. Although histological and immunocytochemical criteria determining the character of pituitary adenoma have been studied extensively, cytogenetic data are scare. This study was conducted to determine genetic alterations unique to this tumor using comparative genomic hybridization (CGH). This technique permits the entire genome survey in one experiment. Fiveteen cases of sporadic macroadenomas were analyzed for their genetic imbalances on all 22 autosomes by CGH. Our material includes 4 GH secreting tumors, 1 prolactinoma, 1 ACTH secreting tumor and 9 nonfunctional adenomas. Multiple aberrations involving entire chromosomes or chromosome arms were detected in 8 (53%) of the 15 macroadenomas. Chromosome losses were more frequent than gains. The chromosomes affected were 1p, 2q, 3q, 4, 5, 6q, 9p, 11, 12q, 13q, 14q, 17, 18q, 19, 20q. In our study chromosomal imbalances were more frequently and mean number was higher in endocrinologically active adenomas than in nonfunctioning cases. Our findings indicate that genetic abnormalities are present in pituitary adenomas at a higher rate than suspected in this benign tumors. Frequent deletions in chromosomes 11q, 13q and 18q as well as amplifications in chromosomes 9p, 17, and 19 imply that candidate genes residing in these locations may be involved in the tumorigenesis of pituitary adenomas. These alternations could be the focus of further investigation in the order to understand the pathogenesis and biological behavior of this tumor type.

P-645

Speed up the healing process of the injured peripheral nerve by low power He-Ne laser radiation

Takzare Nasrin[1], Yaemohammadi Kamran[2], Takzare Alireza[1]
1 Tehran University of Medical Science; Faculty of Medicine

The nervous system has an important and vital role in the human body, but unfortunately damaged nervous tissue can be repaired very slowly. Injury to a mammalian peripheral nerve is accompanied by a restorative process that is manifestes after a delay. Restoration of function occurs when the regenerating fibers reconnect with target organ. The scientists have been searching for the ways to improve the repairment of damaged nervous tissue.
Radiation of low power He-Ne laser has been suggested to slove this problem. In the present study, the efficacy of low power He-Ne laser in treating injured nerves of mammalian was tested.
In our research, 20 rats were divided randomly into control and case groups. The sciatic nerves of all these rats were damaged under general anesthesia and sterile conditions. The day of surgery was considered day zero. Rats of case group received every day laser radiation (λ=65 nm). At 27th day rats were killed and the sciatic nerve was studied histologically.

Data was analysed by t-test and P<0.05 was significant. Results showed that in the case group the repairment was faster. So, low power He-Ne laser radiation on crushed sciatic nerve had accelerated the nerve repair process.
Keywords: Laser; He-Ne; Injured sciatic nerve; Rat; Iran

P-646

Amyotrophic lateral sclerosis: in the search for correlations between pathology and the duration of disease.
Tomik B., Adamek D.*, Pichor A., Kaluza J.*, Szczudlik A.
Dept. of Neurology and Dept. of Neuropathology(*), Institute of Neurology, Jagiellonian University, Medical College, Kraków, Poland

Introduction: Amyotrophic lateral sclerosis (ALS) is clinically and pathologically heterogenetic. A part of numerous pathomorphological findings in ALS may be secondary. The goal of this study was to compare different neuropathological changes (like inclusions, spheroids etc.) with the clinical course of the disease.
Methods: The material includes 24 cases of autopsy-confirmed ALS treated in our center. The detailed evaluation of samples taken from motor cortex, basal ganglia, brain stem (samples from 3 different levels), and spinal cord (at least 3 levels) was focused on the grade of loss of motor neurons ("upper" and "lower"), damage to the cortico-spinal tracts, occurrence of gliosis, infiltrations of macrophages, and different kinds of inclusions (like Bunina bodies, hyalin bodies, Lewy bodies or ubiquitin-positive skein inclusions). The pathological changes were correlated with the duration of the disease (mean duration: 23.5 months, mean age of patients: 57.1 years).
Results: Longer duration of disease was noted in cases with evident degeneration and loss of cortical motor neurons. The cases with numerous macrophages in cortico-spinal tracts had shorter survival as compared with the other cases. In 19/24 cases different types of inclusions were noted, however no correlation with the duration of disease and the occurrence of any kind of inclusion was noted.
Conclusions: The investigations demonstrated morphological heterogeneity of ALS. The degeneration of cortex is rather late change in the course of disease. The intracellular (mainly intraneuronal) inclusions are helpful in post mortem diagnosis (which is not always easy) but in some cases they may be epiphenomenons.

P-647

Morphological and biochemical analysis in different types of mitochondrial myopathy/encephalomyopathy
Török, I[1]., László, A[2]., Zombori, J[1].
[1]Erzsébet City Hospital Pathol. Dep. Hódmezővásárhely,
[2] University of Szeged, A. Szent-györgyi Medical Center, Pediatric Dep., Hungary

Mitochondrial enzyme activity of cytochrome-c oxidase (COX, respiratory enzyme complex IV), NADH-COR (NADH-cytochrome-oxidoreductase, respiratory complex I), carnitine acetyltransferase, citrate synthase, lipoamide-dehydrogenase were measured from 12 patients suffering from progressive myopathy and/or encephalomyopathy.
Among the investigated mitochondrial enzymes COX deficiency was detected in muscle or liver tissues. Eight patients showed cytochrome-c oxidase (COX, complex IV) deficiency, 4 patients had NADH cytochrome-c oxidoreductase (complex I) deficiency. The 3 familiar ataxic children showed decreased activity of carnitine acyl-transferase combined with COX deficiency and 3 other cases had decrased lipoamid-dehydrogenase. According to the onset of symptoms, the distribution of clinical type were 1 neonatal, 7 infantile and 4 adult types. Muscle biopsy revealed diffuse weak or lacking histochemical reaction to COX and muscle atrophy. Three patients had ragged red fibers (RRF) with modified Gomori staining and 1 case showed the signs of MERRF-syndrome (myoclonic epilepsy+RRF).

P-648

Prognostic significance of classic morphologic variables in oligodendrogliomas. A clinicopathologic and image analysis study
Umudum H, Celasun B, Gunhan O, Finci R
Gulhane Military Medical Academy, Department of Pathology, Ankara, Turkey

Introduction: To determine the prognostic significance of radiological, histological, morphometric variables and ploidy in oligodendrogliomas. The presence and degree of variables were correlated with diseases free survival in 26 patients.
Methods: Tumor tissues and archive files were studied in 26 patients with oligodendroglioma. Only patients with documented follow up have been and included in this study. Studies were conducted using morphometry on HE stained sections and Feulgen stained nuclear suspensions.
Results: Prognostically significant factors in order of decreasing importance were low mitotic activity index (MAI<1) (p= 0.008), ploidy (p=0.02), low (mDNA<2.25) meanDNA index (p=0.02), low (5cex DNA<0.3) 5 C exceeding rate (p=0.03), the younger (<30) age (p=0,04).
Conclusions: This investigation provides further evidence that morphometric and ploidy studies as well as standardized histological factors especially mitotic activity index have prognostic value in these erratic behaving tumors. Ploidy studies gain prognostic significance in these tumors, if when they are evaluated with morphometry.

P-649

Skeletal muscle ultrastructural pathology in patients with renal proteinuria
Villalobos J.*, Pulido-Méndez M.*, Márquez A.*, Finol H.J.**, Bello B.**, Febres C.***
Institute of Experimental Medicine, Medicine Faculty*, Center for Electron Microscopy, Sciences Faculty**; Central University of Venezuela, Caracas, Venezuela. Nephrology Department, Military Hospital***

Introduction: Several glomerular diseases exhibit proteinuria whose top levels are found in nephrotic syndrome with a protein loss greater than 3.5g in 24 hours. Extrarenal tissues have metabolic changes associated with massive protein loss, including muscle

tissue which is highly reactive to alterations in protein availability and in the normal balance between protein synthesis and degradation. It is known that progressive renal disease causes motor disturbances. In this study we investigated the skeletal muscle ultrastructural pathology in patients with primary glomerular disease and proteinuria in order to expand the knowledge in this field.

Patients and Methods: Needle biopsies from *quadriceps femoris* muscle were obtained in 4 patients with a pathological diagnosis of primary glomerular disease. All patients presented proteinuria during 5 to 9 years. Muscle clinical examination was normal in all cases. Plasma levels of muscle enzymes were also normal. One case showed neurogenic changes in the EMG. Tissue samples were processed with routine techniques for transmission electron microscopy and observed in a Hitachi H-500 electron microscope.

Results: Fibre atrophy was evident with loss of A band integrity, widening of intermyofibrillar spaces, and swelling of sarcotubular system. Hyperchromatic nuclei, glycogen accumulation, and sarcolemmal foldings were observed. Filamentous bodies were seen. Capillary alterations included endothelial hypertrophy with abundant pinocytotic vesicles and prolongations towards the lumen. Basement membrane looked widened in most capillaries. Macrophages beside muscle fibres were observed.

Conclusions: Long lasting glomerular diseases with proteinuria and no renal failure could be accompanied by ultrastructural alterations in muscle fibres and capillaries. Early changes can be found in absence of patent clinical manifestations. It is noteworthy that vascular changes are similar to those described in several autoimmune diseases (SLE myositis, rheumatoid myositis), this fact could be indicative of the existence of systemic autoimmune processes.

Supported by CDCH of UCV (Nr. O3-10-4169-2000) and CIFMUCV.

P-650

A case of primary T-cell lymphoma of the brain

Kamelija Žarković[1], Jasminka Jakić-Razumović[1], Gordana Jurić[1], Nada Bešenski[2], Josip Paladino[3]
[1]Department of Pathology, [2]Department of Radiology and
[3]Department of Neurosurgery, Zagreb Clinical Hospital Center

Introduction: Primary brain lymphomas of the T-cell origin are extremely rare. These lesions are solitary or multiple cerebral masses, or sometimes may be restricted to the leptomeninges. According to the reported cases primary T-cell lymphomas have a variable histological appearance: small cells, mixed small and large cell, large cell and even unclassifiable tumor cells. Based on their phenotypic similarities with normal lymphocytes, T cell lymphomas are divided into thymic, immature T cell and post-tymic, mature T-cell neoplasms.

Clinical details: This patient was 60-year-old woman who had 10-days history of right-sided weakness and dysphasia. Magnetic resonance imaging revealed a 4×2-cm deep-seated mostly regular mass in the left temporal lobe and left periventricular region with contrast enhancement and associated edema. Differential diagnosis included metastatic tumor without necrotic and haemorrhagic areas or low-grade glioma. There was no evidence of systemic lymphoma or HTLV-1infection. The patient underwent left temporoparietal craniotomy, with gross removal of a soft and grayish tumor.

Neuropathological findings: Microscopic examination of hematoxylin and eosin-stained sections of tumor showed small lymphoid cells with irregular nuclei and scant pale cytoplasm. The cells diffusely involved the parenchyma of the brain; the tumor was composed of solid sheets in that the tumor cells were closely packed. However, in occasional areas the cells were loosely distributed. The tumor cells accumulated also around blood vessels. Silver stain for reticulin demonstrated reticulin concentric reduplication of the vascular walls. Angiocentric pattern of the tumor cells was also found in the areas at the edge of the lesion. Mitoses were absent. The tumor cells expressed LCA, CD3 and CD8. There was no restriction of light chain. Marked infiltration of non-neoplastic cells, including macrophages, plasma cells and B-cells were found.

Conclusion: Based on morphological appearance and immunohistochemical profile this case corresponds to a exceedingly rare primary small T-cell brain lymphoma.

P-651

Etiology of brain lesions in patients died from AIDS

Zinserling V., Chernych M., Vasilieva M., Shevtchenko T.
S. Petersburg, Russia

Introduction: Brain lesions are common in AIDS and can be of different etiology. Succesful treatment of the patients is impossible without its evaluation in single cases.

Methods: On the autopsic material (54 cases) we studied brain lesions caused by different pathogens. The deceased were 4–61 years old; 44 males, 10 females. In 15 cases the homosexual, in 5 cases heterosexual, in 9 parenteral and in 4 cases drug associated ways of infection were prooved. In all cases virological, bacteriological and histological and partly IHC investigation was done.

Results: In all cases we observed lesions due to HIV, in 7 cases playing the leading role in the lethal outcome. Clinical and laboratory data made possible diagnose meningoencephalitis due to HSV and CMV in majority of cases, but the antiviral therapy with zovirax differed strongly in single cases. In majority of cases the degree of lesions on autopsic material was moderate, only in 1 case the lesions due to HSV played the leading role in the lethal outcome. The typical necrotic herpes encephalitis was not observed. In 7 cases with none antiviral therapy the herpes virus lesions were absent.

Virus	Diagnosed clinically	IHC positive
HSV	9	8
CMV	10	3
EBV	0	1

Brain lesions due to criptococci were prominent in 8 cases. In 3 patients focal toxoplasmic encephalitis was present. Brain lymphoma was diagnosed in 5 recent cases. In majority of observations mixed lesions with 2–3 pathogens were seen.

Conclusions: The lesions due to different pathogens can be observed in all lethal cases of AIDS but their etiology and pathogenic role differs strongly and not always depends only on duration of the disease and tactics of antiviral therapy.

P-652

Immunohistochemical expression of c-erbB-2 protein in human astrocytic neoplasms

Zolota V[1], Batistatou A[1], Fratzoglou A[2], Scopa CD[1]
Dept. of Pathology[1] and Neurosurgery[2], University of Patras Medical School, Greece

Introduction: The c-erbB-2 (HER-2/neu) oncogene encodes a 185-kDa transmembrane protein, which is a member of the tyrosine kinase receptor family, with high homology to the epidermal growth factor receptor. c-erbB-2 has been extensively investigated as a prognostic and predictive factor as well as a possible target for therapy in several neoplasms, with emphasis to breast cancer. The aim of the present study has been to determine whether overexpression of c-erbB-2 correlates with progression of human gliomas.
Method: Expression of c-erbB-2 was studied in formalin-fixed, paraffin-embedded sections of 28 astrocytic neoplasms (5 grade I, 6 grade II, 4 grade III and 13 grade IV, WHO classification), using standard immunohistochemical techniques, and the polyclonal antibody c-erbB-2 (A 0485, DAKO, Denmark). Membranous immunostaining of >5% of neoplastic cells was considered positive.
Results: Positive staining for c-erbB-2 was detected in none of grade I, 17% (1/6) of grade II, 25% (1/4) of grade III and 46% (6/13) grade IV astrocytomas. Non-neoplastic brain tissue was negative.
Conclusions: There is molecular heterogeneity of human gliomas, with infrequent overexpression of c-erbB-2 in low-grade astrocytomas and increased expression in high-grade tumors. c-erbB-2 may play a role in the development of at least a subset of more malignant astrocytic tumors. Such patients could benefit from a locally applied anti-HER-2 monoclonal antibody.
Transplantation Pathology

P-653

Liver transplantation from non-heart beating donnors: Patient's survival, primary graft nonfunction and ischemic cholangitis

F. Arnal*, A. Otero**, M.J. Lorenzo*, S. Pita***, F. Suarez**, J. Aguirrezabalaga****, C. Fernandez**, C. Lemos**, M. Gómez**
Department of Pathology*, Liver Transplantation Unit**, Epidemiology Unit***, Department of surgery****, Hospital Juan Canalejo, La Coruña, Spain

Introduction: Sub-optimal donors are used more frequently to alleviate the shortage of organs for transplantation. Our hospital works in a program of liver transplants (LTX) from non-heart beating donors (NHBD). We report our results on liver transplantation from NHBD.
Material and methods: From January 1995 to December 2000 twenty-seven LTX out of a total of 310 (8.7%) were allografts from NHBD. Twenty-three of these donors, suffered an uncontrolled, outside hospital cardiac arrest. All 27 LTX from NHBD and 52 control cases were studied prospectively. A descriptive study of the variables, a Kaplan-Meier curves for survival and Cox's regression for these variables were used as statistical methods.
Results: Patients survival at 12 months was 74.1% in the NHBD group and 82.7% in the control group. At 36 months survival was 74.1% and 76.2%. (log rank test=0.42; p=0.51). Survival of NHBD patients did not change when adjusted for age, creatinine, albumin, bilirrubin and other variables.
On the follow-up 33,3% of NHBD group and only 3,8% of the controls needed a liver retransplatation (RLTX). (OR=12.5 P=0.000). Primary liver nonfunction was the most frequent cause of RLTX (54.5%) followed by ischemic cholangitis (27.3%) and arterial thrombosis (18.2%). Fourteen patients (55.6%) presented ischemic cholangitis and 10 of these needed surgery. Large bile duct necrosis with a cast formation was the characteristic form of biliary damage.
Conclusions: Livers from NHBD did not modify statiscally the survival of receptors but they increased complications of primary nonfunction, retransplatation and ischemic cholangitis.

P-654

Adhesion molecules and angiogenesis in host neoplasia reactions

C.D. Baroni, D. Vitolo
II Pathological Anatomy, University of Rome "La Sapienza", Italy

Introduction: The prognostic significance of vessel quantification in human tumors is debated due to the multiple factors modulating neoangiogenesis and invasiveness of neoplastic cells.
Methods: We have studied in supraglottis squamous carcinomas, non-small cell lung carcinomas and classic (NOS) invasive ductal breast carcinomas, vascularity, immunohistochemical distribution of extracelluar matrix proteins (ECMP) and laminin α2 chain (merosin M chain) in basal membranes of vessels, and gene expression of VEGF, FGF_2, TGFβ1.
Results: Independently of the tumor type and of vascularity, laminin α2 chain was observed in a limited proportion of vessels. In vitro experiments demonstrated laminin α2 chain mainly in early endothelial cell cultures suggesting that laminin α2 chain expression in vivo can be considered a marker of early angiogenesis. Stromal and parenchymal vascularity was associated with laminin α2 chain expression in supraglottis carcinomas, whereas in the other tumors laminin α2 chain+ vessels were observed only in stroma. In supraglottis carcinomas VEGF+ cells were mainly represented by neoplastic cells, whereas in the other tumors the great majority of VEGF+ cells were macrophages and fibroblasts. FGF_2+ and TGFβ1+ cells were macrophages and fibroblasts in all tumors.
Conclusions: Our observations suggest that in addition to quantification and distribution of vessels, evaluation of their maturation may contribute to a better understanding of the role of angiogenesis in the growth and spread potential of solid tumors. In this regard, in supraglottis carcinomas parenchymal angiogenesis seems to be regulated mainly by neoplastic cells; furthermore, in solid tumors of different histogenesis, different cells might be responsible for modulating tumor angiogenesis.

P-655

Post-transplant lymphoproliferative disorders (PTLD) after liver transplantation in Beaujon's Hospital

D. Cazals-Hatem, F. Durand, J. Bernuau, O. Farges, A. Sauvanet, D. Valla, J. Belghiti, C. Degott
Departments of Pathology, Hepatology and Surgery, Hôpital Beaujon, Clichy, France

The overall incidence of PTLD after liver transplantation is variable according to the centers, estimated between 2 and 4%. The experience of one French liver transplant unit is reported.
Patients and methods: The incidence and features of PTLD were studied in 445 patients transplanted between 1989 and 2000 for the following diseases: HCV cirrhosis (21%), acute liver failure (18%), alcoholic cirrhosis (16%), HBV cirrhosis (9.4%), biliary diseases (12.6%), others (22.6%).
Results: Six patients (3 women, 3 men, mean age: 44 year [range 22-65]) developed a PTLD after a median post-transplant period of 7 months (range: 0.5–15 months). Indications of liver transplantation were HCV cirrhosis (2 cases), fulminant autoimmune hepatitis (2 cases), α1-antitrypsin deficiency (1 case) and caustic bilateral cholangitis (1 case). Two patients received anti-lymphocyte globulin to induce immunosuppression. Four patients had episodes of acute rejection treated efficiently with steroids and in one case with anti-CD3 monoclonal antibodies (OKT3). PTLD was located in liver transplants in three cases (after a median delay of 5.5 months). Clinical presentations were otherwise heterogeneous preferentially with extra-nodal involvements (isolated central nervous system or mesenteric location). Histologically, PTLD were polymorphic (3 cases) or monomorphic (2 cases) EBV-driven proliferation of B-cells (five cases examined). Three patients died of PTLD and the last three achieved remission after reduction of immunosuppression alone (1 case), and anti-CD20 antibodies (2 cases).
Conclusion: In our experience we observed: (1) a lower incidence of PTLD, evaluated at 1.4%; (2) the absence of association of HCV infection and PTLD.

P-656

Histologic and immunohistologic features of non-rejection thrombosis in kidney allografts

V. Jurčić, A. Vizjak, T. Perković, D. Ferluga
Institute of Pathology, Medical Faculty, University of Ljubljana, Ljubljana, Slovenia

Thrombosis of the kidney allograft vessels is among the important complications of kidney transplantation. However, the clinical and histological distinction between rejection and non-rejection thrombosis has been poorly investigated. The study included nephrectomy specimens of 8 kidney allografts explanted 2 to 31 days after transplantation due to clinically non-rejection thrombosis of large vessels, and as a control 29 kidney allografts showing histologically acute rejection, with or without signs of chronic rejection. In addition to traditional light microscopy, the expression of cellular markers CD3, CD79a, CD68 and CD31 (DAKO) was determined. Histologically, no signs of acute rejection were found. Nevertheless, reactive vascular changes that should not be confused with rejection vasculitis were seen in 6 allografts, but not in 2 allografts in the early stage of thrombosis. In contrast to mononuclear predominantly T cell rejection vasculitis, cells infiltrating the vessel walls in non-rejection thrombosis were neutrophils, admixted with a variable number of macrophages. The presence of few T lymphocytes together with proliferative vascular changes, found in 2 allografts, explanted more than one week after transplantation, were associated with the organisation of the thrombi. They were characterised by the proliferation of endothelial cells and, to a less extent, of myofibroblasts, while in chronic vascular rejection proliferation of myofibroblasts and sclerosis predominate. Furthermore, vascular changes in non-rejection thrombosis were focal and segmental, limited to the segments with the thrombus, not extending into the nonthrombotic vascular segments as usually seen in vascular rejection. Our common finding of simultaneous multiple thrombi of different age in both extrarenal arteries and veins (5/8 allografts), and intrarenal and extrarenal vessels (4/8 allografts), may be a consequence of local circulatory disturbances and/or release of procoagulant substances following the initially limited large extrarenal vessel thrombotic obstruction.

P-657

Evaluation of biopsies upon extraction and after reperfusion in livers from non-heart beating donnors: Severe ischemia in the reperfusion biopsies and early graft loss

M.J. Lorenzo*, A. Otero**, S. Pita***, F. Suarez**, J. Aguirrezabalaga****, C. Fernandez**, C. Lemos**, M. Gómez**, F. Arnal*
Department of Pathology*, Liver transplantation Unit**, Epidemiology Unit***, Department of surgery****, Hospital Juan Canalejo, La Coruña, Spain

Introduction: Sub-optimal donors are now used in organ transplantation. We work in a program of liver transplantation (LTX) from non-heart beating donors (NHBD) since 1995. Biopsies are used to assess the viability of these organs.
Objective: We analyze the findings on the evaluation and reperfusion liver biopsies and the graft survival.
Material and methods: From January 1995 to December 2000 twenty-seven LTX out of a total of 310 (8.7%) were done from NHBD. Biopsies were taken at the end of liver extraction and studied as frozen sections. When feasible a direct immunfluorescence study for immunoglobulins, complement and fibrinogen was done. Biopsies taken at the end of reperfusion were also studied as rush cases. The Kaplan-Meier curves for survival and Cox's regression were used as statistical methods.
Results: Biopsies taken at the end of the liver extraction showed no signs of significant ischemia and only traces of fibrin deposition were seen. In six cases ischemia was severe at the reperfusion biopsy (22.2%). Graft survival at one- month was 80.4% in cases without severe ischemia and 66.6% in those with severe ischemia. At two months survival of the graft was 80.4% and 44.4% respectively. Donor and recipient's age, creatinine, albumin and other variables did not show statistical significance.
Conclusions: Biopsies studied as frozen sections before transplantation did not correlate with graft outcome. Severe ischemia on biopsies at the end of reperfusion clearly modifies graft survival.

P-658

Significance of total tubular surface area in interstitial cell density assesment during acute and chronic kidney allograft rejection

Smiljanic Radotic K.[1], Basta Jovanovic G.[1], Kostic P.[2], Milosavljevic I.[3]
Institute of Pathology, School of Medicine[1], Faculty of Electrical Engineering[2], University of Belgrade, Military Medical Academy[3], Serbia, Yugoslavia

Introduction: Our previous results indicate that numbers of S-100+ dendritic and S-100+ interstitial tubular epithelial cells

(ITEC) can serve as possible prognostic factors in kidney allograft rejection. The present study was conducted to assess the influence of total tubular surface area on interstitial cell density.

Methods: Fine needle biopsies from 17 patients with transplanted kidneys were in 4% formaldehyde fixed, paraffin embedded, stained on PAS and classified according to the Banff. The numbers of total interstitial cells and tubular surface areas were analyzed on digitalized 0,83mm2 microphotographs (PIXERA digital camera, OLYMPUS microscope, 200×) with CAMIA image analyzer.

Results: Kruskal-Wallis test shows no statistically significant difference in numbers of interstitial cells on 0,83 mm^2 depending on the type/stage of acute/chronic allograft rejection. With 2WAYANOVA test we analyzed the influence of type/stage of acute/chronic rejection on interstitial cell density calculated for 0,83 mm^2 as well as for surface area of the interstitial space. We found statistically significant difference (p=0,034) only in the interstitial cell density calculated for surface area of interstitial space between types 1 and 3 of acute allograft rejection.

Conclusion: Tubular disappearance is statistically highly significant only in acute allograft rejection. Total tubular surface area is important for interstitial cell density assesment only in acute allograft rejection. It means that for chronic allograft nephropathy we can count S-100+DC and S-100+ITEC on 0,83 mm^2 without previous total tubular and interstitial surface areas assesment.

P-659

Pathology of renal transplant in Bulgaria in ten year period

T. Todorov, T. Georgiev ., V. Mincova, E. Paskalev, N.Simeonov, B. Beleva, A. Filev, P. Panchev
Medical Faculty, Department of Pathology, Nephrology and Urology, Sofia, Bulgaria

Aims: The aim of this study is to evaluate the morphology of kidney transplant biopsies in an attempt to answer the clinician (1) is the failure of the graft due to rejection or some unrelated cause and (2) if the rejection is present is the process potentionally reversible with available therapy.

Material and methods: Fifty one core-needle biopsies taken from the lower pole of the kidney transplants, measuring 2–3 mm in diameter, are examined under light microscopy using hemalaun- eosin, van Gieson, PAS, congorot, and Masson's trichrome stains, as well as the silver impregnation technique after Wilder. Immunohistologically frozen and paraffin sections are investigated for the following antigens: immunoglobulins (Ig G, Ig A, Ig M), complements factor (C3, C1q) and fibrin. Eleven cases are studied under electron microscope. Six necropsies from our files are reexamined for comparison.

Results: We find in our material the following forms of rejection based on morphologic criteria:

1. Acute rejection in 8 cases with two reaction patterns: vascular or acute irreversible reaction (2 cases) and interstitial or acute reversible (cellular, tubulointerstitial) reaction (9 cases);
2. Hyperacute rejection in 4 cases with the presence of fibrin thrombi in all renal vessels, including, the glomrular capillaries and peritubular venules, associated with infraction and tubular necrosis. In 2 of the cases a total renal necrosis is found;
3. Chronic rejection or chronic allograft nephropathy in 36 cases showing a picture similar to nephrosclerosis. Transplant glomerulopathy or glomerulonephritis "de novo" is seen in 4 of the cases characterized by thickening and duplication of the peripheral glomerular basement membrane and increase of mesangial matrix.
4. Chronic cyclosporine toxicity in 3 cases consisting of focal fibrosis or so-calle "striped interstitial fibrosis" and tubular atrophy without inflammation.

Conclusion: From the morphologic point of view renal transplant rejection involves different parts of the kidney, the vessels (predominantly in hyperacute and acute rejection), the glomeroli (mainly in chronic rejection) and tubulointerstitial portion (mostly in chronic cyclosporine toxicity). The renal core-needle biopsy is the most reliable method for the clinician to find out the cause of the graft rejection and to foresee the patient's therapy.

P-660

Considerations on helicobacter pylori infection i n a cirrhotic population

Bella MR, Musulen E, Calvet X, Sanfeliu I, Campo R, Brullet E, Gil M, Dalmau B, Orellana R, Pons Ll, Balague O, Combalia N, Rey M
Corporació Parc Taulí, Sabadell, Barcelona, Spain

INTRODUCTION: The aims of this study are: 1) To determine the incidence of Helicobacter pylori (Hp) gastric infection in a cirrhotic population; 2) to determine its location (fundus vs antrum); 3) To compare different diagnostic methods; and 4) to describe associated histopathological findings in gastric mucosa.

METHODOLOGY: Patients: 81 consecutive cirrhotic patients submitted to gastroscopy. Variables: Serology (IgG-antiHp), Breath-test, Urease-test (Clotest®), detection of Hp in fundic and antral mucosal biopsies by Giemsa and by immunohistochemistry (IHC)(1/500, Dako), and histopathological findings according to Sidney's classification. Statistical analysis: χ-square.

RESULTS: Hp infection was detected in 51/81 (63%), all with fundic infection, 7/51 having no infection in antrum. IHC and Giemsa obtain similar results, with only 4 discordant cases. Correlation with Breath-test is good (only 3 discordances) but regular with Urease-test (9 discordances) and serology (23 discordances). Histopathological findings associated to infection with statistical signification were: chronic and acute inflamation both in fundus and antrum, and lymphoid aggregates in antrum. No association was found with other histopathological findings.

CONCLUSIONS: 1) Incidence of Hp infection in this group of cirrhotic population is high (63%), but similar to age-matched population in our country. 2) Immunohistochemistry and Giemsa method obtain quite similar results. 3) Fundus is the most frequent location for Hp infection, being the best site to do one biopsy. 4) Associated findings are acute and chronic inflammation and antral lymphoid aggregates, but no significative association has been found with others.

P-661

Hyalinizing clear cell carcinoma (HCCC) of minor salivary glands vs. other clear cell carcinomas – a case report

Petrushevska G.[1], Cvetkovski P.[1], Jovanovic R. [1], Vasilevski [2]
[1)] Institute of Pathology, Medical Faculty, Skopje, R. Macedonia; [2)] Clinic for Maxillofacial Surgery, Clinical Center, Skopje, R. Macedonia

HCCC is a rare neoplasm of the minor salivary glands which usually apears in adult females' oral cavity, and should be distinguished from the other clear cell tumors of the salivary glands and metastatic renal cell carcinoma. The aim of this paper was to present a case of HCCC in 68 years old female, with clinical local evolution of two years without apparent lymph node metastasis.
A submucosal tumor mass measuring 4×3x×1.5 cm, was found at the inner side of the mandible. On X-ray examination, because of marked atrophy of the bone, an ameloblastoma was suspected. After surgical removal, the tumor tissue with rubbery consistence was formaline fixed and paraffin embedded. Standard histochemical and immunohistochemical stainings were applied. Histological analysis revealed presence of infiltrative tumor consisted of solid cellular masses and nests of polygonal cleear cells, separated by broad hyalinized stromal bands. In the areas, near the stromal brands, smaller cells with an eosinophyllic cytoplasm were found.
These cells were weakly positive on PAS staining and the stromal brands showed mucinous change, positive on Alcian blue staining. On immunohistochemical staining there was positivity for Cytokeratin and ESA, while we found actin and vimentin positive stromal spindle cells. Staining for CEA, S-100, protein were negative, which helps distinguish it from other clear cell neoplasms. We consider that it is important to differentiate this tumor from other clear cell tumors, because of it's special clinical evolution in terms of its slow local infiltrative growth without metastases for a long period of time.

P-662

Oestrogen and progesterone receptors in malignant and benign changes in the thyroid gland (the results of own research).

Iwona Lewy – Trenda
Chair and Dept. of Pathomorphology, University Medical School, Lódž, Poland

The aetiology of thyroid carcinoma is very complex. Among many factors possibly influencing its growth the following ones can be enumerated: iodine deficiency, genetic predisposition, female sex, older age, irradiation in childhood, antigens stimulating the thyroid growth, epidermal growth factor. Some recent reports (among others also epidemiological data) have claimed, that differentiated thyroid carcinoma (papillary, follicular, Hurthle cell) can depend on sex hormones, especially estrogens. Many new research papers describe the presence of oestrogen, progesterone and androgen receptors in normal and malignant thyreocytes and also the contents of estradiol in thyroid tissue. The results of these investigations allow the assume, that thyroid cancer might be oestrogen dependant, but there is no agreement in literature as for the relation between the malignancy of the tumour and the expression of ER, PR and AR adenoma.
In this study 72 thyroid glands were examined by immunohistochemical reactions with ER and PR antigens. The positive expression of examined antigens was obtained primarily in the cell nuclei of differentiated thyroid carcinomas (17 positive ER and 2 positive PR); the lack of expression was exhibited in all cells coming from benign changes and from the tissue surrounding the malignant growth. Moreover, the nuclei of 3 Hurthle cell adenomas and 4 follicular adenomas were ER – positive, while only the 5 nuclei of papillary adenomas were PR – positive. These results correspond with the majority of the data published in bibliography.
Discovering the presence of examined receptors thyreocytes, applying various methods, allows to assume that the sex hormones (mainly estrogens) can directly influence follicular cells of the thyroid an their proliferation.
The presence of ER and PR in thyreocytes can also be associated with the direct influence of estrogens and progesterone on these cells and can pose a serious problem because of the wide usage of medicines containing sex hormones or their derivatives and the increase of concentration of these compounds in the environment.
It appears though, that the data examined by all researchers is too narrow and obtained by various methods of research, so the results cannot be directly compared. According to the above it seems that the results of future investigations will indicate, whether the influence of hormones on the development of changes in the thyroid gland is real and whether the discovery of receptors for sex hormones can help with therapeutic decisions.

P-663

Simultaneous occurrence of Riedel's disease and Hashimoto's thyroiditis: A case report

M. Decaussin[1], M.H. Bernard[2], J.L. Peix[3], C. Crozes[4], N. Berger[4]
[1]Department of Pathology, Centre Hospitalier Lyon Sud,
[2]Department of Endocrinology, [3]Department of Surgery,
[4]Department of Pathology, Hôpital de l'Antiquaille, Lyon, France

Introduction: The simultaneous involvement of the thyroid gland by Hashimoto's thyroiditis and Riedel's disease is a rare entity and less than 10 cases have been described. We report a case of a 40-year-old female.
Methods: the patient presented with a hard and quickly extensive goiter with symptoms of compression. Laboratory investigation revealed hypothyroidism, high titers of thyroid peroxidase and thyroglobulin antibodies. The fine-needle aspiration biopsy was suggestive of lymphocytic thyroiditis. Only a partial thyroidectomy was performed, due to important adherences to the soft tissues around the thyroid gland.
Results: Histopathologic evaluation showed an important fibrosis of the thyroid, extended to the skeletal muscle and the perithyroidal soft tissues. These findings were suggestive of Riedel's disease. However, there were associated with an oncocytic metaplasia of the residual thyroid follicles, and an inflammatory infiltrate. The immunostains showed an equal ratio of T and B cells, associated with a normal κ to λ ratio of plasma cells, consistent with the polyclonal nature of the B cells. The pseudo-inflammatory tumor was eliminated, according to the negativity of the muscular markers. The patient was treated with steroids, without any regression of the hard fibrous mass of the neck.
Conclusions: the clinical, pathological and immunohistochemical features of this case are consistent with an unusual simultaneous involvement of the thyroid gland by Hashimoto's thyroiditis and Riedel's disease, raising the pathogenic origin of this association : two distinct entities or different phases of the same pathology?

P-664

PTOV1, a novel protein overexpressed in prostate cancer, contains a new class of protein modules

Benedit P1, de Torres I 3, Paciucci R1, Reventós J1, Valeri M1, Nadal M2, Càceres C1, Estivill X2, Lozano JJ4, Morote J1,5, Thomson TM1,6
1 Unitat de Recerca Biomèdica, Hospital Materno-Infantil, Hospitals Vall d'Hebrón; 2 Centre de Genètica Molecular, Institut de Recerca Oncològica; 3 Servei d'Anatomia Patològica, Hospitals Vall d'Hebrón; 4 Grup de Recerca en Informàtica Mèdica, Institut Municipal d'Investigació Mèdica i Universitat Pompeu Fabra; 5 Servei d'Urologia, Hospitals Vall d'Hebrón; 6 Institut de Biologia Molecular, CSIC, Barcelona, Spain

We have isolated and characterized a gene and its encoded protein, not described previously, which we have called PTOV1 (prostate tumor overexpressed).
METHODS: The cDNA for PTOV1 was identified in differential display experiments, and shown to be overexpressed in prostate cancer, as determined by semiquantitative RT-PCR. Specific antibodies to PTOV1 were generated, which allowed to study the subcellular localization of this protein, as well as its in situ expression in normal and tumor prostate. The subcellular localization of PTOV1 was further confirmed by means of in vitro expression of chimeric GFP-PTOV1 constructs. Immunohistochemistry with anti-PTOV1 antibodies confirmed its overexpression in prostate tumors, which affected areas of carcinoma cells as well as areas characterized as prostate intraepithelial neoplasia (PIN), the first morphologically recognizable neoplastic lesion in prostate cancer. Therefore, PTOV1 has been found overexpressed both in early and late stages of prostate cancer.
RESULTS: The PTOV1 gene was isolated, sequenced, and its structure characterized. It consists of 12 exons, and it is localized in chromosome 19q13.3. PTOV1 mRNA was found in a range of normal human tissues, including brain, heart, skeletal muscle, kidney and liver, with expectedly low levels in normal prostate. Expression of PTOV was found upregulated by androgens in vitro. The structure of the PTOV1 protein is remarkable, in that it consists almost entirely of a tandemly repeated domain, separated by a short linker peptide. We have identified a Drosophila homolog of PTOV1, which shows also the same repeated domain structure. Furthermore, we have identified a second human gene, and its Drosophila homolog, predicted to encode a protein with a single PTOV domain. We have given the name PTOV2 to this protein. Human and Drosophila PTOV2 contain regions extending towards their amino and carboxy termini which show conservation between both organisms, and containing polyglutamine-rich stretches.
CONCLUSIONS: We found a new family of genes containing the PTOV domain, a new class of protein modules present in human, rodent and fly proteins. PTOV1 gene is regulated by androgens, is not expressed in normal prostate but it is overexpressed in prostate cancer, suggesting its participation in the prostate tumor progression.

P-665

The role of Fas, Fas-l and p27 $^{KIP\ 1}$ expression in carcinogenesis of prostate

Ciftcioglu MA, Kılıcarslan B, Keles N, Gulkesen KH*
Akdeniz University, School of Medicine, Pathology and Bioistatistics* Departments, Antalya, Turkey

Introduction: Impaired regulation of apoptosis is known to be associated with the development of various forms of cancer. Fas (CD 95; APO 1) is a transmembrane protein that mediates apoptosis upon cross-link with Fas Ligand (Fas-L). p27 $^{KIP\ 1}$ is an inhibitor of the cell cycle with potential tumor suppressor function. Decreased level of p27 protein expression have been correlated with tumorogenesis.
Materials and Methods: We evaluated Fas, Fas-L and p27 $^{KIP\ 1}$ expression in 55 patients. The specimens were obtained from 24 patients with prostatic cancer, 21 patients with high grade prostatic intraepithelial neoplasia (H-PIN), and 10 patients with benign prostatic hypertrophy (BPH). Archived paraffin embedded specimens were sectioned and immunostained with Fas, Fas-L and p27 $^{KIP\ 1}$ antibody and scored by two independent observers.
For p27 $^{KIP\ 1}$ at least 300 nuclear stained cells counted and expressed as percentage of positive cells and intensity of staining. For Fas and Fas-L; diffuse cytoplasmic staining was scored by the intensity of staining. Statistical analysis of Fas, Fas-L and p27 $^{KIP\ 1}$ protein expression and the relationship with patient groups were determined using Kruskal Wallis variance analysis and Mann Whitney-U test for pairwise comparisons.
Results: 46.7±28.6% (means±SD) of carcinoma group, 83.0±24.0% of H-PIN group and 100±0.0% of BPH group positive by p27 $^{KIP\ 1}$ immunohistochemistry. There was a significant difference between groups (p:0.0001). Fas and Fas-L stained scores in carcinoma group were the lowest and scores of H-PIN group were lower than BPH grups (p:0.0001) but no significant difference was observed between H-PIN and BPH for Fas staining (p:0.087) by pairwise comparisons.
Conclusion: The results suggest that downregulation of Fas and Fas-L in prostate cancers migth be considered as concomittant with disease progression and loss of the p27 $^{KIP\ 1}$ protein in prostate cancer cells correlates with implicating regulation of p27 $^{KIP\ 1}$ prostate tumor progression.

P-666

Expression of adhesivemolecules in Non Hodgkin`s lymphomas (NHL) classified accordingly to REAL classification

Petrusevska G.*, Hadgi-Pecova L.**, Janevska V.*,
Stojanovic A.**, Georgievski B.**, Jovanovic R.
Institute of Pathology, Clinic for Haematology**, Faculty of medicine, R. Macedonia

It is well established that the angiogenic activity and adhesive molecules have influence on metastatic spreading of malignant tumors. The adhesive molecules contribute to the high tissue specific dissemination patterns of certain lymphoma subtypes.
Fifty cases with diagnosed NHL for the present expression of CD44, CD31, CD34 and Collagen IV were analysed. All cases were classified according to REAL classification using histochemical and immunohistochemical methods. In addition, stainings for CD44, Collagen IV, CD31 and CD34 were done by DAKO En Vision™+ System, Peroxidase (DAB) technique on paraffin sections. The extent of expression of these molecules was measured semiquantitatively and Image Analysing System LUCIA M (NIKON).
Final results showed strongest diffuse expression of CD44 in the group of diffuse large B cell lymphomas (DLCL). The group of small lymphocytic lymphomas showed diffuse weaker staining for

CD44, and lymphoblastic lymphomas cells were positive in the perivascular areas. Collagen IV receptors were found along the vascular basement membranes. CD31 and CD34 followed each other and Collagen IV as well. The highest concentration of vascular spaces was found in the group of DLCL-s, decreasing in the lymphoblastic types, as well as in small lymphocytic lymphomas group. Statistical analyses showed significant difference between the groups of malignant lymphomas respective to control group of reactive lymph nodes. There was significant significant difference between the group of DLCL-s and the other types of lymphomas.
We can conclude that these results should be correlate with clinical stage as well as with survival rate to determine their prognostic significance.

P-667

Human DNA polymerase epsilon in breast cancer

Zhou Q, Elzagheid A, Jalava P, Sundfors C, Huang D, Syväoja JE, Collan Y
Department of Pathology, University of Turku, Turku, Finland

DNA polymerases are potential candidates for cancer genes. The have numerous functions which can be expected to be associated with carcinogenesis of neoplastic progression. These include replication of DNA and DNA repair. Some polymerases have shown cancer association, but there is no data available on polymerase epsilon. To test the potential role of polymerase epsilon in breast cancer 157 DNA samples from human breast cancers and 133 DNA control samples were analysed with the PCR-SSCP methodology for mutation in the highly conserved regions of the polymerase epsilon gene. 14 different primer pairs were used and 35% of all reading frames of the catalytic unit of polymerase epsilon was scanned. Only one mutated triplet was found in a cancer sample, resulting in no change in the deduced amino acid. There were no polymorphisms in the cancer samples. The conclusion is that the conserved areas of the human DNA polymerase epsilon catalytic subunit are improbable candidates for genomic regions causing breast cancer. Rather, the findings suggest that human DNA polymerase epsilon is a housekeeping gene with strictly regulated optimal function. The rest of the genome (65% of reading frames, and introns) is still a potential target for carcinogenetic mutations. The recent sequencing of the smaller subunit of the DNA polymerase epsilon molecule will allow a widening of the study, and give further evidence on the nature of the gene in respect to cancer.
The optimal function of the SSCP methodology was confirmed in the exonuclease I region of the polymerase epsilon gene in 92 cases of breast cancer. There was no evidence of mutation in these samples either in SSCP analysis of in DNA sequencing.

 © Springer-Verlag 2001

ANNOUNCEMENTS

3–5 October 2001
Association for European Cardiovascular Pathology (AECVP)
Academic Medical Center, University of Amsterdam,
The Netherlands

A 2½ day annual meeting with emphasis on educational aspects. On Wednesday, 3 October, the program will include free communications. On Thursday, 4 October, there will be a full-day educational program on "non-atherosclerotic vascular pathology." Topics will include proximal aortic disease, peripheral vascular disease, pathology of hypertension, vasculitis and two keynote lectures on "Ageing in the cardiovascular system" and "Advances in the understanding of vascular genetics." On Friday, 5 October there will be a mini-symposium on microvascular pathology.

This meeting will be submitted to the Royal College of Pathologists, London, and the Dutch Society of Pathology for CPD credits.

Costs: there is no registration fee for the scientific program, except for lunch on Thursday and Friday (NLG 25.00 per day).

For further information: Marsha Schenker, Secretariat: AECVP, Department of Cardiovascular Pathology, Academic Medical Center, Meibrgdreef 9, 1105 AZ Amsterdam, The Netherlands; e-mail: m.i.schenker@amc.uva.nl, Tel.: +31-20-5665646, Fax: +31-20-6914738

5–6 October 2001
Skin and botulinum toxin – First forum of the experts
Munich and Eibsee

This forum is being given by the Gesellschaft für Ärztliche Fortbildung und Wissenschaftliche Forschung at the Clinic and Policlinic for Dermatology and Allergology at Ludwig Maximilian University in Munich.

For further information: Dr. Marc Heckmann (conference leader), Klinik und Poliklinik für Dermatologie und Allergologie, Klinikum der Universität München, Frauenlobstrasse 9–11, 80337 München, Tel.: +49-89-51606391, Fax: +49-89-551606392

Registration: Congress office: Gertrud Hammel, Schmiedberg 6, 86152 Augsburg, Tel.: +49-821-3466219, Fax: +49-821-3466222, e-mail: Gertrud.Hammel@t-online.de, Internet: www.haut-botulinum.de

8 October 2001
Continuing Medical Education
One-day Multi-Disciplinary Update Courses
Nottingham International Breast Education Centre,
Nottingham, UK

For further information: Education Administrators, Nottingham International Breast Education Centre, City Hospital, Hucknall Road, Nottingham NG5 1PB; e-mail: Steph.bury@nibec.co.uk Tel.: +44-115-9691689, Fax: +44-115-9627707

11–12 October 2001
Diagnostic Immunohistochemistry
Treviso, Italy

The Department of Pathology of Treviso is organizing a two-day course on the practical application of immunohistochemistry to surgical pathology as well as the most recent technical advances.

The course is for pathologists and residents in pathology and will include lectures and slide seminar illustrating cases in which immunohistochemistry has played a key role. Cases for the slide seminar will be provided by the faculty. The registrants will receive the cases in CD-ROM along with the clinical histories one month prior to the course.

The number of participants will be limited and therefore early application is advised.

Please contact the organizers before making payment: Tel.: 0422-322707; Fax: 0422-322663. e-mail: apdeitos@ulss.tv.it

Registration fee: Lit. 350.000 (VAT included), comprehensive of slides, handouts and breaks. Members of S.I.A.P.E.C. Lit. 300.000. Residents: Lit. 70.000

Payment should be made by remittance to the: Associazione Trevigiana di Patologia Oncologica, account N. 0015–47382501, CASSAMARCA: ABI: 06035 CAB: 12015.

The registration form and payment should be sent to the following address: Mrs. Eleonora Fonte, Organizing Secretary, Biblioteca Ospedale Civile, Piazza Ospedale, 31100 Treviso, Italy, Tel.: 0422 322743, Fax: 0422 322663

19–21 November 2001
Continuing Medical Education
Multi-Disciplinary Courses on Breast Cancer
Nottingham International Breast Education Centre,
Nottingham, UK

Three-day course. The first part is multi-disciplinary. Thereafter, the different specialties meet to accommodate their own special requirements.

For further information: Education Administrators, Nottingham International Breast Education Centre, City Hospital, Hucknall Road, Nottingham NG5 1PB; e-mail: Steph.bury@nibec.co.uk Tel.: +44-115-9691689, Fax: +44-115-9627707

26–27 October 2001
Bone and Soft-Tissue Tumors
Münster, Germany

This two-day seminar is designed for orthopedists, surgeons, radiologists, and pathologists. The first day will be devoted to the clinical signs, imaging, pathology, and therapy of tumorous lesions of the skeleton. The second day will be a course on operations using the current techniques of reconstruction of the the extremities.

For further information: Klinik und Poliklinik für Allgemeine Orthopädie, Oberarzt Dr. Lindner, Westfälische Wilhelms-Universität Münster, Albert-Schweitzer-Str. 33, 48149 Münster; e-mail: LindneN@uni-muenster.de, Tel.: +49-251-8347901, Fax: +49-251-8347989

Virchows Arch (2001) 439:497–503
DOI 10.1007/s004280100479

REVIEW ARTICLE

Burkhard Helpap

Nonepithelial neoplasms of the urinary bladder

Received: 27 April 2001 / Accepted: 25 May 2001 / Published online: 24 July 2001
© Springer-Verlag 2001

Abstract Nonepithelial tumors are rare in the urinary bladder, but their exact classification is very important in the differential diagnosis between these tumors and epithelial lesions. In the new WHO classification and in the third series of the Armed Forces Institute of Pathology (AFIP) "Atlas of Tumor Pathology" on urinary bladder tumors, various mesenchymal tumors, mixed epithelial and mesenchymal tumors and myofibroblastic proliferations are summarized. In the following we will describe the histology, immunohistology, and cytogenetics of nonepithelial tumors and lesions.

Keywords Urinary bladder · Sarcoma · Mixed tumors · Fibroblastic lesions · Histology · Immunohistology

Introduction

Nonepithelial tumors are quite rare in the urinary bladder, but they are generally more difficult to recognize than epithelial lesions [36, 42, 44]. Whereas nonepithelial tumors account for only 0.51% in the total material examined at the Uropathological Center at the Department of Pathology in Singen, their share is ten times as high in our consultation cases. Only 2% of bladder tumors are nonepithelial in origin. In the renal pelvis and ureter, the percentage is even lower (1.7%). Our data (0.51% nonepithelial tumors in the bladder) are similar to those reported in the literature [31].

The diagnosis is generally based on the assessment of hematoxylin and eosin stained sections. The current subclassifications, however, mostly require additional immunohistochemical stains. For purposes of grading, mitosis rates and sometimes also the Ki67/MIB-1 proliferation index must be determined. In general, low and high grade malignant neoplasms are distinguished. Table 1 shows the immunohistochemical features of epithelial and nonepithelial neoplasms.

B. Helpap (✉)
Department of Pathology, Hegau-Klinikum Singen,
University of Freiburg, Germany
e-mail: pathologie@hegau-klinikum.de
Tel.: +49-7731-892100, Fax: +49-7731-892105

Leiomyomas and leiomyosarcomas

In the lower urinary tract the urinary bladder is the most frequent site of these tumors. Whereas leiomyomas are more frequent in females of all ages and may account for up to 35% of all benign urinary bladder tumors [24], leiomyosarcomas are mainly found in the urinary bladder of males (70%) at an average age of 50 years. Leiomyosarcomas and malignant fibrous histiocytomas can occur as secondary tumors after irradiation of the small pelvis or after chemotherapy [53, 57]. Histologically, the classical spindle cell type and the myxoid type predominate [40] (Fig. 1). The differential diagnosis versus other spindle cell neoplasms has been facilitated by immunohistochemical staining for muscle specific actin and desmin, the former being more frequently positive than the latter (Figs. 2, 3, 4, 5, 6). A high mitotic rate (5/10 HPF), an MIB-1 index over 20%, and extensive necrosis are indicative of a poor prognosis and such neoplasms are therefore considered high-grade tumors, in contrast to low and intermediate grade leiomyosarcomas [40]. Not infrequently, leiomyosarcomas are found in the exterior wall of the urinary bladder. They may extensively infiltrate prostatic tissue, requiring extensive surgical intervention. The risk of bleeding due to the tumor is relatively high. A poor prognosis is related to short-term local recurrence as well as to distant metastases, mainly to the lungs [39] (Table 2).

Epithelioid leiomyosarcoma

This type of leiomyosarcoma is extremely rare in the urinary bladder [31]. Histologically, numerous multinucleated giant cells are found with moderate cellular atypia and frequent mitoses. The MIB-1 labeling index is elevated compared to the usual leiomyosarcomas. Desmin

Table 1 Differential immunohistology of round and spindle cell lesions of the urinary bladder (*A_1CHT* α_1-antichymotrypsin, *LCA* leukocyte common antigen)

	Vimentin	Desmin	SMA	CD 34	F VIII	S 100	NSE	CK	Others
Leiomyoma	+	+	+					–	
Leiomyosarcoma, classic, epithelioid, myxoid	+	+/–	+					–	
Rhabdomyosarcoma	+	+	+			+/–		–/+	
Malignant fibrous histocytoma	+	–/rarely +	–			+/–		–	CD 68 +, A_1CHT+
Rhabdoid tumor	+	+				+	+	+	
Angiosarcoma	+	–	–	+	+	–			CD 31 +
Malignant lymphoma	+	–	–					–	LCA +
Urothelial carcinomas, sarcomatoid	+/–	–	–			–		+	
Postoperative spindle cell nodule	+	–/+	+/–			–		–/rarely +	Myoglobin –
Inflammatory pseudotumor[a]	+	–/+	+/–			–		–/rarely +	Myoglobin –

[a] Syn.: pseudosarcomatous fibromyxoid tumor

is completely negative in epithelioid leiomyosarcomas, whereas muscle specific antigen is focally expressed (Table 1).

Myxoid leiomyosarcoma

The myxoid subtype is more frequent than the epithelioid subtype [40]. Large areas of a myxoid matrix are found between elongated tumor cells with eosinophilic cytoplasm. The matrix is stainable with alcian blue and PAS. Mitoses are very rare [64]. The tumor cells express muscle specific antigen to a variable degree. Even cytokeratins can be expressed causing problems in the differential diagnosis versus epithelial tumors (see below) [31, 39] (Table 1).

Rhabdomyosarcoma

The botryoid type of embryonal rhabdomyosarcoma is the most frequent nonepithelial tumor in children below the age of 10, most of whom are males (over 75%) [13, 33]. Cardinal symptoms are hematuria or bladder neck obstruction. Cystoscopically, polypoid tumor masses are found, which can completely fill the urinary bladder lumen. Much less frequent at this age is the prognostically much less favorable alveolar type of rhabdomyosarcoma [14]. Rhabdomyosarcomas are very rare in adults. Since the establishment of immunohistochemical methods [37] some rhabdomyosarcomas have been reclassified as malignant fibrous histiocytomas, leiomyosarcomas, or liposarcomas (Table 1). Almost 100% of rhabdomyosarcomas are positive for SMA and for desmin. Vimentin is positive in most sarcomas and therefore of little worth in the differential diagnosis. Up to 50% of rhabdomyosarcomas may be positive for cytokeratins [37]. Histologically, embryonal rhabdomyosarcoma cells show typical strongly eosinophilic cytoplasmic protrusions with more or less prominent striation. With decreasing differentiation, the mitotic rate and the MIB-1 proliferative activity increase distinctly, accompanied by loss of striation in the tumor cells and increasing polymorphism. Immunohistochemically, there are no differences between the various grades of differentiation. The same holds for metastases, which are frequently found in paraaortic and iliac lymph nodes.

In the alveolar type of rhabdomyosarcoma, pseudoalveolar clefts are found, which are separated by thin fibrous septa covered by single cell layers of cubic and polygonal tumor cells. Occasionally, atypical multinuclear giant cells can be detected. In addition to the alveolar pattern, solid areas can occur. Actin and desmin are distinctly expressed, focally also S-100 protein and α-1 antichymotrypsin.

Rarely, positive reactions are found with the following antibodies: titin, Z-protein, creatine kinase M, and fetal heavy chain skeletal myosin. Similar to leiomyosarcomas, rhabdomyosarcomas may express epithelial markers, such as cytokeratins and a 58-kDa neurofilament protein [11, 48]. Cytogenetics are of special importance in the diagnosis and subclassification of rhabdomyosarcomas [14, 41]. Two different hyperdiploid basal types are differentiated [7, 45]. Embryonal rhabdomyosarcomas are characterized by loss of heterozygosity at

Fig. 1 Spindle cell leiomyosarcoma of the urinary bladder. (H&E) ▶

Fig. 2 Postoperative spindle cell nodule in the urinary bladder. (H&E)

Fig. 3 Peripheral nerve sheath tumor (MPST). (H&E)

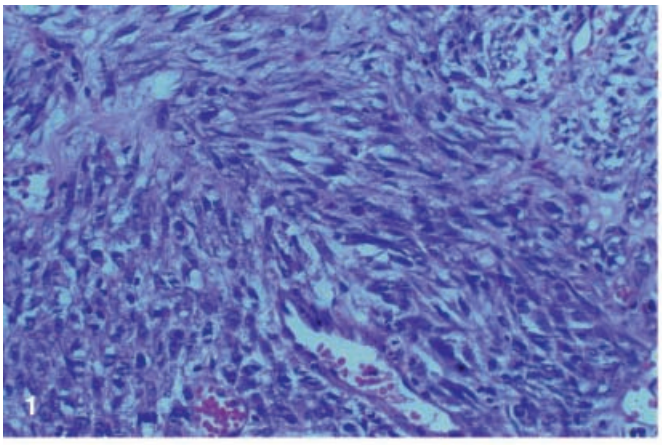
Fig. 4 Myofibroblastic tumor. (H&E)

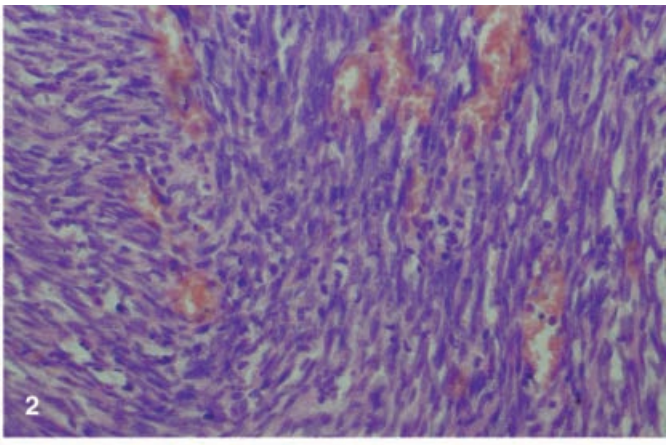
Fig. 5 Spindle cell urothelial carcinoma. (H&E)

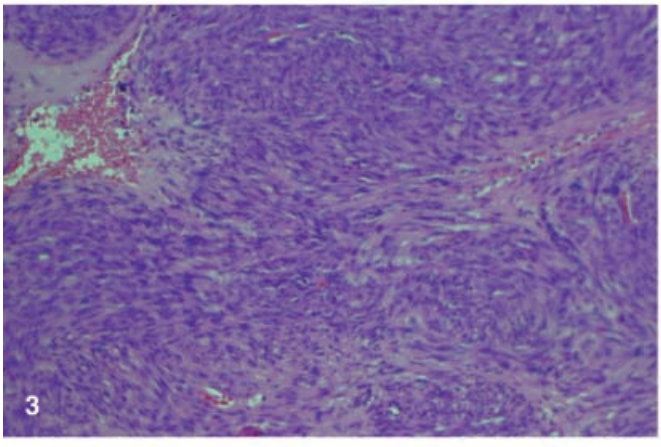
Fig. 6 Muscle invasive angiosarcoma of the urinary bladder. (H&E)

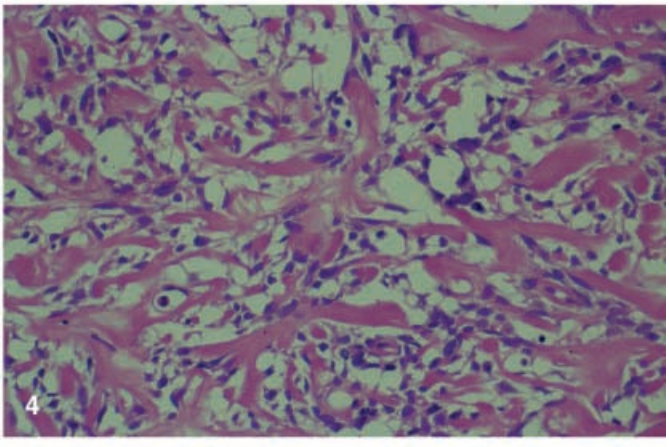
Fig. 7 Iron-negative black-brown pigmentations within the stroma of the urinary bladder wall (melanocytic proliferations). (H&E)

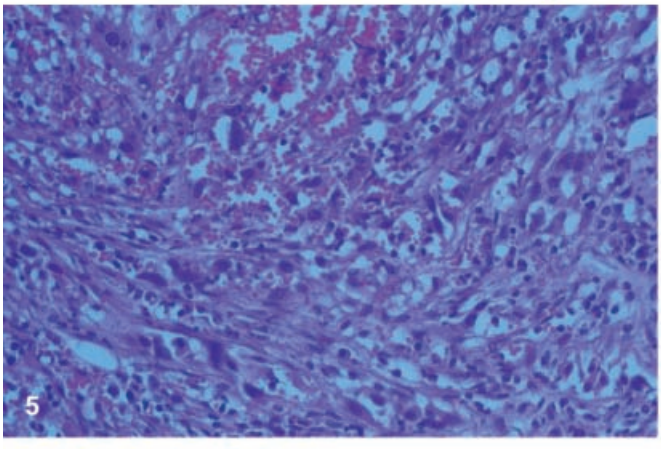
Fig. 8 Malignant melanoma of the urinary bladder with positive HMB 45 expression. (H&E)

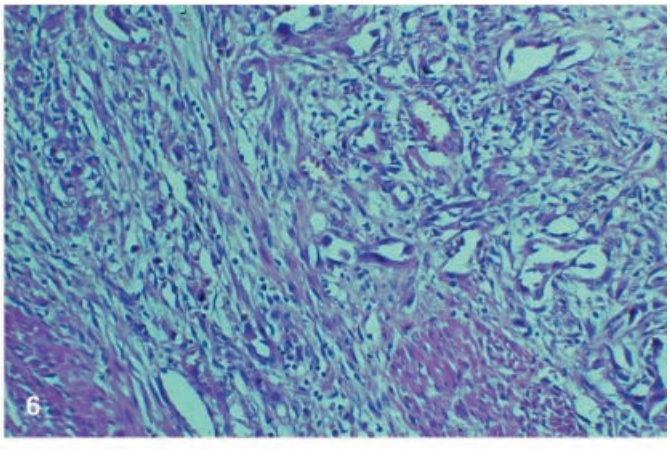

1

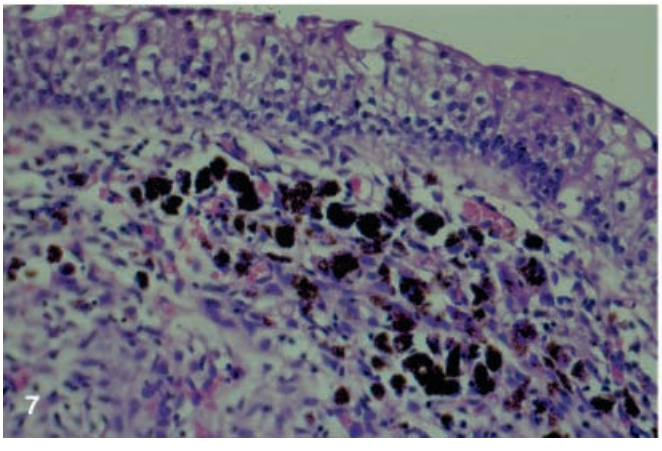

2


3


4


5


6


7

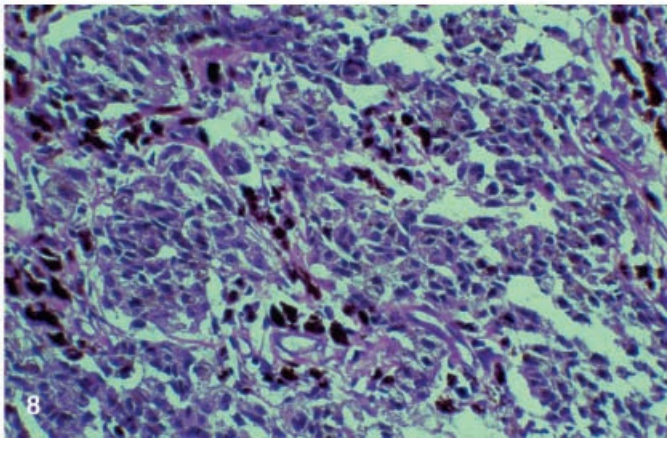

8

Table 2 Five-year survival rates in sarcomas of the bladder

Tumor type	Grade 1	Grade 2	Grade 3	Total
Malignant fibrous histiocytoma	89.8% (33)	76.5% (160)	48.1% (156)	349
Leiomyosarcoma	92.9% (16)	66.6% (65)	44.7% (67)	148
Malignant schwannoma	77.8% (5)	56.1% (26)	52.1% (41)	72
Rhabdomyosarcoma	0% (0)	74.9% (15)	42.1% (45)	60
Undifferentiated sarcomas	0% (0)	66.9% (43)	40.3% (97)	140

chromosome 11p 15.5 [54]. Alveolar rhabdomyosarcomas show a reciprocal chromosome translocation p (2;13) (q37;q14) [8, 59]. In alveolar rhabdomyosarcomas, the gene fusion product PAX 3/FKHR is localized on chromosome 2. PAX is a molecular marker specific for alveolar rhabdomyosarcomas [49].

Whereas the prognosis of untreated rhabdomyosarcomas is poor, modern multimodal therapy concepts have been quite successful [14]. Surgery, chemotherapy, and radiotherapy are applied, depending on the tumor stage [25]. In a review by Bale et al. [2], 72% of patients with urinary bladder rhabdomyosarcomas survived 5 years, while 11 of 31 children (28%) with primary rhabdomyosarcoma died after combined therapy. Unfortunately, advanced tumor stages are usually resistant to treatment (Table 2).

Rhabdoid tumors

Only three rhabdoid tumors have been described in the urinary bladder so far. Two tumors occurred in young girls (6 and 14 years of age) and the third in a 46-year-old woman in combination with high-grade urothelial carcinoma, and sarcoma. Immunohistochemically, vimentin is constantly expressed. Desmin, S-100 protein, and neuron-specific enolase can be focally positive, as can cytokeratins [5, 34] (Table 1). The characteristic morphology consists of spheric eosinophilic cytoplasmic inclusions within very polymorphous tumor cells with hyperchromatic nuclei, large nucleoli, and at times even neurosecretory granules. Malignant rhabdoid tumors can metastasize extensively very rapidly. The main differential diagnosis is versus rhabdomyosarcomas. The tumor cells are myoglobin negative, and striation cannot be detected. The prognosis is very poor.

Fibrohistiocytic tumors

This is a heterogeneous tumor group. Fibrous histiocytomas are very rare in the urinary bladder [26], whereas the storiform, fascicular, and myxoid types of malignant fibrous histiocytoma have been more frequently encountered [10, 46, 56]. These tumor types can develop after radio- or chemotherapy of the urinary bladder [5, 16, 53, 57]. Immunohistochemically, positive reactions have been noted for vimentin and α-1 antichymotrypsin as well as focal positivity for CD68. These reactions are helpful in differentiating these tumors from leiomyosarcomas. Rarely, malignant fibrous histiocytomas show a distinct inflammatory component that makes it difficult to distinguish them from postoperative spindle cell nodules. The cytokeratin positivity in postoperative spindle cell nodules can be helpful (Table 1).

The pleomorphic type of malignant fibrous histiocytoma shows a strongly positive focal reaction for S-100 protein in addition to α-1 antichymotrypsin and CD68. The polygonal, extremely anisomorphic cells have hyperchromatic nuclei and large nucleoli and are interspersed with pleomorphic multinuclear giant cells. Atypical mitoses are frequent. The MIB-1 labeling index is elevated. The very rare pure fibrosarcomas and round cell liposarcomas of the urinary bladder must be differentiated from malignant fibrous histiocytomas [16, 31, 39] (Table 1).

Neurogenic tumors

In patients with generalized neurofibromatosis (von Recklinghausen's disease), neurofibromas have been described in the urinary bladder [39, 51]. Sporadic neurofibromas, however, are extremely rare. Malignant (epithelioid) schwannomas have been described twice in the renal pelvis and twice in the urinary bladder [39, 51]. Granular cell tumors, which are also of neurogenic origin, can be distinguished from rhabdomyosarcomas by means of immunohistochemistry [39].

Vascular tumors

Cavernous, capillary, or plexiform hemangiomas are quite frequent in the urinary bladder [32]. Cavernous hemangiomas are connected with the risk of rupture and life-threatening hemorrhage [62]. Urinary bladder hemangiomas are not infrequently connected with Klippel-Trénaunay or Sturge-Weber syndromes [29]. Much less frequent are malignant angiosarcomas, lymphangiosarcomas, and hemangiopericytomas. Angiosarcomas are often localized in the bladder and in the prostate. The prognosis is poor. The differential diagnosis versus richly vascularized malignant fibrous histiocytomas and also versus plexiform leiomyosarcomas is facilitated by immunohistochemical demonstration of factor VIII-related antigen and CD31 [16] (Fig. 6; Table 1).

Other sarcoma types

Genuine osteo- and chondrosarcomas of the urinary bladder have been described in the older literature [16, 52]. Application of immunohistochemistry, however, has revealed carcinomatous differentiation in some parts of these tumors. It must be concluded that either undifferentiated carcinomas with osteocartilagineous stromal metaplasia or genuine carcinosarcomas were described in these cases [16, 39]. It can be helpful in the differential diagnosis that osseous stromal metaplasms lack severe cytological atypia, in contrast to genuine osteo- and chondrosarcomas [39, 63].

Carcinosarcomas vs. sarcomatoid carcinoma

As mentioned above, not all "carcinosarcomas" of the urinary bladder are true carcinosarcomas [3, 21]. They may be collision tumors of urothelial carcinomas and sarcomas, poorly differentiated urothelial carcinomas with osteocartilaginous stromal metaplasia, or merely undifferentiated sarcomatoid spindle cell urothelial carcinomas [9, 21, 58]. In true carcinosarcomas, epithelial and mesenchymal tumor components are randomly intermingled with the predominant epithelial component. Occasionally, glandular or squamous cell differentiation can be detected. The mesenchymal component consists predominantly of fibro- and leiomyosarcomatous areas. In about 20% of the cases, rhabdomyoblastic, cartilaginous, or osseous differentiation can be found. Immunohistochemically, the epithelial component is characterized by distinct cytoplasmic cytokeratin expression. The urothelial origin is underlined by the positivity for the high-molecular-weight cytokeratin 34ßE12. The sarcomatous component can be stained with vimentin, desmin, and muscle specific actin. Frequently, carcinosarcomas show polypoid exophytic growth. In most cases DNA flow cytometry reveals an aneuploid DNA pattern [58]. The prognosis is extremely poor due to the advanced tumor stage at the time of detection. Radical cystectomy does not yield long-term survival rates [15, 16] (Table 2).

Melanoma and melanosis

Most of the melanomas found in the urinary bladder are metastases of primary melanomas of other organs, mainly the skin. The most frequent localization of primary malignant melanoma in the urogenital tract is the female urethra. Only few cases have been described in the urinary bladder [12, 30, 39]. The histology does not differ from melanomas in other localizations. The histogenesis of malignant melanoma of the urinary bladder remains uncertain. Probably, they originate from melanocytes dispersed from the neural crest. In 1998, de Pinieux and coworkers [6] described the first case of clear cell sarcoma of the bladder. This tumor is a distinct entity within the spectrum of melanotic neuroectodermal tumors. The tumor cells were strongly positive for HMB 45 and S-100 protein.

The prognosis of malignant melanomas of the urinary bladder and urethra is extremely poor, with a high rate of local recurrence even after radical surgery [16, 39].

Melanosis of the urinary bladder is certainly not a precursor of malignant melanoma. Melanin granules can occasionally be found in the cytoplasm of the urothelial cells comparable to that seen in epidermal keratinocytes. Melanin granules can also be found in melanocyte-like cells in the superficial urinary bladder stroma [1] (Figs. 7, 8).

Malignant lymphoma

Malignant lymphomas rank third in frequency among the nonepithelial urinary bladder tumors [43, 47]. The peak incidence is at age 65, with a range from 20 to 85. The tumors form solid polypoid nodules often with intact mucosa. Ulcerations and ureteral obstructions may occur. The submucosal lymph follicles have been discussed as the origin. The main localization is in the trigone, less frequently the lateral walls. Malignant non-Hodgkin's lymphomas of B- and T-cell origin have been found. Increasingly, MALTomas have been being described [28], mainly low-grade B-cell lymphomas. Secondary malignant lymphomas in generalized stages are more frequent than primary malignant lymphomas. The differential diagnosis of signet ring cell lymphomas versus urachus carcinomas can be difficult [55]. Moreover, small cell urothelial carcinomas can be found with plasma cell-like differentiation that can resemble malignant lymphoma [65].

Plasmacytomas are very rare [18] and must be differentiated from benign plasma cell granulomas [60]. Urothelial carcinomas with plasmacytoid features may be confused with lymphomas, from which they can be differentiated by their cytokeratin positivity. Individual cases of Hodgkin's lymphoma have been described in the urinary bladder [23]. Therapy and prognosis do not differ from comparable typical malignant lymphomas.

Differential diagnosis: pseudosarcomas and/or spindle cell lesions of the urinary bladder

In children, sarcoma-like myofibroblastic proliferations are found with a peak incidence between the 2nd and 16th year of age and a female predominance (80%) [19]. Infantile pseudosarcomatous lesions are polypoid with myxoid areas, hemorrhages, and necroses. Histologically, the tumor cells possess eosinophilic to amphophilic cytoplasm with focal dense cellularity and myxoid areas, intermingled with a richly capillarized stroma sparsely infiltrated by lymphocytes. The tumor cells are reminiscent of fibroblasts with occasionally prominent nucleoli. The mitotic rate may be as high as 25/10 HPF especially in adults [50] (Figs. 2, 4; Table 1).

Postoperative spindle cell nodules, which develop about 2–10 months after transurethral resection of the urinary bladder or the prostate, are found mainly in adult males [35]. Histologically, spindle cells predominate some with an increased mitotic rate.

The spindle cell proliferations are occasionally densely infiltrated by lymphocytes, histiocytes, and plasma cells. However, plasma cell granulomas and inflammatory fibrous histiocytomas should be clearly differentiated from postoperative spindle cell nodules or pseudosarcomas. The immunohistochemical characteristics have been described above [21, 22, 35].

Myxoid areas, which are characteristic of leiomyosarcomas, are rare. The immunohistochemical analysis is crucial. Both infantile myofibroblastic proliferations and postoperative spindle cell nodules in adults are focally positive for cytokeratins, in contrast to leiomyosarcomas, and negative for myoglobin. A positive reaction for muscle-specific actin and desmin can be found in either lesion, whereas leiomyosarcomas are usually negative for keratins, with the exception of the myxoid subtype (see above) [20, 35, 39, 46, 61] (Fig. 2; Table 1).

Those pseudosarcomas of the urinary bladder are benign processes which can be locally resected. In contrast to leiomyosarcomas, further measures, such as extensive resection, are unnecessary.

A very rare problem that can occur is differentiating sclerosed thermogranulomas in the urinary bladder after transurethral resection. Usually, a Prussian blue stain reveals macrophages containing carbonized material. This is helpful in distinguishing thermogranulomas from postoperative spindle cell nodules. The reaction for cytokeratin is always negative in thermogranulomas [15].

Tumorlike lesions

In the discussion of the differential diagnosis of spindle cell lesions, leiomyosarcomas, malignant fibrous histiocytomas, and other sarcomas, the inflammatory pseudotumors and pseudosarcomas have already been mentioned. The latter tumors usually have a history of trauma or may develop in the course of long-standing chronic infections of the urinary tract [21]. The typical postoperative spindle cell nodules usually arise subsequent to transurethral resection.

Fibroepithelial polyps occur only sporadically in the urinary bladder, more frequently in the urethra and ureter of males. They are regarded as a hamartomatous lesion [39]. Further lesions are post- transurethral resection and bacillus Calmette-Guérin granulomas of the urinary bladder.

Follicular cystitis is mainly localized in the trigone and can appear as polypoid tumorous structures. Immunohistochemically, a typical reaction pattern is found. IgG is the most frequently encountered product, but IgA and IgM are also found [17]. The above-mentioned plasma cell granulomas must be differentiated from spindle cell tumors with a predominant histiocytic component and from amyloid nodules.

Tumorous malakoplakia of the urinary bladder is a monotonous collection of CD68 positive macrophages with inclusions containing calcium apatite that are referred to as Michaelis-Gutmann bodies. Cytoplasmic iron depositions can also be found. Lymphocytes within the lesion are mainly T-lymphocytes. The changes are caused by an E.coli infection in an individual with reduced macrophage activity.

References

1. Alroy J, Ucci AA, Heany JA, Mitcheson HD, Gravis VE, Woods W (1986) Multifocal pigmentations of prostatic and bladder urothelium. J Urol 136:96–97
2. Bale PMS, Parsons RE, Stevens MM (1986) Pathology and behavior of juvenile rhabdomyosarcoma. In: Finegold M (ed) Pathology of neoplasia in children and adolescents. Saunders, Philadelphia
3. Baschinsky DY, Chen JH, Vadmal MS, Lucas JG, Bahnson RR, Niemann TH (2000) Carcinocarcoma of the urinary bladder – an aggressive tumor with diverse histogenesis. A clinicopathologic study of 4 cases and review of the literature. Arch Pathol Lab Med 124:1172–1178
4. Bhansali SK (1962) Sarcoma botroyides of the bladder in infancy and childhood. J Urol 87:871–875
5. Carter RL, McCarthy KP, Al-Sam SZ, Monagham P, Agrawal M, McElwein TJ (1989) Malignant rhabdoid tumour of the bladder with immunohistochemical and ultrastructural evidence suggesting histiocytic origin. Histopathol 14:179–190
6. De Pinieux G, Chatelain D, Vieillefond A, Arrivets P, de Saint Maur PP (1998) Clear cell sarcoma of tendons and aponeuroses presenting as a bladder mass. J Urol Pathol 9:239–245
7. Dockhorn-Dworniczak B, Schäfer KL, Blasius S, Christiansen H, Koscielniak E, Ritter J, Winkelmann W, Jürgens H, Böcker W (1997) Assessment of molecular genetic detection of chromosome translocations in the differential diagnosis of pediatric sarcomas. Klin Paediat 209:156–164
8. Douglas EC, Valentine M, Etcubans E, Parham D, Webber BL, Houghton PJ, Green AA (1987) A specific chromosomal abnormality in rhabdomyosarcoma. Cytogenet Cell Genet 45: 148–155
9. Eble JN, Young RH (1991) Stromal osseus metaplasia in carcinoma of the bladder. J Urol 145:823–825
10. Egawa S, Uchida T, Koshiba K, et al (1994) Malignant fibrous histiocytoma of the bladder with focal rhabdoid tumor differentiation. J Urol 151:154–156
11. Eusebi V, Rilke F, Cecccarelli C, Fedeli F, Schiaffino S, Bussolati G (1986) Fetal heavy chain skeletal myosin. An oncofetal antigen expressed by rhabdomyosarcoma. Am J Surg Pathol 10:680–686
12. Goldschmidt SJ, Py JM, Kostakopoulos A (1988) Primary malignant melanomas of the urinary bladder. Br J Urol 61: 359–366
13. Harms D, Schmidt D (1997) Solide Tumoren des Kindes- und Adoleszentenalters. In: Remmele W (ed) Pathologie, vol 4, 2nd edn. Springer, Berlin Heidelberg New York, pp 501–549
14. Harms D, Leuschner I, Krams M, Pilgrim TB, Treuner J (1998) Rhabdomyosarcomas (RMS) and extraosseous Ewing's sarcomas. Verh Dtsch Ges Pathol 82:83–98
15. Helpap B (1989) Pathologie der ableitenden Harnwege und der Prostata. Springer, Berlin Heidelberg New York
16. Helpap B (1993) Atlas der Pathologie urologischer Tumoren. Springer, Berlin Heidelberg New York
17. Hill G (1989) Uropathology. Churchill Livingstone, New York
18. Ho DS, Patterson AL, Orozco RE, et al (1993) Extramedullary plasmacytoma of the bladder: case report and review of the literature. J Urol 150:473–474
19. Hojo H, Newton WA, Hamondi Ab, Qualman SJ, Wakasa H, Suzuki S, Jaynes F (1995) Pseudosarcomatous, myofibroblas-

tic tumor of the urinary bladder in children: a study of 11 cases with review of the literature. An Intergroup rhabdomyosarcoma study. Am J Surg Pathol 19:1224–1236
20. Huang W-L, Ro JY, Grignon DJ (1990) Postoperative spindle cell nodule of the prostate and bladder. J Urol 143:824–826
21. Jones EC (1999) Spindle cell lesions of the urinary bladder. J Urol Pathol 10:47–70
22. Jones EC, Clement PB, Young RH (1993) Inflammatory pseudotumor of the urinary bladder. A clinicopathological, immunohistochemical, ultrastructural and flow cytometric study of 13 cases. Am Surg Pathol 17:264–274
23. Jones MW (1989) Primary Hodgkin's disease of the urinary bladder. Br J Urol 63:438
24. Kabalin JN, Freiha FS, Neibel JD (1990) Leiomyoma of the bladder. Urology 35:210–212
25. Kaefer M, Rink RC (2000) Genitourinary rhabdomyosarcoma. Treatment options. Urol Clin North Am 27:471–487
26. Karol JB, Eason AA, Tanagho EA (1977) Fibrous histiocytoma of bladder. Urology 10:593–595
27. Karoly P, Endes P, Krasznai G, et al (1988) Bizarre leiomyoma of the prostate. Virchows Arch A Pathol Anat Histopathol 412:383–387
28. Kempton CL, Kurtin PJ, Inwards DJ, Wollau P, Bostwick DG (1997) Malignant lymphoma of the bladder: evidence from 36 cases that low-grade lymphoma of the MALT-type is the most common primary bladder lymphoma. Am J Surg Pathol 21:1324–1333
29. Klein TW, Kaplan GW (1975) Klippel-Trenaunay syndrome associated with urinary tract hemangiomas. J Urol 114:596–600
30. Kojima T, Tanaka T, Yoshimi N, et al (1992) Primary malignant melanoma of the urinary bladder. Arch Pathol Lab Med 116:1213–1216
31. Kunze E, Theuring F, Krüger G (1994) Primary mesenchymal tumors of the urinary bladder. A histological and immunohistochemical study of 30 cases. Pathol Res Pract 190:311–332
32. Leonhard MP, Nickel JC, Morales A (1988) Cavernous hemangiomas of the bladder in the pediatric age group. J Urol 140: 1503–1504
33. Loughlin KR, Retik AB, Weinstein HJ, et al (1989) Genitourinary rhabdomyosarcoma in children. Cancer 63:1600–1606
34. McBride JA, Ro JY, et al (1994) Malignant rhabdoid tumor of the bladder in an adolescent: case report and discussion of extrarenal rhabdoid tumor. J Urol Pathol 2:255–263
35. Meister P, Heidl G (1991) Postoperativer Spindelzellknoten der Harnblase und Prostata. Pathologe 12:214–219
36. Melamed DE, Choudhury MS, Melamed MR (1999) Multifocal sarcoma of the urinary bladder. Mol Urol 3:381–384
37. Miettinen M (1988) Rhabdomyosarcoma in patients older than 40 years of age. Cancer 62:2060–2065
38. Miettinen M, Rapola J (1989) Immunohistochemical spectrum of rhabdomyosarcoma and rhabdomyosarcoma-like tumors. Expression of cytokeratins and the 68kD Neurofilament protein. Am J Surg Pathol 113:120–132
39. Mikuz G (1993) Non-urothelial tumors of the urinary tract. Verh Dtsch Ges Pathol 77:180–198
40. Mills SE, Bova S, Wice MR, Young RH (1989) Leiomysarcoma of the urinary bladder. A clinicopathological and immunohistochemical study of 15 cases. Am J Surg Pathol 13:480–489
41. Moriyama M, Shuin T, Kubota Y, Satoni Y, Sugio Y, Kurori Y (1986) A case of rhabdomysarcoma of the bladder with a (2;5) chromosomal translocation in peripheral lymphocytes. Cancer Gen Cytogenet 22:177–181
42. Mostofi FK, Davis CJ, Sesterham IA (1999) Histological typing of urinary bladder tumours. In: World Health Organization. International histological classification of tumours. Springer, Berlin Heidelberg New York
43. Mourad WA, Khalie S, Radwi A, Peracha A, Ezzat A (1998) Primary T-cell lymphoma of the urinary bladder. Am J Surg Pathol 22:373–377
44. Murphy WM, Beckwith JB, Farrow GM (1994) Tumors of the kidney, bladder and related urinary structures. In: Atlas of tumorpathology, 3rd series, fascile 11. AFIP, Washington
45. Noguera R (1996) Cytogenetics and tissue culture of small round cell tumors of bone and soft tissue. Semin Diagn Pathol 13:171–183
46. Oesterling JE, Epstein JI, Brendler CB (1990) Myxoid malignant fibrous histiocytoma of the bladder. Cancer 66:1836–1842
47. Ohsawa M, Arozasa K, Horiuchi K, et al (1993) Malignant lymphoma of bladder: report of three cases and review of the literature. Cancer 72:1969–1974
48. Osborn M, Hill C, Altmansberger M, Weber K (1986) Monoclonal antibodies to titin in conjunctioon with antibodies to desmin separates rhabdomyosarcomas from other tumor types. Lab Invest 55:101–108
49. Reichmuth C, Markus MA, Hillemanns M, Atkinsons MJ, Unii KK, Saratzki G, Höfler H (1996) The diagnostic potential of the chromosome translocation t(2;13) in rhabdomyosarcoma: a PCR study of fresh-frozen and paraffin-embedded tumour samples. J Pathol 180:50–57
50. Ro JY, El-Naggar AK, Amin MB, et al (1993) Pseudosarcomatous fibromyxoid tumor of the urinary bladder and prostate. Hum Pathol 24:1203–1210
51. Rober PE, Smith JB, Sakr W, Pierce JM (1991) Malignant peripheral nerve sheath tumor (malignant schwannoma) of urinary bladder in von Recklinghausen neurofibromatosis. Urology 38:473–476
52. Russo P, Brady MS, Conlon K, Hajdu SI, Fair WR, Herr HW, Brennan MF (1992) Adult urological sarcoma. J Urol 147: 1032–1036
53. Schöpp F, Böhm E, Walz PH (1989) Malignes fibröses Histiozytom der Harnblasenwand nach Strahlentherapie eines Urothelcarcinoms. Aktuelle Urol 20:215–217
54. Scrable H, Witte D, Shimada H, Seemayer T, Sheng WW, Soukup S, Koufos A, Houghton P, Lampkin B, Cavenee W (1989) Molecular differential pathology of rhabdomyosarcoma. Genes Chromosom Cancer 1:23–35
55. Siegel RJ, Napoli VM (1991) Malignant lymphoma of the urinary bladder: a case with signet-ring cells simulating urachal adenocarcinoma. Arch Pathol Lab Med 115:635–637
56. Anglada Curado FJ, Lopez Beltran A, Prieto Castro R, Regueiro Lopey JC, Leva Vallejo M, Alameda Aragoneses V, Blanco Espinosa A, Moreno Arcas P, Requena Tapia MJ (2000) Malignant fibrohistiocytoma of the bladder. Actas Urol Esp 24:581–583
57. Thrasher JB, Miller GJ, Wettlaufer JN (1990) Bladder leiomyosarcoma following cylclophosphamide therapy for lupus nephritis. J Urol 143:119–121
58. Torenbeek R, Bloomjous CEM, van Diest PJ, van der Valk P, Meijer CJLM (1997) Sarcomatoid carcinoma vs. carcinosarcoma of the urinary bladder. J Urol Pathol 6:27–42
59. Valentine M, Douglass EC, Look AT (1989) Closely linked loci on the long arm of chromosome 13 flank a specific 2;13 translocation in childhood rhabdomyosarcoma. Cytogenet Cell Genet 52:128–132
60. Weide R, Pflüger KH, Görg C (1990) Multiple myeloma of the bladder and vagina. Cancer 66:989–991
61. Wick MR, Brown BA, Young RH (1988) Spindle cell proliferations of the urinary tract. Am Surg Pathol 12:379–389
62. Winter P, Porst H, Meybehm M, Hermanns M, Köster O (1989) Das kavernöse Hämangiom der Harnblase. Akt Urol 20:48–50
63. Young RH, Rosenberg AE (1987) Osteosarcoma of the urinary bladder: report of a case and review of the literature. Cancer 59:174–178
64. Young RH, Scully RE (1987) Pseudosarcomatous lesions of the urinary bladder, prostate gland and urethra. Arch Pathol Lab Med 111:254–258
65. Zuckerberg LR, Harris NL, Young RH (1991) Carcinomas of the urinary bladder simulating malignant lymphoma. A report of five cases. Am J Surg Pathol 15:569–576

Virchows Arch (2001) 439:504–511
DOI 10.1007/s004280100450

ORIGINAL ARTICLE

Ernst Heinmöller · Birgit Renke · Kurt Beyser
Wolfgang Dietmaier · Cord Langner · Josef Rüschoff

Pitfalls in diagnostic molecular pathology – significance of sampling error

Received: 14 December 2000 / Accepted: 7 March 2001 / Published online: 17 May 2001
© Springer-Verlag 2001

Abstract Today, molecular diagnostic tests are widely used in clinical medicine with polymerase chain reaction (PCR)-based techniques being of particular interest. In tissue specimens, however, false-positive and false-negative results can be obtained if pathomorphological and processing aspects are not considered. We therefore studied the impact of tissue sampling in three widely used diagnostic tests: (1) assessment of clonality in B-cell non-Hodgkin's lymphoma, (2) analysis of microsatellite instability (MSI) in colorectal neoplasia, and (3) demonstration of *mycobacterium tuberculosis*. Tissue sections of routinely formalin-fixed and paraffin-embedded diagnostic specimens were taken, and the significance of sampling was systematically investigated using laser microdissection or processing of the entire section. PCR analyses were done according to standard protocols. False-positive pseudo-monoclonality was obtained in small gastrointestinal biopsies and in laser microdissected lymph follicles of non-neoplastic tonsils. False negativity (pseudo-stability) could be demonstrated in a case with hereditary rectal adenoma if whole tissue sections were taken without microdissection of the most dysplastic subareas. Demonstration of mycobacteria failed in tissue sections of a formalin-fixed lymph node that was positive after complete digestion or in fresh frozen material of the same patient. In diagnostic molecular pathology, sampling error is an important source of false-positive and false-negative results, particularly if disease- and tissue-specific morphological features, such as sample size, type of fixation, and intralesional heterogeneity, are ignored.

E. Heinmöller (✉) · B. Renke · K. Beyser · J. Rüschoff
Institute of Pathology, Klinikum Kassel,
Mönchebergstrasse 41-43, 34125 Kassel, Germany
e-mail: eheinmoeller@klinikum-kassel.de
Fax: +49-561-9806983

W. Dietmaier
Institute of Pathology, University Clinic Regensburg,
Postfach 10-06-42, 93042 Regensburg, Germany

C. Langner
Institute of Pathology, University Clinic Graz,
Auenbruggerplatz 25, 8036 Graz, Austria

Keywords Molecular pathology · Sampling error · B-cell clonality · Microsatellite instability · Tuberculosis

Introduction

Molecular diagnostic tests have become routine in modern clinical medicine and in surgical pathology. They are regarded as a powerful supplement to the conventional histopathologic diagnosis. More and more, therapeutic decisions are based on the molecular analysis of tissue specimens. Minute amounts of DNA can be amplified and specifically analyzed using the polymerase chain reaction (PCR). Although routinely applied molecular diagnostic tests have been proven to be of high technical standard [4], false-negative and false-positive results due to artifacts in amplification technique or sampling still present important pitfalls in molecular diagnostic pathology or basic science [7].

The assessment of clonality in lymphoproliferative disorders, such as B-cell non-Hodgkin's lymphomas (B-NHLs) or T-cell non-Hodgkin's lymphomas (T-NHLs) by amplification of the *IgH* heavy chain gene or the T-cell receptor (*TCR)* genes (β or *Y*), respectively, is well established [15, 22, 24]. The high sensitivity of detecting B-cell clonality using PCR amplification has been demonstrated [13]. Because of the relatively low amount of template DNA that is needed for amplification, PCR-based analysis of clonality is now increasingly performed on small sample sizes, such as small tissue biopsies [20] or microdissected areas from tissue sections [19], fine needle aspiration samples [24], and cytological specimens [1]. However, the results from PCR-based analysis of clonality, especially from small sample sizes, must be evaluated critically because of a high number of false-positive oligoclonal or monoclonal results obtained from such samples [7, 26]. Sampling without precise selection of the lesion of diagnostic interest may lead to false-negative results.

The use of microsatellite markers for screening for microsatellite instability (MSI) or loss of heterozygosity

(LOH) has become one of the most widely used tests in molecular diagnostics and in basic science. The reliability of molecular testing for MSI has been demonstrated thoroughly [2, 6] and is now well established as a screening method in tumor analysis. However, only few data on the reliability of testing for MSI, i.e., for HNPCC (hereditary non-polyposis colorectal cancer) in colonic adenomas, are available yet, and the significance of molecular intralesional heterogeneity as a potential source of false-negative results for MSI has not been taken into account in the present studies [14, 16, 25]. Another aspect that might influence the diagnostic yield in molecular pathology refers to the quality of the material itself. This has to be taken into account, particularly in testing of tissues for the presence of infectious agents. Tests for demonstration of DNA from the *mycobacterium tuberculosis* complex in, for example, sputum [8], peripheral blood [5], and formalin-fixed, paraffin-embedded tissue specimens [23] are frequently used. Particularly in fixed tissues, the density and distribution of bacteria, tissue fixation and access to mycobacterial DNA are critical aspects that may greatly influence the test result. Only few data on these points are available yet [9].

In this study, we tested whether and why tissue sampling from single tissue sections may result in false-positive and false-negative molecular diagnosis. Making use of laser-assisted microdissection and PCR amplification, we report significant pitfalls in selected fields of diagnostic molecular pathology using three commonly applied tests, i.e., demonstration of B-cell monoclonality, MSI, and tuberculosis.

Materials and methods

Tissues

Archival with 4% buffered formalin-fixed, paraffin-embedded tissues or fresh frozen tissue samples obtained from the Institute of Pathology, Klinikum Kassel, were used in this study. Tissue samples analyzed for clonality were taken from hyperplastic tonsils, reactive axillary lymph nodes, the terminal ileum, and the gastric mucosa. For detection of MSI, a HNPCC-related adenoma with a small focus of mucinous adenocarcinoma and one lymph-node metastasis in a 24-year-old male patient were prepared. The molecular diagnostic test for tuberculosis was done in two fresh frozen lymph nodes and in two formalin-fixed, paraffin-embedded lymph nodes from a patient with proven tuberculosis.

Preparation of tissue sections

Preparation of slides for microdissection was performed as described by Schütze et al. [18]. Briefly, 5-µm serial sections of formalin-fixed, paraffin-embedded tissue were mounted onto a polyethylene membrane, which was attached to a glass slide by rubber cement (Marabuwerke, Tamm, Germany). Slides were deparaffinized by incubating the slides in xylene for 2×5 min and rehydrating in 99.9% ethanol for 1 min, in 96% ethanol for 2×2 min, and in 70% ethanol for 2×2 min. Sections were stained with hematoxylin and eosin (HE). Microdissection was performed using a Robot MicroBeam laser (P.A.L.M., Bernried, Germany). Between 50 and 500 cells were harvested and transferred into 10 µl TL buffer [1× *Taq* PCR buffer (Roche, Mannheim, Germany) including 2 mg/ml proteinase K and 0.5% Tween20 (Merck, Darmstadt, Germany)]. Cell lysis was performed by incubation for 16 h at 50°C and a 10-min inactivation step at 90°C.

Samples for analysis of *mycobacterium tuberculosis* were prepared with minor modifications according to Goldmann et al. [9]. Lymph nodes were used either as fresh frozen tissue and cut in half or were formalin-fixed and embedded in paraffin wax. From paraffin blocks, three slides each were cut and mounted on glass slides. The remaining block was deparaffinized by preheating at 64°C for 5 h followed by two 15-min incubations in xylene and rehydrated in 99.9% ethanol for 15 min, in 96% ethanol for 15 min, and in 70% ethanol for 15 min. To gain access to mycobacterial DNA, samples were shock frozen in liquid nitrogen three times. Proteinase K (2 mg/ml) and 0.5% Tween20 was added, and specimens were incubated for 16 h at 50°C. Samples were then shock frozen in liquid nitrogen again three times, followed by a 10-min inactivation step at 90°C. Lysozyme (4 mg/ml) was added and incubated for 30 min at 37°C followed by a DNA purification step (high pure PCR template preparation kit, Roche, Mannheim, Germany).

PCR conditions

The semi-nested PCR for amplification of the immunoglobulin (Ig) genes was performed as described elsewhere [22]. Briefly, first round PCR [0.3 mmol/l of each dinucleotide triphosphate (dNTP), 0.3 µmol/l primers LJH and FR3A, 4 mmol/l $MgCl_2$, 1× PCR buffer, and 0.5 U *Taq* polymerase (Gibco BRL)] was done using 2-µl aliquots of the digested DNA in a final volume of 30 µl in an eppendorf mastercycler gradient thermocycler (Eppendorf, Hamburg, Germany) for 30 cycles: 94°C/30 s, 55°C/30 s, 72°C/1 min followed by a final extension at 72°C for 10 min. Second round PCR was performed using primers VLJH and FR3A. PCR product (5µl) was analyzed using 6% polyacrylamide gel electrophoresis in TBE (tris-borate and ethylene diamine tetraacetic acid) buffer and subsequent ultra violet (UV) light examination after ethidium bromide staining. Microsatellite analysis was performed as described previously [6, 17]. Specific single round PCR [0.3 mmol/l of each dNTP, 2.5 mmol/l $MgCl_2$, 5% DMSO, 1× PCR buffer, 0.3 µmol/l primers MYCL1 or APC55, and 0.5 U *Taq* polymerase (Gibco BRL)] was done using 2-µl aliquots in a final volume of 30 µl for 40 cycles: 94°C/30 s, 53°C (MYCL1) or 55°C (APC55)/30 s, 72°C/1 min, followed by a final extension at 72°C for 10 min. Amplified microsatellites (3 µl) were analyzed using 6.7% polyacrylamide/50% urea gel electrophoresis (1 h, 1500 V, 50°C) in a SequiGen sequencing gel chamber (BioRad, Hercules, Calif.) and using silver nitrate staining. For ABI GeneScan analysis of MSI, the HNPCC MSI test for the determination of the MSI status of colorectal carcinoma research samples (Roche Diagnostics, Mannheim, Germany) was used. MSI diagnosis was done as proposed by National Institutes of Health (NIH) recommendations [3]. Only markers exhibiting clear shifts were diagnosed as microsatellite unstable.

Diagnostic evaluation of tuberculosis was performed as described [5] with modifications. After lysis, DNA was amplified using a semi-nested PCR protocol: first round PCR [0.2 mmol/l of each dNTP, 0.5 µmol/l primers IS6110-U2 (5' GTC CAC GCC GCC AAC TAC GG 3') and IS6110-D, 2.5 mmol/l $MgCl_2$, 5% dimethylsulfoxide (DMSO), 1× PCR buffer, 0.5 U *Taq* polymerase (Gibco BRL)] was done using 3-µl aliquots of the lysed DNA in a final volume of 30 µl in an Eppendorf mastercycler gradient thermocycler (Eppendorf) for 35 cycles: 94°C/30 s, 65°C/30 s, 72°C/1 min followed by a final extension at 72°C for 7 min. Second round PCR was performed using primers IS6110-iU and IS6110-D under the same conditions as the first round PCR. PCR product (5 µl) was analyzed using 6% polyacrylamide gel electrophoresis in TBE buffer and ethidium bromide staining.

ABI sequencing

The PCR product was purified and sequenced using the big dye terminator sequencing kit according to the manufacturer's instructions.

Immunohistochemistry

The colonic tumors and the lymph nodes were evaluated for protein expression of the human mismatch repair genes hMLH1, hMSH2, and hMSH6 using immunohistochemistry. Pretreatment of slides before staining with antibodies MLH1 (dilution 1:600, Pharmingen, San Diego, Calif.) and MSH2 (dilution 1:200, Calbiochem, Bad Soden, Germany) was done by means of microwave (600 W, 20 min) in EDTA buffer pH 8.0. Before staining with antibody MSH6 (1:300 dilution, Becton-Dickinson, San Jose, Calif.), slides were pretreated by pressure cooking at 120°C for 20 min in citrate buffer pH 6.0. Slides were incubated overnight at 4°C. For reliable antigen staining, the polyclonal mirror image complementary antibodies (MICA) kit (The Binding Site LTD, Heidelberg, Germany) was used according to the manufacturer's instructions. Appropriate positive and negative controls were employed for loss of protein expression analysis. Results were confirmed independently by two pathologists (C.L. and J.R.).

Results

PCR analysis of B-cell clonality

From the 11 tissue samples analyzed, a total of 29 foci with lymphatic tissue exhibiting reactive follicular hyperplasia were microdissected (Fig. 1). Between 50 (~0.3 ng DNA) and 300 cells (~2 ng DNA) were collected. Amplification was successful in 27 of the 29 microdissected follicles. In the 27 successfully amplified samples, two (7%) showed a polyclonal pattern, three (11%) had monoclonal bands and 22 (82%) presented with oligoclonal patterns (Fig. 2A). PCR analysis of whole section samples from a monoclonal B-cell non-Hodgkin's lymphoma control gave always a monoclonal band in the expected range. Polyclonal bands or a smear was always seen from whole section samples of reactive follicular hyperplasia.

To determine the reproducibility of PCR amplification of small cell samples, a total of 14 germinal centers from a reactive mammary lymph node and from a hyperplastic reactive tonsil were microdissected, and PCR amplification was performed in duplicate from each sample (Fig. 2B). In four cases, only one of the two PCRs amplified successfully. In seven follicles, at least one prominent band of identical size was found after two independent amplifications. All other samples had either one monoclonal and one oligoclonal PCR product (two cases) or two oligoclonal PCR products. No sample showed two monoclonal bands of identical size after independent amplification.

Analysis of MSI

A resection specimen of a flat villous 3.5-cm width rectal adenoma with a focal carcinoma and a micrometastasis to a regional lymph node was analyzed in an HNPCC patient (Fig. 3). At first, a 5-µm-thick paraffin section of the entire adenoma with the small (<0.5 cm) mucinous carcinoma was scraped off the glass slide and subjected to multiplex PCR microsatellite analysis. Although the highly sensitive ABI GeneScan system was used, no distinct MSI could be detected. Out of ten loci, only one (BAT 25) showed an equivocal shift that is not diagnostic for MSI (Fig. 4). However, immunohistochemistry revealed loss of hMSH2 expression in the adenomatous (Fig. 5) and in the carcinomatous and micrometastatic lesion with positive staining of hMSH6 and hMLH1. Therefore, the lesion was microdissected, taking 50–200 cells from separated regions exhibiting different degrees of dysplasia ranging from low to medium and high grade. Similarly, cells of the carcinoma and of the lymph-node micrometastasis were taken. Single round PCR using primers of the APC and Mycl1 locus showed significant band shifts. Whereas some cell groups taken from low and medium-grade dysplastic areas were still stable at both loci, this was not the case in the severely dysplastic or in the micrometastatic tumor parts (Fig. 6).

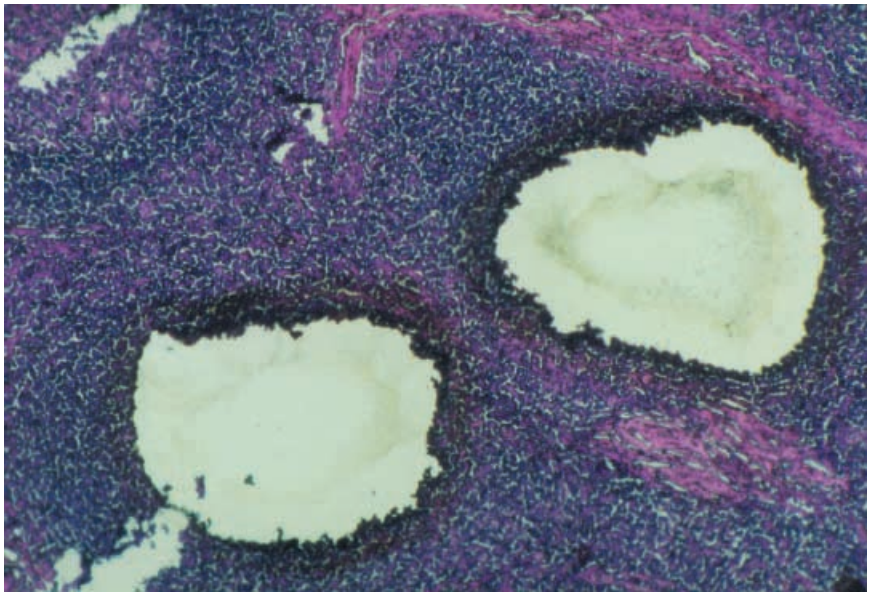


Fig. 1 Microdissection of lymphatic tissue from a reactive tonsil. The microdissected area contains only the germinal center. Hematoxylin and eosin staining (original magnification ×40) of a section from paraffin-embedded tissue

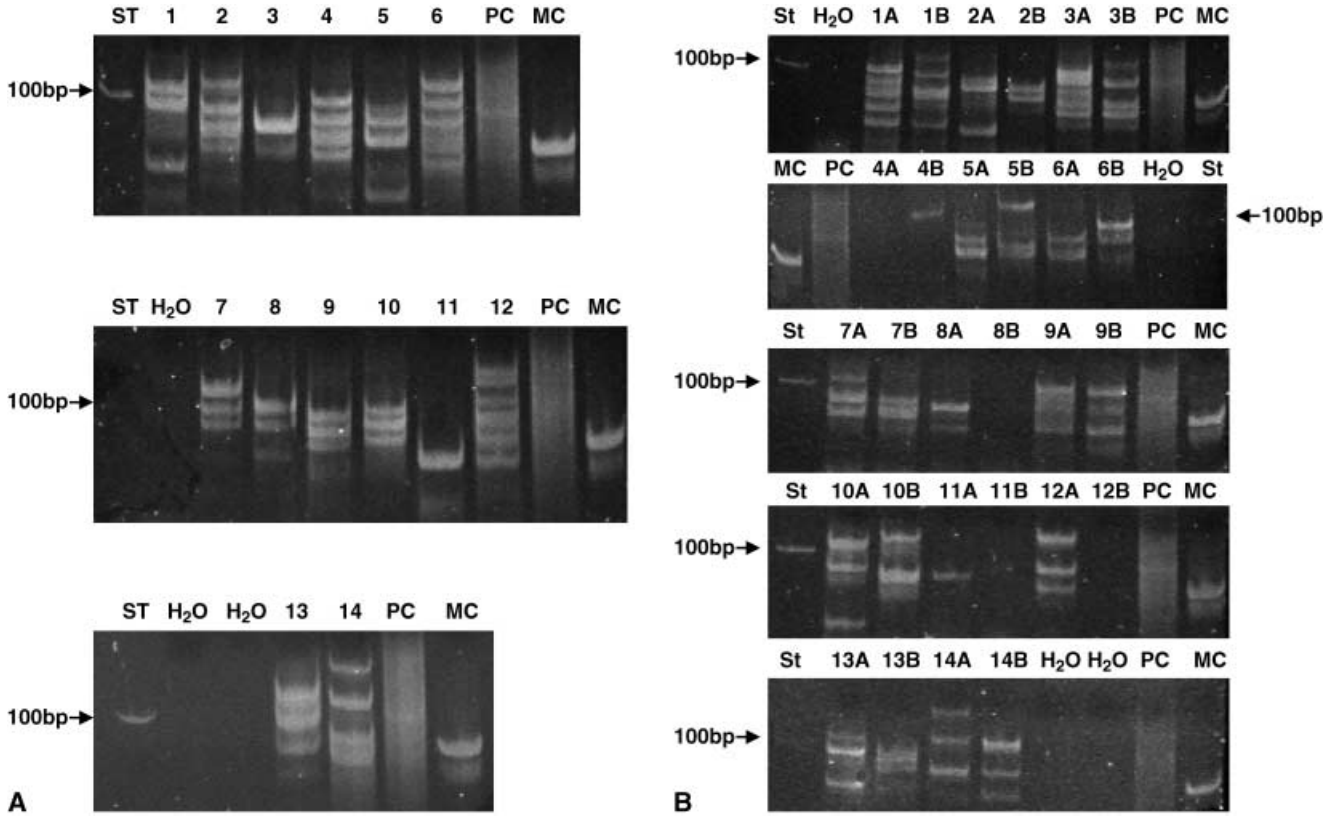


Fig. 2 **A** Examples of polymerase chain reaction (PCR) analysis of B-cell clonality from microdissected germinal centers from a reactive tonsil (*lanes 1–12*) and a reactive mammary lymph node (*lanes 13 and 14*). *ST* (standard) 100-bp ladder molecular weight marker, *PC* polyclonal smear pattern from whole tissue sample, *MC* monoclonal bands from monoclonal B-cell non-Hodgkin's lymphoma control, H_2O negative controls. A pseudo-monoclonal band is seen in *lanes 3 and 11*. *Lanes 1, 2, 4, 5, 7, 8, 9, 10, 13, and 14* exhibit oligoclonal bands. Polyclonal bands are seen in *lanes 6 and 12*. **B** PCR amplification of small cell samples from microdissected germinal centers from a reactive tonsil (*lanes 1A–9B*) and a reactive mammary lymph node (*lanes 10A–14B*) performed in duplicate from the same DNA template (**A** and **B**). *ST* (standard) 100-bp ladder molecular weight marker, *PC* polyclonal smear pattern from whole tissue sample, *MC* monoclonal bands from monoclonal B-cell non-Hodgkin's lymphoma control, H_2O negative control

Diagnosis of tuberculosis

Specimens with tuberculous caseating granulomatous lymphadenitis were tested under different tissue processing conditions. Thereby, one lymph node half of the specimen was fresh frozen, and the other half was routinely formalin-fixed and paraffin-embedded. PCR analysis gave the most distinct amplification products specific for mycobacterium complex when DNA was extracted from tissue sections of the fresh frozen lymph node material. In the formalin-fixed and paraffin-embedded material, a definitive result could only be obtained if DNA of the entire half of the paraffin-embedded lymph node was taken. In the 5-µm-thick paraffin-embedded and formalin-fixed tissue sections, however, usually no amplification products appeared (Fig. 7). In rare cases when equivocal amplification products were found, the specificity of the PCR products could not be confirmed by means of sequence analysis.

Discussion

Rapid progress in the understanding of the molecular basis of disease has led to an increasing demand for molecular diagnostic analyses in medicine. Despite the widespread use of certain PCR techniques for particular diagnostic tests, only very recently studies have been designed to assess technical standards or to systematically look for possible pitfalls, particularly if tissue specimens have to be analyzed [4, 7, 12, 26]. In this study, we have focused on potential hazards in three routinely used tests of diagnostic molecular pathology, especially with respect to tissue sampling and tissue processing. Our results in biopsies taken from the terminal ileum basically confirm previous studies which have found non-reproducible pseudo-oligoclonal or pseudo-monoclonal bands from reactive lymphatic tissues when samples were microdissected or DNA was diluted [7, 21, 26]. In our series, only 2 of 27 microdissected samples (7%), consisting of maximal 500 cells (~3 ng DNA), showed a polyclonal pattern. All others were oligoclonal or monoclonal. However, two samples showed a nearly identical oligoclonal banding pattern when two reactions each were amplified independently (Fig. 2B, lanes 7A and 7B and lanes 9A and 9B), although the amplification product obtained by dissection of a whole serial section of this tissue revealed a polyclonal

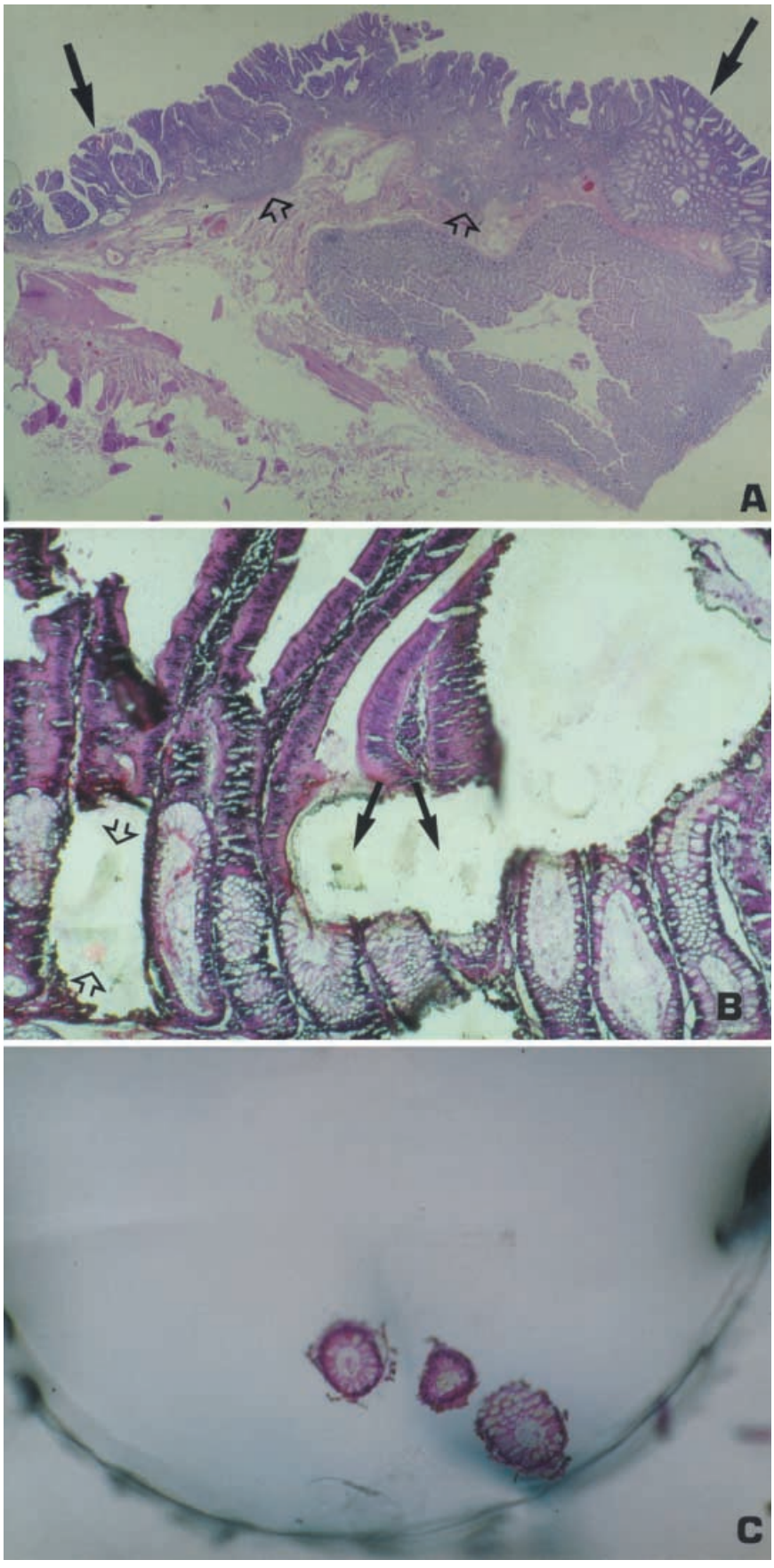


Fig. 3 Microdissection of colonic tissue. **A** Microphotograph taken from the large tubulo-villous rectal adenoma (*solid arrows*) that showed two small foci of early infiltrative carcinoma (*open arrows*; hematoxylin and eosin (HE), original magnification ×25). **B** Villous adenoma after microdissection of dysplastic (*D2*; *solid arrows*) and normal crypt epithelium (open arrows; HE, original magnification ×100). **C** Laser microdissected crypts (~200 cells) from the adenoma captured within the lid of the PCR tube (HE, original magnification ×100)

smear (data not shown). This clearly demonstrates that even independently reproduced monoclonal/oligoclonal bands are not a confident specific indicator of a neoplastic lymphoproliferative disorder. This must be kept in mind, particularly if small biopsies comprising only one or few lymph follicles are subjected for analysis. In cases where histology and immunohistology can not confirm the presence of a neoplastic or clonal lymphoproliferative process, it is recommended to ensure that at least 6–12 ng DNA (~1000–2000 cells) of lympho-cellular origin are dissected and amplified. If PCR analysis still reveals monoclonal/oligoclonal bands, especially in small tissue samples, PCR results should be scored as indeterminate and probably rebiopsy or reevaluation of the patient should be recommended. In case of a rebiopsy, Southern blotting should then be considered as a more reliable technique, especially in the initial phase of lymphoma diagnosis.

Another widely used molecular diagnostic test refers to the assessment of MSI, especially in the context of

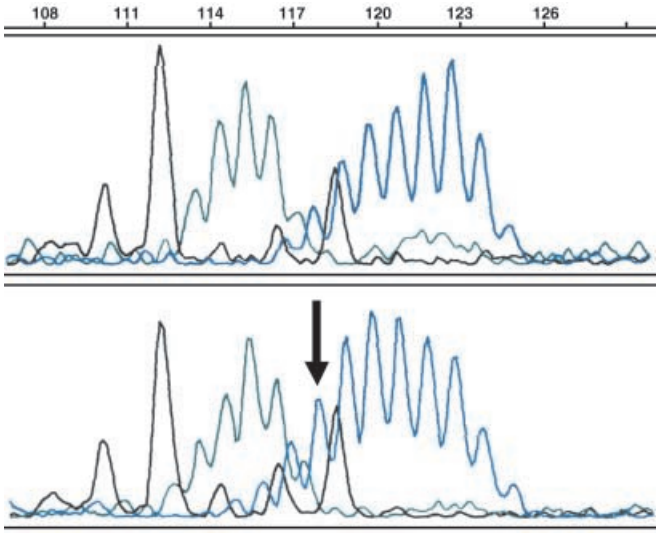


Fig. 4 ABI GeneScan multiplex analysis of microsatellite instability. *Above* Normal tissue from lymph node. *Below* Dissection of the entire colon tumor. *Black curve APC55* microsatellite stable, *green curve MFD15* microsatellite stable, *Blue curve BAT25* discrete instability in the tumor sample (*arrow*)

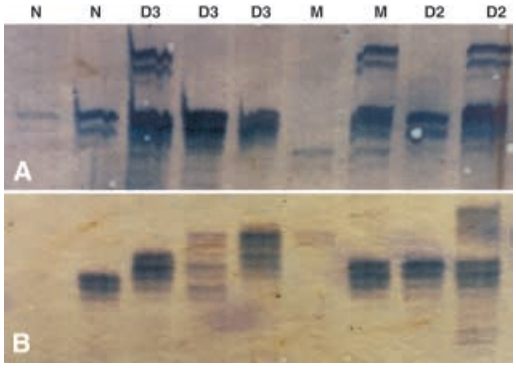


Fig. 6 Examples of genetic heterogeneity detected after microdissection of the colonic tumor visualized using silver nitrate staining. Additional bands or band shifts are seen in various loci with a different grade of cellular dysplasia after amplification of microsatellite markers MYCL1 (**A**) and APC55 (**B**). *N* Normal, *D2* moderate cellular dysplasia, *D3* severe cellular dysplasia, *m* lymph-node metastasis

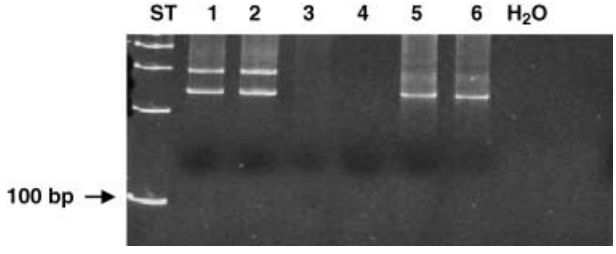


Fig. 7 Assessment of the presence of mycobacterial DNA in tissues of various preparation. *ST* (standard) 100-bp ladder molecular weight marker. *Lanes 1 and 2* fresh frozen tissue. *Lanes 3 and 4* microdissected formalin-fixed paraffin-embedded tissue from slides. *Lanes 5 and 6* tissue from one-half of a formalin-fixed paraffin-embedded lymph node. H_2O negative controls

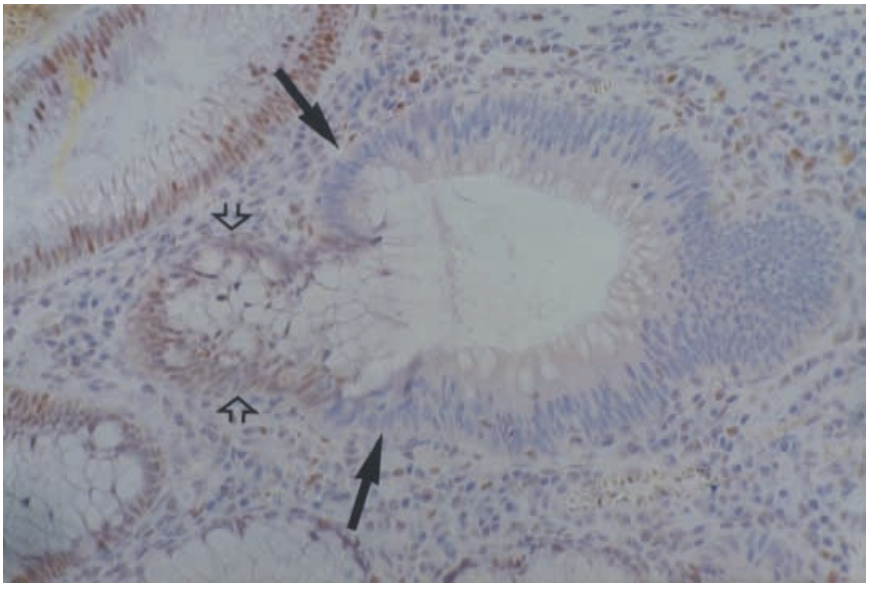


Fig. 5 Immunohistochemical analysis of mismatch repair gene (MSH)2 expression in the colonic adenoma. Nuclear staining (*brown stain*) for human (h)MSH2 protein is seen in normal colonic crypts and in the majority of interstitial cells. A crypt exhibits in part regular nuclear staining for hMSH2 (*open arrow*), whereas in the area of early adenomatous cell growth of the same crypt, the nuclear staining pattern is entirely lost (*solid arrows*; original magnification ×250)

HNPCC. This test has been standardized and is, together with immunohistochemical expression analysis of mismatch repair genes (hMSH2, hMLH1, hMSH6), highly informative for screening of HNPCC [2, 6]. The value of MSI testing has, however, only been shown in apparent carcinomas of affected family members. Whereas MSI prevalence in HNPCC-related carcinomas reaches 80–90%, the corresponding values in HNPCC-related adenomas are much lower. Jass et al. [11] found a high rate of MSI (54%) in adenomas from subjects presenting hyperplastic polyps in addition to a loss of mismatch repair gene expression in these lesions exhibiting high-grade dysplasia. In contrast, Loukola et al. [14] found MSI in only 50% of adenomas from HNPCC patients, which may be a significant underestimation of the prevalence of MSI in adenomas from HNPCC patients and in adenomas from subjects not affected by the HNPCC syndrome. A very recently published study found even 66.7% of HNPCC-related adenomas with high-level MSI [10]. Major drawbacks of the study of Loukola et al. [14] are the lack of microdissection according to polyp type and grade of dysplasia, no use of the standard MSI marker panel recommended by the National Cancer Institute workshop on MSI, December 1997 [3] and no immunohistochemical staining for mismatch repair gene expression. Our molecular analysis of microdissected adenoma and tumor tissue samples from a young HNPCC patient in addition to immunohistochemical analysis of serial tissue sections clearly demonstrated the need for careful histomorphologic grading according to the grade of dysplasia of the adenoma before microdissection. PCR of DNA obtained from the entire tissue section would have masked the presence of instability, resulting in an erroneously false-negative MSI test result. In contrast, microdissection of the adenoma with respect to the degree of dysplasia clearly revealed MSI. More interestingly, even in adenomas, the frequency of unstable cell clones increased with the degree of dysplasia, i.e., tumor progression [10]. Therefore, immunostaining clearly demonstrated that loss of mismatch repair gene expression is one of the earliest events in HNPCC-related neoplasia. Currently, our own studies are under progress to correlate the degree of dysplasia and MSI status in a larger series of HNPCC-related colorectal adenomas.

Molecular diagnosis of mycobacterium tuberculosis is considered especially helpful in those cases when histochemical demonstration of acid-fast bacteria in formalin-fixed paraffin-embedded tissues is not successful and suspicion based on histologic or clinical features needs to be confirmed. A recently published study found false-negative results after PCR amplification of *mycobacterium tuberculosis* from formalin-fixed, paraffin-embedded tissues in 11% to 19% of cases depending on the PCR technique employed [4]. Our data confirm these results and extend the factors of influence to formalin fixation and paraffin embedding in addition to the amount of tissue subjected to *mycobacterium tuberculosis*-specific PCR. We used one of the standard PCR tests for demonstration of *mycobacterium tuberculosis* [5], and we tested a variety of processing techniques in a lymph node that clearly turned out to be positive for *mycobacterium tuberculosis* in the fresh frozen half. In formalin-fixed material, we demonstrate that in addition to the inaccessibility of mycobacterial DNA due to the rigidity of the bacterial wall [9], the amount of tissue template is also crucial for successful confirmation of *mycobacterium tuberculosis* DNA.

Whereas PCR amplification failed from DNA obtained from 5-µm-thick sections of the paraffin-embedded lymph node, the test became positive only after digestion of the whole paraffin-embedded lymph node tissue. We also tried to microdissect granulomas from formalin-fixed, paraffin-embedded tissue slides, but this did not increase the sensitivity, because no PCR products could be obtained from microdissected granulomas (data not shown). A negative tuberculosis test should always be carefully controlled regarding (1) amount of tissue harvested, (2) the method of tissue processing (i.e., fresh frozen vs formalin-fixed and paraffin-embedded), and (3) the correct digestion of samples because of the rigidity of bacterial wall. PCR may also be false positive due to contamination. In addition, positive PCR results of mycobacterium tuberculosis have been reported from sarcoidosis lesions but may have no clinical relevance [23]. Here again, the correct interpretation of positive PCR results should be evaluated in the light of clinical findings and histomorphologic features within the tissues of interest. In questionable cases, sequence analysis of PCR products is recommended as the only technique which ensures 100% specificity.

In summary, our data show that molecular data may largely increase the base of information of conventional histomorphologic and immunohistologic diagnostics, but the interpretation of molecular tests needs to be strictly integrated into (1) the context of pathomorphology, (2) the method of tissue processing, (3) the use of standardized protocols (i.e., choice of primers in MSI diagnostics), and (4) the amount of tissue subjected to molecular analysis. It is essential to closely link molecular data to histomorphologic and clinical data in order to avoid false-negative or false-positive results, which is of great importance for diagnosis and therapy decision and which finally will ensure a high quality standard in molecular pathology.

References

1. Alkan S, Lehman C, Sarago C, Sidawy MK, Karcher DS, Garrett CT (1995) Polymerase chain reaction detection of immunoglobulin gene rearrangement and bcl-2 translocation in archival glass slides of cytologic material. Diagn Mol Pathol 4:25–31
2. Bocker T, Diermann J, Friedl W, Gebert J, Holinski-Feder E, Karner-Hanusch J, von Knebel-Döberitz M, Kölbke K, Möslein G, Schackert HK, Wirtz HC, Fishel R, Rüschoff J (1997) Microsatellite instability analysis: a multicenter study for reliability and quality control. Cancer Res 57:4739–4743
3. Boland CR Thibodeau SN, Hamilton SR, Sidransky D, Eshleman JR, Burt RW, Meltzer SJ, Rodriguez-Bigas MA,

Fodde R, Ranzani GN, Srivastava S (1998) A National Cancer Institute workshop on microsatellite instability for cancer detection and familiar predisposition: development of international criteria for the determination of microsatellite instability in colorectal cancer. Cancer Res 58:5248–5257
4. Cabras AD, Kremer M, Schulz S, Werner M, Hummel M, Komminoth P, Höfler G, Höfler H (2000) Quality assessment in diagnostic molecular pathology: experience from a German-Austrian-Swiss multicenter trial. Virchows Arch 437:46–51
5. Condos R, Mc Clune A, Rom WN, Schluger NW (1996) Peripheral-blood-based PCR assay to identify patients with active pulmonary tuberculosis. Lancet 347:1082–1085
6. Dietmaier W, Wallinger S, Bocker T, Kullmann F, Fishel R, Rüschoff J (1997) Diagnostic microsatellite instability: definition and correlation with mismatch repair protein expression. Cancer Res 57:4749–4756
7. Elenitoba-Johnson KSJ, Bohling SD, Mitchell RS, Brown MS, Robetorye RS (2000) PCR analysis of the immunoglobulin heavy chain gene in polyclonal processes can yield pseudoclonal bands as an artifact of low B cell number. J Mol Diagn 2:92–96
8. Godfry-Frausset P (1995) Molecular diagnosis of tuberculosis: the need for new diagnostic tools. Thorax 50:709–711
9. Goldmann T, Richter E, Galle J, Rüsch-Gerdes S, Vollmer E (1998) Molecular technologies in pathology: detecting mycobacterial DNA in paraffin-embedded tissue. Pathol Res Pract 194:261
10. Iino H, Simms L, Young J, Arnold J, Winship IM, Webb SI, Furlong KL, Leggett B, Jass JR (2000) DNA microsatellite instability and mismatch repair protein loss in adenomas presenting in hereditary non-polyposis colorectal cancer. Gut 47:37–42
11. Jass JR, Iino H, Ruszkiewicz A, Painter D, Solomon MJ, Koorey DJ, Cohn D, Furlong KL, Walsh MD, Palazzo J, Bocker-Edmonston T, Fishel R, Young J, Leggett BA (2000) Neoplastic progression occurs through mutator pathways in hyperplastic polyposis of the colorectum. Gut 47:43–49
12. Kremer M, Cabras AD, Fend F, Schulz S, Schwarz K, Hoefler H, Werner M (2000) PCR analysis of IgH-gene rearrangements in small lymphoid infiltrates microdissected from sections of paraffin-embedded bone marrow biopsy specimens. Hum Pathol 31:847–853
13. Lehman CM, Sarago C, Nasim S**,** Comerford J, Karcher DS, Garrett CT (1995) Comparison of PCR with Southern hybridisation for the routine detection of immumoglobulin heavy chain gene rearrangements. Am J Clin Pathol 103:171–176
14. Loukola A, Salovaara R, Kristo P, Moisio AL, Kääriainen, Ahtola H, Eskelinen M, Härkönen N, Julkunen R, Kangas E, Ojala S, Tulikoura J, Valkamo E, Järvinen H, Mecklin JP, de la Chapelle A, Aaltonen LA (1999) Microsatellite instability in adenomas as a marker for hereditary nonpolyposis colorectal cancer. Am J Pathol 155:1849–1853
15. Medeiros L, Carr J (1999) Overview of the role of molecular methods in the diagnosis of malignant lymphomas. Arch Pathol Lab Med 123:1189–1207
16. Samowitz WS, Slattery ML, Potter JD, Leppert MF (1999) BAT-26 and BAT-40 instability in colorectal adenomas and carcinomas and germ line polymorphisms. Am J Pathol 154: 1637–1641
17. Schlegel J, Bocker T, Zirngibl H, Hofstädter F, Rüschoff J (1995) Detection of microsatellite instability in human colorectal carcinomas using a non-radioactive PCR-based screening method. Virchows Arch 426:223–227
18. Schütze K, Lahr G (1998) Identification of expressed genes by laser-mediated manipulation of single cells. Nat Biotechnol 16:737–742
19. Sukpanichant S, Vnencak-Jones CL, McCurley TL (1993) Detection of clonal immunoglobulin heavy chain gene rearrangements by polymerase chain reaction in scrapings from archival hematoxylin and eosin-stained histologic sections: implications for molecular genetic studies of focal pathologic lesions. Diagn Mol Pathol 2:168–176
20. Sukpanichant S, Vnencak-Jones CL, McCurley TL (1994) Determination of B-cell clonality in paraffin-embedded endoscopic biopsy specimens of abnormal lymphocytic infiltrates and gastrointestinal lymphoma by polymerase chain reaction. Am J Clin Pathol 102:299–305
21. Taylor JM, Spagnolo DV, Kay PH (1997) B-cell target DNA quantity is a critical factor in the interpretation of B-cell clonality by PCR. Pathology 29:309–312
22. Trainor KJ, Brisco MJ, Wan JH, Neoh S, Grist S, Morley AA (1991). Gene rearrangement in B- and T-lymphoproliferative disease detected by the polymerase chain reaction. Blood 78: 192–196
23. Vago L, Barberis M, Gori A, Scarpellini P, Sala E, Nebuloni M, Bonetto S, Cannone M, Marchetti G, Franzetti F, Costanzi G (1998) Nested polymerase chain reaction for mycobacterium tuberculosis IS6110 sequence on formalin-fixed paraffin-embedded tissues with granulomatous diseases for rapid diagnosis of tuberculosis. Am J Clin Pathol 109:411–415
24. Wan JH, Sykes PJ, Orell SR, Morley AA (1992) Rapid method for detecting monoclonality in B cell lymphoma in lymph node aspirates using the polymerase chain reaction. J Clin Pathol 45:420–423
25. Young J, Leggett B, Gustafson C, Ward M, Searle J, Thomas L, Buttenshaw R, Chenevix-Trench G (1993) Genomic instability occurs in colorectal carcinomas but not in adenomas. Hum Mutat 2:351–354
26. Zhou XG, Sandvej K, Gregersen N, Hamilton-Dutoit SJ (1999) Detection of clonal B cells in microdissected reactive lymphoproliferations: possible diagnostic pitfalls in PCR analysis of immunoglobulin heavy chain gene rearrangement. J Clin Pathol Mol Pathol 52:104–110

Virchows Arch (2001) 439:512–522
DOI 10.1007/s004280100477

ORIGINAL ARTICLE

**Thomas Kirchner · Susanne Müller · Takanori Hattori
Kennichi Mukaisyo · Thomas Papadopoulos
Thomas Brabletz · Andreas Jung**

Metaplasia, intraepithelial neoplasia and early cancer of the stomach are related to dedifferentiated epithelial cells defined by cytokeratin-7 expression in gastritis

Received: 10 April 2001 / Accepted: 7 May 2001 / Published online: 24 July 2001
© Springer-Verlag 2001

Abstract Cancer presumably arises from stem cells, preserved in an undifferentiated status since fetal development, or from a dedifferentiation of mature cells that return into a fetal phenotype with the potential for proliferation and renewal. Dedifferentiation in this context could represent a transient phase, passed through by cells, before they switch to redifferentiation, metaplasia or neoplasia. Cytokeratin-7 (CK7) is present in fetal, largely absent in normal adult, and transiently neoexpressed in metaplastic and neoplastic epithelial cells of the stomach according to previous observations. CK7 neoexpression in the stomach could, hence, define a fetal-like, dedifferentiated, cellular phenotype during the development of metaplasia and neoplasia. To test this hypothesis, we investigated CK7 expressions in fetal stomachs, non-neoplastic control stomachs, and neoplastic stomachs exhibiting metaplasia, intraepithelial neoplasia, and early cancer. Proliferation and β-catenin expression of CK7-positive cells were also evaluated. The chronology of CK7 expression was studied during the experimental gastritis–cancer sequence in Mongolian gerbils. Our results show that metaplastic and neoplastic changes in the gastritis–cancer sequence are related to dedifferentiated epithelial cells which are defined by CK7 expression and can phenotypically be linked to fetal cells at the start of gastric pit development. The dedifferentiated cells exhibit a low proliferation and β-catenin accumulation, similar to stem cells. Thus, the "stem cell" and "dedifferentiation" hypotheses for cancer origin could complement one another, and dedifferentiation-redifferentiation processes might be decisive for carcinogenesis in the stomach.

Keywords Dedifferentiation · Carcinogenesis · Gastric cancer · Gastritis · Cytokeratin

Supported by the Johannes and Frieda Marohn-Foundation, Erlangen, Germany, and by the Sander-Foundation, Munich, Germany.

T. Kirchner (✉) · S. Müller · T. Papadopoulos · T. Brabletz
A. Jung
Department of Pathology, University of Erlangen-Nuremberg,
Krankenhausstrasse 8–10, 91054 Erlangen, Germany
e-mail: thomas.kirchner@patho.imed.uni-erlangen.de
Tel.: +49-9131-8522287, Fax: +49-9131-8524745

T. Hattori · K. Mukaisyo
Department of Pathology, Shiga University of Medical Science,
Ohtsu, Japan

Introduction

Neoplasia can follow cellular metaplasia due to chronic inflammation and repair [46]. The process is well documented for the stomach, where *Helicobacter pylori* (*H. pylori*) and/or autoimmunity cause chronic atrophic gastritis, with metaplasia predisposing for gastric cancer [11, 17, 37]. Epidemiologic and molecular studies identified metaplasia, intraepithelial neoplasia (dysplasia), and early cancer as initial morphologic steps of human gastric carcinogenesis [10, 59]. A gastritis-metaplasia-cancer sequence is also described in the experimental *H. pylori* gastritis of Mongolian gerbils [20, 56].

Intestinal metaplasia (IM) is considered to be the most relevant metaplastic change in gastritis, and an incomplete IM, characterized by sulfomucin secretion and classified as IM type III, has been identified as a significant risk factor and potential precursor of the intestinal type cancer [10, 13]. The role of IM in cancer development is also stressed by a rare detection of microsatellite instability, and mutations of p53 and APC genes in the intestinal metaplastic cells [27, 40, 54]. However, the consideration of IM as a precursor lesion of gastric cancer has its limitations. A ciliated metaplasia [35], a metaplastic cell lineage expressing spasmolytic polypeptide [42], and intramucosal cysts [61] were also described to be significantly associated with gastric carcinogenesis. Moreover, gastric cancer is found in a non-atrophic gastritis without IM [23, 45]. Strictly speaking, it is unknown whether the neoplastic cells directly descend from the metaplastic cells, or whether the neoplastic and

metaplastic processes are only indirectly related by a common ancestor.

A widespread concept presently holds that metaplasia and neoplasia are linked to the presence of stem cells [14, 44, 46]. Stem cells are defined as undifferentiated relative to other mature epithelial cells, but not necessarily to immature embryonic or fetal cells [6, 47]. Markers for epithelial stem cells are lacking to a large extent, but certain cytokeratins might be useful for their identification. For example cytokeratin-7 (CK7) and cytokeratin-19 are applied to the characterization of hepatic and pancreatic stem cells [16, 36], and cytokeratin-15 labeling is used to identify hair follicle stem cells [28]. The epidermal stem cells are further characterized by β1-integrin expression, low proliferation, and elevated levels of cytoplasmic β-catenin [29, 60]. It is usually assumed that the undifferentiated stem cells are preserved in a virgin state without further differentiation after early development, and that they generate by asymmetrical division the differentiated cells of tissue regeneration [32]. Other theories, however, suggest the possibility that differentiated or partially differentiated cells dedifferentiate and become stem-like cells [6, 32]. This dedifferentiation could represent a transient phase passed through by cells before the switch to metaplasia or neoplasia. Dedifferentiation in such a context would mean a reversible return of once differentiated cells into an embryonic or fetal phenotype, with the potential for proliferation and renewal [32, 44].

Stosiek and coworkers have previously reported that epithelial cells of the fetal stomach express CK7 [53]. They also found CK7 neoexpressions in the IM and dysplasia during chronic gastritis, whereas the normal gastric mucosa and most of the gastric cancers were CK7 negative [51, 52]. Thus, the transient neoexpression of CK7 could define a phenotype of fetal-like, and possibly dedifferentiated, cells during the development of metaplasia and neoplasia in the adult stomach.

To test this hypothesis, we investigated the presence, distribution, and morphology of CK7-expressing epithelial cells in the fetal, non-neoplastic, and neoplastic stomach. The proliferation and β-catenin expression of CK7-positive epithelial cells were also evaluated. The study focused on resection specimens from gastric intraepithelial neoplasia (GIN) and early gastric cancer (EGC) for an analysis of the initial steps in the gastritis-metaplasia-cancer sequence. The chronology of CK7 expression during the sequence was studied in the experimental *H. pylori* gastritis of Mongolian gerbils.

Materials and methods

Human material

Formalin-fixed and paraffin-embedded human material was derived from the diagnostic files of the Institute of Pathology of the University of Erlangen-Nuremberg. The study of neoplastic stomachs included 25 consecutive gastric specimens resected for GIN (three cases) or EGC (22 cases). Four cases of EGC exhibited GIN in addition. Therefore, seven cases of GIN and 22 cases of EGC were evaluated. All neoplasms – EGC and GIN – were localized in the antrum or body of the stomach. Neoplasms of the cardia were excluded from the study. The neoplasms were classified and graded following the new WHO classification [19] and a recently published consensus called Vienna Classification of Gastrointestinal Neoplasia [41]. Gastritis was diagnosed following the updated Sydney system and divided into a group of atrophic gastritis, including multifocal and corpus predominant types, and a group of non-atrophic gastritis [12]. The Warthin-Starry silver stain was applied for the detection of H. pylori. Data about tumor types, pTNM classification, gastritis type, as well as age and sex of the patients are summarized in Table 1.

The fetal stomach was studied by gastric specimens from autopsies of stillborn fetuses of the 10th week of gestation (one case; crown-rump (CR) length: 45 mm), of the 14th week of gestation (three cases; CR length: 83–91 mm), of the 16th week of gestation (one case; CR length: 120 mm), and of the 19th week of gestation (one case; CR length: 155 mm). Only well preserved gastric specimens were used. Longitudinal and transverse sections of the whole stomach were analyzed.

Samples of non-neoplastic stomachs were studied as controls. These included biopsy cases of normal, uninflamed antral and fundic mucosa (17 cases; 8- to 78-year-old subjects), gastric resection specimens of normal, uninflamed gastric mucosa (three cases; 59- to 66-year-old patients, operated by Whipple's procedure because of pancreatic or periampullary tumors), and gastric resection specimens with non-atrophic *H. pylori* gastritis (three cases; 54- to 69-year-old patients operated by Whipple's procedure because of pancreatic, periampullary, or duodenal tumor).

Typing of IM and mucosal cysts

Sections of neoplasic stomachs and non-neoplastic controls were stained using alcian blue pH 2.5/periodic acid Schiff (AB/PAS) and high iron diamine /alcian blue pH 2.5 (HID/PAS) for the differentiation of mucins according to standard protocols. Based on the mucin expression, the IM was classified as type I, type II, and type III following previous proposals [13]. Using the hematoxylin and eosin stain as well as the mucin stains, mucosal cysts of the stomach were classified. According to previous proposals, foveolar, pyloric, intestinal metaplastic, ciliated, fundic, and non-mucous cysts were distinguished [21, 61].

Table 1 Sample of dysplasias and early gastric carcinomas

Tumor type	Number of cases	Age of patients (years)	Male:female	Atrophic gastritis	Non-atrophic gastritis	Detection of *H. pylori*
Low grade intraepithelial neoplasia	3	42–75	2:1	3	0	1
High grade intraepithelial neoplasia	4	68–79	2:2	4	0	1
Tubular or papillo-tubular adenocarcinoma	12	57–84	2:1	12	0	4
Signet ring cell carcinoma	10	36–72	2:3	4	6	9
Stomachs with two neoplasms	4	42–75	3:1	4	0	2
Total number of neoplastic stomachs	25	36–84	1:1	19	6	13

Immunohistochemistry of human tissues

Sections of neoplastic and fetal stomachs, and non-neoplastic controls were investigated by mouse monoclonal antibodies for the expression of cytokeratin-18 (1:200; Dako, Hamburg, Germany) and of CK7 (1:1000; clone OVTL 12/30; DCS, Hamburg, Germany). Neoplastic specimens and non-neoplastic controls were additionally analyzed by mouse monoclonal antibodies for Mib1 (1:50; Dako, Hamburg, Germany), and β-catenin (1:100; Transduction Lab., Lexington, USA), and by a polyclonal rabbit anti-beta catenin antiserum (1:750, Sigma, Deisenhofen, Germany). The immunostaining of the paraffin sections was performed as previously described [7].

Evaluation of immunostainings

CK7 immunostainings were semiquantitatively evaluated. The categories for GIN and EGC were: *low degree*: less than 30% CK7-positive neoplastic cells; *high degree*: more than 30% CK7-positive neoplastic cells. The categories for non-neoplastic mucosa were: *low score*: CK7 expression of single cells or small cellular foci (single gland, duct-like structure or, cyst); *high score*: CK7 expression of cellular complexes (two and more adjacent glands, duct-like structures, and/or cysts) or total mucosal segments. Boundary and background mucosa were distinguished in neoplastic stomachs. Boundary mucosa was defined as the mucosa immediately adjacent to a neoplasm, either at its lateral or basal margins. The other parts of non-neoplastic mucosa were defined as background mucosa.

Animal model

The animal model of Mongolian gerbils was used for the chronologic study of the gastritis–cancer sequence consecutive to *H. pylori* infection [20, 56]. Five-week-old male Mongolian gerbils weighing 30–40 g (Seac Yoshitomi Co. Ltd., Fukuoka, Japan) were fasted for 24 h and challenged orally with a vehicle of 109 colony-forming units (CFU) *H. pylori* (ATCC-43504) in 1.0 ml of *Brucella* broth with 10% horse serum. Sixty *H. pylori*-infected Mongolian gerbils, in which the IgG anti-*H. pylori* antibody titer increased after 2 months of inoculation, were taken for further studies. Ten animals were killed 2, 6, and 12 months after onset of infection, and their stomachs were histologically studied. Thirty animals were killed 24 months after onset of infection and investigated for the occurrence of gastric cancer. Twenty non-infected Mongolian gerbils served as controls and were killed after the same courses of time. The removed stomachs as well as control tissues from small intestine, kidney, and liver were fixed in 10% formalin, embedded in paraffin, cut in 5-µm serial sections, and stained with hematoxylin and eosin. Control animals showed no inflammatory infiltrates and no metaplastic or cystic changes of gastric mucosa. Two months after infection, mild antral gastritis, a focal loss of specific differentiation, and a duct-like appearance of basal glands were detected. Six months and 12 months after infection animals exhibited moderate to severe antral and mild to moderate corpus gastritis. Mucosal segments now exhibited loss of specific glandular differentiation and duct-like epithelial changes, mucoid (pseudopyloric) cellular metaplasia and hyperplasia of glands, as well as development of intramucosal and submucosal cysts with flat epithelium or mucoid metaplasias. At 24 months these epithelial changes occurred in wide fields of the stomachs. They were associated with severe pangastritis and with foci of IM, mainly in the intra- or submucosal cysts. Two animals had developed infiltrative mucinous adenocarcinomas of the stomach at this stage.

Immunohistochemistry of animal tissues

CK7 expression was studied in tissues of Mongolian gerbils by two mouse monoclonal antibodies (clone OVTL; DCS, Hamburg, Germany; clone RCK 105; Progen, Heidelberg, Germany). Specific binding of the antibody clone RCK105 to CK7 for mouse and hamster had been documented by previous studies [34]. Both antibodies showed selective positive immunostainings of small hepatic bile ducts, known to be CK7 positive, but not with epithelial cells of the small intestine or kidney of Mongolian gerbils. Immunostaining of paraffin sections was done as previously described [7], except that a 30-min incubation with rabbit serum (1:100; Dako, Hamburg, Germany) was performed before the incubation of the secondary antibody to reduce unspecific background staining of gerbils' immunoglobulins. CK7 expression was evaluated in normal gastric mucosa of two control animals, mild gastritis of two animals (2 months after infection), moderate to severe gastritis of seven animals (6, 12, and 24 months after infection), and gastric mucinous adenocarcinoma of two animals (24 months after infection).

Statistical analysis

The non-parametrical Mann-Whitney/U-test was applied. Values for immunostainings were defined as: value 0 for "negative"; value 1 for *low degree* or *low score*; and value 2 for *high degree* or *high score*. The SPSS software (SPSS Standard Software 11.0; SPSS Inc., Chicago, USA) was used for statistical analysis. Resulting *P*-values were not corrected for ties. Significance was assumed for $P<0.05$.

Results

CK7 expression in the fetal stomach

In agreement with previous descriptions of gastric histogenesis, different stages of mucosal development were seen in the stomachs of fetuses from the 10th to the 19th week of gestation [39]: the stomach was lined by pseudostratified columnar epithelium at the 10th week of ges-

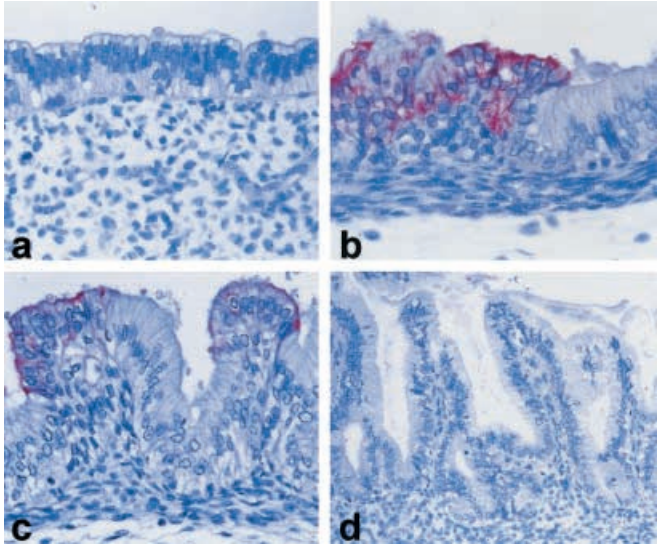


Fig. 1a–d CK7 expression in human fetal stomachs. **a** Pseudostratified epithelium of primitive stomach is negative (10th week of gestation). **b**, **c** Undifferentiated epithelial cells are strongly CK7 positive at the start of gastric pit development, whereas cylindrical cells of the early pits and surface are CK7 negative (14th week of gestation). **d** Different cell types of fetal gastric mucosa after pit development are CK7 negative (16th week of gestation). Original magnification: ×63 (**a–c**); ×40 (**d**)

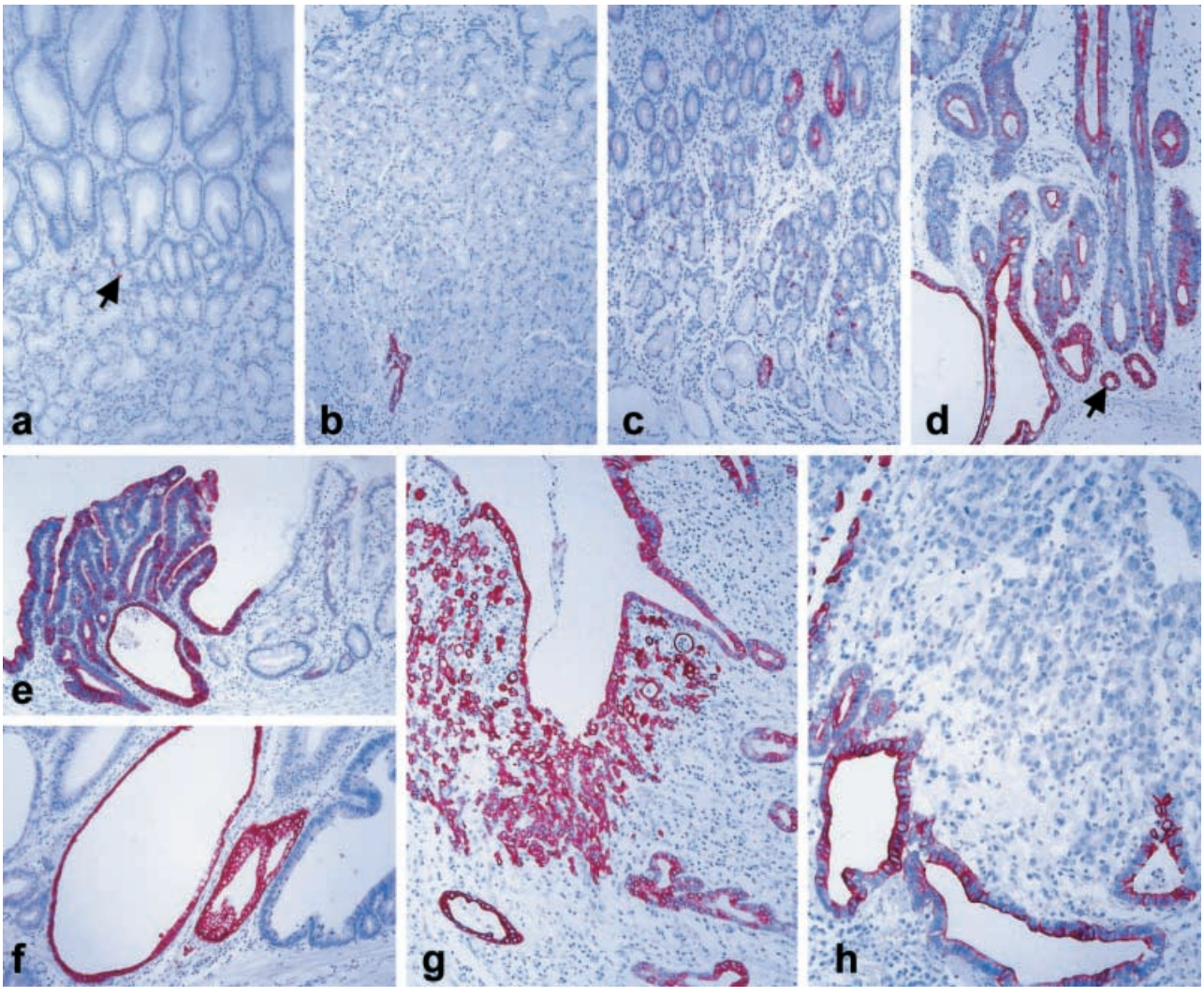


Fig. 2a–h CK7 expression in the non-neoplastic and the neoplastic stomach. **a** Normal antral mucosa with very few CK7 positive cells (*arrow*) at the neck region. **b** Normal corpus mucosa exhibiting a single focus of CK7 positive epithelial cells at the bottom of glands. **c** Antral gastritis with CK7 positivity of focal pits and glands or single neck cells (*low score* CK7 expression). **d** Antral gastritis exhibiting a CK7 positive complex of duct-like structures (*arrow*) and cysts (*high score* CK7 expression); adjacent, partly CK7 positive, IM. **e** Low-grade GIN with *high degree* CK7 expression; adjacent, mainly CK7 negative, IM. **f** CK7-negative high-grade GIN; complex of CK7-positive cysts in adjacent boundary mucosa (*high score* CK7 expression) **g** Signet ring cell carcinoma with *high degree* CK7 positivity; CK7-positive duct-like complex in adjacent boundary mucosa (*high score* CK7 expression). **h** CK7-negative G3-adenocarcinoma bordered by high-grade GIN with *high degree* CK7 expression. Original magnification: ×20 (**a–h**)

tation; development of new gastric pits was seen at the 14th to 16th week of gestation in the cardiac region; and developed gastric pits, neck regions, early glands, and surface epithelium were found at the14th to the 16th week of gestation in most parts of the stomach, except the cardiac region, and at the 19th week of gestation in the whole stomach.

A strong and distinct CK7 expression was detected in undifferentiated fetal cells at the start of gastric pit development (Fig. 1b, c). Only the indifferent fetal cells were positive; the cylindrical fetal cells forming pits and surface epithelium were negative. Moreover, the early pseudostratified epithelium of the primitive stomach before the start of pit development and the different types of epithelial cells of the fetal gastric mucosa after the start of pit development were CK7 negative (Fig. 1a, d). CK18 was expressed by all epithelial cells during all stages of development.

CK7 expression in the non-neoplastic stomach

The normal, uninflamed gastric mucosa was either CK7 negative or contained few CK7-positive epithelial cells. The CK7-positive cells were detected as single cells mainly at the antral (Fig. 2a), and rarely at the corpus neck region. Some controls exhibited also small foci of CK7 positive epithelial cells. Such foci were located mainly at the bottom of antral or corpus glands (Fig. 2b), far from the neck cells, and rarely in other mucosal regions. Non-neoplastic stomachs with non-atrophic *H. py-*

Table 2 CK7 expression in gastric intraepithelial neoplasia and early gastric cancer. *Low degree* <30% CK7-positive neoplastic cells, *High degree* >30% CK7-positive neoplastic cells

Type of gastric neoplasia	Total cases	CK7 expression		
		Negative	*Low degree*	*High degree*
All types	29	3	11	15
Intraepithelial neoplasia	7	1	1	5
Tubular or tubulo-papillary adenocarcinoma	12	1	9*	2*
G1	2	0	2	0
G2	3	0	3	0
G3	7	1	4	2
Signet ring cell carcinoma	10	1	1*	8*
Carcinoma stage pT1m	7	0	5	2
Carcinoma stage pT1sm	15	2	5	8

*P=0.025

Table 4 Detection of *high score* CK7 expression, intramucosal cysts or intestinal metaplasias in background or boundary mucosa of neoplastic stomachs (n=25)

Gastric finding	Background mucosa	Boundary mucosa
High score CK7 expression	9*	23*
Intestinal metaplasia, all types	20*	19*
Type 1 intestinal metaplasia	19	11
Type 2 intestinal metaplasia	13	10
Type 3 intestinal metaplasia	10	13
Cysts, all types	20	24
Foveolar type cysts	15	14
Pyloric type cysts	12	7
Intestinal metaplastic type cysts	11	8
Ciliated cell type cysts	5	0
Non-mucous type cysts	13	18

*P=0.050

lori gastritis constantly exhibited a *low score* of CK7-positive cells in antrum and corpus. *High score* of CK7-positive epithelial cells was not observed.

CK7 expression in the neoplastic stomach

CK7 expression was found in 26 out of 29 gastric epithelial neoplasms (Table 2, Fig. 2e–h). Eleven neoplasms contained *low degree* and 15 neoplasms *high degree* of CK7-positive neoplastic cells. *High degree* was frequent in GIN (five of seven cases), and in EGC of signet ring cell type (eight of ten cases), whereas *low degree* predominated in EGC of tubular or tubulo-papillary type (nine of 12 cases). The CK7 expression was strongly positive in undifferentiated cells, and weaker or negative in mucin containing cells of signet ring cell carcinoma. The difference of CK7 expression between EGC of signet ring cell type and of tubular or tubulo-papillary type was significant (P=0.025). Especially, well- and moderately differentiated (G1 and G2) adenocarcinomas had *low degree* CK7 expression. No correlation was seen between *low* and *high degree* of CK7 expression and the depth of mucosal or submucosal invasion.

High score epithelial CK7 expression occurred in the boundary mucosa of 26 of the 29 neoplasms (Table 3, Fig. 2f, g). *Low score* CK7 expression predominated in the background mucosa. All neoplasms with no or *low degree* CK7 expression and all signet ring cell carcinomas had a *high score* CK7 positivity in the boundary mucosa (Fig. 2f). Four EGCs were bordered by GINs, suggesting a GIN–EGC sequence. Two of these EGCs exhibited *low degree* CK7 expression, but the adjacent GINs exhibited *high degree* CK7 positivity (Fig. 2h). In summary, *high score* epithelial CK7 expression significantly increased from background to boundary mucosa in the neoplastic stomachs (Table 3). This switch from *low score* CK7 expression in background mucosa to a *high score* in boundary mucosa also occurred in non-atrophic gastritis.

Table 3 Low score or high score CK7 expression in background or boundary mucosa of neoplastic stomachs. *Low score* CK7 expression of single cells or small cellular foci, *High score* CK7 expression of cellular complexes or total mucosal segments, *Low degree* <30% CK7-positive neoplastic cells, *High degree* >30% CK7-positive neoplastic cells

Gastric finding	Total cases	Score of CK7 expression			
		Background mucosa		Boundary mucosa	
		Low score	*High score*	*Low score*	*High score*
All types of gastric neoplasia	29	20*	9*	3*	26*
Neoplasias with *low degree* CK7 expression	14	9	5	0	14
Neoplasias with *high degree* CK7 expression	15	11	4	3	12
Intraepithelial neoplasias	7	5	2	2	5
Tubular or tubulo-papillary adenocarcinomas	12	5	7	1	11
Signet ring cell carcinomas	10	9	1	0	10
Gastritis, all types	25	16	9	2	23
Non-atrophic gastritis	6	6	0	0	6
Atrophic gastritis	19	10	9	2	17

*P=0.001

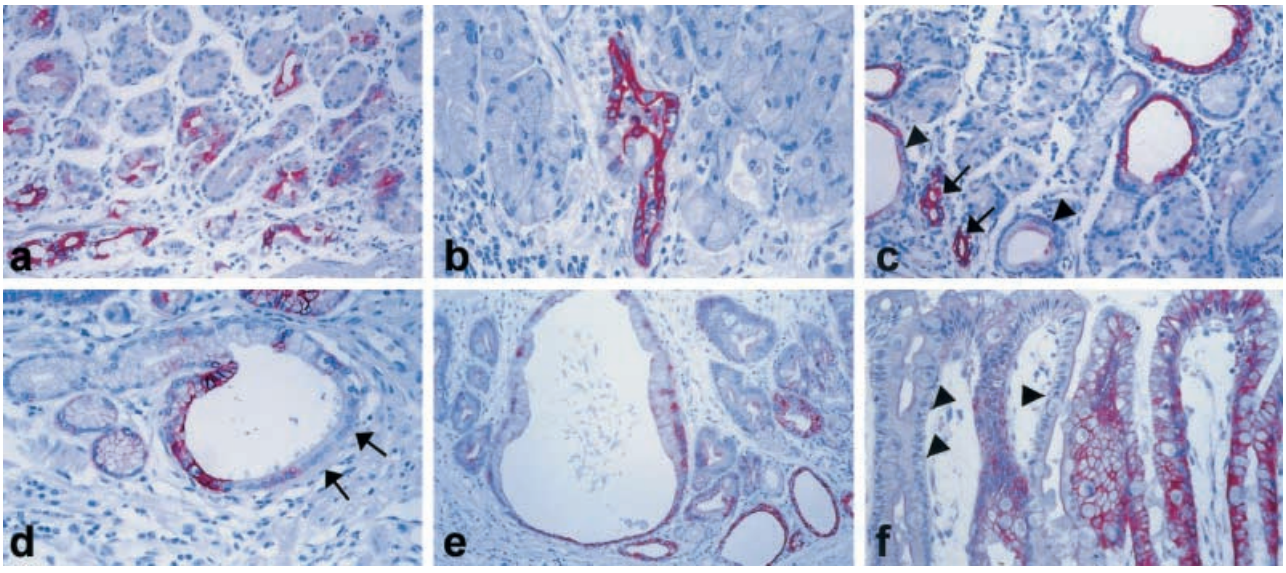


Fig. 3a–f Morphology of gastric CK7-positive dedifferentiated cells, and relationship between them and metaplasia or cysts. **a** CK7-positive dedifferentiated cells with flat and duct-like appearance at the bottom of corpus mucosa in gastritis. **b** Focus of CK7 positive dedifferentiated cells at the bottom of corpus mucosa (detail of Fig. 2b) demonstrating loss of glandular differentiation and epithelial flattening, accompanied by few apoptoses. **c** CK7 positive dedifferentiated cells with duct-like appearance (*arrows*) or cyst formation in basal corpus glands; adjacent pseudopyloric (mucous) metaplastic cells, some with low CK7 expression (*arrowheads*). **d** Intramucosal cyst exhibiting CK7-positive duct-like dedifferentiated cells on the left side, and ciliated metaplastic cells, some with weak CK7 expression, at the right side (*arrows*). **e** Non-mucous cysts with CK7-positive dedifferentiated flat cells; adjacent metaplastic foveolar type cyst with differentiated, weakly CK7-expressing, cylindrical epithelial cells, and tubules of mainly CK7-negative intestinal metaplasia. **f** CK7-positive incomplete intestinal metaplasia, and adjacent CK7-negative complete intestinal metaplasia (*arrowheads*). Original magnification: ×63 (**b**, **d**); ×40 (**a**, **c**, **f**); ×20 (**e**)

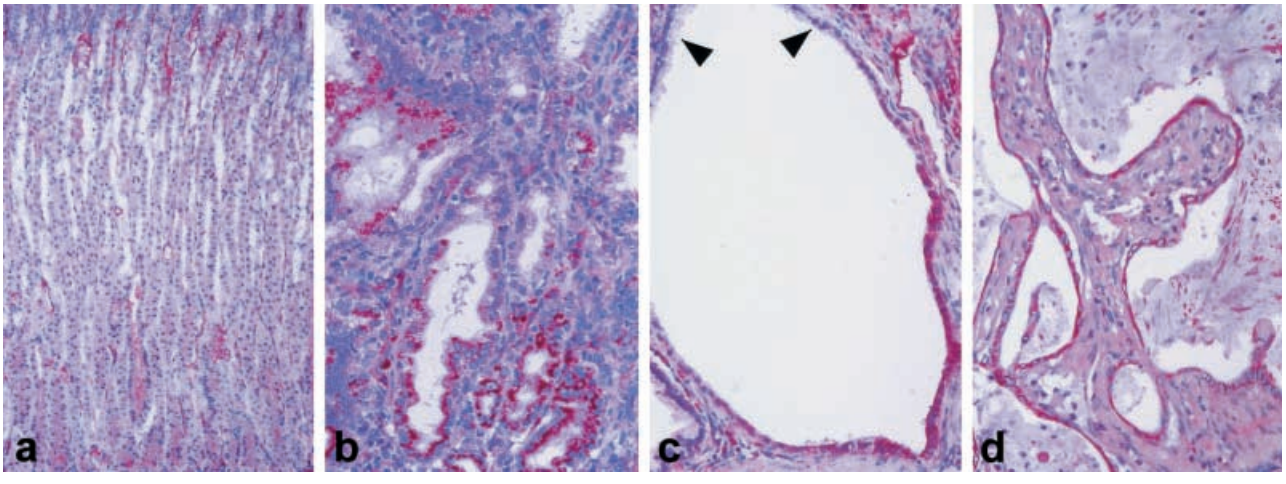


Fig. 4a–d CK7 expression in the gastritis–cancer sequence of *H. pylori*-infected Mongolian gerbils. **a** Normal corpus mucosa without CK7 expression. **b** Loss of specific glandular differentiation and appearance of CK7 positive duct-like epithelial cells at the bottom of mucosa in severe corpus gastritis. **c** Intramucosal cyst with CK7-positive duct-like epithelial cells and some CK7-negative metaplastic mucous cells (*arrowheads*) in severe corpus gastritis. **d** CK7-positive gastric mucinous adenocarcinoma. Slight background staining because of cross-reactivity of secondary antibody with gerbil immunoglobulins in all figures. Original magnification: ×20 (**a**); ×40 (**b–d**)

Relationship between CK7 expression and epithelial morphology, metaplastic or cystic changes

Gastric epithelial cells expressing CK7 were found in antrum and corpus as well as in surface, neck and gland regions (Fig. 2c). A predominance at the neck region was not observed; often, CK7-positive cells were not directly connected to neck cells (Fig. 2b). Epithelial cells with strong CK7-positivity had a flat or simple duct-like appearance (Fig. 3a–c), and formed non-mucous cysts, indicating a loss of specific gastric epithelial features (Figs. 2d, 3e). Flat or simple duct-like appearance was

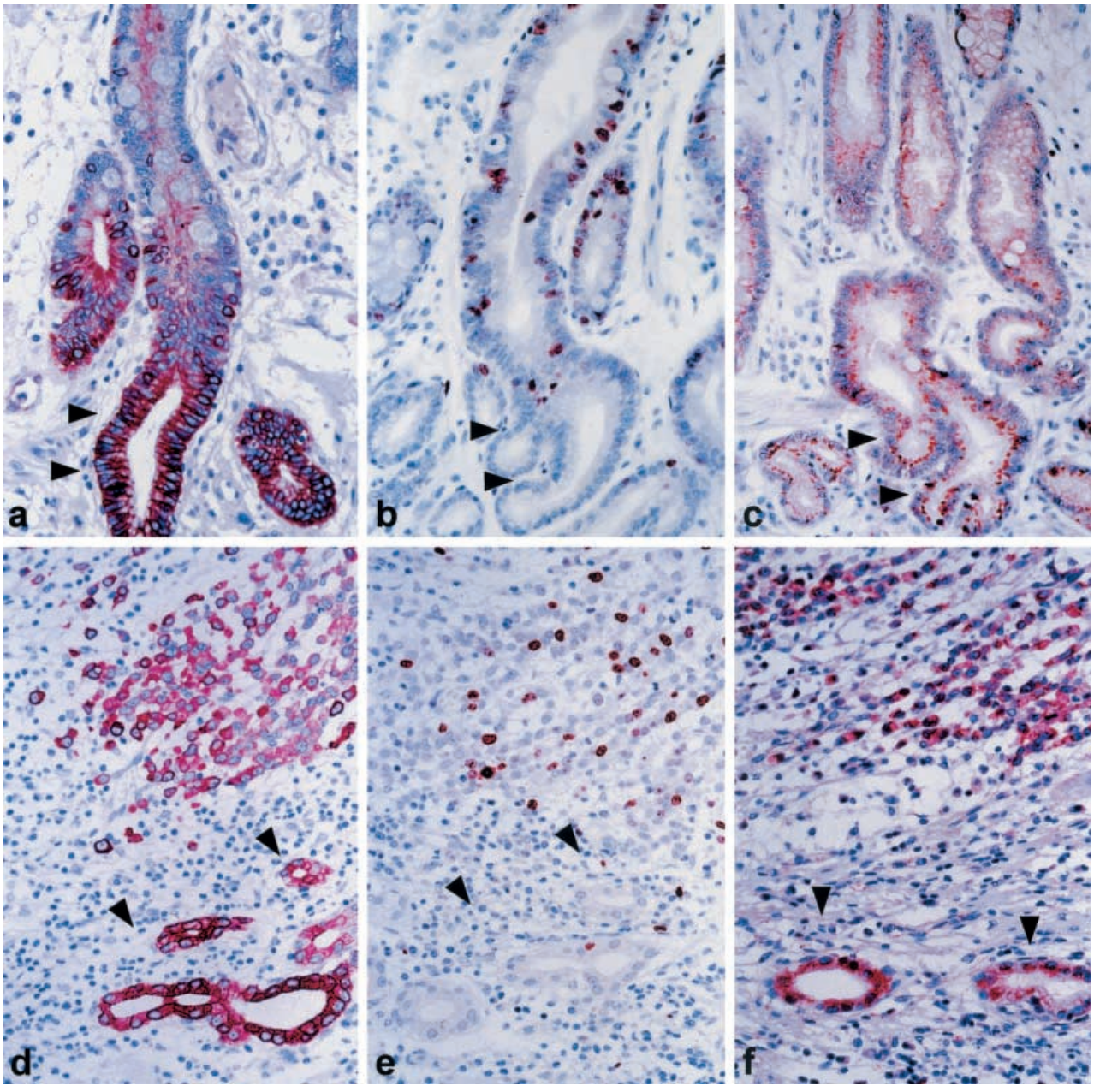


Fig. 5 Serial sections demonstrating Mib1 proliferative activity and β-catenin expression of CK7-positive dedifferentiated epithelial cells adjacent to IM (**a–c**) or to intramucosal signet ring cell carcinoma (**d–f**). **a** Tubule with CK7-positive duct-like dedifferentiated cells at the bottom (*arrowheads*) and complete intestinal metaplasia (IM) with loss of CK7-positive cells in the upper part. **b** Mib1-negative dedifferentiated cells; abrupt transition to many Mib1-positive in IM. **c** Strong dot-like cytoplasmic β-catenin positivity of the dedifferentiated cells; lower and membranous β-catenin expression of IM. **d** Complex of CK7-positive duct-like dedifferentiated cells (*arrowheads*) in boundary mucosa, adjacent to a CK7-positive signet ring cell carcinoma in the upper parts of mucosa. **e** Mainly Mib1-negative dedifferentiated cells (*arrowheads*); abrupt increase of Mib1-positive cells in the carcinoma. **f** Cytoplasmic and nuclear β-catenin positivity of the dedifferentiated duct-like cells and of the neoplastic cells. Original magnification: ×40 (**a–f**)

the most frequent feature of CK7-positive epithelial foci and already seen in some uninflamed stomachs (Figs. 2b, 3b). Flattening was associated with apoptosis of epithelial cells, but not with proliferation (Fig. 3b). CK7-positive complexes or mucosal segments were usually made up of duct-like tubules and cysts (Figs. 2d, 3e).

Metaplasias, including metaplastic cysts generally occurred immediately adjacent to the strongly CK7-positive cells. The CK7 expression became weaker or was lost in the differentiated metaplastic epithelium (Fig. 3c–e). Only incomplete IM (IM type II and III) was mainly, but not constantly, CK7 positive (Fig. 3f). In contrast, complete IM was mainly CK7 negative (Fig. 3e, f), but could be connected to CK7-positive duct-like epithelial cells at the bottom of mucosa (Fig. 5a). The presence of non-mucous cysts with strong CK7 expression showed an increase from background to boundary mucosa. Other cyst

types and IM exhibited no difference in occurrence, or a decrease. Increase in *high score* CK7 expression, but steady presence of IM from background to boundary mucosa, was a significant finding in the neoplastic stomachs (Table 4).

CK7 expression in the gastritis–cancer sequence of *H. pylori*-infected Mongolian gerbils

The normal uninflamed stomach of Mongolian gerbil controls was free of CK7 expression (Fig. 4a). Mild gastritis at 2 months after *H. pylori* infection showed CK7 expression in epithelial cells of basal glands, exhibiting loss of specific differentiation and change to duct-like appearance. Moderate to severe gastritis after 6, 12, and 24 months of *H. pylori* infection was characterized by a loss of differentiated glands and a switch to CK7-positive duct-like structures in large mucosal segments (Fig. 4b). Hyperplastic expansion of branching CK7 positive duct-like tubules was seen. In addition, the formation of numerous small and large intra- and submucosal, cysts, lined by CK7-positive duct-like cells, occurred (Fig. 4c). Some cysts contained metaplastic mucous epithelium without CK7 expression (Fig. 4c). IM was partly CK7 positive and found in the mucosa and in submucosal cysts of three animals. Gastric mucinous adenocarcinomas had developed at 30 months after *H. pylori* infection in two animals and exhibited CK7 positivity in most of the neoplastic cells (Fig. 4d).

Low proliferative activity and accumulation of β-catenin in CK7-positive dedifferentiated epithelial cells

The Mib1 proliferative activity and the β-catenin expression level of CK7-positive dedifferentiated epithelial cells were evaluated on serial sections. The distinct qualitative differences of the two parameters did not require quantification. Thus, the Mib1 labeling was negative or extremely rare in dedifferentiated cells, but abruptly increased in immediately adjacent intestinal metaplastic or neoplastic cells (Fig. 5a–d). β-Catenin showed a distinct and often dot-like cytoplasmic accumulation in most of the CK7-positive dedifferentiated cells, and additional nuclear expressions occurred in some of them (Fig. 5a, c, d, f). Other gastric epithelial cells exhibited only membranous expressions. The metaplastic cells were also characterized by conspiciously lower β-catenin stainings than the adjacent dedifferentiated epithelial cells (Fig. 5c). Low or no β-catenin expression occurred in ten neoplasms. Cytoplasmic and/or nuclear β-catenin accumulations were found in 19 neoplasms (Fig. 5f).

Discussion

Our study extends previous observations about relevant analogies between tumorigenesis and normal tissue development [1, 18, 22]. It suggests that a decisive step for gastric carcinogenesis is dedifferentiation, defining a backward change of differentiated epithelial cells into a fetal-like phenotype. Thus, the CK7 neoexpression links epithelial changes during the gastritis–cancer sequence to a fetal mucosal phase at the start of gastric pit development, when a transient CK7 positivity occurs. CK7 is lost in fetal mucosa after this phase. Only few CK7-positive epithelial cells sometimes occur in the normal, uninflamed stomach. However, CK7 positivity is constantly seen in chronic gastritis and increases to a *high score* expression in the boundary mucosa of gastric neoplasms. Cells with strong CK7 expression in the adult stomach lack the specific glandular differentiation and have a simple flat or duct-like appearance with a frequent cyst formation. Such a phenomenon is called dedifferentiation, and it has been described in a number of experimental studies on tissues or cultured cells [5, 26, 30, 32, 44, 48, 49, 57]. A prototypic process of dedifferentiation, for example, is that iris cells dedifferentiate after the removal of the lens in amphibians, and either differentiate afterwards into a new lens or reform the iris [58]. Therefore, dedifferentiation can be defined as a loss of a differentiated phenotype, with the acquisition of the potential to differentiate into a new phenotype [44].

Spatial and temporal findings from our study accordingly prove a strong relation of the CK7-positive dedifferentiated cells with metaplastic differentiation. Both the dedifferentiated and the metaplastic cells were spatially related by their colocalization in the gastric mucosa and their direct connection in structural units. Moreover, the metaplastic cells expressed CK7, although to a lower degree and with a gradual loss in the differentiated elements compared to the dedifferentiated cells. For instance, the CK7 was still positive in less mature incomplete IM, but negative in differentiated, complete IM. A temporal relationship between the dedifferentiated and metaplastic cells was seen in *H. pylori*-infected Mongolian gerbils: firstly because the loss of specific glandular differentiation and the appearance of duct-like CK7-positive cells occurred before the development of IM, and secondly because IM was found in the newly developed CK7-positive submucosal cysts. Remarkably, the first CK7-positive foci were detected in Mongolian gerbils and in humans at the bottom of the gastric mucosa, far from and without a connection to putative stem cells at the neck region. Metaplastic cells also appeared in basal parts of gastric mucosa and immediately adjacent to CK7-positive dedifferentiated cells, but unrelated to putative neck stem cells.

Dedifferentiation of cells has previously been discussed as one of two hypothetical processes for the development of cancer [44]. Review articles have suggested that malignancy could arise either from stem cells due to a maturation arrest, or from a dedifferentiation of mature cells that regain the ability to proliferate [43, 44]. Although present considerations about gastric carcinogenesis usually prefer the stem cell hypothesis, a definite proof of it is lacking [14].Our study suggests that an origin of gastric carcinomas from dedifferentiated gastric

cells is also possible. The main arguments for the assumption are that GIN and EGC almost constantly occurred in mucosal fields with a *high score* of CK7-positive dedifferentiated cells, and that 90% of the early neoplasms expressed CK7 at least in part of the tumor cells.

Based on these findings, we propose that chronic gastritis could induce long-term repetitive processes of dedifferentiation and redifferentiation. Every redifferentiation would require a new epigenetic coding of the dedifferentiated cells by the mucosal context and inductive environment. Changes in the inductive environment during inflammation could induce alterations of the gene expressions and consecutive metaplasias. The long-term dedifferentiation–redifferentiation processes could favor initiation, accumulation, and clonal expansion of genetic alterations – especially of genes that coordinate and control proliferation and differentiation, such as p53, p21, and cyclins. Such genetic alterations could inhibit or disturb a regular redifferentiation, so that a mitogenic activation of mutated dedifferentiated cells could induce their switch to cancer.

Such a model is able to explain the coincidence of IM and gastric carcinoma [10, 11, 13], as well as the rare detection of genetic alterations already in IM [27, 40, 54]. Otherwise, IM is mostly heterotypic or polyclonal [31]. This was difficult to understand from the idea that IM is derived as lineage from a single permanent stem cell in the niche of a gastric neck [14]. It fits, however, with the assumption that dedifferentiated cells occur at many sites of the gastric mucosa and have a potential for a polyclonal metaplastic redifferentiation induced by the environment. Moreover, the relation of gastric neoplasms to dedifferentiated cells makes it reasonable that signet ring cell carcinomas, or so-called diffuse types of gastric carcinoma, occur without association to IM in non-atrophic and atrophic gastritis, and that both intestinal and diffuse types of cancer are pathogenetically related to *H. pylori* gastritis [23, 45].

Interestingly, signet ring cell carcinomas are immunophenotypically closer to the dedifferentiated cells than the tubular and tubulo-papillary adenocarcinomas, because almost all of them had *high degree* CK7 expression, whereas *low degree* predominated in the latter. Almost all GINs also have *high degree* CK7 positivity. Molecular studies indicate fewer critical steps for the tumorigenesis of diffuse types than intestinal types of carcinoma [38, 59], and intermediate steps of GIN are assumed to occur in the development of the intestinal, but usually not in the diffuse types [59]. Recent findings indicate that intestinalization of signet ring cell carcinomas occurs, but usually as a time-dependent switch starting primarily with a gastric phenotype [3]. Studies of gastric carcinoma without restriction to early stages have reported CK7 positivity in only 28% of the cases [9]. Thus, the neoplastic CK7 expression characterizes the initial steps of malignant transformation, and a loss of it seems to occur with tumor progression.

In contrast to the high proliferation and turnover of epithelial cells in gastritis, a very low proliferative activity is found in the CK7-positive dedifferentiated gastric cells. They further show distinct accumulations of β-catenin in the cytoplasm and sometimes in nuclei, which are not seen in other gastric epithelial cells. We previously reported that nuclear β-catenin accumulations do not correlate with Mib1 proliferative activity, but with morphogenesis in colonic adenomas [8, 22]. An elevated level of cytoplasmic β-catenin was recently described in epidermal stem cells [60], which are characterized by low proliferation, but high proliferative potential [29, 60]. Dedifferentiated cells share some properties with stem cells, for example, fetal-like features, a lack of specific differentiation, and a potential for redifferentiation [32, 44]. The low proliferation and the β-catenin accumulation could be further stem cell-like features of the dedifferentiated cells. Interestingly, an abrupt increase of proliferation takes place at the transition from the CK7-positive dedifferentiated cells to intestinal metaplastic cells or neoplastic cells. Thus, the dedifferentiated cells with β-catenin accumulation could have a proliferative potential that is activated at the switch to differentiation or neoplastic growth. Transient β-catenin stabilization plays a key role in de novo hair follicle morphogenesis and is also involved in hair follicle tumorigenesis in mice [15]. It could be that stabilized β-catenin has a similar morphogenetic and tumorigenic relevance for dedifferentiated gastric cells.

A distinct CK7 expression and β-catenin accumulation, similar to our observations in gastritis, have been described during the metaplasia–dysplasia cancer sequence of Barrett's esophagus in the foregut [2, 4, 33], indicating a putative role of CK7-positive dedifferentiated cells also for the development of distal esophageal adenocarcinoma. A dedifferentiation of acinar cells and occurrence of simple duct-like cells expressing CK7 and cytokeratin-19 have, furthermore, been reported in pancreatitis [26]. In transforming growth factor (TGF)-α transgenic mice the pancreatic acinar cells change into CK7 positive duct-like cells, which form tubular complexes or cysts, and give rise to pancreatic dysplasias and adenocarcinomas [55]. This could correspond to morphologic findings in the gastritis–cancer sequence of *H. pylori*-infected Mongolian gerbils. In pregnant mice both epidermal growth factor (EGF) and TGF α had a dedifferentiating effect on the mammary gland, which was independent of mitogenic properties [50]. The growth factors TGF α and EGF are known to be significantly upregulated in chronic gastritis [24, 25]. Therefore, they are interesting candidates for an induction of epithelial dedifferentiation in gastritis, and for experimental models of dedifferentiation in the stomach.

In summary, our observations demonstrate a relationship between metaplasia, GIN or EGC, and dedifferentiated epithelial cells defined by CK7 expression in chronic gastritis.

The dedifferentiated cells exhibit low proliferation and β-catenin accumulation, similar to stem cells described at other sites. Thus, the "stem cell" and "dedifferentiation" hypotheses for cancer origin might comple-

ment one another, and dedifferentiation–redifferentiation processes could be decisive for carcinogenesis in the stomach.

Acknowledgements We thank C. Egerer-Sieber, G. Herbig, C. Knoll, C. Rudelt, and C. Winkelmann for expert technical assistance, Dr. R. Moll for helpful discussions, and Dr. L. McKenna for proofreading the manuscript.

References

1. Aigner T, Loos S, Müller S, Sandell LJ, Unni KK, Kirchner T (2000) Cell differentiation and matrix gene expression in mesenchymal chondrosarcomas. Am J Pathol 156:1327–1335
2. Bailey T, Biddlestone L, Shepherd N, Barr H, Warner P, Jankowski J (1998) Altered cadherin and catenin complexes in the Barrett's esophagus-dysplasia-adenocarcinoma-sequence: correlation with disease progression and dedifferentiation. Am J Pathol 152:135–144
3. Bamba M, Sugihara H, Kushima R, Okada K, Tsukashita S, Horinouchi M, Hattori T (2001) Time-dependent expression of intestinal phenotype in signet ring cell carcinomas of the human stomach. Virchows Arch 438:49–56
4. Bian YS,Osterheld MC, Bosman FT, Fontolliet C, Benhattar J (2000) Nuclear accumulation of beta-catenin is a common and early event during neoplastic progression of Barrett esophagus. Am J Clin Pathol 114:583–590
5. Blaheta RA, Kronenberger B, Woitaschek D, Auth MK, Scholz M, Weber S, Schuldes H, Encke A, Markus BH (1998) Dedifferentiation of human hepatocytes by extracellular matrix proteins in vitro: quantitative and qualitative investigation of cytokeratin 7, 8, 18, 19 and vimentin filaments. J Hepatol 28:677–690
6. Booth C, Potten CS (2000) Gut instincts: thoughts on intestinal epithelial stem cells. J Clin Invest 105:1493–1499
7. Brabletz T, Jung A, Dag S, Hlubek F, Kirchner T (1999) β-catenin regulates the expression of the matrix metalloproteinase-7 in human colorectal cancer. Am J Pathol 155:1033–1038
8. Brabletz T, Hermann K, Jung A, Faller G, Kirchner T (2000) Expression of nuclear beta-catenin and c-myc is correlated with tumor size but not with proliferative activity of colorectal adenomas. Am J Pathol 156:865–870
9. Chu P, Wu E, Weiss LM (2000) Cytokeratin 7 and cytokeratin 20 expression in epithelial neoplasms: a survey of 435 cases. Mod Pathol 13:962–972
10. Correa P (1992) Human gastric carcinogenesis: a multistep and multifactorial process – First American Cancer Society award lecture on cancer epidemiology and prevention. Cancer Res 52:6735–6740
11. Correa P, Haenszel W, Cuello C, Tannenbaum S, Archer M (1975) A model for gastric cancer epidemiology. Lancet 2: 58–60
12. Dixon MF, Genta RM, Yardley JH, Correa P, participants in the International Workshop on the Histopathology of Gastritis, Houston 1994 (1996) Classification and grading of gastritis. The updated Sydney System. Am J Surg Pathol 20:1161–1181
13. Filipe MI, Muñoz N, Matko I, Kato I, Pompe-Kirn V, Jutersek A, Teuchmann S, Benz M, Prijon T (1994) Intestinal metaplasia types and the risk of gastric cancer: a cohort study in Slovenia. Int J Cancer 57:324–329
14. Garcia SB, Park HS, Novelli M, Wright NA (1999) Field cancerization, clonality, and epithelial stem cells: the spread of mutated clones in epithelial sheets. J Pathol 187:61–81
15. Gat U, DasGupta R, Degenstein L, Fuchs E (1998) De novo hair follicle morphogenesis and hair tumors in mice expressing a truncated β-catenin in Skin. Cell 95:605–614
16. Gmyr V, Kerr-Conte J, Belaich S, Vandewalle B, Leteurtre E, Vantyghem MC, Lecomte-Houcke M, Proye C, Lefebvre J, Pattou F (2000) Adult human cytokeratin 19-positive cells reexpress insulin promoter factor 1 in vitro: further evidence for pluripotent pancreatic stem cells in humans. Diabetes 49: 1671–1680
17. Goldstone AR, Quirke P, Dixon MF (1996) Helicobacter pylori infection and gastric cancer. J Pathol 179:129–137
18. Gottschalk D, Fehn M, Patt S, Saeger W, Kirchner T, Aigner T (2001) Matrix gene expression analysis and cellular phenotyping in chordoma reveals focal differentiation pattern of neoplastic cells mimicking nucleus pulposus development. Am J Pathol 158:1571–1578
19. Hamilton SR, Aaltonen LA (eds) (2000) World Health Organization classification of tumours. Pathology and genetics of tumours of the digestive system. IARC Press, Lyon
20. Honda S, Fujioka T, Tokieda M, Satoh R, Nishizono A, Nasu M (1998) Development of Helicobacter pylori-induced gastric carcinoma in Mongolian gerbils. Cancer Res 58:4255–4259
21. Kato Y, Sugano H, Rubio CA (1983) Classification of intramucosal cysts of the stomach. Histopathol 7:931–938
22. Kirchner T, Brabletz T (2000) Patterning and nuclear β-catenin expression in the colonic adenoma-carcinoma sequence. Analogies with embryonic gastrulation. Am J Pathol 157: 1113–1121
23. Kokkola A, Valle J, Haapiainen R, Sipponen P, Kivilaakso E, Puolakkainen P (1996) Helicobacter pylori infection in young patients with gastric carcinoma. Scand J Gastroenterol 31: 643–647
24. Konturek PC, Ernst H, Konturek SJ, Bobrzynski AJ, Faller G, Klingler C, Hahn EG (1997) Mucosal expression and luminal release of epidermal and transforming growth factors in patients with duodenal ulcer before and after eradication of Helicobacter pylori. Gut 40:463–469
25. Konturek PC, Bobrzynski A, Konturek SJ, Bielanski W, Faller G, Kirchner T, Hahn EG (1998) Epidermal growth factor and transforming growth factor alpha in duodenal ulcer and nonulcer dyspepsia patients before and after Helicobacter pylori eradication. Scand J Gastroenterol 33:143–151
26. Lechene de la Porte P, Iovanna J, Odaira C, Choux R, Sarles H, Berger Z (1991) Involvement of tubular complexes in pancreatic regeneration after acute necrohemorrhagic pancreatitis. Pancreas 6:298–306
27. Leung WK, Kim JJ, Kim JG, Graham DY, Sepulveda AR (2000) Microsatellite instability in gastric intestinal metaplasia in patients with and without gastric cancer. Am J Pathol 156: 537–543
28. Lyle S, Christofidou-Solomidou M, Liu Y, Elder DE, Albelda S, Cotsarelis G (1998) The C8/144B monoclonal antibody recognizes cytokeratin 15 and defines the location of human hair follicle stem cells. J Cell Sci 111:3179–3188
29. Lyle S, Christofidou-Solomidou M, Liu Y, Elder DE, Albelda S, Cotsarelis G (1999) Human hair follicle bulge cells are biochemically distinct and possess an epithelial stem cell phenotype. J Investig Dermatol Symp Proc 4:296–301
30. Mallein-Gerin F, Garrone R, van der Rest M (1991) Proteoglycan and collagen synthesis are correlated with actin organization in dedifferentiating chondrocytes. Eur J Cell biol 56: 364–373
31. Nomura S, Kaminishi M, Sugiyama K. Oohara T, Esumi E (1998) Clonal analysis of isolated intestinal metaplastic glands of stomach using Xk polymorphism. Gut 42:663–668
32. Okada TS (1991) Transdifferentiation, Clarendon Press, Oxford
33. Ormsby AH, Vaezi MF, Richter JE, Goldblum JR, Rice TW, Falk GW, Gramlich TL (2000) Cytokeratin immunoreactivity patterns in the diagnosis of short-segment Barrett's esophagus. Gastroenterology 119:683–690
34. Ramaekers F, Huysmans A, Schaart G, Moesker O, Vooijs P (1987) Tissue distribution of keratin 7 as monitored by a monoclonal antibody. Exp Cell Res 170:235–249
35. Rubio CA, Kato Y (1986) Ciliated metaplasia in the gastric mucosa. Studies on Japanese patients. Jpn J Cancer Res 77: 282–286
36. Ruck P, Xiao JC, Pietsch T, Von Schweinitz D, Kaiserling E (1997) Hepatic stem-like cells in hepatoblastoma: expression of cytokeratin 7, albumin and oval cell associated antigens detected by OV-1 and OV-6. Histopathology 31:324–239

37. Ruddell WSJ, Bone ES, Hill MJ, Walters CL (1978) Pathogenesis of gastric cancer in pernicious anaemia. Lancet 1:521–523
38. Saal K, Vollmers HP, Muller J, Kohler J, Hohn H, Muller-Hermelink HK (1993) Cytogenetic differences between intestinal and diffuse types of human gastric carcinoma. Virchows Arch B Cell Pathol Incl Mol Pathol 64:145–150
39. Salenius P (1962) On the ontogenesis of the human gastric epithelial cells. A histologic and histochemical study. Acta Anatomica 50 [Suppl 46]
40. Sanz-Ortega J, Sanz-Esperona J, Clades T, Gomes de la Concha E, Sobel ME, Merino MJ (1996) LOH at the APC/MCC gene (5Q21) in gastric cancer and pre-neoplastic lesions. Pathol Res Practice 192:1206–1210
41. Schlemper RJ, Riddell RH, Kato Y, Borchard F, Cooper HS, Dawsey SM, Dixon MF, Fenoglio-Preiser CM, Flejou JF, Geboes K, Hattori T, Hirota T, Itabashi M, Iwafuchi M, Iwashita A, Kim YI, Kirchner T, Klimpfinger M, Koike M, Lauwers GY, Lewin KJ, Oberhuber G, Offner F, Price AB, Rubio CA, Shimizu M, Shimoda T, Sipponen P, Solcia E, Stolte M, Watanbe H, Yamabe H (2000) The Vienna classification of gastrointestinal epithelial neoplasia. Gut 47:251–255
42. Schmidt PH, Lee JR, Joshi V, Playford RJ, Poulsom R, Wright NA, Goldenring JR (1999) Identification of a metaplastic cell lineage associated with human gastric adenocarcinoma. Lab Invest 79:639–646
43. Sell S (1993) Cellular origin of cancer: dedifferentiation or stem cell maturation arrest? Environ Health Perspect 101 [Suppl 5]:15–26
44. Sell S, Pierce GB (1994) Maturation arrest of stem cell differentiation is a common pathway for the cellular origin of teratocarcinomas and epithelial cancers. Lab Invest 70:6–22
45. Sipponen P, Riihelä M, Hyvärinen H, Seppälä K (1994) Chronic nonatrophic ('superficial') gastritis increases the risk of gastric carcinoma. Scand J Gastroenterol 29:336–340
46. Slack JMW (1986) Epithelial metaplasia and the second anatomy. Lancet 2:268–271
47. Slack JMW (2000) Stem cells in epithelial tissues. Science 287:1431–1433
48. Slomp J, Gittenberger-de Groot AC, Glukhova MA, Conny van Munsteren J, Kockx MM, Schwartz SM, Koteliansky VE (1997) Differentiation, dedifferentiation, and apoptosis of smooth muscle cells during the development of the human ductus arteriosus. Arterioscler Thromb Vasc Biol 17:1003–1009
49. Sparks RL, Seibel-Ross EI, Wier ML, Scott RE (1996) Differentiation, dedifferentiation, and transdifferentiation of BALB/c 3T3 T mesenchymal stem cells: potential significance in metaplasia and neoplasia. Cancer Res 46:5312–5319
50. Spitzer E, Zschiesche W, Binas B, Grosse R, Erdmann B (1995) EGF and TGF alpha modulate structural and functional differentiation of the mammary gland from pregnant mice in vitro: possible role of the arachidonic acid pathway. J Cell Biochem 57:495–508
51. Stosiek P, Kasper M (1990) Neoexpression von Cytokeratin 7 bei der chronisch-atrophischen Gastritis mit perniziöser Anämie. Pathologe 11:14–17
52. Stosiek P, Kasper M (1993) Transitorisches Auftreten von Zytokeratin 7 bei der Entstehung des Magenkarzinoms. Pathologe 14:71–73
53. Stosiek P, Bräutigam E, Kasper M (1991) Expression of cytokeratin 7 in human glandular epithelium of fetal stomach. Acta Histochem 91:21–23
54. Tahara E (1995) Molecular biology of gastric cancer. World J Surg 19:484–488
55. Wagner M, Lührs H, Klöppel G, Adler G, Schmid RM (1998) Malignant transformation of duct-like cells originating from acini in transforming growth factor α transgenic mice. Gastroenterology 115:1254–1262
56. Watanabe T, Tada M, Nagai H, Sasaki S, Nakao M (1998) Helicobacter pylori infection induces gastric cancer in Mongolian gerbils. Gastroenterology 115:642–648
57. Waters MJ, Tweedale RC, Whip TA, Shaw G, Manley SW, Bourke JR (1987) Dedifferentiation of cultured thyroid cells by epidermal growth factor: some insights into the mechanism. Mol Cell Endocrinol 49:109–117
58. Yamada T, McDevitt DS (1974) Direct evidence for transformation of differentiated iris epitheloid cells into lens cells. Dev Biol 38:104–118
59. Yokozaki H, Kuniyasu H, Semba S, Yasui W, Tahara E (1997) Molecular bases of human stomach carcinogenesis. In: Tahara E (ed) Molecular pathology of gastroenterological cancer: application to clinical practice. Springer, Tokyo, pp 55–70
60. Zhu AJ, Watt FM (1999) beta-catenin signalling modulates proliferative potential of human epidermal keratinocytes independently of intercellular adhesion. Development 126:2285–2289
61. Zhu FG, Deng XJ, Cheng NJ (1987) Intramucosal cysts in gastric mucosa adjacent to carcinoma and peptic ulcer: a histochemical study. Histopathology 11:631–638

Virchows Arch (2001) 439:523–530
DOI 10.1007/s004280100426

ORIGINAL ARTICLE

Frederick C. Koerner · Tetsunari Oyama
Horacio Maluf

Morphological observations regarding the origins of atypical cystic lobules (low-grade clinging carcinoma of flat type)

Received: 17 August 2000 / Accepted: 5 January 2001 / Published online: 19 June 2001
© Springer-Verlag 2001

Abstract This study seeks to define the morphological pathogenesis of a form of cystic transformation of lobules referred to as atypical cystic lobule or low-grade clinging carcinoma of flat type. We collected 25 examples that seem to represent the early stages in the formation of atypical cystic lobules and made a careful study of their morphology. Our observations indicate that this lesion arises from pre-existing, structurally normal terminal duct-lobular units and that it seems to develop by the direct transformation of indigenous luminal cells. The transformed cells first become evident in the small duct or terminal ductule, where they appear as slightly enlarged columnar cells containing atypical nuclei. In more advanced examples, these alterations affect all luminal cells of the terminal duct-lobular unit, but the cells of the terminal ductule continue to show more pronounced changes than the cells lining the acini. The atypical cells within the lobule do not seem to displace the normal acinar cells. Instead, the cells form a continuum, making it impossible to define the point at which atypical cells and normal cells meet. Within the small duct, however, the atypical epithelium comes to an abrupt halt as the duct courses towards the nipple. Considering these observations, we ascribe the formation of atypical cystic lobules to the accumulation of atypical cells in pre-existing terminal duct-lobular units.

Keywords Breast · Ductal carcinoma in situ · Lobule · Cyst · Pathogenesis

F.C. Koerner (✉)
Department of Pathology, Massachusetts General Hospital,
Fruit Street, Boston, MA 02114, USA
e-mail: Fkoerner@Partners.org
Tel.: +1-617-7268572, Fax: +1-617-7267474

T. Oyama
Second Department of Pathology,
Gunma University School of Medicine, Laboratory of Pathology,
Gunma University Hospital, Maebashi, Gunma, Japan

H. Maluf
Lauren V. Ackerman Laboratory of Pathology, Barnes Hospital,
Division of Surgical Pathology,
Washington University School of Medicine, St. Louis, MO, USA

Introduction

In 1979, Dr. Azzopardi described an unusual variety of ductal carcinoma in situ which he called "clinging carcinoma" [1]. He devised this term "to indicate that the neoplastic cells are limited to the periphery of the containing structures, in the sense that they do not fill the lumen in solid or cribriform fashion, nor do they show the numerous cell layers usually seen in comedo cancer." Dr. Azzopardi [1] recognized high- and low-grade types of clinging carcinoma. He believed that the former can progress to comedocarcinoma, whereas the latter represents the forerunner of low-grade micropapillary/cribriform carcinoma in situ. The immunohistochemical studies of *neu* protein expression described by DePotter et al. support this belief [3]. Other authors, too, have described lesions closely related to the low-grade type of clinging carcinoma. Goldstein and O'Malley [7], for instance, describe a type of malignant intraductal proliferation composed of columnar cells growing in a single layer. Rosen refers to the same lesion as "columnar cell (pretubular) hyperplasia" [12], Tavassoli uses the terms "atypical intraductal hyperplasia" [13] and "mammary ductal intraepithelial neoplasia-flat type" [10], Tsuchiya et al. suggest the name "atypical cystic duct" [14], and Fraser et al. call the abnormality "columnar alteration with prominent apical snouts" [6]. We recently called attention to a cystic transformation of terminal duct-lobular units (atypical cystic lobule) [11], which also belongs to this family. We discovered that the cells of atypical cystic lobules display the same cytological and immunohistochemical characteristics as the cells of low-grade micropapillary/cribriform ductal carcinomas in situ and that they frequently merge with low-grade ductal carcinoma in situ. Kusama et al. report similar findings [9]. Genetic studies of Moinfar et al. [10] have established the clonal nature of this lesion as well as its link to more commonplace forms of ductal carcinoma in situ and to invasive ductal carcinoma. The only information regarding the clinical significance of this family of lesions comes from the work of Eusebi and colleagues [5], who fol-

lowed 25 women with low-grade clinging carcinoma of flat type (atypical cystic lobules) for an average of about 19 years. None of the women developed invasive carcinoma and only one suffered a recurrence, which also consisted of low-grade clinging carcinoma of flat type. Taken together, these histopathological, molecular, and clinical observations support Dr. Azzopardi's belief that these lesions represent an early stage in the formation of low-grade ductal carcinoma in situ.

We believe that the foregoing studies have established the (pre)neoplastic nature of this type of lesion but not revealed the early stages in its development or its cell of origin. Three hypotheses regarding the pathogenesis of atypical cystic lobules (low-grade clinging carcinoma of flat type) come to mind. Dr. Azzopardi briefly refers to two: "The malignant cells appear to have originated in situ or perhaps to have spread as a single well-orientated layer of cells by a process of 'creeping replacement.' While the former genesis seems the more likely, it is possible that the latter also plays a part" [1]. Thus, Dr. Azzopardi suggests that the lesion could originate either by the direct (in situ) transformation of the normal cells of the lobule into malignant cells (hypothesis one) or by the displacement (creeping replacement) of pre-existing acinar cells by the malignant population (hypothesis two). Both hypotheses predict that one would observe the earliest changes of this lesion in lobules of normal structure and complexity, but the two proposals differ in one respect: according to the second model, one would observe a juxtaposition of atypical cells and normal cells at the point of displacement, but the first model would not predict the presence of such an abrupt transition. A third hypothesis which Dr. Azzopardi did not mention is that the lesion might represent a growth of new glandular units rather than an alteration of pre-existing lobules (hypothesis three). This model predicts that the earliest atypical cystic lobules would consist of just a few acini populated entirely by atypical cells.

We undertook the following study in the attempt to investigate these three hypotheses and thereby define the pathogenesis of atypical cystic lobules (low-grade clinging carcinoma of flat type). By collecting examples of partially formed atypical cystic lobules and arranging them in a sequence of ever decreasing size, we hoped to identify the earliest steps in the formation of atypical cystic lobules and ultimately the cells from which the lesion arises. We framed our analysis by asking the following questions:

1. Do the earliest recognizable atypical cystic lobules consist of just a few small acini lined entirely by atypical ductal cells, as predicted by hypothesis three above?
2. Can we identify lobules in which at least one acinus shows the features seen in atypical cystic lobules whereas other acini appear unaltered, as predicted by hypotheses one and two?
3. Can we observe the displacement (creeping replacement) of normal acinar cells by atypical ductal cells, as predicted by hypothesis two?

We collected examples of the earliest atypical cystic lobules that we could recognize and made a careful morphological study of their characteristics. We present the results of our observations, answer the questions posed, and speculate on the findings.

Materials and methods

Case selection

While performing routine diagnostic activities, we collected 25 examples of minimal atypical cystic lobules. These were defined as terminal duct-lobular units containing atypical ductal cells characteristic of atypical cystic lobules but not displaying the marked acinar enlargement seen in fully developed examples like that in Fig. 1. Atypical cells appear slightly larger and contain more

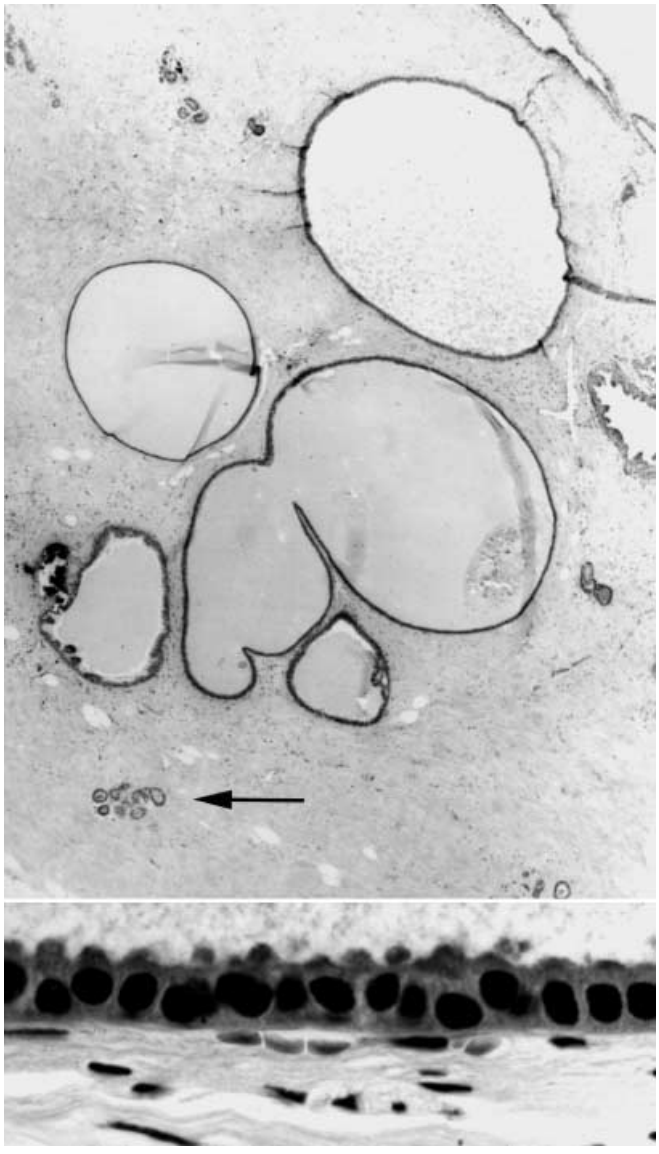
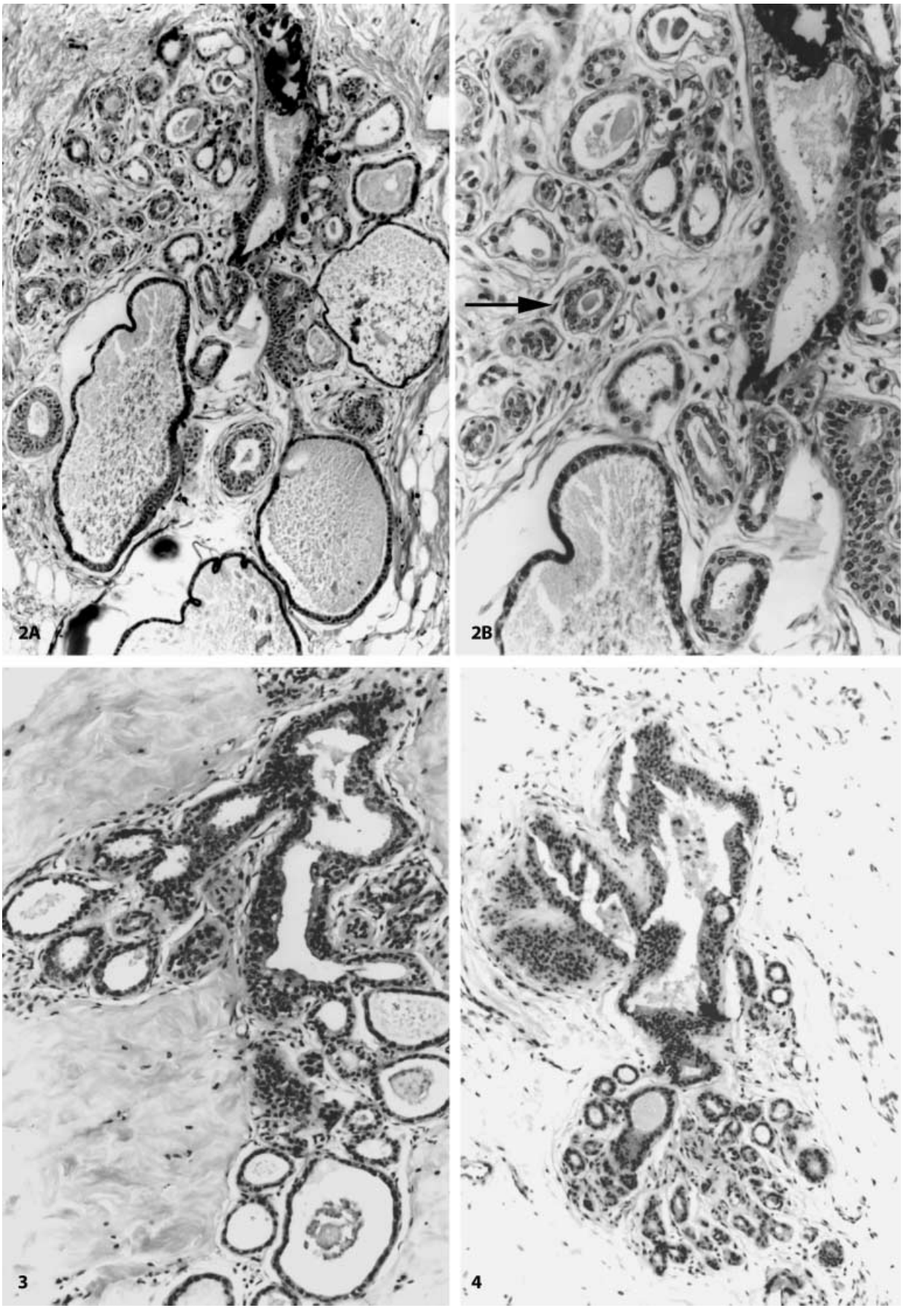


Fig. 1 The acini of this fully developed atypical cystic lobule appear enlarged, and the cells lining them show low-grade cytological atypia (*inset*). *Arrow* marks an uninvolved lobule. ×31, *inset* ×400



Figs. 2–4 Legends see page 526

abundant apical cytoplasm than their normal counterparts. Furthermore, they possess smoothly contoured oval or round nuclei, homogeneous dark chromatin, and inconspicuous nucleoli. We further restricted our study to those minimal atypical cystic lobules in which we could identify the small duct and extralobular terminal ductule adjoining the atypical lobule.

Data collection

After examining H&E-stained tissue sections, we recorded the following information: structural pattern of the lobule (newly formed or pre-existing), appearance of the epithelium (cytological characteristics of the extralobular ducts/terminal ductules, intralobular terminal ductules, and acini), uninvolved acini (present or absent), and the appearance of the transition between altered and unaltered epithelial cells within the lobules and small ducts (gradual or abrupt).

Results

The 25 examples of minimal atypical cystic lobules vary only in the extent of their involvement by the atypical ductal cells and therefore their degree of glandular distension. Figure 2, Fig. 3, and Fig. 4 illustrate typical examples of minimal atypical cystic lobules arranged to demonstrate decreasing degrees of alteration. In Fig. 2, four acini in a single lobule have undergone cystic enlargement and several others appear slightly distended. Figure 3 depicts a small duct and two adjoining lobules in which most acini display a slight degree of enlargement. The focus pictured in Fig. 4 shows involvement of a small duct and minimal distension of a few acini within the adjoining lobules. Despite this variation in extent, the overall pattern of alteration seems constant, and the following seven generalizations apply to most examples:(5, 6, 7, 8, 9)

1. *Luminal cells throughout the terminal duct-lobular unit exhibit nuclear atypicality*. In 22 of the 25 cases studied, all luminal cells of the minimal atypical cystic lobules possess atypical nuclei. Size and shape of the abnormal cells vary according to the degree of proliferation, but nuclear atypicality represents a constant finding. Only in three cases did we observe acini lined by apparently normal epithelial cells. Figure 2 illustrates one such case.
2. *The earliest changes in the acini appear subtle*. Minimally altered acini appear only slightly enlarged and the nuclear atypism of the luminal cells is not obvious (Fig. 5, lower panel). If these acini were encountered in another context, one might either overlook them

◀ **Fig. 2** **A** Four acini of this atypical cystic lobule exhibit prominent enlargement and most of the others show slight distension. Cells of the intralobular terminal ductules exhibit the most extreme changes. ×100. **B** High magnification reveals the columnar shape and atypical nuclei of cells of the terminal ductule. Many small acini appear slightly distended, but that indicated by the *arrow* looks normal. ×200

Fig. 3 Two minimal atypical cystic lobules show only slight enlargement of the acini. The terminal ductule contains crowded, atypical columnar cells. ×125

Fig. 4 A very early atypical cystic lobule. The small duct in the *center* of the field contains atypical columnar cells, and a few acini in the lobule beneath it appear slightly dilated. ×100

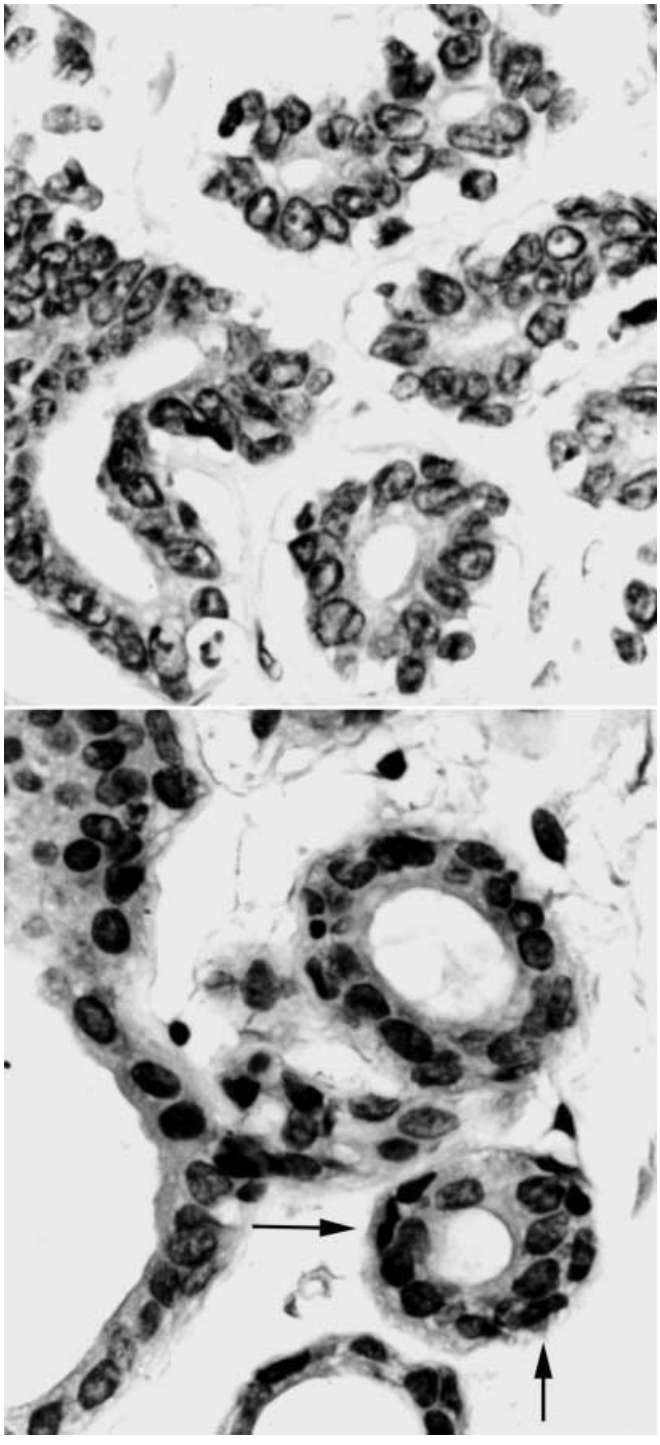
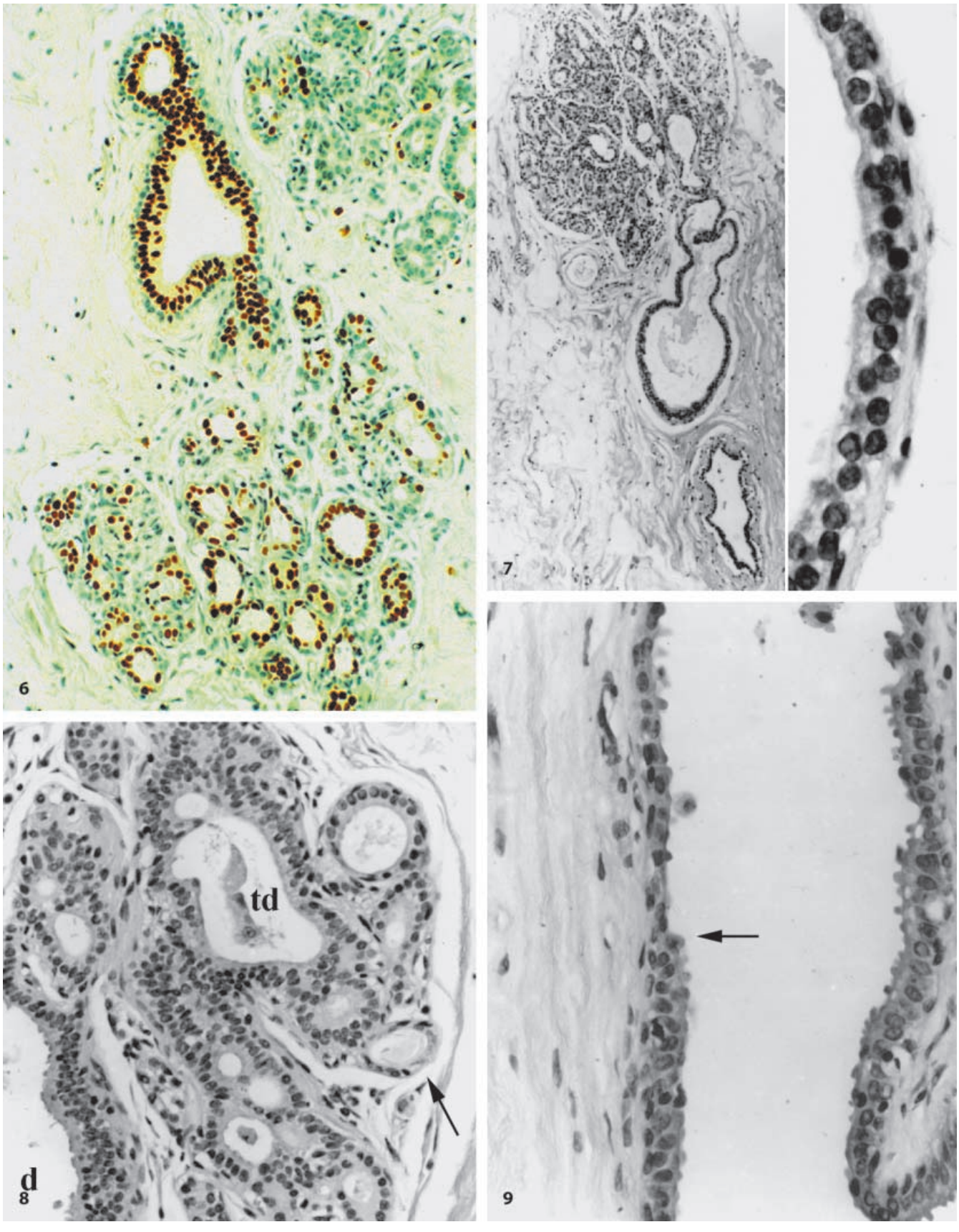


Fig. 5 High magnification of acini from the lobule shown in Fig. 4 and acini from a normal lobule in the same specimen. Those in the former (*lower panel*) show slight distension and minimal cytological atypism when compared with normal acini (*upper panel*). *Arrows* in the lower panel mark myoepithelial cells. ×400



Figs. 6–9 Legends see page 528

entirely or make the diagnosis of early microcyst formation (fibrocystic changes). By comparing the cells of these minimally altered acini with their completely normal counterparts in the same specimen (Fig. 5, upper panel), one can more easily appreciate the nuclear atypicality and slight acinar distension. From this vantage point, one can discern the nuclear hyperchromasia, more homogeneous distribution of the chromatin, and lack of nucleoli. Staining for estrogen or progesterone receptor proteins (Fig. 6) also highlights the abnormal population.

3. *The extralobular and terminal ductules almost always show more obvious changes than the acini*. In most examples of early atypical cystic lobules, the luminal cells of the extralobular terminal ductule appear crowded. The close packing of the cells forces them to assume tall columnar shapes or even to grow in a pseudostratified layer (Fig. 3, Fig. 4). Within the lobule, the cells of the intralobular terminal ductule appear less closely packed and usually have a low columnar shape, and the acinar cell forms range from low columnar through cuboidal to flattened (Fig. 2A, Fig. 3). The acinar cells never look larger, more columnar, or more crowded than the cells of the extralobular ducts.
4. *The cytological changes first become evident in the extralobular ductules.* Figure 7 depicts the earliest stage in the formation of an atypical cystic lobule that we could recognize. One can see that the atypical cells occupy only a short segment of the extralobular ductule and that the nearby terminal duct-lobular units are entirely uninvolved.
5. *Within an affected small duct and terminal duct-lobular unit, the transition from the most altered cells to the least altered takes place gradually.* We could not identify even one example demonstrating atypical cells immediately adjacent to normal luminal cells. Instead, the intralobular epithelium seems to form a continuum. At one extreme, the cells exhibit columnar shapes and crowding and at the other they look cuboid or flattened. Between these two extremes, one appearance gradually and imperceptibly evolves into the other (Fig. 8).
6. *Within the larger duct, the transition from atypical cells to normal cells takes place abruptly.* We found only five examples where we could trace the course of the extralobular ductule as it enlarged and moved toward the nipple. In all five cases, we identified a distinct point at which the population of atypical ductal cells gives way to ductal cells normal in appearance (Fig. 9).
7. *This pattern of morphological change can occur in lobules previously deformed by benign processes.* In two cases, sclerosing adenosis had distorted the underlying architecture of many lobules in the specimens. Several lobules altered in this way also show the changes of early atypical cystic lobules.

◀ **Fig. 6** Immunohistochemical stain for progesterone receptor protein identifies an early stage in the formation of an atypical cystic lobule. Tall columnar cells distend the terminal ductule, and many acini of the adjoining lobule appear slightly dilated. Most of the luminal cells in the small duct and abnormal lobule have progesterone receptors. The acini of a normal lobule in the *upper right corner* do not appear dilated and contain only a few progesterone receptor-positive cells. ×125

Fig. 7 The earliest stage in the formation of an atypical cystic lobule that we could identify. *Left panel*: Atypical ductal cells growing in a single layer distend a short section of a small duct and terminal ductule. The portion of the duct below appears normal. ×50. *Right panel*: The epithelium of the duct shows low grade atypism. ×400

Fig. 8 A minimal atypical cystic lobule showing a continuum of morphological alterations. Cells in the small duct (*d*) show crowding and pseudostratification, those in the intralobular terminal ductule (*td*) have columnar shapes, and certain acini (*arrow*) contain cuboidal or flatted cells. ×200

Fig. 9 Abrupt termination of atypical cells lining a duct. *Arrow* marks the distinct point at which the atypical columnar cells (*below*) abut the normal cuboidal cells (*above*). ×400

Discussion

The results of our study suggest that the formation of atypical cystic lobules (low-grade clinging carcinoma of flat type) begins with the appearance of cytological atypism in the luminal cells of small ducts and terminal duct-lobular units. We acknowledge, however, that these early cytological changes appear subtle and that certain observers might not regard the cells as either abnormal or preneoplastic on purely morphological grounds. Our previously reported immunohistochemical studies [11] and those of Kusama et al. [9] confirm the atypical nature of these subtly atypical cells, and the genetic findings reported by Moinfar et al. [10] reinforce this conclusion even further. The latter authors tested epithelial cells displaying the subtle nuclear atypia that we describe for loss of heterozygosity. Seven of the eight samples showed a loss of heterozygosity at one or more of the eight loci tested, whereas completely normal epithelium from ten women undergoing reduction mammoplasty exhibited no such loss. The authors also studied two cases containing invasive carcinoma, ductal carcinoma in situ, and subtly atypical epithelium. In both cases, the cells of all three components showed inactivation of the same X chromosome, which indicates that the cells of the three lesions constitute a single neoplastic clone. We believe that these molecular studies complement our morphological and immunohistochemical observations and establish the aberrant and neoplastic nature of cells that give rise to atypical cystic lobules.

Our observations lead us to conclude that atypical cystic lobules arise from pre-existing, developmentally normal terminal duct-lobular units. We base this conclusion on four points of similarity between early atypical cystic lobules and normal lobules:

1. The earliest atypical cystic lobules such as those in Fig. 3 and Fig. 4 consist of compact, glandular aggregates clearly demarcated from the surrounding dense

stroma and having the same shape and approximately the same size as normal lobules.
2. The stroma within early atypical cystic lobules shows the cellularity and abundance of myxoid ground substances characteristic of the intralobular, specialized connective tissue of normal lobules.
3. The architectural pattern of the glandular elements of these early atypical lobules recalls the branching pattern of the intralobular terminal ductule and acini of a normal terminal duct-lobular unit.
4. In the most minimally altered acini of an early atypical cystic lobule (Fig. 5, lower panel), one can observe pre-existing myoepithelial cells beneath the atypical luminal cells.

Thus, early atypical cystic lobules display the configuration, stroma, glandular architecture, and cellular components of normal lobules. Moreover, we observed several foci in which early atypical cystic lobules merge with other lobular alterations. Our study group includes two cases in which atypical columnar cells distend terminal duct-lobular units distorted by sclerosing adenosis, and we encountered the same phenomenon in lobules showing blunt duct adenosis and lobular neoplasia. The coexistence of atypical cystic lobules and other lobulocentric lesions reinforces our conclusion that atypical cystic lobules arise by a transformation of pre-existing terminal duct-lobular units.

Although this line of reasoning permits us to reject the hypothesis that atypical cystic lobules represent newly formed glandular units and to regard the atypical cystic lobules as transformed normal lobules, it does not explain how the phenomenon occurs. Like Dr. Azzopardi [1], we believe that the process involves direct transformation of the indigenous lobular cells rather than their displacement (creeping replacement) by the neoplastic population. We prefer the former hypothesis because we never observed a distinct point within a lobule at which atypical cells abut and displace normal acinar cells. We acknowledge that the question remains open for discussion, though, and that the answer requires more compelling evidence than ours.

Since published evidence [5, 9, 10, 11] indicates that atypical cystic lobules represent an early stage in the formation of certain ductal carcinomas and the findings of the current study trace the earliest changes in the formation of atypical cystic lobules to the luminal cells of small ducts, it seems logical to propose that these luminal cells represent the cells of origin of certain low-grade ductal carcinomas. This proposal receives indirect support from studies of rodent breast tissue which reveal that cells in this location differ from the epithelial cells in other parts of the gland in two ways. Firstly, estrogen receptor-positive luminal cells within the small ducts of the mature mouse breast divide only rarely [15]. This kinetic property suggests that these cells might represent either stem cells or closely related primitive cells, which contemporary thinking regards as the likely targets for carcinogenic agents. Secondly, among all the estrogen receptor-positive epithelial cells of the rat breast, only those in the small ducts possess the capacity for estrogen-mediated gene transcription [8]. Cells of the ductal carcinoma cell line MCF-7 also exhibit estrogen-regulated transcription of proteins such as pS2 [2] and c-*myc* [4]. This similarity in cellular physiology suggests a link between these two cell populations. Thus, the unique properties of these cells make them logical candidates as the cells of origin of a group of breast cancers, and the observation that these cells reside within small ducts reinforces the conclusions of our study.

In summary, our findings suggest that the formation of atypical cystic lobules begins with the appearance of cytological atypism in the luminal cells of small ducts and terminal ductules. The cellular alterations appear minimal at first, and one could easily overlook them or dismiss these cells as normal. As the process continues, the cells in the small ducts and terminal ductules become more clearly atypical, and the atypism extends progressively and continuously to involve the luminal cells throughout the lobule. Continued accumulation of atypical cells leads to dilatation of acini, unfolding of the lobule, and creation of the fully developed atypical cystic lobule (low-grade clinging carcinoma of flat type). Stratification of the neoplastic epithelium and the appearance of cribriform spaces or other manifestations of architectural atypism complete the evolution to conventional low-grade ductal carcinoma in situ.

References

1. Azzopardi JG (1979) Problems in breast pathology. In: Bennington JL (ed) Major problems in pathology, vol 11. Saunders, Philadelphia
2. Brown AMC, Jeltsch J-M, Roberts M, Chambon P (1984) Activation of pS2 gene transcription is a primary response to estrogen in the human breast cancer cell line MCF-7. Proc Natl Acad Sci U S A 81:6344–6348
3. DePotter CR, Foschini MP, Schelfhout AM, Schroeter C, Eusebi V (1993) Immunohistochemical study of neu protein overexpression in clinging in-situ duct carcinoma of the breast. Virchows Arch A Pathol Anat 422:375–380
4. Dubik D, Shiu RPC (1988) Transcriptional regulation of c-*myc* oncogene expression by estrogen in hormone-responsive human breast cancer cells. J Biol Chem 263:12705–12708
5. Eusebi V, Feudale E, Foschini MP, Micheli A, Conti A, Riva C, Di Palma S, Rilke F (1994) Long-term follow-up of in situ carcinoma of the breast. Sem Diagn Pathol 11:223–235
6. Fraser JL, Raza S, Chorny K, Connolly JL, Schnitt SJ (1998) Columnar alteration with prominent apical snouts and secretions. A spectrum of changes frequently present in breast biopsies performed for microcalcifications. Am J Surg Pathol 22:1521–1527
7. Goldstein NS, O'Malley BA (1997) Cancerization of small ectatic ducts of the breast by ductal carcinoma in situ cells with apocrine snouts. A lesion associated with tubular carcinoma. Am J Clin Pathol 107:561–566
8. Jeng M-H, Kao C, Sivaraman L, Krnacik S, Chung LWK, Medina D, Conneely OM, O'Malley BW (1998) Reconstitution of estrogen-dependent transcriptional activation of an adenoviral target gene in select regions of the rat mammary gland. Endocrinol 139:2916–2925

9. Kusama R, Fujimori M, Matsuyama I, Fu L, Ishii K, Hama Y, Asanuma K, Shingu K, Kobayashi S, Tsuchiya (2000) Clinicopathological characteristics of atypical cystic duct (ACD) of the breast: assessment of ACD as a precancerous lesion. Pathol Int 50:793–800
10. Moinfar F, Man YG, Brathauer GI, Tavassoli FA (2000) Genetic abnormalities in mammary ductal intraepithelial neoplasia-flat type ("clinging carcinoma in situ"). A simulator of normal mammary epithelium. Cancer 88:2072–2081
11. Oyama T, Maluf H, Koerner F (1999) Atypical cystic lobules. A precursor to low-grade ductal carcinoma in situ. Virchows Archiv Pathol Anat 435:413–421
12. Rosen PP (1997) Rosen's breast pathology. Lippincott-Raven, Philadelphia
13. Tavassoli FA (1992) Pathology of the breast. Appleton Lange, Norwalk
14. Tsuchiya S (1998) Atypical ductal hyperplasia, atypical lobular hyperplasia, and interpretation of a new borderline lesion. Jpn J Cancer Clin 44:548–555
15. Zeps N, Dawkins HJS, Papadimitrou JM, Redmond SL, Walters M-NI (1996) Detection of a population of long-lived cells in mammary epithelium of the mouse. Cell Tissue Res 286:525–536

Virchows Arch (2001) 439:531–539
DOI 10.1007/s004280100434

ORIGINAL ARTICLE

H. Hagedorn · A. Elbertzhagen · I. Ruoss · U. Sauer
A.G. Nerlich

Immunohistochemical analysis of major TGF-β isoforms and their receptors in laryngeal carcinomas

Received: 16 October 2000 / Accepted: 9 February 2001 / Published online: 7 June 2001
© Springer-Verlag 2001

Abstract We analyzed immunohistochemically the tissue distribution of the three major transforming growth factors-β isoforms (TGF-β1,-2,-3) and their receptors (TBR-I, -II and –III) in tissue samples from 38 patients with laryngeal squamous cell carcinomas. Besides a qualitative evaluation, the number of the respectively labeled cells was determined by morphometric analysis. In all tumor samples a significant staining of most tumor cells was seen both for the TGF-β isoforms and the TBRs. Similarly, the majority of stromal cells were labeled. On semiserial sections, there were only minor differences in the distribution pattern and in the number of labeled cells between the three TGF-β isoforms and the TBRs, suggesting that most tumor cells are actively involved in the neosynthesis of TGF-βs and TBRs; accordingly, at least most tumor cells seem to be capable of producing more than one TGF-β form and in parallel several TBRs. With decreasing tumor cell differentiation the number of TGF-β- and TBR-positive tumor cells decreased slightly (but not to a statistically significant degree). Interestingly, the stromal cells were labeled for TGF-βs and TBRs to a lower extent than the epithelial cells, and there was no significant difference between non-tumor-associated control stroma and the immediate peritumoral stroma. Our observations suggest an even, enhanced level of TGF-β production in laryngeal squamous cell carcinomas, which may explain some well-known side-effects of tumor growth, such as stromal desmoplasia. In addition, the presence of immunoreactive TBR-proteins in the vast majority of tumor cells excludes the mere absence of TBRs in those carcinomas as the cause for inappropriate TGF-β function in the tumor cells. This in turn suggests that molecular alterations either of the TBR-proteins non-affecting the synthesis and turnover or downstream alterations of the TGF-β signaling pathway may be main reasons for the loss of response of the tumor cells to the enhanced amounts of TGF-βs.

Keywords TGF-β isoforms · TGF-β receptors · Cell proliferation · Matrix · Formation · Laryngeal cancer

A. Elbertzhagen · I. Ruoss · U. Sauer · A.G. Nerlich (✉)
Institute of Pathology,
Ludwig-Maximilians-Universität München,
Thalkirchnerstrasse 36, 80337 München, Germany
e-mail: Andreas.Nerlich@lrz.uni-muenchen.de
Tel.: +49-89-51604011, Fax: +49-89-51604014

H. Hagedorn
Department of Otolaryngology, Head and Neck Surgery,
University of Munich, Grosshadern Medical Center,
Marchioninistrasse 15, 81377 Munich, Germany

Introduction

Cancer is considered a multi-stage process promoted by nonlethal genetic damage. The main targets, therefore, are the proto-oncogenes which promote growth and proliferation of tumor cells, the inhibiting tumor suppressor genes, and genes controlling cellular apoptosis. Molecular alterations may cause an inappropriate synthesis of the structurally normal growth promoting or inhibiting peptides.

Recent studies have provided clear evidence that regulatory pathways by certain cytokines may directly be involved in carcinogenesis and tumor progression. This holds particularly true for transforming growth factor-β (TGF-β), which is assumed to be associated with one of the most potent tumor suppressing pathways [14].

TGF-β is a family of multifunctional regulatory peptides involved in the control of cell growth and differentiation, morphogenesis, and the remodeling of connective tissues [16, 19, 26]. Up to now, five isoforms of TGF-β have been discovered, although only three isoforms have as yet been identified in mammals. All three isoforms are structurally made up by a 25-kDa homodimer which is composed of two 12.5-kDa biologically active subunits linked by disulfide bonds [3]. All three TGF-β isoforms show a high level of sequence conservation: thus β1/β2 share 74% amino acid identity, β2/β3 82% and β1/β3 78% [17].

TGF-β1 is the most abundant representative. This multifunctional cytokine acts as one of the most potent

inhibitors of cellular replication, suppressing epithelial and vascular smooth muscle cell proliferation by stopping the cell cycle progression from the G1 into the S-phase. Antiproliferative activity is also known for T- and B-lymphocytes, leading to the significant immunosuppressive effects of this cytokine [13, 25]. In contrast, few mesenchymal cell types, such as fibroblasts and articular chondrocytes, show a stimulation of cell replication under the influence of TGF-β1 [15, 29]. Besides many other biological effects, TGF-β1 promotes the neosynthesis and secretion of extracellular matrix proteins, such as collagen III, IV, V and tenascin. By decreasing the synthesis of matrix-degrading enzymes, such as matrix metalloproteinases, the anabolic effect on the extracellular matrix is further increased [17]. TGF-β2 and TGF-β3 do not differ from TGF-β1 in eliciting these different effects, but are spatially and temporally distributed in a different way.

To elicit its effect, TGF-β has to bind to specific trans-membrane receptors [19]. Three major TGF-β receptors (TBR) have been identified so far. TBR I and II are both serine/threonine kinases and appear to be the predominant receptors for the TGF-β signal transduction. TBR III, in contrast, seems not to be directly involved in signal transduction but promotes the presentation in particular of TGF-β2 to TBR II [17]. Binding of either ligand to TBR II at the cell surface results in recruitment of the TBR I into a complex which is subsequently trans-phosphorylated [30].

Since TGF-β plays a key role in controlling epithelial cell proliferation and differentiation, more and more recent studies have focused on the role of TGF-β in malignant tumors. In breast cancer, an upregulation of TGF-β1 protein expression has recently been reported by our own group using molecular morphological investigation [23]. This is well in line with several other studies, e.g., showing that TGF-β has a growth inhibitory effect on tumor cells in colon carcinoma [12].

In parallel, recently published results of our own study demonstrated that invasive laryngeal carcinomas show an increased expression of TGF-β1 mRNA and protein when compared to the normal mucosa [11]. This study also showed that the typical features of enhanced matrix protein production seen under the influence of TGF-β were present in those tumors. In clear contrast to this TGF-β effect, the typical suppression of epithelial cell proliferation by TGF-β was lacking in the tumor cell pool [11]. This dissociation of presumed TGF-β effects may result from a failure of the tumor cells to respond properly to TGF-β while stromal cells seem to have the system maintained. Since the TGF-βs bind to the cell membrane receptors TBR I-III, either a loss of TBR-expression or molecular defects within the receptors at the tumor cell surface may explain the loss of the antiproliferative effect in tumor cells. Certain mutations leading to molecular defects of TBR have previously been described in colorectal carcinomas [18]. Such data are, as yet, scarce for squamous cell carcinomas (SCC) and have been described only in cell lines [10]. Besides these molecular analyses, few reports have investigated the presence/absence of TBRs in SCCs. Thus, Eisma et al. [6] described a complete loss of TBR II in invasive SCC, while Muro-Cacho et al. [20] found a decrease in TBR II expression in poorly differentiated SCC, but without loss of expression of TBR I.

Up to now, no study has been conducted in which the expression of major TGF-βs in parallel to that of the three TBRs in laryngeal carcinomas has been analyzed. We therefore designed the present immunohistochemical study to find out whether significant differences exist in the expression of TGF-β isoforms and that of TBRs in laryngeal cancer.

Material and methods

Study population

The present series was conducted on 38 well-defined cases with laryngeal SCC. Four patients were women, 34 patients were men, and the patient age ranged between 30 and 81 years (mean 59.6±28.4 years). As a common risk factor, all patients had been heavy cigarette smokers for many years.

Five of the SCC were located in the supraglottis, 14 carcinomas were in the glottic area, one tumor was in the subglottic region, and the remaining tumors affected all three laryngeal subsites. The analyzed tumors were mainly large carcinomas (26×T4, 6×T3, 4×T2, and 2×T1) and in only 12 cases was no lymphatic metastasis found. Histopathologically, the degree of tumor cell differentiation revealed in one case a highly differentiated carcinoma, while 14 tumors were classified as moderately differentiated and 23 cases showed poor tumor cell differentiation. The clinical follow-up of the patients ranged between 26 and 48 months. During this period 18 patients died, and their deaths were due to causes related to laryngeal cancer.

From all patients, both tumor and morphologically normal tissue specimens were obtained during surgical treatment of the SCC of the larynx, mostly by laryngectomy. In addition, we analyzed five cases of normal laryngeal mucosa, which served as a control group. These specimens were obtained during routine autopsies performed within 6–10 h after death. Control cases had no anamnesis of significant nicotine or alcohol abuse, the specimens showed a normal histomorphological structure.

All tumor biopsies as well as the tissue samples of the normal laryngeal mucosa were fixed in 4–6% buffered formalin and embedded in paraffin wax for routine diagnostic examination and the subsequent immunohistochemical investigation.

Immunhistochemical analysis (IHC)

For the immunostaining, the tissue sections were deparaffinized in descending concentrations of alcohol and subsequently enzymatically pretreated using 0.1% pronase, as previously described [21] for the enhancement of the immunostaining. Following the application of the monospecific primary antibodies and several washing steps, the antigen-antibody complex was linked to a secondary antibody system coupled with the avidin-biotin system (ABC-complex method, [5]; Vector, Burlingame, Calif., USA). The reaction product was subsequently visualized by chromogene substances (diaminobenzidine; Sigma Chem., Deisenhofen, Germany).

For the present study, we used commercially available monospecific polyclonal antibodies against TGF-β1/-β2/-β3 as well as against the receptor proteins TBR -I/ -II/ -III (all primary antibodies: Santa Cruz Inc., Santa Cruz, Calif., USA). The reaction specificity had earlier been tested by the manufacturer by Western blot-

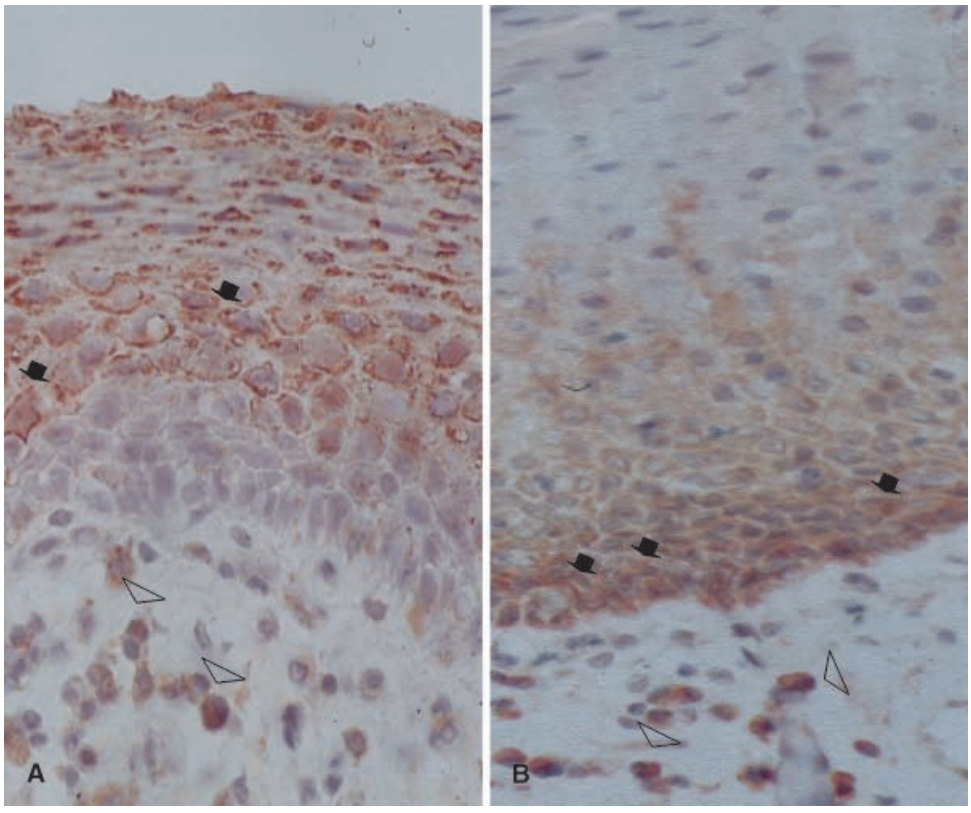


Fig. 1A,B Immunolocalization of TGF-β1 and TBR II in normal laryngeal squamous mucosa. **A** The immunostaining for TGF-β1 shows a labeling of most suprabasally located epithelial cells (*full arrows*). Note the positive labeling of stromal cells (*open arrows*). (Original magnification: ×250) **B** TBR-II is seen exclusively in the basal layers of the normal mucosa with a pericellularly accentuated staining pattern as expected for the receptor (*full arrows*). Please also note that there is also a positive staining for several stromal and endothelial cells (*opened arrows*).(Original magnification: ×200)

ting. In addition, the specificity was tested by control experiments using isotype controls which all yielded negative results.

Morphometric evaluation

All immunostainings were first qualitatively evaluated by light microscopy. Following this assessment of staining quality and distribution, a quantitative morphometric analysis was performed. Therefore, each of the five random fields (the size of each: 0.192 mm^2) covering either tumor or peritumoral stromal areas was counted for the number of positively labeled tumor cells/stromal cells per the total number of tumor/stromal cells, thereby producing the result that, for each specimen, at least 3,500 tumor cells and at least 2,000 stromal cells were evaluated. As a control, a similar analysis was made upon normal epithelia and stroma areas distant from the tumor zone. Furthermore, in each tumor area the degree of tumor cell differentiation was evaluated by use of histopathological criteria. For further analysis, this individual grading of the tumor cell differentiation was then correlated with the number of positively labeled cells. The analysis was performed by two independent observers (H.H. and A.E.), the intra- and inter-observer variability was acceptably low (less than 10%).

Statistical evaluation

In a second step, we correlated the immunohistochemical data with histological parameters, such as the tumor grading (see above), the mode of tumor cell infiltration – as distinguished between finger-like and pushing-border-like infiltration – and clinical prognostic parameters like the tumor stage referring to the TNM classification (UCIC 2000), the occurrence of metastases (both locoregional metastases to lymph nodes and distant hematogenous metastases) and the local tumor recurrence, using the SPSS statistics program and Wilcoxon's test, the Mann-Whitney U test, as well as the Kruskal-Wallis H test, with a level of significance of $P<0.05$ being regarded as statistically significant.

Furthermore, the patterns of overall survival were determined according to the Kaplan-Meier method, and their statistical differences were analyzed by the generalized Wilcoxon's test.

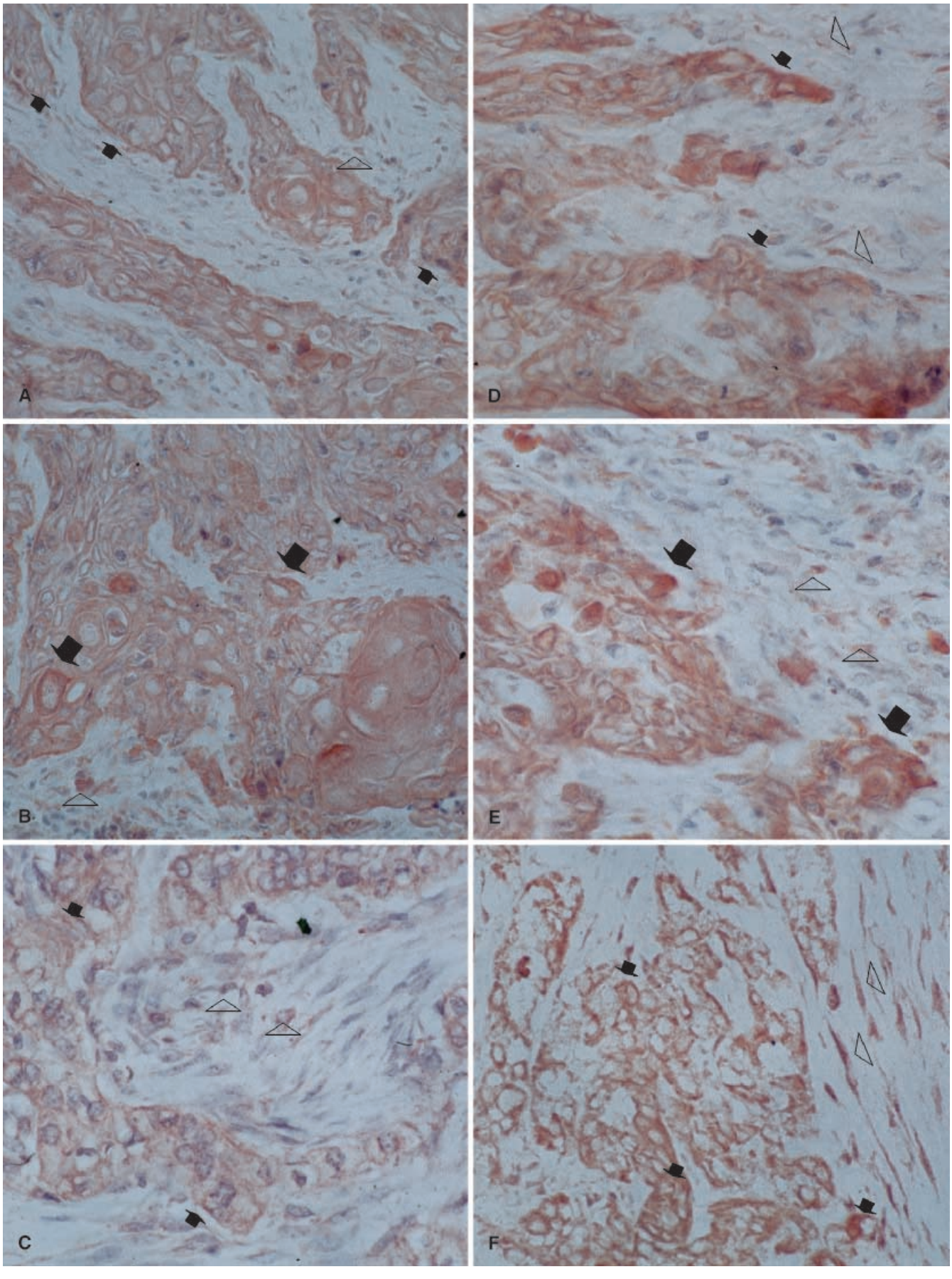
Results

Immunohistochemical distribution of TGF-β isoforms and TBRs in normal laryngeal tissue

Immunohistochemically, all TGF-β isoforms are detected in the suprabasal layer of the normal epithelial cells, occasionally and faintly in the smooth muscle cells of the blood vessels, and also faintly in the normal stroma cells (Fig. 1 A). In these normal tissue samples, we observed no major differences in either the staining pattern or intensity between all three TGF-β isoforms.

A positive signal for all three receptors, TBR I/-II and –III, was also seen in the epithelium of the normal laryngeal mucosa – with a strong expression in the basal and middle epithelial layers and no expression in the upper layer (Fig. 1B). There was also a distinct staining of various stroma cells, such as fibroblasts and endothelial cells, but also of immune effector cells, such as the few lymphocytes and plasma cells seen in the stroma.

The morphometric quantitation confirmed these qualitative observations. Thus, TGF-β1 was detectable in 47.2% (±28%) of the normal epithelial cells, TGF-β2 was seen in 42.5% (±23%) of the epithelia, and TGF-β3 was present in 65.0% (±17%) of all normal epithelial cells. For the stroma cells, we observed for TGF-β1 51%


A
D
B
E
C
F

(±19%), for TGF-β2 57 (±21%), and for TGF-β3 67% (±14%) positively stained cells (all data± SD).

Similar data could be determined for the TBRs. The quantitative analysis, however, revealed more positively labeled epithelial cell than seen for the TGF-β isoforms (TBR-I 68.7% (±16%), TBR-II 72.7% (±20%), TBR-III 55.6% (±17%). The quantitative analysis of the stroma cells demonstrated for TBR-I 65% (±27%) positively labeled cells, for TBR-II 62%(±23%), and for TBR-III 54%(±23%).

Distribution and frequency of TGF-β positive cells in laryngeal carcinomas

In all tumors analyzed, we detected a positive cytoplasmatic staining for the various TGF-β isoforms in both the tumor cells and in adjacent stroma cells (fibroblasts, fibrohistocytes, and endothelial cells). We did not find any significant extracellular staining either along the basement membranes or within the interstitial matrix stroma. The staining was significantly more intense in the tumor cells than in the adjacent stroma cells. This pattern was similar for all three TGF-β isoforms analyzed (Fig. 2 A,B,C). Using semiserial sections, we identified similar distribution patterns for all three TGF-β isoforms tested suggesting the expression of more than one form of this cytokine in the respective cells.

The qualitative observations were confirmed by the morphometric estimation. Thereby, 82.4% (±18%) of the tumor cells were positively stained for TGF-β1, 75.2% (±24%) were positively labeled for TGF-β2, and 83.8% (±19%) cells showed a positive signal for TGF-β3.

For the stromal cells, we observed for TGF-β1 a mean value of positive cells of 54.2% (±21%), for TGF-β2 a mean value of 59.1% (±20%), and for TGF-β3 a value of 65.3% (±23%). Thereby, we observed only minor differences between the quantitative analysis of the stroma cells in the normal tissue and adjacent to laryngeal carcinoma cells (Fig. 3 A,B).

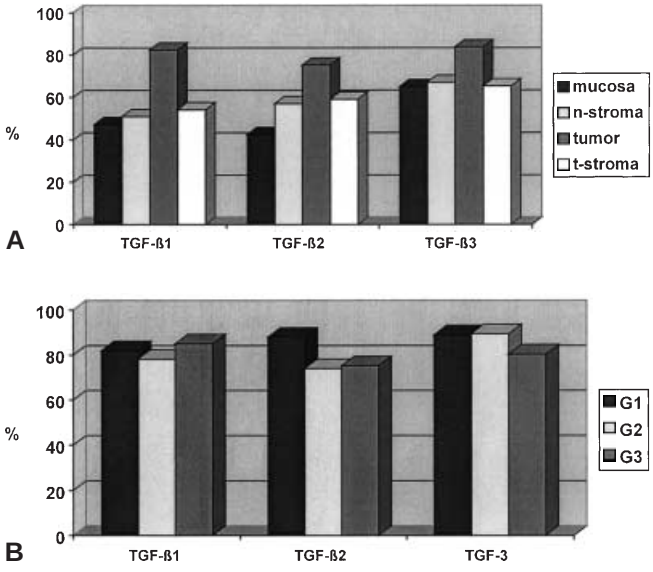


Fig. 3A,B Morphometric evaluation of TGF-β isoforms in laryngeal SCCs. **A** The number (%) of positive normal epithelial (*mucosa*) and stroma (*n-stroma*) cells as well as tumor (*tumor*) and peritumoral stroma (*t-stroma*) cells for TGF-β 1–3 shows an increase in labeled cells in the tumor cell compartment. **B** Expression profile of TGF-β isoforms in tumors of different degrees of tumor cell differentiation, indicating the percentage of positively labeled tumor cells (Degrees of differentiation: *G1* Good, *G2* Moderate, *G3* Poor)

Distribution and frequency of TBR I/ -II and –III in laryngeal carcinomas

As seen for the TGF-β isoforms, we observed in all cases of laryngeal carcinoma a positive staining for the TBRs, again in both the tumor and the stroma cells (Fig. 2 D–F). The staining pattern of those cells revealed an enhanced staining of the cell surface, confirming the expected receptor site. However, there was an additional cytoplasmic staining which was of reduced intensity when compared to the cell surface. There was no preferential expression of TBR-positive tumor cells at any subsite of the tumors, such as the tumor center or the tumor–stroma interface. As seen for the TGF-βs, we observed an obviously increased expression of TBRs in the invasive laryngeal carcinomas when compared to the normal mucosa or the peritumoral stroma cells.

Using semiserial consecutive sections of the tumor samples, we also found a major overlap of labeled cells for the various TBRs and those positive for the TGF-β isoforms, suggesting that the TGF-β-producing cells also contained the corresponding TBRs.

By quantitative morphometric analysis, 82.7% (±19%) of the tumor cells were positive for TBR-I. TBR-II was positively stained in 85.0% (±17%) of all tumor cells, and for TBR-III a mean value of 75.4% (±25%) labeled tumor cells was estimated.

◀ **Fig. 2A–F** Expression of TGF-β isoforms (types 1–3) and TBR I-III in laryngeal squamous cell carcinomas. **A** In invasive SCCs most tumor cells are positively labeled for TGF-β1 (*black arrows*); in addition, several adjacent stroma cells (*opened arrows*) are also specifically stained. (Original magnification:×200). **B** A corresponding area from a moderately differentiated laryngeal carcinoma reveals also for TGF-β2 an extensive labeling of tumor cells (*black arrows*), but also for the stromal cells (*opened arrows*). (Original magnification:×200) **C** Immunohistochemically, TGF-β3 shows also a positive staining of most tumor cells (*black arrows*) as well as for stroma cells (*opened arrows*). (Original magnification: ×200). **D** The TGF-β receptor TBR I is seen in almost all tumor cells of the invasive SCC (*black arrows*) with an accentuated membrane staining. However, several stroma cells are also positively stained for TBR I (*opened arrows*). (Original magnification: ×200). **E** The immunohistochemical staining of TBR II reveals a similar staining pattern as for TBR I, suggesting a parallel expression of both receptors, in the tumor cells (*black arrows*) and the stroma cells (*opened arrows*). (Original magnification: ×200). **F** Also for TBR III, we observed a specific pericellularly accentuated staining for most tumor cells (*black arrows*) and for several stroma cells (*opened arrows*). (Original magnification: ×200)

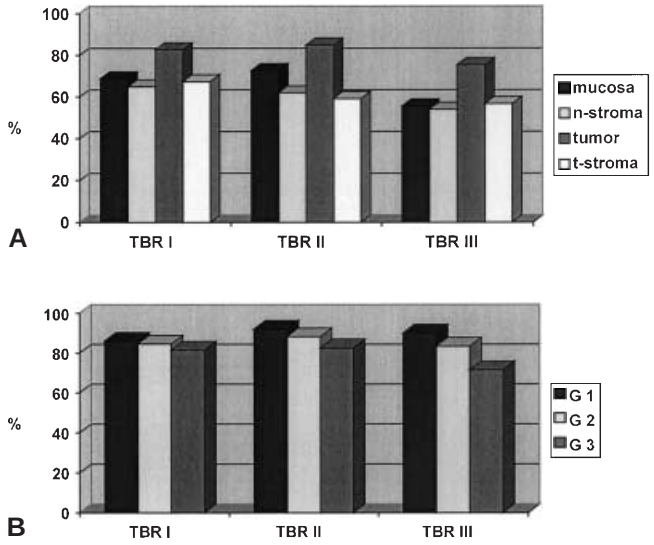


Fig. 4 Morphometric evaluation of the expression of TBRs in laryngeal SCCs. **A** Number of positively labeled cells (%) for the different TGF-β receptors (TBR I-III) in the normal tissue (*mucosa* and *n-stroma*) and in invasive laryngeal carcinomas (*tumor* and *t-stroma*). **B** Morphometric results of labeled cells (%) for TBR I-III in SCCs when compared to different degrees of tumor cell differentiation

The increased frequency of TBR-positive tumor cells was not statistically significantly correlated with the histological grade of tumor cell differentiation. However, we found a decrease in the TBR I/-II and -III expression with a decrease in the tumor cell differentiation. The strongest decrease in the level of TBR expression was found for TBR III and II.

The analysis of the receptors in the peritumoral stroma cell compartment revealed for TBR-I a mean value of 67.4% (±23%) positively stained stroma cells. TBR-II was seen in a lesser frequency, with a mean value of 59.2% (±27%), and for TBR-III an even lower mean value was to be recorded (56.8±25%). Thus, there were again only minor differences in the fraction of labeled stromal cells between normal and peritumoral stroma as seen for the TGF-βs (Fig. 4 A,B).

Statistical correlation between TGF-β isoforms and TBRs

In the next step, we analyzed the statistical association between the amounts of TGF-β and TBR positive tumor and stroma cells. We thus observed a significant correlation between the immunohistochemical expression of the TGF-β isoforms only between TGF-β2 and TGF-β3 (*P*-value 0.006 C: 0.456; Mann-Whitney U test). All other associations, such as TGF-β1 versus TGF-β2 etc., did not provide statistically significant correlations.

In contrast, a statistical correlation between the three TBRs in the tumor cell fraction yielded positive associations between TBR I and TBR II as well as between TBR I and TBR III. Thus, a high level of TBR I-labeled tumor cells was significantly associated with a high number of TBR II-expressing cells (*P*-value: 0.027 C: 0.404; Mann-Whitney U test). Similarly, a high number of positive tumor cells for TBR III correlated positively with that of TBR I (*P*-value: 0.004 C: 0.468; Mann-Whitney U test). However, the expression of TBR II and TBR III was not significantly correlated (*P*-value: 0.169 C: 0.263 Mann-Whitney U test).

The stromal cells adjacent to the tumor revealed a similar significant correlation between all analyzed receptor types (TBR I/II *P*-value; 0.06 C: 0.210; TBR I/III *P*-value: 0.023 C: 0.268 and TBR II/III *P*-value: 0.013 C: 0.428 Mann-Whitney U test). These observations indicate a very similar expression of the different receptor types in the tumor and the stroma compartment of laryngeal carcinomas.

Statistical evaluation of prognostic parameters and TGF-β/TBR expression

Finally, we also correlated the expression of TGF-βs and TBRs with major, well-known prognostic parameters, such as the tumor stage, the rate of tumor recurrence and the occurrence of lymphogenic or haematogenic metastases. There was no statistical association between the expression of TGF-βs and TBRs in tumor cells and the prognostic factors. However, there was a significant correlation between a decreased amount of TGF-β2 in stroma cells and the presence of locoregional lymph node metastases (*P*-value 0.019 C: 0.417, Kruskal-Wallis H test). A similar correlation was seen in the tumor recurrence (*P*-value 0.034 C: 0.308, Kruskal-Wallis H test).Furthermore, an increased amount of TBR-I in the stroma cells was significantly associated with the tumor recurrence (*P*-value 0.014 C: 0.336, Kruskal-Wallis H test).

Discussion

In malignant tumoral growth the proper control of cellular proliferation and decay seems to be dramatically out of balance. Since the cytokines of the TGF-β family are involved as major regulating factors in those processes, recent considerable interest has focused on the impact of TGF-β and its pathway during carcinogenesis and tumor progression. In this regard, it is of particular interest that TGF-β is one of the most potent inhibitors of epithelial cellular proliferation; this it achieves by stopping the cell cycle progression from the G1- into the S-phase [14]. TGF-β exerts its antiproliferative effect through specific cellular receptors, the TBRs. Three major receptors have been identified so far: TBR-I and -II appear to be the predominant receptors for TGF-β signal transduction. The receptor type III (TBR-III) seems not to be directly involved in signal transduction but promotes the presentation of ligand to TBR-II [14].

Our own previous analyses provided evidence for a major upregulation of the expression of TGF-β1 protein,

as well as for the TGF-β1-mRNA in invasive laryngeal carcinomas [11]. This increase in TGF-β1 deposition and neosynthesis affected both the carcinoma cells and the stroma cells, although the labeled tumor cells clearly outnumbered the positively stained stromal cells [11]. These results are in agreement with previous findings in other carcinoma types, such as breast carcinomas, where the increased TGF-β1 expression was also mainly found in the tumor cells, and to a lesser extent in the stroma cells [22]. Similarly, in ovarian carcinomas an overexpression of TGF-β1 and TGF-β3 was seen in the tumor cells [4] and an increased expression of TGF-β2 has been described for pancreatic cancer, glioblastomas, and melanomas. In these cases, the increased amount of TGF-β2 was associated with the progression of the disease [1, 7, 8].

The molecular mechanisms by which the obviously enhanced TGF-β expression failed to exert its strong antiproliferative effect are as yet not completely understood. However, there is growing evidence that molecular alterations of the TGF-β receptors and/or downstream signaling factors may play a pivotal role. Particularly the role of TBR-II has been highlighted, since several observations suggest that TBR-II expression is decreased due to mutations in the TBR-II-gene, such as it has been shown from colorectal cancer [18]. The failure to synthesize an intact TBR-II results in the resistance of the tumor cells to the antiproliferative effect of TGF-β [9, 27, 28]. Similar data as for colorectal carcinomas exist for gastric cancer [24]; however, far less is known for SCCs of the head and neck and, in particular, for laryngeal carcinomas. Garrigue-Antar et al. [10] observed in cell lines from head and neck carcinomas a deficiency in the antiproliferative effect of TGF-β on tumor cells and suggested either the complete loss of the receptor or the presence of mutations in the coding region, leading to inactivation of the kinase activity. However, conflicting data exist concerning the presence of the TGF-β receptors and the interaction between the TGF-β isoforms and these receptors in vivo. Recently, Eisma et al. [6] reported on a complete loss of TBR II expression in invasive SCC, while another group observed, even in poorly differentiated tumor areas close to the luminal surface, a positive staining for TBR II [20]. Accordingly, the data on presence/absence or the reduction of the expression of TBRs in SCCs are still unclear. Since this question, however, seems to be crucial for the understanding of the pathofunction of TBR in SCCs during tumor progression, we designed the present analysis on the immunomorphological expression of the most significant TGF-β isoforms and in parallel with their receptors TBR I-III in a series of laryngeal carcinomas.

In accordance with our previous study [11], we found immunohistochemically in the present analysis a significant increase in the staining for the various TGF-β isoforms in the invasive tumor cells when compared to normal mucosa. Interestingly, there was no evidence of significant differences between the three TGF-β isotypes tested and semi-serial sections suggest that the TGF-β isoforms are synthesized, at least in part, by the same tumor cells. These observations indicate that the tumor cells – and of course the adjacent stromal cells – are obviously able to produce TGF-β in a quantity that should be sufficient to execute typical effects. Indeed, those effects typically induced by TGF-β have at least partly been observed in laryngeal SCCs. In particular, the enhanced neoformation of extracellular matrix components in the peritumoral stroma ("desmoplasia") has been monitored by the increased deposition of tenascin and collagen type III [11]. This may be explained by a proper function of stromal cells which may have been stimulated by the TGF-β to produce enhanced amounts of matrix material.

The observation of enhanced amounts of TGF-β is also consistent with previous biochemical findings in laryngeal carcinomas where an increased amount of TGF-β protein has been recorded [6]. However, in that study the immunohistochemical analysis of TGF-β localization revealed only an extracellular deposition of TGF-β, which is at variance with our observations. It remains unclear at present whether the different antibodies used may explain this difference, although our commercially available antibody provided specific reaction products as indicated by the manufacturer and our own tests. Finally, it is noteworthy that we observed a smaller number of TGF-β-producing cells with decreasing tumor cell differentiation, indicating that the loss of tumor cell differentiation may influence the capability of tumor cells to produce TGF-β isoforms.

A further interesting findings was that the number of TGF-β-positive stromal cells was only slightly different between normal stroma areas (which have been obtained significantly distant from the tumor or from controls without any tumoral process) and the peritumoral stroma zone. A similar observation could be made for the various TBRs tested. These findings suggest that the presence of a tumor does obviously alter the number of positive stromal cells only to a minor extent.

In addition to the TGF-β isoforms, we observed immunohistochemically TBR protein of all three TGF-β receptors in the majority of tumor cells, as well as in most stromal cells. Again, our analysis of semiserial sections provided evidence that all three TBRs are expressed at least in part by the same tumor cells. Therefore, we do not have any evidence that there may be a complete or near-complete loss of any of the TBRs.

In this regard, only very few previous studies have dealt with the presence/absence of TBRs in SCC of the head and neck and have provided differing results. Likewise, Eisma et al. [6] observed a specific expression for TBR-I in only seven out of 47 cases, and an expression of TBR-II in only four out of 43 cases. These observations are clearly in contrast to our findings, in which we observed the expression of both TBRs in most cases of laryngeal SCC. In the study by Muro-Cacho et al. [20] a reduced, present expression of TBR-II was recorded, albeit in well and moderately differentiated carcinomas, and Anderson et al. [2] observed in SCCs of the head

and neck in ten cases a positive reaction, as we have seen in our own study. Interestingly, both Muro-Cacho et al. [20] and Anderson et al. [2] agree with our analysis that the staining was not only membranous but also intracellular, suggesting that stored receptor protein may be detected by this approach. Also in line with the previous analysis by Muro-Cacho et al. [20], we found a positive correlation between a decrease in TBR-expression and the degree of tumor cell differentiation, although not on a statistically significant level.

To date, there has been no study on the expression of TBR III in SCC. As was seen for the other receptors, TBR-III was found extensively in both the stroma and the tumor cells of the invasive laryngeal carcinomas. As also seen for the other receptors, the number of labeled tumor cells was negatively correlated with the degree of tumor cell differentiation.

In a further step, we correlated the expression pattern of TGF-β isoforms and TBRs with clinical prognostic factors such as the tumor stage, tumor recurrence or lymph node metastasis. Interestingly, this statistical analysis did not reveal any statistically significant correlation between the expression pattern for TGF-βs or TBRs in tumor cells and the clinical outcome. However, it was surprising to note that the stroma compartment provided a statistically significant correlation between prognostic parameters and a decreased number of TGF-β2 positive stroma cells. In addition, the increased number of TBR-I stained stroma cells was significantly associated with tumor recurrence and the development of cervical lymph node metastasis. Since we observed only minor differences in the number of positive stromal cells in normal (control) tissue and peritumoral stroma, the significance of this statistical association remains unclear. It may, however, be speculated that even minor alterations in the stroma cell compartment may have a major impact on the spread of the tumor cells. Further analyses on this aspect are required in order to clarify this issue in a larger study group.

In summary, we describe here the immunolocalization of the most important TGF-β isoforms and their receptors in a series of laryngeal carcinomas. We thereby provide clear evidence that both tumor and stromal cells show an even enhanced staining for the three TGF-βs tested. In parallel, we also demonstrate that the majority of tumor cells retain the ability to produce immunoreactive TBRs, although we cannot speculate on the function of the TBR-proteins synthesized. In this regard, it cannot be excluded that any defective receptor protein is retained within the cytoplasm of the cells, although a comparable staining pattern of surrounding stromal cells suggests even more that this staining pattern is not automatically indicative of any defective protein structure. Therefore, subsequent molecular studies on the molecular structure and sequence of TBRs are required in order to identify or rule out any defect of those proteins in laryngeal SCCs.

Acknowledgements This study was supported by a grant from the Wilhelm-Sander-Stiftung (# 95.017.02).

References

1. Albino AP, Davis BM, Nanus DM (1991) Induction of growth factors RNA expression in human malignant melanomas: marker of transformation. Cancer Res 51:4815–4820
2. Anderson M, Muro-Cacho BS, Cordero J, Livingston S, Munoz-Antonia T (1999) Transforming growth factor β receptors in verrucous and squamous cell carcinomas. Arch Otolaryngol Head Neck Surg. 125:849–854
3. Assoian RK, Komoriya A, Meyer CA, Miller DM, Sporn MB (1983) Transforming growth factor-beta in human platelets. Identification of a major storage site, purification and characterization. J Biol Chem 258:7155–7160
4. Bristow R, Baldwin RL, Yamada D, Korc M, Karlan B (1999) Altered expression of transforming growth factor-β ligands and receptors in primary and recurrent ovarian carcinoma. Cancer 85:658–668
5. Cordell FB, Erber WN, Ghosh AH, Abdulaziz Z, MacDonald S, Pulford AF, Stein H, Mason DY (1984) Immunoenzymatic labeling of monoclonal antibodies using immune complex of alkaline phosphatase and monoclonal anti-alkaline phosphatase. J Histochem Cytochem 32:219–225
6. Eisma RJ, Spiro JD, Biberstein SE, Linquist R, Kreutzer D (1996) Decreased expression of TGF-β receptors on head and neck squamous cell carcinoma tumor cells. Am J Surg 101: 641–645
7. Friess H, Yamanaka Y, Buchler M, Ebert M, Beger HG, Gold LI, Kore M (1983) Enhanced expression of transforming growth factor β isoforms in pancreatic cancer correlates with decreased survival. Gastroenterology 105:1846–1856
8. Fontana A, Bodmer S, Frei K, Malipiero U, Siepl C (1991) Expression of TGF-β2 in human glioblastoma; a role in resistance to immune rejection. Ciba Found Symp 157:232–241
9. Grady WM, Rajput A, Myeroff L, Liu DF, Kwon K, Willis J, Markowitz S (1998) Mutations of the type II transforming growth factor-beta is coincident with the transformation of human colon adenomas to malignant carcinomas. Cancer Res 58:3101–3104
10. Garrigue-Antar L, Munoz-Antonia T, Antonio S, Gesmonde J, Vellucci VF, Reiss M (1995) Missense mutations of the transforming growth factor β type II receptor in human head and neck squamous cell carcinoma cells. Cancer Res 15:3982–3987
11. Hagedorn H, Sauer U, Schleicher E, Nerlich A (1999) Expression of TGF-β1 protein and mRNA and the effect on the tissue remodeling in laryngeal carcinoma. Anticancer Res 19:4265–4272
12. Hoosein NM, McKnight MK, Levine AE, Mulder KM, Childress FF, Brattain DE (1989) Differential sensitivity of subclasses of human colon carcinoma cell lines to the growth inhibitory effects of transforming growth factor –β1. Exp Cell Res 181:442–453
13. Kataoka R, Sherlock J, Lanier SM (1993) Signaling events initiated by transforming growth factor-beta 1 that require Gi alpha 1. J Biol Chem 268:19851–19857
14. Kelly DL, Rizzino A (1999) Growth regulatory factors and carcinogenesis: the roles played by transforming growth factor β, its receptors and signaling pathways. Anticancer Res 19: 4791–4808
15. Kim TA, Cutry AF, Kinniburgh AJ, Wenner CE (1993) Transforming growth factor beta 1-induced delay of cell cycle progression and its association with growth-related gene expression in mouse fibroblasts. Cancer Lett 71:125–132
16. Kingsley DM (1994) The TGF-β superfamily: new members, new receptors and new genetic tests of function in different organisms. Genes Dev 8:133–146
17. Lawrence DA (1996) Transforming growth factor-β: a general review. Eur Cytokine Netw 7:363–374

18. Lu SL, Akiyama Y, Nagasaki H, Nomizu T, Ikeda E, Baba S, Ushio K, Iwama T, Maruyama K, Yuasa Y (1996) Loss or somatic mutations of hMSH2 occur in hereditary nonpolyposis colorectal cancers with hMSH2 germline mutations. Jpn J Cancer Res 87:279–287
19. Miyazono K, Ichijo H, Heldin C (1993) Transforming growth factors-β: latent forms, binding proteins and receptors. Growth Factors 8:11
20. Muro-Cacho C, Anderson M, Cordero J, Munoz-Antonia T (1999) Expression of transforming growth factor β type II receptors in the head and neck squamous cell carcinoma. Clin Cancer Res 5:1243–1248
21. Nerlich A, Schleicher E (1991) Immunohistochemical localization of extracellular matrix components in human diabetic glomerular lesions. Am J Pathol 139:889–899
22. Nerlich AG, Wiest I, Wagner E, Sauer U, Schleicher ED (1997) Gene expression and protein deposition of major basement membrane components and TGF-β1 in human breast cancer. Anticancer Res 17:4430–4450
23. Nerlich A, Lebeau A, Hagedorn H, Sauer U, Schleicher E (1998) Morphological aspects of altered basement membrane metabolism in invasive carcinomas of the breast and the larynx. Anticancer Res 18:3515–3520
24. Park K, Kim SJ, Bang YJ, Park JG, Kim NK, Roberts AB, Sporn MB (1994) Genetic changes in the transforming growth factor β (TGF-β) type II receptor gene in human gastric cancer cells: correlation with sensitivity to growth inhibition by TGF-β. Proc Natl Acad Sci USA 91:8772–8776
25. Pennybacker M, Hermann B (1992) Transforming growth factor-beta (TGF-β) induced phosphorylation of myristoylated alanine rich C kinase substrate (MARCKS) protein in ovarian granulosa cells is modulated by follicle stimulating hormone (FSH). Res Commun Chem Pathol Pharmacol 78:359–366
26. Roberts AB, Sporn MB (1990) The transforming growth factors-betas. In: Sporn MB, Roberts AB (eds) Peptide growth factors and their receptors-handbook of experimental pharmacology. Springer, Berlin Heidelberg New York, pp 419–472
27. Shi Long L, Akiyama Y, Nagasaki H, Saitoh K, Yuasa Y (1995) Mutations of the transforming growth factor-β type II receptor gene and genomic instability in hereditary nonpolyposis colorectal cancer. Biochem Biophys Res Commun 216: 452–457
28. Shi Long L, Wen-Cong Z, Akiyama Y, Nomizu T, Yuasa Y (1996) Genomic structure of the transforming growth factor β type II receptor gene and its mutations in hereditary nonpolyposis colorectal cancers. Cancer Res 56:4595–4598
29. Vivien D, Petitfrere E, Martiny L, Sartelet H, Galera P, Haye B, Pujol JP (1993) IPG (inositolphosphate glycan) as a cellular signal for TGF-beta 1 modulation of chondrocyte cell cycle. J Cell Physiol 155:437–444
30. Wrana JL, Attisano L, Wieser R, Ventura F, Massagne J (1994) Mechanism of activation of the TGF-β receptor. Nature 370:341–347

Virchows Arch (2001) 439:540–546
DOI 10.1007/s004280100398

ORIGINAL ARTICLE

M. Kanda · J. Suzumiya · K. Ohshima · S. Haraoka
N. Nakamura · M. Abe · K. Tamura · M. Kikuchi

Analysis of the immunoglobulin heavy chain gene variable region of intravascular large B-cell lymphoma

Received: 6 September 2000 / Accepted: 22 December 2000 / Published online: 11 May 2001
© Springer-Verlag 2001

Abstract Intravascular large B-cell lymphoma (IVLBL) is a rare neoplasm characterized by proliferation of lymphoma cells within the blood vessels. The cell origin of IVLBL has not yet been determined. We examined cell lineage, with immunohistochemical staining and molecular analysis, using polymerase chain reaction (PCR) of the variable region of the immunoglobulin heavy chain (Ig-VH) gene. We also investigated the cell origin using direct sequence analysis of the complementary-determining region 2 (CDR2) and framework region 3 (FR3) in six cases, consisting of two male and four female patients. The sequences in five cases showed frequent mutations. The percent homology to their closest germline genes ranged from 74.7 to 91.8%. However, one case showed a percent homology of 99.4% in CDR2 and FR3 of Ig-VH. All cases showed rearrangements of VH3 family genes. Interestingly, three of the IVLBL cases with hypermutated IgH genes showed the expression of CD5. Therefore, expression of CD5 in lymphoma cells does not indicate that the origin of IVLBL is the same as mantle cell lymphoma having the character of CD5 expression, which develops in pre-germinal center cells. Our results indicate that most IVLBLs may originate in the post-germinal center cells, based on the presence of somatic mutation in VH genes, although some heterogeneous cases are intermingled within IVLBL.

M. Kanda (✉) · J. Suzumiya · K. Ohshima · S. Haraoka
M. Kikuchi
First Department of Pathology, School of Medicine,
Fukuoka University, Nanakuma 7-45-1, Jonan-ku,
Fukuoka 814-0180, Japan
e-mail: kanda@fukuoka-u.ac.jp
Tel.: +81-92-8011011, Fax: +81-92-8617300

M. Kanda · J. Suzumiya · K. Tamura
Internal Medicine, School of Medicine, Fukuoka University,
Fukuoka, Japan

N. Nakamura · M. Abe
First Department of Pathology, Fukushima Medical College,
Fukushima, Japan

Keywords Intravascular large B-cell lymphoma · Direct sequence analysis · CD5 · Ig-VH · Somatic mutation

Introduction

Intravascular large B-cell lymphoma (IVLBL) is a rare neoplasm characterized by proliferation of lymphoma cells within the lumen of small to medium-sized blood vessels. Unlike most lymphomas, in IVLBL, no tumors are found in areas expected to contain malignant tissues, such as the lymph nodes, skin, and gastrointestinal tract. In 1997, we reported that three of four cases with IVLBL expressed the CD5 antigen [12, 13]. Subsequently, Khalidi et al. [16] reported the expression of CD5 in five of ten cases, thus confirming our results. However, the histologic significance of CD5 expression in IVLBL and the cell origin of CD5-positive IVLBL remain to be determined.

IVLBL is often of the large B-cell type, but the cell origin and normal counterpart remain unclear. Examination of somatic mutation of the variable region of the immunoglobulin heavy chain (Ig-VH) gene suggests that the origin of B-cell lymphoma is either the pre-germinal, germinal, or post-germinal center cells [11, 21, 24, 35]. Analysis of VH gene sequences have been used in recent years to provide information about the clonal history of the cell of origin of B-cell lymphomas. Furthermore, characterization of the patterns of somatic mutations within the tumor cell population can also reveal whether the tumor cells continue to mutate after neoplastic transformation [18, 23, 26, 39, 40]. The ability to identify and sequence Ig-VH genes provides information relevant to our understanding of the behavior of B-cell tumors. Using analysis of Ig-VH genes, previous studies have demonstrated that mantle cell lymphomas (MCLs) and B-cell-type chronic lymphocytic leukemia (B-CLLs) have germline VH genes, suggesting that they are derived from pre-germinal center B cells [10, 20]. In contrast, a high frequency of VH somatic mutations is detected in diffuse large B-cell lymphomas (DLBL), suggesting that this type of lymphoma is of post-germinal center origin

[22, 29]. Thus, there is increasing evidence for a somatic mutation of Ig genes. To our knowledge, however, there are no studies that have analyzed the cell origin of IVLBL based on somatic mutation of Ig-VH. Furthermore, it is unclear whether CD5-positive IVLBL are of pre-germinal center or post-germinal center origin. In the present study, we investigated the cell origin and developmental stage of cells from the pre-germinal center and post-germinal center, using direct sequence analysis in six cases of IVLBL.

Materials and methods

Cases

We examined nine IVLBL cases, including four males and five females [13]. Among these, six cases were selected in the present study, including three (cases 2–4) diagnosed by biopsy and three (cases 1, 5, 6) diagnosed at autopsy, as documented in the files maintained at the First Department of Pathology, Fukuoka University, from 1978 to 1996. These case profiles have been reported elsewhere [13].

Specimens

The biopsy or autopsy specimens were fixed in 10% buffered formalin and embedded in paraffin. The anatomic location of the tissues studied were brain (case 1), skin (case 2), nasal cavity mucosa (case 3), kidney (cases 4 and 5), and lung (case 6). For microscopic examination, 4-µm-thick paraffin-embedded sections were prepared and stained with hematoxylin and eosin (HE). Frozen tissues were available in three cases (cases 1, 3, 5) for immunohistochemical and genetic examination.

Immunohistochemical analysis

Monoclonal antibodies (mAbs) used in this study were as follows: CD3 (Leu 4, Becton-Dickinson, Mountain View, Calif.), CD5 (Leu 1, Becton-Dickinson), CD21 (B2, Coulter, Miami, Fla.), and CD23 (Leu 20, Becton-Dickinson). These mAbs were applied to frozen sections. CD3 (PS1, Novocastra Laboratories, Newcastle Upon Tyne, UK), CD5 (4c7, Novocastra Laboratories), CD20 (L26, Becton-Dickinson), CD45RO (UCHL-1, Dako, Glostrup, Denmark), bcl-2 (124, Dako), and bcl-6 (PIF6, Novocastra Laboratories) were applied to paraffin-embedded sections. Biotinylated anti-mouse or anti-rabbit antibodies (Vector Laboratories, Burlingame, Calif.) were used as the secondary antibodies, followed by treatment with alkaline phosphatase-conjugated avidin (Vector Laboratories). New fuchsin and naphthol AS-BI phosphate were also used as substrate chromogen reagents.

Polymerase chain reaction analysis for bcl-2

DNA used in polymerase chain reaction (PCR) analysis was obtained as described previously [13]. PCR was performed in a 50-µl reaction containing 10× buffer (Stratagene, La Jolla, Calif.), 30 pmol each of the primers and dinucleotide triphosphates (dNTP; Takara, Tokyo, Japan), and 1 U of *Taq* polymerase (Perkin-Elmer Cetus, Norwalk, Conn.). PCR amplification was performed for 40 cycles with the primers for the J-region and, for the mbr, synthesized as described previously for bcl-2 (Table 1). Each cycle included denaturation for 1 min at 94°C and extension for 2 min at 72°C. A touch-down PCR technique was used, starting from an annealing temperature of 60°C, which was decreased every other cycle by 2°C for the first eight cycles [5]. DNA amplification commenced with 12 min of denaturation at 95°C and finished with 10 min of final extension at 72°C. Then, 10 µl of PCR products were loaded onto 4% agarose electrophoresis gel, stained with ethidium bromide and visualized under ultraviolet light. DNA was prepared from a lymph node of a patient with follicular cell lymphoma, which revealed translocation (14; 18), and used as a positive control. Bcl-2 rearrangement of the positive case was confirmed by means of Southern blotting, using synthesized oligonucleotide-specific primer labeled with ^{32}P. Distilled water instead of sample DNA was used as a negative control.

IgH-PCR direct sequence

Clonal rearrangement of the IgH gene was examined using seminested PCR amplification, as described previously [12, 13]. Direct sequence analysis of complementary-determining region 2 (CDR2) and framework region 3 (FR3) was performed as described previously [33]. In the first amplification, 1 µl DNA template was applied, and primer LJH was used as the downstream primer. For reamplification, the downstream primer (LJH) was replaced with the nested consensus primer, VLJH, and the amplified product of the first amplification was transferred as a template [4]. The primers of FR2A, LJH and VLJH (Table 1) were synthesized as described previously [37]. In each PCR amplification, the initial denaturation steps were set at 94°C for 8 min in the first round and 5 min in the second round with the addition of enzyme. The PCR condition consisted of five final stringent cycles at 63°C for 30 s for primer annealing, whereas the remaining 35 cycles were performed at 57°C. The conditions for DNA denaturation were similar at 94°C for 15 s and primer extension at 72°C for 30 s in all cycles. For the second PCR, the stringent primer annealing conditions were similar (63°C for 60 s) for 30 cycles. The PCR products were gel-purified and submitted for direct sequencing. Automated direct sequencing was performed using the same FR2A and VLJH primers as described above, using 1 µl of the second round of PCR amplification and fluorescent dideoxynucleotide terminators and the Applied Biosystems 377 sequencer (Weiterstadt, Germany). The results of sequence analysis of CDR2 and FR3 were compared with the germline sequences using the BLAST homology search program (basic local alignment search tool: National Center for Biotechnology Information, Bethesda, Md.). Such an analysis allowed the determination of the usage of VH segments and an estimation of somatic mutations compared with the most proximal germline sequences.

Analysis of mutations

Observed and expected mutations were analyzed using the following calculation: Rexp or Sexp=*n*×(CDR Rf or CDR Sf)×CDRrel,

Table 1 Primers for polymerase chain reaction analysis. *Ig* immunoglobulin

Epstein-Barr Virus	EBW-1: 5′CCAGAGGTAAGTGGACTT3′ EBW-2: 5′GACCGGTGCCTTCTTAGG3′ probe EBW: 5′TTCTGCTAAGCCCAC3′
bcl-2	J-region: 5′AACTGCAGAGGAGACGGTGACC3′ mbr: 5′TTAGAGAGTTGCTTTACGTGGCCTG3′
IgH	FR2A:5′TGG(A/G)TCCG(C/A)CAG(G/C)C(T/C)(T/C)CNGG3′ LJH: 5′TGAGGAGACGGTGACC3′ VLJH: 5′GTGACCAGGGTNCCTTGGCCCCAG3′

where R(S)exp is the number of expected replacement (R) or silent (S) mutations, *n* is the number of observed mutations, R(S)f is the proportion of total possible R or S point mutations inherent in the CDR sequence, and CDRrel is the proportion of CDR in the total VH sequence [4, 33]. This formula was also applied to the analysis of the FR. The number of observed R mutations, expected R mutations, and replacement to noncoding mutation ratio (Ris) for CDR and FR regions are shown. The probability, *P*, that the number of R mutations in the CDR occurred by chance was calculated with the formula of Chang and Casali: $P=\{n!/[k!(n-k)!]\}\, q^k(1-q)^{n-k}$, where *n* is the number of observed mutations, *k* is the number of observed R mutations in the CDR or FR, and q is the number probability that an R mutation will localize to CDR or FR [q=(CDRrel)×(CDR Rf) or (FRrel)×(FR Rf)] [4, 33].

Results

Histologically, all cases exhibited intravascular proliferation of large lymphoma cells (Fig. 1). The clinical findings are summarized in Table 2. Three patients (cases 2, 3 and 4) were diagnosed clinically and received chemo- and radiotherapy. All patients except one died of respiratory failure or gastro-intestinal (GI)-related symptoms.

Immunohistochemical analysis

Some of these results have already been reported [13]. All six cases were positive for CD20 but negative for CD21, CD23, bcl-2, bcl-6, and T-cell markers, including CD45 RO or CD3 (Table 3). CD5 was expressed in three of the six cases.

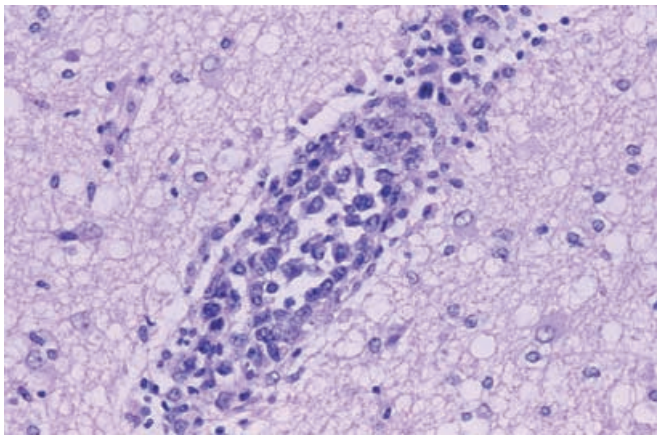


Fig. 1 Case 1. Hematoxylin and eosin-stained brain tissue under low (×98) magnification. Note infiltration of many lymphoma cells within the lumen

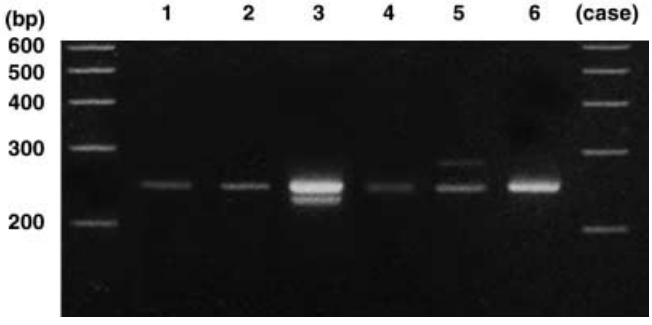


Fig. 2 Polymerase chain reaction analysis of immunoglobulin (Ig)H Fr2 shows a rearranged band (cases 1–6)

Table 2 Summary of clinical findings. *DS* duration of survival after diagnosis, *ND* not done, *RTx* radiotherapy, *PSL* prednisolone; *CHOP* cyclophosphamide, hydroxydaunomycin, vincristine, predisolone; *VEMP* vincristine, cyclophosphamide, methotrexate, predonisolone; *VEPA* vincristine, cyclophosphamide, predonisolone, doxorubicin

Case	Age	Gender	Initial symptoms	Diagnosis	Therapy	DS (months)	Outcome	Cause of death
1	58	Female	Dementia, quadriplegia	Autopsy	ND	3	Deceased	Respiratory failure
2	75	Female	Exanthema	Skin	CHOP, VEMP	63	Deceased	GI bleeding
3	73	Male	Double vision	Nasal cavity	VEPA	84	Deceased	
4	58	Male	Aphasia, Apraxia	Kidney	VEPA, RTx	1	Deceased	Renal failure, GI bleeding
5	71	Female	General fatigue, fever	Autopsy	PSL	4	Deceased	Ileus
6	62	Female	Dyspnea	Autopsy	PSL, RTx	20	Deceased	Respiratory failure

Table 3 Results of immunophenotypic analysis. *PCR* polymerase chain reaction; *EBV* Epstein-Barr virus; *ISH* in situ hybridization

Case	Special stains								PCR
	CD3	CD5	CD20	CD21	CD23	CD45RO	bcl-2	bcl-6	bcl-2
1	–	+	+	–	–	–	–	–	–
2	–	–	+	–	–	–	–	–	–
3	–	+	+	–	–	–	–	–	–
4	–	–	+	–	–	–	–	–	–
5	–	+	+	–	–	–	–	–	–
6	–	–	+	–	–	–	–	–	–

Table 4 Sequence comparison of the amplifiers of intravascular large B-cell lymphoma (IVLBL) with germline sequences. *ISH* in situ hybridization; *R/S* replacememt/silent. *CDR* complementary-determining region; *FR* framework region

Case	Germline usage			R/S	% Homology (%)
1	VH3/DP-42	CDR II	TGG GTC TCA GTT ATT TAT AGC GGT GGT AGC ACA TAC TAC GCA GAC TCC GTC AAG GGC CGA TTC ACC		
			--C --- --- T-G --- --C --- --- --A -AG --- --- --T --- --G --- --- --- --- --- --- ---	5/2	
					85.8
		FR III	ATC TCC AGA GAC AAT TCC AAG AAC ACG CTG TAT CTT CAA ATG AAC AGC CTG AGA GCC GAG GAC ACG GCC GTG TAT TAC TGT GCG AGA		
			G-- --- --- --- --G --- -G- --- --C --- --- --- --G C-- --- --- --A --- C-T --- --T --- --T C-T --- --- --- --- -C-	7/5	
2	VH3/DP 35	CDR III	TAC ATT AGT AGT AGT GGT AGT ACC ATA TAC TAC GCA GAC TCT GTG AAG GGC CGA TTC ACC		
			--- --- --- --- --- --- --- --- --- --T --- T-- --- --G --- G-- --G --- --- ---	2/3	
					91.8
		FR III	ATC TCC AGG GAC AAC GCC AAG AAC TCA CTG TAT CTG CAA ATG AAC AGC CTG AGA GCC GAG GAC ACG GCC GTG TAT TAC TGT GCA AGA		
			--- NT- CA- --- --- --- --- --- --T --- --- --- --C --- --- --- --- --- --- --- --- --- --- T-- --- --- --- --- ---	3/2	
3	VH3/DP-58	CDR II	TGG ATT TCA TAC ATT AGT AGT AGT GGT AGT ACC ATA TAC TAC GCA GAC TCT GTG AAG GGC CGA TTC ACC		
			--A --- --- --T --- --- --- --- --C --- --- --T C-- --T -G- --- --- --- --- --- --- --- ---	3/3	
					87.7
		FR III	ATC TCC AGA GAC AAC GCC AAG AAC TCA CTG TAT CGT CAA ATG AAC AGC CTG AGA GCC GAG GAC ACG GCT GTT TAT TAC TGT GCG AGA		
			--- --- --- --- --A --- --- --T --- T-- -C- --- --- --- G-T GA- --- --- CA- --- --- --- --- --- --- --- --- A-- C--	6/3	
4	VH3/DP-54	CDR II	TGG GTG GCC AAC ATA AAG CAA GAT GGA AGT GAG AAA TAC TAT GTG GAC TCT GTG AAG GGC CGA TTC ACC		
			--- --- --- --- T-G --A --- --- --- --- A-- -TC --- --- --- --- --- --- --- --- --- --- ---	3/1	
					91.5
		FR III	ATC TCC AGA GAC AAC GCC AAG AAC TCA CTG TAT CTG CAA ATG AAC AGC CTG AGA GCC GAG GAC ACG GCT GTG TAT TAC TGT GCG AGA		
			--- --- --- --- --- A-- --- --- --- T-- --- --- --- --- --- --- --- --- -T- --- --- --- --- C-C --- --T --- -T- ---	4/2	
5	VH3/DP-38	CDR II	TGG GTT GGC CGT ATT GAA AGC AAA ACT GAT GGT GGG ACA ACA GAC TAC GCT GCA CCC GTG AAA GGC AGA TTC ACC		
			--- A-A --- -T- --- --- --G G-- -TC --- --- --- -A- GT- T-G -GT AT- -T- G-- --- --C -T- --- --- -T-	15/0	
					74.7
		FR III	ATC TCA AGA GAT GAC TCA AAA AAC ACG CTG TAT CTG CAA ATG AAC AGC CTG AAA ACC GAG GAC ACA GCC GTG TAT TAC TGT ACC ACA		
			G-- --G --- --- --- --- --- G-- C-- A-- G-- --- --G --- --- --- -C- --- G-- --C --- --- -T- --T --- C-- -A- -T- ---	12/3	
6	VH3/DP-54	CDR II	TGG GTG GCC AAC ATA AAG CAA GAT GGA AGT GAG AAA TAC TAT GTG GAC TCT GTG AAG GGC GGA TTC ACC		
			--- ---	0/0	
					99.4
		FR III	ATC TCC AGA GAC AAC GCC AAG AAC TCA TAT CTG CAA ATG AAC AGC CTG AGA GCC GAG GAC ACG GCT GTG TAT TAC TGT GCG AGA	0/1	
			--- --C --- --- --- --- --- ---		

Table 5 Replacement (R) and silent (S) mutations in the variable region of heavy chain (VH) segments of rearranged immunoglobulin genes. *P* probability of obtaining the number of R mutations found in the CDR2 by chance

Case	Germline usage	Homology (%)	CDR2					FR3					p-CDR-2
			Expected		Observed		R/S	Expected		Observed		R/S	
			R	S	R	S	Ratio	R	S	R	S	Ratio	
1	VH3/DP-42	85.8	6.1	2.1	5	2	2.5	8.4	2.4	7	5	1.4	0.1063
2	VH3/DP-35	91.8	3.2	0.9	2	3	0.6	4.6	1.4	3	2	1.5	0.0006
3	VH3/DP-58	87.7	5.1	1.5	3	3	1	6.4	1.9	6	3	2	0.0475
4	VH3/DP-54	91.5	3.5	1.0	3	1	3	4.3	1.3	4	2	2	0.1690
5	VH3/DP-38	74.7	10.4	3.5	15	0	-	12.3	3.8	12	3	4	0.0928
6	VH3/DP-54	99.4	0.3	0.1	0	0	-	0.4	0.1	0	1	0	0.6534

PCR for bcl-2

The bcl-2 rearrangement was not detected using PCR in all cases (data not shown).

PCR for VH and direct sequence analysis

We analyzed six cases in which a complete oligonucleotide sequence of CDR2 and FR3 was identified (Fig. 2). The result of the direct sequence method was compared with the closest germline sequence in the database. Replacement mutations are single base substitutions resulting in amino acid replacement, while silent mutations are single base substitutions without amino acid replacement. The results of direct sequence analysis of CDR2 and FR3 showed that the percent homology ranged from 74.7 to 91.8% in cases 1–5 but was 99.4% in case 6 for CDR2 and FR3 (Table 4). R mutation and the R/S ratio are also shown in Table 4. The distribution of VH gene families used in our IVLBL cases is also shown in Table 4. All cases of IVLBL showed the usage of VH3 in VH gene families.

The R and S mutations in the VH segments are summarized in Table 5. In most cases, the numbers of R mutations in the CDR2 regions and in the FR3 regions were fewer than expected. The R/S ratio in the CDR2 region was less than 3.0 and, in the FR3 regions, was greater than 1.5 in most instances. These findings suggest that IVLBLs are not derived from antigen-selected B cells.

Discussion

IVLBL is a rare systemic lymphoproliferative disorder in which malignant lymphoid cells are confined to the vascular lumina. All IVLBL cases in our study showed B-cell phenotype, and CD5 was expressed in three of the six IVLBL cases examined. The incidence of CD5 expression in our cases with IVLBL was similar to that reported in a previous study [16]. In the present study, none of the patients with CD5-positive IVLBL had a previous history or showed evidence of concomitant chronic lymphocytic leukemia/small lymphocytic lymphoma (CLL/SLL) and, therefore, we considered these cases to be CD5-positive IVLBL. In addition, CD20 expression was detected in all cases but CD23 was negative. Among B-cell lymphomas, MCL and CLL/SLL are well known to express CD5, although the cytological features of these lymphomas differ from those of IVLBL. CD5 is usually expressed in cases with lymphoma of pre-germinal stage, such as MCL and CLL/SLL. Most cases of MCL and CLL/SLL show germline of the VH gene [10, 20, 27, 31], although a few cases show hypermutated VH gene [3, 6, 9, 28, 30]. In comparison, all CD5-positive IVLBL cases in our study showed somatic mutations, suggesting they might be distinct from pregerminal center lymphomas, e.g., MCL and CLL/SLL. In this regard, 5–10% of DLBL are known to express the CD5 antigen [8, 14, 15, 17]. CD5-positive DLBL, which is a unique type of DLBL, exhibits somatic mutation of the Ig gene and seems to originate from post-germinal center cells [14, 19, 34]. Human B cells consist of two distinct subsets, B-1 and B-2 cells. Cells of the former subset are characterized by the expression of CD5 antigen and are distinct from B-2 cells by anatomical localization and gene usage [7, 14, 15, 17]. The majority of antibodies produced by B-1 cells are coded by relatively restricted repertories of Ig-VH genes with little or no somatic mutation [7, 14, 15, 17], although recent analysis of the VH genes of B-1 cells presented controversial results and indicated that B-1 cells are encoded by a hypermutated VH gene [26, 34]. In addition, Taniguchi et al. [34] reported that CD5-positive DLBL might originate from B-1 cells of unique lineages. These findings suggest that CD5-positive IVLBL and CD5-positive DLBL have similar characteristics, such as expression of CD5 and somatic mutation of Ig genes.

Translocation of chromosomes 14 and 18 was not detected using PCR in all of our cases. Previous studies demonstrated that approximately 20–30% of DLBL cases exhibit chromosomal translocation: (14; 18) [1, 38]. Follicular lymphomas originate from follicular center cells and are characterized by chromosomal abnormality: t(14; 18). This translocation is present in up to 85% of cases with follicular lymphoma [36]. Therefore, our results suggest that IVLBL cells are unlikely to originate from follicular center cells.

The percent homology to CDR2 and FW3 of Ig-VH gene ranged from 74.7% to 91.8% in cases 1–5, but was 99.4% in case 6 (Table 4). A low percent homology reflects the presence of somatic mutation and, therefore, the lymphoma cells of IVLBL are likely to be in the post-germinal center stage. The patterns of germline and lymphoma cells in the remaining single case (case 6) with over 99% homology suggested that the lymphoma was in the pre-germinal center stage. However, no differences in various clinicopathological features were identified in IVLBL with and without somatic mutation.

In normal B cells, the germline complexity of VH gene families is reported to be 25–30% for the VH1 family, 5–10% for the VH2 family, 50–55% for the VH3 family, 5–18% for the VH4 family, 1–2% for the VH5 family, and 1% for the VH6 family [2, 32]. Furthermore, the VH4-gene family was found in approximately 50–60% of Japanese cases with CD5+ DLBL [19, 29, 34]. However, in our study, the VH3 family was detected in all IVLBL cases – a pattern similar to that in normal B cells – which are characterized by the predominance of the large VH3 gene family. In general, utilization of the VH gene is roughly proportional to the estimated family size, and the biased VH gene type is thought to be related to antigen selection by auto antigens [25].

The distribution of mutations in the VH regions may reflect the antigen selection of B cells. It has been suggested that (1) the observed numbers of R and S mutations are higher in the CDR regions and lower in the FR region than expected, (2) the R/S ratio in the CDR regions is greater than 3.0 and, in the FR regions, less than 1.5, and (3) the probability of the observed R mutations occurring by chance is very low. This mutation pattern is highly indicative of a derivation from antigen-selected B cells [33]. When the R/S ratio was calculated, none of the IVLBL cases, irrespective of CD5 expression, had a value of more than 3.0 (Table 5). Furthermore, no significant differences were recognized between CD5-positive and CD5-negative IVLBL cases. In most cases with IVLBL, significantly lower R mutations were found in the CDR region and significantly more R mutations were present in the FR region than could be attributed to antigen selection. Taken together, the mutations detected in IVLBL in our study are considered to occur randomly.

IVLBL appear to develop from a pool of B cells, which is similar to how DLBL originate. With respect to the VH family gene, IVLBL was different from DLBL. While the origin of IVLBL remains unclear, most IVLBL have unique characteristics, such as CD5 expression and the presence of somatic mutations in VH genes, which is similar to CD5-positive DLBL. Based on these features, IVLBL could perhaps be included as a subgroup of DLBL, although further studies may identify IVLBL as a separate pathological entity.

Acknowledgements This work was supported in part by a Grant-Aid from the Fukuoka Cancer Society and a Grant-in-Aid for Scientific Research (C) from the Ministry of Education, Science, Sports, and Culture, Japan. We thank Drs. Houjyou, Nozawa, Hashimoto, Mr. Sasaki, Mr. Kuze, and colleague at Fukushima Medical College and Ms. Kubo for giving us permission to examine the direct sequence. We thank Dr. Kume at Akita University School of Medicine for analysis of mutations.

References

1. Aisenberg AC, Wilkes BM, Jacobson JO (1988) The bcl-2 gene is rearranged in many diffuse B-cell lymphomas. Blood 71:969–972
2. Berman JE, Mellis SJ, Pollock R, Smith-CL, Suh H, Heinke B, Kowal C, Surti U, Chess L, Cantor CR (1988) Content and organization of the human Ig VH locus: definition of three new VH families and linkage to the Ig CH locus. EMBO J 7:727–738
3. Cai J, Humphries C, Richardson A, Tucker PW (1992) Extensive and selective mutation of a rearranged VH5 gene in human B cell chronic lymphocytic leukemia. J Exp Med 176:1073–1081
4. Diss TC, Peng H, Wotherspoon AC, Isaacson PG, Pan L (1993) Detection of monoclonality in low-grade B-cell lymphomas using the polymerase chain reaction is dependent on primer selection and lymphoma type. J Pathol 169:291–295
5. Don RH, Cox PT, Wainwright BJ, Baker K, Mattick JS (1991) 'Touchdown' PCR to circumvent spurious priming during gene amplification. Nucleic Acids Res 19:4008
6. Efremov DG, Ivanovski M, Siljanovski N, Pozzato G, Cevreska L, Fais F, Chiorazzi N, Batista FD, Burrone OR (1996) Restricted immunoglobulin VH region repertoire in chronic lymphocytic leukemia patients with autoimmune hemolytic anemia. Blood 87:3869–3876
7. Hardy RR, Hayakawa K (1986) Development and physiology of Ly-1 B and its human homolog, Leu-1 B. Immunol Rev 93:53–79
8. Hardy RR, Carmack CE, Shinton SA, Riblet RJ, Hayakawa K (1989) A single VH gene is utilized predominantly in anti-BrMRBC hybridomas derived from purified Ly-1 B cells. Definition of the VH11 family. J Immunol 142:3643–3651
9. Hashimoto S, Dono M, Wakai M, Allen SL, Lichtman SM, Schulman P, Vinciguerra VP, Ferrarini M, Silver J, Chiorazzi N (1995) Somatic diversification and selection of immunoglobulin heavy and light chain variable region genes in IgG+ CD5+ chronic lymphocytic leukemia B cells. J Exp Med 181:1507–1517
10. Hummel M, Tamaru J, Kalvelage B, Stein H (1994) Mantle cell (previously centrocytic) lymphomas express VH genes with no or very little somatic mutations like the physiologic cells of the follicle mantle. Blood 84:403–407
11. Jacob J, Kelsoe G, Rajewsky K, Weiss U (1991) Intraclonal generation of antibody mutants in germinal centres. Nature 354:389–392
12. Kanda M, Suzumiya J, Ohshima K, Kikuchi M (1997) Angiotropic lymphoma: clinicopathological, immunohistochemical and molecular genetic studies. Proceedings of the fifth Korean-Japanese Lymphoreticular Workshop Kyungju, Korea. Hematolymphoreticular study group/The Korean Society of Pathologists, Seoul, Korea, pp 383–386
13. Kanda M, Suzumiya J, Ohshima K, Tamura K, Kikuchi M (1999) Intravascular large cell lymphoma: clinicopathological, immuno-histochemical and molecular genetic studies. Leuk Lymphoma 34:569–580
14. Kantor AB (1991) The development and repertoire of B-1 cells (CD5 B cells). Immunol Today 12:389–391
15. Kasaian MT, Ikematsu H, Casali P (1991) CD5+ B lymphocytes. Proc Soc Exp Biol Med 197:226–241
16. Khalidi HS, Brynes RK, Browne P, Koo CH, Battifora H, Medeiros LJ (1998) Intravascular large B-cell lymphoma: the CD5 antigen is expressed by a subset of cases. Mod Pathol 11:983–988
17. Kipps TJ (1989) The CD5 B cell. Adv Immunol 47:117–185
18. Klein U, Goossens T, Fischer M, Kanzler H, Braeuninger A, Rajewsky K, Kuppers R (1998) Somatic hypermutation in normal and transformed human B cells. Immunol Rev 162:261–280

19. Kume M, Suzuki R, Yatabe Y, Kagami Y, Miura I, Miura AB, Morishima Y, Nakamura S, Seto M (1997) Somatic hypermutations in the VH segment of immunoglobulin genes of CD5-positive diffuse large B-cell lymphomas. Jpn J Cancer Res 88:1087–1093
20. Kuppers R, Gause A, Rajewsky K (1991) B cells of chronic lymphatic leukemia express V genes in unmutated form. Leuk Res 15:487–496
21. Kuppers R, Zhao M, Hansmann ML, Rajewsky K (1993) Tracing B cell development in human germinal centres by molecular analysis of single cells picked from histological sections. EMBO J 12:4955–4967
22. Kuppers R, Rajewsky K, Hansmann ML (1997) Diffuse large cell lymphomas are derived from mature B cells carrying V region genes with a high load of somatic mutation and evidence of selection for antibody expression. Eur J Immunol 27:1398–1405
23. Levy R, Levy S, Cleary ML, Carroll W, Kon S, Bird J, Sklar J (1987) Somatic mutation in human B-cell tumors. Immunol Rev 96:43–58
24. Liu YJ, Joshua DE, Williams GT, Smith CA, Gordon J, MacLennan IC (1989) Mechanism of antigen-driven selection in germinal centres. Nature 342:929–931
25. Maloum K, Pritsch O, Magnac C, Davi F, Binet JL, Merle Beral H, Dighiero G (1997) VH gene expression in CD5 positive and CD5 negative B cell chronic lymphoid malignancies. Leuk Lymphoma 24:437–448
26. Mantovani L, Wilder RL, Casali P (1993) Human rheumatoid B-1a (CD5+ B) cells make somatically hypermutated high affinity IgM rheumatoid factors. J Immunol 151:473–488
27. Meeker TC, Grimaldi JC, O'Rourke R, Loeb J, Juliusson G, Einhorn S (1988) Lack of detectable somatic hypermutation in the V region of the Ig H chain gene of a human chronic B lymphocytic leukemia. J Immunol 141:3994–3998
28. Nakamura N, Hashimoto Y, Kuze T, Tasaki K, Sasaki Y, Sato M, Abe M (1999a) Analysis of the immunoglobulin heavy chain gene variable region of CD5-positive diffuse large B-cell lymphoma. Lab Invest 79:925–933
29. Nakamura N, Kuze T, Hashimoto Y, Tasaki K, Hojo H, Sasaki Y, Sato M, Abe M (1999b) Analysis of the immunoglobulin heavy chain gene variable region of 101 cases with peripheral B cell neoplasms and B cell chronic lymphocytic leukemia in the Japanese population. Pathol Int 49:595–600
30. Oscier DG, Thompsett A, Zhu D, Stevenson FK (1997) Differential rates of somatic hypermutation in V(H) genes among subsets of chronic lymphocytic leukemia defined by chromosomal abnormalities. Blood 89:4153–4160
31. Pratt LF, Rassenti L, Larrick J, Robbins B, Banks PM, Kipps TJ (1989) Ig V region gene expression in small lymphocytic lymphoma with little or no somatic hypermutation. J Immunol 143:699–705
32. Stewart AK, Schwartz RS (1994) Immunoglobulin V regions and the B cell. Blood 83:1717–1730
33. Tamaru J, Hummel M, Marafioti T, Kalvelage B, Leoncini L, Minacci C, Tosi P, Wright D, Stein-H (1995) Burkitt's lymphomas express VH genes with a moderate number of antigen-selected somatic mutations. Am J Pathol 147:1398–1407
34. Taniguchi M, Oka K, Hiasa A, Yamaguchi M, Ohno T, Kita K, Shiku H (1998) De novo CD5+ diffuse large B-cell lymphomas express VH genes with somatic mutation. Blood 91:1145–1151
35. Tonegawa S (1983) Somatic generation of antibody diversity. Nature 302:575–581
36. Tsujimoto Y, Gorham J, Cossman J, Jaffe E, Croce CM (1985) The t(14;18) chromosome translocations involved in B-cell neoplasms result from mistakes in VDJ joining. Science 229:1390–1393
37. Wan JH, Trainor KJ, Brisco MJ, Morley AA (1990) Monoclonality in B cell lymphoma detected in paraffin wax embedded sections using the polymerase chain reaction. J Clin Pathol 43:888–890
38. Weiss LM, Warnke RA, Sklar J, Cleary ML (1987) Molecular analysis of the t(14;18) chromosomal translocation in malignant lymphomas. N Engl J Med 317:1185–1189
39. Zelenetz AD, Chen TT, Levy R (1991) Histologic transformation of follicular lymphoma to diffuse lymphoma represents tumor progression by a single malignant B cell. J Exp Med 173:197–207
40. Zhu D, Hawkins RE, Hamblin TJ, Stevenson FK (1994) Clonal history of a human follicular lymphoma as revealed in the immunoglobulin variable region genes. Br J Haematol 86:505–512

Virchows Arch (2001) 439:547–551
DOI 10.1007/s004280100424

ORIGINAL ARTICLE

J. Ehrmann Jr · Y. Collan · P. Řiháková · M. Kala
Z. Kolář

Apoptosis, analysed by means of lamin B detection, correlates with grade of astroglial tumours but not with $p27^{Kip1}$/retinoblastoma protein expression

Received: 10 October 2000 / Accepted: 24 January 2001 / Published online: 24 April 2001
© Springer-Verlag 2001

Abstract The aim of our study was to correlate apoptosis, assessed by means of lamin B degradation, with grade of tumour and immunohistochemical expression of $p27^{Kip1}$ and retinoblastoma protein (pRB) in a series of 32 low-grade astrocytomas (LGA) and 43 high-grade astrocytomas (HGA). Determination and analysis of lamin B expression was achieved stereologically with the use of computerised interactive image analysis. The average stereological surface density of the lamin-positive nuclear surface of cells showing evidence of lamin degradation cells was 13.80 mm^2/mm^3 in LGA and 21.02 mm^2/mm^3 in HGA. The average range of immunopositivity of p27 and pRB expression was 2.85 and 2.10, respectively, in LGA and 1.80 and 0.88, respectively, in HGA. The rate of apoptosis indirectly correlated with the expression of both p27 and pRB but was not fully significant ($P \leq 0.09$). Our findings suggest that there may be a loss of function of main cell-cycle regulators and increased uncontrolled cell death in addition to increased cell proliferation in high-grade astrocytomas. Moreover, we believe that the detection of lamin B degradation in astroglial tumours can be an alternative, precise and convenient assay for the detection of a defined set of apoptotic cells. However, before being applied more generally, comparative research should be done on different methods of quantifying apoptosis, with the intent of finding the difference between biologically different methods. Such studies would also be able to find the method associated with the strongest prognostic power.

Keywords Lamin B · Apoptosis · p27 · pRB · Astrogliomas

J. Ehrmann Jr (✉) · Y. Collan
Department of Pathology, University of Turku,
Kiinamyllynkatu 10, 20520 Turku, Finland
e-mail: erman@tunw.upol.cz
Tel.: +420-68-5632455, Fax: +420-68-5632966

J. Ehrmann Jr · P. Řiháková · Z. Kolář
Institute of Pathology,
Faculty of Medicine and Laboratory of Molecular Pathology,
Centre of Molecular Biology and Medicine, Palacký University,
Hněvotínská 3, 775 15 Olomouc, Czech Republic

M. Kala
Department of Neurosurgery, Faculty of Medicine,
Palacký University, I. P. Pavlova 6, 775 15 Olomouc,
Czech Republic

Introduction

Nuclear lamins, the most important proteins of nuclear lamina, are proteins of intermediate filament type, located at the outer rim of the nucleus. They consist of two types of polypeptides, lamin A and lamin B. Two different transcripts of the lamin A gene exist in mammals as lamin A and lamin C, whereas lamin B consists of B1 and B2 lamins. Lamins mechanically stabilise the cell nucleus, and they also play a role in DNA replication and chromatin organisation [2, 37]. Synthesis of lamin B is increased during heating and, hence, lamin B appears to be a member of the prompt heat shock proteins [12]. In several studies, it was also found that phosphorylation of lamin B by protein kinase α or by cdc2 kinase may alter its ability to polymerise and may lead to nuclear membrane disassembly [34, 35]. Lamin B is cleaved by caspase 3 and caspase 6 during the early phases of apoptosis (up to 90 min) and precedes DNA fragmentation. Caspases 3 and 6 are activated mainly downstream to the FAS/FAS-L-mediated apoptotic signalling pathway [8, 18]. Degradation of lamin B allows the detachment of the nuclear envelope from chromatin and the clustering of nuclear pore complexes, both of which are morphological features of apoptosis [3, 14, 25]. The immunohistochemical assessment of lamin B degradation seems to be a good tool for the detection of apoptosis in tissues [16, 24, 27, 33, 38].

Protein $p27^{Kip1}$ (p27), as an inhibitor of cyclin-dependent kinases, can bind to the cyclin E-CDK2 (cyclin dependent kinase) complex, preventing the phosphorylation of the retinoblastoma protein (pRB), an influence that leads to cell cycle arrest [1, 5, 10, 23, 28, 29, 30, 31]. In cooperation with poly (ADP-ribose) polymerase,

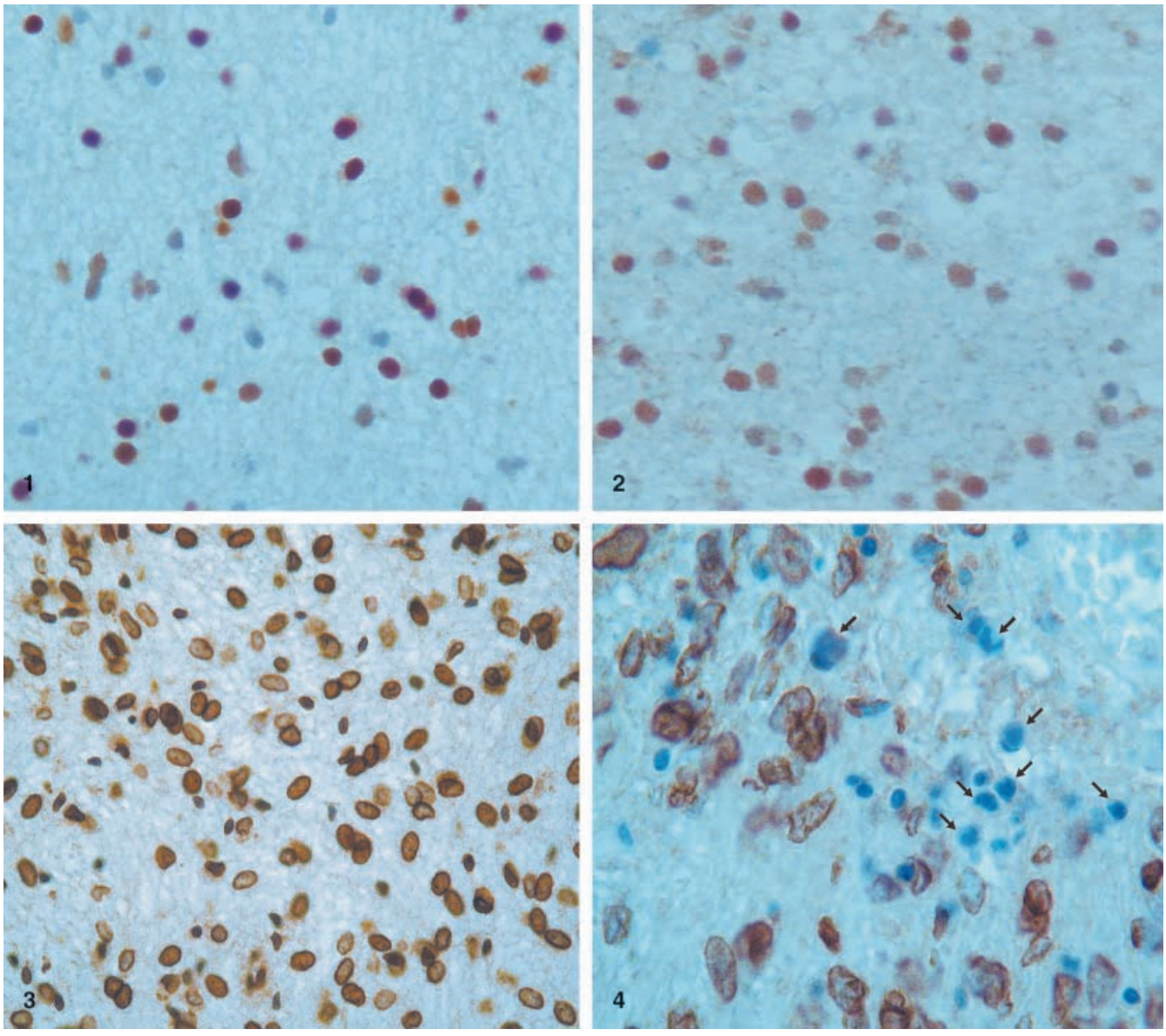


Fig. 1 Expression of p27 in low-grade astrocytoma (magnification ×400)

Fig. 2 Expression of pRB in low-grade astrocytoma (magnification ×400)

Fig. 3 Lamin B expression in low-grade astrocytoma (magnification ×400)

Fig. 4 Degradation of lamin B in high-grade astrocytoma. Apoptotic cells are marked by *arrows* (magnification ×400)

p27 can trigger apoptosis [17]. To study the relationship of p27, pRB and apoptosis as assessed by means of lamin degradation, we decided to study these factors in a series of astrocytic tumours.

Materials and methods

The series consisted of 75 samples from adult patients with astrocytic tumours who underwent surgery at the Department of Neurosurgery, Faculty Hospital, Olomouc, between the years 1986 and 1997. The histopathological diagnosis and grading according to the World Health Organization (WHO) [19] and SAMS (St. Anne Hospital Paris/Mayo Clinic System) [9] were confirmed independently by two pathologists. The series was divided into two groups: a group of low-grade astrocytomas (LGA, 32 cases), including fibrillary astrocytomas, diffuse astrocytomas, gemistocytic astrocytomas and pilocytic astrocytomas, and a group of high-grade astrocytomas (HGA, 43 cases), including anaplastic astrocytomas and glioblastoma multiforme.

A standard indirect immunohistochemical technique using biotinylated secondary anti-mouse and anti-goat antibodies and streptavidin peroxidase (Vectastatin ABC kit, Vector Laboratories) after antigen retrieval (citrate buffer pH 6.0, microwave oven 700 W, 5–10 min) was used for the detection of the lamin B, pRB and p27 proteins (Table 1). As a negative control, the primary antibody was omitted and, as positive controls, we used a sample of liver (for lamin B), a sample of tonsil (for p27) and a sample of breast carcinoma (for pRB). The grade of p27 and pRB immunopositivity was scored semiquantitatively at a magnification of ×400 in the following ranges: 0, up to 10% of positive cells; 1, 11–29% of positive cells; 2, 30–59% of positive cells and 3, 60%

Table 1 Primary antibodies used in study

	Anti-lamin B	anti-p27	anti-pRB
Clone	M-20	1B4	1F8
Dilution	1:100	1:20	1:20
Antigen retrieval	1×5 min	2×5 min	1×5 min
Producer	Santa Cruz Biotechnology (Santa Cruz, Calif.); polyclonal goat	Novocastra Laboratories (Newcastle, UK); monoclonal mouse	Novocastra; monoclonal mouse

and more of positive cells. Determination and analysis of lamin B expression was achieved stereologically with the use of interactive computerised image analysis (system PRODIT, Promis Inc., Almere, Netherland). Sections (5-µm thick) were used, and the stereological surface density (Sv, amount of surface in tissue volume, mm^2/mm^3) of lamin B-positive or -negative nuclei was estimated as Sv=2I/L (where I is the number of intersections of positive nuclei and horizontal lines of the grid and L is the total line length applied on the image) [6, 32]. In each section, 150–200 cells were analysed. The cells with lamin B-negative nuclei, with lamin B disintegration and with nuclear shrinkage and fragmentation were regarded as apoptotic. Moreover, apoptotic cells were also identified by their classical morphology. This includes the presence of crescent-shaped condensation of nuclear chromatin, the rounding up and disintegration of the nucleus and the appearance of apoptotic bodies composed of nuclear fragments and organelles. Any cells not meeting the morphological criteria for apoptosis were not counted. A Mann–Whitney U test, a two-way sample analysis and Pearson $\chi 2$ test with a confidence level of 0.95 and a significance level of 0.05 was used for comparison of the characteristics, lamin B, p27 and pRB between LGA and HGA cases.

Results

We found the following relationships between 32 LGAs and 43 HGAs average range of p27 expression was 2.85 in LGA and 1.80 in HGA ($P \leq 0.0001$; Fig. 1 and Fig. 5A) and the average range of pRB expression was 2.10 in LGA and 0.88 in HGA ($P \leq 0.00002$; Fig. 2 and Fig. 5B). The average surface density (Sv, mm^2/mm^3) of apoptotic, lamin B-fragmented/negative cells was 13.80 in LGA and 21.02 in HGA ($P \leq 0.03$; Figs. 3, 4 and 5C). The average number of cells was 167 per specimen. The rate of lamin B-fragmented/negative cells indirectly correlated with the expression of both p27 and pRB, respectively. However, this correlation was not statistically significant ($P \leq 0.40$ and $P \leq 0.09$, respectively).

Discussion

By stereological analysis of lamin B degradation within tumour cells, we found a higher portion of apoptosis-related cells in HGA when compared with LGA. This finding is similar to the study of Kordek et al. [20]. However, it is contrary to our previous study, where we found a higher terminal deoxynucleotidyl nick end-labelling (TUNEL) index in a group of LGAs [13]. Very careful scrutiny is required to distinguish apoptotic cells from cells in mitosis or necrotic cells, and it is generally accepted that at least two independent methods must be used. In this study, we used the criteria of classical apo-

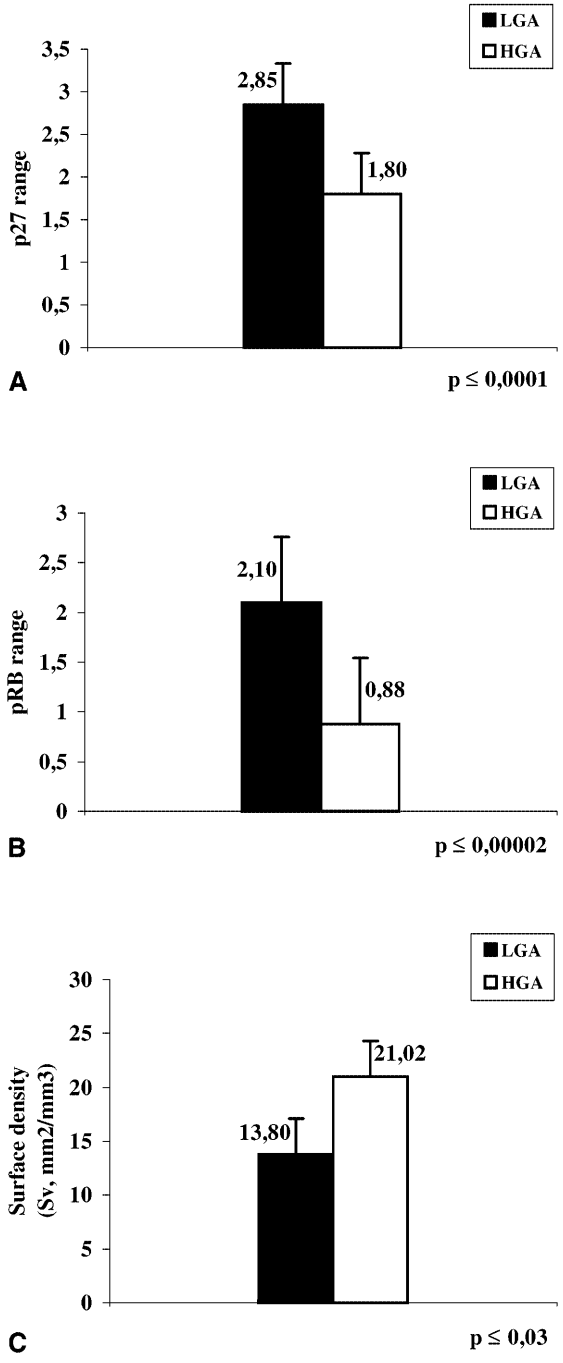


Fig. 5 **A** Relationship between range of p27 expression and tumour grade. **B** Relationship between range of pRB expression and tumour grade. **C** Relationship between surface density Sv (mm^2/mm^3) of fragmented/negative lamin B nuclei and tumour grade

ptotic morphology (nuclear shrinkage, chromatin condensation, etc.) as the additional method. However, based on controversial findings and the knowledge that apoptosis is triggered by various pathways, we believe that the detection of apoptosis in astroglial tumours, even if done using various approaches and methods, has no significant validity in the prediction of grade/biological behaviour of tumours, if the quantitation methods are not similar in comparisons.

Immunohistochemistry of factors responsible for the modulation of apoptosis, such as FAS/FAS-L, caspases, p27, etc. may detect whether cell death is the result of controlled elimination of tumour population, as in low-grade tumours or as the result of massive uncontrolled cell death, as in high-grade tumours [36, 39]. Our finding of an indirect relationship between apoptotic rate and the expression of both p27 and pRB, even if not significant at the 0.05 level (significant at the 0.09 level), may suggest that in HGAs, uncontrolled cell death and increased cell proliferation (which is often parallel to apoptosis, see Huovinen et al. 1993 [15]) may result in a poor prognosis due to the loss of function of these main cell-cycle regulators.

The results also showed significant differences in p27 and pRB expression between LGA and HGA tumours. The finding of a decreased expression of p27 in high-grade tumours is in accordance with other studies [1, 28, 29, 30]. Astrocytoma tumour cells, which do not express p27, retain an active cyclin E/CDK2 complex, allowing them G1 to S progression. However, it was found in several studies that other cell-cycle regulators, such as CDK4, CDK6, $p16^{INK4}$ and pRB are also involved in astrocytoma progression [4, 22, 26]. Our finding of a decreased pRB expression in HGAs is in agreement with the expected inhibition (hyperphosphorylation), mutation and loss of function of the RB gene, resulting in uncontrolled cell cycle progression. Many studies demonstrated that the pRB inactivation in astrocytomas may be due not only to the blockage of the cyclin D1, D2, D3/CDK4, CDK6 complexes via the specific family of INK4 CDK inhibitors (p15, p16, p18 and p19) but also to the blockage of the cyclin E/CDK2 complex via Cip/Kip inhibitors (p21, p27 and p57). The role of the Cip/Kip family in pRB inactivation has been postulated previously [7, 11, 21, 26, 31].

Our findings suggest that there may be a loss of function of main cell-cycle regulators and increased uncontrolled cell death, in addition to increased cell proliferation in HGAs. We also deduce that immunohistochemical analysis of p27 and pRB expression could be a good tool for prediction of the biological behaviour of astrocytomas. Moreover, we believe that the detection of lamin B degradation in astroglial tumours may be an alternative, precise and convenient assay for the detection of a defined set of apoptotic cells. Comparative research of different methods for detection of apoptosis should, however, continue in order to find the best method associated with the greatest prognostic value.

Acknowledgements Supported in part by Internal Grant Agency of Czech Ministry of Health no. 4639–3 and by MSM 151100001. We thank J. Zapletalová from the Department of Biometry, Faculty of Medicine, Palacký University Olomouc, for help with statistical analysis.

References

1. Alleyne CH Jr, He J, Yang J, Hunter SB, Cotsonis G, James CD, Olson JJ (1999) Analysis of cyclin dependent kinase inhibitors in malignant astrocytomas. Int J Oncol 14:1111–1116
2. Bosman FT (1996) Nuclear structure and the lamins. J Pathol 178:3–4
3. Buenida B, Santa-Maria A, Courvalin JC (1999) Caspase-dependent proteolysis of integral and peripheral proteins of nuclear membranes and nuclear pore complex proteins during apoptosis. J Cell Sci 112:1743–1753
4. Burns KL, Ueki K, Jhung SL, Koh J, Louis DN (1998) Molecular genetic correlates of p16, cdk4 and pRb immunohistochemistry in glioblastomas. J Neuropathol Exp Neurol 57:122–130
5. Chen J, Willingham T, Shuford M, Nisen PD (1996) Tumor suppression and inhibition of aneuploid cell accumulation in human brain tumor cells by ectopic overexpression of the cyclin-dependent kinase inhibitor p27KIP1. J Clin Invest 97:1983–1988
6. Collan Y (1984) Introduction to stereology. In: Collan Y (ed) Stereology and morphometry in pathology. Kuopio University Press, Kuopio, pp 21–22
7. Costanzi-Strauss E, Strauss BE, Naviaux RK, Haas M (1998) Restoration of growth arrest by $p16^{INK4}$, p21WAF1, pRB and p53 is dependent in the integrity of the endogenous cell-cycle control pathways in human glioblastoma cell lines. Exp Cell Res 238:51–62
8. Cuvillier O, Rosenthal DS, Smulson ME, Spiegel S (1998) Sphingosine 1-phosphate inhibits activation of caspases that cleave poly(ADP-ribose) polymerase and lamins during Fas- and ceramide-mediated apoptosis in Jurkat T lymphocytes. J Biol Chem 273:2910–2916
9. Daumas-Duport C, Scheithauer B, O'Fallon J (1988) Grading of astrocytomas. A simple and reproducible method. Cancer 62:2152–2165
10. Dirks PB, Hubbard SL, Murakami M, Rutka JT (1997) Cyclin and cyclin-dependent kinase expression in human astrocytoma cell lines. J Neuropathol Exp Neurol 56:291–300
11. Dirks PB, Patel K, Hubbard SL, Ackerley C, Hamel PA, Rutka JT (1997) Retinoic acid and the cyclin dependent kinase inhibitors synergistically alter proliferation and morphology of U343 astrocytoma cells. Oncogene 15:2037–2048
12. Dynlacht JR, Story MD, Zhu WG, Danner J (1999) Lamin B is a prompt heat shock protein. J Cell Physiol 178:28–34
13. Ehrmann J Jr, Rihakova P, Hlobilkova A, Kala M, Kolar Z (2000) The expression of apoptosis-related proteins and the apoptotic rate in glial tumors of the brain. Neoplasma 47:152–156
14. Greidinger EL, Miller DK, Yamin TT, Casciola-Rosen L, Rosen A (1996) Sequential activation of three distinct ICE-like activities in Fas-logated Jurkat cells. FEBS Lett 390:299–303
15. Huovinen R, Warri A, Collan Y (1993) Mitotic activity, apoptosis and TRPM-2 mRNA expression in DMBA-induced rat mammary carcinoma treated with anti-estrogen toremifene. Int J Cancer 55:685–691
16. Huppertz B, Frank HG, Kingdom JC, Reister F, Kaufmann P (1998) Villous cytotrophoblast regulation of the syncytial apoptotic cascade in the human placenta. Histochem Cell Biol 110:495–508
17. Katayose Y, Kim M, Rakkar AN, Li Z, Cowan KH, Seth P (1997) Promoting apoptosis: a novel activity associated with the cyclin-dependent kinase inhibitor p27. Cancer Res 57:5441–5445

18. Kawahara A, Enari M, Talanian RV, Wong WW, Nagata S (1998) Fas-induced DNA fragmentation and proteolysis of nuclear proteins. Genes Cells 3:297–306
19. Kleihues P, Cavenee WK (eds) (2000) Pathology and genetics of tumours of the nervous system. IARC Press, Lyon
20. Kordek R, Hironishi M, Liberski PP, Yanagihara R, Gajdusek DC (1996) Apoptosis in glial tumours as determined by in situ nonradioactive labeling of DNA breaks. Acta Neuropathol 91:112–116
21. Korkopoulou P, Kouzelis K, Christodoulou P, Papanikolaou A, Thomas-Tsagli E (1998) Expression of retinoblastoma gene product and p21 (WAF1/Cip1) protein in gliomas: correlations with proliferation markers, p53 expression and survival. Acta Neuropathol 95:617–624
22. Lin Y, Huang C, Liu D (1997) Relationship between p16 and Rb protein expression in astrocytomas Chung hua Ping Li Hsueh Tsa Chih 26:340–342
23. Lloyd RV, Erickson LA, Jin L, Kulig E, Qian X, Cheville JC, Scheithauer BW (1999) $p27^{kip1}$: a multifunctional cyclin-dependent kinase inhibitor with prognostic significance in human cancers. Am J Pathol 154:313–323
24. Mandal M, Maggirwar SB, Sharma N, Kaufmann SH, Sun SC, Kumar R (1996) Bcl-2 prevents CD95 (Fas/APO-1)-induced degradation of lamin B and poly(ADP-ribose) polymerase and restores the NF-kappa B signalling pathway. J Biol Chem 271:30354–30359
25. Mo H, Elson CE (1999) Apoptosis and cell-cycle arrest in human and murine tumor cells are initiated by isoprenoids. J Nutr 129:804–813
26. Nakamura M, Konishi N, Tsunoda S, Hiasa Y, Tsuzuki T, Inui T, Sakaki T (1997) Retinoblastoma protein expression and MIB-1 correlate with survival of patients with malignant astrocytoma. Cancer 80:242–249
27. Nakamura M, Konishi N, Hiasa Y, Tsunoda S, Nakase H, Tsuzuki T, Aoki H, Sakitani H, Inui T, Sakaki T (1998) Frequent alterations of cell-cycle regulators in astrocytic tumors as detected by molecular genetic and immunohistochemical analyses. Brain Tumor Pathol 15:83–88
28. Nakasu S, Nakajima M, Handa J (1999) Anomalous p27kip1 expression in a subset of malignant gliomas. Brain Tumor Pathol 16:17–21
29. Piva R, Cavalla P, Bortolotto S, Cordera S, Richiardi P, Schiffer D (1997) p27/kip1 expression in human astrocytic gliomas. Neurosci Lett 234:127–130
30. Piva R, Cancelli I, Cavalla P, Bortolotto S, Dominguez J, Draetta GF, Schiffer D (1999) Proteasome-dependent degradation of p27/kip1 in gliomas. J Neuropathol Exp Neurol 58:691–696
31. Rathore A, Kamarajan P, Mathur M, Sinha S, Sarkar C (1999) Simultaneous alteration of retinoblastoma and p53 protein expression in astrocytic tumors. Pathol Oncol Res 5:21–27
32. Reyes MG, Malkin SM, Danon MJ (1983) Stereologic analysis of muscle capillaries in inclusion body myositis. In: Collan Y (ed) Stereology and morphometry in pathology. Kuopio University Press, Kuopio, pp 166–170
33. Saunders PA, Chen RW, Chuang DM (1999) Nuclear translocation of glyceraldehyde-3-phosphate dehydrogenase isoforms during neuronal apoptosis. J Neurochem 72:925–932
34. Schneider U, Mini T, Jeno P, Fischer PA, Stuurman N (1999) Phosphorylation of the major *Drosophila* lamin in vivo: site identification during both M-phase (meiosis) and interphase by electrospray ionization tandem mass spectrometry. Biochemistry 38:4620–4632
35. Shimizu T, Cao CX, Shao RG, Pommier Y (1998) Lamin B phosphorylation by protein kinase alpha and proteolysis during apoptosis in human leukemia HL60 cells. J Biol Chem 273:8669–8674
36. Strand S, Hofmann WJ, Hug H, Müller M, Otto G, Strand D (1996) Lymphocyte apoptosis induced by CD95 (Apo-1/Fas) ligand expression tumor cells – a mechanism of immune evasion? Nat Med 2:1361–1366
37. Stuurman N, Heins S, and Aebi U (1998) Nuclear lamins: their structure, assembly, and interactions. J Struct Biol 122:42–66
38. Wuerzberger SM, Pink JJ, Planchon SM, Byers KL, Bornmann WG, Boothman DA (1998) Induction of apoptosis in MCF-7:WS8 breast cancer cells by beta-lapachone. Cancer Res 58:1876–1885
39. Williams N (1996) Tumor cells fight back to beat immune system. Science 274:1362–1363

Virchows Arch (2001) 439:552–559
DOI 10.1007/s004280100419

ORIGINAL ARTICLE

Eric M. J. Bindels · Marcel Vermey · Nico J. De Both
Theodorus H. van der Kwast

Influence of the microenvironment on invasiveness of human bladder carcinoma cell lines

Received: 22 August 2000 / Accepted: 11 January 2001 / Published online: 22 May 2001
© Springer-Verlag 2001

Abstract To investigate the importance of the microenvironment in bladder cancer invasion, a panel of six bladder carcinoma cell lines (SD, RT112, JON, 1207, T24, and J82) was tested in both in vitro and in vivo invasion assays. Furthermore, invasiveness was correlated with the expression of components of the E-cadherin–catenin complex. The E-cadherin-negative cell lines, T24 and J82, displayed a high in vitro invasive capacity, whereas the E-cadherin-positive cell lines, SD and JON, completely lacked in vitro invasive capacity. In contrast, in vivo invasion was noted for all cell lines, with the exception of cell line JON. Most notably, SD formed highly invasive tumors in vivo. The in vivo invasiveness of the E-cadherin-positive bladder carcinoma cell lines was associated with a heterogeneous expression of the E-cadherin–catenin complex. The discrepancy between in vitro and in vivo invasive behavior implies that, in vivo, the microenvironment plays an important role in the establishment of the invasive phenotype. In addition, it was found that orthotopic xenografting of 1207 and T24 bladder carcinoma cells resulted in site-specific tumor take and an enhanced tumor outgrowth and invasiveness, respectively, compared with heterotopic (i.e., subcutaneous) inoculation. We conclude that the site-specific growth and invasion of the bladder carcinoma cell lines in vivo and the observed assay specific invasion (in vitro vs in vivo) points to an effect of the local (bladder) microenvironment on tumor cell behavior.

Keywords Bladder carcinoma · Microenvironment · Neoplasm invasiveness · E-cadherin · Catenins

T.H. van der Kwast (✉)
Department of Pathology, Josephine Nefkens Institute,
Erasmus University Rotterdam, PO Box 1738,
3000 DR Rotterdam, The Netherlands
e-mail: vanderkwast@path.fgg.eur.nl

E.M.J. Bindels · M. Vermey · N.J. De Both
Department of Pathology, Erasmus University,
Rotterdam, The Netherlands

Introduction

Bladder cancer is the fifth most common malignancy in males in the Western world. From a clinical point of view, bladder cancers can be divided into superficial and deeply invasive tumors. Superficial bladder carcinomas have a relatively good prognosis despite a high recurrence rate after transurethral resection [18]. Only a small proportion of these superficial carcinomas progress to invasive disease, and distant metastases only seldom develop [19]. Invasive bladder carcinoma, however, has a much less favorable prognosis than superficial bladder carcinoma. Despite the use of aggressive therapies, invasive bladder carcinomas have a 5-year survival rate of 50% or less [30]. The key regulators involved in the invasion of bladder tumors into the bladder wall are only partially understood. A further elucidation of these processes requires relevant in vitro and in vivo tumor models.

A currently available in vitro model for tumor invasion is the well-documented embryonic chicken heart invasion assay, which has been used to study several epithelial tumor systems [2, 37, 38]. Since paracrine effects of the host tissue may regulate the expression of invasion promoting or suppressing molecules, it can be anticipated that in vitro observations may not necessarily be identical to in vivo findings. Furthermore, for some tumor systems, it was demonstrated that the site of tumor cell inoculation might influence tumor growth, invasion and metastasis [26]. Particularly, orthotopic xenografting has been shown to enhance tumor take, invasive properties, and metastatic behavior of a number of human carcinoma cell lines [27, 32]. Therefore, we compared the in vitro invasive properties of six human bladder carcinoma cell lines with their invasiveness after orthotopic and heterotopic inoculation in SCID (severe combined immunodeficiency syndrome) mice. SCID mice were chosen as a host strain, since it was demonstrated that these mice were more apt to permit xenograft take than nude mice [6, 8, 16].

An initial step in the invasive process is the detachment of tumor cells from the in situ carcinoma. It has

been proposed that loss of cell–cell adhesions is a prerequisite for detachment of cells from the primary tumor mass. The E-cadherin–catenin complex primarily determines epithelial cell–cell adhesion. In tumor models, loss of E-cadherin expression appears to be associated with the gain of the invasive phenotype. Similarly, loss of the invasion suppressor molecule E-cadherin is predictive for poor survival of patients with bladder cancer [4, 36]. Furthermore, abnormal expression of the cytoplasmatic, E-cadherin-associated proteins (α-, β-, γ-catenin and p120^{cas}) was also correlated with tumor grade, stage, and poor prognosis [35]. Because these studies suggest that the downregulation of the E-cadherin–catenin complex is involved in invasive bladder carcinoma, we also studied the expression of members of the E-cadherin–catenin complex during the in vitro and in vivo invasion assays.

Our results showed that the transitional cell carcinoma (TCC) cell lines which were used demonstrated a different cell biological behavior in the applied bioassays. In vitro, invasion of the TCC cell lines into the embryonic chicken heart fragments was strongly correlated with absent or heterogeneous expression of E-cadherin. However, transplantation of tumor cells into SCID mice resulted in an enhanced invasive capacity of the E-cadherin-positive TCC cell lines. Furthermore, two TCC cell lines (1207 and T24) exhibited site-specific growth and invasion. These results point to a specific influence of the (bladder) microenvironment on tumor growth and invasion.

Materials and methods

Cell lines

The human bladder cancer cell lines T24, SD, RT112, JON, and J82 were kindly provided by Prof. Dr. J.A. Schalken, Urological Research Laboratory, University Hospital Nijmegen, The Netherlands, and have been characterized previously [23, 29]. Bladder carcinoma cell line 1207 was obtained from Dr. W.I. De Boer, GETU Service d'Urologie, Paris, France [10]. Cells were maintained in DMEM supplemented with 10% heat-inactivated fetal calf serum (FCS), 100 IU/ml penicillin and 100 µg/ml streptomycin at 37°C in a 5% CO_2 atmosphere.

Antibodies

Monoclonal antibody RCK108 directed against cytokeratin 19 (Eurodiagnostica, Arnhem, The Netherlands) or monoclonal antibody DC10 directed against cytokeratin 18 (Beckman Coulter, Fullerton, Calif.) was used to distinguish the human bladder carcinoma cells from murine tissue (in vivo assay) or embryonic chicken heart tissue (in vitro assay). This is based on the species specificity of these two antibodies for human cytokeratins. Monoclonal antibody DC10 was used for staining J82 cells, whereas the other cell lines were stained with monoclonal antibody RCK108. Nearly 100% of the bladder carcinoma cells of each cell line were labeled with RCK108 or DC10. The mouse monoclonal anti-bromodeoxyuridine (BrdU) antibody IIB5 (kindly donated by Dr. B. Schutte, University of Maastricht, The Netherlands) was used to visualize cells that had incorporated BrdU during the S-phase of the cell cycle. Expression of E-cadherin was demonstrated with the monoclonal antibody 5H9 (Eurodiagnostica) raised against an 80-kDa tryptic fragment of E-cadherin, derived from human A-431 carcinoma cells. This antibody also detects the 120-kDa mature E-cadherin protein [25]. The monoclonal antibodies against α- and β-catenin were obtained from Transduction Laboratories (Lexington, Ky.).

Immunohistochemistry

E-cadherin, α- and β-catenin expression by bladder tumor cells in vitro was determined as follows: cell lines were cultured on multichamber slides until confluency was reached and fixed in cold acetone (–20°C) for 1 h. After drying, the slides were incubated with the different primary antibodies, followed by visualization with fluorescein isothiocyanate (FITC)-conjugated rabbit anti-mouse immunoglobulins (Dako, Glostrup, Denmark).

For immunohistochemistry on paraffin-embedded tissues, 5-µm-thick paraffin sections were mounted on 3-amino-propyl-triethoxy-silane (Sigma, St. Louis, Mo.) coated slides and dried overnight at 37°C. Sections were deparaffinized, endogenous peroxidase was blocked in 3% H_2O_2 in methanol (20 min), and the sections were then rinsed in phosphate-buffered saline (PBS).

For antigen retrieval, sections were digested for 10 min in 0.1% pronase (Sigma; containing 1% $CaCl_2$ for E-cadherin staining) in PBS. Prior to α- and β-catenin staining, sections were boiled twice for 5 min in a solution of 0.01 M citrate (pH 6.0) in a microwave oven. Paraffin sections of normal human skin were used as positive controls for E-cadherin, α- and β-catenin staining. For BrdU-staining, after the antigen retrieval procedure was performed, slides were incubated in 2 N HCl for 30 min, followed by two 5-min washes with Borax buffer [34]. Prior to the application of the primary antibodies, non-specific binding was blocked with 10% normal goat serum diluted in PBS containing 1% bovine serum albumin. Incubation with the primary antibody was followed by a biotinylated goat anti-mouse antibody (Dako) and, subsequently, a horseradish peroxidase conjugated streptavidin-biotin complex (Biogenex, San Ramon, Calif.). Peroxidase activity was visualized with 0.03% H_2O_2 and 0.02% 3,3,-diaminobenzidine tetrahydrochloride (DAB; Fluka, Basel, Switzerland) diluted in PBS. The slides were counterstained with Mayer's hematoxylin, dehydrated, and mounted.

In vivo tumorigenicity of cell lines

The tumorigenicity of each cell line was tested in 6-week-old female SCID mice (B17/ICR Han Hsd-SCID), obtained from Harlan (Zeist, The Netherlands). Bladder carcinoma cells suspended in Hanks' buffered salt solution were injected both subcutaneously ($\pm 4\times10^6$ cells) in a volume of 200 µl and in the submucosa of the bladder ($\pm 1\times10^6$ cells) in a volume of 50 µl. For inoculation of tumor cells in the bladder wall, an abdominal incision was made in mice anaesthetized with avertine (0.25 mg/g body weight). One hour before the mice were sacrificed, they received an intraperitoneal injection of BrdU (40 mg/kg body weight) in 0.15 M NaCl. Under a dissecting microscope, tumor inoculation sites plus other relevant organs were removed and fixed in 4% phosphate-buffered formalin for 16 h before paraffin embedding.

Determination of the proliferative activity of TCC in vivo

Proliferative activity was determined by counting BrdU-positive nuclei in a total of 1000 nuclei, at four random areas of the tumor. Proliferation is expressed as the labeling index: number of BrdU-positive nuclei/total number of nuclei ×100%.

Morphometry

The size of in vivo-formed tumors was estimated using image analysis. Serial sections were cut, and the estimated largest tumor

area was determined from the immunostainings with the RCK108 or DC10 antibody. Subsequently, these tumor areas were quantitated using a Hitachi CCTV camera equipped with the KS400 image analysis software package (Kontron Elektronik, Eching, Germany).

In vitro invasion assay

Chicken heart invasion assays were performed as described by Mareel et al. [22]. Briefly, human bladder tumor cells were confronted with precultured rounded fragments of embryonic chicken heart on soft agar for 24 h. Next, the fragments with attached bladder tumor cells were kept in suspension culture under gyrotory shaking (120 rpm, 37°C) in MEM REGA 3 medium (GibcoBRL/Life Technologies, Breda, The Netherlands), containing 10% FCS.

After 6 days of cocultivation, fragments were fixed in Bouin-Hollande's solution and embedded in paraffin. Invasion was scored on serial histological sections stained with hematoxylin/eosin. The tumor cells can be discerned from the heart tissue by their more basophilic staining. Additional confirmation of invasion was obtained using selective keratin (RCK108 and DC10) immunostaining of the human bladder carcinoma cells.

Morphology of tumor cells on Matrigel

The morphological appearance of bladder tumor cells on Matrigel was assessed. Therefore, 200 µl growth factor-reduced Matrigel (9.64 mg/ml; Becton Dickinson, Bedford, Mass.) per well was allowed to polymerize for 30 min at 37°C in a 24-well plate. Subsequently, the same Matrigel solution containing 1×10^4 tumor cells was poured on top of the polymerized Matrigel. After the gelation of the second Matrigel solution, standard culture medium was pipetted on top. After 1 week, morphology of the bladder tumor cells (epithelial or fibroblast-like) was recorded using microscopic examination.

Results

In vivo tumorigenicity

Tumor take, tumor size, muscle invasion, and proliferative activity after heterotopic (subcutaneous) and orthotopic inoculation of each of the six cell lines was examined (Table 1). A tumor take of 100% was observed for SD and RT112 bladder carcinoma cells both after orthotopic and heterotopic inoculation. Both cell lines clearly invaded the muscle tissue underlying the skin or bladder mucosa (Fig. 1A, B). The size of the subcutaneous tumors was four- to ten-fold larger than the bladder tumors, possibly reflecting the larger number of cells inoculated subcutaneously. SD and RT112 tumors occasionally penetrated through the bladder mucosa into the bladder lumen.

We observed a high take rate after both heterotopic and orthotopic inoculation of T24 cells in SCID mice (Table 1). Strikingly, subcutaneous T24 tumors were rather small, and no muscle invasion was noted (Table 1 and Fig. 1D). In contrast, T24 tumors, localized in the bladder, were about threefold larger, showed muscle invasion (Fig. 1C), and had a significantly higher proliferative activity than subcutaneous T24 tumors (Table 1).

Site-specific tumor take was seen for cell line 1207. Although in four out of five mice, orthotopically injected with 1207 cells, tumors had developed in the bladder wall (two were muscle-invasive), no tumors were found at the subcutaneous injection sites despite the larger number of subcutaneously inoculated tumor cells. Microscopic examination of the subcutaneous injection sites confirmed this observation. The two muscle invasive 1207 tumors also showed penetration into the bladder lumen.

JON cells demonstrated a high take rate both hetero- and orthotopically, but muscle invasion was completely lacking. The subcutaneous JON tumors showed an expanding growth pattern with sharp tumor borders. These tumors were associated with an inflammatory infiltrate. The tumor take of J82 was low, both after orthotopic and heterotopic inoculation. In one mouse, a large muscle invasive subcutaneous tumor was found.

In none of the injected mice were lymphogenic or distant metastases found, but regional lymph vessels in the loose connective tissue surrounding the bladders of mice injected with SD, RT112, or T24 bladder carcinoma cells occasionally contained isolated small tumor aggregates (Fig. 1A).

In vitro embryonic chicken heart invasion assay and tumor cell morphology on Matrigel

In vitro invasion of bladder carcinoma cells was examined after 4–6 days of cocultivation with embryonic

Table 1 Heterotopic and orthotopic tumorigenicity of bladder carcinoma cell lines. *Htr* heterogeneous; *Hom* homogeneous; *Neg* absent expression at the cell membrane; *labeling index* percentage of BrdU (anti-bromodeoxyuridine)-positive cells; – no subcutaneous tumors

Cell line	Mean follow-up period in days (range)	Bladder		Subcutaneous		E-cadherin in vivo	Labeling index		Estimated largest area	
		Tumor take	Muscle invasion	Tumor take	Muscle invasion		Bladder (mean±SD)	Subcutaneous (mean±SD)	Bladder (mean±SD)	Subcutaneous (mean±SD)
SD	39.5 (35–53)	4/4	4/4	4/4	4/4	Htr	13.4±9.3	16.3±3.4	6.0±6.5	21.2±10.8[a]
RT112	37.5 (27–53)	4/4	3/4	4/4	3/4	Htr	22.0±1.6	19.4	3.5±4.1	34.6±19.3[a]
T24	58 (35–74)	4/4	3/4	3/4	0/3	Neg	10.3±2.9[a]	2.0±0.7	4.0±1.1[a]	1.2±1.6
1207	50.6 (29–53)	4/5	2/4	0/5	0/0	Htr	16.1±3.8	–	2.2±2.6	–
Jon	50.2 (31–57)	5/5	0/5	4/5	0/4	Hom	16.3±2.6	13.2±4.3	1.5±1.5	2.6±1.6
J82	42 (40–53)	2/5	0/2	1/5	1/1	Neg	21.0±0.0	17.3[b]	3.1±4.1	53.2

[a] Significantly different in bladder compared with subcutaneous (*t* test; $P<0.05$)
[b] Only one tumor was available for analysis

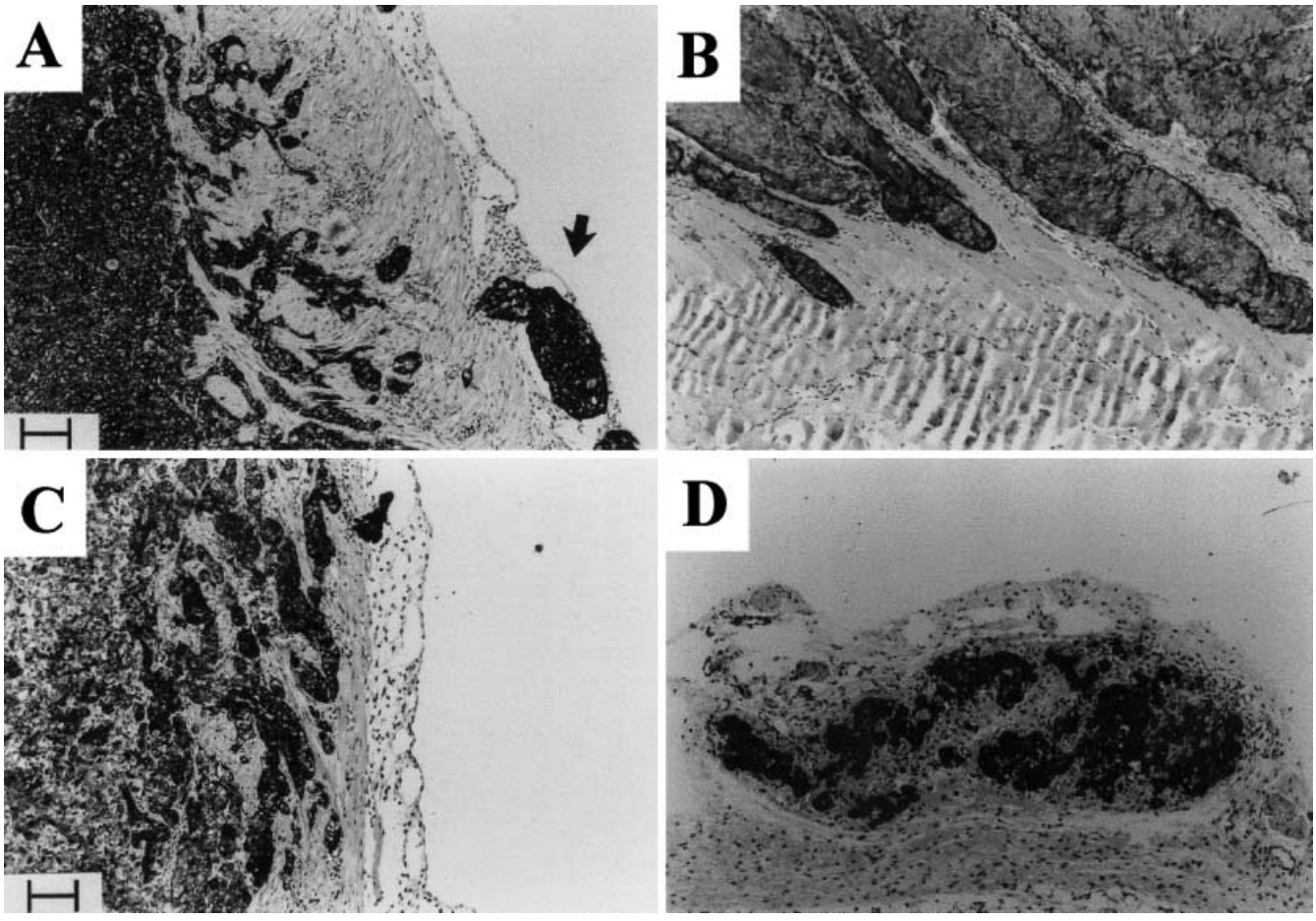


Fig. 1 Tumorigenicity of bladder tumor cells. Tumor cells were selectively stained with RCK108. Invasion of RT112 cells into the submucosa and muscularis of the bladder (**A**) and the skeletal muscle underneath the skin (**B**). Note the clump of RT112 cells in a perivesicular lymph vessel of the bladder (**A**; *arrow*). Part of a large orthotopic tumor of T24 cells in the bladder (**C**) and, as a reference, the small tumor in the subcutis (**D**). *Scale bar* 100 µm

Table 2 In vitro invasion of transitional cell carcinoma (TCC) cell lines. *Htr* heterogeneous; *Hom* homogeneous; *Neg* absent expression at the cell membrane; *cytopl/cell-membr* cytoplasm/cell membrane; *I* invasive; *TC* tight colonies, criteria adapted from [35]

Cell line	E-cadherin expression in vitro	α-catenin expression in vitro	β-catenin expression in vitro	In vitro confronting cultures Adherent[a]	In vitro confronting cultures Invasive[b]	Morphology Matrigel
SD	Hom	Hom	Hom	37/38 (97%)	0/37 (0%)	TC Epithelial
RT112	Hom	Hom	Hom	9/15 (60%)	3/9 (33%)	TC Epithelial
T24	Neg	Htr Cytopl/cell-membr	Hom	18/30 (60%)	16/18 (89%)	I Fibroblastic
1207	Htr	Hom	Hom	28/45 (62%)	11/28 (39%)	TC epithelial
JON	Hom	Hom	Hom	8/15 (53%)	0/8 (0%)	TC Epithelial
J82	Neg	Htr Cytopl/cell-membr	Hom	9/17 (53%)	8/9 (89%)	I Fibroblastic

[a] Number of adherent/total number of confronted embryonic chicken heart cultures
[b] Number of invasive/number of confronted cultures with adherent tumor cells

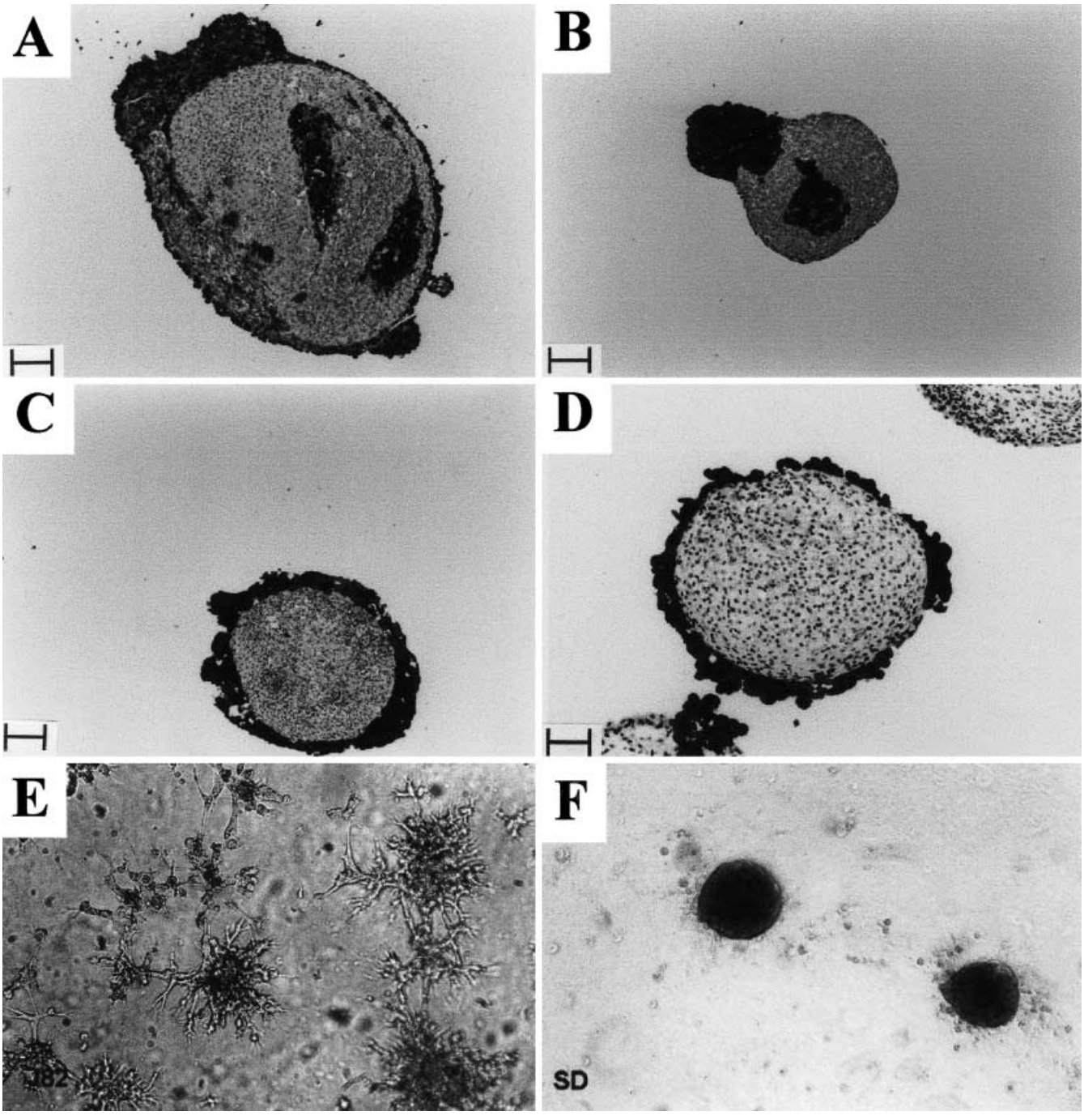


Fig. 2 Confronting cultures of invasive and noninvasive human transitional cell carcinoma (TCC) cells with embryonic chicken heart fragments. Photomicrographs from paraffin sections of embryonic chick heart fragments confronted in organ culture with the cell lines T24 (**A**) and 1207 (**B**) that invaded the fragments and two noninvasive cell lines SD (**C**) and JON (**D**); the former engulfs the chicken heart tissue. Bladder tumor cells could be discerned from the chick tissue using a selective staining with the human-specific antibody RCK108. *Scale bar* 100 µm; except **D,** *scale bar* 50 µm. Phase-contrast photomicrographs of colonies formed in solid Matrigel. Examples of colonies with fibroblastic appearance formed by cell line J82 (**E**) and of epithelioid colonies formed by cell line SD (**F**)

chicken heart fragments. Adhesion of tumor cells to chicken heart fragments varied from 53% of the cases for JON and J82 cells to 97% of the cases for the SD cells (Table 2). T24 and J82 cells showed the strongest invasive capacity. After successful adhesion, nearly all embryonic chicken heart fragments were infiltrated by these E-cadherin-negative tumor cells (Fig. 2A). RT112 and 1207 (Fig. 2B) cells had a moderate capacity (33% and 39% of the cases, respectively) for invading heart fragments, whereas SD (Fig. 2C) and JON (Fig. 2D) cells were not able to invade the embryonic chicken heart fragments at all. The SD cell line formed a clear

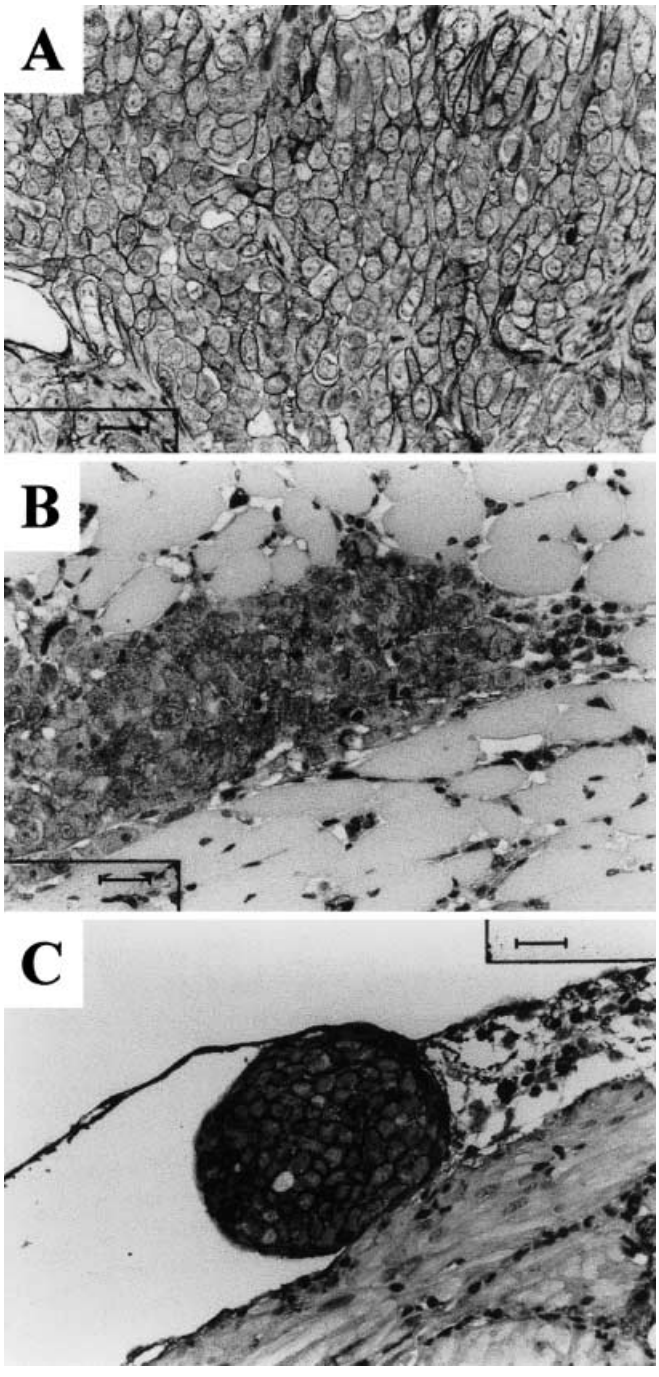


Fig. 3 Expression of E-cadherin in vivo. Normal expression of E-cadherin in a SD tumor (**A**). Reduced expression of E-cadherin in an invasive region of a subcutaneous SD tumor (**B**). RT112 cells in a perivesicular lymph vessel of the bladder, with normal expression of E-cadherin (**C**). *Scale bar* 25 μm

epithelioid cell layer around the embryonic heart tissue (Fig. 2C), a feature characteristic for cells with a functionally intact E-cadherin–catenin complex [37].

To determine the epithelial or mesenchymal morphotype of the used cell lines, cell lines were cultured in solid Matrigel substrate (method adapted from [37]). After 1 week of culture in solid Matrigel (Table 2), the constitutively E-cadherin-negative T24 and J82 (Fig. 2E) cells had a fibroblastic morphology. In contrast, the E-cadherin-positive cell lines, SD (Fig. 2F), RT112, and JON, expressed an epithelial morphology with formation of densely packed colonies. Bladder carcinoma cell line 1207, with a heterogeneous expression of E-cadherin, had an epithelial morphology when cultured in Matrigel.

In vitro and in vivo expression of E-cadherin and α- and β-catenin

Data on expression of E-cadherin and α- and β-catenin on confluent cultures of bladder carcinoma cell lines visualized using immunohistochemistry are summarized in Table 2. Expression patterns of E-cadherin were compared between the in vivo and in vitro assays. Cell lines T24 and J82 lacked E-cadherin expression in vivo and in vitro (Table 1 and Table 2). The cell lines, SD and RT112, which display a homogeneous E-cadherin expression in vitro, displayed a heterogeneous cell membrane immunostaining in vivo both in the subcutaneous tumors and in the tumors located in the bladder wall. Regions with normal expression of E-cadherin were seen in the central areas of these tumors (Fig. 3A). Reduced expression of E-cadherin was primarily seen in the invasive borders of these tumors (Fig. 3B). Strikingly, the isolated small aggregates of SD and RT112 tumor cells in lymph vessels had a normal expression of E-cadherin (Fig. 3C). The expression patterns of either α- or β-catenin was similar to the expression pattern of E-cadherin in the different tumors.

Discussion

The six human bladder carcinoma cell lines studied in this paper display a considerable heterogeneity of cell biological characteristics with respect to their invasive potential both in vitro and in vivo. SCID mice proved to be a very suitable host strain, allowing successful grafting of all six examined human bladder carcinoma cell lines. This was emphasized by xenografting T24 cells in SCID mice. Tumor take of T24 cells in nude mice is poor or absent both after orthotopic and heterotopic inoculation [23; unpublished]. Strikingly, T24 tumor growth, as reflected by tumor size, proliferative activity, and tumor invasiveness, was enhanced by the orthotopic inoculation (Table 1). Cells from cell line 1207 exhibited site-specific outgrowth, since 1207 tumor take only occurred after orthotopic transplantation. No signs of distant metastases for any of the xenografted TCC cell lines were found. Although isolated (RT112, SD, and T24) tumor aggregates were found in the perivesicular loose connective tissue, no lymph-node metastases were found. The short follow-up period of 2 months may account for this.

We compared the in vivo invasiveness of the various TCC cell lines with the results of the in vitro assay. The results of the in vitro embryonic chicken heart invasion

assay did not match the in vivo invasive behavior of some of the tested TCC cell lines, most notably SD. The SD cell line was not invasive in vitro, but after subcutaneous injection and after inoculation in the bladder wall, SD cells developed muscle-invasive tumors. Similar discrepancies between the embryonic chicken heart invasion assay and in vivo invasiveness were reported earlier in a study on colorectal carcinoma cell lines [11, 12]. Our results support the view that the microenvironment may regulate invasive behavior of bladder carcinoma cells in vivo, for instance by influencing the expression of E-cadherin, as suggested by Mareel et al. [21] or by induction of synthesis of extracellular matrix degrading proteins [33]. More recent studies have shown that there is a link between cell–cell adhesion and proteinase production that promotes invasiveness of tumor cells [20, 28].

We studied the immunochemical expression of the E-cadherin–catenin complex in vivo and in vitro and its correlation with invasiveness. The observed in vitro expression of the various members of the E-cadherin–catenin complex in the TCC cell lines was confirmed by means of Western blotting by Giroldi et al. [14]. In vivo, a heterogeneous E-cadherin and catenin expression by SD and RT112 cells was observed, in contrast to their homogeneous E-cadherin–catenin expression in vitro. Loss or reduced expression of the E-cadherin–catenin complex was primarily seen in the invasive regions of these tumors. These findings and the normal E-cadherin and α- and β-catenin expression by small aggregates of SD and RT112 tumor cells in lymph vessels (early sign of metastasis) suggests that the microenvironment may transiently reduce the expression of the E-cadherin–catenin complex during formation of invasive bladder tumors in SCID mice. Transient downregulation of E-cadherin expression in vitro is described previously and could possibly be accomplished through activation of exogenous *c-fos* [31], via c-erb2 [13] or transforming growth factor-β [24]. Furthermore, expression could be regulated by methylation of the E-cadherin gene or via tissue-specific responsive elements in the E-cadherin promoter [9]. Recent investigations have identified the transcription factor Snail, which could bind to E boxes in the human E-cadherin promoter and, thereby, repress transcription of E-cadherin [1, 7]. Furthermore, Keirsebilck et al. described that the in vivo transient downregulation of E-cadherin could be caused by instability of the E-cadherin messenger (m)RNA [17]. Recently, Bringuier et al. showed that abnormal E-cadherin immunoreactivity in bladder tumors is associated with mRNA downregulation or post-transcriptional downregulation of E-cadherin. In the same series of bladder tumors, no structural alterations of the E-cadherin gene were detected [5]. These findings corroborate with our observations on the transient reduction of E-cadherin expression in invasive bladder tumors.

A strong correlation was found between the in vitro expression of E-cadherin of bladder carcinoma cells and their ability to invade embryonic chicken heart fragments. Similar results were reported for cell lines of other origin [2, 37, 38]. The two E-cadherin-negative cell lines T24 and J82 were generally capable of invasion of the embryonic chicken heart, whereas the (in vitro) homogeneously E-cadherin-positive SD and JON cells showed no invasion. The epithelial morphology of these E-cadherin-positive cell lines grown on Matrigel is in accordance with their functionally intact membrane-bound E-cadherin–catenin complex [37].

The in vitro invasive cell lines, T24 and J82, had a fibroblastic morphotype when cultured on solid Matrigel. This is in accordance with the observation that the epithelial-to-mesenchymal transition is correlated with gain of motility and invasive disease [15]. The 1207 cells with a heterogeneous expression of E-cadherin had a rather limited infiltrative capacity in the embryonic chicken heart invasion assay. Surprisingly, RT112 cells with in vitro homogeneous E-cadherin and catenin expression were also capable of embryonic chicken heart invasion in one-third of the samples. Booth et al. showed that RT112 cells could invade the subepithelial capillary bed after culture on urinary tract stroma. In the same paper, they showed that these RT112 cells had partially lost their E-cadherin expression [3]. A similar in vitro mechanism could have occurred in our embryonic chicken heart invasion assay.

In conclusion, we have studied the invasive properties of six bladder carcinoma cell lines with the use of in vitro and in vivo invasion assays. We have shown that the use of SCID mice allows a high tumor take for bladder cancer cell lines, including those which proved to be poorly if at all tumorigenic in nude mice. Bladder tumor cell lines 1207 and T24, on the basis of their site-dependent tumor take and tumor outgrowth, respectively, may be considered to resemble more closely organ-confined human bladder carcinomas with regard to their response to growth-modulating factors and extracellular matrix proteins. The view that the microenvironment influences the induction of bladder tumor invasion is supported by the observation that the results of the in vitro invasion assay of E-cadherin-positive bladder carcinoma cell lines did not correlate well with their invasive properties in vivo. Transient downregulation of the E-cadherin–catenin complex may in part explain the observed invasive capacity in vivo of the latter cell lines.

References

1. Battle E, Sancho E, Franci C, Dominguez D, Monfar M, Baulida J, Garcia de Herreros A (2000) The transcription factor Snail is a repressor of E-cadherin gene expression in epithelial tumour cells. Nat Cell Biol 2:84–89
2. Behrens J, Vakaet L, Friis R, Winterhager E, Van Roy F, Mareel M, Birchmeier W (1993) Loss of epithelial differentiation and gain of invasiveness correlates with tyrosine phosphorylation of the E-cadherin/ß-catenin complex in cells transformed with a temperature-sensitive v-SRC gene. J Cell Biol 120:757–766
3. Booth C, Harnden P, Trejdosiewicz LK, Scriven S, Selby PJ, Southgate J (1997) Stromal and vascular invasion in a human in vitro bladder cancer model. Lab Invest 76:843–857

4. Bringuier PP, Umbas R, Schafsma HE, Karthaus HFM, Debruyne FMJ, Schalken JA (1993) Decreased E-cadherin immunoreactivity correlates with poor survival in patients in bladder cancer. Cancer Res 53:3241–3245
5. Bringuier PP, Giroldi LA, Umbas R, Shimazui T, Schalken JA (1999) Mechanisms associated with abnormal E-cadherin immunoreactivity in human bladder tumors. Int J Cancer 83:591–595
6. Calaf G, Russo J (1993) Transformation of human breast epithelial cells by chemical carcinogens. Carcinogenesis 14:483–492
7. Cano A, Perez-Moreno MA, Rodrigo I, Locascio A, Blanco MJ, del Barrio MG, Portillo F and Nieto MA (2000) The transcription factor Snail controls epithelial-mesenchymal transitions by repressing E-cadherin expression. Nat Cell Biol 2: 76–83
8. Chang SE (1966) In vitro transformation of human epithelial cells. Biochem Biophys Acta 823:161–194
9. Christofori G, Semb H (1999) The role of the cell-adhesion molecule E-cadherin as a tumor-suppressor gene. TIBS 24: 73–76
10. De Boer WI, Houtsmuller AB, Izadifar V, Muscatelli-Groux B, Van Der Kwast TH, Chopin D (1997) Expression and function of EGF, FGF and TGFβ-growth factor family members and their receptors in invasive human transitional-cell-carcinoma cells. Int J Cancer 71:284–291
11. De Both NJ, Vermey M, Dinjens WN, Bosman FT (1999) A comparative evaluation of various invasion assays testing colon carcinoma cell lines. Br J cancer 81:934–941
12. De Vries JE, Dinjens WNM, De Bruyne GK, Verspaget HW, Van Der Linden PM, De Bru AP, Mareel MM, Bosman FT, Ten Kate J (1995) In vivo and in vitro invasion in relation to phenotypic characteristics of human colorectal carcinoma cells. Br J Cancer 71:271–277
13. D'Souza B, Taylor-Papadimitriou J (1994) Overexpression of ERB2 in human mammary epithelial cells signals inhibition of transcription of the E-cadherin gene. Proc Natl Acad Sci USA 91:7202–7206
14. Giroldi LA, Bringuier P-P, Shimazui T, Jansen K, Schalken JA (1999) Changes in cadherin-catenin complexes in the progression of human bladder carcinoma. Int J Cancer 82:70–76
15. Hay ED (1995) An overview of epithelio-mesenchymal transformation. Acta Anat 154:8–20
16. Jankun J, Keck RW, Skrzypcak-Jankun E, Swiercz R (1997) Inhibitors of urokinase reduced size of prostate cancer xenografts in severe combined immunodeficient mice. Cancer Res 57:559–563
17. Keirsebilck A, van Hoorde L, Gao Y, de Bruyne G, Bruyneel E, Vermassen P, Mareel M, van Roy F (1998) Mechanisms of downregulation of transfected E-cadherin cDNA during formation of invasive tumors in syngeneic mice. Invasion Metastasis 18:44–56
18. Kurth KH, Schröder FH, Debruyne F, Senge T, Pavone-Macaluso M, De Pauw M,Ten Kate F, Sylvester R, members of the EORTC Genitourinary Tract Cancer Cooperative Group (1989) Long-term follow-up in superficial transitional cell carcinoma of the bladder: prognostic factors for time to first recurrence, recurrence rate, and survival. Prog Clin Biol Res 303:481–490
19. Liponnen PK (1992) Review of cytometric methods in the assessment of prognosis in transitional cell bladder cancer. Eur Urol 21:177–183
20. Llorens A, Rodrigo I, López-Barcons L, Gonzalez-Garrigues M, Lozano E, Vinyals A, Quintanilla M, Cano A, Fabra A (1998) Down-regulation of E-cadherin in mouse skin carcinoma cells enhances a migratory and invasive phenotype linked to matrix metalloproteinase-9 gelatinase expression. Lab Invest 78:1131–1142
21. Mareel MM, Behrens J, Birchmeier W, De Bruyne GK, Vleminckx K, Hoogewijs A, Fiers WC, van Roy FM (1991) Downregulation of E-cadherin expression in Madin Darby canine kidney (MDCK) cells inside tumors of nude mice. Int J Cancer 47:922–928
22. Mareel M, Kint J, Meyvisch C (1977) Methods of study of the invasion of malignant C3H mouse fibroblasts into embryonic chicken heart in vitro. Virchows Arch 30:95–111
23. Masters JRW, Hepburn PJ, Walker L, Highman WJ, Trejdosiewisz LK, Povey S, Parkar M, Hill BT, Riddle PT, Franks LM (1986) Tissue culture model of transitional cell carcinoma: characterization of twenty-two human urothelial cell lines. Cancer Res 46:3630–3636
24. Mietinnen PJ, Ebner R, Lopez AR, Derynck R (1994) TGF-beta induced transdifferentiation of mammary epithelial cells to mesenchymal cells: involvement of type I receptors. J Cell Biol 127:2021–2036
25. Moll R, Mitze M, FrixenUH, Birchmeier W (1993) Differential loss of E-cadherin expression in infiltrating ductal and lobular breast carcinomas. Am J Pathology 143:1731–1742
26. Morikowa K, Walker SM, Nakajima M, Pathak S, Jessup JM, Fidler IJ (1988) Influence of organ environment on the growth, selection and metastasis of human colon carcinoma cells in nude mice. Cancer Res 48:6863–6871
27. Naito S, Von Eschenbach AC, Giavazzi R, Fidler IJ (1986) Growth and metastasis of tumor cells isolated from a human renal cell carcinoma implanted into different organs of nude mice. Cancer Res 46:4109–4115
28. Noë V, Fingleton B, Jacobs K, Crawford HC, Vermeulen S, Steelant W, Bruyneel E, Matrisian LM, Mareel M (2001) Release of an invasion promoter E-cadherin fragment by matrilysin and stromelysin-1. J Cell Sci 114:111–118
29. Paulie S, Hansson Y, Lundblad ML, Perlmann P (1983) Lectins as probes for identification of tumor associated antigens on urothelial and colonic carcinoma cell lines. Int J Cancer 31:297–303
30. Raghavan D, Shipley WU, Garnick MB, Rusell PJ, Richie JP (1990) Biology and management of bladder cancer. New Engl J Med 322:1129–1138
31. Reichmann E, Schwarz H, Deiner EM, Leitner I, Eilers M, Berger J, Busslinger M, Beug H (1992) Activation of an inducible c-FosER fusion protein causes loss of epithelial polarity and triggers epithelial-fibroblastoid cell conversion. Cell 71:1103–1116
32. Rembrink K, Romijn JC, Van Der Kwast TH, Rüben H, Schröder FH (1997) Orthotopic implantation of human prostate cancer cell lines: a clinically relevant animal model for metastatic prostate cancer. The Prostate 31:168–174
33. Sato H, Takino T, Okada Y, Cao J, Shinagawa A, Yamamoto E, Seiki M (1994) A matrix metalloproteinase expressed on the surface of invasive tumour cells. Nature 370:61–65
34. Schutte B, Reynders MMJ, Van Assche CLMVJ, Hupperts PSGJ, Bosman FT, Blijham GH (1987) Studies with anti-bromodeoxyuridine antibodies. Cytometry 8:372–376
35. Shimazui T, Schalken JA, Giroldi LA, Jansen CFJ, Akaza H, Koiso K, Debruyne FMJ, Bringuier PP (1996) Prognostic value of cadherin-associated molecules (α-, β-, γ-catenins and $p120^{cas}$) in bladder tumors. Cancer Res 56:4154–4158
36. Syrigos KN, Krausz T, Waxman J, Pandha H, Rowlinson-Busza G, Verne J, Epenetos A, Pignatelli M (1995) E-cadherin expression in bladder cancer using formalin-fixed, paraffin-embedded tissues: correlation with histopathological grade, tumor stage and survival. Int J Cancer 64:367–370
37. Vermeulen SJ, Bruyneel EA, Bracke ME, De Bruyne GK, Vennekens KM, Vleminckx KL, Berx GJ, van Roy FM, Mareel MM (1995) Transition from the noninvasive to the invasive phenotype and loss of α-catenin in human colon cancer cells. Cancer Res 55:4722–4728
38. Vleminckx K, Vakaet L, Mareel M, Fiers W, van Roy F (1991) Genetic manipulation of E-cadherin expression by epithelial tumor cells reveals an invasion suppressor. Cell 66:107–119

Virchows Arch (2001) 439:560–570
DOI 10.1007/s004280100420

ORIGINAL ARTICLE

S. Shibata · M. Shigeta · Y. Shu · T. Watanabe
M. Nagata

Initial pathological events in renal dysplasia with urinary tract obstruction in utero

Received: 30 August 2000 / Accepted in revised form: 17 January 2001 / Published online: 15 March 2001
© Springer-Verlag 2001

Abstract Multicystic dysplastic kidneys (MCDK) and obstructive renal dysplasia (ORD) are two different phenotypes of dysplasia commonly associated with urinary tract obstruction. However, the mechanisms whereby obstruction in the developing kidney leads to each dysplasia are unknown. In the present study, 16 fetal MCDKs and 3 fetal ORDs (18–35 weeks of gestation) were analyzed with light microscopy, point-counting morphometry, immunohistochemistry with a podocyte marker, and scanning electron microscopy. Additionally, reconstructions of dysplastic nephrons were done via serial section analysis. Early stages of MCDK and ORD similarly revealed numerous cyst formations, predominantly in the subcapsular nephrogenic zone. Occasionally, glomerular tuft remnants with mature podocyte phenotypes were observed in cysts, suggesting the acquisition of filtration. Three dimensionally, basic nephron structures were installed in the cystic nephrons, namely the macula densa with a primary loop structure. Cysts developed in the once-induced nephrons due to fluid retention in both MCDK and ORD. In utero urinary tract obstruction may cause urine retention in functioning nephrons and lead to glomerular cysts in the nephrogenic zone. These findings were common to MCDK and ORD, albeit at different sites of obstruction. Expansion of glomerular cysts with tubular dilatation (cysts) disturbs the subsequent nephrogenesis and may contribute to the misdevelopment of fetal kidneys.

Keywords Renal dysplasia · Pathogenesis · Urinary tract obstruction · Glomerular cyst

S. Shibata
Department of Pediatrics, First Moriya General Hospital, University of Tsukuba, Ibaraki, 305-8575, Japan

M. Shigeta
Department of Pediatrics, Kinu-Ishikai Hospital, University of Tsukuba, Ibaraki, 305-8575, Japan

Y. Shu · M. Nagata (✉)
Department of Pathology, Institute of Clinical Medicine, University of Tsukuba, Tsukuba, Ibaraki, 305-8575, Japan
e-mail: nagatam@md.tsukuba.ac.jp
Tel.: +81-298-533171, Fax: +81-298-533171

T. Watanabe
Department of Pathology, Institute of Basic Medical Sciences, University of Tsukuba, Ibaraki, 305-8575, Japan

Introduction

Renal dysplasia is a phenotype of renal developmental abnormalities accompanied by heterogeneous disorders. Although it is sometimes associated with malformation syndromes or hereditary disorders [2, 33, 40], the majority of dysplastic kidneys are associated with urinary tract obstruction [5, 32, 35]. Experimental models of ureteral or urethral obstruction in fetal animals resulted in renal dysplasia, and in utero decompression of obstruction prevented the development of this disease [3, 11, 12, 13, 26, 27, 29]. Hence, it is clear that in utero urinary tract obstruction is one of the most important factors in the pathogenesis of renal dysplasia. However, it is still unclear how urinary tract obstruction causes dysplastic changes in the developing kidneys.

There are two types of renal dysplasia associated with urinary tract abnormalities [4, 6, 7]. Obstructive renal dysplasia (ORD) is a phenotype of dysplasia associated with lower urinary tract obstruction. Its pathology is characterized by predominant involvement of the peripheral cortex, typically with peripheral cortical cyst formations. Based on a microdissection study, Osathanondh and Potter suggested ampullary injury of the ureteric buds caused by increased back pressure was the cause of ORD [24, 28].

Multicystic dysplastic kidney (MCDK) is another phenotype of dysplasia associated with pyelocalyceal occlusion and atretic ureters [4, 6, 7]. A microdissection study of MCDK showed little branching of collecting tubules and cystic dilatation of the ampullary portion of the ureteric buds. From these findings, it was suggested that inhibition of ampullary activity causes nephron induction failure [24, 28]. In this context, a question still

remains as to whether phenotypic variations in MCDK and ORD are the result of a different pathogenesis, or if both dysplasias can be explained by a common mechanism based on obstructive uropathy.

Cyst formation is a typical pathology found in renal dysplasia both in MCDK and ORD. Cysts in both dysplasia phenotypes are considered to arise in various portions of the nephrons, namely, the glomeruli, tubuli, and collecting ducts [10, 16]. Of note is that normal nephrogenic areas are sometimes found in fetal dysplastic kidneys. Recently, Matsell et al. demonstrated a normal nephrogenic area expressing molecular markers related to normal nephrogenesis, i.e., WT1 and IGF-II mRNA, in human fetal MCDK after 14 weeks and 19 weeks of gestation [16]. Since obstructive uropathy requires fluid stasis, we hypothesized that the initial glomerular filtration sustained by early nephron induction would have been acquired in fetal dysplastic kidneys and thus are the cause of dysplasia. The present study attempted to investigate in detail the morphology of human fetal MCDK and ORD to determine the pathogenesis of both types of dysplasia.

Materials and methods

Tissues

From 170 fetal autopsy cases at our institute, we selected 11 cases of fetal unilateral or bilateral dysplastic kidneys associated with urinary tract obstruction (18–35 weeks of gestation). The profiles of these cases are summarized in Table 1. Three kidneys from two cases were associated with lower urinary tract obstruction and diagnosed as ORD. The remaining 16 kidneys from nine cases were associated with pyelocalyceal occlusion and ipsilateral ureteral atresia and diagnosed as MCDK. The histological criteria for fetal dysplasia were defined by abnormal spatial organization of nephronic structures associated with an abundance of interstitial mesenchymes and frequent cysts [10]. In addition, primitive ducts, a characteristic structure of dysplasia [5], were confirmed using light microscopy or immunohistochemistry. The pathological findings of both dysplasia phenotypes were consistent with those of MCDK and ORD as defined by Bernstein [6, 7]. The kidneys were fixed with 10% formalin and then embedded in paraffin. Longitudinal sections from all 19 kidneys from 11 cases were used for point-counting morphometry and immunohistochemistry. In addition, five dysplastic kidneys from five cases (case 1 of ORD, cases 3, 4, 6, and 8 of MCDK shown in Table 1) were subjected to serial section analysis to estimate the incidence of glomerular cysts and to perform three-dimensional (3-D) reconstruction of the dysplastic nephrons. The left kidney in case 2 was prepared for scanning electron microscopic observation.

Morphometry

Longitudinal kidney sections were stained with hematoxylin and eosin (HE). Low magnification photographs using a light microscope (×3–8) were taken in each section and developed on photographic paper, size 24.4×18.2 cm. Each picture was covered with a transparent sheet with multiple dots for point-counting morphometry. A standard point-counting method was used to quantitate the respective areas of the whole section area, the area of normal nephrogenesis, and the area of cysts, according to the method described by Weibel [43]. The interstitial area was calculated from the point-counts of the whole area minus the sum of the cystic and normal nephrogenic areas. This analysis was confirmed using concurrent light microscopic inspection. Based on the individual values, the relationships between gestational age and (1) the ratio of the normal nephrogenic area, (2) the ratio of the cystic area, and (3) the ratio of the interstitial area were evaluated using regression analysis for the MCDK cases.

Immunohistochemistry

Glomerular function commences with podocyte differentiation [30]. Thus, we checked whether mature podocytes were present in the initial dysplastic lesions. PHM-5, a specific antibody against differentiated podocytes, was employed to detect the mature podocyte phenotype. The characterization of the antibody and the specific expression in the mature podocytes have been described elsewhere [14, 21]. Alpha-smooth muscle actin (α-SMA, DAKO) immunohistochemistry was performed to identify the primitive ducts, since in fetal cases of dysplasia they can only be identified using periductal expression of α-SMA. All immunohistochemical procedures were performed using the streptavidin–biotin tech-

Table 1 Case profiles. *MCDK* multicystic dysplastic kidney, *Lt* left, *Rt* right

Case no.	Gestational weeks	Gender	Renal pathology	Urinary tract abnormality
Dysplasia with lower urinary tract obstruction				
1[a]	18	Male	Lt: cortical cystic dysplasia Rt: hydronephrosis	Urethral agenesis
2[b]	20	Male	Bilateral cortical cystic dysplasia	Urethral atresia, Lt urteral obstruction
Dysplasia with ureteropelvic occlusion				
3[a]	19	Male	Bilateral MCDK	Bilateral ureteral atresia
4[a]	23	Female	Bilateral MCDK	Bilateral ureteral atresia
5	23	Female	Lt: MCDK Rt: aplastic kidney	Bilateral ureteral atresia
6[a]	26	Male	Bilateral MCDK	Bilateral ureteral atresia
7	32	Female	Bilateral MCDK	Bilateral ureteral atresia
8[a]	32	Male	Bilateral MCDK	Bilateral ureteral atresia
9	35	Male	Bilateral MCDK	Bilateral ureteral atresia
10	35	Female	Lt: aplastic kidney Rt: MCDK	Bilateral ureteral obstruction
11	35	Male	Bilateral MCDK	Bilateral ureteral atresia

[a] Serial section analysis
[b] Scanning electron microscope

nique as previously described [18, 19]. The dilution of each antibody was 1:100 in PHM-5 and 1:50 in α-SMA. The incubation time for the antibodies was 60 min at room temperature. Immunoreactive products were developed with 3,3′-diaminobenzidine in phosphate-buffered saline (PBS) with 1% H_2O_2.

Scanning electron microscopy

To observe cysts in 3-D and to prove the foot process structure in glomerular tuft remnants in the cysts, scanning electron microscopy (SEM) was performed. Dissected dysplastic kidneys from case 2 (ORD) were fixed with 2% glutaraldehyde in 0.1 M PBS (pH 7.4). Randomly cut kidney cubes were rinsed with PBS and post-fixed in 1% osmium tetroxide for 2 h. Tissues were dehydrated in a graded series of ethanol and then freeze-dried with t-butyl-alcohol. The dried specimens were mounted on aluminum stubs with silver conductive paint, spatter-coated with gold (100Å), and examined with a SEM operating at 5 kV with a JSM-6320F scan (JEOL LTD, Tokyo).

Incidence of glomerular cysts

To clarify whether glomerular cysts are the major constituents of the numerous cysts in the early stage of dysplasia, the actual incidence of glomerular cysts is needed. Since cysts were variable in size and glomerular tuft remnants could only be seen in part of a cyst, we analyzed 3-D cyst structures using serial sections.

Five kidney blocks, one ORD and four MCKD, were serially sectioned into 250 sections of 4-μm thickness, and every other section was stained with HE. Immunostaining for PHM-5 was done when appropriate to identify podocytes in cell clusters of the tuft remnants. HE-stained specimens were photographed at low magnification and enlarged by copying. All cysts were assigned consecutive numbers to avoid repeat counting of any cysts. Glomerular cysts were defined by the presence of tuft remnants in the cyst through serial sections with occasional PHM-5 immunostaining. The incidence of glomerular cysts in each kidney was calculated as follows: the number of glomerular cysts/the total number of cysts ×100 (%).

3-D reconstruction

To investigate the background of cystogenesis in renal dysplasia, we reconstructed the nephrons with glomerular cysts via serial section analysis from five kidneys (one case of ORD and four cases of MCDK, Table 1). The reconstruction was expected to demonstrate the basic structure of an entire nephron with cysts. The localization of cysts, presence of intra-nephron obstruction, and luminal continuity of primitive ducts to upper-stream nephrons were additional points to be investigated. Five to ten glomerular cysts in each kidney were selected and traced with serial sections to see whether the entire nephron structure could be reconstructed. As a result, 12 nephrons from 5 kidneys (4 nephrons from ORD and 8 nephrons from MCDK) were completely reconstructed.

Results

Characteristic morphology in fetal dysplastic kidneys

The histology of the early stages of ORD (18 weeks and 20 weeks) revealed dilatation of the pelvis with peripheral cortical cyst formations. Cases of MCDK included various gestational ages, yet virtually all were associated with pyelocalyceal occlusion and diffuse disorganized renal architecture with multiple cyst formations. Metaplastic cartilage was evident in only six kidneys after 32 weeks of gestation in MCDK.

In early gestational cases (18–23 weeks) of both ORD and MCDK, a pathological similarity was found in numerous subcapsular cyst formations which occupied a considerable portion of the nephrogenic zone (Fig. 1A, B). Scattered islands of normal nephrogenesis were found among subcapsular cysts or shifted to the relatively deeper cortex.

Subcapsular cysts were virtually all lined by a flat or columnar epithelium, but not by a hyperplastic epitheli-

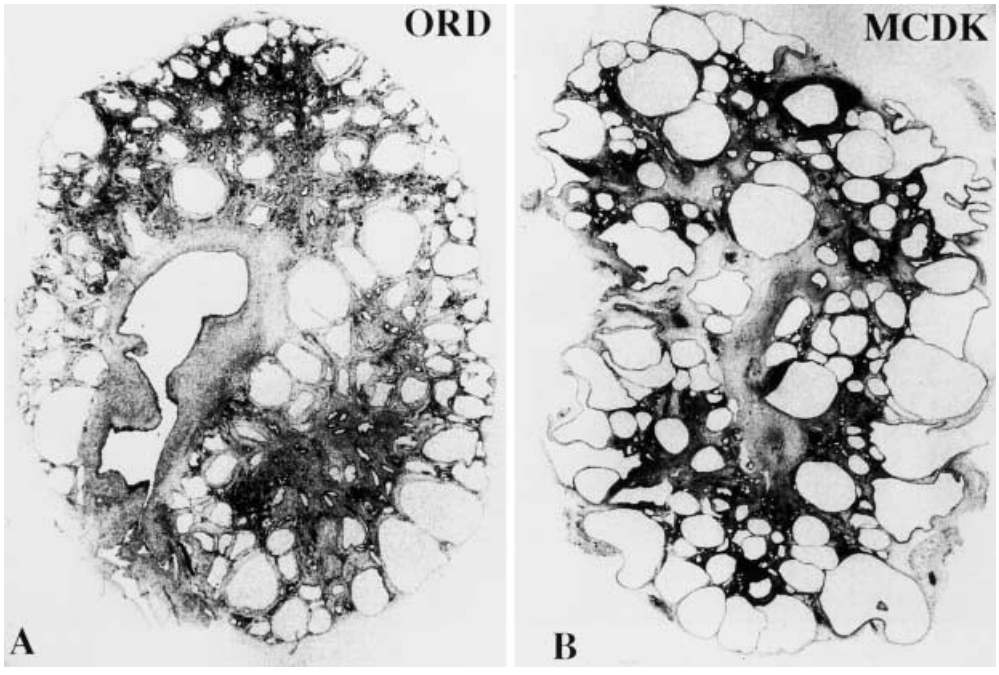


Fig. 1A,B Microscopic view of fetal dysplastic kidneys. **A** An early stage of obstructive renal dysplasia (*ORD*) associated with urethral atresia [case 1 at 18 weeks of gestation, hematoxylin and eosin (HE), ×3.2]. The image reveals pelvic dilatations and peripheral cortical cyst formation. **B** An early stage of multicystic dysplastic kidneys (*MCDKs*) associated with pyelocalyceal occlusion and an atretic ureter (case 3 at 19 weeks of gestation, HE, ×6). Note the numerous cyst formations in the nephrogenic zone with similar pathological changes to that of ORD

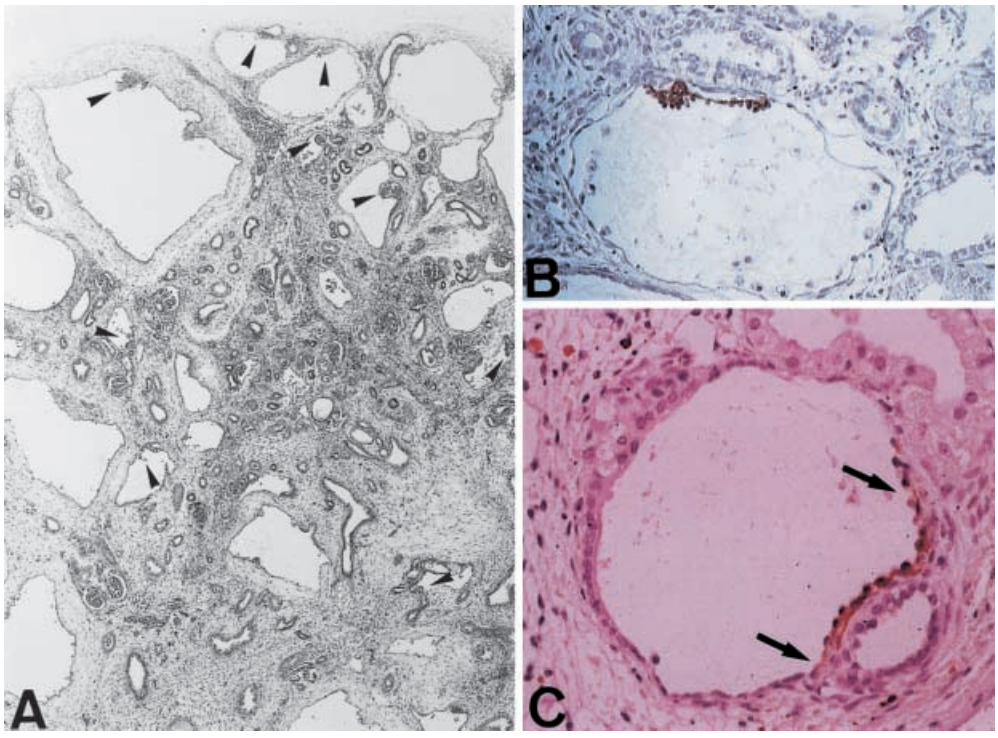


Fig. 2 **A** Microscopic view showing numerous cyst formations under the renal capsule. Note that glomerular tuft remnants (*arrowheads*) are observed in several cysts [case 1 at 18 weeks of gestation, hematoxylin and eosin (HE), ×40]. **B, C** Immunohistochemistry of PHM-5, a mature podocyte marker, in fetal multicystic dysplastic kidneys (MCDKs). PHM-5 is expressed in glomerular tuft remnants (**B** case 4 at 23 weeks of gestation, ×100) and in a part of the cyst wall epithelium (*arrow*) indicating incorporation (**C** case 3 at 19 weeks of gestation, ×200)

um. Cell clusters of glomerular tuft remnants were occasionally noted in subcapsular cysts (Fig. 2A). PHM-5, a mature podocyte marker, was expressed in those cell clusters (Fig. 2B). On some occasions, PHM-5 was only expressed in a part of the cyst wall epithelium without an apparent tuft structure (Fig. 2C). Moreover, SEM revealed distinct foot process formation that was elongated and irregularly arranged, as if the glomerular tufts were stretched due to cyst expansion (Fig. 3). Podocytes with distinct foot processes were transposed to the cyst wall epithelium. These observations provided circumstantial evidence suggesting that the mature glomerulus has been induced before dysplastic changes begin, and then tuft structures disappear due to cyst expansion. In MCDK cases of a later gestational age, the population of cysts apparently decreased and was replaced by fibrosis.

Morphometric analysis

As shown in Fig. 4, point-counting morphometry in MCDK demonstrated an inverse correlation between the cystic area and gestational age ($r=0.81$, $P<0.01$). In contrast, the interstitial area increased with gestational age ($r=0.83$, $P<0.01$). Since the proportion of normal nephrogenic areas varied in each case, no distinct correlation was observed between normal nephrogenic areas and gestational age. Early gestational cases of ORD showed similar values in each area as those of age-matched MCDK cases.

Incidence of glomerular cysts

The incidence of glomerular cysts in all cysts was 48.5% in ORD cases at 18 weeks of gestation, whereas the value was 28.4% and 27.1% in MCDK cases at 19 weeks and 23 weeks of gestation, respectively. In the MCDK cases, the incidence of glomerular cysts tended to decrease with gestational age (Table 2).

Table 2 Incidence of glomerular cysts in total cysts using three-dimensional analysis

Case no.	Gestational ages (weeks)	Number of glomerular cysts	Number of total cysts	Glomerular cysts/total cysts (%)
Dysplasia with lower urinary tract obstruction				
1	18	185	381	48.5
Dysplasia with ureteropelvic occlusion				
3	19	67	236	28.4
4	23	89	328	27.1
6	26	26	171	15.2
8	32	6	94	6.4

Fig. 3A–C Scanning electron microscopy showing glomerular cysts in case 2 at 20 weeks of gestation. **A** Glomerular tuft remnants are seen in the cyst (×230). **B** High-power view of the surrounding area in **A** (×1200). Podocytes with distinct foot process formations are incorporated into the cyst wall. Note that several foot processes are elongated and irregularly arranged. **C** Higher power view of **B** (×3000). *White arrows* in **B** and **C** indicate foot processes of the same podocyte ▶

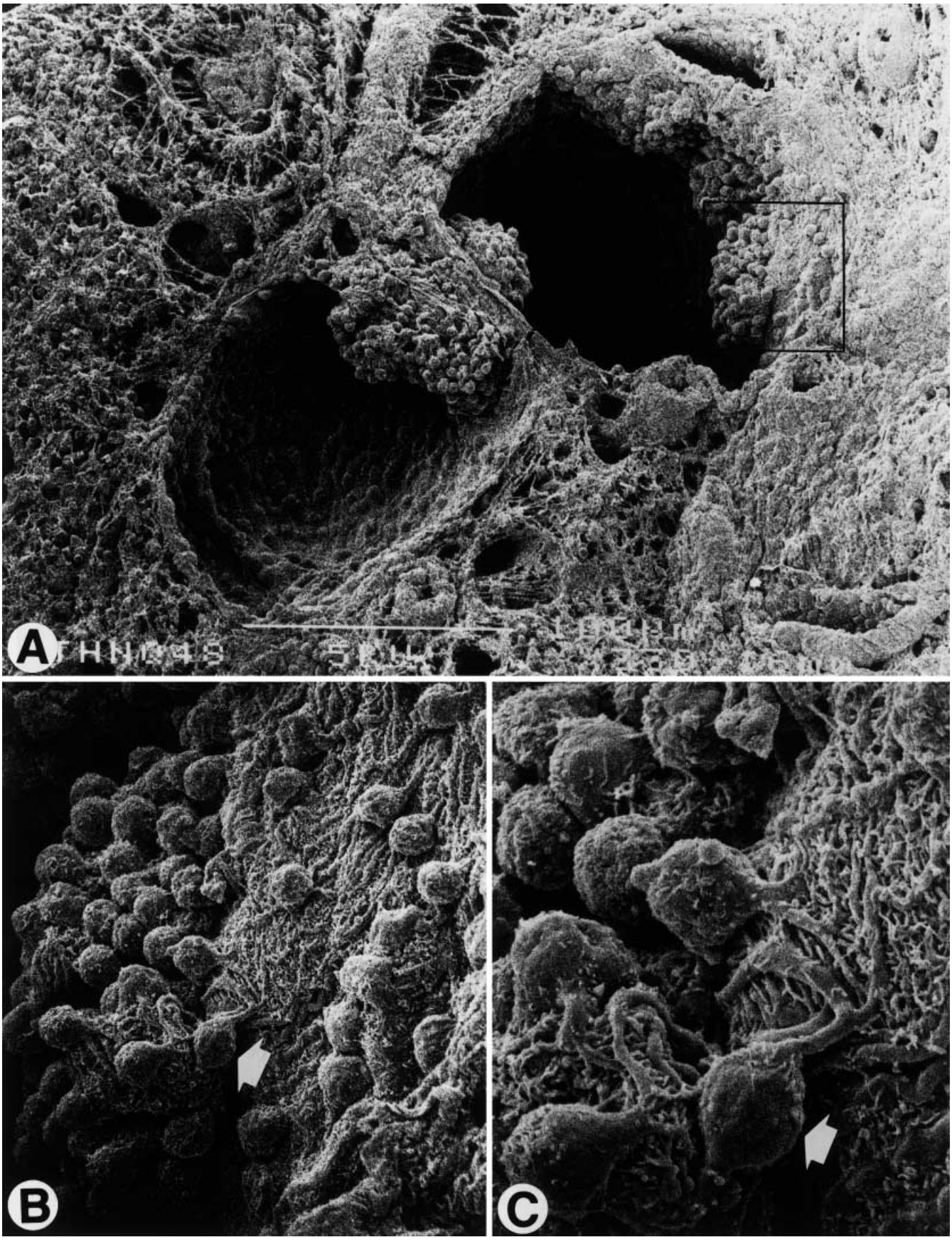


Fig. 3A–C Legend see page 563

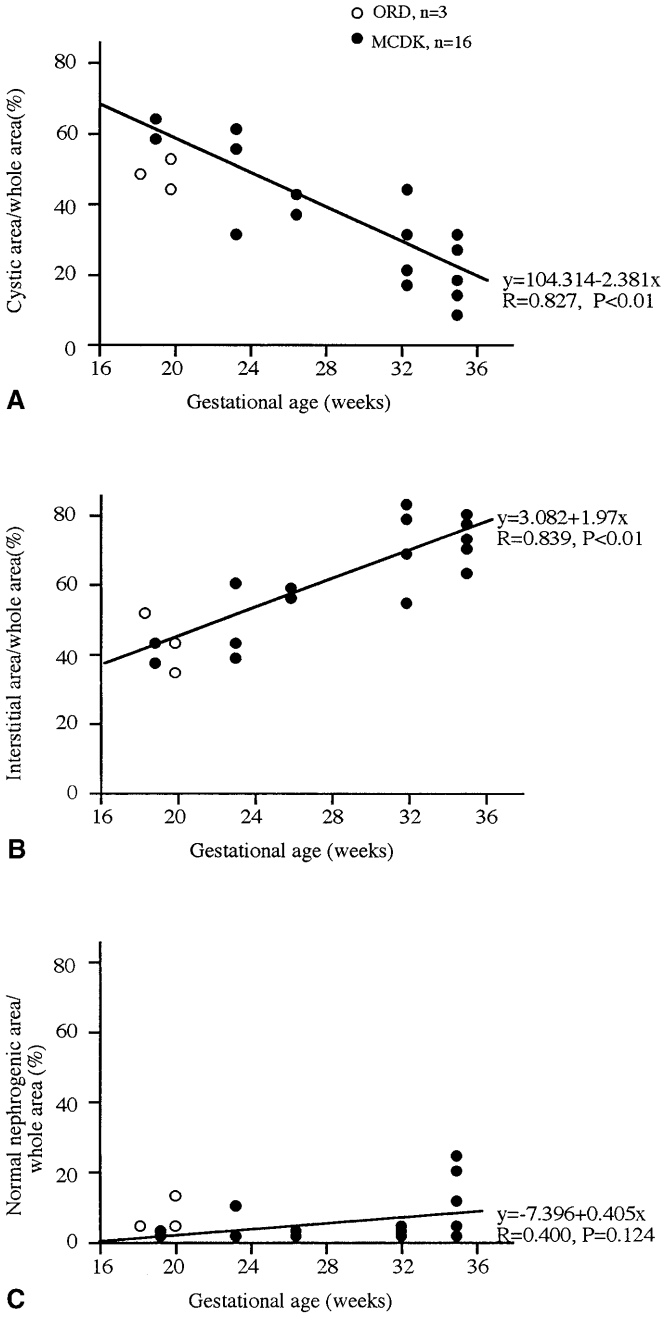


Fig. 4A–C Results of point-counting morphometric analysis. *Closed circles* indicate the value in multicystic dysplastic kidneys (*MCDK*s). Regression analysis between each area and gestational age was done in MCDKs. *Open circles* indicate the value in obstructive renal dysplasias (*ORD*s) associated with lower urinary tract obstruction. **A** The cystic area inversely correlates with gestational age (r=0.827, $P<0.01$). **B** The interstitial area correlates well with gestational age (r=0.839, $P<0.01$). **C** The normal nephrogenic area and gestational age have no significant correlation

3-D reconstruction of early dysplastic nephrons

Among five to ten nephrons per kidney serially traced using microscopic inspection, 12 nephrons (4 nephrons from ORD and 8 nephrons from MCDK) with cysts could be entirely reconstructed. Figures 5 and 6 demonstrate examples of serial section analysis for 3-D reconstruction of the nephrons observed in ORD. Both series of pictures demonstrated that glomerular cysts had a connection with proximal tubules, the distal loop and collecting ducts. No luminal obstruction was observed from the glomerular cyst to the collecting duct. In addition, the basic structure of the macula densa with a primitive loop structure was associated with cystic nephrons. Based on serial section analysis for Fig. 5 and Fig. 6, 3-D reconstructed nephrons are illustrated as Fig. 7A, B, respectively.

Figure 7C–E demonstrates reconstructed nephrons observed in cases of MCDK at 19, 19, and 26 weeks of gestation, respectively. In all the reconstructed nephrons, the basic nephron structure with luminal continuity was installed. In addition, the cysts were not true cysts, but dilatations of nephron segments. These findings were common to MCDK and ORD. Moreover, the two reconstructed nephrons shown in Fig. 7C, E exhibited luminal ends at the collecting duct level. Collecting ducts were occasionally obstructed in MCDK. A serial inspection starting from the primitive ducts showed a distinct continuity between the primitive ducts and upper-stream nephrons. Neither cysts nor primitive ducts were cul-de-sacs in either ORD or MCDK.

Discussion

The present study demonstrated the early pathological events of the two types of renal dysplasia, ORD and MCDK, both of which were associated with urinary tract obstruction in utero. Using morphometry and serial section analysis for 3-D nephrons, we suggested an alternative mechanism for the pathogenesis of dysplasia due to in utero urinary tract obstruction.

In the present study, we showed that an initial nephron induction with a filtration function had been achieved before dysplastic changes commenced in both MCDK and ORD. The histology of early cases of MCDK and ORD (18–23 weeks of gestation) similarly showed numerous cyst formations in the subcapsular nephrogenic zone. PHM-5 immunostaining and SEM clearly showed the presence of mature podocytes in the glomerular tuft remnants. Because glomerular filtration is considered to start at the capillary loop stage with differentiation of podocytes [30, 36], the presence of the

Fig. 5 An example of serial section analysis for three-dimensional reconstruction of a dysplastic nephron [case 1 at 18 weeks of gestation, hematoxylin and eosin (HE), ×240]. The *number* at the *bottom left* in each photograph indicates the section number. The number for each tubule helps to trace the continuity of a single nephron. The glomerular cyst (no. *1*) has a connection with the proximal tubule (nos. *2–6*), distal loop (nos. *7–11*), and collecting duct (no. *19*). In section *142*, the tubular epithelium adjoined to the glomerular tuft remnants has a tall dense columnar epithelium, the macula densa. If the number is traced in numerical order starting from glomerular cyst (*1*) to collecting duct (*19*), the nephron is reconstructed as shown in Fig. 7A ▶

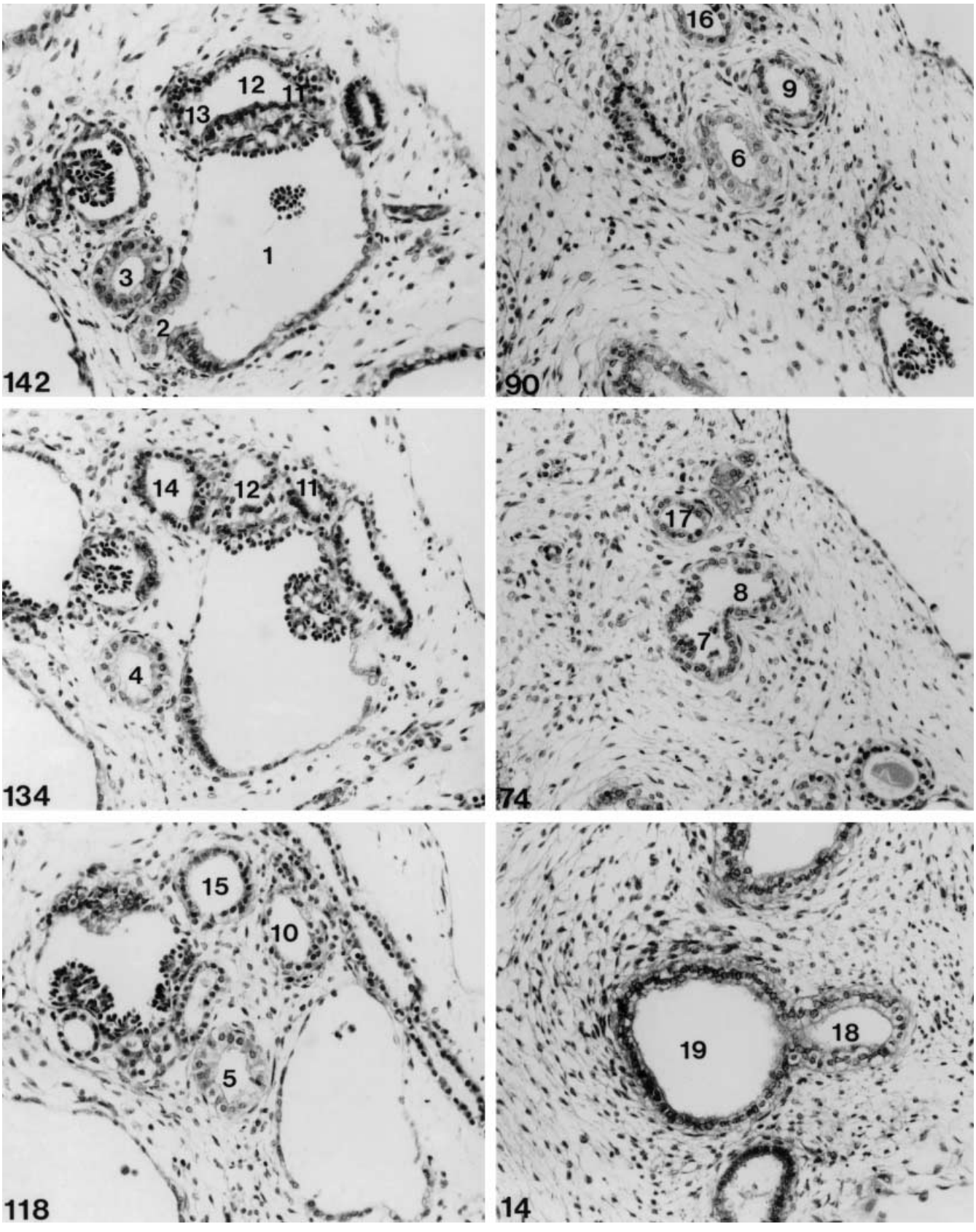


Fig. 5 Legend see page 565

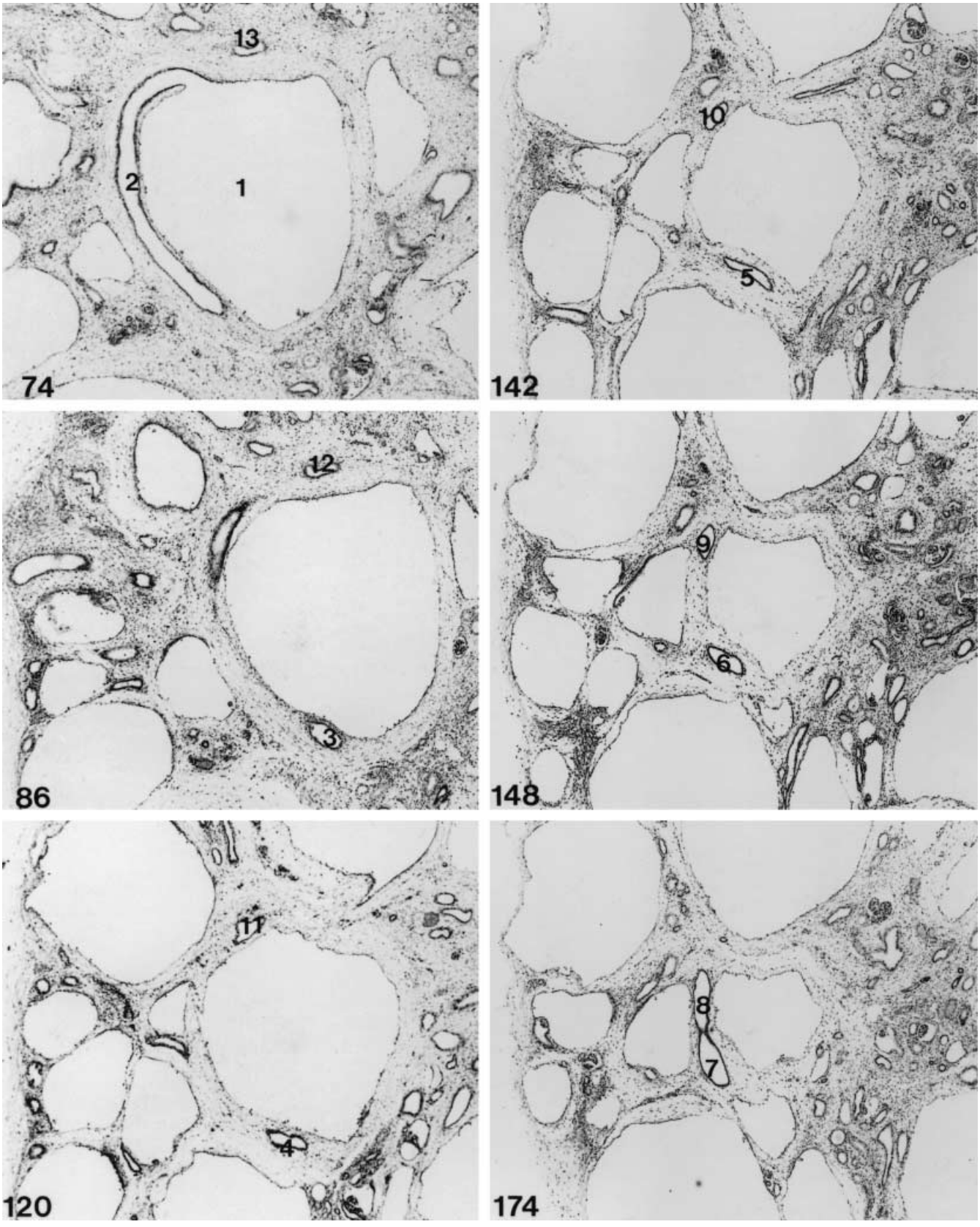


Fig. 6 Another example of serial section analysis for three-dimensional reconstruction of a nephron [case 1 at 18 weeks of gestation, hematoxylin and eosin (HE), ×50]. The *number* at the *bottom left* in each photograph indicates the section number. The number for each tubule helps to trace the continuity of the entire single nephron. The glomerular cyst (no. *1*) has a distinct connection with the proximal tubule (no. *2*), distal loop (nos. *3–10*), and collecting duct (nos. *11–13*). Fig. 7B is the result of the reconstruction

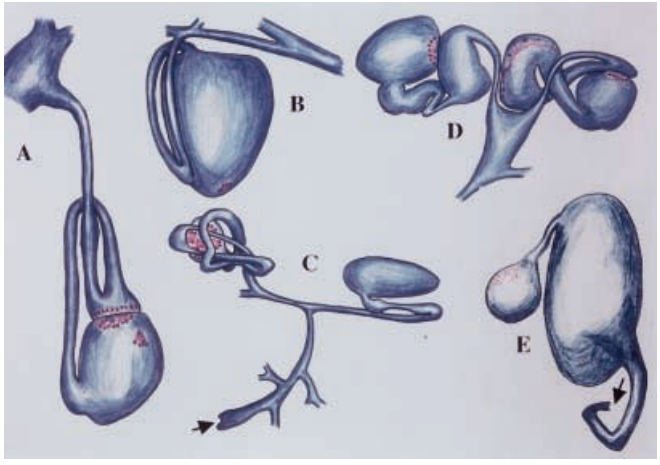


Fig. 7A–E Representative examples of three-dimensional reconstruction of dysplastic nephrons. **A** A reconstructed nephron in obstructive renal dysplasia (ORD) based on the serial section analysis demonstrated in Fig. 5 (case 1, 18 weeks of gestation). The cyst is limited to a glomerular cyst and basic nephron structures; the distal loop and macula densa have been installed. **B** A reconstructed nephron in ORD based on the serial section analysis demonstrated in Figure 6 (case 1). **C** A reconstructed nephron observed in multicystic dysplastic kidneys (MCDKs, case 3, 19 weeks of gestation). Two nephrons flow into the common collecting duct. One nephron has a glomerular cyst and the other nephron has no cystic portions in the entire nephron. This collecting duct has a luminal end (*arrow*). **D** A reconstructed nephron observed in MCDK (case 3, 19 weeks of gestation). Two nephrons with glomerular cysts and cystic segmental tubular dilatations flow into the common collecting duct. Note that these nephrons have macula densa and tubular loops. Cystic dilatation occurs both in the proximal and distal tubuli, but not in the collecting duct. **E** A reconstructed nephron observed in MCDK (case 6, 26 weeks of gestation). The glomerular cyst connects to a larger tubular cyst. This nephron has a luminal end at the collecting duct (*arrow*)

mature podocyte phenotype in the glomerular cysts suggests the acquisition of a filtration function and that this is the cause of cystogenesis.

Serial section analysis to assess glomerular cysts indicated an incidence of 48.5% in ORD at 18 weeks of gestation and 28.4% and 27.1% in MCDK of 19 weeks and 23 weeks of gestation, respectively. Glomerular tufts may have been incorporated into the parietal epithelium as suggested by SEM (Fig. 3) and PHM-5 immunostaining (Fig. 2C), and tuft structures had disappeared in already developed glomerular cysts. Those cysts could not be detected as glomerular cysts using only HE staining. Therefore, we suggest that the actual incidence of glomerular cysts may have been higher than the value in Table 2. Interestingly, the incidence of glomerular cysts in ORD was double that of MCDK. Since the entire space volume of urinary retention in pyelocalyceal occlusion is smaller than that of lower urinary tract obstruction, we surmise that glomerular cysts in MCDK develop earlier than those of ORD.

3-D nephron reconstruction during early pathological events provided a structural background to initiate dysplastic changes. The results indicated that the basic nephron architecture, including the macula densa and primitive loop structure, have been already installed in cystic nephrons. This suggests that cysts in MCDK and ORD develop in once-induced nephrons. Generally, urinary tract obstruction causes urinary stasis in the filtrating nephrons. Although several 3-D nephrons suggested that glomerular cysts were the first cysts in the nephron, fluid retention in developing nephrons could cause cystic formations in various nephron portions. Collecting ducts did not show clear cystic dilatation, despite apparent cysts in upper-stream nephrons. This suggests that urinary tract obstruction may reflect fluid retention at the site where active filtration occurs. The 3-D features of nephrons in both MCDK and ORD closely match the mechanism of obstructive uropathy in general.

MCDK is associated with pyelocalyceal occlusion and ORD with lower urinary tract obstruction. The site of obstruction may determine the morphological differences between MCDK and ORD. Urinary retention in ORD affects the developing nephrons in a somewhat later stage of nephrogenesis than that in MCDK. Thus, the difference in localization of urinary tract obstructions may cause variability of the timing and severity of hydrostatic pressure against the developing nephrons, resulting in the phenotypic difference between MCDK and ORD. Interestingly, two reconstructed nephrons showed luminal obstruction at the collecting-duct level in MCDK. The pelvis and calyces are formed by remodeling of three to five generations of ureteric bud branches at around 12 weeks of gestation [23, 28], just when urine production begins [9]. Hence, intra-renal nephron obstruction may be caused by abnormal papillary development and accelerate cystic formations in MCDK.

Our current hypothesis that dysplastic changes commence after active urine production is supported by the renal manifestations of early fetal Prune-belly syndrome (PBS). This syndrome is defined by the absence of abdominal wall muscles, cryptorchidism, and urogenital abnormalities, including severe urinary tract obstruction [39]. In the majority of cases, the renal phenotype is consistent with ORD. Autopsy cases of PBS at 12 weeks and 14 weeks of gestation revealed normal fetal kidney histology [38, 41]. These cases provide circumstantial evidence for our idea in humans.

Cyst formations in the nephrogenic zone may disturb subsequent nephron induction as a mass effect, resulting in insufficient nephron numbers in dysplasia. The absence of significant increases in the normal nephrogenic area in the later stages of MCDK supports this idea.

Normal kidney development is controlled by the spatial and temporal expression of various genes and molecules [15, 25, 34, 42]. In human and experimental renal dysplasia, deregulated expression of these factors has been reported [1, 17, 44, 45] and was suggested to play an important role in misdevelopment of the kidney. However, experimental dysplasia in fetal animals revealed aberrant molecular expressions caused by urinary tract obstruction [1, 8, 31]. From these observations, it is possible that aberrant molecular expressions in dysplastic kidneys are not necessarily a primary cause, but rather secondary factors promoting dysplastic changes.

Recent molecular technology has demonstrated single gene defects as the cause of renal developmental defects, including renal dysplasia and hypoplasia [20, 22, 37]. It is of interest when a particular gene defect causes ontogenic abnormalities of the urinary tract and causes renal dysplasia. The present study was not aimed at identifying genetic factors contributing to the development of dysplasia. Further investigations are required for a better understanding of the pathological mechanism whereby gene abnormalities lead to dysplasia.

In conclusion, the present study demonstrated the initial pathological events of fetal MCDK and ORD and suggested that both types of dysplasia may be commonly explained by obstructive uropathy. Urinary obstruction in utero may result in fluid stasis at the functioning glomeruli, leading to glomerular cysts and giving rise to the initial pathology of dysplasia. Cysts in the nephrogenic zone may disturb subsequent nephron induction and tubular development and be the direct cause of insufficient nephron numbers and abnormal nephron differentiation.

Acknowledgements The authors wish to thank Dr. R.C. Atkins (Melbourne) for the generous gifts of an antibody. The expert technical support for histology, including electron microscopy, given by T. Mogi and Y. Ohno is gratefully acknowledged. This work was supported by grants from the Ministry of Education, Science and Culture of Japan (no. 10670154) and from University of Tsukuba Research Projects.

References

1. Attar R, Quinn F, Winyard PJD, Mouriquand PDE, Foxall P, Hanson MA, Woolf AS (1998) Short-term urinary flow impairment deregulates PAX2 and PCNA expression and cell survival in fetal sheep kidneys. Am J Pathol 152:1225–1235
2. Barnes EG, Opitz JM (1992) Renal abnormalities in malformation syndromes. In: Edelmann CM (ed) Pediatric kidney disease, 2nd edn. Little Brown, Boston, pp 1067–1119
3. Beck AD (1971) The effect of intra-uterine urinary obstruction upon the development of the fetal kidney. J Urol 105:784–789
4. Becker N, Avner ED (1995) Congenital nephropathies and uropathies. Pediatr Nephrol 42:1319–1341
5. Bernstein J (1958) Developmental abnormalities of the renal parenchyma-renal hypoplasia and dysplasia. Pathol Annu 3:213–247
6. Bernstein J (1992) Renal hypoplasia and dysplasia. In: Edelmann CM (ed) Pediatric kidney disease, 2nd edn. Little Brown, Boston, pp 1121–1137
7. Bernstein J, Barness EG (1994) Congenital malformations of the kidney. In: Tisher CC, Brenner BM (eds) Renal pathology: with clinical and functional correlations, 2nd edn. Lippincott, Philadelphia, pp 1355–1386
8. Chung KH, Chevalier RL (1996) Arrested development of the neonatal kidney following chronic ureteral obstruction. J Urol 155:1139–1144
9. Clapp WL, Abrahamson DR (1994) Development and gross anatomy of the kidney. In: Tisher CC, Brenner BM (eds) Renal pathology: with clinical and functional correlations, 2nd edn. Lippincott, Philadelphia, pp 3–59
10. Daïkha-Dahmane F, Dommergues M, Muller F, Narcy F, Lacoste M, Beziau A, Dumez Y, Gubler MC (1997) Development of human fetal kidney in obstructive uropathy: correlations with ultrasonography and urine biochemistry. Kidney Int 52:21–32
11. Glick PL, Harrison MR, Noall RA, Villa RL (1983) Correction of congenital hydronephrosis in utero. III. Early mid-trimester ureteral obstruction produces renal dysplasia. J Pediatr Surg 18:681–687
12. Glick PL, Harrison MR, Adzick NS, Noall RA, Villa RL (1984) Correction of congenital hydronephrosis in utero. IV. In utero decompression prevents renal dysplasia. J Pediatr Surg 19:649–657
13. Gonzalez R, Reinberg Y, Burke B, Wells T, Vernier RL (1990) Early bladder outlet obstruction in fetal lambs induces renal dysplasia and the prune-belly syndrome. J Pediatr Surg 25:342–345
14. Kerjaschki D, Poczewski H, Dekan G, Horvat R, Balzar E, Kraft N, Atkins RC (1986) Identification of a major sialoprotein in the glycocalyx of human visceral glomerular epithelial cells. J Clin Invest 78:1142–1149
15. Kreidberg JA, Sariola H, Loring JM, Maeda M, Pelletier J, Housman D, Jaenisch R (1993) WT-1 is required for early kidney development. Cell 74:679–691
16. Matsell DG, Bennett T, Goodyer P, Goodyer C, Han VKM (1996) The pathogenesis of multicystic dysplastic kidney disease: insights from the study of fetal kidneys. Lab Invest 74:883–893
17. Matsell DG, Bennett T, Armstrong RA, Goodyer P, Goodyer C, Han VKM (1997) Insulin-like growth factor (IGF) and IGF binding protein gene expression in multicystic renal dysplasia. J Am Soc Nephrol 8:85–94
18. Nagata M, Yamaguchi Y, Ito K (1993) Loss of mitotic activity and expression of vimentin in glomerular epithelial cells of developing human kidneys. Anat Embryol (Berl) 187:275–279
19. Nagata M, Akioka Y, Tsunoda Y, Komatsu Y, Kawaguchi H, Yamaguchi Y, Ito K (1995) Macrophages in childhood IgA nephropathy. Kidney Int 48:527–535
20. Nagata M, Nakauchi H, Nakayama K, Nakayama K, Loh D, Watanabe T (1996) Apoptosis during an early stage of nephrogenesis induces renal hypoplasia in bcl-2-deficient mice. Am J Pathol 148:1601–1611
21. Nagata M, Nakayama K, Terada Y, Hoshi S, Watanabe T (1998) Cell cycle regulation and differentiation in the human podocyte lineage. Am J Pathol 153:1511–1520
22. Nishimura H, Yerkes E, Hohenfellner K, Miyazaki Y, Ma J, Hunley TE, Yoshida H, Ichiki T, Threadgill D, Phillips JA, Hogan BML, Fogo A, Brock III JW, Inagami T, Ichikawa I (1999) Role of the angiotensin type 2 receptor gene in congenital anomalies of the kidney and urinary tract, CAKUT, of mice and men. Mol Cells 3:1–10
23. Osathanondh V, Potter EL (1963) Development of human kidney as shown by microdissection. II. Renal pelvis, calyces, and papillae. Arch Pathol 76:277–289
24. Osathanondh V, Potter EL (1964) Pathogenesis of polycystic kidneys. Arch Pathol 77:459–512
25. Pachnis V, Mankoo B, Costantini F (1993) Expression of the c-ret proto-oncogene during mouse embryogenesis. Development 119:1005–1017
26. Peters CA, Carr MC, Lais A, Retik AB, Mandell J (1992) The response of the fetal kidney to obstruction. J Urol 148:503–509
27. Peters CA (1997) Obstruction of the fetal urinary tract. J Am Soc Nephrol 8:653–663
28. Potter EL (1972) Normal and abnormal development of the kidney. Year Book Medical Publishers, Chicago
29. Pringle KC, Bonsib SM (1988) Development of fetal lamb lung and kidney in obstructive uropathy: a preliminary report. Fetal Ther 3:118–128
30. Reeves W, Caulfield JP, Farquhar MG (1978) Differentiation of epithelial foot processes and filtration slits. Sequential appearance of occluding junctions, epithelial polyanion, and slit membranes in developing glomeruli. Lab Invest 39:90–100
31. Richard MCC, Schlussel RN, Peters CA, Uchida T, Mandell J, Freeman MR (1995) Expression of cell growth regulated genes in the fetal kidney: relevance to in utero obstruction. J Urol 154:242–244
32. Risdon RA (1971) Renal dysplasia. Part I. A clinico-pathological study of 76 cases. J Clin Pathol 24:57–71

33. Roodhooft AM, Birnholz JC, Holmes LB (1984) Familial nature of congenital absence and severe dysgenesis of both kidneys. N Engl J Med 310:1341–1345
34. Rothenpieler UW, Dressler GR (1993) Pax-2 is required for mesenchyme-to-epithelium conversion during kidney development. Development 119:711–720
35. Rubenstein M, Meyer R, Bernstein J (1961) Congenital abnormalities of the urinary system. I. A postmortem survey of developmental anomalies and acquired congenital lesions in a children's hospital. J Pediatr 5:356–366
36. Schnabel E, Dekan G, Miettinen A, Farquhar MG (1989) Biogenesis of podocalyxin – the major glomerular sialoglycoprotein – in the newborn rat kidney. Eur J Cell Biol 48:313–326
37. Schuchardt A, D'Agati V, Pachnis V, Costantini F (1996) Renal agenesis and hypodysplasia in ret-k^- mutant mice result from defects in ureteric bud development. Development 122:1919–1929
38. Shigeta M, Nagata M, Shimoyamada H, Shibata S, Okuno S, Hamada H, Watanabe T (1999) Prune-belly syndrome diagnosed at 14 weeks' gestation with severe urethral obstruction but normal kidneys. Pediatr Nephrol 13:135–137
39. Sutherland RS, Mevorach RA, Kogan BA (1995) The prune-belly syndrome: current insights. Pediatr Nephrol 9:770–778
40. Squiers EC, Morden RS, Bernstein J (1987) Renal multicystic dysplasia: an occasional manifestation of the hereditary renal adysplasia syndrome. Am J Med Genet Suppl 3:279–284
41. Terada S, Suzuki N, Uchide K, Ueno H, Akasofu K (1994) Etiology of prune belly syndrome: evidence of megalocystic origin in an early fetus. Obstet Gynecol 83:865–868
42. Torres M, Gómez-Pardo E, Dressler GR, Gruss P (1995) Pax-2 controls multiple steps of urogenital development. Development 121:4057–4065
43. Weibel ER (1979) Stereological methods. Practical methods for biological morphometry. Academic Press, London
44. Winyard PJD, Nauta J, Lirenman DS, Hardman P, Sams VR, Risdon RA, Woolf AS (1996) Deregulation of cell survival in cystic and dysplastic renal development. Kidney Int 49:135–146
45. Winyard PJD, Risdon RA, Sams VR, Dressler GR, Woolf AS (1996) The PAX2 transcription factor is expressed in cystic and hyperproliferative dysplastic epithelia in human kidney malformations. J Clin Invest 98:451–459

Virchows Arch (2001) 439:571–578
DOI 10.1007/s004280000380

ORIGINAL ARTICLE

Paulo Tambasco de Oliveira
Márcia Martins Marques Jaeger
Sueli Patrícia Harumi Miyagi · Ruy Gastaldoni Jaeger

The effect of a reconstituted basement membrane (Matrigel) on a human salivary gland myoepithelioma cell line

Received: 15 September 2000 / Accepted: 6 December 2000 / Published online: 24 February 2001
© Springer-Verlag 2001

Abstract We have already demonstrated that a reconstituted basement membrane (Matrigel) is a key modulator of morphogenetic changes and cytodifferentiation of pleomorphic adenoma cells in culture. Myoepithelioma is considered to be a neoplasm closely related to pleomorphic adenoma and should experience similar induction processes. Thus, the aim of this study was to investigate whether Matrigel would influence myoepithelioma cells. We used a cell line derived from a human salivary gland plasmacytoid myoepithelioma (M1 cells) grown in a three-dimensional preparation of Matrigel. Phenotype differences were assessed using conventional light microscopy technique (haematoxylin and eosin) and phase and differential interference contrast (Nomarski). Immunofluorescence was carried out to detect smooth-muscle actin, laminin and type-IV collagen. M1 cells exhibited all proteins studied, showing a myoepithelial differentiation. M1 cells grown inside Matrigel presented morphological changes and changes in smooth-muscle actin status. By growing M1 cells inside Matrigel, it was possible to reproduce the tumour architecture with no duct-like structures. Based on our findings, we suggest that myoepithelioma would be derived from a cell with a commitment to myoepithelial differentiation. We also suggest that the mechanical properties of the matrix environment will likely regulate smooth-muscle actin expression in myoepithelioma.

Keywords Salivary gland neoplasms · Myoepithelioma · Extracellular matrix · Smooth-muscle actin · Cell culture

P.T. de Oliveira · M.M.M. Jaeger (✉) · S.P.H. Miyagi · R.G. Jaeger
Department of Oral Pathology, School of Dentistry,
University of São Paulo, Av. Prof. Lineu Prestes 2227,
São Paulo SP 05508-900, Brazil
e-mail: rgjaeger@fo.usp.br
Tel.: +55-11-8187902, Fax: +55-11-2104409

P.T. de Oliveira
Department of Oral Histology, School of Dentistry,
University of São Paulo at Ribeirão Preto, Brazil

Introduction

Myoepithelioma is defined as a rare tumour of myoepithelial cell differentiation [9, 25]. Histopathological growth patterns may be solid, myxoid and reticular [7, 8, 9]. Two main cytological subtypes have been described for this tumour: spindle-shaped and plasmacytoid [23, 24, 25]. Myoepithelioma differs from pleomorphic adenoma in that it has little or no ductal component [24]. For some authors, myoepithelioma is part of the spectrum of pleomorphic adenoma [4, 9, 26].

It has been suggested that the extracellular matrix plays an important role as a regulatory factor of phenotypic differences among salivary gland neoplasms [13, 14, 16]. We have already demonstrated that a three-dimensional preparation of a reconstituted basement membrane (Matrigel), a supramolecular array of extracellular matrix proteins, is a key modulator of morphogenetic changes and cytodifferentiation of pleomorphic adenoma cells in culture [14]. Myoepithelioma is considered to be a neoplasm closely related to pleomorphic adenoma [4, 23, 24, 26] and should experience similar induction processes. Therefore, it would be interesting to study whether basement membrane molecules could influence myoepithelioma cells.

We have previously established a neoplastic myoepithelial cell line (M1 cells) derived from human salivary gland plasmacytoid myoepithelioma [16, 20]. M1 cells were grown in contact with Matrigel in a three-dimensional preparation. Phenotype differences were assessed using conventional light microscopy technique [haematoxylin and eosin (HE)], phase and differential interference contrast (Nomarski) and fluorescence microscopy.

Materials and methods

Cell culture

M1 cells were derived from a human plasmacytoid myoepithelioma [16, 20]. These cells were cultured in high-glucose Dulbecco's Modified Eagle's Medium (DMEM, Sigma Chemical Co., St.

Louis, Mo.) supplemented with 10% fetal bovine serum (Cultilab, Campinas, SP, Brazil) and 1% antibiotic–antimycotic solution (Sigma). The cells were maintained in 25-cm^2 flasks in a humidified atmosphere of 5% CO_2 at 37°C. To study phenotype differentiation, M1 cells were plated on no. 1 round glass coverslips (Ted Pella Inc., Redding, Calif.). Morphology of M1 cells was analysed using phase contrast.

Immunofluorescence

Detection of smooth-muscle actin was carried out to confirm the myogenous differentiation of M1 cells. Labelling of smooth-muscle actin was performed as described previously [16]. For laminin and type-IV collagen immunostaining, M1 cells grown on coverslips were fixed in 1% paraformaldehyde in phosphate-buffered saline (PBS) for 10 min and rinsed in PBS. Cells were then subjected to an immunofluorescence protocol [15] using mouse monoclonal antibodies against laminin (Biogenex Laboratory, San Ramon, Calif.), diluted 1:50 in PBS and type-IV collagen (Biogenex), diluted 1:20 in PBS. An anti-mouse fluorescein (FITC) conjugate (Amersham Co., Arlington Heights, Ill.) was used as a secondary antibody. All incubations were done for 60 min at room temperature. The mounting medium was Pro Long (Molecular Probes, Eugene, Ore.). Replacement of the primary antibody with PBS was used as a negative control.

Immunofluorescence labelling of M1 cells was carried out at least five times, and a minimum of 100 cells was examined each time. The observations and photographic recording were carried out under a Zeiss Axiophot 2 fluorescence microscope (Carl Zeiss Inc, Oberköchen, Germany), using the objectives 40× Plan Neofluar, 1.4 NA and 63× Plan Apochromatic, 1.4 NA.

Three-dimensional preparation of Matrigel

M1 cells were plated on no. 1 round glass coverslips coated with a reconstituted basement membrane (Matrigel, kindly provided by Dr. Matthew Hoffman NIDCR, NIH, Bethesda, Md.). The coating procedure was as follows [14]: we prepared a thick gel for growing cells within a three-dimensional matrix, simulating an intact basement membrane. Matrigel was thawed, homogenised and diluted in cold serum-free DMEM to reach a final concentration of 6 mg/ml (stock solution 13 mg/ml). M1 cells were then harvested from the culture flasks and resuspended inside Matrigel preparation. After that, this Matrigel containing M1 cells was placed (100 µl/cm^2) on cold coverslips. Cells were then incubated at 37°C in a humidified atmosphere of 5% CO_2 in air. M1 cells were grown on this three-dimensional preparation of Matrigel for 1 week. Two controls were used: (1) M1 cells plated on plain glass coverslips and (2) M1 cells plated on coverslips with a thin coating of Matrigel (3 mg/ml; 50 µl/cm^2).

Light microscopy

Coverslips with M1 cells growing within Matrigel were fixed in 10% formalin for 24 h. Then, Matrigel was carefully removed from the coverslips, paraffin-embedded, and stained with HE. Cells growing inside Matrigel were also studied using phase contrast, Nomarski and fluorescence microscopy. For fluorescence microscopy, we used samples immunostained with smooth-muscle actin, in order to access overall morphology of M1 cells inside Matrigel. For comparative analysis between in vitro and in vivo situations, we obtained new HE-stained sections from the tumour that originated the M1-cell line [16, 20].

Results

Phase contrast microscopy showed that M1 cells, when grown on a glass surface, presented a polyedrical morphology with abundant cytoplasm and visible stress fibres (Fig. 1).

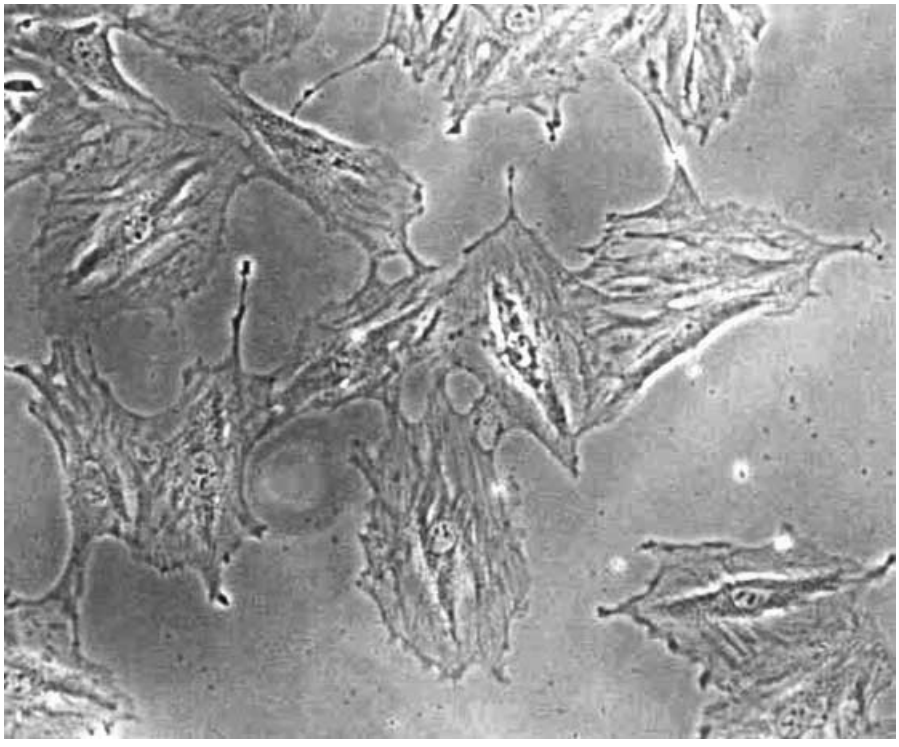


Fig. 1 Phase-contrast microscopy of M1 cells (derived from a human salivary gland plasmacytoid myoepithelioma) grown on a glass surface. A flat monolayer of polyedrical cells is observed. The nuclei are round, with two or three nucleoli. The cytoplasms are abundant, with stress fibres. Magnification 400×

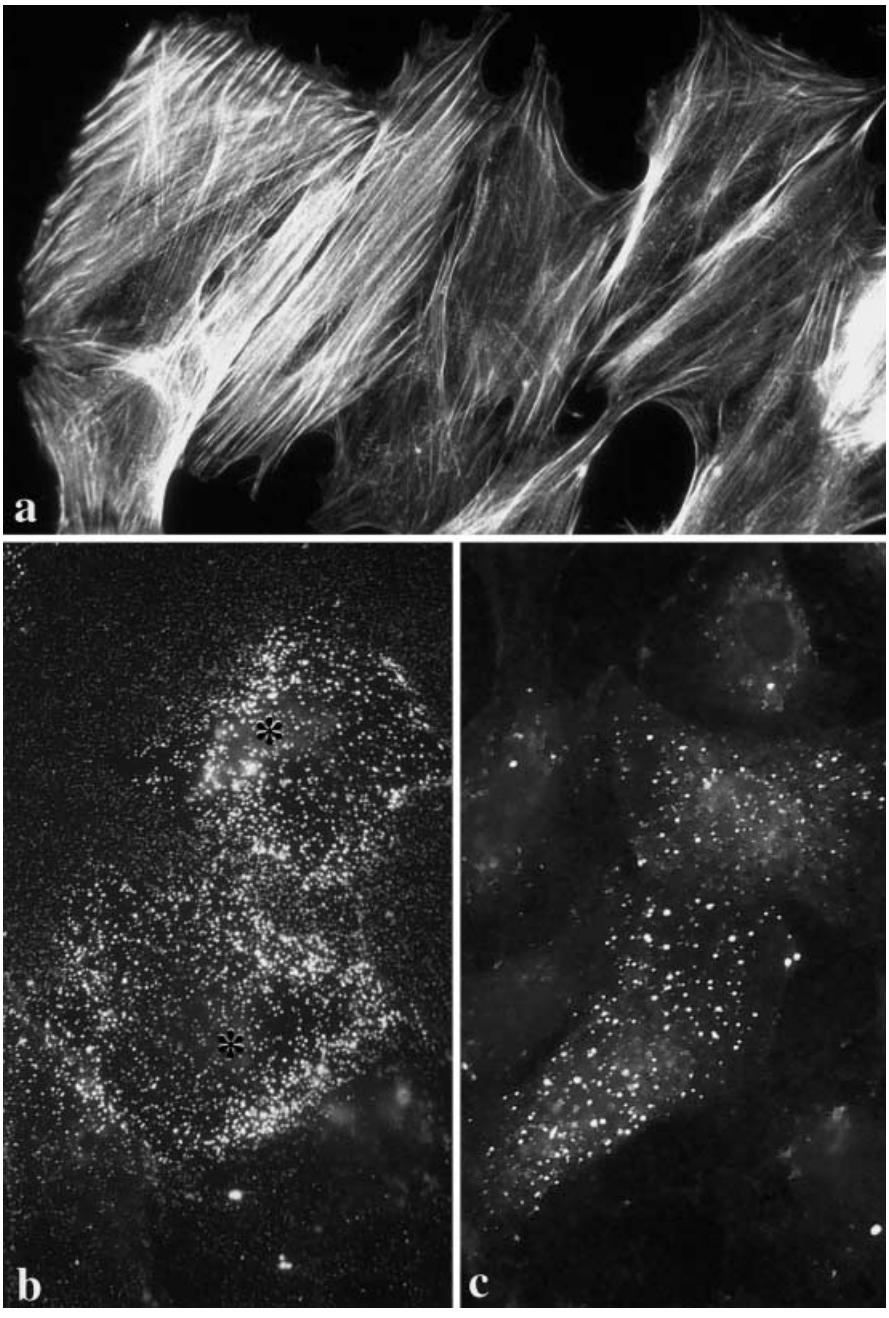


Fig. 2 Characterisation, by means of immunofluorescence, of the M1-cell line (a cell line derived from a human salivary gland plasmacytoid myoepithelioma). These cells express smooth-muscle actin (**a**), mostly as stress fibres. Laminin (**b**) and type-IV collagen (**c**) are also observed, forming multiple dots throughout the cell surface. Laminin label is distributed on the entire surface of M1 cells, making their nuclei (**b**, *) hardly visible. Type-IV collagen expression appears to be weaker when compared with laminin immunostaining. Magnifications 400×

Immunofluorescence

Smooth-muscle actin appeared as parallel bundles of filaments dispersed throughout the cytoplasm (Fig. 2a). Laminin (Fig. 2b) and type-IV collagen (Fig. 2c) exhibited a patchy pattern of distribution throughout the cell surface. Laminin label was more abundant than that of type-IV collagen.

Light microscopy

The M1-cell line, when cultured on a glass surface, formed a flat-cell monolayer composed of juxtaposed cells (Fig. 1). Individually, these cells exhibited a polyedrical shape and abundant cytoplasm. The M1-cell line, when cultured within Matrigel, assumed a new overall morphology, represented by cellular cords in a branching configuration (Fig. 3a–d). No duct-like structures were observed. Individually, M1 cells grown inside Matrigel were mostly spindle-shaped, with a hypercromatic nucleus with a barely discernible nucleolus (Fig. 3e). The plasmacytoid-like phenotype of M1 cells was occasionally observed in this Matrigel preparation (Fig. 3f).

The histopathology of the original tumour was similar to that observed in the three-dimensional preparation of M1 cells in Matrigel. Islands and cords of non-cohesive cells lying in either hyaline or myxoid matrixes

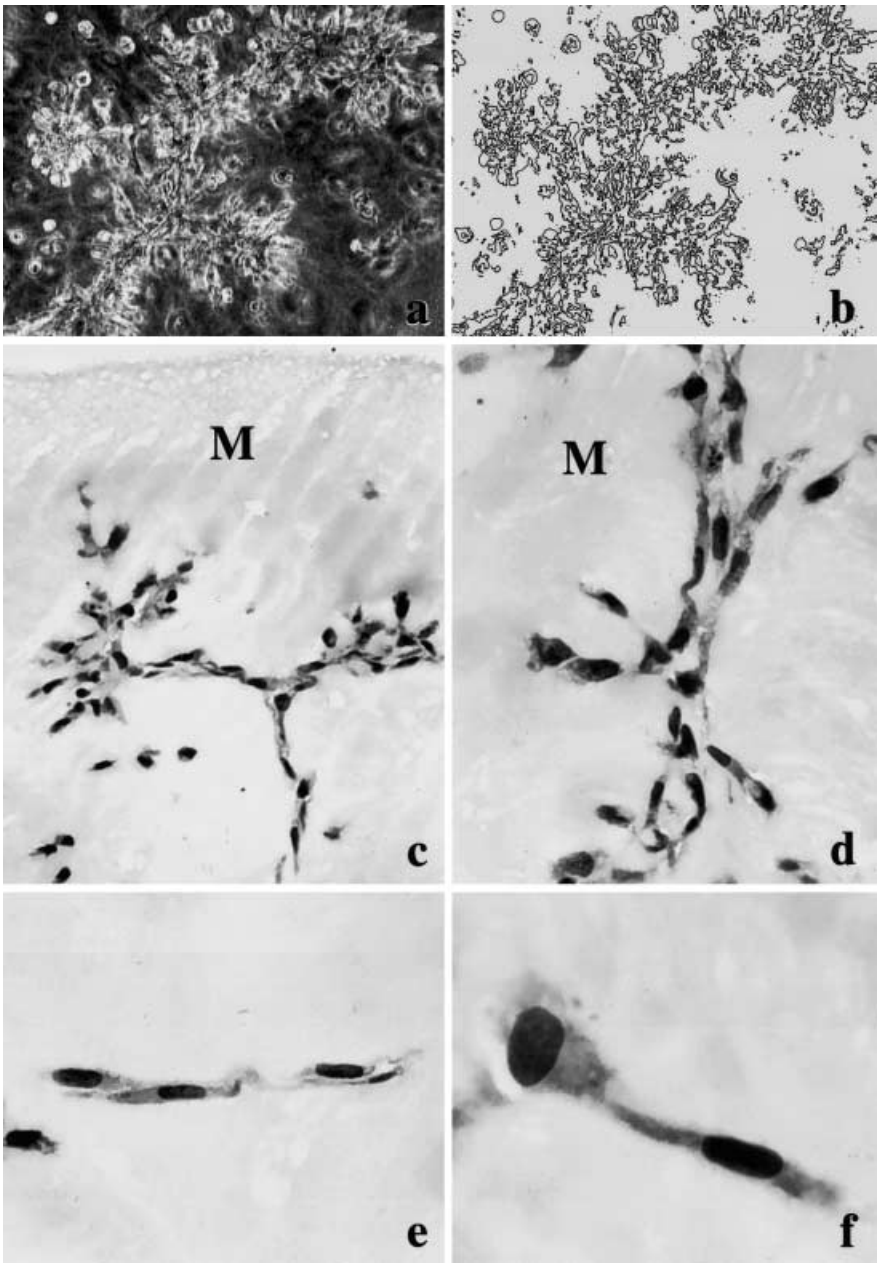


Fig. 3 Morphology of M1 cells (derived from a human salivary gland plasmacytoid myoepithelioma) when grown inside a three-dimensional preparation of Matrigel. Phase contrast shows M1 cells in a branching configuration (**a**). This configuration is clearly depicted when the image shown in (**a**) is processed using the Adobe Photoshop "trace contour" filter (**b**). **c**, **d** Haematoxylin and eosin preparations of M1 cells grown inside Matrigel (*M*). M1 cells are mostly elongated, forming anastomosing cords. Close-up view shows cells with hyperchromatic nucleus with barely discernible nucleoli (**e**). Plasmacytoid-like phenotype was occasionally observed in this Matrigel preparation (**f**). Magnifications **a**, **b** 200×; **c**, **d** 400× and **e**, **f** 800×

(Fig. 4a, b) represented neoplasm architecture. Cells showed glassy and hyaline cytoplasm, and most of them were plasmacytoid in shape. However, the majority of cells facing the extracellular matrix presented an elongated morphology (Fig. 4a, *arrows*).

M1 cells grown within Matrigel revealed a stellate phenotype with long and thin cytoplasmic processes branching out from the cell body (Fig. 5a–c). These elongated multipolar processes established cell–cell contacts (Fig. 5a). The smooth-muscle actin network showed some degree of rearrangement when M1 cells were cultured inside Matrigel. Cells plated on both plain glass coverslips (Fig. 2a) and coverslips with a thin coating of Matrigel (data not shown) presented smooth-muscle actin mostly distributed as bundles of filaments (stress fibres). However, when grown inside Matrigel, M1 cells exhibited mostly globular actin (Fig. 5a). By comparison, the amount of actin in M1 cells grown inside Matrigel (Fig. 5a) was apparently smaller than that of cells grown on plain coverslips (Fig. 2a).

Discussion

A cell line (M1) derived from human plasmacytoid myoepithelioma expressed markers for myoepithelial differentiation, such as smooth-muscle actin, laminin and type-IV collagen. The M1-cell line was cultured inside Matrigel. The culture grew in a branching pattern without formation of duct-like structures. There were confor-

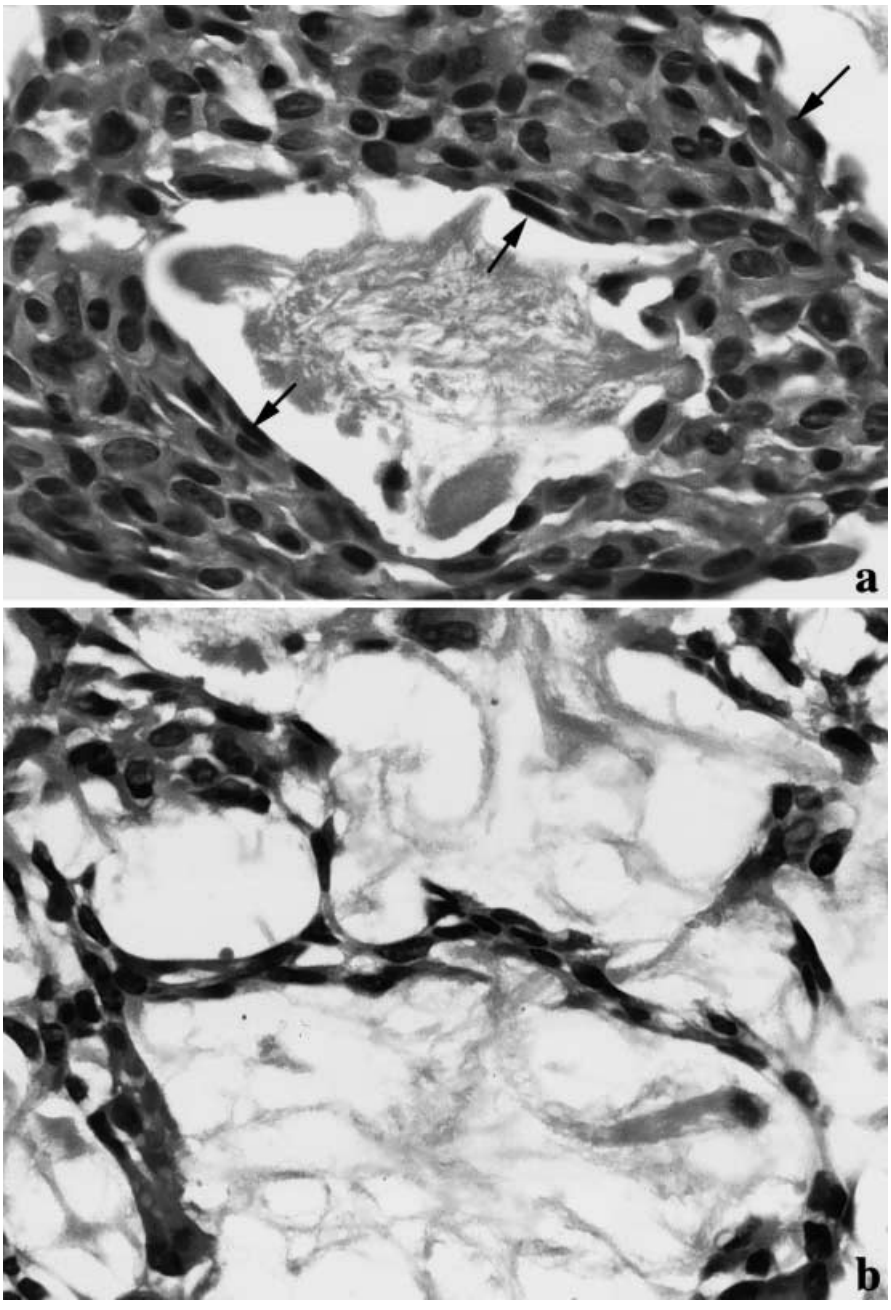


Fig. 4 Morphology (haematoxylin and eosin) of the tumour that originated the M1-cell line (a cell line derived from a human salivary gland plasmacytoid myoepithelioma). The overall picture is similar to the M1-cell line grown inside Matrigel. Islands (**a**) and cords (**b**) of non-cohesive cells lying in either hyaline or myxoid matrix is observed. Most cells are plasmacytoid, with a glassy and hyaline cytoplasm. However, the majority of cells facing the extracellular matrix present an elongated morphology (**a**, *arrows*). Magnifications 400×

mational and molecular changes in these cells, represented by a stellate phenotype and a depolymerisation of smooth-muscle actin, respectively.

We previously described that M1 cells, in addition to smooth-muscle actin, laminin and type-IV collagen, also express vimentin and pan-keratin [16]. Our findings are in agreement with Dundas et al. [10]. These authors demonstrated that clones of cultured myoepithelial cells derived from rat normal mammary gland express variable amounts of cytokeratin 8 and 14, smooth-muscle actin, laminin, type-IV collagen and vimentin.

Morphogenetic studies of normal and neoplastic salivary glands have been carried out through culturing cells in a three-dimensional matrix environment [3, 6, 11, 13, 14, 17, 31, 32, 33]. Most of the studies on neoplastic salivary glands have cultured cells from pleomorphic adenoma [13, 14, 31]. We have used a unique cell line (M1) derived from a rare human salivary gland plasmacytoid myoepithelioma [16, 20]. Moreover, we believe that culturing M1 cells inside Matrigel will provide important information on myoepithelioma biology. This reconstituted basement membrane has been used in many laboratories as a means of preserving, enhancing or inducing phenotypes of a variety of epithelial cells [17, 18, 19, 22, 30]. Matrigel has in its composition important morphoregulatory molecules, such as laminin and type-IV collagen, playing important roles either in cell proliferation or in cell differentiation [19, 30].

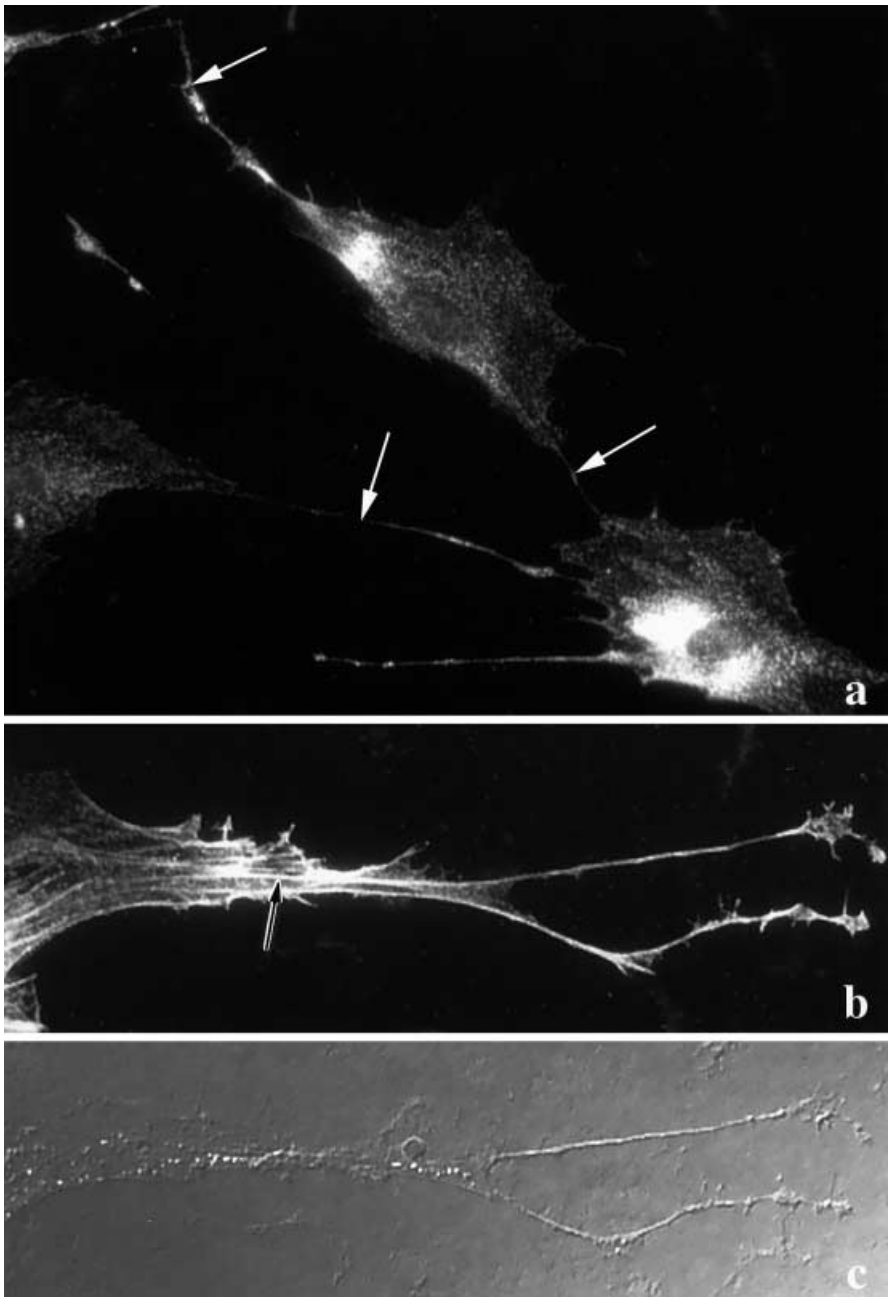


Fig. 5 Cytoplasmic distribution of smooth muscle actin in M1 cells (derived from a human salivary gland plasmacytoid myoepithelioma) grown within Matrigel. Fluorescence microscopy (**a**, **b**) and differential interference contrast (Nomarski, **c**) show cells with stellate phenotype with long and thin cytoplasmic processes branching out from the cell body (**a**–**c**). Cell–cell contacts are noteworthy (**a**, *arrows*). Smooth-muscle actin network shows some degree of rearrangement when M1 cells were cultured inside Matrigel. These cells exhibit mostly globular actin (**a**, **b**) and few stress fibres (**b**, *arrow*). Magnifications **a** 400× and **b**, **c** 630×

The arrangement of M1 cells inside Matrigel mimicked the original tumour in both architectural growth pattern and cytologic subtypes. Islands and cords of noncohesive cells lying in either hyaline or myxoid matrix represented the tumour. Myoepithelioma cells showed glassy and hyaline cytoplasm, and most of them were plasmacytoid in shape. However, the majority of cells facing the extracellular matrix presented elongated morphology, as previously described by Bhaskar and Weinmann [5]. Likewise, M1 cells grown inside Matrigel formed island and cords intermingled in the extracellular matrix. Elongated cells were predominant, growing in direct contact with the extracellular matrix. Plasmacytoid cells, although in smaller amounts, were also present. Duct-like structures were absent in both in vivo and in vitro conditions.

The reproduction of the tumour architecture in our in vitro assay could be due to either the physical or biochemical properties of Matrigel. We have previously shown that spatial arrangement of this reconstituted basement membrane is a key modulator of morphogenetic changes and cytodifferentiation of a pleomorphic adenoma cell line [14]. We showed that M1 cells secrete extracellular matrix molecules, such as laminin and type-IV collagen. Matrigel is basically an enriched preparation of laminin and type-IV collagen [19]. Thus, these molecules may act as autocrine factors, determining the morphogenetic changes of M1 cells.

Differently from the cell line derived from pleomorphic adenoma (AP2 cells) [14], M1 cells exhibited no epithelial differentiation inside Matrigel. M1 cells presented a myoepithelial phenotype with no formation of duct-like structures. Indeed, the myoepithelioma generally lacks duct formation in vivo [7, 8, 9]. Jaeger et al. [14] suggested that pleomorphic adenoma would be derived from a "reserve" cell still capable of differentiation into either direction, epithelial or myoepithelial, depending on the extracellular induction. Based on these findings, we suggest that the myoepithelial cell is the "reserve" cell of the salivary gland myoepithelioma. This should be further emphasised, because it provides evidence that myoepithelioma cells are truly committed to myoepithelial differentiation rather than representing an end of a spectrum of differentiation between ductal and myoepithelial phenotype.

The smooth-muscle actin network showed some degree of rearrangement when M1 cells were cultured inside Matrigel. Cells plated on both plain substrates and on a thin coating of Matrigel presented smooth-muscle actin mostly distributed as bundles of filaments (stress fibres). However, when grown inside Matrigel, M1 cells exhibited mostly globular actin (G-actin). Stress fibres form in response to tension generated across a cell [1]. Cells in culture exhibit different levels of intracellular tension, as shown by the variation in the abundance and distribution of actin stress fibres in different systems [2]. Thus, cells in monolayer cultures on a plastic substrate developed high levels of intracellular tension, whereas in anchored gels, they developed a moderate tension [2]. This could explain the changes in actin status in M1 cells, ranging from stress fibres in cells grown on plain coverslips and on thin coating of Matrigel to mostly G-actin in cells grown inside an anchored Matrigel. Moreover, our results suggest that the amount of actin in cells grown inside the Matrigel was smaller than that of cells grown on plain coverslips. It is in accordance with findings of Arora et al. [2], who showed that smooth-muscle actin transcription is regulated in part by intracellular tension.

In addition to its mechanical properties, Matrigel has chemical factors that may have an impact on actin expression in M1 cells. It has been suggested that a mechanism by which a putative specialised extracellular matrix molecule, under the control of transforming growth factor (TGF)-β, is required for outside–inside signalling and possibly for the development of the intracellular tension necessary for smooth-muscle actin induction [2]. It is known that Matrigel has in its composition TGF-β [30]. Hence, the changes in smooth-muscle actin expression could also be due to this chemical factor.

An increase in smooth-muscle actin leads to retardation of motility. Any reduction in the pool of filamentous actin would increase the rate of motility [21]. Therefore, in cells grown inside Matrigel, the reduction of stress fibres could facilitate the movement of proliferated cells, resulting in the formation of cellular cords in a branching configuration, a finding similar to that reported by Azuma and Sato [3]. The cells grown inside Matrigel would be in a more labile situation capable of remodeling the extracellular matrix by proteolytic enzymes and their inhibitors [27].

In conclusion, we presented the effects of a three-dimensional preparation of Matrigel on cells derived from a human salivary gland plasmacytoid myoepithelioma. The cells grown inside Matrigel presented morphological changes and changes in the smooth-muscle actin status. It was possible to reproduce the tumour architecture with no duct-like formation. Additionally, we showed positivity to smooth-muscle actin. We previously suggested that smooth-muscle actin expression in M1 cells would be regulated by the extracellular matrix [16]. The present investigation is a step further, showing that the plasticity of Matrigel directly influences smooth-muscle actin cytoplasmic organisation. This finding may explain the well-known variations in smooth-muscle actin expression in human salivary gland myoepitheliomas [12, 26, 28, 29].

Acknowledgements This work was supported by grants from Fundação de Amparo à Pesquisa do Estado de São Paulo (FAPESP), Brazil. PTO was supported by Coordenadoria de Aperfeiçoamento de Pessoal de Nível Superior (CAPES), Brazil. SPHM is currently sponsored by Fundação para o Desenvolvimento Científico e Tecnológico da Odontologia (FUNDECTO), Brazil.

References

1. Alberts B, Bray D, Lewis J, Raff M, Roberts K, Watson JD (1994) The cytoskeleton. In: Alberts B, Bray D, Lewis J, Raff M, Roberts K, Watson JD (eds) Molecular biology of the cell, 3rd edn. Garland Publishing Inc., New York, pp 787–861
2. Arora PD, Narani N, McCulloch CAG (1999) The compliance of collagen gels regulates transforming growth factor-β induction of α-smooth muscle actin in fibroblasts. Am J Pathol 154:871–882
3. Azuma M, Sato M (1994) Morphogenesis of normal human salivary gland cells in vitro. Histol Histopathol 9:781–790
4. Barnes L, Appel BN, Perez H, El-Attar AM (1985) Myoepitheliomas of the head and neck: case report and review. J Surg Oncol 28:21–28
5. Bhaskar SN, Weinmann JP (1955) Tumors of the minor salivary glands. A study of twenty-three cases. Oral Surg 8: 1278–1297
6. Burford-Mason AP, Dardick I, MacKay A (1994) Collagen gel cultures of normal salivary gland: conditions for continued proliferation and maintenance of major cell phenotypes in vitro. Laryngoscope 104:335–340
7. Dardick I (1995) Myoepithelioma: definitions and diagnostic criteria. Ultrastruct Pathol 19:335–345
8. Dardick I, Thomas MJ, Van Nostrand AWP (1989) Myoepithelioma. New concepts of histology and classification: a light and electron microscopic study. Ultrastruct Pathol 13:187–224
9. Dardick I, Cavell S, Boivin M, Hoppe D, Parks WR, Stinson J, Yamada S, Burns BF (1989) Salivary gland myoepithelioma variants. Histological, ultrastructural, and immunocytological features. Virchows Arch 416:25–42
10. Dundas SR, Ormerod MG, Gusterson BA, O'Hare MJ (1991) Characterization of luminal and basal cells flow-sorted from the adult rat mammary parenchyma. J Cell Sci 100:459–471
11. Durban EM (1990) Mouse submandibular salivary epithelial cell growth and differentiation in long-term culture: influence

of the extracellular matrix. In Vitro Cell Dev Biol Anim 26:33–43
12. Franquemont DW, Mills SE (1993) Plasmacytoid monomorphic adenoma of salivary glands. Absence of myogenous differentiation and comparison to spindle cell myoepithelioma. Am J Surg Pathol 17:146–153
13. Fujita Y, Yoshida T, Sakakura Y, Sakakura T (1999) Reconstruction of pleomorphic adenoma of the salivary glands in three-dimensional collagen gel matrix culture. Virchows Arch 434:137–143
14. Jaeger MMM, Araújo VC, Kachar B, Jaeger RG (1997) The effect of spatial arrangement of the basement membrane on cultured pleomorphic adenoma cells. Study by immunocytochemistry, electron and confocal microscopy. Virchows Arch 430:467–477
15. Jaeger RG, Jaeger MMM, Araújo VC, Kachar B (1995) Analysis of the interdependent localization of vimentin and microtubules in neoplastic myoepithelial cells. Cell Motil Cytoskeleton 32:289–298
16. Jaeger RG, de Oliveira PT, Jaeger MMM, de Araújo VC (1997) Expression of smooth-muscle actin in cultured cells from human plasmacytoid myoepithelioma. Oral Surg Oral Med Oral Pathol Oral Radiol Endod 84:663–667
17. Kibbey MC, Royce LS, Dym M, Baum BJ, Kleinman HK (1992) Glandular-like morphogenesis of the human submandibular tumor cell line A253 on basement membrane components. Exp Cell Res 198:343–351
18. Kim ND, Oberley TD, Clifton KH (1993) Primary culture of flow cytometry-sorted rat mammary epithelial cell (RMEC) subpopulations in a reconstituted basement membrane, Matrigel. Exp Cell Res 209:6–20
19. Kleinman HK, McGarvey ML, Hassell JR, Star VL, Cannon FB, Laurie GW, Martin GR (1986) Basement membrane complexes with biological activity. Biochemistry 25:312–318
20. Oliveira PT, Jaeger MMM, Loducca FE, Jaeger RG (1996) Myoepithelioma of minor salivary gland. Case report with immunohistochemical, ultrastructural study and propagation of primary culture. Rev Pós-Grad FOUSP (Brazil) 3:234–241
21. Ronnov-Jessen L, Petersen OW (1996) A function for filamentous α-smooth muscle actin: retardation of motility in fibroblasts. J Cell Biol 134:67–80
22. Schnaper HW, Kleinman HK, Grant DS (1993) Role of laminin in endothelial cell recognition and differentiation. Kidney Int 43:20–25
23. Sciubba JJ, Goldstein BH (1976) Myoepithelioma. Review of the literature and report of a case with ultrastructural confirmation. Oral Surg 42:328–338
24. Sciubba JJ, Brannon RB (1982) Myoepithelioma of salivary glands: report of 23 cases. Cancer 49:562–572
25. Seifert G, Sobin LH (1992) The World Health Organization's histological classification of salivary gland tumors. A commentary on the second edition. Cancer 70:379–385
26. Simpson RHW, Jones H, Beasley P (1995) Benign myoepithelioma of the salivary glands: a true entity? Histopathology 27:1–9
27. Sternlicht MD, Safarians S, Rivera SP, Barsky SH (1996) Characterizations of the extracellular matrix and proteinase inhibitor content of human myoepithelial tumors. Lab Invest 74:781–796
28. Takai Y, Mori M, Dardick I, MacKay A, Leung R, Wattimena D, Christensen H, Burford-Mason A (1994) Myofilament localization and immunoelectron microscopic detection of muscle-specific actin in neoplastic myoepithelial cells in pleomorphic adenomas and myoepitheliomas. Ultrastruct Pathol 18:575–591
29. Takai Y, Dardick I, Mackay A, Burford-Mason A, Mori M (1995) Diagnostic criteria for neoplastic myoepithelial cells in pleomorphic adenomas and myoepitheliomas. Immunocytochemical detection of muscle-specific actin, cytokeratin 14, vimentin, and glial fibrillary acidic protein. Oral Surg Oral Med Oral Pathol 79:330–341
30. Vukicevic S, Kleinman HK, Luyten FP, Roberts AB, Roche NS, Reddi AH (1992) Identification of multiple active growth factors in basement membrane Matrigel suggests caution in interpretation of cellular activity related to extracellular matrix components. Exp Cell Res 202:1–8
31. Witsell DL, Weissler MC, Livanos E, Bova-Hill C, Gilmer TM (1993) Unique chromosomal rearrangement and mucin production in a novel salivary myoepithelial cell strain. Arch Otolaryngol Head Neck Surg 119:1151–1157
32. Yang J, Flynn D, Larson L, Hamamoto S (1982) Growth in primary culture of mouse submandibular epithelial cells embedded in collagen gels. In Vitro Cell Dev Biol Anim 18: 435–442
33. Yang J, Larson L, Nandi S (1982) Three-dimensional growth and morphogenesis of mouse submandibular epithelial cells in serum-free primary culture. Exp Cell Res 137:481–485

Virchows Arch (2001) 439:579–585
DOI 10.1007/s004280100422

ORIGINAL ARTICLE

T. Pufe · W. Petersen · B. Tillmann · R. Mentlein

The angiogenic peptide vascular endothelial growth factor is expressed in foetal and ruptured tendons

Received: 30 November 2000 / Accepted: 15 January 2001 / Published online: 29 March 2001
© Springer-Verlag 2001

Abstract The Achilles tendon is one of the most common sites of injury and rupture. Evidence suggests that local vascularisation is involved in this aetiology. We investigated the expression of one important angiogenic factor, the vascular endothelial growth factor (VEGF), in normal and pathologic human Achilles tendons using immunohistochemical, biochemical, molecular and cell biology methods. VEGF could be immunostained in tenocytes of ruptured and foetal Achilles tendons, but not in normal adult ones. In microvessels, the VEGF receptor VEGFR-1 (flt-1) could be visualised as well. High VEGF levels were measured in homogenates from ruptured adult, lower ones in foetal and negligible concentrations in normal adult Achilles tendons using enzyme-linked immunoassay (ELISA) and Western blot experiments. Reverse transcriptase-polymerase chain reaction (RT-PCR) showed that the splice variants $VEGF_{121}$ and $VEGF_{165}$ are exclusively expressed. In tenocytes cultivated from newborn rat Achilles tendons, hypoxia or epidermal growth factor (EGF) raised VEGF production moderately whereas their combination resulted in a strong, synergistic induction. These results prove the presence of an angiogenic peptide and vascularisation in ruptured and foetal tendons and support the view that microtrauma or degeneration in the Achilles tendon precedes its rupture.

Keywords Achilles tendon · Angiogenesis · Hypoxia · Vascular endothelial growth factor (VEGF) · VEGF receptor · Epidermal growth factor (EGF)

Introduction

The formation of new blood vessels is a necessary event during embryogenesis, but occurs rarely in the adult with few exceptions such as the female reproductive system, wound healing and in pathological processes such as cancer or rheumatoid arthritis. Angiogenesis is controlled by a variety of mitogenic, chemotactic or inhibitory peptide and lipid factors that act on invading endothelial and smooth muscle cells. One of the most important angiogenic factors is the vascular endothelial growth factor (VEGF, alternative term: vascular permeability factor VPF), a glycosylated protein of 46–48 kDa composed of two disulphide-linked subunits.

VEGF/VPF is an endothelial cell mitogen that promotes angiogenesis in vivo and renders the microvasculature hyperpermeable to circulating macromolecules [14, 28]. In addition, VEGF is chemotactic for monocytes and a procoagulant. In normal tissues, VEGF is expressed during embryogenesis and in a limited number of sites in adults, e.g. in the circumventricular organs. In the disease state, VEGF can be detected in various tumour cells, the synovial pannus in rheumatoid arthritis or in keratinocytes during wound healing [12, 14]. Five different VEGF isoforms with 121, 145, 165, 189 and 206 amino acids can be generated as a result of alternative splicing from the single VEGF gene. These isoforms differ in their molecular mass and in their biological properties such as their ability to bind to heparin or heparan sulphate proteoglycans and to different VEGF receptors (VEGFR). The splice forms $VEGF_{121}$, $VEGF_{145}$ and $VEGF_{165}$ are secreted, whereas $VEGF_{189}$ is tightly bound to cell surface heparan sulphate and $VEGF_{206}$ is an integral membrane protein. In contrast to the other forms, $VEGF_{121}$ does not bind to heparin or extracellular matrix proteoglycans. The signalling tyrosine kinase receptor VEGFR-1 (flt-1, fms-like tyrosine kinase 1) binds $VEGF_{121}$ and $VEGF_{165}$, and VEGFR-2 (KDR, kinase domain region/flk-1, foetal liver kinase 1) in addition binds $VEGF_{145}$ (apart from certain VEGF-related peptides). The co-receptors neuropilin-1 and -2 bind selectively the 165 residue VEGF isoform [28].

In the majority of patients the Achilles tendon ruptures spontaneously without an apparent adequate trauma [20]. The most frequent localisation for spontaneous Achilles

T. Pufe · W. Petersen · B. Tillmann · R. Mentlein (✉)
University of Kiel, Department of Anatomy, Olshausenstrasse 40, 24098 Kiel, Germany
e-mail: rment@anat.uni-kiel.de
Tel.: +49-431-8802460, Fax: +49-431-8801557

tendon ruptures is located in a region 3–6 cm above the calcanear insertion. Various authors have shown that this region is hypovascular in normal tendons [9, 22]. In contrast, histopathological findings describe an increased vascularity and vascular proliferations in biopsies of patients with spontaneous ruptures [21, 27]. Moreover, animal models of exercise-induced chronic Achilles tendinosis could also demonstrate increased vascularity compared with healthy controls [4, 5]. Since the conditions and factors controlling angiogenesis in tendons are unknown, we elucidated the potential formation of angiogenic factors using the human Achilles tendon as a model. As the most probable candidate for angiogenic peptides we chose VEGF, and determined its presence in ruptured, normal adult and embryonic human Achilles tendons using molecular biology, biochemical and immunocytochemical methods. Furthermore, in a rat cell culture model we elucidated some of the factors responsible for the regulation of the VEGF expression in tenocytes.

Materials and methods

Tissues

Achilles tendons from adults were obtained from orthopaedic surgeries at the "Lubinus Klinik Kiel," Germany. Foetal tendons and controls of healthy tendons were dissected at the Pathological Institute of the University of Kiel. After dissection all tissue biopsies were immediately frozen in liquid nitrogen. All 20 patients (mean age 35 years) had a spontaneous rupture of the Achilles tendon in the region between 3 cm and 6 cm above the calcaneal insertion. In all cases the patient reported about a long history of chronic Achilles tendon pain and the operation was performed within 2 h after rupture.

Immunohistochemistry

For immunohistochemistry, tissue samples were fixed in 3% paraformaldehyde, embedded in paraffin, sectioned, dewaxed, irradiated at 750 W in a microwave oven in 0.01 M sodium citrate buffer (pH 6.0) twice for 5 min. The sections were blocked with 3% hydrogen peroxide (endogenous peroxidases) and subsequently with normal serum (1:5 in Tris-buffered saline) of the species in which the primary antibody was raised. Sections were then immunostained with anti-VEGF (1:40 in Tris-buffered saline, 60 min; sc7269 mouse monoclonal IgG2a, Santa Cruz Biotechnology, Calif., USA) or anti-VEGFR-1 (1:80; sc316-G goat polyclonal antibody; Santa Cruz) followed by biotinylated secondary antibodies and a peroxidase-labelled streptavidin–biotin staining technique. The nuclei were counterstained with hemalum.

Enzyme-linked immunosorbent assay and Western blots

For enzyme-linked immunosorbent assay (ELISA), frozen tissue samples were crushed in an achate mortar under liquid nitrogen, homogenised in 150 mM NaCl 20 mM Tris–HCl buffer (pH 7.4). A soluble fraction was obtained using centrifugation (48,000 *g*, 60 min), and aliquots (100 µl) analysed using a sandwich ELISA (R&D Systems, Minneapolis, Minn., USA) that detects all VEGF splice forms. Human recombinant $VEGF_{165}$ (PreproTech, Rocky Hill, N.J., USA) served as standard. For Western blots, samples were reduced in the presence of 10 mM dithiothreitol, proteins separated using sodium dodecylsulphate–polyacrylamide gel electrophoresis (SDS–PAGE, 10% gels). Samples were transferred onto nitrocellulose membranes that were blocked and incubated with antibodies according to standard techniques as described [18]. Signals were detected using a chemoluminescence reaction (ECL-Plus; Amersham Pharmacia Biotech, Uppsala, Sweden).

Reverse transcription-polymerase chain reaction for VEGF splice variants

For reverse transcription polymerase chain reaction (RT-PCR), frozen samples (1 g) were crushed in an achate mortar under liquid nitrogen. RNA was isolated using the phenol–guanidinium thiocyanate method, and purified with isopropanol and repeated ethanol precipitation. Contaminating DNA was destroyed using digestion with RNase-free DNase I (20 min at 25°C, Boehringer, Mannheim, Germany). After inactivation of the DNase (15 min at 65°C), cDNA was generated with 1 µl (20 pmol) oligo $(dT)_{15}$ primer (Amersham Pharmacia Biotech) and 0.8 µl superscript RNase H^- reverse transcriptase (Gibco, Paisley, UK) for 60 min at 37°C as described [13]. For PCR, 4 µl cDNA was incubated with 30.5 µl water, 4 µl 25 mM $MgCl_2$, 1 µl dNTP, 5 µl 10× PCR buffer and 0.5 µl (2.5 U) Platinum *Taq* DNA polymerase (Gibco) and the following primers (2.5 µl each containing 10 pmol):

1. Nonselective for all VEGF splice variants 5′-ATG-GCA-GAA-GGA-GGG-CAG-CAT-3′ (sense) and 5′-TTG-GTG-AGG-TTT-GAT-CCG-CAT-CAT-3′ (antisense) yielding a 255 bp fragment (40 cycles, annealing temperature 55°C)
2. Selective for VEGF splice variants 5′-CCA-TGA-ACT-TTC-TGC-TGT-CTT-3′ (sense) and 5′-TCG-ATC-GTT-CTG-TAT-CAG-TCT-3′ (antisense) yielding differently sized fragments (40 cycles, annealing temperature 55°C [11])

Culture and stimulation of rat tenocytes

Achilles tendons were dissected from postnatal (2–5-day old) rats, cut into small pieces of less than 0.5 mm, transferred into a small volume (2 ml per 10 cm^2 culture flask, TPP, Switzerland) of Dulbecco's modified Eagle's medium (DMEM) with 50% foetal calf serum (FCS) and left for 24 h at 37°C without enzymatic digestion. Then, a further 3 ml DMEM plus 50% FCS were added and the tissue pieces left for another 24 h at 37°C. During this time, tenocytes migrate out of the tissue and adhere to the bottom of the culture dish. After removing the medium with the remaining tissue pieces floating on top of them, fresh DMEM plus 10% FCS was added and the cells were cultivated for 96 h at 37°C. For subculture, cells were detached using short (about 20 s) trypsin treatment (0.1%, 1:250, Gibco). One million cells were seeded into fresh dishes and cultivated for 24 h in DMEM plus 10% FCS. Then, the medium was replaced with DMEM without FCS and the cells exposed to the stimulators for 72 h. Conditioned medium was withdrawn and aliquots assayed for VEGF content. The cells were washed with phosphate-buffered saline, lysed, the DNA content was measured fluorometrically with the CyQuant reagent (Molecular Probes, Eugene, Ore., USA) and related to a standard number of cells (counted with trypsinised cells). Human recombinant EGF (PreproTech) was used for stimulation.

Results

VEGF can be immunostained in tenocytes of embryonic and ruptured adult, but not in healthy tendons

Using immunocytochemistry, VEGF can be visualised in tenocytes of foetal and ruptured human Achilles tendons, but not in healthy adult ones (Fig. 1a–c). Normally, the cytoplasm of most foetal tenocytes was labelled whereas in ruptured tendons the immunoreactivity was restricted to distinct areas of the tendons. Apart from the cyto-

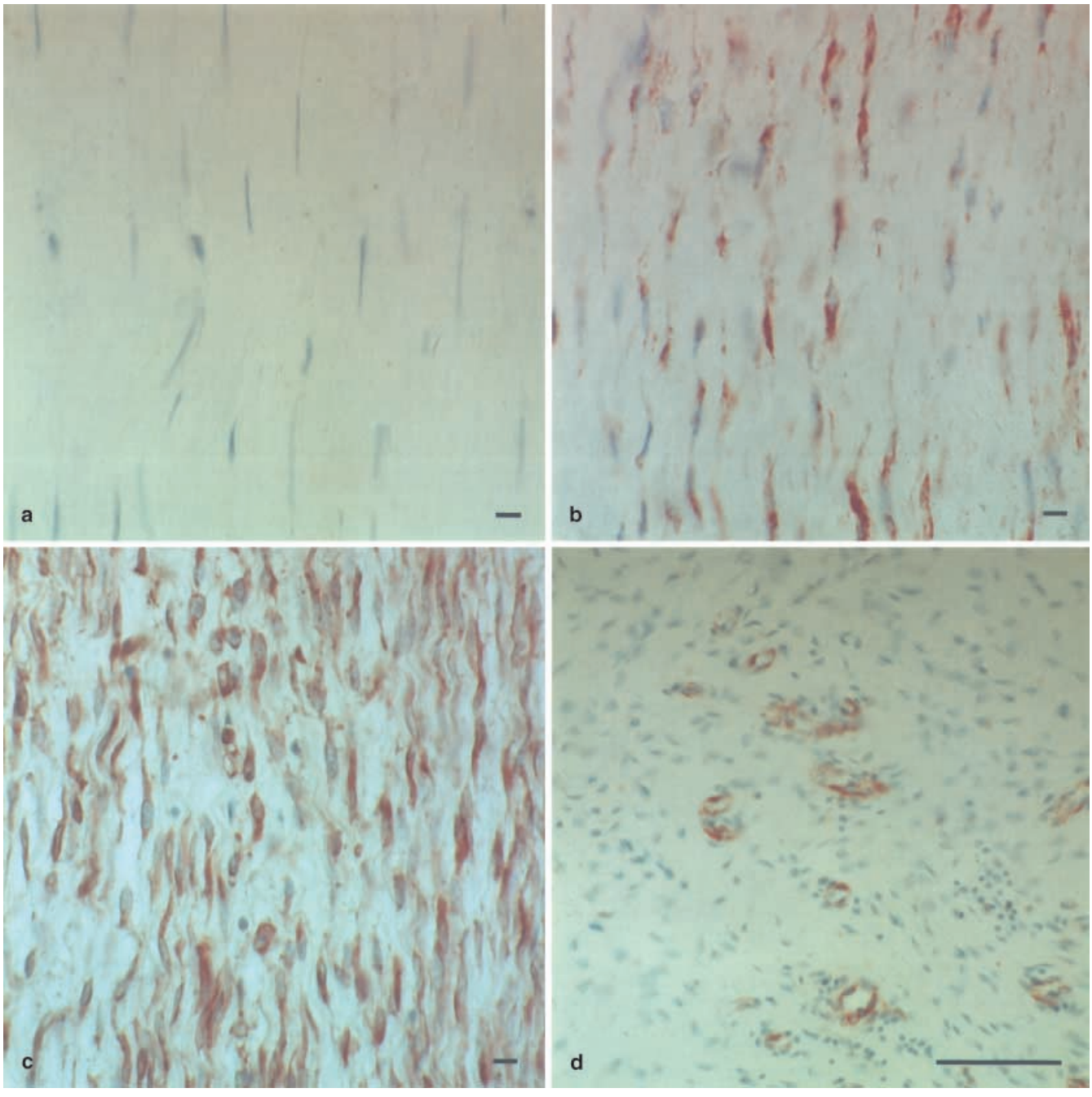


Fig. 1 Immunostaining of vascular endothelial growth factor (VEGF; **a–c**) and its receptor VEGFR-1/flt-1 (**d**) in adult (**a**), ruptured adult (**b, d**), and foetal (**c**; 4 months) human Achilles tendons. Nuclei in the sections were counterstained with Meyer's hemalum. Strong immunoreactivity for VEGF can be detected in ruptured (**b**) and foetal (**c**), but not in normal adult (**a**) samples. In ruptured tendons, the VEGFR-1 is stained on endothelial cells of small blood vessels infiltrating the tissue. The VEGF antibody is cross-reactive with all VEGF splice forms. No immunoreactions were detectable after adsorption of the VEGF antibody to recombinant $VEGF_{165}$ or after omitting the primary antibodies. *Bar*=10 µm (**a–c**) or 100 µm (**d**), original magnifications 360- (**a–c**) or 180-fold (**d**)

plasm of the tenocytes the pericellular space was also immunopositive. To visualise the possible target for the angiogenic peptide, some sections were immunostained for the VEGFR-1/flt-1 (Fig. 1d). Endothelial cells in microvessels of ruptured tendons were intensely stained. At these sites nuclei of invading (VEGFR-1-negative) leukocytes were often detectable.

VEGF concentrations are negligible in healthy adult Achilles tendons, but high in ruptured and embryonic ones

To quantify the VEGF concentrations in Achilles tendons, surgical or pathological samples were homogeni-

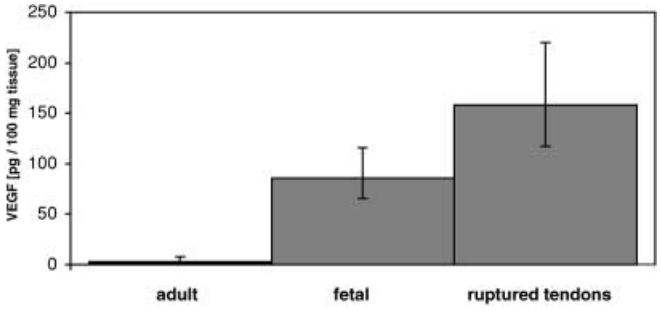


Fig. 2 Vascular endothelial growth factor (VEGF) concentrations are strongly increased in ruptured adult and foetal, but not in normal adult Achilles tendons. Surgical or pathological samples were homogenised in buffer and immunoreactive VEGF determined in the homogenates using an enzyme-linked immunoassay (ELISA) detecting all soluble VEGF splice variants. Means (±SD) from *n*=6 individual patients, foetal tissues were from 4-month-old to 6-month-old embryos

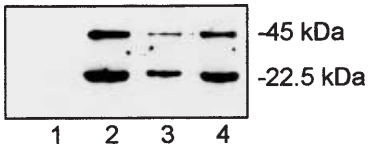


Fig. 3 Vascular endothelial growth factor (VEGF) protein can be detected using Western blot in ruptured (*lanes 1–3*), but not in normal adult (*lane 4*) Achilles tendons. Surgical samples were boiled for 5 min in sample buffer for sodium dodecylsulphate–polyacrylamide gel electrophoresis (SDS–PAGE) in the presence of dithiothreitol. Proteins were separated using SDS-PAGE and transferred onto nitrocellulose membranes that were stained with a VEGF antibody. Chemoluminescence reaction detected two bands of immunoreactive VEGF in ruptured, but not in normal adult tendons with molecular masses of 45 kDa and 22.5 kDa that correspond to the non-reduced VEGF dimer and the reduced VEGF monomer, respectively

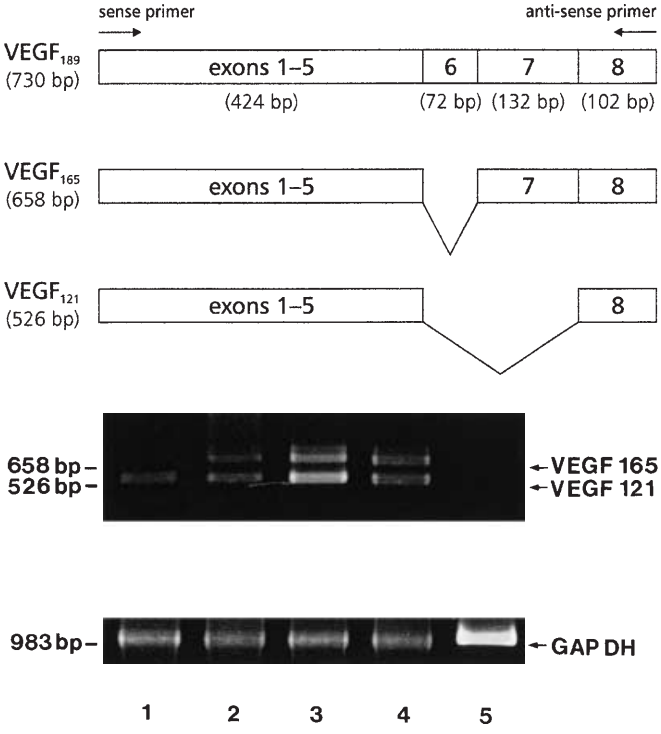


Fig. 4 Reverse transcriptase polymerase chain reaction (RT-PCR) amplification with primers allowing the discrimination of vascular endothelial growth factor VEGF splice variants detect only $VEGF_{121}$ and $VEGF_{165}$ in ruptured (*lanes 1–4*), but not in normal adult (*lane 5*) human Achilles tendons. RNA from the different samples was digested with DNase, reverse transcribed, the cDNA amplified with primers annealing with the VEGF exons 1 (sense) and 8 (antisense), and PCR products were separated on 2% agarose gels that were stained with ethidium bromide. Two products are detectable in ruptured tendons: a 526 bp band derives from $VEGF_{121}$ with exons 6 and 7 spliced out, and a 658 bp band is from $VEGF_{165}$ with exon 6 spliced out. It is easily possible to separate other splice variants, e.g. $VEGF_{189}$ with 730 bp, from the splice forms detected (not shown). A separate RT-PCR for glycerinaldehyde-3-phosphate dehydrogenase (GAPDH) yielding a 983-bp product served as control for intactness of the mRNA applied

sed, and VEGF measured using a sensitive ELISA (Fig. 2). The highest VEGF concentrations were found in ruptured tendons (in areas of the lesion) and lower ones in foetal tendons whereas the VEGF content in healthy adult tendons was negligible. These results could also be verified in Western blotting experiments that further prove the specificity of the immunoreaction. Two bands of 45 kDa (dimer) and 22.5 kDa (monomer) that correspond to the highly glycosylated VEGF protein were heavily stained in ruptured but not in normal tendon samples (Fig. 3).

The splice forms $VEGF_{121}$ and $VEGF_{165}$ can be detected in ruptured tendons

Since the VEGF antibody detects all splice forms and SDS-PAGE lacks resolution to separate variants with 20–40-residue differences due to the high glycosylation of the VEGF protein, we analysed the expression of these differently biological active splice forms using RT-PCR with primers yielding differently sized products (Fig. 4). From all samples of the four ruptured tendons investigated, two PCR products were obtained: one with 526 bp corresponding to $VEGF_{121}$ and one with 658 bp corresponding to $VEGF_{165}$. Both splice products were also obtained with other VEGF-positive human tissues (rheumatoid synovium, gliomas) whereas a human cartilage sample yielded different splice forms ($VEGF_{121}$ and $VEGF_{189}$, not shown) illustrating that the method has the resolution necessary to detect other forms. In conclusion, VEGF mRNA and protein can be detected in tenocytes of ruptured adult, but not in normal human Achilles tendons.

VEGF expression in cultured rat tenocytes is moderately upregulated by hypoxia and growth factors alone, but synergistically by their combination

To address the question of which factors could influence VEGF expression in tenocytes of ruptured tendons, we

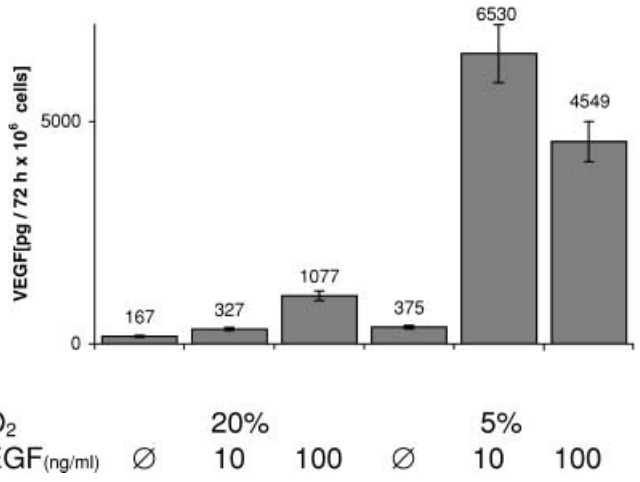


Fig. 5 Influence of hypoxia and growth factors on vascular endothelial growth factor (VEGF) secretion from cultivated tenocytes obtained from rat tail tendons. Conditioned media from tenocytes incubated for 72 h under normoxic (20% O_2) or hypoxic (5% O_2) conditions with or without epidermal growth factor (EGF, 10–100 ng/ml) without foetal calf serum were analysed for VEGF concentration using an enzyme-linked immunoassay (ELISA); values are related to cell numbers determined with DNA measurement after the experiment (mean ±SD from *n*=3 cultures each). VEGF concentrations in the culture supernatants are moderately increased by stimulation with EGF or hypoxia alone, but rise strongly after combined application

challenged primary cultures of rat tenocytes with different stimulators and measured their VEGF secretion. Tenocytes cultivated under normal oxygen pressure released measurable amounts of VEGF into their culture supernatants (Fig. 5). Stimulation with epidermal growth factor (EGF) as an example of a growth factor that activates mitogen-activated protein kinases raised VEGF secretion two- to sixfold. Hypoxic conditions alone (5% O_2) raised VEGF secretion only twofold. However, the combination of EGF and hypoxia increased VEGF production 30- to 40-fold, apparently a synergistic effect.

Discussion

Normal adult human tendons show a relatively low vascularisation due to the low metabolic requirements and rates of this predominantly extracellular tissue. However, they have a well-organised peri- and intratendinous network of blood vessels. Tendons receive their blood supply from vessels coming from the muscle, from the bone or periosteum and especially from vessels surrounding the tendon, in the paratenon, mesotenon and synovial sheets [1, 23, 24]. The number and the diameter of intratendinous vessels varies between different tendons and also within one tendon [29, 30, 31]. Clinical experience has shown that degenerative changes of tendon tissue (tendinosis) occur most frequently within zones of reduced vascularity [20]. Several degenerative and inflammatory pathologic changes of tendons, e.g. “tendinitis” (acute or chronic inflammation within the tendon tissue) result in an enhanced vascularisation [20]. Furthermore, for tendon overuse injuries, e.g. ruptures of the Achilles tendons, pathologic vascular changes accompanied with hypoxia appear to be an important causative factor. Histopathological findings have demonstrated an increased density of vessels in biopsies from patients with tendinosis [2, 21]. Astrom and Westlin [3] demonstrated increased intratendinous blood flow in patients with chronic Achilles tendinopathy using laser Doppler flowmetry. These observations were supported by animal models in the rabbit of exercise-induced acute [10] and chronic tendinosis [4, 5]. The identification of factors regulating the angiogenesis in tendons is therefore an important necessity to understand their pathophysiology.

Using molecular biology and biochemical and immunocytochemical techniques, we could show that VEGF is expressed in injured Achilles tendons at the site of rupture whereas this angiogenic peptide was undetectable in normal tendons. VEGF appears to be one of the most important inducers of angiogenesis despite a variety of other angiogenic factors that have been identified, including members of the fibroblast growth factor family (FGF), transforming growth factors (TGF) α and β, hepatocyte growth factor, tumour necrosis factor (TNF) α, angiogenin, interleukin-8 and others. So far, angiogensis factors have not been identified in embryonic or adult tendons, except mRNA for basic fibroblast growth factor in tenocytes after experimental transfection [25] and – during the experimental work of this study – mRNA for VEGF at the repair site of healing canine flexor tendon in an experimental model [6].

The essential role of VEGF and its receptors, VEGFR-1 and -2 for embryonic vasculogenesis and angiogenesis have been clearly demonstrated using gene knockout studies in mice [8, 16, 33]. However, after birth VEGF also plays a major role in development, e.g. in longitudinal bone growth by stimulating angiogenesis in the epiphyseal growth plate [17]. In the fully grown animal, VEGF is likely to be required for active angiogenesis processes, such as corpus luteum development and wound healing. In addition, several studies have shown that VEGF plays a pivotal role in the angiogenesis of certain tumours, e.g. glioblastomas, and other pathologic conditions associated with high neovascularisation, e.g. diabetic retinopathy, age-related macular degeneration, rheumatoid arthritis [14]. Therefore, the expression of VEGF in embryonic but not normal adult tenocytes points to its function in the development of tendons by stimulation of intratendinous angiogenesis that is needed to supply the growing tendon with oxygen, metabolites and growth factors. Its re-expression in tenocytes of degenerative tendons should likely be induced by a wound-healing or degenerative process. Interestingly, tenocytes produce the two most diffusible splice forms, $VEGF_{121}$ and $VEGF_{165}$, that bind the two signalling receptors VEGFR-1 and VEGFR-2.

We used cultures of postnatal rat tenocytes to elucidate some of the factors responsible for stimulating VEGF expression in adult tendons. Growth factors, as

well as hypoxia, strongly enhanced VEGF secretion from tenocytes and the combination of both showed a synergistic effect. In other cell types oxygen tension and a number of cytokines, hormones and growth factors upregulate VEGF mRNA expression [14, 28]. Their effects, especially in combination, highly depend on the cell type investigated [34]. Induction of VEGF by EGF in tenocytes is an example of the regulation by growth factors that activate mitogen-activated protein kinases (MAPK) p42/p44 and downstream transcription factors such as AP-1 and Sp1 for which binding sites exist in the VEGF promoter region [15, 26]. EGF, TGF-α, platelet-derived growth factor (PDGF) or TNF-β induce VEGF expression in many cell types either by stimulation of a common receptor or activation of identical transcription factors [32]. These cytokines/growth factors are produced during inflammation or wound healing by invading monocytes, thrombocytes, lymphocytes or fibroblasts [7] and could induce – together with hypoxia – VEGF expression in tenocytes. Therefore, microtrauma or inflammatory reactions in tendons resulting in the invasion of leukocytes (Fig. 1d) might be responsible for the observed VEGF production and subsequent angiogenesis.

Indeed, the demonstration of VEGF in tenocytes and VEGFR-1 in endothelial cells of microvessels in ruptured Achilles tendons corroborates the previous histopathological findings of degenerative changes in ruptured tendons [19, 20]. However, the pathophysiological reasons for spontaneous tendon ruptures have been controversial. While a microtrauma or a chronic degeneration of tendon tissue is regarded as a prerequisite for a rupture by most authors, others assume only an excessive and/or uncoordinated movement as the only cause for a tendon rupture [20].

Our findings on the expression of VEGF in tenocytes only of ruptured tendons favour the view that microtrauma or degeneration in the Achilles tendon precedes its rupture. Subsequent angiogenesis contributes to the repair and remodelling of the injured tendon, but may also weaken its mechanically stability by proteolysis of the extracellular matrix by the invading endothelial cells.

Acknowledgements We wish to thank Frank Lichte, Karin Stengel and Regine Worm for their expert technical assistance and Prof. Dr. h.c. D. Harms, Institute of Pathology, University of Kiel, for supplying foetal tendons. This work was supported by a grant from the "Forschungsschwerpunkt Muskel- und Skeletsystem" of the Medical Faculty of the University of Kiel.

References

1. Ahmed IM, Lagopoulos M, McConnel P, Soames RW, Sefton GK (1998) Blood supply of the Achilles tendon. J Orthop Res 16:591–596
2. Astrom M, Rausing A (1995) Chronic Achilles tendinopathy. A survey of surgical and histopathological findings. Clin Orthop 316:151–164
3. Astrom M, Westlin N (1994) Blood flow in chronic Achilles tendinopathy. Clin Orthop 308:166–172
4. Backman C, Boquist L, Friden J, Lorentzon R, Toolanen G (1990) Chronic Achilles paratendinosis with tendinosis: an experimental model in the rabbit. J Orthop Res 8:541–547
5. Backman C, Friden J, Widmark A (1991) Blood flow in chronic Achilles tendinosis: radioactive microsphere study in rabbits. Acta Orthop Scand 62:386–387
6. Bidder M, Towler DA, Gelberman RH, Boyer MI (2000) Expression of mRNA for vascular endothelial growth factor at the repair site of healing canine flexor tendon. J Orthop Res 18:247–252
7. Callard R, Gearing A (1994) The cytokine facts book. Academic Press, London
8. Carmeliet P, Ferreira V, Breier G, Pollefeyt S, Kiekens L, Gerstenstein M, Fahrig M, Vandenhoeck A, Harpal K, Eberhardt C, Declerq C, Pawling J, Moons L, Collen D, Risau W, Nagy A (1996) Abnormal blood vessel development and lethality in embryos lacking a single VEGF allele. Nature 380:435–439
9. Carr AJ, Norris SH (1989) The blood supply of the calcaneal tendon. J Bone Joint Surg 71:100–101
10. Chang J, Most D, Thunder R, Mehrara B, Longaker MT, Lineaweaver WC (1998) Molecular studies in flexor tendon wound healing: the role of basic fibroblast growth factor gene expression. J Hand Surg 23:1052–1058
11. Eckhart L, Ban J, Ballaun C, Weniger W, Tschachler E (1999) Reverse transcription-polymerase chain reaction products of alternatively spliced mRNAs form heteroduplexes and heteroduplex complexes. J Biol Chem 274:2613–2615
12. Fava RA, Olsen NJ, Spencer-Green G, Yeo K-T, Yeo T-K, Berse B, Jackman RW, Senger DR, Dvorak HF, Brown LF (1994) Vascular permeability factor/endothelial growth factor (VPF/VEGF): accumulation and expression in human synovial fluids and rheumatoid synovial tissue. J Exp Med 180:341–346
13. Feindt J, Becker I, Blömer U, Hugo H-H, Mehdorn HM, Krisch B, Mentlein R (1995) Expression of somatostatin receptor subtypes in cultured astrocytes and gliomas. J Neurochem 65:1997–2005
14. Ferrara N (1999) Molecular and biological properties of vascular endothelial growth factor. J Mol Medicine 77:527–543
15. Finkenzeller G, Sparacio A, Technau A, Marme D, Siemeister G (1997) Sp1 recognition sites in the proximal promoter of the human vascular endothelial growth factor gene are essential for platelet-derived growth factor-induced gene expression. Oncogene 15:669–6676
16. Fong DH, Rossant J, Gersenstein M, Breitman ML (1995) Role of the Flt-1receptor tyrosine kinase in regulating the assembly of vascular endothelium. Nature 376:66–70
17. Gerber HP, Vu TH, Ryan AM, Kolwalski J, Werb Z, Ferrara N (1999) VEGF couples hypertrophic cartilage remodeling, ossification and angiogenesis during endochondral bone formation. Nat Med 5:623–628
18. Held-Feindt J, Krisch B, Mentlein R (1999) Molecular and functional analysis of the somatostatin receptor subtype 2 (sst2) in human glioma cells. Mol Brain Res 64:101–107
19. Jarvinen M, Józsa LG, Kannus P, Jarvinen TL, Kvist M, Leadbetter W (1997) Histopathological findings in chronic tendon disorders. Scand J Med Sci Sports 7:86–95
20. Józsa LG, Kannus P (1997) Human tendons – anatomy, physiology, and pathology. Human kinetics, Champain, Ill. USA
21. Kannus P, Józsa LG (1991) Histopathological changes preceding spontaneous rupture of a tendon. A controlled study of 981 patients. J Bone Joint Surg 73:1507–1525
22. Koch S, Tillmann B (1995) The distal tendon of the biceps brachii: structure and clinical correlations. Ann Anat 177:467–474
23. Lang J (1960) Über das Gleitgewebe der Sehnen, Muskeln, Fascien und Gefäße. Z Anat Entwicklungsgeschichte 122: 197–231
24. Lang J (1963) Über die Blutgefäße der Sehnenscheiden. Acta Anat 54:273–309

25. Messner K, Wei Y, Andersson B, Gillquist J, Rasanen T (1999) Rat model of Achilles tendon disorder. A pilot study. Cells Tissues Organs 165:30–39
26. Milanini J, Vinals F, Poussegur J, Pages G (1998) p42/p44 MAP kinase module plays a key role in the transcriptional regulation of the vascular endothelial growth factor gene in fibroblasts. J Biol Chem 273:18165–18172
27. Movin T, Gad A, Reinholt FP, Rolf C (1997) Tendon pathology in long standing achillodynia. Biopsy findings in 40 patients. Acta Orthop Scand 68:170–175
28. Neufeld G, Cohen T, Gengrinovitch S, Poltrak Z (1999) Vascular endothelial growth factor and its receptors. FASEB J 13:9–22
29. Petersen W, Stein V, Tillmann B (1999) Blood supply of the quadriceps tendon. Unfallchirurg 102:543–547
30. Petersen W, Stein V, Tillmann B (1999) Blood supply of the tibialis anterior tendon. Arch Orthop Trauma Surg 119:371–375
31. Petersen W, Bobka T, Stein V, Tillmann B (2000) Blood supply of the peroneal tendons: injection and immunohistochemical studies of cadaver tendons. Acta Orthop Scand 71:168–174
32. Ryuto M, Ono M, Izumi H, Yoshida S, Weich HA, Kohno K, Kuwano M (1999) Induction of vascular endothelial growth factor by tumor necrosis factor alpha in human glioma cells. Possible roles of SP-1. J Biol Chem 271:28220–28228
33. Shalaby F, Rossant J, Yamaguchi TP, Gerstenstein M, Wu XF, Breitman ML, Schuh AC (1995) Failure of blood-island formation and vasculogenesis in Flk-1-deficient mice. Nature 376:62–66
34. Stavri GT, Zachary IC, Baskervillle PA, Martin JF, Erusalimsky JD (1995) Basic fibroblast growth factor upregulates the expression of vascular endothelial growth factor in vascular smooth muscle cells. Synergistic action with hypoxia. Circulation 92:11–14

Virchows Arch (2001) 439:586–592
DOI 10.1007/s004280100465

CASE REPORT

Hajime Umezu · Makoto Naito · Kumiko Yagisawa
Akira Hattori · Yoshifusa Aizawa

An autopsy case of pulmonary capillary hemangiomatosis without evidence of pulmonary hypertension

Received: 23 January 2001 / Accepted: 23 March 2001 / Published online: 13 June 2001
© Springer-Verlag 2001

Abstract We report a case of pulmonary capillary hemangiomatosis (PCH) affecting a 37-year-old woman. PCH is a rare disease accompanying intrapulmonary capillary growth and pulmonary hypertension. In the present case, capillaries infiltrated the alveolar and bronchial walls but not the vascular walls. No signs or symptoms of pulmonary hypertension or right heart hypertrophy/dilatation were present. These findings suggest that vascular involvement in PCH is responsible for the induction of pulmonary hypertension.

Keywords Pulmonary capillary hemangiomatosis · Pulmonary hypertension · Autopsy case · Pathology

Introduction

Pulmonary capillary hemangiomatosis (PCH) is a rare disorder that causes pulmonary hypertension. The most characteristic histological feature is a proliferation of pulmonary capillaries in the alveolar septa, perivascular connective tissue, bronchial wall, and pleura. The proliferating capillaries also surround and invade small pulmonary vessels, which results in a narrowing and occlusion of the vessels. Almost all previously reported cases have been accompanied by pulmonary hypertension and/or right ventricular hypertrophy. However, we experienced a case of PCH without evidence of pulmonary hypertension. Here, we report this unusual case with special reference to pulmonary hypertension in PCH and a review of the literature.

H. Umezu (✉)
Department of Surgical Pathology, Niigata University Hospital,
1-754, Asahimachi-dori, Niigata city, Japan
e-mail: umezu@med.niigata-u.ac.jp
Tel.: +81-25-2272693, Fax: +81-25-2272693

M. Naito
Second Department of Pathology,
Niigata University School of Medicine, Niigata, Japan

K. Yagisawa
First Department of Internal Medicine,
Niigata University School of Medicine, Niigata, Japan

A. Hattori
Department of Internal Medicine, Sado Sogo Hospital,
Niigata, Japan

Y. Aizawa
First Department of Internal Medicine,
Niigata University School of Medicine, Niigata, Japan

Clinical finding

A 37-year-old woman was admitted to Sado General Hospital having suffered from dyspnea and orthopnea for 3 weeks. Approximately 6 years prior, she had had a subarachnoidal hemorrhage and underwent clipping surgery.

The subject was small and markedly obese (143 cm, 79 kg), with high blood pressure (170/120 mmHg). She had had and been treated for hypertension for 10 years. Laboratory data were: red blood cell count (RBC) $395\times10^4/mm^3$, white blood cell count (WBC) $13{,}600/mm^3$, platelet count (Plt) $25\times10^4/mm^3$, Na 144 mEq/l, K 3.5 mEq/l, Cl 104 mEq/l, total bilirubin 0.8 mg/dl, glutamic oxaloacetic transaminase (GOT) 31 IU/l, glutamic pyruvic transaminase (GPT) 31 IU/l, lactate dehydrogenase (LDH) 668 IU/l, cholinesterase (ChE) 3,043 IU/l, uric acid (UA) 10.6 mg/dl, and C-reactive protein (CRP) 0.3 mg/dl. Chest X-ray revealed a diffuse shadow with few air contents.

Echocardiography revealed left ventricular hypertrophy. Antibiotics and an antibronchiectasia agent were administered after admission. Her clinical course improved and the orthopnea disappeared. However, at 6 days after admission, bubbling hemoptysis occurred and was followed by convulsion and syncope. The patient died the next day. An autopsy was performed.

Macroscopic findings

Grossly, the lung was consolidated, heavy, and markedly congested (480 g, 720 g; Fig. 1). The cut surface was dark red and showed a parenchymatous appearance with little air content. There were no infarctions or nodular lesions in the lung.

The heart was enlarged due to marked left ventricular concentric hypertrophy (720 g). The left ventricle and septum were symmetrically hypertrophic (Fig. 2). The right ventricle showed no hypertrophy or dilatation.

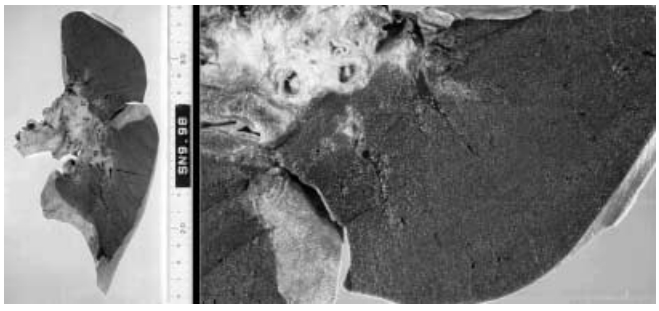


Fig. 1 Macroscopic findings of the lung. The lung is severely congested



Fig. 2 Cut section of the heart. Marked hypertrophy of the left ventricular wall and septum is seen. Note the absence of right ventricular hypertrophy or dilatation

Neither atrium was dilated. There was no infarction, hemorrhage, or fibrosis in the heart. Coronary arteries were smooth with slight atherosclerosis. Cardiac valves showed no remarkable changes. The liver was markedly enlarged (1920 g) with a slightly yellowish discoloration.

Histological findings

At low power examination, the lung field showed marked congestive edema with thickening of alveolar walls (Fig. 3A). At higher magnification, thickened alveolar walls consisted of proliferating thin-walled capillaries. Histologically, these proliferating capillaries showed no cytological atypia. Throughout the lung, the alveolar walls were diffusely thickened by proliferating capillaries occasionally forming a sheet-like mass (Fig. 3B). Capillary proliferation was clearly demonstrated by silver staining. No nodular or patchy growth was detected (Fig. 3A). Collagen fibers did not increase as observed by Azan-Mallory staining. Elastic fibers were disrupted in the area of sheet-like capillary proliferation. The alveolar lumen was filled with serous material accompanying mild hemorrhage and accumulation of hemosiderin-laden macrophages. Immunohistochemically, capillary endothelial cells were positive for factor VIII and CD34 but negative for p53 and Ki-67.

Capillaries invaded the bronchial wall and extended into the bronchial mucosa, resulting in the detachment of bronchial epithelium from the bronchial wall (Fig. 4). However, pulmonary arteries and veins revealed no remarkable changes. No significant compression of the vessel walls or luminal obstruction by the proliferating capillaries was present (Fig. 3). Capillary proliferation in the vascular lumen or in the vascular wall was not

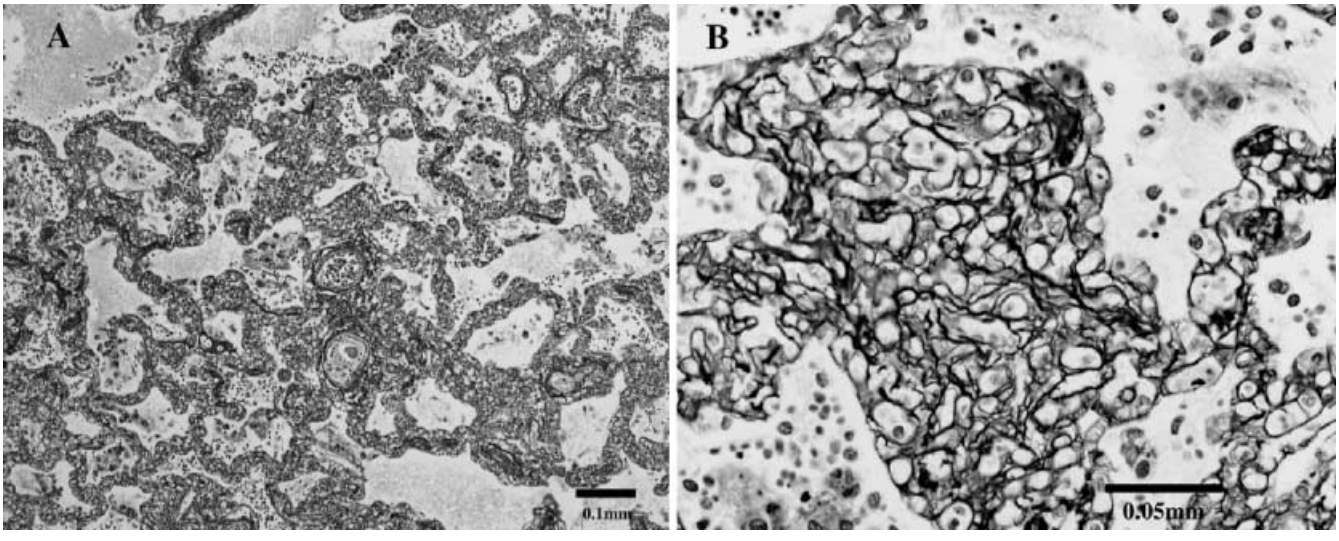


Fig. 3 Histological features of the lung field (silver stain). **A** The lung shows marked edema with diffusely thickened alveolar walls. Capillaries diffusely proliferate in the alveolar wall but do not invade or compress pulmonary arterioles and venules. **B** In some areas, a sheet-like proliferation of capillaries is observed

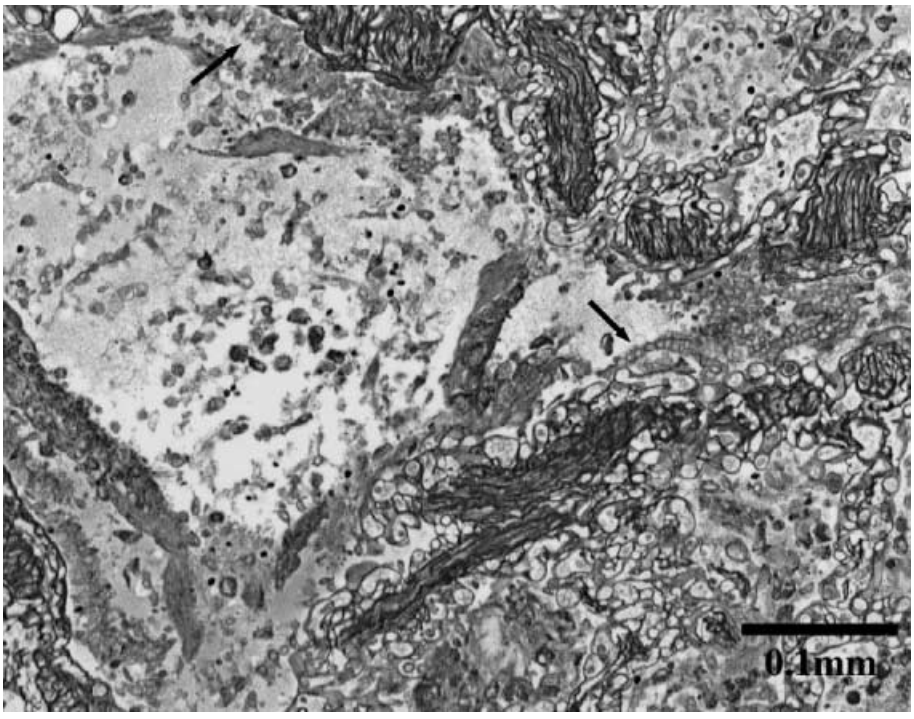


Fig. 4 Capillary growth beneath the bronchial epithelium (silver stain). Bronchial epithelial cells (*arrow*) are desquamated due to the capillary proliferation

detected. Intimal fibrosis or muscular hypertrophy with narrowing of the lumen or occlusion was not observed. Plexiform lesions and thromboemboli were not detected.

Myocardial fibers in the left ventricle and septum were hypertrophic. No pattern of disarray of muscle fibers was found. Coronary arteries showed no remarkable atherosclerotic changes or narrowing. In other organs, no particular finding other than passive congestion was observed.

Discussion

Pulmonary capillary hemangiomatosis is a recently described rare condition [22] and less than 30 cases have been reported in the literature [1, 2, 3, 4, 5, 6, 7, 8, 9, 10, 11, 12, 13, 14, 15, 16, 17, 18, 19, 20, 21, 22, 23, 24]. Age, sex, symptoms, pulmonary artery pressure, and pathological findings of available cases are listed in Table 1. The patients ranged in age from 12 years to 71 years but were predominantly young adults less than 30 years old. The disease affected both sexes. The main symptoms of PCH were dyspnea and hemoptysis. The clinical course was slowly progressive and the patients died after a few years. A correct diagnosis during life is very difficult. Most reported cases were diagnosed at autopsy and three patients were diagnosed at heart–lung transplantation [5].

The nature and pathogenesis of PCH are unknown. PCH has been variously described as a low-grade neoplasm, reactive angioproliferation, and congenital abnormality. Vevaina et al. [20] suggested that the condition is neoplastic, based on the presence of proliferating capillaries in the lung, peritoneum, mediastinum, and lymph nodes. Langleben et al. [14] reported a familial case, suggesting hereditary transmission of an autosomal recessive trait. Prostacyclin was given to the two pulmonary hypertensive patients who were mistakenly thought to have only scleroderma or primary pulmonary hypertension, suggesting that treatment with prostacyclin may have caused the PHC [8, 10]. Some cases were complicated by other diseases, such as scleroderma [8], systemic lupus erythematosus [7], and Takayasu's arthritis [13], implying the autoimmune etiology of PHC. Association of PCH and longstanding hypertrophic cardiomyopathy was also reported [12]. At present, however, this disorder is regarded as a pulmonary angioproliferative disease of unknown etiology.

The most characteristic histologic feature of PCH is the proliferation of thin-walled capillaries with a benign appearance. Proliferating capillaries infiltrate the lung parenchyma, blood vessels, interlobular septa, bronchial walls, pleura, and pericardium. In many cases, lesions are observed as dark-red patches or nodules with patchy hemorrhage in bilateral lungs. In the present case, however, nodular lesions were not detected, and lung parenchyma was diffusely affected, with scarcely a remaining normal lung field. We examined 12 sections from all lobes of both lungs and confirmed that there were diffusely thickened alveolar walls due to capillary proliferation in all sections. There have been no such diffuse lesions in other reported cases. It should be mentioned that Havlik et al. [9] found incidental PCH-like foci in 5.7% of autopsy cases without any symptoms of pulmonary hypertension. The presence of such PCH-like foci may support the view that these foci develop into nodular and, finally, diffuse PCH. However, there is no evidence to judge whether the present case represents the advanced stages of PCH or a peculiar subtype of PCH. More cases must be examined to clarify the natural history of PCH.

Table 1 Review of the literature concerning previously reported pulmonary capillary hemangiomatosis. *H* heart, *L* lung, *PA* pulmonary artery, *RA* right atrium, *RV* right ventricle, *LV* left ventricle, *ND* not described, *PAP* pulmonary artery pressure, *M* mean, *S* systolic, *HLT* heart–lung transplantation, *N* or *D* nodular or diffuse, *PHT* pulmonary hypertension, *M* mean pressure

No.	Age	Sex	Symptom	Chest X-ray, computed tomography, or echocardiogram examination	PAP (mmHg)	Course	Macroscopic finding at autopsy or HLT	N or D	Microscopic findings and other findings	PHT	Reference
1	12	Female	Hemoptysis	H; no congenital abnormality L; minimal signs of interstitial pattern	?	Alive	L; hypoplastic appearance, focally brown in color	D	Left pneumonectomy, diffuse capillary proliferation, little vascular obstruction	–	[21]
2	12	Male	Hemoptysis	H; normal L; dense bilateral interstitial infiltrate	M: 22	Alive	ND		Interferon alfa2a	+?	[23]
3	12	Male	Exertional dyspnea, pulmonary edema, pleural effusion	L; bilateral reticulonodular interstitial marking	ND	Dead 5 Months	H; RV hypertrophy, 230 g L; rt/lt 770, 570 g multiple dark-red patchyes, PA dilated	N	20% of lung fields were affected	+	[11]
4	14	Male	Shortness of breath for 3 years	L; fine interstitial pattern	72/48	Dead 1 Year	H; RV hypertrophy L; focally firm, discrete hemorrhagic area	N		+	[19]
5	19	Male	Hemoptysis Recurrent infection	H; cardiomegaly, PA enlargement L; reticulonodular pattern	100/60 M: 73	Alive (HLT)	H; 560 g/ RV hypertrophy and dilatation L; rt/lt 560, 400 g, nodular consistency with brown hemorrhage. arteriosclerosis, thromboemboli(–)	N	Pulmonary hemosiderosis (pneumonectomy at 11 years) Glomeruloid tuffs in the veins and lymphatics, infiltration into the muscular wall, occlusion of small arteries and venules	+	[5]
6	20	Male	Dyspnea, syncope, RV failure	H; RV hypertrophy and dilatation	M: 75	Dead 1 Month	H; RV hypertrophy and dilatation L; large PA		Oral contraceptive	+	[14]
7	20	Male	Dyspnea	H; RV hypertrophy and dilatation	M: 42	Dead 1 Year	ND			+	[14]
8	21	Male	Dyspnea on excertion	L; diffuse interstitial nodular pattern and a prominent left hilum	ND	Dead 1 Year	H; RV enlargement L; patchy severe congestion, thrombi(–)	N	Capillary proliferation in and around the small venules and arteries, plexiform(–)	+	[19]
9	22	Male	Hemoptysis, pleural effusion	H; enlarged heart L; reticular and micronodular shadowing	M: 15	Dead 7 Years	H; 335 g, RV hypertrophy(–) L; rt/lt 1380, 1190 g		Neoplasm Hospitalization for 7 years	+?	[24]
10	24	Male	Dyspnea, fainting, fever, arthralgia	H; RV hypertrophy L; reticular interstitial infiltrate	ND	Dead 5 Years	H; 650 g L; firm and congestive, multiple small yellow-gray nodules	N	Infiltration and disruption of arteries and venules, intimal and muscular thickening	+	[17]

Table 1 Continued

No.	Age	Sex	Symptom	Chest X-ray, computed tomography, or echocardiogram examination	PAP (mmHg)	Course	Macroscopic finding at autopsy or HLT	N or D	Microscopic findings and other findings	PHT	Reference
11	25	Female	Cough Shortness of breath	L; interstitial reticulonodular infiltrate	ND	Dead	H; 180 g		Capillary infiltration in pericardium and pleura, congenital scoliosis, thromboemboli(–)	?	[20]
12	25	Female	Dyspnea	H; RV hypertrophy and dilatation L; reticulonodular interstitial opacity	M: 69	Dead Few days	ND		Prostacyclin Oral contraceptive	+	[10]
13	25	Female	Dyspnea	H; cardiomegaly, RV predominant L; enlargement PA, focal nodular opacity	M: 69	ND	ND	N		+	[3]
14	27	Male	Hemoptysis, pleural effusion	L; bilateral coarse reticulonodular interstitial disease	M: 74	Dead 4 Days	H; RV hypertrophy, 440 g L; rt/lt 985, 1580 g, patchy hemorrhagic area, organized thrombi(+)	N	Dyspnea on exertion for 12 years Right-lung allogenic transplant, 4 days after died	+	[4]
15	28	Female	Exertional dyspnea	H; right-side cardiomegaly	S: 80	Dead 2.5 Months	H; 300 g L; 1540 g, well defined dark red area	N	SLE, pulmonary vein occlusion by fibrous tissue	+	[7]
16	29	Male	Hemoptysis	H; cardiomegaly, normal PA	105/20	Alive (HLT)	H; 510 g, RV hypertrophy L; patchy hemorrhagic area, organized thrombus(+)	N	ASD, glomeruloid tuffs in the veins and lymphatics, infiltration into the muscular wall, occlusion of small arteries and venules	+	[5]
17	30	Female	Progressive dyspnea	H; RV enlargement L; no pulmonary congestion	M: 55	Dead 1 Year	H; 300 g, RV hypertrophy and dilatation L; rt/lt 900, 850 g, erythematous leion in pleura, thrombi(–)		Oral contraceptive, proliferation inside the vessels, penetrate through venules	+	[14]
18	30	Female	Brown sputum, fatigue Cough	H; PA enlargement L; reticulonodular interstitial marking	60/25	Alive (HLT)	H; 270 g, RV hypertrophy and dilatation L; rt/lt 465, 285 g, patchy hemorrhagic consolidation. thromboemboli(+), intimal fibrosis	N	Glomeruloid tuffs in the veins and lymphatics, infiltration into the muscular wall, occlusion of small arteries and venules	+	[5]
19	34	Female	Dyspnea	H; RV hypertrophy L; patchy reticulonodular interstitial opacity	M: 60	Dead Few days	ND		Prostacyclin Oral contraceptive	+	[10]

Table 1 Continued

No.	Age	Sex	Symptom	Chest X-ray, computed tomography, or echocardiogram examination	PAP (mmHg)	Course	Macroscopic finding at autopsy or HLT	N or D	Microscopic findings and other findings	PHT	Reference
20	34	Male	Exertional dyspnea	H; both ventricle dilatation	ND	Dead	H; 620 g, hypertrophy, septum predominant L; congestion, edema, scattered areas of consolidation		Passive congestion, hypertrophic cardiomyopathy for 18 years, intimal fibrosis (vein), plexiform(–), thrombi(–)	?	[12]
21	34	Female	Dyspnea	L; small, bilateral, diffuse nodular opacities	M: 60	Dead	ND	N		+	[3]
22	35	Female	Pleuritic chest pain Dyspnea	H; RV enlargement L; large PA	44/14	Dead 5 Years	H; 510 g, RV hypertrophy L; rt/lt 570,520 g		Obliteration of small venules, organized thrombi	+	[16]
23	37	Female	Dyspnea, hemoptysis	H; cardiomegaly	ND	Dead	H; 720 g, concentric hypertrophy of left side L; rt/lt 480, 720 g, marked congestive edema	D		–?	Present case
24	38	Female	Shortness of breath Hemoptysis	H; prominent PA	103/39	Dead 1 Year	H; RV hypertrophy L; focally firm, discrete hemorrhagic area	N		+	[19]
25	56	Male	Dyspnea	H; cardiomegaly L; enlarged PA	elevated	Dead	L; patchy area	N	Two brothers died of PPH	+	[18]
26	60	Female	Exertional dyspnea	H; PA enlarge	54/44	Dead	L; firm and congestive, hemorrhage(–), thromboemboli(–)	ND	Breast cancer	+	[2]
				L; diffuse interstitial infiltrates	M: 50	3 Years	H; RV mild hypertrophy and dilatation		Capillaries in lymph nodes		
27	66	Female	Dyspnea	H: mild cardiomegaly, prominent central PA L: clear lung field	M: 52	Dead 6 Days	Thromboemboli(–)		Prostacyclin, scleroderma for 4 years Intimal hyperplasia and fibrosis (PA)	+	[8]
28	71	Female	Exertional dyspnea Hemoptysis	L; diffuse infiltrate	ND	Dead 6 Months	H; RV hypertrophy L; heavy and firm, nodular surface	N	Intimal fibrosis, infiltration in the adventitia and media, occlusion of vein	+	[22]

PCH is generally accompanied by pulmonary hypertension, though their relationship has not been elucidated. An absence of pulmonary hypertension was another peculiar feature of the present case. Although pulmonary arterial pressure has not been measured, the patient showed no signs or symptoms of pulmonary hypertension, hypertrophy, or dilatation of the right heart system. In the literature, there are only a few cases with no pulmonary hypertension and/or right ventricular hypertrophy. In one case, the disease was localized to the left lung [21]. However, the lung lesion was diffuse in the present case, as described above. In most of the reported cases, capillary infiltration of the pulmonary vessels was considered to have caused the clinical pulmonary hyper-

tension. Extensive infiltration of capillaries into the pulmonary vascular wall induces intimal fibrosis, narrowing and occlusion of the pulmonary vessels, and compression of the vessels. The proliferating capillaries around the various classes of pulmonary vessels disrupt and separate the elastic tissue of the media to give rise to pulmonary hemorrhage and hemosiderosis. However, neither the perivascular nor the intravascular proliferation of capillary channels was remarkable in the present case. Thromboembolism and occlusion or narrowing of pulmonary vessels did not occur. The absence of remarkable capillary growth in and around the pulmonary vascular system may have contributed to the maintenance of the pulmonary blood flow.

Veno-occlusive disease, also known to induce pulmonary hypertension, is the most important disease in the differential diagnosis. Secondary thromboembolism appears to be one of the factors responsible for the pulmonary hypertension in PCH. Thromboemboli, mostly in pulmonary arteries, were observed in some [4, 5, 16] but not all cases of PCH [2, 5, 8, 11, 12, 14, 19, 20]. Combining the previously reported data, thromboembolism may not play a major role in the development of pulmonary hypertension in PCH.

In summary, the present case showed unusually diffuse capillary growth in the lung without accompanying pulmonary hypertension. The unusual findings of this case may provide some insight into the pathogenesis of PCH and the PCH-induced pathophysiology.

The case of this 37-year-old with PCH is presented. It is characterized by (1) diffuse proliferation of capillaries in the lung, (2) no capillary infiltration of the vascular lumen or vascular wall, and (3) no evidence of pulmonary hypertension. Perivascular and intravascular proliferation of capillaries rather than thromboembolism appear to be responsible for the development of pulmonary hypertension in PCH.

References

1. Cioffi U, De Simone M, Pavoni G, Poggi L, Pisani D, Ferrero S, Santambrogio L (1999) Pulmonary capillary hemangiomatosis in an asymptomatic elderly patient. Int Surg 84:168–170
2. Domingo C, Encabo B, Roig J, Lopez D, Morera J (1992) Pulmonary capillary hemangiomatosis: report of a case and review of the literature. Respiration 59:178–180
3. Dufour B, Maitre S, Humbert M, Capron F, Simonneau G, Musset D (1998) High-resolution CT of the chest in four patients with pulmonary capillary hemangiomatosis or pulmonary venoocclusive disease. Am J Roentgenol 171:1321–1324
4. Eltorky MA, Headley AS, Winer-Muram H, Garrett HE Jr, Griffin JP (1994) Pulmonary capillary hemangiomatosis: a clinicopathologic review. Ann Thorac Surg 57:772–726
5. Faber CN, Yousem SA, Dauber JH, Griffith BP, Hardesty RL, Paradis IL (1989) Pulmonary capillary hemangiomatosis. A report of three cases and a review of the literature. Am Rev Respir Dis 140:808–813
6. al-Fawaz IM, al Mobaireek KF, al-Suhaibani M, Ashour M (1995) Pulmonary capillary hemangiomatosis: a case report and review of the literature Pediatr Pulmonol 19:243–248
7. Fernandez-Alonso J, Zulueta T, Reyes-Ramirez JR, Castillo-Palma MJ, Sanchez-Roman J (1999) Pulmonary capillary hemangiomatosis as cause of pulmonary hypertension in a young woman with systemic lupus erythematosus (letter). J Rheumatol 26:231–233
8. Gugnani MK, Pierson C, Vanderheide R, Girgis RE (2000) Pulmonary edema complicating prostacyclin therapy in pulmonary hypertension associated with scleroderma: a case of pulmonary capillary hemangiomatosis. Arthritis Rheum 43:699–703
9. Havlik DM, Massie LW, Williams WL, Crooks LA (2000) Pulmonary capillary hemangiomatosis-like foci. An autopsy study of 8 cases. Am J Clin Pathol 113:655–662
10. Humbert M, Maitre S, Capron F, Rain B, Musset D, Simonneau G (1998) Pulmonary edema complicating continuous intravenous prostacyclin in pulmonary capillary hemangiomatosis. Am J Respir Crit Care Med 157:1681–1685
11. Ishii H, Iwabuchi K, Kameya T, Koshino H (1996) Pulmonary capillary hemangiomatosis. Histopathology 29:275–278
12. Jing X, Yokoi T, Nakamura Y, Nakamura M, Shan L, Tomimoto S, Hano T, Kakudo K (1998) Pulmonary capillary hemangiomatosis: a unique feature of congestive vasculopathy associated with hypertrophic cardiomyopathy. Arch Pathol Lab Med 122:94–96
13. Kakkar N, Vasishta RK, Banerjee AK, Singh S, Kumar L (1997) Pulmonary capillary haemangiomatosis as a cause of pulmonary hypertension in Takayasu's aortoarteritis. Respiration 64:381–383
14. Langleben D, Heneghan JM, Batten AP, Wang NS, Fitch N, Schlesinger RD, Guerraty A, Rouleau JL (1988) Familial pulmonary capillary hemangiomatosis resulting in primary pulmonary hypertension. Ann Intern Med 109:106–109
15. Lippert JL, White CS, Cameron EW, Sun CC, Liang X, Rubin LJ (1998) Pulmonary capillary hemangiomatosis: radiographic appearance. J Thorac Imaging 13:49–51
16. Magee F, Wright JL, Kay JM, Peretz D, Donevan R, Churg A (1985) Pulmonary capillary hemangiomatosis. Am Rev Respir Dis 132:922–925
17. Masur Y, Remberger K, Hoefer M (1996) Pulmonary capillary hemangiomatosis as a rare cause of pulmonary hypertension. Pathol Res Pract 192:290–295
18. Rush C, Langleben D, Schlesinger RD, Stern J, Wang NS, Lamoureux E (1991) Lung scintigraphy in pulmonary capillary hemangiomatosis. A rare disorder causing primary pulmonary hypertension. Clin Nucl Med 16:913–917
19. Tron V, Magee F, Wright JL, Colby T, Churg A (1986) Pulmonary capillary hemangiomatosis. Hum Pathol 17: 1144–1150
20. Vevaina JR, Mark EJ (1988) Thoracic hemangiomatosis masquerading as interstitial lung disease. Chest 93:657–659
21. Wagenaar SS, Mulder JJ, Wagenvoort CA, van den Bosch JM (1989) Pulmonary capillary haemangiomatosis diagnosed during life. Histopathology 14:212–214
22. Wagenvoort CA, Beetstra A, Spijker J (1978) Capillary haemangiomatosis of the lungs. Histopathology 2:401–406
23. White CW, Sondheimer HM, Crouch EC, Wilson H, Fan LL (1989) Treatment of pulmonary capillary haemangimatosis with recombinat interferon Alfa-2a. N Engl J Med 320:1197–1200
24. Whittaker JS, Pickering CA, Heath D, Smith P (1983) Pulmonary capillary haemangiomatosis. Diagn Histopathol 6: 77–84

Virchows Arch (2001) 439:593–596
DOI 10.1007/s004280100489

CASE REPORT

Yasunori Takeda · Masanobu Satoh
Shin-ichi Nakamura · Takanori Ohya

Keratoameloblastoma with unique histological architecture: an undescribed variation of ameloblastoma

Received: 20 April 2001 / Accepted: 21 May 2001 / Published online: 24 July 2001
© Springer-Verlag 2001

Abstract Keratoameloblastoma is an extremely rare variant of ameloblastoma, and a review of the English language literature yields only several documented cases of ketatoameloblastoma. This paper reports a keratoameloblastoma showing unique histological architecture. The patient was a 76-year-old Japanese man with a multilocular radiolucent lesion of the mandible extending from the left canine to the second molar area. Microscopically, the lesion was characterized by multicystic spaces lined by papillary projections of proliferating odontogenic epithelium with extensive surface parakeratinization in a lamellar accumulation of keratin. In addition, "hair-like" extensions of keratin were frequently found. There was no ghost cell type keratinization. Histological features of the odontogenic epithelium were similar to those of conventinal ameloblastoma. An additional prominent feature of the present ameloblastoma was formation of hard tissue in continuation, in part, of the accumulated keratin in the fibrous tissue. These hard tissues showed a woven bone- or cellular cementum-like appearance and were not in contact with odontogenic epithelium. The present case was finally diagnosed as "keratoameloblastoma," although such a type of keratoameloblastoma has not been documented previously in the spectrum of ameloblastoma.

This study was supported by Grant-in-Aid for High Performance Bio-Medical Material Research by Ministry of Science, Education, Sports and Culture, Japan.

Y. Takeda (✉) · M. Satoh
Department of Oral Pathology, School of Dentistry,
Iwate Medical University, Uchimaru 19–1,
Morioka 020–8505, Iwate, Japan
e-mail: ytakeda@iwate-med.ac.jp
Tel.: +81-19-6515111
Fax: +81-19-6213321

S. Nakamura
Division of Clinical Pathology, Central Clinical Laboratory,
Iwate Medical University

T. Ohya
Department of Oral and Maxillofacial Surgery,
School of Dentistry, Iwate Medical University

Keywords Keratoameloblastoma · Ameloblastoma · Odontogenic tumor · Jaw bone

Introduction

Ameloblastoma is the most common odontogenic epithelial tumor of the jaw bones. Although most are histologically benign and lack cytological atypia, they are generally considered to be locally aggressive and destructive, exhibiting various rates of recurrence. Histopathologically, there are two main subtypes of ameloblastoma: follicular and plexiform, both of which consist of islands, nests, cords, or strands of odontogenic epithelium rimmed by columnar cells resembling ameloblasts. The center of these epithelial structures contains loosely arranged spindle or stellate shaped cells resembling the stellate reticulum of the enamel organ. Many histological variations of ameloblastoma have been described, and two or more variations may occasionally occur within the same tumor [2]. Although there is no evidence that any histological variation is more aggressive than any



Fig. 1 Radiograph showing a multilocular radiolucent lesion (*arrowheads*) of the mandible extending from the left canine to the second molar area

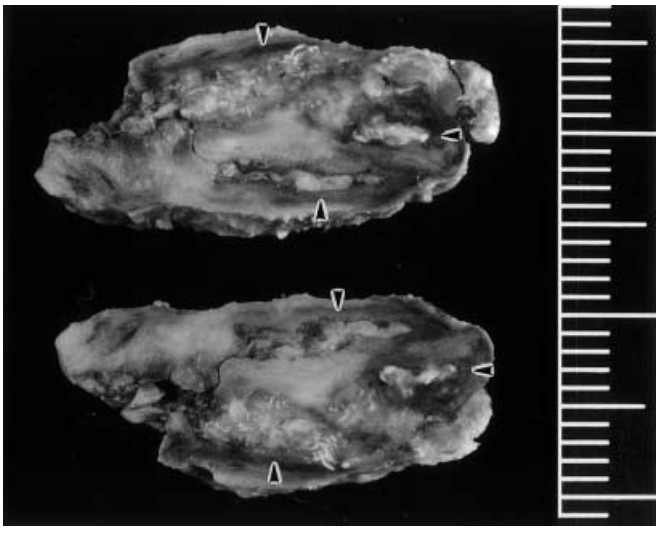


Fig. 2 Cut sections of the surgically resected specimen showing multiple cysts (*arrowheads*) which filled with keratinous material

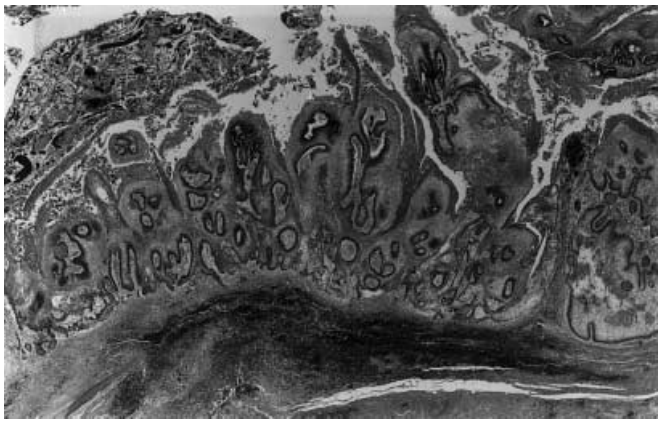


Fig. 3 Cystic tumor consisting of an inner layer of papillary proliferating odontogenic epithelium with marked surface keratinization, and an outer layer of fibrous connective tissue

other, the differential diagnosis from other odontogenic and non-odontogenic tumors has to be made in order to establish appropriate treatment in some variations.

Variations of ameloblastoma that exhibit keratinization in their parenchyma are the acanthomatous ameloblastoma, the keratoameloblastoma (KA), and the papilliferous keratoameloblastoma (PKA) [2]. Of these, KA and PKA are extremely rare tumors, and our review of the English language literature yields only six cases of KA [3, 6, 7] and two cases of PKA [1, 5]. The purpose of this paper is to report a keratoameloblastoma, which has an undescribed histological architecture within the spectrum of ameloblastoma.

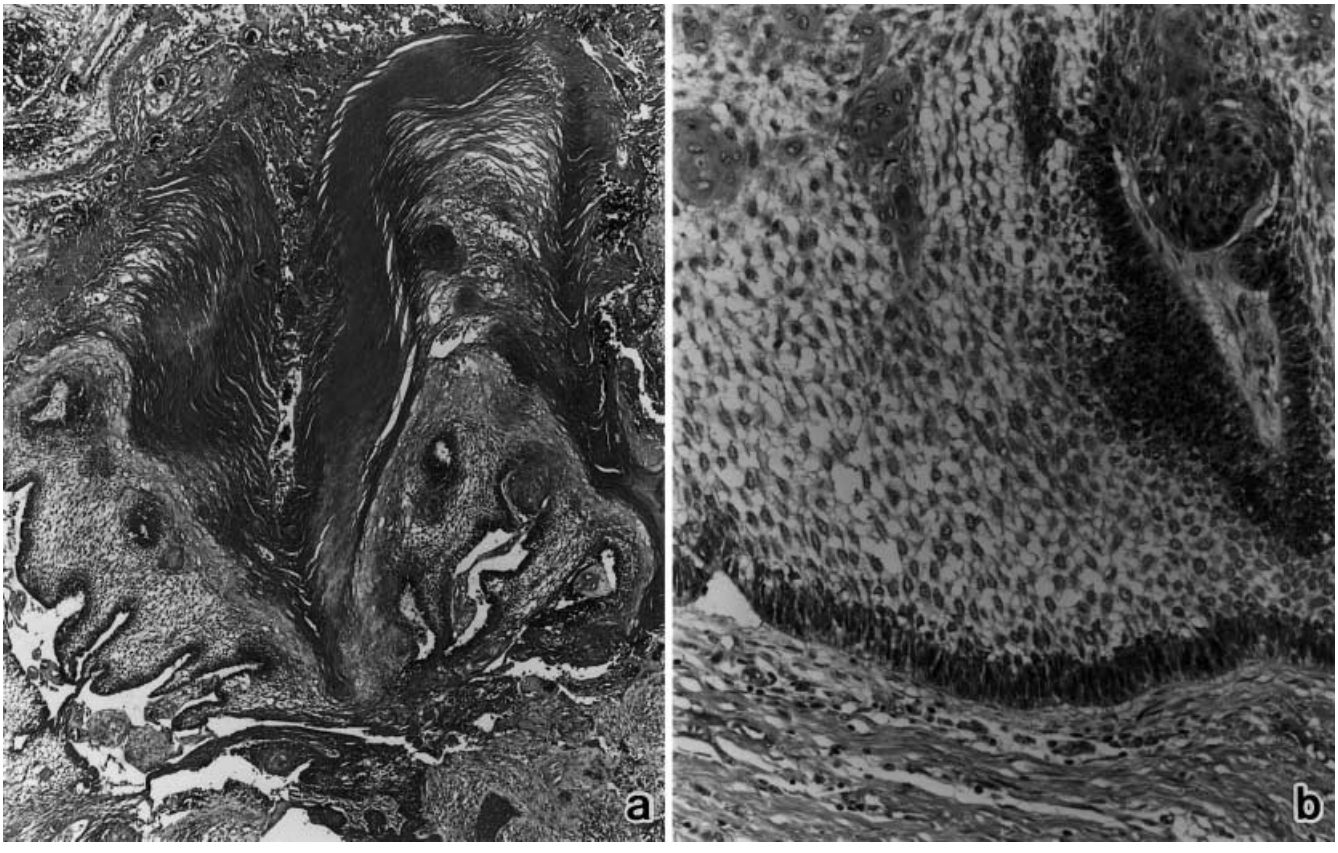


Fig. 4a, b Surface keratinization of proliferating odontogenic epithelium. **a** Extensive surface parakeratinization with lamellar accumulation of keratin in the odontogenic epithelium, resulting in "hair-like" extensions of keratin. **b** Proliferating odontogenic epithelium consisting of loosely arranged polygonal or angular cells resembling stellate reticulum of the enamel organ, and a palisade of tall, columnar, ameloblast-like cells

Case report

A 76-year-old Japanese man was referred to an oral surgeon by his dentist, because of swelling of the mandible. He had no past or familial history of any disease of the head and neck. The patient had first noticed a swelling without pain on the alveolar ridge of the mandibular molar region several months previously. The patient was examined and found to have a diffuse swelling of the mandible from the left canine to the molar region. Radiographic examination showed a multilocular radiolucent lesion extending from the left canine to the second molar area (Fig. 1). The lesion was biopsied and, following a histopathological diagnosis of ameloblastoma with marked keratinization, the patient was admitted soon afterwards and underwent surgical resection of the lesion. At surgery, the lesion was easily removed from the surrounding bone. The postoperative course was uneventful.

Pathological findings

The surgical specimen was a 40×25×15-mm soft tissue mass. Cut sections revealed multiple cysts which were filled with keratinous material and had thickened walls (Fig. 2).

Microscopically, the lesion was characterized by cystic spaces lined by papillary projections of odontogenic epithelium with connective tissue cores (Fig. 3). Extensive surface parakeratinization with lamellar accumulation of keratin was seen in the odontogenic epithelium, and "hair-like" extensions of keratin were frequently found (Figs. 3, 4a). There was no ghost cell type keratinization. The odontogenic epithelium consisted of a loosely arranged polygonal or angular cells resembling the stellate reticulum of the enamel organ and a palisade of tall, columnar, ameloblast-like cells (Fig. 4b).

An additional prominent feature was formation of hard tissue in continuation, in part, with the accumulated keratin in the fibrous tissue (Fig. 5a). These hard tissues showed a cellular cementum- or woven bone-like appearance and were not in contact with odontogenic epithelium (Fig. 5b).

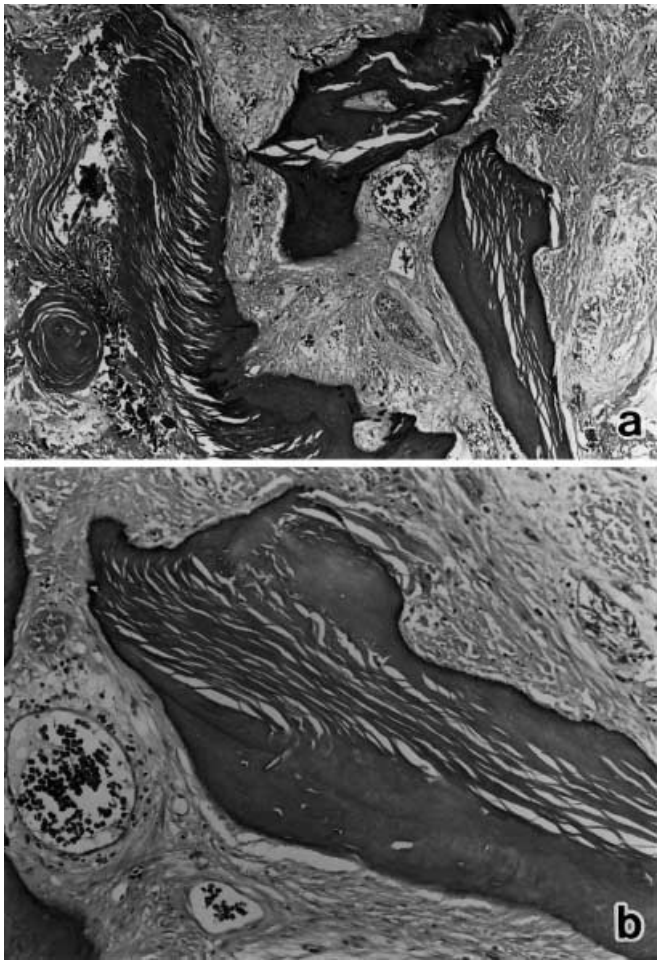


Fig. 5a, b Formation of hard tissue. **a** Hard tissues in continuation with the accumulated keratin in the fibrous stroma. **b** Hard tissue showing woven bone- or cellular cementum-like appearance, and no relation to odontogenic epithelium

Discussion

Histologically, ameloblastoma recapitulates the morphology of the pre-matrix stage of the enamel organ and may assume a variety of histological configurations that have been described in various papers. Clinically, no behavioral difference has been observed among histological and cytological variants. Unicystic tumors in younger patients that arise in conjunction with impacted teeth and exhibit a luminal or mural retiform pattern are generally less aggressive, with a limited tendency to recur following enucleation or curettage.

PKA and KA are extremely rare variants of ameloblastoma [2]. PKA was first described as a subtype of ameloblastoma by Pindborg and Weinmann [5], whose reported a woman with a multilocular radiolucent lesion of the mandible. Histologically, the lesion was composed of microcystic follicles, some of which were keratin-filled cysts lined by parakeratinized stratified squamous epithelium, while others had a non-keratinized epithelium with a papilliferous pattern. Altini et al. [1] reported a second case of PKA, and they suggested that PKA may not be related to ameloblastoma but rather is an unclassified epithelial odontogenic tumor, as none of lesions termed PKA reveal histological features of ameloblastoma, such as nuclear palisading of basal columnar cells and/or stellate reticulum-like cells.

KA was first described by Siar and Ng [7], who reported four examples of a tumor characterized by the simultaneous occurrence of ameloblastoma with pronounced keratinization and cystic components resembling an odontogenic keratocyst. Said-Al-Naief et al. [6] recently presented a new case of KA and reviewed five other cases which he considered to be qualified for the diagnosis (Table 1). Average patient age was 31.8 years (range 26 to 39 years). Four tumors were located in the mandible and two in the maxilla, and there was no gender predominance. Two patients were Chinese, one was African-American, two were Malaysian, and in one case, the race was not described. Histological features of KA are as follows:

1. Scattered cystic and solid epithelial follicles in a dense and mature fibrous connective tissue
2. Epithelial follicles composed of central parakeratin and keratin plugs and peripheral enamel organ-like structure

Table 1 Clinical summary of documented cases diagnosed as "keratoameloblastoma" in the English language literature

Case [references]	Age (years)	Sex	Race	Location	Clinical findings
1 [7]	30	Male	Chinese	Anterior mandible	Painless expansile swelling for 5 years
2 [7]	35	Male	Malay	Left mandible	Hard swelling for 6 months
3 [7]	35	Female	Malay	Right maxilla	Massive, slowly-progressing swelling for 9 months
4 [7]	39	Female	Chinese	Anterior mandible	Cystic lesion
5 [3]	26	Female	Unknown	Right mandible	Firm swelling with pain for 5 years
6 [6]	26	Male	African-American	Right maxilla	Mass protruding from a tooth-extraction wound

3. Some cystic follicles with the epithelial lining suggestive of odontogenic keratocyst [3, 6, 7]

The present lesion, which clinically showed a multilocular radiolucency of the mandible extending from the left canine to the second molar area in a 76-year-old Japanese man, was microscopically characterized by multicystic spaces lined by a papillary projections of odontogenic epithelium with extensive surface parakeratinization in a lamellar accumulation of keratin. In addition, "hair-like" extensions of keratin were frequently found. There was no ghost cell type keratinization. Histological features of proliferating odontogenic epithelium were similar to those of conventional ameloblastoma. The present case was finally diagnosed as "keratoameloblastoma," although such a type of keratoameloblastoma has not been documented previously in the spectrum of ameloblastoma.

As mentioned earlier, no biological behavioral differences have been noted among various histological and cytological variants of ameloblastoma, except for unicystic ameloblastoma. However, pathological knowledge of these variants is important for differential diagnosis. Although keratoameloblastoma is decidedly rare, if excessive keratinization in an ameloblastoma, as presented here, is included in a small biopsy specimen or is aspirated for cytologic diagnosis, the correct diagnosis of ameloblastoma may be confused with other odontogenic tumors or cysts that commonly present with keratinization, such as squamous odontogenic tumor, calcifying odontogenic cyst, odontogenic keratocyst, dentinogenic ghost cell tumor, malignant ameloblastoma, and primary intraosseous carcinoma.

An additional, prominent feature of the present ameloblastoma was formation of hard tissue in continuation, in part, with the accumulated keratin in the fibrous tissue. These hard tissues showed a woven bone- or cellular cementum-like appearance and were not in contact with odontogenic epithelium. There have been a few documented cases of ameloblastoma with formation of hard tissues, which are an inductive formation of dentin or dentinoid [4, 8] or a reactive formation of stromal bone [9]. Hard tissue formation in the present case might be in the nature of pathologic ossification, since transition between accumulated keratin and hard tissue was evident. It is well known that degenerative or necrotic tissues with or without dystrophic calcification may undergo actual conversion to bone, the process being termed pathologic ossification.

References

1. Altini M, Slabbert HV, Johnston T (1991) Papilliferous keratoameloblastoma. J Oral Pathol Med 20:46–48
2. Kramer IRH, Pindborg JJ, Shear M (1992) Histological typing of odontogenic tumours, 2nd edn. Springer, Berlin Heidelberg New York
3. Norval EJG, Thompson IOC, van Wyk CW (1994) An unusual variant of keratoameloblastoma. J Oral Pathol Med 23:465–467
4. Orlowski WA, Doyle JL, Salb R (1991) Unique odontogenic tumor with dentinogenesis and features of unicystic plexiform ameloblastoma. Oral Surg Oral Med Oral Pathol 72:91–94
5. Pindborg JJ, Weinmann JP (1958) Squamous metaplasia with calcification in ameloblastoma. Acta Pathol Microbiol Scand 44:247–252
6. Said-Al-Naief NAH, Lumerman H, Ramer M, Kopp W, Kringstein GJ, Persenchino F, Torno R (1997) Keratoameloblastoma. A case report and review of the literature. Oral Surg Oral Med Oral Pathol Radiol Endod 84:535–539
7. Siar CH, Ng KH (1993) Combined ameloblastoma and odontogenic keratocyst or keratinizing ameloblastoma. Br J Oral Maxillofac Surg 31:183–186
8. Slabbert H, Altini M, Crooks J, Uys P (1992) Ameloblastoma with dentinoid induction: dentinoameloblastoma. J Oral Pathol Med 21:46–48
9. Takeda Y, Kuroda M, Suzuki A (1990) Ameloblastoma with prominent stromal ossification. Acta Pathol Jpn 40:780–784

Virchows Arch (2001) 439:599
DOI 10.1007/s004280100478

ERRATUM

M. Elleder · H. Houštková · J. Zeman · J. Ledvinová
H. Poupětová

Pulmonary storage with emphysema as a sign of Niemann-Pick type C2 disease (second complementation group)

Published online: 9 August 2001
© Springer-Verlag 2001

Virchows Arch (2001) doi10.1007/s004280100407

Two references were incorrect in the Discussion: references [7, 12] should be replaced by [19, 23] in both lines 8 and 16. The references were also incorrect in Table 1, which is reprinted below.

Table 1 Niemann-Pick type-C2 survey of the published cases

	Age (years) involvement	Pulmonary	Reference
1. Infantile, neurological onset	1.66[a]	No	[28]
2. Juvenile, neurological onset[c]	20[b]	No	[28]
3. Infantile, hepatosplenomegaly[d]	0.583[a]	Severe, fatal	[23]
4. Infantile hepatopathic	<1[a]	Severe, fatal	[24]
5. Congenital(hepatomegaly, ascites)	0.6[a]	Severe, fatal	[19]

[a] Age at death
[b] Age of living patient
[c] The patient's sibling suffered from the same disease (identical phenotype)
[d] The patient's sibling, with storage-based neonatal hepatitis, died at 6 weeks with severe, fatal pulmonary involvement

The online version of the original article can be found at http://dx.doi.org/10.1007/s004280100407

M. Elleder (✉) · J. Ledvinová · H. Poupětová
Institute of Inherited Metabolic Disorders, Ke Karlovu 2, Div. B, Building. D, 128 08, Prague 2, Czech Republic
e-mail: melleder@beba.cesnet.cz
Tel.: +420-2-24918283, Fax: +420-2-24919392

H. Houštková · J. Zeman
Pediatric Clinic, Charles University,
First Faculty of Medicine and University Hospital,
Prague, Czech Republic

Virchows Arch (2001) 439:601–603
DOI 10.1007/s004280100412

DIAGNOSTIC STANDARDS

W.D. Lawrence · Association of Directors of Anatomic and Surgical Pathology

ADASP recommendations for processing and reporting of lymph node specimens submitted for evaluation of metastatic disease

Received: 29 November 2000 / Accepted: 21 December 2000 / Published online: 8 June 2001
© Springer-Verlag 2001

Abstract It is well known that different pathologists in different laboratories follow different protocols for the processing and examination of these specimens. There is also extensive literature (some of which is summarized in the references appended to the present report) on the likelihood of identifying metastases of varying sizes with different methods of preparation, as well as on the clinical significance of this identification, which varies not only from site to site but also from report to report on the same site. The Association of Directors of Anatomic and Surgical Pathology (ADASP) has reviewed this literature as well as the personal experience of its own members to present a set of recommendations for lymph node biopsies, lymph node dissections, sentinel node biopsies, lymph node fine needle aspiration (FNA) and core needle biopsies. It should be noted that these recommendations are intended specifically for lymph nodes being studied for metastatic neoplasms, and are not intended to apply to lymph nodes being evaluated for lymphoma, infections, and other disease processes. They are, however, formulated generically enough to apply regardless of whether the primary tumor is a carcinoma of the breast, carcinoma of the prostate, melanoma, or any other malignant, potentially metastasizing tumor. The Association has published numerous documents with recommendations for reporting surgical pathology specimens involving particular organ sites (for example, breast, pancreas, thyroid, etc.) However, the Association has not yet considered the generic question of dealing with lymph node specimens in which the intent is to search for and document the presence of metastatic disease. We are also unaware of guidelines for pathologists published by any other organization on this subject.

Keywords Lymph nodes · Metastasis · Vascular involvement · Therapy · Section numbers · FNA

Lymph node biopsies

In the presence of gross tumor in a biopsy of a single lymph node, one or several routine sections to demonstrate the tumor and its possible extranodal extension will suffice.

In the absence of gross tumor, the entire node should be submitted for microscopic examination, cut into 3- to 4-mm slices in the longitudinal or transverse plane. If the node is so small that it cannot be sliced in this manner, it may be submitted as one piece in toto. If the node is sliced, care should be taken to process different surfaces for microscopic examination. The Association recommends the examination of several levels of each slice, stained with hematoxylin and eosin (H&E) only.

Lymph node dissections

Processing and staining

(a) As mentioned above, the principles presented here are generic, and may vary by site or by institution.
(b) Lymph node dissections are best processed fresh, although other techniques (such as fixation in Bouin's solution) may be used.
(c) No clearing of adipose tissue is necessary, although it may represent an institutional or individual preference.
(d) Submit every node for microscopic examination.
(e) Submit the entire nodes cut as described in section A unless they contain grossly visible tumor, in which case fewer slices are required, or if they are grossly largely replaced by adipose tissue, in which case processing is optional.
(f) Lymph node levels in a dissection specimen should be specified and submitted separately where clinically appropriate (for example, neck dissections, colectomy specimens).

This document was prepared by an ADASP Committee consisting of Drs. Steven G. Silverberg (Chair), James L. Connolly, David Dabbs, Carlos A. Muro-Cacho, David L. Page, Mukunda B. Ray, and Mark R. Wick

W.D. Lawrence (✉)
Dept. of Pathology, The Detroit Medical Center, Hutzel Hospital, 4707 St. Antoine Boulevard, Detroit, MI 48201, USA
Tel.: +1-313-7450831, Fax: +1-313-9938862

(g) The summary of sections in the surgical pathology report should include how many sections of how many nodes are submitted in each cassette. Different color inks may be used to distinguish different nodes submitted in a single cassette.
(h) One H&E slide per cassette is recommended.
(i) Immunohistochemistry and other specialized techniques may be used as part of a research study or for differential diagnosis, but are not now considered mandatory.

Reporting

(a) The number of lymph nodes positive for metastatic disease and the total number of lymph nodes examined microscopically should be reported, with specific levels mentioned when appropriate.
(b) The size of the largest metastasis (measured on the slide) should be reported if clinically indicated.
(c) The presence of extracapsular extension may be reported, depending upon the primary site and institutional preference.
(d) If the only tumor seen is in extranodal vessels, this should be stated.
(e) Deposits of tumor not associated with any structure recognizable as a lymph node should be separately designated.
(f) In rare situations, the grading of nodal metastases may be important.
(g) After preoperative chemotherapy and/or radiotherapy, notation of necrotic versus non-necrotic tumor is recommended.

Sentinel node biopsy

The adequacy of the sentinel node dissection depends upon the skill and experience of the surgeon. At the present time, clinical utility of this technique is still controversial. In many institutions, this is still considered an experimental procedure.

Where this factor has been studied, the level of radiation associated with sentinel node biopsy has not been demonstrated to pose any danger to pathologists or histotechnologists from radioactivity. However, protocols should conform to institutional and state guidelines.

Intraoperative examination, whether by frozen section or scrape/imprint cytology or both, is appropriate only in those clinical situations in which the results will influence immediate therapeutic management. Examination of the intraoperative specimen by other than routine (H&E) stains is experimental at the present time.

The number of nodes received and their sizes should be noted in the gross description of the report. Each node should be processed grossly as mentioned above under "Dissections." If any portion of the sentinel node(s) is not submitted for routine sectioning, this should be specified.

ADASP recommends that more than one section be performed on each block in these cases, if the node or nodes are not positive grossly or at intraoperative pathologic consultation. However, it is not currently clear how many sections (and from what levels of the block) are optimal. It is also unclear whether immunostains add clinically relevant information and whether they may be substituted for additional H&E-stained sections. It should be remembered that false-positive immunostains occur, and these stains should be interpreted in the context of standard histopathology.

If metastases are identified only by immunostains, this should be stated in the final report. Other statements on reporting provided in the section on reporting lymph node dissections of this document are also applicable.

Fine needle aspiration and core needle biopsy

A negative result for tumor does not definitely exclude the presence of a metastatic tumor. Results should be correlated with the clinical situation.

If only FNA is performed, a cell block may be useful for special studies in positive cases.

If only a core needle biopsy is performed, all tissue should be submitted. The number of cores received should be specified in the gross description, and should be correlated with the slides received and examined.

In many cases, it may not be possible to document on an FNA or core needle biopsy specimen that a metastatic tumor is indeed within a lymph node. In such a situation, a comment should be made to that effect.

References

1. Ambrosch P, Kron M, Fischer G, Brinck U (1995) Micrometastases in carcinoma of the upper aerodigestive tract: detection, risk of metastasizing, and prognostic value of depth of invasion. Head Neck 17:473–479
2. Anderson TJ (1999) The challenge of sentinel lymph node biopsy. Histopathology 35:82–84
3. Calaluce R, Miedema BW, Yesus YW (1998) Micrometastases in colorectal carcinoma: a review. J Surg Oncol 67:194–202
4. Carnino F, Fuda G, Ciccone G, Iskra L et al (1997) Significance of lymph node sampling in epithelial carcinoma of the ovary. Gynecol Oncol 65:467–472
5. Cibull ML, for the College of American Pathologists Surgical Pathology Committee (1999) Handling sentinel lymph node biopsy specimens. A work in progress. Arch Pathol Lab Med 123:620–621
6. Cochran AJ (1999) Surgical pathology remains pivotal in the evaluation of "sentinel" lymph nodes. Am J Surg Pathol 23: 1169–1172
7. Cox ED, Pendas S, Cox JM, Joseph E et al. (1998) Guidelines for sentinel node biopsy and lymphatic mapping of patients with breast cancer. Ann Surg 227:645–651
8. Demeure MJ, Doffek KM, Komorowski RA, Wilson SD (1998) Adenocarcinoma of the pancreas: detection of occult metastases in regional lymph nodes by a polymerase chain reaction-based assay. Cancer 83:1328–1334
9. Dobashi K, Sugio K, Osaki T, Oka T, Yasumoto K (1997) Micrometastatic p53-positive cells in the lymph nodes of non-small-cell lung cancer. Prognostic significance. J Thorac Cardiovasc Surg 114:339–346

10. Dowlathshahi K, Fan M, Snide HC, Habib FA (1997) Lymph node mirometastases from breast carcinoma: reviewing the dilemma. Cancer 80:1188–1197
11. Giuliano AE, Jones RC, Brenanan M, Statman R (1997) Sentinel lymphadenectomy in breast cancer. J Clin Oncol 15:2345–2350
12. Hermanek P, Hutter RVP, Sobin LH, Wittekind C (1999) Communication from the International Union Against Cancer. Classification of isolated tumor cells and micrometastasis. Cancer 86:2668–2673
13. Ishida K, Katsuyama T, Sugiyama A, Kawasaki S (1997) Immunohistochemical evaluation of lymph node micrometastases from gastric carcinomas. Cancer 79:1069–1076
14. Jannink I, Fan M, Nagy S, Rayudu G et al. (1998) Serial sectioning of sentinel nodes in patients with breast cancer: a pilot study. Ann Surg Oncol 5:310–314
15. Krag D, Weaver D, Ashikaga T, Moffat F et al. (1998) The sentinel node in breast cancer: a multicenter validation study. N Engl J Med 339:941–946
16. Liberman L (2000) Pathologic analysis of sentinel lymph nodes in breast carcinoma. Cancer 88:971–977
17. Liefers GJ, Cleton-Jansen AM, van de Velde CJH, Hermans J et al. (1998) Micrometastases and survival in stage II colorectal cancer. N Engl J Med 339:223–228
18. Lockett MA, Baron PL, O'Brien PH, Elliott BM et al. (1998) Detection of occult breast cancer micrometastases in axillary lymph nodes using a multimarker reverse transcriptase polymerase chain reaction panel. J Am Coll Surg 187:9–16
19. Maruyama R, Sugio K, Mitsudomi T, Saitoh G et al. (1997) Relationship between early recurrence and micrometastases in the lymph nodes of patients with stage I non-small-cell lung cancer. J Thorac Cardiovasc Surg 114:535–543
20. Natsugoe S, Mueller J, Stein HJ, Feith M et al. (1998) Micrometastasis and tumor cell microinvolvement of lymph nodes from esophageal squamous cell carcinoma: frequency, associated tumor characteristics, and impact on prognosis. Cancer 83: 858–866
21. Niemann TH, Yilmaz AG, Marsh WL Jr, Lucas JG (1998) A half a node or a whole node: a comparison of methods for submitting lymph nodes. Am J Clin Pathol 109:571–576
22. Oberg A, Stenling R, Tavelin B, Lindmark G (1998) Are lymph node micrometastases of any clinical significance in Dukes Stages A and B colorectal cancer? Dis Colon Rectum 41:1244–1249
23. Page DL, Anderson TJ, Carter B (1999) Minimal solid tumor involvement of regional and distant sites. Cancer 86:2589–2592
24. Pelkey TJ, Frierson HF Jr, Bruns DE (1996) Molecular and immunological detection of circulating tumor cells and micrometastases from solid tumors. Clin Chem 42:1369–1381
25. Pfeifer JD (1999) Sentinel lymph node biopsy. Am J Clin Pathol 112:599–602
26. Reintgen D (1996) More rational and conservative surgical strategies for malignant melanoma using lymphatic mapping and sentinel node biopsy techniques. Curr Opin Oncol 8: 152–158
27. Reintgen D, Shivers D (1999) Sentinel lymph node micrometastasis from melanoma. Proven methodology and evolving significance. Cancer 86:551–552
28. Shigaki S, Ohtake K, Nomura T, Nakajima T (1991) The value of single versus multiple sections for detection of lymph node metastasis. J Oral Maxillofac Surg 49:461–463
29. Turner RR, Chu KU, Qi K, Botnick LE et al. (2000) Pathologic features associated with nonsentinel lymph node metastases in patients with metastatic breast carcinoma in a sentinel lymph node. Cancer 89:574–581
30. Van De Brekel MW, van der Waal I, Meijer CJLM, Freeman JL et al. (1996) The incidence of micrometastases in neck dissection specimens obtained from elective neck dissections. Laryngoscope 106:987–991
31. Weaver DL, Krag DN, Ashikaga T, Harlow SP, O'Connell M (2000) Pathologic analysis of sentinel and nonsentinel lymph nodes in breast carcinoma. A multicenter study. Cancer 88: 1099–1107
32. Wilkinson EJ, Hause L (1974) Probability in lymph node sectioning. Cancer 33:1269–1274
33. Yamamoto N, Kato Y, Yanagisawa A, Ohta H et al. (1997) Predictive value of genetic diagnosis for cancer micrometastasis: histologic and experimental appraisal. Cancer 80:1391–1398
34. Yu LL, Flotte TJ, Tanabe KK, Gadd MS et al. (1999) Detection of microscopic melanoma metastases in sentinel lymph nodes. Cancer 86:617–627
35. Yu K, Merrie AEH, Gunn J, Phillips LV, McCall JL (2000) Keratin 20 is a specific marker of submicroscopic lymph node metastases in colorectal cancer: validation by K-RAS mutations. J Pathol 191:21–26
36. Zhang PJ, Reisner RM, Nangia R, Edge SB, Brooks JJ (1998) Effectiveness of multiple-level sectioning in detecting axillary nodal micrometastases in breast cancer: a retrospective study with immunohistochemical analysis. Arch Pathol Lab Med 122:687–690

Virchows Arch (2001) 439:604–608
DOI 10.1007/s004280100503

REVIEW ARTICLE

M. Dietel

The histological diagnosis of endometrial hyperplasia

Is there a need to simplify?

Received: 30 August 2000 / Accepted: 21 June 2001 / Published online: 5 September 2001
© Springer-Verlag 2001

Abstract The intra- and interobserver variability of the histological diagnosis of endometrial hyperplasia, including low-grade carcinomas, is high and thus often causes confusion in the dialogue between pathologists and clinicians. The current classification of the WHO, ISGP, and FIGO is not altogether successful in overcoming this difficulty. New approaches to resolve this unsatisfactory situation have been suggested by two recent simultaneous studies, one by a European group of experts (1999) and the other by Mutter and The Endometrial Collaborative Group (2000). Both studies suggest simplifying the WHO classification by reducing the present four categories to two. The European study names the new histological groups endometrial hyperplasia (EH) and endometrioid neoplasia (EN), while Mutter et al. call them endometrial hyperplasia (EH) and endometrial intraepithelial neoplasia (EIN). Differentiation between the two new categories can be made based on uncomplicated morphological concepts and confirmed morphometrically by the semiquantitative determination of the stromal volume in relation to total tissue volume (stroma+epithelium+gland lumen). This simplification has the advantage of a high degree of reproducibility of histological diagnoses while facilitating understanding by clinicians. Most importantly, there is no decrease in prognostic accuracy, since EH is a benign lesion, easily treated with hormones and almost without risk of progressing to cancer, while EIN/EN is a pre- or already malignant disease with a high risk of progression (≈30%) requiring a more radical treatment. This article summarizes the current discussion on this issue.

Keywords Endometrial hyperplasia · Endometrial carcinoma · Classification · Endometrial intraepithelial neoplasia · Clinical treatment

M. Dietel (✉)
Schumannstr. 20–21, Institute of Pathology, Charité, Humboldt-Universität zu Berlin, 10117 Berlin, Germany
e-mail: manfred.dietel@charite.de

Introduction

Morphological classifications should define criteria which are easy to assess, reproducible, and of clinical, i.e. therapeutic, relevance. WHO classifications, although usually considered as the "gold standard," sometimes do not meet these requirements in everyday practice. The WHO classification for endometrial pathology, analogous to that proposed by the International Society of Gynecological Pathologists and the International Federation of Gynecology and Obstetrics [31] has been seriously challenged lately. The criteria for differential diagnosis of benign, premalignant, and early malignant epithelial lesions of the endometrium given in the WHO Fascicle on Histological Typing of Female Genital Tract Tumors [27] are difficult to sustain since they are associated with an unacceptably high inter- and intraobserver variation [3, 13, 14, 22,30]. Recently, a European group of expert gynecological pathologists [3] reported a poor interobserver (54–73%) and intraobserver (68–73%) agreement in diagnostic curettage material using the four WHO diagnostic categories. Therefore, the question arises: why is it so difficult to define reliable and reproducible histological criteria in order to establish a correct diagnosis?

Firstly, the morphological changes of the endometrium during the normal menstrual cycle are extremely variable and greatly influenced by numerous factors such as age and hormone therapy, and consequently endometrial morphology may show a great number of overlapping features ranging from physiologic variability to true autonomous proliferation.

Secondly, morphology can vary greatly throughout the same endometrium: areas with a more or less normal appearance are found adjacent to simple cystic alterations and/or complex proliferations. The content of the endometrial stroma can also vary from normal to slightly increased or even to reduced, resulting in glands appearing more crowded and angular. The enigma seems to come in deciding which part is of diagnostic importance?

Furthermore, the epithelial cells of any one endometrium may show areas with only slight pseudostratification and

normal gland-lining cells next to areas with pseudopapillary buds, increased proliferation, and polymorphism. The biological relevance of this variability is unclear.

Lastly, the definition and interpretation of atypicality seems to be particularly difficult to define in the endometrium; indeed, one is frequently faced with grade 1 endometrioid invasive adenocarcinomas that have minimal or absent nuclear atypia. This picture is even more complicated in patients undergoing concurrent hormonal treatment [34,35].

There are no clear-cut criteria to differentiate between all these variations, making the weakness of the diagnoses of endometrium hyperplasia not a question of experience versus inexperience but rather a reflection of the lack of a sharp borderline between the different entities. However, this problem has not been considered sufficiently in the WHO classification system.

Non-atypical lesions

For example, in the four category system of the WHO it is difficult to separate a "simple (non-atypical) hyperplasia" from a "complex (non-atypical) hyperplasia" since overlapping histological features often appear within the same lesion. Both the volume of the glands and the stroma are increased with a relative advantage for the glands as stated in the description of Silverberg and Kurman [31]. In a curettage specimen it is practically impossible to determine these criteria with acceptable accuracy and reproducibility. The gland architecture varies from so called "simple," where the glands are more or less normal or slightly cystic or tortuous, with or without outpouching. to "complex," in which the glands are crowded with a higher degree of angularity and lateral glandular buds. With respect to the gland-lining epithelia, the simple hyperplasia shows pseudostratification of otherwise normal cells, while the complex form is characterized by cellular stratification and a slightly higher degree of polymorphism with retention of cellular polarity. These are features which prove very difficult to interpret in the individual case. In the author's experience all these features frequently appear concomitantly in the same specimen, making it difficult to decide what is the diagnostic feature.

In this situation perhaps the question should be raised: is it necessary or useful to divide non-atypical hyperplasias into two categories? The only reason to do so would be if each type requires different clinical treatment. However, there is general agreement among clinicians that both forms of hyperplasia without cellular atypia have only minimal risk of progression into carcinoma, and should both be regarded as benign lesions [8,12]. Treatment of both types is the same: progestagen therapy with a 2–6 weeks post-treatment control of the hormone-induced ablation, which in most patients induced a disappearance of the alterations [34]. Considering that there are no reproducible morphological criteria to differentiate simple from complex hyperplasia without atypia, that there is virtually no risk of malignancy and, above all, the clinical measures are the same, it would seem logical to group them into one main category.

Atypical lesions

The third and fourth categories in the WHO system of nomenclature refer to classification of "atypical" endometrial hyperplasias, dividing these into "simple" and "complex" forms, again presenting us with two groups with broad overlapping of their often heterogeneous morphological appearances. In the corresponding part of the IAP fascicle, Silverberg and Kurman, [31], p. 25, highlight the difficulty of such classification: "Because the two main features distinguishing complex from simple hyperplasia are increased glandular complexity and increased glandular crowding, cases are occasionally encountered in which one but not both of these features may be present....I would classify these examples as complex hyperplasia; but other observers might prefer to place one or both of these examples [given as figures 38 and 39 in the fascicle] into the category of simple hyperplasia."

In the experience of the author and many colleagues, the category of simple atypical hyperplasia, i.e., only slightly disturbed glandular-stromal structures combined with a distinct atypical cytology of the gland-lining epithelial cells, almost never exists, being considered "rara avis."[4]. Even reports that describe cases of simple atypical hyperplasia [34] agree that a clear distinction from complex atypical hyperplasia is often not possible, since crowding of the glands, stratification of the epithelium, and proliferation of the stroma is often intermixed. In particular, Kendall et al. [14] describe the difficulty even to define atypia. Thus, in practical terms, there is only one group with the following morphological characteristics: atypical epithelial cytology (atypia may be focal), nuclear abnormalities with irregular outlines, cellular stratification (but less pronounced than in complex hyperplasia without atypia) and morula metaplasia.

The risk of an atypical hyperplasia to progress to a low-grade carcinoma ranges from 15% to approximately 40% [2, 12, 17, 28,33]. Obviously, such a wide variation reflects different diagnostic criteria and interpretations, but in any case this lesion has to be regarded as premalignant. Consequently, both forms of atypical hyperplasia should be treated as early cancer [6,35], a consideration that constitutes a further argument for classifying them together in one main group. The lack of standardized terminology was found to be the reason for a high uncertainty in the clinical diagnoses of hyperplastic endometrial lesions with undesirable consequences for standardized therapeutic strategies [6,13].

Suggested new classification systems

The confusion in the present diagnostic terminology causes communication problems among pathologists and

Table 1 Comparison between the WHO classification and two recently proposed nomenclatures

WHO – four class system (Scully et al 1994) [27]	EIN group – two class system (Mutter et al. 2000) [22]	European experts – two class system (Bergeron et al. 1999) [3]
Simple non-atypical hyperplasia Complex non-atypical hyperplasia	Endometrial hyperplasia (EH)	Endometrial hyperplasia (EH)
Simple atypical hyperplasia Complex atypical hyperplasia	Endometrial intraepithelial neoplasia (EIN)[a]	Endometrioid neoplasia (EN) [a]

[a] The inclusion of low-grade adenocarcinoma is still under discussion (see text)

clinicians and hinders the comparability of clinical studies. The aim of the current contribution is to discuss the new suggestions that have been recently made to try to solve this dilemma.

Computerized morphometry analyses of the architectural features of endometrial precancerous lesions had prepared the background of a new definition of premalignant endometrial changes [1,7]. A recent report of a group of experienced gynecologic pathologists [22] states "...if the stromal volume is less than approximately half of total tissue volume (stroma+epithelium+gland lumen) the lesion should be diagnosed as endometrial precancer." This definition was shown to be pragmatically relevant since its retrospective application to endometrial biopsies revealed a high rate of progression to carcinoma as well as a high percentage (≈20%) of coexisting carcinomas [1,7]. The authors proposed the term "endometrial intraepithelial neoplasia" (EIN). Since semiquantitative morphometric analysis of the stroma/total tissue ratio can easily be performed in routine diagnostic work either by subjective evaluation, or preferably by using a simple ocular grid, this approach is extremely attractive and provides a more reliable and reproducible classification of hyperplastic endometrial lesions at a practical, everyday level. The recently provided internet based-set of histological images may prove useful in establishing standardized criteria [20] (online at: http://www.endometrium.org). However, the quality of the images should be improved.

Several other approaches have been made in order to discriminate normal and hyperplastic glands without atypia from those with atypia and possible progression to malignancy. Some studies have shown that DNA cytophotometry could be helpful, although more systematic studies evaluating this method are still required since conflicting results have also been reported [25,36]. Recently, Sivridis and coworkers [32] found that the distribution pattern of lectin immunohistochemistry (Con A, LCA, e-PHA, and lPHA) may prove useful in differentiating non-atypical from atypical glandular structures. Proliferation indices, determination of apoptosis, several oncogenic and receptor proteins, nm23 and telomerase expression have been intensively studied, without convincing results, however, in particular with respect to a clearly defined separation between the different forms of hyperplasia [5, 11, 24, 26,29]. Molecular analyses of ras mutations or comparative genomic hybridization [15,21] have shown that endometrial precancers are associated with monoclonal growth of the atypical glands, but this has no relevance yet for diagnostical application. Future investigations using the DNA-microarray technology combined with microdissection may help to clarify the differences between non-malignant and pre-malignant alterations of the endometrium.

Thus, it would seem that hyperplasia can be reliably differentiated from atypical hyperplasia in the reproducible, semiquantitative measures of routine pathology. However, a further question remains: how can atypical hyperplasia be distinguished from low grade, in situ, endometrioid adenocarcinoma? The criteria proposed are: evidence of myometrial invasion; stromal desmoplasia; disappearance of the stroma, stromal necroses, and intraglandular gland cell bridging without stromal support; confluent glandular bridges lacking intervening stroma; and cribriform glandular confluence or gland-within-gland growth pattern [27]. However, these patterns often coexist. Furthermore, metaplasia, in particular squamoid metaplasia, and cytological criteria are of little help. Silverberg [30] excellently reviewed the problems related to the relevance of the criteria for the reproducible differentiation between atypical hyperplasia and low-grade adenocarcinoma. In our experience their subjective interpretation is often the cause of high interobserver variability.

Taking into account that the morphological criteria described above often fail to be reproducible, especially in curettage material, perhaps instead of asking *how* to separate atypical hyperplasia from low-grade endometrioid adenocarcinoma, we should question the *need* to do so, especially considering that the clinical measures are identical in both conditions. Furthermore, in atypical hyperplasia and low-grade carcinomas the measurements of DNA ploidy reveals a diploid histogram and no differences in proliferation can be detected, giving further support for the similarity of these lesions [19]. Harold Fox [10] already stated in 1984: "A true adenocarcinoma in situ of the endometrium is one in which the glands have undergone neoplastic change but in which there is no invasion of the endometrial stroma. It is doubtful if any adenocarcinoma of this type exists or if it could be recognised even if it does exist." Consequently, it should be discussed whether the group of endometrioid intraepithelial neoplasia should include low-grade endometrioid adenocarcinoma as well.

Considering that

- The morphologic recognition of the four WHO categories or FIGO categories suffers from an unacceptably high inter- and intraobserver variation

- There is no clinical reason for the separation of simple versus complex forms in both the non-atypical and the atypical hyperplasia
- The reports of the consensus groups of gynecological pathologists [3,22] provide reliable and reproducible results

it appears logical to subdivide hyperplastic endometrial lesions only into two categories – as suggested by the above cited groups (1):

1. Endometrial hyperplasia (EH) which is exclusively benign without a need for invasive measures
2. Endometrial intraepithelial neoplasia (EIN) which has to be considered as a pre-cancer borderline lesion with a marked risk to progress towards an unquestionable adenocarcinoma with metastasizing potential

Furthermore, it should be discussed whether the category EIN should include low-grade endometrioid carcinoma – as first suggested by H. Fox in 1982 [9] – since the morphology is very similar and the clinical consequences are more or less identical. With respect to the objectivity and reproducibility, as well as to the clinical relevance of histological diagnoses, this merge is strongly suggested.

Conclusions

The classification of hyperplastic endometrial lesions shows the tendency to develop toward a two class system, differentiating endometrial hyperplasia from intraepithelial neoplasia, which in the experience of the author appears to be simple and reproducible, and thus convincing. Further studies are currently being undertaken and their results should be considered before a new classification is launched. The question whether low-grade endometrial adenocarcinomas should additionally be integrated in the EIN/EN group is still a matter for discussion. This tendency to simplify follows that of several other classifications, such as in colon neoplasias, and prostate intraepithelial neoplasia, and may contribute to a better correlation between surgical pathology and clinical management.

Acknowlegment The author is most grateful to Profes. F. Nogales, Universidad de Granada, Spain, and S. Hauptmann, Humboldt-Universität zu Berlin, Germany, for the intensive discussion, and to H. Nogales for linguistic advice.

References

1. Baak JPA, Nauta J, Wisse-Brekelmans E, Bezemer P (1988) Architectural and nuclear morphometrical features together are more important prognosticators in endometrial hyperplasias than nuclear morphometrical features alone. J Pathol 154: 335
2. Baak JP, Wisse-Brekelmans EC, Fleege JC, van der Putten HW, Bezemer PD (1992) Assessment of the risk on endometrial cancer in hyperplasia, by means of morphological and morphometrical features. Pathol Res Pract 188: 856–859
3. Bergeron C, Nogales F, Masseroli M, Abeler V, Duvillard P, Muller-Holzner E, Pickartz H, Wells M (1999) A multicentric European study testing the reproducibility of the WHO classification of endometrial hyperplasia with a proposal of a simplified working classification for biopsy and curettage specimens. Am J Surg Pathol 23: 1102–1108
4. Bergeron C, Nogales F, Masseroli M, Abeler V, Duvillard P, Muller-Holzner E, Pickartz H, Wells M (2000) Reply to letter to the editor by Scully RE and Young RH. Am J Surg Pathol 24: 754–755
5. Brustmann H, Naude S (1999) Expression of nm23 in normal, hyperplastic and neoplastic endometrial tissues. Pathol Res Pract 195: 829–834
6. Burke TW, Tortolero-Luna G, Malpica A, Baker VV, Whittaker L, Follen Mitchell M (1996) Endometrial hyperplasia and endometrial cancer. Obst Gynecol Clin North Am 23: 411–456
7. Dunton C, Baak J, Palazzo J, van Diest P, McHugh M, Widra E (1996) Use of computerized morphometric analyses of endometrial hyperplasias in the prediction of coexistent cancer. Am J Obstet Gynecol 174: 1518,
8. Ferenczy A, Gelfand MM (1986) Hyperplasia vs neoplasia: two tracks for endometrium? Contemp Obstet Gynecol 28: 79–96
9. Fox H, Buckley CH (1982) The endometrial hyperplasia and their relationship to endometrial neoplasia. Histopathology 6: 493–510
10. Fox H. (1984) The endometrial hyperplasia. Obstet Gynecol Annu 13: 197
11. Hernandez E (1993) Pathological findings and prognosis from uterine malignancies. Curr Opin Obstet Gynecol 5: 480–485
12. Huang SJ, Amparo EG, Fu YS (1988) Endometrial hyperplasia. Surg Pathol 1: 215–229
13. Jacques SM, Qureshi F, Munkarah A, Lawrence WD (1998) Interinstitutional surgical pathology review in gynecologic oncology: I. Cancer in endometrial curettings and biopsies. Int J Gynecol Pathol 17: 36–41
14. Kendall BS, Ronnett BM, Isacson C, Cho KR, Hedrick L, Diener-West M, Kurman RJ (1998) Reproducibility of the diagnosis of endometrial hyperplasia, atypical hyperplasia, and well-differentiated carcinoma. Am J Surg Pathol 22: 1012
15. Kiechle M, Hinrichs M, Jacobsen A, Luttges J, Pfisterer J, Kommoss F, Arnold N (2000) Genetic imbalances in precursor lesions of endometrial cancer detected by comparative genomic hybridization. Am J Pathology 156: 1827–1833
16. Kurman RJ, Norris HJ (1982) Evaluation of criteria for distinguishing atypical endometrial hyperplasia from well-differentiated carcinoma. Cancer 49: 2547–2559.
17. Kurman R, Kaminski P, Norris H (1985) The behavior of endometrial hyperplasia: A long term study of “untreated” hyperplasia in 170 patients. Cancer 56: 403
18. Lax SF, Kurman RJ (1997) A dualistic model for endometrial carcinogenesis based on immunhistochemical and molecular genetic analyses. Verh Dtsch Ges Pathol 81: 228–232
19. Michael H, Kotylo PK, Mohr M, Roth LM (1996) DNA ploidy, cell cycle kinetics, and low versus high grade atypia in endometrial hyperplasia. Am J Clin Pathol 106: 22–28
20. Mutter GL (1999) Endometrial precancer type collection. Online at: http://www.endometrium.org
21. Mutter GL, Wada H, Faquin WC, Enomoto T (1999) K-ras mutations appear in the premalignant phase of both microsatellite stable and unstable endometrial carcinogenesis. Mol Pathol 52: 257–262
22. Mutter GL and The Endometrial Collaborative Group (2000) Endometrial intraepithelial neoplasia (EIN): will it bring order to chaos? Gyn Oncol 76: 287–290
23. Mutter GL, Baak JPA, Crum CP, Richart RM, Ferenczy A, Faquin WC (2000) Endometrial precancer diagnosis by histopathology, clonal analysis, and computerized morphometry. J Pathol 190: 462
24. Niikura H, Sasano H., Kaga K, Sato S, Yajima A (1996) Expression of epidermal growth factor family proteins and epidermal growth factor receptor in human endometrium. Hum Pathol 27: 282–289
25. Norris HJ, Becjer RL, v Mikel U(1989) A comparative morphometric and cytophotometric study of endometrial hyperplasia, atypical hyperplasia and carcinoma. Human Path 20: 219–223

26. Palazzo JP, Mercer WE, Kovatich AJ, McHugh M (1997) Immunohistochemical localization of $p21^{WAF1/CIP1}$ in normal, hyperplastic and neoplastic uterine tissue. Hum Pathol 27: 60–66
27. Scully RE, Bonfiglio TA, Kurman RJ, Silverberg SG, Wilkinson EJ (1994) Uterine corpus in Histological Typing of Female Genital Tract Tumors (WHO-Fascicle). Springer, Berlin Heidelberg New York
28. Sherman AI, Brown S (1997) The precursors of endometrial carcinoma. Am J Obstet Gynecol 135: 947–956
29. Shroyer KR, Stephensen JK, Silverberg SG, Marham N, Shroyer AL, Wilson ML (1999) Telomerase expression in normal endometrium, endometrial hyperplasia and endometrial adenocarcinomas. Int J Gynecol Pathol 16: 219–224
30. Silverberg SG (2000) Problems in the differential diagnosis of endometrial hyperplasia and carcinoma. Mod Pathol 13: 309–27
31. Silverberg SG, Kurman RJ (1992) Tumors of the uterine corpus and gestational trophoblastic disease. Atlas of Tumor Pathology, AFIP Fascicle, 3rd Series, Washington DC
32. Sivrides E, Giatromanolaki A, Koukourakis M, Agnatis N (2000) Lectin-binding patter in normal, hyperplastic and neoplastic endometrium: the prognostic value of concanavalin. Virchows Arch 436: 52–58
33. Tavassoli F, Kraus FT (1978) Endometrial lesions in uteri resected for atypical endometrial hyperplasia. Am J Clin Pathol 70: 770–779
34. Terakawa N, Kigawa J, Taketani Y, Yoshikawa H, Yajima A, Noda K, Okada H, Kato J, Yakushiji M, Tanizawa O, Fujimoto S, Nozawa S, Takahashi T, Hasumi K, Furuhashi N, Aono T, Sakamoto A, Furusato M (1997) The behavior of endometrial hyperplasia: a prospective study. Endometrial Hyperplasia Study Group. J Obstet Gynaecol 23: 223–230
35. Trope CG, Marth C, Scheistroen M, Abeler VM (1999) Review Endometrial hyperplasia – diagnosis and treatment. Tidsskr Nor Laegeforen 119: 2030–2034
36. Van der Putten HWHM, Baak JPA, Koenders TJM, Kurver PHJ, Stolk HG, Stolte LAM (1989) Prognostic value of quantitative pathologic features and DNA content in individual patients with stage I endometrial adenocarcinomas. Cancer 63: 1378–1387

Virchows Arch (2001) 439:609–615
DOI 10.1007/s004280100429

ORIGINAL ARTICLE

Ekkehard Kunze · Bernd Francksen · Harald Schulz

Expression of MUC5AC apomucin in transitional cell carcinomas of the urinary bladder and its possible role in the development of mucus-secreting adenocarcinomas

Received: 22 August 2000 / Accepted: 22 January 2001 / Published online: 22 May 2001
© Springer-Verlag 2001

Abstract The histogenesis of primary nonurachal mucus-producing adenocarcinomas of the urinary bladder including signet ring cell carcinomas remains to be elucidated, since the normal bladder contains neither columnar nor mucus-secreting glandular epithelium. Based upon the assumption that adenocarcinomas may develop secondarily from pre-existent transitional cell carcinomas (TCC) by a metaplastic process, it was the purpose of the current immunohistochemical study to analyze whether urothelial carcinomas are capable of secreting MUC5AC apomucin, using the monoclonal antibody 45M1. This antibody has been initially demonstrated to strongly react with the mucus-producing columnar cells of the surface gastric epithelium, recognizing a specific epitope located on the peptide core of glycoproteins as major components of mucins. Nine of 64 uniformly differentiated papillary (14.1%) and 5 of 66 nonpapillary (solid) TCC with a uniform urothelial differentiation (7.6%) expressed the MUC5AC antigen, yielding an overall incidence of 10.8%. Transitional cell carcinomas with a focally altered cellular and structural differentiation (squamous cell, pseudoglandular, true glandular and mixed differentiation) stained positively in a substantially higher percentage of 43.8% (21 of 48 cases). A positive immunoreactivity was also observed in 3 of 19 mixed transitional cell and nonurothelial carcinomas. The tumor-associated resurgence of normally cryptic MUC5AC antigenic determinants in transitional cell carcinomas is considered as a re-expression of oncofetal antigenicity, probably as a result of the embryologic origin of the urinary bladder from the pluripotent tissues of the cloacal endoderm and the mesodermal wolffian ducts. Our findings may help to better understand the histogenetic development of mucus-secreting vesical adenocarcinomas from pre-existent urothelial carcinomas.

E. Kunze (✉) · B. Francksen · H. Schulz
Center of Pathology, University of Göttingen, 37075 Göttingen, Robert-Koch-Strasse 40, Germany
e-mail: EKunze@med.uni-goettingen.de
Tel.: +49-551-396857, Fax: +49-551-392233

Keywords Urinary bladder · Transitional cell carcinomas · Immunohistochemistry · Mucins · MUC5AC apomucin

Introduction

Approximately 2% of primary carcinomas of the urinary bladder account for nonurachal adenocarcinomas with or without mucus production, including signet ring cell carcinomas. Their histogenesis is not clearly understood, since the normal bladder contains neither columnar nor glandular epithelium. Using standard techniques of mucin histochemistry (periodic acid-Schiff, Alcian blue, mucicarmine, periodate borohydride-potassium hydroxide-PAS) both acid and neutral sialylated, sulfated and O-acetylated mucins have been repeatedly identified to be produced by vesical adenocarcinomas and so-called cystitis glandularis of the intestinal (colonic) type as a potential precursor [2, 9, 19, 30,38]. The transitional cell epithelium normally secretes very small amounts of mucous substances, composed of glycosaminoglycans and glycoproteins [17, 24, 25, 31, 32,33]. The mucus forms a thin coat – also known as glycocalyx – on the luminal surface of the urothelium and is assumed to inhibit adherence of uropathogenic bacteria and to protect against irritants in the urine. Since there is a growing body of evidence that nonurachal vesical adenocarcinomas with or without production of mucus may develop histogenetically from pre-existent transitional cell carcinomas by a metaplastic process [27,28], it was the objective of the present study to analyze by immunohistochemistry whether urothelial carcinomas are capable of secreting the MUC5AC apomucin, a specific well-defined mucin detectable with the monoclonal antibody 45 M1. So far, 9 different human mucin genes have been identified encoding distinct mucin glycoproteins, designated MUC1, MUC2, MUC3, MUC4, MUC5AC, MUC5B, MUC6, MUC7, MUC8 and MUC9 [13, 18,22]. The antibody 45M1 was originally obtained by immunization of mice with mucin isolated from the fluid of human ovarian mu-

cinous cysts [7,8] and has been documented to react strongly with the mucus-producing columnar cells of the human surface gastric epithelium (foveolar and mucous neck cells of the antrum and body), recognizing a specific epitope situated on the peptide core of glycoproteins as major components of mucin [7,8].

Materials and methods

Tumors

The study comprised 64 uniformly differentiated papillary transitional cell carcinomas (TCC) of various grades (17×grade 1, 35×grade 2, 12×grade 3) and stages (34×pTa, 16×pT1, 9×pT2a, 1×pT2b; staging not possible in 4 cases), 66 uniformly differentiated nonpapillary (solid) TCC (0×grade 1, 31×grade 2, 35×grade 3; 4×pT1, 18×pT2a, 32×pT2b, 9×pT3, 3×pT4), and 48 papillary or solid TCC with a focally altered cellular and structural differentiation (19 cases with a pseudoglandular, 11 with a true glandular, 10 with a squamous cell and 8 with a mixed differentiation). The phenotypically altered tumor cells within otherwise urothelial differentiated TCC did not manifest any substantial atypia, which distinguishes these tumors from true mixed urothelial and nonurothelial carcinomas. Additionally, 19 pure squamous cell carcinomas, 10 undifferentiated – predominantly small cell – carcinomas, one pure adenocarcinoma and 19 mixed urothelial and nonurothelial carcinomas (7 TCC and squamous cell carcinomas, 5 TCC and undifferentiated carcinomas,3 TCC and adenocarcinomas, one squamous cell carcinoma and undifferentiated carcinoma, one squamous cell carcinoma and adenocarcinoma, two mixed TCC, adenocarcinomas and undifferentiated carcinomas) were included in the study. All cases were retrieved from the files of the "Center of Pathology" of the University of Göttingen between January 1995 and December 1996. Following embedding in paraffin, sections of 4 µm thickness were prepared and stained with hematoxylin and eosin, periodic acid-Schiff (PAS) and Alcian blue (pH 2.5).

Immunohistochemistry

For detection of MUC5AC apomucin, the mouse monoclonal anti-human antibody NCL-HGM-45M1 (Novocastra, Newcastle upon Tyne, Great Britain) was used, applying the alkaline phosphatase anti-alkaline phosphatase (APAAP) method. Sections of 2 µm thickness were prepared from the formalin-fixed and paraffin-embedded tissues, dewaxed in xylene and rehydrated in graded alcohol solutions. Following thorough washing in Tris-buffered saline (TBS; pH 7.4; 0.05 m) the sections were incubated with the primary antibody diluted 1:50 in TBS for 2 h at room temperature. After washing in TBS, the secondary antibody (rabbit anti-mouse immunoglobulins; Dako Diagnostik, Hamburg, Germany) diluted 1:50 in TBS containing 10% nonimmune human serum was applied for 30 min. The sections were then subjected to the APAAP complex (mouse monoclonal alkaline phosphatase anti-alkaline phosphatase; Dako-Diagnostik) at a dilution of 1:100 in TBS for 45 min at room temperature. The color reaction for identifying the sites of immunoprecipitation was developed by treating the sections with a freshly prepared solution of hexazotized new fuchsin as chromogen for 30 min, followed by application of Mayer's haemalaun as counterstain.

Results

Nine of the 64 papillary (14.1%) and five of the 66 nonpapillary (7.6%) transitional cell carcinomas with a uniform urothelial differentiation expressed the MUC5AC apomucin (Table 1), yielding an overall incidence of 10.8%. Compared with the uniformly differentiated uro-

Table 1 Expression of MUC5AC apomucin within uniformly urothelial differentiated papillary and nonpapillary (solid) transitional cell carcinomas of various grades and stages

Pattern of growth	Total number of cases	Number of cases with positive immunoreactivity (%)	Grades of positive cases	Stages of positive cases
Papillary	64	9 (14.1)	2×grade 1 5×grade 2 2×grade 3	5×pTa 2×pT1 2×pT2a
Nonpapillary (solid)	66	5 (7.6)	2×grade 2 3×grade 3	2×pT2a 1×pT2b 1×pT3 1×pT4

Table 2 Expression of MUC5AC apomucin within papillary and nonpapillary (solid) transitional cell carcinomas disclosing a focal altered cellular and structural differentiation

Cellular/structural phenotypes	Total number of cases	Number of cases with positive immunoreactivity (%)	Grades of positive cases	Stages of positive cases
Squamous cell differentiation	10	4 (40)	3×grade 1 1×grade 2	4×pTa
Pseudoglandular differentiation	19	7 (36.8)	1×grade 1 2×grade 2 4×grade 3	2×pTa 2×pT2a 1×pT2b 1×pT3 1×pT4
True glandular differentiation	11	6 (54.5)	6×grade 2	1×pT1 4×pT2a 1×pT2b
Mixed differentiations	8	4 (50)	1×grade 1 3×grade 2	1×pTa 1×pT1 1×pT3 1×pT4

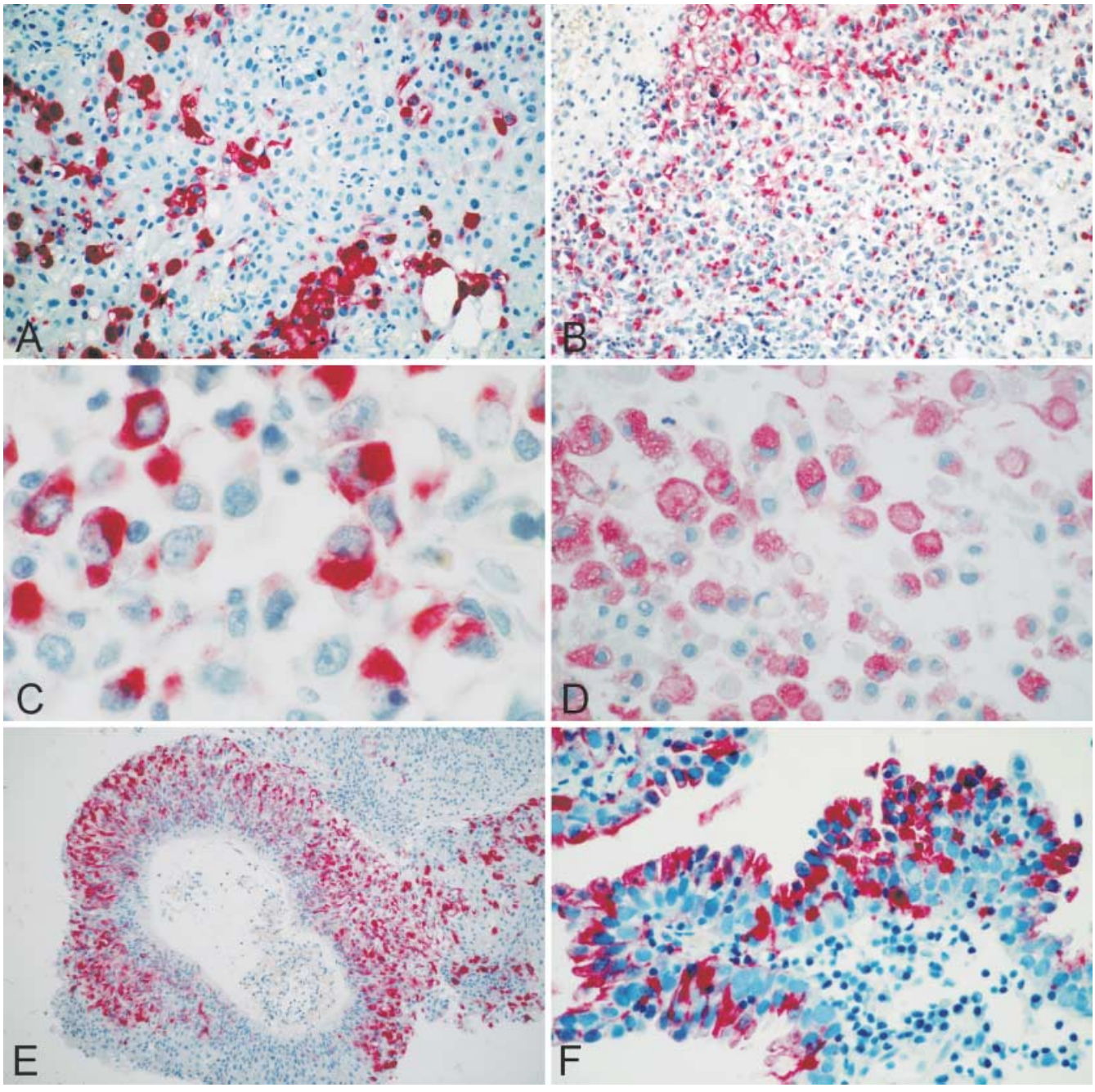


Fig. 1A–F Immunohistochemistry of MUC5AC apomucin in transitional cell carcinomas (TCC) of the urinary bladder. **A** Scattered cells or small clusters of cells strongly positive for MUC5AC within a high-grade and high-stage nonpapillary TCC (original magnification ×180). **B** A large area of densely packed cells in a high-grade and high-stage TCC expressing the MUC5AC gene product (original magnification ×180). **C** Higher magnification of the carcinoma cells shown in figure **B** containing large amounts of MUC5AC within their cytoplasm (original magnification ×900). **D** Positive carcinoma cells resembling signet ring cells, also positive in the PAS and Alcian blue reactions (original magnification ×370). **E** Superficial low-grade and low-stage papillary TCC displaying a large area of cells staining positively for MUC5AC (original magnification ×90). **F** Higher magnification of a papillary TCC with numerous positive cells (original magnification ×370)

thelial carcinomas, TCC with focally altered cellular and structural phenotypes expressed the MUC5AC antigen in a substantially higher overall percentage of 43.8%, those with a true glandular differentiation showing the highest incidence of 54.5% (Table 2). The majority of carcinomas with a positive immunoreactivity represented high-grade and approximately half of them high-stage, muscle invasive tumors (Table 1 and Table 2). Three of the 19 mixed transitional cell and nonurothelial carcinomas (one solid TCC and squamous cell carcinoma, one papillary TCC and adenocarcinoma, one squamous cell carcinoma and adenocarcinoma), the pure adenocarcinoma and one of the 19 squamous cell carcinomas stained focally positive for the MUC5AC gene product, but none

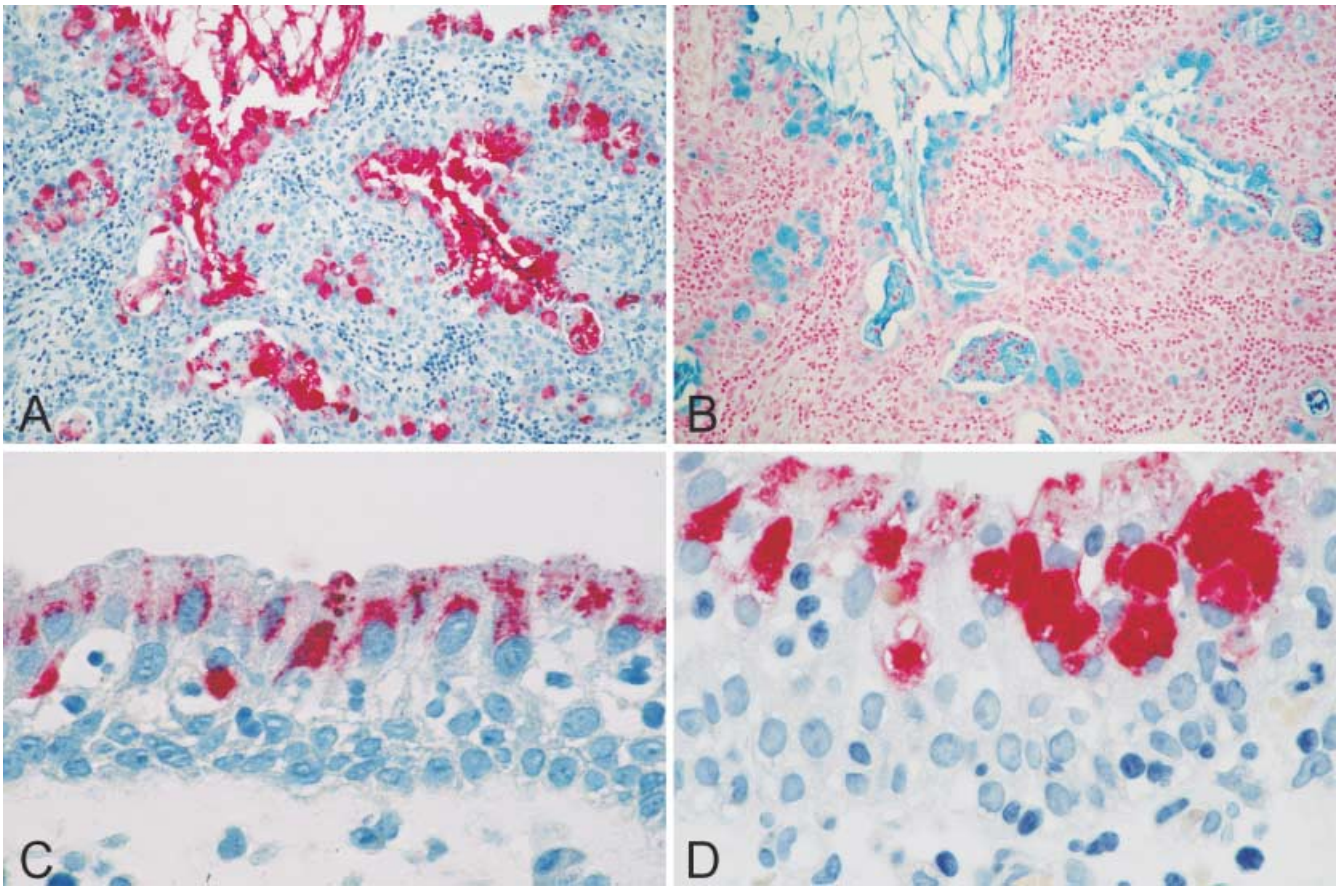


Fig. 2A–D Immunohistochemical expression of MUC5AC apomucin antigenicity in a focally glandular differentiated transitional cell carcinoma (TCC) and within nonneoplastic urothelium adjacent to carcinomas. **A** True glands within a nonpapillary TCC lined by goblet cells with heavy accumulation of MUC5AC (original magnification ×180). **B** Same lesion as seen in figure **A** positive in the Alcian blue reaction (original magnification ×180). **C** Nonneoplastic urothelium adjacent to a TCC with superficial cells containing granular intracytoplasmic deposits of MUC5AC (original magnification ×900). **D** Nonneoplastic transitional cell epithelium bordering a carcinoma with abundant intracytoplasmic MUC5AC apomucin (original magnification ×900)

of the undifferentiated cell carcinomas. The normally appearing nonneoplastic transitional cell epithelium adjacent to the tumors displayed 45M1-positive cells in 15.3% of the cases. MUC5AC apomucin was not detected in the normal urothelium.

The pattern of immunoreactivity was found to be heterogeneous. Most of the TCC with a uniform urothelial differentiation revealed only small clusters of cells and scattered cells which contained densely packed granular deposits of the MUC5AC apomucin within their cytoplasm (Fig. 1 A). In a few other cases, large areas of positive urothelial carcinoma cells were present (Figs. 1B–F), some of them disclosing a signet ring cell configuration (Fig. 1D). None of the carcinomas showed a diffuse immunoreactivity throughout the tumor. Except for the cells resembling signet ring cells, only some of the 45 M1-positive cells also stained positively in the PAS and Alcian blue reaction. As with the uniform TCC, those with an altered cellular and structural differentiation displayed groups of carcinoma cells or interspersed tumor cells expressing the MUC5AC gene product. The columnar cells of true glands and the cells lining pseudoglandular formations proved to be positive in some, but not all cases. Goblet cells, having produced large amounts of mucus positive for PAS and Alcian blue, always strongly expressed the MUC5AC apomucin (Fig. 2 A,B). The nonneoplastic, normally looking transitional cell epithelium adjacent to the carcinomas contained only scattered – predominantly superficial – cells or small groups of cells with a positive immunoreactivity (Fig. 2C and Fig. 2D).

Discussion

Primary nonurachal adenocarcinomas of the urinary bladder may develop directly from the lining transitional cell epithelium or from so-called cystitis glandularis of the intestinal type [20, 26, 27, 28, 29, 35, 36,39], but a stepwise development from pre-existent transitional cell carcinomas by a metaplastic process is assumed to occur more frequently [27,28]. To gain further insights into the histogenetic pathways underlying the formation of mucus-producing vesical adenocarcinomas, including signet ring cell carcinomas from pre-existent urothelial carcinomas, we studied uniformly differentiated transitional cell

carcinomas and those with focally altered cellular and structural differentiations for their ability of secreting the MUC5AC apomucin using the monoclonal antibody 45 M1. This antibody was introduced by Bara and coworkers [7,8] and belongs to a family of 8 different mucin-associated so-called M1 antibodies (1–13 M1, 2–11 M1, 2–12 M1, 9–13 M1, 58 M1, 19 M1 and 96RA) which have all been demonstrated to react strongly with the mucus-producing columnar surface epithelium of the stomach [4, 6, 7,8]. Mucins as major components of mucus are heavily glycosylated high-molecular weight glycoproteins constituting up to 80% of carbohydrate moieties and 20% of a peptide core [9,21]. The various human mucin genes identified to date (MUC1-MUC9) are characterized by repeated domains of peptides, rich in serine and thyreonine residues; MUC5AC gene exhibits a tandem repeat subdomain containing 10 cysteine residues [18,22] and maps to chromosome 11 on the short arm at band 15.5 [18]. Antigenicity of 45 M 1 for MUC5AC is associated with a specific epitope which is situated on the peptide core of mucins [7,8]. The peptidic nature of the 45 M1 epitope was evidenced by its destruction after treatment with papain and β-mercaptoethanol and progressive loss with time following trypsin digestion [8]. Moreover, the 45 M1 epitope was found to be resistant to periodate treatment [7].

We were able – to our knowledge for the first time – to document 14.1% of uniformly differentiated papillary and 7.6% of nonpapillary (solid) transitional cell carcinomas of various grades and stages (overall incidence of papillary and solid TCC=10.8%) expressing the MUC5AC apomucin. Papillary and nonpapillary TCC with focally altered cellular phenotypes showed a secretion of MUC5AC even in 43.8% of the cases. Daher and coworkers using a panel of various M1 antibodies (1–13 M1, 2–11 M1, 2–12 M1, 9–13 M1 and 58 M1) could not detect a positive immunoreactivity in 12 not otherwise specified “bladder carcinomas” [15].

Urothelial carcinomas were found to secrete also some other members of the mucin family. Walsh and coworkers found all TCC tested positive for MUC1, the intensity of which increased with increasing grades and stages [37]. We also found expression of MUC1 mucin in all layers of the normal urothelium and in all the TCC we have studied, including those with altered cellular phenotypes (this information will be published elsewhere). MUC2 glycoprotein is not expressed in the normal transitional cell epithelium, but in 40% of TCC, lacking a correlation with the tumor grades and stages [37]. The monoclonal antibody M344 detecting sialylated carbohydrate epitopes of mucin glycoproteins, which share some common features with MUC2, stained positively in 70–75% of low-grade superficial and in 10–15% of high-grade invasive TCC [10, 11, 12,14]. Expression of MUC5AC apomucin seems to play a more important role during development of mucus-secreting adenocarcinomas from pre-existent transitional cell carcinomas than MUC1 and MUC2, both synthesized by a high percentage of TCC with a predominantly diffuse pattern of immunoreactivity. Whereas MUC1 glycoprotein was found to stain positively in the epithelium of many organs [22] and MUC2 gene product was reported as absent from the gastric mucosa [3], MUC5AC apomucin is strongly expressed by the surface gastric epithelium, indicating a similar quality of gastric and vesical mucus. For these reasons, MUC5AC gene product presumably is of particular significance for metaplastic transformation of urothelial carcinoma cells into mucus-producing adenocarcinomas, including signet ring cell carcinomas as observed in the stomach. Except for potentially detecting early formation of mucus-secreting carcinomas, MUC5AC appears not to be useful for differential diagnosis between the various histopathologic subtypes of bladder cancers, although pure undifferentiated small cell carcinomas never stained positively.

Other tumors known to express the MUC5AC apomucin are all ovarian mucinous cystadenomas and mucinous cystadenocarcinomas [1,23] and a high percentage (60–80%) of gastric carcinomas [34]. Results obtained with colonic adenocarcinomas are conflicting: while Bara and coworkers (1980 and 1984) reported between 13% and 55% expressing gastric M1 mucin gene products [4,5], others did not find expression particularly of MUC5AC apomucin in primary [13] and metastatic [1] adenocarcinomas of the colon. Rectosigmoid villous adenomas stained positively for MUC5AC antigen in all cases [13]. In an experimental study in rats using 1,2-dimethylhydrazine to induce colonic carcinogenesis, Decaens and coworkers (1983) found 78% of mucinous hyperplastic lesions, 58% of dysplastic glandular formations (grades 1 and 2) and most of the adenocarcinomas producing M1 mucins [16].

Unlike the expression of MUC5AC apomucin and other gastric M1 mucin glycoproteins within tumors of the colon and urinary bladder, antigenicity proved to be absent in the normal adult colonic mucosa [3, 6, 7, 13, 16] and the normal adult transitional epithelium, but present in the fetal colonic [6, 7, 16] as well as in the fetal prostatic urethral epithelium and trigonal cells of the bladder, particularly during the sixth month of gestation [15]. Nonneoplastic, normally appearing urothelium adjacent to transitional cell carcinomas was documented in the present study to contain single cells or clusters of cells positive for MUC5AC in 15.3% of cases. Similarly, Buisine and coworkers reported expression of MUC5AC within histologically normal colonic mucosa bordering rectosigmoid villous adenomas [13]. This common phenomenon of a de novo expression of MUC5AC antigenicity in the cancerized urinary bladder and rectum appears understandable from an embryologic point of view, since both organs develop from the sinus urogenitalis. As a conclusion, we regard tumor-associated resurgence of MUC5AC in transitional cell carcinomas as a re-expression of oncofetal antigenicity. This possibility is supported by the well-known capacity of adult urothelium to undergo several pathways of phenotypic cellular and structural differentiations as a result of the embryo-

logic origin of the bladder from the multipotent tissues of the cloacal endoderm (dome and median regions) and the mesodermal Wolffian ducts (trigone). The current new finding of neoexpression of normally cryptic MUC5AC antigenic determinants in urothelial carcinomas may help towards a better understanding of the histogenesis of mucus-secreting adenocarcinomas of the urinary bladder from pre-existent transitional cell carcinomas. Further investigations studying a larger number of vesical adenocarcinomas, including signet ring cell carcinomas, are needed to clarify the significance of MUC5AC apomucin for the histogenetic development of these rarely occurring carcinoma types of the urinary bladder.

Acknowledgement We are indebted to Miss Birgit Jünemann for skilled technical assistance in preparing the immunohistochemical stainings

References

1. Albarracin CT, Jafri J, Montag AG, Hart J, Kuan SF (2000) Differential expression of MUC2 and MUC5AC mucin genes in primary ovarian and metastatic colonic carcinoma. Hum Pathol 31:672–677
2. Alroy J, Roganovic D, Banner BF, Jacobs JB, Merk FB, Ucci AA, Kwan PWL, Coon JS, Miller AW (1981) Primary adenocarcinomas of the human urinary bladder: histochemical, immunological and ultrastructural studies, Virchows Arch 393: 165–181
3. Audié P, Janin A, Porchet N, Copin MC, Gosselin B, Aubert JP (1993) Expression of human mucin genes in respiratory, digestive, and reproductive tracts ascertained by in situ hybridization. J Histochem Cytochem 41:1479–1485
4. Bara J, Loisillier F, Burtin P (1980) Antigens of gastric and intestinal mucous cells in human colonic tumors. Br J Cancer 41:209–221
5. Bara J, Nardelli J, Gadenne C, Prade M, Burtin P (1984) Differences in the expression of mucus-associated antigens between proximal and distal human colon adenocarcinomas. Br J Cancer 49:495–501
6. Bara J, Gautier R, Daher N, Zaghouani H, Decaens C (1986) Monoclonal antibodies against oncofetal mucin M1 antigens associated with precancerous colonic mucosae. Cancer Res 46:3983–3989
7. Bara J, Gautier R, Mouradian P, Decaens C, Daher N (1991) Oncofetal mucin M1 epitope family: characterization and expression during colonic carcinogenesis. Int J Cancer 47:304–310
8. Bara J, Decaens C, Loridon-Rosa B, Oriol R (1992) Immunohistological characterization of mucin epitopes by pre-treatment of gastro-intestinal sections with periodic acid. J Immunol Methods 149:105–113
9. Barresi G, Marafioti T (1990) Mucin histochemistry and lectin binding sites in intestinal metaplasia of the urinary bladder. Histopathologie 17:219–223
10. Bergeron A, Champetier S, LaRue H, Fradet Y (1996) MAUB is a new mucin antigen associated with bladder cancer. J Biol Chem 271:6933–6940
11. Bergeron A, LaRue H, Fradet Y (1997) Biochemical analysis of a bladder-cancer-associated mucin: structural features and epitope characterization. Biochem J 321:889–895
12. Bonner RB, Hemstreet GP, Fradet Y, Rao JY, Min KW, Hurst RE (1993) Bladder cancer risk assessment with quantitative fluorescence image analysis of tumor markers in exfoliated bladder cells. Cancer 72:2461–2469
13. Buisine MP, Janin A, Maunoury V, Audié JP, Delescaut MP, Copin MC, Colombel JF, Degand P, Aubert JP, Porchet N (1996) Aberrant expression of a human mucin gene (MUC5AC) in rectosigmoid villous adenoma. Gastroenterology 110:84–91
14. Cordon-Cardo C, Wartinger DD, Melamed MR, Fair W, Fradet Y (1992) Immunopathologic analysis of human urinary bladder. Characterization of two new antigens associated with low-grade superficial bladder tumors. Am J Pathol 140:375–385
15. Daher N, Gonzales J, Gautier R, Bara J (1990) Evidence of mucin M1 antigens in seminal plasma and normal cells of human prostatic urethra in relation to embryonic development and tumors. Prostate 16:57–69
16. Decaens C, Bara J, Rosa B, Daher N, Burtin P (1983) Early oncofetal antigenic modification during rat colonic carcinogenesis. Cancer Res 43:355–362
17. De Klerk DP (1985) The glycosaminoglycans of human bladder cancers of varying grade and stage. J Urol 134:978–981
18. Desseyn JL, Buisine MP, Porchet N, Aubert JP, Degand P, Laine A (1998) Evolutionary history of the 11p15 human mucin gene family. J Mol Evol 46:102–106
19. Ebel K, Diekhans D (1996) Muzinhistochemische Analysen an schleimbildenden Karzinomen, Metaplasien des Urothels und bei Urachuspersistenz. Pathologe 17:208–212
20. Edwards PD, Hurm RA, Jaeschke WH (1972) Conversion of cystitis glandularis to adenocarcinoma 108:568–570
21. Feizi T, Gooi HC, Childs RA, Picard JK, Uemura K, Loomes LM, Thorpe SJ, Housell EF (1984) Tumour-associated and differentiation antigens on the carbohydrate moieties of mucin-type glycoproteins. Biochem Soc Trans 12:591–596
22. Gendler SJ, Spicer AP (1995) Epithelial mucin genes. Annu Rev Physiol 57:607–634
23. Giuntoli RL, Rodriguez GC, Whitaker RS, Dodge R, Voynow JA (1998) Mucin gene expression in ovarian cancers. Cancer Res 58:5546–5550
24. Grist M, Chakraborty J (1994) Identification of a mucin layer in the urinary bladder. Urology 44:26–33
25. Hurst RE, Rhodes SW, Adamson PB, Parsons CL, Roy JB (1987) Functional and structural characteristics of the glycosaminoglycans of the bladder luminal surface. J Urol 138: 433–437
26. Jacobs LB, Brooks JD, Epstein JI (1997) Differentiation of colonic metaplasia from adenocarcinoma of urinary bladder. Hum Pathol 28:1152–1157
27. Kunze E (1998) Histogenesis of nonurothelial carcinomas in the human and rat urinary bladder. Exp Toxicol Pathol 50: 341–355
28. Kunze E (1998) Formale Pathogenese des Harnblasenkarzinoms. In: Bichler KH, Wilbert D, Wechsel HW, Strohmaier WL (eds) Diagnostik und Therapie des Harnblasenkarzinoms Einhorn-Presse Verlag, Reinbeck, Germany, pp 14–42
29. Lin JI, Tseng CH, Choy C, Yong AS, Marsidi PS, Pilloff B (1980) Diffuse cystitis glandularis. Associated with adenocarcinomatous change. Urology 15:411–415
30. Newbould M, Mc William LJ (1990) A study of vesical adenocarcinoma, intestinal metaplasia and related lesions using mucin histochemistry. Histopathology 17:225–230
31. Parsons CL, Mulholland SG (1978) Bladder surface mucin. Its antibacterial effect against various bacterial species. Am J Pathol 93:423–432
32. Parsons CL, Stauffer C, Schmidt JD (1980) Bladder-surface glycosaminoglycans: an efficient mechanism of environmental adaptation. Science 208:605–607
33. Parsons CL, Greenspan C, Moore S, Mulholland SG (1996) Role of surface mucin in primary antibacterial defense of bladder. Urology 9:48–52
34. Reis CA, David L, Nielsen PA, Clausen H, Mirgorodskaya K, Poepstorff P, Sobrinko-Simoes M (1997) Immunohistochemical study of MUC5AC expression in human gastric carcinomas using a novel monoclonal antibody. Int J Cancer 74: 112–121

35. Shaw JI, Gislason GJ, Imbriglia JE (1958) Transition of cystitis glandularis to primary adenocarcinoma of the bladder. J Urol 79:815–822
36. Susmano D, Rubenstein AB, Dakin AR, Lloyd FA (1971) Cystitis glandularis and adenocarcinoma of the bladder. J Urol 105:671–674
37. Walsh MD, Hohn BG, Thong W, Devine PL, Gardiner RA, Samaratunga MLTH, McGuckin MA (1994) Mucin expression by transitional cell carcinomas of the bladder. J Urol 73:256–262
38. Wells M, Anderson K (1985) Mucin histochemistry of cystitis glandularis and primary adenocarcinoma of the urinary bladder. Arch Pathol Lab Med 109:59–61
39. Young RH, Parkhurst EC (1984) Mucinous adenocarcinoma of bladder. Case associated with extensive intestinal metaplasia of urothelium in patient with nonfunctioning bladder for 12 years. Uropathology 24:192–195

Virchows Arch (2001) 439:616–621
DOI 10.1007/s004280100437

ORIGINAL ARTICLE

Kazumi Suzuki · Akihiko Tokue · Tomoko Kamiakito
Ken Kuriki · Ken Saito · Akira Tanaka

Predominant expression of fibroblast growth factor (FGF) 8, FGF4, and FGF receptor 1 in nonseminomatous and highly proliferative components of testicular germ cell tumors

Received: 21 June 2000 / Accepted: 19 January 2001 / Published online: 27 March 2001
© Springer-Verlag 2001

Abstract Nonseminomatous components within testicular germ cell tumors affect patient prognosis to varying degrees. These components are well known to mimic early embryonic totipotential tissues. Prompted by the recent observation that fibroblast growth factor (FGF) 8, FGF4, and FGF receptor (FGFR) 1 are required for the growth of early postimplantational embryonic tissues, we investigated the expressions of FGF8, FGF4, and FGFR1 in surgically resected specimens of primary testicular germ cell tumors using an immunohistochemical method. All cases of embryonal carcinoma (14 cases), yolk sac tumor (3 cases), and choriocarcinoma (3 cases) showed positive immunostaining for FGF8, FGF4, and FGFR1. In contrast, out of 13 cases of seminoma, immunostaining was negative for FGF8, FGF4, and FGFR1 in 8 cases (61.5%), 6 cases (46.1%), and 7 cases (53.8%), respectively. In 7 cases of mature and immature teratoma, most areas showed negative immunostaining. In addition, the Ki-67 labeling index showed extremely high mitogenic activity in embryonal carcinoma, yolk sac tumor, and choriocarcinoma, which are precisely the carcinomas with the highest expressions of FGF8, FGF4, and FGFR1. It is in keeping with the immunohistochemical result that murine teratocarcinoma P19 cells were shown to express FGF8, FGF4, and FGFR1 only under undifferentiated growth conditions. Taken together, these findings confirm the involvement of FGF8, FGF4, and FGFR1 in highly proliferative conditions of nonseminomatous germ cell tumors.

Keywords Testicular germ cell tumor · FGF8 · FGF4 · FGF receptor 1 · Immunohistochemistry

K. Suzuki · A. Tokue
Department of Urology, Jichi Medical School,
Tochigi 329–0498, Japan

T. Kamiakito · K. Kuriki · K. Saito · A. Tanaka (✉)
Department of Pathology, Jichi Medical School,
Tochigi 329–0498, Japan
e-mail: atanaka@jichi.ac.jp
Tel.: +81-285-587330, Fax: +81-285-448467

Introduction

Primary testicular tumors often show diverse histological heterogeneity [9]. They are believed to originate from a clonally transformed germ cell that has the potency to differentiate into heterogeneous histological subtypes such as seminoma, embryonal carcinoma, yolk sac tumor, choriocarcinoma, and teratoma [9]. The clinical detection of nonseminomatous components within the tumors has been shown to be of prognostic importance [10], implying that nonseminomatous germ cell tumors have a mechanism that affects patient prognosis. However, no such mechanism has been fully elucidated. Recent reports on null-mutant mouse models have clearly shown that fibroblast growth factor (FGF) 8, FGF4, and FGF receptor (FGFR) 1 are required for early postimplantational growth [3, 4, 8, 17]. The histological similarity between nonseminomatous components and embryonic or extra-embryonic tissues at early developmental stages suggests that FGF8, FGF4, and FGFR1 are involved in nonseminomatous germ cell tumors. In this study, we used immunohistochemical methods to investigate the expressions of FGF8, FGF4, and FGFR1 in different types of human testicular germ cell tumors. In addition, FGF4 and FGF8 have been shown to have oncogenic activity, and FGF8 has been shown to form an autocrine loop via FGFR1 in mouse mammary cancer cells [6, 14], strongly suggesting that FGF8, FGF4, and FGFR1 have an important role in proliferative conditions of nonseminomatous germ cell tumors. Therefore, we also estimated mitogenic activity by counting Ki-67 labeling indexes in each histological subtype in relation to FGF8, FGF4, and FGFR1 expression. Finally, differentiation into teratomas is often found during chemotherapy in patients with testicular germ cell tumors [10]. Several human and murine teratocarcinoma cell lines that exhibit mature phenotypes when exposed to retinoic acid or other reagents are used as models for teratoid differentiation [7]. In this study, we also compared *fgf8*, *fgf4*, and *fgfr1* transcripts between undifferentiated and differentiated conditions in murine teratocarcinoma P19 cells.

Table 1 Clinicopathological characteristics of patients

Characteristics	No.	%
No. of patients entered	35	–
Mean age (range)	27.3 (1 month to ~60 years)	–
Histological types		
Seminoma[a]	13	32.5
Embryonal carcinoma[b]	14	35.0
Teratoma[c]	7	17.5
Yolk sac tumor[d]	3	7.5
Choriocarcinoma[e]	3	7.5
Stage		
I	22	62.9
II	9	25.7
III	4	11.4

[a] Combined germ cell tumor: 1 of 13 cases
[b] Combined germ cell tumor: 10 of 14 cases
[c] Combined germ cell tumor: 5 of 7 cases
[d] Combined germ cell tumor: 1 of 3 cases
[e] Combined germ cell tumor: 2 of 3 cases

Materials and methods

Materials

Forty sections of primary testicular germ cell tumors were obtained from 35 specimens taken during high inguinal orchiectomies performed at Jichi Medical School Hospital from 1990 to 1999. None of the patients had been pretreated with irradiation or chemotherapy. The characteristics of these cases are summarized in Table 1.

Antibodies

Isolation of the monoclonal antibody against human FGF8 has been described previously [15]. Polyclonal antibodies against human FGF4 and FGFR1 were purchased from Santa Cruz Biotechnology (Santa Cruz, Calif.). Monoclonal antibody against Ki-67 was purchased from MBL (Nagoya, Japan).

Cells

A murine teratocarcinoma P19 cell line was purchased from Dainippon Pharmacy (Osaka, Japan) and maintained as recommended. Neuronal differentiation of the P19 cells was induced as reported elsewhere [5]. The cells were plated onto a bacteriological grade dish in the presence of 500 nM all-*trans* retinoic acid (tRA) (Wako, Osaka, Japan), cultured for 2 days, and then plated onto a standard culture dish. After another 4 days' incubation, the cells were collected for RNA preparation. The neuronal differentiation of P19 cells was confirmed by the expression of microtubule-associated protein 2 and the neuronal transcription factor, Neuro D, as shown by reverse-transcription polymerase chain reaction (RT-PCR; data not shown).

Immunohistochemistry

The method for immunostaining with anti-FGF8 antibody has been described elsewhere [15]. For immunostaining with anti-FGF4 and anti-FGFR1 antibodies, formalin-fixed and paraffin-embedded sections were boiled in 10 mM citrate buffer in a microwave oven for 10 min, treated with peroxide to block endogenous biotin, and reacted with either anti-FGF4 polyclonal antibody (×200) or anti-FGFR1 polyclonal antibody (×800) at 4°C overnight. The next morning, the sections were further interacted with biotin-labeled secondary antibodies and stained by an avidin–biotin complex method. Nonspecific IgG was used for negative controls. Sections from human adult testis and pituitary gland were used for the positive controls with FGF4 and FGFR1, respectively.

Ki-67 labeling index

Proliferative activity in each human testicular germ cell tumor was estimated by a Ki-67 labeling index as reported previously [11]. Sections of human testicular germ cell tumors were immunostained with Ki-67 at a dilution of 1:100, and ratios of labeled tumor cells were counted.

RNAs

Total RNAs were prepared from P19 cells under undifferentiated or neuronally differentiated conditions by an acid–phenol–chloroform–guanidium method.

Reverse transcription polymerase chain reaction

Single-stranded cDNAs were synthesized with Superscript II (Life Technologies, Rockville, Md.) from 1 µg of total cellular RNAs using an oligo-dT primer according to the manufacturer's instructions. Samples in a total volume of 100 µl were cycled for PCR 35 times at 94°C for 45 s, 55°C for 30 s, and 72°C for 90 s and then put through a final extension at 72°C for 10 min. Then 10 µl of each PCR-amplified sample was electrophoresed in a 2% agarose gel and stained with ethidium bromide. Primer sets used in this study were: mouse FGF4, 5'-TCTACTGCAACGTGGGCATC-3' and 5'-CTTCATGGTAGGCGACACTC-3'; mouse FGF8, 5'-TTTACACAGCATGTGAGGGAG-3' and 5'-GTAGTTGAGGAACTCGAAGCG-3'; mouse FGFR1, 5'-TAACCGCAGAACTGGGATGT-3' and 5'-TCCAGCAGTCTTCAGGATCT-3'.

Statistical analysis

Fisher's exact test and the Mann-Whitney U-test were used for statistical analysis in this study.

Results

Immunohistochemical findings

As summarized in Table 2, FGF8, FGF4, and FGFR1 were expressed in all of the nonseminomatous components except for the teratomas. In FGF8 immunostaining, 8 out of 13 seminoma cases (61.5%) were negative while all cases of embryonal carcinoma (14 cases), yolk sac tumor (3 cases), and choriocarcinoma (3 cases) showed positive staining (Fig. 1A–C, Table 2). In FGF4 and FGFR1 immunostaining, seminomas were negatively stained in 6 out of 13 (46.1%) and 7 out of 13 cases (53.8%), respectively (Table 2). In contrast, all cases of embryonal carcinoma, yolk sac tumor, and choriocarcinoma showed positive staining for FGF4 and FGFR1 (Fig. 1E, F, Table 2). Despite foci of positive tumor cells, most areas of mature and immature teratomas (7 cases)

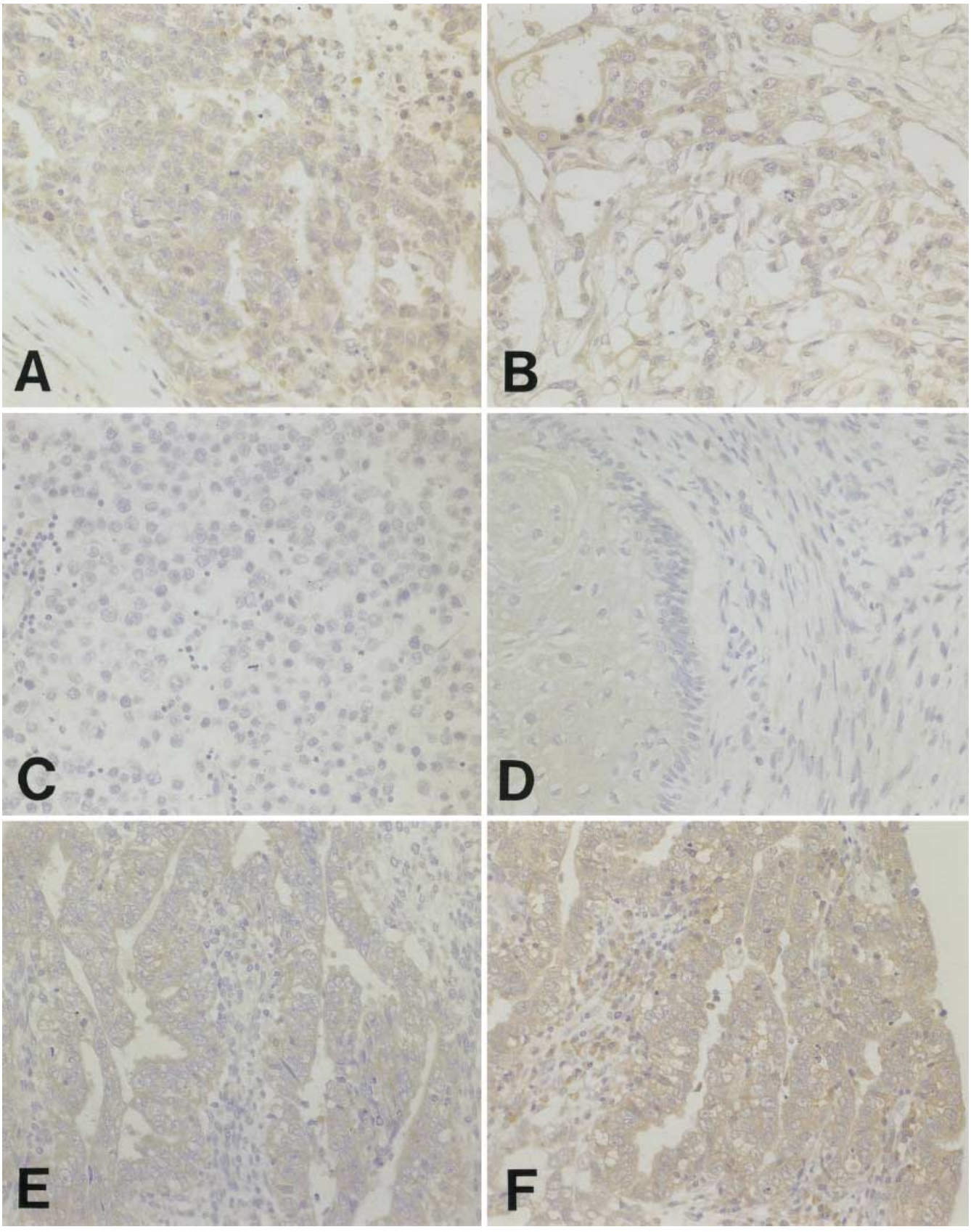
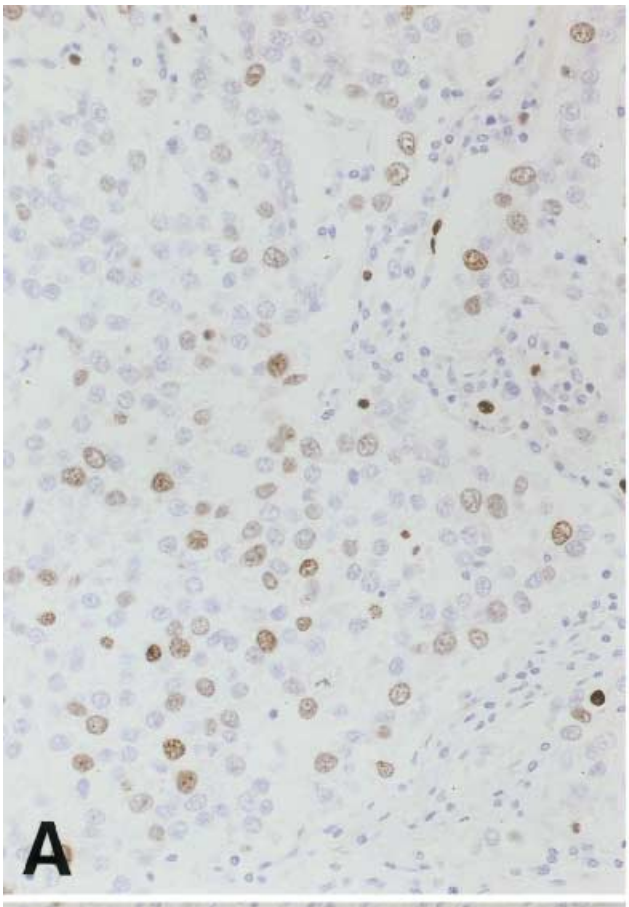
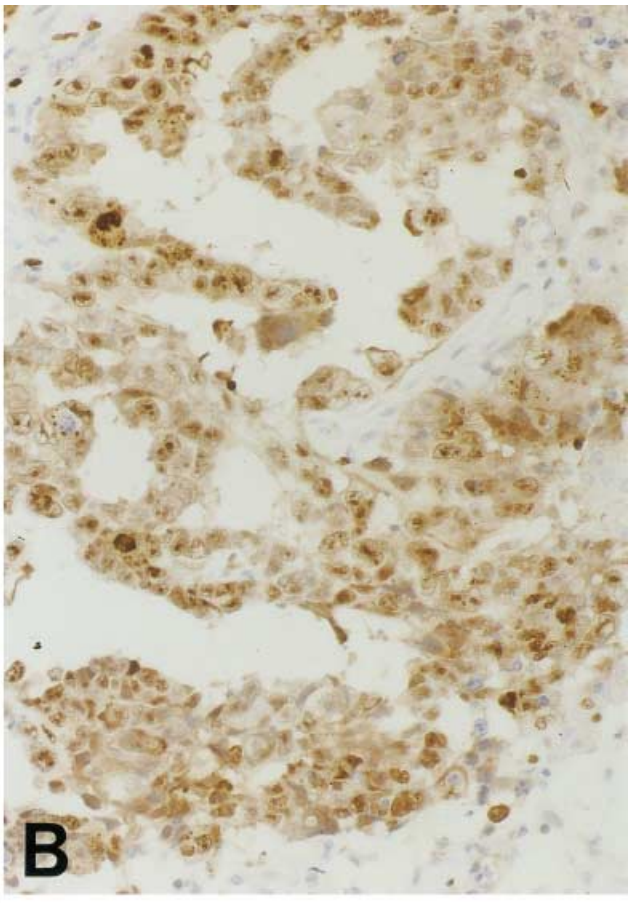


Fig. 1A–F Immunohistochemical findings. FGF8 expression in **A** embryonal carcinoma and **B** yolk sac tumor. Negative immunostaining with FGF8 in **C** seminoma and **D** mature teratoma. **E** FGF4 and **F** FGFR1 expression in embryonal carcinoma. Original magnification ×132





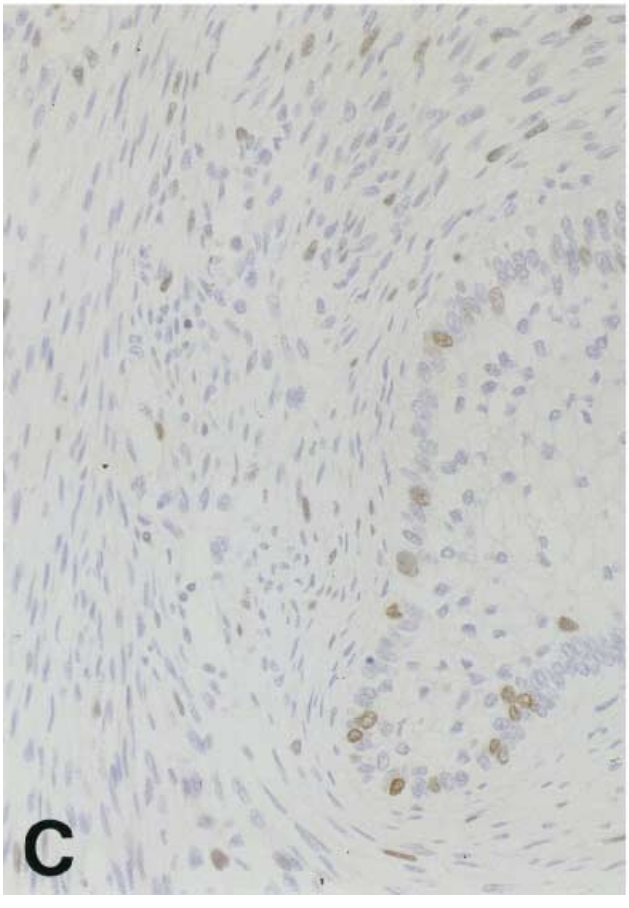


Fig. 2A–C Immunohistochemical staining with Ki-67. Expression of Ki-67 in **A** seminoma, **B** embryonal carcinoma, and **C** teratoma. Original magnification ×200

were negatively immunostained for FGF8, FGF4, and FGFR1 (Fig. 1D, Table 2).

Ki-67 labeling index

A Ki-67 labeling index in each histological tumor section showed counts of 59.5±15.9% (mean±SD) in seminoma, 88.7±8.2% in embryonal carcinoma, 69.2± 16.2% in yolk sac tumor, 85.4±17.3% in choriocarcinoma, and 17.2±10.4% in mature and immature teratomas (Figs. 2A–C, 3). Thus, we can confirm that the expressions of FGF8, FGF4, and FGFR1 are significantly correlated with mitogenic activity in testicular germ cell tumors ($P<0.0001$).

Reverse-transcription polymerase chain reaction

When *fgf8*, *fgf4*, and *fgfr1* transcripts were compared in murine teratocarcinoma P19 cells under undifferentiated and neuronally differentiated conditions, all the transcripts were expressed only in the cells in the undifferentiated condition (Fig. 4).

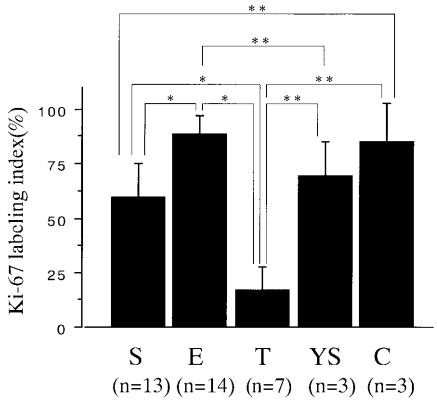


Fig. 3 Ki-67 labeling index in various histological subtypes of testicular germ cell tumors. Percentages of Ki-67-positive tumor cells counted in various histological subtypes of testicular germ cell tumors. Values are expressed as means of total sections in seminoma (*S*), embryonal carcinoma (*E*), teratoma (*T*), yolk sac tumor (*YS*), or choriocarcinoma (*C*). A Ki-67 labeling index was counted three times in different areas in each section. *Bars* represent SD. **P*<0.001; ***P*<0.05

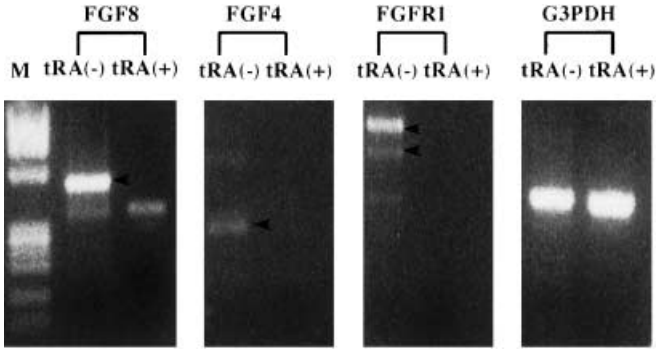


Fig. 4 Comparison of *fgf8*, *fgf4*, and *fgfr1* transcripts between undifferentiated and neuronally differentiated conditions in murine teratoma P19 cells. RT-PCR was carried out with *fgf8* (FGF8), *fgf4* (FGF4), and *fgfr1* (FGFR1) primers using RNAs prepared from undifferentiated P19 cells in the absence of 500 nM all-*trans*-retinoic acid [tRA(–)] or from neuronally differentiated P19 cells in the presence of 500 nM all-*trans*-retinoic acid [tRA(+)]. *Arrowheads* indicate the amplified fragments at the exact calculated size

Table 2 Expression of FGF8, FGF4 and FGFR1 in testicular germ cell tumors

Histological type	No. of specimens	Positive	%	Negative	%	Significance
		FGF8				
Seminoma	13	5	38.5	8	61.5	2* a
Embryonal carcinoma	14	14	100	0	0	5* b
Teratoma	7	0	0	7	100	3* c
Yolk sac tumor	3	3	100	0	0	
Choriocarcinoma	3	3	100	0	0	3* d
		FGF4				
Seminoma	13	7	53.8	6	46.2	* a
Embryonal carcinoma	14	14	100	0	0	4* b
Teratoma	7	0	0	7	100	* c
Yolk sac tumor	3	3	100	0	0	
Choriocarcinoma	3	3	100	0	0	* d
		FGFR1				
Seminoma	13	6	46.2	7	53.8	* a
Embryonal carcinoma	14	14	100	0	0	4* b
Teratoma	7	0	0	7	100	* c
Yolk sac tumor	3	3	100	0	0	
Choriocarcinoma	3	3	100	0	0	* d

P*<0.05; 2P*<0.01; 3**P*<0.005; 4**P*<0.0005; 5**P*<0.0001

[a] Difference between seminoma and embryonal carcinoma

[b] Difference between embryonal carcinoma and teratoma

[c] Difference between teratoma and yolk sac tumor

[d] Difference between teratoma and choriocarcinoma

Discussion

The present immunohistochemical study clearly shows that FGF8, FGF4, and FGFR1 are expressed in all embryonal carcinomas, yolk sac tumors, and choriocarcinomas. In contrast, seminomas and teratomas showed much lower incidences of FGF8, FGF4, and FGFR1 expression. The significant difference in the expressions of these molecules between seminomas and the nonseminomatous tumors other than the teratomas confirms that FGF8, FGF4, and FGFR1 are all preferentially involved in nonseminomatous germ cell tumors. In addition, the embryonal carcinomas, yolk sac tumors, and choriocarcinomas showed extremely high Ki-67 labeling indexes, strongly suggesting that the expressions of these three molecules are related to highly proliferative conditions. These results present strong evidence that FGF8, FGF4, and FGFR1 produce proliferative signals in nonseminomatous germ cell tumors, possibly forming an autocrine loop within tumor cells.

To our knowledge, this is the first report on investigation of FGF8, FGF4, and FGFR1 expression in testicular germ cell tumors using an immunohistochemical method. Previously, Strohmeyer et al. reported finding *fgf4* transcripts in only 1 out of 24 surgically resected specimens of seminoma (4.2%), in contrast to as many as 24 out of 38 nonseminomas (63.2%) [13]. Very few cases were examined in that study, but other investigators have

also reported that *fgf4* and *fgf8* transcripts are found in human testicular tumors, especially in embryonal carcinomas [12, 16, 18]. Apparently, an immunohistochemical approach has great advantages in determining specific tumor cell types from the heterogeneous components of testicular germ cell tumors. From this point of view, the present immunohistochemical data offer a more reliable basis for estimating the incidence of FGF8, FGF4, and FGFR1 expression in nonseminomatous cases. Interestingly, some cases of seminoma also showed FGF8, FGF4, and FGFR1 expression in this study. Given that FGF8, FGF4, and FGFR1 were shown to be expressed in mature testicular germ cells [2], it is not surprising that they were expressed in some cases of pure seminoma. However, there is a possibility that the seminomas that express FGF8, FGF4, and FGFR1 are more liable to develop nonseminomatous components during clinical treatment than those with negative expression. The roles of FGF signals in seminoma are an issue that should be explored in the future.

In vitro models of human and murine teratocarcinoma cell lines provide us with useful information about the molecular basis for growth and differentiation of testicular germ cell tumors. In a human teratocarcinoma cell line, Tera-2, FGF8 and FGF4 expressions were markedly decreased after retinoic acid-induced differentiation [1, 16]. In this study, using murine teratocarcinoma P19 cells, we also showed that the *fgf8*, *fgf4*, and *fgfr1* transcripts all disappeared after neuronal differentiation. Consistent with these in vitro observations, the present immunohistochemical study demonstrated that both mitogenic activity and the expressions of FGF8, FGF4, and FGFR1 are markedly decreased in areas of immature and mature teratomas. Taken together with these findings, the blocking of FGF signals in teratocarcinomas convinced us that the tumor differentiation with decreased levels of mitogenic activity is likely to be induced. If this is indeed the case, the FGF signals might be attractive targets in chemotherapy for teratocarcinoma.

In conclusion, we have shown that FGF8, FGF4, and FGFR1 are expressed predominantly in nonseminomatous and highly proliferative testicular germ cell tumors. To our knowledge, this is the first immunohistochemical study on FGF8, FGF4 and FGFR1 expression in human testicular germ cell tumors.

Acknowledgements This work was supported in part by Grant-in-Aid for Scientific Research (C) no. 09670235 from the Japanese Ministry of Education, Science, and Culture. We thank Y. Haga and M. Hoshino for technical assistance.

References

1. Alanko T, Tienari J, Lehtonen E, Saksela O (1996) FGF-2 inhibits apoptosis in human teratocarcinoma cells during differentiation on collagen substratum. Exp Cell Res 228:306–312
2. Cancilla B, Davies A, Ford-Perriss M, Risbridger GP (2000) Discrete cell- and stage-specific localization of fibroblast growth factors and receptor expression during testis development. J Endocrinol 164:149–159
3. Deng C-X, Wynshaw-Boris A, Shen MM, Daugherty C, Ornitz DM, Leder P (1994) Murine FGFR-1 is required for early postimplantation growth and axial organization. Genes Dev 8:3045–3057
4. Feldman B, Poueymirou W, Papaioannou VE, DeChiara TM, Goldfarb M (1995) Requirement of FGF-4 for postimplantation mouse development. Science 267:246–249
5. Jones-Villeneuve EMV, McBurney MW, Rogers KA, Kalnins VI (1982) Retinoic acid induces embryonal carcinoma cells to differentiate into neurons and glial cells. J Cell Biol 94:253–262
6. Kouhara H, Koga M, Kasayama S, Tanaka A, Kishimoto T, Sato B (1994) Transforming activity of a newly cloned androgen-induced growth factor. Oncogene 9:455–462
7. McBurney MW, Jones-Villeneuve EMV, Edwards MKS, Anderson PJ (1982) Control of muscle and neuronal differentiation in a cultured embryonal carcinoma cell line. Nature 299: 165–167
8. Meyers EN, Lewandoski M, Martin GR (1998) An *Fgf8* mutant allelic series generated by Cre- and Flp-mediated recombination. Nat Genet 18:136–141
9. Mostofi FK (1980) Pathology of germ cell tumors of testis. Cancer 45:1735–1754
10. Richie JP (1998) Neoplasms of the testis. In: Walsh PC, Retik AB, Stamey TA, Vaughan ED Jr, Wein AJ (eds) Campbell's urology. Saunders, Philadelphia, pp 2411–2452
11. Sakurai S, Fukasawa T, Chong J-M, Tanaka A, Fukayama M (1999) Embryonic form of smooth muscle myosin heavy chain (SMemb/MHC-B) in gastrointestinal stromal tumor and interstitial cells of Cajal. Am J Pathol 154:23–28
12. Schofield PN, Ekström TJ, Granerus M, Engström W (1991) Differentiation associated modulation of K-FGF expression in a human teratocarcinoma cell line and in primary germ cell tumours. FEBS Lett 280:8–10
13. Strohmeyer T, Peter S, Hartmann M, Munemitsu S, Ackermann R, Ullrich A, Slamon D (1991) Expression of the *hst-1* and *c-kit* protooncogenes in human testicular germ cell tumors. Cancer Res 51:1811–1816
14. Taira M, Yoshida T, Miyagawa K, Sakamoto H, Terada M, Sugimura T (1987) cDNA sequence of human transforming gene *hst* and identification of the coding sequence required for transforming activity. Proc Natl Acad Sci USA 84:2980–2984
15. Tanaka A, Furuya A, Yamasaki M, Hanai N, Kuriki K, Kamiakito T, Kobayashi Y, Yoshida H, Koike M, Fukayama M (1998) High frequency of fibroblast growth factor 8 expression in clinical prostate cancers and breast tissues, immunohistochemically demonstrated by a newly established neutralizing monoclonal antibody against FGF 8. Cancer Res 58: 2053–2056
16. Wu J, Payson RA, Lang JC, Chiu I-M (1997) Activation of fibroblast growth factor 8 gene expression in human embryonal carcinoma cells. J Steroid Biochem Mol Biol 62:1–10
17. Yamaguchi TP, Harpal K, Henkemeyer M, Rossant J (1994) *fgfr-1* is required for embryonic growth and mesodermal patterning during mouse gastrulation. Genes Dev 8:3032–3044
18. Yoshida T, Tsutsumi M, Sakamoto H, Miyagawa K, Teshima S, Sugimura T, Terada M (1988) Expression of the hst1 oncogene in human germ cell tumors. Biochem Biophys Res Commun 155:1324–1329

Virchows Arch (2001) 439:622–627
DOI 10.1007/s004280100445

ORIGINAL ARTICLE

Sheng-Ben Liang · Mutsuo Furihata
Tamotsu Takeuchi · Hiroshi Sonobe · Yuji Ohtsuki

Reduced human mismatch repair protein expression in the development of precancerous skin lesions to squamous cell carcinoma

Received: 31 October 2000 / Accepted: 17 February 2001 / Published online: 6 July 2001
© Springer-Verlag 2001

Abstract Loss of human mismatch repair (hMSH2) gene function has been linked to hereditary non-polyposis colorectal cancer (HNPCC), Muir-Torre syndrome (MTS), and sporadic cancers, excluding skin cancers unrelated to MTS. We immunohistochemically examined 125 squamous cell carcinomas (SCCs) using a monoclonal antibody to the hMSH2 protein and compared the results with those for 106 precursor lesions of SCC, consisting of actinic keratosis (AK), Bowenoid type of actinic keratosis (BAK), and Bowen's disease (BOD). In contrast to the homogeneous immunoreactivity of proliferating cells composed of AK, BAK, and BOD, heterogeneous and diminished immunostaining to hMSH2 was observed in tumor cells of SCCs examined. In addition, two SCCs (2 of 125; 1.6%) at multiple loci exhibited a complete lack of immunoreaction to hMSH2. Immunohistochemical staining of hMSH2 was semiquantitatively scored as 0 (0% of total cells examined), 1 (less than 10%), 2 (10–50%), or 3 (more than 50%). Percentage preservation of and average score for hMSH2 expression in normal, AK, BAK, BOD, and SCC were 56% and 2.06, 100% and 2.80, 94% and 2.88, 83% and 2.78, 63% and 2.36, respectively. The percentage preservation of and average scores for hMSH2 in AK, BAK, and BOD were significantly higher than those in presumably normal skin ($P<0.01$). There were no significant differences in the percentage preservation of and average scores for hMSH2 between presumably normal skin and SCC. The score for hMSH2 expression was significantly correlated with score for sun exposure in presumably normal skin of each lesion ($R=0.70$). These findings for hMSH2 expression in precursor lesions and SCC suggest that promotion or activation of hMSH2 expression may be induced by the increased DNA damage caused by sun exposure and that diminished expression of it might occur according to the transformation from precancerous lesions to SCC.

Keywords hMSH2 · Skin · Squamous cell carcinoma · Mismatch repair · Immunohistochemistry

S.-B. Liang · M. Furihata (✉) · T. Takeuchi · H. Sonobe
Y. Ohtsuki
Department of Pathology II, Kochi Medical School, Nankoku, Kochi 783-8505, Japan
e-mail: furihata@kochi-ms.ac.jp
Tel.: +81-88-8665811, Fax: +81-88-8802336

Introduction

Repair of DNA damage protects the cell genome from the effects of carcinogenic agents. Mismatch repair (MMR) is an important form of DNA repair. The products of MMR genes play important roles in distinguishing and repairing mispairing and slippage errors in DNA synthesis. In functional abnormalities of MMR genes, hMSH2 alterations are major MMR gene alterations and account for approximately 60% of hereditary nonpolyposis colorectal carcinoma (HNPCC) families [15, 22]. It has been found that Muir-Torre syndrome (MTS), a rare autosomal dominant disorder characterized by the association of visceral malignancies with typical skin lesions, including squamous cell carcinoma (SCC), also shares gene alterations in the MMR system with HNPCC [6, 11, 19].

SCC is the most common malignancy arising in sun-exposed sites of skin, especially in aged individuals [5]. The most commonly accepted exogenous cause of skin SCC is exposure to ultraviolet light with subsequent DNA damage and associated mutagenicity [5]. Prior to the development of overt malignancy of the epidermis, a series of progressively dysplastic changes occur. Because this malignancy is usually the result of chronic exposure to sunlight and is associated with a build-up of excess keratin, its lesions are termed actinic keratosis (AK) and are characterized by basal cell layer atypia and hyperkeratosis and parakeratosis. Progression of nuclear atypia to full thickness, i.e., Bowenoid type of actinic keratosis (BAK), heralds the development of early SCC in situ. Bowen's disease (BOD), which usually develops in sites without sun exposure, is also a common type of carcinoma in situ occurring in skin. Thus, AK, BAK, and

BOD have been considered precursors of skin SCC [2, 18].

It has been demonstrated that microsatellite instability (MSI) secondary to replication errors followed by MMR gene alterations can be detected in various malignant human tumors, including skin cancers and that MSI is an unusual finding in benign and malignant skin tumors [4, 17, 20]. However, the precise associations of in vivo MMR gene status with carcinogenesis have not been studied in sporadic human malignancies. The reasons for this are as follows. In many types of sporadic cancers, mutations of MMR genes are rare, mutations in MMR genes have no marked hot spots [16], and MMR genes sometimes undergo epigenetic silencing [1]. These phenomena discouraged attempts to search for mutations in the expanding panel of MMR genes. An immunohistochemical study is a suitable method for screening for MMR gene status. A lack of hMSH2 gene expression, especially as assessed using immunohistochemistry, correlates with its gene alterations. Because antibody staining is more available than DNA analysis in a clinical setting, the use of immunohistochemistry may offer a relatively convenient and rapid technique for pre-screening tumors for defects in the expression of the hMSH2 gene [12, 21].

In order to examine the roles of defective MMR in sporadic skin cancer, we studied the expression of the hMSH2 product in a large series of cases of non-melanocytic skin cancer using immunohistochemical staining of an antibody against hMSH2. For in vivo modeling of the evolution of skin SCC, the sites examined included presumably normal skin adjacent to skin lesions and the foci of AK, BAK, BOD, and SCC. The results of this study indicated that the promotion of hMSH2 expression in normal skin was related to sun exposure and that reduction and loss of hMSH2 expression might occur according to the transformation from precancerous lesions to SCC.

Materials and methods

Patients

Surgically resected skin lesions of 231 cases in total were obtained from the Department of Pathology II and Clinical Laboratory Medicine of Kochi Medical School and the Matsuyama-Shimin Hospital until the year 2000. These consisted of 48 cases of AK, 18 cases of BAK, 40 cases of BOD, and 125 cases of SCC. We used ten normal skin tissues without preneoplastic or neoplastic lesions as base-line normal controls.

Clinicopathologic variables

Specimens were fixed in 10% buffered formalin and embedded in paraffin. Dewaxed paraffin sections were stained with hematoxylin and eosin (HE). The diagnosis of all cases was doubly checked by expert pathologists. Based on pathological observation, SCC was classified into well, moderately, and poorly differentiated subtypes. Sun exposure was assessed based on the score system reported previously [13, 14].

Briefly, according to the sites, degree of sun exposure was divided into four grades: 0 (no sun exposure even in swimsuit, including vulva, penis and axially fossa, and chest wall and abdomen of female), 1 (only exposed in swimsuit, including legs, feet and shoulders, and chest wall, abdomen, and back of male), 2 (only exposed in summer suit, mainly including arms) and 3 (not covered even in winter suit, that is, head, face, neck, and hands). The grades of 0 and 1 were also termed as weak sun exposure, while the grades of 2 and 3 were termed as strong sun exposure. The following variables were recorded, and some average numbers were calculated: sex, age at the time of diagnosis, sun exposure grade (Table 1), and pathological diagnosis.

Table 1 Clinical features and rate of human mismatch repair (hMSH2) gene immunoreactivity in 231 cases of skin lesions. *AK* actinic keratosis, *BAK* Bowenoid type of actinic keratosis, *BOD* Bowen's disease, *SCC* squamous cell carcinoma, *NS* normal skin

Item	AK	BAK	BOD	SCC	Total
Number of cases	48	18	40	125	231
Gender (male/female)	17/31	9/9	20/20	69/56	115/116
Age					
Average	77.9	80.6	69.3	79.0	77.2
Range	56–100	65–88	41–86	24–105	24–105
Positive rate of hMSH2 (NS, 56%)	100%	94%	83%	63%	85%

Immunohistochemical staining with hMSH2 antibody

In immunohistochemical staining, autoclave pretreatment to strengthen the immune reaction was used before the incubation with anti-hMSH2 mouse monoclonal antibody [hMSH2 (AB-2), 1:10 dilution, Calbiochem, San Diego, Calif.], followed by the application of the labeled streptavidin–biotin method (LSAB Kit, Dako, Kyoto, Japan), as shown in our previous studies [7, 9]. Normal colon mucosa was used as a positive control of immunostaining with hMSH2 antibody.

The immunohistochemical staining of hMSH2 was semiquantitatively scored in each presumably normal skin and skin lesion [9] as follows: 0, 0%; 1, <10%; 2, 10–50%; and 3, >50%. Based on the scoring, all cases were divided into two groups: the reduced group (score 0, 1) and the preserved group (score 2, 3). The observed sites in each case include cancer nests and presumably normal skin if available.

Statistics

The methods for statistical analyses include: Pearson's correlation coefficient for correlation analysis, $\chi 2$ test for difference analysis between positive rate, paired *t*-test for difference analysis between paired groups, Mann-Whitney's *U* test, or student's *t*-test for difference analysis between unpaired groups.

Results

Immunohistochemical staining with hMSH2 antibody

hMSH2-positive cells had brown-stained nuclei (Fig. 1). Presumably normal skin adjacent to the lesions frequently exhibited weak to moderately positive immunostaining in the cells of the basal layer (Fig. 1A). This pattern of staining is the same in that of ten normal controls examined. Preserved expression of hMSH2 was observed

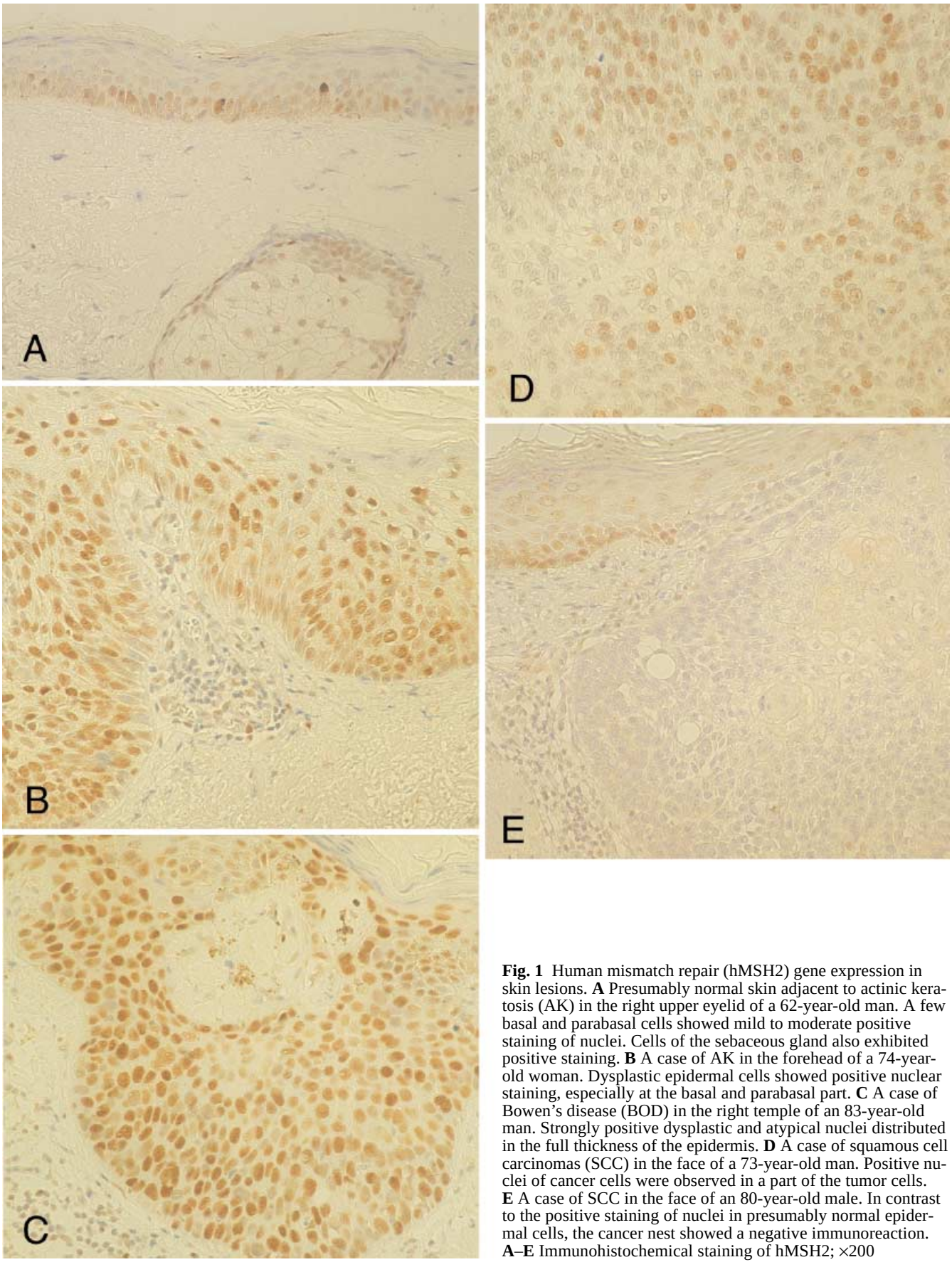


Fig. 1 Human mismatch repair (hMSH2) gene expression in skin lesions. **A** Presumably normal skin adjacent to actinic keratosis (AK) in the right upper eyelid of a 62-year-old man. A few basal and parabasal cells showed mild to moderate positive staining of nuclei. Cells of the sebaceous gland also exhibited positive staining. **B** A case of AK in the forehead of a 74-year-old woman. Dysplastic epidermal cells showed positive nuclear staining, especially at the basal and parabasal part. **C** A case of Bowen's disease (BOD) in the right temple of an 83-year-old man. Strongly positive dysplastic and atypical nuclei distributed in the full thickness of the epidermis. **D** A case of squamous cell carcinomas (SCC) in the face of a 73-year-old man. Positive nuclei of cancer cells were observed in a part of the tumor cells. **E** A case of SCC in the face of an 80-year-old male. In contrast to the positive staining of nuclei in presumably normal epidermal cells, the cancer nest showed a negative immunoreaction. **A**–**E** Immunohistochemical staining of hMSH2; ×200

Table 2 Statistical analyses for human mismatch repair (hMSH2) gene expression associated with sun exposure in skin lesions. *AK* actinic keratosis, *BAK* Bowenoid type of actinic keratosis, *BOD* Bowen's disease, *SCC* squamous cell carcinoma, *NS* no significance (R<0.20 or P^1, P^2>0.05), *Can't* Not to be calculable, *R* correlation value using Pearson's correlation coefficient

Item	AK	BAK	BOD	SCC	Total
Relationship of hMSH2 expression between normal skin and lesion focus					
Difference of preservation (P^1)[a]	0.01	0.02	<0.01	NS	<0.01
Difference of average score (P^2)[b]	<0.01	<0.01	<0.01	NS	<0.01
Average sun exposure score	2.979	2.833	1.275	2.600	2.468
Association with hMSH2 expression and sun exposure (R)					
Presumably normal skin	Can't	0.539	Can't	0.488	0.700
Lesion focus	0.386	NS	NS	NS	NS

[a] P value from $\chi 2$ test for positive rate (%)
[b] P value from paired t-test for score

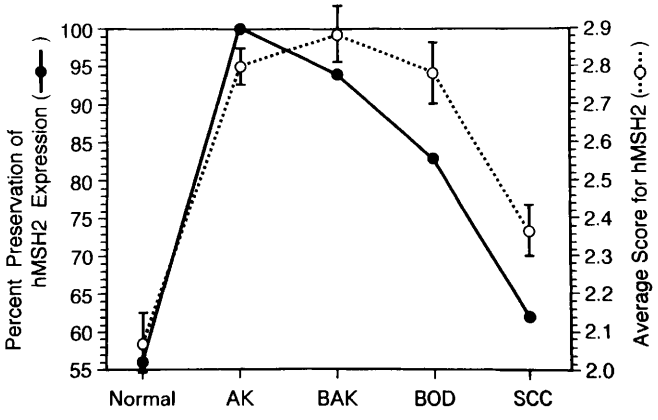


Fig. 2 Comparison of the rate of preservation of expression and average score of positivity for the human mismatch repair (hMSH2; score for hMSH2; 0: 0%, 1: <10%, 2: 10–50%, and 3: >50%) gene in normal, actinic keratosis, Bowenoid type of actinic keratosis, Bowen's disease, and squamous cell carcinomas

in all AKs (Fig. 2), in which dysplastic epidermal cells usually exhibited immunostaining in basal and parabasal layers (Fig. 1B). Most BAKs and BODs exhibited preservation of hMSH2 expression, with stained cells distributed through the entire thickness of the atypical, dysplastic epidermis (Fig. 1C). In contrast, a positive reaction to the hMSH2 antibody was diminished and heterogeneously observed in SCC (Fig. 1D). A complete lack of immunoreaction to hMSH2 antibody in cancer cell nests was found in only two patients with SCC at multiple foci (Fig. 1E).

Scores for hMSH2 expression in skin lesions

Figure 2 demonstrated the rate of preservation of expression and average score of positivity for hMSH2 in presumably normal skin, AK, BAK, BOD, and SCC. Percentage preservation of and average score for hMSH2 expression in normal, AK, BAK, BOD, and SCC were 56% and 2.06, 100% and 2.80, 94% and 2.88, 83% and 2.78, 63% and 2.36, respectively. The rate of preservation of expression and average score of positivity for hMSH2 in AK, BAK, and BOD were higher than in SCC and presumably normal skin (Fig. 2). The score for positivity and rate of preservation of expression of hMSH2 in SCC were close to those in presumably normal skin. In the statistical analysis of hMSH2 expression, the percentage preservation of and average scores for hMSH2 in AK, BAK, and BOD were significantly higher than those in presumably normal skin (Table 2). There were no significant differences in the percentage preservation of and average scores for hMSH2 between presumably normal skin and SCC (Table 2).

Sun exposure and hMSH2 expression

One hundred eighty-five of 231 skin lesions (80.1%) composed of AK, BAK, BOD, and SCC were found in strongly sun-exposed areas. As shown in Table 2, the total score for hMSH2 expression was significantly correlated with score for sun exposure in presumably normal skin adjacent to each lesion (R=0.70). In particular, normal skin lesions of 48 of 48 cases of AK cases (100%) and 17 of 18 cases of BAK (94%), which exhibited the highest rate of preservation of expression and score of positivity for hMSH2, occurred in strongly sun-exposed skin (The statistical significance is not to be calculable). These findings strongly hint that the physiological promotion of hMSH2 expression may be induced by the increased DNA damage caused by sun exposure. SK lesions (R=0.386) exhibited a highly significant correlation between sun exposure and hMSH2 expression (Table 2).

Discussion

Immunohistochemistry is a powerful and commonly used method for study of hMSH2 gene expression in situ [3, 10]. In this study, we immunohistochemically examined the expression of hMSH2 in 231 cases of nonmelanocytic skin cancer and its precursor lesions in order to investigate the roles played by hMSH2 in skin carcinogenesis. The present study showed that the rate of preservation of and average score of positivity for hMSH2 expression in lesions of AK, BAK, and BOD were higher than those in presumably normal skin adjacent to the respective lesions. This result indicates that expression of the hMSH2 product may be promoted in

connection with an increased cell replication rate during the process from normal cells to precancerous cells.

Interestingly, our study revealed a highly significant correlation between sun exposure and the expression of hMSH2 in presumably normal skin adjacent to each lesion. This result supports the hypothesis that ultraviolet radiation plays a role in the generation of genetic instability and that during carcinogenesis, the increased DNA damage caused by sun exposure induces a dose-dependent requirement for promotion of MMR gene expression, including hMSH2.

In the present study, the majority of SCCs and precursor lesions, including AK, BAK, and BOD, exhibited variable degrees of hMSH2 expression in each lesion. The rate of preservation of expression and average score of positivity for hMSH2 in AK, BAK, and BOD were higher than in SCC (Table 2). These findings suggest that the reduced hMSH2 expression occurs as a consequence of the tumor progression during the transformation from precancerous epidermis to SCC. A recent study has indicated that, in contrast to p53 and other randomly selected loci, hMSH2 gene defects are extremely heterogeneous within tumors and that loss of one allele in the hMSH2 gene could affect repair capacity and dose dependently contribute to a replication error (RER) phenotype [23]. In an investigation of RER in sporadic colorectal carcinomas, mild RER (+) carcinomas had concomitantly lost MMR genes through the typical loss of a heterozygosity pathway but exhibited partial preservation of MMR capacity in the remaining normal allele [8]. Thus, it seems likely that the decrease of hMSH2 expression in some cases of SCCs observed in the present study may be associated with the intratumoral heterogeneity of hMSH2 gene defects.

A previous report based on the MSI assay indicated the low frequency of RER in human non-melanoma skin tumors [17]. In the present study, among the 125 cases examined, there were only two SCCs (1.6%) at multiple foci with a complete lack of immunoreaction to the hMSH2 antibody in cancer nests. This also supports the findings of a low RER frequency reported in skin cancers [17]. Although the phenomenon of loss of hMSH2 protein is uncommon in patients with skin SCC, the identification of RER using immunohistochemistry suggests that error-prone replication for hMSH2 may be important in skin SCC development in some individuals. Furthermore, immunohistochemical analysis of skin tumors for RER could also prove useful in the diagnosis of patients genetically predisposed to cancer development due to a MMR defect. Our study, however, also demonstrated the diminished and heterogeneous expression of the hMSH2 protein in most SCCs. In the MSI assay, if only a small fraction of cancer cells had MSI based on the defect of MMR gene expression, the relative population of abnormal-sized bands would be too small to be determined. This theory may explain the phenomena of low RER frequency in skin cancer examined using the MSI assay.

Up to the present, investigations of the relationship between MMR deficiency and carcinogenesis were mainly performed based on the MSI analysis. However, the underlying molecular basis of MSI has not been clearly established. In addition, the detection of MSI usually requires archival paraffin-embedded tissue with potential problems in accessing samples and DNA amplification. The immunohistochemical approach is useful for finding in vivo MMR gene status associated with carcinogenesis of tumors. Further comprehensive studies will be needed to elucidate the involvement of the MMR deficiency in human skin SCCs exhibiting diminished and heterogeneous hMSH2 protein expression.

Acknowledgements We are grateful to Prof. Dr. H. Kodama, Department of Dermatology, and Dr. T. Moriki, Department of Clinical Laboratory Medicine, Kochi Medical School, for providing clinical materials.

References

1. Ahuja N, Mohan AL, Li Q, Stolker JM, Herman JG, Hamilton SR, Baylin SR, Issa JR (1997) Association between CpG island methylation and microsatellite instability in colon cancer. Cancer Res 57:3370–3374
2. Brownstein MH, Rabinowitz AD (1979) The precursors of cutaneous squamous cell carcinoma. Int J Dermatol 18:1–16
3. Dietmaier W, Wallinger S, Bocker T, Kullmann F, Fishel R, Ruschoff J (1997) Diagnostic microsatellite instability: definition and correlation with mismatch repair protein expression. Cancer Res 57:4749–4756
4. Entius MM, Keller JJ, Drillenburg P, Kuypers KC, Giardiello FM, Offerhaus GJA (2000) Microsatellite instability and expression of hMLH-1 and hMSH-2 in sebaceous gland carcinomas as markers for Muir-Torre syndrome. Clin Cancer Res 6:1784–1789
5. Epstein JH (1983) Photocarcinogenesis, skin cancer, and aging. J Am Acad Dermatol 9:487–502
6. Esche C, Kruse R, Lamberti C, Friedl W, Propping P, Lehmann P, Ruzicka T (1997) Muir-Torre syndrome: clinical features and molecular genetic analysis. Br J Dermatol 136: 913–917
7. Furihata M, Shuin T, Takeuchi T, Sonobe H, Ohtsuki Y, Akiyama Y, Yuasa Y (2000) Missense mutation of the hMSH6 and p53 genes in sporadic urothelial transitional cell carcinoma. Int J Oncol 16:491–496
8. Habano W, Sugai T (1998) Nakamura S. Mismatch repair deficiency leads to a unique mode of colorectal tumorigenesis characterized by intratumoral heterogeneity Oncogene 16: 1259–1265
9. Jin TX, Furihata M, Yamasaki I, Kamada M, Liang SB, Ohtsuki Y, Shuin T (1999) Human mismatch repair gene (hMSH2) product expression in relation to recurrence of transitional cell carcinoma of the urinary bladder. Cancer 85: 478–484
10. Kim H, Piao Z, Kim JW, Choi JS, Kim NK, Lee JM, Park JH (1998) Expression of hMSH2 and hMLH1 in colorectal carcinomas with microsatellite instability. Pathol Res Pract 194:3–9
11. Kruse R, Rutten A, Lamberti C, Hosseiny-Malayeri HR, Wang Y, Ruelfs C, Jungck M, Mathiak M, Ruzicka T, Hartschuh W, Bisceglia M, Friedl W, Propping P (1998) Muir-Torre phenotype has a frequency of DNA mismatch-repair-gene mutations similar to that in hereditary nonpolyposis colorectal cancer families defined by the Amsterdam criteria. Am J Hum Genet 63:63–70
12. Leach FS, Polyak K, Burrell M, Johnson KA, Hill D, Dunlop MG, Wyllie AH, Peltomaki P, de la Chapelle A, Hamilton SR, Kinzler KW, Vogelstein B (1996) Expression of the human mismatch repair gene hMSH2 in normal and neoplastic tissues. Cancer Res 56:235–240

13. Liang S-B, Ohtsuki Y, Furihata M, Takeuchi T, Iwata J, Chen BK, Sonobe H (1999) Sunexposure- and aging-dependent p53 protein accumulation results in growth advantage for tumour cells in carcinogenesis of nonmelanocytic skin cancer. Virchows Arch 434:193–199
14. Liang S-B, Furihata M, Takeuchi T, Iwata J, Chen BK, Sonobe H, Ohtsuki Y (2000) Overexpression of cyclin D1 in nonmelanocytic skin cancer. Virchows Arch 436:370–376
15. Marra G, Boland C (1995) Hereditary nonpolyposis colorectal cancer: the syndrome, the genes, and historical perspectives. J Natl Cancer Inst 87:1114–1125
16. Peltomäki P, Chapelle A (1997) Mutations predisposing to hereditary nonpolyposis colorectal cancer. Adv Cancer Res 71: 93–119
17. Quinn AG, Healy E, Rehman I, Sikkink S, Rees JL (1995) Microsatellite instability in human non-melanoma and melanoma skin cancer. J Invest Dermatol 104:309–312
18. Sober AJ, Burstein JM (1995) Precursors to skin cancer. Cancer 75:645–650
19. Suspiro A, Fidalgo P, Cravo M, Albuquerque C, Ramalho E, Leitao CN, Costa Mira F (1998) The Muir-Torre syndrome: a rare variant of hereditary nonpolyposis colorectal cancer associated with hMSH2 mutation. Am J Gastroenterol 93:1572–1574
20. Talwalkar V, Scheiner M, Hedges LK, Butler MG, Schwartz HS (1998) Microsatellite instability in malignant melanoma. Cancer Genet Cytogenet 104:111–114
21. Thibodeau SN, French AJ, Roche PC, Cunningham JM, Tester DJ, Lindor NM, Moslein G, Baker SM, Liskay RM, Burgart LJ, Honchel R, Halling KC (1996) Altered expression of hMSH2 and hMLH1 in tumors with microsatellite instability and genetic alterations in mismatch repair genes. Cancer Res 56:4836–4840
22. Wilson TM, Ewel A, Duguid JR, Eble JN, Lescoe MK, Fishel R, Kelley M (1995) Deferential cellular expression of the human MSH2 repair enzyme in small and large intestine. Cancer Res 55:5146–5150
23. Zaphiropoulos PG, Söderkvist P, Hedblad MA, Toftgard R (1994) Genetic instability of microsatellite markers in region q22.3-q31 of chromosome 9 in skin squamous cell carcinomas. Biochem Biophys Res Commun 201:1495–1501

Virchows Arch (2001) 439:628–635
DOI 10.1007/s004280100451

ORIGINAL ARTICLE

**Balázs Döme · Beáta Somlai · Andrea Ladányi
Károly Fazekas · Margot Zöller · József Tímár**

Expression of CD44v3 splice variant is associated with the visceral metastatic phenotype of human melanoma

Received: 4 December 2000 / Accepted: 8 March 2001 / Published online: 17 May 2001
© Springer-Verlag 2001

Abstract We analyzed the immunohistochemical expression of the metastasis-associated protein, CD44v3, in 46 primary human malignant melanomas (MMs). This is the first time that the v3 splice variant of CD44 was found to be expressed in human melanomas (15 of 46), ranging from 3% to 35% of the cell population in the positive tumors. The expression of CD44v3 was observed in tumors thicker than 1.0 mm, and one-third of these tumors proved to be positive irrespective of the thickness. Patients were followed for a minimum of 61 months. The onset of lymph node or organ metastases occurred not later than 58 months and 60 months, respectively. Of the 15 CD44v3 positive tumors, 14 were observed in the organ metastatic tumor group, comprising the majority of those cases (14 of 21), and this association proved to be statistically significant compared with the non-metastatic (P<0.05) and lymph-node metastatic cases (P<0.01). CD44v3 expression in melanoma was also confirmed at the protein and messenger (mRNA) level in several human melanoma cell lines using flow cytometry and reverse transcriptase polymerase chain reaction analysis. In parallel to CD44v3, MMP-2 expression (determined using immunohistochemistry) was significantly elevated (P<0.05) but only in the organ metastatic group of MM. The 5-year survival of patients having thicker tumors than 1.0 mm (where v3 expression occurred) who had CD44v3+ tumors was significantly lower than those of the negative ones (35.7% versus 68.2%, respectively; P=0.025). Finally, we observed that the CD44v3-expressing tumors were characterized by significantly higher MMP-2 expression than the CD44v3-negative tumors (P<0.001), indicating a possible correlation between CD44v3- and MMP-2-positive phenotype and the organ metastatic potential of MM.

Keywords Malignant melanoma · CD44v3 · MMP-2 · Metastasis · Immunohistochemistry · RT-PCR

J. Tímár (✉)
Department of Tumor Progression, National Institute of Oncology, Ráth Gy. u.7-9., 1122 Hungary
e-mail: jtimar@oncol.hu
Tel.: +36-1-2248786, Fax: +36-1-2248620

B. Döme
First Institute of Pathology and Experimental Cancer Research, Semmelweis University of Medicine, Budapest

B. Somlai
Department of Dermato-Venerology, Semmelweis University, Budapest

A. Ladányi · K. Fazekas
Department of Tumor Progression, National Institute of Oncology, Budapest, Hungary

M. Zöller
Department of Tumor Progression and Immune Defense, German Cancer Research Center, Heidelberg, Germany

Introduction

Tumor metastasis is a cascade of events characterized by proliferative and non-proliferative elements. The latter includes tumor cell matrix interactions (adhesion, degradation, and migration) [33, 34], tumor-induced angiogenesis [22], intra- and extravasation, and immunological interactions. The biological behavior of malignant melanoma (MM) of the skin is heterogeneous, and the best prognostic factor predicting its behavior is still the thickness of the primary tumor. Other features, such as proliferation [2], did not prove to be sensitive enough to predict more precisely the prognosis of the disease. Today, tumor-induced angiogenesis is considered a key determinant of tumor progression. However, in the case of cutaneous MM, there are not enough convincing data to support the positive correlation of angiogenic activity and the progression of the disease [3, 27]. Among the adhesion molecules, only β3 integrin has been conclusively shown to be upregulated in MM [5]. Concerning the matrix-degrading enzymes, both MMP-2 and MMP-9 expressions are detectable in the early stage of melanocytic tumors. Only MMP-2 expression increases with melanoma progression [15, 40, 41], while MMP-9 expression is lost in the vertical growth phase and in metastases [15, 26]. Also, expression of other members of the matrix-

degrading enzyme family, such as uPA [24] or cathepsins [18], could be detected in MM, the clinical significance of which needs further evaluation.

CD44 is a group of heterogeneous cell surface molecules encoded by a single gene but generated by alternative splicing and post-translational modifications. The v6 splice variant was the first metastasis-promoting protein identified and, in certain cases, the expression of this variant was associated with metastatic potential [12]. Studies of CD44 expression in MM have frequently produced controversial results, sometimes indicating even a decreased CD44H expression in metastases [6, 9, 13, 29, 31, 32]. Several splice variants of CD44 (such as v5, v7, v8, and v10) have been reported to be expressed by MM [23, 30, 31], while the expression of others, such as the metastasis-associated form, v6, has been missing [9, 23, 31]. A shift of the expression of v10 to v5 splice variant of CD44 in metastatic MM has been observed in three independent studies [23, 30, 31]. However, expression of the only growth factor binding variant, CD44v3 [16], has not yet been conclusively documented in human melanoma.

More recently, CD44 has been implicated in the regulation of both MMP-2 [35] and MMP-9 [44] expression in human melanoma cells, which suggests a fundamental role for CD44 in regulating the invasive phenotype. Based on these data, we decided to analyze the expression of CD44v3 at the protein and messenger (m)RNA level in human melanoma.

Materials and methods

Patients and tumors

Primary and metastatic melanoma specimens of patients at the Department of Dermatology, Semmelweis University of Medicine, Budapest, were routinely examined for diagnosis. Samples were fixed in 4% buffered formaldehyde and embedded in paraffin. Following diagnostic procedures, the marker expression was evaluated in 5-µm-thick sections of paraffin blocks of 50 primary cutaneous melanomas. Patients were clinically followed until their fatal outcome or for a minimum of 61 months, including as a special aspect, the metastasis-free period. Four patients were not included in the study because of the shorter follow-up time. For diagnostic purposes, tumor thickness and tumor type were determined. The depth of invasion according to Clark ranged from level II to level V (data not shown), and the Breslow index varied between 0.5 mm and 10.0 mm (Table 1). Patients were treated by means of surgery and, in two cases, they were treated by means of chemotherapy [dacarbazine (DTIC)] as well.

Immunohistochemistry

For immunohistochemistry, paraffin sections were mounted onto Superfrost+ slides, deparaffinized, and an antigen retrieval technique was applied using microwave exposure [19]. Endogenous peroxidase activity was blocked with 3% H_2O_2 in methanol, and non-specific binding sites were blocked with 20% rabbit or goat serum. The primary antibodies, diluted in phosphate-buffered saline (PBS), pH 7.5 were applied to the slides for 60 min at 37°C. The CD44v3 domain was detected using a mouse monoclonal anti-CD44v3 antibody (R&D, Abingdon, UK; diluted 1:100). MMP-2 collagenase was detected with a rabbit anti-MMP-2-peptide antibody (Research Genetics, Huntsville, Ala.; diluted 1:100) [38]. The slides were washed in PBS, and biotinylated rabbit anti-mouse immunoglobulin IgG (Amersham, Little Chalfont, UK; diluted 1:100) or biotinylated goat anti-rabbit IgG (Amersham; diluted 1:100) was applied as secondary antibody. After washings with PBS, the slides were incubated in streptavidin–peroxidase complex solution (Amersham; diluted 1:200). Samples were then washed again, and the antibody reactions were visualized using 3-amino-9-ethylcarbazole (AEC, Shandon, Nottingham, UK).

After counterstaining with hematoxylin, the immunoreaction was quantified at three areas of each tumor by two independent observers, who determined the percentage of positive tumor cells by counting 100 cells per field. Data were analyzed using analysis of variance (ANOVA) single factor method. We also determined the expression as percentage of positive cells. Due to the rare and low incidence of CD44v3 expression, all positive tumors were considered as high expressors.

Tumor cell lines and culture conditions

The HT168 and HT168-M1 melanoma lines [21, 37] are derivatives of the A2058 cell line [39]. The HT199 line was established from a primary melanoma in our laboratory [20]. The WM983A, WM983B, and WM35 melanoma lines were kindly provided by M. Herlyn (Wistar Institute, Philadelphia, Penn.) [14]. The cell lines were maintained in vitro in RPMI 1640 medium (Sigma, St. Louis, Mo.) supplemented with 5% fetal calf serum (Sigma), 0.1 mM non-essential amino acids, 1 mM sodium pyruvate, and 50 mg/ml gentamycin sulfate (all from Gibco BRL, Life Technologies, Paisley, Scotland) at 37°C in a 5% CO_2 atmosphere.

Flow cytometry of the expression of CD44

The anti-human CD44H (IgG2a), anti-human CD44v3 (IgG2b), and anti-human CD44v6 (IgG1) monoclonal antibodies [11] were purchased from R&D Systems, and used at a concentration of 10 µg/ml. Isotype control IgGs were from Sigma and were applied at the same concentration.

Cells were detached from plastic using 0.02% ethylene diamine tetraacetic acid (EDTA; Sigma), washed, and fixed in 4% paraformaldehyde (surface staining) or, following fixation, were permeabilized in 0.1% saponin (cellular labeling). Non-specific protein binding sites were blocked by incubation for 20 min in 1% bovine serum albumin (BSA)/PBS (Sigma), then 2×10^5 cells per sample were incubated with the primary antibodies for 45 min at room temperature and washed three times in PBS. Fluorescein isothiocyanate-conjugated goat anti-mouse IgG (Amersham) was used as a secondary antibody at a dilution of 1:100 for 45 min on ice, followed by washing three times in PBS. The cells were then analyzed on a FACStar flow cytometer (Becton Dickinson, Sunnyvale, Calif.). Cells were considered positive when the fluorescence intensity was above that of 99% of the control cells labeled with the appropriate isotype control Ig.

PCR analysis of reverse transcribed CD44 mRNAs

Primer sequences used in this study had been previously published [43]. Single cell suspension was prepared from cultured WM35 and HT168 human melanoma cell lines. 10^6 cells were lysed in guanidin isothiocyanate buffer (80% guanidin isothiocyanate, 0.045 M Na-citrate, 0.9% Na-lauryl-sarcosinate, and 0.001% mercaptoethanol). Nucleic acid was extracted from the lysate using a phenol:chloroform:isoamylalcohol (25:24:1) mixture and isopropanol. Total cellular RNA (1 g) was subjected to reverse transcription under the following conditions: MuLV reverse transcriptase (Promega, Madison, Wis.) 2.5 U/l, 5 mM $MgCl_2$, dGTP, dATP, dCTP, dTTP 1 mM each, oligo $d(T)_{16}$ 2.5 M, RNase inhibitor (MBI Fermentas, Sacramento, Calif.) 1 U/l, 1× RT buffer (Promega). CD44 complementary (c)DNA (5 µl) was amplified using the 5′ primer of the standard CD44 (CD44H) cDNA and the variant exon-specific 3′ primers under the following conditions: 35 cycles

Table 1 Clinical data of patients with primary malignant melanoma. *LN* lymph node metastasis, *V* visceral metastasis, *E* exitus letalis within 60 months, *SSM* superficial spreading melanoma, *NM* nodular melanoma, *ALM* acral lentiginous melanoma

Case no.	Gender	Thickness (mm)	Type	Metastasis onset (months)	Survival (months)
1	Female	0.5	SSM		124
2	Female	0.6	SSM		63
3	Female	0.6	SSM	LN	149
4	Male	0.6	SSM		66
5	Male	0.85	SSM		173
6	Female	1	SSM	LN	89
7	Male	1	SSM		144
8	Male	1.2	SSM	LN	136
9	Male	1.3	SSM		65
10	Male	0.75	SSM		66
11	Female	0.75	SSM		96
12	Female	0.9	SSM		97
13	Female	1.6	SSM		63
14	Male	1.6	AM	LN	E
15	Male	1.7	SSM	LN+V	E
16	Male	1.8	SSM		62
17	Male	1.8	SSM	LN+V	E
18	Female	2.2	SSM	LN+V	E
19	Male	2.3	SSM	LN+V	E
20	Female	2.8	NM	LN	89
21	Male	2.9	SSM		62
22	Male	3	NM	LN+V	E
23	Male	3	NM	LN	61
24	Female	3	SSM	LN+V	E
25	Male	3.1	NM	LN+V	E
26	Female	3.2	NM	LNV	60
27	Male	3.2	SSM	LN	67
28	Female	3.6	NM	LN+V	E
29	Female	3.6	NM	LN+V	E
30	Female	3.6	NM	LN	57
31	Female	3.6	NM	LN+V	E
32	Female	3.7	SSM		144
33	Male	3.8	SSM		83
34	Female	4	NM	LN+V	E
35	Female	4.1	ALM	LN	74
36	Male	4.3	NM	LN	76
37	Female	4.5	NM	LN	102
38	Male	4.7	SSM	LN+V	E
39	Male	5.0	SSM	LN+V	E
40	Female	5.2	NM	LN	89
41	Female	6	SSM		54
42	Male	6	NM	LN+V	E
43	Male	6.9	NM	LN+V	E
44	Female	8	NM	LN+V	E
45	Female	9.9	NM	LN+V	E
46	Male	10.0	NM	LN+V	E

(94°C for 30 s, 65°C for 30 s, 72°C for 2 min), 1 U *Taq* polimerase, 0.2 M of each primer, 250 M deoxynucleotide triphosphate (dNTP) mixture, and 1.5 mM Mg^{2+} in a Perkin Elmer GeneAmp PCT system 2400 thermocycler. PCR products were electrophoresed in 1.2% agarose gel supplemented with ethidium bromide.

Statistical analysis

Experimental data were evaluated using either ANOVA single factor analysis, $\chi 2$ test, or Mantel-Cox generalized savage method.

Results

Primary skin melanoma

The 46 skin melanoma cases were heterogeneous regarding the age and gender of the patients, the thickness, and the biological behavior of the tumor (Table 1). The invasive potential of the tumors varied from non-metastatic through regional or distant lymph-node metastatic to visceral-metastatic cases. Local skin recurrence was not considered metastasis. Visceral metastasis was defined as clinical detection of metastasis at least in one of the following organs; lung, liver, brain, bone, spleen, intestine, pancreas, adrenal gland, or heart.

Immunohistochemical labeling of the paraffin sections of the primary skin tumors for CD44v3 was performed. Epithelial cells of the skin constitutively expressing CD44v3 served as an inner positive control throughout the study (Fig. 1a). Immunohistochemical positivity for CD44v3 was defined when more than 1% of melanoma cells were found to be reactive. CD44v3 was rarely expressed by the primary MMs and, when it

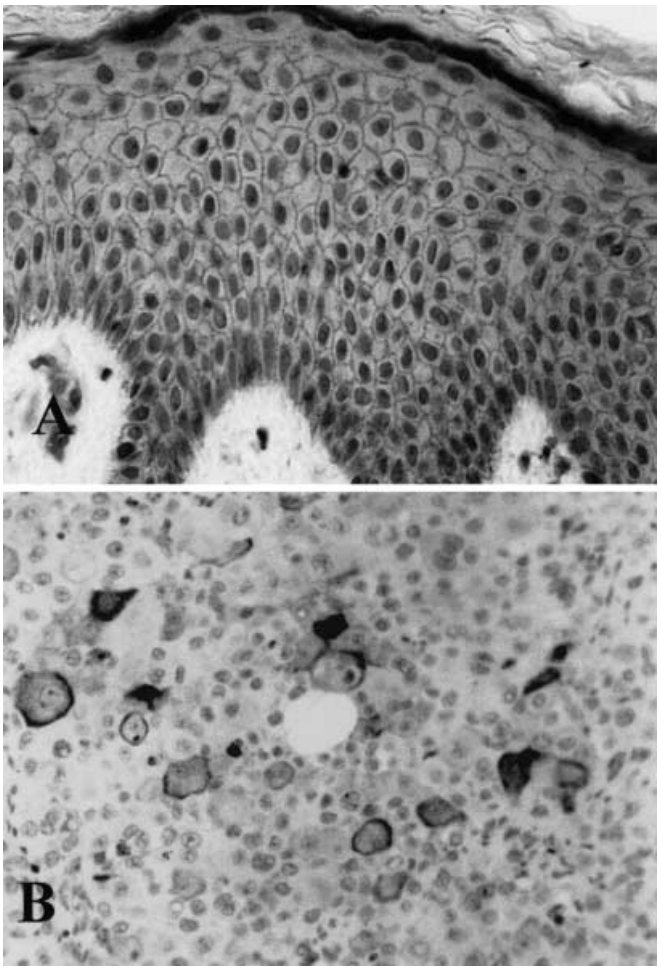


Fig. 1 Immunohistochemical labeling of CD44v3 in human skin. **A** Epithelial cells exhibit constitutive expression of v3 at the cell surface (200×). **B** CD44v3 staining of primary melanoma (case no. 16). Note the scattered positive cells in a tumor nodule (300×)

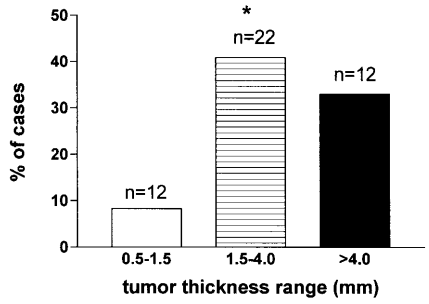


Fig. 2 Expression of CD44v3 in human malignant melanomas in relation to the thickness of the primary. *P<0.05 (χ^2 test)

was expressed, it was only present in a small proportion of tumor cells (3–35%), localized to the periphery of the cytoplasm or to the plasma membrane (Fig. 1b). Due to the relatively low percentage of CD44v3+ melanoma cells, we have categorized the cases as positive or negative irrespective of the intensity of the immunoreactions.

First, we compared the immunohistochemical expression of CD44v3 to the thickness of the tumors, where we used thin (<1.5 mm; n=12), medium thick (1.5–4.0 mm; n=22), and thick (>4.0 mm; n=12) tumor categories. CD44v3-positive tumors occurred only in tumors thicker than 1.0 mm and was accidental in the thinnest group (<1.5 mm) but significantly increased in the medium thick and thick tumor categories (Fig. 2). These data indicated a weak association between CD44v3 positivity of MM and tumor thickness.

In the following, samples were re-grouped according to the metastatic behavior of the tumors (non-metastatic, n=15; lymph-node metastatic, n=10; and visceral + lymph-node metastatic tumors, n=21). The minimum follow-up period of patients was 61 months. Lymph-node metastases were detected not later than 58 months, while organ metastases were diagnosed not later than 60 months following the removal of the primary tumor. The thickness of the tumors increased gradually with the more advanced stage of the disease as expected, and all of the cases of fatal outcome occurred in the organ metastatic group (Table 1.).

The immunohistochemical expression of CD44v3 was not detected in the non-metastatic and lymph-node metastatic tumors (except one case), but it was significantly prevalent (P<0.05 and 0.01, respectively) in the organ metastatic tumor group (Table 2). Previous studies indicated an association of MMP-2 expression to melanoma progression. Therefore, we have also analyzed the percent of MMP-2-expressing tumor cells in MM of various clinical categories. The immunohistochemical expression level of MMP-2 was similar in the non-metastatic and lymph-node metastatic tumor group but proved to be significantly higher in the organ metastatic group (P<0.05, P<0.001, respectively; Table 2).

Since the immunohistochemical expression of CD44v3 was detectable only in tumors thicker than 1.0 mm, we analyzed the 5-year survival of these stage-II melanoma patients and the influence of CD44v3 expression. Analysis of the survival of 38 patients revealed that the CD44v3-positive patient group is associated with a significantly poorer survival rate than the group of negative patients (35.7% vs 68.2%; P=0.025, Fig. 3). Finally, we compared the MMP-2 expression levels of the same stage-II MMs having a different CD44v3 phenotype (+/–). The analysis indicated that the CD44v3+ phenotype of skin melanoma was associated with a significantly higher MMP-2 expression level too (P=0.0013, Fig. 3).

Human melanoma cell lines

Immunohistochemical analysis of CD44v3 only reflects the presence of an extracellular antigenic domain in biopsy samples. Therefore, we attempted to prove the expression of the authentic gene using human melanoma cell lines, since mRNA isolation from the biopsy sample could be very misleading due to the constitutive expression of CD44v3 in the human skin epithelia. Flow cytometry, using the same antibody used for the clinical

Table 2 Comparison of CD44v3 and MMP-2 phenotype of malignant melanoma (MM). Progression categories were based on the minimal 61-month follow-up period of patients, except for those who died previously. Locoregional lymph node (LN) metastases developed no later than 58 months, and visceral metastases developed no later than 60 months. Data are expressed as incidence of positive tumors (CD44v3) or as mean percentage of positive tumor cells±SEM (MMP-2). Statistical analysis was performed using the χ^2 test (incidence) or analysis of variance (ANOVA) single factor analysis

Progression category	CD44v3 (percentage positive cells)	MMP-2 (percentage positive cells)
Non-metastatic	0	6
	0	92
	0	9
	0	97
	0	0
	0	9
	0	13
	7	100
	0	7
	0	0
	0	59
	0	0
	0	0
	0	0
	0	0
n=15	1/15	26.13±10.12
LN-metastatic	0	0
	0	59
	0	17
	0	80
	0	9
	0	0
	0	18
	0	21
	0	38
	0	83
n=10	0/10	32.50±9.88
Visceral metastatic	4	78
	0	81
	0	6
	0	100
	0	78
	0	9
	8	86
	3	60
	12	100
	16	88
	3	0
	0	11
	21	83
	0	0
	35	55
	15	70
	27	65
	24	56
	27	77
	15	58
	14	100
n=21	14/21[a, b]	60.05±7.47[c, d]

[a] $P<0.01$ (relative to LN-metastatic group)
[b] $P<0.05$ (relative to the non-metastatic group)
[c] $P<0.05$ (relative to LN-metastatic group)
[d] $P<0.01$ (relative to non-metastatic group)

Table 3 Immunocytochemical expression of CD44v3 in human melanoma cell lines (flow cytometry). Data are expressed as percentage of positive cells. In vitro cultured cell lines were detached from plastic surfaces, fixed in paraformaldehyde (surface expression) and permeabilized with saponin to detect cellular expression. A minimum of 10^4 cells were measured from each cell population, where 99% of the negative control population served to gate out the unstained cells. *n.t.* not tested

Cell lines	CD44v3 – cellular	CD44v3 – cell surface
A431 carcinoma (positive control)	75	n.t.
WM35	90	54
WM983B	85	16
HT168	n.t.	24
HT168M1/9	81	11
HT199	61	17

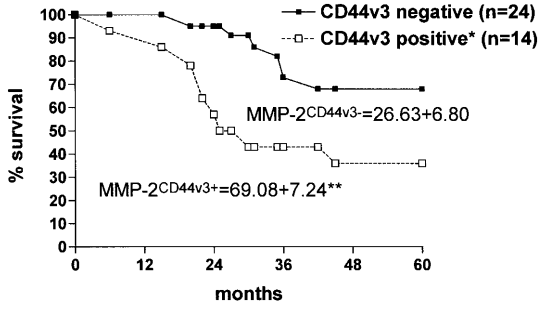


Fig. 3 Survival analysis of stage-II malignant melanoma (MM) patients in relation to the CD44v3 expression. Five-year survival was analyzed in 36 patients grouped according to the positivity (*n*=14) or negativity (*n*=22) of their tumors for CD44v3. Statistical analysis was performed using Mantel-Cox generalized savage analysis; *$P<0.025$. Note that the MMP-2 expression level (% of positive cells in the individual tumors, mean±SEM) is also significantly different between the two patient groups (**$P<0.025$; analysis of variance single factor analysis)

studies, indicated that all of the studied cell lines express cytoplasmic CD44v3 protein in the majority of the cell population (61–90%), and the adhesion molecule is also present at the cell surface to a variable extent (11–54%; Table 3). These studies also indicated that, other than CD44v3, the standard isoform, CD44H, is also strongly expressed in the cytoplasm and at the cell surface of all of the studied cell lines (data not shown).

The CD44 mRNA exon pattern of two human melanoma cell lines, WM35 and HT168, was analyzed using reverse transcriptase polymerase chain reaction (RT-PCR) analysis (Fig. 4). It is important to mention that in our setup, besides the particular exon, we could also identify the downstream positioned additional exons of CD44 (i.e., the expression of exon combinations if any). In the case of the WM35 human melanoma cell line, we demonstrated the expression of each variable exon (2–10), including v3 (and v6), but only v2, 4, 5, 7, 8, 9, and 10 occurred in combinations (Fig. 4, Table 4 a). In the case of HT168 human melanoma cell line, a more restricted exon expression pattern was detected (v3, 6, 7, and 8), where again, v3 (and v6) did not occur in combi-

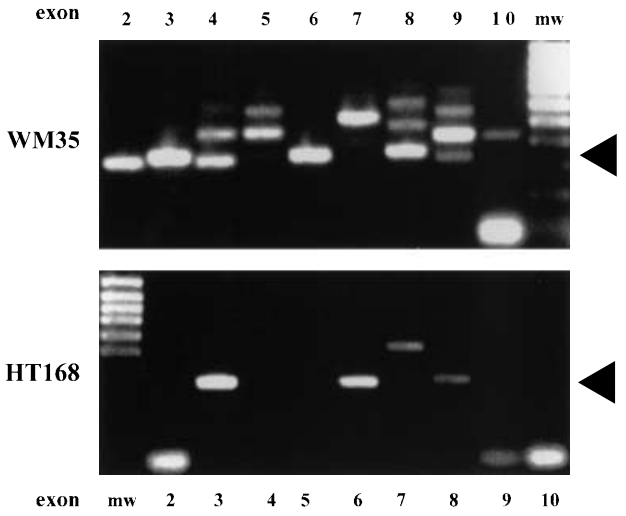


Fig. 4 Reverse transcriptase polymerase chain reaction (RT-PCR) detection of CD44 message in two human melanoma cell lines, WM35 and HT168. Agarose gel electrophoretic analysis of CD44 RT-PCR products. For each amplification, the 5′ primer was the standard sequence of CD44. The 3′ primers were from exons 2, 3, 4, 5, 6, 7, 8, 9, and 10. The standard is the 100-bp DNA ladder. A 150-bp band corresponds to a PCR product containing one additional exon to the standard CD44 (*arrow*), a 300-bp band corresponds to a PCR product containing two additional exons, and a 450-bp band corresponds to a PCR product containing three additional exons. Note the positive signal in the case of using the 3′ primer of exon3 in both tumor cell lines. See Table 4 and Table 5 for an explanation of exon patterns

Table 4 Analysis of CD44 exon pattern of the complementary (c)DNA of WM35 human melanoma cell lines on the basis of Fig. 4

	Exon combinations							
	Single	e2–3	e2–4	e2–5	e2–6	e2–7	e2–8	e2–9
Exon 2	+							
Exon 3	+	0						
Exon 4	+	2						
Exon 5	+		2					
Exon 6	+			0				
Exon 7	+				1			
Exon 8	+					2		
Exon 9	+						2	
Exon 10	+							1

Table 5 Analysis of CD44 exon pattern of the complementary (c)DNA of HT168 human melanoma cell lines on the basis of Fig. 4

	Exon combinations							
	Single	2–3	2–4	2–5	2–6	2–7	2–8	2–9
Exon 2	–							
Exon 3	+	0						
Exon 4	–							
Exon 5	–							
Exon 6	+			0				
Exon 7	+				2			
Exon 8	+					0		
Exon 9	–							
Exon 10	–							

nations (Fig. 4, Table 5). These data let us conclude that human melanoma expresses CD44v3 at the mRNA and protein level both in vitro and in vivo.

Discussion

There is no doubt that the best prognosticator of the outcome of skin melanoma is still the thickness of the primary tumor. Therefore, identification of geno- or phenotypic markers that could be responsible for the metastatic behavior have great clinicopathologic significance. In contrast to the initial expectations, oncogene expression or proliferation-related markers proved to be insufficient as prognostic markers [2].

Analysis of the expression of metastasis-associated gene products produced controversial results. A typical example is the expression of NM23 metastasis suppressor gene in skin MMs and their metastases. Analysis of the NM23 gene expression at the mRNA level showed decreased expression in the metastases [4, 10]. However, analysis of the NM23 protein gave more controversial results [7, 8, 17, 25, 28].

Data on the expression of the metastasis gene CD44 in MM of the skin is also controversial. A decreased expression of the standard isoform (CD44H) has been reported to correlate with the metastatic potential [13]. Studies on the expression of the CD44 splice variants in MM demonstrated the presence of v5, 7, 8, and 10 without a clear correlation to the biological behavior [23, 31]. In this study, we show for the first time the protein expression of CD44v3 in the MM of the skin using immunohistochemistry. Previous studies attempted to detect the v3 splice variant in MM without much success. We not only used a different monoclonal antibody compared with the previous studies, but we also applied a powerful antigen retrieval technique [19]. As an internal control, skin epithelial cells, constitutively expressing CD44v3 were used [30]. To confirm our observation made on archival materials, we analyzed the CD44v3 expression in human melanoma cell lines as well. All of the six human melanoma cell lines expressed v3 protein epitope both intracellularly and, to a lower extent, at the cell surface. More importantly, RT-PCR analysis of mRNA isolated from two representative cell lines (HT168 and WM35) confirmed the expression of exon 3 without combination with other exons.

The expression level of the CD44v3 splice variant was low in MM, ranging between 3% and 35% of the tumor cell populations. CD44v3 appeared in melanomas thicker than 1 mm and characterized one-third of these tumors. The induction of the expression of CD44v3 in primary MM seems to have biological significance, since 14 out of 15 positive tumors produced organ metastases. The association of CD44v3 expression with the metastatic behavior was further supported by our observation that the expression was induced in the corresponding regional lymph-node metastases of CD44v3-negative primary tumors (3 of 4 cases; data not shown). Furthermore, the

5-year survival of stage-II melanoma patients (n=38) with CD44v3+ tumors proved to be significantly poorer than those of the negative cases.

What could be the function of CD44v3 on the surface of melanoma cells? Since the v3 splice variant is the only CD44 isoform able to bind heparin-binding growth factors and cytokines through heparan sulfate side chains [1, 36, 42], cells expressing the v3 variant have a better chance to accumulate matrix-bound growth factors upon arrival to a new matrix or organ environment and to improve the chance for survival and growth.

The matrix-degrading potential of invasive tumors is another key determinant of the invasive phenotype, and matrix metalloproteinases are major contributors to this process. Our observations could help to understand the development of the metastatic phenotype of MM. It seems that the generation of the MMP-2-positive phenotype takes place at an earlier phase of melanoma genesis [15, 40, 41]. However, it is not a universal phenomenon since only half of the tumors used in our study are characterized by high MMP-2 expression. The expression of MMP-2 was frequently reported as an independent prognosticator in cutaneous MM [15, 40, 41]. These observations were confirmed in this study as well; we showed a significant increase of MMP-2 expression in the visceral metastatic tumors. It is interesting in this respect, that although a smaller proportion of MM expresses CD44v3, these tumors are characterized by a significantly higher MMP-2 expression. The recent findings on the cross talk between CD44 and MMPs [35,44] in tumor invasion further suggest a non-accidental correlation between CD44 and MMP-2 expressions in human melanoma.

Because in our study only one-half of organ metastatic MMs expressed CD44v3, it is obvious that other invasion/metastasis-associated gene products are also involved in shaping the aggressive phenotype of MM, such as motility factors and their receptors, which also have to be tested on clinical samples to improve the progression-predicting potential of the currently available markers.

Acknowledgements This work was supported by the Ministry of Welfare (ETT 445/2000, J.T., and a core grant from the Semmelweis Medical University (J.T.). The authors appreciate the excellent technical help of J. Bocsi, PhD, and A. Tamássy (First Institute of Pathology and Experimental Cancer Research, Semmelweis University of Medicine, Budapest) throughout the study.

References

1. Bennett KL, Jackson DG, Simon JC, Tanczos E, Peach R, Modrell B, Stamenkovic I, Plowman G, Aruffo A (1995) CD44 isoforms containing exon V3 are responsible for the presentation of heparin-binding growth factor. J Cell Biol 128:687–698
2. Bishop NJA (1997) Molecular pathology of melanoma. Cancer Metastasis Rev 16:141–154
3. Busam KJ, Berwick M, Blessing K, Fandrey K, Kang S, Karaoli T, Fine J, Cochran AJ, White WL, Rivers J, et al (1995) Tumor vascularity is not a prognostic factor for malignant melanoma of the skin. Am J Pathol 147:1049–1056
4. Caligo MA, Grammatico P, Cipollini G, Varesco L, Del Porto G, Bevilacqua G (1994) A low NM23.H1 gene expression identifying high malignancy human melanomas. Melanoma Res 4:179–184
5. De Wit PE, Van Muijen GN, De Waal RM, Ruiter DJ (1996) Pathology of malignant melanoma, including new markers and techniques in diagnosis and prognosis. Curr Opin Oncol 8: 143–151
6. Dietrich A, Tanczos E, Vanscheidt W, Schopf E, Simon JC (1997) The cell surface glycoprotein CD44 has been implicated in the progression and metastasis of certain human tumours including malignant melanoma (MM). Eur J Cancer 33:926–930
7. Dome B, Somlai B, Timar J (2000) The loss of NM23 protein in malignant melanoma predicts lymphatic spread without affecting survival. Anticancer Res 20:3971–3974
8. Easty DJ, Maung K, Lascu I, Veron M, Fallowfield ME, Hart IR, Bennett DC (1996) Expression of NM23 in human melanoma progression and metastasis. Br J Cancer 74:109–114
9. Fernandez-Figueras MT, Ariza A, Calatrava A, Puig L, Fernandez-Vasalo A, Ferrandiz C (1996) CD44 and melanocytic tumors: a possible role for standard CD44 in the epidermotropic spread of melanoma J Cutan Pathol 23:133–139
10. Florenes VA, Aamdal S, Myklebost O, Maelandsmo GM, Bruland OS, Fodstad O (1992) Levels of nm23 messenger RNA in metastatic malignant melanomas: inverse correlation to disease progression. Cancer Res 52:6088–6091
11. Fox SB, Fawcett J, Jackson DG, Collins I, Gatter KC, Harris AL, Gearing A, Simmons DL (1994) Normal human tissues, in addition to some tumors, express multiple different CD44 isoforms. Cancer Res 54:4539–4546
12. Gunthert U, Hofmann M, Rudy W, Reber S, Zoller M, Haussmann I, Matzku S, Wenzel A, Ponta H, Herrlich P (1991) A new variant of glycoprotein CD44 confers metastatic potential to rat carcinoma cells. Cell 65:13–24
13. Harwood CA, Green MA, Cook MG (1996) CD44 expression in melanocytic lesions: a marker of malignant progression? Br J Dermatol 135:876–882
14. Herlyn M (1990) Human melanoma: development and progression. Cancer Metastasis Rev 9:101–112
15. Hofmann UB, Westphal JR, Van Muijen GN, Ruiter DJ (2000) Matrix metalloproteinases in human melanoma. J Invest Dermatol 115:337–344
16. Jackson DG, Bell JI, Dickinson R, Timans J, Shields J, Whittle N (1995) Proteoglycan forms of the lymphocyte homing receptor CD44 are alternatively spliced variants containing the v3 exon. J Cell Biol 128:673–685
17. Kanitakis J, Euvrard S, Bourchany D, Faure M, Claudy A (1997) Expression of the nm23 metastasis-suppressor gene product in skin tumors. J Cutan Pathol 24:151–156
18. Kos J, Stabuc B, Schweiger A, Krasovec M, Cimerman N, Kopitar-Jerala N, Vrhovec I (1997) Cathepsins B, H, and L and their inhibitors stefin A and cystatin C in sera of melanoma patients. Clin Cancer Res 3:1815–1822
19. Kovacs L, Szende B, Elek G, Lapis K, Horvath O, Hiszek I, Tamasi A, Schmidt O (1996) Working experience with a new vacuum-accelerated microwave histoprocessor. J Pathol 180: 106–110
20. Ladanyi A, Timar J, Bocsi J, Tovari J, Lapis K (1995) Sex-dependent liver metastasis of human melanoma lines in SCID mice. Melanoma Res 5:83–86
21. Ladanyi A, Timar J, Paku S, Molnar G, Lapis K (1990) Selection and characterization of human melanoma lines with different liver-colonizing capacity. Int J Cancer 46:456–461
22. Liotta LA, Steeg PS, Stetler-Stevenson (1991) Cancer metastasis and angiogenesis: an imbalance of positive and negative regulation. Cell 64:327–336
23. Manten-Horst E, Danen EH, Smit L, Snoek M, Le Poole IC, Van Muijen GN, Pals ST, Ruiter DJ (1995) Expression of CD44 splice variants in human cutaneous melanoma and melanoma cell lines is related to tumor progression and metastatic potential. Int J Cancer 64:182–188

24. Montgomery AM, De Clerck YA, Langley KE, Reisfeld RA, Mueller BM (1993) Melanoma-mediated dissolution of extracellular matrix: contribution of urokinase-dependent and metalloproteinase-dependent proteolytic pathways. Cancer Res 53:693–700
25. van den Oord JJ, Maes A, Stas M, Nuyts J, De Wever I, De Wolf-Peeters C (1997) Prognostic significance of nm23 protein expression in malignant melanoma. An immunohistochemical study. Melanoma Res 7:121–128
26. van den Oord JJ, Paemen L, Opdenakker G, de Wolf-Peeters C (1997) Expression of gelatinase B and the extracellular matrix metalloproteinase inducer EMMPRIN in benign and malignant pigment cell lesions of the skin. Am J Pathol 151:665–670
27. Rongioletti F, Miracco C, Gambini C, Pastorino A, Tosi P, Rebora A (1996) Tumor vascularity as a prognostic indicator in intermediate-thickness (0.76–4 mm) cutaneous melanoma. A quantitative assay. Am J Dermatopathol 18:474–477
28. Reichrath J, Seyfried P, Braun R, Muller SM, Baum HP, Bahmer FA (1997) Expression of NM23 protein in acquired melanocytic nevi, malignant melanoma and metastases of malignant melanoma: an immunohistological assessment in human skin. Dermatology 194:136–139
29. Schaider H, Soyer HP, Heider KH, Hofmann-Wellenhof R, Zatloukal K, Smolle J, Kerl H (1998) CD44 and variants in melanocytic skin neoplasms. J Cutan Pathol 25:199–203
30. Seelentag WK, Gunthert U, Saremaslani P, Futo E, Pfaltz M, Heitz PU, Roth J (1996) CD44 standard and variant isoform expression in normal human skin appendages and epidermis. Histochem Cell Biol 106:283–289
31. Seiter S, Schadendorf D, Herrmann K, Schneider M, Rosel M, Arch R, Tilgen W, Zoller M (1996) Expression of CD44 variant isoforms in malignant melanoma. Clin Cancer Res 2: 447–456
32. Simon JC, Heider KH, Dietrich A, Wuttig C, Schopf E, Adolf GR, Ponta H, Herrlich P (1996) Expression of CD44 isoforms in human skin cancer. Eur J Cancer 32A:1394–1400
33. Starkey JR (1990) Cell-matrix interactions during tumor invasion. Cancer Metastasis Rev 9:113–123
34. Stetler-Stevenson WG, Liotta LA, Kleiner DE Jr (1993) Extracellular matrix 6: role of matrix metalloproteinases in tumor invasion and metastasis. FASEB J 7:1434–1441
35. Takahashi K, Eto H, Tanabe KK (1999) Involvement of CD44 in matrix metalloproteinase-2 regulation in human melanoma cells. Int J Cancer 80:387–395
36. Tanaka Y, Adams DH, Hubscher S, Hirano H, Siebenlist U, Shaw S (1993) T-cell adhesion induced by proteoglycan-immobilized cytokine MIP-1 beta. Nature 361:79–82
37. Timar J, Kovalszky I, Paku S, Lapis K, Kopper L (1989) Two human melanoma xenografts with different metastatic capacity and glycosaminoglycan pattern. J Cancer Res Clin Oncol 115: 554–557
38. Timar J, Tovari J, Pogany G, Ladanyi A, Paku S, Rso E, Bocsi J, Jeney A, Lapis K (1996) The antimetabolite Tiazofurin (TR) inhibits glycoconjugate biosynthesis and invasiveness of tumour cells. Eur J Cancer 32A:152–159
39. Todaro GJ, Fryling C, De Larco JE (1980) Transforming growth factors produced by certain human tumor cells: polypeptides that interact with epidermal growth factor receptors. Proc Natl Acad Sci U S A 77:5258–5262
40. Vaisanen A, Tuominen H, Kallioinen M, Turpeenniemi-Hujanen T (1996) Matrix metalloproteinase-2 (72 kD type IV collagenase) expression occurs in the early stage of human melanocytic tumour progression and may have prognostic value. J Pathol 180:283–289
41. Vaisanen A, Kallioinen M, Taskinen PJ, Turpeenniemi-Hujanen T (1998) Prognostic value of MMP-2 immunoreactive protein (72 kD type IV collagenase) in primary skin melanoma. J Pathol 186:51–58
42. Van der Voort R, Taher TE, Wielenga VJ, Spaargaren M, Prevo R, Smit L, David G, Hartmann G, Gherardi E, Pals ST (1999) Heparan sulfate-modified CD44 promotes hepatocyte growth factor/scatter factor-induced signal transduction through the receptor tyrosine kinase c-Met. J Biol Chem 274:6499–6506
43. Woerner SM, Givehchian M, Durst M, Schneider A, Costa S, Melsheimer P, Lacroix J, Zoller M, Doeberitz MK (1995) Expression of CD44 splice variants in normal, dysplastic, and neoplastic cervical epithelium. Clin Cancer Res 1:1125–1132
44. Yu Q, Stamenkovic I (1999) Localization of matrix metalloproteinase 9 to the cell surface provides a mechanism for CD44-mediated tumor invasion. Genes Dev 13:35–48

Virchows Arch (2001) 439:636–639
DOI 10.1007/s004280100449

ORIGINAL ARTICLE

**Véronique Winnepenninckx · Maria Debiec-Rychter
Mark Jorissen · Sophie Bogaerts · Raf Sciot**

Aneurysmal bone cyst of the nose with 17p13 involvement

Received: 27 December 2000 / Accepted: 15 March 2001 / Published online: 16 May 2001
© Springer-Verlag 2001

Abstract We report on a 6-year-old girl with a polypoid mass, filling up the entire right nasal cavity as shown on a magnetic resonance imaging scan. Histologically, the tumor had the characteristics of an aneurysmal bone cyst, which is extremely rare in this location. Cytogenetic analysis disclosed a single (6;17)(p21;p13) translocation, confirming a specific genetic involvement in the development of aneurysmal bone cysts. Fluorescent in situ hybridization analysis mapped the putative gene between the p53 (17p13.1) and the Mieller-Dieker gene (17p13.3) loci.

Keywords Aneurysmal bone cyst · Nose · Cytogenetics · t(6;17)(p21; p13)

Introduction

An aneurysmal bone cyst (ABC) is a benign, often rapidly expanding osteolytic multicystic lesion, first described in 1942 by Jaffe and Lichtenstein [7]. ABC usually affects young patients [2, 8, 9, 14, 16] and is most frequently found in the metaphysial region of long bones and vertebrae [8, 14, 23]. This lesion rarely occurs in the skull (3–6% of cases) [8, 9, 15, 22] and is relatively rarely encountered in the facial bones and jaws [1, 2, 6, 16, 18, 20, 22, 25]. ABC occasionally occurs in soft tissues [9, 13, 19, 21, 24]. Primary nasal (ethmoidal) ABC is extremely rare, with only five cases reported so far [2, 9, 15, 22, 26]. We report on an ABC obstructing the nose of a 6-year-old girl and stress the cytogenetic findings on which there are only limited data in the literature [23].

V. Winnepenninckx · R. Sciot (✉)
University Hospital St-Raphael, Department of Pathology,
Katholieke Universiteit Leuven, Minderbroedersstraat 12,
3000 Leuven, Belgium
e-mail: Raf.Sciot@uz.kuleuven.ac.be
Tel.: +32-16-336593, Fax: +32-16336548

M. Jorissen · S. Bogaerts
Departments of Pathology, Otorhinolaryngology,
University Hospitals, Katholieke Universiteit Leuven, Belgium

M. Debiec-Rychter
Center of Human Genetics, University Hospitals,
Katholieke Universiteit Leuven, Belgium

Clinical history

A 6-year-old girl consulted in February 2000 for a 1-month continuous nasal secretion from the right nostril and a total nasal obstruction at that side. A supratentorial neuroblastoma grade-IV of the right frontal lobe was diagnosed 2 years earlier. Screening for metastatic localizations was negative. The patient was treated with an extensive partial resection followed by chemo- and radiotherapy. The treatment was achieved in February 1999. Afterwards, the evolution seemed clinically and radiologically favorable.

At clinical examination, a polypoid mass was seen in the right nasal cavity, obstructing the nasal passage and deviating the nasal septum to the left.

A magnetic resonance imaging (MRI) scan of the maxillofacial massive showed an expansive polylocular mass filling up the entire right nasal cavity without evidence of connection with the intracranial space (Fig. 1). The nose shelves and the ethmoidal structures were no longer well-defined at that side. The medial wall of the right maxillary sinus and the right lamina papyracea were deviated to the right, and the nasal septum was deviated to the left. Retrograde obstructive inflammation was seen in all right paranasal sinuses. The whole mass was endoscopically resected piece meal under general anesthesia. The swelling seemed to originate from the right lateral nasal wall under the ground lamella of the middle turbinate and had a gray cystic aspect. The girl recovered uneventfully.

Materials and methods

The piece-meal resection specimen was received fresh. The tissue was fixed in 10% buffered formalin and stained with hematoxylin and eosin. Cytogenetic analysis was performed on a 4-day-old culture using collagenase-disaggregated tumor cells, according to the procedure published previously [12]. The karyotype was described using International System for Cytogenetic Nomenclature (ISCN) criteria [10].

For better characterization of the translocation breakpoints, fluorescent in situ hybridization (FISH) was performed on metaphase cells from the tumor specimen following GTG-banding of the same metaphase spreads. The subsequent probe sets were used: biotin-labeled PAC-59-C23 clone [containing the HMGI (Y) gene that maps to 6p21.3 region] [11], together with the Spectrum-

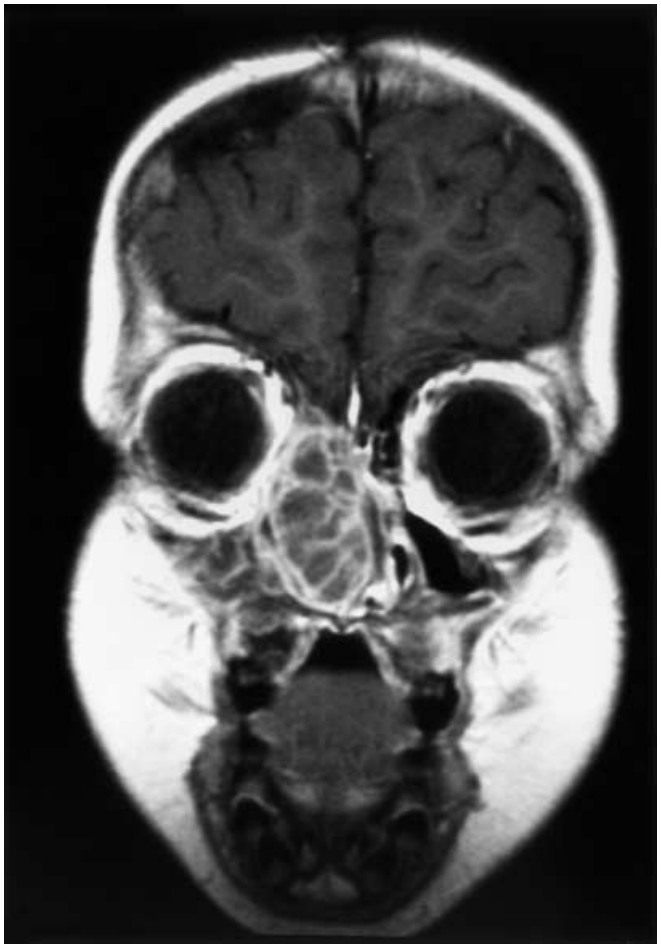


Fig. 1 T1 weighed magnetic resonance imaging (MRI) image, showing the polycular mass in the right nose cavity. Note the post-operative sequelae in the right upper frontal lobe



Fig. 2 Aneurysmal bone cyst showing the characteristic blood-filled channels, bordered by a thin layer of spindle-shaped cells and surrounded by connective tissue containing numerous multi-nucleated giant cells. (Hematoxylin and eosin, ×125)



Fig. 3 Cytogenetic analysis revealing a 46,XX,t(6;17)(p21;p13)/46,XX (*arrowheads*)

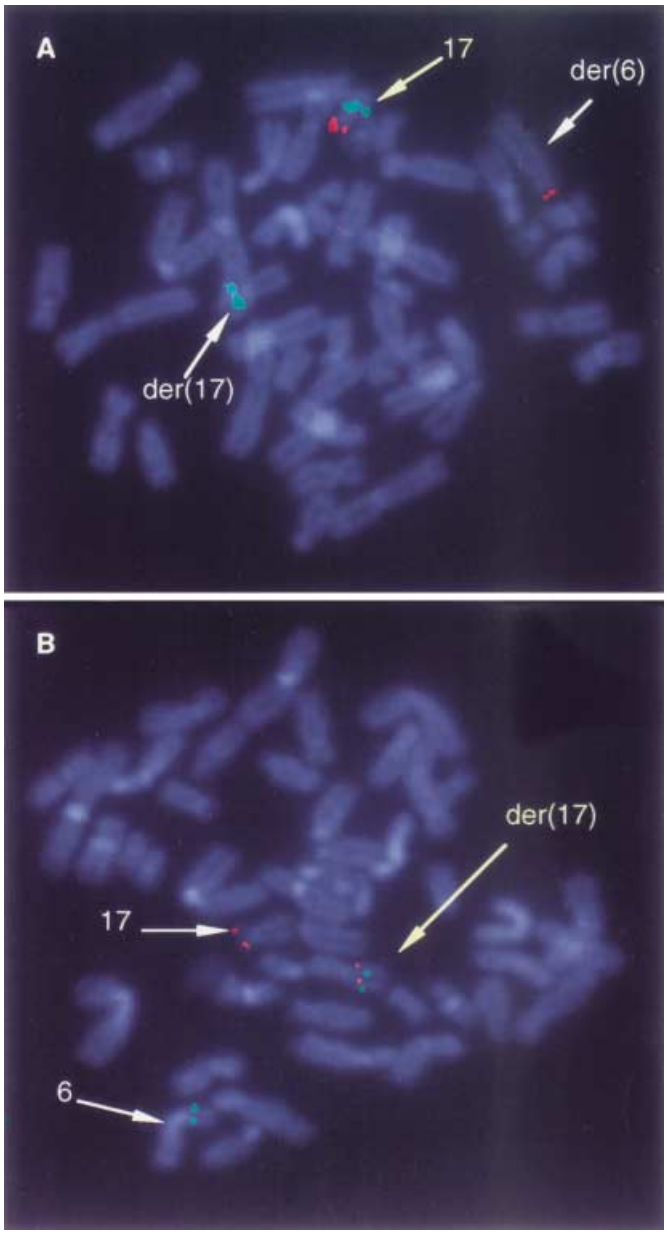


Fig. 4 Fluorescent in situ hybridization analysis of metaphase chromosomes from aneurysmal bone cyst tumor showing t(6;17)(p21;p13) translocation. **A** The mixture of Spectrum Orange-labeled Miller-Dieker (17p13.3) gene-specific probe and a control Spectrum Green-labeled RARA loci (17q11)-specific probe was used for hybridization. The presence of a *red signal* on the der(6) chromosome 17p breakpoint is proximal to the Mieler-Dieker gene loci. **B** The mixture of Spectrum Orange-labeled PAC S9C23 clone that maps to the HMGI(Y) gene (6p21) was used as a probe. The presence of a *red signal* on der(17) chromosome localizes the chromosome 17p breakpoint distally to the p53 gene loci

Orange LSI p53/17p13.1 (Vysis Inc., Stuttgart, Germany) probe and dual-color Spectrum Orange Mieller-Dieker (LIS1 loci; 17p13.3)/Spectrum Green LSI RARA (17q12) probe (Vysis Inc., Stuttgart, Germany).

Hybridization and detection were performed as previously described [5]. Hybridization signals were analyzed using an Axioplan 2 fluorescence microscope equipped with a cooled CCD camera and run using the Cytogen TM System for capture and analysis (Imstar S.A., Paris, France).

Results

Gross examination revealed multiple fragment reddish-brown tissue showing cystic spaces, filled with unclotted viscous material. Histology showed that the lesion was composed of blood-filled anastomosing cavernous vascular spaces, separated by relatively cellular fibrous septa, containing spindle cells, fibroblasts, and multiple osteoclast-like giant cells and a various amount of mineralizing structures, including osteoid-like material and immature bone (Fig. 2).

Deposits of hemosiderin were seen within the stromal matrix. The lesion was focally surrounded by sinus mucosa. Cytogenetic analysis demonstrated a 46,XX,t(6;17)(p21;p13)[8]/46,idem,t(1;5)(p32;q31)[1]/46,XX[9] karyotype in 18 metaphases analyzed from the tumor specimen (Fig. 3). Using FISH analysis using PAC-59-C23, the signal was present on normal chromosome 6 and derivative chromosome 17, indicating that the chromosome 6 breakpoint was proximal to the HMGI(Y) gene. Using LSI p53 (17p13.1) and LSI Mieller-Dieker/LSI1 (17p13.3) probes, FISH revealed signals on both normal and derivative chromosomes 17 in the former and on the normal chromosome 17 and derivative chromosome 6 in the later hybridization (Fig. 4). These results allowed for the assignment of the chromosome 17 breakpoint to the region between both tested loci.

Discussion

ABC rarely occurs in facial bones and is exceptionally seen in the ethmoid sinus. To our knowledge, only five primary cases have been reported in the literature. All of them occurred in young children between 5 years and 15 years old, consulting for either nasal obstruction, epistaxis, or tearing with conjunctivitis and blurred vision [2, 9, 15, 22, 26]. Coscina et al. described a case of an ethmoidal ABC, concurring with an osteoblastoma [3].

ABCs have radiologic characteristics that may suggest the diagnosis [2]. They appear as expansile and sometimes multilocar radiolucencies, having a ‘honeycomb’ or ‘soap bubble’ appearance. Computed tomography (CT) and MRI may be useful to determine the (bony) extent of the lesion and to further delineate the lesion from overlying tissues [2, 13, 15, 23].

Some lesions (giant cell granuloma, osteosarcoma, etc.) may mimic the clinical and radiographic presentation of (craniomaxillofacial) ABC, and the presence of abundant edema (especially in ABC of soft tissue) may lead to the erroneous diagnosis of an aggressive process [2, 24]. Therefore, a definitive diagnosis should be based solely on the histopathology of the lesion. In addition, about 50% of ABC are ‘secondary’, i.e., associated with other entities, the most frequent being giant cell tumor, chondroblastoma, and fibrous dysplasia [14, 23].

The pathogenesis of ABC remains undetermined. ABC is generally considered to be of a reactive nature, caused by trauma or a ‘local disturbance’ (venous throm-

bosis, arteriovenous aneurysm, etc.), leading to an increase in venous pressure and the development of a dilated and engorged vascular bed [1, 2, 14, 16, 20]. In our case, there was no evidence of a previous trauma or a preexisting lesion. It is unlikely but unclear if the chemo- and radiotherapy could have played a role in the pathogenesis of the lesion.

The presence of chromosomal changes in our case and recent cytogenetic reports suggest that at least some of the ABCs are neoplastic. The existing cytogenetic data on ABC indicate that the occurrence of chromosomal aberrations involving 17p13 and/or 16q22 are characteristic of this entity. Among the seven published cases, two specimens revealed a distinctive t(16;17)(q22;p13), while in three other tumors, 17p13 was involved with other chromosomal segments as the translocation partners [4, 17, 23]. Solitary involvement of 16q22 was seen in two cases [4, 17]. The case of an aneury-smal bone cyst presently reported disclosed a single t(6;17)(p21;p13) translocation. Our finding confirms that a yet unknown gene involved in the development of an aneurysmal bone cyst maps to the 17p13 region. FISH analysis allowed sublocalization of this gene between the p53 (17p13.1) and the Mieller-Dieker gene (17p13.3) loci.

The mechanism leading to ABC development and the histopathological and clinical significance of the involvement of specific genes in their tumorigenesis are presently unknown and warrant further studies. The refinement of the chromosomal region of interest may pave the way for the characterization of the putative gene(s) involved.

References

1. Carmichael F, Malcolm AJ, Ord RA (1989) Aneurysmal bone cyst of the zygomatic bone. Oral Surg 68:558–562
2. Citardi MJ, Janjua T, Abrahams JJ, Sasaki CT (1996) Orbito-ethmoid aneurysmal bone cyst. Otolaryngol Head Neck Surg 114:466–470
3. Coscina WF, Lee BC (1985) Concurrent osteoblastoma and aneurysmal bone cyst of the ethmoid sinus. J Comput Tomogr 9:347–350
4. Dal Cin P, Kozakewich HP, Goumnerova L, Mankin HJ, Rosenberg AE, Fletcher JA (2001) Variant translocations involving 16q22 and 17p13 in solid and extraosseous forms of aneurysmal bone cyst. Genes Chromosomes Cancer (in press)
5. Dierlamm J, Wlodarska I, Michaux L, La Starza R, Zeller W, Mecucci C, Van den Berghe H (1996) Successful use of the same slide for consecutive fluorescence in situ hybridization experiments. Genes Chromosomes Cancer 16:261–264
6. Giddings NA, Kennedy TL, Knipe KL, Levine HL, Smith JD (1989) Aneurysmal bone cyst of the mandible. Arch Otolaryngol Head Neck Surg 115:865–870
7. Jaffe HL, Lichtenstein L (1942) Solitary unicameral bone cyst with emphasis on the roentgen picture, the pathologic appearances and the pathogenesis. Arch Surg 44:1004–1025
8. Johnson TE, Bergin DJ, Mc Cord CD (1988) Aneurysmal bone cyst of the orbit. Ophthalmol 95:86–89
9. Jordan RC, Osguthorpe JD, Saunders RA (1983) Aneurysmal bone cyst of the ethmoid sinus. Otolaryngol Head Neck surgery 91:562–565
10. Karger S (ed) (1995) ISCN guidelines for cancer cytogenetics, supplement to an international system for human cytogenetic nomenclature. Karger, Basel
11. Kazmierczak B, Bol S, Wanschura S, Bartnitzke S, Bullerdiek J (1996) PAC clone containing the HMGI(Y) gene spans the breakpoint of a 6p21 translocation in a uterine leiomyoma cell line. Genes Chromosomes Cancer 17:191–193
12. Limon J, Dal Cin P, Sandberg AA (1986) Application of long-term collagenase disaggregation for the cytogenetic analysis of human solid tumors. Cancer Genet Cytogenet 23:305–313
13. Lopez-Barera F, Rodriguez-Peralto JL, Burgos-Lizaldez E, Alvarez-Linera J, Sanchez-Herrera S (1996) Primary aneurysmal cyst of soft tissue. Virchows Arch 428:125–129
14. Martinez V, Sissons HA (1988) Aneurysmal bone cyst. A review of123 cases including primary lesions and those secondary to other bone pathology. Cancer 61:2291–2304
15. Mouchon Y, Pharaboz Ch, Garcia JF, Rigaud A, Bassoulet J, Cosnard G (1988) Kyste osseux anévrysmal de l'ethmo. Radiol 69:103–107
16. Nik-Hussein NN, Boon LC (1989) Aneurysmal bone cyst of the mandible. J Pedodontics 13:366–372
17. Panoutsakopoulos G, Pandis N, Kyriazoglou I, Gustafson P, Mertens F, Mandahl N (1999) Recurrent t(16;17)(q22;p13) in aneurysmal bone cysts. Genes Chromosomes Cancer 26:265–266
18. Patel BC, Sabir DI, Flaharty PM, Anderson RL (1993) Aneursymal bone cyst of the orbit and ethmoid sinus. Arch Ophtalmol 111:586–587
19. Petrik PK, Findlay JM, Sherlock RA(1993) Aneurysmal cyst, bony type, primary in artery. Am J Surg Pathol 17:1062–1066
20. Reychler H (1988) Revue des pseudo-kystes et lacunes osseuses des maxillaires. Rev Stomatol Chir maxillofac 89:190–198
21. Rodriguez-Peralto JL, Lopez-Barea F, Sanchez-Herrera S, Atienza M (1994) Primary aneurysmal cyst of soft tissues (extraosseous aneurysmal cyst). Am J Surg Pathol 18:632–636
22. Saito K, Fukuto K, Takahashi M, Seki Y, Yoshida Y (1988) Benign fibroosseous lesions involving the skull base, paranasal sinuses, and nasal cavity. J Neurosurg 88:1116–1119
23. Sciot R, Dorfman H, Brys P, Dal Cin P, De Wever I, Fletcher DM, Jonson K, Mandahl N, Mertens F, Mitelman F, Rosai J, Rydholm A, Samson I, Tallini G, Van den Berghe H, Vanni R, Willén H (2000) Cytogenetic-morphologic correlations in aneurysmal bone cyst, giant cell tumor of bone and combined lesions. A report from the Champ study group. Mod Pathol 13:1206–1210
24. Shannon P, Bédard Y, Bell R, Kandel R (1997) Aneurysmal cyst of soft tissue: report of a case with serial magnetic resonance imaging and biopsy. Human Pathol 28:255–257
25. Watzke I, Chiari FM (1988) Die aneurysmatische Knochenzyste. Dtsch Z Mund Kiefer Gesichts Chir 12:477–480
26. Zielnik B, Gutkowska J (1995) A case of aneurysmal cyst of the ethmoid sinus. Otolaryngol Pol 49:169–172

Virchows Arch (2001) 439:640–644
DOI 10.1007/s004280100427

ORIGINAL ARTICLE

Masayuki Shintaku · Akiko Sangawa
Akihito Yonezawa · Kaori Nasu

Aortic lesions in aspergillosis: histopathological study of two autopsy cases

Received: 26 May 2000 / Accepted: 4 January 2001 / Published online: 30 March 2001
© Springer-Verlag 2001

Abstract The involvement of the aorta in aspergillosis is relatively rare, and its histopathological features have not been described in detail. In two autopsy cases of invasive aspergillosis in immunologically compromised patients with hematological disorders, the aspergillotic lesions of the aorta showed different characteristic histopathological features depending on the three layers of aortic wall. Intimal lesions were formations of the mural thrombus composed of aggregates of numerous fungal hyphae arranged perpendicularly to the aortic wall. In the media, smooth muscle cells were completely necrotic (anemic infarct of the media), while the framework of elastic fibers was well preserved, with only a few fungal hyphae detected. In the adventitia, an intense, partly granulomatous chronic inflammatory change with fibrosis was observed in association with mycotic embolic occlusion of the vasa vasorum. These histopathological changes were considered to represent one of the typical tissue reaction patterns in the wall of an elastic artery in aspergillosis.

Keywords Aorta · Aspergillosis · Histopathology

Introduction

Aspergillosis, which is usually caused by *Aspergillus fumigatus* infection, is one of the most common opportunistic fungal infections affecting immunologically compromised patients [17]. The primarily affected organ is the lung, and the invasive form of pulmonary aspergillosis frequently shows extensive local spread and further results in widespread hematogenous dissemination into various organs [14, 17].

M. Shintaku (✉) · A. Sangawa
Department of Pathology, Osaka Red Cross Hospital,
5–53 Fudegasaki, Tennoji, Osaka 543-8555, Japan
Tel.: +81-6-67715131 ext 357, Fax: +81-6-67743239

A. Yonezawa · K. Nasu
Department of Internal Medicine, Osaka Red Cross Hospital,
Osaka, Japan

Aspergillus fungal hyphae exhibit a remarkable propensity for the invasion of arterial walls with embolic occlusion of the lumina, and an anemic or hemorrhagic infarct is occasionally produced [14]. Among the organs, the heart is involved infrequently [1, 16, 17]. The incidence of involvement of great vessels, including the aorta, is even lower.

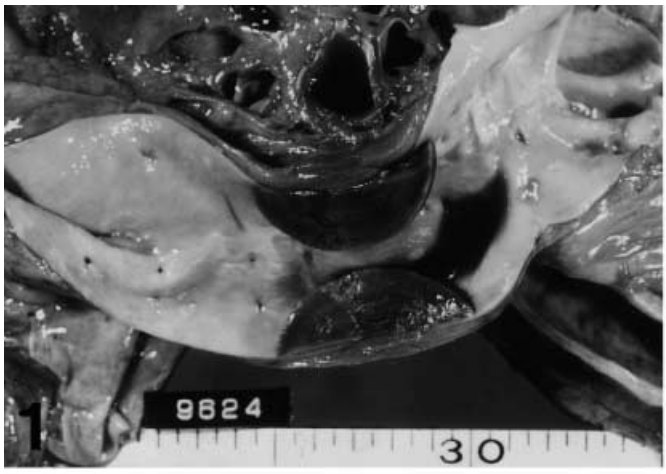
We report here two autopsy cases showing involvement of the aorta by aspergillosis in patients with hematological disorders. In the first case, the aspergillus infection involved the bilateral lungs and mediastinum extensively and formed a large, dome-shaped, mural thrombus in the thoracic aorta. In the second case, the aspergillus infection was disseminated into various organs, and a mass lesion was found within the wall of the thoracic aorta. Although detailed radiographic and hemodynamic studies were not performed antemortem because of the rapid disease progression and poor general condition of the patients, we describe the histopathological findings of the aortic lesions in these cases and discuss briefly the pathological aspects of the aortic involvement due to aspergillosis.

Case report

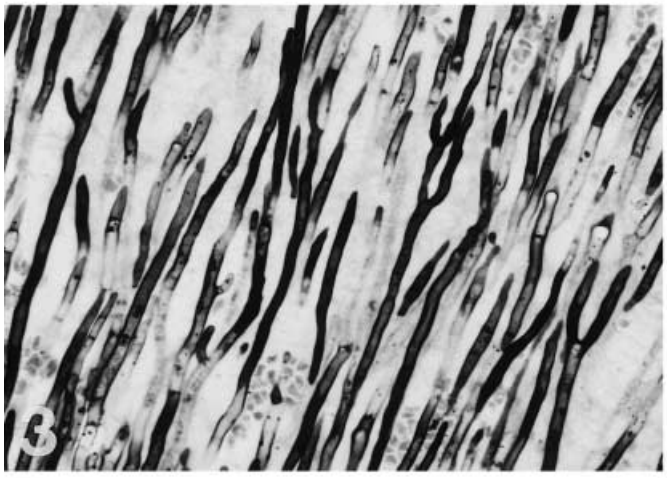
Case 1

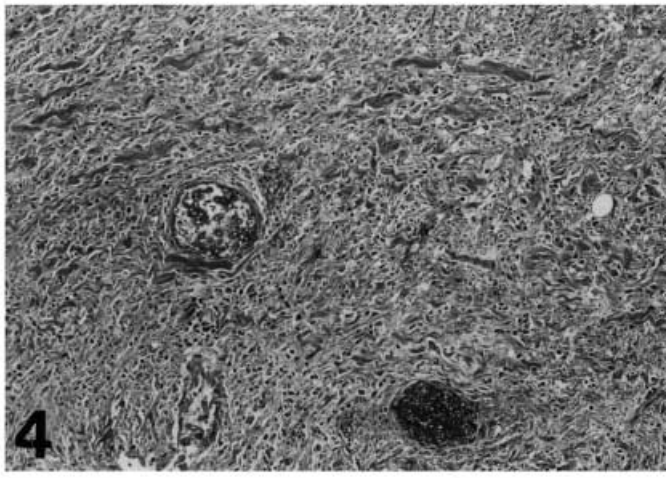
The patient was a 63-year-old male factory worker with a history of chronic pancreatitis due to excessive alcohol intake who had undergone subtotal gastrectomy for gastric cancer at the age of 55. He presented to our hospital on 12 June 1996 with a 2-week history of dyspnea on exertion, palpitation, and dizziness. On admission, high fever and purpura of lower extremities were also noted. Hematological examination revealed pancytopenia (erythrocytes 196×10^4/μl, leukocytes 1700/μl with 3% neutrophils and 97% lymphocytes, and platelets 5.2×10^4/μl). The myelogram showed marked hypoplasia (13,100 nucleated cells/μl). Chest X-ray on admission did not reveal any significant abnormalities.

Intensive treatment with antibiotics and antifungal drugs and the administration of granulocyte colony-stimulating factor were commenced immediately. Because the clinical symptoms did not improve, steroid pulse therapy was added from 19 June. On 25 June, severe chest pain developed suddenly, but chest X-ray and electrocardiographic examination at that time disclosed no









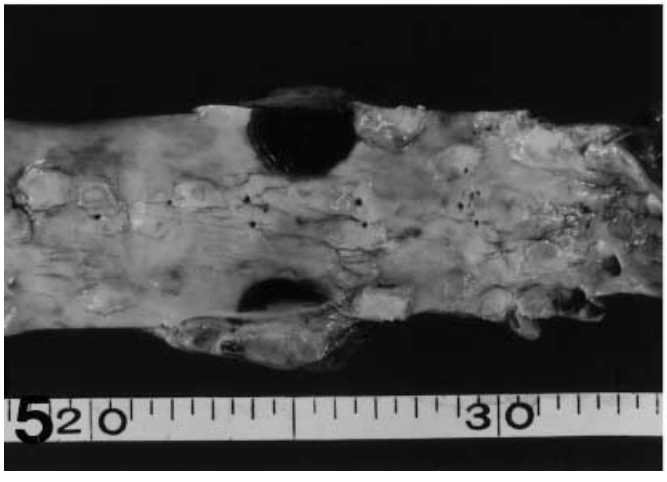




Fig. 1 A dome-shaped mural thrombus (bisected) just below the aortic arch, whose cut surface revealed a dark red laminated structure. The pericardium and the pulmonary hilus adhered firmly to the adventitia

Fig. 2 The mural thrombus contained numerous fungal hyphae showing a fan-like or "sunburst" appearance. (Grocott-Gomori methenamine-silver nitrate, ×10)

Fig. 3 Higher magnification of septate fungal hyphae showing variable staining intensity and dichotomous branching. (Grocott-Gomori methenamine-silver nitrate, ×100)

Fig. 4 The adventitia at the portion of the mural thrombus showed severe chronic inflammatory cell infiltration with fibrosis. Occlusion of the lumina of the vasa vasorum by fungal emboli was seen. (H&E, ×25)

Fig. 5 A mass lesion involving the wall of the thoracic aorta (bisected). The intimal surface of the lesion formed a plaque-like dark red mural thrombus

Fig. 6 Numerous fungal hyphae were arranged perpendicularly to the aortic wall. Although the hyphae penetrated the intima (*I*), few were found in the media (*M*). (Grocott-Gomori methenamine-silver nitrate, ×10)

causative abnormalities. Dry cough and tachypnea supervened on 30 June, and chest X-ray revealed extensive infiltrative shadows over the right upper lung field and left hilar region. Respiratory distress increased progressively and the patient died of respiratory failure on 12 July.

Pathological findings

The bone marrow exhibited severe hypoplasia with lymphoplasmacytic infiltration, confirming the diagnosis of aplastic anemia (panmyelophthisis). The lungs (r: 1070 g, l: 700 g) showed a whitish diffuse consolidation of the bilateral upper lobes and marked congestion and edema of the other lobes. The upper lobes also contained several ill-defined, hemorrhagic nodules of up to thumb-tip size which showed typical histopathological features of invasive pulmonary aspergillosis. These nodules were composed of the central necrotic hemorrhagic areas and the peripheral areas of intra-alveolar exudation showing organizing processes.

Numerous septate fungal hyphae exhibiting the dichotomous branching characteristic of *Aspergillus* species were found throughout the lesions. Fungal hyphae had extensively invaded the walls of pulmonary arteries, and large areas of anemic infarct of the lung parenchyma were noted in the upper lobes.

One of these aspergillotic nodules involved the left hilar region and spread from there contiguously into the pericardium. The pericardium and epicardium were markedly thickened, their surfaces being very hyperemic and shaggy, and the pericardial space was filled with about 500 ml of fibrin-rich exudate, which had caused cardiac tamponade. Histologically, the pericardium showed extensive aspergillosis involvement. The epicardium also showed marked fibrinofibrous inflammation, but fungal hyphae were not found on the epicardial surface. The myocardium had no aspergillotic lesions.

Just below the aortic arch, the adventitia of the aorta adhered firmly to the thickened pericardium and the pulmonary hilus, and a large, dome-shaped mural thrombus measuring 4.8×3.0×1.5 cm was found (Fig. 1). Its cut surface exhibited a dark red laminated structure. This mural thrombus contained numerous fungal hyphae arranged perpendicularly to the aortic wall showing a fan-like or "sunburst" appearance (Fig. 2). Most of the hyphae had degenerated and showed only pale staining with periodic acid-Schiff and Grocott-Gomori methenamine-silver nitrate stains (Fig. 3). The atherosclerosis of the intima was minimal. The media beneath the thrombus showed coagulation necrosis of the smooth muscle cells, but elastic fibers were well preserved.

Neither inflammatory cell infiltration nor fibrosis was noted in the media, and only a few hyphae were present. The adventitia at that portion was necrotic and showed intense inflammatory changes with fibrosis. Numerous hyphae were found in the lumina of the vasa vasorum (Fig. 4).

The spread of aspergillotic lesions was confined to the mediastinal and intrathoracic organs. The deposition of calcium oxalate crystals was not detected in the aspergillotic lesions. The intra-abdominal and retroperitoneal organs showed no remarkable abnormalities.

Case 2

The patient was a 59-year-old nurse who presented with cough, sore throat, weight loss, and superficial lymph node swelling in 1995. Radiographic examination disclosed remarkable lymph node swelling in the deep cervical, mediastinal, intra-abdominal, and retroperitoneal regions. Biopsy of one of the cervical nodes revealed immunoblastic lymphadenopathy-like T cell lymphoma, and chemotherapy was instituted.

Her clinical course thereafter included remissions and relapses for about 3 years, during which time herpes zoster and cytomegalovirus enterocolitis developed. A peripheral blood stem cell transplantation was performed twice. On the final admission in April 1998, the patient was febrile and emaciated, and a skin rash of reddish color was seen on the chest. Skin biopsy revealed perivascular infiltration of lymphoma cells in the dermis.

Hematological examination revealed severe pancytopenia secondary to the chemotherapy (erythrocytes 262×10^4/μl, leukocytes 1000/μl with 51% neutrophils and 32% lymphocytes, and platelets 7000/μl). The skin rash subsided after administration of steroids, cyclosporin, and etoposide. On 24 May, a high fever developed, and a culture of venous blood yielded *Escherichia coli* growth. In early June, chest X-ray disclosed infiltrative shadows in the bilateral lung fields which gradually changed into ill-defined multinodular shadows. On 7 June, she suddenly lost consciousness, and involuntary movements of the right upper and lower extremities were noted. She died on 19 June.

Pathological findings

At autopsy, no lymph node swelling was noted, but infiltration of lymphoma cells was found histologically in the liver, spleen, bone marrow, kidneys, and adrenals. The lungs (r: 500 g, l: 400 g) contained multiple nodular foci of invasive aspergillosis less than 3 cm in diameter which were associated with anemic infarct and distributed over the entirety of both lungs with a background of congestion and edema. The central areas of the nodules showed coagulation necrosis and contained numerous fungal hyphae. The peripheral areas consisted of inflammatory granulation tissue containing numerous neutrophils. The hyphae exhibited morphological features similar to those of case 1. The invasion of hyphae into the arterial walls was a prominent feature. A vegetation measuring 12 mm in maximal diameter and composed mostly of fungal hyphae was found on the tip of papillary muscle of the tricuspid valve. Disseminated aspergillotic lesions were observed in the cerebrum, kidneys, and thyroid.

The cerebrum was the most severely involved site, and multiple foci of the anemic infarct associated with the vascular invasion of hyphae were noted.

In the thoracic aorta, 10 cm below the arch, a mass lesion measuring 3×2.5×1.5 cm was found to involve the wall transmurally. The intimal surface formed an elevated, plaque-like, dark red mural thrombus (Fig. 5). Histological findings of the aortic lesion were essentially similar to those in case 1. Numerous degenerated hyphae arranged perpendicularly to the aortic wall protruded from the intima and formed a thin, plaque-like mural thrombus (Fig. 6). The intima showed moderate atherosclerosis. Infiltration of neutrophils was found in the boundary zone between the intima and media, and the smooth muscle cells of the media showed coagulation necrosis. Elastic fibers of the media were well preserved, and only a few hyphae were found. In the adventitia, granulomatous lesions surrounding necrotic foci and composed of histiocytes, multinucleated giant cells, and lymphocytes were found. The lumina of the vasa vasorum were occluded by hyphae. The outer layers of the media were partly eroded by the granulomatous lesions. No oxalate deposits were found in the aortic lesions or the other organs.

The other notable pathological findings were necrotizing tubulointerstitial nephritis due to adenovirus infection, transfusional hemosiderosis of the liver, spleen, bone marrow, and pancreas, and hypoplasia of the bone marrow.

Discussion

Cardiovascular involvement due to fungal infections is relatively infrequent [1, 14, 16]. Various debilitating disorders, congenital and acquired immunological deficiencies, and history of open heart surgery [4, 15] or intravenous drug abuse [10] are considered to be important factors predisposing to the development of cardiovascular mycosis. It is usually associated with a disseminated fungal infection and leads to a fatal outcome in most pa-

tients [1, 2, 9, 10, 14, 15, 16, 17]. *Candida* is the most frequent pathogenic fungus, followed by *Aspergillus* [1, 16]. Among the aspergillotic cardiac lesions, myocardial involvement is the most common, while aspergillus endocarditis and pericarditis are relatively rare [1, 16, 17].

In the two cases reported here, the pathogenic *Aspergillus* could not be determined in terms of species, because cultures of the blood or lesional foci were not attempted and conidial heads of specific morphology were not found in the tissue sections. However, the pathogens were most likely *Aspergillus fumigatus*, since this is by far the most common in invasive aspergillosis affecting immunologically compromised hosts [14, 17].

Although the involvement of great vessels, including the aorta, with aspergillosis is even more rare than cardiac involvement, several reports have described various forms of aspergillotic lesions in the aorta. They include the formation of a mural thrombus [8], embolic occlusion of the aortic lumen [2, 10], aortic aspergilloma [15], mycotic aneurysm [4, 11, 12] or pseudoaneurysm [3], rupture of the sinus of Valsalva [7], and aspergillus aortitis [6, 11, 15]. These aortic lesions have been discussed with particular reference to their clinical and hemodynamic aspects, but there are very few detailed descriptions and analysis of histopathological findings.

The two cases reported here showed essentially the same histopathological features, and in each layer of the aortic wall a pathological alteration with characteristic appearance was found. In the intima, a dome-shaped or plaque-like mural thrombus was found which was composed mostly of numerous degenerated hyphae showing a fan-like or “sunburst” appearance and which was not accompanied by tissue reaction.

On the other hand, the adventitia showed an intense inflammatory cellular reaction and fibrosis, and many small vessels in the adventitia (vasa vasorum) contained emboli of fungal hyphae. The alterations found in the media were interesting. Smooth muscle cells in the media showed coagulation necrosis, while no inflammatory cellular reaction was found. In contrast, the elastic fibers of the media were well preserved. These different histopathological features in the three layers of the aorta seem to represent one of the typical tissue reaction patterns of the aortic wall in aspergillus infection, although other reaction patterns such as granuloma formation in the media [11] have also been reported.

In the first case, the pathological process in the aortic wall evidently began in the adventitia by the direct spread from the aspergillus pericarditis. The severe chest pain which developed suddenly 17 days before death was most likely due to the invasion of the aortic wall, and the transmural spread from the adventitia to the intima seems to have proceeded rapidly. A similar case was reported by Kluin-Nelemans et al. [8]. The large, dome-shaped mural thrombus must have caused a severe derangement of blood flow. In the second case, aortic involvement also most likely started in the adventitia, probably as a result of the fungal embolization of the vasa vasorum, since the mass lesion in the aortic wall protruded to the adventitial surface, many adventitial small vessels contained fungal emboli, and the adventitial lesion showed remarkable inflammatory changes and fibrosis.

In the media of elastic arteries, the aggregation and organization of elastic fibers produced by the smooth muscle cells form multiple layers of lamellae enclosing numerous fenestrae [5]. These fenestrae are relatively large, and cytoplasmic processes of the medial smooth muscle cells traverse them. In the present cases, fungal hyphae seem to have insinuated rapidly into the intima through the fenestrae of elastic lamellae in the media without severely destroying the framework of elastic fibers. This is probably why elastic fibers in the media were well preserved in spite of almost complete coagulation necrosis of the smooth muscle cells. Necrosis of the smooth muscle cells was probably the result of embolic occlusion of the vasa vasorum by the hyphae (anemic infarct of the media). The direct cytotoxic effects of the hyphae to muscle cells should also be considered, although the deposition of calcium oxalate crystals, a characteristic finding in aspergillus infection (especially of *Aspergillus niger*) [13] was not found in the aortic lesions. The absence of a cellular reaction in the media may also be related to the immunocompromised state of the patients and the rapid clinical course which is characteristic of invasive aspergillosis [14]. If the patients had survived longer, the elastic lamellae of the media may also have been destroyed by the aspergillotic processes.

In summary, these two cases showed that aspergillotic involvement of the wall of the aorta or other elastic arteries exhibits characteristic histopathological features depending on each layer of the vascular wall.

References

1. Atkinson JB, Connor DH, Robinowitz M, McAllister HA, Virmani R (1984) Cardiac fungal infections. Review of autopsy findings in 60 patients. Human Pathol 15:935–942
2. Byard RW, Jimenez CL, Carpenter BF, Hsu E (1987) Aspergillus-related aortic thrombosis. Can Med Ass J 136:155–156
3. Corrigan C, Horner SM (1988) Aspergillus endocarditis in association with a false aortic aneurysm. Clin Cardiol 11:430–432
4. Doshi R (1971) Aspergillus fumigatus endocarditis of an aortic homograft with aneurysm of the ascending aorta. J Pathol 103:263–265
5. Fawcett DW (1994) Blood and lymph vascular systems. In: Bloom and Fawcett (eds) A textbook of histology, 12th edn. Chapman and Hall, New York, pp 368–409
6. Hadorn VW (1960) Aortenruptur durch Aspergillusinfektion nach Operation einer Aortenstenose. Endaortitis polyposa mycotica. Schweiz Med Wochenschr 90:929–934
7. Hurley J, McGovern E (1994) Rupture of a sinus of Valsalva aneurysm due to aspergillus endocarditis. J Cardiovasc Surg 35:75–77
8. Kluin-Nelemans JC, Koelma IA, van der Merwe PC, Peetermans WEC (1991) Fulminant pulmonary aspergillus infection occluding the aortic arch after high-dose antileukemic chemotherapy. Cancer 67:3123–3126
9. Kuijer PMM, Kuijper EJ, van den Tweel JG, van der Lelie J (1992) Aspergillus fumigatus, a rare cause of fatal coronary artery occlusion. Infection 20:49–51

10. Light JT, Hendrickson M, Sholes WM, Portnoy DA, Bell WH, Kerstein MD (1991) Acute aortic occlusion secondary to aspergillus endocarditis in an intravenous drug abuser. Ann Vasc Surg 5:271–275
11. Malcolm AD, Bakerspigel A, Enriquez AA (1971) Aspergillus flavus endaortitis following aortic valvotomy. Thorax 26:435–442
12. Myerowitz RL, Friedman R, Grossman WL (1971) Mycotic "mycotic aneurysm" of the aorta due to aspergillus fumigatus. Am J Clin Pathol 55:241–246
13. Nime FA, Hutchins GM (1973) Oxalosis caused by aspergillus infection. Hopkins Med J 133:183–194
14. Rinaldi MG (1983) Invasive aspergillosis. Rev Infect Dis 5:1061–1077
15. Robbins JA, Mohanty PK, Mohanty LB (1983) Aortic aspergilloma resulting in supravalvular aortic stenosis after aortocoronary bypass surgery. Am Heart J 106:163–166
16. Walsh TJ, Hutchins GM, Bulkley BH, Mendelsohn G (1980) Fungal infections of the heart. Analysis of 51 autopsy cases. Am J Cardiol 45:357–366
17. Young RC, Bennett JE, Vogel CL, Carbone PP, DeVita VT (1970) Aspergillosis. The spectrum of the disease in 98 patients. Medicine 49:147–173

Virchows Arch (2001) 439:645–652
DOI 10.1007/s004280100464

ORIGINAL ARTICLE

**Bernhard Hemmerlein · Alexander Kugler
Rehyan Özisik · Rolf-Hermann Ringert
Heinz-Joachim Radzun · Paul Thelen**

Vascular endothelial growth factor expression, angiogenesis, and necrosis in renal cell carcinomas

Received: 4 December 2000 / Accepted: 10 April 2001 / Published online: 18 August 2001
© Springer-Verlag 2001

Abstract Rapidly growing tumors often develop necrosis. In the present study the expression of vascular endothelial growth factor (VEGF) was investigated and compared to microvessel density and necrosis of renal cell carcinomas. In the tumor-host interface the microvessel density was significantly increased compared to central tumor areas. Tumor necrosis was associated with a decrease of microvessel density and an increase of the VEGF protein expression within the perinecrotic rim. VEGF protein was focally upregulated in vital tumor tissue. An increase of the apoptotic rate of endothelia and vital tumor tissue in tumors with necrosis could not be detected. $VEGF_{(121,165)}$ mRNA was decreased in proliferatively active carcinomas compared to less proliferative tumors. Multicellular renal cell cancer spheroids as a model of chronic hypoxia developed central apoptosis but no necrosis. VEGF was upregulated in the spheroid. Tumor microvessels expressed matrix metalloproteinase –2 and –9 and an incomplete pericyte covering in comparison to tumor-free tissue indicating immature active angiogenesis. We conclude that highly proliferative renal cell carcinomas outgrow their vascular supply and develop chronic hypoxia inducing a decrease of proliferation and an increase of VEGF expression. However, chronic hypoxia does not cause significant necrosis or apoptosis. Tumor necrosis is more likely induced by acute hypoxia due to immature microvessels. Furthermore, VEGF expression associated with concomitant tumor necrosis may help identify renal cell carcinomas susceptible to antiangiogenic therapy.

This work was supported by the grant Ku 1204/1–1 of the Deutsche Forschungsgemeinschaft, Bonn, Germany

B. Hemmerlein (✉) · R. Özisik · H.-J. Radzun
Department of Pathology, Georg-August University,
Medizinische Fakultät, Robert-Koch-Str. 40,
37075 Göttingen, Germany
e-mail: hemmer@med.uni-goettingen.de
Fax: +49 551-398633

A. Kugler · R.-H. Ringert · P. Thelen
Department of Urology, Georg-August University,
Medizinische Fakultät, 37075 Göttingen, Germany

Keywords Microvessel density · Tumor necrosis · VEGF expression

Introduction

Angiogenesis is an essential step during embryogenesis and organogenesis for the physiological turnover of tissues [5, 8, 20, 21] and for the growth of transformed tissues. Most studies confirm the hypothesis that metastasis of a large variety of solid tumors such as cancer of the lung, breast, urinary bladder, and prostate is closely associated with angiogenesis [9, 27, 28, 29]. Nevertheless, malignant tumors frequently show spontaneous tumor necrosis which in most cases of soft tissue tumors and malignant gliomas represents an essential component for histological grading. Recently it could be shown that aggressive breast carcinomas, although inducing high levels of angiogenesis, outgrow their vascular supply which leads to chronic hypoxia and necrosis [16].

Among numerous pleiotropic angiogenic growth factors that have been identified, the vascular endothelial growth factor (VEGF) seems to be the most potent mediator, acting on endothelial cells via specific receptor tyrosine kinases that are upregulated during angiogenesis. VEGF mRNA was shown to be upregulated in tumor tissue compared to tumor-free tissue and to be highly increased in renal cell cancer [2], inducing a high microvessel density (MVD) [4]. Induction of VEGF expression could be attributed to hypoxia [12, 24, 25].

Microvessel plasticity and recruitment of pericytes were investigated in experimental animal models of the retina and ovarian cycle, and it is assumed that intratumoral microvessel remodeling follows similar principles [1, 10]. Because angiogenesis requires remodeling of basement membranes, matrix metalloproteinases (MMP) are involved in this process, the expression of which in endothelia can be stimulated by VEGF [15, 26]. During angiogenesis, mature vessels develop a pericyte covering which enables them to react with vasoactive substances

and which stabilizes them against increased tissue pressure and tensional forces.

In the present study we analyzed the expression of VEGF in comparison to angiogenesis and necrosis in renal cell cancer. For this purpose immunohistochemical detection of corresponding antigens as well as qualitative and quantitative analyses of mRNA such as in situ hybridization and competititve reverse transcription-polymerase chain reaction (cRT-PCR) were applied. It is shown that highly proliferative tumors express lower levels of VEGF mRNA than slowly proliferating tumors. It is likely that rapidly proliferating tumors outgrow their vascular supply, leading to chronic hypoxia, a decrease of cell proliferation, and an expression of hypoxia-inducible genes such as VEGF. Tumor necrosis, however, is caused by acute but not chronic hypoxia due to immature microvessels which are susceptible to tensional forces that induce vessel obturation.

Material and Methods

Patients

Analyzed were renal cell carcinoma specimens from 58 patients who underwent total nephrectomy without prior adjuvant therapy. Histological type, grade, and tumor stage were determined on hematoxylin and eosin stained sections as proposed by Thoenes et al. [23] and according to the UICC classification. Carcinomas in progress (≥pT3) and all cases with positive lymph nodes or distant metastases were regarded as advanced, whereas tumors without metastasis (≤pT2, N0, M0) were classified as organ-confined.

Analysis of microvessel density, tumor cell density and proliferation

Microvessel count, tumor cell density, and tumor cell proliferation were assessed by light microscopy within the tumor-host interface (invasive area) and tumor areas. Necrotic areas and those with prominent hyalinization were excluded. At 400x magnification and using an optical grid (Zeiss, Göttingen, Germany), a minimum of 500 tumor cells and vessel profiles in identical areas were analyzed in regard to MIB-1 expression. Tumor cell density and MVD were expressed in tumor cells/0.1 mm^2 and microvessels/0.1 mm^2, respectively.

Double-immunostaining for microvessels (CD31) and tumor cell proliferation (MIB-1)

The streptavidin-biotin labeling technique was used for double-immunostaining (Biogenex, Hamburg, Germany). Three micron thick paraffin sections of representative tissues were mounted on organo-silane coated slides. After deparaffination and rehydration endogeneous peroxidase activity was quenched with 3% hydrogen peroxide in bidistilled water. For antigen retrieval, slides were microwaved in 10 mM citrate buffer (pH 6.0) at 700 Wfor at least 15 min. After blocking with 5% bovine serum albumin (BSA)/5% fetal calf serum (FCS) for 20 min, slides were incubated overnight (4°C) with the monoclonal mouse anti-CD31 antibody JC/70 A (DAKO Diagnostica, Hamburg, Germany) diluted 1:50 in Tris-buffered solution (50 mM Tris-HCl, 150 mM NaCl, pH 7.4) (TBS) containing 5% BSA and for 30 min with a biotinylated goat-anti-mouse antibody (1:50 in TBS containing 5% BSA). Finally, slides were incubated with streptavidin-peroxidase (1:50) for 30 min. Peroxidase reaction was developed using 3,3′-diaminobenzidine tetrahydrochloride (DAB; Roche, Mannheim, Germany) for 15 min. After labeling with anti-CD31, slides were immersed again in citrate buffer and microwaved at 700 W for 2 min, incubated for 2 h with the MIB-1 antibody (DAKO Diagnostica, Hamburg, Germany) diluted 1:100 in TBS containing 5% BSA, and subsequently incubated for 30 min with biotinylated goat-anti-mouse antibody (1:50 in TBS containing 5% BSA). Afterwards, sections were labeled with streptavidin–alkaline phosphatase (1:50) for 30 min. Chromogen detection was performed using Fast Red for 20 min (Biogenex).

Immunostaining for smooth muscle actin and matrix metalloproteinase-2 and –9

Paraffin sections were prepared as described above and incubated for 2 h with a prediluted monoclonal mouse anti-smooth muscle actin antibody (Immunotech, Hamburg, Germany), the monoclonal mouse antibody anti-MMP-2 (Clone CA4002, Quartett, Berlin, Germany) or with a mouse monoclonal MMP-9 antibody (Oncogene, Hamburg, Germany) diluted 1:50 in TBS containing 5% BSA and 5% FCS. After incubation with Envision-peroxidase (DAKO Diagnostica) for 1 h, peroxidase activity was developed as described above. All steps were performed at room temperature in a humid chamber. For immunostaining of MMP-9 slides were microwaved at 700 W for 15 min and incubated for 2 h. Endothelial expression of MMP-2 and –9 was semiquantitatively scored: negative (no positive endothelia), weak (positive endothelia <10%), moderate (positive endothelia 10–50%), and high expression (positive endothelia >50%).

In situ hybridization of MMP-9 mRNA

Three-micron-thick paraffin sections were mounted on organo-silane coated slides under RNase-free conditions. In situ hybridization was performed using a digoxigenin-labeled riboprobe of 263 nucleotides (1438 b–1700 b) corresponding to the published mRNA sequence of the human MMP-9 gene [31]. Sections were deparaffinized and rehydrated, digested with Proteinase K (DAKO), and incubated with labeled riboprobes at 55°C overnight. In a first step, sections were washed at 55°C in 1% sodium dodecyl sulfate (SDS) in 2× saline sodium citrate (SSC) for 15 min at room temperature followed by a second washing step (1% SDS in 1×SSC; 20 min, room temperature). Sections were incubated with TBS containing 1% FCS and 0.1% (vol/vol) Tween 20 (Sigma, Deisenhofen, Germany). RNA hybrids were detected with a sheep polyclonal anti-digoxigenin antibody $F(ab)_2$ fragment conjugated with alkaline phosphatase (Roche, Mannheim, Germany). Signals were detected using 5-bromo-4-chloro-indolyl phosphate and nitro tetrazolium blue. Slides were mildly counterstained with Mayer´s hematoxylin and mounted in glycerin gelatin.

Analysis of VEGF expression

VEGF was detected with the polyclonal rabbit anti-VEGF antibody (Zymed, San Francisco, USA) at a 1:200 dilution in TBS at 4°C overnight after microwave pretreatment and visualized with the anti-rabbit Envision-peroxidase (DAKO) and DAB as described above.

In 20 cases tumor-free tissue and tumor tissue of the same nephrectomy specimen were snap-frozen in liquid nitrogen immediately after removal. Total RNA was extracted according to Chomczyinski and Sacchi [6] and purified with RNeasy Mini Kit (Qiagen, Hilden, Germany). RNA quality was proven by denaturating formaldehyde-gel electrophoresis. cRT-PCR was performed using antisense primer 5′-TCG GGC CTC CGA AAC CAT GA-3′ and sense primer 5′-CCT GGT GAG AGA TCT GGT TC-3′ detecting the isoforms VEGF121 and VEGF165. For construction of the competitor a nested mutagenic primer 3′-CCG CTC CGT

CGA ACT CAA TTT GCT TGG TCT AGA GAG TGG TCC-5′ was used to generate a shortened cDNA variant of the VEGF165 cDNA, which was cloned into the TOPO cloning vector (Invitrogen, Groningen, The Netherlands) and transcribed to cRNA. Competitor cRNA was added in various dilutions (10–500 attomol) and RT-PCR was performed using the GeneAmp RNA-PCR kit (PERKIN ELMER, Weiterstadt, Germany) according to the manufacturers' instructions. The resulting products were separated by agarose gel electrophoresis, densitometrically evaluated (E.A.S.Y. win 32, HEROLAB, Wiesloch, Germany) and plotted against the competitor quantities in a logarithmic scale [22].

In situ end-labeling

Sections were deparaffinized, rehydrated, microwaved in citrate buffer as described above, and washed in ice-cold TBS for 5 min. Subsequently, slides were incubated under cover slips with ISEL mixture containing 160 U/ml terminal transferase, terminal transferase buffer (Promega, Mannheim, Germany), and digoxigenin-dNTP labeling mixture (Roche) at 37°C for 1 h. Slides were washed in TBS, blocked with 10% FCS for 15 min at room temperature, and subsequently incubated with a polyclonal anti-digoxigenin $F(ab)_2$ fragment conjugated with alkaline phosphatase (Roche) diluted 1:250 in TBS for 2 h at room temperature. All incubation steps were performed in a humid chamber. After washing twice with TBS, a color reaction was performed with 5-bromo-4-chloro-indolyl phosphate and nitro tetrazolium blue under microscopic control to prevent overstaining. Slides were counterstained with nuclear Fast Red (Merck, Darmstadt, Germany) and mounted in glycerin gelatin. In some cases immunohistochemistry of smooth muscle actin was performed prior to in situ end-labeling.

Tumor spheroid culture

A primary tumor cell line derived from a grade 2 clear cell type of renal cell carcinoma was cultivated in RPMI 1640 containing 10% FCS, 10 mM L-glutamine, and amino acid solution at 37°C in 5% CO_2. For spheroid generation tumor cells in the exponential growth phase were trypsinated, collected by centifugation, and seeded in concentrations of 2.5 and 4×10^4 cells per 200 µl medium in multiwells coated with 1% agarose. After 3, 5, 7, and 9 days spheroids were harvested, fixed in 4% neutral-buffered formalin, and embedded in paraffin. Three-micron-thick sections were mounted on organo-silane coated slides and stained with hematoxylin-eosin and immunohistochemically with the anti-VEGF antibody as described above.

Statistics

For statistical analyses the Spearman rank correlation coefficient, the Wilcoxon rank sum test, and the U-test were applied.

Results

Microvessel density, tumor cell density and tumor proliferation

Anti-CD31 and MIB-1 immunolabeled microvessels were counted at the tumor–host interface and in tumor tissue. The mean MVD within the tumor was 17.1/0.1mm^2 (SD±11.7). The mean MVD at the tumor–host interface was significantly increased up to 22.9/0.1 mm^2 (SD±15.3) in comparison to tumor areas (P<0.0001) (Fig. 1 A, B). MVD correlated negatively with tumor diameter (Spearman r = – 0.37; P=0.0055). The mean MVD in grade 1 and 2 carcinomas was 25.5/0.1 mm^2 (SD±16.4). In grade 3 carcinomas the mean MVD was decreased 12.3/0.1 mm^2 (SD±6.6) (p=0.033). The highest MVD of 60/0.1 mm^2 was found in a well-differentiated clear cell type renal cell carcinoma with a diameter of 1 cm, the lowest MVD of 2/0.1 mm^2 in a grade 2 clear cell type tumor with a diameter of 12 cm.

No difference was seen between tumor cell density within the tumor (mean 101.7 cells/0.1 mm^2 ; SD±69) and at the tumor–host interface (mean 92 cells/0.1 mm^2; SD±44.7) (P>0.05). There was a close positive correlation of MVD and tumor cell density of the tumor–host interface and tumor tissue (Spearman r=0.5; P<0.0001).

Analysis of the tumor proliferation index based on the evaluation of a minimum of 500 tumor cells at the tumor–host interface (mean 5.9%; SD±7.7) and within the tumor (mean 9.9%; SD±7.7) did not show a significant difference. A correlation between tumor proliferation index and the MVD was therefore not observed.

Microvessels, tumor necrosis, and apoptosis

To determine a possible association between MVD and tumor viability, renal cell carcinomas with and without necrosis were compared. In 12 cases focal or extended necrosis could be demonstrated (Fig. 2A). The mean MVD in carcinomas without necrosis (19.2/mm^2 ; SD±11.8) was significantly higher than in tumors with necrosis (8.2/mm^2; SD±4) (P=0.0014). In accordance with the increased MVD, necrosis could never be found at the tumor–host interface.

Because some avital tumor areas showed fragmented nuclei resembling tumor cell apoptosis, and hypoxia is known to induce apoptosis, in situ end-labeling was performed to distinguish them from one another. In situ end-labeling revealed only singular apoptotic endothelial cells within vital tumor tissue. Apoptotic tumor cells were detected at the rim and within avital areas. Even in cases with focal or large tumor necrosis only few apoptotic tumor cells were detected in vital tissue areas (Fig. 2B).

Expression of VEGF

In 20 cases mRNA expression of $VEGF_{121}$ and $VEGF_{165}$ could be analyzed in tumor-free tissue and tumor tissue of the same nephrectomy specimen by cRT-PCR. In tumor-free tissue the amount of $VEGF_{121}$ and $VEGF_{165}$ mRNA amounted to 37 attomol/µg total RNA (mean 6.3 attomol/µg total RNA; SD±8). Within tumor tissue the VEGF mRNA was highly upregulated up to 142 attomol/µg total RNA (mean 48.8 attomol/µg total RNA; SD±40.6) (P<0.0001).

Comparison with the tumor cell proliferation index revealed a lower VEGF mRNA expression in tumors with a MIB-1 index above 10% (20.33 attomol/µg total

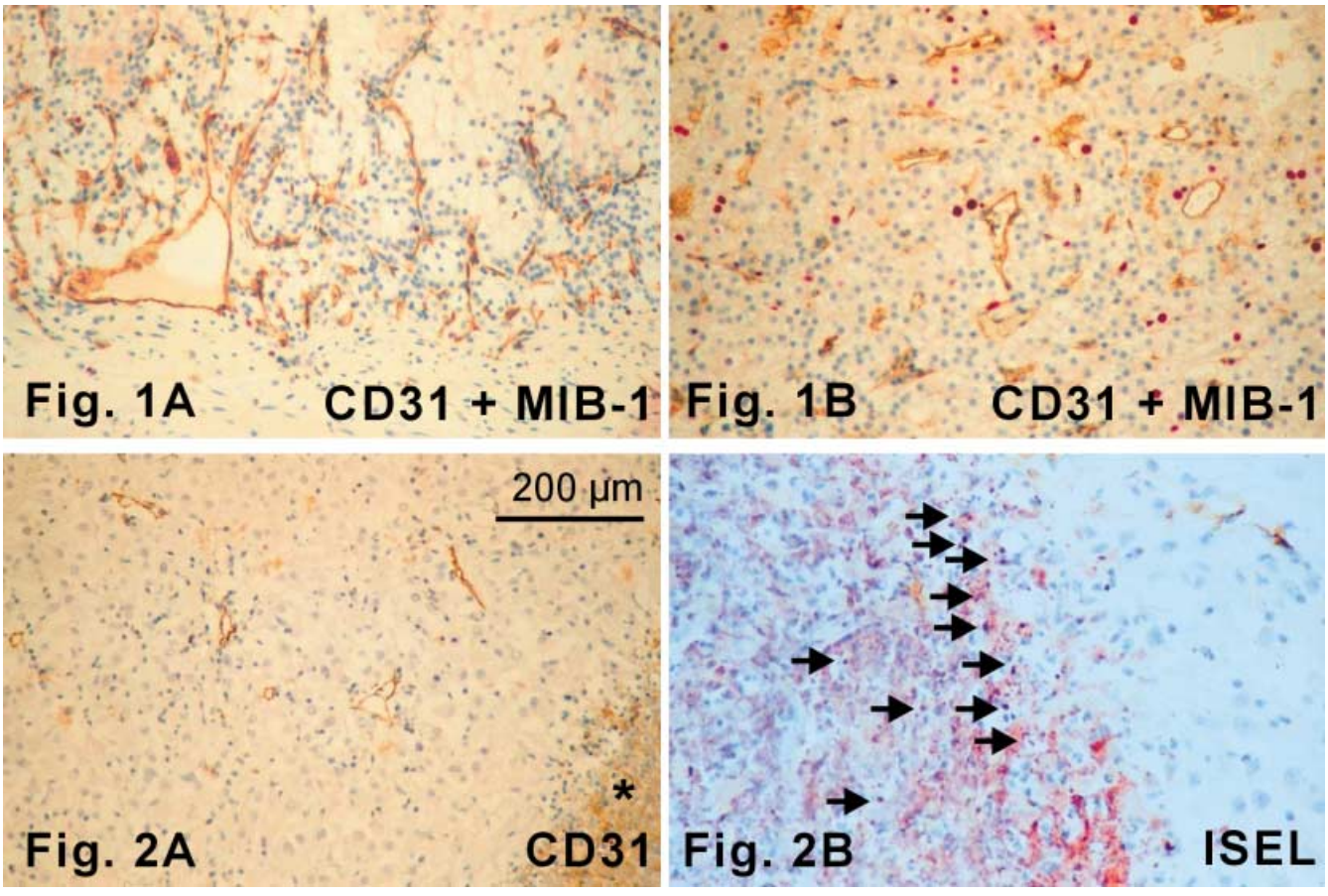


Fig. 1A,B Immunohistochemical detection of microvessels (CD31) and proliferating tumor cells (MIB-1). An increased vascular density with a large sinusoidal vessel at the tumor–host interface is observed (**A**) compared to central tumor microvessels (**B**). In contrast to numerous tumor cells no endothelia express MIB-1 antigen (magnification 100×)

Fig. 2A,B Comparative analysis of vessel density, necrosis and apoptosis, and VEGF expression. Within tumor tissue necrosis (*) is located in a distance of 200 µm away from microvessels (**A**, magnification 100×). Apoptotic bodies (➔) can be observed at the rim of avital tumor tissue (**B**; magnification 400×)

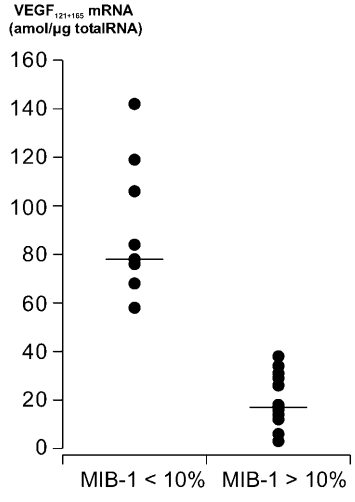


Fig. 3 Comparison of VEGFmRNA expression. Renal cell carcinomas with a MIB –1 index below 10% express higher amounts of $VEGF_{121+165}$ mRNA. Single values with median are demonstrated (P<0.0001)

RNA; SD±11.16) than in tumors with a MIB-1 index under 10% (91.37 attomol/µg total RNA; SD±28.46; P<0.0001; Fig.3).

At the rims of necrosis VEGF was upregulated. In vital tumor tissue VEGF was expressed in a patchy staining pattern (Fig. 4A).

Multicellular tumor spheroids imitate the intervascular space and develop chronic hypoxia independently of a microvessel supply. This static model is therefore useful for analyzing pure and chronic hypoxic effects on VEGF expression and induction of cell damage. Multicellular spheroids were generated up to a diameter of 600 µm, which is 1.5 times the widest intervascular distance within tumor tissue. In contrast to tumor tissues, necrosis could not be found within the spheroid center. However, a significant number of apoptotic bodies with the highest density within the spheroid center could be identified (Fig. 5A, B). Accordingly, VEGF protein expression was found highly upregulated in the spheroid center as compared to the outer spheroid rim (Fig. 4 B).

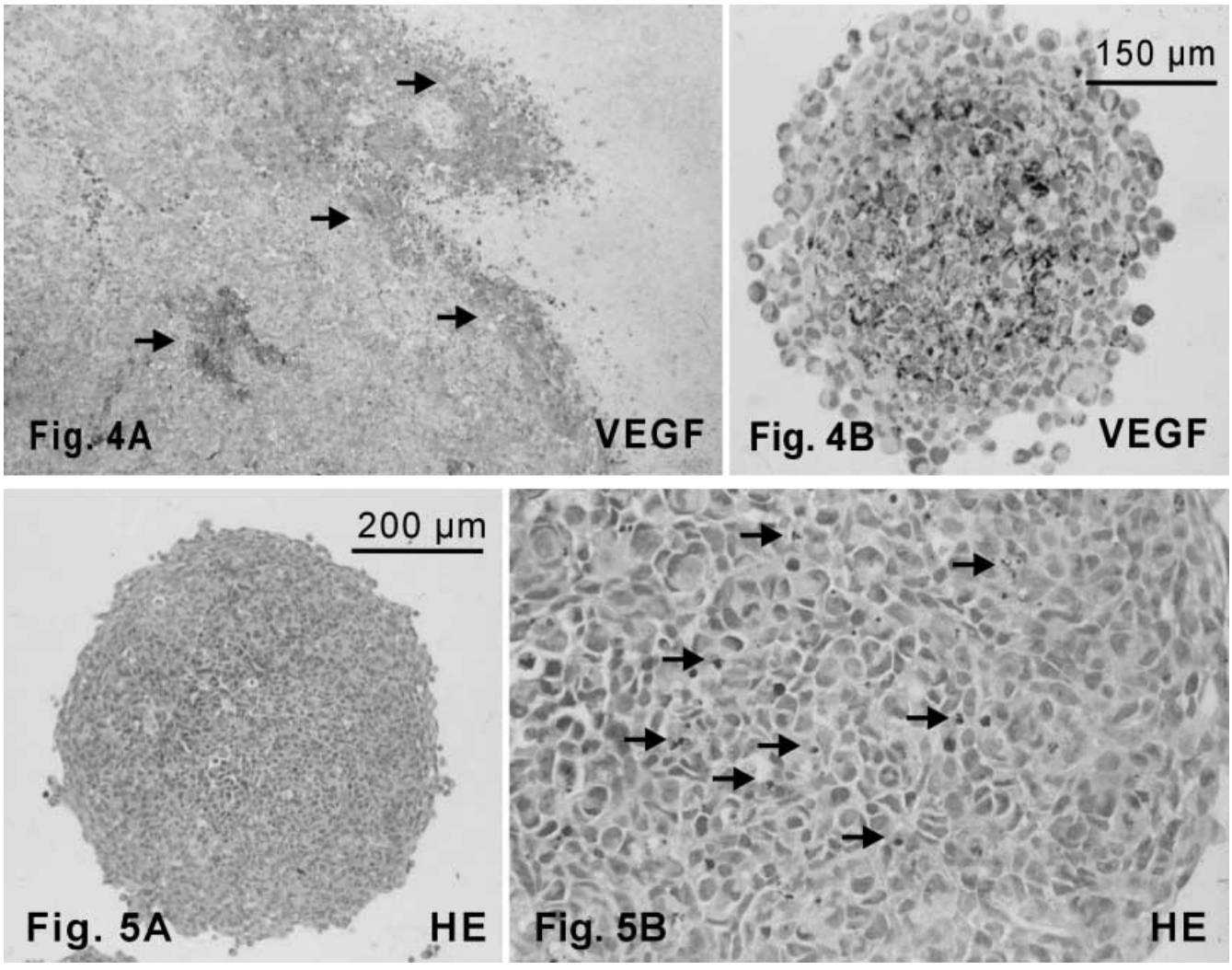


Fig. 4A,B VEGF expression in tumor tissue and multicellular tumor spheroids. Intratumoral VEGF expression is not only increased at the rims (➔) of necrosis but also in areas without necrosis or apoptosis (➔)(**A**; magnification 100×). Within the spheroid center VEGF is upregulated (**B**, magnification 200×).

Fig. 5A,B Tumor cell spheroids and apoptosis. Tumor spheroids extending the intervascular space of tumor tissue (**A**, magnification 100×) do not develop central necrosis but apoptosis (➔) in a centripedal pattern. Nuclear fragmentation and condensation can already be seen in hematoxylin-eosin stains (**B**; magnification 400×).

Matrix metalloproteinase expression and microvessel plasticity

The analysis of the expression of MMP-2 and -9, and the pericyte covering in 10 randomly selected cases revealed significant differences between tumor-free and tumor tissue.

In tumor tissue, in four cases endothelial MMP-2 expression was high, in two cases moderate, and in four cases weak. In nine cases the MMP-9 expression was weak and one case was negative. Because MMP-9 protein immunohistochemistry revealed faint signals, the expression was confirmed by mRNA in situ hybridization. In capillaries of unaffected, tumor-free renal tissue endothelial MMP-2 and -9 expression was not found (Fig. 6 A, B).

Nearly all capillaries of tumor-free renal tissue were covered by smooth muscle actin-positive pericytes. In contrast, only a mean of 44.2% of CD31 positive microvessels within tumor tissue exhibited a pericyte covering (minimum 16.7%, maximum 70.6%; $P<0.0001$; Fig. 6C, D).

Discussion

The aim of the present study was to analyze the relationship between VEGF expression, MVD, and tumor necrosis in renal cell cancer. The relevance of chronic hypoxia for angiogenesis has been interpreted in various ways. Tumor necrosis in invasive breast cancer has been shown to be associated with focal areas of high vascular density situated remotely from the actual sites of necrosis. Furthermore, it has been suggested that chronic hypoxia is a

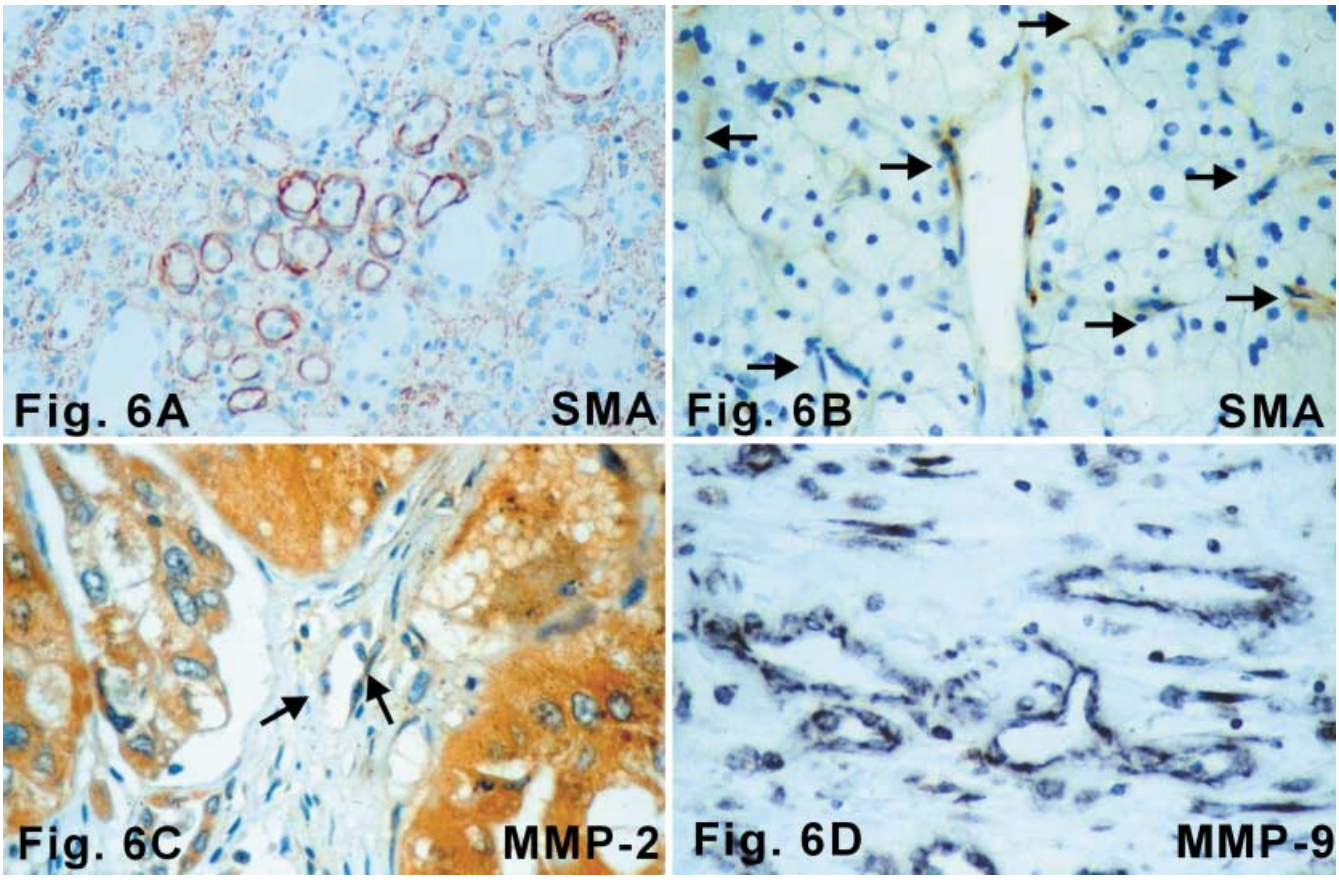


Fig. 6A–D Pericyte recruitment of microvessels and matrixmetalloproteinase expression in endothelia of tumor and tumor-free tissue. Microvessels within tumor tissue (➔) showing a discontinuous pericyte covering (**B**) and capillaries within tumor-free tissue with a complete covering (**A**, magnification 400×). Within tumor tissue capillary endothelia (➔) expressed MMP-2 (**C**, immunohistochemistry, magnification 400×). High MMP-9 mRNA levels in endothelia of microvessels at the tumor–host interface (**D**, non radioactive in situ-hybridization, magnification 400×)

main cause of tumor necrosis observed in aggressive tumors which outgrow their vascular supply [16]. In contrast to breast cancer [16], in renal cell carcinoma a significantly reduced MVD could be observed within vital areas of tumors exhibiting necrosis in comparison to tumors without necrosis. This implies that in renal cell carcinomas angiogenesis is not stimulated between necrotic foci. Since necrosis is often seen in highly proliferative tumors we compared VEGF mRNA levels with the tumor proliferation index. Highly proliferating tumors are likely to develop hypoxia, which is a strong stimulus of VEGF. However, a reduced VEGF mRNA expression in tumors with high proliferative activity was found. We speculate that the early stage of tumor formation is accompanied by a high MVD. At this stage highly proliferating tumors induce a high level of angiogenesis. This is supported by the finding that small tumors show a higher MVD than large tumors. High proliferative activity of tumor cells results in a faster increase of the tumor diameter. At this stage the tumor tissue is less hypoxic, inducing low levels of VEGF. The increase of the tumor volume is accompanied by a reduced MVD. Tumors outgrow their vascular supply and develop chronic hypoxia, leading to a decrease in tumor proliferation and an increase in the VEGF mRNA expression level. Our recent observations in a dorsal skinfold chamber model in nude mice revealed that implanted tumor spheroids show an increase in spheroid diameter and MVD until day 6 after implantation; thereafter microvessel density and spheroid growth decreases (data not shown). We therefore assume that antiangiogenic factors may hinder endothelial growth or induce microvessel regression. As shown in a previous study macrophages contribute a major component of the tumor-associated immune infiltrate and their density is positively correlated with the tumor grade [13]. It is known that macrophages do not only secrete VEGF but also factors such as reactive oxygen intermediates suppressing cellular proliferation. Consequently, tumor cell and vessel proliferation decreases and VEGF expression increases. Furthermore, in vitro within spheroids tumor cell proliferation and VEGF expression are mainly located at the rim and within the center, respectively. Hypoxia therefore constitutes the major functional link for suppression of tumor cell proliferation, on the one hand, and induction of VEGF gene expression, on the other.

As shown in the present study and by other authors, VEGF protein expression could be localized at the rims of necrotic tumor areas [7, 14, 17, 19] and in a patchy

fashion in tumor areas in which neither necrosis nor apoptosis could be detected. We used large multicellular spheroids extending the intervascular distance of tumor tissue as a model of continuous chronic hypoxia. In these spheroids the VEGF expression was upregulated within the hypoxic spheroid center. This has also been described by Waleh et al. [25], who found that within spheroids hypoxic conditions resulted in an expression of $VEGF_{165}$ mRNA. Within these spheroids no central necrosis but apoptosis could be detected. According to tumor biopsy specimens, cell proliferation was predominantly found at the periphery of spheroids expressing low levels of VEGF. Corresponding to the VEGF expression pattern within spheroids, locally upregulated VEGF expression within tumor tissue can be regarded as an indicator of hypoxia. However, the degree of hypoxia is not sufficient to induce a marked amount of tumor cell apoptosis as could be seen in spheroids. We therefore conclude that the duration and degree of hypoxia in tumors differs between tumor regions and does not necessarily lead to apoptosis or necrosis of tumor cells as long as a sudden break-down of the local perfusion does not disrupt the oxygen supply. This assumption is supported by Wijffels et al [30] who found large hypoxic viable tumor areas at distances even larger than 200 µm from the vessels. Microvascular regression itself induced by a deprivation of VEGF, as demonstrated by Meeson et al [18], could not be established as a cause of such a reduction of perfusion because only few apoptotic endothelia in vital tumor tissue could be detected. Therefore, focal necroses are more likely induced by acute disturbances of the perfusion and a lack of maturity of microvessels. The endothelial expression of MMP-2 and -9 found in this study indicates active angiogenesis, the expression of which can be induced by VEGF or TNF-α derived from renal cancer cells or tumor-associated macrophages [11, 12, 17]. Within tumor tissue we found an increased expression of endothelial MMP and a higher degree of pericyte-deficient microvessels compared with tumor-free tissue, which supports the hypothesis of structural weakness in immature vessels [3] and increased susceptibility of microvessels to intratumoral pressure and tensional forces. The latter might be the prerequisite of a sudden perfusion stop leading to necrosis.

In summary, the development of necrosis in renal cell carcinomas depends on acute hypoxia supported by a decreased density of immature microvessels. Therefore, chronic hypoxia does not necessarily lead to necrosis but may support the selective growth of hypoxia-resistant tumor cell clones. Furthermore, tumor necrosis may help to identify candidates for antiangiogenic therapy.

References

1. Benjamin LE, Hemo I, Keshet E (1998) A plasticity window for blood vessel remodelling is defined by pericyte coverage of the preformed endothelial network and is regulated by PDGF- B and VEGF. Development 125:1591–1598
2. Berger DP, Herbstritt L, Dengler WA, Marme D, Mertelsmann R, Fiebig HH (1995) Vascular endothelial growth factor (VEGF) mRNA expression in human tumor models of different histologies. Ann Oncol 6:817–825
3. Blood CH, Zetter BR (1990) Tumor interactions with the vasculature: angiogenesis and tumor metastasis. Biochim Biophys Acta 1032:89–118
4. Boldrini L, Calcinai A, Silvestri V, Basolo F, Lucchi M, Mussi A, Angeletti CA, Bevilacqua G, Fontanini G (1999) Quantitation by competitive PCR assay of vascular endothelial growth factor in non-small cell lung carcinomas. Int J Oncol 14:161–168
5. Breier G, Damert A, Plate KH, Risau W (1997) Angiogenesis in embryos and ischemic diseases. Thromb Haemost 78:678–683
6. Chomczynski P, Sacchi N (1987) Single-step method of RNA isolation by acid guanidinium thiocyanate-phenol-chloroform extraction. Anal Biochem 162:156–159
7. Damert A, Machein M, Breier G, Fujita MQ, Hanahan D, Risau W, Plate KH (1997) Up-regulation of vascular endothelial growth factor expression in a rat glioma is conferred by two distinct hypoxia-driven mechanisms. Cancer Res 57: 3860–3864
8. Feucht M, Christ B, Wilting J (1997) VEGF induces cardiovascular malformation and embryonic lethality. Am J Pathol 151:1407–1416
9. Fontanini G, Lucchi M, Vignati S, Mussi A, Ciardiello F, De Laurentiis M, De Placido S, Basolo F, Angeletti CA, Bevilacqua G (1997) Angiogenesis as a prognostic indicator of survival in non-small-cell lung carcinoma: a prospective study. J Natl Cancer Inst 89:881–886
10. Goede V, Schmidt T, Kimmina S, Kozian D, Augustin HG (1998) Analysis of blood vessel maturation processes during cyclic ovarian angiogenesis. Lab Invest 78:1385–1394
11. Gogusev J, Augusti M, Chretien Y, Droz D (1993) Interleukin-6 and TNF alpha production in human renal cell carcinoma. Kidney Int 44:585–592
12. Harmey JH, Dimitriadis E, Kay E, Redmond HP, Bouchier-Hayes D (1998) Regulation of macrophage production of vascular endothelial growth factor (VEGF) by hypoxia and transforming growth factor beta-1. Ann Surg Oncol 5:271–278
13. Hemmerlein B, Markus A, Wehner M, Kugler A, Zschunke F, Radzum HJ (2000) Expression of acute and late-stage inflammatory antigens, c-fms, CSF-1, and human monocytic serine esterase 1, in tumor-associated macrophages of renal cell carcinomas. Cancer Immunol Immunother 49:485–492
14. Jonjic N, Valkovic T, Lucin K, Iternicka Z, Krstulja M, Mustac E, Dobi-Babic R, Sasso F, Melato M (1998) Comparison of microvessel density with tumor associated macrophages in invasive breast carcinoma. Anticancer Res 18:3767–3770
15. Lamoreaux WJ, Fitzgerald ME, Reiner A, Hasty KA, Charles ST (1998) Vascular endothelial growth factor increases release of gelatinase A and decreases release of tissue inhibitor of metalloproteinases by microvascular endothelial cells in vitro. Microvasc Res 55:29–42
16. Leek RD, Landers RJ, Harris AL, Lewis CE (1999) Necrosis correlates with high vascular density and focal macrophage infiltration in invasive carcinoma of the breast. Br J Cancer 79:991–995
17. Lewis CE, Leek R, Harris A, McGee JO (1995) Cytokine regulation of angiogenesis in breast cancer: the role of tumor- associated macrophages. J Leukoc Biol 57:747–751
18. Meeson AP, Argilla M, Ko K, Witte L, Lang RA (1999) VEGF deprivation-induced apoptosis is a component of programmed capillary regression. Development 126:1407–1415
19. Plate KH, Warnke PC (1997) Vascular endothelial growth factor. J Neurooncol 35:365–372
20. Risau W (1998) Development and differentiation of endothelium. Kidney Int Suppl 67:S3-S6
21. Smith SK (1998) Angiogenesis, vascular endothelial growth factor and the endometrium. Hum Reprod Update 4:509–519
22. Thelen P, Hemmerlein B, Kugler A, Seiler T, Ozisik R, Kallerhoff M, Ringert RH (1999) Quantification by competitive

quantitative RT-PCR of VEGF121 and VEGF165 in renal cell carcinoma. Anticancer Res 19:1563–1565
23. Thoenes W, Storkel S, Rumpelt HJ (1986) Histopathology and classification of renal cell tumors (adenomas, oncocytomas and carcinomas). The basic cytological and histopathological elements and their use for diagnostics. Pathol Res Pract 181: 125–143
24. Tohma Y, Gratas C, Van Meir EG, Desbaillets I, Tenan M, Tachibana O, Kleihues P, Ohgaki H (1998) Necrogenesis and Fas/APO-1 (CD95) expression in primary (de novo) and secondary glioblastomas. J Neuropathol Exp Neurol 57:239–245
25. Waleh NS, Brody MD, Knapp MA, Mendonca HL, Lord EM, Koch CJ, Laderoute KR, Sutherland RM (1995) Mapping of the vascular endothelial growth factor-producing hypoxic cells in multicellular tumor spheroids using a hypoxia-specific marker. Cancer Res 55:6222–6226
26. Wang H, Keiser JA (1998) Vascular endothelial growth factor upregulates the expression of matrix metalloproteinases in vascular smooth muscle cells: role of flt-1. Circ Res 83:832–840
27. Weidner N (1996) Intratumoral vascularity as a prognostic factor in cancers of the urogenital tract. Eur J Cancer 32A:2506–2512
28. Weidner N, Carroll PR, Flax J, Blumenfeld W, Folkman J (1993) Tumor angiogenesis correlates with metastasis in invasive prostate carcinoma. Am J Pathol 143:401–409
29. Weidner N, Semple JP, Welch WR, Folkman J (1991) Tumor angiogenesis and metastasis–correlation in invasive breast carcinoma. N Engl J Med 324:1–8
30. Wijffels KI, Kaanders JH, Rijken PF, Bussink J, van den Hoogen FJ, Marres HA, de Wilde PC, Raleigh JA, van der Kogel AJ (2000) Vascular architecture and hypoxic profiles in human head and neck squamous cell carcinomas. Br J Cancer 83:674–683
31. Wilhelm SM, Collier IE, Marmer BL, Eisen AZ, Grant GA, Goldberg GI (1989) SV40-transformed human lung fibroblasts secrete a 92-kDa type IV collagenase which is identical to that secreted by normal human macrophages. J Biol Chem 264: 17213–17221

Virchows Arch (2001) 439:653–660
DOI 10.1007/s004280100411

ORIGINAL ARTICLE

Peter Loogna · Lennart Franzén · Pentti Sipponen
Lennart Domellöf

Helicobacter pylori, N-methyl-N′-nitro-N′-nitrosoguanidine, and bile modulate gastric cell kinetics in experimental cancer

Received: 1 December 2000 / Accepted: 9 January 2001 / Published online: 27 March 2001
© Springer-Verlag 2001

Abstract *Helicobacter pylori* infection is a risk factor for gastric cancer. How the bacterium contributes to this process is still unclear. We present a new Wistar rat model that was used to evaluate the effect of *H. pylori* on early preneoplastic events as judged from epithelial cell turnover and histopathological changes. One hundred and four rats were colonized with *H. pylori* and exposed to MNNG (N-methyl-N′-nitro-N′-nitrosoguanidine) and/or taurocholic acid. Inflammation, goblet cell-like metaplasia, atrophy, dysplasia, and adenocarcinoma were scored in a blinded manner. Apoptotic cells were counted after staining with terminal uridine deoxynucleotidyl nick end labeling, and epithelial cell proliferation was determined by means of the Ki-67 labeling index. No early tumor enhancement with *H. pylori* could be found in ordinary histology. However, *H. pylori* significantly enhanced the epithelial cell proliferation compared with the control group, and the combination with taurocholic acid appeared to have a synergistic effect. MNNG significantly increased the normal gastric epithelial apoptosis. This increase was reduced in antral mucosa with *H. pylori* infection. The findings suggest that *H. pylori*, especially when combined with bile, has an influence on cell kinetics, contributing to the development of gastric cancer. The reduced apoptosis of MNNG also observed in infected animals indicates a dual function of *H. pylori*.

Keywords Wistar rat · Stomach carcinogenesis · *Helicobacter pylori* · Cell proliferation · Apoptosis

P. Loogna · L. Domellöf (✉)
Department of Surgery, Örebro Medical Centre Hospital, 701 85 Örebro, Sweden
e-mail: lennart.domellof@orebroll.se
Tel.: +46-19-6021796, Fax: +46-19-125439

L. Franzén
Department of Pathology, Örebro Medical Centre Hospital, Örebro, Sweden

P. Sipponen
Department of Pathology, Jorvi Hospital, Espoo, Finland

Introduction

Helicobacter pylori infection was classified by the World Health Organization (WHO) and the International Agency for Research on Cancer (IARC) in 1994 as a group-1 carcinogen in humans [12]. This conclusion was based mainly on epidemiological findings [7, 27, 30, 29, 41]. Some reports have claimed a lack of association between *H. pylori* and risk of gastric cancer [2, 46]. IARC stressed the importance of developing animal models of *H. pylori* infection to address mechanisms of carcinogenesis.

Gastric cancer is a multifactorial disease, where environmental, genetic factors and *H. pylori* may interact in a complex way. Consequently, the mechanisms by which the *H. pylori* infection may lead to cancer have not yet been determined. It is obvious that the bacterial infection alone cannot explain the pathogenesis of gastric cancer. Only a minority of *H. pylori*-infected individuals develop gastric cancer. Furthermore, it has been shown that this bacterium is not directly mutagenic in an Ames test [19]. However, it has been proposed that *H. pylori* may act as a tumor promoter by changing proliferation and apoptosis of the gastric epithelium [32]. The promoting mechanisms could be that an increased cell proliferation leads to an increased susceptibility for DNA damage and mutagenesis and a decreased apoptosis, which may result in the accumulation of potentially malignant cells.

In studies on the role of *H. pylori* in gastric carcinogenesis, several animal models have been developed. Recently, spontaneous development of gastric carcinoma has been observed in the Mongolian gerbil infected with *H. pylori* [36, 37, 38, 45]. Experimental chemical gastric carcinogenesis has previously been successful in dogs, hamsters, rabbits, rats [40], and mice [43].

So far, no study has been performed on the association between *H. pylori* infection and chemical gastric carcinogens in the rat species. In the present study, the influence of *H. pylori* infection on N-methyl-N′-nitro-N′-nitrosoguanidine (MNNG)-induced stomach carcinogenesis in Wistar rats was examined. The possible pro-

moting role of *H. pylori* gastritis and bile acids on MNNG-induced carcinogenesis was investigated. We focused in particular on cell proliferation, apoptosis, histological alterations, and cell damage in the gastric mucosa.

Materials and methods

Animals

One hundred and four 8-week-old male Wistar rats, weighing about 200 g, were used. The animals were housed in Macrolon cages, two rats per cage, in a room with regulated temperature (20–22°C), humidity (50–60%), and a 12/12 h light/dark cycle. The rats were allowed at least 1 week of acclimatization before the experiment. The animals had free access to drinking water and rat and mouse diet no. 2 (BK Universal, Sollentuna, Sweden). Body weight was controlled every second week. Termination and autopsies were performed when the rats were sick or after experimental week 37. The care of the animals and the experimental procedures were carried out according to accepted standards and with approval of the regional ethical committee.

H. pylori strain

The *H. pylori* strain (He l73,vacA+,cagA+) used in this study had been isolated from a patient with duodenal ulcer. The strain was rat-adapted [18].

Chemicals

A stock solution of MNNG (Aldrich Chemicals, Inc., Milwauke, Wis.) was prepared every second week with distilled water to a concentration of 1 g/l. The solution was kept in the dark at 4°C. Every other day, an aliquot of this stock solution was diluted with tap water to a concentration of 100 mg/l. The solution was provided in light-shielded bottles ad libitum to MNNG animals as the drinking water. Control animals were given only tap water.

Taurocholic acid (Sigma Chemicals, Sweden) was added to the ground meal at a concentration of 0.25%, which was then pelleted.

Study design

The animals were randomly divided into two groups. Sixty-two rats were given the *H. pylori* suspension (about 5×10^8 CFU/ml) by gavage (2 ml/rat) four times over a 5-day period. The rats were given omeprazole (Astra Hässle AB, Mölndal, Sweden) 400 mol/kg, suspended in carbonate-buffered 0.5% HPMC (Hydroxypropylmethylcellulose, Shinyetsu, Japan), pH 9, by gavage [17], 3 h before the first inoculation. The control groups, consisting of 42 animals, were kept for the same period of time, but they were not inoculated. The *H. pylori*-treated rats and the controls were divided into eight subgroups 4 weeks after the inoculation (Fig. 1).

At sacrifice, blood was sampled, and serum was separated and stored at –20°C until analysis. The stomach was opened along the greater curvature and was carefully examined, as were all other organs. All subsequent investigations were performed by operators blinded with regard to the different treatment groups.

Histopathological examination

The stomach was fixed in 10% neutral-buffered formalin for 48 h at room temperature and embedded in paraffin. Sections (5-µm thick) were stained with hematoxylin and eosin (HE), Giemsa, and periodic acid–Schiff (PAS) and examined for morphological lesions and the presence of bacteria. Histological parameters included assessment of degree of inflammation, erosions, presence of goblet-like cells, focal atrophy, dysplasia, and adenocarcinoma. The inflammation score was based on criteria described by Mohammadi et al. [25]. Briefly, the score equals the sum of the grade of intensity of inflammation in the most inflamed area (0–3), the longitudinal extent (0–3), and depth of inflammation (0–3), giving a maximum score of nine.

Erosions were defined as epithelial defects that did not extend through the muscularis mucosae. Areas where gastric glands were sparse and separated by connective tissue stroma with a few inflammatory cells were classified as atrophy. Goblet cell metaplasia was defined as areas with goblet-like cells intermixed with normal foveolar epithelial cells but with no absorptive intestinal cells. Dysplastic epithelium were defined as areas with prominent cellular and architectural abnormalities of the epithelium and glands. Lesions were categorized as adenocarcinoma by the presence of atypical glands that showed invasion and destroyed the original mucosal architecture.

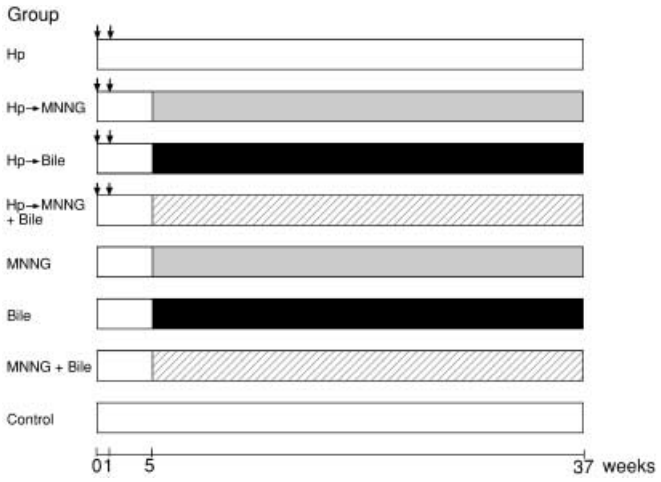


Fig. 1 Experimental design. *Arrows* indicate inoculations over a 5-day period with *Helicobacter pylori*. All rats were sacrificed 37 weeks after the study commenced

Detection of *H. pylori*

Samples, 5×5 mm, from macroscopically normal antrum mucosa, were homogenized. The material was placed on gonococcus (GC) agar plates and incubated for 4–14 days in micro-aerobic conditions at 37°C. *H. pylori* were identified by colony morphology, typical curved Gram-negative rods, and by urease, catalase, and oxidase tests.

One in-house enzyme-linked immunosorbent assay (ELISA) was used to demonstrate serum immunoglobulin (Ig)G anti-*H. pylori* antibodies as described by Mohammadi et al.[24]. The titer of the antibody was expressed by way of an arbitrary index; values greater than 1.0 were accepted as indicating positive detection of *H. pylori*. For histological detection of *H. pylori*, Giemsa stain was used. The definition of a *H. pylori*-positive animal was at least one positive test with histology, serology, or culture.

Immunohistochemistry

Gastric epithelial cell proliferation in the antrum mucosa was assessed using the ABC method (avidin–biotin peroxidase complex; Dako, Glostrup, Denmark). The monoclonal antibody used was MIB-5, specific for rat Ki-67 antigen (Dianova, Hamburg, Germa-

ny)[10]. For each primary antibody and tissue, negative controls were run by replacing the primary antibody with nonimmune serum.

Proliferation was assessed by counting 1000 epithelial cells in the antrum mucosa, approximately 400 µm from the gastroduodenal junction. A 310-µm wide swath, perpendicular to the mucosal surface and comprising the entire thickness of the mucosa, was used. Within the swath, all labeled and unlabeled epithelial cells were counted. Special attention was paid to assessing these measurements only in slides containing vertical cuts. Areas with artifacts, such as foldings of the tissue sections, were omitted from the counting. The results were expressed as labeling index (LI), which is the percentage of labeled cell nuclei over the total number of counted epithelial cell nuclei [16].

Quantification of apoptosis

Apoptotic cells were stained using TUNEL terminal deoxynucleotidyl nick end labeling), with the In situ Apoptosis Detection Kit (Oncor, Gaithersburg, Md.). Sections from rat spleen served as positive controls. For negative controls, terminal deoxynucleotidyl transferase was omitted [9]. The epithelial apoptotic cells were counted in one contiguous area, starting from the gastroduodenal junction to 3 mm proximally in the antrum. The results were expressed as apoptotic index, which is the number of apoptotic cells/mm mucosal length [18].

Thickness of the antrum mucosa

The thicknesses of the different compartments of the antrum mucosa (crypts, proliferative zone, and foveolae) were assessed in images (290×) captured with a Leica DC 200 digital camera mounted on a Leica DMRXE microscope (Leica Microsystems Wetzlar GmbH, Wetzlar, Germany). Each image spanned the whole thickness of mucosa. A length of 1 mm, starting from the gastroduodenal junction, was analyzed. The proliferative zone was identified by the staining of nuclei with the antibody MIB-5 against Ki-67 antigen. The area and lateral length of the different compartments were measured, and the mean thickness was calculated using the Leica Q-Win (Leica Microsystems Imaging Solutions Ltd., Cambridge, UK) image analysis program.

Statistics

The nonparametric Mann–Whitney U test was used for pairwise comparisons, while the Kruskal–Wallis test was used for overall comparisons between the groups. Spearman R correlation coefficients were calculated to analyze the relationship between apoptotic index and atrophy. Significance was defined as $P<0.05$.

Results

General findings

All animals developed and behaved normally during the experiment. The median body weight was significantly lower ($P<0.004$) at sacrifice only in the groups receiving MNNG (535.5 g) and *H. pylori* and MNNG (555.0 g) compared with the uninfected controls (646.0 g). There was no significant difference in survival between the different groups. Eight animals (one control, three MNNG+bile, and four *H. pylori*+MNNG+bile) that died of pneumonia before the termination of the experiment were excluded from analysis due to autolytic changes in the stomach.

Histopathological findings

Two cases of adenocarcinoma in the antrum were found in the MNNG+bile group (Table 1). No adenocarcinoma was found in the other groups. Dysplasia was found in three animals (two MNNG+bile and one MNNG). Focal scar-like atrophy, where there are atypic, irregular proliferation of mucosal glands, was seen in more than 50% of all animals in all MNNG groups (Fig. 2). These groups also showed goblet-like cell metaplasia in 10–50% of the cases. *H. pylori* did not significantly influence these frequence rates. There was a significant correlation between areas of atrophy and goblet cell metaplasia ($R=0.37$, $P<0.0003$). The thickness of the antrum mucosa was not significantly changed by *H. pylori* infection (Fig. 3). All animals exposed to MNNG had, however, a significantly thicker antrum mucosa compared with the controls ($P=0.0000$). One case of hepatocellular cancer was found in the MNNG+bile group, one case of malignant skin fibrosarcoma was found in the MNNG group, and a benign abdominal lipoma was found in the *H. pylori*+MNNG group. Control animals had no pathological changes.

H. pylori colonized 57 out of 62 rats inoculated with the bacteria at the study entry. The later administration

Table 1 Histopathological changes in the glandular stomach of Wistar rats. *Hp* Helicobacter pylori; *MNNG* N-methyl-N′-nitro-N′-nitrosoguanidine

Group	Effective numbers	Inflammation score[a]	Erosions	Goblet cell metaplasia	Focal atrophy	Dysplasia	Adenocarcinoma
Hp	11	4.3±1.3[b]	1	0	0	0	0
Hp+MNNG	17	3.4±0.6[b]	7	7[b]	9[b]	0	0
Hp+Bile	12	3.2±1.3[b]	0	0	0	0	0
Hp+MNNG+Bile	13	3.9±1.0[b]	0	6[b]	8[b]	0	0
MNNG	10	3.8±1.0[b]	4	1	8[b]	1	0
Bile	10	2.0±1.8	0	0	0	0	0
MNNG+Bile	9	4.2±1.1[b]	1	1	6[b]	2	2
Control	9	1.0±1.5	0	0	0	0	0

[a] Mean±SD maximum score 9
[b] Significantly different from control group ($P<0.005$)

of bile or MNNG did not affect the colonization. All non-infected rats were excluded from the subsequent investigations. Microscopy demonstrated the presence of *H. pylori* in 56% of inoculated rats at the end of the experiment. The bacteria were only confined to the antrum mucosa. *H. pylori* were mainly observed in the lumen of the gastric pits and, to a lesser extent, attached to the surface of the epithelial cells. Very few *H. pylori* were found in the corpus–antrum transition zone. No *H. pylori* were observed in the sections from the corpus, in the cardia-equivalent region adjacent to the squamo–columnar junction, or in the duodenum. The mucosal inflammation was mild in the *H. pylori*-infected animals and was dominated by infiltration of lymphocytes and macrophages. No case of severe inflammation was noted. The inflammation was localized to the antrum and the corpus/antrum transition zone. There was no visible inflammation in the corpus mucosa.

The results of *H. pylori* serology and histological findings of *H. pylori* infection correlated well (Spearman's correlation coefficient r=0.50, P<0.00001). All cases with positive microscopic findings were also positive for serum anti-*H. pylori*. *H. pylori* was never observed by bacterial culture or by microscopy in the control animals, and serology was negative.

Epithelial proliferation

With immunohistochemical staining of the Ki-67 protein, we could easily demonstrate proliferating antrum epithelial cells (Fig. 4). Increased LI significantly correlated with increased arbitrary index for *H. pylori* serology (Spearman's correlation coefficient r=0.51 and

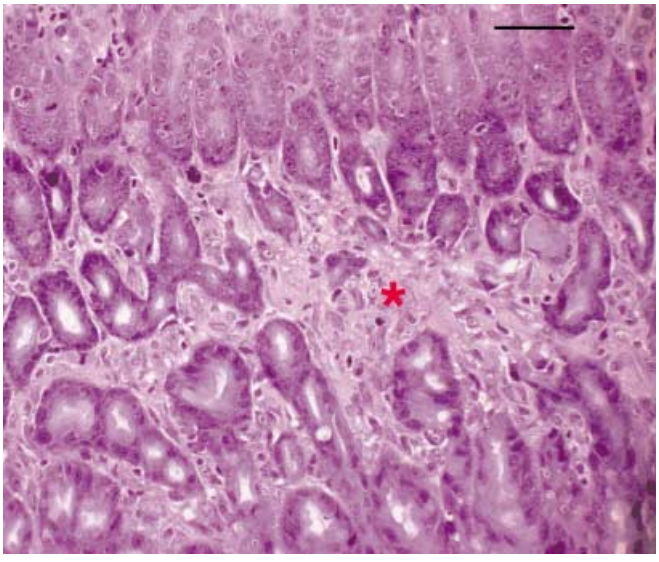


Fig. 2 A focal antral scar (*red asterix*) after treatment with *Helicobacter pylori*, N-methyl-N′-nitro-N′-nitrosoguanidine, and bile. Giemsa stain; *bar* 50 μm

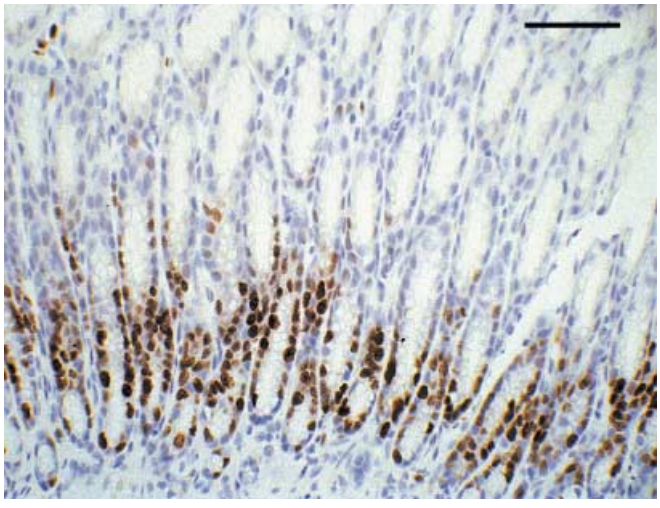
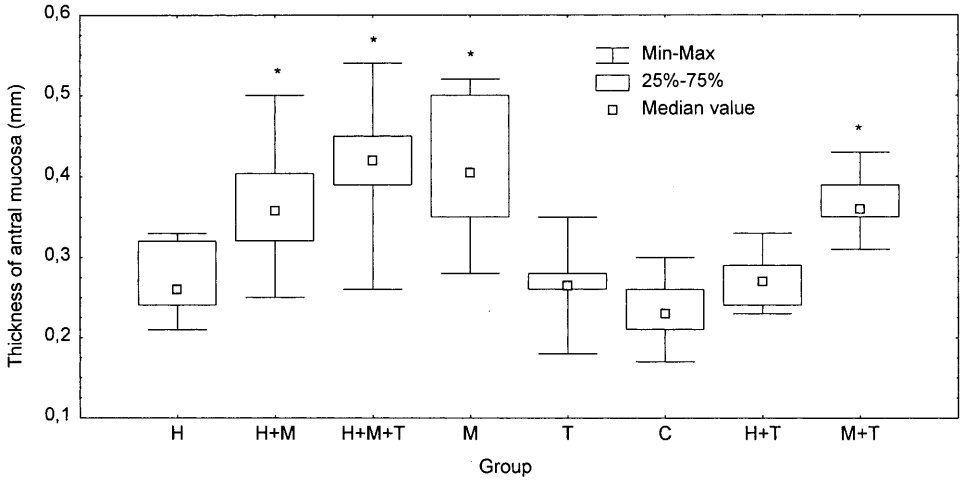


Fig. 4 Immunohistochemical staining of Ki-67 protein in proliferating cells in antral mucosa after treatment with N-methyl-N′-nitro-N′-nitrosoguanidine and taurocholic acid. The proliferative zone is easily discerned in the lower part of the mucosa. *Bar* 50 μm

Fig. 3 Thickness of antral mucosa (mm) in the different groups (*H Helicobacter pylori*; *M* N-methyl-N′-nitro-N′-nitrosoguanidine; *T* taurocholic acid; *C* control). Data are expressed as median. *P=0.000



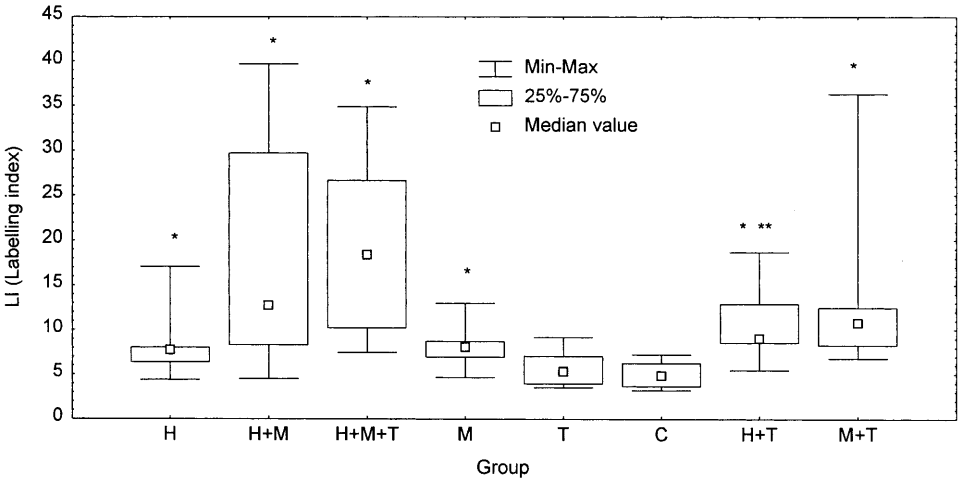


Fig. 5 Labeling index of antral epithelial cells in the different groups (*H Helicobacter pylori*; *M* N-methyl-N′-nitro-N′-nitrosoguanidine; *T* taurocholic acid; *C* control). Data are expressed as median. **P*<0.004 (significant difference from *C*); ***P*<0.002 (significant difference from *T*)

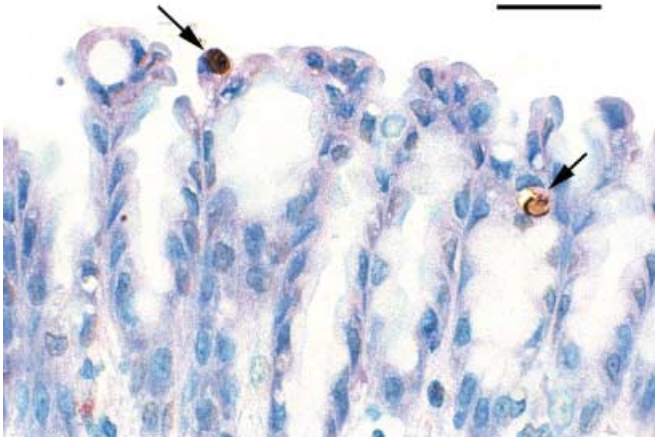


Fig. 6 Apoptotic epithelial cell nuclei at the surface of the antral mucosa (*arrows*) in a rat treated with *Helicobacter pylori* and N-methyl-N′-nitro-N′-nitrosoguanidine. TUNEL staining; *bar* 25 µm

P=0.00000) and antral inflammation (*r*=0.23 and *P*<0.023) and focal atrophy (*r*=0.42 and *P*<0.00003). *H. pylori* enhanced the LI in the *H. pylori*+bile group compared with bile group alone (*P*<0.002) but not significantly in the *H. pylori*+MNNG group compared with MNNG alone (*P*=0.063; Fig. 5). Furthermore, *H. pylori* enhanced the thickness of the proliferative zone in the *H. pylori*+MNNG+bile group compared with MNNG+bile (*P*<0.002). The control and bile groups had a significantly lower LI than all other groups (*P*<0.004 and *P*<0.05, respectively).

Apoptosis of the gastric epithelium

The apoptotic epithelial cells were found at the surface of the upper part of the antrum mucosa (Fig. 6). The number of apoptotic cells was higher in the MNNG group than in the *H. pylori*+MNNG group (*P*<0.01; Fig. 7). Increased apoptosis correlated positively to inflammation score, atrophy, and dysplasia (*P*<0.05) but negatively to body weight (*P*<0.0008). No correlation

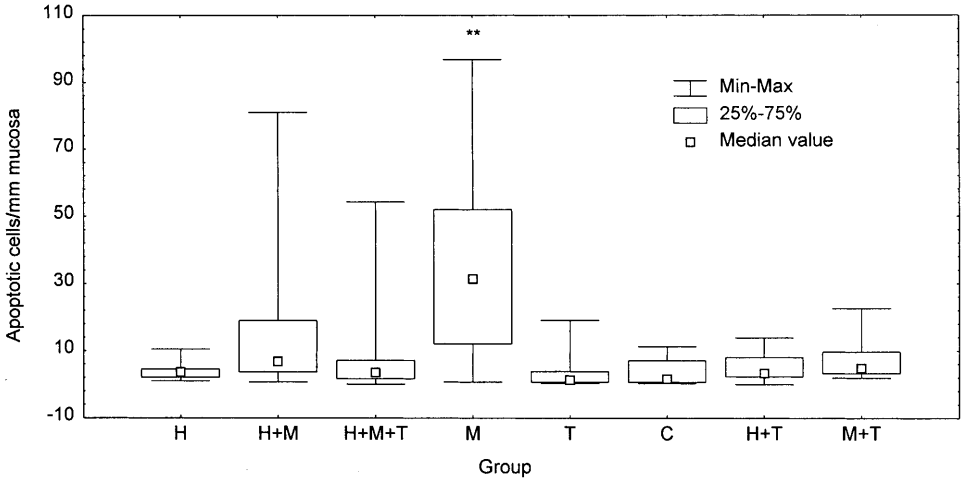


Fig. 7 Apoptotic index of antral epithelial cells in the different groups (*H Helicobacter pylori*; *M* N-methyl-N′-nitro-N′-nitrosoguanidine; *T* taurocholic acid; *C* control). Data are expressed as median. ***P*<0.01 (significant difference from *H+M*)

could be seen between increased LI and increased apoptosis (r=0.12, P=0.27).

Discussion

Gastric cancer is the second most common neoplasm in the world [28]. Although *H. pylori* infection is classified as a group-I carcinogen, there is a need for using animal models to elucidate this association and specific carcinogenic mechanisms. The rat model has several advantages, because rats are inexpensive, easily housed, and well-defined biologically and genetically. Many pioneering works in gastric carcinogenesis have particularly been done in rats [1]. The Wistar strain has been regarded as the gold standard in such experiments.

Only one study has been found that focuses on a possible association between *H. pylori* and gastric cancer in rats [14]. However, in this study, *H. pylori* was inoculated three times per week for 40 weeks, and the study did not control the colonization of the stomach mucosa by *H. pylori*. We have applied the only verified rat model of *H. pylori* infection described by Li et al. [17] on Sprague–Dawley rats. Wistar rats do not normally carry urease-positive spiral bacteria in the gastric mucosa [22]. This was also confirmed in our control animals. Ratified *H. pylori* were successfully colonizing Wistar rats, which are a standard model for MNNG-induced cancer. The *H. pylori* colonization was not altered by the later addition of MNNG and/or bile. In this study, we used taurocholic acid, which is known to be the most potent bile acid, to break the gastric mucosal barrier [33, 39]. Furthermore, it has a verified low toxicity to *H. pylori* [13].

In the present study, the carcinogen was given to young animals after infection with *H. pylori*, mimicking the clinical situation where the infection may start in childhood, after which the stomach is exposed to a variety of exo- and endogenous carcinogens. In this study, we used a defined cagA- and vacA-positive strain of *H. pylori*. The cagA gene is used as a marker for the presence of the cag pathogenicity island. Strains positive for the cagA gene have been shown to associate with an increased gastric cell proliferation but not with apoptosis [34]. There is accumulating evidence that humans infected with strains of *H. pylori* that express VacA and/or cagA (type-I strain) are more likely to have a more aggressive gastritis than those with non-cytotoxic strains. These subjects are more likely to develop a peptic ulcer or gastric cancer than subjects infected with other strains [31]. Contrary to humans, the *H. pylori* colonization in Wistar rats caused a mild gastritis, dominated by infiltration of lymphocytes and macrophages, with only few polymorphonuclear neutrophils. The differences in the inflammatory patterns between man and Wistar rats may be due to different host responses.

In the present study, we could not find an early tumor enhancement or atrophic gastritis with *H. pylori* in ordinary histology. This is in accordance with the only previous study in Wistar rats [14]. However, these results are in discrepancy with the findings in Mongolian gerbils. Tokieda et al. demonstrated that *H. pylori* infection enhanced the carcinogenic action of MNNG after 52 weeks [44]. The relatively mild degree of *H. pylori* gastritis obtained in Wistar rats against the severe gastritis of Mongolian gerbils might explain this difference. The focal atrophy that was seen in 50% of all animals receiving MNNG has previously been described [15]. This alteration was not found in the other groups. We could also demonstrate an increased cell proliferation and apoptosis in these lesions, confirming earlier studies [23]. The focal atrophy with irregular proliferation of the glands could at most be classified as a lesion indefinite for dysplasia.

No complete intestinal metaplasia was found in the present study, but goblet-like cells were quite frequently seen in the MNNG groups. These cells have previously been reported as intestinal metaplasia after treatment with MNNG [21, 42]. However, in our study, the columnar cells between and around goblet-like cells are normal foveolar cells without any metaplastic features. We found that the goblet cell metaplasia was always correlated with mucosal atrophy. Both these findings are part of the events leading to gastric cancer, as suggested by Correa [5]. A further support for this sequence was that the early cases with dysplasia and adenocarcinoma that we observed also had these carcinogen-induced mucosal alterations. Although some groups have found intestinal metaplasia in control animals, we could not demonstrate goblet-like cell metaplasia in any of our controls [21, 42].

MNNG-induced apoptosis, as a possible cause of mucosal atrophy in the rat, has been reported as early as after 8 weeks [23]. In our study, MNNG was given for 32 weeks in order to better observe any promotional effect of *H. pylori*. A longer experiment may have decreased the differences between the MNNG groups, since the majority of animals will develop adenocarcinomas [35]. Recently, the importance of studying preneoplastic events has also received attention [26].

Increased cell proliferation and/or alteration in apoptosis are characteristic findings in cancer. While some authors have reported increased proliferative rates in *H. pylori*-infected mucosa in man [8] that will be normalized after eradication [3], others have observed no effect or even decreased proliferation rates in infected animals [4]. These discrepancies could be due to difficulties in evaluating the proliferative activity [11]. In this study, the proliferative cells are easily identified using the antibody MIB-5-detecting Ki-67 antigen as a marker for cell proliferation and for the LI. It has been claimed that the epithelial hyperproliferation is due to either altered apoptosis or is a direct effect of *H. pylori* on epithelial cells [20]. We could not, however, see any obvious compensatory epithelial proliferation with increased apoptosis in the different groups.

The present study verifies that *H. pylori* infection significantly enhanced the LI of the epithelium compared with that in the control group. Bile had no enhancing ef-

fect on proliferation. However, the combination of *H. pylori* and bile appeared to act synergistically, resulting in a significant increase of LI. The latter finding is in line with the increased risk for development of cancer in the stomach remnant exposed to bile reflux following partial gastrectomy [6].

In accordance, the addition of *H. pylori* induces an extension of the proliferative zone when combined with bile and MNNG. Interestingly, *H. pylori*, when combined with MNNG, decreased the apoptotic index, while MNNG alone significantly increased apoptosis in the antral mucosa.

In summary, the results indicate a dual influence of *H. pylori* on gastric cell kinetics. It may act as a tumor promoter by increasing proliferation (especially in combination with bile acid) and thereby increasing the chance of mutation and reducing the time for DNA repair [11]. Furthermore, *H. pylori* reduce the MNNG-enhanced apoptosis, thus impairing the elimination of cells mutated by this carcinogen. The Wistar rat model will be of value in studying which role different strains of *H. pylori* have in the multifactorial development of gastric cancer.

Acknowledgements This work was financially supported by grants from the Research Committe of Örebro County Council and the Örebro Medical Centre Research Foundation. We thank Angela Steen and Vivianne Lindén-Sjökvist for excellent technical assistance and Hong Li (PhD) for providing us with the Helicobacter strain (He 173).

References

1. Bralow SP (1972) Experimental gastric carcinogenesis. Digestion 5:290–310
2. Bresalier RS (1998) *Helicobacter pylori* and gastric cancer: a not so simple association. Gastroenterology 114:408–409
3. Cahill RJ, Kilgallen C, Beattie S, Hamilton H, O'Morain C (1996) Gastric epithelial cell kinetics in the progression from normal mucosa to gastric carcinoma. Gut 38:177–181
4. Chow KW, Bank S, Ahn J, Roberts J, Blumstein M,Kranz V (1995) *Helicobacter pylori* infection does not increase gastric antrum mucosal cell proliferation. Am J Gastroenterol 90:64–66
5. Correa P (1988) A human model of gastric carcinogenesis. Cancer Res 48:3554–3560
6. Domellöf L (1993) Remnant stomach and gastric cancer. In: Nishi M, et al (eds) Gastric cancer. Springer, Berlin Heidelberg New York, pp 168–182
7. Eurogast study group (1993) An international association between *Helicobacter pylori* infection and gastric cancer. Lancet 341:1359–1362
8. Fan XG, Kelleher D, Fan XJ, Xia HX, Keeling PW (1996) *Helicobacter pylori* increases proliferation of gastric epithelial cells. Gut 38:19–22
9. Gavrieli Y, Sherman Y, Ben-Sasson SA (1992) Identification of programmed cell death in situ via specific labeling of nuclear DNA fragmentation. J Cell Biol 119:493–501
10. Gerlach C, Golding M, Larue L, Alison MR, Gerdes J (1997) Ki-67 immunoexpression is a robust marker of proliferative cells in the rat. Lab Invest 77:697–698
11. Honig A, Witte F, Mirecka J, Binder C, Schauer A (2000) *Helicobacter pylori*-induced hyperproliferation: relevance for gastric cancer development in connection with mutagenic factors. Anticancer Res 20:1641–1648
12. IARC (1994) Infection with *Helicobacter pylori*. IARC Monogr Eval Carcinog Risks Hum 61:177–240
13. Itoh M, Wada K, Tan S, Kitano Y, Kai J, Makino I (1999) Antibacterial action of bile acids against *Helicobacter pylori* and changes in its ultrastructural morphology: effect of unconjugated dihydroxy bile acid (see comments). J Gastroenterol 34:571–576
14. Kawaura A, Yamamoto I, Tanida N, Inouye H, Takahashi A, Tonokatsu Y, Sawada Y, Sawada K, Shimoyama T (1991) *Helicobacter pylori* is not a co-carcinogen in N-methyl-N′-nitro-N-nitrosoguanidine-induced rat gastric carcinogenesis. Tokushima J Exp Med 38:71–75
15. Kobori O, Gedigk P, Totovic V (1976) Early changes of glandular stomach in Wistar rats ingesting N-methyl-N′-nitro-N-nitrosoguanidine (MNNG): with special reference to light microscopic, electron microscopic, and enzyme histochemical study of the regenerating epithelium induced by MNNG. Z Krebsforsch Klin Onkol Cancer Res Clin Oncol 87:127–138
16. Li H, Helander HF (1996) Hypergastrinemia increases proliferation of gastroduodenal epithelium during gastric ulcer healing in rats. Dig Dis Sci 41:40–48
17. Li H, Kalies I, Mellgard B, Helander HF (1998) A rat model of chronic *Helicobacter pylori* infection. Studies of epithelial cell turnover and gastric ulcer healing. Scand J Gastroenterol 33:370–378
18. Li H, Andersson EM, Helander HF (1999) Reactions from rat gastric mucosa during one year of *Helicobacter pylori* infection. Dig Dis Sci 44:116–124
19. Loogna P, Domellöf L (2001) *Helicobacter pylori* is not mutagenic in Ames test (in press)
20. Lynch DA, Axon AT (1995) *Helicobacter pylori*, gastric cancer and gastric epithelial kinetics: a review. Eur J Gastroenterol Hepatol 7[Suppl 1]:S17–S23
21. Matsukura N, Kawachi T, Sasajima K, Sano T, Sugimura T, Hirota T (1978) Induction of intestinal metaplasia in the stomachs of rats by N-methyl-N′-nitro-N-nitrosoguanidine. J Natl Cancer Inst 61:141–144
22. Mendes EN, Queiroz DM, Coimbra RS, Moura SB, Barbosa AJ, Rocha GA (1996) Experimental infection of Wistar rats with 'Gastrospirillum suis'. J Med Microbiol 44:105–109
23. Miwa H, Endo K, Wada R, Hirai S, Hirose M, Misawa H, Nagahara A, Ohta K, Watanabe S, Sato N (1997) Cellular proliferation and differentiation in rat atrophic gastric mucosa induced by N′-methyl-N′-nitro-N-nitrosoguanidine. J Clin Gastroenterol 25[Suppl 1]:S116–1121
24. Mohammadi M, Czinn S, Redline R, Nedrud J (1996) Helicobacter-specific cell-mediated immune responses display a predominant Th1 phenotype and promote a delayed-type hypersensitivity response in the stomachs of mice. J Immunol 156:4729–4738
25. Mohammadi M, Redline R, Nedrud J, Czinn S (1996) Role of the host in pathogenesis of Helicobacter-associated gastritis: H. felis infection of inbred and congenic mouse strains. Infect Immun 64:238–245
26. Moss SF (1998) Review article: Cellular markers in the gastric precancerous process. Aliment Pharmacol Ther 12 [Suppl 1]: 91–109
27. Nomura A, Stemmermann GN, Chyou PH, Kato I, Perez-Perez GI, Blaser MJ (1991) *Helicobacter pylori* infection and gastric carcinoma among Japanese Americans in Hawaii [see comments]. N Engl J Med 325:1132–1136
28. Parkin DM, Pisani P, Ferlay J (1999) Estimates of the worldwide incidence of 25 major cancers in 1990. Int J Cancer 80:827–841
29. Parsonnet J, Vandersteen D, Goates J, Sibley RK, Pritikin J,Chang Y (1991) *Helicobacter pylori* infection in intestinal- and diffuse-type gastric adenocarcinomas (published erratum appears in J Natl Cancer Inst 1991 Jun 19;83:881). J Natl Cancer Inst 83:640–643
30. Parsonnet J, Friedman GD, Vandersteen DP, Chang Y, Vogelman JH, Orentreich N, Sibley RK (1991) *Helicobacter*

pylori infection and the risk of gastric carcinoma [see comments]. N Engl J Med 325:1127–1131
31. Parsonnet J, Friedman GD, Orentreich N,Vogelman H (1997) Risk for gastric cancer in people with CagA positive or CagA negative *Helicobacter pylori* infection (see comments). Gut 40:297–301
32. Peek RM, Jr., Moss SF, Tham KT, Perez-Perez GI, Wang S, Miller GG, Atherton JC, Holt PR,Blaser MJ (1997) *Helicobacter pylori* cagA+ strains and dissociation of gastric epithelial cell proliferation from apoptosis [see comments]. J Natl Cancer Inst 89:863–868
33. Ritchie WP Jr (1977) Bile acids, the "barrier," and reflux-related clinical disorders of the gastric mucosa. Surgery 82:192–200
34. Rokkas T, Ladas S, Liatsos C, Petridou E, Papatheodorou G, Theocharis S, Karameris A, Raptis S (1999) Relationship of *Helicobacter pylori* CagA status to gastric cell proliferation and apoptosis. Dig Dis Sci 44:487–493
35. Salmon RJ, Laurent M, Thierry JP (1984) Effect of taurocholic acid feeding on methyl-nitro-N-nitroso-guanidine induced gastric tumors. Cancer Lett 22:315–320
36. Shimizu N, Inada KI, Tsukamoto T, Nakanishi H, Ikehara Y, Yoshikawa A, Kaminishi M, Kuramoto S, Tatematsu M (1999) New animal model of glandular stomach carcinogenesis in Mongolian gerbils infected with *Helicobacter pylori* and treated with a chemical carcinogen. J Gastroenterol 34[Suppl 11]:61–66
37. Shimizu N, Inada K, Nakanishi H, Tsukamoto T, Ikehara Y, Kaminishi M, Kuramoto S, Sugiyama A, Katsuyama T, Tatematsu M (1999) *Helicobacter pylori* infection enhances glandular stomach carcinogenesis in Mongolian gerbils treated with chemical carcinogens. Carcinogenesis 20:669–676
38. Shimizu N, Ikehara Y, Inada K, Nakanishi H, Tsukamoto T, Nozaki K, Kaminishi M, Kuramoto S, Sugiyama A, Katsuyama T, Tatematsu M (2000) Eradication diminishes enhancing effects of *Helicobacter pylori* infection on glandular stomach carcinogenesis in Mongolian gerbils. Cancer Res 60:1512–1514
39. Silen W, Forte JG (1975) Effects of bile salts on amphibian gastric mucosa. Am J Physiol 228:637–644
40. Sugimura T, Terada M (1998) Experimental chemical carcinogenesis in the stomach and colon. Jpn J Clin Oncol 28:163–167
41. Talley NJ, Zinsmeister AR, Weaver A, DiMagno EP, Carpenter HA, Perez-Perez GI, Blaser MJ (1991) Gastric adenocarcinoma and *Helicobacter pylori* infection. J Natl Cancer Inst 83:1734–1739
42. Tatematsu M, Furihata C, Katsuyama T, Hasegawa R, Nakanowatari J, Saito D, Takahashi M, Matsushima T, Ito N (1983) Independent induction of intestinal metaplasia and gastric cancer in rats treated with N-methyl-N′-nitro-N-nitrosoguanidine. Cancer Res 43:1335–1341
43. Tatematsu M, Ogawa K, Hoshiya T, Shichino Y, Kato T, Imaida K, Ito N (1992) Induction of adenocarcinomas in the glandular stomach of BALB/c mice treated with N-methyl-N-nitrosourea. Jpn J Cancer Res 83:915–918
44. Tokieda M, Honda S, Fujioka T, Nasu M (1999) Effect of *Helicobacter pylori* infection on the N-methyl-N′-nitro-N-nitrosoguanidine-induced gastric carcinogenesis in mongolian gerbils. Carcinogenesis 20:1261–1266
45. Watanabe T, Tada M, Nagai H, Sasaki S, Nakao M (1998) *Helicobacter pylori* infection induces gastric cancer in mongolian gerbils (see comments). Gastroenterology 115:642–648
46. Webb PM, Yu MC, Forman D, Henderson BE, Newell DG, Yuan JM, Gao YT, Ross RK (1996) An apparent lack of association between *Helicobacter pylori* infection and risk of gastric cancer in China. Int J Cancer 67:603–607

Virchows Arch (2001) 439:661–667
DOI 10.1007/s004280100456

ORIGINAL ARTICLE

Peter Loogna · Lennart Franzén · Pentti Sipponen
Lennart Domellöf

Effects of *Helicobacter pylori* and bile on N-methyl-N′-nitro-N′-nitrosoguanidine exposed antral mucosa of C57BL/6 mice

Received: 31 January 2001 / Accepted: 28 March 2001 / Published online: 17 July 2001
© Springer-Verlag 2001

Abstract The aim of this study was to evaluate the early influence of *Helicobacter pylori* infection on cell kinetics in the antral mucosa of mice exposed to N-methyl-N′-nitro-N′-nitrosoguanidine (MNNG) and bile alone or in combinations. Four hundred and one C57BL/6 male and female mice were assigned into seven treatment groups and one non-treated control group. The gastric antrums were assessed by histology and immunohistochemistry for studies of cell proliferation and apoptosis at 32 and 44 weeks. One female and one male mouse had developed dysplastic adenomas in the pylorus mucosa and one male animal had dysplastic proliferation in the antrum. Only one of these lesions occurred in a *H. pylori* colonized animal. *H. pylori* infection significantly increased the cell proliferation at 32 weeks and promoted the cell proliferation in the MNNG and bile group at 44 weeks. Female mice showed less increase in cell proliferation than did the males. No change in apoptosis was seen in any of the groups. Bile had no promotional effect on cell proliferation. These results indicate that *H. pylori* infection has the potential to alter epithelial cell kinetics as well as antrum mucosa of an animal species that is regarded as resistant to MNNG. However, this change is not sufficient to promote the early development of neoplastic lesions.

Keywords Stomach carcinogenesis · *Helicobacter pylori* · Cell proliferation · Apoptosis

This work was supported by grants from the Research Committe of Örebro County Council, the Örebro Medical Centre Research Foundation and Lions cancer foundation Uppsala-Örebro

P. Loogna · L. Domellöf (✉)
Department of Surgery, Örebro Medical Centre Hospital, 70185 Örebro, Sweden
e-mail: lennart.domellof@orebroll.se
Tel.: +46-19-6021796, Fax: +46-19-125439

L. Franzén
Department of Pathology, Örebro Medical Centre Hospital, Örebro, Sweden

P. Sipponen
Department of Pathology, Jorvi Hospital, Espoo, Finland

Introduction

Gastric cancer in man most often occurs in middle and old age, making it possible for both tumor initiators and promoters to play a role in gastric carcinogenesis over a considerable period of time. Several environmental factors, including *Helicobacter pylori*, excessive intake of salt, bile reflux, N-nitroso compounds, and a deficiency of antioxidants, have been linked with different stages of gastric carcinogenesis [5, 11].

In 1994, the International Agency for Research on Cancer (IARC) classified *H. pylori* as an important risk factor for gastric cancer [14]. However, the mechanisms by which *H. pylori* infection increases the risk for gastric carcinoma remain unknown.

Increased cell proliferation is a common finding in preneoplasia and cancer. An increased rate of cell proliferation increases the number of cells in S-phase. Dividing cells are more sensitive to mutagenic factors such as food components and oxidative radicals than are cells which are not dividing [1]. Changes in cell proliferation may reveal an abnormality even before any microscopic pathology is visible, and increased cell proliferation has recently been proposed as an early biomarker for colonic cancer [8]. It has also been proposed that *H. pylori* may act as a tumor promoter by changing proliferation and apoptosis of the gastric epithelium [31]. However, *H. pylori* is not mutagenic in the Ames test [21].

MNNG is a direct-acting mutagenic and carcinogenic compound that induces adenocarcinomas in rats [38], hamsters [10], and dogs [39]. However, the glandular stomach of mice has generally been found to be resistant to this carcinogen [17].

The present investigation was undertaken to study whether the normally MNNG-resistant mouse mucosa becomes more sensitive to MNNG when it is colonized with *H. pylori*. Recent studies have shown that *H. pylori* [31, 42] can increase the cell proliferation in the gastric mucosa and therefore the number of cells at risk of MNNG-induced carcinogenesis. The carcinogen has to pass through the surface mucus and the cell layer in or-

der to reach the proliferating neck cells. Detergent bile acid was used for increasing the permeability of the mucosa. The induction time for experimental cancer is generally 50% of the animal's median life span, or about 1 year. The present study intended to explore possible early effects in relation to cell kinetics. C57BL/6 mice were studied to investigate whether *H. pylori* and/or bile could promote the effect of MNNG, resulting in more preneoplastic lesions in the glandular stomach. The gastric mucosa was examined for histological alterations. Special emphasis was laid on cell proliferation using the Ki-67 labeling index and on apoptosis as detected by TUNEL.

Materials and methods

Animals

Six-week-old male and female C57BL/6 mice were used (B&K Universal Company, Sollentuna, Sweden). The animals were housed in Macrolon cages, 10 mice per cage, with a 12-h light–dark schedule, temperature (20–22°C) and humidity (40–60%). The animals had free access to drinking water and Rat and mouse diet No. 2 (RM2, B&K Universal Company, Sollentuna, Sweden). Body weight was measured every second week. Terminations (using CO_2) and autopsies were performed when the mice were sick and after experimental weeks 32 and 44. The care of the animals and the experimental procedures were carried out according to accepted standards and with approval of the regional ethical committee.

H. pylori strains

H. pylori strains (553/93, 83/95, 87/95, 105/95, 116/95, 119/95, 122/96, 125/96 and 131/96) were used in a mixture with all the strains in equal amounts [41]. Strain 553/93 was CagA and VacA negative, 83/95 was CagA positive but VacA negative. All other strains were CagA and VacA positive.

Chemicals

A stock solution of MNNG (Aldrich Chemicals, Inc.,USA) was prepared every second week with distilled water to a concentration of 1 g/l. The solution was kept dark at 4°C. Every other day an aliquot of this solution was diluted with tap water to a concentration of 100 mg/l. The solution was provided in light-shielded bottles ad libitum to MNNG-animals as their drinking water. Animals in the other groups were given only tap water.

Taurocholic acid (Sigma Chemicals, Sweden) was added to the ground meal at a concentration of 0.25% which was then pelleted.

Study design

The male animals were randomly divided in two groups. One hundred and seventy-six mice were given equal amounts of a mixture of the *H. pylori* strains (about 10^9 CFU/ml) by gavage (0.1 ml) three times at 2-day intervals. The control groups consisting of 166 animals were kept for the same period of time but they were not inoculated. Three months after the last inoculation the *H. pylori*-treated mice as well as the controls were divided into eight subgroups and given different combinations of MNNG, bile, and *H. pylori* (Fig. 1). Half the number of mice in each group was killed at 32 and 44 weeks after *H. pylori* inoculation. However, the animals in the bile group were not killed until after 44 weeks, because of the limited number of animals.

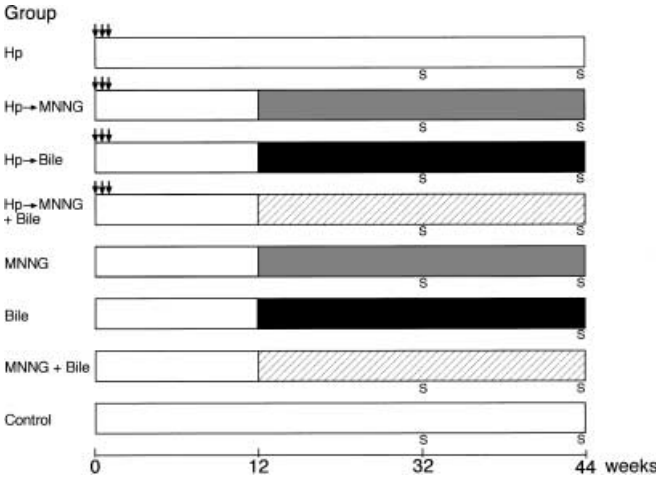


Fig. 1 Experimental design (male mice). *Arrows* indicate inoculations over a 6-day period with *H. pylori*. Half the mice were sacrificed (*S*) 32 and 44 weeks after *H. pylori* inoculation

At death, blood was sampled, and serum was separated and stored at –20°C until analyzed. The stomach was opened along the greater curvature and was carefully examined, as were all other organs. All subsequent investigations were performed by operators blinded with regard to the different treatment groups.

In an additional experiment, designed to study possible sex differences, female C57BL/6 mice were used. Forty-five of those were inoculated with *H. pylori* and 14 animals served as controls. The infected animals were divided into an *H. pylori* group (n=30) and a *H. pylori*+MNNG+bile group (n=15). The same study design as for the male mice was followed.

Histopathological examination

The stomach was fixed in 10% neutral buffered formalin, cut in longitudinal stripes parallel to the minor curvature, and embedded in paraffin. Sections 4 µm thick were stained with hematoxylin and eosin (H&E), Giemsa, and periodic acid-Schiff (PAS) and examined for morphological lesions and the presence of bacteria.

Histological parameters included assessment of degree of inflammation, presence of indefinite dysplasia and presence of adenoma. The inflammation score was based on criteria described by Mohammadi et al. [27]. Briefly, the score equals the sum of the grade of intensity of inflammation in the most inflamed area (0 to 3), the longitudinal extent (0 to 3), and the depth of inflammation (0 to 3), giving a maximum score of 9.

Detection of *H. pylori*

One sample, 4×4 mm in size, was homogenized from macroscopically normal antrum mucosa of each animal. The material was placed on GC agar plates and incubated for 4–14 days in microaerobic conditions at 37°C. *H. pylori* were identified by colony morphology (typical curved, Gram-negative rods) and by urease, catalase, and oxidase tests.

One in-house enzyme-linked immunosorbent assay (ELISA) was used to demonstrate serum IgG anti-*H. pylori* antibodies as described by Mohammadi et al. [26]. The titer of the antibody was expressed by means of an arbitrary index; values >1.0 were accepted as indicating positive detection of *H. pylori*. For histological detection of *H. pylori*, Giemsa stain was used. The definition of an *H. pylori*-positive animal was at least one positive test with histology, serology, or culture.

Immunohistochemistry

Gastric epithelial cell proliferation in the antral mucosa was assessed by identification of Ki-67 positive cells using the monoclonal antibody TEC-3, specific for mouse Ki-67 antigen (Dianova, Hamburg, Germany). The ABC-method (Dako, Glostrup, Denmark) was used for visualization of the antigen-binding sites.

For each primary antibody and tissue, negative controls were run by replacing the primary antibody with nonimmune serum. Proliferation was assessed by counting at least 1000 epithelial cells in antrum mucosa approximately 400 µm from the gastroduodenal junction. A 310-µm-wide swath, perpendicular to the mucosal surface and comprising the entire thickness of the mucosa, was used. Within the swath, all labeled as well as unlabeled epithelial cells were counted. Special attention was paid to assessing these measurements only in slides containing vertical cuts. Areas with artifacts such as foldings of the tissue were omitted from counting.

The results were expressed as labeling index (LI), which is the percentage of labeled cell nuclei in the total number of counted epithelial cell nuclei [19].

Quantification of apoptosis

Apoptotic cells were stained by TUNEL with the In situ Apoptosis Detection Kit (Oncor, Gaithersburg, MD, USA). Sections from mouse spleen served as positive controls. For negative controls, terminal deoxynucleotidyl transferase was omitted [13].

The epithelial apoptotic cells were counted in one contiguous area, starting from the gastroduodenal junction to 3 mm proximally in the antrum. The results were expressed as apoptotic index, which is the number of apoptotic cells per millimeter mucosal length [20].

Thickness of antrum mucosa

The thickness of the different compartments of the antrum mucosa (crypts, proliferative zone, and foveolae) was assessed in images (740×) captured with a Leica DC 200 digital camera mounted on a Leica DMRXE microscope (Leica Microsystems Wetzlar GmbH,Wetzlar, Germany). Each image spanned the whole thickness of mucosa. A length of 1 mm starting from the gastroduodenal junction was analyzed. The proliferative zone was well demarcated with many Ki-67 positive cells. Occasionally, single positive nuclei were seen above the proliferative zone and they were not included. The area and lateral length of the different compartments were measured and the mean thickness calculated using the Leica Q-Win (Leica Microsystems Imaging Solutions Ltd.,Cambridge, United Kingdom) image analysis program.

Statistics

The nonparametric Mann-Whitney U test was used for pairwise comparisons while the Kruskal-Wallis test was used for overall comparisons between the groups. Spearman's rank correlation was used to test for associations between variables. Significance was defined as $P<0.05$.

Results

Male mice

Reduced median body weight ($P<0.05$) was observed at 44 weeks in treated mice (average 43.9 g) compared to the controls (48.2 g) The bile group (46.7 g), however, did not differ from the controls. Clinical signs of disease were not observed. There was no significant difference in survival. Nine animals (one *H. pylori*, one MNNG + *H. pylori*, three MNNG, two MNNG + bile, two bile) that died before the termination of the experiment were excluded from analysis due to autolytic changes in the stomach. The cause of death in these nine was not attributed to gastric cancer or any other type of malignancy.

Histopathological findings

One adenoma with dysplasia of low grade was found in the pylorus after 8 months in MNNG + bile group. Dysplastic proliferation (indefinite for dysplasia) was seen after 8 months in the duodenal bulb from one animal from the MNNG + bile group and in the antrum from an-

Table 1 Histopathological changes in the antral stomach of male C57BL/6 mice at 32 weeks

Group	Effective numbers	Inflammation score[a]	Indefinite for dysplasia	Adenoma
Hp	26	3.7±1.6*	0	0
Hp + MNNG	22	4.1±1.3*	0	0
Hp + bile	9	4.3±2.2*	0	0
Hp + MNNG + bile	5	4.2±1.3*	0	0
MNNG	30	0.6±1.2	0	0
MNNG + bile	15	1.7±1.8	0	0
Control	30	0.9±1.8	0	0

[a] Mean±SD, maximum score 9
* Significantly different from control and MNNG group ($P<0.002$)

Table 2 Histopathological changes in the antral stomach of male C57BL/6 mice at 44 weeks

Group	Effective numbers	Inflammation score[a]Π	Indefinite for dysplasia	Adenoma
Hp	15	4.1±1.2*	0	0
Hp + MNNG	25	3.9±1.8*, **	0	0
Hp + bile	3	2.0±1.7	0	0
Hp + MNNG + bile	4	3.5±1.0*	0	0
MNNG	27	1.0±1.8	1	0
MNNG + bile	14	1.6±1.7	1	1
Control	27	0.6±1.2	0	0

[a] Mean±SD, maximum score 9
* Significantly different from control group ($P<0.006$)
** Significantly different from MNNG group ($P<0.000$)

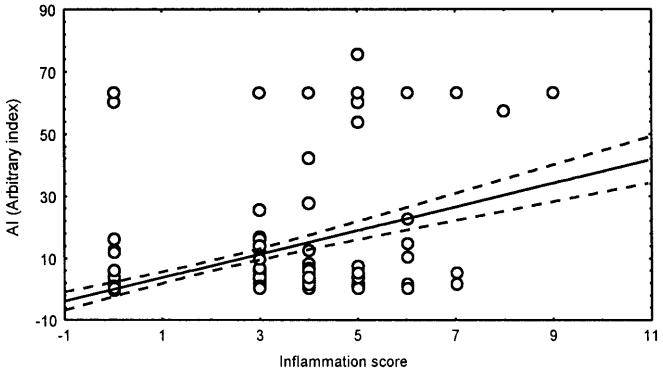


Fig. 2 The correlation between AI (arbitrary index) for *H. pylori* antibody titer and inflammation in the glandular stomach in male mice. Each *dot* may represent several observations

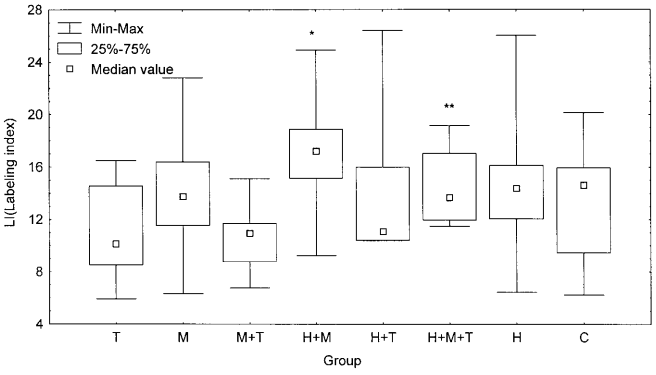


Fig. 4 Labeling index of antral epithelial cells in the different male groups at 44 weeks (*H H. pylori*, *M* MNNG, *T* taurocholic acid, *C* control). Data are expressed as median. * $P<0.03$ (significant difference from C); ** $P<0.03$ (significant difference from M+T)

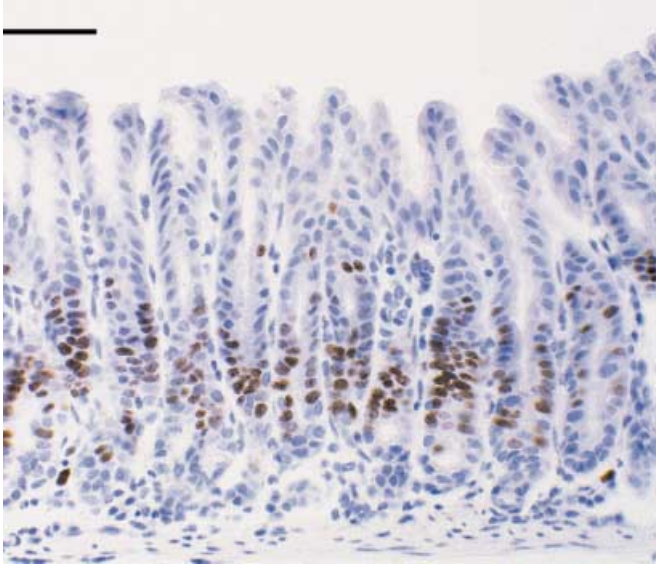


Fig. 3 Immunohistochemical staining of Ki-67 protein in proliferating cells in antral mucosa after treatment with *H. pylori* and MNNG in male mice at 44 weeks. The proliferative zone is easily discerned in the lower part of the mucosa. *Bar*=50 μm

other animal of the bile group. There were no animals with ulcer, atrophy, metaplasia, or malignant tumor. Stones in thin-walled gallbladders developed in 45% of the bile treated mice but not in the controls.

H. pylori colonized 62 out of 90 (68.9%) inoculated male mice at 32 weeks and 47 out of 84 (55.9%) at 44 weeks as judged by the defined criteria. The lowest level of colonization was found in the bile or MNNG treated groups, however, this difference was not significant. All noninfected animals were excluded from the subsequent investigation. When colonization was verified by mucosal culture, it was positive in 53.2% at 32 weeks and in 89% at 44 weeks. Spiral bacteria were visualized at histology in 18 mice. The bacteria were found in both antrum and body mucosa but not in the squamo-columnar junction, which would be equivalent to human cardia. When present, the colonization was most intense in the antrum. Bacteria were observed along the length of the gastric crypts and within the mucus which overlies the surface epithelium. The inflammation was mild to moderate in the *H. pylori*-infected animals and was dominated by infiltration of lymphocytes and macrophages. The inflammation was localized to the antrum, corpus, and cardia regions.

There was no significant difference in inflammation score or dysplasia between male animals sacrificed at 32 weeks and 44 weeks after *H. pylori* inoculation (Tables 1 and 2). All infected mice had significantly ($P<0.001$) higher levels of serum antibody response to *H. pylori* than the uninfected mice. The levels of antibody increased with time after the infection and there was a positive correlation between the severity of inflammatory response and the level of antibody (Spearman's correlation coefficient R=0.51, $P<0.001$) (Fig. 2).

The results of *H. pylori* serology and culture correlated well (R=0.57, $P<0.001$). All cases with positive microscopy were also positive for serum anti-*H. pylori*. All bacterial cultures, serology and microscopy were negative in control animals.

Epithelial proliferation. With immunohistochemical staining of the Ki-67 protein we could easily demonstrate proliferating antral epithelial cells (Fig. 3). The *H. pylori* group (32 weeks) and the *H. pylori* + MNNG (44 weeks) had significantly higher LI compared with the control group ($P<0.05$). Furthermore, *H. pylori* enhanced the LI at 44 weeks in the *H. pylori*+MNNG + bile group compared with the MNNG + bile group ($P<0.03$) (Fig. 4).

Increased LI significantly correlated with increased arbitrary index for *H. pylori* serology (R=0.22, $P<0.01$) as well as with mucosa inflammation (R=0.26, $P<0.004$).

There was no significant difference in antral mucosal thickness in *H. pylori*-challenged and control mice and at any time in the study. The thickness of the proliferative zone correlated to LI (R=0.5, $P<0.001$).

Apoptosis of the gastric epithelium. The apoptotic epithelial cells were found at the surface of the upper part of

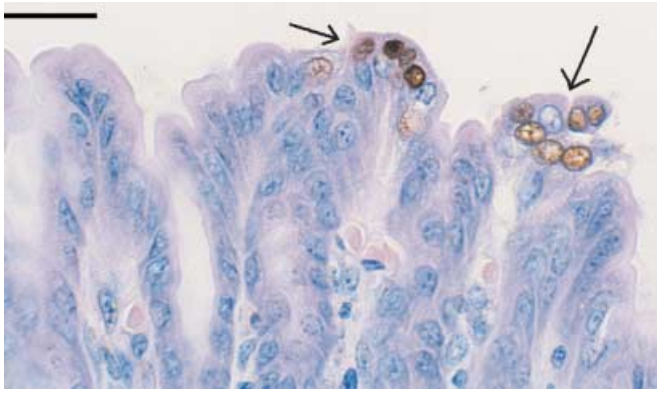


Fig. 5 Apoptotic epithelial cell nuclei at the surface of the antral mucosa (*arrows*) in a male mouse at 32 weeks treated with *H. pylori*, MNNG and taurocholic acid. TUNEL-staining. *Bar*=25 µm

the antrum mucosa (Fig. 5). There was no difference in apoptosis between *H. pylori*-inoculated and control animals. The addition of MNNG or bile did not significantly alter the number of apoptotic cells, and no correlation could be seen between LI and apoptosis (R=0.07, $P<0.5$).

Female mice

H. pylori colonized the stomach mucosa in 16 out of 21 (76.2%) inoculated mice at 32 weeks and in 7 out of 24 (29.2%) at 44 weeks. In total, 23 female mice were infected, with 31% culture positive at 32 weeks and 57% at 44 weeks. All non-infected animals and two animals that died (one *H. pylori* and one MNNG + *H. pylori*) were excluded from subsequent analysis.

One adenoma with dysplasia of low grade was found in the prepyloric antral mucosa after 5 months in *H. pylori* + MNNG + bile group. Thus, there was no sex difference in the development of neoplasia.

H. pylori-inoculated female mice at 32 weeks had a significantly lower inflammation score ($P<0.029$), LI ($P<0.037$) and lesser width of proliferative zone ($P<0.033$) than the male group. This sex difference in inflammation score disappeared at 44 weeks, but still the female mice had lower LI ($P<0.040$).

Even in the female *H. pylori* + MNNG + bile group at 44 weeks there was significantly less LI ($P<0.025$) and proliferation ($P<0.030$) than in the similar male group. These differences were not seen at 32 weeks. There was no difference in apoptosis between female and male mice.

Discussion

The present study shows that the number of proliferating cells in the antrum of *H. pylori* infected C57BL/6 mice at 32 weeks was significantly increased by the presence of *H. pylori*. This finding is in agreement with observations of other groups in man, mice, and Mongolian gerbils [4, 23, 40, 42]. Most often stomach cancer in man develops in the antrum [3], which also is a common localization for *H. pylori* colonization. However, the mechanisms by which *H. pylori* contributes to the development of gastric cancer have not yet been determined. It is known that *H. pylori* is not mutagenic [21]. In man, infection alone appears insufficient as a causative agent, because the majority of *H. pylori*-infected individuals do not develop gastric cancer.

H. pylori strains with CagA positivity have been associated with an increased risk for gastric cancer [9, 30]. However, in Asia where most individuals are CagA positive the associations with disease are not readily apparent [25]. C57BL/6 mice do not normally carry urease-positive spiral bacteria in the gastric mucosa [18]. This was also confirmed in our controls that were free from bacteria histologically and at culture. We used a mixture of nine different *H. pylori* strains known to give moderate to severe gastritis in C57BL/6 mice [41]. In this study it was shown that the strain 119/95 (CagA+,VacA+) infected most mice, with only a few animals infected with other strains. This was also confirmed in our study where one CagA- and VacA-positive strain dominated in all tested animals (data not presented). Of interest, the increased cell proliferation rate in the *H. pylori*-infected group was not accompanied by an increase in apoptosis. This finding in mice confirms the results by Peek et al. [31], who showed that CagA-positive strains have increased cell proliferation but unaltered apoptosis in humans. They hypothesized that this discrepancy between proliferation and apoptosis could explain the increased risk for gastric cancer with CagA positive strains.

The host response to *H. pylori* infection might also contribute to the pathogenicity. It is known that *H. pylori* can cause varying degrees of gastritis and colonization in different mouse strains. The C57BL/6 mice generally exibit good colonization and inflammation by *H. pylori* [18] and *H. felis* [27]. In contrast to these studies, we saw only a mild to moderate gastritis. This might have been due to different *H. pylori* strains and diets used in the studies. In contrast to its occurrence in humans, the gastritis in the C57BL/6 mice was dominated by infiltration of lymphocytes and macrophages, with few polymorphonuclear neutrophils, and thus a lesser production of reactive oxygen metabolites. We could, however, demonstrate a strong correlation between antral mucosal cell proliferation and the inflammation score. This is in accordance with the study of Lynch et al. [24], who also hypothesized that increased cell proliferation could partly be due to increased mucosal inflammatory response.

We have recently shown [22] that a ratified *H. pylori* strain, also CagA- and VacA-positive, significantly enhanced the epithelial cell proliferation in the antrum of Wistar rats. This confirms that similar *H. pylori* strains may act in the same way in different species.

Interestingly, there was a significantly lesser degree of inflammation and LI in female mice with *H. pylori*

gastritis than in male mice at 32 weeks and LI at 44 weeks. The cell proliferation was also lower in the female *H. pylori* and MNNG and bile group at 44 weeks compared with the corresponding male group. It has previously been shown that male rats are more susceptible to induction of gastric carcinoma by MNNG [12, 29]. Furthermore, it is well known that, in humans, the female sex is associated with a lesser risk of gastric cancer. However, the number of culture positive female animals was lower in the 32 weeks group compared with the group at 44 weeks, and this may reflect the difference in inflammation score.

The stomach is continuously exposed to different endo-and exogenous carcinogens. MNNG is a nitrosamide with mutagenic and carcinogenic properties. In the extremely sensitive Wistar rats adenocarcinomas were obtained in 73% at the 83 mg/l dose within 1 year [2]. In contrast, the mouse is relatively resistant to the carcinogenic actions of MNNG. There is only one study that has reported that long-term use of MNNG in drinking water for 68 weeks resulted in the development of gastric adenocarcinoma, mainly in the antrum, in five out of 69 non-infected Swiss albino mice [36]. The reason for this genetic difference is unknown, but gastric emptying, metabolism, and composition of gastric contents may differ.

The increased risk of gastric remnant cancer following peptic ulcer surgery has been attributed to the promotion by bile reflux [7, 28]. Bile acids in the stomach have a detergent effect on the mucosal barrier and facilitate the action of carcinogens on mucosal cells. In this study we used taurocholic acid, which is known to be the most potent bile acid to break the gastric mucosal barrier [32, 37]. Furthermore, it has a verified low toxicity to *H. pylori* [15]. The tumor-enhancing effects of bile and bile acids on MNNG-induced gastric carcinogenesis in rats have been confirmed in several studies [16, 33, 34]. However, no promoting effect of bile on MNNG-induced alterations was found in the present mouse model. On the other hand, we found that *H. pylori* infection had a promoting effect on gastric mucosal proliferation when MNNG and bile was combined. Unfortunately, the number of animals in this group was small, which is why these data should be interpreted with great care. The combination of MNNG and bile also resulted in an increased cell proliferation compared to the controls. However, only three early pre/neoplastic lesions occurred and only one of them was found in a *H. pylori*-infected animal. This is in agreement with the only previous study on the association of MNNG and *H. heilmanni* in mice [6]. In this 18-month study *H. heilmanni* infected BALB/c mice were given MNNG without any tumor enhancement by the infection. In contrast, *H. pylori* promoted the development of pepsinogen-altered pyloric glands in BALB/c mice exposed to another carcinogen N-methyl-N-nitrosurea [35]. Recently, Tokieda et al. [40] found that *H. pylori* enhanced the carcinogenic action of MNNG in Mongolian gerbils after 52 weeks. The relatively mild degree of gastritis obtained in the C57BL/6 mice, with respect to the severe gastritis in Mongolian gerbils, might explain this difference. The development of cancer in the mouse model may require either additional mutations or a longer time period of infection in the gastric mucosa. Furthermore, age of the animals could be of importance. Young cells have been found resistant to transformation, and intraperitoneal administration of MNU to C57BL/6 J mice resulted in significantly less cancers when given to young compared to older animals [43]. A study of MNNG administered to older animals would be of interest.

In summary, this is the first study in mice using combinations of *H. pylori*, MNNG and bile. We could demonstrate that *H. pylori* infection in C57BL/6 mice resulted in an increased gastric cell proliferation with unchanged apoptosis. However, these results were not accompanied by an increased development of gastric neoplastic lesions. This could be explained by genetic species differences and the age of the animal at the time of carcinogen administration.

Acknowledgments We thank Angela Steen and Vivianne Lindén-Sjökvist for excellent technical assistance, Pär Aleljung and Torkel Wadström for providing us with the Helicobacter strains, and Lars Engstrand for analyzing CagA and VacA expression.

References

1. Ames BN, Gold LS (1990) Chemical carcinogenesis: too many rodent carcinogens. Proc Natl Acad Sci USA 87:7772–7726
2. Bralow SP, Gruenstein M, Meranze DR (1973) Host resistance to gastric adenocarcinomatosis in three strains of rats ingesting N-methyl-N'-nitro-N-nitrosoguanidine. Oncology 27:168–180
3. Breaux JR, Bringaze W, Chappuis C, Cohn I Jr (1990) Adenocarcinoma of the stomach: a review of 35 years and 1710 cases [see comments]. World J Surg 14:580–586
4. Brenes F, Ruiz B, Correa P, Hunter F, Rhamakrishnan T, Fontham E, Shi TY (1993) Helicobacter pylori causes hyperproliferation of the gastric epithelium: pre- and post-eradication indices of proliferating cell nuclear antigen. Am J Gastroenterol 88:1870–1875
5. Correa P (1992) Human gastric carcinogenesis: a multistep and multifactorial process – First American Cancer Society Award Lecture on Cancer Epidemiology and Prevention. Cancer Res 52:6735–6740
6. Danon SJ, Eaton KA (1998) The role of gastric Helicobacter and N-methyl-N'-nitro-N-nitrosoguanidine in carcinogenesis of mice. Helicobacter 3:260–268
7. Domellöf L (1993) Remnant stomach and gastric cancer. In: Nishi M, Ichikawa H, Nakajima T, Maruyama K, Tahara E (eds) Gastric cancer. Springer, Hong Kong, pp 168–182
8. Einspahr JG, Alberts DS, Gapstur SM, Bostick RM, Emerson SS, Gerner EW (1997) Surrogate end-point biomarkers as measures of colon cancer risk and their use in cancer chemoprevention trials. Cancer Epidemiol Biomarkers Prev 6:37–48
9. Enroth H, Kraaz W, Engstrand L, Nyrén O, Rohan T (2000) Helicobacter pylori strain types and risk of gastric cancer: a case-control study. Cancer Epidemiol Biomarkers Prev 9:981–985
10. Fujimura S, Kogure K, Oboshi S, Sugimura T (1970) Production of tumors in glandular stomach of hamsters by N-methyl-N'-nitro-N-nitrosoguanidine. Cancer Res 30:1444–1448
11. Furihata C, Takezawa R, Matsushima T, Tatematsu M (1987) Potential tumor-promoting activity of bile acids in rat glandular stomach. Jpn J Cancer Res 78:32–39
12. Furukawa H, Iwanaga T, Koyama H, Taniguchi H (1982) Effect of sex hormones on carcinogenesis in the stomachs of rats. Cancer Res 42:5181–5182

13. Gavrieli Y, Sherman Y, Ben-Sasson SA (1992) Identification of programmed cell death in situ via specific labeling of nuclear DNA fragmentation. J Cell Biol 119:493–501
14. International Agency for Research on Cancer (1994) Infection with Helicobacter pylori. IARC Monogr Eval Carcinog Risks Hum 61:177–240
15. Itoh M, Wada K, Tan S, Kitano Y, Kai J, Makino I (1999) Antibacterial action of bile acids against Helicobacter pylori and changes in its ultrastructural morphology: effect of unconjugated dihydroxy bile acid [see comments]. J Gastroenterol 34: 571–576
16. Kobori O, Shimizu T, Maeda M, Atomi Y, Watanabe J, Shoji M, Morioka Y (1984) Enhancing effect of bile and bile acid on stomach tumorigenesis induced by N-methyl-N'-nitro-N-nitrosoguanidine in Wistar rats. J Natl Cancer Inst 73:853–861
17. Kodama M, Kodama T, Fukami H, Ogiu T (1992) Comparative genetics of host response to N-methyl 1-N'-nitro-N-nitrosoguanidine. I. A lack of tumor production in the glandular stomach of Swiss mouse. Anticancer Res 12:441–449
18. Lee A, O'Rourke J, De Ungria MC, Robertson B, Daskalopoulos G, Dixon MF (1997) A standardized mouse model of Helicobacter pylori infection: introducing the Sydney strain [published erratum appears in Gastroenterology 1997 Aug 113(2):732]. Gastroenterology 112:1386–1397
19. Li H, Helander HF (1996) Hypergastrinemia increases proliferation of gastroduodenal epithelium during gastric ulcer healing in rats. Dig Dis Sci 41:40–48
20. Li H, Andersson EM, Helander HF (1999) Reactions from rat gastric mucosa during one year of Helicobacter pylori infection. Dig Dis Sci 44:116–124
21. Loogna P, Domellöf L (2001) Helicobacter Pylori is not mutagenic in Ames test. Cancer Res Ther Control 11:167–174
22. Loogna P, Franzén L, Sipponen P, Domellöf L (2001) Helicobacter pylori, MNNG and bile modulate gastric cell kinetics in experimental cancer. Virchows Arch. DOI 10.1007/s004280100411
23. Lynch DA, Mapstone NP, Clarke AM, Jackson P, Dixon MF, Quirke P, Axon AT (1995) Cell proliferation in the gastric corpus in Helicobacter pylori associated gastritis and after gastric resection. Gut 36:351–353
24. Lynch DA, Mapstone NP, Clarke AM, Jackson P, Moayyedi P, Dixon MF, Quirke P, Axon AT (1999) Correlation between epithelial cell proliferation and histological grading in gastric mucosa. J Clin Pathol 52:367–371
25. Mitchell HM, Hazell SL, Li YY, Hu PJ (1996) Serological response to specific Helicobacter pylori antigens: antibody against CagA antigen is not predictive of gastric cancer in a developing country. Am J Gastroenterol 91:1785–1788
26. Mohammadi M, Czinn S, Redline R, Nedrud J (1996) Helicobacter-specific cell-mediated immune responses display a predominant Th1 phenotype and promote a delayed-type hypersensitivity response in the stomachs of mice. J Immunol 156: 4729–4738
27. Mohammadi M, Redline R, Nedrud J, Czinn S (1996) Role of the host in pathogenesis of Helicobacter-associated gastritis: H. felis infection of inbred and congenic mouse strains. Infect Immun 64:238–245
28. Northfield TC, Hall CN (1990) Carcinoma of the gastric stump: risks and pathogenesis. Gut 31:1217–1219
29. Ohgaki H, Kawachi T, Matsukura N, Morino K, Miyamoto M, Sugimura T (1983) Genetic control of susceptibility of rats to gastric carcinoma. Cancer Res 43:3663–3667
30. Parsonnet J, Friedman GD, Orentreich N, Vogelman H (1997) Risk for gastric cancer in people with CagA positive or CagA negative Helicobacter pylori infection [see comments]. Gut 40:297–301
31. Peek RM Jr, Moss SF, Tham KT, Perez-Perez GI, Wang S, Miller GG, Atherton JC, Holt PR, Blaser MJ (1997) Helicobacter pylori cagA+ strains and dissociation of gastric epithelial cell proliferation from apoptosis [see comments]. J Natl Cancer Inst 89:863–868
32. Ritchie WP Jr (1975) Acute gastric mucosal damage induced by bile salts, acid, and ischemia. Gastroenterology 68:699–707
33. Salmon RJ, Laurent M, Thierry JP (1984) Effect of taurocholic acid feeding on methyl-nitro-N-nitroso-guanidine induced gastric tumors. Cancer Lett 22:315–320
34. Salmon RJ, Merle S, Zafrani B, Decosse JJ, Sherlock P, Deschner EE (1985) Gastric carcinogenesis induced by N-methyl-N'-nitro-N-nitrosoguanidine: role of gastrectomy and duodenal reflux. Jpn J Cancer Res 76:167–172
35. Shimizu N, Kaminishi M, Tatematsu M, Tsuji E, Yoshikawa A, Yamaguchi H, Aoki F, Oohara T (1998) Helicobacter pylori promotes development of pepsinogen-altered pyloric glands, a preneoplastic lesion of glandular stomach of BALB/c mice pretreated with N-methyl-N-nitrosourea. Cancer Lett 123:63–69
36. Sigaran MF, Con-Wong R (1979) Production of proliferation lesions in gastric mucosa of albino mice by oral administration of N-methyl-N'-nitro-N-nitrosoguanidine. Gann 70:343–352
37. Silen W, Forte JG (1975) Effects of bile salts on amphibian gastric mucosa. Am J Physiol 228:637–644
38. Sugimura T, Fujimura S (1967) Tumour production in glandular stomach of rat by N-methyl-N'-nitro-N-nitrosoguanidine. Nature 216:943–944
39. Sugimura T, Tanaka N, Kawachi T, Kogure K, Fujimura S (1971) Production of stomach cancer in dogs by N-methyl-N'-nitro-N-nitrosoguanidine. Gann 62:67
40. Tokieda M, Honda S, Fujioka T, Nasu M (1999) Effect of Helicobacter pylori infection on the N-methyl-N'-nitro-N-nitrosoguanidine-induced gastric carcinogenesis in mongolian gerbils. Carcinogenesis 20:1261–1266
41. Wang X, Willén R, Wadstrom T, Aleljung P (1998) RAPD-PCR, Histopathological and serological analysis of four mouse strains infected with multiple strains of Helicobacter pylori. Microb Ecol Health Dis 10:148–154
42. Yamaguchi T, Nakajima N, Kuwayama H, Ito Y, Iwasaki A, Arakawa Y (2000) Gastric epithelial cell proliferation and apoptosis in Helicobacter pylori-infected mice. Aliment Pharmacol Ther 14:68–73
43. Zimmerman JA, Trombetta LD, Carter TH, Weisbroth SH (1982) Pancreatic carcinoma induced by N-methyl-N'-nitrosourea in aged mice. Gerontology 28:114–120

Virchows Arch (2001) 439:668–674
DOI 10.1007/s004280100452

ORIGINAL ARTICLE

**Andreas Gaumann · Peter Petrow · Thomas Mentzel
Eckhard Mayer · Manfred Dahm · Mike Otto
C. James Kirkpatrick · Jörg Kriegsmann**

Osteopontin expression in primary sarcomas of the pulmonary artery

Received: 14 December 2000 / Accepted: 28 February 2001 / Published online: 13 June 2001
© Springer-Verlag 2001

Abstract Primary tumors of the great vessels (aorta, pulmonal artery, and inferior vena cava) are rare and represent in most cases vascular leiomyosarcomas. Furthermore, there also exists a group of sarcomas arising from the intima, known as intimal sarcomas, associated with early metastasis and a very poor prognosis. Osteopontin (OPN) is an extracellular matrix protein that binds to αv integrins, thereby promoting cell attachment, chemotaxis, and signal transduction. The reported association of OPN with malignancy and metastasis prompted us to examine the expression of this protein in seven sarcomas of the pulmonary artery. Strong OPN-specific staining could be detected in tumor cells and the adjacent extracellular matrix. Using a double labeling procedure, proliferating cells showed a strong positive reaction with antibodies against OPN. In addition, this protein could be demonstrated in the cytoplasm of macrophages. CD44, a putative receptor of OPN, was expressed on the cellular surface of tumor-associated lymphocytes. The expression of OPN in macrophages and tumor cells indicates that this molecule could possibly mediate cellular adhesion of both cell types in pulmonary sarcomas. The detection in the extracellular matrix shows that OPN is actively secreted and may interact with the corresponding receptor, CD44, on the surface of lymphocytes. Although the function of OPN is not yet fully understood, our data indicate that strong expression of this molecule in poorly differentiated sarcomas could play a role in the progression of malignancy and metastasis as described previously for carcinomas.

Keywords Pulmonary artery sarcoma · Osteopontin · CD44 · Invasion

A. Gaumann (✉)
MPI für Physiologische und Klinische Forschung,
W.G. Kerckhoff Institut, Abt. für Molekulare Zellbiologie,
Parkstr. 1, 61231 Bad Nauheim, Germany
e-mail: andreas-gaumann@gmx.de
Tel.: +49-6032-7051, Fax: +49-6032-705211

A. Gaumann · M. Otto · C.J. Kirkpatrick · J. Kriegsmann
Department of Pathology, University of Mainz, Langenbeckstr. 1,
55101 Mainz, Germany

E. Mayer · M. Dahm
Department of Cardiovascular Surgery, University of Mainz,
Langenbeckstr. 1, 55101 Mainz, Germany

P. Petrow
Department of Pathology, University of Jena, Ziegelmühlenweg 1,
07743 Jena, Germany

T. Mentzel
Institute of Dermatohistopathology, Siemensstr. 6/1,
88048 Friedrichshafen, Germany

Introduction

Primary sarcomas of major blood vessels (aorta, pulmonal artery, and inferior vena cava) are rare, and only about 300 cases have been reported in the literature [30]. Sarcomas of great arteries are generally intimal tumors with divergent types of cellular differentiation, whereas those of the inferior vena cava are usually mural, well-differentiated vascular leiomyosarcomas [5, 6, 26]. Based on immunohistochemical examinations, intimal sarcomas show an endothelial, fibroblastic, or myofibroblastic differentiation [18, 20, 24, 30]. While some investigators describe a positive staining for smooth muscle actin (sm-actin), [5] others [24] propose that intimal sarcomas are only positive for vimentin but not for desmin or sm-actin. Typical clinical presentations of these sarcomas are recurrent pulmonary emboli [16, 23] and a rapidly progressive clinical course with fatal outcome as a result of pulmonary metastasis [22, 24].

Osteopontin (OPN) is a secreted phosphoprotein that was primarily defined in bone [10, 35] and was also demonstrated in normal epithelium [3] in different tumor types [1, 4] and in inflammatory lesions [32].

Several reports have shown that OPN is able to promote cell attachment and spreading through its Gly-Arg-Gly-Asp-Ser cell binding domain [9, 39]. The cell attachment is mediated by the cell surface αv integrin family [21], serving as a receptor for several other adhesive ligands [11]. Examination of the β3 subunit

Table 1 Immunohistochemical examination was performed using the following antibodies

Antibody	Source	Clone	Dilution	Pretreatment
OPN	Mrs. Farrach-Carson	–	1:100	Trypsin
CD68	Dako	K11/EBM11	1:50	Trypsin
CD44s	Dako	DF1485	1:50	Microwave
CD44 v3–10	R&D	BBA10	1:500	Microwave
Ki-67	Dianova	MIB-1	1:50	Microwave
Cytokeratin 19	Boehringer	CAM 5.2	1:200	Trypsin
Cytokeratin 8	B&D		1:25	
Vimentin	Progen	3B4	1:200	Trypsin
Desmin	Dako	D33	1:200	–
Sm-actin	Progen	asm-1	1:500	Trypsin
Factor VIII	Dako	Polyclonal	1:1000	Trypsin
CD 34	Immunotech	QBEND10	1:200	Trypsin
CD 31	Dako	JC/70A	1:50	Trypsin
UEA-1	EY Laboratories	–	1:800	Trypsin

revealed that this receptor plays a substantial role in the tumor development in mice, whereas the inhibition of this receptor by an antibody inhibits the tumorigenicity of melanoma cells [27]. Thus, there is evidence that the integrin receptors and their ligand, OPN, may promote tumor development and progression. OPN is markedly expressed in experimental tumor cell lines in vitro [7, 36], and elevated OPN expression was demonstrated in T24-H-ras transfected NIH3T3 cells [8]. The same results were obtained with a murine melanoma cell line, showing a correlation with the metastatic potential of these tumor cells [13]. In addition, it has been shown that patients with various tumors displayed significantly higher OPN levels in blood samples of patients with metastatic cancer than in healthy volunteers. [37]

OPN expression has also been studied in primary human epithelial tumors and their metastases. Some carcinomas showed strong OPN protein and messenger RNA expression but, in most cases, OPN could only be detected in numerous tumor-associated macrophages [4]. Thus, OPN may be involved in tumor development, progression, and metastases of carcinomas. However, to our knowledge, no data are available about the role of OPN in sarcomas. Since pulmonary vessel sarcomas are clinically very aggressive with an extraordinary high metastatic potential, we investigated the OPN expression in these tumors.

In addition, the role of CD44, which has been described as an alternative receptor for binding secreted OPN protein, is controversially discussed. While Somerman and coworkers have found that OPN binds to CD44 [39], a recent publication denied an interaction between both molecules [38]. Thus, we investigated the expression of CD44 in vessel sarcomas to clarify if this molecule could be involved in an interaction with OPN in pulmonary vessel sarcomas.

Materials and methods

Tissues were obtained from seven patients undergoing total pneumonectomy or partial artery or vein resection. All tissue samples were provided by the department of cardiovascular surgery of the Johannes Gutenberg University at Mainz. Immediately after surgery, tissue samples were fixed in 4% formaldehyde, embedded in paraffin, and processed routinely for tissue sections.

Diaminobenzidine immunohistochemical staining

Immunohistology was performed using antibodies as shown in Table 1. The sections were dewaxed according to a standard protocol and pretreated with 2% H_2O_2 in methanol for 30 min. After intervening washing steps in phosphate buffered saline (PBS), the slides were placed in 10 mM citrate buffer, pH 6.0 (in the case of MIB-1 and CD44v3-10) and treated for 15 min in a microwave oven or incubated with trypsin (Sigma-Aldrich, Deisenhofen, Germany; 1 mg/ml) for 20 min at 37°C (in the case of vimentin, factor VIII-associated antigen, α-smooth muscle actin, CD34, CD31, UEA-1, and cytokeratin) or received no pretreatment (desmin). Nonspecific binding was blocked with 2% horse serum or 2% goat serum (Vector Laboratories) at room temperature (RT) for 30 min and then incubated with the primary antibodies at RT for 1 h. The secondary anti-mouse antibody or anti-rabbit antibody (raised in horse, Vector Laboratories; 1:200) was applied for 30 min (RT) and followed by incubation with the avidin–biotin peroxidase complex (1:25; Vectastatin ABC-Kit, Vector Laboratories) for 30 min (RT). Finally, the sections were stained with the diaminobenzidine (DAB) substrate, rinsed for 10 min in running tap water, stained with hematoxylin, and mounted in glycerol–gelatin medium. The results of the DAB labeling are shown in Table 2.

Alkaline phosphatase–antialkaline phosphatase immunohistochemical staining

The antibodies used are shown in Table 1. The sections were preincubated in trypsin (Sigma-Aldrich; 1 mg/ml) for 30 min (for CD68) or treated with the microwave three times for 5 min in citrate buffer (for MIB-1, CD44 s) respectively. The alkaline phosphatase–antialkaline phosphatase (APAAP) technique was performed as previously described [19]. In control sections, the primary antibodies were either omitted, or non-specific mouse immunoglobulins were applied.

Double labeling with immunogold–silver detection of OPN protein

The double labeling with immunogold–silver method was performed according to our previously published protocol [19]. The primary OPN rabbit anti-human antibody (donated by Dr. Farrach-Carson, Houston Tex.), diluted in Tris-NaCl buffer pH 7.6 (1:100) for 90 min at RT, was used. The immunoglobulin fraction of serum from healthy non-immunized rabbits (Dako) was used as a control. Finally, slides were counterstained with hematoxylin and mounted in Kaiser's glycerol gelatin.

In control sections, the primary antibody was either omitted or substituted with non-specific rabbit or mouse immunoglobulins. A colon carcinoma and lung tissue specimens served as positive

Table 2 Clinical and pathological characteristics of pulmonary vessel sarcoma. *PT* pulmonary trunk, *PA* pulmonary artery, *RV* right ventricle

Patient no.	Age (years)	Gender	Relationship to vessel, size	Procedure	Histologic type	Follow-up	Treatment	Recurrence metastases
1	55	Male	Pulmonary trunk pericardium luminal	PT resection and reconstruction	Leiomyosarcoma	Died 18 months postoperatively	Radiation	Local lung
2	49	Female	Bifurcation right PA branch luminal	Resection PA replacement	Leiomyosarcoma	Died 9 months postoperatively	None	Lung
3	59	Male	Bifurcation right PA branch luminal	Endarterectomy right pneumonectomy	Intimal sarcoma	Died 7 months postoperatively	Radiation chemotherapy	Local
4	30	Male	RV outflow tract luminal	RV outflow resection valve/trunk reconstruction	Leiomyosarcoma	Alive 70 months postoperatively	Chemotherapy	None
5	49	Female	Pulmonary trunk luminal	Resection failed	Leiomyosarcoma	Died 18 months postoperatively	Chemotherapy	Local lung
6	60	Male	Pulmonary trunk luminal	Endarterectomy failed, left pneumonectomy	Intimal sarcoma	Alive 45 months postoperatively	Chemotherapy	Lung
7	60	Male	Pulmonary trunk luminal	PA resection reconstruction	Leiomyosracoma	Alive 31 months postoperatively	Chemotherapy	None

controls for OPN. A breast carcinoma was used as a positive control for MIB1, and lymph node and tonsillar tissue were used as controls for CD44.

Results

Clinical findings

In our patients, there was a male predominance (5:2) with a mean age of 52 years at time of presentation (30–60 years). The main clinical symptoms were recurrent pulmonary emboli, dyspnea, and chest pain. In all cases, the sarcomas were located in the pulmonary trunk and/or the right pulmonary artery and were diagnosed using a computed tomography (CT) scan, angiography, and pathology. The follow-up time ranged from 7 months to 48 months (mean 20 months). Four patients died within 18 months. Two patients received radiation, and five received chemotherapy. During the follow-up, three patients developed lung metastasis and two of them had a second operation (for details, see Table 2)

Gross findings

The examined vessel specimens ranged in diameter from 2.3 cm to 19 cm (mean 5.6 cm) with soft to firm, red–brown to yellow–gray crumbly necrotic tumor masses infiltrating vessel walls and adjacent soft tissues. The vessel lumen was usually partially obliterated by tumor thrombi. In two cases, the resected vessel tumors were accompanied by pneumonectomy specimens, showing up to 7-cm necrotic lesions.

Histological findings

Histological examination showed blood vessel structures with prominent fibrosis in the intima and media, foci of intramural hemorrhage, and a varying degree of reactive inflammation. The neoplastic tissue was composed of large atypical polygonal cells with little to abundant eosinophilic cytoplasm. There was a moderate to marked nuclear pleomorphism (Fig. 1). Sometimes, multinucleated giant tumor cells were seen. The tumor cells were arranged in a fascicular to storiform growth pattern with abundant myxoid intercellular matrix in two cases. One case showed some areas of metaplastic ossification. The mitotic count was elevated up to 25 mitoses/10 HPF (objective, 40×), including atypical mitoses. Moderate to abundant coagulative tumor necrosis was noted in all cases. According to the criteria of histopathologic grading of soft tissue sarcomas, four of the present tumors were classified as G2 sarcomas, and three were classified as G3 sarcomas [12] (see Table 3).

Immunohistochemical findings

The results of the immunohistochemical staining are summarized in Table 3. Tumor cells in all cases stained

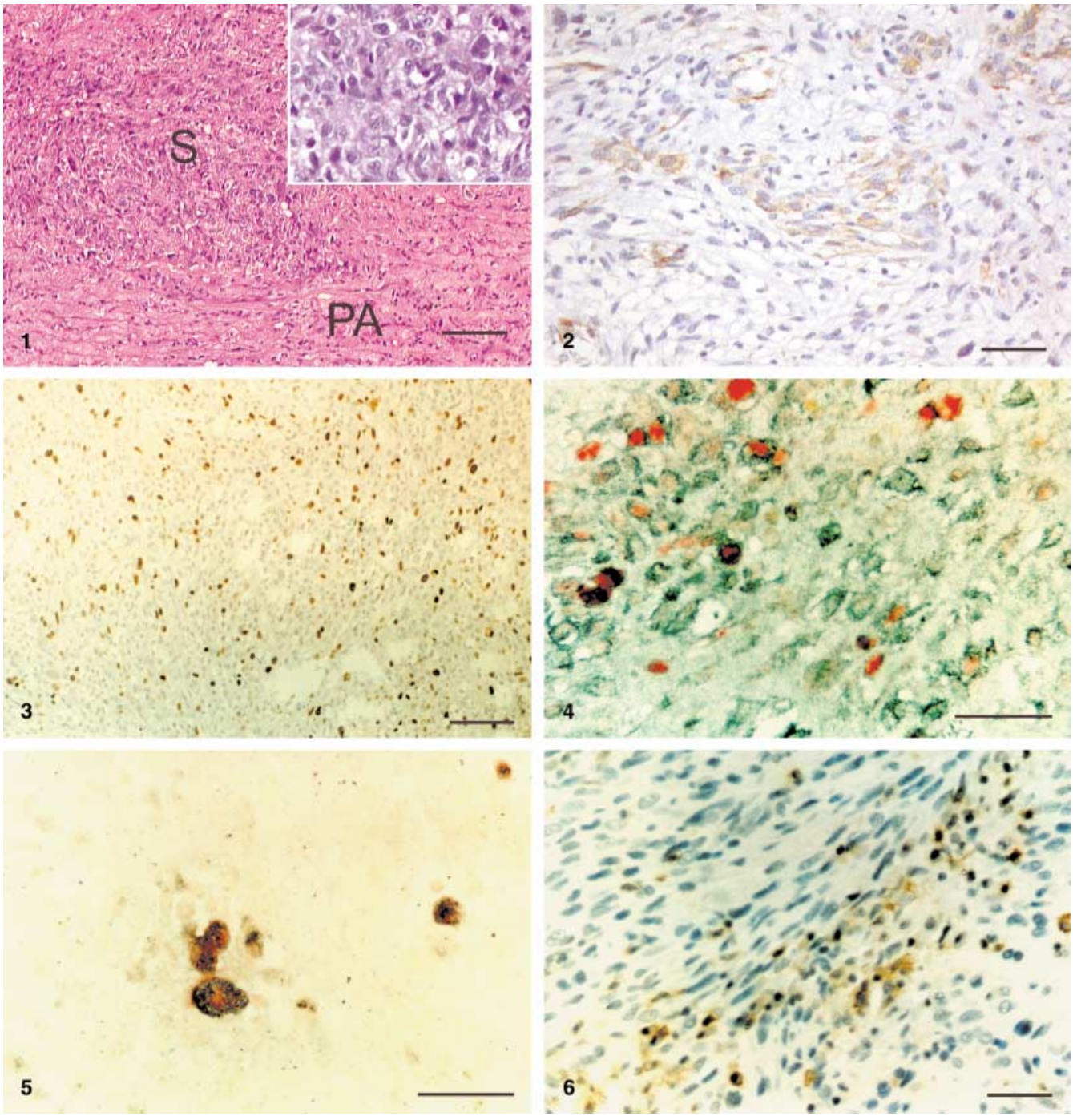


Fig. 1 Hematoxylin and eosin staining, showing sarcoma formation with marked nuclear pleomorphism (see *inset*) infiltrating the vessel wall of the pulmonary artery. Case 5; magnification 100× (*bar* 100 µm)

Fig. 2 Leiomyosarcoma with focally positive tumor cells for smooth muscle actin. Case 1; magnification 200× (*bar* 50 µm)

Fig. 3 Abundant nuclear expression of Ki-67 in sarcoma cells. Case 3; magnifciation 100× (*bar* 100 µm)

Fig. 4 Some spindle-shaped sarcoma cells show expression of Ki67 (*red*) in the nucleus and osteopontin (*black*) at the cellular surface and the cytoplasm. Case 4; magnification 400× (*bar* 50 µm)

Fig. 5 Intracellular accumulation of osteopontin (*black*) in CD68-positive macrophages (*red*). Case 4; magnification 400× (*bar* 50 µm)

Fig. 6 CD 44 is expressed at the surface of some tumor cells but also in numerous tumor-associated lymphocytes. Case 5; magnification 200× (*bar* 50 µm)

Table 3 Results of the immunohistochemical examinations of the seven pulmonary artery sarcoma cases. The positive reactions are graded as follows: + slight reaction, ++ moderate reaction, +++ strong reaction, and ++++ intense reaction. – negative reaction, *v* reaction in vessel structures

Case	Cytokeratin	Vimentin	Desmin	Actin	FVIII	CD34	CD31	UEA-1	Differentiation	Grade
1	–	++	++	+	–, v	–, v	–, v	–, v	Leiomyosarcoma	G2
2	–	+++	–	++	–, v	–, v	–, v	–, v	Leiomyosarcoma	G2
3	–	+	–	–	–, v	–, v	–, v	–, v	Intimal sarcoma	G3
4	–	++	+++	++	–, v	–, v	–, v	–, v	Leiomyosarcoma	G2
5	–	+++	+	+	–, v	–, v	–, v	–, v	Leiomyosarcoma	G2
6	–	++++	–	–	–, v	–, v	–, v	–, v	Intimal sarcoma	G3
7	–	+++	+++	++	–, v	–, v	–, v	–, v	Leiomyosarcoma	G3

positively for vimentin and, in five cases, myogenic differentiation was identified by a slight positivity of either desmin and/or sm-actin. Endothelial markers were completely negative in all tumor specimens, except for tumor-associated vessels (Fig. 2). In summary, five neoplasms were diagnosed as leiomyosarcomas and two as intimal sarcomas. The examination of Ki-67 revealed 20–60% positive tumor cells (Fig. 3).

The majority of the spindle-shaped polymorphous tumor cells stained strongly positive for OPN protein, and most of these cells could be double labeled with MIB1 (Fig. 4). The OPN protein staining was accentuated at the surface of the tumor cells. OPN expression was pronounced at sites of invasion or at the border of necrosis. An intracellular accumulation of OPN protein could be detected in CD68-positive macrophages (Fig. 5). In addition to the tumor cells and macrophages, the extracellular matrix stained prominently for OPN in all examined cases. Since some of the pulmonary artery sarcomas had adjacent lung tissue, we were able to show a marked staining at the apical surface of the bronchiolar epithelium, which served as an internal control. Control sections from pulmonary arteries were negative for OPN protein.

In addition, we examined the CD44 standard form and splicing variants in order to determine whether this receptor could be a possible binding site for OPN, besides the αv integrins. The immunohistochemistry could not demonstrate a significant expression of CD44 for the standard form but revealed a focally positive membrane expression for the antibody detecting the splicing variants in tumor-associated lymphocytes (Fig. 6). Control sections from lymph nodes and tonsils were positive for both standard and isoform variants of CD44.

Discussion

Primary sarcomas of the pulmonary artery are characterized by rapid progression and early hematogenous metastasis. Since OPN is known to be associated with cell attachment and metastatic spread in tumors, it is of particular interest to investigate the distribution of this molecule in pulmonary artery sarcomas.

The present cases lacked an endothelial differentiation demonstrated by a negative staining for CD31, CD34, factor VIII-associated antigen, and UEA-1. Concordant with the literature, only few cases have been described showing endothelial differentiation of these tumors [5, 18, 20]. Most reported cases were positive for vimentin, desmin, and/or α-smooth muscle actin, thus resembling typical leiomyosarcomas. [14] Five cases in our series had abundant vimentin staining and a slight to moderate positivity for desmin and α-smooth muscle actin and were therefore classified as leiomyosarcomas. Two cases could only be stained with vimentin and were classified as intimal sarcomas. Interestingly, one case showed focal metaplastic ossification, which may sometimes occur in this entity [5, 6]. The proliferation rate varied between 20% and 60%, reflecting a rapid progression of these tumors.

The examination of OPN protein expression showed abundant staining for tumor cells and also for the extracellular matrix. Since OPN has been described as a putative cellular adhesion molecule which promotes cell attachment and invasion in tumors [4], our data support the conclusion that the OPN protein could play a substantial role in tumor progression in vessel sarcomas. Although the "origin" of the sarcoma cells is controversially discussed by several authors, it seems to be most likely that these tumors originate from fibroblasts or myofibroblasts of the inner vessel wall [5, 18]. It has been reported that rat aortic smooth muscle cells in culture expressed high levels of OPN messenger RNA [15], whereas others found no evidence of OPN or OPN transcripts in various human organs containing smooth muscle [3, 29]. This may explain why expression of this molecule differs between rodents and humans. In our series, we could not see an expression of OPN in adjacent normal smooth muscle cells, thus supporting the opinion of Newman and coworkers.

It has been shown that ras transfection of the fibroblast cell line NIH3T3 may be responsible for the elevation of the OPN transcript and protein through a ras-mediated signal transduction pathway [2, 8]. Interestingly, Guo and coworkers reported a possible interaction of OPN and ets-related transcription factors in ras-activated cells and a correlation with their metastatic potential [17]. The relationship between OPN and ras is not restricted to malignant conditions, as reports have shown that rastransfected smooth muscle cells are able to overexpress OPN and may have an impact in the development of atherogenesis [33, 34]. However, Brown and coworkers were able to demonstrate OPN protein and tran-

scripts only in carcinomas of the endometrium and the kidney, whereas most other carcinomas showed only OPN mRNA in tumor-associated macrophages. A possible explanation for this discrepancy could be that most studies used ras-transfected cell lines or serially passaged experimental tumors, whereas Brown et al. examined routine tumor specimens [4]. Another reason for the difference between the in vitro and in vivo observations could be that mutation of ras is required for the overexpression of OPN in tumor cells. This has not been tested in the study of Brown et al. Since we do not know whether there is any ras mutation in our series, it will be important to investigate this oncogene at the molecular level in pulmonary vessel sarcomas.

In our series, we were able to find prominent OPN expression at the cell surface of sarcoma cells and in the extracellular matrix. A possible explanation for this finding could be that OPN is secreted into the extracellular matrix and binds to the surface of tumor cells, as has been previously described [4]. Although we have no data about OPN mRNA so far, it is conceivable that the protein is released from some tumor cells into the extracellular matrix. However, this still remains speculative at present. Most likely, OPN binds to other tumor cells, thus mediating cell signaling in a paracrine fashion. In addition, we could show that OPN is present in the majority of macrophages, suggesting that these cells seem to be the main source for OPN in these tumors. The pathomechanism of OPN production, secretion, and paracrine function through macrophages has been suggested by several investigators in a variety of different pathologic conditions, such as wound healing, myocardial infarction and coronary disease [15, 25, 28, 31].

The focal expression of the CD44 splice variant but not the standard form in tumor-associated lymphocytes suggests that these cells are the target for OPN. It is possible that OPN regulates cell trafficking and adhesion of inflammatory cells as a signal peptide. In addition, cellular adhesion between tumor cells and lymphocytes may be mediated through OPN/CD44 interaction, although the functional role is still unknown.

In summary, we have shown that OPN was strongly expressed in pulmonary vessel sarcomas, especially at the site of invasion. Since it is known that OPN affects cell adhesion and tumor cell invasion, these data suggest that OPN may contribute to the poor prognosis and high incidence of metastasis of these tumors.

Acknowledgements We would like to thank Sandra Gerecht and Antonietta Rastiello for excellent technical support and Peter Pulkowski and Thomas Boehm for their photographic support.

References

1. Bellahcène A, Castronovo V (1995) Increased expression of osteonectin and osteopontin, two bone matrix proteins, in human breast cancer. Am J Pathol 146:95–100
2. Bondy GP, Wilson S, Chambers AF (1985) Experimental metastatic ability of H-ras-transformed NIH3T3 cells. Cancer Res 45:6005–6009
3. Brown LF, Berse B, Van de Water L, Papadopoulos-Sergiou A, Perruzzi CA, Manseau EJ, Dvorak HF, Senger DR (1992) Expression and distribution of osteopontin in human tissues: widespread association with luminal epithelial surfaces. Mol Biol Cell 3:1169–1180
4. Brown LF, Papadopoulos-Sergiou A, Berse B, Manseau EJ, Tognazzi K, Perruzzi CA, Dvorak HF, Senger DR (1994) Osteopontin expression and distribution in human carcinomas. Am J Pathol 145:610–623
5. Burke AP, Vermani R (1993) Sarcomas of the great vessels. Cancer 71:1761–1773
6. Burke AP, Vermani R (1996) Tumors of the heart and great vessels. In: Rosai J, Sobin LH (eds) Atlas of tumor pathology, vol III. Armed Forces Institute of Pathology, Washington D.C. pp 211–220
7. Chambers AF (1995) Regulation and function of osteopontin in ras-transformed cells. Ann N Y Acad Sci 21:101–108
8. Chambers AF, Behrend EI, Wilson SM, Denhardt D (1992) Induction of expression of osteopontin (OPN; secreted phosphoprotein) in metastatic, ras-transformed NIH 3T3 cells. Anticancer Res 12:43–47
9. Chambers AF, Hota C, Prince CW (1993) Adhesion of metastatic, ras-transformed NIH 3T3 cells to osteopontin, fibronectin, and laminin. Cancer Res 53:701–706
10. Chen J, Singh K, Mukherjee BB, Sodek J (1993) Developmental expression of osteopontin (OPN) mRNA in rat tissues: evidence for a role for OPN in bone formation and resorption. Matrix 13:113–123
11. Cheresh DA (1991) Structure, function and biological properties of integrin $\alpha_v\beta_3$ on human melanoma cells. Cancer Met Rev 10:3–10
12. Coindre JM, Nguyen BB, Bonichon F, de Mascarel I, Trojani M (1988) Histopathologic grading in spindle cell soft tissue sarcomas. Cancer 61:2305–2309
13. Craig AM, Bowden GT, Chambers AF, Spearman MA, Greenberg AH, Wright JA et al (1990) Secreted phosphoprotein mRNA is induced during multi-stage carcinogenesis in mouse skin and correlates with the metastatic potential of murine fibroblasts. Int J Cancer 46:133–137
14. Eng J, Murday AJ (1992) Leiomyosarcoma of the pulmonary artery. Ann Thorac Surg 53:905–906
15. Giachelli CM, Lombardi D, Johnson RJ, Murry CE, Almeida M (1998) Evidence for a role of osteopontin in macrophage infiltration in response to pathological stimuli in vivo. Am J Pathol 152:353–358
16. Gosalbez F, Gudin C, Miralles M, Naya J, Valle JM (1993) Intimal sarcoma of the left pulmonary artery: diagnosis, treatment and survival. Cardivasc Surg 1:447–448
17. Guo X, Zhang YP, Mitchell DA, Denhardt DT, Chambers AF (1995) Identification of a ras-activated enhancer in the mouse osteopontin promoter and its interaction with a putative ETS-related transcription factor whose activity correlates with the metastatic potential of the cell. Mol Cell Biol 15: 476–487
18. Haber LM, Truong L (1988) Immunohistochemical demonstration of the endothelial nature of aortic intimal sarcoma. Am J Surg Pathol 12:798–802
19. Hansen T, Petrow PK, Gaumann A, Keyszer GM, Eysel P, Eckardt A, Kriegsmann J (2000) Cathepsin B and its endogenous inhibitor cystatin C in rheumatoid arthritis synovium. J Rheumatol 27:859–865
20. Hottenrott G, Mentzel T, Peters A, Schroder A, Katenkamp D (1999) Intravascular ("intimal") epithelioid angiosarcoma: clinicopathological and immunohistochemical analysis of three cases. Virchows Arch 435:473–478
21. Hu DD, Lin EC, Kovach NL, Hoyer JR, Smith JW (1995) A biochemical characterization of the binding of osteopontin to integrins $\alpha v\beta 1$ and $\alpha v\beta 5$. J Biol Chem 270: 26232–26238
22. Klinke WP, Gelfand ET, Baron L (1985) Primary sarcoma of the pulmonary trunk: successful surgical intervention and prolonged survival. Clin Cardiol 8:437–440

23. Krüger I, Borowski A, Horst M, de Vivie R, Theissen P, Gross-Fengels W (1990) Symptoms, diagnosis and therapy of primary sarcomas of the pulmonary artery. Thorac Cardiovasc Surg 38:91–95
24. McGlennen RC, Manivel JC, Stanley SJ, Slater DL, Wick MR, Dehner LP (1989) Pulmonary artery trunk sarcoma: a clinicopathologic, ultrastructural, and immunohistochemical study of four cases. Mod Pathol 2:486–494
25. McKee MD, Nanci A (1996) Secretion of osteopontin by macrophages and its accumulation at tissue surfaces during wound healing in mineralized tissues: a potential requirement for macrophage adhesion and phagocytosis. Anat Rec 245:394–409
26. Mingoli A, Cavallaro A, Sapienza P, di Marzo L, Feldhaus RJ, Cavallari N (1996) International registry of inferior vena cava leiomyosarcoma: analysis of a world series on 218 patients. Anticancer Res 16:3201–3206
27. Mitjans F, Sander D, Adan J, Sutter A, Martinez JM, Jaggle CS, Moyano JM, Kreysch HG, Piulats J, Goodman SL (1995) An anti-alpha v-integrin antibody that blocks integrin function inhibits the development of a human melanoma in nude mice. J Cell Sci 108:2825–2838
28. Murry CE, Giachelli CM, Schwartz SM, Vracko R (1994) Macrophages express osteopontin during repair of myocardial necrosis. Am J Pathol 145:1450–1462
29. Newman CM, Bruun BC, Mistry PK, Weissberg PL, Shanahan CM (1995) High expression of osteopontin mRNA in human macrophages but not human vascular smooth muscle cells in culture. Ann N Y Acad Sci 21:381–382
30. Nonomura A, Kurumaya H, Kono N, Nakanuma Y, Ohta G, Terahata S, Matsubara F, Matsuda T, Asaka T, Nishino T (1988) Primary pulmonary artery sarcoma. Report of two autopsy cases studied by immunohistochemistry and electron microscopy, and review of 110 cases reported in the literature. Acta Pathol Jpn 38:883–896
31. O'Brien ER, Garvin MR, Stewart DK, Hinohara T, Simpson JB, Schwartz SM, Giachelli CM (1994) Osteopontin is synthesized by macrophage, smooth muscle, and endothelial cells in primary and restenotic human coronary atherosclerotic plaques. Arterioscler Thromb 14:1648–1656
32. O'Brien KD, Kuusisto J, Reichenbach DD, Ferguson M, Giachelli C, Alpers CE, Otto CM (1995) Osteopontin is expressed in human aortic valvular lesions. Circulation 92: 2163–2168
33. Parrish AR, Weber TJ, Ramos KS (1997) Osteopontin overexpression in vascular smooth muscle cells transfected with the c-Ha-ras oncogene. In Vitro Cell Dev Biol Anim 33: 584–587
34. Ramos KS (1999) Redox regulation of c-Ha-ras and osteopontin signaling in vascular smooth muscle cells: implications in chemical atherogenesis. Annu Rev Pharmacol Toxicol 39: 243–265
35. Reinholt FP, Hultenby K, Oldberg A, Heinegard D (1990) Osteopontin – a possible anchor of osteoclasts to bone. Proc Natl Acad Sci U S A 87:4473–4475
36. Saitoh Y, Kuratsu J, Takeshima H, Yamamoto S, Ushio Y (1995) Expression of osteopontin in human glioma. Its correlation with the malignancy. Lab Invest 72:55–63
37. Senger DR, Peruzzi CA, Gracey CF, Papadopoulos A, Tenen DG (1988) Secreted phosphoproteins associated with neoplastic transformation: close homology with plasma proteins cleaved during blood coagulation. Cancer Res 48:5770–5774
38. Smith LL, Greenfield BW, Aruffo A, Giachelli CM (1999) CD44 is not an adhesive receptor for osteopontin. J Cell Biochem 73:20–30
39. Somerman MJ, Prince CW, Butler WT, Foster RA, Moehring JM, Sauk JJ (1989) Cell attachment activity of the 44 kDa bone phosphoprotein is not restricted to bone cells. Matrix 9:49–5

Virchows Arch (2001) 439:675–682
DOI 10.1007/s004280100432

ORIGINAL ARTICLE

N. Rinaldi · M. Willhauck · D. Weis · B. Brado
P. Kern · M. Lukoschek · M. Schwarz-Eywill
T.F.E. Barth

Loss of collagen type IV in rheumatoid synovia and cytokine effect on the collagen type-IV gene expression in fibroblast-like synoviocytes from rheumatoid arthritis

Received: 6 September 2000 / Accepted: 25 January 2001 / Published online: 7 July 2001
© Springer-Verlag 2001

Abstract Collagen type IV is a structural matrix protein which contributes to the structural organization of the synovia. In order to characterize the distribution of this protein in synovia with chronic synovitis, collagen type IV was detected by immunochemistry in normal synovia and in synovia from patients with osteoarthritis (OA) and rheumatoid arthritis (RA). A decrease of collagen type IV was observed in synovial layers of rheumatoid synovia, which statistically correlated with the grade of inflammation and with the thickness of the synovial layer. In vitro, we found no differences in the gene expression of collagen type IV in cultures of fibroblast-like synoviocytes (FLS) derived from OA and RA using a reverse-transcriptase polymerase chain reaction. Nevertheless, we observed a downregulating effect of tumor necrosis factor-α and interleukin (IL)-1β on the gene expression of collagen type IV only in FLS isolated from patients with RA. The effect of IL-1β was dose dependent. In summary, we observed an inflammation-associated decrease of collagen type IV in the synovial layer of rheumatoid synovia. Inflammatory cytokines may play a role in regulating the synthesis of collagen type IV in the rheumatoid process in vivo.

N. Rinaldi (✉) · P. Kern
Abteilung Innere Medizin III, Robert-Kochstraße 8,
89081 Ulm, Germany
e-mail: nadia.rinaldi@medizin.uni-ulm.de
Tel.: +49-731-5024429, Fax: +49-731-5024422

M. Willhauck · D. Weis · B. Brado
Medizinische Klinik und Poliklinik V, Universität Heidelberg, Germany

M. Lukoschek
Orthopädische Klinik, Vincentius Krankenhaus, Konstanz, Germany

M. Schwarz-Eywill
Medizinische Klinik, Evangelisches Krankenhaus, Oldenburg, Germany

T.F.E. Barth
Pathologisches Institut, Universität Ulm, Albert-Einstein-Allee 11,
89081 Ulm, Germany

Keywords Collagen type IV · Basement membrane · Rheumatoid arthritis · Osteoarthritis

Introduction

Extracellular matrix proteins play an important role in maintaining the integrity of tissues [2, 17]. Although normal synovia lacks a basement membrane, there is a clearly defined distribution of extracellular matrix proteins such as collagen type IV and laminin in the synovia. This suggests that this network of extracellular matrix components contributes to the organization of the synovia [19, 23, 24]. One of the most striking aspects of chronic synovitis is the remodeling of the connective tissue matrix. The concomitant degradation of the normal synovial tissue and the replacement of this tissue by inflammatory cells and fibrous tissue results in joint destruction and loss of function. Potential effectors of this destructive process are synovial lining cells (SLCs), which have been shown to synthesize extracellular matrix proteins [28] and proteolytic enzymes [18]. In chronic synovitis, cytokines may induce a degradative phenotype in SLCs [15]. In situ and in vitro studies have shown that fibroblast-like synovial cells (FLSs) synthesize collagen type IV [19, 28]. Since collagen type IV is regarded as a major structural component of the basement membrane, we investigated the in situ distribution of this structural protein using immunochemistry in synovia with chronic synovitis from patients with osteoarthritis (OA) and rheumatoid arthritis (RA). In order to characterize the regulating factors of the remodeling process of the extracellular matrix in vivo, we detected the effect of cytokines on the collagen type-IV gene expression using reverse-transcription polymerase chain reaction (RT-PCR) in FLS in vitro from patients with OA and RA.

Materials and methods

Synovial tissue

Synovial tissues were obtained at arthroplasty from different joints of 23 patients with RA and 16 patients with OA (according to the criteria of the "American College of Rheumatology", formerly the "American Association of Rheumatology" [4, 6]). Control specimens were obtained at autopsy from two patients without arthritis who died of unrelated causes. Autopsy specimens were taken within 6 h of death. Control specimens, 19 specimens of patients with RA and 12 synovia specimens of patients with OA, were quick-frozen in liquid nitrogen and stored at –70°C until the immunostaining procedure was performed. Laboratory tests, erythrocyte sedimentation rate (ESR) and rheumatoid factor are reported in Table 1. The specimens from four patients with OA and from four patients with RA were processed immediately after excision and prepared for FLS culture.

Reagents

The anti-collagen type-IV monoclonal antibody (mAb) CIV22 (IgG1) was purchased from Dako (Hamburg, Germany). A polyclonal biotinylated sheep antibody to mouse immunoglobulin (Ig; reactive with all mouse and rat isotypes) and a streptavidin-biotinylated peroxidase complex were purchased from Amersham (High Wycombe, UK). 3-Amino-9-ethylcarbazole (AEC) and *N′N*-dimethylformamide (DMF) were obtained from Sigma Chemical (St. Louis, Mo.). An anti-cytomegalovirus antibody (clone CCH2; IgG1) was used as a negative control and was obtained from Dako (Glostrup, Denmark).

Immunostaining procedure

Serial frozen sections of approximately 1 cm^2 in area and 5 µm in thickness were air-dried overnight, fixed in acetone for 10 min at room temperature, and immunostained immediately or after stor-

Table 1 Inflammation score, clinical, and immunostaining data in synovial lining cells of normal, osteoarthritis (OA), and rheumatoid arthritis (RA) synovia. Scoring of cell reaction: 4+, 75–100% cells positive; 3+, 50–75% cells positive; 2+, 25–50% cells positive; 1+, 1–25% cells positive; (), low level of antigen expression; –, all cells negative. Scoring of synovial lining layers: 1, 1–3 cell layers; 2, 4–5 cell layers; 3, 6–8 cell layers; 4, 9 cell layers. *ESR* erythrocyte sedimentation rate, *RF* rheumatoid factor, *NSAID* non-steroidal anti-inflammatory drug, n.d. not determined

	ESR	RF	Antirheumatic treatment	Site of synovia	Inflammation score	Synoviocyte hyperplasia	Collagen type IV
Normal synovia							
Sample 1	–		–	Knee	3	1	4+
Sample 2	–		–	Knee	3	1	4+
OA synovia							
Sample 3	7		No	Knee	5	2	3+
Sample 4	2		No	Knee	8	2	(1+)
Sample 5	20		No	Hip	7	1	4+
Sample 6	2		No	Hip	11	1	3+
Sample 7	30		No	Hip	4	1	3+
Sample 8	3		No	Hip	4	1	3+
Sample 9	20		No	Hip	6	1	3+
Sample 10	n.d.		No	Knee	4	1	3+
Sample 11	6		NSAID	Hip	8	1	(3+)
Sample 12	2		NSAID	Hip	7	1	(4+)
Sample 13	18		No	Hip	6	2	(2+)
Sample 14	3		NSAID	Hip	4	1	3+
mean value ±SD					6.2 (2.1)	1,2 (0.4)	2.9 (0.7)
RA synovia							
Sample 15	18	+	Gold	Knee	7	1	(2+)
Sample 16	22	+	Gold	Wrist	11	1	1+
Sample 17	9	n.d.	Methotrexate	Wrist	15	4	–
Sample 18	20	+	Methotrexate	Wrist	9	2	4+
Sample 19	35	–	Methotrexate	Wrist	9	1	(2+)
Sample 20	n.d.	+	Gold	Knee	11	1	1+
Sample 21	16	+	NSAID	Wrist	12	1	2+
Sample 22	44	+	Methotrexate	Knee	9	2	–
Sample 23	40	n.d.	Methotrexate	Hip	8	2	(2+)
Sample 24	34	+	Gold	Knee	13	2	(1+)
Sample 25	4	–	Methotrexate	Hip	4	3	(2+)
Sample 26	54	+	Methotrexate	Knee	6	1	(2+)
Sample 27	21	–	Methotrexate	Elbow	15	1	(1+)
Sample 28	17	n.d.	Methotrexate	Knee	10	2	3+
Sample 29	33	–	NSAID	Wrist	12	4	–
Sample 30	80	+	Penicillamine	Knee	15	4	–
Sample 31	20	n.d.	Gold	Knee	15	4	–
Sample 32	14	+	Methotrexate	Hip	10	2	(1+)
Sample 33	20	n.d.	Penicillamine	Knee	8	1	3+
Mean value ±SD					10.6±3.2	2.1±1.1	1.3±1.13

age at –20°C for 1–3 weeks. Immunostaining procedures were carried out according to standard methods as previously described [25]. Briefly, for immunohistochemistry, following rehydration with phosphate-buffered saline solution (PBS; pH 7.5), the frozen sections were incubated for 1 h with primary mAbs. The primary mAb was used in a protein concentration of about 5 µg/ml PBS. The sections were then incubated with biotinylated anti-mouse antibody (20 µg/ml protein) and a streptavidin–biotin–peroxidase complex (10 µg/ml protein) for 30 min, respectively. All incubation steps were carried out in a humid chamber at room temperature. Between each incubation step, the sections were rinsed twice in PBS. Using AEC as the chromogen (0.4 mg/ml in 0.1 mol/l acetate buffer, pH 5.0, with 5% DMF and 0.01% hydrogen peroxide for about 20 min), the peroxidase reaction caused an intense-red precipitate. The sections were then rinsed in tap water, counterstained with Harris' hematoxylin, and mounted with glycerol gelatin. Each series of frozen sections contained a negative control without the primary reagent and the control anti-cytomegalovirus antibody. No staining was observed in the control slides except for scattered granulocytes whose endogenous peroxidase was not blocked in order to permit optimal antigenicity. This reactivity was disregarded during evaluation. In tissue sections, strongly stained endothelial cells served as intrinsic positive controls.

Controls and evaluation of antigen expression

SLC staining in tissue sections was evaluated in a semi-quantitative manner: ''+'' indicates strong intensity of the detected antigen; ''(+)'' is regarded as weak intensity of antigen detected. The absence of antigen was symbolized as ''–''. A simple semi-quantitative statement was made for the staining intensity within SLCs: ''4+'', meaning 75–100% cells positive; ''3+'', meaning 50–75% cells positive; ''2+'', meaning 25–50% cells positive; and ''1+'', meaning 1–25% cells positive.

Degree of inflammation

Hematoxylin-eosin-stained sections from each synovial specimen were scored for the degree of inflammation by two independent observers, according to Rooney et al. [27]. SLC depth was determined, and the results were recorded as 1 (1–3 cell layers), 2 (4–5 cell layers), 3 (6–8 cell layers), and 4 (=9 cell layers). Proliferating blood vessels were determined by immunostaining using anti-von Willebrand Factor (Dako) and recorded as 1+ [0–5 vessels/high power field (HPF)], 2+ (5–10 vessels/HPF), 3+ (10–20 vessels/HPF), and 4+ (>20 vessels/HPF). The size of lymphoid aggregates on stained sections was recorded as 0+ (no aggregates), 1+ (1–20 cells/HPF), and 2+ (>20 cells/HPF). The number of vessels showing perivascular infiltrates was determined for the final score and regarded as 1+ (1–25% of the vessels involved), 2+ (25–50% of the vessels involved), 3+ (50–75% of the vessels involved), and 4+ (75–100% of the vessels involved). The degree of fibrosis and the presence of necrosis were assessed. Sections containing less than 10% fibrous tissue in the membrane sublining layers were considered normal and graded 1. Sections containing 10–50% fibrous tissue were scored as 2+, whereas sections with 50% fibrous tissue were graded as 3+. The absence of necrosis was scored as 0. The presence of necrosis was scored as 2+. The scores of the individual items were added, and the sum was used as an estimate of the overall intensity of inflammation using histological criteria (range of possible values 3–19).

FLS isolation

In vitro cultures of FLS were obtained using standard methods, as previously described [1]. The tissue was minced into small pieces and digested with collagenase type Ia (Sigma Chemical) in serum-free basal Iscove medium (Seromed-Biochrom, Berlin, Germany). The samples were washed and suspended in basal Iscove medium, supplemented with 10% fetal calf serum (FCS, Bio Pro, Karlsruhe, Germany) and penicillin–streptomycin–amphotericin B (10 U/ml, 10 mg/ml, and 0.25 mg/ml). Finally, isolated cells were cultured in a humidified 5% carbon dioxide atmosphere. After overnight culture, non-adherent cells were removed. Fresh medium was added and the incubation continued. At confluence, cells were trypsinized, split at a ratio of 1:3 and re-cultured. The medium was changed twice weekly. At the end of in vitro incubation, FLS cultures were washed with PBS, detached with ethylene diamine tetraacetic acid (EDTA; 0.02%) and centrifuged at 1000 rpm for 5 min. The cultured cells comprised a homogeneous population of FLSs with respect to morphological and immunocytochemical criteria (<1% CD11b+, <1% CD11a+, <1% CD11c+, <1% CD53+, <1% CD3+, <1% factor VIII+).

FLS cultures for RT-PCR

Collagen type-IV gene expression was investigated in 3 OA-FLS and 3 RA-FLS cultures at different culture times (from passages 1 to 5) and in two other FLS-cultures (1 OA-FLS and 1 RA-FLS from passages 3 to 9) after stimulation with interleukin (IL-1β; Genzyme; Cambridge, Mass.; 40 U/ml, 100 U/ml, and 1000 U/ml), tumor necrosis factor (TNF)-α (Knoll; Ludwigshafen, Germany; 10 ng/ml), and transforming growth factor (TGF)-β (Boehringer; Mannheim, Germany; 10 ng/ml). FLS cultures were incubated for 72 h in serum-free conditions with these cytokines, used alone or in combination (IL-1β and TNF-α, IL-1β and TNF-α, TGF-β and IL-1β), or with medium alone as a negative control. Each FLS culture (4–5×10^5 cells) was lysed using a guanidinium thiocyanate buffer and stored at –70°C until RNA extraction.

Preparation of RNA and complementary (c)DNA synthesis

Total RNA was extracted from cultured FLSs using the method described by Chomczynski and Sacchi [8], based on a guanidinium thiocyanate buffer. The amount of RNA obtained was photometrically determined and 0.2 µg total RNA used for cDNA synthesis with the following reagents (total volume of 25 µl): 8 µM random hexamers (Pharmacia, Freiburg, Germany) 1 mM deoxyribonucleoside triphosphate (dNTP; Promega, Madison, Wis.), 20 U AMV reverse transcriptase (Promega), 40 U RNasin (Promega), 50 mM KCl, 5 mM Tris-HCl, and 10 mM $MgCl_2$. After incubation for 1 h at 42°C, newly synthesized cDNA was stored at –20°C until further use.

Semi-quantitative PCR analysis of collagen type-IV mRNA expression

Primers of collagen type-IV cDNA were devised from published sequences [14, 30]: sense 5′-GCTCACCAGGACCAGTGGGT-3′, antisense 5′-TCACCTTTAGGTCCTGGCTG-3′. Primers for cDNA of the housekeeping gene β2-microglobulin were used that closely matched the melting temperature of collagen type-IV primers: sense 5′-CTCGCGCTACTCTCTCTTTCT-3′, antisense 5′-TGTCGGATTGATGAAACCCAG-3′.

The PCR reaction of a 2-µl cDNA aliquot contained: 2 U *Taq* polymerase (Promega), 0.83 µM of the respective PCR primers, 3 mM $MgCl_2$, 200 µM dNTP, 1×PCR buffer (Promega; total volume of 50 µl). Thirty PCR cycles were performed at temperatures of 94°C, 60°C, and 72°C, each for 1.5 min. Previous experiments had shown that, under these conditions, the PCR reaction was in the exponential phase. PCR products were separated according to size in 2% agarose gel and transferred onto a nylon membrane (Boehringer). PCR from collagen type-IV cDNA yielded a 310-bp product.

To confirm the identity of the amplification products and to determine the amounts of PCR products, nylon filters were simulta-

neously hybridized with the following 3′-digoxigenin-labelled oligonucleotide probes specific to internal collagen type IV (5′-AAAGGTGATAAGGGGGATGTCGGTCTG-3′) and β2-microglobulin sequences (5′-ATTCTCTGCTGGATGACGTGAGTAAACCTG-3′). Prehybridization with a buffer described by Church and Gilbert [9] containing 5×SSC (sodium saline citrate), 2.0% blocking solution (Boehringer), 0.1% *N*-lauroylsarcosyl (Serva, Germany), 7% sodium dodecylsulphate (Sigma Chemical), 50 mM sodium phosphate, pH 7.0, and 50 µg/ml yeast tRNA (Boehringer) was performed for 2 h in a hybridization flask with continuous rolling (Bachofer, Germany). Subsequent hybridization was performed for approximately 15 h using 2.5 ml per 100 cm^2 filter surface of the same buffer with 10 pmol/ml digoxygenin (DIG)-labeled oligonucleotide probes specific to the β2m and the collagen type-IV gene. Washing conditions and chemoluminescence reaction with CSPD (disodium 3-(methoxyspiro{1,2-dioxetane-3,2′-(5′-chloro)tricyclo[3.3.1.13,7]decan}-4-yl) phenyl phosphate) as substrate were performed using instructions and reagents of a commercially available chemoluminescence detection kit (Boehringer). Emission of light was detected by exposition of X-ray films. Signals on the exposed films were quantified after scanning (Macintosh Color One Scanning) using IMAGE 1.41 software (National Cancer Institute, Bethesda, Md.). Relative collagen type-IV mRNA expression was calculated from the ratio of collagen type IV to β2-microglobulin strength. To confirm the reproducibility of collagen type-IV/β2m gene expression, the RT-PCR of one synovial cell culture was repeated three times. Results showed a maximum variability of 15% (data not shown). Therefore, only differences of collagen type-IV expression of 15% or more were considered relevant.

Statistical analysis

Correlations between collagen type-IV staining and inflammation score/therapy were calculated using the rank correlation Spearman test.

Results

Inflammation score, clinical, and immunostaining data

Histologic scores of inflammation, immunohistochemical results, and patient data are listed in Table 1. Normal synovial membranes were histologically devoid of inflammatory changes, and the synovial lining layer was generally 1–3 cells in thickness. We found a strong positivity for collagen type IV both in all synovial layer cells and in the subintimal arterial and venular vessels (Fig. 1a, b).

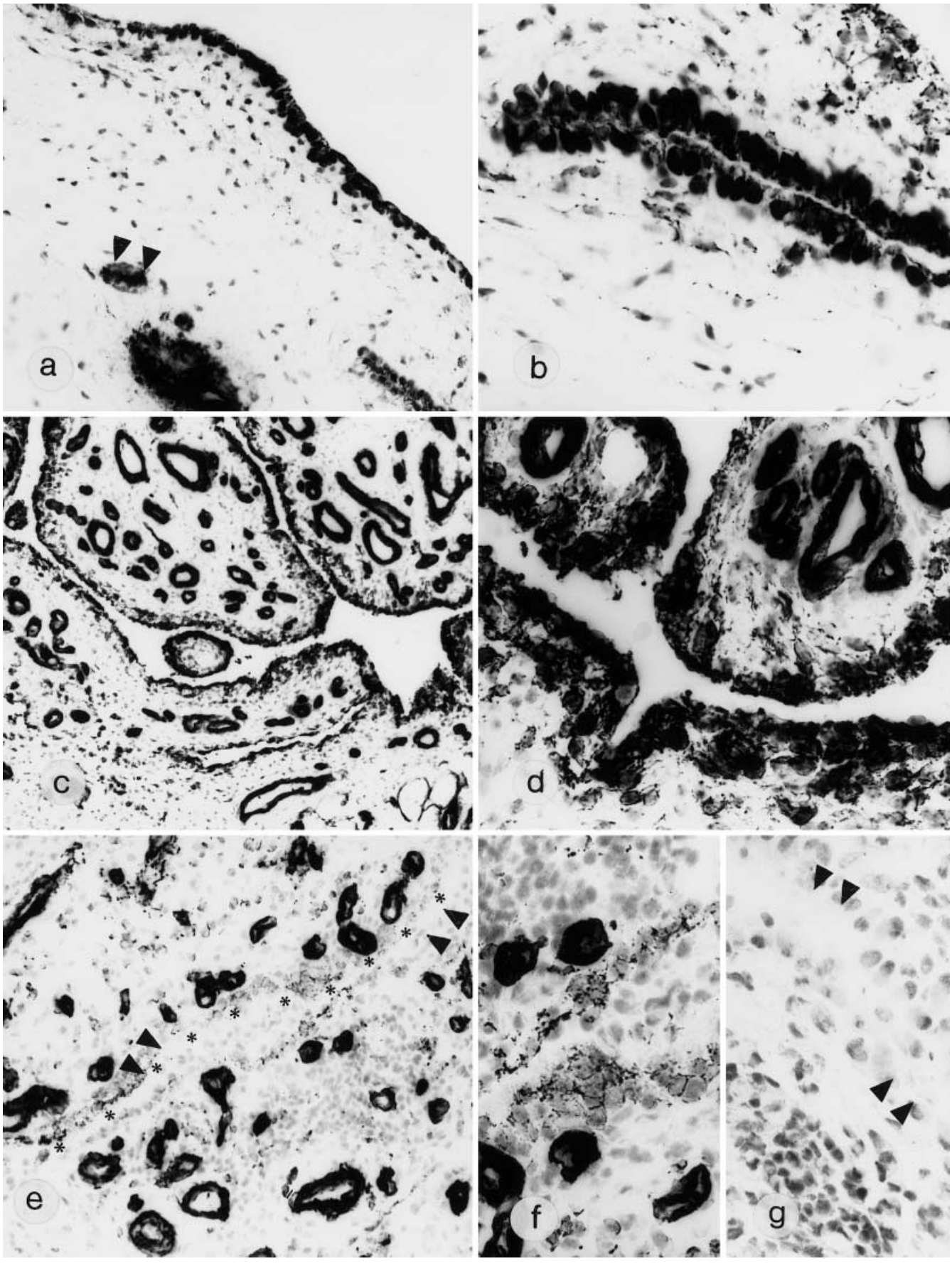
In OA synovia, the mean inflammation score was higher (mean±SD 6.2±2.1) than that of normal synovia. In only 1 of the 12 synovia samples was the inflammation score greater than 10. In 9 of 12 OA samples, SLCs were distributed in 1–3 cell layers, whereas in 3 of 12 OA samples the cell layer number was comprised within 4 and 5 cell layers. No correlation was found between the inflammation score and the synoviocyte hyperplasia. These parameters did not correlate with the laboratory test ESR. In 9 of 12 OA samples, the majority (samples 3, 6, 7, 8, 9, 10, and 14) or all (samples 5 and 12) SLCs showed collagen type-IV staining (Fig. 1c, d). In two samples (samples 4 and 11), a faint positivity for collagen type IV was distributed in 25–50% of SLCs. Only in one case (sample 13) was a weak collagen type-IV staining found in a low number of SLCs. Collagen type-IV staining did not correlate with the inflammation score or with the thickness of the synovial layer.

RA samples showed a high grade of inflammation (10.6±3.2). The degree of inflammation correlated statistically with the synovial lining hyperplasia. Collagen type-IV staining was heterogeneous in RA samples. Only in 3 of 19 RA samples did all (sample 18) or the majority (samples 28 and 33) of the SLCs show a collagen type-IV staining. In 6 (samples 15, 19, 21, 23, 25, and 26) and in 5 (16, 20, 24, 27, and 32) of 19 RA samples, collagen type-IV staining was found in 25–50% and in 1–25% of SLCs, respectively (Fig. 1e, f, g). The staining was mostly weak and distributed in the superficial synovial lining layers. In the other 5 RA samples (samples 17, 22, 29, 30, and 31), no collagen type-IV staining was found, whereas vessels were strongly collagen type-IV positive. The distribution of collagen type-IV staining inversely correlated with the degree of inflammation (P=0.002) and with the thickness of the synovial membrane (P=0.026).

Semi-quantitative RT-PCR of collagen type-IV gene expression

In order to investigate the factors playing a role in the synthesis of collagen type IV, RT-PCR analysis was performed in FLS isolated from synovia of patients with OA and RA. In pilot experiments, we established optimal reaction conditions for a semi-quantitative non-radioactive RT-PCR of collagen type-IV mRNA using a β2-microglobulin-specific PCR reaction as an internal control. In order to test the specificity of the PCR fragment, we blotted and hybridized the PCR products with digoxigenated oligonucleotide probes specific to collagen type IV and β2-microglobulin cDNA, which yielded one sharp, distinctive band of the expected size for each pair of primers (Fig. 3a). Since in situ results have shown differences in collagen type-IV staining related to the origin of the synovial membrane, we investigated the gene expression of collagen type IV in FLS from OA and RA. To determine whether the culture time influences the gene expression of collagen type IV, we established the RT-PCR analysis for FLS cultures after 1, 3, 5, and 8 weeks. Signal

Fig. 1 Detection of collagen type IV in normal synovia (**a**, **b**), osteoarthritis (**c**, **d**), and rheumatoid arthritis (**e**, **f**, **g**). Normal synovia (sample 1): (**a**, **b**) synovial lining cells (SLCs) are organized in a monolayer and show strong pericellular staining for collagen type IV; small vessels are strongly collagen type-IV positive (*arrowheads*). Osteoarthritis (sample 5): (**c**, **d**) SLCs form a pluricellular layer and a marked vascularization is noted. SLCs show the same strong collagen type-IV staining as the numerous intermingled small vessels. Rheumatoid arthritis (sample 23): (**e**) the synovia is hyperplastic with interspersed lymphoid aggregates. *Asterisks* mark the synovial cleft. Collagen type IV is detected only in a weak fashion in the synovial layers (*arrowheads*). At higher magnification, the hyperplastic SLCs show a weak and granular staining for collagen type IV (**f**) or are completely negative for collagen type IV (**g**); (original magnification **a**, **c**, **e**: ×71; **b**, **d**, **f**, **g**: ×140) ▶


a
b
c
d
e
f
g

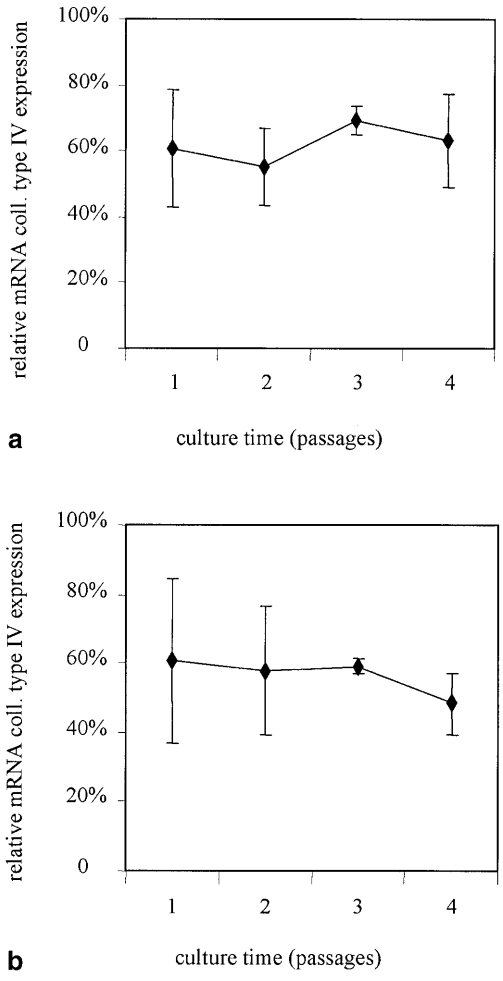


Fig. 2 Collagen type-IV mRNA expression of cultures of three fibroblast-like synoviocytes from osteoarthritis patients (OA-FLS; **a**) and three fibroblast-like synoviocytes from rheumatoid arthritis patients (RA-FLS; **b**) over a period of 6 weeks. mRNA expression is indicated as a mean value of the three cell cultures after normalization to β2-microglobulin signal. There are no relevant differences in the gene expression of collagen type IV between OA-FLS and RA-FLS at the indicated passages

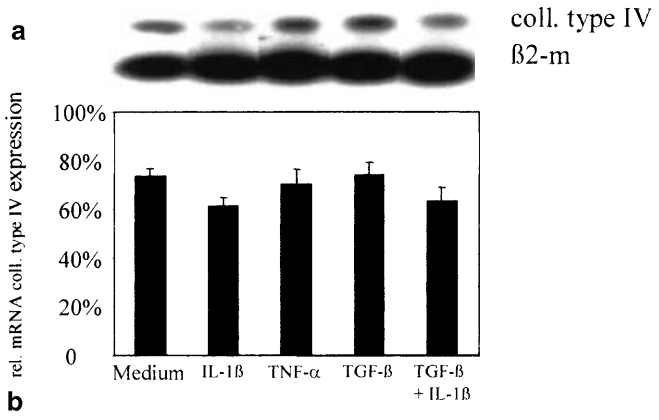


Fig. 3 mRNA collagen type-IV expression after cytokine stimulation in fibroblast-like synoviocytes from osteoarthritis patients (OA-FLS). **a** Southern-blot analysis of collagen type IV and β2-microglobulin mRNA expression in a representative experiment. No difference is seen in collagen type-IV expression relative to β2-microglobulin. **b** mRNA collagen type-IV expression is given as a mean value of three independent experiments after normalization to β2-microglobulin signal. Cytokines have no or only a minimal effect on the gene expression of collagen type IV in OA-FLS

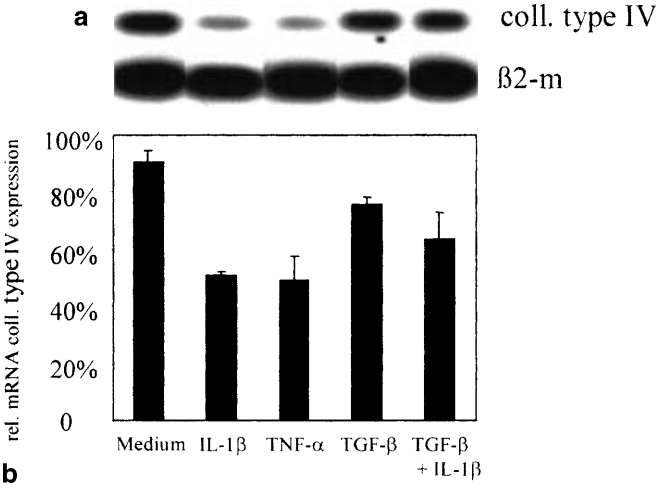


Fig. 4 mRNA collagen type IV expression after cytokine stimulation in fibroblast-like synoviocytes from rheumatoid arthritis patients (RA-FLS). **a** Southern-blot analysis of collagen type IV and β2-microglobulin mRNA expression in a representative experiment. The bands for collagen type IV are weaker for stimulation with interleukin (IL)-1β, tumor necrosis factor (TNF)-α, and for transforming growth factor (TGF)-β plus IL-1β when compared with the control. **b** mRNA collagen type-IV expression is given as a mean value of three independent experiments after normalization to β2-microglobulin signal. IL-1β, TNF-α used alone or in combination show a downregulating effect on the gene expression of collagen type IV in RA-FLS, whereas no effect is shown after treating RA-FLS with TGF-β alone

strength of the collagen type-IV products obtained were compared with each other after normalization to the housekeeping gene β2-microglobulin.

As shown in Fig. 2a, b, we observed no relevant differences in the mRNA expression for collagen type IV between OA-FLS and RA-FLS. No differences in the collagen type-IV expression level were detectable between OA-FLS and RA-FLS, leading to the assumption of a comparable constitutional collagen type-IV mRNA expression.

OA-FLS and RA-FLS were treated with the cytokines IL-1β, TNF-α, and TGF-β, either alone or in combination to assess the influence on collagen type-IV gene expression. As shown in Fig. 3a, b, no relevant differences (=15%) were found for the gene expression of collagen type IV in cytokine-stimulated OA-FLS when compared with control cells. A relevant effect was shown by treatment of the RA-FLS with IL-1β and TNF-α (Fig. 4a, b). A decrease of collagen type-IV gene expression of circa 50% was found on adding IL-1β and TNF-α relative to the control (81.8%).

No synergistic effect was observed by adding IL-1β and TNF-α. Treatment of RA-FLS with TGF-β had no

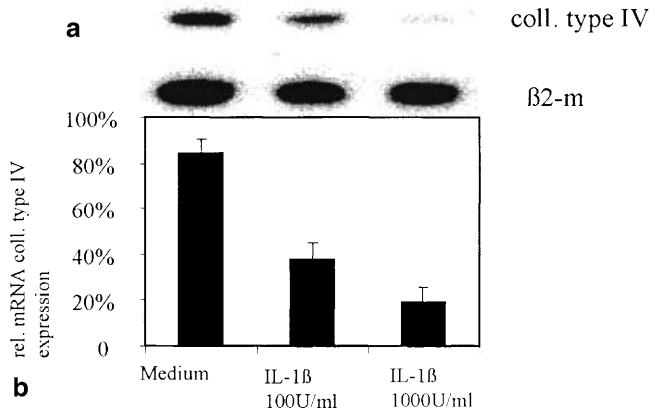


Fig. 5 mRNA collagen type-IV expression after stimulation in fibroblast-like synoviocytes from rheumatoid arthritis patients (RA-FLS) with various concentrations of interleukin (IL)-1β. **a** Southern-blot analysis of collagen type IV and β2-microglobulin mRNA expression. **b** A representative experiment shows weaker bands in correlation to the high concentration of IL-1β used. mRNA collagen type-IV expression is indicated as a mean value of three independent experiments after normalization to β2-microglobulin signal. Dose-dependent effect of IL-1β on the gene expression of collagen type IV is evident

relevant effect on the collagen type-IV gene expression (72.7%). However, the combination of IL-1β and TGF-β led to a decrease in collagen type-IV gene expression (63.9%). In the same FLS cultures stimulated with various concentrations of IL-1β, we showed that the effect on RA-FLS was dose dependent. As shown in Fig. 5, the original collagen type-IV gene expression (s. medium 85%) was downregulated by IL-1β used at a concentration of 100 U/ml to 38% and by IL-1β used at a concentration of 1000 U to 25% (Fig. 5a, b), whereas no relevant differences were observed in the collagen type-IV gene expression in OA-FLS by IL-1β used at higher concentrations.

Discussion

In agreement with other immunohistological studies, we observed that SLC in normal synovia in situ show a pericellular staining for the structural protein collagen type IV, suggesting that this protein may contribute to the structural organization of the synovial membrane [19, 24]. This study revealed a loss of collagen type IV in SLC of rheumatoid synovia. The decrease of collagen type IV in rheumatoid synovia correlated statistically with the grade of inflammation of the rheumatoid synovia and with the hyperplasia of the synovial cell layer. The loss of collagen type IV and of other basement membrane components may facilitate the infiltration of inflammatory cells in the synovial lining layer contributing to the pannus formation in the rheumatoid process [26, 31]. Previous in situ studies showed that collagen type IV is found surrounding the fibroblast-like synoviocytes in normal, OA and RA synovia [19, 29], suggesting that these cells may be responsible for the decrease of collagen type IV in rheumatoid arthritis.

This study revealed, that FLS in vitro, independent of origin, show a constitutive gene expression for collagen type IV. This finding is in agreement with immunofluorescence studies showing a collagen type-IV staining in cultured FLS [28]. In vitro, no differences in the baseline gene expression for collagen type IV were observed between RA-FLS and OA-FLS.

Since the presence of collagen type IV in rheumatoid synovia in situ correlated with the grade of inflammation and with the thickness of the synovial layer, we stimulated OA-FLS and RA-FLS with the cytokines involved in the inflammatory process in vivo [5, 10]. While TGF-β had no effect on the mRNA expression of collagen type IV, TNF-α and IL-1β downregulated the gene expression of collagen type IV in RA-FLS. The increase of the concentration of IL-1β led to a further downregulation of the gene expression of this protein. Since IL-1β is not only produced by inflammatory cells but also by synovial lining cells [13], this may explain the in situ findings, showing an inverse correlation between collagen type IV and the hyperplasia of the synovial lining cells. IL-1β and TNF-α are strong stimuli for the production of arachidonic acid metabolites, such as PGE2 in fibroblast-like synoviocytes [12]. Since PGE2 may decrease collagen synthesis, the downregulating effect by IL-1β and TNF-α on collagen type-IV gene expression may be mediated by PGE2 [20]. A downregulating effect on collagen gene expression was also observed in cultured human condrocytes by TNF-α and interferon (IFN)-γ [21]. However, IL-1β used at various concentrations showed a marginal effect on the gene expression of collagen type IV in OA-FLS. This suggests that the consistent presence of collagen type IV observed in SLC of OA-synovia may not only be due to a low grade of inflammation. The data suggest that the different regulation of the gene expression of collagen type IV by IL-1β in RA-FLS and OA-FLS may be caused by a different reactivity of these cells. The hypothesis of a different functional state of RA-FLS is supported by experimental evidence showing genetic mutations and different gene regulation in cultured RA-FLS [3, 7, 22, 32]. Previous data have shown enhanced serum concentrations of 7s-collagen, a marker of type-IV collagen metabolism, in patients with RA [11]. Therefore, apart from the direct effect of cytokines on the synthesis of collagen type IV, the presence of proteolytic enzymes for this matrix component like metalloproteinases may contribute to the degradation of this extracellular matrix protein [16].

In conclusion, the loss of collagen type IV in SLCs of rheumatoid synovia in situ correlates with the degree of inflammation and with the thickness of the synovial layer. Our in vitro results show that IL-1β and TNF-α have a downregulating effect on the gene expression of collagen type IV, suggesting that these cytokines may control the synthesis of collagen type IV in the rheumatoid process in vivo.

Acknowledgements We thank U. Braun and U. Fabian for technical assistance and A. Jellen Ritter for methodological advice. Supported by a grant from the Hochschulsonderprogramm III, University of Ulm.

References

1. Abrahamsen TG, Froland SS, Natvig JB, Pahle J (1975) Elution and characterization of lymphocytes from rheumatoid inflammatory tissue. Scand J Immunol 4:822–830
2. Adachi E, Hopkinson I, Hayashi T (1997) Basement-membrane stromal relationships: interactions between collagen fibrils and the lamina densa. Int Rev Cytol 173:73–156
3. Aicher WK, Heer AH, Trabandt A, Bridges SL, Schroeder HW, Stransky G, Gay RE, Eibel H, Peter HH, Siebenlist U (1994) Overexpression of zinc-finger transcription factor Z-225/Egr-1 in synoviocytes from rheumatoid arthritis patients. J Immunol 152:5940–5948
4. Altman R, Asch E, Bloch D, Bole G, Borenstein D, Brandt K, Christy W, Cooke TD, Greenwald R, Hochberg M, Howell D, Kaplan D, Koopman W, Longley S, Mankin H, McShane DJ, Medsger T, Meenan R, Mikkelsen W, Moskowitz R, Murphy W, Rothschild B, Segal M, Sokoloff L, Wolfe F (1988) Development of criteria for the classification and reporting of osteoarthritis: classification of osteoarthritis of the knee. Arthritis Rheum 29:1039–1049
5. Arend WP, Dayer JM (1990) Cytokines and cytokine inhibitors or antagonists in rheumatoid arthritis. Arthritis Rheum 33:305–315
6. Arnett FC, Edworthy SM, Bloch DA, McShane DJ, Fries JF, Cooper NS, Healy LA, Kaplan SR, Liang MH, Luthra HS, Medsger TA, Mitchell DM, Neustadt DH, Pinals RS, Schaller Sharp JT, Wilder RL, Hunder GG (1988) The American Rheumatism Association 1987 revised criteria for the classification of rheumatoid arthritis. Arthritis Rheum 31:315–324
7. Aupperle KR, Boyle DL, Hendrix M, Seftor EA, Zvaifler NJ, Barbosa M, Firestein GS (1998) Regulation of synoviocyte proliferation, apoptosis, and invasion by the p53 tumor suppression gene. Am J Pathol 152:1091–1098
8. Chomczynski P, Sacchi N (1987) Single-step method of RNA isolation by acid guanidinium thiocyanate-phenol-chloroform extraction. Anal Biochem 162:156–159
9. Church MG, Gilbert W (1984) Genomic sequencing. Proc Natl Acad Sci U S A 81:1991–1995
10. Feldmann M, Brennan FM, Chantry D, Haworth C, Turner M, Katsikis P, Londei M, Abney E, Buchan G, Barrett K (1991) Cytokine assays: role in evaluation of the pathogenesis of autoimmunity. Immunol Rev 119:105–123
11. Gabazza EC, Osamu T, Yamakami T, Ibata H, Sato T, Sato Y, Shima T (1994) Correlation between clotting and collagen metabolism markers in rheumatoid arthritis. Thromb Haemost 71: 199–202
12. Gitter BD, Labus JM, Lees SL, Scheetz ME (1989) Characteristics of human synovial fibroblast activation by IL-1 beta and TNF alpha. Immunology 66:196–200
13. Goto M, Okamoto M, Sasano M, Yanagisawa S, Miyamoto T, Nishioka K (1990) Adherent synovial cells from non-rheumatoid arthritis do not release interleukin-1 beta and prostaglandin E2 spontaneously in long term culture. J Rheumatol 17:1299–1302
14. Hostikka SL, Tryggvason K (1988) The complete primary structure of the alpha 2 chain of human type IV collagen and comparison with the alpha 1(IV) chain. J Biol Chem 263: 19488–19493
15. Khalkhali Ellis Z, Seftor EA, Nieva DR, Seftor RE, Samaha HA, Bultman L, De Larco JE, Ince A, Moore TL, Hendrix MJ (1997) Induction of invasive and degradative phenotype in normal synovial fibroblasts exposed to synovial fluid from patients with juvenile rheumatoid arthritis: role of mononuclear cell population. J Rheumatol 24:2451–2460
16. Martel Pelletier J, McCollum R, Fujimoto N, Obata K, Cloutier JM, Pelletier JP (1994) Excess of metalloproteases over tissue inhibitor of metalloproteinase may contribute to cartilage degradation in osteoarthritis and rheumatoid arthritis. Lab Invest 70:807–815
17. McCarthy JB, Vachhani B, Iida J (1996) Cell adhesion to collagenous matrices. Biopolymers 40:371–381
18. Okada Y, Morodomi T, Enghild JJ, Suzuki K, Yasui A, Nakanishi I, Salvesen G, Nagase H (1990) Matrix metalloproteinase 2 from human rheumatoid synovial fibroblasts. Purification and activation of the precursor and enzymic properties. Eur J Biochem 194:721–730
19. Pollock LE, Lalor P, Revell PA (1990) Type IV collagen and laminin in the synovial intimal layer: an immunohistochemical study. Rheumatol Int 9:277–280
20. Raisz LG, Pilbeam CC, Fall PM (1993) Prostaglandins: mechanisms of action and regulation of production in bone. Osteoporos Int 3[Suppl 1]:136–140
21. Reginato AM, Sanz-Rodriguez C, Diaz A, Dharmavaram RM, Jimenez SA (1993) Transcriptional modulation of cartilage-specific gene expression by interferon gamma and tumor necrosis factor alpha in cultured human condrocytes. Biochem J 294:761–769
22. Reme T, Travaglio A, Gueydon E, Adla L, Jorgensen C, Sany J (1998) Mutation of the p53 tumor suppressor gene in erosive rheumatoid synovial tissue. Clin Exp Immunol 111:353–358
23. Revell PA (1989) Synovial lining cells. Rheumatol Int 9:49–51
24. Revell PA, Al-Saffar N, Fish S, Osei D (1995) Extracellular matrix of the synovial intimal cell layer. Ann Rheum Dis 54: 404–407
25. Rinaldi N, Barth T, Henne C, Mechtersheimer G, Möller P (1994) Synoviocytes in chronic synovitis in situ and cytokine stimulated synovial cells in vitro neo-express α1, α3 and α5 chains of ß1 integrins. Virchows Arch 425:171–180
26. Rinaldi N, Barth TFE, Weis D, Schwarz-Eywill M, Pezzutto A, Lukoschek M, Brocai D, Brado B (1998) Loss of laminin and of the laminin receptor integrin subunit α6 in situ correlates with cytokine induced down-regulation of α6 on fibroblast-like synoviocytes from rheumatoid arthritis. Ann Rheum Dis 57:559–565
27. Rooney M, Condell D, Quinlan W, Daly L, Whelan A, Feighery C, Bresnihan B (1988) Analysis of the histologic variation of synovitis in rheumatoid arthritis. Arthritis Rheum 31: 956–963
28. Schneider M, Voss B, Rauterberg J, Menke M, Pauly T, Miehlke RK, Friemann J, Gerlach U (1994) Basement membrane proteins in synovial membrane: distribution in rheumatoid arthritis and synthesis by fibroblast-like cells. Clin Rheumatol 13:90–97
29. Smith SC, Folefac VA, Osei DK, Revell PA (1998) An immunocytochemical study of the distribution of proline-4-hydroxylase in normal, osteoarthritic and rheumatoid arthritic synovium at both the light and electron microscopic level. Br J Rheumatol 37:287–291
30. Soininen R, Haka-Risku T, Prockop DJ, Tryggvason K (1987) Complete primary structure of the alpha 1-chain of human basement membrane (type IV) collagen. FEBS Lett 225: 188–194
31. Suzuki M, Uetsuka K, Suzuki M, Shinozuka J, Nakayama H, Doi K (1997) Immunohistochemical study on type II collagen-induced arthritis in DBA/1J mice. Exp Anim 46:259–267
32. Trabandt A, Aicher WK, Gay RE, Sukhatme VP, Fassbender HG, Gay S (1992) Spontaneous expression of immediately-early response genes c-fos and egr-1 in collagenase-producing rheumatoid synovial fibroblasts. Rheumatol Int 12:53–59

Virchows Arch (2001) 439:683–690
DOI 10.1007/s004280100425

ORIGINAL ARTICLE

Sylvie Cantet · Marjorie Fanjul · François Brémont
Véronique Midy · Etienne Hollande

Cytological characterization of apatitic calcium phosphate structures in bronchial epithelial tissue cultured from a child with cystic fibrosis (ΔF508)

Received: 14 September 2000 / Accepted: 11 January 2001 / Published online: 25 April 2001
© Springer-Verlag 2001

Abstract Patients with cystic fibrosis homozygous for the ΔF508 mutation have marked disturbances in ion exchanges in a variety of tissues. Alterations in intra- or extracellular levels of Ca^{2+} and calcifications have been observed in numerous tissues from such patients, although the nature and origin of such calcifications have yet to be elucidated. In this study, we investigated the formation of calcifications in the respiratory tract of a ΔF508 homozygous child and attempted to establish their origin. Samples of bronchial epithelium from this patient were subjected to cytophysiological analysis ex vivo and in vitro. The defect of targeting of the cystic fibrosis transmembrane conductance regulator (CFTR) to the apical plasma membrane of epithelial cells was verified. Cytochemical and ultrastructural analysis revealed the presence of crystalline aggregates in fine needles in the respiratory tract. Cytochemical analysis, X-ray spectrometry, and electron diffraction showed that these aggregates corresponded to crystals of calcium phosphate in an apatite-like structure. Ultrastructural study of primary cultures of bronchial epithelium showed the presence of calcium phosphate crystals in granules from Golgi apparatus and in mitochondria. These observations indicated that modifications of ionic exchanges due to a defect in targeting of CFTR ΔF508 to the apical plasma membrane led to the formation of crystals of calcium phosphate in the cytoplasm of pulmonary cells. These crystals could enhance inflammation of the lung in patients with cystic fibrosis.

S. Cantet · M. Fanjul · V. Midy · E. Hollande (✉)
Laboratoire de Biologie Cellulaire et Moléculaire des Epithéliums, Université Paul Sabatier, 38 rue des 36 ponts, 31400 Toulouse, France
e-mail: hollande@lmtg.ups-tlse.fr
Tel.: +33-5-61556515, Fax: +33-5-61556515

F. Brémont
Service de Pneumologie Allergologie Pédiatrique, Hôpital des Enfants, 330 Avenue de Grande Bretagne, 31026 Toulouse, France

Keywords Cystic fibrosis · Lung · Tissue culture · Calcium phosphate crystals

Introduction

Cystic fibrosis (CF) is a hereditary disease affecting a variety of organs, especially the respiratory tract and pancreas. The disease is the consequence of various mutations of the cystic fibrosis transmembrane conductance regulator (CFTR) gene, the most common being the ΔF508 mutation [22, 33]. The CFTR protein is a low conductance chloride channel that regulates other ion channels, such as outwardly rectifying chloride channels (ORCC) [37], epithelial sodium channels (ENaC) [40], and potassium channels (ROMK) [27]. The expression of a mutated CFTR protein gives rise to significant physiological alterations: decrease in secretion of Cl^- [23] and HCO_3^- [39] ions, excessive absorption of Na^+ [5], modification of intracellular pH [13], defect in acidification of the trans-Golgi network and prelysosomes [2], alteration of sialylation, and fucosylation [36] or sulfation of proteins [7]. Furthermore, the expression of a mutated CFTR in various cell types gives rise to alterations in the metabolism of Ca^{2+}. Elevated intracellular levels of Ca^{2+} have been found in acinar cells from the parotid gland [28], in skin fibroblasts maintained in culture [14], in lymphocytes [43], and in the mucous cells of the bronchial epithelium and submucosal glands [34]. Abnormalities in the transport of Ca^{2+}, which are thought to stem from a decrease in Ca^{2+}-ATPase (adenosine triphosphatase) activity, have been observed in erythrocytes [20] and skin fibroblasts [21]. In addition, high concentrations of Ca^{2+} have been found in tears [4], nasal [26], tracheobronchial [8] and duodenal secretions, and in seminal fluid [35] from CF patients. Blomfield et al. [3] have described the formation ex vivo of hydroxyapatite in saliva. In CF patients in an advanced stage of the disease, calcification has been observed in blood vessels, pineal body, renal epithelium, gastric mucosa [24], pancreas [10, 16, 32], and intestine [25]. Calcifications have

also been observed in the lungs of CF patients, especially in the cartilage of the trachea and bronchi [24, 29] and in the walls of alveoli [24]. All of these observations would indicate that calcification is a late manifestation of cystic fibrosis, but the chemical composition and origin of such calcifications have yet to be determined.

In the present study, we investigated the nature and origin of crystalline structures from lung tissue removed from a child homozygous for the ΔF508 mutation. We demonstrated the presence in the bronchial epithelium of calcium phosphate crystals in an apatite-like structure. We also showed how such crystals formed in intracellular compartments of epithelial cells from CF lung maintained in culture.

Materials and methods

Pulmonary tissue

Fragments of segmental bronchi, bronchioles, and alveoli were removed after a right upper lobectomy in an 8-year-old child with CF, homozygous for the ΔF508 mutation. Prior to surgery, the patient had been treated with daily nebulization of rhDNase (recombinant human deoxyribonuclease) for 2 years and inhalation of corticoids (budesonide dry powder 400 mg/day) for 1 year. Pulmonary tissue was colonized by *Pseudomonas aeruginosa* and *Staphylococcus aureus*. The patient was treated with oral theophylline (slow release), pancreatic extracts, vitamins, and selenium. After removal of the pulmonary lobe, fragments of tissue were kept for 2 h at +4°C in RPMI 1640 medium (Gibco, Grand Island, N.Y.) supplemented with 20% fetal calf serum (FCS; Gibco).

Histology

Fragments of segmental bronchi, bronchioles, and alveoli were fixed in Bouin, Carnoy fluids, in 10% isotonic formalin, 2.5% paraformaldehyde or 95% alcohol, dehydrated, and then embedded in paraffin. Thin sections of tissue were stained with hemalum–eosin or Mallory trichrome. Mucins were revealed by staining with PAS (periodic acid–Schiff reagent) or periodic acid–thiocarbohydrazide–silver proteinate (PATAg) [41]. On sections, blood cells were stained with Giemsa solution.

Tissue culture

Epithelium of fragments of segmental bronchi, bronchioles, and alveoli was cultured. Briefly, fragments were cut lengthways and then washed several times in Earle's saline solution. The epithelia were scraped off and explanted in 25-cm^2 culture flasks (Nunc, Roskilde, Denmark), 35-mm diameter Petri dishes (Nunc), or coverslips in Leighton tubes in a mixture of RPMI 1640 (50%)-Ham F12 (50%) (Gibco), supplemented with 20% FCS and antibiotics [piperilline (8 µg/ml), penicillin (200 U/ml), streptomycin (200 µg/ml), and fungizone (0.5 µg/ml); all from Gibco]. Cultures were incubated at 37°C in a 95% air, 5% CO_2 atmosphere. Culture media were renewed 7 days after explantation and then every other day thereafter with the same medium but containing only 10% FCS and half the previous concentrations of antibiotics. The growth of cultures was monitored by examination of live cells using phase contrast microscopy. Cell growth was estimated by calculation of the mitotic index on 9-day-old to 70-day-old cultures and using planimetry. Mycoplasmic contamination was checked after seeding on selective medium and further passage or using the polymerase chain reaction (PCR; Mycoplasma PCR primer set, Stratagene, La Jolla, Calif.).

Ultrastructural analysis

Fragments of lung tissue before explantation and the 16-day-old to 70-day-old primary cultures were examined using electron microscopy after fixation in a mixture of 2.5% glutaraldehyde–2% paraformaldehyde in 0.1 M cacodylate buffer, pH 7.2 (1 h at 4°C), post-fixed with 1% osmium tetroxide, dehydrated, and embedded in Epon–Araldite. Zones of interest were selected from semi-thin sections stained with toluidine blue. Ultra-thin sections contrasted with uranyl acetate and lead citrate were examined using a Hitachi HU 11C electron microscope.

Expression of CFTR

The expression of CFTR protein was analyzed using immunofluorescence or immunoperoxidase reaction on: (1) sections of lung tissue fixed in 2.5% paraformaldehyde or by freezing, (2) 13-day-old to 39-day-old primary cultures fixed in paraformaldehyde and permeabilized with methanol (–20°C), and (3) living cells from 8-day-old to 30-day-old primary cultures. The following anti-CFTR antibodies were used: polyclonal ECL-885 directed against a sequence of the fourth extra-cellular loop of the protein (885–904) [18] (dilution 1:100), monoclonal MATG 1031, directed against a sequence of the first extracellular loop (107–117; Transgène, Strasbourg, France; 1:20 to 1:400) and monoclonal anti-R domain, directed against the sequence 703–712 [11] (1:25) in Tris-HCl buffer (0.5 M pH 7.6) containing 0.1% of bovine serum albumin (BSA; fixed cells) or in RPMI 1640 medium pH 7.4 with 10% FCS (living cells). Fixed cells were preincubated in a solution of 0.5 M NH_4Cl and then in Tris-HCl with 0.1% BSA and incubated with anti-CFTR antibody for 1 h at 22°C or overnight at +4°C in a moist chamber. Antigen–antibody complexes were revealed with rabbit or mouse anti-immunoglobulins coupled either with peroxidase (dilution 1:20 to 1:400) or with fluorescein isothiocyanate (FITC; dilution 1:20 to 1:300). Peroxidase activity was revealed with 3-amino-9-ethylcarbazole (AEC) as the substrate in the presence of H_2O_2. Living cells were incubated with anti-CFTR antibody (30 min, 37°C), rinsed in RPMI 1640 medium, incubated with FITC-coupled anti-immunoglobulins (dilution 1:100) and then fixed for 7 min at –20°C in a mixture of 95% methanol–5% acetic acid. Immunofluorescence was observed using a Diaplan episcopic microscope or with a laser scanning confocal microscope (argon laser at 488 nm; LSM 410, Carl Zeiss, Oberkochen, Germany) fitted with a ×63 objective.

Characterization of epithelial type of cultured cells

The epithelial type was characterized by means of immunocytochemistry using the monoclonal anti-cytokeratin gp56KD antibody, clone KL1 (Immunotech S.A., Westbrook, Me.) directed against a pool of cytokeratins [42] diluted to 1:100 (1 h, 22°C). Antigen–antibody complexes were revealed using mouse anti-immunoglobulins coupled with tetramethyl rhodamine isothiocyanate (1 h, 1:100). The specimens were observed by means of confocal microscopy using a helium laser (wavelength 543 nm).

Characterization of crystalline deposits

The crystalline deposits were characterized using various methods. Refringence was observed using polarization microscopy, and their calcium phosphate content was determined using the Von Kossa reaction. Their chemical composition was analyzed using X-ray spectrometry on a JEOL 200 CX microscope equipped with a EDAX 9100 microanalyzer at 100 KeV, cooled with liquid nitrogen. In this case, fragments of bronchial segments and primary cultures were fixed in 2% paraformaldehyde–2.5% glutaraldehyde (1 h, +4°C), dehydrated, and embedded in Epon–Araldite. Ultra-thin sections were placed on gold carbon-coated formvar grids. The crystalline structure was determined by means of electron diffrac-

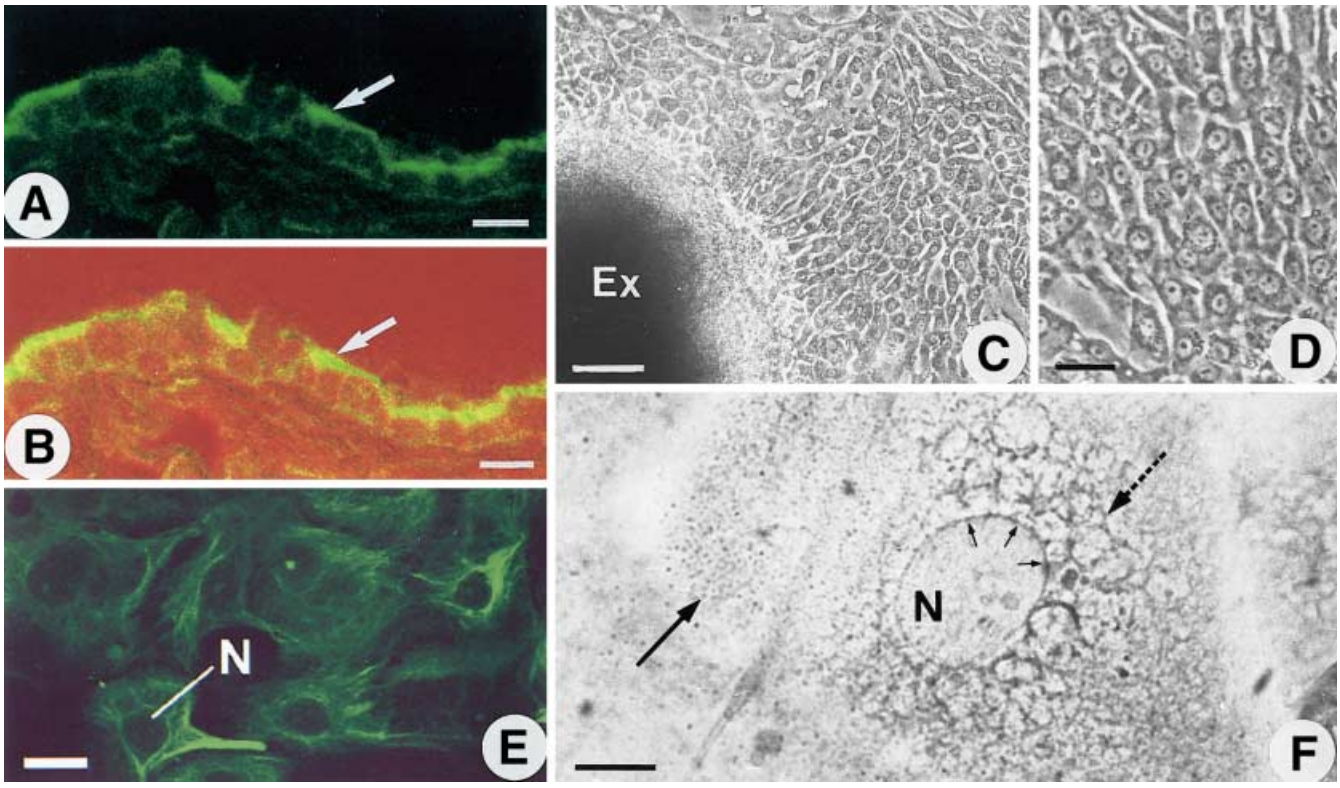


Fig. 1 Localization of cystic fibrosis transmembrane conductance regulator (CFTR) in lung cells in vivo and in vitro and morphological characteristics of cells in culture. **A, B** Intracytoplasmic CFTR immunoreactivity in CF bronchiolar epithelial cells. **B** Superimposition of the confocal microscopic image of CFTR immunoreactivity onto that of the same cells observed using interference microscopy. CFTR-immunoreactive cubic ciliated cells can be seen (*arrows*). ×700; *bar* 10 µm. **C** General appearance of growth area of living cells (7-day-old culture). *Ex* explant; ×90; *bar* 100 µm. **D** Detail of epithelial-type cells in central zones of a growth area. ×220; *bar* 40 µm. **E** Confocal microscopic image showing cytokeratin-immunoreactive cells in a growth area (9-day-old culture). *N* nucleus; ×700; *bar* 10 µm. **F** Visualization of granules (*arrow*) and CFTR immunoreactivity in an intracytoplasmic network (*dotted arrow*) in an epithelial cell (13-day-old culture). *Small arrows* show CFTR immunoreactivity in nuclear membrane. *N* nucleus; ×1100; *bar* 10 µm

tion with a camera length of 137 cm. The d-spacing of the electron diffraction pattern was compared with those obtained from synthetic hydroxyapatite crystals. The possible presence of crystalline deposits of calcium phosphate derived from nanobacteria [19] was checked using monoclonal anti-nanobacteria antibodies (a gift from Dr E. Olavi Kajander, Kuopio, Finland). Two antibodies (dilution 1:5000), antibody 5/2, directed against a carbohydrate epitope and antibody 8/0, directed against a protein epitope [9], were used on CF lung tissues or on primary cultures fixed in Carnoy solution, paraformaldehyde, or by freezing. Positive controls (smears of heat-dried nanobacteria) were run at the same time.

Results

Pathological examination

Marked inflammation of epithelial structures was observed in all the fragments of CF lung tissue. Modification of the pseudostratified epithelium, accompanied by desquamation of ciliated and mucous cells, leaving a thickened basement membrane either bare or covered with numerous basal cells was noted. The cilia at the apices of intact ciliated cells were embedded in a thick layer of mucus containing polynuclear cells, macrophages, and much cellular debris. There was an approximately 25% increase in number of mucous cells compared with that of a healthy lung. Some mucous cells contained agglutinated PAS+ elements. There was marked alteration of alveolar structure that was covered with an epithelium of cuboidal cells. There was marked fibrosis, especially between alveoli where wide bands of connective tissue oriented in all directions were observed.

CFTR was detected with all of the anti-CFTR immunsera in ciliated cells of bronchi and bronchioles, in alveolar cuboidal cells, and in basal cells. Immunoreactivity was mostly confined to the cytoplasm (Fig. 1A, B, arrows). CFTR immunoreactivity was also noted at the apex of some ciliated cells.

Characterization of crystalline aggregates

Refringent Von Kossa-positive elements were observed in the surface epithelium of fragments of segmental bronchi, indicating the presence of a calcium salt with a periodic structure. Electron microscopic examination of segmental bronchi and alveoli confirmed the presence of crystalline deposits close to zones of damaged epithelium. These deposits were isolated or in clusters extending over more than 10 µm (Fig. 2A). They mostly comprised

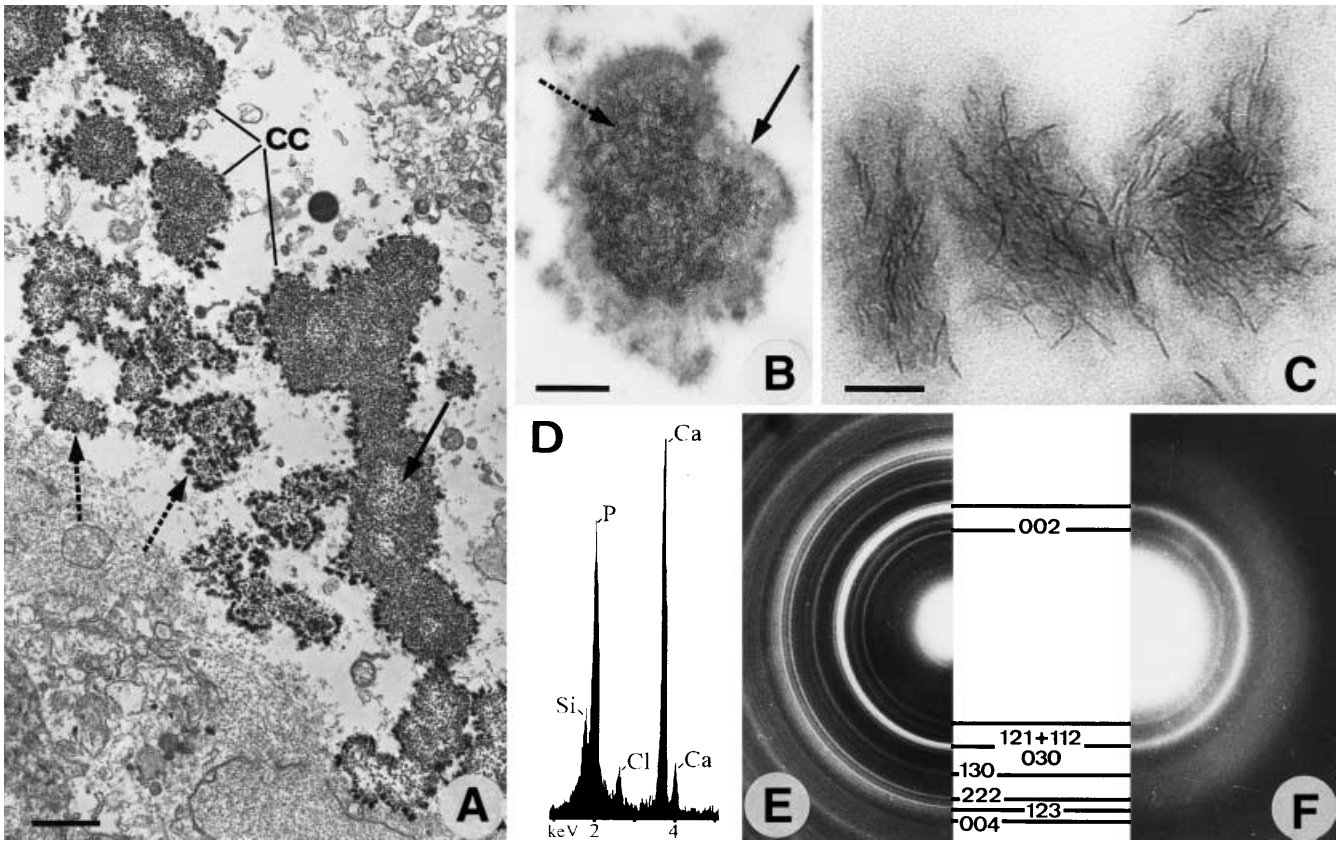


Fig. 2 Structure and characterization of crystalline aggregates in cystic fibrosis (CF) lung. **A**, **B** General appearance of an extracellular zone with abundant crystalline concretions (*cc*). *Full arrows* indicate amorphous regions, and the *dotted arrows* the crystalline regions. **A** ×6000; *bar* 1.5 µm; **B** ×31000; *bar* 0.3 µm. **C** Detail of needles. ×170,000; *bar* 0.06 µm. **D** X-ray emission spectrum of needles shown in Fig. 2C. Note the characteristic peaks of calcium (*Ca*) and phosphorus (*P*). *Si* silicon; *Cl* chlorine. **E**, **F** Electron diffraction diagrams. Note the 002 and 121+112+030 Debye–Scherrer rings (**F**) characteristic of calcium phosphate in apatite structure. The indices of the principle rings of synthetic hydroxyapatite (**E**) are shown in the lower part of the diagram

an amorphous central zone of granulo-fibrillary material (Fig. 2A, arrow), an intermediate granular zone of high electron density, surrounded by a tangle of needles (Fig. 2A, dotted arrows). In contrast, some aggregates contained abundant needles in the center (Fig. 2B, dotted arrow), surrounded with an amorphous material (Fig. 2B, arrow). The needles (44.53±11.94 nm long, n=300 and 2.59±0.66 nm in diameter, n=300) had no preferential orientation (Fig. 2C). X-ray diffraction analysis (Fig. 2D) revealed the presence of calcium and phosphorus, confirming their Von Kossa positivity with a calcium/phosphorus ratio of 1.4. The pattern of electron diffraction (Fig. 2F) compared with that of a synthetic hydroxyapatite control (Fig. 2E) demonstrated the presence of crystals with Debye–Scherrer 002 and 121+112+030 rings, characteristic of hydroxyapatite.

Formation of crystalline aggregates in primary cultures of lung cells

Growing tissue cultures were obtained from fragments of surface epithelium mechanically dissociated from segmental bronchi, bronchioles, or alveoli. In many cultures, the explants floated for 2–6 days. On their surface, ciliated cells were identified by their cilial movements. After adherence to the bottom of the flasks, epithelial-type cells were observed to migrate. After 4 days in culture, small colonies of polygonal cells formed, followed by growth areas extending over 48 mm^2 after 16 days in culture. Cellular proliferation was observed until the 31st day (mitotic index 1.6%). The cells ranged from 15 µm to 30 µm in diameter (Fig. 1C, D). After 15 days in culture, cells became more voluminous. Up to day 70, all cells in growth areas were cytokeratin-immunoreactive and exhibited wide bands of immunoreactive filaments throughout the cytoplasm and cytoplasmic extensions (Fig. 1E). Many cells contained PAS+ granules.

No CFTR immunoreactivity was detected in living cells. After fixation and permeabilization, CFTR-immunoreactive elements were observed (Fig. 1F). Numerous CFTR-immunoreactive granules were seen in the exoplasm of most cells (Fig. 1F, arrow). In perinuclear cytoplasm, a network of highly immunoreactive, anastomosed filaments was observed (Fig. 1F, dotted arrow).

Analysis of ultra-thin sections on 9-day-old to 70-day-old growth areas identified at least three cell types, all containing abundant microfilaments: (1) ciliated cells

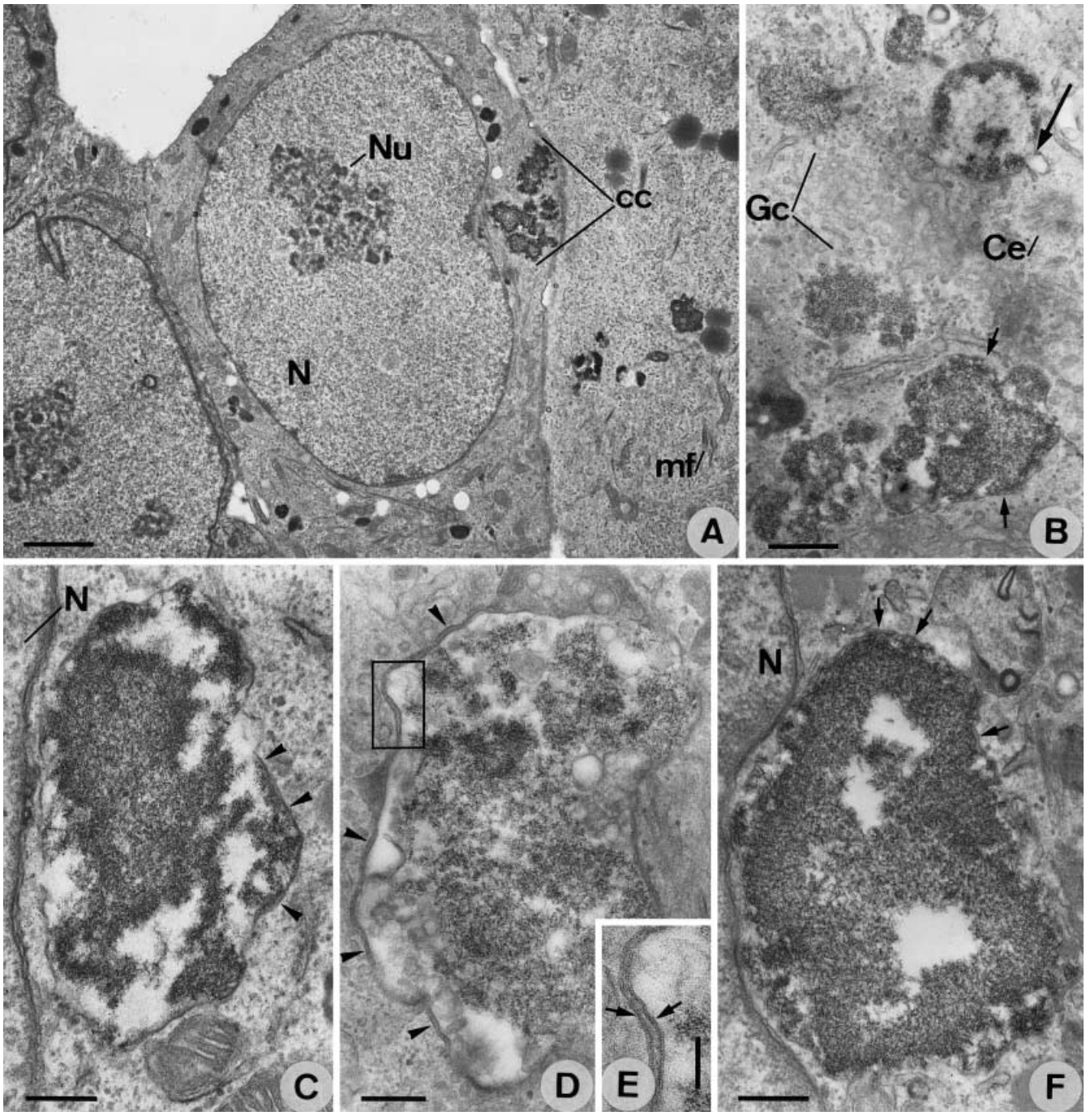


Fig. 3 Intracytoplasmic crystalline aggregates in cystic fibrosis (CF) lung epithelial cells in culture (16 days). **A** Intracytoplasmic crystalline concretions (*cc*) in an undifferentiated cell. *N* nucleus; *Nu* nucleolus; *mf* microfilaments; ×6000; *bar* 2 µm. **B** Appearance of dense bodies around Golgi apparatus. The *arrow* shows fusion of an immature dense body and a small vesicle. The *small arrows* indicate crystals outside the matrix. *Gc* Golgi compartments; *Ce* centrosome; ×22,000; *bar* 0.5 µm. **C** Large dense body containing numerous crystalline structures. The *arrowheads* indicate the boundary membrane. *N* nucleus; ×37,000; *bar* 0.3 µm. **D** Body containing crystals bounded by a double membrane (*arrowheads*). ×34,000; *bar* 0.3 µm. **E** Higher magnification of the inset in **D** showing the structure of two boundary membranes. Each membrane is indicated by an *arrow*. ×80,000; *bar* 0.1 µm. **F** Intracytoplasmic crystalline formations in perinuclear cytosol. The *small arrows* indicate remnants of boundary membrane. *N* nucleus; ×31,000; *bar* 0.35 µm

joined together by tight junctions with microvilli, cilia, and mitochondria-rich cytoplasm, (2) mucous cells with cytoplasm characterized by developed Golgi apparatus with dilated cisternae on their *cis* side and numerous PATAg-positive secretory granules on their *trans* side, and (3) small undifferentiated cells containing a large nucleus and a poorly developed cytoplasm rich in polyribosomes (Fig. 3A). In these different types, some cells presented dense bodies of variable size dispersed throughout their cytoplasm. Small dense bodies (0.2 µm) were abundant in the Golgi apparatus zone, and there were signs of fusion (Fig. 3B, arrow). In these three cell types, crystalline aggregates were observed, being more

frequent in the cells with abundant dense bodies. The stages of formation of crystals could be observed in such cells. Some dense bodies, bounded by a single membrane, were seen in the Golgi apparatus zone. Other larger bodies (0.4 µm) exhibited crystals elongated in all directions around their matrix (Fig. 3B, small arrows). Large vacuoles contained crystals in contact with the external nuclear membrane (Fig. 3C) and were bounded by a membrane which was sometimes disrupted by the crystalline structures (Fig. 3C, arrowheads). We observed other bodies (2.5-µm diameter) containing abundant crystalline material, remnants of membranes, and vesicles of various sizes (Fig. 3D). These bodies were bounded by a double membrane (Fig. 3D, arrowheads), whose fine structure is shown in Fig. 3E. Each membrane (Fig. 3E, small arrows) was 5–6 nm thick, and the two membranes were separated by a regular spacing of 15 nm. Finally, sheets of hyaloplasmic crystalline structures attaining 5 µm in diameter were observed (Fig. 3F) with membrane remnants in the periphery (Fig. 3F, small arrows). Cells with high crystalline content appeared to be in the process of degeneration. Some extracellular aggregates were also observed. X-ray spectrometry and electron diffraction analysis of the intracellular crystalline aggregates produced identical spectra and diffraction patterns to those observed in the lung tissue before explantation. Immunocytochemical reactions using anti-nanobacteria antibodies were consistently negative.

Discussion

In this study, we showed the existence of crystals of calcium phosphate in an apatite-like structure in the lung of a CF patient. Their intracellular origin was demonstrated in vitro. A detailed cytological analysis of pulmonary epithelia from a CF child homozygous for the ΔF508 mutation could be carried out due to the relatively large amount of tissue removed by a partial lobectomy of the right lung. At the pathological level, we observed essentially the same features as described in the literature. Nevertheless, the marked hyperplasia of the basement membrane and the existence of a cuboidal epithelium in alveoli has only rarely been described in cases of cystic fibrosis [12].

The defect of targeting of the ΔF508 CFTR in pulmonary surface epithelial cells [30] was confirmed using three different anti-CFTR antibodies. However, we described for the first time crystalline calcium phosphate aggregates in segmental bronchi near zones of lysis of the surface epithelia from the lung of a CF patient. The physicochemical properties of these crystalline formations, such as their refringence under polarized light, the identification of phosphorus and calcium in the X-ray spectra, the positive Von Kossa reaction, and the characteristic Debye–Scherrer rings on the electron diffraction pattern demonstrated that these formations were calcium phosphate in an apatite structure. PAS-positive elements corresponding to a viscous and thick mucus were assumed to indicate the presence of a calcification matrix like that observed for glycoproteins in many calcified tissues [44]. The amorphous calcium phosphate identified in this study may represent an early phase of tissue mineralization [31], with the presence of crystalline structures reflecting an on-going process of mineralization. Indeed, the calcium/phosphorus ratio of 1.4, which is below that of the stoichiometric ratio for hydroxyapatite (1.67), and the formation of needle-shaped crystals were indicative of an octacalcium phosphate (OCP) phase (calcium/phosphorus: 1.33). It has been suggested that OCP is involved in the initial phase of mineralization of normal bone tissue [6].

The demonstration of the existence of these crystalline formations in the respiratory tract raises the question of their origin. An exogenous origin for the formation of these crystals was ruled out by a number of arguments. The inhalation of therapeutic agents known to favor fibrosis of lung tissue could possibly have been responsible for the crystal formations. Nevertheless, neither the active principle administered to the patient, nor the excipients contained compounds leading to formation of calcium phosphate crystals. Furthermore, we checked for the absence of nanobacteria, which have been reported to lead to hydroxyapatite deposits on their surface [19]. There is no description to date of the presence of calcium phosphate crystals in an apatite structure in CF tissues, although Blomfield et al. demonstrated the existence of non-crystalline calcium phosphate in zymogen granules from submandibular salivary glands [3].

Thorough analysis of the primary cultures obtained from the lung epithelium demonstrated a cellular origin for the crystals. Epithelial cells of high purity were isolated by means of mechanical scraping of the epithelium. Cellular migration appeared early in culture; the rapid formation of growth areas and cellular proliferation lasting for more than 30 days were evidence for the quality of the tissue culture. After checking the epithelial nature of cells in the growth areas by detection of cytokeratins, we investigated expression of the CFTR protein. Immunocytochemical tests on living cells showed an absence of CFTR on plasma membranes. However, immunoperoxidase reactions after permeabilization of cells evidenced CFTR in some granules but essentially in a network of filamentous, anastomosed, and perinuclear structures. These images resembled the tubulo-vesicular structure of the endoplasmic reticulum–Golgi intermediate compartment (ERGIC), where ΔF508 CFTR is sequestrated [15]. In the lung epithelial cells studied, the defect in targeting of CFTR in the cultured cells was assumed to have altered ion exchanges in intracellular media and thus enhanced modifications in intracellular pH [2, 13]. It is of interest that a rather high calcium content has been described in secretory granules of goblet cells from the bronchial epithelium of CF patients [34]. It is also known that calcium phosphate can precipitate if there is an over-saturation of Ca^{2+} and HPO_4^{2-} ions [31]. In our primary cultures, the crystalline structures observed in intracellular membrane compartments that

were identical to those observed in vivo, were thought to have stemmed from a defect in ion exchanges. Crystals were observed in two types of organelles:

1. Dense bodies, bounded by a single membrane and probably of Golgi origin. An increase in Ca^{2+} ions in the matrix of these bodies, as described in secretory granules in CF cells [34], was assumed to have favored the formation of crystals of calcium phosphate, especially because some granules contained mucins.
2. Bodies surrounded by a double membrane whose structure resembled that of mitochondria. In cystic fibrosis, mitochondria are known to accumulate and sequestrate Ca^{2+} ions [43] due to an increase in electron transfer activity [38]. Moreover, the accumulation of Ca^{2+} in cytoplasm [14, 28, 34, 43] due to a fall in activity of the plasma membrane Ca^{2+}-ATPase [20, 21] could increase the calcium content of mitochondria. Furthermore, phospholipids resulting from the degradation of membranes of mitochondrial cristae could have induced crystallization in the matrix of these bodies, as described in pathologic calcifications [1].

We concluded that the crystals of calcium phosphate were initially formed in intracellular compartments, such as the Golgi apparatus or mitochondria. Demonstration of the presence of these crystals in the cytoplasm of CF epithelial cells in culture and their detection during growth of cells in different cellular compartments point to an intracellular origin for the crystals observed in the CF lung analyzed in the present study.

The crystalline structures observed in CF tissues [10, 16, 24, 25, 29, 32] may well have been calcium phosphate in an apatite-like structure. It is likely that such crystals form at a late stage of cystic fibrosis as has been observed in other diseases [1, 17, 32]. The crystalline aggregates in bronchial segments and alveoli that we observed could be accounted for by the fact that the tissue came from a child with an advanced stage of the disease.

Nevertheless, further study will be required to demonstrate that CF cells synthesize calcium phosphate crystals in response to alterations of ionic exchanges due to the ΔF508 mutation. Such observations would account for the crystalline aggregates of calcium phosphate that probably enhance the pulmonary inflammation in CF patients.

Acknowledgements We are grateful to Drs G. Ratovo and J. Puech for constant advice and discussion and to C. Baritaud and F. Stéfani for their technical assistance. This study was funded by the "Association Française de Lutte contre la Mucoviscidose" (AFLM) and the Ministère de l'Enseignement Supérieur et de la Recherche (MESR).

References

1. Anderson HC (1988) Mechanisms of pathologic calcification. Rheum Dis Clin North Am 14:303–319
2. Barasch J, Kiss B, Prince A, Saiman L, Gruenert D, Al-Awqati Q (1991) Defective acidification of intracellular organelles in cystic fibrosis. Nature 352:70–73
3. Blomfield J, Van Lennep EW, Shorey CD, Malin AS, Dascalu J, Brown JM (1974) Ultrastructure of the in vitro formation of hydroxyapatite in submandibular saliva of children with cystic fibrosis. Arch Oral Biol 19:1153–1160
4. Botelho SY, Goldstein AM, Rosenlund ML (1973) Tear sodium, potassium, chloride, and calcium at various flow rates: children with cystic fibrosis and unaffected siblings with and without corneal staining. J Pediatr 83:601–606
5. Boucher RC, Stutts MJ, Knowles MR, Cantley L, Gatzy JT (1986) Na^+ transport in cystic fibrosis respiratory epithelia. Abnormal basal rate and response to adenylate cyclase activation. J Clin Invest 78:1245–1252
6. Brown WE (1962) Crystal structure of octacalcium phosphate. Nature 196:1048–1050
7. Cheng P-W, Boat TF, Cranfill K, Yankaskas JR, Boucher RC (1989) Increased sulfation of glycoconjugates by cultured nasal epithelial cells from patients with cystic fibrosis. J Clin Invest 84:68–72
8. Chernick WS, Barbero GJ (1959) Composition of tracheobronchial secretions in cystic fibrosis of the pancreas and bronchiectasis. Pediatrics 24:739–745
9. Çiftçioglu N, Kajander EO (1998) Interaction of nanobacteria with cultured mammalian cells. Pathophysiology 4:259–270
10. Daneman A, Gaskin K, Martin DJ, Cutz E (1983) Pancreatic changes in cystic fibrosis: CT and sonographic appearances. Am J Roentgenol 141:653–655
11. Djelidi S, Fay M, Cluzeaud F, Thomas-Soumarmon A, Bonvalet JP, Farman N, Blot-Chabaud M (1999) Vasopressin stimulates long-term net chloride secretion in cortical collecting duct cells. FEBS Lett 460:533–538
12. Dovey M, Wisseman CL, Roggli VL, Roomans GM, Shelburne JD, Spock A (1989) Ultrastructural morphology of the lung in cystic fibrosis. J Submicrosc Cytol Pathol 21:521–534
13. Elgavish A (1991) High intracellular pH in CFPAC: a pancreas cell line from a patient with cystic fibrosis is lowered by retrovirus-mediated CFTR gene transfer. Biochem Biophys Res Commun 180:342–348
14. Feigal RJ, Shapiro BL (1979) Altered intracellular calcium in fibroblasts from patients with cystic fibrosis and heterozygotes. Pediatr Res 13:764–768
15. Gilbert A, Jadot M, Leontieva E, Wattiaux-De Coninck S, Wattiaux R (1998) ΔF508 CFTR localizes in the endoplasmic reticulum-Golgi intermediate compartment in cystic fibrosis cells. Exp Cell Res 242:144–152
16. Haller JO, Heffer ET, Kassner EG, Pinck RL (1977) Unusual radiographic manifestations of cystic fibrosis. Rev Interam Radiol 2:41–42
17. Hollande E, Levrat di Donato J-H, Fanjul M, Palevody C, Daumas M, Puech J, Ratovo G (1990) Calcium phosphate deposits in domes of human pancreatic adenocarcinoma (Capan-1) cell cultures. Biol Cell 69:191–203
18. Hollande E, Fanjul M, Chemin-Thomas C, Devaux C, Demolombe S, Van Rietschoten J, Guy-Crotte O, Figarella C (1998) Targeting of CFTR protein is linked to the polarization of human pancreatic duct cells in culture. Eur J Cell Biol 76:220–227
19. Kajander EO, Çiftçioglu N (1998) Nanobacteria: an alternative mechanism for pathogenic intra- and extracellular calcification and stone formation. Proc Natl Acad Sci U S A 95:8274–8279
20. Katz S (1978) Calcium and sodium transport processes in patients with cystic fibrosis. I. A specific decrease in Mg^{2+}-dependent, Ca^{2+}-adenosine triphosphatase activity in erythrocyte membranes from cystic fibrosis patients. Pediatr Res 12:1033–1038
21. Katz S, Ansah T-A (1980) (Mg^{2+}+ Ca^{2+})-ATPase activity in plasma membrane enriched preparations of human skin fibroblasts: decreased activity in fibroblasts derived from cystic fibrosis patients. Clin Chim Acta 100:245–252
22. Kerem B-S, Rommens JM, Buchanan JA, Markiewicz D, Cox TK, Chakravarti A, Buchwald M, Tsui L-C (1989) Identification of the cystic fibrosis gene: genetic analysis. Science 245:1073–1080

23. Kopelman H, Corey M, Gaskin K, Durie P, Weizman Z, Forstner G (1988) Impaired chloride secretion, as well as bicarbonate secretion, underlies the fluid secretory defect in the cystic fibrosis pancreas. Gastroenterology 95:349–355
24. Kuhn JP, Rosenstein BJ, Oppenheimer EH (1970) Metastatic calcification in cystic fibrosis. Radiology 97:59–64
25. Lang I, Daneman A, Cutz E, Hagen P, Shandling B (1997) Abdominal calcification in cystic fibrosis with meconium ileus: radiologic-pathologic correlation. Pediatr Radiol 27:523–527
26. Lorin MI, Gaerlan PF, Mandel ID, Denning CR (1976) Composition of nasal secretion in patients with cystic fibrosis. J Lab Clin Med 88:114–117
27. Loussouarn G, Demolombe S, Mohammad-Panah R, Escande D, Baró I (1996) Expression of CFTR controls cAMP-dependent activation of epithelial K^+ currents. Am J Physiol 271:C1565–C1573
28. Mangos JA, Donnelly WH (1981) Isolated parotid acinar cells from patients with cystic fibrosis. Morphology and composition. J Dent Res 60:19–25
29. Ogrinc G, Kampalath B, Tomashefski JF (1998) Destruction and loss of bronchial cartilage in cystic fibrosis. Hum Pathol 29:65–73
30. Puchelle E, Gaillard D, Ploton D, Hinnrasky J, Fuchey C, Boutterin MC, Jacquot J, Dreyer D, Pavirani A, Dalemans W (1992) Differential localization of the cystic fibrosis transmembrane conductance regulator in normal and cystic fibrosis airway epithelium. Am J Respir Cell Mol Biol 7:485–491
31. Posner AS (1987) Bone mineral and the mineralization process. In: Peck WA (ed) Bone and mineral research, 5. Elsevier Science Publishers BV, Amsterdam, pp 65–116
32. Ring EJ, Eaton SB, Ferrucci JT, Short WF (1973) Differential diagnosis of pancreatic calcification. Am J Roentgenol Radium Ther Nucl Med 117:446–452
33. Riordan JR, Rommens JM, Kerem B-S, Alon N, Rozmahel R, Grzelczak Z, Zielenski J, Lok S, Plavsic N, Chou J-L, Drumm ML, Iannuzzi MC, Collins FS, Tsui L-C (1989) Identification of the cystic fibrosis gene: cloning and characterization of complementary DNA. Science 245:1066–1073
34. Roomans GM, von Euler AM, Müller RM, Gilljam H (1986) X-ray microanalysis of goblet cells in bronchial epithelium of patients with cystic fibrosis. J Submicrosc Cytol 18:613–615
35. Rule AH, Kopito L, Shwachman H (1970) Chemical analysis of ejaculates from patients with cystic fibrosis. Fertil Steril 21:515–520
36. Scanlin TF, Voynow JA, Thomas EJ, Glick MC (1982) Glycoproteins in culture medium: a comparison from cystic fibrosis and control skin fibroblasts. Biochemistry 21:491–497
37. Schwiebert EM, Egan ME, Hwang T-H, Fulmer SB, Allen SS, Cutting GR, Guggino WB (1995) CFTR regulates outwardly rectifying chloride channels through an autocrine mechanism involving ATP. Cell 81:1063–1073
38. Shapiro BL (1989) Evidence for a mitochondrial lesion in cystic fibrosis. Life Sci 44:1327–1334
39. Smith JJ, Welsh MJ (1992) cAMP stimulates bicarbonate secretion across normal, but not cystic fibrosis airway epithelia. J Clin Invest 89:1148–1153
40. Stutts MJ, Canessa CM, Olsen JC, Hamrick M, Cohn JA, Rossier BC, Boucher RC (1995) CFTR as a cAMP-dependent regulator of sodium channels. Science 269:847–850
41. Thiéry J-P (1967) Mise en évidence des polysaccharides sur coupes fines en microscopie électronique. J Microscopie 6:987–1018
42. Viac J, Reano A, Brochier J, Staquet MJ, Thivolet J (1983) Reactivity pattern of a monoclonal antikeratin antibody (KL1). J Invest Dermatol 81:351–354
43. Waller RL, Brattin WJ, Dearborn DG (1984) Cytosolic free calcium concentration and intracellular calcium distribution in lymphocytes from cystic fibrosis patients. Life Sci 35:775–781
44. Weiner S (1984) Organization of organic matrix components in mineralized tissues. Am Zool 24:945–951

Virchows Arch (2001) 439:691–696
DOI 10.1007/s004280100471

CASE REPORT

M. Rodriguez-Justo · T. Fisher · A.C. Wotherspoon

Hodgkin's disease with an intrasinusoidal pattern of infiltration

A report of two cases

Received: 31 August 2000 / Accepted: 5 April 2001 / Published online: 7 June 2001
© Springer-Verlag 2001

Abstract The histological distinction between Hodgkin's disease (HD) and anaplastic large cell lymphoma (ALCL) may be difficult but is important as the two conditions have different clinical behaviours, prognoses and responses to therapy. Morphological appearances that have been emphasised as favouring the diagnosis of ALCL rather than HD include the identification of neoplastic cells permeating sinusoidal spaces. We document two cases of Hodgkin's disease with classical morphological and immunohistochemical features of nodular-sclerosis subtype (HDNS) but with striking sinusoidal involvement by neoplastic cells. In each case, the CD30 positive/CD15 positive immunophenotype of the neoplastic cells was characteristic of HD without expression of any of the other antigens normally associated with ALCL. HD is generally considered to be a morphological diagnosis and, in those laboratories in which it is not possible to use wide panels of antibodies for the confirmation of the diagnosis, the identification of sinusoidal infiltration by the neoplastic cells in HD may lead to the mistaken impression of ALCL.

Keywords Hogkin's disease · Anaplastic large cell lymphoma · Immunophenotype · Differential diagnosis · ALCL Hodgkin's like · Pathology

M. Rodriguez-Justo (✉)
Department of Pathology, Hospital Universitario de Getafe,
28905 Getafe-Madrid, Spain
e-mail: lolo_rj@teleline.es
Tel.: +34-91-6830241, Fax: +34-91-5332405

M. Rodriguez-Justo · A.C. Wotherspoon
Department of Histopathology, Royal Marsden NHS Trust,
London, UK

T. Fisher
Lymphoma Unit-Department of Medicine,
Royal Marsden NHS Trust, London, UK

Introduction

The histological distinction between Hodgkin's disease (HD) and anaplastic large cell lymphoma (ALCL) may be difficult but is important as the two conditions have different clinical behaviours, prognoses and therapeutic options. There is considerable overlap in the morphological appearances of these two conditions, and this is particularly recognised by the recent description of a Hodgkin's-like variant of ALCL [14]. Traditionally, sinusoidal involvement by pleomorphic large cells and Reed-Sternberg (RS)-like cells is considered to be characteristic of ALCL, and considerable weight is often given to this finding when distinguishing HD from ALCL [4, 6, 12, 13, 19, 23].

We report two cases of classical HD which show characteristic morphological and immunohistochemical features of the nodular-sclerosis type but in which the neoplastic cells are clearly situated within sinusoidal spaces in a way more reminiscent of ALCL. This morphology is unusual in HD. The aim of this study was to highlight this pattern of involvement in classical cases of HD and to point out that this does not exclude that diagnosis in favour of ALCL.

Materials and methods

Cases of HD were sought in the surgical files of the Department of Histopathology of the Royal Marsden Hospital, London, diagnosed in the year 1998. A total of 50 cases were retrieved (45 nodular sclerosis; 5 mixed cellularity), of which two showed a striking infiltration of preserved lymph node sinuses. These two cases provide the substance of the current report.

Lymph node biopsies were fixed in formalin and embedded in paraffin wax, sectioned and stained with haematoxylin and eosin (HE). Immunohistochemical studies were performed using a streptavidin–biotin technique and employing a panel of antibodies including: CD20, CD79a, CD3, CD15, CD30, EMA, CD43, CD45, BNH-9, CD68 (KP1 and PGM1), EBV-LMP1, CBF.78 and ALK1. Appropriate pre-treatment was performed for each antibody as required, and the signal was developed by application of substrate for alkaline phosphatase to react with the covalent conjugate of streptavidin and alkaline phosphatase which gives a permanent red signal.

Clinical data

Case 1

A 21-year-old single male presented with a 2-week history of right supraclavicular lymphadenopathy. He had no other symptoms (no fever, sweats, loss of appetite or weight loss). Clinically, he had a firm 3.0×2.0-cm right supraclavicular node with a second small 1-cm node just beside it. There was another very small node in the left axilla but, otherwise, examination was unremarkable. A chest X-ray showed a probable mediastinal mass. This was confirmed by a computed tomography (CT) scan that showed a large anterior mediastinal mass containing areas of solid tumour with cystic change. There was also evidence of paratracheal lymphadenopathy. The supraclavicular node was excised and the histology showed nodular sclerosis HD (HDNS). A bone-marrow aspirate and trephine biopsy were unremarkable.

Case 2

A 35-year-old female presented with a 2-month history of general malaise, night sweats and pruritus. Approximately 4 weeks prior to presentation, she had developed a lump in the right supraclavicular fossa. On examination, she had a fixed right supraclavicular fossa mass measuring 1.0×2.0 cm. Cardiovascular, respiratory and abdominal examinations were unremarkable. A chest X-ray showed widening of the mediastinum. A CT scan demonstrated disease in the supraclavicular fossa, the mediastinum, the coeliac nodes and the para-aortic regions. Biopsy of a supraclavicular node was performed and this showed HDNS. Bone-marrow aspirate and trephine biopsy were unremarkable.

Results

Histopathology

Macroscopically, the first case consisted of a matted mass of lymph nodes, individually measuring between

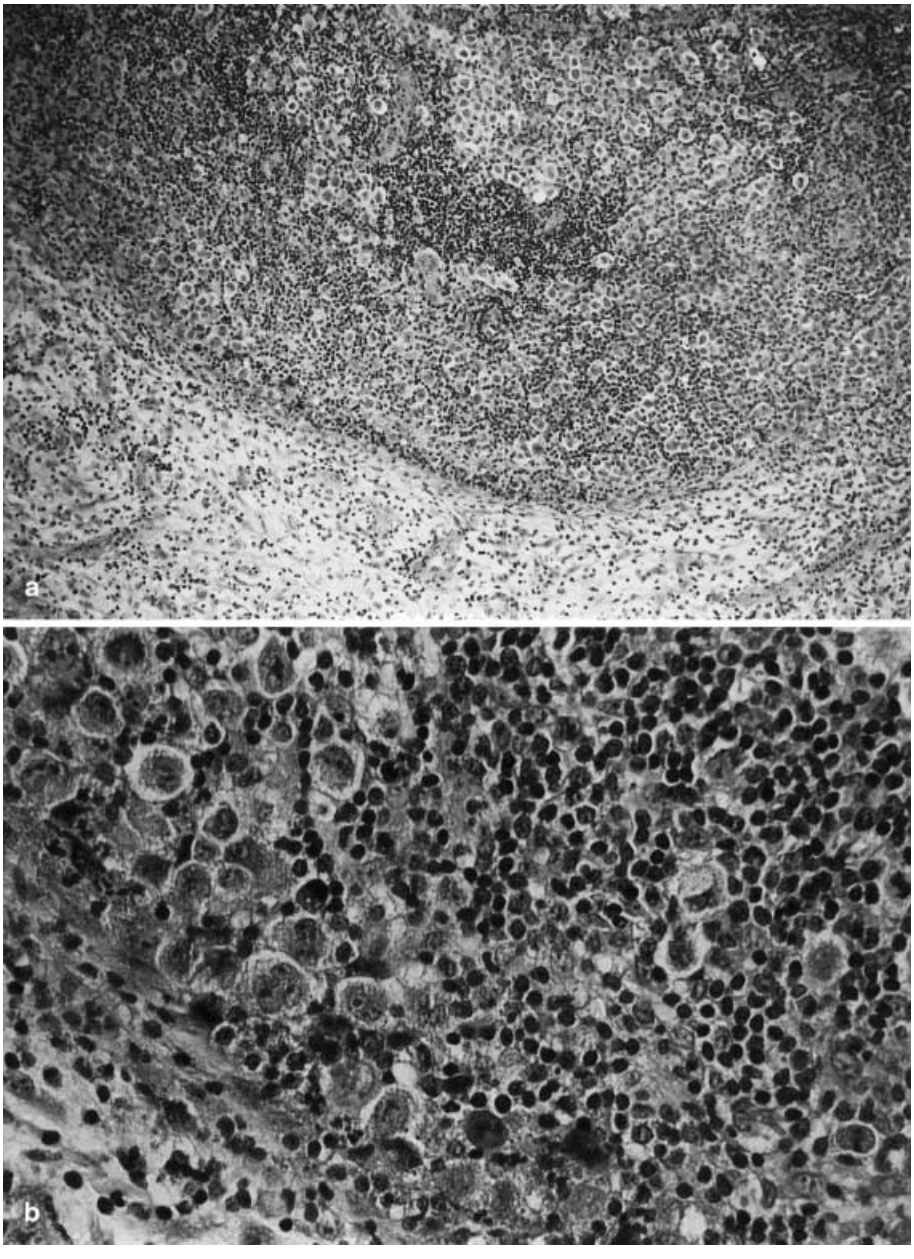


Fig. 1 Case number 1. Low (**a**) and high (**b**) power view of sinusoidal infiltration by sheets of neoplastic Hodgkin's and Reed-Sternberg cells (HE 200× and 400×)

0.5 cm and 1.1 cm, and together measuring 4.2×2.3× 1.3 cm. The HE sections showed the characteristic features of classical HDNS. The nodes had thickened capsules with an architecture that was effaced by a population of cells which, for the most part, was divided into nodules by collagenous fibrous bands. However, in some areas at the periphery of the nodal mass lymphoid follicles were present with partially preserved architecture. Within the cellular population, there was a great number of classical Reed-Sternberg cells. These were large cells with bilobed nuclei, prominent inclusion-like eosinophilic nucleoli, marginal chromatin and abundant eosinophilic cytoplasm. Mononuclear Hodgkin's cells and lacunar-type RS cells – large cells with a multilobed nucleus, one or more prominent eosinophilic nucleoli and abundant pale cytoplasm retracted from the surrounding cells – were also present. An appropriate background of lymphocytes, histiocytes, plasma cells and eosinophils was seen. Focal necrosis was noted in some of the nodules. In some areas, the neoplastic cells showed a striking pattern of sinusoidal infiltration. This was mainly present in areas in which the architecture of the lymph nodes was preserved. Occasional confluent clusters of Hodgkin/RS cells were also seen (Fig. 1)

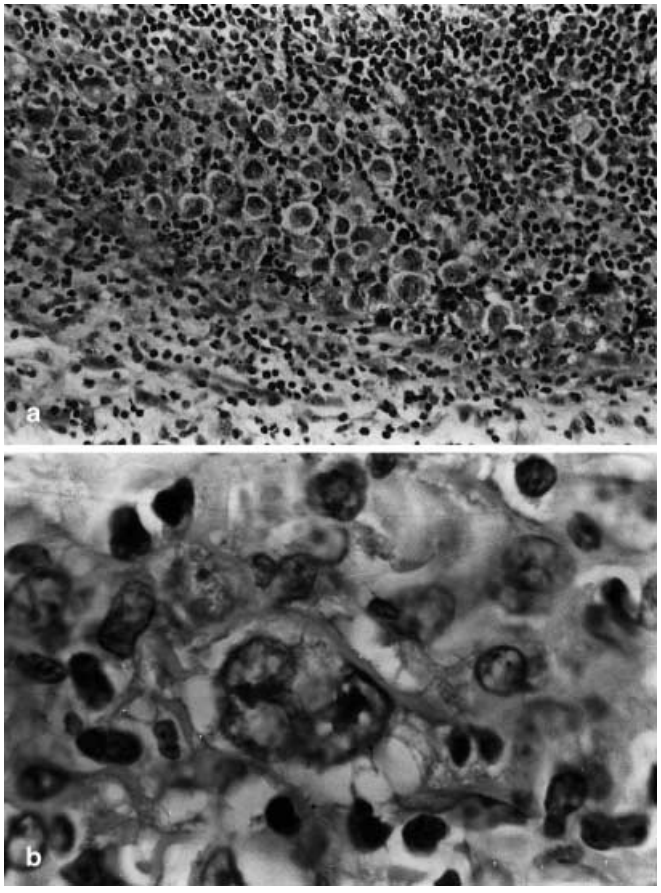


Fig. 2 Case number 2. **a** Scattered Hodgkin's and Reed-Sternberg cells within sinusoidal spaces (HE 200×). **b** High-power view of an intrasinusoidal Reed-Sternberg cell (HE 1000×)

The second case (Fig. 2) again showed the morphological features of HDNS. The morphological changes were similar to the first case although the nodular growth pattern was less evident. There was a major degree of capsular sclerosis with fibrous bands that extended into the nodes. In this case, there were Hodgkin's and Reed-Sternberg cells clearly situated within sinusoidal spaces, although no confluent sheets of these cells were noted. There were no areas of necrosis.

Immunohistochemistry

The immunophenotype of the neoplastic Hodgkin's/RS cells in each case is summarised in Table 1. In both cases, the cells were positive for anti-CD30 with both paranuclear and membrane staining (Fig. 3 and Fig. 4). Staining with anti-CD15 was positive in 50–75% of cells

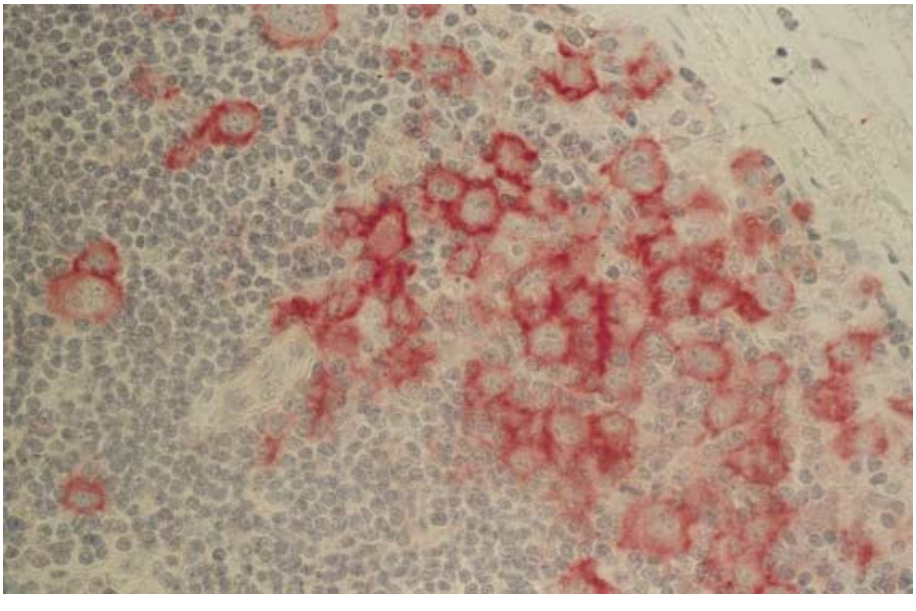


Fig. 3 Case number 1. CD30 immunohistochemical staining showing positive cells in a subcapsular sinus (Ber-H2 antibody, 200×)

Table 1 Immunohistochemical features. +++ 75–100% positive cells, ++ 50–75% positive cells, + 25–50% positive cells, – negative

Case	CD20	CD79a	CD3	CD43	CD45	CD30	CD15	EMA	BNH9	CBF78	ALK1	LMP1	CD68
1	–	–	–	–	–	+++	++	–	–	–	–	–	–
2	–	–	–	–	–	+++	+	–	–	–	–	–	–

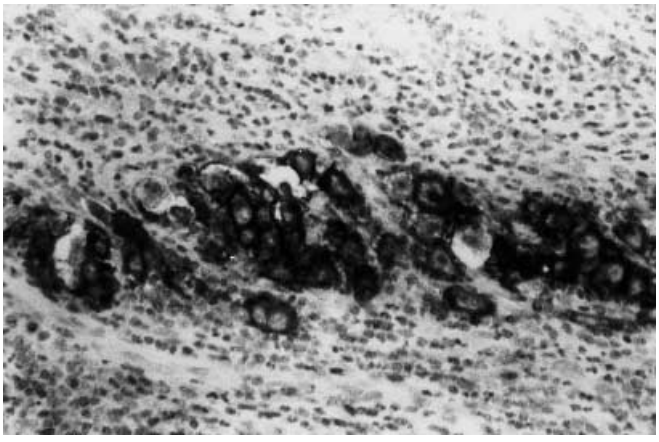


Fig. 4 Case number 2. Neoplatic cells with marked positivity for CD30 (Ber-H2 antibody 200×)

in case number 1 and 25–50% in case number 2. In each case, the staining pattern was juxtanuclear.

All cases were negative for B-cell markers (CD20, CD79a), CD3, leucocyte common antigen (CD45), CD43, epithelial membrane antigen (EMA), BNH-9, CBF.78 and histiocytic markers (CD68; both KP1 and PGM1). In case number 1, staining for CD68 showed a great number of epithelioid histiocytes around areas of focal necrosis No expression of Epstein-Barr virus was detected by staining for the latent membrane protein 1 (LMP1), but studies to detect Epstein-Barr-encoded nuclear RNA (EBERs) and Epstein-Barr nuclear antigens (EBNAs) were not performed. No staining for the monoclonal antibody ALK1 was obtained in either case.

Discussion

The distinction between classical HD and ALCL can be problematic but is important as they have a different clinical behaviour and prognosis and are associated with different therapeutic options [4, 6, 12, 13, 19]. Histologically, HDNS usually has at least a partially nodular pattern, with fibrous bands separating the nodules. Focal necrosis may be seen. The nodules contain the characteristic mixed background population seen in HD – histiocytes, lymphocytes, plasma cells and eosinophils. Within this background are found the classical RS cells, mononuclear Hodgkin's cells and their variants. The characteristic variant of the RS cell found in HDNS is the so-called lacunar cell which shows a multilobated nuclei and small nucleoli, as well as abundant pale cytoplasm which retracts in formalin-fixed sections producing an empty lacuna. In some cases, the nodules show relative lymphocyte depletion in the background and the RS cells and their variants may be seen in syncytial sheets [3, 27]. In the early phases, the nodularity may not be pronounced and the diagnosis is confirmed by the identification of the lacunar variant of the RS cell [26]. Diagnostic RS cells are also present.

In contrast, ALCL is characterised by large malignant pleomorphic cells with prominent nucleoli and abundant cytoplasm (Table 2). These may resemble mononuclear or multinucleated RS cell variants. In addition, the cells are usually smaller than RS cells and often have eccentric horseshoe-shaped nuclei and a prominent paranuclear hof. The neoplastic cells characteristically grow in cohesive sheets, frequently involve sinusoids within the lymph nodes, and may show a perivascular pattern of infiltration [2].

Several different morphological variants of ALCL have been proposed, including a Hodgkin's-like/Hodgkin's-related type. This is a variant of ALCL first recognised in 1987, and this has been included in the REAL classification as a provisional subtype [14], although the upcoming World Health Organization classification does not consider ALCL-HD like as a real entity [15]. The Clinical Advisory Committee recommends that cases that cannot be classified as HD or ALCL (by a combination of morphology – immunohistochemistry and genetic studies) should be reported as unclassifiable, because there is no borderline between HL and ALCL (T/null type). ALCL-HD like is morphologically characterised by a background of neutrophils, histiocytes, eosinophils, plasma cells and fibrosis. The tumour cells tend to be found in nodules and there is capsular thickening. Overall, the reactive cells tend to be in the minority. Intrasinusoidal spread is present but may be less marked than is seen in common ALCL [22]. In the European Association of Haematopathology Workshop held in Toledo (Spain, 1994), the intrasinusoidal spread of the tumour cells was regarded as a very important criterion in favour of Hodgkin's-like ALCL or true ALCL. The immunophenotype is essentially the same as that found in common ALCL and this is a reliable distinguishing feature between this type of ALCL and HD. Indeed, Kadin [18] has proposed that the distinction between the two entities relies heavily on the immunophenotypic profile of the neoplastic cells with expression of antigens not associated with HD (EMA, BNH9, CBF78) favouring the diagnosis of ALCL. It is widely accepted that HD and ALCL have many similarities and this variant may represent an area of overlap between the two entities. Clinically, patients with Hodgkin's-like ALCL are older than those with common ALCL and present more frequently with a

Table 2 Anaplastic large cell lymphoma and Hodgkin's disease/Hodgkin's lymphoma: differential diagnosis. *EBER* Epstein-Barr-encoded nuclear RNA, *EMA* epithelial membrane antigen

	Anaplastic large cell lymphoma	Nodular sclerosis Hodgkin's disease
Morphology	Cohesive sheets, prominent sinusoidal spread, perivascular infiltration	Partially nodular pattern
	Pleomorphic large cells (smaller than Reed-Sternberg cells): eccentric horseshoe-shaped nuclei and a prominent paranuclear hof	Characteristic mixed background population (histiocytes, plasma cells, eosinophils...)
		Classical Reed-Sternberg cells, mononuclear Hodgkin's cells and their variants
Immunophenotype	T/null EMA+(60–100%) BNH9+(50–80%) CBF78+(80%) CD15–/+ (0–20%) CD45 usually + CD43+ ALK1+(60–80%)	B-cell (CD20, CD79a)+(60%) EMA–(0–5%+) BNH9–(0–5%+) CBF78–(10%+) CD15+(80%) CD45 usually – CD43 usually – ALK1–
Genetic studies	EBER+(4.5–20%)* t(2,5)–NPM/ALK rearrangement T-cell receptor gene	EBER+(15–30%)

*4.5% by Southern blot and 20% by polymerase chain reaction

mediastinal mass [13, 14, 19]. Overall survival is similar for both Hodgkin's-like and common types of ALCL [28].

The immunophenotype of the Hodgkin's and RS cells is well established [6]. They are CD30 positive and about 80% express CD15. Hodgkin's and RS cells are usually CD45 negative but up to 60% express B cell antigens (CD20/CD79a) [17]. Of the antigens associated with ALCL, EMA is expressed in 0–5%, BNH9 in about 5% (occasional cells) [16, 17] and CBF78 in less than 10% of cases of classical HD [1]. The neoplastic cells of ALCL also express CD30. The reported incidence of CD15 staining in cases of ALCL varies from 0% to 20%. CD45 reactivity in ALCL is variable. Of the antigens characteristically associated with ALCL rather than HD, EMA is positive in 60–100%, BNH9 in 50–80% [5, 7] and CBF78 in up to 80% of ALCL [1]. Another antibody that may aid in the distinction between HD and ALCL is anti-CD43 which, although not lineage specific, is thought to favour ALCL rather than HD [12, 20]. P53 was found less frequently in ALCL than in HD and the same appeared to be true for EBER [25].

Staining with the antibody ALK-1 indicates the presence of a t(2;5) translocation and can be found in about 80% of adult cases of ALCL [2]. Orscheschek et al. [21] found, using reverse-transcriptase polymerase chain reaction, the translocation t(2;5) in 11 of 13 cases of HD (nodular sclerosis and mixed cellularity types); but the majority of studies have found that this translocation is absent in cases of HD and Hodgkin's-like ALCL [6, 11, 14, 16, 23, 24]. Classically, it was well documented that ALK-1 staining indicated the diagnosis of ALCL [6, 23] and negative ALCL cases still expressed the characteristic immunophenotype of ALCL (EMA+BNH9+) [6]. However, recent studies have shown that 40% of ALCL cases do not express ALK (interestingly common and Hodgkin's-like types more frequently) [8]. The authors have suggested that ALK positivity appears to define a clinicopathological entity (ALK lymphomas) that shows a much wider spectrum of morphological pattern than has been appreciated previously, and they show a better prognosis than ALK-negative ALCL. Moreover, it seems to be that HD, Hodgkin's-like ALCL and ALK-1-negative ALCL cases might be more closely related to each other than to the ALK1+ subgroup [9, 10].

We have reported two cases showing the classical features of HDNS although with different degrees of nodular growth pattern, capsular thickening and number of lymphoid follicles partially preserved. In each case, sinusoidal infiltration by neoplastic cells was clearly seen, sometimes in confluent sheets in a pattern more commonly associated with that of ALCL. In neither case was there any other suggestion that the diagnosis could be ALCL and the features were not typical even of the Hodgkin's-like variant of this condition. In each case, the immunophenotype was clearly that of HD with no aberrant antigen expression to suggest ALCL. In each case, the intrasinusoidal pattern was seen in small adjacent nodes or in areas of the node showing partial involvement. If these had been the only areas sampled, then the potential for confusion may have arisen. Cases of classical HD with such an unequivocal sinusoidal pattern are rare but might lead to a mistaken morphological diagnosis if too much reliance is placed on this histological feature. Chittal and Delsol [6] have reported this pattern of infiltration in cases that showed morphological overlap of HD and ALCL, but in their conclusions the cases were actually considered Hodgkin's-like ALCL rather than true HD, whereas our cases are classical HDNS.

We conclude that while sinusoidal infiltration by pleomorphic large cells is characteristically seen in ALCL, it is not pathognomonic of that disease, and this feature may be seen in cases of otherwise typical HD. The finding of morphological features of ALCL in such cases highlights the relationship between the two conditions, but it remains important to distinguish the two entities as they have different clinical behaviours. It should be pointed out that, while this appearance may not trouble a specialist haematopathologist, it is a potential area of confusion for the general pathologist that should be highlighted.

Acknowledgements We would like to acknowledge the help of Alex Javed and Keith Miller in performing the immunocytochemical stains and Professor Peter Isaacson for his help and advice.

References

1. Al-Saati T, Tkaczuk J, Kjrissansen G, Print C, et al (1995) A novel antigen detected by the CBF.78 antibody further distinguishes anaplastic large cell lymphoma from Hodgkin's disease. Blood 86:2741–46
2. Benharroch D, Meguerian-Bedoyan Z, Lamant L, Amin C, et al (1998) ALK-Positive lymphoma: a single disease with a broad spectrum of morphology. Blood 91:2076–2084
3. Ben-Yehuda-Salz D, Ben-Yehuda A, Polliack A, Ron N, Okon E (1990) Syncytial variant of nodular sclerosing Hodgkin's disease. A new clinicopathologic entity. Cancer 65:1167–1172
4. Braziel RM, Oyama K (1997) Mistaken diagnoses of Hodgkin's disease. Hematol Oncol Clin North Am 11:863–892
5. Carbone A, Gloghini A, Volpe R (1992) Immunohistochemistry of Hodgkin and Non-Hodgkin lymphomas with emphasis on the diagnostic significance of the BNH9 antibody reactivity with anaplastic large cell (CD30+) lymphomas. Cancer 70: 2691–2698
6. Chittal SM, Delsol G (1997) The Interface of Hodgkin's disease and anaplastic large cell lymphoma. Cancer Surv 30: 87–105
7. Delsol G, Blancher A, Saati A, Ralfkiaer E, et al (1991) Antibody BNH9 detects red blood cell-related antigens on anaplastic large cell (CD30+) lymphomas. Br J Cancer 64:321–326
8. Falini B, Bigerna B, Fizzotti M, Pulford K, et al (1998) ALK expression defines a distinct group of T/Null lymphomas ("ALK lymphomas") with a wide morphological spectrum. Am J Pathol 153:875–886
9. Falini B, Pileri S, Zinzani PL, Carbone A, et al (1999) ALK+ lymphoma: clinico-pathological findings and outcome. Blood 93:2697–2706
10. Falini B, Poulford K, Pucciarini A, Carbone A, et al (1999) Lymphomas expressing ALK fusion protein(s) other than NPM-ALK. Blood 94:3509–3515
11. Flippa DA, Ladany M, Wollner N, Straus DJ, et al (1996) CD30 (Ki-1)-positive malignant lymphomas: clinical, immunophenotypic, histologic, and genetic characteristics and differences with Hodgkin's disease. Blood 87:2905–2917
12. Frizzera G (1992) The distinction of Hodgkin's disease from anaplastic large cell lymphoma. Semin Diagn Pathol 9:291–296
13. Harris NL (1999) Hodgkin's disease: classification and differential diagnosis. Mod Pathol 12:159–176
14. Harris NL, Jaffe ES, Stein H, et al (1994) A revised European-American classification of lymphoid neoplasms: a proposal from the International Lymphoid Study Group. Blood 84: 1361–1392
15. Harris NL, Jaffe ES, Diebold J, Flandrin G, Muller-Hermelink HK, Vardiman J, Lister TA, Bloomfield CD (2000) The World Health Organization classification of neoplastic diseases of the haematopoietic and lymphoid tissues: report of the Clinical Advisory Committee Meeting, Airlie House, Virginia, November 1997. Histopathology 36:69–89
16. Herbst H, Anagnostopoulous J, Heinze B, Dürkop H, et al (1995) ALK gene products in anaplastic large cell lymphomas and Hodgkin's disease. Blood 86:1694–1700
17. Isaacson PG, Ashton-Key M (1996) Phenotype of Hodgkin and Reed-Sternberg cells. Lancet 347:481
18. Kadin ME (1997) Anaplastic large cell lymphoma and its morphological variants. Cancer Surv 30:77–86
19. Kinney MC, Kadin ME (1999) The pathologic and clinical spectrum of anaplastic large cell lymphoma and correlation with ALK gene dysregulation. Am J Clin Pathol 111[Suppl1]: S56–S67
20. Leoncini L, Del-Vecchio MT, Kraft R, Megha T, et al (1990) Hodgkin's disease and CD30-positive anaplastic large cell lymphomas: a continuous spectrum of malignant disorders. Am J Pathol 137:1047–1057
21. Orscheschek K, Merz H, Hell J, Binder T, et al (1995) Large-cell anaplastic lymphoma-specific translocation (t[2;5] [p23;q35]) in Hodgkin's disease: indication of a common pathogenesis? Lancet 345:87–90
22. Pileri SA, Bocchi M, Baroni CD, Martelli M, et al (1994) Anaplastic large cell lymphoma (CD30+/Ki1+): results of a prospective clinicopathological study of 69 cases. Br J Hematol 86:513–523
23. Pileri SA, Pittaluga A, Poggi S, Sabatini E, et al (1995) Anaplastic large cell lymphoma: update of findings. Leuk Lymphoma 18:17–25
24. Pittaluga S, Wlodarska I, Pulford K, Campo E, Morris S, et al (1997) The monoclonal antibody ALK1 identifies a distinct morphological subtype of anaplastic large cell lymphoma associated with 2p23/ALK rearrangements. Am J Pathol 151: 343–351
25. Stein H (1999) Diagnosis of Hodgkin's disease, Hodgkin's-like anaplastic large cell lymphoma, and T cell/histiocyte-rich B cell lymphoma. In: Masson DY, Harris NL (eds) Human lymphoma: clinical implications of the REAL classification. Springer, Berlin Heidelberg New York, pp 52.1–52.4
26. Strauchen JA (1998) Diagnostic histopathology of the lymph node. Oxford University Press, New York
27. Strickler JG, Michie SA, Warnke RA, Dorman RF (1986) The syncytial variant of nodular sclerosing Hodgkin's disease. Am J Surg Pathol 10:470–477
28. Zinzani PL, Bendandi M, Marteli M, Falini B, et al (1996) Anaplastic large-cell lymphoma: clinical and prognostic evaluation of 90 adult patients. J Clin Oncol 14:955–962

Virchows Arch (2001) 439:697–699
DOI 10.1007/s004280100492

LETTER TO THE EDITOR

Ji Shin Lee · Hyung Seok Kim · Jong Jae Jung
Sang Woo Han · Young Bog Kim

Ancient schwannoma of the pancreas mimicking a cystic tumor

Received: 30 March 2001 / Accepted: 28 May 2001 / Published online: 7 August 2001
© Springer-Verlag 2001

Sir,

Schwannoma of the pancreas is an extremely rare lesion; only 29 cases have been reported in the present era [1, 4, 6]. In the literature, pancreatic schwannomas are reported as often showing cystic features, clinically mimicking pseudocysts or cystic tumors. Ancient schwannoma is a variant of schwannoma displaying pronounced degenerative changes; these include cyst formation, calcification, hemorrhage, hyalinization, and xanthomatous infiltration [3]. Degenerative nuclear atypia is also noted. According to a PubMeD search, ancient pancreatic schwannoma has not been previously reported. We report a case of ancient schwannoma of the pancreas mimicking a cystic tumor. A 63-year-old previously healthy woman presented with a 6-month history of upper abdominal discomfort. A pertinent physical examination revealed a large mass in the left upper quadrant. All laboratory data were normal, including tumor markers. An abdominal computed tomography (CT) revealed a 10-cm multicystic mass in the tail of the pancreas (Fig. 1A), which was suspected to be a cystic tumor of the pancreas. A distal pancreatectomy with a splenectomy was performed. The resected tail of the pancreas contained a 10.5×10×9 cm mass that was well demarcated and partially covered by stretched but otherwise normal pancreatic parenchyma. The cut surfaces of the mass showed a well-circumscribed, septate, cystic mass with a thick fibrous capsule (Fig. 1B). The cystic areas were filled with old and new hemorrhage. Microscopically, the tumor was surrounded by thick fibrous tissue and normal pancreatic parenchyma (Fig. 2A). The peripheral portion of the mass was partially solid and composed of sheets of spindle cells that occasionally formed interlacing fascicles. The spindle cells had twisted nuclei and occasional vacuolar cytoplasm (Fig. 2B). Some of the tumor cells showed nuclear atypia, but lacked mitotic figures. Most of the tumor showed extensive degenerative changes, including cyst formation, hemorrhage, and perivascular hyalinization (Fig. 2C). The tumor was abundantly infiltrated by histiocytes and siderophages. The tumor also had deposits of cholesterol in clefts and calcification in the degenerative areas. Immunostains showed the tumor cells to be strongly and diffusely positive for S-100 protein (DAKO, USA) and vimentin (DAKO, USA) (Fig. 2D). There was no positive staining for actin (DAKO, USA) or for CD34 (Novocastra, UK). The tumor was diagnosed as an ancient schwannoma of the pancreas. After 6 months of follow-up, the patient had no specific complaints regarding this disorder.

In the literature, only 29 cases of intrapancreatic schwannoma have been previously reported [1, 4, 6]. These 29 cases demonstrated that schwannoma of the pancreas is a tumor generally found in older adults, in a nearly equal ratio of men to women. The majority of tumors are located in the body of the pancreas, but a few have been present in the head or tail. In all instances, a simple excision was adequate where this was technically feasible. In our case, the patient was a 63-year-old woman, and the tumor was located in the tail of the pancreas. Upon follow-up 6 months after the excising the mass, the patient was doing well.

The group of nonepithelial tumors of the pancreas with spindle cell features can have a histopathologic resemblance to pancreatic schwannoma. Leiomyoma and solitary fibrous tumor have to be differentiated from pancreatic schwannoma [5]. The tumor of our case showed immunohistochemical reactivity for S-100 protein, ruling out leiomyoma and solitary fibrous tumor.

J.S. Lee (✉) · H.S. Kim · J.J. Jung
Department of Pathology, Seonam University,
College of Medicine, 720 Kwangchi-Dong Namwon,
Chollabuk-Do, 590-711, Korea
e-mail: jshinlee@hanmail.net
Tel.: +82–63–620–0352, Fax: +82–63–620–0355

S.W. Han
Department of Internal Medicine, Seonam University,
College of Medicine, Namwon, Korea

Y.B. Kim
Department of General Surgery, Seonam University,
College of Medicine, Namwon, Korea

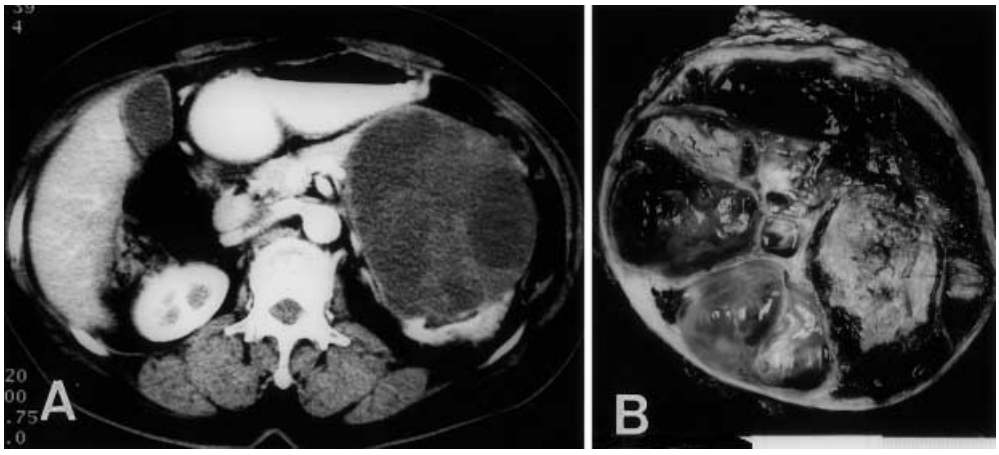


Fig. 1 A computed tomography (CT) scan (**A**) and cut surface of the mass (**B**). The CT scan shows a 10-cm multicystic mass in the tail of the pancreas. Grossly, the tumor is well demarcated and covered by thick fibrous tissues and normal pancreatic parenchyma. There is extensive cyst formation and hemorrhage

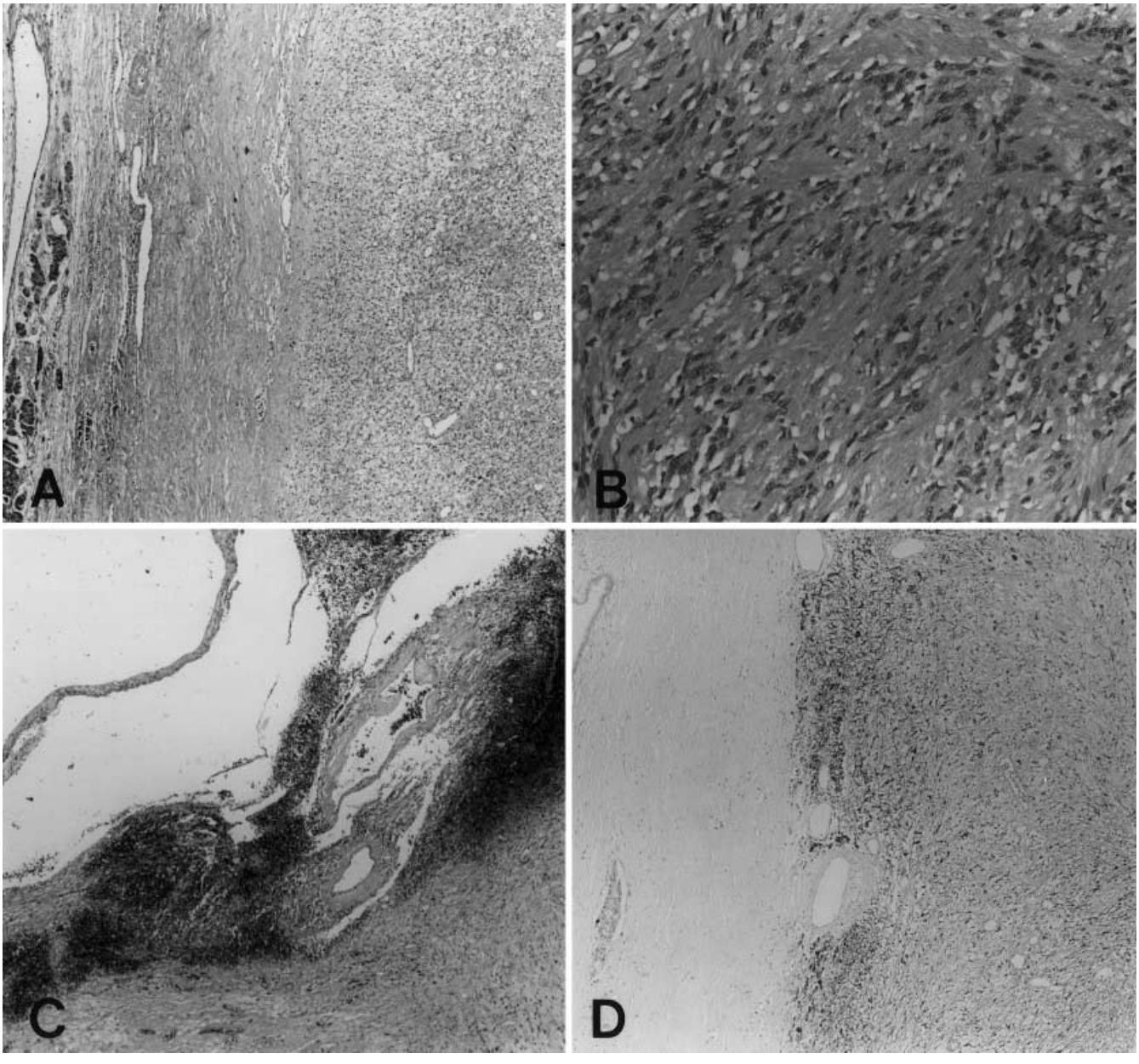


Fig. 2A–D Microscopic and immunohistochemical findings. The tumor, which is surrounded by fibrous tissues and normal pancreatic parenchyma (**A**, hematoxylin-eosin, original magnification ×20), is partially composed of spindle cells that have twisted nuclei and vacuolated cystoplasm (**B**, hematoxylin-eosin, original magnification ×200). The tumor has cyst formation, hemorrhage, and perivascular hyalinization (**C**, hematoxylin-eosin, original magnification ×100). The tumor displays an intensely positive reaction for S-100 protein, whereas the surrounding pancreatic duct fails to react (**D**, anti-S-100 protein, avidin-biotin-immunoperoxidase, original magnification ×40)

Ancient schwannoma is a neurilemmoma that displays pronounced degenerative changes [3]. A significant percentage of this tumor is located in deep structures such as the retroperitoneum [2]. The degenerative changes include cyst formation, calcification, hemorrhage, and hyalinization. Degenerative nuclear atypia is also another peculiar finding. According to the review of the literature of pancreatic schwannoma, approximately two-thirds are partially cystic and some, particularly the larger ones, can mimic a pancreatic pseduocyst or cystic pancreatic tumor in a radiographic examination [4]. Using CT, the tumor mass in our patient was initially suspected to be a cystic tumor of the pancreas, but the morphological features are typical of ancient schwannoma found elsewhere in the body. A PubMeD search failed to reveal any reports of ancient schwannoma of the pancreas. Thus, to the best our knowledge, this is the first report describing an ancient pancreatic schwannoma. Definitive diagnosis of ancient pancreatic schwannoma was only established by pathological examination. It is suggested that ancient schwannoma of the pancreas be considered as one possibility in the differential diagnosis of cystic masses in the pancreas.

References

1. Brown SZ, Owen DA, O'Connell JX, Scudamore CH (1998) Schwannoma of the pancreas: a report of two cases and a review of the literature. Mod Pathol 11: 1178–1182
2. Dahl I (1977) Ancient neurilemmoma (schwannoma). Acta Pathol Microbiol Scand [A] 85: 812–818
3. Enzinger FM, Weiss SM (1995) Benign tumors of peripheral nerves. In: Enzinger FM, Weiss SM (eds) Soft tissue tumors. Mosby Year Book, St. Louis, pp 821–888
4. Hsiao WC, Lin PW, Chang KC (1998) Benign retroperitoneal schwannoma mimicking a pancreatic cystic tumor: case report and literature review. Hepato-Gastroenterology 45: 2418–2420
5. Lüttges J, Mentzel T, Hübner G, Klöppel G (1999) Solitary fibrous tumour of the pancreas: a new member of the small group of mesenchymal pancreatic tumours. Virchows Arch 435:37–42
6. Morita S, Okuda J, Sumiyoshi K, Taketani M, Moriguchi A, Katsu K, Tanigawa N (1999) Pancreatic schwannoma: report of a case. Surg Today 29: 1093–1097

Virchows Arch (2001) 439:725–751
DOI 10.1007/s004280100516

REVIEW ARTICLE

E. Van Aken · O. De Wever · A. S. Correia da Rocha
M. Mareel

Defective E-cadherin/catenin complexes in human cancer

Received: 11 April 2001 / Accepted: 25 July 2001 / Published online: 14 September 2001
© Springer-Verlag 2001

Abstract Cancer is caused by a series of genomic changes leading directly or indirectly to disturbance of growth, differentiation and tissue integrity. Genomic, transcriptional or posttranscriptional alterations of E-cadherin/catenin complexes that are implicated in various steps of cancer development comprise mutational inactivation, transcriptional downregulation of E-cadherin sometimes accompanied by upregulation of N-cadherin, proteolysis of E-cadherin and posttranslational stabilisation of β-catenin and plakoglobin. The E-cadherin/catenin complex serves not only cell–cell adhesion but also transduces signals to the nucleus and to the cytoskeleton, either directly or through its connections with multiple other complexes. We review here the expression of E-cadherin/catenin in human cancers, emphasising methods of observation and prognostic interpretation of results. This is illustrated in thyroid lesions from the benign follicular adenoma to the extremely malignant anaplastic carcinoma. The eye is an organ largely neglected by students of cadherins and catenins. The implication of a variety of members of these molecular families in the embryonic development of the eye strongly suggests that disturbances of cadherin/catenin complexes are crucial also in the development of ocular tumours.

Keywords Cancer · Cadherin · Catenin · Thyroid · Eye

E. Van Aken
Department of Ophthalmology, Ghent University Hospital,
De Pintelaan 185, 9000 Gent, Belgium

O. De Wever · M. Mareel (✉)
Laboratory of Experimental Cancerology,
Ghent University Hospital, De Pintelaan 185, 9000 Gent, Belgium
e-mail: marc.mareel@rug.ac.be
Tel.: +32-9-2403078, Fax: +32-9-2404991

A.S.C. da Rocha
Institute of Molecular Pathology and
Immunology of University of Porto, Rua Roberto Frias s/n°,
4200 Porto, Portugal

M. Mareel
Laboratory of Experimental Cancerology,
Ghent University Hospital, De Pintelaan 185, 9000 Gent, Belgium

The E-cadherin/catenin complex in cancer development

Cancer is a disease of growth, differentiation and tissue organisation. These cellular activities are crucial for embryonic development and for the maintenance of the proper structure and function of the adult organism; disturbances cause accumulation of cells, loss of tissue differentiation, and gain of invasion and metastasis (Fig. 1). In most patients, the disease goes from bad to worse and, in absence of treatment, causes death. Clinical and experimental observations indicate that reversion of at least part of the cancer cell population is possible. Metastases sometimes show a high degree of differentiation and grow without invasion; in culture, human colon cancer cells are able to form M cells, a specially differentiated type of absorptive enterocytes covering Peyer's patches [151]. The cause of cancer is a series of alterations in the genome, leading to activation of oncogenes and repression of tumour-suppressor genes [90]. Stage specificity of genetic alterations has previously led to the concept that oncogenes and tumour-suppressor genes were implicated in growth disturbance and that they differed from genes promoting or suppressing differentiation or invasion [182]. The growing list of cancer genes, however, comprises several examples of oncogenes and tumour-suppressor genes that are implicated in earlier stages of growth disturbance as well as in later stages of gain of invasion, either in the same or in different types of tumours [22]. The majority of molecules that are implicated in the expression of the cancer phenotypes are products of normal wild-type genes. They are indicated further as tumour-promoter or tumour-suppressor molecules. Examples given in the present review pertain to the E-cadherin/catenin complex or to signalling pathways related to this complex.

The E-cadherin/catenin complex

E(pithelial)-cadherin is a transmembrane glycoprotein of the type-I cadherin superfamily [210]. Its cytoplasmic

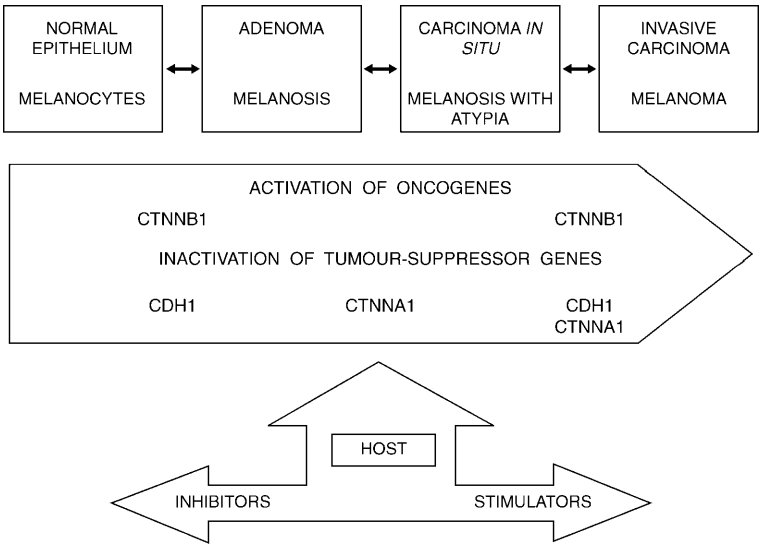


Fig. 1 Schematic of cancer development. The activation of promoter genes, also called oncogenes, or the inactivation of suppressor genes underlies the development of cancer. Examples given are genes encoding E-cadherin (*CDH1*), α-catenin (*CTNNA1*) and β-catenin (*CTNNB1*). The cancer phenotypes (*second row*) result from the effect exerted by stimulatory and inhibitory host factors (*bottom row*) on the genetically altered cells. Where do cadherins and catenins play a crucial role? Adapted from [181]

part is linked to the actin cytoskeleton via the catenins, α-, β- and γ-catenin (the same as plakoglobin). Homophilic interaction of the extracellular part of E-cadherin mediates cell–cell adhesion, mainly homotypic, i.e. epithelial cell to epithelial cell, but also heterotypic, e.g. melanocytes or dendritic cells to keratinocytes [272, 273]. Heterophilic–heterotypic interactions occur between E-cadherin and the $\alpha_E\beta_7$ integrin, respectively, on enterocytes and T lymphocytes [54] and between E-cadherin and internalin, respectively, on enterocytes and enteric bacteria [166]. These heterophilic interactions regulate, respectively, the retention of lymphocytes in the target epithelium and invasion of bacteria into vertebrate cells. The E-cadherin/catenin complex is implicated also in directed migration during epithelial wound healing presumably through contact inhibition of membrane ruffling [6]. It is by now quite clear that E-cadherin is not only a cell–cell adhesion molecule [281] but is also pivotal in signal transduction from the outer cell surface to the cytoskeleton. In differentiated cells, the minus ends of microtubules that are released from the centrosome are stabilised by signalling from cadherins through cell–cell contact [58]. Connections between the E-cadherin/catenin complex and multiple other receptor and nonreceptor signal-transducing systems may contribute to the complexity of the cancer phenotypes [206]. Figure 2 presents a current view on the structure of the complex and its connections.

The E-cadherin gene *CDH1*: an invasion-suppressor gene

CDH1, the gene on chromosome 16q22.1 encoding E-cadherin, was recognised as an invasion-suppressor gene through in vitro genetic manipulation of human and animal cell lines [24, 91, 292]. The causal relationship between E-cadherin and invasion in vivo was demonstrated by Perl et al. [225]. Seventy-four percent of transgenic mice expressing the tumourigenic SV40T antigen under the insulin promoter (*Rip1Tag*) developed pancreatic β-cell adenomas and 26% developed invasive adenocarcinomas. Overexpression of E-cadherin under the same promoter (*Rip1E-cad*) did not cause tumours. *Rip1Tag* × *Rip1E-cad* crosses had a lower (8%) ratio of adenocarcinomas, showing that overexpression of E-cadherin counteracted the acquisition of the invasive phenotype. By contrast, crosses of *Rip1Tag* mice with mice expressing dominant negative E-cadherin that lack the extracellular domain (*Rip1dnE-cad*) had invasive and metastatic carcinomas in 50% of the cases. Interestingly, *Rip1dnE-cad* mice show a transient perturbation of β-cell aggregation during islet development but did not form pancreatic tumours, indicating that the loss of E-cadherin alone is not sufficient for tumour development [66].

Immunohistochemical changes in E-cadherin expression and localisation in human cancers are compatible with *CDH1* as an invasion-suppressor gene but obviously do not prove it. The evidence from immunohistochemical studies is at best circumstantial, and loss of E-cadherin expression may also occur at the posttranscriptional level. Gastrointestinal cancers provide early examples [75, 193, 284]. A positive correlation is observed between cancer aggressiveness and E-cadherin disturbance, but this does not permit conclusions about cause and effect. Indeed, a normal pattern of E-cadherin is hard to imagine in a cancer that has lost the epithelial structure of its tissue of origin. Later, abnormal patterns of E-cadherin expression were found in most invasive human tumours, including melanomas [41, 67, 75].

The E-cadherin gene *CDH1*: a tumour-suppressor gene

CDH1 sometimes acts as a tumour-suppressor gene, as shown in lobular breast cancer and diffuse gastric cancer. The first indications that *CDH1* could act as a tumour-

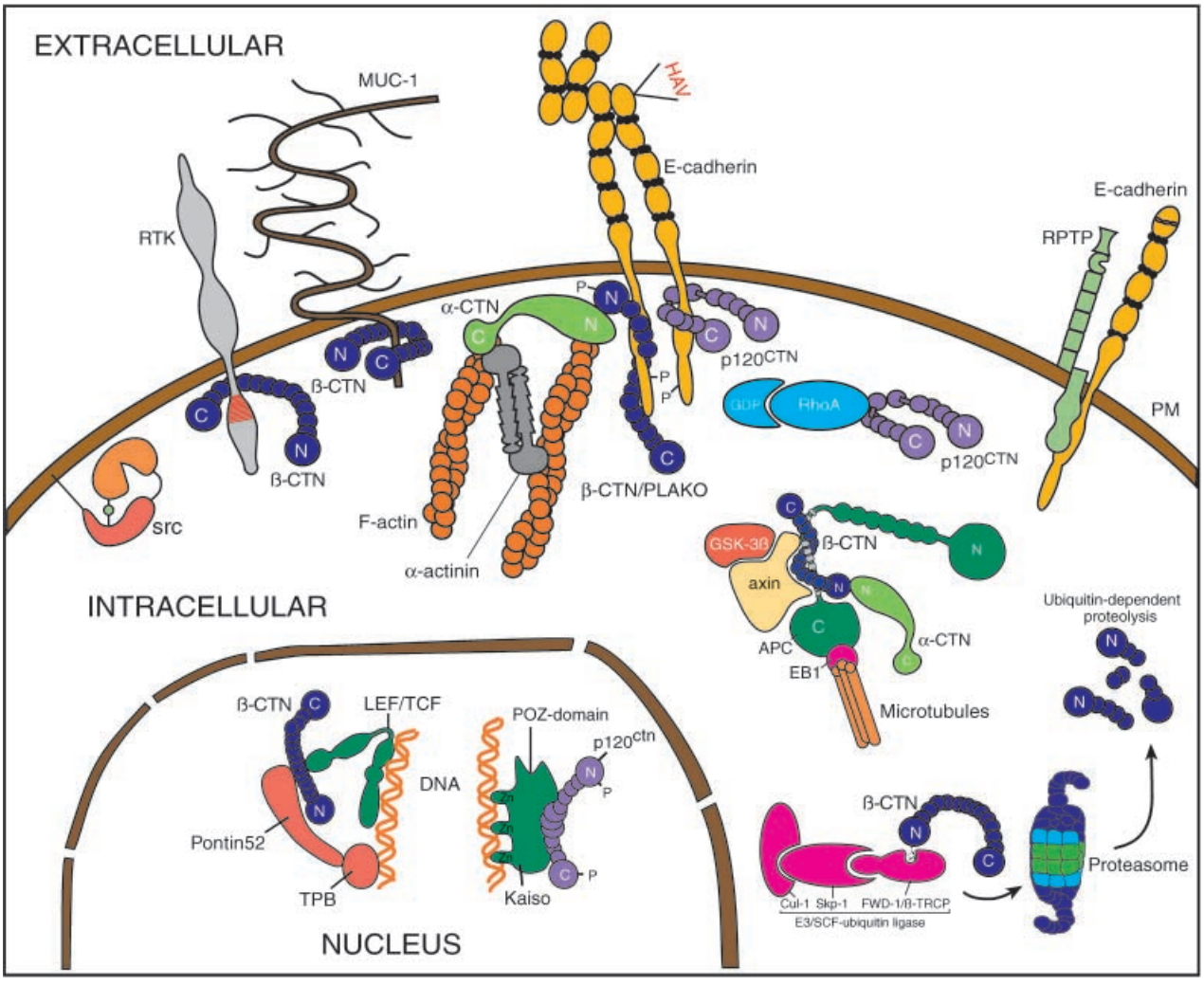


Fig. 2 Schematic overview of regulation of the E-cadherin/catenin complex at the protein level and of nuclear protein complexes containing β-catenin (*β-CTN*) or p120 catenin (*p120*^{CTN}). E-cadherin serves homotypic homophilic adhesion through a histidine–alanine–valine (HAV) sequence, characteristic of the first extracellular domain of type-I cadherins. Binding of E-cadherin via the catenins to the actin cytoskeleton directly or via α-actinin (actin cross-linking protein, belonging to the calponin homology-domain family) is essential for cell–cell adhesion. α-Catenin (α-CTN) binds via its aminoterminal end (N) to β-CTN or to plakoglobin (*PLAKO*). The E-cadherin/catenin complex is a substrate for receptor tyrosine kinases (RTKs), e.g. c-erbB2 (oncogenic tyrosine kinase receptor from the EGFR family), c-met (receptor for plasminogen related growth factor 1, PRGF-1, previously termed scatter factor/hepatocyte growth factor), EGFR (epidermal growth factor receptor), of non-receptor tyrosine kinases, e.g. src, of receptor protein tyrosine phosphatases (RPTP), and of MUC-1 (a nonsecretory mucin also called episialin). β-CTN that is not associated with E-cadherin binds to a macromolecular complex containing APC (adenomatous polyposis coli protein), the adaptor protein axin, GSK-3β (glycogen synthase kinase-3β) and EB1 (microtubule end binding protein). GSK-3β phosphorylates (P) β-CTN, triggering in this way β-CTN interaction with the E3/SCF-ubiquitin ligase complex, comprising Skp1–Cullin–FWD-1 (F-box protein)/β-TRCP (beta-transducin repeat-containing protein). Ubiquinated β-CTN is then degraded via proteasomes. Mutation in the phosphorylation sites of β-CTN or in the β-CTN binding site of APC leads to the accumulation of β-CTN in the nucleus. Pontin52 may act as a bridge protein between β-CTN and TBP (TATA box binding protein) in complex with LEF/TCF (lymphocyte enhancer factor/ T cell factor). Transcription is activated when nuclear β-CTN interacts with the aminoterminal end of LEF/TCF. P120^{CTN} (p120catenin) promotes cadherin clustering by binding to the juxtamembrane region of E-cadherin. Cytosolic p120^{CTN} is complexed (directly or indirectly) with RhoA (small GTPase). The interaction of p120^{CTN} with Kaiso, belonging to the Pox virus and zinc-finger (POZ/ZF) superfamily of transcription factors, is of yet unknown biological significance. *PM* plasma membrane, *N* and *C* respectively, amino- and carboxy-terminal residues. *Filled circles* indicate the position of Ca^{2+} ions at the cell surface proximal end of cadherin protomers. Tandemly repeated circles in β-CTN, p120^{CTN} and APC indicate arm domains in these molecules. Adapted from [4, 206, 209]

suppressor in lobular breast cancer were provided using immunohistochemistry. Lower E-cadherin expression correlated with higher grade and stage breast carcinomas [213]. E-cadherin expression was found in all (88) ductal breast carcinomas, only in 6 of 35 invasive lobular breast carcinomas and in zero of the 9 lobular breast carcinomas in situ [231], in line with the negative correlation between the lobular type of the breast tumour and E-cadherin expression [98, 196]. In lobular breast cancer, inactivating mutations in *CDH1* were associated with tu-

mour-specific loss of heterozygosity of 16q22.1 [29]. In this study, all cancers examined were invasive. Therefore, *CDH1* might have been inactivated either at the transition between the noninvasive to the invasive stage or earlier and was considered as a tumour/invasion-suppressor gene. The same truncating mutations associated with loss of heterozygosity were also found in sporadic lobular carcinoma in situ, in line with a tumour-suppressor function of *CDH1* [296]. In gastric cancer, absence of E-cadherin expression is correlated not only with higher grade, but also with histological type [20]. In four diffuse-type gastric carcinomas, the amplification product of E-cadherin cDNA was shorter than the expected 630 bp due to skipping of exon 9 or exon 8. E-cadherin mutations were found in 13 of 26 diffuse gastric carcinomas and in 1 of 7 mixed carcinomas. The 2 mutations found in 26 intestinal-type gastric carcinomas were silent [21]. Inactivating germline mutations were found in families suffering from a high incidence of diffuse gastric cancer. Interestingly, the mother of one of the gastric cancer patients suffered from metachronous lobular breast cancer and diffuse gastric cancer and had the same *CDH1* germline mutation [150].

The α-CATENIN gene *CTNNA1*: a differentiation gene?

The *CTNNA1* gene encoding α-catenin is localised on chromosome 5q3.1 [208]. In a family of human colon cancer cell lines HCT-8, loss of α-catenin causes the transition from an E (epithelioid) to an R (round) morphotype [289, 290]. Noteworthy, DNA fingerprinting suggests that the HCT-8, HRT-18, DLD-1 and HCT-15 cell lines probably originate from the same patient [290]. The HCT-8 family carries a heterozygous mutation in a *CTNNA1* gene and mutation or loss of the remaining wild-type allele causes loss of α-catenin and the above-mentioned E to R transition [291]. *CTNNA1* is, therefore, considered as a tumour-suppressor gene in accordance with Knudson's criteria [159]. A suppressor of what? In the chick heart invasion assay, α-catenin-positive E-type HCT-8 cells are not or are poorly invasive, in contrast with the α-catenin-negative R-type cells which are fully invasive. These experiments led to the conclusion that *CTNNA1* is an invasion-suppressor gene [289]. Differentiation constituted another striking difference between the two cell types, E-type cells forming an epithelioid structure around the heart tissue and R-type cells producing an unorganised mass inside the heart tissue. When confronted with collagen type-I gels, both types of cells fail to invade unless cancer-associated myofibroblasts are admixed to the collagen (our unpublished results). In the latter situation, both E- and R-type cells do invade, the former as epithelioid strands and the latter as loose files. It is, therefore, justified to consider *CTNNA1* as a differentiation gene, influencing invasion only in a quantitative way and, possibly, as a consequence of changes in differentiation. When injected orthotopically into the caecum wall of nude mice, genotypic differences in *CTNNA1* between E- and R-type cells were conserved, but phenotypic differences could not be seen any more; both produced moderately differentiated invasive adenocarcinomas that were indistinguishable from one another [287]. Re-expression of α-catenin in an E-cadherin-positive prostate cancer cell line PC-3 however suppressed tumourigenicity in nude mice [87].

New data suggest that α-catenin not only functions through maintenance of cell–cell adhesion but also through interference with β-catenin/Tcf/DNA complex formation and β-catenin signalling in the nucleus [104].

The β-CATENIN gene *CTNNB1*: an oncogene

β-Catenin was originally described as an element of the E-cadherin/catenin complex [218]. It is, however, as an element of the Wnt (wingless/int) signalling pathway that β-catenin may be tumourigenic [27, 239, 303]. In normal cells, β-catenin is associated not only with cadherins but also with the APC (adenomatous polyposis coli) multi-protein complex. Here, it is normally phosphorylated by the serine/threonine kinase GSK (glycogen synthase kinase)-3β and directed to the ubiquitine proteasome pathway for degradation (Fig. 2). Mutations in these phosphorylation sites (coded on exon 3 of the β-catenin gene) stabilise β-catenin and so lead to its accumulation in the nucleus in association with LEF/TCF (lymphocyte enhancer factor/T-cell factor; Fig. 3). In 39 oesophageal squamous cell carcinomas [73], 55 squamous cell carcinomas of the head and neck [110], 21 gastric carcinomas (16 diffuse- and 5 intestinal-type) and 11 breast carcinomas (9 lobular and 2 ductal) [50], β-catenin mutations could not be found. In a series of 58 colorectal tumours without APC mutation, there were no point mutations, but 7 tumours showed a deletion of 234–760 bp, each of which included all or part of exon 3 [143]. Nuclear accumulation of β-catenin may result also from mutations in the β-catenin binding site of APC [201]. Target genes of the β-catenin/TCF transactivator complex comprise, among others, the gene encoding for MMP-7 (matrix metalloproteinase-7; matrilysin) [64], *myc* [123], *cyclin D1* [174], *MDR1* (multi-drug resistance gene 1) [308], two components of the AP-1 transcription complex *jun* and *fra-1* [180], all of which are genes that are implicated in cancer development as they modulate growth, differentiation, invasion and response to therapy. In fibroblasts, a LEF/TCF binding site is described in the fibronectin promoter [111].

An overview of β-catenin mutations in human tumours is depicted by Nollet et al. [209]. Remarkably, such mutations are characteristic also of desmoid tumours, locally invasive outgrowths of mesenchymal cells that do not produce metastases [275]. There is not much evidence to interpret *CTNNB1* as an invasion-suppressor gene. In contrast with α-catenin, there are only few cell lines with inactivating mutations in the gene encoding for β-catenin. An in-frame deletion in the αE-cat-

| TUMOUR TYPE | MUTATION 17 | | |

Table 1 Levels of downregulation of the E-cadherin/catenin complex in cancer; selected examples

Level	Example	Reference
Genes		
Inactivating mutation	*CDH1* in lobular breast cancer	[30]
Hypermethylation	*CDH1* promoter in thyroid cancer	[85]
Transcriptional regulation		
Repression	*CDH1* by Snail, SIP1	[51, 60]
Loss of transactivators of *CDH1*	RB, Myc, WT1	[18, 132, 184]
Transactivation of other cadherins	N-cadherin	[121]
Proteins		
Phosphorylation	Of armadillo proteins by tyrosine kinases	[254, 260]
Sterical hindrance	Of extracellular part of E-cadherin by MUC-1	[126, 267, 293]
Proteolysis	Ectodomain shedding of E-cadherin by MMPs	[207]
Endocytosis		[35]

trast, transfection of K562 leukaemia cells with a construct encoding E-cadherin with a deletion of the juxtamembrane domain favoured cell–cell adhesion [217]. The most likely hypothesis is that $p120^{CTN}$, existing in an "active" form, induces cadherin clustering and cell–cell adhesion by binding to the juxtamembrane part of E-cadherin, and that intracellular signalling can induce an "inactive" form of $p120^{CTN}$. Although it has not yet been proven that activation of $p120^{CTN}$ is due to phosphorylation, tyrosine phosphorylation of $p120^{CTN}$ increases its affinity for the juxtamembrane domain of type-I cadherins and lowers its affinity for RhoA. Hypothetically, RhoA, uncoupled from 120^{CTN} subsequently could be activated by GEF (guanine nucleotide-exchange factor) and further downstream RhoA signalling would promote cadherin clustering and junction [5, 277]. The phosphorylation of $p120^{CTN}$ can also be modulated by binding to the protein tyrosine phosphatase (hematopoietic cell phosphatase) SHP-1 [148] or to PTPμ (protein tyrosine phosphatase μ) [314]. SHP-1 also inhibits phosphorylation of β-catenin and tumour formation in nude mice [200]. In the nucleus, $p120^{CTN}$ binds to the zinc finger transcription factor Kaiso [69, 285].

Reversible downregulation of E-cadherin

The E-cadherin/catenin complex can be structurally and functionally downregulated at various levels, and this phenomenon may well be reversible (Table 1). During embryonic development, E-cadherin is first expressed at the morula stage, hence its former name uvomoruline, at which it serves compaction [138, 164, 227]. Later during development it is expressed in a temporo-spatial manner with well-regulated and reversible modulation. Reversible expression of E-cadherin was also shown in an experimental tumour model with a MDCK (Madin-Darby Canine Kidney) cell line transformed by a mutated *ras* oncogene [183]. E-cadherin-positive MDCK-*ras* variants were noninvasive in vitro but produced invasive and metastatic cancers after injection into nude mice. Immunohistochemistry of the nude mouse tumours revealed loss of E-cadherin. Ex vivo culture of the MDCK tumours resulted in rapid re-expression of E-cadherin and loss of invasiveness. In E-cadherin-negative human breast cancers, E-cadherin is re-expressed in the metastases [46].

CDH1 gene silencing through hypermethylation

Inactivating mutations of E-cadherin, as described above, are limited to a few types of cancer, namely lobular breast cancer, diffuse gastric cancer and endometrial cancer.

Methylation is a common type of transcriptional modification in mammals. It normally occurs during genomic imprinting and X-chromosome inactivation. Highly methylated DNA is found in genetically silent regions of chromosomes, and hypermethylation of CpG islands in the promoter region of the genes leads to transcriptional silencing. This mechanism of downregulation occurs in several tumour-suppressor genes such as *APC*, *VHL*, *Rb* and *CDH1* [85]. Germline mutations in *CDH1* without loss of heterozygosity at the *CDH1* locus are suggestive for hypermethylation. Indeed, in hereditary diffuse gastric cancer, with a mutation in one *CDH1* allele, hypermethylation constitutes the second hit eliminating the expression of E-cadherin [112]. In a gastric cancer cell line, the expression of E-cadherin could be restored by treatment with the demethylating agent 5-azacytidine. In diffuse gastric cancer and also in oesophagus cancer, hypermethylation may occur as early as the intramucosal, i.e. noninvasive, stage, underscoring the tumour-suppressor function of E-cadherin [80, 271]. Caution is needed when interpreting hypermethylation in terms of tumour development, since this phenomenon may be a reflection rather than a cause of gene inactivation in cancer [89]. The expression of E-cadherin is not restricted to epithelial cells. In normal bone marrow, it is expressed on erythroid precursors, CD34+ stem cells and stromal cells, albeit at low level and with unknown function [63]. In leukaemic bone marrow and cell lines derived therefrom, hypermethylation is a frequent event [188] and is

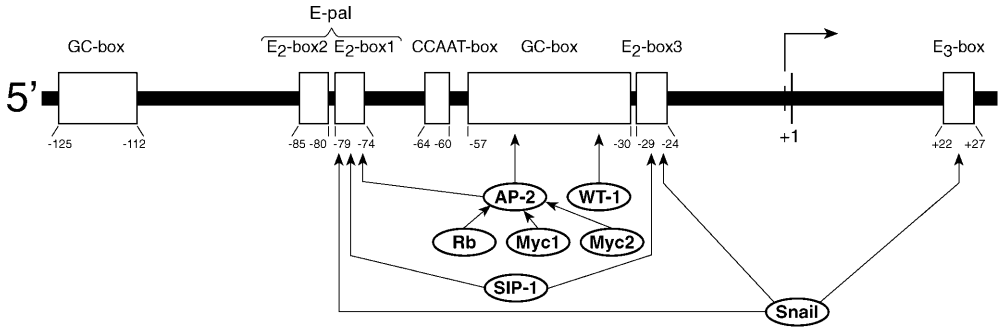


Fig. 4 Overview of the E-cadherin promoter. Basal expression is conferred by the CCAAT box (–64 to –60) and the GC-box (–57 to –30). The palindromic element E-pal consists of E2-box 2 (–85 to –80) and E2-box 1 (–79 to –74) and is responsible for the cell-type specificity of the promoter, acting positively in epithelial cells and negatively in undifferentiated cells. E2-box 1 (–79 to –74) and E2-box 3 (–29 to –24) regulate the promoter negatively. RB is a coactivator for binding of the AP-2 transcription factor to the GC-box (–57 to –29) and the E-pal element. Myc1 and Myc2 act as coactivators of AP-2 when expressed together, and as inhibitors of AP-2 when expressed alone. WT1 activates the E-cadherin promoter by binding to the GC-box. The binding sites of HNF-4 and Pax-2 in the E-cadherin promoter are yet unknown. SIP1 downregulates E-cadherin expression by binding to E2-box 1 (–79 to –74) and E2-box 3 (–29 to –24). The former two E2-boxes cooperate with an E3-box upstream of the transcription initiation site (+22 to +27) in Snail-mediated E-cadherin repression. Adapted from [16, 18, 60, 132, 209]

reversible after treatment with 5-azacytidine. Reactivation of tumour-suppressor genes using such a potent and specific inhibitor of DNA methylation would be an interesting adjuvant for cancer treatment [197].

Transcriptional regulation of E-cadherin

The E-cadherin promoter contains positive regulatory elements including a CCAAT box and a GC box as well as two E-boxes (CANNTG) to which a repressor role is ascribed [25, 107] (Fig. 4). Proteins acting directly or indirectly on the E-cadherin promoter include the tumour-suppressor RB (retinoblastoma), implicated in the control of the cell cycle and in epithelial differentiation [184]; the WT1 transcription factor encoded by the tumour-suppressor gene associated with Wilms' tumour of the kidney [132]; the hepatocyte nuclear factor 4 (HNF4), a morphogen in liver development [266]; Snail, a zinc-finger transcriptional repressor implicated in the transition from epithelium to mesenchyme (EMT) during embryonic development [51]; the transcription factor Pax-2 implicated in kidney development [279]; and the Smad-interacting multi-zinc-finger protein SIP1 [60]. The SV40 large T antigen, encoded by a viral oncogene, inactivates RB and, in MDCK cells, causes EMT associated with loss of epithelial markers, including E-cadherin, and with loss of expression of the oncogene *myc* [184]. The latter encodes two distinct Myc proteins, acting as transcription factor [17]. Transfection experiments with dog MDCK and human HaCat cells show that RB and Myc specifically activate transcription of the E-cadherin promoter and that this is mediated by the transcription factor AP-2 [18]. Transactivation of the E-cadherin promoter is strongly dependent on the ratio between the two Myc proteins and is cell-type specific [17]. This specificity is confirmed by the finding that inactivation of RB by HPV16E7 infection of primary human mammary epithelial explants in reconstituted extracellular matrix does not interfere with the correct expression of E-cadherin [264]. In such cultures, viral inactivation of RB causes loss of the differentiation markers lactoferrin and cytokeratin 19. These experiments illustrate the complexity of oncogenic pathways: a viral tumour promoter binds to and inactivates a cellular tumour suppressor that indirectly counteracts invasion in one type of cells and maintains differentiation in another type. The WT1 can directly transactivate *CDH1* through binding to the proximal GC-rich sequence in the promoter as evidenced by transfection of 3T3 fibroblasts [132]. In hepatocytes, the morphogenetic activity of HNF-4 is explained by the activation of *CDH1* [266], while, in the thyroid, E-cadherin mRNA levels increase upon stimulation by thyroid stimulating hormone (TSH) [37]. During the metanephrogenic mesenchyme to epithelium transition (MET), there is a loss of Pax-2 expression and a gain of E-cadherin and β-catenin expression [279]. Snail is a strong repressor that interacts specifically with E-boxes in the E-cadherin promoter and represses transcription of E-cadherin; in this way it causes EMT and invasion [16, 51]. Snail is expressed in fibroblasts, some E-cadherin deficient cell lines and in invasive regions of experimental carcinomas.

Transcriptional stimulation of other (e.g. N-) cadherins

The synchronic in- and decrease of respectively N- and E-cadherin expression in mesodermal cells during gastrulation, associated with loss of epithelial structure and gain of migratory characteristics [119], suggests a role for N-cadherin in invasion. Indeed, loss of E-cadherin expression in cancer cells may be associated with gain of N-cadherin expression, leading to a fibroblastic phenotype with increased motility and invasive potential in vitro and in vivo (Table 2). Increase of cadherin-11 expres-

Table 2 Expression of N-cadherin in human cancer cell lines and tumour biopsies; relationship with E-cadherin expression and invasive phenotype. The non-invasive or invasive phenotype of cancer cell lines was characterised by an epitheloid morphotype (*E*), dedifferentiated, fibroblastic, non-epithelial morphotype (*F*), by increased motility (*M*) or by increased invasion in vitro or in vivo (*I*). The invasive phenotype of tumour biopsies was characterised by histological grade. E-cadherin (*E-cad*) and N-cadherin (*N-cad*) were evaluated: + present, – absent, decrease/increase compared with normal tissue, *ND* not determined, *G* grade, *T* stage

Tumour type	Cell line or biopsy	E-cad/N-cad expression	Invasive phenotype	Reference
Squamous cell carcinoma of head and neck	UM-SCC-11B, SCC-9	–/+	F	[142, 171]
	UM-SCC-11A	+/+	F	
	Biopsy	–/+	ND	
Anaplastic thyroid carcinoma	HTh7, HTh74, C643, SW1736	–/+	F	[137]
Oesophageal squamous cell carcinoma	Biopsy	–/+	ND	[244]
Melanoma	SBcl2, WM35, WM98–1, WM115, WM793, WM1631A, WM1152C, WM239, WM852, WM1232, WM1617, WM3214, MeWo, A375	–/+	I	[133, 187, 245, 246, 298]
	1205Lu	+/+	ND	
	Biopsy	–/+	ND	
Breast carcinoma	BT549, HS578 t, HS578 N, MDA-MB-435, MDA-MB-436, SUM159PT	–/+	F, I, M	[84, 121, 204, 228, 241]
	MA-11	+/+	I	
	Biopsy	–/+	ND	
Prostate carcinoma	PC-3 N, TSU-pr1, PPC-1, JCA-1	–/+	F, I	[49, 278, 280]
	ALVA31	+/+	F	
	Biopsy	Decrease/increase	Gleason score ≥7. Lymph-node metastases	
Bladder carcinoma	253 J, 5637, J82, SW800, SW1710, T24, VMCub2, TCCSUP	–/+	F	[108, 191, 232]
	SW780, RT112	+/+	E	
	Biopsy	+/+	G2/T1, G2/T3	
		Decrease/increase	G3/T1, G3/T2	

sion, another mesenchymal cadherin, has also been associated with cancer cell invasion [49, 204, 228, 248, 255, 278]. Formation of the human placenta, where foetal cytotrophoblast cells invade the vasculature of the uterus, is marked by a switch from E- to VE-cadherin expression [312]. Immunohistochemical studies indicate that increased P-cadherin expression, together with maintenance or loss of E-cadherin expression, may be associated, on the one hand, with growth disturbance during early stages of tumour development in the gastrointestinal tract [118, 144, 258], oral epithelium [306] and breast [220] and, on the other hand, with invasiveness in tumours of the cervix [117], gastrointestinal tract [11] and breast [220, 224].

Most epithelial cancer cell lines that express N-cadherin have lost E-cadherin (Table 2). Some do, however, express both E- and N-cadherin. The latter cell types have a tendency towards invasiveness and this is confirmed by transfection experiments. A weakly metastatic E-cadherin expressing breast cancer cell line, MCF-7, yielded, upon successful transfection with N-cadherin, cells that co-expressed E- and N-cadherin and that were highly metastatic [122]. E-cadherin transfection in N-cadherin-expressing breast cancer cells did not revert their invasive phenotype [263]. How the invasion-promoter function of N-cadherin dominates the invasion-suppressor function of E-cadherin is an open question.

N-cadherin expression may also reflect the origin of certain tumours. Examples are pleural mesotheliomas, glioblastoma, renal cell carcinoma, ovarian tumours and astrocytoma [116, 222, 223, 256, 259, 274, 307]. A decrease in N-cadherin expression was related to aggressiveness in some of these tumours [8, 70].

Repressors of E-cadherin may also transactivate the gene encoding for N-cadherin. Snail not only represses genes, such a E-cadherin, but might also transactivate other genes, such as the gene encoding N-cadherin, required for the acquisition of the fibroblastic phenotype [16, 51]. E- and N-cadherin expression are inversely regulated in squamous carcinoma cells. When N-cadherin was transfected, E-cadherin expression decreased; when N-cadherin expression was decreased by introduction of an antisense construct, E-cadherin expression increased [142]. Decreased N-cadherin expression upon transfection with L-CAM, the chicken homologue of E-cadherin, was not due to decreased N-cadherin mRNA synthesis but of N-cadherin protein instability [171]. Progesterone regulates inversely the expression of cadherin-6 and cad-

herin-11 in endometrial stromal cells, supporting the hypothesis that steroids can be considered as key regulators of cadherin expression [103]. Increased N-cadherin expression by gonadal steroids has been observed in the adult hippocampus [198]. In postmenopausal women, oestrogen deficiency leads to excessive production of tumour necrosis factor-α (TNF-α) and interleukin-1 (IL-1), cytokines that downregulate N-cadherin expression in osteoblasts, facilitating the direct adhesion of osteoclasts on the calcified bone matrix surface and thus osteoporosis [282]. Overexpression of Wnt-1 is associated with increased N-cadherin expression in AtT20 cells [127] and increased E-cadherin expression in PC12 cells [42]. Inverse regulation of E-cadherin and cadherin-6 expression, in response to the expression of β-catenin mutants, which activate the Wnt-1/Wg signalling pathway, has been observed in MDCK cells [268]. Transforming growth factor-β1 (TGF-β1) causes a RhoA-dependent EMT of mouse mammary cells, and this phenotypic transition is accompanied by a decrease in E-cadherin expression and an increase in N-cadherin expression [31, 156]. In chicken epiblast cells in vitro, the switch from E- to N-cadherin expression was induced by plasminogen-related growth factor-1 (PRGF-1, formerly called scatter factor/hepatocyte growth factor [61]) [76]. To understand further the molecular cross talk between host cells and cancer cells, it would be of interest to know whether or not host cells can cause the switch from E- to N-cadherin expression in cancer cells. Many cancer cells of different origin express the PRGF-1 receptor c-Met, and tumour-associated (myo)fibroblasts are a source of PRGF-1. N-cadherin expressing cancer cells become spindle shaped and more motile, invade into the extracellular matrix and adhere dynamically to other N-cadherin expressing cells, such as myofibroblasts [121, 280, 286], and endothelial cells [243]. Such interactions might shield the cancer cells from the immune response [173], create gap-junction communication [134], or assist intravazation [246].

The extracellular and the juxtamembrane domains of N-cadherin are implicated in signalling. The histidine–alanine–valine (HAV) binding sequence in the fourth extracellular domain may interact in *cis* with the HAV sequence in the fibroblast growth factor receptor (FGFR), activating a signalling pathway that leads to neurite outgrowth (reviewed in [79]). From the activated FGFR, multiple signalling pathways may start, leading either to an increase in motility via activation of diacylglycerol lipase [204] or to an increase in MMP-9 production via activation of the MAPK pathway [122]. These cellular responses are potentiated by FGF2 [122]. The role of FGFR in N-cadherin-dependent cell motility and invasion is still uncertain. Crystallographic studies revealed that the histidine and valine side chains of the HAV sequence in FGFR1 are involved in intradomain contacts and are, therefore, not available for interaction with other molecules [229]. In contrast, the side chains of the amino acids in the HAV sequence in cadherins are all solvent exposed and free for homophilic interaction [253]. From observations with chimeric molecules, comprising selected domains of E- and N-cadherin, Kim et al. [152] concluded that the HAV-binding region of the fourth extracellular domain of N-cadherin was necessary and sufficient to promote both EMT and increased cell motility. The juxtamembrane domain of N-cadherin regulates neurite outgrowth [233] and the selective exclusion of N-cadherin from cell–cell contacts by VE-cadherin in endothelial cells [202]. $P120^{ctn}$ [277] and the nonreceptor tyrosine kinase Fer [238] are potential regulatory molecules associated either directly or indirectly with the juxtamembrane domain of cadherins. Immunohistochemical analysis of cadherin expression in prostate tumours demonstrated E- and N-cadherin expression in the same cells. N-cadherin showed a dotted pattern and seemed to be excluded from the cell–cell contacts by E-cadherin [278]. In some tumours the isoform of $p120^{ctn}$ varied with the type of cadherin at the cell–cell contacts [108, 137, 280]. $P120^{ctn}$ may influence the activity of Rho family GTPases, thereby influencing motility and invasion [5, 211]. The increase of N-cadherin expression and/or the shift in $p120^{ctn}$ isoform expression can disrupt the delicate balance between cadherins, $p120^{ctn}$ and Rho family GTPases, leading to a change in morphology and increased motility and invasion. Trojan peptides, designed to interfere with the juxtamembrane domain of N-cadherin, release Fer kinase from N-cadherin. This is accompanied with an accumulation of Fer kinase in the integrin complex and results in inhibition of neurite outgrowth [7]. Whether Fer kinase plays a role in N-cadherin-mediated invasion is presently unknown. A better understanding of the downstream signalling pathways is needed to elucidate the mechanisms by which N-cadherin stimulates invasion in tumour and embryonic development. From a therapeutic point of view, it is interesting to note that N-cadherin may have been involved in thalidomide teratogenicity. Thalidomide may disturb cellular recognition and migration by binding to the N-terminal domain of N-cadherin and so mimic a tryptophan residue critical for the homodimerization of N-cadherin [276]. Small cyclic peptide antagonists that inhibit N-cadherin functions offer another therapeutic possibility [305].

Posttranslational modification of the E-cadherin/catenin complex

The structure and function of the E-cadherin/catenin complex is sensitive also to posttranslational modification. Catenins with Armadillo repeats, namely β-catenin, plakoglobin and $p120^{CTN}$, are good substrates for tyrosine kinases [68]. Tyrosine phosphorylation of β-catenin by nonreceptor kinases, such as Src [26], and receptor kinases such as epidermal growth factor receptor (EGFR) [260], c-Met [254] and possibly others (Fig. 2), perturbs the E-cadherin/catenin complex. Suggested mechanisms include alterations of the binding of the complex to actin which is necessary for the organisation

Table 3 The effect of stimulators and inhibitors on E-cadherin/catenin complexes. *AMF* autocrine motility factor, *EGF* epidermal growth factor, *EMT* epithelium to mesenchyme transition, *IGF-I* insulin-like growth factor-I, *Il-12* interleukin-12, *ND* effect is not determined, *PHF* precultured chick heart fragment, *PRGF-1* plasminogen-related growth factor-1, *PTH* parathyroid hormone, *sE-CAD* soluble E-cadherin fragments, *TFF3* intestinal trefoil factor, *TGF-β* transforming growth factor-β, *TNF-α* tumour necrosis factor-α, *TSH* thyroid stimulating hormone, *Wnt-1* protooncogene-encoded protein homologous to the product of the Drosophila gene wingless

Agent		Effect		Reference
Family	Name	Functional	Structural	
Cytokines	EGF	Loss of adhesion Gain of chemotaxis (uncoated) Gain of invasion (collagen type I)	β-Catenin tyrosine phosphorylation	[260]
	IGF-I	Gain of migration (wound healing)	β-Catenin tyrosine phosphorylation	[6]
		Gain of adhesion Inhibition of invasion	Exocytosis of E-cadherin	[35]
	PRGF-1	Loss of adhesion	β-Catenin tyrosine phosphorylation	[254]
	TNF-α	Loss of adhesion	Dotted pattern of E-cadherin	[269]
	AMF	Gain of motility	Loss of E-cadherin expression	[141]
	Il-12	Loss of chemotaxis (Matrigel)	Gain of E-cadherin expression	[129]
	Wnt-1	Gain of adhesion	Gain of E-cadherin expression	[42]
	TFF3	Loss of adhesion	β-Catenin tyrosine phosphorylation	[175]
Ectodomains	sE-CAD	Loss of adhesion	ND	[301]
		Loss of adhesion Gain of invasion (collagen type I)		[207]
Hormones	TSH	ND	Transactivation of *CDH1*	[37]
	PTH	ND	Endocytosis of E-cadherin	[10]
	Relaxin	ND	Gain of E-cadherin expression	[14]
	Insulin	Gain of adhesion; loss of invasion (PHF)	ND	[38]
	17-β estradiol	ND	Gain of E-cadherin expression	[178]
	Dihydrotestosteron	ND	Gain of E-cadherin expression	[53]
Irradiation		Loss of chemotaxis (Matrigel)	Gain of E-cadherin expression	[1]
Pharmacological agents	Adriamycin	Gain of adhesion	Transactivation of *CDH1*	[310]
	Docetaxel	ND	Gain of E-cadherin expression	[81]
	Tamoxifen	Gain of adhesion; inhibition of invasion (PHF)	ND	[40]
	Carbachol	Gain of adhesion	ND	[304]
	Tangeretin	Gain of adhesion; inhibition of invasion (PHF)	ND	[39]
Proteases	Stromelysin-1	Gain of invasion (Matrigel/nude mice)	Loss of E-cadherin expression	[177]
	Matrilysin	Loss of adhesion; gain of invasion (collagen type I)	Ectodomain shedding of E-cadherin	[207]

of the adherens junctions; disturbance of the signalling function of the complex through conformational changes by an increase in negative charge that hamper the cross talk with other proteins; recruitment of new partner proteins that possess phosphotyrosine-specific binding domains.

For some molecules, such as c-ErbB-2, different mechanisms for modulating the E-cadherin/catenin complex are described: tyrosine phosphorylation of β-catenin [255] and repression of *CDH1* [65]. The β-catenin binding site of E-cadherin shows PEST (Pro-Glu-Ser-Thr) sequences, candidates for degradation by the ubiquitine/proteasome pathway. Binding of β-catenin prevents the cytoplasmic tail of E-cadherin from degradation [135].

The expression of large proteoglycans such as episialin, also called MUC-1, may sterically hinder the homophilic interactions of E-cadherin and so contribute to invasion of cancer cells [126, 267, 293]. The argument to accept that sterical hindrance is the mechanism of action is the restoration of E-cadherin-dependent functions, such as cellular aggregation, by antibodies that cause capping of MUC-1 [299]. Direct or indirect association of the small cytoplasmic part of MUC-1 with β-catenin suggest other mechanisms as well [309].

Proteolysis of the extracellular part of E-cadherin results in the release of a stable 80-kDa fragment into the medium and a 40-kDa fragment that remains associated with the plasma membrane [207]. Proteases able to perform such cleavage include stromelysin-1, matrilysin and plasmin (our unpublished results). Interestingly, the 80-kDa fragment, coined sE-cad (s, for soluble), inhibits the function of the E-cadherin/catenin complex in a paracrine manner, inducing invasion into collagen type I of cells that do express an intact complex. How the sE-cad signal is received by the cell, how the signal is transduced and how the cell responds to become invasive is not known.

Endocytosis is another way to lose expression of the E-cadherin/catenin complex [35]. Treatment of human mammary cancer cells of the MCF-7 family with conditioned medium of the human skin cancer cell line COLO 16 caused EMT and loss of aggregation, and this was associated with the translocation of the elements of the complex into the cytoplasm as evidenced by confocal laser scanning and by Western blotting after biotinylation [35]. Insulin-like growth factor-1 counteracts the effect of the conditioned medium, but the factor responsible for loss of expression of the E-cadherin/catenin complex remains unknown.

The effect of host factors on E-cadherin/catenin complexes

MET and EMT are not only mediated by, respectively, up- and downregulation of E-cadherin, but are even enhanced by host factors. Embryonic corneal fibroblasts express cytokeratin and vimentin and are connected to each other by zonulae adherentes and desmosomes upon transfection with E-cadherin. Seeded on collagen, the transfected fibroblasts lose vimentin and gain basement membrane-like material and, thus, even enhance their epithelial phenotype [120]. The purpose of Table 3 is to summarise host factors that may stimulate or inhibit invasion of cells by (in)direct action on the E-cadherin/catenin complex. The inhibitors and stimulators of E-cadherin/catenin complexes are numerous and of various nature. Their functional effect is evaluated by a gain or loss of chemotaxis (in the Boyden chamber with uncoated or Matrigel-coated filter), adhesion (by aggregation assays), and invasion (into collagen type I or precultured chick heart fragment). Soluble E-cadherin fragments (sE-cad), released from the cancer cell surface by tumour proteases, inhibit E-cadherin function probably by signal transduction pathways in the cancer cell. Cancer cells can also switch E-cadherin expression to N- or VE-cadherin expression [121, 312]. As a result, homophilic heterotypic cadherin interactions between the cancer cells and N-cadherin expressing fibroblasts or VE-cadherin expressing endothelial cells are established and would facilitate invasion of cancer cells into the surrounding stroma.

Trefoil peptides are produced in the mammalian gastrointestinal tract by mucus-secreting cells and are expressed at abnormal levels in gastrointestinal tumours [82]. Recently, some molecular aspects of the role of trefoil peptides in tumour development have been unravelled. Transfection of pS2 (spasmolytic peptide) results in invasion of MDCK cells and HCT-8/E11 cells in collagen type I and is dependent on PI3-kinase, phospholipase C and protein kinase C [82].

In epidermal cells in culture, exogenous okadaic acid hyperphosphorylates β-catenin on serine and threonine residues [251]. Okadaic acid treated epidermal cells also show a translocation of E-cadherin from the plasmamembrane to the cytoplasm, associated with a decrease in its CK2 (casein kinase 2) mediated serin/threonin phosphorylation and a decrease in aggregation of the cells in vitro [252].

E-cadherin/catenin expression in human cancers

Publication of the experimental evidence in favour of the invasion-suppressor function of E-cadherin was rapidly followed by a growing number of reports concerning the aberrant expression in human cancers of E-cadherin and later also of the catenins. One of the aims of such investigations is the improvement of staging and grading and, as a consequence, refinement of prognosis and selection of subgroups of patients with more malignant tumours that may profit from more aggressive forms of treatment. Staging is routinely based on the volume of the primary tumour and on its depth of invasion, grading in accordance with proliferative activity and loss of differentiation [262]. Methods to evaluate, qualitatively or quantitatively, protein expression in biopsies from human tumours have serious limitations because of sampling from heterogeneous tissue, non-stoichiometric labelling and subjective evaluation. Computerised image analysis and tissue micro-arrays might solve some of the problems, but these methods have not been largely applied to cadherin/catenin analysis [128, 131]. We, therefore, favour a rather rough categorisation with a high reproducibility and a low degree of interobserver variation. Such categorisation, based on a comparison with the normal tissue from which the cancer cells derive, is presented in Table 4. Examples were chosen from recent publications mentioning numerical data (for earlier examples, see [41]). Immunohistochemical staining intensity is the appreciation of the intensity of the signal independent of cellular localisation or tissue distribution. Tissue distribution is categorised in eu-expression (the number of cancer cells, positive for an element, is equal to the number of cells of normal tissue, positive for that element) and underexpression (the number of cancer cells, positive for an element, is less than the number of cells of normal tissue), both independent of staining intensity. Immunohistochemistry was only infrequently combined with densitometric measurement of the signal for E-cadherin and the catenins on Western blot or Northern blot [205, 311]. One has to bear in mind that these methods can give accurate numerical information about the down-

Table 4 Selected examples of the methods used for the immunohistochemical evaluation of cadherin/catenin complexes in human cancers. For technical details and interpretations, see references

Feature	Category	Element	Tumour type	Frequency*	Reference
Staining intensity	Similar to normal	E-cadherin	Oesophageal squamous cell carcinoma	9/39 (23%)	[73]
			Ductal breast carcinoma	33/33 (100%)	[168]
			Cervical adenocarcinoma	2/10 (20%)	[52]
			Wilms' tumour	6/30 (20%)	[248]
			Renal cell carcinoma	13/43 (30%)	[257]
		α-Catenin	Cervical adenocarcinoma	1/10 (10%)	[52]
	Decreased to normal	E-cadherin	Oesophageal squamous cell carcinoma	30/39 (77%)	[73]
			Cervical adenocarcinoma	2/10 (20%)	[52]
			Wilms' tumour	17/30 (57%)	[248]
		α-Catenin	Cervical adenocarcinoma	1/10 (10%)	[52]
Cellular localisation	Lateral plasma membrane	E-cadherin	Ductal breast carcinoma	33/33 (100%)	[168]
			Wilms' tumour	15/30 (50%)	[248]
		β-Catenin	Oesophageal squamous cell carcinoma	32/39 (82%)	[73]
				15/22 (68%)	[205]
			Basal cell carcinoma	195/195 (100%)	[34]
	Apical plasma membrane	E-cadherin	Wilms' tumour	6/30 (20%)	[248]
	Cytoplasm	E-cadherin	Wilms' tumour	2/30 (7%)	[248]
		β-Catenin	Oesophageal squamous cell carcinoma	7/22 (32%)	[205]
	Nucleus	β-Catenin	Oesophageal squamous cell carcinoma	7/39 (18%)	[73]
Tissue distribution	Eu-expression	E-cadherin	Tongue carcinoma	13/85 (15%)	[59]
			Colorectal carcinoma	22/105 (21%)	[139]
			Synovial sarcoma	7/57 (12%)	[242]
			Breast carcinoma	35/90 (39%)	[45]
				81/168 (48%)	[125]
			Cervical adenocarcinoma	0/10 (0%)	[52]
			Prostate adenocarcinoma	2/7 (29%)	[297]
		α-Catenin	Tongue carcinoma	5/85 (6%)	[59]
			Synovial sarcoma	3/57 (5%)	[242]
			Breast carcinoma	14/90 (16%)	[45]
			Cervical adenocarcinoma	0/10 (0%)	[52]
			Prostate adenocarcinoma	3/7 (43%)	[297]
		β-Catenin	Tongue carcinoma	9/85 (11%)	[59]
			Synovial sarcoma	5/57 (9%)	[242]
			Breast carcinoma	23/90 (26%)	[45]
			Prostate adenocarcinoma	5/7 (71%)	[297]
		Plakoglobin	Tongue carcinoma	14/85 (16%)	[59]
			Synovial sarcoma	1/57 (2%)	[242]
			Breast carcinoma	30/90 (33%)	[45]
	Underexpression	E-cadherin	Tongue carcinoma	72/85 (85%)	[59]
			Colorectal carcinoma	83/105 (79%)	[139]
			Synovial sarcoma	50/57 (88%)	[242]
			Breast carcinoma	55/90 (61%)	[45]
				87/168 (52%)	[125]
			Cervical adenocarcinoma	4/10 (40%)	[52]
			Endometrial adenocarcinoma	24/33 (73%)	[165]
			Prostate adenocarcinoma	4/7 (57%)	[297]
		α-Catenin	Tongue carcinoma	80/85 (95%)	[59]
			Synovial sarcoma	54/57 (95%)	[242]
			Breast carcinoma	76/90 (84%)	[45]
			Cervical adenocarcinoma	2/10 (20%)	[52]
			Prostate adenocarcinoma	4/7 (57%)	[297]
		β-Catenin	Tongue carcinoma	76/85 (89%)	[59]
			Synovial sarcoma	52/57 (91%)	[242]
			Breast carcinoma	67/90 (74%)	[45]
			Prostate adenocarcinoma	2/7 (29%)	[297]
		Plakoglobin	Tongue carcinoma	71/85 (84%)	[59]
			Synovial sarcoma	56/57 (98%)	[242]
			Breast carcinoma	60/90 (67%)	[45]
	Absent	E-cadherin	Lobular breast carcinoma	15/15 (100%)	[168]
			Cervical adenocarcinoma	6/10 (60%)	[52]
			Endometrial adenocarcinoma	9/33 (27%)	[165]
			Prostate adenocarcinoma	1/7 (14%)	[297]
			Wilms' tumour	7/30 (23%)	[248]
			Renal cell carcinoma	30/43 (70%)	[257]
		α-Catenin	Cervical adenocarcinoma	8/10 (80%)	[52]

*n/n or %, number of tumours belonging to the category over total number of specified tumour type examined

regulation of the E-cadherin/catenin complex, but that these accurate values come from inaccurate sampling: as tumours are far from homogeneous, it is difficult to localise areas representative for the whole tumour. Comparing the numerical values between different studies is also difficult because of the variance in definition of eu- and underexpression which is in turn dependent of the authors' view of the number of positive cells in normal tissue. One would expect that the higher the number of positive cells needed for defining eu-expression, the fewer tumours will fulfil this criteria, but Heimann et al. showed E-cadherin eu-expression in 81 of 168 (48%) breast carcinomas [125] (criteria of 75%: 75% of all cancer cells must show positive E-cadherin staining for defining E-cadherin eu-expression) compared with 35 of 90 (39%) breast carcinomas by Bukholm et al. [45] (criteria of 50%: 50% of all cancer cells must show positive E-cadherin staining for defining E-cadherin eu-expression). The inclusion criteria in both studies are, however, completely different: the breast specimens in the study of Bukholm comprise grade 2 and grade 3 tumours, with or without lymph-node metastases. Heimann's group only included breast tumours without lymph-node metastases. A striking difference is also seen between Lehr's study [168], examining E-cadherin expression in lobular breast carcinoma and Berx' study [30]. E-cadherin was expressed only in ductal breast carcinomas (33 of 33) and in none of the 15 lobular breast carcinomas, from which the authors assign a diagnostic role to E-cadherin. Berx et al. [30], however, showed clear membranous expression of E-cadherin in 5 of 31 (16%) lobular breast carcinomas. In neither of these studies was the stage or grade of the breast carcinomas defined.

As a rule, the less a carcinoma is differentiated, the less E-cadherin is expressed in the tissue. This holds true for example for bladder carcinoma [230], pancreas carcinoma [145] and also for hepatocellular carcinoma [83], which shows a concomitant decrease of α-catenin, β-catenin and plakoglobin. In an early example from our group, frozen sections from colorectal cancers selected for differences in grade were immunostained with an antibody against E-cadherin [284]. Well-differentiated cancers, such as colon polyps and normal colon mucosa, show a honeycomb pattern of staining; moderately differentiated cancers show heterogeneity with areas of irregularly stained structures and interruptions in the honeycomb pattern; in poorly differentiated tumours, many E-cadherin-negative cancer cells are found in the stroma. The important question is, however, whether or not the pattern of E-cadherin staining has any additional prognostic value? A review of the literature reveals a strong positive correlation between disturbance of E-cadherin and poor prognosis for a variety of tumours (Fig. 5). Moreover, in some cancers matched for grade and stage, E-cadherin had significant independent prognostic value [230]. Attempts to correlate the presence of E-cadherin fragments in the serum with disease met with variable success [146, 157].

Not all these studies meet the stringent criteria put forward by Peto et al. [226]. In a study of 108 breast

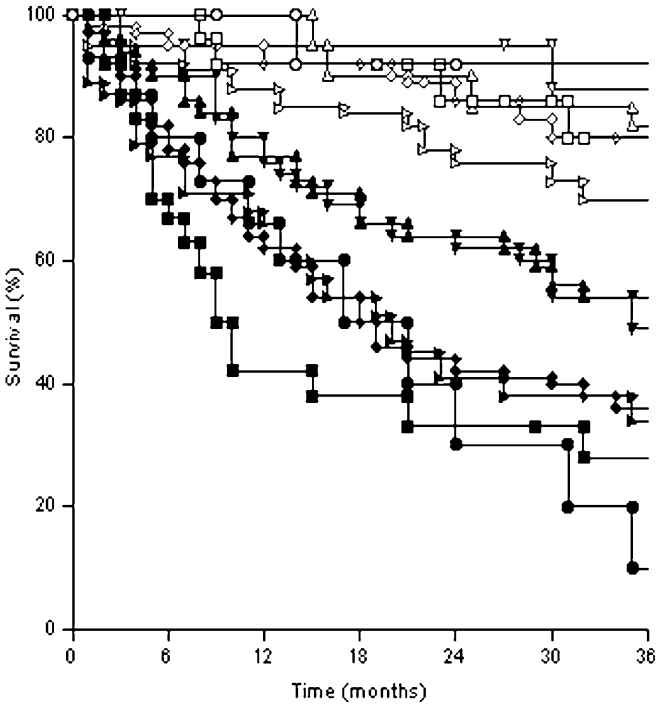


Fig. 5 Compilation of selected Kaplan-Meyer survival curves of patients bearing tumours of the prostate (*circles*; *n*=47; [106]), urinary bladder (*squares*; *n*=111; [44] and confirmed by [230]), stomach (*diamonds*; *n*=92; [311]), colon (*upward pointing triangles*; *n*=105; [139]), liver (*right-handed triangles*; *n*=107; [83]) and synovial membrane (*downward pointing triangles*; *n*=72; [242]) that had either a normal (*open symbols*) or an abnormal (*closed symbols*) E-cadherin expression. Methods used here for the evaluation of E-cadherin were immunohistochemistry, Western blotting and reverse-transcription polymerase chain reaction

cancers, a trend for lower disease-free survival was found in case of absence of E-cadherin, but significance was not reached [9]. For some tumours, e.g. of the oesophagus, the relationship between E-cadherin expression and prognosis remains controversial [283]; interestingly, in the latter study radiochemotherapy enhanced the expression of E-cadherin (Table 3). Combinations with other criteria may enhance the prognostic value of E-cadherin. Gastric cancers expressing S100A4, a member of the S100 family of calcium-binding proteins implicated in cell motility, together with reduced E-cadherin had a worse prognosis than their S100A4 negative counterparts [311]. Other examples are bladder cancers with reduced E-cadherin and expression of gp78, the receptor for AMF (autocrine motility factor) a tumour-derived motility factor [215]; E-cadherin-deficient breast cancers with high microvessel density and low Nm-23H1, a metastasis-suppressor [125]. E-cadherin also has a diagnostic application in gastric cancer where there is a correlation between the mutation in *CDH1* and the subtype of gastric cancer. Mutations in *CDH1* are not yet described for the intestinal type of gastric cancer but they predispose for diffuse-type gastric cancer. Here, E-cadherin mutation screening can identify high-risk persons with subsequent clinical surveillance [22]. The relationship

between E-cadherin expression and tumour stage has been studied so far only in cutaneous melanoma [67, 203].

For the catenins fewer data are available. Translocation of β-catenin from the lateral membrane to the cytoplasm is described for less differentiated oral squamous carcinoma [176] and is correlated with staging in cutaneous melanoma [245]. Nuclear expression of β-catenin significantly correlates with poor prognosis in synovial sarcoma [242]. Simultaneous loss of E-cadherin and β-catenin immunoreactivity in bladder carcinoma is associated with poor survival [99]. Clinical data show an inverse relationship between the presence of the α-catenin protein and the depth of invasion [109] or correlate a high α-catenin expression to a better survival in patients with colorectal cancer [237]. Loss of p120 catenin as well as overexpression has been linked to tumour aggressiveness, which might be partially explained by the multiple isoforms of p120 catenin [4].

Cadherins are by no means the only cell surface molecules that have been correlated with tumour staging and patient survival. Other examples are described for colon carcinoma. There is evidence of a correlation between staging of colon carcinoma and lost expression of α6, β1 and β4 integrins or more intense expression of the intercellular adhesion molecule-1 (ICAM-1) and the proteoglycan receptor CD44. Levels of the sLe^x lectin, HER-2/neu, vascular endothelial growth factor (VEGF) and urokinase-type plasminogen activator (uPA) and its receptor (uPAR) and its inhibitor (PAI-1) are inversely correlated with survival in colon cancer [114].

Cadherins/catenins in the thyroid

The thyroid is of endodermal origin and, although no data are available concerning cadherin expression in the foetal thyroid, in the adult thyroid follicles cadherin expression profile reflects this embryonic origin, with E-cadherin as the sole member of this family being expressed [55, 250, 261]. Immunohistochemical staining patterns of α-, β-catenin and plakoglobin are similar to those of E-cadherin.

The thyroid shows a spectrum of benign and malignant lesions; the first group includes multinodular goitres, diffuse toxic goitres and follicular thyroid adenomas (FTA), while the second comprises differentiated carcinomas such as papillary thyroid carcinomas (PTC), follicular thyroid carcinomas (FTC) and poorly differentiated carcinomas (PDC) and undifferentiated carcinomas (anaplastic carcinomas). Although the histological grade is a most useful prognostic marker [2], further research is needed to understand the behaviour of these various types of thyroid cancers. PTC frequently produces metastases in the regional lymph nodes, regardless of the size of the primary cancer, whereas distant metastases are rare [261]. FTC rarely forms lymph-node metastases but locally invasive types do metastasise to lungs and bone. Undifferentiated carcinomas, typically composed of varying proportions of spindle-shaped, polygonal and giant cells, are extremely malignant with a 10-year survival rate of 14% [136].

Changes in the E-cadherin/catenin complex observed in thyroid lesions are summarised in Table 5. In thyroid cancer, like in many other cancers, E-cadherin is reduced in poorly differentiated lesions and lost in undifferentiated tumours. Differentiated tumours present a very heterogeneous expression pattern of E-cadherin, both at the protein and mRNA level. There have been, however, reports that in this group of tumours loss of E-cadherin is associated with loss of differentiation. This feature can be further observed in the undifferentiated carcinomas where expression becomes highly heterogeneous and strongly reduced. Anaplastic carcinomas represent the final stage of the dedifferentiation process of the thyroid neoplastic transformation and, as a rule, they show lack of E-cadherin and the catenins expression. These patterns of expression in the various lesions are compatible with the concept that, also in the thyroid, E-cadherin counteracts invasion and maintains differentiation. Indeed, in cultured thyrocytes, Northern blotting shows a positive correlation between the expression of E-cadherin and that of the thyrotropin receptor, another marker of differentiation [36]. Moreover, during neoplastic transformation by a *ras* oncogene, loss of growth control occurred without disturbance of the differentiation markers including E-cadherin [105].

β-Catenin membrane staining is discontinuous in PDCs with clear-cut immunopositivity in the cytoplasm; the better-differentiated areas in these carcinomas maintained the honeycomb-staining pattern (Table 5). *CTNNB1* mutations at the Ser/Thr phosphorylation sites on exon 3, which were implicated in ubiquitination and degradation of β-catenin, were to some extent positively correlated with nuclear localisation of β-catenin, in anaplastic carcinoma [100]. These observations are in line with the role of *CTNNB1* as an oncogene. Nuclear positivity in the anaplastic but not in differentiated parts of the same cancers indicates that the exon-3 mutation is a late event and that nuclear localisation of β-catenin favours aggressiveness, possibly through transactivation of oncogenes. Garcia-Rostan et al. [101] even showed that low membrane β-catenin expression as well as its nuclear localisation or *CTNNB1* exon 3 mutations are associated with poor prognosis, independent of conventional prognostic indicators of thyroid cancer. More studies are needed to understand the expression of β-catenin and plakoglobin for which controversial data appeared [236]. The same holds true for the prognostic value of loss of E-cadherin expression in differentiated cancers [39, 261, 295]. Note that TSH increased E-cadherin mRNA levels in cultures of dedifferentiated dog and human thyrocytes via cAMP-dependent pathways and restored differentiation [37].

As to the molecular basis of aberrant E-cadherin expression, only one missense *CDH1* mutation is found in 1 of 27 PTCs. This particular tumour was, however, E-cadherin positive in both the primary and the metastasis

Table 5 E-cadherin/catenin complexes in tumours of the thyroid

Lesion	Feature	Category	Element	Frequency*	Reference
Follicular adenoma	Cellular localisation	Plasma membrane	E-cadherin	5/5, 2/2	[36, 261]
		Cytoplasm	E-cadherin	1/5, 1/2	[36, 261]
	Tissue distribution	Eu-expression	E-cadherin	4/5	[36]
		Underexpression	E-cadherin	1/5, 2/2	[36, 261]
Follicular thyroid carcinoma	Cellular localisation	Plasma membrane	E-cadherin	8/8	[261]
		Cytoplasm	E-cadherin	4/8	[261]
	Tissue distribution	Eu-expression	E-cadherin	0/6, 3/7, 5/8, 4/24	[36, 55, 261, 295]
			α-Catenin	16/33	[33]
			β-Catenin	18/33, 4/7	[33, 55]
			Plakoglobin	8/33, 0/7	[33, 55]
		Underexpression	E-cadherin	6/6, 4/7, 3/8, 20/24	[36, 55, 261, 295]
			α-Catenin	17/33	[33]
			β-Catenin	15/33, 3/7	[33, 55]
			Plakoglobin	25/33	[33]
Papillary thyroid carcinoma	Cellular localisation	Plasma membrane	Plakoglobin	7/7	[55]
		Cytoplasm	E-cadherin	17/17	[261]
	Tissue distribution	Eu-expression	E-cadherin	1/16, 5/15, 2/17, 23/88	[36, 55, 261, 295]
			α-Catenin	124/173	[33]
			β-Catenin	137/173, 12/15	[33, 55]
			Plakoglobin	94/173, 2/15	[33, 55]
		Underexpression	E-cadherin	15/16, 10/15, 15/17, 65/88	[36, 55, 261, 295]
			α-Catenin	49/173	[33]
			β-Catenin	36/173, 3/15	[33, 55]
			Plakoglobin	79/173, 13/15	[33, 55]
Poorly differentiated thyroid carcinoma	Cellular localisation	Plasma membrane	E-cadherin	2/3, 0/3	[55, 261]
			β-Catenin	3/3	[55]
		Cytoplasm	E-cadherin	3/3	[261]
			β-Catenin	0/3	[55]
		Nucleus	β-Catenin	1/3, 6/28	[55, 101]
	Tissue distribution	Eu-expression	E-cadherin	0/3, 0/3	[55, 261]
			β-Catenin	1/3	[55]
			Plakoglobin	0/3	[55]
		Underexpression	E-cadherin	3/3, 3/3	[55, 261]
			β-Catenin	0/3	[55]
			Plakoglobin	3/3	[55]
Anaplastic thyroid carcinoma	Cellular localisation	Nucleus	β-Catenin	14/29	[101]
	Tissue distribution	Absence of expression	E-cadherin	6/6, 5/5	[36, 55]
			β-Catenin	5/5	[55]
			Plakoglobin	5/5	[55]

*n/n or %, number of tumours belonging to the category over total number of specified lesion examined

and showed no obvious differences to other PTCs [261]. *CDH1* mutations are rare events in thyroid cancers [236]. Aberrant methylation of CpG islands in the E-cadherin promoter is associated with loss of expression of the protein in cell lines and primary cancers, particularly of the PTC type [113, 236]. With respect to the stages of tumour development at which E-cadherin modifications do occur, it should be noted that promoter methylation has been observed in FTA. In thyroid cancer cell lines derived from human PDC, upregulation of N-cadherin accompanies the loss of E-cadherin [137] (Table 2).

Neo-expression of P-cadherin, with changes of E-cadherin protein localisation was observed in areas of PTC showing squamous metaplasia [236]. Posttranslational modifications observed in neoplastic thyroid tissue comprise decreased tyrosine phosphorylation of E-cadherin and its deconnection from the cytoskeleton [250]. Increased expression of EGFR in thyroid cancers [3] and of c-Met in PTC [77] possibly mediate aggressiveness of the cancer cells through tyrosine phosphorylation of β-catenin.

Cadherins/catenins in the eye

Morphogenesis involves dynamic rearrangements of cells and cell layers. The classical cadherins are considered to be regulators of these processes [270]. At the implantation stage, E-cadherin is expressed in all cells of the embryo. According to the type of differentiation, E-cadherin either remains on the cell surface or disappears. As a rule, E-cadherin is expressed in those ectodermal and endodermal cells that undergo epithelial differentiation, except for terminally differentiated epithelial cells such as the lens cells, which will lose their E-cadherin [270]. Loss of E-cadherin expression occurs in mesodermal cells migrating through the primitive streak into the space between the ectoderm and the endoderm, in neural

Table 6 Distribution of cadherins in the eye. *b* bovine, *c* chick, *r* rabbit, *ra* rat, *hu* human, *m* mouse. The type of cadherin (*-cad*) is characterised by immunocytochemistry (*IC*), immunohistochemistry (*IH*), in situ hybridisation (*ISH*), reverse transcriptase-polymerase chain reaction (*RT-PCR*), Western blot (*WB*) or is not determined (*ND*)

Tissue	Cell type	Cadherin		Method	Reference
		Embryonic	Postnatal		
Conjunctiva	Epithelium	ND	E-cad (hu)	IH	[92, 249]
Cornea	Endothelium	N-cad (c)	ND	IH	[23, 169]
	Epithelium	B-cad (c)	ND	IH	[169]
	Keratocytes	cad-11 (ra)	ND	ISH	[88]
Lens	Anterior epithelium	N-cad (c)	ND	IH, WB	[119, 169]
	Fibres	N-cad (c)	ND	IH	[119, 169]
		B-cad (c)		IH, WB	[169]
Retina	Retinal pigment epithelium	ND	N-cad (hu), E-cad (hu)	IH, WB	[47]
			E-cad (b), P-cad (b)	IH	[48, 270]
	Outer limiting membrane	ND	N-cad (c)	IH, WB	[12, 13, 167]
	Ganglion cells	cad-7 (m)	cad-7 (m)	IH, ISH	[88]
		N-cad (c)		IH, WB	[12, 13, 167]
		cad-6 (m)	ISH	[130, 140]	
	Amacrine cells	cad-7 (m)	cad-7 (m)	IH, ISH	[88]
		N-cad (c)		IH, WB	[12, 13, 167]
			cad-6 (m), cad-8 (m), R-cad (m)	ISH	[130, 140]
	Horizontal cells	cad-7 (m)		IH, ISH	[88]
		N-cad (c)		IH, WB	[12, 13, 167]
			R-cad (m)	ISH	[130, 140]
	Müller cells	ND	N-cad (m), cad-11 (m)	ISH	[130, 140]
	Bipolar cells	cad-7 (m)	ND	IH, ISH	[88]
		N-cad (c)		IH, WB	[12, 13, 167]
	Pericytes	cad-7 (m)	ND	IH, ISH	[88]
		N-cad (c)		IH, ISH, WB	[102, 172, 221]
	Endothelium	N-cad (c)		IH, ISH, WB	[102, 172, 221]
			VE-cad (hu)	IH	[71]
Sclera	Fibroblasts	cad-11 (ra)	ND	ISH	[88]
Cell lines	Corneal keratocytes	ND	N-cad (r), cad-11(r)	IC, WB	[185]
	Corneal epithelium	ND	E-cad (r)	RT-PCR	[195]
	Lens fibres	N-cad (c)	ND	IC	[28, 169]
		B-cad (c)			
	Retinal ganglion cells	N-cad (c)	ND	IC	[78, 233]
	Retinal pigment epithelium	ND	N-cad (hu), E-cad (hu)	IC, WB, RT-PCR	[47, 72]

cells invaginating from the neural plate and in cells forming the lens vesicle. In all three cases, cells invaginate from the surface ectoderm [270]. As the expression of N-cadherin coincides with the segregation of cells from other cell layers, invaginating cells transiently express both E-cadherin and N-cadherin. After this stage, E-cadherin and N-cadherin are expressed on a mutually exclusive basis [121] at least in normal cells. Moreover, migrated mesodermal cells that differentiate further into epithelial cells keep N-cadherin at their surface or will re-express E-cadherin, as is the case for the proximal and the distal tubules, respectively, of the developing and adult nephrons [212]. Similarly, most of the renal cell carcinomas are derived from the N-cadherin positive proximal tubule, but a certain percentage of these tumours have regained E-cadherin expression [257], which reflects the embryological situation. Another analogy between morphogenesis and neoplasia can be seen in the colon [154]. Intense nuclear staining for β-catenin is found during colon cancer cell invasion, which resembles gastrulation, and also during tubular branching of adenomas and adenocarcinomas, which resembles endodermal invagination.

The developing neuroretina in the eye has been used as a model for neurite outgrowth. Expression of N-cadherin during neural development is under dynamic spatio-temporal regulation. N-cadherin is initially expressed in all undifferentiated retinal cells in mouse [130] and chick [167] embryos. It stimulates the axonal outgrowth from retinal neurons. This neurite outgrowth is mediated by activation of the FGFR1. Through later embryological development, there is a steady loss of N-cadherin expression until it is localised only at the outer limiting membrane in avian species [186, 270] or at the inner nuclear layer in the mouse [130]. N-cadherin expression is modulated by transcriptional activation and repression [235] and by dephosphorylation/phosphorylation, the balance of which determines whether N-cadherin remains stably expressed or is targeted for proteolytic production of N-cadherin fragments [167]. N-cadherin-

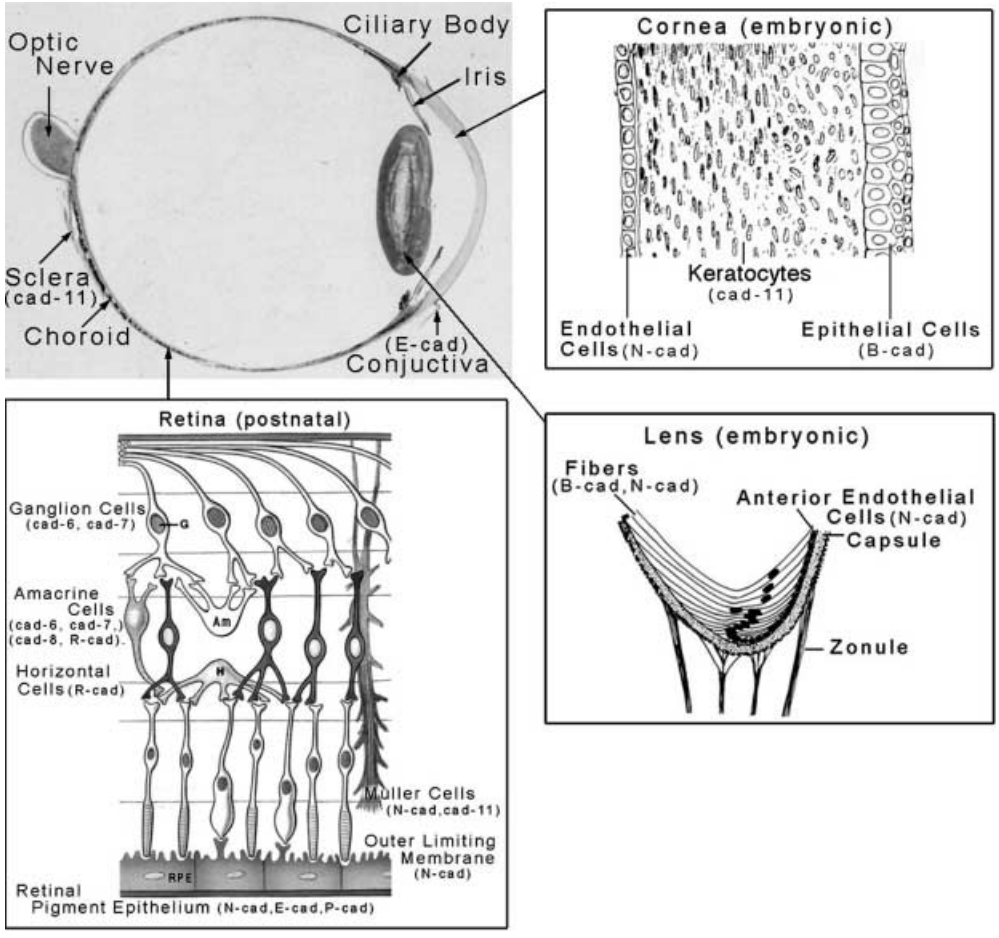


Fig. 6 Illustration of cadherin (*-cad*) distribution in the eye mentioned in Table 6 [95, 300]

mediated neurite outgrowth does not stop because of the proteolytic breakdown of N-cadherin, as one might expect, since the N-cadherin fragments substitute for the intact molecule [221]. A cell-surface N-acetylgalactosaminyl-phosphotransferase (GalNAcPTase) specifically associates with N-cadherin and is a critical component of a regulatory circuit that coordinates the inhibitory activity of β1 integrin on neurite outgrowth [170]. N-cadherin is also transiently expressed on vascular endothelial cells and pericytes of the developing chick eye, where they may be involved in the commitment of early blood vessels to form the blood–retina barrier [102].

The distribution of cadherins in the eye is summarised in Table 6 and illustrated in Fig. 6. A heterophilic interaction between E-cad of the epithelial cells and $\alpha_E\beta_7$ integrin of lymphocytes is described in the conjunctiva and the lacrimal gland in patients with Sjögren's syndrome [92, 249]. A *pax-6* (paired box 6) knock-out mouse shows reduced R-cadherin, cadherin-6 and cadherin-8 expression in the brain and the eye, leading to a S(mall) E(ye) phenotype [32, 288]. The *pax-2* knock-out mouse has an, as yet, unknown cadherin dysregulation with coloboma and failure to form the optic chiasma [93]. Interestingly, null mutation of the *prox1* gene in mice causes persistent E-cadherin expression in the lens epithelial cells, which then fail to differentiate into lens fibres [302].

All (neuro)epithelial tissues of the human eye can give rise to tumours, except for the lens [179]. Lens cells are however not refractive to tumour development, as evidenced by transgenic mice containing the simian virus 40 T antigen [179] and by prolonged time in vitro maintenance [190].

In humans, retinoblastoma and melanoma are the most frequent intraocular cancers in children [247] and adults, respectively. Moreover, retinoblastoma is the prototype embryonal tumour on which Knudson has based his two-hit theory for tumour-suppressor genes [158]. To explain why cancer emerges specifically in the human developing retina in the absence of functional retinoblastoma protein (RB–/–), Gallie et al. [97] hypothesised that the non-tumourous neuroretina is built by a balance between RB+/+ neuroblasts that undergo terminal differentiation or that die. Retinocytoma would occur when proliferating RB–/– neuroblasts keep on proliferating instead of differentiating but are still susceptible to programmed cell death. A retinoblastoma would occur when the RB–/– neuroblasts are not susceptible any more to programmed cell death because of constitutively activated anti-apoptotic genes, such as *Notch 1*. Cadherins have

hardly been analysed in retinoblastoma [247]. We set out to analyse invasion of retinoblastoma cell lines in vitro in collagen type I, and preliminary results indicate that this is mediated by N-cadherin. Moreover, there is a clear difference in N-cadherin pattern between retinoblastoma specimens and non-tumourous neuroretina: the regular honeycomb pattern of N-cadherin, and the catenins is disturbed in retinoblastoma, showing a dotted pattern at the cell–cell contacts. Currently, we are investigating the structure and function of the whole N-cadherin/catenin complex in retinoblastoma relative to normal neuroretina. In line with the fact that N-cadherin is seen as an invasion promoter in tumourigenesis (Table 2) and morphogenesis, tumour cell lines derived from cells that express E-cadherin are not invasive in vitro unless transfection with or transactivation of the gene encoding for N-cadherin takes place. Neuroblastoma and retinoblastoma cell lines, however, are derived from N-cadherin expressing cells and are accordingly already invasive in vitro.

Uveal melanoma cell lines do not contain E-cadherin [67]. Kim et al. [153] showed that invasive uveal melanoma cell lines contain little or no APC from which one might expect β-catenin to localise in the nucleus. Invasive behaviour in uveal melanoma cell lines can, however, be linked to a substantial amount of cytoplasmic instead of nuclear unphosphorylated β-catenin. In cutaneous melanoma cell lines, GSK3-β is unable to phosphorylate mutated β-catenin which results in constitutively upregulated β-catenin/TCF-mediated transcriptional activity [62, 240]. Uveal melanomas, unlike cutaneous melanomas, are rarely familial and are not due to mutations in RB and p53, but to mutational inactivation of other elements in their pathway, e.g. cyclin D1 [43, 199]. There are major differences between uveal and cutaneous melanomas concerning the inactivation of the RB pathway [189]. Nuclear overexpression of Myc is associated with a better prognosis for survival in uveal melanoma and a worse prognosis in cutaneous melanoma [57]. This can be explained by the fact that Myc increases the susceptibility to apoptosis in cells subjected to stress through a p53-dependent mechanism [86]. The p53 pathway on its turn is intact in uveal melanoma, proning cells to apoptosis, but p53 mutation can occur as a late event in cutaneous melanoma, thus predisposing cells to survive and metastasise. Considering RB and Myc as inducers of the expression of E-cadherin [18], it would be interesting to see whether the difference in prognosis between uveal and cutaneous melanoma could also be linked to differences in E-cadherin expression.

Conclusions

The E-cadherin/catenin and its associated complexes participate at tumour development as suppressors or stimulators of growth, differentiation and invasion. E-cadherin is downregulated in the majority of cancers, mostly at the invasive stage; its CDH1 gene acts as a tumour-suppressor gene in lobular breast cancer and in diffuse gastric cancer. Downregulation of E-cadherin and its associated proteins also occurs at the posttranslational level, through phosphorylation, sterical hindrance, proteolysis and internalisation. β-catenin, when protected from proteolysis by lack of GSK3β- and APC-mediated phosphorylation, acts as a tumour-promoter through transactivation of stimulators of growth and invasion. The present review shows the fundamental character of E-cadherin/catenin changes as they are found in all human cancers. To better define prognosis, quantitative and sometimes qualitative changes in marker molecules have been put forward. One of these is the E-cadherin/catenin complex, downregulation of which may serve as a marker of poor prognosis in various tumours. Future research in this field is warranted to understand the role of other members of the growing families of cadherins, catenins and their downstream signalling targets in the development and the clinical manifestations of human cancer.

Acknowledgments We gratefully acknowledge Dr. M. Bracke for critical reading of the manuscript, G. De Bruyne and G. Desmet for technical assistance, and J. Roels for preparation of the illustrations. E. Van Aken is a research assistant with the F.W.O. (Fonds voor Wetenschappelijk Onderzoek)-Flanders, Brussels, Belgium, and is supported by the F.R.O.(Fonds voor Research in Oftalmologie), Leuven, Belgium. O. De Wever is a fellow of the I.W.T.(Vlaams Instituut voor bevordering van het wetenschappelijk-technologisch onderzoek in de industrie), Brussels, Belgium. A.S. Correia da Rocha is a fellow of the F.C.T. from the Portuguese Ministery for Science and Technology (PRAXXIS XXI BD 21775/99), Lisbon, Portugal.

References

1. Akimoto T, Mitsuhashi N, Saito Y, Ebara T, Niibe H (1998) Effect of radiation on the expression of E-cadherin and α-catenin and invasive capacity in human lung cancer cell line in vitro. Int J Radiat Oncol Biol Phys 41:1171–1176
2. Akslen LA, LiVolsi VA (2000) Prognostic significance of histologic grading compared with subclassification of papillary thyroid carcinoma. Cancer 88:1902–1908
3. Akslen LA, Varhaug JE (1995) Oncoproteins and tumor progression in papillary thyroid carcinoma. Presence of epidermal growth factor receptor, c-erbB-2 protein, estrogen receptor related protein, p21-ras protein, and proliferation indicators in relation to tumor recurrences and patient survival. Cancer 76:1643–1654
4. Anastasiadis PZ, Reynolds AB (2000) The p120 catenin family: complex roles in adhesion, signaling and cancer. J Cell Sci 113:1319–1334
5. Anastasiadis PZ, Moon SY, Thoreson MA, Mariner DJ, Crawford HC, Zheng Y, Reynolds AB (2000) Inhibition of RhoA by p120 catenin. Nat Cell Biol 2:637–644
6. André F, Rigot V, Thimonier J, Montixi C, Parat F, Pommier G, Marvaldi J, Luis J (1999) Integrins and E-cadherin cooperate with IGF-I to induce migrartion of epithelial colonic cells. Int J Cancer 83:497–505
7. Arregui C, Pathre P, Lilien J, Balsamo J (2000) The nonreceptor tyrosine kinase Fer mediates cross-talk between N-cadherin and β1-integrins. J Cell Biol 149:1263–1273
8. Asano K, Kubo O, Tajika Y, Takakura K, Suzuki S (2000) Expression of cadherin and CSF dissemination in malignant astrocytic tumors. Neurosurg Rev 23:39–44

9. Ásgeirsson KS, Jónasson JG, Tryggvadóttir L, Ólafsdóttir K, Sigurgeirsdóttir JR, Ingvarsson S, Ögmundsdóttir HM (2000) Altered expression of E-cadherin in breast cancer: patterns, mechanisms and clinical significance. Eur J Cancer 36:1098–1106
10. Babich M, Foti LR (1994) E-cadherins identified in osteoblastic cells: effects of parathyroid hormone and extracellular calcium on localization. Life Sci 54:PL201–PL208
11. Bailey T, Biddlestone L, Shepherd N, Barr H, Warner P, Jankowski J (1998) Altered cadherin and catenin complexes in the Barrett's esophagus-dysplasia-adenocarcinoma sequence. Am J Pathol 152:135–144
12. Balsamo J, Lilien J (1990) N-cadherin is stably associated with and is an acceptor for a cell surface *N*-acetylgalactosaminylphosphotransferase. J Biol Chem 265:2923–2928
13. Balsamo J, Thiboldeaux R, Swaminathan N, Lilien J (1991) Antibodies to the retina N-acetylglactosaminylphosphotransferase modulate N-cadherin-mediated adhesion and uncouple the N-cadherin transferase complex from the actin-containing cytoskeleton. J Cell Biol 113:429–436
14. Bani Sacchi T, Bani D, Brandi ML, Falchetti A, Bigazzi M (1994) Relaxin influences growth, differentiation and cell-cell adhesion of human breast-cancer cells in culture. Int J Cancer 57:129–134
15. Barker N, Clevers H (2000) Catenins, Wnt signaling and cancer. Bioessays 22:961–965
16. Batlle E, Sancho E, Franci C, Dominguez D, Monfar M, Baulida J, Garcia de Herreros A (2000) The transcription factor Snail is a repressor of E-cadherin gene expression in epithelial tumour cells. Nat Cell Biol 2:84–89
17. Batsché E, Crémisi C (1999) Opposite transcriptional activity between the wild type c-myc gene coding for c-Myc1 and c-Myc2 proteins and c-Myc1 and c-Myc2 separately. Oncogene 18:5662–5671
18. Batsché E, Muchardt C, Behrens J, Hurst HC, Crémisi C (1998) RB and c-Myc activate expression of the E-cadherin gene in epithelial cells through interaction with transcription factor AP-2. Mol Cell Biol 18:3647–3658
19. Bauer A, Chauvet S, Huber O, Usseglio F, Rothbächer U, Aragnol D, Kemler R, Pradel J (2000) Pontin52 and Reptin52 function as antagonistic regulators of β-catenin signaling activity. EMBO J 19:6121–6130
20. Becker K-F, Atkinson MJ, Reich U, Huang HH, Nekarda H, Siewert JR, Höfler H (1993) Exon skipping in the E-cadherin gene transcript in metastatic human gastric carcinomas. Hum Mol Genet 2:803–804
21. Becker K-F, Atkinson MJ, Reich U, Becker I, Nekarda H, Siewert JR, Höfler H (1994) E-cadherin gene mutations provide clues to diffuse type gastric carcinomas. Cancer Res 54:3845–3852
22. Becker K-F, Keller G, Hoefler H (2000) The use of molecular biology in diagnosis and prognosis of gastric cancer. Surg Oncol 9:5–11
23. Beebe DC, Coats JM (2000) The lens organizes the anterior segment: specification of neural crest cell differentiation in the avian eye. Dev Biol 220:424–431
24. Behrens J, Mareel MM, Van Roy FM, Birchmeier W (1989) Dissecting tumor cell invasion: epithelial cells acquire invasive properties following the loss of uvomorulin-mediated cell-cell adhesion. J Cell Biol 108:2435–2447
25. Behrens J, Löwrick O, Klein-Hitpass L, Birchmeier W (1991) The E-cadherin promoter: functional analysis of a GC-rich region and an epithelial cell-specific palindromic regulatory element. Proc Natl Acad Sci U S A 88:11495–11499
26. Behrens J, Vakaet L, Friis R, Winterhager E, Van Roy F, Mareel MM, Birchmeier W (1993) Loss of epithelial morphotype and gain of invasiveness correlates with tyrosine phosphorylation of the E-cadherin/β-catenin complex in cells transformed with a temperature-sensitive v-src gene. J Cell Biol 120:757–766
27. Behrens J, von Kries JP, Kühl M, Bruhn L, Wedlich D, Grosschedl R, Birchmeier W (1996) Functional interaction of ß-catenin with the transcription factor LEF-1. Nature 382:638–642
28. Berthoud VM, Bassnett S, Beyer EC (1999) Cultured chicken embryo lens cells resemble differentiating fiber cells in vivo and contain two kinetic pools of connexin56. Exp Eye Res 68:475–484
29. Berx G, Cleton-Jansen A-M, Nollet F, de Leeuw WJF, van de Vijver MJ, Cornelisse C, Van Roy F (1995) E-cadherin is a tumour/invasion suppressor gene mutated in human lobular breast cancers. EMBO J 14:6107–6115
30. Berx G, Cleton-Jansen A-M, Strumane K, de Leeuw WJF, Nollet F, Van Roy F, Cornelisse C (1996) E-cadherin is inactivated in a majority of invasive human lobular breast cancers by truncation mutations throughout its extracellular domain. Oncogene 13:1919–1925
31. Bhowmick NA, Ghiassi M, Bakin A, Aakre M, Lundquist CA, Engel ME, Arteaga CL, Moses HL (2001) Transforming growth factor-ß1 mediates epithelial to mesenchymal transdifferentiation through a RhoA-dependent mechanism. Mol Biol Cell 12:27–36
32. Bishop KM, Goudreau G, O'Leary DDM (2000) Regulation of area identity in the mammalian neocortex by Emx2 and Pax6. Science 288:344–349
33. Böhm J, Niskanen L, Kiraly K, Kellokoski J, Eskelinen M, Hollmen S, Alhava E, Kosma V-M (2000) Expression and prognostic value of α-, ß-, and γ-catenins in differentiated thyroid carcinoma. J Clin Endocrinol Metab 85:4806–4811
34. Boonchai W, Walsh M, Cummings M, Chenevix-Trench G (2000) Expression of ß-catenin, a key mediator of the WNT signaling pathway, in basal cell carcinoma. Arch Dermatol 136:937–938
35. Boterberg T, Vennekens KM, Thienpont M, Mareel MM, Bracke ME (2000) Internalization of the E-cadherin/catenin complex and scattering of human mammary carcinoma cells MCF-7/AZ after treatment with conditioned medium from human skin squamous carcinoma cells COLO 16. Cell Adhes Commun 7:299–310
36. Brabant G, Hoang-Vu C, Cetin Y, Dralle H, Scheumann G, Mölne J, Hansson G, Jansson S, Ericson LE, Nilsson M (1993) E-cadherin: a differentiation marker in thyroid malignancies. Cancer Res 53:4987–4993
37. Brabant G, Hoang-Vu C, Behrends J, Cetin Y, Pötter E, Dumont JE, Maenhaut C (1995) Regulation of the cell-cell adhesion protein, E-cadherin, in dog and human thyrocytes in vitro. Endocrinology 136:3113–3119
38. Bracke ME, Vyncke BM, Bruyneel EA, Vermeulen SJ, De Bruyne GK, Van Larebeke NA, Vleminckx K, Van Roy FM, Mareel MM (1993) Insulin-like growth factor I activates the invasion suppressor function of E-cadherin in MCF-7 human mammary carcinoma cells in vitro. Br J Cancer 68:282–289
39. Bracke ME, Bruyneel EA, Vermeulen SJ, Vennekens K, Van Marck V, Mareel MM (1994) Citrus flavonoid effect on tumor invasion and metastasis. Food Technol 48:121–124
40. Bracke ME, Charlier C, Bruyneel EA, Labit C, Mareel MM, Castronovo V (1994) Tamoxifen restores the E-cadherin function in human breast cancer MCF-7/6 cells and suppresses their invasive phenotype. Cancer Res 54:4607–4609
41. Bracke ME, Van Roy FM, Mareel MM (1996) The E-cadherin/catenin complex in invasion and metastasis. In: Günthert U, Birchmeier W (eds) Attempts to understand metastasis formation I. Springer, Berlin, pp 123–161
42. Bradley RS, Cowin P, Brown AM (1993) Expression of Wnt-1 in PC12 cells results in modulation of plakoglobin and E-cadherin and increased cellular adhesion. J Cell Biol 123:1857–1865
43. Brantley MA Jr, Harbour JW (2000) Inactivation of retinoblastoma protein in uveal melanoma by phosphorylation of sites in the COOH-terminal region. Cancer Res 60:4320–4323
44. Bringuier PP, Umbas R, Schaafsma HE, Karthaus HFM, Debruyne FMJ, Schalken JA (1993) Decreased E-cadherin immunoreactivity correlates with poor survival in patients with bladder tumors. Cancer Res 53:3241–3245
45. Bukholm IK, Nesland JM, Kåresen R, Jacobsen U, Børresen-Dale A-L (1998) E-cadherin and α-, ß-, and γ-catenin protein expression in relation to metastasis in human breast carcinoma. J Pathol 185:262–266

46. Bukholm IK, Nesland JM, Børresen-Dale A-L (2000) Re-expression of E-cadherin, α-catenin and ß-catenin, but not of γ-catenin, in metastatic tissue from breast cancer patients. J Pathol 190:15–19
47. Burke JM, Cao F, Irving PE, Skumatz CMB (1999) Expression of E-cadherin by human retinal pigment epithelium: delayed expression in vitro. Invest Ophthalmol Vis Sci 40:2963–2970
48. Burke JM, Cao F, Irving PE (2000) High levels of E-/P-cadherin: correlation with decreased apical polarity of Na/K ATPase in bovine RPE cells in situ. Invest Ophthalmol Vis Sci 41:1945–1952
49. Bussemakers MJG, Van Bokhoven A, Tomita K, Jansen CFJ, Schalken JA (2000) Complex cadherin expression in human prostate cancer cells. Int J Cancer 85:446–450
50. Candidus S, Bischoff P, Becker KF, Höfler H (1996) No evidence for mutations in the α- and ß-catenin genes in human gastric and breast carcinomas. Cancer Res 56:49–52
51. Cano A, Pérez-Moreno MA, Rodrigo I, Locascio A, Blanco MJ, del Barrio MG, Portillo F, Nieto MA (2000) The transcription factor Snail controls epithelial-mesenchymal transitions by repressing E-cadherin expression. Nat Cell Biol 2:76–83
52. Carico E, Atlante M, Bucci B, Nofroni I, Vecchione A (2001) E-cadherin and α-catenin expression during tumor progression of cervical carcinoma. Gynecol Oncol 80:156–161
53. Carruba G, Miceli D, D'Amico D, Farruggio R, Comito L, Montesanti A, Polito L, Castagnetta LAM (1995) Sex steroids up-regulate E-cadherin expression in hormone-responsive LNCaP human prostate cancer cells. Biochem Biophys Res Commun 212:624–631
54. Cepek KL, Shaw SK, Parker CM, Russell GJ, Morrow JS, Rimm DL, Brenner MB (1994) Adhesion between epithelial cells and T lymphocytes mediated by E-cadherin and the αEß7 integrin. Nature 372:190–193
55. Cerrato A, Fulciniti F, Avallone A, Benincasa G, Palombini L, Grieco M (1998) Beta- and gamma-catenin expression in thyroid carcinomas. J Pathol 185:267–272
56. Chan EF, Gat U, McNiff JM, Fuchs E (1999) A common human skin tumour is caused by activating mutations in ß-catenin. Nat Genet 21:410–413
57. Chana JS, Wilson GD, Cree IA, Alexander RA, Myatt N, Neale M, Foss AJE, Hungerford JL (1999) c-myc, p53, and Bcl-2 expression and clinical outcome in uveal melanoma. Br J Ophthalmol 83:110–114
58. Chausovsky A, Bershadsky AD, Borisy GG (2000) Cadherin-mediated regulation of microtubule dynamics. Nat Cell Biol 2:797–804
59. Chow V, Yuen APW, Lam KY, Tsao GSW, Ho WK, Wei WI (2001) A comparative study of the clinicopathological significance of E-cadherin and catenins (α, ß, γ) expression in the surgical management of oral tongue carcinoma. J Cancer Res Clin Oncol 127:59–63
60. Comijn J, Berx G, Vermassen P, Verschueren K, van Grunsven L, Bruyneel E, Mareel M, Huylebroeck D, van Roy F (2001) The two-handed E box binding zinc finger protein SIP1 down-regulates E-cadherin and induces invasion. Mol Cell 7:1267–1278
61. Comoglio PM, Tamagnone L, Boccaccio C (1999) Plasminogen-related growth factor and semaphorin receptors: a gene superfamily controlling invasive growth. Exp Cell Res 253:88–99
62. Compagni A, Christofori G (2000) Recent advances in research on multistage tumorigenesis. Br J Cancer 83:1–5
63. Corn PG, Smith BD, Ruckdeschel ES, Douglas D, Baylin SB, Herman JG, (2000) E-cadherin expression is silenced by 5' CpG island methylation in acute leukemia. Clin Cancer Res 6:4243–4248
64. Crawford HC, Fingleton BM, Rudolph-Owen LA, Heppner Goss KJ, Rubinfeld B, Polakis P, Matrisian LM (1999) The metalloproteinase matrilysin is a target of ß-catenin transactivation in intestinal tumors. Oncogene 18:2883–2891
65. D'Souza B, Taylor-Papadimitriou J (1994) Overexpression of ERBB2 in human mammary epithelial cells signals inhibition of transcription of the E-cadherin gene. Proc Natl Acad Sci U S A 91:7202–7206
66. Dahl U, Sjödin A, Semb H (1996) Cadherins regulate aggregation of pancreatic ß-cells in vivo. Development 122:2895–2902
67. Danen EHJ, de Vries TJ, Morandini R, Ghanem GG, Ruiter DJ, van Muijen GNP (1996) E-cadherin expression in human melanoma. Melanoma Res 6:127–131
68. Daniel JM, Reynolds AB (1997) Tyrosine phosphorylation and cadherin/catenin function. Bioessays 19:883–891
69. Daniel JM, Reynolds AB (1999) The catenin $p120^{ctn}$ interacts with Kaiso, a novel BTB/POZ domain zinc finger transcription factor. Mol Cell Biol 19:3614–3623
70. Dara E, Scoazec J-Y, Walker-Combrouze F, Mlika-Cabanne N, Feldmann G, Madelenat P, Potet F (1997) Expression of cadherins in benign, borderline, and malignant ovarian epithelial tumors: a clinicopathologic study of 60 cases. Hum Pathol 28:922–928
71. Davidson MK, Russ PK, Glick GG, Hoffman LH, Chang MS, Haselton FR (2000) Reduced expression of the adherens junction protein cadherin-5 in a diabetic retina. Am J Ophthalmol 129:267–269
72. Davis AA, Bernstein PS, Bok D, Turner J, Nachtigal M, Hunt RC (1995) A human retinal pigment epithelial cell line that retains epithelial characteristics after prolonged culture. Invest Ophthalmol Vis Sci 36:955–964
73. De Castro J, Gamallo C, Palacios J, Moreno-Bueno G, Rodríguez N, Feliu J, González-Barón M (2000) ß-Catenin expression pattern in primary oesophageal squamous cell carcinoma. Relationship with clinicopathologic features and clinical outcome. Virchows Arch 437:599–604
74. De La Coste A, Romagnolo B, Billuart P, Renard C-A, Buendia M-A, Soubrane O, Fabre M, Chelly J, Beldjord C, Kahn A, Perret C (1998) Somatic mutations of the ß-catenin gene are frequent in mouse and human hepatocellular carcinomas. Proc Natl Acad Sci U S A 95:8847–8851
75. Debruyne P, Vermeulen S, Mareel M (1999) The role of the E-cadherin/catenin complex in gastrointestinal cancer. Acta Gastroenterol Belg LXII:393–403
76. DeLuca SM, Gerhart J, Cochran E, Simak E, Blitz J, Mattiacci-Paessler M, Knudsen K, George-Weinstein M (1999) Hepatocyte growth factor/scatter factor promotes a switch from E- to N-cadherin in chick embryo epiblast cells. Exp Cell Res 251:3–15
77. Di Renzo MF, Olivero M, Ferro S, Prat M, Bongarzone I, Pilotti S, Belfiore A, Costantino A, Vigneri R, Pierotti MA, et al. (1992) Overexpression of the c-MET/HGF receptor gene in human thyroid carcinomas. Oncogene 7:2549–2553
78. Doherty P, Walsh FS (1991) The contrasting roles of N-CAM and N-cadherin as neurite outgrowth-promoting molecules. J Cell Sci Suppl 15:13–21
79. Doherty P, Walsh FS (1996) CAM-FGF receptor interactions: a model for axonal growth. Mol Cell Neurosci 8:99–111
80. Eads CA, Lord RV, Kurumboor SK, Wickramasinghe K, Skinner ML, Long TI, Peters JH, DeMeester TR, Danenberg KD, Danenberg PV, Laird PW, Skinner KA (2000) Fields of aberrant CpG island hypermethylation in Barrett's esophagus and associated adenocarcinoma. Cancer Res 60:5021–5026
81. Eckert K, Fuhrmann-Selter T, Maurer HR (1997) Docetaxel enhances the expression of E-cadherin and carcinoembryonic antigen (CEA) on human colon cancer cell lines in vitro. Anticancer Res 17:7–12
82. Emami S, Le Floch N, Bruyneel E, Thim L, May F, Westley B, Rio M-C, Mareel M, Gespach C (2001) Induction of scattering and cellular invasion by trefoil peptides in src- and RhoA-transformed kidney and colonic epithelial cells. FASEB J 15:351–361
83. Endo K, Ueda T, Ueyama J, Ohta T, Terada T (2000) Immunoreactive E-cadherin, alpha-catenin, beta-catenin, and gamma-catenin proteins in hepatocellular carcinoma: relationships with tumor grade, clinicopathologic parameters, and patients' survival. Hum Pathol 31:558–565

84. Engebraaten O, Fodstad Ø (1999) Site-specific experimental metastasis patterns of two human breast cancer cell lines in nude rats. Int J Cancer 82:219–225
85. Esteller M (2000) Epigenetic lesions causing genetic lesions in human cancer: promoter hypermethylation of DNA repair genes. Eur J Cancer 36:2294–2300
86. Evan GI, Wyllie AH, Gilbert CS, Littlewood TD, Land H, Brooks M, Waters CM, Penn LZ, Hancock DC (1992) Induction of apoptosis in fibroblasts by c-myc protein. Cell 69:119–128
87. Ewing CM, Ru N, Morton RA, Robinson JC, Wheelock MJ, Johnson KR, Barrett JC, Isaacs WB (1995) Chromosome 5 suppresses tumorigenicity of PC3 prostate cancer cells: correlation with re-expression of α-catenin and restoration of E-cadherin function. Cancer Res 55:4813–4817
88. Faulkner-Jones BE, Godinho LNM, Reese BE, Pasquini GF, Ruefli A, Tan S-S (1999) Cloning and expression of mouse cadherin-7, a type-II cadherin isolated from the developing eye. Mol Cell Neurosci 14:1–16
89. Fearon ER (2000) BRCA1 and E-cadherin promoter hypermethylation and gene inactivation in cancer – association or mechanism? J Natl Cancer Inst 92:515–517
90. Fearon ER, Vogelstein B (1990) A genetic model for colorectal tumorigenesis. Cell 61:759–767
91. Frixen UH, Behrens J, Sachs M, Eberle G, Voss B, Warda A, Löchner D, Birchmeier W (1991) E-cadherin-mediated cell-cell adhesion prevents invasiveness of human carcinoma cells. J Cell Biol 113:173–185
92. Fujihara T, Fujita H, Tsubota K, Saito K, Tsuzaka K, Abe T, Takeuchi T (1999) Preferential localization of $CD8^+$ $\alpha_E ß_7^+$ T cells around acinar epithelial cells with apoptosis in patients with Sjögren's syndrome. J Immunol 163:2226–2235
93. Fujimori T, Takeichi M (1993) Disruption of epithelial cell-cell adhesion by exogenous expression of a mutated nonfunctional N-cadherin. Mol Biol Cell 4:37–47
94. Fukuchi T, Sakamoto M, Tsuda H, Maruyama K, Nozawa S, Hirohashi S (1998) ß-catenin mutation in carcinoma of the uterine endometrium. Cancer Res 58:3526–3528
95. Fundamentals and Principles of Ophthalmology (1999) Basic and clinical science course 1999–2000. American Academy of Ophthalmology, San Francisco, CA
96. Gallet A, Angelats C, Erkner A, Charroux B, Fasano L, Kerridge S (1999) The C-terminal domain of Armadillo binds to hypophosphorylated Teashirt to modulate Wingless signalling in Drosophila. EMBO J 18:2208–2217
97. Gallie BL, Campbell C, Devlin H, Duckett A, Squire JA (1999) Developmental basis of retinal-specific induction of cancer by RB mutation. Cancer Res Suppl 59:1731s-1735s
98. Gamallo C, Palacios J, Suarez A, Pizarro A, Navarro P, Quintanilla M, Cano A (1993) Correlation of E-cadherin expression with differentiation grade and histological type in breast carcinoma. Am J Pathol 142:987–993
99. Garcia del Muro X, Torregrosa A, Muñoz J, Castellsagué X, Condom E, Vigués F, Arance A, Fabra A, Germà JR (2000) Prognostic value of the expression of E-cadherin and ß-catenin in bladder cancer. Eur J Cancer 36:357–362
100. Garcia-Rostan G, Tallini G, Herrero A, D'Aquila TG, Carcangiu ML, Rimm DL (1999) Frequent mutation and nuclear localization of ß-catenin in anaplastic thyroid carcinoma. Cancer Res 59:1811–1815
101. Garcia-Rostan G, Camp RL, Herrero A, Carcangiu ML, Rimm DL, Tallini G (2001) ß-catenin dysregulation in thyroid neoplasms. Down-regulation, aberrant nuclear expression, and CTNNB1 exon 3 mutations are markers for aggressive tumor phenotypes and poor prognosis. Am J Pathol 158:987–996
102. Gerhardt H, Liebner S, Redies C, Wolburg H (1999) N-cadherin expression in endothelial cells during early angiogenesis in the eye and brain of the chicken: relation to blood-retina and blood-brain barrier development. Eur J Neurosci 11:1191–1201
103. Getsios S, Chen GTC, Stephenson MD, Leclerc P, Blaschuk OW, MacCalman CD (1998) Regulated expression of cadherin-6 and cadherin-11 in the glandular epithelial and stromal cells of the human endometrium. Dev Dyn 211:238–247
104. Giannini AL, Vivanco MdM, Kypta RM (2000) α-Catenin inhibits ß-catenin signaling by preventing formation of a ß-catenin T-cell factor DNA complex. J Biol Chem 275:21883–21888
105. Gire V, Wynford-Thomas D (2000) RAS oncogene activation induces proliferation in normal human thyroid epithelial cells without loss of differentiation. Oncogene 19:737–744
106. Giroldi LA, Bringuier P-P, Schalken JA (1994–95) Defective E-cadherin function in urological cancers: clinical implications and molecular mechanisms. Invasion Metastasis 14:71–81
107. Giroldi LA, Bringuier PP, de Weijert M, Jansen C, van Bokhoven A, Schalken JA (1997) Role of E boxes in the repression of E-cadherin expression. Biochem Biophys Res Commun 18:453–458
108. Giroldi LA, Bringuier P-P, Shimazui T, Jansen K, Schalken JA (1999) Changes in cadherin-catenin complexes in the progression of human bladder carcinoma. Int J Cancer 82:70–76
109. Gofuku J, Shiozaki H, Tsujinaka T, Inoue M, Tamura S, Doki Y, Matsui S, Tsukita S, Kikkawa N, Monden M (1999) Expression of E-cadherin and α-catenin in patients with colorectal carcinoma. Correlation with cancer invasion and metastasis. Am J Clin Pathol 111:29–37
110. González MV, Pello MF, Ablanedo P, Suárez C, Alvarez V, Coto E (1998) Chromosome 3p loss of heterozygosity and mutation analysis of the FHIT and ß-cat genes in squamous cell carcinoma of the head and neck. J Clin Pathol 51:520–524
111. Gradl D, Kühl M, Wedlich D (1999) The Wnt/Wg signal transducer ß-catenin controls fibronectin expression. Mol Cell Biol 19:5576–5587
112. Grady WM, Willis J, Guilford PJ, Dunbier AK, Toro TT, Lynch H, Wiesner G, Ferguson K, Eng C, Park J-G, Kim S-J, Markowitz S (2000) Methylation of the CDH1 promoter as the second genetic hit in hereditary diffuse gastric cancer. Nat Genet 26:16–17
113. Graff JR, Greenberg VE, Herman JG, Westra WH, Boghaert ER, Ain KB, Saji M, Zeiger MA, Zimmer SG, Baylin SB (1998) Distinct patterns of E-cadherin CpG island methylation in papillary, follicular, Hurthle's cell, and poorly differentiated human thyroid carcinoma. Cancer Res 58:2063–2066
114. Haier J, Nasralla M, Nicolson GL (2000) Cell surface molecules and their prognostic values in assessing colorectal carcinomas. Ann Surg 231:11–24
115. Hakimelahi S, Parker HR, Gilchrist AJ, Barry M, Li Z, Bleackley RC, Pasdar M (2000) Plakoglobin regulates the expression of the anti-apoptotic protein BCL-2. J Biol Chem 275:10905–10911
116. Han AC, Peralta-Soler A, Knudsen KA, Wheelock MJ, Johnson KR, Salazar H (1997) Differential expression of N-cadherin in pleural mesotheliomas and E-cadherin in lung adenocarcinomas in formalin-fixed, paraffin-embedded tissues. Hum Pathol 28:641–645
117. Han AC, Edelson MI, Peralta Soler A, Knudsen KA, Lifschitz-Mercer B, Czernobilsky B, Rosenblum NG, Salazar H (2000) Cadherin expression in glandular tumors of the cervix. Aberrant P-cadherin expression as a possible marker of malignancy. Cancer 89:2053–2058
118. Hardy RG, Sanders DSA, Morton DG, Matthews GM, Adams C, Pretlow TP, Jankowski JAZ (1999) Transient P-cadherin expression is important in the early stages of exophytic growth and clonal expansion within the colon. J Pathol 189:12A
119. Hatta K, Takeichi M (1986) Expression of N-Cadherin adhesion molecules associated with early morphogenetic events in chick development. Nature 320:447–449
120. Hay ED, Zuk A (1995) Transformations between epithelium and mesenchyme: normal, pathological, and experimentally induced. Am J Kidney Dis 26:678–690

121. Hazan RB, Kang L, Whooley BP, Borgen PI (1997) N-cadherin promotes adhesion between invasive breast cancer cells and the stroma. Cell Adhes Commun 4:399–411
122. Hazan RB, Phillips GR, Fang Qiao R, Norton L, Aaronson SA (2000) Exogenous expression of N-cadherin in breast cancer cells induces cell migration, invasion, and metastasis. J Cell Biol 148:779–790
123. He T-C, Sparks AB, Rago C, Hermeking H, Zawel L, da Costa LT, Morin PJ, Vogelstein B, Kinzler KW (1998) Identification of c-MYC as a target of the APC pathway. Science 281:1509–1512
124. Hecht A, Vleminckx K, Stemmler MP, van Roy F, Kemler R (2000) The p300/CBP acetyltransferases function as transcriptional coactivators of ß-catenin in vertebrates. EMBO J 19:1839–1850
125. Heimann R, Lan F, McBride R, Hellman S (2000) Separating favorable from unfavorable prognostic markers in breast cancer: the role of E-cadherin. Cancer Res 60:298–304
126. Hilkens J, Ligtenberg MJL, Vos HL, Litvinov SV (1992) Cell membrane-associated mucins and their adhesion-modulating property. Trends Biol Sci 17:359–363
127. Hinck L, Nelson WJ, Papkoff J (1994) Wnt-1 modulates cell-cell adhesion in mammalian cells by stabilizing ß-catenin binding to the cell adhesion protein cadherin. J Cell Biol 124:729–741
128. Hippo Y, Yashiro M, Ishii M, Taniguchi H, Tsutsumi S, Hirakawa K, Kodama T, Aburatani H (2001) Differential gene expression profiles of scirrhous gastric cancer cells with high metastatic potential to peritoneum or lymph nodes. Cancer Res 61:889–895
129. Hiscox S, Hallett MB, Puntis MCA, Jiang WG (1995) Inhibition of cancer cell motility and invasion by interleukin-12. Clin Exp Metastasis 13:396–404
130. Honjo M, Tanihara H, Suzuki S, Tanaka T, Honda Y, Takeichi M (2000) Differential expression of cadherin adhesion receptors in neural retina of the postnatal mouse. Invest Ophthalmol Vis Sci 41:546–551
131. Hooper LV, Wong MH, Thelin A, Hansson L, Falk PG, Gordon JI (2001) Molecular analysis of commensal host-microbial relationships in the intestine. Science 291:881–884
132. Hosono S, Gross I, English MA, Hajra KM, Fearon ER, Licht JD (2000) E-cadherin is a WT1 target gene. J Biol Chem 275:10943–10953
133. Hsu M-Y, Wheelock MJ, Johnson KR, Herlyn M (1996) Shifts in cadherin profiles between human normal melanocytes and melanomas. J Invest Dermatol Symp Proc 1:188–194
134. Hsu M-Y, Andl T, Li G, Meinkoth JL, Herlyn M (2000) Cadherin repertoire determines partner-specific gap junctional communication during melanoma progression. J Cell Sci 113:1535–1542
135. Huber AH, Stewart DB, Laurents DV, Nelson WJ, Weiss WI (2001) The cadherin cytoplasmic domain is unstructured in the absence of ß-catenin. A possible mechanism for regulating cadherin turnover. J Biol Chem 276:12301–12309
136. Hundahl SA, Cady B, Cunningham MP, Mazzaferri E, McKee RF, Rosai J, Shah JP, Fremgen AM, Stewart AK, Hölzer S (2000) Initial results from a prospective cohort study of 5583 cases of thyroid carcinoma treated in the United States during 1996. Cancer 89:202–217
137. Husmark J, Heldin N-E, Nilsson M (1999) N-cadherin-mediated adhesion and aberrant catenin expression in anaplastic thyroid-carcinoma cell lines. Int J Cancer 83:692–699
138. Hyafil F, Morello D, Babinet C, Jacob F (1980) A cell surface glycoprotein involved in the compaction of embryonal carcinoma cells and cleavage stage embryos. Cell 21:927–934
139. Ikeguchi M, Taniguchi T, Makino M, Kaibara N (2000) Reduced E-cadherin expression and enlargement of cancer nuclei strongly correlate with hematogenic metastasis in colorectal adenocarcinoma. Scand J Gastroenterol 35:839–846
140. Inuzuka H, Miyatani S, Takeichi M (1991) R-Cadherin: a novel Ca^{2+} -dependent cell-cell adhesion molecule expressed in the retina. Neuron 7:69–79
141. Ishisaki A, Oida S, Momose F, Amagasa T, Rikimaru K, Ichijo H, Sasaki S (1994) Identification and charaterization of autocrine-motility-factor-like activity in oral squamous-cell-carcinoma cells. Int J Cancer 59:783–788
142. Islam S, Carey TE, Wolf GT, Wheelock MJ, Johnson KR (1996) Expression of N-cadherin by human squamous carcinoma cells induces a scattered fibroblastic phenotype with disrupted cell-cell adhesion. J Cell Biol 135:1643–1654
143. Iwao K, Nakamori S, Kameyama M, Imaoka S, Kinoshita M, Fukui T, Ishiguro S, Nakamura Y, Miyoshi Y (1998) Activation of the ß-catenin gene by interstitial deletions involving exon 3 in primary colorectal carcinomas without adenomatous polyposis coli mutations. Cancer Res 58:1021–1026
144. Jankowski JAZ, Bedford FK, Boulton RA, Cruickshank N, Hall C, Elder J, Allan R, Forbes A, Kim YS, Wright NA, Sanders DSA (1998) Alterations in classical cadherins associated with progression in ulcerative and Crohn's colitis. Lab Invest 78:1155–1167
145. Karayiannakis AJ, Syrigos KN, Chatzigianni E, Papanikokalou S, Alexiou D, Kalahanis N, Rosenberg T, Bastounis E (1998) Aberrant E-cadherin expression associated with loss of differentiation and advanced stage in human pancreatic cancer. Anticancer Res 18:4177–4180
146. Katayama M, Hirai S, Kamihagi K, Nakagawa K, Yasumoto M, Kato I (1994) Soluble E-cadherin fragments increased in circulation of cancer patients. Br J Cancer 69:580–585
147. Kawanishi J, Kato J, Sasaki K, Fujii S, Watanabe N, Niitsu Y (1995) Loss of E-cadherin-dependent cell-cell adhesion due to mutation of the ß-catenin gene in a human cancer cell line, HSC-39. Mol Cell Biol 15:1175–1181
148. Keilhack H, Hellman U, van Hengel J, van Roy F, Godovac-Zimmermann J, Böhmer F-D (2000) The protein-tyrosine phosphatase SHP-1 binds to and desphosphorylates p120 catenin. J Biol Chem 275:26376–26384
149. Keirsebilck A, Bonné S, Staes K, van Hengel J, Nollet F, Reynolds A, Van Roy F (1998) Molecular cloning of the human $p120^{ctn}$ catenin gene (CTNND1): expression of multiple alternatively spliced isoforms. Genomics 50:129–146
150. Keller G, Vogelsang H, Becker I, Hutter J, Ott K, Candidus S, Grundei T, Becker K-F, Mueller J, Siewert JR, Höfler H (1999) Diffuse type gastric and lobular breast carcinoma in a familial gastric cancer patient with an E-cadherin germline mutation. Am J Pathol 155:337–342
151. Kernéis S, Bogdanova A, Kraehenbuhl J-P, Pringault E (1997) Conversion by Peyer's patch lymphocytes of human enterocytes into M cells that transport bacteria. Science 277:949–952
152. Kim J-B, Islam S, Kim YJ, Prudoff RS, Sass KM, Wheelock MJ, Johnson KR (2000) N-Cadherin extracellular repeat 4 mediates epithelial to mesenchymal transition and increased motility. J Cell Biol 151:1193–1206
153. Kim K, Daniels KJ, Hay ED (1998) Tissue-specific expression of ß-catenin in normal mesenchyme and uveal melanomas and its effect on invasiveness. Exp Cell Res 245:79–90
154. Kirchner T, Brabletz T (2000) Patterning and nuclear ß-catenin expression in the colonic adenoma-carcinoma sequence. Analogies with embryonic gastrulation. Am J Pathol 157:1113–1121
155. Kitaeva MN, Grogan L, Williams JP, Dimond E, Nakahara K, Hausner P, DeNobile JW, Soballe PW, Kirsch IR (1997) Mutations in ß-catenin are uncommon in colorectal cancer occurring in occasional replication error-positive tumors. Cancer Res 57:4478–4481
156. Knudsen KA, Frankowski C, Johnson KR, Wheelock MJ (1998) A role for cadherins in cellular signaling and differentiation. J Cell Biochem Suppl 30/31:168–176
157. Knudsen KA, Lin CY, Johnson KR, Wheelock MJ, Keshgegian AA, Soler AP (2000) Lack of correlation between serum levels of E- and P-cadherin fragments and the presence of breast cancer. Hum Pathol 31:961–965
158. Knudson AG (1971) Mutation and cancer: statistical study of retinoblastoma. Proc Natl Acad Sci U S A 68:820–823

159. Knudson AG (1997) Hereditary cancer: theme and variations. J Clin Oncol 15:3280–3287
160. Koch A, Denkhaus D, Albrecht S, Leuschner I, von Schweinitz D, Pietsch T (1999) Childhood hepatoblastomas frequently carry a mutated degradation targeting box of the ß-catenin gene. Cancer Res 59:269–273
161. Kolligs FT, Kolligs B, Hajra KM, Hu G, Tani M, Cho KR, Fearon ER (2000) γ-Catenin is regulated by the APC tumor suppressor and its oncogenic activity is distinct from that of ß-catenin. Genes Dev 14:1319–1331
162. Korinek V, Barker N, Morin PJ, van Wichen D, de Weger R, Kinzler KW, Vogelstein B, Clevers H (1997) Constitutive transcriptional activation by a ß-catenin-Tcf complex in $APC^{-/-}$ colon carcinoma. Science 275:1784–1787
163. Labbé E, Letamendia A, Attisano L (2000) Association of Smads with lymphoid enhancer binding factor 1/T cell-specific factor mediates cooperative signaling by the transforming growth factor-ß and Wnt pathways. Proc Natl Acad Sci U S A 97:8358–8363
164. Larue L, Antos C, Butz S, Huber O, Delmas V, Dominis M, Kemler R (1996) A role for cadherins in tissue formation. Development 122:3185–3194
165. Leblanc M, Poncelet C, Soriano D, Walker-Combrouze F, Madelenat P, Scoazec JY, Darai E (2001) Alteration of CD44 and cadherins expression: possible association with augmented aggressiveness and invasiveness of endometrial carcinoma. Virchows Arch 438:78–85
166. Lecuit M, Dramsi S, Gottardi C, Fedor-Chaiken M, Gumbiner B, Cossart P (1999) A single amino acid in E-cadherin responsible for host specificity towards the human pathogen Listeria monocytogenes. EMBO J 18:3956–3963
167. Lee MM, Fink BD, Grunwald GB (1997) Evidence that tyrosine phosphorylation regulates N-cadherin turnover during retinal development. Dev Genet 20:224–234
168. Lehr H-A, Folpe A, Yaziji H, Kommoss F, Gown AM (2000) Cytokeratin 8 immunostaining pattern and E-cadherin expression distinguish lobular from ductal breast carcinoma. Am J Clin Pathol 114:190–196
169. Leong L, Menko AS, Grunwald GB (2000) Differential expression of N- and B-cadherin during lens development. Invest Ophthalmol Vis Sci 41:3503–3510
170. Li H, Leung T-C, Hoffman S, Balsamo J, Lilien J (2000) Coordinate regulation of cadherin and integrin function by the chondroitin sulfate proteoglycan neurocan. J Cell Biol 149:1275–1288
171. Li Z, Gallin WJ, Lauzon G, Pasdar M (1998) L-CAM expression induces fibroblast-epidermoid transition in squamous carcinoma cells and down-regulates the endogenous N-cadherin. J Cell Sci 111:1005–1019
172. Liebner S, Gerhardt H, Wolburg H (2000) Differential expression of endothelial β-catenin and plakoglobin during development and maturation of the blood-brain and blood-retina barrier in the chicken. Dev Dyn 217:86–98
173. Lieubeau B, Heymann M-F, Henry F, Barbieux I, Meflah K, Grégoire M (1999) Immunomodulatory effects of tumor-associated fibroblasts in colorectal-tumor development. Int J Cancer 81:629–636
174. Lin S-Y, Xia W, Wang JC, Kwong KY, Spohn B, Wen Y, Pestell RG, Hung M-C (2000) β-Catenin, a novel prognostic marker for breast cancer: its roles in cyclin D1 expression and cancer progression. Proc Natl Acad Sci USA 97:4262–4266
175. Liu D, El-Hariry I, Karayiannakis AJ, Wilding J, Chinery R, Kmiot W, McCrea PD, Gullick WJ, Pignatelli M (1997) Phosphorylation of β-catenin and epidermal growth factor receptor by intestinal trefoil factor. Lab Invest 77:557–563
176. Lo Muzio L, Staibano S, Pannone G, Grieco M, Mignogna MD, Cerrato A, Testa NF, De Rosa G (1999) Beta- and gamma-catenin expression in oral squamous cell carcinoma. Anticancer Res 19:3817–3826
177. Lochter A, Srebrow A, Sympson CJ, Terracio N, Werb Z, Bissell MJ (1997) Misregulation of stromelysin-1 expression in mouse mammary tumor cells accompanies acquisition of stromelysin-1-dependent invasive properties. J Biol Chem 272:5007–5015
178. MacCalman CD, Farookhi R, Blaschuk OW (1994) Estradiol regulates E-cadherin mRNA levels in the surface epithelium of the mouse ovary. Clin Exp Metastasis 12:276–282
179. Mahon KA, Chepelinsky AB, Khillan JS, Overbeek PA, Piatigorsky J, Westphal H (1987) Oncogenesis of the lens in transgenic mice. Science 235:1622–1628
180. Mann B, Gelos M, Siedow A, Hanski ML, Gratchev A, Ilyas M, Bodmer WF, Moyer MP, Riecken FO, Buhr HJ, Hanski C (1999) Target genes of β-catenin-T cell-factor/lymphoid-enhancer-factor signaling in human colorectal carcinomas. Proc Natl Acad Sci U S A 96:1603–1608
181. Mareel MM, Bracke ME (2001) Molecular mechanisms of cancer invasion. In: Encyclopedia of cancer. Academic Press, San Diego (in press)
182. Mareel MM, Van Roy FM (1986) Are oncogenes involved in invasion and metastasis? Anticancer Res 6:419–436
183. Mareel MM, Behrens J, Birchmeier W, De Bruyne GK, Vleminckx K, Hoogewijs A, Fiers WC, Van Roy FM (1991) Downregulation of E-cadherin expression in Madin Darby canine kidney (MDCK) cells inside nude mice tumors. Int J Cancer 47:922–928
184. Martel C, Harper F, Cereghini S, Noë V, Mareel M, Crémisi C (1997) Inactivation of retinoblastoma family proteins by SV40 T antigen results in creation of a hepatocyte growth factor/scatter factor autocrine loop associated with an epithelial-fibroblastoid conversion and invasiveness. Cell Growth Differ 8:165–178
185. Masur SK, Conors RJ Jr, Cheung JK-H, Antohi S (1999) Matrix adhesion characteristics of corneal myofibroblasts. Invest Ophthalmol Vis Sci 40:904–910
186. Matsunaga M, Hatta K, Nagafuchi A, Takeichi M (1988) Guidance of optic nerve fibres by N-cadherin adhesion molecules. Nature 334:62–64
187. Matsuyoshi N, Tanaka T, Toda K-i, Imamura S (1997) Identification of novel cadherins expressed in human melanoma cells. J Invest Dermatol 108:908–913
188. Melki JR, Vincent PC, Brown RD, Clark SJ (2000) Hypermethylation of E-cadherin in leukemia. Blood 95:3208–3213
189. Merbs SL, Sidransky D (1999) Analysis of p16 (CDKN2/MTS-1/INK4A) alterations in primary sporadic uveal melanoma. Invest Ophthalmol Vis Sci 40:779–783
190. Messiaen L, Qian S, De Bruyne G, Boghaert E, Moens T, Rabaey M, Van Roy F, Mareel M (1991) Spontaneous acquisition of tumorigenicity and invasiveness by mouse lens explant cells during culture in vitro. In Vitro 27:369–380
191. Mialhe A, Levacher G, Champelovier P, Martel V, Serres M, Knudsen K, Seigneurin D (2000) Expression of E-, P-, N-cadherins and catenins in human bladder carcinoma cell lines. J Urol 164:826–835
192. Mirabelli-Primdahl L, Gryfe R, Kim H, Millar A, Luceri C, Dale D, Holowaty E, Bapat B, Gallinger S, Redston M (1999) β-Catenin mutations are specific for colorectal carcinomas with microsatellite instability but occur in endometrial carcinomas irrespective of mutator pathway. Cancer Res 59:3346–3351
193. Miyata M, Shiozaki H, Kobayashi K, Yano H, Tamura S, Tahara H, Mori T (1990) Correlation between expression of E-cadherin and metastases in human esophageal cancer: preliminary report. Nippon Geka Gakkai Zasshi 91:1761
194. Miyoshi Y, Iwao K, Nagasawa Y, Aihara T, Sasaki Y, Imaoka S, Murata M, Shimano T, Nakamura Y (1998) Activation of the β-catenin gene in primary hepatocellular carcinomas by somatic alterations involving Exon 3. Cancer Res 58:2524–2527
195. Mohan R, Lee B, Panjwani N (1995) Molecular cloning of the E-cadherin cDNAs from rabbit corneal epithelium. Curr Eye Res 14:1135–1145
196. Moll R, Mitze M, Frixen UH, Birchmeier W (1993) Differential loss of E-cadherin expression in infiltrating ductal and lobular breast carcinomas. Am J Pathol 143:1731–1742
197. Momparler RL, Bovenzi V (2000) DNA methylation and cancer. J Cell Physiol 183:145–154

198. Monks DA, Getsios S, MacCalman CD, Watson NV (2001) N-cadherin is regulated by gonadal steroids in the adult hippocampus. Proc Natl Acad Sci U S A 98:1312–1316
199. Mouriaux F, Maurage C-A, Labalette P, Sablonnière B, Malecaze F, Darbon J-M (2000) Cyclin-dependent kinase inhibitory protein expression in human choroidal melanoma tumors. Invest Ophthalmol Vis Sci 41:2837–2843
200. Müller T, Choidas A, Reichmann E, Ullrich A (1999) Phosphorylation and free pool of β-catenin are regulated by tyrosine kinases and tyrosine phosphatases during epithelial cell migration. J Biol Chem 274:10173–10183
201. Munemitsu S, Albert I, Souza B, Rubinfeld B, Polakis P (1995) Regulation of intracellular β-catenin levels by the adenomatous polyposis coli (APC) tumor-suppressor protein. Proc Natl Acad Sci U S A 92:3046–3050
202. Navarro P, Ruco L, Dejana E (1998) Differential localization of VE- and N-cadherins in human endothelial cells: VE-cadherin competes with N-cadherin for junctional localization. J Cell Biol 140:1475–1484
203. Nesbit M, Herlyn M (1994–95) Adhesion receptors in human melanoma progression. Invasion Metastasis 14:131–146
204. Nieman MT, Prudoff RS, Johnson KR, Wheelock MJ (1999) N-cadherin promotes motility in human breast cancer cells regardless of their E-cadherin expression. J Cell Biol 147:631–643
205. Ninomiya I, Endo Y, Fushida S, Sasagawa T, Miyashita T, Fujimura T, Nishimura G, Tani T, Hashimoto T, Yagi M, Shimizu K, Ohta T, Yonemura Y, Inoue M, Sasaki T, Miwa K (2000) Alteration of β-catenin expression in esophageal squamous-cell carcinoma. Int J Cancer 85:757–761
206. Noë V, Bruyneel E, Mareel M, Bracke M (1999) The E-cadherin/catenin complex in invasion: the role of ectodomain shedding. In: Jiang WG, Mansel RE (eds) Cancer metastasis, molecular & cellular mechanisms and clinical interventons. Kluwer Academic Publishers, Dordrecht, The Netherlands, pp 75–119
207. Noë V, Fingleton B, Jacobs K, Crawford HC, Vermeulen S, Steelant W, Bruyneel E, Matrisian LM, Mareel M (2001) Release of an invasion promotor E-cadherin fragment by matrilysin and stromelysin-1. J Cell Sci 114:111–118
208. Nollet F, Van Hengel J, Berx G, Molemans F, Van Roy F (1995) Isolation and characterization of a human pseudogene (CTNNAP1) for αE-catenin (CTNNA1): assignment of the pseudogene to 5q22 and the αE-catenin gene to 5q31. Genomics 26:410–413
209. Nollet F, Berx G, Van Roy F (1999) The role of the E-cadherin/catenin adhesion complex in the development and progression of cancer. Mol Cell Biol Res Commun 2:77–85
210. Nollet F, Kools P, van Roy F (2000) Phylogenetic analysis of the cadherin superfamily allows identification of six major subfamilies besides several solitary members. J Mol Biol 299:551–572
211. Noren NK, Liu BP, Burridge K, Kreft B (2000) p120 Catenin regulates the actin cytoskeleton via Rho family GTPases. J Cell Biol 150:567–579
212. Nouwen EJ, Dauwe S, Van Der Biest I, De Broe ME (1993) Stage- and segment-specific expression of cell-adhesion molecules N-CAM, A-CAM, and L-CAM in the kidney. Kidney Int 44:147–158
213. Oka H, Shiozaki H, Kobayashi K, Inoue M, Tahara H, Kobayashi T, Takatsuka Y, Matsuyoshi N, Hirano S, Takeichi M, Mori T (1993) Expression of E-cadherin cell adhesion molecules in human breast cancer tissues and its relationship to metastasis. Cancer Res 53:1696–1701
214. Omholt K, Platz A, Ringborg U, Hansson J (2001) Cytoplasmic and nuclear accumulation of β-catenin is rarely caused by CTNNB1 exon 3 mutations in cutaneous malignant melanoma. Int J Cancer 92:839–842
215. Otto T, Birchmeier W, Schmidt U, Hinke A, Schipper J, Rübben H, Raz A (1994) Inverse relation of E-cadherin and autocrine motility factor receptor expression as a prognostic factor in patients with bladder carcinomas. Cancer Res 54:3120–3123
216. Oyama T, Kanai Y, Ochiai A, Akimoto S, Oda T, Yanagihara K, Nagafuchi A, Tsukita S, Shibamoto S, Ito F, Takeichi M, Matsuda H, Hirohashi S (1994) A truncated β-catenin disrupts the interaction between E-cadherin and α-catenin: a cause of loss of intercellular adhesiveness in human cancer cell lines. Cancer Res 54:6282–6287
217. Ozawa M, Kemler R (1998) The membrane-proximal region of the E-cadherin cytoplasmic domain prevents dimerization and negatively regulates adhesion activity. J Cell Biol 142:1605–1613
218. Ozawa M, Baribault H, Kemler R (1989) The cytoplasmic domain of the cell adhesion molecule uvomorulin associates with three independent proteins structurally related in different species. EMBO J 8:1711–1717
219. Palacios J, Gamallo C (1998) Mutations in the β-catenin gene (CTNNB1) in endometrioid ovarian carcinomas. Cancer Res 58:1344–1347
220. Palacios J, Benito N, Pizarro A, Suarez A, Espada J, Cano A, Gamallo C (1995) Anomalous expression of P-cadherin in breast carcinoma. Am J Pathol 146:605–612
221. Paradies NE, Grunwald GB (1993) Purification and characterization of NCAD90, a soluble endogenous form of N-cadherin, which is generated by proteolysis during retinal development and retains adhesive and neurite-promoting function. J Neurosci Res 36:33–45
222. Peralta Soler A, Knudsen KA, Jaurand M-C, Johnson KR, Wheelock MJ, Klein-Szanto AJP, Salazar H (1995) The differential expression of N-cadherin and E-cadherin distinguishes pleural mesotheliomas from lung adenocarcinomas. Hum Pathol 26:1363–1369
223. Peralta Soler A, Knudsen KA, Tecson-Miguel A, McBrearty FX, Han AC, Salazar H (1997) Expression of E-cadherin and N-cadherin in surface epithelial-stromal tumors of the ovary distinguishes mucinous from serous and endometrioid tumors. Hum Pathol 28:734–739
224. Peralta Soler A, Knudsen KA, Salazar H, Han AC, Keshgegian AA (1999) P-Cadherin expression in breast carcinoma indicates poor survival. Cancer 86:1263–1272
225. Perl A-K, Wilgenbus P, Dahl U, Semb H, Christofori H (1998) A causal role for E-cadherin in the transition from adenoma to carcinoma. Nature 392:190–193
226. Peto R, Pike MC, Armitage P, Breslow NE, Cox DR, Howard SV, Mantel N, McPherson K, Peto J, Smith PG (1977) Design and analysis of randomized clinical trials requiring prolonged observation of each patient. II. Analysis and examples. Br J Cancer 35:1–39
227. Peyriéras N, Hyafil F, Louvard D, Ploegh HL, Jacob F (1983) Uvomorulin: a nonintegral membrane protein of early mouse embryo. Proc Natl Acad Sci U S A 80:6274–6277
228. Pishvaian MJ, Feltes CM, Thompson P, Bussemakers MJ, Schalken JA, Byers SW (1999) Cadherin-11 is expressed in invasive breast cancer cell lines. Cancer Res 59:947–952
229. Plotnikov AN, Schlessinger J, Hubbard SR, Mohammadi M (1999) Structural basis for FGF receptor dimerization and activation. Cell 98:641–650
230. Popov Z, Gil-Diez de Medina S, Lefrere-Belda M-A, Hoznek A, Bastuji-Garin S, Abbou CC, Thiery JP, Radvanyi F, Chopin DK (2000) Low E-cadherin expression in bladder cancer at the transcriptional and protein level provides prognostic information. Br J Cancer 83:209–214
231. Rasbridge SA, Gillett CE, Sampson SA, Walsh FS, Millis RR (1993) Epithelial (E-) and placental (P-) cadherin cell adhesion molecule expression in breast carcinoma. J Pathol 169:245–250
232. Rieger-Christ KM, Cain JW, Braasch JW, Dugan JM, Silverman ML, Bouyounes B, Libertino JA, Summerhayes IC (2001) Expression of classic cadherins type I in urothelial neoplastic progression. Hum Pathol 32:18–23
233. Riehl R, Johnson K, Bradley R, Grunwald GB, Cornel E, Lilienbaum A, Holt CE (1996) Cadherin function is required for axon outgrowth in retinal ganglion cells in vivo. Neuron 17:837–848

234. Rimm DL, Caca K, Hu G, Harrison FB, Fearon ER (1999) Frequent nuclear/cytoplasmic localization of β-catenin without exon 3 mutations in malignant melanoma. Am J Pathol 154:325–329
235. Roark EF, Paradies NE, Lagunowich LA, Grunwald GB (1992) Evidence for endogenous proteases, mRNA level and insulin as multiple mechanisms of N-cadherin down-regulation during retinal development. Development 114:973–984
236. Rocha AS, Soares P, Seruca R, Máximo V, Matias-Guiu X, Cameselle-Teijeiro J, Sobrinho-Simões M (2001) Abnormalities of the E-cadherin/catenin adhesion complex in classical papillary thyroid carcinoma and in its diffuse sclerosing variant. J Pathol 194:358–366
237. Ropponen KM, Eskelinen MJ, Lipponen PK, Alhava EM, Kosma V-M (1999) Reduced expression of α catenin is associated with poor prognosis in colorectal carcinoma. J Clin Pathol 52:10–16
238. Rosato R, Veltmaat JM, Groffen J, Heisterkamp N (1998) Involvement of the tyrosine kinase Fer in cell adhesion. Mol Cell Biol 18:5762–5770
239. Rubinfeld B, Souza B, Albert I, Muller O, Chamberlain SH, Masiarz FR, Munemitsu S, Polakis P (1993) Association of the APC gene product with beta-catenin. Science 262:1731–1734
240. Rubinfeld B, Robbins P, El-Gamil M, Albert I, Porfiri E, Polakis P (1997) Stabilization of β-catenin by genetic defects in melanoma cell lines. Science 275:1790–1792
241. Rye PD, Norum L, Olsen DR, Garman-Vik S, Kaul S, Fodstad O (1996) Brain metastasis model in athymic nude mice using a novel MUC1-secreting human breast-cancer cell line, MA11. Int J Cancer 68:682–687
242. Saito T, Oda Y, Sakamoto A, Tamiya S, Kinukawa N, Hayashi K, Iwamoto Y, Tsuneyoshi M (2000) Prognostic value of the preserved expression of the E-cadherin and catenin families of adhesion molecules and of β-catenin mutations in synovial sarcoma. J Pathol 192:342–350
243. Salomon D, Ayalon O, Patel-King R, Hynes RO, Geiger B (1992) Extrajunctional distribution of N-cadherin in cultured human endothelial cells. J Cell Sci 102:7–17
244. Sanders DSA, Bruton R, Darnton SJ, Casson AG, Hanson I, Williams HK, Jankowski J (1998) Sequential changes in cadherin-catenin expression associated with the progression and heterogeneity of primary oesophageal squamous carcinoma. Int J Cancer 79:573–579
245. Sanders DSA, Blessing K, Hassan GAR, Bruton R, Marsden JR, Jankowski J (1999) Alterations in cadherin and catenin expression during the biological progression of melanocytic tumours. J Clin Pathol 52:151–157
246. Sandig M, Voura EB, Kalnins VI, Siu CH (1997) Role of cadherins in the transendothelial migration of melanoma cells in culture. Cell Motil Cytoskeleton 38:351–364
247. Schiffman JS, Grunwald GB (1992) Differential cell adhesion and expression of N-cadherin among retinoblastoma cell lines. Invest Ophthalmol Vis Sci 33:1568–1574
248. Schulz S, Becker K-F, Braungart E, Reichmuth C, Klamt B, Becker I, Atkinson M, Gessler M, Höfler H (2000) Molecular analysis of E-cadherin and cadherin-11 in Wilms' tumours. J Pathol 191:162–169
249. Scott RA, Lauweryns B, Snead DM, Haynes RJ, Mahida Y, Dua HS (1997) E-Cadherin distribution and epithelial basement membrane characteristics of the normal human conjunctiva and cornea. Eye 11:607–612
250. Serini G, Trusolino L, Saggiorato E, Cremona O, De Rossi M, Angeli A, Orlandi F, Marchisio PC (1996) Changes in integrin and E-cadherin expression in neoplastic versus normal thyroid tissue. J Natl Cancer Inst 88:442–449
251. Serres M, Grangeasse C, Haftek M, Durocher Y, Duclos B, Schmitt D (1997) Hyperphosphorylation of β-catenin on serine-threonine residues and loss of cell-cell contacts induced by calyculin A and okadaic acid in human epidermal cells. Exp Cell Res 231:163–172
252. Serres M, Filhol O, Lickert H, Grangeasse C, Chambaz EM, Stappert J, Vincent C, Schmitt D (2000) The disruption of adherens junctions is associated with a decrease of E-cadherin phosphorylation by protein kinase CK2. Exp Cell Res 257:255–264
253. Shapiro L, Fannon AM, Kwong PD, Thompson A, Lehmann MS, Grübel G, Legrand JF, Als-Nielsen J, Colman DR, Hendrickson WA (1995) Structural basis of cell-cell adhesion by cadherins. Nature 374:327–337
254. Shibamoto S, Hayakawa M, Takeuchi K, Hori T, Oku N, Miyazawa K, Kitamura N, Takeichi M, Ito F (1994) Tyrosine phosphorylation of β-catenin and plakoglobin enhanced by hepatocyte growth factor and epidermal growth factor in human carcinoma cells. Cell Adhes Commun 1:295–305
255. Shibata T, Ochiai A, Kanai Y, Akimoto S, Gotoh M, Yasui N, Machinami R, Hirohashi S (1996) Dominant negative inhibition of the association between β-catenin and c-erbB-2 by N-terminally deleted β-catenin suppresses the invasion and metastasis of cancer cells. Oncogene 13:883–889
256. Shimazui T, Giroldi LA, Bringuier PP, Oosterwijk E, Schalken JA (1996) Complex cadherin expression in renal cell carcinoma. Cancer Res 56:3234–3237
257. Shimazui T, Oosterwijk-Wakka J, Akaza H, Bringuier PP, Ruijter E, Debruyne FMJ, Schalken JA, Oosterwijk E (2000) Alterations in expression of cadherin-6 and E-cadherin during kidney development and in renal cell carcinoma. Eur Urol 38:331–338
258. Shimoyama Y, Hirohashi S (1991) Expression of E- and P-cadherin in gastric carcinomas. Cancer Res 51:2185–2192
259. Shinoura N, Paradies NE, Warnick RE, Chen H, Larson JJ, Tew JJ, Simon M, Lynch RA, Kanai Y, Hirohashi S, Hemperly JJ, Menon AG, Brackenbury R (1995) Expression of N-cadherin and α-catenin in astrocytomas and glioblastomas. Br J Cancer 72:627–633
260. Shiozaki H, Kadowaki T, Doki Y, Inoue M, Tamura S, Oka H, Iwazawa T, Matsui S, Shimaya K, Takeichi M, Mori T (1995) Effect of epidermal growth factor on cadherin-mediated adhesion in a human oesophageal cancer cell line. Br J Cancer 71:250–258
261. Soares P, Berx G, Van Roy F, Sobrinho-Simões M (1997) E-cadherin gene alterations are rare events in thyroid tumors. Int J Cancer 70:32–38
262. Sobin LH, Wittekind C (eds) (1997) TNM classification of malignant tumours, 5th edn. John Wiley & Sons, Inc, New York
263. Sommers CL, Thompson EW, Torri JA, Kemler R, Gelmann EP, Beyers SW (1991) Cell adhesion molecule uvomorulin expression in human breast cancer cell lines: relationship to morphology and invasive capacities. Cell Growth Differ 2:365–372
264. Spancake KM, Anderson CB, Weaver VM, Matsunami N, Bissell M, White RL (1999) E7-transduced human breast epithelial cells show partial differentiation in three-dimensional culture. Cancer Res 59:6042–6045
265. Sparks AB, Morin PJ, Vogelstein B, Kinzler KW (1998) Mutational analysis of the APC/β-catenin/Tcf pathway in colorectal cancer. Cancer Res 58:1130–1134
266. Späth GF, Weiss MC (1998) Hepatocyte nuclear factor 4 provokes expression of epithelial marker genes, acting as a morphogen in dedifferentiated hepatoma cells. J Cell Biol 140:935–946
267. Steelant WFA, Goeman JL, Philippé J, Oomen LCJM, Hilkens J, Krzewinski-Recchi M-A, Huet G, Van der Eycken J, Delannoy P, Bruyneel EA, Mareel MM (2001) The alkyl-lysophospholipid 1-O-octadecyl-2-O-methyl-glycerophosphocholine induces invasion through episialin-mediated neutralization of E-cadherin in human mammary MCF-7 cells in vitro. Int J Cancer 92:527–536
268. Stewart DB, Barth AIM, Nelson WJ (2000) Differential regulation of endogenous cadherin expression in Madin-Darby canine kidney cells by cell-cell adhesion and activation of ß-catenin signaling. J Biol Chem 275:20707–20716

269. Tabibzadeh S, Kong QF, Kapur S, Satyaswaroop PG, Aktories K (1995) Tumour necrosis factor-α-mediated dyscohesion of epithelial cells is associated with disordered expression of cadherin/β-catenin and disassembly of actin filaments. Hum Reprod 10:994–1004
270. Takeichi M (1988) The cadherins: cell-cell adhesion molecules controlling animal morphogenesis. Development 102:639–655
271. Tamura G, Yin J, Wang S, Fleisher AS, Zou T, Abraham JM, Kong D, Smolinski KN, Wilson KT, James SP, Silverberg SG, Nishizuka S, Terashima M, Motoyama T, Meltzer SJ (2000) E-cadherin gene promoter hypermethylation in primary human gastric carcinomas. J Natl Cancer Inst 92:569–573
272. Tang A, Amagai M, Granger LG, Stanley JR, Udey MC (1993) Adhesion of epidermal Langerhans cells to keratinocytes mediated by E-cadherin. Nature 361:82–85
273. Tang A, Eller MS, Hara M, Yaar M, Hirohashi S, Gilchrest BA (1994) E-cadherin is the major mediator of human melanocyte adhesion to keratinocytes in vitro. J Cell Sci 107:983–992
274. Tani T, Laitinen L, Kangas L, Lehto V-P, Virtanen I (1995) Expression of E- and N-cadherin in renal cell carcinomas, in renal cell carcinoma cell lines in vitro and in their xenografts. Int J Cancer 64:407–414
275. Tejpar S, Nollet F, Li C, Wunder JS, Michils G, dal Cin P, Van Cutsem E, Bapat B, Van Roy F, Cassiman JJ, Alman BA (1999) Predominance of beta-catenin mutations and beta-catenin dysregulation in sporadic aggressive fibromatosis (desmoid tumor). Oncogene 18:6615–6620
276. Thiele A, Thormann M, Hofmann HJ, Naumann WW, Eger K, Hauschildt S, (2000) A possible role of N-cadherin in thalidomide teratogenicity. Life Sci 67:457–461
277. Thoreson MA, Anastasiadis PZ, Daniel JM, Ireton RC, Wheelock MJ, Johnson KR, Hummingbird DK, Reynolds AB (2000) Selective uncoupling of p120^{ctn} from E-cadherin disrupts strong adhesion. J Cell Biol 148:189–201
278. Tomita K, van Bokhoven A, van Leenders GJLH, Ruijter ETG, Jansen CFJ, Bussemakers MJG, Schalken JA (2000) Cadherin switching in human prostate cancer progression. Cancer Res 60:3650–3654
279. Torban E, Goodyer PR (1998) Effects of PAX2 expression in a human fetal kidney (HEK293) cell line. Biochim Biophys Acta 1401:53–62
280. Tran NL, Nagle RB, Cress AE, Heimark RL (1999) N-cadherin expression in human prostate carcinoma cell lines. An epithelial-mesenchymal transformation mediating adhesion with stromal cells. Am J Pathol 155:787–798
281. Tselepis C, Chidgey M, North A, Garrod D (1998) Desmosomal adhesion inhibits invasive behavior. Proc Natl Acad Sci U S A 95:8064–8069
282. Tsutsumimoto T, Kawasaki S, Ebara S, Takaoka K (1999) TNF-alpha and IL-1beta suppress N-cadherin expression in MC3T3-E1 cells. J Bone Miner Res 14:1751–1760
283. Turner JR, Torres CM, Wang HH, Shahsafaei A, Richards WG, Sugarbaker D, Odze RD (2000) Preoperative chemoradiotherapy alters the expression and prognostic significance of adhesion molecules in Barrett's-associated adenocarcinoma. Hum Pathol 31:347–353
284. Van Aken J, Cuvelier CA, De Wever N, Gao Y, Mareel MM, Roels HJ (1993) Immunohistochemical analysis of E-cadherin expression in human colorectal tumours. Pathol Res Pract 189:975–978
285. Van Hengel J, Vanhoenacker P, Staes K, van Roy F (1999) Nuclear localization of the p120^{ctn} Armadillo-like catenin is counteracted by a nuclear export signal and by E-cadherin expression. Proc Natl Acad Sci U S A 96:7980–7985
286. Van Hoorde L, Braet K, Mareel M (1999) The N-cadherin/catenin complex in colon fibroblasts and myofibroblasts. Cell Adhes Commun 7:139–150
287. Van Hoorde L, Pocard M, Maryns I, Poupon M-F, Mareel M (2000) Induction of invasion in vivo of α-catenin-positive HCT-8 human colon-cancer cells. Int J Cancer 88:751–758
288. van Raamsdonk CD, Tilghman SM (2000) Dosage requirement and allelic expression of PAX6 during lens placode formation. Development 127:5439–5448
289. Vermeulen SJ, Bruyneel EA, Bracke ME, De Bruyne GK, Vennekens KM, Vleminckx KL, Berx GJ, Van Roy FM, Mareel MM (1995) Transition from the noninvasive to the invasive phenotype and loss of α-catenin in human colon cancer cells. Cancer Res 55:4722–4728
290. Vermeulen SJ, Chen TR, Speleman F, Nollet F, Van Roy FM, Mareel MM (1998) Did the four human cancer cell lines DLD-1, HCT-15, HCT-8, and HRT-18 originate from one and the same patient? Cancer Genet Cytogenet 107:76–79
291. Vermeulen SJ, Nollet F, Teugels E, Vennekens KM, Malfait F, Philippé J, Speleman F, Bracke ME, Van Roy FM, Mareel MM (1999) The αE-catenin gene (CTNNA1) acts as an invasion-suppressor gene in human colon cancer cells. Oncogene 18:905–915
292. Vleminckx K, Vakaet L Jr, Mareel M, Fiers W, Van Roy F (1991) Genetic manipulation of E-cadherin expression by epithelial tumor cells reveals an invasion suppressor role. Cell 66:107–119
293. Vleminckx KL, Deman JJ, Bruyneel EA, Vandenbossche GMR, Keirsebilck AA, Mareel MM, Van Roy FM (1994) Enlarged cell-associated proteoglycans abolish E-cadherin functionality in invasive tumor cells. Cancer Res 54:873–877
294. Voeller HJ, Truica CI, Gelmann EP (1998) β-Catenin mutations in human prostate cancer. Cancer Res 58:2520–2523
295. von Wasielewski R, Rhein A, Werner M, Scheumann GFW, Dralle H, Pötter E, Brabant G, Georgii A (1997) Immunohistochemical detection of E-cadherin in differentiated thyroid carcinomas correlates with clinical outcome. Cancer Res 57:2501–2507
296. Vos CBJ, Cleton-Jansen AM, Berx G, de Leeuw WJF, ter Haar NT, van Roy F, Cornelisse CJ, Peterse JL, van de Vijver MJ (1997) E-cadherin inactivation in lobular carcinoma in situ of the breast: an early event in tumorigenesis. Br J Cancer 76:1131–1133
297. Wang J, Krill D, Torbenson M, Wang Q, Bisceglia M, Stoner J, Thomas A, DeFlavia P, Dhir R, Becich MJ (2000) Expression of cadherins and catenins in paired tumor and non-neoplastic primary prostate cultures and corresponding prostatectomy specimens. Urol Res 28:308–315
298. Welch DR, Bisi JE, Miller BE, Conaway D, Seftor EA, Yohem KH, Gilmore LB, Seftor RE, Nakajima M, Hendrix MJ (1991) Characterization of a highly invasive and spontaneously metastatic human malignant melanoma cell line. Int J Cancer 21:227–237
299. Wesseling J, van der Valk SW, Hilkens J (1996) A mechanism for inhibition of E-cadherin-mediated cell-cell adhesion by the membrane-associated mucin episialin/MUC1. Mol Biol Cell 7:565–577
300. Wheater PR, Burkitt HG, Daniels VG (eds) (1987) Functional histology: a text and colour atlas, 2nd edn. Churchill Livingstone, Edinburgh, London, Melbourne, New York
301. Wheelock MJ, Buck CA, Bechtol KB, Damsky CH (1987) Soluble 80-kd fragment of cell-CAM 120/80 disrupts cell-cell adhesion. J Cell Biochem 34:187–202
302. Wigle JT, Chowdhury K, Gruss P, Oliver G (1999) Prox1 function is crucial for mouse lens-fibre elongation. Nat Genet 21:318–322
303. Willert K, Nusse R (1998) β-Catenin: a key mediator of Wnt signaling. Curr Opin Genet Dev 8:95–102
304. Williams CL, Hayes VY, Hummel AM, Tarara JE, Halsey TJ (1993) Regulation of E-cadherin-mediated adhesion by muscarinic acetylcholine receptors in small cell lung carcinoma. J Cell Biol 121:643–654
305. Williams E, Williams G, Gour BJ, Blaschuk OW, Doherty P (2000) A novel family of cyclic peptide antagonists suggests that N-cadherin specificity is determined by amino acids that flank the HAV motif. J Biol Chem 275:4007–4012
306. Williams HK, Sanders DSA, Jankowski JAZ, Landini G, Brown AMS (1998) Expression of cadherins and catenins in

oral epithelial dysplasia and squamous cell carcinoma. J Oral Pathol Med 27:308–317
307. Wong AST, Maines-Bandiera SL, Rosen B, Wheelock MJ, Johnson KR, Leung PCK, Roskelley CD, Auersperg N (1999) Constitutive and conditional cadherin expression in cultured human ovarian surface epithelium: influence of family history of ovarian cancer. Int J Cancer 81:180–188
308. Yamada T, Takaoka AS, Naishiro Y, Hayashi R, Maruyama K, Maesawa C, Ochiai A, Hirohashi S (2000) Transactivation of the multidrug resistance 1 gene by T-cell factor 4/β-catenin complex in early colorectal carcinogenesis. Cancer Res 60:4761–4766
309. Yamamoto M, Bharti A, Li Y, Kufe D (1997) Interaction of the DF3/MUC1 breast carcinoma-associated antigen and β-catenin in cell adhesion. J Biol Chem 272:12492–12494
310. Yang S-Z, Kohno N, Kondo K, Yokoyama A, Hamada H, Hiwada K, Miyake M (1999) Adriamycin activates E-cadherin-mediated cell-cell adhesion in human breast cancer cells. Int J Oncol 15:1109–1115
311. Yonemura Y, Endou Y, Kimura K, Fushida S, Bandou E, Taniguchi K, Kinoshita K, Ninomiya I, Sugiyama K, Heizmann CW, Schafer BW, Sasaki T (2000) Inverse expression of S100A4 and E-cadherin is associated with metastatic potential in gastric cancer. Clin Cancer Res 6:4234–4242
312. Zhou Y, Fisher SJ, Janatpour M, Genbacev O, Dejana E, Wheelock M, Damsky CH (1997) Human cytotrophoblasts adopt a vascular phenotype as they differentiate. A strategy for successful endovascular invasion? J Clin Invest 99:2139–2151
313. Zhurinsky J, Shtutman M, Ben-Ze'ev A (2000) Plakoglobin and β-catenin: protein interactions, regulation and biological roles. J Cell Sci 113:3127–3139
314. Zondag GCM, Reynolds AB, Moolenaar WH (2000) Receptor protein-tyrosine phosphatase RPTPμ binds to and dephosphorylates the catenin $p120^{ctn}$. J Biol Chem 275:11264–11269
315. Zorn AM, Barish GD, Williams BO, Lavender P, Klymkowsky MW, Varmus HE (1999) Regulation of Wnt signaling by Sox proteins: XSox17α/β and XSox3 physically interact with β-catenin. Mol Cell 4:487–498
316. Zurawel RH, Chiappa SA, Allen C, Raffel C (1998) Sporadic medulloblastomas contain oncogenic β-catenin mutations. Cancer Res 58:896–899

Virchows Arch (2001) 439:752–755
DOI 10.1007/s004280100467

ORIGINAL ARTICLE

Maria P. Foschini · Luca Morandi · Sandro Macchia
Pier Roberto DalMonte · Annalisa Pession

TT virus-related acute recurrent hepatitis

Histological features of a case and review of the literature

Received: 28 February 2001 / Accepted: 20 April 2001 / Published online: 5 September 2001
© Springer-Verlag 2001

Abstract TT virus is a recently discovered virus, of which the pathogenetic potential is still uncertain. The present paper describes the histopathological features of a case of TT virus-related acute recurrent hepatitis. The patient is a 28-year-old woman with no history of drug or alcohol abuse, presenting with repeated episodes of hypertransaminasemia evidenced during the last 4 years. No other markers of viral or autoimmune disease were found. On histological analysis, the liver parenchyma showed a preserved architecture. The histological features were those of a mild acute hepatitis. The clinicopathological findings suggest that TT virus might be responsible for a mild form of liver disease.

Keywords Liver biopsy · Histology · TTV · Acute recurrent hepatitis

Note added in proof. Since the submission of the present paper, an additional case was seen by us. The patient was a 30-year-old lady who had repeated episodes of hypertransaminasemia, with serum alanine transferase levels ranging from normal to 204 U\l. Episodes of hypertransaminasemia presented with intervals of 2–3 months and had been present for the last 3 years. The patient had no history of drug abuse; viral markers tested (HBV and HCV) were negative as were markers of autoimmune disease. The liver biopsy showed a preserved architecture. Portal tracts contained mild lymphoid infiltrate. No features of piecemeal necrosis were observed. The liver parenchyma showed small foci of hepatocellular necrosis. TTV DNA was detected in the liver tissue. This second case had clinical history and pathologic features superimposable to those discussed in the present paper, thus reinforcing the suggestion that TTV can be responsible for a mild form of liver damage.

M.P. Foschini (✉) · L. Morandi · A. Pession
Department of Oncology, Section of Pathology,
University of Bologna, Bologna, Italy
e-mail: mariapia.foschini@ausl.bologna.it
Tel.: +39-051-6225523, Fax: +39-051-6225759

S. Macchia · P.R. DalMonte
Department of Gastroenterology, Ospedale Bellaria, Bologna, Italy

M.P. Foschini
Anatomia Patologica, Ospedale Bellaria, Via Altura 3,
40139 Bologna, Italy

Introduction

TT virus (TTV) was recently isolated in Japanese patients with acute non-A/non-G hepatitis [14]. TTV is a circular single-stranded DNA virus of 3852 bp which belongs to a new family named "circinoviridae" [13]. TTV is a heterogeneous virus. Based on sequence analysis, at least six different genotypes and several subtypes, with 30% and 11–15% nucleotide sequence divergences, have been described [18]. Series of TTV infections have been initially reported in Japan [24] and in the United States [3]. Subsequently, the incidence and distribution of TTV infection has been studied in Europe [1, 4, 7]. The possibility that TTV is responsible of non-A/non-G chronic and acute hepatitis and for hepatocellular carcinoma arising in cryptogenic cirrhosis was initially suggested [14, 16, 19] but recently questioned [5, 24]. More recent data indicate that TTV is a widespread virus with low pathogenicity, which might be responsible for a proportion of cases of non-A/non-G acute and chronic hepatitis [25].

The distribution and incidence of TTV have been the subject of numerous papers; nevertheless, histological features of TTV-related liver damage has been rarely described. The purpose of the present paper was to report the histopathological features of a case of TTV-related liver damage in order to further document the possible pathogenetic role of this newly discovered virus.

Case history

The patient discussed is a 28-year-old woman, with no history of alcohol or drug abuse. She presented herself in 1996 complaining of episodes of weakness. During clinical work-up, the serum alanine transferase (ALT) level was found to be 198 U\l (normal ranges 5–40 U\l). The remaining liver function tests were within normal ranges. Measurements of serum hepatitis B virus (HBV) DNA and hepatitis C virus (HCV) RNA were negative using polymerase chain reaction. Tests for HBV surface antigen (HbsAg), anti-HBc (hepatitis B core), and anti-HCV were negative. No autoimmunity was demonstrated. Cholesterol levels were within normal ranges. No therapy was administered, and the ALT level returned to normal value within 2 months. The patient remained well until June 2000 when she had a new episode of hypertransaminasemia (ALT

198 U\l). In September 2000, the ALT level was normal again, but at a further control in November 2000 it was 190 U\l. No markers of viral infection or of autoimmune disease have ever been found. On echography, the liver was unremarkable. No clinical signs of portal hypertension were present. A liver biopsy was performed to grade and stage the disease. In addition, as no causes of liver disease were evident, TTV DNA was sought in the liver tissue.

Materials and methods

The liver biopsy was obtained using a 14-G needle and was immediately fixed in formalin. The tissue was then paraffin embedded, following routine procedures. From the paraffin block, sections were obtained and stained with hematoxylin and eosin, Sirius red, periodic acid–schiff base after diastase digestion and Perls methods for histological diagnosis. Histological grading and staging were performed according to a previously reported system [22]. In addition, from the paraffin tissue block, five 5-µm sections were cut for DNA extraction, using a method described previously [6] and summarized here.

DNA extraction

Tissues were dewaxed in xylene and alcohol and treated with proteinase K (100 µg) in 100 µl digestion buffer [50 mM Tris HCl, pH 8.0; 5 mM ethylene diamine tetraacetic acid (EDTA), pH 8.0; 0.5% Tween 20] for 72 h at 37°C. Genomic DNA was extracted using column technology (Alphagenics Diaco Biotechnology Trieste, Italy) and diluted in 100 µl TE buffer (10 mM Tris HCl, pH 8.0; 1 mM EDTA, pH 8.0).

Outer and nested polymerase chain reaction

A 10-µl aliquot served as a template for amplification by means of manual hot-start polymerase chain reaction (PCR). TTV DNA was detected using a method described previously [17, 18, 19] with some modifications. Outer 5′UTR (untranslated region) PCR was performed with primers NG133 5′-GTAAGTGCACTTCCGAATGGCTGAG-3′ and NG147 5′-GCCAGTCCCGAGCCCGAATTGCC-3′ in the first round of PCR for 30 cycles (94°C 4 min; 94°C 30 s, 65°C 30 s, 72°C 30 s; with an additional 7 min for the last cycle). Nested 5'UTR PCR was carried out with primers NG134 5′-AGTTTTCCACGCCCGTCCGCAGC-3′ and NG132 5′-AGCCCGAATTGCCCCTTGAC-3′ for 30 cycles under the same conditions. The amplification products of the first round of PCR were 143-bp long, and those of the second round were 110-bp long. PCR mixes consisted of 10 mM Tris HCl, pH 8.3, 50 mM KCl, 1.5 mM $MgCl_2$, 200 µM dNTPs, 2.5 U Ampli *Taq* polymerase (Perkin Elmer), and 40 pmol each primer. The amplicons were visualized on an ethidium bromide-stained agarose gels (2%) in a conventional electrophoresis apparatus.

Sequence analysis

Direct sequencing of nested amplicons was carried out using fluorescence-labeled ddNTPs and analyzed in a CEQ2000 (Beckman Coultear) automatic capillary sequence analyzer. Nucleotide sequence comparisons were made by BLAST 2 and Advance BLAST (http://www.ncbi.nlm.nih.gov/gorf/bl2.html) with nucleotide sequence data of the TTV complete genome deposited in GeneBank under accession number NC_002076 [4].

Results

Histology

The liver biopsy showed a preserved architecture (Fig. 1). A periportal fibrosis was seen and graded as mild [22] (Fig. 2). No portal inflammation was present.

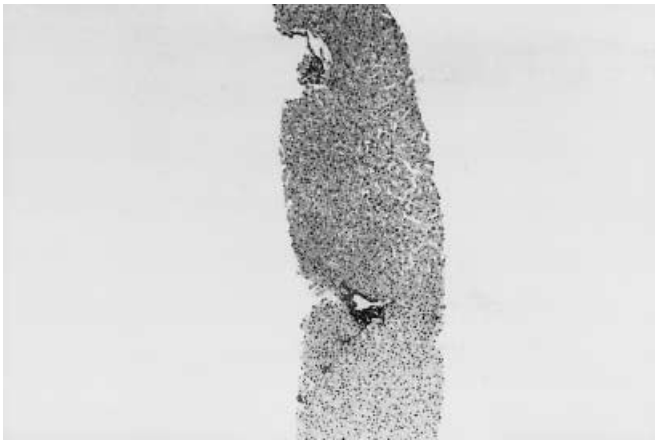


Fig. 1 The liver biopsy showed a preserved architecture (Sirius red ×25)

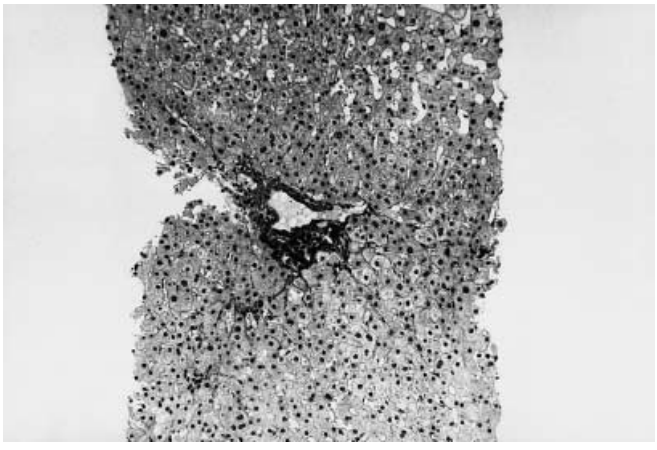


Fig. 2 A mild periportal fibrosis was evidenced by Sirius red staining (×125)

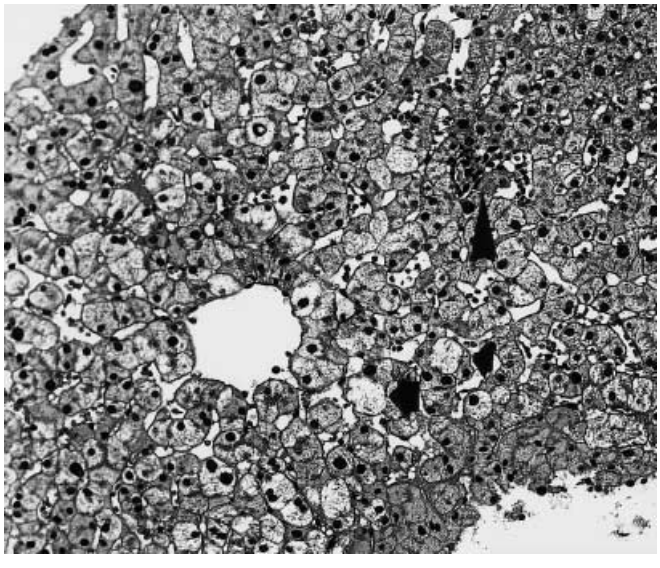


Fig. 3 Hepatocytes present swollen cytoplasm (*arrow*). A small focus of spotty necrosis is visible (*arrowhead*) (hematoxylin and eosin ×250)

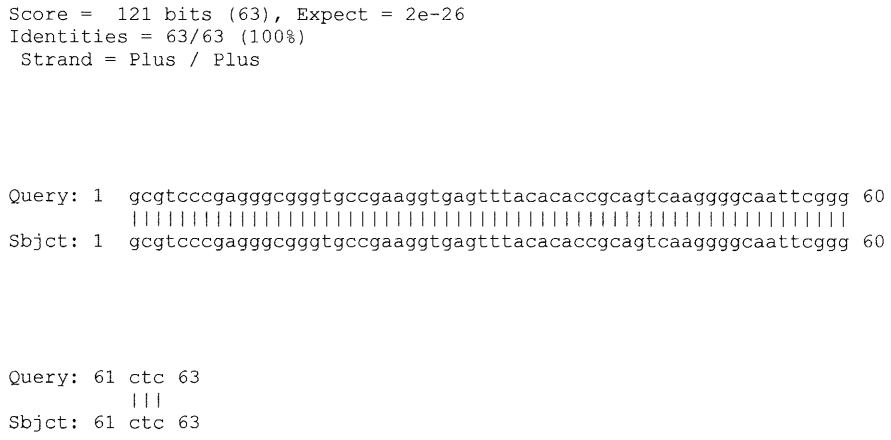


Fig. 4 The alignment of the 5′UTR fragment obtained from our sample confirmed the specificity of the polymerase chain reaction product

Portal bile ducts were preserved. In the liver parenchyma, a mild [22] lobular activity was observed, characterized by rare foci of spotty necrosis (Fig. 3) with rare apoptotic bodies. Ballooning degeneration of hepatocytes and mild intracellular cholestasis were present, mainly in zone-3 hepatocytes. In addition, features of regeneration were present as, focally, hepatocytes were organized in two-cell thick trabeculae, and binucleated hepatocytes appeared.

PCR results

A PCR product of the expected size was detected demonstrating the presence of TTV genome in the liver tissue. The alignment, by BLAST2, of the 5′UTR fragment obtained from our sample confirmed the specificity of PCR amplification by perfect alignment (100%) with TTVsan-S039 strain (accession number AB038620). The statistics (bitscore and expect value) were calculated based on the size of non-redundant database (Fig. 4).

Discussion

The present case presented histological features of mild acute hepatitis. Only mild periportal fibrosis was present, presumably as a sequel from previous hepatitis episodes. Despite extensive clinical and laboratory searches, no other possible causes of liver injury were detected, thus proposing TTV as the most plausible cause of the repeated episodes of hypertransaminasemia.

TTV is a widespread virus, having been found in a large proportion of the general population. Its incidence varies in different countries, being higher in Japan [10, 24]. In Western countries it has been found in 1–22% [1, 3, 4, 25] of healthy blood donors, without transaminase elevation. TTV is present in blood and blood products [23], thus being implicated as a possible cause of post-transfusion hepatitis. TTV has been found also in saliva, bile, and semen [8, 15], thus allowing for the possibility of an oro–faecal route of transmission. In view of the large diffusion of TTV and of the possible multiple transmission routes, its pathogenetic role is under evaluation.

Where TTV is localized and replicates in liver tissue is an open question. TTV is present inside the hepatocytes, as demonstrated using in situ hybridization [11, 21]. It has been shown that TTV titers in liver tissue are 10–100 times higher than in serum [19]. In addition replicative intermediates have been demonstrated in liver tissue by Okamoto et al. [20]. Finally, TTV is excreted in the bile [15]. All these data point toward the elective localization and replication of TTV in liver tissue.

A second point to be clarified is the pathogenetic potential of TTV. Despite the diffusion among the general population, studies comparing the incidence of TTV infection in healthy and diseased patients found a prevalence of TTV in the second group. Charlton et al. [3] found TTV in 1% of healthy blood donors, compared with 15% positivity obtained in cases of cryptogenic cirrhosis and 27% of patients with idiopathic hepatic failure. Tuveri et al. [25] studied a large series of patients composed of three groups: healthy blood donors and those with non-viral liver diseases and non-A/non-G hepatitis. The incidence of TTV was 2% and 4.4%, respectively, in the first two groups compared with 11.8% in the group with non-A/non-G hepatitis. These latter investigators suggested that TTV is a widespread agent with weak pathogenicity, but it might be responsible for a small proportion of hepatitis of unknown etiology.

Data on tissue damage are needed in order to further assess the pathologic potential of the virus. Only few histopathological studies on liver tissues in patients with TTV infection have been published [2, 11, 12, 21], and part of them deal with cases of multiple infections or with cases of TTV associated with non-viral liver disease [2, 21]. Bruno et al. [2] compared histological features of HCV infection and of HCV–TTV infection in patients with human immunodeficiency virus. They found no differences between the two groups, thus suggesting that TTV is not associated with a distinct type of liver injury. Similar data have been described by Rodriguez Inigo et al. [21]. Nevertheless, the latter group, studying TTV distribution in liver tissue by in situ hybridization, found that the percentage of infected hepatocytes significantly correlated with the levels of serum ALT. A histological description of liver biopsies from patients carrying TTV

infection alone, not associated with other possible causes of hepatitis, has been provided by Luo et al. [12] who found a mild liver cell damage, similar to that observed in the present case.

The patient described here went through repeated episodes of elevated levels of ALT. Only a few data are available on the follow-up of TTV-infected patients. Kangxian et al. [9] followed up a series of 381 patients with enterically transmitted TTV infection and found that ALT levels remained elevated for 6 months after the onset of the disease in 29.7% of the patients, and for 18 months in 13.9% of the patients.

These data suggest that, even if most of the TTV-infected patients are asymptomatic, a mild form of liver disease may appear and persist for a long period in a minority of cases.

Acknowledgements We thank Prof. V. Eusebi for critical review of the manuscript.

References

1. Biagini P, Gallian P, Tounissi M, Cantaloube JF, Zapitelli J, de Lamball X, de Micco P (2000) High prevalence of TT virus infection in French blood donors revealed by the use of three PCR systems. Transfusion 40:590–595
2. Bruno R, Sacchi P, Debiaggi M, Patruno SFA, Zara F, Ciappina V, Brunetti E, Filice C, Zocchetti C, Maffezini E, Pistorio A, Filice G (2000) Prevalence and histologic features of transfusion transmitted virus and hepatitis C coinfection in a group of HIV patients. Digest Liver Dis 32:617–620
3. Charlton M, Adjei P, Poterucha J, Zein N, Moore B, Therneau T, Krom R, Wiesner R (1998) TT virus infection in North American blood donors, patients with fulminant hepatic failure and cryptogenetic cirrhosis. Hepatology 28:839–842
4. Colombatto P, Brunetto MR, Kansopon J, Oliveti F, Maina A, Argon U, Bortoli ML, Scatena F, Baicchi U, Houghton M, Bonino F, Weiner AG (1999) High prevalence of G1 and G2 TT-virus infection in subjects with high and low exposure risk. Identification of G4 isolates in Italy. J Hepatol 31:990–996
5. Del Carmen Parquet M, Yatsuhashi H, Koga M, Inoue O, Matsumoto T, Hamada R, Igarashi A, Yano M (1999) Prevalence and characteristics of TT virus (TTV) in patients with sporadic acute hepatitis of unknown etiology. J Hepatol 31: 985–989
6. Foschini MP, Morandi L, Macchia S, DalMonte PR, Pession A (2001) Demonstration of TT virus in formalin fixed and paraffin embedded liver tissue. Pathologica 93:112–117
7. Gallian P, Biagini P, Zhong S, Tounissi M, Yeo W, Cantaloube JF, Atton, De Micco P, Johnson PJ, de Lamballerie X (2000) TT virus: a study of molecular epidemiology and transmission of genotypes 1, 2 and 3. J Clin Virol 17:43–49
8. Inami T, Konomi N, Arakawa Y, Abe K (2000) High prevalence of TT virus DNA in human saliva and semen. J Clin Microbiol 38:2407–2408
9. Kangxian L, Weifgang L, Lian Z, Zhiying C (2000) Epidemiological survey and follow-up of transfusion-transmitted virus after an outbreak of enterically transmitted infection. J Viral Hepatitis 7:309–312
10. Kato T, Mizokami M, Orito E, Nakano T, Tanaka Y, Ueda R, Hirashima N, Iijima Y, Kato T, Sagauchi F, Mukaide M, Shimamatsu K, Kage M, Kojiro M (1999) High prevalence of TT virus infection in Japanese patients with liver disease and in blood donors. J Hepatol 31:221–227
11. Jiang XJ, Luo X, He HT (2000) Intrahepatic transfusion – transmitted virus detected by in situ hybridization in patients with liver disease. J Viral Hepatitis 7:292–296
12. Luo KX, Zhang L, Wang SS, Nie J, Yang SC, Liu DX, Liang WF, He HT (1999) An outbreak of enterically transmitted non-A, non-E viral hepatitis. J Viral Hepatitis 6:59–64
13. Mushahwar IK, Erker JC, Muerhoff AS, Leary TP, Simons JN, Birkenmeyer LG, Chalmers ML, Pilot-Matias TJ, Dexai SM (1999) Molecular and biophysical characterization of TT virus: evidence for a new virus family infecting humans. Proc Natl Acad Sci U S A 96:3177–3182
14. Nagakawa N, Ikoma J, Ishikara T, Yasui N, Iwasa M, Kaito M, Watanabe S, Adachi Y (1999) High prevalence of transfusion transmitted virus among patients with non B, non C hepatocellular carcinoma. Cancer 86:1437–1440
15. Nakagawa N, Ikoma J, Ishikara T, Yasui-Kawamura N, Fuijita N, Iwasa Kaito M, Watanabe S, Adachi Y (2000) Biliary excretion of TT virus (TTV). J Med Virol 61:462–467
16. Nishizawa T, Okamoto H, Konishi K, Yoshizawa H, Miyakawa Y, Mayumi M (1997) A novel DNA virus (TTV) associated with elevated transaminase levels in post-transfusion hepatitis of unknown aetiology. Biochem Biophys Res Commun 241:92–97
17. Okamoto H, Fukuda M, Tawara A, Nishizawa T, Itoh Y, Hayasaka I, Tsuda F, Tanaka T, Miyakawa Y, Mayumi M (2000) Species-specific TT viruses and cross-species infection in nonhuman primates. J Virol 74:1132–1139
18. Okamoto H (1999) Marked genomic heterogeneity and frequent mixed infection of TT virus demonstrated by PCR with primers from coding and non coding regions. Virology 259: 428–436
19. Okamoto H, Nishizawa T, Kato N, Ukita M, Ikeda H, Iizuka H, Miyakawa Y, Mayumi M (1998) Molecular cloning and characterization of a novel DNA virus (TTV) associated with post transfusion hepatitis of unknown etiology. Hepatology Res 10:1–16
20. Okamoto H, Ukita M, Nishizawa T, Kishimoto J, Hoshi Y, Mizuo H, Tanaka T, Miyakawa Y, Mayumi M (2000) Circular double-stranded forms of TT virus DNA in the liver. J Virol 74:5161–5167
21. Rodriguez-Inigo E, Casqueiro M, Bartolome J, Ortiz-Movilla N, Lopez-Alcorocho JM, Herreo M, Monzarbeitia F, Oliva H, Carreno V (2000) Detection of TT virus DNA in liver biopsies by in situ hybridization. Am J Pathol 156:1227–1234
22. Scheuer PJ (1991) Classification of chronic viral hepatitis: a need for a reassessment. J Hepatol 13:372–374
23. Simmonds P, Davidson F, Lycett C, Prescott LE, MacDonald DM, Ellender J, Yap PL, Ludlam CA, Haydon GH, Gillon J, Jarvis LM (1998) Detection of a novel DNA virus (TTV) in blood donors and blood products. Lancet 352:191–195
24. Takahashi K, Hoshino H, Ohta Y, Yoshida N, Mishiro S (1998) Very high prevalence of TT virus (TTV) infection in the general population in Japan revealed by a new set of PCR primers. Hepatol Res 12:233–239
25. Tuveri R, Jaffredo F, Lunel F, Nalpas B, Pol S, Feray C, Marcellin P, Thibault V, Delagneau JF, Opolon P, Scarpa B, Brechot C, Thiers V (2000) Impact of TT virus infection in acute and chronic, viral and non viral related liver disease. J Hepatol 33:121–127

Virchows Arch (2001) 439:756–761
DOI 10.1007/s004280100468

ORIGINAL ARTICLE

Janusz Wlodarczyk · Birgit Bethke · Elke Mueller
Manfred Stolte · James Mueller

A comparative study of E-cadherin and stromelysin-3 expression in de novo and ex adenoma carcinoma of the colorectum

Received: 10 November 2000 / Accepted: 19 April 2001 / Published online: 5 October 2001
© Springer-Verlag 2001

Abstract An apparent exception to the colorectal adenoma-carcinoma carcinogenetic pathway is the so-called "de novo" carcinoma which has no evidence of adenoma in its vicinity. Despite the fact that they are often quite small, these lesions appear to be more aggressive (i.e., greater likelihood of lymph-node metastases) than carcinomas that clearly arise from surrounding adenomas ex-adenoma carcinoma. The purpose of the present comparative immunohistochemical study was to compare rates of cell adhesion molecule (E-cadherin) and protease [stromelysin-3 (ST-3)] expression in groups of de novo (n=64) and ex adenoma (n=42) lesions in order to see whether their more aggressive behavior is associated with decreased cell adhesion and increased protease expression. The rates of extensive ST-3 expression and decreased E-cadherin expression were significantly higher in the de novo group (P=0.014 and 0.005, respectively). Histopathologically, the de novo group also had a significantly higher percentage of cases with an infiltrative invasion pattern. These differences highlight the more aggressive phenotype of the de novo colorectal carcinoma and fit with their greater invasive potential.

Keywords De novo colorectal carcinoma · E-cadherin · Stromelysin-3 · Immunohistochemistry

J. Wlodarczyk
Chirurgische Klinik und Poliklinik,
Technische Universität München, Klinikum rechts der Isar,
Ismaninger Straße 22, 81675 Munich, Germany

B. Bethke · E. Mueller · M. Stolte
Institut für Pathologie, Klinikum Bayreuth,
Preuschwitzer Straße 101, 95445 Bayreuth, Germany

J. Mueller (✉)
Department of Pathology, Brigham and Women's Hospital,
75 Francis Street, Boston, MA, USA 02115
e-mail: jmueller@rics.bwh.harvard.edu
Tel.: +1-617-7325984, Fax: +1-617-7326177

Introduction

The development of colorectal carcinoma from a pre-existing adenoma is widely accepted as the predominant pathway of colorectal carcinogenesis. This concept is based on a large body of histomorphologic and molecular biologic data that has accumulated over the past several decades [7, 15, 16, 32]. Several years ago, however, primarily in Japan, small colorectal carcinomas were described that did not appear to have arisen from an adenoma, since no remnants of adenomatous tissue were found in their vicinity [14, 26]. These lesions were given the name "de novo" carcinomas, since it appeared that they arose de novo from normal mucosa. Along with their unusual appearance in which there is a sharp transition from normal to carcinomatous tissue, reports from Japan also emphasized that they appeared to be more aggressive than the conventional ex adenoma carcinomas, since they had a tendency to more deeply invade the colonic wall at a smaller size [13, 26].

E-cadherin is a 120-kDa transmembrane glycoprotein that belongs to a large superfamily of calcium-dependent cadherin adhesion molecules [24] and plays an important role in embryogenesis and in mature epithelia [6]. Abnormalities of E-cadherin expression have been described in colorectal carcinoma [31] and have been correlated with increased invasiveness, metastatic potential and poor patient prognosis in this tumor type [27].

Stromelysin-3 (ST-3) is a member of the metalloprotease family of proteases that also includes collagenases and gelatinases [1] and has been found to be especially strongly expressed in those tumors that have a pronounced locally invasive growth pattern [17]. In our own previous studies of ST-3 expression in colorectal carcinoma, we found that it was frequently expressed and was associated with an infiltrative invasion pattern [19, 28].

The aim of the present study was to determine whether the immunohistochemical expression of the cell adhesion molecule E-cadherin and the protease ST-3 differed significantly between groups of de novo and ex adenoma

Table 1 Clinicopathologic data for the two groups, de novo and ex adenoma

Significant differences were found between the two groups, de novo and ex adenoma carcinoma, comparing * size (P<0.0001, t-test), ** grade G1,2 vs G3 (P=0.003), and *** tumor-cell dissociation (P=0.003)

Group	De novo	Ex adenoma	Total
n	64	42	106
Sex (male:female)	39:25	18:24	57:49
Age (years; mean, range)	67.7 (45–91)	68.1 (33–92)	67.9 (33–92)
Site (right colon:left colon, rectum)	2:62	4:38	6:100
Mean lesion size (cm; range)*	0.72 (0.3–1.0)	1.88 (0.4–4.5)	1.18 (0.3–4.5)
Grade (G1:G2: G3)**	15:37:12	6:36:0	21:73:12
Tumor-cell dissociation (%)***	32 (50)	9 (21.4)	41 (38.7)
Lymph-vessel invasion (%)	18 (28.1)	9 (21.4)	27 (25.5)

carcinoma and could help explain the greater invasive and metastatic potential of de novo carcinoma.

Materials and methods

Specimens

The lesions for study consisted of 106 pT1 colorectal carcinomas (TNM classification of the UICC [30]), which were obtained from 106 patients (49 female, 57 male), with a mean age of 67.9 years (range 33–92 years) as shown in Table 1. None of the patients in either group had a known familial colon carcinoma syndrome such as familial adenomatous polyposis (FAP) or hereditary non-polyposis colon carcinoma (HNPCC). The tissue samples consisted of formalin-fixed, paraffin-embedded samples, most of which (103) were removed by endoscopic polypectomy. All but six of the lesions were found in the left colon or rectum.

Based on a previously published set of criteria [18, 20, 21], the lesions were classified as either de novo or ex adenoma carcinomas. The de novo cases showed definite invasion into, but not beyond, the submucosa, were 1.0 cm or less in diameter, and lacked adenoma elements in the vicinity of the tumor. The ex adenoma cases also invaded the submucosa, but not beyond, and had definite adenoma elements on the edge of the tumor. On the basis of these criteria, there were 64 de novo and 42 ex-adenoma colorectal carcinoma cases. The average size of the de novo cases was 0.72 cm (range 0.3–1.0 cm) and of the polyps in the ex adenoma group 1.88 cm (range 0.4–4.5 cm).

Immunohistochemistry

E-cadherin immunohistochemistry was carried out as previously described [25] with the E-cadherin specific HEC-D1 monoclonal antibody (Takara Biomedicals, Takara Shuzo, Japan). Briefly, 6-µm-thick tissue sections were placed onto silanized slides which were then deparaffinized and rehydrated. Antigen retrieval was performed by means of a citric acid solution (pH 6.0) which was heated with a microwave (1×15 min at 650 W). Endogenous peroxidase activity was blocked with a 0.2% hydrogen peroxide solution. The primary HEC-D1 antibody was incubated for 1.5 h at room temperature at a dilution of 1:1000. Detection of the bound antibody was carried out with the avidin–biotin complex peroxidase method (ABC Elite kit, Vector Burlingame, Calif.), followed by staining with the peroxidase substrate 3,3-diaminobenzidine tetrachloride (DAB; Sigma GmbH, Deisenhofen, Germany). A light hematoxylin stain was used as the counterstain. As a negative control, the primary antibody was replaced with phosphate-buffered saline. Normal colonic mucosa in the tissue sections served as the positive control. Staining for E-cadherin was classified as normal (3+) when it was similar to non-malignant mucosa, as reduced (2+) when the staining was somewhat less than in normal mucosa, as weak (1+) in the case of barely visible staining, and as negative (0) when there was no visible reaction.

Immunohistochemistry for ST-3 was also carried out as previously described [19, 23] using the monoclonal antibody 5ST-4A9, which was kindly provided by P. Chambon (Strasbourg, France) [29]. The 5ST-4A9 antibody was used at a dilution of 1:2000, and the reaction was developed using the ABC method followed by DAB staining with a light hematoxylin as the counterstain. The positive control consisted of a case of colon carcinoma known to be positive for ST-3 expression, and the negative control was the omission of the primary antibody on this case. Staining for ST-3 was scored according to percentage of the tumor stroma showing staining as negative (0), focal (1+ or ≤33% of the tumor–stroma interface), moderate (2+, >33%; 2, 67% of the tumor–stroma interface), or extensive (3+, >67% of the tumor–stroma interface).

Statistics

The results of the immunohistochemical reactions for E-cadherin and ST-3 in the de novo and ex adenoma groups were statistically compared using the Chi^2 test or the Fisher test (two sided) when appropriate. Additional comparisons were made between the antibodies and in comparison with selected histological features, including vessel invasion, tumor-cell dissociation at the invasion front and degree of differentiation. A P value <0.05 (two sided) was considered to be statistically significant.

Results

Histopathology

A comparison of the histological features of the two groups of carcinomas (Table 1) showed that there were significant differences in size (P<0.0001), due primarily to the definition of de novo carcinoma which required that they be 1.0 cm or less in diameter, in degree of differentiation (P=0.003), by which 12 of the de novo but none of the ex adenoma cases were poorly differentiated, and in tumor-cell dissociation on the invasion front (P=0.003), which was significantly more frequent in the de novo group. According to the extent of tumor-cell dissociation as described by Gabbert et al. [8], among the seven cases with extensive tumor-cell dissociation, six were in the de novo group, and three of the four cases with moderate tumor-cell dissociation were also in the de novo group. Lymph-vessel invasion was slightly more frequent in the de novo group (28% vs 21%), but this was not statistically significant. Of the 18 de novo cases with lymph-vessel invasion, 15 had low-grade and 3 high-grade invasion, compared with 7 low-grade and 2 high-grade of the 9 ex adenoma cases with lymph-vessel invasion.

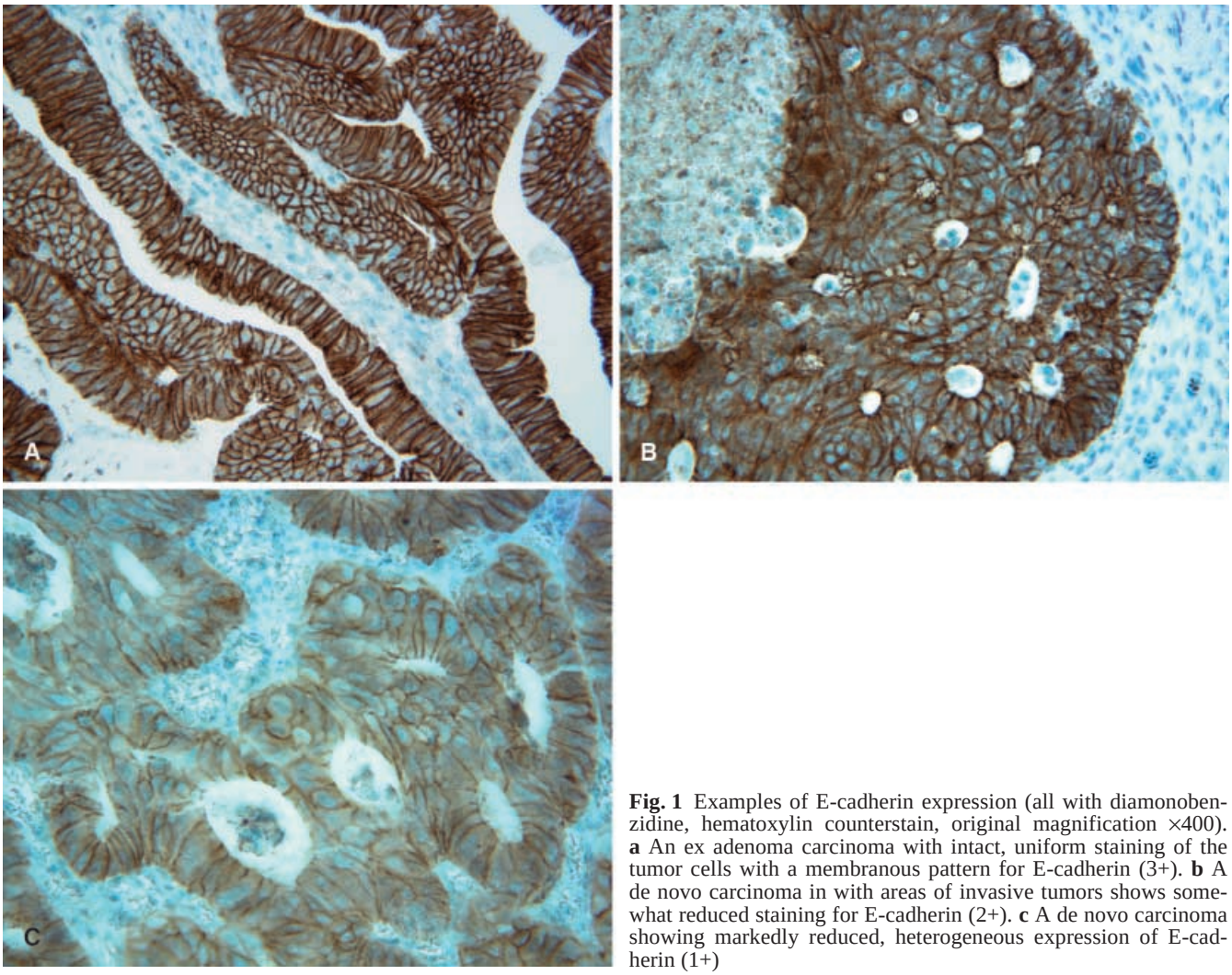


Fig. 1 Examples of E-cadherin expression (all with diamonobenzidine, hematoxylin counterstain, original magnification ×400). **a** An ex adenoma carcinoma with intact, uniform staining of the tumor cells with a membranous pattern for E-cadherin (3+). **b** A de novo carcinoma in with areas of invasive tumors shows somewhat reduced staining for E-cadherin (2+). **c** A de novo carcinoma showing markedly reduced, heterogeneous expression of E-cadherin (1+)

Table 2 Results of the immunohistochemistry

Group	De novo	Ex adenoma	Total
E-cadherin			
Normal- 3+	33 (51.6)	33 (78.6)	66 (62.3)
Reduced- 2+	29 (45.3)	8 (19.0)	37 (34.9)
Weak- 1+	2 (3.1)	1 (2.4)	3 (2.8)
Negative- 0	0	0	0
ST-3			
Extensive- 3+	5 (7.8)	1 (2.4)	6 (5.7)
Moderate- 2+	10 (15.6)	1 (2.4)	11 (10.4)
Focal- 1+	26 (40.6)	18 (42.9)	44 (41.5)
Negative- 0	23 (35.9)	22 (52.4)	45 (42.5)

Results of the immunohistochemistry

Table 2 shows the results of immunohistochemistry. All 106 lesions showed at least some staining for E-cadherin. Of both groups, 33 cases had normal expression of E-cadherin, which was a higher percentage (79% vs 52%) in the ex adenoma group. An example of a de novo carcinoma with reduced staining for E-cadherin is shown in Fig. 1. Only 3 cases of the entire group of 106 showed markedly reduced staining for E-cadherin. When E-cadherin expression was classified as either normal (3+) or reduced (2+ or 1+) (Table 3), reduced expression was found to show a significant correlation with the de novo type (P=0.005) and with tumor-cell dissociation (P=0.023). No correlation was seen with grade, lymphatic vessel invasion, or with the expression of ST-3. Within the de novo and ex adenoma groups, the significant difference between cases with or without tumor-cell dissociation was no longer seen, probably due to the very low number of cases in some categories.

Approximately half of the cases of both groups showed at least focal expression of ST-3 (49% de novo, 51% ex adenoma). As has been described in previous reports, the expression of ST-3 was seen only in fibroblasts directly adjacent to tumor-cell nests and not in tumor cells themselves [1] (Fig. 2). Significant differences in expression were seen between the de novo and ex adenoma tumors when the degree of expression was consid-

Table 3 *P* values (two sided) for the comparison of the immunohistochemistry with selected features in the de novo and ex adenoma tumors

Feature	Type	Grade	Tumor-cell dissociation	Lymphatic vascular invasion
Expression of:	(De novo vs ex adenoma)	(G1,2 vs G3)		
E-cadherin (normal vs reduced or weak)	0.005	n.s.	0.023	n.s.
ST-3 (extensive or moderate vs focal or absent)	0.0138	n.s.	0.0032	0.0015

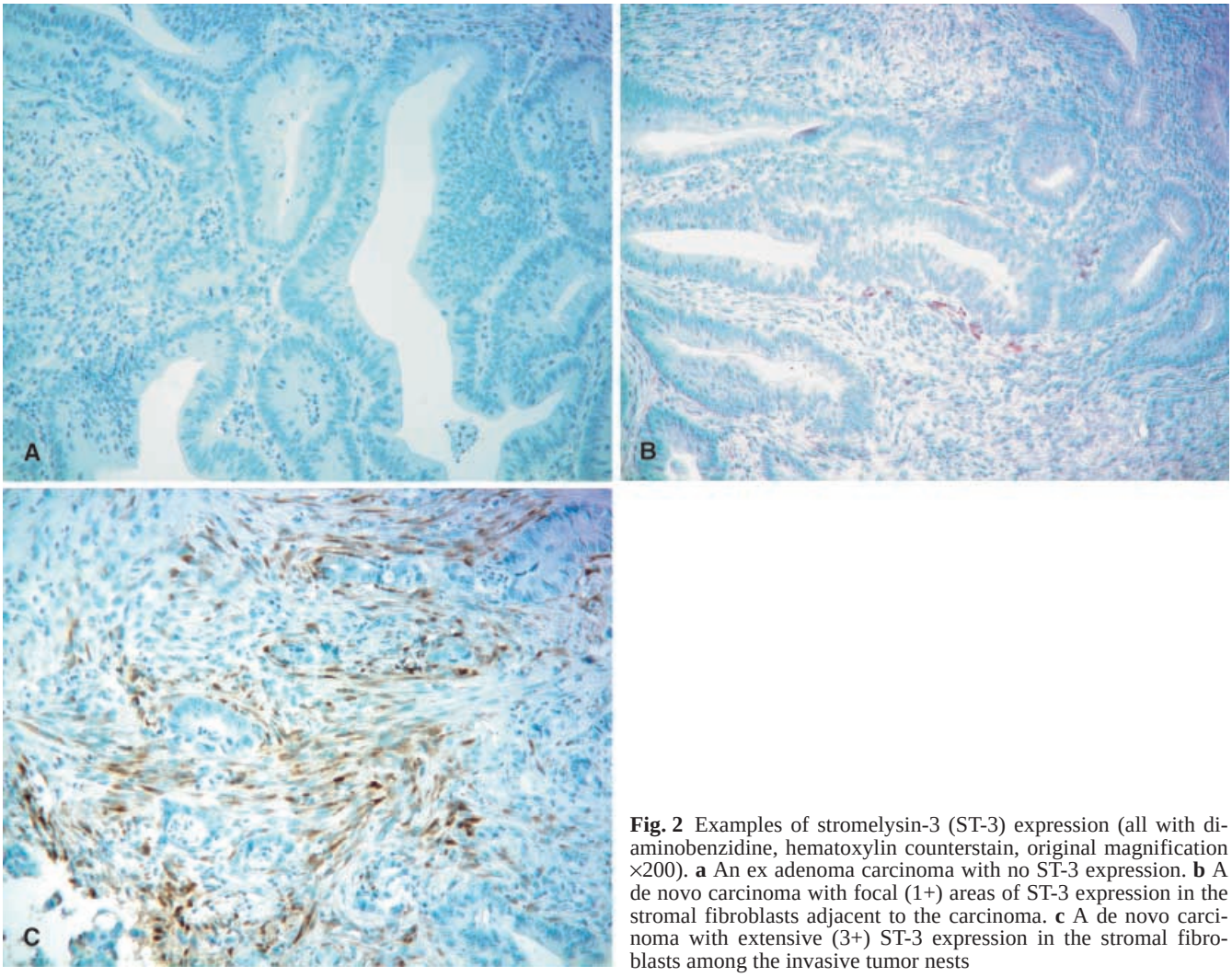


Fig. 2 Examples of stromelysin-3 (ST-3) expression (all with diaminobenzidine, hematoxylin counterstain, original magnification ×200). **a** An ex adenoma carcinoma with no ST-3 expression. **b** A de novo carcinoma with focal (1+) areas of ST-3 expression in the stromal fibroblasts adjacent to the carcinoma. **c** A de novo carcinoma with extensive (3+) ST-3 expression in the stromal fibroblasts among the invasive tumor nests

ered. Among the de novo cases, there were 15 (23%) that showed moderate or extensive expression of ST-3 compared with only 2 (5%) of the ex adenoma cases, a statistically significant difference (P=0.01). Comparison of strong or moderate ST-3 expression found even stronger statistical correlation with tumor-cell dissociation (P=0.0032), and lymphatic vessel invasion (P=0.0015). No correlation was found, however, with tumor grade or E-cadherin expression. Within the de novo and ex adenoma groups, a significant difference was still seen for lymphatic vessel invasion and ST-3 expression for the de novo (P=0.022) and ex adenoma groups (P=0.042). Tumor-cell dissociation was only significantly related to ST-3 expression within the ex adenoma group (P=0.042). This difference was no longer significant within the de novo group, probably due to the low numbers of cases in some categories.

Discussion

E-cadherin is a calcium-dependent, transmembrane molecule which is important in the maintenance of cell–cell adhesion in normal epithelia, including the mucosa of

the colorectum [6]. Several previous studies have demonstrated that the development of dysplasia and then carcinoma in the colorectum is not infrequently associated with a reduction in the expression of E-cadherin [31]. However, unlike the situation in other organs, most notably the breast and stomach, in most cases reduced or absent expression of E-cadherin in colorectal carcinoma cannot be attributed to mutations of the E-cadherin gene itself, but rather to decreased expression of normal protein, probably through regulatory mechanisms [25]. The biologic effect of decreased E-cadherin expression is that the invasiveness and metastatic potential of the tumor cells is increased [4] and some studies have found that patients with colorectal tumors with decreased E-cadherin expression have a greater likelihood of developing recurrent tumor [12]. In the present study, we found that the de novo type of early colorectal carcinoma had both a statistically greater rate of decreased E-cadherin expression and a greater rate of tumor-cell dissociation at the invasion front than the ex adenoma group. It is not surprising, given the function of E-cadherin, that these two factors were also closely associated with one another. These results suggest that, at this early stage, de novo colorectal carcinoma has diminished cell adhesion and thus a greater invasive potential than carcinomas arising ex adenoma.

ST-3 expression has been described in a wide variety of carcinomas, including the colorectum [11, 28] and has the interesting property of being expressed only by fibroblasts in the direct vicinity of invading carcinoma nests [2]. In a few carcinoma types (e.g., tumors of the head and neck), the expression of ST-3 has been related to the degree of local invasiveness [17], and in breast carcinoma high levels of ST-3 expression, as determined by semiquantitative immunohistochemistry, have been correlated with a poor prognosis [5]. In our own previous study of early (pT1) colorectal carcinomas, we found that the expression of ST-3 had a close association with an infiltrative pattern of tumor-cell invasion at the invasion front and was not expressed in tumors or in areas where the invasion was of the pushing, broad-based type [19]. This association of ST-3 expression with an infiltrative invasion pattern was confirmed by the present study; however, in addition, a very strong correlation with lymph-vessel invasion was also found. In another study of a set of urinary bladder neoplasms, we also found a very strong correlation with lymph-vessel invasion [22], indicating that extensive ST-3 expression may be a useful indicator of a high likelihood of vascular invasion in at least some carcinoma types. Another aspect of our data is the fact that although both extensive ST-3 expression and decreased expression of E-cadherin correlated with the de novo type, they did not correlate with one another, indicating that these two molecules are involved in two separate processes that are both more likely to be abnormal in the de novo type and both promote the invasiveness of these tumors.

In summary, the results of the present study demonstrate that de novo carcinoma has a higher rate of abnormality with respect to cell adhesion (E-cadherin) and protease expression (ST-3) that fit with a more aggressive biologic profile and are related to the histopathologic findings of tumor-cell dissociation at the invasion front and vascular invasion. Together with our previous findings showing that de novo carcinomas have a greater rate of p53 abnormalities at the protein and genomic levels, these data all indicate that this tumor type may be more aggressive, fitting well with clinicopathologic data that indicate that these de novo tumors metastasize more readily to regional lymph nodes [3, 9, 10].

Acknowledgements Supported by a grant from the Deutsche Krebshilfe 70–1950-Mu-1.

References

1. Basset P, Wolf C, Chambon P (1993) Expression of the stromelysin-3 gene in fibroblastic cells of invasive carcinomas of the breast and other human tissues: a review. Breast Cancer Res Treat 24:185–193
2. Basset P, Bellocq JP, Lefebvre O, Noel A, Chenard MP, Wolf C, Anglard P, Rio MC (1997) Stromelysin-3: a paradigm for stroma-derived factors implicated in carcinoma progression. Crit Rev Oncol Hematol 26:43–53
3. Bethke B, Walter T, Stolte M (1995) Endoskopische Polypektomie: vergleich der Häufigkeit kolorektaler Ex-Adenoma- und De-novo-Frühkarzinome. Coloproctology 17:176–183
4. Birchmeier W (1995) E-cadherin as a tumor (invasion) suppressor gene. Bioessays 17:97–99
5. Chenard MP, O'Siorain L, Shering S, Rouyer N, Lutz Y, Wolf C, Basset P, Bellocq JP, Duffy MJ (1996) High levels of stromelysin-3 correlate with poor prognosis in patients with breast carcinoma. Int J Cancer 69:448–451
6. El-Bahrawy MA, Pignatelli M (1998) E-cadherin and catenins: molecules with versatile roles in normal and neoplastic epithelial cell biology. Microsc Res Tech 43:224–232
7. Fearon ER, Vogelstein B (1990) A genetic model for colorectal tumorigenesis. Cell 61:759–767
8. Gabbert HE, Meier S, Gerharz CD, Hommel G (1992) Tumor-cell dissociation at the invasion front: a new prognostic parameter in gastric cancer patients. Int J Cancer 50:202–207
9. Herrera L, Hanna S, Castillo N, Petrelli NJ (1991) Primary de novo adenocarcinoma of the colon measuring 8 mm in diameter with lymph node metastases. Report of a case. Dis Colon Rectum 34:275–279
10. Jelinek GP, Nava HR, Nime F (1983) Small primary de novo adenocarcinoma of the colon with mesenteric lymphatic metastasis. J Surg Oncol 23:185–188
11. Johnson LD, Hunt DM, Kim K, Nachtigal M (1996) Amplification of stromelysin-3 transcripts from carcinomas of the colon. Hum Pathol 27:964–968
12. Kitadai Y, Ellis LM, Tucker SL, Greene GF, Bucana CD, Cleary KR, Takahashi Y, Tahara E, Fidler IJ (1996) Multiparametric in situ mRNA hybridization analysis to predict disease recurrence in patients with colon carcinoma. Am J Pathol 149:1541–1551
13. Kuramoto S (1989) Flat early cancers of the large intestine. Cancer 64:950–955
14. Kuramoto S, Oohara T (1987) Minute cancers arising de novo in the human large intestine. Cancer 61:829–834
15. Morson B (1974) The polyp-cancer sequence in the large bowel. Proc R Soc Med 67:451–457
16. Morson BC (1976) Genesis of colorectal cancer. Clin Gastroenterol 5:505–525
17. Muller D, Wolf C, Abecassis J, Millon R, Engelmann A, Bronner G, Rouyer N, Rio MC, Eber M, Methlin G (1993) Increased stromelysin 3 gene expression is associated with in-

creased local invasiveness in head and neck squamous cell carcinomas. Cancer Res 53:165–169
18. Mueller JD, Mueller E, Hoepner I, Jutting J, Bethke B, Stolte M, Hofler H (1996) Expression of bcl-2 and p53 in de novo and ex-adenoma colon carcinoma: a comparative immunohistochemical study. J Pathol 180:259–265
19. Mueller JD, Mueller E, Arras E, Bethke B, Stolte M, Hofler H (1997) Stromelysin-3 expression in early (pT1) carcinomas and pseudoinvasive lesions of the colorectum. Virchows Arch 430:213–219
20. Mueller JD, Haegele N, Keller G, Mueller E, Saretzky G, Bethke B, Stolte M, Höfler H (1998) Loss of heterozygosity and microsatellite instability in de-novo versus ex-adenoma carcinomas of the colorectum. Am J Pathol 153:1977–1984
21. Mueller JD, Heider KH, Oberhuber G, Mueller E, Bethke B, Stolte M, Höfler H (1998) Comparison of CD44 expression in early colorectal carcinomas of the de novo and ex-adenoma types. Virchows Arch 433:407–414
22. Mueller JD, Steiner C, Höfler H (2000) Stromelysin-3 expression in noninvasive and invasive neoplasms of the urinary bladder. Hum Pathol 31:860–865
23. Mueller JD, Brebeck B, Schmalfeldt B, Kuhn W, Graeff H, Höfler H (2000) Stromelysin-3-expression in invasive ovarian carcinomas and tumors of low malignant potential. Virchows Arch 437:618–624
24. Nollet F, Kools P, van Roy F (2000) Phylogenetic analysis of the cadherin superfamily allows identification of six major subfamilies besides several solitary members. J Mol Biol 299:551–572
25. Schuhmacher C, Becker I, Oswald S, Atkinson M, Nekarda H, Becker KF, Mueller JD, Siewert JR, Höfler H (1999) Loss of immunohistochemical E-cadherin expression in colon cancer is not due to structural gene alterations. Virchows Arch 434:489–495
26. Shimoda T, Ikegami M, Fusisaki J, Matsui T, Aizawa S, Ishikawa E (1989) Early colorectal carcinoma with special reference to its development de novo. Cancer 64:1138–1146
27. Streit M, Schmidt R, Hilgenfeld RU, Thiel E, Kreuser ED (1996) Adhesion receptors in malignant transformation and dissemination of gastrointestinal tumors. Recent Results Cancer Res 142:19–50
28. Thewes M, Pohlmann G, Atkinson M, Mueller JD, Putz B, Hofler H (1996) Stromelysin-3 (ST-3) mRNA expression in colorectal carcinomas. Localization and clinicopathologic correlations. Diagn Mol Pathol 5:284–290
29. Santavicca M, Noel A, Chenard MP, Lutz Y, Stoll I, Segain JP, Rouyer N, Rio MC, Wolf C, Belloco JP, et al (1995) Characterization of monoclonal antibodies against stromelysin-3 and their use to evaluate stromelysin-3 levels in breast carcinoma by semi-quantitative immunohistochemistry. Int J Cancer 64:336–341
30. UICC-International Union Against Cancer (1997)TNM classification of malignant tumours, 5th edn. J. Wiley and Sons, New York
31. Van Aken J, Cuvelier CA, De Wever N, Roels J, Gao Y, Mareel MM (1993) Immunohistochemical analysis of E-cadherin expression in human colorectal tumours. Pathol Res Pract 189:975–978
32. Vogelstein B, Fearon ER, Hamilton SR, Kern SE, Preisinger AC, Leppert M, Nakamura Y, White R, Smits AM, Bos JL (1988) Genetic alterations during colorectal-tumor development. N Engl J Med 319:525–532

Virchows Arch (2001) 439:762–767
DOI 10.1007/s004280100469

ORIGINAL ARTICLE

Alena Skálová · Ivo Stárek · Roderick HW Simpson
Vladislava Kučerová · Jana Dvořáčková
Romuald Čuřík · Milada Dušková

Spindle cell myoepithelial tumours of the parotid gland with extensive lipomatous metaplasia

A report of four cases with immunohistochemical and ultrastructural findings

Received: 27 November 2000 / Accepted: 19 March 2001 / Published online: 30 June 2001
© Springer-Verlag 2001

Abstract We report four cases of parotid gland tumours composed predominantly of spindle-shaped myoepithelial cells and mature adipocytes. The central portion of one tumour showed extensive adipose differentiation, whereas in the peripheral parts there were small foci of ductal epithelium arranged in cords and tubules within an abundant myxoid stroma. The other cases were adipose spindle cell myoepitheliomas without an obvious glandular component. Under high-power examination, a transition between modified spindle-shaped myoepithelial cells and adipocytes was observed, and this was confirmed with immunohistochemistry. Ultrastructurally, the modified myoepithelial cells showed intracytoplasmic tonofilaments, bundles of actin microfilaments and lipid droplets. A possible pathogenesis is proposed of true metaplastic transformation of myoepithelial cells to adipocytes. This lesion is important to identify correctly, as inadequate surgery can lead to recurrence.

A. Skálová (✉)
Šikl's Department of Pathology,
Medical Faculty Hospital, dr. E. Beneše 13,
305 99 Plzeň, Czech Republic
e-mail: skalova@fnplzen.cz
Tel.: +420-19-7402545, Fax: +420-19-7421561

I. Stárek
Department of Otorhinolaryngology,
Medical Faculty, Palacký University,
Olomouc, Czech Republic

R.H. Simpson
Department of Pathology, Postgraduate Medical School,
University of Exeter, UK

V. Kučerová · M. Dušková
Department of Pathology, Medical Faculty,
Palacký University, Olomouc, Czech Republic

J. Dvořáčková
Private Cytological and Bioptical Laboratory,
Ostrava, Czech Republic

R. Čuřík
Department of Pathology, Faculty Hospital,
Ostrava, Czech Republic

Keywords Lipomatous · Adipose metaplasia · Salivary gland tumour · Myoepithelial · Pleomorphic adenoma

Introduction

Epithelial tumours of the salivary gland display great pathomorphological variation. In some neoplasms, this variation is due to the participation of neoplastic myoepithelial cells, which may take several forms, including epithelioid, spindle shaped, plasmacytoid or clear. The most common salivary neoplasm with significant myoepithelial cell participation is pleomorphic adenoma; in it, the ductal and myoepithelial cellular structures are embedded in a myxochondroid matrix. The extent of the myoepithelial element also varies, and it may be a minor, a major or even an exclusive component. Therefore, most authors accept that pleomorphic adenoma and myoepithelioma are part of the same biological spectrum, the main morphological difference being the relative proportions of the myoepithelial and ductal elements [19].

Recently, the spectrum has been expanded to include basal cell adenoma and canalicular adenoma, the latter displaying no significant myoepithelial population [26]. The availability of new markers, such as α smooth muscle actin, smooth muscle myosin heavy chain and calponin, for smooth muscle differentiation provided a new opportunity to study a diversity of modified myoepithelial neoplastic cells [17]. A further variation in the appearance of pleomorphic adenoma is that sporadically, squamous [4], mucous, sebaceous [6], oncocytic [21] or osteoid metaplasia can be seen. Lipomatosis, in the form of isolated small islands or scattered single lipocytes, is uncommon [22], and a large amount of adipose tissue in a pleomorphic adenoma and myoepithelioma is a rarity [12, 14]. Here, we present four cases of spindle cell myoepithelial-rich adenomas of the parotid gland with extensive adipose metaplasia.

Case reports

Case 1

A 73-year-old woman presented with a large recurrent tumour in her left preauricular region. A primary tumour of the parotid gland had been removed 30 years previously. Physical examination showed a soft elastic and freely mobile recurrent tumour 5 cm in diameter. There were no clinical signs of infiltrative growth. Ultrasonography revealed a hyperechoic, heterogeneous, well-delineated spherical mass. The tumour was removed by subtotal conservative parotidectomy. The postoperative course was uneventful and 12 months after surgery there are no signs of recurrence.

Case 2

A 57-year-old woman presented with painless swelling of her left parotid gland present for many years and which had recently enlarged over 9 months. The tumour measured 1.8 cm in diameter, and it was removed by superficial parotidectomy. The patient had no recurrence in the 18 years and 4 months after surgery; however, she died suddenly of a cerebral haemorrhage. Permission for autopsy was not obtained. This lesion was reported by one of us (RHWS) as case 1 in a series of benign myoepitheliomas [19], but no consideration was given to the lipomatous component.

Case 3

A 48-year-old woman presented with a slowly growing tumour of the left parotid gland. The tumour measured 2.5 cm in diameter, and it was surgically removed by means of conservative superficial parotidectomy.

Case 4

A 55-year-old man presented with a 1-year history of a slowly enlarging non-tender mass of the left parotid gland. The tumour was hard in consistency, well circumscribed and partly cystic on cut section.

Materials and methods

The specimens were immediately fixed in 10% formalin, embedded in paraffin and routinely stained. For electron microscopy, formalin-fixed wet tumour tissue samples of case 1 were washed in phosphate buffer, fixed briefly in 4% paraformaldehyde, postfixed in 1% osmium tetraoxide and embedded in epoxy resin (Durcupan-Epon). Sections 1-μm thick were stained with uranyl acetate and lead citrate, and examined under an electron microscope. Immunohistochemistry was performed on paraffin sections using the supersensitive streptavidin–biotin method. The antibodies used are listed in Table 1.

Pathological findings

Gross examination of the case 1 showed a multilobular tumour mass measuring 5 cm in diameter. Sectioning revealed an elastic consistency and a homogeneous yellow greasy cut surface. A minor part of the tumour, comprising less than 10% of the total mass, was more gelatinous, harder and grey–white in colour. In the cases 2 and 3, the superficial parotidectomy specimens contained well-circumscribed yellow nodules 1.8 cm and 2.5 cm in diameter, respectively. The tumour in case 4 was partly cystic on cut section.

Histological examination of all cases showed a well-circumscribed, partly encapsulated tumour that consisted of anastomosing bundles of spindle-shaped cells intermingled with abundant mature adipose tissue (Fig. 1). In case 1, the lesion was divided into indistinct nodules by thin bundles of collagenous tissue with scant foci of myxoid transformation. In the central portion, the tumour was composed predominantly of mature, univacuolated adipocytes and spindle-shaped myoepithelial cells. A gradual transition between spindle-shaped cells and adipocytes was observed (Fig. 2). These transitional cell elements were spindle in shape and contained multiple intracytoplasmic fat vacuoles. The cells displayed elongated bland nuclei without polymorphism. Mitotic figures were not identified. The other neoplastic cells exhibited more advanced lipomatous differentiation with a spectrum from immature-appearing multivacuolated adipocytes with nuclear scalloping (lipoblast-like cells) to mature univacuolar fat cells. At the periphery of the tumour, there were foci comprising no more than 10% of the total tumour mass, within which the tumour was

Table 1 Immunohistochemical findings. *neg.* no staining, *%* percentage of stained cells, * staining not performed

Antibody	Specificity	Source	Dilution	Case 1	Case 2	Case 3	Case 4
AE1–AE3[a]	CK 5, 8, 10, 14, 19	Boehringer-Mannheim	1:500	70%	60%	60%	50%
MNF116	CK 5, 6, 8, 17, 19(±)	Dako	1:400	*	15%	*	*
Cytokeratin 7	CK 7	Dako	1:50	*	10%	*	*
Cytokeratin 20	CK 20	Dako	1:50	*	neg.	*	*
LP 34	CK 5, 6, 18	Dako	1:4000	*	10%	*	*
CAM 5.2	CK 8, 18	Becton-Dickinson	1:50	15%	40%	20%	30%
S-100 protein (polyclonal)		Dako	1:1000	80%	100%	100%	90%
113–1	Anti-mitochondrial antigen	Biogenex	1:100	neg.	neg.	neg.	10%
HHF35	Muscle-specific actin	Dako	1:400	60%	35%	70%	60%
1A4	α Smooth muscle actin	Dako	1:1000	40%	30%	70%	60%
CALP	Calponin	Menarini	1:20	60%	50%	60%	65%
SMMS-1	Smooth muscle myosin heavy chain	Menarini	1:200	*	5%	*	*
MIB1	Ki67	Immunotech	1:100	2%	1%	2%	1%

[a] AE1–3 reacts with 65–67, 64, 49, 58, 56.2, 52, 50, 48, and 40-kDa proteins (based on data from Dako 2000 Catalogue)

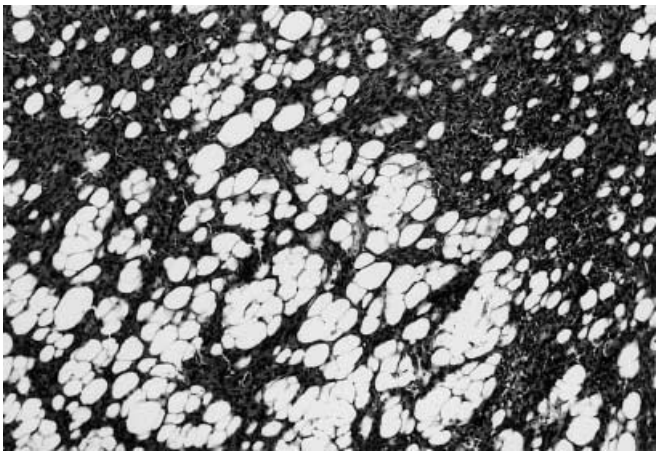


Fig. 1 Low-power view shows extensive lipomatous component intermingled with spindle-shaped myoepithelial cells. Haematoxylin-eosin, ×36

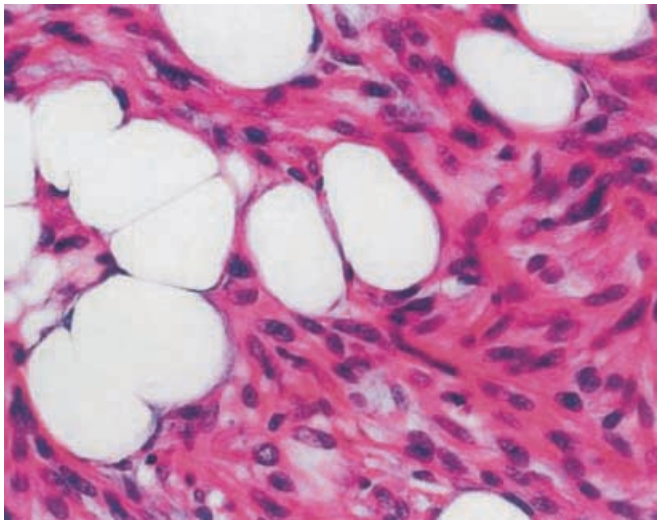


Fig. 2 High-power examination showing transition between spindled myoepithelial cells and well-developed adipocytes. Haematoxylin-eosin, original magnification, ×180

composed of ductal and myoepithelial cells arranged in trabeculae, cords and tubules embedded in a loose myxoid stroma as typically seen in pleomorphic adenomas (Fig. 3). No chondroid differentiation was noted. There were few adipocytes scattered in this peripheral area of the tumour. Histopathological examination of the original tumour in case 1 showed identical features to the recurrence, the only exception being fewer adipose cells in the former. In other cases, the tumours were composed only of spindle-shaped myoepithelial cells with extensive adipose metaplasia without any obvious glandular component and no foci with chondromyxoid stroma. A few tiny barely perceptible small ducts were, however, identified in the slides stained for cytokeratins. There was small area with oncocytic metaplasia of epithelioid myoepithelial cells in the case 4.

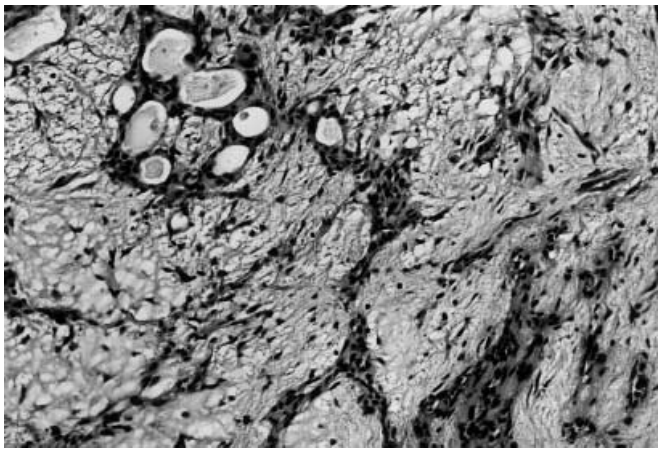


Fig. 3 A minor peripheral portion of the tumour was composed of tubular and trabecular structures within a loose myxoid stroma. Haematoxylin-eosin, ×90

Immunohistochemical examination

The results are summarised in Table 1. Most spindle-shaped cells were strongly positive for cytokeratins (Fig. 4A), both actins (Fig. 4B), calponin and S-100 protein. Smooth muscle myosin heavy chain was positive in approximately 5% of spindle cells. In addition, approximately 10% of spindle cells expressed cytokeratin 7, whereas positive staining of these cells with other cytokeratins ranged between 10% and 70% (both AE1–3, CAM5.2, MNF116 and LP34). This immunophenotype was typical of myoepithelial cells. Some spindle cells with cytoplasmic vacuoles were positive with S-100 protein, αSMA and calponin. We interpret these cells as myoepithelial cells undergoing lipid accumulation. Mature fat cells reacted with S-100 protein and vimentin only. In case 1, cytokeratin was particularly strongly expressed in ductal, tubular and trabecular structures in the peripheral part of the tumour. These epithelial cells were mostly positive for S-100 protein and negative for actins. Strong reactivity for cytokeratins was also observed in the central portion of the tumour in case 1 and within the whole tumours in cases 2–4, where it was localised to tiny tubules, hardly discernable on haematoxylin and eosin-stained sections; these were scattered between spindle-shaped myoepithelial cells and abundant adipocytes (Fig. 5). Anti-mitochondrial antibody staining was focally positive in spindle-shaped and epithelioid myoepithelial cells in case 4. Proliferative activity in all four tumours was low, with MIB1 indices between 1% and 2%.

Ultrastructural examination of case 1 confirmed myoepithelial differentiation of the spindle-shaped cells. These contained abundant tonofilaments in the cytoplasm and bundles of actin microfilaments with focal densities close to the cell membrane (Fig. 6). There was a transition between these cells and the adipocytes. The latter were also spindle shaped and contained clumps of tonofilaments in the perinuclear region and myofilaments along the plasma membrane. In addition, a mesh-

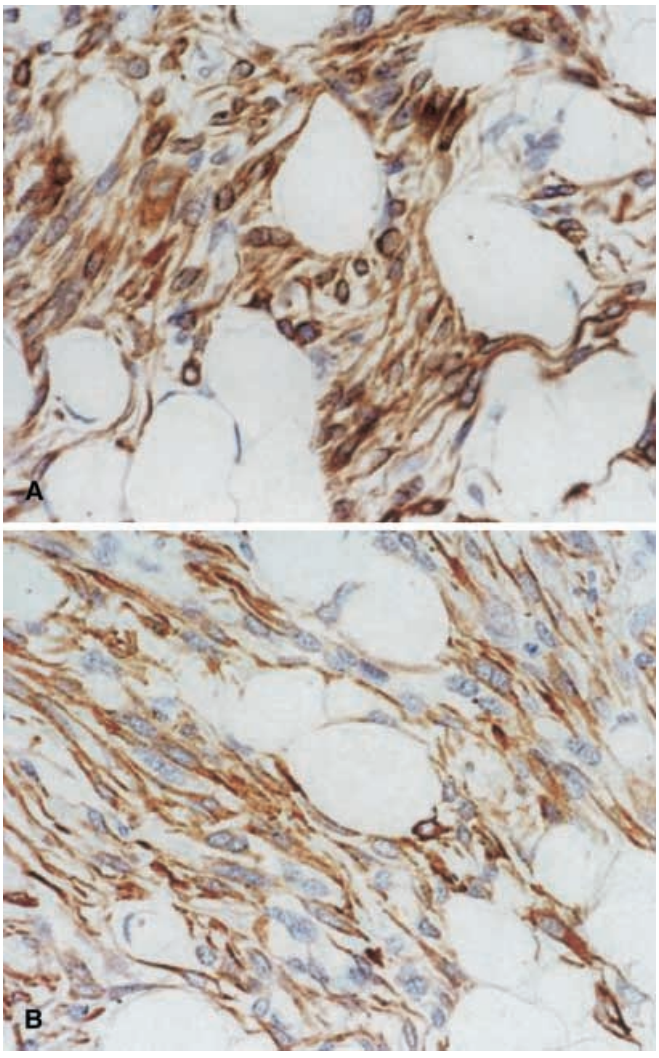


Fig. 4 Most spindle-shaped myoepithelial cells demonstrated co-expression of cytokeratins, actins and calponin. **A** A positive staining for AE1–3. **B** A positive staining for actin. Immunohistochemical stain and haematoxylin counterstain. Original magnification, ×180

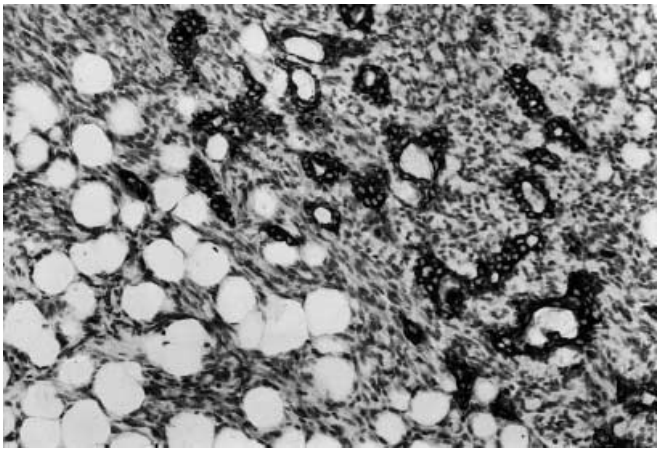


Fig. 5 Cytokeratins AE1–3 are strongly expressed by neoplastic ductal epithelial cells in the tubular structures. Immunohistochemical stain and haematoxylin counterstain. Original magnification, ×90

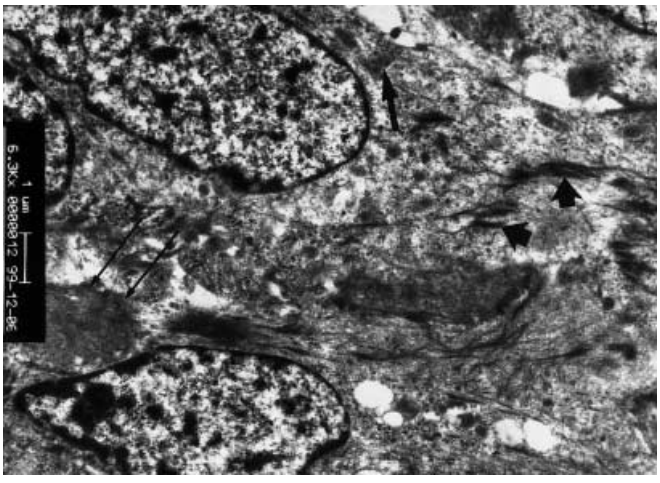


Fig. 6 Neoplastic spindle myoepithelial cells contain microfilaments with dense bodies (*arrow*) and abundant tonofilaments (*short arrows*). Fat droplet can be seen close to the nucleus (*thin arrows*). Magnification, ×6300

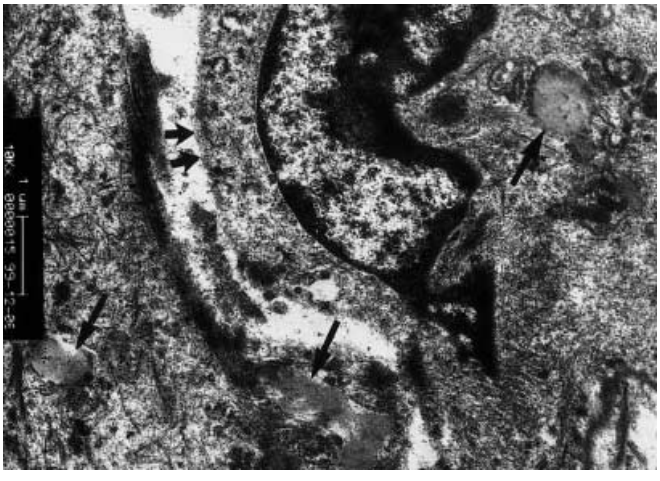


Fig. 7 The cytoplasm is focally packed with a dense meshwork of haphazardly arranged intermediate filaments. There are few mitochondria and fat droplets in the cytoplasm (*arrows*). Interrupted basal lamina is seen on the cell surface (*short arrows*). Magnification, ×10,000

work of haphazardly arranged intermediate filaments and small lipid droplets in the cytoplasm was noted (Fig. 7). The adipocytes, transitional cells and myoepithelial cells were each surrounded by an interrupted basal lamina (Fig. 7).

Discussion

Abundant adipose tissue in epithelial salivary gland tumours is rare, although elsewhere in the head and neck region it can be encountered in benign thyroid and parathyroid lipoadenomas [7, 10, 13, 23, 24]. Extensive adipose metaplasia in an otherwise typical pleomorphic adenoma is only rarely mentioned in the literature [12, 14,

18]. In two cases [12, 18], the central portion of the tumour was composed of sheets of adipose tissue with some compressed epithelial cords arranged in a septum-like pattern. Chondromyxoid and epithelial structures typical of pleomorphic adenoma of usual type were located at the periphery, and projected into the centre in narrow trabeculae, thus dividing the central fatty tissue into vague lobules. In these tumours, spindle cell myoepithelial proliferation was not a feature and, thus, they seem to be different from our cases [12, 18]. The only other case in the literature of extensive adipose metaplasia in an otherwise typical pleomorphic adenoma is different to the first two [12, 18], but seems similar to ours; it comprised a pleomorphic adenoma with predominantly spindle-shaped myoepithelial cells and mature adipocytes [14]. The authors postulated a direct metaplastic transition of the myoepithelial cells to adipocytes. In our cases, we have also demonstrated the existence of transitional cells with the immunophenotypic and ultrastructural features both of myoepithelial cells and adipocytes. Thus, it seems reasonable to expect that abundant adipose tissue in both these pleomorphic adenoma/myoepitheliomas is a result of lipomatous metaplasia of the neoplastic myoepithelial cells rather than a simple entrapment of surrounding adipose tissue by the adenoma. The ultrastructural characteristics of the adipocytes (i.e. remnants of the basal lamina) and the presence of cells with immunohistochemical and electron microscopic features between myoepithelial and adipose ones (with lipid droplets and actin microfilaments in the cytoplasm) support Dardick's histogenetic model of pleomorphic adenoma [3], in which the neoplastic myoepithelial cells play the key role in tumour morphogenesis, particularly the synthesis and deposition of the extracellular matrix [5, 20]. The proliferation of neoplastic modified myoepithelial cells may be linked to differentiation pathways leading to morphologically very diverse metaplastic changes, both in the epithelial and mesenchymal components. In the former, this can take the form of squamous and (less commonly) oncocytic change [21], and, in the latter chondroid, osseous or rarely lipomatous metaplasia.

Similar phenomenon of presence of an abundant adipose tissue admixtured with proliferating myofibroblasts and fibroblasts has been described recently in mammary myofibroblastomas [8] and soft tissue lipomatous hemangiopericytomas [2, 15], respectively. Myofibroblastoma of the breast is a benign mesenchymal spindle cell tumour [8] that can display a spectrum of light microscopic and immunohistochemical features including abundant adipose cells in most cases. This situation seems similar to that encountered in salivary gland tumours composed of modified myoepithelial cells, which range from myoid to epithelioid imunophenotypically, and which are prone to heterogeneous metaplastic changes. Hemangiopericytoma of soft tissue is a controversial pathologic entity that is believed to originate from the pericytes [1]. Pericytes are myogenic cells that are involved in the regulation of the capillary blood flow and may also function as progenitor cells for developing adipocytes [11]. In 1995, Nielsen et al. [15] reported a series of three previously undescribed lipomatous hemangiopericytomas that exhibited an admixture of spindle cells and mature adipocytes in a growth pattern similar to that of our cases. The authors hypothesised that adipocyte component of lipomatous hemangiopericytoma arises from the population of pericyte cells undergoing direct adipocytic differentiation [15].

The significance of extensive lipomatous metaplasia in pleomorphic adenoma/myoepithelioma lies primarily in the differential diagnosis. From the histopathological point of view, a correct diagnosis is not difficult, provided the islets of typical ductal and myxochondroid structures are found, although ducts can be inconspicuous as in our cases 2, 3, and 4. Problems may arise when a FNA specimen produces only adipose cells, the tumour thus may be misdiagnosed as a lipoma. A false cytologic diagnosis may further be supported by the clinical finding of a soft elastic mass which is common to both the lipoma and the pleomorphic adenoma with extensive lipometaplasia. True lipomas of the salivary glands are encapsulated and characterised by a soft consistency and a yellow cut surface and, as at other sites, histologically by lobules of uniform differentiated adipocytes. Spindle cell lipoma is characterised by an admixture of mature adipocytes and undifferentiated spindle cells with uniform nuclei set in variably fibromyxoid stroma and may histologically closely resemble lipomatous myoepithelioma. Spindle cell lipoma can be, however, distinguished by absence of immunoreactivity for S-100 protein and cytokerations in the spindle cells. Moreover, spindle cell lipomas show consistent chromosomal aberrations of 13q and 16q [16].

The recently described lipoadenoma of the salivary glands is another rare entity which should be distinguished from lipomatous myoepithelial cell rich pleomorphic adenoma and spindle cell myoepithelioma [9, 25]. Hirokawa [9] reported a tumour of the submandibular gland, composed *ana partes* of lipocytes and oncocytic cells with an acinar and a microglandular architectural pattern of the latter. In a similar lesion [25], the glandular component consisted of bilayered ductal/basal cell tubular structures, and adipose tissue constituted 60% of the total tumour mass. In contrast to our cases, both lipoadenomas lacked myoepithelial differentiation and a myxoid stroma merging with the ductal/myoepithelial cell component. The source of the adipose cells in these tumours is obscure. It may be due to metaplastic stromal change, a hamartomatous process or even metaplasia of the adenomatous component.

Preoperative identification of lipomatous pleomorphic adenoma/myoepithelioma from other benign lipomatous tumours is crucial for planning surgical intervention. Whilst lipomas and lipoadenomas can be removed by simple enucleation, this procedure is insufficient for a pleomorphic adenoma/myoepithelioma and would most probably result in tumour recurrence, as indeed happened with our case 1. Ultrasonography may help to differentiate these tumours, in that fat in both lipomas

and lipomatous pleomorphic adenoma/myoepitheliomas causes them to be hyperechoic, in comparison with "usual" benign tumours of salivary glands, which are hypoechoic. The hyperechogeneity of lipomas, of which one of the characteristics is a "feathered" homogeneous appearance, is not as high as it is in extensively lipomatous pleomorphic adenomas in which the myxochondroepithelial component causes a heterogeneous pattern. In this paper, we described a rare variant of a common tumour, which needs to be recognised, perhaps even preoperatively, so that inadequate surgery might be avoided.

Acknowledgements The authors are grateful to Michal Pavlovský, M.D. (Department of Pathology, Hospital in Most), who contributed the case 4. The authors also appreciate a skilful assistance of Petr Mukenšnabl, M.D., who prepared the photomicrographs, and of Mr. Dostál, who helped with electron microscopy examination.

References

1. Battifora H (1973) Hemangiopericytoma: ultrastructural study of five cases. Cancer 31:1481–1432
2. Ceballos KM, Munk PL, Masri BA, O'Connell JX (1999) Lipomatous hemangiopericytoma. A morphologically distinct soft tissue tumor. Arch Pathol Lab Med 123:941–945
3. Dardick I (1985) A role for electron microscopy in salivary gland neoplasms. Ultrastruct Pathol 9:151–161
4. Dardick I, Van Nostrand P, Jeans MTD, et al. (1983) Pleomorphic adenoma: I. Ultrastructural organization of "epithelial" regions. Hum Pathol 14:780–797
5. Dardick I, Nostrand AWPV, Jeans MTD, et al (1983) Pleomorphic adenoma II: Ultrastructural organization of "stromal" regions. Hum Pathol 14:798–809
6. Ellis GL, Auclair PL (1996) Atlas of tumor pathology, 3rd series, fascicle 17. Tumors of the salivary glands. AFIP, Washington DC, pp 39–57
7. Gnepp DR, Ogorzalek JM, Heffes CS (1989) Fat-containing lesions of the thyroid gland. Am J Surg Pathol 13:605–612
8. Hamele-Bena D, Cranor ML, Sciotto C, Erlandson R (1996) Uncommon presentation of mammary myofibroblastoma. Mod Pathol 9:786–790
9. Hirokawa M, Shimizu M, Manabe T, et al (1998) Oncocytic lipoadenoma of the submandibular gland. Hum Pathol 29:410–412
10. Hjorth L, Thomsen LB, Nielsen VT (1986) Adenolipoma of the thyroid gland. Histopathology 10:91–96
11. Iyama KI, Ohzono K, Usuku G (1979) Electron microscopical studies on the genesis of white adipocytes: differentiation of immature pericytes into adipocytes in transplanted preadipose tissue. Virchows Arch 31:143–155
12. Jin ZT, Lian JD, Yan JJ, et al (1996) Pleomorphic adenoma with extensive adipose content. Histopathology 28:87–89
13. Mizukami Y, Michigishi T, Nonomura A, Noguchi M, Nakamura S (1995) Adenolipoma of the thyroid gland. Pathol Int 45:247–249
14. Ng WK, Ma L (1995) Pleomorphic adenoma with extensive lipometaplasia. Histopathology 27:285–288
15. Nielsen GP, Dickersin GR, Provenzal JM, Rosenberg AE (1995) Lipomatous hemangiopericytoma: a histologic, ultrastructural and immunohistochemical study of a unique variant of hemangiopericytoma. Am J Surg Pathol 19:748–756
16. Rubin BP, Fletcher CDM (1997) The cytogenetics of lipomatous tumours. Histopathology 30:507–511
17. Savera AT, Gown AM, Zarbo RJ (1997) Immunolocalization of three novel smooth muscle-specific proteins in salivary gland pleomorphic adenoma: assessment of the morphogenetic role of myoepithelium. Mod Pathol 10:1093–1100
18. Seifert G, Donath K, Schafer R (1999) Lipomatous pleomorphic adenoma of the parotid gland. Classification of lipomatous tissue in salivary glands. Path Res Pract 195:247–252
19. Simpson RHW, Jones H, Beasley P (1995) Benign myoepithelioma of the salivary glands: a true entity? Histopathology 27:1–9
20. Skálová A, Leivo I, Michal M, Saksela E (1992) Analysis of collagen isotypes in crystalloid structures of salivary gland tumors. Hum Pathol 23:748–754
21. Skálová A, Michal M, Ryška A, Simpson RWH, Kinkor Z, Walter J, Leivo I (1999) Oncocytic myoepithelioma and pleomorphic adenoma of the salivary gland. Virchows Arch 434: 537–546
22. Thackray AC, Lucas RB (1974). Pleomorphic adenoma (mixed tumor). In: Thackray AC, Lucas RB (eds) Atlas of tumor pathology. Tumors of the major salivary glands, 2nd series, fascicle 10. AFIP, Washington, DC, pp 16–39
23. Van Hoeven KH, Brennan MF (1993) Lipothymoadenoma of the parathyroid. Arch Pathol Lab Med 17:247–249
24. Weiland LH, Garrison RC, ReMine WH et al (1978) Lipoadenoma of the parathyroid gland. Am J Surg Pathol 2:3–7
25. Yau KC, Tsang ChB, Chan JKC (1997) Lipoadenoma of the parotid gland with probable striated duct differentiation. Mod Pathol 10:242–246
26. Zarbo RJ, Prasad AR, Regezi JA, Gown AM, Savera AT (2000) Salivary gland basal cell and canalicular adenomas: immunohistochemical demonstration of myoepithelial cell participation and morphogenetic considerations. Arch Pathol Lab Med 124: 401–405

Virchows Arch (2001) 439:768–775
DOI 10.1007/s004280100470

ORIGINAL ARTICLE

Aleš Ryška · Carol Reynolds · Gary L. Keeney

Benign tumors of the breast with multinucleated stromal giant cells

Immunohistochemical analysis of six cases and review of the literature

Received: 5 December 2000 / Accepted: 24 March 2001 / Published online: 17 July 2001
© Springer-Verlag 2001

Abstract The authors present six cases of benign tumors of the breast with numerous multinucleated stromal giant cells (MSGC). All six patients were women aged 37–70 years (mean 48 years), presenting clinically with a breast mass 1.0–3.8 cm in size (mean 1.9 cm; median 1.5 cm). By standard H&E examination, all cases showed the presence of numerous MSGC haphazardly dispersed within the tumor stroma. Three cases revealed MSGC merging into the surrounding adipose tissue simulating infiltrative growth. The MSGC appeared to have multiple nuclei (5 to 25) with fine chromatin and sporadic small nucleoli. Their cytoplasm was inconspicuous. The MSGC expressed vimentin only and to lesser extent CD34. These cells were negative for muscle markers, keratins, S-100 protein, vascular markers, CD68 and hormone receptors. Interestingly, the majority of MSGC and mononuclear stromal cells showed reactivity for p53 protein and Ki-67 proliferation antigen. All patients were treated by simple excision and remain free of recurrence (mean 70 months, median 48 months.). The reactivity of p53 in MSGC and mononuclear stromal cells may play a key role in linking these two cell types. Nonetheless, the presence of MSGC does not alter prognosis of otherwise typical benign lesions.

Keywords Breast · Benign tumor · Multinucleated stromal giant cell · p53 · Ki-67 · Prognosis

This work was supported in part by grant IGA MZ CR No. 4559–3 of Ministry of Health, Czech Republic.

A. Ryška (✉)
Department of Pathology,
Charles University Medical Faculty Hospital,
500 05 Hradec Králové, Czech Republic
e-mail: ryskaale@fnhk.cz
Tel.: +420-49-5833748, Fax: +420-49-5832004

C. Reynolds · G.L. Keeney
Department of Laboratory Medicine and Pathology, Mayo Clinic,
Rochester, MN, USA

Introduction

Multinucleated stromal giant cells (MSGC) have been well documented in several anatomic locations, including lower female genital tract, testis, urinary bladder, and anus [7, 9, 10, 17, 18].

MSGC in the breast were first described in 1979 by Rosen [21] in patients treated for breast carcinoma. The foci containing MSGC were located in otherwise normal mammary gland and were usually widely separated from the carcinoma. Since appearance of this article, only several reports described similar cells in both benign and malignant epithelial and fibroepithelial tumors of the breast for a total of 17 cases [2, 4, 6, 16, 18, 19]. However, the histogenesis of MSGC still remains obscure. Their origin has been linked to myoepithelial cells [16], fibroblastic elements of interlobular stroma [2, 4, 6, 18], and stromal fibrohistiocytic cells [19].

We present a series of six benign breast tumors containing abundant MSGC. In hopes to elucidate the histogenesis of MSGC, we utilized a broad panel of immunohistochemical markers and electron microscopy. The immunohistochemical markers included epithelial, myoepithelial, myogenic, vascular, fibrohistiocytic, and hormonal, plus expression of p53 oncoprotein and Ki-67 proliferation antigen.

Material and methods

Six benign breast lesions containing MSGC were retrieved from the surgical pathology files of Mayo Clinic, Rochester, MN, between 1983 and 1999. In all cases, the H&E slides and paraffin blocks were available. Deparaffinized sections were examined immunohistochemically using antibodies specific for the following antigens: vimentin (monoclonal, 3B4), 1:500, DAKO Carpinteria, CA, USA; CD34, (monoclonal, HPCA), 1:20, Becton Dickinson, San Jose, CA, USA; cytokeratin (monoclonal, AE1/AE3), 1:400, Boehringer-Mannheim, Indianapolis, IN, USA; high-molecular-weight keratin K903 (HMW) (monoclonal, 34βE12), 1:10, DAKO; cytokeratin CAM5.2, (monoclonal, CAM 5.2), 1:50, Becton Dickinson; S100, polyclonal, 1:2000, HSC, Toronto, Ontario, Canada; α smooth muscle actin (SMA), (monoclonal, 1A4),

1:150, DAKO; factor VIII related antigen (FVIII), polyclonal, 1:1000, DAKO; CD31, (monoclonal, JC/70A), 1:25, DAKO; CD68, (monoclonal, KP1), 1:200, DAKO; estrogen receptor (monoclonal, 6F11), prediluted, Ventana Tucson, AZ, USA; progesterone receptor (monoclonal, 1A6), prediluted, Ventana; p53, (monoclonal, DO7), 1:200, DAKO; and Ki-67, (monoclonal, MIB1), 1:400, Immunotech, Westbrook, ME, USA. An avidin-biotin complex detection system was used [11]. Appropriate tissue specimens were used as positive controls. In addition, structures within the examined slide, known as expressing detected antigen, also served as an internal positive control. Staining with omission of the primary antibody (replaced by PBS buffer) was used as a negative control.

In one case, material retrieved from the paraffin block was used for ultrastructural studies. Briefly, tissue was deparaffinized in xylene, rehydrated in alcohol, and then transferred into glutaraldehyde fixative. Tissue was then processed and embedded in Epon. Grids were cut and stained with lead citrate and uranyl acetate. Sections were examined with a Phillips CM-10 transmission electron microscope.

Clinical information and follow up data were obtained from pathology reports, referring pathologists, or referring primary physicians.

Results

Clinical data

A total of six cases were identified. The clinical data are summarized in Table 1. All six were women and ranged in age from 37 to 70 years (mean 48 years). All patients were treated by simple excision; they are alive and remain free of recurrence (mean 70 months, median 48 months.). To our knowledge, there had been no prior fine-needle aspiration cytology or surgical procedure in any of our patients.

Light microscopy

Based on the overall architecture, growth pattern and cellular features (excluding MSGC from consideration), the six cases were classified as follows: fibroadenoma – two cases (one with partly tubular pattern, the other one with features of complex fibroadenoma); adenosis tumor – two cases (one with focal atypical ductal hyperplasia); intraductal papilloma – one case; adenomyoepithelioma – 1 case (see Table 1).

All cases shared a common feature, the presence of numerous MSGC within the tumor stroma (Fig. 1A–D). The MSGC were haphazardly and relatively diffusely dispersed. Five cases (83%) revealed more than 10 MSGC/HPF; one case (17%) revealed 5–10 MSGC/HPF. We did not observe a significant difference in numbers of MSGC in different types of lesions.

The cells appeared to have multiple, often hyperchromatic nuclei (5 to 25), which usually showed moderate to marked atypia, fine chromatin structure, and sporadic small nucleoli. Sometimes, nuclear pseudoinclusions were a prominent feature (Fig. 3A). The nuclei were usually aggregated, forming a grape-like cluster, less often they were arranged in a floret pattern. Occasionally the nuclei were bizarre, lobulated with multiple nucleoli. Mitotic figures were exceedingly rare; we observed only several unequivocal mitotic figures in MSGC in about 120 slides. The cytoplasm of MSGC was inconspicuous, forming a thin rim around the clustered nuclei. Less commonly the cytoplasm was more abundant, eosinophilic with a coarsely granular pattern.

Occasionally the cells appeared to line lacunar spaces simulating vascular lumina, thus strongly resembling features of giant cell fibroblastoma or pseudoangiomatous stromal hyperplasia of the mammary gland. These spaces with MSGC at the edge were optically empty, devoid of erythrocytes or other cellular elements (Fig. 1C).

Three cases showed MSGC permeating the surrounding adipose and fibrous tissue simulating an infiltrative growth pattern (Fig. 1D). This pattern was observed mainly in the vicinity of small duct-like spaces protruding from the lesion itself into the surrounding tissue, giving the impression of periductal spread of MSGC. In all cases, MSGC were present close to the surgical margin.

Immunocytochemistry

The results of the immunohistochemical studies are summarized in Table 2. Despite the broad range of antibodies

Table 1 Clinicopathological features of benign tumors with multinucleated stromal giant cells (*r* right, *l* left, *ADH* atypical ductal hyperplasia, *NR* no recurrence)

Case number	Age (years)	Clinical impression	Side (r/l)	Size (cm)	Gross description	Histological diagnosis	Follow-up (months/status)
1	43	Breast mass	r	2.5	Bosselated, circumscribed	Adenomyoepithelioma	36/NR
2	55	Breast mass	r	1.0	Rubbery, gray-white	Adenosis tumor	26/NR
3	42	Cystic breast mass	l	1.3	Rubbery white cystic mass	Intraductal papilloma	96/NR
4	37	Breast mass	l	3.8	Circumscribed nodule	Complex fibroadenoma	59/NR
5	70	Breast mass	l	1.7	No description	Adenosis tumor with focal ADH	189/NR
6	41	Fibroadenoma	r	1.2	Well circumscribed tan nodule	Fibroadenoma with tubular pattern	11/NR

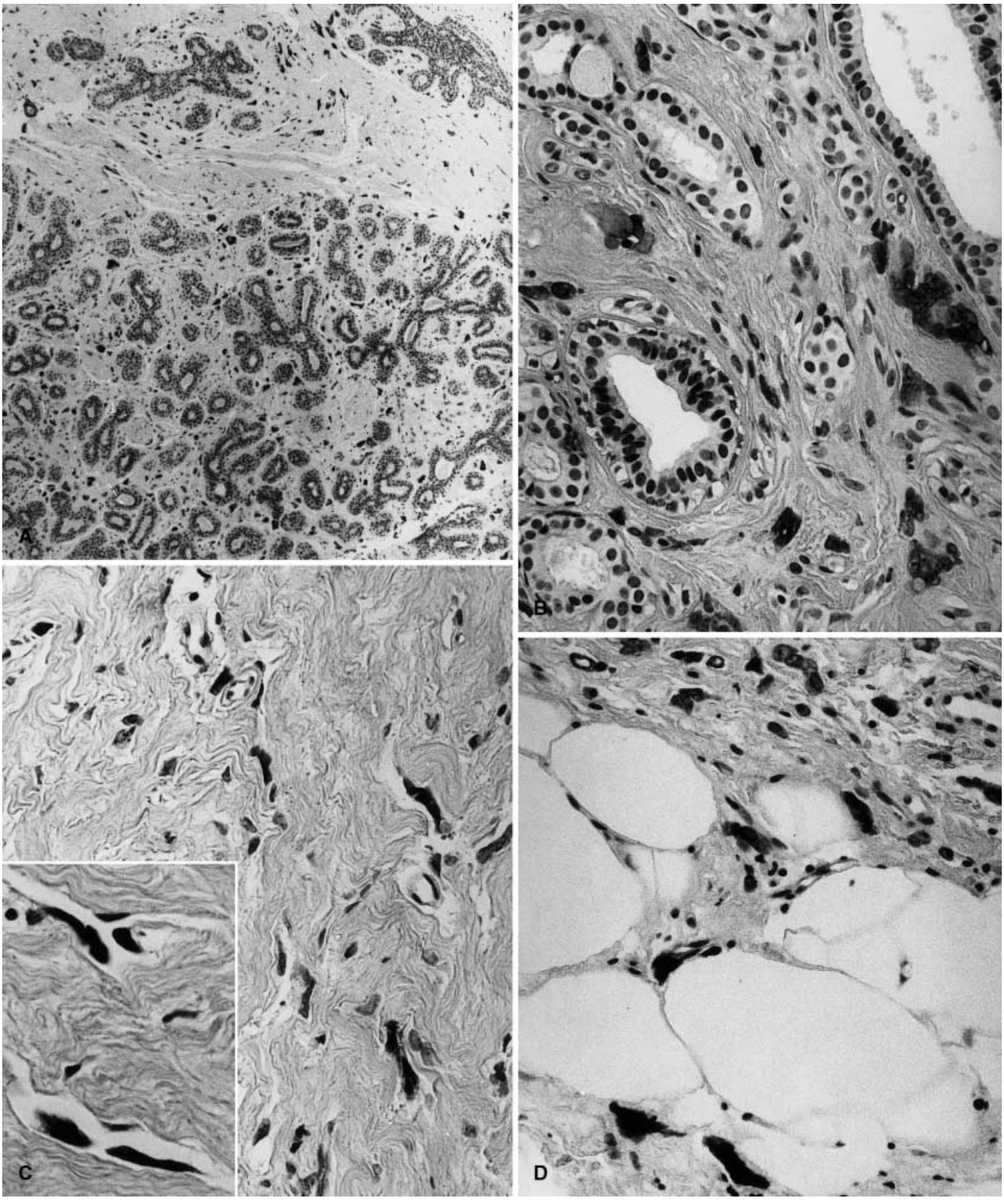


Fig. 1 **A** Fibroadenoma with partial tubular growth pattern. Numerous multinucleated stromal giant cells (MSGC) were dispersed throughout the tumor and were well visible in low-power magnification (Case 6) (×50). **B** Adenosis tumor with numerous MSGC haphazardly dispersed within the collagenous stroma. They contained multiple nuclei, with fine chromatin and sporadic nucleoli, forming a grape-like cluster or arranged in a floret. Sometimes the nuclei were hyperchromatic (Case 5) (×250). **C** MSGC appeared to line lacunar spaces simulating vascular lumina, superficially resembling appearance of giant cell fibroblastoma or pseudoangiomatous stromal hyperplasia (Case 4) (×250, inset ×470). **D** MSGC permeated the surrounding adipose and fibrous tissue, mimicking a malignant lesion with an infiltrative growth pattern. (Case 5) (×470)

Table 2 Immunohistochemical findings in MSGC [*MSGC* multinucleated stromal giant cells, – negative. *1+* weakly positive (less than 25% of MSGC), *2+* moderately positive (25–50% of MSGC), *3+* strongly positive (more than 50% of MSGC), *ER* estrogen receptor, *PR* progesterone receptor]

Case number	1	2	3	4	5	6
Vimentin	1+	3+	3+	2+	3+	3+
CD34	1+	–	1+	2+	2+	3+
AE1/AE3	–	–	–	–	–	–
34ßE12	–	–	–	–	–	–
CAM5.2	–	–	–	–	–	–
S-100	–	–	–	–	–	–
Actin	–	–	–	–	–	–
FVIII	–	–	–	–	–	–
CD31	–	–	–	–	–	–
CD68	–	–	–	–	–	–
ER	–	–	–	–	–	–
PR	–	–	–	–	–	–
P53	2+	3+	3+	3+	3+	–
Ki-67	1+	1+	1+	1+	1+	–

used to elucidate the histogenetic origin of MSGC, the MSGC showed strong reactivity for vimentin in six (100%) cases and in four (67%) cases revealed variable positivity for CD34 (Fig. 2A). Staining for epithelial markers (broad spectrum cytokeratin AE1/AE3, HMW keratin, CAM 5.2), myoepithelial markers (S-100 protein, SMA), myogenic markers (actin), vascular markers (FVIII, CD31), histiocytic markers (CD68), and hormonal receptors (ER, PR) were all negative. Interestingly, in all but one case the majority of the mononuclear cells and MSGC showed diffuse moderate to strong reactivity for p53 protein (Fig. 2B). The vast majority of stromal cells were positive in each case. The epithelial and myoepithelial elements were uniformly negative, as well as the structures of adjacent normal mammary gland (both stromal and epithelial cells) and fibrofatty tissue. Case no. 6 revealed inverse staining pattern with p53; stromal cells (both mononucleated and MSGC) were uniformly negative, but the vast majority of both epithelial and myoepithelial cells were weakly to moderately positive for p53.

In addition to sporadic epithelial and myoepithelial cells, many mononuclear cells and some MSGC revealed Ki-67 antigen expression (Fig. 2C). The number of Ki-67 positive cells was similar in all cases, with the exception of case no. 6, where only epithelial and myoepithelial cells and sporadic mononuclear cells were positive; MSGC were uniformly Ki-67 negative.

Electron microscopy

The MSGC were embedded within a collagenous matrix. They had multiple, often multilobated nuclei (Fig. 3A) with conspicuous isolated nucleoli (Fig. 3B). Their cytoplasm was scanty, containing abundant granular endoplasmic reticulum with numerous ribosomes (Fig. 3B). Basal lamina, pinocytic vesicles, desmosomes, and microfila-

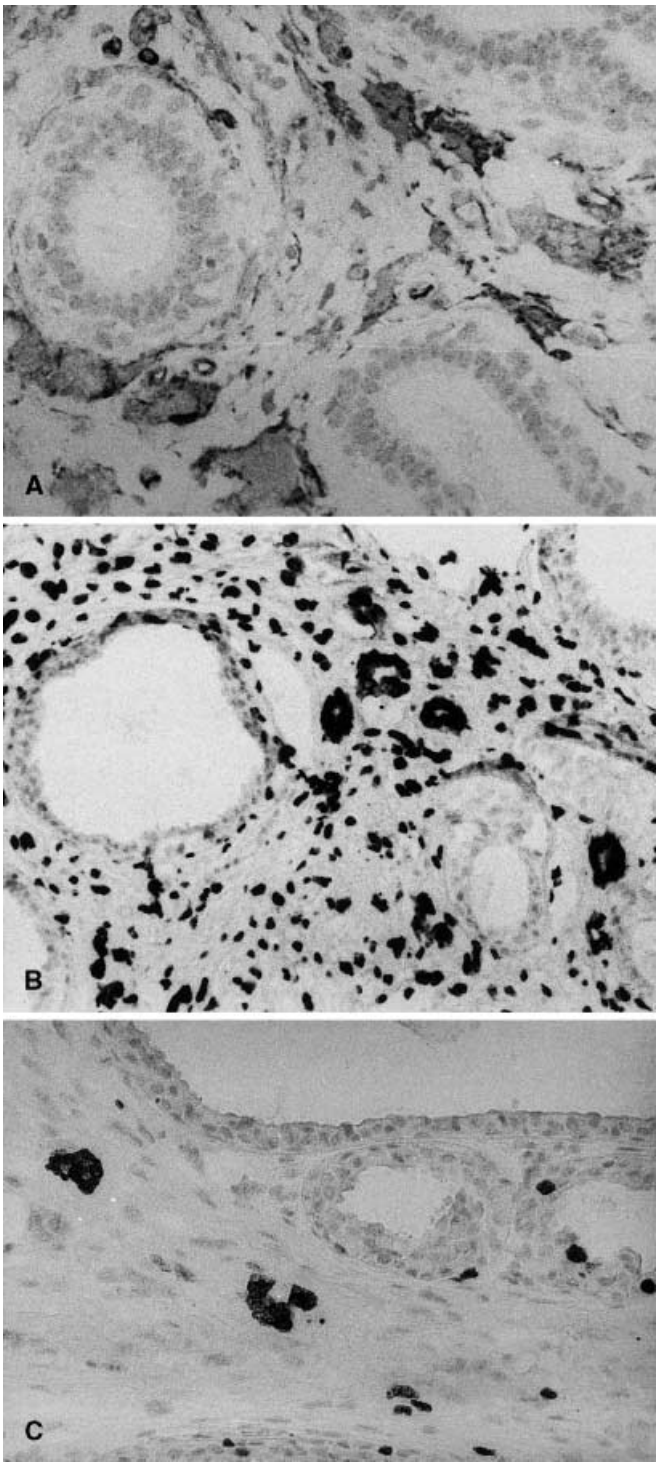


Fig. 2 **A** Multinucleated stromal giant cells (MSGC) showed variable reactivity for CD34. The staining highlighted the otherwise inconspicuous cytoplasm with irregular margin and numerous thin cytoplasmic processes (Case 4) (×250). **B** The vast majority of both mononuclear stromal cells and MSGC showed diffuse moderate to strong reactivity for p53 protein. The epithelial and myoepithelial elements were uniformly negative (Case 2) (×120). **C** Some MSGC, as well as sporadic epithelial and myoepithelial cells and mononuclear cells revealed Ki-67 antigen expression (Case 2) (×120)

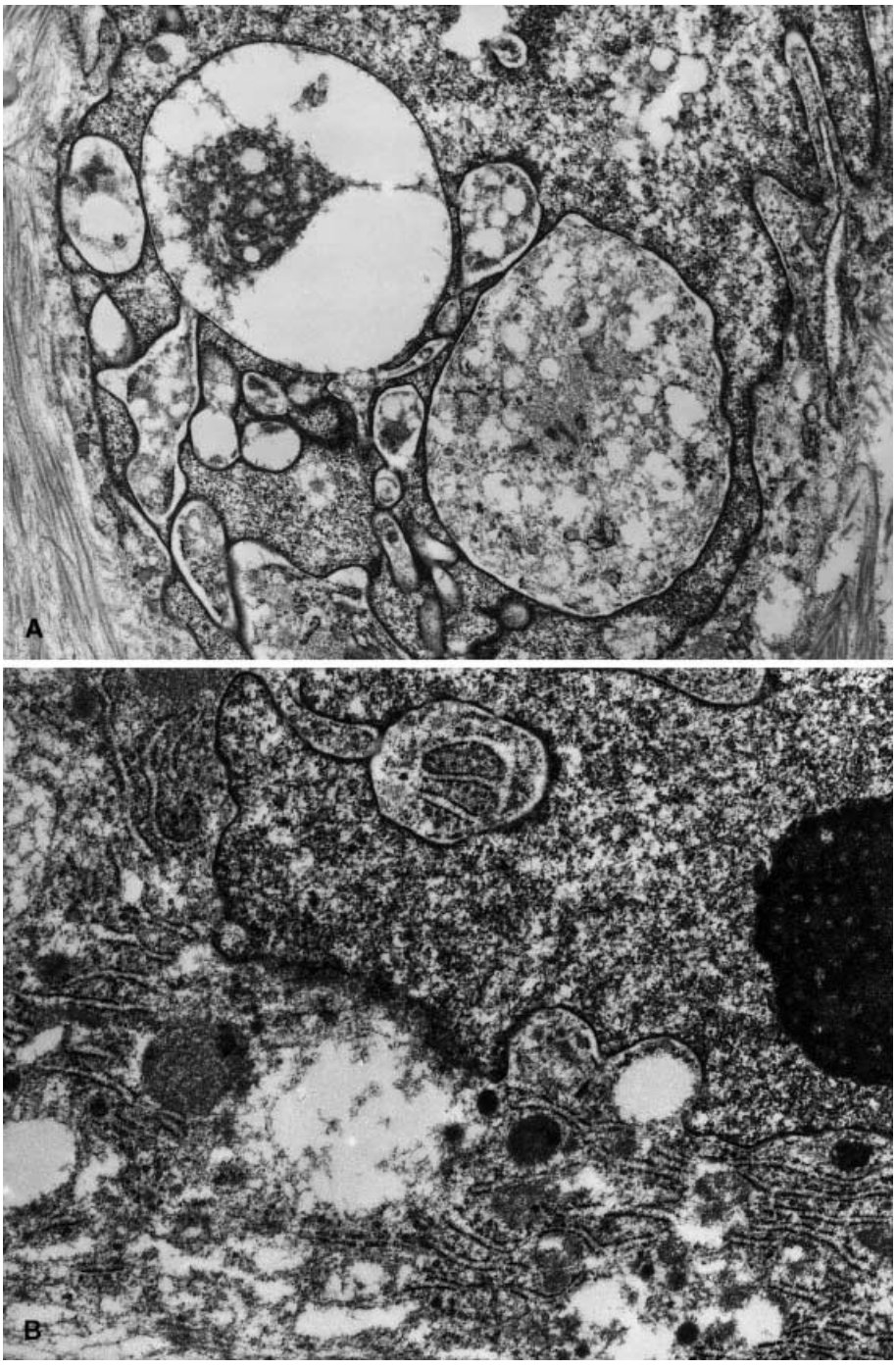


Fig. 3 **A** Some multinucleated stromal giant cells (MSGC) had bizarre multilobated nuclei with multiple intranuclear pseudoinclusions (Case 4) (×16,000). **B** Cytoplasm of MSGC was scanty, containing abundant granular endoplasmic reticulum with numerous ribosomes. Basal lamina, pinocytic vesicles, desmosomes, and microfilaments with dense bodies were not seen. Note prominent isolated nucleolus (Case 4) (×17,640)

ments with dense bodies were not seen. These ultrastructural findings support MSGC to be of fibroblastic origin.

Discussion

We report herein the second largest series of mammary fibroepithelial tumors with MSGC. To the best of our knowledge, only 17 cases have been published previously [2, 4, 6, 16, 18, 19], indicating that this peculiar lesion is extremely rare. Originally, Rosen described MSGC in otherwise normal breast parenchyma in mastectomy specimens [21]. In the series of 200 consecutive mastectomies for carcinoma, he observed MSGC in nine cases (4.5%). He interpreted them as a sign of probable reparative process, possibly linked to hormonal changes, as the majority of patients in this series were in their 40s. The predominant interlobular localization, usually not adjacent to carcinoma, was stressed.

The cases reported here are exceptional in two aspects:

1. The abundance of MSGC in each case. Based on our personal experience (unpublished data), MSGC are

occasionally present in various breast lesions. However, their number is usually limited to several cells per slide.
2. Absence of any accompanying pathological changes, which are usually described in MSGC in other locations [9, 10, 17, 18] – namely, moderate to severe inflammation and/or edema.

History of irradiation was stressed in several reported cases, but none of our patients had undergone irradiation. Some authors pointed out the occurrence of numerous mast cells in close contact with MSGC. This led to assumptions about a possible pathogenetic linkage between mast cells and MSGC. Nevertheless, in none of our cases were mast cells observed.

In the study of Coyne [7], documenting the occurrence of MSGC within the interstitium of the testis, the number of MSGC correlated with increasing age; all patients with numerous MSGC were in their 70s or 80s. This does not seem to be the case in breast. Age of the patients in our series, together with the other reported cases, ranged between 23 and 70 years (average 43 years, median 42 years). We also did not observe any differences in the number of MSGC in different ages.

The origin of MSGC remains obscure. Theoretically, they could be derived from four different stem cells – epithelial, myoepithelial, (myo)fibroblastic, and histiocytic. Whereas in the majority of reports, MSGC are supposed to originate from fibrous or fibrohistiocytic elements [4, 14, 18, 19, 21]. Nielsen and Ladefoged in their case report [16] hypothesized that they could be derived from myoepithelial cells. However, their conclusions are based on the unconvincing results of ultrastructural examination of poorly preserved paraffin embedded material only; no immuhohistochemistry confirming this hypothesis (actin, SMA, S-100 protein) was performed.

The results of immunohistochemistry and electron microscopy in our series indicate that MSGC are probably derived from periductal stromal fibroblasts. No signs of myofibroblastic or histiocytic differentiation were present. In cases with an infiltrative growth pattern, we have seen the periductal localization of MSGC as was emphasized by Rosen in his original report [21]. None of our cases showed positivity of stromal cells in hormonal receptor examination.

The presence of MSGC in breast tumors is a phenomenon of uncertain significance. None of the reported cases has recurred or metastasized. The uniform and constant positivity of p53 protein in the stromal elements (both mononuclear cells and MSGC) in five of our six cases is a rather surprising finding. It was detected neither in normal mammary gland nor in benign breast lesions (both tumors and fibrocystic changes) in series of 95 benign breast lesions [3]. However, detection of p53 overexpression seems to be strongly dependent on the type of primary antibody and fixative used. In another series of 275 obviously benign breast specimens [28], a minority of cases (16%) showed unequivocal positivity of p53. Unfortunately, the authors do not mention whether there was positivity both in glandular (epithelial and myoepithelial) as well as in stromal cells. In this series, patients with p53 positivity in benign lesions were not at any greater risk of breast cancer when compared with those with p53 negative benign lesions.

p53 is a tumor supressor gene encoding a 53-kDa nuclear phosphoprotein, present at normal circumstances as a wild-type form, which has a very short half-life and attains such a low intranuclear level that it is not detectable using immunohistochemical techniques. Through the induction of protein p21, which is the inhibitor of both cyclin dependent kinases and proliferating cell nuclear antigen, p53 induces (in cells with unreparable DNA defects) either growth arrest at the G1 phase or apoptosis. Whether a cell would undergo growth arrest or apoptosis appears to depend on a variety of factors, mainly environmental conditions and cell type [27]. In the case of p53 point mutation, which is one of the most common events in human malignancies, the gene is able to act as a dominant transforming oncogene. Moreover, the gene product (mutant p53 protein), which is synthesized, is much more stable and has an extended half-life, so it can be readily detected immunohistochemically. Thus, one could suppose that the appearance of the bizarre MSGC is a result of inability of their mechanism of self-destruction by programmed cell death. However, in the experimental study of human fibroblasts cultured in vitro, despite the much higher DNA binding activity of p53 in senescent fibroblasts, the levels of total p53 mRNA and protein did not differ between low-passage (young) and high-passage (old) cells [1]. Thus, the significance of p53 positivity of MSGC in our series remains unexplained.

Unlike the cases from urinary bladder [17], where MSGC have been shown to express proliferating cell nuclear antigen (PCNA) but not Ki-67, 5/6 of our cases revealed positivity of Ki-67 in the nuclei of stromal cells, including MSGC. The presence of Ki-67 in the nuclei of MSGC indicates that these cells are not just a degenerative phenomenon of senescence, as in the case of symplastic uterine leiomyomas or ancient schwannomas. Ki-67 is a fairly specific marker for proliferating cells, expressed during the whole cell cycle with the exception of the G0 phase. Unlike PCNA, Ki-67 is not involved in DNA repair [25]. MSGC show proliferative activity, although by standard H&E examination the finding of mitoses was an extremely rare event in our series. Powell et al. described the occasional presence of hyperchromatic nuclei of MSGC in their cases, appearing to be mitotic figures [19]; however, distinguishing their presented examples in the microphotographs from apoptotic changes seems to be extremely difficult.

In three of our cases, and in one tumor from another series [19], infiltration of the MSGC into the adjacent fat was observed. The importance of this finding lies mainly in the possibility of mimicking the growth pattern of invasive carcinoma. Despite the fact that in all of our cases MSGC were present at the surgical margin, we did not observe any recurrence or metastasis during the extended

follow-up period (11–189 months; median 48 months). This indicates the probable indolent nature of MSGC.

The peculiar presence of MSGC within lacunar, vascular-like spaces was not stressed previously [4, 16, 19] with one exception [2]. However, we consider this to be highly significant and constant feature, as it was observed in all of our cases and is also visible in some figures in previous reports [16, 19]. In some areas the stroma strongly resembled the appearance of giant cell fibroblastoma (GCF), where a pseudoangiomatous pattern is a feature [12, 23]. Another lesion featuring spaces reminiscent of vascular lumina is pseudoangiomatous stromal hyperplasia of the mammary gland (PASH) [2, 20, 26]. This rather common tumor-like condition is characterized by the presence of cleft-like spaces, discontinuously lined by slender spindle cells of fibroblastic or myofibroblastic origin. Presence of these spaces was observed even in frozen sections of PASH, which excludes the hypothesis about their artifactual origin during formaldehyde fixation.

MSGC should be distinguished from other multinucleated stromal elements in breast tumors – osteoclast-like giant cells. Osteoclast-like giant cells are a rare finding in poorly differentiated or metaplastic carcinomas of breast, thyroid, pancreas, and other organs [5, 8, 13, 15, 22, 24, 29]. They most likely represent reactive stromal elements of histiocytic origin, microscopically indistinguishable from true osteoclasts. The cells have numerous small uniform nuclei and copious cytoplasm. They frequently express histiocytic markers, like lysozyme, α-1-antitrypsin or CD68. The morphology of MSGC is essentially different from osteoclasts and none of our cases showed CD68 positivity in the MSGC, despite the staining of a variable number of macrophages in the background.

In conclusion, we report six cases of benign tumors of the breast with numerous MSGC. It is difficult to explain their histogenesis; we assume the positivity of p53 (either result of mutation or overexpression) in both mononuclear stromal cells and MSGC may play a key role in linking together these two cell types. MSGC could presumably originate from mononuclear stromal cells. The absence of p53 staining in the stromal elements within the surrounding normal mammary gland accentuates the true neoplastic nature of these lesions. All patients were treated by simple excision of the lesion and they remain free of recurrence for from 11 to 189 months (mean and median follow up 70 and 48 months, respectively), indicating that the presence of MSGC does not alter the prognosis of an otherwise typical benign lesion.

Acknowledgments We gratefully acknowledge the help to this study of the following physicians who provided follow-up information on the patients: P.S. Fekete, Gwinnett Medical Center, Lawrenceville, GA; D. Baitlon, Parkview Episcopal Medical Center, Pueblo, CO; J.E. Hasson, Alexian Brothers Hospital, San Jose, CA; C. Branch, Olmsted Community Hospital, Rochester, MN; J.S. Welch, Methodist Hospital, Rochester, MN; R.D. Lawrence, Delta Pathology Associates Med. Group, Stockton, CA. We also thank K. Wettleson for her secretarial assistance and B. Šepsová for her preparation of photographs.

References

1. Atadja P, Wong H, Garkavtsev I, Veillette C, Raibowol K (1995) Increased activity of p53 in senescing fibroblasts. Proc Natl Acad Sci USA 92:8348–8352
2. Badve S, Sloane JP (1995) Pseudoangiomatous hyperplasia of male breast. Histopathology 26:463–466
3. Bartek J, Bartkova J, Vojtesek B, Staskova Z, Rejthar A, Kovarik J, Lane DP (1990) Patterns of expression of the p53 tumour suppressor in human breast tissues and tumours in situ and in vitro. Int J Cancer 46:839–844
4. Berean K, Tron VA, Churg A, Clement PB (1986) Mammary fibroadenoma with multinucleated stromal giant cells. Am J Surg Pathol 10:823–827
5. Bocklage TJ, Dail D, Colby TV (1998) Primary lung tumors infiltrated by osteoclast-like giant cells. Ann Diagn Pathol 2:229–240
6. Campbell AP (1992) Multinucleated stromal giant cells in adolescent gynaecomastia. J Clin Pathol 45:443–444
7. Coyne JD, Dervan PA (1997) Multinucleated stromal giant cells of testis. Histopathology 31:381–383
8. Esmaili JH, Hafez GR, Warner TF (1983) Anaplastic carcinoma of the thyroid with osteoclast-like giant cells. Cancer 52:2122–2128
9. Groisman GM, Polak-Charcon S (1998) Fibroepithelial polyps of the anus: a histologic, immunohistochemical, and ultrastructural study, including comparison with the normal anal subepithelial layer. Am J Surg Pathol 22:70–76
10. Groisman GM, Amar M, Polak-Charcon S (2000) Multinucleated stromal cells of the anal mucosa: a common finding. Histopathology 36:224–228
11. Hsu SM, Raine L, Fanger H (1981) Use of avidin-biotin-peroxidase complex (ABC) in immunoperoxidase technique: a comparison between ABC and unlabeled antibody (PAP) procedures. J Histochem Cytochem 29:577–580
12. Kanai Y, Mukai M, Sugiura H, et al (1991) Giant cell fibroblastoma. Acta Pathol Jpn 41:552–560
13. Molberg KH, Heffess C, Delgado R, Albores-Saavedra J (1998) Undifferentiated carcinoma with osteoclast-like giant cells of the pancreas and periampullary region. Cancer 82:1279–1287
14. Nesland JM, Johannessen JV (1985) Fibroadenoma of the female breast with multinucleated giant cells – letter to the case. Path Res Pract 180:724–725
15. Nielsen BB, Kiaer HW (1985) Carcinoma of the breast with stromal multinucleated giant cells. Histopathology 9:183–193
16. Nielsen BB, Ladefoged C (1985) Fibroadenoma of the female breast with multinucleated giant cells. Path Res Pract 180:721–724
17. Ohtsuki Y, Furihata M, Iwata J, Takeuchi T, Sonobe H, Chen BK, Liang SB, Kuwahara M, Ochi K, Terao N (2000) Multinucleated giant cells in submucosal layer of human urinary bladder: an immunohistochemical and electron microscopic study. Pathol Res Pract 196:293–298
18. Pitt MA, Roberts IS, Agbamu DA, Eyden BP (1993) The nature of atypical multinucleated stromal cells: a study of 37 cases from different sites. Histopathology 23:137–145
19. Powell CM, Cranor ML, Rosen PP (1994) Multinucleated stromal giant cells in mammary fibroepithelial neoplasms. A study of 11 patients. Arch Pathol Lab Med 118:912–916
20. Powell CM, Cranor ML, Rosen PP (1995) Pseudoangiomatous stromal hyperplasia (PASH): a mammary stromal tumor with myofibroblastic differentiation. Am J Surg Pathol 19:270–277
21. Rosen PP (1979) Multinucleated mammary stromal giant cells. A benign lesion that simulates invasive carcinoma. Cancer 44:1305–1308
22. Rosen PP, Oberman HA (1992) Tumors of the mammary gland. Atlas of tumor pathology. Fascicle 7 (3rd series). Armed Forces Institute of Pathology, Washington, D.C., pp 115–117
23. Shmookler BM, Enzinger FM, Weiss SW (1989) Giant cell fibroblastoma. A juvenile form of dermatofibrosarcoma protuberans. Cancer 64:2154–2161

24. Stracca-Pansa V, Menegon A, Donisi PM, Bozzola L, Fedeli F, Quarto F, Nappi O, Pettinato G (1995) Gastric carcinoma with osteoclast-like giant cells. Report of four cases. Am J Clin Pathol 103:453–459
25. van Diest PJ, Brugal G, Baak JPA (1998) Proliferation markers in tumours: interpretation and clinical value. J Clin Pathol 51:716–724
26. Vuitch MF, Rosen PP, Erlandson RA (1986) Pseudoangiomatous hyperplasia of mammary stroma. Hum Pathol 17:185–191
27. Yonish-Rouach E (1997) A question of life or death: the p53 tumor suppressor gene. Path Biol (Paris) 45:815–823
28. Younes M, Lebovitz RM, Bommer KE, Cagle PT, Morton D, Khan S, Laucirica R (1995) p53 accumulation in benign breast biopsy specimens. Hum Pathol 26:155–158
29. Zukerberg LR, Armin AR, Pisharodi L, Young RH (1990) Transitional cell carcinoma of the urinary bladder with osteoclast-type giant cells: a report of two cases and review of the literature. Histopathology 17:407–411

Virchows Arch (2001) 439:776–781
DOI 10.1007/s004280100475

ORIGINAL ARTICLE

A. Ubiali · A. Benetti · M. Papotti · V. Villanacci
G. Rindi

Genetic alterations in poorly differentiated endocrine colon carcinomas developing in tubulo-villous adenomas: a report of two cases

Received: 14 March 2001 / Accepted: 25 April 2001 / Published online: 12 July 2001
© Springer-Verlag 2001

Abstract The genetic study of two cases of tubulo-villous adenoma associated with poorly differentiated endocrine carcinoma (PDEC) is reported. Aim of this work was to assess whether the exocrine and endocrine growths share a common genotype. The analysis entailed the search for allelic loss (LOH) or imbalances of polymorphic microsatellite markers at the corresponding chromosomal loci of the genes *MEN-1* (11q13), *p53* (17p13), Deleted in Colorectal Carcinoma (*DCC*) (18q21) and hMSH-2 (*BAT26*) (2p21–22). Additionally, the exons 5–8 of the *p53* gene were sequenced in the two PDECs only. One of the two cases investigated showed LOH for 18q *DCC* markers in the tubulo-villous adenoma while a point mutation of the *p53* gene was observed in the PDEC component. No genetic abnormality was observed in both adenoma and PDEC components of the other case. In the two cases *p53* protein accumulation was observed in both PDEC and adenoma cells. These data indicate that only the *p53* gene abnormality is shared by both colon cancer and PDEC in the two cases reported. The lack of other common genetic defect may suggest a different histogenesis for the two tumor types. The development of colon PDEC implies the defect of *p53* gene.

Keywords PDEC · SCC · Tubulo-villous adenoma · LOH · DCC · p53 · hMSH-2

Introduction

Colorectal endocrine tumors present a wide range of aggressiveness [23]. Among them, the poorly differentiated (small-cell) endocrine carcinoma (PDEC) represents a subgroup with poor prognosis due to its wide and rapid dissemination. PDEC cells are small with hyperchromatic nuclei, even though larger elements can be found, and are characterized by immunohistochemical and ultrastructural features of neuroendocrine differentiation [2, 9, 20]. It has been reported that colon PDEC may be associated with a conventional exocrine adenocarcinoma [7, 20]. This observation led to the speculation that both tumors originate from the same transformed precursor cell, thus implying common genetic events leading to both exocrine and endocrine carcinoma. Recent genetic data support this view [24].

Here we report two cases of metastatic PDEC developing within tubulo-villous adenoma with high-grade epithelial dysplasia. To understand the natural history and evolution of both tumors we assessed the allelic status of chromosomal loci of genes potentially involved in the exocrine and endocrine tumorigenesis. The gene loci investigated comprised the *MEN-1* on 11q13 [4, 18], *p53* on 17p13 [16] and *DCC* (Deleted in Colorectal Carcinoma) on 18q21 [15]. The pattern of the *hMSH-2* gene locus on 2p21–22 (*BAT26*) was investigated since it is an informative genetic marker of the replication error phenotype (RER) [14] in colorectal carcinoma in its sporadic and hereditary non-polyposis associated (HPCC) forms [12]. Additionally, in PDECs' DNA only, the exons 5–8 of *p53* gene were direct-sequenced in search for point mutations.

Clinical history

Patient A

A 66-year-old man presented in December 1998 to the hospital Spedali Civili of Brescia, Italy, with fever in absence of other signs or symptoms. Abdominal ultrasound examination showed the liver to be almost entirely replaced by multiple metastases that were found to be poorly differentiated carcinoma upon cyto-histological examination. At colonoscopy a large, polypoid and ulcerated lesion was observed in the right colon. Biopsies were taken and were consistent with a tubulo-villous adenoma with

Source of support: University of Brescia (GR and AB), MURST COFIN 99, N.99062198982 (GR).

A. Ubiali · A. Benetti · V. Villanacci · G. Rindi (✉)
Pathology Service 2 University of Brescia and Spedali Civili,
Piazza Spedali Civili, 1, 25124 Brescia, Italy
e-mail: rindi@master.cci.unibs.it
Tel.: +39-030-3995830, Fax: +39-030-3995053

M. Papotti
Surgical Pathology III, University of Turin, Turin, Italy

moderate to high-grade dysplasia upon histological examination. A right hemicolectomy was performed for palliation and the surgical specimen revealed 9 polyps, two of which were 4 cm in size, one macroscopically infiltrating the colon wall. The patient died of sudden cardiovascular complications 28 days after surgery. Autopsy was not performed.

Patient B

A 45-year-old woman presented in September 1998 to the Hospital San Giovanni Battista of Turin, Italy, with abdominal pain and occult blood in the stool. Abdominal ultrasound investigation showed multiple liver metastases, and a CT scan revealed a tumor in the right colon. At colonoscopy a polypoid lesion of 5 cm in size was observed in the cecum, 3 cm distal to the ileocecal valve. A right hemicolectomy was performed and samples from two liver metastases were taken for diagnostic purposes. The patient was discharged home with persistent metastatic liver disease in October 1998. A right liver lobectomy with concurrent resection of three metastases in the left lobe was subsequently performed at the Hospital Beaujon of Clichy, France, in March 1999. The patient is alive and well at 24 months of follow-up.

Materials and methods

Histology

After fixation in 10% buffered formalin for 48 h, all tumor growths, lymph nodes and liver metastases (patient B only) were sampled and processed into paraffin. Serial sections 4 µm thick were stained with hematoxylin-eosin (H&E) and Alcian blue pH 2.5 and periodic acid–Schiff (PAS) for mucin detection. Mitoses were counted in ten high power fields (HPF, ×400). Immunoperoxidase tests were performed using a universal peroxidase streptavidin-biotin complex (SABC) (StreptHRP 6100, Biospa, Milan, Italy) [13]. The primary antibodies included: cytokeratin (Becton Dickinson, Milan Italy; CAM-5, mouse 1:20), neuron-specific enolase (NSE) (Biogenex, San Ramon, CA, USA; MIG-N3, mouse 1:80), PGP 9.5 (Histoline Labs, Milan, Italy; mouse 1:500), synaptophysin (Dako, Glostrup, Denmark; rabbit 1:100), chromogranin A (CgA) (Biogenex; LK2H10 mouse, 1:800), *p53* (Neomarkers, Union City, CA, USA; mouse DO7, 1:50). Protease or microwave pretreatment was performed for cytokeratin, CgA, Synaptophysin, PGP9.5, and *p53* before applying the primary antibody [3]. Controls consisted of omission of the first layer and use of tissue with or without the pertinent antigen.

Genetic analysis

Sections of 3 µm on glass slides were dewaxed and briefly stained with eosin. Adenoma, PDEC, and normal tissue from both the primary and metastatic sites were isolated and microdissected under direct light microscope for ~90% tumor cell enrichment [25]. Low-molecular-weight DNA was extracted by proteinase K digestion (Sigma Chemicals, Milan, Italy), phenol-purified, ethanol-precipitated, and resuspended in water. For polymerase chain reaction (PCR) amplification the following microsatellite markers were investigated: PYGM, D11S4946, and D11S913 for *MEN-1* [18]; TP53, D17S513, and D17S804 for *p53* [10, 16]; D18S69, D18S61, D18S55, and D18S58 for *DCC* [15] and BAT26 for *HMSH-2* [12]. When possible one of the selected microsatellite markers was located within or close to the investigated gene, and at least one in centromeric and telomeric position, respectively. Specific primers were designed from sequences published by Genebank (http://www.ncbi.hlm.nih.gov) and purchased from Gibco-BRL, Milan, Italy. PCR conditions were set as follows: PYGM 35 cycles, denaturation 1 min at 94°C, annealing 1 min at 58°C, elongation 2 min at 72°C; D11S4946 35 cycles, denaturation 30 s at 94°C, annealing 30 s at 60°C, elongation 1 min at 72°C, D11S913 35 cycles, denaturation 30 s at 94°C, annealing 30 s at 55°C, elongation 30 s at 72°C, TP53 and D17SXXX*:* 35 cycles, denaturation at 94°C for 1 min, annealing at 55°C for 1 min and elongation at 72 °C for 90 s, D18SXX*:* 30 cycles, denaturation at 94°C for 30 s, annealing at 50°C for 1 min and elongation at 72°C for 1 min, BAT26*:* 35 cycles, denaturation at 94°C for 30 s, annealing at 54°C for 1 min and elongation at 72°C for 1 min. A 3-min pre-heating step at 94°C and a final elongation at 72°C for 30 min was performed for all PCR reactions. The quality of the amplification was evaluated on 2% agarose gel electrophoresis. For LOH analysis 1–5 µl of each PCR product was resolved on a non-denaturing, 9.5% acrylamide sequencing gel. The gels were silver-stained with a method modified from Allen et al. 1989 [1]. In brief, the gels were fixed with 10% ethanol, saturated with 1% nitric acid, stained with 1 M silver nitrate and developed with 300 mM sodium carbonate and 0.02% formalin. Gels were finally fixed in 10% acetic acid, dried, and visually evaluated for allelic loss. In addition, bands were quantified by scanning densitometry with the PhotoPrint III System (Euroclone-Celbio, Milan, Italy). The peak area was assessed using the software PhotoCaptMW 99.03 (Vilber-Lourmat, Marne-La Vallee, France) to determine the ratio $(\text{lower allele/higher allele})^{\text{tumor}}/(\text{lower allele/higher allele})^{\text{normal}}$. Alleles were considered lost when this ratio was below 0.6, thus identifying a 40% loss of the signal.

Sequence analysis of *p53* gene was performed on amplified sequences from exons 5–8 where most point mutations have been reported [11]. The primers used were: exon 5 forward 5’ TTC CAC ACC CCC GCC CGG CA 3’, reverse 5’ GCC CCA GCT GCT CAC CAT C 3’; exon 6 forward 5’ GAG ACG ACA GGG CTG GTT 3’, reverse: 5’ CCA CTG ACA ACC ACC CTT 3’; exon 7 forward 5’ GGT CTC CCC AAG GCG CAC TGG 3’, reverse: 5’ AGG CTG GGG CAC AGC AGG CC 3’; exon 8 forward 5’ ATT TCC TTA CTG CCT CTT GC 3’, reverse 5’ TCC ACC GCT TCT TGT CCT GC 3’. The PCR conditions were set as follows: exon 5, 35 cycles, denaturation at 94°C for 30 s, annealing at 60°C for 90 s and elongation at 72°C for 2 min, exon 6, 35 cycles, denaturation at 94°C for 30 s, annealing at 55°C for 90 s and elongation at 72°C for 2 min, exons 7 and 8, 35 cycles, denaturation at 94°C for 30 s, annealing at 68°C for 90 s and elongation at 72°C for 2 min. All PCR reactions were preceded by a 3-min denaturation step at 94°C and followed by a final elongation of 30 min at 72°C. The efficiency and stringency of the PCR was verified on 2% agarose gels. Both strands of the amplified fragments were direct sequenced on ABI Prism 377 Genetic Sequencer using the ABI Prism BigDye Terminator Cycle Sequencing Ready Reaction kit, with AmpliTaq DNA Polymerase, FS (Perkin-Elmer, USA).

Results

Histology

Of the nine growths observed in patient A, one was a hyperplastic polyp and eight were adenomas, with various degree of epithelial dysplasia. Of the two largest adenomas, one showed high-grade epithelia dysplasia and was superimposed on a neoplastic growth with solid structure, abundant central necrosis, composed by atypical, small to intermediate round cells with a very high mitotic index (42 mitoses, often atypical, per ten HPF). The histology was consistent with a poorly differentiated (small cell) endocrine carcinoma (PDEC) of the colon (Fig. 1A). The differential diagnosis of colon PDEC includes the undifferentiated colon carcinoma and non-Hodgkin lymphomas. The PDEC was deeply infiltrating the colon wall and invaded the surrounding adipose tissue.

In patient B the polyp growth was a tubulo-villous adenoma with high-grade epithelial dysplasia in the

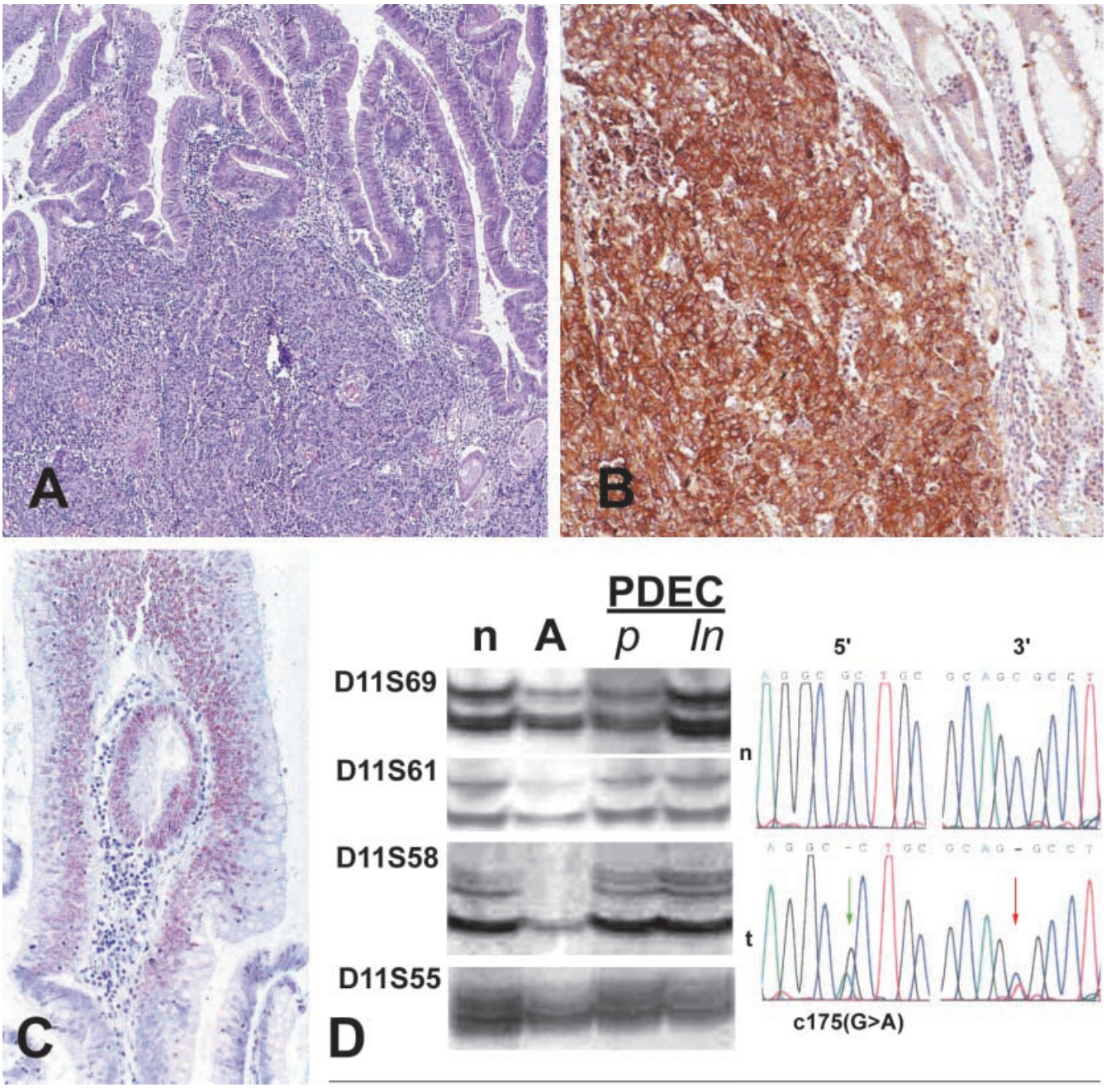


Fig. 1A–D Patient A: histopathological findings. **A** The typical solid structure with focal necrosis of the poorly differentiated endocrine carcinoma (PDEC, *lower part* of the micrograph) growing within the tubulo-villous adenoma (*upper part* of the micrograph). **B** The intense and diffuse immunoreactivity for synaptophysin of the PDEC cells: note the absence of significant immunoreactivity in the adenoma cells. **C** *p53* overexpression/accumulation in the nuclei of the adenoma cells: note that some cells at the base of the villous growth are negative. **A** H&E; **B**, **C** immunoperoxidase, SABC method. Molecular genetic findings. **D** (*left part*) Allelic status of four microsatellite markers on 18q in DNA from normal tissue (*n*), adenoma (*A*), PDEC primary (*p*) and lymph-node metastasis (*ln*). In **A** samples all the four microsatellite markers show signal reduction indicative for allelic loss; this is evident for D11S61 and D11S58, but also appreciable for D11S69 and D11S55, as demonstrated after quantification (not shown). **D** (*right part*) Sequence analysis of *p53* exon 5 in normal tissue (*n*) and in PDEC cells (*t*) showing the G>A substitution at codon 175, (c175(G>A), *arrows*); note that the electropherogram shows also a normal signal for both strands (5' and 3'), indicative of mixed amplified DNA, possibly due either to double tumor cell population or to normal cell contamination

absence of clear-cut lamina propria invasion. Solid nests, sometimes with central necrosis, of atypical, small to intermediate round carcinoma cells with a high mitotic index (18 mitosis, often atypical, per ten HPF) were observed within the mucosa and submucosa of the polyp fibrous stalk and at its base, in the absence of deep wall invasion (Fig. 2A). This lesion too was interpreted as PDEC.

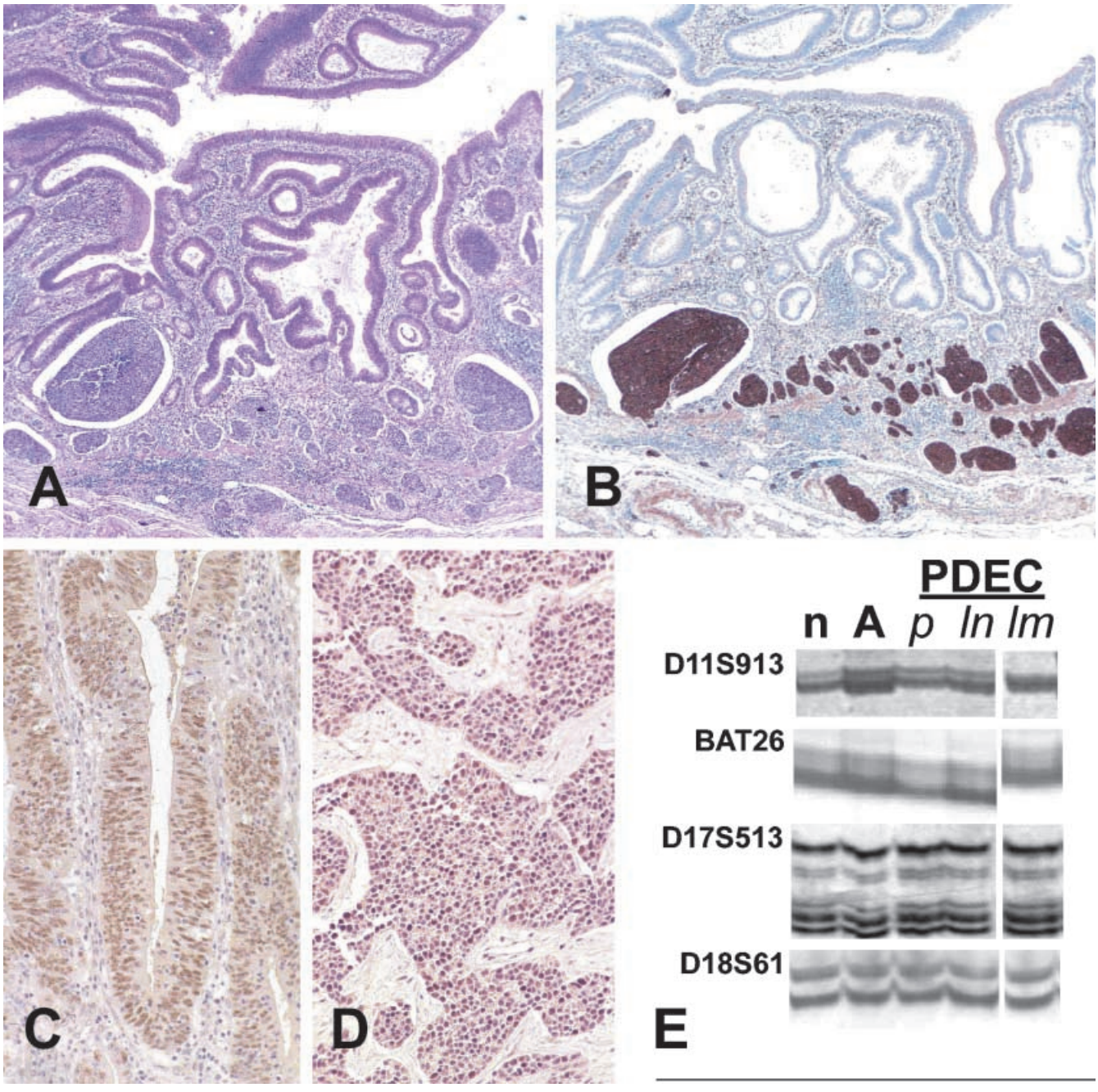


Fig. 2A–E Patient B: histopathological findings. **A** Several solid islets of the poorly differentiated endocrine carcinoma (PDEC) located in the lamina propria with initial infiltration of the colon submucosa; the overlying colon epithelium is entirely substituted by the tubulo-villous adenoma complex growth. **B** The intense and diffuse immunoreactivity for PGP9.5 of the PDEC nests: note the absence of immunoreactivity in the adenoma cells. **C, D** *p53* overexpression/accumulation is diffusely present in the nuclei of the adenoma cells (**C**) and in PDEC cells of a liver metastasis (**D**). **A** H&E; **B**–**D** immunoperoxidase, SABC method. Molecular genetic findings. **E** Representative examples of the allelic status for microsatellite markers on 11q (D11S913), 3p (BAT26), 17p (D17S513), and 18q (D18S61) in the DNA from normal tissue (n), adenoma (A), PDEC primary (*p*), lymph-node (*ln*), and liver metastasis (*lm*). In all samples no loss is detected; the migration pattern observed for all amplified fragments is unchanged in different tissues' DNA (note the gel for D17S513 where higher fragments are also shown)

Extensive lymphatic and blood vessel embolization by PDEC cells was observed in both cases. Massive PDEC metastasis involved four and eight local lymph nodes (patient A and B, respectively) and the liver (surgical samples available only for patient B). By histochemistry, PDEC cells were PAS-AB negative, strongly positive for cytokeratin and for the neuroendocrine markers synaptophysin (Fig. 1B), NSE, or PGP9.5 (Fig. 2B), though negative for chromogranin A. These findings were consistent with a diagnosis of PDEC. The

tubulo-villous adenoma cells were consistently negative for all the neuroendocrine markers investigated, though faintly to moderately positive for *p53* nuclear accumulation in 60–80% of the cells (Fig. 1C and 2C). *p53* nuclear staining of moderate intensity was observed in 90% of PDEC cells in both the primary tumors and related metastases of the two cases (Fig. 2D).

Genetic analysis

DNA samples from four tissues (normal colon, tubulo-villous adenoma, PDEC primary, PDEC lymph-node metastasis) for patient A and from six tissues (normal liver, PDEC liver metastasis, normal colon, tubulo-villous adenoma, PDEC primary, and PDEC lymph-node metastasis) for patient B were investigated. All DNA samples were informative for the microsatellite markers in use except for D11S4946 (*MEN1* intragenic marker), homozygous in both patients, and for D11S913 (*MEN1*, telomeric marker) homozygous in patient B only. Patient A showed LOH for three out of four microsatellite markers used for the *DCC* gene locus on 18q21 (Fig. 1D). Such abnormalities were found consistently in the adenoma DNA only and were not observed in the PDEC DNA. No LOH for the other markers and no pattern abnormality for BAT26 were observed. Patient B showed no allelic loss for any of the markers in any of the four tumor DNA samples investigated (Fig. 2E). Additionally, in both patients no abnormal pattern of fragments, including longer or shorter fragments or appearance of alleles of different size, was observed for any of the informative markers used. Sequence analysis of exons 5–8 of the *p53* gene revealed a single substitution mutation of exon 5 at codon 175 (CGC>CAG) in patient A (Fig. 1D). This mutation resides in a so-called hot spot of exon 5, frequently found to be mutated in various human tumors [11]. No mutation of *p53* exons 5–8 was detected in the PDEC DNA of patient B.

Discussion

We have described two cases of (small cell) PDEC of the colon developing within a tubulo-villous adenoma with high-grade epithelial dysplasia. The simultaneous occurrence of both tumors suggested a common histogenesis. Aim of this work was to assess whether the exocrine and endocrine growths shared some genetic aberrance. Here, the LOH analysis for multiple markers of four chromosomal loci did not reveal common genetic imbalances; however, *p53* immunohistochemical abnormalities were observed in both tumor types.

p53 protein accumulation was demonstrated in the two PDECs investigated, one of which (patient A) also showed a mutation of *p53* at exon 5, codon 175 (CGC>CAG) upon sequencing analysis. To our knowledge this is the only p53 mutation analysis reported so far in colon PDEC. The absence of *p53* mutation in one PDEC in the presence of *p53* protein accumulation may be due to several reasons, including mutation in exons other than 5–8, and is a relatively common finding in several human tumors [6, 19]. Similarly, the discrepancy between immunohistochemistry and LOH finding for *p53* locus markers may reflect technical problems, including the relatively low sensitivity of the detection method used. Notably, allelic loss for 17p markers was reported in gastric PDEC; colon PDEC showed Tp53 LOH; and accumulation of *p53* protein was observed in pancreatic and gastric PDEC [17, 21, 22, 24]. Overall, these data and the present findings indicate that *p53* gene defect is involved in the genesis of PDEC in the gastrointestinal tract and pancreas.

p53 protein accumulation was also observed in the severely dysplastic adenoma cells of both cases. Despite the absence of LOH for 17p markers, this finding suggests an abnormal status of *p53*, consistent with the accepted adenoma-carcinoma sequence for colon cancer [5, 8].

LOH for 18q21 (*DCC* gene locus) was observed in one of the two tubulo-villous adenomas investigated (patient A). The fact that only one of the two cases showed LOH for 18q21 markers lies within the expected frequency of this defect in colon cancer [15] and is consistent with the late adenoma phase of the colon adenoma-carcinoma sequence [5, 8]. The two PDECs analyzed here did not show LOH for any of the four 18q microsatellite markers used. However, frequent loss for unspecified 18q marker(s) has been previously reported in nine colon PDECs and seven synchronous adenoma/adenocarcinomas [24]. In this series only one of the two informative adenoma/PDECs analyzed, and thus comparable with the present cases, showed LOH for DCC marker(s) in both tumor types [24]. The absence of such a defect in the two present cases might reflect a difference for the DCC markers in use [24].

We did not find any abnormality using the marker for the replication error phenotype (RER) BAT26 [12] in the PDECs and adenomas investigated. This finding is in keeping with the absence of abnormal pattern of amplified fragments for all the chromosome markers here used and, as regarding the adenomas, may reflect the low frequency of the RER+ status in sporadic colon cancer [12]. The present data are the only available for colon PDEC and, although limited, may suggest that the RER mechanism is not involved in the development of colon PDEC.

In conclusion, only the *p53* gene abnormality as assessed by immunohistochemistry is common to both colon adenoma and PDEC cells of the two cases here investigated. Within the limits inherent in the small number of chromosomal loci studied, the lack of common genetic defect would imply a different genetic mechanism of tumor development and may suggest a different histogenesis for the two types of tumor. Our data indicate that the development of colon PDEC requires the defect of the *p53* gene, as observed in poorly differentitaed endocrine carcinomas developing in other sites of the gastrointestinal tract and pancreas.

References

1. Allen RC, Graves G, Budowle B (1989) Polymerase chain reaction amplification products separated on rehydratable polyacrylamide gels and stained with silver. Biotechniques 7: 736–744
2. Burke AB, Shekitka KM, Sobin LH (1991) Small cell carcinoma of the large intestine. Clin Pathol 95:315–321
3. Cattoretti G, Pileri S, Parravicini C, Becker MHG, Poggi S, Bifulco C, Göran K, D'Amato LS, Feudale E, Reynolds F, Gereds J, Rilke F (1993) Antigen unmasking on formalin-fixed paraffin-embedded tissue sections. J Pathol 171:83–98
4. Chandrasekharappa SC, Guru SC, Manickam P, Olufemi SE, Collins FS, Emmert-Buck MR, Debelenko LV, Zhuang Z, Lubensky IA, Liotta LA, Crabtree JS, Wang Y, Roe BA, Weisemann J, Boguski MS, Agarwal SK, Kester MB, Kim YS, Heppner C, Dong Q, Spiegel AM, Burns AL, Marx SJ (1997) Positional cloning of the gene for multiple endocrine neoplasia-type 1. Science 276:404–407
5. Chung DC (2000) The genetic basis of colorectal cancer: insights into critical pathways of tumorigenesis. Gastroenterology 119:854–865
6. Cripps KJ, Purdie CA, Carder PJ, White S, Komine K, Bird CC, Wyllie AH (1994) A study of stabilization of p53 protein *versus* point mutation in colorectal carcinoma. Oncogene 9:2739–2743
7. Damjanov I, Amenta PS, Bosman F (1983) Undifferentiated carcinoma of the colon containing exocrine, neuroendocrine and squamous cells. Virchows Arch 401:57–66
8. Fearon ER, Vogelstein BA (1990) A genetic model for colorectal tumorigenesis. Cell 61:759–767
9. Gould VE, Chejfec G (1978) Neuroendocrine carcinomas of the colon. Ultrastructural and biochemical evidence of their secretory function. Am J Surg Pathol 2:31–38
10. Group TNCCM (1992) A comprehensive genetic linkage map of the human genome. Science 258:67–86
11. Hernandez-Boussard T, Rodriguez-Tome P, Montesano R, Heinaut P (1999) IARC p53 mutation database: a reliable database to compile and analyze p53 mutations in human tumors and cell lines. Hum Mutat 14:1–8
12. Hoang JM, Cottu PH, Thuille B, Salmon RJ, Thomas G, Hamelin R (1997) BAT-26, an indicator of the replication error phenotype in colorectal cancers and cell lines. Cancer Res 57:300–303
13. Hsu SM, Raine L, Fanger H (1981) Use of avidin-biotin-peroxidase complex (ABC) in immunoperoxidase technique. J Histochem Cytochem 29:577–580
14. Ionov Y, Peinado MA, Malkhosian S, Shibata D, Perucho M (1993) Ubiquitous somatic mutations in simple repeated sequences reveal a new mechanism of colonic carcinogenesis. Nature 363:5581–5561
15. Jen J, Kim HK, Piantadosi SP, Liu Z-F, Levitt RC, Sistonen P, Kinzler KW, Vogelstein BA, Hamilton SR (1994) Allelic loss of chromosome 18q and prognosis in colorectal cancer. N Engl J Med 331:213–221
16. Jones MH, Nakamura Y (1992) Detection of loss of heterozygosity at the human TP53 locus using a dinucleotide repeat polymorphism. Genes Chrom Cancer 5:89–90
17. Lang FF, Miller DC, Pisharody S, Koslow M, Newcomb EW (1994) High frequency of p53 protein accumulation without *p53* gene mutation in human pilocytic, low grade and anaplastic astrocytomas. Oncogene 9:949–954
18. La Rosa S, Sessa F, Capella C, Riva C, Leone BE, Klersy C, Rindi G, Solcia E (1996) Prognostic criteria in nonfunctioning pancreatic endocrine tumours. Virchows Arch 429:323–333
19. Larsson K, Skogseid B, Öberg K, Nakamura Y, Nordenskjöld M (1988) Multiple endocrine neoplasia type 1 gene maps to chromosome 11 and is lost in insulinoma. Nature 332:85–87
20. Mills SE, Allen MSJ, Cohen AR (1983) Small-cell undifferetiated carcinoma of the colon. A clinicopathological study of five cases and their association with colonic adenomas. Am J Surg Pathol 7:643–651
21. Rindi G, Alberizzi P, Candusso M, LaRosa S, Capella C, Solcia E (1999) Loss of heterozygosity for chromosome 17p, P53 gene, and chromosome 18q, DCC gene, in aggressive endocrine tumors of the stomach. Gastroenterology 116: G2156 (abstract)
22. Rindi G, Azzoni C, La Rosa S, Klersy C, Paolotti D, Rappel S, Stolte M, Capella C, Bordi C, Solcia E (1999) ECL cell tumor and poorly differentiated endocrine carcinoma of the stomach: prognostic evaluation by pathological analysis. Gastroenterology 116:532–542
23. Solcia E, Sobin LH (2000) Histological typing of endocrine tumours, 2nd edn. Springer, New York Berlin Heidelberg
24. Vortmeyer AO, Lubensky IA, Merino MJ, Wang CY, Pham T, Furth EE, Zhuang Z (1997) Concordance of genetic alterations in poorly differentiated colorectal neuroendocrine carcinomas and associated adenocarcinomas. J Natl Cancer Inst 89: 1448–1453
25. Zhuang Z, Bertheau P, Emmert-Buck MR, Liotta L, Gnarra J, Linehan WM, Lubensky IA (1995) A microdissection technique for archival DNA analysis of specific cell populations in lesions <1 mm in size. Am J Pathol 146: 620–625

Virchows Arch (2001) 439:782–786
DOI 10.1007/s004280100483

ORIGINAL ARTICLE

G. C. Behrendt · M. L. Hansmann

Carcinomas of the anal canal and anal margin differ in their expression of cadherin, cytokeratins and p53

Received: 22 January 2001 / Accepted: 8 May 2001 / Published online: 20 July 2001
© Springer-Verlag 2001

Abstract Carcinomas of the anus are subdivided into those of the anal canal and those of the anal margin. It has been postulated that the various types of tumours of the anal canal represent a spectrum of differentiation rather than tumours of a separate origin. We compared the expression of Pan-cadherin, cytokeratins (CKs) 5/6, 7, 13, 18 and 19, p53 and MIB-1 in 17 cases of carcinoma of the anal canal and 5 cases of carcinoma of the anal margin. Expression of Pan-cadherin was decreased in 70% of carcinomas of the anal canal but preserved in all five carcinomas of the anal margin. Most of the carcinomas of the anal canal expressed all of the CKs studied. Carcinomas of the anal margin showed expression of CK 5/6 and CK 13, whereas CK7, CK18 and CK19 were rarely expressed. Loss of expression of CK 18 and 19, but not CK 7, is a marker of dedifferentiation in anal canal carcinoma. Of the carcinomas of the anal canal and anal margin, 46% and 80%, respectively, expressed p53. The immunhistochemical findings support the opinion that the various subtypes of carcinoma of the anal canal represent variants in differentiation of squamous cell carcinomas of the anal canal. They confirm the separate histogenetic origin of tumours from the anal canal and anal margin.

Keywords Anus · Carcinoma · Cadherins · Cytokeratins · p53

G.C. Behrendt (✉)
Department of Histopathology, University College London,
Rockefeller Building, University Street, London WC1E 6JJ, UK
e-mail: Gabriele@behrendt.fsnet.co.uk
Tel.: +44-207-6796033, Fax: +44-207-3873674

M.L. Hansmann
Senckenbergisches Institut für Pathologie,
Klinikum der Johann Wolfgang Goethe-Universität,
Theodor-Stern Kai 7, 60590 Frankfurt/Main, Germany

Introduction

Carcinoma of the anus is a rare neoplasm. Current estimates give an incidence of 0.67–0.74 per 100,000 for women and 0.38–0.53 per 100,000 for men [5]. Evidence from epidemiological studies conducted in Denmark and the United States shows a nearly 3-fold increase in the incidence for women and a 1.5- to 2-fold increase for men during the past three decades [5, 11]. This increase is thought to be the result of changes in sexual behaviour in combination with the spread of high-risk papillomavirus [5, 6]. The exact role of human papillomavirus in the aetiology of anal cancer has yet to be determined.

Anal carcinomas are separated into carcinomas of the anal canal and the anal margin. In practice, the assessment of tumour site can be difficult or impossible, especially as pathologists, anatomists and surgeons use different definitions regarding the limitations of the anal canal [4, 12]. The histology of carcinoma of the anal canal shows a variety of different features (i.e. squamous, transitional, basaloid, cloacogenic, glandular), and there has been a long debate about the classification of these tumours. Current opinion is that squamous morphology, basaloid features or glandular differentiation with mucin production are variants of squamous cell carcinoma [9, 22].

Clinical differences between squamous cell carcinoma of the anal canal and the anal margin are considerable: Carcinoma of the anal margin occurs more commonly in men (male:female = 4:1), and the histology is usually a well-differentiated, keratinizing squamous cell carcinoma. Treatment by local excision carries a good prognosis. Carcinoma of the anal canal is three times more common than carcinoma of the anal margin and shows a marked female preponderance. It is usually less well differentiated with little keratinization, and the prognosis is less favourable [2, 12, 22]. Our aim was to characterise the properties of carcinomas of the anal canal and anal margin with relevance to cellular differentiation and proliferation.

Differentiation of epithelial cells is characterised by the expression of a specific cytokeratin (CK) profile and

the expression of intercellular adhesion molecules (Cadherins). Cadherins are cell membrane proteins mediating calcium-dependent intercellular adhesion. In epithelial cells, they form part of the E-cadherin/catenin-complex and loss of their function within this complex is thought to be a prerequisite for tumour invasion and metastasis [8, 16]. The expression of cadherins has not previously been investigated in anal carcinoma.

Normal mucosa of the anal canal is known to express a variety of different CKs [23]. The CK profile of anal carcinoma has also been investigated, although in this study no distinction was made between carcinomas of the anal canal and anal margin [24].

Based on these results, we included the stratification marker CK 5/6 and CK13 and the simple cytokeratins CK7, CK18 and CK19 in our study. Overexpression of p53 has been found in anal carcinomas, and there is a possible association with an increased risk of local recurrence [3]. The mitotic rate as determined by MIB-1 (Ki-67) was also included.

Materials and methods

The clinical data and histology of 24 patients diagnosed with anal carcinoma between 1 October 1996 and 31 March 1999 were reviewed. We found 17 cases of carcinoma of the anal canal. These specimens were 13 pre-treatment-biopsies, 2 local excisions and 2 pre-treatment biopsies and subsequent anorectal resection specimens. In two cases, material from metastases (liver core biopsy, paraaortical lymph node) was also available and included into the analyses. Carcinoma of the anal margin was found in five specimens consisting of a local excision of the tumour.

The haematoxylin and eosin sections and diastase resistant periodic acid Schiff (PAS) stains were reviewed and morphology classified according to the current World Health Organization (WHO) classification. It was noted if more than one subtype of squamous cell carcinoma of the anal canal was present, but the tumour was classified according to the predominating morphological features. Tumour grade was assessed by comparison of tumour morphology with the tissue of origin. None of the sections from the tumours from the anal margin showed striated or smooth muscle.

After reassessment of the slides for the presence of a representative tumour sample, further sections were cut from the paraffin blocks for immunohistochemical analysis. The following panel of antibodies was used: CK5/6 (Boehringer Mannheim GmbH; dilution 1:100, no pretreatment), CK7 (Dako; dilution 1:100, pretreatment with protease digestion), CK13 (Progen, dilution 1:10, pretreatment with a pressure cooker), CK18 (Dako; dilution 1:20, pretreatment with protease digestion), Pan-cadherin (Sigma; dilution 1:500 no pretreatment), MIB-1 (dianova; dilution 1:50, pretreatment pressure cooker), CK 19 (Progen, dilution 1:5, pretreatment with protease digestion) and p53 (Novocastra, pretreatment with microwave).

A section of the anal canal taken from a specimen with a rectal carcinoma was used as a control. Furthermore, most sections contained some areas of adjacent normal epithelium, which was used as an additional internal control. Slides stained with CK antibodies were evaluated as to the presence or absence of staining. The proportion of nuclei staining positive for Ki-67 was determined starting in a region with the highest proliferation and counting 200 nuclei or as many as possible, if it was a small biopsy. The proportion of nuclei expressing p53 was assessed similarly, each case being allocated to one of four groups: none, less than 5%, 5–15% and more than 15%.

The expression of cadherins has not previously been studied in benign or malignant anal epithelium. We therefore used an antibody binding to an epitope common to all cadherins. Optimal dilution and pretreatment was determined in preliminary experiments. Background staining was still present, but only staining that was apparent at intercellular junctions was evaluated. It was compared with the staining of the adjacent normal epithelium or the staining of the control slide. Cadherin expression was judged as preserved if there was no or little change and as decreased if no more than faint granular staining at presumed intercellular junctions was seen.

Results

Twenty-two cases of anal carcinoma occurring over a period of 2.5 years were studied. Seventeen were carcinomas of the anal canal. Median age was 58 years (range 41–94 years) and the sex distribution was 3.25:1 (female:male). Two patients had evidence of metastases (liver, para aortic lymph node).

Five patients had carcinoma of the anal margin. Median age was 63 years (range 35–74 years) and the sex distribution was 3:2 (male:female).

The 17 cases of carcinoma of the anal canal were classified according to their predominant morphology into large-cell keratinizing (*n*=4), large-cell non-keratinizing (*n*=7) and basaloid (*n*=6) carcinomas. In seven cases (41%), a mixed histological appearance was seen. None of these cases showed larger areas of ductal or glandular differentiation. Very small foci of glandular differentiation with droplets of diastase-resistant PAS positive mucin production could be observed in five cases. The two

Table 1 Cytokeratins, Pan-cadherin and p53 in carcinomas of the anal canal and anal margin

	Carcinomas of the anal canal (*n*=17)	Carcinomas of the anal margin (*n*=5)
Cytokeratins		
5/6	17/17 (100%)	5/5 (100%)
7	14/17 (82%)	0/5 (0%)
13	17/17 (100%)	3/4* (75%)
18	12/17 (71%)	1/5 (20%)
19	11/17 (64%)	0/5 (0%)
Pan-cadherin		
Reduced/little staining at intercellular junctions	12/17 (70%)	0
Normal or near-normal staining pattern	4/17 (30%)	5
p53		
No nuclear staining	9 (53%)	1 (20%)
Positive nuclear staining:		
<5%	4	3
5–10%	0	1
Presence of tumour islands with >70% of nuclei staining positive	4	0

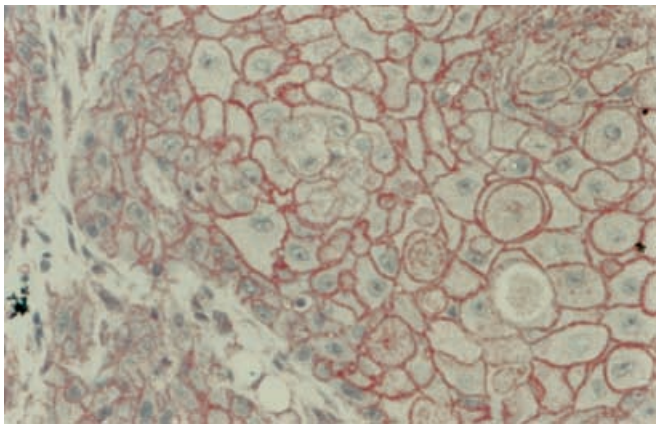


Fig. 1 Carcinoma of the anal canal. Staining for Pan-cadherin is preserved (haematoxylin and eosin, ×400)

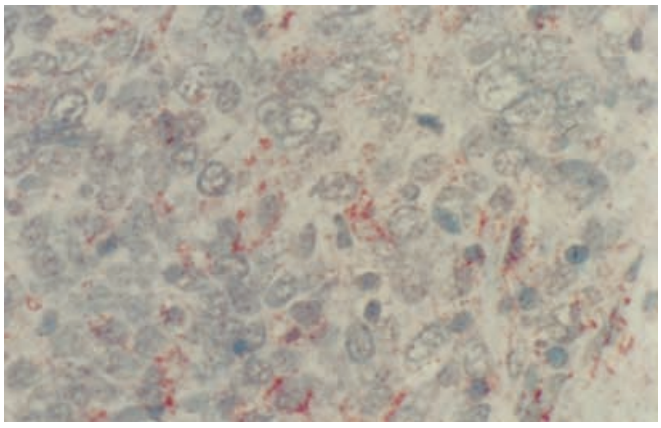


Fig. 2 Carcinoma of the anal canal. Staining for Pan-cadherin is reduced (haematoxylin and eosin, ×400)

metastases showed basaloid (para aortic lymph node) and large-cell non-keratinizing (liver) morphology. All tumours were either moderately (*n*=8) or poorly (*n*=9) differentiated.

There were five tumours of the anal margin. All of them had been treated with local excision and all were squamous cell carcinomas. One of them was a minimally invasive carcinoma arising on the background of extensive carcinoma in situ (Bowen's disease). Two of the tumours were well differentiated and three were moderately differentiated.

The expression of CKs 5/6, 7, 13, 18 and 19 was investigated (Table 1). The majority of tumours of the anal canal expressed all of these CKs, although considerable variation concerning the intensity and pattern of the staining was noted. There were no differences among the three histological subtypes. The metastases showed a similar CK profile to the corresponding primary tumours. In three of four tumours with large-cell keratinizing morphology, areas with apparent stratification were noted and the expression of CKs seemed to recapitulate a basal/suprabasal staining pattern.

All five tumours of the anal margin were positive for CK 5/6 and negative for CK 7. Four of five tumours stained positive for CK 13. The fifth tumour was a minimally invasive carcinoma showing no invasive component on this slide. Expression of CK 18 and CK19 was infrequent.

The CK 18 and CK 19 were expressed in almost all of the tumours of the anal canal which were moderately differentiated (they were positive in seven of eight cases). In comparison, only about half of the carcinomas of the anal canal, which were poorly differentiated, demonstrated expression of CK 18 (four of nine cases) and CK 19 (five of nine cases).

All tumours of both sites stained positive with the antibody against Pan-cadherin (Table 1). However, in comparison with normal epithelium, the expression of cadherins was decreased in 12 of 17 (70%) carcinomas of the anal canal and similar/preserved in four cases. The two metastastic tumours did not differ from their primary tumours and showed decreased staining for Pan-cadherin. There were no differences in expression between the three histological subtypes (Fig. 1 and Fig. 2). All five carcinomas of the anal margin had preserved expression of cadherins.

Expression of p53 was found in eight carcinomas of the anal canal (47%). Different nuclear staining patterns for p53 were observed. There was either no expression of p53 at all (*n*=9) or there was staining of less than 5% of nuclei (*n*=4). Four tumours contained islands in which the majority of nuclei (>70%) stained positive for p53. These islands were usually found at the border of the lesion and the remainder of the tumour contained occasional, i.e. less than 5%, positive nuclei. Carcinoma of the anal margin showed diffuse staining of less than 15% of nuclei in four of five cases.

In carcinoma of the anal canal, the nuclear staining of MIB-1 ranged from 20% to more than 90% of nuclei. No correlation with the histological subtype, tumour grade or any of the other parameters was observed. The mitotic rate of carcinoma of the anal margin ranged from 5% to 60% and no correlation with any of the other parameters was observed.

Discussion

We investigated the expression of Pan-cadherin, various CKs, MIB-1 and p53 in 17 cases of carcinoma of the anal canal and 5 cases of carcinoma of the anal margin. Age and sex distribution of the cases conformed to the epidemiological data in the literature [2, 12, 22]. Histological typing showed that a large proportion (41%) of carcinoma of the anal canal in our series were mixed tumours. This confirms an observation made by Williams et. al., although in this study more than two-thirds of carcinomas of the anus showed more than one morphological feature [22]. In addition to that, four of seven carcinomas with a mixed morphology in our series had only

evidence of small foci of glandular differentiation. The majority of our specimens were biopsies, which may account for an underestimation of the presence of different morphological areas. This, however, will be the case in most future instances, as first-line treatment of carcinomas of the anal canal has changed from abdominoperineal resection to primary radiochemotherapy, with surgical treatment only in a small number of cases with residual disease [1, 10, 14, 19].

We investigated the expression of cadherins, as these are mediators of cellular adhesion and involved in tumour invasion and metastatic spread [18]. There are several subclasses. Most notably in this context are E- (epithelial) and P-(placental) cadherins. E-cadherins are transmembraneous glycoproteins forming part of the E-cadherin/catenin complex. Loss of function of this complex is considered a central element of tumorigenesis, as it permits invasion of the underlying tissue. It is now known that its function can be impaired by several intracellular mechanisms, the most frequent probably being inactivation of β-catenin by phosphorylation [8, 16]. A preserved cadherin expression is therefore not necessarily indicative of a preserved function of epithelial adhesion. Most studies of carcinomas are limited to the investigation of expression and/or function of E-cadherin. As no previous study has investigated the expression of cadherins on normal or malignant anal epithelia, we chose an antibody that covered all subclasses of cadherins.

In summary, we found preserved expression of cadherins in carcinomas of the anal margin but decreased expression in the majority of carcinomas of the anal canal. It is assumed that perianal skin is similar to that of the skin elsewhere. In normal skin, E-cadherin is expressed in suprabasal layers and the expression of P-cadherin is confined to basal cells [13]. Previous studies have reported a decreased expression of E-cadherin in squamous cell carcinoma of the skin [7, 17], whereas in our study carcinoma of the anal margin stained positive with an antibody against Pan-cadherin. However, one recent study found a decrease in E-cadherin expression and preserved P-cadherin in well-differentiated squamous cell carcinomas [15]. It is possible that, similarly, the staining of our tumours is mainly due to a preserved or increased expression of P-cadherin and loss or decrease of E-cadherin. However, it is also possible that carcinoma of the anal margin differs from squamous cell carcinoma of the skin elsewhere. Further studies on this subject will be needed.

In our study, the majority of cancers of the anal canal showed decreased expression of pan-cadherins. Carcinoma of the anal canal is frequently compared to carcinoma of the uterine cervix, as both tumours originate at junctions between different types of epithelium and the infection with high-risk human papillomavirus is a key element in their aetiology [3].

Decreased expression of E-cadherin in cervical carcinoma has been reported and there is further, more recent evidence from HPV-immortalised keratinocyte cell lines suggesting a close interaction between parts of the HPV genome and decreased membrane expression of E-cadherin [20, 21].

The epithelium of the anal canal is known to express a variety of CKs, including CKs 4, 6, 7, 8, 13, 14, 16, 17, 18 and 19 [23]. We have limited our investigation to include the stratification markers CK 5/6 and CK 13 and the simple CKs 7, 18 and 19. We found that most carcinomas of the anal canal expressed all of the CKs studied (CK 5/6, 7, 13, 18, 19), whereas carcinoma of the anal margin expressed the stratification markers CK 5/6 and CK 13 and only very rarely simple CKs 7, 18 and 19. Comparison of moderately and poorly differentiated carcinomas of the anal canal revealed that poorly differentiated tumours were less likely to express CK 18 and CK 19. Expression of stratification markers and CK 7 was similar in both groups. As there were only five carcinomas of the anal margin in our series, the correlation with tumour grade could not be assessed.

The CK profile of anal carcinomas has been studied previously [24]. In this study, tumours were not separated according to site of origin. Williams et al. found that the expression of CK18 and CK 19 was less frequently seen in carcinomas that were poorly differentiated than in carcinomas that were moderately differentiated. Conversely, expression of CK 7 correlated with dedifferentiation. We could confirm the correlation between expression of CK 18 and CK 19 and differentiation in carcinoma of the anal canal. However, there is no correlation between expression of CK 7 and differentiation. CK 7 is expressed in carcinomas of the anal canal regardless of differentiation and not in carcinomas of the anal margin. As a group, carcinomas of the anal margin are better differentiated than those of the anal canal [2, 12]; a fact which may have led to misleading results in the study by Williams et al.

Expression of p53 was seen in 47% of carcinomas of the anal canal and 80% of those of the anal margin. In one clinical study, overexpression of p53 was shown to correlate with an increased frequency of local tumour recurrence and shortened survival [3]. We have noted four anal canal carcinomas with tumour islands staining positive for p53, but the significance of this observation must yet be determined.

Acknowledgements The authors are indebted to Fr. Albrecht and Hr. Lieberz for their assistance.

References

1. Bartelink H, Roelofsen F, Eschwege F et al (1997) Concomitant radiotherapy and chemotherapy is superior to radiotherapy alone in the treatment of locally advanced anal cancer: results of a phase III randomised trial of the European Organisation for Research and Treatment of Cancer Radiotherapy and gastrointestinal cooperative groups. J Clin Oncol 15:2040–2049
2. Beahrs OH, Wilson SM (1976) Carcinoma of the anus. Ann Surg 184:422–428
3. Bonin SR, Pajak TF, Russell AH, Coia LR, Paris KR, Flam MS, Sauter ER (1999) Overexpression of p53 protein and outcome of patients treated with chemoradiation for carcinoma of the anal canal. Cancer 85:1226–1233

4. Fenger C (1988) Histology of the anal canal. Histology for pathologists. Am J Surg Pathol 12:41–55
5. Frisch M, Melbye M, Møller H (1993) Trends in incidence of anal cancer in Denmark. BMJ 3:419–422
6. Frisch M, Fenger C, van den Bruule AJC, Sørensen P, Meijer CJLM, Walboomers JMM, Adami HO, Melbye M, Glimelius B (1999) Variants of squamous cell carcinoma of the anal canal and perianal skin and their relation to human papillomavirus. Cancer Res 59:753–757
7. Koseki S, Aoki T, Ansai S, Hozumi Y, Mitsuhashi Y, Kondo S (1999) An immunohistochemical study of E-cadherin expression in human squamous cell carcinoma of the skin: relationship between decreased expression of E-cadherin in the primary lesion and regional lymph node metastasis. J Dermatol 26:416–422
8. Ilyas M, Tomlinson IPM (1997) The interactions of APC, E-cadherin and β-catenin in tumour development and progression. J Pathol 182:128–137
9. Jass JR, Sobin LH (1989) Histological typing of intestinal tumours, 2nd edn. Springer, Berlin Heidelberg New York, pp 41–47
10. McConnell EM (1970) Squamous carcinoma of the anus – a review of 96 cases. Br J Surg 57:89–92
11. Melbye M, Rabkin C, Frisch M, Biggar RJ (1994) Changing patterns of anal cancer incidence in the United States. Am J Epidemiol 139:772–780
12. Morson BC, Dawson IMP, Day DW (eds) (1990) Morson & Dawson's gastrointestinal pathology, 3rd edn. Blackwell Scientific Publications, Oxford, p 675
13. Pizarro A, Gamallo C, Benito N, Palacios J, Quintanilla M, Cano A, Contreras F (1995) Differential patterns of placental and epithelial cadherin expression in basal cell carcinoma and in the epidermis overlying tumours. Br J Cancer 72:327–332
14. Ryan DP, Compton CC, Mayer RJ (2000) Medical progress: carcinoma of the anal canal. N Engl J Med 342:792–800
15. Shirahama S. Furukawa F, Wakita H, Takigawa M (1996) E- and P-cadherin expression in tumor tissues and soluble E-cadherin levels in sera of patients with skin cancer. J Dermatol Sci 13:30–36
16. Smith MEF, Pignatelli M (1997) The molecular histology of neoplasia: the role of the cadherin/catenin complex. Histopathology 31:107–111
17. Tada H, Hatokoko M, Muramatsu T, Shirai T (1996) Expression of E-cadherin in skin carcinomas. J Dermatol 23:104–110
18. Takeichi M (1991) Cadherin cell adhesion receptors as a morphogenetic regulator. Science 251:1451
19. UKCCCR Anal Cancer Trial Working Party (1996) Epidermoid anal cancer: results from the UKCCCR randomised trial of radiotherapy alone versus radiotherapy, 5-fluorouracil, and mitomycin. Lancet 348:1049–1054
20. Vessey CJ, Wilding J, Folarin N, Hirano S, Takeichi M, Soutter P, Stamp GW, Pignatelli M (1995) Altered expression and function of E-cadherin in cervical intraepithelial neoplasia and invasive squamous cell carcinoma. J Pathol 176:151–159
21. Wilding J, Vousden KH, Soutter WP, McCrea PD, Del Buono R, Pignatelli M (1996) E-cadherin transfection down-regulates the epidermal growth factor receptor and reverses the invasive phenotype of human papilloma virus-transfected keratinocytes. Cancer Res 56:5285–5292
22. Williams GR, Talbot IC (1994) Anal carcinoma – a histology review. Histopathology 25:507–516
23. Williams GR, Talbot IC, Northover JMA, Leigh IM (1995) Keratin expression in the normal anal canal. Histopathology 26:39–44
24. Williams GR, Talbot IC, Leigh IM (1997) Keratin expression in anal carcinoma: an immunohistochemical study. Histopathology 30:443–450

Virchows Arch (2001) 439:787–797
DOI 10.1007/s004280100494

ORIGINAL ARTICLE

Mauro Papotti · Sabrina Croce · Marilena Bellò
Massimo Bongiovanni · Elena Allìa
Marcus Schindler · Gianni Bussolati

Expression of somatostatin receptor types 2, 3 and 5 in biopsies and surgical specimens of human lung tumours

Correlation with preoperative octreotide scintigraphy

Received: 20 February 2001 / Accepted: 28 May 2001 / Published online: 7 August 2001
© Springer-Verlag 2001

Abstract The increasingly popular use of somatostatin analogs in clinical practice for both diagnostic and therapeutic purposes prompted extensive investigations on somatostatin receptor (sst) expression in human tumors by autoradiography, nucleic acid analysis and, recently, immunohistochemistry (IHC). The currently employed radiotracer for scintigraphy (Octreoscan) is octreotide, a somatostatin analog having a high affinity for sst types 2, 3, and 5. In this study on 25 patients, we compared sst 2, 3, and 5 expression in surgical and biopsy specimens of lung tumors, as revealed by immunohistochemical and reverse transcriptase polymerase chain reaction (RT-PCR), with the octreoscan outcome (which was positive in 20/25 cases). By IHC, the tumors mainly expressed sst2 (17/25, 68%) at the cell membrane level, while sst 3 and 5 were detected in a fraction of cases (24% and 20%, respectively). Comparing RT-PCR and IHC data, a correlation was found in 83.3% of cases, while octreoscan findings and sst expression were correlated in 22/25 cases (88%). In addition, cytological and biopsy specimens expressed the same sst type found in the corresponding surgical sample, thus indicating that a cell membrane sst immunoreactivity in a biopsy reliably predicts the tumor–receptor profile before its resection. Finally, sst expression was not restricted to neuroendocrine lung tumors, but was also a feature of some non-neuroendocrine carcinomas, although to a lesser extent. The occasional expression of sst subtypes in intratumoral lymphocytes, endothelia and necrotic areas is an additional feature to be considered in the interpretation of Octreoscan findings, since the in vivo procedure does not allow to define the sst cellular distribution. IHC can therefore be usefully coupled to radionuclear investigations to better characterize the sst cellular location and subtype in lung tumors.

Keywords Lung · Tumors · Somatostatin receptors · Immunohistochemistry · Octreotide scintigraphy

Work supported by grants from the Italian Ministry of University and Research (MURST, Rome), Ministry of Health (Rome, contract no. ICS030.12/RF99.28.) and the Italian Association for Cancer Research (AIRC, Milan).

M. Papotti (✉) · S. Croce · M. Bongiovanni · E. Allìa
G. Bussolati
Department of Biomedical Sciences and Oncology,
University of Turin, Via Santena 7, 10126 Torino, Italy
e-mail: papotti@molinette.unito.it
Tel.: +39011 6706514, Fax: +39011 6635267

M. Bellò
Department of Nuclear Medicine, University of Turin,
Ospedale Molinette, C. Bramante 88, 10126 Torino, Italy

M. Schindler
Glaxo Institute of Applied Pharmacology,
University of Cambridge, UK

Present address:
M. Schindler,
Cardiovascular Research Boehringer Ingelheim Pharma KG,
Birkendorfer Str 65, 88397 Biberach, Germany

Introduction

The importance of somatostatin receptor (sst) analysis in lung tumors is related to widespread clinical applications of somatostatin analogs for diagnostic and therapeutic purposes [18, 21]. Radiolabeled octreotide is used for localizing tumors of suspected neuroendocrine nature and for radiotherapy, based on the high affinity of octreotide for sst type 2 (the most commonly encountered receptor type in endocrine tumors) and also for types 3 and 5 [12, 18, 41, 44]. Different radiotracers were recently found to display a different affinity for single receptor subtypes [33, 35], and therefore the future applications of somatostatin analogs for diagnosis and treatment will need detailed information on the exact sst subtype profile of each tumor. Radiolocalization is an in vivo, indirect demonstration of functional receptor status, but does not prove the existence of a given subtype of sst, nor does it define sst localization in the tumor (i.e., neoplastic cells versus other non-neoplastic cell populations). Autoradiography is a more accurate procedure to demonstrate so-

matostatin binding sites and to localize them in their relationship with anatomic structures or cells [23, 28, 32]. By these means, lymphoid cells and peritumoral vessels of several human neoplasms were found to bear a high amount of receptors [5], possibly contributing to in vivo positive scintigraphic findings. Other recent techniques allowed the demonstration of sst mRNA [24, 31, 40] or –more accurately – the receptor protein itself, which is the ultimate target of the ligand, either somatostatin or its analogs.

After the original report of Reubi et al [29] in small cell lung carcinomas (SCLC). several data have appeared regarding sst expression in endocrine neoplasms in lung tumors. In the same tumors, sst binding sites were reported by means of in vivo studies based on octreotide scintigraphy [1, 2, 22, 26, 47]. The tissue localization of sst in lung tumors was analyzed by means of autoradiography [29, 32], in situ hybridization [10, 25, 31] and immunohistochemistry [9, 11, 25, 32, 34]. These studies showed the presence of sst type 2 in a fraction of SCLC and in the majority of typical carcinoids, all tumors having a preferential cell membrane distribution of the receptor.

While analyzing the sst2 expression in a series of neuroendocrine tumors of the lung, as detected by reverse transcriptase polymerase chain reaction (RT-PCR) and immunohistochemistry [25], we noticed that individual patients had a positive pre-operative octreotide scintigraphy, but had only a focal expression of sst2. In addition, control cases of non-endocrine carcinomas had a positive octreotide scintigraphy, but no sst2 expression in tumor cells.

This prompted a further study of different sst subtypes expression in lung tumors, selecting patients who underwent pre-operative octreotide scintigraphy in our hospital and were subsequently biopsied and/or operated upon in the same Institution. To this aim, RT-PCR and immunohistochemistry with anti-receptor antibodies were performed to reveal sst types 2, 3, and 5, which are the receptor types having the highest affinity for octreotide. We show here that a correlation was observed between radiolabeled octreotide uptake and the presence of at least one sst subtype in individual tumors and that octreotide scintigraphy positive cases also include non-neuroendocrine lung carcinomas. Moreover, sst immunoreactivity was also detectable in small pre-operative biopsy samples.

Materials and methods

Case selection, Octreoscan procedure, and clinical data

Twenty-five patients affected by lung tumor, who underwent pre-operative octreotide scintigraphy at the Institute of Nuclear Medicine of the University of Turin, were selected for this study. All patients were subsequently operated in the same Institution and each surgical specimen was available for review and further investigations (see below). All cases were reviewed applying currently accepted criteria of classification [42, 46] and included 19 endocrine tumors, namely, 11 cases of well differentiated endocrine tumors (typical carcinoids, TC), three cases of well differentiated endocrine carcinomas (atypical carcinoids, AC), four cases of large cell neuroendocrine carcinoma (LCNeC), one case of SCLC, and six additional cases of non-neuroendocrine lung carcinomas, namely, three of squamous cell carcinoma, two of large cell anaplastic carcinoma, and one of adenocarcinoma. Eight of these cases had been included in the previous study on sst type 2 expression [25]. In 12 cases, fresh frozen tissue was available for RNA analysis. Paraffin blocks of formalin-fixed surgical specimens were collected from all cases for immunohistochemistry. In six cases, the pre-operative cytological or biopsy material was also retrieved and studied in parallel with the corresponding surgical sample. Clinico-pathological data and follow-up information were obtained for all patients. Octreotide scintigraphy (Octreoscan, Mallincrodt Medical, Holland) was performed, injecting intravenously 220 Mbq of ^{111}In-labeled [diethylenetriamine pentaacetic acid (DTPA)-DPhe1]-octreotide. The images (total body and planar scans) were collected with acquisitions of 10 min each, at 4 and 24 h, with a G.E. 400T scintillation camera (General Electric Medical Systems, Milwaukee, WI, USA). The study was performed in accordance with the ethical standards laid down in the 1964 Declaration of Helsinki and informed consent was obtained from the patients included in this study.

Reverse transcriptase-polymerase chain reaction for sst2, 3 and 5

Total RNA was extracted using the guanidine thiocyanate–cesium chloride method [3]. The concentration of RNA was estimated by spectrophotometry, and RNA degradation was assessed by 1% agarose gel electrophoresis, as previously reported [40]. Total RNA (1 µg) was first digested with 10 units of RNase-free DNase (Boehringer, Mannheim, Germany) in a 10-µl solution containing 2 mM $MgCl_2$ to avoid DNA contamination. The solution was kept at room temperature for 10 min, then heated for 5 min at 70°C to inactivate DNases; 40 pM of oligodeoxythymidine primer (oligo dT_{16}) were added and the solution heated at 70°C for 10 min, then chilled on ice to allow primer hybridization. The final solution was reverse transcribed using 100 units of Superscript Reverse Transcriptase (Gibco BRL, Gaitersburg,MD, USA) and complementary DNA (cDNA) was generated in a 50 µl final reaction volume containing 50 mM Tris-HCl pH 8.3, 75 mM KCl, 3 mM $MgCl_2$, 10 mM DTT, 1 mM dNTPs and 20 units of RNasin (Promega, Madison, WI, USA). The solution was heated at 37°C for 90 min and then the enzymes inactivated by heating at 70°C for 10 min. RNA integrity was determined by performing a PCR reaction for β_2-microglobulin. PCR experiments were carried out in a 10-µl final reaction volume containing 1 µl of cDNA template, 1 pM of sense and antisense oligonucleotide primers, 10 mM Tris-HCl pH 8.3, 50 mM KCl, 200nM deoxynucleotide triphosphates (dNTPs), 1 mM of from 1.5 mM (β2 microglobulin, sst2 and sst3) to 3.5 mM $MgCl_2$ (sst5) and 0.5 U of Taq polymerase (GeneAmp, Perkin Elmer, Roche, NJ, USA). Amplification reactions were performed under the following conditions: 35 cycles, each cycle consisting of denaturation at 94°C for 1 min, annealing at specific temperatures for 2 min and extension at 72°C for 2 min. The characteristics of the primers used for RT-PCR [7, 20 40] together with the specific annealing temperatures are reported in Table 1. PCR products were visualized in 1% agarose gel, containing 0.5 µg/ml ethidium bromide. Strict precautions against contamination were undertaken [17]. Negative controls (a no template control and a no RT control and distilled water to replace the RNA) were included. The RNA extracted from H716 neuroendocrine colon carcinoma cell line (known to express sst [40]) served as positive controls. To confirm the specificity of sst2, sst3, and sst5 PCR reactions, PCR products were agarose gel purified (CONCERT Gel Extraction Systems,Gibco BRL, Life Technologies, Milan, Italy) and ethanol precipitated, then subjected to nucleic acid direct sequencing by a fluorescence-based sequencing kit (ABI Prism BigDye Terminator Sequencing kit, Applied Biosystems, Weiterstadt, Germany); electrophoresis and data analysis were carried out in an automated DNA sequencer ABI PRISM 377 (Applied Biosystems), following the manufacturer's recommendations.

Table 1 Sequences of primers used for reverse trancriptase polymerase chain reaction

	Size of PCR product (bp)	GenBank accession no.	Position	Annealing temperature	Reference
β2-microglobulin sense 5′ ACCCCCACTGAAAAAGATGA 3′	114	XM_007650	284–303	55°C	Gussow at al. [7]
β2-microglobulin antisense 5′ ATCTTCAAACCTCCATGATG 3′			378–397		
Sst2 sense 5′ CAGTCATGAGCATCGACCGA 3′	283	NM_001050	402–421	61°C	Sestini et al. [40]
Sst2 antisense 5′GCAAAGACAGATGATGGTGA 3′			665–684		
Sst3 sense 5′ TCATCTGCCTCTGCTACCTG 3′	221	NM_001051	662–681	57°C	Mato et al. [20]
Sst3 antisense 5′ GAGCCCAAAGAAGGCAGGCT 3′			863–882		
Sst5 sense 5′GCCGGCCTCTACTTCTTCGTG 3′	153	NM_001053	847–866	60°C	Mato et al. [20]
Sst5 antisense 5′CCGTGGCGTCAGCGTCCTTGG 3′			980–999		

Antibodies

Two different antibodies specific for sst2 were employed. One was a commercially available antiserum purchased by Gramsch Laboratories (Schwabhausen, Germany) and characterized elsewhere [38]. It was raised from a sequence of the C-terminal portion of the sst2A (amino acids 355–369). A second polyclonal antibody anti-sst2 was produced and characterized by one of us (MS) [36, 37]. This antibody (coded K230) was raised in sheep and was specific for a sequence of the C-terminal portion of the sst2A (KSRLNETTETQRTLLNEDLQ, amino acids 347–366). Antibodies to sst3 were purchased from the same source (Gramsch Laboratories) [38]. Antiserum anti-sst5 was produced by one of us (MS) using the sequence CGAKDADATEPRPDR, corresponding to a carboxy-terminal fragment of the human sst5 receptor. The full characterization is reported elsewhere (Papotti et al.submitted). Briefly, after injection of the peptide into one rabbit, the serum (coded MK 86) was obtained from bleedings after each booster injection and tested by means of immunohistochemistry on normal pituitary gland tissue and pre-adsorption experiments with the antigenic peptide, which completely removed the immunostaining. In addition, western blotting was carried out as previously described [36] on membranes from different CHO-cells, each expressing the recombinant somatostatin receptor types 1, 2, 3, 4, and 5. No cross-reactivity was observed, and the serum anti-sst5 was found to be positive only in sst5-transfected cell membranes.

Immunohistochemistry

Four- or five-micron-thick sections, adjacent to those used for conventional histopathological examination and immunostaining for neuroendocrine markers, were collected onto poly-L-lysine-coated slides. Primary antibodies to sst2, 3, and 5 were applied to tissue sections with prior antigen retrieval (three 3-min passages in microwave oven at 800 W in citrate buffer pH 6.0), for 30 min at room temperature, at dilutions of 1/20000, 1/40000, and 1/35000, respectively. The antiserum anti-sst2A coded K230 was applied overnight at a dilution of 1:300 with no prior antigen retrieval. The immune reactions were then revealed with the immunoperoxidase technique using the streptavidin-peroxidase kit (Dako, Glostrup, Denmark) and a further amplification with biotinylated-tyramide (Genpoint, Dako, diluted 1/5) with the subsequent washing step performed in PBS at 95°C to reduce the background and increase the sensitivity, as described by Volante et al. [48]. Diaminobenzidine was used as chromogen, followed by a weak nuclear counterstain (or no counterstain in selected cases). Control stainings for all antibodies included immunoperoxidase reaction on serial sections, using pre-immune serum or buffer instead of the primary antibody.

Results

Octreotide scintigraphy and clinico-pathological data

The octreotide scintigraphy was positive in 20/25 patients and gave a variable intensity of the signal from very strong (nine cases) (Fig. 1) to rather weak (one patient, case 2). These findings were apparently not related to the histological type of the tumor since the five negative cases included three carcinoids and two non-neuroendocrine carcinomas. Conversely, in the positive tumor group, the four non-neuroendocrine carcinomas displayed a highly variable uptake of the radiotracer, exactly as occurred in the endocrine tumor group. The current study group included 17 males and eight female patients, median age 58 years. The lung tumors detected by octreotide scintigraphy measured 1–8 cm (mean 3.5). Pathological examination showed the presence of areas of necrosis in approximately half cases (13/25) and a prominent intratumoral lymphocyte infiltrate in 12/25 cases. Neither sex, age, tumor size and type, or clinical

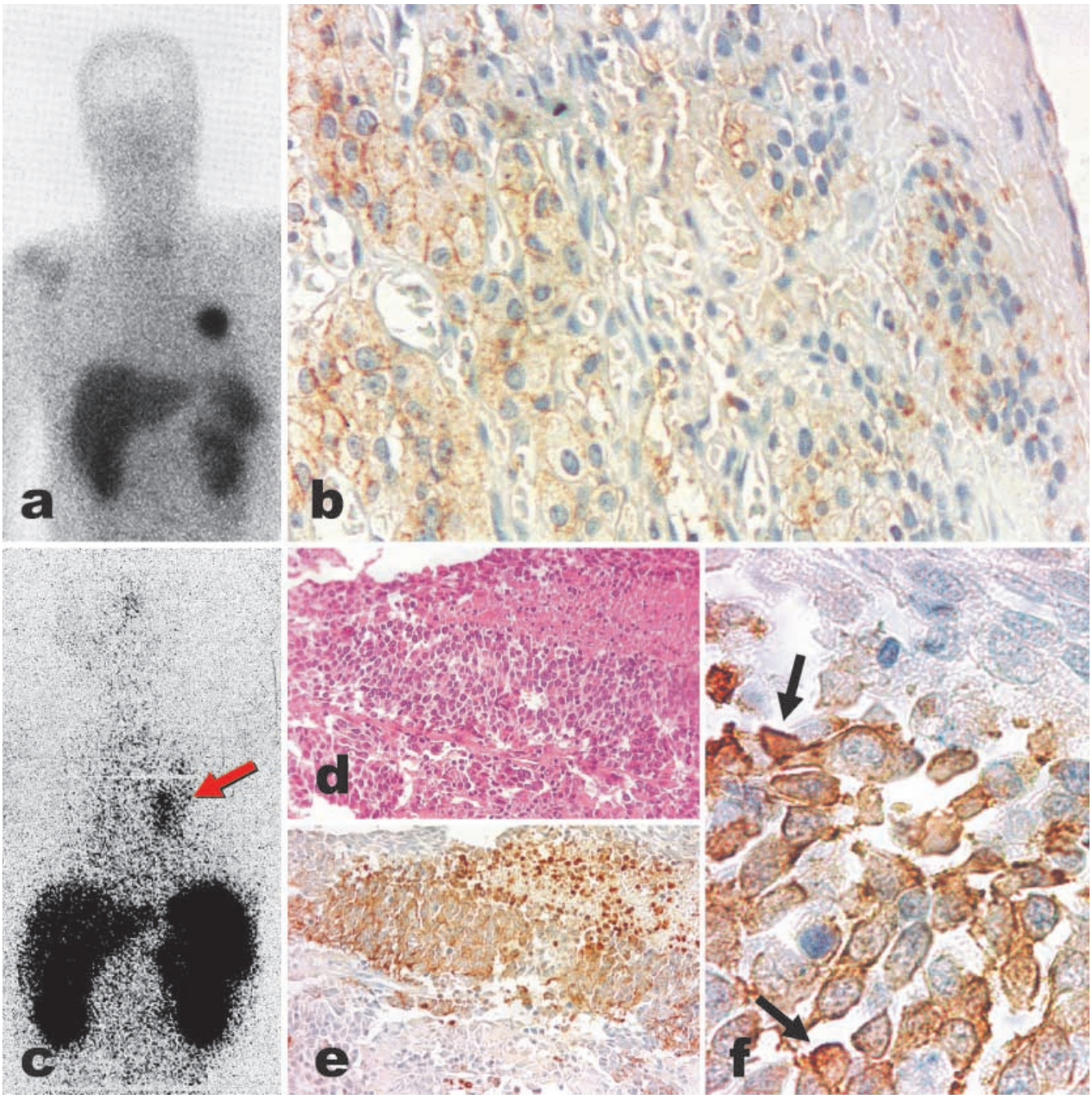


Fig. 1 Case 1: Typical bronchial carcinoid detected by Octreoscan in the left lung (**a**). The resected specimen is strongly positive for sst2 with a cell membrane reactivity (**b**, ×400). Case 12: A large cell neuroendocrine carcinoma of the lung was found by octreotide scintigraphy in the left lung hilus (*red arrow*; **c**). The tumor is made of medium or large-size cells and is extensively necrotic (**d**, H&E, ×200). A serial section stained for sst2 shows a diffuse positivity (**e**, ×200), with predominant cell membrane reactivity (*arrows*; **f**, x1000)

evolution was apparently related to octreotide scintigraphy outcome.

Reverse transcriptase polymerase chain reaction

In 12 cases RT-PCR was performed to reveal sst2, 3 and 5 mRNAs (Table 2). All cases expressed the "house keeping gene" β-2-microglobulin mRNA. All but one (no. 6, a large cell neuroendocrine carcinoma) case expressed sst2 mRNA, as opposed to mRNA of sst types 3 and 5, which was detected in two and zero cases, respectively (Fig. 2). No amplification was obtained in no-template or no-reverse transcriptase experiments.

Table 2 Clinico-pathological data, octreotide scintigraphy results and somatostatin receptor (sst) expression in 25 lung tumors. *M* male, *F* female, *mos* months, *f* focal, *n.a.* not available, *Octreoscan* octreotide scintigraphy, *NED* no evidence of disease, *AWD* alive with disease, *DOD* died of disease, *TC* typical carcinoid, *AC* atypical carcinoid, *LCNeC* large cell neuroendocrine carcinoma, *AdCa* adenocarcinoma, *SqCa* squamous cell carcinoma, *SCLC* small-cell lung carcinoma, *LCACa* large cell anaplastic carcinoma, *LC* prominent intratumoral lymphoid infiltrate, *IHC* immunohistochemistry, *PCR* polymerase chain reaction, *N* necrosis

	Sex and age	Diagnosis	Pathological features			Octreoscan	sst2		sst3		sst5	
			Size (cm)	LC	N		PCR	IHC	PCR	IHC	PCR	IHC
1	M 58	TC	3.8	–	–	+++	+	+	+	+f	–	–
2	M 65	SqCa	3.3	+	+	+	+	–	–	–	–	–
3	M 58	LCACa	8	–	+	+++	+	+f	–	–	–	–
4	F 29	TC	2	–	–	++	+	+	–	–	–	+f
5	M 41	TC	1.3	–	–	+++	+	+	–	–	–	–
6	M 57	LCNeC	5	+	+	++	–	–	–	–[a,b]	–	+f[b]
7	M 66	AC	8	–	+	++	+	+	–	–	–	–
8	M 65	SqCa	5.5	+	+	++	+	–[b]	–	+[b]	–	–
9	F 25	TC	4	+	–	++	+	+f	–	–	–	–
10	F 31	TC	1	–	–	–	+	+f	–	–	–	–
11	F 32	TC	3	–	–	+++	+	+	–	–	–	–
12	M 62	LCNeC	8	+	+	+++	+	+	+	–	–	–[b]
13	M 41	LCACa	3	+	+	+++	n.a.	–[b]	n.a.	+f[a]	n.a.	+
14	M 47	SCLC	3	–	+	+++	n.a.	+f	n.a.	–	n.a.	–
15	F 68	AC	1	–	–	–	n.a.	–	n.a.	–	n.a.	–
16	F 61	TC	3.5	–	–	–	n.a.	+f	n.a.	–	n.a.	–
17	M 42	TC	1	–	–	++	n.a.	–	n.a.	–	n.a.	+f
18	M 79	AdCa	4.2	+	+	–	n.a.	–[b]	n.a.	–[a]	n.a.	+f[b]
19	M 69	SqCa	2.5	+	+	–	n.a.	–[c]	n.a.	–[c,b]	n.a.	–
20	F 54	TC	1	–	–	+++	n.a.	+	n.a.	–	n.a.	–
21	M 68	AC	5	+	+	+++	n.a.	+	n.a.	+	n.a.	–
22	M 49	TC	3.5	–	–	++	n.a.	+	n.a.	+f	n.a.	–
23	F 31	TC	2.5	+	–	++	n.a.	+f	n.a.	–	n.a.	–
24	M 62	LCNeC	3.5	+	+	++	n.a.	+f	n.a.	–[b]	n.a.	–
25	M 67	LCNeC	1.2	+	+	++	n.a.	+	n.a.	+f	n.a.	–

[a] Blood vessels focally positive [b] Intratumoral lymphocytes focally positive [c] Necrotic areas focally positive

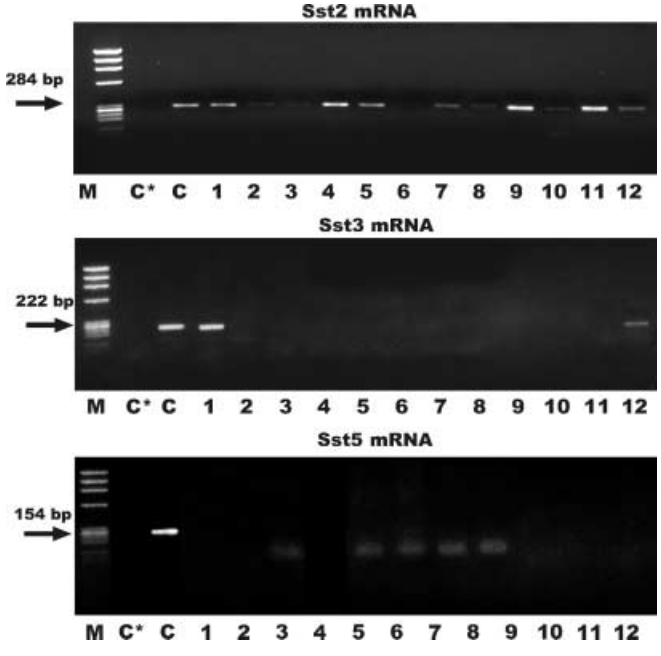


Fig. 2 Reverse transcriptase polymerase chain reaction for sst2, 3, and 5 mRNA in 12 cases of lung tumors. *Numbers* in each *lane* correspond to case numbers in Table 2. The *first column to the left* represents the molecular weight marker. *C** and *C* stand for negative and positive controls, respectively. Sst2 mRNA was amplified in 11/12 cases, sst3 mRNA in 2/12 cases, and sst5 mRNA in no case

Immunohistochemistry

The two antibodies to sst2A gave overlapping results. Positive immunoreaction was observed in 17/25 cases (68%). Six of these were only focally (less than 10% of tumor cells) positive. The staining had a membrane-bound distribution (Fig. 3) and was better outlined in slides lacking nuclear counterstain. The immunohistochemical results were concordant with those of RT-PCR in 10/12 cases. Cases 2 and 8 were RT-PCR-positive, but no positive tumor cells were detected by immunohistochemistry. Antibodies to sst3 and sst5 positively immunostained 6/25 (24%) and 5/25 (20%) cases, respectively. Four of these cases each had a focal staining. The subcellular distribution was predominantly membrane-bound, although in single cells and in single cases a cytoplasmic reactivity was also found (Fig. 3). The immunohistochemical results were concordant with those of RT-PCR in 10/12 cases for both sst3 and sst5. Case 8 had a positive sst3 immunohistochemical reaction but no RT-PCR signal and the opposite was true for case 12. A focal immunostaining was observed with antibodies to sst5 in cases 4 and 6, which were both negative by RT-PCR.

Special attention was paid to the immunostaining of non-tumoral cells and tissues after sst immunohistochemistry. Several cells in peritumoral tissues were occa-

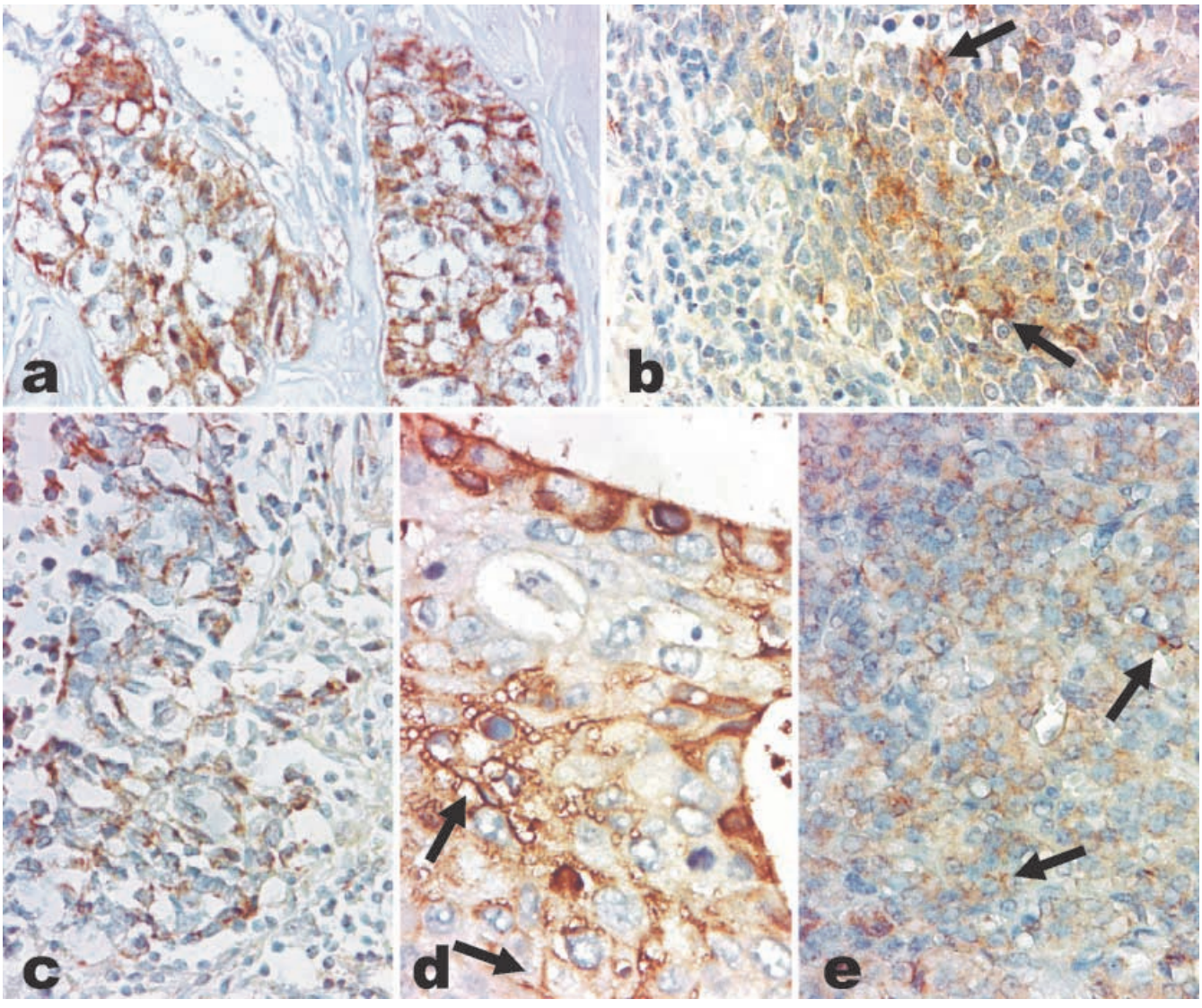


Fig. 3 Immunostaining for sst2 in a Reverse transcriptase polymerase chain reaction-positive atypical carcinoid (case 7; **a**) and in a typical carcinoid (case 20: **b**). Most cells have a strong cell membrane reactivity (*arrows*). Sst3 was expressed in an atypical carcinoid (case 21; **c**) and also in a squamous cell carcinoma (case 8). The latter had cytoplasmic and cell membrane (*arrows*) reactivity (**d**). A typical carcinoid was focally positive for sst5 immunoperoxidase with a faint cytoplasm and also membrane staining (*arrows*; **e**). (**a–e,** ×400)

sionally stained with all antibodies. Ciliated cells of bronchial mucosa focally had a peripheral staining at the cilia border with sst2 antibodies. The endothelial cells of peritumoral and occasionally intratumoral vessels were positive for antibodies to sst3 (three cases). Necrotic areas in a squamous cell carcinoma had sst2 and sst3 immunoreactive cells of probable inflammatory nature. Finally, intratumoral lymphocytes were occasionally stained by antibodies to sst2 (three cases), sst3 (four cases), and 5 (three cases) (Fig. 4). These findings may have in part contributed to the positive octreotide scintigraphy signal, although, in general, the extension of the immunostaining of non-tumoral cells was rather limited. Lymphocytes of peritumoral lung parenchyma, bronchial wall, or regional lymph nodes were generally unreactive, with the exception of one peribronchial lymph node (case 7) which showed positive germinal center cells for sst2 and two cases of sst3 reactivity in interstitial lymphocytes.

Biopsy material

Six pre-operative biopsy cases were studied in parallel with the corresponding surgical specimens. These included one cytological specimen (a bronchoalveolar lavage) and five endoscopic bronchial biopsies. In all cases (nos. 4, 7, 20–23), the corresponding surgical specimen was positive for sst2 as shown by immunohistochemistry (and also by RT-PCR in two cases). Overlapping results were found in all biopsy specimens, in which the tumor cell membrane was strongly stained by the sst2 antibody in a variable percentage of the tumor cell (Fig. 5).

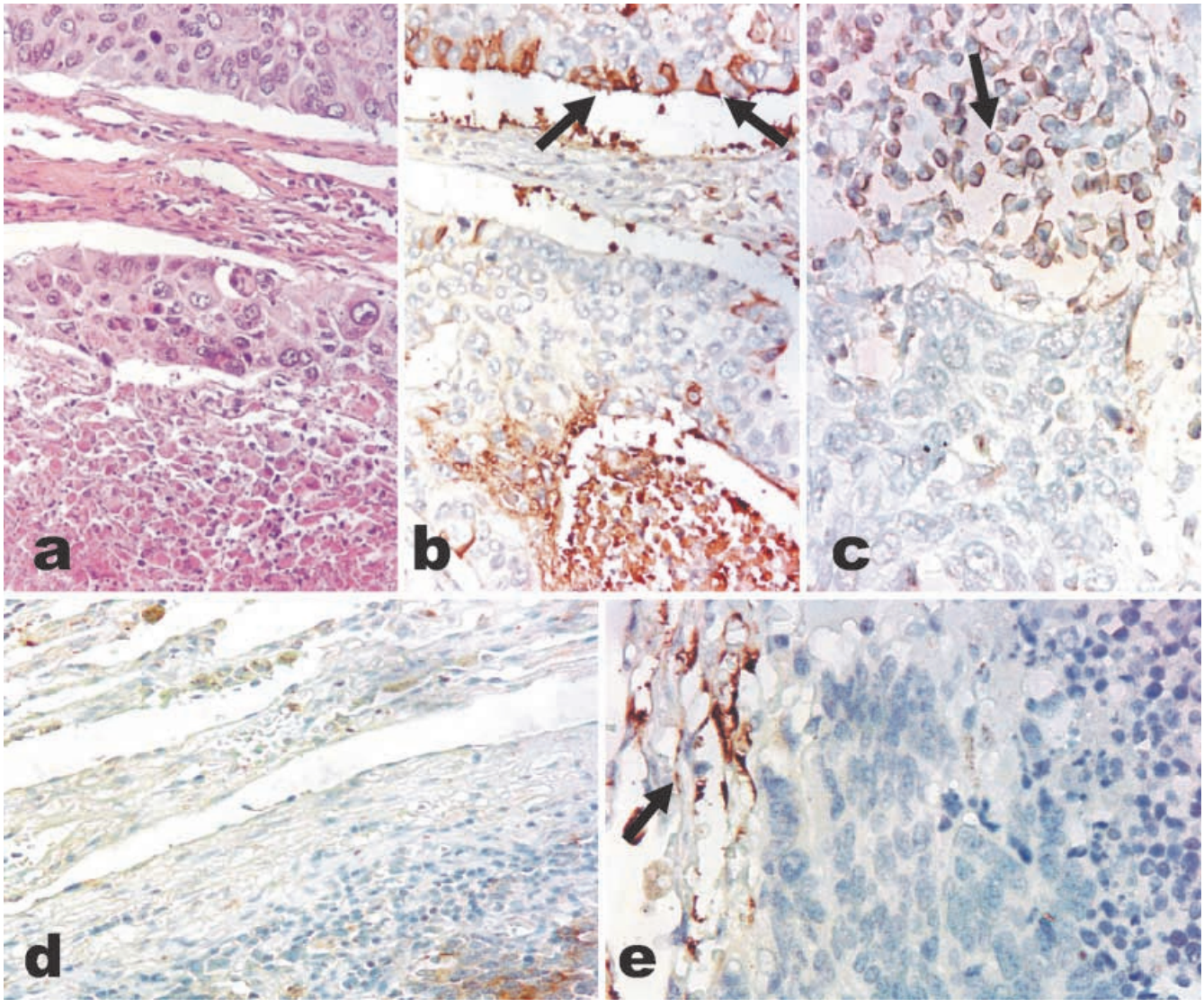


Fig. 4 Sst expression in non-neoplastic cells: sst3 is present in necro-inflammatory areas of a squamous cell carcinoma (case 8) (**a, b**, ×400) and in intratumoral lymphocytes of a squamous cell carcinoma (case 19; **c**, ×400). Peritumoral blood vessels are negative in a sst2-positive (*lower right*) large cell neuroendocrine carcinoma (case 25; **d**, ×200), but are immunostained by sst3 antibodies in a large cell neuroendocrine carcinoma (case 6; **e**, ×400)

Correlations

Overall, completely overlapping results of sst detection with the three methods (i.e. Octreoscan, RT-PCR, and immunohistochemistry) was obtained in 11/12 cases (91.7%), having at least one sst subtype expressed in individual tumors. Taking into account the whole case series, and comparing Octreoscan findings and sst expression data, it appeared that 22/25 cases (88%) had concordant in vivo octreotide scintigraphy findings and immunohistochemical localization of one or more sst subtypes in tumor specimens. Most commonly observed was sst2 in the present series. In this respect, it should be noticed that this same antibody to sst2 also detected sst2-positive cells in two of three Octreoscan-negative tumors (the third case had a focal sst5 immunoreactivity). Since these antibodies appeared highly specific, it is possible that the in vivo procedure failed to identify small areas of sst expression. Conversely, no "false-positive" (absent sst expression in tumor tissue) octreotide scintigraphies were observed. Presence of sst in the four octreoscan-positive non-neuroendocrine carcinomas was not related to a particular subtype (two expressed sst2 and the other two sst3).

Discussion

In this study, we analyzed the sst subtype expression in a series of lung tumors that were preoperatively evaluated by means of octreotide scintigraphy. The tissue expression of sst was correlated with octreoscan findings in most cases (88%), sst2 being the predominantly expressed receptor subtype. The observed discrepancies in

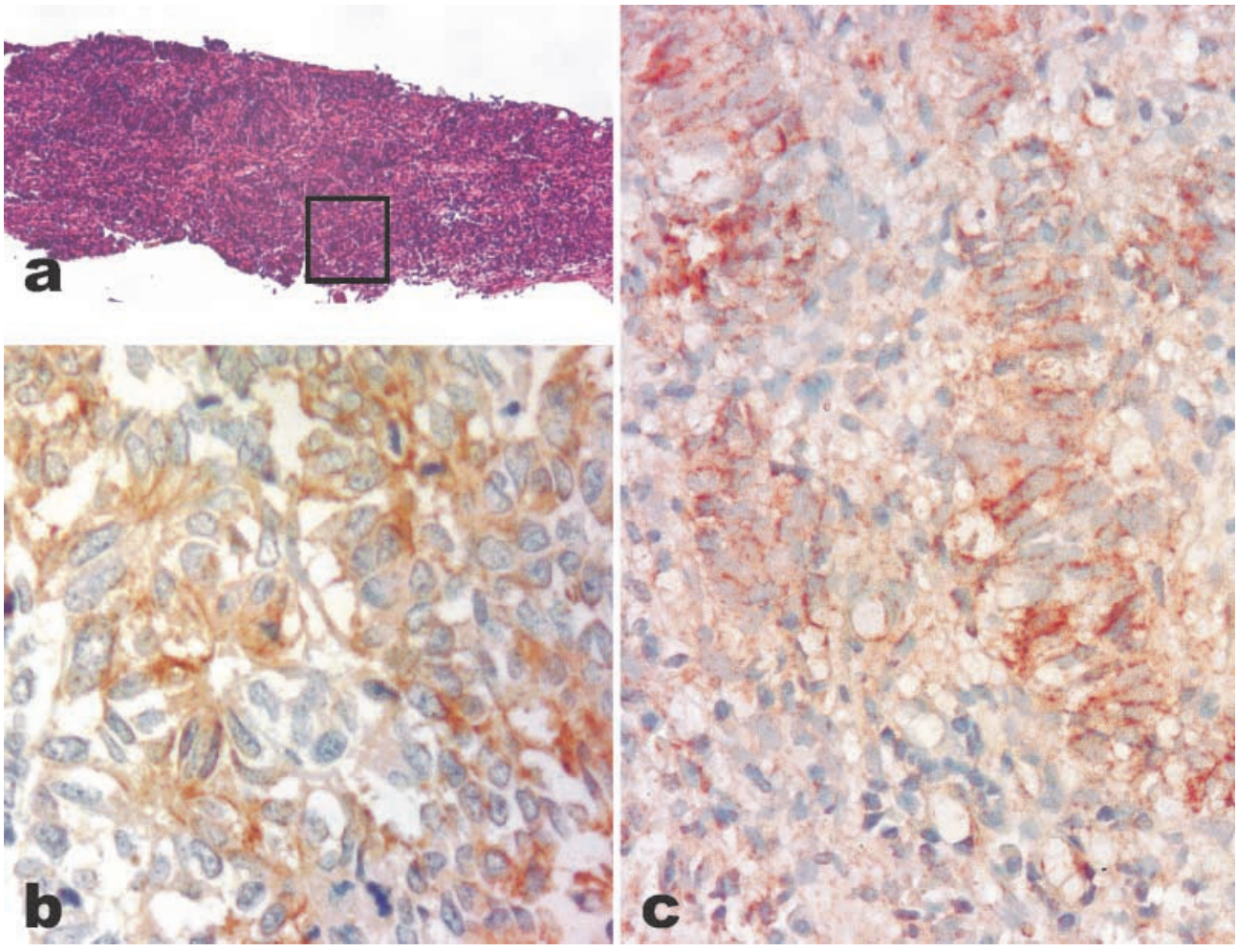


Fig. 5 Case 21: This atypical carcinoid has a strong cell membrane reactivity for sst2 in both the preoperative bronchial biopsy (**a,b**) and the corresponding surgical specimen (**c**) (**a,** ×100; **b, c,** ×400)

three cases were probably related to tumor heterogeneity or to a focal sst expression below the threshold of detectability of the in vivo scintigraphy. These findings are in part confirmatory of previous literature data on sst type 2 only, obtained in small case series (Table 3). However, this study provides several items of new information, which include: (a) the correlation of octreotide scintigraphy with cellular localization of the sst, either in tumor cells or in non-tumoral tissues; (b) the analysis of other receptor subtypes, namely, sst3 and sst5, known to have high affinity for octreotide, too; (c) the validation of immunohistochemical methods to reveal sst subtypes in comparison with the highly sensitive RT-PCR procedure; (d) the reliability of immunohistochemical detection of sst in pre-operative biopsy material; and (e) the occasional expression of sst by non-neuroendocrine lung carcinomas. This new information will be briefly commented on.

Octreotide scintigraphy has a definite role in the diagnosis of primary and metastatic sst positive tumors [18, 21]. This procedure provides information on sst presence, functionality, and affinity for the (radio)ligand. Discrepancies between in vivo and tissue sst detection have been occasionally observed [11, 25], possibly related to sensitivity of the radiotracers and/or to methods of sst localization. With regard to the former, DOTA (tetraazacyclododecane-tetra-acetic acid)-labeled radiotracers were found to be superior to DTPA labeling and to be related to the peptide amount used [4, 16]. In addition, new radioligands [19] may display a different sst subtype affinity, as compared with octreotide [33, 35]. As for the sst detection methods, RT-PCR is certainly the most sensitive procedure, but does not provide information on the cell distribution of the receptors. In situ hybridization or immunohistochemistry may overcome this problem, but are less sensitive, and the specificity needs to be strictly controlled (see below). In the present study, positive octreotide scintigraphy cases were all positive for one or more sst subtype by immunohistochemistry. Conversely, three Octreoscan-negative cases had sst2 or sst5 focal expression, probably to an extent below the threshold of scintigraphic detectability. Sst2 was the predominantly expressed receptor subtype, while sst types 3 and 5 were poorly represented in lung tumors.

Table 3 Reported data on somatostatin receptor (sst) expression in tumors of the lung. *SCLC* small-cell lung carcinoma, *TC* typical carcinoid, *NET* neuroendocrine lung tumor, *NSCLC* non-small-cell lung carcinoma, *AR* autoradiography, *IHC* immunohistochemistry, *ISH* in situ hybridisation, *RT-PCP* reverse transcriptase polymerase chain reaction, *+ve* positive, *n.a.* not available

Author (Reference)	Tumor (+ve/total cases)	Method	sst Type	Material
Reubi [29]	SCLC (2/4) NSCLC (0/12)	AR	2	Tissues
Reubi [31]	SCLC (2/2)	AR, ISH	2	Tissues
Reubi [32]	TC (2/5)	AR, IHC	2	Tissues
Janson [11]	TC (1/5)	IRC, ISH octreoscan	2	Tissues
Kimura [13]	SCLC (1/2)	IHC	2	Tissues
Reubi [34]	SCLC (11/18)	AR, IHC	2	Tissues
Papotti [25]	NET (22/26)	RT-PCR, IHC, ISH	2	Tissues
Denzler [5]	NSCLC (4/13)	AR	2	Peritumoral vessels
Kirsch [14]	SCLC (22/25) NSCLC (10/13)	Octreoscan	n.a.	Clinical study
Semprebene [39]	SCLC (19/22)	Octreoscan	n.a.	Clinical study
Bombardieri [2]	SCLC (20/2 1)	Octreoscan	n.a.	Clinical study
Berenger [11]	SCLC (19/19)[a]	Octreoscan	n.a.	Clinical study
Reisinger [26]	SCLC (96/100) [a]	Octreoscan	n.a.	Clinical study
Vaccarili [47]	SCLC (15/21)	Octreoscan	n.a.	Clinical study
Fujita [6]	SCLC and NSCLC	RT PCR	1–2	Tumor cell lines
Taylor [45]	SCLC	AR	2	Tumor cell lines
Zhang [49]	SCLC	RT-PCR	2	Tumor cell lines

[a] Primary tumors (method less effective for metastatic deposits)

In cases having either sst-negative or sst-positive tumor cells, non-neoplastic cells were occasionally immunostained by sst antibodies. Endothelial cells of peritumoral vessels were focally sst3 immunoreactive in three cases. Conversely, several tumors had more or less extensive lymphocytic infiltrates and necrotic areas, both of which appeared occasionally sst positive. It is known that lymphoreticular tissue [27, 30] and pulmonary fibrosis [43] may express sst. Therefore, a positive octreotide scintigraphy may well be due (at least in part) to radiotracer binding to non-neoplastic cells or tissues (namely, inflammatory or necrotic areas in lung tumors), thus providing information not directly related to the true tumor content of sst.

The above data therefore indicate that immunohistochemical detection of sst has proven advantages, as compared with all the other methods, because it allows a precise localisztion of the sst subtypes in the cell compartments. Unfortunately, the availability of antibodies for the individual sst types is limited and the interpretation criteria of the immunostaining are still debated. A strong cell membrane reactivity is the “gold standard” for sst2 antibodies [11, 32, 36]. Antibodies to other receptor showed either a cytoplasm or a cell membrane reactivity [8, 15, 38]. Different patterns of reactivity were observed in different tumor typesand also in relationship to the receptor saturation by its endogenous ligand somatostatin [34].

Most of earlier studies and the present one validated the reliability of immunohistochemical detection of sst subtypes in archival pathological material by comparing the immunostainings with the results of other methods. In the 12 cases in which frozen material was available, we were able to confirm a good correlation between RT-PCR and immunohistochemical results, provided that the subcellular distribution is (predominantly) at the cell membrane level. A major problem is the interpretation of weak immunohistochemical reactions, especially when amplification, tyramide-based systems are used. We generally employ dilute tyramide solutions (1/5 that of the manufacturer) and extremely dilute antibodies, plus a wash at 95°C after the tyramide incubation steps, to obtain a much clearer background [48]. In general, the good correlation with octreotide scintigraphy and RT-PCR findings indicates that immunohistochemical detection of sst subtypes is feasible and reliable (it correlates with presence of specific sst mRNA and with a functional receptor) in terms of expected response to treatment with somatostatin analogs.

Additional information provided by this study is that indicating the applicability of sst immunohistochemistry to pre-operative biopsy material. Immunohistochemistry is the only technique applicable to small biopsy samples together with in situ hybridization. In six cases of the present series, a pre-operative (cytological or bioptic) diagnostic evaluation was performed. All cases had overlapping features in biopsy and surgical materials, in terms of tumor cell membrane distribution and amount of reactive tumor cells for sst. These findings are in agreement with those of Reubi et al. [34], on small cell carcinoma biopsies, but extend the observation to cytological material, too. The diagnostic work-up of a patient affected by a lung tumor may therefore benefit from a rapid assessment of the sst status, as early as at the time of pre-operative histo-cytological evaluation.

Finally, six non-neuroendocrine lung carcinomas were also studied. Interestingly and contrary to earlier reports [29], four of six cases had positive octreotide scintigraphy. All of them expressed one or more sst subtypes by RT-PCR or immunohistochemistry. The tumor cells of these cases were, however, only focally immunoreactive to sst antibodies, although at least two cases had

a strongly positive scintigraphic signal. In some cases (nos. 8,13), necrotic areas as well as intratumoral lymphocytes and endothelial cells were sst immunoreactive, a finding that may have in part contributed to the uptake of the radiotracer. These data indicate that a positive octreotide scintigraphy, at least with the currently employed radiotracers and labeling procedures, does not necessarily indicate the presence of a neuroendocrine tumor, in agreement with the scintigraphic findings of Kirsch and coworkers [14] for bronchogenic carcinoma.

In conclusion, we have shown that immunohistochemical methods may be useful to characterize the sst expression profile of a lung tumor, and that a good correlation exists between octreoscan and IHC (and also with RT-PCR) data in both surgical and cytological or bioptic material.

Acknowledgements We are grateful to Prof G. Bisi (University of Turin) for helpful discussion, to Dr C. Pecchioni and Miss S. Chiappone for skillful technical assistance and to Mr A. Grua for the photographs.

References

1. Berenger N, Moretti JL, Boaziz C, Vigneron N, Morere JF, Breau JL (1996) Somatostatin receptor imaging in small cell lung cancer. Eur J Cancer 32:1429–1431
2. Bombardieri E, Crippa F, Cataldo I, Chiti A, Seregni E, Soresi E, Boffi R, Invernizzi G, Buraggi GL (1995) Somatostatin receptor imaging of small cell lung cancer (SCLC) by means of 111 In-DTPA octreotide scintigraphy. Eur J Cancer 31:184–188
3. Chirgwin JM, Przybyla AE, Mac Donald RJ and Rutter W (1979) Isolation of biologically active RNA from sources enriched in ribonuclease. Biochemistry 18:5294–5297
4. de Jong M, Breeman WA, Bernard BF, van Gameren A, de Bruin E, Bakker WH, van der Pluijm ME, Visser TJ, Macke HR, Krenning EP (1999) Tumour uptake of the radiolabelled somatostatin analogue [DOTA0, TYR3]octreotide is dependent on the peptide amount. Eur J Nucl Med 26:693–698
5. Denzler B, Reubi JC (1999) Expression of somatostatin receptors in peritumoral veins of human tumors. Cancer 85:189–198
6. Fujita T, Yamaji Y, Sato M, Murao K, Takahara J (1994) Gene expression of somatostatin receptor subtypes, SSTR1 and SSTR2, in human lung cancer cell lines. Life Sci 55:1797–1806
7. Gussow D, Rein R, Ginjaar I, Hochstenbach F, Seemann G, Kottman A, Ploegh HL (1987) The human beta 2-microglobulin gene. Primary structure and definition of the transcriptional unit. J Immunol 139: 3132–3138
8. Helboe L, Moller M, Norregaard L, Schiodt M, Stidsen CE (1997) Development of selective antibodies against the human somatostatin receptor subtypes sst1-sst5. Brain Res Mol Brain Res 49:82–88
9. Hofland LJ, Liu Q, Van Koetsveld PM, Zuijderwijk J, Van Der Ham F, De Krijger RR, Schonbrunn A, Lamberts SWJ (1999) Immunohistochemical detection of somatostatin receptor subtypes sst1 and sst2A in human somatostatin receptor positive tumors. J Clin Endocrinol Metabol 84:775–780
10. Janson ET, Gobl A, Kalkner KM, Oberg K (1996) A comparison between the efficacy of somatostatin receptor scintigraphy and that of in situ hybridization for somatostatin receptor subtype 2 messenger RNA to predict therapeutic outcome in carcinoid patients. Cancer Res 56:2561–2565
11. Janson ET, Stridsberg M, Gobl A, Westlin JE, Oberg K (1998) Determination of Somatostatin receptors subtype 2 in carcinoid tumors by immunohistochemical investigation with somatostatin receptor subtype 2 antibodies. Cancer Res 58: 2375–2378
12. Janson ET, Westlin JE, Ohrvall U, Oberg K, Lukinius A (2000) Nuclear localisation of 111-In after intravenous injection of [111In-DTPA-D-Phe1]-octreotide in patients with neuroendocrine tumors. J Nucl Med 41:1514–1518
13. Kimura N, Pilichowska M, Date F, Kimura I, Schindler M (1999) Immunohistochemical expression of somatostatin type 2A receptor in neuroendocrine tumors. Clin Cancer Res 5:3483–3487
14. Kirsch CM, von Pawel J, Grau I, Tatsch K (1994) Indium-111 pentetreotide in the diagnostic work-up of patients with bronchogenic carcinoma. Eur J Nucl Med 21:1318–1325
15. Kumar U, Laird D, Srikant CB, Escher E, Patel YC (1997) Expression of the five somatostatin receptors (SSTR1–5) subtypes in rat pituitary somatotrophes: quantitative analysis by double-label immunofluorescence confocal microscopy. Endocrinology 138:4473–4476
16. Kwekkeboom DJ, Kooij PP, Bakker WH, Macke HR, Krenning EP (1999) Comparison of 111In-DOTA-TYR3-octreotide and 111In-DTPA-octreotide in the same patients: biodistribution, kinetics, organ and tumor uptake. J Nucl Med 40:762–767
17. Kwok, S, Higuchi R (1989) Avoiding false positives with PCR. Nature 339: 237–238
18. Lamberts SWJ, Hofland LJ, Koetsveld PM, Reubi JC, Bruining HA, Bakker WH, Krenning EP (1990) Parallel in vivo and in vitro detection of functional somatostatin receptors in human endocrine pancreatic tumors: consequences with regard to diagnosis, localization and therapy. J Clin Endocrinol Metab 71:566–574
19. Lau SK, Johnson DS, Coel MN (2000) Imaging of non-small-cell lung cancer with indium-111 pentetreotide. Clin Nucl Med 25:24–28
20. Mato E, Matias-Guiu X, Chico A, Webb SM, Cabezas R, Berna L, De Leiva A (1998) Somatostatin and somatostatin receptor subtype gene expression in medullary thyroid carcinoma. J Clin Endocrinol Metab 83:2417–2420
21. Nilsson O, Kolby L, Wängberg B, Wigander A, Billig H, William Olsson L, Fjälling M, Forssell Aronsson E, Ahlman H (1998) Comparative studies on the expression of somatostatin receptor subtypes, outcome of octreotide scintigraphy and response to octreotide treatment in patients with carcinoid tumours. Br J Cancer 77:632–637
22. O'Byrne KJ, Halmos J, Pinski J, Groot K, Szepeshazi K, Schally AV, Carney DN (1994) Somatostatin receptor expression in lung cancer. Eur J Cancer 30: 1682–1687
23. Papotti M, Macrì L, Bussolati G, Reubi JC (1989) Correlative study on neuroendocrine differentiation and presence of somatostatin receptors in breast carcinomas. Int J Cancer 43: 365–369
24. Papotti M, Macrì L, Pagani A, Aloi F, Bussolati G (1999) Quantitation of somatostatin receptor type 2 in neuroendocrine (Merkel cell) carcinoma of the skin by competitive RT-PCR. Endocr Pathol 10:1–10
25. Papotti M, Croce S, Macrì L, Funaro A, Pecchioni C, Schindler M, Bussolati G (2000) Correlative immunohistochemical and reverse transcriptase-polymerase chain reaction analysis of somatostatin receptor type 2 in neuroendocrine tumors of the lung. Diagn Mol Pathol 9:47–57
26. Reisinger I, Bohuslavtzki KH, Brenner W, Braune S, Dittrich I, Geide A, Kettner B, Otto HJ, Schmidt S, Munz DL (1998) Somatostatin receptor scintigraphy in small-cell lung cancer: results of a multicenter study. J Nucl Med 39:224–227
27. Reubi JC (1998) What is a false-positive somatostatin receptor scintigraphy? J Nucl Med 39:2193–2194
28. Reubi JC, Maurer R, von Werder K, Torhorst J, Klijin JGM, Lamberts SWJ (1987) Somatostatin receptors in human endocrine tumors. Cancer Res 47:551–558
29. Reubi JC, Waser B, Sheppard M, Macaulay V (1990) Somatostatin receptors are present in small-cell but not in non-

small-cell primary lung carcinomas: relationship to EGF receptors. Int J Cancer 45:269–274
30. Reubi JC, Waser B, Horisberger U, Krenning E, Lamberts SWJ, Gebers JO, Gerschbach P, Laissue JA (1993) In vitro autoradiographic and in vivo scintigraphic localisation of somatostatin receptors in human lymphatic tissues. Blood 82: 2143–2151
31. Reubi JC, Schaer JC, Waser B, Mengod G (1994) Expression and localization of somatostatin receptors SSTR1, SSTR2, SSTR3 messenger RNA in primary human tumors using in situ hybridisation. Cancer Res 54:3455–3459
32. Reubi JC, Kappeler A, Wsaer B, Laissue J, Hipkin R W, Schonbrunn A (1998) Immunohistochemical localization of Somatostatin receptors sst2A in human tumors. Am J Pathol 153:233–245
33. Reubi JC, Schaer JC, Wenger S, Hoeger C, Erchegyi J, Waser B, Rivier J (2000) sst3-selective potent peptidic somatostatin receptor antagonists. Proc Natl Acad Sci USA 97:13973–13978
34. Reubi JC, Waser B, Liu Q, Laissue JA, Schonbrunn A (2000) Subcellular distribution of somatostatin sst2A receptors in human tumors of the nervous and neuroendocrine systems: membranous versus intracellular location. J Clin Endocrinol Metab 85:3882–3891
35. Reubi JC, Schaer JC, Waser B, Wenger S, Heppeler A, Schmitt JS, Macke HR (2000) Affinity profiles for human somatostatin receptor subtypes sst1-sst5 of somatostatin radiotracers selected for scintigraphic and radiotherapeutic use. Eur J Nucl Med 27:273–282
36. Schindler M, Sellers LA, Humphrey PPA, Emson PC (1997) Immunohistochemical localization of the somatostatin sst2(A) receptor in the rat brain and spinal cord. Neuroscience 76: 225–240
37. Schindler M, Holloway S, Humphrey PPA, Waldvogel H, Faull RLM, Berger W, Emson PC (1998) Localization of the somatostatin sst2a receptor in human cerebral cortex, hippocampus and cerebellum. Neuroreport 9 521–525
38. Schulz So, Schulz St, Schmitt J, Wiborny D, Schmitt H, Olbricht S, Weise W, Roessner A, Gramsch C, Hollt V (1998) Immunocytochemical detection of somatostatin receptors sst_1, sst_{2A}, sst_{2B} and sst_3 in paraffin-embedded breast cancer tissue using subtype-specific antibodies. Clin Cancer Res 4:2047–2052
39. Semprebene A, Ferraironi A, Franciotti G, Venturo I, Giunta S, Lopez M, Maini CL (1995) 111 In-octreotide scintigraphy in small cell lung cancer. Q J Nucl Med 39:108–110
40. Sestini R, Orlando C, Peri A, Tricarico C, Pazzagli M, Serio M, Pagani A, Bussolati G, Granchi S, Maggi M (1996) Quantification of Somatostatin receptor type 2 gene expression in neuroblastoma cell lines and primary tumors using competitive reverse transcription-polymerase chain reaction. Clin Cancer Res 2:1757–1765
41. Slooter GD, Mearadji A, Breeman WA, Marquet RL, De Jong M, Krenning EP, Wan Eijck CH (2001) Somatostatin receptor imaging, therapy and new strategies in patients with neuroendocrine tumors. Br J Surg 88:31–40
42. Solcia E, Kloppel G, Sobin LH (eds) (2000) Histological typing of endocrine tumors, 2nd edn. Springer, Berlin Heidelberg New York (WHO international classification of tumors)
43. Stoffel M, Jamar F, Donckier J, Hainaut P, Decoster P, Beckers C, Pauwels S (1996) Increased uptake of indium-111 pentetreotide up to ten years after external thoracic irradiation: report of two cases. Eur J Nucl Med 23:723–726
44. Stokkel MP, Kwa BM, Pauwels EK (1995) Imaging and staging of small-cell lung cancer: is there a future role for octreotide scintigraphy? Br J Clin Pract 49:235–238
45. Taylor JE, Theveniau MA, Bashirzadeh R, Reisine T, Eden PA (1994) Detection of somatostatin receptor subtype 2 (SSTR2) in established tumors and tumor cell lines: evidence for sst2 heterogeneity. Peptides 15:1229–1236
46. Travis WD, Colby TV, Corrin B, Shimosato Y, Brambilla E (eds) (1999) Histological typing of lung and pleural tumors, 3rd edn. Springer, Berlin Heidelberg New York (WHO international classification of tumors)
47. Vaccarili M, Lococo A, Fabiani F, Staffilano A (2000) Clinical diagnostic application of 111In-DTPA-octreotide scintigraphy in small cell lung cancer. Tumori 86:224–228
48. Volante M, Pecchioni C, Bussolati G (2000) Post-incubation heating significantly improves tyramide signal amplification. J Histochem Cytochem 48:1583–1585
49. Zhang CY, Yokogoshi Y, Yoshimoto K, Fujinaka Y, Matsumoto K, Saito S (1995) Point mutation of the somatostatin receptor 2 gene in the human small cell lung cancer cell line COR-L103. Biochem Biophys Res Commun 210:805–815

Virchows Arch (2001) 439:798–802
DOI 10.1007/s004280100474

ORIGINAL ARTICLE

**Patrick S. Moore · Bence Sipos · Simonetta Orlandini
Claudio Sorio · Francisco X. Real
Nicholas R. Lemoine · Thomas Gress · Claudio Bassi
Günter Klöppel · Holger Kalthoff
Hendrik Ungefroren · Matthias Löhr · Aldo Scarpa**

Genetic profile of 22 pancreatic carcinoma cell lines

Analysis of K-*ras*, *p53*, *p16* and *DPC4/Smad4*

Received: 26 May 2000 / Accepted: 23 April 2001 / Published online: 27 June 2001
© Springer-Verlag 2001

Abstract The K-*ras*, *p53*, *p16* and *DPC4* genes are among those most frequently altered in pancreatic ductal carcinoma. We analyzed 22 cell lines for alterations in these genes by direct sequence analysis and methylation-specific polymerase chain reaction. These cell lines showed mutations in K-*ras* and *p53* at frequencies of 91% and 95%, respectively. Alterations in $p16^{INK4a}$ were found in all cases and included nine homozygous deletions, seven mutations and promoter methylation in six cases. Eight cell lines (36%) had an alteration of *DPC4*, including one mutation and seven homozygous deletions. The most typical mutational profile involved K-*ras*, *p53*, and $p16^{INK4a}$, concurrently aberrated in 20 cases (91%). Eight cell lines had alterations in all four genes. Inactivation of *DPC4* was always accompanied by alteration of all of the other three genes. This comprehensive data regarding the cumulative genetic alterations in pancreatic carcinoma cell lines will be of great value for studies involving drug sensitivity or resistance that may be associated with inactivation of a particular gene or molecular pathway.

Keywords Pancreas · Carcinoma cell lines · K-*ras* · *P16* · *P53* · *DPC4/Smad4*

P.S. Moore · S. Orlandini · C. Sorio · A. Scarpa (✉)
Department of Pathology, University of Verona, Strada Le Grazie, I-37134 Verona, Italy
e-mail: scarpa@anpat.univr.it
Tel.: +39-45-8074822, Fax: +39-45-8027136

C. Bassi
Department of Surgery, University of Verona, Italy

T. Gress
Department of Internal Medicine I, University of Ulm, Germany

N.R. Lemoine
ICRF Molecular Oncology Unit, Department of Cancer Medicine, Imperial College School of Medicine, London, UK

F.X. Real
Unitat de Biologia Cellular i Molecular, Institut Municipal d'Investigació Mèdica, Barcelona, Spain

B. Sipos · G. Klöppel · H. Kalthoff · H. Ungefroren
Department of Pathology and Molecular Oncology of Clinic of General Surgery University of Kiel, Germany

M. Löhr
IV Department of Internal Medicine, Medical Faculty of Mannheim, University of Heidelberg, Mannheim, Germany

Introduction

Information regarding the mutational status of multiple genes in cancer will aid not only in a greater understanding of the molecular processes involved in tumorigenesis but may also be valuable in the design of molecular diagnosis strategies, in studies in which certain genetic alterations may be related to drug resistance and in the molecular epidemiology of pancreatic cancer. This would therefore have dramatic implications for therapeutic intervention. One such example is the recent demonstration that the low efficacy of 5-fluorouracil is causally related to the inactivation of the *p53* gene by mutation [4, 22].

Pancreatic ductal adenocarcinoma represents a unique opportunity to study multigenic mutational status, as it is characterized by a relatively unique molecular fingerprint comprising activating point mutations at codon 12 of the K-*ras* oncogene in 80% of cases and inactivation of the tumor suppressor genes $p16^{INK4a/(CDKN2/MTS1)}$ and *p53* in 90% and 60% of cases, respectively [1, 5, 19, 25, 32, 35, 36, 37, 41]. More recently, the *DPC4/Smad4* gene has been reported to be altered in about 50% of xenografted cancers [11].

Molecular studies in primary ductal carcinoma of the pancreas are problematic because of the tumor's conspicuous desmoplastic stroma, which makes the isolation of cells difficult. Such studies are therefore much easier to perform in tumor cell lines and xenografts [42]. While the former are easily handled, the latter are not readily

available to all researchers, as they require special and costly facilities. The use of both cell lines and xenografts is limited by the potential acquisition of additional mutations by tumor cells during their manipulation [33]. Cell lines nonetheless represent a commonly used source of material, and some of these have been characterized for a number of different chromosomal and gene anomalies. While data regarding the cumulative genetic alterations in pancreatic carcinoma xenografts have been reported [34], a comprehensive analysis of commonly used pancreatic ductal carcinoma cell lines has not been performed. In this report, we present the results of the analysis of 22 pancreatic cancer cell lines for alterations in the K-*ras*, *p53*, *p16* and *DPC4* genes.

Materials and methods

Cell lines

A total of 24 human pancreatic ductal carcinoma cell lines were originally analyzed in this study (Table 1). Two cell lines, SW850 and SW979, were excluded, because a recent analysis revealed that these cell lines most likely are derived from cervix carcinomas. In particular, testing of the original cell lines received from Memorial Sloan-Kettering Cancer Center in the mid 1980s revealed that SW850 and SW979 contain the same HPV16 sequences as the cervix carcinoma cell lines C4–1 and C4–2 (H. Kalthoff, personal communication). Because of these findings – the fact that they lack any K-*ras*, *p53*, *p16* and *DPC4* mutations and the uncertain documentation of their origin – these cell lines should not be regarded as pancreatic carcinoma cell lines. All cell lines were cultured in RPMI 1640 medium supplemented with 10% heat-inactivated fetal calf serum (Gibco BRL, Life Technologies) and were *Mycoplasma* free.

Analysis of K-*ras*, *p16*, *p53* and *DPC4*

All samples were analyzed for mutations in exon 1 of the K-*ras* gene, exons 1 and 2 of *p16*, exons 5–9 of *p53* and exons 8–11 of *DPC4* by direct sequencing of polymerase chain reaction (PCR)-amplified DNA fragments. Primers for amplification of the *p53* [36], *p16* [49], K-*ras* [37] and *DPC4* genes [12] were as described. Methylation-specific PCR for the 5′ CpG island of the *p16* gene was carried out as described [13].

H. Kalthoff, personal communication

Testing of the original cell lines 1983, received from Dr. Jørgen Fogh, Sloan-Kettering Institute for Cancer Research, revealed that SW850 and SW979 contain the same HPV18 sequences as the cervix carcinoma cell line C4-I (E. Schwarz, DKFZ, Heidelberg; J. Schwarte-Waldhoff, IML, Bochum). Because of these findings, the fact that they lack any K-*ras*, *p53*, *p16* and *DPC4* mutations and the uncertain documentation of their origin, these cell lines should not be regarded as pancreatic carcinoma cell lines.

Results and discussion

The 22 cell lines were analyzed for mutations in exon 1 of K-*ras*, exons 5–9 of *p53* and in highly conserved exons 8–11 of *DPC4*. The *p16* gene was examined for alterations in exons 1 and 2 as well as for methylation of its 5′ CpG island by methylation-specific PCR. The results are summarized in Table 2. Activating mutations in K-*ras* at codon 12 were found in 20 samples (91%); twelve of these were G to A transitions. Inactivating mutations of *p53* were found in 21 of 22 (95%) cases, with G to A transitions being the most common type of nucleotide change (6 of 21, 28.5%). The *p16* gene was altered

Table 1 Origin of pancreatic ductal carcinoma cell lines

Cell line	Synonym (misnomer)	Established by	Source of tumor cells	Provided by
A818–4		H. Kalthoff (Germany)	Ascites	H. Kalthoff
ASPC-1		Chen and M.H Tan (USA) [6]	Ascites	American Type Culture Collection
BI		A. Andren-Sandberg (Sweden)[a]		A. Andren-Sandberg
BJ		A. Andren-Sandberg (Sweden)[a]		A. Andren-Sandberg
CFPAC1		R.A. Schoumacher (USA) [38]	Liver metastasis	N. Lemoine
FA6		N. Nagata (Japan) [29]		N. Lemoine
Ger		A.G. Grant (Great Britain) [9]	Primary tumor	N. Lemoine
HPAF-II		R.S. Metzgar (Germany) [28]	Ascites	N. Lemoine
IMIM-PC2		M. R. Vila (Spain) [44]	Primary tumor	F.X. Real
MDAPanc3		M. Frazier (USA) [8]	Liver metastasis	N. Lemoine
MiaPaCa-2		A. Yunis (USA) [48]	Primary tumor	American Type Culture Collection
Paca3	Pc3	M. v Bülow (Germany)[b]	Primary tumor	M. v Bülow
Paca44	Patu8902	M. v Bülow (Germany)[b]		M. v Bülow
Panc1		M. Lieber (USA) [26]	Primary tumor	American Type Culture Collection
PancTuI	PaCa2 (originally by M. Bülow) PancTuII PaTu-I Panc2, Pc2	M. v Bülow (Germany)[b]	Primary tumor	M. v Bülow
PC		A. Andren-Sandberg (Sweden)[a]		A. Andren-Sandberg
PSN1		H. Yamada (Japan) [47]	Primary tumor	N. Lemoine
PT45P1		H. Kalthoff (Germany)	Primary tumor	H. Kalthoff
RWP1		D.L. Dexter, P. Calabresi (USA) [7]	Liver metastasis	N. Lemoine
SK-PC1		M. R. Vila (Spain) [44]	Primary tumor	F.X. Real
SUIT-2		T. Iwamura (Japan) [17]	Liver metastasis	T. Iwamura
T3M4	Panc89	T. Okabe (Japan) [31]	Lymph node metastasis	N. Lemoine

[a] A. Andren-Sandberg, personal communication
[b] G. Klöppel, personal communication

Table 2 Molecular alterations of K-*ras*, *p53*, *p16* and *DPC4* in pancreatic ductal carcinoma cell lines. *HD* homozygous deletion, *Wt* wild type

	K-*ras*		*p53*		*p16*		*DPC4*		No. of genes mutated
	Alteration	Predicted product	Alteration	Predicted product	Alteration	Predicted product	Alteration	Predicted product	
A818.4	12 GGT-CGT	Gly to arg	Mutated in tetramerization domain *	Shorter protein	HD	Absent	None	Wt	3
AsPc1**	12 GGT-GAT	Gly to asp	135 TGC-GC	Frameshift	77 ACT-A	Frameshift	None	Wt	3
BI	12 GGT-GAT	Gly to asp	197 GTG-TTG	Val to leu	Methylated	Absent	HD	Absent	4
BJ	12 GGT-GAT	Gly to asp	275 TGT-TAT	Cys to tyr	44 TAC-TAAC	Tyr to stop	HD	Absent	4
CFPAC1	12 GGT-GTT	Gly to val	242 TGC-CGC	Cys to arg	Methylated	Absent	HD	Absent	4
FA6***	12 GGT-GAT	Gly to asp	149, 840bp del	Truncated	58 CGA-TGA	Arg to stop	HD	Absent	4
Ger	12 GGT-GAT	Gly to asp	272 GTG-TTG	Val to leu	HD	Absent	HD	Absent	4
HPAF II	12 GGT-GAT	Gly to asp	151 CCC-TCC	Pro to ser	29–34 del	In-frame deletion	None	Wt	3
IMIM-PC2	12 GGT-GAT	Gly to asp	306 CGA-TGA	Arg to stop	HD	Absent	None	Wt	3
MDAPanc3	12 GGT-GCT	Gly to ala	273 CGT-TGT	Arg to cys	–36 to (+5)-C	Absent	None	Wt	3
MiaPaCa2	12 GGT-TGT	Gly to cys	248 CGG-TGG	Arg to trp	HD	Absent	None	Wt	3
PaCa3	None	Wt	None	Wt	Methylated	Absent	None	Wt	1
PaCa44	12 GGT-GTT	Gly to val	176 TGC-AGC	Cys to ser	Methylated	Absent	None	Wt	3
PANC1	12 GGT-GAT	Gly to asp	273 CGT-CAT	Arg to his	HD	Absent	None	Wt	3
PancTu-I	12 GGT-GTT	Gly to val	176 TGC-AGC	Cys to ser	Methylated	Absent	None	Wt	3
PC	12 GGT-GTT	Gly to val	175 CGC-CAC	Arg to his	HD	Absent	355 GAC-GGC	Asp to gly	4
PSN1	12 GGT-CGT	Gly to arg	132 AAG-CAG	Lys to gln	HD	Absent	HD	Absent	4
PT45P1	13 GGC-GAC	Gly to asp	280 AGA-AAA	Arg to lys	HD	Absent	None	Wt	3
RWP1	12 GGT-GAT	Gly to asp	175 CGC-CAC	Arg to his	58 CGA-TGA	Arg to stop	None	Wt	3
SK-PC 1	12 GGT-GAT	Gly to asp	282 CGG-CTG	Arg to leu	HD	Absent	HD	Absent	4
Suit-2	12 GGT-GAT	Gly to asp	273 CGT-CAT	Arg to his	69 GAG-TAG	Glu to stop	None	Wt	3
T3M4	None	Wt	220 TAT-TGT	Tyr to cys	methylated	Absent	None	Wt	2

* Personal communication from H. Kalthoff
** AsPc1 is reported to have a mutation in exon 2 of DPC4 (24)
*** FA6 also has the A148T polymorphism in p16

in all of the cell lines; homozygous deletions were seen in nine (41%) tumors, seven (32%) contained mutations or small deletions, while six other cell lines (27%) had methylation of the 5′ CpG island. For the cases that showed methylation, transcriptional inactivation of the *p16* gene was verified by reverse-transcription (RT)-PCR (data not shown). Homozygous deletion of the *DPC4* gene was observed in seven cell lines (32%), while only one mutation was found (4.5%). Thus, 36% of cases had alterations of *DPC4*. All eight cell lines showing abnormalities in *DPC4* had concurrent alteration of all the other three genes analyzed.

Pancreatic ductal adenocarcinomas share the high rate of K-*ras*, *p53* and *p16* alterations with a number of cancers from other organs [2, 3, 11, 12, 16, 20, 21, 23, 24, 27, 30, 34, 39]. *DPC4* changes, however, are rarely seen in extrapancreatic cancers (except for colorectal carcinomas) at the same high frequency as in pancreatic ductal carcinoma [34, 43]. The reported frequency of homozygous deletion of *DPC4* in cell lines and xenografts from ductal adenocarcinoma ranges from 20% to 53% [11, 45]. *DPC4* mutations, in contrast, were either not found [3] or were detected at a much lower frequency (16%) [34]. These data compare well with our results. Since only one study found that *DPC4* mutations (4 of 12 short-term cultured pancreatic carcinoma cell lines) were more frequent than homozygous deletions (1 of 12) [18], it seems that homozygous deletion is the preferred inactivation mechanism for *DPC4* in pancreatic carcinoma. Compared with other genetic changes in pancreatic ductal carcinoma, loss of heterozygosity on chromosome 18q is one of the most frequent genetic events [40]. Given the fact that these deletions are usually very large and may involve the entire chromosome [10], there may be additional deletional targets in addition to *DPC4*. This possibility has been explored in more detail in recent reports [14, 15].

The frequencies of genetic alteration for each individual gene are those largely expected from existing data. Multigenic analysis showed that 20 of the 22 cell lines (91%) had concurrent alterations in K-*ras*, *p53* and *p16*. These patterns of accumulated gene inactivation are detailed in Table 3. A previous multigenic analysis of 41 xenografts observed mutation of K-*ras* in all samples [34]. A trend was also seen between mutation of *DPC4* and *p16* in that alteration of the former was always accompanied by alteration of the latter [34]. In this panel of cell lines, alteration of *DPC4* was only seen in those cases having alterations in all three of the other genes. This might indicate that alteration of *DPC4* is a late pathogenetic event, a possibility further suggested by a recent study [46].

In summary, the molecular alterations present in this series of cell lines represent the variety of alterations

Table 3 Accumulation of genetic alterations in pancreatic ductal carcinoma cell lines

Altered genes	Number of affected cell lines
K-*ras*, *p53*, *p16*, *DPC4*	8
K-*ras*, *p53*, *p16*	12
p*53*, *p16*	1
p16	1

present in primary pancreatic carcinomas. The comprehensive data regarding the multigenic alterations in this large series of cell lines should prove valuable for studies involving drug sensitivity or resistance that may be associated with inactivation of a particular gene or molecular pathway.

Acknowledgements This study was supported by grants from the Associazione Italiana Ricerca Cancro (AIRC) to A.S., Milan, Italy; Consorzio Studi Universitari di Verona, Italy; Ministero Università e Ricerca Scientifica e Tecnologica (MURST, Cofin MM06158571–9906195987), Rome, Italy; and European Community grant BIOMED 2 CA-Contract no. BMH4-CT98–3805.

References

1. Almoguera C, Shibata D, Forrester K, Martin J, Arnheim N, Perucho M (1988) Most human carcinomas of the exocrine pancreas contain mutant c-K-ras genes. Cell 53:549–554
2. Barrett MT, Schutte M, Kern SE, Reid BJ (1996) Allelic loss and mutational analysis of the DPC4 gene in esophageal adenocarcinoma. Cancer Res 56:4351–4353
3. Bartsch D, Barth P, Bastian D, Ramaswamy A, Gerdes B, Chaloupka B, Deiss Y, Simon B, Schudy A (1999) Higher frequency of DPC4/Smad4 alterations in pancreatic cancer cell lines than in primary pancreatic adenocarcinomas. Cancer Lett 139:43–49
4. Bunz F, Hwang PM, Torrance C, Waldman T, Zhang Y, Dillehay L, Williams J, Lengauer C, Kinzler KW, Vogelstein B (1999) Disruption of p53 in human cancer cells alters the responses to therapeutic agents. J Clin Invest 104:263–269
5. Caldas C, Hahn SA, da Costa L, Redston MS, Schutte M, Seymour AB, Weinstein CL, Hruban RH, Yeo CJ, Kern SE (1994) Frequent somatic mutations and homozygous deletions of the p16 (MTS1) gene in pancreatic adenocarcinoma. Nat Genet 8:27–32
6. Chen WH, Horoszewicz JS, Leong SS, Shimano T, Penetrante R, Sanders WH, Berjian R, Douglass HO, Martin EW, Chu TM (1982) Human pancreatic adenocarcinoma: in vitro and in vivo morphology of a new tumor line established from ascites. In Vitro 18:24–34
7. Dexter DL, Matook GM, Meitner PA, Bogaars HA, Jolly GA, Turner MD, Calabresi P (1982) Establishment and characterization of two human pancreatic cancer cell lines tumorigenic in athymic mice. Cancer Res 42:2705–2714
8. Frazier ML, Pathak S, Wang ZW, Cleary K, Singletary SE, Olive M, Mackay B, Steck PA, Levin B (1990) Establishment of a new human pancreatic adenocarcinoma cell line, MDA-Panc-3. Pancreas 5:8–16
9. Grant AG, Duke D, Hermon-Taylor J (1979) Establishment and characterization of primary human pancreatic carcinoma in continuous cell culture and in nude mice. Br J Cancer 39:143–151
10. Hahn SA, Seymour AB, Hoque AT, Schutte M, da Costa LT, Redston MS, Caldas C, Weinstein CL, Fischer A, Yeo CJ (1995) Allelotype of pancreatic adenocarcinoma using xenograft enrichment. Cancer Res 55:4670–4675
11. Hahn SA, Schutte M, Hoque AT, Moskaluk CA, da Costa LT, Rozenblum E, Weinstein CL, Fischer A, Yeo CJ, Hruban RH, Kern SE (1996) DPC4, a candidate tumor suppressor gene at human chromosome 18q21.1. Science 271:350–353
12. Hahn SA, Bartsch D, Schroers A, Galehdari H, Becker M, Ramaswamy A, Schwarte-Waldhoff I, Maschek H, Schmiegel W (1998) Mutations of the DPC4/Smad4 gene in biliary tract carcinoma. Cancer Res 58:1124–1126
13. Herman JG, Graff JR, Myohanen S, Nelkin BD, Baylin SB (1996) Methylation-specific PCR: a novel PCR assay for methylation status of CpG island. Proc Natl Acad Sci USA 93:9821–9826
14. Hilgers W, Su GH, Groot Koerkamp B, Tang DJ, Shekher MC, Sugar AY, Yeo CJ, Hruban RH, Kern SE (1999) Novel homozygous deletions of chromosomal band 18q22 in pancreatic adenocarcinoma identified by STS marker scanning. Genes Chromosomes Cancer 25:370–375
15. Hilgers W, Song JJ, Haye M, Hruban RR, Kern SE, Fearon ER (2000) Homozygous deletions inactivate DCC, but not MADH4/DPC4/SMAD4, in a subset of pancreatic and biliary cancers. Genes Chromosomes Cancer 27:353–357
16. Hoque AT, Hahn SA, Schutte M, Kern SE (1997) DPC4 gene mutation in colitis associated neoplasia. Gut 40:120–122
17. Iwamura T, Katsuki T, Ide K (1987) Establishment and characterization of a human pancreatic cancer cell line (SUIT-2) producing carcinoembryonic antigen and carbohydrate antigen 19–9. Jpn J Cancer Res 78:54–62
18. Jonson T, Gorunova L, Dawiskiba S, Andren-Sandberg A, Stenman G, ten Dijke P, Johansson B, Hoglund M (1999) Molecular analyses of the 15q and 18q SMAD genes in pancreatic cancer. Genes Chromosomes Cancer 24:62–71
19. Kalthoff H, Schmiegel W, Roeder C, Kasche D, Schmidt A, Lauer G, Thiele HG, Honold G, Pantel K, Riethmüller G, Scherer E, Maurer J, Maacke H, Deppert W (1993) p53 and K-RAS alterations in pancreatic epithelial cell lesions. Oncogene 8:289–298
20. Kaneko H, Horiike S, Sasai Y, Iwai T, Nakao M, Yokota S, Taniwaki M, Kashima K, Misawa S (1998) Rare alteration of genomic structure or expression of the DPC4 gene in myelogenous leukemias. Acta Haematol 99:187–190
21. Kim SK, Fan Y, Papadimitrakopoulou V, Clayman G, Hittelman WN, Hong WK, Lotan R, Mao L (1996) DPC4, a candidate tumor suppressor gene, is altered infrequently in head and neck squamous cell carcinoma. Cancer Res 56:2519–2521
22. Komarov PG, Komarova EA, Kondratov RV, Christov-Tselkov K, Coon JS, Chernov MV, Gudkov AV (1999) A chemical inhibitor of p53 that protects mice from the side effects of cancer therapy. Science 285:1733–1737
23. Kong XT, Choi SH, Inoue A, Xu F, Chen T, Takita J, Yokota J, Bessho F, Yanagisawa M, Hanada R, Yamamoto K, Hayashi Y (1997) Expression and mutational analysis of the DCC, DPC4, and MADR2/JV18–1 genes in neuroblastoma. Cancer Res 57:3772–3778
24. Lei J, Zou TT, Shi YQ, Zhou X, Smolinski KN, Yin J, Souza RF, Appel R, Wang S, Cymes K, Chan O, Abraham JM, Harpaz N, Meltzer SJ (1996) Infrequent DPC4 gene mutation in esophageal cancer, gastric cancer and ulcerative colitis-associated neoplasms. Oncogene 13:2459–2462
25. Lemoine NR, Jain S, Hughes CM, Staddon SL, Maillet B, Hall PA, Klöppel G (1992) Ki-*ras* oncogene activation in preinvasive pancreatic cancer. Gastroenterology 102:230–236
26. Lieber M, Mazzetta J, Nelson-Rees W, Kaplan M, Todaro G (1975) Establishment of a continuous tumor-cell line (panc-1) from a human carcinoma of the exocrine pancreas. Int J Cancer 15:741–747
27. MacGrogan D, Pegram M, Slamon D, Bookstein R (1997) Comparative mutational analysis of DPC4 (Smad4) in prostatic and colorectal carcinomas. Oncogene 15:1111–1114
28. Metzgar RS, Gaillard MT, Levine SJ, Tuck FL, Bossen EH, Borowitz MJ (1982) Antigens of human pancreatic adenocarcinoma cells defined by murine monoclonal antibodies. Cancer Res 42:601–608

29. Nagata N, Akatsu T, Kugai N, Yasutomo Y, Kinoshita T, Kosano H, Shimauchi T, Takatani O, Ueyama Y (1989) The tumor cells (FA-6) established from a pancreatic cancer associated with humoral hypercalcemia of malignancy: a simultaneous production of parathyroid hormone-like activity and transforming growth factor activity. Endocrinol Jpn 36:75–85
30. Nagatake M, Takagi Y, Osada H, Uchida K, Mitsudomi T, Saji S, Shimokata K, Takahashi T (1996) Somatic in vivo alterations of the DPC4 gene at 18q21 in human lung cancers. Cancer Res 56:2718–2720
31. Okabe T, Yamaguchi N, Ohsawa N (1983) Establishment and characterization of a carcinoembryonic antigen (CEA)-producing cell line from a human carcinoma of the exocrine pancreas. Cancer 51:662–668
32. Redston MS, Caldas C, Seymour AB, Hruban RH, da Costa L, Yeo CJ, Kern SE (1994) p53 mutations in pancreatic carcinoma and evidence of common involvement of homocopolymer tracts in DNA microdeletions. Cancer Res 54:3025–3033
33. Reyes G, Villanueva A, Garcia C, Sancho FJ, Piulats J, Lluis F, Capella G (1996) Orthotopic xenografts of human pancreatic carcinomas acquire genetic aberrations during dissemination in nude mice. Cancer Res 56:5713–5719
34. Rozenblum E, Schutte M, Goggins M, Hahn SA, Panzer S, Zuhurak M, Goodman SN, Sohn TA, Hruban RH, Yeo CJ, Kern SE (1997) Tumor-suppressive pathways in pancreatic carcinoma. Cancer Res 57:1731–1734
35. Ruggeri B, Zhang SY, Caamano J, DiRado M, Flynn SD, Klein-Szanto AJ (1992) Human pancreatic carcinomas and cell lines reveal frequent and multiple alterations in the p53 and Rb-1 tumor-suppressor genes. Oncogene 7:1503–1511
36. Scarpa A, Capelli P, Mukai K, Zamboni G, Oda T, Iacono C, Hirohashi S (1993) Pancreatic adenocarcinomas frequently show p53 gene mutations. Am J Pathol 142:1534–1543
37. Scarpa A, Capelli P, Villaneuva A, Zamboni G, Lluis F, Accolla R, Mariuzzi G, Capella G (1994) Pancreatic cancer in Europe: Ki-ras gene mutation pattern shows geographical differences. Int J Cancer 57:167–171
38. Schoumacher RA, Ram J, Iannuzzi MC, Bradbury NA, Wallace RW, Hon CT, Kelly DR, Schmid SM, Gelder FB, Rado TA (1990) A cystic fibrosis pancreatic adenocarcinoma cell line. Proc Natl Acad Sci USA 87:4012–4016
39. Schutte M, Hruban RH, Hedrick L, Cho KR, Nadasdy GM, Weinstein CL, Bova GS, Isaacs WB, Cairns P, Nawroz H, Sidransky D, Casero RA, Meltzer PS, Hahn SA, Kern SE (1996) DPC4 gene in various tumor types. Cancer Res 56: 2527–2530
40. Seymour AB, Hruban RH, Redston M, Caldas C, Powell SM, Kinzler KW, Yeo CJ, Kern SE (1994) Allelotype of pancreatic adenocarcinoma. Cancer Res 54:2761–2764
41. Smit VTBH, Boot AJM, Smits AMM, Focuren GJ, Cornelasse CJ, Bos JL (1988) K-*ras* codon 12 mutations occur very frequently in pancreatic adenocarcinoma. Nucleic Acids Res 16:7773-7782
42. Sorio C, Bonora A, Orlandini S, Moore PS, Capelli P, Cristofori P, Dal Negro G, Marchiori P, Gaviraghi G, Falconi M, Pederzoli P, Zamboni G, Scarpa A (2001) Successful xenografting of cryopreserved primary pancreatic cancers. Virchows Arch 438:154–158
43. Thiagalingam S, Lengauer C, Leach FS, Schutte M, Hahn SA, Overhauser J, Willson JK, Markowitz S, Hamilton SR, Kern SE, Kinzler KW, Vogelstein B (1996) Evaluation of candidate tumour suppressor genes on chromosome 18 in colorectal cancers. Nat Genet 13:343–346
44. Vila MR, Lloreta J, Schussler MH, Berrozpe G, Welt S, Real FX (1995) New pancreas cancers cell lines that represent distinct stages of ductal differentiation. Lab Invest 72:395–404
45. Villanueva A, Garcia C, Paules AB, Vicente M, Megias M, Reyes G, de Villalonga P, Agell N, Lluis F, Bachs O, Capella G (1998) Disruption of the antiproliferative TGF-beta signaling pathways in human pancreatic cancer cells. Oncogene 17:1969–1978
46. Wilentz RE, Iacobuzio-Donahue CA, Argani P, McCarthy DM, Parsons JL, Yeo CJ, Kern SE, Hruban RH (2000) Loss of expression of Dpc4 in pancreatic intraepithelial neoplasia: evidence that DPC4 inactivation occurs late in neoplastic progression. Cancer Res 60:2002–2006
47. Yamada H, Yoshida T, Sakamoto H, Terada M, Sugimura T (1986) Establishment of a human pancreatic adenocarcinoma cell line (PSN-1) with amplifications of both c-myc and activated c-Ki-ras by a point mutation. Biochem Biophys Res Commun 140:167–173
48. Yunis AA, Arimura GK, Russin DJ (1977) Human pancreatic carcinoma (MIA PaCa-2) in continuous culture: sensitivity to asparaginase. Int J Cancer 19:218–235
49. Zhang SY, Klein-Szanto AJ, Sauter ER, Shafarenko M, Mitsunaga S, Nobori T, Carson DA, Ridge JA, Goodrow TL (1994) Higher frequency of alterations in the p16/CDKN2 gene in squamous cell carcinoma cell lines than in primary tumors of the head and neck. Cancer Res 54:5050–5053

Virchows Arch (2001) 439:803–807
DOI 10.1007/s004280100509

ORIGINAL ARTICLE

**Wolfgang Hartmann · Andreas Waha · Arend Koch
Steffen Albrecht · Steven G. Gray · Tomas J. Ekström
Dietrich von Schweinitz · Torsten Pietsch**

Promoter-specific transcription of the *IGF2* gene: a novel rapid, non-radioactive and highly sensitive protocol for mRNA analysis

Received: 15 January 2001 / Accepted: 18 June 2001 / Published online: 2 October 2001
© Springer-Verlag 2001

Abstract The human insulin-like growth factor-II (IGF2) is a regulatory peptide which is critical in normal fetal growth. *IGF2* gene transcription is controlled by the usage of four promoters P1–P4 of which promoters P2–P4 are genomically imprinted. Disruption of imprinting and the resulting increase of gene dosage have been shown to be implicated in tumor progression in a variety of human tumors. Due to the need for high amounts of tissue material for conventional methods such as Northern blotting or ribonuclease protection assay (RPA), studies on *IGF2* expression have most often been limited to the detection of total *IGF2* transcript, though different dysregulatory events can be responsible for the abundance of *IGF2* mRNA found in many tumors. We established a highly sensitive competitive RT-PCR assay for the four different transcripts of the *IGF2* gene with transcript-specific external RNA competitors in which we take advantage of fluorescence-based quantification on a semiautomated sequencer. The amount of total RNA needed is approximately 100 times lower than the amounts required for Northern blotting or RPA, so that even cytological samples can be analyzed. We applied the assay to a series of eleven hepatoblastomas (HB) in which normal adjacent liver tissue could also be analyzed.

W. Hartmann · A. Waha · A. Koch · T. Pietsch (✉)
Department of Neuropathology,
University of Bonn Medical Center,
Sigmund-Freud-Strasse 25, 53105 Bonn,Germany
e-mail: pietsch-t@uni-bonn.de
Tel.: +49-228-287-4398, Fax: +49-228-287-4331

S. Albrecht
Department of Pathology,
Sir Mortimer B. Davis Jewish General Hospital,
McGill University, Montreal, Canada

S.G. Gray · T.J. Ekström
Laboratory of Molecular Development and Tumor Biology,
Experimental Alcohol and Drug Addiction Research Section,
Department of Clinical Neuroscience, Karolinska Institute,
Stockholm, Sweden

D. von Schweinitz
Department of Pediatric Surgery,
University of Basel Medical Center, Switzerland

Keywords Insulin-like growth factor · Imprinting · 11p15.5 · Liver cancer

Introduction

The human insulin-like growth factor-II (IGF2) is a regulatory peptide which is critical in normal fetal growth and which has been shown to be implicated in tumor progression in a variety of human tumors [7], e.g. in breast cancer [6]. The *IGF2* gene transcription is controlled by four promoters P1–P4 [8]. Generally, promoters P2–P4 are imprinted whereas P1-dependent transcripts are always derived from both parental alleles [1, 9]. The different transcriptional activity of these promoters allows subtly differentiated regulation of *IGF2* transcription in different tissues. An example of the fine regulatory activity of the different promoters is the situation in human liver development: P4 shows its highest activity in the fetal stage, activity of P3 and P2 peak shortly after birth, and P1 is increasingly responsible for *IGF2* transcription in the aging liver [5]. So, the frequently found abundance of *IGF2* mRNA in tumors can be caused by different dysregulatory events affecting one or more of the promoters. A good assay for identifying the nature of the dysregulatory events is to differentiate between the different promoter-specific transcripts.

Reverse-transcription polymerase chain reaction (RT-PCR) is a powerful tool for analyzing mRNA expression [11, 12]. Multiplex PCR of *IGF2* using one common downstream primer and labeling with radioisotopes [10] allows relative conclusions in one sample but does not provide quantitative comparability, e.g., between a tumor and its matching normal tissue. Differential PCR introduces an internal reference by equalizing the result to a housekeeping gene, but it faces criticism concerning its value as a quantitative method. The ribonuclease protection assay [5] and Northern blotting require high amounts of tissue material or RNA, which are rarely available in all cases, and both frequently involve

considerable exposure to radioisotopes. Therefore, we established a competitive RT-PCR assay for the four different transcripts of the *IGF2* gene with transcript-specific external RNA competitors. In this assay we circumvent the need for isotopes and take advantage of fluorescence-based quantification on a semiautomated sequencer employing only one labeled reverse primer for all four transcripts. Here, we present the results of our analysis of promoter-specific *IGF2* expression in a series of 11 hepatoblastomas (HB) in which normal adjacent liver tissue could also be analyzed. HB represent the most frequent malignant liver tumor of childhood and *IGF2* overexpression for this tumor has been documented before [4].

Materials and methods

Tissue samples were first examined by frozen section to verify their composition. To establish the system and to generate RNA competitors, total cellular RNA was extracted by lysis in guanidinium thiocyanate and ultracentrifugation through a cesium chloride cushion [3] or by extraction with the Trizol reagent (Life Technologies, Inc.) according to the manufacturer's instructions. DNase treatment of 5 µg RNA was performed in a total volume of 30 µl using 10U RNase free DNase I (Roche, Mannheim, Germany), 3 µl DNase buffer and 40U RNasin (Promega). DNase was removed by an additional round of Trizol extraction. Total RNA of a pool of normal tissue samples was reverse transcribed using the Superscript II preamplification system and random hexamers (Life Technologies, Inc.) according to the manufacturer's instructions. Template cDNA product was created by PCR with primers for all four described *IGF2* transcripts and β_2-*microglobulin* (*B2M*), a housekeeping gene. PCR reactions were carried out on a Uno Thermoblock cycler (Biometra) in a final volume of 30 µl containing 200 µM of each deoxyribonucleoside triphosphate (Life Tech-

Table 1 Primer sequences, PCR conditions and fragment sizes (target transcript / competitor). All primer pairs span intronic sequence so that accidential DNA contamination would not interfere with the reaction's kinetics

Primer designation	Sequence 5′–3′	PCR conditions	Fragment size
IGF2-P1-f	GCTCCCAGAACTGAGGCTGG	1.0 mM $MgCl_2$, 10% DMSO	147 bp / 122 bp
IGF2-P1-T7	GGATCCTAATACGACTCACTATAGGGAGGGCTCCCAGAACTGAGGCTGG	40 cycles 94°C× 35 s / 55°C× 40 s / 72°C 40 s	
IGF2-P2-f	TGCCACAGAGCGTTCGATCG	1.5 mM $MgCl_2$, 10% DMSO	158 bp / 133 bp
IGF2-P2-T7	GGATCCTAATACGACTCACTATAGGGAGGTGCCACAGAGCGTTCGATCG	40 cycles 94°C× 35 s / 59°C× 40 s /72°C 40 s	
IGF2-P3-f	GCTGTTCGGTTTGCGACACG	1.0 mM $MgCl_2$, 10% DMSO	144 bp / 119 bp
IGF2-P3-T7	GGATCCTAATACGACTCACTATAGGGAGGGCTGTTCGGTTTGCGACACG	40 cycles 94°C×35 s / 59°C×40 s / 72°C 40 s	
IGF2-P4-f	GCTTCTCCTGTGAAAGAGAC	1.0 mM $MgCl_2$, 10% DMSO	174 bp / 149 bp
IGF2-P4-T7	GGATCCTAATACGACTCACTATAGGGAGGGCTTCTCCTGTGAAAGAGAC	40 cycles 94°C× 35 s / 57°C× 40 s / 72°C 40 s	
IGF2-P1-P4-r	GCGGTAAGCAGCAATGCAGC		
IGF2-P1-P4-mut	GCGGTAAGCAGCAATGCAGCAAGCACCAGCATCGACTTCC		
IGF2-all-f	TGCTGCATTGCTGCTTACCG	1.0 mM $MgCl_2$	153 bp / 145 bp
IGF2-all-T7	GGATCCTAATACGACTCACTATAGGGAGGTGCTGCATTGCTGCTTACCG	40 cycles 94°C× 35 s / 52°C× 40 s / 72°C 40 s	
IGF2-all-r	ACAGCACTCCTCAACGATGC		
IGF2-all-mut	ACAGCACTCCTCAACGATGCCGACGGCTCACACGGCTTGC		
β_2-microglobulin-f	TGTCTTTCAGCAAGGACTGG	1.5 mM $MgCl_2$	148 bp / 130 bp
β_2-microglobulin-r	GATGCTGCTTACATGTCTCG	40 cycles 94°C× 30 s / 57°C× 40 s / 72°C 40 s	
β_2-microglobulin-T7	GGATCCTAATACGACTCACTATAGGGAGGTGTCTTTCAGCAAGGACTGG		
β_2-microglobulin-mut	GATGCTGCTTACATGTCTCGGCTGTGACAAAGTCACATGG		

nologies, Inc.), 15 pmol of each primer, 0.75 unit of *Taq* Polymerase (Life Technologies, Inc.) (for primer information, detailed PCR conditions, and fragment sizes see Table 1 and Fig. 1). Mutagenesis and T7 promoter addition were performed in a single PCR reaction with one single reverse primer for mutagenesis for all four *IGF2* transcripts and the promoter-specific forward primers with a T7 promoter sequence added at the 5′ end. PCR conditions were the same as used in the first round of PCR. The mutation inserted in the 3′ region of the fragments was a deletion of 25 bp within exon 7 (bases 43 to 67 referred to the first 5′ base of the exon). This meant a size reduction of 14–17% compared to the corresponding wild type product.

These templates for in vitro transcription were column-purified (QIAquick PCR Purification kit; Qiagen, Inc.), and 0.5 µg were transcribed with 10U T7 polymerase (Stratagene, Heidelberg, Germany) and the reagents provided by the manufacturer in a total volume of 25 µl. After DNase digestion of the DNA template (performed as described above), samples were subjected to purification with RNeasy Quickspin columns (Qiagen, Inc.) and eluted in 30 µl DEPC-treated water. Spectrophotometric determination of the concentrations of the homologous exogenous competitors followed. To ensure coverage of the equimolar range of the competitors and the corresponding RNA transcripts in the final assay, we set up a titration experiment. Reverse transcription of serial dilutions of the competitors (5×10^{-10}–5×10^{-6} mg) was performed with 250 ng of the RNA pool from tumor and liver tissue and subsequent PCR amplification of all products with the fluorescent labeled reverse primer was carried out. Products were separated and analyzed on a 6% denaturing acrylamide gel on a semiautomated DNA Sequencer (ABI 373A) using the Genescan software (ABI). Optimal titration was defined as the point of equal signal intensity of exogenous competitor and target transcript.

Eventually, 250 ng of RNA from each tumor or normal liver sample were reverse transcribed together with preevaluated amounts of the exogenous standards (for *IGF2-P1*, *-P2*, *-P3* and *-P4*: 500 pg, 100 pg, 10 pg, 2 pg, 200 fg, 20 fg and for *B2M* ten times as much in each dilution) using the same system as above. The wider range of competitor concentrations was applied to ensure optimal coverage of even higher fluctuations. Amplification and analysis were done as described for the titration experiment. RNA expression levels were calculated by the following algorithm: $(\text{TARGET}_{\text{sample}}/\text{TARGET}_{\text{standard}})$ / $(\beta_2\text{-microglobulin}_{\text{sample}}/\beta_2\text{-microglobulin}_{\text{standard}})$

Division of the ratio obtained for the target by the ratio of the housekeeper gene was performed to take into account possible differences in the amounts of tissue RNA subjected to reverse transcription. As only the relative amounts of housekeeping gene expression were of interest, $(\beta_2\text{-microglobulin}_{\text{sample}}/\beta_2\text{-microglobulin}_{\text{standard}})$ could be divided by the mean of β_2-microglobulin expression in all samples. All measurements were done in triplicates, mean expression and standard deviation were calculated. Optimal titration for the genes in most of the samples was found to be 100 pg for *B2M*, approximately 200 fg for *IGF2-P1* and *-P2*, about 100 pg for *IGF2-P3*, and 2 pg for *IGF2-P4*.

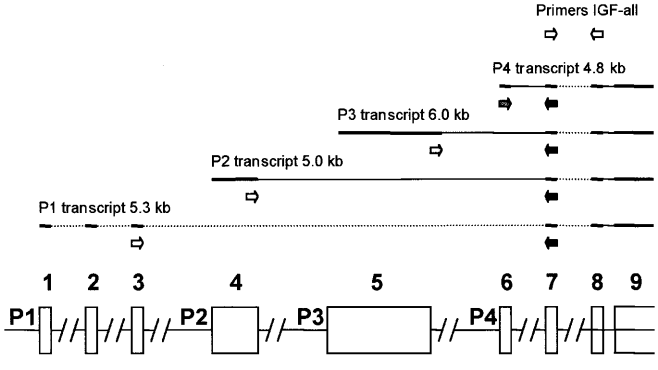


Fig. 1 Schematic structure of the *IGF2* gene with the positions of the primers

Results and discussion

Expression of the different promoter-specific transcripts was analyzed in 11 cases of hepatoblastoma. All cases had shown elevated total *IGF2* mRNA expression in another experiment (Hartmann et al., data not shown). The P1-dependent transcript was significantly downregulated in the tumor in most of the cases, while the P2-dependent transcript showed clear upregulation versus the matching normal liver. With only two exceptions the P3-transcript was also found to be dramatically upregulated, while the analysis of the P4-dependent transcript did not reveal such consistent results. Nonetheless, a trend towards upregulation can be suggested (Table 2, Fig. 2a, b).

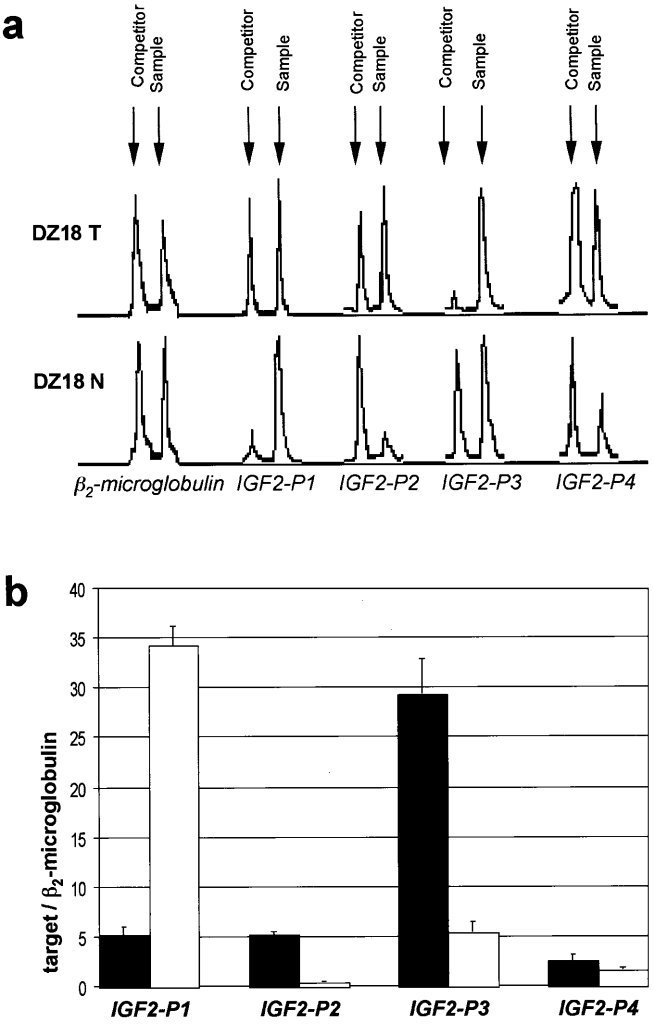


Fig. 2 **a** Graphs showing representative results of one measurement of competitive PCR in a pair of matching tumor and normal liver sample. Equal amounts of competitor RNA were present in both tissue samples of the case DZ18. **b** *Solid bars* tumor, *open bars* matching normal liver tissue, chart with results after equalization to β_2-*microglobulin*

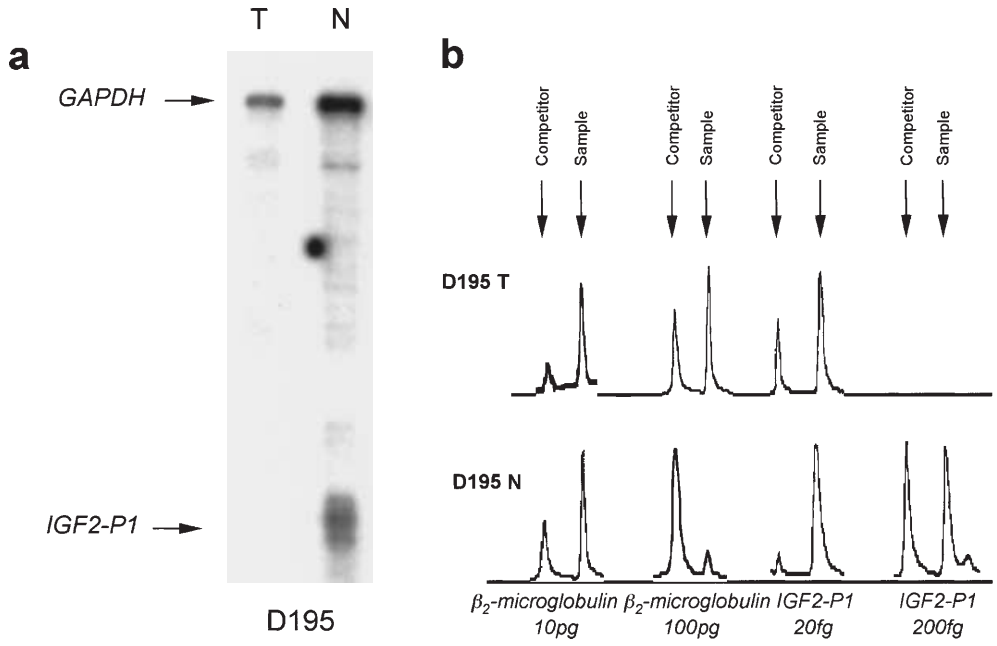


Fig. 3 **a** Ribonuclease protection assay for the *IGF2-P1* transcript and *GAPDH* as a housekeeping gene for the case D195. *IGF2-P1* RNA is not detectable in the tumor sample. **b** Graphs obtained for the case D195 with different amounts of competitors as indicated below the gene's name. The final results were calculated with the area-under-peak ratios for the following competitor concentrations: β_2-*microglobulin*: D195 T, 100 pg; D195 N, 10 pg; *IGF2-P1* D195 T, 20 fg; D195 N: 200 fg

Table 2 Eleven cases of hepatoblastoma, clinical data and the results of the expression study for each of the four transcripts. Expression of the promoter-specific transcripts relative to β_2-microglobulin and the standard deviation (SD) is indicated for tumor and matching normal liver tissue. In addition, the ratio (expression tumor/expression in the corresponding liver) is calculated

Sample	Age (months/ sex)	Histology	IGF2-P1			IGF2-P2		
			Tumor (±SD)	RATIO	Liver (±SD)	Tumor (±SD)	RATIO	Liver (±SD)
D269	9/F	mixed	4.10 (±4.18)	0.13	32.00 (±3.34)	12.78 (±1.06)	32.43	0.39 (±0.01)
D272	12/M	mixed	1.15 (±0.64)	0.45	2.59 (±0.23)	1.80 (±0.12)	80.40	0.02 (±0.01)
D266	8/F	mixed	3.71 (±3.82)	0.01	52.39 (±8.02)	7.00 (±0.32)	6.66	1.05 (±0.05)
D263	12/M	epithelial	7.08 (±4.14)	–	0.00	12.04 (±1.59)	34.98	0.34 (±0.09)
D166	48/M	epithelial multifocal	0.00	–	23.97 (±12.11)	13.82 (±0.21)	208.32	0.07 (±0.01)
D23II	22/M	epithelial	0.13 (±0.13)	0.01	13.52 (±2.63)	0.22 (±0.02)	1.34	0.16 (±0.06)
D195	19/M	epithelial	0.51 (±0.18)	0.03	17.77 (±1.21)	0.19 (±0.01)	1.71	0.11 (±0.002)
D197	54/M	epithelial	5.44 (±2.26)	0.09	60.31 (±32.37)	0.21 (±0.02)	31.02	0.01 (±0.002)
DZ18	6/M	epithelial	5.22 (±0.79)	0.15	34.23 (±1.87)	5.25 (±0.29)	10.35	0.51 (±0.03)
M12	13/M	epithelial	0.74 (±0.13)	0.04	20.23 (±13.62)	6.07 (±0.29)	8.31	0.73 (±0.11)
M14	20/M	epithelial	1.59 (±0.26)	1.61	0.98 (±1.06)	4.83 (±0.55)	22.01	0.22 (±0.02)
Sample			IGF2-P3			IGF2-P4		
			Tumor (±SD)	RATIO	Liver (±SD)	Tumor (±SD)	RATIO	Liver (±SD)
D269			80.67 (±10.83)	11.48	7.02 (±1.71)	5.22 (±0.57)	4.05	1.29 (±0.39)
D272			5.47 (±1.67)	15.43	0.35 (±0.06)	1.48 (±0.14)	14.04	0.11 (±0.01)
D266			52.62 (±3.53)	10.05	5.24 (±0.62)	3.67 (±0.20)	0.59	6.23 (±0.06)
D263			32.09 (±1.74)	3.82	8.40 (±0.59)	1.72 (±0.25)	3.20	0.54 (±0.10)
D166			104.30 (±39.40)	44.01	2.37 (±1.00)	9.52 (±1.14)	104.97	0.09 (±0.01)
D23II			4.16 (±0.76)	0.68	6.13 (±2.38)	2.07 (±0.02)	2.32	0.89 (±0.17)
D195			0.88 (±0.47)	0.36	2.47 (±0.79)	0.06 (±0.01)	0.15	0.38 (±0.06)
D197			3.16 (±0.34)	7.02	0.45 (±0.07)	0.36 (±0.13)	0.58	0.62 (±0.12)
DZ18			29.32 (±3.54)	5.40	5.43 (±1.09)	2.60 (±0.64)	1.54	1.69 (±0.22)
M12			7.55 (±1.62)	2.22	3.39 (±0.63)	1.75 (±0.28)	3.23	0.54 (±0.03)
M14			3.83 (±0.84)	1.45	2.64 (±0.50)	0.53 (±0.02)	1.32	0.40 (±0.06)

The upregulation of *IGF2-P3* must be considered as the quantitatively most important one regarding the concentration of the competitor applied. The highest relative level of tumor-specific activation was found for the P2 promoter. The P1 promoter which physiologically takes over control of *IGF2* transcription with increasing age shows clearly lower activity in the tumors than in the corresponding livers. So far, the data found here fit very well with data published before [4]. However, to our knowledge, this was the first time that P1-derived tran-

scripts could be detected and quantitatively analyzed in hepatoblastoma. In order to demonstrate this superior sensitivity of our assay we performed an RPA for the P1-specific transcript and *GAPDH* as a housekeeping gene in 5 of our cases as described before [1]. Indeed, *IGF2-P1*-transcript was not detectable in any of the tumor cases by RPA, while the corresponding liver showed clear expression (Figure 3).

In a further step beyond the protocol presented here, promoter-specific transcription could be compared to the levels of total *IGF2* transcripts that can be measured by amplification of a region present in all transcripts (Fig. 1, Table 1).

The competitive RT-PCR assay for the analysis of promoter-specific *IGF2*-expression has marked advantages. Only very small amounts of tissue material are required for analysis: the necessary amount of total RNA is approximately 100 times lower than the amounts required for Northern blotting or RPA. Therefore, cytological samples can also be analyzed, and studies of tumor heterogeneity with microdissected material can be approached. In addition, this method allows the simultaneous quantification of several other mRNA species as different competitors can be added before RT. The efficiency of RT is controlled since the competitors are reverse transcribed together with the RNA samples to be analyzed. This cannot be achieved by the use of cDNA standards employed in other approaches. RNA input in the RT reaction and RNA integrity are controlled by the simultaneous analysis of a housekeeping gene. Contamination derived from residual genomic DNA cannot affect the expression data because the amplicons span introns.

Our method takes into account the problem of larger deviations from the titration point or of major differences in the expression profile of specific genes in tumors and matching normal tissues by establishing optimal titration steps. It allows a rather precise idea of the absolute amount of RNA transcripts present in a sample, since it includes the addition of a preevaluated amount of exogenous competitor. Clearly, this permits exact comparability between expression levels of different samples. This feature is not provided by real-time PCR assays which give good information about cycling kinetics, but which do not allow the incorporation of preevaluated amounts of RNA standards [2]. Fluorescence labeling and sequencer-based analysis replace probe production and exposure of gels to PhosphorImager screens and thus the analyst is not exposed to isotopes.

In conclusion, our results are in good agreement with data produced by other methods for the analysis of RNA expression, but obviously our protocol is more sensitive and more comfortable. The design of this competitive RT-PCR assay allows sensitive, reliable, and fast screening of large panels of tumors or other tissues for dysregulated *IGF2* transcription.

Acknowledgements This work was supported by the Deutsche Forschungsgemeinschaft (grant Pi 191/9–1). We would like to thank T. Eriksson for excellent technical assistance and U. Klatt for photographic work.

References

1. Ekström TJ, Cui H, Li X, Ohlsson R (1995) Promoter-specific IGF2 imprinting status and its plasticity during human liver development. Development 121: 309–316
2. Freeman WM, Walker SJ, Vrana KE (1999) Quantitative RT-PCR: pitfalls and potentials. Biotechniques 26: 112–125
3. Koch A, Tonn J, Kraus JA, Sorensen N, Albrecht NS, Wiestler OD, Pietsch T (1996) Molecular analysis of the lissencephaly gene 1 (LIS-1) in medulloblastomas. Neuropathol Appl Neurobiol 22: 233–242
4. Li X, Adam G, Cui H, Sandstedt B, Ohlsson R, Ekström TJ (1995) Expression, promoter usage and parental imprinting status of insulin-like growth factor II in human hepatoblastoma: uncoupling of IGF2 and H19 imprinting. Oncogene 11: 221–229
5. Li X, Cui H, Sandstedt B, Norlinder H, Larsson E, Ekström TJ (1996) Expression levels of the insulin-like growth factor-II gene (IGF2) in the human liver: developmental relationships of the four promoters. J Endocrinol 149: 117–124
6. McCann AH, Miller NA, O'Meara A, Pedersen I, Keogh K, Gorey T, Dervan PA (1996) Biallelic expression of the IGF2 gene in human breast disease. Hum Mol Genet 5:1123–1127
7. Toretsky JA, Helman LJ (1996) Involvement of IGF-II in human cancer. J Endocrinol 149: 367–372
8. van Dijk MA, van Schaik FMA, Bootsma HJ, Holthuizen P, Sussenbach JS (1991) Initial characterization of the four promoters of the human insulin-like growth factor II gene. Mol Cell Endocrinol 81: 81–94
9. Vu TH, Hoffman AR (1994) Promoter-specific imprinting of the human insulin-like growth factor-II gene. Nature 371: 714–717
10. Vu TH, Hoffman AR (1996) Alterations in the promoter-specific imprinting of the insulin-like growth factor-II gene in Wilms' tumor. J Biol Chem 271: 9014–9023
11. Waha A, Watzka M, Koch A, Pietsch T, Przkora R, Peters N, Wiestler OD, von Deimling A (1998) A rapid and sensitive protocol for competitive reverse transcriptase PCR analysis of cellular genes. Brain Pathol 8: 13–18
12. Zimmermann K, Mannhalter JW (1996) Technical aspects of quantitative competitive PCR. Biotechniques 21: 268–272

Virchows Arch (2001) 439:808–817
DOI 10.1007/s004280100454

ORIGINAL ARTICLE

**Kuniaki Nakanishi · Fumiko Tajima · Hiroshi Itoh
Yasuko Nakata · Hiroshi Osada · Norio Hama
Osamu Nakagawa · Kazuwa Nakao · Toshiaki Kawai
Kunio Takishima · Takashi Aurues · Tomosumi Ikeda**

Changes in atrial natriuretic peptide and brain natriuretic peptide associated with hypobaric hypoxia-induced pulmonary hypertension in rats

Received: 8 November 2000 / Accepted: 5 March 2001 / Published online: 12 May 2001
© Springer-Verlag 2001

Abstract Experimental pulmonary hypertension induced in a hypobaric hypoxic environment (HHE) is characterized by structural remodeling of the heart and pulmonary arteries. Atrial natriuretic peptide (ANP) and brain natriuretic peptide (BNP) both have diuretic, natriuretic, and hypotensive effects, and both are involved in cardiovascular homeostasis as cardiac hormones. To study the effects of HHE on the natriuretic peptide synthesis system, 170 male Wistar rats were housed in a chamber at the equivalent of the 5500-m altitude level for 1–12 weeks. After 1 week of HHE, pulmonary arterial pressure was significantly raised, and the ratio of left ventricle plus septum over right ventricle of the heart showed a significant decrease (compared with those of ground-level control rats). In both ventricular tissues, the expression of ANP messenger (m)RNA and BNP mRNA increased after exposure to HHE. The amounts of ANP and BNP had decreased significantly in right atrial tissue at 12 weeks of HHE (compared with those of the controls), whereas in ventricular tissues at the same time point, both levels had increased significantly. In in situ hybridization and immunohistochemical studies, the staining of the mRNAs for ANP and BNP and of ANP and BNP themselves was more intense in both ventricular tissues after exposure to HHE than before (i.e., in the controls). The results suggest that, in response to HHE, the changes in ventricular synthesis are similar for ANP and BNP. These changes may play a role in modulating pulmonary hypertension in HHE. However, under our conditions, pulmonary hypertension increased progressively throughout the HHE period.

Keywords Natriuretic peptide · Pulmonary hypertension · Hypoxia

K. Nakanishi (✉) · T. Aurues · T. Ikeda
Division of Environmental Medicine,
National Defense Medical College Research Institute,
Tokorozawa 359-8513, Japan
e-mail: nknsknak@res.ndmc.ac.jp
Tel.: +81-429-951626, Fax: +81-429-911612

F. Tajima · Y. Nakata · H. Osada
Biochemical Division, Aeromedical Laboratory,
Japan Air Self-Defense Force, Tachikawa 190-0003, Japan

H. Itoh · N. Hama · O. Nakagawa · K. Nakao
Department of Medicine and Clinical Science,
Kyoto University Graduate School of Medicine,
Kyoto 606-8507, Japan

T. Kawai
Department of Pathology, National Defense Medical College,
Tokorozawa 359-8513, Japan

K. Takishima
Department of Biochemistry, National Defense Medical College,
Tokorozawa 359-8513, Japan

Introduction

High altitude hypoxia is known to cause pulmonary hypertension in both humans and animals [8, 21, 25, 28, 35]. This hypobaric hypoxia-induced pulmonary hypertension has been shown to be accompanied by such structural remodeling of the heart and pulmonary arteries as right ventricular hypertrophy, hypertrophy of muscular pulmonary arteries, and muscularization of partially muscular and nonmuscular pulmonary arteries [21, 25, 28, 35)]. Over the last decade or so, there have been many studies dealing with the changes in cardiovascular hormones that occur in people with high altitude disease [4, 19] and in animals exposed to acute [1, 3, 45] or chronic hypoxia [9, 14, 17, 20, 32, 33, 38]. Several investigators [1, 3, 9, 13, 17, 20, 32, 33, 38, 45] have reported alterations in atrial natriuretic peptide (ANP) and brain natriuretic peptide (BNP) in the plasma and cardiac tissues of animals exposed to hypoxia, and these peptides may play a role in the pathophysiology of hypoxia-induced pulmonary hypertension.

ANP was originally isolated from the mammalian heart, and it plays an important role in body fluid ho-

meostasis and blood pressure control by virtue of its diuretic, natriuretic, and vasodilator activity [15, 16, 30, 42]. BNP, a second natriuretic peptide, was originally isolated from the porcine brain, and it has been reported to elicit pharmacological effects similar to those of ANP [11, 12, 23, 36, 40]. A close relationship has been revealed between increased plasma levels of these two peptides and increased degrees of overload in patients with congestive heart failure [43, 46]. In the present study, in order better to understand the effects of long-term exposure to a hypobaric hypoxic environment (HHE) on natriuretic peptides, such as ANP and BNP, rats were housed in a mechanical chamber at the equivalent of an altitude of 5500 m for 12 weeks, a period longer than those studied in previously reported chronic hypoxia experiments. We measured pulmonary arterial pressure and the expressions of ANP and BNP messenger (m)RNAs in cardiac tissues and the concentrations of ANP and BNP themselves in plasma and cardiac tissues, and we examined the possible causes of the morphologic changes occurring in cardiac tissues using in situ hybridization and immunohistochemical methods.

Materials and methods

One hundred and seventy male Wistar rats, approximately 8 weeks old and weighing 210–240 g, were divided into six groups of 15–87 rats each, and then housed in a hypobaric chamber. This mechanical chamber was maintained at a simulated altitude of 5500 m (380 mmHg=50.6 kPa) as previously described [24, 25, 26, 27, 28, 29]. The chamber, measuring 5.6×3.0×3.0 m, was composed of two rooms: a main room as the animals' living area and an accessory room for the insulation and preparation of animals in HHE. The partial pressure of oxygen in the main room was maintained constant at a fractional inspired oxygen (F_IO_2) of 0.105 (to mimic the 5500-m level). The age of the rats at the initiation of HHE was chosen so that all rats were approximately 20 weeks old at the termination of the experiment. All rats were given commercial chow and tap water ad libitum. An additional 15 rats kept in the ground level environment served as controls. This experimental study was carried out in accordance with the recommendations in the Guide for the Care and Use of Laboratory Animals of the National Institutes of Health. The protocol was approved by the Committee on the Ethics of Animal Experiments in the Aeromedical Laboratory, Japan Air Self-Defense Force.

Measurement of pulmonary arterial pressure

At 1, 2, 4, 6, 8, and 12 weeks of HHE, five rats in each group (except in the group at 12 weeks of HHE for which n=1) were subjected to measurement of mean pulmonary arterial pressure (PAPm) under anesthesia produced by an intramuscular injection of ketamine hydrochloride (60 mg/kg body weight) as previously described [25, 28]. First, a polyethylene catheter [0.28 mm inside diameter (ID) and 0.61 mm outside diameter (OD)] was inserted into the right jugular vein. Then, while pressure was monitored, the catheter was advanced to the pulmonary artery through the right ventricle. PAPm was recorded after the rats had recovered from the anesthesia.

Blood sampling and autopsy

Before autopsy, the rats were decapitated, and blood samples were taken from rats not subjected to PAPm measurement for the determination of hematocrit and natriuretic peptides. The blood samples were placed in chilled tubes containing ethylenediaminetetraacetic acid (EDTA; 2 mg/ml) and aprotinin (10^6 IU/ml; Peptide Institute, Osaka, Japan), and then centrifuged [2, 7, 31]. The plasma was frozen immediately and stored at –80°C until the assay.

At autopsy, the heart was removed and dissected on ice into bilateral atrial and ventricular tissues. The apical half of the ventricular tissue was used as the ventricular sample so as to prevent atrial contamination [2, 31]. Tissues were weighed, frozen in liquid nitrogen, and stored at –80°C until use. The cardiac tissues so obtained were subjected to RNA and peptide extractions. Then, the ratio of left ventricle plus septum over right ventricle (LV+S/RV) was calculated for the assessment of right ventricular hypertrophy. The cardiac tissues from the remaining four rats in each group (one rat in the group at 12 weeks of HHE) were fixed with periodate–lysine–paraformaldehyde (PLP) solution for in situ hybridization and immunohistochemistry.

Total RNA extraction and Northern-blot analysis

The expression of ANP and BNP mRNAs in cardiac tissues from three rats of each group was examined using the Northern-blotting method [28]. The total RNA in the cardiac tissues was isolated using acid guanidinium isothiocyanate–phenol–chloroform extraction and ethanol precipitation [6]. Following extraction, 20 µg of total RNA was electrophoresed on a 1.5% agarose gel containing 8% formaldehyde. The electrophoresed RNA was transferred onto a nylon membrane using capillary action. The rat ANP and BNP complimentary (c)DNAs used as probes encoded 368 bp and 386 bp, respectively [33, 34, 35]. After hybridization with 20 ng/ml biotin-labeled DNA probes in 50% (vol/vol) deionized formamide, 5× Denhardt's solution, 1% (vol/vol) sodium dodecyl sulfate (SDS), 5× standard saline citrate (SSC, 1× SSC, NaCl 150 mM, Na citrate 15 mM), and 0.1 mg/ml salmon sperm DNA for 16 h at 42°C, the membrane was washed three times in 1× SSC with 0.1% SDS for 20 min each time at 42°C. The blot was detected using immunoluminescence and then exposed to X-ray film at room temperature for 2 h.

Extraction of tissues and determination of ANP and BNP

Tissue samples were boiled for 10 min in ten volumes of 0.1 M acetic acid containing 0.1% Triton X-100 to avoid intrinsic proteolysis and then homogenized using a polytron homogenizer (Kinematica AG, Lucerne, Switzerland). The homogenate was centrifuged at 15000×g for 30 min at 4°C, and the supernatant was stored at –80°C until the radioimmunoassay (RIA). The concentrations of ANP and BNP were measured using their respective RIAs [7]. The minimum detection limits for ANP and BNP concentrations were 40 pg/ml and 16 fmol/ml, respectively.

Measurement of the plasma levels of ANP and BNP

The plasma concentrations of ANP and BNP were measured in 50 µl and 100 µl rat plasma using the RIAs described above.

In situ hybridization

In situ hybridization was performed essentially as previously described [26, 27, 28]. Briefly, sections from four rats (one rat in the group at 12 weeks of HHE) were treated with 0.2 N HCl for 20 min. Next, they were incubated first in 2× SSC for 10 min at 37°C and then in 1 µg/ml proteinase K for 10 min at 37°C. Sections were subsequently post-fixed in 4% paraformaldehyde for 5 min and then incubated in 0.1 mol/l triethanolamine buffer, pH 8.0, containing 0.25% (vol/vol) acetic anhydride for 10 min to prevent nonspecific binding due to oxidation of the tissue. Hybridization was carried out overnight at 42°C in 50% (vol/vol) deion-

ized formamide, 5× Denhardt's solution, 5% (wt/vol) dextran sulfate, 2× SSC, 0.3 mg/ml salmon sperm DNA, 5 mM EDTA, and 10 ng/ml digoxigenin-labeled probe. After performing a final stringency wash at 55°C for 20 min, hybridization was detected immunologically (Genpoint: Dako, Glostrup, Denmark). The rat ANP cDNA was inserted as 368 bp within the *Hin*cII site of pGEM3Zf(+/–), and the rat BNP cDNA was inserted as 386 bp within the *Pst*I site of pSPT18 (Boehringer Mannheim, Mannheim, Germany). The antisense digoxigenin-labeled probe was 368 bp of rat ANP cDNA or 386 bp of rat BNP cDNA under an SP6 or T7 promoter, respectively, and the corresponding sense probe was under a T7 or SP6 promoter, respectively (procedures carried out using an RNA labeling kit: Boehringer Mannheim). For the negative control, the sense probe was used.

Immunohistochemistry

The indirect immunoperoxidase method was applied to PLP-fixed, 4-µm-thick frozen sections [7]. The antibodies used were: primary rabbit polyclonal antibodies against α-ANP 1–28 (human) and BNP-32 (rat; Peninsula Laboratories, Inc., Belmont, Calif.) diluted at 1:200, and horseradish peroxidase-labeled secondary antibody against rabbit immunoglobulins (Chemicon International, Temecula, Calif.) diluted at 1:250. For the negative control, the incubation step with the primary antibody was omitted.

Statistical analysis

The results are expressed as mean±SEM. Fisher's PLSD (protected least significant difference) test was applied to the data when significant *F* ratios were obtained in an analysis of variance (ANOVA). Differences were considered significant at $P<0.05$.

Results

Animal growth

Rats exposed to the equivalent of the 5500-m level showed a significant decrease in body weight by comparison with ground-level rats with no hypobaric exposure (control rats; $P<0.05$, Table 1). In the period after 4 weeks of exposure to HHE, 80 of the 87 rats scheduled for a 12-week exposure to HHE became weak and died.

Pulmonary hypertension

After one or more weeks of exposure to HHE, the PAPm of HHE rats was significantly higher than in control rats ($P<0.05$, Table 1).

Hematocrit

The hematocrit of HHE rats was increased after one or more weeks of exposure to HHE by comparison with the values for control rats ($P<0.05$, Table 1). The values stabilized after 4–6 weeks of exposure to HHE.

Cardioventricular measurements

The ratio of LV+S over RV (LV+S/RV) was significantly lower for HHE rats than for control rats ($P<0.05$,

Table 1 Body weight, mean pulmonary arterial pressure (PAPm), cardioventricular measurements, and plasma levels of atrial natriuretic peptide (ANP) in rats exposed to a hypobaric hypoxic environment (HHE). *RV* right ventricle, *LV* left ventricle, *BW* body weight, *LV+S* left ventricle with septum, *RV/BW* ratio of RV over BW, *LV/BW* ratio of LV over BW, *LV+S/RV* ratio of LV+S over RV, n.a. not available

	Hypobaric period (weeks)						
	0[a]	1	2	4	6	8	12
Body weight (g; *n*=7–10)	419±7	*P*<0.05[c] 379±10	*P*<0.05[c] 371±7	*P*<0.05[c] 341±6	*P*<0.05[c] 325±11	*P*<0.05[c] 318±11	*P*<0.05[c] 278±8
PAPm (mmHg; *n*=5[b])	12.6±0.4	*P*<0.05[c] 21.9±1.3	*P*<0.05[c] 26.3±0.8	*P*<0.05[c] 30.3±3.0	*P*<0.05[c] 29.0±1.7	*P*<0.05[c] 38.5±2.7	43.7
Hematocrit (%; *n*=7–10)	42.2±0.8	*P*<0.05[c] 53.5±1.0	*P*<0.05[c] 60.9±1.0	*P*<0.05[c] 68.6±1.3	*P*<0.05[c] 73.4±2.2	*P*<0.05[c] 73.0±1.8	*P*<0.05[c] 69.0±3.6
Cardioventricular measurements							
RV/BW (%; *n*=5)	0.049±0.001	*P*<0.05[c] 0.066±0.002	*P*<0.05[c] 0.077±0.004	*P*<0.05[c] 0.104±0.005	*P*<0.05[c] 0.122±0.006	*P*<0.05[c] 0.124±0.003	*P*<0.05[c] 0.153±0.008
LV+S/BW (%; *n*=5)	0.140±0.002	0.140±0.006	0.144±0.005	0.165±0.008	*P*<0.05[c] 0.172±0.019	*P*<0.05[c] 0.168±0.006	*P*<0.05[c] 0.221±0.007
LV+S/RV (*n*=5)	4.1±0.1	*P*<0.05[c] 3.2±0.1	*P*<0.05[c] 2.8±0.1	*P*<0.05[c] 2.4±0.1	*P*<0.05[c] 2.3±0.2	*P*<0.05[c] 2.1±0.1	*P*<0.05[c] 2.2±0.1
Plasma[d]							
ANP (pg/ml; *n*=4–7)	180.0±29.8	82.7±12.9	111.1±13.9	232.4±48.7	113.3±21.7	186.0±44.7	n.a.

[a] Ground-level rats with no hypobaric exposure (controls)
[b] Five rats in each group, except for 12 week HHE treatment (where *n*=1)
[c] $P<0.05$ vs control rats
[d] If plasma concentration of ANP was under the minimum detectable level (40 pg/ml) in a given rat, a value of 40 pg/ml was used for the calculation of mean±SEM

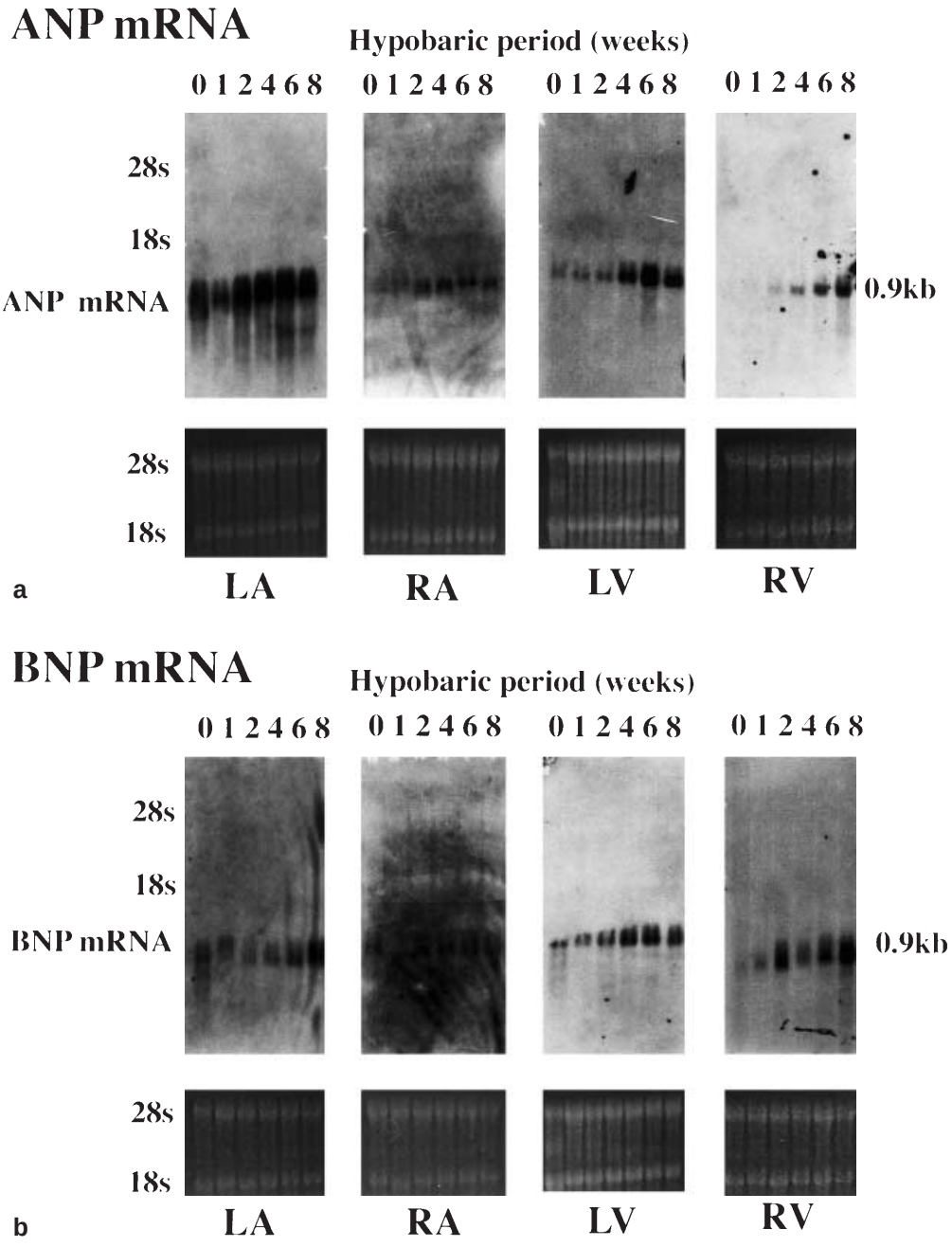


Fig. 1 Northern-blot analysis of atrial natriuretic peptide (ANP) messenger (m)RNA (**a**) and brain natriuretic peptide (BNP) mRNA (**b**) from cardiac tissues of rats exposed to a hypobaric hypoxic environment. The signals for ANP mRNA and BNP mRNA were identified at 0.9 kb

Table 1), indicating right ventricular hypertrophy. The LV+S/RV values stabilized after 4 weeks of exposure to HHE. By comparison with the values in control rats: (1) the ratio of LV+S over body weight (BW) was significantly raised after 6 weeks or more of exposure to HHE, and (2) RV/BW was significantly raised after 1 week or more of exposure to HHE.

Expression of ANP and BNP mRNAs in cardiac tissues

ANP and BNP mRNAs in the cardiac tissues of control rats were each present on the gel as one band of 0.9 kb (Fig. 1a, b). ANP mRNA was markedly induced in the ventricular tissues of HHE rats, especially after 6 weeks or more (right ventricle) or 4 weeks or more (left ventricle) of exposure to HHE. BNP mRNA was also markedly induced in the right and left ventricular tissues of HHE rats, especially after 2 weeks or more of exposure to HHE. However, ANP and BNP mRNAs were not changed in either the right or left atrial tissues of HHE rats.

The concentrations of ANP and BNP in cardiac tissues

In right atrial tissue from 4 weeks to 12 weeks and in left atrial tissue at 12 weeks of HHE, ANP levels were sig-

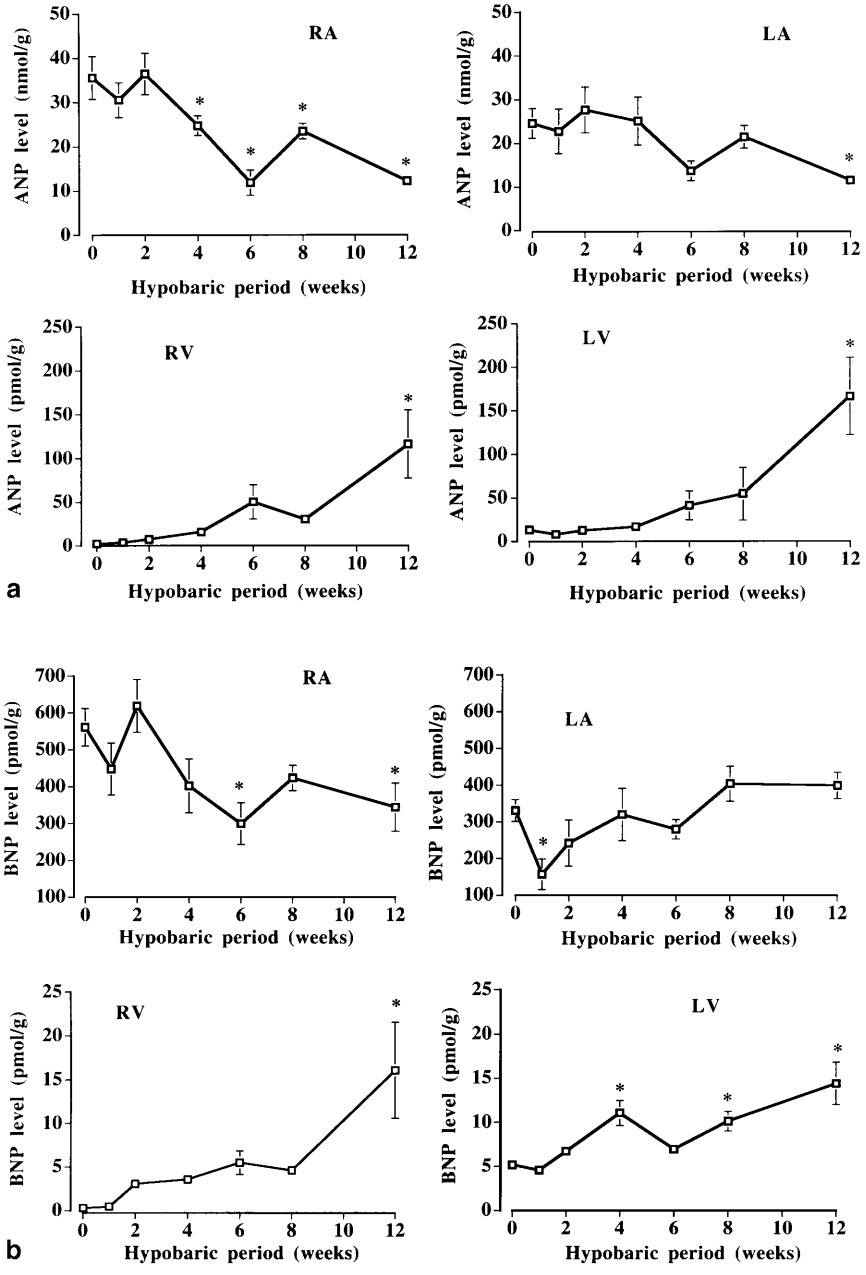


Fig. 2 Concentrations of atrial natriuretic peptide (ANP; **a**) and brain natriuretic peptide (BNP; **b**) in the cardiac tissues of rats exposed to a hypobaric hypoxic environment

nificantly lower than in control rats ($P<0.05$, Fig. 2a). In contrast, ANP levels in right and left ventricular tissues were significantly higher than in control rats, although only at 12 weeks of exposure to HHE ($P<0.05$).

In right atrial tissue at 6 weeks and 12 weeks and in left atrial tissue at 1 week of HHE, BNP levels were significantly lower than in control rats (Fig. 2b). In contrast, BNP levels in ventricular tissues were significantly higher than in control rats at 12 weeks (right ventricle) or at 4, 8, and 12 weeks (left ventricle) of HHE ($P<0.05$).

Plasma levels of ANP and BNP

The plasma levels of ANP in HHE rats were unchanged by comparison with those of control rats (Table 1). The plasma levels of BNP were minimal (<16 fmol/ml) in all rats.

In situ hybridization and immunohistochemistry

In control rats, tissues from both atria were stained strongly positive for the mRNAs for ANP and BNP and for ANP and BNP themselves, whereas in tissues from the two ventricles, such staining was barely detectable

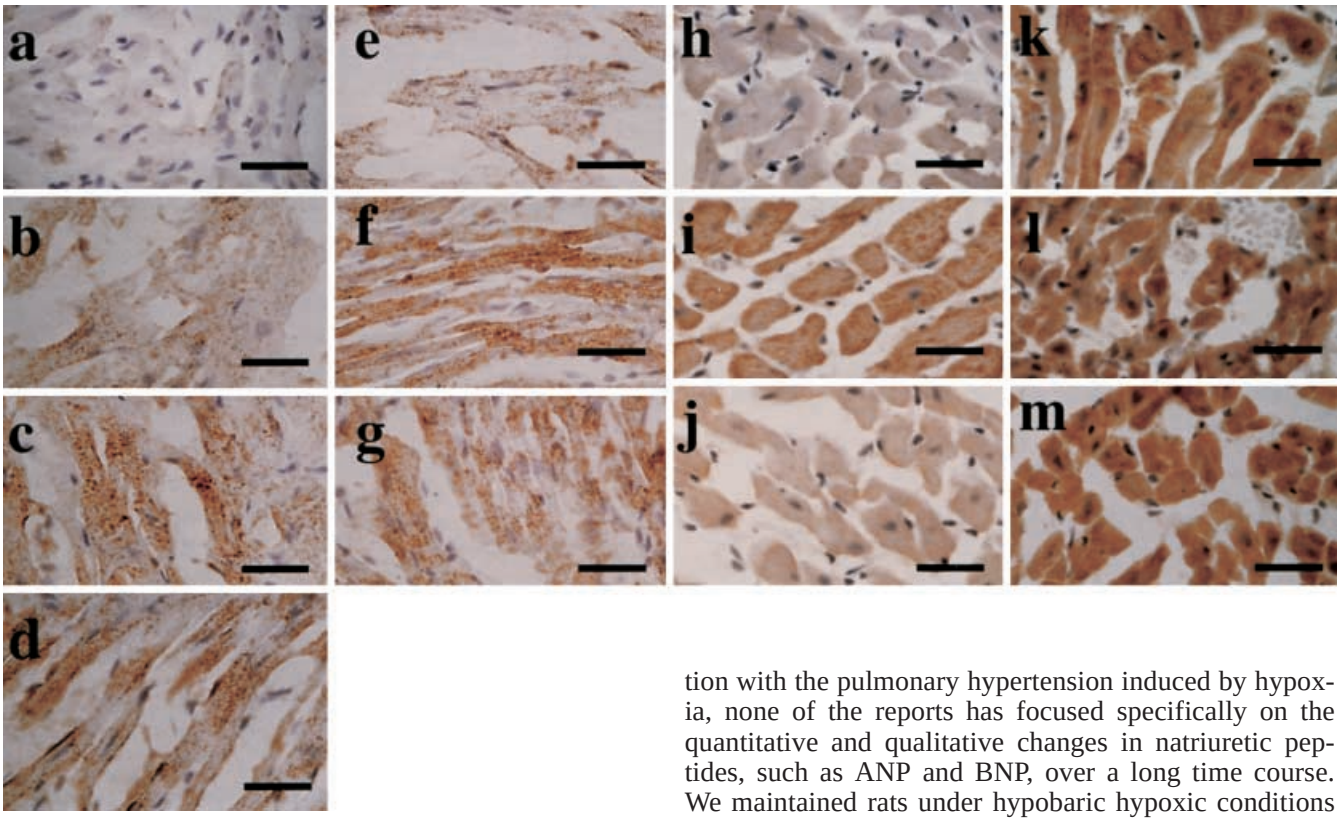


Fig. 3 Localization of messenger (m)RNA for atrial natriuretic peptide (ANP) and of ANP itself in the cardiac tissues of rats exposed to a hypobaric hypoxic environment (HHE). Hybridization with an ANP mRNA sense probe (**a**) revealed weak levels of background grains in all preparations. In control rats, hybridization with the ANP mRNA antisense probe (**b**) revealed little ANP mRNA in right ventricular tissues. Following a 12-week exposure to HHE (**c**), ANP mRNA was abundant in right ventricular tissues. Following an 8-week exposure to HHE (**d**), ANP mRNA was abundant in left ventricular tissues, but it was present in only small amounts in left ventricular tissues in control rats (**e**). In control rats, ANP mRNA was abundant in right atrial (**f**) and left atrial (**g**) tissues. In control rats (**h**), ANP was barely detectable in right ventricular tissues. Following a 6-week exposure to HHE (**i**), ANP was abundant in right ventricular tissues. In control rats (**j**), ANP was barely detectable in left ventricular tissues. Following an 8-week exposure to HHE (**k**), ANP was abundant in left ventricular tissues. In control rats, ANP was abundant in right (**l**) and left (**m**) atrial tissues. *Scale bars* 100 µm

(Fig. 3 and Fig. 4). The staining for both of the mRNAs and for the two peptides was observed as granules in the cytoplasm of myocardial cells. In tissues from both ventricles, the staining for both of the mRNAs and for ANP and BNP was more intense after exposure to HHE than in the controls. In contrast, in tissues from both atria, the staining for both of the mRNAs and for ANP and BNP remained unchanged throughout the exposure to HHE.

Discussion

Although there have been several studies of the alterations in natriuretic peptides that occur in rats in association with the pulmonary hypertension induced by hypoxia, none of the reports has focused specifically on the quantitative and qualitative changes in natriuretic peptides, such as ANP and BNP, over a long time course. We maintained rats under hypobaric hypoxic conditions for 12 weeks, a period longer than those used in previously reported chronic hypoxic experiments. We examined (1) the expression levels of ANP and BNP mRNAs using Northern-blotting analysis, (2) the concentrations of ANP and BNP in cardiac tissues using a RIA, and (3) the expression levels of the two mRNAs using in situ hybridization analysis and those of the peptides using immunohistochemistry. We also measured PAPm and assessed the degree of cardiac hypertrophy. In both right and left ventricular tissues after exposure to HHE, especially at 8 weeks and 12 weeks of HHE, we observed overexpression of ANP and BNP mRNAs (using Northern-blotting analysis and in situ hybridization methods) and increases in the amounts of ANP and BNP (using RIA and immunohistochemical methods). Moreover, during HHE, the change in the expression of BNP mRNA and that in the concentration of BNP in both ventricular tissues paralleled the changes in the expression of ANP mRNA and the concentration of ANP. Therefore, these results suggest that in response to HHE, the change in the synthesis of ANP is similar to the change in the synthesis of BNP (in each ventricular tissue). Possibly, these changes may play an important role in modulating the pulmonary hypertension induced by HHE (however, see below).

ANP is secreted predominantly from atrial tissues in normal states [2, 31, 42], and its secretion is mainly regulated by atrial stretch [42]. During exposure to normobaric [33, 45] or hypobaric [9, 20] hypoxia, previous investigators have reported an increased plasma concentration of ANP. Furthermore, a decreased concentration of ANP in right atrial tissues and an increased concentra-

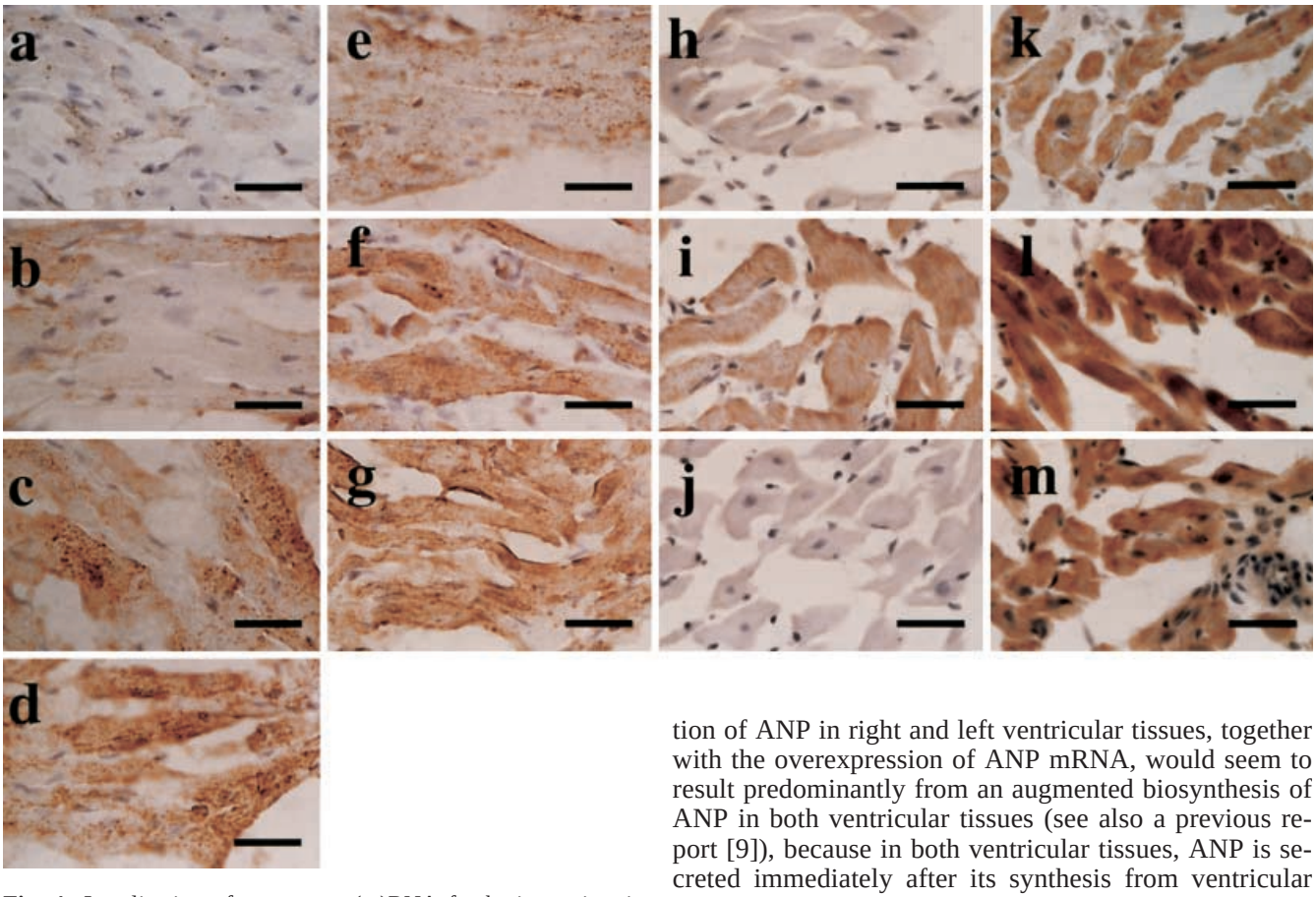


Fig. 4 Localization of messenger (m)RNA for brain natriuretic peptide (BNP) and of BNP itself in the cardiac tissues of rats exposed to a hypobaric hypoxic environment (HHE). Hybridization with a BNP mRNA sense probe (**a**) revealed weak levels of background grains in all preparations. In control rats, hybridization with the BNP mRNA antisense probe (**b**) revealed little BNP mRNA in right ventricular tissues. Following a 12-week exposure to HHE (**c**), BNP mRNA was abundant in right ventricular tissues. Following an 8-week exposure to HHE (**d**), BNP mRNA was abundant in left ventricular tissues, while BNP mRNA was present in only small amounts in left ventricular tissues in control rats (**e**). In control rats, BNP mRNA was abundant in right atrial (**f**) and left atrial (**g**) tissues. In control rats (**h**), BNP was barely detectable in right ventricular tissues. Following a 6-week exposure to HHE (**i**), BNP was abundant in right ventricular tissues. In control rats (**j**), BNP was barely detectable in left ventricular tissues. Following an 8-week exposure to HHE (**k**), BNP was abundant in left ventricular tissues. In control rats, BNP was abundant in right (**l**) and left (**m**) atrial tissues. *Scale bars* 100 μm

tion of ANP in right ventricular tissues has been reported in rats exposed to normobaric hypoxia (10% oxygen) for 3 weeks [38] or to hypobaric hypoxia (0.5 atm) for 3 weeks [20]. Further, an overexpression of ANP mRNA in both ventricular tissues was reported in rats exposed to hypobaric hypoxia (0.5 atm) for 3 weeks [9]. In our experiment, the plasma ANP concentration did not change. However, the concentration of ANP showed a decrease in both right and left atrial tissues at 12 weeks of exposure to HHE, whereas the concentrations in the right and left ventricular tissues were both increased at 12 weeks of exposure to HHE. This increased concentration of ANP in right and left ventricular tissues, together with the overexpression of ANP mRNA, would seem to result predominantly from an augmented biosynthesis of ANP in both ventricular tissues (see also a previous report [9]), because in both ventricular tissues, ANP is secreted immediately after its synthesis from ventricular cardiocytes (which have only a small capacity for storage) [2, 31]. Ogawa et al. [31] reported that the level of plasma ANP in SHR rats is determined by the synthesis and secretion of ANP from ventricular tissues. Although plasma ANP levels were not changed by HHE in our experiment, it is still possible that the plasma ANP present in rats after exposure to hypobaric hypoxia is mainly derived from its synthesis and secretion from right and left ventricular tissues.

There are several reports indicating that an attenuation of hypoxia-induced pulmonary hypertension occurs following ANP infusions [1, 13, 14, 34, 47]. Despite the increased concentration of ANP and overexpression of ANP mRNA in both ventricular tissues during HHE in our experiment, pulmonary hypertension developed rapidly and was most severe at 12 weeks of HHE, perhaps indicating that the pulmonary hypertension induced by HHE leads to a condition in which demand for ANP (with respect to its moderating effect on pulmonary hypertension) exceeds its production capacity. Moreover, 80 of the 87 rats scheduled for a 12-week exposure to HHE died before the end of the experiment. This may indicate that during the later part of the period of exposure to HHE, especially at nearly 12 weeks, the rats suffered from severe failure of both ventricles. Conceivably, if ANP and BNP had not increased, as described here, the pulmonary hypertension at a given stage would have been even worse; however, at present we have no way of knowing whether this is true.

In normal adult rats, no substantial difference in the distribution of ANP or BNP has been observed between right and left atrial tissues [20, 31]. However, Ogawa et al. reported a differential distribution of these peptides between atrial and ventricular tissues, ANP being produced mainly by the atrial tissues and BNP mainly by the ventricular tissues [10, 31]. In addition, they also found that the expression levels of the mRNAs and the concentrations of ANP and BNP were higher in the left ventricular tissues of Wistar–Kyoto rats than in the right ventricular tissues. These findings were taken to indicate that left ventricular tissue is a major source of BNP as a cardiac hormone. In the present study, the BNP concentration increased in both ventricular tissues during HHE, and the levels were roughly equal in the two ventricular tissues at 12 weeks of HHE. However, in control rats, BNP was at least ten times higher in the left ventricular tissues than in the right. Therefore, in HHE rats, substantial BNP synthesis may take place not only in the left ventricular tissues but also in the right. In addition, we found right and left ventricular hypertrophy (increase in LV+S/body weight and RV/body weight and decrease in LV+S/RV) during HHE. These findings are consistent with the hypothesis of Ogawa et al. that BNP synthesis in ventricular tissues may be accounted for in part by increased wall stress [31]. Some other findings may cast light on the possible link between the ventricular BNP concentration and the development of pulmonary hypertension and ventricular failure. Our previous study [28] revealed that mean systemic blood pressure was not changed by a 4-week exposure to HHE (0.5 atm; although ventricular end-diastolic pressure as an indicator of ventricular heart failure was not measured). Furthermore, Suarez et al. reported that during a 40-day acclimatization to a chamber-simulated altitude of 29,000 feet, all three indices of LV systolic function examined – ejection fraction, ratio of peak systolic pressure to end systolic volume and mean normalized systolic ejection rate at rest – remained constant in all seven of a group of healthy young men despite the development of pulmonary hypertension and severe hypoxemia [39]. However, in the present study, we observed that the BNP concentration in LV was increased significantly at a 4-week exposure to HHE (by comparison with control rats). On this basis, we suggest that BNP synthesis by LV may possibly be a reflection of left ventricular overload during the period before ventricular heart failure becomes overt.

A number of investigators have demonstrated that the plasma BNP level is higher in patients with heart failure than in normal control subjects, increased secretion from ventricular tissues seemingly being the major source [22, 40, 44]. One report noted an elevated plasma BNP level in rats with pulmonary hypertension induced by hypobaric hypoxia (0.5 atm for 3 weeks); however, the BNP concentration in the right atrial tissues was not affected [9]. In the present study, while the BNP concentration in the right atrial tissues was significantly decreased at 12 weeks of HHE, it was not affected in the early period (the first 4 weeks) of HHE. Our results are thus consistent with the earlier report [9], and we suggest that right atrial tissues may not play a significant role in BNP release during the first few weeks of HHE. During the later part of the period of HHE, the release of BNP from right atrial tissues may increase in proportion to the severity of the pulmonary hypertension. However, another possibility is that the explanation for the lack of a detectable rise in the atrial concentrations of ANP and BNP after a 4-week exposure to HHE may be that although it occurs, it is masked by hypertrophy and an increase in the mass of the contractile elements.

In our in situ hybridization and immunohistochemical studies in control rats, the mRNAs for ANP and BNP and the peptides themselves were strongly represented in right and left atrial tissues but barely detectable in ventricular tissues. During the 12-week exposure to HHE, the staining for the mRNAs and for the peptides remained unchanged or declined in the two atrial tissues, whereas the staining became progressively stronger in the two ventricular tissues. These findings were supported by the changes in regional ANP and BNP (both mRNA and peptide) in the two ventricular tissues that were detected using Northern-blotting analysis and RIA.

In conclusion, we have demonstrated that during a 12-week exposure to HHE, the changes in the synthesis of ANP are similar to those occurring in the synthesis of BNP (in both right and left ventricular tissues). It is possible that these changes play an important role in modulating pulmonary hypertension in HHE. However, it should be noted that in our experiment, mean pulmonary arterial pressure rose progressively throughout the 12-week period of HHE, perhaps suggesting that the levels of these peptides were insufficient to produce a major moderating effect under our conditions. Two distinct types of natriuretic peptide receptor have been identified [5, 37]. The ANP-A receptor has a ligand selectivity with a rank order of potency for cyclic guanosine monophosphate (cGMP) production that is ANP ≥ BNP >> C-type natriuretic peptide (CNP), while for the ANP-B receptor the rank order of ligand selectivity is CNP > ANP ≥ BNP [18, 41]. Further studies will be needed to identify the effects of HHE exerted via the ANP-A receptor in the cardiovascular system.

Acknowledgements The authors are indebted to S. Tominaga and M. Uenoyama for technical assistance and to Dr. R. Timms for correcting the English version of the manuscript.

References

1. Adnot S, Chabrier PE, Brun-Buisson C, Viossat I, Braquet P (1988) Atrial natriuretic factor attenuates the pulmonary pressor response to hypoxia. J Appl Physiol 65:1975–1983
2. Arai H, Nakao K, Saito Y, Morii N, Sugawara A, Yamada T, Itoh H, Shiono S, Mukoyama M, Ohkubo H, Nakanishi S, Imura H (1988) Augmented expression of atrial natriuretic polypeptide gene in ventricles of spontaneously hypertensive rats (SHR) and SHR-stroke prone. Circ Res 62:926–930

3. Baertschi AJ, Adams JM, Sullivan MP (1988) Acute hypoxemia stimulates atrial natriuretic factor secretion in vivo. Am J Physiol 255 (Heart Circ Physiol 24):H295–H300
4. Bärtsch P, Shaw S, Franciolli M, Gnädinger MP, Weidmann P (1988) Atrial natriuretic peptide in acute mountain sickness. J Appl Physiol 65:1929–1937
5. Chang M, Lowe DG, Lewis M, Hellmiss R, Chen E, Goeddel DV (1989) Differential activation by atrial and brain natriuretic peptides of two different receptor guanylate cyclases. Nature 341:68–72
6. Chomczyski P, Sacchi N (1987) Single-step method of RNA isolation by acid guanidium thiocyanate–phenol–chloroform extraction. Anal Biochem 162:156–159
7. Hama N, Itoh H, Shirakami G, Nakagawa O, Suga S, Ogawa Y, Masuda I, Nakanishi K, Yoshimasa T, Hashimoto Y, Yamaguchi M, Hori R, Yasue H, Nakao K (1995) Rapid ventricular induction of brain natriuretic peptide gene expression in experimental acute myocardial infarction. Circulation 92: 1558–1564
8. Heath D, Williams DR (1981) Man at high altitude. The pathophysiology of acclimatization and adaptation. Churchill Livingstone, Edinburgh
9. Hill NS, Klinger JR, Warburton RR, Pietras L, Wrenn DS (1994) Brain natriuretic peptide:possible role in the modulation of hypoxic pulmonary hypertension. Am J Physiol 266 (Lung Cell Mol Physiol 10):L308–L315
10. Hosoda K, Nakao K, Mukoyama M, Saito Y, Jougasaki M, Shirakami G, Suga S, Ogawa Y, Yasue H, Imura H (1991) Expression of brain natriuretic peptide gene in human heart: production in the ventricle. Hypertension 17:1152–1156
11. Itoh H, Nakao K, Yamada T, Shirakami G, Kangawa K, Minamino N, Matsuo H, Imura H (1988) Antidipsogenic action of a novel peptide, 'brain natriuretic peptide', in rats. Eur J Pharmacol 150:193–196
12. Itoh H, Nakao K, Kambayashi Y, Hosoda K, Saito Y, Yamada T, Mukoyama M, Arai H, Shirakami G, Suga S, Yoshida I, Inouye K, Imura H (1989) Occurrence of a novel cardiac natriuretic peptide in rats. Biochem Biophys Res Commun 161: 732–739
13. Jin H, Yang R, Chen Y, Jackson RM, Oparil S (1990) Atrial natriuretic peptide attenuates the development of pulmonary hypertension in rats adapted to chronic hypoxia. J Clin Invest 85:115–120
14. Jin H, Yang R, Chen Y, Jackson RM, Itoh H, Mukoyama M, Nakao K, Imura H, Oparil S (1991). Atrial natriuretic peptide in acute hypoxia-induced pulmonary hypertension in rats. J Appl Physiol 71:807–814
15. Kangawa K, Matsuo H (1984) Purification and complete amino acid sequence of α-human atrial natriuretic polypeptide (α-hANP). Biochem Biophys Res Commun 118:131–139
16. Kangawa K, Tawaragi Y, Oikawa S, Mizuno A, Sakuragawa Y, Nakazato H, Fukuda A, Minamino N, Matsuo H (1984) Identification of rat γ atrial natriuretic polypeptide and characterization of the cDNA encoding its precursor. Nature 312: 152–155
17. Klinger JR, Wrenn DR, Warburton RR, Pietras L, Ou L, Hill NS (1997) Atrial natriuretic peptide expression in rats with different pulmonary hypertensive responses to hypoxia. Am J Physiol 273 (Heart Circ Physiol 42):H411–H417
18. Koller KJ, Lowe DG, Bennett GL, Minamino N, Kangawa K, Matsuo H, Goeddel DV (1991) Selective activation of the B natriuretic peptide receptor by C-type natriuretic peptide (CNP). Science 252:120–123
19. Liu L, Cheng H, Chin W, Jin H, S. Oparil S (1989) Atrial natriuretic peptide lowers pulmonary arterial pressure in patients with high altitude disease. Am J Med Sci 298:397–401
20. Mckenzie JC, Tanaka I, Inagami T, Misono KS, Klein RM (1986) Alterations in atrial and plasma atrial natriuretic factor (ANF) content during development of hypoxia-induced pulmonary hypertension in the rat. Proc Soc Exp Biol Med 181: 459–463
21. Meyrick B, Reid L (1978). The effect of continued hypoxia on rat pulmonary arterial circulation: an ultrastructural study. Lab Invest 38:188–200
22. Mukoyama M, Nakao K, Saito Y, Ogawa Y, Hosoda K, Suga S, Shirakami G, Jougasaki M, Imura H (1990) Human brain natriuretic peptide, a novel cardiac hormone. Lancet 335: 801–802
23. Mukoyama M, Nakao K, Hosoda K, Suga S, Saito Y, Ogawa Y, Shirakami G, Jougasaki M, Obata K, Yasue H, Kambayashi Y, Inouye K, Imura H (1991) Brain natriuretic peptide (BNP) as a novel cardiac hormone in humans: evidence for an exquisite dual natriuretic peptide system, atrial natriuretic peptide and brain natriuretic peptide. J Clin Invest 87:1402–1412
24. Nakanishi K, Tajima F, Nakamura A, Yagura S, Ookawara T, Yamashita H, Suzuki K, Taniguchi N, Ohno H (1995) Effects of hypobaric hypoxia on antioxidant enzymes in rats. J Physiol 489:869–876
25. Nakanishi K, Tajima F, Osada H, Nakamura A, Yagura S, Kawai T, Suzuki M, Torikata C (1996) Pulmonary vascular responses in rats exposed to chronic hypobaric hypoxia at two different altitude levels. Pathol Res Pract 192:1–12
26. Nakanishi K, Tajima F, Nakata Y, Osada H, Sugiyama K, Maruta H, Kawai T, Suzuki M, Torikata C (1997) Hypercoagulable state in a hypobaric, hypoxic environment causes nonbacterial thrombotic endocarditis in rats. J Pathol 181:338–346
27. Nakanishi K, Tajima F, Nakata Y, Osada H, Ogata K, Kawai T, Torikata C, Suga T, Takishima K, Aurues T, Ikeda T (1998) Tissue factor is associated with the nonbacterial thrombotic endocarditis induced by a hypobaric hypoxic environment in rats. Virchows Arch 433:375–379
28. Nakanishi K, Tajima F, Nakata Y, Osada H, Tachibana S, Kawai T, Torikata C, Suga T, Takishima K, Aurues T, Ikeda T (1999) Expression of endothelin-1 in rats developing hypobaric hypoxia-induced pulmonary hypertension. Lab Invest 79: 1347–1357
29. Nakanishi, K, Tajima F, Nakata Y, Osada H, Kato T, Miyazaki H, Kawai T, Torikata C, Suga T, Takishima K, Aurues T, Ikeda T (1999) Thrombopoietin expression in normal and hypobaric hypoxia-induced thrombocytopenic rats. Lab Invest 79:679–688
30. Nakao K, Ogawa S, Suga S, Imura H (1992) Molecular biology and biochemistry of the natriuretic peptide system, I: natriuretic peptides. J Hypertension 10:907–912
31. Ogawa Y, Nakao K, Mukoyama M, Hosoda K, Shirakami G, Arai H, Saito Y, Suga S, Jougasaki M, Imura H (1991) Natriuretic peptides as cardiac hormones in normotensive and spontaneously hypertensive rats: the ventricle is a major site of synthesis and secretion of brain natriuretic peptide. Circ Res 69:491–500
32. Perhonen M, Takala TES, Vuolteenaho O, Mäntymaa P, Leppäluoto J, Ruskoaho H (1997) Induction of cardiac natriuretic peptide gene expression in rats trained in hypobaric hypoxic conditions. Am J Physiol 273 (Regulatory Integrative Comp Physiol 42):R344–R352
33. Raffestin B, Adnot S, Mercadier JJ, Levame M, Duc P, Braquet P, Viossat I, Chabrier PE (1990) Synthesis and secretion of atrial natriuretic factor during chronic hypoxia: a study in the conscious instrumented rat. Clin Sci 78:597–603
34. Raffestin B, Eddahibi LS, Braquet P, Chabrier PE, Cantin M, Adnot S (1992) Pulmonary vasodilatory action of endogenous atrial natriuretic factor in rats with hypoxic pulmonary hypertension: effects of monoclonal atrial natriuretic factor antibody. Circ Res 70:184–192
35. Reid LM (1986) Structure and function in pulmonary hypertension; new perceptions. Chest 89:279–288
36. Saito Y, Nakao K, Itoh H, Yamada T, Mukoyama M, Arai H, Hosoda K, Shirakami G, Suga S, Minamino N, Kangawa K, Matsuo H, Imura H (1989) Brain natriuretic peptide is a novel cardiac hormone. Biochem Biophys Res Commun 158:360–368

37. Schulz S, Singh S, Bellet RA, Singh G, Tubb DJ, Chin H, Garbers DL (1989) The primary structure of a plasma membrane guanylate cyclase demonstrates diversity within this new receptor family. Cell 58:1155–1162
38. Stockmann PT, Will DH, Sides SD, Brunnert SR, Wilner GD, Leahy KM, Wiegand RC, Needleman P (1988) Reversible induction of right ventricular atriopeptin synthesis in hypertrophy due to hypoxia. Circ Res 63:207–213
39. Suarez L, Alexander JK, Houston CS (1987) Enhanced left ventricular systolic performance at high altitude during Operation Everest II. Am J Cardiol 60:137–142
40. Sudoh T, Kangawa K, Minamino N, Matsuo H (1988) A new natriuretic peptide in porcine brain. Nature 332:78–81
41. Suga S, Nakao K, Hosoda K, Mukoyama M, Ogawa Y, Shirakami G, Arai H, Saito Y, Kambayashi Y, Inouye K, Imura H (1992) Receptor selectivity of natriuretic peptide family, atrial natriuretic peptide, brain natriuretic peptide, and C-type natriuretic peptide. Endocrinology 130:229–239
42. Sugawara A, Nakao K, Morii N, Sakamoto M, Suda M, Shimokura M, Kiso Y, Kihara M, Yamori Y, Nishimura K, Soneda J, Ban T, Imura H (1985) α-Human atrial natriuretic polypeptide is released from the heart and circulation in the body. Biochem Biophys Res Commun 129:439–446
43. Takahashi T, Allen PD, Izumo S (1992) Expression of A-, B-, and C-type natriuretic peptide genes in failing and developing human ventricles: correlation with expression of the Ca^{2+}-ATPase gene. Circ Res 71:9–17
44. Wei C, Heublein DM, Perrlla MA, Lerman A, Rodeheffer RJ, McGregor CGA, Edwards WD, Schaff HV, Burnett JC (1993) Natriuretic peptide system in human heart failure. Circulation 88:1004–1009
45. Winter RJD, Meleagros L, Pervez S, Jamal H, Krausz T, Polak JM, Bloom SR (1989) Atrial natriuretic peptide levels in plasma and in cardiac tissues after chronic hypoxia in rats. Clin Sci 76:95–101
46. Yoshimura M, Yasue H, Okumura K, Ogawa H, Jougasaki M, Mukoyama M, Nakao K, Imura H (1993) Different secretion patterns of atrial natriuretic peptide and brain natriuretic peptide in patients with congestive heart failure. Circulation 87:464–469
47. Zhao L, Winter RJD, Krausz T, Hughes JMB (1991) Effects of continuous infusion of atrial natriuretic peptide on the pulmonary hypertension induced by chronic hypoxia in rats. Clin Sci 81:379–385

Virchows Arch (2001) 439:818–822
DOI 10.1007/s004280100473

CASE REPORT

**M. Ebnöther · R. A. Schoenenberger
A. P. Perruchoud · M. Solèr · F. Gudat · P. Dalquen**

Severe bronchiolitis in acute *Mycoplasma pneumoniae* infection

Received: 20 December 2000 / Accepted: 12 April 2001 / Published online: 6 September 2001
© Springer-Verlag 2001

Abstract We report on a 17-year-old patient with severe bronchiolitis due to *Mycoplasma pneumoniae* infection. Despite an early 10-day course of clarithromycin, she developed progressive dyspnea, cough, fever, and severe obstructive ventilatory impairment. Sixteen days after onset of the disease a severe hemolytic anemia developed with only cold agglutinins positive at serologic screening. Thoracoscopic lung biopsy revealed diffuse bronchiolitis with suppurative intrabronchiolar inflammation, lymphohistiocytic "cuffing" of the bronchioli, and foam cell aggregates within neighboring alveoli. The infiltrate consisted mainly of $CD3^+$, $CD8^+$ lymphocytes and $CD68^+$ macrophages. The diagnosis of *Mycoplasma pneumoniae* bronchiolitis was based on repeated complement fixation tests, which turned strongly positive only at day 74 after onset of the disease. Pulmonary function improved slowly under long-term prednisone treatment.

Keywords *Mycoplasma pneumoniae* · Bronchiolitis · Inflammation · Pathogenesis · Bronchoalveolar lavage

Introduction

Mycoplasma pneumoniae (MP) infections are common. The infection provokes flue-like symptoms in most cases, but in up to 30% of the patients pulmonary and other complications may develop [24]. The pulmonary complications include pneumonia, tracheobronchitis, obliterative bronchitis, bronchiectasis, Swyer-James syndrome, pleural effusions, interstitial fibrosis, lung abscess, and exacerbation or, possibly, initiation of reactive airway disease [4, 8, 10, 15, 17, 20, 25].

MP disease is usually self-limiting. Therefore, the knowledge of the pathology of the lung lesions is based mainly on autopsy findings in rare fatal cases and on findings in animals. Histology of acute MP-induced bronchiolitis in humans has been described in less than 20 autopsies and biopsy specimens [4, 20]. We describe in detail the histological and immunohistochemical findings in a patient with MP bronchiolitis who underwent open lung biopsy because of initial clinical treatment failure and non-diagnostic serological tests.

M. Ebnöther · A.P. Perruchoud · M. Solèr
Medizinische Klinik des Kantonsspitals, Universität Basel, Switzerland

R.A. Schoenenberger
Medizinische Klinik, Bürgerspital Solothurn, Switzerland

F. Gudat · P. Dalquen (✉)
Institute of Pathology, Kantonsspital, University of Basel, 4003 Basel, Switzerland
e-mail: pdalquen@uhbs.ch
Tel.: +41-61-2652851, Fax: +41-61-2653194

Case study

Clinical history

A 17-year old girl was admitted to hospital in November 1999 with a 12-day history of fever and dry cough. Progressive dyspnea developed despite a complete 10-day course of clarithromycin (2×500 mg per day) before admission. The patient was previously healthy except for a mild macrocytic anemia of unknown origin diagnosed in 1985. She had no history of asthma, allergies, recurrent infections, toxic exposure, or recent travel. On physical examination the patient presented with fever of 39°C and markedly diminished breath sounds over the lower right lung field. Arterial blood gas examination revealed a decreased pO_2 of 7.36 kPa and a normal pCO_2 of 4.53 kPa while breathing room air. Blood tests showed a moderately decreased hemoglobin of 104 g/l with a normal reticulocyte count of 136×10^9/l, a low white blood count (1.8×10^9/l with 68% neutrophils), and a normal platelet count (205×10^9/l). Liver transaminases were slightly increased (ASAT 46 U/l, ALAT 61 U/l; normal range for both 11–41 U/l). The lactate dehydrogenase (LDH) was 588 U/l (normal range 230–430 U/l), and bilirubin was normal with 16 µ mol/l. The C-reactive protein was 50 mg/l. A chest radiograph revealed a disseminated reticulo-micronodular pattern over the whole right lung and over the lower lobe of the left lung. A computer tomograph (CT) disclosed a pattern of airspace consolidation and prominence of bronchovascular structures (1).

Bronchoalveolar lavage

Fluid recovery was 60/150 ml (40%), total cell count 1197.5×10^6/l (normal $50–300\times10^6$/l), macrophages 15%=179.6×10^6/l (50–300),



Fig. 1 High resolution computed tomographic scan of the lungs: strikingly prominent bronchovascular structures

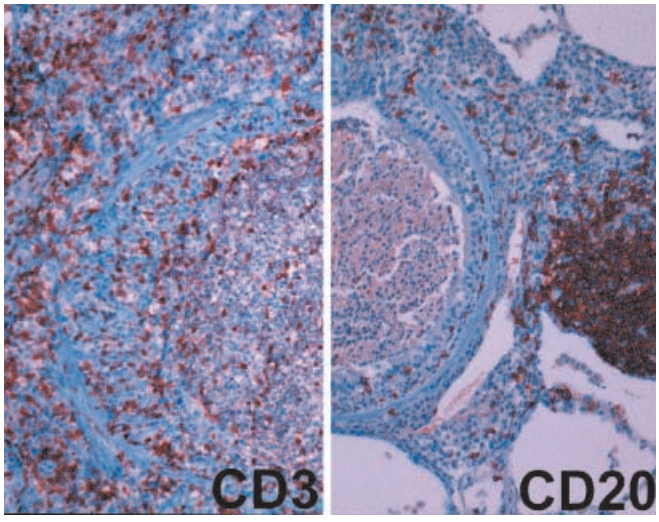
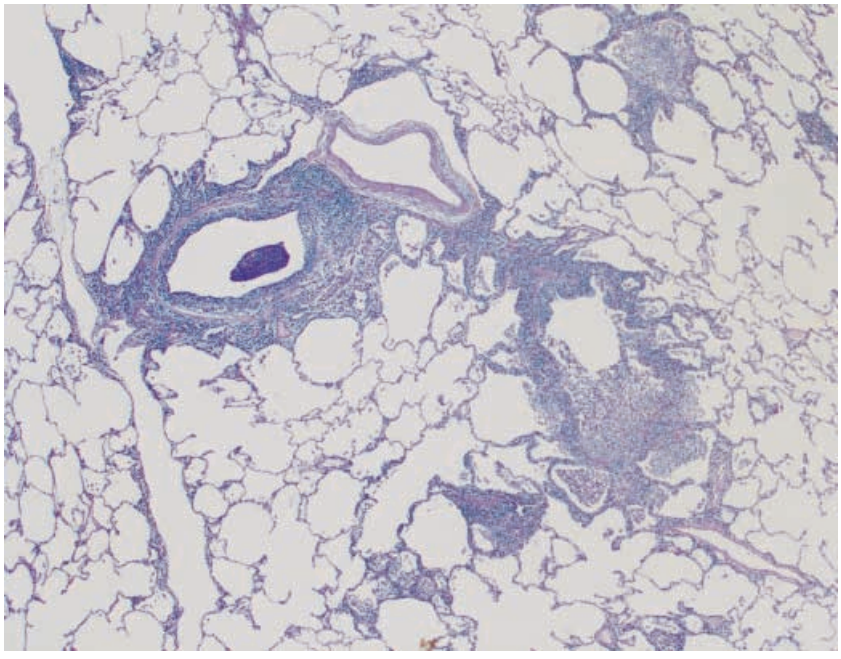


Fig. 3 Left side: Distribution of the $CD3^+$ T-lymphocytes within the bronchiolar infiltrate. Right side: Infiltration of the bronchiolar epithelium by $CD20^+$ T-lymphocytes (DAB/ Mayer's hemalaun, both 62.5 ×)

Fig. 2 Open lung biopsy: Generalized lymphohistiocytic bronchiolitis (PAS, 15×)



lymphocytes 37%=443.1×10^6/l (<10), neutrophils 48%=574×10^6/l (<10); eosinophils and mast cells were within normal limits. There was a considerable mucus admixture such that the subpopulations of lymphocytes could not be differentiated. Immunocytochemically, cytomegalovirus (CMV) infection could not be demonstrated with antibodies against early and immediate early antigen. No other opportunistic germ was detected with special stains. Pulmonary function tests revealed a predominant, non-reversible obstruction (1, day 28).

Table 1 Course of pulmonary function tests (before inhalation with β2 mimetics). *FVC* forced vital capacity, *FEV_1* forced expiratory volume in 1 s

	Predicted	Day 28	Day 74	Day 151	Day 310
FEV_1 (L)	2.64	1.10	2.06	1.87	2.14
FVC (L)	3.10	2.01	2.88	2.59	2.96
FEV_1/FVC (%)		55	68	66	68

Preoperative treatment and evolution

Initial cefepime therapy had no effect on clinical and laboratory parameters. The patient was therefore switched to clarithromycin

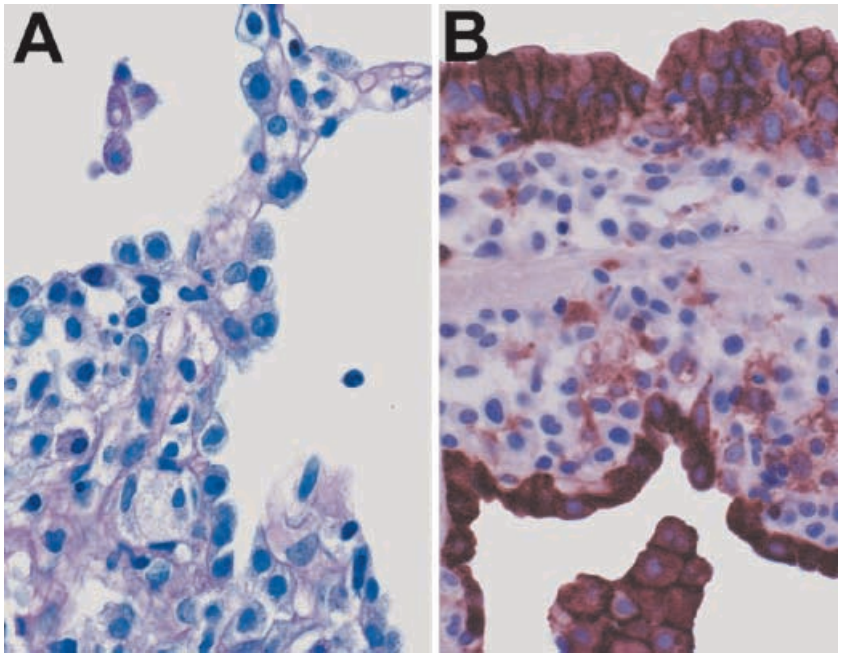


Fig. 4 **A** Predominantly lymphohistiocytic infiltrate of a bronchiolar wall encroaching upon neighboring alveolar septa. Note foam cells (Giemsa, 250×). **B** Overexpression of HLA-DR of macrophages and bronchiolar and alveolar epithelia (DAB/Mayer's hemalaun, 62.5×)

(3×500 mg/day) after 3 days. Laboratory tests 2 days later showed a further decrease of hemoglobin to 59 g/l, reticulocytosis, and a positive complement-specific antiglobulin test, all interpreted as signs of immunohemolysis. The presence of cold agglutinins suggested an infection with MP, but at the same time serological tests for MP, respiratory syncytial virus, adenovirus, influenza, *Coxiella*, *Chlamydia pneumoniae*, and *Legionella pneumophila* were negative. In view of the unfavorable course, open lung biopsy was performed. Histology (see below) was suggestive of diffuse panbronchiolitis or bronchiolitis due to *Mycoplasma*.

Pathologic findings

The cut surface of the lung specimen showed macroscopically fine, partly confluent whitish speckles, which corresponded to cross sections of bronchioli. Histologically, the bronchiolar lumina were obturated by debris, mucus-like material, neutrophils, and by $CD68^+$ macrophages showing a finely vacuolated cytoplasm (Fig. 2). The bronchiolar epithelium was partly destroyed or replaced by a layer of regenerative cells. No giant cells were seen. All bronchiolar and alveolar epithelia were strongly positive for HLA-DR $(LN3)^+$. Where the epithelium was destroyed, discrete fibroblast proliferation was seen. The bronchiolar walls were densely infiltrated. As shown by immunohistochemistry, the infiltrate consisted mainly of $CD3^+$ lymphocytes (35% of mononucleated cells) and $CD68^+$ macrophages (30%). There were also some scattered plasma cells and minor follicle-like spots of $CD20^+$ B-lymphocytes (Fig. 3). The T-lymphocytes were mostly $CD8^+$ (21%) intruding into the bronchiolar epithelium. The $CD4^+$ lymphocytes and macrophages were less than half as frequent as $CD8^+$ cells. $CD56^+$ and $CD57^+$ cytolytic lymphocytes were strikingly rare. The few plasma cells were mainly immunoglobulin A positive (IgA^+) and IgM^+, whereas IgG^+ plasma cells were extremely rare. $CD21^+$ and $S100^+$ dendritic cells were only sporadically seen within the bronchiolar walls. Forty percent (320/800) of nuclei within the bronchiolar wall tissue stained positive with MIB-1, indicating high proliferative activity of the lymphocytic cells. The peribronchiolar lymphocytes and foam cells were encroaching upon the septa of surrounding alveoli (Fig. 4a). Most foam cells were seen within the alveolar lumina, sometimes intermingled with granulocytes and debris. Most foam cells and all bronchiolar and alveolar epithelia showed an overexpression of HLA-DR (Fig. 4b). Necroses were absent.

Postoperative course

A second complement fixation test after 12 days was still not conclusive for MP or respiratory syncytial virus. In view of the histological findings and despite the unproven infectious etiology, treatment with clarithromycin for 10 days was started again in combination with 50 mg prednisone per day. The condition of the patient improved and she was discharged from the hospital. A follow-up examination on day 74 after the beginning of symptoms still showed a mild obstructive airway disorder (1). The complement fixation titer for MP was 1:10,240. At this time the prednisone was tapered gradually to 5 mg per day. On day 151 hemoglobin was normal and the antiglobulin test was negative, but arterial blood gases still showed a low pO_2 of 8.9 kPa and pulmonary function was still diminished as shown by tests FEV_1, FVC, and FEV_1/FVC(1), whereas the chest radiograph was normal. The titer of complement fixation test was again positive (1:5,120). At day 310 the patient was feeling well, although mild reversible airway obstruction still existed (1).

Materials and methods

The lung specimen measuring 3.5×2.5×1.0 cm was fixed in an unfolded state by infiltration with 4% formalin. Immunohistochemistry was done on 4-µm-thick paraffin sections. The following monoclonal antibodies were used: CD3/A0452(Dako), CD4, (Novocastra), CD8/M7103 (Dako), CD21/M0784 (Dako), CD56/CMA361 (Cell Marque), CD57/347390 (Becton Dickinson), CD68-KP1/M0814, CD68-PG-M_1/M876 (Dako), MIB-1/0505 (Immunotech), HLA-DR/812235 (Biotest). Additionally the following polyclonal antibodies were applied: S100/z311 (Dako), IgA, IgG, M/A0426, A0262, A0423 (Dako). The portion of stained/unstained mononuclear cells was assessed within two areas of bronchiolar wall by counting 400 cells per area at magnification 1000× to quantify the subtypes of lymphocytes and $CD68^+$ macrophages.

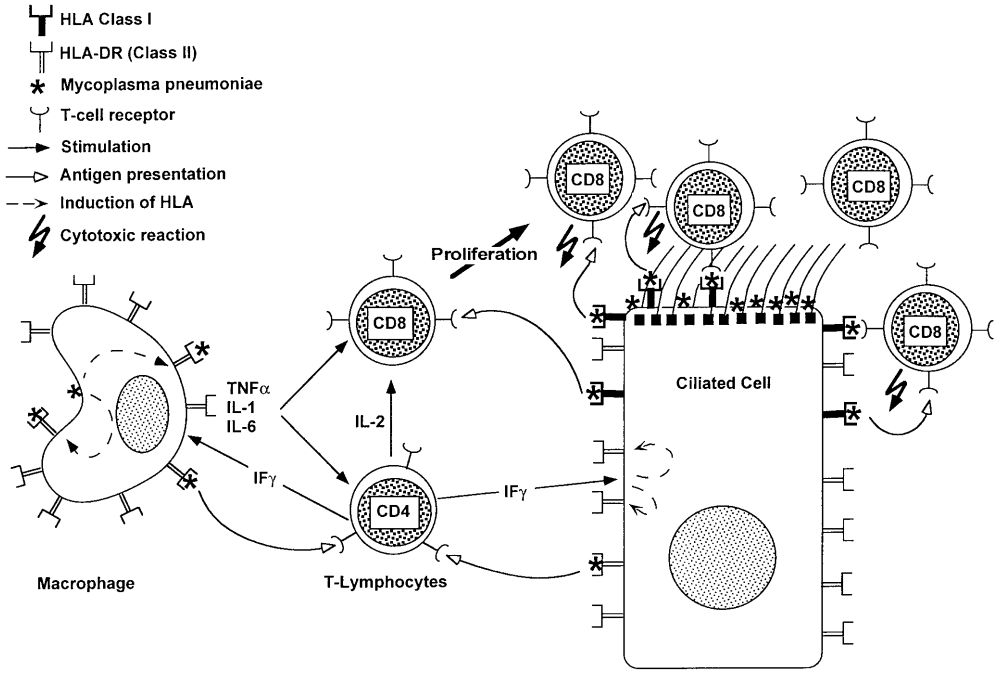


Fig. 5 Simplified delineation of the pathogenesis of MP bronchiolitis: Antigen (MP)-stimulated macrophages present antigen (MP) associated with HLA-class II (HLA-DR) molecules and release of tumor necrosis factor alpha (*TNFα*), interleukin 1 (*IL-1*) and interleukin 6 (*IL-6*). These cytokines stimulate T-cells. $CD4^+$ cells produce interferon gamma (*IFγ*) and interleukin 2 (*IL-2*), which induces proliferation of $CD8^+$ cells. Secretion of IFγ provokes HLA-DR-expression on surface of ciliated cells and macrophages. Ciliated cells present antigen (MP) in association with HLA-class I molecules. This leads to a cytotoxic reaction of stimulated $CD8^+$ cells against ciliated cells, while antigen presentation by ciliated cells in association with HLA-class II molecules stimulate $CD4^+$ cells in proliferation and cytokine release

Discussion

In this patient with bronchiolitis the first signs suggesting MP infection were high titers of cold hemagglutinins and hemolytic anemia, which are typical in mycoplasmal infection [16]. The initial lack of clinical response to macrolide therapy and the delayed rise of the complement fixation titer made open lung biopsy necessary. Lymphohistiocytic bronchiolitis was found.

Although lymphohistiocytic bronchiolitis has been observed in few humans with MP infection or in animals naturally or experimentally infected with various *Mycoplasma* species [9, 14, 19], the biopsy alone did not solve the diagnostic problem. Similar pathologic findings may also occur in several other disorders [11].

The cytogram of the bronchoalveolar lavage (BAL) fluid with raised neutrophils and lymphocytes reflected exactly the composition of the inflammatory infiltration of the bronchioli. Although the CD4/CD8 ratio of BAL lymphocytes could not be determined, immunohistochemistry showed that most lymphocytes within the bronchiolar tissue were of the $CD3^+$ type and that $CD8^+$ lymphocytes clearly outnumbered $CD4^+$ lymphocytes as seen in experimental Mycoplasma infection [13] and in several other forms of human bronchiolitis [7, 26]. The similarity of morphological features irrespective of the underlying disease may only indicate that bronchiolar lesions of different origin share a common pathway.

Mycoplasms are extracellular parasites with a high affinity for respiratory cells. As repeatedly shown, they attach to the surface of bronchiolar and alveolar epithelia [18] via a specific high molecular protein (P-1) that binds to neuraminic acid receptor sites at the cell surface [6]. The histological findings suggest that the ciliary cells are destroyed during MP infection and that the cellular debris is cleared by neutrophilic granulocytes and macrophages. The epithelia may directly be damaged by the organisms' secretion of toxic substances. The pronounced infiltration of the bronchiolar walls by T-lymphocytes, however, supports the hypothesis first suggested by Fernald [12] that immunological mechanisms may be mainly responsible for the development of MP bronchiolitis. The decisive role of T-cell mediated immunity is suggested by several observations: (1) High levels of circulating antibodies do not prevent recurrent disease in case of MP reinfection, in either humans or other animals [12, 21]. One study showed that more than two thirds of individuals developing MP lung infiltrates had antibodies before exposure to the organisms [1]. Moreover, vaccination does not prevent MP pneumonia [22]. (2) Immunosuppressed individuals rarely develop MP pneumonia [25]. Severe pulmonary lesions develop only in immunocompetent mice when inoculated with MP [21]. (3) In MP-infected mice the peribronchiolar and perivascular lymphohistiocytic infiltrate is exacerbated by interleukin (IL)-2 and reduced by cyclosporin A [23]. (4) MP bronchiolitis rapidly improves under corticosteroid therapy which suppresses mainly the T-lymphocytic reaction [4]. The suppression of the lymphocytic reaction

by corticosteroids probably favors the proliferation of the MP organisms and may prolong their presence on the epithelium for many weeks [3]. Their persistence here could explain why, as in our patient, an early withdrawal of the corticosteroid dose may provoke relapse.

The immunohistological findings suggest that the destruction of the epithelia is mainly mediated by actively proliferating cytotoxic $CD8^+$ T-cells, whereas $CD56^+$ or $CD57^+$ natural killer cells seem not to play a major role in the elimination of the organisms. HLA-DR expression by the epithelia is probably also a consequence of the stimulation of T-lymphocytes.

The immunologic reaction may be modulated by the specific properties of the mycoplasma organisms. They may evade the immune response of the host by a variation of surface-exposed membrane proteins resulting in a masking of some epitopes and demasking of others [5]. Why some individuals develop disease despite the presence of serum antibodies is not clear. The antibodies may have been induced by cross reactive antigens present in vegetables or bacteria [1], or they may not cover the whole antigenic spectrum of the organisms. Animal experiments [2] and observations in humans [10] have shown that humoral antibodies may prevent extrapulmonary colonization by MP, whereas cellular immune responses may be important in exacerbation of MP lung disease.

In conclusion, the histological and immunohistological findings in this case, together with observations of others, suggest that the pathogenesis and clinical presentation of mycoplasma bronchiolitis correspond to those of a non-cytopathogenic T-cell reaction stimulating agent [Fig. 5]. Individual factors responsible for delayed or insufficient humoral immune response and the special properties of the mycoplasma organism apparently play a role in the pathogenesis of MP-associated bronchiolitis.

References

1. Brunner H (1997) Models of mycoplasma respiratory and genital tract infections. Wien Klin Wochenschr 109:569–573
2. Cartner SC, Lindsey JR, Gibbs-Erwin J, Cassell GH, Simecka JW (1998) Roles of innate and adaptative immunity in respiratory mycoplasmosis. Infect Immun 66:3485–3491
3. Cassell GH, Lindsey JR, Baker HJ (1974) Immune response of pathogen-free mice inoculated intranasally with Mycoplasma pulmonis. J Immunol 112:124–136
4. Chan ED, Kalayanamit T, Lynch DA, Tuder R, Arndt P, Winn R, Schwarz MI (1999) Mycoplasma pneumoniae-associated bronchiolitis causing severe restrictive lung disease in adults: report of three cases and literature review. Chest 115:1188–1194
5. Citti C, Rosengarten R (1997) Mycoplasma genetic variation and its implication for pathogenesis. Wien Klin Wochenschr 109:562–568
6. Clyde WAJr, Hu PC (1984) Mycoplasma pneumoniae infections of man: integration of attachment mechanism, cellular responses and clinical manifestations. Ann Microbiol (Paris) 135A:125–128
7. Costabel U, Teschler H, Guzman J (1992) Bronchiolitis obliterans organizing pneumonia (BOOP): the cytological and immunocytological profile of bronchoalveolar lavage. Eur Respir J 5:791–797
8. Coultas DB, Samet JM, Butler C (1986) Bronchiolitis obliterans due to Mycoplasma pneumoniae. West J Med 144:471–474
9. Davis JK, Cassell GH (1982) Murine respiratory mycoplasmosis in LEW and F344 rats: strain differences in lesion severity. Vet Pathol 19:280–293
10. Doucet V, Bourliere-Najean B, Petit P, Panuel M, Faure F, Devred P (1998) Infection à Mycoplasma pneumoniae: présentation thoracique inhabituelle et localisaions osseuses. J Radiol 79:1398–1400
11. Ezri T, Kunichezky S, Eliraz A, Soroker D, Halperin D, Schattner A (1994) Bronchiolitis obliterans – current concepts. Q J Med 87:1–10
12. Fernald GW (1969) Immunologic aspects of experimental Mycoplasma pneumoniae infection. J Infect Dis 119:255–266
13. Gaunson JE, Philip CJ, Whithear KG, Browning GF (2000) Lymphocytic infiltration in the chicken trachea in response to Mycoplasma gallisepticum infection. Microbiology 146:1223–1229
14. Kirchner BK, Port CD, Magoc TJ, Sidor MA, Ruben Z (1990) Spontaneous bronchopneumonia in laboratory dogs infected with untyped Mycoplasma spp. Lab Anim Sci 40:625–628
15. Leong MA, Nachajon R, Ruchelli E, Allen JL (1997) Bronchitis obliterans due to Mycoplasma pneumonia. Pediatr Pulmonol 23:375–381
16. Lind K, Benzon MW, Skov Jensen J, Clyde WA (1997) A seroepidemiological study of Mycoplasma pneumoniae infections in Denmark over the 50-year period 1946–1995. Eur J Epidemiol 13:581–586
17. Mlczoch F, Witek F (1976) Miliary mycoplasmal pneumonia: a report of six cases. Infection 4:64–67
18. Penner JD, Jacobson ER, Brown DR, Adams HP, Besch-Williford CL (1997) A novel Mycoplasma sp. associated with proliferative tracheitis and pneumonia in a Burmese python (Python molurus bivittatus). J Comp Pathol 117:283–288
19. Rodriguez JL, Gutierrez C, Brooks DL, Damassa AJ, Oros J, Fernandez A (1998) A pathological and immunohistochemical study of goat kids undergoing septicaemic disease caused by Mycoplasma capricolum subsp. capricolum, Mycoplasma mycoides subsp. capri and Mycoplasma mycoides subsp. mycoides (large colony type). Zentralbl Veterinarmed [B] 45:141–149
20. Rollins S, Colby T, Clayton F (1986) Open lung biopsy in Mycoplasma pneumoniae pneumonia. Arch Pathol Lab Med 110:34–41
21. Sandstedt K, Berglof A, Feinstein R, Bolske G, Evengard B, Smith CI (1997) Differential susceptibility to Mycoplasma pulmonis intranasal infection in X-linked immunodeficient (xid), severe combined immunodeficient (scid), and immunocompetent mice. Clin Exp Immunol 108:490–496
22. Smith CB, Friedewald WT, Chonock RM (1967) Inactivated Mycoplasma pneumoniae vaccine; evaluation in volunteers. JAMA 199:103–108
23. Tanaka H, Honma S-I, Abe S, Tamura H (1996) Effects of interleukin-2 and cyclosporin A on pathologic features in mycoplasma pneumonia. Am J Respir Crit Care Med 154: 1908–1912
24. Taylor-Robinson D (1996) Infections due to species of Mycoplasma and ureoplasma: an update. Clin Infect Dis 23:671–686
25. Theile A, Karg O, Wex P, Muller KM (1994) Bronchiolitis obliterans nach Mycoplasmenpneumonie. Pneumologie 48:491–494
26. Tiroke AH, Bewig B, Haverich A (1999) Bronchoalveolar lavage in lung transplantation. State of the art. Clin Transplant 13:131–157

Virchows Arch (2001) 439:823–826
DOI 10.1007/s004280100517

CASE REPORT

Daniela Mihic-Probst · Jianming Zhao
Parvin Saremaslani · Angela Baer · Paul Komminoth
Philipp U. Heitz

Spitzoid malignant melanoma with lymph-node metastasis

Is a copy-number loss on chromosome 6q a marker of malignancy?

Received: 9 April 2001 / Accepted: 25 July 2001 / Published online: 5 September 2001
© Springer-Verlag 2001

Abstract Distinction of spitzoid malignant melanomas (SMM) from Spitz nevi may be difficult or even impossible on the basis of conventional histology. In this report, a patient suffering from a primary lesion diagnosed as a Spitz nevus and a metastatic malignant melanoma approximately 4 years thereafter is described. A diagnosis of SMM was made subsequently upon review of the primary lesion. In the present analysis, we used comparative genomic hybridization (CGH) to define markers characteristic of SMM. The primary lesion revealed deletions on chromosomes 6q and 9p. In the metastasis, additional deletions on chromosomes 10p and 10q and gains of chromosome 7 were found. To our knowledge, no chromosomal aberration on chromosome 6 was hitherto demonstrated in benign melanocytic nevi. Findings reported in the literature suggest that human melanoma metastasis suppressor gene maps to 6q. In contrast, losses on chromosome 9p seem to be an early event in the development of melanoma. However, they are not only found in melanomas but are occasionally present in Spitz nevi as well as in atypical nevi. The CGH result with deletion of 6q in this difficult to diagnose primary melanocytic lesion strongly supports the diagnosis of malignant melanoma. To demonstrate the reliability of loss on chromosome 6q as a marker of SMM, a larger number of lesions must be investigated.

Keywords Melanoma · Spitzoid malignant melanoma · Spitz nevus · Comparative genomic hybridization · Tumor suppressor gene

D. Mihic-Probst (✉) · J. Zhao · P. Saremaslani · A. Baer
P.U. Heitz
Department of Pathology, University Hospital,
Schmelzbergstrasse 12, 8091 Zürich, Switzerland
e-mail: daniela.mihic@pty.usz.ch
Tel.: +41-1-2552595, Fax: +41-1-2554397

P. Komminoth
Institute of Pathology, Cantonal Hospital, Baden, Switzerland

Introduction

Spitzoid malignant melanoma (SMM) is a rare form of malignant melanoma [21]. Its morphology closely resembles that of Spitz nevus. Correspondingly, histological distinction of SMM from Spitz nevus is difficult or even impossible on the basis of conventional histology [2, 19]. Spitz nevus is a benign lesion, while SMM is malignant. A reliable distinction of the two lesions is therefore relevant – however, it is notoriously difficult. Reliable criteria are therefore required for establishing a precise diagnosis of these lesions.

We tried to identify chromosomal markers that could help in discriminating SSM from Spitz nevus using the relatively simple and straightforward technique of comparative genomic hybridization (CGH). This technique allows an investigation of the entire genome, revealing chromosomal regions affected by copy number gains or losses. It has been widely used to analyze a variety of human tumors, including Spitz nevi [4, 9].

The purposes of this study were (i) to explore the molecular genetic background of SMM, (ii) to look for reliable diagnostic markers of malignancy at the genetic level, and (iii) to compare molecular damage of a primary SMM and its metastasis.

History of the patient

In 1999, a 16-year-old girl was found to have enlarged inguinal lymph nodes on the left side. A local excision was performed. Histological examination showed a large lymph-node metastasis of a poorly differentiated tumor with extranodal involvement and invasion of a perinodal vein.

The history of the patient revealed the occurrence of a tumor at the left ankle in 1996. This tumor had been diagnosed as Spitz nevus. Upon a histological review, we made the diagnosis of childhood SMM.

Materials and methods

Samples of the primary tumor and the metastasis were fixed in formaldehyde, embedded in paraffin, cut at 2 µm, and stained with

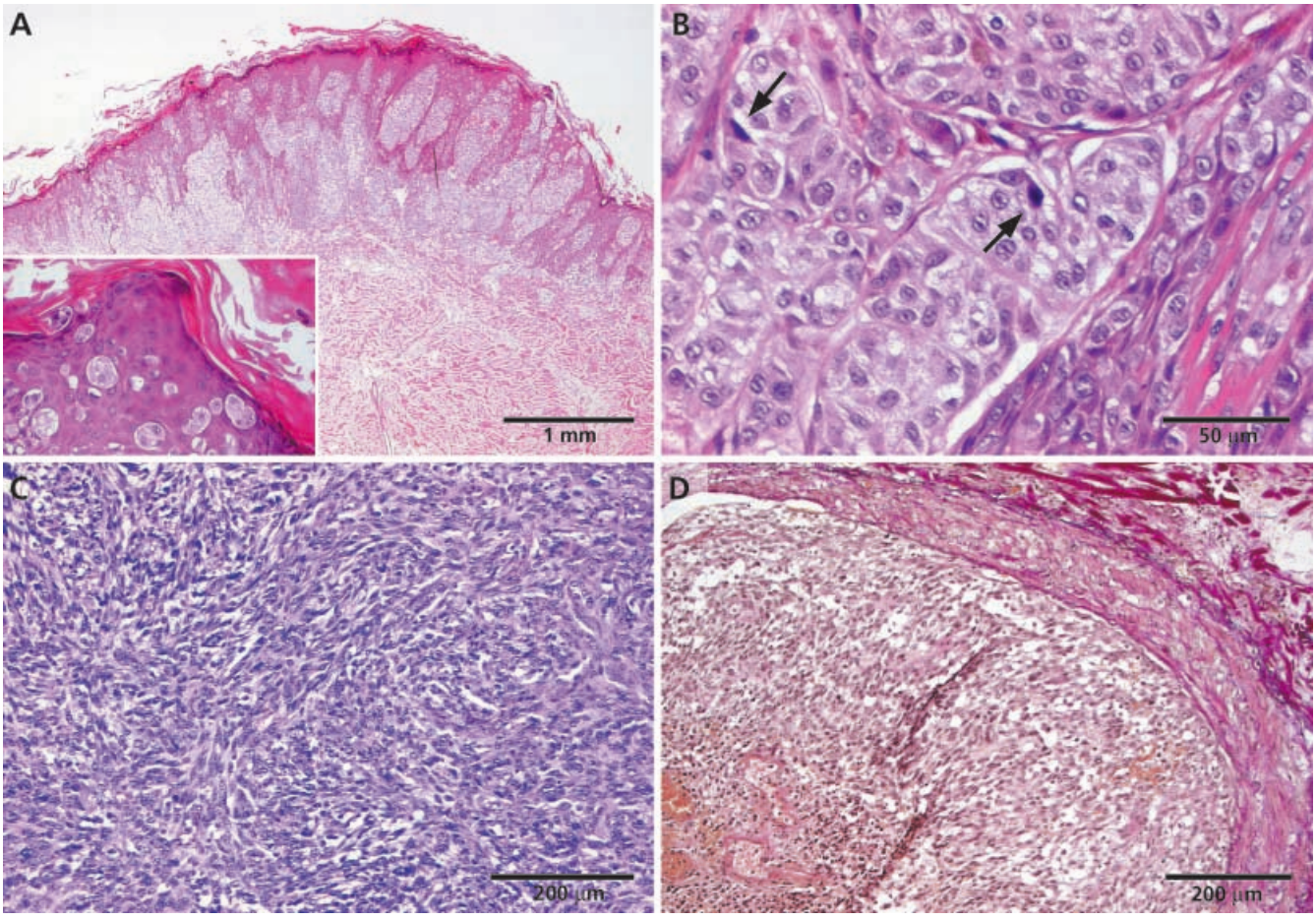


Fig. 1 Histology of the spitzoid malignant melanoma and its metastasis. **A** Slightly asymmetrical dome-shaped epidermal and dermal melanocytic lesion. Hyperplastic epidermis with pagetoid infiltration (*inset*). Hematoxylin-eosin ×17, inset ×125. **B** Spindle and epitheloid cells with mitotic figures. Hematoxylin-eosin ×350. **C** Lymph-node metastasis displaying an architecture resembling a malignant peripheral nerve sheath tumor. Hematoxylin-eosin ×100. **D** Tumor invasion of a perinodal vein. Elastin-van Gieson's stain ×90

hematoxylin-eosin. Immunohistochemical reactions were carried out on deparaffinized sections, using the Ventana NexES automated staining system (Ventana Medical Systems, Tucson, Ariz.), including appropriate positive and negative controls. For antigen retrieval, slides were heated in citrate buffer for 3 min, using a pressure cooker (except for neuron-specific enolase and melanoma-specific antigen). Primary antibodies against the following antigens were applied: S-100 protein (rabbit affinity-purified antibodies; dilution 1:500), synaptophysin (rabbit affinity-purified antibodies; dilution 1:150), neuron-specific enolase (clone BBS/NC/VI-H14; dilution 1:100), vimentin (clone 3B4; dilution 1:500) – all from Dako (Glostrup, Denmark) – and melanoma specific antigen (clone HMB45; dilution 1:50, Enzo Diagnostics, Farmingdale, N.Y.). Peroxidase was detected using diaminobenzidine or alkaline phosphatase with new fuchsin as substrates. Slides were counterstained with hemalum.

DNA preparation for CGH

Paraffin embedded tissue (10-µm-thick sections) were cut and placed on glass slides. An area of interest was microdissected without deparaffinizing. Microdissection was carried out manually under a light microscope. Twenty sections were used, and regions with a high density of tumor cells were separated from normal cells. The percentage of tumor cells was at least 80%. The dissected tumor parts were collected in tubes and deparaffinized by washing with xylene and ethanol.

Genomic DNA was isolated as described previously [22]. Direct fluorescence labeling of DNA was performed by nick translation using a commercial kit (BioNick kit, Life Technologies, Gaithersburg, Md.).

CGH analysis

CGH was performed as described previously [22]. The hybridization mixture consisted of 200–400 ng spectrum green-labeled tumor DNA, 200 ng spectrum red-labeled normal reference DNA, and 10 µg unlabeled human Cot-1 DNA dissolved in 10 µl hybridization buffer (50% formamide, 10% dextran sulfate, 2× sodium saline citrate, pH 7.0). Hybridization took place over 3 days at 37°C to sex-matched normal metaphase spreads (Vysis, Downer Grove, Ill.). Digital images were collected from six to seven metaphases using a cooled charge-coupled device (CCD) camera (Microimager 1400, Xillix Technologies, Vancouver, British Columbia, Canada). The software program QUIPS (Vysis) was used to calculate average green to red ratio profiles for each chromosome. At least five observations per autosome and three observations per sex chromosome were included in each analysis.

Thresholds used for definition of DNA sequence copy-number gains and losses were based on the results of CGH analyses of normal tissues. A gain of DNA sequences was assumed at chromosomal regions where the hybridization resulted in a green to red ratio of 1.2 or greater. Over-representations were considered amplifications if fluorescence ratio values exceeded 1.5 or greater in a subregion of a chromosome arm. A loss of DNA se-

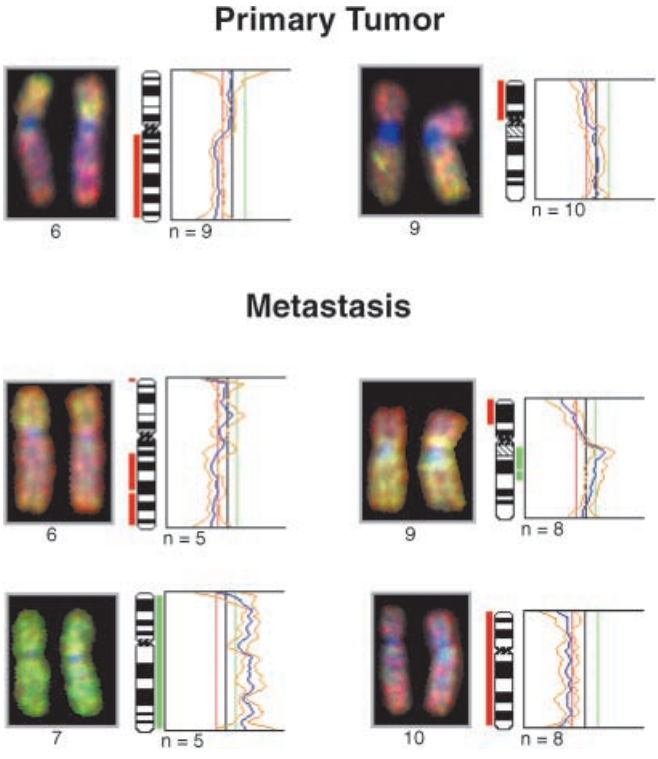


Fig. 2 Representative comparative genomic hybridization digital images and corresponding profiles illustrating losses on chromosome 6q and 9p in the primary tumor. Metastasis with the same chromosomal aberrations and additional gains of chromosome 7 and losses of chromosome 10. Tumor DNA was labeled using green dUTP and normal reference DNA with red dUTP. The color ratio values 0.8, 1.2, and 1.5 were used as thresholds for chromosomal losses, gains, and amplifications, respectively

quences was presumed at chromosomal regions where the tumor to normal ratio was 0.8 or less. Since some false-positive results were found in normal tissues at chromosomes 1p, 16p, 19, and 22, gains at these G–C-rich regions were excluded from all analyses.

Results

Histology and immunohistochemistry

At histology, the primary tumor consisted of a slightly asymmetrical dome-shaped epidermal and dermal melanocytic lesion composed of large spindle and epitheloid cells, displaying a prominent pagetoid pattern. The epidermis was hyperplastic. The mitotic rate was 7/mm^2. Mitoses were also found in deeper parts of the lesion (Fig. 1).

The metastasis was composed of spindle and epitheloid cells. The mitotic rate was 5/mm^2. The architecture resembled that of a malignant peripheral nerve sheath tumor (Fig. 1). Immunohistochemistry showed a strong reaction for vimentin and S-100 protein. The results of immunostaining for HMB 45 and synaptophysin were negative.

Comparative genomic hybridization

CGH analysis of the primary tumor revealed losses on chromosomes 6q and 9p. In the metastasis, the same chromosomal aberrations and additional losses on chromosome 10 as well as gains of chromosome 7 were found (Fig. 2).

Discussion

To our knowledge, this is the first report dealing with CGH analysis of SSM. The finding of chromosomal loss on chromosome 6q in SMM is interesting, as no chromosomal aberrations on chromosome 6 in benign melanocytic lesions, atypical nevi, or Spitz nevi have been demonstrated to date [4, 7]. By contrast, in cutaneous melanoma, analyses using CGH or loss of heterozygosity (LOH) have shown deletions involving 6q in 28% [3], in 40% [14], and in 31% [7]. In addition, translocations and/or deletions involving 6q have been found in over 80% of melanomas at a later stage, i.e., metastatic disease [20]. These results parallel those obtained in CGH studies of uveal melanomas (6q:26%) [15]. One study compared primary nonmetastasizing with metastasizing uveal tumors, and metastasis thereof. Deletions on 6q were found in 7%, 40%, and 83%, respectively. They were associated with poor overall survival [1]. Previously published data suggest that, in human melanoma, a metastasis tumor suppressor locus maps to 6q16.3-q23 [10, 11, 13]. Genes on chromosome 6q appear therefore to be involved in the progression of malignant melanoma.

Our finding of chromosome 10 deletion in the metastasis in contrast to the primary melanoma is surprising, because the deletion on 10q has been found in between 30% and over 60% of primary sporadic melanomas [3, 7, 8, 18]. A role of the 10q deletion in tumor progression is however conceivable since additional germline mutations in the PTEN gene (on chromosome 10q23) have been shown to be present in Crowden's disease [12]. A recent study [17] underlines that mutations of PTEN are not an essential early event in the onset of sporadic malignant melanoma, but could exert an important impact on tumor progression.

Our finding of chromosomal aberrations of 6q, 9p, 10q, 10p, 7q, and 7p in the metastasis is in agreement with cytogenetic studies of metastatic melanoma [20]. In a previous study of 17 Spitz nevi, using CGH analysis, 13 lesions did not show any chromosomal aberrations [4]. Three of four additional lesions with chromosomal aberrations involved chromosome 11, and one lesion showed aberrations on chromosome 7. In another study using LOH, only 2 of 27 Spitz nevi showed interstitial deletions on chromosome 9p. Two of 32 benign melanocytic nevi with atypical histological features demonstrated genetic alterations: loss in chromosome 9p and allelic losses at 8p, 11q and 12p and additional band shifts at multiple loci respectively [7].

One gene among currently characterized melanoma loci resides on chromosome 9p and encodes a tumor sup-

pressor designated p16 [5, 16]. This gene is either mutated or deleted in the large majority of melanoma cell lines, as well as in many in vivo melanoma cells and in the germ line of melanoma kindreds. The p16 locus encodes for two separate gene products transcribed in alternative reading frames. Both products function as negative regulators of cell cycle progression. Inherited and acquired deletions or point mutations in the p16 gene increase the probability of escape to repair of potentially mutagenic DNA damage prior to cell division.

As mentioned above, losses of chromosome 9p are not only found in melanomas but are occasionally present in Spitz nevi [7] and in atypical nevi (sometimes classified as dysplastic nevi) [6]. Changes in chromosome 9 appear to be a very early event in melanoma formation.

Experimental data suggest that loss on chromosome 6q strongly supports the diagnosis of malignant melanoma [10, 11, 13]. In the presented difficult to diagnose SMM of a very young person, our finding of loss on chromosome 6q would therefore have strongly supported the diagnosis of malignancy, i.e., CGH analysis would have been a useful additional diagnostic procedure.

Loss on chromosome 6q as detected by CGH is possibly a reliable marker to differentiate between SMM and Spitz nevus. It will however be necessary to investigate a larger number of SMM cases in order to support this hypothesis, to answer the question whether this loss of genetic material is an early event during progression of melanoma, and to define more precisely the genetic defect.

Acknowledgements We thank Prof. H.J. Altermatt, Private Institute for Pathology, Bern, and Dr. Ch. Sigg, Private Institute for Dermatohistology, Zürich, for supplying the tumor tissue. We are grateful to N. Wey for photographic and computer-assisted reproductions.

References

1. Aalto Y, Eriksson L, Seregard S, Larsson O, Knuutila S (2001) Concomitant loss of chromosome 3 and whole arm losses and gains of chromosome 1, 6, or 8 in metastasizing primary uveal melanoma. Invest Ophthalmol Vis Sci 42:313–317
2. Barnhill RL, Argenyi ZB, From L, Glass LF, Maize JC, Mihm MC, Jr., Rabkin MS, Ronan SG, White WL, Piepkorn M (1999) Atypical Spitz nevi/tumors: lack of consensus for diagnosis, discrimination from melanoma, and prediction of outcome. Hum Pathol 30:513–520
3. Bastian BC, LeBoit PE, Hamm H, Brocker EB, Pinkel D (1998) Chromosomal gains and losses in primary cutaneous melanomas detected by comparative genomic hybridization. Cancer Res 58:2170–2175
4. Bastian BC, Wesselmann U, Pinkel D, Leboit PE (1999) Molecular cytogenetic analysis of Spitz nevi shows clear differences to melanoma. J Invest Dermatol 113:1065–1069
5. Cannon-Albright LA, Goldgar DE, Meyer LJ, Lewis CM, Anderson DE, Fountain JW, Hegi ME, Wiseman RW, Petty EM, Bale AE, et al. (1992) Assignment of a locus for familial melanoma, MLM, to chromosome 9p13-p22. Science 258: 1148–1152
6. Cowan JM, Halaban R, Francke U (1988) Cytogenetic analysis of melanocytes from premalignant nevi and melanomas. J Natl Cancer Inst 80:1159–1164
7. Healy E, Belgaid CE, Takata M, Vahlquist A, Rehman I, Rigby H, Rees JL (1996) Allelotypes of primary cutaneous melanoma and benign melanocytic nevi. Cancer Res 56:589–593
8. Herbst RA, Weiss J, Ehnis A, Cavenee WK, Arden KC (1994) Loss of heterozygosity for 10q22–10qter in malignant melanoma progression. Cancer Res 54:3111–3114
9. Kallioniemi A, Kallioniemi OP, Sudar D, Rutovitz D, Gray JW, Waldman F, Pinkel D (1992) Comparative genomic hybridization for molecular cytogenetic analysis of solid tumors. Science 258:818–821
10. Lee JH, Welch DR (1997) Identification of highly expressed genes in metastasis-suppressed chromosome 6/human malignant melanoma hybrid cells using subtractive hybridization and differential display. Int J Cancer 71:1035–1044
11. Lee JH, Miele ME, Hicks DJ, Phillips KK, Trent JM, Weissman BE, Welch DR (1996) KiSS-1, a novel human malignant melanoma metastasis-suppressor gene. J Natl Cancer Inst 88:1731–1737
12. Liaw D, Marsh DJ, Li J, Dahia PL, Wang SI, Zheng Z, Bose S, Call KM, Tsou HC, Peacocke M, Eng C, Parsons R (1997) Germline mutations of the PTEN gene in Cowden disease, an inherited breast and thyroid cancer syndrome. Nat Genet 16:64–67
13. Miele ME, Jewett MD, Goldberg SF, Hyatt DL, Morelli C, Gualandi F, Rimessi P, Hicks DJ, Weissman BE, Barbanti-Brodano G, Welch DR (2000) A human melanoma metastasis-suppressor locus maps to 6q16.3-q23. Int J Cancer 86:524–528
14. Millikin D, Meese E, Vogelstein B, Witkowski C, Trent J (1991) Loss of heterozygosity for loci on the long arm of chromosome 6 in human malignant melanoma. Cancer Res 51: 5449–5453
15. Naus NC, van Drunen E, de Klein A, Luyten GP, Paridaens DA, Alers JC, Ksander BR, Beverloo HB, Slater RM (2001) Characterization of complex chromosomal abnormalities in uveal melanoma by fluorescence in situ hybridization, spectral karyotyping, and comparative genomic hybridization. Genes Chromosomes Cancer 30:267–273
16. Piepkorn M (2000) Melanoma genetics: an update with focus on the CDKN2A(p16)/ARF tumor suppressors. J Am Acad Dermatol 42:705–722 (quiz 723–726)
17. Poetsch M, Dittberner T, Woenckhaus C (2001) PTEN/MMAC1 in malignant melanoma and its importance for tumor progression. Cancer Genet Cytogenet 125:21–26
18. Reifenberger J, Wolter M, Bostrom J, Buschges R, Schulte KW, Megahed M, Ruzicka T, Reifenberger G (2000) Allelic losses on chromosome arm 10q and mutation of the PTEN (MMAC1) tumour suppressor gene in primary and metastatic malignant melanomas. Virchows Arch 436:487–493
19. Spatz A, Ruiter D, Hardmeier T, Renard N, Wechsler J, Bailly C, Avril MF, Kwee H, Bastian BC, Hill C, De Potter C, Prade M (1996) Melanoma in childhood: an EORTC-MCG multicenter study on the clinico-pathological aspects. Int J Cancer 68:317–324
20. Thompson FH, Emerson J, Olson S, Weinstein R, Leavitt SA, Leong SP, Emerson S, Trent JM, Nelson MA, Salmon SE, et al. (1995) Cytogenetics of 158 patients with regional or disseminated melanoma. Subset analysis of near-diploid and simple karyotypes. Cancer Genet Cytogenet 83:93–104
21. Walsh N, Crotty K, Palmer A, McCarthy S (1998) Spitz nevus versus spitzoid malignant melanoma: an evaluation of the current distinguishing histopathologic criteria. Hum Pathol 29: 1105–1112
22. Zhao J, Richter J, Wagner U, Roth B, Schraml P, Zellweger T, Ackermann D, Schmid U, Moch H, Mihatsch MJ, Gasser TC, Sauter G (1999) Chromosomal imbalances in noninvasive papillary bladder neoplasms (pTa). Cancer Res 59:4658–4661